



## Comprehensive Organometallic Chemistry III

Elsevier, 2007

### Volume 4: Compounds of Groups 3 to 5 and the f elements

- 4.01 Complexes of Group 3 and Lanthanide Elements**, Pages 1-190, F.T. Edelmann
- 4.02 Complexes of Actinide Elements**, Pages 191-242, F.T. Edelmann
- 4.03 Complexes of Titanium in Oxidation States 0 to II**, Pages 243-279, P.J. Chirik and M.W. Bouwkamp
- 4.04 Complexes of Titanium in Oxidation State III**, Pages 281-322, P. Mountford and N. Hazari
- 4.05 Complexes of Titanium in Oxidation State IV**, Pages 323-695, T. Cuenca
- 4.06 Complexes of Zirconium and Hafnium in Oxidation States 0 to II**, Pages 697-739, P.J. Chirik and C.A. Bradley
- 4.07 Complexes of Zirconium and Hafnium in Oxidation State III**, Pages 741-757, S.J. Lancaster
- 4.08 Complexes of Zirconium and Hafnium in Oxidation State IV**, Pages 759-1004, E.Y.-X. Chen and A. Rodriguez-Delgado
- 4.09 Olefin Polymerizations with Group IV Metal Catalysts**, Pages 1005-1166, L. Resconi, J.C. Chadwick and L. Cavallo

# 4.01

## Complexes of Group 3 and Lanthanide Elements

---

F T Edelmann, Otto-von-Guericke-Universität Magdeburg, Magdeburg, Germany

© 2007 Elsevier Ltd. All rights reserved.

<b>4.01.1</b>	<b>Introduction</b>	<b>2</b>
<b>4.01.2</b>	<b>Carbonyls</b>	<b>3</b>
<b>4.01.3</b>	<b>Hydrocarbyls</b>	<b>4</b>
4.01.3.1	Neutral Homoleptic Compounds	4
4.01.3.2	Anionic Homoleptic Compounds	7
4.01.3.3	Heteroleptic Compounds	7
<b>4.01.4</b>	<b>Alkenyl and Alkynyl Compounds</b>	<b>17</b>
<b>4.01.5</b>	<b>Allyls</b>	<b>19</b>
<b>4.01.6</b>	<b>Cyclopentadienyl Compounds</b>	<b>21</b>
4.01.6.1	CpLnX Compounds	21
4.01.6.2	Cp <sub>2</sub> Ln Compounds	25
4.01.6.2.1	Synthesis	25
4.01.6.3	CpLnX <sub>2</sub> Compounds	29
4.01.6.4	Cp <sub>2</sub> LnX Compounds	41
4.01.6.4.1	Cp <sub>2</sub> LnX compounds with X = halide	42
4.01.6.4.2	Cp <sub>2</sub> LnX compounds with C and OH ligands	45
4.01.6.4.3	Cp <sub>2</sub> LnX compounds with chelating Cp ligands	46
4.01.6.4.4	Cp <sub>2</sub> LnX compounds with alkoxide, carboxylate, and related ligands	49
4.01.6.4.5	Cp <sub>2</sub> LnX compounds with amide and related N-donor ligands	52
4.01.6.4.6	Cp <sub>2</sub> LnX compounds with P ligands	55
4.01.6.4.7	Cp <sub>2</sub> LnX compounds with alkyl and silyl ligands	56
4.01.6.4.8	Cp <sub>2</sub> LnX compounds with borohydride and hydride ligands	57
4.01.6.5	Cp <sub>3</sub> Ln Compounds	58
4.01.6.6	Cp <sub>3</sub> LnL and Cp <sub>3</sub> LnL <sub>2</sub> Compounds	60
4.01.6.7	Cp <sub>3</sub> LnX Compounds	61
4.01.6.8	Pentamethylcyclopentadienyl Compounds	62
4.01.6.8.1	Cp <sup>+</sup> MX compounds	62
4.01.6.8.2	Cp <sup>+</sup> <sub>2</sub> M compounds	63
4.01.6.8.3	Mono(pentamethylcyclopentadienyl)lanthanide(III) compounds	66
4.01.6.8.4	Bis(pentamethylcyclopentadienyl)lanthanide(III) compounds	69
4.01.6.8.5	Tris(pentamethylcyclopentadienyl)lanthanide(III) compounds	81
4.01.6.9	Compounds with Ring-bridged Cyclopentadienyl Ligands	83
4.01.6.9.1	Lanthanide(II) compounds	83
4.01.6.9.2	Lanthanide(III) compounds	84
4.01.6.10	Indenyl and Fluorenyl Compounds	91
4.01.6.10.1	Lanthanide(II) compounds	91
4.01.6.10.2	Lanthanide(III) compounds	95
4.01.6.10.3	ansa-Indenyl and fluorenyl compounds	100
<b>4.01.7</b>	<b>Cyclopentadienyl-Like Compounds</b>	<b>105</b>
4.01.7.1	Compounds with Heteroatom Five-membered Ring Ligands	106
4.01.7.2	Compounds with Carboranyl Ligands	110

<b>4.01.8 Arene Complexes</b>	<b>118</b>
<b>4.01.9 Cycloheptatrienyl Compounds</b>	<b>122</b>
<b>4.01.10 Cyclooctatetraenyl Compounds</b>	<b>122</b>
4.01.10.1 Cyclooctatetraenyl Lanthanide(II) Compounds	122
4.01.10.2 Mono(cyclooctatetraenyl) Lanthanide(III) Compounds	124
4.01.10.3 Bis(cyclooctatetraenyl) Lanthanide(III) Compounds	129
4.01.10.4 Bis(cyclooctatetraenyl)cerium Compounds ("Cerocenes")	130
<b>4.01.11 Metallofullerenes</b>	<b>130</b>
<b>4.01.12 Heterobimetallic Compounds</b>	<b>131</b>
4.01.12.1 Metal–Metal Bonded Compounds	131
4.01.12.2 Heterobimetallic Compounds without Direct Metal–Metal Bonds	131
<b>4.01.13 Organolanthanide Catalysis</b>	<b>136</b>
4.01.13.1 Organolanthanide-catalyzed Hydrogenation Reactions	136
4.01.13.2 Organolanthanide-catalyzed Oligomerization Reactions	137
4.01.13.3 Organolanthanide-catalyzed Cyclization Reactions	138
4.01.13.4 Organolanthanide-catalyzed Polymerization Reactions	138
4.01.13.4.1 Reviews	138
4.01.13.4.2 Monoolefins	138
4.01.13.4.3 Diene polymerization	144
4.01.13.4.4 Ring-opening polymerization of cyclic esters and amides	145
4.01.13.4.5 Polymerization of acrylic monomers	147
4.01.13.4.6 Other monomers (isocyanates, stannanes, etc.)	152
4.01.13.5 Organolanthanide-catalyzed Hydroboration Reactions	152
4.01.13.6 Organolanthanide-catalyzed Hydrosilylation Reactions	153
4.01.13.7 Organolanthanide-catalyzed Hydroamination Reactions	155
4.01.13.8 Other Organolanthanide-catalyzed Reactions	160
<b>4.01.14 Organolanthanides in Organic Synthesis</b>	<b>163</b>
<b>4.01.15 Organolanthanides in Materials Science</b>	<b>173</b>
<b>References</b>	<b>173</b>

## 4.01.1 Introduction

This chapter summarizes the progress in organolanthanide chemistry during the period 1993–2005. Earlier developments in this area from the beginning of organolanthanide chemistry in 1954, when Birmingham and Wilkinson discovered the tris(cyclopentadienyl)lanthanide complexes  $\text{Cp}_3\text{Ln}$ ,<sup>1</sup> have been fully outlined in COMC (1982) and COMC-II (1995).<sup>2,3</sup> The sections in this chapter are subdivided according to ligand types, while the last three sections are devoted to organolanthanide catalysis, and the use of organolanthanide complexes in organic synthesis and materials science. Several review articles on different aspects of organolanthanide chemistry have been published since 1993. An overview on the progress in this area can be found in the annual reviews published regularly in *Coordination Chemistry Reviews*.<sup>4–11</sup>

In addition to reviews presenting a general survey of organolanthanide chemistry, several review articles on special aspects involving organolanthanide complexes have also been published since 1993. Schumann *et al.* reviewed organometallic  $\pi$ -complexes of scandium, yttrium, and lanthanides in the oxidation state  $\text{Ln}^{3+}$  with aromatic ligands.<sup>12</sup> The review focused on the most successful methods for preparation of the compounds and their molecular structures. Organometallic complexes of rare earth metals with cyclopentadienyl, cyclooctatetraenyl, indenyl, fluorenyl, and other aromatic  $\pi$ -ligands were considered in the review.<sup>12,13,13a</sup> Evans described an approach of ancillary ligand sets via heterometallic stabilization as alternative to the bis(pentamethylcyclopentadienyl) coordination in organometallic lanthanide chemistry. The purpose of the review article was to encourage development of new non-cyclopentadienyl ligand environments for yttrium and lanthanides.<sup>14</sup> In 1996 Deacon published a review on complexes of lanthanides

with neutral  $\pi$ -donor ligands. The synthesis, structures, and reactions of lanthanide complexes with alkenes, alkynes, and arenes have been described. Whilst the discussion focused on neutral  $\pi$ -donors, including intramolecular  $\pi$ -arene–lanthanide bonding, some formal  $[\text{Sm}^{\text{III}}\text{Cp}^*_2(\pi\text{-donor})^-]$  complexes, derived from  $\text{SmCp}^*_2$  and neutral  $\pi$ -donors, have been included, especially examples which readily dissociate into the reactants.<sup>15</sup> Edelmann published a review on rare earth cyclooctatetraenyl complexes. Various types of mono- and bis( $\eta^8$ -cyclooctatetraenyl)lanthanide complexes with metals in formal 2+, 3+, and 4+ oxidation states were considered. Synthesis, reactivity, and structural aspects of the compounds were discussed in detail.<sup>16</sup> Mikami reviewed “Asymmetric catalysis with lanthanide complexes,” including organometallic catalysts.<sup>17,17a</sup> Researches on non-classical organolanthanide chemistry have been highlighted by Lappert *et al.* in 2003.<sup>18</sup> A review entitled: “Product class 12: organometallic complexes of scandium, yttrium and the lanthanides” was published by Hou and Wakatsuki in 2003.<sup>19</sup>

In 2002 both *Chemical Reviews* (*Frontiers in Lanthanide Chemistry*)<sup>20</sup> and the *Journal of Organometallic Chemistry* published special issues devoted to (organo)lanthanide chemistry. Thus, various important special aspects of organolanthanide chemistry have been covered recently in excellent review articles. Among the topics were “Chiral lanthanide complexes: coordination chemistry and applications” (Aspinall),<sup>21</sup> “Synthesis, arrangement, and reactivity of arene–lanthanide compounds” (Bochkarev),<sup>22</sup> “Bis(pentafluorophenyl)mercury – a versatile synthon in organo-, organooxo-, and organoamido–lanthanoid chemistry” (Deacon *et al.*),<sup>23</sup> “Synthesis and structural chemistry of non-cyclopentadienyl organolanthanide complexes” (Edelmann *et al.*),<sup>24</sup> “Chemistry of tris(pentamethylcyclopentadienyl) *f*-element complexes, ( $\text{C}_5\text{Me}_5$ )<sub>3</sub>M” (Evans and Davis),<sup>25</sup> “The expansion of divalent organolanthanide reduction chemistry via new molecular divalent complexes and sterically induced reduction reactivity of trivalent complexes” (Evans),<sup>26</sup> “Recent advances in *f*-element reduction chemistry” (Evans),<sup>27</sup> “DFT studies of some structures and reactions of lanthanides complexes” (Eisenstein and Maron),<sup>28</sup> “[ $(\text{Tp}^{\text{tBu,Me}}\text{Yb}(\mu\text{-H}))_2$ : a fecund precursor to a host of divalent, hydrotris(pyr-azolyl)borate supported *f*-element complexes” (Ferrence and Takats),<sup>29</sup> “Lanthanide(II) complexes bearing mixed linked and unlinked cyclopentadienyl – monodentate-anionic ligands” (Hou and Wakatsuki),<sup>30</sup> “Asymmetric catalysis and amplification with chiral lanthanide complexes” (Inanaga *et al.*),<sup>31</sup> “A new era in divalent organolanthanide chemistry?” (Izod),<sup>32,33</sup> “Aspects of non-classical organolanthanide chemistry” (Lappert *et al.*),<sup>34</sup> “Organolanthanide chemistry in the gas phase” (Marçalo and Pires de Matos),<sup>35</sup> “Chemistry of the lanthanides using pyrazolylborate ligands” (Marques *et al.*),<sup>36</sup> “Lanthanocene catalysts in selective organic synthesis” (Molander and Romero),<sup>37</sup> “Mono(cyclopentadienyl) complexes of the rare-earth metals” (Okuda and Arndt),<sup>38</sup> “Organolanthanides  $\text{RLnX}$  ( $\text{R}$  = alkyl, aryl,  $\text{X}$  = halogen) and lanthanide complexes with aromatic hydrocarbon dianions: synthesis, structure, and reactivity” (Petrov *et al.*),<sup>39</sup> “Intramolecular coordination of  $\text{Ln-O}$  and  $\text{Ln-N}$  bonds in some new substituted lanthanocene complexes” (Qian and Huang),<sup>40</sup> “Synthesis, structural characterization and catalytic behavior of one-atom bridged fluorenyl cyclopentadienyl lanthanocene complexes with  $\text{C}_s$ - or  $\text{C}_1$ -symmetry” (Qian *et al.*),<sup>41</sup> “Synthesis and reactivity of organolanthanoid complexes containing N and S ligands” (Shen and Yao),<sup>42</sup> “Organo-rare-earth-metal initiated living polymerizations of polar and nonpolar monomers” (Yasuda),<sup>43</sup> and “Insertions into lanthanide–ligand bonds in organolanthanide chemistry” (Zhou and Zhu).<sup>44</sup>

#### 4.01.2 Carbonyls

Isolable binary lanthanide carbonyls remained elusive until now (several complexes of the type  $\text{Cp}_2\text{Ln}(\text{CO})$  have been reported, cf. Section 4.01.6.2). Thus, most of the work in this area is of theoretical nature or deals with highly unstable intermediates. A comparative density functional study on metal–ligand ( $\text{M-L}$ ) interaction has been performed on  $\text{X}_3\text{Ln}(\text{CO})$  ( $\text{X} = \text{F}, \text{I}$ ;  $\text{Ln} = \text{La}, \text{Nd}$ ) species including scalar relativistic effects by means of the zero-order regular approximation (ZORA) Hamiltonian. The role of the halogen atoms in modeling the  $\text{M-L}$  interactions has been discussed for the  $\pi$ -ligand CO.<sup>45,46</sup> The characterization of the structure and the spectra of holmium complexes formed in a CO matrix have been reported. The equilibrium geometry configurations and high-frequency IR spectra for the complex  $\text{HoCO}$  were characterized by *ab initio* quantum chemical calculations.<sup>47</sup> The geometry, electronic structure, and bonding of  $\text{LaCO}$  have been studied with SCM-DV- $\text{X}_a$  methods. From the results it was certified that  $\text{LaCO}$  is a linear molecule, in which the bond lengths of  $\text{La-C}$  and  $\text{C-O}$  are 2.273 Å and 1.179 Å, respectively, and that a  $\sigma$ -coordinated bond and a  $\pi$ -back bond are formed between La and CO. It was also shown that the  $\text{La-C}$  bond has more than about 90% covalent character and the 4*f* orbitals play a certain role in the bonding of  $\text{LaCO}$ .<sup>48</sup> The equilibrium geometry for the low-lying high-spin electronic state of  $\text{ScCO}$  was studied with the *ab initio* method. Restricted Hartree–Fock, multireference configuration interactions, and perturbation calculations were performed by employing flexible basis sets. The equilibrium geometry of the  $\text{ScCO}$  molecule was found to be linear.<sup>49–51</sup> Reactions of neutral, ground-state yttrium atoms with formaldehyde, acetaldehyde, and acetone ( $\text{Y} + \text{RR}^1\text{CO}$ , where  $\text{R}, \text{R}^1 = \text{H}, \text{Me}$ )



were studied in crossed molecular beams, and carbonyl species of the type  $(R)(R^1)Y(CO)$  and  $YCO$  have been discussed.<sup>52,53</sup> The interaction between La, Gd, or Lu atoms and carbon monoxide has been studied by means of the density functional method with gradient correction and quasi-relativistic correction. Three linkage isomers,  $Ln-CO$ ,  $Ln-OC$ , and  $Ln-(\eta^2-CO)$  have been obtained through full geometric optimization. The vibrational frequencies and the dissociation energies for decomposition into  $Ln$  atoms and  $CO$  have been calculated.<sup>54</sup> In a related study, the reaction of ground-state  $Y$  atoms with ketene ( $H_2CCO$ ) with the formation of  $YCH_2$ ,  $YCCO$ , and  $YCHCO$  has been investigated.<sup>55</sup> The structure, binding energy, and vibrational frequencies have been determined for  $ScCO_2^+$ . The inserted  $OSc^+CO$  structure in the  $^1A'$  state is the most stable isomer and lies  $43.2 \text{ kcal mol}^{-1}$  below the ground-state  $Sc^+ + CO_2$  asymptote. The stability of the insertion product arises from the very strong  $MO^+$  bond that is formed.<sup>56,57</sup>

### 4.01.3 Hydrocarbyls

Whereas complexes of unsubstituted and substituted cyclopentadienyl ligands represent the vast majority of all published compounds in organolanthanide chemistry, examples of isolated and fully characterized (including X-ray structural analyses) compounds containing only  $\sigma$ -bonded alkyl and aryl ligands are still fairly rare. The first structurally characterized homoleptic lanthanide alkyls became available through the use of bulky mono-, bis-, and tris(trimethylsilyl)-substituted methyl ligands. Simple unsolvated alkyls of the rare earth elements have not yet been synthesized.

An *ab initio* study on the reaction of the ground state (3D) and the excited state (1D) of  $Sc^+$  with methane leading to  $Sc^+-CH_2$  and  $H_2$  as well as with ethane and propane has been performed.<sup>58-60,60a</sup> Related studies concerned the reactions of yttrium with dihydrogen, methane, and ethylene,<sup>61-63</sup> the reaction of yttrium with cyclopropane,<sup>64</sup> as well as the  $Sc^+$ -alkyl bond strengths.<sup>65,66</sup> Density functional B3LYP calculations have been employed to investigate potential energy surfaces for the reaction of scandium oxide with methane.  $ScO$  is not reactive with respect to methane at low and ambient temperatures. At elevated temperatures, the  $ScO + CH_4$  reaction can proceed via a barrier of  $22.4 \text{ kcal mol}^{-1}$  to form an  $MeScOH$  molecule with exothermicity of  $9.8 \text{ kcal mol}^{-1}$ .  $MeScOH$  is not likely to decompose to the methyl radical and  $ScOH$  because this process is  $58.9 \text{ kcal mol}^{-1}$  exothermic.<sup>67</sup> Intermediates containing  $Sc-C$  bonds have also been discussed for the reaction mechanism of  $CO_2$  hydrogenation to formic acid in the presence of scandium oxide.<sup>68</sup> Hybrid methods such as a mixing of Hartree-Fock exchange and density functional exchange have been applied to the cationic methyl complexes  $LnMe^+$  ( $Ln = Sc, La$ ). The methods were shown to be a promising alternative to rigorous high-level *ab initio* theory for the description of singly bonded open-shell transition metal complexes. According to these methods, bond dissociation energies for  $ScMe^+$  and for  $LaMe^+$  range from  $51.5$  to  $76.1$  and from  $52.7$  to  $59.3 \text{ kcal mol}^{-1}$ , respectively.<sup>69</sup> Density functional theory (DFT) (B3PW91) calculations on the activation of  $CH_4$  by models ( $Cl_2LnZ$ ) of  $Cp^*_2LnZ$  ( $Z = H, Me$ ) have been carried out for the entire lanthanide series.  $Cl_2LnZ$  appears to be a good model for  $Cp^*_2LnZ$ . It reproduces well the coordination around the lanthanide.<sup>70</sup> Reactions of  $Y^{2+}$  with  $C_1$ - $C_6$  alkanes have been examined using a Fourier transform mass spectrometer. There is no observable reaction with methane. The predominant product from the reactions with ethane, propane, and butane is  $YC_2H_4^{2+}$ .<sup>71</sup> The potential energy surface and reaction mechanism corresponding to the reaction of the ytterbium monocation with fluoromethane, involving  $MeYbF^+$  as an intermediate, has been investigated using DFT. The reaction represents a prototype of the activation of the C-F bond in fluorohydrocarbons by bare lanthanide cations.<sup>72</sup>

#### 4.01.3.1 Neutral Homoleptic Compounds

The europium(II) and ytterbium(II) alkyls  $EuR_2$  ( $R = C(SiMe_3)_3$ ) and  $YbR_2$  ( $R = [C(SiMe_3)_2(SiMe_2X)]$ ;  $X = Me, CH=CH_2$ , or  $CH_2CH_2OEt$ ) have been obtained from reactions between  $KR$  and  $MI_2$ ,<sup>73</sup> and the ytterbium analogs of Grignard reagents,  $Yb[C(SiMe_3)_2(SiMe_2X)]I \cdot OEt_2$  ( $X = Me, CH=CH_2, Ph$ , or  $OMe$ ) from reactions between  $RI$  and  $Yb$  metal. Single crystals of  $Eu[C(SiMe_3)_3]_2$ ,  $Yb[C(SiMe_3)_2(SiMe_2CH=CH_2)]I \cdot OEt_2$ , and  $Yb[C(SiMe_3)_2(SiMe_2OMe)]I \cdot OEt_2$  were used to determine the structures of the compounds in the solid state. The compounds  $YbR_2$  and  $EuR_2$  crystallize as solvent-free monomers with  $C-M-C = 136-137^\circ$ . The alkylytterbium iodides crystallize from diethyl ether as solvated iodide-bridged dimers in which the coordination at  $Yb$  is 4 when  $X = Me$  but is increased to 5 by chelation from the group  $X$  when  $X = OMe$ . When  $X = CH=CH_2$ , the  $Yb \cdots X$  interaction is weak. The reaction  $2 RYbI = R_2Yb + YbI_2$  is not observed when  $X = Me$ , but takes place readily when  $X = Ph, CH=CH_2$ , or  $OMe$ , and provides a route to the dialkyls  $MR_2$  when the alkylpotassium  $KR$  cannot be obtained, for example, when  $X = OMe$ . The dialkyl  $Yb[C(SiMe_3)_2(SiMe_2X)]_2$  with  $X = Me$  reacts with ethers  $R^1OEt$  ( $R^1 = Et, Bu^n, Bu^t$ ) to give ethene and alkoxides  $RYbOR^1$ . The corresponding reaction does not take place when  $X = OMe$  and is very slow when  $X = CH=CH_2$ .<sup>74</sup>

The ytterbium(II) alkyl complexes  $\text{Yb}(\text{CHR}_2)_2(\text{OEt}_2)_2$  and  $\text{Na}[\text{Yb}(\text{CHR}_2)_3]$  ( $\text{R} = \text{SiMe}_3$ ) were synthesized by reactions of  $\text{YbI}_2$  with 2 and 3 equiv. of  $\text{Na}(\text{CHR}_2)$ .<sup>75</sup> Treatment of  $\text{Yb}(\text{OR}^1)_2(\text{OEt}_2)_2$  ( $\text{R}^1 = \text{C}_6\text{H}_2\text{Bu}^t\text{-2,6-Me-4}$ ) with 2 equiv. of  $\text{K}(\text{CHR}_2)$  led to a mixture of the products  $\text{Yb}(\text{CHR}_2)_2(\text{OEt}_2)_2$  and  $\text{Yb}(\text{CHR}_2)(\text{OR}^1)(\text{OEt}_2)_2$ . The complex  $\text{Yb}(\text{CHR}_2)_2(\text{TMEDA})$  was obtained by the reaction of  $\text{Cp}^*\text{Yb}(\text{OEt}_2)_2$  with  $\text{Li}(\text{CHR}_2)$  in the presence of TMEDA ( $=\text{Me}_2\text{NCH}_2\text{CH}_2\text{NMe}_2$ ) (Scheme 1).

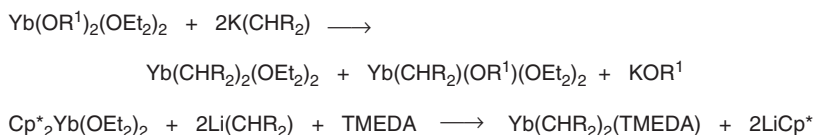
The compound  $\text{Yb}(\text{CHR}_2)_2(\text{OEt}_2)_2$  reacted readily with 1,2-bis(dimethylphosphino)ethane (DMPE) or with  $\text{C}_6\text{H}_4(\text{NHR})_{2-1,4}$  (Scheme 2).<sup>75</sup>

The complex  $[\text{Yb}(\text{CR}_3)(\mu\text{-OEt})(\text{OEt}_2)]_2$  was synthesized by the reaction of  $\text{YbI}_2$  with  $\text{K}(\text{CR}_3)$ . The  $\text{OEt}^-$  ligand apparently resulted from the cleavage of  $\text{OEt}_2$  by  $\text{K}(\text{CR}_3)$  or  $\text{Yb}(\text{CR}_3)_2$  (Scheme 3).

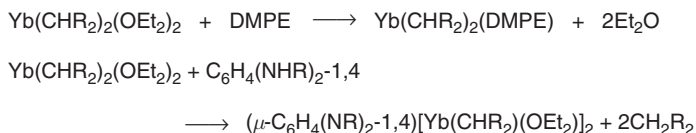
Lewis base adducts of  $[\text{Yb}(\text{NR}_2)(\mu\text{-NR}_2)]_2$  were obtained by treatment with  $\text{NC}_5\text{H}_4(\text{CH}_2\text{R})\text{-2}$  or  $\text{NC}_5\text{H}_4(\text{CHR}_2)\text{-2}$  in hexane (Scheme 4).

Complexes  $\text{Yb}[\text{NC}_5\text{H}_4(\text{CHR})\text{-2}]_2(\text{DME})$  and  $\text{K}[\text{Yb}[\text{NC}_5\text{H}_4(\text{CHR})\text{-2}]_3](\text{DME})_2$  were also synthesized by the reactions of  $\text{YbI}_2$  with 2 or 3 equiv. of  $\text{K}[\text{NC}_5\text{H}_4(\text{CHR})\text{-2}](\text{DME})(\text{OEt}_2)$ , accordingly. The complex  $[\text{Yb}(\text{C}(\text{SiMe}_3)_3)(\mu\text{-OEt})(\text{OEt}_2)]_2$  was characterized by X-ray crystallography. The molecule is an ethoxo-bridged dimer, with each Yb atom in a distorted-tetrahedral geometry.<sup>75</sup> Reaction of 2 equiv. of  $\text{KN}(\text{SiMe}_3)_2$  and a mixture of  $\text{CH}_2(\text{Ph}_2\text{P}=\text{NC}_6\text{H}_2\text{Me}_3\text{-2,4,6})_2$  and  $\text{SmI}_2$  in THF resulted in the formation of the stable samarium dialkyl  $\text{Sm}[\text{CH}(\text{Ph}_2\text{PNC}_6\text{H}_2\text{Me}_3\text{-2,4,6})_2]$  without additional solvent coordination. The deep purple-black crystals were isolated in 72% yield and structurally characterized by X-ray methods.<sup>76</sup>

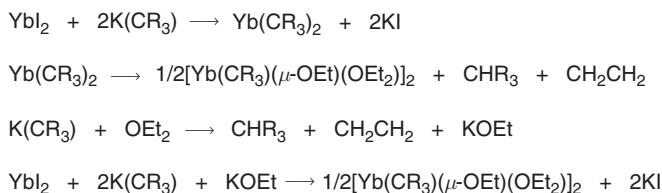
Anhydrous  $\text{SmCl}_3$  reacts with  $\text{LiCH}_2\text{SiMe}_3$  in THF yielding  $\text{Sm}(\text{CH}_2\text{SiMe}_3)_3(\text{THF})_3$  as yellow crystals in 50% yield. The single crystal structural analyses of the Sm compound as well as those of  $\text{Er}(\text{CH}_2\text{SiMe}_3)_3(\text{THF})_2$ ,  $\text{Yb}(\text{CH}_2\text{SiMe}_3)_3(\text{THF})_2$ , and  $\text{Lu}(\text{CH}_2\text{SiMe}_3)_3(\text{THF})_2$  showed the Sm atom in a *fac*-octahedral coordination and the heavier lanthanides Er, Yb, and Lu trigonal bipyramidally coordinated with the three alkyl ligands in equatorial, and



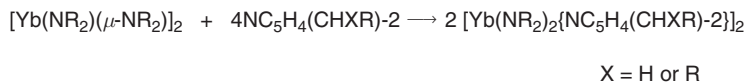
Scheme 1



Scheme 2



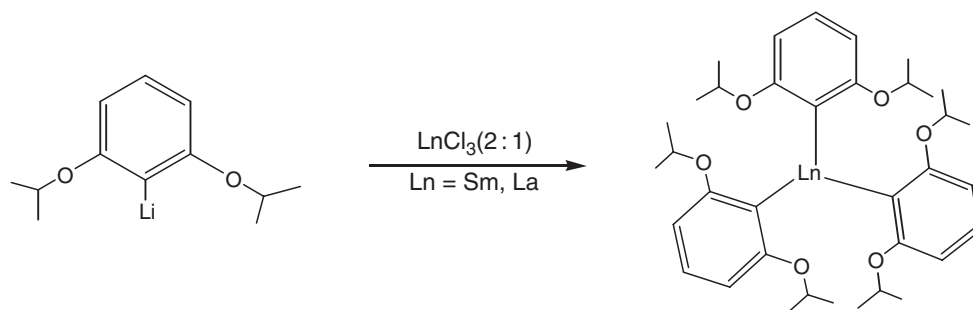
Scheme 3



Scheme 4

two THF molecules in axial position.<sup>77,78</sup> The structural and electronic properties of  $\text{LnMe}_3$  species have been studied by DFT calculations<sup>79</sup> as well as electron localization function studies.<sup>80</sup> DFT calculations have also been carried out on the compounds  $\text{Ln}[\text{CH}(\text{SiR}_2\text{R}^1)(\text{SiR}_3)]_3$  for  $\text{Ln} = \text{La}, \text{Sm}$  and (i)  $\text{R} = \text{R}^1 = \text{Me}$ , (ii)  $\text{R} = \text{H}$ ,  $\text{R}^1 = \text{Me}$ , and (iii)  $\text{R} = \text{R}^1 = \text{H}$ . The results were compared with the X-ray structures that are available from the literature for both metals and  $\text{R} = \text{R}^1 = \text{Me}$ . The calculations correctly reproduced the experimental structural features in these complexes exhibiting the peculiar pyramidal coordination geometry. The results show significant increases in the Si–C bond lengths associated with  $\beta$ -Si–C agostic interactions, whereas little structural change was found for  $\gamma$ -C–H agostic interactions. The latter are in fact repulsive.<sup>81,82</sup> Recent DFT calculations showed that  $\text{La}[\text{CH}(\text{SiMe}_3)_2]_3$ , the X-ray structure of which had previously been determined, should be considered as having a  $\beta$ -agostic Si–C bond and not a  $\gamma$ -agostic C–H bond.<sup>83</sup> Large transparent single crystals of  $\text{Ln}[\text{CH}(\text{SiMe}_3)_2]_3$  ( $\text{Ln} = \text{Pr}, \text{Nd}, \text{Sm}$ ) were obtained by slowly lowering the temperature of nearly saturated solutions in *n*-pentane, isopentane, or methylcyclohexane from  $-5$  to  $-40^\circ\text{C}$  within 3 days.<sup>84,85</sup> The linear dichroism spectrum of an oriented single crystal of tris[bis(trimethylsilyl)methyl]erbium was measured at room temperature and low temperatures. From the spectra thus obtained, a truncated crystal field (CF) splitting pattern was derived and simulated by fitting the parameters of an empirical Hamiltonian. The parameters derived allowed the estimation of the CF strength produced by the bis(trimethylsilyl)methyl ligand, the insertion of this ligand into truncated empirical nephelauxetic and relativistic nephelauxetic series, and the construction of experimentally based non-relativistic and relativistic molecular orbital schemes in the *f*-range.<sup>86</sup> The CF parameters of base-free  $(\text{Me}_3\text{SiC}_5\text{H}_4)_3\text{Pr}$ ,  $\text{Cp}_3\text{Pr}\cdot\text{NCCH}_3$ , praseodymium-doped  $\text{Cp}_3\text{La}(\text{NCCH}_3)_2\cdot\text{Pr}$ ,  $[\text{Pr}(\text{COT})]^+$ , and  $\text{Nd}[\text{N}(\text{SiMe}_3)_2]_3$  as model compounds for  $\text{Nd}[\text{CH}(\text{SiMe}_3)_2]_3$  were inserted into the corresponding energy matrices of a model spin-free *f*<sup>1</sup>-system. By diagonalizing these matrices the CF splitting patterns of the *f*-orbitals were calculated. These experimentally based molecular orbital schemes were compared with the results of previous model calculations.<sup>87</sup> Reactions of  $\text{Ln}[\text{CH}(\text{SiMe}_3)_2]_3$  ( $\text{Ln} = \text{Y}, \text{La}$ ) with 4 equiv. of nonafluorobiphenyl-2-ol (PBOH) in pentane results in rapid and quantitative formation of  $\text{Ln}(\text{PBO})_3(\text{PBOH})$  complexes.<sup>88</sup> The metallation of  $\text{HP}(\text{SiMe}_3)_2$  with  $\text{Y}[\text{CH}(\text{SiMe}_3)_2]_3$  gave homoleptic, dimeric  $[\text{Y}\{\text{P}(\text{SiMe}_3)_2\}_2]_2$ .<sup>89</sup> Homoleptic phosphinomethanide samarium complexes such as  $\text{Sm}[\text{CH}(\text{PPh}_2)_2]^{90}$  and  $\text{Sn}[\text{CH}(\text{PMe}_2)_2]_3^{91}$  also contain lanthanide–carbon bonds. Different reactions of the di- and triphenyllanthanides  $\text{Ph}_2\text{Yb}(\text{THF})_2$  and  $\text{Ph}_3\text{Ln}(\text{THF})_3$  ( $\text{Ln} = \text{Ho}, \text{Tm}, \text{Yb}$ ) have been investigated. Reactions with  $\text{H}_2\text{O}$ ,  $\text{PhC}\equiv\text{CH}$ ,  $\text{C}_5\text{H}_6$ ,  $\text{HgX}_2$ , and  $\text{I}_2$  were performed. The phenyl derivatives of the lanthanides are highly reactive towards these agents and form the expected products in high yields.<sup>92</sup> The synthesis of the 2,6-dialkoxyphenyllanthanide complexes  $[\text{C}_6\text{H}_3(\text{O}^i\text{Pr})_2-2,6]_3\text{Ln}$  ( $\text{Ln} = \text{Sm}, \text{La}, \text{Yb}$ ) has been reported (Scheme 5). The complexes of Sm and La were obtained in the 1 : 1 and 2 : 1 equimolar reaction of  $\text{Li}[\text{C}_6\text{H}_3(\text{O}^i\text{Pr})_2-2,6]$  with anhydrous  $\text{LnCl}_3$  in THF or  $\text{LnCl}_3(\text{THF})_2$ , while the 3 : 1 reaction gave  $\text{Li}[\text{Sm}(\text{C}_6\text{H}_3(\text{O}^i\text{Pr})_2-2,6)_4]$  as the major product.<sup>93</sup>

In a 2 : 1 reaction,  $\text{Yb}^{3+}$ , the smallest of the three cations, reacted with the Li salt and formed  $[\text{2,6-(Pr}^i\text{O)}_2\text{C}_6\text{H}_3]_2\text{YbCl}$  which produced  $[\text{2,6-(Pr}^i\text{O)}_2\text{C}_6\text{H}_3]_2\text{Yb}[\text{CH}(\text{SiMe}_3)_2]_2\text{Li}$  by reaction with  $\text{LiCH}(\text{SiMe}_3)_2$ .<sup>93</sup> The synthesis and characterization of the solvated ytterbium alkyl complex  $\text{Yb}(\text{CH}_2\text{Bu}^t)_3(\text{THF})_2$  have been published. The complex was obtained in moderate yield from the reaction of ytterbium metal with neopentyl iodide. The ruby-red air-sensitive crystals were fully characterized by including X-ray crystallography. The ytterbium atom is situated in the center of a trigonal bipyramid with the neopentyl groups and the THF ligands occupying the equatorial and axial positions, respectively.<sup>94</sup> Still very little is known about the higher homologs of the homoleptic lanthanide alkyls, that is, germlys, stannyls, etc. Reactions of bis(triphenylmethyl)ytterbium and bis(triphenylgermyl)ytterbium with  $\text{HgCl}_2$ ,  $\text{BiPh}_3$ ,  $\text{I}_2$ ,  $\text{Bu}^t\text{OH}$ ,  $\text{HC}\equiv\text{CPh}$ , and  $\text{CpH}$  have been studied.<sup>95</sup>



Scheme 5

### 4.01.3.2 Anionic Homoleptic Compounds

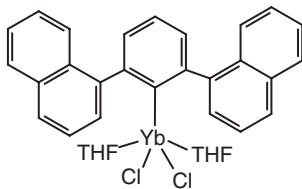
The first homoleptic three-coordinate lanthanide(III) alkyl anions have been successfully prepared with the use of the sterically demanding bis(trimethylsilyl)methyl ligand. Red  $[\text{K}(\text{YbR}_3)]_\infty$  was obtained in 87% yield by reacting ytterbium diiodide with KR in benzene ( $\text{R} = \text{CH}(\text{SiMe}_3)_2$ ). Mixing LiR,  $\text{YbI}_2$ , and 2 equiv. of KR in a mixture of diethyl ether and a small amount of THF yielded the red lithium salt  $[\text{Li}(\text{THF})_4][\text{YbR}_3]$  in 52% yield. Both compounds have been structurally characterized.<sup>96</sup> The homoleptic yttrium trimethylsilylmethyl complex  $\{(\text{Me}_3\text{SiCH}_2)_x(\text{Bu}^t\text{O})_{5-x}\text{Y}(\mu\text{-OBu}^t)_4[\text{Li}(\text{THF})]_4(\mu_4\text{-Cl})\}^+ [\text{Y}(\text{CH}_2\text{SiMe}_3)_4]^-$  was obtained by the reaction of  $\text{YCl}_3$  with 2 equiv. of  $\text{LiCH}_2\text{SiMe}_3$  and 2 equiv. of  $\text{LiOCMe}_3$ . In the  $[\text{Y}(\text{CH}_2\text{SiMe}_3)_4]^-$  anion the yttrium atom has a tetrahedral arrangement with C–Y–C angles ranging from  $105.9(3)^\circ$  to  $113.2(3)^\circ$  and with an average Y–C bond distance of  $2.42(2) \text{ \AA}$ . The geometry of the cation  $\{(\text{Me}_3\text{SiCH}_2)_x(\text{Bu}^t\text{O})_{5-x}\text{Y}(\mu\text{-OBu}^t)_4[\text{Li}(\text{THF})]_4(\mu_4\text{-Cl})\}^+$  is a distorted bicapped square antiprism with the Y and Cl atoms in the capping positions, four Li atoms in one square face of the antiprism and four OBu<sup>t</sup> groups in the other square face. The average Y–O( $\mu\text{-OBu}^t$ ) and Y–Cl distances in the cation are  $2.270(5)$  and  $3.263(2) \text{ \AA}$ , respectively.<sup>97</sup> Several anionic scandium complexes containing 3-borane-1-alkyl-imidazol-2-ylidene derivatives have been prepared and structurally characterized.<sup>98</sup>

### 4.01.3.3 Heteroleptic Compounds

Synthesis and structural chemistry of non-cyclopentadienyl organolanthanide complexes have been reviewed by Edelmann and Schumann *et al.*<sup>13,13a,24</sup> Marques *et al.* have published a review on the chemistry of the lanthanide using pyrazolylborate ligands.<sup>36</sup> Theoretical investigations on lanthanide alkyls have been published by Eisenstein *et al.* under the title “Lanthanide complexes: electronic structure and H–H, C–H, and Si–H bond activation from a DFT perspective.”<sup>99</sup>

Compounds of the type  $\text{LnF}_2\text{Me}$  have been given as examples of the application of computational methods to organometallic complexes for accurate prediction of molecular and vibrational structures (“X-ray diffraction without X-rays”).<sup>100</sup> The dimerization, unimolecular methane ejection, and bimolecular methane metathesis reactions of  $\text{L}_2\text{LnMe}$  species ( $\text{L} = \text{H}, \text{Cl}, \text{Cp}, \text{Cp}^*$ ;  $\text{Ln} = \text{Sc}, \text{Y}, \text{Lu}$ ) have been modeled at the density functional level (B3LYP) using a relativistic effective core potential basis set.<sup>101</sup> The use of very bulky terphenyl-type ligands allowed the isolation and structural characterization of several monoaryllanthanide dihalides.<sup>102,103</sup> Reactions of  $\text{dmpLi}$  ( $\text{dmp} = 2,6\text{-dimesitylphenyl}$ ) with  $\text{LnCl}_3$  ( $\text{Ln} = \text{Sc}, \text{Y}, \text{Yb}$ ) in a 1 : 1 molar ratio in THF at room temperature followed by crystallization from toluene/hexane at  $-30^\circ\text{C}$  produced  $\text{DmpLnCl}_2(\text{THF})_2$  ( $\text{Ln} = \text{Sc}, \text{Yb}$ ) and  $\text{DmpYCl}_2(\text{THF})_3$ , respectively. The molecular structures of these materials feature monomeric complexes with distorted bipyramidal ( $\text{Ln} = \text{Sc}, \text{Yb}$ ) or octahedral ( $\text{Ln} = \text{Y}$ ) coordination geometry around the metal atom, with the two chlorine ligands occupying the axial positions.<sup>102</sup> The molecular structures of the terphenyl derivatives  $\text{DnpLnCl}_2(\text{THF})_2$  ( $\text{Dnp} = 2,6\text{-di}(1\text{-naphthyl})\text{phenyl}$ ;  $\text{Ln} = \text{Y}, \text{Tm}, \text{Yb}$ ) have been reported (Scheme 6).<sup>104</sup> Reaction of  $\text{LiDpp}$  ( $\text{Dpp} = 2,6\text{-diphenylphenyl}$ ) with  $\text{SmCl}_3$  in THF afforded the *ate*-complex  $(\text{Dpp})_2\text{Sm}(\mu\text{-Cl})_2\text{Li}(\text{THF})_3$ ,<sup>105</sup> while with the 2,6-di(*o*-anisyl)phenyl ligand (= Danip) several organolanthanide amides such as  $\text{DanipYb}[\text{N}(\text{SiMe}_3)_2]_2$  and  $\text{DanipLn}[\text{N}(\text{SiMe}_2\text{H})_2]_2$  ( $\text{Ln} = \text{Sm}, \text{Yb}$ ) have been isolated and structurally characterized.<sup>106</sup>

The synthesis and structure of an  $(\text{Et}_2\text{O})_3\text{LiCl}$  adduct of  $\text{Y}[\text{CH}(\text{SiMe}_3)_2]_3$  have been reported (Scheme 7). In the structure of  $(\text{Et}_2\text{O})_3\text{Li}(\mu\text{-Cl})\text{Y}[\text{CH}(\text{SiMe}_3)_2]_3$  the Y and Li atoms are tetrahedrally coordinated and are connected via



Scheme 6



Scheme 7

the  $\mu_2$ -Cl bridge. The Y-Cl-Li fragment is almost linear ( $175.9^\circ$ ). The Y-C bond distances range from 2.415(7) to 2.435(7) Å.<sup>107</sup>

The homoleptic alkyls  $\text{Ln}[\text{CH}(\text{SiMe}_3)_2]_3$  ( $\text{Ln} = \text{Y}, \text{Ce}$ ) react with nitriles forming adducts rather than  $\beta$ -diketiminato-metal insertion products.<sup>108</sup> Reaction of rare earth metal-alkyl complexes  $\text{Ln}(\text{CH}_2\text{SiMe}_3)_3(\text{THF})_3$  ( $\text{Ln} = \text{Y}, \text{Lu}$ ) with  $\text{B}(\text{C}_6\text{X}_5)_3$  ( $\text{X} = \text{H}, \text{F}$ ) in the presence of crown ethers gave the ion pairs  $[\text{Ln}(\text{CH}_2\text{SiMe}_3)(\text{CE})(\text{THF})_n][\text{B}(\text{CH}_2\text{SiMe}_3)(\text{C}_6\text{X}_5)_3]$  ( $\text{CE} = 12\text{-crown-4}, n = 1$ ;  $\text{CE} = 15\text{-crown-5}, 18\text{-crown-6}, n = 0$ ). The compound  $[\text{Lu}(\text{CH}_2\text{SiMe}_3)_2(12\text{-crown-4})(\text{THF})][\text{B}(\text{CH}_2\text{SiMe}_3)\text{Ph}_3]$  was the first structurally characterized cationic lanthanide alkyl complex.<sup>109</sup> In the absence of  $\text{B}(\text{C}_6\text{X}_5)_3$  the thermally stable trialkyls (12-crown-4) $\text{Ln}(\text{CH}_2\text{SiMe}_3)_3$  ( $\text{Ln} = \text{Sc}, \text{Y}, \text{Sm}, \text{Gd}, \text{Tb}, \text{Dy}, \text{Ho}, \text{Er}, \text{Tm}, \text{Yb}, \text{Lu}$ ) can be isolated, of which the yttrium complex was structurally characterized.<sup>110</sup> The unusual cationic yttrium alkyl complexes  $[\text{YMe}(\text{THF})_6][\text{BPh}_4]_2$  and  $[\text{Y}(\text{CH}_2\text{SiMe}_3)_2(\text{THF})_4][\text{Al}(\text{CH}_2\text{SiMe}_3)_4]$  have been synthesized and structurally characterized.<sup>111,111a</sup>

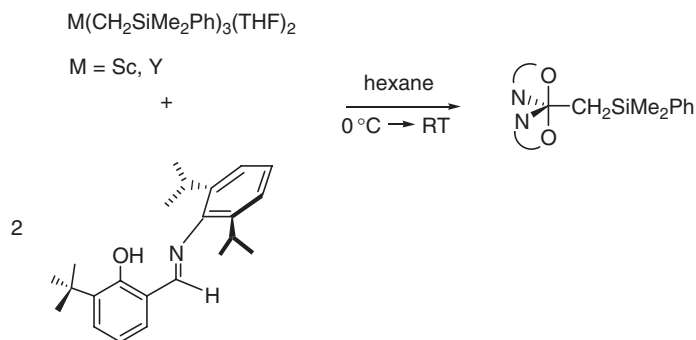
Alkali-benzyl compounds react via metathesis with lanthanide halides to give benzyl complexes of the rare earths. The reaction of  $\text{YBr}_3$  with  $\text{PhCH}_2\text{Li}(\text{TMEDA})$  afforded  $(\text{TMEDA})\text{Y}(\text{CH}_2\text{Ph})_2(\mu\text{-Br})_2\text{Li}(\text{TMEDA})$ , in which yttrium and lithium are linked via two bromide bridges. The analogous reaction with  $\text{SmBr}_3$  led to reduction of samarium to the divalent oxidation state and formation of  $(\text{TMEDA})_2\text{SmBr}(\mu\text{-Br})_2\text{Li}(\text{TMEDA})$  with no  $\sigma$ -bonded benzyl ligands.<sup>112</sup>

Similar reactions of  $\text{Ln}(\text{CH}_2\text{SiMe}_3)_3(\text{THF})_2$  ( $\text{Ln} = \text{Sc}, \text{Y}$ ) with a bulky salicylaldiminato ligand as depicted in Scheme 8 led to diastereoselective formation of highly thermally stable  $\text{L}_2\text{LnR}$  complexes whose reactivity with dihydrogen to form Group 3 metal hydrides has been investigated. For the Y derivative smooth and clean reaction with  $\text{H}_2$  (4 atm, RT) was observed, leading to the formation of the dimeric hydride.<sup>113</sup> A series of mono(salicylaldiminato) bis-alkyls of scandium and yttrium have been prepared analogously.<sup>114,115</sup>

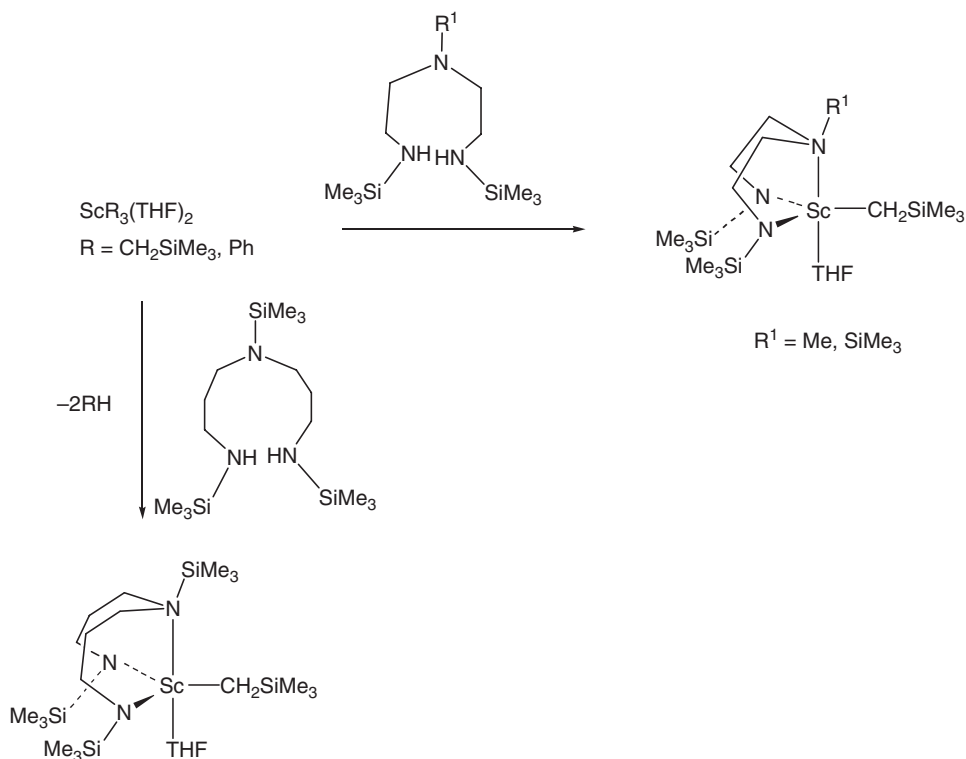
Sterically demanding chelating diamide ligands have also been employed in the synthesis of monoalkyl lanthanide complexes. Yttrium triiodide reacts with the potassium salt  $\text{K}_2[\text{ArN}(\text{CH}_2)_3\text{NAr}]$  ( $\text{Ar} = 2,6\text{-Pr}^i_2\text{C}_6\text{H}_3$ ) to yield a monoiodide complex and, by further reaction with  $\text{KCH}(\text{SiMe}_3)_2$ , the corresponding alkyl complex  $[\text{ArN}(\text{CH}_2)_3\text{NAr}]\text{Y}[\text{CH}(\text{SiMe}_3)_2](\text{THF})$ , which has been structurally characterized by X-ray crystallography.<sup>116</sup> Chelating diamides of the type  $[\text{ArN}(\text{CH}_2)_3\text{NAr}]^{2-}$  have been shown to be highly useful ligands for the stabilization of yttrium alkyl and hydride complexes.<sup>117</sup> Several scandium hydrocarbyl complexes stabilized by diamido-donor ligands have been synthesized according to Scheme 9. The most suitable synthetic route is protonation of alkyl or aryl precursors by the free amines. Both monoorganoscandium complexes form thermally sensitive yellow solids.<sup>118</sup>

Related bis(alkyl) complexes of scandium and yttrium have become accessible with the use of a specially designed bulky iminophenolato ligand. The reaction of equimolar amounts of 2-(2,4,6-Me<sub>3</sub>C<sub>6</sub>H<sub>2</sub>N=CH)(6-Bu<sup>t</sup>)C<sub>6</sub>H<sub>3</sub>OH (=HL) with  $\text{Ln}(\text{CH}_2\text{SiMe}_3)_3(\text{THF})_2$  ( $\text{Ln} = \text{Sc}, \text{Y}$ ) under mild conditions gave  $\text{Ln}(\text{CH}_2\text{SiMe}_3)_3(\text{THF})(\text{L})$  (Scheme 10). The trigonal bipyramidal structure of these dialkyls was conformed crystallographically for  $\text{Ln} = \text{Sc}$ . Whereas the scandium complex is stable in solution at room temperature, the yttrium derivative slowly disproportionates to give  $\text{YL}_3$  which is also accessible from  $\text{Y}(\text{CH}_2\text{SiMe}_3)_3(\text{THF})_2$  and three HL.<sup>119</sup>

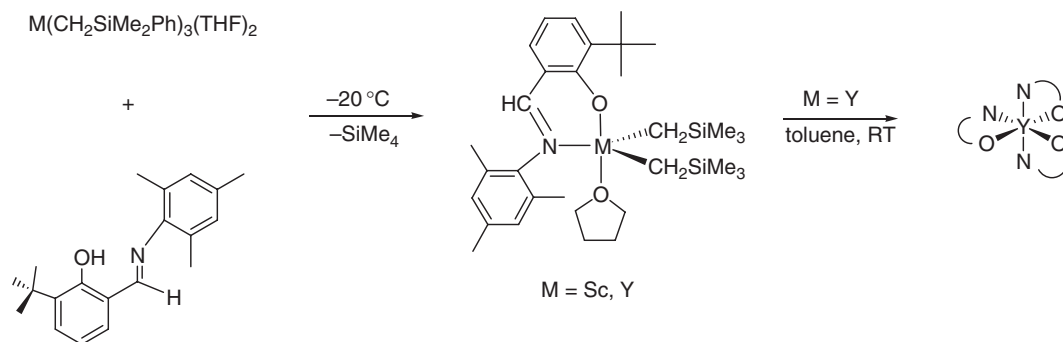
The cyclopentadienyl-free dialkyl-diaryloxide complexes  $[(\text{Me}_3\text{SiCH}_2)_2\text{Ln}(\text{OC}_6\text{H}_3\text{Bu}^t_{2-2,6})_2]^-$  ( $\text{Ln} = \text{Y}, \text{Lu}$ ) were prepared and their reactivity studied and compared with cyclopentadienyl-containing organolanthanide complexes.  $[(\text{Me}_3\text{SiCH}_2)_2\text{Y}(\text{OC}_6\text{H}_3\text{Bu}^t_{2-2,6})_2][[(\text{THF})_3\text{Li}]_2\text{Cl}]$  was obtained from the reaction of  $\text{YCl}_3$  with 2 equiv. of  $\text{LiCH}_2\text{SiMe}_3$  and 2 equiv. of  $\text{LiOC}_6\text{H}_3\text{Bu}^t_{2-2,6}$  and crystallized with a cation which can be viewed as an  $\text{LiCl}$  adduct of  $[\text{Li}(\text{THF})_x]^+$ . The lutetium complex  $[\text{Li}(\text{THF})_4][(\text{Me}_3\text{SiCH}_2)_2\text{Lu}(\text{OC}_6\text{H}_3\text{Bu}^t_{2-2,6})_2](\text{THF})_2$  was prepared analogously. Both complexes have distorted tetrahedral coordination geometries around the metals.<sup>120</sup>



Scheme 8



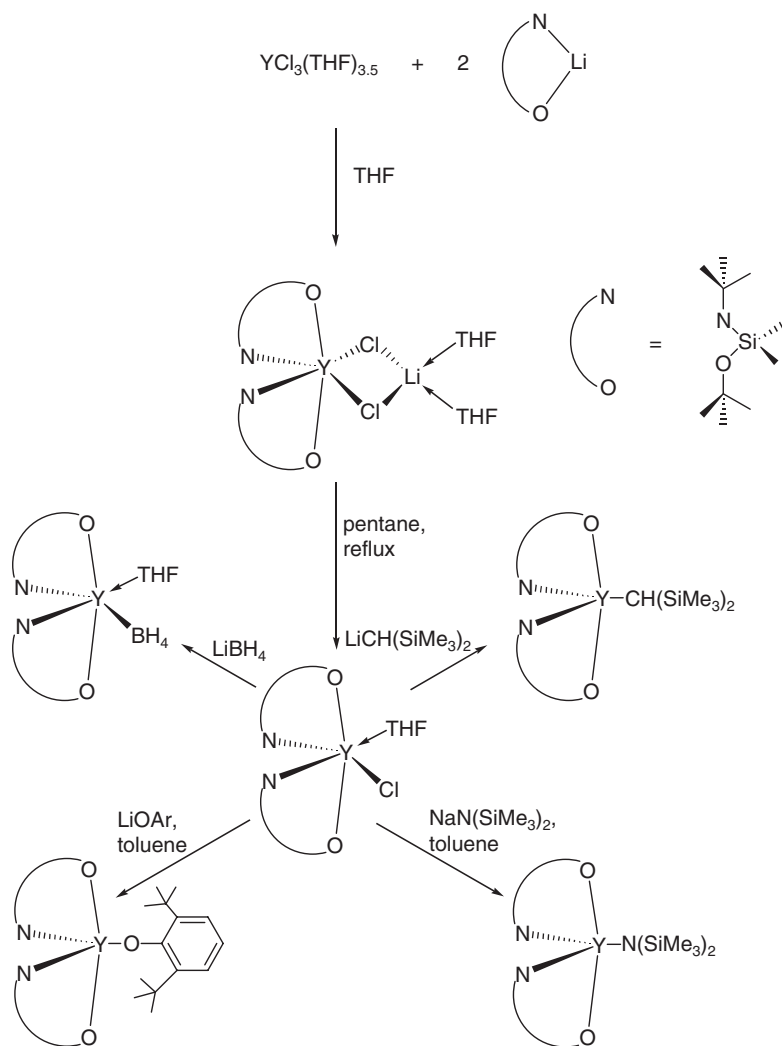
Scheme 9



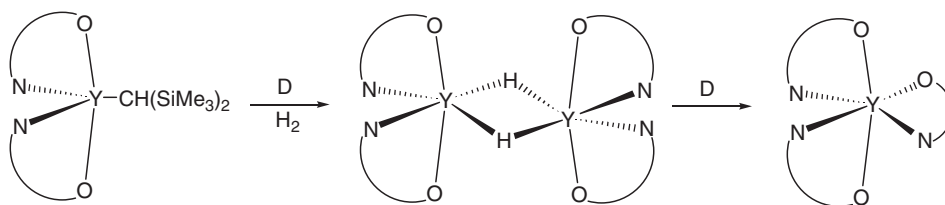
Scheme 10

The chemistry of bis[*N,O*-bis(*tert*-butyl)alkoxydimethylsilyl]amido]yttrium complexes, including hydrocarbyl derivatives, has been investigated in detail. Reaction of  $\text{YCl}_3(\text{THF})_{3,5}$  with 2 equiv. of  $\text{Li}[\text{Me}_2\text{Si}(\text{NBu}^t)(\text{OBu}^t)]$  produces  $[\text{Me}_2\text{Si}(\text{NBu}^t)(\text{OBu}^t)]_2\text{Y}(\mu\text{-Cl})_2\text{Li}(\text{THF})_2$ , which easily loses  $\text{LiCl}$  to give  $[\text{Me}_2\text{Si}(\text{NBu}^t)(\text{OBu}^t)]_2\text{YCl}(\text{THF})$ . Salt metathesis of the latter precursor with  $\text{LiBH}_4$ ,  $\text{LiOAr}$  ( $\text{OAr} = \text{O}-2,6\text{-Bu}_2\text{C}_6\text{H}_3$ ),  $\text{NaN}(\text{SiMe}_3)_2$ , and  $\text{LiCH}(\text{SiMe}_3)_2$  gave the corresponding yttrium bis[*N,O*-bis(*t*-butyl)alkoxydimethylsilyl]amido] derivatives  $[\text{Me}_2\text{Si}(\text{NBu}^t)(\text{OBu}^t)]_2\text{YR}$  ( $\text{R} = \text{BH}_4(\text{THF})$ ,  $\text{OAr}$ ,  $\text{N}(\text{SiMe}_3)_2$ ,  $\text{CH}(\text{SiMe}_3)_2$ ) (Scheme 11).<sup>121</sup>

The alkyl compound  $[\text{Me}_2\text{Si}(\text{NBu}^t)(\text{OBu}^t)]_2\text{YCH}(\text{SiMe}_3)_2$  reacts with  $\text{H}_2$  in  $\text{THF}$  to give an unstable dimeric hydride, which readily disproportionates forming the homoleptic alkoxysilylamide complex  $[\text{Me}_2\text{Si}(\text{NBu}^t)(\text{OBu}^t)]_3\text{Y}$  (Scheme 12).<sup>121</sup>  $[\text{Me}_2\text{Si}(\text{NBu}^t)(\text{OBu}^t)]_2\text{YCH}(\text{SiMe}_3)_2$  also reacts with pyridine and alkylpyridines under C–H activation to give pyridyl and  $\alpha$ -picolyl derivatives.<sup>122</sup>



Scheme 11



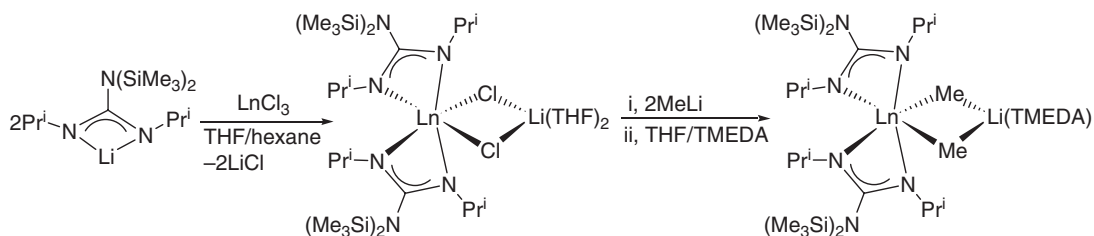
Scheme 12

Guanidinate lanthanide methyl complexes of the type  $[(\text{Me}_3\text{Si})_2\text{NC}(\text{NPr}^i)_2]_2\text{Ln}(\mu\text{-Me})_2\text{Li}(\text{TMEDA})$  ( $\text{Ln} = \text{Nd}, \text{Yb}$ ) are accessible in good yields by reacting the chloro-bridged precursors with methyllithium (Scheme 13).<sup>123</sup>

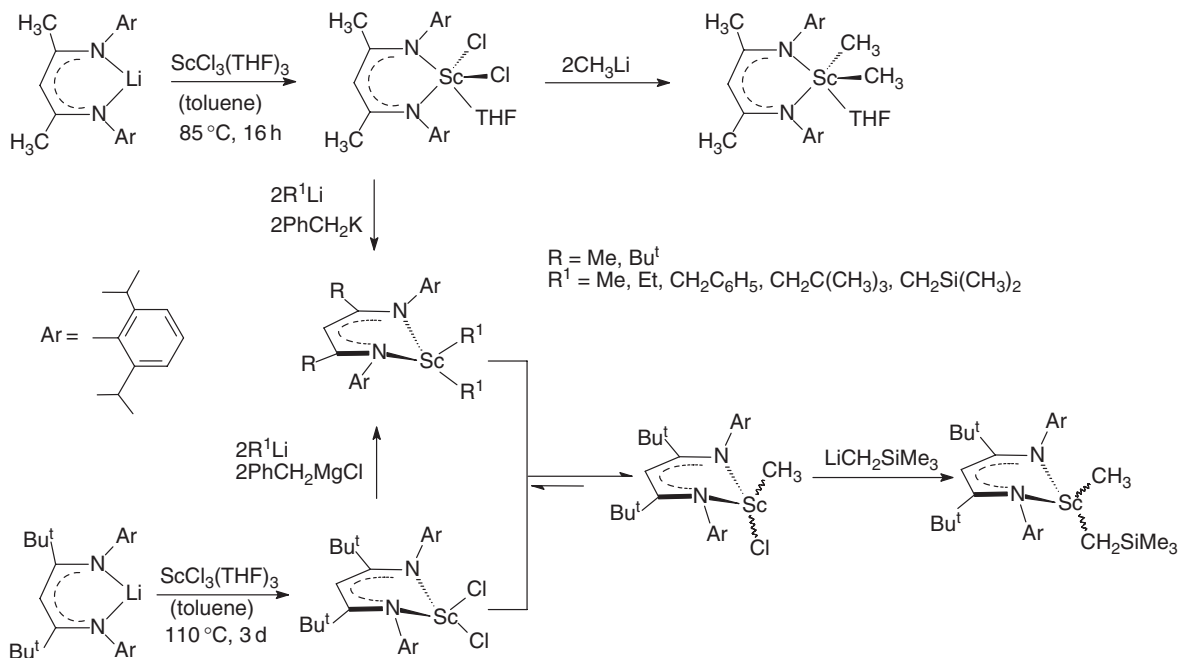
$\beta$ -Diketiminato (“nacnac”) ligands are becoming increasingly popular as ancillary ligands in organolanthanide chemistry.<sup>108,124–126</sup> Scheme 14 summarizes typical synthetic routes leading to diorganoscandium complexes stabilized by bulky  $\beta$ -diketiminato ligands.<sup>127,128,128a</sup>

Unusual cationic scandium methyl complexes supported by a  $\beta$ -diketiminato ligand (=  $\text{L}^{\text{Bu}^i}$ ) have also recently been reported. As depicted in Scheme 15, the monomeric dimethylscandium precursor reacts with varying





Scheme 13

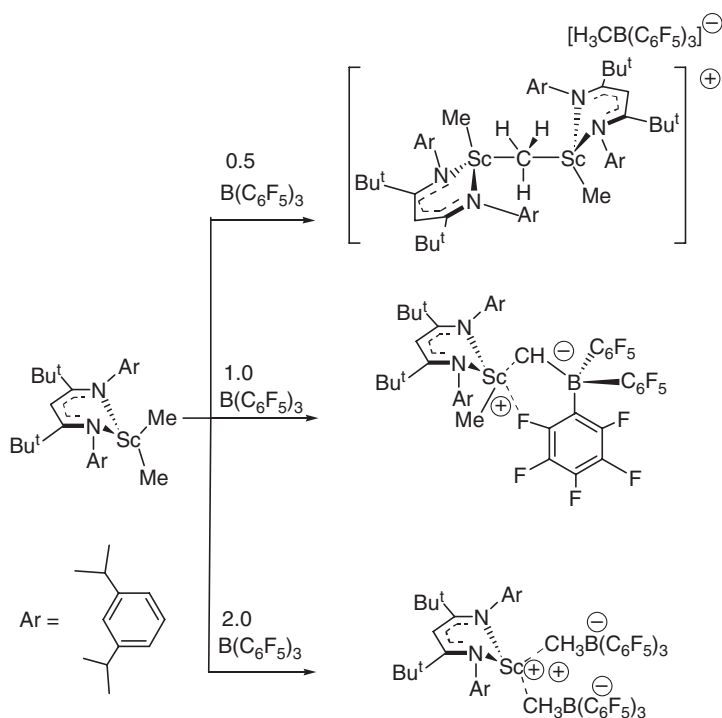


Scheme 14

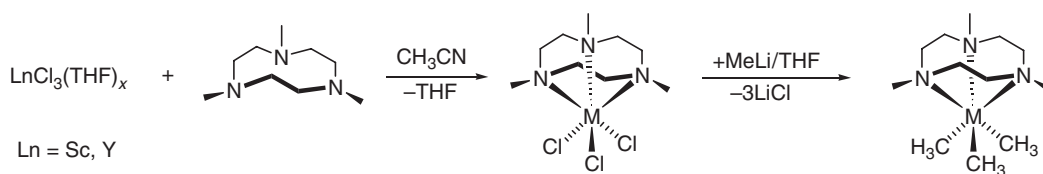
equivalents of B(C<sub>6</sub>F<sub>5</sub>)<sub>3</sub> to form different ion pairs. Upon reaction with 0.5 equiv. of borane, a  $\mu$ -methyl dimer is formed, which is quite unstable and slowly evolves methane. When the dimethyl complex is treated with a full equivalent of B(C<sub>6</sub>F<sub>5</sub>)<sub>3</sub>, however, a monomeric ion pair [LBu<sup>t</sup>ScMe][MeB(C<sub>6</sub>F<sub>5</sub>)<sub>3</sub>] is produced in excellent yield as a yellow, crystalline solid when precipitated from hexane. Even the second scandium methyl group can be abstracted to form the dicationic species as an analytically pure white solid.<sup>129</sup>

One of the most remarkable achievements was the stabilization of a diamagnetic Sc<sup>I</sup>Br molecule in a sandwich-like structure. The reaction of the  $\beta$ -diketiminato scandium derivative LScBr<sub>2</sub> (L = Et<sub>2</sub>NCH<sub>2</sub>CH<sub>2</sub>NC(Me)-CHC(Me)NCH<sub>2</sub>CH<sub>2</sub>NEt<sub>2</sub>) with (C<sub>3</sub>H<sub>5</sub>)MgBr gave the unexpected blue-green scandium complex (LMgBr)<sub>2</sub>ScBr, the structure of which was established by X-ray analysis, liquid- and solid-state NMR, EPR, UV-vis, and magnetic measurements as well as DFT calculations. Correlation of all the results led to the conclusion that the formal oxidation state of scandium in this complex is "one" (Sc(I)) having no unpaired electrons.<sup>130,131</sup> The same tetradentate  $\beta$ -diketiminato ligand has recently been utilized for the synthesis of LLnBr<sub>2</sub> (Ln = Y, Sm, Er, Yb) and the bis(alkyl)erbium complex LEr(CH<sub>2</sub>SiMe<sub>3</sub>)<sub>2</sub>.<sup>132,133</sup> Silyl-substituted  $\beta$ -diketiminato ligands have been shown to be highly useful for the preparation of divalent ytterbium complexes.<sup>134</sup>

Reaction of the neutral ligand 1,4,7-trimethyl-1,4,7-triazacyclononane (Me<sub>3</sub>[9]aneN<sub>3</sub>) with LnCl<sub>3</sub>(THF)<sub>3</sub> (Ln = Sc, Y) in acetonitrile afforded the novel trihalide complexes (Me<sub>3</sub>[9]aneN<sub>3</sub>)LnCl<sub>3</sub>. Subsequent alkylation with LiMe in



Scheme 15



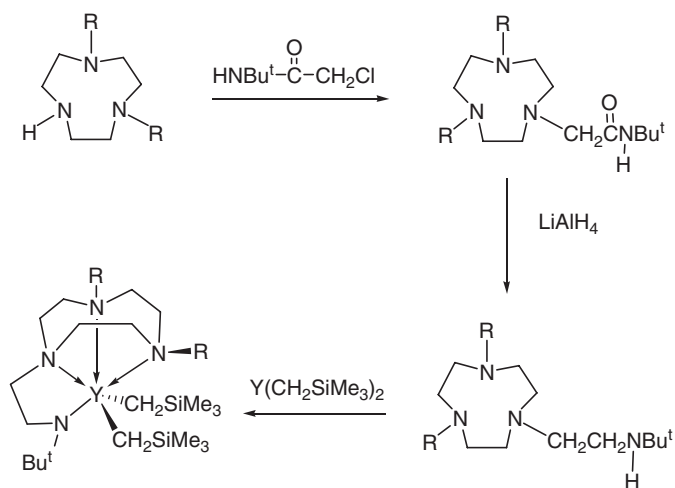
Scheme 16

THF cleanly gave the corresponding trimethyl species  $(\text{Me}_3[9]\text{aneN}_3)\text{LnMe}_3$  (Scheme 16). Reactivity studies revealed that the metal carbon bonds of these highly coordinatively unsaturated  $12e^-$ ,  $d^0$  complexes are remarkably unreactive toward insertion chemistry with typical unsaturated substrates such as alkenes and alkynes.<sup>135</sup> The neutral trialkyl complexes  $(\text{Me}_3[9]\text{aneN}_3)\text{Ln}(\text{CH}_2\text{SiMe}_3)_3$  ( $\text{Ln} = \text{Sc}, \text{Y}$ ) were made by reacting the free ligand with  $\text{Ln}(\text{CH}_2\text{SiMe}_3)_3(\text{THF})_2$ .<sup>136</sup>

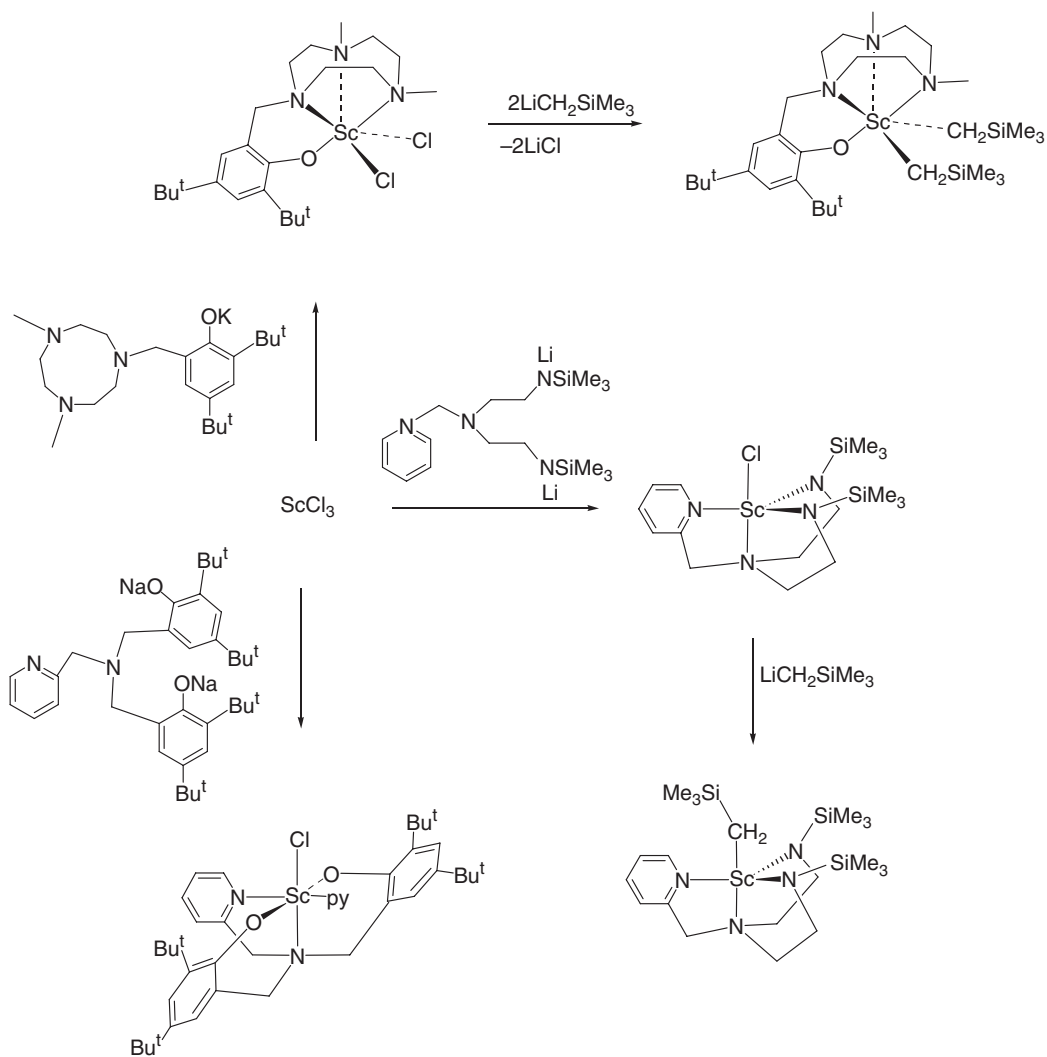
Neutral and cationic yttrium and lanthanum alkyl complexes have also been prepared with related linked 1,4,7-triazacyclononane-amide monoanionic ancillary ligands as illustrated in Scheme 17.<sup>137,138</sup>

Related new ligand sets for the stabilization of scandium and yttrium alkyls have been introduced. Typical reactions are summarized in Scheme 18.<sup>139–141</sup>

Closely related is a series of triamino-amide ligands, which has been utilized to stabilize yttrium bis(alkyl) complexes.<sup>142</sup> The yttrium dialkyl *trans*- $\text{Y}(\text{MAC})(\text{CH}_2\text{SiMe}_3)_2$  ( $\text{MAC}$  = deprotonated aza-18-crown-6) has been isolated and characterized. The colorless crystalline compound is formed in high yield by a protonation reaction between  $\text{Y}(\text{CH}_2\text{SiMe}_3)_3(\text{THF})$  and  $\text{HMAC}$ . The dialkyl complex exhibits high stability toward ligand redistribution and metallation, reacts with  $\text{CO}$  to form a *trans*-bis(enolate),  $\text{trans-Y}(\text{MAC})[\text{OC}(\text{SiMe}_3)=\text{CH}_2]_2$ , by silyl migration, and undergoes alkyl abstraction by  $\text{B}(\text{C}_6\text{F}_5)_3$  to generate the highly unstable cation  $[\text{Y}(\text{MAC})(\text{CH}_2\text{SiMe}_3)]^+$ .<sup>143</sup> An yttrium alkyl adduct with deprotonated 4,13-diaza-18-crown-6 (DAC) has been prepared by reacting  $\text{Y}(\text{CH}_2\text{SiMe}_3)_3(\text{THF})_2$  with  $\text{H}_2\text{DAC}$ . The complex  $\text{Y}(\text{DAC})(\text{CH}_2\text{SiMe}_3)$  was characterized by X-ray diffraction. In the monomeric structure the yttrium arrangement can be considered as consisting of primary trigonal planar coordination of alkyl and two amido groups with secondary coordination of the four ether oxygens. The analysis of



Scheme 17

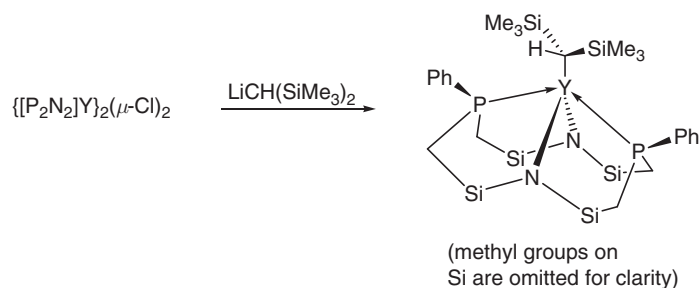


Scheme 18

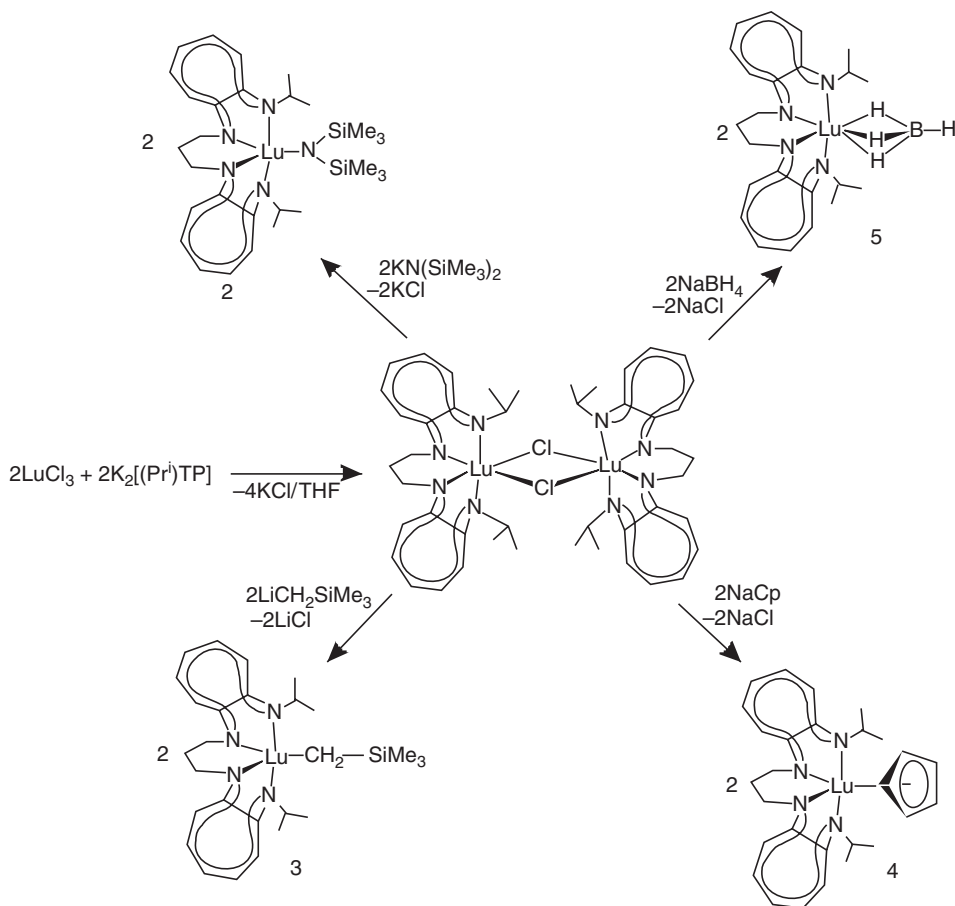
the X-ray structure revealed that this compound has no agostic interactions with the alkyl group. The complex  $\text{Y}(\text{DAC})(\text{CH}_2\text{SiMe}_3)$  decomposes slowly in the solid state at room temperature and decomposes more rapidly to produce TMS in benzene solution.<sup>144</sup>

More recently, a tetradentate bis(phenoxy) ligand has been used to stabilize an yttrium alkyl complex of the type  $[\text{L}]\text{Y}(\text{CH}_2\text{SiMe}_3)(\text{THF})$ .<sup>145,145a</sup> A phosphorus-containing macrocycle, *syn*- $[\text{P}_2\text{N}_2]$  ( $[\text{P}_2\text{N}_2] = [\text{PhP}(\text{CH}_2\text{SiMe}_2\text{NSiMe}_2\text{CH}_2)_2\text{PPh}]$ ), has been successfully employed in the synthesis of monoalkyl lanthanide complexes. Addition of the very bulky  $\text{LiCH}(\text{SiMe}_3)_2$  to the chloro-bridged dimer led to the formation of  $[\text{P}_2\text{N}_2]\text{YCH}(\text{SiMe}_3)_2$  in 92% yield (Scheme 19).<sup>146</sup>

The first bridged aminotroponiminato complexes of lutetium were synthesized by the reaction of dipotassium-1,3-di[2-(isopropylamino)troponiminato]propane,  $\text{K}_2[(\text{Pr}^i)\text{TP}]$ , with lutetium trichloride (Scheme 20). The complex was



Scheme 19



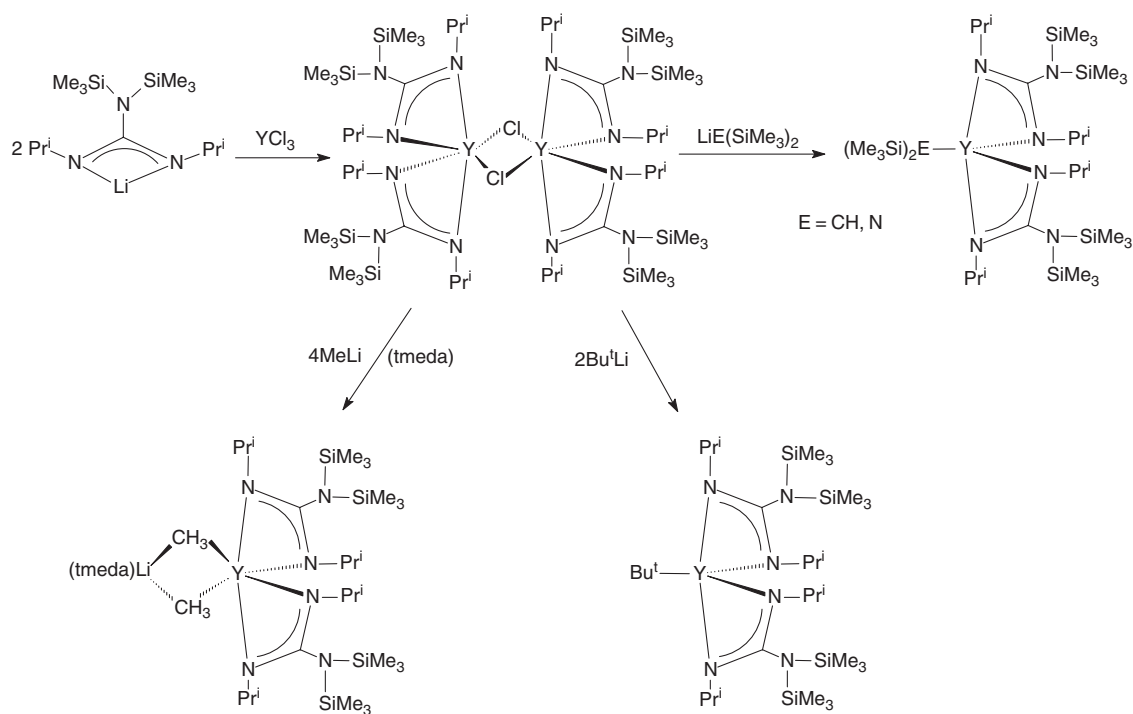
Scheme 20

characterized by single crystal X-ray crystallography and its derivative chemistry with some selected ligands such as alkyl, amide, cyclopentadienyl, and  $\eta^3$ -borohydride has been investigated.<sup>147</sup>

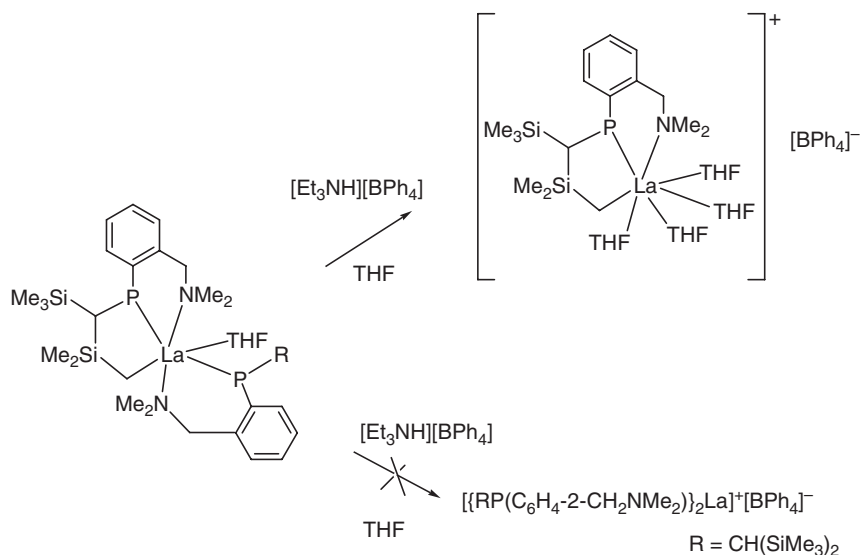
Bulky guanidinato ligands have been successfully employed in the stabilization of yttrium alkyl complexes. Typical synthetic procedures are depicted in Scheme 21.<sup>148</sup>

Heteroleptic lanthanide alkyls containing one or two  $\text{CH}_2\text{SiMe}_3$  ligands have also been stabilized with the use of pyrrolylaldiminato ligands,<sup>149</sup> chelating tridentate diamide ligands,<sup>150</sup> bulky anilido-imine ligands,<sup>151</sup> sterically demanding benzamidinate ligands,<sup>152</sup> multidentate anilido-pyridine-imine ligands,<sup>153</sup>  $C_2$ -symmetric fluorous diamino-dialkoxide ligands,<sup>154</sup> and triamino-diamide ligands.<sup>142</sup> Treatment of  $\text{SmI}_2(\text{THF})_2$  with the potassium salt of the methylphenyl dipyrromethanyl dianion in THF resulted in a rapid reaction with the formation of  $[[\text{MePhC}(\text{C}_4\text{H}_3\text{N})_2]\text{Sm}]_5(\mu\text{-I})][\text{K}(\text{THF})_6]$ . Single crystal X-ray determinations showed that the complex is formed by a pentanuclear anion consisting of five  $[[\text{MePhC}(\text{C}_4\text{H}_3\text{N})_2]\text{Sm}]_5$  units with the five samarium atoms pentagonally arranged around a central iodine atom. Each ligand bridges two samarium atoms with the pyrrole rings being in turn  $\pi$ -bonded to one samarium and  $\sigma$ -bonded to a second.<sup>155</sup>

The chemistry of organolanthanide complexes containing pyrazolylborate ancillary ligands has recently been reviewed by Marques *et al.*<sup>36</sup> Reactions between  $(\text{Tp}^{\text{Me,Me}})\text{ScCl}_2(\text{THF})$  and  $(\text{Tp}^{\text{tBu,Me}})\text{ScCl}_2$  ( $\text{Tp}^{\text{Me,Me}}$  = tris(3,5-dimethylpyrazolyl)borate;  $\text{Tp}^{\text{tBu,Me}}$  = tris(3-*t*-butyl-5-methylpyrazolyl)borate) with alkyl lithium reagents  $\text{RLi}$  ( $\text{R} = \text{Me}$ ,  $\text{CH}_2\text{SiMe}_3$ ,  $\text{CH}(\text{SiMe}_3)_2$ ) mostly gave the lithium salts of the Tp ligands as the major products. Only the heteroleptic alkyl complex  $(\text{Tp}^{\text{Me,Me}})\text{Sc}(\text{CH}_2\text{SiMe}_3)_2(\text{THF})$  could be obtained contaminated with at least 10%  $\text{Li}(\text{Tp}^{\text{Me,Me}})$  via this method. However, a salt-free elimination route involving reaction between *in situ* generated  $\text{Sc}(\text{CH}_2\text{SiMe}_3)_3(\text{THF})_2$  and the protonated ligands  $\text{Tp}^{\text{R,MeH}}$  ( $\text{R} = \text{Me}$ ,  $\text{Bu}^t$ ) gave the desired dialkyl complexes  $(\text{Tp}^{\text{Me,Me}})\text{Sc}(\text{CH}_2\text{SiMe}_3)_2(\text{THF})$  and unsolvated  $(\text{Tp}^{\text{tBu,Me}})\text{Sc}(\text{CH}_2\text{SiMe}_3)_2$  in 67% and 87% yield, respectively.<sup>36</sup> Addition of a stoichiometric amount of  $\text{KR}$  ( $\text{R} = \text{CH}_2\text{C}_6\text{H}_4\text{-}o\text{-NMe}_2$ ,  $\text{C}_6\text{H}_4\text{-}o\text{-CH}_2\text{NMe}_2$ ,  $\text{CH}_2\text{Ph}$ ) to a solution of  $\text{SmI}_2$  in toluene or THF led to the immediate formation of the insoluble, purple  $\text{Sm}(\text{Tp}^{\text{Me}_2})_2$  compound. However, when these reactions were carried out in the presence of protic substrates such as  $\text{CpH}$  or  $\text{HC}\equiv\text{CPh}$ , the compounds  $(\text{Tp}^{\text{Me,Me}})_2\text{SmCp}$  and  $(\text{Tp}^{\text{Me}_2})_2\text{SmC}\equiv\text{CPh}$  were readily formed and isolated in good yields.<sup>156</sup> The use of the neutral tris(pyrazolyl)methane ligand  $\text{HC}(\text{Me}_2\text{pz})_3$  allowed the synthesis of the trialkyls  $[\text{HC}(\text{Me}_2\text{pz})_3]\text{Ln}(\text{CH}_2\text{SiMe}_3)_3$  ( $\text{Ln} = \text{Sc}$ ,  $\text{Y}$ ) directly from  $\text{Ln}(\text{CH}_2\text{SiMe}_3)_3(\text{THF})_2$ . Further reaction of the trialkyls with  $[\text{CPh}_3][\text{B}(\text{C}_6\text{F}_5)_4]$  afforded the cationic species  $[\{\text{HC}(\text{Me}_2\text{pz})_3\}\text{Ln}(\text{CH}_2\text{SiMe}_3)_2(\text{THF})][\text{B}(\text{C}_6\text{F}_5)_4]$ .<sup>136</sup>



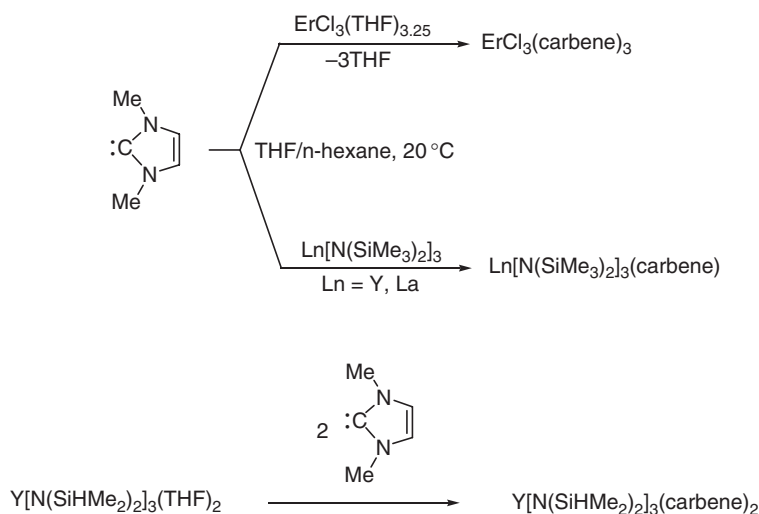
Scheme 21



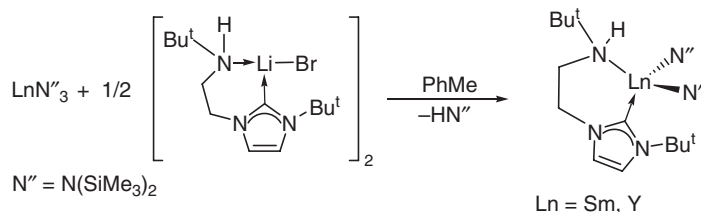
Scheme 22

Protonation of a heteroleptic, cyclometallated lanthanum phosphide complex with  $[\text{NEt}_3\text{H}][\text{BPh}_4]$  was shown to occur at the La–P and not at the La–C bond, which allowed the isolation of a cationic lanthanum alkyl complex as shown in Scheme 22.<sup>157,158</sup>

The reaction of  $\text{Ln}[\text{N}(\text{SiMe}_3)_2]_3$  ( $\text{Ln} = \text{Y, La, Ce, Pr, Nd, Sm, Eu, Tb, Dy, Ho, Tm, Yb}$ ) with 2 equiv. of cyclohexylisocyanide gave good yields of complexes of the composition  $\text{Ln}[\text{N}(\text{SiMe}_3)_2]_3(\text{CNC}_6\text{H}_{11})_2$ . The crystal, molecular, and electronic structure of the neodymium derivative have been investigated in detail. The structure of  $\text{Nd}[\text{N}(\text{SiMe}_3)_2]_3(\text{CNC}_6\text{H}_{11})_2$  shows the five-coordinate  $\text{Nd}^{3+}$  ion in a nearly exact trigonal bipyramidal environment with two  $\text{CNC}_6\text{H}_{11}$  molecules in the axial and the three  $\text{N}(\text{SiMe}_3)_2$  ligands in the equatorial positions.<sup>159</sup> The same investigations have also been carried out on the corresponding praseodymium species  $\text{Pr}[\text{N}(\text{SiMe}_3)_2]_3(\text{CNR})_2$  ( $\text{R} = \text{Bu}^t, \text{C}_6\text{H}_{11}$ ).<sup>160</sup> Several lanthanide complexes containing heterocyclic carbenes as ligands have been prepared. Typical syntheses are outlined in Scheme 23. The donor capability of the strongly nucleophilic carbene ligand is expressed by the displacement of both THF ligands in the precursor  $\text{Y}[\text{N}(\text{SiHMe}_2)_2]_3(\text{THF})_2$  to form the related bis(carbene) complex  $\text{Y}[\text{N}(\text{SiHMe}_2)_2]_3(\text{carbene})_2$ .<sup>161</sup>



Scheme 23



Scheme 24

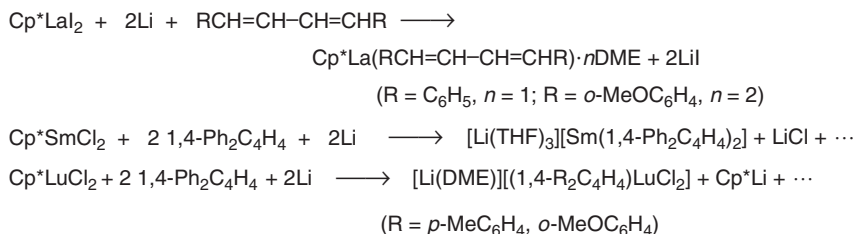
Lanthanide complexes containing anionic amido *N*-heterocyclic carbenes as ligands have been synthesized as illustrated in Scheme 24.<sup>162,162a</sup>

#### 4.01.4 Alkenyl and Alkynyl Compounds

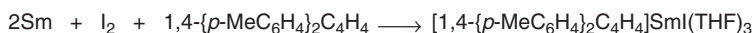
The first spectroscopic identification and characterization of ytterbium monoacetylide,  $\text{YbC}\equiv\text{CH}$ , in the gas phase was reported in 1997.<sup>163</sup> Reaction pathways for the Y-induced acetylene( $\text{HCCH}$ )-vinylidene( $\text{CCH}_2$ ) rearrangement in the gas phase have been identified by density functional and coupled cluster calculations with basis set extrapolations.<sup>164,165</sup> The reaction of  $\text{LnI}_2$  or  $\text{LnI}_3$  with  $\text{PhC}\equiv\text{CNa}$  in tetrahydrofuran was used for the preparation of the phenylethynyl derivatives  $(\text{PhC}\equiv\text{C})_2\text{Ln}(\text{THF})_x$  ( $\text{Ln} = \text{Sm}, \text{Yb}; x = 1, 2$ ) and  $(\text{PhC}\equiv\text{C})_3\text{Ln}(\text{THF})_x$  ( $\text{Ln} = \text{Pr}, \text{Nd}, \text{Dy}, \text{Ho}, \text{Er}, \text{Lu}; x = 1, 2$ ), respectively.<sup>166</sup> The ytterbium(II) phenylethynyl complex  $(\text{PhC}\equiv\text{C})_2\text{Yb}(\text{THF})_4$  reacts with  $\text{Me}_3\text{SiCl}$ ,  $\text{Ph}_3\text{GeCl}$ , and  $\text{Ph}_3\text{SnCl}$  to give a mixture of  $(\text{PhC}\equiv\text{C})\text{YbCl}(\text{THF})_2$  and  $\text{YbCl}_2(\text{THF})_2$ .<sup>95</sup> Reactions of some halides, cyclopentadienyl dichlorides, and bis(cyclopentadienyl) chlorides of lanthanides with *trans*-stilbene adducts of alkali metals  $\text{M}^+[\text{PhCHCHPh}]^-$  ( $\text{M} = \text{Li}, \text{Na}$ ) have been studied. At first the reaction of  $\text{SmI}_2(\text{THF})_2$  with metallic lithium and *trans*-stilbene in 1:2.2 ratio in dimethoxyethane (DME) gives a stilbene complex of divalent samarium  $(\text{PhCHCHPh})\text{Sm}(\text{DME})_2$ . This complex then reacts with hydrogen in THF to give  $\text{SmH}_2(\text{THF})_2$  and 1,2-diphenylethane. This stilbene complex of divalent samarium  $(\text{PhCHCHPh})\text{Sm}(\text{DME})_2$  reacts with hexamethyldisilazane in DME to the divalent samarium amide  $[(\text{Me}_3\text{Si})_2\text{N}]_2\text{Sm}(\text{DME})_2$  and *trans*-stilbene.<sup>167</sup>

The 1,4-diaryl-1,3-butadiene lanthanide complexes  $\text{Cp}^*\text{La}(1,4\text{-Ph}_2\text{C}_4\text{H}_4)\cdot\text{DME}$ ,  $\text{Cp}^*\text{La}(1,4\text{-}o\text{-MeOC}_6\text{H}_4)_2\text{C}_4\text{H}_4\cdot 2\text{DME}$ ,  $[\text{Li}(\text{THF})_3][\text{Sm}(1,4\text{-Ph}_2\text{C}_4\text{H}_4)_2]$ ,  $[\text{Li}(\text{DME})][(1,4\text{-}p\text{-MeC}_6\text{H}_4)_2\text{C}_4\text{H}_4]\text{LuCl}_2$ , and  $[\text{Li}(\text{DME})][(1,4\text{-}o\text{-MeOC}_6\text{H}_4)_2\text{C}_4\text{H}_4]\text{LuCl}_2$  were prepared by reactions of appropriate (cyclopentadienyl)lanthanide halides with 1,4-diaryl-1,3-butadienes in the presence of alkali metals (Scheme 25).<sup>168</sup>

Reaction of  $\text{SmCl}_3(\text{THF})_3$  with lithium and 1,4-diphenyl-1,3-butadiene led to  $[\text{Li}(\text{THF})_4][\text{Sm}(1,4\text{-Ph}_2\text{C}_4\text{H}_4)_2]$ . One more samarium complex  $(1,4\text{-}p\text{-MeC}_6\text{H}_4)_2\text{C}_4\text{H}_4\text{SmI}(\text{THF})_3$  was obtained by reaction of metallic samarium with 1,4- $\{p\text{-MeC}_6\text{H}_4\}_2\text{C}_4\text{H}_4$  in the presence of iodine (Scheme 26).<sup>168</sup>



Scheme 25



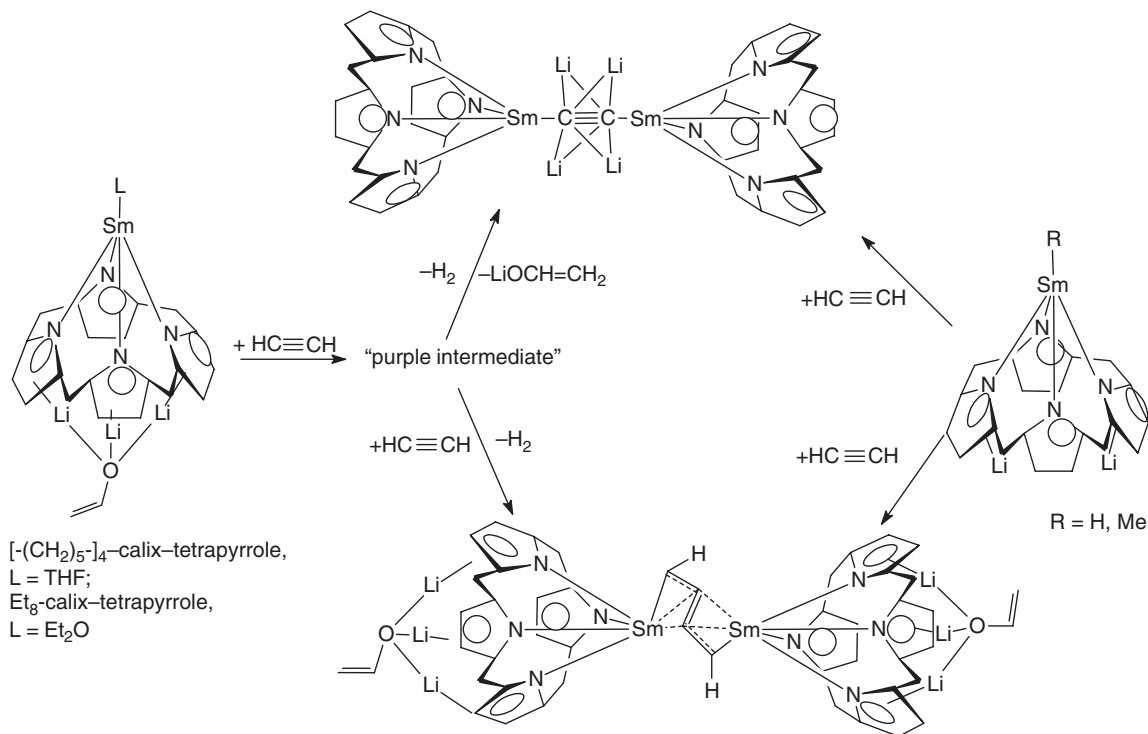
Scheme 26



An analogous reaction between  $\text{GdCl}_3$  and diphenylbutadiene potassium afforded low yields of the red diphenylbutadiene-bridged gadolinium complex  $(\mu\text{-Ph}_2\text{C}_4\text{H}_4)[\text{GdCl}_2(\text{THF})_3]_2(\text{THF})_3$ .<sup>169</sup> In the case of lutetium, the polymeric 1,4-diphenylbutadiene complex  $\text{K}(\text{THF})_2(\mu\text{-Ph}_2\text{C}_4\text{H}_4)_2\text{Lu}(\text{THF})_2$  has been isolated and structurally characterized,<sup>170</sup> while for lanthanum the diene complex  $(\mu\text{-}\eta^4\text{:}\eta^4\text{-PhCH=CHCH=CHPh})[\text{LaI}_2(\text{THF})_3]_2$  has been reported.<sup>171</sup> Trivalent methyl and vinyl samarium derivatives supported by a calixpyrrole ligand system ( $\text{Et}_8\text{-calixpyrrol})(\text{R})\text{Sm}(\mu^3\text{-Cl})[\text{Li}(\text{THF})]_2[\text{Li}_2(\text{THF})_3]$  ( $\text{R} = \text{Me}, \text{CH=CH}_2$ ) were prepared via the reaction of  $(\text{Et}_8\text{-calixpyrrol})(\text{Cl})\text{Sm}[\text{Li}_2(\text{THF})_3]$  with the corresponding organolithium reagent. The dinuclear complex  $(\text{Et}_8\text{-calixpyrrol})\text{Sm}_2\{(\mu\text{-Cl})_2[\text{Li}(\text{THF})_2]\}_2$  was alkylated in diethyl ether, resulting in the formation of the isostructural alkyl complex  $(\text{Et}_8\text{-calixpyrrol})\text{Sm}_2\{(\mu\text{-CH}_3)_2[\text{Li}(\text{THF})_2]\}_2$ .<sup>172,173</sup> The nature of the substituents present on the calixtetrapyrrole tetraanion ligand  $\{[\text{R}_2\text{C}(\text{C}_4\text{H}_2\text{N})_4]^{4-}$  ( $\text{R} = \{-\text{CH}_2\}_5\text{-}, \text{Et}$ ) has been reported to greatly influence the type of reactivity of the corresponding  $\text{Sm}(\text{II})$  compounds with acetylene, as illustrated in Scheme 27.<sup>174</sup>

Butyne reacts with  $(\text{Me}_3[9]\text{aneN}_3)\text{YMe}_3$  ( $\text{Me}_3[9]\text{aneN}_3 = 1,4,7\text{-trimethyl-1,4,7-triazacyclononane}$ ) by C–H activation to give a compound that is characterized as a major allenyl isomer,  $(\text{Me}_3[9]\text{aneN}_3)\text{YMe}_2[\sigma\text{-C}(\text{Me})=\text{C}=\text{CH}_2]$ , in equilibrium with a minor propargyl isomer  $(\text{Me}_3[9]\text{aneN}_3)\text{YMe}_2(\sigma\text{-CH}_2\text{C}\equiv\text{CMe})$ .<sup>135</sup> Treatment of  $\text{Sm}(\text{Tp}^{\text{Me,Me}})_2$  with  $\text{Hg}(\text{C}\equiv\text{CPh})_2$  in THF has been shown to afford the monomeric, base-free lanthanide alkynide complex  $(\text{Tp}^{\text{Me,Me}})_2\text{Sm}(\text{C}\equiv\text{CPh})$ .<sup>175</sup> The reaction of ethynylbenzene with the tris(amides)  $\text{Ln}[\text{N}(\text{SiMe}_3)_2]_3$  ( $\text{Ln} = \text{Ce}, \text{Sm}, \text{Eu}$ ) in the presence of  $\text{NaN}(\text{SiMe}_3)_2$  in THF proceeds with the formation of the complexes  $\text{Na}(\text{THF})_3\text{Ln}[\text{N}(\text{SiMe}_3)_2]_3(\text{C}\equiv\text{CPh})$ .<sup>176</sup>

A single crystal X-ray structure determination of  $\text{Na}(\text{THF})_3\text{Sm}[\text{N}(\text{SiMe}_3)_2]_3(\text{C}\equiv\text{CPh})$  revealed the presence of an ion pair in which the terminal carbon atom of the  $\text{C}\equiv\text{CPh}^-$  ligand is connected with the samarium atom of the  $\text{Sm}[\text{N}(\text{SiMe}_3)_2]_3$  group. The sodium ion is side-on connected with the acetylido group. The distance between the Sm center and the terminal C of the acetylido ligand is 2.485 Å and is understandable as a strongly polar  $\text{Sm}\cdots\text{C}$  bond.  $\text{Na}(\text{THF})_3\text{Sm}[\text{N}(\text{SiMe}_3)_2]_3(\text{C}\equiv\text{CPh})$  does not polymerize methyl metacrylate but catalyzes the ring-opening polymerization of  $\epsilon$ -caprolactone or  $\delta$ -valerolactone.<sup>176</sup> Ytterbium and samarium–benzophenone complexes react with 1-alkynes to generate lanthanide(II) acetylides having diphenylmethoxo ligands. It has been found that these acetylides act as reductants as well as nucleophiles, depending on the electrophiles used. The reaction of Yb with



Organic substituents (either Et or  $-(\text{CH}_2)_5\text{-}$ ) and THF coordinated to the Li atoms have been omitted for clarity.

Scheme 27

benzophenone in THF/1,3-dimethylimidazolidinone followed by treatment with  $\text{Bu}^n\text{C}\equiv\text{CH}$  yielded  $\text{Ph}_2\text{CHOYbC}\equiv\text{CBu}^n$ . Reaction of  $\text{Ph}_2\text{CHOYbC}\equiv\text{CBu}^n$  with  $\text{Pr}^n\text{CHO}$  in the same solvent system gave 88%  $\text{Pr}^n\text{CH}(\text{OH})\text{C}\equiv\text{CBu}^n$ .<sup>177</sup>

#### 4.01.5 Allys

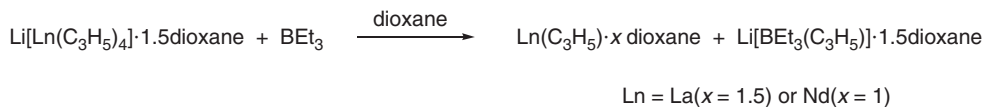
The first neutral tris(allyl)lanthanide complexes  $\text{La}(\eta^3\text{-C}_3\text{H}_5)_3 \cdot 1.5\text{dioxane}$  and  $\text{Nd}(\eta^3\text{-C}_3\text{H}_5)_3 \cdot \text{dioxane}$  were synthesized in 1996 and tested as “single-site” catalysts for the stereospecific polymerization of butadiene. These complexes were obtained by the reaction of tetrakis(allyl)lanthanate(III) complexes  $\text{Li}[\text{Ln}(\text{C}_3\text{H}_5)_4] \cdot 1.5\text{dioxane}$  ( $\text{Ln} = \text{La}$  or  $\text{Nd}$ ) with  $\text{BEt}_3$  in dioxane (Scheme 28). The addition of  $\text{BEt}_3$  led to the abstraction of allyllithium.<sup>178</sup>

In both complexes the three allyl anions are  $\eta^3$ -coordinated. By the coordination of THF in the case of lanthanum the dimeric structure  $[(\mu\text{-THF})_2\text{La}(\eta^3\text{-C}_3\text{H}_5)_3(\eta^1\text{-THF})_2]_2$  and with neodymium a polymeric structure  $[\text{Nd}(\eta^3\text{-C}_3\text{H}_5)_3(\mu\text{-THF})_2]_\infty$  is formed. The dioxane can be split off easily at 40 °C in *n*-hexane without further decomposition to give yellow-green unsolvated  $\text{Nd}(\eta^3\text{-C}_3\text{H}_5)_3$  in 93% yield.<sup>178,179</sup> A more straightforward preparation of the dioxane adduct of tris(allyl)neodymium involves the reaction of  $\text{NdI}_3(\text{THF})_{3.5}$  with 3 equiv. of  $\text{C}_3\text{H}_5\text{MgBr}$  in THF, followed by recrystallization from dioxane. This procedure affords the halide-free product in more than 70% yield.<sup>179</sup> The dimeric tris(allyl)-lanthanum dioxane complex  $[\text{La}(\eta^3\text{-C}_3\text{H}_5)_3(\text{C}_4\text{H}_8\text{O}_2)_{1.5}]_2$  can be transformed by a reaction with other donor ligands into monomeric complexes of the type  $\text{La}(\eta^3\text{-C}_3\text{H}_5)_3\text{L}$  ( $\text{L} = \text{DME}$ , TMEDA, hexamethyl phosphoric triamide (HMPA)).<sup>180</sup>

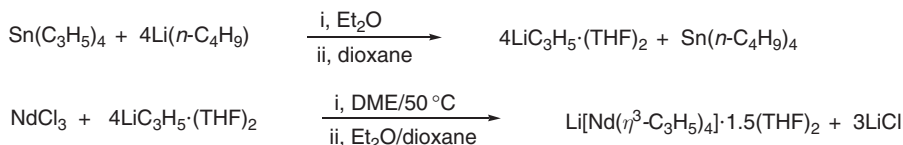
<sup>139</sup>La NMR chemical shifts were measured for several anionic complexes of formulas  $[\text{Li}(\text{THF})_{1.5}][\text{La}(\eta^3\text{-C}_3\text{H}_5)_4]$ ,  $[\text{Li}(\text{THF})_2][\text{Cp}'_n\text{La}(\eta^3\text{-C}_3\text{H}_5)_{4-n}]$  ( $\text{Cp}' = (\eta^5\text{-C}_5\text{H}_5)$ ,  $n = 1, 2$  and  $\text{Cp}' = (\eta^5\text{-Cp}^*)$ ,  $n = 1$ ), and  $[\text{Li}[\text{R}_n\text{La}(\eta^3\text{-C}_3\text{H}_5)_{4-n}]]$  ( $\text{R} = \text{N}(\text{SiMe}_3)_2$ ,  $n = 1, 2$  and  $\text{R} = \text{C}\equiv\text{CSiMe}_3$ ,  $n = 4$ ), and as well as for neutral compounds of formulas  $\text{La}(\eta^3\text{-C}_3\text{H}_5)_3\text{L}_n$  ( $\text{L}_n = (\text{THF})_{1.5}$ ,  $(\text{HMPA})_2$ , TMEDA),  $\text{Cp}'_n\text{La}(\eta^3\text{-C}_3\text{H}_5)_{3-n}$  ( $\text{Cp}' = \text{Cp}$ ,  $\text{Cp}^*$ ,  $n = 1, 2$ ) and  $\text{La}(\eta^3\text{-C}_3\text{H}_5)_3\text{X}(\text{THF})_2$  ( $\text{X} = \text{Cl}$ ,  $\text{Br}$ ,  $\text{I}$ ). Typical ranges of the <sup>139</sup>La NMR shifts were found for the different types of complexes independent of the number and kind of organyl groups directly bonded to lanthanum.<sup>181</sup>

The synthesis and characterization of anionic allylneodymium(III) complexes and their use as catalysts for the stereospecific polymerization of butadiene have been reported. For the already known tetrakis(allyl) complex  $\text{Li}[\text{Nd}(\eta^3\text{-C}_3\text{H}_5)_4] \cdot 1.5\text{dioxane}$  a significantly improved method of preparation from anhydrous  $\text{NdCl}_3$  and  $\text{LiC}_3\text{H}_5 \cdot \text{dioxane}$  in DME was found (Scheme 29).<sup>182</sup>

An anionic tetrakis(allyl)lanthanum complex has been synthesized analogously.<sup>183</sup> By partial protolysis of  $\text{Li}[\text{Nd}(\eta^3\text{-C}_3\text{H}_5)_4] \cdot 1.5\text{THF}_2$  with cyclopentadiene and pentamethylcyclopentadiene the complexes  $\text{Li}[\text{CpNd}(\eta^3\text{-C}_3\text{H}_5)_3] \cdot 2\text{THF}_2$  and  $\text{Li}[\text{Cp}^*\text{Nd}(\eta^3\text{-C}_3\text{H}_5)_3] \cdot 3\text{DME}$  were obtained.<sup>184</sup> Both compounds were also synthesized from the appropriate  $\text{CpNdCl}_2(\text{THF})_3$ . The new compounds  $\text{Li}[\text{CpNd}(\eta^3\text{-C}_3\text{H}_5)_3] \cdot 2\text{THF}_2$  and  $\text{Li}[\text{Cp}^*\text{Nd}(\eta^3\text{-C}_3\text{H}_5)_3] \cdot 3\text{DME}$  were characterized by elemental analyses, IR and <sup>1</sup>H NMR spectroscopy, and  $\text{Li}[\text{Cp}^*\text{Nd}(\eta^3\text{-C}_3\text{H}_5)_3] \cdot 3\text{DME}$  also by X-ray crystal structure analysis.<sup>182</sup> The synthesis of a cationic allylneodymium complex has also been achieved. In the first step, a comproportionation reaction between  $\text{Nd}(\eta^3\text{-C}_3\text{H}_5)_3(\text{dioxane})$  and  $\text{NdCl}_3(\text{THF})_2$  (molar ratio 2:1) gave the bis(allyl)neodymium chloride complex  $(\eta^3\text{-C}_3\text{H}_5)_2\text{NdCl}(\text{THF})_x$ , which was not isolated but treated *in situ* with  $[\text{Me}_3\text{NH}][\text{BPh}_4]$  to afford grass-green  $[(\eta^3\text{-C}_3\text{H}_5)_2\text{NdCl}(\text{THF})_5][\text{BPh}_4] \cdot \text{THF}$ , which has been structurally characterized by an X-ray analysis.<sup>179</sup> The protolysis of  $[\text{La}(\eta^3\text{-C}_3\text{H}_5)_3(\kappa^1\text{-dioxane})]_2(\mu\text{-dioxane})$  and  $[\text{Ln}(\eta^3\text{-C}_3\text{H}_5)_3(\mu\text{-dioxane})]_\infty$  with the diketimine ligand



Scheme 28



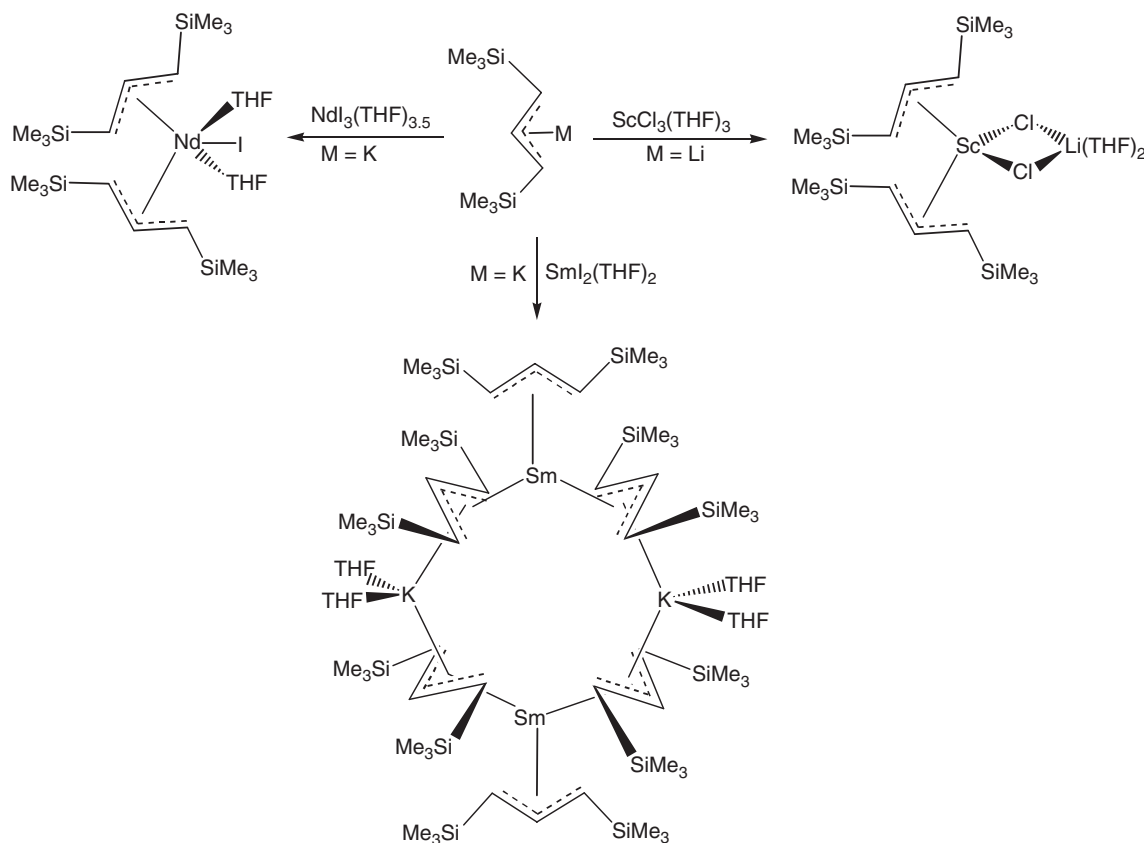
Scheme 29

2-(2,6-diisopropylphenyl)amino-4-(2,6-diisopropylphenyl)imino-2-pentene in THF generates the  $\beta$ -diketiminato complexes  $\text{Ln}(\eta^3\text{-C}_3\text{H}_5)_2\{\kappa^2\text{-HC(MeCNAr)}_2\}$ , ( $\text{Ar} = 2,6\text{-C}_6\text{H}_3\text{iPr}_2$ ;  $\text{Ln} = \text{La, Y, Sm, Nd}$ ). The crystal structure of the Sm derivative showed a distorted tetrahedral  $\text{SmN}_2(\text{allyl})_2$  core, with the samarium atom positioned about  $1.4 \text{ \AA}$  out of the  $\text{C}_3\text{N}_2$  ligand plane. These complexes are highly effective single-component catalysts for the ring-opening polymerization of  $\epsilon$ -caprolactone and *rac*-lactide.<sup>185</sup>

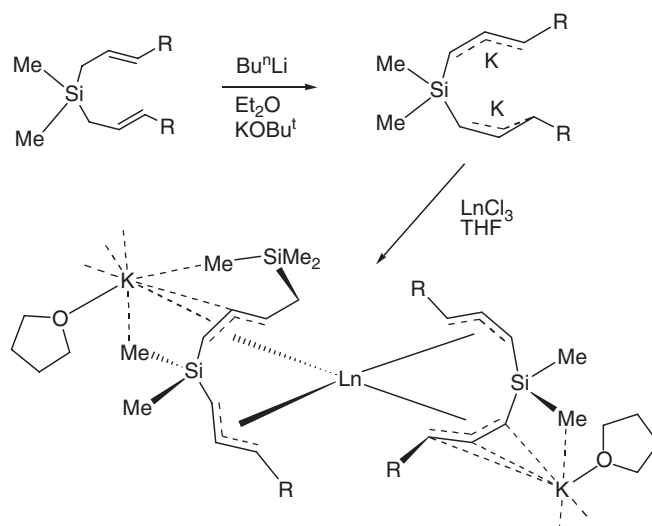
More recent contributions to the chemistry of lanthanide allyl complexes were based on silyl-substituted allyl ligands.<sup>186,186a,187</sup> For example,  $\text{K}(\text{CH}_2\text{CHCHSiMe}_3)_3$  ( $\text{R} = \text{Me, Bu}^t$ ) reacts with  $\text{YCl}_3$  in tetrahydrofuran to afford  $\text{Y}(\text{CH}_2\text{CHCHSiMe}_3)_3$  and  $\text{Y}(\text{CH}_2\text{CHCHSiMe}_2^t\text{Bu})_3(\text{THF})_{1.5}$ , respectively. The reaction of the bulky allyl  $\text{Li}[1,3\text{-C}_3\text{H}_3(\text{SiMe}_3)_2]$  with  $\text{ScCl}_3(\text{THF})_{3.5}$  gave  $\{1,3\text{-C}_3\text{H}_3(\text{SiMe}_3)_2\}_2\text{Sc}(\mu\text{-Cl})_2\text{Li}(\text{THF})_2$ . The potassium reagent  $\text{K}[1,3\text{-C}_3\text{H}_3(\text{SiMe}_3)_2]$  combined with  $\text{YCl}_3(\text{THF})_{3.5}$  and  $\text{LaCl}_3$  furnished  $\text{Y}\{1,3\text{-C}_3\text{H}_3(\text{SiMe}_3)_2\}_2\text{Cl}$  and  $\text{La}\{1,3\text{-C}_3\text{H}_3(\text{SiMe}_3)_2\}_2\text{Cl}(\text{THF})$ , respectively, while with  $\text{SmI}_2(\text{THF})_2$  the allyl-bridged dimer  $[\mu\text{-K}(\text{THF})_2]_2[\text{Sm}\{1,3\text{-C}_3\text{H}_3(\text{SiMe}_3)_2\}_2]$  was obtained as dark green crystals in 62% yield, the first structurally authenticated Sm(II) allyl complex (Scheme 30).<sup>186,186a</sup>

Similar treatment of  $\text{NdI}_3(\text{THF})_{3.5}$  with 2 equiv. of the potassium salt gave a mixture of products, including  $\text{NdI}_2\{1,3\text{-C}_3\text{H}_3(\text{SiMe}_3)_2\}(\text{THF})_{1.25}$  and the crystallographically characterized  $[1,3\text{-C}_3\text{H}_3(\text{SiMe}_3)_2]_2\text{NdI}(\text{THF})_2$  (Scheme 30). These allyl complexes undergo ligand exchange with  $\text{AlBu}_3$  and on activation with methylalumoxane (MAO) catalyze the polymerization of butadiene; the neodymium complexes proved particularly active.<sup>185–187,187a</sup>

A new class of anionic allyl-lanthanide complexes of the type  $[\text{K}(\text{THF})_4][\{1,3\text{-C}_3\text{H}_3(\text{SiMe}_3)_2\}_3\text{LnI}]$  ( $\text{Ln} = \text{Ce, Pr, Nd, Gd, Tb, Dy, Er}$ ) have been prepared and isolated by the reaction of 3 equiv. of the 1,3-bis(trimethylsilyl)allyl anion with  $\text{LnI}_3$ . The neutral complex  $[1,3\text{-C}_3\text{H}_3(\text{SiMe}_3)_2]_3\text{Nd}(\text{THF})$  (green crystals) has been isolated from the reaction of the triflate precursor  $\text{Nd}(\text{O}_3\text{SCF}_3)_3$  with 3 equiv. of  $\text{K}[1,3\text{-C}_3\text{H}_3(\text{SiMe}_3)_2]$ . These complexes have been structurally characterized using single crystal X-ray diffraction.<sup>187,187a</sup> The synthetic route has been extended to the preparation of the first *ansa*-bis(allyl)lanthanide complexes (Scheme 31). The crystal structure determination of the



Scheme 30



Scheme 31

La derivative revealed the presence of a coordination polymer with potassium bridging two allyl moieties of two neighboring lanthanide units and close  $K \cdots CH_3Si$  contacts.<sup>188</sup>

A novel class of lanthanide(II) and lanthanide(III) heteroallyl complexes containing the 1,3-bis(trimethylsilyl)-1-aza-allyl ligand,  $\eta^3-N(SiMe_3)C(Bu^t)CHSiMe_3^- (=LL')$ , has been explored. Complexes of the formula  $Sm(LL')_2(THF)$ ,  $Yb(LL')_2$ , and  $Ln(LL')_2X(THF)_n$  ( $Ln = Ce, Nd, X = Cl, n = 1$ ;  $Ln = Sm, X = I, n = 1$ ;  $Ln = Yb, X = I, n = 0$ ) have been synthesized by the reaction of the appropriate lanthanide(II) or lanthanide(III) halides with 2 equiv. of 1,3-bis(trimethylsilyl)-1-aza-allyl-potassium  $K(LL')_n$ . X-ray structural analyses of several representatives revealed  $\eta^3$ -coordination of the heteroallylic ligand in all cases.<sup>189</sup>

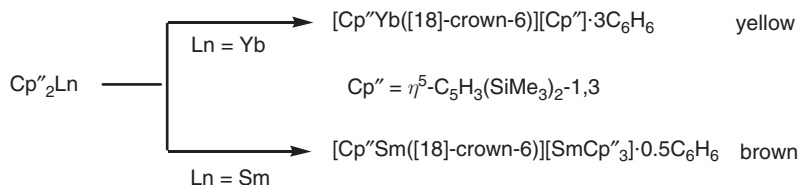
#### 4.01.6 Cyclopentadienyl Compounds

Mono(cyclopentadienyl) complexes of the rare earth metals have been comprehensively reviewed by Okuda and Arndt.<sup>38</sup>

##### 4.01.6.1 $CpLnX$ Compounds

Cationic lanthanide complexes of samarium and ytterbium,  $[Cp''Sm([18]\text{-crown-6})][SmCp''_3] \cdot 0.5C_6H_6$  and  $[Cp''Yb([18]\text{-crown-6})][Cp''] \cdot 3C_6H_6$  [ $Cp'' = \eta^5-C_5H_3(SiMe_3)_{2-1,3}$ ], have been prepared by the reaction between bis(cyclopentadienyl) lanthanide and [18]-crown-6 in benzene (Scheme 32).<sup>190</sup>

The samarium complex consists of two separate ions. The cation  $[Cp''Sm([18]\text{-crown-6})]^+$  has a sandwich-like structure and the samarium is located within the cavity of the quasi-parallel  $Cp''$  and the crown ether ligand. The centroid of the  $Cp''$  ring and the six oxygen atoms of the crown ether form a strongly distorted pentagonal bipyramidal arrangement around Sm. The anion  $[SmCp''_3]^-$  forms an almost trigonal planar arrangement with respect to the centroids of the three  $Cp''$  ligands, as in the neutral molecule  $SmCp''_3$ .<sup>190</sup>

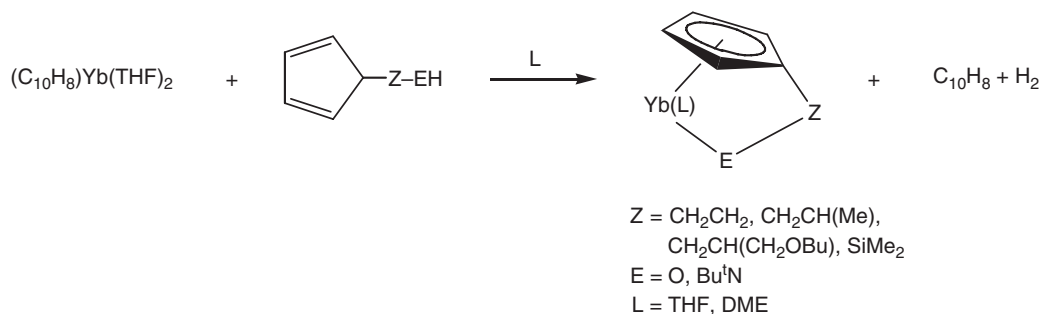


Scheme 32

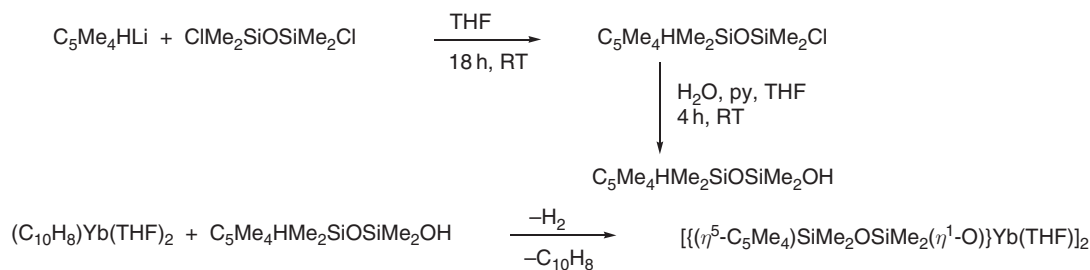
Reactions of ytterbium naphthalene,  $(C_{10}H_8)Yb(THF)_2$ , with 2-cyclopentadienyl ethanol, 1-cyclopentadienylpropan-2-ol, and 3-cyclopentadienyldimethylsilyl-*t*-butylamine have been studied as a convenient synthetic route to half-sandwich complexes of divalent ytterbium.<sup>191</sup> The divalent ytterbium complexes with chelating bifunctional cyclopentadienyl ligands  $(C_5H_4CH_2CH_2O)Yb(THF)$ ,  $(C_5H_4CH_2CH_2O)Yb(DME)$ ,  $[C_5H_4CH_2CH(Me)O]Yb(THF)$ ,  $[C_5H_4CH_2CH(CH_2OC_4H_9)O]Yb(THF)$ , and  $[C_5H_4SiMe_2(NBu^t)]Yb(THF)$  were obtained and characterized (Scheme 33).<sup>191</sup>

The dimeric half-sandwich complex  $[(C_5Me_4SiMe_2OSiMe_2O)Yb(THF)]_2$  was obtained in a similar manner from the interaction of  $(C_{10}H_8)Yb(THF)_2$  with  $C_5Me_4SiMe_2OSiMe_2OH$  in THF at room temperature, affording  $H_2$  and  $C_{10}H_8$  (Scheme 34). The complex possesses inversion symmetry imposing the central four-membered ring  $(Yb-O)_2$  to be planar with ytterbium oxygen distances of 2.274 Å and 2.319 Å and a Yb–Cp(centroid) distance of 2.41 Å.<sup>192</sup>

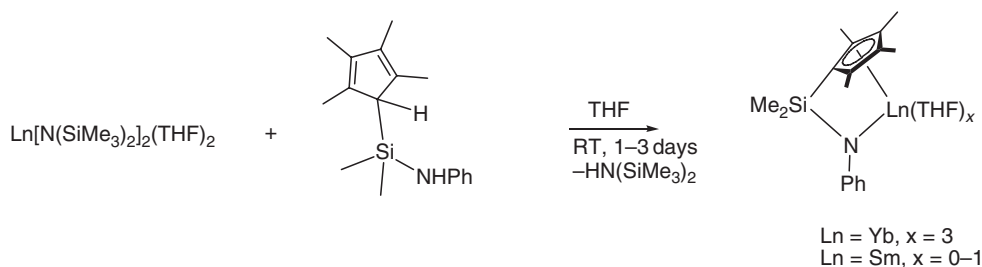
In the case of the ligand 3-cyclopentadienyl-1-butoxy-2-propanol,  $C_5H_4CH_2CH(OH)OBu^n$ , the reaction with  $(C_{10}H_8)Yb(THF)_2$  afforded the unusual tetranuclear, cubane-like complex  $\{[C_5H_4CH_2CH(O)OBu^n]Yb\}_4$  in the form of ruby-red crystals, which have been characterized by an X-ray diffraction analysis.<sup>193</sup> Reactions of  $Ln[N(SiMe_3)_2]_2(THF)_2$  ( $Ln = Sm, Yb$ ) with 1 equiv. of  $(C_5Me_4H)SiMe_2NHPH$  afforded the first linked cyclopentadienyl-anilido (or amido) lanthanide(II) complexes,  $[Me_2Si(C_5Me_4)(NPh)]Ln(THF)_x$  ( $Ln = Sm, x = 0, 1$ ;  $Ln = Yb, x = 3$ ) in 75–84% isolated yields (Scheme 35).<sup>194</sup>



Scheme 33



Scheme 34



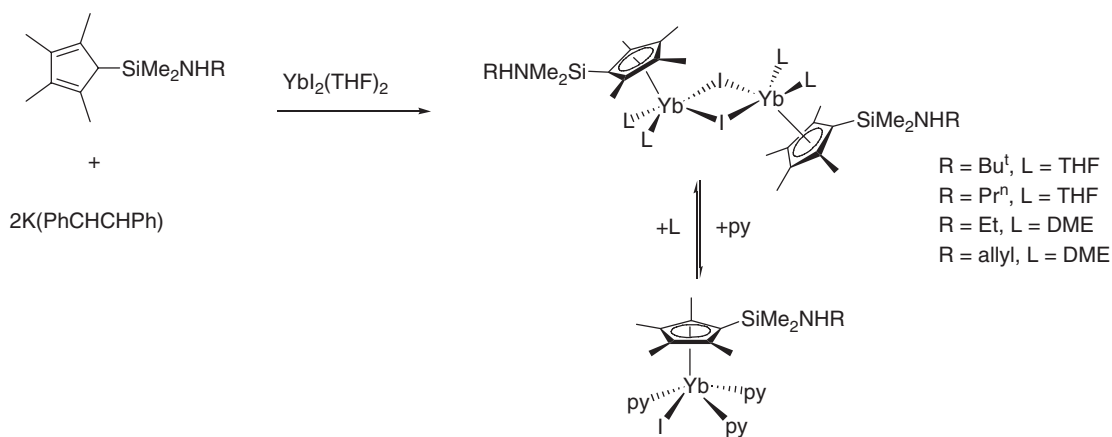
Scheme 35

Reactions of the aminosilylcyclopentadienes  $(C_5Me_4H)SiMe_2NHR$  ( $R = Et, allyl, Pr^i, Bu^t$ ) with  $YbI_2(THF)_2$  in the presence of 2 equiv. of potassium 1,2-diphenylethylenide in THF at room temperature gave the diamagnetic half-sandwich complexes  $[(C_5Me_4SiMe_2NHR)YbL_n(\mu-I)]_2$  ( $L = THF, n = 2$ ;  $L = DME, n = 1$ ) (Scheme 36). The *t*-butylamido complex was characterized by X-ray structural analysis as a binuclear complex containing a non-chelating aminosilylcyclopentadienyl ligand. In pyridine partial dissociation into a mononuclear species occurs (Scheme 36).<sup>195</sup>

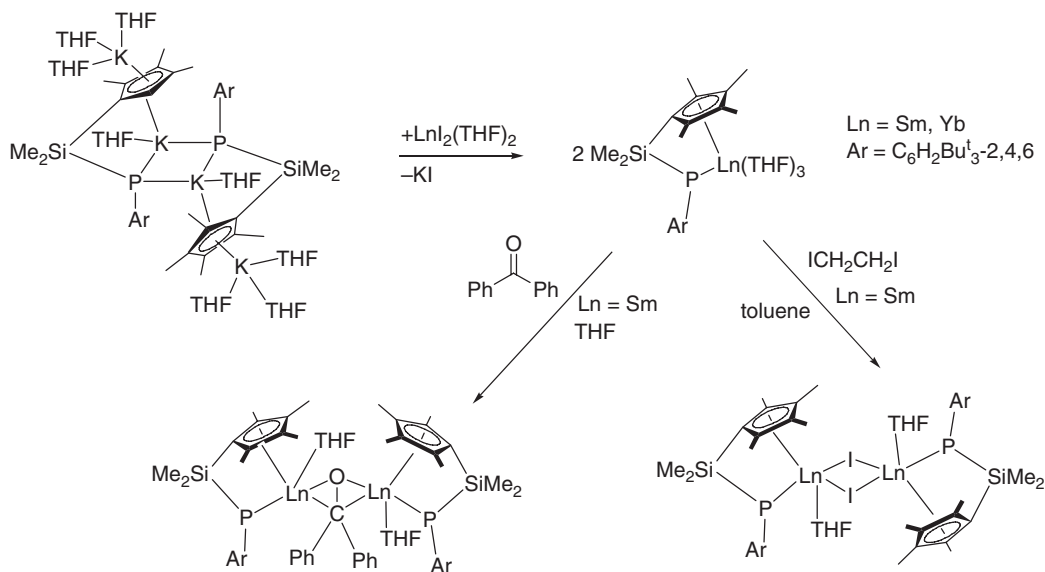
The synthesis, structures, and reactivity of the related silylene-linked cyclopentadienyl-phosphido lanthanide complexes has been studied. Scheme 37 illustrates the synthesis of the ligand precursors and the corresponding lanthanide(II) derivatives as well as reactions of the latter with 1,2-diiodoethane and benzophenone, which lead to binuclear lanthanide(III) species.<sup>196</sup>

Synthetic routes leading to  $\sigma$ -alkyl complexes containing the silylene-linked cyclopentadienyl-phosphido ligand are outlined in Scheme 38.<sup>197</sup>

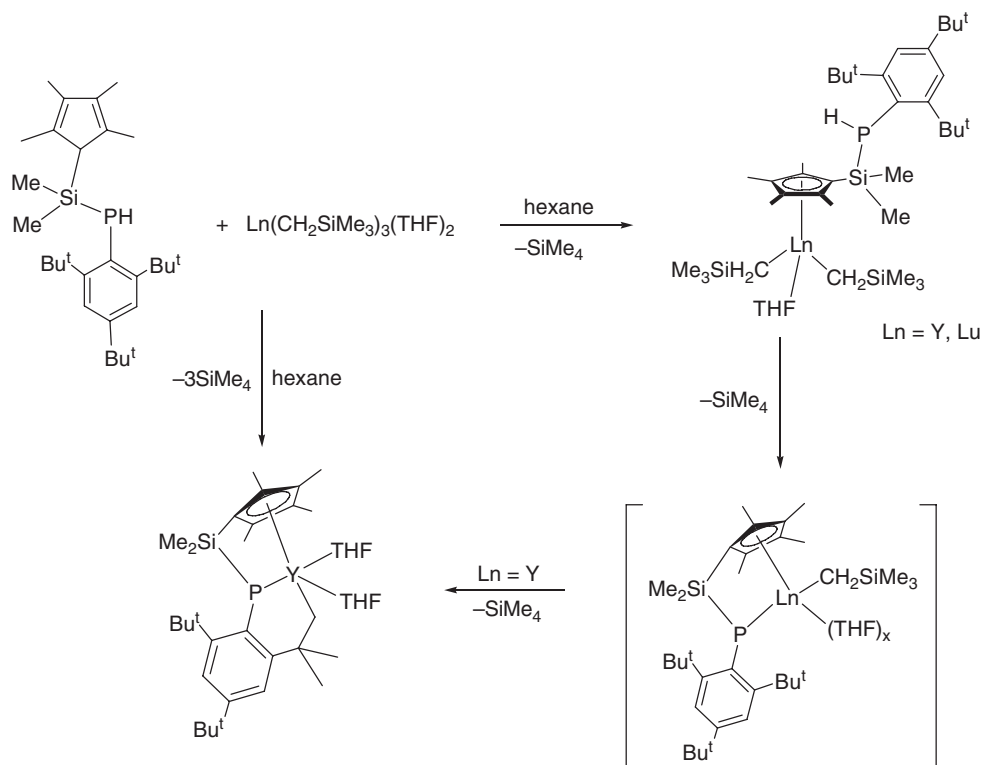
Two different synthetic routes leading to the iodo-bridged dimer  $[(C_5HPr^i_4)Sm(\mu-I)(THF)]_2$  have been reported.<sup>198</sup> A mixture of 1,2- and 1,3-disubstituted isomers of potassium cyclopentadienide with two



Scheme 36



Scheme 37



Scheme 38

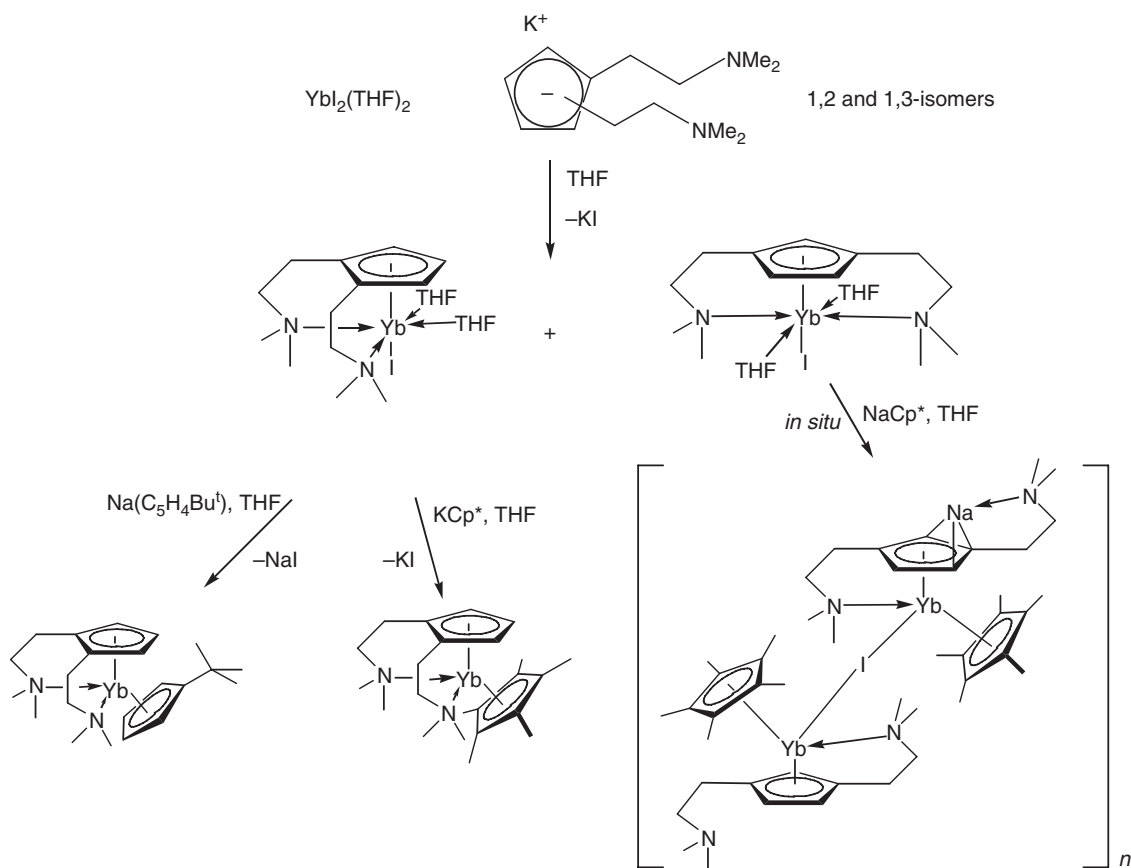
dimethylaminoethyl side chains was reacted with  $\text{YbI}_2(\text{THF})_2$  to form only  $[\eta^5:\eta^1\text{-C}_5\text{H}_3(\text{CH}_2\text{CH}_2\text{NMe}_2)_2\text{-1,2}]\text{Yb}(\text{THF})_2$  crystals. The non-crystallizing 1,3-isomer left in solution reacts with  $\text{NaCp}^*$  forming the polymeric mixed metallocene *-ate* complex (Scheme 39). The reaction of  $[\eta^5:\eta^1\text{-C}_5\text{H}_3(\text{CH}_2\text{CH}_2\text{NMe}_2)_2\text{-1,2}]\text{Yb}(\text{THF})_2$  with  $\text{Cp}^*\text{K}$  or  $\text{Na}(\text{C}_5\text{H}_4\text{Bu}^t)$  results in the formation of the sandwich complexes  $[\eta^5:\eta^1\text{-C}_5\text{H}_3(\text{CH}_2\text{CH}_2\text{NMe}_2)_2\text{-1,2}]\text{YbCp}^*$  and  $[\eta^5:\eta^1\text{-C}_5\text{H}_3(\text{CH}_2\text{CH}_2\text{NMe}_2)_2\text{-1,2}]\text{Yb}(\text{C}_5\text{Me}_4\text{Bu}^t)$ , respectively.<sup>199</sup>

The synthesis and characterization of divalent lanthanide complexes of a triazacyclononane-functionalized tetramethylcyclopentadienyl ligand have been reported.<sup>200,201</sup> Addition of  $\text{LnI}_2(\text{THF})_2$  ( $\text{Ln} = \text{Sm, Yb}$ ) to  $\text{K}[\text{C}_5\text{Me}_4\text{SiMe}_2(\text{Pr}^i\text{-tacn})]$  ( $\text{Pr}^i\text{-tacn} = 1,4\text{-diisopropyl-1,4,7-triazacyclononane}$ ) in THF yielded the monomeric organolanthanide  $[\text{C}_5\text{Me}_4\text{SiMe}_2(\text{Pr}^i\text{-tacn})]\text{SmI}$  (dark red crystals, 85% yield) and  $[\text{C}_5\text{Me}_4\text{SiMe}_2(\text{Pr}^i\text{-tacn})]\text{YbI}$  (red blocks, 80% yield) (Scheme 40). The crystal structures of both compounds have been explored.<sup>200</sup>

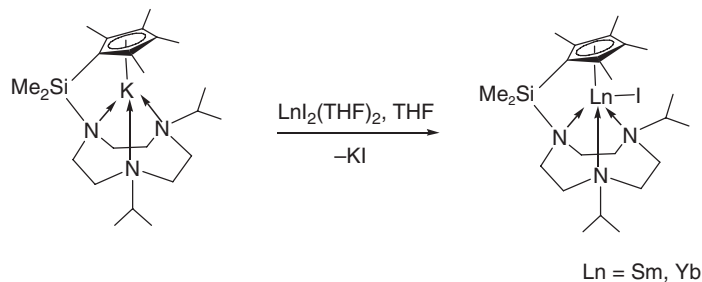
The ytterbium(II) complex  $\text{Yb}[\text{C}_5\text{H}_3(\text{SiMe}_3)_2\text{-1,3}](\text{OAr})(\text{THF})_x$  ( $\text{OAr} = \text{OC}_6\text{H}_2\text{Bu}^t\text{-2,6-Me-4}$ ) was obtained from the reaction of either  $\text{Na}[\text{C}_5\text{H}_3(\text{SiMe}_3)_2\text{-1,3}]$  or  $\text{Yb}[\text{C}_5\text{H}_3(\text{SiMe}_3)_2\text{-1,3}]_2(\text{THF})$  with  $\text{Yb}(\text{OAr})_2(\text{THF})_3$ .<sup>202</sup> Donor-functionalized amide ligands such as *N*-(methoxyphenyl)-*N*-(trimethylsilyl)amide have been employed as ancillary ligands in the preparation of dimeric mono(cyclopentadienyl)lanthanide chloride complexes.<sup>203</sup>

The synthesis and characterization of mixed pyrazolylborate/cyclopentadienyl derivatives of divalent lanthanides have been reported.<sup>204</sup> Reaction of  $[(\text{Tp}^{\text{tBu,Me}})\text{YbH}]_2$  ( $\text{Tp}^{\text{tBu,Me}} = \text{hydrotris}(3\text{-}t\text{-butyl-5-methylpyrazolyl})\text{borate}$ ) with cyclopentadiene ( $\text{C}_5\text{H}_6$ ) and trimethylsilylcyclopentadiene ( $\text{C}_5\text{H}_5\text{SiMe}_3$ ) resulted in the formation of the corresponding mixed ligand complexes  $(\text{Tp}^{\text{tBu,Me}})\text{Yb}(\text{C}_5\text{H}_4\text{R})$  ( $\text{R} = \text{H, SiMe}_3$ ) in quantitative yield. The complexes were characterized by multinuclear NMR spectroscopy. The complex  $(\text{Tp}^{\text{tBu,Me}})\text{Yb}(\text{C}_5\text{H}_4\text{SiMe}_3)$  was characterized by single crystal X-ray diffraction. This complex consists of well-separated monomeric units with a  $\text{C}_5\text{H}_4\text{SiMe}_3$  ring, but the  $\text{Tp}^{\text{tBu,Me}}$  ligands exhibit an unusual distortion. One of the pyrazolyl rings is rotated in such a way as to bring both pyrazolyl nitrogens in bonding contact with ytterbium, while two of the pyrazolyl moieties interact the usual way (lone-pair donation from 2-N). This is evidenced by the large  $\text{Yb-N12-N11-B}$  torsional angle,  $75.3(3)^\circ$ , compared with  $14.9(3)^\circ$  and  $14.3(3)^\circ$  for the other two pyrazolyl rings.<sup>204</sup>





Scheme 39



Scheme 40

#### 4.01.6.2 $\text{Cp}_2\text{Ln}$ Compounds

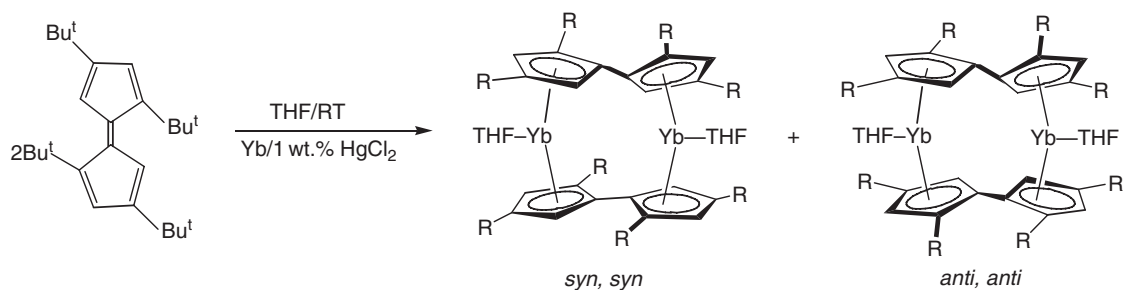
##### 4.01.6.2.1 Synthesis

The solubility of bis(cyclopentadienyl)samarium(II) in THF/ether mixtures has been studied, showing that bis(cyclopentadienyl)samarium(II), also formed in the reaction of samarium with  $\text{Cp}_2\text{Hg}$ , is not soluble in a THF/ether mixture.<sup>205</sup> The one-pot reaction between  $\text{SmX}_2$  ( $\text{X} = \text{Cl}, \text{I}$ ) and  $\text{Bu}^t\text{Li}$  in THF at  $-40^\circ\text{C}$ , followed by the addition of  $\text{NaCp}$  resulted in a dark red solution, from which X-ray quality crystals of  $\text{Cp}_2\text{Sm}(\text{THF})_2$  could be obtained.<sup>206</sup> High yields of  $\text{Cp}_2\text{Yb}$  have been obtained from the reaction of  $\text{YbI}_2$  with  $\text{CpCuPPh}_3$ .<sup>207</sup> The complex  $\text{NaYbCp}_3$ , prepared from  $\text{Cp}_3\text{Yb}$  and sodium naphthalenide in THF and crystallized by sublimation at ca.  $400^\circ\text{C}$  ( $<10^{-4}$  mm Hg), is a three-dimensional polymer in which  $\mu\text{-}\eta^5\text{:}\eta^5\text{-Cp}$  groups link sodium and ytterbium with each

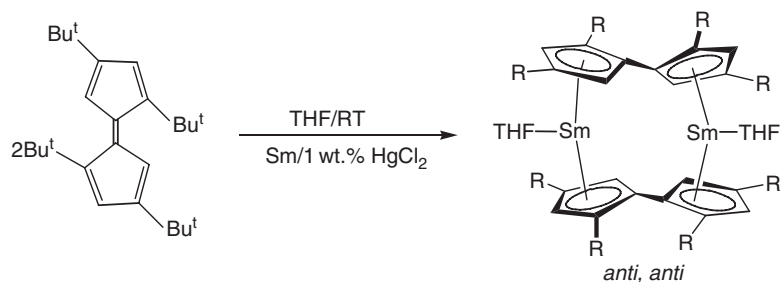
metal having a pseudo-trigonal arrangement of Cp ligands. Unsolvated  $\text{Cp}_2\text{Yb}$ , similarly crystallized as red crystals by sublimation at  $420^\circ\text{C}$  ( $4 \times 10^{-5}$  mm Hg), has a polymeric chain structure with one terminal and two bridging Cp ligands per ytterbium, and there is  $\eta^1$ -bonding between adjacent chains.<sup>208</sup> Polymeric  $(\text{Cp}_2\text{Yb} \cdot \text{THF})_n$ , the ionic *ate*-complex  $\text{Cp}_3\text{YbNa}$ , and the mono-adduct  $(\text{Bu}^t_2\text{C}_5\text{H}_3)_2\text{Yb} \cdot \text{THF}$  were prepared through reactions of  $\text{CpNa}$  or  $\text{Bu}^t_2\text{C}_5\text{H}_3\text{Na}$  with  $\text{YbI}_2$  in THF.<sup>209</sup> In a new synthetic route leading to  $\text{Cp}_2\text{Yb}(\text{THF})_2$  the complex was obtained by reduction of the  $\text{Cp}_2\text{YbCl}(\text{THF})$  with cyclooctadienyl potassium.<sup>210</sup> A tetramethylurea adduct of bis(cyclopentadienyl) ytterbium(II),  $\text{Cp}_2\text{Yb}(\text{TMU})_2$  (TMU = 1,1,3,3-tetramethylurea), was obtained by addition of  $\text{Me}_2\text{NCONMe}_2$  to  $\text{Cp}_2\text{Yb}(\text{THF})_2$ , which was previously synthesized by reduction of  $\text{Cp}_2\text{YbCl}(\text{THF})$  with sodium naphthalenide. In the structure, the ytterbium atom has a distorted tetrahedral arrangement formed by the two Cp rings and two oxygen atoms of the TMU ligand.<sup>211</sup> The synthesis and crystal structure of  $(\text{C}_5\text{H}_4\text{Me})_2\text{Yb}(\text{DME})$  have been reported, which was prepared through reduction of the chloro precursor  $[(\text{C}_5\text{H}_4\text{Me})_2\text{Yb}(\mu\text{-Cl})]_2$  with metallic sodium in THF followed by crystallization from DME.<sup>212</sup> The  $\text{Ln}(\text{II})$ -complexes  $(\text{C}_5\text{Me}_4\text{H})_2\text{Ln}(\text{THF})_2$  ( $\text{Ln} = \text{Sm}, \text{Yb}$ ) were synthesized by the reactions of the appropriate  $\text{LnI}_2$  with  $\text{Na}(\text{C}_5\text{Me}_4\text{H})$  in THF.<sup>213</sup> Similarly, the mono-THF solvates  $\text{Cp}^*\text{Sm}(\text{THF})$  and  $[\text{C}_5\text{H}_2(\text{SiMe}_3)_3][\text{C}_5\text{H}_3(\text{SiMe}_3)_2]\text{Sm}(\text{THF})$  were prepared and structurally characterized.<sup>214</sup> The sodium salt of the ethyltetramethylcyclopentadienyl ligand has been used for the synthesis of the corresponding samarium(II) and ytterbium(II) complexes  $(\text{C}_5\text{Me}_4\text{Et})_2\text{Ln}(\text{THF})$  ( $\text{Ln} = \text{Sm}$  or  $\text{Yb}$ ). The compounds were characterized by NMR and mass spectrometry. The structure of  $(\text{C}_5\text{Me}_4\text{Et})_2\text{Yb}(\text{THF})$  was determined by X-ray diffraction. The ytterbium complex has a typical bent metallocene structure in which the Yb atom is coordinated by two  $\text{C}_5\text{Me}_4\text{Et}$  ligands and one oxygen atom of the solvating THF.<sup>215</sup>

In a one-step treatment of the zero-valent metals a *t*-butyl substituted pentafulvalene derivative yielded pentafulvalenyl dilanthanide(II) sandwich complexes ( $\text{Ln} = \text{Sm}, \text{Yb}$ ). A two-electron transfer of a lanthanide to the pentafulvalene ( $= \text{Pf}$ ), a system with 10  $\pi$ -electrons, gave a  $\text{Pf}^{2-}$  dianion (Scheme 41).<sup>216</sup>

In the ytterbium case, a 60:40 mixture of two  $\text{Yb}(\text{II})$  isomers could be isolated in 68% yield. The isomers differ from one another by the alignment of the  $\text{Bu}^t$  substituents on both Cp rings of the Pf ligands. In the major isomer of the Yb complex the  $\text{Bu}^t$  substituents on both Cp rings of the Pf ligands are eclipsed. In neither isomer is there a metal interaction  $\text{Yb}-\text{Yb}$  (4.94, 5.00 Å). In the samarium case, only the *anti,anti*-compound similar to the *anti,anti*-ytterbium compound was obtained (Scheme 42). In the samarium complex there is also no  $\text{Sm}-\text{Sm}$  metal interaction (4.93 Å).<sup>216</sup>



Scheme 41



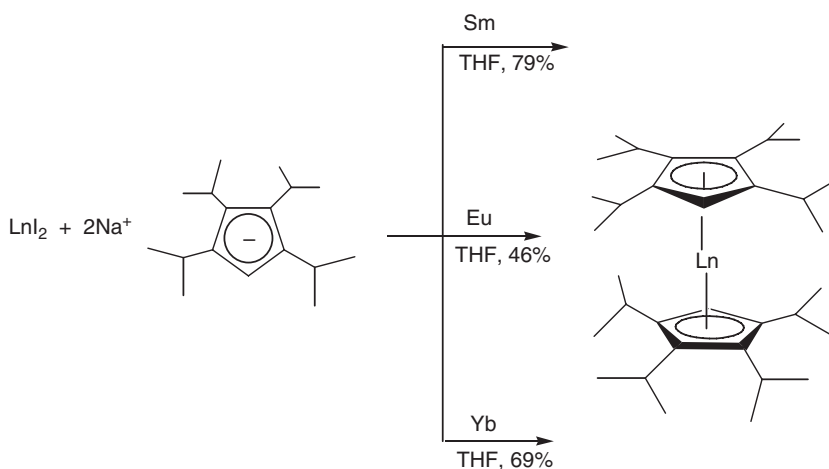
Scheme 42

The synthesis of several new metallocenes of divalent samarium, europium, and ytterbium has been achieved with the use of the especially bulky cyclopentadienyl ligands tetraisopropylcyclopentadienide ( $\text{C}_5\text{HPr}_4^{\text{I}}^-$ ), 1,2,4-tri(*t*-butyl)cyclopentadienide ( $\text{C}_5\text{H}_2\text{Bu}_3^{\text{I}}^-$ ), and penta-isopropylcyclopentadienide ( $\text{C}_5\text{Pr}_5^{\text{I}}^-$ ). Octaisopropylmetallocenes of the lanthanides Sm, Eu, Yb can be obtained easily from the diiodides of the rare earth elements according to Scheme 43. The Cp–Sm–Cp angle in unsolvated octaisopropylsamarocene is  $152^\circ$ , which is larger than in the permethylated analog.<sup>217,218</sup>

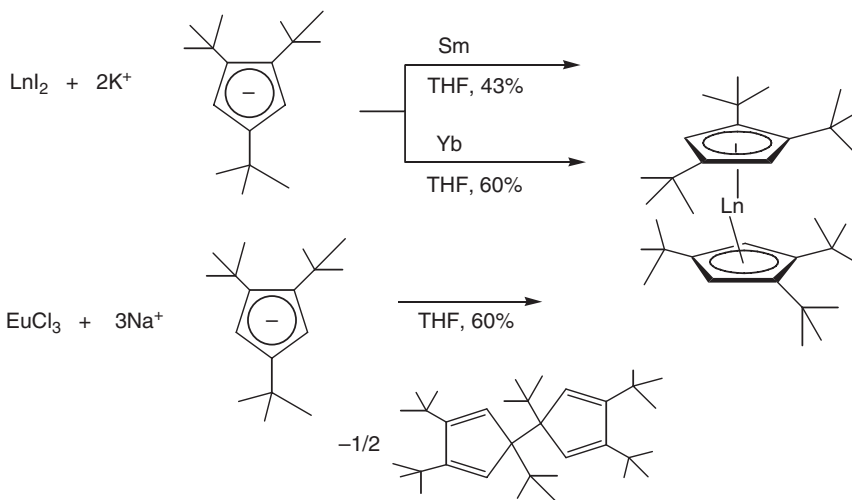
The hexa(*t*-butyl)metallocenes of Sm, Eu, and Yb have been prepared following the routes depicted in Scheme 44. Adducts of the samarocene with THF and of the samarocene and ytterbocene with 2,6-Me<sub>2</sub>C<sub>6</sub>H<sub>3</sub>NC have also been prepared and characterized.<sup>218,219</sup> The deca-*i*-propylmetallocenes have been synthesized from the metal and the free penta-*i*-propylcyclopentadienyl radical (Scheme 45).<sup>218</sup>

The three europocenes octa(*i*-propyl)europocene, hexa(*t*-butyl)europocene, and deca(*i*-propyl)europocene show fluorescence in daylight or under UV irradiation (336 nm). The europocenes octa(*i*-propyl)europocene and hexa(*t*-butyl)europocene are bent-sandwich complexes, whereas for the deca(*i*-propyl)europocene axial symmetry with parallel five-membered rings has been observed.<sup>218</sup>

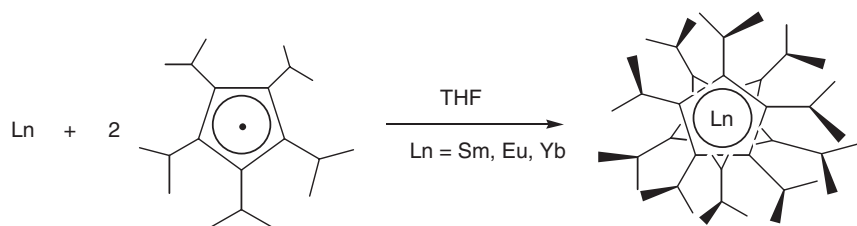
The reaction of CO (cf. Section 4.01.2) with the divalent lanthanide decamethylmetallocenes  $\text{Cp}^*_2\text{Ln}$  (Ln = Sm, Eu, Yb) has been studied in toluene or methyleyclohexane solution in a high pressure infrared cell. In all cases, the



Scheme 43



Scheme 44



Scheme 45

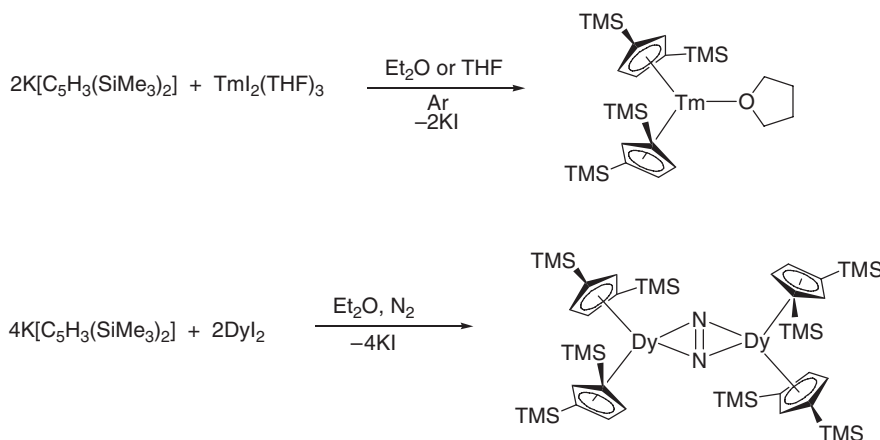
monocarbonyl complex  $\text{Cp}^*_2\text{LnCO}$  was observed to form under CO pressure. The CO stretching frequencies for  $\text{Cp}^*_2\text{SmCO}$  ( $2153\text{ cm}^{-1}$ ) and  $\text{Cp}^*_2\text{EuCO}$  ( $2150\text{ cm}^{-1}$ ) are greater than that of free CO ( $2134\text{ cm}^{-1}$  in toluene or methylcyclohexane). In contrast,  $\text{Cp}^*_2\text{YbCO}$  has  $\nu\text{CO}$   $2114\text{ cm}^{-1}$ , below that of free CO. This 1 : 1 complex is formed at low CO pressure ( $<2$  bar), while at higher CO pressures the 1 : 2 adduct  $\text{Cp}^*_2\text{Yb}(\text{CO})_2$  with an even lower  $\nu\text{CO}$  value at  $2072\text{ cm}^{-1}$  predominates.<sup>220–222</sup>

Coordination of carbon monoxide and isocyanides to divalent ytterbocenes have been studied in detail. In the course of these investigations, the crystal structures of  $(\text{C}_5\text{H}_3\text{Bu}^t_{2-1,3})_2\text{Yb}(\text{2,6-Me}_2\text{C}_6\text{H}_3\text{NC})_2$  and  $[\text{C}_5\text{H}_3(\text{SiMe}_3)_2-1,3]_2\text{Yb}(\text{2,6-Me}_2\text{C}_6\text{H}_3\text{NC})_2$  have been determined.<sup>222</sup>

The reaction between  $\text{YbI}_2$  and  $\text{NaC}_5\text{H}_3\text{Bu}^t_{2-1,3}$  in diethyl ether or 1,2-DME afforded the divalent bulky substituted bis(di-*t*-butylcyclopentadienyl)ytterbium complexes  $(\text{C}_5\text{H}_3\text{Bu}^t_{2-1,3})_2\text{Yb}(\text{OEt}_2)$  and  $(\text{C}_5\text{H}_3\text{Bu}^t_{2-1,3})_2\text{Yb}(\text{DME})$ , respectively. The compound  $(\text{C}_5\text{H}_3\text{Bu}^t_{2-1,2})_2\text{Yb}(\text{DME})$  was also formed. Both  $(\text{C}_5\text{H}_3\text{Bu}^t_{2-1,3})_2\text{Yb}(\text{OEt}_2)$  and  $(\text{C}_5\text{H}_3\text{Bu}^t_{2-1,2})_2\text{Yb}(\text{DME})$  were structurally characterized by X-ray methods.<sup>223</sup> The synthesis of  $(\text{C}_5\text{H}_3\text{Bu}^t_{2-1,3})_2\text{Eu}(\text{THF})$  has been achieved via the reaction of  $\text{EuI}_2$  with 2 equiv. of  $\text{NaC}_5\text{H}_3\text{Bu}^t_{2-1,3}$  in THF. The mixed cyclopentadienyl complex  $(\text{C}_5\text{H}_3\text{Bu}^t_{2-1,3})\text{Cp}^*\text{Yb}(\text{THF})$  was obtained from the subsequent reaction of  $\text{YbI}_2$  with  $\text{NaCp}^*$  and  $\text{NaC}_5\text{H}_3\text{Bu}^t_{2-1,3}$  in THF. Single crystal X-ray determinations revealed the monomeric structures of  $(\text{C}_5\text{H}_3\text{Bu}^t_{2-1,3})_2\text{Eu}(\text{THF})$  and  $(\text{C}_5\text{H}_3\text{Bu}^t_{2-1,3})\text{Cp}^*\text{Yb}(\text{THF})$ .<sup>224</sup> The crystal and molecular structure of  $[\text{C}_5\text{H}_3(\text{SiMe}_3)_2]_2\text{Yb}(\text{THF})$  has been determined. The formally seven-coordinate  $\text{Yb}(\text{II})$  ion is symmetrically coordinated to the 1,3- $\text{C}_5\text{H}_3(\text{SiMe}_3)_2$  ligands with a centroid–Yb–centroid angle of  $136^\circ$ .<sup>225</sup>

The *i*-propyltetramethylcyclopentadienyl samarium complexes  $(\text{C}_5\text{Me}_4\text{Pr}^i)_2\text{Sm}(\text{THF})$  and  $[(\text{C}_5\text{Me}_4\text{Pr}^i)_2\text{Sm}]_2(\mu\text{-Cl})$  were synthesized and characterized. The complex  $(\text{C}_5\text{Me}_4\text{Pr}^i)_2\text{Sm}(\text{THF})$  has a  $141.6^\circ$  ring centroid–Sm–ring centroid angle. In the mixed valence complex  $[(\text{C}_5\text{Me}_4\text{Pr}^i)_2\text{Sm}]_2(\mu\text{-Cl})$  the two bent metallocene units of the complex are connected by an asymmetrical chloride bridge. In the 1 : 2 reaction of  $\text{LnI}_2(\text{THF})_x$  ( $\text{Ln} = \text{Sm}, \text{Yb}$ ) with  $\text{Na}[\text{C}_5\text{Me}_4\text{Pr}^i]$  in THF the divalent metallocene complexes  $(\text{C}_5\text{Me}_4\text{Pr}^i)_2\text{Ln}(\text{THF})$  were formed.<sup>226</sup> The divalent lanthanide complexes  $[\text{Li}(\text{DME})_3]_2[(\text{C}_5\text{H}_4(\text{CMe}_2\text{Ph}))_2\text{Ln}(\mu\text{-X})_2]$  ( $\text{Ln} = \text{Sm}, \text{X} = \text{I}$  (black crystals);  $\text{Ln} = \text{Yb}, \text{X} = \text{Cl}$  (dark red crystals)) consist of two  $[\text{Li}(\text{DME})_3]^+$  cations and halide-bridged dimeric anions in the solid state.<sup>227</sup> In a successful attempt to expand divalent organolanthanide chemistry, the synthesis and structural characterization of the first organothulium(II) complex has been achieved. While the reaction of  $\text{TmI}_2(\text{THF})_3$  with  $\text{KCp}^*$  under argon led to diethyl ether decomposition, the use of  $\text{KCp}''$  [ $\text{Cp}'' = 1,3\text{-(Me}_3\text{Si)}_2\text{C}_5\text{H}_3$ ] in THF allowed the isolation of the organothulium(II) complex  $\text{Cp}''_2\text{Tm}(\text{THF})$  in 90% yield. The purple crystalline compound was structurally characterized. An attempt to isolate the corresponding divalent dysprosium complex led to the formation of the dark-orange dysprosium(III) dinitrogen complex  $[\text{Cp}''_2\text{Dy}]_2(\mu\text{-N}_2)$  (Scheme 46).<sup>228,228a</sup>

More recently another thulium(II) metallocene complex,  $\text{Tm}(\text{C}_5\text{H}_3\text{Bu}^t_{2-1,3})_2$ , has been synthesized analogously from  $\text{TmI}_2(\text{THF})_3$  and 2 equiv. of  $\text{Na}[\text{C}_5\text{H}_3\text{Bu}^t_{2-1,3}]$ , and isolated as a reddish-purple solid.<sup>229</sup> The reaction of  $\text{YbI}_2$  with 2 equiv. of  $\text{NaCp}''$  in boiling toluene afforded  $\text{Na}[(\text{Cp}''_2\text{Yb})_2(\mu\text{-I})]$  as black crystals in 71% yield. The crystal unit cell contains  $\text{Na}^+$  cations and the complex anions  $[(\text{Cp}''_2\text{Yb})_2(\mu\text{-I})]^-$ .<sup>230</sup> The synthesis of unsolvated  $(\text{C}_5\text{H}_4\text{CH}_2\text{CH}_2\text{OMe})_2\text{Sm}$  and  $(\text{C}_5\text{H}_4\text{CH}_2\text{CH}_2\text{OMe})_2\text{Yb}$  was achieved through a reaction of  $\text{LnI}_2$  ( $\text{Ln} = \text{Sm}, \text{Yb}$ ) with  $\text{K}(\text{C}_5\text{H}_4\text{CH}_2\text{CH}_2\text{OMe})$  in a 1 : 2 molar ratio in THF.<sup>231</sup> The interaction of  $\text{LnCl}_3$  ( $\text{Ln} = \text{Sm}, \text{Yb}$ ) and 1,1'-(3-oxa-pentamethylene)dicyclopentadienyl disodium salt in THF provided trivalent complexes  $[\text{O}(\text{CH}_2\text{CH}_2\text{C}_5\text{H}_4)_2]\text{LnCl}$  ( $\text{Ln} = \text{Sm}, \text{Yb}$ ). The chlorides were then reduced with sodium metal in THF at room temperature for 3 days and purple-black ( $\text{Ln} = \text{Sm}$ ) and red-black ( $\text{Ln} = \text{Yb}$ ) solutions were being formed, respectively, from which new divalent organolanthanide complexes, that is, the purple compound  $[\text{O}(\text{CH}_2\text{CH}_2\text{C}_5\text{H}_4)_2]\text{Sm}(\text{THF})_2$  and the red-orange compound  $[\text{O}(\text{CH}_2\text{CH}_2\text{C}_5\text{H}_4)_2]\text{Yb}(\text{THF})_2$ , were obtained in good yield. Another method was also used to synthesize the Sm compound.  $\text{SmI}_2$  reacted with  $\text{K}_2[\text{O}(\text{CH}_2\text{CH}_2\text{C}_5\text{H}_4)_2]$  in THF to give  $[\text{O}(\text{CH}_2\text{CH}_2\text{C}_5\text{H}_4)_2]\text{Sm}(\text{THF})_2$  in good yields. Both compounds are soluble



Scheme 46

in THF and DME, but insoluble in aromatic and aliphatic solvents. The Yb complex dissolves in DME to give a red-green solution. Recrystallization from DME gave red single crystals of  $[\text{O}(\text{CH}_2\text{CH}_2\text{C}_5\text{H}_4)_2]\text{Yb}(\text{DME})$ .<sup>232</sup>

The donor-functionalized chiral cyclopentadienyl ytterbium(II) complex  $\text{Yb}[(\text{S})-\eta^5\text{-}\eta^1\text{-C}_5\text{H}_4\text{CH}_2\text{CH}(\text{Me})\text{NMe}_2]_2$  has been synthesized and structurally characterized.<sup>233</sup> The new bis(cyclopentadienyl)ytterbium complex  $[\text{C}_5\text{H}_4(\text{CH}_2)_2\text{NMe}_2]_2\text{Yb}$  was obtained by treatment of  $\text{K}[\text{C}_5\text{H}_4(\text{CH}_2)_2\text{NMe}_2]$  with  $\text{YbI}_2$  in THF at room temperature. Crystals of the complex are dark red (almost black). The coordination geometry may be described as a distorted tetrahedron formed by two nitrogen atoms and two cyclopentadienyl centroids.<sup>234</sup> In a similar manner, the synthesis of  $(\text{C}_5\text{Me}_4\text{CH}_2\text{CH}_2\text{NMe}_2)_2\text{Sm}$  was achieved by the reaction of  $\text{K}(\text{C}_5\text{Me}_4\text{CH}_2\text{CH}_2\text{NMe}_2)$  with  $\text{SmI}_2(\text{THF})_2$  in THF solution. The solvent-free complex is stabilized by additional intramolecular coordination of the nitrogen atoms in the side chains of the ligands.<sup>235</sup> Cyclopentadienyl ligands bearing pendant pyridyl groups have also been utilized to prepare ytterbocene(II) derivatives.<sup>236</sup> The divalent ytterbium complex  $(\text{C}_5\text{H}_4\text{PPh}_2)_2\text{Yb}(\text{DME})$  was obtained by a reaction between the thallium derivative  $[(\eta^5\text{-}\eta^5\text{-C}_5\text{H}_4\text{PPh}_2)\text{Tl}]_\infty$  and excess of metallic ytterbium in THF with the following extraction by DME. According to the X-ray structure, the Yb atom in  $(\text{C}_5\text{H}_4\text{PPh}_2)_2\text{Yb}(\text{DME})$  is coordinated to the two Cp rings and two oxygen atoms of the solvated DME molecule, but not to the phosphorus substituents.<sup>237</sup> The analogous reaction of  $\text{Tl}(\text{C}_5\text{H}_4\text{PPh}_2)$  with metallic europium or ytterbium powder in THF at  $60^\circ\text{C}$  in the presence of metallic mercury, followed by crystallization from a mixture of DME and diethylene glycol dimethyl ether (diglyme) (10:1), afforded  $(\text{C}_5\text{H}_4\text{PPh}_2)_2\text{Eu}(\text{diglyme})$  and  $(\text{C}_5\text{H}_4\text{PPh}_2)_2\text{Yb}(\text{diglyme})$ , respectively.<sup>238</sup> The compounds  $(\text{C}_5\text{H}_4\text{PPh}_2)_2\text{Eu}(\text{DME})$  and  $(\text{C}_5\text{H}_4\text{PPh}_2)_2\text{Sm}$  were made analogously. Treatment of the Sm and Yb derivatives with  $\text{Ph}_3\text{PO}$  in DME afforded the triphenylphosphine oxide adducts  $(\text{C}_5\text{H}_4\text{PPh}_2)_2\text{Sm}(\text{OPPh}_3)$  and  $(\text{C}_5\text{H}_4\text{PPh}_2)_2\text{Yb}(\text{OPPh}_3)$ , respectively.<sup>239</sup>

The olefin-substituted cyclopentadienyl ligand  $[\text{C}_5\text{Me}_4\text{SiMe}_2\text{CH}_2\text{CH}=\text{CH}_2]^-$  forms unsolvated metallocenes,  $[\text{C}_5\text{Me}_4\text{SiMe}_2\text{CH}_2\text{CH}=\text{CH}_2]_2\text{Ln}$  ( $\text{Ln} = \text{Sm}, \text{Eu}, \text{Yb}$ ), from  $\text{K}[\text{C}_5\text{Me}_4\text{SiMe}_2\text{CH}_2\text{CH}=\text{CH}_2]$  and  $\text{LnI}_2(\text{THF})_2$  in good yield. In the solid state, the tethered olefins are oriented toward the metal center, with the  $\text{Ln}-\text{C}(\text{terminal alkene carbon})$  distances  $0.2\text{--}0.3\text{ \AA}$  shorter than the  $\text{Ln}-\text{C}(\text{internal alkene carbon})$  distances.<sup>240</sup> This asymmetric  $\text{C}=\text{C}$  bonding is reminiscent of alkene bonding in group 4 metallocene catalysts.

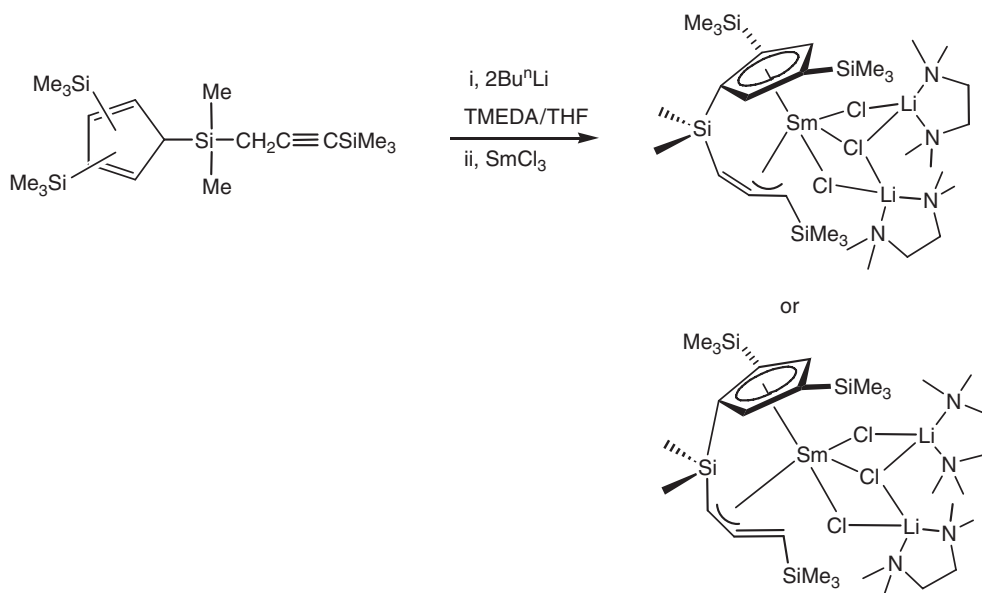
#### 4.01.6.3 $\text{CpLnX}_2$ Compounds

The reduced lanthanide iodides of the composition  $\text{LnI}_x$  ( $\text{Ln} = \text{Sc}, \text{Y}, \text{La}, \text{Ce}, \text{Pr}, \text{Nd}, \text{Gd}, \text{Dy}, \text{Ho}, \text{Er}; x < 3$ ), obtained by the reaction of an excess of the appropriate metal with iodine at high temperature, react with cyclopentadiene to afford the complexes  $\text{CpLnI}_2(\text{THF})_3$  with yields up to 60%.<sup>241,242</sup>  $\text{CpHoCl}_2(\text{THF})_3$  was made in a one-pot synthesis from  $\text{HoCl}_3$ , cyclopentadiene, and metallic sodium (molar ratio 1:5:1).<sup>243</sup> High yields of  $\text{CpSmI}_2(\text{THF})_2$  have been obtained from the reaction of  $\text{SmI}_2(\text{THF})_4$  with  $\text{CpCuPPh}_3$ .<sup>207</sup> Crystal structure analyses have been reported for  $\text{CpYCl}_2(\text{THF})_3$ <sup>244</sup> and  $\text{CpEuCl}_2(\text{THF})_3$ .<sup>245</sup>  $\text{CpTbCl}_2$  has been reported to form adducts with pyrazole and triphenylphosphine.<sup>246</sup> An alternative method leading to mono-Cp derivatives is the substitution of a Cp ligand in  $\text{Cp}_2\text{LnX}$  complexes. For example,  $\text{CpSmBr}_2(\text{THF})_3$  and  $\text{CpSmI}_2(\text{THF})_3$  have been obtained from

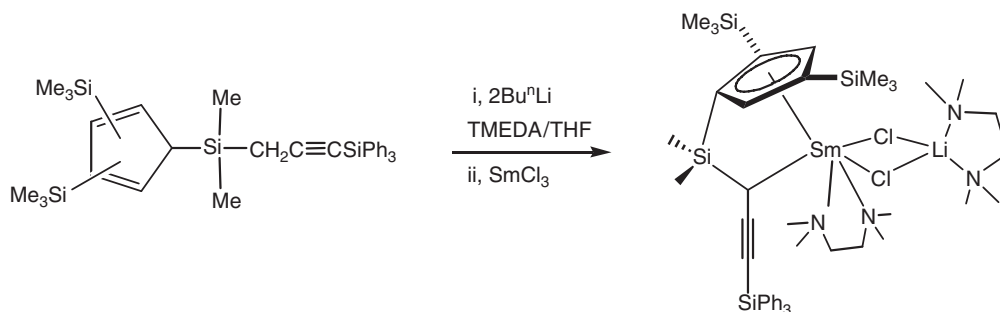
$\text{Cp}_2\text{Sm}(\text{THF})$  and 1,2-dibromoethane and 1,2-diiodoethane, respectively. The reaction of  $\text{Cp}_2\text{Sm}(\text{THF})$  with  $\text{C}_2\text{Cl}_6$  forms the corresponding  $\text{CpSmCl}_2(\text{THF})_3$ . The molecular structure shows a distorted pseudo-octahedral arrangement in which the centroid of the Cp ring and one THF molecule occupy the apical positions, while both halide ions are transoid in the equatorial plane. The Sm–I bonds are significantly different [3.143 Å and 3.168 Å] and are relatively long compared to other terminal  $\text{Sm}^{\text{III}}$ –I bond lengths. This and the likewise long Sm–THF distances show the relative steric crowding of the  $\text{CpSmI}_2(\text{THF})_3$  complex.<sup>247</sup>

Addition of vinylcyclopentadienyl lithium in a molar ratio  $[\text{LnCl}_3]:[\text{Li}(\text{C}_5\text{H}_4\text{CH}=\text{CH}_2)]$  of 1:1 to  $\text{LnCl}_3$  ( $\text{Ln}=\text{La}$ ,  $\text{Sm}$ ,  $\text{Eu}$ ,  $\text{Gd}$ ,  $\text{Dy}$ , and  $\text{Er}$ ) afforded mono(vinylcyclopentadienyl) complex of the type  $(\text{C}_5\text{H}_4\text{CH}=\text{CH}_2)\text{LnCl}_2$ .<sup>248</sup> Complexes of the type  $[\text{C}_5\text{H}_4\text{C}(\text{Et})_2\text{CH}_2\text{CH}=\text{CH}_2]\text{LnCl}_2\cdot\text{MgCl}_2\cdot\text{THF}$  have been reported for  $\text{Ln}=\text{La}$ ,  $\text{Nd}$ , and  $\text{Gd}$ .<sup>249</sup> Oxidative reactions of the ytterbium(II) thiocyanate complex  $\text{Yb}(\text{NCS})_2(\text{THF})_2$  with  $\text{TiCp}$  or  $\text{Ti}(\text{C}_5\text{H}_4\text{Me})$  yielded the mono(cyclopentadienyl)ytterbium(III) derivatives  $\text{CpYb}(\text{NCS})_2(\text{THF})_3$  and  $(\text{C}_5\text{H}_4\text{Me})\text{Yb}(\text{NCS})_2(\text{THF})_3$ , respectively, in the form of orange crystals.<sup>250</sup>

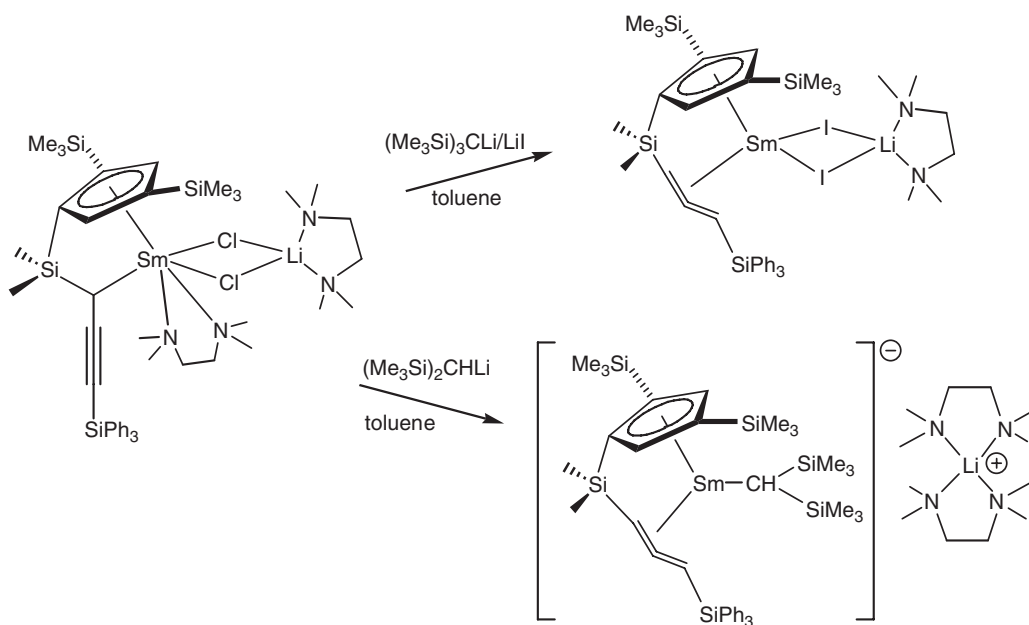
The synthesis and crystal structures of samarium complexes incorporating bridged  $\text{Cp}'\text{-SiMe}_2\text{allenyl/propargyl}$  ligands ( $\text{Cp}'=\text{C}_5\text{H}_2(\text{SiMe}_3)_2$ ) have been published. The complex  $[\text{C}_5\text{H}_2(\text{SiMe}_3)_2\text{SiMe}_2(\eta^3\text{-C}=\text{C}=\text{C}[H]\text{SiMe}_3)]\text{SmCl}_3\text{Li}_2(\text{TMEDA})_2$  (TMEDA = *N,N,N',N'*-tetramethylethylenediamine) was obtained as depicted in Scheme 47 by the reaction of a dilithium salt of  $[(\text{Me}_3\text{Si})_2(\text{C}_5\text{H}_3)]\text{SiMe}_2\text{CH}_2\text{C}\equiv\text{CSiMe}_3$  with  $\text{SmCl}_3$ , while the  $\text{SiPh}_3$  analog  $[\text{C}_5\text{H}_3(\text{Me}_3\text{Si})_2]\text{SiMe}_2\text{CH}_2\text{C}\equiv\text{CSiPh}_3$  leads to an  $\eta^1$ -propargyl complex  $[\text{C}_5\text{H}_2(\text{SiMe}_3)_2]\text{SiMe}_2(\eta^1\text{-CHC}\equiv\text{CSiPh}_3)]\text{Sm}(\text{TMEDA})[\text{Cl}_2\text{Li}(\text{TMEDA})]$  (Scheme 48).<sup>251</sup>



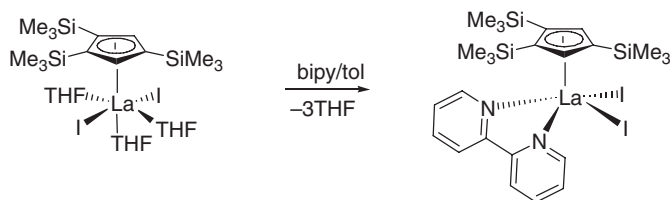
Scheme 47



Scheme 48



Scheme 49



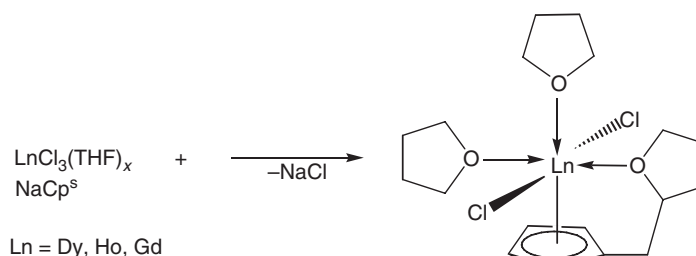
Scheme 50

A conversion of the bonding mode from  $\eta^1$ -propargyl to  $\eta^3$ -allenyl was observed by removing the coordinated TMEDA molecule on the Sm center and exchanging two chlorides in  $[\text{C}_5\text{H}_2(\text{SiMe}_3)_2]\text{SiMe}_2(\eta^1\text{-CHC}\equiv\text{CSiPh}_3)\text{Sm}(\text{TMEDA})(\mu\text{-Cl})_2\text{Li}(\text{TMEDA})$  for two iodide anions (Scheme 49).<sup>251</sup>

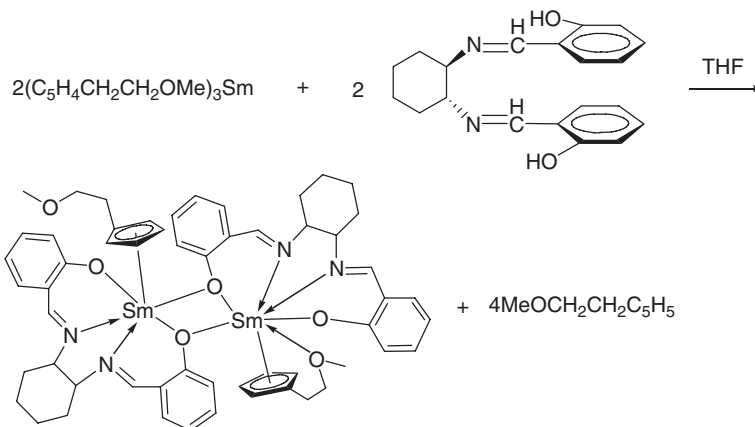
Mono(cyclopentadienyl)lanthanide diiodides are readily accessible utilizing the very bulky 1,2,4-tris(trimethylsilyl)cyclopentadienyl ligand (= Cp<sup>'''</sup>). A typical example is depicted in Scheme 50.<sup>252</sup> Cp<sup>'''</sup>LaI<sub>2</sub>(THF)<sub>3</sub> also served as a useful starting material for the preparation of a series of mono(cyclopentadienyl)lanthanum-anilido complexes.<sup>253</sup>

The (+)-neomenthylcyclopentadienyl complexes Cp<sup>R</sup>LnX<sub>2</sub>(THF)<sub>3</sub> [X = Cl, Ln = Sm, Gd, Yb, Y, Lu; X = I, Ln = Sm, Yb] have been prepared by metathetical reactions of lanthanide halides with appropriate alkali metal (+)-neomenthylcyclopentadienides. The syntheses of mono-(+)-neomenthylcyclopentadienyl lanthanide dichloride complexes were accomplished by the reaction of lanthanide trichlorides with 1 equiv. of sodium (+)-neomenthylcyclopentadienide in THF. <sup>1</sup>H NMR spectroscopic studies showed the coordination of three THF molecules.<sup>254</sup> Alternatively, lanthanide triiodides have been treated with 1 equiv. of potassium (+)-neomenthylcyclopentadienide in THF at room temperature to obtain the mono-(+)-neomenthylcyclopentadienyl lanthanide diiodides.<sup>254</sup> A single crystal X-ray diffraction study of Cp<sup>R</sup>SmI<sub>2</sub>(THF)<sub>3</sub> revealed a pseudo-octahedral geometry with the iodine atoms bonded to the samarium in a *trans*-fashion and the THF molecules in a *mer*-conformation. The bond distances of Sm–I (3.139 Å and 3.140 Å) and Sm–Cp<sup>centroid</sup> (2.453 Å) are relatively long compared to known bond lengths in analogous compounds which demonstrates the steric crowding in this compound. Optical rotation values of the mono-(+)-neomenthylcyclopentadienyl lanthanide dichlorides and diiodides are all in the same range of 9–10°, which suggests that a similar coordination sphere exists around the metal center among all the mono-(+)-neomenthylcyclopentadienyl lanthanide dihalides.<sup>254</sup> Mono(tetrahydrofurylcyclopentadienyl) lanthanide dichlorides were formed by the reaction of lanthanide trichlorides with 1 equiv. of tetrahydrofurylcyclopentadienyl (Cp<sup>s</sup>) sodium salt in THF





Scheme 51



Scheme 52

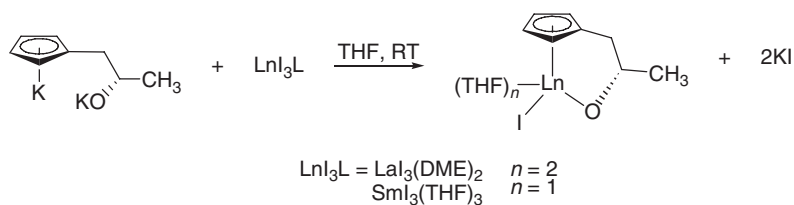
to give  $\text{Cp}^s\text{LnCl}_2(\text{THF})_2$  ( $\text{Ln} = \text{Dy, Ho, Gd}$ ) (Scheme 51). The complex  $\text{Cp}^s\text{DyCl}_2(\text{THF})_2$  reacts with 1 equiv. of  $\text{NaCp}$  to yield the mixed ring complex  $[\text{Cp}^s\text{CpDy}(\mu\text{-Cl})]_2$ .<sup>255</sup>

$\text{SmCl}_3$  reacted with 3 equiv. of methoxyethylcyclopentadienyl potassium in THF, followed by treatment with *trans*-(±)-2,2'-[1,2-cyclohexanediylbis(iminomethyl)]diphenol to give the binuclear mono(methoxyethylcyclopentadienyl)samarium complex  $[\eta^5\text{-}\eta^1\text{-Cp}'\text{Sm}][(\mu\text{-}\eta\text{-OC}_{20}\text{H}_{20}\text{N}_2\text{O})_2][\eta^5\text{-Cp}'\text{Sm}]$  ( $\text{Cp}' = \text{MeOCH}_2\text{CH}_2\text{C}_5\text{H}_4$ ) (Scheme 52). X-ray crystallographic studies showed that the molecule is a dimer in which two  $(\text{MeOCH}_2\text{CH}_2\text{C}_5\text{H}_4)\text{Sm}(\mu\text{-}\eta\text{-C}_{20}\text{H}_{20}\text{N}_2\text{O}_2)$  units are connected to two bridging oxygen atoms of the Schiff base ligands.<sup>256</sup>

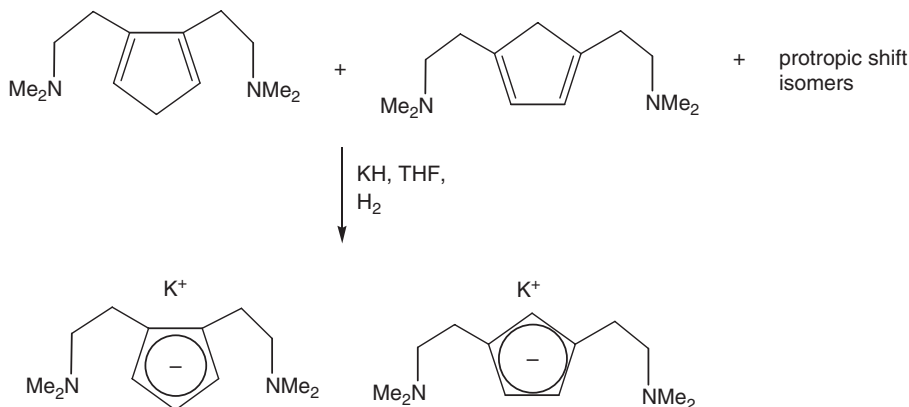
The analogous dysprosium complex  $[(\text{C}_5\text{H}_4\text{CH}_2\text{CH}_2\text{OMe})\text{Dy}(\text{OC}_{20}\text{H}_{20}\text{N}_2\text{O})]_2$  can be obtained from the reaction of  $\text{Cp}'\text{DyCl}$  ( $\text{Cp}' = \text{C}_5\text{H}_4\text{CH}_2\text{CH}_2\text{OMe}$ ) with the disodium salt of *trans*-(±)-2,2'-[1,2-cyclohexanediylbis(iminomethyl)]diphenol.<sup>256</sup> The reaction of a 1 : 2 molar ratio of  $\text{Cp}_3\text{Pr}$  with diethyl malonate in *n*-hexane results in the formation of  $\{\text{CpPr}[\text{CH}(\text{COOC}_2\text{H}_5)_2][\mu\text{-CH}(\text{COOC}_2\text{H}_5)_2]\}_2$ . The complex is a dimer and the two praseodymium atoms are bridged by two oxygen atoms of the independent diethyl malonate ligands. The bridging ligands coordinate with praseodymium in a bidentate mode.<sup>257</sup>

A series of monocyclopentadienyl lanthanoid complexes has been realized with new asymmetric  $\beta$ -hydroxycyclopentadienyl ligands. The novel ligands  $\text{C}_5\text{H}_4\text{CH}_2\text{CH}(\text{R})\text{OH}$  ( $\text{R} = \text{Me, CH}_2\text{OMe, Ph}$ ) were obtained by the nucleophilic ring-opening reaction of enantiopure epoxides by cyclopentadienyl anions. The metallation of these ligands with sodium or potassium or with *n*-butyllithium led to the formation of the alkali metal derivatives  $\text{M}_2[\text{C}_5\text{H}_4\text{CH}_2\text{CH}(\text{R})\text{O}]$  ( $\text{M} = \text{Li, Na, K}$ ). The complexes  $(S)\text{-C}_5\text{H}_4\text{CH}_2\text{CH}(\text{Me})\text{OLaI}(\text{THF})_2$  and  $(S)\text{-C}_5\text{H}_4\text{CH}_2\text{CH}(\text{Me})\text{OSmI}(\text{THF})$  were synthesized from the bis(potassium) salt and lanthanum or samarium iodides in THF (Scheme 53).<sup>258</sup> The related asymmetric cyclopentadienyl ligand  $\text{C}_5\text{H}_4\text{CH}_2\text{CH}(\text{Me})\text{OCH}_2\text{Ph}$  ( $= \text{Cp}'$ ) has been employed to prepare the corresponding monomeric mono(cyclopentadienyl) diiodides  $\text{Cp}'\text{LnI}_2(\text{THF})_n$  ( $\text{Ln} = \text{La, } n = 2; \text{Ln} = \text{Sm, } n = 3$ ).<sup>259</sup>

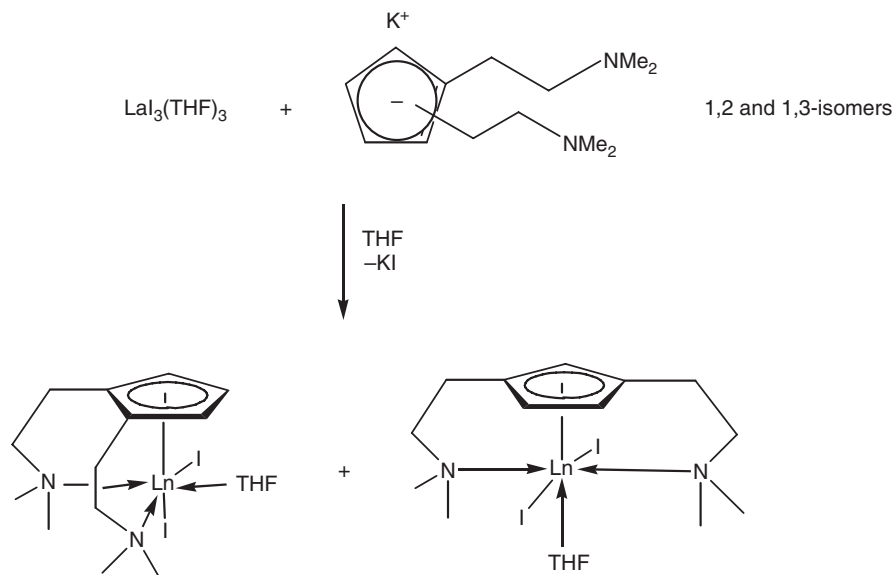
The dimeric chloro complex  $[(\eta^5\text{-}\eta^1\text{-C}_5\text{Me}_4\text{SiMe}_2\text{NCMe}_2\text{R})\text{Y}(\text{THF})(\mu\text{-Cl})]_2$  could be synthesized by reacting *in situ* formed " $\text{Y}(\text{CH}_2\text{SiMe}_3)_2\text{Cl}(\text{THF})_n$ " with the aminocyclopentadiene  $(\text{C}_5\text{Me}_4\text{H})\text{SiMe}_2\text{NHCMe}_2\text{R}$  in a  $\sigma$ -bond metathesis reaction.<sup>260</sup> Bis(donor)-substituted cyclopentadienyl ligands have been employed to synthesize new



Scheme 53



Scheme 54



Scheme 55

half-sandwich complexes of lanthanum(III) and ytterbium(II). The ligand was obtained as a 1.5 : 1 mixture of 1,2- and 1,3-disubstituted isomers with two dimethylaminoethyl side chains (Scheme 54).<sup>199</sup>

Addition of  $\text{LaI}_3(\text{THF})_3$  to the mixture in THF caused the formation of the half-sandwich complexes  $[\eta^5:\eta^1:\eta^1\text{-C}_5\text{H}_3(\text{CH}_2\text{CH}_2\text{NMe}_2)_2\text{-1,2}]\text{LaI}_2(\text{THF})$  and  $[\eta^5:\eta^1:\eta^1\text{-C}_5\text{H}_3(\text{CH}_2\text{CH}_2\text{NMe}_2)_2\text{-1,3}]\text{LaI}_2(\text{THF})$ , which were successfully separated because of their different crystal shapes (Scheme 55).<sup>199</sup>

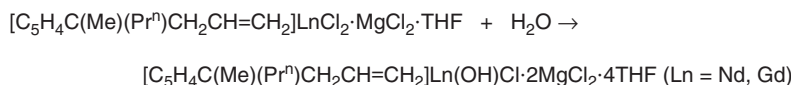
Well-defined partially hydrolyzed organolanthanide complexes have been synthesized from mono(cyclopentadienyl) precursors. The trichlorides of lanthanum, neodymium, samarium, and gadolinium react with 1 equiv. of a substituted cyclopentadienyl Grignard reagent in THF to give the mono(cyclopentadienyl) lanthanide species  $[\text{C}_5\text{H}_4\text{C}(\text{Me})(\text{Pr}^n)\text{CH}_2\text{CH}=\text{CH}_2]\text{LnCl}_2 \cdot \text{MgCl}_2 \cdot \text{THF}$  coordinated with magnesium dichloride and THF.<sup>261</sup> Subsequent recrystallization of the neodymium and the gadolinium complexes from moist THF/hexane afforded hydrolysis products in which one chloride is exchanged by a hydroxy group (Scheme 56). Single crystal X-ray determinations of the partially hydrolyzed Nd and Gd complexes revealed distorted geometries around the lanthanide, with the lanthanide center being coordinated to three magnesium bonded chlorides in addition to the coordination to the hydroxy group, one chloride, and the cyclopentadienyl ligand. The THF molecules are coordinated to the magnesium atoms which have a coordination number of 6.<sup>261</sup>

In the complex  $(\text{C}_5\text{H}_4\text{Me})\text{Yb}(\text{OC}_6\text{H}_2\text{-2,6-Bu}^t_2\text{-4-Me})_2(\text{THF})$  the ytterbium atom is coordinated by one methylcyclopentadienyl ligand and three O atoms. The formal coordination number around the Yb atom is 6 (Scheme 57).<sup>262</sup>

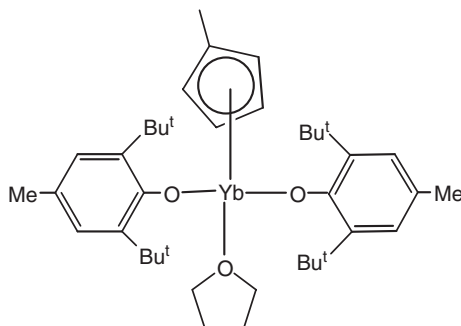
Reduction of 2,5-di-*t*-butylcyclopentadienone with 2 equiv. of thulium diiodide in THF gave a binuclear thulium(III) complex containing a cyclopentadienyl oxide ligand  $[\eta^5\text{-(C}_5\text{H}_2\text{Bu}^t_2\text{O)TmI}_2(\text{THF})_3]\text{TmI}_2(\text{THF})_2$  as orange crystals.<sup>263</sup>  $[\{\text{Zr}_2(\text{OPr}^i)_9\}\text{LnI}]_2$  reacts with NaCp to give the hexane-soluble complexes  $[\text{Zr}_2(\text{OPr}^i)_9]\text{LnCp}$  (Ln = Yb, Sm).  $[\text{Zr}_2(\text{OPr}^i)_9]\text{SmCp}$  was the first reported soluble cyclopentadienyl complex of Sm<sup>II</sup>. Neither complex forms isolable adducts with THF, Et<sub>2</sub>O, or DME, but NMR spectra in [D<sub>8</sub>]-THF show two distinct THF environments, suggesting coordination of THF in solution. Single X-ray determinations revealed that the samarium and ytterbium complexes are isostructural. The  $[\text{Zr}_2(\text{OPr}^i)_9]^-$  ligand is comparable to cyclopentadienyl and enhances the solubility of divalent lanthanide organometallic species in comparison with Cp analogs.<sup>264</sup>

The preparation and reaction chemistry of  $\beta$ -diketiminato ytterbium complexes containing an additional cyclopentadienyl ligand have been investigated. Reaction of  $\text{Li}[(\text{DIPPh})_2\text{nacnac}]$  ( $(\text{DIPPh})_2\text{nacnac} = N,N$ -diisopropylphenyl-2,4-pentanediiiminate anion) with 1 equiv. of anhydrous  $\text{YbCl}_3$  in THF afforded the dark red monomeric complex  $[(\text{DIPPh})_2\text{nacnac}]\text{YbCl}_2(\text{THF})_2$  in high yield. Further treatment of this complex with  $\text{Na}(\text{C}_5\text{H}_4\text{Me})$  in a 1 : 1 molar ratio in THF gave the mixed ligand ytterbium chloride  $(\text{C}_5\text{H}_4\text{Me})[(\text{DIPPh})_2\text{nacnac}]\text{YbCl}$  as red crystals in 84% yield. This compound readily exchanges chloride with  $\text{LiNR}_2$  in THF to form the compounds  $(\text{C}_5\text{H}_4\text{Me})[(\text{DIPPh})_2\text{nacnac}]\text{YbNR}_2$  (R = Ph, Pr<sup>*i*</sup>).<sup>265–267</sup> Sterically demanding chelating diamide ligands have also been employed in the synthesis of mono(cyclopentadienyl)lanthanide complexes. A typical synthetic route is outlined in Scheme 58. The structure of the product in solution and in the solid state is best described as a distorted tetrahedron.<sup>268</sup>

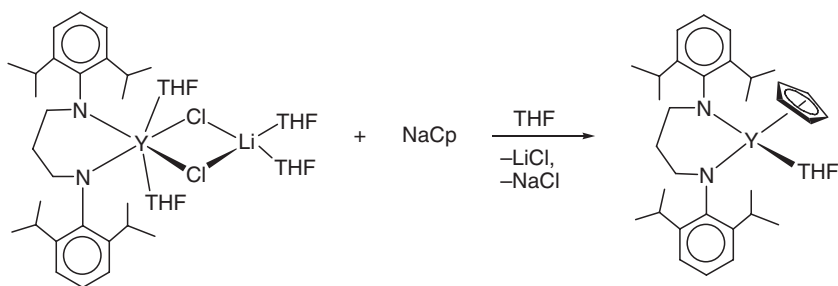
The first mono(cyclopentadienyl)ytterbium Schiff base complex was obtained from the reaction of  $\text{YbCl}_3$  with 3 equiv. of NaCp in THF, followed by treatment with *trans*-( $\pm$ )-*N,N'*-bis(salicylidene)-1,2-cyclohexanediamine to give dimeric  $[\text{CpYb}(\mu\text{-C}_{20}\text{H}_{20}\text{N}_2\text{O}_2)]_2(\mu\text{-THF})(\text{THF})$ .<sup>269</sup> Bis(cyclopentadienyl)samarium chloride reacted with 0.5 equiv. of disodium salts of *trans*-( $\pm$ )-*N,N'*-bis(salicylidene)-1,2-cyclohexanediamine to give the



Scheme 56



Scheme 57

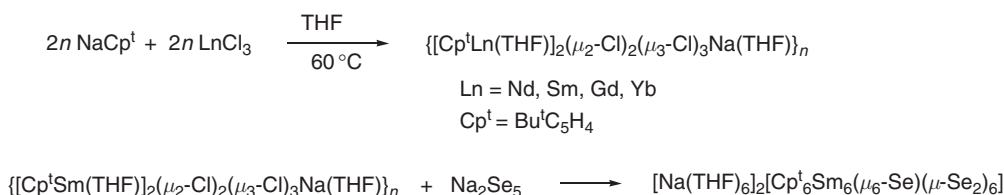


Scheme 58

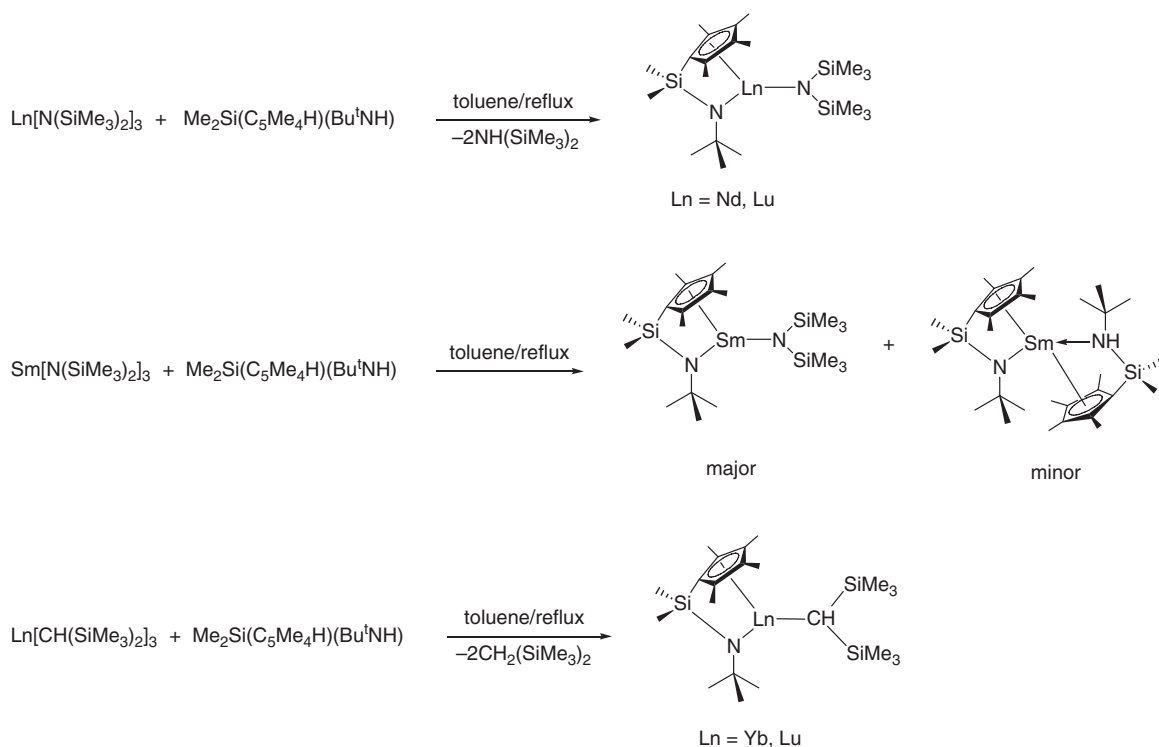
mono(cyclopentadienyl)samarium complex  $[\text{CpSm}(\mu\text{-C}_{20}\text{H}_{20}\text{N}_2\text{O}_2)]_2(\mu\text{-THF})(\text{THF})_2$ . X-ray crystal determination showed that the molecule is a dimer in which two  $\text{CpSm}(\mu\text{-C}_{20}\text{H}_{20}\text{N}_2\text{O}_2)$  units are connected via a THF oxygen and two bridging oxygen atoms of the Schiff base ligands.<sup>270</sup> Mono(cyclopentadienyl)lanthanide derivatives have also been isolated from reactions of  $\text{Cp}_3\text{Ln}$  with salicylaldehyde thiosemicarbazone.<sup>271</sup> A  $\mu$ -hydroxo-bridged mono(cyclopentadienyl)lanthanide Schiff base complex was obtained as a partial hydrolysis product when  $\text{Cp}_3\text{Pr}$  was reacted with bis(acetylacetonate)ethylenediamine.<sup>272,273</sup> The samarium complex  $\text{CpSm}[\text{N}(\text{PPh}_2)_2](\text{THF})$  contains two diphosphinoamide ligands in the coordination sphere of Sm.<sup>274</sup>

The reaction of the half-sandwich *t*-butylcyclopentadienyl neodymium complex  $[(\text{C}_5\text{H}_4\text{Bu}^t)\text{NdCl}_2(\text{THF})_2]_2$  with  $\text{Na}_2\text{Se}_5$  was reported to give the organoneodymium polyselenide complex  $[\text{Na}(\text{THF})_6][(\text{C}_5\text{H}_4\text{Bu}^t)_6\text{Nd}_6\text{Se}_{13}]$ , which has been characterized by X-ray crystallography.<sup>275</sup> In the solid-state structure of the anion in  $[\text{Na}(\text{THF})_6][\text{Cp}^t_6\text{Nd}_6\text{Se}_{13}]$ , each Nd atom is coordinated with six Se atoms. The distances between Nd and the Se atoms are between 2.888 Å and 3.214 Å, whereas the Se atoms can be divided into three types: a central Se atom which is coordinated to six Nd atoms, six pairs of bridging  $\text{Se}_2$  units in which one Se atom is coordinated to three Nd atoms, and the other one is connected with only two Nd atoms.<sup>275</sup> The corresponding organosamarium polyselenide cluster has been prepared via the reaction sequence shown in Scheme 59.<sup>276</sup>

$(\text{C}_5\text{Me}_4\text{SiMe}_2\text{NBu}^t)\text{LnN}(\text{SiMe}_3)_2$  ( $\text{Ln} = \text{Nd}, \text{Lu}, \text{Sm}$ ) and  $(\text{C}_5\text{Me}_4\text{SiMe}_2\text{NBu}^t)\text{LnCH}(\text{SiMe}_3)_2$  ( $\text{Ln} = \text{Yb}, \text{Lu}$ ) complexes were synthesized by the reaction of the corresponding homoleptic amides or alkyls with  $\text{C}_5\text{Me}_4\text{HSiMe}_2\text{NHBu}^t$  (Scheme 60).<sup>277,278</sup> The amine elimination does not lie completely on the product side and must be driven to completion by  $\text{HN}(\text{SiMe}_3)_2$  removal. A single crystal X-ray determination of  $(\text{C}_5\text{Me}_4\text{SiMe}_2\text{NBu}^t)\text{SmN}(\text{SiMe}_3)_2$  revealed a monomeric structure with a relatively long  $\text{Sm}-\text{N}(\text{SiMe}_3)_2$  distance of 2.320 Å while the  $\text{Sm}-\text{NBu}^t$  distance (2.257 Å) is substantially shorter than usual, presumably due to the chelating structure. The structure of  $(\text{C}_5\text{Me}_4\text{SiMe}_2\text{NBu}^t)\text{YbCH}(\text{SiMe}_3)_2$  shows the typical close  $\text{Ln}-\text{CH}_3-\text{Si}$  contact of 2.657 Å which is observed in numerous organolanthanide  $-\text{CH}(\text{SiMe}_3)_2$  complexes.<sup>277</sup> An unusual binuclear azobenzene complex,  $[\text{CpLu}(\text{THF})(\mu\text{-}\eta^2\text{-}\eta^2\text{-PhNNPh})]_2(\text{THF})_2$ , was synthesized by reacting cyclopentadienyllutetium anthracene,  $\text{CpLu}(\text{C}_{14}\text{H}_{10})(\text{THF})_2$ , with azobenzene. The molecular structure of the complex was verified by an X-ray analysis.<sup>279</sup> The reaction of  $\text{TlCp}$  with a slurry of  $\text{Sm}(\text{Tp}^{\text{Me}_2})_2$  in THF [ $\text{Tp}^{\text{Me}_2} = \text{tris}(3,5\text{-dimethylpyrazolyl})\text{hydroborate}$ ] resulted in the formation of thallium metal and  $\text{CpSm}(\text{Tp}^{\text{Me}_2})_2$ . NMR data indicate different coordination modes of the two  $\text{Tp}^{\text{Me}_2}$  ligands.<sup>280</sup> Moderate yields (55%) of the related mixed ligand complex  $(\text{C}_5\text{H}_4\text{PPh}_2)\text{Sm}(\text{Tp}^{\text{Me}_2})(\text{i})(\text{THF})$  (green-yellow crystals) were obtained from the redox reaction between  $\text{SmI}_2$  and  $\text{Tl}(\text{C}_5\text{H}_4\text{PPh}_2)$  in THF at ambient temperature followed by direct treatment with  $\text{K}(\text{Tp}^{\text{Me}_2})$ .<sup>281</sup> Heating of  $\text{CpSm}(\text{Tp}^{\text{Me}_2})_2$  overnight in a sealed tube at 165 °C gave two products: one is the result of an unprecedented transformation of the Tp ligand to the mixed pyrazolylborate  $[\text{HB}(3,5\text{-Me}_2\text{pz})_2(\text{C}_5\text{H}_4)]$ , the second product is



Scheme 59

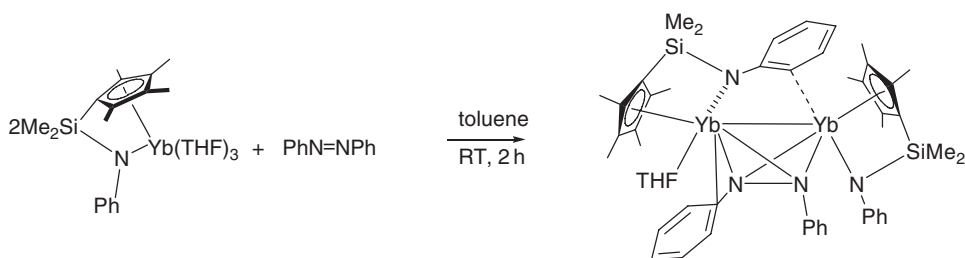


Scheme 60

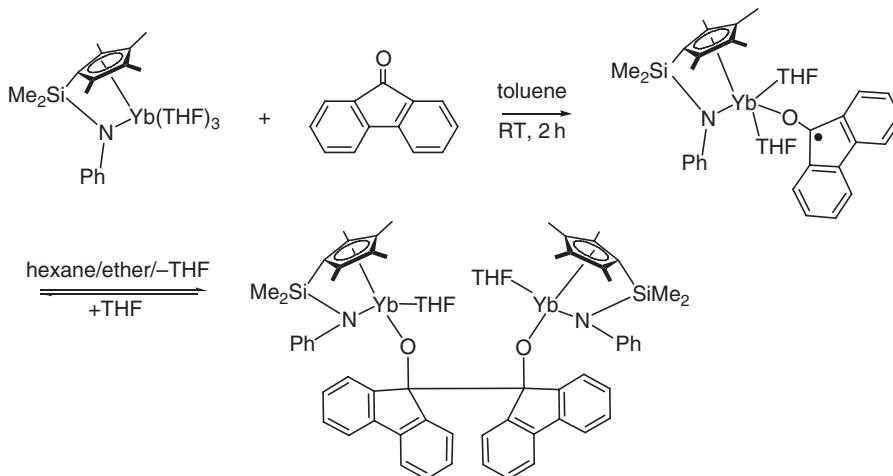
$\text{Sm}(\text{Tp}^{\text{Me}_2})_2(3,5\text{-Me}_2\text{pz})$ , which was also generated from the reaction of  $\text{CpSm}(\text{Tp}^{\text{Me}_2})_2$  with 3,5-dimethylpyrazole. The thermally induced intramolecular C–H activation in  $\text{CpSm}(\text{Tp}^{\text{Me}_2})_2$  is a useful method for the preparation of the new  $[\text{HB}(3,5\text{-Me}_2\text{pz})_2(\text{C}_5\text{H}_4)]$  ligand and opens the way for the synthesis of an extended family of heteroscorpionates with different organic functional groups.<sup>280</sup>

The synthesis of cyclopentadienyl lanthanide pyrazolate complexes and their reactivity towards dimethylsilicone has been reported. Reactions of  $\text{Cp}_3\text{Ln}$  ( $\text{Ln} = \text{Ho}, \text{Dy}, \text{Yb}, \text{Sm}$ ) with 2 equiv. of  $\text{HPzMe}_2$  ( $\text{HPzMe}_2 = 3,5\text{-dimethylpyrazole}$ ) in THF at room temperature yield complexes of the type  $\text{CpLn}(\text{PzMe}_2)_2$  ( $\text{Ln} = \text{Ho}, \text{Dy}$ ), and  $\text{Cp}_2\text{Yb}(\text{PzMe}_2)(\text{HPzMe}_2)$ , and  $\text{Sm}(\text{PzMe}_2)_3$ , respectively. Similar reactions have been carried out with the methylcyclopentadienyl lanthanide precursors  $(\text{C}_5\text{H}_4\text{Me})_3\text{Ln}$  ( $\text{Ln} = \text{Nd}, \text{Gd}, \text{Dy}$ ).<sup>282–284</sup> The different products indicate that the number of cyclopentadienyl groups liberated from a  $\text{Cp}_3\text{Ln}$  moiety is influenced by the size of the lanthanide ion.  $\text{CpHo}(\text{PzMe}_2)_2$  and  $\text{CpDy}(\text{PzMe}_2)_2$  react with silicone grease to give the corresponding  $\text{Me}_2\text{SiO}$  insertion products  $[\text{CpLn}(\text{PzMe}_2)(\text{OSiMe}_2\text{PzMe}_2)]_2$  ( $\text{Ln} = \text{Ho}, \text{Dy}$ ). Only the monocyclopentadienyl-type organolanthanide pyrazolates show the insertion of dimethylsilicone into the  $\text{Ln}–\text{N}$  bond. X-ray diffraction studies revealed  $[\text{CpHo}(\text{PzMe}_2)(\text{OSiMe}_2\text{PzMe}_2)]_2$  to be a centrosymmetric dimer in which each holmium is coordinated to one cyclopentadienyl group, two bridging oxygen atoms, and three nitrogen atoms, two from the chelating  $\text{PzMe}_2$  ligand and one from the bridging 3,5-dimethylpyrazolyl siloxide ligand to form a distorted octahedron.<sup>282,283</sup> The syntheses and structures of phosphorane iminato complexes of ytterbium, yttrium, and samarium have been reported, including another case of silicon grease reacting with an organolanthanide complex. Thus,  $\text{Cp}_2\text{YbBr}$  and  $\text{LiNPPH}_3$  in boiling toluene give  $\text{Cp}_3\text{Yb}_2(\text{NPPH}_3)_3$ . The single crystal X-ray structure of  $\text{Cp}_3\text{Yb}_2(\text{NPPH}_3)_3$  shows two Cp rings bonded to one ytterbium and one Cp ligand bonded to the second ytterbium atom which also binds one terminal  $(\text{NPPH}_3)^-$  ligand. The other two  $(\text{NPPH}_3)^-$  groups are linked to both ytterbium atoms to form a non-planar  $\text{Yb}_2\text{N}_2$  four-membered ring.<sup>285</sup>

The reaction of  $\text{CpLu}(\text{C}_{10}\text{H}_8)(\text{THF})_2$  with azobenzene in THF led to a diphenylhydrazido complex  $[\text{CpLu}(\text{THF})]_2(\mu\text{-Ph}_2\text{N}_2)_2$ .<sup>286</sup> The reaction of the linked cyclopentadienyl-anilido ytterbium(II) complex  $(\text{C}_5\text{Me}_4\text{SiMe}_2\text{NPh})\text{Yb}(\text{THF})_3$  has also been studied. It yields the binuclear ytterbium(III) complex  $(\text{C}_5\text{Me}_4\text{SiMe}_2\text{NPh})\text{Yb}(\text{THF})(\mu\text{-}\eta^2\text{-}\eta^3\text{-Ph}_2\text{N}_2)\text{Yb}(\text{C}_5\text{Me}_4\text{SiMe}_2\text{NPh})$  (Scheme 61), which contains a *cis*-oriented azobenzene dianion bonding in an  $\eta^3$ -fashion to one Yb atom and in  $\eta^2$ -fashion to the other Yb atom. The similar reaction of  $(\text{C}_5\text{Me}_4\text{SiMe}_2\text{NPh})\text{Yb}(\text{THF})_3$  with



Scheme 61



Scheme 62

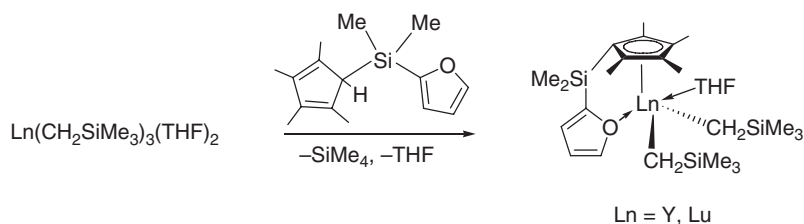
1 equiv. of fluorenone gave the corresponding Yb(III) ketyl complex  $(\text{C}_5\text{Me}_4\text{SiMe}_2\text{NPh})\text{Yb}(\text{THF})_2(\text{OC}_{13}\text{H}_8)$  in 75% yield (Scheme 62).<sup>194</sup>

The new multidentate ligand  $\text{Me}_2\text{NCH}_2\text{CH}_2\text{C}_5\text{H}_4\text{SiMe}_2\text{NHBu}^t$  was prepared in 71% yield as a mixture of 1,3- and 1,2-isomers ( $\sim 7:3$ ) in one step from  $\text{LiC}_5\text{H}_4\text{CH}_2\text{CH}_2\text{NMe}_2$ ,  $\text{Me}_2\text{SiCl}_2$ , and *t*-butylamine. The ligand was attached to scandium in an efficient alkane elimination reaction by treatment of *in situ* generated  $\text{Sc}(\text{CH}_2\text{SiMe}_3)_3(\text{THF})_2$  with  $\text{Me}_2\text{NCH}_2\text{CH}_2\text{C}_5\text{H}_4\text{SiMe}_2\text{NHBu}^t$ , yielding the alkylscandium species  $(\text{Me}_2\text{NCH}_2\text{CH}_2\text{C}_5\text{H}_3\text{SiMe}_2\text{NHBu}^t)\text{ScCH}_2\text{SiMe}_3$  in 52% yield. Treatment of  $(\text{Me}_2\text{NCH}_2\text{CH}_2\text{C}_5\text{H}_3\text{SiMe}_2\text{NHBu}^t)\text{ScCH}_2\text{SiMe}_3$  with  $\text{H}_2$  gave two of the four possible diastereomeric  $\mu$ -dihydrides. The  $C_i$ -symmetric 1*R*-*trans*-1'*S* diastereomer  $[(\text{Me}_2\text{NCH}_2\text{CH}_2\text{C}_5\text{H}_3\text{SiMe}_2\text{NHBu}^t)\text{Sc}(\mu\text{-H})]_2$  was characterized crystallographically. Thermolysis of  $(\text{Me}_2\text{NCH}_2\text{CH}_2\text{C}_5\text{H}_3\text{SiMe}_2\text{NHBu}^t)\text{ScCH}_2\text{SiMe}_3$  at  $70^\circ\text{C}$  for 3 days resulted in the metallation of an N-methyl group and loss of  $\text{SiMe}_4$ . A mixture of two dimeric compounds with bridging methylene units was formed, one of which was identified as the  $C_i$ -symmetric 1*R*-*trans*-1'*S* diastereomer by X-ray crystallography.<sup>287</sup>

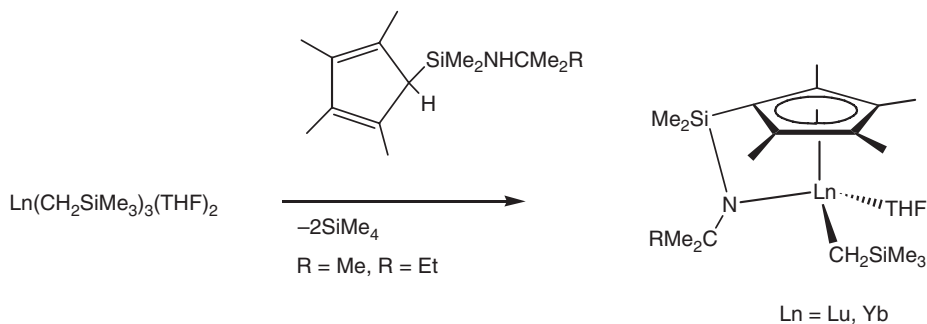
Rare earth metal dialkyls of the type  $[\text{C}_5\text{Me}_4\text{SiMe}_2(\text{C}_4\text{H}_3\text{O}-2)]\text{Ln}(\text{CH}_2\text{SiMe}_3)_2(\text{THF})$  ( $\text{Ln}=\text{Y}, \text{Lu}$ ) have been prepared by  $\sigma$ -bond metathesis of  $\text{Ln}(\text{CH}_2\text{SiMe}_3)_3(\text{THF})$  with the 2-furyl-substituted tetramethylcyclopentadiene  $(\text{C}_5\text{Me}_4\text{H})\text{SiMe}_2(\text{C}_4\text{H}_3\text{O}-2)$  (Scheme 63).<sup>288</sup>

Pendant-arm amido-cyclopentadienyl ligands have also been shown to be useful in the stabilization of highly reactive mono(cyclopentadienyl)lanthanide alkyl and hydrido complexes. When the tris(trimethylsilylmethyl) complexes of lutetium and ytterbium,  $\text{Ln}(\text{CH}_2\text{SiMe}_3)_3(\text{THF})_2$ , were treated in pentane solution with 1 equiv. of  $(\text{C}_5\text{Me}_4\text{H})\text{SiMe}_2\text{NHCMe}_2\text{R}$  ( $\text{R}=\text{Me}, \text{Et}$ ) at  $0^\circ\text{C}$ , the new complexes  $(\eta^5\text{-}\eta^1\text{-C}_5\text{Me}_4\text{SiMe}_2\text{NHCMe}_2\text{R})\text{Ln}(\text{CH}_2\text{SiMe}_3)(\text{THF})$  were formed (Scheme 64).<sup>260,278</sup>

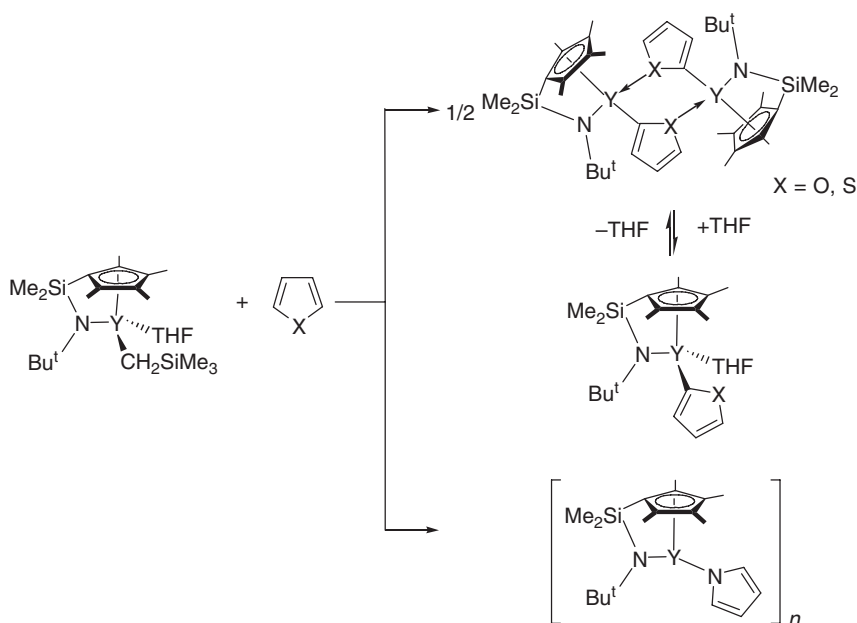
The half-sandwich alkyl complex  $(\eta^5\text{-}\eta^1\text{-C}_5\text{Me}_4\text{SiMe}_2\text{NHCMe}_2\text{R})\text{Y}(\text{CH}_2\text{SiMe}_3)(\text{THF})$  reacts with furan and thiophene to give the metallation products  $[\text{Ln}(\eta^5\text{-}\eta^1\text{-C}_5\text{Me}_4\text{SiMe}_2\text{NHCMe}_2\text{R})(\mu\text{-}2\text{-C}_4\text{H}_3\text{X})]_2$  ( $\text{X}=\text{O}, \text{S}$ ) (Scheme 65) which are sparingly soluble in hydrocarbons due to the dimeric structure. Single crystal X-ray structure analysis of the 2-thienyl complex confirmed a six-membered core with bridging sulfur atoms and *trans*-disposed



Scheme 63



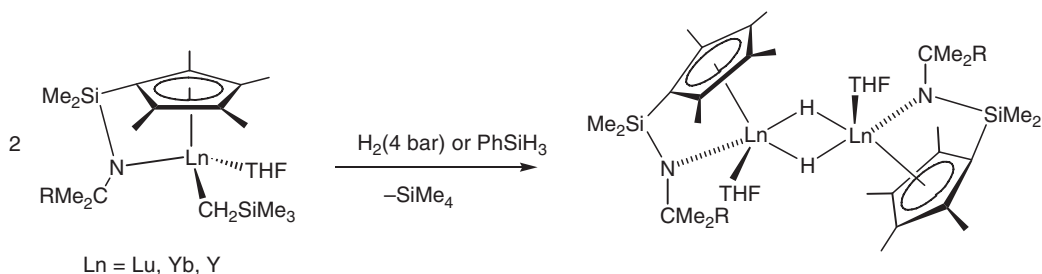
Scheme 64



Scheme 65

amido-tetramethylcyclopentadienyl ligands. In contrast to THF and pyridine, 1,2-DME was found to form isolable, crystalline adducts ( $\eta^5:\eta^1\text{-C}_5\text{Me}_4\text{SiMe}_2\text{NCMe}_2\text{R})\text{Y}(\text{2-C}_4\text{H}_3\text{X})(\text{DME})$ . A structure determination of the 2-furyl derivative showed a four-legged piano stool configuration.<sup>289,290</sup>

Similar *ortho*-metallation products have been obtained from reactions of  $(\eta^5:\eta^1\text{-C}_5\text{Me}_4\text{SiMe}_2\text{NBu}^t)\text{Y}(\text{CH}_2\text{SiMe}_3)(\text{THF})$  with anisole and 3- and 4-methylanisole.<sup>290</sup> Both the lutetium and ytterbium alkyl complexes were subjected to hydrogenolysis with dihydrogen or with phenylsilane in pentane at room temperature to give the



Scheme 66

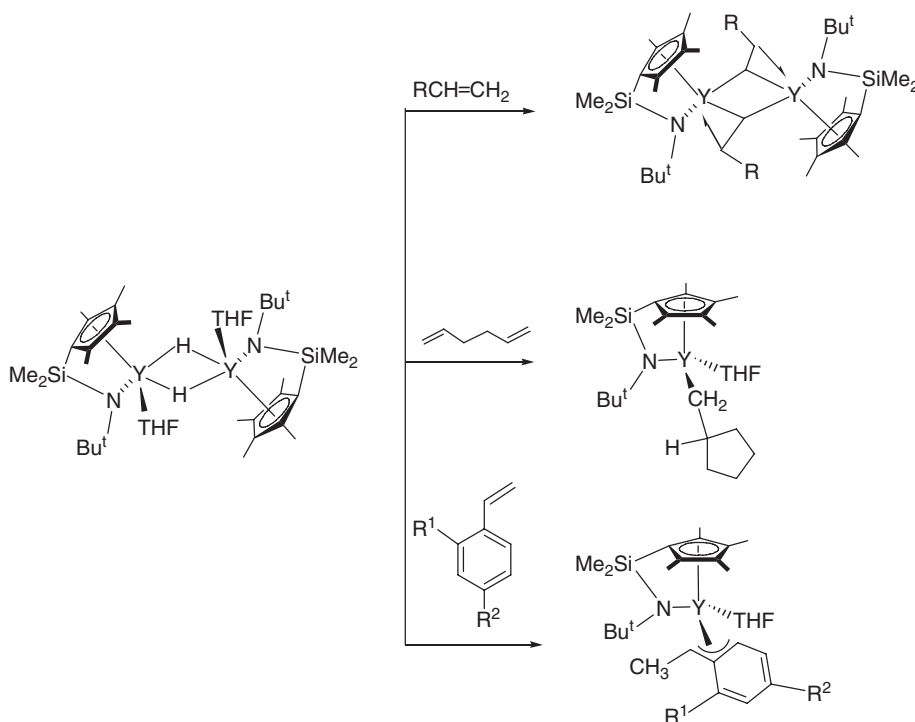
dimeric hydrides  $[(\eta^5\text{-C}_5\text{Me}_4\text{SiMe}_2\text{NCMe}_2\text{R})\text{Ln(THF)}(\mu\text{-H})_2]$  ( $\text{Ln} = \text{Lu, Yb, Y}$ ) (Scheme 66). Because of the thermal instability of the alkyl complexes of lutetium and ytterbium, it proved advantageous to prepare the hydride complexes in a one-pot procedure without isolating the alkyl complexes.<sup>260,278,291</sup>

When the dimeric lutetium and ytterbium hydrides are treated with excess  $\text{PMe}_3$ , exchange against THF occurs. By mixing equimolar amounts of the lutetium and ytterbium hydrido complexes in  $\text{C}_6\text{D}_6$ , the mixed Y/Lu binuclear complexes were formed as a statistical 1:2:1 mixture.<sup>260</sup> Closely related scandium chemistry with the  $[\text{C}_5\text{Me}_4\text{SiMe}_2\text{NBu}^t]^-$  ligand has also been investigated in detail.<sup>292</sup>

The hydrido complex  $[(\eta^5\text{-C}_5\text{Me}_4\text{SiMe}_2\text{NCMe}_2\text{R})\text{Y(THF)}(\mu\text{-H})_2]$  smoothly reacts with stoichiometric amounts of olefinic substrates such as ethylene,  $\alpha$ -olefins, butadiene, and styrenes to give the corresponding alkyl or allyl complexes, respectively (Scheme 67).<sup>278,291</sup>

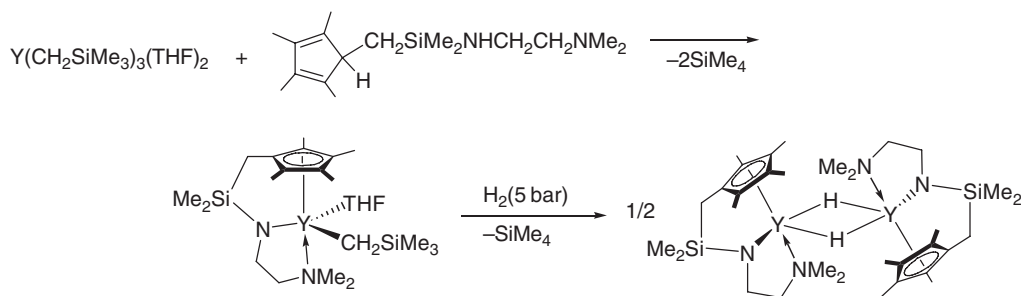
More recently the chemistry has been extended to yttrium alkyl and hydrido complexes stabilized by tridentate-linked amido-cyclopentadienyl ligands. A typical synthetic route is illustrated in Scheme 68.<sup>293</sup>

Synthesis and reactivity of the yttrium hydride dimer  $[\text{Cp}^*\text{Y(OAr)}(\mu\text{-H})_2]$  ( $\text{Ar} = 2,6\text{-Bu}_2\text{C}_6\text{H}_3$ ) have been investigated in detail.<sup>294,295</sup> Synthetic routes leading to tetranuclear yttrium and lutetium hydride clusters have been worked out. The complexes are accessible by reacting precursors of the type  $(\text{C}_5\text{Me}_4\text{SiMe}_2\text{R})\text{Ln}(\text{CH}_2\text{SiMe}_3)_2(\text{THF})$

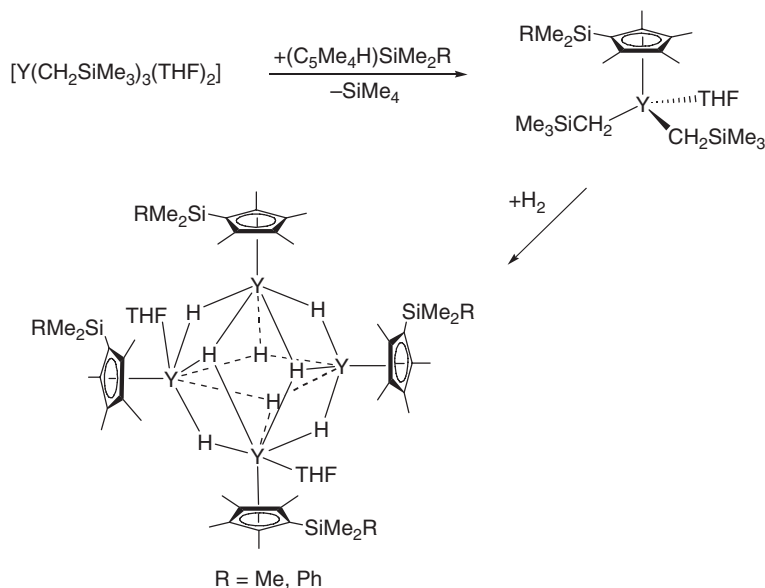


Scheme 67





Scheme 68

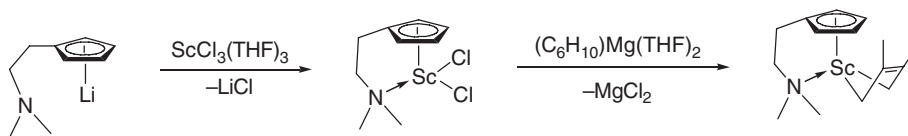


Scheme 69

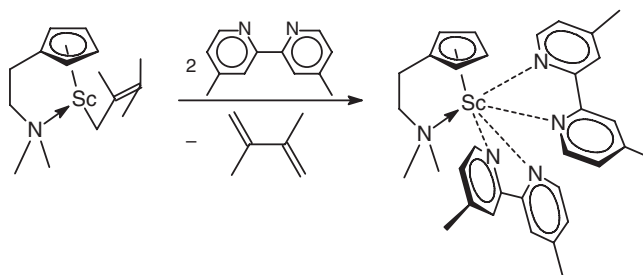
( $\text{R} = \text{Me}, \text{Ph}$ ;  $\text{Ln} = \text{Y}, \text{Lu}$ ) with either  $\text{H}_2$  (Scheme 69)<sup>296,297</sup> or  $\text{PhSiH}_3$ ,<sup>298</sup> and their reactivity has been studied.<sup>297,299,300</sup> This includes, for example, hydrogenation of carbon dioxide and aryl isocyanates.<sup>301</sup> The effective group potentials (EGP) method has been used for predicting the properties of the trinuclear hydride clusters  $\text{Cp}_6\text{Lu}_3\text{H}_3$  and  $\text{Cp}_6\text{Lu}_3\text{H}_4^-$ .<sup>302</sup>

A redox transmetalation reaction of the tetranuclear cubane-like cluster complex  $[\{\text{C}_5\text{H}_4\text{CH}_2\text{CH}(\eta^1\text{-O})\text{OBu}^n\}\text{Yb}]_4$  with  $\text{Me}_2\text{Hg}$  produced a monomeric  $\sigma$ -methyl complex of trivalent ytterbium  $[\text{C}_5\text{H}_4\text{CH}_2\text{CH}(\eta^1\text{-O})\text{OBu}^n]\text{YbMe}(\text{THF})$  in nearly quantitative yield.<sup>193</sup> Related half-sandwich complexes have been synthesized utilizing the tridentate ligands  $[\text{C}_5\text{H}_4\text{CH}_2\text{CH}(\text{O})\text{CH}_2\text{OBu}^n]^{2-}$ . Treatment of the  $\text{CpLu}(\text{C}_{10}\text{H}_8)(\text{DME})$  with diphenylacetylene in DME yielded a binuclear complex  $[\text{CpLu}(\text{DME})]_2\{1,1-\mu-4,4-\mu\text{-PhC}(\text{Ph})\text{C}\equiv\text{C}(\text{Ph})\text{CPh}\}$ , which was structurally characterized. In the structure, two Lu atoms of  $\text{CpLu}(\text{DME})$  fragments are bound by the bridging  $[\text{C}_4\text{Ph}_4]^{4-}$  ligand. The central  $\text{C}_4$  fragment is planar (within 0.03 Å), and the  $\text{Lu}-\mu_2\text{-C}(\text{C}_4\text{Ph}_4)$   $\sigma$ -bond lengths are 2.280(7) and 2.336(7) Å. The  $\text{C}_4\text{Ph}_4$  ligand has an asymmetrical propeller-like structure, which provides chirality to the molecule of the complex on the whole. The unit cell contains both enantiomeric forms.<sup>286</sup> The (cyclopentadienyl)lanthanide 1,3-butadiene complexes  $(\text{C}_5\text{H}_3\text{Bu}^t\text{-1,3})\text{Nd}(\text{C}_4\text{H}_6)\cdot\text{MgCl}_2\cdot 2\text{THF}$ ,  $\text{CpEr}(\text{C}_4\text{H}_6)\cdot\text{MgCl}_2\cdot 2\text{THF}$ , and  $(\text{C}_5\text{H}_3\text{Bu}^t\text{-1,3})\text{Lu}(\text{C}_4\text{H}_6)\cdot\text{MgCl}_2\cdot 2\text{THF}$  have been prepared by the reaction of appropriate cyclopentadienyl lanthanide dihalides with  $(\text{C}_4\text{H}_6)\text{Mg}(\text{THF})_2$ .<sup>303</sup> The scandium 2,3-dimethyl-1,3-butadiene complex  $[\eta^5\text{-}\eta^1\text{-C}_5\text{H}_4(\text{CH}_2)_2\text{NMe}_2]\text{Sc}(\text{C}_6\text{H}_{10})$  has been obtained as red crystals in 48% yield by the two-step procedure outlined in Scheme 70.<sup>304</sup>

The scandium diene complex reacts with  $\text{PhCN}$  via initial nitrile insertion into the  $\text{Sc}$ -diene bond to give a dimeric  $\eta^2$ -imido species, but with a 2,2'-bipyridine under elimination of the free diene (Scheme 71). The latter reaction



Scheme 70



Scheme 71

shows that  $[\eta^5\text{-C}_5\text{H}_4(\text{CH}_2)_2\text{NMe}_2]\text{Sc}(\text{C}_6\text{H}_{10})$  can be used to generate the reactive fragment  $[\eta^5\text{-}\eta^1\text{-C}_5\text{H}_4(\text{CH}_2)_2\text{NMe}_2]\text{Sc}^\dagger$ .<sup>304</sup>

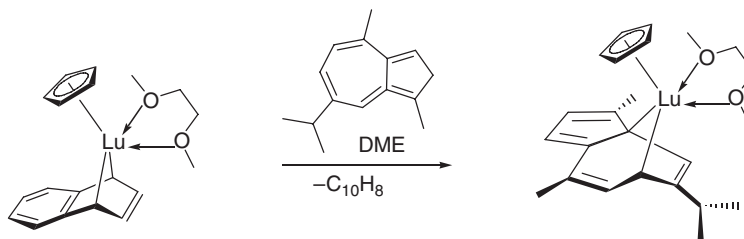
The mono(cyclopentadienyl)lutetium complex  $\text{CpLu}(2\eta^1\text{-}\eta^2\text{-guaiazulene})(\text{DME})$  has been prepared in the form of blue crystals by reduction of guaiazulene with the naphthalene–lutetium complex  $\text{CpLu}(\eta^1\text{-}\eta^2\text{-C}_{10}\text{H}_8)(\text{DME})$  in DME (Scheme 72). According to an X-ray analysis, the molecule has a skewed pseudo-sandwich structure in which the Lu atom is  $2\eta^1\text{-}\eta^2$ -coordinated by the seven-membered ring of the guaiazulene dianion ligand.<sup>304,305</sup>

Unexpected results have been obtained by investigating the chemistry of yttrium  $\text{C}_5\text{Me}_4\text{Si}(\text{Me})_2\text{CH}_2\text{CH}=\text{CH}_2^-$  (Scheme 73). The neutral diene reacts with  $\text{Y}(\text{CH}_2\text{SiMe}_3)_3(\text{THF})_2$  forming a bright yellow mono(cyclopentadienyl) dialkyl derivative. While insertion of  $\text{CO}_2$  produced the expected insertion product, thermolysis at  $65^\circ\text{C}$  led to a dark red compound resulting from double metallation of the ligand and formation of a new type of trianionic cyclopentadienyl allyl ligand  $[\text{C}_5\text{Me}_4\text{SiMe}_2\text{C}_3\text{H}_3]^{3-}$ .<sup>306</sup>

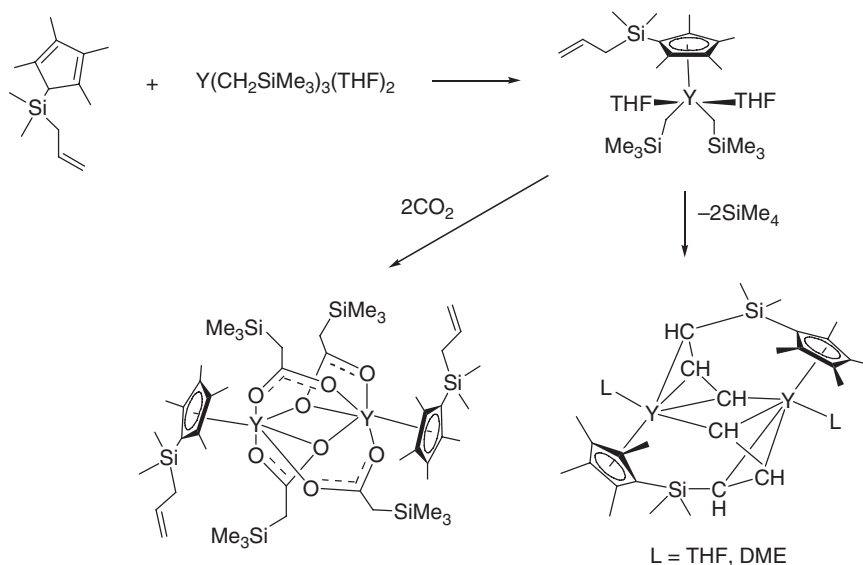
The synthesis of the first half-metallocene bis(borohydrides) of lanthanide elements has been achieved by a reaction of the tetraisopropylcyclopentadienyl sodium salt  $\text{Na}(\text{C}_5\text{HPr}_4)$  with  $\text{Ln}(\text{BH}_4)_3(\text{THF})_3$  ( $\text{Ln} = \text{Sm}, \text{Nd}$ ) at room temperature to afford the monocyclopentadienyl complexes  $(\text{C}_5\text{HPr}_4)\text{Sm}(\text{BH}_4)_2(\text{THF})$  and  $(\text{C}_5\text{HPr}_4)\text{Nd}(\text{BH}_4)_2(\text{THF})$  in 50–60% yield. These complexes are thermally stable and melt without decomposition at around  $170^\circ\text{C}$ .<sup>307</sup> Analogous compounds have also been synthesized with the use of the  $[\text{C}_5\text{Me}_4\text{Pr}^n]^-$  ligand.<sup>308</sup>

#### 4.01.6.4 $\text{Cp}_2\text{LnX}$ Compounds

Electron density calculations have been carried out on  $\text{Cp}_2\text{ScR}$  ( $\text{R} = \text{H}, \text{Me}, \text{Et}, \text{Pr}^n, \text{vinyl}, \text{acetylide}$ ). Geometry optimizations revealed an agostic interaction for  $\text{R} = \text{Et}$ , whereas Me and Pr are bonded to the metal center without agostic interactions.<sup>309</sup> Other density functional studies have been carried out on the complexes  $\text{Cp}_2\text{LnCl}$  and  $\text{Cp}_2\text{LnX}(\text{THF})$  ( $\text{Ln} = \text{La-Lu}$ ;  $\text{X} = \text{F}, \text{Cl}, \text{Br}, \text{I}$ ). In these mixed ligand complexes,  $\text{Ln-Cp}$  and  $\text{Ln-THF}$  bonds are



Scheme 72



Scheme 73

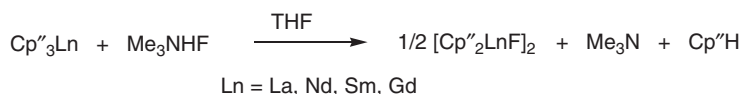
more covalent compared to  $Ln-X$ .<sup>310,311</sup> DFT calculations have been performed on the lanthanidocene complexes  $Cp_2LnX(THF)$  ( $Ln = La, Gd, Lu$ ;  $X = F, Cl, Br, I$ ), and the calculated geometries were in good agreement with the available experimental data.<sup>312</sup> DFT calculations have also been carried out to elucidate the coordination geometry in the olefin-pendant-arm cyclopentadienyl scandium complexes  $CpSc[C_5H_4SiMe_2(CH_2-\eta^2-CH=CH_2)](CH_2Ph)$ .<sup>313</sup> The reaction of  $CF_4$  with  $Cp_2LnH$  has been studied with DFT(B3PW91) calculations for the entire lanthanide series. The reaction paths for H/F exchange (formation of  $CF_3H$  and  $Cp_2LnF$ ) and alkylation (formation of  $Cp_2LnCF_3$  and  $HF$ ) have been determined. Even though a transition state for the formation of  $Cp_2LnCF_3$  has been located,  $Cp_2LnCF_3$  reacts with no energy barrier with  $HF$  to give  $Cp_2LnF$  and  $CF_3H$ .<sup>314</sup>

The “Lewis base-free” cationic lanthanide metallocene complexes of the type  $[Cp''_2Ln]Y$  ( $Y = BPh_4^-, CB_{11}Br_6H_6^-, Cp'' = C_5H_3(SiMe_3)_{2-1,3}$ ) were synthesized by treatment of unsolvated  $Cp''_2Ln(II)$  or  $[Cp''_2LnI]_2$  with 1 equiv. of  $Ag(I)Y$  or with two molar equivalents of  $Ag(CB_{11}Br_6H_6)$  in toluene at room temperature. The reactivity of these complexes with respect to the coordinating nature of the counter ions was investigated.<sup>315</sup>

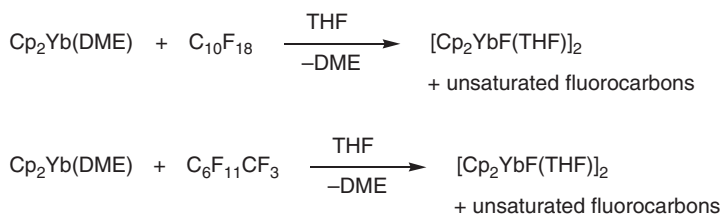
#### 4.01.6.4.1 $Cp_2LnX$ compounds with $X = \text{halide}$

Several organolanthanide fluoride complexes have been prepared by treatment of  $[C_5H_3(SiMe_3)_{2-1,3}]_3Ln$  ( $Cp''_3Ln$ ) or  $Cp_3Ln$  with the new useful fluorinating reagent  $Me_3NHF$  in an equimolar ratio (Scheme 74). This way  $[Cp''Ln(\mu-F)]_2$  ( $Ln = La, Nd, Sm, Gd$ ) and  $[Cp_2LnF(THF)]_2$  ( $Ln = Y, Yb$ ) were obtained.<sup>316</sup>

To investigate the effect of substituents at the Cp ring on the formation and molecular structure of organolanthanide fluoride compounds, compounds of the type  $Cp_2LnF(THF)$  were also prepared.<sup>316</sup> Sodium was shown to reduce  $[Cp''_2Sm(\mu-F)]_2$  to  $Cp''_2Sm(THF)$ . Upon treatment of  $[Cp''_2Sm(\mu-F)]_2$  with an excess amount of  $NaCp''$  in THF no  $Cp''_3Sm$  was isolated. Reaction of this complex with 1 equiv. of anhydrous  $AlCl_3$  gave  $[Cp''_2Sm(\mu-Cl)]_2$ . The bimetallic compound  $Cp''_2Sm(\mu-F)(\mu-Cl)AlCl_2$  was not isolated.  $[Cp''_2Sm(\mu-F)]_2$  reacted with 1 equiv. of  $Ph_3SiOH$  or 2,6- $Pr^i_2C_6H_3OH$  in THF to give the unexpected products  $Sm(OSiPh_3)_3(THF)_3$  and  $Sm(2,6-Pr^i_2C_6H_3O)_3(THF)_3$ , respectively.<sup>316</sup> A facile new synthetic route to obtain  $[Cp_2Yb(\mu-F)(THF)]_2$ , which involves the reaction of  $Cp_2Yb(DME)$  with perfluorodecalin or perfluoro(methylcyclohexane) in THF, has been discovered. These are the first examples of C–F activation of saturated perfluorocarbons by a lanthanide organometallic (Scheme 75).<sup>317</sup>



Scheme 74



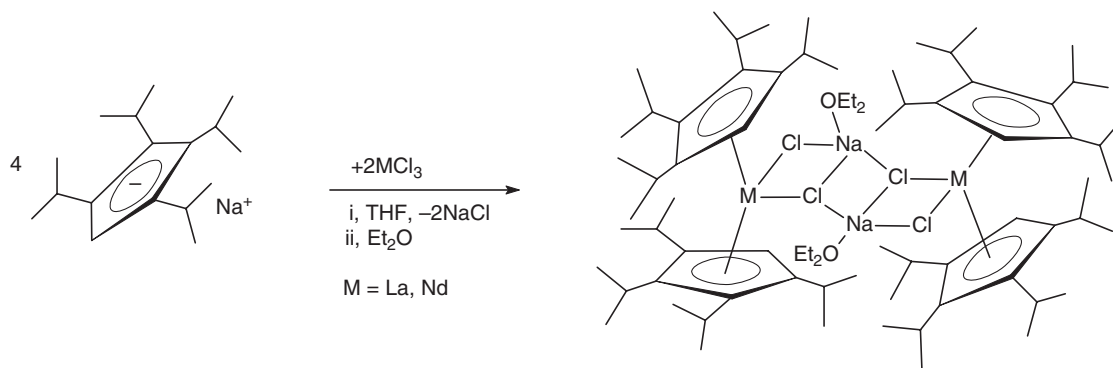
Scheme 75

The bis(cyclopentadienyl)fluoroytterbium(III) complexes  $[\text{Cp}_2\text{Yb}(\mu\text{-F})]_3$ ,  $[(\text{C}_5\text{H}_4\text{Me})_2\text{Yb}(\mu\text{-F})]_4$ ,  $[\text{Cp}_2\text{Yb}(\mu\text{-F})(\text{OPh}_3)]_2$ , and  $[(\text{C}_5\text{H}_4\text{Me})_2\text{Yb}(\mu\text{-F})(\text{THF})]_4$  have been prepared analogously starting with ytterbocene(II) precursors. Oxidation of bis(cyclopentadienyl)ytterbium(II) with perfluoro(methylcyclohexane) or perfluorodecalin in DME gives unsolvated  $[\text{Cp}_2\text{Yb}(\mu\text{-F})]_3$ . The analogous reaction of bis(methylcyclopentadienyl)ytterbium(II) yields unsolvated  $[(\text{C}_5\text{H}_4\text{Me})_2\text{Yb}(\mu\text{-F})]_4$ , while in THF the oxidation provides  $[(\text{C}_5\text{H}_4\text{Me})_2\text{Yb}(\mu\text{-F})(\text{THF})]_4$ .<sup>205</sup>  $\text{Cp}_2\text{Yb}(\text{DME})$  has also been used as a reagent for the regiospecific replacement of fluorine by hydrogen in an aromatic ring.<sup>318</sup> The net reaction of monomeric  $(\text{C}_5\text{H}_2\text{Bu}^t\text{-1,3,4})_2\text{CeH}$  with  $\text{C}_6\text{F}_6$  in  $\text{C}_6\text{D}_6$  is  $(\text{C}_5\text{H}_2\text{Bu}^t\text{-1,3,4})_2\text{CeF}$ ,  $\text{H}_2$ , and tetrafluorobenzene. The pentafluorophenylmetallocene  $(\text{C}_5\text{H}_2\text{Bu}^t\text{-1,3,4})_2\text{Ce}(\text{C}_6\text{F}_5)$  is formed as an intermediate that decomposes slowly to  $(\text{C}_5\text{H}_2\text{Bu}^t\text{-1,3,4})_2\text{CeF}$  (orange crystals) and  $\text{C}_6\text{F}_4$  (tetrafluorobenzene), and the latter is trapped by the solvent  $\text{C}_6\text{D}_6$  as a [2+4]-cycloadduct.<sup>319</sup> Treatment of  $\text{Cp}_2\text{YbF}(\text{THF})$  with triphenylphosphine oxide gave  $[\text{Cp}_2\text{Yb}(\mu\text{-F})(\text{OPPh}_3)]_2$ .<sup>205</sup> X-ray structure determinations revealed that  $[\text{Cp}_2\text{Yb}(\mu\text{-F})]_3$  is trimeric with formal eight-coordination for ytterbium and a planar  $(\text{YbF})_3$  ring, whereas  $[(\text{C}_5\text{H}_4\text{Me})_2\text{Yb}(\mu\text{-F})]_4$  is an eight-coordinated tetramer having a puckered  $(\text{YbF})_4$  ring with  $\text{F-Yb-F}$  angles of ca.  $90^\circ$  and  $\text{Yb-F-Yb}$  angles close to  $180^\circ$ . Both  $[(\text{C}_5\text{H}_4\text{Me})_2\text{Yb}(\mu\text{-F})(\text{THF})]_4$  and  $[\text{Cp}_2\text{Yb}(\mu\text{-F})(\text{OPPh}_3)]_2$  are nine-coordinate fluoride-bridged dimers.<sup>205</sup> The methylcyclopentadienyl samarium chloro complex  $[(\text{C}_5\text{H}_4\text{Me})\text{Sm}(\mu\text{-Cl})]_2$ , prepared in the usual manner from  $\text{SmCl}_3$  and  $\text{K}(\text{C}_5\text{H}_4\text{Me})$ , is a THF-solvated dimer in the solid state.<sup>320</sup> Mixed-ring bis(cyclopentadienyl)lanthanide complexes of the type  $\text{Cp}(\text{C}_5\text{H}_4\text{Me})\text{LnCl}$  ( $\text{Ln} = \text{Y, Gd, Er, Yb}$ ) have been synthesized by reacting  $\text{LnCl}_3$  with  $\text{Na}(\text{C}_5\text{H}_4\text{Me})$  followed by addition of 1 equiv. of  $\text{NaCp}$ . Further reaction of the Yb derivative with excess  $\text{HCp}$  led to ring displacement and the formation of  $\text{Cp}_2\text{YbCl}(\text{THF})$ .<sup>321</sup> The crystal structures of  $\text{Cp}_2\text{YbX}(\text{THF})$  ( $\text{X} = \text{Cl, Br}$ ) have been determined. The ligand arrangements around the formally eight-coordinate Yb atom are pseudo-tetrahedral. These two structure determinations completed the first series of  $\text{Cp}_2\text{LnX}(\text{L})$  ( $\text{X} = \text{F, Cl, Br, I}$ ) structures covering all halogens for one lanthanide element.<sup>322</sup> The deuterated complex  $[(\text{C}_5\text{D}_5)_2\text{Dy}(\mu\text{-Br})]_2$  has been prepared and structurally characterized. The synthesis involved the reaction of anhydrous  $\text{DyBr}_3$  with 2 equiv. of  $\text{TIC}_5\text{D}_5$  in benzene- $d_6$ .<sup>323</sup> The crystal structure of  $[\text{Cp}_2\text{Sc}(\mu\text{-Cl})]_2$  has been found to be isomorphous with that of  $[\text{Cp}_2\text{Dy}(\mu\text{-Br})]_2$ . A series of organolanthanide triphenylphosphine adducts,  $\text{Cp}_2\text{LnCl}(\text{PPh}_3)$  ( $\text{Ln} = \text{La, Nd, Eu, Yb, Lu}$ ), were characterized by elemental analysis and IR spectroscopy.<sup>324</sup> Addition of vinylcyclopentadienyl lithium in a molar ratio of  $[\text{LnCl}_3]:[\text{Li}(\text{C}_5\text{H}_4\text{CH}=\text{CH}_2)]$  of 1:2 to  $\text{LnCl}_3$  ( $\text{Ln} = \text{Nd, Tb}$ ) afforded bis(vinylcyclopentadienyl) complexes of the type  $(\text{C}_5\text{H}_4\text{CH}=\text{CH}_2)_2\text{LnCl}$ .<sup>248</sup> More recently the chemistry of organolanthanide complexes containing the bulky vinyltetramethylcyclopentadienyl ligand and its homologs has been thoroughly investigated.<sup>325</sup> The bis(butenylcyclopentadienyl)lanthanide chlorides  $(\text{C}_5\text{H}_4\text{CH}_2\text{CH}_2\text{CH}=\text{CH}_2)_2\text{LnCl}(\text{THF})_2$  ( $\text{Ln} = \text{Sm, Y, Dy, Er}$ ) have been synthesized as air- and moisture-sensitive, free-flowing oils. No evidence of intramolecular coordination of the butenyl side chain was observed.<sup>326</sup> Numerous bis(cyclopentadienyl)lanthanide complexes containing the 1-(but-3-enyl)-2,3,4,5-tetramethylcyclopentadienyl ligand have been synthesized and structurally characterized.<sup>327</sup> The reaction of  $\text{LnCl}_3$  ( $\text{Ln} = \text{Sm, Yb}$ ) with  $\text{Li}(\text{C}_5\text{H}_3\text{Bu}^t\text{-1,3})$  afforded the  $(\text{C}_5\text{H}_3\text{Bu}^t\text{-1,3})_2\text{Ln}(\mu\text{-Cl})_2\text{Li}(\text{THF})_2$  ate-complexes.<sup>328</sup> In  $[(\text{C}_5\text{H}_4\text{Me})_2\text{Tb}(\mu\text{-Cl})(\text{THF})]_2$ , the  $\text{Tb}^{3+}$  ion is coordinated by two  $\text{C}_5\text{H}_4\text{Me}$  groups, two chloride ions, and one O atom from THF to form a distorted trigonal bipyramidal geometry.<sup>329</sup> An analogous structure was found for  $[(\text{C}_5\text{H}_4\text{Me})_2\text{Sm}(\mu\text{-Cl})(\text{THF})]_2$ .<sup>330</sup>  $[(\text{C}_5\text{H}_4\text{Bu}^t)_2\text{Ln}(\mu\text{-Cl})]_2$  ( $\text{Ln} = \text{Gd, Er}$ ) complexes were prepared from  $\text{Na}(\text{C}_5\text{H}_4\text{Bu}^t)$  and  $\text{LnCl}_3$  in THF and characterized by X-ray crystallography.<sup>331,332</sup> The cyanoethyl-substituted bis(cyclopentadienyl) samarium complex  $\text{Cp}(\text{C}_5\text{H}_4\text{CH}_2\text{CH}_2\text{CN})\text{SmCl}$  has been reported.<sup>333</sup> The trichlorides of yttrium, samarium, and lutetium reacted with 2 equiv. of  $\text{Na}(\text{C}_5\text{Me}_4\text{Pr}^i)$  in THF to form  $(\text{C}_5\text{Me}_4\text{Pr}^i)_2\text{LnCl}(\text{THF})$  containing two bulky tetramethyl-isopropylcyclopentadienyl ligands.<sup>334</sup> Reactions of  $\text{LnCl}_3$  ( $\text{Ln} = \text{Ho, Tm, Lu}$ ) with  $\text{Na}(\text{C}_5\text{Me}_4\text{H})$  in THF gave the corresponding dicyclopentadienyl complexes  $(\text{C}_5\text{Me}_4\text{H})_2\text{LnCl}(\text{THF})$ ,<sup>213</sup> while those of  $\text{LnCl}_3(\text{THF})_x$  ( $\text{Ln} = \text{Y, Nd, Sm, Lu}$ ) with  $\text{Na}(\text{C}_5\text{Me}_4\text{Et})$  in THF gave the analogous  $(\text{C}_5\text{Me}_4\text{Et})_2\text{LnCl}(\text{THF})$  complexes.<sup>335</sup> Bis(cyclopentylcyclopentadienyl)lanthanide chlorides,  $[(\text{C}_5\text{H}_4\text{C}_5\text{H}_9)_2\text{Ln}(\mu\text{-Cl})(\text{THF})]_2$  ( $\text{Ln} = \text{Nd, Sm}$ )

and  $[(C_5H_4C_5H_9)_2Ln(\mu-Cl)]_2$  ( $Ln = Er, Yb$ ), have been prepared by the usual metathetical reactions.<sup>336</sup> The crystal structures of the complexes  $(C_5Me_4Pr^i)_2LuCl(THF)$  and  $(C_5Me_4Pr^i)_2LuMe(THF)$  were determined. These structures are typical of bent metallocene species and the central lutetium atom is tetrahedrally surrounded by two cyclopentadienyl ring centroids, the oxygen atom and the chlorine atom.<sup>334</sup> The ytterbium complex  $[(C_5H_4SiMe_3)_2Yb(\mu-Cl)]_2$  was prepared by the reaction of  $YbCl_3$  with  $Li(C_5H_4SiMe_3)$  in THF. According to X-ray diffraction, the compound has a typical dimeric structure with two bridging chlorine atoms.<sup>337</sup> In the crystal structure of the dimeric compound  $[(C_5H_4SiMe_3)_2Sm(\mu-Cl)]_2$ , the Sm atom has pseudo-tetrahedral coordination geometry like the corresponding Yb derivative. The four centroids of the monosubstituted cyclopentadienyl rings adopt a square planar arrangement.<sup>338</sup> The ytterbocene(III) iodide  $Cp''_2YbI(THF)$  was prepared by the reaction of 2 equiv. of  $NaCp''$  with  $YbI_3(THF)_2$ , which was obtained from Yb metal and an excess of 1,2-diiodoethane in THF ( $Cp'' = C_5H_3(SiMe_3)_2-1,3$ ). In contrast to  $NaCp''$ , the reaction of  $LiCp''$  with  $YbCl_3$  formed a heterobimetallic complex  $Cp''_2Yb(\mu-Cl)_2Li(THF)_2$ .<sup>202</sup>

Several bis(cyclopentadienyl)iodide complexes with lanthanum, samarium, yttrium, erbium, and lutetium were synthesized by halide exchange reactions between  $[Cp''_2Ln(\mu-Cl)]_2$  and NaI in THF. The starting materials  $[Cp''_2Ln(\mu-Cl)]_2$  were synthesized by treatment of anhydrous  $LnCl_3$  with 2 equiv. of  $Cp''Na$  in THF. Subsequent treatment of  $[Cp''_2Ln(\mu-Cl)]_2$  with excess of NaI at room temperature produced the organolanthanide iodide complexes  $Cp''_2LnI(THF)$  in 50–69% yield. The five monomeric complexes  $Cp''_2LnI(THF)$  were fully characterized by elemental analysis, IR, MS,  $^1H$  NMR spectroscopy, and single crystal X-ray diffraction. In the complexes the metal atom is enclosed in distorted tetrahedral environment with the  $C_5$  rings of  $Cp''$ , an oxygen atom of THF, and an iodide ligand.<sup>339</sup> Upon heating of  $Cp''LnI(THF)$  at  $50^\circ C$  under vacuum, the THF molecule was reversibly removable forming the dimeric complexes  $[Cp''Ln(\mu-I)]_2$ . The iodo complexes have a dimeric structure similar to their chloro analogs. Also reported was a more convenient and less time-consuming one-pot reaction method for making these iodide complexes.  $Cp''Na$  was added to a mixture of  $LnCl_3$  and NaI in THF at room temperature.<sup>339</sup>

The spontaneous self-assembly of a hexanuclear ytterbium(II) octaiodo dianion in the complex  $[Li(THF)_4]_2[Yb_6(C_5Me_4(SiMe_2Bu^t))_6I_8]$  has been investigated. The reaction of 1 equiv. of  $Li[C_5Me_4(SiMe_2Bu^t)]$  with  $YbI_2$  affords the novel half-sandwich polyatomic species; the molecular structures and solid- and solution-state  $^{171}Yb$  NMR data for  $[Li(THF)_4]_2[Yb_6(C_5Me_4(SiMe_2Bu^t))_6I_8]$  and, for comparison, the dimeric half-sandwich derivatives  $[Cp^*Yb(\mu-I)L_n]_2$  ( $L = THF, n = 2$ ;  $L = DME, n = 1$ ) have been presented. The molecular structure of  $[Li(THF)_4]_2[Yb_6(C_5Me_4(SiMe_2Bu^t))_6I_8]$  comprises two  $Li^+$  cations, each tetrahedrally coordinated by four THF molecules, and a  $[Yb_6(C_5Me_4(SiMe_2Bu^t))_6I_8]^{2-}$  dianion. Each face of the  $I_8$  cube is bridged in a  $\mu_4$ -fashion by a  $Yb[C_5Me_4(SiMe_2Bu^t)]$  moiety.<sup>340</sup> The organolanthanide oxide cluster complex  $(C_5H_4Me)_3Yb_4(\mu-Cl)_6(\mu_3-Cl)(\mu_4-O)(THF)_3$  was obtained from the reaction of  $Na(C_5H_4Me)$  with  $YbCl_3$  and  $YbOCl$  in THF. In the structure of  $(C_5H_4Me)_3Yb_4(\mu-Cl)_6(\mu_3-Cl)(\mu_4-O)(THF)_3$  the four Yb atoms form a distorted tetrahedron. The three Yb atoms are coordinated by one bridging oxygen atom, four bridging chlorine atoms, and a  $C_5H_4Me$  group to give a distorted octahedral geometry, while the fourth Yb atom is coordinated by one bridging oxygen atom, three bridging chlorine atoms, and three tetrahydrofuran molecules. The average Yb–C( $Cp$ -ring) distance is  $2.59(2) \text{ \AA}$ , the triply bridging Yb–Cl distances are  $2.79(4)$ – $2.81(4) \text{ \AA}$ , the doubly bridging Yb–Cl lengths are  $2.60(4)$ – $2.71(4) \text{ \AA}$ , and the Yb–O( $\mu_4$ -oxide) distances are  $2.13(1)$ – $2.29(1) \text{ \AA}$ .<sup>341</sup>  $[(C_5H_3CH=CHCH_2C=CHC_5H_4)_2Ho_2Cl_2]_\infty$  was obtained by sublimation of  $Cp_2HoCl$  at  $235^\circ C$ . The polymeric two-dimensional infinite network of the compound consists of the  $(C_5H_3CH=CHCH_2C=CHC_5H_4)_2Ho_2Cl_2$  units, in which each holmium atom is coordinated by a monosubstituted  $\eta^5$ -Cp group, a disubstituted  $\eta^5$ -Cp group, and two bridging chlorine atoms. The cyclopentadienyl groups are cross-linked together by  $\mu_3$ -“open cyclopentadiene” trialkenyl chains.<sup>342</sup> Treatment of 2 equiv. of  $NaCp^R$  ( $Cp^R = (+)$ -neomenthylcyclopentadienyl) with anhydrous lanthanide trichlorides in THF at room temperature afforded the organolanthanide chlorides  $[Cp^R_2Ln(\mu-Cl)]_2$  ( $Ln = Sm, Yb, Y, Lu$ ). Single crystal X-ray diffraction studies of  $[Cp^R_2Sm(\mu-Cl)]_2$  and  $[Cp^R_2Y(\mu-Cl)]_2$  revealed that both compounds are chloro-bridged dimers, with the  $Ln_2Cl_2$  plane being almost perpendicular to the plane described by the four cyclopentadienyl ring centroids. The  $(+)$ -neomenthyl groups attached to the cyclopentadienyl rings in each  $Cp^R_2Sm$  unit are positioned in a *trans* orientation with respect to each other in order to minimize the steric interaction.<sup>254</sup> Treatment of  $LnCl_3$  with 2 equiv. of  $Cp^RLi$  in THF gave the ionic compounds  $[Li(THF)_4][Cp''_2LnCl_2]$  ( $Ln = Er, Yb$ ) in good yield. The complexes consist of well-separate, alternating layers of discrete tetrahedral anions  $[Cp''_2LnCl_2]^-$  and tetrahedral cations  $[Li(THF)_4]^+$  in a typical ionic lattice. Recrystallization of the ytterbium complex from a toluene solution afforded the *ate*-compound  $Cp''_2Yb(\mu-Cl)_2Li(THF)_2$ .<sup>343</sup> Solvent-free  $[Cp''_2Tm(\mu-Cl)]_2$  was made from  $TmI_2(THF)_2$  and  $Cp''MgCl$ .<sup>344</sup> The  $Yb^{3+}$  ion in  $Cp''_2Yb(\mu-Cl)_2Li(THF)_2$  is  $\eta^5$ -bound to two cyclopentadienyl rings and  $\sigma$ -bound to two doubly bridging chloride ions in a distorted tetrahedral geometry. The Cl–Yb–Cl angle of  $84.89(3)^\circ$  is smaller than that in  $[Cp''_2Nd(\mu-Cl)_2Li(THF)]$ , but is significantly smaller than that of  $102.77(3)^\circ$  in  $[Li(THF)_4][Cp''_2YbCl_2]$  probably



Scheme 76

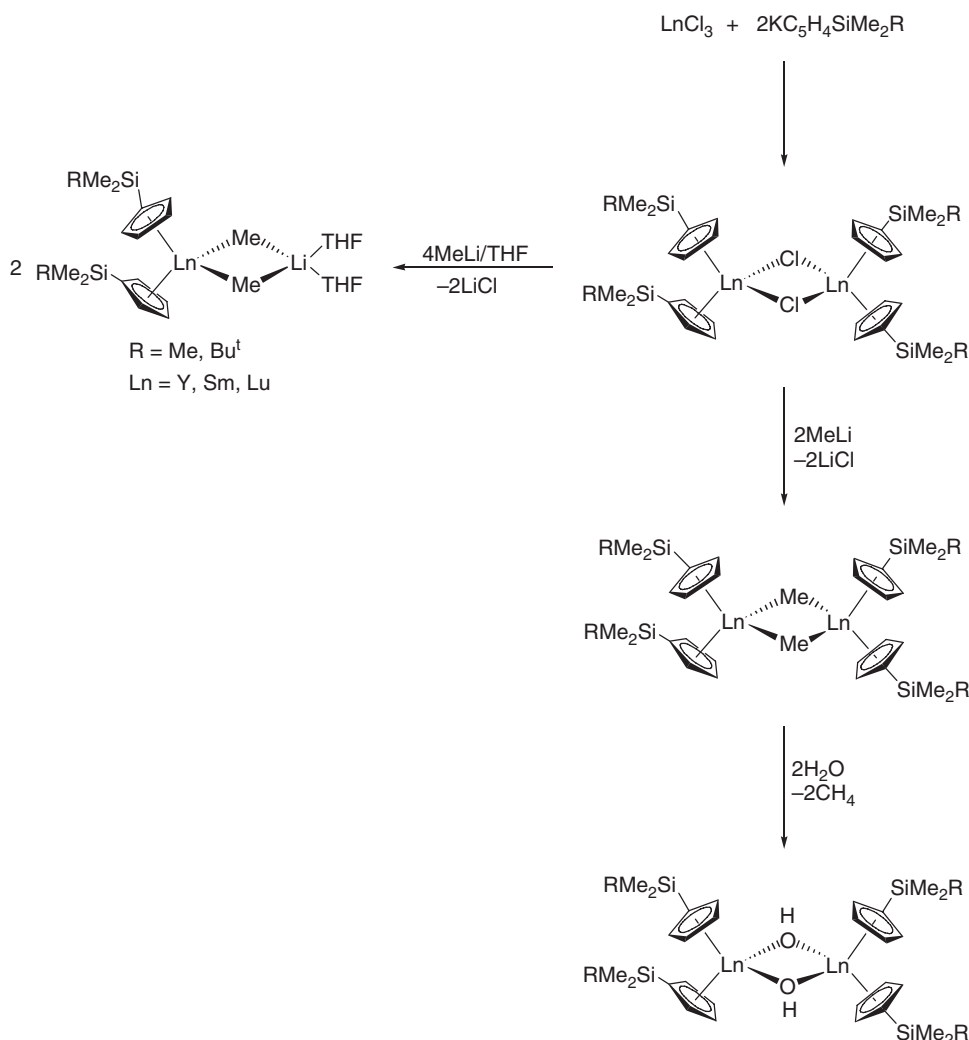
due to the bridging unit  $\text{Yb}(\mu\text{-Cl})_2\text{Li}$  that forces the  $\text{Cl}\text{--}\text{Yb}\text{--}\text{Cl}$  angle to be smaller.<sup>343</sup> The trichlorides of yttrium, samarium, and lutetium react with 2 equiv. of  $\text{K}(\text{C}_5\text{H}_4\text{SiEt}_3)$  to form the dimeric compounds  $[(\text{C}_5\text{H}_4\text{SiEt}_3)_2\text{Ln}(\mu\text{-Cl})]_2$  ( $\text{Ln} = \text{Y}, \text{Sm}, \text{Lu}$ ).<sup>345</sup> Reaction of 2 equiv. of 1,3-dimesitylimidazolium chloride with  $\text{Cp}_3\text{Yb}$  in refluxing THF afforded the golden-orange salt  $[\text{Imid}_2\text{Cp}]^+[\text{Cp}_2\text{YbCl}_2]^-$ .<sup>346</sup> The bis(substituted cyclopentadienyl)lanthanide(III) halides  $[\text{LnCp}^{\text{R}1}_2(\mu\text{-Cl})]_2$  ( $\text{Ln} = \text{Pr}, \text{Nd}, \text{Sm}, \text{Dy}, \text{Tb}, \text{Y}$ ),  $[\text{LnCp}^{\text{R}2}_2(\mu\text{-X})]_2$  ( $\text{X} = \text{Cl}, \text{Ln} = \text{La}, \text{Nd}$ ;  $\text{X} = \text{I}, \text{Ln} = \text{Tm}$ ), and  $[\text{Nd}(\text{Cp}^{\text{R}1}_2\text{SiMe}_2)(\mu\text{-Cl})]_2$ , and bis(substituted cyclopentadienyl)lanthanide(II) complexes  $\text{LnCp}^{\text{R}2}_2(\text{THF})_2$  ( $\text{Ln} = \text{Sm}, \text{Eu}, \text{Yb}$ ),  $\text{YbCp}^{\text{R}2}_2(\text{THF})_2$ ,  $\text{LnCp}^{\text{R}2}_2(\text{THF})_2$  ( $\text{Ln} = \text{Sm}, \text{Yb}$ ),  $\text{LnCp}^{\text{R}2}_2(\text{Ln} = \text{Sm}, \text{Eu}, \text{Yb})$ ,  $\text{YbCp}^{\text{R}2}_2$ ,  $\text{LnCp}^{\text{R}2}_2$  ( $\text{Ln} = \text{Sm}, \text{Yb}$ ), and  $\text{Yb}(\text{Cp}^{\text{R}1}_2\text{SiMe}_2)(\text{THF})_2$  [ $\text{Cp}^{\text{R}} = \text{C}_5\text{H}_4\text{CH}(\text{SiMe}_3)_2$ ,  $\text{Cp}^{\text{I}} = \text{C}_5\text{H}_4\text{SiMe}_2\text{Bu}^{\text{I}}$ ,  $\text{Cp}^{\text{II}} = \text{C}_5\text{H}_3(\text{SiMe}_2\text{Bu}^{\text{I}})_2\text{-1,3}$ ,  $\text{Cp}^{\text{R}1} = \text{C}_5\text{H}_3\text{CH}(\text{SiMe}_3)_2\text{-3}$ ] have been synthesized from the appropriate  $\text{LnCl}_3$ ,  $\text{TmI}_3$ , or  $\text{LnI}_2$  with the selected sodium or potassium cyclopentadienide. The molecular structures of  $[\text{Cp}^{\text{R}2}_2\text{Nd}(\mu\text{-Cl})]_2$ ,  $[\text{Cp}^{\text{R}2}_2\text{Tm}(\mu\text{-I})]_2$ , and  $(\text{Cp}^{\text{R}1}_2\text{SiMe}_2)_2\text{Yb}(\text{THF})_2$  have been determined by X-ray diffraction.<sup>347</sup> Complexes of the type  $\text{Cp}_2\text{LnCl}$  have been isolated with the very bulky tetraisopropylcyclopentadienyl ligand. Even in this case incorporation of alkali metal halide leads to the formation of *ate*-complexes (Scheme 76).<sup>348</sup> Substitution reactions leading to the corresponding lanthanide silylamide complexes have recently been described.<sup>349</sup> The cationic complex  $[(\text{C}_5\text{H}_4\text{Bu}^{\text{I}})_2\text{Yb}(\text{THF})_2][\text{BPh}_4] \cdot x\text{THF}$  has been synthesized by a one-electron oxidation of  $(\text{C}_5\text{H}_4\text{Bu}^{\text{I}})_2\text{Yb}(\text{THF})_2$  with  $\text{AgBPh}_4$ .<sup>350</sup>

#### 4.01.6.4.2 $\text{Cp}_2\text{LnX}$ compounds with C and OH ligands

The dimeric dicyclopentadienyl lanthanide chlorides react with 2 equiv. of methyl lithium in diethyl ether to give the dimeric lanthanide methyl complexes  $[(\text{C}_5\text{H}_4\text{SiMe}_2\text{R})_2\text{Ln}(\mu\text{-Me})]_2$  ( $\text{R} = \text{Me}, \text{Bu}^{\text{I}}$ ;  $\text{Ln} = \text{Y}, \text{Sm}, \text{Lu}$ ) which are moderately stable in atmospheric moisture. The reaction of the monochlorides  $[(\text{C}_5\text{H}_4\text{SiMe}_3)_2\text{Ln}(\mu\text{-Cl})]_2$  ( $\text{Ln} = \text{Y}, \text{Sm}, \text{Lu}$ ) with methyl lithium in a 1:4 ratio in THF afforded the monomeric lanthanidocene methyl complexes  $(\text{C}_5\text{H}_4\text{SiMe}_3)_2\text{Ln}(\mu\text{-Me})_2\text{Li}(\text{THF})_2$  ( $\text{Ln} = \text{Y}, \text{Sm}, \text{Lu}$ ). Treatment of  $[(\text{C}_5\text{H}_4\text{SiMe}_2\text{R})_2\text{Ln}(\mu\text{-Me})]_2$  ( $\text{R} = \text{Me}, \text{Bu}^{\text{I}}$ ;  $\text{Ln} = \text{Y}, \text{Sm}, \text{Lu}$ ) with stoichiometric amounts of  $\text{H}_2\text{O}$  in toluene yields the dimeric lanthanidocene hydroxy complexes  $[(\text{C}_5\text{H}_4\text{SiMe}_2\text{R})_2\text{Ln}(\mu\text{-OH})]_2$  ( $\text{R} = \text{Me}, \text{Bu}^{\text{I}}$ ;  $\text{Ln} = \text{Y}, \text{Sm}, \text{Lu}$ ) (Scheme 77).<sup>351</sup>

It was also shown that the decomposition reaction of the dicyclopentadienyl lanthanidocene methyl complexes  $[(\text{C}_5\text{H}_4\text{SiMe}_2\text{R})_2\text{Ln}(\mu\text{-Me})]_2$  ( $\text{R} = \text{Me}, \text{Bu}^{\text{I}}$ ;  $\text{Ln} = \text{Y}, \text{Sm}, \text{Lu}$ ) in moist air depends on the ionic radius of the lanthanoid center and on the steric demand of the cyclopentadienyl ligand. The hydroxo complexes  $[(\text{C}_5\text{H}_4\text{SiMe}_2\text{R})_2\text{Ln}(\mu\text{-OH})]_2$  ( $\text{R} = \text{Me}, \text{Bu}^{\text{I}}$ ;  $\text{Ln} = \text{Y}, \text{Sm}, \text{Lu}$ ) were found to be intermediate products in the decomposition process. Single crystal X-ray determinations of  $[(\text{C}_5\text{H}_4\text{SiMe}_2\text{Bu}^{\text{I}})_2\text{Lu}(\mu\text{-Cl})]_2$ ,  $[(\text{C}_5\text{H}_4\text{SiMe}_3)_2\text{Y}(\mu\text{-Me})]_2$ ,  $[(\text{C}_5\text{H}_4\text{SiMe}_2\text{R})_2\text{Lu}(\mu\text{-OH})]_2$  showed the dimeric structure of these compounds.<sup>351</sup> Partial hydrolysis of the cationic organolanthanide compounds  $[\text{Cp}^{\text{R}2}_2\text{Sm}][\text{B}(\text{C}_6\text{H}_5)_4]$  and  $[\text{Cp}^{\text{R}2}_2\text{Sm}][\text{CB}_{11}\text{H}_6\text{Br}_6]$  in toluene at  $-30^\circ\text{C}$  gave  $(\text{Cp}^{\text{R}2}_2\text{Sm})_2(\mu\text{-O})(\mu\text{-OH}_2)$  and two distinct crystalline forms of  $[\text{Cp}^{\text{R}2}_2\text{Sm}(\mu\text{-OH})]_2$ , respectively. The two crystalline forms are not crystallographically interconvertible, and they are clearly distinguishable from one another. These observations imply that there may be a continuous process leading from organosamarium hydroxo to oxo compounds. The solid-state IR spectrum of  $(\text{Cp}^{\text{R}2}_2\text{Sm})_2(\mu\text{-O})(\mu\text{-OH}_2)$  displays a broad band at  $3300\text{ cm}^{-1}$  attributable to the O–H stretching frequency of the coordinated  $\text{H}_2\text{O}$  molecule, while the spectra of the two forms of  $[\text{Cp}^{\text{R}2}_2\text{Sm}(\mu\text{-OH})]_2$  exhibit one sharp band at  $3668\text{ cm}^{-1}$  that is assigned to the O–H stretching mode of the  $\text{Ln}(\text{OH})\text{Ln}$  unit. Single crystal X-ray determinations on  $(\text{Cp}^{\text{R}2}_2\text{Sm})_2(\mu\text{-O})(\mu\text{-OH}_2)$  and  $[\text{Cp}^{\text{R}2}_2\text{Sm}(\mu\text{-OH})]_2$  confirmed their dimeric structures. The samarium centers in



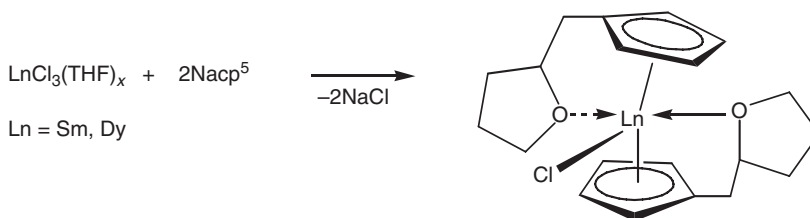


Scheme 77

$[\text{Cp}''_2\text{Sm}(\mu\text{-OH})_2]$  are coordinated by two cyclopentadienyl rings and the OH groups with Sm–O distances of 2.308 Å to 2.41 Å for the different forms of the molecule.  $(\text{Cp}''_2\text{Sm})_2(\mu\text{-O})(\mu\text{-OH}_2)$  shows a dimeric structure as well with one oxygen bridge with Sm–O distances of 2.25 Å/2.32 Å and one  $\text{H}_2\text{O}$  bridge (Sm–O = 2.61 Å/2.63 Å).<sup>352</sup>

#### 4.01.6.4.3 $\text{Cp}_2\text{LnX}$ compounds with chelating Cp ligands

Bis(tetrahydrofurylmethylcyclopentadienyl)lanthanide chloride complexes have been synthesized with  $\text{Ln} = \text{Sm}$  and  $\text{Dy}$  (Scheme 78). In the complex  $\text{Cp}^s_2\text{SmCl}$  the Sm atom is surrounded by two  $\text{Cp}^s$  rings, one chlorine atom, and two oxygen atoms of the side chain to form a distorted trigonal bipyramid. Treatment of the complex  $\text{Cp}^s_2\text{SmCl}$  with 1 equiv. of  $\text{NaPzMe}_2$  ( $\text{PzMe}_2 = 3,5\text{-dimethylpyrazolate}$ ) formed  $\text{Cp}^s_2\text{SmPzMe}_2$ .<sup>255</sup> X-ray structural analyses showed that the complexes  $\text{Cp}^s_2\text{SmCl}$  and  $\text{Cp}^s_2\text{SmPzMe}_2$  are unsolvated monomers. In the latter complex the Sm atom is coordinated by two  $\text{Cp}^s$  rings, two nitrogen atoms of 3,5-dimethylpyrazolate, and two oxygen atoms of the side chain in a distorted tetragonal bipyramidal geometry. The coordination number at the Sm atom is 10. The strong intramolecular chelating coordination and the high steric crowding result in a lower activity of  $\text{Cp}^s_2\text{SmPzMe}_2$  towards methyl methacrylate (MMA) polymerization.<sup>353</sup> Numerous monomeric and dimeric  $\text{Cp}_2\text{LnX}$ -type complexes, including chlorides, iodides, borohydrides, and hydrides containing the pendant-arm 2-methoxyethylcyclopentadienyl ligand,  $[\text{C}_5\text{H}_4\text{CH}_2\text{CH}_2\text{OMe}]^-$ , have been investigated for almost all members of the lanthanide series, and several examples



Scheme 78

have been structurally characterized by X-ray analyses.<sup>354–358</sup> The alkoxy-functionalized cyclopentadienyl ligand  $\text{C}_5\text{H}_5\text{CH}_2\text{CH}_2\text{C}(\text{Ar}_\text{F})_2\text{OH}$  ( $\text{Ar}_\text{F} = 3,5\text{-(CF}_3)_2\text{C}_6\text{H}_3$ ) has been employed in the synthesis of the corresponding bis(cyclopentadienyl)yttrium complexes, including halide precursors as well as aryloxide, silylamide, and alkyl derivatives.<sup>359</sup> A chloro-bridged dimeric bis(amino)-functionalized cyclopentadienyl yttrium complex has been synthesized in high yield by the reaction of  $\text{YCl}_3$  with 2 equiv. of  $\text{NaC}_5\text{H}_4\text{CH}[(\text{CH}_2)_2]_2\text{NMe}$ .<sup>360</sup> Bis(donor)-substituted monomeric  $(\text{C}_5\text{H}_4\text{CH}_2\text{CH}_2\text{NMe}_2)_2\text{TmI}$  has been made from  $\text{TmI}_3(\text{THF})_3$  and  $\text{K}(\text{C}_5\text{H}_4\text{CH}_2\text{CH}_2\text{NMe}_2)$ .<sup>344</sup> Novel chiral non-racemic metallocenes of yttrium, samarium, and lutetium with *N*- or *O*-substituted side chain as ligands were obtained by a metathetical reaction and oxidation of the corresponding divalent compound. Using the stabilizing influence of the donor-substituted ligands, it was possible to isolate lanthanide sandwich complexes with two different cyclopentadienyl ligands.<sup>361</sup> Similar chemistry has been investigated with the use of the *N*-functionalized cyclopentadienyl ligand  $[(S)\text{-C}_5\text{H}_4\text{CH}(\text{Ph})\text{CH}_2\text{NMe}_2]^-$ .<sup>362</sup> The asymmetric cyclopentadienyl ligand  $\text{C}_5\text{H}_4\text{CH}_2\text{CH}(\text{Me})\text{OCH}_2\text{Ph}$  ( $= \text{Cp}^\text{R}$ ) has been employed analogously to prepare the corresponding monomeric bis(cyclopentadienyl) iodides  $\text{Cp}^\text{R}_2\text{LnI}$  ( $\text{Ln} = \text{La, Sm}$ ).<sup>259</sup>

Several lanthanide complexes ( $\text{Ln} = \text{Y, Sm, Yb, Lu}$ ) containing sulfur-functionalized cyclopentadienyl ligands have been reported. For example, yttrium trichloride reacted with 2 equiv. of  $\text{Na}(\text{C}_5\text{H}_4\text{CH}_2\text{CH}_2\text{SEt})$  in THF to form  $(\text{C}_5\text{H}_4\text{CH}_2\text{CH}_2\text{SEt})_2\text{YCl}$  (Scheme 79). The stepwise reaction of lutetium trichloride with 1 equiv. each of  $\text{Na}(\text{C}_5\text{H}_4\text{CH}_2\text{CH}_2\text{SEt})$  and 1 equiv.  $\text{NaCp}^*$  yielded  $\text{Cp}^*(\text{C}_5\text{H}_4\text{CH}_2\text{CH}_2\text{SEt})\text{LuCl}$ . Alkylation of  $(\text{C}_5\text{H}_4\text{CH}_2\text{CH}_2\text{SEt})_2\text{YCl}$  and  $\text{Cp}^*(\text{C}_5\text{H}_4\text{CH}_2\text{CH}_2\text{SEt})\text{LuCl}$  with  $\text{MeLi}$  in toluene gave the lanthanide alkyls  $(\text{C}_5\text{H}_4\text{CH}_2\text{CH}_2\text{SEt})_2\text{YMe}$  and  $\text{Cp}^*(\text{C}_5\text{H}_4\text{CH}_2\text{CH}_2\text{SEt})\text{LuMe}$ , respectively.<sup>363–365</sup>

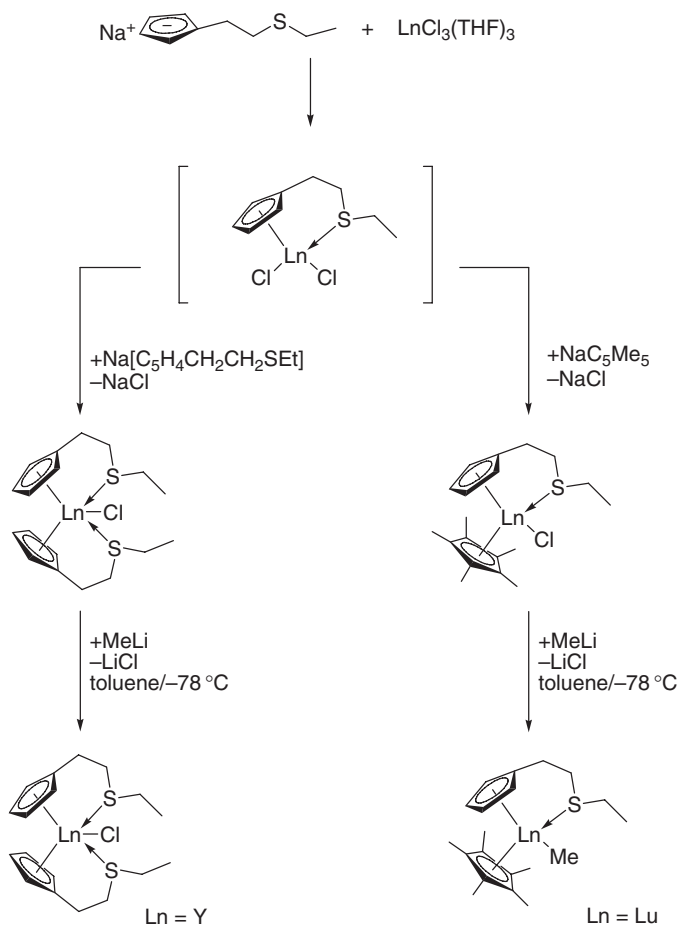
Single crystal X-ray determinations of  $(\text{C}_5\text{H}_4\text{CH}_2\text{CH}_2\text{SEt})_2\text{YCl}$  and  $\text{Cp}^*(\text{C}_5\text{H}_4\text{CH}_2\text{CH}_2\text{SEt})\text{LuCl}$  exhibited monomeric structures for both complexes. The geometry around the metal center in  $(\text{C}_5\text{H}_4\text{CH}_2\text{CH}_2\text{SEt})_2\text{YCl}$  is a distorted bipyramid where the cyclopentadienyl centers and the chlorine atom are in equatorial and the sulfur atoms are in axial position. The solid-state structure of  $\text{Cp}^*(\text{C}_5\text{H}_4\text{CH}_2\text{CH}_2\text{SEt})\text{LuCl}$  shows a distorted tetrahedral coordination sphere with an  $\text{Lu-S}$  bond distance of 2.79 Å, revealing sulfur–lutetium coordination.<sup>363</sup>

The reaction of  $\text{Li}[\text{C}_5\text{H}_4(\text{CH}_2)_2\text{PMe}_2]$  and yttrium triflate formed bis(dimethylphosphinoethylcyclopentadienyl) yttrium triflate with an intramolecular coordination of the phosphinoethyl chain. The ligand  $\text{Li}[\text{C}_5\text{H}_4(\text{CH}_2)_2\text{PMe}_2]$  was synthesized from spiro[2.4]hepta-4,6-diene upon treatment with  $\text{LiPMe}_2$  according to Scheme 80.<sup>366</sup>

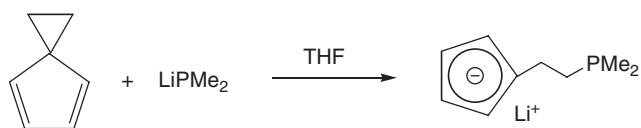
The reaction of 2 equiv. of  $\text{Li}[\text{C}_5\text{H}_4(\text{CH}_2)_2\text{PMe}_2]$  with 1 equiv. of  $\text{Y}(\text{CF}_3\text{SO}_3)_3$  in the presence of  $\text{LiBr}$  afforded the disubstituted yttrium bromide derivative (Scheme 81).<sup>366</sup>

The stabilization by intramolecular coordination of the phosphino functionalities prevents both the dimerization of the system and the coordination of donor solvents. Temperature-dependent NMR spectra showed that the system is not involved in any dynamic processes. The Y atom is surrounded in a slightly distorted trigonal bipyramidal fashion and the two phosphorus atoms occupy the apical positions. The Y–P bond lengths are 2.960(1) and 2.933(1) Å. The distances are only slightly longer than in non-cyclopentadienyl-stabilized Y–P complexes.<sup>366</sup> Two equivalents of phosphinoethylcyclopentadienyl lithium reacted similarly with Sc, Y, La, Lu trichlorides to give monomeric, solvent-free complexes. In the yttrium derivative the central Y atom is surrounded in a trigonal bipyramidal geometry by two axial phosphino groups and two equatorial cyclopentadienyl groups, and the third equatorial site is occupied by the halide ligand.<sup>367</sup> The closely related ytterbium complex  $[(\text{C}_5\text{H}_4\text{PPh}_2)_2\text{Yb}(\mu\text{-Cl})_2]$  was prepared by oxidation of the divalent precursor  $(\text{C}_5\text{H}_4\text{PPh}_2)_2\text{Yb}(\text{THF})$  with  $\text{HgCl}_2$  in THF,<sup>368</sup> whereas treatment of  $\text{YbCl}_3$  with the sodium salt of diphenylphosphino-cyclopentadiene gave the *ate*-complex  $(\text{C}_5\text{H}_4\text{PPh}_2)_2\text{Yb}(\mu\text{-Cl})_2\text{Na}(\text{Et}_2\text{O})_2$ .<sup>369</sup> Monomeric  $(\text{C}_5\text{H}_4\text{CH}_2\text{CH}_2\text{PPh}_2)_2\text{LuCl}$  was made from  $\text{LuCl}_3(\text{THF})_3$  and  $\text{Li}(\text{C}_5\text{H}_4\text{CH}_2\text{CH}_2\text{PPh}_2)$ . NMR studies revealed that in this complex both phosphino groups are coordinated to the lutetium center.<sup>370</sup> Using the dianionic ligand  $\text{Li}_2[(\text{C}_5\text{H}_4\text{CH}_2\text{CH}_2)_2\text{PMe}]$  phosphino-bridged *ansa*-metallocene derivatives  $[(\text{C}_5\text{H}_4\text{CH}_2\text{CH}_2)_2\text{PMe}]\text{LnX}$  ( $\text{Ln} = \text{Y, Lu}$ ;  $\text{X} = \text{Cl}^-, \text{CF}_3\text{SO}_3^-$ ) were isolated (Scheme 82). The complexes are soluble in toluene, monomeric and free of coordinated solvent ligands.<sup>367</sup>

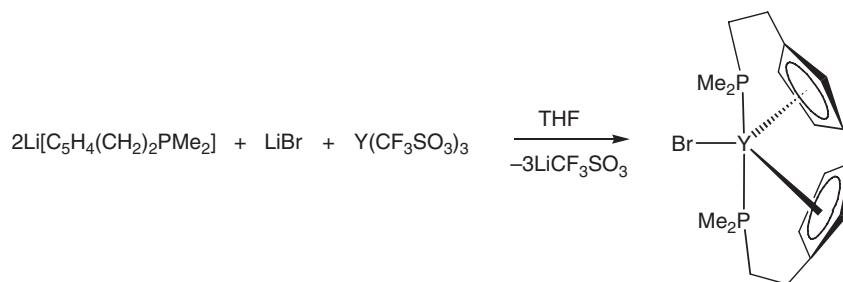




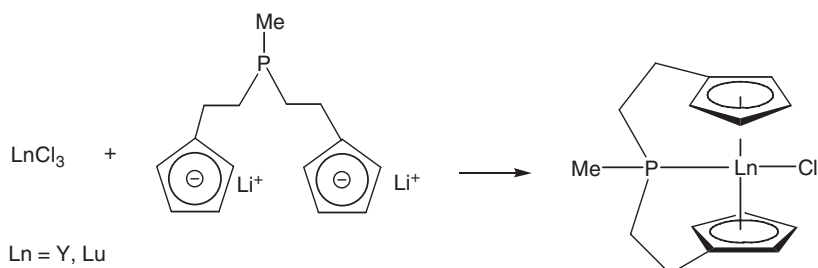
Scheme 79



Scheme 80



Scheme 81



Scheme 82

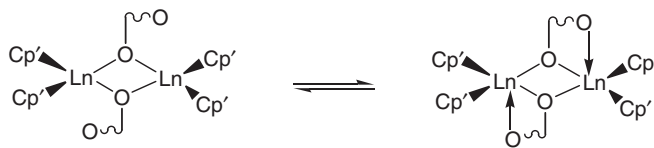
#### 4.01.6.4.4 $\text{Cp}_2\text{LnX}$ compounds with alkoxide, carboxylate, and related ligands

A bis(cyclopentadienyl)ytterbium nitrite complex,  $\text{Cp}_2\text{Yb}(\text{NO}_2)(\text{THF})$ , was prepared by the reaction of  $[\text{Cp}_2\text{Yb}(\mu\text{-Cl})_2]$  with  $\text{NaNO}_2$  in THF at room temperature. The nitrite anion acts as a chelating ligand in this complex.<sup>371</sup> The organoerbium cluster  $[\text{Na}(\text{DME})_3]^+[(\text{C}_5\text{H}_4\text{PPh}_2)_3(\mu_3\text{-O})(\mu\text{-OH})_2]^-$  was obtained by the reaction of  $\text{ErCl}_3$  with  $\text{Na}(\text{C}_5\text{H}_4\text{PPh}_2)$  in the presence of traces of water. The structure consists of discrete cation  $[\text{Na}(\text{DME})_3]^+$  and anion  $[(\text{C}_5\text{H}_4\text{PPh}_2)_3(\mu_3\text{-O})(\mu\text{-OH})_2]^-$  pairs. In the anion three  $(\text{C}_5\text{H}_4\text{PPh}_2)_2\text{Er}$  fragments are linked by one  $\mu_3$ -oxygen and two  $\mu_2$ -hydroxy groups in a trigonal array. Two erbium atoms have the coordination number 8, while the third erbium atom is nine-coordinated.<sup>372</sup>

Dimeric bis(cyclopentadienyl)lanthanide complexes containing  $\mu$ -alkoxide ligands form a large and well-investigated class of organolanthanide complexes. A review article titled “Unusually structured organolanthanoid(III) dimers with two chiral, but not strictly equivalent, nitrogen-functionalized alkoxide bridges” has been published by Fischer *et al.*<sup>373</sup> An interesting route leading to bis(cyclopentadienyl)samarium(III) alkoxides involves oxidation of samarium(II) precursors such as  $(\text{C}_5\text{HPr}^i)_2\text{Sm}(\text{THF})$  with di-*t*-butylperoxide.<sup>198</sup> Reaction of  $\text{LnCp}_3$  ( $\text{Ln} = \text{Sm, Yb}$ ) with cyclohexanol in a 1 : 1 molar ratio afforded the dimeric alkoxide complexes  $[\text{Cp}_2\text{Ln}(\mu\text{-OC}_6\text{H}_{11})_2]$ , of which the Yb derivative was structurally characterized.<sup>374</sup> Analogous dimeric alkoxides containing *N*-functionalized  $\mu$ -alkoxide ligands have been prepared from  $\text{Ln}(\text{C}_5\text{H}_4\text{Me})_3$  or  $\text{YbCp}_3(\text{THF})$  and  $\text{HOCH}_2\text{CH}_2\text{NR}_2$  ( $\text{R} = \text{Me, Et}$ ) in THF.<sup>375,376</sup> Binuclear organolanthanide alkoxides,  $[\text{Cp}_2\text{Yb}(\mu\text{-OCH}_2\text{CH}_2\text{CH}_2\text{CH}_2\text{CH}_3)_2]$  and  $[\text{Cp}_2\text{Ln}(\mu\text{-OCH}_2\text{CH}_2\text{CH}(\text{Me})_2)_2]$  ( $\text{Ln} = \text{Dy, Yb}$ ), were prepared by the reaction of  $\text{LnCp}_3$  with an equimolar amount of the alcohol HOR ( $\text{R} = \text{CH}_2\text{CH}_2\text{CH}_2\text{CH}_2\text{CH}_3$  or  $\text{OCH}_2\text{CH}_2\text{CH}(\text{Me})_2$ ).<sup>377,378</sup> The complexes  $[\text{Cp}_2\text{Yb}(\mu\text{-OCH}_2\text{CH}_2\text{CH}_2\text{CH}_2\text{CH}_3)_2]$ ,  $[\text{Cp}_2\text{Yb}(\mu\text{-OCH}_2\text{CH}=\text{CHCH}_3)_2]$ ,  $[\text{Cp}_2\text{Yb}(\mu\text{-OCH}(\text{CH}_2)_3\text{O})_2]$ , and  $[\text{Cp}_2\text{Yb}(\mu\text{-OCH}_2\text{CH}_2\text{CH}(\text{Me})_2)_2]$  were characterized by X-ray crystallography. In all these dimeric structures the ytterbium atom is coordinated by two Cp ligands and two oxygen atoms of alkoxide ligands to form a distorted tetrahedral geometry. The central  $\text{Yb}_2\text{O}_2$  metallacycles in these molecules are completely planar. Similar reactions were carried out using  $\text{Cp}_3\text{Yb}$  and (R)-(+)-, (S)-(–)-isobutyl lactate, or (S)-(+)-2-butanol.<sup>377,378</sup> The reaction of  $\text{Cp}_3\text{Yb}$  with  $\text{CH}_2=\text{CHCH}_2\text{OH}$  and  $\text{Pr}^n\text{OH}$  in THF at room temperature afforded the dimeric alkoxide-bridged complexes  $[\text{Cp}_2\text{Yb}(\mu\text{-OCH}_2\text{CH}=\text{CH}_2)_2]$  and  $[\text{Cp}_2\text{Yb}(\mu\text{-OPr}^n)_2]$ , respectively, which are dehydrogenated in refluxing THF to yield the complex  $[\text{Cp}_2\text{Yb}(\mu\text{-OCH}=\text{C}=\text{CH}_2)_2]$ .<sup>379</sup>

The interaction of  $\text{Ce}(\text{C}_5\text{H}_3\text{Bu}^t\text{-1,3})_3$  or  $\text{LnCp}^n_3$  ( $\text{Ln} = \text{La, Ce, Nd}$ ) with metallic lithium or potassium in DME led to alkoxide complexes  $[\text{Cp}^n_2\text{Ln}(\mu\text{-OMe})_2]$  and  $[\text{Cp}^n_2\text{Nd}(\mu\text{-OMe})_2\text{Li}(\text{DME})]$ . The latter complex and  $[(\text{C}_5\text{H}_3\text{Bu}^t\text{-1,3})_2\text{Ce}(\mu\text{-OMe})_2]$  were characterized by X-ray crystallography. In the dimeric structure of  $[(\text{C}_5\text{H}_3\text{Bu}^t\text{-1,3})_2\text{Ce}(\mu\text{-OMe})_2]$  two  $(\text{C}_5\text{H}_3\text{Bu}^t\text{-1,3})_2\text{Ce}$  fragments are bound by two bridging OMe groups. The structure of  $[\text{Cp}^n_2\text{Nd}(\mu\text{-OMe})_2\text{Li}(\text{DME})]$  contains one  $[\text{Cp}^n_2\text{Nd}]$  fragment bound with Li ion by two OMe bridges. The metallacycle  $\text{NdO}_2\text{Li}$  is almost planar.<sup>380</sup> The formation of the lanthanocene(III) methoxide proceeds via persistent paramagnetic lanthanum(II) intermediates.<sup>381</sup>  $[\text{K}\{\mu\text{-Cp}\}_2\text{Nd}(\mu\text{-O-C}_6\text{H}_3\text{Me}_{2-2,6})_2]_n$  was obtained by the reaction of  $\text{KCp}$  with  $[\text{Nd}(\text{OAr})_3(\text{THF})_2]_2$  ( $\text{Ar} = \text{C}_6\text{H}_3\text{Me}_{2-2,6}$ ) in THF. According to X-ray diffraction studies, in the complex  $[\text{Cp}_2\text{Nd}(\text{OAr})_2]^-$  anions are connected into a two-dimensional layered structure by  $\text{K}^+$  cations bridged by arene and cyclopentadienyl rings. Each potassium atom connects four different  $[\text{Cp}_2\text{Nd}(\text{OAr})_2]^-$  anions and is surrounded by two bridging Cp groups and two bridging arenes. The neodymium atom in the  $[\text{Cp}_2\text{Nd}(\text{OAr})_2]^-$  anion has a distorted tetrahedral arrangement.<sup>380</sup>

New organolanthanide complexes of the general type  $[\text{Cp}'_2\text{Ln}(\mu\text{-OCHR}^{(1)}\text{Z})_2]$  ( $\text{Cp}' = \text{Cp}$  or  $\text{C}_5\text{H}_4\text{Me}$ ,  $\text{R}^{(1)} = \text{H}$  or  $\text{Me}$ ) containing exclusively chiral, oxygen-functionalized alkoxide ligands with  $\text{Z} = \text{CHR}^{(2)}\text{OMe}$  ( $\text{R}^{(2)} = \text{Me}$  or  $\text{Ph}$ ),  $\text{Z} = \text{COOBu}^i$ , and  $\text{Z} = \text{CH}_2\text{COOE}$  were obtained at low temperature in toluene using a selected tris(cyclopentadienyl)lanthanide(III) system ( $\text{LnCp}'_3$ ) with the corresponding oxygen-functionalized alcohol. All

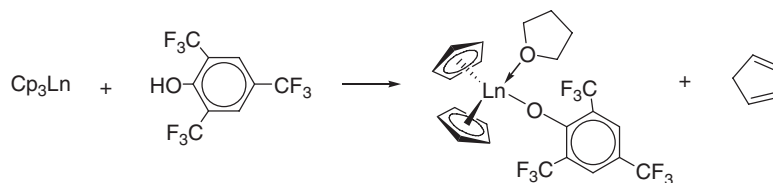


Scheme 83

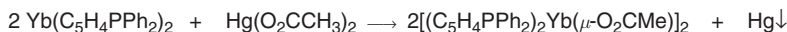
alcohols were chiral and used enantiomerically pure.  $^1\text{H}$  NMR studies of the complexes revealed that a new type of species existed (Scheme 83).<sup>382</sup>

The dimeric bis(cyclopentadienyl)lanthanide furyl methoxide complexes  $[\text{Cp}_2\text{Ln}(\mu\text{-OCH}_2\text{C}=\text{CHCH}=\text{CH})]_2$  ( $\text{Ln} = \text{Nd}, \text{Sm}, \text{Dy}, \text{Yb}$ ) were obtained by the metathetical reaction of the appropriate  $\text{Cp}_3\text{Ln}$  with furfuryl alcohol in THF. Investigation of the thermal stability of the compounds has shown that they decompose into  $\text{Cp}_3\text{Ln}$  and  $\text{Ln}(\text{OR})_3$ .<sup>383</sup> The alkoxide complexes  $\text{Cp}_2\text{Yb}(\text{THF})(\text{OR}_\text{F})$  [ $\text{Ln} = \text{Nd}, \text{Sm}, \text{Yb}$ ;  $\text{R}_\text{F} = 2,4,6\text{-tris(trifluoromethyl)phenyl}$ ] were obtained by the reaction of the appropriate  $\text{LnCp}_3$  with 2,4,6-tris(trifluoromethyl)phenol ( $\text{R}_\text{F}\text{OH}$ ) (Scheme 84). The thiolate complex  $\text{Cp}_2\text{Yb}(\text{THF})(\text{SR}_\text{F})$  was prepared analogously from  $\text{Cp}_3\text{Yb}$  and  $\text{R}_\text{F}\text{SH}$ . According to X-ray diffraction studies, the  $\text{Cp}_2\text{Yb}(\text{THF})(\text{SR}_\text{F})$  is a monomer, in which the ytterbium atom is coordinated by two Cp rings, one sulfur of  $\text{SC}_6\text{H}_2(\text{CF}_3)_3\text{-2,4,6}$  ligand, and one oxygen of solvating THF molecule. Thus, the ytterbium has pseudotetrahedral arrangement and a formal coordination number of 8.<sup>384</sup>

The reaction of  $\text{LnCp}_3$  ( $\text{Ln} = \text{Pr}, \text{Gd}, \text{Dy}, \text{and Yb}$ ) with equimolar amounts of acetoxime can be used to synthesize bis(cyclopentadienyl)lanthanide acetoximate derivatives  $[\text{Cp}_2\text{Ln}(\mu, \eta^2\text{-ONCMe}_2)]_2$ . The complex  $[\text{Cp}_2\text{Gd}(\mu, \eta^2\text{-ONCMe}_2)]_2$  was characterized by X-ray diffraction. In the binuclear structure each Gd atom is coordinated by two Cp ligands, two oxygen atoms, and one nitrogen atom of  $\text{ONCMe}_2$ , to form a distorted trigonal bipyramidal arrangement (oxygen and nitrogen atoms in the axial positions).<sup>385,386</sup> Benzophenone oxime reacts analogously to afford the dimeric complexes  $[\text{Cp}_2\text{Ln}(\mu, \eta^2\text{-ONCPh}_2)]_2$  ( $\text{Ln} = \text{Pr}, \text{Nd}, \text{Sm}, \text{Gd}, \text{Tb}, \text{Dy}, \text{Ho}, \text{Er}, \text{Tm}, \text{Yb}$ ).<sup>387,388</sup> Organolanthanide chlorides  $\text{Cp}'_2\text{Ln}(\mu\text{-Cl})_2\text{M}(\text{L})_2$  ( $\text{Cp}' = \text{Cp}, \text{C}_5\text{HMe}_4$ ,  $\text{Cp}^*$ ;  $\text{M} = \text{Na}, \text{Li}$ ;  $\text{L} = \text{THF}, \text{Et}_2\text{O}$ ) react with sodium acetate yielding the corresponding dimeric organo-rare-earth acetates  $[\text{Cp}_2\text{Ln}(\mu\text{-O}_2\text{CMe})]_2$  ( $\text{Ln} = \text{Sc}, \text{Y}, \text{Sm}, \text{Lu}$ ),  $[(\text{C}_5\text{HMe}_4)_2\text{Ln}(\mu\text{-O}_2\text{CMe})]_2$  ( $\text{Ln} = \text{Y}, \text{La}, \text{Sm}, \text{Lu}$ ), and  $[(\text{Cp}^*)_2\text{Ln}(\mu\text{-O}_2\text{CMe})]_2$  ( $\text{Ln} = \text{Y}, \text{La}, \text{Sm}, \text{Lu}$ ). The dimeric structure of the complexes  $[(\text{C}_5\text{HMe}_4)_2\text{Y}(\mu\text{-O}_2\text{CMe})]_2$ ,  $[(\text{C}_5\text{HMe}_4)_2\text{La}(\mu\text{-O}_2\text{CMe})]_2$ , and  $[(\text{C}_5\text{HMe}_4)_2\text{Sm}(\mu\text{-O}_2\text{CMe})]_2$  could be verified by X-ray crystallography. There are bidentate bridging acetate groups in the yttrium and samarium compounds, with eight-coordinate  $\text{Y}^{3+}$  and  $\text{Sm}^{3+}$ , and tridentate bridging acetate ligands in the nine-coordinate  $\text{La}^{3+}$  in the lanthanum complex.<sup>389</sup> The synthesis and single crystal structure analysis of the monomeric organolanthanide acetates  $(\text{C}_5\text{Me}_4\text{Bu}^t)_2\text{Ln}(\text{O}_2\text{CMe})$  ( $\text{Ln} = \text{La}, \text{Lu}$ ) have also been reported. The monomeric structures are due to the sterically demanding  $\text{Bu}^t$  substituents of the cyclopentadienyl ligands. The single crystal X-ray structure analysis of  $(\text{C}_5\text{Me}_4\text{Bu}^t)_2\text{Lu}(\text{O}_2\text{CMe})$  as well as the cryoscopic molecular weight determination of  $(\text{C}_5\text{Me}_4\text{Bu}^t)_2\text{La}(\text{O}_2\text{CMe})$  verify the monomeric structure of these complexes.<sup>390</sup> The ytterbium benzoate complexes  $[(\text{C}_5\text{H}_4\text{Me})_2\text{Yb}(\mu\text{-O}_2\text{CPh})]_2$  (orange-red needles),<sup>391</sup>  $[(\text{C}_5\text{H}_4\text{Me})_2\text{Yb}(\mu\text{-O}_2\text{CC}_6\text{F}_5)]_2$  (orange plates), and  $[(\text{C}_5\text{H}_4\text{Me})_2\text{Yb}(\mu\text{-O}_2\text{CC}_6\text{F}_4\text{H-}o)]_2$  (orange plates) are dimeric.<sup>392</sup> The acetato complex  $[(\text{C}_5\text{H}_4\text{PPh}_2)_2\text{Yb}(\mu\text{-O}_2\text{CMe})]_2$  was obtained by the oxidation of  $\text{Yb}(\text{C}_5\text{H}_4\text{PPh}_2)_2$  with  $\text{Hg}(\text{O}_2\text{CCH}_3)_2$  in THF (Scheme 85). The structures



Scheme 84

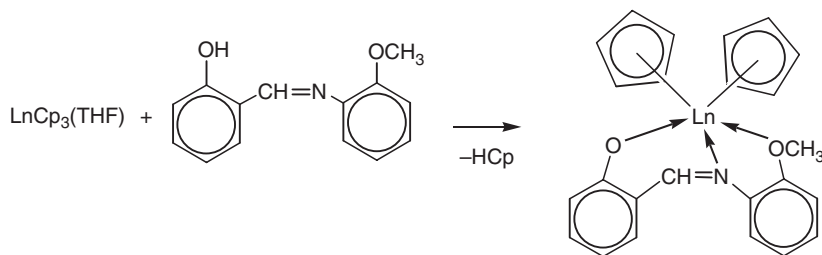


Scheme 85

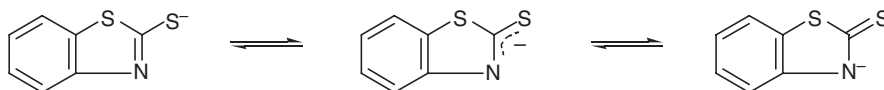
of  $[(C_5H_4PPh_2)_2Yb(\mu-O_2CMe)]_2$  and analogously obtained  $[Cp_2Yb(\mu-O_2CMe)]_2$  were determined by X-ray diffraction. Both complexes have a dimeric structure with two acetate bridges. However, the crystal structure of  $[(C_5H_4PPh_2)_2Yb(\mu-O_2CMe)]_2$  contains one dimer, while the  $[Cp_2Yb(\mu-O_2CMe)]_2$  has two similar independent dimers A and B. Each ytterbium atom of the two complexes is formally nine-coordinated by two cyclopentadienyl ligands, two oxygen atoms from the one chelating and bridging acetate ligands and one oxygen atom from the other. Thus, the  $O_2CMe$  ligand gives bridging tridentate coordination.<sup>393</sup>

New bis(cyclopentadienyl)lanthanide complexes with the 2-naphthoyltrifluoroacetato chelate ligand,  $Cp_2Ln[C_{10}H_7C(O)CHC(O)CF_3](THF)$  ( $Ln = Ho, Er$ ) and  $Cp_2Ln[C_{10}H_7C(O)CHC(O)CF_3]$  ( $Ln = Pr, Sm$ ), have been prepared. In the structure of  $Cp_2Ho[C_{10}H_7C(O)CHC(O)CF_3](THF)$  the central Ho atom is coordinated by two Cp ligands, two oxygen atoms of the 2-naphthoyltrifluoroacetato ligand, and one oxygen of the solvated THF molecule.<sup>394</sup> The closely related 1,1,1-trifluoroacetylacetonato ytterbium complex  $Cp_2Yb\{MeC(O)CH(O)CF_3\}$  is readily accessible by protonation of  $YbCp_3$  with the free ligand in THF.<sup>395</sup> Complexes of the type  $Cp_2Ln(PhCONHO)$  ( $Ln = Pr, Gd, Dy, Ho, Er, Tm, Yb$ ) have been obtained by reacting the corresponding tris(cyclopentadienyl)lanthanides with benzohydroxamic acid.<sup>396</sup> A similar series of complexes,  $Cp_2Ln(PhCONOPh)$  ( $Ln = Pr, Nd, Sm, Gd, Dy, Ho, Er, Yb$ ), has been synthesized with the use of the *N*-phenylbenzohydroxamic acid ligand,<sup>397</sup> and related compounds with  $Ln = La, Pr, Sm, Dy$ , and  $Yb$  have been made starting from piperonal dimethylacetal.<sup>398</sup>  $Cp_2Ln(III)$  derivatives have been obtained from the reactions of  $LnCp_3$  with 8-hydroxyquinoline, benzophenoneoxime or 2-aminophenol.<sup>294,399</sup> Dimerization of phenylisocyanate and formation of the binuclear complex  $[\mu-(PhN)OCCO(NPh)][(MeC_5H_4)_2Sm(THF)]_2$  occurs when the divalent precursor  $(C_5H_4Me)_2Sm(THF)$  is treated with  $PhNCO$  in a 1:1 molar ratio.<sup>400,401</sup> Monomeric complexes have been obtained from the reactions of  $[(C_5H_4Me)_2Ln(\mu-Cl)]_2$  with the lithium salt of  $\epsilon$ -caprolactam in toluene at 0 °C.<sup>400</sup> Reaction of  $NdCl_3$  with 3.3 equiv. of  $NaCp$  in THF followed by subsequent treatment with (S)-(+)-*N*-(1-phenylethyl)salicylideneamine afforded a chiral bis(cyclopentadienyl)neodymium complex.<sup>402</sup> The corresponding Sm derivative was prepared in an analogous manner.<sup>403</sup> The reaction of tris(cyclopentadienyl)lanthanide with the tridentate Schiff base *N*-1-(*ortho*-methoxyphenyl)salicylideneamine in THF at room temperature afforded the monomeric lanthanocene Schiff base complexes  $Cp_2Ln(OC_{14}H_{13}NO)$  ( $Ln = Sm, Er, Dy, Y$ ) (Scheme 86).<sup>404,405</sup>

$[Cp'_2Yb]_2(OC_{20}H_{20}N_2O)$  ( $Cp' = C_5H_4CH_2CH_2OMe$ ) has been prepared from  $YbCp'_3$  and *trans*-( $\pm$ )-2,2'-[1,2-cyclohexanediyl-bis(iminomethyl)]diphenol in THF, which is in contrast to the previously described (Section 4.01.6.3) reaction of  $SmCp'_3$  with *trans*-( $\pm$ )-2,2'-[1,2-cyclohexanediyl-bis(iminomethyl)]diphenol giving the mono(methoxyethylcyclopentadienyl)samarium complex  $[\eta^5:\eta^1-Cp'Sm][(\mu:\eta-OC_{20}H_{20}N_2O)]_2[\eta^5-Cp'Sm]$ .<sup>256</sup> The reaction of  $Cp_3Yb$  with equimolar amounts of *n*-propanethiol in THF at room temperature resulted in the formation of the new complex  $[Cp_2Yb(\mu-SPr^n)]_2$  in good yield. The bridging unit  $Yb_2S_2$  is planar. The ytterbium atom is coordinated by two Cp groups and two bridging sulfur atoms to form a distorted tetrahedral geometry.<sup>406</sup> The trivalent lanthanide metallocenes  $LnCp_3$  ( $Ln = Dy, Yb$ ) react with thiols, HSR ( $R = Pr^n, Bu^n$ ), to give the dimeric complexes  $[Cp_2Ln(\mu-SR)]_2$  in THF at room temperature.<sup>407</sup> A large number of dimeric bis(*t*-butylcyclopentadienyl)-lanthanide complexes of the type  $[(C_5H_4Bu^t)_2Ln(\mu-ER)]_2$  have been synthesized, and  $[(C_5H_4Bu^t)_2Y(\mu-SePh)]_2$  has been structurally characterized.<sup>408</sup> The reaction of  $LnCp_3$  ( $Ln = Yb, Dy, Sm, Y$ ) with an equimolar amount of 2-mercapto-benzothiazole (HSBT) in THF at room temperature yields the monomeric bis(cyclopentadienyl) complexes  $Cp_2Ln(SBT)(THF)$  ( $Ln = Yb, Dy, Sm, Y$ ).<sup>409–411</sup> The crystal structure analysis showed that in  $Cp_2Yb(SBT)(THF)$  and  $Cp_2Dy(SBT)(THF)$  each lanthanide ion is coordinated by two cyclopentadienyl groups, one oxygen atom of THF, and one sulfur and one nitrogen atom from the chelating benzothiazole-2-thiolate ligand to form a distorted trigonal bipyramidal coordination geometry. The Yb–S distance of 2.84 Å is longer than those found in related compounds, while the Yb–N distance of 2.39 Å is relatively short compared with analogous compounds. Presumably, the



Scheme 86



Scheme 87

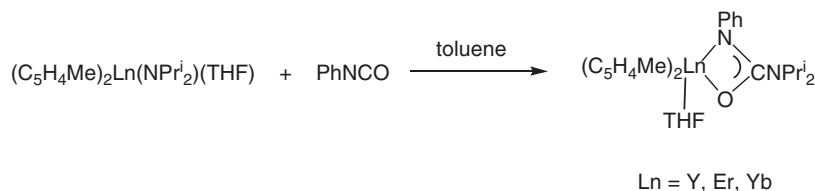
rather long Ln–S and the rather short Ln–N bond distances result from the fact that the benzothiazole-2-thiolate group has a resonance structure as shown in [Scheme 87](#) where the negative charge is partially delocalized to the N atom.<sup>409</sup> Closely related benzothiazole-2-thiolate complexes have also been prepared starting from the chloride-bridged precursor  $[(C_5H_4SiMe_2Bu^t)_2Gd(\mu-Cl)]_2$ .<sup>412</sup>

A similar series of complexes with  $Ln = Pr, Gd, Dy, Ho, Er, Tm,$  and  $Yb$  has been prepared with the anion of benzotriazole as ligand.<sup>413,414</sup> The complexes  $Cp_2Ln[N(QPPh_2)_2]$  ( $Ln = La, Gd, Er, Yb$  for  $Q = Se$ ;  $Ln = Yb$  for  $Q = S$ ) have been synthesized from the corresponding lanthanide tris(cyclopentadienyl) compounds and  $H[N(QPPh_2)_2]$ . The structures of the complexes of  $La, Gd,$  and  $Er$  with  $Se$  and  $Yb$  with  $S$  consist of a  $Cp_2Ln$  fragment, coordinated  $\eta^3$  through two chalcogen atoms and an N atom of the imidodiphosphinochalcogenido ligand  $[N(QPPh_2)_2]^-$ . In the complex  $Cp_2Yb[N(SePPh_2)_2]$  the  $Cp_2Yb$  moiety is coordinated  $\eta^2$  through the two  $Se$  atoms of the  $[N(SePPh_2)_2]^-$  ligand.<sup>415</sup> The imidodiphosphinochalcogenido complexes  $Cp_2Y[\eta^3-N(SPPPh_2)_2]$  and  $Cp_2Y[\eta^3-N(SePPh_2)_2]$  have been synthesized analogously in THF via a protonolysis reaction between  $Cp_3Y$  and the amines  $HN(SPPPh_2)_2$  and  $HN(SePPh_2)_2$ , respectively. In both compounds, the  $[N(QPPh_2)_2]^-$  ligand ( $Q = S, Se$ ) is bonded to the  $Y$  center in an  $\eta^3$ -fashion. Additionally, the  $Y$  atom is coordinated to two cyclopentadienyl ligands which leads to the formal coordination number 9. Single crystal X-ray determinations of both compounds showed the  $Y$  atom coordinated to the nitrogen atom of the  $[N(QPPh_2)_2]^-$  ligand ( $Q = S, Se$ ) and to both  $S$  atoms and  $Se$  atoms, respectively. The molecules possess an approximate twofold symmetry with  $Y-S$  distances of 2.93 Å and  $Y-Se$  distances of 3.05 Å.<sup>416</sup> Metallocenes of yttrium and the lanthanides with bis(phosphinimino)methanides in the coordination sphere have been reported. Reaction of  $[(CH(PPh_2NSiMe_3)_2)LnCl(\mu-Cl)]_2$  ( $Ln = Y, Sm, Er$ ) with  $NaCp$  in a 1:4 molar ratio in THF afforded the corresponding metallocenes  $Cp_2Ln[CH(PPh_2NSiMe_3)_2]$ . The structures of these compounds have been investigated in solution and in the solid state. Single crystal X-ray structures showed that both imine groups and the central methine carbon are bonded to the lanthanide atom.<sup>417</sup>

#### 4.01.6.4.5 $Cp_2LnX$ compounds with amide and related N-donor ligands

Neutral heteroleptic diphenylamido complexes of ytterbium,  $(C_5H_4Me)_2Yb(NPh_2)(THF)$ ,  $(C_5H_4Bu^t)_2Yb(NPh_2)(THF)$ , and  $Cp^*_2Yb(NPh_2)$ , were obtained by the reaction of ytterbocene chlorides with  $NaNPh_2$  in THF or THF/toluene at 0°C.<sup>418</sup> The crystal structures of  $(C_5H_4Me)_2Yb(NPh_2)(THF)$  and  $Cp^*_2Yb(NPh_2)$  were determined by X-ray diffraction analysis. The complex  $(C_5H_4Me)_2Yb(NPh_2)(THF)$  has a distorted tetrahedral arrangement around ytterbium by two  $C_5H_4Me$  groups, one oxygen atom, and one nitrogen atom. The crystal structure of the complex  $Cp^*_2Yb(NPh_2)$  shows a triangular array of two  $Cp^*$  ligands and one nitrogen atom surrounding ytterbium with additional intramolecular  $Yb-\eta^2-Ph$  chelate interactions.<sup>418</sup> The reactivity of  $(C_5H_4Me)_2Yb(NPh_2)(THF)$  ( $Ln = Y, Yb$ ) has been studied, and the corresponding products resulting from heterocumylene insertion into the  $Ln-N$  bond have been isolated.<sup>419</sup> (Diisopropylamido)bis(methylcyclopentadienyl) lanthanides ( $Ln = Y, Er, Yb$ ) were synthesized in a two-step reaction from  $LnCl_3$ ,  $Na(C_5H_4Me)$ , and  $LiNPr_2$ .<sup>420</sup> The resulting lanthanide amides were subsequently reacted with a stoichiometric amount of phenylisocyanate ([Scheme 88](#)). The first insertion product was isolated and the crystal structure was investigated ( $Ln = Y$ ).<sup>420</sup>

In a similar manner, treatment of  $Cp_2LnBu^n$  ( $Ln = Y, Dy, Er$ ) with  $N,N'$ -di-*t*-butylcarbodiimide resulted in monoinsertion of carbodiimide into the  $Ln-C$  bond to yield the amidinate complexes



Scheme 88

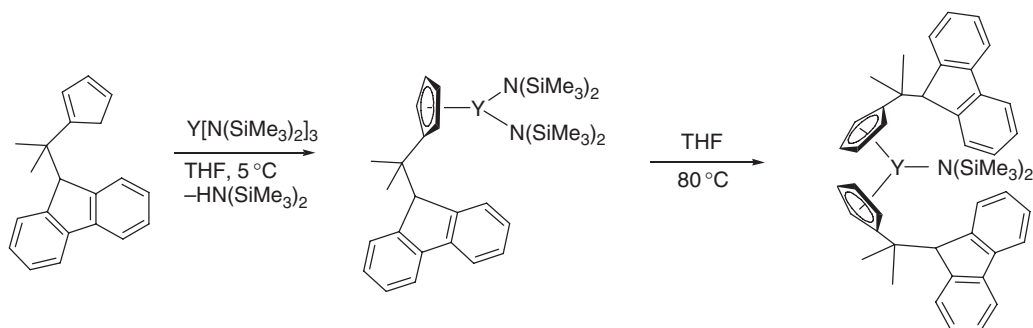
$\text{Cp}_2\text{Ln}[\text{Bu}^n\text{NC}(\text{Bu}^n)\text{NBu}^n]$ ,<sup>421</sup> while insertion of  $\text{PhNCO}$  led to the formation of  $[(\text{C}_5\text{H}_4\text{Me})_2\text{Ln}(\mu\text{-OC}(\text{R})\text{NPh})]_2$  ( $\text{R} = \text{Bu}^n$ ,  $\text{Ln} = \text{Sm}$ ,  $\text{Dy}$ ,  $\text{Er}$ ;  $\text{R} = \alpha$ -naphthyl;  $\text{Ln} = \text{Dy}$ ).<sup>422</sup> Treatment of  $(\text{C}_5\text{H}_4\text{Me})_2\text{LnCl}$  with  $\text{NaNPh}_2$  in THF afforded the supramolecular amide complexes  $[\text{Na}(\text{THF})_2(\mu\text{-}\eta^5\text{-C}_5\text{H}_4\text{Me})_2\text{Ln}(\text{NPh}_2)_2]_n$  ( $\text{Ln} = \text{Sm}$ ,  $\text{Er}$ ). Both complexes have an alternating  $\text{-Cp-Ln-Cp-Na-}$  chain structure, and each lanthanide atom is coordinated with two  $\text{C}_5\text{H}_4\text{Me}$  rings and two  $\text{NPh}_2$  ligands, while  $\text{Na}$  is coordinated by two  $\text{C}_5\text{H}_4\text{Me}$  rings and two THF ligands without interacting with any amido ligands.<sup>423</sup> Similar treatment of neodymium trichloride with a mixture of  $\text{NaCp}$  and  $\text{LiNPh}_2$  in DME produced the anionic bis(amido) complex  $[\text{Li}(\text{DME})_3][\text{Cp}_2\text{Nd}(\text{NPh}_2)_2]$ , which consists of separated ions in the solid state.<sup>424</sup> Lanthanide amido complexes of the general formula  $\text{Cp}_2\text{Ln}(\text{DPA})(\text{THF})$  ( $\text{Ln} = \text{Pr}$ ,  $\text{Sm}$ ,  $\text{Ho}$ ,  $\text{Yb}$ ;  $\text{DPA} = \text{dipyridylamide}$ ) were synthesized by reacting tris(cyclopentadienyl)lanthanide with equimolar amounts of 2,2'-dipyridylamine in THF at room temperature.<sup>425</sup> Amine elimination reactions between homoleptic silylamide lanthanide complexes and an isopropylidene-bridged cyclopentadiene-fluorene system led to unusual bis(cyclopentadienyl) complexes in which the fluorene unit does not participate in coordination to the central lanthanide atom. A typical reaction sequence is outlined in Scheme 89.<sup>426</sup>

The chemistry of organolanthanide imido complexes still awaits exploration, and the reactions of lanthanide-imido complexes have remained almost unexplored to date. Only very recently it was found that compounds containing the novel  $\text{Ln}_4\text{N}_4$  cubane core structure exhibit unprecedented reactivity (Scheme 90).<sup>427,427a</sup> The starting materials  $[(\text{C}_5\text{H}_4\text{SiMe}_3)\text{Ln}(\mu_3\text{-NCH}_2\text{R})]_4$  ( $\text{Ln} = \text{Y}$ ,  $\text{Lu}$ ) were made by reacting the tetranuclear lanthanide polyhydrido complexes  $[(\text{C}_5\text{H}_4\text{SiMe}_3)\text{Ln}(\mu\text{-H})_2]_4(\text{THF})$  with nitriles  $\text{RCN}$ . This reaction involves double addition of the  $\text{Ln-H}$  units across the  $\text{C}\equiv\text{N}$  bond.<sup>299,427,427a</sup> In their high reactivity the lanthanide-imido complexes differ from their  $d$ -transition metal counterparts. Depending on the stoichiometries of the starting materials, the cubane clusters add different amounts of benzonitrile (Scheme 90). The products catalyze the trimerization of benzonitrile.<sup>427,427a</sup>

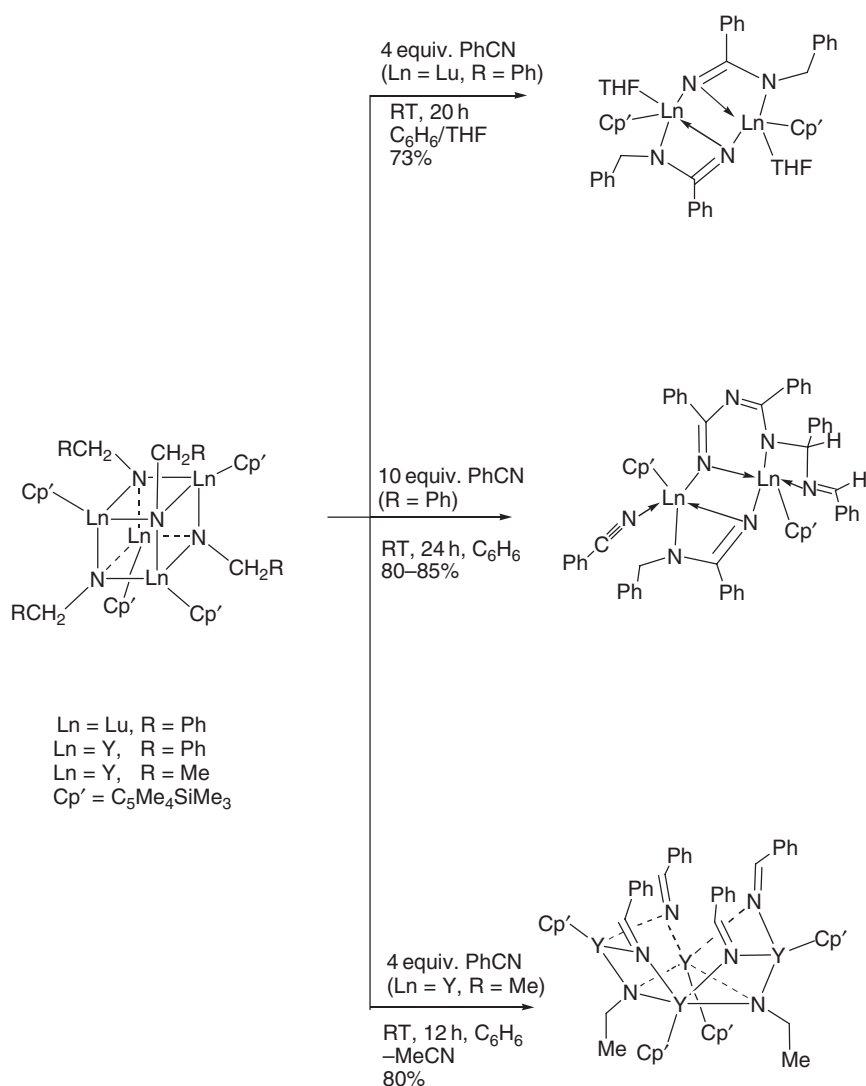
The reaction of 2 equiv. of dilithium amido-cyclopentadienides  $\text{Li}_2(\text{C}_5\text{R}_4\text{SiMe}_2\text{NCH}_2\text{CH}_2\text{X})$  ( $\text{C}_5\text{R}_4 = \text{C}_5\text{Me}_4$ ,  $\text{C}_5\text{H}_3\text{Bu}^t$ ;  $\text{X} = \text{OMe}$ ,  $\text{NMe}_2$ ) with anhydrous  $\text{LnCl}_3$  ( $\text{Ln} = \text{Y}$ ,  $\text{Lu}$ ) gave heterobimetallic complexes of the type  $\text{Li}[\text{Ln}(\eta^5\text{-C}_5\text{R}_4\text{SiMe}_2\text{NCH}_2\text{CH}_2\text{X})_2]$ . In the case of the complexes  $\text{Li}[\text{Y}(\eta^5\text{-}\eta^1\text{-C}_5\text{Me}_4\text{SiMe}_2\text{NCH}_2\text{CH}_2\text{OMe})_2]$ ,  $(R,S)\text{-Li}[\text{Y}(\eta^5\text{-}\eta^1\text{-C}_5\text{H}_3\text{Bu}^t\text{SiMe}_2\text{NCH}_2\text{CH}_2\text{OMe})_2]$ , and  $(R,R)\text{-Li}[\text{Y}(\eta^5\text{-}\eta^1\text{-C}_5\text{H}_3\text{Bu}^t\text{SiMe}_2\text{NCH}_2\text{CH}_2\text{NMe}_2)_2]$  the molecular structures were determined by single crystal X-ray analyses.<sup>428</sup>

Phosphoraneiminato complexes of ytterbium, dysprosium, and erbium were prepared by reactions of the cyclopentadienyl lanthanide chlorides  $[\text{LnCp}_2(\mu\text{-Cl})]_2$  with  $\text{LiNPPH}_3$  in boiling toluene. Two of the three phosphoraneiminato groups link the metal atoms via  $\mu_2\text{-N}$  bridges to form almost planar  $\text{Ln}_2\text{N}_2$  four-membered rings. The third  $\text{NPPH}_3$  group is terminally bonded. In the dimeric molecules  $[\text{Ln}_2\text{Cp}_3(\text{NPPH}_3)_2]$ , the metal atoms together with two N atoms form slightly distorted  $\text{Ln}_2\text{N}_2$ -four ring. One of the two metal atoms is coordinated by cyclopentadienyl and one  $\text{NPPH}_3^-$  forming nearly a straight line. The second metal atom is coordinated by two cyclopentadienyl ligands in an  $\eta^5$ -coordination mode.<sup>429</sup> Monomeric bis(cyclopentadienyl)(1,3-diphenyltriazenido)(4-*t*-butylpyridine) complexes of erbium and lutetium have been prepared via the reaction of the tris(cyclopentadienyl) complexes with 1,3-diphenyltriazene in the presence of 4-*t*-butylpyridine (Scheme 91). The presence of 4-*t*-butylpyridine is essential because of the insolubility of tris(cyclopentadienyl)erbium and -lutetium in toluene.<sup>430</sup>

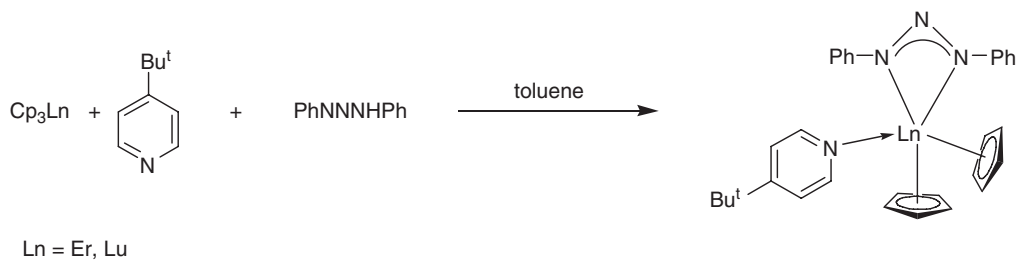
Three equivalents of 1,3-diphenyltriazene react with 1 equiv. of the tris(cyclopentadienyl)lanthanides in the presence of pyridine to afford tris(1,3-diphenyltriazenido)(pyridine) lanthanide complexes. Single crystal X-ray determinations of bis(cyclopentadienyl)(1,3-diphenyltriazenido)(4-*t*-butylpyridine)erbium revealed a monomeric species with two cyclopentadienyl ligands, one bidentate 1,3-diphenyltriazenido ligand, and one 4-*t*-butylpyridine



Scheme 89



Scheme 90



Scheme 91

donor. The erbium–nitrogen bond lengths within the 1,3-diphenyltriazenido ligand are 2.423 Å (N(1)), 2.447 Å (N(3)), and 2.958 Å (N(2)), indicating idealized bidendate bonding of the 1,3-diphenyltriazenido ligand, with N(2) not being bonded to erbium.<sup>430</sup> Reaction of  $\text{ErCp}_3$  with 1 equiv. of  $\text{HPzMe}_2$  ( $\text{HPzMe}_2 = 3,5\text{-dimethylpyrazol}$ ) in THF at room temperature gives the complex  $\text{Cp}_2\text{Er}(\text{PzMe}_2)(\text{THF})$ . Abstraction of only one cyclopentadienyl ligand



occurred by reacting  $\text{Cp}_3\text{Yb}$  with 2 equiv. of  $\text{HPzMe}_2$  in THF leading to the bis(cyclopentadienyl)monopyrazolate  $\text{Cp}_2\text{Yb}(\text{PzMe}_2)(\text{HPzMe}_2)$  where the coordination sphere of the ytterbium is saturated by one  $\text{HPzMe}_2$  molecule. Presumably, the formation of  $\text{Cp}_2\text{Yb}(\text{PzMe}_2)(\text{HPzMe}_2)$  is due to the enhanced covalence of the  $\text{Ln}-\text{Cp}$  bond in the series  $\text{LnCp}_3$  ( $\text{Ln} = \text{Sm}, \text{Dy}, \text{Ho}, \text{Yb}$ ), as a result of the lanthanide contraction, and because the acidity of  $\text{HCp}$  is relatively high. Thus,  $\text{HPzMe}_2$  is not a strong enough acid to liberate the second Cp group from the more covalent  $\text{Cp}_3\text{Yb}$  moiety to give  $\text{CpYb}(\text{PzMe}_2)_2$ . The structures of  $\text{Cp}_2\text{Er}(\text{PzMe}_2)(\text{THF})$  and  $\text{Cp}_2\text{Yb}(\text{PzMe}_2)(\text{HPzMe}_2)$  in the solid state show monomeric molecules with a coordination geometry which is typical for bent metallocenes.<sup>282</sup>

Reactions of  $[\text{Cp}_2\text{Ln}(\mu\text{-Cl})_2]$  with  $\text{LiN}=\text{C}(\text{NMe}_2)_2$  proceeded at room temperature in THF to yield the lanthanocene guanidinate complexes  $[\text{Cp}_2\text{Ln}\{\mu\text{-}\eta^1\text{:}\eta^2\text{-N}=\text{C}(\text{NMe}_2)_2\}]_2$  ( $\text{Ln} = \text{Gd}, \text{Er}$ ). Treatment of these complexes with phenylisocyanate resulted in monoinsertion of  $\text{PhNCO}$  into the  $\text{Ln}-\text{N}$  bond to yield the corresponding insertion products  $[\text{Cp}_2\text{Ln}\{\mu\text{-}\eta^1\text{:}\eta^2\text{-OC}(\text{N}=\text{C}(\text{NMe}_2)_2)\text{NPh}\}]_2$ . Monomeric guanidinoacetimidate complexes of the type  $\text{Cp}_2\text{Ln}[\text{Pr}^i\text{N})_2\text{C}(\text{N}=\text{C}(\text{NMe}_2)_2)]$  ( $\text{Ln} = \text{Dy}, \text{Er}, \text{Yb}$ ) were obtained by reacting  $[\text{Cp}_2\text{Ln}(\mu\text{-Cl})_2]$  with  $\text{Li}[(\text{Pr}^i\text{N})_2\text{C}(\text{N}=\text{C}(\text{NMe}_2)_2)]$ .<sup>431</sup> Lanthanocene guanidinate complexes of the type  $\text{Cp}_2\text{Ln}[\text{Pr}^i\text{NC}(\text{NPr}^i)_2\text{NPr}^i]$  have also been obtained by insertion of  $N,N'$ -diisopropylcarbodiimide into the  $\text{Ln}-\text{N}$  bond of  $\text{Cp}_2\text{Ln}(\text{NPr}^i)_2$ <sup>432,433</sup> and  $\text{Cp}_2\text{Yb}(\text{Cbz})(\text{THF})$  ( $\text{Cbz} = \text{carbazolate}$ ).<sup>434</sup> Similar insertion chemistry with  $\text{PhNCO}$  and  $\text{PhNCS}$  into an  $\text{Ln}-\text{S}$  bond has been reported for the thiolate-bridged dimeric neodymium complex  $[(\text{C}_5\text{H}_4\text{Me})_2\text{Nd}(\mu\text{-SPh})(\text{THF})]_2$ ,<sup>435</sup> and the first examples of ketene insertion into an  $\text{Ln}-\text{S}$  bond have also recently been described.<sup>436</sup> By treatment of  $\text{Ln}(\text{C}_5\text{H}_4\text{Me})_3$  ( $\text{Ln} = \text{Yb}, \text{Er}, \text{Dy}, \text{Gd}$ ) with 5-phenyl-1H-tetrazole ( $\text{TzH}$ ) 5-phenyltetrazolate organolanthanide complexes of the type  $[(\text{C}_5\text{H}_4\text{Me})_2\text{Ln}(\mu\text{-Tz})]_2$  were obtained. The molecules are centrosymmetric dimers in which each ytterbium atom is coordinated by two methylcyclopentadienyl groups and three nitrogen atoms of the bridging Tz ligands to form a distorted trigonal bipyramidal geometry. The complexes  $[(\text{C}_5\text{H}_4\text{Me})_2\text{Ln}(\mu\text{-Tz})]_2$  with Dy and Gd have two disconnected structural units  $[(\text{C}_5\text{H}_4\text{Me})\text{CpLn}(\mu\text{-Tz})]_2$  and  $[(\text{C}_5\text{H}_4\text{Me})_2\text{Ln}(\mu\text{-Tz})]_2$  when there was a small amount of  $(\text{C}_5\text{H}_4\text{Me})_2\text{LnCp}$  present in the  $\text{Ln}(\text{C}_5\text{H}_4\text{Me})_3$ . The complex crystallized in one asymmetrical unit, with each of the tetrazolate-bridged dimers having an inversion center. The bridging unit  $\text{Ln}_2\text{N}_6$  is planar and all three structures reveal an unusual bonding mode of the tetrazolate ligand, in which the tetrazolate group acts as both a bridging and chelating ligand, with the nitrogen atoms at 1, 2, and 3 position taking part in bonding.<sup>437</sup> The neutral bis(methylcyclopentadienyl)piperidino complexes  $(\text{C}_5\text{H}_4\text{Me})_2\text{Ln}(\text{C}_5\text{H}_{10})(\text{HNC}_5\text{H}_{10})$  with  $\text{Ln} = \text{Yb}, \text{Er}, \text{Y}$  were obtained by the reaction of anhydrous  $\text{LnCl}_3$  with  $\text{Na}(\text{C}_5\text{H}_4\text{Me})$  followed by treatment with  $\text{LiNC}_5\text{H}_{10}$ . In the erbium complex the  $\text{Er}-\text{N}(1)$  and  $\text{Er}-\text{N}(2)$  distances are 2.464(7) and 2.159(8) Å. The large disparity in the  $\text{Er}-\text{N}$  bond lengths showed that the complex exhibits two different  $\text{Er}-\text{N}$  bonding modes: donor bond for the bond distance 2.464(7), and the lanthanide amido bond.<sup>438</sup>

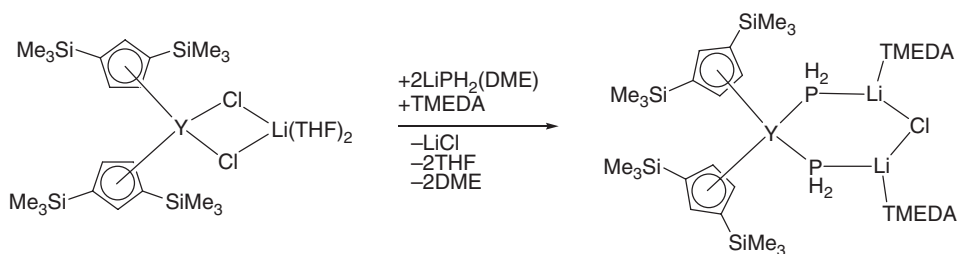
The trivalent ytterbium diazadiene complex  $\text{Cp}_2\text{Yb}(\text{DAD})$  ( $\text{DAD} = \text{Bu}^t\text{N}=\text{CHCH}=\text{NBu}^t$ ) was obtained using three different procedures, namely, by oxidation of  $\text{Cp}_2\text{Yb}(\text{THF})_2$  with the diazadiene in THF, by reaction of  $\text{Cp}_2\text{YbCl}$  with  $\text{Na}_2^+\text{DAD}^{2-}$  in a ratio of 2:1, and by the reaction of  $\text{Cp}_2\text{YbCl}(\text{THF})$  with  $\text{K}^+\text{DAD}^-$  taken in a ratio of 1:1.<sup>225</sup> The solid-state structure shows  $\text{Cp}_2\text{Yb}(\text{DAD})$  to be monomeric with average  $\text{Yb}-\text{N}$  distances of 2.31 Å.  $\text{Cp}_2\text{Yb}(\text{DAD})$  exhibits a magnetic moment at room temperature of 4.8  $\mu_B$ , which is slightly higher than the average value observed for  $\text{Yb}^{\text{III}}$  derivatives (4.3–4.5  $\mu_B$ ). This can be explained taking into account the radical anionic character of the DAD ligand and its contribution to the total magnetic moment of the molecule.<sup>225</sup>

The bis(ethyltetramethylcyclopentadienyl)lanthanide chlorides  $(\text{C}_5\text{Me}_4\text{Et})_2\text{LnCl}(\text{THF})$  were converted into the amide  $(\text{C}_5\text{Me}_4\text{Et})_2\text{LnN}(\text{SiMe}_3)_2$  or alkyl  $(\text{C}_5\text{Me}_4\text{Et})_2\text{LnCH}(\text{SiMe}_3)_2$  complexes by reaction in toluene with equimolar amounts of either  $\text{NaN}(\text{SiMe}_3)_2$  or  $\text{LiCH}(\text{SiMe}_3)_2$ , respectively. The compounds  $(\text{C}_5\text{Me}_4\text{Et})_2\text{YN}(\text{SiMe}_3)_2$  and  $(\text{C}_5\text{Me}_4\text{Et})_2\text{SmCH}(\text{SiMe}_3)_2$  were characterized by X-ray crystallography. In  $(\text{C}_5\text{Me}_4\text{Et})_2\text{Y}[\text{N}(\text{SiMe}_3)_2]$  the yttrium atom is coordinated by two  $\text{C}_5\text{Me}_4\text{Et}$  ligands and one bis(trimethylsilyl)amide ligand, and has a pseudo-trigonal planar arrangement. In  $(\text{C}_5\text{Me}_4\text{Et})_2\text{Sm}[\text{CH}(\text{SiMe}_3)_2]$  the samarium atom also has a pseudo-trigonal planar coordination sphere from two  $\text{C}_5\text{Me}_4\text{Et}$  ligands and one  $\text{CH}(\text{SiMe}_3)_2$  ligand. The  $\text{SmC}(\text{alkyl})$   $\sigma$ -bond length is 2.502(3) Å. The authors presumed  $\gamma$ -agostic bonds between the methyl groups of the amide  $\text{N}(\text{SiMe}_3)_2$  or  $\text{CH}(\text{SiMe}_3)_2$  ligands and the lanthanide center in both structures.<sup>430</sup>

#### 4.01.6.4.6 $\text{Cp}_2\text{LnX}$ compounds with P ligands

A series of bis[1,3-bis(trimethylsilyl)cyclopentadienyl]yttrium phosphido complexes has been synthesized and structurally characterized. The chloro-bridges in  $\text{Cp}''_2\text{Y}(\mu\text{-Cl})\text{Li}(\text{THF})_2$  ( $\text{Cp}'' = \text{C}_5\text{H}_3(\text{SiMe}_3)_2\text{-1,3}$ ) can be selectively replaced by one or two triisopropylsilylphosphide substituents. The metathesis reaction of the yttrium precursor with  $\text{LiPH}_2(\text{DME})$  followed by treatment with TMEDA gave a colorless bis(phosphido)yttriate as shown in Scheme 92. The central  $\text{YP}_2\text{Li}_2\text{Cl}$  cycle is nearly planar with  $\text{Y}-\text{P}$  bond lengths of 2.849 Å.<sup>439</sup>





Scheme 92

In a similar manner, the metathesis reaction of  $\text{Cp}''_2\text{YCl}$  with  $\text{KPHSiBu}_3$  afforded monomeric  $\text{Cp}''_2\text{YPHSiBu}_3$  as colorless crystals in 65% yield. The compound was structurally characterized by X-ray methods.<sup>89</sup>

#### 4.01.6.4.7 $\text{Cp}_2\text{LnX}$ compounds with alkyl and silyl ligands

The reaction of  $(\text{C}_5\text{H}_9\text{C}_5\text{H}_4)_2\text{ErCl}$  with  $\text{LiMe}$  in  $\text{Et}_2\text{O}/\text{THF}$  at room temperature gave bis[bis(cyclopentylcyclopentadienyl)methylerybium],  $[(\text{C}_5\text{H}_9\text{C}_5\text{H}_4)_2\text{Er}(\mu\text{-Me})]_2$ . A structure analysis showed that the complex is a dimer. Two cyclopentylcyclopentadienyl and two methyl groups are bonded to  $\text{Er}^{3+}$  to form a tetrahedron around it. Each cyclopentyl in  $[(\text{C}_5\text{H}_9\text{C}_5\text{H}_4)_2\text{Er}(\mu\text{-Me})]_2$  has two conformations, and the two cyclopentyl substituents in the cyclopentylcyclopentadienyls on the same erbium atom are located on the opposite sides.<sup>440</sup> An unusual  $\mu$ -peroxo organolanthanide complex,  $[(\text{C}_5\text{H}_4\text{C}_5\text{H}_9)_2\text{Yb}(\text{THF})_2(\mu\text{-O}_2)]$ , was serendipitously obtained from a reaction between  $\text{YbI}_2$  and cyclopentylcyclopentadienyl sodium,  $\text{Na}(\text{C}_5\text{H}_4\text{C}_5\text{H}_9)$ , in the presence of trace amounts of oxygen. In the molecular structure of  $[(\text{C}_5\text{H}_4\text{C}_5\text{H}_9)_2\text{Yb}(\text{THF})_2(\mu\text{-O}_2)]$ , the ytterbium atoms and the asymmetric  $\text{O}_2$  unit define a plane that contains a  $C_i$ -symmetry center.<sup>441</sup> In metathesis reactions of  $(\text{C}_5\text{Me}_4\text{Pr}^i)_2\text{LnCl}(\text{THF})$  with  $\text{LiMe}$  and  $\text{LiCH}(\text{SiMe}_3)_2$  the corresponding complexes  $(\text{C}_5\text{Me}_4\text{Pr}^i)_2\text{LnMe}(\text{THF})$  ( $\text{Ln} = \text{Y}, \text{Lu}$ ) and  $(\text{C}_5\text{Me}_4\text{Pr}^i)_2\text{LnCH}(\text{SiMe}_3)_2$  ( $\text{Ln} = \text{Y}, \text{Sm}$ ) were formed.<sup>334</sup> In the crystal structure of  $[(\text{C}_5\text{H}_4\text{Bu}^t)_2\text{Tb}(\mu\text{-Me})]_2$  the metal atom adopts a tetrahedral geometry, and the complex has  $C_{2h}$ -symmetry.<sup>442</sup>  $[(\text{C}_5\text{H}_4\text{Bu}^t)_2\text{Y}(\mu\text{-Me})]_2$  was synthesized analogously from  $[(\text{C}_5\text{H}_4\text{Bu}^t)_2\text{Tb}(\mu\text{-Me})]_2$  and  $\text{MeLi}$  and structurally characterized.<sup>443</sup> Reactions of  $\text{Ce}(\text{C}_5\text{H}_4\text{Bu}^t)_3$  or  $[(\text{C}_5\text{H}_4\text{Bu}^t)_2\text{Ce}(\mu\text{-SPR}^i)]_2$  with  $\text{MeLi}$  in hydrocarbon solvents produced the cerium analog  $[(\text{C}_5\text{H}_4\text{Bu}^t)_2\text{Ce}(\mu\text{-Me})]_2$ . The dimeric methyl complexes  $[(\text{C}_5\text{H}_4\text{Bu}^t)_2\text{Ln}(\mu\text{-Me})]_2$  ( $\text{Ln} = \text{Nd}, \text{Gd}$ ) react with  $\text{PhC}\equiv\text{CH}$  to form the dimeric alkynide-bridged complexes  $[(\text{C}_5\text{H}_4\text{Bu}^t)_2\text{Ln}(\mu\text{-C}\equiv\text{CPh})]_2$ .<sup>444</sup> The dimeric compounds  $[(\text{C}_5\text{H}_4\text{SiEt}_3)_2\text{Ln}(\mu\text{-Cl})]_2$  ( $\text{Ln} = \text{Y}, \text{Sm}, \text{Lu}$ ) react with 1 equiv. of methylolithium to give the corresponding dimeric lanthanocene methyl complexes  $[(\text{C}_5\text{H}_4\text{SiEt}_3)_2\text{Ln}(\mu\text{-Me})]_2$ . Monomeric methyl complexes of the type  $\text{Cp}''_2\text{LnMe}(\text{THF})$  ( $\text{Ln} = \text{Sm}, \text{Lu}$ ) were obtained by the reaction of  $\text{SmCl}_3$  and  $\text{LuCl}_3$ , respectively, with 2 equiv. of  $\text{KCp}''$ .<sup>345</sup> A monomeric structure has also been found for the phenyl complex  $\text{Cp}_2\text{SmPh}(\text{THF})$ .<sup>445</sup> New alkyl and allyl derivatives of cyclopentadienyl samarium complexes were synthesized from  $[(\text{C}_5\text{H}_4\text{Bu}^t)_2\text{Sm}(\mu\text{-Cl})]_2$  and the magnesium derivative  $(\text{C}_5\text{H}_4\text{Bu}^t)_2\text{SmCl}\cdot\text{MgCl}_2(\text{THF})_4$ . In the presence of the Lewis base 1,3-diisopropylimidazoline-2-ylidene  $\text{C}(\text{NPr}^i)_2(\text{CMe})_2$  crystals of the monoadduct  $(\text{C}_5\text{H}_4\text{Bu}^t)_2\text{Sm}(\text{C}_3\text{H}_5)[\text{C}(\text{NPr}^i)_2(\text{CMe})_2]$  were obtained.<sup>446</sup>

The interaction of  $(\text{C}_5\text{H}_4\text{Bu}^t)_2\text{YbCl}\cdot\text{LiCl}$  with 1 equiv. of  $\text{Li}[(\text{CH}_2)_2\text{PPh}_2]$  in tetrahydrofuran at room temperature gave white crystals of the stoichiometry  $[\text{Ph}_2\text{PMe}_2][\text{Li}(\text{C}_5\text{H}_4\text{Bu}^t)_2]$  and yellow crystals of the stoichiometry  $(\text{C}_5\text{H}_4\text{Bu}^t)_2\text{YbCl}[\text{CH}_2\text{P}(\text{Me})\text{Ph}_2]$  in 10% and 30% yields, respectively, after successive recrystallization from a THF/toluene mixture. The molecular structure of  $(\text{C}_5\text{H}_4\text{Bu}^t)_2\text{YbCl}[\text{CH}_2\text{P}(\text{Me})\text{Ph}_2]$  can be described as a distorted tetrahedron if one considers that the metal is coordinated to the centroid of the *t*-butylcyclopentadienyl rings. The  $\text{Yb}\text{--}\text{C}(\text{ylide})$  distance is 2.51(3) Å. The  $\text{P}\text{--}\text{C}(19)$  distance of 1.71(2) Å is between the range of a  $\text{P}=\text{C}$  double bond distance (1.665 Å) and a  $\text{P}\text{--}\text{C}$  single bond distance (1.872 Å).<sup>447,448</sup> The reaction of  $\text{CpLuCl}_2(\text{THF})_3$  with  $[\text{PhCHCHPh}]^-\text{Na}^+$  in a molar ratio of 1:2 in DME gave the ate-complex  $[\text{Cp}_2\text{Lu}\{\mu\text{-CH}(\text{Ph})\text{CH}(\text{Ph})\text{CH}(\text{Ph})\text{CH}(\text{Ph})\}]\text{Na}(\text{DME})_3$  in 47% yield.<sup>167</sup>

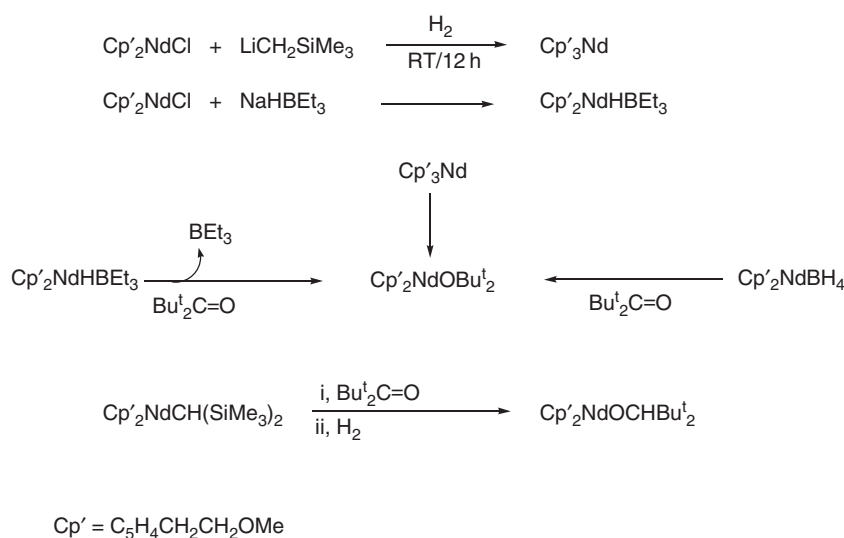
Organolanthanide complexes containing a  $\sigma$ -bonded 1,3-dithiane,  $(\text{C}_5\text{H}_4\text{Bu}^t)_2\text{Ln}(\text{C}_4\text{H}_7\text{S}_2\text{-1,3})(\mu\text{-Cl})\text{Li}(\text{THF})_2$  ( $\text{Ln} = \text{Lu}, \text{Y}$ ), have been characterized by single crystal X-ray diffraction. In  $(\text{C}_5\text{H}_4\text{Bu}^t)_2\text{Lu}(\text{C}_4\text{H}_7\text{S}_2\text{-1,3})(\mu\text{-Cl})\text{Li}(\text{THF})_2$  the Lu atom is coordinated by two  $\text{C}_5\text{H}_4\text{Bu}^t$  rings, bridging chloride ligand and a  $\sigma$ -bonded carbon atom of 1,3-dithiane to form a pseudo-tetrahedral arrangement. The central fragment of the structure is a pentagon, formed by the Lu atom, 1,3-dithiane, and a molecule of  $\text{LiCl}$ .<sup>449</sup>

The scandocene silyl and germyl complexes  $\text{Cp}_2\text{Sc}[\text{Si}(\text{SiMe}_3)_3](\text{THF})$ ,  $\text{Cp}_2\text{Sc}[\text{Si}(\text{SiMe}_3)_2\text{Ph}](\text{THF})$ ,  $\text{Cp}_2\text{Sc}[\text{SiBu}^t\text{Ph}_2](\text{THF})$ ,  $\text{Cp}_2\text{Sc}[\text{SiPh}_3](\text{THF})$ , and  $\text{Cp}_2\text{Sc}[\text{Ge}(\text{SiMe}_3)_3](\text{THF})$  have been prepared by addition of the appropriate silyl- or germyllithium reagents to  $[\text{Cp}_2\text{Sc}(\mu\text{-Cl})_2]$  in THF. The crystal structure of  $\text{Cp}_2\text{Sc}[\text{Si}(\text{SiMe}_3)_3](\text{THF})$  revealed no unusual distortions in the molecule and an Sc–Si bond length of 2.86 Å. These unusually reactive  $d^0$ -silyl complexes polymerize ethylene.  $\text{Cp}_2\text{Sc}[\text{Si}(\text{SiMe}_3)_3](\text{THF})$  reacts with phenylacetylene via  $\sigma$ -bond metathesis to give  $\text{HSi}(\text{SiMe}_3)_3$  and the known acetylide species  $[\text{Cp}_2\text{Sc}(\mu\text{-C}\equiv\text{CPh})_2]$ . The complexes  $\text{Cp}_2\text{Sc}[\text{Si}(\text{SiMe}_3)_3](\text{THF})$ ,  $\text{Cp}_2\text{Sc}[\text{SiBu}^t\text{Ph}_2](\text{THF})$ , and  $\text{Cp}_2\text{Sc}[\text{Ge}(\text{SiMe}_3)_3](\text{THF})$  react with CO via CO–CO coupling processes to yield the scandoxyketene derivatives  $\text{Cp}_2\text{ScO}(\text{ER}_3)(\text{C}=\text{C}=\text{O})$ , which were trapped as the adducts  $\text{Cp}_2\text{Sc}[\text{O}(\text{L})\text{C}(\text{ER}_3)\text{CO}]$  ( $\text{ER}_3 = \text{Si}(\text{SiMe}_3)_3$ ,  $\text{SiBu}^t\text{Ph}_2$ ,  $\text{Ge}(\text{SiMe}_3)_3$ ;  $\text{L} = \text{THF}$ ,  $\text{Me-THF}$ ,  $\text{PMc}_2\text{Ph}$ ). In non-polar media, carbonylations of  $\text{Cp}_2\text{Sc}[\text{Si}(\text{SiMe}_3)_3](\text{THF})$ ,  $\text{Cp}_2\text{Sc}[\text{SiBu}^t\text{Ph}_2](\text{THF})$ , and  $\text{Cp}_2\text{Sc}[\text{Ge}(\text{SiMe}_3)_3](\text{THF})$  afforded the enedionediolate structures  $[\text{Cp}_2\text{ScOC}(\text{ER}_3)\text{CO}]_2$  ( $\text{ER}_3 = \text{Si}(\text{SiMe}_3)_3$ ,  $\text{SiBu}^t\text{Ph}_2$ ,  $\text{Ge}(\text{SiMe}_3)_3$ ). Insertion of 2,6-xylyl isocyanide ( $\text{XylNC}$ ) into the Sc–Si bond of  $\text{Cp}_2\text{Sc}[\text{Si}(\text{SiMe}_3)_3](\text{THF})$  yielded the stable  $\eta^2$ -iminosilaacyl complex  $\text{Cp}_2\text{Sc}[\eta^2\text{-CN}(\text{Xyl})\text{Si}(\text{SiMe}_3)_3]$ , which reacts with  $\text{PhC}\equiv\text{CH}$  to afford  $[\text{Cp}_2\text{Sc}(\mu\text{-C}\equiv\text{CPh})_2]$  and the formimidoylsilane  $\text{HC}(\text{=N-2,6-Me}_2\text{C}_6\text{H}_3)\text{Si}(\text{SiMe}_3)_3$ .<sup>450</sup>

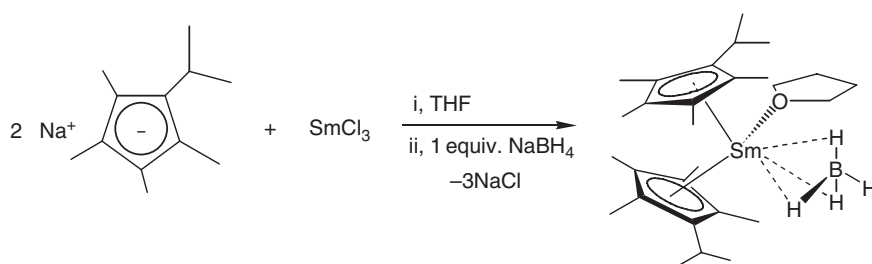
#### 4.01.6.4.8 $\text{Cp}_2\text{LnX}$ compounds with borohydride and hydride ligands

The bis(cyclopentadienyl)neodymium triethylborohydrides  $(\text{C}_5\text{H}_4\text{CH}_2\text{CH}_2\text{OCH}_3)_2\text{NdHBEt}_3$  and  $(\text{C}_5\text{H}_4\text{Bu}^t)_2\text{NdHBEt}_3 \cdot n\text{THF}$  were obtained by addition of  $\text{NaHBEt}_3$  to the corresponding chlorides. The Nd–H NMR signals are found at 200 ppm ( $\omega_{1/2} = 1000$  Hz). The reactivity of these moderately stable complexes is similar to that of the known dimeric cyclopentadienyl lanthanide hydrides.<sup>451</sup> The trialkylborohydride  $\text{Cp}'_2\text{NdHBEt}_3$  ( $\text{Cp}' = \text{C}_5\text{H}_4\text{CH}_2\text{CH}_2\text{OMe}$ ) obtained by the reaction of  $\text{NaHBEt}_3$  with  $\text{Cp}'_2\text{NdCl}$  (Scheme 93) is fairly stable in benzene solution whereas the hydride  $\text{Cp}'_2\text{NdH}$  formed from  $\text{Cp}'_2\text{NdCl}$  and  $\text{NaH}$  or by hydrogenolysis of  $\text{Cp}'_2\text{NdR}$  ( $\text{R} = \text{CH}_2\text{SiMe}_3$  or  $\text{CH}(\text{SiMe}_3)_2$ ) is a species of very short life, undergoing rearrangement to  $\text{NdCp}'_3$  (Scheme 93). The transient hydride can be trapped with ketones, for example, acetone or pivalone, leading to the alkoxides  $\text{Cp}'_2\text{NdOCHR}'_2$  ( $\text{R}' = \text{Me}$  or  $\text{Bu}^t$ ) (Scheme 93).  $\text{Cp}'_2\text{NdOPr}^i$  is not isolable, but was detected by its NMR spectra. In contrast, the use of the sterically hindered ketone pivalone afforded the stable alkoxide  $\text{Cp}'_2\text{NdOCHBu}^t_2$ ; the latter is also produced by the reaction of pivalone with the borohydrides  $\text{Cp}'_2\text{NdHBEt}_3$  and  $\text{Cp}'_2\text{NdBH}_4$ , as well as by alcoholysis of  $\text{NdCp}'_3$  with pivalic alcohol (Scheme 93).<sup>452</sup>

The trichlorides of yttrium, samarium, and lutetium react with 2 equiv. of  $\text{Na}(\text{C}_5\text{H}_4\text{Bu}^t)$  followed by 1 equiv. of  $\text{NaBH}_4$  to give monomeric complexes of the type  $(\text{C}_5\text{H}_4\text{Bu}^t)_2\text{LnBH}_4(\text{THF})$ . The methyl derivatives of the complexes  $(\text{C}_5\text{H}_4\text{Bu}^t)_2\text{LnBH}_4(\text{THF})$  were also formed by the same procedure with 2 equiv. of  $\text{Na}(\text{C}_5\text{Me}_4\text{R})$  and 1 equiv. of  $\text{NaBH}_4$ .<sup>453</sup> Treatment of  $\text{SmCl}_3$  and  $\text{NaC}_5\text{Me}_4\text{Pr}^i$  in refluxing THF followed by addition of 1 equiv. of  $\text{NaBH}_4$  afforded  $(\text{C}_5\text{Me}_4\text{Pr}^i)_2\text{Sm}^{\text{III}}(\text{BH}_4)(\text{THF})$  (Scheme 94). The complex shows a distorted tetrahedral arrangement around



Scheme 93



Scheme 94

the central Sm(III) atom. It consists of two *i*-propyltetramethylcyclopentadienyl ligands, one tetrahydroborato ( $\text{BH}_4^-$ ) ligand bridging via H atoms to the lanthanide atom and one coordinating THF molecule. The  $\text{BH}_4^-$  unit of the complex coordinates as a tridentate ligand with three bridging H atoms and one terminal H atom. The  $\eta^5\text{-C}_5\text{Me}_4\text{Pr}^i$  ligands of this bent-sandwich complex adopt staggered conformation.<sup>454</sup>

DFT(B3PW91) calculations have been used to propose models for  $\text{C}_5\text{H}_5$  (Cp) in lanthanides at low computational cost. The hydrogen exchange reaction,  $\text{Cp}_2\text{LnH}^* + \text{H}_2 \rightarrow \text{Cp}_2\text{LnH} + \text{HH}^*$ , previously studied with  $\text{C}_5\text{H}_5$  has been used as a benchmark.<sup>455</sup>

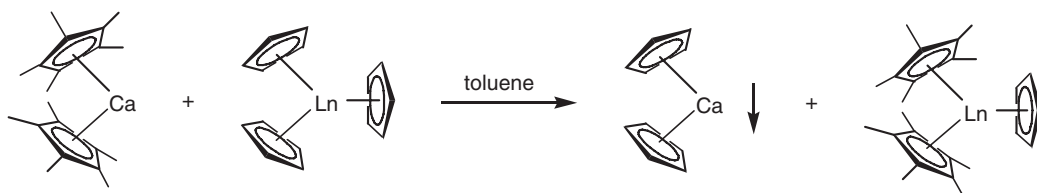
A conclusion of studies relating the stability of lanthanide hydrides including the bis(cyclopentadienyl) lanthanide hydrides  $(\text{C}_5\text{H}_4\text{Bu}^i)_2\text{SmH}$  and  $(\text{C}_5\text{H}_4\text{Bu}^i)_2\text{NdH}$  has been published.<sup>353</sup> The dimeric complex  $[\text{Cp}'_2\text{Sm}(\mu\text{-H})]_2$  and monomeric  $\text{Cp}'_2\text{SmHBEt}_3(\text{THF})_n$  ( $\text{Cp}' = \text{C}_5\text{H}_4\text{Bu}^i$ ) trialkylborohydride were obtained from the starting dimeric  $[\text{Cp}'\text{Sm}(\mu\text{-Cl})]_2$  by a reaction with the hydride reagent  $\text{NaHBEt}_3$ . A monomeric hydride,  $\text{Cp}'_2\text{SmH}(\text{PMe}_3)_2$ , was also obtained in the presence of a catalytic amount of  $\text{PMe}_3$  by hydrogenolysis of  $\text{Cp}'_2\text{SmR}$  ( $\text{R} = \text{CH}_2\text{SiMe}_3$  or  $\text{CH}(\text{SiMe}_3)_2$ ). The trialkylborohydride was the most stable in solution as compared to other hydrides of samarium. All hydrides reacted with acetone to give the corresponding dimeric alkoxide derivative  $[\text{Cp}'\text{Sm}(\mu\text{-OCHMe}_2)]_2$ .<sup>456</sup>

#### 4.01.6.5 $\text{Cp}_3\text{Ln}$ Compounds

Non-relativistic and relativistic discrete variational- $X\alpha$  calculations have been performed on  $\text{CeCp}_3$ . Metal ligand covalent interactions in  $\text{CeCp}_3$  are dominated by metal *d*-orbital participation in the  $(\eta\text{-C}_5\text{H}_5)$   $\pi_2$ -based 2e and 3e molecular orbitals, and an *f*-orbital contribution to the 1a<sub>2</sub> level. The non-relativistic calculations predict a formal ground-state configuration of  $4f^1$  and  $5f^1$  for  $\text{CeCp}_3$ . The 4*f*-based molecular orbitals of  $\text{CeCp}_3$  are found to be little altered from those of free Ce(III).<sup>457</sup> The mean dipole polarizability of the tris(cyclopentadienyl)lanthanides  $\text{NdCp}_3$ ,  $\text{SmCp}_3$ , and  $\text{ErCp}_3$  has been exactly determined by means of refractive index measurements in the vapor phase.<sup>160</sup>  $\text{GdCp}_3$  has been reported to show a green luminescence in ether solution.<sup>458</sup>

Tris(cyclopentadienyl)lanthanides,  $\text{LnCp}_3$  ( $\text{Ln} = \text{Nd}, \text{Yb}$ ), were prepared by the reaction of anhydrous lanthanide(III) triflates,  $\text{Ln}(\text{O}_3\text{SCF}_3)_3$ , with  $\text{NaCp}$  in THF.<sup>459</sup> High yields of  $\text{LnCp}_3$  ( $\text{Ln} = \text{Pr}, \text{Er}, \text{Yb}$ ) have been obtained from the reaction of the metallic lanthanides with  $\text{CpCuPPh}_3$ .<sup>207</sup> The molecular structure of base-free  $\text{Pr}(\text{C}_5\text{H}_4\text{Me})_3$  has been determined and found to be nearly identical with that of the La, Ce, and Nd analogs.<sup>460</sup> The electronic structure of organometallic complexes, especially  $\eta^5$ -cyclopentadienyl complexes, of the *f*-elements has been further investigated. Because of the polymeric nature of the base-free  $\text{Cp}_3\text{Ln}$  compounds, monomeric homo-leptic cyclopentadienyl lanthanide complexes of the type  $\text{LaCp}_3$  using sterically demanding substituted  $\eta^5$ -cyclopentadienyl ligands such as  $(\text{C}_5\text{H}_4\text{SiMe}_3)$  and  $\text{Cp}''$  are more suitable. For example, the molecular structure of the complex  $\text{CeCp}''_3$  displays a pseudo-trigonal planar geometry. The CF splitting pattern of  $\text{PrCp}''_3$  was obtained on the basis of absorption, magnetic circular dichroism (MCD), and luminescence measurements. By fitting the experimental parameters of an empirical Hamiltonian the authors obtained the splitting pattern and could estimate the CF strength of  $\text{C}_5\text{H}_4(\text{SiMe}_3)$  ligand.<sup>461</sup>

The use of alkaline earth metallocenes  $\text{Cp}^*_2\text{Ca}(\text{THF})_x$  ( $x = 0\text{--}2$ ) as cyclopentadienyl ring metathesis (CRM) reagents with lanthanide and the main group metal complexes has been propagated. The CRM reaction provided a controllable route to mixed ring cyclopentadienyl species and allowed to study the effect of changes in the ligand environment around a metal center in a systematic manner. The type of product formed depended on whether unsolvated or solvated lanthanocene derivatives were employed. In the CRM reaction between unsolvated



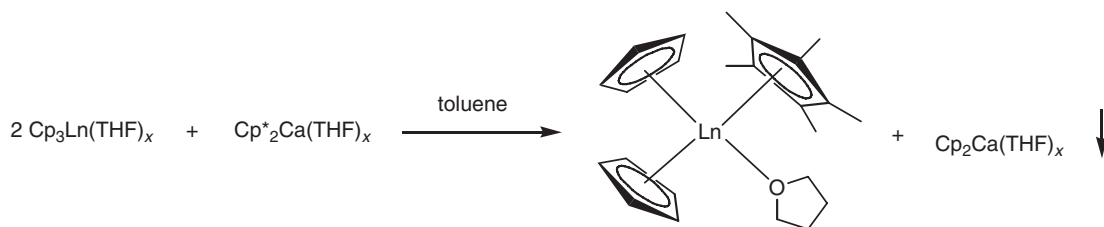
Scheme 95

lanthanocene and  $\text{CaCp}^*_2$  50% of excess of the co-reagent was used to overcome the low solubility of  $\text{LnCp}_3$  in toluene. The excess did not generate any  $\text{LnCp}^*_3$  but  $\text{LnCp}^*_2\text{Cp}$  instead (Scheme 95). According to X-ray diffraction crystallography, the complex  $\text{NdCp}^*_2\text{Cp}$  consists of monomeric units, in which the Nd atom is coordinated by two  $\eta^5\text{-Cp}^*$  and one  $\eta^5\text{-Cp}$  rings.<sup>462,463</sup>

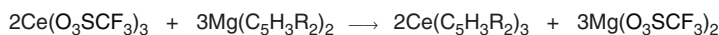
The CRM reaction took an appreciably different course when solvated starting materials were used. Only one  $\text{Cp}^*$  exchange at the lanthanide center was observed. When  $\text{KCp}^*$  was reacted with  $\text{LnCp}_3(\text{THF})$  in excess or in three times more than the equimolar ratio, no  $\text{Cp}^*$  ring transfer to the lanthanum center was observed (Scheme 96).<sup>463</sup>

The reaction of bis(vinylcyclopentadienyl)mercury(II) with powdered dysprosium in THF afforded the tris(vinylcyclopentadienyl)dysprosium complex  $(\text{C}_5\text{H}_4\text{CH}=\text{CH}_2)_3\text{Dy}$ .<sup>248</sup> Anhydrous lanthanide trichlorides were reacted with an excess amount of  $\text{NaCp}''$ . For the metals La, Nd, Sm, Gd, and Dy tris(ligand) complexes of the type  $\text{LnCp}''_3$ , and for the metals Gd, Dy, Y, Er, and Yb bis(ligand) complexes of the type  $[\text{Cp}''_2\text{Ln}(\mu\text{-Cl})_2]$  were formed.<sup>464</sup> The new tris(cyclopentadienyl)lanthanide(III) complexes  $\text{LaCp}''_3$  and  $\text{PrCp}''_3$  with  $\text{Cp}''$  were made from the appropriate anhydrous lanthanide(III) triflates or chlorides and  $3/2 \text{ MgCp}''_2$  or  $3 \text{ KCp}''$  in THF at ambient temperature.<sup>465</sup> The synthesis of a series of homoleptic tris(substituted-cyclopentadienyl)lanthanide(III) complexes  $\text{LnCp}_3^{\text{R}}$  ( $\text{Ln} = \text{La, Ce, Pr, Nd, Sm, Gd, Tb, Dy, Er, Tm, Yb}$ ) [ $\text{Cp}_3^{\text{R}} = \text{C}_5\text{H}_4\text{CH}(\text{SiMe}_3)_2$ ] has been described. The complexes were synthesized from the appropriate lanthanide trichlorides or  $\text{TmI}_3$  in the case of thulium with 3 equiv. of  $\text{KCp}^{\text{R}}$  in THF. Single crystal X-ray determinations show the isostructural complexes of  $\text{NdCp}_3^{\text{R}}$  and  $\text{TmCp}_3^{\text{R}}$  to be monomeric with bond lengths and angles in the expected areas. No short M–C agnostic interactions were observed. As potential starting materials for organoneodymium(II) complexes,  $\text{NdCp}^{\text{f}}_3$  and  $\text{NdCp}^{\text{t}}_3$  as well as  $\text{CeCp}^{\text{t}}_3$  were synthesized [ $\text{Cp}^{\text{f}} = \text{C}_5\text{H}_4\text{SiMe}_2\text{Bu}^{\text{f}}$ ,  $\text{Cp}^{\text{t}} = \text{C}_5\text{H}_3(\text{SiMe}_2\text{Bu}^{\text{f}})_{2-1,3}$ ] from the related lanthanide trichlorides and 3 equiv. of  $\text{Cp}^{\text{f}}\text{Na}$  or  $\text{Cp}^{\text{t}}\text{K}$ , respectively.  $\text{Cp}_3^{\text{f}}\text{Nd}$ ,  $\text{Cp}_3^{\text{t}}\text{Nd}$ , and  $\text{Cp}_3^{\text{t}}\text{Ce}$  are monomeric with  $\eta^5$ -bonded cyclopentadienyl ligands. Due to the bulky substituents, all complexes are highly soluble in hydrocarbons. The X-ray structure determination of single crystals of  $\text{Cp}_3^{\text{t}}\text{Ce}$  revealed an approximate  $C_3$ -symmetry with Ce–C(centroid) distances of  $2.55^\circ$ .<sup>466</sup>  $(\text{C}_5\text{H}_3\text{Bu}^{\text{f}}_{2-1,3})_3\text{Yb}$  was also obtained in high yield. The catalytic reaction of 1-hexene with  $(\text{C}_5\text{H}_3\text{Bu}^{\text{f}}_{2-1,3})_3\text{Yb}\cdot\text{OEt}_2$  and  $\text{AlBu}^{\text{f}}_3$  also gave this product in high yield.<sup>467</sup> The cerium complexes  $(\text{C}_5\text{H}_3\text{Bu}^{\text{f}}_{2-1,3})_3\text{Ce}$  and  $\text{Cp}^{\text{f}}_3\text{Ce}$  were obtained by the reaction of  $\text{Ce}(\text{O}_3\text{SCF}_3)_3$  with the corresponding  $\text{Mg}(\text{R}_2\text{C}_5\text{H}_3)_2$  ( $\text{R} = \text{SiMe}_3, \text{Bu}^{\text{f}}$ ) in THF (Scheme 97). According to X-ray diffraction the  $(\text{C}_5\text{H}_3\text{Bu}^{\text{f}}_{2-1,3})_3\text{Ce}$  has a monomeric structure with three ordered  $\text{C}_5\text{H}_3\text{Bu}^{\text{f}}_{2-1,3}$  rings and  $C_{3h}$ -symmetry.<sup>468</sup>

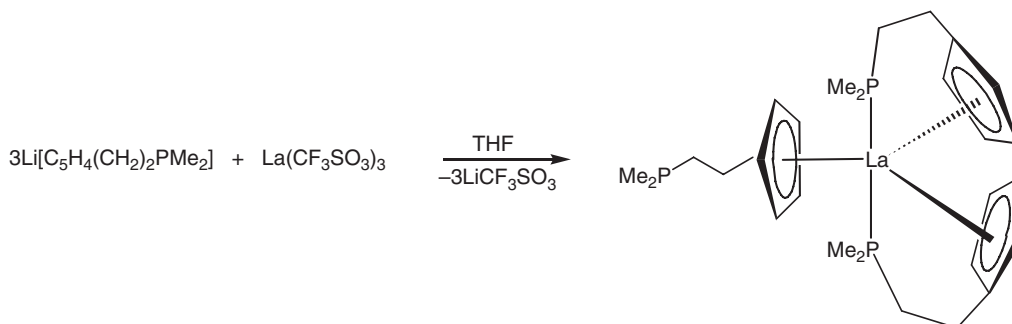
Homoleptic tris(cyclopentadienyl) complexes of the type  $\text{Ln}(\text{C}_5\text{Me}_4\text{H})_3$  ( $\text{Ln} = \text{La, Nd, Sm, Tb}$ ) were formed by the reaction of  $\text{LnCl}_3$  with  $\text{Na}(\text{C}_5\text{Me}_4\text{H})$  in THF. The complexes  $\text{Ln}(\text{C}_5\text{Me}_4\text{H})_3$  ( $\text{Ln} = \text{La, Sm}$ ) were characterized by X-ray crystallography. The compounds have typical monomeric structures.<sup>213,469</sup> The readily sublimable homoleptic complexes  $(\text{C}_5\text{H}_4\text{CH}_2\text{CH}_2\text{OMe})_3\text{Nd}$  and  $(\text{C}_5\text{H}_4\text{CH}_2\text{CH}_2\text{NMe}_2)_3\text{Nd}$  have been obtained by reacting  $\text{NdCl}_3$  with  $\text{K}(\text{C}_5\text{H}_4\text{CH}_2\text{CH}_2\text{R})$  ( $\text{R} = \text{OMe, NMe}_2$ ) in THF. These compounds are easily isolated solvent-free due to internal coordination of the donor groups. Under the same conditions,  $\text{K}(\text{C}_5\text{H}_4\text{Bu}^{\text{i}})$  gave the adduct



Scheme 96



Scheme 97



Scheme 98

$(\text{C}_5\text{H}_4\text{Bu}^t)_3\text{Nd}(\text{THF})$ , which could be desolvated by vacuum sublimation. A silylamide route was applied to synthesize the homoleptic neopentylcyclopentyl derivative  $(\text{C}_5\text{H}_4\text{CH}_2\text{Bu}^t)_3\text{Nd}$ . The alkyl-substituted complexes, particularly the isobutyl derivative, show a remarkable volatility. The first solvent-free, monomeric complex of the type  $\text{Cp}_2\text{LnCl}$ , namely  $(\text{C}_5\text{H}_4\text{CH}_2\text{CH}_2\text{NMe}_2)_2\text{NdCl}$ , was obtained from  $\text{NdCl}_3$  and 2 equiv. of  $\text{Na}(\text{C}_5\text{H}_4\text{CH}_2\text{CH}_2\text{NMe}_2)$ .<sup>470</sup> A tris(amino)-functionalized cyclopentadienylttrium complex has been synthesized in high yield by the reaction of  $\text{YCl}_3$  with 3 equiv. of  $\text{Na}[\text{C}_5\text{H}_4\text{CH}((\text{CH}_2)_2)_2\text{NMe}]$ .<sup>360</sup> Internal coordination of a donor functionality was also found in the mixed tris(cyclopentadienyl)complexes  $\text{Cp}_2\text{Ln}(\text{C}_5\text{H}_4\text{CH}_2\text{CH}_2\text{OMe})$  ( $\text{Ln} = \text{Y}, \text{La}, \text{Sm}, \text{Gd}, \text{Er}, \text{Yb}$ ).<sup>471</sup> The reaction of 3 equiv. of  $\text{Li}[\text{C}_5\text{H}_4(\text{CH}_2)_2\text{PMe}_2]$  with 1 equiv. of  $\text{La}(\text{CF}_3\text{SO}_3)_3$  led to the formation of the homoleptic compound  $\text{La}[\text{C}_5\text{H}_4(\text{CH}_2)_2\text{PMe}_2]_3$  (Scheme 98).<sup>446</sup> Oxidation of  $(\text{C}_5\text{H}_4\text{PPh}_2)_2\text{Sm}$  with  $\text{Ti}(\text{C}_5\text{H}_4\text{PPh}_2)_2$  in toluene yielded solvent-free  $(\text{C}_5\text{H}_4\text{PPh}_2)_3\text{Sm}$ .<sup>239</sup> The absorption spectra of the pseudo-trigonal bipyramidally coordinated complexes  $(\text{C}_5\text{H}_4\text{CH}_2\text{CH}_2\text{OMe})_3\text{Nd}$  and  $(\text{C}_5\text{H}_4\text{CH}_2\text{CH}_2\text{PMe}_2)_3\text{Nd}$  have been measured.<sup>472</sup>

#### 4.01.6.6 $\text{Cp}_3\text{LnL}$ and $\text{Cp}_3\text{LnL}_2$ Compounds

The absorption spectrum of  $\text{Cp}_3\text{Er}(\text{CNC}_6\text{H}_{11})$  has been measured at room temperature. From the spectra obtained a truncated CF splitting pattern was derived, and simulated by fitting the parameters of an empirical Hamiltonian. Making use of the calculated wave functions and eigenvalues the experimentally determined dependence of  $\mu_{\text{eff}}^2$  of powdered  $\text{Cp}_3\text{Er}(\text{CNC}_6\text{H}_{11})$  could be reproduced.<sup>473</sup> Absorption and MCD spectra have also been measured for the THF adduct  $\text{Cp}_3\text{Tm}(\text{THF})$ ,<sup>474</sup> the methyl-THF derivative  $\text{Cp}_3\text{Er}(\text{Me}^t\text{THF})$ ,<sup>475</sup> the samarium tris(cyclopentadienyl) complexes  $(\text{C}_5\text{H}_4\text{Bu}^t)_3\text{Sm}$ ,  $(\text{C}_5\text{H}_4\text{Bu}^t)_3\text{Sm}(\text{THF})$ , and  $\text{Cp}_3\text{Sm}(\text{CNC}_6\text{H}_{11})$ ,<sup>476</sup>  $\text{Cp}_3\text{Nd}(\text{methylacetate})$ ,<sup>477</sup> as well as  $(\text{C}_5\text{H}_4\text{Bu}^t)_3\text{Nd}$ ,  $(\text{C}_5\text{H}_4\text{Bu}^t)_3\text{Nd}(\text{THF})$ , and  $(\text{C}_5\text{H}_4\text{SiMe}_3)_3\text{Nd}$ .<sup>478</sup> The electronic structure of  $\text{Pr}^{3+}$  in pseudo-trigonal bipyramidal organic coordination has been published. By doping a  $\text{Cp}_3\text{La}(\text{NCCH}_3)_2$  matrix with different amounts of  $\text{Pr}^{3+}$ , relatively stable  $\text{Cp}_3\text{La}_{1-x}\text{Pr}_x(\text{NCCH}_3)_2$  ( $x = 0.6, 0.3, 0.1$ ) single crystals have been grown. On the basis of absorption, luminescence and, in part, magnetic CD spectroscopic measurements, the CF splitting pattern of  $\text{Cp}_3\text{La}_{1-x}\text{Pr}_x(\text{NCCH}_3)_2$  and also of  $(\text{CH}_3\text{OCH}_2\text{CH}_2\text{C}_5\text{H}_4)_3\text{Pr}$  could be derived.<sup>479</sup> The cerium and neodymium derivatives  $\text{Cp}_3\text{Ln}(\text{NCMe})_2$  ( $\text{Ln} = \text{Ce}, \text{Nd}$ ) were analyzed analogously. Large blue-purple crystals of the neodymium compound could be obtained by slow cooling of a solution of  $\text{Cp}_3\text{Nd}$  in acetonitrile.<sup>480</sup> The isotropic NMR shifts of various paramagnetic compounds of the type  $\text{Cp}_3\text{Ln}(\gamma\text{-picoline})$  ( $\text{Ln} = \text{Pr}, \text{Nd}, \text{Tm}, \text{Yb}$ ) were quantitatively interpreted in terms of dipolar and contact shifts.<sup>481,482</sup> Trialkylphosphate adducts of the type  $\text{Cp}_3\text{Ln}[\text{OP}(\text{OR})_3]$  ( $\text{Ln} = \text{Pr}, \text{R} = \text{Me}; \text{Ln} = \text{La}, \text{Pr}, \text{R} = \text{Et}$ ) have been prepared and their electronic structures investigated.<sup>483</sup>

A novel ring displacement reaction of  $(\text{C}_5\text{H}_4\text{Me})_3\text{Ln}(\text{THF})$  ( $\text{Ln} = \text{Sm}, \text{Tb}, \text{Ho}, \text{Yb}$ ) with cyclopentadiene has been reported to give the parent tris(cyclopentadienyls)  $\text{Cp}_3\text{Ln}(\text{THF})$  in high yields.<sup>484</sup> The crystal structures of

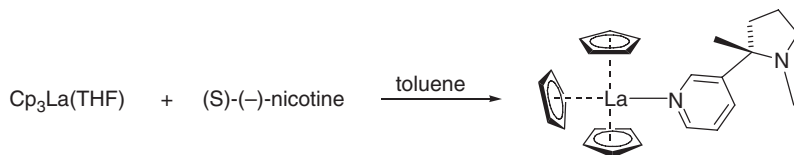
$\text{Cp}_3\text{Ce}(\text{THF})$ ,<sup>485</sup>  $\text{Cp}_3\text{Pr}(\text{THF})$ ,<sup>486</sup>  $\text{Cp}_3\text{Sm}(\text{THF})$ ,<sup>487,488</sup>  $(\text{C}_5\text{H}_4\text{Me})_3\text{Sm}(\text{THF})$ ,<sup>489</sup>  $\text{Cp}_3\text{Dy}(\text{THF})$ ,<sup>490</sup> and  $\text{Cp}_3\text{Er}(\text{THF})$ <sup>485</sup> have been determined. The  $^{151}\text{Eu}$  Mössbauer spectrum of  $\text{Cp}_3\text{Eu}(\text{THF})$  revealed a weak but definite covalent interaction between the 4f-orbitals of Eu(III) and the ligands.<sup>245</sup> Synthesis and characterization of the tris(cyclopentylcyclopentadienyl)lanthanide complexes  $(\text{C}_5\text{H}_4\text{C}_5\text{H}_9)_3\text{Nd}(\mu\text{-Br})\text{Li}(\text{THF})_3$  and  $(\text{C}_5\text{H}_4\text{C}_5\text{H}_9)_3\text{Sm}(\text{THF})$  have been reported.<sup>491</sup> The compound  $\text{Cp}_3\text{Dy}(\text{O}=\text{CPh}_2)$  is a distorted tetrahedral complex with the central Dy atom  $\eta^5$ -bonded to three cyclopentadienyl groups and  $\eta^1$ -bonded to one benzophenone molecule.<sup>492</sup> From a mixture solution of  $\text{Cp}_3\text{Nd}$  and  $(\text{C}_5\text{H}_4\text{Me})_3\text{Nd}$  in THF, crystals of a new form of  $\text{Cp}_3\text{Nd}(\text{THF})$  were obtained. The new structure differs markedly from the previously reported data for the same compound in cell dimension parameters, space group, and Z-value.<sup>493</sup> Numerous adducts of  $(\text{C}_5\text{H}_4\text{Bu}^t)_3\text{Ce}$  with six-membered N-heterocycles have been prepared and structurally characterized.<sup>494</sup> The synthesis of triphenylphosphine oxide complexes of the tris(cyclopentadienyl)lanthanides with  $\text{Ln} = \text{La}, \text{Nd}, \text{Sm}, \text{Yb}, \text{Gd}$  has been reported. By treatment of  $\text{Cp}_3\text{Ln}(\text{THF})$  with  $\text{OPR}_3$  ( $\text{R} = \text{Ph}, o\text{-tolyl}, \text{Bu}^n$ ) the formation of different products was observed. While with  $\text{Ln} = \text{La}, \text{Nd}, \text{Sm}, \text{Yb}$  the complexes  $\text{Cp}_3\text{Ln}(\text{OPPh}_3)$  were formed, the unsolvated  $\text{Cp}_3\text{Gd}$  was obtained with gadolinium, as well as a small amount of  $\text{Cp}_3\text{Gd}(\text{OPPh}_3)$ . An attempted synthesis of  $\text{Cp}_3\text{Yb}(\text{OPBu}^n)_3$  yielded  $[\text{Cp}_2\text{Yb}(\text{OPBu}^n)_3]_2(\mu\text{-O})$ . The crystal structure of  $\text{Cp}_3\text{Yb}(\text{OPPh}_3)$  was determined by single crystal X-ray structure determination. The complex contains formally 10-coordinated ytterbium with distorted pseudo-tetrahedral coordinating geometry.  $\text{Cp}_3\text{Nd}(\text{OPBu}^n)_3$  contains 10-coordinate neodymium with a trigonal arrangement of the oxygen atom and the Cp ring centroids.<sup>495</sup> A series of tris(cyclopentadienyl)lanthanide(III) sulfoxide adducts has been investigated using variable-temperature NMR and circular dichroism. This new class of adducts was prepared by the reaction of the THF adducts of the tris(cyclopentadienyl)lanthanides with the sulfoxides  $\text{MTSO}$  ( $\text{OS}(\text{Me})\text{C}_6\text{H}_4\text{Me}-4$ ) or  $\text{DPSO}$  ( $\text{OSPh}_2$ ) in toluene. As expected for the strongly oxophilic  $\text{Ln}^{3+}$  ions, the sulfoxide ligand is coordinated exclusively through its oxygen atom.  $\text{Ln}-\text{O}$  distances are shorter by about 10 pm than in the corresponding THF adducts.<sup>496</sup> Other  $\text{Cp}_3\text{Ln}$  adducts which have been investigated include those with various esters such as butylacetate ( $\text{Ln} = \text{La}, \text{Pr}, \text{Sm}, \text{Tb}, \text{Er}, \text{Tm}$ ),<sup>497</sup> tetramethylurea ( $\text{Ln} = \text{La}, \text{Ce}, \text{Nd}, \text{Sm}, \text{Eu}, \text{Yb}$ ),<sup>498</sup> cyclohexylisocyanide ( $\text{Ln} = \text{Eu}$ ),<sup>499</sup> and (S)-(–)-nicotine (Scheme 99).<sup>500</sup>

The neodymium-ylide complexes  $(\text{C}_5\text{H}_4\text{R})_3\text{Nd}[\text{CH}_2\text{P}(\text{Me})\text{Ph}_2]$  ( $\text{R} = \text{H}, \text{Bu}^t$ ) were synthesized by refluxing  $[(\text{C}_5\text{H}_4\text{R})_3\text{NdCl}\cdot\text{LiCl}]$  with 1 equiv. of  $\text{Li}[(\text{CH}_2)_2\text{PPh}_2]$  in THF. The compounds were characterized by single crystal X-ray diffraction. In  $\text{Cp}_3\text{Nd}[\text{CH}_2\text{P}(\text{Me})\text{Ph}_2]$  the Nd has distorted tetrahedral geometry formed by three Cp rings and by one carbon atom of  $\text{CH}_2\text{P}(\text{Me})\text{Ph}_2$  ligand. The mean  $\text{Nd}-\text{C}(\text{Cp})$  distances are 2.76, 2.78, and 2.79 Å, and the  $\text{Nd}-\text{C}(\text{CH}_2\text{P}(\text{Me})\text{Ph}_2)$  distance is 2.64(2) Å. The complex  $(\text{C}_5\text{H}_4\text{Bu}^t)_3\text{Nd}[\text{CH}_2\text{P}(\text{Me})\text{Ph}_2]$  has the same structure.<sup>501</sup> Room-temperature transmetalation of  $\text{Tl}(\text{C}_5\text{H}_4\text{PPh}_2)_3$  with neodymium metal gave the organolanthanide(III) compound  $(\text{C}_5\text{H}_4\text{PPh}_2)_3\text{Nd}(\text{THF})$ .<sup>239</sup>  $\text{Cp}_3\text{Ln}(\text{THF})$ -type complexes containing 1,2-phenylenedioxyborylcyclopentadienyl ligands have been reported for  $\text{Ln} = \text{La}, \text{Ce},$  and  $\text{Yb}$ .<sup>502</sup>

#### 4.01.6.7 $\text{Cp}_3\text{LnX}$ Compounds

The electronic structures of the cerium(IV) alkoxide complexes  $\text{Cp}_3\text{Ce}(\text{OR})$  have been investigated by He I and He II UV photoelectron spectroscopy combined with SCF  $X\alpha\text{-DVM}$  calculations.<sup>503</sup>

The crystal structure of the *ate*-complex tris(*t*-butylcyclopentadienyl)praseodymium- $\mu$ -bromo-tris(tetrahydrofuran)lithium has been determined. The complex  $(\text{C}_5\text{H}_4\text{Bu}^t)_3\text{Pr}(\mu\text{-Br})\text{Li}(\text{THF})_3$  has a distorted pseudo-tetrahedral geometry around the 10-coordinated Pr atom.<sup>504</sup> Synthesis and X-ray structure determination of the analogous lanthanum complex  $(\text{C}_5\text{H}_4\text{Bu}^t)_3\text{La}(\mu\text{-Cl})\text{Li}(\text{THF})_3$  had been reported earlier.<sup>505</sup> The interaction of  $\text{Li}[(\text{CH}_2)_2\text{PPh}_2]$  with  $(\text{C}_5\text{H}_4\text{Bu}^t)_2\text{Sm}(\mu\text{-Cl})_2\text{Li}$  in a molar ratio of 1:1 afforded the anionic lanthanide *ate*-complex  $[\text{PMe}_2\text{Ph}_2][(\text{C}_5\text{H}_4\text{Bu}^t)_3\text{SmCl}]$ .<sup>448</sup>



Scheme 99



### 4.01.6.8 Pentamethylcyclopentadienyl Compounds

#### 4.01.6.8.1 Cp\*MX compounds

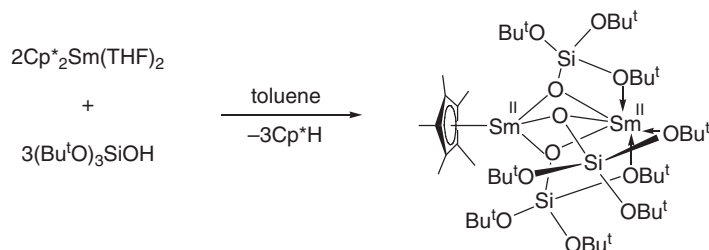
Novel chemistry has been developed around binuclear samarium(II) complexes containing one pentamethylcyclopentadienyl ligand and bulky siloxide ligands. The reaction of  $\text{Cp}^*\text{Sm}(\text{THF})_2$  with 1.5 equiv. of  $(\text{Bu}^t\text{O})_3\text{SiOH}$  in toluene gave the unsymmetrical binuclear Sm(II) complex  $\text{Cp}^*\text{Sm}[\mu\text{-OSi}(\text{OBu}^t)_3]_3\text{Sm}$  as green crystals in 93% yield (Scheme 100).<sup>506</sup>

Addition of 4 equiv. of HMPA to a toluene solution of  $\text{Cp}^*\text{Sm}[\mu\text{-OSi}(\text{OBu}^t)_3]_3\text{Sm}$  afforded purple  $\text{Cp}^*\text{Sm}[\text{OSi}(\text{OBu}^t)_3](\text{HMPA})_2$  as the only isolable product (Scheme 101).<sup>506</sup>

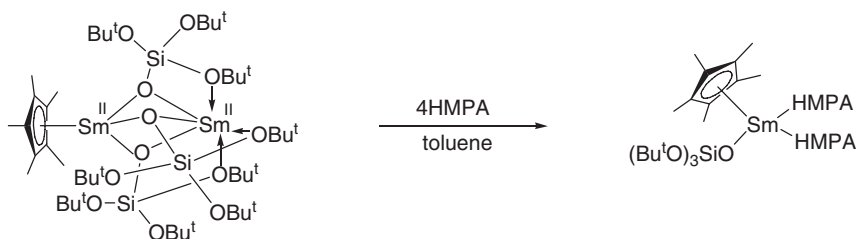
Other interesting reactions of  $\text{Cp}^*\text{Sm}[\mu\text{-OSi}(\text{OBu}^t)_3]_3\text{Sm}$  led to novel samarium(III) species. For example, treatment with 1 equiv. of azobenzene in toluene gave the corresponding binuclear Sm(III) azobenzene dianion complex as red-brown crystals in 64% yield (Scheme 102).<sup>506</sup>

A highly unusual trinuclear Sm(II)/Sm(III) mixed valence “inverse sandwich” was obtained when  $\text{Cp}^*\text{Sm}[\mu\text{-OSi}(\text{OBu}^t)_3]_3\text{Sm}$  was treated with either phenylacetylene or 4-Me-2,6- $\text{Bu}^t_2\text{C}_6\text{H}_2\text{OH}$  ( $=\text{ArOH}$ ) in toluene (Scheme 103). Most of the products were structurally characterized by X-ray analyses, and the reactions illustrated in Schemes 100 to 103 represent only part of the interesting chemistry discovered with this system.<sup>506</sup>

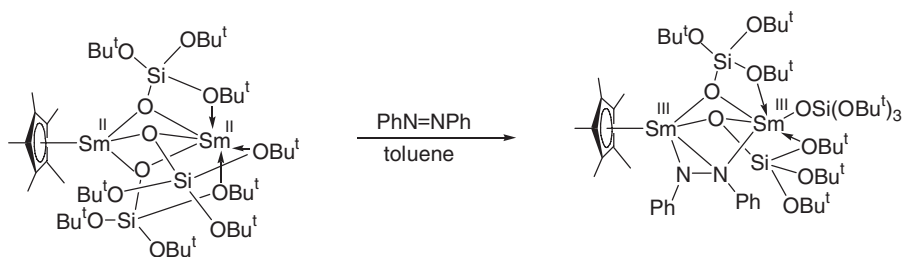
Red  $\text{Cp}^*\text{Yb}[\text{N}(\text{SiMe}_3)_2](\text{THF})_2$  can be generated from  $\text{KN}(\text{SiMe}_3)_2$  and  $[\text{Cp}^*\text{Yb}(\mu\text{-I})(\text{THF})_2]_2$  in THF (79% yield) and crystallizes from toluene with a distorted piano stool geometry.<sup>507</sup> Ytterbium metal reacts with  $\text{HgPh}(\text{C}_6\text{F}_5)$  and  $\text{HCp}^*$  in THF to give the seven-coordinate monomeric perfluoroorganoytterbium(II) complex  $\text{Cp}^*\text{Yb}(\text{C}_6\text{F}_5)(\text{THF})_3$



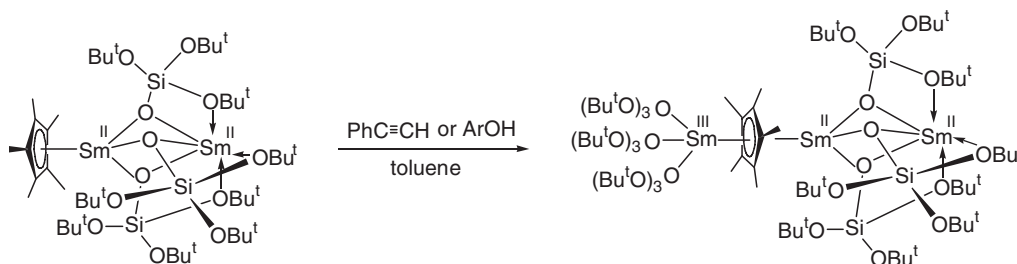
Scheme 100



Scheme 101



Scheme 102



Scheme 103

(red-orange crystals), which is presumed to be formed by protolysis of a transitory “YbPh(C<sub>6</sub>F<sub>5</sub>)” species with HCp\*.<sup>508</sup> The reaction of Cp\*<sub>2</sub>Yb(OEt)<sub>2</sub> with 1 equiv. of Li[Si(SiMe<sub>3</sub>)<sub>3</sub>](THF)<sub>3</sub> in toluene afforded Cp\*Yb[Si(SiMe<sub>3</sub>)<sub>3</sub>](THF)<sub>2</sub> in high yields (75%). The title compound was initially characterized by its <sup>171</sup>Yb NMR spectrum in toluene solution, which displayed a single resonance at  $\delta$  421 ppm with satellites corresponding to  $^1J(^{171}\text{Yb}-^{29}\text{Si}) = 829$  Hz. The molecular structure of Cp\*Yb[Si(SiMe<sub>3</sub>)<sub>3</sub>](THF)<sub>2</sub> was determined from a single crystal X-ray diffraction study. The ligand geometry around the Yb atom is distorted tetrahedral, with the angle between the bulky silyl substituent and the Cp\* centroid, Cp\*-Yb-Si, expanded to 128° and a corresponding compression of the angle O(THF1)-Yb-O(THF2) to 89°. The Yb-Si distance, 3.032(3) Å, is somewhat shorter than that reported for the other previously recorded Yb<sup>II</sup>-Si compounds.<sup>509</sup>

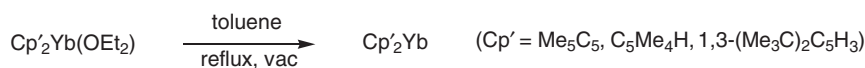
#### 4.01.6.8.2 Cp\*<sub>2</sub>M compounds

The molecular conformations of the bent-sandwich metallocenes Cp<sub>2</sub>M including Cp\*<sub>2</sub>Ln (Ln = Sm, Eu, Yb) have been studied.<sup>510,511</sup> The molecular mechanics calculations were carried out with the MM3 program, using standard optimization procedures. The calculations have shown that the bending is mainly a result of non-bonding interactions, especially attraction between the Cp ligands. Crystal packing forces are not a major factor in determining the degree of bending. When the interplanar distances between the planes of Cp rings are short (the metals with small radius), the ligands have parallel orientation. When the metal atom in Cp<sub>2</sub>M has a large radius, the interplanar distances are longer and the ligand planes do not stay parallel. The influence of bulky substituents on the bending angle was also shown.<sup>511</sup> It was predicted (and later verified experimentally) that the bis(pentaisopropylcyclopentadienyl) complexes of Sm, Eu, and Yb should be linear.<sup>510</sup> In another theoretical study, relativistic, gradient-corrected DFT was used to establish the equilibrium geometries of Cp\*<sub>2</sub>Yb. The molecule is significantly bent with a Cp\*-Yb-Cp\* angle of 160°. The bent structure is 5 kJ mol<sup>-1</sup> more stable than the linear structure. The agreement between the calculated structure of Cp\*<sub>2</sub>Yb and that detected experimentally in the gas phase is excellent. The origins of the deviation from linearity have been discussed in detail and placed in the context of previous, contrasting explanations for bending in metallocenes. Evidence was found for both valence and core metal electron participation in the bending process. The metal-ligand bonding Cp\*<sub>2</sub>Yb is predominantly ionic, with small amounts of *d*- and (to a lesser extent) *f*-orbital covalency.<sup>512</sup> The results of DFT calculations have been used to define trends in the interactions of H<sub>2</sub>, N<sub>2</sub>, C<sub>2</sub>H<sub>4</sub>, and C<sub>2</sub>Me<sub>2</sub> with the divalent lanthanide metallocenes Cp<sub>2</sub>Ln and Cp\*<sub>2</sub>Ln (Ln = Sm, Eu, Yb).<sup>513</sup>

A series of ytterbium(II) cyclopentadienyl derivatives has been studied by high resolution solid-state <sup>171</sup>Yb CP MAS (cross-polarization magic angle spinning) NMR spectroscopy. The principal components of the chemical shift tensors have been determined from spinning sideband analysis. Examining the <sup>171</sup>Yb NMR data reveals that: (i) with the exception of Cp\*<sub>2</sub>Yb(py)<sub>2</sub>, the isotropic chemical shifts are in general in good agreement with the solution data, thereby providing strong support for the retention of very similar structures in solution, (ii) the addition of the *O*-centered Lewis base to Cp\*<sub>2</sub>Yb (which exhibits two magnetically inequivalent Yb atoms within the unit cell) results in a high frequency shift of some 40–60 ppm, and (iii) the difference between solid- and solution-state <sup>171</sup>Yb NMR chemical shifts for Cp\*<sub>2</sub>Yb(py)<sub>2</sub> (some 160 ppm) is too large to be explained by magnetic susceptibility changes alone. This high frequency shift is presumably due to a solution equilibrium between the bis- and tris-pyridine adducts. Support for this conclusion also came from the large temperature dependence of the <sup>171</sup>Yb resonance displayed by pyridine solutions of Cp\*<sub>2</sub>Yb.<sup>514–516</sup>

The base-free ytterbocenes Cp\*<sub>2</sub>Yb, (C<sub>5</sub>Me<sub>4</sub>H)<sub>2</sub>Yb, and (C<sub>5</sub>H<sub>3</sub>Bu<sup>t</sup>-1,3)<sub>2</sub>Yb have been prepared from their diethyl ether adducts by the toluene reflux method, where a toluene solution must be refluxing vigorously before the system is exposed to dynamic vacuum (Scheme 104).<sup>517</sup>





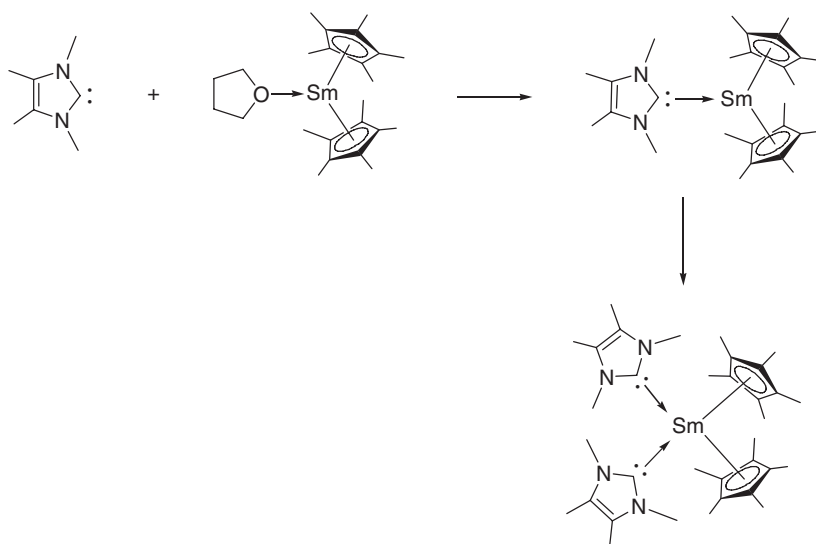
Scheme 104

In order to get the ether-free ytterbocene derived from  $(\text{C}_5\text{Me}_4\text{H})_2\text{Yb}(\text{OEt}_2)$ , the complex was dissolved in toluene and crystallized slowly at  $-40^\circ\text{C}$ . The structures of these base-free molecules have been determined by X-ray crystallography. The complexes exhibit bent structures in the solid state with centroid–metal–centroid angles ranging from  $132^\circ$  to  $147^\circ$ .<sup>517</sup> Coordination of carbon monoxide and isocyanides to  $\text{Cp}^*_2\text{Yb}$  and related divalent ytterbocenes has been studied in detail. In the course of these investigations, the crystal structures of  $\text{Cp}^*_2\text{Yb}(\text{2,6-Me}_2\text{C}_6\text{H}_3\text{NC})_2$  have been determined.<sup>222</sup> Interactions of  $\text{Cp}^*_2\text{Yb}$  with trialkylphosphines ( $\text{Me}_3\text{P}$ ,  $\text{Et}_3\text{P}$ , and  $1,2\text{-(Me}_2\text{P)}_2\text{C}_6\text{H}_4$ ) and  $\text{R}_3\text{PX}$  complexes ( $\text{Me}_3\text{PO}$ ,  $\text{Et}_3\text{PNH}$ ,  $\text{Me}_2\text{PhPCHSiMe}_3$ ,  $\text{Me}_2\text{PhPCH}_2$ ) in solution have been investigated. The interactions and the obtained adducts,  $\text{Cp}^*_2\text{Yb}(\text{PMe}_3)_2$ ,  $\text{Cp}^*_2\text{Yb}(\text{PMe}_3)$ ,  $\text{Cp}^*_2\text{Yb}(\text{PET}_3)$ ,  $\text{Cp}^*_2\text{Yb}(\text{Me}_2\text{PCH}_2\text{PMe}_2)$ ,  $\text{Cp}^*_2\text{Yb}(1,2\text{-(Me}_2\text{P)}_2\text{C}_6\text{H}_4)$ ,  $\text{Cp}^*_2\text{Yb}(\text{OPMe}_3)$ ,  $\text{Cp}^*_2\text{Yb}(\text{HNPEt}_3)$ ,  $\text{Cp}^*_2\text{Yb}(\text{OPMe}_3)_2$ ,  $\text{Cp}^*_2\text{Yb}(\text{HNPEt}_3)_2$ ,  $\text{Cp}^*_2\text{Yb}(\text{Me}_2\text{PhPCHSiMe}_3)$ , and  $\text{Cp}^*_2\text{Yb}(\text{Me}_2\text{PhPCH}_2)$ , have been investigated by  $^1\text{H}$ ,  $^{13}\text{C}$ ,  $^{31}\text{P}$ ,  $^{171}\text{Yb}$ , and variable-temperature NMR spectroscopy. It was found that  $^1J_{\text{YbP}}$  is significantly reduced for 1 : 2 phosphine adducts, relative to the 1 : 1 adducts. The barrier to intermolecular exchange for phosphine oxide and imine adducts is much higher and the  $^1J_{\text{YbP}}$  values for 1 : 1 adducts are one order of magnitude less than the analogous one-bond values for the phosphine derivatives. The ylide adduct  $\text{Cp}^*_2\text{Yb}(\text{Me}_2\text{PhPCHSiMe}_3)$  was also characterized by X-ray crystallography. In the structure the Yb–C distance ( $2.69(2) \text{ \AA}$ ) and other parameters indicate a direct Yb–C interaction, supplemented by a secondary  $\gamma\text{-CH}_3$  interaction.<sup>518</sup>

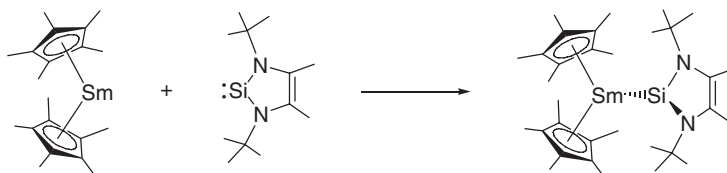
Organolanthanide carbene complexes have been elusive for a long time. With the use of Arduengo-type heterocyclic carbenes this interesting class of compounds has become readily available. The (imidazol-2-ylidene) samarium complexes shown in Scheme 105 were obtained from 1,3,4,5-tetramethylimidazol-2-ylidene and  $\text{Cp}^*_2\text{Sm}(\text{THF})$  in different molar ratios.<sup>519</sup>

An  $\text{Ln}(\text{II})$  silylene complex,  $\text{Cp}^*_2\text{Sm}[\text{Si}(\text{Bu}^t\text{NCH})_2]$ , has been synthesized as purple crystals in 90% yield by the reaction of the free silylene with  $\text{Cp}^*_2\text{Sm}$  in toluene (Scheme 106). The silylene ligand is located asymmetrically in the metallocene wedge with one *t*-butyl group ( $\text{Sm}–\text{C}(\text{Me}) = 3.396(4) \text{ \AA}$ ) much closer to the metal than the other ( $\text{Sm}–\text{C}(\text{Me}) = 4.741(4) \text{ \AA}$ ). The  $\text{Sm}(\text{II})$ –Si distance is  $3.1910(1) \text{ \AA}$ .<sup>520</sup>

In the presence of 2 equiv. HMPA, the reaction of  $[(\text{ArO})\text{Sm}(\mu\text{-I})(\text{THF})_3]_2$  with 2 equiv. of  $\text{KCp}^*$  in THF yielded  $\text{Cp}^*_2\text{SmOAr}(\text{HMPA})_2$  as dark brown crystals. When  $[(\text{ArO})\text{Sm}(\mu\text{-I})(\text{THF})_3]_2$  was mixed with 2 equiv. of  $\text{KCp}^*$  in THF, polymeric  $[\text{ArOSm}(\mu\text{-Cp}^*)\text{K}(\mu\text{-Cp}^*)(\text{THF})_2]_\infty$  was obtained. The  $\text{KCp}^*$  unit acted as a neutral ligand and could be easily removed by addition of HMPA to give  $\text{Cp}^*_2\text{SmOAr}(\text{HMPA})_2$ . An X-ray analysis of



Scheme 105

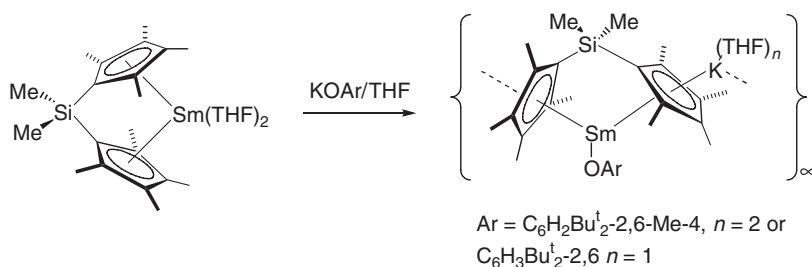


Scheme 106

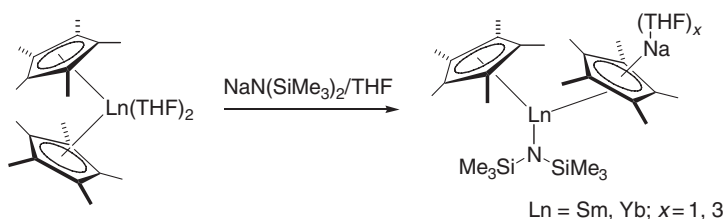
$\text{Cp}^*\text{SmOAr}(\text{HMPA})_2$  revealed that the central  $\text{Sm}(\text{II})$  ion is bonded to one  $\text{Cp}^*$ , one  $\text{ArO}$ , and two  $\text{HMPA}$  ligands in a distorted tetrahedral form.<sup>521,522</sup> Reactions of  $\text{Cp}^*_2\text{Sm}(\text{THF})_2$  with 1 equiv. of  $\text{ArOH}$  ( $\text{Ar} = \text{C}_6\text{H}_2\text{Bu}^t_{2-2,6}\text{-R-4}$ ,  $\text{R} = \text{H}$ ,  $\text{Me}$ ,  $\text{Bu}^t$ ) or  $\text{Sm}(\text{OAr})_2(\text{THF})_3$  in toluene gave quantitatively the corresponding heteroleptic dimeric  $\text{Sm}(\text{II})$  complexes  $[\text{Cp}^*\text{Sm}(\mu\text{-OAr})]_2$ . The crystal structures of the new complexes were investigated by X-ray diffraction.<sup>523</sup> Besides alcoholysis, the metathesis reaction of  $\text{Sm}(\text{OAr})_2$  with  $\text{KCp}^*$  also afforded the heteroleptic samarium(II) aryloxide/pentamethylcyclopentadienyl complexes. In this reaction the product was coordinated with a neutral unit “ $(\mu, \eta^5\text{-Cp}^*)\text{K}(\text{THF})_2$ ”. The intermolecular  $\text{K} \cdots \text{Cp}^*$  interactions constituted a polymeric structure in which each  $\text{Cp}^*$  was bonded in a  $\mu, \eta^5$ -fashion to an  $\text{Sm}$  atom on one side and to a  $\text{K}^+$  ion on the other side. The complex has a mirror plane, which is orientated along the polymer chain.<sup>523</sup> The reaction of  $\text{Cp}^*_2\text{Yb}(\text{THF})_2$  with 1 equiv. of  $\text{KN}(\text{SiMe}_3)_2$  yielded the corresponding  $\text{Yb}(\text{II})$  complex  $[\text{Cp}^*\text{Yb}\{\text{N}(\text{SiMe}_3)_2\}(\mu\text{-Cp}^*)\text{K}(\text{THF})_2]_\infty$ . The reaction of the dimethylsilyl-bridged bis(tetramethylcyclopentadienyl) samarium(II) complex  $\text{Me}_2\text{Si}(\text{C}_5\text{Me}_4)_2\text{Sm}(\text{THF})_2$  with 1 equiv. of  $\text{KOAr}$  in  $\text{THF}$  gave  $[\text{Me}_2\text{Si}(\text{C}_5\text{Me}_4)(\mu\text{-C}_5\text{Me}_4)\text{K}(\text{THF})_n\text{Sm}(\text{OAr})]_\infty$ , which can be viewed as a  $\text{C}_5\text{Me}_4/\text{OAr}$ -ligated  $\text{Sm}(\text{II})$  species coordinated by the dimethylsilyl-bridged, neutral “ $\text{C}_5\text{Me}_4\text{K}$ ” ligand (Scheme 107).<sup>524,525</sup>

Using  $\text{NaN}(\text{SiMe}_3)_2$  instead of  $\text{KN}(\text{SiMe}_3)_2$  in the reaction with  $\text{Cp}^*_2\text{Ln}(\text{THF})_2$  afforded the “ $\text{Cp}^*\text{Na}(\text{THF})_3$ ”-coordinated  $\text{Sm}(\text{II})$  and  $\text{Yb}(\text{II})$  complexes. In contrast to the “ $\text{Cp}^*\text{K}$ ”-coordinated complexes, which adopt a polymeric structure through intermolecular  $\text{K} \cdots \text{Cp}^*$  interactions, the “ $\text{Cp}^*\text{Na}$ ”-coordinated complexes are monomers due to the coordination of  $\text{THF}$  to the sodium ion (Scheme 108).<sup>524,525</sup>

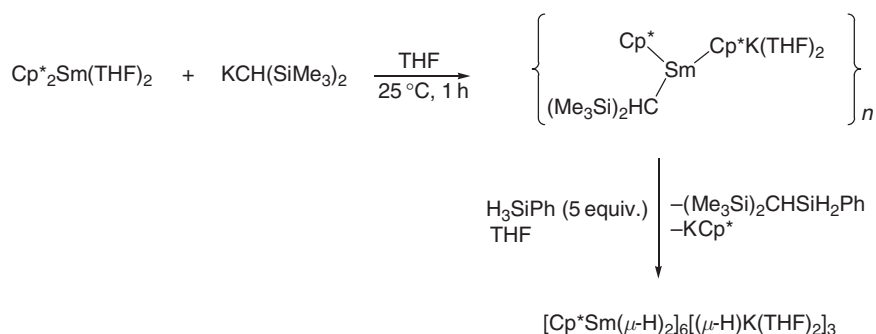
The synthesis and polymerization reactions of a series of  $\text{Cp}^*/\text{ER}$ -ligated lanthanide(II) complexes ( $\text{ER} = \text{OAr}$ ,  $\text{SAr}$ ,  $\text{NR}^1\text{R}^2$ ) have been described. Reactions of  $\text{Cp}^*_2\text{Sm}(\text{THF})_2$  with 1 equiv. of  $\text{K}(\text{ER})$  in  $\text{THF}$  gave the  $\text{Sm}(\text{II})$  complexes  $[\text{Cp}^*\text{Sm}(\text{THF})_m(\text{ER})(\mu\text{-Cp}^*)\text{K}(\text{THF})_n]_\infty$  ( $m = 0$  or  $1$ ;  $n = 1$  or  $2$ ;  $\text{ER} = \text{OC}_6\text{H}_2\text{Bu}^t_{2-2,6}\text{-Me-4}$ ,  $\text{OC}_6\text{H}_3\text{Pr}^i_{2-2,6}$ ,  $\text{SC}_6\text{H}_2\text{Pr}^i_{3-2,4,6}$ ,  $\text{NHC}_6\text{H}_2\text{Bu}^t_{2-2,4,6}$ , or  $\text{N}(\text{SiMe}_3)_2$ ) in high yields. This type of heteroleptic samarium(II) complexes act as a unique catalytic system, which can not only polymerize styrene and ethylene, but also co-polymerize these monomers into styrene–ethylene block co-polymers.<sup>524,525</sup> These complexes are stable in toluene solution and do not undergo ligand redistribution. Addition of 4 equiv. of  $\text{HMPA}$  to a  $\text{THF}$  solution afforded



Scheme 107



Scheme 108



Scheme 109

the corresponding HMPA-coordinated monomeric complexes. In the complex  $[\text{Cp}^*\text{Sm}(\mu\text{-OC}_6\text{H}_2\text{Bu}^t\text{-2,4,6})_2]$  the two Sm atoms are bridged by two  $\text{OC}_6\text{H}_2\text{Bu}^t\text{-2,4,6}$ -ligands, and the  $\text{Sm}(\mu\text{-O})_2\text{Sm}$  unit is exactly planar.<sup>523</sup> A similar reaction sequence (Scheme 109) was successfully employed to synthesize the first dihydrido lanthanide(III) complex. The orange-red crystalline product was isolated in 42% yield and structurally characterized by X-ray diffraction.<sup>526</sup> Related  $\text{Cp}^*\text{Ln}^{\text{II}}$  alkyl and silyl complexes have been prepared in a similar manner.<sup>527</sup>

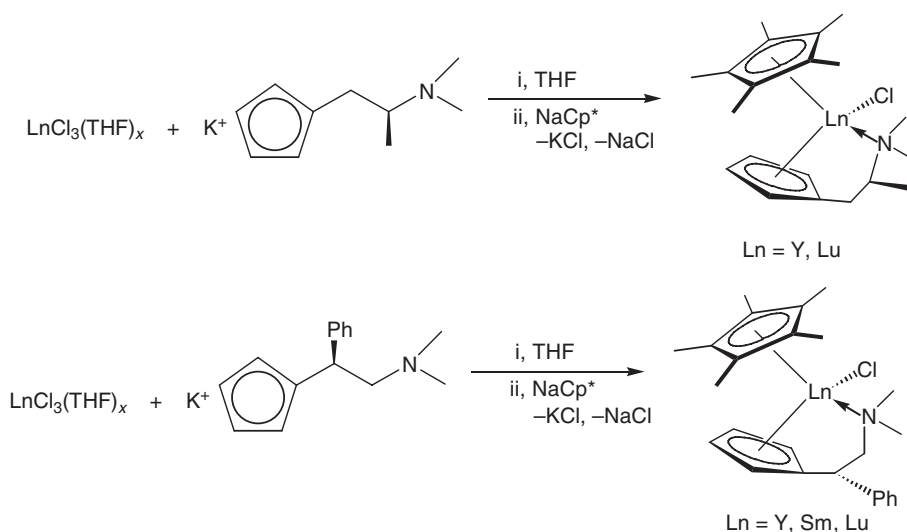
#### 4.01.6.8.3 Mono(pentamethylcyclopentadienyl)lanthanide(III) compounds

The synthesis of the mono(pentamethylcyclopentadienyl) derivative  $\text{Cp}^*\text{NdI}_2(\text{THF})_3$  has been accomplished by the reaction of  $\text{NdI}_3(\text{THF})_x$  with 1 equiv. of  $\text{KCp}^*$  in THF.  $\text{NdI}_3(\text{THF})_x$  was generated from neodymium metal with 1.5 equiv. of elemental iodine in *i*-propanol, followed by crystallization from THF.<sup>528</sup> Treatment of  $\text{Cp}^*\text{NdI}_2(\text{THF})_3$  with an excess of pyridine in toluene leads to displacement of the THF ligands and formation of the tris(pyridine) adduct  $\text{Cp}^*\text{NdI}_2(\text{py})_3$ . According to a single crystal X-ray diffraction study,  $\text{Cp}^*\text{NdI}_2(\text{py})_3$  adopts a pseudo-octahedral geometry in the solid state, with the cyclopentadienyl ligand occupying one coordination site, the three pyridine ligands being arranged in a *mer*-conformation, and the iodide ligands *trans* to one another. The Nd–I distance is 3.1603 Å, while the Nd–N bond lengths to the pyridine ligands are 2.631 and 2.678 Å.<sup>528</sup> Hydrated neodymium nitrates can be readily transformed to anhydrous ether solvates which react with cyclopentadienyl reagents to give organometallic nitrate complexes (e.g.,  $\text{Cp}^*\text{Nd}(\text{NO}_3)_3(\text{THF})\text{Na}(\text{THF})_x$  derivatives).<sup>529</sup> Controlled hydrolysis of the divalent organosamarium complex  $\text{Cp}^*_2\text{Sm}(\text{THF})_2$  formed the hexametallal organosamarium oxide hydroxide cluster  $[\text{Cp}^*\text{Sm}]_6\text{O}_9\text{H}_6$  as brown crystals in 40% yield. The compound has a solid-state structure consisting of a distorted octahedral array of six  $\text{Cp}^*\text{Sm}^{2+}$  units connected by eight triply bridging oxygens and a central oxygen.<sup>530</sup> Dimeric mono(pentamethyl)cyclopentadienyl yttrium alkoxides such as  $[\text{Cp}^*\text{Y}(\mu\text{-OBu}^t)(\text{OBu}^t)]_2$  have been synthesized by reacting the alkoxide cluster precursor  $\text{Y}_3(\text{OBu}^t)_7\text{Cl}_2(\text{THF})_2$  with  $\text{KCp}^*$  in toluene, thereby disrupting the trimetallic structure of the starting material.<sup>531</sup> The reaction of  $\text{SmCl}_3$  with 3 equiv. of  $\text{KO-2,6-Bu}^t_2\text{C}_6\text{H}_3$  in THF leads to the tris(aryloxide) complex  $\text{Sm}(\text{O-2,6-Bu}^t_2\text{C}_6\text{H}_3)_3(\text{THF})$  which undergoes clean metathesis reaction with 1 equiv. of  $\text{LiCp}^*$  to form the mono(pentamethylcyclopentadienyl) aryloxide derivative  $\text{Cp}^*\text{Sm}(\text{O-2,6-Bu}^t_2\text{C}_6\text{H}_3)_2(\text{THF})$ . Single crystal X-ray diffraction studies showed that the complex features a three-legged piano stool geometry with Sm–O distances to the aryloxide ligands of 2.133 Å and 2.188 Å and an Sm–O(THF) distance of 2.435 Å.<sup>532</sup> In contrast, the analogous reaction of  $\text{LiCp}^*$  with the 2,6-di-isopropylphenoxide complex  $\text{Sm}(\text{O-2,6-Pr}^i_2\text{C}_6\text{H}_3)_3(\text{THF})_2$  gave the lithium containing *ate*-complex  $[\text{Cp}^*\text{Sm}(\text{O-2,6-Pr}^i_2\text{C}_6\text{H}_3)(\mu\text{-O-2,6-Pr}^i_2\text{C}_6\text{H}_3)_2\text{Li}(\text{THF})]$ . The complex possesses a similar three-legged piano stool geometry like the  $\text{O-2,6-Bu}^t_2\text{C}_6\text{H}_3$  analog, with two of the aryloxide oxygen atoms coordinated to a lithium metal center. A THF ligand completes the coordination sphere of the lithium. The Sm–O bond lengths to the lithium-coordinated aryloxide oxygens (2.250 Å and 2.247 Å) are somewhat longer than the distance to the terminal aryloxide (Sm–O = 2.144 Å), presumably due to a loss of electron density at the oxygen upon forming the Sm–O–Li bridges.<sup>532</sup> When a green toluene solution of  $[\text{Cp}^*\text{Sm}(\mu\text{-OC}_6\text{H}_2\text{Bu}^t\text{-2,4,6})_2]$  was exposed to trace amounts of air, the trivalent samarium complex  $[\text{Cp}^*_2\text{Sm}(\mu\text{-OC}_6\text{H}_2\text{Bu}^t\text{-2,4,6})]$  was obtained in the form of orange-red crystals in 35% yield.<sup>523</sup> Other structurally characterized mono- $\text{Cp}^*$  lanthanide complexes containing group 16 co-ligands include  $[\text{Cp}^*\text{Eu}(\text{OBu}^t)(\mu\text{-OBu}^t)]_3$ <sup>533</sup> and  $[\mu\text{-S}_2\text{P}(\text{OMe})_2]_2[\text{Cp}^*\text{Sm}\{\text{S}_2\text{P}(\text{OMe})_2\}]_2$ .<sup>534</sup>

Single crystal neutron diffraction studies on  $\text{Cp}^*\text{Y}(\text{OAr})[\text{CH}(\text{SiMe}_3)_2]$  ( $\text{Ar} = \text{O-2,6-Bu}^t_2\text{C}_6\text{H}_3$ ) and  $\text{Cp}^*\text{La}[\text{CH}(\text{SiMe}_3)_2]_2$  have been performed in order to get conclusive evidence for the nature of the close intramolecular contacts between  $\text{CH}(\text{SiMe}_3)_2$  and the lanthanide center in these complexes. These intramolecular

contacts are often described in the literature and can be caused by  $\alpha_{\text{CH}}$ ,  $\alpha_{\text{CSi}}$ ,  $\beta_{\text{SiC}}$ , and  $\gamma_{\text{CH}}$  interactions. The molecular structures of both compounds as determined by neutron diffraction show distorted  $\text{CH}(\text{SiMe}_3)_2$  groups with the metal–silicon and metal–oxygen distances well within the sum of their van der Waals radii. The yttrium complex shows interaction with the  $\text{CH}(\text{SiMe}_3)_2$  group ( $\text{Y} \cdots \text{Si}(1) = 3.281 \text{ \AA}$ ,  $\text{Y} \cdots \text{C}(2) = 2.972 \text{ \AA}$ ). The coordinative unsaturation around the La in the lanthanum complex is relieved by interaction with two Si–Me bonds, one from each  $\text{CH}(\text{SiMe}_3)_2$  group ( $\text{La} \cdots \text{Si}(2) = 3.346 \text{ \AA}$ ,  $\text{La} \cdots \text{C}(17) = 2.964 \text{ \AA}$ ,  $\text{La} \cdots \text{Si}(4) = 3.416 \text{ \AA}$ ,  $\text{La} \cdots \text{C}(22) = 2.973 \text{ \AA}$ ). None of the short  $\text{C-H} \cdots \text{M}$  intramolecular contacts shows a significant elongation of the C–H bonds. In contrast, the elongation of the agostic  $\text{Si}_\beta\text{-C}_\gamma$  bonds is significant ( $0.037 \text{ \AA}$  in average). The metal center interacts mainly with the  $\beta$ -Si–C bond, but not with the  $\gamma$ -C–H bonds. The results were supported by theoretical calculations.<sup>535</sup> Using  $\text{Cp}^*\text{Yb}[\text{N}(\text{PPh}_2)_2]_2$ , a mono- $\text{Cp}^*$  lanthanide complex with two diphosphinoamide ligands has been synthesized and structurally characterized.<sup>274</sup> An unprecedented C–H activation of a 2,2'-bipyridine ligand has been found when  $\text{Cp}^*\text{Lu}(\text{bipy})(\text{CH}_2\text{SiMe}_3)(\text{NHAr})$  ( $\text{Ar} = 2,6\text{-Pr}_2\text{C}_6\text{H}_3$ ) was reacted with carbon monoxide.<sup>536</sup> The chloride complex  $[(\text{salen}')\text{Y}(\mu\text{-Cl})(\text{THF})]_2$  ( $\text{salen}' = N,N'$ -bis(3,5-di-*t*-butylsalicylidene)ethylenediamine) is a useful precursor to organometallic derivatives of this ancillary ligand. The mono(pentamethylcyclopentadienyl) derivative could be prepared by a reaction with  $\text{KCp}^*$ . The yellow solid was isolated in 75% yield, and its structure was verified by an X-ray analysis.<sup>537</sup> The mono(pentamethylcyclopentadienyl)yttrium bis(amide) complex  $\text{Cp}^*\text{Y}[\text{N}(\text{SiHMe}_2)_2]_2$  is accessible as an unsolvated, monomeric species by reacting  $\text{Y}[\text{N}(\text{SiHMe}_2)_2]_3$  with  $\text{Cp}^*\text{H}$  (40% yield).<sup>538</sup> The reaction of the mono(pentamethylcyclopentadienyl) derivative  $\text{Cp}^*\text{NdI}_2(\text{py})_3$  with  $\text{KC}_5\text{H}_4\text{SiMe}_3$  in THF led to the mixed bis(cyclopentadienyl) complex  $\text{Cp}^*(\text{C}_5\text{H}_4\text{SiMe}_3)\text{NdI}(\text{py})$ . The monomeric  $\text{Cp}^*(\text{C}_5\text{H}_4\text{SiMe}_3)\text{NdI}(\text{py})$  features a typical bent metallocene  $\text{Cp}_2\text{MX}_2$  geometry with Nd–I and Nd–N distances of  $3.066 \text{ \AA}$  and  $2.555 \text{ \AA}$ , respectively, which is in both cases shorter than in  $\text{Cp}^*\text{NdI}_2(\text{py})_3$ .<sup>528</sup>  $\text{ScCl}_3$  and the lanthanide trichlorides  $\text{LnCl}_3$  ( $\text{Ln} = \text{Nd}, \text{Sm}, \text{Ho}, \text{Lu}$ ) were allowed to react stepwise first with (dimethylaminoethyl)cyclopentadienyl potassium ( $\text{KCp}^{\text{Do}}$ ) and then with tetramethylcyclopentadienyl sodium ( $\text{NaCp}_5\text{Me}_4\text{H}$ ) or pentamethylcyclopentadienyl sodium ( $\text{NaCp}^*$ ), respectively, to yield the mixed sandwich complexes  $\text{Cp}^{\text{Do}}(\text{C}_5\text{Me}_4\text{H})\text{ScCl}$ ,  $\text{Cp}^{\text{Do}}(\text{C}_5\text{Me}_4\text{H})\text{LnCl}$  ( $\text{Ln} = \text{Nd}, \text{Sm}, \text{Ho}, \text{Lu}$ ), and  $\text{Cp}^{\text{Do}}\text{Cp}^*\text{LuCl}$ . Treatment of these precursors with methyllithium in  $\text{Et}_2\text{O}$  afforded the chiral alkyl derivatives  $\text{Cp}^{\text{Do}}(\text{C}_5\text{Me}_4\text{H})\text{ScMe}$  and  $\text{Cp}^{\text{Do}}(\text{C}_5\text{Me}_4\text{H})\text{LnMe}$  ( $\text{Ln} = \text{Nd}, \text{Sm}, \text{Ho}, \text{Lu}$ ), respectively. Reaction of  $\text{Cp}^{\text{Do}}\text{Cp}^*\text{LuCl}$  with  $\text{LiCH}_2\text{SiMe}_3$  yielded the corresponding alkyl derivative  $\text{Cp}^{\text{Do}}\text{Cp}^*\text{LuCH}_2\text{SiMe}_3$ .<sup>539</sup> Novel chiral non-racemic metallocenes of yttrium, samarium, and lutetium with two different cyclopentadienyl ligands were synthesized analogously (Scheme 110).<sup>361</sup>

Single crystal X-ray structures of  $\text{Cp}^{\text{Do}}\text{Cp}^*\text{HScCl}$  and  $\text{Cp}^{\text{Do}}\text{Cp}^*\text{HScMe}$  were published. Both molecules showed a similar structure. The Cl complex is one of the very few examples of a di(cyclopentadienyl)scandium chloride without bridging chlorine atoms. This terminal Sc–Cl distance is  $2.4574(12) \text{ \AA}$  shorter than in a scandium chloride complex with bridging chlorine atoms like  $[\text{Cp}''_2\text{Sc}(\mu\text{-Cl})]_2$  with  $2.58 \text{ \AA}$ . The scandium metal atom is surrounded by four ligands in a distorted tetrahedral geometry. The coordinated dimethylamino group decreases the Lewis acidity



Scheme 110

of the scandium atom resulting in a weakening of the bond strength between scandium and the carbon atom of the methyl group.<sup>539</sup> Calculations via the quasi-relativistic self-consistent modified extended Hückel MO method (QR-SCMEH MO) were conducted on the model cluster  $[\text{Cp}^*\text{Sm}]_4^{8+}$  and the known cluster compound  $[\text{Cp}^*\text{Sm}]_4(\text{N}_2\text{H}_2)_2(\text{N}_2\text{H}_3)_4(\text{NH}_3)_2$ .<sup>540</sup>

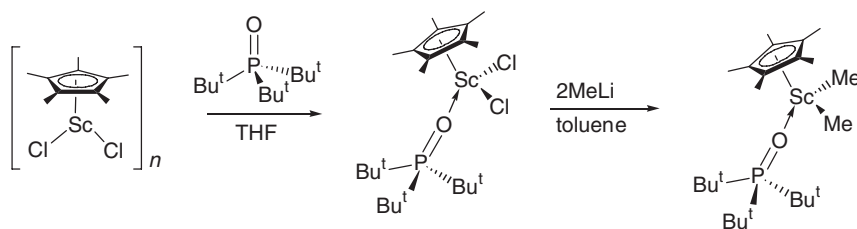
The mono(pentamethylcyclopentadienyl)lutetium bis(alkyl) complex  $\text{Cp}^*\text{Lu}(\text{CH}_2\text{SiMe}_3)_2(\text{THF})$  has been synthesized from  $\text{Lu}(\text{CH}_2\text{SiMe}_3)_3(\text{THF})_2$  and  $\text{HCp}^*$ , and its derivative chemistry has been investigated.<sup>541</sup> A new family of mono(cyclopentadienyl) organoscandium bis(alkyls) supported by a bulky trialkylphosphine oxide ancillary ligand has been reported. Treatment of the oligomeric precursor  $[\text{Cp}^*\text{ScCl}]_n$  with tri-*t*-butylphosphine oxide in THF led to the mono(cyclopentadienyl)scandium dichloride  $\text{Cp}^*\text{ScCl}_2(\text{OPBu}^t_3)$  as a monomeric, THF-free solid in 72% yield. Facile alkylation with MeLi gave the dimethyl derivative  $\text{Cp}^*\text{ScMe}_2(\text{OPBu}^t_3)$  (Scheme 111).<sup>542</sup>

Treatment of  $\text{Cp}^*\text{ScMe}_2(\text{OPBu}^t_3)$  with 1 equiv. of  $\text{B}(\text{C}_6\text{F}_5)_3$  in toluene led to the soluble contact ion pair  $[\text{Cp}^*\text{ScMe}(\text{OPBu}^t_3)][\text{MeB}(\text{C}_6\text{F}_5)_3]$  (Scheme 112), demonstrating that the  $\text{Cp}^*/\text{OPBu}^t_3$  ligand combination can deliver a stable platform for organoscandium chemistry.<sup>542</sup>

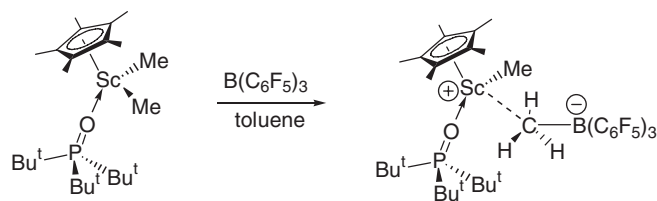
To investigate the potential role of  $\text{Sm-Ph}$  species as intermediates in the samarium-catalyzed redistribution of  $\text{PhSiH}_3$  to  $\text{Ph}_2\text{SiH}_2$  and  $\text{SiH}_4$ , the samarium phenyl complex  $[\text{Cp}^*_2\text{SmPh}]_2$  was prepared by oxidation of  $\text{Cp}^*_2\text{Sm}$  with  $\text{HgPh}_2$ .  $[\text{Cp}^*_2\text{SmPh}]_2$  thermally decomposes to yield benzene and the phenylene-bridged disamarium complex  $\text{Cp}^*_2\text{Sm}(\mu\text{-}1,4\text{-C}_6\text{H}_4)\text{SmCp}^*_2$ . This decomposition reaction appears to proceed through dissociation of  $[\text{Cp}^*_2\text{SmPh}]_2$  into monomeric  $\text{Cp}^*_2\text{SmPh}$  species which then react with unimolecular and bimolecular pathways, involving rate-limiting  $\text{Cp}^*$  metallation and direct C–H activation (Scheme 113).<sup>543</sup>

The mono(pentamethylcyclopentadienyl)gadolinium benzyl complex  $\text{Cp}^*\text{Gd}(\text{CH}_2\text{C}_6\text{H}_5)_2(\text{THF})$  was synthesized from  $\text{GdBr}_3$ ,  $\text{KCp}^*$ , and  $\text{KCH}_2\text{C}_6\text{H}_5$ , and its structure was determined by X-ray methods.<sup>544</sup> The ligand geometry around the Gd atom in  $\text{Cp}^*\text{Gd}(\text{CH}_2\text{C}_6\text{H}_5)_2(\text{THF})$  is distorted tetrahedral. The angles  $\text{Gd-C-C}_{\text{ipso}}(\text{benzyl})$  in  $[\text{Cp}^*_2\text{Sm}(\text{CH}_2\text{C}_6\text{H}_5)_2\text{K}(\text{THF})_2]_\infty$  and  $\text{Cp}^*\text{Gd}(\text{CH}_2\text{C}_6\text{H}_5)_2(\text{THF})$ . Additionally the  $\text{Gd-C}_{\text{ipso}}(\text{benzyl})$  distance is shorter than observed in the other benzyl complexes. This result of the X-ray crystal structure analysis indicates a weak interaction of the Gd atom with the  $\text{C}_{\text{ipso}}(\text{benzyl})$  in the solid state.<sup>544</sup> 9-Pentamethylcyclopentadienyl-9-lanthanofluorene complexes were obtained by the one-pot reaction of  $\text{LnCl}_3$  ( $\text{Ln} = \text{Sm}, \text{Yb}, \text{Lu}$ ) with  $\text{NaCp}^*$  and then with the TMEDA adduct of 2,2'-dilithio-biphenyl (Scheme 114).<sup>545</sup>

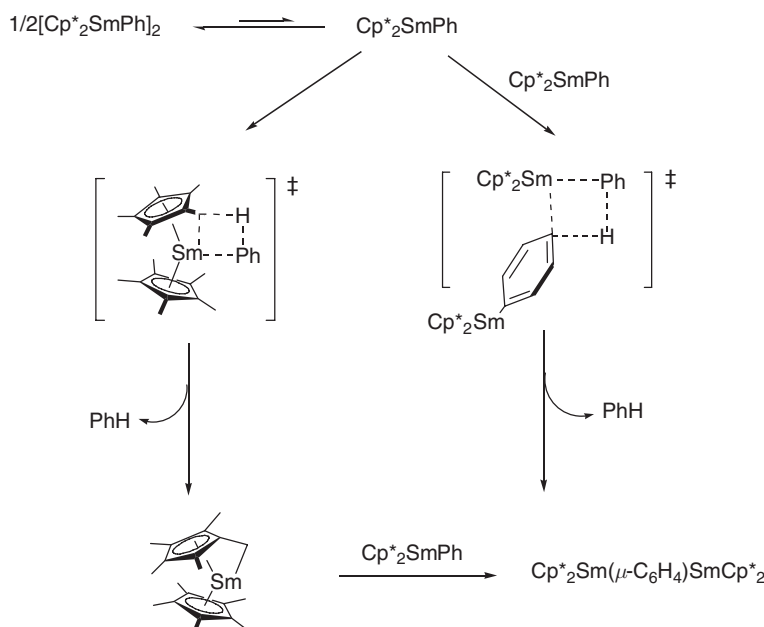
The synthesis of a mono(pentamethylcyclopentadienyl)neodymium allyl complex, green  $\text{Cp}^*\text{Nd}(\eta^3\text{-C}_3\text{H}_5)_2(\text{dioxane})$ , has been achieved by protonation of  $\text{Nd}(\eta^3\text{-C}_3\text{H}_5)_3(\text{dioxane})$  with pentamethylcyclopentadiene. The ease of this protolytic reaction is due to the predominantly ionic nature of the tris(allyl) precursor.<sup>179</sup> The (cyclopentadienyl)lanthanide 1,3-butadiene complexes,  $\text{Cp}^*\text{La}(\text{C}_4\text{H}_6)\cdot\text{MgI}_2\cdot 3\text{THF}$ ,  $\text{Cp}^*\text{Ce}(\text{C}_4\text{H}_6)\cdot\text{MgBr}_2\cdot 2\text{THF}$ , and  $\text{Cp}^*\text{Nd}(\text{C}_4\text{H}_6)\cdot\text{MgCl}_2\cdot 2\text{THF}$  have been prepared by the reaction of appropriate (pentamethylcyclopentadienyl)-lanthanide dihalides with  $(\text{C}_4\text{H}_6)\text{Mg}(\text{THF})_2$ . Reactions of the  $\text{Cp}^*\text{Nd}(\text{C}_4\text{H}_6)\cdot\text{MgCl}_2\cdot 2\text{THF}$  with diphenylamine and  $\text{Cp}^*\text{Ce}(\text{C}_4\text{H}_6)\cdot\text{MgBr}_2\cdot 2\text{THF}$  with carbon dioxide were also investigated.<sup>303</sup>



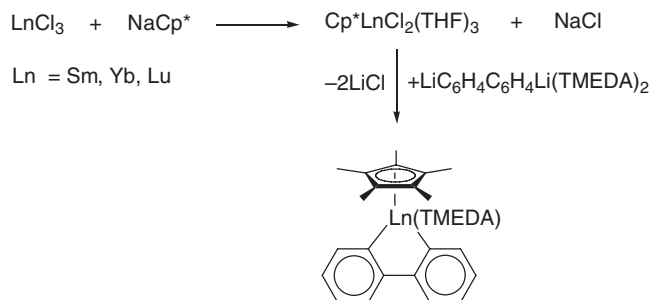
Scheme 111



Scheme 112



Scheme 113



Scheme 114

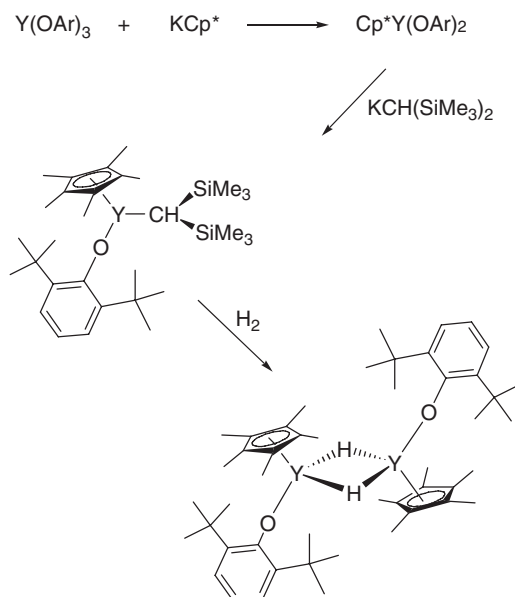
The well-known chlorolanthanide bis(tetrahydroborates) have been employed as starting materials for the preparation of organolanthanide complexes. Treatment of  $\text{LnCl}(\text{BH}_4)_2$  with 1 equiv. of  $\text{KCp}^*$  produced the new organolanthanide tetrahydroborates  $\text{Cp}^*\text{Ln}(\text{BH}_4)_2$  ( $\text{Ln} = \text{Sm, Dy, Yb}$ ). A similar reaction of  $\text{SmCl}(\text{BH}_4)_2$  with  $\text{K}[\text{HB}(3,5\text{-Me}_2\text{pz})_3]$  ( $\text{pz} = \text{pyrazolyl}$ ) afforded the disubstituted pyrazolylborate derivative  $[\text{HB}(3,5\text{-Me}_2\text{pz})_3]_2\text{SmCl}$ .<sup>546</sup> In a similar manner,  $\text{Nd}(\text{BH}_4)_3(\text{THF})_3$  reacts with  $\text{KCp}^*$  to give the organometallic derivative  $\text{Cp}^*\text{Nd}(\text{BH}_4)_2(\text{THF})$ .<sup>547</sup>

A dimeric mono(pentamethylcyclopentadienyl)yttrium hydride has been synthesized through the reaction sequence illustrated in Scheme 115. The hydrogenation of  $\text{Cp}^*\text{Y}(\text{OAr})\text{CH}(\text{SiMe}_3)_2$  ( $\text{Ar} = 2,6\text{-Bu}^t_2\text{C}_6\text{H}_3$ ) in hexane under 10 bar of  $\text{H}_2$  yielded  $[\text{Cp}^*\text{Y}(\text{OAr})(\mu\text{-H})]_2$ .<sup>295,548</sup>

#### 4.01.6.8.4 Bis(pentamethylcyclopentadienyl)lanthanide(III) compounds

##### 4.01.6.8.4.(i) $\text{Cp}^*_2\text{Ln}$ halides and $\text{Cp}^*_2\text{Ln}^+$ salts

Semi-empirical molecular orbital calculations using the INDO/S method have been carried out for organoscandium complexes of the general formula  $\text{Cp}^*_2\text{ScX}$  ( $\text{X} = \text{Cl, I, Me, CH}_2\text{Ph, NHPH}$ ).<sup>549</sup> The utility of electrospray mass spectrometry for the characterization of air-sensitive organolanthanides and related species has been demonstrated.<sup>550</sup> A wide variety of lanthanide complexes, including divalent and trivalent compounds, neutral and



Scheme 115

cationic species, and complexes with cyclopentadienyl as well as alternative ancillary ligands was studied. The spectra are sensitive to the composition of the complex and the oxidation potential of the lanthanide ion. The  $[\text{Cp}^*_2\text{Ln}][\text{BPh}_4]$  ( $\text{Ln} = \text{Nd}, \text{Sm}, \text{Y}, \text{Tm}$ ) complexes form the solvated parent ions  $[\text{Cp}^*_2\text{Ln}(\text{MeCN})_x]^+$ , whereas  $[\text{Zr}_2(\text{OPr}^i)_9]\text{LnCp}$  ( $\text{Ln} = \text{Sm}, \text{Yb}$ ) forms the unsolvated parent ion  $\{[\text{Zr}_2(\text{OPr}^i)_9]\text{LnCp}\}^+$ . The ions  $[\text{Cp}^*_2\text{Ln}(\text{MeCN})_x]^+$  are also observed in the spectra of  $\text{Cp}^*_2\text{Ln}(\text{C}_3\text{H}_5)$  ( $\text{Ln} = \text{Sm}, \text{Y}$ ) and  $\text{Cp}^*_2\text{Ln}(\text{THF})_x$  ( $\text{Ln} = \text{Sm}, \text{Eu}, \text{Yb}$ ).  $[\text{Cp}^*_2\text{Ln}(\mu\text{-I})(\text{THF})_2]_2$  ( $\text{Ln} = \text{Sm}, \text{Yb}, \text{Eu}$ ) and  $\text{LnI}_2(\text{THF})_2$  ( $\text{Ln} = \text{Sm}, \text{Yb}, \text{Eu}$ ) gave differing sets of ions, depending on the specific metal. The spectra of bimetallic compounds,  $[\text{Cp}^*_2\text{Ln}(\text{THF})_x]_2(\text{COT})$  ( $\text{Ln} = \text{Sm}, \text{Yb}$ ), were also investigated.<sup>550</sup>

The crystal structure of  $\text{Cp}^*_2\text{Sm}(\mu\text{-Cl})_2\text{Li}(\text{Et}_2\text{O})_2$  was found to be isomorphous with its long-known  $\text{Ce}(\text{III})$  and  $\text{Yb}(\text{III})$  analogs.<sup>551</sup> Synthetic routes to unsolvated lanthanide metallocene cations isolated as  $[\text{Cp}^*_2\text{Ln}][\text{BPh}_4]$  have been published. Divalent  $\text{Cp}^*_2\text{Sm}$  reacted with  $\text{AgBPh}_4$  in toluene to yield  $[\text{Cp}^*_2\text{Sm}][\text{BPh}_4]$ . The crystal structure of this complex consists of a trivalent  $\text{Cp}^*_2\text{Sm}$  bent metallocene unit with a 2.702(3) Å average  $\text{Sm}-\text{CCp}^*$  distance that is oriented toward two of the phenyl rings of the  $[\text{BPh}_4]^-$  anion with 2.8525(3) and 2.917(3) Å  $\text{Sm}-\text{C}(o\text{-Ph})$  distances.<sup>552</sup> More recently, the unsolvated salt-like species  $[\text{Cp}^*_2\text{Ln}][\text{B}(\text{C}_6\text{F}_5)_4]$  ( $\text{Ln} = \text{Pr}, \text{Nd}, \text{Gd}$ ) have become available by reacting the bimetallic precursors  $[\text{Cp}^*_2\text{Ln}(\mu\text{-Me})_2\text{AlMe}_2]_2$  with 2 equiv. of  $[\text{CPh}_3][\text{B}(\text{C}_6\text{F}_5)_4]$ .<sup>553</sup> The cationic organo-lanthanide compounds  $[(\text{C}_5\text{H}_4\text{R})_2\text{Sm}(\text{THF})_2][\text{BPh}_4]$  ( $\text{R} = \text{Bu}^t, \text{SiMe}_3$ ),  $[\text{Pyr}^*_2\text{Sm}(\text{THF})][\text{BPh}_4]$  ( $\text{Pyr}^* = \text{NC}_4\text{H}_2\text{Bu}^t_{2-2,5}$ ),  $[\text{Cp}^*_2\text{Ln}(\text{THF})_2][\text{BPh}_4]$  ( $\text{Ln} = \text{Y}, \text{Yb}$ ), and  $[(\text{C}_5\text{Me}_4\text{Et})_2\text{Ln}(\text{THF})_2][\text{BPh}_4]$  ( $\text{Ln} = \text{Sm}, \text{Y}$ ) have been synthesized by oxidation of the divalent metallocenes  $[(\text{C}_5\text{H}_4\text{R})_2\text{Sm}(\text{THF})_2]$ ,  $[\text{Pyr}^*_2\text{Sm}(\text{THF})]$ ,  $[\text{Cp}^*_2\text{Yb}(\text{THF})]$ , and  $[(\text{C}_5\text{Me}_4\text{Et})_2\text{Sm}(\text{THF})]$  with  $\text{Ag}[\text{BPh}_4]$  and by protolysis of the lanthanide alkyls  $\text{Cp}^*_2\text{LnMe}(\text{THF})$ ,  $\text{Cp}^*_2\text{YbCH}(\text{SiMe}_3)_2$ , and  $(\text{C}_5\text{Me}_4\text{Et})_2\text{LnCH}(\text{SiMe}_3)_2$  ( $\text{Ln} = \text{Y}, \text{Sm}$ ) by  $[\text{NEt}_3\text{H}][\text{BPh}_4]$ .  $[\text{Cp}^*_2\text{Yb}(\text{THF})_2][\text{BPh}_4]$  was characterized by X-ray crystal structure analysis.<sup>554</sup> The unsolvated bimetallic yttrium complex  $\text{Cp}^*_2\text{Y}(\mu\text{-Cl})\text{YCp}^*_2\text{Cl}$  has been utilized as a convenient platform upon which to compare the coordination chemistry of oxygen-donor ligands and monomers with Lewis-acidic metal ions. Reactions of  $\text{Cp}^*_2\text{Y}(\mu\text{-Cl})\text{YCp}^*_2\text{Cl}$  with 2 equiv. of oxygen-containing substrates formed the monomeric complexes  $\text{Cp}^*_2\text{YCl}(\text{L})$  ( $\text{L} = \text{THF}$ , benzophenone, MMA,  $\varepsilon$ -caprolactone, HMPA,  $\varepsilon$ -caprolactam, 1-methyl-2-pyrrolidone, and  $N,N'$ -dimethylpropyleneurea). Each of these readily crystallize, which allowed comparison of the  $\text{Y}-\text{O}$  interaction in the solid state.<sup>555</sup> Adduct formation between  $\text{Cp}^*_2\text{Nd}(\mu\text{-Cl})_2\text{Li}(\text{OEt}_2)_2$  and  $\text{Cp}^*_2\text{Nd}(\mu\text{-Cl})(\mu\text{-Me})\text{Li}(\text{OEt}_2)_2$  and phosphine oxides has also been observed.<sup>556</sup>

The polymeric structure of the pentamethylcyclopentadienyl complex of thulium  $[\text{Cp}^*_2\text{Tm}(\mu_3\text{-Cl})_2\text{K}(\text{THF})]_n$  is generated by triply bridging chloride ligands, with each chloride being connected to one  $\text{Cp}^*_2\text{Tm}$  bent metallocene unit and two  $\text{K}(\text{THF})$  moieties in a T-shaped geometry around the chloride.<sup>557</sup>  $\text{Cp}^*_2\text{Tm}(\text{III})$  complexes have also been isolated from reactions of  $\text{TmI}_2(\text{THF})_2$  with  $\text{KCp}^*$ .<sup>344</sup>  $\text{Cp}^*_2\text{Nd}(\mu\text{-Cl})_2\text{Na}(\text{DME})_2$  was obtained by the reaction

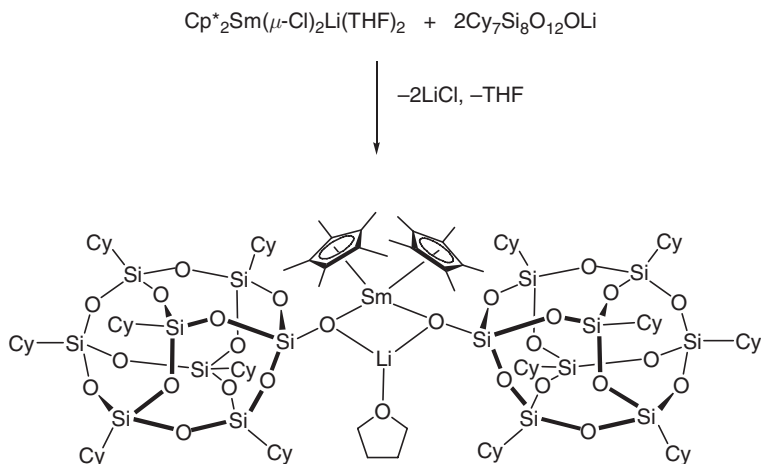


of  $\text{NdCl}_3$  with  $\text{NaCp}^*$ . Methoxylation of  $\text{Cp}^*_2\text{Nd}(\mu\text{-Cl})_2\text{Na}(\text{DME})_2$  led to methoxide derivative  $\text{Cp}^*_2\text{Nd}(\mu\text{-OMe})_2\text{Na}(\text{DME})_2$ . Both complexes were structurally characterized.<sup>558</sup> The reaction of  $\text{Cp}^*_2\text{Sm}(\text{CH}_2\text{C}_6\text{H}_5)(\text{THF})$  with  $\text{N}_2\text{O}$  in toluene leads to  $[\text{Cp}^*_2\text{Sm}(\text{C}_6\text{H}_5\text{CH}_2\text{NNO})]_2$  via an unusual insertion reaction of  $\text{N}_2\text{O}$  into the  $\text{Sm}-\text{C}$   $\sigma$ -bond. Single X-ray determinations revealed a dimeric structure with two samarium centers linked via an ( $\eta^1:\eta^2$ ) bridge by two benzyldiazotato ligands forming a nearly planar  $\text{Sm}_2\text{N}_2\text{O}_2$  ring. The distorted tetrahedral coordination geometry is completed by two  $\eta^5$ -bonded pentamethylcyclopentadienyl ligands. In contrast, the reaction of  $\text{Cp}^*_2\text{Yb}(\text{CH}_2\text{C}_6\text{H}_5)(\text{THF})$  with  $\text{KSCN}$  and 18-crown-6 shows a substitution of the benzyl group with  $\text{NCS}^-$  giving  $[\text{K}(18\text{-crown-6})][\text{Cp}^*_2\text{Yb}(\text{NCS})_2]$ . The solid-state structure shows a polymeric chain structure where two  $\text{Cp}^*_2\text{Yb}$  units are connected through a  $[\text{K}(18\text{-crown-6})(\text{NCS})]$  bridge with tetrahedrally coordinated  $\text{Yb}^{\text{III}}$  ions.<sup>559</sup> Monomeric iminoacetylacetonato complexes of the type  $\text{Cp}^*_2\text{Ln}[\text{OC}(\text{Me})=\text{CHC}(\text{Me})=\text{NR}]$  ( $\text{Ln} = \text{Y, La, Lu}$ ;  $\text{R} = \text{Ph, MeC}_6\text{H}_4$ ) have been synthesized by treatment of the chloro precursors  $\text{Cp}^*_2\text{Ln}(\mu\text{-Cl})_2\text{ML}_2$  ( $\text{Ln} = \text{Y, La, Lu}$ ;  $\text{M} = \text{Li, K}$ ;  $\text{L} = \text{Et}_2\text{O, THF}$ ) with  $\text{Na}[\text{OC}(\text{Me})=\text{CHC}(\text{Me})=\text{NR}]$ . For the complex  $\text{Cp}^*_2\text{La}[\text{OC}(\text{Me})=\text{CH}(\text{Me})=\text{NC}_6\text{H}_4\text{Me}]$  the chelating structure was confirmed by an X-ray structure analysis.<sup>560</sup>

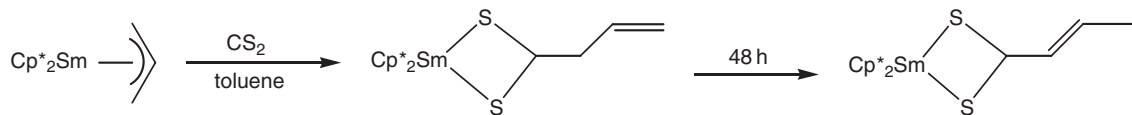
#### 4.01.6.8.4.(ii) $\text{Cp}^*_2\text{Ln}$ compounds with bonds to chalcogens

Examination of the chemistry of sterically crowded  $(\text{C}_5\text{Me}_4\text{R})_3\text{Ln}$  complexes has provided access to a series of oxo-bridged complexes:  $[\text{Cp}^*_2\text{La}]_2(\mu\text{-O})$ ,  $[\text{Cp}^*_2\text{Nd}(\text{NC}_5\text{H}_4\text{NC}_4\text{H}_8)]_2(\mu\text{-O})$ ,  $[(\text{C}_5\text{Me}_4\text{Pr})_2\text{Sm}]_2(\mu\text{-O})$ ,  $[(\text{C}_5\text{Me}_4\text{Et})_2\text{Gd}]_2(\mu\text{-O})$ , and  $[\text{Cp}^*_2\text{Gd}(\text{NC}_5\text{H}_5)]_2(\mu\text{-O})$ . X-ray crystallographic data on these complexes provided information on the effect of metal and cyclopentadienyl ring size on  $\text{Ln}-\text{O}$  bond lengths and  $\text{Ln}-\text{O}-\text{Ln}$  angles, which vary between  $173^\circ$  and  $180^\circ$  in these complexes.<sup>561</sup> Yellow  $\text{Cp}^*_2\text{Sm}[\mu\text{-Cy}_7\text{Si}_8\text{O}_{12}\text{O}]_2$  ( $\text{Cy} = \text{c-C}_6\text{H}_{11}$ ), the first organolanthanide silsesquioxane complex, has been obtained in 68% yield by treatment of the *ate*-complex  $\text{Cp}^*_2\text{Sm}(\mu\text{-Cl})_2\text{Li}(\text{THF})_2$  with  $\text{Cy}_7\text{Si}_8\text{O}_{12}\text{OLi}$  in a molar ratio of 1:2. In this complex, samarium and lithium are bridged by two silsesquioxane silanolate ligands (Scheme 116).<sup>562</sup>

$\text{CO}_2$  insertion chemistry of organoallylsamarium compounds has been investigated.  $\text{CO}_2$  reacted with  $\text{Cp}^*_2\text{Sm}(\eta^3\text{-CH}_2\text{CHCH}_2)$  and  $\text{Cp}^*_2\text{SmPh}$  to form  $[\text{Cp}^*_2\text{Sm}(\mu\text{-O}_2\text{CCH}_2\text{CHCH}_2)]_2$  and  $[\text{Cp}^*_2\text{Sm}(\mu\text{-O}_2\text{CPh})]_2$ , respectively, in  $>90\%$  yield.  $\text{Cp}^*_2\text{Sm}(\mu^2\text{-O}_2\text{CCH}_2\text{CHCH}_2)$  exists as a solvated species in THF. The sulfur analog  $\text{CS}_2$  reacted with  $\text{Cp}^*_2\text{Sm}(\eta^3\text{-CH}_2\text{CHCH}_2)$  to form  $\text{Cp}^*_2\text{Sm}(\eta^2\text{-S}_2\text{CCH}_2\text{CH}=\text{CH}_2)$ , which subsequently isomerized to  $\text{Cp}^*_2\text{Sm}(\eta^2\text{-S}_2\text{CCH}=\text{CH}_2\text{CH}_2)$  (Scheme 117).<sup>563</sup>

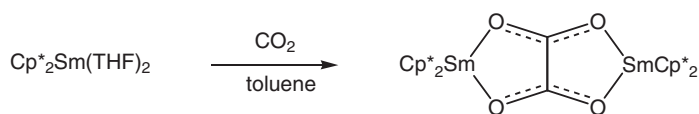


Scheme 116



Scheme 117





Scheme 118

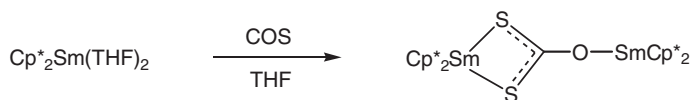
The reactivity of  $\text{CO}_2$  and  $\text{COS}$  towards divalent and trivalent organosamarium complexes has also been investigated.  $\text{Cp}^*_2\text{Sm}(\text{THF})_2$  reductively couples  $\text{CO}_2$  in THF at room temperature to form an oxalate complex,  $(\mu\text{-}\eta^2\text{:}\eta^2\text{-O}_2\text{CCO}_2)[\text{Cp}^*_2\text{Sm}]_2$ , in which the samarium metal is formally eight-coordinated (Scheme 118).<sup>563</sup>

The reaction of  $\text{COS}$  with  $\text{Cp}^*_2\text{Sm}(\text{THF})_2$  is more complicated and generated a disproportionation product,  $\text{Cp}^*_2\text{Sm}(\mu\text{-}\eta^2\text{:}\eta^1\text{-S}_2\text{CO})\text{SmCp}^*_2(\text{THF})$ , which has one  $\text{Cp}^*_2\text{Sm}$  unit involved in a four-membered  $\text{SmSCS}$  ring, while the other  $\text{Cp}^*_2\text{Sm}$  unit is bound to THF and the oxygen of the  $\text{S}_2\text{CO}$  ligand (Scheme 119).<sup>563</sup>

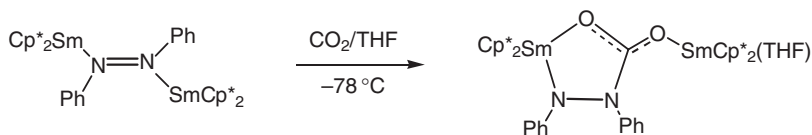
The reaction of the samarium complex  $[\text{Cp}^*_2\text{Sm}]_2(\mu\text{-}\eta^1\text{:}\eta^1\text{-N}_2\text{Ph}_2)$  with excess  $\text{CO}_2$  at  $-78^\circ\text{C}$  in THF gave  $\text{Cp}^*_2\text{Sm}[\mu\text{-}\eta^2\text{:}\eta^1\text{-PhNN}(\text{CO}_2)\text{Ph}]\text{Sm}(\text{THF})\text{Cp}^*_2$  in  $>90\%$  yield (Scheme 120).<sup>563</sup>

The reaction of 1 equiv. of tris(pentamethylcyclopentadienyl) neodymium or tris(pentamethylcyclopentadienyl) samarium (cf. following section) with 1 equiv. of  $\text{Ph}_3\text{P}=\text{Se}$  leads to the  $\text{Se}_2^{2-}$ -bridged dimers  $[\text{Cp}^*_2\text{Nd}]_2(\mu\text{-}\eta^2\text{:}\eta^2\text{-Se}_2)$  and  $[\text{Cp}^*_2\text{Sm}]_2(\mu\text{-}\eta^2\text{:}\eta^2\text{-Se}_2)$ , respectively (Scheme 121).<sup>564</sup>

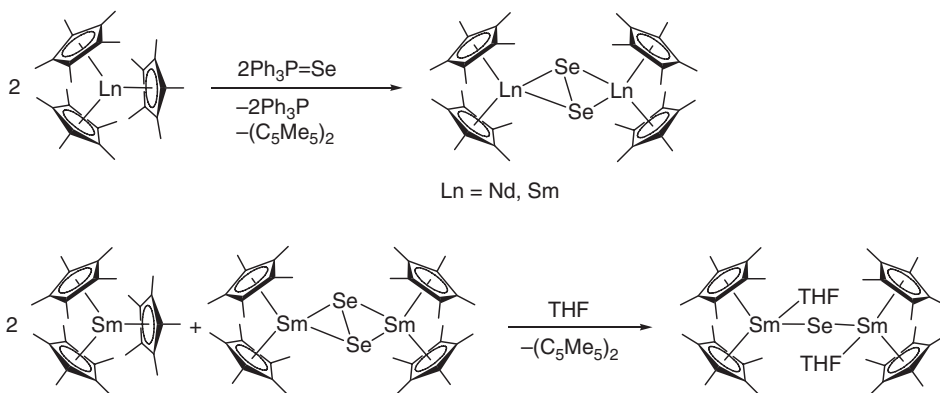
$\text{Cp}^*_3\text{Ln}$  complexes act like one-electron reducing agents.  $\text{Se}=\text{PPh}_3$  is reduced to  $\text{Ph}_3\text{P}$  and  $[\text{Cp}^*_2\text{Nd}]_2(\mu\text{-}\eta^2\text{:}\eta^2\text{-Se}_2)$ . As a byproduct,  $(\text{C}_5\text{Me}_5)_2$  is isolated, which is in good agreement with a one-electron reduction. Single X-ray determinations revealed the dimeric structure of  $[\text{Cp}^*_2\text{Nd}]_2(\mu\text{-}\eta^2\text{:}\eta^2\text{-Se}_2)$  with a symmetric  $\text{Se}-\text{Se}^{2-}$  bridge between both neodymium centers. The  $\text{Se}-\text{Se}$  distance is  $2.389 \text{ \AA}$  and is in good agreement to known  $\text{Se}-\text{Se}$  single bonds.<sup>564</sup> The reaction behavior of  $\text{Cp}^*_3\text{Sm}$  is slightly different. An equimolar reaction of  $\text{Cp}^*_3\text{Sm}$  with  $\text{SePPh}_3$  led to the



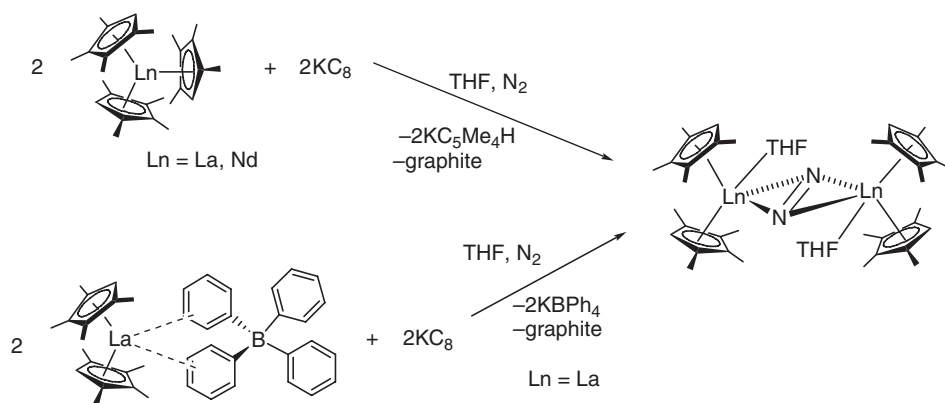
Scheme 119



Scheme 120



Scheme 121



Scheme 122

homologous Se–Se<sup>2−</sup>-bridged dimer [Cp<sup>\*</sup><sub>2</sub>Sm]<sub>2</sub>(μ-η<sup>2</sup>:η<sup>2</sup>-Se<sub>2</sub>). In contrast to Cp<sup>\*</sup><sub>3</sub>Nd, where [Cp<sup>\*</sup><sub>2</sub>Nd]<sub>2</sub>(μ-η<sup>2</sup>:η<sup>2</sup>-Se<sub>2</sub>) and unreacted Cp<sup>\*</sup><sub>3</sub>Nd could be isolated, the reaction of 2 equiv. Cp<sup>\*</sup><sub>3</sub>Sm with 1 equiv. of Se=PPh<sub>3</sub> in THF gave the Se<sup>2−</sup>-bridged dimer [Cp<sup>\*</sup><sub>2</sub>Sm(THF)]<sub>2</sub>(μ-Se), which is also the product of the reaction of Cp<sup>\*</sup><sub>3</sub>Sm with [Cp<sup>\*</sup><sub>2</sub>Sm]<sub>2</sub>(μ-η<sup>2</sup>:η<sup>2</sup>-Se<sub>2</sub>) (Scheme 121). The different reaction behavior is presumably caused by the different ionic radii of Nd<sup>3+</sup> and Sm<sup>3+</sup>.<sup>564</sup> Other decamethylsamarocene complexes containing group 16 element anions include the series [Cp<sup>\*</sup><sub>2</sub>Sm(THF)]<sub>2</sub>(μ-E), [Cp<sup>\*</sup><sub>2</sub>Sm]<sub>2</sub>(μ-E<sub>3</sub>)(THF) (E = S, Se, Te), and [Cp<sup>\*</sup><sub>2</sub>Sm]<sub>2</sub>(μ-Te<sub>2</sub>).<sup>565</sup> The synthesis of the permethylsamarocene tellurolates Cp<sup>\*</sup><sub>2</sub>Sc(TeCH<sub>2</sub>SiMe<sub>3</sub>) and Cp<sup>\*</sup><sub>2</sub>Sc(TeCH<sub>2</sub>Ph) has been achieved by insertion of tellurium into the scandium–carbon bonds of the corresponding alkyl complexes. These tellurolates were found to be thermally unstable with respect to the elimination of TeR<sub>2</sub> and the formation of the dimeric μ-telluride [Cp<sup>\*</sup><sub>2</sub>Sc]<sub>2</sub>(μ-Te). In the latter complex the Se–Te distance is 2.75 Å, and the Sc–Te–Sc angle is 172.1°, indicating significant π-bonding between scandium and tellurium.<sup>566–569</sup>

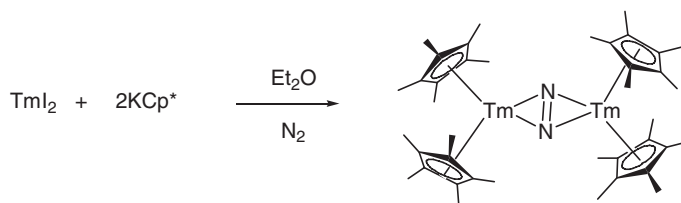
#### 4.01.6.8.4.(iii) Cp<sup>\*</sup><sub>2</sub>Ln compounds with bonds to pnictides

μ-Dinitrogen-bis(pentamethylcyclopentadienyl) complexes of lanthanum and neodymium have recently become readily accessible through the use of potassium graphite as reducing agent. The synthetic routes are illustrated in Scheme 122.<sup>570</sup>

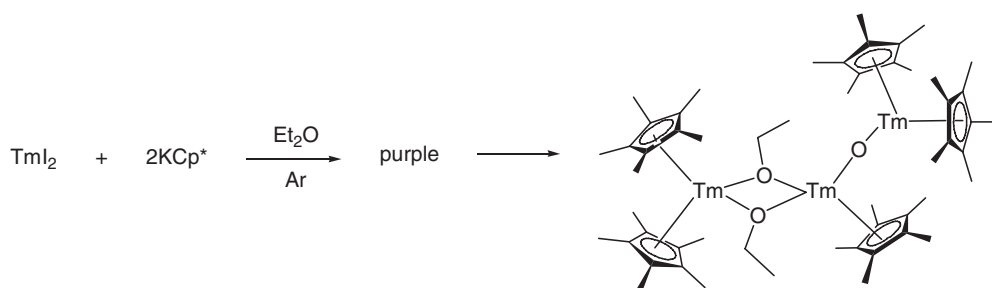
Facile dinitrogen reduction via organometallic Tm(II) chemistry has also been reported. TmI<sub>2</sub>, prepared directly from Tm and I<sub>2</sub>, reacts with KCp<sup>\*</sup> in Et<sub>2</sub>O under nitrogen to form a white precipitate and a reddish-orange solution from which (μ-N<sub>2</sub>)[TmCp<sup>\*</sup><sub>2</sub>]<sub>2</sub> could be crystallized in 55% yield (Scheme 123).<sup>571</sup>

Notably, a control reaction of TmI<sub>2</sub> with KCp<sup>\*</sup> in Et<sub>2</sub>O under argon proceeded differently. It formed a purple solution that changed color to orange when nitrogen was added. In the absence of nitrogen, the purple solution slowly changed to yellow-orange over a period of hours. From this solution yellow crystals of Cp<sup>\*</sup><sub>2</sub>Tm(μ-OEt)<sub>2</sub>TmCp<sup>\*</sup>(μ-O)TmCp<sup>\*</sup><sub>2</sub> could be isolated, which resulted from diethyl ether cleavage (Scheme 124).<sup>571</sup>

The reaction of Cp<sup>\*</sup><sub>2</sub>La(μ-Cl)<sub>2</sub>K(DME)<sub>2</sub> with 1 equiv. of Na<sub>2</sub>(DAD) [DAD = PhN=C(Ph)C(Ph)=NPh] in the presence of DAD or with 2 equiv. of Na(DAD) gave the ionic complex [Na(DAD)]<sup>+</sup>[Cp<sup>\*</sup><sub>2</sub>La(DAD)]<sup>−</sup>. The interaction of Cp<sup>\*</sup><sub>2</sub>Y(μ-Cl)<sub>2</sub>Li(OEt)<sub>2</sub> with Na(DAD) led to the Cp<sup>\*</sup><sub>2</sub>Y(DAD) complex, which was structurally characterized. The DAD ligand in the complex is reduced to the radical anion. In the structure the yttrium atom has pseudo-tetrahedral arrangement formed by the two Cp<sup>\*</sup> groups and two N atoms of the *cis*-1,4-diazadiene. The



Scheme 123



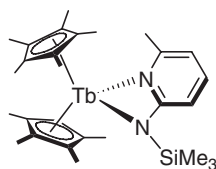
Scheme 124

metallacycle  $\text{Y}(\text{N}-\text{C}-\text{C}-\text{N})$  is planar.<sup>572</sup> Binuclear complexes have been obtained from the related reactions of  $\text{Cp}^*_2\text{La}(\mu\text{-Cl})_2\text{K}(\text{DME})_2$  with the anions of 2,3-dimethylquinoxaline or phenazine.<sup>573</sup> Oxidation of  $\text{Cp}^*_2\text{Yb}(\text{THF})_2$  with the diazadiene  $\text{Bu}^t\text{N}=\text{CHCH}=\text{NBu}^t$  also afforded a diazadiene complex,  $\text{Cp}^*_2\text{Yb}(\text{DAD})$ , in 72% yield. An X-ray diffraction study confirmed the trivalent state of the ytterbium ion and the radical nature of the DAD ligand in this complex.<sup>574</sup>

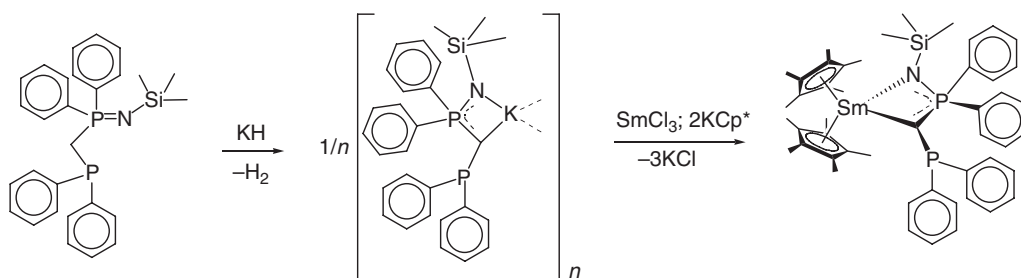
Adduct formation between  $\text{Cp}^*_2\text{Yb}(\text{THF})_2$  with 2,2'-bipyridine and 1,10-phenanthroline<sup>575,576</sup> as well as various nitrogen heterocycles involving diazadiene systems<sup>577</sup> has been studied in detail. In all cases, deeply colored adducts of the type  $\text{Cp}^*_2\text{Yb}(\text{L})$  were formed (1:1 adducts with 2,2'-bipyridine, 1,10-phenanthroline, pyrazine, quinoxaline, 1,5- and 1,8-naphthyridine, phthalazine, azobenzene, and 4,4'-bipyridine; 1:2 adducts with phenazine, 2,2'-azopyridine, 2,2'-bipyrimidine, and 2,3-bis(2-pyridino)quinoxaline), which all have to be formulated as  $\text{Cp}^*_2\text{Yb}^{\text{III}}(\text{L}^{\cdot-})$  ( $\text{L}^{\cdot-}$  = radical anion).<sup>577</sup> In a similar manner,  $\text{Cp}^*_2\text{Yb}(\text{Et}_2\text{O})$  reacts with terpyridine and tetrapyridinylpyrazine.<sup>578</sup> Various lanthanide(III) complexes with pyrazolate ligands have been described. The tris(pyrazolate) complexes  $\text{Ln}(\text{Ph}_2\text{pz})_3(\text{THF})_n$  ( $\text{Ph}_2\text{pz}$  = 3,5-diphenylpyrazolate, Ln = Sc, Y, Gd, Er) contain just N–Ln bonds whereas the complexes  $\text{Cp}_2\text{Ln}(\text{Me}_2\text{pz})(\text{THF})_n$  (Ln = Y, Lu; pz = pyrazolate, Mepz = 3-methylpyrazolate,  $\text{Me}_2\text{pz}$  = 3,5-dimethylpyrazolate),  $\text{Cp}^*_2\text{Y}(\text{pz})(\text{THF})$ ,  $\text{Cp}^*_2\text{Y}(\text{Mepz})(\text{THF})$ ,  $\text{Cp}^*_2\text{Y}(\text{Me}_2\text{pz})(\text{THF})_2$  also have  $\eta^5$ -bonded Cp ligands. These compounds were synthesized by the reactions of  $\text{Cp}^*_2\text{LnCl}$  derivatives with the corresponding sodium pyrazolates.<sup>579</sup> Oxidative synthetic routes leading to pyrazolates and pseudo-pyrazolates of lanthanides have been reported.  $\text{Cp}^*_2\text{Yb}$  reacted with  $\text{Ti}(\text{Ph}_2\text{pz})$  and  $\text{Ti}(\text{azin})$  ( $\text{Ph}_2\text{pz}$  = 3,5-diphenylpyrazolate, azin = 7-azaindolate) to yield  $\text{Cp}^*_2\text{Yb}(\text{Ph}_2\text{pz})$  and  $\text{YbCp}^*_2(\text{azin})$ . The X-ray crystal structures of  $\text{Cp}^*_2\text{Yb}(\text{Ph}_2\text{pz})$  and  $\text{Cp}^*_2\text{Yb}(\text{azin})$  show to be eight-coordinated monomers with the Cp\* ligands  $\eta^5$ -bound to the ytterbium atom and the diaza ligand chelating edge-on through the nitrogen atoms.<sup>580</sup> The potassium salt of the 2,3-dimethylindolide anion (= DMI),  $[\text{K}(\text{DMI})(\text{THF})]_n$ , reacts with  $\text{Cp}^*_2\text{Ln}(\mu\text{-Cl})_2\text{K}(\text{THF})_2$  (Ln = Sm, Y) to form unsolvated amide complexes  $\text{Cp}^*_2\text{Ln}(\text{DMI})$ , in which DMI attaches primarily through nitrogen, although the edge of the arene ring is oriented toward the metals at long distances.<sup>581</sup> Lanthanidocene silylamide complexes of the type  $\text{Cp}'_2\text{LnN}(\text{SiHMe}_2)_2$  ( $\text{Cp}' = \text{Cp}^*$ ,  $\text{C}_5\text{HMe}_4$ ,  $\text{C}_5\text{HPh}_4$ ) have been prepared by reacting the precursors  $\text{Y}[\text{N}(\text{SiHMe}_2)_2]_3(\text{THF})_2$  with the highly substituted cyclopentadiene derivatives  $\text{Cp}^*\text{H}$ ,  $\text{C}_5\text{H}_2\text{Me}_4$ , and  $\text{C}_5\text{H}_2\text{Ph}_4$ .<sup>538</sup> Heteroleptic lanthanide complex containing a monoanionic 2-amidopyridine ligand has been reported for terbium (Scheme 125).<sup>582</sup>

Monoanionic phosphine(phosphinimino)methanide ligands have recently been introduced in organolanthanide chemistry. Scheme 126 illustrates the ligand synthesis and the preparation of a  $\text{Cp}^*_2\text{Sm}(\text{III})$  derivative, which is monomeric in the solid state and contains the ligand in  $\eta^3$ -heteroallylic fashion.<sup>583</sup>

$\text{Cp}^*_2\text{Sm}$  and  $\text{Cp}^*_2\text{Sm}(\text{THF})_2$  react with  $\text{EPh}_3$  or  $\text{Ph}_3\text{E}-\text{EPh}_3$  (E = P, As, Sb, Bi) in three different ways: coordination, E–C cleavage, and E–E cleavage. E–C cleavage is most common for the heavier congeners, which have weaker E–C bonds. Hence,  $\text{Cp}^*_2\text{SmPh}$  products were found in reactions with Sb and Bi but not with P and As (Scheme 127).<sup>584</sup>



Scheme 125



Scheme 126



Scheme 127

E–E cleavage occurs with all of the systems studied: P, As, Sb, Bi. For the lighter congeners with stronger E–C bonds, the E–E cleavage products were isolated as the  $\text{EPh}_2$  complexes  $\text{Cp}^*_2\text{SmPPh}_2$  and  $\text{Cp}^*_2\text{SmAsPh}_2$  (Scheme 128).<sup>584</sup>

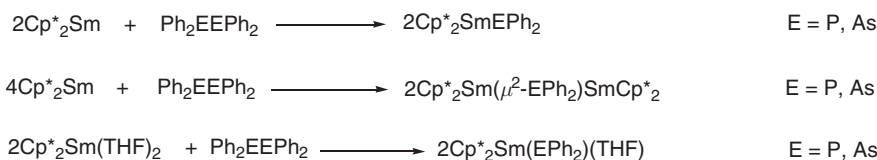
The THF adducts display further chemistry and provide a system in which THF coordination and ring opening can be separately defined. This ring opening occurs over a period of days at room temperature in benzene, toluene, hexane, or THF (Scheme 129).<sup>584</sup>

#### 4.01.6.8.4.(iv) $\text{Cp}^*_2\text{Ln}$ carbene compounds

$\text{Cp}^*_2\text{Sm}(\text{THF})_2$  reacts with 1,3-diisopropyl-4,5-dimethylimidazoline-2-ylidene,  $\text{C}_3\text{N}_2\text{Me}_2\text{Pr}^i_2$  (=  $\text{Pr}^i$ -carben), forming  $\text{Cp}^*_2\text{Sm}(\text{Pr}^i\text{-carben})$ . In the carbene ring the values for the C–N distances alternate between 1.395(4) and 1.348(4) Å. The Sm–C, C–C, and the exocyclic N–C bond lengths are in the normal range.<sup>585</sup> Several related samarium(II) and ytterbium(II) carbene complexes have been synthesized analogously.<sup>586</sup>

#### 4.01.6.8.4.(v) $\text{Cp}^*_2\text{Ln}$ hydrides and alkyls

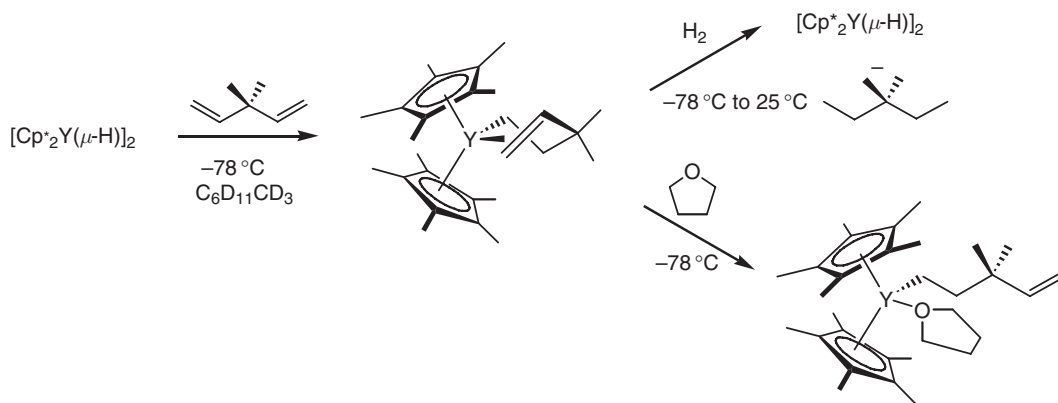
The dissociation of the dimer  $[\text{Cp}^*_2\text{Y}(\mu\text{-H})]_2$  to the  $\text{Cp}^*_2\text{YH}$  monomer is an important process in the reactions of the dimer with alkenes. The kinetics and formation of yttrium alkyl complexes from  $[\text{Cp}^*_2\text{Y}(\mu\text{-H})]_2$  and alkenes have been investigated.<sup>587</sup> *In situ* prepared dimeric bis(pentamethylcyclopentadienyl)yttrium hydride reacted rapidly with 3,3-dimethyl-1,4-pentadiene in methylcyclohexane- $d_{14}$  at  $-78^\circ\text{C}$  and formed a bright yellow solution of the  $d^0$ -yttrium(III)pentenyl chelate complex  $\text{Cp}^*_2\text{Y}[\eta^1, \eta^2\text{-CH}_2\text{CH}_2\text{CMe}_2\text{CH=CH}_2]$  in 98% yield (Scheme 130). This pentenyl chelate complex was also prepared in toluene- $d_8$  in 84% yield. The chelate complex was stable for about 2 weeks at  $-78^\circ\text{C}$  but decomposed after a few hours at  $-50^\circ\text{C}$ . The complex was characterized without isolation by  $^1\text{H}$  and  $^{13}\text{C}$  NMR spectroscopy at  $-100^\circ\text{C}$ ; such complexes can be regarded as models for the coordination of alkenes to lanthanide and isoelectronic group 4 polymerization catalysts.<sup>588</sup> Agostic interactions in yttrium alkyls of the type  $\text{Cp}^*_2\text{YR}$  have been studied in detail.<sup>589</sup>



Scheme 128



Scheme 129



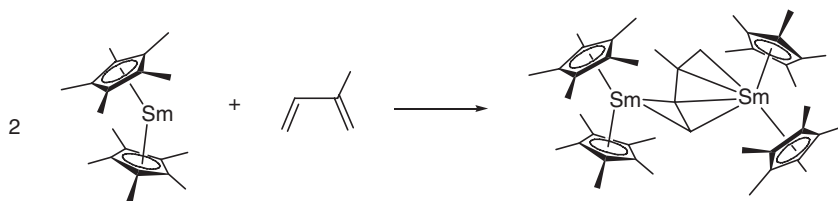
Scheme 130

The new benzyl complexes  $\text{Cp}^*_2\text{Y}(\text{CH}_2\text{C}_6\text{H}_5)(\text{THF})$  and  $[\text{Cp}^*_2\text{Sm}(\text{CH}_2\text{C}_6\text{H}_5)_2\text{K}(\text{THF})_2]_\infty$  were synthesized by reacting  $\text{LnBr}_3$  with  $\text{KCp}^*$  and  $\text{KCH}_2\text{C}_6\text{H}_5$  in different molar ratios. The structures of the new benzyl complexes were determined by X-ray single crystal structure analysis. The structure of  $\text{Cp}^*_2\text{Y}(\text{CH}_2\text{C}_6\text{H}_5)(\text{THF})$  is unexceptional for bis(cyclopentadienyl) compounds of the rare earth metals. The polymer chain of  $[\text{Cp}^*_2\text{Sm}(\text{CH}_2\text{C}_6\text{H}_5)_2\text{K}(\text{THF})_2]_\infty$  is formed by  $\eta^6$ -coordination of the  $\text{K}(\text{THF})_2$  fragment with two benzyl ligands of different  $\text{Cp}^*_2\text{Sm}(\text{CH}_2\text{C}_6\text{H}_5)_2$  units. The  $\text{Cp}^*$ (centroid)–Sm bond length is  $2.50\text{ \AA}$ , whereas the  $\text{C}_6\text{H}_5$ (centroid)–K distance was determined to be  $2.88\text{--}2.90\text{ \AA}$ .<sup>544</sup>

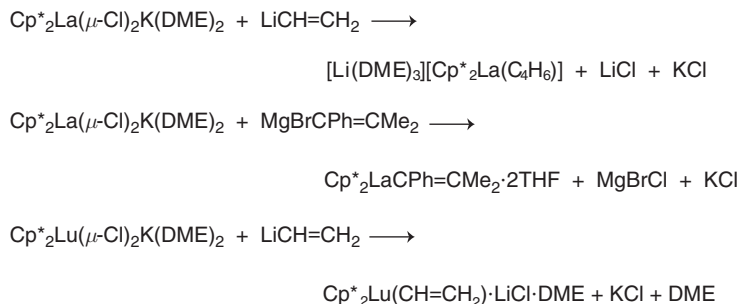
The well-known lanthanocene alkyls  $\text{Cp}^*_2\text{LnCH}(\text{SiMe}_3)_2$  ( $\text{Ln} = \text{La, Ce, Nd, Sm, Lu}$ ) have been investigated by relativistic *ab initio* and DV- $X\alpha$  calculations and gas-phase UV photoelectron spectroscopy.<sup>590</sup> DFT and QM/MM calculations have been carried out to model  $\text{Cp}^*$  for reactivity studies in  $\text{Cp}^*_2\text{LnR}$  complexes.<sup>591</sup> The reaction of  $\text{Cp}^*_2\text{LaCH}(\text{SiMe}_3)_2$  with  $\text{PhC}\equiv\text{CH}$  at room temperature yielded the coupled product  $(\mu\text{-PhC}_4\text{Ph})[\text{Cp}^*_2\text{La}]_2$  besides  $\text{CH}_2(\text{SiMe}_3)_2$ . At  $0^\circ\text{C}$ ,  $\text{Cp}^*_2\text{LaCH}(\text{SiMe}_3)_2$  reacts with  $\text{Bu}^t\text{C}\equiv\text{CH}$  forming the dimeric acetylide  $[\text{Cp}^*_2\text{La}(\mu\text{-C}\equiv\text{CBu}^t)]_2$ , which, in toluene solution at  $50\text{--}60^\circ\text{C}$  undergoes clean unimolecular conversion to the coupled dimer  $(\mu\text{-Bu}^t\text{C}_4\text{Bu}^t)[\text{Cp}^*_2\text{La}]_2$ . Both  $\mu$ -butatrienediyl complexes have been structurally characterized.<sup>592</sup> Various other acetylides and  $\mu$ -butatrienediyl complexes of this type have been thoroughly investigated. These include  $[\text{Cp}^*_2\text{Ce}(\mu\text{-C}\equiv\text{CR})]_n$  ( $\text{R} = \text{Me, Bu}^t$ ),  $[\text{Cp}^*_2\text{La}(\mu\text{-C}\equiv\text{CMe})]_n$ ,<sup>593</sup> and  $\text{Cp}^*_2\text{Sm}(\text{C}\equiv\text{CPh})(\text{THF})$ <sup>594</sup> as well as  $(\mu\text{-MeC}_4\text{Me})[\text{Cp}^*_2\text{La}]_2$ ,  $(\mu\text{-RC}_4\text{R})[\text{Cp}^*_2\text{Ce}]_2$  ( $\text{R} = \text{Me, Bu}^t$ ),<sup>593</sup> and  $(\mu\text{-PhC}_4\text{Ph})[\text{Cp}^*_2\text{Sm}]_2$ .<sup>593</sup> Several members of these two classes of compounds have been structurally characterized by X-ray diffraction. The bis(alkynide) complexes  $[\text{Cp}^*_2\text{Ln}(\mu\text{-C}\equiv\text{CPh})_2\text{K}]_n$  ( $\text{Ln} = \text{Ce, Nd, Sm}$ ) do not undergo the coupling reaction, but butatrienediyl complexes have been obtained by thermolysis of  $\text{Cp}^*_2\text{Ln}(\text{C}\equiv\text{CPh})(\text{THF})$  ( $\text{Ln} = \text{Ce, Nd}$ ). The latter complexes were synthesized by metathetical reactions between  $\text{Cp}^*_2\text{LnN}(\text{SiMe}_3)_2$  and  $\text{HC}\equiv\text{CPh}$ . The coupled butatrienediyl products  $[\text{Cp}^*_2\text{Sm}]_2(\mu\text{-Ph}(\text{CH}_2)_2\text{C}_4(\text{CH}_2)_2\text{Ph})$  and  $[\text{Cp}^*_2\text{Sm}]_2(\mu\text{-Me}_2\text{CH}(\text{CH}_2)_2\text{C}_4(\text{CH}_2)_2\text{CHMe}_2)$  have also been obtained by treatment of  $\text{Cp}^*_3\text{Sm}$  with  $\text{HC}\equiv\text{C}(\text{CH}_2)_2\text{Ph}$  and  $\text{HC}\equiv\text{C}(\text{CH}_2)_2\text{CHMe}_2$ , respectively. The NMR spectra and crystal structures of these products show agostic interactions involving methylene groups. The reaction of  $[\text{Cp}^*_2\text{Sm}(\mu\text{-H})_2]$  with  $\text{HC}\equiv\text{CBu}^t$  generated the loosely associated dimeric alkynide  $[\text{Cp}^*_2\text{Sm}(\mu\text{-C}\equiv\text{CBu}^t)]_2$  and the unusual insertion product  $\text{Cp}^*_2\text{Sm}[\text{Bu}^t\text{CCH}=\text{CC}(\text{Bu}^t)=\text{CH}_2]$ . Both products as well as the bis(alkynide)  $[\text{Cp}^*_2\text{Sm}(\mu\text{-C}\equiv\text{CPh})_2\text{K}]_n$  have been structurally characterized by X-ray analyses.<sup>594</sup> The precise mechanism of the reaction of butadiene with  $\text{Cp}^*_2\text{SmH}$  to give the known insertion product  $\text{Cp}^*_2\text{Sm}(\eta^3\text{-CH}_2\text{CHCHMe})$  has been investigated on the basis of DFT calculations.<sup>595</sup> The interaction of the substituted diene monomers isoprene and myrcene with  $\text{Cp}^*_2\text{Sm}$  has been studied. In both cases binuclear complexes with bridging diene ligands were obtained. Scheme 131 illustrates the formation of the isoprene derivative as an example.<sup>596</sup>

A series of permethylanthanocene and -lutetiocene vinyl complexes,  $[\text{Li}(\text{DME})_3][\text{Cp}^*_2\text{La}(\text{C}_4\text{H}_6)]$ ,  $\text{Cp}^*_2\text{LaCPh}=\text{CMe}_2\cdot 2\text{THF}$ ,  $\text{Cp}^*_2\text{Lu}(\text{CH}=\text{CH}_2)\cdot\text{LiCl}\cdot\text{DME}$ , and  $\text{Cp}^*_2\text{LuCPh}=\text{CMe}_2\cdot 2\text{MgCl}_2\cdot\text{DME}$ , has been described. The compounds were obtained by reactions of the appropriate  $\text{Cp}^*_2\text{Ln}(\mu\text{-Cl})_2\text{K}(\text{DME})_2$  ( $\text{Ln} = \text{La}$  or  $\text{Lu}$ ) precursors with  $\text{LiCH}=\text{CH}_2$  or with  $\text{MgBrCPh}=\text{CMe}_2$  (Scheme 132).<sup>597</sup>

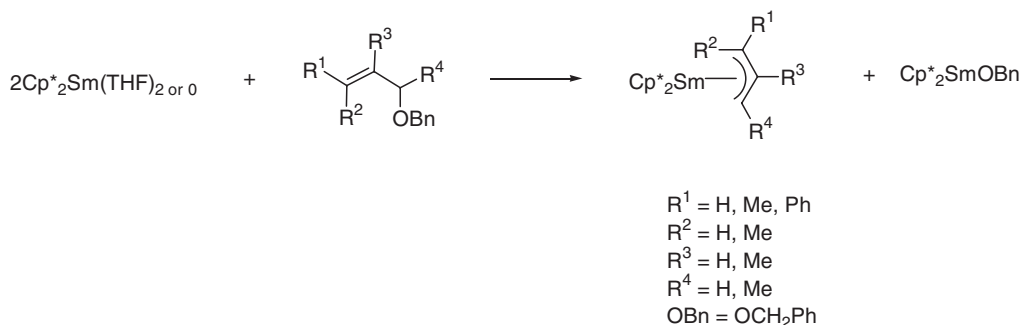
The generation of organosamarium  $\eta^3$ -allyl complexes by reductive cleavage of allylic ethers with  $\text{Cp}^*_2\text{Sm}(\text{THF})_n$  has been reported (Scheme 133). The second product of the reactions is samarium benzyloxide  $\text{Cp}^*_2\text{SmOCH}_2\text{Ph}$ .<sup>598</sup>



Scheme 131



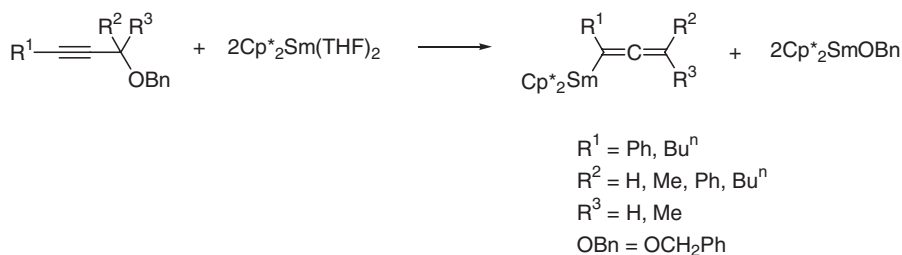
Scheme 132



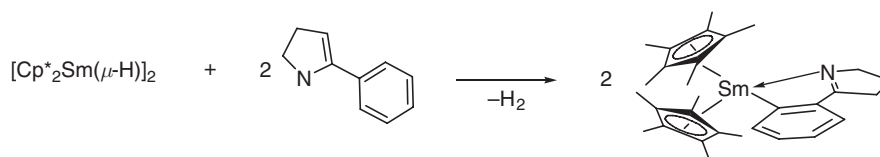
Scheme 133

Allenic samarium complexes have been generated from propargylic benzyl ethers and  $\text{Cp}^*_2\text{Sm}(\text{THF})_2$  (Scheme 134).<sup>599</sup>

Aromatic imines react with  $[\text{Cp}^*_2\text{Sm}(\mu\text{-H})_2]$  via *ortho*-metallation, rather than the anticipated 1,2-insertion of the imine into the  $\text{Sm-H}$  bond to form an amide complex. The facile conversion to the *ortho*-metallated complex (Scheme 135) was observed when the reaction with  $[\text{Cp}^*_2\text{Sm}(\mu\text{-H})_2]$  was followed by  $^1\text{H}$  NMR spectroscopy.<sup>600</sup>



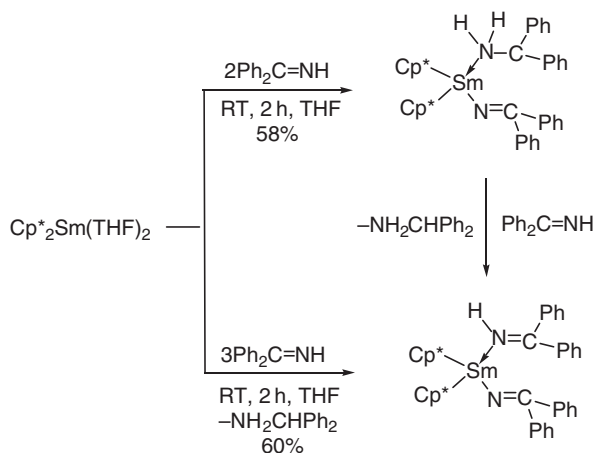
Scheme 134



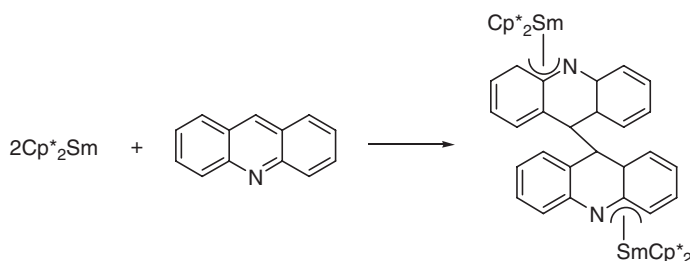
Scheme 135

The  $\text{Cp}^*_2\text{Sm}(\text{2-phenyl-1-pyrroline})$  complex was characterized spectroscopically and by single crystal X-ray diffraction. The *ortho*-metallation pathway is not limited to cyclic imines. This reaction also occurs with acyclic imines, halogen-containing ketimine substrates, and aldimines.<sup>600</sup> The reaction of  $\text{Cp}^*_2\text{Sm}(\text{THF})_2$  with 2 equiv. of benzophenone imine ( $\text{Ph}_2\text{C}=\text{NH}$ ) in THF at room temperature gave the samarocene(III) amine/ketimido complex  $\text{Cp}^*_2\text{Sm}(\text{N}=\text{CPh}_2)(\text{NH}_2\text{CHPh}_2)$  (Scheme 136), while an excess of  $\text{Ph}_2\text{C}=\text{NH}$  led to the formation of the imine-coordinated complex  $\text{Cp}^*_2\text{Sm}(\text{N}=\text{CPh}_2)(\text{HN}=\text{CPh}_2)$ .<sup>601</sup>

A reaction between  $\text{Cp}^*_2\text{Sm}$  and acridine produced the binuclear complex  $[\text{Cp}^*_2\text{Sm}]_2[\mu\text{-}\eta^3:\eta^3\text{-(C}_{13}\text{H}_9\text{N})_2]$  (Scheme 137) which, according to an X-ray diffraction analysis, contains non-planar  $\text{C}_{13}\text{H}_9\text{N}$  units. The Sm–N distance is 2.380(5) Å.<sup>602</sup> In a similar manner,  $\text{Cp}^*_2\text{Sm}(\text{THF})_2$  reacts with 1,2-bis(2-pyridyl)ethylene forming the binuclear product  $[\text{Cp}^*_2\text{Sm}]_2[\mu\text{-}\eta^2:\eta^2\text{-pyCHCHpy}]$  in 80% yield, when the reaction stoichiometry is 2:1. Combination of the same reagents in a 1:1 molar ratio gave  $[\text{Cp}^*_2\text{Sm}]_2[\mu\text{-}\eta^3:\eta^3\text{-1,2,3,4-(py)}_4\text{C}_4\text{H}_4]$  (78% yield) which contains a dimerized ligand system.<sup>603</sup> Closely related binuclear decamethylsamarocene derivatives with polycyclic aromatic hydrocarbon ligands have been obtained from reactions of  $\text{Cp}^*_2\text{Sm}$  with anthracene, 9-methylantracene, 2,3-benzanthracene, acenaphthylene, and phenazine.<sup>602</sup>



Scheme 136



Scheme 137

4.01.6.8.4.(vi)  $\text{Cp}^*_2\text{Ln}$  compounds with bonds to silicon

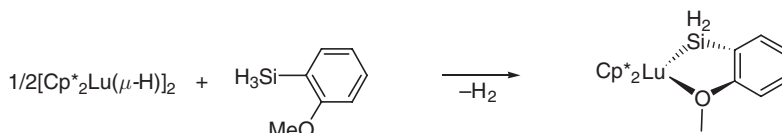
Activation of the Si–C bond of  $\text{C}_6\text{F}_5\text{SiH}_3$  with  $[\text{Cp}^*_2\text{Lu}(\mu\text{-H})]_2$  yielded the lutetium aryl complex  $\text{Cp}^*_2\text{LuC}_6\text{F}_5$  and oligosilanes. In contrast, the reaction of  $[\text{Cp}^*_2\text{Lu}(\mu\text{-H})]_2$  with *o*- $\text{MeOC}_6\text{H}_4\text{SiH}_3$  resulted in the formation of dihydrogen and a neutral lutetium silyl complex as shown in Scheme 138.<sup>604</sup>

The samarium-mediated redistribution of silanes and formation of trinuclear samarium–silicon clusters has been reported. Reaction of  $\text{Cp}^*_2\text{SmCH}(\text{SiMe}_3)_2$  with  $\text{PhSiH}_3$  (1 equiv.) in  $\text{D}_6$ -benzene occurs rapidly after a variable induction time (5–20 min) to produce a deep red solution. By  $^1\text{H}$  NMR spectroscopy, this reaction gives a quantitative yield of  $\text{CH}_2(\text{SiMe}_3)_2$ , along with  $\text{H}_2$  (26%),  $\text{PhSiH}_2\text{-SiH}_2\text{Ph}$  (11%),  $\text{Ph}_2\text{SiH}_2$  (46%), and  $\text{Ph}_3\text{SiH}$  (trace). Quantitative transfer of the deuterium label from  $\text{PhSiD}_3$  to the alkyl group (to produce  $\text{CHD}(\text{SiMe}_3)_2$ ) implies that the first step in the reaction is the formation of  $\text{Cp}^*_2\text{SmSiH}_2\text{Ph}$ , but this species has not been identified as an intermediate. In contrast,  $\text{Cp}^*_2\text{SmCH}(\text{SiMe}_3)_2$  reacts slowly with  $\text{Ph}_2\text{SiH}_2$  via redistribution at silicon to give  $\text{PhSiH}_3$  (10% after 2 d) and unidentified silicon-containing compounds, but no  $\text{PhSiH}_3$  or  $\text{Ph}_2\text{HSiSiHPh}_2$ . Crystals from such reactions over 2 days contain the cluster  $[(\text{Cp}^*_2\text{Sm})_3(\mu\text{-SiH}_3)(\mu^3\text{-}\eta^1, \eta^1, \eta^2\text{-SiH}_2\text{SiH}_2)]$  (Scheme 139).<sup>605</sup>

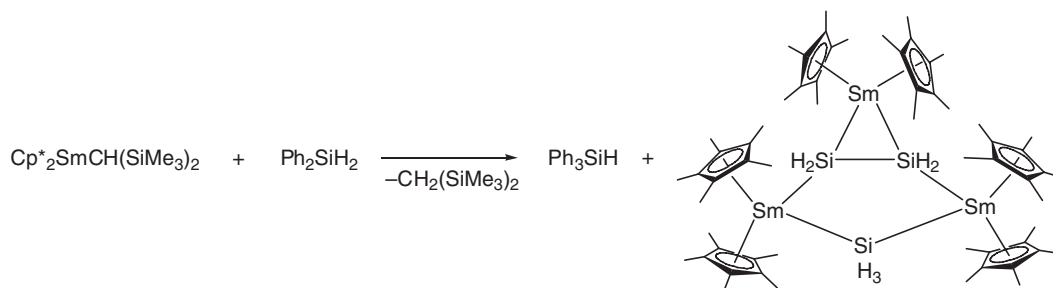
Metal–silicon bond disruption enthalpies have been measured for a series of metallocene complexes including  $\text{Cp}^*_2\text{SmSiH}(\text{SiMe}_3)_2$ . The complexes were studied by iodolytic titration calorimetry. The treatment of  $\text{Cp}^*_2\text{SmSiH}(\text{SiMe}_3)_2$  with stoichiometric amounts of  $\text{MeI}$  gave  $\text{MeSiH}(\text{SiMe}_3)_2$  and  $[\text{Cp}^*_2\text{SmI}]_x$  (Scheme 140).<sup>606</sup>

The chemistry of  $\text{Cp}^*_2\text{SmSiH}_3$  complexes has been investigated. Reaction of  $\text{PhSiH}_3$  with  $[\text{Cp}^*_2\text{Sm}(\mu\text{-H})]_2$  leads to redistribution at silicon, yielding benzene, silane,  $\text{Ph}_2\text{SiH}_2$ ,  $\text{Ph}_3\text{SiH}$ , and dehydrocoupling products (Scheme 141).<sup>607</sup>

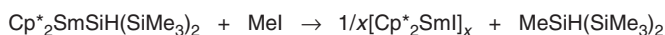
$[\text{Cp}^*_2\text{SmSiH}_3]_3$  is a rare example of a lanthanide silyl complex and represents the first example of an *f*-element  $\text{SiH}_3$  derivative. This complex activates the S–O bond of dimethyl sulfoxide (DMSO) to form the bridged species  $\text{Cp}^*_2\text{Sm}(\text{DMSO})\text{OSiH}_2\text{OSm}(\text{DMSO})\text{Cp}^*_2$  (Scheme 141). The hard Lewis bases  $\text{Ph}_3\text{PO}$  and HMPA ( $\text{HMPA} = (\text{Me}_2\text{N})_3\text{PO}$ ) react with the  $\text{Sm-SiH}_3$  complex to produce the base adducts  $\text{Cp}^*_2\text{SmSiH}_3(\text{OPPh}_3)$  and  $\text{Cp}^*_2\text{SmSiH}_3(\text{HMPA})$ , respectively.<sup>607</sup> The alkyl complexes  $\text{Cp}^*_2\text{LnCH}(\text{SiMe}_3)_2$  ( $\text{Ln} = \text{Sm}, \text{Nd}, \text{Y}$ ) and  $(\text{C}_5\text{Me}_4\text{Et})_2\text{LnCH}(\text{SiMe}_3)_2$  ( $\text{Ln} = \text{Sm}, \text{Nd}$ ) react with neat  $\text{H}_2\text{Si}(\text{SiMe}_3)_2$  (ca. 5 equiv.) at  $85^\circ\text{C}$  to give the new silyl complexes  $\text{Cp}^*_2\text{LnSiH}(\text{SiMe}_3)_2$  ( $\text{Ln} = \text{Sm}, \text{Nd}, \text{Y}$ ) and  $(\text{C}_5\text{Me}_4\text{Et})_2\text{LnSiH}(\text{SiMe}_3)_2$  ( $\text{Ln} = \text{Sm}, \text{Nd}$ ).<sup>608,609</sup> These neutral silyl complexes have been characterized, and are monomeric in pentane solution at room temperature. The



Scheme 138

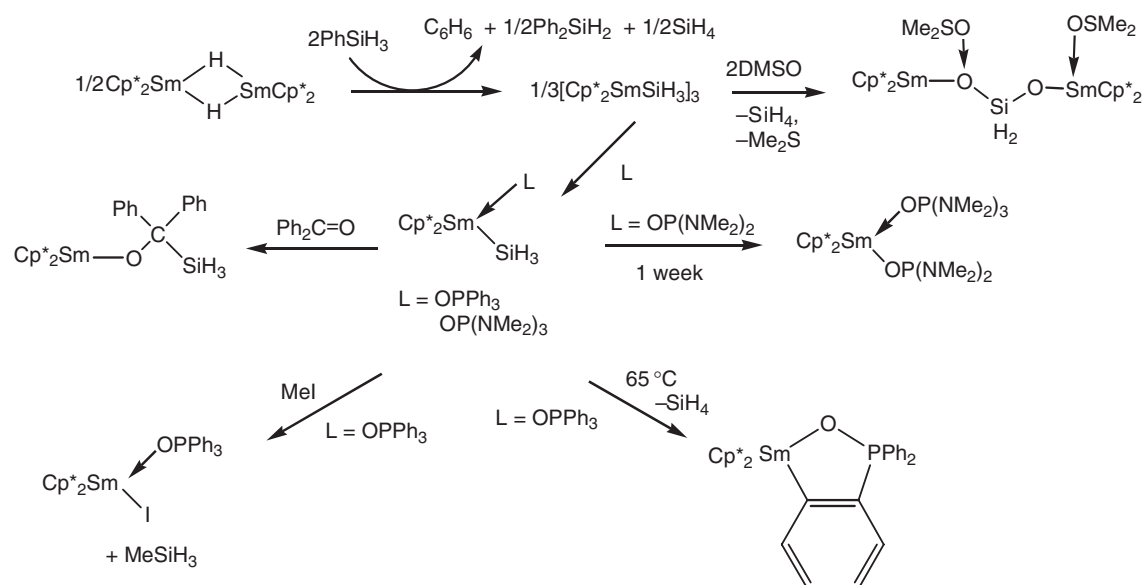


Scheme 139



Scheme 140





Scheme 141

structure of  $\text{Cp}^*_2\text{SmSiH}(\text{SiMe}_3)_2$  reveals that this compound forms dimers in the solid state via intramolecular  $\text{Sm} \cdots \text{CH}_3\text{-Si}$  interactions. The  $\text{Sm-Si}$  bond length in  $\text{Cp}^*_2\text{LnSiH}(\text{SiMe}_3)_2$  is  $3.052(8) \text{ \AA}$ . Initial reactivity studies characterized the  $\text{Ln-Si}$  bonds as being highly reactive.<sup>609</sup> The closely related scandium dihydrosilyl complexes  $\text{Cp}^*_2\text{ScSiH}_2\text{R}$  ( $\text{R} = \text{Mes}$ ,  $\text{Trip}$ ,  $\text{SiPh}_3$ ,  $\text{Si}(\text{SiMe}_3)_3$ ;  $\text{Trip} = 2,4,6\text{-Pri}_3\text{C}_6\text{H}_2$ ) have been synthesized by addition of the appropriate hydrosilane to  $\text{Cp}^*_2\text{ScMe}$ . Studies of these complexes in the context of hydrocarbon activation led to the discovery of catalytic processes for the dehydrogenative silylation of hydrocarbons (including methane, isobutene and cyclopropane) with  $\text{Ph}_2\text{SiH}_2$  via  $\sigma$ -bond metathesis.<sup>610</sup>

#### 4.01.6.8.4.(vii) $\text{Cp}^*_2\text{Ln}$ hydroborates

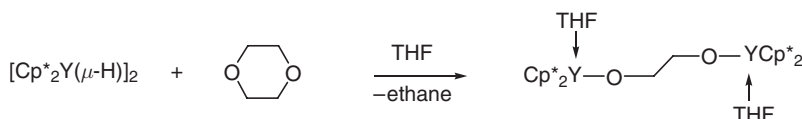
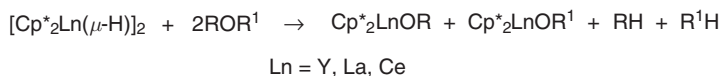
The crystal structures of the complexes  $\text{Cp}^*_2\text{SmBH}_4(\text{THF})$  and  $(\text{C}_5\text{Me}_4\text{Et})_2\text{YBH}_4(\text{THF})$  were determined. The samarium ion is coordinated by the two pentamethylcyclopentadienyl ring centroids, the THF oxygen atom, and the boron atom in an approximately tetrahedral fashion. The molecular structure of the Y complex shows two hydroborate hydrogen atoms bridging yttrium and boron. Bidentate coordination of tetrahydroborate is very common for analogous compounds of metals which are comparable in size to Y or smaller than Y.<sup>453</sup> The borohydride complexes  $\text{Cp}^*_2\text{Ln}(\mu\text{-H})_2$  ( $\text{Ln} = \text{Y}$ ,  $\text{Sm}$ ;  $\text{Mes} = \text{mesityl}$ ) have been synthesized from  $[\text{Cp}^*_2\text{Ln}(\mu\text{-H})]_2$  and  $(\text{HBMes}_2)_2$ .<sup>608</sup>

#### 4.01.6.8.4.(viii) Reactivity of $\text{Cp}^*_2\text{Ln}$ hydrides

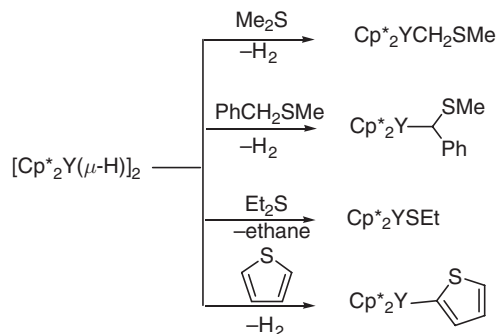
The organolanthanide hydrides  $[\text{Cp}^*_2\text{Ln}(\mu\text{-H})]_2$  ( $\text{Ln} = \text{Y}$ ,  $\text{La}$ ,  $\text{Ce}$ ) cleave dialkyl ethers  $\text{ROR}^1$  to form alkoxides  $\text{Cp}^*_2\text{LnOR}$  and  $\text{Cp}^*_2\text{LnOR}^1$ , and alkanes. The interactions of  $[\text{Cp}^*_2\text{Ln}(\mu\text{-H})]_2$  with  $\text{Et}_2\text{O}$ ,  $\text{Bu}^t\text{OMe}$ ,  $\text{Bu}^t\text{OEt}$ ,  $\text{Bu}^n\text{OEt}$ , THF, 1,4-dioxane, furan, vinyl ethyl ether, and allyl ethyl ether were studied. NMR tube experiments were used for monitoring the reactions. The product of reaction between the  $[\text{Cp}^*_2\text{Y}(\mu\text{-H})]_2$  and 1,4-dioxane (Scheme 142),  $(\mu\text{-OCH}_2\text{CH}_2\text{O})[\text{Cp}^*_2\text{Y}(\text{THF})]_2$ , was characterized by X-ray crystallography. In the structure two  $\text{Cp}^*_2\text{Y}(\text{THF})$  units with distorted tetrahedral arrangement are bridged by the glycolate ligand.<sup>611</sup>

$\text{C-O}$  bonds of the alkoxides  $\text{Cp}^*_2\text{LnOEt}$  were cleaved also by  $[\text{Cp}^*_2\text{Ln}(\mu\text{-H})]_2$  to give bimetallic complexes  $[\text{Cp}^*_2\text{Ln}]_2(\mu\text{-O})$ . The structure of the THF adduct  $[\text{Cp}^*_2\text{Ce}(\text{THF})]_2(\mu\text{-O})$  was determined by X-ray diffraction. The complex consists of two  $\text{Cp}^*_2\text{Ce}$  fragments linked by a nearly linear oxygen bridge. In contrast to ethers, activation of organic sulfides by  $[\text{Cp}^*_2\text{Y}(\mu\text{-H})]_2$  led to the corresponding metallation products (Scheme 143).<sup>611</sup>

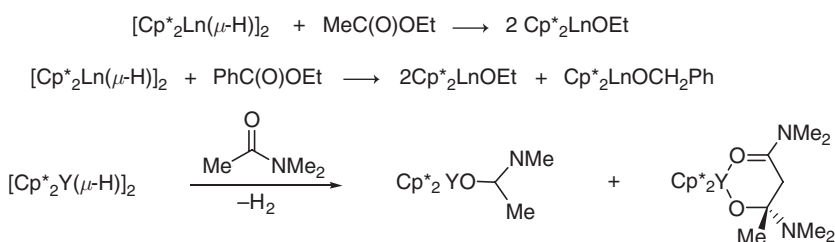
Metallation reactions of  $[\text{Cp}^*_2\text{Y}(\mu\text{-H})]_2$  with pyridine derivatives have been investigated in detail.<sup>612</sup> Thermolysis of  $[\text{Cp}^*_2\text{Y}(\mu\text{-H})]_2$  in octane, cyclohexane, or benzene was reported to yield the thermodynamically favored tetramethylfulvene product  $\text{Cp}^*_2\text{Y}(\mu\text{-H})(\mu\text{-}\eta^1, \eta^5\text{-CH}_2\text{C}_5\text{Me}_4)\text{YCp}^*$ . In reactions of  $[\text{Cp}^*_2\text{Y}(\mu\text{-H})]_2$  with substituted benzene  $\text{PhX}$  ( $\text{X} = \text{OMe}$ ,  $\text{SMe}$ ,  $\text{NMe}_2$ ,  $\text{CH}_2\text{NMe}_2$ ,  $\text{PMe}_2$ ,  $\text{PPh}_2=\text{CH}_2$ ) *ortho*-metallation of the phenyl group is the



Scheme 142



Scheme 143



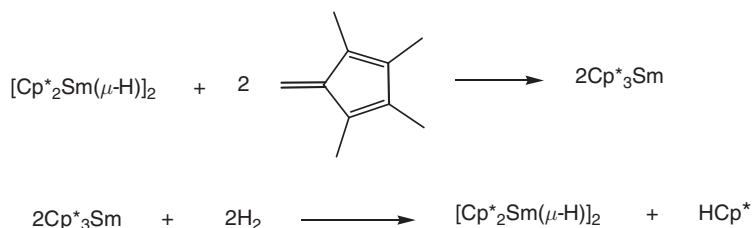
Scheme 144

predominant reaction, although formation of  $\text{Cp}^*_2\text{Y}(\mu\text{-H})(\mu\text{-}\eta^1, \eta^5\text{-CH}_2\text{C}_5\text{Me}_4)\text{YCp}^*$  was also observed ( $\text{X} = \text{NMe}_2$ ,  $\text{CH}_2\text{NMe}_2$ ). The crystal structure of  $\text{Cp}^*_2\text{Y}(\text{o-C}_6\text{H}_4\text{PPh}_2=\text{CH}_2)$  has been determined.<sup>613</sup> Reactions of  $[\text{Cp}^*_2\text{Ln}(\mu\text{-H})]_2$  ( $\text{Ln} = \text{Y, La}$ ) and  $\text{Cp}^*_2\text{Y}(2\text{-C}_6\text{H}_4\text{CH}_2\text{NMe}_2)$  with esters (ethyl acetate, ethyl benzoate, ethyl acrylate, ethyl 2-methylpropanoate) and amides (*N,N*-dimethylacetamide) have also been studied (Scheme 144). The molecular structure of  $[\text{Cp}^*_2\text{Y}(\mu\text{-OCMe}=\text{CHC}(\text{OEt})\text{O})]_2$ , the product of the reaction of  $\text{Cp}^*_2\text{Y}(2\text{-C}_6\text{H}_4\text{CH}_2\text{NMe}_2)$  with ethyl acetate, has been determined by X-ray diffraction. The dimer contains two equivalent  $\text{Cp}^*_2\text{Y}(\mu\text{-OCMe}=\text{CHC}(\text{OEt})\text{O})$  fragments.<sup>614</sup>

#### 4.01.6.8.5 Tris(pentamethylcyclopentadienyl)lanthanide(III) compounds

The more recently discovered tris(pentamethylcyclopentadienyl)lanthanides and their fascinating chemistry have been summarized in several review articles by Evans.<sup>25–27</sup> A four-step procedure to synthesize  $\text{Cp}^*_3\text{La}$  has been developed. The same synthetic route could also be successfully applied to the preparation of the highly crowded tris(peralkylcyclopentadienyl)lanthanum complexes  $(\text{C}_5\text{Me}_4\text{Et})_3\text{La}$ ,  $(\text{C}_5\text{Me}_4\text{Pr}^i)_3\text{La}$ , and  $(\text{C}_5\text{Me}_4\text{SiMe}_3)_3\text{La}$ , which have all been structurally characterized by X-ray analyses.<sup>615</sup> A new synthetic method to tris(pentamethylcyclopentadienyl) samarium has been reported. It involves the reaction of tetramethylfulvene with the samarocene hydride  $[\text{Cp}^*_2\text{Sm}(\mu\text{-H})]_2$ . The reagent  $[\text{Cp}^*_2\text{Sm}(\mu\text{-H})]_2$  was in turn produced by the reaction of  $\text{Cp}^*_3\text{Sm}$  and  $\text{H}_2$  under hydrogenolysis (Scheme 145).<sup>616,616a</sup>

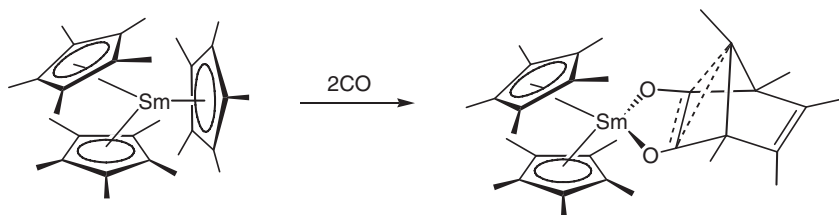
The complex  $[\text{Cp}^*_2\text{Sm}][\text{BPh}_4]$  reacts with  $\text{KCp}^*$  in benzene to yield the sterically crowded complex  $\text{Cp}^*_3\text{Sm}$ . This reaction provides a convenient way to make  $\text{Cp}^*_3\text{Ln}$  complexes of lanthanide elements which do not have a readily



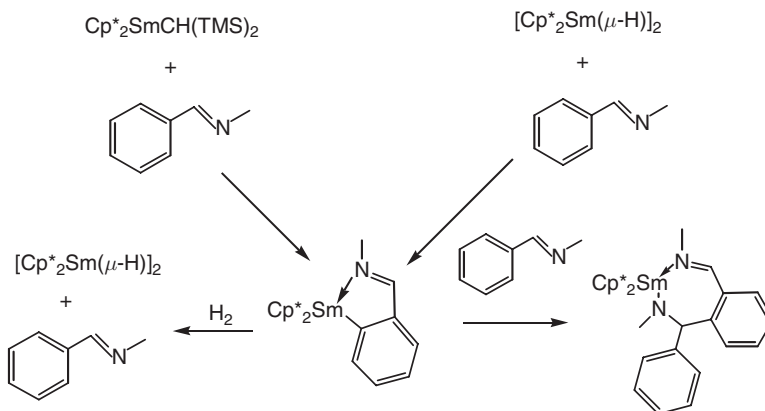
Scheme 145

accessible divalent oxidation state.  $\text{Cp}^*_3\text{Nd}$  was also synthesized from  $[\text{Cp}^*_2\text{Nd}][\text{BPh}_4]$  in the reaction with  $\text{LiCH}(\text{SiMe}_3)_3$  and  $\text{KCp}^*$ . This complex has an  $(\eta^5\text{-Cp}^*)_3\text{Nd}$  structure with a 2.86(6) Nd–C(Cp<sup>\*</sup>) distance.<sup>552</sup> The reactivity of sterically crowded  $\text{Cp}^*_3\text{Sm}$  with a variety of substrates including CO, THF, ethylene, hydrogen, nitriles, isonitriles, isocyanates, 1,3,5,7-cyclooctatetraene (COT), azobenzene, and  $\text{Ph}_3\text{P}=\text{E}$  (E = O, S, Se) has been investigated (cf. preceding Section). The reactions include polymerization, insertion, ring-opening, and reduction. Depending on the substrate  $\text{Cp}^*_3\text{Sm}$  can react as if it were a bulky alkyl complex of the formula  $\text{Cp}^*_2\text{SmR}$  in which R is an  $\eta^1\text{-Cp}^*$  group, or as if it were the zwitterionic species  $[\text{Cp}^*_2\text{Sm}]^+[\text{Cp}^*]^-$  in which the  $[\text{Cp}^*]^-$  component is a one-electron reductant. In the former mode, the samarium compound reacted with CO to form  $\text{Cp}^*_2\text{Sm}(\text{O}_2\text{C}_7\text{Me}_5)$ , which has a ligand containing a non-classical carbocationic center, originating from the five-ring carbon atoms of a  $\text{Cp}^*$  moiety and the carbon atoms of two CO molecules. The seven non-methyl carbon atoms of the ligand adopt a norbornadiene structure. The symmetry-equivalent Sm–O bonds are 2.347(2) Å, the average Sm–CCp<sup>\*</sup> distance is 2.73 Å (Scheme 146).<sup>617,618</sup> This unexpected formation of a non-classical carbocation has been highlighted by Krishnamurthy.<sup>619</sup>

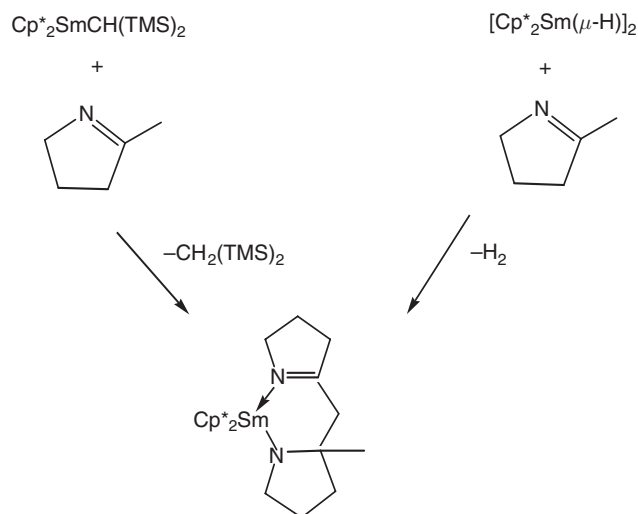
$\text{Cp}^*_3\text{Sm}$  reacts with  $\text{H}_2$  to form  $[\text{Cp}^*_2\text{Sm}(\mu\text{-H})_2]_2$ , opens the ring of THF to form  $\text{Cp}^*_2\text{Sm}[\text{O}(\text{CH}_2)_4\text{Cp}^*](\text{THF})$ , and reacts with  $\text{PhNCO}$  to form  $\text{Cp}^*_2\text{Sm}[\text{OCCp}^*\text{N}(\text{Ph})\text{C}(\text{NPh})\text{O}]$ .  $\text{Cp}^*_3\text{Sm}$  reduces  $\text{Ph}_3\text{PO}$  to form  $\text{PPh}_3$ ,  $(\text{C}_5\text{Me}_5)_2$ , and  $[\text{Cp}^*_2\text{Sm}]_2(\mu\text{-O})$ . In general  $\text{Cp}^*_3\text{Sm}$  reduces  $\text{Ph}_3\text{PE}$  (E = S, Se) to form  $\text{Cp}^*_2$  and  $[\text{Cp}^*_2\text{Sm}(\text{THF})_2]_2(\mu\text{-E})$ . With COT this samarium complex reacts to form  $\text{Cp}^*\text{Sm}(\text{COT})$  and  $(\text{C}_5\text{Me}_5)_2$ .<sup>618</sup> The stoichiometric reaction of *N*-benzylidene(methyl)amine with  $\text{Cp}^*_2\text{SmCH}(\text{SiMe}_3)_2$  or  $[\text{Cp}^*_2\text{Sm}(\mu\text{-H})_2]_2$  yields an *ortho*-metallated  $\text{Cp}'_2\text{Sm}$  substrate complex which undergoes either hydrogenolysis/hydrogenation or competing C=N insertion of a second substrate molecule to yield a  $\text{Cp}^*_2\text{Sm}$ -imine-amido complex with a seven-membered chelate ring (Scheme 147).<sup>620</sup>



Scheme 146



Scheme 147



Scheme 148

The stoichiometric reaction of 2-methylen-1-pyrroline results in the formation of a  $\text{Cp}_2^*\text{Sm}$ -imine-amido complex in which two substrate molecules have been coupled to form a six-membered chelate ring (Scheme 148).<sup>620</sup>

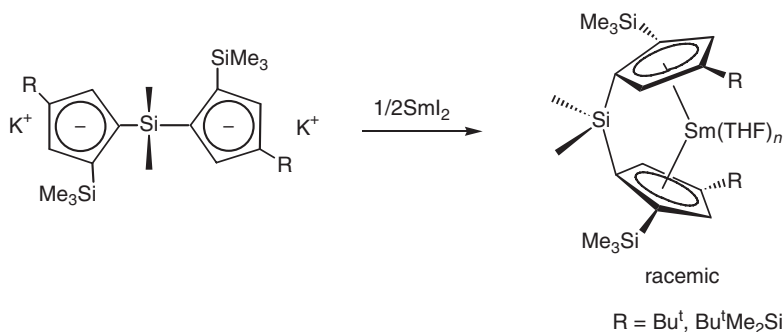
The stoichiometric reaction of *N*-benzylidene(trimethylsilyl)amine with  $[\text{Cp}_2^*\text{Sm}(\mu\text{-H})]_2$  yields a  $\text{Cp}_2^*\text{Sm}$ -imine-amido complex with a four-membered  $\text{Sm}(\text{NSiMe}_3)(\text{CPh})\text{N}=\text{CHPh}$  chelate ring. Heating of this product under  $\text{H}_2$  gave  $S_6$ -symmetric  $[\text{Cp}_2^*\text{SmCN}]_6$ , which contains an unusual chair-like 18-membered  $(\text{SmCN})_6$  ring.<sup>620</sup>

#### 4.01.6.9 Compounds with Ring-bridged Cyclopentadienyl Ligands

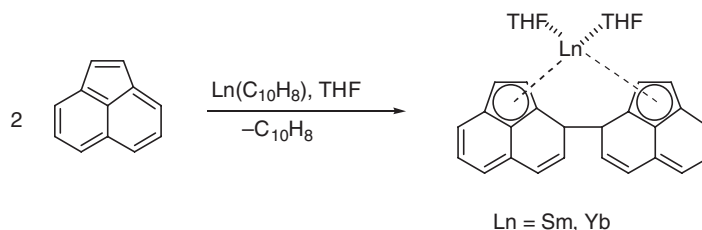
##### 4.01.6.9.1 Lanthanide(II) compounds

2-*t*-Butyl-6,6,-dimethylfulvene reacts with samarium metal to give the *ansa*-samarocene(II) complex  $[\text{Me}_4\text{C}_2(\text{C}_5\text{H}_3\text{Bu}^t)_2]\text{Sm}$ .<sup>621</sup> Several new divalent samarium complexes with bridged bis(cyclopentadienyl) ligands were synthesized by the reaction of the dipotassium salt of the corresponding ligand with  $\text{SmI}_2$ . A typical example is shown in Scheme 149.<sup>622</sup>

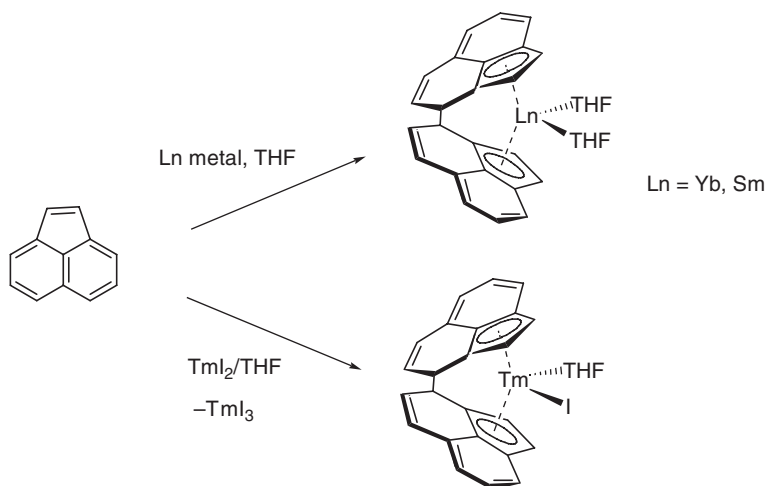
These bridged bis(cyclopentadienyl) samarium complexes exhibit various structures with regard to the bridging group and the position of substituents on the Cp rings.<sup>622</sup> *ansa*-Metalloenes of the formula  $(\eta^5:\eta^5\text{-C}_{24}\text{H}_{16})\text{Ln}(\text{THF})_2$



Scheme 149



Scheme 150



Scheme 151

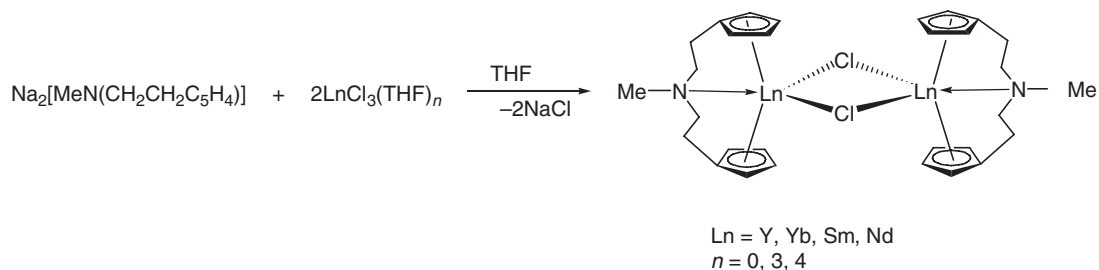
( $\text{Ln} = \text{Sm, Yb}$ ) were prepared in 80–90% yields by the *in situ* reactions of 2 equiv. of potassium acenaphthylenide,  $\text{KC}_{12}\text{H}_8$ , with  $\text{LnI}_2$  or by reacting the naphthalene complexes of Sm and Yb with acenaphthylene (Scheme 150).<sup>623–625</sup>

The same compounds are also readily accessible via reductive coupling of acenaphthylene with activated ytterbium or samarium as depicted in Scheme 151.<sup>626,626a</sup>

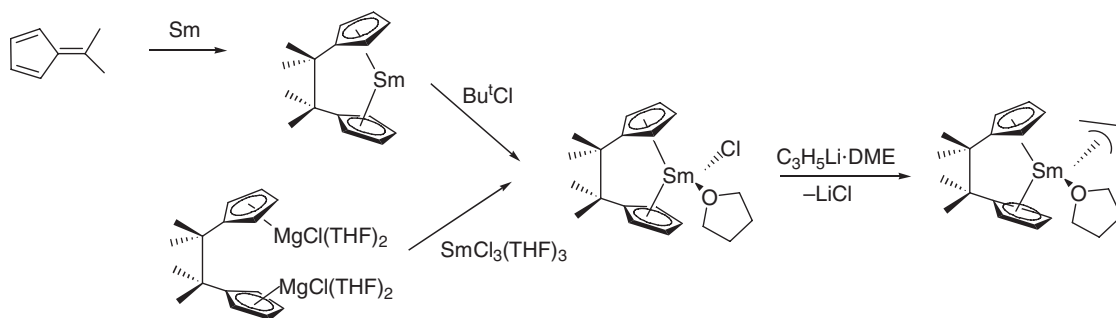
Guaiazulene reacts with ytterbium metal in the same manner to give an *ansa*-bis(guaiazulene)ytterbium(II) complex.<sup>627</sup> The powerful reducing agent thulium(II) diiodide also reacts directly with acenaphthylene in THF solution to give orange crystals of *ansa*- $[(\eta^5\text{-C}_{12}\text{H}_8)_2]\text{TmI}(\text{THF})$  in 82% yield (Scheme 151).<sup>628</sup>

#### 4.01.6.9.2 Lanthanide(III) compounds

The synthesis of  $[\{\text{MeN}(\text{CH}_2\text{CH}_2\text{C}_5\text{H}_4)_2\}\text{Ln}(\mu\text{-Cl})_2]$  ( $\text{Ln} = \text{Y, Nd, Sm, Yb}$ ) in high yields has been achieved by treatment of anhydrous  $\text{LnCl}_3(\text{THF})_n$  ( $n = 0, 3, \text{ or } 4$ ) with  $\text{Na}_2[\text{MeN}(\text{CH}_2\text{CH}_2\text{C}_5\text{H}_4)_2]$  (Scheme 152).<sup>629</sup> Closely related dimeric *ansa*-lanthanocene chlorides have been reported with pyridine-bridged<sup>630,631</sup> and furan-bridged<sup>505</sup> bis(cyclopentadienyl) ligands.



Scheme 152

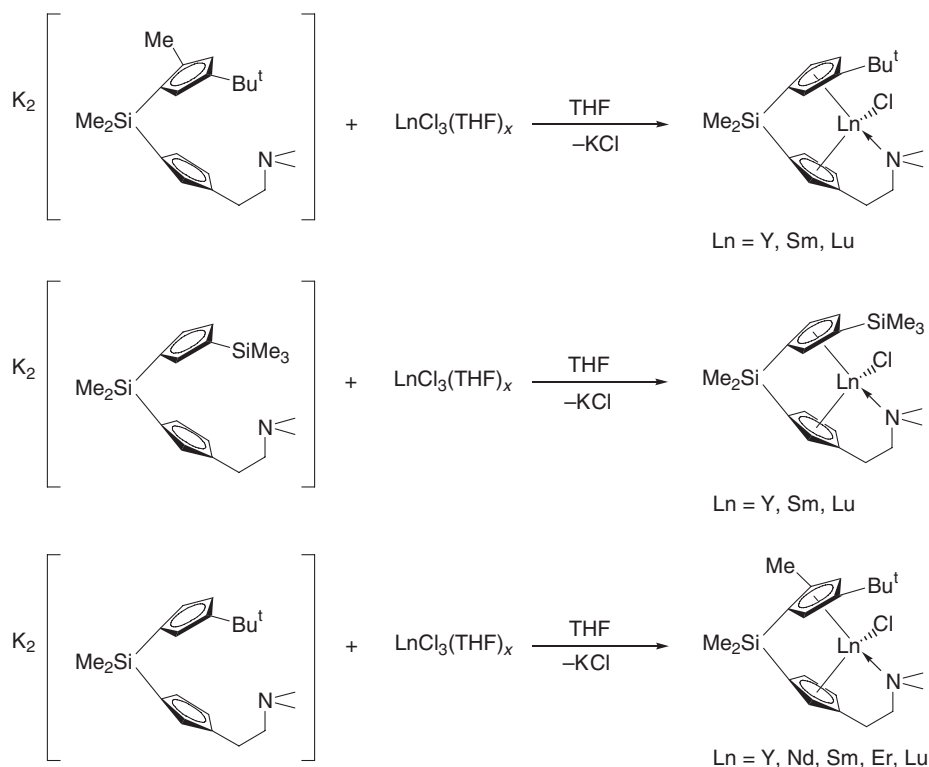


Scheme 153

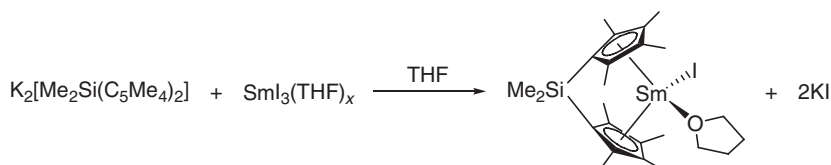
*ansa*-Metalloenes of the formula  $(\eta^5\text{-C}_{24}\text{H}_{16})\text{LnI}(\text{THF})$  ( $\text{Ln} = \text{Dy}, \text{Er}, \text{Tm}, \text{Lu}$ ) were prepared in 50–90% yields by the *in situ* reactions of 2 equiv. of potassium acenaphthylenide,  $\text{KC}_{12}\text{H}_8$ , with  $\text{LnI}_3$ .<sup>624</sup> The divalent *ansa*-metalloenes  $[\text{Me}_4\text{C}_2(\text{C}_5\text{H}_4)_2]\text{Ln}$  ( $\text{Ln} = \text{Sm}, \text{Yb}$ ) have been shown to be useful starting materials for trivalent organolanthanide complexes containing this bridged ligand system. Oxidation of  $[\text{Me}_4\text{C}_2(\text{C}_5\text{H}_4)_2]\text{Yb}$  with  $\text{Bu}^t\text{Cl}$  afforded the chloro-bridged binuclear ytterbium(III) complex  $[\{\text{Me}_4\text{C}_2(\text{C}_5\text{H}_4)_2\}\text{Yb}(\mu\text{-Cl})]_2$ . In contrast, treatment of  $[\text{Me}_4\text{C}_2(\text{C}_5\text{H}_4)_2]\text{Sm}$  with  $\text{Bu}^t\text{Cl}$  yielded the mononuclear derivative  $[\text{Me}_4\text{C}_2(\text{C}_5\text{H}_4)_2]\text{SmCl}(\text{THF})$  (Scheme 153). An organosamarium(III) selenolate,  $[\text{Me}_4\text{C}_2(\text{C}_5\text{H}_4)_2]\text{Sm}(\text{SeMes})$ , was prepared from  $[\text{Me}_4\text{C}_2(\text{C}_5\text{H}_4)_2]\text{Sm}$  and dimesityl diselenide via reductive cleavage of the Se–Se bond. Similarly, the dithiocarbamates and dithiophosphates  $[\text{Me}_4\text{C}_2(\text{C}_5\text{H}_4)_2]\text{Ln}(\text{S}_2\text{CNMe}_2)$  and  $[\text{Me}_4\text{C}_2(\text{C}_5\text{H}_4)_2]\text{LnS}_2\text{P}(\text{OMe})_2$  ( $\text{Ln} = \text{Sm}, \text{Yb}$ ) have been prepared by treatment of  $[\text{Me}_4\text{C}_2(\text{C}_5\text{H}_4)_2]\text{Ln}$  ( $\text{Ln} = \text{Sm}, \text{Yb}$ ) with the corresponding disulfides.<sup>621</sup> In a similar manner, catalytically active (isoprene polymerization) non-hindered *ansa*-dicyclopentadienyl allyl complexes of samarium have been synthesized either starting from the magnesium salt of the ligand or by dimerization of 6,6-dimethylfulvene in the presence of samarium followed by oxidation (Scheme 153).<sup>632,633</sup> The reaction of  $\text{SmCl}_3$  with the magnesium reagents  $\text{Me}_4\text{C}_2(\text{C}_5\text{H}_4\text{MgCl})_2(\text{THF})_4$  has been reported by other authors to give the bimetallic *ansa*-samarocene derivative  $[\{\text{Me}_4\text{C}_2(\text{C}_5\text{H}_4\text{MgCl})_2\}_2\text{SmClMgCl}_2(\text{THF})_4]_2$  (Scheme 153).<sup>634</sup>

The reaction of  $\text{Me}_2\text{SiCl}_2$  with  $\text{K}[\text{C}_5\text{H}_4\text{Bu}^t]$ ,  $\text{Li}[\text{C}_5\text{H}_4\text{SiMe}_3]$ , or  $\text{K}[\text{C}_5\text{H}_3\text{Bu}^t\text{Me-3}]$  followed by treatment with  $\text{K}[\text{C}_5\text{H}_4\text{CH}_2\text{CH}_2\text{NMe}_2]$  yields mixed substituted dicyclopentadienyldimethylsilanes, which after double deprotonation with potassium hydride afforded the dipotassium salts  $\text{K}_2[\text{Me}_2\text{Si}(\text{C}_5\text{H}_3\text{Bu}^t\text{-3})(\text{C}_5\text{H}_3\text{CH}_2\text{CH}_2\text{NMe}_2\text{-3})]$ ,  $\text{K}_2[\text{Me}_2\text{Si}(\text{C}_5\text{H}_3\text{SiMe}_3\text{-3})(\text{C}_5\text{H}_3\text{CH}_2\text{CH}_2\text{NMe}_2\text{-3})]$ , and  $\text{K}_2[\text{Me}_2\text{Si}(\text{C}_5\text{H}_2\text{Bu}^t\text{-3-Me-5})(\text{C}_5\text{H}_3\text{CH}_2\text{CH}_2\text{NMe}_2\text{-3})]$ , respectively.<sup>635</sup> The reaction of the dipotassium salts with lanthanide trichlorides in a 1:1 molar ratio gave the *ansa*-lanthanidocenes according to Scheme 154. Asymmetrical substitution of the cyclopentadiene ligands leads to the possible formation of four different isomers. However, the NMR spectra implied the presence of a racemic mixture of just one enantiomeric form. The NMR spectra in benzene showed two signals for the methyl protons of the amino function indicating the coordination of the nitrogen to the metal. Single crystal X-ray determinations of  $[\text{Me}_2\text{Si}(\text{C}_5\text{H}_2\text{Bu}^t\text{-3-Me-5})(\text{C}_5\text{H}_3\text{CH}_2\text{CH}_2\text{NMe}_2\text{-3})]\text{SmCl}$  and  $[\text{Me}_2\text{Si}(\text{C}_5\text{H}_2\text{Bu}^t\text{-3-Me-5})(\text{C}_5\text{H}_3\text{CH}_2\text{CH}_2\text{NMe}_2\text{-3})]\text{LuCl}$  revealed their monomeric structure with pseudo-tetrahedrally coordinated metal centers. The metal centers are coordinated by the cyclopentadienyl ligands, chlorine, and the nitrogen atom of the dimethylamino group. The metal–Cp and metal–N distances of both complexes are in good agreement with those of related complexes.<sup>635</sup> Closely related donor-substituted *ansa*-lanthanidocenes have been prepared by reacting anhydrous  $\text{LnCl}_3(\text{THF})_n$  ( $\text{Ln} = \text{Y}, \text{Sm}, \text{Ho}, \text{Er}, \text{Lu}$ ) with the dipotassium salt  $\text{K}_2[\text{Me}_2\text{Si}(\text{C}_5\text{Me}_4)(\text{C}_5\text{H}_3\text{CH}_2\text{CH}_2\text{NMe}_2)]$  (Scheme 154).<sup>636</sup> Alkylation of some of the lanthanidocene monochlorides with  $\text{LiMe}$ ,  $\text{LiCH}_2\text{SiMe}_3$ , and  $\text{LiCH}(\text{SiMe}_3)_2$  led to the corresponding alkylmetalloenes. The alkylated species  $[\text{Me}_2\text{Si}(\text{C}_5\text{H}_3\text{Bu}^t\text{-3})(\text{C}_5\text{H}_3\text{CH}_2\text{CH}_2\text{NMe}_2\text{-3})]\text{LnR}$  ( $\text{R} = \text{Me}$ ,  $\text{Ln} = \text{Sm}, \text{Y}$ ;  $\text{R} = \text{CH}_2\text{SiMe}_3$ ,  $\text{Ln} = \text{Y}$ ),  $[\text{Me}_2\text{Si}(\text{C}_5\text{H}_3\text{SiMe}_3\text{-3})(\text{C}_5\text{H}_3\text{CH}_2\text{CH}_2\text{NMe}_2\text{-3})]\text{YMe}$ , and  $[\text{Me}_2\text{Si}(\text{C}_5\text{H}_2\text{Bu}^t\text{-3-Me-5})(\text{C}_5\text{H}_3\text{CH}_2\text{CH}_2\text{NMe}_2\text{-3})]\text{LnR}$  ( $\text{R} = \text{CH}_3$ ,  $\text{Ln} = \text{Lu}$ ;  $\text{R} = \text{CH}_2\text{SiMe}_3$ ,  $\text{Ln} = \text{Lu}$ ;  $\text{R} = \text{CH}(\text{SiMe}_3)_2$ ,  $\text{Ln} = \text{Nd}, \text{Lu}$ ) show several signal sets in the NMR spectra indicating the existence of an enantiomeric mixture like in case of the homologous monochloride complexes. NMR spectroscopic determinations in pyridine suggested dissociation of the dimethylamino group in strongly basic solvents.<sup>635</sup>

$\text{SmI}_3$  was reacted with  $\text{Me}_2\text{Si}(\text{C}_5\text{Me}_4)_2$  to obtain  $[\text{Me}_2\text{Si}(\text{C}_5\text{Me}_4)_2]\text{SmI}(\text{THF})$  (Scheme 155). A single crystal X-ray determination showed a monomeric structure for  $(\text{C}_5\text{Me}_4)_2\text{SmI}(\text{THF})$  with normal Sm–Cp, Sm–I, and Sm–O(THF) distances.<sup>637</sup>



Scheme 154



Scheme 155

The *ansa*-ytterbium *ate*-complex  $\text{rac-}[\text{Me}_2\text{C}(\text{C}_5\text{H}_3\text{Me}_3\text{Si-3})_2]\text{Yb}(\mu_2\text{-Cl})_2\text{Li}(\text{OEt})_2$  was obtained in ether from the dilithium salt of 2,2-bis(3-trimethylsilylcyclopentadienyl)propane  $\text{Li}_2[\text{Me}_2\text{C}(\text{C}_5\text{H}_3\text{Me}_3\text{Si-3})_2]$  and ytterbium(III) chloride (Scheme 156).<sup>638</sup>

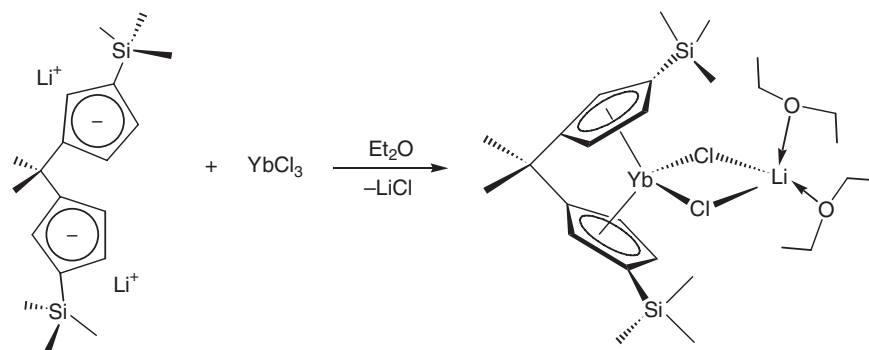
The *ansa*-ytterbocene complex  $\text{meso-}[\text{Me}_2\text{Si}(\text{C}_5\text{H}_3\text{Me}_3\text{Si-3})_2]\text{YbCl}(\text{THF})$  undergoes desolvation during recrystallization from toluene to give the dimeric complex  $\text{meso-}[\{\text{Me}_2\text{Si}(\text{C}_5\text{H}_3\text{Me}_3\text{Si-3})\}_2\text{Yb}(\mu_2\text{-Cl})_2]$ . The monomeric complex  $[\text{meso-}\text{Me}_2\text{Si}(\text{C}_5\text{H}_3\text{Me}_3\text{Si-3})_2]\text{YbCl}(\text{THF})$  reacts with  $\text{LiBH}_4$  in diethyl ether, yielding the borohydride complex  $\text{meso-}[\text{Me}_2\text{Si}(\text{C}_5\text{H}_3\text{Me}_3\text{Si-3})_2]\text{YbBH}_4(\text{THF})$  with a tridentate  $\text{BH}_4$  group, while in similar lanthanide borohydrides the  $\text{BH}_4$  group is often bonded in a bidentate fashion with B–H bond length typical for such compounds.<sup>639</sup> Sterically more congested dimethylsilylen-bis(cyclopentadienyl) ligands containing four bulky substituents have been employed in the synthesis of *ansa*-neodymocenes as illustrated in Scheme 157.<sup>640,641</sup>

The complexes  $[\text{MeRSiCp}''_2]\text{LnCH}(\text{SiMe}_3)_2$  ( $\text{Ln} = \text{Y, Sm}$ ) containing a new ligand functionalized with a donor group, which is appended through varying chain length to the silicon bridge, were synthesized to investigate the influence of the tethered ether group on the reactivity and catalytic properties of the products (Scheme 158).<sup>642</sup>

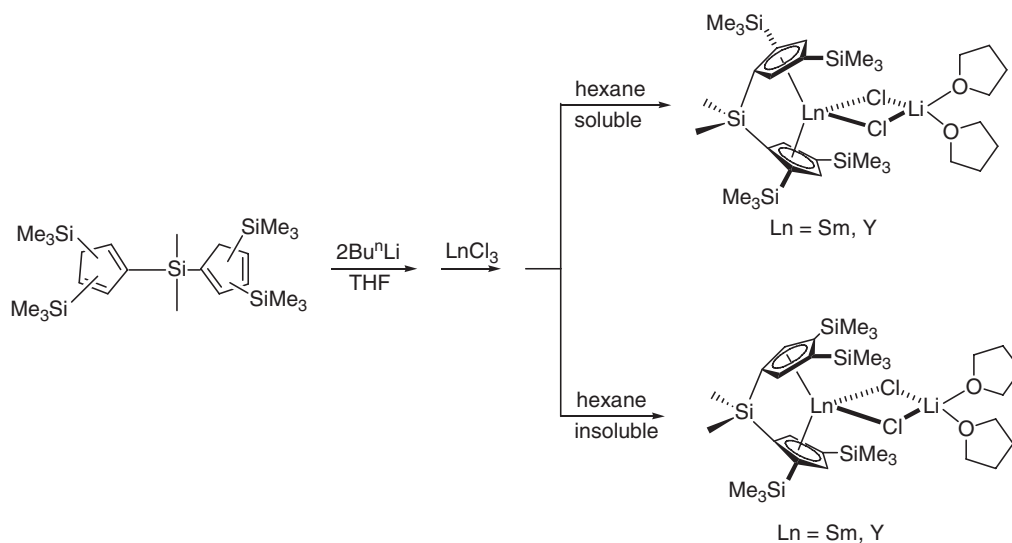
The chiral silicon-bridged lanthanidocene chlorides  $[\text{MeRSi}(\text{C}_5\text{H}_4)(\text{C}_5\text{Me}_4)\text{LnCl}]_2$  ( $\text{R} = \text{Et, Ph}$ ;  $\text{Ln} = \text{Y, La, Sm, Lu}$ ) were made according to Scheme 159 from the disodium salts  $\text{Na}_2[\text{MeRSi}(\text{C}_5\text{H}_4)(\text{C}_5\text{Me}_4)]$  ( $\text{R} = \text{Et, Ph}$ ) and the corresponding lanthanide trichlorides in THF.<sup>643</sup>

The  $^1\text{H}$  NMR spectra indicate the presence of monomeric THF-containing complexes of the type  $[\text{MeRSi}(\text{C}_5\text{H}_4)(\text{C}_5\text{Me}_4)]\text{LnCl}(\text{THF})$  as primary products which on vacuum-drying lose their THF forming the

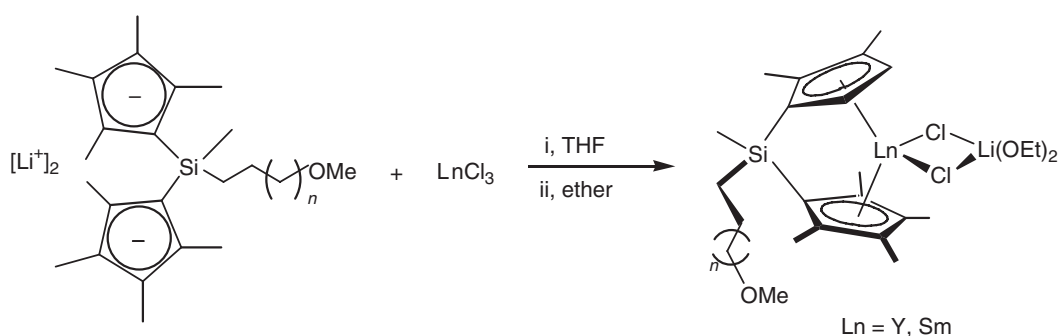




Scheme 156

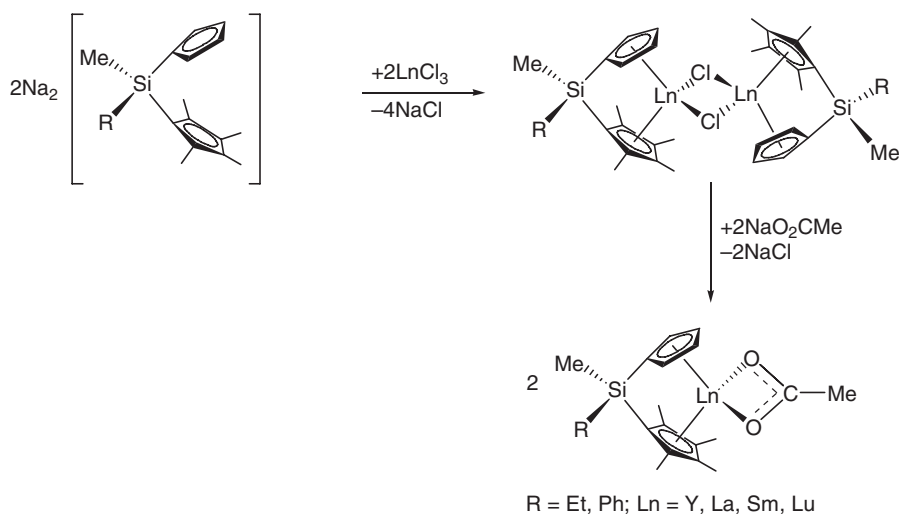


Scheme 157



Scheme 158

dimers. Single crystal X-ray determination of  $[\{\text{MeEtSi}(\text{C}_5\text{H}_4)(\text{C}_5\text{Me}_4)\}\text{Sm}(\mu\text{-Cl})(\text{THF})]_2$  showed a dinuclear complex. One THF molecule is coordinated to each samarium. Distances and angles are roughly similar to that of known compounds of the same type.<sup>643</sup> Five homologs of the new *ansa*-lanthanidocene series  $[\text{LnL}(\mu\text{-OTf})]_2$  with Ln = Y, Pr, Nd, Sm, Yb have been prepared from Ln(OTf)<sub>3</sub> (OTf = trifluoromethanesulfonate) and Na<sub>2</sub>L, where L designates two cyclopentadienyl rings tethered by a 2,6-bis(methylene)pyridyl unit.<sup>644</sup>



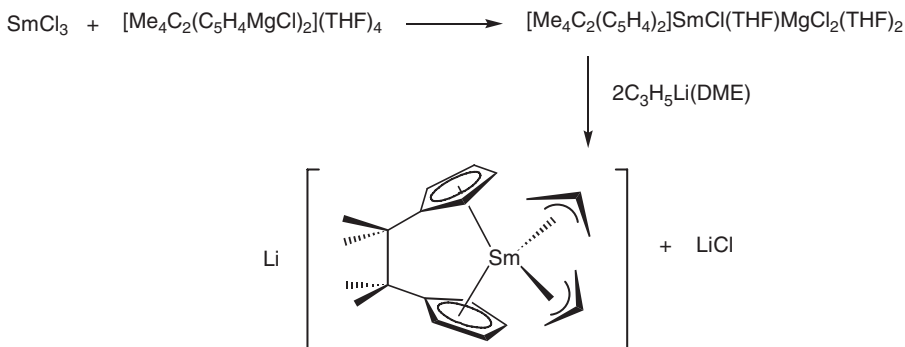
Scheme 159

The reaction of  $[\text{Me}_2\text{Si}(\text{C}_5\text{Me}_4)_2]\text{SmI}(\text{THF})$  with  $\text{KCp}^*$  in toluene yielded the base-free complex  $[\text{Me}_2\text{Si}(\text{C}_5\text{Me}_4)_2]\text{SmCp}^*$ , whereas the same reaction in THF produced the THF adduct  $[\text{Me}_2\text{Si}(\text{C}_5\text{Me}_4)_2]\text{SmCp}^*(\text{THF})$ .<sup>637</sup> The crystal structure of the *ansa*-tris(cyclopentadienyl) samarium complex  $[\text{O}(\text{SiMe}_2\text{C}_5\text{H}_4)_2]\text{Sm}(\text{C}_5\text{H}_4\text{SiMe}_2\text{NMe}_2)$  has been determined.<sup>645</sup> Various other silylene-bridged *ansa*-cyclopentadienyl lanthanide complexes, which have been thoroughly investigated, contain the bis(cyclopentadienyl) ligands  $[\text{Me}_2\text{Si}(\text{C}_5\text{H}_3\text{Bu}^t)_2]^{2-}$  and  $[\text{Me}_2\text{Si}(\text{C}_5\text{H}_3\text{SiMe}_3)_2]^{2-}$ ,<sup>646</sup>  $[\text{O}(\text{SiMe}_2\text{C}_5\text{H}_4)_2]^{2-}$  (Ln = Pr, Yb),<sup>647</sup>  $[\text{Me}_2\text{Si}(\text{C}_5\text{H}_3\text{Bu}^t)(\text{C}_5\text{Me}_4)]^{2-}$  (Ln = La, Nd, Lu),<sup>648</sup> and  $[\text{Me}_2\text{Si}(\text{C}_5\text{Me}_4)_2]^{2-}$  (Ln = Sc).<sup>649</sup>

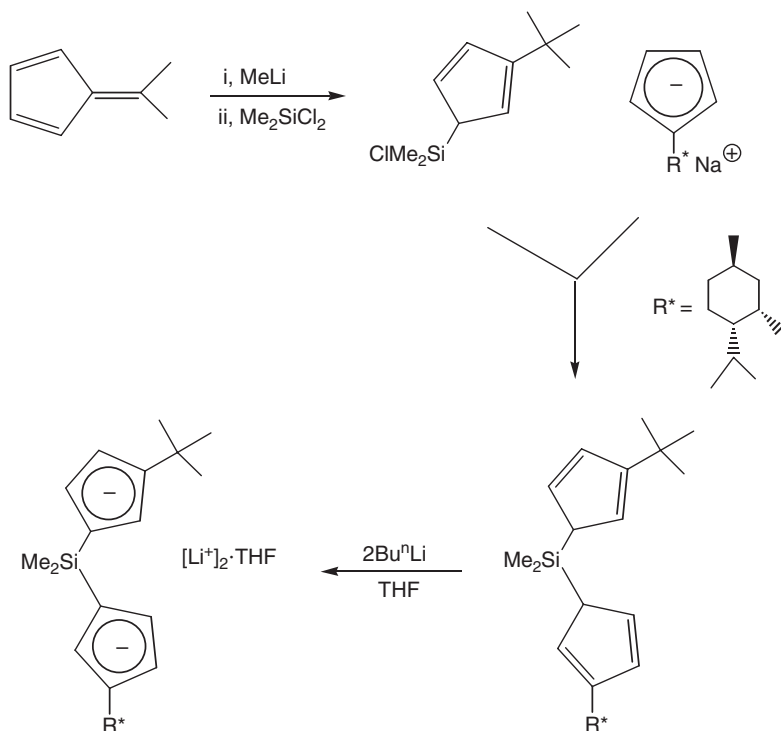
From the reaction between  $\text{SmCl}_3(\text{THF})_3$  and  $\text{Me}_4\text{C}_2(\text{C}_5\text{H}_4\text{MgCl})_2(\text{THF})_4$  under sonification the bimetallic *ansa*-cyclopentadienyl samarium complex  $[\text{Me}_4\text{C}_2(\text{C}_5\text{H}_4)_2]\text{SmCl}(\text{THF})\text{MgCl}_2(\text{THF})_2$  was obtained as a brick-red powder. This complex reacts with 2 equiv. of  $\text{C}_3\text{H}_5\text{Li}(\text{DME})$  to give an anionic bis(allyl) derivative (Scheme 160).<sup>446</sup>

The synthesis and characterization of enantiomerically pure *ansa*-cyclopentadienyl organolanthanides  $\text{Me}_2\text{Si}(\text{Bu}^t\text{Cp})[(+)\text{-}neo\text{-Men-Cp}]\text{Ln}(\text{CH}(\text{SiMe}_3)_2)$  and their use as precatalysts for asymmetric olefin hydrogenation have been reported. In a one-pot reaction starting from 6,6-dimethylfulvene, methyllithium, and dimethyldichlorosilane the desired product  $\text{Me}_2\text{Si}(\text{Bu}^t\text{Cp})\text{Cl}$  was obtained, which was alkylated with  $\text{Na}[(+)\text{-}neo\text{-Men-Cp}]$  to afford the neutral ligand. Reaction with  $\text{Bu}^n\text{Li}$  afforded the dilithium salt as a colorless crystalline solid (Scheme 161).<sup>650</sup>

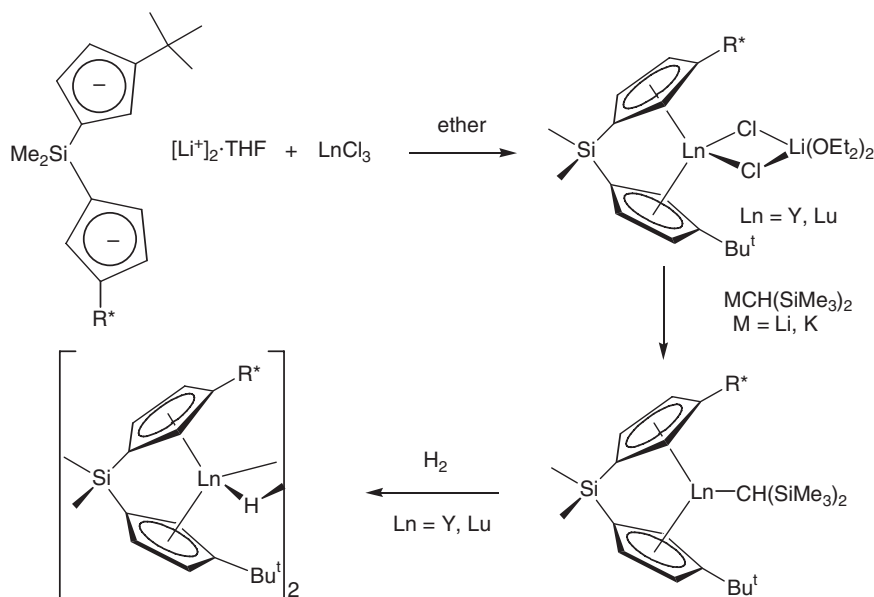
The synthesis of the corresponding organolanthanide chlorides was performed by transmetalation of the dilithium salt with anhydrous lutetium or yttrium trichloride. Metallocene dichloro complexes  $[(R,S)\text{-Me}_2\text{Si}(\text{C}_5\text{H}_3\text{Bu}^t)(+)\text{-}neo\text{-Men-Cp}]\text{Ln}(\mu\text{-Cl}_2)\text{Li}(\text{OEt}_2)_2$  (Ln = Y, Lu) were synthesized by treatment of the corresponding lanthanide trichlorides with the dilithium salt of the ligand and isolated isomerically pure by crystallization from diethyl ether (Scheme 162).<sup>650</sup>



Scheme 160



Scheme 161



Scheme 162

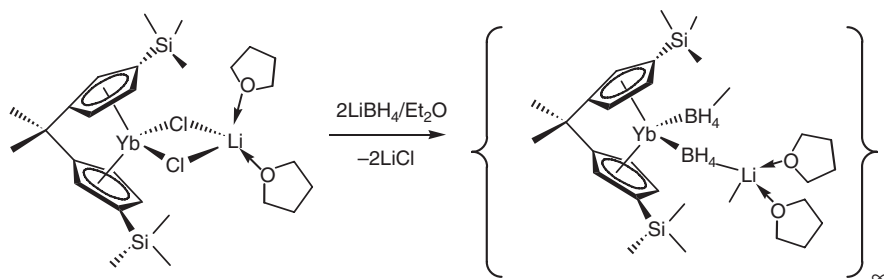
Similarly to the reaction with KCp<sup>\*</sup>, treatment of [Me<sub>2</sub>Si(C<sub>5</sub>Me<sub>4</sub>)<sub>2</sub>]SmI(THF) with KC<sub>5</sub>Me<sub>4</sub>R (R = Et, Pr<sup>n</sup>, Pr<sup>i</sup>) in toluene afforded the base-free tris(cyclopentadienyl) systems. Single crystal X-ray determinations revealed a pseudo-tetrahedral coordination sphere for [Me<sub>2</sub>Si(C<sub>5</sub>Me<sub>4</sub>)<sub>2</sub>]SmCp<sup>\*</sup>(THF) and a pseudo-trigonal one for [Me<sub>2</sub>Si(C<sub>5</sub>Me<sub>4</sub>)<sub>2</sub>]SmCp<sup>\*</sup> and [Me<sub>2</sub>Si(C<sub>5</sub>Me<sub>4</sub>)<sub>2</sub>]Sm(C<sub>5</sub>Me<sub>4</sub>Pr<sup>n</sup>), respectively. Bond lengths and angles are in the same range as in similar compounds. The (ring centroid)–metal–(ring centroid) angles of the Me<sub>2</sub>Si(C<sub>5</sub>Me<sub>4</sub>)<sub>2</sub> units in each structure range from 115.2°

to 123.3°. The  $\beta$ -carbon of the propyl substituent in  $\text{Me}_2\text{Si}(\text{C}_5\text{Me}_4)_2\text{Sm}(\text{C}_5\text{Me}_4\text{Pr}^n)$  is orientated to the samarium at a distance of 3.36 Å. In contrast to  $\text{Cp}^*_3\text{Sm}$  the complexes  $[\text{Me}_2\text{Si}(\text{C}_5\text{Me}_4)_2]\text{SmCp}^*(\text{THF})$  and  $[\text{Me}_2\text{Si}(\text{C}_5\text{Me}_4)_2]\text{Sm}(\text{C}_5\text{Me}_4\text{R})$  ( $\text{R} = \text{Me}, \text{Et}, \text{Pr}^n, \text{Pr}^i$ ) do not show the reductive ring-opening reaction of THF and consistently no polymerization of ethylene or reduction chemistry as observed for  $\text{Cp}^*_3\text{Sm}$ .<sup>637</sup>

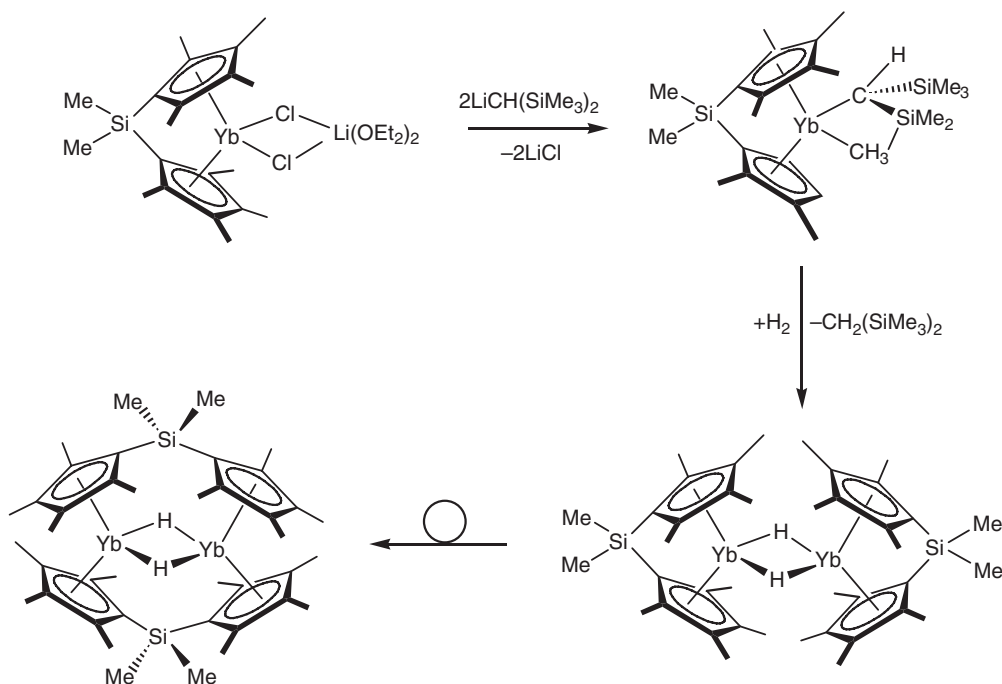
The reaction between the ytterbium *ate*-complex  $[\text{rac-Me}_2\text{C}(\text{C}_5\text{H}_3\text{-3-SiMe}_3)_2]\text{Yb}(\mu_2\text{-Cl})_2\text{Li}(\text{OEt}_2)_2$  and a 50% excess of  $\text{LiBH}_4$  afforded the borohydride *ansa*-ytterbocene complex  $\{\text{rac-Me}_2\text{C}[\text{C}_5\text{H}_3\text{-3-SiMe}_3)_2]\text{Yb}[(\mu_2\text{-H})_2\text{B}(\mu_2\text{-H})_2\text{Li}(\text{THF})_2]_\infty$  (Scheme 163).<sup>651</sup>

The *ansa*-ytterbocene borohydride complex crystallizes in the triclinic space group  $\text{P}\bar{1}$ . Average Yb–B, Yb–Cp bond lengths and B–Yb–B, Cp–Yb–Cp angles are 2.59 Å and 2.33 Å, 96.3° and 111.0°, respectively. The same research group published the synthesis and crystal structure of *ansa*-ytterbocenes with a short bridge and bulky substituents.  $\text{Li}_2[\text{Me}_2\text{E}(\text{C}_5\text{H}_3\text{EMe}_3)_2]$  ( $\text{E} = \text{C}, \text{Si}$ ), the lithium salts of the ligands, reacted with  $\text{YbCl}_3$  to yield the complexes *rac*- $[\text{Me}_2(\text{C}_5\text{H}_3\text{Bu}^t)_2]\text{Yb}(\mu\text{-Cl})_2\text{Li}(\text{OEt}_2)_2$  and the monosolvated *meso*- $[\text{Me}_2\text{Si}(\text{C}_5\text{H}_3\text{SiMe}_3)_2]\text{YbCl}(\text{THF})$ , respectively.<sup>651</sup>

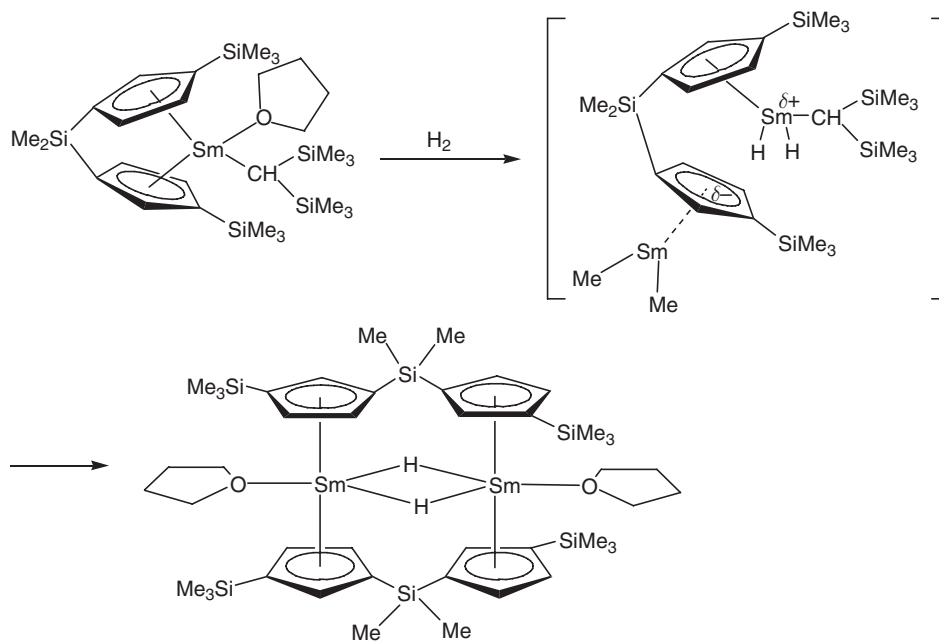
The synthesis and structural characterization of  $[\text{Me}_2\text{Si}(\text{C}_5\text{Me}_4)_2]\text{YCH}(\text{SiMe}_3)_2$ , hydrogenation to  $[\{\text{Me}_2\text{Si}(\text{C}_5\text{Me}_4)_2\}\text{Y}]_2(\mu\text{-H})_2$  and its facile ligand redistribution to  $\text{Y}_2[\mu_2\text{-}\{(\text{C}_5\text{Me}_4)\text{SiMe}_2(\text{C}_5\text{Me}_4)\}]_2(\mu\text{-H})_2$  have been reported. Alkylation of  $[\{\text{Me}_2\text{Si}(\text{C}_5\text{Me}_4)_2\}\text{Y}]_2(\mu\text{-Cl})_2\text{Li}(\text{OEt}_2)_2$  with  $\text{LiCH}(\text{SiMe}_3)_2$  proceeds readily in toluene. Removal of the toluene *in vacuo*, followed by extraction of the product from  $\text{LiCl}$  with petroleum ether affords  $[\text{Me}_2\text{Si}(\text{C}_5\text{Me}_4)_2]\text{YCH}(\text{SiMe}_3)_2$  in moderate yields (Scheme 164).<sup>652</sup>



Scheme 163



Scheme 164



Scheme 165

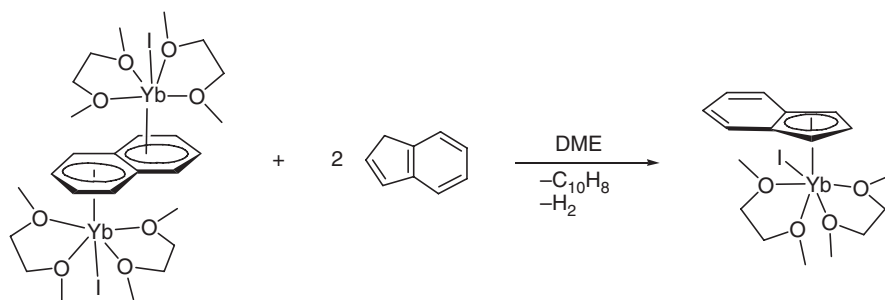
The structure of  $[\text{Me}_2\text{Si}(\text{C}_5\text{Me}_4)_2]\text{YCH}(\text{SiMe}_3)_2$  has been examined. The bis(trimethylsilyl)methyl ligand is distorted in the equatorial plane, such that one of the methyl groups of the  $[\text{CH}(\text{SiMe}_3)_2]$  bridges yttrium and a silicon in a three-center, two-electron bridging fashion. Hydrogenolysis of  $[\text{Me}_2\text{Si}(\text{C}_5\text{Me}_4)_2]\text{YCH}(\text{SiMe}_3)_2$  results, initially, in the formation of the *ansa*-yttrocene hydride dimer  $[\{\text{Me}_2\text{Si}(\text{C}_5\text{Me}_4)_2\text{Y}\}_2(\mu\text{-H})_2]$ . This compound is unstable with respect to ligand redistribution affording the hydride- and  $\{(\text{C}_5\text{Me}_4)_2\text{SiMe}_2\}$ -bridged (“flyover”) hydride dimer  $\text{Y}_2[\mu_2\{(\text{C}_5\text{Me}_4)_2\text{SiMe}_2(\text{C}_5\text{Me}_4)_2\}]_2(\mu\text{-H})_2$ .<sup>652</sup> The related complexes  $[\{\text{Me}_2\text{Si}(\text{C}_5\text{H}_4)_2\}\text{Ln}(\mu\text{-H})]_2$  and  $[\{\text{Me}_2\text{Si}(\text{C}_5\text{H}_4)_2\}\text{Ln}(\text{THF})]_2(\mu\text{-H})(\mu\text{-Cl})$  have been synthesized by the reaction of  $[\{\text{Me}_2\text{Si}(\text{C}_5\text{H}_4)_2\}\text{Ln}(\mu\text{-Cl})]_2$  ( $\text{Ln} = \text{Y}, \text{Yb}$ ) with NaH in THF.<sup>653</sup> The alkyl complex  $\text{Me}_2\text{Si}(\text{C}_5\text{H}_3\text{-3-R})_2\text{SmCH}(\text{SiMe}_3)_2$  and the corresponding lanthanide hydride,  $[\text{Me}_2\text{Si}(\text{C}_5\text{H}_3\text{-3-R})_2\text{Sm}(\mu\text{-H})]_2$ , have been synthesized and structurally characterized by single crystal X-ray analyses. Detailed studies were performed to explain the catalytic activity of this complex in the process of block co-polymerization of ethylene with polar monomers. The first step is the reaction of the monomeric  $[\text{Me}_2\text{Si}(\text{C}_5\text{H}_3\text{-3-R})_2]\text{SmCH}(\text{SiMe}_3)_2$  with  $\text{H}_2$  forming the dimeric hydride (Scheme 165).<sup>654</sup>

#### 4.01.6.10 Indenyl and Fluorenyl Compounds

##### 4.01.6.10.1 Lanthanide(II) compounds

Ruby-red  $(\text{C}_9\text{H}_7)\text{YbI}(\text{DME})_2$  has been prepared in 76% yield according to Scheme 166 as the first indenyl half-sandwich complex of divalent ytterbium. The complex is a monomer in the solid state and stable in DME solution.<sup>655</sup>

Bis(indenyl) and bis(fluorenyl) complexes of divalent samarium have been prepared from  $\text{SmI}_2(\text{THF})_2$  and 2 equiv. of the potassium reagents. The series includes  $(\text{C}_9\text{H}_7)_2\text{Sm}(\text{THF})$ ,  $(\text{C}_9\text{H}_7)\text{Sm}(\text{THF})_2$ ,  $(\text{C}_9\text{H}_7)_2\text{Sm}(\text{THF})_3$ , and  $(\text{C}_{13}\text{H}_9)_2\text{Sm}(\text{THF})_2$ .<sup>656</sup> The reactivity of samarium(II) in a bis(indenyl) coordination environment has been investigated and compared with that of  $\text{Cp}^*\text{Sm}(\text{THF})_2$ . Reaction of the organosamarium(II) indenyl complex  $(\text{C}_9\text{H}_7)_2\text{Sm}(\text{THF})_x$  with excess  $\text{N}_2\text{O}$  yielded  $(\mu\text{-O})[(\text{C}_9\text{H}_7)_2\text{Sm}(\text{THF})]_2$  and  $(\text{C}_9\text{H}_7)_3\text{Sm}(\text{THF})$ . Treatment of 2 equiv. of  $(\text{C}_9\text{H}_7)_2\text{Sm}(\text{THF})_x$  with 1,2-diiodoethane gave  $(\text{C}_9\text{H}_7)_3\text{Sm}(\text{THF})$  and  $(\text{C}_9\text{H}_7)\text{SmI}_2(\text{THF})_2$  complexes. These two compounds could be synthesized also by the reaction of  $\text{SmCl}_3$  with 3 equiv. of  $\text{KC}_9\text{H}_7$  in THF for  $(\text{C}_9\text{H}_7)_3\text{Sm}(\text{THF})$  and by reaction of  $\text{SmI}_3$  with 1 equiv. of  $\text{KC}_9\text{H}_7$  in THF for  $(\text{C}_9\text{H}_7)\text{SmI}_2(\text{THF})_2$ , respectively. Two equivalents of  $(\text{C}_9\text{H}_7)_2\text{Sm}(\text{THF})_x$  also react with 1 equiv. of 1,3,5,7-COT to form  $(\text{C}_9\text{H}_7)_3\text{Sm}(\text{THF})$  and  $(\text{C}_9\text{H}_7)\text{Sm}(\text{COT})(\text{THF})_x$ . Reaction of  $(\text{C}_9\text{H}_7)_2\text{Sm}(\text{THF})_x$  with azobenzene led to  $(\text{C}_9\text{H}_7)_3\text{Sm}(\text{THF})$  and  $[(\text{C}_9\text{H}_7)\text{Sm}(\text{N}_2\text{Ph}_2)(\text{THF})]_x$ . The complexes  $[(\text{C}_9\text{H}_7)_2\text{Sm}(\text{THF})]_2(\mu\text{-O})$ ,  $(\text{C}_9\text{H}_7)_3\text{Sm}(\text{THF})$ ,  $(\text{C}_9\text{H}_7)\text{SmI}_2(\text{THF})_3$ ,

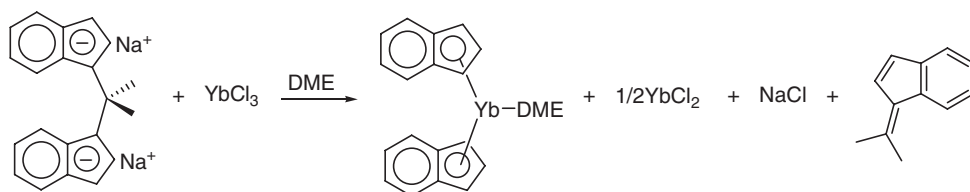


Scheme 166

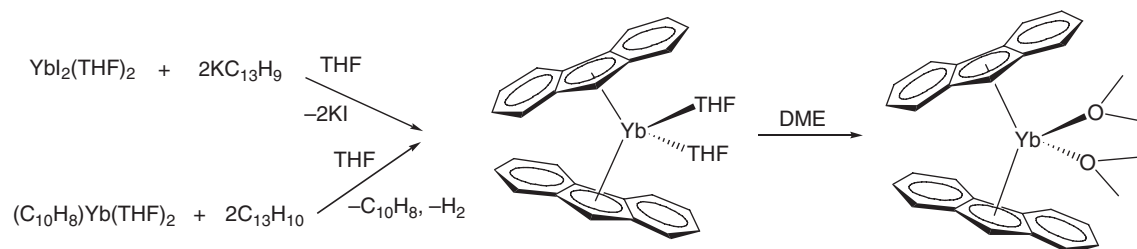
and the 2,2'-bipyridine adduct of  $(\text{C}_9\text{H}_7)\text{Sm}(\text{COT})(\text{THF})_x$ ,  $(\text{C}_9\text{H}_7)\text{Sm}(\text{COT})(\text{C}_{10}\text{H}_8\text{N}_2)$  were characterized by X-ray diffraction.<sup>657</sup> Protonolysis of  $(\text{C}_9\text{H}_7)_2\text{Sm}(\text{THF})_3$  with  $[\text{NEt}_3\text{H}][\text{BPh}_4]$  has been reported to yield the Cp-free salt-like species  $[\text{Sm}(\text{THF})_7][\text{BPh}_4]_2$ .<sup>658</sup> Metallation of 2,2-bis(1'-indenyl)propane by sodium hydride and subsequent reaction of the sodium derivative with  $\text{YbCl}_3$  yielded the Yb(II) indenyl complex  $(\text{C}_9\text{H}_7)_2\text{Yb}(\text{DME})$  besides a benzofulvene byproduct (Scheme 167). Single crystal X-ray data showed a rather unusual orientation of the indenyl ligands with their benzene rings directed towards the oxygen atoms of the coordinated DME.<sup>659</sup>

Fluorenyl complexes of divalent ytterbium,  $(\text{C}_{13}\text{H}_9)_2\text{Yb}(\text{L})_n$  ( $\text{L} = \text{THF}$ ,  $n = 2$ ;  $\text{L} = \text{DME}$ ,  $n = 1$ ), have been prepared by reaction of  $\text{YbI}_2(\text{THF})_2$  with 2 equiv. of  $\text{KC}_{13}\text{H}_9$  as well as by reaction of  $(\text{C}_{10}\text{H}_8)\text{Yb}(\text{THF})_2$  with fluorene in THF (Scheme 168).<sup>260</sup>

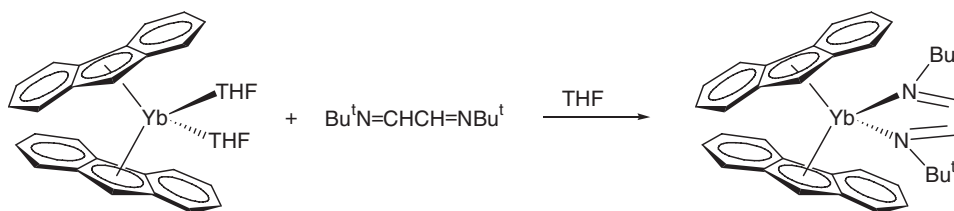
Reaction of  $(\text{C}_{13}\text{H}_9)_2\text{Yb}(\text{THF})_2$  with  $\text{Bu}^t\text{N}=\text{CHCH}=\text{NBu}^t$  (DAD) resulted in the formation of  $(\text{C}_{13}\text{H}_9)_2\text{Yb}(\text{DAD})$ , which was isolated as deep-green crystals in virtually quantitative yield (98%) (Scheme 169).<sup>660</sup>



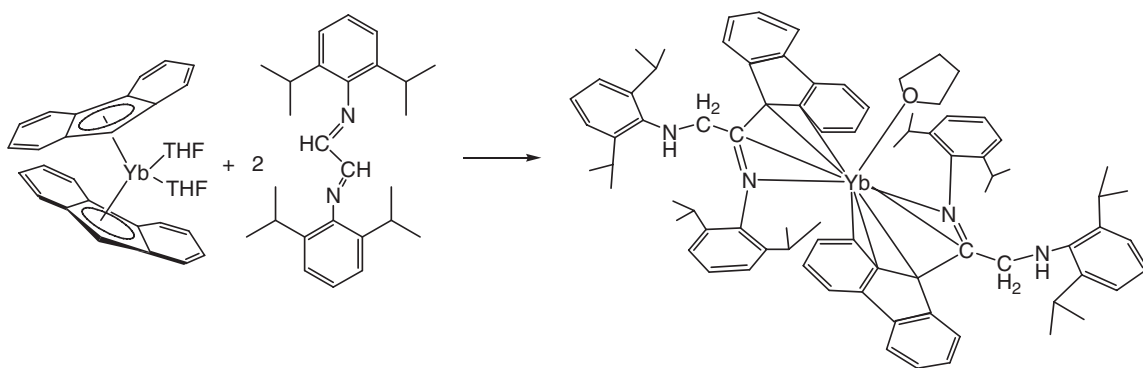
Scheme 167



Scheme 168



Scheme 169



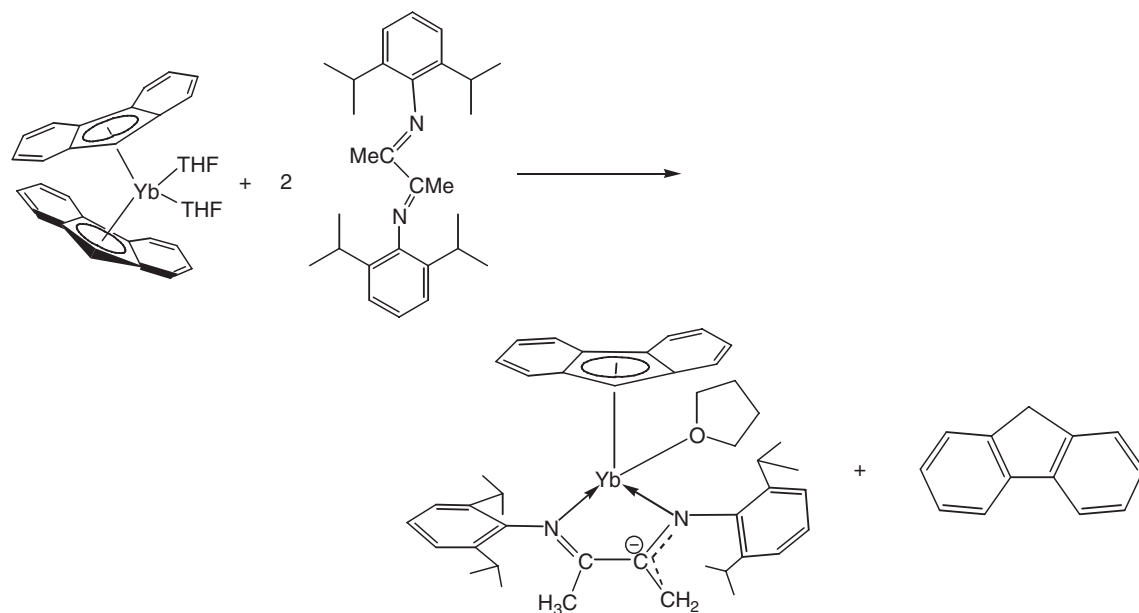
Scheme 170

Unexpected pathways including C–C coupling and C–H bond activation have been found for reactions of  $(C_{13}H_9)_2Yb(THF)_2$  with sterically demanding diazadienes. Scheme 170 illustrates the formation of a novel multi-functional ligand system in the reaction with the bulky ligand  $(2,6-Pr^iC_6H_3)N=CHCH=N(2,6-Pr^iC_6H_3)$ .<sup>661,661a</sup>

It was found that replacement of the imino hydrogen atoms in the DAD ligand by methyl groups dramatically influenced the reaction pathway and led to the formation of a totally different product (Scheme 171) which was isolated as a deep-green crystalline solid in 64% yield. The novel ytterbium(II) complex contains a new ligand resulting from proton abstraction from a methyl substituent on the imino group.<sup>661,661a</sup>

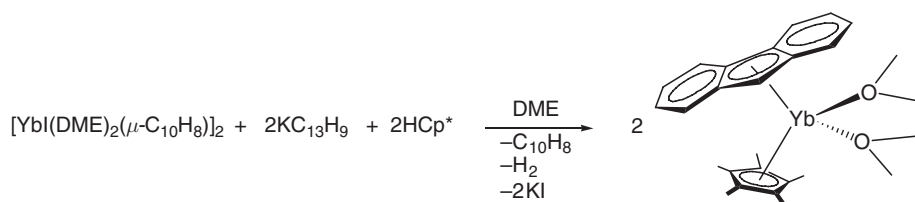
The first mixed-ligand sandwich complex of a divalent lanthanide metal, yellow  $(C_{13}H_9)Cp^*Yb(DME)$ , was synthesized in a one-pot reaction of  $[YbI(DME)_2]_2(\mu-C_{10}H_8)$  with  $Cp^*H$  and  $KC_{13}H_9$  in DME (Scheme 172).<sup>660</sup>

The substituted indenyl ytterbium(II) complex  $(C_9H_6C_5H_9)_2Yb(THF)_2$  was obtained by the reaction of  $YbI_2$  with 2 equiv. of 1-cyclopentylindenyl lithium  $Li(C_9H_6C_5H_9)$ .<sup>441</sup> Complexes of the type  $(C_9H_6C_5H_9)_2Ln(THF)_n$  ( $Ln=Sm$ ,  $n=1$ , black crystals;  $Ln=Yb$ ,  $n=2$ , purple crystals) were also prepared by the reaction between  $K(C_9H_6C_5H_9)$  and anhydrous  $LnCl_3$  ( $Ln=Sm$ ,  $Yb$ ) in a molar ratio of 2:1 in THF and subsequent treatment with Na–K alloy.<sup>662</sup> A series of europium(II) and ytterbium(II) metallocenes containing methoxyethyl-functionalized indenyl ligands have been synthesized by reacting suitable lanthanide silylamide precursors with the free ligands.<sup>663</sup> Indenyl-derived ytterbocene(II) complexes  $[1-(SiHR_2)-2-R^1-C_9H_5]_2Yb(L)_2$  ( $R=Me, C_6H_5$ ;  $R^1=H, Me$ ;  $L=$  donor ligand) have also been synthesized via silylamine elimination from  $Yb[N(SiMe_3)_2]_2(THF)_2$ .<sup>664</sup>



Scheme 171

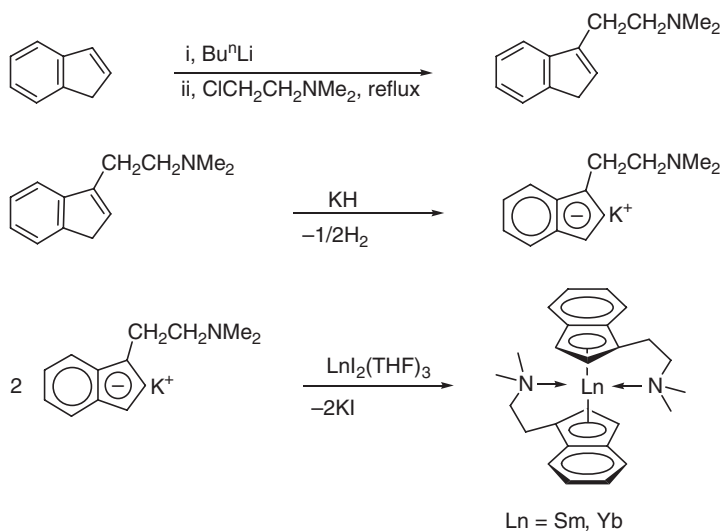




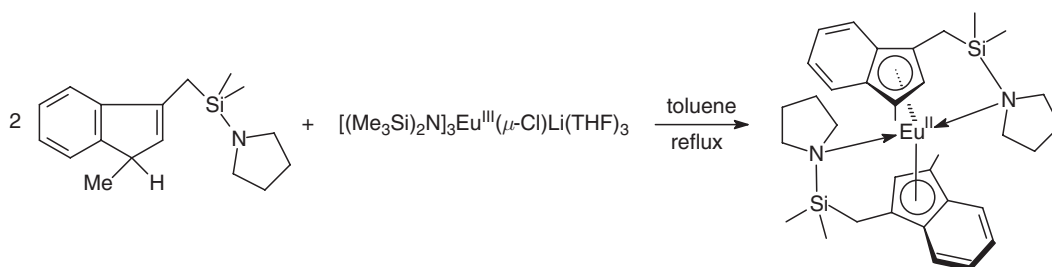
Scheme 172

The first examples of racemic bis(2-dimethylaminoethylindenyl) divalent unsolvated organolanthanide complexes,  $(\text{Me}_2\text{NCH}_2\text{CH}_2\text{C}_9\text{H}_6)_2\text{Sm}$  and  $(\text{Me}_2\text{NCH}_2\text{CH}_2\text{C}_9\text{H}_6)_2\text{Yb}$ , were synthesized according to [Scheme 173](#) by the reaction of  $\text{K}(\text{Me}_2\text{NCH}_2\text{CH}_2\text{C}_9\text{H}_6)$  with  $\text{LnI}_2$  ( $\text{Ln} = \text{Sm}, \text{Yb}$ ) in THF at room temperature or alternatively by reacting the Yb(III) silylamide  $\text{Yb}[\text{N}(\text{SiMe}_3)_2]_3$  with 2 equiv. of the free ligand.<sup>665–667</sup>

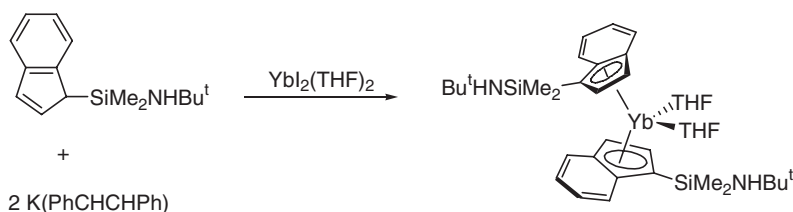
The molecular structure of the ytterbium complex as determined by single crystal X-ray diffraction revealed the intermolecular coordination of both dimethylaminoethyl groups with  $\text{Yb-N}$  distances of 2.58 Å and 2.608 Å. Only one possible diastereomeric conformation with *trans*-arrangement of both indenyl rings and coordinated side-arms is present.<sup>665</sup> Divalent lanthanide metallocenes of Sm and Yb have also been prepared using the pendant-arm 3-(2-pyridylmethyl)indenyl ligand.<sup>668</sup> A novel europium(II) complex containing a pendant-arm pyrrolidinyl-indenyl ligand has been synthesized according to [Scheme 174](#). The yellow compound was isolated in 75% yield.<sup>669</sup>



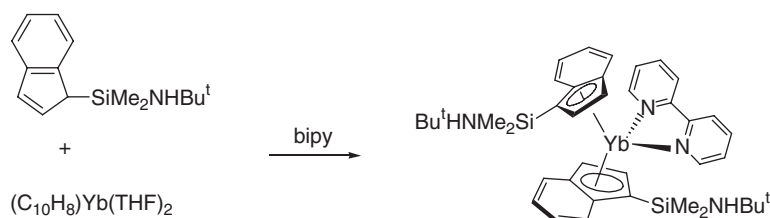
Scheme 173



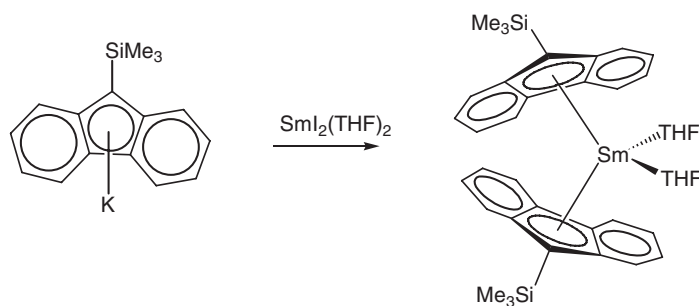
Scheme 174



Scheme 175



Scheme 176



Scheme 177

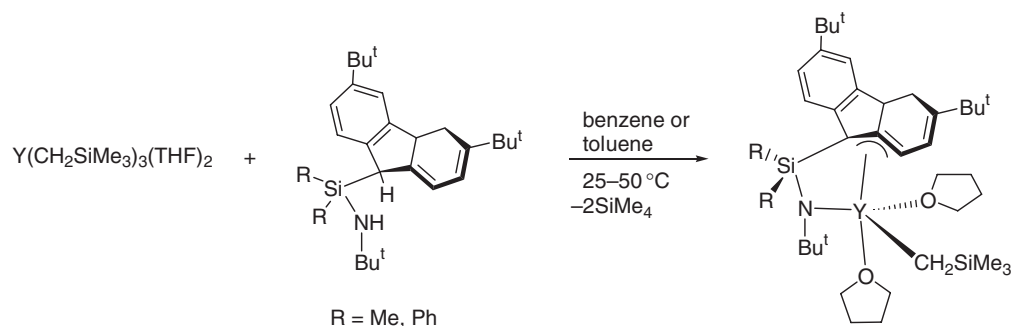
The reaction of  $YbI_2(THF)_2$  with the aminosilylindene ligand  $(C_9H_7)SiMe_2NHBu^t$  in the presence of potassium 1,2-diphenylethylenide, through a different course, yielded a divalent ytterbocene complex with non-chelating aminosilylindenyl ligands (Scheme 175).<sup>670</sup>

The corresponding 2,2'-bipyridine adduct has been prepared directly from the free ligand and ytterbium naphthalenide, followed by addition of 2,2'-bipyridine (Scheme 176). The black crystalline material has been structurally characterized by X-ray analysis.<sup>670</sup>

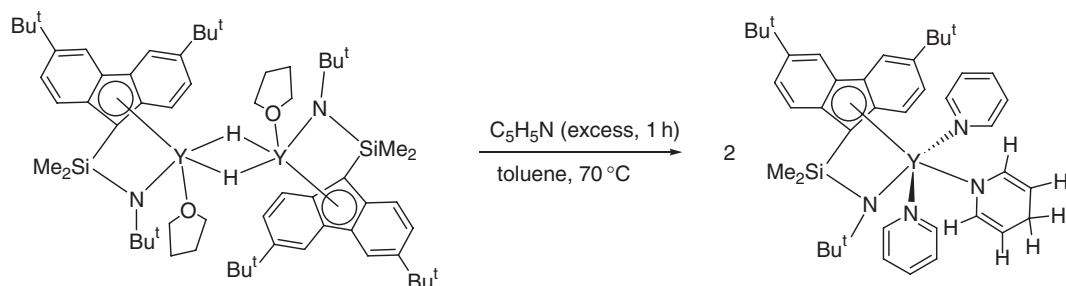
$\eta^5$ -Bis( $Me_3Si$ -fluorenyl) $Sm(THF)_2$  was synthesized by the reaction of  $Me_3Si$ -fluorenylpotassium with  $SmI_2(THF)_2$ , and its structure was analyzed by X-ray diffraction (Scheme 177).<sup>671</sup>

#### 4.01.6.10.2 Lanthanide(III) compounds

Dichloro(indenyl)tris(tetrahydrohydrofuran)holmium(III) was synthesized from  $C_9H_7Na$  and  $HoCl_3$  in 0.8:1 mole ratio in THF. The holmium atom has a distorted octahedral geometry with one five-membered ring centroid of an indenyl ligand, three THF oxygen atoms, and two chloride anions.<sup>672</sup> Upon treatment of anhydrous  $PrCl_3$  with  $Na(C_9H_7)$  (1:2) and  $LaCl_3$  with  $Na(C_9H_7)$  (1:3 molar ratio) in THF, the indenyl complexes  $[(C_9H_7)_2Pr(\mu-Cl)(THF)]_2$  and  $(C_9H_7)_3La(THF)$  were obtained.<sup>673</sup> Complexes of the types  $(C_9H_7)_2LnCl(THF)$  and  $[(C_9H_7)_2Ln(\mu-H)]_2 \times 4THF \times NaCl$  have been reported for  $Ln = Sm, Gd$ , and  $Dy$ .<sup>674</sup> Interesting “constrained-geometry” lanthanide complexes have been synthesized with the use of the fluorenyl-based ligands  $[(3,6-Bu^t_2Flu)SiR_2NBu^t]^{2-}$  ( $R = Me, Ph$ ) (Scheme 178).<sup>675</sup>



Scheme 178



Scheme 179

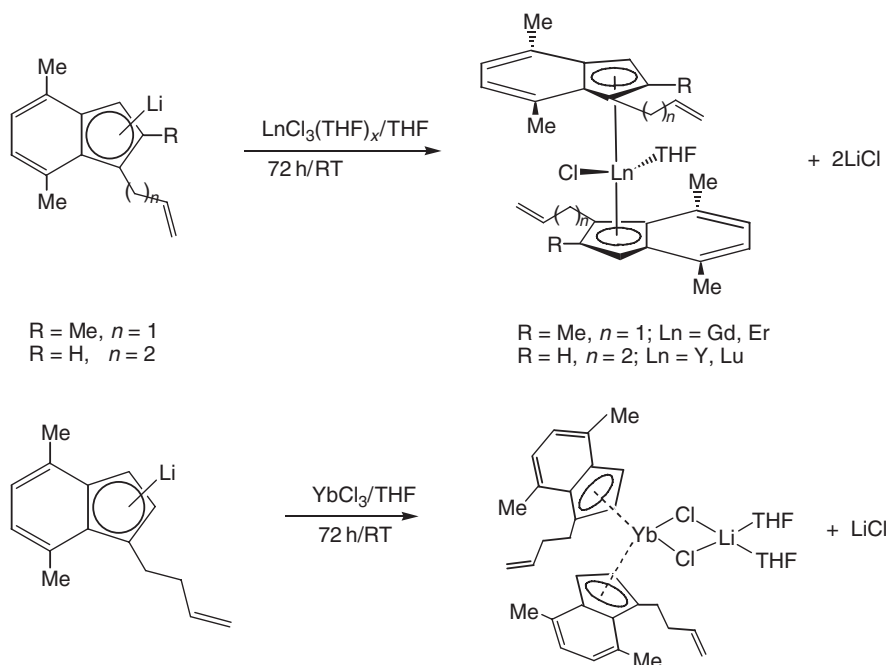
Reaction of pyridine with the corresponding fluorenyl(hydrido)yttrium complex  $[(3,6\text{-Bu}^t\text{Flu})\text{SiR}_2\text{NBu}^t]\text{Y}(\mu\text{-H})(\text{THF})_2$  selectively gave the 1,4-addition product, which was characterized by single crystal X-ray diffraction (Scheme 179).<sup>676</sup>

The synthesis and characterization of the first bis- and tris[1-( $\omega$ -alken-1-yl)indenyl]lanthanide complexes ( $\text{Ln} = \text{Gd}, \text{Er}, \text{Y}, \text{Lu}$ ) have been reported. 1-Allyl-2,4,7-trimethyl-1H-indene and 1-(3-buten-1-yl)-4,7-dimethyl-1H-indene were prepared from (2,4,7-trimethylindenyl)lithium and allyl chloride or from (4,7-dimethylindenyl)lithium and 4-bromo-1-butene.<sup>677</sup> The reactions of the trichlorides of gadolinium, erbium, yttrium, lutetium, and ytterbium in molar ratios in THF produce the bis(1-allyl-2,4,7-trimethylindenyl)lanthanide chloride complexes  $\text{L}_2\text{LnCl}(\text{THF})$  ( $\text{Ln} = \text{Gd}, \text{Er}$ ), bis(1-buten-1-yl-4,7-dimethylindenyl)lanthanide complexes ( $\text{Ln} = \text{Y}, \text{Lu}$ ) or the heterometallic complexes bis(1-buten-1-yl-4,7-dimethylindenyl) $\text{Yb}(\mu\text{-Cl})_2\text{Li}(\text{THF})_2$  (Scheme 180).<sup>677</sup>

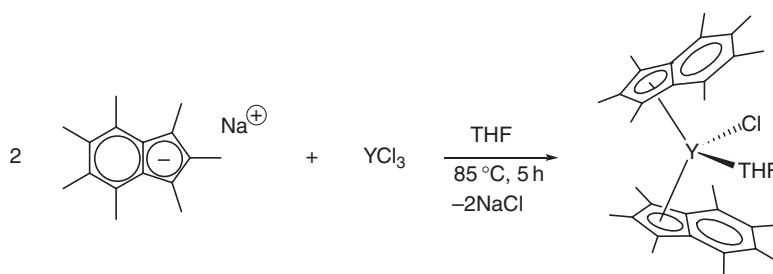
The sterically demanding heptamethylindenyl ligand has recently been introduced into organolanthanide chemistry. The chloride complex  $\text{Ind}^*\text{YCl}(\text{THF})$  ( $\text{Ind}^* = \text{heptamethylindenyl}$ ) was prepared according to Scheme 181 and served as valuable starting material for a series of new alkyl, silyl, and hydride derivatives.<sup>678</sup>

The cyclopentyl-substituted bis(indenyl)lanthanide complexes  $(\text{C}_9\text{H}_6\text{C}_5\text{H}_9)_2\text{Ln}(\mu\text{-Cl})_2\text{Li}(\text{Et}_2\text{O})_2$  ( $\text{Ln} = \text{Y}, \text{Yb}$ )<sup>679,680</sup> and the bis[(tetrahydrofurfuryl)indenyl]lanthanide chlorides  $(\text{C}_6\text{H}_6\text{CH}_2\text{OC}_4\text{H}_7)_2\text{LnCl}$  ( $\text{Ln} = \text{Y}, \text{La}, \text{Pr}, \text{Gd}, \text{Lu}$ )<sup>681,682</sup> have been prepared by standard methods. The tris(indenyl)lanthanide complexes  $(\text{C}_9\text{H}_7)_3\text{Ln}(\text{THF})$  ( $\text{Ln} = \text{Pr}, \text{Nd}$ ) reacted with equimolar amounts of 2-tetrahydrofurfuryl methanol at room temperature to afford binuclear bis(indenyl)lanthanide alkoxides. The crystal structure of the Nd complex showed that the oxygen atoms of the tetrahydrofurfuryl methoxide ligand act as both a bridging and a chelating group in the complex. The Nd atom is coordinated by two  $\eta^5\text{-C}_9\text{H}_7$  rings, two oxygen atoms of tetrahydrofurfuryl methoxide ligands, and an oxygen atom of a tetrahydrofuran ring to give the formal coordination number 9.<sup>683</sup> The reaction of  $(\text{C}_9\text{H}_7)_3\text{Pr}(\text{THF})$  with 8-hydroxyquinoline ( $\text{C}_9\text{H}_6\text{NOH}$ ) or 2-aminophenol ( $\text{H}_2\text{NC}_6\text{H}_4\text{OH}$ ) in THF gave the thermally stable complexes  $(\text{C}_9\text{H}_7)_2\text{Ln}(\text{OC}_9\text{H}_6\text{N})$ ,  $(\text{C}_9\text{H}_7)\text{Pr}(\text{OC}_6\text{H}_6\text{N})_2$ , and  $(\text{C}_9\text{H}_7)_2\text{Pr}(\text{OC}_6\text{H}_4\text{NH}_2)$ , as well as the mixed-ligand derivative  $(\text{C}_9\text{H}_7)\text{Ln}(\text{OC}_9\text{H}_6\text{N})(\text{OC}_6\text{H}_4\text{NH}_2)$ .<sup>399</sup>

Bis(indenyl)lanthanide thiolate complexes of the type  $(\text{C}_9\text{H}_7)_2\text{LnSR}(\text{THF})$  are formed in the reaction of tris(indenyl)lanthanide with equimolar amounts of thiols (Scheme 182). The complexes were characterized by elemental



Scheme 180



Scheme 181

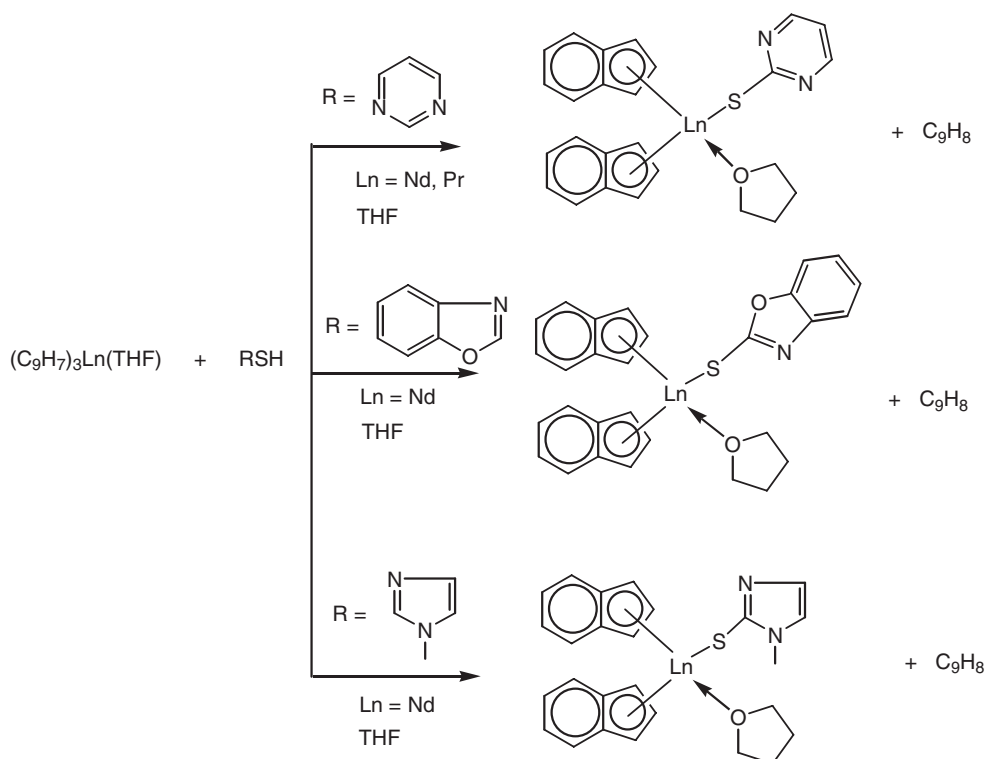
analyses, IR spectroscopy, and MS spectrometry. The thermal stability of the complexes has been studied by the temperature dependence of their ESR spectra as well as TG and DTA measurements.<sup>684</sup>

The ESR spectra show that, at low temperature, the  $g$ -value, which is close to the free electron spin value, may be assigned to the  $4f \text{Nd}^{3+}$  ion. When the temperature is higher than 400 K, the  $g$ -value and relative intensity change, probably owing to the paramagnetism of decomposed organic ligand radicals.

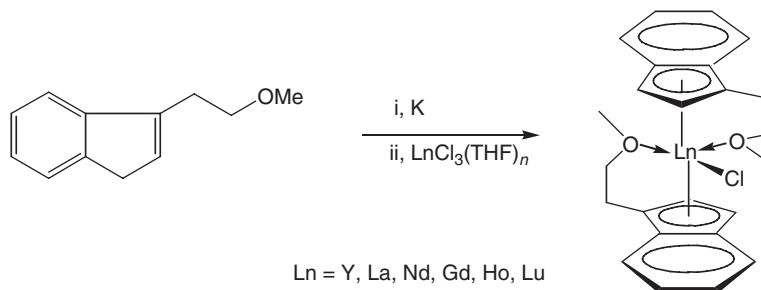
Chiral lanthanocene chlorides with an ether-functionalized indenyl ligand were obtained by the reaction of 1-(2-methoxyethylindenyl) potassium (*in situ*) with the corresponding anhydrous lanthanide chlorides in THF ( $\text{Ln} = \text{Y}, \text{La}, \text{Nd}, \text{Gd}, \text{Ho}, \text{Lu}$ ) (Scheme 183).<sup>685</sup>

X-ray crystal structure analyses of these complexes showed that they are unsolvated monomeric complexes with a *trans*-arrangement of both the sidearm and indenyl rings in the solid state. All complexes are *rac*-isomers and have similar structures in the solid state. The approximately planar indene rings are  $\eta^5$ -bonded to the central metals, and the two indene rings and sidearms adopt a *trans*-configuration.<sup>685</sup> Reaction of anhydrous lanthanide trichlorides with tetrahydrofurfurylindenyl lithium in THF afforded bis(tetrahydrofurfurylindenyl)lanthanocene chloride complexes  $(\text{C}_4\text{H}_7\text{OCH}_2\text{C}_9\text{H}_6)_2\text{LnCl}$  ( $\text{Ln} = \text{Nd}, \text{Sm}, \text{Dy}, \text{Ho}, \text{Er}, \text{Yb}$ ). The crystal structures of all six complexes have been determined. They are all unsolvated nine-coordinated monomeric complexes with a *trans*-arrangement of both the sidearm and indenyl rings in the solid state.<sup>686</sup>

The base-free tris(indenyl) lanthanide(III) complexes  $(\text{C}_9\text{H}_7)_3\text{Ln}$  ( $\text{Ln} = \text{Nd}, \text{Pr}, \text{La}$ ) were prepared from the corresponding tetrahydrofuran adducts  $(\text{C}_9\text{H}_7)_3\text{Ln}(\text{THF})$ . The strictly THF-free complexes are obtained when the



Scheme 182



Scheme 183

thermal degradation is carried out at higher temperatures between 120–150 °C and a better vacuum ( $1 \times 10^{-3}$  mbar) for sufficiently long periods of at least 5 h. The base-free complexes are extremely sensitive to air and moisture. Interestingly, the base-free systems differ notably in color from their THF adducts (Table 1). While base-free (C<sub>9</sub>H<sub>7</sub>)<sub>3</sub>Pr and (C<sub>9</sub>H<sub>7</sub>)<sub>3</sub>Nd are isostructural, the La complex adopts a different structural pattern. The positions of the metal ion and the centers of the six-membered rings are close to the plane spanned by the centers of the three five-membered ring fragments of the indenyl ligands.<sup>687</sup>

**Table 1** Comparison of tris(indenyl)lanthanide complexes and their THF adducts

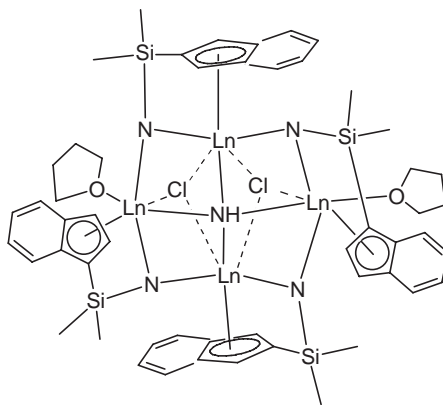
<i>Base-free system: color</i>	<i>THF adducts: color</i>
(C <sub>9</sub> H <sub>7</sub> ) <sub>3</sub> Nd: violet-red	(C <sub>9</sub> H <sub>7</sub> ) <sub>3</sub> Nd(THF): green
(C <sub>9</sub> H <sub>7</sub> ) <sub>3</sub> Pr: deep red	(C <sub>9</sub> H <sub>7</sub> ) <sub>3</sub> Pr(THF): pale green
(C <sub>9</sub> H <sub>7</sub> ) <sub>3</sub> La: faintly yellow	(C <sub>9</sub> H <sub>7</sub> ) <sub>3</sub> La(THF): almost colorless

The complex  $[\text{Na}(\text{THF})_6][(\text{C}_9\text{H}_7)_3\text{Pr}(\mu\text{-Cl})\text{Pr}(\text{C}_9\text{H}_7)_3]$  was obtained by the reaction of  $\text{PrCl}_3$  with sodium indenide (in 1:0.8 molar ratio) in THF. The structure consists of the  $[(\text{C}_9\text{H}_7)_3\text{Pr}(\mu\text{-Cl})\text{Pr}(\text{C}_9\text{H}_7)_3]^-$  anion and  $[\text{Na}(\text{THF})_6]^+$  cation. In the anion each Pr atom is coordinated by three indenyl and one chloride ligands to form a distorted tetrahedral geometry.<sup>688</sup> Tris(indenyl)(tetrahydrofuran)praseodymium,  $(\text{C}_9\text{H}_7)_3\text{Pr}(\text{THF})$ , was prepared analogously by the reaction of  $\text{PrCl}_3$  with sodium indenide in THF.<sup>689</sup> The crystal structures of four homologous tris(indenyl)lanthanide(THF) adducts of the type  $(\text{C}_9\text{H}_7)_3\text{Ln}(\text{THF})$  with  $\text{Ln} = \text{La}, \text{Pr}, \text{Nd}, \text{Sm}$  have been investigated. Some structural differences in the conformations were found for these molecules.<sup>690,690a</sup> In analogy to the tris(cyclopentadienyl)lanthanide(III) sulfoxide adducts, several tris(indenyl)lanthanide(III) sulfoxide adducts were investigated using single crystal X-ray analysis, variable-temperature NMR, and circular dichroism. The 1:1 adducts have been prepared in toluene from the homologous THF adducts and MTSO ( $\text{OS}(\text{Me})\text{C}_6\text{H}_4\text{Me}-4$ ) and DPSO ( $\text{OSPh}_2$ ), respectively, yielding the complexes  $(\text{C}_9\text{H}_7)_3\text{Ln}(\text{MTSO})$  and  $(\text{C}_9\text{H}_7)_3\text{Ln}(\text{DPSO})$ .<sup>496,691,691a</sup> The triphenylphosphineoxide adduct  $(\text{C}_9\text{H}_7)_3\text{La}(\text{OPPh}_3)$ <sup>691,691a</sup> and the trialkylphosphate complex  $(\text{C}_9\text{H}_7)_3\text{Pr}[\text{OP}(\text{OEt})_3]$ <sup>483</sup> have been prepared analogously. Other Lewis base adducts of tris(indenyl)lanthanide include those with (S)-(-)-nicotine and various substituted pyridine ligands.<sup>692</sup> The trichlorides of the comparatively large samarium and lanthanum ions react with different molar amounts of bis[(1-buten-1-yl)-4,7-dimethylindenyl]lithium (LLi) in THF exclusively to give tris(indenyl) complexes of type  $\text{L}_3\text{Sm}$  or  $\text{L}_3\text{La}(\mu\text{-Cl})\text{Li}(\text{Et}_2\text{O})_3$ .<sup>677</sup>

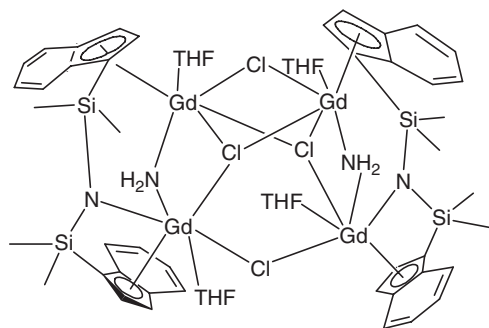
Treatment of  $\text{Me}_2\text{Si}(\text{C}_9\text{H}_7)(\text{C}_2\text{B}_{10}\text{H}_{11})$  with 4 equiv. of  $\text{NaNH}_2$  in THF, followed by reaction with 1 equiv. of  $\text{LnCl}_3$  at room temperature, afforded  $[(\eta^5\text{-}\mu^2\text{-C}_9\text{H}_6\text{SiMe}_2\text{NH})\text{Ln}]_2(\mu^3\text{-Cl})(\text{THF})_2(\mu^4\text{-NH})(\text{THF})_n$  ( $n = 1, \text{Ln} = \text{Gd}, \text{Er}; n = 0, \text{Ln} = \text{Dy}$ ), which represent the first examples of organometallic clusters containing a central  $\mu^4$ -imido group, as well as indenyl ligands. The solid-state structure of the Er complex revealed a butterfly arrangement of four metals which are connected by four doubly bridging  $\mu^2$ -NHSiMe<sub>2</sub>(indenyl) units over the edges, by two triply bridging  $\mu^3$ -Cl atoms spanning three Er atoms in each case, and by a quadruply bridging  $\mu^4$ -NH group located on the crystallographic twofold axis (Scheme 184).<sup>693,694</sup>

Another type of tetranuclear cluster,  $[(\eta^5\text{-C}_9\text{H}_6\text{SiMe}_2)_2\text{N}](\mu^2\text{-NH}_2)\text{Ln}_2(\text{THF})_2(\mu^3\text{-Cl})_2(\mu^2\text{-Cl})_2\cdot\text{THF}$  ( $\text{Ln} = \text{Gd}, \text{Y}$ ), was obtained when the above reactions were carried out at reflux temperature. The solid-state structure of  $[(\eta^5\text{-C}_9\text{H}_6\text{SiMe}_2)_2\text{N}](\mu^2\text{-NH}_2)\text{Gd}_2(\text{THF})_2(\mu^3\text{-Cl})_2(\mu^2\text{-Cl})_2\cdot\text{THF}$  derived from single X-ray analysis revealed that the cluster consists of a distorted tetrahedral arrangement of four Gd atoms from two  $[(\eta^5\text{-C}_9\text{H}_6\text{SiMe}_2)_2\text{N}](\mu^2\text{-NH}_2)\text{Gd}_2(\text{THF})_2^{2+}$  units that are connected by two doubly bridging  $\mu^2$ -Cl atoms spanning two Gd atoms in each case (Scheme 185). Each metal is both  $\eta^5$ -bonded to one indenyl group and  $\sigma$ -bonded to one oxygen atom, one nitrogen atom, and three chloro ligands. Treatment of  $\text{Me}_2\text{Si}(\text{C}_9\text{H}_7)(\text{C}_2\text{B}_{10}\text{H}_{11})$  with 8 equiv. of  $\text{NaNH}_2$  in THF, followed by reaction with 1 equiv. of  $\text{LnCl}_3$  at room temperature, gave the trinuclear clusters  $[(\eta^5\text{-C}_9\text{H}_6\text{SiMe}_2)_2\text{N}][\mu^2, \mu^2\text{-Me}_2\text{Si}(\text{NH})_2](\eta^5\text{-}\mu^2\text{-C}_9\text{H}_6\text{SiMe}_2\text{NH})(\mu^2\text{-Cl})_2\text{Ln}_3(\text{THF})_3$  ( $\text{Ln} = \text{Gd}, \text{Er}$ ). These results indicate that  $\text{NaNH}_2$  serves as both base and nucleophile in the reactions. The *o*-carborane can be recovered by sublimation under vacuum.<sup>693,694</sup>

The reaction of  $(\text{C}_9\text{H}_7)_2\text{LnCl}(\text{THF})$  with NaH in THF generates the dimeric bis(indenyl)lanthanide hydrides  $[(\text{C}_9\text{H}_7)_2\text{Ln}(\mu\text{-H})]_2\cdot 4\text{THF}\cdot\text{NaCl}$ .<sup>695</sup> The stereoselective synthesis and structural characterization of *rac*-planar chiral bis(2-methoxyethylindenyl)lanthanum and yttrium tetrahydroborate complexes has been achieved. The complexes



Scheme 184



Scheme 185

(MeOCH<sub>2</sub>CH<sub>2</sub>C<sub>9</sub>H<sub>6</sub>)<sub>2</sub>LnBH<sub>4</sub> (Ln = Y, La) were synthesized in high yield by the reaction of their chloride precursors (MeOCH<sub>2</sub>CH<sub>2</sub>C<sub>9</sub>H<sub>6</sub>)<sub>2</sub>LnCl with excess NaBH<sub>4</sub> in THF at room temperature.<sup>696</sup>

Both complexes are *rac*-planar chiral lanthanocenes with *trans*-orientation of the  $\eta^5$ -indenyl planes as well as the coordinated sidearms. The two molecular structures are essentially identical except for the coordination mode of BH<sub>4</sub><sup>−</sup>. The Ln–O bond distances are longer than those of the cyclopentadienyl analogs. The two bridging Y–H distances 2.33(5) and 2.39(6) Å are comparable to those in the cyclopentadienyl analogs of 2.26(6) and 2.27(5) Å. In contrast, the three hydrogen atom bridges between the lanthanum and the boron atoms have significantly different La–H distances with 2.38(5), 2.50(6), and 2.60(6) Å. Thus, the tetrahydroborate ion has been identified as slipped bidentate ( $\mu_2$ -H)<sub>2</sub>BH<sub>2</sub> and tridentate ( $\mu_2$ -H)<sub>3</sub>BH ligands in the complexes.<sup>696</sup>

#### 4.01.6.10.3 *ansa*-Indenyl and fluorenyl compounds

The synthesis, structural characterization, and catalytic behavior of one-atom-bridged fluorenyl cyclopentadienyl lanthanocene complexes with *C<sub>s</sub>*- or *C<sub>1</sub>*-symmetry have been reviewed by Qian *et al.*<sup>41</sup> Two Yb(II) *ansa*-indenyl complexes were synthesized by the reaction between Li<sub>2</sub>[(CH<sub>2</sub>)<sub>2</sub>(1-Ind')<sub>2</sub>] and YbCl<sub>3</sub> in diethyl ether and subsequent reduction of the product with sodium metal in THF yielding [*rac*-(CH<sub>2</sub>)<sub>2</sub>(1-Ind')<sub>2</sub>]Yb(THF)<sub>2</sub> where Ind' = C<sub>9</sub>H<sub>6</sub> and 4,7-(CH<sub>3</sub>)<sub>2</sub>C<sub>9</sub>H<sub>4</sub>. Solid-state structural data of both complexes are basically identical to each other with values in the expected areas.<sup>659</sup>

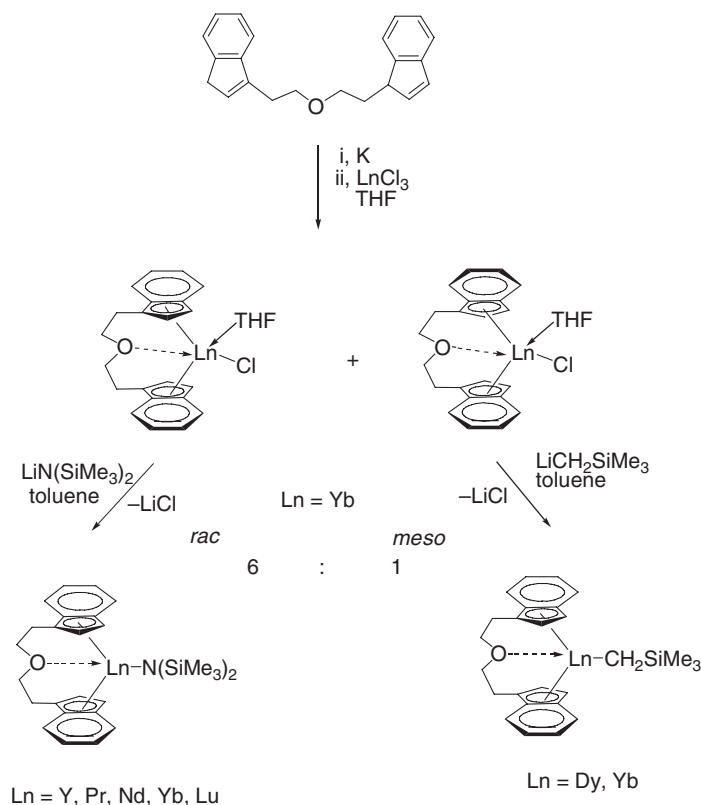
A series of chiral 1,1'-(3-oxapentamethylene)-bridged bis(indenyl) *ansa*-lanthanidocenes have been synthesized with high stereoselectivity. The synthetic routes are illustrated in Scheme 186.<sup>697,698</sup>

*ansa*-[Me<sub>2</sub>Si(C<sub>13</sub>H<sub>9</sub>)<sub>2</sub>]Yb(THF) and *ansa*-[Me<sub>2</sub>Si(C<sub>13</sub>H<sub>9</sub>)<sub>2</sub>]Sm(THF)<sub>4</sub> have been obtained in 75–85% yield by treatment of the appropriate lanthanide diiodides with K<sub>2</sub>[Me<sub>2</sub>Si(C<sub>13</sub>H<sub>9</sub>)<sub>2</sub>] in THF according to Scheme 187.<sup>660</sup>

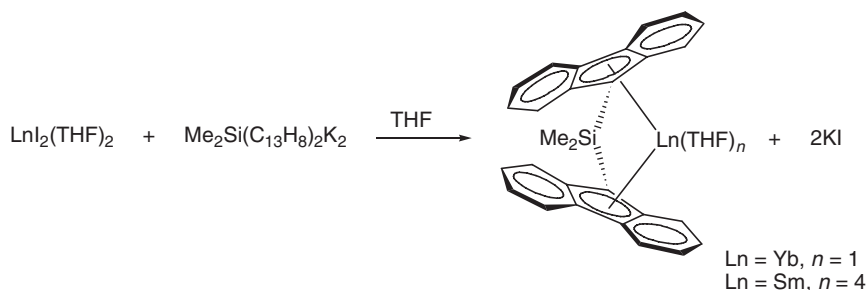
YCl<sub>3</sub> and LuCl<sub>3</sub> react with the ligand bis(2-methyl-4,5,6,7-tetrahydroinden-1-yl)dimethylsilane to form *meso/dl* stereoisomeric mixtures in ratios from 1 : 1 to 2 : 1 *dl*: *meso* (Scheme 188).<sup>699</sup>

A series of donor-functionalized *ansa*-cyclopentadienyl-indenyl and *ansa*-bis(indenyl) complexes of yttrium, samarium, thulium, and lutetium has been synthesized by stepwise reaction of Me<sub>2</sub>SiCl<sub>2</sub> with K[C<sub>5</sub>H<sub>3</sub>Bu<sup>t</sup>-3-Me-5] or Li[C<sub>9</sub>H<sub>7</sub>] followed by the reaction with K[C<sub>9</sub>H<sub>6</sub>CH<sub>2</sub>CH<sub>2</sub>NMe<sub>2</sub>-1] and subsequent deprotonation with KH or Bu<sup>n</sup>Li, yielding the two dimethylsilyl-bridged complexes K<sub>2</sub>[(C<sub>5</sub>H<sub>2</sub>Bu<sup>t</sup>-3-Me-5)SiMe<sub>2</sub>(1-C<sub>9</sub>H<sub>5</sub>CH<sub>2</sub>CH<sub>2</sub>NMe<sub>2</sub>-3)] and Li<sub>2</sub>[(1-C<sub>9</sub>H<sub>6</sub>)SiMe<sub>2</sub>(1-C<sub>9</sub>H<sub>5</sub>CH<sub>2</sub>CH<sub>2</sub>NMe<sub>2</sub>-3)], respectively (Scheme 189).<sup>700</sup>

The reaction of the lithium precursor with LuCl<sub>3</sub> according to Scheme 189 afforded [(1-C<sub>9</sub>H<sub>6</sub>)SiMe<sub>2</sub>(1-C<sub>9</sub>H<sub>5</sub>CH<sub>2</sub>CH<sub>2</sub>NMe<sub>2</sub>-3)]LuCl. Treatment of K<sub>2</sub>[(C<sub>5</sub>H<sub>2</sub>Bu<sup>t</sup>-3-Me-5)SiMe<sub>2</sub>(1-C<sub>9</sub>H<sub>5</sub>CH<sub>2</sub>CH<sub>2</sub>NMe<sub>2</sub>-3)] with the THF adducts of YCl<sub>3</sub>, SmCl<sub>3</sub>, and LuCl<sub>3</sub>, or the DME adduct of TmI<sub>3</sub> gave the mixed *ansa*-metallocenes [(C<sub>5</sub>H<sub>2</sub>Bu<sup>t</sup>-3-Me-5)SiMe<sub>2</sub>(1-C<sub>9</sub>H<sub>5</sub>CH<sub>2</sub>CH<sub>2</sub>NMe<sub>2</sub>-3)]LnX (X = Cl, Ln = Y, Sm, Lu; X = I, Ln = Tm) (Scheme 189). <sup>1</sup>H NMR spectra of all complexes in polar solvents (except for the thulium one) at room temperature showed the magnetic non-equivalence of the protons of the dimethylamino group and hence proved the existence of a strong N→M coordination even in polar solvents like pyridine. 2D NMR spectroscopic determinations led to the assumption that only one set of enantiomers exists in solution. Single crystal X-ray determinations of [(C<sub>5</sub>H<sub>2</sub>Bu<sup>t</sup>-3-Me-5)SiMe<sub>2</sub>(1-C<sub>9</sub>H<sub>5</sub>CH<sub>2</sub>CH<sub>2</sub>NMe<sub>2</sub>-3)]LnX (X = Cl, Ln = Lu) and (X = I, Ln = Tm) showed the monomeric complexes with short Ln–N bonds (2.45 Å for Lu, 2.50/2.47 Å for Tm). In addition to the halide atom, both the cyclopentadienyl and the indenyl part of the *ansa*-ligand are  $\eta^5$ -coordinated to the lanthanide atom with nearly equal bond lengths.<sup>700</sup> The synthesis and structure of *meso*-[ethylene-bis( $\eta^5$ -indenyl)]ytterbium(III) bis(trimethylsilyl)amide and the syntheses



Scheme 186

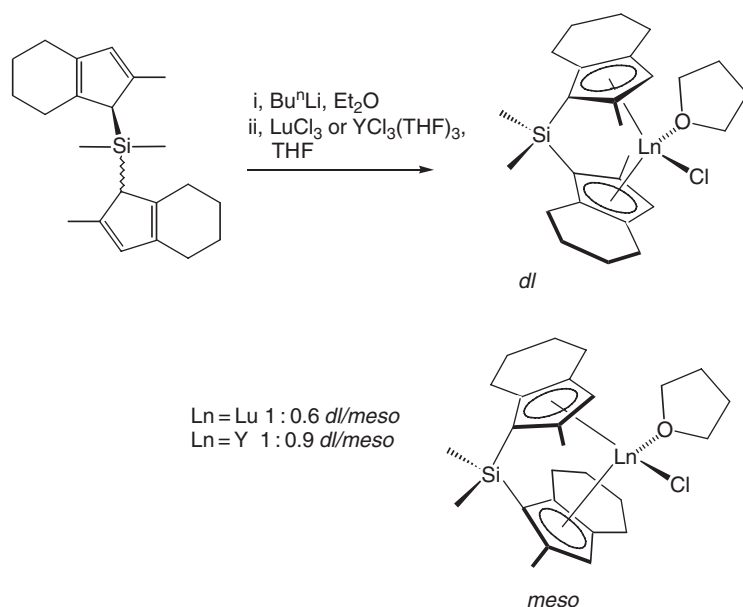


Scheme 187

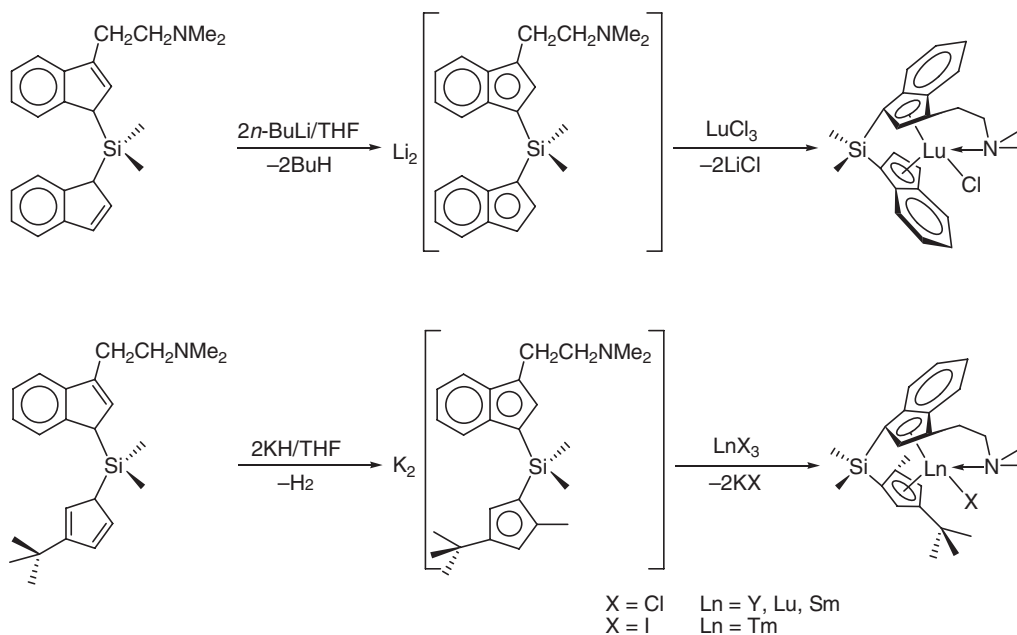
of *rac*- and *meso*-[ethylene-bis( $\eta^5$ -indenyl)ytterbium(III)chloride][LiCl(Et<sub>2</sub>O)<sub>2</sub>] and *rac*- and *meso*-[ethylene-bis( $\eta^5$ -indenyl)lutetium(III)chloride][LiCl(Et<sub>2</sub>O)<sub>2</sub>] were reported. The complexes were synthesized by metathesis of dilithiated 1,2-bis(indenylethane) with either YbCl<sub>3</sub> or LuCl<sub>3</sub> in THF followed by solvent exchange with diethyl ether to give the *rac/meso* mixture of [ethylene-bis( $\eta^5$ -indenyl)Ln(III)chloride][LiCl(Et<sub>2</sub>O)<sub>2</sub>] (Ln = Yb, Lu) (Scheme 190).<sup>701</sup>

In the Yb case, the major diastereomer formed is *meso*, while in the lutetium reaction, the *rac*-diastereomer is the predominant species. The amide complex *meso*-[ethylene-bis( $\eta^5$ -indenyl)ytterbium(III)-bis(trimethylsilyl)amide] was synthesized by the reaction of *meso*-[ethylene-bis( $\eta^5$ -indenyl)ytterbium(III)chloride][LiCl(Et<sub>2</sub>O)<sub>2</sub>] with Na[N(SiMe<sub>3</sub>)<sub>2</sub>] in diethyl ether. Single crystal X-ray determinations revealed a small centroid–Yb–centroid angle of 122.0° caused by the constraining effect of the ethyl bridge.<sup>701</sup> A series of new silylene-bridged fluorenyl cyclopentadienyl *ansa*-lanthanocene chlorides with *C<sub>s</sub>*-symmetry, [(R<sub>2</sub>Si(Flu)(C<sub>5</sub>H<sub>3</sub>R<sup>1</sup>))Ln( $\mu$ -Cl)]<sub>2</sub> (Flu = C<sub>13</sub>H<sub>8</sub>, (R = Me, R<sup>1</sup> = H, Ln = Y, Lu, Dy, Er) and R = Ph, R<sup>1</sup> = Bu<sup>t</sup>, Ln = Dy), has been described. The complexes were synthesized by the reaction of anhydrous lanthanide chloride with the dilithium salt of the ligand Me<sub>2</sub>Si(FluH)(C<sub>5</sub>H<sub>4</sub>R). The





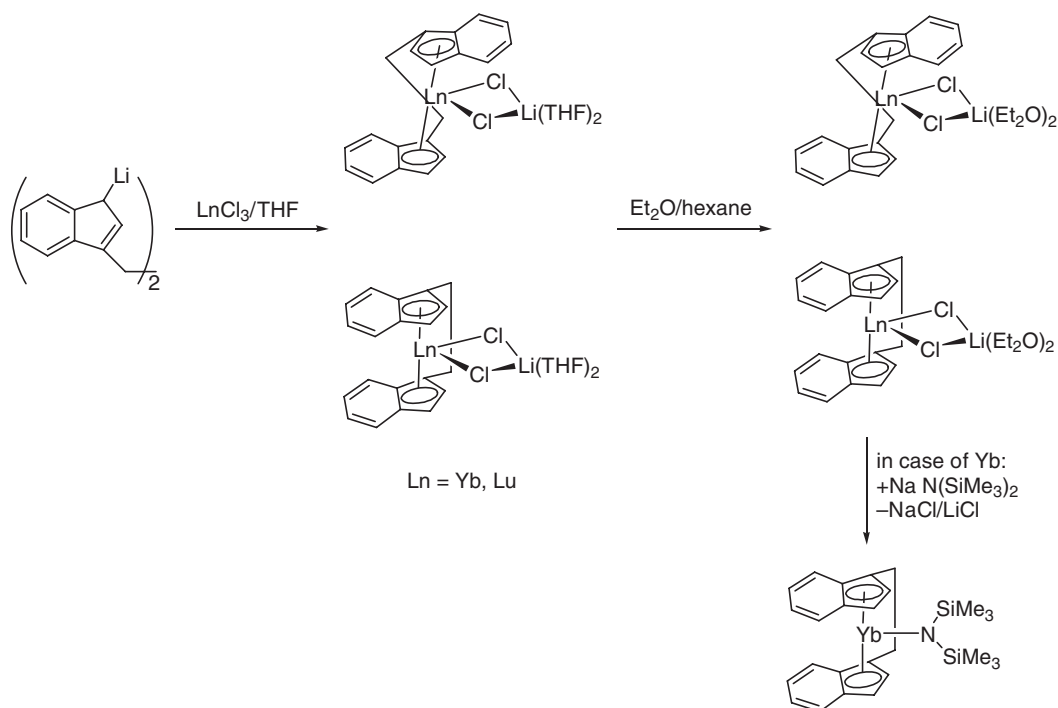
Scheme 188



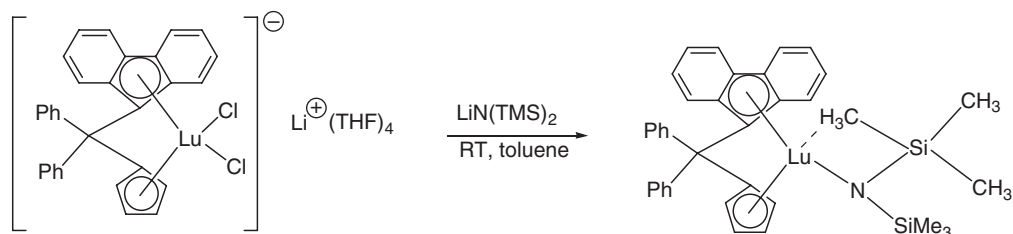
Scheme 189

complexes were characterized by X-ray diffraction studies.<sup>702</sup> The silyl-bridged organolanthanide complexes  $[\text{Me}_2\text{Si}(\text{Flu})_2]\text{LnCl}$  ( $\text{Ln} = \text{La, Pr, Nd, Sm, Yb}$ ) were synthesized by the reaction of  $\text{LnCl}_3$  with  $\text{Li}_2[\text{Me}_2\text{Si}(\text{Flu})_2]$  in THF.<sup>703</sup> The series  $[\text{MePhSi}(\text{Flu})_2]\text{LnCl}$  ( $\text{Ln} = \text{La, Pr, Nd, Sm, Dy, Yb}$ ) was made analogously.<sup>704</sup> The one-carbon-atom-bridged amide complex  $[\text{Ph}_2\text{C}(\text{Flu})(\text{C}_5\text{H}_4)]\text{LuN}(\text{SiMe}_3)_2$  has been synthesized analogously by a reaction of its chloride precursor with  $\text{LiN}(\text{SiMe}_3)_2$  in toluene (Scheme 191). An X-ray structural analysis showed an intramolecular  $\beta$ -Si–C agostic interaction with Lu.<sup>705</sup>

Treatment of chloride precursors with  $\text{ME}(\text{SiMe}_3)_2$  ( $\text{M} = \text{Li or K}$ ;  $\text{E} = \text{N, CH}$ ) gave the amide and hydrocarbyl derivatives  $[\text{Me}_2\text{Si}(\text{Flu})(\text{C}_5\text{H}_4)]\text{LnE}(\text{SiMe}_3)_2$  ( $\text{E} = \text{N}$ ,  $\text{Ln} = \text{Dy, Er}$ ;  $\text{E} = \text{CH}$ ,  $\text{Ln} = \text{Dy}$ ) (cf. Scheme 190). All amide

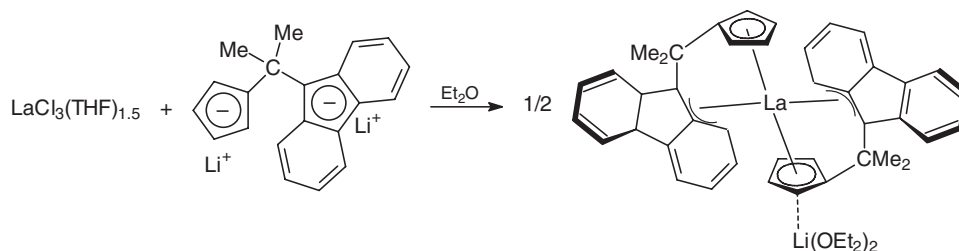


Scheme 190



Scheme 191

and hydrocarbyl complexes show normal chelating structures and exhibit apparently intramolecular agostic Ln–Me–Si interaction.<sup>702</sup> An  $\eta^3$ -coordinated fluorenyl moiety has been found in *ansa*-metallocenes of the general formula  $[\text{Li}(\text{Et}_2\text{O})_2][\text{Ln}\{\text{Me}_2\text{C}(\text{Flu})(\text{C}_5\text{H}_4)\}]$  ( $\text{Ln} = \text{Y, La}$ ) (Scheme 192, see also Scheme 178).<sup>706,707</sup> Various other  $C_2$ -symmetric *ansa*-lanthanidocene amides have been synthesized via silylamine elimination.<sup>708</sup>

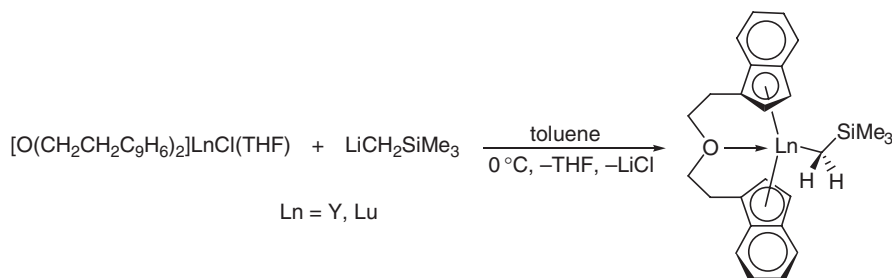


Scheme 192

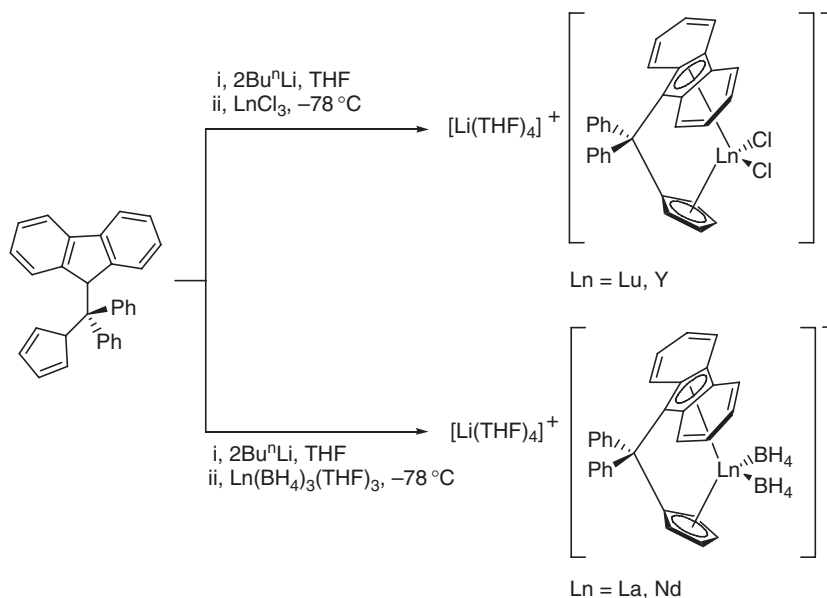
The synthesis of *ansa*-metallocene alkyl complexes of yttrium and lutetium with an ether-bridged indenyl ligand has been reported. The reaction of the corresponding monochlorides with  $\text{LiCH}_2\text{SiMe}_3$  in THF afforded the pure *rac*-, *ansa*-lanthanocene alkyl complexes  $[\text{O}(\text{CH}_2\text{CH}_2\text{C}_9\text{H}_6)_2]\text{LnCH}_2\text{SiMe}_3$  ( $\text{Ln} = \text{Y}, \text{Lu}$ ) (Scheme 193). The authors claimed, that only the *rac*-diastereomer was formed due to the non-bonded interactions between the six-membered fragment of the indenyl moiety and the alkyl group.<sup>709</sup>

The synthesis of diphenylmethylene-bridged fluorenyl cyclopentadienyl lanthanocene complexes with  $C_s$ -symmetry has been reported. The reaction of lanthanide chlorides  $\text{LnCl}_3$  with the dilithium salt of  $[(\text{C}_{13}\text{H}_9)\text{CPh}_2\text{C}_5\text{H}_4]^{2-}$  in THF at ambient temperature led to the formation of the *ate* complexes  $[\text{Li}(\text{THF})_4][\text{LnCl}_2\{(\text{C}_{13}\text{H}_8)\text{CPh}_2(\text{C}_5\text{H}_4)\}]$  ( $\text{Ln} = \text{Lu}, \text{Y}$ ) (Scheme 194).<sup>710</sup>

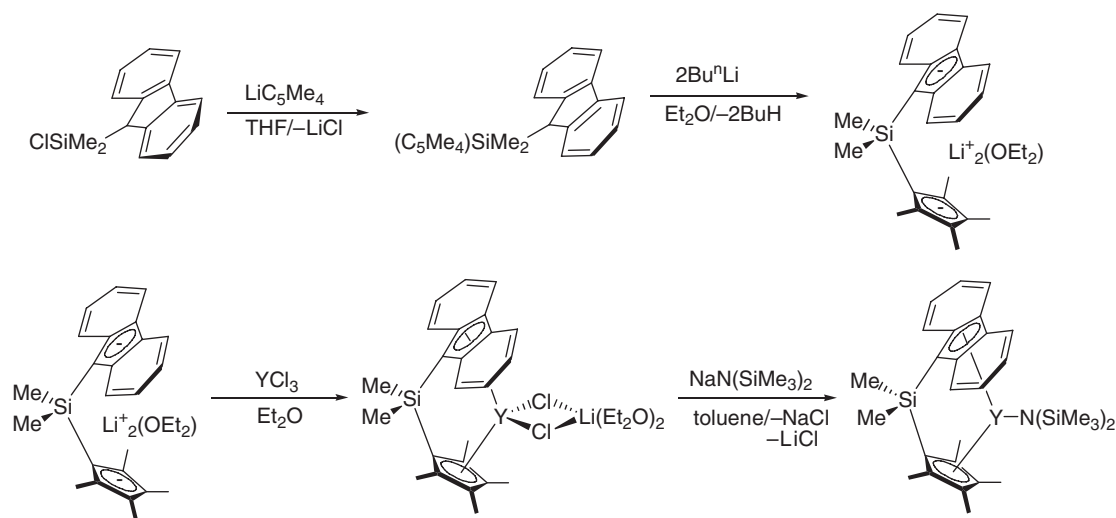
Treatment of  $\text{Ln}(\text{BH}_4)_3(\text{THF})_3$  with 3 equiv. of  $\text{Li}_2[(\text{C}_{13}\text{H}_8)\text{CPh}_2(\text{C}_5\text{H}_4)]$  in THF solution gave the anionic complexes  $[\text{Li}(\text{THF})_4][\text{Ln}(\text{BH}_4)_2\{(\text{C}_{13}\text{H}_8)\text{CPh}_2(\text{C}_5\text{H}_4)\}]$  ( $\text{Ln} = \text{La}, \text{Nd}$ ). Single crystal X-ray determinations of  $[\text{Li}(\text{THF})_4][\text{Ln}(\text{BH}_4)_2\{(\text{C}_{13}\text{H}_8)\text{CPh}_2(\text{C}_5\text{H}_4)\}]$  ( $\text{Ln} = \text{La}, \text{Nd}$ ) and  $[\text{Li}(\text{THF})_4][\text{LuCl}_2\{(\text{C}_{13}\text{H}_8)\text{CPh}_2(\text{C}_5\text{H}_4)\}]$  revealed the existence of discrete cation/anion pairs. The  $\text{Ln}-\text{C}$  (Cp ring) distances in these complexes are within the range expected for *ansa*-lanthanocenes. The  $\text{Ln}-\text{C}$  (fluorenyl ring) distances show differences of up to  $0.3 \text{ \AA}$  probably due to the inclined rigid planar fluorenyl ligation.<sup>710</sup> A novel  $C_s$ -symmetric fluorenyl *ansa*-yttrocene, *ansa*- $\text{Me}_2\text{Si}(\eta^3\text{-Flu})(\eta^5\text{-Cp'})\text{YCl}_2\text{Li}(\text{OEt})_2$  ( $\text{Flu} = \text{C}_{13}\text{H}_8$ ,  $\text{Cp}' = \text{C}_5\text{Me}_4$ ), has been prepared via salt metathesis reaction from  $\text{YCl}_3$  and the dilithium salt of the ligand  $\text{Me}_2\text{Si}(\text{FluH})(\text{Cp}'\text{H})$  (Scheme 195). Treatment of *ansa*- $\text{Me}_2\text{Si}(\eta^3\text{-Flu})(\eta^5\text{-Cp'})\text{YCl}_2\text{Li}(\text{OEt})_2$  with  $\text{NaN}(\text{SiMe}_3)_2$  afforded the corresponding bis(trimethylsilyl)amide derivative *ansa*- $\text{Me}_2\text{Si}(\eta^3\text{-Flu})(\eta^5\text{-Cp'})\text{YN}(\text{SiMe}_3)_2$ .<sup>711</sup>



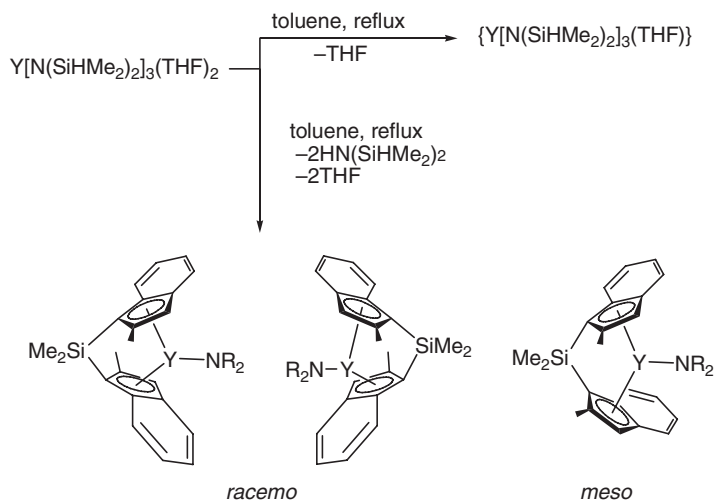
Scheme 193



Scheme 194



Scheme 195



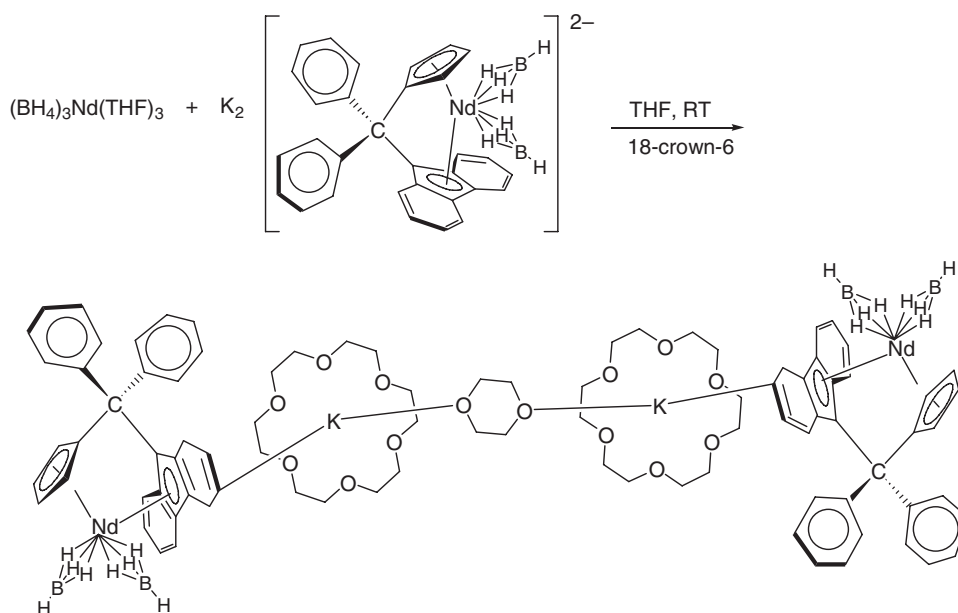
Scheme 196

In the bis(trimethylsilyl)amide complex, the Y–Flu bonding is partially slipped towards  $\eta^3$ . Furthermore, a  $\pi$ -dative bond nature of the Y–N bond and an additional interaction between the Y center and one methyl group of the  $\text{N}(\text{SiMe}_3)_2$  fragment have been discussed. The amide complex was found to be active in the polymerization of MMA.<sup>711</sup> The *ansa*-ytrocene complex  $[(\text{C}_9\text{H}_5-2\text{-Me})_2\text{SiMe}_2]\text{YN}(\text{SiHMe}_2)_2$ , derived from a linked bis(indenyl) ligand, has been prepared by an amine elimination reaction as depicted in Scheme 196.<sup>712</sup> Treatment of  $[(\text{C}_9\text{H}_5-2\text{-Me})_2\text{SiMe}_2]\text{YN}(\text{SiHMe}_2)_2$  with  $\text{AlHBU}_2^i$  ( $=\text{DIBAH}$ ) led to the formation of a dimeric hydride species.<sup>713,713a</sup>

A dinuclear anionic lanthanocene compound containing an *ansa*-fluorenyl ligand has been obtained by the reaction of  $\text{Nd}(\text{BH}_4)_3(\text{THF})_3$  with  $\text{K}_2[\text{Ph}_2\text{C}(\text{Flu})(\text{C}_5\text{H}_4)]$  in THF solution (Scheme 197). The crystallographically characterized product contains a dioxane ligand bridging the two potassium cations.<sup>714</sup>

#### 4.01.7 Cyclopentadienyl-Like Compounds

An excellent comprehensive review of heterocyclopentadienyl complexes of the group 3 and lanthanide metals was published in 2001 by Nief.<sup>715</sup> It covers complexes of monocyclic pyrrolyl, phospholyl, and arsolyl ligands, ring-fused



Scheme 197

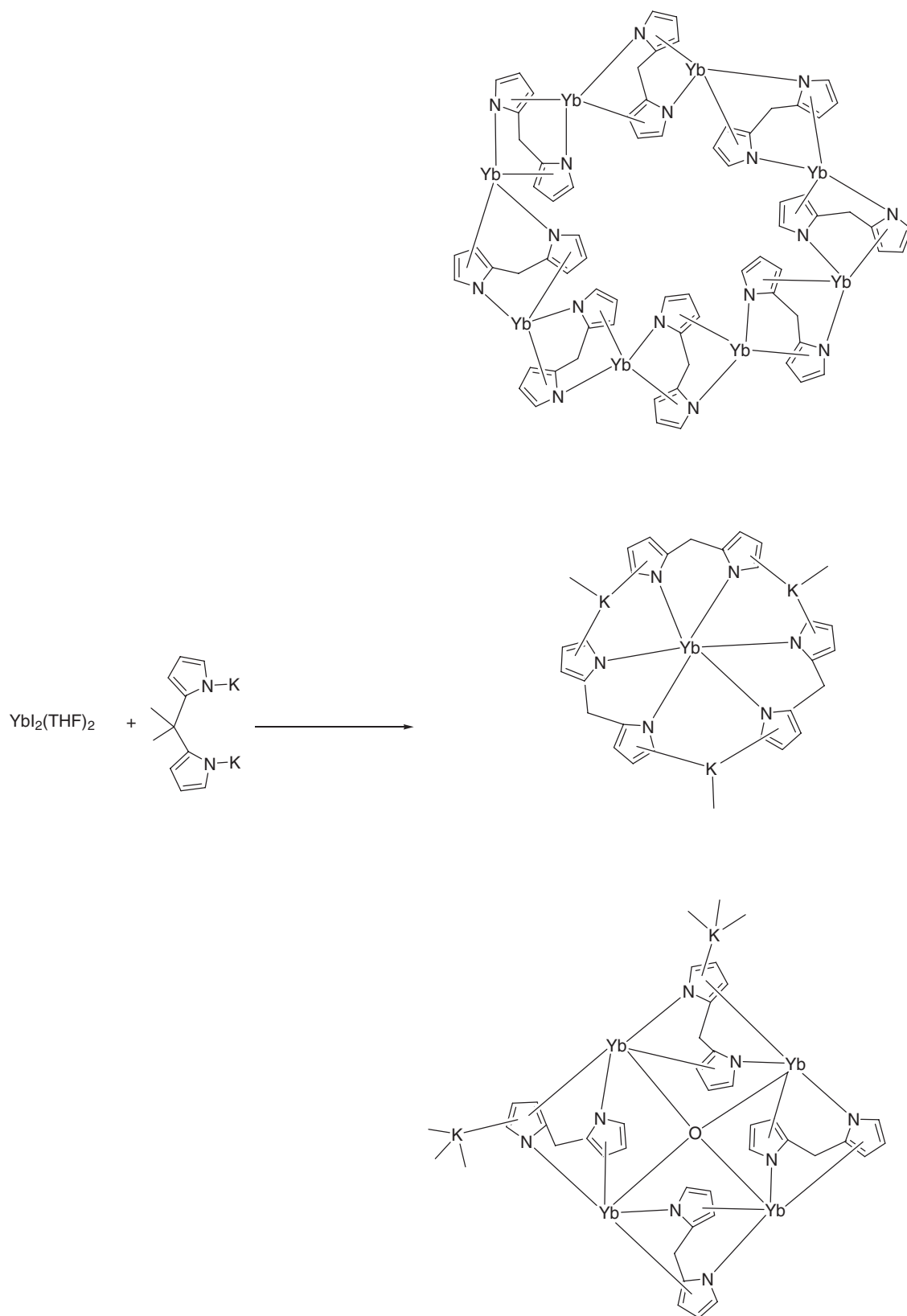
pyrrolyl and phospholyl ligands, pyrazolyl, triphospholyl, and stibadiphospholyl ligands, as well as those containing bridged pyrrolyl ligands (dipyrrolyl complexes and macrocyclic tetrapyrrolyl complexes). Almost all compounds of the latter two classes display  $\sigma, \pi$ -complexation of the pyrrolyl rings to the lanthanide centers and should thus be considered true organometallic compounds.

#### 4.01.7.1 Compounds with Heteroatom Five-membered Ring Ligands

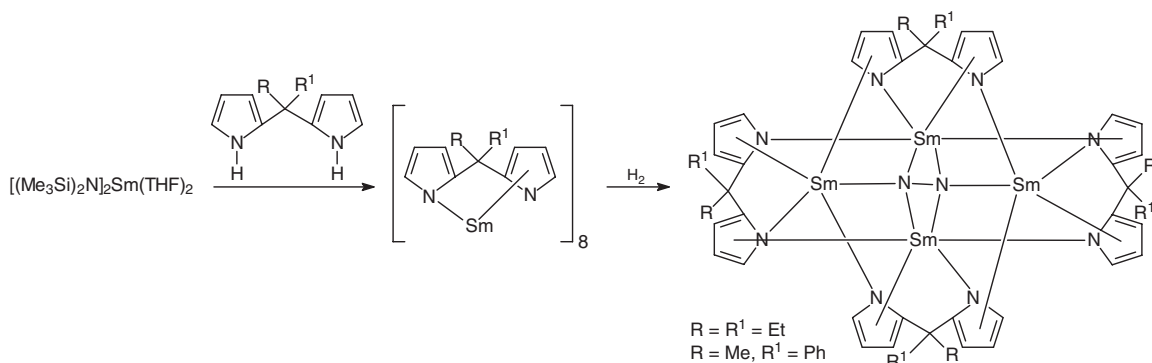
Synthesis and crystal structure of the monopyrrolyl complex  $(\text{pyr}^*)\text{YbCl}_2(\text{THF})_2$  ( $\text{pyr}^* = \text{NC}_4\text{H}_2\text{Bu}^t_{2-2,5}$ ) have been reported. The compound was obtained by the reaction of  $\text{YbCl}_3(\text{THF})_3$  with  $\text{Na}[\text{pyr}^*]$  in THF. In the structure the Yb atom is coordinated by the azacyclopentadienyl ligand ( $\text{NC}_4\text{H}_2\text{Bu}^t_{2-2,5}$ ) in  $\pi$ -fashion, two chlorine ligands, and two THF molecules. The Yb has a distorted trigonal bipyramidal environment with both chloride and pyrrolyl ligands in equatorial and the THF ligands in axial positions. The Yb–pyr(cent.) distance is 232.6 pm.<sup>716</sup> Reactions of  $\text{SmI}_2(\text{THF})_2$  and  $\text{YbI}_2(\text{THF})_2$  with the alkali metal salts of 2,5-dimethylpyrrole, or the reaction of  $\text{SmCl}_3(\text{THF})_3$  and  $\text{YbCl}_3(\text{THF})_3$  with the same ligand followed by reduction with the appropriate alkali metals, led to the formation of divalent mono- and polynuclear complexes. Structural analyses of these complexes indicated that the bonding mode adopted by the ligand depends on the nature of the alkali metal cation retained in the structure.<sup>717</sup> Dipyrrolide dianions were formed by a transient divalent Tm complex via fragmentation of the  $(\text{Et}_8\text{-calix}[4]\text{tetrapyrrole})[\text{K}(\text{DME})]_4$  ligand during the reaction with  $\text{TmI}_2(\text{DME})_3$ .<sup>718</sup> The related reaction of  $\text{YbI}_2(\text{THF})_2$  with diphenyldipyrrolylmethanide led to a complex reaction from which a dark red octameric ytterbium(II) macrocyclic complex,  $[(\text{diphenyldipyrromethanediyl})\text{Yb}]_8$ , was obtained as a major product (Scheme 198). A tetrameric cyclic Yb(II)-oxo complex,  $[\text{K}(\text{THF})_3]_2[(\text{diphenyldipyrrolyl}(\mu\text{-O}))\text{Yb}]_4(\mu\text{-O})(\text{THF})_2$ , arising from solvent deoxygenation, and a monomeric Yb(III) complex,  $[\text{K}(\text{THF})_3]\text{Yb}(\text{diphenyldipyrrolyl}(\mu\text{-O}))_3$ , were also isolated as byproducts of this complex reaction. All three products have been unambiguously characterized by X-ray structural analyses.<sup>719</sup>

Samarium chemistry with polydentate pyrrolyl ligands is also very diverse. Divalent and trivalent dinuclear samarium complexes supported by pyrrole-based tetradentate Schiff bases<sup>720</sup> as well as  $\text{Ln}(\text{II})$  and  $\text{Ln}(\text{III})$  meso-octaethylporphyrinogen complexes<sup>721</sup> have been investigated, which all involve coordination of the pyrrolyl rings to the lanthanide metals. The same is true for a recently reported series of homoleptic lanthanide pyrazolates<sup>722,723</sup> and the europium indolate  $\text{Eu}_2(\text{indolate})_4(\text{NH}_3)_6$ .<sup>724</sup> Transamination reactions of  $\text{Sm}[\text{N}(\text{SiMe}_3)_2]_2(\text{THF})_2$  with dipyrrolylmethanes under nitrogen as illustrated in Scheme 199 produced unusual tetranuclear dinitrogen complexes.<sup>725</sup>

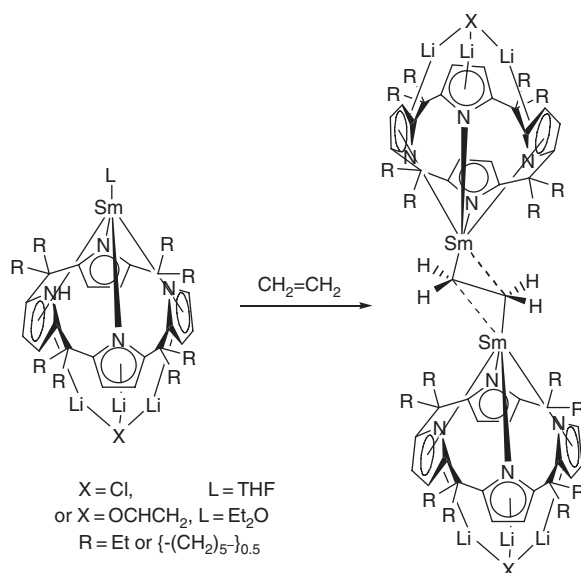
A reversible fixation of ethylene at a samarium center in a calixpyrrol-samarium complex has also been reported. Reduction of the  $\text{Sm}(\text{III})$  complexes  $[(\text{R}_8\text{-calixpyrrol})\text{ClSm}\{\text{Li}(\text{THF})\}_2\{\text{Li}(\text{THF})_2\}(\mu_3\text{-Cl})]$  ( $\text{R} = \text{Et}$  or  $\{-\text{CH}_2\}_{5-}\}_{0.5}$ )



Scheme 198



Scheme 199

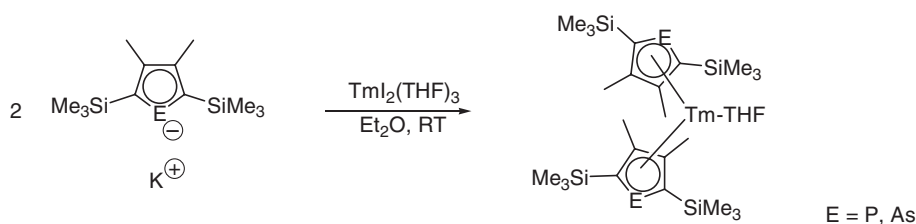


Scheme 200

with lithium gave dark green solutions in both cases (Scheme 200). The resulting complex is dependent on the aliphatic substitution at the calixpyrrol ring. The compounds  $[(\text{R}_8\text{-calixpyrrol})(\text{L})\text{Sm}\{\text{Li}(\text{THF})\}_2\{\mu_3\text{-X}(\text{Et}_2\text{O})_{1.5}\}]$  ( $\text{R} = \{-(\text{CH}_2)_5-\}_{0.5}$ ,  $\text{X} = \text{Cl}$ ,  $\text{L} = \text{THF}$ ;  $\text{R} = \text{Et}$ ,  $\text{X} = \text{OCH}=\text{CH}_2$ ,  $\text{L} = \text{Et}_2\text{O}$ ) react with ethylene forming the ethylene-bridged complexes  $\{[(\text{R}_8\text{-calixpyrrol})[(\text{CH}_2=\text{CHO})\text{Li}][\text{Li}(\text{THF})]_2\text{Sm}](\mu\text{-CH}_2\text{CH}_2)\}$  ( $\text{R} = \{-(\text{CH}_2)_5-\}_{0.5}$  or  $\text{R} = \text{Et}$ ). The magnetical moment of the compound  $\text{R} = \{-(\text{CH}_2)_5-\}_{0.5}$  shows the complete oxidation to a  $\text{Sm}(\text{III})$  species. Single crystal X-ray determinations revealed an  $\text{Sm}-\text{C}-\text{C}-\text{Sm}$  center with a relatively long carbon-carbon distance of 1.487 Å.<sup>726</sup>

Treatment of thulium diiodide with substituted phospholide and arsolide salts afforded stable bis(phospholyl)- and bis(arsolyl)thulium(II) complexes (Scheme 201) as green solids, that were characterized by multinuclear NMR and X-ray crystal structures. The latter clearly revealed the beneficial effects of the steric and electronic properties of crowded phospholyl and arsolyl ligands for the stabilization of divalent thulium.<sup>727</sup> Several other homoleptic samarium(II) and thulium(II) phospholyl sandwich complexes containing the 2,5-di-*t*-butyl-3,4-dimethylphospholide (= dtp) or 2,5-bis(trimethylsilyl)-3,4-dimethylphospholide (= dsp) ligand have been synthesized and structurally characterized. X-ray studies revealed that  $[\text{Sm}(\text{dtp})_2]_2$  and  $[\text{Sm}(\text{dsp})_2]_2$  are both dimeric in the solid state due to coordination of the phosphorus lone pairs to samarium.<sup>728,729</sup>

Like the decamethylanthanidocenes, the bis(phospholyl)lanthanide(II) sandwich complexes exhibit an interesting derivative chemistry. For example, addition of azobenzene to the samarium(II) and thulium(II) complexes resulted in



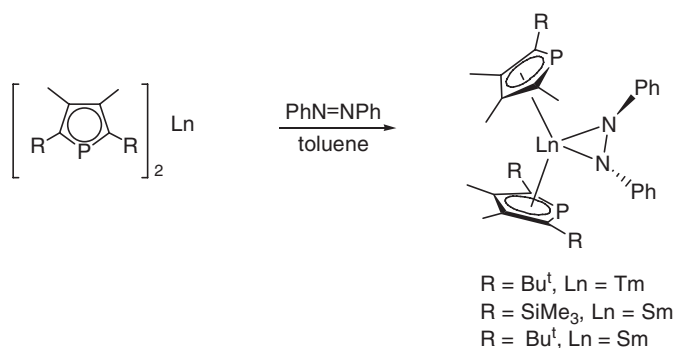
Scheme 201

the immediate formation of dark blue solutions from which the adducts  $(dtp)_2Tm(N_2Ph_2)$ ,  $(dsp)_2Sm(N_2Ph_2)$ , and  $(dtp)_2Sm(N_2Ph_2)$  could be isolated, in which the azobenzene is  $\eta^2$ -coordinated (Scheme 202).<sup>728</sup>

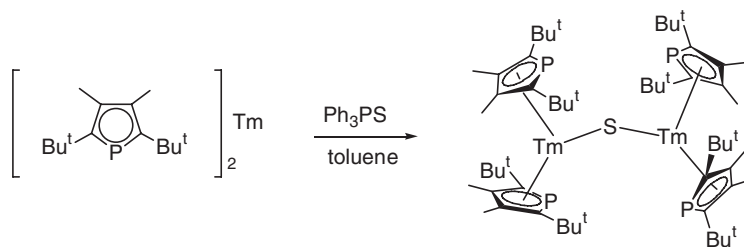
Triphenylphosphine sulfide ( $Ph_3PS$ ) reacts with  $Tm(dtp)_2$  to give the sulfido-bridged binuclear complex  $[(dtp)_2Tm]_2(\mu-S)$  (Scheme 203), whereas the samarium(II) phospholyl complexes have been found to be unreactive towards  $Ph_3PS$ .<sup>728</sup>

Bis(pentamethylcyclopentadienyl) phospholyl and arsolylsamarium(III) complexes have been synthesized from decamethylsamarocene via two different synthetic routes, which are illustrated in Schemes 204 and 205.<sup>727</sup>

Reaction of  $KTmp$  ( $Tmp = 2,3,4,5$ -tetramethylphospholyl) with  $SmCl_3$  in a 3:1 molar ratio in toluene yielded the phosphonylsamarium(III) complex  $[(Tmp)_6Sm_2(KCl)_2(C_7H_8)_3]_n$ . According to X-ray crystallography the compound has a polymeric structure comprising two crystallographically different eight-membered  $[Sm-P-K-Cl]_2$  rings connected by  $[Sm-P-K]$  links. Each Sm atom is coordinated by two Tmp ligands in  $\pi$ -fashion, one Tmp ligand through the phosphorus atom and one bridging Cl atom to give a pseudo-tetrahedral arrangement. The Sm-P bond lengths range from 2.92 to 2.95 Å. The K atom also has pseudo-tetrahedral environment formed by one  $\pi$ -coordinated Tmp ligand, one  $\pi$ -toluene ligand, one bridging chlorine atom, and one phosphorus atom of Tmp ligand from another unit. The complex  $[(\eta^5-Dmp)_4(\mu-(\eta^5, \eta^1)-Dmp)_2Sm_2]$  ( $Dmp = 3,4$ -dimethylphospholyl) was synthesized in a similar manner from KDmp and  $SmCl_3$  in 3:1 molar ratios in toluene. According to an X-ray diffraction study, the compounds have a dimeric structure in which two  $(\eta^5-Dmp)_2Sm$  fragments are bridged by two  $\mu-(\eta^5, \eta^1)-Dmp$  ligands. Each Sm atom also has pseudo-tetrahedral arrangement.<sup>730,730a</sup>

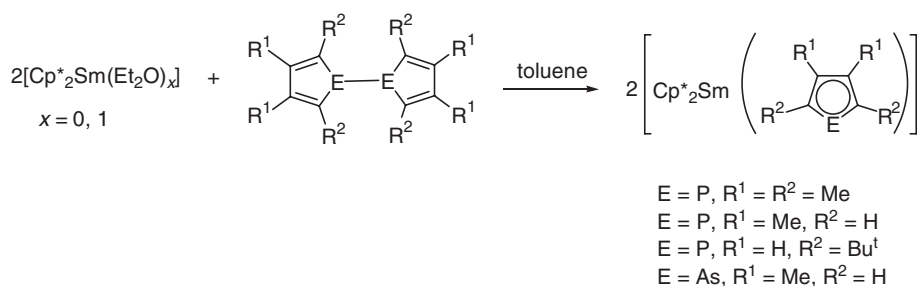


Scheme 202

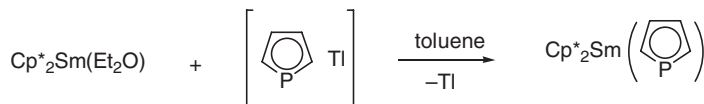


Scheme 203

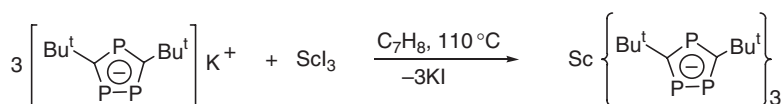




Scheme 204



Scheme 205



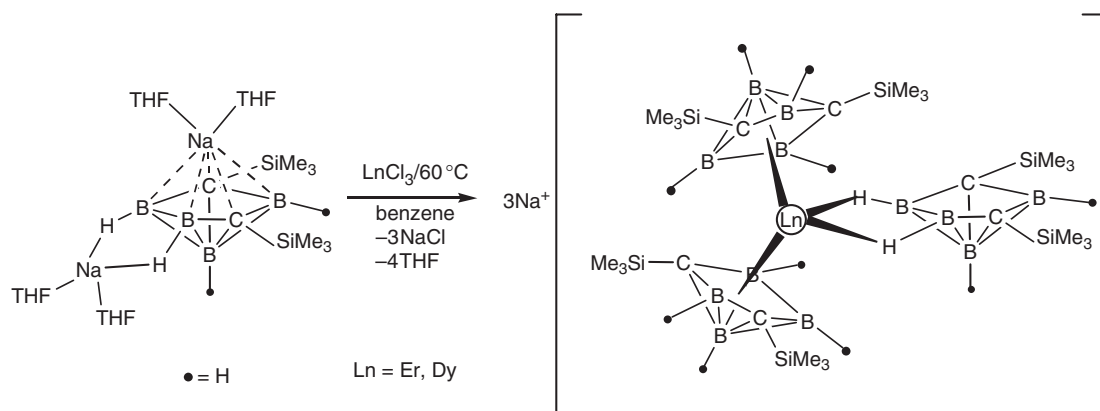
Scheme 206

The novel bis(tetramethylphospholyl)ytterbium carbene complexes ( $\text{Tmp})_2\text{Yb}(\text{carbene})$  (carbene =  $\text{C}_2\text{Me}_2(\text{NPr}^i)_2\text{C}$  and  $\text{C}_2\text{Me}_2(\text{NMe}_2\text{C})$ ) have been synthesized from  $[\text{Yb}(\text{Tmp})_2]_n$  and the free carbenes. Both compounds are not stable in THF solution.<sup>731</sup>  $\text{Nd}(\text{BH}_4)_3(\text{THF})_3$  reacts with  $\text{KC}_4\text{Me}_4\text{P}$  to give the organometallic derivative and  $[\text{K}(\text{THF})][(\text{C}_4\text{Me}_4\text{P})_2\text{Nd}(\text{BH}_4)_2]$ .<sup>547</sup> The molecular structure of  $[\text{K}(18\text{-crown-6})(\text{THF})_2][(\text{C}_4\text{Me}_4\text{P})_2\text{Nd}(\text{BH}_4)_2]$  has been determined by X-ray diffraction analysis.<sup>732</sup> Oxidation of  $\text{SmCp}^*_2$  with  $[\text{Ti}(1,4,2\text{-P}_2\text{SbC}_2\text{Bu}^t_2)]/[\text{Ti}(1,2,4\text{-P}_3\text{C}_2\text{Bu}^t_2)]$  (approximately 4:1) gave a mixture of  $[\text{SmCp}^*_2(1,2,4\text{-P}_3\text{C}_2\text{Bu}^t_2)]$  and  $[\text{SmCp}^*_2(1,4,2\text{-P}_2\text{SbC}_2\text{Bu}^t_2)]$ .<sup>580</sup> The former was shown to be a nine-coordinate monomer with novel pseudopyrazolate  $\eta^2\text{-}[1,2,4\text{-P}_3\text{C}_2\text{Bu}^t_2]$  coordination of the triphosphacyclopentadienide ligand. After metathesis routes to  $\text{Ln}(1,4,2\text{-P}_2\text{SbC}_2\text{Bu}^t_2)_n$  complexes failed, redox transmetalation between ytterbium metal and  $\text{Ti}(1,4,2\text{-P}_2\text{EC}_2\text{Bu}^t_2)$  ( $\text{E} = \text{Sb}, \text{P}$ ) containing a substantial impurity of  $[\text{Li}(\text{tmeda})_2][1,4,2\text{-P}_2\text{EC}_2\text{Bu}^t_2]$  yielded the first lanthanide diphosphastibacyclopentadienide complex in a mixture with  $1,2,4\text{-P}_3\text{C}_2\text{Bu}^t_2$  species.<sup>580</sup> Prolonged heating of base-free  $\text{K}(\text{P}_3\text{C}_2\text{Bu}^t)$  and  $\text{ScI}_3$  in toluene or mesitylene resulted in the formation of a deep red solution from which red crystals of  $\text{Sc}(\text{P}_3\text{C}_2\text{Bu}^t)_3$  could be isolated (Scheme 206).<sup>733,733a</sup>

Further treatment of  $\text{Sc}(\text{P}_3\text{C}_2\text{Bu}^t)_3$  with  $\text{KC}_8$  in toluene at low temperature ( $-78^\circ\text{C}$ ) produced a very deep blue solution, the color of which persisted at room temperature. Sublimation of the residue after removal of the volatiles gave very dark blue crystals of  $[\text{Sc}(\text{P}_3\text{C}_2\text{Bu}^t)_2]_n$  containing formally divalent scandium. The complex is dimeric in the solid state and should best be described as a mixed oxidation state complex containing both  $\text{Sc}^{\text{I}}$  and  $\text{Sc}^{\text{III}}$  centers.<sup>733,733a</sup>

#### 4.01.7.2 Compounds with Carboranyl Ligands

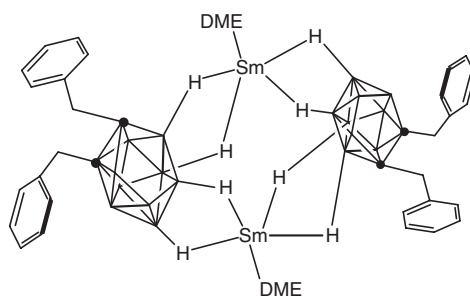
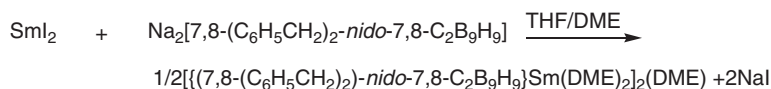
The complex  $\text{Cp}^*_2\text{Yb}$  forms complexes with *ortho*-, *meta*-, and 1,2-dimethyl-*ortho*-carborane. The sterically and electronically unsaturated ytterbium center in this complex is expected to coordinate any molecule with a permanent dipole moment. The dipole moment of *ortho*-carborane is 4.31 D. When *ortho*-carborane and  $\text{Cp}^*_2\text{Yb}$  are mixed in hexane, an immediate precipitation of a green solid is observed. The solid can be recrystallized from hot toluene to give dark green needles in good yield. This complex shows thermochromism: at lower temperatures the complex is green and turns reversibly orange at  $130^\circ\text{C}$ . Carboranes with smaller dipole moments like *meta*-carborane and 2-dimethyl-*ortho*-carborane also form complexes with  $\text{Cp}^*_2\text{Yb}$ , which are more soluble and can be crystallized from hexane at  $-25^\circ\text{C}$ .<sup>517</sup>



Scheme 207

The reaction between 1,1-( $\text{SiMe}_3$ )<sub>2</sub>-*closo*-1,2- $\text{C}_2\text{B}_4\text{H}_4$ ,  $\text{ErCl}_3$ , and K in a 2:1:4 molar ratio, in the absence of an outside electron-transfer agent, produced the erbacarborane sandwich 2,2',4,4'-( $\text{SiMe}_3$ )<sub>4</sub>-3,6'-[( $\mu\text{-H}$ )<sub>2</sub>K(THF)<sub>2</sub>]-1,1'-*commo*-Er( $\eta^5\text{-2,4-C}_2\text{B}_4\text{H}_4$ )<sub>2</sub> as light orange crystals in 82% yield. All experimental observations were consistent with a process in which the erbium metal is acting as both the capping group and an electron-transfer agent.<sup>734</sup> In a similar manner, the reaction of *closo-exo*-5,6-Na(THF)<sub>2</sub>-1-Na(THF)<sub>2</sub>-2,4-( $\text{SiMe}_3$ )<sub>2</sub>-2,4- $\text{C}_2\text{B}_4\text{H}_4$  and anhydrous  $\text{LnCl}_3$  in a molar ratio of 3:1 in dry benzene at  $60^\circ\text{C}$  produced novel lanthanocene analogs of metallacarborane complexes of the formula  $\text{Na}_3[1,1'\text{-}\{5,6\text{-}(\mu\text{-H})_2\text{-nido-2,4-(SiMe}_3)_2\text{-2,4-C}_2\text{B}_4\text{H}_4\}\text{-2,2',4,4'-(SiMe}_3)_4\text{-1,1'-commo-Ln-(}\eta^5\text{-2,4-C}_2\text{B}_4\text{H}_4)_2]$  ( $\text{Ln} = \text{Er, Dy}$ ) as yellow crystalline solids in 82% and 78% yields, respectively, thus establishing a new structural pattern for lanthanacarboranes (Scheme 207).<sup>735</sup> The analogous reaction of *closo-exo*-5,6-Na(THF)<sub>2</sub>-1-Na(THF)<sub>2</sub>-2,4-( $\text{SiMe}_3$ )<sub>2</sub>-2,4- $\text{C}_2\text{B}_4\text{H}_4$  with anhydrous  $\text{LuCl}_3$  in a molar ratio of 2:1 in dry benzene at  $60^\circ\text{C}$  produces the first full-sandwiched lutetiacarborane complex, 2,2',4,4'-( $\text{SiMe}_3$ )<sub>4</sub>-3,5',6'-[( $\mu\text{-H}$ )<sub>3</sub>Na(THF)<sub>2</sub>]-1,1'-*commo*-Ln-( $\eta^5\text{-2,4-C}_2\text{B}_4\text{H}_4$ )<sub>2</sub>, as an off-white crystalline solid in 88% yield.<sup>736</sup> The same synthetic route has later been extended to a series of homologous complexes with  $\text{Ln} = \text{Nd, Gd, Dy, Ho, Er, Tb, Lu}$ ,<sup>737,738</sup> while in the case of  $\text{Ln} = \text{La, Nd, Gd, Tb, Ho, and Lu}$  oxide ion-encapsulating tetralanthanide clusters have also been isolated,<sup>739,740</sup> and with neodymium an unsolvated “carbons apart” neodymacarborane sandwich stabilized by bis( $\eta^6\text{-benzene}$ ) potassium cation has been obtained.<sup>741</sup> For terbium and erbium novel sandwich complexes derived from mixed  $\eta^5\text{-pentadienyl}$  and  $\text{C}_2\text{B}_4$  carborane ligands have been also described.<sup>742</sup>

Treatment of  $\text{SmI}_2$  with an equimolar amount of  $\text{Na}_2[7,8\text{-(C}_6\text{H}_5\text{CH}_2)_2\text{-nido-7,8-C}_2\text{B}_9\text{H}_9]$  in THF at room temperature accompanied by a solvent exchange from THF to DME gave the dark red dimeric complex  $[\{(7,8\text{-(C}_6\text{H}_5\text{CH}_2)_2\text{-nido-7,8-C}_2\text{B}_9\text{H}_9\}\text{Sm}(\text{DME})_2\}_2(\text{DME}) + 2\text{NaI}$  (Scheme 208).<sup>743</sup>



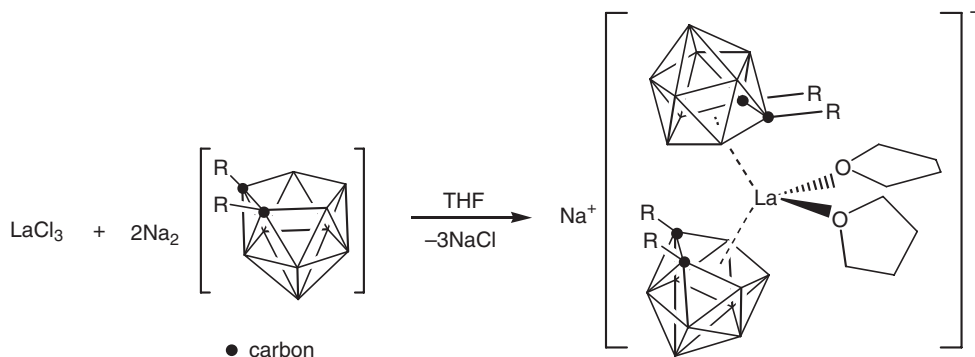
Scheme 208

In the dimeric samarium complex each of the two dibenzylidicarbollide ligands serves as a bridging ligand for two samarium atoms. The main feature of this structure is the presence of exclusive Sm–H–B bonding between Sm(II) and the dibenzylidicarbollide anions. This was the first example of a structurally characterized *exo-nido*-lanthanacarborane of the C<sub>2</sub>B<sub>9</sub> system.<sup>743</sup> The synthesis of the scandium dicarbollide complex Cp<sup>\*</sup>Sc(C<sub>2</sub>B<sub>9</sub>H<sub>11</sub>)(THF)<sub>3</sub> was achieved by the reactions of [Cp<sup>\*</sup>ScCl<sub>2</sub>]<sub>x</sub> with Na<sub>2</sub>(C<sub>2</sub>B<sub>9</sub>H<sub>11</sub>) or [Cp<sup>\*</sup>Sc(μ-Me)<sub>2</sub>]<sub>x</sub> with C<sub>2</sub>B<sub>9</sub>H<sub>13</sub>, followed by treatment with THF. Alkylation of Cp<sup>\*</sup>Sc(C<sub>2</sub>B<sub>9</sub>H<sub>11</sub>)(THF)<sub>3</sub> with LiCH(SiMe<sub>3</sub>)<sub>2</sub> afforded the anionic alkyl derivatives [Li(THF)<sub>3</sub>][Cp<sup>\*</sup>Sc(C<sub>2</sub>B<sub>9</sub>H<sub>11</sub>)(CH(SiMe<sub>3</sub>)<sub>2</sub>)] and [Li(THF)<sub>3</sub>][Li(Cp<sup>\*</sup>Sc(C<sub>2</sub>B<sub>9</sub>H<sub>11</sub>)(CH(SiMe<sub>3</sub>)<sub>2</sub>))<sub>2</sub>]. These alkyls slowly react with H<sub>2</sub> to give the unreactive scandium hydride dimer [Li(THF)<sub>n</sub>]<sub>2</sub>[Cp<sup>\*</sup>Sc(C<sub>2</sub>B<sub>9</sub>H<sub>11</sub>)(μ-H)]<sub>2</sub>.<sup>744</sup> Treatment of LnCl<sub>3</sub> with 1 equiv. of Na<sub>2</sub>[*nido*-7,8-C<sub>2</sub>B<sub>9</sub>H<sub>11</sub>] in THF gave the half-sandwich lanthanacarborane chloride compounds (η<sup>5</sup>-C<sub>2</sub>B<sub>9</sub>H<sub>11</sub>)Ln(THF)<sub>2</sub>(μ-Cl)<sub>2</sub>Na(THF)<sub>2</sub> (Ln = Y, Er, Yb, Lu).<sup>745</sup> Recrystallization of the yttrium and ytterbium complexes from a wet THF/toluene solution gave the ionic compounds [LnCl<sub>2</sub>(THF)<sub>5</sub>][*nido*-C<sub>2</sub>B<sub>9</sub>H<sub>12</sub>] (Ln = Y, Yb). Reaction of (η<sup>5</sup>-C<sub>2</sub>B<sub>9</sub>H<sub>11</sub>)Ln(THF)<sub>2</sub>(μ-Cl)<sub>2</sub>Na(THF)<sub>2</sub> (Ln = Y, Yb) with Na<sub>2</sub>[*nido*-7,8-C<sub>2</sub>B<sub>9</sub>H<sub>11</sub>] in a molar ratio of 1 : 1 in THF afforded the full-sandwich lanthanacarboranes {(η<sup>5</sup>-C<sub>2</sub>B<sub>9</sub>H<sub>11</sub>)<sub>2</sub>Ln(THF)<sub>2</sub>}[Na(THF)<sub>2</sub>] (Ln = Y, Yb).<sup>746</sup> Treatment of anhydrous LaCl<sub>3</sub> with 1 equiv. of Na<sub>2</sub>[7,8-*nido*-7,8-C<sub>2</sub>B<sub>9</sub>H<sub>9</sub>] (R = H, C<sub>6</sub>H<sub>5</sub>CH<sub>2</sub>) afforded the colorless sandwich complexes *closo*-[(THF)<sub>2</sub>Na][(R<sub>2</sub>C<sub>2</sub>B<sub>9</sub>H<sub>9</sub>)<sub>2</sub>La(THF)<sub>2</sub>] (Scheme 209).<sup>743</sup>

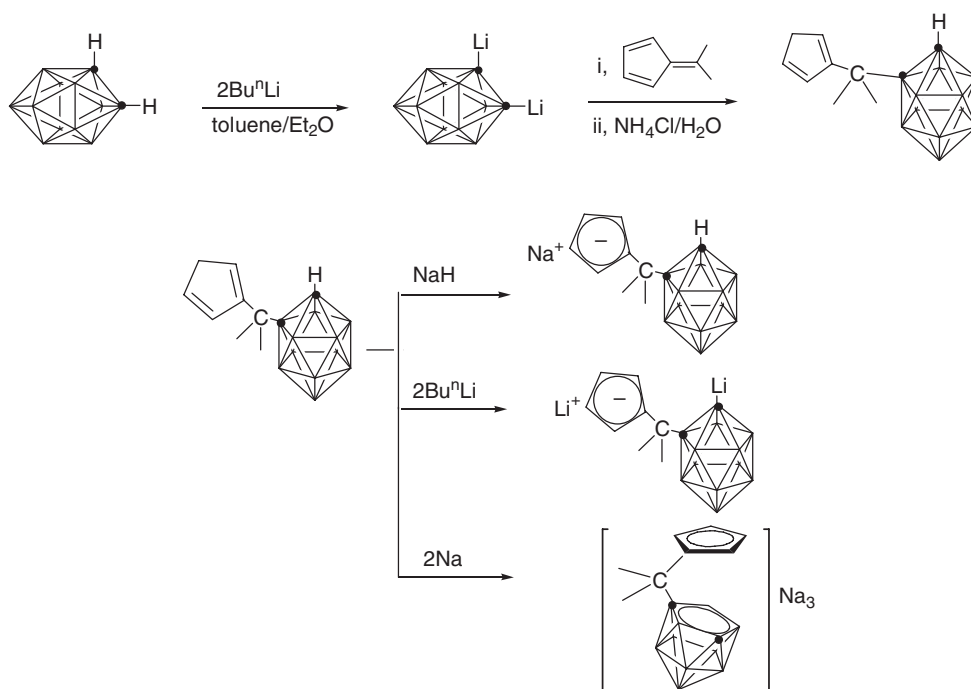
The mono-, di-, and trianions of the compound Me<sub>2</sub>C(Cp)(C<sub>2</sub>B<sub>10</sub>H<sub>11</sub>), [Me<sub>2</sub>C(C<sub>5</sub>H<sub>4</sub>)(C<sub>2</sub>B<sub>10</sub>H<sub>11</sub>)]<sup>−</sup>, [Me<sub>2</sub>C(C<sub>5</sub>H<sub>4</sub>)(C<sub>2</sub>B<sub>10</sub>H<sub>10</sub>)]<sup>2−</sup>, and [Me<sub>2</sub>C(C<sub>5</sub>H<sub>4</sub>)(*nido*-C<sub>2</sub>B<sub>10</sub>H<sub>11</sub>)]<sup>3−</sup>, have been synthesized according to Scheme 210.<sup>747</sup>

Reactions of LnCl<sub>3</sub> with the monoanion in molar ratios of 1 : 1, 1 : 2, and 1 : 3 generated the mono-, bis-, and tris-ligated organolanthanide compounds [η<sup>5</sup>-Me<sub>2</sub>C(C<sub>5</sub>H<sub>4</sub>)(C<sub>2</sub>B<sub>10</sub>H<sub>11</sub>)]LnCl<sub>2</sub>(S)<sub>n</sub> ((S)<sub>n</sub> = (THF)<sub>3</sub>, Ln = Er, Sm, (S)<sub>n</sub> = (DME)<sub>2</sub>, Ln = Nd), [η<sup>5</sup>-Me<sub>2</sub>C(C<sub>5</sub>H<sub>4</sub>)(C<sub>2</sub>B<sub>10</sub>H<sub>11</sub>)]<sub>2</sub>SmCl(THF)<sub>2</sub>, and [η<sup>5</sup>-Me<sub>2</sub>C(C<sub>5</sub>H<sub>4</sub>)(C<sub>2</sub>B<sub>10</sub>H<sub>11</sub>)]<sub>3</sub>Sm·0.5C<sub>7</sub>H<sub>8</sub>, respectively. Reactions of LnCl<sub>3</sub> with 1 or 2 equiv. of the dianion gave the same compounds [(η<sup>5</sup>:σ-Me<sub>2</sub>C(C<sub>5</sub>H<sub>4</sub>)(C<sub>2</sub>B<sub>10</sub>H<sub>10</sub>))<sub>2</sub>Ln][Li(DME)<sub>3</sub>] (Ln = Sm, Yb).<sup>747</sup> (Scheme 211).

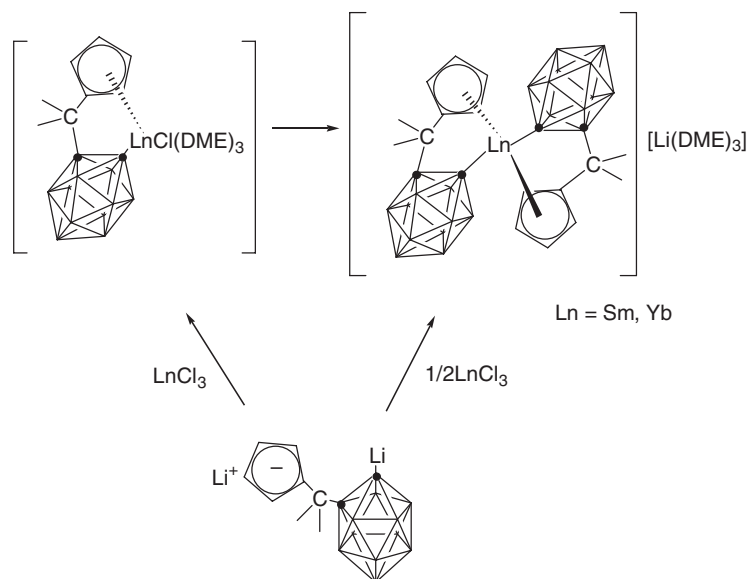
The first organolanthanide compound containing an η<sup>7</sup>-carboranyl ligand, [(η<sup>5</sup>:η<sup>7</sup>-Me<sub>2</sub>C(C<sub>5</sub>H<sub>4</sub>)(C<sub>2</sub>B<sub>10</sub>H<sub>11</sub>))Er]<sub>2</sub>[Na<sub>4</sub>(THF)<sub>9</sub>]<sub>n</sub>, has been achieved by treatment of [η<sup>5</sup>-Me<sub>2</sub>C(C<sub>5</sub>H<sub>4</sub>)(C<sub>2</sub>B<sub>10</sub>H<sub>11</sub>)]ErCl<sub>2</sub>(THF)<sub>3</sub> or [(η<sup>5</sup>:η<sup>6</sup>-Me<sub>2</sub>C(C<sub>5</sub>H<sub>4</sub>)(C<sub>2</sub>B<sub>10</sub>H<sub>11</sub>))Er]<sub>2</sub>(THF)<sub>2</sub> with excess Na metal in THF. The Na<sup>+</sup> ions in [(η<sup>5</sup>:η<sup>7</sup>-Me<sub>2</sub>C(C<sub>5</sub>H<sub>4</sub>)(C<sub>2</sub>B<sub>10</sub>H<sub>11</sub>))Er]<sub>2</sub>[Na<sub>4</sub>(THF)<sub>9</sub>]<sub>n</sub> can be replaced by Er<sup>3+</sup> ions, giving the tetranuclear cluster [(η<sup>5</sup>:η<sup>7</sup>-Me<sub>2</sub>C(C<sub>5</sub>H<sub>4</sub>)(C<sub>2</sub>B<sub>10</sub>H<sub>11</sub>))Er<sub>2</sub>(μ-Cl)(THF)<sub>3</sub>]<sub>2</sub>. The polymeric nature of [(η<sup>5</sup>:η<sup>7</sup>-Me<sub>2</sub>C(C<sub>5</sub>H<sub>4</sub>)(C<sub>2</sub>B<sub>10</sub>H<sub>11</sub>))Er]<sub>2</sub>[Na<sub>4</sub>(THF)<sub>9</sub>]<sub>n</sub> has been confirmed by a single crystal X-ray analysis, which reveals two [(η<sup>5</sup>:η<sup>7</sup>-Me<sub>2</sub>C(C<sub>5</sub>H<sub>4</sub>)(C<sub>2</sub>B<sub>10</sub>H<sub>11</sub>))Er]<sub>2</sub><sup>2−</sup> structural motifs in each asymmetrical unit. The asymmetrical units are linked to each other via B–H–Er bonds to form an infinite polymeric chain.<sup>747–750</sup> The Me<sub>2</sub>Si-bridged cyclopentadienyl/carboranyl ligand systems can be generated by the reaction of Me<sub>2</sub>SiCpCl with 1 equiv. of Li<sub>2</sub>C<sub>2</sub>B<sub>10</sub>H<sub>10</sub> and subsequent hydrolysis, giving Me<sub>2</sub>SiCp(C<sub>2</sub>B<sub>10</sub>H<sub>11</sub>). Me<sub>2</sub>SiCp(C<sub>2</sub>B<sub>10</sub>H<sub>11</sub>) can be conventionally converted into the monoanion Na[Me<sub>2</sub>Si(C<sub>5</sub>H<sub>4</sub>)(C<sub>2</sub>B<sub>10</sub>H<sub>11</sub>)], the dianion Li<sub>2</sub>[Me<sub>2</sub>SiCp(C<sub>2</sub>B<sub>10</sub>H<sub>10</sub>)], and the trianion K<sub>3</sub>[Me<sub>2</sub>Si(C<sub>5</sub>H<sub>4</sub>)(C<sub>2</sub>B<sub>10</sub>H<sub>11</sub>)] by treatment with NaH, MeLi, and K metal in THF at room temperature, respectively. Na[Me<sub>2</sub>Si(C<sub>5</sub>H<sub>4</sub>)(C<sub>2</sub>B<sub>10</sub>H<sub>11</sub>)] reacts with 1 equiv. of LnCl<sub>3</sub> in THF yielding the dichlorides [η<sup>5</sup>-Me<sub>2</sub>Si(C<sub>5</sub>H<sub>4</sub>)(C<sub>2</sub>B<sub>10</sub>H<sub>11</sub>)]LnCl<sub>2</sub>(THF)<sub>3</sub> (Ln = Nd, Sm, Er, Yb). Single crystal X-ray studies reveal a monomeric structure for the dichloro complexes. The cyclopentadienyl ligand is bonded to the Yb center in η<sup>5</sup>-fashion. The coordination sphere of the metal center is saturated by the two chlorine atoms and three THF molecules.<sup>749–751</sup> Treatment of LnCl<sub>3</sub> with 2 equiv. of Na[Me<sub>2</sub>Si(C<sub>5</sub>H<sub>4</sub>)(C<sub>2</sub>B<sub>10</sub>H<sub>11</sub>)] or reaction of the dichloro complexes



Scheme 209



Scheme 210



Scheme 211

$[\eta^5\text{-Me}_2\text{Si}(\text{C}_5\text{H}_4)(\text{C}_2\text{B}_{10}\text{H}_{11})]\text{LnCl}_2(\text{THF})_3$  with an equimolar amount of  $\text{Na}[\text{Me}_2\text{Si}(\text{C}_5\text{H}_4)(\text{C}_2\text{B}_{10}\text{H}_{11})]$  in THF results in the isolation of the monochlorides  $[\text{Me}_2\text{Si}(\text{C}_5\text{H}_4)(\text{C}_2\text{B}_{10}\text{H}_{11})]_2\text{LnCl}(\text{THF})_2$  ( $\text{Ln} = \text{Nd}, \text{Sm}, \text{Y}, \text{Gd}, \text{Yb}$ ). The solid-state structure of  $[\eta^5\text{-Me}_2\text{Si}(\text{C}_5\text{H}_4)(\text{C}_2\text{B}_{10}\text{H}_{11})]_2\text{SmCl}(\text{THF})_2$  reveals a distorted trigonal bipyramidal geometry at the metal center with two  $\eta^5$ -bonded cyclopentadienyl rings, one chloride ion, and two THF molecules.<sup>751</sup> Interaction of  $\text{Li}_2[\text{Me}_2\text{SiCp}(\text{C}_2\text{B}_{10}\text{H}_{10})]$  with  $\text{LnCl}_3$  in THF in a molar ratio 1:1 or 2:1 or reaction of  $[\text{Me}_2\text{Si}(\text{C}_5\text{H}_4)(\text{C}_2\text{B}_{10}\text{H}_{11})]_2\text{LnCl}(\text{THF})_2$  with 2 equiv. of MeLi in THF gives the same compounds  $[\text{Li}(\text{THF})_4][\{\eta^5\text{-}\sigma\text{-Me}_2\text{Si}(\text{C}_5\text{H}_4)(\text{C}_2\text{B}_{10}\text{H}_{11})\}_2\text{Ln}]$ .

(C<sub>2</sub>B<sub>10</sub>H<sub>10</sub>)]<sub>2</sub>Ln] (Ln = Nd, Y, Er, Yb). The solid-state structure of [Li(THF)<sub>4</sub>][{ $\eta^5$ : $\sigma$ -Me<sub>2</sub>Si(C<sub>5</sub>H<sub>4</sub>)(C<sub>2</sub>B<sub>10</sub>H<sub>10</sub>))<sub>2</sub>Er] shows well-separated, alternating layers of the discrete tetrahedral cation Li(THF)<sub>4</sub><sup>+</sup> and anion [{ $\eta^5$ : $\sigma$ -Me<sub>2</sub>Si(C<sub>5</sub>H<sub>4</sub>)(C<sub>2</sub>B<sub>10</sub>H<sub>10</sub>))<sub>2</sub>Er]<sup>−</sup>. In the anion, the Er center is  $\eta^5$ -bonded to each of the two cyclopentadienyl rings and  $\sigma$ -bonded to each of the two carbon atoms from two carborane cages in a distorted tetrahedral arrangement.<sup>749–751</sup>

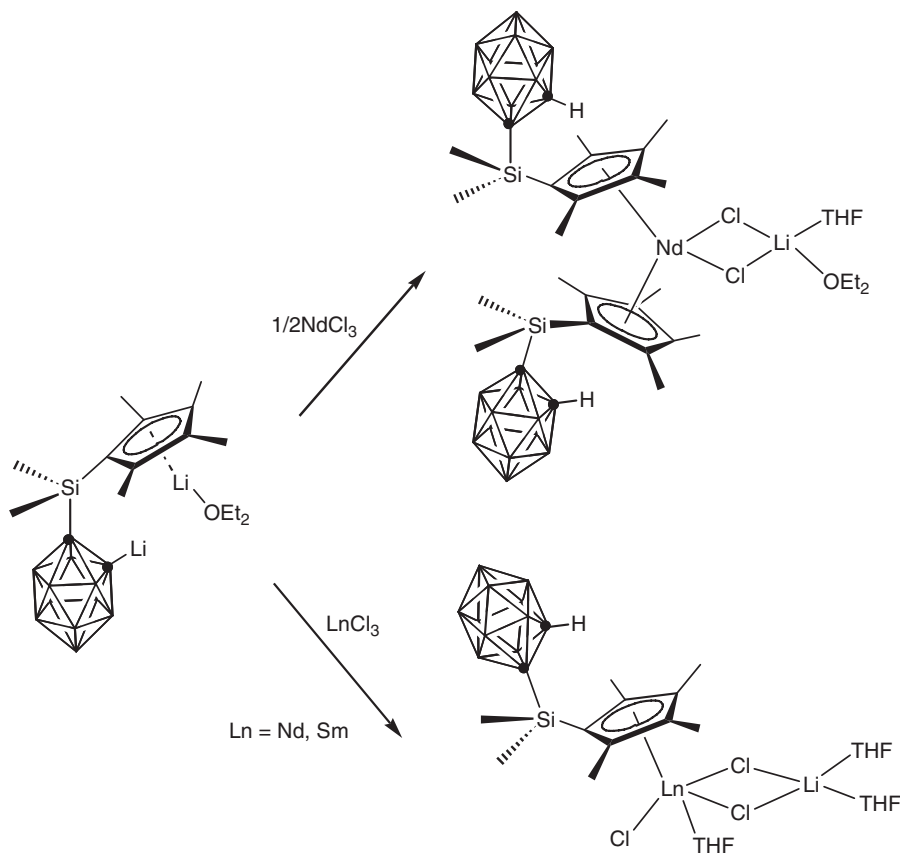
Treatment of NdCl<sub>3</sub> with an equimolar amount of K<sub>3</sub>[Me<sub>2</sub>Si(C<sub>5</sub>H<sub>4</sub>)(C<sub>2</sub>B<sub>10</sub>H<sub>11</sub>)] in THF produces [ $\eta^5$ : $\eta^6$ -Me<sub>2</sub>Si(C<sub>5</sub>H<sub>4</sub>)(C<sub>2</sub>B<sub>10</sub>H<sub>11</sub>)]Nd(THF)<sub>2</sub>. The samarium analogous [ $\eta^5$ : $\eta^6$ -Me<sub>2</sub>Si(C<sub>5</sub>H<sub>4</sub>)(C<sub>2</sub>B<sub>10</sub>H<sub>11</sub>)]Sm(THF)<sub>2</sub> was prepared from an unprecedented redox reaction of SmI<sub>2</sub> with 2 equiv. of Na[Me<sub>2</sub>Si(C<sub>5</sub>H<sub>4</sub>)(C<sub>2</sub>B<sub>10</sub>H<sub>11</sub>)] in THF. The reaction of LnCl<sub>3</sub> (Sm, Yb) with K<sub>3</sub>[Me<sub>2</sub>Si(C<sub>5</sub>H<sub>4</sub>)(C<sub>2</sub>B<sub>10</sub>H<sub>11</sub>)] in THF afforded the organolanthanide(II) compounds [{ $\eta^5$ : $\eta^6$ -Me<sub>2</sub>Si(C<sub>5</sub>H<sub>4</sub>)(C<sub>2</sub>B<sub>10</sub>H<sub>11</sub>)]Ln(II)(THF)<sub>2</sub>][K(THF)<sub>2</sub>]. The solid-state structure of [ $\eta^5$ : $\eta^6$ -Me<sub>2</sub>Si(C<sub>5</sub>H<sub>4</sub>)(C<sub>2</sub>B<sub>10</sub>H<sub>11</sub>)]Sm(THF)<sub>2</sub> revealed every Sm atom  $\eta^5$ -bonded to the cyclopentadienyl ring and  $\eta^6$ -bonded to the hexagonal C<sub>2</sub>B<sub>4</sub> face of the C<sub>2</sub>B<sub>10</sub>H<sub>11</sub> cage and two THF molecules in a distorted tetrahedral geometry.<sup>749–751</sup> In a comparative study, closely related chemistry has been investigated using the tetramethylcyclopentadienyl-substituted carborane ligand Me<sub>2</sub>Si(C<sub>5</sub>Me<sub>4</sub>H)(C<sub>2</sub>B<sub>10</sub>H<sub>11</sub>). Reaction of (C<sub>5</sub>Me<sub>4</sub>H)Cl with 1 equiv. of Li<sub>2</sub>C<sub>2</sub>B<sub>10</sub>H<sub>11</sub> gave a monoanionic salt, which could be converted into the dianionic salt by treatment with Bu<sup>n</sup>Li. Both lithium salts have been employed in the preparation of organolanthanide complexes containing these ligands (Scheme 212).<sup>752</sup>

A new versatile ligand for organolanthanide chemistry, Me<sub>2</sub>C(C<sub>9</sub>H<sub>7</sub>)(C<sub>2</sub>B<sub>10</sub>H<sub>11</sub>), has been prepared by treatment of Li<sub>2</sub>C<sub>2</sub>B<sub>10</sub>H<sub>10</sub> with 1 equiv. of 6,6-dimethylbenzofulvene followed by hydrolysis with saturated NH<sub>4</sub>Cl aqueous solution (Scheme 213).<sup>753</sup>

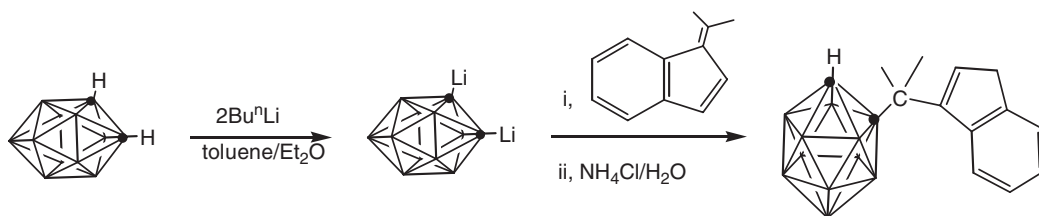
This ligand can conveniently be converted into the monoanion Li[Me<sub>2</sub>C(C<sub>9</sub>H<sub>6</sub>)(C<sub>2</sub>B<sub>10</sub>H<sub>11</sub>)] and the dianion Li<sub>2</sub>[Me<sub>2</sub>C(C<sub>9</sub>H<sub>7</sub>)(C<sub>2</sub>B<sub>10</sub>H<sub>10</sub>)] by treatment with 1 or 2 equiv. of Bu<sup>n</sup>Li, respectively (Scheme 214).<sup>753</sup>

The dianion reacted with 1 equiv. of SmI<sub>2</sub>, followed by reaction (without isolation) with 1 equiv. of the monoanion, to the redox product *rac*-[Li(DME)<sub>2</sub>][{ $\eta^5$ : $\sigma$ -Me<sub>2</sub>C(C<sub>9</sub>H<sub>6</sub>)(C<sub>2</sub>B<sub>10</sub>H<sub>10</sub>))<sub>2</sub>Sm] (Scheme 215).<sup>753</sup>

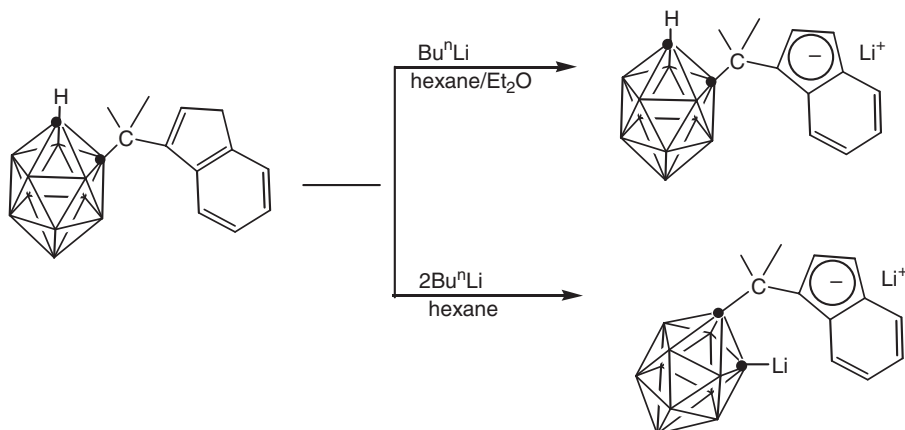
Unlike the SmI<sub>2</sub> case, an equimolar reaction between the dianion and YbI<sub>2</sub> afforded the Yb(II) compound [ $\eta^5$ : $\sigma$ -Me<sub>2</sub>C(C<sub>9</sub>H<sub>6</sub>)(C<sub>2</sub>B<sub>10</sub>H<sub>10</sub>))<sub>2</sub>Yb(DME)<sub>2</sub>. Reaction of LnCl<sub>3</sub> with 1 or 2 equiv. of the dianion yielded organolanthanide



Scheme 212



Scheme 213

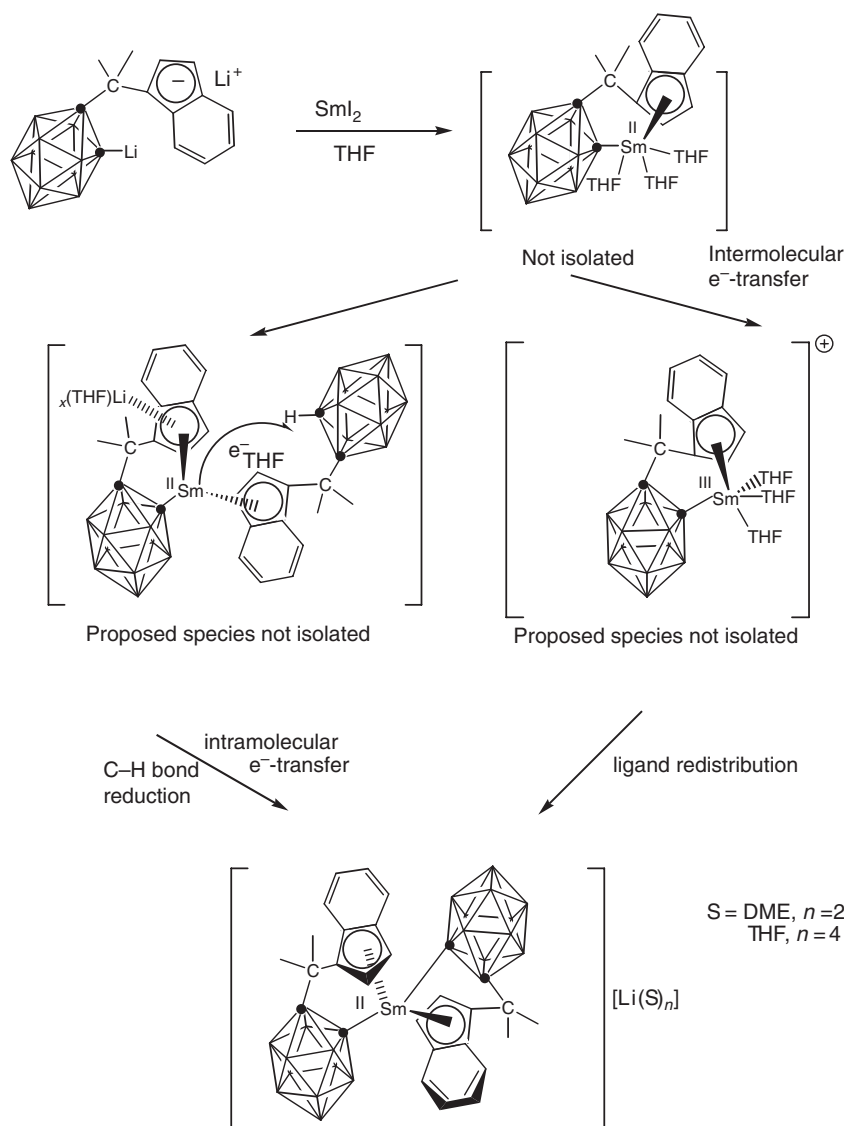


Scheme 214

dichloride and monochloride compounds, respectively,  $[\eta^5\text{-Me}_2\text{C}(\text{C}_9\text{H}_6)(\text{C}_2\text{B}_{10}\text{H}_{11})]\text{GdCl}_2(\text{THF})_2$  and  $[\eta^5\text{-Me}_2\text{C}(\text{C}_9\text{H}_6)(\text{C}_2\text{B}_{10}\text{H}_{11})]_2\text{LnCl}(\text{THF})(\text{OEt}_2)$  ( $\text{Ln} = \text{Y}, \text{Yb}$ ). Reaction of  $\text{LnCl}_3$  with 2 equiv. of the dianion afforded ionic compounds  $\text{rac-}[\text{Li}(\text{DME})_2][\{\eta^5\text{-}\sigma\text{-Me}_2\text{C}(\text{C}_9\text{H}_6)(\text{C}_2\text{B}_{10}\text{H}_{10})\}_2\text{Ln}]$  ( $\text{Ln} = \text{Yb}, \text{Nd}, \text{Er}$ ).<sup>753</sup>

The new versatile ligand  $\text{Me}_2\text{Si}(\text{C}_9\text{H}_6)(\text{C}_2\text{B}_{10}\text{H}_{11})$  can conveniently be converted into the monoanion  $[\text{Me}_2\text{Si}(\text{C}_9\text{H}_6)(\text{C}_2\text{B}_{10}\text{H}_{11})]^-$  and the dianion  $[\text{Me}_2\text{Si}(\text{C}_9\text{H}_6)(\text{C}_2\text{B}_{10}\text{H}_{11})]^{2-}$  with 1 equiv. or excess amounts of  $\text{NaH}$ , respectively. Treatment of  $\text{SmI}_2$  with  $\text{Na}[\text{Me}_2\text{Si}(\text{C}_9\text{H}_6)(\text{C}_2\text{B}_{10}\text{H}_{11})]$  in THF gave the redox product  $[\eta^5\text{-}\eta^6\text{-Me}_2\text{Si}(\text{C}_9\text{H}_6)(\text{C}_2\text{B}_{10}\text{H}_{11})]\text{Sm}(\text{THF})_2$ . The Sm atom is  $\eta^5$ -bonded to the indenyl and  $\eta^6$ -bonded to the hexagonal  $\text{C}_2\text{B}_4$  face of the  $\text{C}_2\text{B}_{10}\text{H}_{11}$  cage and two THF molecules in a distorted tetrahedral geometry. Reaction of  $\text{SmI}_2$  with 1 equiv. of the sodium salt of the dianion  $[\text{Me}_2\text{Si}(\text{C}_9\text{H}_6)(\text{C}_2\text{B}_{10}\text{H}_{11})]^{2-}$  afforded the C–H bond reduction product  $[\{\eta^5\text{-}\sigma\text{-Me}_2\text{Si}(\text{C}_5\text{H}_4)(\text{C}_2\text{B}_{10}\text{H}_{10})\}_2\text{Sm}][\text{Na}(\text{THF})_6](\text{THF})_2$ . Its solid-state structure consists of alternating layers of discrete tetrahedral anions and  $[\text{Na}(\text{THF})_6]^+$  cations. In the anion the Sm atom sits on a  $C_2$ -axis and is  $\eta^5$ -bonded to each of the two indenyl rings and  $\sigma$ -bonded to the two carbon atoms from two carborane cages in a distorted tetrahedral geometry.<sup>754</sup> In contrast, reaction of  $\text{YbI}_2$  with 1 or 2 equiv.  $\text{Na}[\text{Me}_2\text{Si}(\text{C}_9\text{H}_6)(\text{C}_2\text{B}_{10}\text{H}_{11})]$  afforded  $[\{\eta^5\text{-Me}_2\text{Si}(\text{C}_9\text{H}_6)(\text{C}_2\text{B}_{10}\text{H}_{11})\}]\text{Yb}(\mu\text{-I})(\text{THF})_2]_2$  or  $[\eta^5\text{-Me}_2\text{Si}(\text{C}_9\text{H}_6)(\text{C}_2\text{B}_{10}\text{H}_{11})]_2\text{Yb}(\text{THF})_2$ , respectively, which demonstrates the differences of Yb and Sm chemistry. More studies on  $\text{Me}_2\text{Si}(\text{C}_9\text{H}_7)(\text{C}_2\text{B}_{10}\text{H}_{11})$  led to the indication that in this type of bridging ligand the carboranyl and cyclic organic groups communicate with each other. The authors discussed that the acidity of the CH group of the carborane is dependent upon the substituents on the cyclopentadienyl ring, which in turn affects the properties of the resulting complex. Besides the known monoanion and dianion, they described the synthesis of the trianion  $\text{K}_3[\text{Me}_2\text{Si}(\text{C}_9\text{H}_6)(\text{C}_2\text{B}_{10}\text{H}_{11})]$  from  $\text{Me}_2\text{Si}(\text{C}_9\text{H}_6)(\text{C}_2\text{B}_{10}\text{H}_{11})$  and K metal in THF.<sup>754</sup>

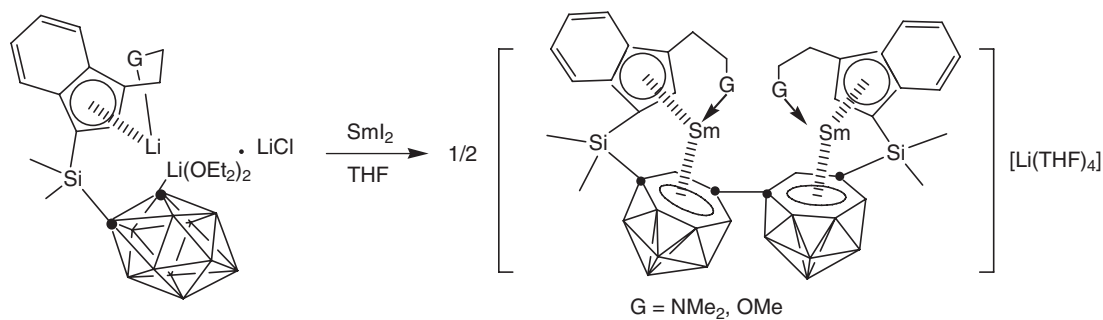
The reaction of  $\text{LnCl}_3$  with 1 equiv. of  $\text{Na}[\text{Me}_2\text{Si}(\text{C}_9\text{H}_6)(\text{C}_2\text{B}_{10}\text{H}_{11})]$  gave the dichloride complexes  $[\eta^5\text{-Me}_2\text{Si}(\text{C}_9\text{H}_6)(\text{C}_2\text{B}_{10}\text{H}_{11})]\text{LnCl}_2(\text{THF})_3$  ( $\text{Ln} = \text{Nd}, \text{Er}$ ). They can further react with another equivalent of  $\text{Na}[\text{Me}_2\text{Si}(\text{C}_9\text{H}_6)(\text{C}_2\text{B}_{10}\text{H}_{11})]$  to afford the monochloride complexes  $[\eta^5\text{-Me}_2\text{Si}(\text{C}_9\text{H}_6)(\text{C}_2\text{B}_{10}\text{H}_{11})]_2\text{LnCl}(\text{THF})_3$  ( $\text{Ln} = \text{Ce}, \text{Nd}, \text{Sm}, \text{Er}$ ), which can also be prepared by treatment of  $\text{LnCl}_3$  with 2 equiv. of  $\text{Na}[\text{Me}_2\text{Si}(\text{C}_9\text{H}_6)(\text{C}_2\text{B}_{10}\text{H}_{11})]$  in one step. Furthermore, the authors described detailed reactivity studies of the monochloride and dichloride lanthanide complexes with  $\text{NaH}$  and K metal. For example, treatment of  $[\eta^5\text{-Me}_2\text{Si}(\text{C}_9\text{H}_6)(\text{C}_2\text{B}_{10}\text{H}_{11})]\text{ErCl}_2(\text{THF})_3$  with 2 equiv. of K metal at room temperature yielded  $[\eta^5\text{-}\eta^6\text{-Me}_2\text{Si}(\text{C}_9\text{H}_6)(\text{C}_2\text{B}_{10}\text{H}_{11})]\text{Er}(\text{THF})_2$ . The new bis(carborane) compound  $[\text{LnCl}_2(\text{THF})_5][\mu\text{-CH-}(\text{closo-C}_2\text{B}_{10}\text{H}_{11})\text{-nido-CB}_{10}\text{H}_{11}]$



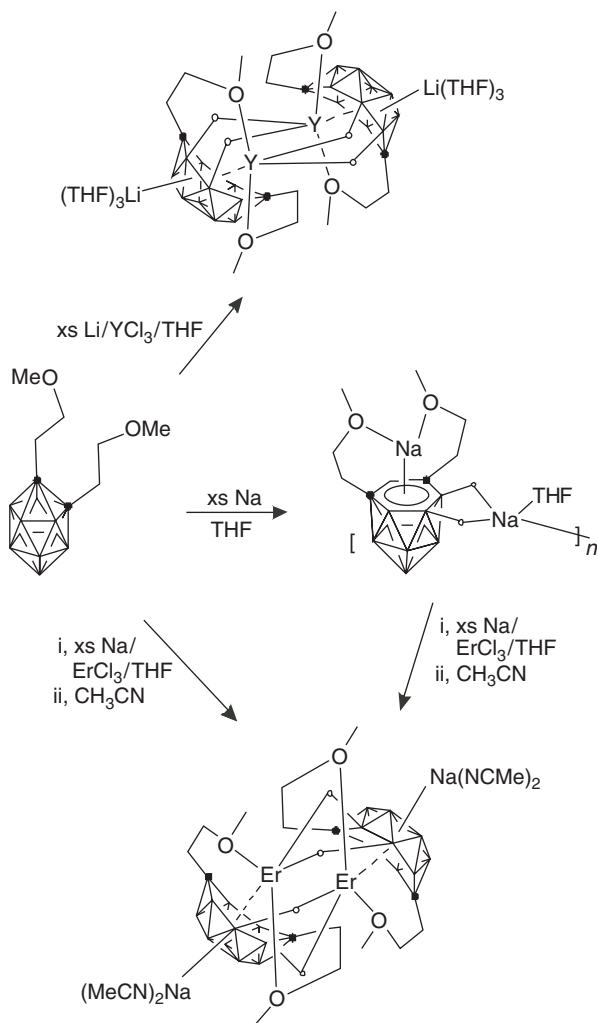
Scheme 215

(Ln = Er, Y) was isolated. The solid-state structure of  $[\text{ErCl}_2(\text{THF})_5][\mu\text{-CH-(}closo\text{-C}_2\text{B}_{10}\text{H}_{11}\text{)-}nido\text{-CB}_{10}\text{H}_{11}]$  consists of well-separated, alternating layers of discrete cations  $[\text{ErCl}_2(\text{THF})_5]^+$  and bis(carborane) monoanions  $[\mu\text{-CH-(}closo\text{-C}_2\text{B}_{10}\text{H}_{11}\text{)-}nido\text{-CB}_{10}\text{H}_{11}]^-$ . The cation adopts a pentagonal bipyramidal geometry with two chloro ligands in the axial positions and the five THF molecules in the equatorial positions. The anion consists of two carborane cages that are connected through a C–C single bond.<sup>755</sup> Various lanthanacarboranes incorporating the so-called “carbons-adjacent” *nido*- and *arachno*-carborane anions of the  $\text{C}_2\text{B}_{10}$  system have also been synthesized and structurally characterized.<sup>756</sup> Among the new classes of lanthanide metallacarboranes are also several examples containing  $\eta^7$ -carboranyl ligands.<sup>757</sup> An interesting variation of the indenyl/carborane ligand system is the introduction of additional donor-functionalized side chains. New metallacarboranes bearing a  $(nido\text{-RC}_2\text{B}_{10}\text{H}_{10})_2^{4-}$  ligand,  $[\{\eta^5:\eta^1:\eta^6\text{-Me}_2\text{Si}(\text{C}_9\text{H}_5\text{CH}_2\text{CH}_2\text{G})(\text{C}_2\text{B}_{10}\text{H}_{10})\text{Sm}\}_2(\mu\text{-Cl})][\text{Li}(\text{THF})_4]$  (G = NMe<sub>2</sub>, OMe), have been prepared and structurally characterized by treatment of  $\text{SmI}_2(\text{THF})_x$  with an unexpected samarium-mediated ligand coupling reaction (Scheme 216).<sup>758–760</sup>

A recent addition to organolanthanide carborane chemistry is the use of hydroxyethyl- and alkoxyethyl-*o*-carborane ligands. Scheme 217 illustrates typical synthetic routes leading to lanthanide derivatives of such ligands.<sup>761</sup>



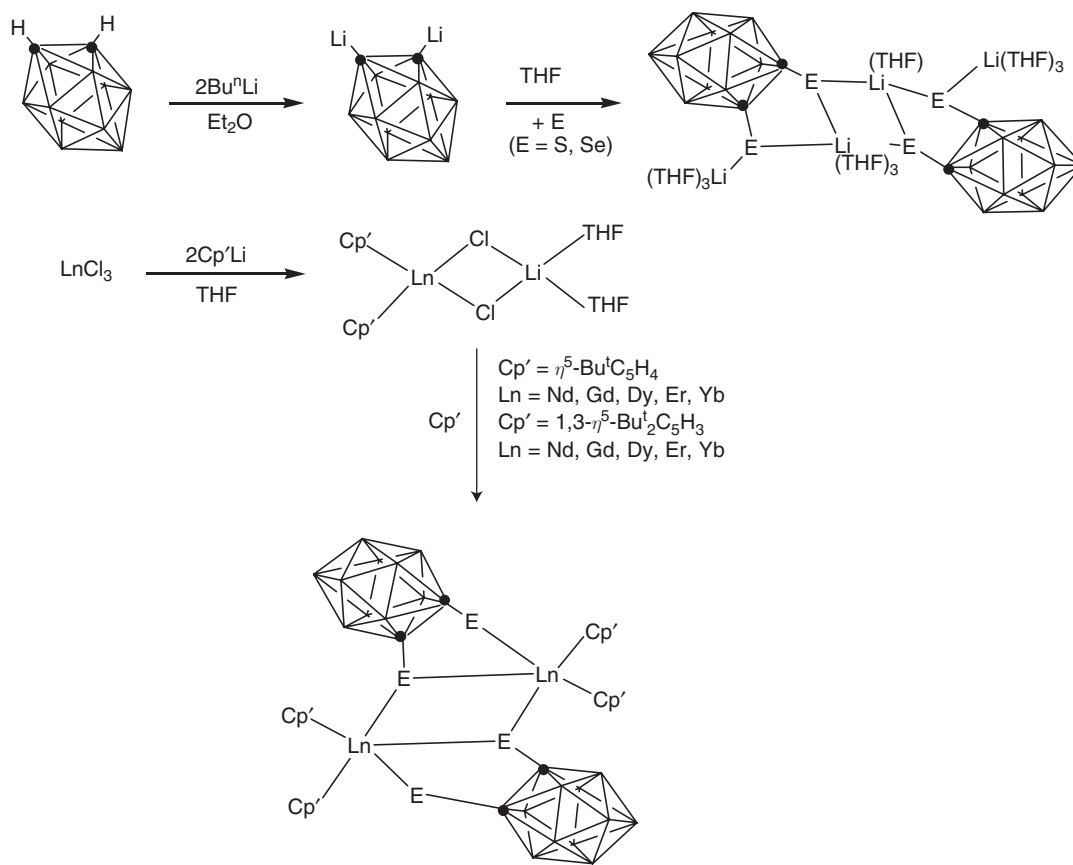
Scheme 216



Scheme 217

Numerous organolanthanide complexes are derived from the new versatile boron-bridged ligand  $\text{Pr}_2^i\text{NB}(\text{C}_9\text{H}_7)(\text{C}_2\text{B}_{10}\text{H}_{11})$ .<sup>762,763</sup> A series of bis(cyclopentadienyl)lanthanide complexes containing bridging 1,2-dicarba-*closo*-dodecaborane-1,2-dichalcogenolate ligands has been synthesized and structurally characterized. Scheme 218 illustrates the preparation of the starting materials as well as the products. The dimeric carborane





Scheme 218

precursors are accessible via insertion of elemental chalcogen  $\text{E}$  ( $\text{E} = \text{S}, \text{Se}$ ) into the  $\text{Li}-\text{C}$  bonds of dilithium *o*-carborane in  $\text{THF}$  solution. The central  $\text{Ln}_2\text{E}_2$  four-membered ring in the products is not planar.<sup>764,765</sup>

#### 4.01.8 Arene Complexes

The synthesis, arrangement, and reactivity of arene-lanthanide compounds have recently been comprehensively reviewed by Bochkarev.<sup>22</sup> The nature of the metal–ligand bond in trivalent neodymium complexes with neutral  $\pi$ -donor ligands, including benzene, has been the subject of a theoretical study.<sup>766</sup> Organometallic clusters in the gas phase containing scandium or lanthanide metals and aromatic ligand systems such as benzene,  $\text{C}_{60}$ , or COT have been studied in detail. Novel network structures were found in organometallic clusters between metal atoms produced by laser ablation and organic ligand molecules. The size and structure of the clusters were determined using time-of-flight mass spectrometric techniques. For scandium–benzene clusters,  $\text{Sc}_n(\text{C}_6\text{H}_6)_m$ , a multiple-decker sandwich structure was found ( $n, m$ ) = ( $n, n + 1$ ) in which the metal atoms and benzene are alternatively piled up. A similar multiple-decker sandwich structure was formed between lanthanide metal atoms and the organic ligand COT consisting of positively charged lanthanide ions and negatively charged COT.<sup>767</sup> In related studies the scandium–benzene complexes  $\text{ScC}_6\text{H}_6^-$ ,  $\text{ScC}_6\text{H}_6$ , and  $\text{Sc}_n(\text{C}_6\text{H}_6)_m$  ( $n = 1\text{--}3$ ,  $m = 2\text{--}4$ ) have been successfully synthesized using a laser vaporization method.<sup>768–770</sup> Mono- and bis-adducts of benzene of the type  $\text{Ln}(\text{C}_6\text{H}_6)_{1,2}^+$  ( $\text{Ln} = \text{Sc}, \text{Y}, \text{Ln}$ ) have been generated in the gas phase, and their reactivities toward molecular oxygen have been measured using an inductively coupled plasma/selected-ion flow tube tandem mass spectrometer.<sup>771,771a</sup> Theoretical calculations have been carried out on the binding between  $\text{Sc}^+$  and phenol<sup>772</sup> as well as of  $\text{ScX}_n$  ( $\text{X} = \text{Cl}, \text{Br}$ ;  $x = 1\text{--}3$ ) with benzene.<sup>773</sup>

Co-deposition of a monoatomic lanthanide vapor ( $\text{Sm}, \text{Eu}, \text{Tm}, \text{Yb}$ ) and tri-*i*-butylbenzene,  $1,3,5\text{-Bu}^t_3\text{C}_6\text{H}_3$ , onto a cold (77 K) surface afforded matrices that contained zero-valent bis( $\eta^6$ -arene)lanthanide complexes of the form  $\text{Ln}(\eta^6\text{-C}_6\text{H}_3\text{Bu}^t_3\text{-}1,3,5)_2$  as formed in macroscale co-condensation reactions using metal vapor synthetic (MVS)

techniques.<sup>774</sup> Holmium vapor reacts with 2,4,6-tri-*t*-butylphosphorine to afford the zero-valent heteroarene lanthanide complex  $\text{Ho}(\eta^6\text{-PC}_5\text{H}_2\text{Bu}^t\text{-2,4,6})_2$ , the first structurally characterized complex of this class. Gram quantities of the compound are formed in 45% yield as extremely air- and moisture-sensitive, purple iridescent crystals, which can be recrystallized from pentane. The novel sandwich complex sublimates at 160 °C ( $10^{-5}$  mbar) with 90% recovery.<sup>774,775</sup>

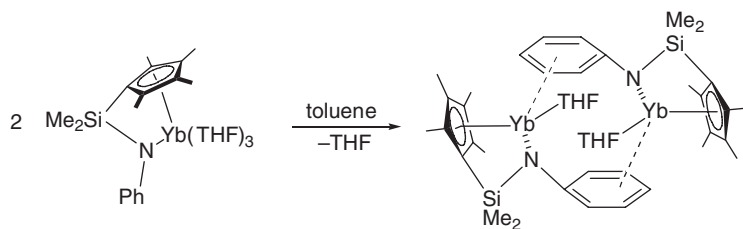
Recrystallization of the linked cyclopentadienyl-anilido ytterbium(II) complex  $[\text{Me}_2\text{Si}(\text{C}_5\text{Me}_4)(\text{NPh})]\text{Yb}(\text{THF})_3$  from toluene/hexane yielded the less solvated complex  $[\{\text{Me}_2\text{Si}(\text{C}_5\text{Me}_4)(\text{NPh})\}\text{Ln}(\text{THF})]_2$  as brown crystals in 91% yield (Scheme 219). The compound forms a dimeric structure through an intermolecular Yb–Ph  $\pi$ -interaction.<sup>194</sup>

The reaction of  $\text{CpLnCl}_2(\text{THF})_3$  (Ln = Y, Gd, Er, Tm, Lu) with sodium naphthalenide in 1,2-DME led to the formation of mononuclear complexes  $\text{CpLnC}_{10}\text{H}_8(\text{DME})$ .<sup>776,777,777a</sup> Binuclear complexes  $(\text{CpLn})_2\text{C}_{10}\text{H}_8(\text{THF})_4$  (Ln = Sm and Yb) containing the Ln atoms in the oxidation state +II were formed in similar reactions of Sm and Yb complexes. The structure of  $\text{CpYC}_{10}\text{H}_8(\text{DME})$  was determined by X-ray diffraction. The coordinated naphthalene ring linked to the Y atom is non-planar and bent by an angle of 26.1° over the  $\text{C}(1)\cdots\text{C}(4)$  line. The existence of two short,  $\text{Y}(1)\cdots\text{C}(1)$  and  $\text{Y}(1)\cdots\text{C}(4)$  [2.438(6) and 2.452(6) Å],  $\text{Y}\cdots\text{C}(\text{C}_{10}\text{H}_8)$  bonds verifies the  $2\eta^1:\eta^2$ -interaction of the Y atom with the naphthalene dianion. The same yttrium complex was formed in a mixture with  $\text{Cp}_3\text{Y}$  in the reaction of  $\text{Cp}_2\text{YCl}$  with sodium naphthalenide.<sup>777,777a</sup> The analogous reaction of  $\text{Cp}^*\text{LuCl}_2$  with sodium naphthalenide in DME solution afforded the mononuclear complex  $\text{Cp}^*\text{LuC}_{10}\text{H}_8(\text{DME})$  in 48% besides naphthalene and NaCl. The same reaction in THF solution produced a series of products:  $\text{Cp}^*\text{Li}(\text{C}_{10}\text{H}_8)_2\text{Na}(\text{THF})_3$ ,  $\{[\text{Cp}^*\text{Lu}]_3(\text{C}_{10}\text{H}_8)(\text{C}_{10}\text{H}_7)(\text{H})\}[\text{Na}(\text{THF})_3]_2(\text{C}_{10}\text{H}_8)$ , and  $[\text{Cp}^*\text{LuH}(\text{THF})]_3(\text{C}_{10}\text{H}_7)$ .<sup>777,777a</sup> The reaction of thulium(II) iodide with 2 equiv. of lithium naphthalenide in DME yields a binuclear thulium(III) complex with one bridging and two terminal dianions of naphthalene,  $(\mu^2\text{-}\eta^4:\eta^4\text{-C}_{10}\text{H}_8)[\text{Tm}(\eta^2\text{-C}_{10}\text{H}_8)(\text{DME})]_2$ , in the form of black crystals.<sup>778</sup>

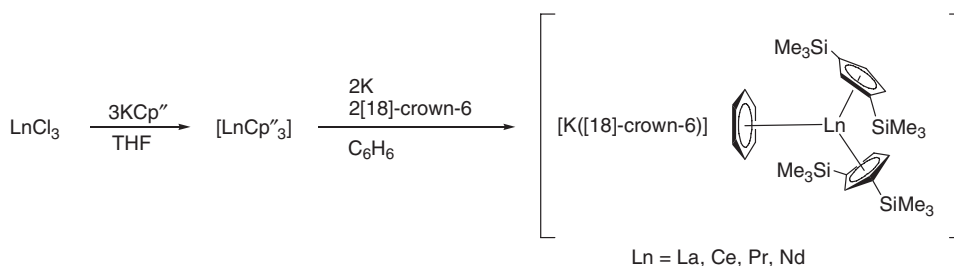
Treatment of  $[\text{Ln}\{\eta^5\text{-C}_5\text{H}_3(\text{SiMe}_3)_2\text{-1,3}\}_3]$  or  $[\text{Ln}\{\eta^5\text{-C}_5\text{H}_3(\text{SiMe}_3)_2\text{-1,3}\}_2(\mu\text{-Cl})_2]$  with a potassium mirror or  $\text{C}_8\text{K}$  and 18-crown-6 in benzene under similarly mild conditions afforded the tight ion pairs  $[\text{K}(18\text{-crown-6})][\text{Ln}\{\eta^5\text{-C}_5\text{H}_3(\text{SiMe}_3)_2\text{-1,3}\}_2(\text{C}_6\text{H}_6)]$  (Ln = La, Ce) containing the remarkable anions  $[\text{Ln}\{\eta^5\text{-C}_5\text{H}_3(\text{SiMe}_3)_2\text{-1,3}\}_2(\text{C}_6\text{H}_6)]^-$ , which in principle can be regarded as either (benzene)lanthanocene(II) or (1,4-cyclohexa-2,5-dienyl)lanthanocene(III) anion. The latter representation is the more appropriate and supported by X-ray crystallographic, UV–VIS, and NMR spectroscopic data, as well as by their hydrolysis products which included cyclohexa-1,4-diene and a smaller proportion of benzene. The lanthanum and the cerium complexes are isomorphous.<sup>779</sup>

The first synthesis of a subvalent organolanthanum complex  $[\text{K}([18\text{-crown-6})(\eta^2\text{-C}_6\text{H}_6)_2][(\text{LaCp}^{\text{tr}})_2(\mu\text{-}\eta^6\text{-}\eta^6\text{-C}_6\text{H}_6)]\cdot\text{C}_6\text{H}_6$  ( $\text{Cp}^{\text{tr}} = \eta^5\text{-C}_5\text{H}_3\text{Bu}^t\text{-2,1,3}$ ) was reported in 1998. The complex can be formulated as a salt containing as anion two  $\text{Cp}^{\text{tr}}_2\text{La}(\text{II})$  moieties bridged by an  $\eta^6$ -benzenide monoanionic ligand. The compound was formed by the reaction between an excess of K in  $\text{C}_6\text{H}_6$  and [18]-crown-6 at 20 °C.<sup>780</sup> Later it was reported that treatment of the appropriate compounds  $\text{LaCp}^{\text{tr}}_3$ ,  $\text{CeCp}^{\text{tr}}_3$ ,  $\text{PrCp}^{\text{tr}}_3$ , or  $\text{NdCp}^{\text{tr}}_3$  with 2 equiv. each of [18]-crown-6 and potassium in benzene at ambient temperature affords the red or red-brown crystalline salts  $[\text{K}([18\text{-crown-6})][\text{LnCp}^{\text{tr}}_2(\mu\text{-C}_6\text{H}_6)]]$  (Ln = La, Ce, Pr, Nd;  $\text{Cp}^{\text{tr}} = \eta^5\text{-C}_5\text{H}_3(\text{SiMe}_3)_2\text{-1,3}$ ) with  $[\text{K}([18\text{-crown-6})][\text{Cp}^{\text{tr}})]$  as a byproduct (Scheme 220).<sup>465</sup>

Proton NMR spectra in benzene- $d_6$  show the lanthanum species to be diamagnetic, consistent with the presence of a lanthanate(III) anion. The signals of the [18]-crown-6 moiety in the spectra of the Ce, Pr, and Nd complexes are only slightly paramagnetically shifted. Hydrolysis of these lanthanide complexes yields cyclohexa-1,4-diene. The molecular structures of the isomorphous salts  $[\text{K}([18\text{-crown-6})][\text{LnCp}^{\text{tr}}_2(\mu\text{-C}_6\text{H}_6)]]$  (Ln = La, Ce, Nd) reveal that each comprises a tight ion pair with a  $\text{C}_6\text{H}_6$  ligand bridging the K and Ln atoms. The potassium has close contacts to the six crown ether oxygen atoms and the centroids of the 2,3- and 5,6-carbon atoms of the  $\text{C}_6\text{H}_6$  ligand. The latter is boat-shaped with the shortest C–Ln distances being those to the 1- and 4-carbon atoms (2.62 Å/2.65 Å for La, 2.59 Å/2.61 Å, for Ce, and 2.56 Å/2.57 Å for Nd). The endocyclic bond angles at the 1- and 4-carbon atoms are narrower ( $110.65 \pm 1.15^\circ$ ) than those at the other four ( $122.4 \pm 1.2^\circ$ ), while the four C–C bonds to the 1- and 4-carbon atoms



Scheme 219

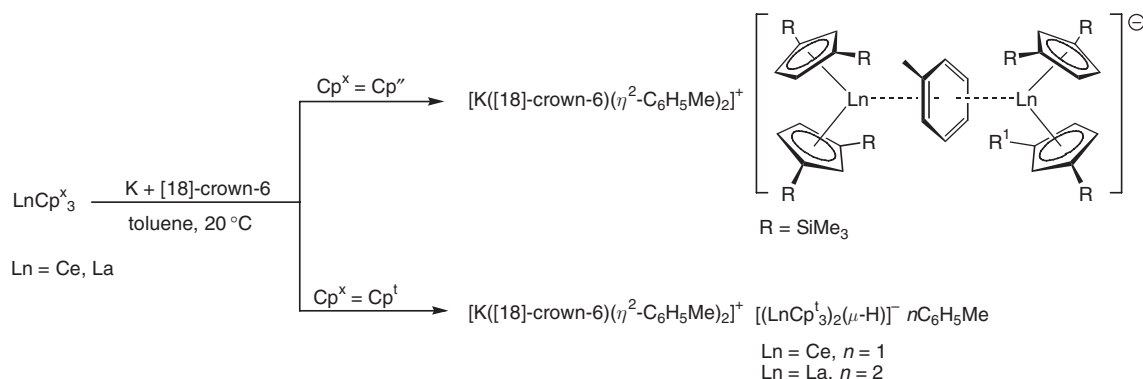


Scheme 220

are longer ( $1.46 \pm 0.02 \text{ \AA}$ ) than the remaining two ( $1.35 \pm 0.013 \text{ \AA}$ ). EPR studies of the reaction of  $\text{LaCp}''_3$  with K and [18]-crown-6 in benzene show the presence of at least four La(II) paramagnetic intermediate species prior to the formation of  $[\text{K}([18]\text{-crown-6})][\text{LaCp}''_2(\mu\text{-C}_6\text{H}_6)]$ .<sup>465</sup> Upon treatment of  $\text{LnCp}^t_3$  or  $\text{LnCp}''_3$  ( $\text{Cp}^t = \eta^5\text{-C}_5\text{H}_4\text{SiMe}_2\text{Bu}^t$ , Ln = La, Ce) with potassium and [18]-crown-6 in toluene the potassium salts  $[\text{K}([18]\text{-crown-6})(\eta^2\text{-PhMe})_2][(\text{LnCp}^t_3)_2(\mu\text{-H})]$  and  $[\text{K}([18]\text{-crown-6})(\eta^2\text{-PhMe})_2][(\text{LnCp}''_2)_2(\mu\text{-}\eta^6\text{-}\eta^6\text{-PhMe})]$  were obtained (Scheme 221).<sup>781</sup>

Treatment of  $\text{Cp}^*\text{LaCl}(\mu\text{-Cl})_2\text{Li}(\text{THF})_2$  with pyrene and potassium in toluene formed red-violet crystals of  $(\text{Cp}^*\text{LaCl})_3(\text{C}_{16}\text{H}_{10})$  as the first organolanthanide complex with a pyrene ligand. In the complex, there is an unusual coordination between La atoms and the pyrene ligand.<sup>782,782a</sup> The organolutetium anthracene derivatives  $\text{CpLu}(\text{C}_{14}\text{H}_{10})(\text{THF})$  and  $[\text{Na}(\text{diglyme})][\text{Cp}_2\text{Lu}(\text{C}_{14}\text{H}_{10})]$  were formed in the reaction of  $\text{CpLuCl}_2(\text{THF})_3$  or  $\text{Cp}_2\text{LuCl}$  with dianionic  $\text{Na}_2(\text{C}_{14}\text{H}_{10})$  or radical anionic  $\text{Na}(\text{C}_{14}\text{H}_{10})$  sodium anthracenide, respectively. An interesting structural feature of  $[\text{Na}(\text{diglyme})][\text{Cp}_2\text{Lu}(\text{C}_{14}\text{H}_{10})]$  is the conformation of the coordinated anthracenide dianion. The central six-membered ring of the ligand has lost its aromatic character and acquires a boat conformation.<sup>783</sup> Bridging acenaphthylene was found in the binuclear lanthanum complex  $[\text{LaI}_2(\text{THF})_3]_2(\mu\text{-C}_{12}\text{H}_8)$ .<sup>784</sup> Bis(decamethylanthanocene)–anthracene,  $[\text{Cp}^*_2\text{La}]_2(\mu\text{-}\eta^3\text{-}\eta^3\text{-C}_{14}\text{H}_{10})\cdot 2\text{C}_6\text{H}_5\text{CH}_3$ , was obtained as black-green crystals via the reaction of  $\text{Cp}^*_2\text{La}(\mu\text{-Cl})_2\text{K}(\text{DME})_2$  with disodium anthracenide in toluene in the molar ratio 2:1. The molecule contains two  $\text{Cp}^*_2\text{La}$  moieties which are  $\eta^3$ -coordinated to two of the aromatic rings from opposite sides of the anthracene ligand.<sup>785</sup> The formation of the “ate” complex  $[\text{Li}(\text{THF})_4][\text{Nd}\{\text{Me}_2\text{C}(\text{C}_5\text{H}_4)(\text{C}_{14}\text{H}_{10})\}_2]$  from neodymium trichloride and 2 equiv. of the lithium salt of 9-(cyclopentadienyl-1-methylethyl)-9,10-dihydroanthracene has been reported. The C(10) atoms of the dihydroanthracene moieties are  $\sigma$ -bonded to the central neodymium atom.<sup>786</sup> Reaction of a freshly prepared solution of lithium anthracenide,  $\text{Li}(\text{C}_{14}\text{H}_{10})$ , in DME to a suspension of  $\text{TmI}_2$  (1:1 molar ratio) produced a dark red-brown solution from which red crystals of  $(\eta^2\text{-C}_{14}\text{H}_{10})\text{TmI}(\text{DME})_2$  could be isolated in about 80% yield.<sup>628</sup>

Arene complexes of the type  $(\eta^6\text{-C}_6\text{Me}_6)\text{Ln}(\text{AlCl}_4)_3\cdot\text{toluene}$  have been reported for Ln = Nd, Sm, Gd, Yb.<sup>787</sup> The complexes  $(\eta^6\text{-C}_6\text{H}_5\text{Me})\text{Ln}(\text{AlCl}_3\text{Me})_3$  (Ln = Nd, Sm, or Y),  $(\eta^6\text{-C}_6\text{H}_5\text{Me})\text{Ln}(\text{AlCl}_3\text{Et})_3$  (Ln = Pr or Nd),  $(\eta^6\text{-C}_6\text{H}_5\text{Me})\text{Gd}(\text{AlBr}_3\text{Me})_3$ ,  $(\eta^6\text{-C}_6\text{H}_5\text{Me})\text{Nd}(\text{AlX}_3\text{Me})_3$  (X = Br or I), and  $(\eta^6\text{-C}_6\text{H}_2\text{Me}_4)\text{Nd}(\text{AlCl}_3\text{R})_3$  (R = Me or Et) were synthesized by the reaction of appropriate  $(\eta^6\text{-arene})\text{Ln}(\text{AlX}_4)_3$  precursors with the corresponding  $\text{AlR}_3$  in



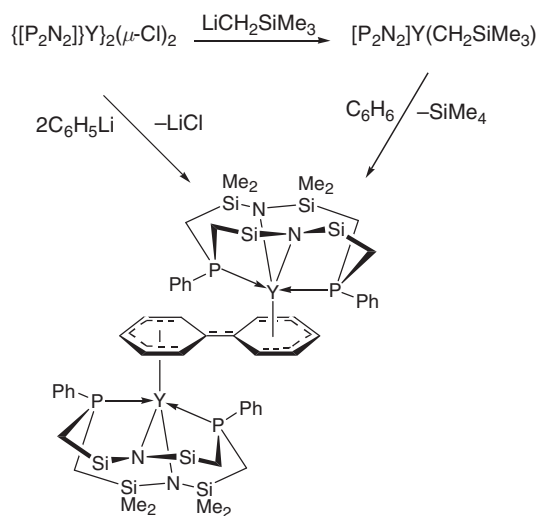
Scheme 221

toluene.<sup>788</sup> The molecular structure of  $(\eta^6\text{-C}_6\text{H}_5\text{Me})\text{Nd}(\text{AlCl}_3\text{Me})_3$  was studied by X-ray diffraction. The Nd atom is located on the center of the basal plane formed by the five Cl atoms and has distorted pentagonal bipyramidal arrangement. The Nd–C bond distances are in the range from 2.91(1) to 3.03(1) Å. Catalytic activity of the  $(\eta^6\text{-arene})\text{Ln}(\text{AlX}_3\text{R})_3$  derivatives in the polymerization of butadiene and ethylene has been also studied.<sup>788</sup> Metal- $\pi$ -arene interactions were reported for the solid-state structures of two Lewis-donor-free aryl bis(cyclopentadienyl)-lanthanides.  $\text{Ar}'\text{Yb}(\text{C}_5\text{H}_4\text{Me})_2$  and  $\text{Ar}'\text{SmCp}_2$  ( $\text{Ar}' = 2,6\text{-Me}_2\text{C}_6\text{H}_3$ ) have been obtained by the reaction of  $\text{LiAr}'$  with  $\text{Yb}(\text{C}_5\text{H}_4\text{Me})_3$  or  $\text{SmCp}_3$  in toluene. Single crystal X-ray determinations reveal  $\eta^5$ -coordination of the cyclopentadienyl ligands to the metal centers in both cases and  $\eta^1$ -coordination to the *ipso*-carbon atom of the aryl groups. Additional  $\pi$ -arene contacts to one mesityl group give rise to a different pyramidalization of the metal centers, which depends on the size of the central lanthanide ion.<sup>789</sup>  $\eta^6$ -Arene coordination has recently been reported for a series of cationic scandium complexes containing  $\beta$ -diketiminato ligands.<sup>790</sup>

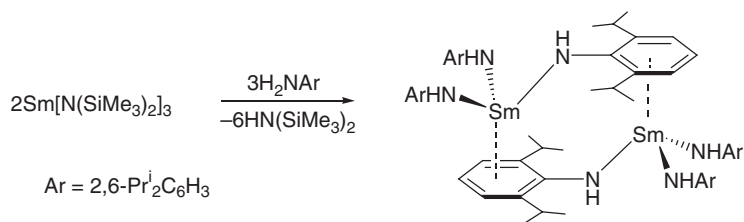
The formation of highly colored yttrium arene complexes with macrocyclic ancillary ligands has been reported.<sup>791,792</sup> The compound  $[\{\text{P}_2\text{N}_2\}\text{Y}(\mu\text{-Cl})_2]$  ( $\{\text{P}_2\text{N}_2\} = [\text{PhP}(\text{CH}_2\text{SiMe}_2\text{NSiMe}_2\text{CH}_2)_2\text{PPh}]^{2-}$ ) reacts with phenyllithium to give a dark blue product with the empirical formula  $\{\text{P}_2\text{N}_2\}\text{Y}(\text{C}_6\text{H}_5)$ . The same product was obtained in a C–H activation reaction between  $\{\text{P}_2\text{N}_2\}\text{YCH}(\text{SiMe}_3)_2$  and benzene. An X-ray structure determination revealed the presence of unusual dimeric complexes of the composition  $[\{\text{P}_2\text{N}_2\}\text{Y}]_2(\mu\text{-}\eta^6\text{:}\eta^6\text{-C}_6\text{H}_5\text{C}_6\text{H}_5)$  as depicted in Scheme 222.

While the same type of dark blue compound could be generated using *m*-tolyllithium, the reaction of  $[\{\text{P}_2\text{N}_2\}\text{Y}(\mu\text{-Cl})_2]$  with *p*-tolyllithium had a different outcome, affording a dark brown crystalline product. In this case an X-ray diffraction study showed again the presence of a dinuclear complex containing a bridging bi-*p*-tolyl ligand, although here the two  $\{\text{P}_2\text{N}_2\}\text{Y}$  fragments are sandwiching one tolyl group, leaving the second uncoordinated.<sup>791,792</sup> Closely related dinuclear  $\pi$ -complexes of yttrium and lutetium with sandwiched naphthalene and anthracene ligands have been reported more recently. The synthetic route involved treatment of the chloro precursors  $[\{\text{P}_2\text{N}_2\}\text{Ln}(\mu\text{-Cl})_2]$  ( $\text{Ln} = \text{Y}, \text{Lu}$ ) with the respective polyarenes in the presence of potassium graphite ( $\text{C}_8\text{K}$ ) in toluene/diethyl ether.<sup>793,793a</sup>

The influence of intramolecular lanthanide- $\pi$ -arene interactions on the structural architecture of homoleptic aryloxolanthanide complexes was studied by Deacon *et al.* The homoleptic binuclear aryloxolanthanide(II) complexes  $[\text{Eu}_2(\text{Odpp})(\mu\text{-Odpp})_3]$ ,  $[\text{Yb}_2(\text{Odpp})_2(\mu\text{-Odpp})_2]$ , and  $[\text{Yb}_3(\text{Odpp})_7]$  ( $^-\text{Odpp} = 2,6\text{-diphenylphenolate}$ ) have been prepared by direct reactions of ytterbium or europium metal with 2,6-diphenylphenol in the presence of mercury at elevated temperatures in sealed tubes.<sup>793,793a</sup> X-ray diffraction studies of  $[\text{Eu}_2(\text{Odpp})_4]$  and  $[\text{Yb}_2(\text{Odpp})_4]$  revealed different binuclear structures. In the europium complex three aryloxide oxygens bridge two Eu ions, with a terminal Odpp and three  $\eta^1$ - $\pi$ -bonded substituent phenyl groups also being attached to one europium, and three  $\eta^2$ - $\pi$ -bonded phenyl groups to the other. By contrast, both Yb atoms of  $[\text{Yb}_2(\text{Odpp})_4]$  have one terminal and two bridging Odpp ligands in a pyramidal arrangement and the coordination sphere is completed by  $\pi$ -interactions of pendant phenyl



Scheme 222



Scheme 223

groups (one  $\eta^4$  and one  $\eta^3$  to one Yb, and an  $\eta^6$  and an  $\eta^1$ -Ph group to the other). The structure of  $[\text{Yb}_3(\text{Odpp})_7]$  comprises an unprecedented  $[\text{Yb}(\text{II})_2(\text{Odpp})_3]^+$  cation and a  $[\text{Yb}(\text{III})(\text{Odpp})_4]^-$  anion.<sup>794</sup>

Reaction of 3 equiv. of 2,6-diisopropylaniline with  $\text{Sm}[\text{N}(\text{SiMe}_3)_2]_3$  afforded the dimeric species  $[\text{Sm}(\text{NHAr})_3]_2$  (Scheme 223). X-ray crystallography revealed that each metal center engages in an  $\eta^6$ -arene interaction with the aryl ring of an amide ligand attached to an adjacent samarium.<sup>795</sup> Arene coordination has also been observed in the analogous lanthanide tris(aryloxides)  $[\text{Ln}(\text{OAr})_3]_2$  ( $\text{Ln} = \text{Nd}, \text{Sm}, \text{Er}$ ;  $\text{Ar} = 2,6\text{-Pr}_2\text{C}_6\text{H}_3$ ).<sup>796</sup>

The bis(boratabenzene)samarium complexes  $[\text{SmCl}(\text{C}_5\text{H}_5\text{BMe}_2)_2]_2$ ,  $[\text{SmCl}(3,5\text{-Me}_2\text{C}_5\text{H}_3\text{BNMe}_2)_2]_2$ , and  $\text{SmCl}(3,5\text{-Me}_2\text{C}_5\text{H}_3\text{BN}(\text{SiMe}_3)_2)_2$  were synthesized from the solvent-free lithium boratabenzenes and  $\text{SmCl}_3$  in toluene.<sup>797</sup> The complex  $[\text{SmCl}(\text{C}_5\text{H}_5\text{BMe}_2)_2]_2$  possesses a doubly chloro-bridged dinuclear structure with four facially coordinated boratabenzene ligands. The structure of  $[\text{SmCl}(3,5\text{-Me}_2\text{C}_5\text{H}_3\text{BNMe}_2)_2]_2$  differs in that each samarium atom binds to one boratabenzene in an unprecedented N–B–C–two-coordination mode and facially to the second boratabenzene ligand. In solution  $[\text{SmCl}(3,5\text{-Me}_2\text{C}_5\text{H}_3\text{BNMe}_2)_2]_2$  is fluxional, displaying only one type of boratabenzene ligand.  $\text{SmCl}(3,5\text{-Me}_2\text{C}_5\text{H}_3\text{BN}(\text{SiMe}_3)_2)_2$  is mononuclear, because of the bulkiness of the boratabenzene.<sup>797</sup> The chemistry of boratabenzene group 3 complexes has later been extended to yttrium as well as differently substituted boratabenzene ligands.<sup>798</sup> The reaction of yttrium trichloride with lithium 1-methylboratabenzene (1 : 2) in toluene (110 °C, 3 days) afforded the donor-free dinuclear sandwich complex  $[(\text{C}_5\text{H}_5\text{BMe}_2)_2\text{Y}(\mu\text{-Cl})_2]$  in 85% yield as pale yellow crystals. By means of single crystal and powder diffraction methods, three conformational polymorphs of this complex were characterized in the solid state.<sup>799</sup>

#### 4.01.9 Cycloheptatrienyl Compounds

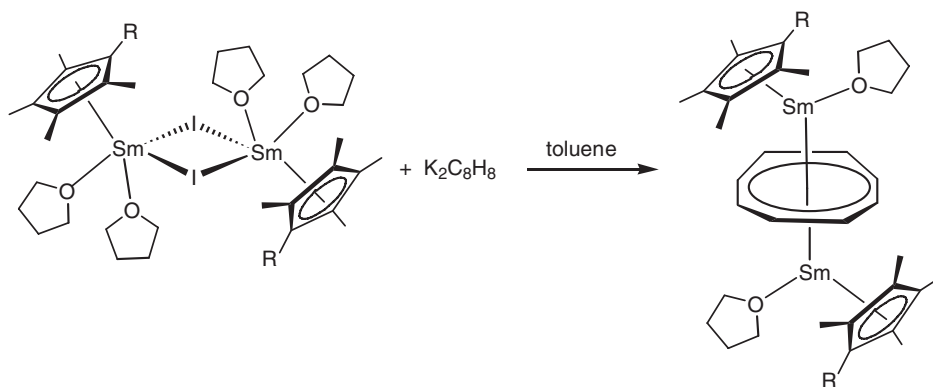
Treatment of  $\text{Nd}(\text{BH}_4)_3(\text{THF})_2$  with  $\text{KC}_7\text{H}_9$  gave the first cycloheptatrienyl compound of a 4f element,  $[\text{Nd}(\text{BH}_4)_2(\text{THF})_2](\mu\text{-}\eta^7\text{-C}_7\text{H}_7)$ , as green microcrystals in 77% yield. The formation of the cycloheptatrienyl resulted from the disproportionation reaction  $3\text{C}_7\text{H}_9^- \rightarrow \text{C}_7\text{H}_7^{3-} + 2\text{C}_7\text{H}_{10}$ . Its crystal structure has been determined.<sup>800</sup>

#### 4.01.10 Cyclooctatetraenyl Compounds

The use of neodymium borohydride complexes as precursors for (COT)lanthanide complexes has been reviewed by Ephritikhine *et al.* A comparison has been made to the corresponding uranium chemistry.<sup>801</sup>

##### 4.01.10.1 Cyclooctatetraenyl Lanthanide(II) Compounds

Triple decked bent metallocenes of europium and ytterbium were reported by Evans *et al.* The europium(II) compound  $[\text{Cp}^*\text{Eu}(\text{THF})_2]_2(\mu\text{-COT})$  was synthesized from the reaction of  $\text{K}_2\text{COT}$  with  $\text{EuCl}_3$  followed by interaction with  $\text{KCp}^*$  in THF. According to X-ray diffraction, the complex has an inverse sandwich structure in which the COT ring is located symmetrically between two Eu(II) atoms. Each europium is coordinated by one  $\eta^8$ -COT ring, one  $\text{Cp}^*$  group, and two solvating THF molecules, and has a formal coordination number of 10. The planar COT ring is nearly perpendicular to the Eu–Eu vector, and the (COT-cent.)–Eu–( $\text{Cp}^*$ -cent.) angles are 139.1° and 137.9°. <sup>802</sup>  $\text{YbI}_2(\text{THF})_2$  reacts with  $\text{KCp}^*$  and  $\text{K}_2\text{COT}$  in THF to form  $(\mu\text{-}\eta^8\text{-}\eta^8\text{-COT})[\text{Cp}^*\text{Yb}(\text{THF})]_2$ , which can be desolvated at 30 °C and  $10^{-7}$  torr to afford the solvent-free complex  $[\text{Cp}^*\text{Yb}]_2(\mu\text{-}\eta^8\text{-}\eta^8\text{-COT})$ . The molecular structure shows two divalent  $[\text{Cp}^*\text{Yb}]^+$  moieties bridged by a  $(\text{COT})^{2-}$  unit.  $[\text{Cp}^*\text{Eu}(\text{THF})_2]_2(\mu\text{-}\eta^8\text{-}\eta^8\text{-COT})$  can be desolvated



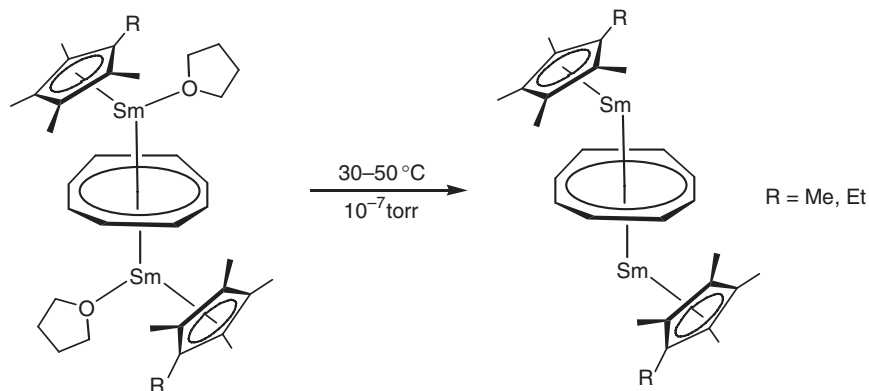
Scheme 224

analogously at 55 °C and  $10^{-7}$  torr to afford  $[Cp^*Eu]_2(\mu-\eta^8:\eta^8-COT)$ , which shows (Cp\* ring centroid)–Yb–(COT ring centroid) angles of 149.3° and 148.9°.  $[Cp^*Yb]_2(\mu-\eta^8:\eta^8-COT)$  reacts with 1,3,5,7-COT to form  $Cp^*Yb(COT)$ .<sup>803</sup> An analogous new series of bimetallic triple-decker sandwich samarium complexes containing two cyclopentadienyl and one cyclooctatetraenyl ligand,  $[(C_5Me_4R)Sm(THF)]_2(\mu-\eta^8:\eta^8-COT)$  ( $R = Me, Et$ ), has been prepared by allowing  $[(C_5Me_4R)Sm(\mu-I)(THF)_2]_2$  to react with 1 equiv. of  $K_2COT$  in toluene (Scheme 224).<sup>804</sup>

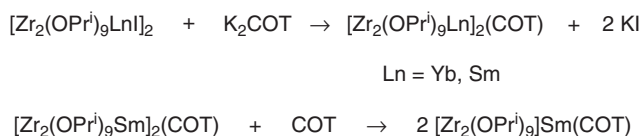
In the diglyme adduct of the complex  $[(C_5Me_4R)Sm(THF)]_2(\mu-\eta^8:\eta^8-COT)$ , the dianion  $(COT)^{2-}$  is sandwiched between two  $[(C_5Me_4R)Sm(THF)]^+$  cations with an angle of 137.6°. This bent triple-decked metallocene has Sm–C(Cp\*) and Sm–C(COT) average distances of 2.91(2) Å and 2.96(5) Å, respectively. Both the THF and diglyme complexes could be desolvated at 30–50 °C under high vacuum (Scheme 225). However, no metallocene structures with parallel rings like  $(COT)_2U$  and  $[(COT)_2Ce]^-$  were formed.<sup>804</sup>

Inverse sandwich complexes containing a COT ligand bridging lanthanide bis(silylamide) units have been reported for divalent samarium and ytterbium. Blue-green  $[Sm\{N(SiMe_3)_2\}(THF)]_2(\mu-COT)$  can be obtained from  $Sm[N(SiMe_3)_2](THF)_2$ ,  $SmI_2(THF)_2$ , and  $K_2COT$  in THF (83% yield). The analogous red-brown  $[Yb\{N(SiMe_3)_2\}(THF)]_2(\mu-COT)$  can be generated from  $KN(SiMe_3)_2$ ,  $YbI_2(THF)_2$ , and  $K_2COT$  in THF (86% yield). The Sm derivative has been structurally characterized.<sup>507</sup>

Evans *et al.* also reported the synthesis of the divalent lanthanide COT complexes  $[Zr_2(OPr^i)_9Ln]_2(COT)$  ( $Ln = Yb, Sm$ ) from  $[Zr_2(OPr^i)_9Ln]_2$  and  $K_2COT$  (Scheme 226). The monoanionic  $[Zr_2(OPr^i)_9]^-$  unit is used as a cyclopentadienyl analog. X-ray diffraction studies show the bimetallic Ln(II) complexes with the Sm centers coordinated to the bridging COT ligand in an  $\eta^8$ -fashion.<sup>264</sup>  $[Zr_2(OPr^i)_9Sm]_2(COT)$  reacts with 1,3,5,7-COT to form the hexane-soluble Sm(III) complex  $[Zr_2(OPr^i)_9]Sm(COT)$ , in a manner analogous to the reduction of COT by  $Cp^*Sm(COT)$ . The molecular structure shows the monomeric complex with one  $\eta^8$ -coordinated COT ligand and the monoanionic  $[Zr_2(OPr^i)_9]^-$  unit attached to the Sm in a tetradentate fashion.<sup>264</sup>



Scheme 225



Scheme 226

#### 4.01.10.2 Mono(cyclooctatetraenyl) Lanthanide(III) Compounds

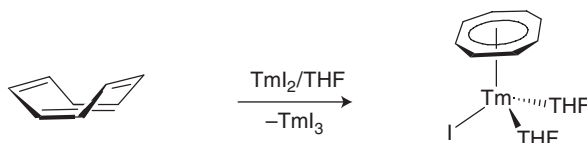
The dimeric mono(cyclooctatetraenyl)lanthanide chlorides  $[(\text{COT})\text{Ln}(\mu\text{-Cl})(\text{THF})_2]_2$  are long known and still represent the most useful precursors in  $(\text{COT})\text{Ln}$  chemistry. A recently reported alternative preparation of the Sm derivative involves the reaction of samarium metal with COT in THF in the presence of a small amount of  $\text{HgCl}_2$ . The molecular structure of  $[(\text{COT})\text{Sm}(\mu\text{-Cl})(\text{THF})_2]_2$  has been determined.<sup>805,806</sup> Iodo-(cyclooctatetraenyl)lanthanide iodides of the type  $(\text{COT})\text{LnI}(\text{THF})_n$  ( $\text{Ln} = \text{La, Ce, Pr, } n = 3$ ;  $\text{Ln} = \text{Nd, } n = 2$ ;  $\text{Ln} = \text{Sm, } n = 1$ ) are readily accessible in a one-pot reaction of metallic lanthanides with COT in the presence of an equimolar amount of iodine. Bromo- and chloro-bridged binuclear complexes of samarium,  $[(\text{COT})\text{Sm}(\mu\text{-X})(\text{THF})_2]_2$  ( $\text{X} = \text{Br, Cl}$ ), were also prepared by the reaction of samarium metal with COT in the presence of 1,2-dibromoethane or  $\text{Ph}_3\text{PCl}_2$ , respectively.<sup>807</sup> Alternatively, the iodo complexes  $(\text{COT})\text{LnI}(\text{THF})_3$  ( $\text{Ln} = \text{Nd, Sm}$ ) can be synthesized directly from the lanthanide triiodides and  $\text{K}_2\text{COT}$ . The molecular structure of  $(\text{COT})\text{NdI}(\text{THF})_3$  has been determined by X-ray diffraction.<sup>808</sup> A clean preparation of the monomeric half-sandwich complex  $(\text{COT})\text{TmI}(\text{THF})_2$  involves treatment of  $\text{TmI}_2$  with equimolar amounts of COT in THF at room temperature (Scheme 227). The product was isolated as red crystals in 75% yield.<sup>628</sup>

A series of binuclear complexes with bridging alkoxide ligands has been prepared of which three representatives,  $[(\text{COT})\text{Y}(\mu\text{-OPh})(\text{THF})]_2$ ,  $[(\text{COT})\text{Nd}(\mu\text{-OEt})(\text{THF})]_2$  (pale blue crystals), and  $[(\text{COT})\text{Dy}\{\mu\text{-O}(\text{CH}_2)_3\text{CH}=\text{CH}_2\}(\text{THF})]_2$  (bright yellow crystals), have been structurally characterized. With the use of sterically more demanding alkoxide and siloxide ligands the monomeric compounds  $(\text{COT})\text{Ln}(\text{OCBu}^t_3)(\text{THF})$  ( $\text{Ln} = \text{Y, Lu}$ ) and  $(\text{COT})\text{Ln}(\text{OSiPh}_3)(\text{THF})$  ( $\text{Ln} = \text{Y, Lu}$ ) have been prepared.<sup>809,810</sup> The reaction of  $\text{NdCl}_3$  with  $\text{C}_6\text{H}_5\text{CH}_2\text{C}_5\text{H}_4\text{Na}$  in the ratio 1:1 at  $-78^\circ\text{C}$  affords  $(\text{C}_6\text{H}_5\text{CH}_2\text{C}_5\text{H}_4)\text{NdCl}_2 \cdot n\text{THF}$ , which on treatment with  $\text{K}_2\text{COT}/\text{THF}$  gives  $\text{Nd}_2(\text{COT})_3(\text{C}_6\text{H}_5\text{CH}_2\text{C}_5\text{H}_4)\text{K}(\text{THF})_3$  ( $\text{C}_6\text{H}_5\text{CH}_2\text{C}_5\text{H}_4 = \text{benzyl cyclopentadienyl}$ ). The crystal structure of the Nd complex revealed that the complex consists of the two parts of  $[(\eta^8\text{-COT})\text{Nd}(\eta^8\text{-COT})]^-$  and  $[(\text{C}_6\text{H}_5\text{CH}_2\text{C}_5\text{H}_4)\text{Nd}(\text{THF})_2(\eta^8\text{-COT})]$  connected by the  $\text{K}^+$  ion, to which the  $\eta^3\text{-C}_6\text{H}_5$  ring of a benzyl cyclopentadienyl and a THF molecule are coordinated.<sup>811</sup>

The electronic features of the COT ligand in the complex  $(\text{COT})\text{Nd}^{\text{III}}[\text{HB}(3,5\text{-Me}_2\text{pz})_3]$  have been investigated. The absorption spectrum has been measured at different temperatures, and the bands were assigned by applying the selection rules for  $C_{8v}$ -symmetry. The CF parameters found for  $[\text{COT}]^{2-}$  were the same as in the praseodymium case.<sup>812</sup>

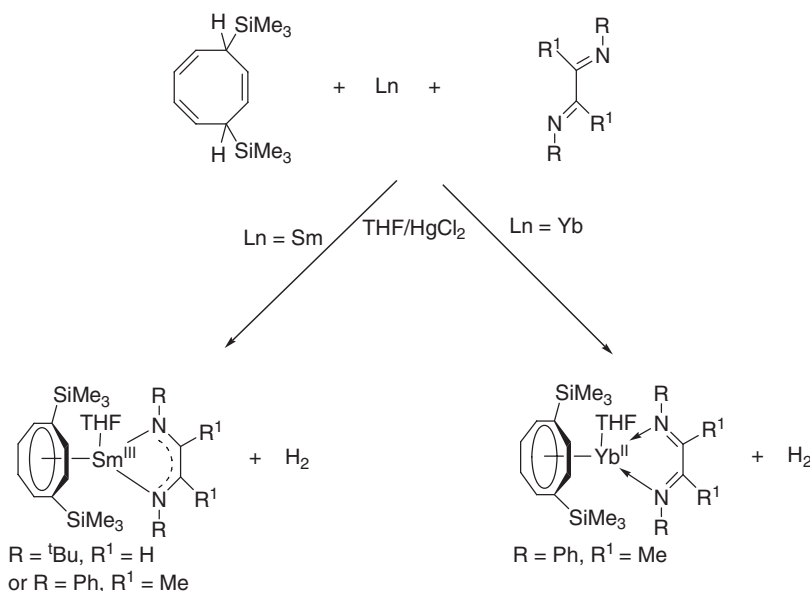
Complexes of the type  $(\text{COT}^*)\text{Ln}(\text{DAD}(\text{THF}))$  ( $\text{Ln} = \text{Sm, Yb}$ ;  $\text{COT}^* = \text{C}_8\text{H}_6(\text{SiMe}_3)_2\text{-1,4}$ ;  $\text{DAD} = 1,4\text{-diazadienes}$ ) have been prepared in a one-pot reaction by treatment of elemental Sm or Yb with equimolar amounts of 1,4-bis(trimethylsilyl)cyclooctatriene and 1,4-diazadiene ligands (Scheme 228).  $^1\text{H}$  and  $^{171}\text{Yb}$  NMR data show that the Sm derivatives contain  $\text{Sm}^{3+}$  ions and coordinated DAD radical anions, while in the case of Yb the neutral DAD ligand is coordinated to divalent ytterbium.<sup>813</sup>

The (cyclooctatetraenyl)lanthanide borohydride,  $[(\text{COT})\text{Nd}(\mu\text{-BH}_4)(\text{THF})_2]_2$ , was obtained by treatment of  $\text{Nd}(\text{BH}_4)_3(\text{THF})$  with  $\text{K}_2\text{COT}$  in THF. This complex could be transformed into  $[(\text{COT})\text{Nd}(\text{THF})_4][\text{BPh}_4]$  and  $(\text{COT})\text{Nd}(\text{Cp}^*)(\text{THF})$  with  $\text{NHET}_3\text{BPh}_4$  and  $\text{KCp}^*$ , respectively. Both the cyclooctatetraenyl complex and the cation reacted with  $\text{KCp}^*$  to form  $(\text{COT})\text{Nd}(\text{Cp}^*)(\text{THF})_2$ .<sup>814</sup> The complex  $[(\text{COT})\text{Nd}(\mu\text{-BH}_4)(\text{THF})_2]_2$  consists of two



Scheme 227





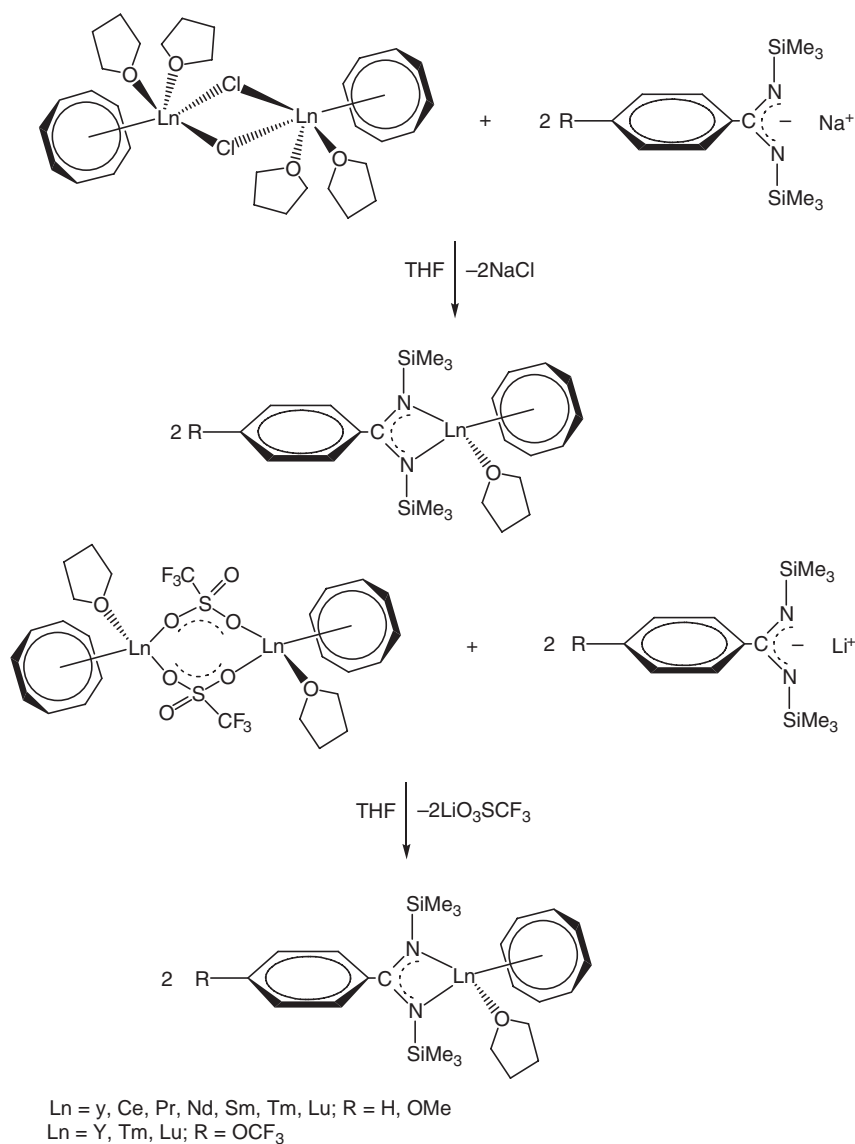
Scheme 228

mononuclear units bridged by two  $\text{BH}_4$  groups. Each Nd atom is in a three-legged piano stool environment, defined by the boron, the oxygen atom, and the COT ligand. The boron atom is linked to each metal center via  $\mu_2$ -hydrogens, the other two H atoms bridge the B and both Nd atoms in a  $\mu_3$  fashion. This coordination type of the borohydride ligand was encountered only once before in the cerium compound  $[(\text{C}_5\text{H}_3\text{Bu}^t)_2\text{Ce}(\text{BH}_4)]_2$ . In the  $[(\text{COT})\text{Nd}(\text{THF})_4]^+$  cation the Nd atom is situated in a slightly distorted square pyramidal environment.<sup>814</sup>

The alkoxide  $[(\text{COT})\text{Nd}(\text{OEt})(\text{THF})]_2$ , and the thiolates  $\text{Na}[(\text{COT})\text{Nd}(\text{S}^t\text{Bu})_2]$  and  $[\text{Na}(\text{THF})_2][(\text{COT})\text{Nd}_2(\text{S}^t\text{Bu})_3]$  were synthesized by treating  $(\text{COT})\text{Nd}(\text{BH}_4)(\text{THF})$  or  $[(\text{COT})\text{Nd}(\text{THF})_4][\text{BPh}_4]$  with the alkali metal salt of the corresponding anionic reagent.<sup>547</sup> In the crystal structure of a toluene solvated  $[\text{Na}(\text{THF})_2][(\text{COT})\text{Nd}_2(\text{S}^t\text{Bu})_3]$  the two  $(\text{COT})\text{Nd}$  fragments are bridged by three  $\text{S}^t\text{Bu}$  groups. Each Nd atom has a pseudo-tetrahedral arrangement, if the cyclooctatetraenyl group is considered as a monodentate ligand. The two tetrahedra share the common trigonal basis defined by the S atoms. This basal plane is parallel to the planar COT rings and perpendicular to the COT(centroid)–Nd–Nd–COT(centroid) axis. The COT ligation is quite similar to that found in the complex  $[(\text{COT})\text{Nd}(\text{OEt})(\text{THF})]_2$ , with an average Nd–C bond length of 2.67(3) Å. The Nd–S–Nd angles range from 88.50(5)° to 91.0(3)°; the S(1)–Nd–S(2) angles vary from 71.3(2)° to 87.0(2)°, due to coordination of S(1) and S(2) to the sodium atom.<sup>547</sup>

Half-sandwich complexes of the types  $(\text{COT})\text{Ln}(\text{HBpz}_3)$ ,  $(\text{COT})\text{Ln}[\text{HB}(3,5\text{-Me}_2\text{pz})_3]$ ,  $(\text{COT})\text{Ln}[\text{CpCo}[\text{P}(\text{O})(\text{OEt})_2]_3]$ ,  $(\text{COT})\text{Ln}[\text{Ph}_2\text{P}(\text{NSiMe}_3)_2](\text{THF})$ , and  $(\text{COT})\text{Ln}[4\text{-MeOC}_6\text{H}_4\text{C}(\text{NSiMe}_3)_2](\text{THF})$  ( $\text{Ln} = \text{Y}, \text{Ce}, \text{Pr}, \text{Nd}, \text{Sm}$ ) are readily accessible through metathetical reactions of  $[(\text{COT})\text{Ln}(\mu\text{-Cl})(\text{THF})_2]_2$  with the appropriate anionic ligands.<sup>815,816</sup> The monomeric (cyclooctatetraenyl)lanthanide benzamidinate complexes  $(\text{COT})\text{Ln}[4\text{-RC}_6\text{H}_4\text{C}(\text{NSiMe}_3)_2](\text{THF})$  ( $\text{R} = \text{H}, \text{OMe}$ ;  $\text{Ln} = \text{Y}, \text{Ce}, \text{Pr}, \text{Nd}, \text{Sm}, \text{Tm}, \text{Lu}$ ;  $\text{R} = \text{CF}_3$ ,  $\text{Ln} = \text{Y}, \text{Tm}, \text{Lu}$ ) were synthesized by the reactions of  $[(\text{COT})\text{Ln}(\mu\text{-Cl})(\text{THF})_2]_2$  or  $[(\text{COT})\text{Ln}(\mu\text{-O}_3\text{SCF}_3)(\text{THF})_2]_2$  with  $\text{Na}[4\text{-RC}_6\text{H}_4\text{C}(\text{NSiMe}_3)_2]$  ( $\text{R} = \text{H}, \text{OMe}, \text{CF}_3$ ) or  $\text{Li}[\text{PhC}(\text{NSiMe}_3)_2]$  in THF (Scheme 229).  $[(\text{COT})\text{Ln}(\mu\text{-Cl})(\text{THF})_2]_2$  ( $\text{Ln} = \text{Ce}, \text{Pr}, \text{Nd}, \text{Sm}$ ) reacted also with  $\text{Li}[\text{Ph}_2\text{P}(\text{NSiMe}_3)_2]$  in THF to give the corresponding (cyclooctatetraenyl)[diphenyl(trimethylsilylimido)phosphinato] complexes  $(\text{COT})\text{Ln}[\text{Ph}_2\text{P}(\text{NSiMe}_3)_2](\text{THF})$ . Structures of  $(\text{COT})\text{Tm}[\text{PhC}(\text{NSiMe}_3)_2](\text{THF})$ ,  $(\text{COT})\text{Lu}[4\text{-MeOC}_6\text{H}_4\text{C}(\text{NSiMe}_3)_2](\text{THF})$ , and  $(\text{COT})\text{Nd}[\text{Ph}_2\text{P}(\text{NSiMe}_3)_2](\text{THF})$  were studied by X-ray single crystal diffraction. Crystal structures of  $(\text{COT})\text{Tm}[\text{PhC}(\text{NSiMe}_3)_2](\text{THF})$  and  $(\text{COT})\text{Lu}[4\text{-MeOC}_6\text{H}_4\text{C}(\text{NSiMe}_3)_2](\text{THF})$  are similar with the exception that the thulium compound contains solvent molecules (toluene) in the unit cell. In both complexes  $\text{Ln}^{3+}$  ion is coordinated by one  $\eta^8$ -COT ring, two nitrogen atoms of chelating benzamidinate ligand, and one THF molecule. In the structure of  $(\text{COT})\text{Nd}[\text{Ph}_2\text{P}(\text{NSiMe}_3)_2](\text{THF})$  the neodymium is also coordinated by one  $\eta^8$ -COT ring, two nitrogens of chelating diphenylbis(trimethylsilylimido)phosphinate anion, and one THF molecule. The  $\text{PN}_2\text{Nd}$  cycle is almost planar.<sup>817</sup>





Scheme 229

Diphosphinoamide complexes of the type  $(\text{COT})\text{Ln}[\text{N}(\text{PPh}_2)_2](\text{THF})$  have been prepared with  $\text{Ln} = \text{La}$  and  $\text{Sm}$ , and both complexes have been structurally characterized.<sup>818</sup> The crystal structures of  $[(\text{COT})\text{Ln}(\mu\text{-O}_3\text{SCF}_3)(\text{THF})_2]_2$  ( $\text{Ln} = \text{Nd}, \text{Ce}$ ) have been determined. Together with the bridging triflate ligands the lanthanide atoms form eight-membered  $\text{Ln}_2\text{O}_4\text{S}_2$  rings.<sup>808,819</sup> Several dimeric  $(\text{COT})\text{Sm}$  complexes containing bridging thiolate and selenolate have been prepared directly from metallic samarium, COT, and disulfides or diselenides. The molecular structure of the benzeneselenolato complex  $[(\text{COT})\text{Sm}(\mu\text{-SePh})(\text{THF})_2]_2$  as a typical representative has been determined.<sup>807</sup>

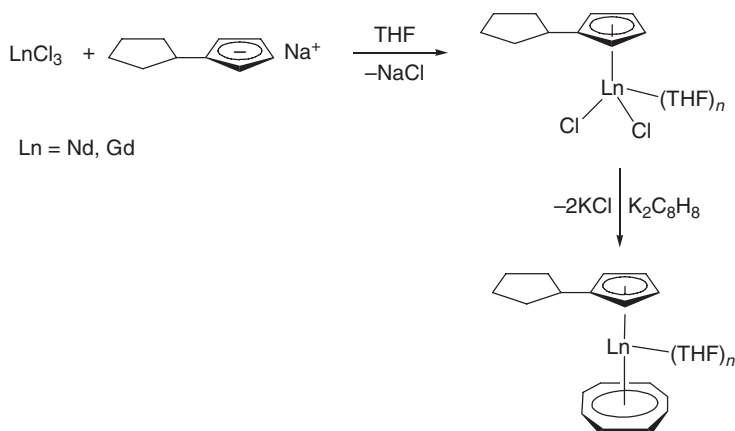
The complex  $[(\text{COT})\text{Ce}(\mu\text{-O}_3\text{SCF}_3)(\text{THF})_2]_2$  reacts with 2 equiv. of  $\text{K}[1,3\text{-Bu}^t_2\text{C}_5\text{H}_3]$  to give the mixed sandwich complex  $(\text{COT})\text{Ce}(1,3\text{-Bu}^t_2\text{C}_5\text{H}_3)$ .<sup>819</sup> The variability of (ring centroid)–Ln–(ring centroid) angles in the mixed ligand  $\text{C}_5\text{Me}_5/\text{COT}$  complexes  $\text{Cp}^*\text{Ln}(\text{COT})$  and  $[\text{Cp}^*\text{Yb}(\text{THF})][\text{YbCp}^*](\mu\text{-}\eta^8\text{:}\eta^8\text{-COT})$  has been investigated.<sup>820</sup> The solid-state structures of  $\text{Cp}^*\text{Sm}(\text{COT})$ ,  $\text{Cp}^*\text{Dy}(\text{COT})$ ,  $\text{Cp}^*\text{Er}(\text{COT})$ , and  $\text{Cp}^*\text{Yb}(\text{COT})$  were determined for comparison with that of  $\text{Cp}^*\text{Lu}(\text{COT})$ . The Ln–C( $\text{Cp}^*$ ) and Ln–C(COT) distances decrease from Sm to Lu with changes that follow the differences in eight-coordinate metal radii. The complex  $[\text{Cp}^*\text{Yb}(\text{THF})][\text{YbCp}^*](\mu\text{-}\eta^8\text{:}\eta^8\text{-COT})$  was

obtained from a reaction of 0.5 equiv. of  $\text{Al}_2\text{Et}_6$  with 1 equiv. of  $(\mu\text{-}\eta^8\text{-COT})[\text{Cp}^*\text{Yb}(\text{THF})]_2$ . The  $\text{Yb}(1)\text{-C}(\text{Cp}^*)$  average distance is 2.683(3) Å on the solvated side versus 2.615(3) Å for the unsolvated  $\text{Yb}(2)\text{-C}(\text{Cp}^*)$ .<sup>820</sup>

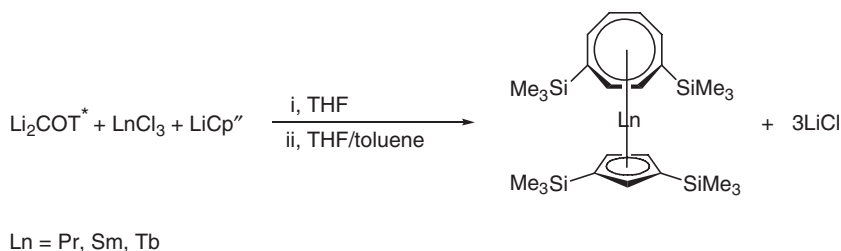
Reactions of  $[(\text{COT})\text{Ln}(\mu\text{-Cl})(\text{THF})_n]_2$  ( $\text{Ln} = \text{Y}, \text{La}, \text{Pr}, \text{Sm}, \text{Gd}, \text{Dy}, \text{Er}, \text{Lu}$ ;  $n = 1, 2$ ) with  $\text{Na}(\text{C}_5\text{Me}_4\text{H})$  in THF yielded the sandwich complexes  $(\text{COT})\text{Ln}(\text{C}_5\text{Me}_4\text{H})(\text{THF})_x$  ( $x = 0, 1, 2$ ), of which  $(\text{COT})\text{La}(\text{C}_5\text{Me}_4\text{H})(\text{THF})_2$  and  $(\text{COT})\text{Lu}(\text{C}_5\text{Me}_4\text{H})$  have been structurally characterized.<sup>821</sup> The complexes  $(\text{COT})\text{Nd}(\text{C}_5\text{H}_9\text{C}_5\text{H}_4)(\text{THF})_2$  and  $[(\text{COT})\text{Gd}(\text{C}_5\text{H}_9\text{C}_5\text{H}_4)(\text{THF})][(\text{COT})\text{Gd}(\text{C}_5\text{H}_9\text{C}_5\text{H}_4)(\text{THF})_2]$  were obtained by the reaction between the appropriate  $\text{LnCl}_3$  ( $\text{Ln} = \text{Nd}, \text{Gd}$ ) and  $\text{C}_5\text{H}_9\text{C}_5\text{H}_4\text{Na}$  (or  $\text{K}_2\text{COT}$ ) in THF ( $\text{C}_5\text{H}_9\text{C}_5\text{H}_4 = \text{cyclopentylcyclopentadienyl}$ ) followed by reaction with  $\text{K}_2\text{COT}$  (or  $\text{C}_5\text{H}_9\text{C}_5\text{H}_4\text{Na}$ ) in THF (Scheme 230). In the structure of  $(\text{COT})\text{Nd}(\text{C}_5\text{H}_9\text{C}_5\text{H}_4)(\text{THF})_2$  Nd is coordinated by one  $\eta^8\text{-COT}$  ring, one  $\eta^5\text{-C}_5\text{H}_9\text{C}_5\text{H}_4$  ligand, and two oxygen atoms of solvating THF molecules. The Nd atom has a twisted tetrahedral coordination geometry. The crystals of  $[(\text{COT})\text{Gd}(\text{C}_5\text{H}_9\text{C}_5\text{H}_4)(\text{THF})][(\text{COT})\text{Gd}(\text{C}_5\text{H}_9\text{C}_5\text{H}_4)(\text{THF})_2]$  consist of two independent units  $(\text{COT})\text{-Gd}(\text{C}_5\text{H}_9\text{C}_5\text{H}_4)(\text{THF})$  and  $(\text{COT})\text{Gd}(\text{C}_5\text{H}_9\text{C}_5\text{H}_4)(\text{THF})_2$ ; the latter complex has a similar structure with the above-mentioned neodymium analog.<sup>822</sup>

The complexes  $(\text{COT}^*)\text{LnCp}''$  [ $\text{COT}^* = 1,4\text{-(Me}_3\text{Si)}_2\text{C}_8\text{H}_6$ ;  $\text{Cp}'' = 1,3\text{-(Me}_3\text{Si)}_2\text{C}_5\text{H}_3$ ] with  $\text{Ln} = \text{Pr}, \text{Sm}, \text{Tb}$  have been synthesized in a one-pot reaction by simultaneous treatment of anhydrous lanthanide trichlorides with equimolar amounts of  $\text{Li}_2\text{COT}^*$  and  $\text{LiCp}''$  (Scheme 231).<sup>823</sup>

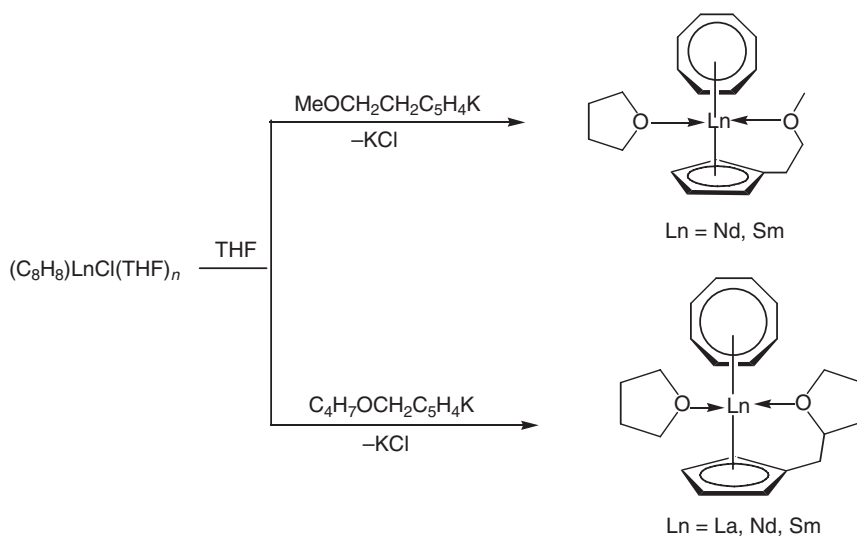
The synthesis of THF-free metallocenes of early lanthanides with highly substituted cyclopentadienyl and cyclooctatetraenyl ligands has been investigated. The complexes were obtained by the reaction of  $(\text{COT})\text{LnCl}(\text{THF})_2$  ( $\text{Ln} = \text{Sm}, \text{Nd}$ ) with 1 equiv. of  $\text{NaCp}^{4i}$  ( $\text{Cp}^{4i} = \text{C}_5\text{H}(\text{Pr}^i)_4$ , tetraisopropylcyclopentadienyl) in high yield of the corresponding lanthanide(III) metallocenes  $\text{COTLn}(\text{Cp}^{4i})$ . The molecular structure of  $(\text{COT})\text{NdCp}^{4i}$  shows a slight bending;  $170.4^\circ$  for the  $\text{Cp}\text{-Sm}\text{-COT}$  angle in  $(\text{COT})\text{SmCp}^{4i}$ ,  $165^\circ$  in one independent conformer of  $(\text{COT})\text{NdCp}^{4i}$ , and  $173^\circ$  in the other.<sup>217</sup> Lanthanide mixed sandwich complexes with a cyclooctatetraenyl ligand and cyclopentadienyl with a chelating ether side chain have been synthesized.  $\text{LnCl}_3$  reacted with  $\text{K}_2\text{COT}$  in THF in the ratio 1 : 1 at room temperature and formed  $(\text{COT})\text{LnCl}\cdot n\text{THF}$ , which was then treated with



Scheme 230



Scheme 231

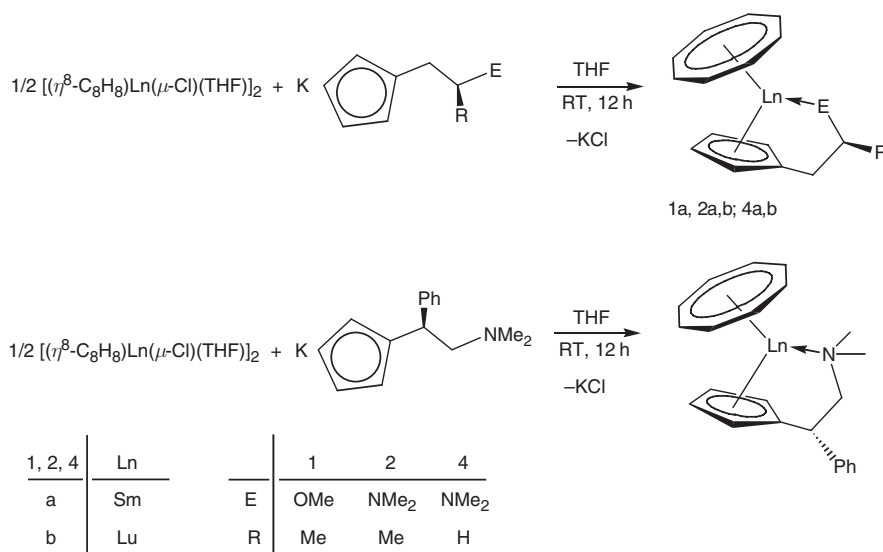


Scheme 232

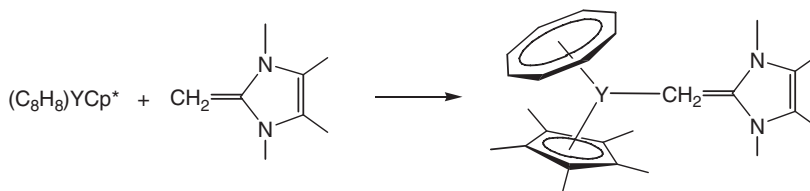
$RCpK-THF$  ( $RCp = MeOCH_2CH_2C_5H_4$  or  $C_4H_7OCH_2CH_2C_5H_4$ ) to yield the complexes  $(RCp)Ln(COT)(THF)$  ( $Ln = Nd, Sm$ ,  $RCp = MeOCH_2CH_2C_5H_4$ ;  $Ln = La, Nd, Sm$ ,  $RCp = C_4H_7OCH_2C_5H_4$ ) (Scheme 232).<sup>824</sup>

Enantiomerically pure sandwich complexes of samarium and lutetium have been synthesized with the use of donor-functionalized cyclopentadienyl ligands. The reaction of  $[K\{(S)-C_5H_4CH_2CH(Me)OMe\}]$ ,  $[K\{(S)-C_5H_4CH_2CH(Me)NMe_2\}]$ , and  $[K\{(S)-C_5H_4CH(Ph)CH_2NMe_2\}]$  with the cyclooctatetraenyl lanthanide chlorides  $[(COT)Ln(\mu-Cl)(THF)]_2$  ( $Ln = Sm, Lu$ ) yield the mixed cyclooctatetraenyl cyclopentadienyl lanthanide complexes  $[(COT)Sm\{(S)-\eta^5:\eta^1-C_5H_4CH_2CH(Me)OMe\}]$ ,  $[(COT)Ln\{(S)-\eta^5:\eta^1-C_5H_4CH_2CH(Me)NMe_2\}]$  ( $Ln = Sm, Lu$ ), and  $[(COT)Ln\{(S)-\eta^5:\eta^1-C_5H_4CH(Ph)CH_2NMe_2\}]$  ( $Ln = Sm, Lu$ ) (Scheme 233). The X-ray crystal structures of  $[(COT)Lu\{(S)-\eta^5:\eta^1-C_5H_4CH(Ph)CH_2NMe_2\}]$  and the achiral compound  $[(COT)Ln\{\eta^5:\eta^1-C_5H_4CH_2CH_2NMe_2\}]$  have been determined.<sup>825</sup>

Two types of indenyl/cyclooctatetraenyl mixed sandwich complexes,  $(MeOCH_2CH_2C_9H_6)Ln(COT)(THF)_n$  ( $Ln = La, Nd$ ,  $n = 0$ ;  $Ln = Sm, Dy, Er$ ,  $n = 1$ ) and  $(C_4H_7OCH_2C_9H_6)Ln(COT)(THF)$  ( $Ln = La, Nd, Sm, Dy, Er$ ),



Scheme 233



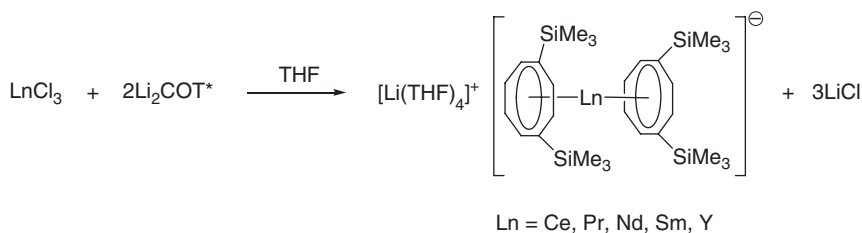
Scheme 234

have been synthesized by the reactions of LnCl<sub>3</sub> with 1 equiv. of K<sub>2</sub>COT, followed by treatment with the corresponding potassium salt of the ether-substituted indenide anion.<sup>826</sup> The novel mixed phospholyl/cyclooctatetraenyl lanthanide sandwich complexes (COT)Sm(Tmp)(THF), (COT)Sm(Dsp), and (COT)Nd(Dsp)(THF) (Tmp = 2,3,4,5-tetramethylphospholyl; Dsp = 3,4-dimethyl-2,5-bis(trimethylsilyl)phospholyl) have been prepared by metathesis of phospholylpotassium salts with the dimeric cyclooctatetraenyllanthanide chloride precursors [(COT)Ln(μ-Cl)(THF)<sub>2</sub>] (Ln = Nd, Sm). The neodymium derivative has been structurally characterized.<sup>805</sup>

Terphenyl cyclooctatetraenyl samarium complexes of the type (COT)Sm(Dpp)(μ-Cl)Li(THF)<sub>3</sub>, (COT)Sm(Dmp)(THF), and (COT)Sm(Danip)(THF) (Dpp = 2,6-diphenylphenyl; Dmp = 2,6-dimesitylphenyl; Danip = 2,6-di(*o*-anisyl)phenyl) have been synthesized in a one-pot reaction from SmCl<sub>3</sub>, K<sub>2</sub>COT, and the corresponding terphenyllithium derivative.<sup>105</sup> (COT)Tm(Dmp)(THF) displays an analogous molecular structure.<sup>827</sup> The ylidic olefin complex (COT)YCp\*[CH<sub>2</sub>=CN(Me)C(Me)=C(Me)N(Me)] has been prepared by the reaction of (COT)YCp\* with 1,3,4,5-tetramethyl-2-methylenimidazoline (Scheme 234). In the structure the yttrium atom is coordinated by one η<sup>8</sup>-COT and one η<sup>5</sup>-Cp\* ring, and one carbon atom of the 1,3,4,5-tetramethyl-2-methylenimidazoline ligand (C<sub>8</sub>H<sub>14</sub>N<sub>2</sub>). The Y-(COT-cent.), Y-(Cp\*-cent.), and Y-C(C<sub>8</sub>H<sub>14</sub>N<sub>2</sub>) distances are 1.895(15), 2.410(13), and 2.624(11) Å, respectively.<sup>828</sup>

#### 4.01.10.3 Bis(cyclooctatetraenyl) Lanthanide(III) Compounds

Structural investigations have been carried out on the anionic sandwich complexes [Li(THF)<sub>4</sub>][Ce(COT)<sub>2</sub>] and (THF)<sub>3</sub>Na(μ-COT)Ce(COT),<sup>829</sup> as well as [Li(THF)<sub>3</sub>][Tm(COT)<sub>2</sub>]<sup>830</sup> and [Li(THF)<sub>2</sub>][Sc(COT)<sub>2</sub>].<sup>831</sup> The ionic samarium bis(cyclooctatetraenyl) complex [(COT)Sm(HMPA)<sub>3</sub>][Sm(COT)<sub>2</sub>] was obtained by the reaction of metallic samarium with COT in the presence of a catalytic amount of iodine in THF containing HMPA.<sup>832</sup> The anionic sandwich complexes [Li(THF)<sub>4</sub>][Ln(COT\*)<sub>2</sub>] (Ln = Ce, Pr, Nd, Sm, Y; COT\* = C<sub>8</sub>H<sub>6</sub>(SiMe<sub>3</sub>)<sub>2</sub>-1,4) have been prepared by treatment of anhydrous lanthanide trichlorides with 2 equiv. of Li<sub>2</sub>COT\* (Scheme 235). The structure of the Sm derivative has been determined. Ion exchange of [Li(THF)<sub>4</sub>][Sm(COT\*)<sub>2</sub>] with [PPN]Cl afforded the derivative [PPN][Sm(COT\*)<sub>2</sub>]. In a similar manner, the hexasilylated sandwich salt [K(THF)<sub>3</sub>][Tb(COT\*\*) <sub>2</sub>] (COT\*\* = C<sub>8</sub>H<sub>5</sub>(SiMe<sub>3</sub>)<sub>3</sub>-1,3,6) has been obtained by reacting anhydrous TbCl<sub>3</sub> with K<sub>2</sub>COT\*\* in a 1:2 molar ratio. Treatment of anhydrous lanthanide trichlorides with Li<sub>2</sub>COT\* in a 2:3 molar ratio afforded the first well-defined organolanthanide triple-decker sandwich complexes Ln<sub>2</sub>(COT\*)<sub>3</sub> (Ln = Ce, Nd, Sm).<sup>833,833a</sup>



Scheme 235

#### 4.01.10.4 Bis(cyclooctatetraenyl)cerium Compounds (“Cerocenes”)

Large-scale state-average multiconfiguration self-consistent field, configuration interaction, averaged coupled-pair functional, and spin-orbit configuration interaction calculations have been carried out for the cerocene sandwich complex  $\text{Ce}(\text{COT})_2$  as well as the Nd, Tb, and Yb analogs.<sup>834,835</sup> On the basis of the calculations, it was concluded that the  $\text{Ce}(\text{COT})_2$  is essentially a  $\text{Ce}(\text{III})$  compound, that is, a  $\text{Ce}^{3+}$  ion with a  $4f^1$  configuration and two  $\text{COT}^{1.5-}$  ligands. The covalent contributions to metal–ring bonding in  $\text{Ce}(\text{COT})_2$  result mainly from the cerium  $5d$  orbitals, whereas the  $4f$  orbitals retain an atomic-like character in the molecular environment. The calculated  $\text{Ce}$ – $\text{COT}(\text{ring})$  distance of 2.05 Å still shows a substantial error with the experimental value of 1.97 Å.<sup>834</sup> The assignment of the oxidation state as  $\text{Ce}(\text{III})$  has been confirmed by X-ray absorption near-edge structure (XANES) measurements. The XANES spectra indicate that  $\text{Ce}$  in substituted cerocenes is also trivalent. The  $\text{Ce}$  ion in the substituted cerocenes appears to be less electron-rich than in their alkali metal salts, as shown by a 4.5 eV shift toward higher oxidation state of their X-ray K-edges. This argument is supported by structural data which show the  $\text{Ce}$  ring centroid distance for the substituted cerocenes is  $\sim 1.97$  Å as compared to  $\sim 2.07$  Å for the  $\text{K}[\text{Ce}(\text{COT})_2]$  diglyme salt. The experimental results therefore support the conclusion of the sophisticated *ab initio* calculations that the cerocene ground configuration should be formulated primarily as a  $4f^{12}e_u^0e_g^0n^0$  singlet.<sup>836</sup> In 2004, an efficiently modified synthesis for the long-known parent cerocene which involves oxidation of  $\text{K}[\text{Ce}(\text{COT})_2]$  with allyl bromide was published. An electrochemical study of cerocene showed redox with the cerate ion  $[\text{Ce}(\text{COT})_2]^-$  to be reversible with a relatively low reduction potential ( $-0.6$  V vs. NHE). The corresponding praseodymium salt,  $\text{K}[\text{Pr}(\text{COT})_2]$ , does not undergo comparable reversible oxidation.<sup>837</sup> Polysilylated cerocenes have also been reported;  $[1,3,6-(\text{Me}_3\text{Si})_3\text{C}_8\text{H}_5]_2\text{Ce}$  forms permanganate-colored, low melting crystals, while  $[1,4-(\text{Me}_3\text{Si})_2\text{C}_8\text{H}_6]_2\text{Ce}$  has been isolated in the form of a purple oil.<sup>838</sup>

#### 4.01.11 Metallofullerenes

A lanthanum fullerene complex of the composition  $\text{C}_{60}[\text{La}(\text{Gly})_2]_2(\text{ClO}_4)_6$  has been reported to contain  $\eta^2$ -coordinated  $\text{C}_{60}$ , though structural evidence is lacking.<sup>839</sup> Bochakarev *et al.* described the synthesis of the first  $\text{C}_{60}$ -fullerenide complexes of (cyclopentadienyl)ytterbium and -lutetium. By treatment of  $\text{Cp}^\#_2\text{Yb}$  ( $\text{Cp}^\# = \text{C}_5\text{H}_4(\text{CH})_2\text{NMe}_2$ ) with  $\text{C}_{60}$  the fullerenide complex  $[\text{Cp}^\#_2\text{Yb}]_2\text{C}_{60}$  was obtained in 57% yield. In the same way fullerenide complexes of lutetium,  $\text{Cp}^\#\text{Lu}(\text{C}_{60})(\text{DME})$  and  $\text{Cp}^\#\text{Lu}(\text{C}_{60})(\text{DME})(\text{C}_6\text{H}_5\text{CH}_3)$ , were synthesized.<sup>234</sup>

The La-containing carbon clusters  $\text{LaC}_n^+$  and  $\text{La}_2\text{C}_n^+$  were generated by the laser vaporization of a composite  $\text{LaC}_2/\text{graphite}$  rod, then the clusters were mass-selected and injected into a drift tube.<sup>840–842</sup> Three families of ring isomers, La-containing graphite sheets and metallofullerenes were observed for the  $\text{LaC}_n^+$  clusters. The suggested geometries for the ring isomers are: an La inserted into carbon ring, an La inside a carbon ring, and various  $\text{LaC}_n$  and  $\text{C}_m$  rings fused together.  $\text{LaC}_{36}^+$  and all  $\text{LaC}_n^+$  fullerenes with  $n = 38$ – $90$  were found to be endohedral, while  $\text{LaC}_{29}^+$ – $\text{LaC}_{36}^+$  fullerenes were non-endohedral. Annealing processes in the  $\text{LaC}_n^+$  fullerenes for larger clusters led to the formation of fullerenes and graphite sheets. The graphite sheet was found to be the main isomerization product for clusters with 30–34 carbon atoms, while for clusters with more than 38 atoms >90% of the rings are converted into metallofullerenes.<sup>840</sup> In the case of  $\text{La}_2\text{C}_n^+$  the efficiency of encapsulation of a second La atom inside a fullerene cage was found to be substantially lower than that of the first.<sup>842</sup> Both di-endohedral fullerenes and fullerenes with one non-endohedral metal atom were observed for  $\text{La}_2\text{C}_n^+$  clusters. Authors suggested that the reduced efficiency for encapsulating the second La could also result from stabilization of the  $\text{La}(\text{La}@\text{C}_n)^+$  or  $\text{La}@\text{C}_n\text{La}^+$  geometry by the endohedral La atom.<sup>840–842</sup> Three isomers of  $\text{Y}_2\text{C}_2@\text{C}_{82}$  have been synthesized and chromatographically isolated.<sup>843</sup> Quantized rotational states of a diatomic  $\text{C}_2$  unit have been observed in solid endohedral fullerene  $\text{C}_2\text{Sc}_2@\text{C}_{84}$ .<sup>844</sup>

A photofragmentation study of metal fullerenes  $\text{C}_{60}\text{Ln}_x$  ( $\text{Ln} = \text{Y}, \text{La}, \text{Sm}$ ) by excimer laser ablation–TOF mass spectrometry showed that many kinds of metallofullerenes have been observed in both the positive and negative ionic modes. For  $\text{C}_{60}\text{Sm}_x$ , the metal atom is incorporated into the network of the fullerene cage to replace one carbon atom of the cage forming substitutional metallofullerenes. In the case of the metal fullerenes  $\text{C}_{60}\text{Ln}_x$  ( $\text{Ln} = \text{Y}, \text{La}$ ), evidence of the encapsulation of Y and La atoms in the fullerene cages forming endohedral fullerenes has been observed.<sup>333,845–847</sup> The configuration of La ions of  $\text{La}_2@\text{C}_{80}$  in the [80]fullerene cage has been investigated by using quantum chemical calculations.<sup>848</sup> An improved high-pressure toluene extraction of the lanthanum-containing fullerenes  $\text{La}@\text{C}_n$  for even  $n$  from 74 to 90 has been described.<sup>849</sup> The isolation and characterization of an endohedral metallofullerene encapsulating three lanthanide atoms inside a nanoscale  $\text{C}_{80}$  cage,  $\text{Lu}_3\text{N}@\text{C}_{80}$ , has been reported. Also described were mixed metal species of gadolinium/lutetium and holmium/lutetium,  $\text{Lu}_{3-x}\text{Ln}_x\text{N}@\text{C}_{80}$  ( $\text{Ln} = \text{Gd}, \text{Ho}; x = 0$ – $2$ ), which may prove useful as multifunctional contrast agents for X-ray, MRI, and radiopharmaceuticals.<sup>850</sup>

## 4.01.12 Heterobimetallic Compounds

### 4.01.12.1 Metal–Metal Bonded Compounds

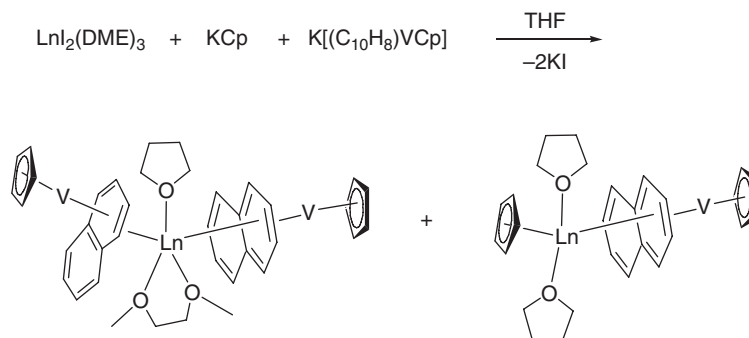
The gas-phase reactions of lanthanide ( $\text{Ln}^+ = \text{La}^+ - \text{Lu}^+$ , except  $\text{Pm}^+$ ) cations with iron pentacarbonyl,  $\text{Fe}(\text{CO})_5$ , and with ferrocene,  $\text{Cp}_2\text{Fe}$ , have been studied by Fourier transform ion cyclotron resonance mass spectrometry (FT-ICR/MS). In the case of  $\text{Fe}(\text{CO})_5$ , the observed primary products were of the type  $\text{LnFe}(\text{CO})_x^+$  ( $\text{Ln} = \text{La}, \text{Ce}, \text{Pr}, \text{Nd}, \text{Gd}, \text{Tb}$ ;  $x = 3$ ;  $\text{Ln} = \text{Ho}, \text{Er}, \text{Lu}$ ;  $x = 3$  and  $4$ ;  $\text{Ln} = \text{Sm}, \text{Eu}, \text{Dy}, \text{Tm}, \text{Yb}$ ;  $x = 4$ ), and evidence was obtained for the presence of direct  $\text{Ln}-\text{Fe}$  bonds in these species. With  $\text{Cp}_2\text{Fe}$  the majority of the  $\text{Ln}^+$  cations reacted by metal exchange, yielding  $\text{Ln}$  bis(cyclopentadienyl) ions  $\text{Cp}_2\text{Ln}^+$ , while the less reactive  $\text{Ln}^+$  cations formed the “adduct” ions  $\text{LnFeCp}_2^+$ .<sup>851</sup>

Still very little is known about isolable organolanthanide complexes containing direct  $\text{Ln}-\text{M}$  ( $\text{M}$  = transition metal) bonds. In 1993, Beletskaya *et al.* reported the synthesis of the heterobimetallic complexes  $\text{Cp}_2\text{Lu}[\text{Ru}(\text{CO})_2\text{Cp}](\text{THF})$ ,  $[\text{C}_5\text{H}_3(\text{SiMe}_3)_2]_2\text{Lu}[\text{Ru}(\text{CO})_2\text{Cp}](\text{THF})$ ,  $\text{Cp}^*_2\text{Lu}[\text{Ru}(\text{CO})_2\text{Cp}](\text{THF})$ , and  $[\text{Ru}(\text{CO})_2\text{Cp}]\text{LaI}_2(\text{THF})_3$  by metathetical reactions of the corresponding chlorolanthanide precursors with the salt  $\text{Na}[\text{Ru}(\text{CO})_2\text{Cp}]$ .<sup>852</sup> The molecular structure of  $\text{Cp}_2\text{Lu}[\text{Ru}(\text{CO})_2\text{Cp}](\text{THF})$  has been established by X-ray structure analysis. The complex was the first example of a structurally characterized compound in which there is a direct lanthanide–transition metal bond ( $\text{Lu}-\text{Ru}$  2.955 Å) without additional bridging ligands. According to IR and NMR evidence the  $\text{Ln}-\text{Ru}$  bond in all these complexes is stable in solution. The reactivity of the bimetallic compounds towards  $\text{HCl}$ ,  $\text{H}_2\text{O}$ ,  $\text{HgCl}_2$ , acetone,  $\text{MeI}$ ,  $\text{H}_2$ ,  $\text{CO}$ ,  $\text{PhMeSiH}_2$ , and  $\text{Me}_3\text{SiC}\equiv\text{CSiMe}_3$  has been investigated. Reactions of  $[\text{C}_5\text{H}_3(\text{SiMe}_3)_2]_2\text{Lu}[\text{Ru}(\text{CO})_2\text{Cp}](\text{THF})$  with  $\text{HCl}$  and  $\text{H}_2\text{O}$  led to  $\text{Lu}-\text{Ru}$  bond scission and formation of  $[\text{C}_5\text{H}_3(\text{SiMe}_3)_2]_2\text{Lu}(\mu\text{-Cl})_2$  and  $[\text{C}_5\text{H}_3(\text{SiMe}_3)_2]_2\text{Lu}(\mu\text{-OH})_2$ , respectively.<sup>852</sup>

### 4.01.12.2 Heterobimetallic Compounds without Direct Metal–Metal Bonds

The (phenylethynyl)cuprate europium complex  $\{[(\text{PhC}\equiv\text{C})_3\text{Cu}][\text{Eu}(\text{py})(\text{THF})_2]\}_2$  was synthesized by a reaction of metallic  $\text{Eu}$  with  $\text{PhC}\equiv\text{CCu}$  in pyridine. The pale yellow-brown crystals were isolated in 70% yield and structurally characterized by X-ray diffraction. In a similar manner, the ytterbium cuprate complex  $\{[(\text{PhC}\equiv\text{C})_3\text{Cu}][\text{Yb}(\text{THF})_2]\}_2$  was synthesized by the reaction of  $\text{Yb}$  metal with  $\text{PhC}\equiv\text{CCu}$  in THF in the presence of catalytic amounts of  $\text{YbI}_2$  and also by the reaction of  $(\text{PhC}\equiv\text{C})_2\text{Yb}$  with  $\text{PhC}\equiv\text{CCu}$ . The ytterbium cuprate forms red, diamagnetic crystals.<sup>853</sup> The synthesis and characterization of  $\text{Eu}(\text{II})$  and  $\text{Sm}(\text{II})$  complexes containing the (cyclopentadienyl)vanadiumnaphthalene anion have been reported. The compounds were prepared by the reaction of  $\text{LnI}_2(\text{DME})_3$  with an equimolar mixture of  $\text{KCp}$  and  $\text{KCpV}(\text{C}_{10}\text{H}_8)$  in DME followed by treatment with THF (Scheme 236). The trinuclear complexes  $[\text{CpV}(\mu_2\text{-}\eta^6\text{:}\eta^6\text{-C}_{10}\text{H}_8)]_2\text{Ln}(\text{THF})(\text{DME})$  ( $\text{Ln} = \text{Eu}, \text{Sm}$ ) consists of two  $[\text{CpV}(\text{C}_{10}\text{H}_8)]$  sandwiches, bonded  $\eta^6$  to the europium atom via the naphthalene bridges; there is no interaction between the cyclopentadienyl group and the europium or samarium. The angle  $\text{V}-\text{Eu}-\text{V}$  is  $126^\circ$ . The naphthalene ligands remain planar. The distances of the europium atoms to the carbon atoms of both  $\eta^6$ -coordinating rings are in the range of 2.84–3.02 Å. The C–C bonds in the naphthalene ring coordinated to europium are elongated and equalized compared with free naphthalene.<sup>854</sup>

Complexes of the composition  $[\text{CpV}(\mu_2\text{-}\eta^6\text{:}\eta^6\text{-C}_{10}\text{H}_8)]_2\text{Ln}(\mu_2\text{-}\eta^5\text{:}\eta^5\text{-C}_5\text{H}_5)(\text{THF})_n$  ( $\text{Ln} = \text{Sm}, \text{Eu}$ ) have first been observed as side-products in the reactions to prepare  $[\text{CpV}(\mu_2\text{-}\eta^6\text{:}\eta^6\text{-C}_{10}\text{H}_8)]_2\text{Ln}(\text{THF})(\text{DME})$ . The reaction of



Scheme 236

(C<sub>10</sub>H<sub>8</sub>)Ln(DME)<sub>2</sub> with equimolar amounts of dicyclopentadienylniobium in THF–DME results in better yields in the formation of [CpV(μ<sub>2</sub>-η<sup>6</sup>:η<sup>2</sup>-C<sub>10</sub>H<sub>8</sub>)Ln(μ<sub>2</sub>-η<sup>5</sup>:η<sup>5</sup>-C<sub>5</sub>H<sub>5</sub>)(THF)]<sub>n</sub> (Ln = Sm, Eu) (Scheme 236).<sup>854</sup>

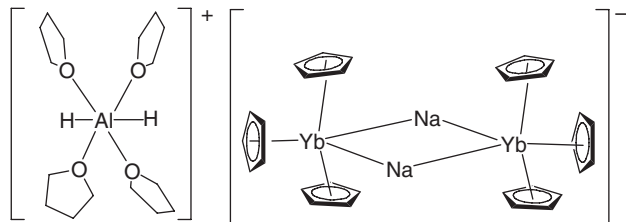
The X-ray crystal structure analysis of [CpV(μ<sub>2</sub>-η<sup>6</sup>:η<sup>2</sup>-C<sub>10</sub>H<sub>8</sub>)Ln(μ<sub>2</sub>-η<sup>5</sup>:η<sup>5</sup>-C<sub>5</sub>H<sub>5</sub>)(THF)]<sub>n</sub> shows a polymer structure, built from infinite zig-zag chains formed by Ln(μ<sub>2</sub>-η<sup>5</sup>:η<sup>5</sup>-C<sub>5</sub>H<sub>5</sub>) units. Each europium atom of this chain is further coordinated η<sup>2</sup> by the naphthalene of the [CpV(C<sub>10</sub>H<sub>8</sub>)] unit and by the oxygen of the THF.<sup>854</sup> The novel heterotrimetallic complex Li[Cp<sub>2</sub>Y(FcN)<sub>2</sub>] (FcN = 2-dimethylaminomethylferrocenyl) was obtained by the reaction of [Cp<sub>2</sub>YCl]<sub>2</sub> with 2 equiv. of 2-dimethylaminomethylferrocenyl lithium in THF. In the structure the Y atom is pseudo-tetrahedral coordinated by two η<sup>5</sup>-Cp ligands and by two η<sup>1</sup>-σ-bound cyclopentadienyl rings from the dimethylaminomethylferrocenyl groups. The Y–C(η<sup>1</sup>-σ-Cp) distance is 2.534(3) Å and the angle (η<sup>1</sup>-σ-Cp)C–Y–C(η<sup>1</sup>-σ-Cp) is 89.37(11)°. The lithium atom also has a tetrahedral arrangement formed by the two N atoms of Me<sub>2</sub>NCH<sub>2</sub> substituents and by the two C atoms of the Cp rings.<sup>855</sup>

The synthesis of the Yb/Al heterobimetallic complex [AlH<sub>2</sub>(THF)<sub>4</sub>][(μ-Na)(YbCp<sub>3</sub>)<sub>2</sub>] has been reported<sup>856</sup> (Scheme 237).

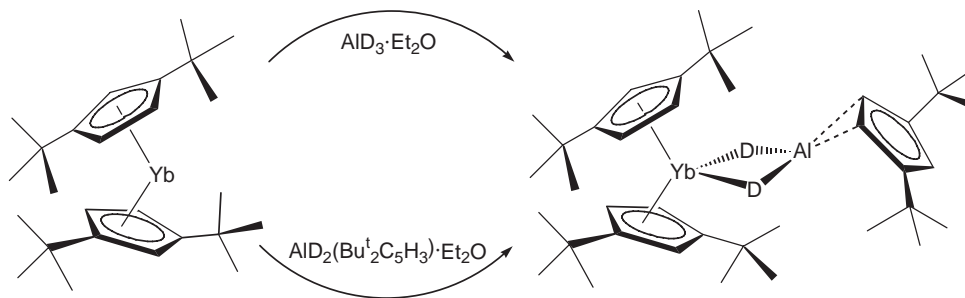
Synthetic routes to the Yb/Al complexes Cp<sup>\*</sup><sub>2</sub>Yb(AlMe<sub>4</sub>) and [Cp<sup>\*</sup><sub>2</sub>Yb(ER)(AlMe<sub>3</sub>)<sub>2</sub>]<sub>2</sub> (ER = OBu<sup>t</sup>, SPh, SC<sub>6</sub>H<sub>4</sub>Me-*p*, TePh) have been developed.<sup>857</sup> Heterometallic complexes of divalent ytterbium, Cp'<sub>2</sub>Yb (Cp' = Bu<sup>t</sup><sub>2</sub>C<sub>5</sub>H<sub>2</sub>, Cp<sup>\*</sup>), and alanes AlH<sub>3</sub>(L) (L = NEt<sub>3</sub>, THF, Et<sub>2</sub>O) have been obtained without changing the oxidation state of the ytterbium atom.<sup>858</sup> The novel heterometallic complex (η<sup>5</sup>-1,3-Bu<sup>t</sup><sub>2</sub>C<sub>5</sub>H<sub>3</sub>)<sub>2</sub>Yb(μ-D)<sub>2</sub>Al(η<sup>2</sup>-1,3-Bu<sup>t</sup><sub>2</sub>C<sub>5</sub>H<sub>3</sub>) was obtained by the reaction of (η<sup>5</sup>-1,3-Bu<sup>t</sup><sub>2</sub>C<sub>5</sub>H<sub>3</sub>)<sub>2</sub>Yb·OEt<sub>2</sub> with AlD<sub>3</sub>·Et<sub>2</sub>O or AlD<sub>2</sub>(η<sup>2</sup>-1,3-Bu<sup>t</sup><sub>2</sub>C<sub>5</sub>H<sub>3</sub>)·Et<sub>2</sub>O in diethyl ether (Scheme 238). This complex containing a Yb<sup>2+</sup> and a three-coordinated Al cation is stable due to the interaction of π-electrons of the allyl group of the η<sup>2</sup>-bonded Cp ring with an unoccupied orbital of the aluminum atom.<sup>467</sup>

The heterobimetallic complex [(C<sub>5</sub>Me<sub>4</sub>Et)<sub>2</sub>Sm(μ-Me)AlMe<sub>3</sub>]<sub>2</sub> is easily formed by the reaction of the THF adduct of bis[(ethyltetramethylcyclopentadienyl)]samarium(II) with AlMe<sub>3</sub> (Scheme 239).<sup>585</sup>

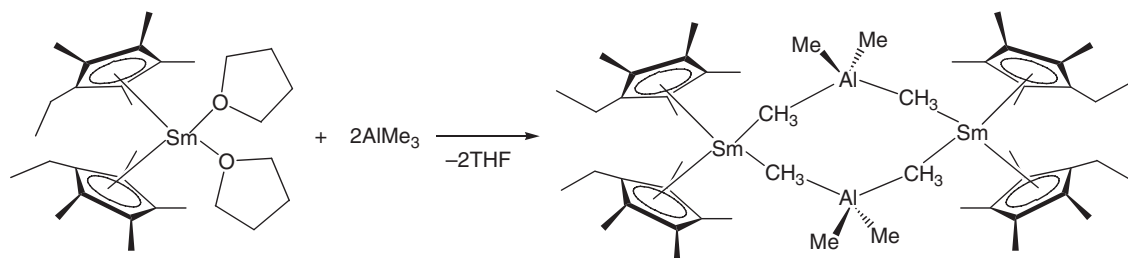
Similarly, C<sub>2</sub>-symmetric tetraalkylaluminate complexes *rac*-[Me<sub>2</sub>(2-MeC<sub>9</sub>H<sub>5</sub>)<sub>2</sub>]Y(μ-R)AlR<sub>2</sub> (R = Me, Et, Bu<sup>i</sup>) are quantitatively formed upon treatment of the corresponding indenyl-derived *ansa*-lanthanidocene bis(dimethylsilylamides) with AlR<sub>3</sub>.<sup>859</sup> The homoleptic rare earth carboxylate complexes [Ln(O<sub>2</sub>CC<sub>6</sub>H<sub>2</sub>Pr<sup>i</sup><sub>3-2,4,6</sub>)<sub>3</sub>]<sub>n</sub> (Ln = Y, La, Nd, Lu) react with trimethylaluminum to yield hexane-soluble monolanthanide complexes featuring an η<sup>2</sup>-coordinated tetraalkylaluminate ligand and a novel ancillary AlMe<sub>2</sub>-bridged bis(carboxylate) ligand (Scheme 240). The Nd derivative has been structurally characterized by X-ray diffraction.<sup>860</sup>



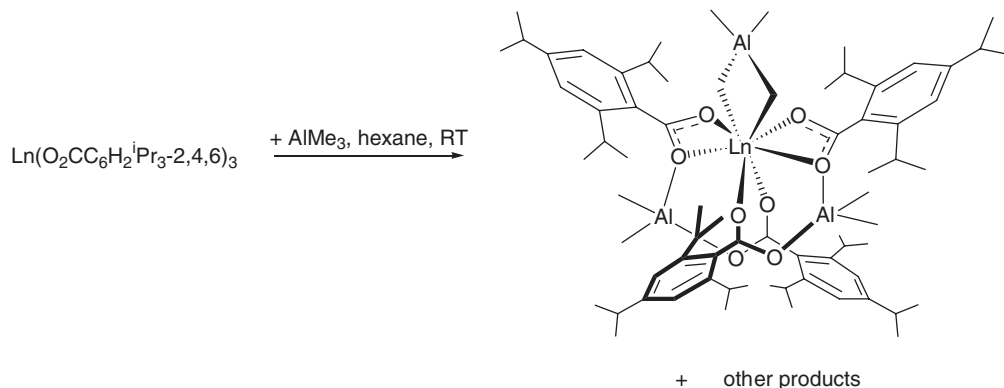
Scheme 237



Scheme 238



Scheme 239

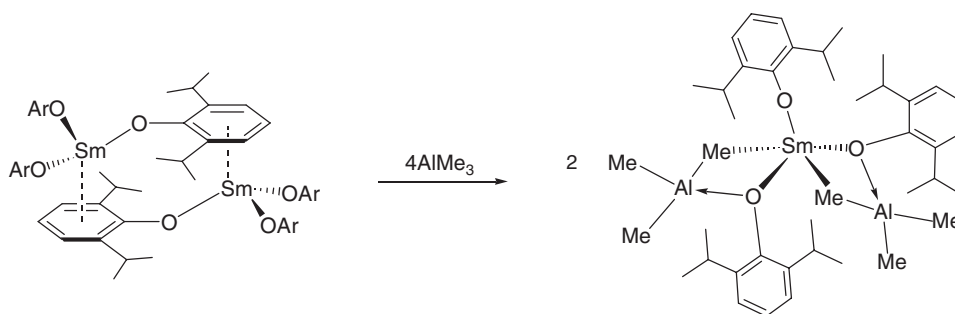


Scheme 240

Bimetallic Ln/Al complexes of the type Ln[(μ-OBu<sup>t</sup>)(μ-Me)AlMe<sub>2</sub>]<sub>3</sub> have been obtained from the reaction of Ln(Obu<sup>t</sup>)<sub>3</sub> with 3 equiv. of trimethylaluminum.<sup>861</sup> Treatment of the homoleptic aryloxides Ln(OAr)<sub>3</sub> (Ar = 2,6-Bu<sup>t</sup>-4-MeC<sub>6</sub>H<sub>2</sub>) with 4 equiv. of trialkylaluminum leads to the formation of the bis-trialkylaluminum adducts (ArO)Ln[(μ-OAr)(μ-R)AlR<sub>2</sub>]<sub>2</sub> (Ln = La, R = Me; Ln = La, Sm, R = Et), which have been structurally characterized by X-ray analyses.<sup>862</sup> The analogous reaction of Sm(OAr)<sub>3</sub> (Ar = 2,6-Pr<sup>i</sup>-4-MeC<sub>6</sub>H<sub>2</sub>) with 4 equiv. of trimethylaluminum led to the formation of the bis-trimethylaluminum adduct (ArO)Sm[(μ-OAr)(μ-Me)AlMe<sub>2</sub>]<sub>2</sub> (Scheme 241), which exhibits very short Sm–C(bridging) distances of 2.620(5) and 2.632(5) Å. A reduced <sup>1</sup>J<sub>C–H</sub> coupling constant of 106 Hz and a low ν(C–H) stretch in the solution, and solid-state IR spectrum are indicative of a strong agostic Sm···H–C interaction in solution.<sup>863</sup>

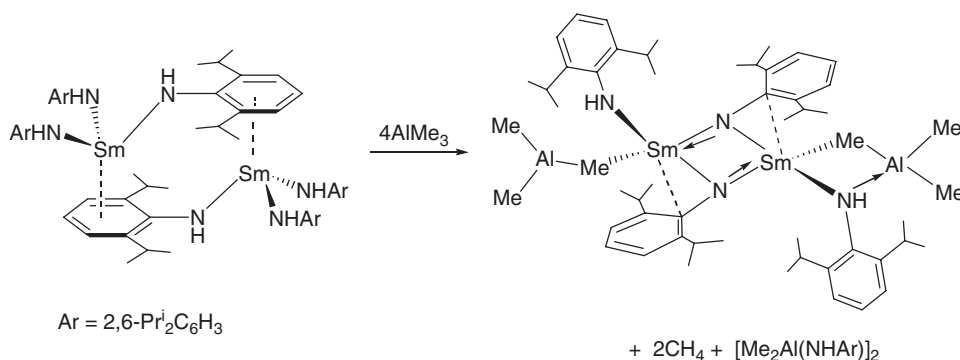
Similar treatment of the dimeric arylimido complex [Sm(NHAr)<sub>3</sub>]<sub>2</sub> (Ar = 2,6-Pr<sup>i</sup>-4-MeC<sub>6</sub>H<sub>2</sub>) with trimethylaluminum resulted in an unusual imido-bridged heterobimetallic samarium–aluminum complex (Scheme 242).<sup>795,864</sup>

A novel type of metallotropic tautomerism, that is, reversible and equilibrium isomerization of η<sup>5</sup>-bis(Me<sub>3</sub>Si-fluorenyl)-rare earth metal complexes to η<sup>5</sup>-bis(Me<sub>3</sub>Si-fluorene-AIR<sub>3</sub>)-rare earth metal complexes, has been reported.



Scheme 241



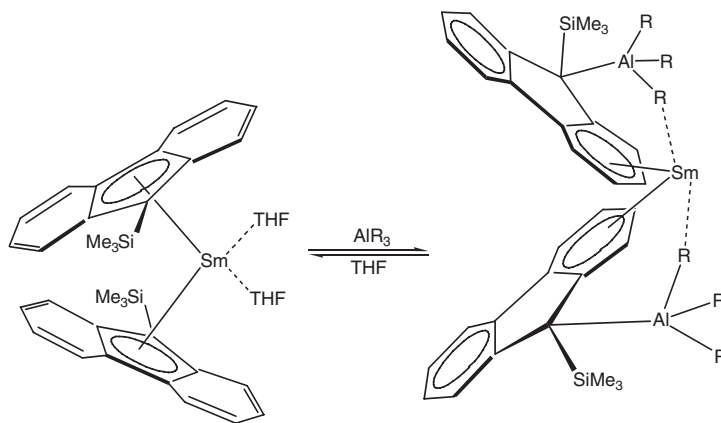


Scheme 242

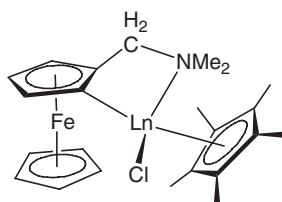
This metallotropic tautomerism was realized by the addition of AlR<sub>3</sub> to the former complexes.  $\eta^6$ -Bis(Me<sub>3</sub>Si-fluorenyl)-AlMe<sub>3</sub>Sm was synthesized by the reaction of  $\eta^5$ -bis(Me<sub>3</sub>Si-fluorenyl)Sm(THF)<sub>2</sub> with excess AlMe<sub>3</sub>. The corresponding reaction of excess AlEt<sub>3</sub> with  $\eta^5$ -bis(Me<sub>3</sub>Si-fluorenyl)Sm(THF)<sub>2</sub> gave  $\eta^6$ -bis(Me<sub>3</sub>Si-fluorenyl)-AlEt<sub>3</sub>Sm (Scheme 243).<sup>671,865</sup>

The mixed metal complexes [PPh<sub>4</sub>][(Cp\*<sub>2</sub>Sm)<sub>2</sub>Mo(μ-S)<sub>4</sub>] and [PPh<sub>4</sub>][Cp\*<sub>2</sub>Sm(μ-S)<sub>2</sub>WS<sub>2</sub>] were obtained by the reaction of Cp\*<sub>2</sub>Sm(THF)<sub>2</sub> with (PPh<sub>4</sub>)<sub>2</sub>MoS<sub>4</sub> and (PPh<sub>4</sub>)<sub>2</sub>WS<sub>4</sub>. According to the X-ray structure, the anion [(Cp\*<sub>2</sub>Sm)<sub>2</sub>Mo(μ-S)<sub>4</sub>]<sup>−</sup> contains two essentially identical Cp\*<sub>2</sub>Sm(μ-S)<sub>2</sub> units with eight-coordinated Sm(III) atoms. The Sm–S distances are 2.784(2)–2.796(2) Å. In the structure of [Cp\*<sub>2</sub>Sm(μ-S)<sub>2</sub>WS<sub>2</sub>]<sup>−</sup> the Sm atom is bound with the tungsten center by two bridging sulfur atoms. The Sm–S distances are 2.817(8)–2.841(7) Å.<sup>866</sup> Reactions of 2-(dimethylaminomethyl)ferrocenyl-lithium (=Li(FcN)) with various cerium(IV) precursors led to the formation of heterobimetallic organocerium(III) complexes. The compounds Li<sub>3</sub>[(FcN)<sub>2</sub>CeF<sub>4</sub>(THF)<sub>3</sub>], (FcN)<sub>2</sub>CeF(DME)<sub>2</sub>, Li<sub>4</sub>[(FcN)CeCl<sub>6</sub>], and Li[(FcN)CeCl<sub>3</sub>(DME)] have been isolated from such redox reactions. Several mono(pentamethylcyclopentadienyl) lanthanide complexes containing the FcN ligand have also been synthesized and characterized. Treatment of Cp\*<sub>2</sub>Ln(μ-Cl)<sub>2</sub>K(THF)<sub>2</sub> with 1 equiv. of Li(FcN) afforded the neutral heterobimetallic species Cp\*<sub>2</sub>Ln(FcN)Cl (Ln = Ce, Pr, Nd, Sm; Scheme 244) via displacement of one Cp\* ligand. These lanthanide FcN complexes have been studied by Mößbauer spectroscopy.<sup>867</sup> In a similar manner the thermally stable heterobimetallic FcN derivatives CpSm(FcN)Cl, Cp<sub>2</sub>Sc(FcN), Cp\*Y(FcN)Cl, and Cp\*<sub>2</sub>Sm(FcN) have been prepared by a reaction of the corresponding chloro precursors with Li(FcN).<sup>868,869</sup>

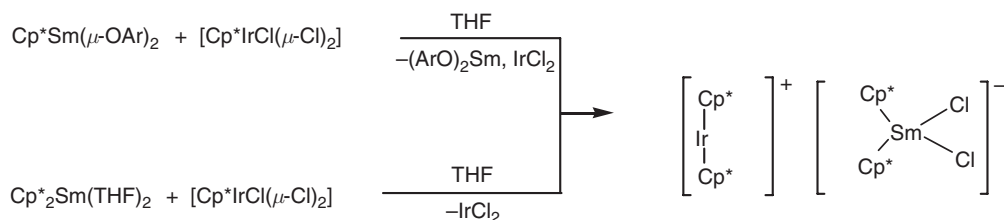
The reaction of Cp\*<sub>2</sub>Sm(μ-OAr)<sub>2</sub> (Ar = 2,6-Bu<sup>t</sup>-4-MeC<sub>6</sub>H<sub>2</sub>) or Cp\*<sub>2</sub>Sm(THF)<sub>2</sub> with equivalent amounts of [Cp\*<sub>2</sub>IrCl(μ-Cl)]<sub>2</sub> in THF gave the heterometallic dimer “ate” complex iridocenium dichloro-bis(pentamethylcyclopentadienyl)samarate [Cp\*<sub>2</sub>Ir]<sup>+</sup>[Cp\*<sub>2</sub>SmCl<sub>2</sub>]<sup>−</sup> (Scheme 245). The complex represents the first example of a structurally characterized “free” metallocenium lanthanocene dihalide complex which consists of a [Cp\*<sub>2</sub>SmCl<sub>2</sub>]<sup>−</sup> anion and a [Cp\*<sub>2</sub>Ir]<sup>+</sup> cation.<sup>870</sup>



Scheme 243



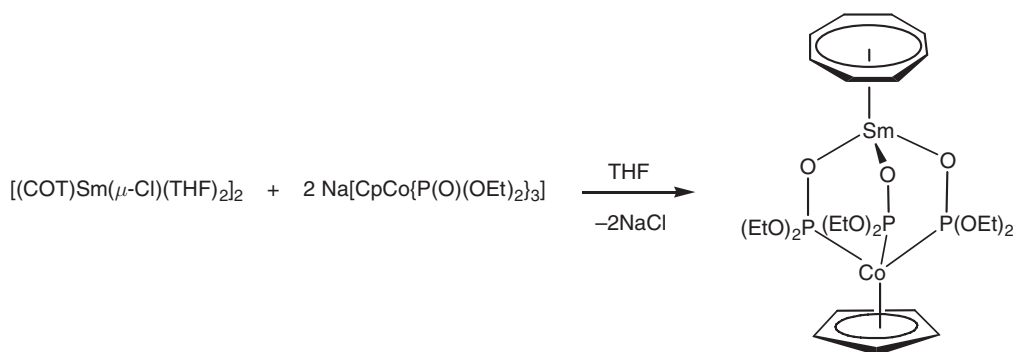
Scheme 244



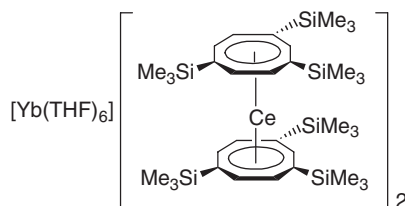
Scheme 245

Reactions of  $\text{Cp}^*_2\text{Yb}$  with  $\text{cis-P}_2\text{PtX}_2$  complexes ( $\text{P}_2$ =chelating phosphine;  $\text{X}=\text{H}, \text{Me}$ ) have been carried out. The complexes  $(\text{cis-Bu}^i_2\text{PCH}_2\text{CH}_2\text{P}^i\text{Bu}^i_2)\text{Pt}(\mu\text{-H})_2\text{YbCp}^*_2$ ,  $(\text{cis-Cy}_2\text{PCH}_2\text{CH}_2\text{PCy}_2)\text{Pt}(\mu\text{-H})_2\text{YbCp}^*_2$ ,  $(\text{cis-Pr}^i_2\text{PCH}_2\text{CH}_2\text{PP}^i\text{R}^i_2)\text{Pt}(\mu\text{-Me})_2\text{YbCp}^*_2$ ,  $(\text{cis-Pr}^i_2\text{PCH}_2\text{CH}_2\text{PP}^i\text{R}^i_2)\text{Pt}(\mu\text{-Me})(\mu\text{-H})\text{YbCp}^*_2$  have been investigated by NMR spectroscopy. The two latter compounds were characterized also by their X-ray structures. In the structure of  $(\text{cis-Pr}^i_2\text{PCH}_2\text{CH}_2\text{PP}^i\text{R}^i_2)\text{Pt}(\mu\text{-Me})_2\text{YbCp}^*_2$  the Pt and Yb atoms are bound by the two bridging methyl groups. The  $\text{Pt} \cdots \text{Yb}$  separation is 4.0391(5) Å, the  $\text{Yb-C}(\mu\text{-CH}_3)$  distances are 2.908(8) and 2.88(1) Å, and the  $\text{Pt-C-Yb}$  angles are 106.8(3)° and 107.5(4)°. An agostic  $\text{C-H} \cdots \text{Yb}$  bonding mode has been found for the bridging methyl groups. The  $\text{Yb-H}(\mu\text{-CH}_3)$  distances are ranging from 2.30 to 3.80 Å. For the structure of  $(\text{cis-Pr}^i_2\text{PCH}_2\text{CH}_2\text{PP}^i\text{R}^i_2)\text{Pt}(\mu\text{-Me})(\mu\text{-H})\text{YbCp}^*_2$  the hydrogen atoms on the bridging methyl group and the hydride ligand were not located. In the structure the  $\text{Pt-Yb}$  separation is 3.388(9) Å and the  $\text{Yb-C}(\mu\text{-Me})$  distance is 2.79(2) Å. In contrast to the agostic interactions observed for the previous structure, structural parameters for the  $(\text{cis-Pr}^i_2\text{PCH}_2\text{CH}_2\text{PP}^i\text{R}^i_2)\text{Pt}(\mu\text{-Me})(\mu\text{-H})\text{YbCp}^*_2$  were found to be consistent with a  $\text{Pt-C-Yb}$  interaction.<sup>871</sup> The weak interactions of  $\text{Cp}^*_2\text{Yb}$  and  $\text{cis-dihydrido}$  platinum complexes in solution have been investigated using multinuclear NMR spectroscopy.  $\text{Cp}^*_2\text{Yb}$  formed 1:1 adducts with the  $\text{cis-dihydrido}$  complexes  $\text{P}_2\text{PtH}_2$  [ $\text{P}_2 = \text{Cy}_2\text{P}(\text{CH}_2)_2\text{PCy}_2$ ,  $\text{Cy}_2\text{P}(\text{CH}_2)_3\text{PCy}_2$ ] that undergo slow intermolecular exchange at 25 °C on the NMR timescale. There are significant perturbations in the spectral values from those of the free  $\text{P}_2\text{PtH}_2$  complexes, and JYBX coupling ( $\text{X} = {}^1\text{H}, {}^{31}\text{P}, {}^{195}\text{Pt}$ ) is present. The interactions of  $\text{Cp}^*_2\text{Yb}$  with  $\text{Ph}_2\text{P}(\text{CH}_2)_2\text{PPh}_2\text{PtMe}_2$  and  $\text{Ph}_2\text{P}(\text{CH}_2)_2\text{PPh}_2\text{Pt}(\text{H})\text{Me}$  have also been investigated.<sup>872</sup>

The bis(tetramethylphospholyl)ytterbium carbene complex  $(\text{Tmp})_2\text{Yb}[\text{C}_2\text{Me}_2(\text{NPr}^i)_2\text{C}]$  reacts in benzene- $d_6$  with  $\text{RuH}_4(\text{PPh}_3)_3$  to give the moderately stable heterobimetallic dihydride  $(\text{PPh}_3)_2\text{RuH}_2(\mu\text{-Tmp})_2\text{Yb}[\text{C}_2\text{Me}_2(\text{NPr}^i)_2\text{C}]$ .<sup>731</sup> The diphenylphosphinocyclopentadienyl ligand has been established as a useful tool for the assembly of heterobimetallic lanthanide/transition metal complexes. The synthesis of three bis(diphenylphosphinocyclopentadienyl)yttrium chloride complexes and the heterobimetallic derivative  $[(\text{CO})_4\text{Mo}(\text{C}_5\text{H}_4\text{PPh}_2)_2\text{Y}(\mu\text{-Cl})]_2$  has been reported. The X-ray structure of  $[(\text{C}_5\text{H}_4\text{PPh}_2)_2\text{Y}(\mu\text{-Cl})]_2$  is remarkable in that the crystal exhibits two independent chloride-bridged dimers that differ in the arrangement (*syn*, *anti*) of the diphenylphosphino groups.<sup>873</sup> The ionic Ln/Co heterobimetallic complexes  $[(\text{C}_5\text{H}_4\text{CH}_2\text{CH}_2\text{OMe})_2\text{Ln}(\text{THF})][\text{Co}(\text{CO})_4]$  ( $\text{Ln} = \text{Sm}, \text{Yb}$ ) have been obtained either by the reaction of  $[(\text{C}_5\text{H}_4\text{CH}_2\text{CH}_2\text{OMe})_2\text{LnI}]$  with  $\text{K}[\text{Co}(\text{CO})_4]$  or by the one-electron oxidation of  $(\text{C}_5\text{H}_4\text{CH}_2\text{CH}_2\text{OMe})_2\text{Ln}(\text{THF})$  with  $\text{Co}_2(\text{CO})_8$ .<sup>874</sup> The reaction of bis(diphenylphosphinocyclopentadienyl)ytterbium(II) with tungsten hexacarbonyl in THF yielded  $\text{Yb}(\text{THF})_3(\text{C}_5\text{H}_4\text{PPh}_2)_2\text{W}(\text{CO})_4 \cdot 0.5\text{THF}$  as red crystals, whereas dark red  $\text{Yb}(\text{THF})(\text{C}_5\text{H}_4\text{PPh}_2)_2(\mu\text{-OC})\text{W}(\text{CO})_3$  was obtained when the same reaction was carried out in boiling toluene. Heating of  $\text{Yb}(\text{THF})_3(\text{C}_5\text{H}_4\text{PPh}_2)_2\text{W}(\text{CO})_4 \cdot 0.5\text{THF}$  also led to elimination of two THF molecules and conversion to the isocarbonyl-bridged compound.<sup>875</sup> Treatment of an equimolar mixture of  $\text{Na}_2\text{W}(\text{CO})_5$  and  $\text{Na}_2\text{W}_2(\text{CO})_{10}$  in DME unexpectedly resulted in the formation of  $[\text{Na}(\text{DME})_3]_2[\text{W}_3(\text{CO})_{14}]$  without incorporation of lutetium.<sup>876</sup> Reactions



Scheme 246



Scheme 247

of  $[\text{Cp}^*_2\text{Ln}(\mu\text{-H})_2]$  ( $\text{Ln}=\text{Y}, \text{Sm}$ ) with  $\text{Cp}_2\text{WH}_2$  afforded bimetallic complexes of the type  $\text{Cp}^*_2\text{Ln}(\mu\text{-C}_5\text{H}_4)(\mu\text{-H})_2\text{WCp}$  containing a metallated cyclopentadienyl ring.<sup>608</sup>

The reaction of  $[(\text{COT})\text{Sm}(\mu\text{-Cl})(\text{THF})_2]_2$  with  $\text{Na}[\text{CpCo}\{\text{P}(\text{O})(\text{OEt})_2\}_3]$  in a molar ratio of 1:2 in THF solution afforded orange  $(\text{COT})\text{Sm}[\text{CpCo}\{\text{P}(\text{O})(\text{OEt})_2\}_3]$  as the first organolanthanide containing Kläui's tripod ligand (Scheme 246).<sup>877,877a</sup>

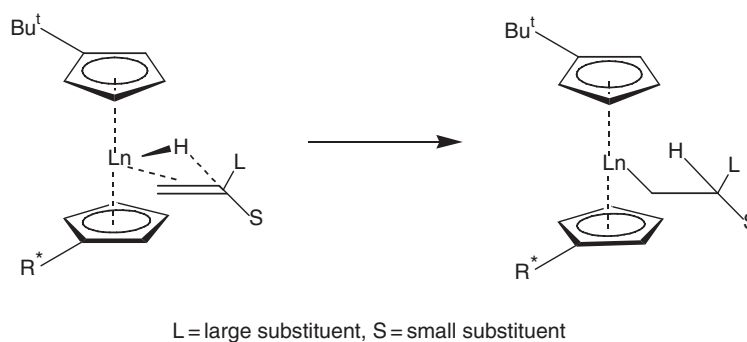
The first heterobimetallic organolanthanide complex containing two different rare earth elements  $[\text{Yb}(\text{THF})_6][\text{Ce}(\text{COT}')_2]_2$  ( $\text{COT}' = \eta^8\text{-C}_8\text{H}_5(\text{SiMe}_3)_3\text{-1,3,6}$ ) (Scheme 247) has been prepared in the form of a bright green crystalline solid by reacting the neutral cerocene derivative  $(\text{COT}')_2\text{Ce}$  with ytterbium metal in THF.<sup>877,877a</sup>

#### 4.01.13 Organolanthanide Catalysis

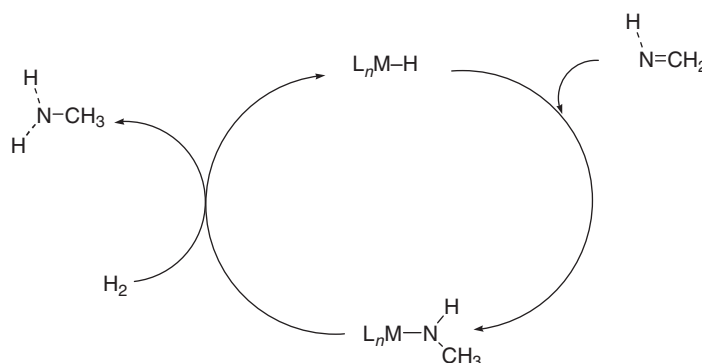
Asymmetric catalysis with lanthanide complexes, including organometallic compounds, has been reviewed by Mikami *et al.*<sup>17,17a</sup> A review on asymmetric catalysis and amplification with chiral lanthanide complexes has been published by Inanaga *et al.*<sup>31</sup> Organo-rare-earth-metal initiated living polymerizations of polar and non-polar monomers have been highlighted by Yasuda.<sup>43</sup> An account on synthesis, structural characterization, and catalytic behavior of one-carbon-bridged fluorenyl cyclopentadienyl lanthanocene complexes with  $C_s$ - and  $C_1$ -symmetry has been published by Qian *et al.*<sup>41</sup> Molander *et al.* reviewed the use of lanthanocene catalysts in selective organic synthesis.<sup>37</sup> Okuda reported on rare earth metal-based catalysts for the polymerization of non-polar and polar monomers.<sup>278</sup> "Lanthanide metallocenes in homogeneous catalysis" have been reviewed by Edelmann.<sup>878</sup>

##### 4.01.13.1 Organolanthanide-catalyzed Hydrogenation Reactions

A DFT study of H-H activation by  $\text{Cp}_2\text{LnH}$   $d_0$ -complexes has been published.<sup>879</sup> Asymmetric hydrogenation of unfunctionalized olefins by enantiomerically pure organolanthanides of the type  $(R,S)\text{-Me}_2\text{Si}(\text{Bu}^t\text{C}_5\text{H}_4)[(+)\text{-neomenthylC}_5\text{H}_4]\text{LnCH}(\text{SiMe}_3)_2$  ( $\text{Ln}=\text{Y}, \text{Lu}$ ) has been investigated.<sup>650,880</sup> These complexes represent a second generation of asymmetric organolanthanide catalysts employing a new type of potentially pseudo- $C_2$ -symmetric ligation, and the results of this study offer an interesting contrast to the other known classes of diastereomerically pure asymmetric organolanthanide catalysts. The unfunctionalized olefins are typically difficult substrates to



Scheme 248



Scheme 249

hydrogenate/deuterate with substantial enantioselectivity. In the frontal approach of the olefin, the large substituent (L) of olefin would be oriented *syn* to the Bu<sup>t</sup> substituent and *anti* to the bulkier (+)-neomenthyl group. The ee values obtained for 1-pentene were up to 63% (Scheme 248).<sup>650</sup>

The Cp'<sub>2</sub>Ln/Me<sub>2</sub>SiCp''<sub>2</sub>Ln-catalyzed hydrogenation of acyclic imines has been reported to yield the corresponding amines (Scheme 249).<sup>620</sup>

Selective hydrogenation of conjugated diolefin polymers, especially co-polymers with alkenylaromatic hydrocarbons, has been achieved by treatment of the polymers with hydrogen in the presence of a catalyst comprising Cp\*<sub>2</sub>LnR (R = H, alkyl, aryl) and an alkali metal promoter.<sup>881</sup>

#### 4.01.13.2 Organolanthanide-catalyzed Oligomerization Reactions

Ethylene oligomers with  $\bar{M}_n$  up to 2500 Da and narrow molecular weight distributions have been prepared using *in situ* combinations between a chloroneodymocene precursor such as Cp\*<sub>2</sub>Nd(μ-Cl<sub>2</sub>)Li(OEt<sub>2</sub>)<sub>2</sub> and a dialkylmagnesium reagent.<sup>882</sup> Selective dimerization of butanal to butyl butyrate is catalyzed by (C<sub>5</sub>H<sub>4</sub>Bu<sup>t</sup>)<sub>2</sub>LnCl (Ln = Yb, Er), (C<sub>5</sub>H<sub>4</sub>Me)<sub>2</sub>YbCl, (C<sub>5</sub>H<sub>4</sub>Bu<sup>t</sup>)LnCl<sub>2</sub> (Ln = Yb, Nd), or (C<sub>5</sub>H<sub>4</sub>Me)YbCl<sub>2</sub> together with *n*-BuLi at 0 °C. The yields of butyl butyrate were found to be dependent on the lanthanocene complex structures.<sup>883</sup> A wide variety of aldehydes are efficiently dimerized to esters by a catalytic amount of Cp\*<sub>2</sub>LnCH(SiMe<sub>3</sub>)<sub>2</sub> (Ln = Nd, La). The neodymium catalysts were also applied to polyester synthesis starting with aromatic dialdehydes.<sup>884</sup> Organolanthanide complexes such as (MeC<sub>5</sub>H<sub>4</sub>)<sub>3</sub>Yb, (MeC<sub>5</sub>H<sub>4</sub>)<sub>2</sub>YbOR, and (MeC<sub>5</sub>H<sub>4</sub>)<sub>2</sub>SmSPh have been found to serve as efficient catalyst precursors for the Aldol–Tishchenko reaction of butanal to give 2-ethyl-1,3-hexanediol monobutyrate in good to high yields under mild conditions. The yields are influenced by the structure of the organolanthanide complexes and the reaction conditions. The yield of trimerization of butanal can reach 85% under certain conditions.<sup>885</sup> The oligomerization of 2-cycloalken-1-ones is catalyzed by organolanthanide hydrides of the type [Cp\*<sub>2</sub>LnH]<sub>2</sub> (Ln = Y, La). It was found that [Cp\*<sub>2</sub>La(μ-H)]<sub>2</sub> showed a higher activity (≥150 mmol monomer per mol precatalyst per hour at 25 °C) than the yttrium analog (≤100 h<sup>-1</sup>). The average degree of oligomerization of 2.7–3.5 at 25 °C increased at higher reaction temperature (by 15 at 100 °C). The

hydrides  $[\text{Cp}^*_2\text{Ln}(\mu\text{-H})_2]$  ( $\text{Ln}=\text{Y}, \text{La}$ ) are active catalysts for the oligomerization of 2-cyclohexen-1-one.<sup>886</sup> Silyl-substituted *ansa*-neodymocenes have been utilized as catalysts for the oligomerization of ethylene ( $\bar{M}_n=400\text{--}5000$  Da) and 1-octene ( $\bar{M}_n=400\text{--}1300$  Da).<sup>641</sup> Different types of organolanthanide complexes have been found to catalyze the oligomerization of phenylisocyanate.<sup>887</sup> A novel Z-selective head-to-head dimerization of terminal alkynes has been achieved with the use of “constrained-geometry” lanthanide half-sandwich complexes as catalysts.<sup>888</sup>

#### 4.01.13.3 Organolanthanide-catalyzed Cyclization Reactions

In the presence of  $\text{Cp}_2\text{LnX}\text{--}\text{HgCl}_2$ , the treatment of  $\text{RC}\equiv\text{CCH}_2\text{Br}$  with Mg leads to the formation of benzene derivatives  $\text{C}_6\text{H}_4\text{R}_2\text{--}1,2$  ( $\text{R}=\text{H}, \text{Ph}$ ) in moderate yield. This reaction provides a new method for the construction of the benzene ring skeleton. A plausible reaction pathway is given in Scheme 250.<sup>889</sup>

Samarium(II) complexes or  $\text{Sm}(\text{II})/n$ -hexylamine systems were found to be efficient catalysts for cyclotrimerization of aryl nitriles. A variety of nitriles can be converted into the corresponding substituted *s*-triazines under mild conditions in good to high yields by using  $\text{Sm}(\text{II})$  complexes/*n*-hexylamine as catalysts. The same reaction catalyzed by samarium(II) complexes alone gives *s*-triazines in moderate yields. Among the  $\text{Sm}(\text{II})$  catalysts employed were  $\text{SmI}_2$  (Scheme 251) and  $(\text{C}_5\text{H}_4\text{Me})_2\text{Sm}$ .<sup>890</sup>

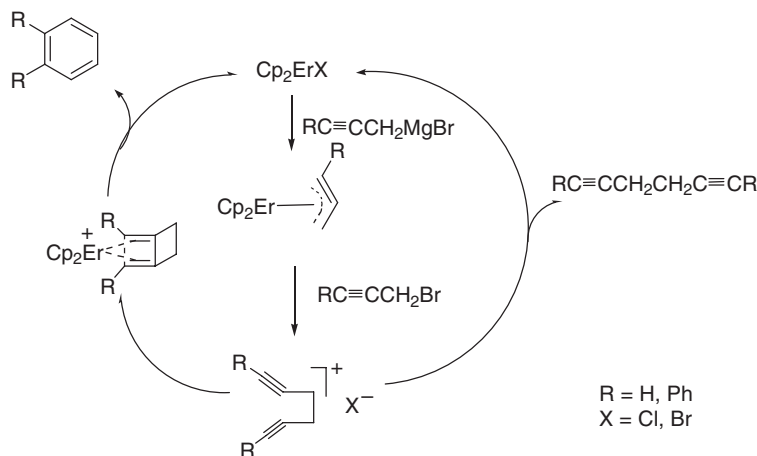
#### 4.01.13.4 Organolanthanide-catalyzed Polymerization Reactions

##### 4.01.13.4.1 Reviews

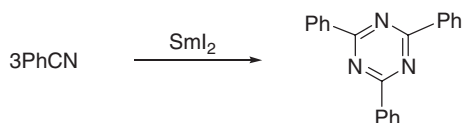
Organolanthanides of several classes were examined by Bochkarev *et al.* as potential styrene and propene polymerization catalysts.<sup>891</sup> “Developments of rare earth metal catalysts for olefin polymerization” have been highlighted by Yasuda *et al.*<sup>195</sup>

##### 4.01.13.4.2 Monoolefins

Quantum chemical investigations of the initial steps of the yttrium-mediated polymerization of ethylene and propene have been presented. The authors investigated the mechanistic details of the initial step of the polymerization brought about by a di(cyclopentadienyl)yttriumhydride catalyst using approximate DFT. In accord with the experimental



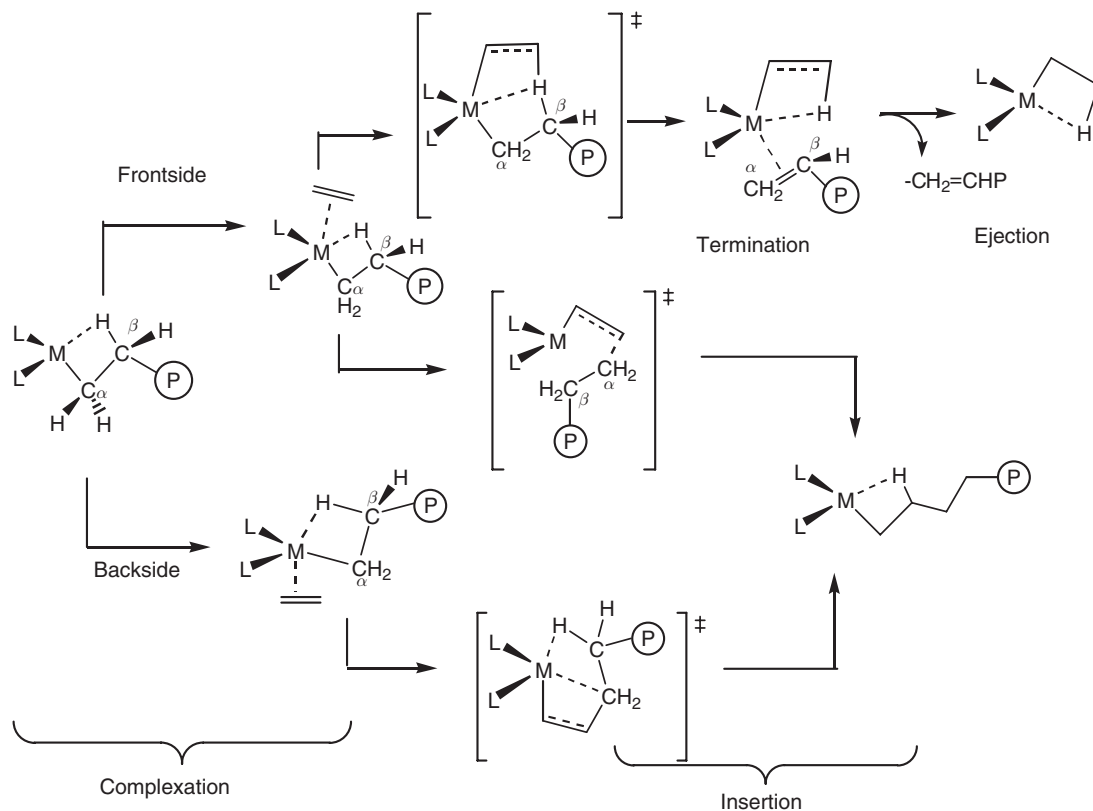
Scheme 250



Scheme 251

information, the overall reaction sequences  $\text{Cp}_2\text{YH} + \text{C}_2\text{H}_4 \rightarrow \text{Cp}_2\text{Y}-\text{C}_2\text{H}_5$  and  $\text{Cp}_2\text{YH} + \text{C}_3\text{H}_6 \rightarrow \text{Cp}_2\text{Y}-\text{C}_3\text{H}_7$  were computed to be exothermic by approximately 22.2 and 20.8 kcal mol<sup>-1</sup>, respectively.<sup>892</sup> Ethylene insertion into the Sm–C bond of  $\text{H}_2\text{SiCp}_2\text{SmCH}_3$ , a model reaction of an olefin polymerization propagation step, has been studied using *ab initio* molecular orbital methods. The low electronegativity of the samarium atom makes the Sm–C bond ionic, the methyl group being charged by –0.75. The reaction passes through a loose ethylene complex with a binding energy of 15 kcal mol<sup>-1</sup> and then a tight four-centered transition state with an agostic interaction between the Sm atom and one of the methyl CH bonds. A small activation energy of 14 kcal mol<sup>-1</sup> is required to pass through this transition state, indicating that this is an easy reaction. Compared with reactions involving group 4 cationic silylene-bridged metallocenes the activation energy is higher, and the reaction is less exothermic.<sup>893</sup>

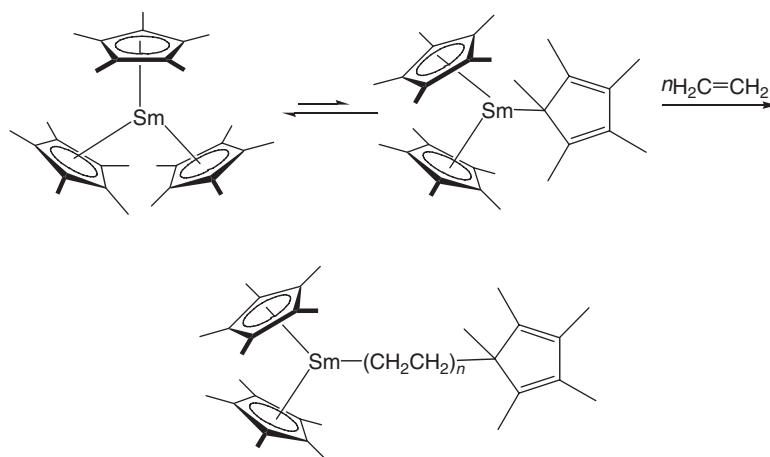
A detailed study addressed the question why propene is not polymerized by  $[\text{Cp}^*_2\text{Y}(\mu\text{-H})]_2$ . Yttrium alkyl complexes of the type  $\text{Cp}^*_2\text{YR}$  react with C–H bonds of 1-alkenes to form either yttrium allyl or yttrium vinyl complexes. Less substituted alkenes react faster, consistent with prior alkene coordination. The selectivity of the reaction of  $\text{Cp}^*_2\text{YR}$  with C–H bonds is allylic  $\text{CH}_3 \gg$  vinyl C–H  $\gg$  allylic  $\text{CH}_2$ . Propene is readily metallated by  $\text{Cp}^*_2\text{YR}$  giving the  $\eta^3$ -allyl complex  $\text{Cp}^*_2\text{Y}(\eta^3\text{-CH}_2\text{CHCH}_2)$ , which does not react further with propene. This explains why the complexes  $\text{Cp}^*_2\text{YR}$  (R = H, alkyl) make poor propene polymerization catalysts.<sup>894</sup> The same problem has also been investigated using approximate DFT.<sup>895</sup> Molecular modeling has been utilized to study the regioselectivity in the propene polymerization with *ansa*-metallocenes of scandium and yttrium.<sup>896</sup> Various other theoretical investigations on lanthanide-based olefin polymerization catalysts have been carried out.<sup>897–899</sup> A systematic study of ethylene polymerization catalyzed by  $d^0$  and  $d^0f^n$  transition metals has been carried out on the complexation of ethylene to a number of  $d^0$   $[\text{L}]\text{MC}_2\text{H}_5^{0,+2+}$  fragments [M = Y(III), La(III), Lu(III), Ce(IV), and Th(IV)]; L =  $\text{Cp}_2^{2-}$ , where a hydrogen atom on the  $\beta$ -carbon of the ethyl unit is bound to the metal by an agostic interaction. The relative preference for front side (ethylene *syn* to  $\beta$ -agostic bond) versus backside (ethylene *anti* to  $\beta$ -agostic bond) coordination by the olefin as a function of the central atom, the auxiliary ligand set L, and the strength of the  $\beta$ -agostic bond has been discussed. It was found that the  $\beta$ -agostic bond strength in the  $[\text{L}]\text{MC}_2\text{H}_5$  precursor follows the order  $\text{Y} \geq \text{La} > \text{Lu}$  (Scheme 252).<sup>900</sup>



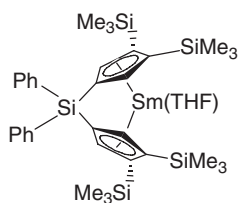
Scheme 252

The samarium-catalyzed polymerization of ethylene under hydrogen has been studied using field desorption mass spectrometry (FD-MS). The complexes  $\text{Cp}^*_2\text{Sm}$ ,  $\text{Cp}^*_2\text{Sm}(\text{THF})_2$ ,  $[\text{Cp}^*_2\text{Sm}(\mu\text{-H})]_2$ ,  $[\text{Cp}^*_2\text{Sm}]_2(\mu\text{-PhCHCHPh})$ ,  $[\text{Cp}^*_2\text{Sm}]_2(\mu\text{-PhC}_2\text{Ph})$ , and  $(\mu\text{-PhC}_4\text{Ph})[\text{Cp}^*_2\text{Sm}]_2(\mu\text{-PhC}_4\text{Ph})$  were investigated as catalysts. Polymerization reactions of propene, 1-pentene, *cis*- and *trans*-2-pentene, 1-heptene, *trans*-2-heptene, *trans*-3-heptene, 1-octene, and 1-nonadecene with ethylene under  $\text{H}_2$  and with  $\text{CD}_2=\text{CD}_2$  under  $\text{D}_2$  were studied as well as reactions of ethylene with propene- $d_6$  and 3,3,3-propene- $d_3$  using  $\text{Cp}^*_2\text{Sm}$  and  $\text{Cp}^*_2\text{Sm}(\eta^3\text{-CH}_2\text{CHCHR})$  precursors, where  $\text{R} = \text{H}$ ,  $\text{Et}$ , and  $\text{Bu}^n$ . According to FD-MS, the variety of precursors gave the same FD-MS data, which confirmed the existence of one common primary catalytic cycle for all of these samarium complexes. The FD-MS and NMR data on the formation of  $\text{D}-(\text{CH}_2\text{CH}_2)_n\text{-D}$  from  $\text{CH}_2=\text{CH}_2$  under  $\text{D}_2$  and  $\text{H}-(\text{CD}_2\text{CD}_2)_n\text{-H}$  from  $\text{CD}_2=\text{CD}_2$  under  $\text{H}_2$  were consistent with the termination of the polymerization by hydrogenolysis. The  $\beta$ -hydrogen elimination is not competing with hydrogenolysis as a termination mechanism. The data showed also no evidence for radical-based polymerization in the system. 2-Pentene and 2-heptene do not incorporate as readily as their  $\alpha$ -olefin analogs and 3-heptene incorporation was not detectable, but these internal olefins are effective termination agents via metallation. Styrene was not polymerized by these compounds but could be incorporated into polyethylene.<sup>901,902</sup> Surprisingly,  $\text{Cp}^*_3\text{Sm}$  is also active for the polymerization of ethylene, even though the sterically overcrowded complex has no potential center of activity like  $\text{Sm}^{\text{II}}$ , hydride, or alkyl. The initiation of ethylene polymerization is thought to proceed through a  $\eta^1\text{-C}_5\text{Me}_5$  intermediate (Scheme 253).<sup>616,616a</sup>

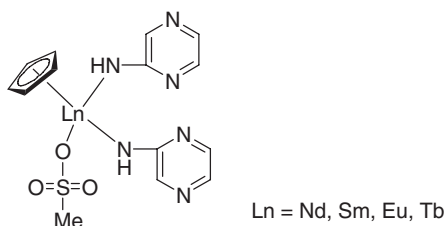
The neutral dialkyl-aryloxide complex  $(\text{Me}_3\text{SiCH}_2)_2\text{Y}(\text{OC}_6\text{H}_3\text{Bu}^t_{2-2,6})(\text{THF})_2$  has been found to polymerize ethylene.<sup>120</sup> Ethylene polymerization by using the *racemic*  $[(2\text{-SiMe}_3\text{-4-Bu}^t\text{C}_5\text{Me}_2)_2\text{SiMe}_2]\text{Sm}(\text{THF})_2$ , *meso*- $[(3\text{-Bu}^t\text{C}_5\text{H}_2)_2\text{SiMe}_2(\text{SiMe}_2\text{OSiMe}_2)]\text{Sm}(\text{THF})_2$ , and  $C_1$ -symmetric  $[\{2,4\text{-(SiMe}_3)_2\text{C}_5\text{H}_2\}\{3,4\text{-(SiMe}_3)_2\text{C}_5\text{H}_2\}]\text{SiMe}_2]\text{Sm}(\text{THF})_2$  in the absence of MAO has been explored. The *meso*-isomer exhibits highest initiating activity but the number-average molecular weight is relatively low ( $\bar{M}_n = 50,000$  Da). In contrast to these complexes, the  $C_1$ -symmetric complex provides the highest molecular weight of polyethylene,  $\bar{M}_n > 10^6$  Da, with relatively narrow molecular weight distribution ( $\bar{M}_w/\bar{M}_n = 1.6$ ). Only the *racemic* complex exhibits good activity for the polymerization of propylene, 1-pentene, and 1-hexene.<sup>903</sup> The same authors reported the synthesis and polymerization activities of the *ansa*-samarocene complexes (Scheme 254), monocyclopentadienyl samarium complexes with allyl or benzyl groups on the cyclopentadienyl ring, and the use of 2,6-dialkoxyphenyl groups as new ligands for samarium polymerization initiators.



Scheme 253



Scheme 254



Scheme 255

Mono(cyclopentadienyl)lanthanide compounds of the types  $\text{CpLn}(\text{O}_3\text{SCF}_3)(\text{PzA})_2$  and  $\text{CpLnBr}_2(\text{PzA})_2$  ( $\text{Ln} = \text{Nd}, \text{Sm}, \text{Eu}, \text{Tb}$ ;  $\text{PzA} = \text{pyrazinamide}$ ) (Scheme 255) have been found to be active in ethylene polymerization when MAO was used as co-catalyst producing low crystalline polyethylene.<sup>904,904a,906</sup>

A series of lanthanide metallocene catalysts are active in the regioselective ring-opening polymerization of strained *exo*-methylenecycloalkanes to yield *exo*-methylene-functionalized polyethylenes.<sup>907,907a,910</sup> Methylenecyclobutane affords the polymer  $[-\text{CH}_2\text{CH}_2\text{CH}_2\text{C}(\text{=CH}_2)-]_n$  under the catalytic action of  $[(1,2-(\text{CH}_3)_2\text{C}_5\text{H}_3)_2\text{ZrCH}_3]^+[\text{CH}_3\text{B}(\text{C}_6\text{F}_5)_3]^-$ , while  $[\text{Cp}^*_2\text{Lu}(\mu\text{-H})_2]$  catalyzes the polymerization of methylenecyclopropane to give  $[-\text{CH}_2\text{CH}_2\text{C}(\text{=CH}_2)-]_n$ . In the latter case reversible catalyst deactivation is ascribed to the formation of an Lu-allyl species, based on  $\text{D}_2\text{O}$  quenching experiments. In contrast,  $[\text{Cp}^*_2\text{Sm}(\mu\text{-H})_2]$  and  $[\text{Cp}^*_2\text{La}(\mu\text{-H})_2]$  dimerize methylenecyclopropane to give 1,2-dimethylene-3-methylcyclopentane with high chemoselectivity. The mechanism of dimerization is proposed to involve the intermediacy of 3-methylene-1,6-heptadiene and is supported by the observation that independently synthesized 3-methylene-1,6-heptadiene is smoothly converted to 1,2-dimethylene-3-methylcyclopentane under catalytic conditions. The co-polymerization of methylenecyclopropane with ethylene is catalyzed by  $[\text{Cp}^*_2\text{Lu}(\mu\text{-H})_2]$  and  $[\text{Cp}^*_2\text{Sm}(\mu\text{-H})_2]$  and yields high molecular weight  $[-\text{CH}_2\text{CH}_2]_x[-\text{CH}_2\text{CH}_2\text{C}(\text{=CH}_2)]_y$ , with an exclusively ring-opened microstructure. When  $[\text{Cp}^*_2\text{La}(\mu\text{-H})_2]$  is used as the catalyst, more than 50% of the methylenecyclopropane is located at the chain ends in a dienyne structure. The only zirconium polymerization catalyst which incorporates methylenecyclopropane in the ring-opened form in a moderate percentage is  $[(\text{Me}_4\text{C}_5)\text{SiMe}_2(\text{NBu}^t)\text{ZrCH}_3]^+[\text{B}(\text{C}_6\text{F}_5)_4]^-$ .<sup>907,907a</sup> The ring opening of methylenecyclopropane catalyzed by the lanthanocene  $\text{Cp}_2\text{LaH}$  has been simulated by quantum chemical molecular dynamics.<sup>911</sup>

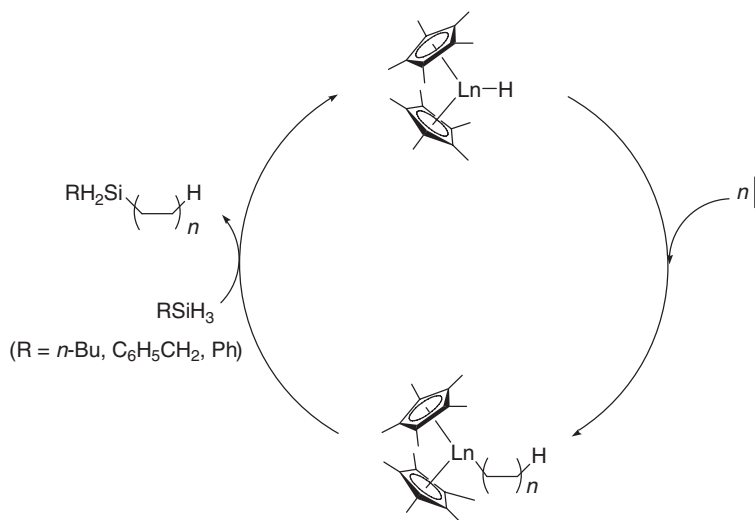
$\text{PhSiH}_3$  is an efficient and selective chain-transfer agent in  $\alpha$ -olefin polymerization and co-polymerization catalyzed by  $[\text{Cp}^*_2\text{Ln}(\mu\text{-H})_2]$  ( $\text{Ln} = \text{Y}, \text{La}, \text{Sm}, \text{Lu}$ ), and  $\text{Me}_2\text{Si}(\text{C}_5\text{Me}_4)_2\text{LnCH}(\text{SiMe}_3)_2$  ( $\text{Ln} = \text{Sm}, \text{Nd}$ ). Organolanthanide-catalyzed ethylene-1-hexene and ethylene-styrene co-polymerization processes were also studied.<sup>912</sup> Silanolytic ( $\text{PhSiH}_3$ ,  $\text{Bu}^n\text{SiH}_3$ ,  $\text{PhCH}_2\text{SiH}_3$ ) chain transfer in organolanthanide-catalyzed ethylene polymerization and ethylene co-polymerization with several  $\alpha$ -olefins leads to a series of silyl-capped polyolefins. In  $[\text{Cp}^*_2\text{Ln}(\mu\text{-H})_2]$  ( $\text{Ln} = \text{Y}, \text{La}, \text{Sm}, \text{Lu}$ ) and  $[\text{Me}_2\text{Si}(\text{C}_5\text{Me}_4)_2\text{Ln}(\mu\text{-H})_2]$ -mediated ethylene homopolymerization and ethylene co-polymerization, both primary arylsilanes ( $\text{PhSiH}_3$ ) and alkylsilanes ( $\text{Bu}^n\text{SiH}_3$ ,  $\text{C}_6\text{H}_5\text{CH}_2\text{SiH}_3$ ) function as efficient chain-transfer agents. In the case of ethylene polymerization mediated by  $[\text{Cp}^*_2\text{Sm}(\mu\text{-H})_2]$ , the mechanism of chain transfer is supported by the observation that  $\bar{M}_n$  of the capped polyethylenes formed at constant concentrations of catalyst,  $\text{PhSiH}_3$ , and ethylene is inversely proportional to the concentration of  $\text{PhSiH}_3$  (Scheme 256). It was also found that the use of silane-activated  $\text{Me}_2\text{Si}(\text{C}_5\text{Me}_4)_2\text{LnCH}(\text{SiMe}_3)_2$  precatalysts was efficient in producing silyl-endcapped ethylene/1-hexene and ethylene/styrene co-polymers.<sup>913</sup>

A method for synthesizing polyolefins having a silyl group at one terminus has been patented. These polymerizations were carried out in the presence of a metallocene catalyst using silanes (e.g.,  $\text{PhSiH}_3$ ) as a chain-transfer agent.  $\text{Cp}_2\text{LnH}$ ,  $\text{Cp}^*_2\text{LnCH}(\text{SiMe}_3)_2$ ,  $\text{Cp}^*_2\text{LnH}$ ,  $[\text{Me}_2\text{Si}(\text{C}_5\text{Me}_4)_2]\text{LnCH}(\text{SiMe}_3)_2$  ( $\text{Ln} = \text{Sc}, \text{Y}, \text{La}, \text{Ac}, \text{Ce-Lu}$ ), and several Ti, Zr, and Hf complexes were claimed as catalytic active compounds. The activities of the organolanthanide complexes and molecular weights of the polyolefins are inversely proportional to the silane concentration, showing that the silane is a true chain-transfer agent.<sup>914</sup>

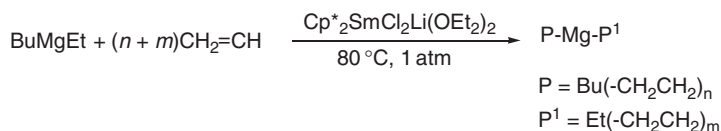
Ethylene insertion into an  $\text{Mg-C}$  bond is possible under very mild conditions by an alkyl chain transfer via chain-growing polymerization catalyzed by a lanthanocene. This new reaction is an efficient method for the synthesis of  $\text{P-Mg-P}^1$  compounds ( $\text{P} = \text{C}_4\text{-C}_{200}$  alkyl chain) (Scheme 257).<sup>915,915a</sup>

The experiments were usually performed in hydrocarbons at  $80^\circ\text{C}$ . The ethylene reacted immediately and was consumed constant until the alkyl chain of the dialkyl magnesium compounds grew too long and the products began to precipitate. The treatment of the  $\text{P-Mg-P}^1$  compounds with  $\text{CO}_2$  followed by hydrolysis gave acids with odd carbon chain lengths of between 5 and 13 C atoms ( $\text{FAB}^+\text{-MS}$ ,  $m/z$  101–213).<sup>915,915a,916</sup> Direct alkylation of the





Scheme 256

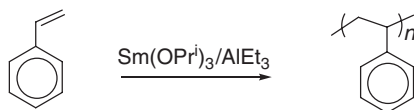


Scheme 257

neodymium precatalyst  $\text{Cp}^*_2\text{Nd}(\mu\text{-Cl}_2)\text{Li}(\text{OEt}_2)_2$  by butylethylmagnesium produced efficient homogeneous catalytic species for ethylene polymerization with a very high productivity. The polymers were highly linear, vinyl-terminated, and possessed narrow molecular weight distributions ( $\bar{M}_w/\bar{M}_n = 2$ ).<sup>917</sup>

Polymerization of styrene in the presence of dialkylmagnesium or a combination of chlorolanthanocene and dialkylmagnesium has been studied.<sup>918</sup> In the presence of butylethylmagnesium or *n,s*-dibutylmagnesium, the styrene polymerization proceeds via thermal self-initiation, but is accompanied by a reversible transfer to dialkylmagnesium compounds giving oligostyrylmagnesium species. When the dialkylmagnesium is combined with a lanthanocene such as  $\text{Cp}^*_2\text{Nd}(\mu\text{-Cl}_2)\text{Li}(\text{OEt}_2)_2$ , an increase in activity is obtained which is ascribed to additional styrene polymerization initiated by *in situ* generated alkyl(hydrido)lanthanocene species. The influence of various reaction parameters on the performance of this system has been investigated. The oligostyrenes have a relatively narrow molar mass distribution which can be explained by an efficient transfer between the chain-growing lanthanide and the oligostyrylmagnesium species. Finally, the combination of butylethylmagnesium and  $\text{Cp}^*_2\text{Nd}(\mu\text{-Cl}_2)\text{Li}(\text{OEt}_2)_2$  has been used to achieve (styrene-co-ethylene) block co-polymers.<sup>918</sup> The cationic complex  $[(\text{Bu}^t\text{C}_5\text{H}_4)_2\text{Yb}(\text{THF})_2][\text{BPh}_4] \cdot x\text{THF}$  shows catalytic activity for the polymerization of styrene at high temperatures.<sup>350</sup> The guanidinate lanthanide methyl complexes  $[(\text{Me}_3\text{Si})_2\text{NC}(\text{NPr}^i)_2]_2\text{Ln}(\mu\text{-Me})_2\text{Li}(\text{TMEDA})$  ( $\text{Ln} = \text{Nd, Yb}$ ) as well as  $\beta$ -diketiminato complexes of  $\text{Yb}(\text{II})$  have been established as effective single-component initiators for styrene polymerization.<sup>919</sup> The heterometallic complexes  $\text{Cp}'\text{YbAlH}_3(\text{L})$  ( $\text{Cp}' = \text{Bu}^t_2\text{C}_5\text{H}_3$ ,  $\text{Cp}^*$ ;  $\text{L} = \text{NEt}_3$ ,  $\text{THF}$ ,  $\text{Et}_2\text{O}$ ) have been shown to be moderately active in styrene polymerization, producing atactic polystyrene. The results provided some evidence for a heterometallic mechanism of styrene polymerization.<sup>859</sup> The catalytic activity in the polymerization of styrene has been examined using commercially available simple rare earth metal compounds such as  $\text{Sm}(\text{OPr}^i)_3$ ,  $\text{Sm}(\text{acac})_3$ ,  $\text{Sm}(\text{O}_2\text{CMe})_3$ ,  $\text{SmI}_2(\text{THF})_2$ , or  $\text{SmCl}_3$  coupled with  $\text{Et}_3\text{Al}$  or MAO. Among these compounds, the  $\text{Sm}(\text{OPr}^i)_3/\text{AlEt}_3$  system shows the highest catalytic activity, especially in the presence of minor amounts of toluene at  $60^\circ\text{C}$  (Scheme 258).<sup>920</sup>

Anionic or neutral allylic samarium or neodymium species as catalysts polymerize styrene without addition of any co-catalysts (catalyst/styrene ratio = 1 : 1000). Random syndiotactic-rich material was obtained from tetra(allyl)lanthanates, whereas the neutral tris(allyl)lanthanides or anionic *ansa*-bis(cyclopentadienyl)bis(allyl)lanthanates afforded



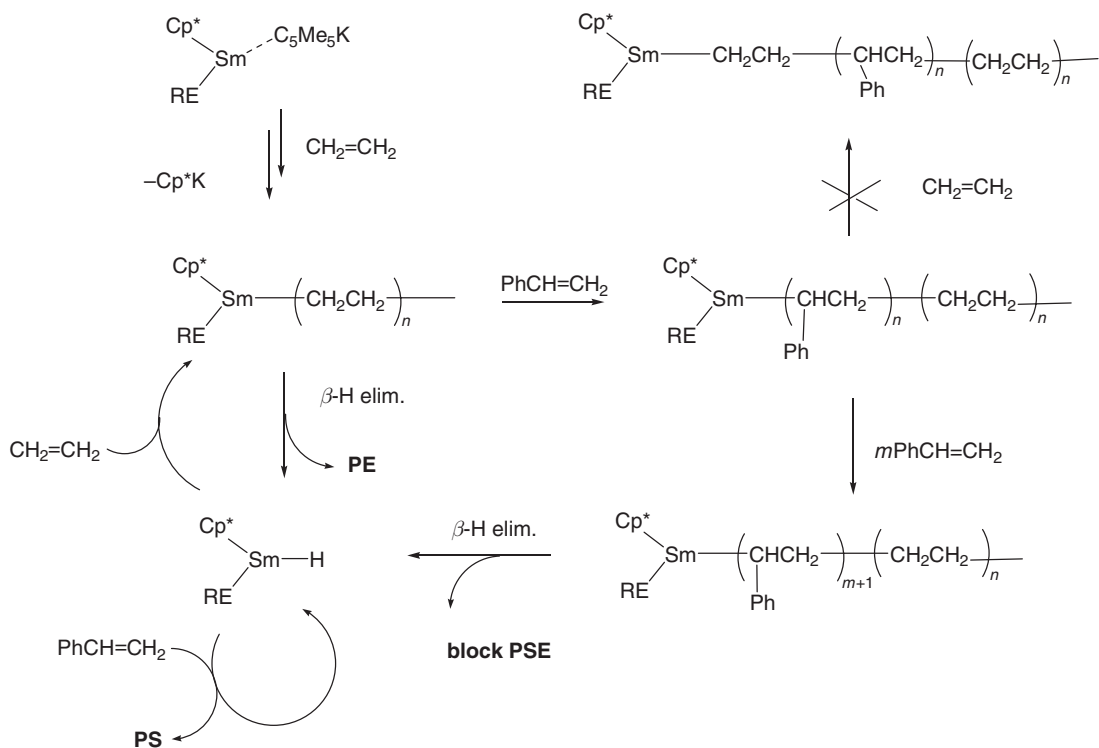
Scheme 258

isotactic-rich polystyrene.<sup>921</sup> Highly syndiospecific polymerization has also recently been achieved by allyl lanthanide complexes of the type  $[\text{Me}_2\text{C}(\text{Flu})(\text{C}_5\text{H}_4)]\text{Ln}(\eta^3\text{-C}_3\text{H}_5)$  ( $\text{Ln} = \text{Y}, \text{La}, \text{Sm}$ )<sup>864</sup> and with scandium half-metallocenes such as  $(\text{C}_5\text{Me}_4\text{SiMe}_3)\text{Sc}(\text{CH}_2\text{SiMe}_3)_2(\text{THF})$ .<sup>922</sup> Rare earth metal complexes containing silylated Cp ligands and the 3-(2,6-dimethoxyphenyl)allyl ligand have been found to catalyze the polymerization of ethylene and MMA.<sup>923</sup> The organolanthanide hydrides  $[\text{Cp}^*_2\text{Ln}(\mu\text{-H})_2]$  ( $\text{Ln} = \text{Sm}, \text{Lu}$ ) have been patented as catalysts for co-polymerization of methylenecyclopropane and simple olefins (ethylene, propylene, or styrene). The polymerization goes via a lanthanide-mediated  $\beta$ -alkyl shift ring-opening process and results in exomethylene-functionalized polyolefins  $\{-(\text{CH}_2\text{CHR})_x-[\text{CH}_2\text{CH}_2\text{C}(\text{CH}_2)]_y-\}$  ( $\text{R} = \text{H}, \text{CH}_3$ , or  $\text{Ph}$ ).<sup>924</sup>  $\text{Cp}^*/\text{ER}$ -ligated  $\text{Sm}(\text{II})$  complexes are easily obtained by the reaction of  $\text{Cp}^*_2\text{Sm}(\text{THF})_2$  with 1 equiv. of  $\text{KER}$  ( $\text{ER} = \text{OC}_6\text{H}_3\text{Pr}^i_{2-2,6}, \text{OC}_6\text{H}_2\text{Bu}^t_{2-2,6}\text{-Me-4}, \text{SC}_6\text{H}_2\text{Pr}^i_{3-2,4,6}$ ) in THF in yields of 85–90%; they catalyze the one-step block co-polymerization of ethylene with styrene. This was apparently the first example of a block co-polymerization of two different simple olefin monomers in a mixture (Scheme 259).<sup>925–927</sup>

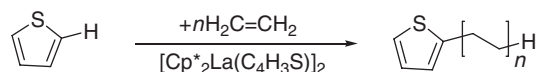
$[\text{Cp}^*_2\text{La}(\mu\text{-C}_4\text{H}_3\text{S})_2]$  was found to be able to combine ethylene polymerization and C–H activation of thiophene to result in catalytic formation of polyethylene with 2-thienyl end groups (Scheme 260).<sup>928</sup>

Recently, diphenylphosphine has been shown to be an efficient chain-transfer agent in organolanthanide-catalyzed ethylene polymerization, yielding phosphine-terminated polyethylenes. This reaction is a versatile, efficient way of incorporating an electron-rich functional group into an otherwise inert polymer.<sup>929</sup>

Lanthanide complexes without  $\pi$ -ligands were also found to be highly active catalysts. The alkyls  $\text{Ln}(\text{CH}_2\text{SiMe}_3)_3(\text{THF})_2$  in the presence of  $\text{AlBu}^i_3$  and activated with  $[\text{HNMe}_2\text{Ph}][\text{B}(\text{C}_6\text{F}_5)_4]$  polymerize ethylene with good activity to give polymers of medium molecular weight. The activities increased with increasing ionic radius



Scheme 259

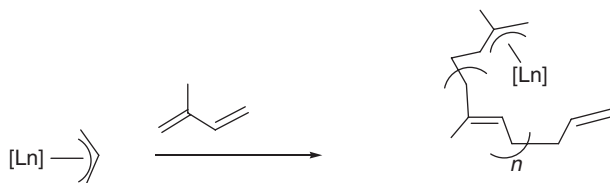


Scheme 260

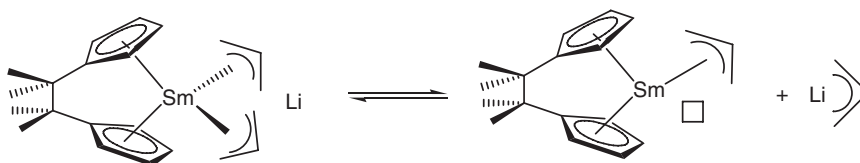
of the lanthanide metal,  $\text{Sc} = \text{Lu} = \text{Yb} < \text{Tm} < \text{Er} < \text{Y}$ ,  $\text{Ho} \ll \text{Dy} < \text{Tb}$ . An excess of the ammonium salt is required for high activity. The suggestion that dications  $[\text{Ln}(\text{CH}_2\text{SiMe}_3)(\text{solvent})_x]^{2+}$  may be the active species was supported by the isolation of  $[\text{Y}(\text{CH}_2\text{SiMe}_3)(\text{THF})_5]^{2+}$  and  $[\text{YMe}(\text{THF})_6]^{2+}$  as  $\text{BPh}_4^-$  salts.<sup>930</sup>

#### 4.01.13.4.3 Diene polymerization

The stereospecific polymerization of 1,3-butadiene with  $\text{Li}[\text{Nd}(\eta^3\text{-C}_3\text{H}_5)_4] \cdot 1.5$  dioxane,  $\text{Li}[\text{Cp}^*\text{Nd}(\eta^3\text{-C}_3\text{H}_5)_3] \cdot 2$  THF,  $\text{Li}[\text{Cp}^*\text{Nd}(\eta^3\text{-C}_3\text{H}_5)_3] \cdot 3$  DME and  $(\eta^3\text{-C}_3\text{H}_5)_2\text{Nd}(\mu\text{-Cl})_2\text{MgCl}(\text{THF})$  as catalysts has been reported.<sup>182,184,931,932</sup> The catalytic reactivity of these compounds depends obviously on how far a dissociation of the complexes with the formation of  $\text{LiC}_3\text{H}_5$  takes place under the reaction conditions. By addition of proper acceptor or donor molecules, like  $\text{BEt}_3$ ,  $\text{Ph}_2\text{SnCl}_2$ ,  $\text{Et}_2\text{AlCl}$ , and THF, or dipiperidylethane, the reactivity can be controlled accordingly.<sup>182</sup> The same authors also published the results on the synthesis of neutral tris(allyl)lanthanide complexes  $\text{La}(\eta^3\text{-C}_3\text{H}_5)_3 \cdot 1.5$  dioxane and  $\text{Nd}(\eta^3\text{-C}_3\text{H}_5)_3 \cdot \text{dioxane}$  and their test as “single-site” catalysts for the stereospecific polymerization of butadiene. The title complexes were obtained by a reaction of tetrakis(allyl)lanthanide(III) complexes  $\text{Li}[\text{Ln}(\text{C}_3\text{H}_5)_4] \cdot 1.5$  dioxane ( $\text{Ln} = \text{La}$  or  $\text{Nd}$ ) with  $\text{BEt}_3$  in dioxane. The compounds catalyzed the 1,4-*trans*-polymerization of butadiene in toluene with high selectivity. By addition of Lewis acids such as  $\text{Et}_2\text{AlCl}$ ,  $\text{EtAlCl}_2$ , or  $(\text{MeAlO})_3$ , catalysts for the 1,4-*cis*-polymerization are obtainable. The results allowed first conclusions on the mechanism of the lanthanide complex-catalyzed butadiene polymerization.<sup>178,931</sup> Various other mono-, di-, and triallyl neodymium complexes in combination with trialkylaluminums have also been investigated as highly active single-site catalysts for the 1,4-*cis*-polymerization of butadiene,<sup>933</sup> as have supported La and Nd allyl complexes.<sup>934</sup> Solvate-free  $\text{Nd}(\eta^3\text{-C}_3\text{H}_5)_3$  catalyzes the 1,4-*trans*-polymerization of butadiene in toluene at 50 °C (*trans*-selectivity 80–85%),<sup>935</sup> whereas the activation of the neutral neodymium allyl complex  $\text{Nd}(\eta^3\text{-C}_3\text{H}_5)_3 \cdot \text{dioxane}$  with alkylaluminumoxanes (MAO or HIBAO) results in highly selective catalysts for the 1,4-*cis*-polymerization of butadiene (*cis*-selectivity  $\leq 80\%$ ).<sup>936</sup> Polymerizations of butadiene and isoprene were carried out using various rare earth metallocenes such as  $(\text{C}_5\text{H}_9\text{C}_5\text{H}_4)_2\text{NdCl}$ ,  $(\text{C}_5\text{H}_9\text{C}_5\text{H}_4)_2\text{NdCl}$  ( $\text{C}_5\text{H}_9$  = cyclopentyl),  $(\text{MeC}_5\text{H}_4)_2\text{NdOAr}$  ( $\text{Ar} = 2,6\text{-Bu}^t_2\text{-4-Me-C}_6\text{H}_2$ ),  $(\text{C}_9\text{H}_7)_2\text{NdCl}$ ,  $\text{Me}_2\text{Si}(\text{C}_9\text{H}_6)_2\text{NdCl}$ , and  $(\text{Flu})_2\text{NdCl}$  in the presence of MAO.<sup>937</sup> In the presence of  $\text{AlMe}_2\text{Cl}$ , heterobimetallic complexes of the composition  $\text{LnAl}_3\text{Me}_8(\text{O}_2\text{CC}_6\text{H}_2\text{Pr}^t_3\text{-2,4,6})_4$  (cf. Section 4.01.12.2) transform isoprene to a high-*cis* polymer ( $>99\%$  stereoselectivity).<sup>860</sup> (Allyl)neodymium intermediates have been discussed for the butadiene polymerization and co-polymerization of butadiene with styrene and glycidyl methacrylate using well-defined neodymium alkoxides/aryloxides in combination with dialkylmagnesium reagents as catalysts,<sup>938</sup> while the *ansa*-metallocenes  $\text{Me}_2\text{Si}(\text{C}_5\text{H}_3\text{SiMe}_3\text{-3})_2\text{NdCl}$  or  $\text{Me}_2\text{Si}(\text{C}_{13}\text{H}_8)_2\text{NdCl}$  in combination with  $\text{Bu}^n\text{Li}$  and  $\text{AlHBu}^i_2$  have been found to be efficient and unique catalysts for the co-polymerization of ethylene with butadiene.<sup>939,940</sup> The polymerization of an equimolar mixture of isoprene and 1-hexene led to a co-polymer (1-hexene/isoprene = 1:10) essentially formed of 1,4-*trans*-polyisoprene blocks separated by only one inserted hexyl group. The tetra(allyl)-lanthanate complexes  $[\text{Li}(\text{dioxane})_{1.5}][\text{Ln}(\text{allyl})_4]$  ( $\text{Ln} = \text{Sm}$ ,  $\text{Nd}$ ) showed no hexene insertion under the same polymerization conditions and formed a mixture of *cis*- and *trans*-poly(isoprene).<sup>941</sup> The bis(allyl)-*ansa*-lanthanate complexes  $\text{Me}_2\text{C}(\text{C}_5\text{H}_4)_2\text{Ln}(\text{allyl})_2\text{Li}(\text{DME})$  ( $\text{Ln} = \text{Sm}$ ,  $\text{Nd}$ ) act as single-component catalysts of diene polymerization (Scheme 261). These anionic allyl *ansa*-cyclopentadienyl samarium complexes exhibited especially good activity for the stereospecific 1,4-*trans*-polymerization of isoprene. The dissociation of an allylic ligand in this compound is easy and allows the coordination of the diene (Scheme 262).<sup>446</sup> The same system was found to be an efficient initiator



Scheme 261



Scheme 262

which not only polymerizes 1,3-dienes, but also co-polymerizes dienes and long-chain  $\alpha$ -olefins or  $\alpha,\omega$ -dienes to give functionalizable polymers. It also polymerizes caprolactone and allows the controlled diblock co-polymerization of isoprene or isoprene/ $\alpha$ -olefin co-polymer and caprolactone.<sup>633,942–944</sup>

The stereospecific polymerization of 1,3-butadiene has also been achieved with samarocene catalysts. The single-site catalyst system  $\text{Cp}^*_2\text{Sm}(\text{THF})_2$  activated with modified methylaluminoxane (MMAO) containing isobutylaluminoxane as a co-catalyst (1:200) induces the rapid polymerization of butadiene at 50 °C in toluene, with the conversion of 2500 equiv. of butadiene reaching to 65% in 5 min (TON: 20 000 butadiene (mol Sm)<sup>−1</sup>h<sup>−1</sup>). The resulting polybutadiene possesses a very high 1,4-*cis*-microstructure (98.8%), high molecular weight ( $\bar{M}_n = 400\,900$ ), and narrow MWD ( $\bar{M}_w/\bar{M}_n = 1.8$ ).<sup>945</sup> The activity of arene complexes  $\text{Ln}(\eta^6\text{-arene})(\text{AlX}_3)_3$  for the polymerization of butadiene and ethylene has been investigated, using  $\text{AlHBu}^i_2$  and  $\text{MgBu}^n_2$  as co-catalysts.<sup>168</sup>

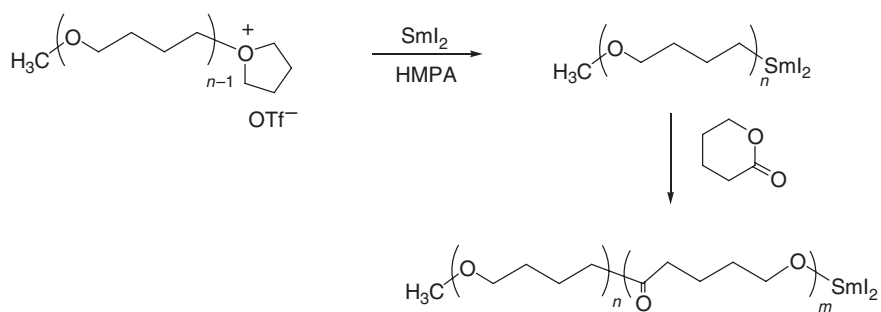
Catalytic systems containing an *ansa*-bis(cyclopentadienyl)lanthanide core and lithium and/or magnesium salts have been obtained by the reaction of the chloride precursors with allyllithium. These allyl complexes lead to the same active species which polymerizes 1,3-dienes, co-polymerizes 1,3-dienes and  $\alpha$ -olefins or  $\alpha,\omega$ -dienes, or allows the controlled diblock polyisoprene/polycaprolactone co-polymerization.<sup>946</sup> Ethylene and butadiene are co-polymerized with neodymocene catalysts. The microstructure of the resulting ethylene/butadiene co-polymers has been investigated by <sup>1</sup>H and <sup>13</sup>C NMR.<sup>947</sup> Random and block-co-polymerization of 1,3-butadiene with styrene has been achieved on the stereospecific system  $\text{Cp}^*_2\text{Sm}(\mu\text{-Me})_2\text{AlMe}_2/\text{AlBu}^i_3/[\text{Ph}_3\text{C}][\text{B}(\text{C}_6\text{F}_5)_4]$ . Such random co-polymers of butadiene and styrene are utilized commercially as styrene–butadiene rubbers (SBR).<sup>948</sup> Addition of appropriate co-catalysts such as MMAO or  $\text{AlR}_3/[\text{Ph}_3\text{C}][\text{B}(\text{C}_6\text{F}_5)_4]$  to the samarocene complexes  $\text{Cp}^*_2\text{Sm}(\text{THF})_2$  or  $\text{Cp}^*_2\text{Sm}(\mu\text{-Me})_2\text{AlMe}_2$  also afforded catalytic systems for stereospecific 1,4-*cis* living polymerization of butadiene and co-polymerization of butadiene with styrene.<sup>927,949</sup> Stereospecific polymerization of isoprene with molecular and MCM-48-grafted lanthanide(III) tetraalkylaluminates such as  $\text{Ln}[(\mu\text{-Me})_2\text{AlMe}_2]_3$  has been reported.<sup>950,950a,951</sup>

The metallocenium salts  $[\text{Cp}^*_2\text{Ln}][\text{B}(\text{C}_6\text{F}_5)_4]$  ( $\text{Ln} = \text{Pr}, \text{Nd}, \text{Gd}$ ) in combination with  $\text{AlBu}^i_3$  efficiently induce highly 1,4-*cis*-specific polymerization of butadiene. The activity of the Gd complex/ $\text{AlBu}^i_3$  system is high enough to exhibit good catalytic activity even at low temperature. Polymerization at −78 °C gave polybutadiene with nearly perfect 1,4-*cis*-microstructure (>99.9%) with narrow molecular weight distribution ( $\bar{M}_w/\bar{M}_n = 1.45$ ) and in reasonable yield.<sup>553</sup> Other organolanthanide complexes which have been reported to effectively catalyze diene polymerization include the divalent samarocenes  $(\text{C}_5\text{Me}_4\text{Pr}^n)_2\text{Sm}(\text{THF})$  and  $(\text{C}_5\text{H}_2\text{Ph}_{2-1,2,4})_2\text{Sm}(\text{THF})$ ,<sup>952</sup> mixed cyclopentadienyl/ $\beta$ -diketiminate complexes of Sm and Nd,<sup>953</sup> and Nd complexes supported by a dianionic modification of the 2,6-diiminopyridine ligand.<sup>953</sup>

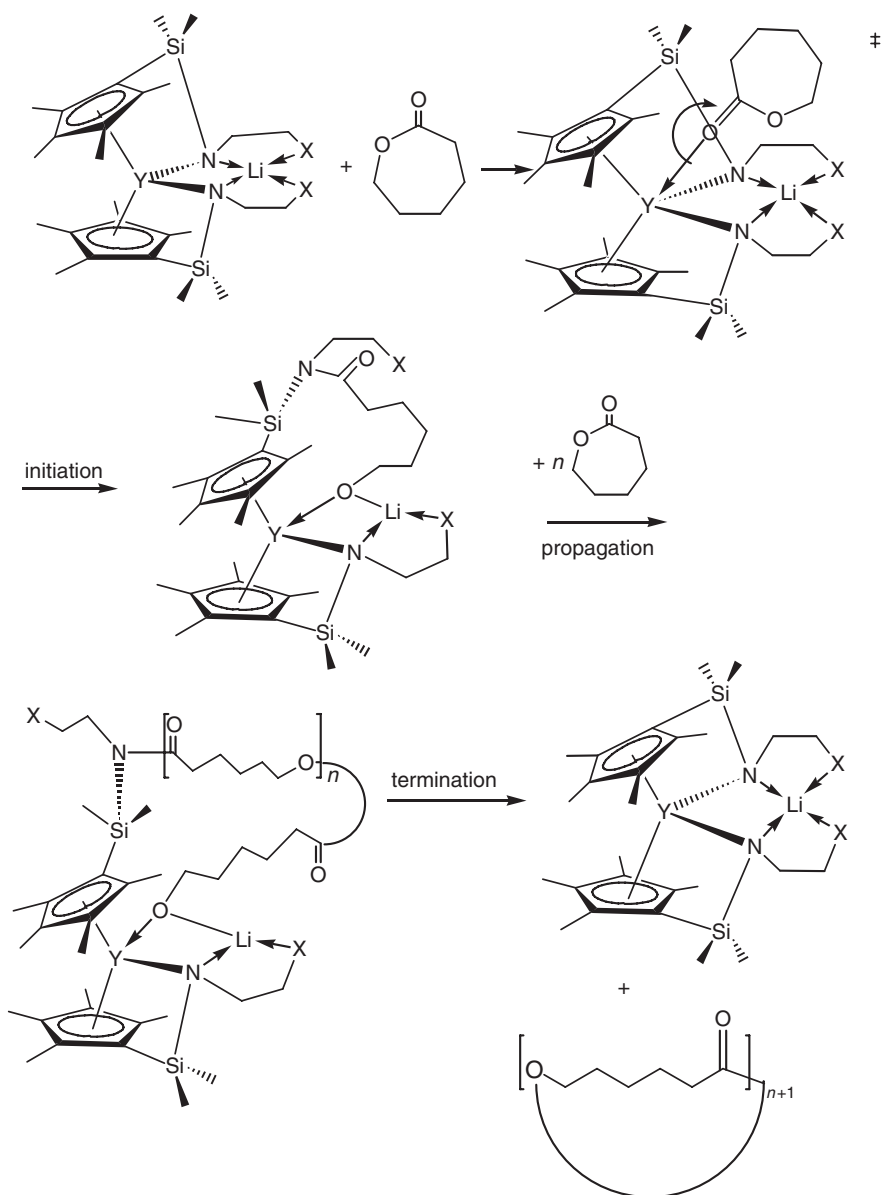
#### 4.01.13.4.4 Ring-opening polymerization of cyclic esters and amides

The polymerization behavior of  $\delta$ -valerolactone with alkylsamarium reagents ( $\text{RSmI}_2$ ) was studied, and its application to the block co-polymerization of tetrahydrofuran with  $\delta$ -valerolactone was examined. Polymerization of  $\delta$ -valerolactone by butylsamarium gave the corresponding polyvalerolactone; the yield increased with increasing concentration of valerolactone and decreasing polymerization temperature, due to the equilibrium between  $\delta$ -valerolactone and polyvalerolactone. The decrease in the molecular weight of polyvalerolactone at longer polymerization times indicated backbiting to form cyclic oligomers. The polymerization of  $\delta$ -valerolactone with polytetrahydrofuran macroanion obtained by the two-electron reduction of the propagation center of living polytetrahydrofuran with  $\text{SmI}_2$  led to a block co-polymer of THF with  $\delta$ -valerolactone (Scheme 263). The initiation efficiency of valerolactone polymerization was almost quantitative, and the unit ratio of THF and  $\delta$ -valerolactone segments could be controlled by both the polymerization time of THF and the amounts of  $\delta$ -valerolactone.<sup>954</sup>

The heterobimetallic complexes  $\text{Li}[\text{Ln}(\eta^5\text{-}\eta^1\text{-C}_5\text{R}_4\text{SiMe}_2\text{NCH}_2\text{CH}_2\text{X})_2]$  catalyze the ring-opening polymerization of  $\epsilon$ -caprolactone (Scheme 264). The product of this polymerization had a high molecular weight  $\bar{M}_n > 30\,000$  Da and moderate polydispersity ( $\bar{M}_w/\bar{M}_n < 2.0$ ). The polymerization was carried out in toluene or dichloromethane at room



Scheme 263



Scheme 264

temperature. The lutetium complex was found to be the least effective catalyst. The homoleptic tris(amide)  $\text{Y}[\text{N}(\text{SiMe}_3)_2]_3$  was also found to polymerize  $\epsilon$ -caprolactone. As the initial step of the polymerization, one can anticipate a nucleophilic attack by one of the nucleophilic amido-nitrogen atoms at the lactone carbonyl carbon atom, followed by acyl bond cleavage and formation of an alkoxide.<sup>428,955</sup>

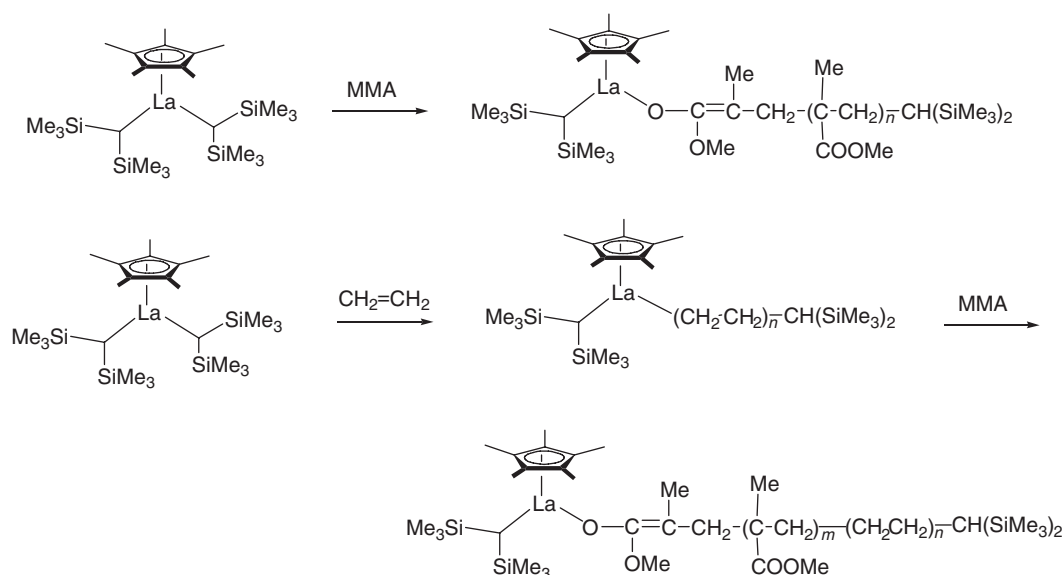
Successful room temperature ring-opening polymerization of  $\epsilon$ -caprolactone and  $\delta$ -valerolactone has also been carried out using  $\text{SmX}_2$  ( $\text{X} = \text{I}, \text{Br}, \text{Cp}$ ) catalysts.  $\text{SmI}_2$  in the presence of metallic Sm was found to have enhanced reactivity at room temperature in ring-opening polymerization processes as compared to pure  $\text{SmI}_2$ .  $\text{SmBr}_2$  and  $\text{SmCp}_2$  showed increased reactivity compared with the  $\text{Sm}/\text{SmI}_2$  system due to their higher reductive power. The catalyst concentration and time of polymerization showed a remarkable effect on number-average molecular weight ( $\bar{M}_n$ ). A decrease in  $\bar{M}_n$  on increasing reaction time and decreasing catalyst concentration was observed.<sup>956</sup>  $[\text{Cp}^* \text{Sm}(\mu\text{-OC}_6\text{H}_2\text{Bu}^t_{2-2,6-\text{Me}-4})_2]$  was also shown to exhibit an extremely high activity for the ring-opening polymerization of  $\epsilon$ -caprolactone and  $\delta$ -valerolactone.<sup>957</sup> The substituted indenyl ytterbium(II) complex  $(\text{C}_9\text{H}_6\text{C}_5\text{H}_9)_2\text{Yb}(\text{THF})_2$  shows high activity to ring-opening polymerization of lactones.<sup>441</sup> Scandium dialkyl complexes containing bulky iminophenolato ligands have been found to be efficient catalysts for the ring-opening polymerization of  $\epsilon$ -caprolactone.<sup>119</sup> The ring-opening polymerization of cyclic esters ( $\epsilon$ -caprolactone and  $L$ -lactide) and the cyclic carbonate 1,3-dioxan-2-one (TMC) is initiated by  $\text{Cp}_3\text{Ln}$  complexes ( $\text{Ln} = \text{Ce}, \text{Pr}, \text{Sm}, \text{Gd}, \text{Er}$ ). Polycarbonate (poly-TMC) was obtained without  $\text{CO}_2$  elimination using  $\text{LnCp}_3$  as initiator.<sup>958</sup> Ring-opening polymerization and block co-polymerization of  $L$ -lactide has also been achieved with the divalent samarocene complexes  $(\text{C}_5\text{H}_4\text{C}_5\text{H}_9)_2\text{Sm}(\text{THF})_2$  as catalyst,<sup>959</sup> while  $D,L$ -lactide is effectively polymerized using  $\text{Cp}^* \text{SmMe}(\text{THF})$ .<sup>960</sup> The complexes  $[(\text{C}_5\text{H}_4\text{SiMe}_3)_2\text{Sm}(\mu\text{-Me})]_2$  and  $[(\text{C}_5\text{H}_3(\text{SiMe}_3)_2-1,3-)_2\text{Ln}(\mu\text{-Me})]_2$  ( $\text{Ln} = \text{Nd}, \text{Sm}$ ) perform the block co-polymerization of  $L$ -lactide with  $\epsilon$ -caprolactone in high yields in the absence of any co-catalysts.<sup>961</sup> The guanidinate lanthanide methyl complexes  $[(\text{Me}_3\text{Si})_2\text{NC}(\text{NPr}^i)_2]_2\text{Ln}(\mu\text{-Me})_2\text{Li}(\text{TMEDA})$  ( $\text{Ln} = \text{Nd}, \text{Yb}$ ) have been established as effective single-component initiators for  $\epsilon$ -caprolactone polymerization.<sup>123</sup> The preparation of block-co-polymers of an olefin and a terminally unsaturated monomer ( $\alpha$ -olefins with three and more C-atoms, vinyl, and vinylidene compounds) or lactone using bis-cyclopentadienyl complexes of lanthanides, scandium, and yttrium with bridged Cp ligands has been patented.<sup>962</sup> Organolanthanide thiolate complexes have been examined as polymerization catalysts for lactones. The compounds  $(\text{COT})\text{Sm}(\text{SAr})(\text{HMPA})$  ( $\text{SAr} = \text{pyridine-2-thiolate}, 2,4,6\text{-triisopropylbenzenethiolate}$ ) have been found to be highly active catalyst precursors for lactone polymerization.<sup>963</sup> Other organolanthanide complexes which have been reported to catalyze the (co-)polymerization of  $\epsilon$ -caprolactone and/or ethylenecarbonate include divalent samarocenes,<sup>964,965</sup>  $\text{Cp}^* \text{LnX}$ -type complexes ( $\text{X} = \text{H}, \text{alkyl}, \text{SiMe}_3$ ),<sup>966</sup> homoleptic lanthanide guanidinate complexes,<sup>967</sup>  $\text{Cp}^* \text{Sm}(\text{BH}_4)(\text{THF})$ ,<sup>968</sup> and sterically hindered lanthanide allyl complexes.<sup>187,187a</sup>

Optically active poly(ester carbonate)s have been synthesized by co-polymerization of substituted trimethylene-carbonate with  $\epsilon$ -caprolactone using organolanthanides among others as catalysts. The homopolymerization of optically active  $(R)$ -1-methyltrimethylenecarbonate (1-MTC) was performed in toluene solution using various types of initiators including  $\text{Cp}^* \text{Sm}(\text{THF})_2$  and  $\text{Cp}^* \text{SmMe}(\text{THF})$ . While all other catalysts for the ring-opening polymerization required relatively high temperatures (60–100 °C), the samarium complexes initiated polymerization processes at room temperature and below.  $\text{Cp}^* \text{Sm}(\text{THF})_2$  and  $\text{Cp}^* \text{SmMe}(\text{THF})$  brought about higher yields and lower polydispersities when the ring-opening polymerization was carried out at 0 °C. These complexes also catalyze the homopolymerization of  $(R,R)$ -1,3-dimethyltrimethylenecarbonate;  $\text{Cp}^* \text{Sm}(\text{THF})_2$  was also used as an initiator for the co-polymerization of  $(R,R)$ -,  $(S,S)$ -, or *rac*-1,3-dimethyltrimethylene carbonate with  $\epsilon$ -caprolactone. All polymers exhibited high molecular weights, low polydispersities, and high polymer yields. The polymers were subjected to detailed biodegradation studies.<sup>969</sup> Other complexes which have been found to exhibit high catalytic activity in the ring-opening polymerization of  $\epsilon$ -caprolactone include  $\text{Cp}_3\text{Dy}_2(\text{NPPH}_3)_3$ .<sup>970</sup>

#### 4.01.13.4.5 Polymerization of acrylic monomers

The half-sandwich complex,  $\text{Cp}^* \text{La}[\text{CH}(\text{SiMe}_3)_2]_2(\text{THF})$ , showed a dual function of performing the controlled polymerizations of non-polar monomers such as ethylene and styrene as well as polar monomers like MMA, hexylisocyanate, and acrylonitrile in high yields (Scheme 265).<sup>971</sup>

More recently, block co-polymers of higher 1-olefins with traditional polar monomers have been made using metallocene-type single-component lanthanide initiators.<sup>972</sup>  $\text{Cp}^* \text{SmMe}(\text{THF})$  and  $\text{Cp}^* \text{YMe}(\text{THF})$  were used as catalysts for living polymerizations and co-polymerizations of alkyl acrylates and alkyl methacrylates.  $\text{Cp}^* \text{SmMe}(\text{THF})$  also initiated the random living co-polymerization of methyl acrylate with *n*-butyl acrylate and block-co-polymerization of alkyl acrylates with MMA to give triblock co-polymers of MMA/*n*-butyl acrylate/MMA.



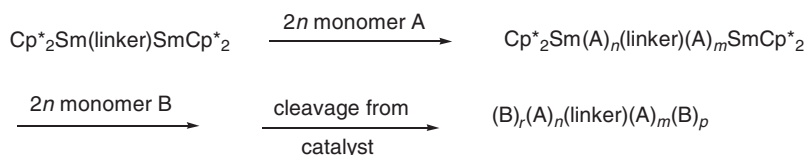
Scheme 265

These co-polymers exhibited good mechanical properties. Monomodal block-co-polymers of alkyl acrylate with  $\epsilon$ -caprolactone were obtained with  $\text{Cp}^*_2\text{SmMe}(\text{THF})$ ; they contained mainly caprolactone.<sup>973–975</sup> Reports and patents have also appeared on the living polymerization and a two-step method for the formation of triblock co-polymers containing both acrylate and methacrylate segments, using bimetallic, bis-lanthanoid initiators  $\text{M-L-M}$  ( $\text{M}$ =organolanthanide complex,  $\text{L}$ =functionalized linking group that is covalently bound to each of the two metal atoms). The catalyst  $\text{Cp}^*_2\text{Sm}(\mu\text{-}\eta^3\text{-allyl})(\mu\text{-}\eta^3\text{-allyl})\text{SmCp}^*_2$  polymerized acrylate esters or lactones (**A**) to give polymers of formula  $(\text{A})_n(\text{L})(\text{A})_m(\text{L}-(\text{CH}_2)_6)$  with a narrow molecular weight distribution. The addition of a second monomer (**B**) led to triblock co-polymer  $(\text{B})_r(\text{A})_n(\text{L})(\text{A})_m(\text{B})_p$  (Scheme 266).<sup>976–978</sup>

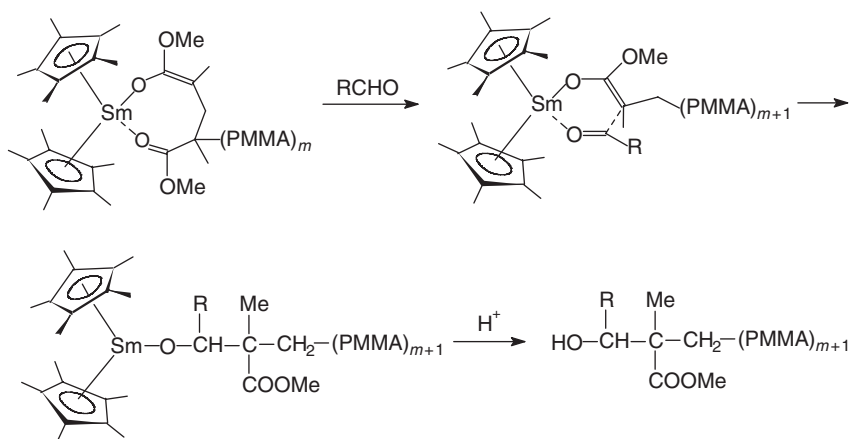
In association with  $\text{AlBu}_3^i$ , the complexes  $(\text{C}_5\text{H}_4\text{CH}_2\text{CH}_2\text{CH}=\text{CH}_2)_2\text{LnCl}(\text{THF})_2$ <sup>326</sup> as well as an ethylene-bridged heterodinuclear metallocene of samarium and titanium<sup>979</sup> have shown high activity for the bulk polymerization of MMA. No co-catalyst is required when allyl-functionalized lanthanocenes containing the 2-propenylcyclopentadienyl ligand are used.<sup>980</sup>  $\text{Cp}^*_2\text{SmMe}(\text{THF})$  acts as initiator in the syntheses of monodispersed MMA oligomers ( $\bar{M}_n$  2500 Da;  $\bar{M}_w/\bar{M}_n < 1.10$ ). The oligomerization proceeds via a samarium enolate as the propagating species, and the reaction of the living oligomer with *p*-tolualdehyde produced *p*-tolyl hydroxymethyl-terminated oligo-MMA (Scheme 267).<sup>981</sup>

The stereocontrol in the polymerization of MMA mediated by chiral organolanthanide metallocenes has been investigated. Hydride, hydrocarbyl, and amido bis(cyclopentadienyl) complexes (Scheme 268) were used as pre-catalysts for the processes. The achiral hydride precatalysts yielded syndiotactic PMMA with narrow polydispersities ( $\bar{M}_w/\bar{M}_n = 1.02\text{--}1.05$ ). The polydispersities of PMMA from the chiral and achiral hydrocarbyl precatalysts are larger than those from the hydride precatalysts, and amide precatalysts gave the largest polydispersities.<sup>982</sup>

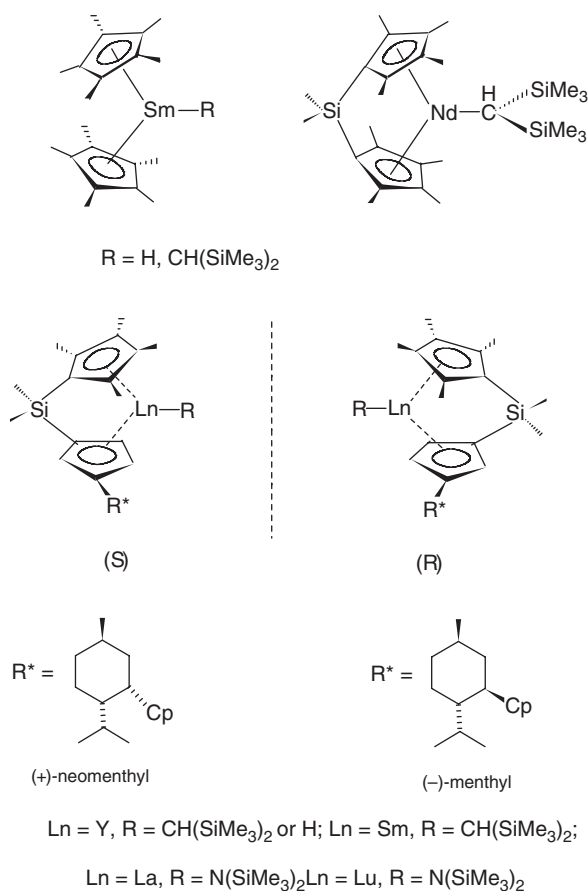
A novel transformation reaction of living poly(tetrahydrofuran) from cationic into anionic propagation species has been published. This species was formed by end-capping of living poly(THF) with potassium iodide followed by the reduction with bis(pentamethylcyclopentadienyl)samarium ( $\text{Cp}^*_2\text{Sm}$ ). The formed terminal anionic carbanion is



Scheme 266



Scheme 267

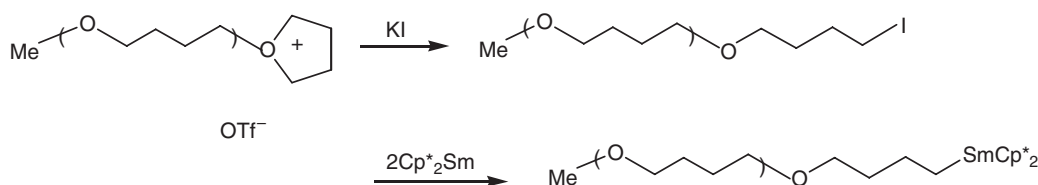


Scheme 268

active for the polymerization of *t*-butyl methacrylate (TBMA),  $\epsilon$ -caprolactone (CL),  $\delta$ -valerolactone (L) and leads to the selective formation of unimodal block-co-polymers (Scheme 269).<sup>983</sup>

The synthesis of “link-functionalized” (LFP) poly(methyl methacrylate) (PMMA), and poly( $\epsilon$ -caprolactone) (PCL), using bimetallic complexes of the type  $\text{Cp}^*_2\text{Sm}-\text{R}-\text{SmCp}^*_2$  has been reported. Bis-initiated polymerization





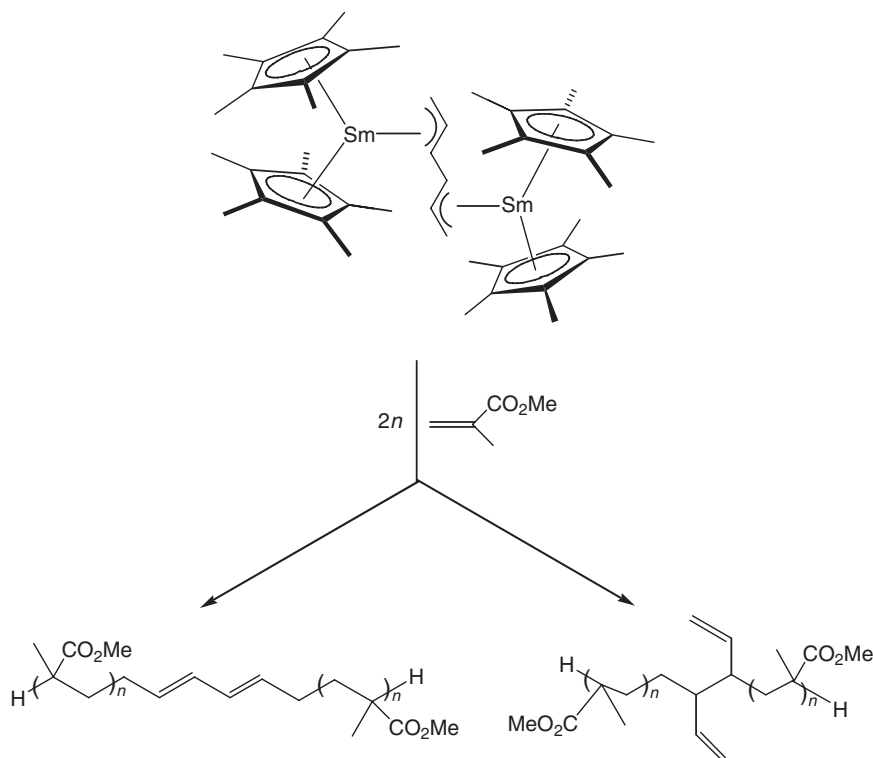
Scheme 269

of MMA and  $\epsilon$ -caprolactone through the bimetallic complexes  $\text{Cp}^*_2\text{Sm}-\text{R}-\text{SmCp}^*_2$  gave polymers with discrete functionalities at the center of the backbone, the LFP polymers (Scheme 270).<sup>984</sup>

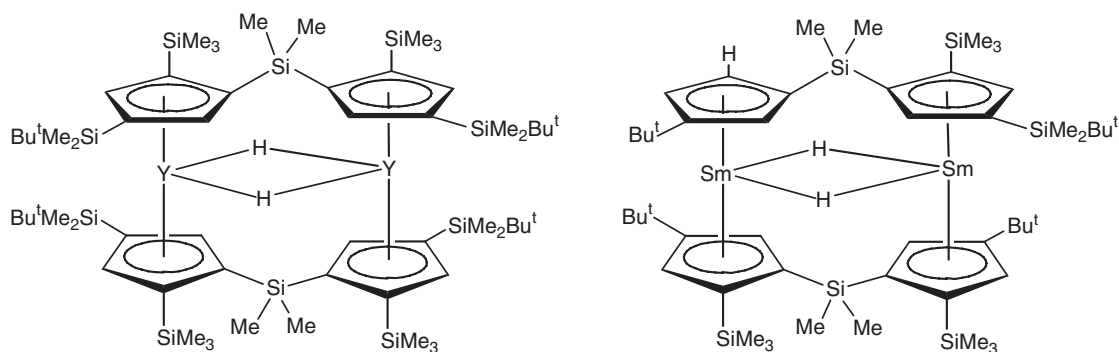
Well-controlled block co-polymerization of 1-olefins with MMA or  $\epsilon$ -caprolactone using the unique dual catalytic function of organolanthanide complexes which are active toward polymerization reactions of polar and non-polar monomers has been achieved with bridged  $[\text{Me}_2\text{Si}(\text{C}_5\text{R}_4)_2]\text{LnH}$  ( $\text{Ln} = \text{Y}, \text{Sm}$ ) type complexes. These initiators are highly active in co-polymerization processes without the presence of any co-catalyst (Scheme 271).<sup>985</sup>

The dimeric yttrium and samarium hydride complexes are converted into monomers in the first step of the reaction. The preparation of block-co-polymers of 1-hexene or 1-pentene with MMA and  $\epsilon$ -caprolactone, respectively, has also been reported. The polymerization of ethylene with MMA,  $\epsilon$ -caprolactone and 2,2-dimethyltrimethylenecarbonate was studied in detail; racemic  $\text{Me}_2\text{Si}(\text{C}_5\text{H}_2-2-\text{SiMe}_3-4-\text{Bu}^t)_2\text{Sm}(\text{THF})_2$  or *meso*- $\text{Me}_2\text{Si}(\text{Me}_2\text{SiOSiMe}_2)(\text{C}_5\text{H}_2-3-\text{Bu}^t)\text{Sm}(\text{THF})$  were active in the ABA-type triblock-co-polymerization.<sup>986</sup>

The catalytic activity of divalent organolanthanides with unbridged substituted indenyl or fluorenyl ligands,  $(\text{C}_9\text{H}_6\text{SiMe}_3-1)_2\text{Yb}(\text{THF})$ ,  $(\text{C}_{13}\text{H}_8\text{SiMe}_3-9)_2\text{Yb}(\text{THF})$ , in the stereoregular polymerization of MMA has been investigated. The formation of isotactic-rich PMMAs from the  $(\text{C}_{13}\text{H}_8\text{SiMe}_3-9)_2\text{Yb}(\text{THF})$  complex was proposed to be associated with the fluctuation of the 9-trimethylfluorenyl ligands around a  $C_2$ -symmetric twisted conformation. The formation of multi (syndio-PMMA-block-iso-PMMA) polymers from the mixture of *rac*- and *meso*-isomers of  $(\text{C}_9\text{H}_6\text{SiMe}_3-1)_2\text{Yb}(\text{THF})$  was rationalized on the basis of competing conjugate addition and inversion of the metallocene conformation.<sup>987</sup> The alkyl-bridged dimer  $[(\text{C}_5\text{H}_4\text{Bu}^t)_2\text{Y}(\mu-\text{Me})]_2$  was found to show good catalytic



Scheme 270

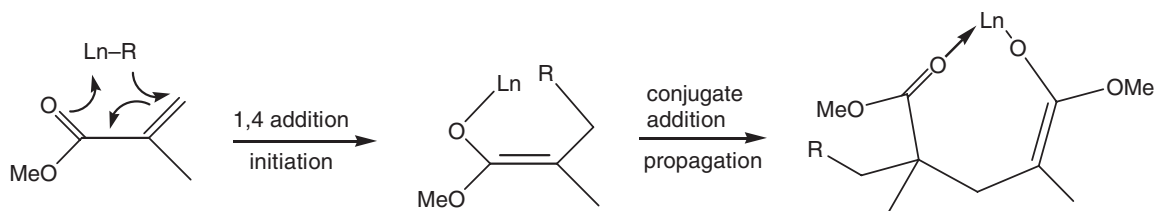


Scheme 271

activity for the polymerization of MMA at  $-78^{\circ}\text{C}$  to  $-40^{\circ}\text{C}$ . The conversion of MMA increased with increasing catalyst and monomer concentrations. The catalytic activity of  $[(\text{C}_5\text{H}_4\text{Bu}^t)_2\text{Y}(\mu\text{-Me})]_2$  for different methacrylates decreased in the following order: MMA > ethyl methacrylate > butyl methacrylate.<sup>443</sup> Catalytic activity for MMA polymerization has also been reported for the neodymium analog  $[(\text{C}_5\text{H}_4\text{Bu}^t)_2\text{Nd}(\mu\text{-Me})]_2$ .<sup>988</sup> The *ansa*-fluorenyl-cyclopentadienyl complex  $\text{Ph}_2\text{C}(\text{Flu})(\text{Cp})\text{LuN}(\text{SiMe}_3)_2$  has been found to catalyze the polymerization of MMA and lactones.<sup>705</sup> MMA is also polymerized by alane complexes of bivalent ytterbocenes  $\text{L}_2\text{YbAlH}_3(\text{NEt}_3)$  ( $\text{L} = \text{Cp}^*$ , 1-SiMe<sub>3</sub>Ind, 9-SiMe<sub>3</sub>Flu). The polymerization was shown to proceed via the formation of a catalytically active intermediate  $\text{L}_2\text{YbAlH}_2[\text{OC}(\text{OMe})=\text{C}(\text{Me})\text{CH}_2\text{C}(\text{Me})_2(\text{CO}_2\text{Me})]$  which was proposed to exist in various forms. At low temperatures the stereochemistry is controlled by the metallocene architecture, with the complexes  $\text{L}_2\text{YbAlH}_3\cdot\text{NEt}_3$  producing more stereoregular polymers than  $\text{L}_2\text{Yb}(\text{THF})$  catalysts (Scheme 272).<sup>989</sup>

Bis(methylcyclopentadienyl)lanthanide diisopropylamides  $(\text{C}_5\text{H}_4\text{Me})_2\text{Ln}(\text{NPr}^i)_2(\text{THF})$  ( $\text{Ln} = \text{Yb}$ , Er, Y) polymerize MMA. The activity increases with increasing ionic radii of the metal elements,  $\text{Y} > \text{Er} > \text{Yb}$ . The polymerization reactions can be carried out over a broad range of polymerization temperatures from  $-78$  to  $40^{\circ}\text{C}$ .<sup>990,990a</sup> MMA is also polymerized by single-component catalysts of the type  $[\text{O}(\text{C}_2\text{H}_4\text{C}_5\text{H}_3\text{CH}_3)_2]\text{LnCl}$  ( $\text{Ln} = \text{Y}$ , Nd, Sm). The effects of temperature, time, and molar ratio (MMA/catalyst) on the polymerization behavior were studied in detail; the results showed that higher temperature and longer time increased the catalytic activities.<sup>991</sup>

Lanthanidocene amide complexes have been established as single-component initiators for the polymerization of (dimethylamino)ethyl methacrylate (DMAEMA), which is one of the most useful nitrogen-functionalized methacrylates.<sup>992</sup> Block co-polymerizations of MMA with butyl acrylate (BuA), trimethylsilyl methacrylate (TMSMA) with MMA, and TMSMA with BuA have been performed in the presence of the organosamarium catalyst  $\text{Cp}^*_2\text{SmMe}(\text{THF})$ .<sup>993</sup> A novel chain-transfer polymerization mediated by  $\text{Cp}^*_2\text{Sm}(\text{III})$  species and organic acids has been achieved. The studied chain polymerization involves the reaction of organic acids such as thiols or ketones with an active bond between samarium(III) and the enolate at the living end of poly(methyl methacrylate). This chain-transfer reaction resulted in termination of the living chain end and the regeneration of the active initiator which would consist of  $\text{Cp}^*_2\text{Sm}(\text{III})$  and deprotonated organic acids.<sup>994</sup> The polymerization of acrylate-based macromonomers by organolanthanide catalysts furnishes polymers with the structure of cylindrical brushes.<sup>995,996,996a</sup> Other catalysts for MMA polymerization are different mixed ligand lanthanocenes  $\text{CpLnCl}(\text{Schiff base})$  ( $\text{Ln} = \text{Sm}$ , Dy, Y, and Er), where the Schiff base is deprotonated *N*-(2-methoxyphenyl)salicylideneamine ( $\text{C}_{14}\text{H}_{13}\text{NO}_2$ ). On activation with  $\text{AlBu}^i_3$ , poly-MMA with narrow molecular weight distribution was made.<sup>997</sup> Other examples of MMA polymerization catalysts include  $(\text{C}_9\text{H}_6)_2\text{Y}(\mu\text{-Et})_2\text{AlEt}_2$  and  $(\text{C}_9\text{H}_6)_2\text{LnNPr}^i_2$  ( $\text{Ln} = \text{Y}$ , Yb),<sup>998</sup> the samarocene derivatives



Scheme 272

$\text{Cp}^*_2\text{SmMe}(\text{THF})$  supported on MCM-41,<sup>999</sup> mesoporous silicates<sup>1000</sup> or silica gel grade 995,<sup>1001</sup> the *ansa*-neodymocene amide  $\text{Me}_2\text{Si}(\text{Flu})(\text{C}_5\text{H}_4)\text{Nd}(\text{NPr}^i)_2(\text{THF})_m$ ,<sup>1002</sup> permethylanthanocene hydrides and methyl derivatives,<sup>1003</sup> 1,1'-(3-oxapentamethylene)-bridged bis(indenyl) *ansa*-lanthanidocenes,<sup>697</sup> carbene complexes derived from permethylsamarocene and permethylytterbocene,<sup>1004</sup>  $\text{Yb}[\text{C}(\text{SiMe}_3)_3]_2$ ,<sup>1005</sup> bis(pyrrolylaldiminato)samarium hydrocarbyl complexes,<sup>149</sup> divalent ytterbium complexes containing  $\beta$ -diketiminato ligands,<sup>267</sup> an Sm(II) allyl complex,<sup>185</sup> *ansa*-bis(allyl)lanthanide complexes,<sup>189</sup> bis- and tetrakis(trimethylsilyl)-substituted lanthanocene methyl complexes such as  $[(\text{C}_5\text{H}_4\text{SiMe}_3)_2\text{Sm}(\mu\text{-Me})]_2$  and  $[(\text{C}_5\text{H}_3(\text{SiMe}_3)_2\text{-1,3})_2\text{Ln}(\mu\text{-Me})]_2$  ( $\text{Ln} = \text{Nd}, \text{Sm}$ ),<sup>961</sup> guanidinate lanthanide methyl complexes of the type  $[(\text{Me}_3\text{Si})_2\text{NC}(\text{NPr}^i)_2]_2\text{Ln}(\mu\text{-Me})_2\text{Li}(\text{TMEDA})$  ( $\text{Ln} = \text{Nd}, \text{Yb}$ ),<sup>123</sup> bis(arylamido)lanthanide methyl complexes,<sup>1006</sup>  $\text{Cp}_2\text{Ln}$  complexes containing piperonal dimethylacetal as ligand,<sup>1007</sup> silylene-bridged *ansa*-bis(fluorenyl)lanthanide complexes,<sup>1008</sup> pendant phenyl cyclopentadienyl lanthanide complexes,<sup>1009</sup> sterically hindered allyl lanthanide complexes,<sup>187,187a</sup> and benzyl-substituted cyclopentadienyl lanthanide complexes.<sup>1010</sup>

Several 1-cyclopentylindenyl lanthanide(II) complexes have been found to be active for the polymerization of acrylonitrile.<sup>662,1011–1013</sup> In the case of  $(\text{C}_5\text{H}_4\text{Bu}^t)_2\text{Sm}(\text{THF})_2$  the catalytic activity can be greatly increased by adding certain sodium phenoxide derivatives.<sup>1013</sup> The catalytic activity of  $[(\text{C}_5\text{H}_4\text{Bu}^t)_2\text{Nd}(\mu\text{-Me})]_2$  was found to be greatly increased by adding quaternary ammonium salts or sodium phenoxides.<sup>1014</sup> The heterobimetallic bis(indenyl) complexes  $(\text{C}_9\text{H}_6)_2\text{Y}(\mu\text{-Et})_2\text{AlEt}_2$  and  $(\text{C}_9\text{H}_6)_2\text{LnNPr}^i_2$  ( $\text{Ln} = \text{Y}, \text{Yb}$ ) have been used as single-component catalysts for the polymerization of acrylonitrile. These complexes can produce polyacrylonitrile (PAN) with molecular weights from 10 000 to 30 000.<sup>1015,1016</sup>

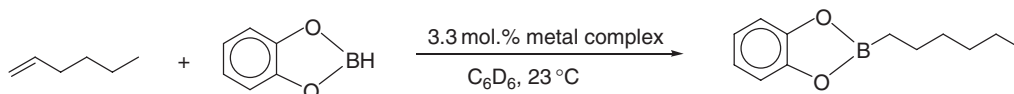
#### 4.01.13.4.6 Other monomers (isocyanates, stannanes, etc.)

Lanthanide amides of the type  $(\text{C}_5\text{H}_4\text{Me})_2\text{Ln}\{\text{OCN}(\text{Pr}^i)_2\text{NPh}\}(\text{THF})$ ,  $\text{Ln} = \text{Y}, \text{Er}, \text{Yb}$ , have been synthesized and their activity in the polymerization of  $\text{PhNCO}$  tested. The Y complex showed good activity at 30 °C and yielded yellow solid polymers which consisted of 43% methanol-insoluble and 57% methanol-soluble fractions.<sup>420</sup> The regio- and stereoselective polymerization of aromatic diynes catalyzed by lanthanide metallocenes such as  $\text{Cp}^*_2\text{PrCH}(\text{SiMe}_3)_2$  has been investigated.<sup>1017</sup>

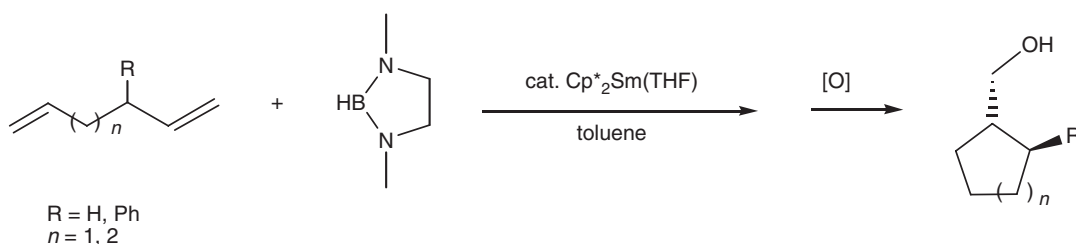
Metallocene complexes including  $\text{Cp}^*_2\text{SmCH}(\text{SiMe}_3)_2$  catalyze the dehydropolymerization of secondary stannanes to polymers and oligomers.<sup>1018</sup>

#### 4.01.13.5 Organolanthanide-catalyzed Hydroboration Reactions

The samarium(III)-catalyzed olefin hydroboration reaction using *ab initio* methods has been investigated. The stationary structures on the model reaction path considering ethylene as alkene,  $\text{Cp}_2\text{SmH}$  as an active catalyst, and  $\text{HB}(\text{OH})_2$  as model borane were obtained at the RHF and MP2 levels, and the MP4SDQ energy calculations were carried out at the MP2 structure. In the reaction, ethylene initially coordinates to the active catalyst to form a  $\pi$ -complex. Then, ethylene insertion into the  $\text{Sm-H}$  bond takes place leading to stable  $\text{Cp}_2\text{SmC}_2\text{H}_5$  after passing through the barrier of 4.2 kcal mol<sup>-1</sup>. In the following step the model borane adds to  $\text{Cp}_2\text{SmC}_2\text{H}_5$  to form a borane complex which thereafter passes through the smaller barrier of 1.1 kcal mol<sup>-1</sup> giving rise to a product complex. In the final step, the dissociation of the hydroborated product,  $\text{C}_2\text{H}_5\text{B}(\text{OH})_2$ , takes place with a large endothermicity of 40.4 kcal mol<sup>-1</sup>.<sup>1019</sup> The organolanthanide complexes  $\text{Cp}^*_2\text{LnCH}(\text{SiMe}_3)_2$  ( $\text{Ln} = \text{Y}, \text{La}$ ),  $\text{Cp}^*_2\text{YMe}(\text{THF})$ ,  $[\text{Cp}^*_2\text{Y}(\mu\text{-H})]_2$ ,  $\text{Cp}_2\text{YCH}(\text{SiMe}_3)_2$ , and  $\text{Cp}_2\text{YCH}(\text{SiMe}_3)_2\cdot\text{Et}_2\text{O}$  have been investigated as catalysts for hydroboration of 1-hexene using catecholborane as boration agent (Scheme 273). The complex  $\text{Cp}^*_2\text{LaCH}(\text{SiMe}_3)_2$  showed the highest activity but the yttrium analog was found to be much less active. Other permethyltrocene compounds,  $\text{Cp}^*_2\text{YMe}(\text{THF})$  and  $[\text{Cp}^*_2\text{Y}(\mu\text{-H})]_2$ , were moderately active, while the sterically more accessible  $\text{Cp}_2\text{YCH}(\text{SiMe}_3)_2$  and  $\text{Cp}_2\text{YCH}(\text{SiMe}_3)_2\cdot\text{Et}_2\text{O}$  showed an increasing activity. The benzamidinato complexes  $[\text{PhC}(\text{NSiMe}_3)_2]_2\text{YCH}(\text{SiMe}_3)_2$ ,  $[\text{PhC}(\text{NSiMe}_3)_2]_2\text{YCH}_2\text{Ph}\cdot\text{THF}$ , and  $[\text{PhC}(\text{NMe}_3)_2]_2\text{YCH}(\text{SiMe}_3)_2$  were also catalytically active but the activity was substantially lower than that of the  $\text{Cp}^*_2\text{LaCH}(\text{SiMe}_3)_2$ .<sup>1020</sup> The



Scheme 273



Scheme 274

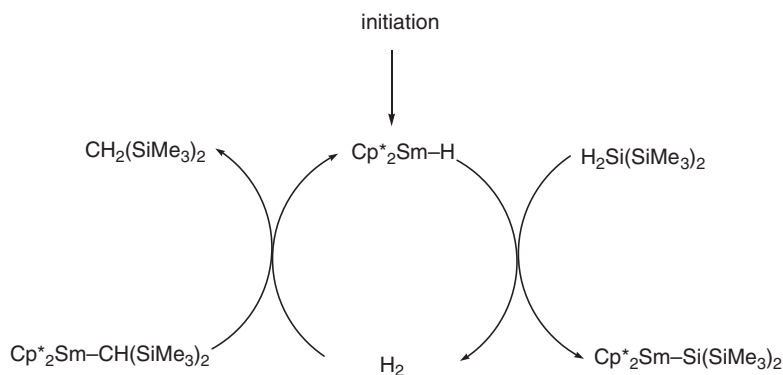
catalytic activities of  $[\text{Cp}^*_2\text{Sm}(\mu\text{-OAr})_2]$  and  $[(\mu\text{-Cp}^*)\text{Sm}(\text{OAr})\text{K}(\mu\text{-Cp}^*)(\text{THF})_2]_\infty$  ( $\text{Ar} = 2,6\text{-Bu}^t_2\text{-4-MeC}_6\text{H}_2$ ) in the hydroboration of alkenes have been investigated.<sup>925</sup>

The 1,5- and 1,6-dienes undergo a cyclization/boration reaction in the presence of a catalytic amount of  $\text{Cp}^*_2\text{Sm}(\text{THF})$ . The resulting organoboranes can be oxidized to the corresponding primary cyclic alcohols using standard conditions (Scheme 274).<sup>1021</sup>

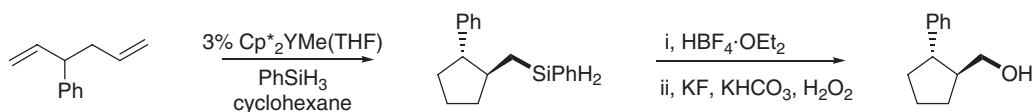
#### 4.01.13.6 Organolanthanide-catalyzed Hydrosilylation Reactions

A theoretical study of  $\text{SiH}_4$  activation by  $\text{Cp}_2\text{LnH}$  complexes for the entire series of lanthanides has been carried out at the DFT-B3PW91 level of theory. The reaction paths corresponding to H/H exchange and silylation, formation of  $\text{Cp}_2\text{Ln}(\text{SiH}_3)$ , have been computed. They both occur via a single-step  $\sigma$ -bond metathesis mechanism. Both pathways are thermally accessible. The H/H exchange path was calculated to be kinetically more favorable, whereas the silylation reaction is thermodynamically preferred. The reactivity of this family of lanthanide complexes with  $\text{SiH}_4$  contrasts strongly with that obtained previously with  $\text{CH}_4$ . The considerably lower activation barrier for silylation relative to methylation was attributed to the ability of Si to become hypervalent.<sup>1022</sup> Various lanthanide alkyl complexes have been utilized as catalysts for hydrosilylation in the reaction of phenylsilane with selected commercially available alkenes and alkynes. The catalytic reaction takes place with high regioselectivity, and the silyl group is delivered preferentially to the less hindered carbon atom of the double or triple bond.<sup>539</sup> The mechanism of  $\sigma$ -bond metathesis reactions of  $\text{Cp}^*_2\text{SmCH}(\text{SiMe}_3)_2$  with silicon-hydrogen bonds has been investigated. The study showed that a seemingly simple  $\sigma$ -bond metathesis reaction proceeds in fact by a more complex autocatalytic mechanism mediated by a reactive hydride complex (Scheme 275).<sup>1023</sup>

The dimeric lanthanide methyl complexes  $[(\text{C}_5\text{H}_4\text{SiMe}_2\text{R})_2\text{Ln}(\mu\text{-Me})_2]$  ( $\text{R} = \text{Me, Bu}^t$ ;  $\text{Ln} = \text{Y, Sm, Lu}$ ) have been found to be effective precatalysts for the hydrosilylation of a series of alkenes and alkynes using phenylsilane as the hydrosilylation agent.<sup>351</sup> Dimeric lanthanides (Tb, Yb, Lu) and yttrium hydrides,  $[(\text{C}_5\text{H}_4\text{Bu}^t)_2\text{Ln}(\mu\text{-H})_2]$  and hydrocarbyls  $[(\text{C}_5\text{H}_4\text{Bu}^t)_2\text{Ln}(\mu\text{-Me})_2]$ , as well as hydrido-alkyl compounds  $(\text{C}_5\text{H}_4\text{Bu}^t)_2\text{Ln}(\mu\text{-H})(\mu\text{-Me})\text{Ln}(\text{C}_5\text{H}_4\text{Bu}^t)_2$  are efficient and selective catalysts for the hydrosilylation of 1-octene. Binuclear complexes with  $\text{Ln}(\mu\text{-H})_2\text{Ln}$  and  $\text{Ln}(\mu\text{-H})(\mu\text{-alkyl})\text{Ln}$  bridges were found to be the key intermediates in 1-octene hydrosilylation catalyzed by both the



Scheme 275



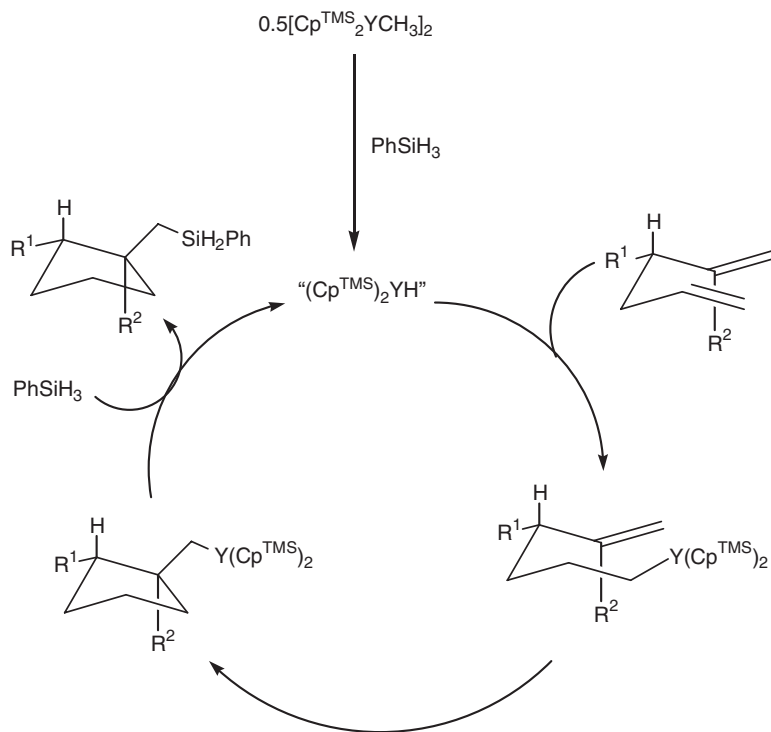
Scheme 276

hydrides and the mixed compounds in benzene at 75 °C. It was argued therefore that in this case the dissociation of the starting dimeric organolanthanide into monomeric species is not required for the catalytic reaction to proceed.<sup>1024</sup>

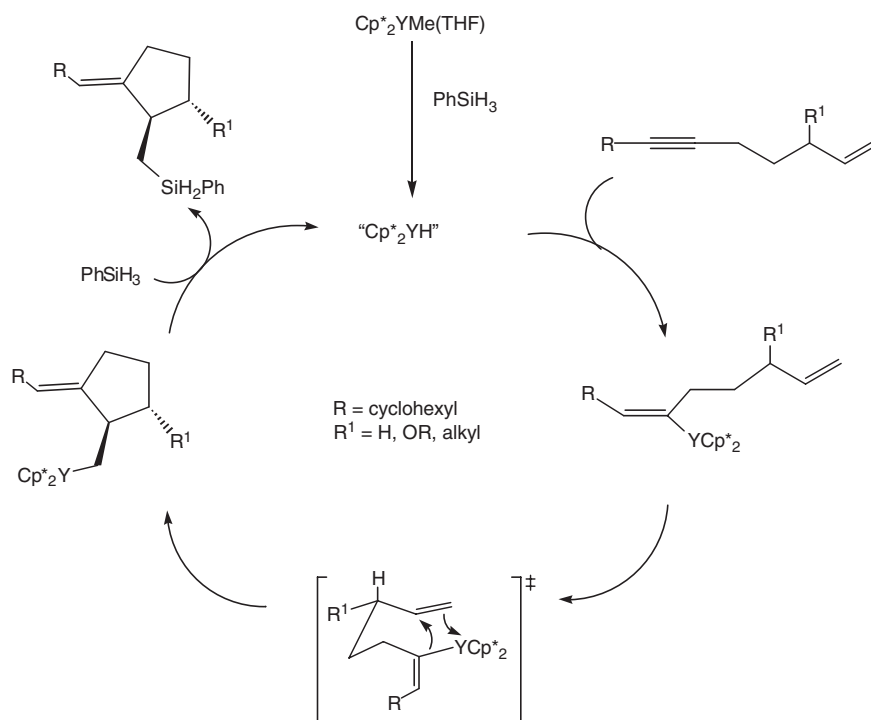
The sequential cyclization/silylation reactions of 1,5-dienes and 1,6-dienes are catalyzed by  $\text{Cp}^*_2\text{YMe}(\text{THF})$ . The reaction tolerates a number of functional groups and proceeds with good yields and diastereoselectivities to give phenylsilane products which can be converted easily to synthetically more versatile alcohols (Scheme 276).<sup>1025</sup> The hydrosilylation of dienes is also effectively catalyzed by the neodymium alkyl complex  $\text{Cp}^*_2\text{NdCH}(\text{SiMe}_3)_2$ .<sup>1026</sup>

Cyclization/silylation reactions of nitrogen-containing enynes catalyzed by the complexes  $\text{Cp}^*_2\text{LnMe}(\text{THF})$  ( $\text{Ln} = \text{Y}, \text{Lu}$ ) have been investigated. Using standard conditions, the  $\text{Cp}^*_2\text{YMe}(\text{THF})$  complex suffers from poor reactivity at room temperature with nitrogen positioned in  $\alpha$ -position to the alkyne. This can be overcome by either slow catalyst addition or by using  $\text{Cp}^*_2\text{LuMe}(\text{THF})$  as the catalyst, which contains the smaller  $\text{Lu}(\text{III})$  ion. The use of  $\text{Cp}^*_2\text{LuMe}(\text{THF})$  allowed the preparation of various nitrogen-containing ring systems in excellent yields with good to excellent diastereoselectivities at room temperature. The results of these studies highlight the ability to tune the reactivity of an organolanthanide complex by changing the metal center.<sup>1027</sup>

The catalytic cyclization/silylation reaction of sterically hindered dienes with  $\text{PhSiH}_3$  is catalyzed by relatively non-hindered complexes  $\text{Me}_2\text{Si}(\text{C}_5\text{H}_3\text{SiMe}_3)_2\text{YCH}(\text{SiMe}_3)_2$  and  $[(\text{C}_5\text{H}_4\text{SiMe}_3)_2\text{Ln}(\mu\text{-Me})]_2$  ( $\text{Ln} = \text{Y}, \text{Lu}$ ) (Scheme 277). The precatalyst reacts with the silane via a  $\sigma$ -bond metathesis reaction to generate an organolanthanide hydride, releasing the alkyl group. This hydride then inserts the least hindered olefin, placing the metal at the terminus of the carbon chain. The hydrocarbyl thus formed undergoes intramolecular olefin insertion through a chairlike transition structure before reacting with the silane via  $\sigma$ -bond metathesis.<sup>1028</sup>



Scheme 277



Scheme 278

The selective sequential cyclization/silylation of 1,6- and 1,7-enynes is catalyzed by the organoyttrium complex  $\text{Cp}^*_2\text{YMe}(\text{THF})$  (Scheme 278).<sup>1029</sup>

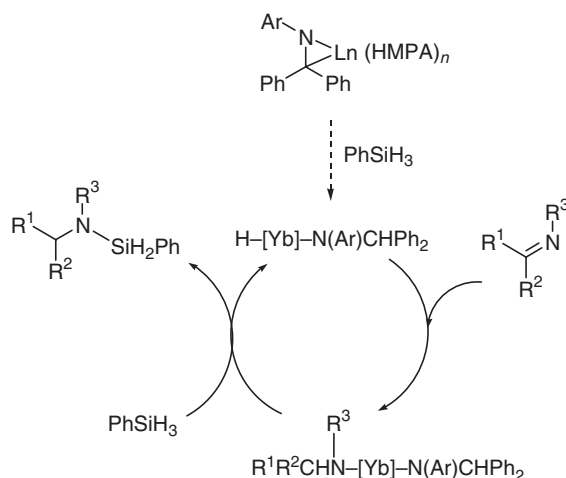
It was proposed that the catalytic cycle is initiated by  $\sigma$ -bond metathesis between  $\text{Cp}^*_2\text{YMe}(\text{THF})$  and  $\text{PhSiH}_3$ , producing a catalytically active metal hydride species " $\text{Cp}^*_2\text{YH}$ ". In the next step, the catalyst inserts preferentially at the alkyne sites. This intermediate undergoes cyclization via an intramolecular olefin insertion and produces a second intermediate alkylttrium species. In the reaction with silane this intermediate undergoes a subsequent  $\sigma$ -bond metathesis to generate the cyclized product.<sup>1029</sup>

Commercially available lanthanum tris[bis(trimethylsilyl)amide] has been shown to be a very effective catalyst for the hydrosilylation of representative alkenes and dienes in the presence of  $\text{PhSiH}_3$ .<sup>1030</sup> The organolanthanide metallocene-catalyzed hydrosilylation of alkynylsilanes has been found to provide (Z)-1,1-bis(silyl)alkenes. In particular,  $\text{Cp}^*_2\text{YMe}(\text{THF})$ ,  $[(\text{C}_5\text{H}_4\text{SiMe}_3)_2\text{Y}(\mu\text{-Me})_2]$ , and  $[(\text{C}_5\text{H}_4\text{SiMe}_3)_2\text{Lu}(\mu\text{-Me})_2]$  were shown to be regioselective for the hydrosilylation of various alkynylsilanes. The process was evaluated for diverse substitution patterns and functional groups on the pendant alkyl chain. Silyl ethers and halogens are stable to the catalytic process, affording excellent chemo- and regioselectivities. Competition between "aryl-directed" and "silyl-directed" processes was observed upon hydrosilylation of (phenylethynyl)dimethylsilane.<sup>1031</sup> Dimeric yttrium hydrido complexes containing the pendant-arm cyclopentadienyl ligand  $[\text{C}_5\text{Me}_4\text{CH}_2\text{SiMe}_2\text{NBu}^t]^-$  have been found to catalyze the hydrosilylation of 1,5-hexadiene, 1,7-octadiene, and vinylcyclohexene by  $\text{PhSiH}_3$ .<sup>1032</sup>

Lanthanide(II)-imine complexes, obtained by reduction of aromatic ketimines with samarium and ytterbium metal, effectively catalyze the hydrosilylation of imines. The proposed catalytic cycle for the imine hydrosilylation is outlined in Scheme 279.<sup>961,1033</sup>

#### 4.01.13.7 Organolanthanide-catalyzed Hydroamination Reactions

Organo-*f*-element-catalyzed hydroaminations have been extensively investigated for more than 10 years.<sup>1034–1038</sup> Lanthanide metallocenes catalyze the regiospecific intermolecular addition of primary amines to acetylenic, olefinic, and diene substrates at rates which are  $\sim 1/1000$  those of the most rapid intramolecular analogs. Kinetic and mechanistic data argue for turnover-limiting  $\text{C}\equiv\text{C}/\text{C}=\text{C}$  insertion into an  $\text{Ln}-\text{N}$  bond, followed by protonolysis of



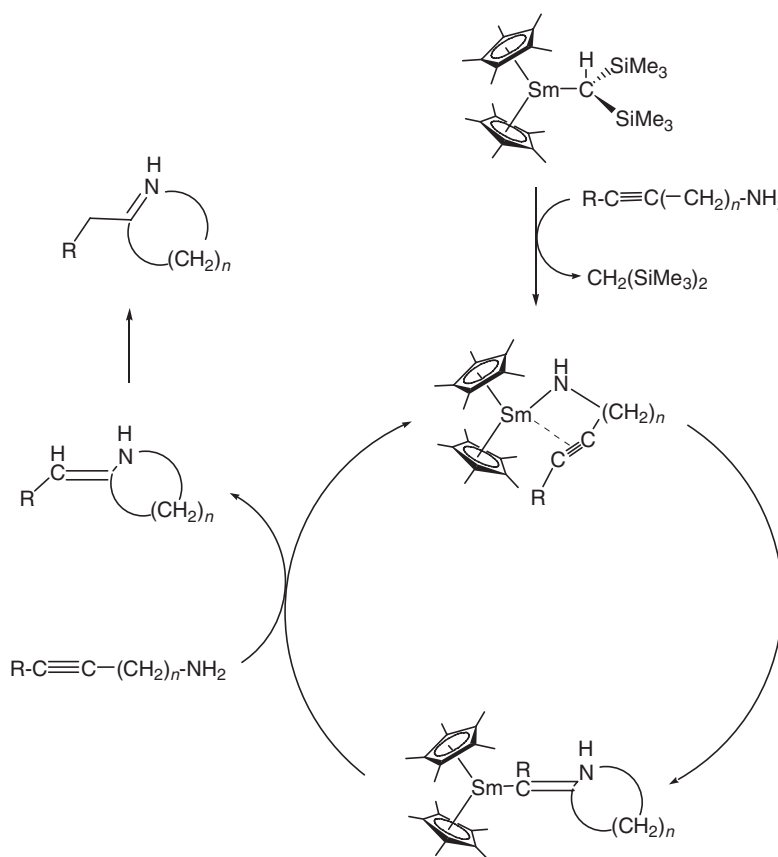
Scheme 279

the resulting Ln–C bond. The rigorously anhydrous/anaerobic reaction of primary alkyl amines (0.30 M) with various alkynes, alkenes, and dienes (1.2 M) was carried out in hydrocarbon solvents using  $\text{Cp}^*_2\text{LnCH}(\text{SiMe}_3)_2$  and  $\text{Me}_2\text{Si}(\text{C}_5\text{Me}_4)_2\text{LnCH}(\text{SiMe}_3)_2$  ( $\text{Ln} = \text{Sm}, \text{Nd}$ ) as precatalysts. The reactions proceed with >95% regioselectivity.<sup>1039</sup> The efficient and regioselective hydroamination/cyclization of aliphatic and aromatic aminoalkynes of the formula  $\text{RC}\equiv\text{C}(\text{CH}_2)_n\text{NH}_2$  catalyzed by  $\text{Cp}^*_2\text{LnCH}(\text{SiMe}_3)_2$  ( $\text{Ln} = \text{La}, \text{Nd}, \text{Sm}, \text{Lu}$ ) and  $[\text{Me}_2\text{Si}(\text{C}_5\text{Me}_4)_2\text{LnCH}(\text{SiMe}_3)_2]$  ( $\text{Ln} = \text{Nd}, \text{Sm}$ ) yields the corresponding cyclic imines  $\text{RCH}_2\text{C}=\text{N}(\text{CH}_2)_{n-1}\text{CH}_2$ , and that of aliphatic secondary aminoalkynes of the formula  $\text{RC}\equiv\text{C}(\text{CH}_2)_3\text{NHR}^1$  generates the corresponding cyclic enamines  $\text{RCH}=\text{CNR}^1(\text{CH}_2)_2\text{CH}_2$ . Kinetic and mechanistic evidence argues that the turnover-limiting step is an intramolecular alkyne insertion into the Ln–N bond followed by rapid protonolysis of the resulting Ln–C bond (Scheme 280). The use of metals with larger ionic radius (e.g.,  $\text{Cp}^*_2\text{LnCH}(\text{SiMe}_3)_2$ ) and more open  $\text{Me}_2\text{Si}(\text{C}_5\text{Me}_4)_2\text{LnCH}(\text{SiMe}_3)_2$  complexes as the precatalysts results in a decrease in the rate of hydroamination/cyclization, arguing that the steric demands in the  $-\text{C}\equiv\text{C}$ -insertive transition state are relaxed compared to those of the analogous aminoolefin hydroamination/cyclization. The process provides an efficient method for the catalytic synthesis of pyrrole, pyridine, and azepin derivatives.<sup>1040</sup>

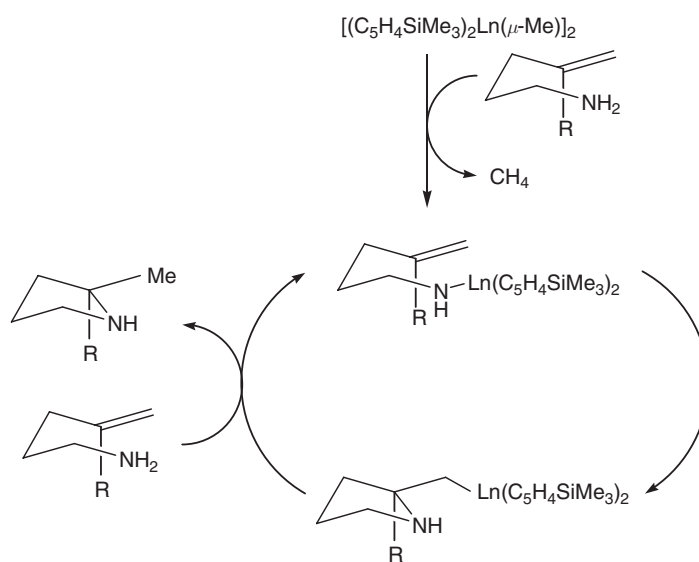
Investigations of the intramolecular hydroamination of sterically hindered alkenes using organolanthanide complexes have been made. The non-hindered catalyst system  $[(\text{C}_5\text{H}_4\text{SiMe}_3)_2\text{Ln}(\mu\text{-Me})_2]$  is able to add to hindered alkenes providing products containing quaternary centers. This process tolerates a wide variety of substitution patterns, allowing the construction of monocyclic as well as fused and bridged bicyclic heterocycles. The organometallic complex enters the catalytic cycle with metallation of the amine nitrogen. This is followed by an intramolecular olefin insertion to generate a hydrocarbyl intermediate which undergoes  $\sigma$ -bond metathesis with another primary amine to complete the cycle (Scheme 281).<sup>1041</sup>

The organolanthanides  $[\text{Me}_2\text{Si}(\text{C}_5\text{Me}_4)(\text{NBu}^t)]\text{LnN}(\text{SiMe}_3)_2$  ( $\text{Ln} = \text{Nd}, \text{Lu}, \text{Sm}$ ) and  $[\text{Me}_2\text{Si}(\text{C}_5\text{Me}_4)(\text{NBu}^t)]\text{LnCH}(\text{SiMe}_3)_2$  ( $\text{Ln} = \text{Yb}, \text{Lu}$ ) have been found to be significantly more active as precatalysts for the aminoalkene hydroamination/cyclization than the corresponding bis(cyclopentadienyl) complexes  $\text{Cp}^*_2\text{LnN}(\text{SiMe}_3)_2$  and  $\text{Cp}^*_2\text{LnCH}(\text{SiMe}_3)_2$ .<sup>277</sup> In another contribution the organolanthanide-catalyzed intramolecular hydroamination/cyclization of amines tethered to 1,2-disubstituted alkenes to afford the corresponding mono- and disubstituted pyrrolidines and piperidines (Scheme 282) by using coordinatively unsaturated complexes of the type  $\text{Cp}^*_2\text{LnCH}(\text{SiMe}_3)_2$  ( $\text{Ln} = \text{La}, \text{Sm}$ ),  $\text{Me}_2\text{Si}(\text{C}_5\text{Me}_4)_2\text{NdCH}(\text{SiMe}_3)_2$ ,  $[\text{Et}_2\text{Si}(\text{C}_5\text{Me}_4)(\text{C}_5\text{H}_4)]\text{NdCH}(\text{SiMe}_3)_2$ , and  $[\text{Me}_2\text{Si}(\text{C}_5\text{Me}_4)(\text{Bu}^t\text{N})]\text{LnE}(\text{SiMe}_3)_2$  ( $\text{Ln} = \text{Y}, \text{Sm}, \text{Yb}, \text{Lu}; \text{E} = \text{N}, \text{CH}$ ) as precatalysts has been reported.<sup>1042</sup> More recently, the organolanthanide-catalyzed hydroamination/cyclization has been extended to conjugated amino-dienes<sup>1043</sup> and amine-tethered unactivated 1,2-disubstituted alkenes.<sup>1044</sup>

Diastereoselective hydroamination/cyclization reactions found their application in the total synthesis of the pyrrolidine alkaloid (+)-197B and pyrrolizidine alkaloid (+)-xenovenine.<sup>1045</sup> The organolanthanide precatalysts  $\text{Cp}^*_2\text{LnCH}(\text{SiMe}_3)_2$  and  $[\text{Me}_2\text{Si}(\text{C}_5\text{Me}_4)(\text{NBu}^t)]\text{LnCH}(\text{SiMe}_3)_2$  ( $\text{Ln} = \text{La}, \text{Nd}, \text{Sm}$ ) catalyze the regio- and stereoselective cyclohydroamination of the aminoallenes (5S,8S)-5-amino-trideca-8,9-diene and the aminoallene (5S)-5-amino-pentadeca-1,8,9-triene, which are the key steps of the total synthesis of the above-mentioned molecules.<sup>1045</sup>

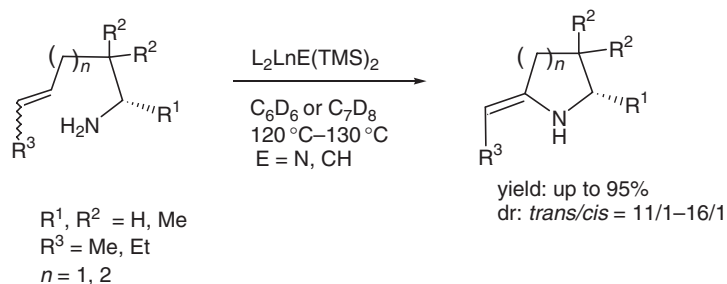


Scheme 280



Scheme 281





Scheme 282

The scope of the lanthanide-mediated, intramolecular amination/cyclization reaction has been determined for the formation of substituted quinolizidines, indolizidines, and pyrrolizidines,<sup>1046</sup> as well as tricyclic and tetracyclic aromatic nitrogen heterocycles.<sup>1047</sup> The amide derivative *meso*-[ethylene-bis(indenyl)]ytterbium(III) bis(trimethylsilyl)amide catalyzes the hydroamination of primary olefins in excellent yields.<sup>701</sup> A facile intramolecular hydroamination process catalyzed by  $[(\text{C}_5\text{H}_4\text{SiMe}_3)_2\text{Nd}(\mu\text{-Me})_2]$  has also been reported. The lanthanide-catalyzed hydroamination enables a rapid access to 10,11-dihydro-5*H*-dibenzo[*a,d*]cyclohepten-5,10-imines (Scheme 283).<sup>1048</sup>

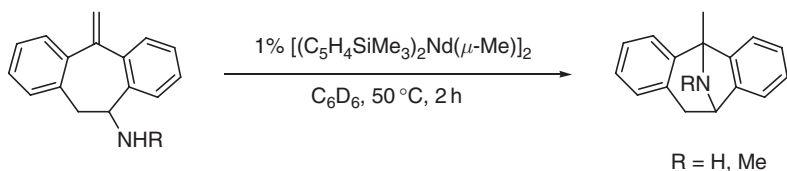
A series of organolanthanide complexes of the general type  $\text{Cp}^*_2\text{LnCH}(\text{SiMe}_3)_2$  ( $\text{Ln} = \text{La, Sm, Y, Lu}$ ) have been reported to be effective as precatalysts for the rapid, regioselective, and highly diastereoselective intramolecular hydroamination/cyclization of aminoallenes.<sup>1049</sup> The hydroamination of aminoallenes with the general formula  $\text{RCH}=\text{C}=\text{CH}(\text{CH}_2)_n\text{CHR}^1\text{NH}_2$  yields the corresponding heterocycles  $\text{RCH}=\text{CHCHNHCH}(\text{R}^1)(\text{CH}_2)_{n-1}\text{CH}_2$  ( $\text{R} = \text{Me, Pr}^n, n\text{-C}_5\text{H}_{11}$ ;  $\text{R}^1 = \text{H, Me, Bu}^n, \text{CH}_2=\text{CHCH}_2\text{CH}_2$ ;  $n = 2, 3$ ). The mono- and disubstituted pyrrolidines and piperidines produced bear an  $\alpha$ -alkenyl functionality available for further synthetic manipulation. Kinetic and mechanistic data parallel organolanthanide-mediated intramolecular aminoalkene and aminoalkyne hydroamination/cyclizations, implying turnover-limiting allene insertion into the  $\text{Ln-N}$  bond followed by rapid protonolysis of the resulting  $\text{Ln-C}$  bond (Scheme 284).<sup>1049,1050</sup>

In principle, two regioisomeric products are possible starting from aminoallenes (Scheme 285).<sup>1049</sup>

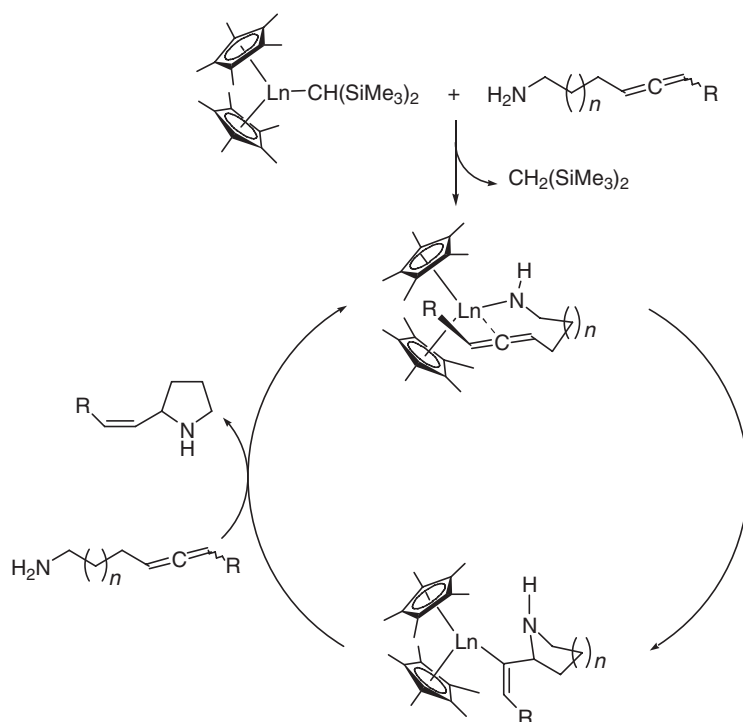
Catalytic tandem C–N and C–C bond-forming reactions involving the intramolecular hydroamination/bicyclization and intermolecular hydroamination/cyclization of olefins and alkynes using the organolanthanide complexes  $\text{Cp}^*_2\text{LnCH}(\text{SiMe}_3)_2$  and  $\text{Me}_2\text{Si}(\text{C}_5\text{Me}_4)_2\text{LnCH}(\text{SiMe}_3)_2$  ( $\text{Ln} = \text{Sm, Nd}$ ) as precatalysts have also been described (Scheme 286).<sup>1051</sup>

Recently, novel  $C_2$ -symmetric bis(oxazolinato)lanthanide catalysts have been introduced as precatalysts for the efficient enantioselective intramolecular hydroamination/cyclization of aminoalkenes and aminodienes.<sup>1052</sup> Chiral binaphtholate yttrium aryl complexes have been reported to be highly active and enantioselective catalysts for the asymmetric hydroamination of aminoalkenes, as well as the kinetic resolution of  $\alpha$ -substituted 1-aminopent-4-enes to give *trans*-2,5-disubstituted pyrrolidines with good enantiomeric excess and high  $k_{\text{rel}}$ .<sup>1053</sup> Intramolecular hydroamination of alkenes and alkynes has also been reported for yttrium catalysts bearing diamidoamine ligands,<sup>141</sup> and a cationic  $\beta$ -diketiminato scandium alkyl complex.<sup>1054</sup>

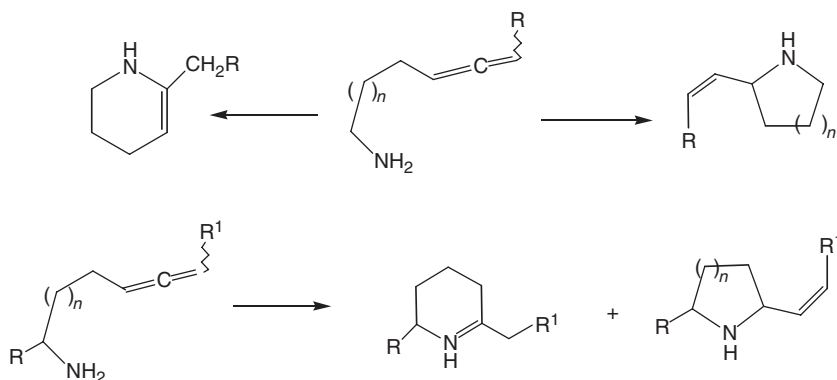
Homoleptic lanthanide alkyls of the form  $\text{Ln}[\text{CH}(\text{SiMe}_3)_2]_3$  ( $\text{Ln} = \text{Y, La, Nd, Sm, Lu}$ ) serve as efficient precatalysts for intramolecular homogeneous hydrophosphination. Both phosphinoalkenes and phosphinoalkynes undergo cyclization to the corresponding heterocyclic structures.<sup>1055</sup> The catalytic intramolecular hydrophosphination/cyclization of phosphinoalkenes and phosphinoalkynes using organolanthanide precatalysts of the type



Scheme 283



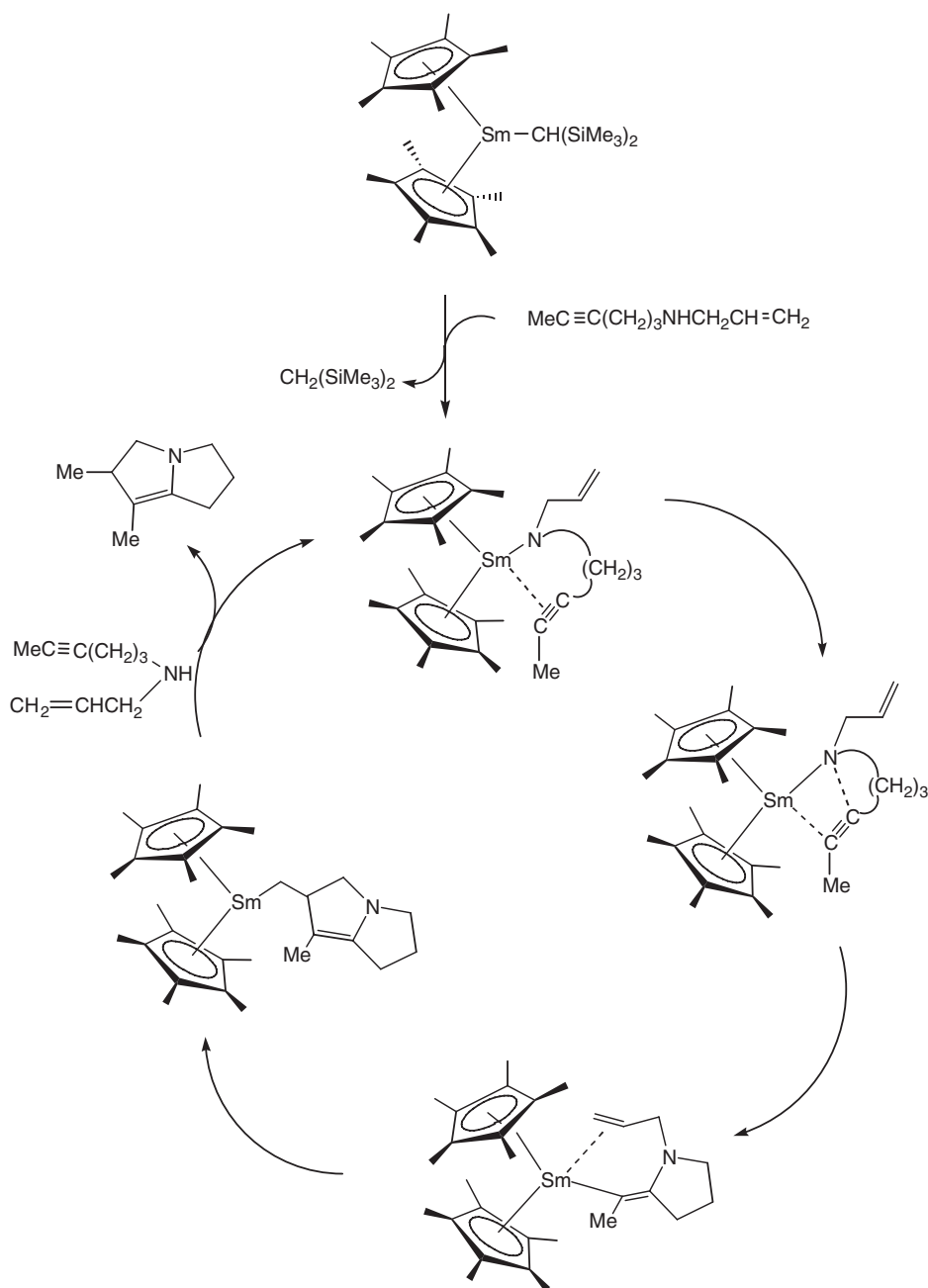
Scheme 284



Scheme 285

$\text{Cp}^*_2\text{LnCH}(\text{SiMe}_3)_2$  ( $\text{Ln} = \text{Y}, \text{La}, \text{Sm}, \text{Lu}$ ) and  $[\text{Me}_2\text{Si}(\text{Me}_4\text{C}_5)(\text{NBu}^t)]\text{SmN}(\text{SiMe}_3)_2$  has been studied in detail (Scheme 287).<sup>1056,1057</sup>

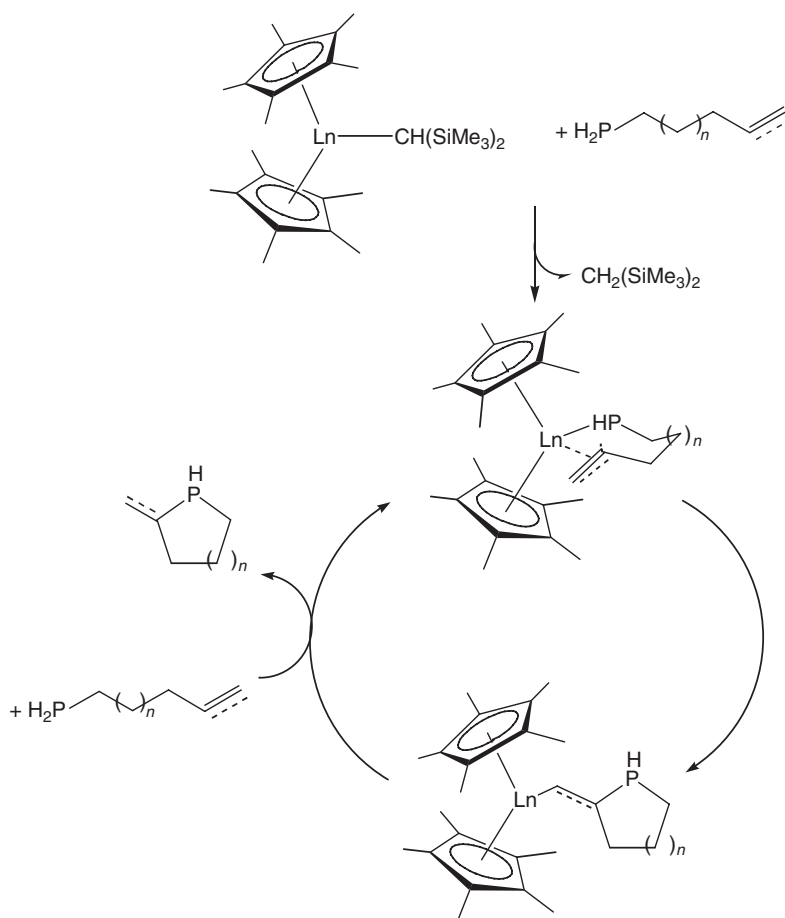
More recently, new chiral  $C_1$ -symmetric organolanthanide catalysts of the type  $[\text{Me}_2\text{Si}(\text{OHf})(\text{CpR}^*)]\text{LnN}(\text{SiMe}_3)_2$  ( $\text{OHf} = \eta^5$ -octahydrofluorenyl;  $\text{CpR}^* = (-)$ -menthyl- $\text{C}_5\text{H}_3$ ;  $\text{Ln} = \text{Y}, \text{Sm}, \text{Lu}$ ) have been synthesized, characterized, and implemented in the enantioselective and diastereoselective cyclizations of aminoalkenes and phosphinoalkenes.<sup>1058</sup> Intermolecular hydrophosphination of alkynes with diphenylphosphine is catalyzed by a Yb-imine complex,  $\text{Yb}(\eta^2\text{-Ph}_2\text{CNPh})(\text{HMPA})_3$ , to give alkenylphosphines and phosphine oxides after oxidative workup in good yields under mild conditions (Scheme 288). This reaction is also applicable to various carbon–carbon multiple bonds such as conjugated diynes and dienes, allenes, and styrene derivatives. The reaction takes place through insertion of alkynes to a Yb–PPh<sub>2</sub> bond, followed by protonation.<sup>696</sup>



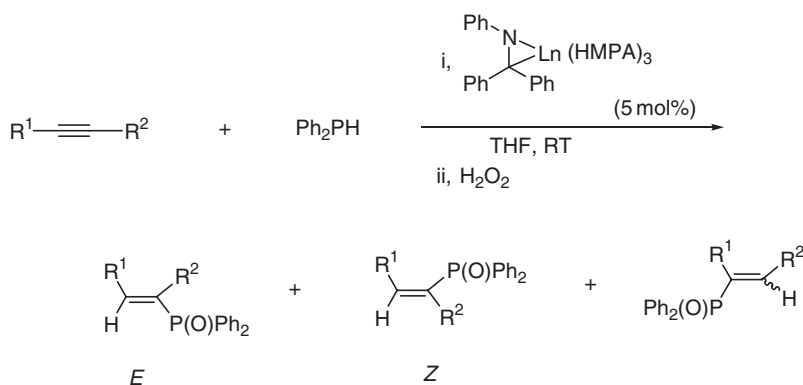
Scheme 286

#### 4.01.13.8 Other Organolanthanide-catalyzed Reactions

An exciting new approach for the selective, catalytic conversion of methane has been described. Heating a cyclohexane solution of  $\text{Ph}_2\text{SiH}_2$  and  $\text{Cp}^*_2\text{ScMe}$  to  $80^\circ\text{C}$  under 150 atm of methane produced 5 equiv. of  $\text{Ph}_2\text{MeSiH}$  after 1 week, 1 equiv. of which was derived directly from  $\text{Cp}^*_2\text{ScMe}$ .<sup>1059,1059a</sup> The related scandium alkyl  $\text{Cp}^*_2\text{ScCH}_2\text{Bu}^t$  was synthesized by the addition of a pentane solution of  $\text{LiCH}_2\text{Bu}^t$  to  $\text{Cp}^*_2\text{ScCl}$  at low temperature.  $\text{Cp}^*_2\text{ScCH}_2\text{Bu}^t$  reacts with the C–H bonds of hydrocarbons including methane, benzene, and cyclopropane to yield the corresponding hydrocarbyl complex and  $\text{CMe}_4$ . High selectivity toward methane activation suggested the participation of this



Scheme 287



Scheme 288

chemistry in a catalytic hydromethylation, which was observed in the slow,  $\text{Cp}^*_2\text{ScMe}$ -catalyzed addition of methane across the double bond of propene to form isobutene.<sup>1060</sup>

The monomeric lanthanocene Schiff base complexes  $\text{Cp}_2\text{Ln}(\text{OC}_{14}\text{H}_{13}\text{NO})$  ( $\text{Ln} = \text{Sm}, \text{Er}, \text{Dy}, \text{Y}$ ) in the presence of  $\text{NaH}$  have been found to catalyze the isomerization of 1,5-hexadiene. The isomerization results in a mixture of 1,4-hexadiene, 2,4-hexadiene, 1,3-hexadiene, methylenecyclopentane, and methylcyclopentane. The ratio of linear to

cyclic product depends upon the amount of catalyst used.<sup>405</sup> The reactions between lanthanide ( $\text{Ln} = \text{Tb}, \text{Yb}, \text{Lu}, \text{Y}$ ) hydrocarbyls and various organosilicon, -germanium, -tin, -aluminum, and -gallium hydrides in hydrocarbon solution did not produce the expected compounds with lanthanide element bonds but the corresponding unsolvated dimeric lanthanide and yttrium hydrides  $[\text{Cp}^*_2\text{Ln}(\mu\text{-H})]_2$ . The progress of the reactions of  $\text{PhMeSiH}_2$  with  $[\text{Cp}^*_2\text{Lu}(\mu\text{-Me})]_2$  and  $[\text{Cp}^*_2\text{Y}(\mu\text{-Me})]_2$  was followed by  $^1\text{H}$  NMR spectroscopy at  $20^\circ\text{C}$  and showed that the dihydrido complexes of lanthanides were formed via intermediates containing both  $\mu\text{-Me}$  and  $\mu\text{-H}$  bridges. Dimeric compounds of the type  $[\text{Cp}^*_2\text{Ln}(\mu\text{-H})(\mu\text{-Me})\text{LnCp}^*_2]$  were isolated. This reaction is a convenient and effective method for the synthesis of yttrium and lanthanide hydrides. The same authors also investigated the reactivity of lanthanide hydrides toward organosilicon hydrides and related compounds. The catalytic reaction of dimeric yttrium hydrides in the H/D exchange reaction in silanes was reported (Scheme 289).<sup>442</sup>

The lutetium hydride complex  $[\text{Cp}^*_2\text{Lu}(\mu\text{-H})]_2$  efficiently cleaves the Si-C bond of  $\text{PhSiH}_3$  to produce benzene and cross-linked polysilanes  $(\text{SiH}_x)_y$  (Scheme 290).<sup>604</sup> Formation of  $\text{Ph}_2\text{SiH}_2$  and  $\text{SiH}_4$  has also been observed during the samarium-catalyzed redistribution of  $\text{PhSiH}_3$ .<sup>543</sup>

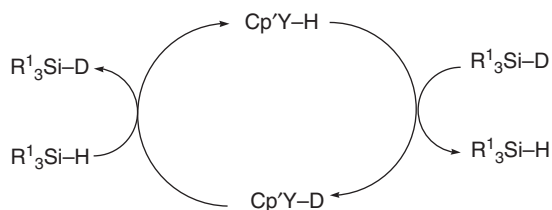
The Si-C bond cleavage appears to proceed via the lutetium phenyl complex  $\text{Cp}^*_2\text{LuPh}$ . This is supported by the reaction of  $\text{PhSiH}_3$  with  $\text{Cp}^*_2\text{LuPh}$ , which results in the formation of benzene. A plausible reaction pathway is outlined in Scheme 291.<sup>604</sup>

The organosamarium complex  $\text{Cp}^*_2\text{Sm}(\text{THF})_2$  was found to be active as catalyst for a new type of coupling reactions of vinyl esters with aldehydes (Scheme 292). The reactions led to the corresponding diesters with good yields. The proposed mechanism might involve an eight-membered alkoxy samarium intermediate with the subsequent intramolecular hydride shift reaction to give the diesters and regenerated samarium species.<sup>1061</sup>

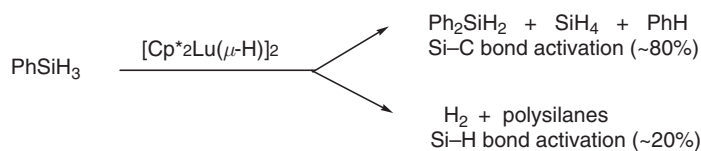
Dimeric bis(indenyl)lanthanide hydrides  $[(\text{C}_9\text{H}_7)_2\text{Ln}(\mu\text{-H})]_2 \cdot 4\text{THF} \cdot \text{NaCl}$  have been found to promote the Claisen rearrangement and selectively reduce carbonyl functions. For example, organolanthanide-catalyzed Claisen rearrangement of  $\text{PhCH}_2\text{C}(\text{O})\text{OCH}_2\text{CH}=\text{CH}_2$  in THF gave  $\text{PhCH}(\text{CHO})(\text{CH}_2\text{CH}=\text{CH}_2)$  in 61% yield.<sup>695</sup> *N*-(1-Allyl-3-butenyl)-*N*-arylamines were prepared for the first time in good yields via the direct diallylation reaction of formamides with an organosamarium reagent under mild conditions.<sup>1062</sup> The acetylcyanation of aldehydes with acetone cyanohydrin and isopropenylacetate is catalyzed by  $\text{Cp}^*_2\text{Sm}(\text{THF})_2$  (Scheme 293).<sup>1063,1063a</sup>

$\text{Cp}^*_2\text{Sm}(\text{THF})_2$  was found to catalyze the regioselective acylation of tertiary alcohols under acid-free conditions in the presence of an oxime ester. Scheme 294 illustrates the supposed catalytic process. The alcohol reacts with the oxime ester in the presence of  $\text{Cp}^*_2\text{Sm}(\text{THF})_2$  to produce the ester and cyclohexanone oxime which subsequently reacts with isopropenylacetate to regenerate cyclohexanone oxime acetate.<sup>1064</sup>

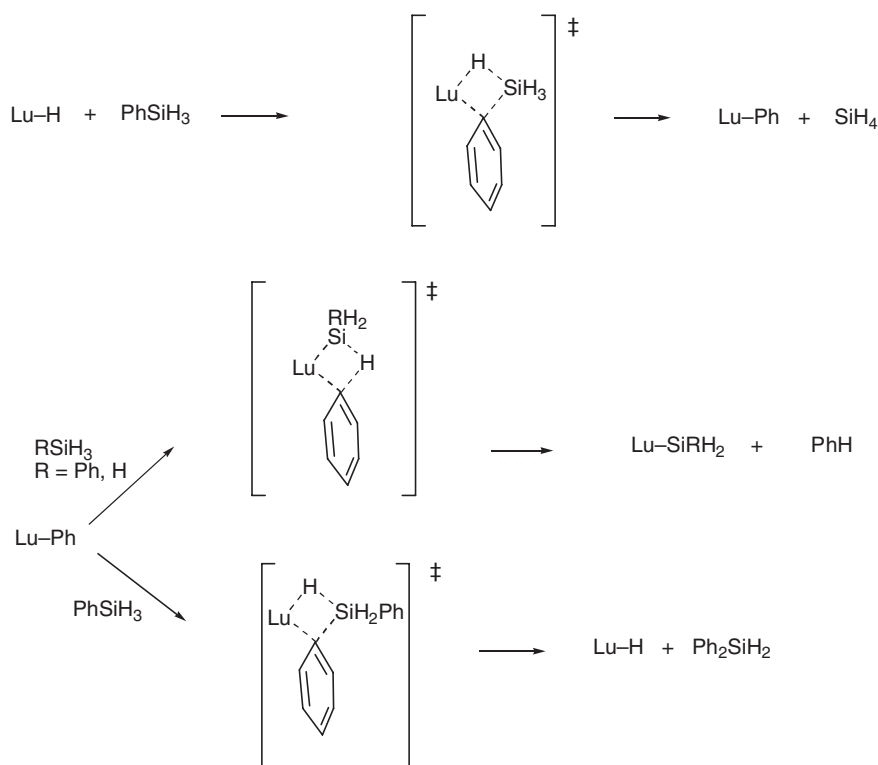
Cross silyl-benzoin additions have been reported by an *in situ* prepared “ $\text{LaBu}_3^{\text{III}}/\text{Me}_3\text{SiCN}^-$ ” catalyst system.<sup>1065</sup> The Friedel-Crafts acylation of anisole with acetanhydride using ytterbium(III) tris[tris(nonafluorobutanesulfonyl)methide] has been studied with respect to catalyst loading. A strong inhibitory effect due to the product became apparent from doping experiments and from examination of the kinetic data. This understanding allowed catalyst loadings to be reduced to as little as 0.1 mol% for effective acylation under a suitable temperature and pressure regime.<sup>680</sup>



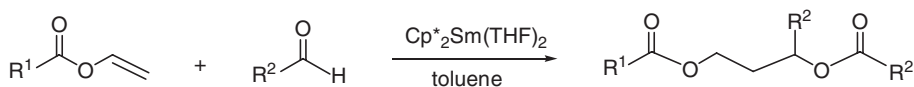
Scheme 289



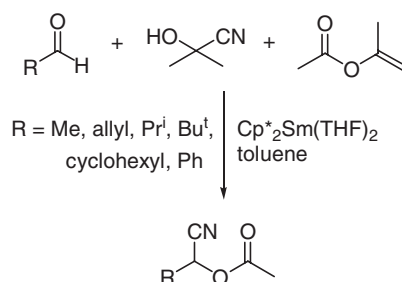
Scheme 290



Scheme 291



Scheme 292

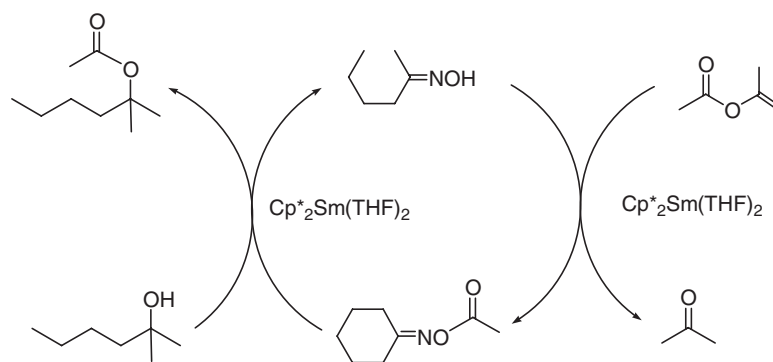


Scheme 293

#### 4.01.14 Organolanthanides in Organic Synthesis

A comprehensive review on lanthanocene catalysts in selective organic synthesis has been published by Molander and Romero.<sup>37</sup> Petrov *et al.*<sup>39</sup> have reviewed the synthesis, structure, and reactivity organolanthanides  $\text{RLnX}$  ( $\text{R}$  = alkyl, aryl;  $\text{X}$  = halogen) and lanthanide compounds with aromatic hydrocarbon dianions.

A computational study of cyclopropanation reactions of the divalent samarium carbenoid  $\text{ISmCH}_2\text{I}$  with ethylene has been presented. The  $\text{ISmCH}_2\text{I}$  species was found to have a “samarium carbene complex” character with



Scheme 294

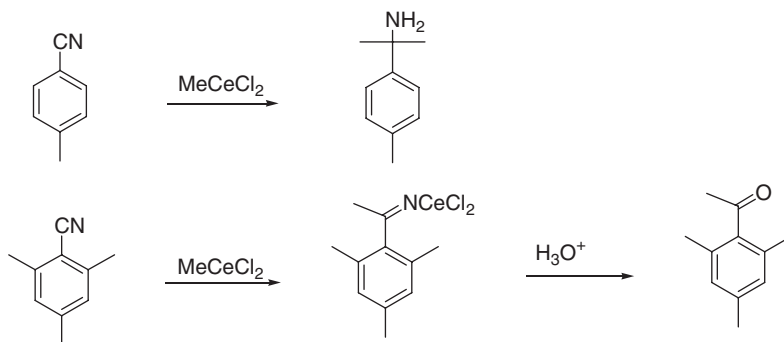
properties similar to previously investigated lithium carbenoids  $\text{LiCH}_2\text{X}$  ( $\text{X} = \text{Cl}, \text{Br}, \text{I}$ ). The  $\text{ISmCH}_2\text{I}$  carbenoid was found to be noticeably different in structure with more electrophilic character and higher chemical reactivity than the closely related classical Simmons–Smith ( $\text{IZnCH}_2\text{I}$ ) carbenoid.<sup>1066,1067</sup> The reaction of  $\text{RYbI}$  ( $\text{R} = \text{Me}, \text{Ph}$ ) with acid bromides,  $\text{R}^1\text{COBr}$  ( $\text{R}^1 = \text{Ph}, \text{Me}$ ), gave acetophenone and the corresponding tertiary alcohols, with the latter predominating when  $\text{R} = \text{Ph}$ . This addition reaction is analogous to the Grignard reaction. For example, reaction of 4 equiv.  $\text{PhYbI}$  with  $\text{MeCOBr}$  at  $20^\circ\text{C}$  in THF gave 87%  $\text{Ph}_2\text{MeCOH}$ . Acid bromides in reaction with  $\text{Yb(0)}$  are converted into  $\alpha$ -diketone which, in the presence of the  $\text{YbBr}_2$  formed in the reaction, gave some products from their partial reduction.<sup>1068</sup> The alkylation system  $\text{LnCl}_3/\text{RLi}$  has been studied in detail. Until a few years ago, “ $\text{RLnCl}_2$ ” was written as the active species, but the general drying method for preparing anhydrous  $\text{CeCl}_3$  did not remove all solvated water and led to monosolvated  $[\text{CeCl}_3(\text{H}_2\text{O})]_n$ . This complicated the reaction since at least some of the  $\text{RLi}$  could react with the water to form  $\text{Ce}_n\text{Cl}_b\text{R}_c(\text{OH})_d\text{O}_e\text{Li}_f$ . To determine the precise nature of the  $[\text{CeCl}_3(\text{H}_2\text{O})]_n/\text{RLi}$ , diamagnetic  $^{89}\text{Y}$  was used as a model. The anhydrous  $\text{YCl}_3$  was obtained by the usual method of dehydrating by heating. Recrystallization at  $25^\circ\text{C}$  from a THF solution gave crystals of  $[\text{YCl}_2(\text{H}_2\text{O})_6]\text{Cl}$ .<sup>1069</sup> Methylcerium reagents have been employed for additions to pentodialdo-1,4-furanoses. The addition of methylcerium reagents to incorporate the branching methyl group at C3 in a 2-deoxyfuranosid-3-ulose was found to be superior to either Grignard reagents or methyl lithium.<sup>1070</sup> Organocerium reagents have been employed in a simple and efficient process for the direct conversion of benzamides and thiobenzamides into tertiary carbinamines,<sup>1071</sup> as well as the formation of  $\alpha$ -silyl alcohols from  $\alpha$ -epoxytriisopropylsilane,<sup>1072</sup> the preparation of trisubstituted allylphosphine boranes,<sup>1073</sup> and other alkylation reactions.<sup>1074</sup>

The stereoselective nucleophilic addition of organocerium reagents such as  $\text{RCeCl}_2$  or  $\text{RMgBr/CeCl}_3$  ( $\text{R} = \text{Me}, \text{Ph}$ ) to the 1-imino-*E,E*-butadiene-irontricarboxyl complex  $(\text{MeCH}=\text{CHCH}=\text{CHCH}=\text{NBn})\text{Fe}(\text{CO})_3$  ( $\text{Bn} = \text{benzyl}$ ) has been studied.<sup>1075</sup> The allylcerium reagent  $(\text{CH}_2=\text{CHCH}_2)\text{CeCl}_2$  has been prepared *in situ* by stirring allylmagnesium chloride with cerium trichloride, and used for allylation reactions.<sup>1076</sup> Conjugate allylation of  $\alpha,\beta$ -unsaturated aldehydes was successfully accomplished with a new amphiphilic alkylation system, aluminum-tris(2,6-diphenylphenoxide) (ATPH)/allylcerium reagents. Diallylcerium chloride was found to be the most satisfactory among several allylcerium reagents. For example, treatment of cinnamaldehyde with  $(\text{CH}_2=\text{CHCH}_2)_2\text{CeCl}/\text{ATPH}$  in toluene gave 91% overall yield of 1,4- and 1,2-adducts in 87:13 ratio.<sup>1077</sup> The *in situ* preparation of  $\text{Me}_3\text{SiC}\equiv\text{CCeCl}_2$  and its reactions with aldehydes have been described.<sup>1078,1079</sup> The use of  $\text{MeCeCl}_2$  for the preparation of 2-(2,4,6-trimethylphenyl)-2-propanol and 2,4,6-trimethylacetophenone has been reported. It was found that only a single addition of  $\text{MeCeCl}_2$  to 2,4,6-trimethylbenzonitrile led to an imine, while it was necessary to add  $\text{MeCeCl}_2$  twice to *p*-methylbenzonitrile in order to obtain the corresponding imine (Scheme 295).<sup>1080</sup>

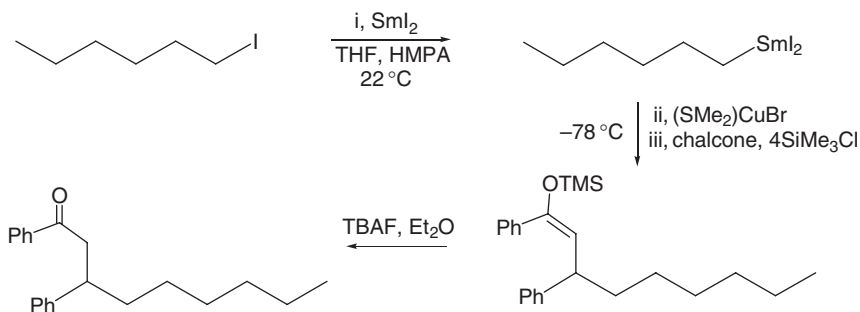
It was found that  $\text{Me}_3\text{SiCl}$  accelerates the conjugate addition of *in situ* prepared organosamarium reagents to  $\alpha,\beta$ -unsaturated carbonyl compounds and nitriles in the presence of HMPA and catalytic amounts of  $\text{Cu(I)}$  salts (Scheme 296). HMPA is also necessary for the *in situ* preparation of the organosamarium species from alkyl halide and  $\text{SmI}_2$ .<sup>1081</sup>

Homoallylic amines (*Z*-diastereomers) are formed from the appropriate imines in the presence of vinylcerium dichloride (Scheme 297). The  $\text{CH}_2=\text{CHCeCl}_2$  reagent was prepared from  $\text{CH}_2=\text{CHMgBr}$  and  $\text{CeCl}_3$ . Using  $\text{CH}_2=\text{CHCeCl}_2$  some chiral imines could also be transformed into *l*-products with high diastereoselectivity.<sup>1082</sup>

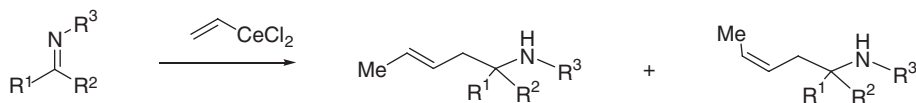
The reaction of dichlorocerium trimethylsilylacetylide with a  $\beta,\gamma$ -unsaturated ketone as shown in Scheme 298 has been reported. The reaction was followed by  $\text{Pd(0)}$ -assisted construction of the acyclic enediyne.<sup>1083</sup>



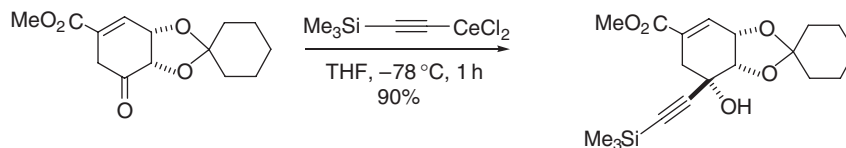
Scheme 295



Scheme 296



Scheme 297



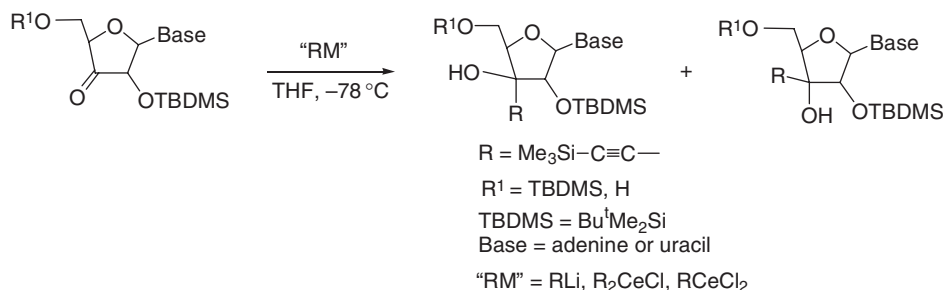
Scheme 298

Additions of cerium trimethylsilylacetylides to 3'-ketonucleosides have also been investigated (Scheme 299). The ethynylcerium reagents (RCeCl<sub>2</sub>) gave the best yield and a highest degree of diastereoselectivity for the *ribo*- and *xylo*-derivatives, respectively.<sup>1084</sup>

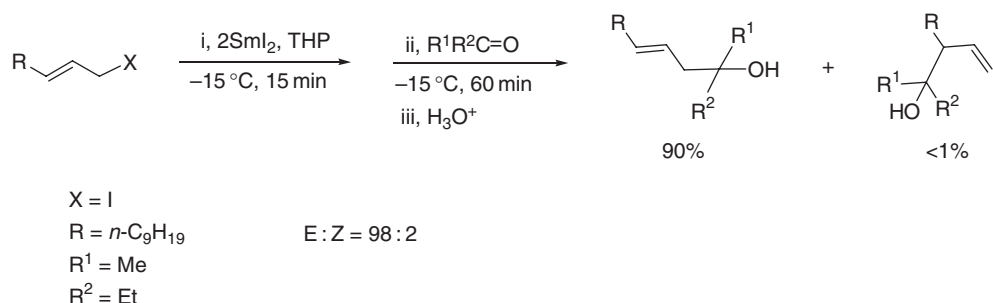
Isolable allyl samarium species are formed in tetrahydropyran at -15 °C by the reaction of SmI<sub>2</sub> with (*E*)-1-iodo-2-dodecene (Scheme 300).<sup>1085</sup>

A THF ring can be opened by *in situ* generated (acyloxy)phosphonium bromide using allylsamarium bromide as catalyst to afford 4-bromobutyl esters under mild conditions in good to excellent yields.<sup>1086</sup> Allylsamarium bromide reacts with acyl azides to give the corresponding *gem*-diallylation products, 4-alkyl-1,6-heptadiene-4-ol derivatives, in good to excellent yields. This novel reaction has been described to proceed within a few minutes at room temperature.<sup>1087</sup> The nucleophilic substitution of the benzotriazolyl group in the *N*-( $\alpha$ -benzotriazol-1-ylalkyl)amides





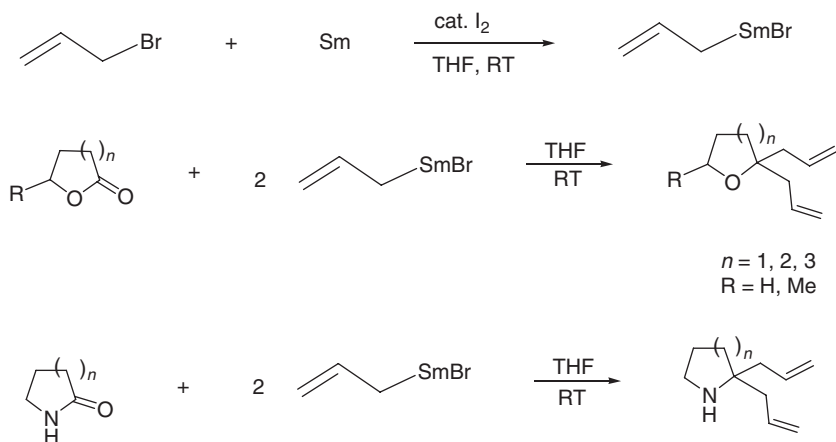
Scheme 299



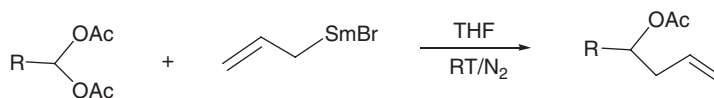
Scheme 300

and *N*-( $\alpha$ -benzotriazol-1-ylalkyl)sulfonamides with allylsamarium bromide has been investigated, and the corresponding homoallylamides or homoallylsulfonamides have been obtained in good to excellent yields.<sup>1088</sup> Direct geminal diallylation of ketones, lactams, and acyclic amides containing an N-H bond has been achieved in the presence of allylsamarium bromide (Scheme 301). By applying this method, quaternary carbons have been constructed, and 2,2-diallylated cyclic ethers, 2,2-diallylated nitrogen heterocycles, and diallylated amides were synthesized in moderate to good yields under mild conditions.<sup>1089</sup>

The substitution reaction between *gem*-diacetates and allylsamarium bromide has also been investigated. Homoallylic alcohol acetates were obtained in moderate to good yields (Scheme 302).<sup>1090</sup>



Scheme 301



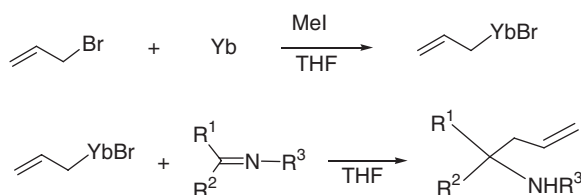
Scheme 302

In the presence of methyl iodide, metallic ytterbium can easily react with allylbromide in anhydrous THF to form allylytterbium bromide, which reacts readily with imines to give the corresponding bromoallylamines in satisfactory yields under mild and neutral conditions (Scheme 303).<sup>1091</sup>

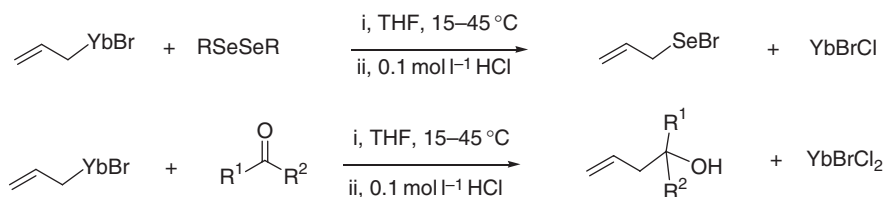
Allylytterbium bromide has also been reported to react with diselenides, aldehydes, and ketones to afford allyl selenides and homoallylic alcohols, respectively, in good yields under neutral and mild conditions (Scheme 304).<sup>1092</sup>

The preparation and use of hexenylsamarium diiodide has been studied.<sup>1093</sup> Three methods for generating alkynylsamarium complexes for use in organic synthesis have been developed: (i) reduction of iodoalkynes with  $\text{SmI}_2$  in the presence of HMPA, (ii) deprotonation at the terminal position of 1-alkynes either by tetrahydrofurysamarium generated by  $\text{PhI}$  and  $\text{SmI}_2$  in THF, or, (iii) undergo coupling with carbonyl compounds under both Barbier and Grignard conditions in benzene–HMPA or THF–HMPA as a solvent system. Tetrahydrofurysamarium generated from iodobenzene and  $\text{SmI}_2$  in THF can deprotonate terminal alkynes to yield alkynylsamariums whereas other alkylsamariums, such as ethyl-, isopropyl-, cyclohexyl-, and cyclopentylsamarium do not work well. Metal–metal exchange between an alkynyllithium and  $\text{SmI}_3$  is also effective; the reactive species in this case would be alkynylsamarium rather than alkynyllithium compounds. To reveal the properties of alkynylsamariums, their stability and reactivity toward various electrophiles have been examined.<sup>1094</sup> A cerium acetylido compound (Scheme 305) has been used for a C–C coupling reaction at a ring carbonyl center.<sup>1095</sup>

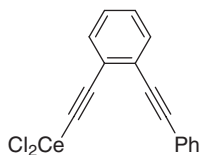
Alkynylsamarium species have also been found to be involved as intermediates in the  $\text{SmI}_2$ -mediated coupling reactions between iodoalkynes and ketones or aldehydes (Scheme 306). The reactions led to propargyl alcohols.<sup>1096</sup>



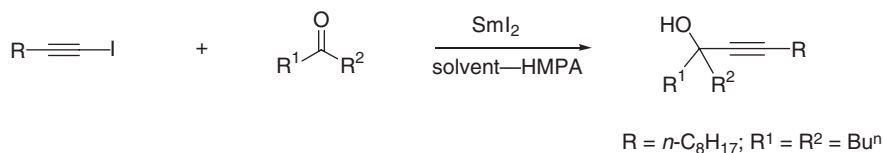
Scheme 303



Scheme 304



Scheme 305



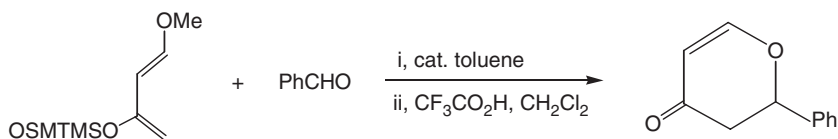
Scheme 306

*L*-Iduronyl synthons catalyzed by a vinyl cerium reagent have been shown to open a way to an efficient preparation of 1,2,4-tri-*O*-acetyl-3-*O*-benzyl-*L*-iduronyl derivatives.<sup>1097</sup> The synthetic utility of the cationic lanthanide complex  $[\text{Cp}^*_2\text{Ce}][\text{BPh}_4]$  as an effective Lewis acid catalyst for the hetero-Diels–Alder reaction between Danishefsky's diene and substituted benzaldehydes has been demonstrated (Scheme 307).<sup>1098</sup>

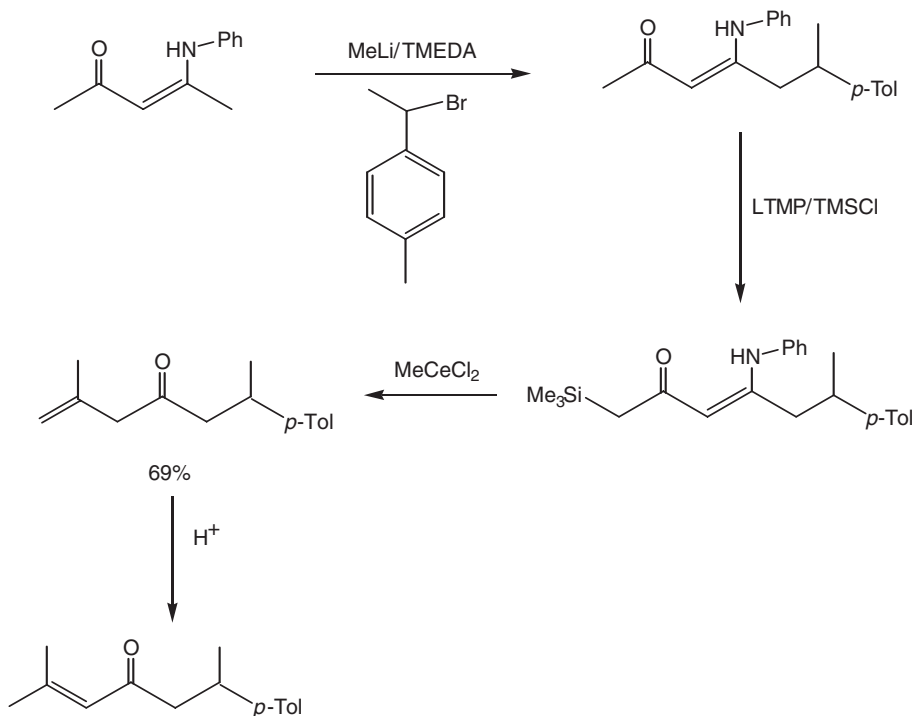
The synthesis of  $\beta,\gamma$ -unsaturated ketones is often complicated by a tendency toward rearrangement to produce mixtures of conjugated and unconjugated ketones. The use of “dry” cerium(III) chloride allowed the regiocontrolled addition of organolithium to enaminones (Scheme 308).<sup>1099</sup>

The facile and convenient synthesis of  $\beta,\gamma$ -unsaturated ketones via silanol elimination of silylated enaminones has also been published. Quenching the reaction with HCl gave exclusively the desired compound (Scheme 309).<sup>1099</sup>

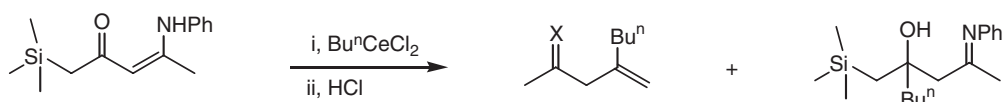
An alkenylcerium reagent (Scheme 310) has been utilized in the total synthesis of sesterpenic acids.<sup>1100</sup>



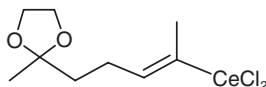
Scheme 307



Scheme 308



Scheme 309

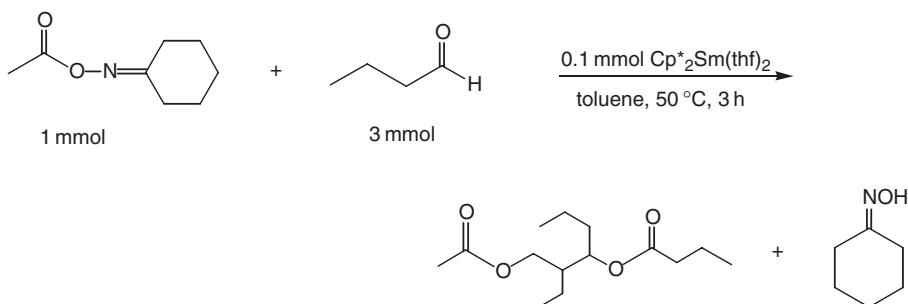


Scheme 310

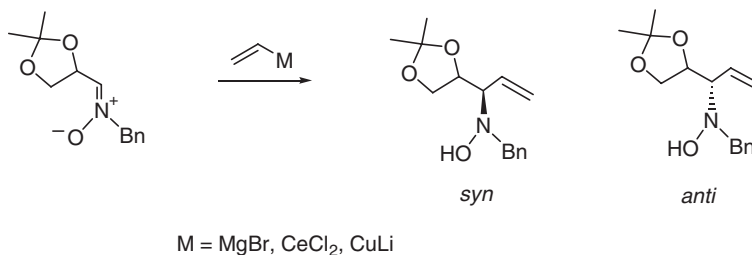
The synthesis of 1,3-diol diesters through a coupling reaction with aldehydes and oxime esters catalyzed by bis(pentamethylcyclopentadienyl)samarium has been reported (Scheme 311).<sup>1101</sup>

Methylcerium reagents formed by the reaction of  $\text{CeCl}_3$  and methylolithium add cleanly to morpholine amides to give the corresponding methyl ketones. In the presence of a large excess of methylolithium, no tertiary alcohol formation was observed. The  $\text{MeCeCl}_2$  acts as a Lewis acid, coordinating to the oxygen atom, decreasing the basicity of nitrogen and thereby increasing the electrophilicity of the amide carbonyl function.<sup>1102</sup> The direct vinylation and ethynylation of nitrones for the stereodivergent synthesis of allyl and propargyl amines according to Scheme 312 has been investigated. The best result for preparing the *syn*-hydroxylamine was obtained using 1.2 equiv. of vinylmagnesium bromide at  $0^\circ\text{C}$  in THF as a solvent. The stereoselective course of the reaction changes dramatically when several Lewis acids were used for precomplexing nitrones. Similar results were obtained with vinylcerium and vinylcuprate derivatives.<sup>1103</sup>

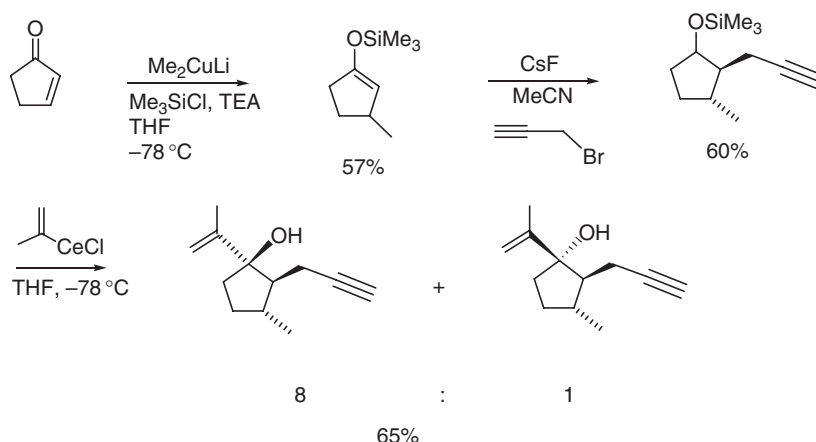
Reactions of a vinylcerium species,  $\text{Cl}_2\text{CeC}(\text{=CH}_2)\text{Me}$ , have been employed in the synthesis of vinyl-substituted 4-alkyn-1-ols. The reaction sequence shown in Scheme 313 is part of an efficient synthesis of the biologically active compound ( $\pm$ )-7-*epi*- $\beta$ -bulnesene.<sup>1104</sup>



Scheme 311



Scheme 312



Scheme 313

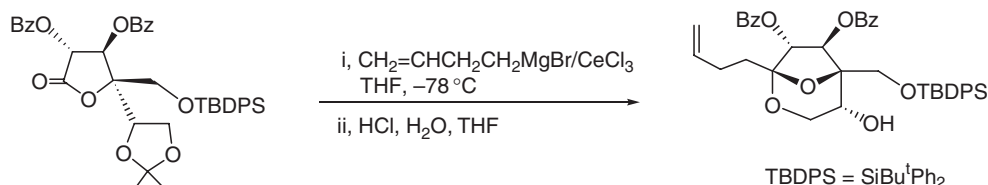
*In situ* generated organo-Ce(III) compounds have been used as selective reagents in steps of the total synthesis of zaragozic acid A (squalstatin S1) (Scheme 314). Addition of the Grignard reagent prepared from 4-bromo-1-butene and magnesium led to elimination of the benzyloxy group  $\beta$  to the carbonyl. This problem was circumvented by transmetalation to the cerium reagent  $\text{CH}_2=\text{CHCH}_2\text{CH}_2\text{CeCl}_2$ .<sup>1105</sup>

( $\alpha$ -Iminoalkyl)samarium has been generated by treatment of mixtures of alkyl halides and 2,6-xylyl isocyanide with  $\text{SmI}_2$ . Addition of carbonyl compounds to the reaction mixtures led to the formation of  $\alpha$ -hydroxyimines.<sup>1106</sup> Ytterbium and samarium metals reduce aromatic ketimines to give directly divalent azalanthanacyclopropane complexes quantitatively (Scheme 315), the structures of which were characterized by X-ray analysis.<sup>961</sup>

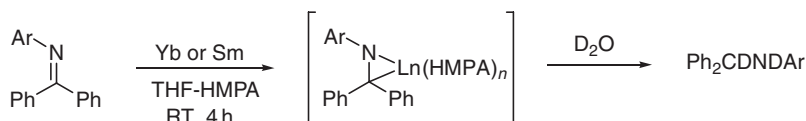
The imine complexes have been found to catalyze dehydrogenative silylation of terminal alkynes, hydrosilylation of imines and alkenes, and intermolecular hydrophosphination of alkynes. Moreover, dehydrogenative double silylation of conjugated dienes was achieved with these reagents.<sup>961</sup> Metallation of 1,3-diphenyl-2-benzylpropene by diphenylytterbium followed by addition of  $\text{Ph}_3\text{SnCl}$  afforded  $(\text{PhCHSnPh}_3)_2\text{C}=\text{CHPh}$ .<sup>1107</sup>

The use of  $\text{Cp}_2\text{Sm}$  as a valuable reagent for the addition of alkyl-, allyl-, benzyl-, and acyl moieties to carbonyl compounds has been summarized.  $\text{Cp}_2\text{Sm}$  and  $\text{SmI}_2$  have been successfully used in Barbier-type reactions involving organic halides and carbonyl compounds;  $\text{Cp}_2\text{Sm}$  proved to be in some instances superior (Scheme 316). It also offers the unique advantage of being able to produce, via radical intermediates, soluble and stable organosamarium derivatives, which can be further reacted with electrophile. These stepwise conditions proved to be crucial for the success of several reactions involving allyl-, benzyl-, and acid halides.<sup>1108</sup>

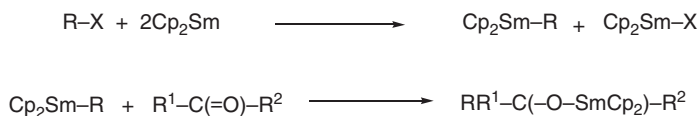
$\text{Cp}^*\text{Sm}(\text{THF})_2$  has been used as an efficient catalyst for the acylation of alcohols with vinyl esters to give the corresponding esters in moderate to good yields (Scheme 317). In addition,  $\text{SmI}_2$  was found to catalyze an aldol-type reaction of imines in the presence of a formate to the corresponding  $\alpha,\beta$ -unsaturated imines in satisfactory yields.<sup>1109</sup>



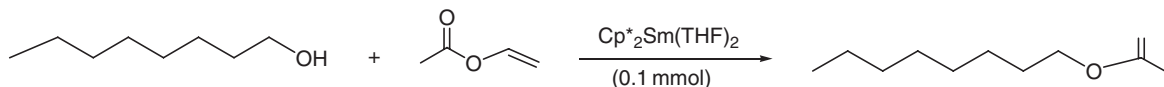
Scheme 314



Scheme 315



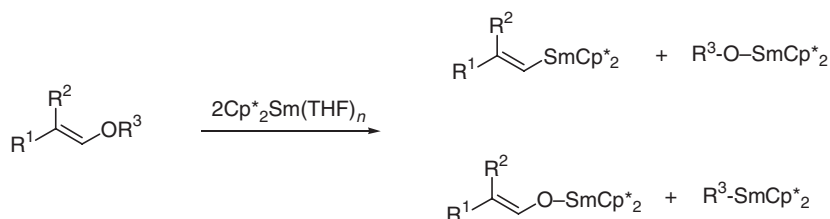
Scheme 316



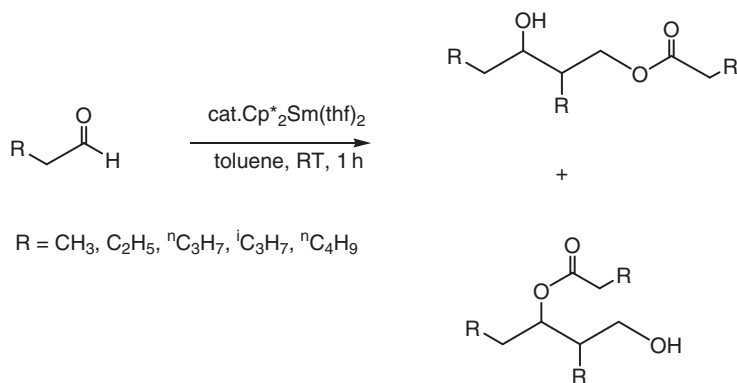
Scheme 317

The regioselectivity of the reductive cleavage of alkyl vinyl ethers with  $\text{Cp}^*_2\text{Sm(THF)}_n$ , that is, competition (Scheme 318) between (i)  $sp^2$  C–O fission leading to vinyl species and alkoxides and (ii)  $sp^3$  C–O fission to enolates and alkyl complexes has been studied. Interestingly, it was found that the selectivity depends on the substituent  $\text{R}^3$ . The path (i) was observed for  $\text{R}^3 = \text{Me}$  ( $\text{R}^1 = \text{Ph}$ ,  $\text{R}^2 = \text{H}$ ), while (ii) was found for  $\text{R}^3 = \text{benzyl}$ . The reactions were detected by  $^1\text{H}$  NMR spectroscopy. Hydrolysis, deuterolysis, and electrophilic trapping of the intermediates were used to prove the kind of bond cleavage.<sup>1110</sup>

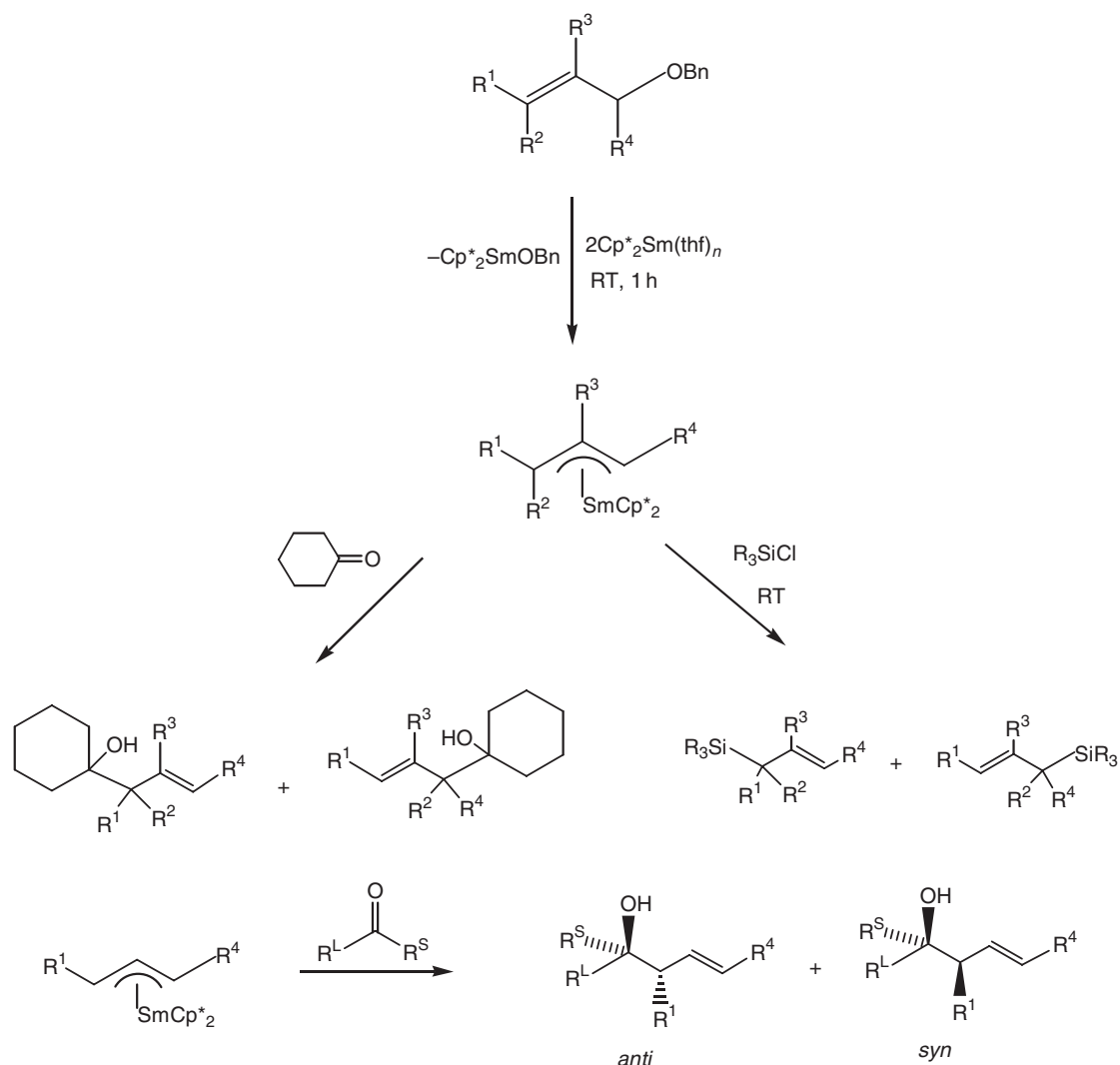
The reductive C–O bond cleavage of allylic and propargylic benzyl ethers with 2 equiv. of  $\text{Cp}^*_2\text{Sm(THF)}_n$  ( $n = 0-2$ ) gives allylic and allenic samarium complexes, respectively, in high yields along with equimolar amounts of  $\text{Cp}^*_2\text{SmOBn}$  ( $\text{Bn} = \text{benzyl}$ ). The stereoselectivity of the electrophilic trapping of these complexes has been studied. Reactions of the allylic complexes with acetophenone and pivalaldehyde afford selectively more substituted *anti*-homoallylic alcohols. With aldimines, *syn*-homoallylic alcohols were obtained predominantly. The allenic samarium complexes react with acetophenone to yield *anti*-homopropargylic alcohols with high regio- and stereoselectivities.<sup>1111</sup> Coupling reactions of aliphatic aldehydes catalyzed by  $\text{Cp}^*_2\text{Sm(THF)}_2$  afford 1,3-diol monoesters in good yields (Scheme 319).<sup>1112</sup>



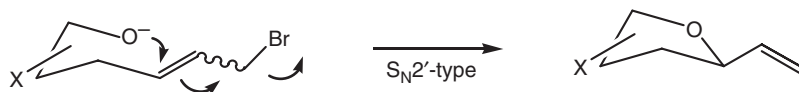
Scheme 318



Scheme 319



Scheme 320



Scheme 321

An investigation of the regio- and stereochemistry effects of  $\text{Cp}^*_2\text{Sm}(\text{THF})_n$  on the electrophilic trapping of allylic compounds showed that the nature of the electrophiles has a remarkable influence on the regio- and stereochemistry of the electrophilic trapping (Scheme 320).<sup>1113</sup>

An efficient method for the preparation of mono-heterocyclic compounds such as substituted tetrahydrofurans with high stereoselectivity via intramolecular  $\text{S}_{\text{N}}2'$  O-cyclization of alkoxides has been reported. This is a nucleophilic displacement with a simultaneous allylic rearrangement (Scheme 321).<sup>1114</sup>

#### 4.01.15 Organolanthanides in Materials Science

A review article covering the topic “Organolanthanides in Materials Science” has been published by Edelmann and Gun'ko in 1997.<sup>1115</sup>

Surface functionalization with polymer and block-co-polymer films using organometallic catalysts has been reported. A layer of 5-hexenylsilane was generated on a silicon surface by the reaction of a 5-hexenyltrichlorosilane precursor with pretreated surfaces. These functionalized silicon substrates were exposed to a THF solution of  $\text{Cp}^*_2\text{Sm}(\text{THF})_2$ .<sup>1116</sup> Tris(isopropylcyclopentadienyl)lanthanum,  $\text{La}(\text{C}_5\text{H}_4\text{Pr}^i)_3$ , has been employed as a precursor for the preparation of ferroelectric lanthanum modified lead zirconate titanate (PLZT) thin films by metalorganic chemical vapor deposition (MOCVD).  $\text{La}(\text{C}_5\text{H}_4\text{Pr}^i)_3$  is a promising precursor for the MOCVD because it is a liquid and it is very easy to control the vapor pressure in the process.<sup>1117</sup> Erbium-doped GaAs films have been prepared by MOCVD using tris(*n*-butylcyclopentadienyl)erbium,  $(\text{C}_5\text{H}_4\text{Bu}^n)_3\text{Er}$ , as liquid precursor. The growth parameters (Ga/As ratio, temperature, and Er-vapor flow) were also studied.<sup>1118</sup> Several new source materials for doping AlGaAs films have been developed.  $\text{Cp}_3\text{Er}$  and  $\text{Er}[\text{N}(\text{SiMe}_3)_2]_3$  have been compared in terms of purity, kinetics, and doping of germanium films deposited from  $\text{GeMe}_4$  in a hydrogen atmosphere.  $\text{Cp}_3\text{Er}$  left large amounts of carbon in pure metal films and in the germanium film at low pressure and temperatures up to 850 °C.  $\text{Er}[\text{N}(\text{SiMe}_3)_2]_3$  decomposed without incorporating carbon, nitrogen, or silicon in the deposited film.<sup>1119</sup> Different III–V semiconductors have been doped with Er, Tm, and Yb using atmospheric pressure MOCVD. Best results were obtained using the isopropylcyclopentadienyl complexes  $(\text{C}_5\text{H}_4\text{Pr}^i)_3\text{Ln}$  ( $\text{Ln} = \text{Er}, \text{Tm}, \text{Yb}$ ) as precursors which have an acceptable vapor pressure and can be used as liquids at bubbler temperatures of 60–90 °C.<sup>1120</sup> Quartz glasses doped with rare earth elements has been produced by thermal decomposition of porous glass preforms containing dopants (Ge, P, B, Al, Ni) and cyclopentadienyl lanthanide complexes.<sup>1121</sup> Mesoporous niobium oxide with a pore size of 22 Å was treated with excess  $\text{Cp}^*_2\text{Sm}(\text{THF})_2$  in THF to give a new mesoporous niobium oxide composite with a mixed-oxidation-state organosamarium phase in the pores.<sup>1122,1123</sup>

Rare earth oxides could represent a valuable alternative to  $\text{SiO}_2$  in complementary metal-oxide-semiconductor devices. In this context, the growth of lutetium oxide ( $\text{Lu}_2\text{O}_3$ ) films by atomic-layer deposition using the dimeric  $[(\text{C}_5\text{H}_4\text{SiMe}_3)_2\text{Lu}(\mu\text{-Cl})]_2$  precursor complex and  $\text{H}_2\text{O}$  has been described. The films were found to be stoichiometric, with  $\text{Lu}_2\text{O}_3$  composition, and amorphous. Annealing in nitrogen at 950 °C led to crystallization in the cubic bixbyite structure.<sup>1124</sup>

Rare earth (RE)–group V (RE–V) compounds are of great interest in realizing new functions of high-speed magnetoelectronic, magneto-optical devices, semi-metal-base transistors, etc. Erbium phosphide,  $\text{ErP}$ , has been grown on  $\text{In}(001)$  substrates by organometallic vapor phase epitaxy (OMVPE) using the new liquid organolanthanide precursor tris(ethylcyclopentadienyl)erbium  $(\text{C}_5\text{H}_4\text{Et})_3\text{Er}$ .<sup>1125</sup>

## References

1. Wilkinson, G.; Birmingham, J. M. *J. Am. Chem. Soc.* **1954**, *76*, 6210.
2. Marks, T. J.; Ernst, R. D. In *Comprehensive Organometallic Chemistry I*; Wilkinson, G., Stone, F. G. A., Abel, E. W., Eds.; Pergamon: Oxford, UK, 1982; pp 173–270.
3. Edelmann, F. T. In *Comprehensive Organometallic Chemistry II*; Abel, E. W., Stone, F. G. A., Wilkinson, G., Eds.; Elsevier: Oxford, UK, 1995; pp 11–212.
4. Richter, J.; Edelmann, F. T. *Coord. Chem. Rev.* **1996**, *147*, 373.
5. Gun'ko, Yu. K.; Edelmann, F. T. *Coord. Chem. Rev.* **1996**, *156*, 1.
6. Edelmann, F. T.; Gun'ko, Yu. K. *Coord. Chem. Rev.* **1997**, *165*, 163.
7. Edelmann, F. T.; Lorenz, V. *Coord. Chem. Rev.* **2000**, *209*, 99.
8. Hyeon, J.-Y.; Edelmann, F. T. *Coord. Chem. Rev.* **2003**, *241*, 249.
9. Hyeon, J.-Y.; Edelmann, F. T. *Coord. Chem. Rev.* **2003**, *247*, 21.
10. Gottfriedsen, J.; Edelmann, F. T. *Coord. Chem. Rev.* **2005**.
11. Hyeon, J.-Y.; Gottfriedsen, J.; Edelmann, F. T. *Coord. Chem. Rev.* **2005**.
12. Schumann, H.; Meese-Marktscheffel, J. A.; Esser, L. *Chem. Rev.* **1995**, *95*, 865.
13. Edelmann, F. T. *Angew. Chem.* **1995**, *107*, 2647.
- 13a. Edelmann, F. T. *Angew. Chem. Int. Ed.* **1995**, *34*, 2466.
14. Evans, W. J. *New J. Chem.* **1995**, *19*, 525.
15. Deacon, G. B.; Shen, Q. *J. Organomet. Chem.* **1996**, *511*, 1.
16. Edelmann, F. T. *New J. Chem.* **1995**, *19*, 535.
17. Mikami, K.; Terada, M.; Matsuzawa, H. *Angew. Chem.* **2002**, *114*, 3704.
- 17a. Mikami, K.; Terada, M.; Matsuzawa, H. *Angew. Chem. Int. Ed.* **2002**, *41*, 3554.
18. Hitchcock, P. B.; Hulkes, A. G.; Khvostov, A. V.; Lappert, M. F.; Protchenko, A. V. *Spec. Publ. – R. Soc. Chem.* **2003**, *287*, 86.
19. Hou, Z.; Wakatsuki, Y. *Sci. Synth.* **2003**, *2*, 849.



20. Kagan, H. B. *Chem. Rev.* **2002**, *102*, 1805.
21. Aspinall, H. C. *Chem. Rev.* **2002**, *102*, 1807.
22. Bochkarev, M. N. *Chem. Rev.* **2002**, *102*, 2089.
23. Deacon, G. B.; Forsyth, C. M.; Nickel, S. J. *Organomet. Chem.* **2002**, *647*, 50.
24. Edelmann, F. T.; Freckmann, D. M. M.; Schumann, H. *Chem. Rev.* **2002**, *102*, 1851.
25. Evans, W. J.; Davis, B. L. *Chem. Rev.* **2002**, *102*, 2119.
26. Evans, W. J. *J. Organomet. Chem.* **2002**, *647*, 2.
27. Evans, W. J. *J. Organomet. Chem.* **2002**, *652*, 61.
28. Eisenstein, O.; Maron, L. *J. Organomet. Chem.* **2002**, *647*, 190.
29. Ferrence, G. M.; Takats, J. *J. Organomet. Chem.* **2002**, *647*, 84.
30. Hou, Z.; Wakatsuki, Y. *J. Organomet. Chem.* **2002**, *647*, 61.
31. Inanaga, J.; Furuno, H.; Hayano, T. *Chem. Rev.* **2002**, *102*, 2211.
32. Izod, K. *Angew. Chem.* **2002**, *114*, 769.
33. Izod, K. *Angew. Chem. Int. Ed.* **2002**, *41*, 743.
34. Cassani, M. C.; Gun'ko, Y. K.; Hitchcock, P. B.; Hulkes, A. G.; Khvostov, A. V.; Lappert, M. F.; Protchenko, A. V. *J. Organomet. Chem.* **2002**, *647*, 71.
35. Marçalo, J.; Pires de Matos, A. J. *Organomet. Chem.* **2002**, *647*, 216.
36. Marques, N.; Sella, A.; Takats, J. *Chem. Rev.* **2002**, *102*, 2137.
37. Molander, G. A.; Romero, J. A. C. *Chem. Rev.* **2002**, *102*, 2161.
38. Arndt, S.; Okuda, J. *Chem. Rev.* **2002**, *102*, 1953.
39. Petrov, E. S.; Roitershtein, D. M.; Rybakova, L. F. *J. Organomet. Chem.* **2002**, *647*, 21.
40. Qian, Y.; Huang, J. *J. Organomet. Chem.* **2002**, *647*, 100.
41. Nie, W.; Qian, C.; Chen, Y.; Jie, S. *J. Organomet. Chem.* **2002**, *647*, 114.
42. Shen, Q.; Yao, Y. *J. Organomet. Chem.* **2002**, *647*, 180.
43. Yasuda, H. *J. Organomet. Chem.* **2002**, *647*, 128.
44. Zhou, X.; Zhu, M. *J. Organomet. Chem.* **2002**, *647*, 28.
45. Vetere, V.; Maldivi, P.; Adamo, C. *J. Comp. Chem.* **2003**, *24*, 850.
46. Vetere, V.; Maldivi, P.; Adamo, C. *Int. J. Quant. Chem.* **2003**, *91*, 321.
47. Ermilov, A. Y.; Nemukhin, A. V.; Kovba, V. M. *Mendeleev Commun.* **1999**, *9*, 88.
48. Yositaka, Y.; Oguro, I. *Appl. Phys. Lett.* **1996**, *69*, 586.
49. Fournier, R. *J. Chem. Phys.* **1993**, *99*, 1801.
50. Jeung, G.-H.; Haettel, S. *Int. J. Quant. Chem.* **1997**, *61*, 547.
51. Pilme, J.; Silvi, B.; Alikhani, M. E. *J. Phys. Chem. A* **2003**, *107*, 4506.
52. Schrodén, J. J.; Teo, M.; Davis, H. F. *J. Chem. Phys.* **2002**, *117*, 9258.
53. Bayse, C. A. *J. Phys. Chem. A* **2002**, *106*, 4226.
54. Hong, G.; Lin, X.; Li, L.; Xu, G. *J. Phys. Chem. A* **1997**, *101*, 9314.
55. Schroeden, J. J.; Teo, M.; Davis, H. F. *J. Phys. Chem. A* **2002**, *106*, 11695.
56. Sodupe, M.; Branchadell, V.; Oliva, A.; Bertran, J. *Int. J. Quant. Chem.* **1997**, *63*, 523.
57. Sodupe, M.; Branchadell, V.; Rosi, M.; Bauschlicher, C. W., Jr., *J. Phys. Chem. A* **1997**, *101*, 7854.
58. Ye, S.; Shi, N.; Huang, J.; Dai, S. *Int. J. Quant. Chem.* **1997**, *62*, 23.
59. Zhang, D.; Liu, C.; Bi, S.; Yuan, S. *Chem. Eur. J.* **2003**, *9*, 484.
60. Siegbahn, P. E. M.; Blomberg, M.; Svensson, M. *J. Am. Chem. Soc.* **1993**, *115*, 4191.
- 60a. Ding, F.-J. *Huaxue Xuebao* **2003**, *61*, 161.
61. Siegbahn, P. E. M.; Blomberg, M.; Svensson, M. *J. Am. Chem. Soc.* **1993**, *115*, 1952.
62. Siegbahn, P. E. M.; Svensson, M. *Chem. Phys. Lett.* **1993**, *216*, 147.
63. Siegbahn, P. E. M. *Chem. Phys. Lett.* **1993**, *205*, 290.
64. Hinrichs, R. Z.; Schrodén, J. J.; Davis, H. F. *J. Am. Chem. Soc.* **2003**, *125*, 860.
65. Perry, J. K.; Goddard, W. A. *J. Am. Chem. Soc.* **1994**, *116*, 5013.
66. Crellin, K. C.; Geribaldi, S.; Beauchamp, *Organometallics* **1994**, *13*, 3733.
67. Hwang, D.-Y.; Mebel, A. M. *J. Phys. Chem. A* **2002**, *106*, 12072.
68. Hwang, D.-Y.; Mebel, A. M. *Chem. Phys. Lett.* **2004**, *396*, 75.
69. Holthausen, M. C.; Heinemann, C.; Cornehl, H. H.; Koch, W.; Schwarz, H. *J. Chem. Phys.* **1995**, *102*, 4931.
70. Maron, L.; Perrin, L.; Eisenstein, O. *J. Chem. Soc., Dalton Trans.* **2002**, 534.
71. Hill, Y. D.; Huang, Y.; Ast, T.; Freiser, B. S. *Rapid Commun. Mass Spectrom.* **1997**, *11*, 148.
72. Zhang, D. J.; Liu, C. B. *Chin. Chem. Lett.* **2002**, *13*, 359.
73. Eaborn, C.; Hitchcock, K.; Izod, K.; Smith, J. D. *J. Am. Chem. Soc.* **1994**, *116*, 12071.
74. Eaborn, C.; Hitchcock, P. B.; Izod, K.; Lu, Z.-R.; Smith, L. D. *Organometallics* **1996**, *15*, 4783.
75. van den Hende, J. R.; Hitchcock, P. B.; Holmes, S. A.; Lappert, M. F.; Tian, S. *J. Chem. Soc., Dalton Trans.* **1995**, 3933.
76. Collin, J.; Daran, J.-C.; Schulz, E.; Trifonov, A. *Chem. Commun.* **2003**, 3048.
77. Niemeyer, M. *Acta Crystallogr., Sect. E: Struct. Rep. Online* **2001**, *57*, m553.
78. Schumann, H.; Freckmann, D. M. M.; Dechert, S. Z. *Anorg. Allg. Chem.* **2002**, *628*, 2422.
79. Perrin, L.; Maron, L.; Eisenstein, O. *Faraday Discuss.* **2003**, *124*, 25.
80. Gillespie, R. J.; Noury, S.; Pilme, J.; Silvi, B. *Inorg. Chem.* **2004**, *43*, 3248.
81. Clark, D. L.; Gordon, J. C.; Hay, P. J.; Martin, R. L.; Poli, R. *Organometallics* **2002**, *21*, 5000.
82. Brady, E. D.; Clark, D. L.; Gordon, J. C.; Hay, P. J.; Keogh, D. W.; Poli, R.; Scott, B. L.; Watkin, J. G. *Inorg. Chem.* **2003**, *42*, 6682.
83. Perrin, L.; Maron, L.; Eisenstein, O.; Lappert, M. F. *New J. Chem.* **2003**, *27*, 121.
84. Guttenberger, C.; Amberger, H.-D. *J. Organomet. Chem.* **1997**, *545–546*, 601.
85. Guttenberger, C.; Unrecht, B.; Reddmann, H.; Amberger, H.-D. *Inorg. Chim. Acta* **2003**, *348*, 165.
86. Reddmann, H.; Guttenberger, C.; Amberger, H. D. *J. Organomet. Chem.* **2000**, *602*, 65.
87. Jank, S.; Amberger, H. D. *Acta Phys. Pol., A* **1996**, *90*, 21.

88. Metz, M. V.; Sun, Y.; Stern, C. L.; Marks, T. J. *Organometallics* **2002**, *21*, 3691.
89. Westerhausen, M.; Schmeiderbauer, S.; Hartmann, M.; Warchhold, M.; Nöth, H. Z. *Anorg. Allg. Chem.* **2002**, *628*, 330.
90. Hao, S.; Song, J.; Aghabozorg, H.; Gambarotta, S. *J. Chem. Soc., Chem. Commun.* **1994**, 157.
91. Karsch, H. H.; Ferazin, G.; Bissinger, P. *J. Chem. Soc., Chem. Commun.* **1994**, 505.
92. Zheleznova, T. A.; Bochkarev, L. N.; Safronova, A. V.; Zhil'tsov, S. F. *Russ. J. Gen. Chem.* **1999**, *69*, 784.
93. Ihara, E.; Adachi, Y.; Yasuda, H.; Hashimoto, H.; Kanehisa, N.; Kai, Y. *J. Organomet. Chem.* **1998**, *569*, 89.
94. Niemeyer, M. Z. *Anorg. Allg. Chem.* **2000**, *626*, 1027.
95. Pimanova, N. A.; Zhil'tsov, S. F.; Druzhova, O. N. *J. Gen. Chem.* **2003**, *73*, 1188.
96. Hitchcock, P. B.; Khvostov, A. V.; Lappert, M. F. *J. Organomet. Chem.* **2002**, *663*, 263.
97. Evans, W. J.; Shreeve, J. L.; Broomhall-Dillard, R. N. R.; Ziller, J. W. *J. Organomet. Chem.* **1995**, *501*, 7.
98. Wacker, A.; Yan, C. G.; Kaltenpoth, G.; Ginsberg, A.; Arif, A. M.; Ernst, R. D.; Pritzkow, H.; Siebert, W. *J. Organomet. Chem.* **2002**, *641*, 195.
99. Perrin, L.; Maron, L.; Eisenstein, O. *ACS Symp. Ser.* **2004**, *885*, 116.
100. Cundari, T. R.; Moody, E. W.; Raby, P. D.; Ignarra, E. S.; Sommerer, S. O. *Trans. Am. Cryst. Assoc.* **1997**, *31*, 23.
101. Sherer, E. C.; Cramer, C. J. *Organometallics* **2003**, *22*, 1682.
102. Rabe, G. W.; Bérubé, C. D.; Yap, G. P. A.; Lam, K.-C.; Concolino, T. E.; Rheingold, A. L. *Inorg. Chem.* **2002**, *41*, 1446.
103. Rabe, G. W.; Rhatigan, B.; Golen, J. A.; Rheingold, A. L. *Acta Crystallogr., Sect. E: Struct. Rep. Online* **2003**, *59*, m99.
104. Rabe, G. W.; Berube, C. D.; Yap, G. P. A. *Inorg. Chem.* **2001**, *40*, 2682.
105. Rabe, G. W.; Zhang-Presse, M.; Riederer, F. A.; Golen, J. A.; Incarvito, C. D.; Rheingold, A. L. *Inorg. Chem.* **2003**, *42*, 7587.
106. Rabe, G. W.; Zhang-Presse, M.; Riederer, F. A.; Yap, G. P. A. *Inorg. Chem.* **2003**, *42*, 3527.
107. Westerhausen, M.; Hartmann, M.; Pfitzner, A.; Schwarz, W. Z. *Anorg. Allg. Chem.* **1995**, *621*, 837.
108. Avent, A. G.; Caro, C. F.; Hitchcock, P. B.; Lappert, M. F.; Li, Z.; Wei, X.-H. *Dalton Trans.* **2004**, 1567.
109. Arndt, S.; Spaniol, T. P.; Okuda, J. *Chem. Commun.* **2002**, 896.
110. Arndt, S.; Zeimentz, P. M.; Spaniol, T. P.; Okuda, J.; Honda, M.; Tatsumi, K. *Dalton Trans.* **2003**, 3622.
111. Arndt, S.; Spaniol, T. P.; Okuda, J. *Angew. Chem.* **2003**, *115*, 5229.
- 111a. Arndt, S.; Spaniol, T. P.; Okuda, J. *Angew. Chem. Int. Ed.* **2003**, *42*, 5075.
112. Mandel, A.; Magull, J. Z. *Anorg. Allg. Chem.* **1997**, *623*, 1542.
113. Emslie, D. J. H.; Piers, W. E.; McDonald, R. *J. Chem. Soc., Dalton Trans.* **2002**, 293.
114. Emslie, D. J. H.; Piers, W. E.; Parvez, M.; McDonalds, R. *Organometallics* **2002**, *21*, 4226.
115. Emslie, D. J. H.; Piers, W. E.; Parvez, M. *Dalton Trans.* **2003**, 2615.
116. Cloke, F. G. N.; Elvidge, B. R.; Hitchcock, P. B.; Lamarche, V. M. E. *J. Chem. Soc., Dalton Trans.* **2002**, 2413.
117. Avent, A. G.; Cloke, F. G. N.; Elvidge, B. R.; Hitchcock, P. B. *J. Chem. Soc., Dalton Trans.* **2004**, 1083.
118. Ward, B. D.; Dubberley, S. R.; Maise-François, A.; Gade, L. H.; Mountford, P. *J. Chem. Soc., Dalton Trans.* **2002**, 4649.
119. Lara-Sanchez, A.; Rodriguez, A.; Hughes, L.; Schormann, M.; Bochmann, M. *J. Organomet. Chem.* **2002**, *663*, 63.
120. Evans, W. J.; Broomhall-Dillard, R. N. R.; Ziller, J. W. *J. Organomet. Chem.* **1998**, *569*, 89.
121. Duchateau, R.; Tuinstra, T.; Brussee, E. A. C.; Meetsma, A.; van Duijn, P. T.; Teuben, J. H. *Organometallics* **1997**, *16*, 3511.
122. Duchateau, R.; Bruessee, E. A. C.; Meetsma, A.; Teuben, J. H. *Organometallics* **1997**, *16*, 5506.
123. Lou, Y.; Yao, Y.; Shen, Q.; Yu, K.; Weng, L. *Eur. J. Inorg. Chem.* **2003**, 318.
124. Eisenstein, O.; Hitchcock, P. B.; Khvostov, A. V.; Lappert, M. F.; Maron, L.; Perrin, L.; Protchenko, A. V. *J. Am. Chem. Soc.* **2003**, *125*, 10790.
125. Harder, S. *Angew. Chem.* **2004**, *116*, 2768.
- 125a. Harder, S. *Angew. Chem. Int. Ed.* **2004**, *43*, 2714.
126. Luo, Y.-J.; Yao, Y.-M.; Zhang, Y.; Shen, Q.; Yu, K.-B. *Chin. J. Chem.* **2004**, *22*, 187.
127. Hayes, P. G.; Piers, W. E.; Lee, L. W.; Knight, L. K.; Parvez, M.; Elsegood, M. R. J.; Clegg, W. *Organometallics* **2001**, *20*, 2533.
128. Basuli, F.; Tomaszewski, J.; Huffman, J. C.; Mindiola, D. J. *Organometallics* **2003**, *22*, 4705.
- 128a. Knight, L. K.; Piers, E. W.; Fleurat-Lessard, P.; Parvez, M.; McDonald, R. *Organometallics* **2004**, *23*, 2087.
129. Hayes, P. G.; Piers, W. E.; McDonald, R. *J. Am. Chem. Soc.* **2002**, *124*, 2132.
130. Neculai, A. M.; Neculai, D.; Roesky, H. W.; Magull, J.; Baldus, M.; Andromesi, O.; Jansen, M. *Organometallics* **2002**, *21*, 2590.
131. Neculai, A.-M.; Cummins, C. C.; Neculai, D.; Roesky, H. W.; Bunkóczi, G.; Walford, B.; Stalke, D. *Inorg. Chem.* **2003**, *42*, 8803.
132. Neculai, D.; Roesky, H. W.; Mirela, A.; Magull, J.; Herbst-Irmer, R.; Walford, B.; Stalke, D. *Organometallics* **2003**, *22*, 2279.
133. Neculai, A. M.; Neculai, D.; Roesky, H. W.; Magull, J. *Polyhedron* **2004**, *23*, 183.
134. Avent, A. G.; Hitchcock, P. B.; Khvostov, A. V.; Lappert, M. F.; Protchenko, A. V. *J. Chem. Soc., Dalton Trans.* **2004**, 2272.
135. Hajela, S.; Schaefer, W. P.; Bercaw, J. E. *J. Organomet. Chem.* **1997**, *532*, 45.
136. Lawrence, S. C.; Ward, B. D.; Dubberley, S. R.; Kozak, C. M.; Mountford, P. *Chem. Commun.* **2003**, 2880.
137. Bambirra, S.; van Leusen, D.; Meetsma, A.; Hessen, B.; Teuben, J. H. *J. Chem. Soc., Chem. Commun.* **2001**, 637.
138. Tazelaar, C. G. J.; Bambirra, S.; van Leusen, D.; Meetsma, A.; Hessen, B.; Teuben, J. H. *Organometallics* **2004**, *23*, 936.
139. Skinner, M. E. G.; Tyrrell, B. R.; Ward, B. D.; Mountford, P. *J. Organomet. Chem.* **2002**, *647*, 145.
140. Skinner, M. E. G.; Mountford, P. *J. Chem. Soc., Dalton Trans.* **2002**, 1694.
141. Hultsch, K. C.; Hampel, F.; Wagner, T. *Organometallics* **2004**, *23*, 2601.
142. Bambirra, S.; Boot, S. J.; van Leusen, D.; Meetsma, A.; Hessen, B. *Organometallics* **2004**, *23*, 1891.
143. Lee, L.; Berg, D. J.; Einstein, F. W.; Batchelor, R. J. *Organometallics* **1997**, *16*, 1819.
144. Lee, L.; Berg, D. J.; Bushnell, G. W. *Organometallics* **1995**, *14*, 8.
145. Cai, C.-X.; Toupet, L.; Lehmann, C. W.; Carpentier, J.-F. *J. Organomet. Chem.* **2003**, *683*, 131.
- 145a. Nakayama, Y.; Yasuda, H. *J. Organomet. Chem.* **2004**, *689*, 4489.
146. Fryzuk, M. D.; Love, J. B.; Rettig, S. J. *J. Am. Chem. Soc.* **1997**, *119*, 9071.
147. Roesky, P. W. *J. Organomet. Chem.* **2000**, *603*, 161.
148. Lu, Z.; Yap, G. P. A.; Richeson, D. S. *Organometallics* **2001**, *20*, 706.
149. Cui, C.; Shafir, A.; Reeder, C. L.; Arnold, J. *Organometallics* **2003**, *22*, 3357.
150. Estler, F.; Eicklerling, G.; Herdtweck, E.; Anwender, R. *Organometallics* **2003**, *22*, 1212.
151. Hayes, P. G.; Welch, G. C.; Emslie, D. J. H.; Noack, C. L.; Piers, W. E.; Parvez, M. *Organometallics* **2003**, *22*, 1577.
152. Bambirra, S.; van Leusen, D.; Meetsma, A.; Hessen, B.; Teuben, J. T. *Chem. Commun.* **2003**, 522.

153. Cameron, T. M.; Gordon, J. C.; Michalczyk, R.; Scott, B. L. *Chem. Commun.* **2003**, 2282.
154. Lavanant, L.; Chou, T.-Y.; Chi, Y.; Lehmann, C. W.; Toupet, L.; Carpentier, J.-F. *Organometallics* **2004**, *23*, 5450.
155. Dubé, T.; Conoci, S.; Gambarotta, S.; Yap, G. P. A. *Organometallics* **2000**, *19*, 1182.
156. Lopes, I.; Monteiro, B.; Lin, G.; Domingos, A.; Marques, N.; Takats, J. J. *Organomet. Chem.* **2001**, *632*, 119.
157. Izod, K.; Liddle, S. T.; Clegg, W. *Chem. Commun.* **2004**, 1748.
158. Izod, K.; Liddle, S. T.; McFarlane, W.; Clegg, W. *Organometallics* **2004**, *23*, 2734.
159. Jank, S.; Hanss, J.; Reddmann, H.; Amberger, H.-D.; Edelstein, N. M. Z. *Anorg. Allg. Chem.* **2002**, *628*, 1355.
160. Amberger, H.-D.; Jank, S.; Reddmann, H.; Edelstein, N. M. *Spectrochim. Acta, Part A* **2002**, *58*, 379.
161. Herrmann, W. A.; Munck, F. C.; Artus, G. R. J.; Runte, O.; Anwander, R. *Organometallics* **1997**, *16*, 682.
162. Arnold, P. L.; Mungur, S. A.; Blake, A. J.; Wilson, C. *Angew. Chem.* **2003**, *115*, 6163.
- 162a. Arnold, P. L.; Mungur, S. A.; Blake, A. J.; Wilson, C. *Angew. Chem. Int. Ed.* **2003**, *42*, 5981.
163. Loock, H.-P.; Bérces, A.; Simard, B. J. *Chem. Phys.* **1997**, *107*, 2720.
164. Glendening, E. D.; Strange, M. L. *J. Phys. Chem. A* **2002**, *106*, 7338.
165. Glendening, E. D. *J. Phys. Chem. A* **2004**, *108*, 10165.
166. Druzhkova, O. N.; Pimanova, N. A.; Bochkarev, L. N. *Russ. J. Gen. Chem.* **1999**, *69*, 784.
167. Trifonov, A. A.; Fedorova, E. A.; Kirillov, E. N.; Bochkarev, M. N.; Girgsdies, F.; Schumann, H. *Russ. Chem. Bull. Int. Ed.* **2000**, *49*, 1436.
168. Kretschmer, W.; Thiele, K.-H. Z. *Anorg. Allg. Chem.* **1995**, *621*, 1304.
169. Emelyanova, N. S.; Trifonov, A. A.; Zakharov, L. N.; Shestakov, A. F.; Struchkov, Y. T.; Bochkarev, M. N. *J. Organomet. Chem.* **1997**, *540*, 1.
170. Trifonov, A. A.; Zakharov, L. N.; Bochkarev, M. N.; Shestakov, A.; Struchkov, Y. *Metalloorg. Khim.* **1993**, *6*, 363.
171. Mashima, K.; Sugiyama, H.; Nakamura, A. J. *Chem. Soc., Chem. Commun.* **1994**, 1581.
172. Dubé, T.; Gambarotta, S.; Yap, G. P. A. *Organometallics* **2000**, *19*, 121.
173. Dubé, T.; Gambarotta, S.; Yap, G. P. A. *Organometallics* **2000**, *19*, 817.
174. Dube, T.; Guan, J.; Gambarotta, S. *Chem. Eur. J.* **2001**, *7*, 374.
175. Lin, G.; McDonald, G. R.; Takats, J. *Organometallics* **2000**, *19*, 1814.
176. Karl, M.; Seybert, G.; Massa, W.; Harms, K.; Agarwal, S.; Maleika, R.; Stelter, W.; Greiner, A.; Heitz, W.; Neumüller, B., *et al.* *Z. Anorg. Allg. Chem.* **1999**, *625*, 1301.
177. Makioka, Y.; Takaki, K.; Taniguchi, Y.; Fujiwara, Y. *Nippon Kagaku Kaishi* **1996**, 424.
178. Taube, R.; Windisch, H.; Maiwald, S.; Hemling, H.; Schumann, H. *J. Organomet. Chem.* **1996**, *513*, 49.
179. Taube, R.; Maiwald, S.; Sieler, J. *J. Organomet. Chem.* **2001**, *621*, 327.
180. Taube, R.; Windisch, H.; Weißenborn, H.; Hemling, H.; Schumann, H. *J. Organomet. Chem.* **1997**, *548*, 229.
181. Windisch, H.; Scholz, J.; Taube, R.; Wrackmeyer, B. *J. Organomet. Chem.* **1996**, *520*, 23.
182. Taube, R.; Maiwald, S.; Sieler, J. *J. Organomet. Chem.* **1996**, *513*, 37.
183. Taube, R.; Windisch, H.; Görlitz, F. H.; Schumann, H. *J. Organomet. Chem.* **1993**, *445*, 85.
184. Taube, R.; Windisch, H. *J. Organomet. Chem.* **1994**, *472*, 71.
185. Sánchez-Barba, L. F.; Hughes, D. L.; Humphrey, S. M.; Bochmann, M. *Organometallics* **2005**, *24*, 3792.
186. Woodman, T. J.; Schormann, M.; Bochmann, M. *Isr. J. Chem.* **2003**, *42*, 283.
- 186a. Woodmann, T. J.; Schormann, M.; Hughes, D. L.; Bochmann, M. *Organometallics* **2003**, *22*, 3028.
187. Woodman, T. J.; Schormann, M.; Hughes, D. L.; Bochmann, M. *Organometallics* **2004**, *23*, 2972.
- 187a. Kuehl, C. J.; Simpson, C. K.; John, K. D.; Sattelberger, A. P.; Carlson, C. N.; Hanusa, T. P. *J. Organomet. Chem.* **2003**, *683*, 149.
188. Woodman, T. J.; Schormann, M.; Bochmann, M. *Organometallics* **2003**, *22*, 2938.
189. Hitchcock, P. B.; Lappert, M. F.; Tian, S. J. *Organomet. Chem.* **1997**, *549*, 1.
190. Gun'ko, Y. K.; Hitchcock, P. B.; Lappert, M. F. *Chem. Commun.* **1998**, 1843.
191. Trifonov, A. A.; Kirillov, E. N.; Kurskii, Y. A.; Bochkarev, M. N. *Russ. Chem. Bull. Int. Ed.* **2000**, *4*, 744.
192. Trifonov, A. A.; Kirillov, E. N.; Fischer, A.; Edelmann, F. T.; Bochkarev, M. N. *J. Chem. Soc., Chem. Commun.* **1999**, 2203.
193. Trifonov, A. A.; Kirillov, E. N.; Fischer, A.; Edelmann, F. T.; Bochkarev, M. N. *J. Organomet. Chem.* **2002**, *647*, 94.
194. Hou, Z.; Koizumi, T.; Nishiura, M.; Wakatsuki, Y. *Organometallics* **2001**, *20*, 3323.
195. Spaniol, T. P.; Okuda, J.; Kitamura, M.; Takahashi, T. *J. Organomet. Chem.* **2003**, *684*, 194.
196. Tardif, O.; Hou, Z.; Nishiura, M.; Koizumi, T.; Wakatsuki, Y. *Organometallics* **2001**, *20*, 4565.
197. Tardif, O.; Nishiura, M.; Hou, Z. *Tetrahedron* **2003**, *59*, 10525.
198. Barbier-Baudry, D.; Heiner, S.; Kubicki, M. M.; Vigier, E.; Visseaux, M. *Organometallics* **2001**, *20*, 4207.
199. Fedushkin, I. L.; Dechert, S.; Schumann, H. *Organometallics* **2000**, *19*, 4066.
200. Giesbrecht, G. R.; Cui, C.; Shafir, A.; Schmidt, J. A. R.; Arnold, J. *Organometallics* **2002**, *21*, 3841.
201. Wang, D.; Zhao, C.; Phillips, D. L. *Organometallics* **2004**, *23*, 1953.
202. Hitchcock, P. B.; Lappert, M. F.; Prashar, S. J. *Organomet. Chem.* **2000**, *613*, 105.
203. Deacon, G. B.; Forsyth, C. M.; Scott, N. M. *Dalton Trans.* **2003**, 3216.
204. Ferrence, G. M.; McDonald, R.; Morissette, M.; Takats, J. J. *Organomet. Chem.* **2000**, *596*, 95.
205. Deacon, G. B.; Stellfeldt, D.; Meyer, G. Z. *Anorg. Allg. Chem.* **2000**, *626*, 623.
206. Jagannatha, S. S. *Indian J. Chem., Sect A* **2002**, *41*, 1850.
207. Shoshkin, A. N.; Bochkarev, L. N.; Khorshev, S. Y. *Russ. J. Gen. Chem.* **2002**, *72*, 715.
208. Apostolidis, C.; Deacon, G. B.; Dornberger, E.; Edelmann, F. T.; Kanellakopulos, B.; MacKinnon, P.; Stalke, D. *J. Chem. Soc., Chem. Commun.* **1997**, 1047.
209. Trifonov, A. A.; Fedorova, E. A.; Kirillov, E. N.; Nefedov, S. E.; Eremenko, I. L.; Kurskii, Y. A.; Shavyrin, A. S.; Bochkarev, M. N.; Razuvaev, G. A. *Russ. Chem. Bull.* **2002**, *51*, 684.
210. Xia, J. S.; Wei, G. C.; Jin, Z. S.; Chen, W. Q.; Xue, W. C. *Report* **1995**, *95*, 724.
211. Silva-Valenzuela, M. G.; Zinner, L. B.; Domingos, A.; Marques, N.; Pires de Matos, A. J. *Alloys Compd.* **1995**, *225*, 331.
212. Jiang, T.; Shen, Q.; Lin, Y.; Jin, S. J. *Organomet. Chem.* **1993**, *450*, 121.
213. Schumann, H.; Glanz, M.; Hemling, H.; Hahn, F. E. Z. *Anorg. Allg. Chem.* **1995**, *621*, 341.
214. Evans, W. J.; Kociok-Köhne, G.; Foster, S.; Ziller, J.; Doedens, R. J. *Organomet. Chem.* **1993**, *444*, 61.
215. Schumann, H.; Glanz, M.; Hemling, H. *New J. Chem.* **1995**, *19*, 491.
216. Nief, F.; Ricard, L. *J. Organomet. Chem.* **1998**, *553*, 503.

217. Visseaux, M.; Barbier-Baudry, D.; Blacque, O.; Hafid, A.; Richard, P.; Weber, F. *New J. Chem.* **2000**, *24*, 939.
218. Sitzmann, H.; Dezimmer, T.; Schmitt, O.; Weber, F.; Wolmershäuser, G. *Z. Anorg. Allg. Chem.* **2000**, *626*, 2241.
219. Weber, F.; Sitzmann, H.; Schultz, M.; Sofield, C. D.; Andersen, R. A. *Organometallics* **2002**, *21*, 3139.
220. Selg, P.; Brintzinger, H. H.; Schultz, M.; Andersen, R. A. *Organometallics* **2002**, *21*, 3100.
221. Maron, L.; Perrin, L.; Eisenstein, O.; Andersen, R. A. *J. Am. Chem. Soc.* **2002**, *124*, 5614.
222. Schultz, M.; Burns, C. J.; Schwartz, D. J.; Andersen, R. A. *Organometallics* **2001**, *20*, 5690.
223. Khvostov, A. V.; Sizov, A. I.; Bulychev, B. M.; Knjazhanski, S. Y. *J. Organomet. Chem.* **1998**, *559*, 97.
224. Khvostov, A. V.; Bulychev, B. M.; Belsky, V. K.; Sizov, A. I. *Russ. Chem. Bull.* **1999**, *48*, 2162.
225. Trifonov, A. A.; Kirillov, E. N.; Bochkarev, M. N.; Schumann, H.; Mühle, S. *Russ. Chem. Bull.* **1999**, *48*, 382.
226. Evans, W. J.; Forrestal, K. J.; Ziller, J. W. *Polyhedron* **1998**, *17*, 4015.
227. Deng, M.; Yoa, Y.; Shen, Q.; Zhang, Y.; Lang, J.; Zhou, Y. *J. Organomet. Chem.* **2003**, *681*, 174.
228. Evans, W. J.; Allen, N. T.; Ziller, J. W. *Angew. Chem.* **2002**, *114*, 369.
- 228a. Evans, W. J.; Allen, N. T.; Ziller, J. W. *Angew. Chem. Int. Ed.* **2002**, *41*, 359.
229. Evans, W. J.; Perotti, J. M.; Ziller, J. W. *J. Am. Chem. Soc.* **2005**, *127*, 1068.
230. Voskoboynikov, A. Z.; Agarkov, A. Y.; Shetakova, A. K.; Beletskaya, I. P.; Kuz'mina, L. O.; Howard, J. A. K. *J. Organomet. Chem.* **1997**, *544*, 65.
231. Deng, D.; Qian, C.; Song, F.; Wang, Z.; Wu, G.; Zheng, P. *J. Organomet. Chem.* **1993**, *443*, 79.
232. Qian, C.; Zhu, C.; Lin, Y.; Xing, Y. *J. Organomet. Chem.* **1996**, *507*, 41.
233. Molander, G. A.; Schumann, H.; Rosenthal, E. C. E.; Demtschuk, J. *Organometallics* **1996**, *15*, 3817.
234. Bochkarev, M. N.; Fedushkin, I. L.; Nevodchikov, V. I.; Protchenko, A. V.; Schumann, H.; Girsdsies, F. *Inorg. Chim. Acta* **1998**, *280*, 138.
235. Jutzi, P.; Dahlhaus, J.; Kristen, M. *J. Organomet. Chem.* **1993**, *450*, C1.
236. van den Hende, J. R.; Hitchcock, P. B.; Lappert, M. F. *J. Organomet. Chem.* **1994**, *472*, 79.
237. Lin, G.; Wong, W.-T. *J. Organomet. Chem.* **1995**, *495*, 203.
238. Lin, G.; Wong, W.-T. *J. Organomet. Chem.* **1996**, *523*, 93.
239. Deacon, G. B.; Forsyth, C. M.; Gatehouse, B. M.; Philosofo, A.; Skelton, B. W.; White, A. H.; White, P. A. *Aust. J. Chem.* **1997**, *50*, 959.
240. Evans, W. J.; Perotti, J. M.; Brady, J. C.; Ziller, J. W. *J. Am. Chem. Soc.* **2003**, *125*, 5204.
241. Khorosheńkov, G. V.; Petrovskaya, T. V.; Fedushkin, I. L.; Bochkarev, M. N. *Z. Anorg. Allg. Chem.* **2002**, *628*, 1355.
242. Khorosheńkov, G. V.; Fagin, A. A.; Bochkarev, M. N.; Dechert, S.; Schumann, H. *Russ. Chem. Bull.* **2003**, *52*, 1358.
243. Xu, Z.; You, X.; Zhou, X.; Wang, H.; Yang, Y. *Polyhedron* **1993**, *12*, 795.
244. Zhou, X.; Wu, Z.; Ma, H.; Xu, Z.; You, X. *Polyhedron* **1994**, *13*, 375.
245. Depaoli, G.; Russo, U.; Valle, G.; Grandjean, F.; Williams, A. F.; Long, G. J. *J. Am. Chem. Soc.* **1994**, *116*, 5999.
246. Maia, A.; Sampaio Paulino, I.; Schuchardt, U.; de Oliveira, W. *Inorg. Chem. Commun.* **2003**, *6*, 304.
247. Stelfeldt, D.; Meyer, G.; Deacon, G. B. *Z. Anorg. Allg. Chem.* **1999**, *625*, 1252.
248. Alves, N. P.; de Souza Maia, A.; de Oliveira, W. *J. Alloys Compd.* **2000**, *303–304*, 178.
249. Lin, J.; Zhao, R.; Wang, Z. *Rare Earth Mater. Eng.* **2001**, *30*, 238.
250. Deacon, G. B.; Forsyth, C. M.; Wilkinson, D. L. *Chem. Eur. J.* **2001**, *7*, 1784.
251. Ihara, E.; Tanaka, M.; Yasuda, H.; Kanehisa, N.; Maruo, T.; Kai, Y. *J. Organomet. Chem.* **2000**, *613*, 26.
252. Giesbrecht, G. R.; Clark, D. L.; Gordon, J. C.; Scott, B. L. *Appl. Organomet. Chem.* **2003**, *17*, 473.
253. Giesbrecht, G. R.; Collis, G. E.; Gordon, C. J.; Clark, D. L.; Scott, B. L.; Hardman, N. J. *J. Organomet. Chem.* **2004**, *689*, 2177.
254. Leung, W.-P.; Song, F.-Q.; Xue, F.; Zhang, Z.-Y.; Mak, T. C. W. *J. Organomet. Chem.* **1999**, *582*, 292.
255. Zhang, L.; Zhou, X.; Cai, R.; Weng, L. *J. Organomet. Chem.* **2000**, *612*, 176.
256. Liu, Q.; Huang, J.; Qian, Y.; Chan, A. S. C. *Polyhedron* **1999**, *18*, 2345.
257. Shen, F.; Zhang, W.; Hu, J.; Wang, S.; Huanh, X. *J. Organomet. Chem.* **1996**, *523*, 121.
258. Trifonov, A. A.; Ferri, F.; Collin, J. *J. Organomet. Chem.* **1999**, *582*, 211.
259. Trifonov, A. A.; Van de Weghe, P.; Collin, J.; Domingos, A.; Santos, I. *J. Organomet. Chem.* **1997**, *527*, 225.
260. Arndt, S.; Voth, P.; Spaniol, T. P.; Okuda, J. *Organometallics* **2000**, *19*, 4690.
261. Lin, J.; Wang, Z. *J. Organomet. Chem.* **1999**, *589*, 127.
262. Yao, Y.; Shen, Q.; Sun, J.; Xue, F. *Acta Crystallogr., Sect. C: Cryst. Struct. Commun.* **1998**, *54*, 625.
263. Fedushkin, I. L.; Nevodchikov, V. I.; Bochkarev, M. N.; Dechert, S.; Schumann, H. *Russ. Chem. Bull.* **2003**, *52*, 154.
264. Evans, W. J.; Greci, M. A.; Johnston, M. A.; Ziller, J. W. *Chem. Eur. J.* **1999**, *5*, 3482.
265. Yao, Y.; Zhang, Y.; Shen, Q.; Yu, K. *Organometallics* **2002**, *21*, 819.
266. Zhang, Y.; Yao, Y.-M.; Luo, Y.-J.; Shen, Q.; Cui, Y.; Yu, K.-B. *Polyhedron* **2003**, *22*, 1241.
267. Yao, Y.; Zhang, Y.; Zhang, Z.; Shen, Q.; Yu, K. *Organometallics* **2003**, *22*, 2876.
268. Roesky, P. W. *Organometallics* **2002**, *21*, 4756.
269. Liu, Q.; Ding, M. *J. Organomet. Chem.* **1998**, *553*, 179.
270. Liu, Q.; Ding, M.; Lin, Y.; Xing, Y. *Polyhedron* **1998**, *17*, 555.
271. Zhang, L.-J.; Lu, X.-J.; Ma, H.-Z.; Zhang, W. *Hecheng Huaxue* **2003**, *11*, 363.
272. Cia, Y.-P.; Ma, H.-Z.; Kang, B.-S.; Su, C.-Y.; Zhang, W.; Sun, J.; Xiong, Y.-L. *J. Organomet. Chem.* **2001**, *628*, 99.
273. Zhang, W.; Cai, Y.-P.; Li, H.-X.; Ma, H.-Z. *Jiegou Huaxue* **2002**, *21*, 378.
274. Gamer, M. T.; Roesky, P. W. *Inorg. Chem.* **2004**, *43*, 4903.
275. Jin, G.-X.; Cheng, Y.; Lin, Y. *Organometallics* **1999**, *18*, 947.
276. Cheng, Y.; Jin, G.-X.; Shen, Q.; Lin, Y. *J. Organomet. Chem.* **2001**, *631*, 94.
277. Tian, S.; Arredondo, V. M.; Stern, C. L.; Marks, T. J. *Organometallics* **1999**, *18*, 2568.
278. Okuda, J.; Arndt, S.; Beckerle, K.; Hultsch, K. C.; Voth, P.; Spaniol, T. P. *Pure Appl. Chem.* **2001**, *73*, 351.
279. Roitershtein, D. M.; Lyssenko, K. A.; Belyakov, P. A.; Antipin, M. Y. *Russ. Chem. Bull.* **1997**, *46*, 1590.
280. Lopes, I.; Lin, G. Y.; Domingos, A.; McDonald, R.; Marques, N.; Takats, J. *J. Am. Chem. Soc.* **1999**, *121*, 8110.
281. Lin, G.; McDonald, R.; Takats, J. *J. Organomet. Chem.* **2001**, *626*, 76.
282. Zhou, X.; Huang, Z.; Cai, R.; Zhang, L.; Huang, X. *Organometallics* **1999**, *18*, 4128.
283. Zhou, X.-G.; Ma, W.-W.; Huang, Z.-E.; Cai, R.-F.; You, X.-Z.; Huang, X.-Y. *J. Organomet. Chem.* **1997**, *545–546*, 309.
284. Zhu, M.; Li, Y.; Luo, J.; Zhou, X. *Chin. Sci. Bull.* **2003**, *48*, 2041.
285. Anfang, S.; Gröb, T.; Harms, K.; Seybert, G.; Massa, W.; Greiner, A.; Dehnicke, K. *Z. Anorg. Allg. Chem.* **1999**, *625*, 1853.



286. Bochkarev, M. N.; Protchenko, A. V.; Zakharov, L. N.; Fukin, G. K.; Struchkov, Y. T. *J. Organomet. Chem.* **1995**, *501*, 123.
287. Mu, Y.; Piers, W. E.; MacQuarrie, D. C.; Zaworotko, M. J.; Young, V. G. *Organometallics* **1996**, *15*, 2720.
288. Arndt, S.; Spaniol, T. P.; Okuda, J. *Organometallics* **2003**, *22*, 775.
289. Arndt, S.; Trifonov, A.; Spaniol, T. P.; Okuda, J.; Kitamura, M.; Takahashi, T. *J. Organomet. Chem.* **2002**, *647*, 158.
290. Arndt, S.; Spaniol, T. P.; Okuda, J. *Eur. J. Inorg. Chem.* **2001**, 73.
291. Voth, P.; Arndt, S.; Spaniol, T. P.; Okuda, J. *Organometallics* **2003**, *22*, 65.
292. Shapiro, P. J.; Cotter, W. D.; Schaefer, W. P.; Labinger, J. A.; Bercaw, J. E. *J. Am. Chem. Soc.* **1994**, *116*, 4623.
293. Voth, P.; Spaniol, T. P.; Okuda, J. *Organometallics* **2003**, *22*, 3921.
294. Shen, X.; Xie, Y.; Jiang, H.; Li, Q. *Pol. J. Chem.* **1994**, *68*, 1303.
295. Schaverien, C. J. *Organometallics* **1994**, *13*, 69.
296. Hultsch, K. C.; Voth, P.; Spaniol, T. P.; Okuda, J. *Z. Anorg. Allg. Chem.* **2003**, *629*, 1272.
297. Tardif, O.; Kurazumi, J.; Nishiura, M.; Horiuchi, A.; Hou, Z. *Kidorui* **2003**, *42*, 50.
298. Tardif, O.; Nishiura, M.; Hou, Z. *Organometallics* **2003**, *22*, 1171.
299. Cui, D.; Tardif, O.; Hou, Z. *J. Am. Chem. Soc.* **2004**, *126*, 1312.
300. Tardif, O.; Hashizume, D.; Hou, Z. *J. Am. Chem. Soc.* **2004**, *126*, 8080.
301. Barnea, E.; Andrea, T.; Kapon, M.; Eisen, M. S. *J. Am. Chem. Soc.* **2004**, *126*, 5066.
302. Alary, F.; Heully, J.-L.; Poteau, R.; Maron, L.; Trinquier, G.; Daudey, J.-P. *J. Am. Chem. Soc.* **2003**, *125*, 11051.
303. Kretschmer, W.; Thiele, K.-H. *Z. Anorg. Allg. Chem.* **1995**, *621*, 1093.
304. Beetstra, D.; Meetsma, A.; Hessen, B.; Teuben, J. H. *Organometallics* **2003**, *22*, 4372.
305. Fedushkin, I. L.; Bochkarev, M. N.; Muehle, S.; Schumann, H. *Russ. Chem. Bull.* **2003**, *52*, 2005.
306. Evans, W. J.; Brady, J. C.; Ziller, J. W. *J. Am. Chem. Soc.* **2001**, *123*, 7711.
307. Barbier-Baudry, D.; Blacque, O.; Hafid, A.; Nyassi, A.; Sitzmann, H.; Visseaux, M. *Eur. J. Inorg. Chem.* **2000**, 2333.
308. Bonnet, F.; Visseaux, M.; Barbier-Baudry, D.; Hafid, A.; Vigier, E.; Kubicki, M. M. *Inorg. Chem.* **2004**, *43*, 3682.
309. Ziegler, T.; Folga, E.; Berces, A. J. *J. Am. Chem. Soc.* **1993**, *115*, 636.
310. Luo, Y.; Selvam, P.; Ito, Y.; Endou, A.; Kubo, M.; Miyamoto, A. *J. Organomet. Chem.* **2003**, *679*, 84.
311. Luo, Y.; Selvam, P.; Koyama, M.; Kubo, M.; Miyamoto, A. *Inorg. Chem. Commun.* **2004**, *7*, 566.
312. Lou, Y.; Selvam, P.; Ito, Y.; Kubo, M.; Miyamoto, A. *Inorg. Chem. Commun.* **2003**, *6*, 1243.
313. Nicolas, P.; Royo, P.; Galakhov, M. V.; Blacque, O.; Jacobsen, H.; Berke, H. *J. Chem. Soc., Dalton Trans.* **2004**, 2943.
314. Maron, L.; Perrin, L.; Eisenstein, O. *J. Chem. Soc., Dalton Trans.* **2003**, 4313.
315. Xie, Z.; Liu, Z.; Zhou, Z. Y.; Mak, T. C. W. *J. Chem. Soc., Dalton Trans.* **1998**, 3367.
316. Xie, Z.; Chui, K.; Yang, Q.; Mak, T. C. W.; Sun, J. *Organometallics* **1998**, *17*, 3937.
317. Deacon, G. B.; Harris, S. C.; Meyer, G.; Stellfeldt, D.; Wilkinson, D. L.; Zelesny, G. J. *Organomet. Chem.* **1998**, *552*, 165.
318. Deacon, G.; Forsyth, G. M.; Sun, J. *Tetrahedron Lett.* **1994**, *35*, 1095.
319. Maron, L.; Werkema, E. L.; Perrin, L.; Eisenstein, O.; Andersen, R. A. *J. Am. Chem. Soc.* **2005**, *127*, 279.
320. Evans, W. J.; Keyer, R.; Ziller, J. *J. Organomet. Chem.* **1993**, *450*, 115.
321. Zhou, X.-G.; Zhang, C.-M.; Luo, J.; Chen, Y.-H.; Shao, Z.-H.; Li, Q. *Fudan Xuebao, Ziran Kexueban* **2003**, *42*, 1025.
322. Stellfeldt, D.; Meyer, G.; Deacon, G. B. *Z. Anorg. Allg. Chem.* **2001**, *627*, 1659.
323. Wehausen, P.; Borgmeier, O.; Furrer, A.; Fischer, P.; Allenspach, P.; Henggeler, W.; Schilder, H.; Lueken, H. *J. Alloys Compd.* **1997**, *246*, 139.
324. Gatti, P. M.; da Luz, M. A.; de Oliveira, W. *Quim. Nova* **2000**, *23*, 191.
325. Schumann, H.; Heim, A.; Demtschuk, J.; Mühle, S. H. *Organometallics* **2003**, *22*, 118.
326. Bala, M. D.; Huang, J.; Zhang, H.; Qian, Y.; Sun, J.; Liang, C. J. *Organomet. Chem.* **2002**, *647*, 105.
327. Schumann, H.; Heim, A.; Demtschuk, J.; Mühle, S. H. *Organometallics* **2002**, *21*, 3334.
328. Cheng, Y.-X.; Jin, G.-X.; Jia, H.-Q.; Xing, Y.; Lin, Y.-H. *Chin. J. Struct. Chem.* **2001**, *20*, 31.
329. Wu, Z.-Z.; Huang, Z.-E.; Cai, R.-F.; Zhou, X.-G.; Xu, Z.; You, X.-Z.; Huang, X.-Y. *Jiegou Huaxue* **1996**, *15*, 367.
330. Jiang, T.; Shen, Q. *J. Ocean Univ. Qiangdao* **2001**, *31*, 173.
331. Song, S.; Jin, S.; Lin, Y.; Shen, Q. *Yingyong Huaxue* **1993**, *10*, 80.
332. Ren, J.-S.; Shen, Q.; Hu, J.-Y.; Lin, Y.-H.; Xing, Y. *Jiegou Huaxue* **1996**, *15*, 379.
333. Liang, C.-F.; Sun, J.-Q.; Hu, W.-Q.; Yang, Y.-R.; Schumann, H. *Zhejiang Daxue Xuebao Gongxueban* **2002**, *36*, 109.
334. Schumann, H.; Keitsch, M. R.; Winterfeld, J.; Mühle, S.; Molander, G. A. *J. Organomet. Chem.* **1998**, *559*, 181.
335. Schumann, H.; Rosenthal, E. C. E.; Kociok-Koehn, G.; Molander, G. A.; Winterfeld, J. *J. Organomet. Chem.* **1995**, *496*, 233.
336. Jin, J.; Jin, Z.; Wie, G.; Chen, W. *Chin. Sci. Bull.* **1993**, *38*, 526.
337. Spirlet, M.-R.; Goffart, J. *J. Organomet. Chem.* **1995**, *493*, 149.
338. Spirlet, M. R.; Goffart, J. *Acta Crystallogr., Sect. C: Cryst. Struct. Commun.* **1998**, *54*, 1624.
339. Xie, Z.; Liu, Z.; Xue, F.; Zhang, Z.; Mak, T. C. W. *J. Organomet. Chem.* **1997**, *542*, 285.
340. Constantine, S. P.; De Lima, G. M.; Hitchcock, P. B.; Keates, J. M.; Lawless, G. A. *Chem. Commun.* **1996**, 2421.
341. Zhou, X.; Ma, H.; Wu, Z.; You, X.; Xu, Z.; Huang, X. *J. Organomet. Chem.* **1995**, *503*, 11.
342. Zhou, X.; Ma, H.; Wei, G.; Jin, Z.; Wu, Z.; Xu, Z.; You, X. *Chin. Sci. Bull.* **1995**, *40*, 552.
343. Chan, H.-S.; Yang, Q.; Mak, T. C. W.; Xie, Z. *J. Organomet. Chem.* **2000**, *601*, 160.
344. Fedushkin, I. L.; Girgsdies, F.; Schumann, H.; Bochkarev, M. N. *Eur. J. Inorg. Chem.* **2001**, 2405.
345. Schumann, H.; Kreitsch, M. R.; Mühle, S. H. *Z. Anorg. Allg. Chem.* **2002**, *628*, 1311.
346. Abernethy, C. D.; Macdonald, C. L. B.; Clyburne, J. A. C.; Cowley, A. H. *J. Chem. Soc., Chem. Commun.* **2001**, 61.
347. Hitchcock, P. B.; Lappert, M. F.; Tian, S. *Organometallics* **2000**, *19*, 3420.
348. Sitzmann, H.; Schmitt, O.; Weber, F.; Wolmershäuser, G. *Z. Anorg. Allg. Chem.* **2001**, *627*, 12.
349. Schmitt, O.; Wolmershäuser, G.; Sitzmann, H. *Eur. J. Inorg. Chem.* **2003**, 3105.
350. Yuan, F.; Shen, Q.; Sun, J. *J. Organomet. Chem.* **1997**, *538*, 241.
351. Schumann, H.; Keitsch, M. R.; Demtschuk, J.; Molander, G. A. *J. Organomet. Chem.* **1999**, *582*, 70.
352. Xie, Z.; Liu, Z.; Chui, K.; Xue, F.; Mak, T. C. W. *J. Organomet. Chem.* **1999**, *588*, 78.
353. Barbier-Baudry, D.; Dormond, A.; Visseaux, M. *J. Organomet. Chem.* **2000**, *609*, 21.
354. Qian, C. T.; Wang, B.; Deng, D. L.; Hu, J. Q. *Inorg. Chem.* **1994**, *33*, 3382.

355. Qian, C.; Zheng, X.; Wang, B.; Deng, D.; Sun, J. *J. Organomet. Chem.* **1994**, *466*, 101.
356. Zhang, S.; Zhuang, X.; Wei, G.; Chen, W. *Polyhedron* **1994**, *13*, 2867.
357. Deng, D.; Jiang, Y.; Qian, Ch.; Wu, G.; Zheng, P. *J. Organomet. Chem.* **1994**, *470*, 99.
358. Deng, D.; Zheng, X.; Qian, C.; Sun, J.; Zhang, L. *J. Organomet. Chem.* **1994**, *466*, 95.
359. Gendron, R. A. L.; Berg, D. J.; Barclay, T. *Can. J. Chem.* **2002**, *80*, 1285.
360. Corradi, M. M.; McGowan, M. A. D.; McGowan, P. C.; Thornton-Pett, M. *Eur. J. Inorg. Chem.* **2002**, 2362.
361. Schumann, H.; Rosenthal, E. C. E.; Demtschuk, J. *Organometallics* **1998**, *17*, 5324.
362. Schumann, H.; Herrmann, K.; Erbstein, F. *Z. Naturforsch., B: Chem. Sci.* **2003**, *58*, 832.
363. Schumann, H.; Herrmann, K.; Demtschuk, J.; Mühle, S. H. *Z. Anorg. Allg. Chem.* **1999**, *625*, 1107.
364. Schumann, H.; Herrmann, K.; Mühle, S. H.; Dechert, S. *Z. Anorg. Allg. Chem.* **2003**, *629*, 1184–1194.
365. Zhu, M.; Zhang, L.-B.; Chen, Y.-H.; Zhou, X.-G.; Cai, R.-F.; Weng, L.-H. *Chin. J. Chem.* **2004**, *22*, 935.
366. Karsch, H. H.; Graf, V.; Reisky, M.; Witt, E. *Eur. J. Inorg. Chem.* **1998**, 1403.
367. Karsch, H. H.; Graf, V. W.; Scherer, W. *J. Organomet. Chem.* **2000**, *604*, 72.
368. Deacon, G. B.; Fallon, G. D.; Forsyth, C. M. *J. Organomet. Chem.* **1993**, *462*, 183.
369. Lin, G.; Wong, W.-T. *Polyhedron* **1994**, *13*, 3027.
370. Roitershtein, D. M.; Krut'ko, D. P.; Veksler, E. N.; Lemenovskii, D. A.; Nie, W.; Qian, C. *Russ. Chem. Bull.* **2001**, *50*, 1295.
371. Xu, Z.; You, X.; Wang, H.; Wu, Z.; Zhou, X.; Sheng, F.; Hu, J. *J. Organomet. Chem.* **1993**, *455*, 93.
372. Lin, G.; Wong, W.-T. *Polyhedron* **1995**, *14*, 3167.
373. Schierwater, K.; Hanika-Heidl, H.; Bollmann, M.; Fischer, D. R.; Harris, R. K.; Apperley, D. C. *Coord. Chem. Rev.* **2003**, *242*, 15.
374. Yuan, F.-G.; Chen, L.; Wen, L.-H.; Yang, J. *Youji Huaxue* **2003**, *23*, 646.
375. Deng, M.; Zhou, Y.; Yao, Y.; Shen, Q.; Weng, L. *Zhongguo Xitu Xuebao* **2003**, *21*, 626.
376. Hahn, T.; Hey-Hawkins, E.; Hilder, M.; Junk, P. C.; Smith, M. K. *Inorg. Chim. Acta* **2004**, *357*, 2125.
377. Massarweh, G.; Fischer, R. D. *J. Organomet. Chem.* **1993**, *444*, 67.
378. Wu, Z.-Z.; Huang, Z.-E.; Cai, R.-F.; Hu, Z.; You, X.-Z.; Huang, X.-Y. *Polyhedron* **1995**, *15*, 13.
379. Wu, Z.; Xu, Z.; You, X.; Zhou, X.; Xing, Y.; Jin, Z. *J. Chem. Soc., Chem. Commun.* **1993**, 1494.
380. Gun'ko, Y. K.; Hitchcock, P. B.; Lappert, M. F. *J. Organomet. Chem.* **1995**, *499*, 213.
381. Cassani, M. C.; Lappert, M. F.; Laschi, F. *J. Chem. Soc., Chem. Commun.* **1997**, 1563.
382. Steudel, A.; Stehr, J.; Siebel, E.; Fischer, R. D. *J. Organomet. Chem.* **1998**, *570*, 89.
383. Wu, Z.-Z.; Huang, Z.-E.; Cai, R.-F. *Synth. React. Inorg. Met.-Org. Chem.* **1995**, *25*, 1401.
384. Poremba, P.; Noltemeyer, M.; Schmidt, H.-G.; Edelmann, F. T. *J. Organomet. Chem.* **1995**, *501*, 315.
385. Wu, Z.; Zhou, X.; Zhang, W.; Xu, Z.; You, X.; Huang, X. *J. Chem. Soc., Chem. Commun.* **1994**, 813.
386. Wu, Z.-Z.; Fan, D.-M.; Huang, Z.-E.; Cai, R.-F. *Polyhedron* **1995**, *15*, 127.
387. Weng, X.; Shen, X.; Du, B. *Synth. React. Inorg. Met.-Org. Chem.* **1993**, *23*, 419.
388. Shen, X.; Xie, Y. *Synth. React. Inorg. Met.-Org. Chem.* **1994**, *24*, 267.
389. Schumann, H.; Zietzke, K.; Weimann, R. *Eur. J. Solid State Inorg. Chem.* **1996**, *33*, 121.
390. Schumann, H.; Zietzke, K.; Erbstein, F.; Weimann, R. *J. Organomet. Chem.* **1996**, *520*, 265.
391. Deacon, G. B.; Quitmann, C. C.; Müller-Buschbaum, K.; Meyer, G. *Z. Anorg. Allg. Chem.* **2001**, *627*, 1431.
392. Deacon, G. B.; Quitmann, C. C.; Müller-Buschbaum, K.; Meyer, G. *Z. Anorg. Allg. Chem.* **2003**, *629*, 589.
393. Deacon, G. B.; Fallon, G. D.; Gatehouse, B. M.; Rabinovich, A.; Skelton, B. W.; White, A. J. *J. Organomet. Chem.* **1995**, *501*, 23.
394. Shen, F.; Hu, J.; Xie, M.; Wang, S.; Huang, X. *J. Organomet. Chem.* **1995**, *485*, C6.
395. Ye, Z.; Yu, Y.; Wang, S.; Jin, X. *J. Organomet. Chem.* **1993**, *448*, 91.
396. Sun, Y.-M.; Ling, Q.; Wan, Y.-B.; Wang, X.-R.; Yu, H.-Y. *Chin. J. Chem.* **2002**, *20*, 996.
397. Ling, Q.; Shen, G.-X.; Yu, H.-Y.; Zhang, Y.; Sun, Y.-M. *Hecheng Huaxue* **2002**, *10*, 263.
398. Luo, M.; Ma, H.-Z.; Su, Q.-D.; Li, Q.-R.; Hu, N.-L. *Asian J. Chem.* **2002**, *14*, 1463.
399. Wu, Z.; Xu, Z.; You, X. *Synth. React. Inorg. Met.-Org. Chem.* **1993**, *23*, 155.
400. Wang, Y.; Shen, Q.; Wu, L.; Zhang, Y.; Sun, J. *J. Organomet. Chem.* **2001**, *626*, 176.
401. Yuan, F.-G.; Shen, Q.; Sun, J. *Chem. J. Chin. Univ.* **2001**, *22*, 1501.
402. Liu, Q.; Ding, M.; Lin, Y.; Xing, Y. *J. Organomet. Chem.* **1997**, *548*, 139.
403. Liu, Q.; Ding, M.; Lin, Y.; Xing, Y. *Polyhedron* **1998**, *17*, 2327.
404. Yousaf, M.; Liu, Q.; Huang, J.; Qian, Y.; Chan, A. S. C. *Inorg. Chem. Commun.* **2000**, *3*, 105.
405. Muhammad, Y.; Huang, J.; Feng, Z.; Qian, Y. *Huadong Ligong Daxue Xuebao* **2001**, *27*, 211.
406. Wu, Z.-Z.; Ma, W.-W.; Huang, Z.-E.; Cai, R.-F.; Xu, Z.; You, X.-Z.; Sun, J. *Polyhedron* **1996**, *15*, 3427.
407. Wu, Z.-Z.; Huang, Z.-E.; Cai, R.-F.; Zhou, X.-G.; Xu, Z.; You, X.-Z.; Huang, X.-Y. *J. Organomet. Chem.* **1996**, *506*, 25.
408. Beletskaya, I. P.; Voskoboynikov, A. Z.; Shestakova, A. K.; Yanovsky, A. I.; Fukin, G. K.; Zacharov, L. N.; Struchkov, Yu. T.; Schumann, H. *J. Organomet. Chem.* **1994**, *468*, 121.
409. Zhang, L.-X.; Zhou, X.-G.; Huang, Z.-E.; Cai, R.-F.; Huang, X.-Y. *Polyhedron* **1999**, *18*, 1533.
410. Zhang, L.-G.; Zhou, X.-G.; Huang, Z.-E.; Cai, R.-F.; Zhang, L.-B. *Chin. J. Struct. Chem.* **2001**, *20*, 40.
411. Zhang, L.-X.; Xie, M.-H.; Ma, H.-Z. *Hecheng Huaxue* **2001**, *9*, 156.
412. Zhou, X.-G.; Zhang, L.-X.; Zhang, C.-M.; Zhang, J.; Zhu, M.; Cai, R.-F.; Huang, Z.-E.; Huang, Z.-X.; Wu, Q.-J. *J. Organomet. Chem.* **2002**, *655*, 120.
413. Wan, Y.-B.; Wang, X.-R. *J. Anhui Univ. Technol.* **2001**, *18*, 235.
414. Wang, X. R.; Wan, Y.-B.; Hu, J.-P. *Hecheng Huaxue* **2001**, *9*, 452.
415. Pernin, C. G.; Ibers, J. A. *Inorg. Chem.* **2000**, *39*, 1216.
416. Pernin, C. G.; Ibers, J. A. *Inorg. Chem.* **1999**, *38*, 5478.
417. Gamer, M. T.; Roesky, P. W. *J. Organomet. Chem.* **2002**, *647*, 123.
418. Wang, Y.; Shen, Q.; Xue, F.; Yu, K. *J. Organomet. Chem.* **2000**, *598*, 359.
419. Li, H.; Yao, Y.; Shen, Q.; Weng, L. *Organometallics* **2002**, *21*, 2529.
420. Mao, L.; Shen, Q.; Xue, M. *Organometallics* **1997**, *16*, 3711.
421. Zhang, J.; Ruan, R.; Shao, Z.; Cai, R.; Weng, L.; Zhou, X. *Organometallics* **2002**, *21*, 1420.
422. Zhou, X.-G.; Zhang, L.-B.; Zhu, M.; Cai, R.-F.; Weng, L.-H. *Organometallics* **2001**, *20*, 5700.

423. Wang, Y.; Shen, Q.; Xue, F.; Yu, K. *Organometallics* **2000**, *19*, 357.
424. Guan, J.; Shen, Q.; Jin, S.; Lin, Y. *Polyhedron* **1994**, *13*, 1695.
425. Fan, D.; Ma, W.; Wu, Z.; Cai, R.; Huang, Z. *Fudan Xuebao, Ziran Kexueban* **1997**, *36*, 59.
426. Dash, A. K.; Razavi, A.; Mortreux, A.; Lehmann, C. W.; Carpentier, J.-F. *Organometallics* **2002**, *21*, 3238.
427. Cui, D.; Nishiura, M.; Hou, Z. *Angew. Chem.* **2005**, *117*, 981.
- 427a. Cui, D.; Nishiura, M.; Hou, Z. *Angew. Chem. Int. Ed.* **2005**, *44*, 959.
428. Hultsch, K. C.; Spaniol, T. P.; Okuda, J. *Organometallics* **1997**, *16*, 4845.
429. Anfang, S.; Harms, K.; Weller, F.; Borgmeier, O.; Lueken, H.; Schilder, H.; Dehnicke, K. Z. *Anorg. Allg. Chem.* **1998**, *624*, 159.
430. Pfeiffer, D.; Guzei, I. A.; Liable-Sands, L. M.; Heeg, M. J.; Rheingold, A. L.; Winter, C. H. *J. Organomet. Chem.* **1999**, *588*, 167.
431. Zhang, J.; Zhou, X.; Cai, R.; Weng, L. *Inorg. Chem.* **2005**, *44*, 716.
432. Zhang, J.; Cai, R.; Weng, L.; Zhou, X. *J. Organomet. Chem.* **2003**, *672*, 94.
433. Zhang, J.; Cai, R.; Weng, L.; Zhou, X. *Organometallics* **2004**, *23*, 3303.
434. Zhang, J.; Cai, R.; Weng, L.; Zhou, X. *Organometallics* **2003**, *22*, 5385.
435. Shen, Q.; Li, H.; Yao, C.; Yao, Y.; Zhang, L.; Yu, K. *Organometallics* **2001**, *20*, 3070.
436. Zhang, C.; Liu, R.; Zhou, X.; Chen, Z.; Weng, L.; Lin, Y. *Organometallics* **2004**, *23*, 3246.
437. Zhou, X. G.; Huang, Z. E.; Cai, R. F.; Zhang, L. X.; Hou, X. F.; Feng, X. J.; Huang, X. Y. *J. Organomet. Chem.* **1998**, *563*, 101.
438. Mao, L.; Shen, Q.; Sun, J. *J. Organomet. Chem.* **1998**, *566*, 9.
439. Westerhausen, M.; Schneiderbauer, S.; Makropoulos, N.; Warchhold, M.; Nöth, H.; Piotrowski, H.; Karaghiosoff, K. *Organometallics* **2002**, *21*, 4335.
440. Jin, J.; Zhuang, X.; Wei, G.; Chen, W. *Jiegou Huaxue* **1996**, *15*, 261.
441. Cui, D.; Tang, T.; Cheng, J.; Hu, N.; Chen, W.; Huang, B. *J. Organomet. Chem.* **2002**, *650*, 84.
442. Voskoboinikov, A. Z.; Parhina, I. N.; Schestakova, A. K.; Butin, K. P.; Beletskaya, I. P.; Kuz'mina, L. G.; Howard, J. A. K. *Organometallics* **1997**, *16*, 4041.
443. Hu, J.; Ren, J.; Shen, Q. *Yingyong Huaxue* **1997**, *14*, 86.
444. Ren, J.; Hu, J.; Lin, Y.; Xing, Y.; Shen, Q. *Polyhedron* **1996**, *15*, 2165.
445. Wang, S.; Yu, Y.; Ye, Z.; Qian, C.; Jin, X. *J. Chem. Soc., Chem. Commun.* **1994**, 1097.
446. Baudry-Barbier, D.; Andre, N.; Dormond, A.; Pardes, C.; Richard, P.; Visseaux, M.; Zhu, C. J. *Eur. J. Inorg. Chem.* **1998**, 1721.
447. Wong, W.-K.; Zhang, L.; Wong, W.-T.; Xue, F.; Mak, T. C. W. *Polyhedron* **1996**, *15*, 4593.
448. Wong, W.-K.; Zhang, L.; Xue, F.; Mak, T. C. W. *Polyhedron* **1997**, *16*, 2013.
449. Vinogradov, S. A.; Mistrukov, A. E.; Beletskaya, I. P. *J. Chem. Soc., Dalton Trans.* **1995**, 2679.
450. Campion, B.; Heyn, R.; Tilley, T. D. *Organometallics* **1993**, *12*, 2584.
451. Visseaux, M.; Baudry, D.; Dormond, A.; Qian, C. T. C. *R. Acad. Sci. Ser. IIB* **1996**, *323*, 415.
452. Visseaux, M.; Baudry, D.; Dormond, A.; Qian, C. J. *Organomet. Chem.* **1999**, *574*, 213.
453. Schumann, H.; Keitsch, M. R.; Demtschuk, J.; Mühle, S. Z. *Anorg. Allg. Chem.* **1998**, *624*, 1811.
454. Schumann, H.; Keitsch, M. R.; Mühle, S. H. *Acta Crystallogr., Sect. C: Cryst. Struct. Commun.* **2000**, *56*, 48.
455. Maron, L.; Eisenstein, O.; Alary, F.; Poteau, R. *J. Phys. Chem. A* **2002**, *106*, 1797.
456. Baudry, D.; Dormond, A.; Lachlot, B.; Visseaux, M.; Zucchi, G. *J. Organomet. Chem.* **1997**, *547*, 157.
457. Kaltsayannis, N.; Bursten, B. E. *J. Organomet. Chem.* **1997**, *528*, 19.
458. Strasser, A.; Vogler, A. *Chem. Phys. Lett.* **2003**, *379*, 287.
459. de Oliveira, W.; Bazito, R.; Gatti, P. M. *J. Braz. Chem. Soc.* **1995**, *6*, 243.
460. Zhou, X.-G.; Huang, Z.-E.; Cai, R.-F.; Yu, S.-N.; Huang, X.-Y. *Jiegou Huaxue* **1997**, *16*, 384.
461. Jank, S.; Reddmann, H.; Amberger, H. D. *J. Alloys Compd.* **1997**, *250*, 387.
462. Tanner, P. S.; Burke, D. J.; Hanusa, T. P. *Polyhedron* **1995**, *14*, 331.
463. Tanner, P. S.; Overby, J. S.; Henein, M. M.; Hanusa, T. P. *Chem. Ber. Rec.* **1997**, *130*, 155.
464. Xie, Z.; Chui, K.; Liu, Z.; Xue, F.; Zhang, Z.; Mak, T. C. W.; Sun, J. *J. Organomet. Chem.* **1997**, *549*, 239.
465. Cassani, M. C.; Gun'ko, Y. K.; Hitchcock, P. B.; Lappert, M. F.; Laschi, F. *Organometallics* **1999**, *18*, 5539.
466. Al-Juaid, S.; Gun'ko, Y. K.; Hitchcock, P. B.; Lappert, M. F.; Tian, S. *J. Organomet. Chem.* **1999**, *582*, 143.
467. Khvostov, A. V.; Bulyshev, B. M.; Belsky, V. K.; Sizov, A. I. *J. Organomet. Chem.* **1998**, *568*, 113.
468. Chadwick, D. C.; Andersen, R. A. *J. Organomet. Chem.* **1995**, *501*, 271.
469. Schumann, H.; Glanz, M.; Hemling, H. *J. Organomet. Chem.* **1993**, *445*, C1.
470. Herrmann, W. A.; Anwender, R.; Munck, F.; Scherer, W. *Chem. Ber.* **1993**, *126*, 331.
471. Qian, C.; Wang, B.; Deng, D.; Jin, X. *Polyhedron* **1993**, *12*, 2265.
472. Amberger, H.-D.; Reddmann, H.; Karsch, H. H.; Graf, V. W.; Quian, C.; Wang, B. *J. Organomet. Chem.* **2003**, *677*, 35.
473. Reddmann, H.; Schultze, H.; Amberger, H. D.; Edelstein, N. M. *J. Organomet. Chem.* **2000**, *604*, 296.
474. Amberger, H.-D.; Reddmann, H.; Jank, S.; Zhang, L.; Edelstein, N. M. *J. Organomet. Chem.* **2002**, *656*, 18.
475. Reddmann, H.; Jank, S.; Schultze, H.; Amberger, H.-D.; Edelstein, N. M. *Inorg. Chim. Acta* **2003**, *344*, 243.
476. Amberger, H.-D.; Reddmann, H.; Jank, S.; Lopes, M. I.; Marques, N. *Eur. J. Inorg. Chem.* **2004**, 98.
477. Schulz, H.; Hagen, C.; Reddmann, H.; Amberger, H.-D. *Z. Allg. Anorg. Chem.* **2004**, *630*, 268.
478. Jank, S.; Reddmann, H.; Amberger, H.-D.; Apostolidis, C. *J. Organomet. Chem.* **2004**, *689*, 3143.
479. Amberger, H.-D.; Schulz, H.; Reddmann, H.; Jank, S.; Edelstein, N.; Qian, C.; Wang, B. *Spectrochim. Acta Part A* **1996**, *52*, 429.
480. Amberger, H.-D.; Reddmann, H.; Schultze, H.; Jank, S.; Kanellakopoulos, B.; Apostolidis, C. *Spectrochim. Acta, Part A* **2003**, *59*, 2527.
481. Schulz, H.; Reddmann, H.; Amberger, H.-D. *J. Organomet. Chem.* **1993**, *461*, 69.
482. Reddmann, H. *Magn. Reson. Chem.* **1997**, *35*, 403.
483. Apostolidis, C.; Morgenstern, A.; Walter, O.; Reddmann, H.; Amberger, H.-D. *Z. Allg. Anorg. Chem.* **2004**, *630*, 928.
484. Liu, T.-Q.; Ding, F.-C.; Lin, Y.-H.; Yu, J.-X.; Shi, Q.-S.; Shen, Q. *Youji Huaxue* **2003**, *23*, 1029.
485. Chen, W.; Lin, G.; Xia, J.; Wie, G.; Zhang, Y.; Jin, Z. *J. Organomet. Chem.* **1994**, *467*, 75.
486. Junk, P. C. *Appl. Organomet. Chem.* **2003**, *17*, 875.
487. Wang, S.; Yu, Y.; Ye, Z.; Qian, C.; Huang, X. *J. Organomet. Chem.* **1993**, *464*, 55.
488. Wang, S.; Yu, Y.; Ye, Z.; Qian, C. *J. Organomet. Chem.* **1994**, *464*, 55.
489. Liu, T. *Crystallogr. Rep.* **2002**, *47*, 425.

490. Wu, Z.; Xu, Z.; You, X.; Zhou, X.; Huang, X.; Chen, J. *Polyhedron* **1994**, *13*, 379.
491. Cui, D.-M.; Cheng, J.-H.; Zhuang, X.-L.; Hu, N.-H.; Jin, J.-Z.; Chen, W.-Q.; Tang, T.; Huang, B.-T. *Jiegou Huaxue* **2002**, *21*, 78.
492. Zhou, X.; Ma, H.; Wu, Z.; You, X.; Xu, Z.; Zhang, Y.; Huang, X. *Acta Crystallogr., Sect. C: Cryst. Struct. Commun.* **1996**, *52*, 1875.
493. Huang, X. Y.; Zhou, X. G.; Ma, H. Z.; Zhen, Y. P.; Yu, Y. Q.; You, X.-Z.; Xu, Z. *Jiegou Huaxue* **1996**, *15*, 223.
494. Mehddoui, T.; Berthet, J.-C.; Thuery, P.; Ephritikhine, M. *Dalton Trans.* **2004**, 579.
495. Deacon, G. B.; Fallon, G. D.; Forsyth, C. M.; Gatehouse, B. M.; Junk, P. C.; Philosofo, A.; White, P. A. *J. Organomet. Chem.* **1998**, *565*, 201.
496. Guan, J.; Stehr, J.; Fischer, R. D. *Chem. Eur. J.* **1999**, *5*, 1992.
497. Schulz, H.; Amberger, H.-D. *J. Organomet. Chem.* **1993**, *443*, 71.
498. Domingos, A.; Marques, N.; Pires de Matos, A.; Silva-Valenzuela, M. G.; Zinner, L. B. *Polyhedron* **1993**, *12*, 2545.
499. Hagen, C.; Reddmann, H.; Amberger, H.-D.; Edelmann, F. T.; Pegelow, U.; Shalimoff, G.; Edelstein, N. M. *J. Organomet. Chem.* **1993**, *462*, 69.
500. Guan, J.; Fischer, R. D. *Eur. J. Inorg. Chem.* **2001**, 2497.
501. Wong, W.-K.; Guan, J.; Chen, Q.; Zhang, L.; Lin, Y.; Wong, W.-T. *Polyhedron* **1995**, *14*, 277.
502. Cassani, M. C.; Davies, M. J.; Hitchcock, P. B.; Lappert, M. F. *Inorg. Chim. Acta* **2005**, *358*, 1595.
503. Gulino, A.; Di Bella, S.; Fragalá, I.; Casarin, M.; Seyam, A.; Marks, T. J. *Inorg. Chem.* **1993**, *32*, 3873.
504. Luo, Y.; Yao, Y.; Shen, Q.; Sun, J.; Xue, F. *Acta Crystallogr., Sect. C: Cryst. Struct. Commun.* **1998**, *54*, 711.
505. Ren, J.; Guan, J.; Jin, S. *Polyhedron* **1994**, *13*, 2979.
506. Nishiura, M.; Hou, Z.; Wakatsuki, Y. *Organometallics* **2004**, *23*, 1359.
507. Evans, W. J.; Johnston, M. A.; Clark, R. D.; Anwender, R.; Ziller, J. W. *Polyhedron* **2001**, *20*, 2483.
508. Deacon, G. B.; Forsyth, C. M. *Organometallics* **2003**, *22*, 1349.
509. Corradi, M. M.; Frankland, A. D.; Hitchcock, P. B.; Lappert, M. F.; Lawless, G. A. *Chem. Commun.* **1996**, 2323.
510. Hollis, T.; Burdett, J.; Bosnich, B. *Organometallics* **1993**, *12*, 3385.
511. Timofeeva, T. V.; Lii, J.-H.; Allinger, N. L. *J. Am. Chem. Soc.* **1995**, *117*, 7452.
512. Kaltsayannis, N.; Russo, M. R. *J. Nucl. Sci. Technol.* **2002**, 393.
513. Perrin, L.; Maron, L.; Eisenstein, O.; Schwartz, D. J.; Burns, C. J.; Andersen, R. A. *Organometallics* **2003**, *22*, 5447.
514. Keates, J. M.; Lawless, G. A.; Waugh, M. P. *Chem. Commun.* **1996**, 1627.
515. Rabe, G. W.; Sebald, A. *Solid State Nucl. Magn. Reson.* **1996**, *6*, 197.
516. Keates, J. M.; Lawless, G. A. *Organometallics* **1997**, *16*, 2842.
517. Schultz, M.; Burns, C. J.; Schwartz, D. J.; Andersen, R. A. *Organometallics* **2000**, *19*, 781.
518. Schwartz, D. J.; Andersen, R. A. *Organometallics* **1995**, *14*, 4308.
519. Arduengo, A. J. III; Tamm, M.; McLain, S. J.; Calabrese, J. C.; Davidson, F.; Marshall, W. J. *J. Am. Chem. Soc.* **1994**, *116*, 7927.
520. Evans, W. J.; Perotti, J. M.; Ziller, J. W.; Moser, D. F.; West, R. *Organometallics* **2003**, *22*, 1160.
521. Hou, Z.; Fujita, A.; Yoshimura, T.; Jesorka, A.; Zhang, Y.; Yamazaki, H.; Wakatsuki, Y. *Inorg. Chem.* **1996**, *35*, 7190.
522. Hou, Z.; Yoshimura, T.; Wakatsuki, Y. *Kidorui* **1996**, *28*, 290.
523. Hou, Z.; Zhang, Y.; Yoshimura, T.; Wakatsuki, Y. *Organometallics* **1997**, *16*, 2963.
524. Hou, Z.; Zhang, Y.; Tezuka, H.; Xie, P.; Tardif, O.; Koizumi, T. A.; Yamazaki, H.; Wakatsuki, Y. *J. Am. Chem. Soc.* **2000**, *122*, 10533.
525. Hou, Z.; Wakatsuki, Y. *J. Alloys Compd.* **2000**, *303–304*, 75.
526. Hou, Z.; Zhang, Y.; Tardif, O.; Wakatsuki, Y. *J. Am. Chem. Soc.* **2001**, *123*, 9216.
527. Hou, Z.; Zhang, Y.; Nishiura, M.; Wakatsuki, Y. *Organometallics* **2003**, *22*, 129.
528. Clark, D. L.; Gordon, J. C.; Scott, B. L.; Watkin, J. G. *Polyhedron* **1999**, *18*, 1389.
529. Evans, W. J.; Giarikos, D. G.; Workman, P. S.; Ziller, J. W. *Inorg. Chem.* **2004**, *43*, 5754.
530. Evans, W. J.; Allen, N. T.; Greci, M. A.; Ziller, J. W. *Organometallics* **2001**, *20*, 2936.
531. Evans, W. J.; Boyle, T. J.; Ziller, J. W. *Organometallics* **1993**, *12*, 3998.
532. Butcher, R. J.; Clark, D. L.; Gordon, J. C.; Watkin, J. G. *J. Organomet. Chem.* **1999**, *577*, 228.
533. Evans, W. J.; Shreeve, J. L.; Ziller, J. W. *Organometallics* **1994**, *13*, 731.
534. Rieckhoff, M.; Noltemeyer, M.; Edelmann, F. T. *J. Organomet. Chem.* **1994**, *469*, C19.
535. Klooster, W. T.; Brammer, L.; Schaverien, C. J.; Budzelaar, P. H. M. *J. Am. Chem. Soc.* **1999**, *121*, 1381.
536. Cameron, T. M.; Gordon, J. C.; Scott, B. L.; Tumas, W. *Chem. Commun.* **2004**, 1398.
537. Evans, W. J.; Fujimoto, C. H.; Ziller, J. W. *Polyhedron* **2002**, *21*, 1683.
538. Klimpel, M. G.; Görlitzer, H. W.; Tafipolsky, M.; Spiegler, M.; Scherer, W.; Anwender, R. *J. Organomet. Chem.* **2002**, *647*, 236.
539. Schumann, H.; Erbstein, F.; Herrmann, K.; Demtschuk, J.; Weimann, R. *J. Organomet. Chem.* **1998**, *562*, 255.
540. Boudreaux, E. A.; Baxter, E. *Int. J. Quant. Chem.* **1997**, *62*, 23.
541. Cameron, T. M.; Gordon, J. C.; Scott, B. L. *Organometallics* **2004**, *23*, 2995.
542. Henderson, L. D.; MacInnis, G. D.; Piers, W. E.; Parvez, M. *Can. J. Chem.* **2004**, *82*, 162.
543. Castillo, I.; Tilley, T. D. *J. Am. Chem. Soc.* **2001**, *123*, 10526.
544. Mandel, A.; Magull, J. Z. *Anorg. Allg. Chem.* **1996**, *622*, 1913.
545. Swamy, S. J.; Schumann, H. *Indian J. Chem., Sect A* **1995**, *34*, 396.
546. Richter, J.; Edelmann, F. T. *Eur. J. Solid State Inorg. Chem.* **1996**, *33*, 1063.
547. Cendrowski-Guillaume, S. M.; Le Gland, G.; Nierlich, M.; Ephritikhine, M. *Organometallics* **2000**, *19*, 5654.
548. Schaverien, C. J. *J. Mol. Catal. Catal. B* **1994**, *90*, 177.
549. Pfennig, B. W.; Thompson, M. E.; Bocarsly, A. B. *Organometallics* **1993**, *12*, 649.
550. Evans, W. J.; Johnston, M. A.; Fujimoto, C. H.; Greaves, J. *Organometallics* **2000**, *19*, 4258.
551. Junk, P. C.; Smith, M. K. *Appl. Organomet. Chem.* **2004**, *18*, 252.
552. Evans, W. J.; Seibel, C. A.; Ziller, J. W. *J. Am. Chem. Soc.* **1998**, *120*, 6745.
553. Kaita, S.; Hou, Z.; Nishiura, M.; Doi, Y.; Kurazumi, J.; Horiuchi, A. C.; Wakatsuki, Y. *Macromol. Rapid Commun.* **2003**, *24*, 179.
554. Schumann, H.; Winterfeld, J.; Keitsch, M. R.; Herrmann, K.; Demtschuk, J. Z. *Anorg. Allg. Chem.* **1996**, *622*, 1457.
555. Evans, W. J.; Fujimoto, C. H.; Johnston, M. A.; Ziller, J. W. *Organometallics* **2002**, *21*, 1825.
556. Viseaux, M.; Dormond, A.; Baudry, D. *Bull. Soc. Chim. Fr.* **1993**, *130*, 173.
557. Evans, W. J.; Broomhall-Dillard, R. N. R.; Foster, S. E.; Ziller, J. W. *J. Coord. Chem.* **1998**, *43*, 199.
558. Lin, Y. H.; Zeng, D. S.; Shen, Q. *Report* **1995**, *95*, 706.



559. Labahn, T.; Mandel, A.; Magull, J. Z. *Anorg. Allg. Chem.* **1999**, 625, 1273.
560. Thiele, K.-H.; Scholz, A.; Scholz, J.; Böhme, U. Z. *Naturforsch., B: Chem. Sci.* **1993**, 48, 1753.
561. Evans, W. J.; Davis, B. L.; Nyce, G. W.; Perotti, J. M.; Ziller, J. W. J. *Organomet. Chem.* **2003**, 677, 89.
562. Lorenz, V.; Fischer, A.; Edelmann, F. T. J. *Organomet. Chem.* **2002**, 647, 245.
563. Evans, W. J.; Seibel, C. A.; Ziller, J. W.; Doedens, R. J. *Organometallics* **1998**, 17, 2103.
564. Evans, W. J.; Nyce, G. W.; Clark, R. D.; Doedens, R. J.; Ziller, J. W. *Angew. Chem. Int. Ed.* **1999**, 38, 1801.
565. Evans, W. J.; Rabe, G. W.; Ziller, J. W.; Doedens, R. J. *Inorg. Chem.* **1994**, 33, 2719.
566. Piers, W. E.; MacGillivray, L. R.; Zaworotko, M. J. *Organometallics* **1993**, 12, 4723.
567. Piers, W. E.; Parks, D. J.; MacGillivray, L. R.; Zaworotko, M. J. *Organometallics* **1994**, 13, 4547.
568. Piers, W. E. *J. Chem. Soc., Chem. Commun.* **1994**, 309.
569. Piers, W. E.; Ferguson, G.; Gallagher, J. F. *Inorg. Chem.* **1994**, 33, 3784.
570. Evans, J. W.; Lee, D. S.; Lie, C.; Ziller, J. W. *Angew. Chem.* **2004**, 116, 5633.
- 570a. Evans, J. W.; Lee, D. S.; Lie, C.; Ziller, J. W. *Angew. Chem. Int. Ed.* **2004**, 43, 5517.
571. Evans, W. J.; Allen, N. T.; Ziller, J. W. *J. Am. Chem. Soc.* **2001**, 123, 7927.
572. Scholz, A.; Thiele, K.-H.; Scholz, J.; Weimann, R. J. *Organomet. Chem.* **1995**, 501, 195.
573. Scholz, J.; Scholz, A.; Weimann, R.; Janiak, C.; Schumann, H. *Angew. Chem.* **1994**, 106, 1221.
574. Trifonov, A. A.; Kurskii, Y. A.; Bochkarev, M. N.; Muehle, S.; Dechert, S.; Schumann, H. *Russ. Chem. Bull.* **2003**, 52, 601.
575. Schultz, M.; Boncella, J. M.; Berg, D. J.; Tilley, T. D.; Andersen, R. A. *Organometallics* **2002**, 21, 460.
576. Da Re, R. E.; Kuehl, C. J.; Brown, M. G.; Rocha, R. C.; Bauer, E. D.; John, K. D.; Morris, D. E.; Shreve, A. P.; Sarrao, J. L. *Inorg. Chem.* **2003**, 42, 5551.
577. Berg, D. J.; Boncella, J. M.; Andersen, R. A. *Organometallics* **2002**, 21, 4622.
578. Kuehl, C. J.; Da Re, R. E.; Scott, B. L.; Morris, D. E.; John, K. D. *Chem. Commun.* **2003**, 2336.
579. Cosgriff, J. E.; Deacon, G. B.; Gatehouse, B. M.; Lee, P. R.; Schumann, H. Z. *Anorg. Allg. Chem.* **1996**, 622, 1399.
580. Deacon, G. B.; Delbridge, E. E.; Fallon, G. D. *Organometallics* **2000**, 19, 1713.
581. Evans, W. J.; Brady, J. C.; Ziller, J. W. *Inorg. Chem.* **2002**, 41, 3340.
582. Cole, M. L.; Junk, P. C. *New J. Chem.* **2003**, 27, 1032.
583. Gamer, M. T.; Roesky, P. W. *Organometallics* **2004**, 23, 5540.
584. Evans, W. J.; Leman, J. T.; Ziller, J. W.; Khan, S. I. *Inorg. Chem.* **1996**, 35, 4283.
585. Glanz, M.; Dechert, S.; Schumann, H.; Wolff, D.; Springer, J. Z. *Anorg. Allg. Chem.* **2000**, 626, 2467.
586. Schumann, H.; Glanz, M.; Winterfeld, J.; Hemling, H.; Kuhn, N.; Kratz, T. *Chem. Ber.* **1994**, 127, 2369.
587. Casey, C. P.; Tunge, J. A.; Lee, T.-Y.; Carpenetti, D. W. II *Organometallics* **2002**, 21, 389.
588. Casey, C. P.; Hallenbeck, S. L.; Wright, J. M.; Landis, C. R. J. *Am. Chem. Soc.* **1997**, 119, 9680.
589. Casey, C. P.; Tunge, J. A.; Lee, T.-Y.; Fagan, M. A. J. *Am. Chem. Soc.* **2003**, 125, 2641.
590. Di Bella, S.; Gulino, A.; Lanza, G.; Fragala, I.; Stern, D.; Marks, T. J. *Organometallics* **1994**, 13, 3810.
591. Perrin, L.; Maron, L.; Eisenstein, O. *New J. Chem.* **2004**, 28, 1255.
592. Forsyth, C. M.; Nolan, S.; Stern, C.; Marks, T. J. *Organometallics* **1993**, 12, 3618.
593. Heeres, H. J.; Nijhoff, J.; Teuben, J. H. *Organometallics* **1993**, 12, 2609.
594. Evans, W. J.; Keyer, R.; Ziller, J. *Organometallics* **1993**, 12, 2618.
595. Kaita, S.; Koga, N.; Hou, Z.; Doi, Y.; Wakatsuki, Y. *Organometallics* **2003**, 22, 3077.
596. Evans, W. J.; Giarikos, D. G.; Robledo, C. B.; Leong, V. S.; Ziller, J. W. *Organometallics* **2001**, 20, 5648.
597. Thiele, K.-H.; Seifert, R. Z. *Anorg. Allg. Chem.* **1995**, 621, 2089.
598. Takaki, K.; Kusodo, T.; Uebori, S.; Makioka, Y.; Taniguchi, Y.; Fujiwara, Y. *Tetrahedron Lett.* **1995**, 36, 1505.
599. Makioka, Y.; Koyama, K.; Nishiyama, T.; Takaki, K. *Tetrahedron Lett.* **1995**, 36, 6283.
600. Radu, N. S.; Buchwald, S. L.; Scott, B.; Burns, C. J. *Organometallics* **1996**, 15, 3913.
601. Hou, Z.; Yoda, C.; Koizumi, T.; Nishiura, M.; Wakatsuki, Y.; Fukuzawa, S.; Takats, J. *Organometallics* **2003**, 22, 3586.
602. Evans, W. J.; Gonzales, Sh. L.; Ziller, J. W. *J. Am. Chem. Soc.* **1994**, 116, 2600.
603. Evans, W. J.; Keyer, R.; Rabe, G.; Drummond, D.; Ziller, J. *Organometallics* **1993**, 12, 4664.
604. Castillo, I.; Tilley, T. D. *Organometallics* **2001**, 20, 5598.
605. Radu, N. S.; Hollander, F. J.; Tilley, T. D.; Rheingold, A. L. *Chem. Commun.* **1996**, 2459.
606. King, W. A.; Marks, T. J. *Inorg. Chim. Acta* **1995**, 229, 343.
607. Castillo, I.; Tilley, T. D. *Organometallics* **2000**, 19, 4733.
608. Radu, N. S.; Tilley, T. D. *Phosphorus Sulfur Silicon* **1994**, 87, 209.
609. Radu, N. S.; Tilley, T. D.; Rheingold, A. L. *J. Organomet. Chem.* **1996**, 516, 41.
610. Sadow, A. D.; Tilley, T. D. *J. Am. Chem. Soc.* **2005**, 127, 643.
611. Deelman, B.-J.; Booi, M.; Meetsma, A.; Teuben, J. H.; Kooijman, H.; Spek, A. L. *Organometallics* **1995**, 14, 2306.
612. Deelman, B.-J.; Stevels, W. M.; Teuben, J. H.; Lakin, M. T.; Spek, A. L. *Organometallics* **1994**, 13, 3881.
613. Booi, M.; Deelman, B.-J.; Duchateau, R.; Postma, D.; Meetsma, A.; Teuben, J. H. *Organometallics* **1993**, 12, 3531.
614. Deelman, B.-J.; Wierda, F.; Meetsma, A.; Teuben, J. H. *Appl. Organomet. Chem.* **1995**, 9, 483.
615. Evans, W. J.; Davis, B. L.; Ziller, J. W. *Inorg. Chem.* **2001**, 40, 6341.
616. Evans, W. J.; Forrestal, K. J.; Ziller, J. W. *Angew. Chem.* **1997**, 109, 798.
- 616a. Evans, W. J.; Forrestal, K. J.; Ziller, J. W. *Angew. Chem. Int. Ed.* **1997**, 36, 798.
617. Evans, W. J.; Forrestal, K. J.; Ziller, J. W. *J. Am. Chem. Soc.* **1995**, 117, 12635.
618. Evans, W. J.; Forrestal, K. J.; Ziller, J. W. *J. Am. Chem. Soc.* **1998**, 120, 9273.
619. Krishnamurthy, S. S. *Curr. Sci.* **1996**, 70, 769.
620. Obora, Y.; Ohta, T.; Stern, C. L.; Marks, T. J. *J. Am. Chem. Soc.* **1997**, 119, 3745.
621. Edelmann, F. T.; Rieckhoff, M.; Haiduc, I. *J. Organomet. Chem.* **1993**, 447, 203.
622. Ihara, E.; Nodono, M.; Katsura, K.; Adachi, Y.; Yasuda, H.; Yamagashira, M.; Hashimoto, H.; Kanehisa, N.; Kai, Y. *Organometallics* **1998**, 17, 3945.
623. Fedushkin, I. L.; Petrovskaya, T. V.; Bochkarev, M. N.; Dechert, S.; Schumann, H. *Angew. Chem.* **2001**, 40, 2540.
- 623a. Fedushkin, I. L.; Petrovskaya, T. V.; Bochkarev, M. N.; Dechert, S.; Schumann, H. *Angew. Chem. Int. Ed.* **2001**, 40, 2474.

624. 2002/48
625. Fedushkin, I. L.; Kurskii, Y. A.; Nevodchikov, V. I.; Bochkarev, M. N.; Mühle, S.; Schumann, H. *Russ. Chem. Bull.* **2002**, *51*, 160.
626. Fedushkin, I. L.; Dechert, S.; Schumann, H. *Angew. Chem.* **2001**, *40*, 584.
- 626a. Fedushkin, I. L.; Dechert, S.; Schumann, H. *Angew. Chem. Int. Ed.* **2001**, *40*, 561.
627. Fedushkin, I. L.; Kurskii, Y. A.; Balashova, T. V.; Bochkarev, M. N.; Mühle, S.; Dechert, S.; Schumann, H. *Russ. Chem. Bull.* **2003**, *52*, 1363.
628. Fedushkin, I. L.; Bochkarev, M. N.; Dechert, S.; Schumann, H. *Chem. Eur. J.* **2001**, *7*, 3558.
629. Qiao, C.; Zhu, D. *J. Organomet. Chem.* **1993**, *445*, 79.
630. Paolucci, G.; D'Ippolito, R.; Ye, Ch.; Gräper, J.; Fischer, R. D. *J. Organomet. Chem.* **1994**, *471*, 97.
631. Paolucci, G.; Vignola, M.; Coletto, L.; Pitteri, B.; Benetollo, F. *J. Organomet. Chem.* **2003**, *687*, 161.
632. Sun, Ch.; Wei, G.; Jin, Zh.; Chen, W. *Polyhedron* **1994**, *13*, 1483.
633. Barbier-Baudry, D.; Bonnet, F.; Dormond, A.; Hafid, A.; Nyassi, A.; Visseaux, M. *J. Alloys Compd.* **2001**, *323–324*, 592.
634. Sun, C.; Wei, G.; Jin, Z.; Chen, W. *J. Organomet. Chem.* **1993**, *453*, 61.
635. Schumann, H.; Erbstein, F.; Demtschuk, J.; Weimann, R. *Z. Anorg. Allg. Chem.* **1999**, *625*, 1457.
636. Schumann, H.; Erbstein, F.; Weimann, R.; Demtschuk, J. *J. Organomet. Chem.* **1997**, *536–537*, 541.
637. Evans, W. J.; Cano, D. A.; Greci, M. A.; Ziller, J. W. *Organometallics* **1999**, *18*, 1381.
638. Khvostov, A. V.; Belsky, V. K.; Sizov, A. I.; Bulychev, B. M.; Ivchenko, N. B. *J. Organomet. Chem.* **1998**, *564*, 5.
639. Khvostov, A. V.; Nesterov, V. V.; Bulychev, B. M.; Sizov, A. I.; Antipin, M. Y. *J. Organomet. Chem.* **1999**, *589*, 222.
640. Ihara, E.; Yoshioka, S.; Furo, M.; Katsura, K.; Yasuda, H.; Mohri, S.; Kanehisa, N.; Kai, Y. *Organometallics* **2001**, *20*, 1752.
641. Bogaert, S.; Chenal, T.; Mortreux, A.; Nowogrocki, G.; Lehmann, C. W.; Carpentier, J.-F. *Organometallics* **2001**, *20*, 199.
642. Roesky, P. W.; Stern, C. L.; Marks, T. J. *Organometallics* **1997**, *16*, 4705.
643. Schumann, H.; Zietzke, K.; Weimann, R.; Demtschuk, J.; Kaminski, W.; Schauenwienold, A.-M. *J. Organomet. Chem.* **1999**, *574*, 228.
644. Paolucci, G.; Zanon, J.; Lucchini, V.; Damrau, W.-E.; Siebel, E.; Fischer, R. D. *Organometallics* **2002**, *21*, 1088.
645. Schumann, H.; Erbstein, F.; Hemling, H. *Z. Kristallogr.* **1997**, *212*, 319.
646. Molander, G. A.; Dowdy, E. D.; Noll, B. C. *Organometallics* **1998**, *17*, 3754.
647. Gräper, J.; Fischer, R. D.; Paolucci, G. *J. Organomet. Chem.* **1994**, *471*, 85.
648. Schumann, H.; Glanz, M.; Hemling, H. *Chem. Ber.* **1994**, *127*, 2363.
649. Hajela, Sh.; Bercaw, J. E. *Organometallics* **1994**, *13*, 1147.
650. Roesky, P. W.; Denniger, U.; Stern, C. L.; Marks, T. J. *Organometallics* **1997**, *16*, 4486.
651. Khvostov, A. V.; Belsky, V. K.; Bulychev, B. M.; Sizov, A. I.; Ustinov, B. M. *J. Organomet. Chem.* **1998**, *571*, 243.
652. Coughlin, E. B.; Henling, L. M.; Bercaw, J. E. *Inorg. Chim. Acta* **1996**, *242*, 205.
653. Qiao, C.; Fischer, R. D.; Paolucci, G. *J. Organomet. Chem.* **1993**, *456*, 185.
654. Desurmont, G.; Li, Y.; Yasuda, H.; Maruo, T.; Kanehisa, N.; Kai, Y. *Organometallics* **2000**, *19*, 1811.
655. Trifonov, A. A.; Kirillov, E. N.; Dechert, S.; Schumann, H.; Bochkarev, M. N. *Eur. J. Inorg. Chem.* **2001**, 3055.
656. Evans, W. J.; Gummersheimer, T. S.; Boyle, T. J.; Ziller, J. W. *Organometallics* **1994**, *13*, 1281.
657. Evans, W. J.; Gummersheimer, T. S.; Ziller, J. W. *Appl. Organomet. Chem.* **1995**, *9*, 437.
658. Evans, W. J.; Johnston, M. A.; Greci, M. A.; Gummersheimer, T. S.; Ziller, J. W. *Polyhedron* **2003**, *22*, 119.
659. Khvostov, A. V.; Bulychev, B. M.; Belsky, V. K.; Sizov, A. I. *J. Organomet. Chem.* **1999**, *584*, 164.
660. Trifonov, A. A.; Kirillov, E. N.; Dechert, S.; Schumann, H.; Bochkarev, M. N. *Eur. J. Inorg. Chem.* **2001**, 2509.
661. Trifonov, A. A.; Fedorova, E. A.; Fukin, G. K.; Druzhkov, N. O.; Bochkarev, M. N. *Angew. Chem.* **2004**, *116*, 5155.
- 661a. Trifonov, A. A.; Fedorova, E. A.; Fukin, G. K.; Druzhkov, N. O.; Bochkarev, M. N. *Angew. Chem. Int. Ed.* **2004**, *43*, 5045.
662. Qi, M.-H.; Shen, X.-Q.; Gong, X.-Q.; Shen, Z.-Q.; Weng, L.-H. *Chin. J. Chem.* **2002**, *20*, 564.
663. Zhang, K.; Zhang, W.; Wang, S.; Sheng, E.; Yang, G.; Xie, M.; Zhou, S.; Feng, Y.; Mao, L.; Huang, Z. *Dalton Trans.* **2004**, 1029.
664. Klimpel, M. G.; Herrmann, W. A.; Anwender, R. *Organometallics* **2000**, *19*, 4666.
665. Qian, C.; Li, H.; Sun, J.; Nie, W. *J. Organomet. Chem.* **1999**, *585*, 59.
666. Sheng, E.; Wang, S.; Yang, G.; Zhou, S.; Cheng, L.; Zhang, K.; Huang, Z. *Organometallics* **2003**, *22*, 684.
667. Sheng, E.; Zhou, S.; Wang, S.; Yang, G.; Wu, Y.; Feng, Y.; Mao, L.; Huang, Z. *Eur. J. Inorg. Chem.* **2004**, 2923.
668. Cheng, J.; Cui, D.; Chen, W.; Hu, N.; Tang, T.; Huang, B. *J. Organomet. Chem.* **2004**, *689*, 2646.
669. Wang, S.; Zhou, S.; Sheng, E.; Xie, M.; Zhang, K.; Cheng, L.; Feng, Y.; Mao, L.; Huang, Z. *Organometallics* **2003**, *22*, 3546.
670. Trifonov, A. T.; Spaniol, T. P.; Okuda, J. *Eur. J. Inorg. Chem.* **2003**, 926.
671. Nakamura, H.; Nakayama, Y.; Yasuda, H.; Maruo, T.; Kanehisa, N.; Kai, Y. *Organometallics* **2000**, *19*, 5392.
672. Kong, D.; Wang, S.; Zhu, Q.; Xie, Y.; Hang, X. *Synth. React. Inorg. Met.-Org. Chem.* **1998**, *28*, 1455.
673. Shen, Q.; Qi, M.; Song, S.; Zhang, L.; Lin, Y. *J. Organomet. Chem.* **1997**, *549*, 95.
674. Ge, Y.; Yue, Z.-Y.; Gao, J.-S.; Yan, P.-F. *Chem. Res. Chin. Univ.* **2001**, *17*, 338.
675. Kirillov, E.; Toupet, L.; Lehmann, C. W.; Razavi, A.; Carpentier, J.-F. *Organometallics* **2003**, *22*, 4467.
676. Kirillov, E.; Lehmann, C. W.; Razavi, A.; Carpentier, J.-F. *Eur. J. Inorg. Chem.* **2004**, 943.
677. Schumann, H.; Karasiak, D. F.; Mühle, S. H. *Z. Anorg. Allg. Chem.* **2000**, *626*, 1434.
678. Gavenonis, J.; Tilley, D. T. *J. Organomet. Chem.* **2004**, *689*, 870.
679. Cui, D.-M.; Tang, T.; Cheng, J.-H.; Chen, W.-Q.; Huang, B.-T. *Chin. J. Chem.* **2003**, *21*, 153.
680. Barrett, A. G. M.; Bouloc, N.; Braddock, C. D.; Chadwick, D.; Henderson, D. A. *Synlett* **2002**, 653.
681. Cheng, J.-H.; Cui, D.-M.; Chen, W.-Q.; Hu, N.-H.; Tang, T.; Huang, B.-T. *Gaodeng Xuexiao Huaxue Xuebao* **2003**, *24*, 973.
682. Cheng, J.; Cui, D.; Chen, W.; Tang, T.; Huang, B. *Polyhedron* **2004**, *23*, 1075.
683. Ma, W. W.; Wu, Z. Z.; Cai, R. F.; Huang, Z. E.; Sun, J. *Polyhedron* **1997**, *16*, 3723.
684. Ma, W.; Huang, Z.; Zhou, X.; Cai, R. *Synth. React. Inorg. Met.-Org. Chem.* **1998**, *28*, 1469.
685. Qian, C.; Zou, G.; Sun, J. *J. Organomet. Chem.* **1998**, *566*, 21.
686. Cheng, J.; Cui, D.; Chen, W.; Tang, T.; Huang, B. *J. Organomet. Chem.* **2002**, *658*, 153.
687. Guan, J.; Fischer, R. D. *J. Organomet. Chem.* **1998**, *564*, 167.
688. Ye, Z.; Wang, S.; Kong, D.; Huang, X. *J. Organomet. Chem.* **1995**, *491*, 57.
689. Wang, S.; Kong, D.; Ye, Z.; Huang, X. *J. Organomet. Chem.* **1995**, *496*, 37.
690. Alcaraz, C.; Groth, U. *Angew. Chem.* **1997**, *109*, 2590.
- 690a. Alcaraz, C.; Groth, U. *Angew. Chem. Int. Ed.* **1997**, *36*, 2480.

691. Guan, J.; Fischer, R. D. *J. Organomet. Chem.* **1997**, 532, 147.
- 691a. Guan, J.; Shen, Q.; Fischer, R. D. *J. Organomet. Chem.* **1997**, 549, 203.
692. Parker, D.; Dickins, R. S.; Puschmann, H.; Crossland, C.; Howard, J. A. K. *Chem. Rev.* **2002**, 102, 1977.
693. Xie, Z.; Wang, S.; Yang, Q.; Mak, T. C. W. *Organometallics* **1999**, 18, 1578.
694. Wang, S.; Yang, Q.; Mak, T. C. W.; Xie, Z. *Organometallics* **1999**, 18, 5511.
695. Sun, H.-Y.; Du, J.; Xie, X.-M.; Gao, T.; Yue, Z.-Y.; Yan, P.-F. *Heilongjiang Daxue Ziran Kexue Xuebao* **2003**, 20, 108.
696. Takaki, K.; Koshiji, G.; Komeyama, K.; Takeda, M.; Shishido, T.; Kitani, A.; Takehira, K. *J. Org. Chem.* **2003**, 68, 6554.
697. Qian, C.; Zou, G.; Chen, Y.; Sun, J. *Organometallics* **2001**, 20, 3106.
698. Qian, C.; Zou, G.; Jiang, W.; Chen, Y.; Sun, J.; Li, N. *Organometallics* **2004**, 23, 4980.
699. Haltermann, R. L.; Schumann, H.; Dübner, F. *J. Organomet. Chem.* **2000**, 604, 12.
700. Schumann, H.; Erbstein, F.; Karasiak, D. F.; Fedushkin, I. L.; Demtschuk, J.; Girgsdies, F. *Z. Anorg. Allg. Chem.* **1999**, 625, 781.
701. Gilbert, A. T.; Davis, B. L.; Emge, T. J.; Broene, R. D. *Organometallics* **1999**, 18, 2125.
702. Qian, C.; Nie, W.; Sun, J. *Organometallics* **2000**, 19, 4134.
703. Zhang, W.; Cai, Y.-P.; Li, H.-X.; Ma, H.-Z. *Hecheng Huaxue* **2002**, 10, 268.
704. Luo, M.; Ma, H.-Z.; Su, Q.-D.; Hu, N.-L.; Du, B.-J. *Asian J. Chem.* **2002**, 14, 1469.
705. Qian, C.; Nie, W.; Chen, Y.; Sun, J. *J. Organomet. Chem.* **2002**, 645, 82.
706. Kirillov, E.; Toupet, L.; Lehmann, C. W.; Razavi, A.; Kahlal, S.; Saillard, J.-Y.; Carpentier, J.-F. *Organometallics* **2003**, 22, 4038.
707. Kirillov, E.; Lehmann, C. W.; Razavi, A.; Carpentier, J.-F. *Organometallics* **2004**, 23, 2768.
708. Eppiger, J.; Spiegler, M.; Hierlinger, W.; Hermann, W. A.; Anwender, R. *J. Am. Chem. Soc.* **2000**, 122, 3080.
709. Qian, C.; Zou, G.; Sun, J. *J. Chem. Soc., Dalton Trans.* **1999**, 519.
710. Qian, C.; Nie, W.; Sun, J. *J. Chem. Soc., Dalton Trans.* **1999**, 3283.
711. Lee, M. H.; Hwang, J.-W.; Kim, Y.; Kim, J.; Han, Y.; Do, Y. *Organometallics* **1999**, 18, 5124.
712. Herrmann, W. A.; Eppinger, J.; Spiegler, M.; Runte, O.; Anwender, R. *Organometallics* **1997**, 16, 1813.
713. Klimpel, M. G.; Sirsch, P.; Scherer, W.; Anwender, R. *Angew. Chem.* **2003**, 115, 594.
- 713a. Klimpel, M. G.; Sirsch, P.; Scherer, W.; Anwender, R. *Angew. Chem. Int. Ed.* **2003**, 42, 574.
714. Qian, C.; Nie, W.; Sun, J. *J. Organomet. Chem.* **2001**, 626, 171.
715. Nief, F. *Eur. J. Inorg. Chem.* **2001**, 891.
716. Schumann, H.; Rosenthal, E. C. E.; Winterfeld, J.; Kociok-Köhn, G. *J. Organomet. Chem.* **1995**, 495, C12.
717. Ganesan, M.; Bérubé, C. D.; Gambarotta, S.; Yap, G. P. A. *Organometallics* **2002**, 21, 1707.
718. Korobkov, I.; Aharonian, G.; Gambarotta, S.; Yap, G. P. A. *Organometallics* **2002**, 21, 4899.
719. Freckmann, D. M. M.; Dubé, T.; Bérubé, C. D.; Gambarotta, S.; Yap, G. P. A. *Organometallics* **2002**, 21, 1240.
720. Bérubé, C. D.; Gambarotta, S.; Yap, G. P. A.; Cozzi, P. G. *Organometallics* **2003**, 22, 434.
721. Wang, J.; Dick, A. K. J.; Gardiner, M. G.; Yates, B. F.; Peacock, E. J.; Skelton, B. W.; White, A. H. *Eur. J. Inorg. Chem.* **2004**, 1992.
722. Deacon, G. B.; Forsyth, C. M.; Gidlis, A.; Skelton, B. W.; White, A. H. *Dalton Trans.* **2004**, 1239.
723. Quitmann, C. C.; Mueller-Buschbaum, K. *Z. Naturforsch., B: Chem. Sci.* **2004**, 59, 562.
724. Mueller-Buschbaum, K. *Z. Allg. Anorg. Chem.* **2004**, 630, 895.
725. Bérubé, C. D.; Yazdanbakhsh, M.; Gambarotta, S.; Yap, G. P. A. *Organometallics* **2003**, 22, 3742.
726. Dubé, T.; Gambarotta, S.; Yap, G. P. A. *Angew. Chem. Int. Ed.* **1999**, 38, 1432.
727. Nief, F.; Ricard, L. *Organometallics* **2001**, 20, 3884.
728. Turcitu, D.; Nief, F.; Ricard, L. *Chem. Eur. J.* **2003**, 9, 4916.
729. Nief, F.; de Borms, B. T.; Ricard, L.; Carmichael, D. *Eur. J. Inorg. Chem.* **2005**, 637.
730. Gosink, H.-J.; Nief, F.; Ricard, L.; Mathey, F. *Inorg. Chem.* **1995**, 34, 1306.
- 730a. Lopez, R. G.; Boisson, C.; D'Agosto, F.; Spitz, R.; Boisson, F.; Bertin, D.; Tordo, P. *Macromolecules* **2004**, 37, 3540.
731. Desmurs, P.; Dormond, A.; Nief, F.; Baudry, D. *Bull. Soc. Chim. Fr.* **1997**, 134, 683.
732. Cendrowski-Guillaume, S. M.; Le Gland, G.; Ephritikhine, M.; Nierlich, M. *Z. Kristallogr.-New Cryst. Struct.* **2002**, 217, 35.
733. Clentsmith, G. K. B.; Cloke, F. G. N.; Green, J. C.; Hanks, J.; Hitchcock, P. B.; Nixon, J. F. *Angew. Chem.* **2003**, 115, 1068.
- 733a. Clentsmith, G. K. B.; Cloke, F. G. N.; Green, J. C.; Hanks, J.; Hitchcock, P. B.; Nixon, J. F. *Angew. Chem. Int. Ed.* **2003**, 42, 1038.
734. Wang, J.; Li, S.; Zheng, C.; Maguire, J. A.; Hosmane, N. S. *Organometallics* **2002**, 21, 5149.
735. Wang, J.; Li, S.; Zheng, C.; Maguire, J. A.; Hosmane, N. S. *Organometallics* **2002**, 21, 3314.
736. Wang, J.; Li, S.; Zheng, C.; Maguire, J. A.; Hosmane, N. S. *Inorg. Chem. Commun.* **2002**, 5, 602.
737. Wang, J.; Li, S.; Zheng, C.; Maguire, J. A.; Sarkar, B.; Kaim, W.; Hosmane, N. S. *Organometallics* **2003**, 22, 4334.
738. Wang, J.; Li, S.; Zheng, C.; Maguire, J. A.; Kaim, W.; Hosmane, N. S. *Inorg. Chem. Commun.* **2003**, 6, 1220.
739. Wang, J.; Li, S.; Zheng, C.; Hosmane, N. S.; Maguire, J. A.; Roesky, H. W.; Cummins, C. C.; Kaim, W. *Organometallics* **2003**, 22, 4390.
740. Wang, J.; Li, S.; Zheng, C.; Li, A.; Hosmane, N. S.; Maguire, J. A.; Roesky, H. W.; Cummins, C. C.; Kaim, W. *Organometallics* **2004**, 23, 4621.
741. Wang, J.; Li, S.; Zheng, C.; Maguire, J. A.; Hosmane, N. S. *Inorg. Chem. Commun.* **2003**, 6, 549.
742. Li, A.; Wang, J.; Zheng, C.; Maguire, J. A.; Hosmane, N. S. *Organometallics* **2004**, 23, 3091.
743. Xie, Z.; Liu, Z.; Chiu, K. Y.; Xue, F.; Mak, T. C. W. *Organometallics* **1997**, 16, 2460.
744. Bazan, G. C.; Schaefer, W.; Bercaw, J. E. *Organometallics* **1993**, 12, 2126.
745. Xie, Z. *Kidorui* **1997**, 30, 98.
746. Chia, K. Y.; Zhang, Z.; Mak, T. C. W.; Xie, Z. *J. Organomet. Chem.* **2000**, 614–615, 107.
747. Chui, K.; Yang, Q.; Mak, T. C. W.; Xie, Z. *Organometallics* **2000**, 19, 1391.
748. Xie, Z.; Chui, K.; Yang, Q.; Mak, T. C. W. *Organometallics* **1999**, 18, 3947.
749. Xie, Z.; Wang, S.; Zhou, Z. Y.; Xue, F.; Mak, T. C. W. *Organometallics* **1998**, 17, 489.
750. Xie, Z.; Wang, S.; Zhou, Z. Y.; Mak, T. C. W. *Organometallics* **1998**, 17, 1907.
751. Xie, Z.; Wang, S.; Zhou, Z.-Y.; Mak, T. C. W. *Organometallics* **1999**, 18, 1641.
752. Zi, G.; Yang, Q.; Mak, T. C. W.; Xie, Z. *Organometallics* **2001**, 20, 2359.
753. Wang, S.; Yang, Q.; Mak, T. C. W.; Xie, Z. *Organometallics* **2000**, 19, 334.
754. Xie, Z.; Wang, S.; Yang, Q.; Mak, T. C. W. *Organometallics* **1999**, 18, 2420.
755. Wang, S.; Yang, Q.; Mak, T. C. W.; Xie, Z. *Organometallics* **1999**, 18, 4478.

756. Zi, G.; Li, H.-W.; Xie, Z. *Organometallics* **2002**, *21*, 3464.
757. Wang, S.; Wang, Y.; Cheung, M.-S.; Chan, H.-S.; Xie, Z. *Tetrahedron* **2003**, *59*, 10373.
758. Wang, S.; Li, H.-W.; Xie, Z. *Organometallics* **2001**, *20*, 3624.
759. Wang, S.; Li, H.-W.; Xie, Z. *Organometallics* **2004**, *23*, 3780.
760. Wang, S.; Li, H.-W.; Xie, Z. *Organometallics* **2004**, *23*, 2469.
761. Cheung, M.-S.; Chan, H.-S.; Xie, Z. *Organometallics* **2004**, *23*, 517.
762. Zi, G.; Li, H.-W.; Xie, Z. *Organometallics* **2002**, *21*, 1136.
763. Wang, H.; Wang, H.; Li, H.-W.; Xie, Z. *Organometallics* **2004**, *23*, 875.
764. Yu, X.-Y.; Jin, G.-X.; Wenig, L.-H. *Chin. J. Chem.* **2002**, *20*, 1256.
765. Yu, X.-Y.; Jin, G.-X.; Hu, N.-H.; Weng, L.-H. *Organometallics* **2002**, *21*, 5540.
766. Tobisch, S.; Nowak, T.; Bögel, H. *J. Organomet. Chem.* **2001**, *619*, 24.
767. Nakajima, A.; Kaya, K. *J. Phys. Chem. A* **2000**, *104*, 176.
768. Kurikawa, T.; Takeda, H.; Nakajima, A.; Kaya, K. *Z. Phys. D* **1997**, *40*, 65.
769. Rabilloud, F.; Rayane, D.; Allouche, A. R.; Antoine, R.; Aubert-Frèçon, M.; Broyer, M.; Compagnon, I.; Dugourd, P. *J. Phys. Chem. A* **2003**, *107*, 11347.
770. Kambalapalli, S.; Ortiz, J. V. *J. Phys. Chem. A* **2004**, *108*, 2988.
771. Roszak, S.; Majumdar, D. *J. Chem. Phys.* **2002**, *116*, 10238.
- 771a. Caraiman, D.; Bohme, D. K. *J. Phys. Chem. A* **2002**, *106*, 9705.
772. Dunbar, R. C. *J. Phys. Chem. A* **2002**, *106*, 7328.
773. Gapeev, A.; Dunbar, R. C. *J. Am. Soc. Mass Spectrom.* **2002**, *13*, 477.
774. Arnold, P. L.; Cloke, F. G. N.; Hitchcock, P. B. *J. Chem. Soc., Chem. Commun.* **1997**, 481.
775. Arnold, P. L.; Petrukhina, M. A.; Bochenkov, V. E.; Shabatina, T. I.; Zagorskii, V. V.; Sergeev, G. B.; Cloke, F. G. N. *J. Organomet. Chem.* **2003**, *688*, 49.
776. Protchenko, A. V.; Zakharov, L. N.; Bochkarev, M. N.; Struchkov, Y. T. *J. Organomet. Chem.* **1993**, *447*, 209.
777. Protchenko, A. V.; Zakharov, L. N.; Fukin, G. K.; Struchkov, Y. T.; Bochkarev, M. N. *Izv. Akad. Nauk, Ser. Khim.* **1996**, *4*, 993.
- 777a. Protchenko, A. V.; Almazova, O. G.; Zakharov, L. N.; Fukin, G. K.; Struchkov, Y.; Bochkarev, M. N. *J. Organomet. Chem.* **1997**, *536–537*, 457.
778. Bochkarev, M. N.; Fedushkin, I. L.; Fagin, A. A.; Schumann, H.; Demtschuk, J. *J. Chem. Soc., Chem. Commun.* **1997**, 1783.
779. Cassani, M. C.; Gun'ko, Y. K.; Hitchcock, P. B.; Lappert, M. F. *Chem. Commun.* **1996**, 1987.
780. Cassani, M. C.; Duncalf, D. J.; Lappert, M. F. *J. Am. Chem. Soc.* **1998**, *120*, 12958.
781. Gun'ko, Y. K.; Hitchcock, P. B.; Lappert, M. F. *Organometallics* **2000**, *19*, 2832.
782. Thiele, K.-H.; Bambirra, S.; Sieler, J.; Yelonek, S. *Angew. Chem.* **1998**, *110*, 3016.
- 782a. Thiele, K.-H.; Bambirra, S.; Sieler, J.; Yelonek, S. *Angew. Chem. Int. Ed.* **1998**, *37*, 2886.
783. Roitershtein, D. M.; Rybakova, L.; Petrov, E.; Ellern, A.; Yu, M. *J. Organomet. Chem.* **1993**, *460*, 39.
784. Fedushkin, I. L.; Khoroshen'kov, G. V.; Bochkarev, M. N.; Mühle, S.; Schumann, H. *Russ. Chem. Bull.* **2003**, *52*, 1358.
785. Thiele, K.-H.; Bambirra, S.; Schumann, H.; Hemling, H. *J. Organomet. Chem.* **1996**, *517*, 161.
786. Chauvin, Y.; Heyworth, H.; Olivier, H.; Robert, F.; Saussine, L. *J. Organomet. Chem.* **1993**, *455*, 89.
787. Liang, H.; Shen, Q.; Guan, J.; Lin, Y. *J. Organomet. Chem.* **1994**, *474*, 113.
788. Biagini, P.; Lugli, G.; Abis, L.; Millini, R. *New. J. Chem.* **1995**, *19*, 713.
789. Niemeyer, M.; Hauber, S.-O. *Z. Anorg. Allg. Chem.* **1999**, *625*, 137.
790. Hayes, P. G.; Piers, W. E.; Parvez, M. *J. Am. Chem. Soc.* **2003**, *125*, 5622.
791. Fryzuk, M. D.; Jafarpour, L.; Kerton, F. M.; Love, J. B.; Patrick, B. O.; Rettig, S. J. *Organometallics* **2001**, *20*, 1387.
792. Fryzuk, M. D.; Love, J. B.; Rettig, S. J. *J. Am. Chem. Soc.* **1997**, *119*, 1819.
793. Fryzuk, M. D.; Jafarpour, L.; Kerton, F. M.; Love, J. B.; Rettig, S. J. *Angew. Chem.* **2000**, *112*, 783.
- 793a. Fryzuk, M. D.; Jafarpour, L.; Kerton, F. M.; Love, J. B.; Rettig, S. J. *Angew. Chem. Int. Ed.* **2000**, *39*, 767.
794. Deacon, G. B.; Forsyth, C. M.; Junk, P. C.; Skelton, B. W.; White, A. H. *Chem. Eur. J.* **1999**, *5*, 1452.
795. Gordon, J. C.; Giesbrecht, G. R.; Clark, D. L.; Hay, P. J.; Keogh, D. W.; Poli, R.; Scott, B. L.; Watkin, J. G. *Organometallics* **2002**, *21*, 4726.
796. Barnhart, D. M.; Clark, D. L.; Gordon, J. C.; Huffmann, J. C.; Vincent, R. L.; Watkin, J. G.; Zwick, B. D. *Inorg. Chem.* **1994**, *33*, 3487.
797. Herberich, G. E.; Engler, U.; Fischer, A.; Ni, J.; Schmitz, A. *Organometallics* **1999**, *18*, 5496.
798. Wang, B.; Zheng, X.; Herberich, G. E. *Eur. J. Inorg. Chem.* **2002**, 31.
799. Zheng, X.; Wang, B.; Englert, U.; Herberich, G. E. *Inorg. Chem.* **2001**, *40*, 3117.
800. Arliguie, T.; Lance, M.; Nierlich, M.; Ephritikhine, M. *J. Chem. Soc., Dalton Trans.* **1997**, 2501.
801. 2002/187
802. Evans, W. J.; Shreeve, J. L.; Ziller, J. W. *Polyhedron* **1995**, *14*, 2945.
803. Evans, W. J.; Johnston, M. A.; Greci, M. A.; Ziller, J. W. *Organometallics* **1999**, *18*, 1460.
804. Evans, W. J.; Clark, R. D.; Ansari, M. A.; Ziller, J. W. *J. Am. Chem. Soc.* **1998**, *120*, 9555.
805. Visseaux, M.; Nief, F.; Ricard, L. *J. Organomet. Chem.* **2002**, *647*, 139.
806. Yao, Y.; Qi, G.; Shen, Q.; Hu, J.; Lin, Y. *Chin. Sci. Bull.* **2003**, *48*, 2164.
807. Mashima, K.; Nakayama, Y.; Nakamura, A. *J. Organomet. Chem.* **1994**, *473*, 85.
808. Kilimann, U.; Schäfer, M.; Herbst-Irmer, R.; Edelmann, F. T. *J. Organomet. Chem.* **1994**, *469*, C10.
809. Schumann, H.; Winterfeld, J.; Köhn, R. D.; Esser, L.; Sun, J.; Dietrich, A. *Chem. Ber.* **1993**, *126*, 907.
810. Zhang, S.; Wie, G.; Chen, W. *Polyhedron* **1994**, *13*, 1927.
811. Xia, J.; Zhuang, X.; Jin, Z.; Chen, W. *Polyhedron* **1996**, *15*, 3399.
812. Utrecht, B.; Jank, S.; Reddmann, H.; Amberger, H. D.; Edelmann, F. T.; Edelstein, N. M. *J. Alloys Compd.* **1997**, *250*, 383.
813. Poremba, P.; Edelmann, F. T. *J. Organomet. Chem.* **1997**, *549*, 101.
814. Cendrowski-Guillaume, S. M.; Nierlich, M.; Lance, M.; Ephritikhine, M. *Organometallics* **1998**, *17*, 768.
815. Kilimann, U.; Edelmann, F. T. *J. Organomet. Chem.* **1993**, *444*, C15.
816. Kilimann, U.; Edelmann, F. T. *J. Organomet. Chem.* **1994**, *469*, C5.
817. Schumann, H.; Winterfeld, J.; Hemling, H.; Hahn, F. E.; Reich, P.; Brzezinka, K.-W.; Edelmann, F. T.; Kilimann, U.; Schäfer, M.; Herbst-Irmer, R. *Chem. Ber.* **1995**, *128*, 395.



818. Roesky, P. W.; Gamer, M. T.; Marinos, N. *Chem. Eur. J.* **2004**, *10*, 3537.
819. Reißmann, U.; Poremba, P.; Noltemeyer, M.; Schmidt, H. G.; Edelmann, F. T. *Inorg. Chim. Acta* **2000**, *303*, 156.
820. Evans, W. J.; Johnsten, M. A.; Clark, R. D.; Ziller, J. W. *J. Chem. Soc., Dalton Trans.* **2000**, 1609.
821. Schumann, H.; Glanz, J.; Winterfeld, J.; Hemling, H. *J. Organomet. Chem.* **1993**, *456*, 77.
822. Jin, J.; Zhuang, X.; Jin, Z.; Chen, W. *J. Organomet. Chem.* **1995**, *490*, C8.
823. Poremba, P.; Edelmann, F. T. *Polyhedron* **1997**, *16*, 2067.
824. Liu, Q.; Shen, X.; Huang, J.; Qian, Y.; Chan, A. S. C.; Wong, W. T. *Polyhedron* **2000**, *19*, 453.
825. Schumann, H.; Rosenthal, E. C. E.; Demtschuk, J.; Mühle, S. H. *Z. Anorg. Allg. Chem.* **2000**, *626*, 2161.
826. Huang, J.-L.; Shen, X.-Q.; Liu, Q.-C.; Qian, Y.-L.; Chan, A. S.-C. *Chin. J. Chem.* **2001**, *19*, 102.
827. Rabe, G. W.; Zhang-Presse, M.; Golen, J. A.; Rheingold, A. L. *Acta Crystallogr., Sect. E: Struct. Rep. Online* **2003**, *59*, m1102.
828. Schumann, H.; Glanz, M.; Winterfeld, J.; Hemling, H.; Kuhn, N.; Bohnen, H.; Bläser, D.; Boese, R. *J. Organomet. Chem.* **1995**, *490*, C14.
829. Kilimann, U.; Schäfer, M.; Herbst-Irmer, R.; Edelmann, F. T. *J. Organomet. Chem.* **1994**, *469*, C15.
830. Rabe, G. W.; Zhang-Presse, M.; Golen, J. A.; Rheingold, A. L. *Acta Crystallogr., Sect. E: Struct. Rep. Online* **2003**, *59*, m255.
831. Rabe, G. W.; Zhang-Presse, M.; Yap, G. P. A. *Inorg. Chim. Acta* **2003**, *348*, 245.
832. Mashima, K.; Fukumoto, H.; Oshiki, T.; Tani, K.; Nakayama, Y.; Nakamura, A. *Kidorui* **1997**, *30*, 96.
833. Poremba, P.; Reißmann, U.; Noltemeyer, M.; Schmidt, H.-G.; Brüser, W.; Edelmann, F. T. *J. Organomet. Chem.* **1997**, *544*, 1.
- 833a. Poremba, P.; Edelmann, F. T. *J. Organomet. Chem.* **1998**, *553*, 393.
834. Dolg, M.; Fulde, P.; Stoll, H.; Preuss, H.; Chang, A.; Pitzer, R. M. *Chem. Phys.* **1995**, *195*, 71.
835. Liu, W.; Dolg, M.; Fulde, P. *J. Chem. Phys.* **1997**, *107*, 3584.
836. Edelstein, M. M.; Allen, P. G.; Bucher, J. J.; Shuh, D. K.; Sofield, C. D.; Kaltsoyannis, N.; Maunder, G. H.; Russo, M. R.; Sella, A. J. *Am. Chem. Soc.* **1996**, *118*, 13115.
837. Streitwieser, A.; Kinsley, S. A.; Jenson, C. H.; Rigsbee, J. T. *Organometallics* **2004**, *23*, 5169.
838. Kilimann, U.; Herbst-Irmer, R.; Stalke, D.; Edelmann, F. T. *Angew. Chem., Int. Ed. Engl.* **1994**, *33*, 1618.
839. Li, J.-L.; Lin, Y.-S.; Wu, Z.-Y.; Yang, S.-G.; Cheng, D.-D.; Zhan, M.-X. *Xiamen Daxue Xuebao Ziran Kexueban* **2002**, *41*, 453.
840. Shelimov, K. B.; Clemmer, D. E.; Jarrold, M. F. *J. Phys. Chem.* **1995**, *99*, 11376.
841. Shelimov, K. B.; Clemmer, D. E.; Jarrold, M. F. *Proc. Electrochem. Soc.* **1995**, *95*, 1437.
842. Shelimov, K. B.; Jarrold, M. F. *J. Am. Chem. Soc.* **1995**, *117*, 6404.
843. Inoue, T.; Tomiyama, T.; Sugai, T.; Okazaki, T.; Suenatsu, T.; Fujii, N.; Utsumi, H.; Nojima, K.; Shinohara, H. *J. Phys. Chem. B* **2004**, *108*, 7573.
844. Krause, M.; Hulman, M.; Kuzmany, H.; Dubay, O.; Kresse, G.; Vietze, K.; Seifert, G.; Wang, C. *Phys. Rev. Lett.* **2004**, *93*.
845. Kong, Q.; Shen, Y.; Zhao, L.; Zhuang, J.; Qian, S.; Li, Y.; Lin, R.; Cai, R. *J. Chem. Phys.* **2002**, *116*, 128.
846. Kong, Q.; Zhuang, J.; Li, X.; Cai, R.; Zhao, L.; Qian, S.; Li, Y. *Appl. Phys. A: Mater. Sci. Process.* **2002**, *75*, 367.
847. Kong, Q.; Zhuang, J.; Xu, J.; Shen, Y.; Li, Y.; Zhao, L.; Cai, R. *J. Phys. Chem. A* **2003**, *107*, 3670.
848. Shimotani, H.; Ito, T.; Iwasa, Y.; Taninaka, A.; Shinohara, H.; Nishibori, E.; Takata, M.; Sakata, M. *J. Am. Chem. Soc.* **2004**, *126*, 364.
849. Capp, C.; Wood, T. D.; Marshall, A. G.; Coe, J. V. *J. Am. Chem. Soc.* **1994**, *116*, 4987.
850. Iezzi, E. B.; Duchamp, J. C.; Fletcher, K. R.; Glass, T. E.; Dorn, H. C. *Nano Lett.* **2002**, *2*, 1187.
851. da Conceicao Vieira, M.; Marcalo, J.; Pires de Matos, A. *J. Organomet. Chem.* **2001**, *632*, 126.
852. Beletskaya, I. P.; Voskoboinikov, A.; Chuklanova, E.; Kirillova, N. *J. Am. Chem. Soc.* **1993**, *115*, 3156.
853. Bochkarev, L. N.; Druzhkova, O. N.; Zhiltsov, S. F.; Zakharov, L. N.; Fukin, G. K.; Khorshev, S. Y.; Yanovsky, A. I.; Struchkov, Y. T. *Organometallics* **1997**, *16*, 500.
854. Fedushkin, I. L.; Nevodchikov, V. K.; Cherkasov, V. K.; Bochkarev, M. N.; Schumann, H.; Girgsdies, F.; Görlitz, F.; Kociok-Köhn, G.; Pickardt, J. *J. Organomet. Chem.* **1996**, *511*, 157.
855. Jacob, K.; Schäfer, M.; Steiner, A.; Sheldrick, G. M.; Edelmann, F. T. *J. Organomet. Chem.* **1995**, *487*, C18.
856. Knjazhansky, S. Ya.; Nomerotsky, I. Yu.; Bulychev, B. M.; Bel'sky, V. K.; Soloveichik, G. L. *Organometallics* **1994**, *13*, 2075.
857. Berg, D. J.; Andersen, R. A. *Organometallics* **2003**, *22*, 627.
858. Knjazhanski, S. Y.; Kalyuzhnaya, E. S.; Herrera, L. E. E.; Bulychev, B. M.; Khvostov, A. V.; Sizov, A. I. *J. Organomet. Chem.* **1997**, *531*, 19.
859. Klimpel, M. G.; Eppinger, J.; Sirsch, P.; Scherer, W.; Anwender, R. *Organometallics* **2002**, *21*, 4021.
860. Fischbach, A.; Perdihi, F.; Sirsch, P.; Scherer, W.; Anwender, R. *Organometallics* **2002**, *21*, 4569.
861. Biagini, P.; Lugli, G.; Abis, L. *J. Organomet. Chem.* **1994**, *474*, C16.
862. Giesbrecht, G. R.; Gordon, J. C.; Brady, J. T.; Clark, D. L.; Keogh, D. W.; Michalczyk, R.; Scott, L.; Watkin, J. G. *Eur. J. Inorg. Chem.* **2002**, *723*.
863. Gordon, J. C.; Giesbrecht, G. R.; Brady, J. T.; Clark, D. L.; Keogh, D. W.; Scott, B. L.; Watkin, J. G. *Organometallics* **2002**, *21*, 127.
864. Kirillov, E.; Lehmann, C. W.; Razavi, A.; Carpentier, J.-F. *J. Am. Chem. Soc.* **2004**, *126*, 12240.
865. Yasuda, H. *Spec. Publ. - R. Soc. Chem.* **2003**, *287*, 152.
866. Evans, W. J.; Ansari, M. A.; Ziller, J. W. *Organometallics* **1995**, *14*, 3.
867. Jacob, K.; Edelmann, F. T.; Pietzsch, C. *Monatsh. Chem.* **1997**, *128*, 165.
868. Jacob, K.; Pavlik, I.; Edelmann, F. T. *Z. Anorg. Allg. Chem.* **1993**, *619*, 1957.
869. Thiele, K.-H.; Baumann, H. *Z. Anorg. Allg. Chem.* **1993**, *619*, 1111.
870. Zhang, Y.; Hou, Z.; Wakatsuki, Y. *Bull. Chem. Soc. Jpn.* **1998**, *71*, 1381.
871. Schwartz, D. J.; Ball, G. E.; Andersen, R. A. *J. Am. Chem. Soc.* **1995**, *117*, 6027.
872. Schwartz, D. J. Ph.D. Dissertation, University of California, Berkeley, CA, USA, 1995, (*Diss. Abstr. Int.* **1996**, B57(3), 1791).
873. Broussier, R.; Delmas, G.; Perron, P.; Gautheron, B.; Petersen, J. L. *J. Organomet. Chem.* **1996**, *511*, 185.
874. Deng, D.; Zheng, X.; Qian, Ch.; Sun, J.; Dormond, A.; Baudry, D.; Visseaux, M. *J. Chem. Soc., Dalton Trans.* **1994**, 1665.
875. Müller-Buschbaum, K.; Deacon, G. B.; Forsyth, C. M. *Eur. J. Inorg. Chem.* **2002**, 3172.
876. Beletskaya, I. P.; Voskoboinikov, A. Z.; Chuklanova, E.; Kisin, A. *J. Organomet. Chem.* **1993**, *454*, 1.
877. Reißmann, U.; Edelmann, F. T. *Z. Anorg. Allg. Chem.* **2003**, *629*, 2433.
- 877a. Reißmann, U.; Lameyer, L.; Stalke, D.; Poremba, P.; Edelmann, F. T. *Chem. Commun.* **1999**, 1865.
878. Edelmann, F. T. *Top. Curr. Chem.* **1996**, *179*, 247.
879. Maron, L.; Eisenstein, O. *J. Am. Chem. Soc.* **2001**, *123*, 1036.
880. Giardello, M. A.; Conticello, V. P.; Brard, L.; Sabat, M.; Rheingold, A. L.; Stern, Ch. L.; Marks, T. J. *J. Am. Chem. Soc.* **1994**, *116*, 10212.

881. Chamberlain, L.; Gibler, C.; Kemp, R. A.; Wilson, S.; Brownscombe, T. F. US Pat. 5, 177, 155.
882. Bogaert, S.; Chenal, T.; Morttreux, A.; Carpentier, J.-F. *J. Mol. Catal. A* **2002**, *190*, 207.
883. Xu, F.; Zhang, L. L.; Yao, Y. M.; Ding, Y. C.; Bai, Z. M.; Shen, Q. *Chin. Chem. Lett.* **1995**, *6*, 617.
884. Onozawa, S.; Sakakura, T.; Tanaka, M. *Chem. Lett.* **1994**, 531.
885. Chen, J.; Zhang, Y.-M. *Chin. J. Chem.* **2002**, *20*, 103.
886. Deelman, B.-J.; Bijpost, E. A.; Teuben, J. H. *J. Chem. Soc., Chem. Commun.* **1995**, 1741.
887. Deng, M.-Y.; Yoa, Y.-M.; Zhou, Y.-F.; Zhang, L.-F.; Shen, Q. *Chin. J. Chem.* **2003**, *21*, 574.
888. Nishiura, M.; Hou, Z.; Wakatsuki, Y.; Yamaki, T.; Miyamoto, T. *J. Am. Chem. Soc.* **2003**, *125*, 1184.
889. Ruan, R.; Zhou, X.; Cai, R. *Chem. Commun.* **2002**, 538.
890. Xu, F.; Zhu, X.-H.; Shen, Q.; Lu, J.; Li, J.-Q. *Chin. J. Chem.* **2002**, *20*, 1334.
891. Kirillov, E. N.; Fedorova, A. E.; Trifonov, A. A.; Bochkarev, M. N. *Appl. Organometal. Chem.* **2001**, *15*, 151.
892. Sändig, N.; Dargel, T. K.; Koch, W. Z. *Anorg. Allg. Chem.* **2000**, *626*, 392.
893. Koga, N. *Theor. Chem. Acta* **1999**, *102*, 285.
894. Casey, C. P.; Tunge, J.; Fagan, M. A. *J. Organomet. Chem.* **2002**, *663*, 91.
895. Sändig, N.; Koch, W. *Organometallics* **2002**, *21*, 1861.
896. Cavallo, L.; Talarico, G. *Polym. Mater. Sci. Eng.* **2002**, *87*, 38.
897. Woo, T. K.; Fan, L.; Ziegler, T. *Organometallics* **1994**, *13*, 2252.
898. Woo, T. K.; Fan, L.; Ziegler, T. *Organometallics* **1994**, *13*, 432.
899. Bierwagen, E. P.; Bercaw, J. E.; Goddard, W. A., III *J. Am. Chem. Soc.* **1994**, *116*, 1481.
900. Margl, P.; Deng, L.; Ziegler, T. *Organometallics* **1998**, *17*, 933.
901. Evans, W. J.; DeCoster, D. M.; Greaves, J. *Organometallics* **1996**, *15*, 3210.
902. Evans, W. J.; DeCoster, D. M.; Greaves, J. *Macromolecules* **1995**, *28*, 7929.
903. Ihara, E.; Nodono, M.; Yasuda, H.; Kanchisa, N.; Kai, Y. *Macromol. Chem. Phys.* **1996**, *197*, 1909.
904. Miotti, R. D.; de Souza Maia, A.; Paulino, I. S.; Schuchardt, U.; de Oliveira, W. *J. Alloys Compd.* **2002**, *344*, 92.
- 904a. Miotti, R. D.; de Souza Maia, A.; de Oliveira, W.; Paulino, I. S.; Schuchardt, U. *Quim. Nova* **2002**, *25*, 762.
905. Lavini, V.; de Souza Maia, A.; Paulino, I. S.; Schuchardt, U.; de Oliveira, W. *Inorg. Chem. Commun.* **2001**, *4*, 582.
906. Geerts, R. L. US Pat. 5,244,991 (*Chem. Abstr.* **1994**, *120*, 218830p).
907. Jia, L.; Yang, X.; Seyam, A. M.; Albert, I. D. L.; Fu, P.-F.; Yang, S.; Marks, T. J. *J. Am. Chem. Soc.* **1996**, *118*, 7900.
- 907a. Yang, X.; Seyam, A. M.; Fu, P. F.; Marks, T. J. *Macromolecules* **1994**, *27*, 4625.
908. Jensen, T. R.; Marks, T. J. *Macromolecules* **2003**, *36*, 1775.
909. Luo, Y.; Selvam, P.; Endou, A.; Kubo, M.; Miyamoto, A. *J. Am. Chem. Soc.* **2003**, *125*, 16210.
910. Jensen, T. R.; O'Donnell, J. J., III; Marks, T. J. *Organometallics* **2004**, *23*, 740.
911. Luo, Y.; Selvam, P.; Ito, Y.; Takami, S.; Kubo, M.; Imamura, A.; Miyamoto, A. *Organometallics* **2003**, *22*, 2181.
912. Fu, P.-F.; Marks, T. J. *J. Am. Chem. Soc.* **1995**, *117*, 10747.
913. Koo, K.; Fu, P.-F.; Marks, T. J. *Macromolecules* **1999**, *32*, 981.
914. Marks, T. J.; Fu, P.-F. *Eur. Patent EP 739,910*, October 30, 1996.
915. Pelletier, J.-F.; Mortreux, A.; Olonde, X.; Bujadoux, K. *Angew. Chem.* **1996**, *108*, 1980.
- 915a. Pelletier, J.-F.; Mortreux, A.; Olonde, X.; Bujadoux, K. *Angew. Chem. Int. Ed.* **1996**, *35*, 1854.
916. Pelletier, J.-F.; Bujadoux, K.; Olonde, X.; Adisson, E.; Mortreux, A. *Eur. Patent EP 736,536*, October 9, 1996.
917. Olonde, X.; Mortreux, A.; Petit, F. *J. Mol. Catal.* **1993**, *82*, 75.
918. Bogaert, S.; Carpentier, J. F.; Chenal, T.; Mortreux, A.; Ricart, G. *Macromol. Chem. Phys.* **2000**, *201*, 1813.
919. Lou, Y.; Yao, Y.; Shen, Q. *Macromolecules* **2002**, *35*, 8670.
920. Hayakawa, T.; Nakayama, Y.; Yasuda, H. *Polym. Int.* **2001**, *50*, 1260.
921. Baudry-Barbier, D.; Camus, E.; Dormond, A.; Visseaux, M. *Appl. Organomet. Chem.* **1999**, *13*, 813.
922. Luo, Y.; Baldamus, J.; Hou, Z. *J. Am. Chem. Soc.* **2004**, *126*, 13910.
923. Tanaka, M.; Sekiya, K.; Ihara, E.; Yasuda, H.; Kanchisa, N.; Kai, Y. *Kidorui* **1997**, *30*, 304.
924. Yang, X.; Seyam, A. M.; Marks, T. J. US Pat. 5,422,406, June 6, 1995.
925. Hou, Z.; Zhang, Y.; Wakatsuki, Y. *Kidorui* **1997**, *30*, 40.
926. Hou, Z.; Tezuka, H.; Zhang, Y.; Yamazaki, H.; Wakatsuki, A. *Macromolecules* **1998**, *31*, 8650.
927. Hou, Z.; Kaita, S.; Wakatsuki, Y. *Pure Appl. Chem.* **2001**, *73*, 291.
928. Ringelberg, S. N.; Meetsma, A.; Hessen, B.; Teuben, J. H. *J. Am. Chem. Soc.* **1999**, *121*, 6082.
929. Kawaoka, A. M.; Marks, T. J. *J. Am. Chem. Soc.* **2004**, *126*, 12764.
930. Arndt, S.; Spaniol, T. P.; Okuda, J. *Angew. Chem. Int. Ed.* **2003**, *42*, 5075.
931. Nekhaeva, L. A.; Bondarenko, G. N.; Frolov, V. M. *Kinet. Catal.* **2003**, *44*, 631.
932. Nekhaeva, L. A.; Frolov, V. M.; Konovalenko, N. A.; Vyshinskaya, L. I.; Tikhomirova, I. N.; Khodzhaeva, V. L.; Shklyaruk, B. F.; Antipov, E. M. *Vysokomolekulyarnye Soedineniya, Seriya A i Seriya B* **2003**, *45*, 540.
933. Maiwald, S.; Sommer, C.; Müller, G.; Taube, R. *Macromol. Chem. Phys.* **2002**, *203*, 1029.
934. Berndt, H.; Landmesser, H. *J. Mol. Catal. A: Chem.* **2003**, *197*, 245.
935. Maiwald, S.; Weissenborn, H.; Sommer, C.; Müller, G.; Taube, R. *J. Organomet. Chem.* **2001**, *640*, 1.
936. Maiwald, S.; Weissenborn, H.; Windisch, H.; Sommer, C.; Müller, G.; Taube, R. *Macromol. Chem. Phys.* **1997**, *198*, 3305.
937. Cui, L.; Jin, Y.; Sun, J.; Li, K.; Ba, X.; Teng, H. *Hecheng Xiangjiao Gongye* **1997**, *20*, 79.
938. Gromada, J.; le Pichon, L.; Mortreux, A.; Leising, F.; Carpentier, J.-F. *J. Organomet. Chem.* **2003**, *683*, 44.
939. Boisson, C.; Monteil, V.; Ribour, D.; Spitz, R.; Barbotin, F. *Macromol. Chem. Phys.* **2003**, *204*, 1747.
940. Anwander, R.; Klimpel, M. G.; Dietrich, H. M.; Shorokhov, D. J.; Scherer, W. *Chem. Commun.* **2003**, 1008.
941. Barbier-Baudry, D.; Dormond, A.; Desmurs, P. C. R. *Acad. Sci., Ser. IIc: Chim.* **1999**, *2*, 375.
942. Barbier-Baudry, D.; Bonnet, F.; Dormond, A.; Visseaux, M. *Entropie* **2001**, 96.
943. Bonnet, F.; Barbier-Baudry, D.; Dormond, A.; Visseaux, M. *Polym. Int.* **2002**, *51*, 986.
944. Bonnet, F.; Visseaux, M.; Barbier-Baudry, D.; Dormond, A. *Macromolecules* **2002**, *35*, 1143.
945. Kaita, S.; Hou, Z.; Wakatsuki, Y. *Macromolecules* **1999**, *32*, 9078.
946. Barbier-Baudry, D.; Bonnet, F.; Domenichini, B.; Dormond, A.; Visseaux, M. *J. Organomet. Chem.* **2002**, *647*, 167.

947. Llauro, M. F.; Monnet, C.; Barbotin, F.; Monteil, V.; Spitz, R.; Boisson, C. *Macromolecules* **2001**, *34*, 6304.
948. Kaita, S.; Hou, Z.; Wakatsuki, Y. *Macromolecules* **2001**, *34*, 1536.
949. Kaita, S.; Takeguchi, Y.; Hou, Z.; Nishiura, M.; Doi, Y.; Wakatsuki, Y. *Macromolecules* **2003**, *36*, 7923.
950. Fischbach, A.; Klimpel, M. G.; Widenmeyer, M.; Herdtweck, E.; Scherer, W.; Anwender, R. *Angew. Chem.* **2004**, *116*, 2284.
- 950a. Fischbach, A.; Klimpel, M. G.; Widenmeyer, M.; Herdtweck, E.; Scherer, W.; Anwender, R. *Angew. Chem. Int. Ed.* **2004**, *43*, 2234.
951. Kaita, S.; Doi, Y.; Kaneko, K.; Horiuchi, A. C.; Wakatsuki, Y. *Macromolecules* **2004**, *37*, 5860.
952. Bonnet, F.; Visseaux, M.; Barbier-Baudry, D. *J. Organomet. Chem.* **2004**, *689*, 264.
953. Bonnet, F.; Visseaux, M.; Barbier-Baudry, D.; Vigier, E.; Kubicki, M. M. *Chem. Eur. J.* **2004**, *10*, 2428.
- 953a. Sugiyama, H.; Gambarotta, S.; Yap, G. P. A.; Wilson, D. R.; Thiele, S. K.-H. *Organometallics* **2004**, *23*, 5054.
954. Nomura, R.; Shibasaki, Y.; Endo, T. *Polym. Bull.* **1996**, *37*, 597.
955. Hultsch, K. C.; Okuda, J. *Macromol. Rapid Commun.* **1997**, *18*, 809.
956. Agarwal, S.; Brandukova-Szmikowski, N. E.; Greiner, A. *Macromol. Rapid Commun.* **1999**, *20*, 274.
957. Nishiura, M.; Hou, Z.; Koizumi, T.-A.; Imamoto, T.; Wakatsuki, Y. *Macromolecules* **1999**, *32*, 8245.
958. Agarwal, S.; Puchner, M. *Eur. Polym. J.* **2002**, *38*, 2365.
959. Cui, D.; Tang, T.; Bi, W.; Cheng, J.; Chen, W.; Huang, B. *J. Polym. Sci., Part A: Polym. Chem.* **2003**, *41*, 2667.
960. Tsutsumi, C.; Nakagawa, K.; Shirahama, H.; Yasuda, H. *Polym. Int.* **2003**, *52*, 439.
961. Satoh, Y.; Ikitake, N.; Nakayama, Y.; Okuno, S.; Yasuda, H. *J. Organomet. Chem.* **2003**, *667*, 42.
962. Yasuda, H.; Ihara, E. *Eur. Pat. Appl. EP 634429 A1*, January 18, 1995.
963. Shibahara, T.; Nakayama, Y.; Mashima, K.; Nakamura, A. *Kidorui* **1997**, *30*, 302.
964. Evans, W. J.; Katsumata, H. *Macromolecules* **1994**, *27*, 2330.
965. Evans, W. J.; Katsumata, H. *Macromolecules* **1994**, *27*, 4011.
966. Yasuda, H. *Jpn. Kokai Tokkyo Koho JP 05247184 (Chem. Abstr.* **1994**, *120*, 135475a).
967. Chen, J.-L.; Yao, Y.-M.; Luo, Y.-J.; Zhou, L.-Y.; Zhang, Y.; Shen, Q. *J. Organomet. Chem.* **2004**, *689*, 1019.
968. Palard, I.; Soum, A.; Guillaume, S. M. *Chem. Eur. J.* **2004**, *10*, 4054.
969. Yasuda, H.; Aludin, M.-S.; Kitamura, N.; Tanabe, M.; Sirahama, H. *Macromolecules* **1999**, *32*, 6047.
970. Ravi, P.; Gröb, T.; Dehnicke, D.; Greiner, A. *Macromol. Chem. Phys.* **2001**, *202*, 2641.
971. Tanaka, K.; Furo, M.; Ihara, E.; Yasuda, H. *J. Polym. Sci., Part A: Polym. Chem.* **2001**, *39*, 1382.
972. Yasuda, H.; Desurmont, G. *Polym. Intern.* **2004**, *53*, 1017.
973. Ihara, E.; Morimoto, M.; Yasuda, H. *Macromolecules* **1995**, *28*, 7886.
974. Ihara, E.; Morimoto, M.; Yasuda, H. *Proc. Jpn. Acad., Ser. B* **1995**, *71B*, 126.
975. Tanabe, M.; Sugimura, T.; Yasuda, H. *React. Funct. Polym.* **2002**, *52*, 135.
976. Novak, B. M.; Boffa, L. S. *PCT Int. Appl. WO 9521873 A1*, August 17, 1995.
977. Boffa, L. S.; Novak, B. M. *Tetrahedron* **1997**, *53*, 15367.
978. Novak, B. M.; Boffa, L. S. *Polym. Prepr.* **1997**, *38*, 442.
979. Sun, J.; Pan, Z.; Hu, W.; Yang, S. *Eur. Polym. J.* **2002**, *38*, 545.
980. Qian, Y.; Bala, M. D.; Yousaf, M.; Zhang, H.; Huang, J.; Liang, C. *J. Mol. Catal. A: Chem.* **2002**, *188*, 1.
981. Ihara, E.; Taguchi, M.; Yasuda, H. *Appl. Organomet. Chem.* **1995**, *9*, 427.
982. Giardello, M. A.; Yamamoto, Y.; Brard, L.; Marks, T. J. *J. Am. Chem. Soc.* **1995**, *117*, 3276.
983. Nomura, R.; Shibasaki, Y.; Endo, T. *J. Polym. Sci., Part A: Polym. Chem.* **1998**, *36*, 2209.
984. Boffa, L. S.; Novak, B. M. *Macromolecules* **1997**, *30*, 3494.
985. Desurmont, G.; Tokimitsu, T.; Yasuda, H. *Macromolecules* **2000**, *33*, 7679.
986. Desurmont, G.; Tanaka, M.; Li, Y.; Yasuda, H.; Tokimitsu, T.; Tone, S.; Yanagase, A. *J. Polym. Sci., Part A: Polym. Chem.* **2000**, *38*, 4095.
987. Knjazhanski, S. Y.; Elizalde, L.; Cadenas, G.; Bulychev, B. M. *J. Polym. Sci.* **1998**, *36*, 1599.
988. Zhang, Y.; Yao, Y.-M.; Shen, Q.; Meng, Q.-J.; Ren, J.-S.; Lin, Y.-H. *Yingyong Huaxue* **2002**, *19*, 173.
989. Knjazhanski, S. Y.; Elizalde, L.; Cadenas, G.; Bulychev, B. M. *J. Organomet. Chem.* **1998**, *568*, 33.
990. Mao, L.; Shen, Q. *J. Polym. Sci.* **1998**, *36*, 1593.
- 990a. Shen, Q.; Yao, Y.-M. *Chin. J. Org. Chem.* **2001**, *21*, 1018.
991. Junquan, S.; Zhida, P.; Yu, Z.; Weiqiu, H.; Shilin, Y. *Eur. Polym. J.* **2000**, *36*, 2375.
992. Shen, Q.; Wang, Y.; Zhang, K.; Yao, Y. *J. Polym. Sci.* **2002**, *40*, 612.
993. Kakehi, T.; Yamashita, M.; Yasuda, H. *Reac. Funct. Polym.* **2000**, *46*, 81.
994. Nodono, M.; Tokimitsu, T.; Tone, S.; Makino, T.; Yanagase, A. *Macromol. Chem. Phys.* **2000**, *201*, 2282.
995. Neiser, M. W.; Okuda, J.; Schmidt, M. *Macromolecules* **2003**, *36*, 5437.
996. Neiser, M. W.; Muth, S.; Kolb, U.; Harris, J. R.; Okuda, J.; Schmidt, M. *Angew. Chem.* **2004**, *116*, 3255.
- 996a. Neiser, M. W.; Muth, S.; Kolb, U.; Harris, J. R.; Okuda, J.; Schmidt, M. *Angew. Chem. Int. Ed.* **2004**, *43*, 3192.
997. Yousaf, M.; Huang, J.-L.; Feng, Z.-F.; Qian, Y.-L.; Sun, J.-Q.; Pan, Z.-D. *Chin. J. Chem.* **2000**, *18*, 759.
998. Ying, L.-Q.; Ba, X.-W.; Zhao, Y.-Y.; Li, G.; Tang, T.; Jin, Y.-T. *Chin. J. Polym. Sci.* **2001**, *19*, 85.
999. Ni, X. F.; Shen, Z. Q.; Yasuda, H. *Chin. Chem. Lett.* **2001**, *12*, 821.
1000. Yasuda, H.; Nakayama, Y.; Satoh, Y.; Shen, Z.; Ni, X.; Inoue, M.; Namba, S. *Polym. Intern.* **2004**, *53*, 1682.
1001. Zhang, Y.-F.; Ni, X.-F.; Shen, Z.-Q. *Chem. J. Chin. Univ.* **2001**, *22*, 1778.
1002. Teng, H.-X.; Ying, L.-Q.; Han, S.-C.; Tang, W.-H.; Ba, X.-W.; Zhao, Y. Y.; Li, G.; Tang, T.; Jin, Y.-T. *Chin. J. Appl. Chem.* **2001**, *18*, 246.
1003. Yasuda, H.; Yamamoto, H.; Yamashita, M.; Yokota, K. *Macromolecules* **1993**, *26*, 7134.
1004. Schumann, H.; Glanz, M.; Gottfriedsen, J.; Dechert, S.; Wolff, D. *Pure Appl. Chem.* **2001**, *73*, 279.
1005. Qi, G.; Nitto, Y.; Saiki, A.; Tomohiro, T.; Nakayama, Y.; Yasuda, H. *Tetrahedron* **2003**, *59*, 10409.
1006. Lou, Y.; Yao, Y.; Li, W.; Chen, J.; Zhang, Z.; Zhang, Y.; Shen, Q. *J. Organomet. Chem.* **2003**, *679*, 125.
1007. Mei, L.; Ma, H.-Z.; Su, Q.-D.; Li, Q.-R. *Asian J. Chem.* **2003**, *15*, 259.
1008. Mei, L.; Ma, H.-Z.; Su, Q.-D. *Asian J. Chem.* **2003**, *15*, 497.
1009. Xie, X.; Huang, J. *Appl. Organomet. Chem.* **2004**, *18*, 282.
1010. Qian, Y.-L.; Bala, M. D.; Xie, X.-M.; Huang, J.-L. *Chin. J. Chem.* **2004**, *22*, 568.
1011. Qi, M.; Qi, S.; Shen, Z. *Zhongguo Xitu Xuebao* **2002**, *20*, 279.
1012. Cui, D.-M.; Tang, T.; Cheng, J.-H.; Hu, N.-H.; Chen, W.-Q.; Huang, B. *Gaodeng Xuexiao Huaxue Xuebao* **2002**, *23*, 188.

1013. Yao, Y.; Shen, Q.; Zhang, L. *Chin. Sci. Bull.* **2001**, *46*, 1443.
1014. Luo, Y.-J.; Yao, Y.-M.; Shen, Q. *Chin. J. Appl. Chem.* **2001**, *18*, 392.
1015. Ying, L.-Q.; Ba, X.-W.; Zhao, Y.-Y.; Li, G.; Tang, T.; Jin, Y.-T. *Chin. J. Polym. Sci.* **2001**, *19*, 89.
1016. Ying, L.-Q.; Li, G.; Zhao, Y.-Y.; Ba, X.-W.; Cui, D.-M.; Tang, T.; Jin, Y.-T. *J. Chin. Rare Earth Soc.* **2001**, *19*, 275.
1017. Nishiura, M.; Tanikawa, M.; Hoshino, M.; Miyamoto, T.; Hou, Z. *Kidorui* **2003**, *42*, 54.
1018. Imori, T.; Lu, V.; Cai, H.; Tilley, T. D. *J. Am. Chem. Soc.* **1995**, *117*, 9931.
1019. Kulkarni, S. A.; Koga, N. *Theochem* **1999**, *461–462*, 297.
1020. Bijpost, E. A.; Duchateau, R.; Teuben, J. H. J. *Mol. Catal. A: Chem.* **1995**, *95*, 121.
1021. Molander, G. A.; Pfeiffer, D. *Org. Lett.* **2001**, *3*, 361.
1022. Perrin, L.; Maron, L.; Eisenstein, O. *Inorg. Chem.* **2002**, *41*, 4355.
1023. Radu, N. S.; Tilley, T. D. *J. Am. Chem. Soc.* **1995**, *117*, 5863.
1024. Voskoboinikov, A. Z.; Shestakova, A. K.; Beletskaya, I. P. *Organometallics* **2001**, *20*, 2794.
1025. Molander, G. A.; Nicols, P. J. *J. Am. Chem. Soc.* **1995**, *117*, 4415.
1026. Onozawa, S.; Sakakura, T.; Tanaka, M. *Tetrahedron Lett.* **1994**, *35*, 8177.
1027. Molander, G. A.; Corrette, C. P. *J. Org. Chem.* **1999**, *64*, 9697.
1028. Molander, G. A.; Dowdy, E. D. *J. Org. Chem.* **1998**, *63*, 3386.
1029. Molander, G. A.; Retsch, W. H. *J. Am. Chem. Soc.* **1997**, *119*, 8817.
1030. Horino, Y.; Livinghouse, T. *Organometallics* **2004**, *23*, 12.
1031. Molander, G. A.; Romero, J. A. C.; Corrette, C. P. *J. Organomet. Chem.* **2002**, *647*, 225.
1032. Trifonov, A. A.; Spaniol, T. P.; Okuda, J. *Dalton Trans.* **2004**, 2245.
1033. Takaki, K.; Komeyama, K.; Koshiji, G.; Takehira, K. *Kidorui* **2003**, *42*, 52.
1034. Li, Y.; Fu, P.-F.; Marks, T. J. *Organometallics* **1994**, *13*, 439.
1035. Giardello, M. A.; Conticello, V. P.; Brard, L.; Gagne, M. R.; Marks, T. J. *J. Am. Chem. Soc.* **1994**, *116*, 10241.
1036. Ryu, J.-S.; Li, G. Y.; Marks, T. J. *J. Am. Chem. Soc.* **2003**, *125*, 12584.
1037. Seyam, A. M.; Stubbert, B. D.; Jensen, T. R.; O'Donnell, J. J., III; Stern, C.; Marks, T. J. *Inorg. Chim. Acta* **2004**, *357*, 4029.
1038. Motta, A.; Lanza, G.; Fraga, I. L.; Marks, T. J. *Organometallics* **2004**, *23*, 4097.
1039. Li, Y.; Marks, T. J. *Organometallics* **1996**, *15*, 3770.
1040. Li, Y.; Marks, T. J. *J. Am. Chem. Soc.* **1996**, *118*, 9295.
1041. Molander, G. A.; Dowdy, E. D. *J. Org. Chem.* **1998**, *63*, 8983.
1042. Ryu, J.-S.; Marks, T. J.; McDonald, F. E. *Org. Lett.* **2001**, *3*, 3091.
1043. Hong, S.; Kawaoka, A. M.; Marks, T. J. *J. Am. Chem. Soc.* **2003**, *125*, 15878.
1044. Ryu, J.-S.; Marks, T. J.; McDonald, F. E. *J. Org. Chem.* **2004**, *69*, 1038.
1045. Arredondo, V. M.; Tian, S.; McDonald, F. E.; Marks, T. J. *J. Am. Chem. Soc.* **1999**, *121*, 3633.
1046. Molander, G. A.; Pack, S. K. *J. Org. Chem.* **2003**, *68*, 9214.
1047. Molander, G. A.; Pack, S. K. *Tetrahedron* **2003**, *59*, 10581.
1048. Molander, G. A.; Dowdy, E. D. *J. Org. Chem.* **1999**, *64*, 6515.
1049. Arredondo, V. M.; McDonald, F. E.; Marks, T. J. *J. Am. Chem. Soc.* **1998**, *120*, 4871.
1050. Arredondo, V. M.; McDonald, F. E.; Marks, T. J. *Organometallics* **1999**, *18*, 1949.
1051. Li, Y.; Marks, T. J. *J. Am. Chem. Soc.* **1998**, *120*, 1757.
1052. Hong, S.; Tian, S.; Metz, M. V.; Marks, T. J. *J. Am. Chem. Soc.* **2003**, *125*, 14768.
1053. Gribkov, D. V.; Hultsch, K. C. *Chem. Commun.* **2004**, 730.
1054. Lauterwasser, F.; Hayes, P. G.; Braese, S.; Piers, W. E.; Schafer, L. L. *Organometallics* **2004**, *23*, 2234.
1055. Kawaoka, A. M.; Douglass, M. R.; Marks, T. J. *Organometallics* **2003**, *22*, 4630.
1056. Douglass, M. R.; Marks, T. J. *J. Am. Chem. Soc.* **2000**, *122*, 1824.
1057. Douglass, M. R.; Stern, C. L.; Marks, T. J. *J. Am. Chem. Soc.* **2001**, *123*, 10221.
1058. Douglass, M. R.; Ogasawara, M.; Hong, S.; Metz, M. V.; Marks, T. J. *Organometallics* **2002**, *21*, 283.
1059. Sadow, A. D.; Tilley, T. D. *Angew. Chem.* **2003**, *115*, 827.
- 1059a. Sadow, A. D.; Tilley, T. D. *Angew. Chem. Int. Ed.* **2003**, *42*, 803.
1060. Sadow, A. D.; Tilley, T. D. *J. Am. Chem. Soc.* **2003**, *125*, 7971.
1061. Takeno, M.; Kikuchi, S.; Morita, K.-I.; Nishiyama, Y.; Ishii, Y. *J. Org. Chem.* **1995**, *60*, 4974.
1062. Li, Z.; Zhang, Y. *J. Chem. Res., Synop.* **2002**, 297.
1063. Kawasaki, Y.; Fujii, A.; Nakano, Y.; Sakaguchi, S.; Ishii, Y. *J. Org. Chem.* **1999**, *64*, 4214.
- 1063a. Tashiro, D.; Nishiyama, Y.; Sakaguchi, S.; Ishii, Y. *Kidorui* **1997**, *30*, 296.
1064. Wang, D.; Zhao, C.; Phillips, D. L. *J. Org. Chem.* **2004**, *69*, 5512.
1065. Bausch, C. C.; Johnson, J. S. *J. Org. Chem.* **2004**, *69*, 4283.
1066. Zhao, C.; Wang, D.; Phillips, D. L. *J. Am. Chem. Soc.* **2003**, *125*, 15200.
1067. Wang, X.; Li, J.; Zhang, Y. *Synth. Commun.* **2003**, *33*, 3575.
1068. Rybakova, L. F.; Syutkina, O. P.; Starostina, T. A.; Petrov, E. S. *Zh. Obshch. Khim.* **1996**, *65*, 1600.
1069. Evans, W. J.; Ansari, M. A.; Feldman, J. D.; Doedens, R. J.; Ziller, J. W. *J. Organomet. Chem.* **1997**, *545–546*, 157.
1070. Giuliano, R. M.; Villani, F. J., Jr. *J. Org. Chem.* **1995**, *60*, 202.
1071. Calderwood, D. J.; Davis, R. V.; Rafferty, P.; Twigger, H. L.; Whelan, H. M. *Tetrahedron Lett.* **1997**, *38*, 1241.
1072. Lipshutz, B. H.; Lindsley, C.; Susfalk, R.; Gross, T. *Tetrahedron Lett.* **1994**, *35*, 8999.
1073. Cacatian, S. T.; Fuchs, P. L. *Tetrahedron* **2003**, *59*, 7177.
1074. Wee, A. G. H.; McLeod, D. D. *J. Org. Chem.* **2003**, *68*, 6268–6273.
1075. Takemoto, Y.; Takeuchi, J.; Iwata, C. *Tetrahedron Lett.* **1993**, *34*, 6069.
1076. Felpin, F.-X.; Boubekeur, K.; Lebreton, J. *Eur. J. Org. Chem.* **2003**, 4518.
1077. Ooi, T.; Miura, T.; Kondo, Y.; Maruoka, K. *Tetrahedron Lett.* **1997**, *38*, 3947.
1078. Arndt, H.-D.; Welz, R.; Mueller, S.; Ziemer, B.; Koert, U. *Chem. Eur. J.* **2004**, *10*, 3945.
1079. Wada, A.; Takakura, Y.; Yamazaki, K.; Takahashi, T.; Ito, M. *Lett. Org. Chem.* **2004**, *1*, 59.
1080. Timberlake, J. W.; Pan, D.; Murray, J.; Jursic, B. S.; Chen, T. *J. Org. Chem.* **1995**, *60*, 5295.



1081. Wipf, P.; Venkatraman, S. *J. Org. Chem.* **1993**, *58*, 3455.
1082. Betz, J.; Heuschmann, M. *Tetrahedron Lett.* **1995**, *36*, 4043.
1083. Ulibarri, G.; Nadler, W.; Skrydstrup, T.; Audrain, H.; Chirani, A.; Riche, C.; Grierson, D. S. *J. Org. Chem.* **1995**, *60*, 2753.
1084. Jung, P. M. J.; Burger, A.; Biellmann, J.-F. *Tetrahedron Lett.* **1995**, *36*, 1031.
1085. Hamann-Gaudinet, B.; Namy, J.-L.; Kagan, H. B. *J. Organomet. Chem.* **1998**, *567*, 39.
1086. Liu, Y.; Zhang, Y. *J. Chem. Res., Synop.* **2002**, 15.
1087. Li, J.; Liu, Y.; Zhang, Y. *J. Chem. Res., Synop.* **2003**, 438.
1088. Wang, X.; Li, J.; Zhang, Y. *Synth. Commun.* **2003**, *33*, 3575.
1089. Li, Z.; Zhang, Y. *Tetrahedron* **2002**, *58*, 5301.
1090. Wang, X. X.; Zhang, Y. M. *Chin. Chem. Lett.* **2001**, *12*, 943.
1091. Su, W.-K.; Zhang, Y.-M.; Li, Y.-S. *Chin. J. Chem.* **2001**, *19*, 205.
1092. Su, W.-K.; Zhang, Y.-M.; Li, Y.-S. *Chin. J. Chem.* **2001**, *19*, 381.
1093. Hasegawa, E.; Curran, D. P. *Tetrahedron Lett.* **1993**, *34*, 1717.
1094. Kunishima, M.; Nakata, D.; Tanaka, S.; Hioki, K.; Tani, S. *Tetrahedron* **2000**, *56*, 9927.
1095. Zhang, H.-R.; Wang, K. K. *J. Org. Chem.* **1999**, *64*, 7996.
1096. Kunishima, M.; Tanaka, S.; Kono, K.; Hioki, K.; Tani, S. *Tetrahedron Lett.* **1995**, *36*, 3707.
1097. Lubineau, A.; Gavard, O.; Alais, J.; Bonnafe, D. *Tetrahedron Lett.* **2000**, *41*, 307.
1098. Molander, G. A.; Rzasa, R. M. *J. Org. Chem.* **2000**, *65*, 1215.
1099. Dalpozzo, R.; De Nino, A. *J. Org. Chem.* **1998**, *63*, 3745.
1100. Hsu, D.-S.; Liao, C.-C. *Org. Lett.* **2003**, *5*, 4741.
1101. Kawasaki, Y.; Tashiro, D.; Sakaguchi, S.; Ishii, Y. *Chem. Lett.* **1998**, 53.
1102. Kurosu, M.; Kishi, Y. *Tetrahedron Lett.* **1998**, *39*, 4793.
1103. Merino, P.; Anoro, S.; Castillo, E.; Merchan, F.; Jejero, T. *Tetrahedron: Asymmetry* **1996**, *7*, 1887.
1104. Ravi Kumar, J. S.; O'Sullivan, M. F.; Reismann, S. E.; Hulford, C. A.; Ovaska, T. V. *Tetrahedron Lett.* **2002**, *43*, 1939.
1105. Caron, S.; Stoermer, D.; Mapp, A. K.; Heathcock, C. H. *J. Org. Chem.* **1996**, *61*, 9126.
1106. Murakami, M.; Ito, Y. *J. Organomet. Chem.* **1994**, *473*, 93.
1107. Rybakova, L. F.; Tsygankova, S. V.; Roitershtein, D. M.; Petrov, E. S. *Russ. J. Gen. Chem.* **2004**, *74*, 141.
1108. Krief, A.; Laval, A.-M.; Shastri, B. E.; Badaoui, E. *Acros. Org. Acta* **1996**, *2*, 20.
1109. Kawasaki, Y.; Shiraishi, H.; Yakeno, M.; Nishiyama, Y.; Sakaguchi, S.; Ishii, Y. *Kidorui* **1996**, *28*, 320.
1110. Takaki, K.; Maruo, M.; Kamata, T.; Makioka, Y.; Fujiwara, Y. *J. Org. Chem.* **1996**, *61*, 8332.
1111. Kamata, T.; Nishiyama, T.; Maruo, M.; Takaki, K.; Taniguchi, Y.; Fujiwara, Y. *Kidorui* **1996**, *28*, 320.
1112. Miyano, A.; Tashiro, D.; Kawasaki, Y.; Sakaguchi, S.; Ishii, Y. *Tetrahedron Lett.* **1998**, *39*, 6901.
1113. Takaki, K.; Kusudo, T.; Uebori, S.; Nishiyama, T.; Kamata, T.; Yokoyama, M.; Takehira, K.; Makioka, Y.; Fujiwara, Y. *J. Org. Chem.* **1998**, *63*, 4299.
1114. Li, P.; Wang, T.; Emge, T.; Zhao, K. *J. Am. Chem. Soc.* **1998**, *120*, 7391.
1115. Gun'ko, Yu. K.; Edelmann, F. T. *Comments Inorg. Chem.* **1997**, *19*, 153.
1116. Ingall, M. D. K.; Joray, S. J.; Duffy, D. J.; Long, D. P.; Bianconi, P. A. *J. Am. Chem. Soc.* **2000**, *122*, 7845.
1117. Shimizu, M.; Fujisawa, H.; Shiosaki, T. *Microelectron. Eng.* **1995**, *29*, 173.
1118. Langer, D. W.; Li, Y.; Fang, X.; Conn, V. *Mater. Res. Soc. Symp. Proc.* **1993**, *301*, 15.
1119. Greenwald, A. C.; Lay, U. W. *Mater. Res. Soc. Symp. Proc.* **1993**, *301*, 21.
1120. Scholz, F.; Weber, J.; Pressel, K.; Doernen, A. *Mater. Res. Soc. Symp. Proc.* **1993**, *301*, 3.
1121. Edakawa, N.; Yoshida, H.; Kamya, K.; Taya, M. *Jpn. Kokai Tokkyo Koho* JP 05279050.
1122. He, X.; Trudeau, M.; Antonelli, D. J. *Mater. Chem.* **2003**, *13*, 75.
1123. He, X.; Trudeau, M.; Antonelli, D. J. *Mater. Chem.* **2003**, *13*, 75.
1124. Scarel, G.; Bonera, E.; Wiemer, C.; Tallarida, G.; Spiga, S.; Fanciulli, M.; Fedushkin, I. L.; Schumann, H.; Lebedinski, Y.; Zenkevich, A. *Appl. Phys. Lett.* **2004**, *85*, 630.
1125. Akane, T.; Jinno, S.; Yang, Y.; Kuno, T.; Hirata, T.; Isogai, Y.; Watanabe, N.; Fujiwara, Y.; Nakamura, A.; Takeda, Y. *Appl. Surf. Sci.* **2003**, *216*, 537.

## 4.02

# Complexes of Actinide Elements

---

F T Edelmann, Otto-von-Guericke-Universität Magdeburg, Magdeburg, Germany

© 2007 Elsevier Ltd. All rights reserved.

<b>4.02.1</b>	<b>Introduction</b>	<b>192</b>
<b>4.02.2</b>	<b>Carbonyls</b>	<b>192</b>
<b>4.02.3</b>	<b>Hydrocarbyls</b>	<b>192</b>
4.02.3.1	Homoleptic Compounds	192
4.02.3.2	Heteroleptic Compounds	193
<b>4.02.4</b>	<b>Allyls</b>	<b>197</b>
<b>4.02.5</b>	<b>Cyclopentadienyl Compounds</b>	<b>198</b>
4.02.5.1	Compounds of Trivalent Actinides: $\text{Cp}_2\text{AnX}$ , $\text{Cp}_3\text{An}$ , and $\text{Cp}_3\text{AnL}$ Compounds	198
4.02.5.2	$\text{CpAnX}_3$ and $\text{Cp}_2\text{AnX}_2$ Compounds	200
4.02.5.3	$\text{Cp}_3\text{AnX}$ and $\text{Cp}_3\text{AnX(L)}$ Compounds	204
4.02.5.4	$\text{Cp}_4\text{An}$ Compounds	206
4.02.5.5	Pentamethylcyclopentadienyl Compounds	206
4.02.5.5.1	$\text{Cp}^*\text{AnX}_2$ and $\text{Cp}^*_2\text{AnX}$ compounds	206
4.02.5.5.2	$\text{Cp}^*_3\text{An}$ compounds	207
4.02.5.5.3	Mono(pentamethylcyclopentadienyl) actinide(IV) compounds	207
4.02.5.5.4	Bis(pentamethylcyclopentadienyl) actinide(IV), (V), and (VI) compounds	210
4.02.5.5.5	Tris(pentamethylcyclopentadienyl) actinide(IV) compounds	219
4.02.5.6	Compounds with Ring-bridged Cyclopentadienyl Ligands	220
4.02.5.7	Indenyl and Pentalenediyl Compounds	221
<b>4.02.6</b>	<b>Cyclopentadienyl-like Compounds</b>	<b>224</b>
4.02.6.1	Compounds with Heteroatom Five-membered Ring Ligands	224
4.02.6.2	Compounds with Carboranyl Ligands	224
<b>4.02.7</b>	<b>Arene Complexes</b>	<b>225</b>
<b>4.02.8</b>	<b>Cycloheptatrienyl Compounds</b>	<b>226</b>
<b>4.02.9</b>	<b>Cyclooctatetraenyl Compounds</b>	<b>227</b>
4.02.9.1	Cyclooctatetraenyl Actinide(III) Compounds	227
4.02.9.2	Mono(cyclooctatetraenyl) Actinide(IV) and -(V) Compounds	227
4.02.9.3	Bis(cyclooctatetraenyl) Actinide(IV) Compounds	231
<b>4.02.10</b>	<b>Heterobimetallic Compounds</b>	<b>232</b>
4.02.10.1	Metal–Metal Bonded Compounds	232
4.02.10.2	Heterobimetallic Compounds without Direct Metal–Metal Bonds	232
<b>4.02.11</b>	<b>Organoactinide Catalysis</b>	<b>233</b>
4.02.11.1	Organoactinide-catalyzed Hydrogenation Reactions	233
4.02.11.2	Organoactinide-catalyzed Oligomerization Reactions	234
4.02.11.3	Organoactinide-catalyzed Polymerization Reactions	235
4.02.11.4	Organoactinide-catalyzed Hydrosilylation Reactions	236
4.02.11.5	Organoactinide-catalyzed Hydroamination Reactions	237
4.02.11.6	Other Organoactinide-catalyzed Reactions	238
	<b>References</b>	<b>239</b>

---

### 4.02.1 Introduction

This chapter summarizes the progress in organoactinide chemistry during the period 1993–2005. Earlier developments in this area from the beginning of organoactinide chemistry in 1956, when Reynolds and Wilkinson discovered  $\text{Cp}_3\text{UCl}$ ,<sup>1</sup> have been fully outlined in COMC(1982) and COMC(1995).<sup>2,3</sup> The sections in this chapter are subdivided according to ligand types, while the last section is devoted to organoactinide catalysis. Several review articles on different aspects of organoactinide chemistry have been published since 1993. An overview on the progress in this area can be found in the annual reviews which are published regularly in *Coordination Chemistry Reviews*.<sup>4–11</sup> A general survey of organoactinide chemistry covering mainly the years 1985–1992 has been published by Ephritikhine.<sup>12</sup> In 2003, Dormond *et al.* published a comprehensive review under the title: “Product Class 23: Organometallic Complexes of the Actinides.”<sup>13</sup>

In general, there was a decrease in research activities in the field of organoactinide chemistry in the past 12 years. This is, presumably in part, due to more restrictive safety regulations and increasing bureaucracy involved in the handling of actinide elements and their organometallic compounds. Nevertheless, organoactinide chemistry continues to be an exciting field of organometallic chemistry where spectacular novel structures and unprecedented reaction pathways can still be discovered. The uniqueness of the organoactinide compounds becomes immediately apparent in the section on organoactinide catalysis. This is an area where significant progress has been made since 1993.

### 4.02.2 Carbonyls

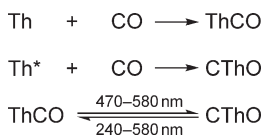
While stable binary actinide carbonyls are still unknown, research in this area focused mainly on the detection and theoretical investigation of unstable molecules such as the monocarbonyl complexes of thorium and uranium. The possible molecular structures  $\text{U-CO}$ ,  $\text{U-OC}$ , and  $\text{CUO}$  of carbon monoxide interacting on a uranium metal surface have been studied by density functional theory (DFT).<sup>14</sup>  $\text{CUO}$  has been produced experimentally by reaction of laser-ablated U atoms with CO in excess argon and trapped in a triplet state in solid argon at 7 K.<sup>15</sup> Studies of the reaction of thorium atoms with CO have been carried out. The reaction of laser-ablated thorium atoms with carbon monoxide in excess neon gave the first thorium carbonyl complex,  $\text{Th-CO}$ , which rearranges photochemically to  $\text{CThO}$  (Scheme 1).<sup>16</sup>

In a closely related study, the same authors also reported the first identification of the molecules  $\text{CThO}^-$ ,  $\text{OThCCO}$ ,  $\text{OTh}(\eta^3\text{-CCO})$ , and  $\text{Th}(\text{CO})_n$  ( $n = 1\text{--}6$ ). The complexes  $\text{Th}(\text{CO})_n$  ( $n = 1\text{--}6$ ) were formed on deposition or on annealing. Relativistic DFT calculations showed that  $\text{CThO}$  is an unprecedented actinide–carbene molecule with a triplet ground state and an unusual bent structure ( $\angle\text{CThO} = 109^\circ$ ). The  $\text{CThCCO}$  molecule has a bent structure while its rearranged product  $\text{OTh}(\eta^3\text{-CCO})$  is found to have a unique exocyclic structure with side-bonded  $\text{CCO}$  group. It was also found that both  $\text{Th}(\text{CO})_2$  and  $\text{Th}(\text{CO})_2^-$  are, surprisingly, highly bent, with the  $\angle\text{CThC}$  bond angle being close to  $50^\circ$ . The unusual geometries are the result of extremely strong Th-to-CO back-bonding, which causes significant three-centered bonding among the Th atom and the two C atoms.<sup>17</sup> A comparative density functional study on metal–ligand (M–L) interaction has been performed on  $\text{X}_3\text{U}(\text{CO})$  ( $\text{X} = \text{F}, \text{I}$ ) species including scalar relativistic effects by means of the zero-order regular approximation (ZORA) hamiltonian. The role of the halogen atoms in modeling the M–L interactions has been discussed for the  $\pi$ -ligand CO.<sup>18</sup>

### 4.02.3 Hydrocarbyls

#### 4.02.3.1 Homoleptic Compounds

A theoretical investigation of structural and vibrational properties of the gas-phase molecule  $\text{U}(\text{CH}_3)_3$  by density functional methodologies or with a post-Hartree–Fock MP2 perturbative approach has been published. The optimized geometries for  $\text{U}(\text{CH}_3)_3$  have been compared with the experimental solid-state structural data for  $\text{U}[\text{CH}(\text{SiMe}_3)_2]_3$ .<sup>19</sup> A novel gas-phase technique, MPCA, employing the reaction between co-ablated metal ions



Scheme 1

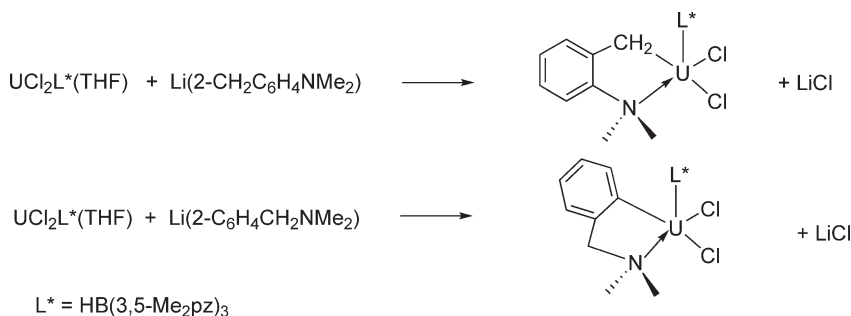
and polymer radical fragments, was used for the production of labile gas-phase organoactinide complexes to the first transplutonium element Am. This technique is applicable to highly radioactive elements not amenable to conventional methods. Laser ablation into vacuum of a dilute dispersion of  $\text{AmO}_2$  in polyimide produced organoamericium ions of the general formula  $\text{AmC}_x\text{H}_y\text{N}_z^+$ . Comparisons of product abundances with previous results for lanthanides (Ln) and lighter actinides (An) suggest amounts of  $\text{MC}_2\text{H}^+$  and  $\text{MC}_4\text{H}^+$ . In addition to the carbide/hydrocarbide complex ions,  $\text{Am}^+$  hydroxide, cyanide, cyanate, and nitrile ions were produced.<sup>20</sup> Similarly, organoberkelium and organocalifornium ions were produced for the first time by laser ablation of  $^{249}\text{Bk}_2\text{O}_3$  and  $^{249}\text{Cf}_2\text{O}_3$  dispersions in polyimide, followed by time-of-flight mass spectrometry. The primary organometallic products were  $\text{BkCH}_3^+$ ,  $\text{AnC}_2\text{H}^+$ , and  $\text{AnC}_4\text{H}^+$  (An = Bk, Cf).<sup>21</sup> Gas-phase reactions of the bare berkelium monocation,  $\text{Bk}^+$ , with several reagents have been examined by a mass spectrometric technique adapted for the highly radioactive transuranium actinides. Organometallic products were observed with several alkenes such as ethylene, propene, 1- and 2-butene, isobutene, cyclohexene, 1,5-cyclooctadiene, cyclooctatetraene, and pentamethylcyclopentadiene. The products included  $\pi$ -bonded organoberkelium ions such as  $\text{BkCOT}^+$ , presumably the berkelium-cyclooctatetraenyl half-sandwich complex ion.<sup>22</sup>

The homoleptic tetrabenzylthorium derivative  $\text{Th}(\text{1,3,5-CH}_2\text{C}_6\text{H}_3\text{Me}_2)_4$  was straightforwardly prepared in the form of pale yellow crystals by the reaction of  $\text{ThCl}_4$  with 1,3,5-Li $\text{CH}_2\text{C}_6\text{H}_3\text{Me}_2$  in THF, followed by extraction with toluene and recrystallization from pentane.<sup>23</sup> The oxidation of the tetrabenzyluranium complex  $(\text{C}_6\text{H}_5\text{CH}_2)_4\text{U}\cdot\text{MgCl}_2$  with  $\text{O}_2$  or  $\text{Me}_3\text{COOH}$  in organic solvents at room temperature gives products of different composition depending on the oxidizing reagent and the stoichiometry. The reaction yielded mainly uranium(IV) benzyloxy derivatives, and in the case of oxygen the so-called peroxide mechanism took place. The novel heteroleptic complex  $(\text{C}_6\text{H}_5\text{CH}_2)_2\text{U}(\text{OCH}_2\text{C}_6\text{H}_5)_2\cdot\text{MgCl}_2$  was obtained.<sup>24</sup>

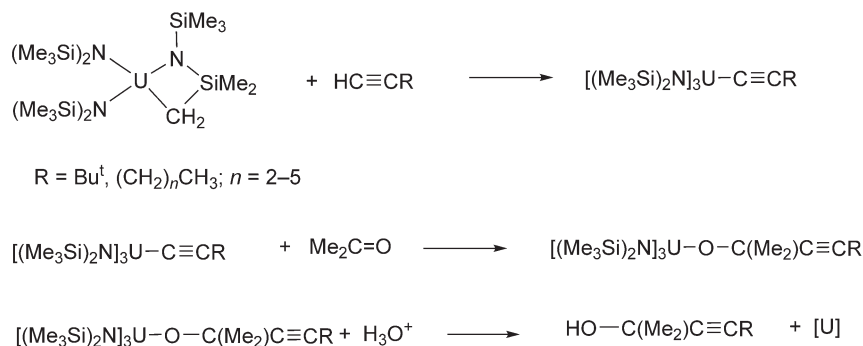
#### 4.02.3.2 Heteroleptic Compounds

Various mostly *N*-coordinated multidentate ancillary ligands have been successfully employed in the stabilization of uranium hydrocarbyl species. This is an area of active research where interesting results have been achieved. Hydrocarbyl derivatives of  $\text{UCl}_2[\text{HB}(\text{pz})_3]_2$  have been synthesized, and their reactivity toward protic substrates and ketones has been studied. The reaction of  $\text{UCl}_2[\text{HB}(\text{pz})_3]_2$  with lithium alkyls  $\text{LiR}$  (R = Me,  $\text{CH}_2\text{SiMe}_3$ ,  $\text{C}_6\text{H}_4$ -*o*- $\text{CH}_2\text{NMe}_2$ ) in a 1:1 or 1:2 molar ratio afforded the compounds  $\text{UClR}[\text{HB}(\text{pz})_3]_2$  (R = Me,  $\text{CH}_2\text{SiMe}_3$ ,  $\text{C}_6\text{H}_4$ -*o*- $\text{CH}_2\text{NMe}_2$ ) and  $\text{UR}_2[\text{HB}(\text{pz})_3]_2$  (R = Me,  $\text{CH}_2\text{SiMe}_3$ ), respectively, in 60–80% yield.<sup>25</sup> The hydrocarbyl compounds  $[\text{HB}(3,5\text{-Me}_2\text{pz})_3]\text{UCl}_2\{\text{CH}(\text{SiMe}_3)_2\}$  and  $[\text{HB}(3,5\text{-Me}_2\text{pz})_3]\text{UCl}_{3-x}(\text{CH}_2\text{SiMe}_3)_x$  ( $x = 1, 2, 3$ ) have been obtained analogously.<sup>26</sup> Hydro-tris(pyrazolyl)borate  $\sigma$ -hydrocarbyl-uranium(IV) complexes of the type  $\text{UCl}_2(2\text{-CH}_2\text{C}_6\text{H}_4\text{NMe}_2)\text{L}^*$  and  $\text{UCl}_2(2\text{-C}_6\text{H}_4\text{CH}_2\text{NMe}_2)\text{L}^*$  ( $\text{L}^* = \text{HB}(3,5\text{-Me}_2\text{pz})_3$ ) were synthesized by reaction of  $\text{UCl}_2\text{L}^*(\text{THF})$  with  $\text{Li}(2\text{-CH}_2\text{C}_6\text{H}_4\text{NMe}_2)$  and  $\text{Li}(2\text{-C}_6\text{H}_4\text{CH}_2\text{NMe}_2)$ , respectively (Scheme 2).<sup>27</sup> The complexes  $\text{UCl}_2(2\text{-CH}_2\text{C}_6\text{H}_4\text{NMe}_2)\text{L}^*$  and  $\text{UCl}_2(2\text{-C}_6\text{H}_4\text{CH}_2\text{NMe}_2)\text{L}^*$  were found to exhibit fluxional behavior in  $\text{C}_6\text{D}_6$  solution at room temperature.

The synthesis and reactivity of alkynyl(silylamido)uranium complexes of the type  $[(\text{Me}_3\text{Si})_2\text{N}]_3\text{U-C}\equiv\text{CR}$  (R =  $\text{Bu}^t$ ,  $(\text{CH}_2)_n\text{CH}_3$ ;  $n = 2\text{--}5$ ) was achieved by reaction of  $[(\text{Me}_3\text{Si})_2\text{N}]_2\text{UCH}_2\text{SiMe}_2\text{NSiMe}_3$  with the appropriate terminal alkynes.<sup>28</sup> Treatment of the alkynyl(silylamido)uranium complexes with stoichiometric amount of acetone



Scheme 2



Scheme 3

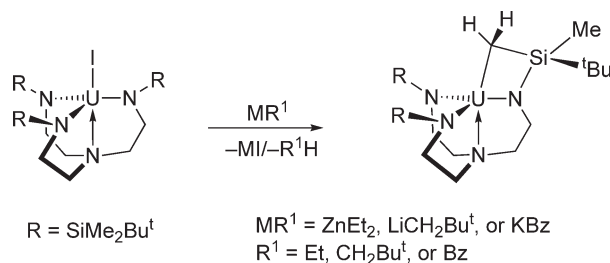
led to the corresponding uranium alkoxides  $[(\text{Me}_3\text{Si})_2\text{N}]_3\text{U}-\text{O}-\text{C}(\text{Me}_2)\text{C}\equiv\text{CR}$  via insertion of acetone into the U–C bond. Subsequent hydrolysis of the latter complexes with aqueous HCl afforded the  $\alpha$ -acetylenic alcohols (Scheme 3).

The surprisingly fast reaction of  $\text{U}(\text{NN}'_3)\text{I}$  ( $\text{NN}'_3 = \text{N}(\text{CH}_2\text{CH}_2\text{NSiMe}_2\text{Bu}^t)_3$ ) with group 1 and 2 metal alkyls gives, via metallation of a methylsilyl group, a metallocycle  $\text{U}(\text{bit-NN}'_3)$  (Scheme 4). The analogous  $\text{Th}(\text{bit-NN}'_3)$  was prepared from  $\text{Th}(\text{NN}'_3)\text{Cl}$  using the same procedure or through reduction of  $\text{Th}(\text{NN}'_3)\text{I}$  with a potassium film. A similar reaction of  $\text{U}(\text{NN}'_3)\text{I}$  with potassium in toluene resulted in formation of the dimeric U(III) complex  $[\{\text{K}(\eta^6\text{-C}_6\text{H}_5\text{Me})\}\text{U}(\text{bit-NN}'_3)]_2$ .<sup>29</sup>

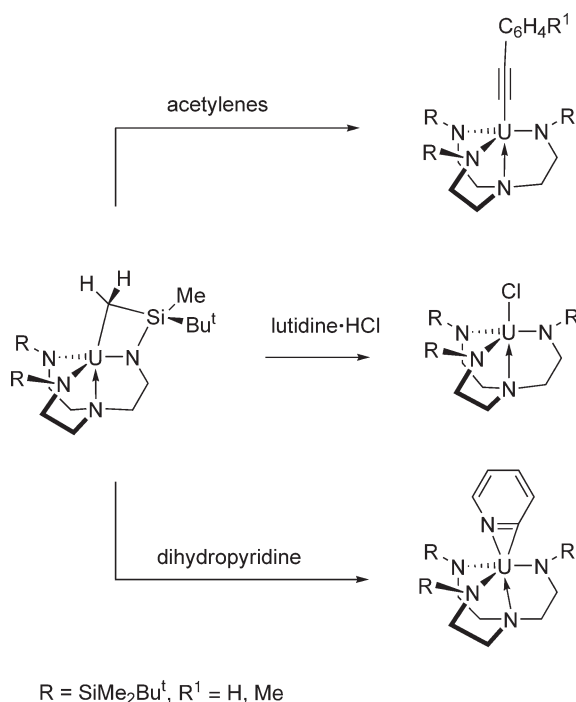
Oxidation of  $\text{U}(\text{bit-NN}'_3)$  with air or other oxygen sources led to formation of an oxo-bridged dimer with intermolecularly metalated methylsilyl groups. Reaction of H-acidic compounds HX like lutidine·HCl, diethylamine, or *t*-butanol gave the  $\text{U}(\text{NN}'_3)\text{X}$  complexes under reprotonation of the previously metalated methylsilyl group (Scheme 5). Pyridines and monosubstituted alkynes reacted in a similar manner to give  $\eta^2$ -dehydropyridyl complexes and  $\eta^1$ -alkynyls, respectively.<sup>29</sup>

Reduction of  $\text{U}(\text{NN}'_3)\text{I}$  ( $\text{NN}'_3 = \text{N}(\text{CH}_2\text{CH}_2\text{NSiMe}_2\text{Bu}^t)_3$ ) with potassium in pentane gave the purple trivalent monomer  $\text{U}(\text{NN}'_3)$ , this compound having previously been synthesized via fractional vacuum sublimation of mixed-valent  $[\text{U}(\text{NN}'_3)]_2(\mu\text{-Cl})$ . The chemistry of  $\text{U}(\text{NN}'_3)$  toward various reagents (pyridine, HMPA, trimethylsilylazide, trimethylsilyldiazomethane,  $\text{Me}_3\text{NO}$ ) has been studied in detail. While the reaction products in these cases should not be considered as metallorganic compounds, the reaction with methylenetriethylphosphorane led to formation of the adduct  $\text{U}(\text{NN}'_3)(\text{CH}_2\text{PMe}_3)$  containing a uranium–carbon bond. Reaction of this complex with air gave a few crystals of the unusual hydroxo complex  $\text{U}(\text{NN}'_3)(\text{OH})(\text{CH}_2\text{PMe}_3)$ , which was structurally characterized.<sup>30</sup> The doubly deprotonated diamidosilyl ether ligand  $(\text{Bu}^t\text{NHSiMe}_2)_2\text{O}^{2-}$  ( $[\text{Bu}^t\text{NON}]^{2-}$ ) has been successfully employed in the stabilization of heteroleptic organoactinide complexes. Scheme 6 depicts the preparation of the dimeric halide precursors, which have subsequently been treated with  $\text{C}_3\text{H}_5\text{MgCl}$  or  $\text{LiCH}_2\text{SiMe}_3$  to afford the stable disubstituted diallyl and dialkyl complexes.<sup>31</sup>

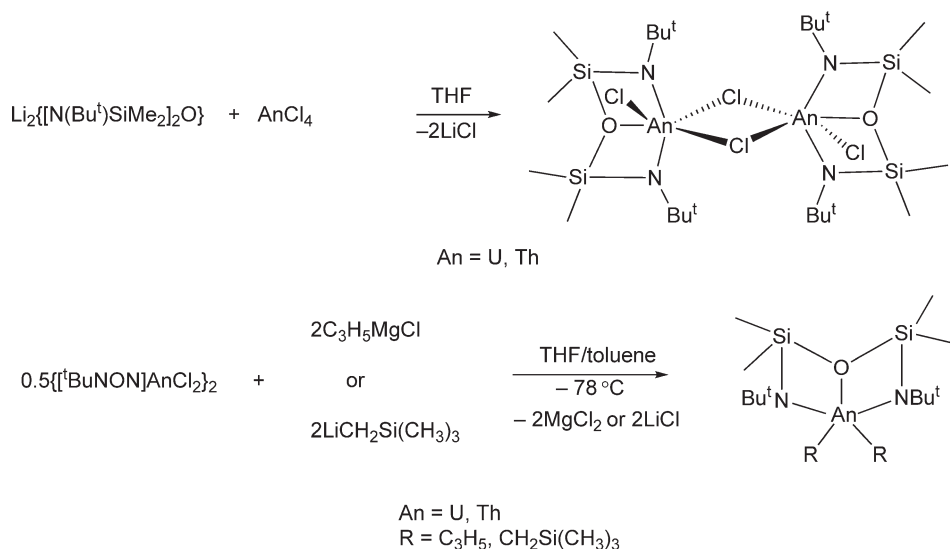
The first examples of compounds with an *N*-heterocyclic carbene ligand coordinated to a low-valent uranium center were reported in 2004. The synthetic procedures are illustrated in Schemes 7 and 8. Notably, the silylamide derivative (Scheme 8) was isolated in the form of dark blue crystals in excellent yield (>90%). DFT studies indicated a significant degree of  $\pi$ -bonding in the U(III) carbene entity.<sup>32</sup>



Scheme 4



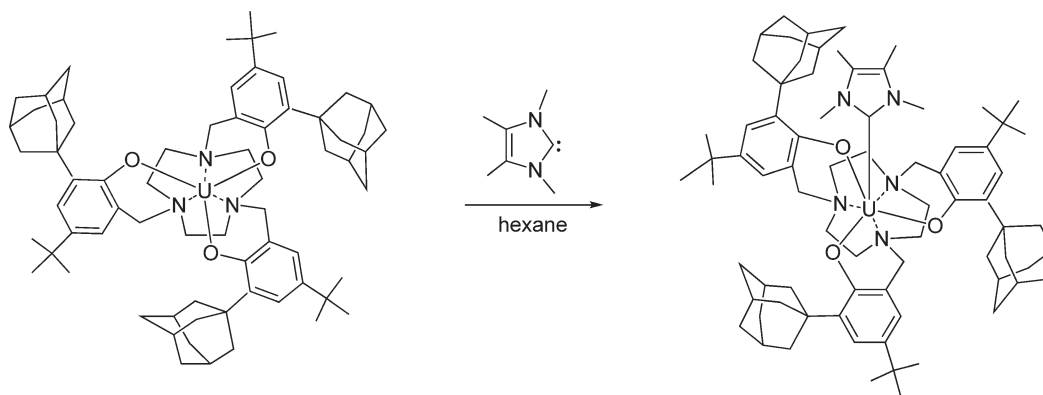
Scheme 5



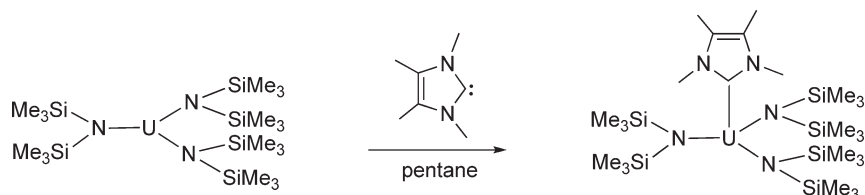
Scheme 6

Treatment of  $\text{UO}_2\text{Cl}_2(\text{THF})_3$  in THF with 1 equiv. of  $\text{Na}[\text{CH}(\text{Ph}_2\text{P}=\text{NSiMe}_3)_2]$  led to formation of an unusual red uranyl chloro-bridged dimer (70% yield) containing a uranium(vi)–carbon bond as part of a tridentate bis(imino-phosphorano)methanide chelate complex (Scheme 9). This was the first example of a uranyl–methine carbon bond. The methine carbon is displaced significantly from the uranyl equatorial plane.<sup>33</sup>

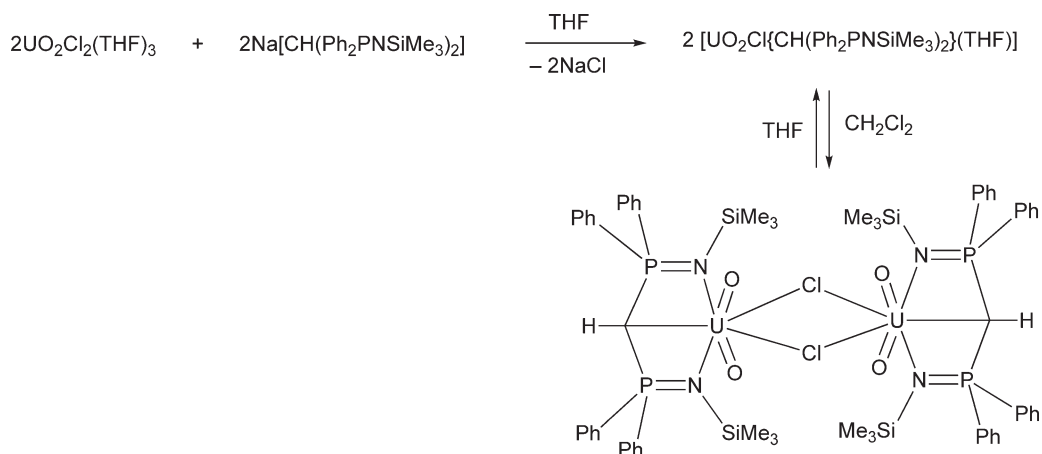
A uranyl–carbon bond is also present in the adducts of  $[\text{PhC}(\text{NSiMe}_3)_2]_2\text{UO}_2$  with *t*-butylisocyanide. Treatment of a toluene solution of the precursor with  $\text{Bu}^t\text{NC}$  cleanly formed  $[\text{PhC}(\text{NSiMe}_3)_2]_2\text{UO}_2(\text{CNBu}^t)$



Scheme 7



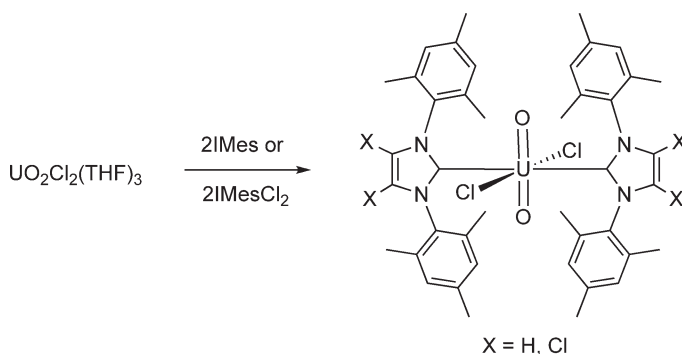
Scheme 8



Scheme 9

as the first uranyl complex containing a coordinated isonitrile.<sup>34</sup> Treatment of  $\text{UO}_2\text{Cl}_2(\text{THF})_3$  in THF with 2 equiv. of 1,3-dimesitylimidazole-2-ylidene (IMes) or 1,3-dimesityl-4,5-dichloroimidazole-2-ylidene (IMesCl<sub>2</sub>) as depicted in Scheme 10 afforded novel monomeric uranyl *N*-heterocyclic carbene complexes. The complexes were isolated in 74% and 62% yield, respectively, as pale yellow crystalline solids, which were both structurally characterized by X-ray diffraction. The uranium–carbon bond lengths are 2.626(7) and 2.609(4) Å, respectively.<sup>35</sup>



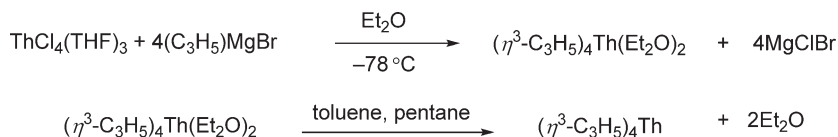


Scheme 10

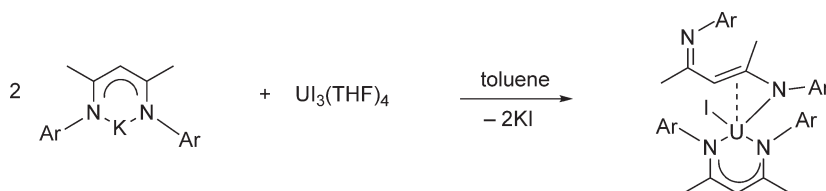
#### 4.02.4 Allyls

Tetraallylthorium,  $(\eta^3\text{-C}_3\text{H}_5)_4\text{Th}$ , was prepared according to [Scheme 11](#) by the low-temperature reaction of  $\text{ThCl}_4(\text{THF})_3$  with an excess of allylmagnesium bromide in diethyl ether.<sup>23</sup>

Tetraallylthorium is stereochemically non-rigid in solution, with the exchange of *syn*- and *anti*- $\eta^3$ -allyl protons observable by variable-temperature dynamic  $^1\text{H}$  NMR spectroscopy.<sup>23</sup> Recently, significant progress in actinide allyl chemistry has been made through the use of bulky silyl-substituted allyl ligands. Reactions of 4 equiv. of  $\text{K}[\text{C}_3\text{H}_4\text{SiMe}_3\text{-1}]$  or  $\text{K}[\text{C}_3\text{H}_3(\text{SiMe}_3)_2\text{-1,3}]$  with  $\text{ThBr}_4(\text{THF})_4$  in THF at  $-78^\circ\text{C}$  cleanly produced the bright yellow complexes  $[\text{C}_3\text{H}_4\text{SiMe}_3\text{-1}]_4\text{Th}$  and  $[\text{C}_3\text{H}_3(\text{SiMe}_3)_2\text{-1,3}]_4\text{Th}$ , respectively, in high yields. In both complexes the central Th atom is tetrahedrally coordinated by four  $\eta^3$ -allyl ligands.<sup>36</sup> Bis(allyl)actinide complexes containing the doubly deprotonated diamidosilyl ether ligand  $(\text{Bu}^t\text{NHSiMe}_2)_2\text{O}^{2-}$  ( $[\text{Bu}^t\text{NON}]^{2-}$ ) have been described in the preceding section.<sup>31</sup> The chemistry of 1-aza allyl complexes of thorium has been investigated. Treatment of  $\text{ThCl}_4$  with  $\text{K}(\text{LL}')_n$  ( $\text{LL}' = \text{N}(\text{SiMe}_3)\text{C}(\text{Bu}^t)\text{CH}(\text{SiMe}_3)$ ) afforded the heterobimetallic bis(aza allyl)dichlorothorium(IV)–KCl complex  $[\text{Th}(\text{LL}')_2(\mu_3\text{-Cl})(\mu\text{-Cl})_2\text{K}(\text{OEt}_2)]_\infty$  in good yield (72%). The compound was found to be resistant to reduction by Na–K alloy.<sup>37</sup> An uncommon  $\eta^3\text{-(N,C,C')}$ -1-aza allyl bonding mode for a  $\beta$ -diketiminato ligand has been reported for a bis( $\beta$ -diketiminato)uranium(III) iodide complex. As shown in [Scheme 12](#), reaction of  $\text{UI}_3(\text{THF})_4$  with 2 equiv. of the sterically demanding  $\text{K}(\text{Nacnac})$  ( $\text{Nacnac} = \text{ArNC}(\text{Me})\text{CHC}(\text{Me})\text{NAr}$ ,  $\text{Ar} = 2,6\text{-Pr}_2\text{C}_6\text{H}_3$ ) in toluene solution at room temperature afforded a bis( $\beta$ -diketiminato)uranium(III) complex as a dark blue crystalline solid in 42% isolated yield. The molecule features one  $\beta$ -diketiminato ligand bound to the U(III) center in an unusual  $\eta^3\text{-(N,C,C')}$ -1-aza allyl mode and possesses close  $\text{U}\cdots\text{C}_{\text{alkene}}$  contacts.<sup>38</sup>



Scheme 11



Scheme 12

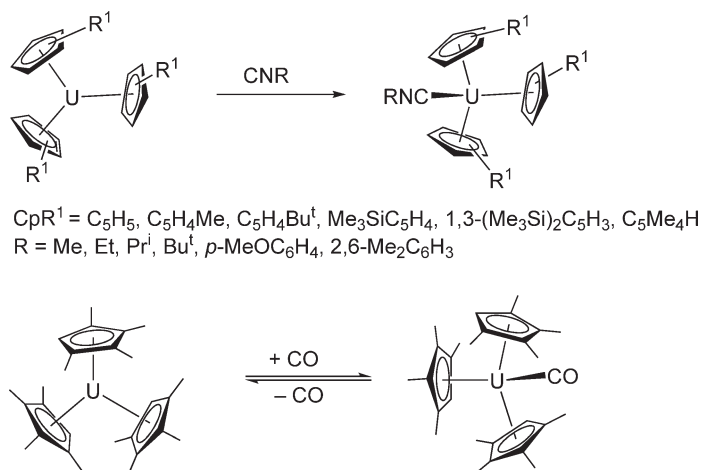
## 4.02.5 Cyclopentadienyl Compounds

### 4.02.5.1 Compounds of Trivalent Actinides: $\text{Cp}_2\text{AnX}$ , $\text{Cp}_3\text{An}$ , and $\text{Cp}_3\text{AnL}$ Compounds

Non-relativistic and relativistic discrete variational- $X\alpha$  calculations have been performed on  $\text{Cp}_3\text{Th}$  and  $\text{Cp}_3\text{Pa}$ . M–L covalent interactions in  $\text{Cp}_3\text{Th}$  are dominated by metal  $d$ -orbital participation in the  $(\eta\text{-C}_5\text{H}_5)$   $\pi_2$ -based 2e and 3e molecular orbitals, and an  $f$ -orbital contribution to the 1a<sub>2</sub> level. The non-relativistic calculations predict a formal ground configuration of  $4f^1$  and  $5f^1$  for  $\text{Cp}_3\text{Th}$ , while the destabilization of the  $nf$  and slight stabilization of the  $(n+1)d\sigma$  level, on the incorporation of relativistic effects, result in a  $6d^1$  electronic configuration for  $\text{Cp}_3\text{Th}$ .  $\text{Cp}_3\text{Pa}$  was found to have a  $5f^1$  ground configuration in both non-relativistic and relativistic calculations, and both the  $6d$  and  $5f$  metal orbitals participate significantly in M–L covalent bonding.<sup>39</sup>

The voltammetric behavior of  $\text{Cp}_2\text{U}(\text{BH}_4)_2$  and  $\text{Cp}_3\text{U}(\text{BH}_4)$  has been studied using a conventional Pt microelectrode or a Pt ultramicroelectrode in a  $[\text{NBu}_4]\text{PF}_6/\text{THF}$  medium. The results showed that both compounds were reduced in accordance with a rapid one-electron process to afford the uranium(III) species,  $\text{Cp}_2\text{U}(\text{BH}_4)_2^-$  and  $\text{Cp}_3\text{U}(\text{BH}_4)^-$ .<sup>40</sup> Studies of the solution structure and the behavior of dimeric uranium(III) metallocene halides were performed on the complexes,  $[\text{Cp}''_2\text{U}(\mu\text{-X})_2]$  and  $[\text{Cp}^+_2\text{U}(\mu\text{-X})_2]$  ( $\text{X} = \text{F}, \text{Cl}, \text{Br}, \text{or I}$ ;  $\text{Cp}'' = \text{C}_5\text{H}_3(\text{SiMe}_3)_{2-1,3}$ ; and  $\text{Cp}^+ = \text{C}_5\text{H}_3\text{Bu}^t_{2-1,3}$ ).<sup>41</sup> The synthesis of these complexes was achieved by reacting the corresponding bis(cyclopentadienyl)uranium(IV) halides with  $t$ -butyllithium. The variable-temperature  $^1\text{H}$  NMR behavior of the uranium(III) dimers  $[\text{Cp}''_2\text{U}(\mu\text{-X})_2]$  and  $[\text{Cp}^+_2\text{U}(\mu\text{-X})_2]$  was examined in a range of  $-90$  and  $100^\circ\text{C}$ . At low temperature, the number of inequivalent  $\text{Bu}^t$  or  $\text{SiMe}_3$  groups implies that the solution structure is the same as the solid-state structure in all of these complexes. The barriers of ring rotation in the  $\text{Cp}''$  series are strongly dependent on the U–X distances, but all of the barriers of ring rotation in the  $\text{Cp}^+$  series are the same. The trends in ring rotation barriers are explained by the different conformation of the Cp ligands in the dimers. In addition to the homohalide dimers, the variable-temperature NMR behavior of the hetero-halide dimers  $\text{Cp}_4\text{U}_2(\mu\text{-X})(\mu\text{-Y})$ , where Cp is  $\text{Cp}''$  or  $\text{Cp}^+$  and X and Y are halides where  $\text{X} \neq \text{Y}$ , was examined. Above room temperature, the halide atoms exchange sites rapidly on the NMR timescale.<sup>41</sup> The structure of (substituted-cyclopentadienyl)uranium(III) dimers and related uranium metallocenes was deduced by EXAFS, and the crystal structures of  $[\text{Cp}''_2\text{U}(\mu\text{-F})_2]$  and  $[\text{Cp}^+_2\text{U}(\mu\text{-O})_2]$  were reported.<sup>42</sup> Both complexes have idealized  $C_{2h}$  symmetry, and their U···U distances are 3.85 and 3.39 Å, respectively. The X-ray spectra of several uranium metallocene complexes, and the numerical results from fitting the EXAFS spectra, were reported. For  $[\text{Cp}^+_2\text{U}(\mu\text{-F})_2]$ , the U···U distance was found by EXAFS to be similar to that in  $[\text{Cp}''_2\text{U}(\mu\text{-F})_2]$ , implying that  $[\text{Cp}^+_2\text{U}(\mu\text{-F})_2]$  is dimeric. A structural model was advanced that correlates the U···U distances with the orientation of the cyclopentadienyl rings; the orientation depends on a subtle combination of steric repulsions between ligands on adjacent metal centers.<sup>42</sup> The methyl-bridged bis(cyclopentadienyl) complex  $[(\text{C}_5\text{H}_4\text{Bu}^t)_2\text{U}(\mu\text{-Me})_2]$  has been prepared by reaction of  $(\text{C}_5\text{H}_4\text{Bu}^t)_3\text{U}$  with MeLi. The compound is unstable in the gas phase and in benzene solution and rearranges to give  $(\text{C}_5\text{H}_4\text{Bu}^t)_3\text{U}$  and other materials.<sup>43</sup> The uranium(III) nitrile complexes  $\text{Cp}_3\text{U}(\text{NCR})$  ( $\text{R} = \text{Me}, \text{Pr}^n, \text{Pr}^i, \text{Bu}^t$ ) have been prepared by treatment of  $\text{Cp}_3\text{U}(\text{THF})$  with the corresponding nitrile. Similar reaction of  $\text{Cp}_3\text{U}(\text{THF})$  with benzonitrile at room temperature or thermolysis of the adducts  $\text{Cp}_3\text{U}(\text{NCMe})$  or  $\text{Cp}_3\text{U}(\text{NCP}^n)$  afforded an equimolar mixture of the uranium(IV) compounds  $\text{Cp}_3\text{UCN}$  and  $\text{Cp}_3\text{UR}$  ( $\text{R} = \text{Me}, \text{Pr}^n, \text{Ph}$ ).<sup>44</sup> Organic isocyanide complexes of trivalent uranium metallocenes of the type  $\text{Cp}^x_3\text{U}(\text{CNR})$  have been prepared, where  $\text{Cp}^x = \text{C}_5\text{H}_5, \text{C}_5\text{H}_4\text{Me}, \text{C}_5\text{H}_4\text{Bu}^t$ , and  $\text{C}_5\text{H}_4\text{SiMe}_3$  and  $\text{R} = \text{Et}$ ;  $\text{Cp}'' = \text{C}_5\text{H}_3(\text{SiMe}_3)_{2-1,3}$  and  $\text{R} = \text{Bu}^t$ ;  $\text{Cp}' = \text{C}_5\text{Me}_4\text{H}$  and  $\text{R} = p\text{-MeOC}_6\text{H}_4$  and  $\text{C}_6\text{H}_3\text{Me}_{2-2,6}$ . For  $\text{Cp}^x = \text{C}_5\text{H}_4\text{Me}$  and  $\text{R} = \text{C}_6\text{H}_3\text{Me}_{2-2,6}$ , both 1:1 and 1:2 adducts were obtained. The IR spectra of the complexes showed that  $\tilde{\nu}_{\text{CN}}$  increases slightly for the alkyl isocyanide complexes and decreases slightly for the aryl isocyanide complexes relative to  $\tilde{\nu}_{\text{CN}}$  for the free ligands.<sup>45,46</sup> Numerous adducts of  $(\text{C}_5\text{H}_4\text{Bu}^t)_3\text{U}$  with pyridine derivatives and other six-membered  $N$ -heterocycles have been prepared and structurally characterized.<sup>47</sup> This reaction also allowed a clear lanthanide(III)/actinide(III) differentiation between  $(\text{C}_5\text{H}_4\text{Bu}^t)_3\text{Ce}$  and  $(\text{C}_5\text{H}_4\text{Bu}^t)_3\text{U}$ . In contrast to  $(\text{C}_5\text{H}_4\text{Bu}^t)_3\text{Ce}$ , which reacts with pyrazine to give the Lewis base adduct  $(\text{C}_5\text{H}_4\text{Bu}^t)_3\text{Ce}(\text{pyrazine})$ , the uranium analog was oxidized by the azine molecule to the binuclear U(IV) complex  $[(\text{C}_5\text{H}_4\text{Bu}^t)_3\text{U}]_2(\mu\text{-pyrazine})$ .<sup>48</sup>

The uranium metallocenes also form carbon monoxide adducts in which  $\tilde{\nu}_{\text{CO}}$  moves to lower wave numbers upon coordination by  $155\text{--}266\text{ cm}^{-1}$ . In only one case a carbon monoxide adduct could be isolated in crystalline form. The synthesis and crystal structure of the first stable uranium carbonyl complex,  $(\text{C}_5\text{Me}_4\text{H})_3\text{U}(\text{CO})$ , is certainly one of the highlights in recent organoactinide chemistry. The compound was prepared by treatment of the uranium(III) complex  $(\text{C}_5\text{Me}_4\text{H})_3\text{U}$  with CO under ca. 1 atm at room temperature (Scheme 13). A single-crystal X-ray determination of  $(\text{C}_5\text{Me}_4\text{H})_3\text{U}(\text{CO})$  revealed a monomeric structure with a U–C(CO) bond length of 2.383 Å with an almost linear U–C–O arrangement ( $175.2^\circ$ ). The  $\tilde{\nu}_{\text{CO}}$  stretching frequencies decrease in the order

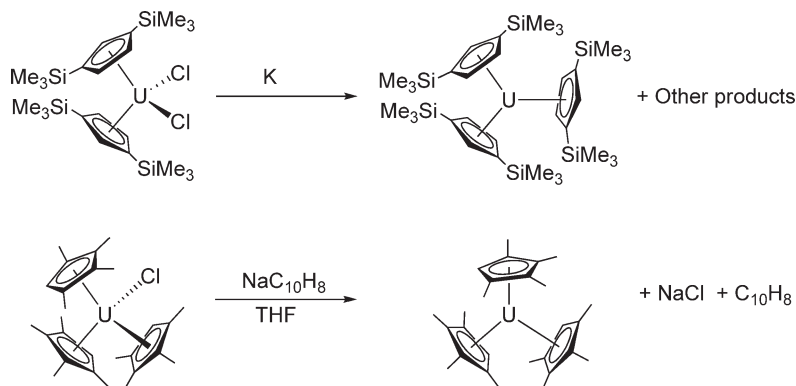


Scheme 13

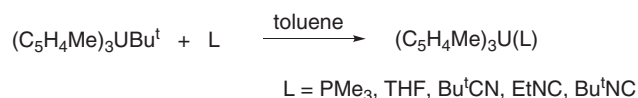
$1,3-(\text{Me}_3\text{Si})_2\text{C}_5\text{H}_3 > \text{Me}_3\text{SiC}_5\text{H}_4 > \text{Bu}^t\text{C}_5\text{H}_4 > \text{C}_5\text{Me}_4\text{H}$ .  $(\text{C}_5\text{Me}_4\text{H})_3\text{U}$  was shown to be the best  $\pi$ -donor in this series of metallocenes. Solution  $^1\text{H}$  NMR spectra showed that the adducts are fluxional, and in the case of  $(\text{C}_5\text{Me}_4\text{H})_3\text{U}(\text{L})$ , with  $\text{L} = \text{CO}$  or  $4\text{-MeOC}_6\text{H}_4\text{NC}$ , two fluxional processes were observed: dissociation of  $\text{L}$  at relatively high temperature and cessation of ring rotation at low temperature.<sup>45</sup>

The tris(cyclopentadienyl)uranium(III) complexes  $\text{Cp}^{*3}\text{U}$  and  $(\text{C}_5\text{Me}_4\text{H})_3\text{U}$  were prepared by synthetic routes that involve the reduction of the appropriate tetravalent uranium metallocene precursors with potassium metal and  $\text{NaC}_{10}\text{H}_8$ , respectively (Scheme 14). The molecular structure of  $(\text{C}_5\text{Me}_4\text{H})_3\text{U}$  shows a perfectly trigonal structure with a threefold axis (all  $\text{Cp}^*$  (centroid)– $\text{U}$ – $\text{Cp}^*$  (centroid) angles equal to  $120^\circ$ ).<sup>46</sup>

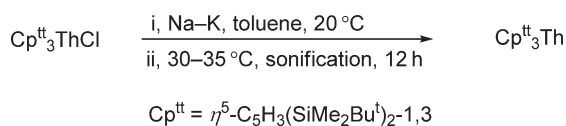
Treatment of  $(\text{C}_5\text{H}_4\text{Me})_3\text{UBu}^t$  with Lewis bases ( $\text{L} = \text{PMe}_3, \text{THF}, \text{Bu}^t\text{CN}, \text{EtNC}, \text{Bu}^t\text{NC}$ ) led to the reduced uranium(III) base derivatives  $(\text{MeC}_5\text{H}_4)_3\text{U}(\text{L})$  (Scheme 15).<sup>49</sup>



Scheme 14



Scheme 15



Scheme 16

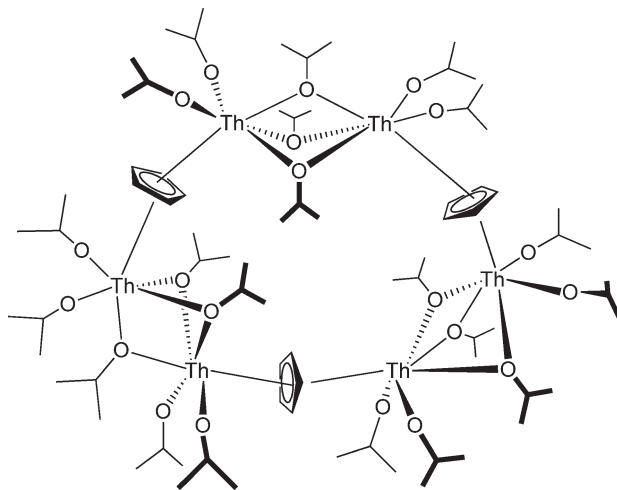
A remarkable achievement was the synthesis and characterization of tris(cyclopentadienyl)thorium(III) complexes. The homoleptic dark blue, crystalline (disubstituted-cyclopentadienyl)thorium(III) complexes  $[\text{C}_5\text{H}_3(\text{SiMe}_2\text{R})_{2-1,3}]_3\text{Th}$  ( $\text{R} = \text{Me}, \text{Bu}^t$ ) were obtained in good yield from the appropriate tris(cyclopentadienyl)thorium(IV) chloride by treatment with an excess of Na–K alloy in toluene at 20–35 °C with sonication (Scheme 16). The complex with  $\text{R} = \text{Me}$  is also accessible by a similar reduction of  $\text{Cp}^{\text{t}}_2\text{ThCl}_2$ .<sup>50</sup>

#### 4.02.5.2 CpAnX<sub>3</sub> and Cp<sub>2</sub>AnX<sub>2</sub> Compounds

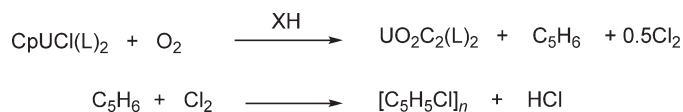
The mono(cyclopentadienyl)thorium(IV) compounds  $[(\text{Cp}^{\text{'''}}\text{ThCl}_3)_2\text{NaCl}(\text{OEt}_2)]_2$  and  $\text{Cp}^{\text{'''}}\text{ThCl}_3(\text{PMDETA})$  ( $\text{Cp}^{\text{'''}} = \text{C}_5\text{H}_2(\text{SiMe}_3)_{3-1,2,4}$ ;  $\text{PMDETA} = \text{MeN}(\text{CH}_2\text{CH}_2\text{NMe}_2)_2$ ) were synthesized by reaction of  $\text{ThCl}_4$  with  $\text{NaCp}^{\text{'''}}$  or  $\text{NaCp}^{\text{'''}}$  (PMDETA). The structure of  $[(\text{Cp}^{\text{'''}}\text{ThCl}_3)_2\text{NaCl}(\text{OEt}_2)]_2$  is tetranuclear (two Th and two Na atoms) and contains eight  $\mu_2$ - and two  $\mu_3$ -bridging chloride ligands. Each thorium atom adopts a distorted octahedral arrangement in which Th is coordinated by a  $\text{Cp}^{\text{'''}}$  and one triply bridging chloride ligand in axial positions and by four  $\mu_2$ -bridging chlorides in equatorial positions.<sup>51</sup>

The monocyclopentadienyl Th complex  $[\text{CpTh}_2(\text{OPr}^i)_7]_3$  was synthesized by the reaction between  $\text{ThBr}_4(\text{THF})_4$  and 1 equiv. of  $\text{TiCp}$  in THF followed by addition of 3 equiv. of  $\text{KOPr}^i$  to the mixture. The hexanuclear complex has a cyclic structure in which three binuclear  $[\text{CpTh}_2(\text{OPr}^i)_7]$  units are linked together by bridging ( $\mu\text{-}\eta^5\text{:}\eta^5$ )-cyclopentadienyl ligands. Each thorium is coordinated by an  $\eta^5$ -cyclopentadienyl ring, three bridging and two terminal *i*-propoxide ligands to give a distorted octahedral geometry (Scheme 17).<sup>52</sup>

Mono(cyclopentadienyl)uranium(IV) complexes can also be stabilized by  $\beta$ -diketonate and certain alkoxide ligands, as shown by the synthesis of the series  $\text{CpUX}_3$  with  $\text{X} = \text{CH}_3\text{C}(\text{O})\text{CHC}(\text{O})\text{CF}_3$ ,  $\text{C}_4\text{H}_3\text{SC}(\text{O})\text{CHC}(\text{O})\text{CF}_3$ ,  $\text{CF}_3\text{C}(\text{O})\text{CHC}(\text{O})\text{CF}_3$ ,  $\text{C}_3\text{HF}_6\text{O}$ , and  $\text{C}_3\text{H}_3\text{F}_4\text{O}$ . In a similar manner, a bis(cyclopentadienyl)uranium(IV) complex with a fluorinated diketonate ligand,  $\text{Cp}_2\text{U}[\text{C}_4\text{H}_3\text{SC}(\text{O})\text{CHC}(\text{O})\text{CF}_3]_2$ , has been prepared.<sup>53</sup> Monocyclopentadienyl uranium(IV) complexes of the type  $\text{CpUCl}_3(\text{L})_2$  ( $\text{L} = \text{THF}, (\text{Bu}^n\text{O})_3\text{P}=\text{O}$ ) react with molecular oxygen at 298 K in organic solvents to give uranyl dichloride complexes  $\text{UO}_2\text{Cl}_2(\text{L})_2$  and free cyclopentadiene (Scheme 18,  $\text{XH} = \text{solvent}$



Scheme 17



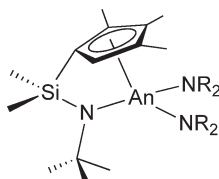
Scheme 18

or metalorganic compound as proton source). The latter was easily halogenated under the reaction conditions to give polymeric products. Possible routes for the transformation of the cyclopentadienyl ligand have been proposed.<sup>54</sup>

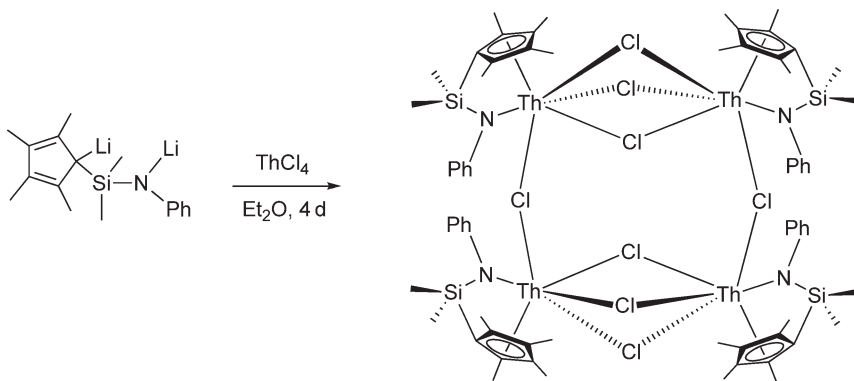
Constrained-geometry monocyclopentadienyl actinide complexes  $[\text{Me}_2\text{Si}(\text{C}_5\text{Me}_4)(\text{NBu}^t)]\text{An}(\text{NRR}^1)_2$  (Scheme 19, An = Th, U; R = R<sup>1</sup> = Me; R = Me, R<sup>1</sup> = Et; R = R<sup>1</sup> = Et) were synthesized in high yields and excellent purity, and  $[\text{Me}_2\text{Si}(\text{C}_5\text{Me}_4)(\text{NBu}^t)]\text{U}(\text{NMe}_2)_2$  was structurally characterized by an X-ray analysis.<sup>55</sup>

Starting from  $\text{ThCl}_4$ , two new thorium complexes, a tetramer of  $[\{\text{Me}_2\text{Si}(\text{C}_5\text{Me}_4)(\text{NPh})\}\text{ThCl}]_4$  (Scheme 20) and a dimer of  $[\text{Li}(\text{Et}_2\text{O})_2\{\text{Me}_2\text{Si}(\text{C}_5\text{Me}_4)(\text{NBu}^t)\}\text{ThCl}_3]_2$  (Scheme 21) have been synthesized and structurally characterized.<sup>56</sup>

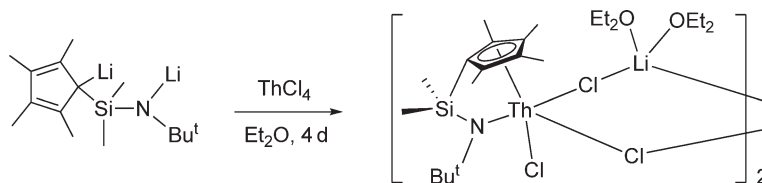
Methyl derivatives of monocyclopentadienyl hydro-tris(pyrazolyl)borate uranium complexes  $\text{CpUCl}_{2-x}\text{Me}_x\text{L}^*$  ( $\text{L}^* = \text{HB}(3,5\text{-Me}_2\text{pz})_3$ ,  $x = 1, 2$ ) were prepared by the reaction of  $\text{CpUCl}_2\text{L}^*$  with appropriate amounts of MeLi in toluene (Scheme 22).<sup>27</sup>



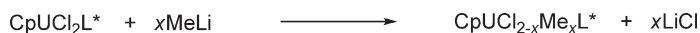
Scheme 19



Scheme 20



Scheme 21



Scheme 22

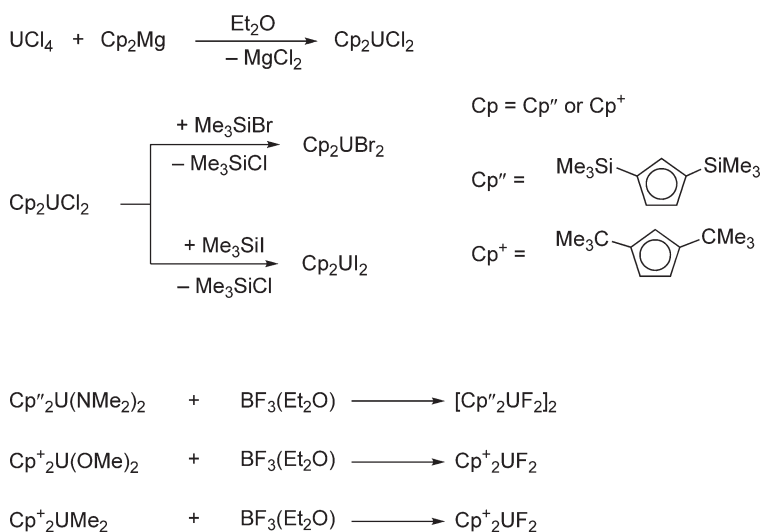
A series of monocyclopentadienyl uranium borohydrides,  $\text{Cp}'\text{U}(\text{BH}_4)_3$  ( $\text{Cp}' = \text{Cp}$ ,  $\text{C}_5\text{H}_4\text{PPh}_2$ ,  $\text{C}_5\text{Me}_4\text{PPh}_2\cdot\text{BH}_3$ ,  $\text{C}_5\text{H}_4\text{PPh}_2\cdot\text{BH}_3$ ,  $\text{C}_5\text{Me}_4\text{H}$ ,  $\text{C}_5\text{Me}_4\text{PPh}_2$ ), was synthesized and characterized by  $^1\text{H}$  and  $^{11}\text{B}$  NMR spectroscopy. A correlation between the electronic density around the uranium and the chemical shifts of the complying nuclei were studied. The shift ( $\delta$ , ppm) of the  $\text{BH}_4$  groups for both the  $^1\text{H}$  and  $^{11}\text{B}$  nuclei was found to increase in the series  $\text{Cp}^* < \text{C}_5\text{Me}_4\text{H} < \text{C}_5\text{Me}_4\text{PPh}_2 < \text{Cp}$ ,  $\text{C}_5\text{H}_4\text{PPh}_2 < \text{C}_5\text{Me}_4\text{PPh}_2\cdot\text{BH}_3 < \text{C}_5\text{H}_4\text{PPh}_2\cdot\text{BH}_3$ .<sup>57</sup>

The bulky 1,3-bis(trimethylsilyl)cyclopentadienyl ligand has proved to be very useful in organoactinide chemistry. Synthetic routes to  $\text{Cp}''_2\text{MCl}_2$  ( $\text{M} = \text{Th}$  or  $\text{U}$ ) and  $\text{Cp}''_2\text{UX}_2$  ( $\text{X} = \text{Br}$ ,  $\text{I}$ , or  $\text{BH}_4$ ) have been developed. The complexes  $\text{Cp}''_2\text{MCl}_2$  and  $\text{Cp}''_2\text{UX}_2$  ( $\text{X} = \text{Br}$  or  $\text{BH}_4$ ) are monomeric, isostructural, and have a typical bis(cyclopentadienyl)actinide(IV) halide bent-sandwich structure. The iodo complex  $\text{Cp}''_2\text{UI}_2$  is also monomeric but has non-equivalent  $\eta\text{-C}_5\text{H}_3(\text{SiMe}_3)_2$ -1,3 and iodide ligands.  $^1\text{H}$  and  $^{11}\text{B}$  NMR investigations of  $\text{Cp}''_2\text{U}(\text{BH}_4)_2$  complexes revealed fluxional processes for these compounds in solution.<sup>58</sup> The same synthetic approach was used for the preparation of new bis(cyclopentadienyl)thorium(IV) compounds  $\text{Cp}_2''' \text{ThCl}_2(\text{OEt}_2)$ ,  $\text{Cp}_2''' \text{ThCl}_2$ ,  $\text{Cp}_2'' \text{ThCl}_2$ ,  $\text{Cp}_2'' \text{ThCl}_2(\text{DMPE})$ ,  $\text{Cp}_2'' \text{Th}(\text{Cl})[\text{CH}(\text{SiMe}_3)_2]$  and  $\text{Cp}_2'' \text{Th}(\text{acac})\text{Cl}$  ( $\text{Cp}''' = \text{C}_5\text{H}_2(\text{SiMe}_3)_3$ -1,2,4;  $\text{Cp}_2'' = \text{C}_5\text{H}_3(\text{SiMe}_2\text{Bu}^t)_2$ -1,3;  $\text{DMPE} = (\text{Me}_2\text{PCH}_2)_2$  and  $\text{acacH} = \text{MeC}(\text{O})\text{CH}_2\text{C}(\text{O})\text{Me}$ ). The complexes  $\text{Cp}_2''' \text{ThCl}_2(\text{OEt}_2)$  and  $\text{Cp}_2''' \text{ThCl}_2$ , were obtained by reaction of  $\text{ThCl}_4$  and  $\text{LiCp}'''$  in  $\text{Et}_2\text{O}$  followed by sublimation of the evaporated reaction mixture in vacuo. Thorium complexes with the  $\text{C}_5\text{H}_3(\text{SiMe}_2\text{Bu}^t)_2$ -1,3 ( $= \text{Cp}''$ ) ligand have been prepared;  $\text{Cp}_2'' \text{ThCl}_2(\text{dmpe})$  (disordered) and  $\text{Cp}_2'' \text{Th}(\text{Cl})\text{CH}(\text{SiMe}_3)_2$  were studied by X-ray diffraction. In the crystal structure of  $\text{Cp}_2'' \text{Th}(\text{Cl})\text{CH}(\text{SiMe}_3)_2$ , the thorium has a distorted tetrahedral environment formed by two  $\text{Cp}''$  ring centroids, the carbon atom of the  $\text{CH}(\text{SiMe}_3)_2$  ligand and one chloride.<sup>51</sup>

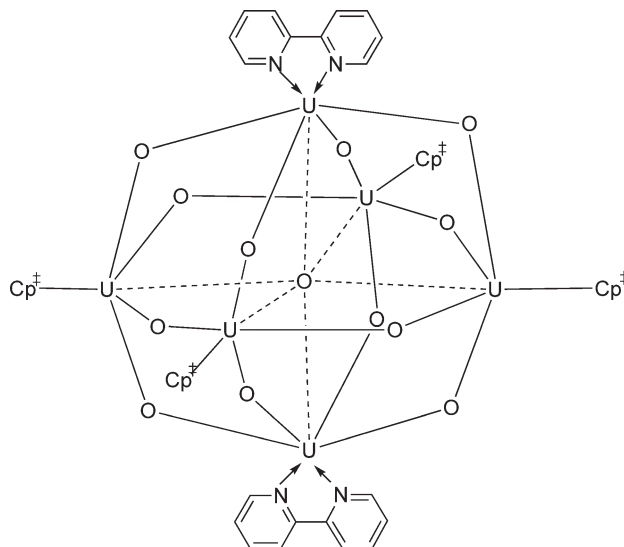
1,2-Di-*t*-butylcyclopentadienyllithium has been used to prepare bis(1,2-di-*t*-butylcyclopentadienyl)uranium dichloride and the corresponding compounds of titanium and zirconium for comparison. The bent metallocene structures of these compounds have been confirmed by X-ray crystallography and illustrate that the 1,2-di-*t*-butylcyclopentadienyl ligands are arranged with all four *t*-butyl groups in the open part of the wedge between the two canted cyclopentadienyl rings, but that steric interactions between the substituents afford a conformationally dictated  $C_2$  symmetry for the molecules.<sup>59</sup> Detailed studies on substituted-bis(cyclopentadienyl) complexes of U(IV) have been carried out.<sup>41,42,60</sup> Besides common analytical methods variable-temperature NMR determinations and EXAFS studies were used to characterize the monomeric and dimeric complexes as well as their dynamic behavior. High-yield preparations of the uranium metallocenes  $\text{Cp}''_2\text{UCl}_2$  and  $\text{Cp}^+_2\text{UCl}_2$  ( $\text{Cp}^+ = \text{C}_5\text{H}_3\text{Bu}^t$ -1,3) have been developed from the reaction of  $\text{UCl}_4$  and the corresponding magnesocenes  $\text{Cp}''_2\text{Mg}$  and  $\text{Cp}^+_2\text{Mg}$  in diethyl ether.<sup>60</sup> The chloride ligands were exchanged with either  $\text{Me}_3\text{SiBr}$  or  $\text{Me}_3\text{SiI}$  to give the uranium metallocene bromides,  $\text{Cp}''_2\text{UBr}_2$  and  $\text{Cp}^+_2\text{UBr}_2$  or iodides,  $\text{Cp}''_2\text{UI}_2$  and  $\text{Cp}^+_2\text{UI}_2$  (Scheme 23).

The corresponding fluorides  $[\text{Cp}''_2\text{UF}_2]_2$  and  $\text{Cp}^+_2\text{UF}_2$  were prepared by the reaction of  $\text{BF}_3\cdot\text{OEt}_2$  with  $\text{Cp}''_2\text{U}(\text{NMe}_2)_2$ ,  $\text{Cp}^+_2\text{U}(\text{OMe})_2$ , or  $\text{Cp}^+_2\text{UMe}_2$ . Crystal structure determinations show monomeric structures for  $\text{Cp}''_2\text{UCl}_2$ ,  $\text{Cp}^+_2\text{UCl}_2$ ,  $\text{Cp}''_2\text{UMe}_2$ ,  $\text{Cp}^+_2\text{UF}_2$  and a dimeric one for  $[\text{Cp}''_2\text{UF}_2]_2$ . The idealized symmetry of the monomers  $\text{Cp}''_2\text{UX}_2$ ,  $\text{Cp}^+_2\text{UCl}_2$  was found to be  $C_{2v}$  when  $\text{X} = \text{F}$ ,  $\text{Cl}$ , or  $\text{Br}$  and  $C_2$  when  $\text{X}$  is  $\text{I}$  or  $\text{Me}$ ; in the dimer, the idealized symmetry is  $C_2$ . The preferences can be rationalized by intramolecular and intermolecular steric effects. The solution ring conformation and intramolecular exchange process have been studied by variable-temperature  $^1\text{H}$  NMR spectroscopy which showed that a monomer–dimer equilibrium is present in solution of both difluoride complexes  $(\text{Cp}''_2\text{UF}_2)_2$  and  $\text{Cp}^+_2\text{UF}_2$ .<sup>41,42,60</sup> The reaction of the uranium(IV) triflate  $\text{U}(\text{OTf})_4$  ( $\text{OTf} = \text{OSO}_2\text{CF}_3$ ) with 2 equiv. of  $\text{KCp}$  afforded a mixture of  $\text{Cp}_3\text{U}(\text{OTf})$  and  $\text{Cp}_2\text{U}(\text{OTf})_2$  in a ratio of 73:27. Thus, pure  $\text{Cp}_2\text{U}(\text{OTf})_2$  could not be obtained by this synthetic route.<sup>61</sup>

The synthesis and structural characterization of the first uranium cluster containing an isopolyoxometalate core has been achieved. Reduction of  $(\text{C}_5\text{H}_2\text{Bu}^t)_3$ -1,2,4) $_2\text{UCl}_2$  with 2 equiv. of  $\text{KC}_8$  in THF, followed by addition of 2 equiv. of pyridine *N*-oxide was conducted in an attempt to produce the organometallic dioxo species  $(\text{C}_5\text{H}_2\text{Bu}^t)_3$ -1,2,4) $_2\text{UO}_2$ . However, the cluster compound  $(\text{C}_5\text{H}_2\text{Bu}^t)_3$ -1,2,4) $_4\text{U}_6\text{O}_{13}(\text{bipy})_2$  ( $\text{py} = \text{pyridine}$ ) was isolated as the main product (54% yield) from this reaction. In the molecular structure, six uranium atoms are arranged in approximate octahedral symmetry, with an interstitial  $\mu_6$ -oxo group situated in the center of the cluster. Twelve other oxo ligands form  $\mu_2$ -O bridging interactions to uranium centers around the cluster framework to furnish the  $\text{U}_6\text{O}_{13}$  core that mimics the isopolyoxometalate Lindqvist structure (Scheme 24).<sup>62,62a</sup>



Scheme 23



Scheme 24

The chemistry of organoactinide complexes containing chelating phosphoylide ligands has been further explored. The complex  $\text{Cp}_2\text{Th}[(\text{CH}_2)_2\text{PPh}_2]_2$  was obtained by the reaction of  $\text{Cp}_3\text{ThCl}$  with  $\text{Li}[(\text{CH}_2)_2\text{PPh}_2]$ . However, as was previously reported, the analogous reaction between  $\text{Cp}_3\text{UCl}$  and  $\text{Li}[(\text{CH}_2)_2\text{PPh}_2]$  led to  $\text{Cp}_3\text{U}=\text{CHPPh}_2\text{Me}$ . In  $\text{Cp}_2\text{Th}[(\text{CH}_2)_2\text{PPh}_2]_2$  the thorium is coordinated by two Cp rings and two bidentate ylide chelates. The Th atom has a distorted tetrahedral arrangement. The Th-C(CH<sub>2</sub>) bond lengths are 2.77(2) and 2.67(1) Å.<sup>63</sup> The organouranium(IV)triflate complex was prepared by protonation of an amide precursor with pyridinium triflate.<sup>64</sup>

The synthesis and reactivity of mono(diphenylphosphinocyclopentadienyl)uranium tris(borohydrides),  $\text{C}_5\text{R}_4\text{PPh}_2\text{U}(\text{BH}_4)_3$  (R = H or Me) and of their borane adducts has been reported. The reactivity of the monocyclopentadienyl complex  $(\text{C}_5\text{H}_4\text{PPh}_2)\text{U}(\text{BH}_4)_3$  and of its borane adduct  $(\text{C}_5\text{H}_4\text{PPh}_2\cdot\text{BH}_3)\text{U}(\text{BH}_4)_3$  strongly suggests that in solution these complexes are in equilibrium with the bis(cyclopentadienyl) complexes  $(\text{C}_5\text{H}_4\text{PPh}_2)_2\text{U}(\text{BH}_4)_2$ ,  $(\text{C}_5\text{H}_4\text{PPh}_2\cdot\text{BH}_3)_2\text{U}(\text{BH}_4)_2$ , and  $\text{U}(\text{BH}_4)_4$ , which is the most reactive species in such systems. Both species rearrange in the presence of neutral ligands and are only characterizable in solution. The analogous





Scheme 25



Scheme 26

tetramethylcyclopentadienyl compound  $(\text{C}_5\text{Me}_4\text{PPh}_2\cdot\text{BH}_3)\text{U}(\text{BH}_4)_3$ , a model of monolinked bimetallic complexes, is stable and has been isolated (Scheme 25).<sup>65</sup>

The successful synthesis of the stable half-metallocene uranium tris(borohydride),  $(\text{C}_5\text{HPr}^i_4)\text{U}(\text{BH}_4)_3$ , was achieved by employing the sterically encumbered tetra(*i*-propyl)cyclopentadienyl ligand (Scheme 26).<sup>66</sup>

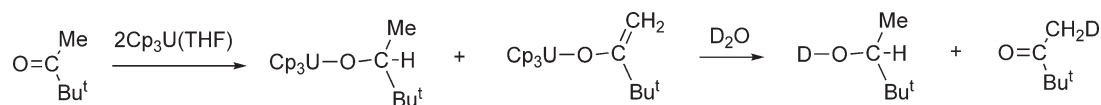
#### 4.02.5.3 $\text{Cp}_3\text{AnX}$ and $\text{Cp}_3\text{AnX(L)}$ Compounds

The electronic structure of the alkoxide complexes  $\text{Cp}_3\text{U(OR)}$  and  $\text{Cp}_3\text{Th(OR)}$  has been investigated by He(I) and He(II) UV photoelectron spectroscopy combined with SCF  $X\alpha$ -DVM calculations. Full relativistic Dirac–Slater calculations were also carried out for the thorium complexes.<sup>67</sup> Comparative relativistic effective core potential *ab initio* calculations have been reported for both Th(IV) and U(IV)  $\text{Cp}_3\text{AnL}$  ( $\text{L} = \text{Me}, \text{BH}_4$ ) complexes.<sup>68</sup>

The reaction of  $(\text{C}_5\text{H}_4\text{Me})_3\text{UBu}^t$  with  $\text{C}_6\text{F}_6$  or  $\text{PhCF}_3$  in toluene yielded  $(\text{C}_5\text{H}_4\text{Me})_3\text{UF}$  in quantitative yields as the first example of intermolecular C–F activation of a saturated fluorocarbon by a neutral *f*-element complex.<sup>69</sup> Metathesis reactions between  $\text{AnCl}_4$  ( $\text{An} = \text{Th}, \text{U}$ ) have been employed for the preparation of the tris(tetramethylcyclopentadienyl) derivatives  $(\text{C}_5\text{Me}_4\text{H})_3\text{An}$ .<sup>70</sup> The first organouranium(IV) triflates, including  $\text{Cp}_3\text{U(OTf)}$  ( $\text{OTf} = \text{OSO}_2\text{CF}_3$ ), have been prepared by protonation of amide or alkyl precursors with pyridinium triflate. The crystal structure of  $\text{Cp}_3\text{U(OTf)(CNBu}^t\text{)}$  was determined.<sup>64</sup>  $\text{Cp}_3\text{U(OTf)}$  is also accessible from  $\text{U(OTf)}_4$  and  $\text{KCp}$ .<sup>61</sup> The same authors also prepared the cationic tris(cyclopentadienyl)uranium(IV) complex  $[\text{Cp}_3\text{U(THF)}][\text{BPh}_4]$  by protonolysis of the correspondent neutral amide  $\text{Cp}_3\text{U(NEt}_2\text{)}$  with  $[\text{NHEt}_3][\text{BPh}_4]$ .<sup>71</sup> The synthesis and characterization of tris(cyclopentadienyl)uranium(IV) complexes with fluorinated ligands  $\text{Cp}_3\text{U(L)}$  ( $\text{L} = \text{CF}_3\text{C(O)CHC(O)CF}_3^-$ ,  $\text{MeC(O)CHC(O)CF}_3^-$ ,  $\text{C}_4\text{H}_3\text{SC(O)CHC(O)CF}_3^-$ ) has been reported.<sup>53</sup> Reactions of saturated ketones  $\text{RC(O)CH}_2\text{R}^1$  with the trivalent uranium complex  $\text{Cp}_3\text{U(THF)}$  gave equimolar mixtures of the U(IV) alkoxide derivatives  $\text{Cp}_3\text{UOCHR(CH}_2\text{R}^1\text{)}$  and  $\text{Cp}_3\text{UOCR(=CHR}^1\text{)}$ . The hydrolysis of the products with  $\text{D}_2\text{O}$  afforded the *O*-deuterated pinacolyl alcohol and the pinacolone, respectively (Scheme 27).<sup>72</sup>

The geometry of  $\text{Cp}_3\text{Np(OPh)}$  has been compared with that of the isostructural uranium analog. The molecular structure consists of one Np atom coordinated by the O atom of the phenoxide and by three  $\eta^5$ -coordinated cyclopentadienyl rings. If the coordination polyhedron is considered to be formed by the O atom and the centres of the cyclopentadienyl rings, the coordination around the Np atom displays approximate  $\text{C}_{3v}$  symmetry, with the O atom at the apex and the cyclopentadienyl rings at the base of a flattened tetrahedron. Thus the  $\text{Cp}_3\text{MY}$  geometry is maintained in this complex; the Cp–Np–Cp angles are nearly identical and significantly smaller than  $109^\circ$ . The deviation of the structure from a regular tetrahedron is also shown by the distance of the Np atom from the plane defined by the centers of the three cyclopentadienyl rings. If one assumes tetrahedral geometry around the Np atom and an average Np to ring-center distance of  $2.47(1) \text{ \AA}$ , then the Np atom should be located  $0.823 \text{ \AA}$  above the plane. The distance in the compound is  $0.452(4) \text{ \AA}$  and is a measure for the trigonal distortion from tetrahedral geometry.<sup>73</sup>

The U(IV) hydroxo complexes  $(\text{C}_5\text{H}_4\text{SiMe}_3)_3\text{UOH}$  and  $(\text{C}_5\text{H}_4\text{Bu}^t)_3\text{UOH}$  have been prepared either by controlled hydrolysis of the corresponding hydrides or by treatment of the cationic compounds  $[(\text{C}_5\text{H}_4\text{R})_3\text{U}][\text{BPh}_4]$  ( $\text{R} = \text{SiMe}_3, \text{Bu}^t$ ) with sodium hydroxide. Further reaction of  $(\text{C}_5\text{H}_4\text{SiMe}_3)_3\text{UOH}$  with  $(\text{C}_5\text{H}_4\text{SiMe}_3)_3\text{UH}$  yielded the  $\mu$ -oxo



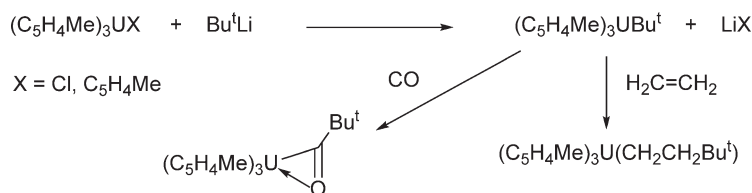
Scheme 27

derivative  $[(C_5H_4SiMe_3)_3U]_2(\mu-O)$ , and thermolysis of the hydroxo complexes afforded the trinuclear compounds  $[(C_5H_4SiMe_3)_2U(\mu-O)]_3$  and  $[(C_5H_4Bu^t)_2U(\mu-O)]_3$ , of which the  $C_5H_4SiMe_3$  derivative was structurally characterized.<sup>74</sup> Oxidation of  $Cp_3U^{III}(THF)$  with oxygen in THF afforded the linear-bridged complex  $[Cp_3U]_2(\mu-O)$ . Three cyclopentadienyl rings are  $\eta^5$ -bonded to each uranium atom to form a distorted tetrahedron with one bridging oxygen atom. The U–O–U angle is  $180^\circ$  with the oxygen atom located on a center of inversion. The U–O distance, 2.0881(4) Å, is among the shortest ever observed. The temperature-dependent paramagnetic susceptibility of the compound was measured in the temperature range between 4.2 and 300 K and was discussed in comparison with the magnetic susceptibilities of  $Cp_3UOH$ ,  $Cp_3USH$ , and  $(\mu-S)[Cp_3U]_2$ . The magnetic moment of the  $\mu-O$  bridged complex is remarkably lower than the magnetic moment of the OH compound. From the low magnetic moment and the absence of any indication for a temperature-independent paramagnetic behavior at low temperatures, as well as from the slight field dependence of the susceptibility at low temperatures, it was suggested that a slight long-range  $U \cdots U$  magnetic interaction via the bridging oxygen atom within the molecule is present.<sup>75</sup> The “absolute” bond disruption enthalpies  $D(U-S)$  for the formation of the organouranium(IV) thiolates  $Cp'_3USET$  from  $Cp'_3U$  derivatives ( $Cp' = Cp, Cp^*, C_9H_7$ ) and  $EtSSEt$  have been determined by batch-titration solution calometry in toluene.<sup>76</sup> Related tris(cyclopentadienyl)uranium(IV) thiolates were prepared by two principal methods, namely (i) substitution of the chloride group of  $Cp_3UCl$  by  $SR^-$  and (ii) oxidation of the trivalent precursors  $Cp_3U(THF)$ ,  $(C_5H_4SiMe_3)_3U$ , and  $(C_5H_4Bu^t)_3U$  with the disulfides  $RSSR$  ( $R = Me, Et, Pr^i, Bu^t$ , or  $Ph$ ). Similar treatment with  $MeSeSeMe$  afforded  $Cp_3USeMe$  and  $(C_5H_4SiMe_3)_3USeMe$ . The thiolate  $Cp_3USMe$  shows a U–S bond length of 2.695(4) Å, U–Cp(centroid) distances of 2.48(1) and 2.39(1) Å and U–S–C(Me) angle of  $107.2(5)^\circ$ . Several reactions of these complexes were reported, that is, cleavage of the U–S bond by acidic substrates or iodine, insertion of  $CS_2$  and  $CO_2$  into the U–S bond, and reduction to afford the corresponding U(III) anions. The synthesis, structure and reactivity of the thiolate compounds were compared with those of the alkoxide analogs.<sup>77</sup>

Various new mixed tris(cyclopentadienyl)thorium(IV) and uranium(IV) complexes have been reported. Three of these complexes were obtained as mixed tris(cyclopentadienyl)thorium(IV) complexes by treatment of  $Cp''_2ThCl_2$  and  $Cp^t_2ThCl_2$  with the lithium or potassium (cyclopentadienyl) reagent:  $Cp''_2(Cp^*)ThCl$ ,  $Cp^t_2(Cp^R)ThCl$ , and  $Cp^t_2(Cp^+)ThCl$  ( $Cp'' = C_5H_3(SiMe_3)_2-1,3$ ;  $Cp^R = C_5H_4CH(SiMe_3)_2$ ;  $Cp^t = C_5H_3(SiMe_2Bu^t)_2-1,3$ ;  $Cp^+ = C_5H_3Bu^t_2-1,3$ ). Other tris(cyclopentadienyl) thorium and uranium complexes were prepared by transmetalation between  $MCl_4$  and the corresponding lithium cyclopentadienyl derivatives.<sup>78</sup>

The crystal structure of  $Cp_3UNCS$  has been determined. The U–N bond lengths in this thiocyanate derivative is 2.34 Å.<sup>79</sup> The tertiary alkyl complex  $(MeC_5H_4)_3UBu^t$  was prepared by reaction of  $(C_5H_4Me)_3UX$  ( $X = Cl, C_5H_4Me$ ) with  $Bu^tLi$  in toluene (Scheme 28); it reacts with CO under 1 atm to give the uranium(IV) acyl complex  $(C_5H_4Me)_3U[C(O)Bu^t]$  and slowly with ethylene (210 psi pressure) to form the monoinsertion product  $(C_5H_4Me)_3U(CH_2CH_2Bu^t)$ . Treatment of various thorium complexes  $(C_5H_4Me)_3ThX$  ( $X = Cl, I, MeC_5H_4, O-2,6-Me_2C_6H_3$ ) with  $Bu^tLi$  in toluene led to intractable products only. However, the ionic complexes  $[(C_5H_4R)_3Th][BPh_4]$  ( $R = Me_3Si, Bu^t$ ) reacted with  $Bu^tLi$  to give the thorium hydrides  $(C_5H_4R)_3ThH$ .<sup>49</sup>

Metal–silicon bond disruption enthalpies have been measured for a series of metallocene complexes including  $Cp_3USi(SiMe_3)_3$ . This complex was synthesized by reaction of  $Cp_3UCl$  with  $LiSi(SiMe_3)_3(THF)_3$  in diethyl ether. The thermodynamic data were obtained by titration calorimetry with  $I_2$  (Scheme 29).<sup>80</sup>



Scheme 28



Scheme 29

$$D[\text{Cp}_3\text{U-Si}(\text{SiMe}_3)_3] = D[\text{Cp}_3\text{U-I}] + D[(\text{SiMe}_3)_3\text{Si-I}] + \Delta H_{\text{rxn}} - D[\text{I-I}]$$

(where  $\Delta H_{\text{rxn}} = -58(1) \text{ kcal mol}^{-1}$ )

Scheme 30

The resulting  $D[\text{Cp}_3\text{U-Si}(\text{SiMe}_3)_3]$  value of  $37(3) \text{ kcal mol}^{-1}$  was calculated from the equation shown in Scheme 30.<sup>80</sup>

The reactivity of U–H and U–C bonds in electron-poor tris(cyclopentadienyl)uranium complexes has been investigated. The compounds  $(\text{C}_5\text{H}_4\text{PPh}_2\cdot\text{BH}_3)_3\text{UX}$  ( $\text{X} = \text{Cl}, \text{Me}$ ) have been synthesized.<sup>81</sup> The series of new tris(cyclopentadienyl)uranium complexes also includes the borohydride derivatives  $\text{Cp}'_3\text{U}(\text{BH}_4)$  ( $\text{Cp}' = \text{Cp}, \text{C}_5\text{H}_4\text{PPh}_2, \text{C}_5\text{Me}_4\text{PPh}_2\cdot\text{BH}_3, \text{C}_5\text{H}_4\text{PPh}_2\cdot\text{BH}_3, \text{C}_5\text{Me}_4\text{H}, \text{C}_5\text{Me}_4\text{PPh}_2$ ).<sup>57,81</sup>

#### 4.02.5.4 $\text{Cp}_4\text{An}$ Compounds

The crystal structure of  $\text{Cp}_4\text{Th}$  has been investigated by single-crystal X-ray diffraction. The average Th–C(centroid) distance is  $2.606 \text{ \AA}$ .<sup>82</sup> Reactions of  $\text{Cp}_4\text{U}$  with CO and  $\text{CO}_2$  have been investigated. Interaction occurred by a migratory insertion mechanism of the small molecules into the uranium–carbon bond. Treatment of  $\text{Cp}_4\text{U}$  with CO in benzene afforded the binuclear complex  $[\text{Cp}_2\text{U}(\text{C}_5\text{H}_4\text{CO})]_2$  (Scheme 31).<sup>83</sup>

#### 4.02.5.5 Pentamethylcyclopentadienyl Compounds

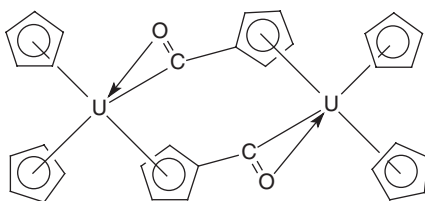
The pentamethylcyclopentadienyl ligand remains the most important ligand in organoactinide chemistry. It has been very successfully employed in the stabilization of novel organoactinide complexes and in organoactinide catalysis.

##### 4.02.5.5.1 $\text{Cp}^*\text{AnX}_2$ and $\text{Cp}^*_2\text{AnX}$ compounds

The synthesis and characterization of a series of mono(pentamethylcyclopentadienyl)uranium(III) complexes has been explored. The uranium(III) triiodide precursor  $\text{UI}_3(\text{THF})_4$  reacts at ambient temperature with 1 equiv. of sodium or potassium pentamethylcyclopentadienide in THF to form the monocyclopentadienyl complex(III)  $\text{Cp}^*\text{UI}_2(\text{THF})_3$  (Scheme 32).<sup>84</sup>

In the solid state the complex exhibits a *pseudooctahedral mer-, trans-*ligand geometry with the  $\text{Cp}^*$  ligand occupying one axial position. This monocyclopentadienide complex also provides a convenient entry into a variety of other monoring complexes of uranium(III). In the presence of excess pyridine, the coordinated THF ligands of  $\text{Cp}^*\text{UI}_2(\text{THF})_3$  were readily displaced to form the tris(pyridine) adduct  $\text{Cp}^*\text{UI}_2(\text{py})_3$ , which exhibits a *mer-, trans-*ligand geometry in the solid state similar to that of THF adduct.<sup>84</sup>

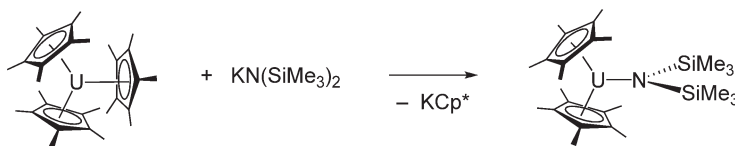
Oxidation of the sterically crowded complex  $\text{Cp}^*_3\text{U}$  provided access to  $[\text{Cp}^*_2\text{U}]_2(\mu\text{-O})$  as the first molecular trivalent uranium oxide. The U–O–U angle in this molecule is  $171.5(6)^\circ$ .<sup>85</sup> Reduction of the uranium(IV) thiolates



Scheme 31



Scheme 32



Scheme 33

$\text{Cp}^*_2\text{U}(\text{SR})_2$  ( $\text{R} = \text{Me}, \text{Pr}^i, \text{Bu}^t, \text{Ph}$ ) with sodium amalgam afforded the corresponding U(III) complexes  $\text{Na}[\text{Cp}^*_2\text{U}(\text{SR})_2]$  or the U(IV) sulfide  $\text{Na}[\text{Cp}^*_2\text{U}(\text{SBU}^t)(\text{S})]$ . C–S bond cleavage of a thiolate ligand was also observed during the thermal decomposition of  $\text{Na}[\text{Cp}^*_2\text{U}(\text{SPr}^i)_2]$ , whereas  $\text{Na}[\text{Cp}^*_2\text{U}(\text{SMe})_2]$  was transformed in refluxing THF into the thiametallacyclopropane complex  $\text{Na}[\text{Cp}^*_2\text{U}(\text{SMe})(\text{SCH}_2)]$ , resulting from C–H bond activation of a SMe group. The X-ray crystal structures of  $[\text{Na}(18\text{-crown-6})(\text{THF})_2][\text{Cp}^*_2\text{U}(\text{SPr}^i)_2]$ ,  $[\text{Na}(18\text{-crown-6})][\text{Cp}^*_2\text{U}(\text{SBU}^t)(\text{S})]$ , and  $[\text{Na}(18\text{-crown-6})(\text{THF})_2][\text{Cp}^*_2\text{U}(\text{SMe})(\text{SCH}_2)]$  have been determined.<sup>86</sup>

Metathesis of the iodide ligands in  $\text{Cp}^*\text{UI}_2(\text{THF})_3$  with 2 equiv. of  $\text{KN}(\text{SiMe}_3)_2$  afforded the bis(amido) complex  $\text{Cp}^*\text{U}[\text{N}(\text{SiMe}_3)_2]_2$ . An X-ray diffraction study of this molecule revealed that methyl groups from both amido ligands are involved in agostic interactions with the uranium(III) center.<sup>84</sup> More recently, the same compound has been obtained in nearly quantitative yield by reacting the sterically crowded  $\text{Cp}^*_3\text{U}$  with  $\text{KN}(\text{SiMe}_3)_2$  (Scheme 33).<sup>87</sup>

Whereas the mixed amide complex  $\text{U}(\text{NEt}_2)_2[\text{N}(\text{SiMe}_3)_2]_2$  reacts with  $[\text{NHEt}_3][\text{BPh}_4]$  in THF to give the cation  $[\text{U}(\text{NEt}_2)\{\text{N}(\text{SiMe}_3)_2\}_2]^+$ , the  $\text{Cp}^*$  complex  $\text{Cp}^*\text{U}[\text{N}(\text{SiMe}_3)_2]_2$  is inert toward  $[\text{NHEt}_3][\text{BPh}_4]$  but is protolyzed by  $\text{NH}_4[\text{BPh}_4]$  to afford the cationic complex  $[\text{Cp}^*_2\text{U}(\text{THF})_2][\text{BPh}_4]$  as an orange microcrystalline solid in 79% yield, the first cationic cyclopentadienyl compound of uranium(III). Its molecular structure was determined by X-ray diffraction.<sup>88</sup>

#### 4.02.5.5.2 $\text{Cp}^*_3\text{An}$ compounds

The first tris(pentamethylcyclopentadienyl) complex of uranium was synthesized in 50% yield by hydrogenation of tetramethylfulvene with  $\text{Cp}^*_2\text{UH}(\text{dmpe})$  (Scheme 34) and characterized by common analytical methods (IR,  $^1\text{H}$ ,  $^{13}\text{C}$  NMR, magnetic susceptibility and elemental analysis).<sup>89,89a</sup>

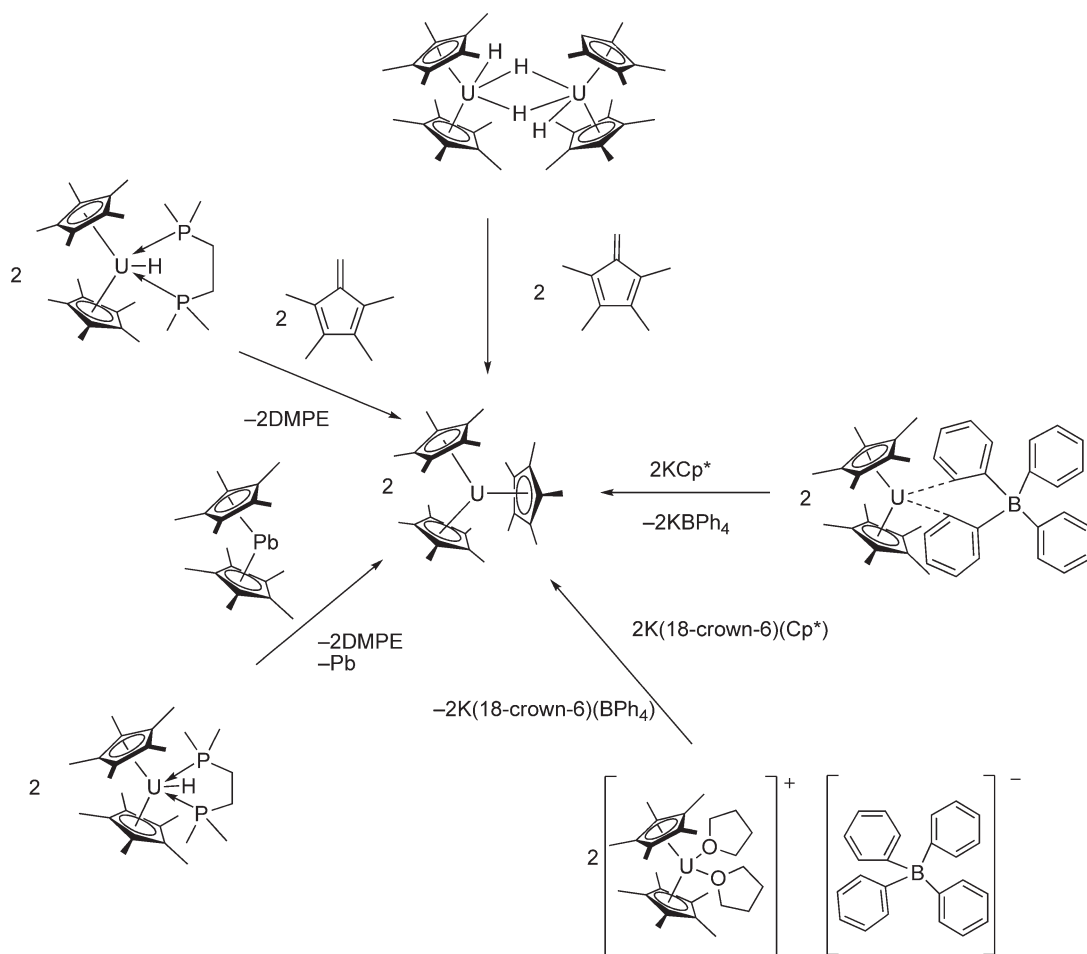
Crystals of  $\text{Cp}^*_3\text{U}$  and  $\text{Cp}^*_3\text{Sm}$  are isostructural. In the uranium complex, there are three different bond lengths with an average length of 2.84(4) Å, but the angles between the three  $\text{Cp}^*$  ligands are exactly 120°. The three  $\text{Cp}^*$  ligands are orientated in such a way that the steric interaction between them is minimized.<sup>89,89a</sup> More recently several new methods leading to the sterically crowded  $\text{Cp}^*_3\text{U}$  complex have been developed (Scheme 34), including (i) reaction of  $[\text{Cp}^*_2\text{U}(\mu\text{-H})_2]$  with tetramethylfulvene, (ii) reduction of  $\text{Cp}^*_2\text{Pb}$  with  $\text{Cp}^*_2\text{UH}(\text{dmpe})$ , (iii) reaction of  $[\text{Cp}^*_2\text{U}(\text{L})]^+$  ( $\text{L} = \text{THF}, \text{dmpe}$ ) with  $\text{K}(18\text{-crown-6})\text{Cp}^*$ , and (iv) reaction of  $[\text{Cp}^*_2\text{U}][\text{BPh}_4]$  with  $\text{KCp}^*$ .<sup>90</sup>

$\text{Cp}^*_3\text{U}$  reacts with  $\text{N}_2$  to give the first *f*-element complex binding a formally neutral  $\text{N}_2$  ligand end-on. Solutions of  $\text{Cp}^*_3\text{U}$  under  $\text{N}_2$  at 80 psi darken slightly and produce hexagonal crystals of  $\text{Cp}^*_3\text{U}(\eta^1\text{-N}_2)$ . The U–N( $\text{N}_2$ ) bond length in this spectacular molecule is 2.492(10) Å.<sup>91</sup> In a similar manner,  $\text{Cp}^*_3\text{U}$  reacts with CO to form the uranium carbonyl complex  $\text{Cp}^*_3\text{U}(\text{CO})$ , which shows a CO stretching frequency  $\nu_{\text{CO}} = 1922\text{ cm}^{-1}$  and a U–C(CO) distance of 2.485(9) Å.<sup>92</sup>

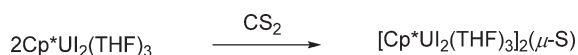
#### 4.02.5.5.3 Mono(pentamethylcyclopentadienyl) actinide(IV) compounds

Reactions of the monopositive actinide ions  $\text{An}^+$  with pentamethylcyclopentadiene,  $\text{HCp}^*$ , have been studied by mass spectrometry. This was the first study of the  $\text{An}^+/\text{HCp}^*$  reaction for  $\text{An}^+ = \text{Am}^+, \text{Cm}^+, \text{Bk}^+, \text{Cf}^+, \text{Es}^+$ . Each of the actinide ions reacted with  $\text{HCp}^*$  to produce  $[\text{AnCp}^*]^+ (+\text{H})$ , as well as additional products. Both  $\text{Cf}^+$  and  $\text{Es}^+$  have previously been found to be inert toward most alkenes, but efficiently reacted with  $\text{HCp}^*$  to induce (i) H-loss and  $[\text{AnCp}]^+$ , (ii)  $\text{H}_2$ -loss and  $[\text{An}(\text{C}_5\text{Me}_4\text{CH}_2)]^+$ , and (iii)  $\text{CH}_3$ -loss and  $[\text{An}(\text{C}_5\text{Me}_4\text{H})]^+$  ( $\text{An} = \text{Cf}, \text{Es}$ ). These were the first organoeinsteinium complexes derived from activation of an organic substrate. Secondary products included  $[\text{Cp}^*_2\text{An}]^+$  ( $\text{An} = \text{Am}, \text{Cm}, \text{Bk}, \text{Cf}, \text{Es}$ ), the compositions of which correspond to the metallocene sandwich complexes.<sup>93</sup>

The mono(pentamethylcyclopentadienyl) uranium(IV) sulfido complex  $[\text{Cp}^*\text{UI}_2(\text{THF})_3]_2(\mu\text{-S})$  was synthesized by the oxidation of  $\text{Cp}^*\text{UI}_2(\text{THF})_3$  with 1 or 2 equiv. of  $\text{CS}_2$  in toluene (Scheme 35).<sup>94</sup> After prolonged standing of a solution of  $[\text{Cp}^*\text{UI}_2(\text{THF})_3]_2(\mu\text{-S})$  in THF, crystals of  $\text{Cp}^*_3\text{U}_3\text{I}_3(\mu_3\text{-I})(\mu_3\text{-S})(\mu_2\text{-I})_3$  were obtained. X-ray structural characterization of the latter compound has shown that this is a triangular homometallic cluster, in which three U atoms are linked by one triply bridging sulfido ligand, three doubly bridging and one triply bridging iodide ligands.



Scheme 34

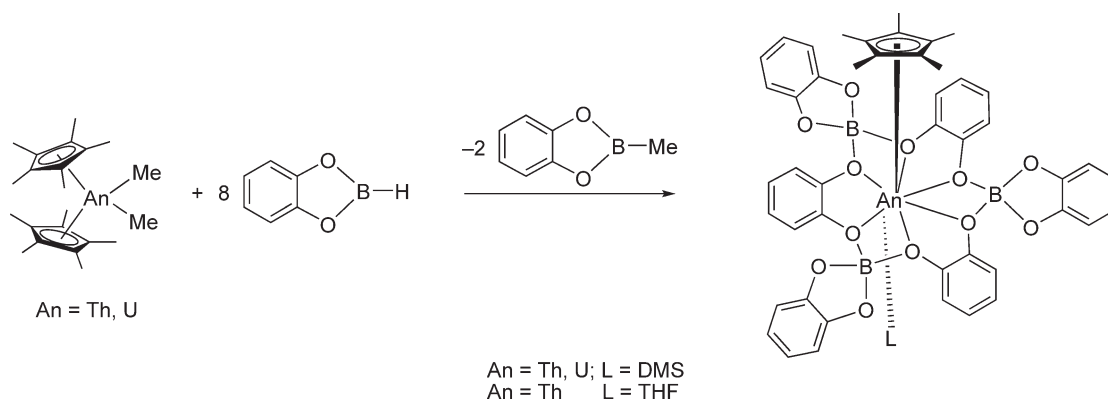


Scheme 35

Each uranium atom has a distorted octahedral geometry formed by coordination of one  $\text{Cp}^*$  ring, one  $\mu_3$ -sulfido ligand, two  $\mu_2$ -, one  $\mu_3$ - and one terminal iodide ligands. The average  $\text{U}-\text{C}(\text{Cp}^*)$  and  $\text{U}-\mu_3\text{-S}$  bond lengths are 2.71 and 2.75(2) Å respectively. The  $\text{U}-\text{I}(\text{term.})$  distances with an average value of 2.952(5) Å are shorter than the  $\text{U}-\mu_2\text{-I}$  distances with an average of 3.096(8) Å. The  $\text{U}-\mu_3\text{-I}$  distances were found to be significantly different for the three uranium atoms (3.240(5), 3.289(5), and 3.353(4) Å).<sup>94</sup>

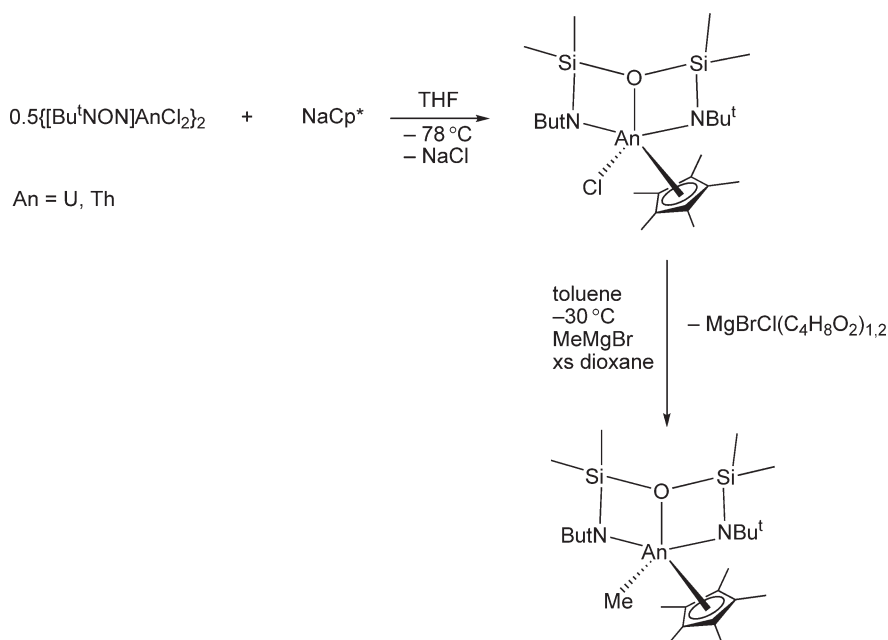
Unusual mono(pentamethylcyclopentadienyl)actinide complexes containing a 15-membered trianionic hexaaxo ligand built from catechol and catecholborate have been prepared and structurally characterized. As depicted in Scheme 36, the synthesis of these complexes has been achieved by reacting  $\text{Cp}^*_2\text{AnMe}_2$  ( $\text{An} = \text{Th}, \text{U}$ ) with an excess of catecholborane that contains 5% dimethylsulfide (DMS) in benzene at room temperature for 24 h. The DMS ligand could be replaced by THF.<sup>95</sup>

Amino(triamido)-pentamethylcyclopentadienyluranium and thorium complexes of the type  $(\text{C}_5\text{R}_5)\text{ML}$  ( $\text{M} = \text{U}, \text{Th}$ ;  $\text{R} = \text{H}, \text{Me}$ ,  $\text{L} = \text{N}(\text{CH}_2\text{CH}_2\text{NSiMe}_3)_3$ ) were prepared by reaction of the corresponding dimeric chlorides  $[\text{ML}(\text{Cl})]_2$  with the appropriate  $\text{Na}(\text{C}_5\text{R}_5)$  salts in THF. The complex  $\text{Cp}^*\text{UL}$  was characterized by single-crystal X-ray diffraction. In the structure, the uranium atom is coordinated by one  $\text{Cp}^*$  ring and four nitrogens of the  $\text{N}(\text{CH}_2\text{CH}_2\text{NSiMe}_3)_3$  ligand. The  $\text{U}-\text{Cp}^*(\text{cent.})$  distance is 2.58 Å while the  $\text{U}-\text{N}$  distances range from 2.25–2.264(15) Å. The complexes  $(\text{C}_5\text{R}_5)\text{ML}$  were found to be fluxional exhibiting apparent threefold symmetry on the NMR timescale in solution at room

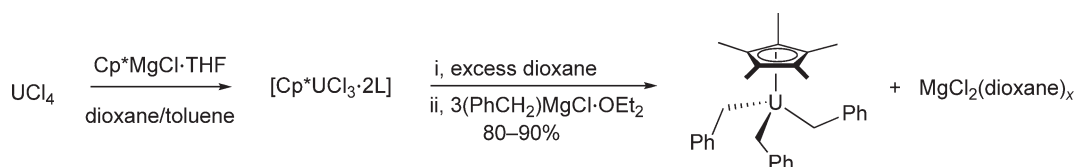


Scheme 36

temperature.<sup>96</sup> Interesting cationic mono(pentamethylcyclopentadienyl)uranium amido complexes have also been investigated. The uranium(v) complex  $[\text{Cp}^* \text{U}(\text{NMe}_2)_3(\text{THF})][\text{BPh}_4]$  was prepared by oxidation of the neutral tetravalent precursor  $\text{Cp}^* \text{U}(\text{NMe}_2)_3$  with  $\text{Ag}[\text{BPh}_4]$  in THF. The crystal structure of  $[\text{Cp}^* \text{U}(\text{NMe}_2)_3(\text{THF})][\text{BPh}_4]$  consists of discrete cation–anion pairs. In the cation  $[\text{Cp}^* \text{U}(\text{NMe}_2)_3(\text{THF})]^+$  the uranium atom is in a pseudotrigonal bipyramidal arrangement formed by the centroid of the  $\text{Cp}^*$  ring and an oxygen atom of THF in apical positions and three nitrogen atoms of the amide groups in equatorial positions.<sup>97</sup> The cationic uranium(IV) complex  $[\text{Cp}^* \text{U}(\text{NEt}_2)_2(\text{THF})_2][\text{BPh}_4]$  was obtained by protonolysis of the neutral amide precursor  $\text{Cp}^* \text{U}(\text{NEt}_2)_3$  with  $[\text{NEt}_3\text{H}][\text{BPh}_4]$ . In the structure of the cation  $[\text{Cp}^* \text{U}(\text{NEt}_2)_2(\text{THF})_2]^+$  the uranium atom is five-coordinated by one  $\text{Cp}^*$  ring, two nitrogen atoms of the amido groups and two oxygen atoms of solvating THF molecules. The geometry of the cation can be described as a distorted trigonal bipyramid with the  $\text{Cp}^*$  ring centroid and two nitrogen atoms of  $\text{NEt}_2$  groups in the equatorial and two oxygen atoms of the THF molecules in the axial positions.<sup>97</sup> Mono(pentamethylcyclopentadienyl)actinide complexes containing the doubly deprotonated diamidosilyl ether ligand  $(\text{Bu}^t\text{NHSiMe}_2)_2\text{O}^{2-}$  ( $[\text{Bu}^t\text{NON}]^{2-}$ ) have been prepared according to Scheme 37.<sup>31</sup>



Scheme 37



Scheme 38

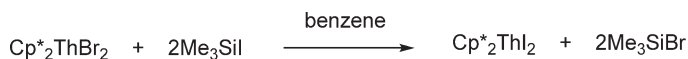
A high-yield one-pot synthesis of the tribenzyl complex  $\text{Cp}^*\text{U}(\text{CH}_2\text{Ph})_3$  has been developed (Scheme 38). It circumvents the isolation of  $\text{Cp}^*\text{UCl}_3$  and employs the commercially available reagent benzylmagnesium chloride. Dark brown  $\text{Cp}^*\text{U}(\text{CH}_2\text{Ph})_3$  can be isolated in typically 80–90% yield using this synthetic route. The reaction of  $\text{Cp}^*\text{U}(\text{CH}_2\text{Ph})_3$  with excess cyclopentadiene led to elimination of 2 equiv. of toluene and formation of  $\text{Cp}^*\text{Cp}_2\text{UCH}_2\text{Ph}$  (black crystals, 89%).<sup>98</sup>

#### 4.02.5.5.4 Bis(pentamethylcyclopentadienyl) actinide(IV), (V), and (VI) compounds

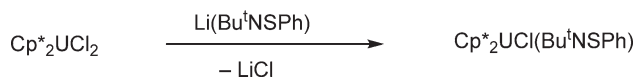
Detailed cyclic voltammetric and UV–VIS–near-IR electronic absorption spectral data have been published for a series of  $\text{Cp}^*_2\text{An}$  ( $\text{An} = \text{Th}, \text{U}$ ) complexes.<sup>99</sup> Bis(pentamethylcyclopentadienyl)thorium(IV) dibromide,  $\text{Cp}^*_2\text{ThBr}_2$ , has been prepared by reacting  $\text{ThBr}_4(\text{THF})_4$  with 2 equiv. of  $\text{Cp}^*\text{MgCl} \cdot \text{THF}$  and was structurally characterized.<sup>100</sup> The THF adduct  $\text{Cp}^*_2\text{ThBr}_2(\text{THF})$  was synthesized by reaction of  $\text{Cp}^*_2\text{ThCl}_2$  and  $\text{LiCp}^*$  and subsequent treatment of the product with  $\text{BBr}_3$ .<sup>51</sup> Bis(pentamethylcyclopentadienyl)thorium(IV) diiodide,  $\text{Cp}^*_2\text{ThI}_2$ , was synthesized from the dibromo derivative  $\text{Cp}^*_2\text{ThBr}_2$  using a slight excess of trimethylsilyl iodide as a halide exchange reagent (Scheme 39). The structurally characterized thorium complex  $\text{Cp}^*_2\text{ThI}_2$  exhibits the typical bent metallocene structure.<sup>101</sup>

The synthesis of the uranium(IV) triflate  $\text{Cp}^*_2\text{U}(\text{OTf})_2(\text{py})$  was achieved by protonation of amide or alkyl precursors with pyridinium triflate.<sup>64</sup> The uranium sulfimine derivative  $\text{Cp}^*_2\text{UCl}_2(\text{HNSPh}_2)$  was prepared by the reaction of  $\text{Cp}^*_2\text{UCl}_2$  with  $\text{HNSPh}_2$ . According to an X-ray analysis, the U atom is coordinated by two  $\text{Cp}^*$  rings, two chloride ligands and one nitrogen of the sulfimine ligand. Hydrolysis of  $\text{Cp}^*_2\text{UCl}_2(\text{HNSPh}_2)$  with  $\text{HNSPh}_2 \cdot \text{H}_2\text{O}$  led to crystals of the unusual mixed-valent U(IV)/U(V) complex  $[\text{Cp}^*(\text{Cl})(\text{HNSPh}_2)\text{U}(\mu_3\text{-O})(\mu_2\text{-O})_2\text{U}(\text{Cl})(\text{HNSPh}_2)_2]_2$ . This compound is a cluster formed by four co-planar uranium atoms, which are linked by two  $\mu_3$ - and four  $\mu_2$ -oxygen atoms. There are two types of uranium atoms in the cluster. Two uranium atoms are bound each to one  $\mu_3$ - and two  $\mu_2$ -oxygen atoms, one  $\text{Cp}^*$  ring, one chloride ligand and one  $\text{HNSPh}_2$  ligand to give a coordination number of 8. The two other uranium atoms in the cluster have the coordination number 7 caused by the coordination of one chloride ligand, one  $\mu_3$ - and two  $\mu_2$ -oxygen atoms and two  $\text{HNSPh}_2$  ligands to each metal atom.<sup>102</sup> Under different reaction conditions, the reaction of  $\text{Cp}^*_2\text{UCl}_2$  with  $\text{HNSPh}_2 \cdot \text{H}_2\text{O}$  in 1:1 stoichiometry produced  $\text{Cp}^*_2\text{UCl}(\text{OH})(\text{HNSPh}_2)$  as green crystals in good yield. This was the first structurally characterized *f*-element metallocene complex containing a terminal hydroxy ligand.<sup>103</sup> A related bis(pentamethylcyclopentadienyl) complex of uranium with a sulfenamido ligand has been prepared according to Scheme 40.<sup>104</sup>

Among the major achievements in recent organoactinide chemistry is the synthesis of the first high-valent organouranium complexes containing terminal monooxo functional groups. The precursors  $\text{Cp}^*_2\text{U}(\text{O}-2,6\text{-Pr}^i_2\text{C}_6\text{H}_3)(\text{THF})$  and  $\text{Cp}^*_2\text{U}(\text{N}-2,6\text{-Pr}^i_2\text{C}_6\text{H}_3)(\text{THF})$  were prepared by reaction of  $\text{Cp}^*_2\text{UI}(\text{THF})$  or  $\text{Cp}^*_2\text{UMe}_2$  with  $\text{K}(\text{O}-2,6\text{-Pr}^i_2\text{C}_6\text{H}_3)$  or  $\text{H}_2\text{N}-2,6\text{-Pr}^i_2\text{C}_6\text{H}_3$ , respectively, in THF. Reactions of  $\text{Cp}^*_2\text{U}(\text{O}-2,6\text{-Pr}^i_2\text{C}_6\text{H}_3)(\text{THF})$  and  $\text{Cp}^*_2\text{U}(\text{N}-2,6\text{-Pr}^i_2\text{C}_6\text{H}_3)(\text{THF})$  with  $\text{C}_5\text{H}_5\text{NO}$  afforded the novel oxo complexes  $\text{Cp}^*_2\text{U}(\text{O}-2,6\text{-Pr}^i_2\text{C}_6\text{H}_3)(\text{O})$  and  $\text{Cp}^*_2\text{U}(\text{N}-2,6\text{-Pr}^i_2\text{C}_6\text{H}_3)(\text{O})$ , which have both been structurally characterized by X-ray analyses (Scheme 41).<sup>105</sup>

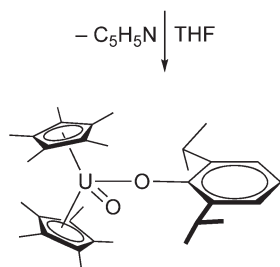
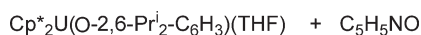


Scheme 39



Scheme 40

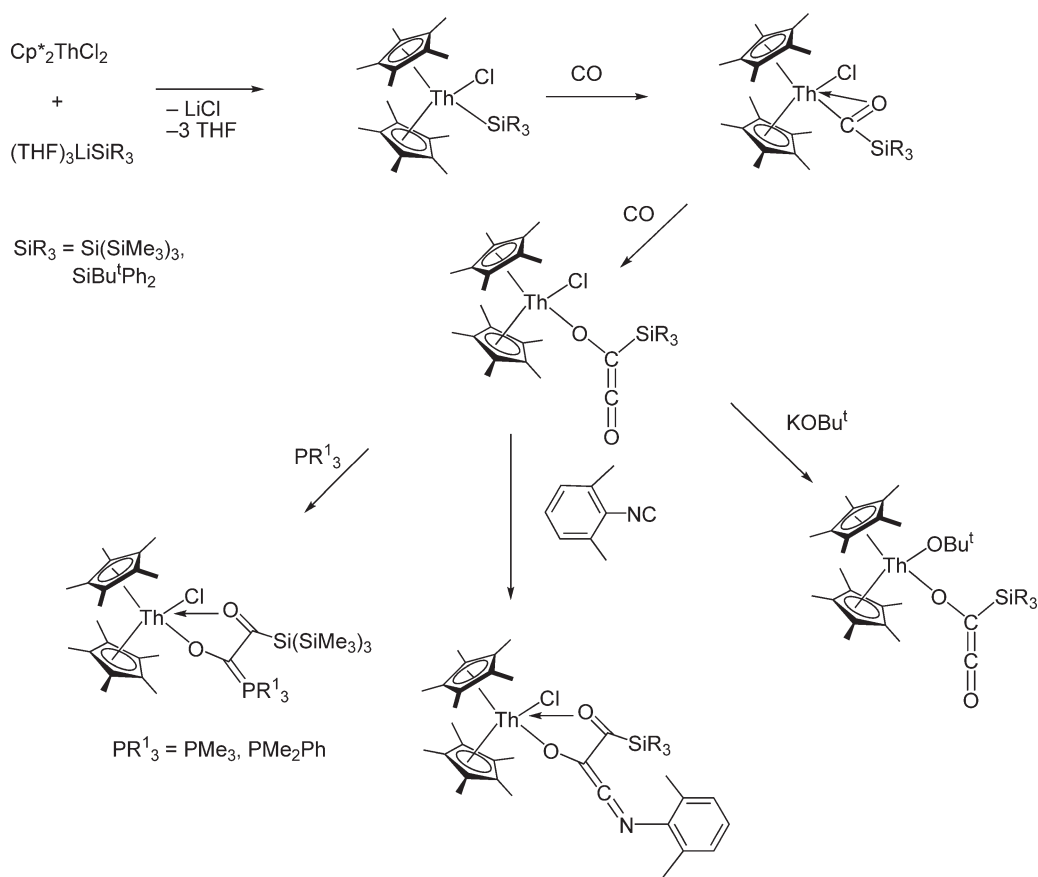




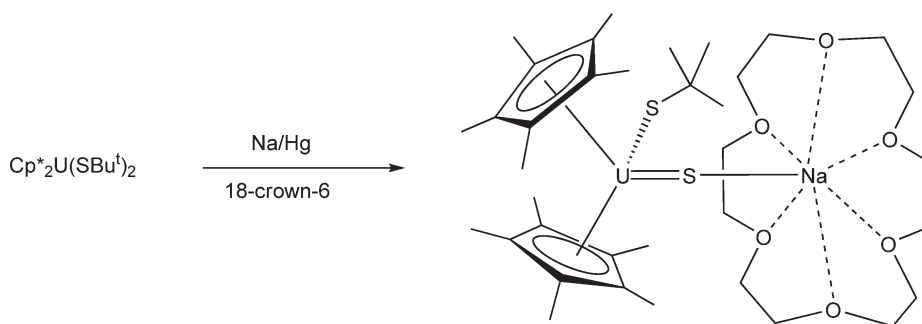
Scheme 41

Unusual metaloxoketene thorium complexes have been prepared via “double insertion” of carbon monoxide into thorium–silicon bonds (Scheme 42). In the structure of  $\text{Cp}^*_2\text{Th}(\text{Cl})[\text{OC}(=\text{C}=\text{O})\text{Si}(\text{SiMe}_3)_3]$  the ketene unit is oriented roughly in the plane bisecting the  $\text{Cp}^*$  rings. The Th–Cl and Th–O bond distances are 2.651(5) and 2.15(1) Å respectively.<sup>106</sup>

The synthesis of  $[\text{Na}(18\text{-crown-6})][\text{Cp}^*_2\text{U}(\text{SBU}^i)(\text{S})]$ , which is the first *f*-element compound containing a metal–sulfur double bond, has been reported in 1999.<sup>107</sup> The C–S bond cleavage of a thiolate ligand of  $\text{Cp}^*_2\text{U}(\text{SBU}^i)_2$  was induced by treatment with Na(Hg), and  $[\text{Na}(18\text{-crown-6})][\text{Cp}^*_2\text{U}(\text{SBU}^i)(\text{S})]$  was isolated after addition of 18-crown-6. Single-crystal X-ray determinations exhibited the unsupported U–S–Na linkage of the molecular complex with a U–S bond distance of 2.462 Å (Scheme 43).<sup>107</sup>



Scheme 42



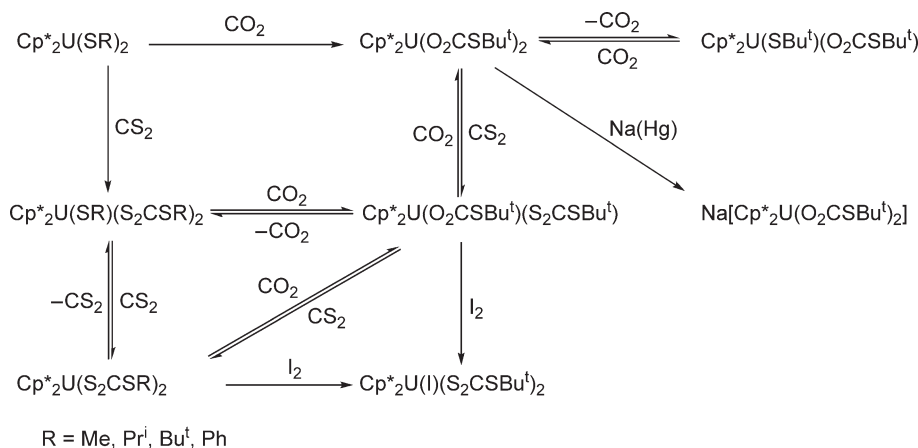
Scheme 43

The synthesis of bis(pentamethylcyclopentadienyl)uranium(IV) thiolate compounds and their reactions with  $\text{CO}_2$  and  $\text{CS}_2$  have been investigated.<sup>108</sup> The bis(thiolato) complexes  $\text{Cp}^*_2\text{U}(\text{SR})_2$  ( $\text{R} = \text{Me}, \text{Pr}^i, \text{Bu}^t, \text{Ph}$ ) were synthesized by treatment of  $\text{Cp}^*_2\text{UCl}_2$  with  $\text{NaSR}$  in toluene or THF. Their reactions with  $\text{CO}_2$  and  $\text{CS}_2$  gave the insertion derivatives  $\text{Cp}^*_2\text{U}(\text{SR})(\text{E}_2\text{CSR})$  ( $\text{E} = \text{O}$  and  $\text{R} = \text{Bu}^t$ ;  $\text{E} = \text{S}$  and  $\text{R} = \text{Me}, \text{Pr}^i$ , or  $\text{Bu}^t$ ) and  $\text{Cp}^*_2\text{U}(\text{E}_2\text{CSR})_2$  ( $\text{E} = \text{O}$  and  $\text{R} = \text{Bu}^t$ ;  $\text{E} = \text{S}$  and  $\text{R} = \text{Me}$  or  $\text{Bu}^t$ ) (Scheme 44). Treatment of  $\text{Cp}^*_2\text{U}(\text{SBu}^t)(\text{S}_2\text{CSBu}^t)$  with  $\text{CO}_2$  gave the mixed insertion complex  $\text{Cp}^*_2\text{U}(\text{O}_2\text{CSBu}^t)(\text{S}_2\text{CSBu}^t)$ . Thermolysis of the insertion compounds led to the reverse elimination reaction of  $\text{CO}_2$  and  $\text{CS}_2$ . Reduction of  $\text{Cp}^*_2\text{U}(\text{O}_2\text{CSBu}^t)_2$  with  $\text{Na}(\text{Hg})$  afforded the corresponding anionic U(III) complex. Single-crystal X-ray structure determinations of  $\text{Cp}^*_2\text{U}(\text{SBu}^t)(\text{S}_2\text{CSBu}^t)$  revealed a classical bent-sandwich structure.<sup>108</sup>

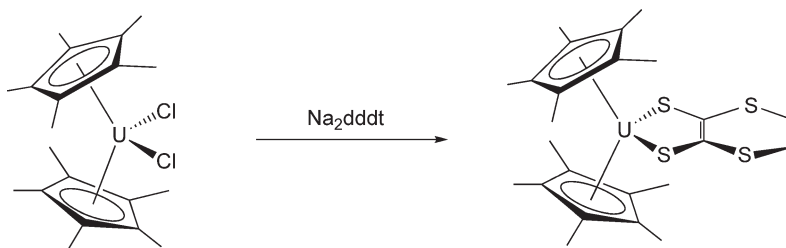
The synthesis and characterization of the first dithiolene complexes of uranium(IV) was achieved by treatment of either  $\text{Cp}^*_2\text{UCl}_2$  or  $[(\text{COT})\text{UX}_2(\text{THF})_n]$  ( $\text{X} = \text{BH}_4$ ,  $n = 0$ ;  $\text{X} = \text{I}$ ,  $n = 2$ ) with  $\text{Na}_2\text{dddt}$  ( $\text{dddt} = 5,6\text{-dihydro-1,4-dithiin-2,3-dithiolate}$ ) to afford the compounds  $\text{Cp}^*_2\text{U}(\text{dddt})$  and  $[\text{Na}(\text{18-crown-6})]_2[(\text{COT})\text{U}(\text{dddt})_2]$  (cf. Section 4.02.0.2) (Scheme 45).<sup>109</sup>

The cationic bis(pentamethylcyclopentadienyl)uranium(V) complex  $[\text{Cp}^*_2\text{U}(\text{NEt}_2)_2][\text{BPh}_4]$  was obtained by oxidation of neutral tetravalent precursor  $\text{Cp}^*_2\text{U}(\text{NEt}_2)_2$  by  $\text{AgBPh}_4$  in THF. The crystal structure of  $[\text{Cp}^*_2\text{U}(\text{NEt}_2)_2][\text{BPh}_4]$  consists of discrete cation–anion pairs. The cation  $[\text{Cp}^*_2\text{U}(\text{NEt}_2)_2]^+$  exhibits pseudotetrahedral geometry. The uranium atom is coordinated by two  $\text{Cp}^*$  rings and two nitrogen atoms of the  $\text{NEt}_2$  ligands.<sup>97</sup> The synthesis of the cationic bis(pentamethylcyclopentadienyl)uranium(IV) complexes  $[\text{Cp}^*_2\text{U}(\text{NEt}_2)(\text{THF})][\text{BPh}_4]$  ( $\text{R} = \text{H}$  or  $\text{Me}$ ) and  $[\text{Cp}^*_2\text{U}(\text{NMe}_2)(\text{THF})][\text{BPh}_4]$  was achieved by protonolysis of the correspondent neutral amide precursors  $[\text{Cp}^*_2\text{U}(\text{NR}'_2)_2]$  ( $\text{R}' = \text{Me}$  or  $\text{Et}$ ) with  $[\text{NHET}_3][\text{BPh}_4]$ . The compound  $[\text{Cp}^*_2\text{U}(\text{NMe}_2)(\text{THF})][\text{BPh}_4]$  was prepared readily in THF according to Scheme 46 and was isolated in high yields.<sup>71,110</sup>

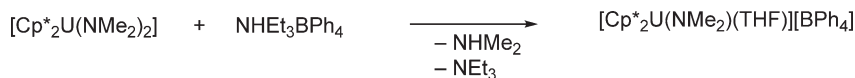
However, when the reaction mixture was kept at room temperature for a longer period of time, the red solution of  $[\text{Cp}^*_2\text{U}(\text{NMe}_2)(\text{THF})][\text{BPh}_4]$  progressively deposited a yellow microcrystalline powder. The result was a novel



Scheme 44



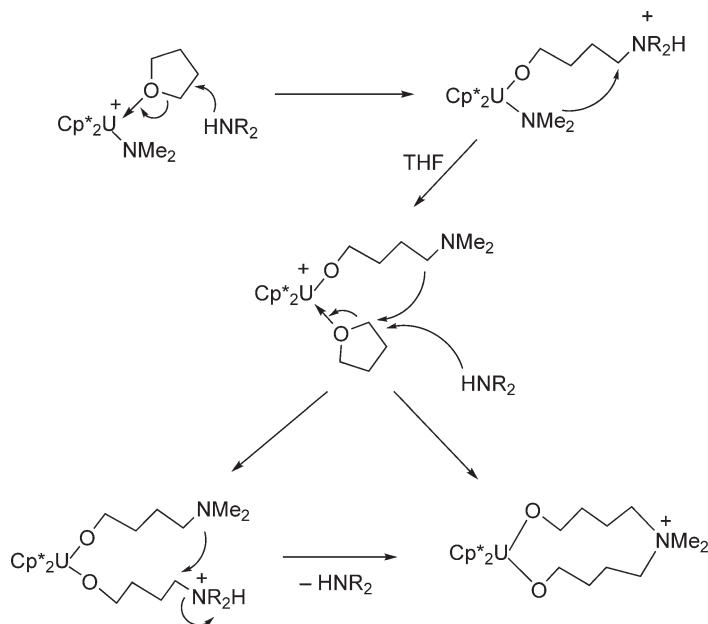
Scheme 45



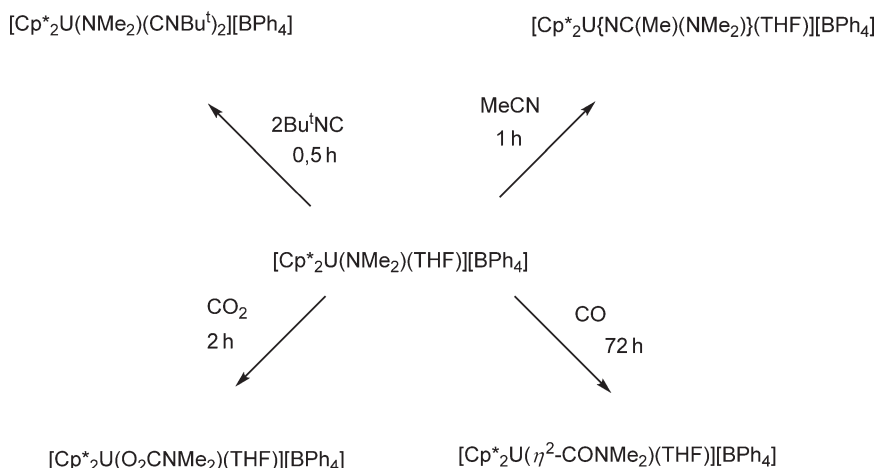
Scheme 46

ring-opening reaction of THF promoted by  $[\text{Cp}^*_2\text{U}(\text{NMe}_2)(\text{THF})][\text{BPh}_4]$  and the presence of free amine. This reaction product,  $[\text{Cp}^*_2\text{U}\{\text{O}(\text{CH}_2)_4\text{NMe}_2(\text{CH}_2)_4\text{O}\}][\text{BPh}_4](\text{THF})_{0.5}$ , was identified by  $^1\text{H}$  NMR and by X-ray diffraction analysis of the solvate obtained by crystallization from pyridine.  $[\text{Cp}^*_2\text{U}(\text{NMe}_2)(\text{THF})][\text{BPh}_4]$  was transformed slowly into  $[\text{Cp}^*_2\text{U}\{\text{O}(\text{CH}_2)_4\text{NMe}_2(\text{CH}_2)_4\text{O}\}][\text{BPh}_4](\text{THF})_{0.5}$  (ca. 20% after 4 days) by reaction with two molecules of THF (Scheme 47). In fact, pure  $[\text{Cp}^*_2\text{U}(\text{NMe}_2)(\text{THF})][\text{BPh}_4]$  was found to be inert toward THF, except in the presence of free amine; the reactivity sequence was  $\text{NHMe}_2 > \text{NHEt}_2 > \text{NEt}_3$ .<sup>110</sup>

In the molecular structure of the cation in the pyridine-solvated salt  $[\text{Cp}^*_2\text{U}\{\text{O}(\text{CH}_2)_4\text{NMe}_2(\text{CH}_2)_4\text{O}\}][\text{BPh}_4](\text{NC}_5\text{H}_5)$  the uranium atom is in a pseudotetrahedral environment which is quite familiar for complexes of the type  $\text{Cp}^*_2\text{MX}_2$ . The short U–O distances of 2.08(1), 2.09(1) Å and the large U–O–C angles 170.2(5)° and 172.8(5)° reflect the strong bonding interaction between the uranium and oxygen atoms.<sup>110</sup> Treatment of  $[\text{Cp}^*_2\text{U}(\text{NMe}_2)(\text{THF})][\text{BPh}_4]$  with  $\text{Bu}^t\text{NC}$  afforded the isocyanide adduct  $[\text{Cp}^*_2\text{U}(\text{NMe}_2)(\text{CNBu}^t)_2][\text{BPh}_4]$ , whereas reactions with MeCN,  $\text{CO}_2$ , and



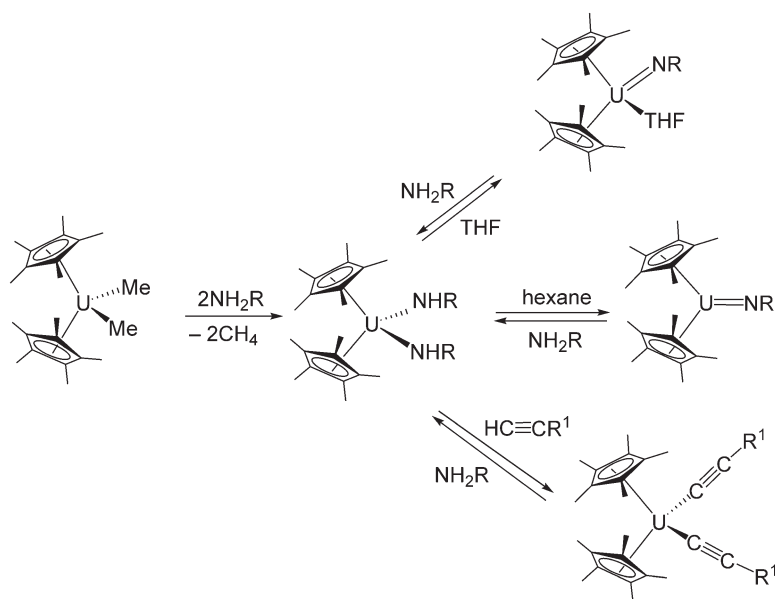
Scheme 47



Scheme 48

$\text{CO}$  gave the insertion compounds  $[\text{Cp}^*_2\text{U}\{\text{NC}(\text{Me})(\text{NMe}_2)\}(\text{THF})][\text{BPh}_4]$ ,  $[\text{Cp}^*_2\text{U}(\text{O}_2\text{CNMe}_2)(\text{THF})][\text{BPh}_4]$ , and  $[\text{Cp}^*_2\text{U}(\eta^2\text{-CONMe}_2)(\text{THF})][\text{BPh}_4]$  (Scheme 48).<sup>111</sup>

The crystal structure of  $[\text{Cp}^*_2\text{U}(\text{NMe}_2)(\text{CNBu}^t)_2][\text{BPh}_4]$  has been determined. It consists of discrete cation–anion pairs. The cation  $[\text{Cp}^*_2\text{U}(\text{NMe}_2)(\text{CNBu}^t)_2]^+$  adopts the classical bent-sandwich structure of  $[(\eta\text{-C}_5\text{R}_5)_2\text{M}(\text{X})_2(\text{Y})]$  compounds. The arrangement of the amide and two isocyanide ligands in the equatorial girdle is symmetrical. The uranium–nitrogen distance of 2.22 Å is in the range of U–N bond lengths for terminally coordinated amide ligands and the geometry of the  $\text{UNC}_2$  fragment is planar; these structural parameters are indicative of a  $\pi$ -interaction between the U and N atoms.<sup>111</sup> Reactions of  $\text{Cp}^*_2\text{U}(\text{NMe}_2)_2$  with primary aromatic or aliphatic amines led to the rapid formation of monomeric uranium(IV) complexes  $\text{Cp}^*_2\text{U}(\text{NHR})_2$  ( $\text{R} = 2,6\text{-dimethylphenyl, Et, Bu}^t$ ). The compounds were characterized by standard techniques, and  $\text{Cp}^*_2\text{U}(\text{NH-C}_6\text{H}_3\text{Me}_2\text{-2,6})_2$  by X-ray diffraction. In coordinating solvents like THF,  $\text{Cp}^*_2\text{U}(\text{NH-C}_6\text{H}_3\text{Me}_2\text{-2,6})_2$  reacted intramolecularly releasing one primary amine and forming the imidouranium(IV)  $\text{Cp}^*_2\text{U}(\text{=NC}_6\text{H}_3\text{Me}_2\text{-2,6})(\text{THF})$ , whereas in non-coordinating solvents the base-free compound  $\text{Cp}^*_2\text{U}(\text{=NC}_6\text{H}_3\text{Me}_2\text{-2,6})$  was obtained (Scheme 49).<sup>112</sup> The solid-state structure of chloro(*p*-chloroanilido-*N*)bis( $\eta^5$ -pentamethylcyclopentadienyl)uranium(IV) has been reported.<sup>113</sup>

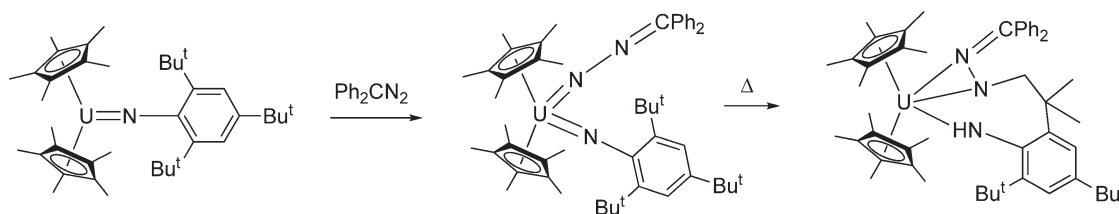


Scheme 49

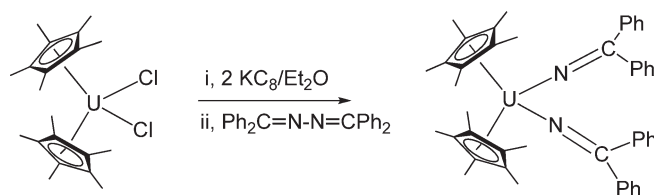
$\sigma$ -Bond metathesis reactions of bis(amido) and/or imido complexes with terminal alkynes produced the bis(acetylide) complexes  $\text{Cp}^*_2\text{U}(\text{C}\equiv\text{CR})_2$  ( $\text{R} = \text{Ph}$  or  $\text{Bu}^t$ ) as active species for the regioselective oligomerization of terminal alkynes, which can be prepared also from the reaction of  $\text{Cp}^*_2\text{UMe}_2$  with 2 equiv. of the corresponding terminal alkyne. Reactivity studies showed the possible interconversion among these bis(amido), imido, and bis(acetylide) complexes.<sup>112</sup> Diphenyldiazomethane effected a two-electron oxidation of the uranium(IV) monoimido complex  $\text{Cp}^*_2\text{U}=\text{NC}_6\text{H}_2\text{Bu}^t_{3-2,4,6}$  to give the uranium(VI) mixed bis(imido) complex  $\text{Cp}^*_2\text{U}(=\text{NC}_6\text{H}_2\text{Bu}^t_{3-2,4,6})(=\text{N}-\text{N}=\text{CPh}_2)$  (brown crystals, 97% yield), which undergoes a rare cyclometallation reaction upon mild thermolysis to afford a cherry red uranium(IV) bis(amide) complex that results from net addition of a C–H bond of an *ortho*-*t*-butyl group across the  $\text{N}=\text{U}=\text{N}$  core (Scheme 50).<sup>114</sup>

The first example of a 5f-element ketimido complex has been prepared by the reaction sequence shown in Scheme 51. The product is surprisingly unreactive and displays unusual electronic properties. The physical properties and chemical stability of this complex suggest higher U–N bond order due to significant ligand to metal  $\pi$ -bonding in the uranium ketimido interactions.<sup>115</sup> Electronic absorption and resonance-enhanced Raman spectra have been recorded for the uranium(IV) ketimido complexes  $\text{Cp}^*_2\text{U}[\text{N}=\text{C}(\text{Ph})(\text{R})]_2$  ( $\text{R} = \text{Me}$ ,  $\text{Ph}$ ,  $\text{CH}_2\text{Ph}$ ). The observations of both charge-transfer transitions and resonance enhancement of Raman vibrational bands are exceedingly rare for tetravalent actinide complexes and reflect the strong bonding interactions between the uranium 5f/6d-orbitals and those on the ketimido ligands.<sup>116</sup>

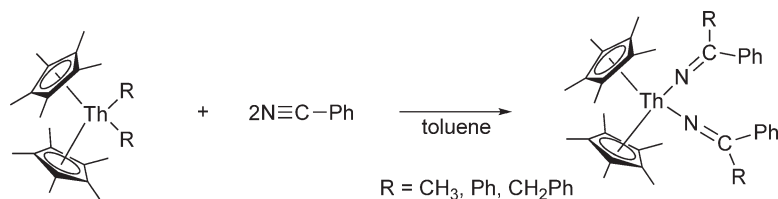
Migratory insertion of benzonitrile into both An–C bonds of the bis(alkyl) and bis(aryl) complexes  $\text{Cp}^*_2\text{AnR}_2$  ( $\text{An} = \text{Th}$ ,  $\text{U}$ ;  $\text{R} = \text{Me}$ ,  $\text{CH}_2\text{Ph}$ ) afforded the actinide ketimido complexes  $\text{Cp}^*_2\text{An}[\text{N}=\text{C}(\text{Ph})\text{R}]_2$ . Thus, for example, treatment of a colorless toluene solution of  $\text{Cp}^*_2\text{ThPh}_2$  with excess benzonitrile instantly generated the highly iridescent orange-colored thorium(IV) bis(ketimido) complex  $\text{Cp}^*_2\text{Th}[\text{N}=\text{C}(\text{Ph})\text{R}]_2$ , which was isolated as an orange crystalline solid in 82% yield (Scheme 52).<sup>117</sup>



Scheme 50



Scheme 51



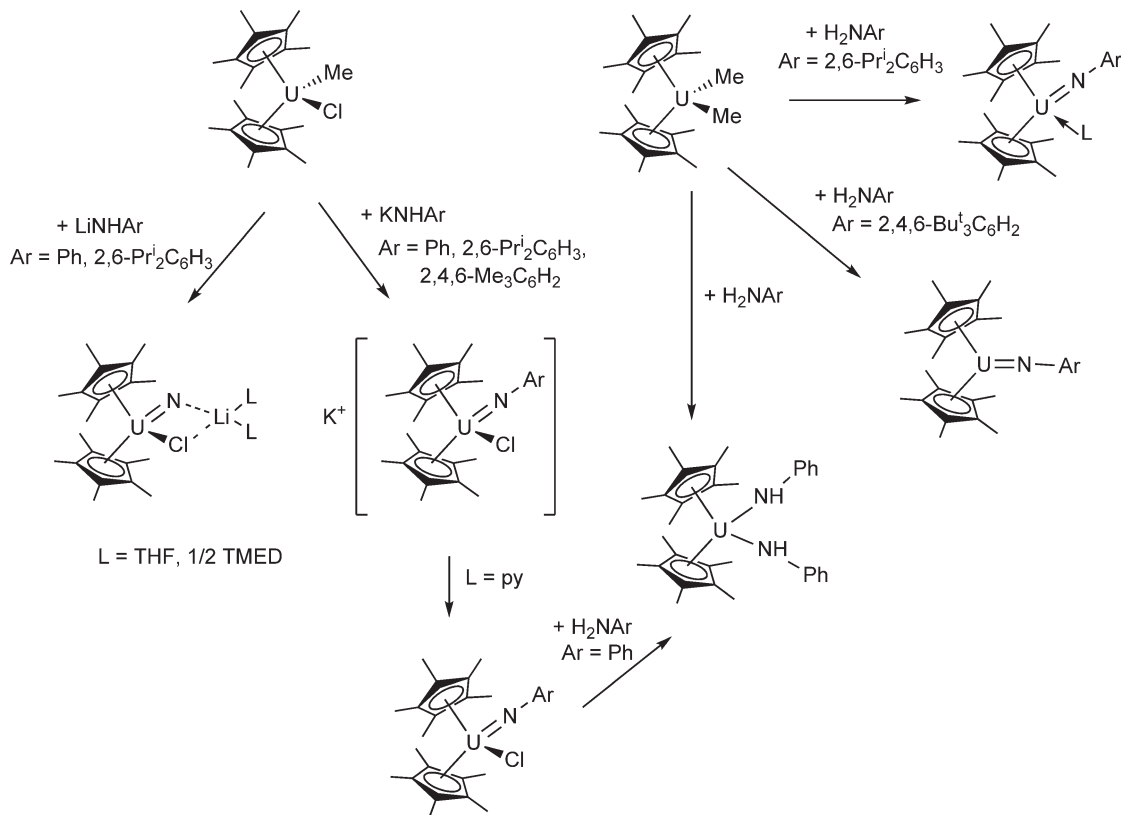
Scheme 52

Closely related are the sulfinimido complexes  $\text{Cp}^*_2\text{UCl}(\text{N}=\text{SPh}_2)$  and  $\text{Cp}^*_2\text{U}(\text{N}=\text{SPh}_2)_2$ , which have been prepared in high yield from  $\text{Cp}^*_2\text{UCl}_2$  and various stoichiometry amounts of  $\text{LiNSPh}_2$ . The same compounds can also be synthesized by treating  $\text{Cp}^*_2\text{UCl}[(\text{CH}_2)_2\text{PPh}_2]$  with anhydrous  $\text{HNSPh}_2$ . Its short U–N distance suggests significant uranium-imido multiple-bond character.<sup>118</sup>

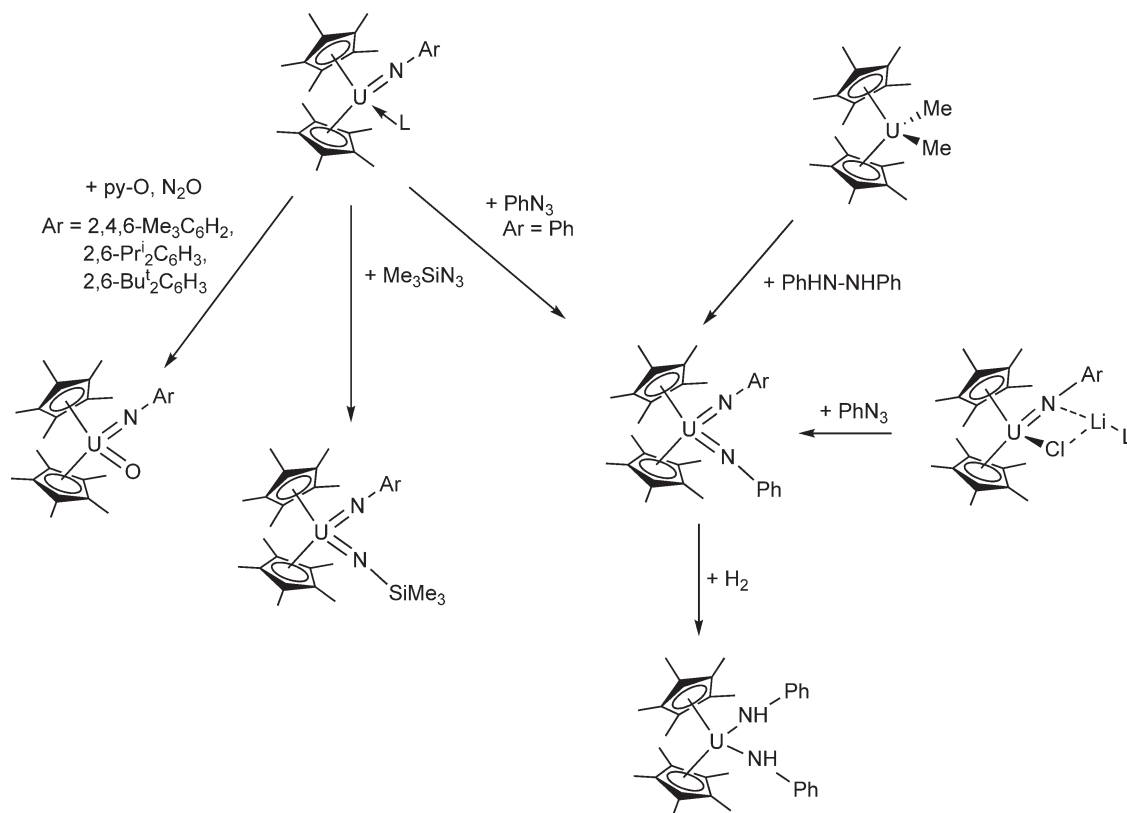
Among the highlights in recent organoactinide chemistry is the successful synthesis of high-valent organouranium imido complexes.<sup>119,120</sup> Density functional calculations have been used to investigate the structure and bonding in several unusual cyclopentadienyl complexes with nitrogen-containing ligands. The U(vi) imido complex Cp<sub>2</sub>U(NPh)<sub>2</sub> and the U(iv) amido complex Cp<sub>2</sub>U(NHPh)<sub>2</sub> were examined and important orbitals involved in the U–N bonds analyzed.<sup>121</sup> Monoimido complexes of uranium(iv) were synthesized by metathesis or direct protonation reactions (Scheme 53). The orange-brown complex [Li(TMEDA)][Cp<sup>\*</sup><sub>2</sub>U(=NC<sub>6</sub>H<sub>5</sub>)Cl] obtained from Cp<sup>\*</sup><sub>2</sub>UmeCl and lithium anilide in the presence of tetramethylethylenediamine (TMEDA) has been characterized by X-ray diffraction. It exhibits a typical “bent metallocene” structure with an average U–C(η<sup>5</sup>-Cp<sup>\*</sup>) distance of 2.77(2) Å and an angle Cp<sup>\*</sup>(cent.)–U–Cp<sup>\*</sup>(cent.) of 132.4°. The U–Cl and U–N(NC<sub>6</sub>H<sub>5</sub>) bond lengths are 2.690(5) and 2.051(14) Å, respectively. The complex Cp<sup>\*</sup><sub>2</sub>U(N-2,4,6-Bu<sup>t</sup><sub>3</sub>C<sub>6</sub>H<sub>2</sub>), prepared by protonation of Cp<sup>\*</sup><sub>2</sub>Ume<sub>2</sub> with H<sub>2</sub>N-2,4,6-Bu<sup>t</sup><sub>3</sub>C<sub>6</sub>H<sub>2</sub>, was also structurally characterized. The most interesting feature of this molecule is the very short U–N bond length of 1.952(12) Å.<sup>119–121</sup>

Organometallic complexes of uranium(vi) with organoimido and oxo functional groups  $\text{Cp}^*_2\text{U}(=\text{NR})(=\text{E})$  ( $\text{E}=\text{NR}$  or  $\text{O}$ ) have also been prepared by two-electron oxidative atom transfer using organic azides, amine *N*-oxides or nitrous oxide. Another way of generating the compounds is reductive cleavage of 1,2-disubstituted hydrazines (Scheme 54).<sup>119–121</sup>

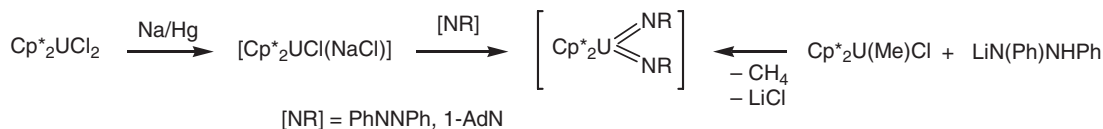
The synthesis of the bis(imido)uranium(vi) complexes Cp<sup>\*</sup>U(NR)<sub>2</sub> (R = Ph, 1-adamantyl (1-Ad)) was achieved according to [Scheme 55](#) in a one-pot reaction with high yield.<sup>122,122a</sup> In this reaction the N=N double bond is cleaved by the uranium metal center. This is only possible if the *f*-orbital is involved in the cleavage of the double bond. For the *d*-transition metals such a cleavage is symmetry forbidden.<sup>122,122a</sup> Yet another preparation of the



### Scheme 53



Scheme 54



Scheme 55

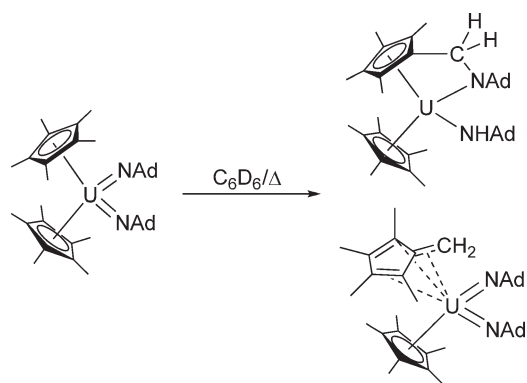
uranium(vi) bis(phenylimido) complex was achieved by the reaction of 1-lithio-1,2-diphenylhydrazine with  $\text{Cp}^*_2\text{U}(\text{Me})\text{Cl}$  in diethyl ether.<sup>119</sup>

Thermolysis of  $\text{Cp}^*_2\text{U}(=\text{NAd})_2$  in benzene or hexane resulted in the intramolecular C–H bond activation of a methyl group on a pentamethylcyclopentadienyl ligand across the imido functional groups.<sup>123</sup> The activation product is a reduced U(IV) metallocene bis(amide) complex with an *N*-bonded methylene unit derived from the methyl group attached to one amide group. Scheme 56 shows the formation of the ring bite uranium complex with the two possible structures that are consistent with the <sup>1</sup>H NMR data.<sup>123</sup>

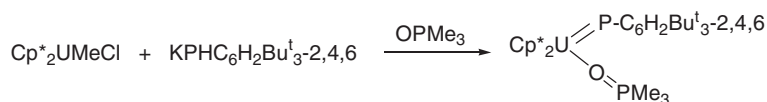
A single-crystal X-ray structure determination revealed a constrained geometry of the bifunctional amide–cyclopentadienide ligand, that gives rise to the distortions in the metallocene geometry. The *N*-bonded methylene derived from a  $\text{Cp}^*$  methyl group is pulled out of the plane of the C<sub>5</sub> ring toward the metal center by 0.52 Å.<sup>123</sup>

The reaction of  $\text{Cp}^*_2\text{U}(\text{Me})_2$  with  $\text{HPPH}_2$  afforded the first uranium diphenylphosphide compounds.<sup>124</sup> The reaction of  $\text{Cp}^*_2\text{U}(\text{Me})_2$  with  $\text{HPPH}_2$  was found to be the best route to the uranium(IV) diphenylphosphide compounds  $\text{Cp}^*_2\text{U}(\text{PPh}_2)(\text{Me})$  and  $\text{Cp}^*_2\text{U}(\text{PPh}_2)_2$ . Thermolysis of  $[\text{Cp}^*_2\text{U}(\text{PPh}_2)(\text{Me})]$  afforded the *ortho*-metallated complex  $\text{Cp}^*_2\text{U}[\text{PPh}(o\text{-C}_6\text{H}_4)]$  after 24 h in refluxing toluene. Reduction of  $\text{Cp}^*_2\text{U}(\text{PPh}_2)_2$  with KH gave the first U(III) phosphide  $\text{K}[\text{Cp}^*_2\text{U}(\text{PPh}_2)_2]$ .<sup>124</sup> The preparation of the first actinide phosphinidene complexes as well as the





Scheme 56



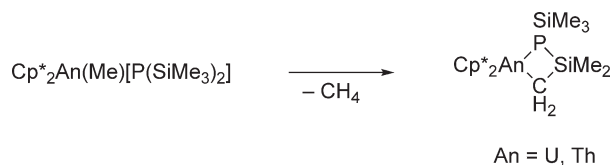
Scheme 57

steric control of their reactivity has been reported. The reaction of  $\text{KPH-2,4,6-Bu}^t_3\text{C}_6\text{H}_2$  with  $\text{Cp}^*_2\text{UMeCl}$  at room temperature in toluene in the presence of trimethylphosphine oxide afforded the complex  $\text{Cp}^*_2\text{U}(\text{=PC}_6\text{H}_2\text{Bu}^t_{3-2,4,6})(\text{O=PMe}_3)$  as black crystals in 62% yield (Scheme 57). In the absence of added base, intractable product mixtures result, possibly due to reduction of the metal center or reaction of the formed phosphinidene ligand with the solvent or ancillary ligand.<sup>125</sup>

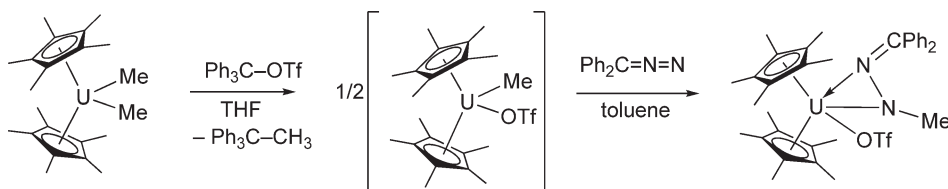
The organoactinide diorganophosphido complexes  $\text{Cp}^*_2\text{U}[\text{P}(\text{SiMe}_3)_2]\text{Cl}$ ,  $\text{Cp}^*_2\text{Th}[\text{P}(\text{SiMe}_3)_2]\text{Cl}$ ,  $\text{Cp}^*_2\text{U}[\text{P}(\text{SiMe}_3)_2]\text{Me}$ , and  $\text{Cp}^*_2\text{Th}[\text{P}(\text{SiMe}_3)_2]\text{Me}$  have been synthesized by reaction of  $\text{Cp}^*_2\text{AnCl}_2$  or  $\text{Cp}^*_2\text{AnCl}(\text{Me})$  ( $\text{An} = \text{Th, U}$ ) with  $\text{KP}(\text{SiMe}_3)_2$  in THF. Thermal decomposition of  $\text{Cp}^*_2\text{U}[\text{P}(\text{SiMe}_3)_2]\text{Me}$  and  $\text{Cp}^*_2\text{Th}[\text{P}(\text{SiMe}_3)_2]\text{Me}$  resulted in formation of the metallacycles  $\text{Cp}^*_2\text{An}[\text{P}(\text{SiMe}_3)\text{SiMe}_2\text{CH}_2]$  ( $\text{An} = \text{Th, U}$ ), accompanied by the liberation of methane (Scheme 58). Several representatives of this interesting class of compounds have been structurally characterized by X-ray diffraction.<sup>126</sup>

The reaction of tris(2,2',2''-nonafluorobiphenyl)borane (PBB) with  $\text{Cp}^*_2\text{ThMe}_2$  has been reported to afford the base-free cationic complex  $[\text{Cp}^*_2\text{ThMe}]^+[\text{MePBB}]^-$ .<sup>127</sup> A bis(pentamethylcyclopentadienyl)uranium triflate has been established as a new reagent for uranium metallocene chemistry. The synthesis and characterization of the first actinide hydrazonato complex,  $\text{Cp}^*_2\text{U}[\eta^2-(N,N')\text{-MeNN=CPh}_2](\text{OTf})$  has been made possible by the use of the organouranium(IV)trifluoromethanesulfonate (triflate) complex  $[\text{Cp}^*_2\text{UMe}(\text{OTf})]_2$  ( $\text{OTf} = \text{OSO}_2\text{CF}_3$ ), which is derived from the reaction between  $\text{Cp}^*_2\text{UMe}_2$  and  $\text{Ph}_3\text{COTf}$  (Scheme 59).<sup>128</sup>

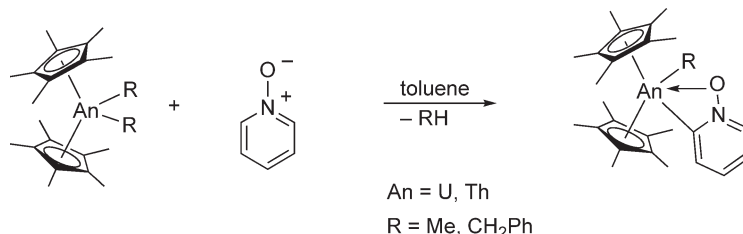
An unusual case of C–H activation with uranium(IV) and thorium(IV) bis(alkyl) complexes has been discovered for pyridine *N*-oxide. As shown in Scheme 60, addition of 1 equiv. of pyridine *N*-oxide to a toluene solution of the uranium(IV) bis(alkyl) complexes  $\text{Cp}^*_2\text{UR}_2$  ( $\text{R} = \text{Me, CH}_2\text{Ph}$ ) unexpectedly resulted in activation of an  $sp^2$  hybridized



Scheme 58



Scheme 59



Scheme 60

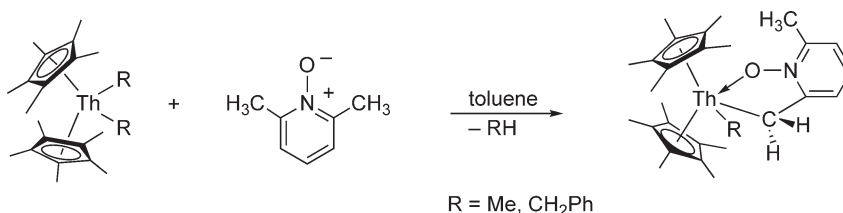
C–H bond, with loss of alkane and formation of novel cyclometalated pyridine *N*-oxide complexes in greater than 70% yield. The same reactions could be carried out with the analogous thorium(IV) bis(alkyls).<sup>129</sup>

This chemistry is not limited to  $sp^2$  hybridized C–H bonds. As depicted in Scheme 61, reaction of 1 equiv. of 2,6-lutidine *N*-oxide with the Th(IV) bis(alkyls) at room temperature afforded the cyclometalated complexes in 70–80% yield, whereas the analogous uranium(IV) complexes did not form even at elevated temperatures.<sup>129</sup>

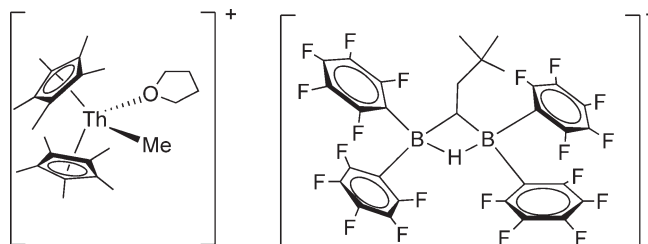
The uranium(IV) carbene complex  $\text{Cp}^*_2\text{U}(\text{O})[\text{C}(\text{NMeCMe}_2)_2]$  has been synthesized in the form of red-brown crystals from  $\text{Cp}^*_3\text{U}$  and the free carbene. It represents a rare example of a monometallic uranium monooxo compound.<sup>85</sup> Recently, the crystal structures of the known thorium and uranium complexes  $\text{Cp}^*_2\text{Th}(\text{CH}_2\text{Ph})_2$ ,  $\text{Cp}^*_2\text{ThMe}_2$ ,  $\text{Cp}^*_2\text{U}(\text{CH}_2\text{Ph})_2$ , and  $\text{Cp}^*_2\text{UMe}_2$  have been determined.<sup>117</sup> New syntheses of  $\text{Cp}^*_2\text{ThPh}_2$  and  $\text{Cp}^*_2\text{Th}(\text{Me})(\text{aryl})$  ( $\text{aryl} = o\text{-MeC}_6\text{H}_4$ ,  $2,5\text{-Me}_2\text{C}_6\text{H}_3$ ,  $o\text{-MeOC}_6\text{H}_4$ ) derivatives have been reported. The complex  $\text{Cp}^*_2\text{ThPh}_2$  was obtained from  $\text{Cp}^*_2\text{ThCl}_2$  and  $\text{PhMgBr}$  in the presence of dioxane.<sup>130</sup> The cationic metallocene complex  $[\text{Cp}^*_2\text{ThMe}][(\mu\text{-H})(\mu\text{-CHCH}_2\text{Bu}^t)\{\text{B}(\text{C}_6\text{F}_5)_2\}]$  was obtained by the protolytic reaction of  $[\text{NBu}^t_3\text{H}][(\mu\text{-H})(\mu\text{-CHCH}_2\text{Bu}^t)\{\text{B}(\text{C}_6\text{F}_5)_2\}]$  with  $\text{Cp}^*_2\text{ThMe}_2$ . The monoTHF adduct  $[\text{Cp}^*_2\text{ThMe}(\text{THF})][(\mu\text{-H})(\mu\text{-CHCH}_2\text{Bu}^t)\{\text{B}(\text{C}_6\text{F}_5)_2\}]$  has been characterized by X-ray diffraction. The complex consists of well-separated ions (Scheme 62).<sup>131</sup> The synthesis,  $^1\text{H}$  and  $^{11}\text{B}$  NMR study, and X-ray crystal structure determination of the bis(pentamethylcyclopentadienyl)uranium borohydride  $\text{Cp}^*_2\text{U}(\text{BH}_4)_2$  has been reported.<sup>57,132</sup>

#### 4.02.5.5.5 Tris(pentamethylcyclopentadienyl) actinide(IV) compounds

The question of how much steric crowding is possible in tris( $\eta^5$ -pentamethylcyclopentadienyl)actinide complexes has been addressed by the synthesis of the hitherto unknown compounds  $\text{Cp}^*_3\text{UCl}$  and  $\text{Cp}^*_3\text{UF}$ . Reaction of  $\text{Cp}^*_3\text{U}$  with 1 equiv. of  $\text{PhCl}$  gives  $\text{Cp}^*_3\text{UCl}$  as the primary product (Scheme 63). Upon addition of another equivalent of  $\text{PhCl}$  this



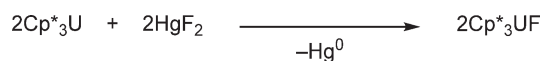
Scheme 61



Scheme 62



Scheme 63



Scheme 64

complex transformed over several days into  $\text{Cp}^*_2\text{UCl}_2$ . The latter complex can also be made in good yield using directly 2 equiv. of  $\text{PhCl}$ . In this case,  $\text{Cp}^*_3\text{U}$  is functioning as a two-electron reductant.<sup>133</sup>

The complex  $\text{Cp}^*_3\text{UCl}$  crystallizes in the same  $P6_3/m$  space group as  $\text{Cp}^*_3\text{U}$  and both have similar unit cell constants. A molecular mirror plane bisects the three symmetry-equivalent  $\text{Cp}^*$  rings, and the chloride ligand is disordered on either side. The  $\text{U}-\text{C}(\text{Cp}^*)$  distances are equivalent within experimental error to those of  $\text{Cp}^*_3\text{U}$ . Thus, the chloride ligand in  $\text{Cp}^*_3\text{UCl}$  does not appear to perturb the  $\text{U}-\text{CCp}^*$  parameters, and with  $2.90(1)\text{Å}$  the  $\text{U}-\text{Cl}$  bond is exceptionally long. The homologous fluoro derivative  $\text{Cp}^*_3\text{UF}$  could be synthesized from  $\text{Cp}^*_3\text{U}$  and  $\text{HgF}_2$  (Scheme 64).<sup>133</sup>

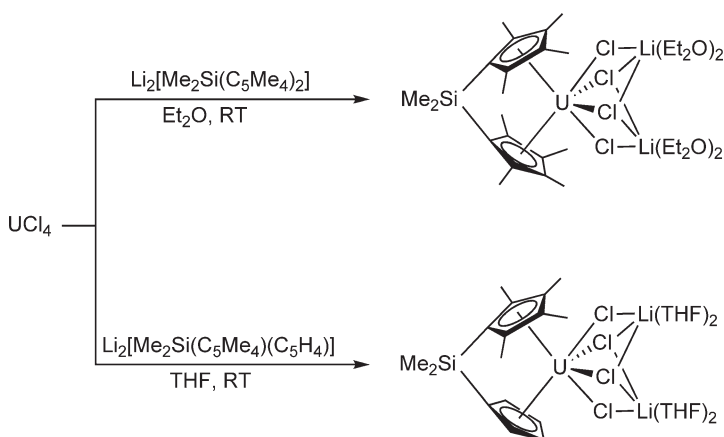
In order to determine if tris(pentamethylcyclopentadienyl) chemistry could be extended to thorium, the reaction of a cationic organothorium hydride,  $[\text{Cp}^*_4\text{Th}_2\text{H}_2(\text{DMPE})][\text{BPh}_4]$  with 2 equiv. of  $\text{K}(18\text{-crown-6})\text{Cp}^*$  was examined and found to produce  $\text{Cp}^*_3\text{ThH}$  as a pale yellow powder in 70% yield. The precursor was obtained by protonation of  $[\text{Cp}^*_2\text{ThH}(\mu\text{-H})_2]$  with  $[\text{Et}_3\text{NH}][\text{BPh}_4]$ . Preliminary reactivity studies of  $\text{Cp}^*_3\text{ThH}$  showed that its chemistry is surprisingly limited.<sup>134</sup>

#### 4.02.5.6 Compounds with Ring-bridged Cyclopentadienyl Ligands

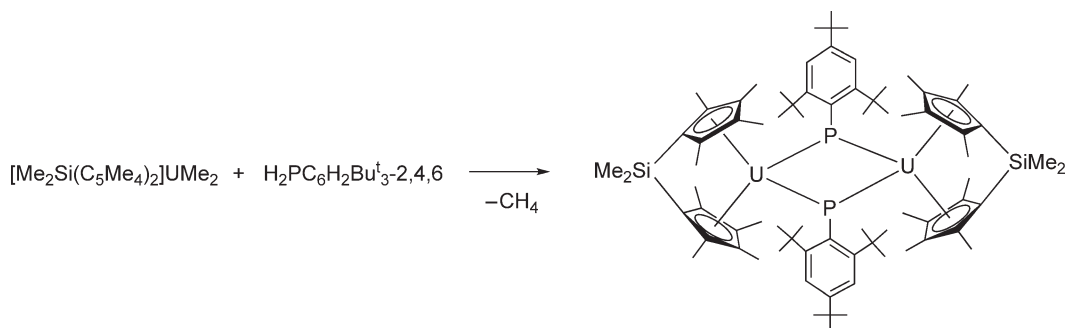
Complexes of  $\text{U}(\text{IV})$  employing the chelating bis(cyclopentadienyl) ligand sets  $[\text{Me}_2\text{Si}(\text{C}_5\text{Me}_4)_2]^{2-}$  and  $[\text{Me}_2\text{Si}(\text{C}_5\text{Me}_4)(\text{C}_5\text{H}_4)]^{2-}$  have been prepared in order to examine their utility in generating organoamido complexes of uranium (Scheme 65).<sup>135</sup>

The chloride complexes  $[\text{Me}_2\text{Si}(\text{C}_5\text{Me}_4)_2]\text{U}(\mu\text{-Cl})_2(\text{LiCl})_2(\text{Et}_2\text{O})_4$  and  $[\text{Me}_2\text{Si}(\text{C}_5\text{Me}_4)(\text{C}_5\text{H}_4)]\text{U}(\mu\text{-Cl})_2(\text{LiCl})_2(\text{Et}_2\text{O})_4$  were generated by reaction of  $\text{UCl}_4$  with the corresponding bis(cyclopentadienyl) dilithio salt in diethyl ether and tetrahydrofuran, respectively. The chloro precursors were alkylated by Grignard reagents.  $[\text{Me}_2\text{Si}(\text{C}_5\text{Me}_4)_2]\text{UMe}_2$  and the benzyl derivatives employing both ligand sets have been prepared.  $[\text{Me}_2\text{Si}(\text{C}_5\text{Me}_4)(\text{C}_5\text{H}_4)]\text{UMe}_2$  was not isolable because it appears to be thermally unstable. The alkyl complexes  $[\text{Me}_2\text{Si}(\text{C}_5\text{Me}_4)_2]\text{UR}_2$  ( $\text{R} = \text{Me}, \text{Bz}$ ) were protonated by  $N,N'$ -diphenylhydrazine yielding the expected  $\text{U}(\text{VI})$  complex  $[\text{Me}_2\text{Si}(\text{C}_5\text{Me}_4)_2]\text{U}(\text{NPh})_2$ . Reaction of  $[\text{Me}_2\text{Si}(\text{C}_5\text{Me}_4)(\text{C}_5\text{H}_4)]\text{UBz}_2$  with  $N,N'$ -diphenylhydrazine gave the  $\text{U}(\text{VI})$  monoimido dimer  $\{[\text{Me}_2\text{Si}(\text{C}_5\text{Me}_4)(\text{C}_5\text{H}_4)]\text{U}(\mu\text{-NPh})\}_2$ . The molecular structure of this complex revealed the dimeric structure with asymmetric organoimido bridging ligands.<sup>135</sup>

The reaction of the *ansa*-uranocene dimethyl complex  $[\text{Me}_2\text{Si}(\text{C}_5\text{H}_4)_2]\text{UMe}_2$  with  $\text{H}_2\text{PC}_6\text{H}_2\text{Bu}^t_{3-2,4,6}$  led to  $[\text{Me}_2\text{Si}(\text{C}_5\text{H}_4)_2]\text{U}(\mu\text{-PC}_6\text{H}_2\text{Bu}^t_{3-2,4,6})_2$ , a complex containing two  $\text{U}-\text{P}$  bridge bonds (Scheme 66). The dimer is



Scheme 65



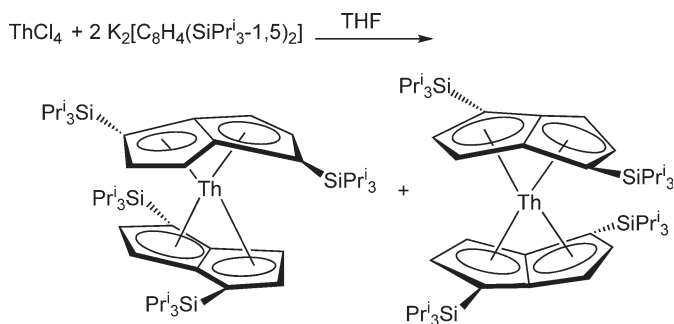
Scheme 66

readily disrupted by the addition of 1 equiv. of phosphine oxide as an Lewis base, yielding a product that may be formulated on the basis of NMR spectroscopy as the analog of the compound  $\text{Cp}^*_2\text{U}=\text{PC}_6\text{H}_2\text{Bu}^t_{3-2,4,6}(\text{O}=\text{PMe}_3)$ .<sup>125</sup>

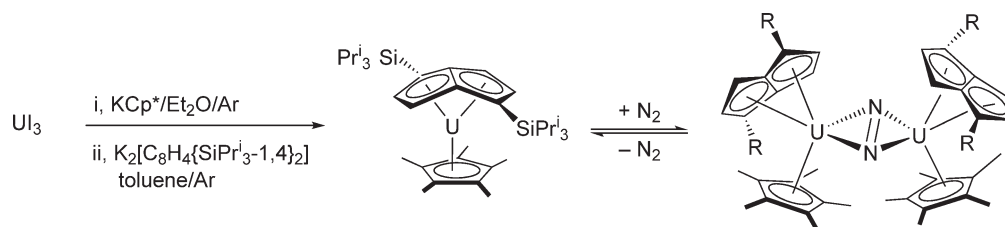
#### 4.02.5.7 Indenyl and Pentalenediyl Compounds

In 1997, the synthesis of a fascinating new class of actinide “sandwich” complexes with pentalene ligands has been reported. Tris(alkylsilyl)-substituted pentalene rings act like the  $\eta^8$ -membered ring system cyclooctatetraenyl. The dipotassium salt of the 1,5-bis(tri-*i*-propylsilyl)pentalene dianion reacted with  $\text{ThCl}_4$  under salt elimination to afford the bis( $\eta^8$ -pentalene)thorium complex (Scheme 67). The compound was characterized by UV/VIS,  $^1\text{H}$ ,  $^{13}\text{C}$ , and  $^{29}\text{Si}$  NMR, and the crystal structure was determined by X-ray diffraction.<sup>136</sup> The yield of the deep orange crystals was 70%. The crystals contain a mixture of staggered and eclipsed isomers. The two isomers differ in the relative orientation of the pentalene rings facing the thorium and in the twist angles (defined by the angles between the two bridgehead C–C vectors) of the two pentalene rings. The latter were  $83^\circ$  and  $38^\circ$ . The silicon atoms are  $17^\circ$  bent out of the planes of the five-membered rings away from the metal centre. The thorium–ring carbon distances range from  $2.543(10)\text{ \AA}$  for the bridgehead carbon to  $2.908(11)\text{ \AA}$  for the “wingtip” carbon. The pentalene ring C–C bond lengths range from  $1.36(2)$  to  $1.49(2)\text{ \AA}$ .<sup>136</sup>

Later the preparation of the bis(pentalene) uranium complex  $\text{U}[\eta^8\text{-C}_8\text{H}_4(\text{SiPr}^i_3)_2\text{-1,4}]_2$  and studies of the binding properties by DFT and photoelectron spectra have also been reported. Geometry optimization of  $\text{M}(\eta^8\text{-C}_8\text{H}_6)_2$ ,  $\text{M}=\text{Th}$ , with  $D_{2d}$  and  $D_2$  symmetry constraints gives structures in good agreement with the X-ray structure found for  $\text{Th}[\eta^8\text{-C}_8\text{H}_4(1,4\text{-SiPr}^i_3)_2]_2$ ; in particular, the folded nature of the ligand is well reproduced by the calculation. Examination of the barrier of relative rotation of the two ligands only showed a significant energy rise when the



Scheme 67

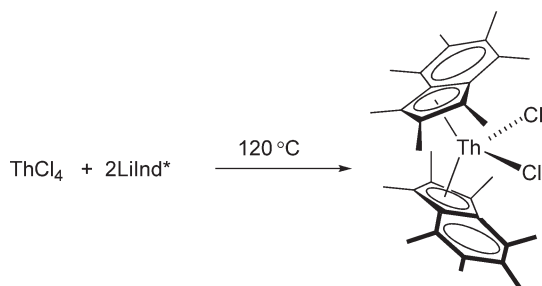


Scheme 68

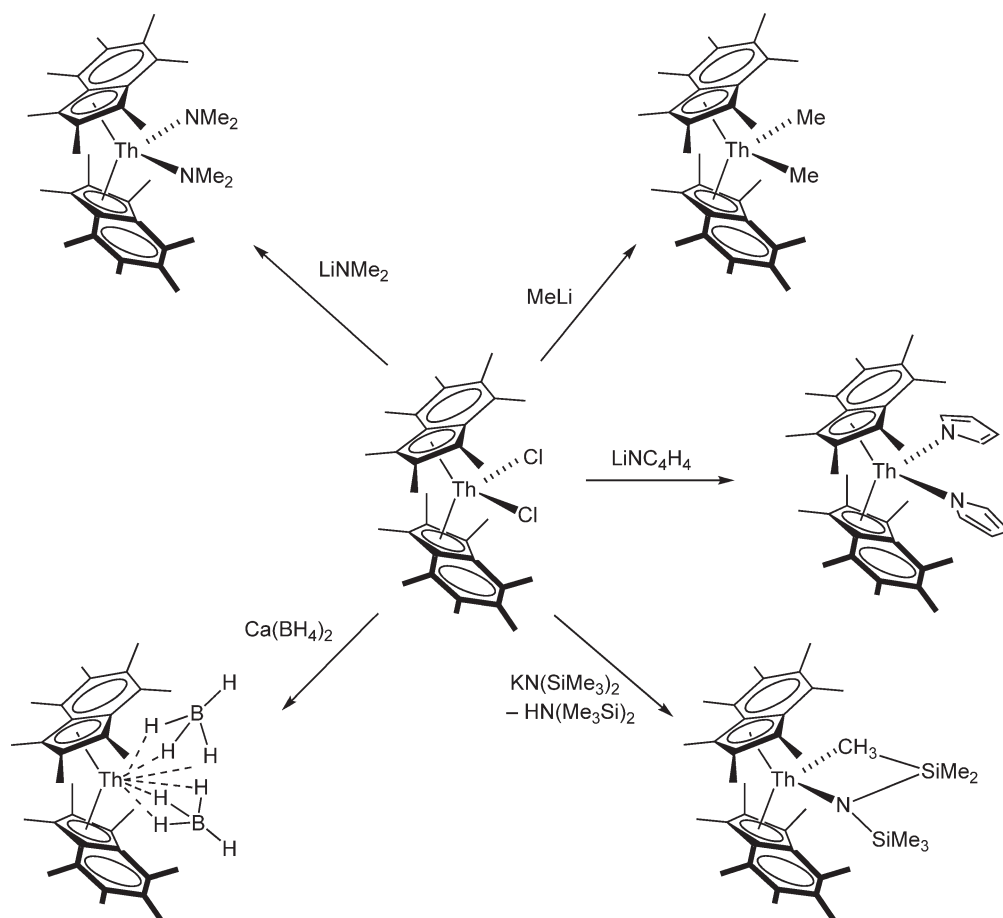
two rings were eclipsed.<sup>137</sup> Exciting uranium (III) chemistry has also been developed around the silyl-substituted pentalene ligand. The reaction of  $\text{U}^{\text{III}}$  with 1 equiv. of  $\text{KCp}^*$  in diethyl ether afforded a dark green material assumed to be  $[\text{Cp}^*\text{U}]_2$  or an etherate thereof. This material was not isolated but reacted directly with  $\text{K}_2[\text{C}_8\text{H}_4(\text{SiPr}^i_3)_{2-1,4}]$  in toluene under argon to afford purple-black, crystalline  $\text{Cp}^*\text{U}[\eta^8\text{-C}_8\text{H}_4(\text{SiPr}^i_3)_{2-1,4}]$  in moderate yield (40%) (Scheme 68). According to an X-ray diffraction study, the compound adopts a slightly bent-sandwich structure. Exposure of a sample of  $\text{Cp}^*\text{U}[\eta^8\text{-C}_8\text{H}_4(\text{SiPr}^i_3)_{2-1,4}]$  led to formation of an  $\text{N}_2$  complex which could be isolated as green-black crystals from a pentane solution of  $[\text{Cp}^*\text{U}[\eta^8\text{-C}_8\text{H}_4(\text{SiPr}^i_3)_{2-1,4}]]_2(\mu\text{-N}_2)$  under a 5 psi overpressure of  $\text{N}_2$  at  $-20^\circ\text{C}$ .  $[\text{Cp}^*\text{U}[\eta^8\text{-C}_8\text{H}_4(\text{SiPr}^i_3)_{2-1,4}]]_2(\mu\text{-N}_2)$  has a binuclear structure, in which two units of the precursor are bridged by a sideways-bound dinitrogen unit. The key structural feature of the latter is the N–N bond length of 1.232(10) Å, consistent with an N–N double bond. The complex loses dinitrogen extremely easily both in solution and the solid state.<sup>138</sup> The electronic structure of  $[\text{Cp}^*\text{U}[\eta^8\text{-C}_8\text{H}_4(\text{SiPr}^i_3)_{2-1,4}]]_2(\mu\text{-N}_2)$  has been investigated by density functional calculations.<sup>139</sup>

A variety of thorium complexes incorporating the bulky permethylindenyl ligand ( $\text{Ind}^* = \text{C}_9\text{Me}_7$ ) have been synthesized and characterized. Specifically, the dichloride  $\text{Ind}^*_2\text{ThCl}_2$  was obtained by reaction of  $\text{ThCl}_4$  with  $\text{LiInd}^*$  in toluene (Scheme 69). The yellow, crystalline product was isolated in 67% yield.<sup>140</sup>

With  $\text{Ind}^*_2\text{ThCl}_2$  as precursor, the derivatives  $\text{Ind}^*_2\text{ThMe}_2$ ,  $\text{Ind}^*_2\text{Th}(\text{NC}_4\text{H}_4)_2$ , and  $\text{Ind}^*_2\text{Th}(\text{BH}_4)_2$  could be obtained by metathesis with  $\text{MeLi}$ ,  $\text{LiNC}_4\text{H}_4$ , and  $\text{Ca}(\text{BH}_4)_2$ , respectively. In the same manner,  $\text{Ind}^*_2\text{ThCl}_2$  reacted with 2 equiv. of  $\text{LiNMe}_2$  to give the regular bis(dimethylamide)  $\text{Ind}^*_2\text{Th}(\text{NMe}_2)_2$  (Scheme 70). In contrast to simple



Scheme 69

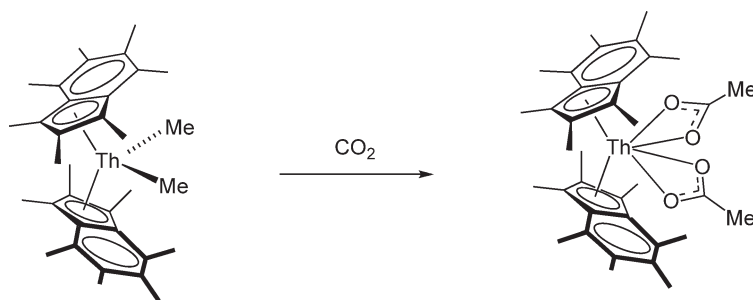


Scheme 70

metathesis, reaction of  $\text{Ind}^*_2\text{ThCl}_2$  with  $\text{KN}(\text{SiMe}_3)_2$  yielded the metallacycle  $\text{Ind}^*_2\text{Th}(\eta^2\text{-CH}_2\text{SiMe}_2\text{NSiMe}_3)$ . X-Ray crystal structure determination on several bis(permethylinindenyl)thorium complexes indicated that the permethylinindenyl ligands in these complexes exhibit a variety of conformations.<sup>140</sup>

$\text{Ind}^*_2\text{ThMe}_2$  undergoes several insertion reactions. For example, it reacts rapidly with  $\text{CO}_2$  to yield the acetate complex  $\text{Ind}^*_2\text{Th}(\eta^2\text{-O}_2\text{CMe})_2$  as a pale orange solid in 88% yield (Scheme 71).<sup>140</sup>

Bond disruption enthalpies have been determined for the complexes  $(\text{C}_9\text{H}_6\text{SiMe}_3)_3\text{ThH}$ ,  $(\text{C}_9\text{H}_6\text{SiMe}_3)_3\text{ThD}$ , and  $(\text{C}_5\text{H}_4\text{SiMe}_3)_3\text{ThH}$ . The thermodynamic data were obtained by iodolysis batch-titration calorimetry.<sup>141</sup>



Scheme 71

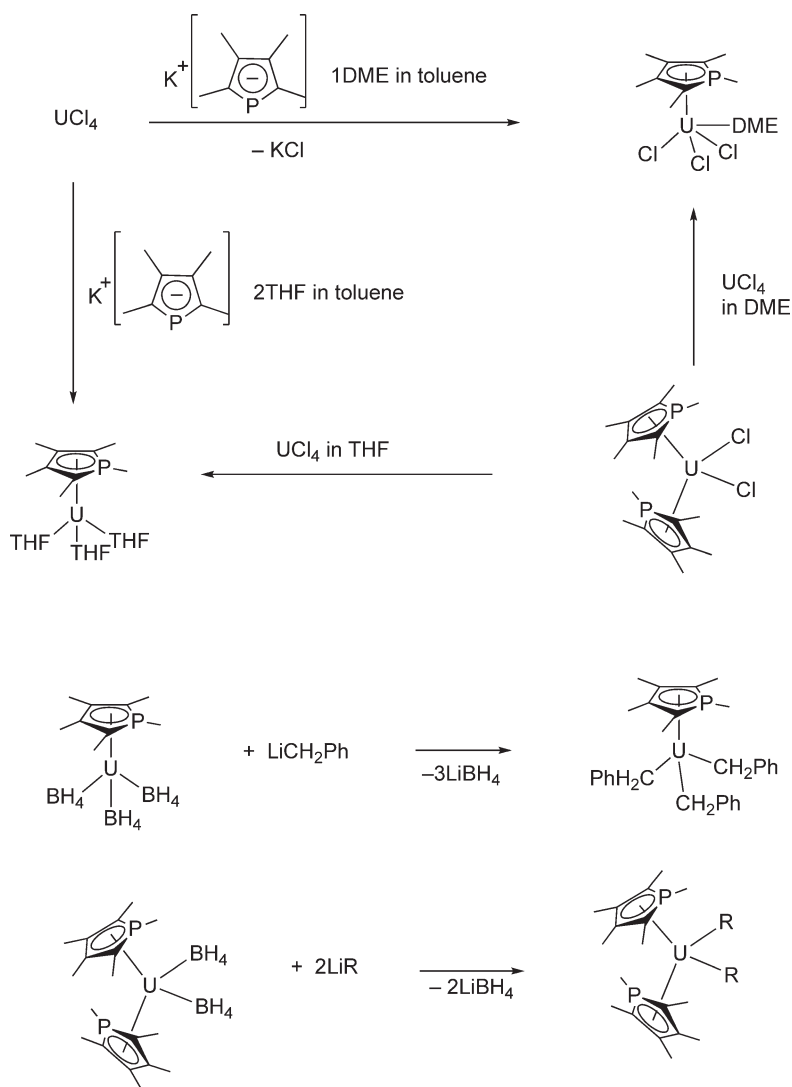
## 4.02.6 Cyclopentadienyl-like Compounds

### 4.02.6.1 Compounds with Heteroatom Five-membered Ring Ligands

A highly reactive uranium complex supported by the  $\text{Et}_8\text{-calix-[4]-tetrapyrrole}$  tetraanion ligand has been reported. The compound was found to effect dinitrogen cleavage, solvent desoxygenation, and polysilanol depolymerization. These compounds are mentioned here because they involve  $\pi$ -bonding interactions between the pyrrole units and the uranium centers.<sup>142,142a</sup> The synthesis of a series of mono- and bis(tmp)uranium (tmp = tetramethylphospholyl) complexes has been reported. The synthetic procedures are illustrated in [Scheme 72](#).<sup>132</sup>

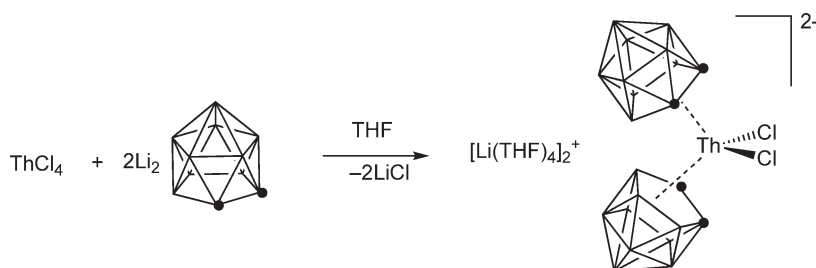
### 4.02.6.2 Compounds with Carboranyl Ligands

Synthesis and characterization of the first dicarbollide thorium complexes have been reported in 1997. A THF suspension of  $\text{ThCl}_4$  or a THF solution of  $\text{ThCl}_4(\text{TMEDA})_2$  was reacted with 2 equiv. of lithium dicarbollide ( $\text{Li}_2\text{C}_2\text{B}_9\text{H}_{11}$ ) to form the anionic bis(dicarbollide) complex  $[\text{Th}(\eta^5\text{-C}_2\text{B}_9\text{H}_{11})_2\text{Cl}_2]^{2-}$  ([Scheme 73](#)). By fractional

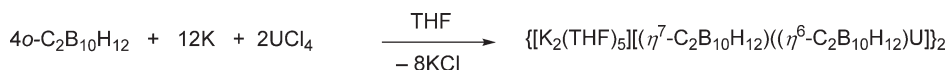


Scheme 72





Scheme 73



Scheme 74

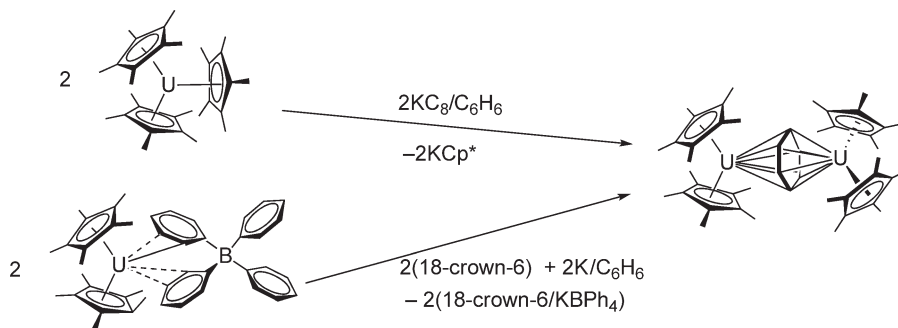
crystallization the lithium salt of the complex was isolated in a yield of 39%. The yield of the corresponding bromo complex was 75%.<sup>143</sup>

The synthesis of  $\{[K_2(THF)_5][(\eta^7-C_2B_{10}H_{12})(\eta^6-C_2B_{10}H_{12})U]\}_2$ , a metallocarborane with a novel  $(\eta^7-C_2B_{10}H_{12})^{4-}$  ligand has been reported (Scheme 74).<sup>144,144a</sup> A single-crystal X-ray determination revealed a centrosymmetrical dimer with a bent-sandwich structure involving  $\eta^6$ -coordination of the uranium atom to the *nido*- $C_2B_{10}H_{12}^{2-}$  ligand and  $\eta^7$ -bonding to the *arachno*-type  $C_2B_{10}H_{12}^{4-}$  ligand. Furthermore, a coordination of two B–H bonds of the  $C_2B_5$  layer of the *arachno*- $C_2B_{10}H_{12}^{4-}$  is observable. The most interesting feature of the structure is the boat conformation of the  $C_2B_5$  layer described above with short U–C distances of 2.41 and 2.44 Å lying in the range of U–C  $\sigma$ -bonds.<sup>144,144a</sup>

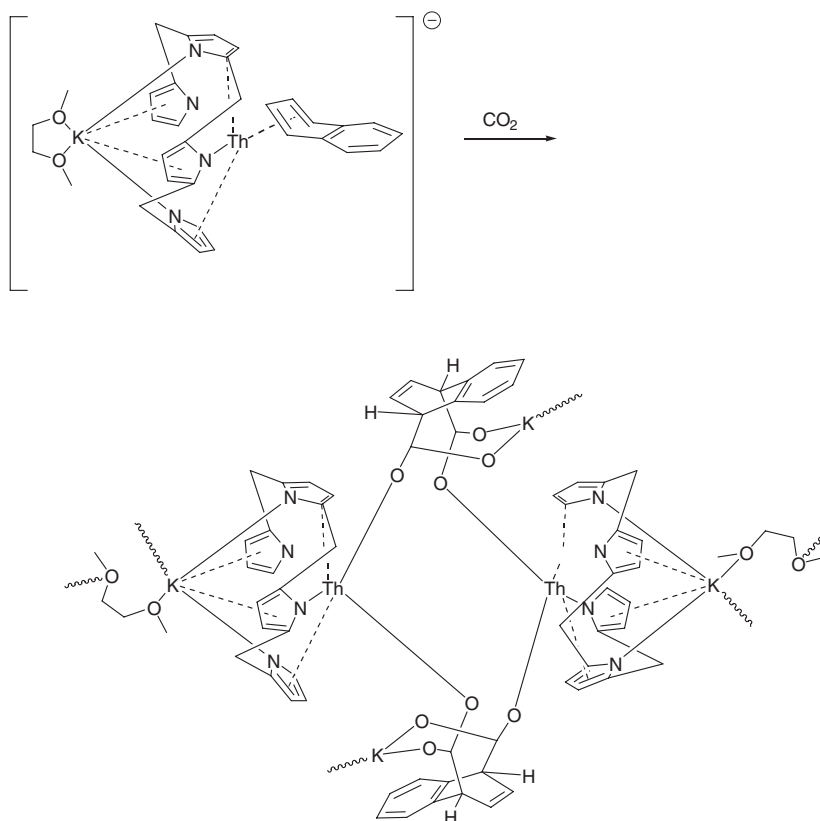
#### 4.02.7 Arene Complexes

The U(III) complex  $Cp^*_3U$  reacts with  $KC_8$  or K/18-crown-6 in benzene to form the novel U(II)  $\mu$ -benzene complex  $[Cp^*_2U]_2(\mu-\eta^6-C_6H_6)$  as a brown solid in nearly quantitative yield. An alternative preparation involves the use of  $[Cp^*_2U][(\mu-Ph)_2BPh_2]$  as the starting material (Scheme 75).  $[Cp^*_2U]_2(\mu-\eta^6:\eta^6-C_6H_6)$  reacts with  $KN(SiMe_3)_2$  to afford the amide-substituted analog  $[Cp^*_2UN(SiMe_3)_2]_2(\mu-\eta^6:\eta^6-C_6H_6)$ . Both compounds have non-planar  $C_6H_6$  rings sandwiched between the two uranium atoms.<sup>87</sup>

By reducing the tetravalent  $[K(DME)]_2[(Et_8\text{-calix-[4]-tetrapyrrole})Th(\mu-Cl)]_2$  with K(naphthalene), it was possible to obtain a unique example of the Th arene complex  $\{[(Et_8\text{-calix-[4]-tetrapyrrole})ThK(DME)](\mu,\mu'-\eta^4:\eta^6-C_{10}H_8)-(\mu-K)\}_n$ . Exposure of a deep red toluene solution of the naphthalene complex to  $CO_2$  at room temperature



Scheme 75



Scheme 76

and 1 atm afforded colorless crystals of the new compound  $[(\text{Et}_8\text{-calix-[4]-tetrapyrrole})\text{ThK}(\text{DME})]_2[\mu\text{-}cis\text{-}1,4\text{-(CO}_2)_2\text{C}_{10}\text{H}_6\text{K}(\text{DME})_{1.5}]_2$ , resulting from the *cis*-insertion of two molecules of CO<sub>2</sub> at the 1- and 4-positions of the coordinated naphthalene ring (Scheme 76).<sup>145</sup>

#### 4.02.8 Cycloheptatrienyl Compounds

The cycloheptatrienyl actinide sandwich complexes  $(\eta^7\text{-C}_7\text{H}_7)_2\text{An}^q$  ( $\text{An} = \text{Th-Am}$ ;  $q = 2-, 1-, 0, 1+$ ) have been studied using local and gradient-corrected density functional methods, with the inclusion of scalar (mass-velocity and Darwin) relativistic effects. It was found that the staggered conformer of  $[(\eta^7\text{-C}_7\text{H}_7)_2\text{U}]^-$  is more stable than the eclipsed one by about  $0.6 \text{ kcal mol}^{-1}$ . The bonding analysis indicated that  $[(\eta^7\text{-C}_7\text{H}_7)_2\text{U}]^-$  and  $(\eta^7\text{-C}_7\text{H}_7)_2\text{U}$  are best considered as complexes of U(III) and U(IV), respectively.<sup>146</sup> Novel cycloheptatrienyl sandwich complexes of actinide elements have also been explored experimentally.<sup>147</sup> For example, reaction between UCl<sub>4</sub>, metallic potassium, and an excess of cycloheptatriene in THF gave the anionic complex  $\text{K}[\text{U}(\text{C}_7\text{H}_7)_2]$ . Subsequent treatment of the  $\text{K}[\text{U}(\text{C}_7\text{H}_7)_2]$  with 18-crown-6 in THF yielded crystals of  $[\text{K}(18\text{-crown-6})][\text{U}(\text{C}_7\text{H}_7)_2]$ . The complex was also alternatively prepared from the UCl<sub>4</sub> or U(BH<sub>4</sub>)<sub>4</sub> and 4 equiv. of  $\text{KC}_7\text{H}_9$  in THF followed by addition of 18-crown-6 to the filtered solution. According to X-ray diffraction crystallography the complex consists of discrete  $[\text{K}(18\text{-crown-6})]^+$  cations and  $[\text{U}(\text{C}_7\text{H}_7)_2]^-$  anions. The anion  $[\text{U}(\text{C}_7\text{H}_7)_2]^-$  has a sandwich structure with two parallel cycloheptatrienyl rings in a staggered conformation. The U–C distances are equal within experimental error with average value of  $2.53(2) \text{ \AA}$ . The question of the uranium oxidation state in the complex has been discussed.<sup>147</sup> Inverse cycloheptatrienyl uranium complexes have been prepared by a similar synthetic route. Reactions of  $\text{UX}_4$  ( $\text{X} = \text{NEt}_2, \text{BH}_4$ ) with  $\text{KC}_7\text{H}_9$  gave the anionic complexes  $\text{K}[\text{X}_3\text{U}(\mu\text{-}\eta^7\text{:}\eta^7\text{-C}_7\text{H}_7)\text{UX}_3]$  and  $[\text{K}(18\text{-crown-6})][(\text{NEt}_2)_3\text{U}(\mu\text{-}\eta^7\text{:}\eta^7\text{-C}_7\text{H}_7)\text{U}(\text{NEt}_2)_3]$ .<sup>148,149</sup>

### 4.02.9 Cyclooctatetraenyl Compounds

The investigation of actinide cyclooctatetraenyl complexes continued to be an area of active research in recent years. Especially notable among the more recent developments is the synthesis and derivative chemistry of various cationic mono(cyclooctatetraenyl) uranium(IV) and (V) complexes.<sup>71,97</sup> The chemistry of mono(cyclooctatetraenyl)uranium complexes has been reviewed by Ephritikhine *et al.*<sup>150</sup> A highly interesting essay on the discovery and chemistry of uranocene has been published by Seyferth under the title: "Uranocene. The First Member of a New Class of Organometallic Derivatives of the *f* Elements."<sup>151</sup>

#### 4.02.9.1 Cyclooctatetraenyl Actinide(III) Compounds

The synthesis of the mixed-ring uranium(III) complex (COT)Cp<sup>\*</sup>U(THF) has been achieved by reaction of Cp<sup>\*</sup>UI<sub>2</sub>(THF)<sub>3</sub> with K<sub>2</sub>(COT) in THF. Further treatment of (COT)Cp<sup>\*</sup>U(THF) with 4,4'-dimethyl-2,2'-bipyridine (Me<sub>2</sub>bipy) in toluene yielded the formally 10-coordinate complex (COT)Cp<sup>\*</sup>U(Me<sub>2</sub>bipy), which was structurally characterized by an X-ray analysis.<sup>152</sup> The mixed-sandwich uranium(III) complex (COT)Cp<sup>\*</sup>U(HMPA) was isolated from the reaction of the uranium cation complex [(COT)U(HMPA)<sub>3</sub>][BPh<sub>4</sub>] with KCp<sup>\*</sup> (70% yield). The analogous tmp derivative (COT)U(tmp)(HMPA)<sub>2</sub> was obtained upon reduction of the cationic uranium(IV) complex [(COT)U(tmp)(HMPA)<sub>2</sub>][BPh<sub>4</sub>] with sodium amalgam.<sup>153</sup>

#### 4.02.9.2 Mono(cyclooctatetraenyl) Actinide(IV) and -(V) Compounds

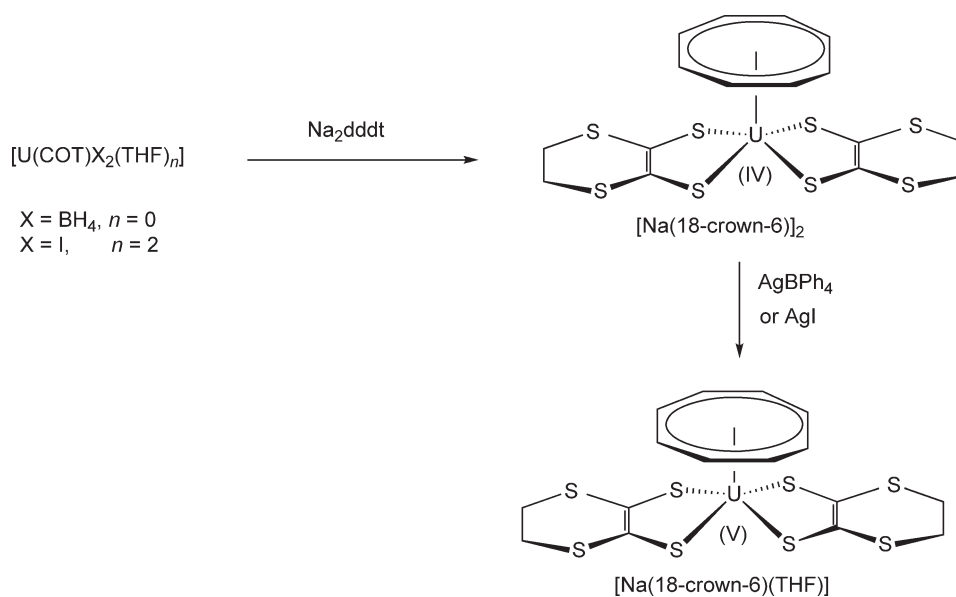
Gas-phase reactions of the bare monocationic berkelium ion, Bk<sup>+</sup>, with several reagents including cyclooctatetraene have been examined by a mass spectrometric technique adapted for the highly radioactive transuranium actinides. The products included  $\pi$ -bonded organoberkelium ions such as BkCOT<sup>+</sup>, presumably, the berkelium-cyclooctatetraenyl half-sandwich complex ion.<sup>22</sup>

The thiolate complexes [(COT)U( $\mu$ -SR)<sub>2</sub>]<sub>2</sub> (R = Pr<sup>i</sup>, Bu<sup>n</sup>, Bu<sup>t</sup>) were obtained by treating (COT)U(BH<sub>4</sub>)<sub>2</sub> with an excess of the corresponding thiol RSH or NaSR in toluene. In the molecular structure of [(COT)U( $\mu$ -SP<sup>r</sup>)<sub>2</sub>]<sub>2</sub>, two (COT)U units are connected via four bridging thiolate ligands. The analogous reaction of (COT)U(BH<sub>4</sub>)<sub>2</sub> with 3 equiv. of NaSBu<sup>t</sup> afforded the anionic tris(thiolate) complex Na[(COT)U(SBu<sup>t</sup>)<sub>3</sub>].<sup>154</sup> The synthesis of the first dithiolene complex of uranium with a COT ligand was achieved through the reaction of (COT)UX<sub>2</sub>(THF)<sub>*n*</sub> with Na<sub>2</sub>dddt affording the (dithiolene)uranium(IV) compound [Na(18-crown-6)]<sub>2</sub>[(COT)U(dddt)<sub>2</sub>]. This complex was oxidized in THF with AgBPh<sub>4</sub> to the corresponding U(V) monoanion [Na(18-crown-6)(THF)][(COT)U(dddt)<sub>2</sub>] (Scheme 77). The uranium atom is five coordinate in a distorted-square-pyramidal arrangement (if the cyclooctatetraenyl is considered a monodentate ligand).<sup>109</sup>

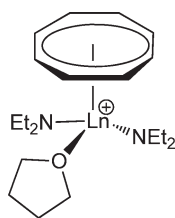
In a related study, reaction of (COT)U(BH<sub>4</sub>)<sub>2</sub>(THF) with the dithiocarbonates dddtCO and dmioCO (dmio = 1,3-dithiole-2-one-4,5-dithiolate) gave the neutral dithiolene compounds [(COT)U(dithiolene)]<sub>2</sub> in good yields (dithiolene = dddt, dmio, or 1,3-dithiole-4,5-dithiolate (mdt)). The reactions are accompanied by elimination of formaldehyde and borane. The X-ray crystal structures of [(COT)U(mdt)]<sub>2</sub> and monomeric (COT)U(mdt)(pyridine)<sub>2</sub> showed an interaction between the C=C double bond of the mdt ligand and the uranium atom, and the <sup>1</sup>H NMR spectra revealed a facile dithiolene ring inversion process in solution.<sup>155</sup>

The cationic cyclooctatetraenyluranium(V) complex [(COT)U(NEt<sub>2</sub>)<sub>2</sub>(THF)][BPh<sub>4</sub>] has been prepared by oxidation of the neutral tetravalent precursor (COT)U(NEt<sub>2</sub>)<sub>2</sub> with 1 equiv. of AgBPh<sub>4</sub> in THF. Treatment of (COT)U(NEt<sub>2</sub>)<sub>2</sub> with TiCp gave the mixed neutral cyclopentadienyl–cyclooctatetraenyl uranium complex (COT)CpU(NEt<sub>2</sub>)<sub>2</sub>.<sup>97</sup> X-ray absorption spectroscopy (XAS) has been used to study mono(cyclooctatetraenyl) uranium compounds in the oxidation states IV and V, including the cationic complex [(COT)U(NEt<sub>2</sub>)<sub>2</sub>(THF)][BPh<sub>4</sub>] (Scheme 78).<sup>156</sup>

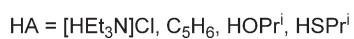
The same authors reported the synthesis of the cationic uranium(IV) cyclooctatetraenyl and cyclopentadienyl–cyclooctatetraenyl complexes [(COT)U(NEt<sub>2</sub>)(THF)<sub>2</sub>][BPh<sub>4</sub>] and [(COT)Cp<sup>\*</sup>U(THF)<sub>2</sub>][BPh<sub>4</sub>] (R = H, Me). The compounds were obtained by protonolysis of the corresponding neutral amide precursors with [NH<sub>4</sub>Et<sub>3</sub>][BPh<sub>4</sub>] (Scheme 79). The complex [(COT)Cp<sup>\*</sup>U(THF)<sub>2</sub>][BPh<sub>4</sub>] was characterized by single-crystal X-ray diffraction. The structure consists of discrete cation–anion pairs. In the cation [(COT)Cp<sup>\*</sup>U(THF)<sub>2</sub>]<sup>+</sup>, the U atom has a pseudo-tetrahedral environment. The average U–C(Cp<sup>\*</sup>) and U–C(COT) distances are 2.74(1) and 2.65(2) Å, respectively, and the angle Cp<sup>\*</sup>(cent.)–U–COT(cent.) is 139.6(5)°. <sup>71,148</sup> The first cyclooctatetraenyl uranium(IV) triflate complex, (COT)U(OTf)<sub>2</sub>(py),<sup>64</sup> is accessible from the uranium(IV) triflate precursor U(OTf)<sub>4</sub> and K<sub>2</sub>COT in pyridine.<sup>61</sup>



Scheme 77



Scheme 78



Scheme 79

The anionic mono(cyclooctatetraenyl)uranium complexes  $M[(COT)U(NEt_2)_3]$  were obtained by treatment of the amide precursor  $[U(NEt_2)_3][BPh_4]$  with  $M_2COT$  ( $M = Li, Na, K$ ). Oxidation of  $M[(COT)U(NEt_2)_3]$  with  $TiBPh_4$  afforded the neutral uranium(v) half-sandwich complex  $(COT)U(NEt_2)_3$ , which in turn reacts with sodium amalgam to give back  $Na[(COT)U(NEt_2)_3]$ . Protonation of  $(COT)U(NEt_2)_3$  with  $[NEt_3H][BPh_4]$  led to formation of the cationic uranium(v) complex  $[(COT)U(NEt_2)_2(THF)][BPh_4]$ .<sup>157</sup> The reactivity of the cationic uranium amide compound  $[(COT)U(NEt_2)_2(THF)_2][BPh_4]$  has been studied in detail. The reactions are summarized in Scheme 79.<sup>158</sup>

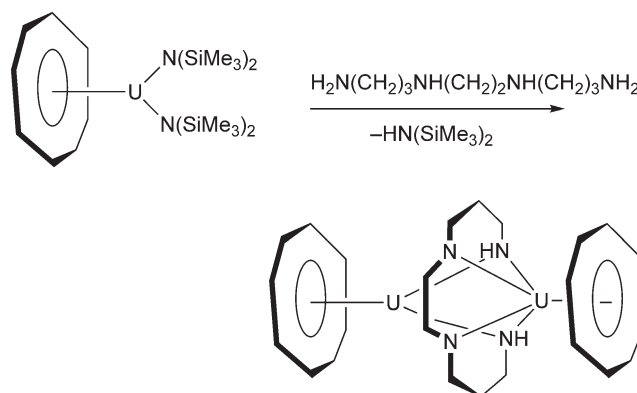
The chloro- and tetrahydroborato amide complexes  $(COT)U(NEt_2)(THF)_x(BH_4)$ ,  $(COT)U(NEt_2)(THF)_x(X)$ , which were readily formed upon addition of  $LiCl$  or  $KBH_4$ , were stable in THF solution. They could, however, not be isolated in solid form and decomposed into  $U(COT)_2$  and other unidentified species by desolvation. Treatment of  $[U(COT)(NEt_2)(THF)_2][BPh_4]$  with  $CO_2$ ,  $CS_2$ , or acetonitrile led to insertion of these small molecules into the U–N bond to form the carbamate or dithiocarbamate complex, respectively (Scheme 79).<sup>158</sup>

The reaction of  $[(COT)U(NEt_2)(THF)_2][BPh_4]$  with proton acidic substrates HA provides a straightforward route to U–A derivatives (Scheme 79). The complexes  $[(COT)U(NEt_2)(THF)_3][BPh_4]$  and  $[(COT)U(S_2CNEt_2)(THF)_2][BPh_4]$  have been crystallographically characterized.<sup>158</sup>

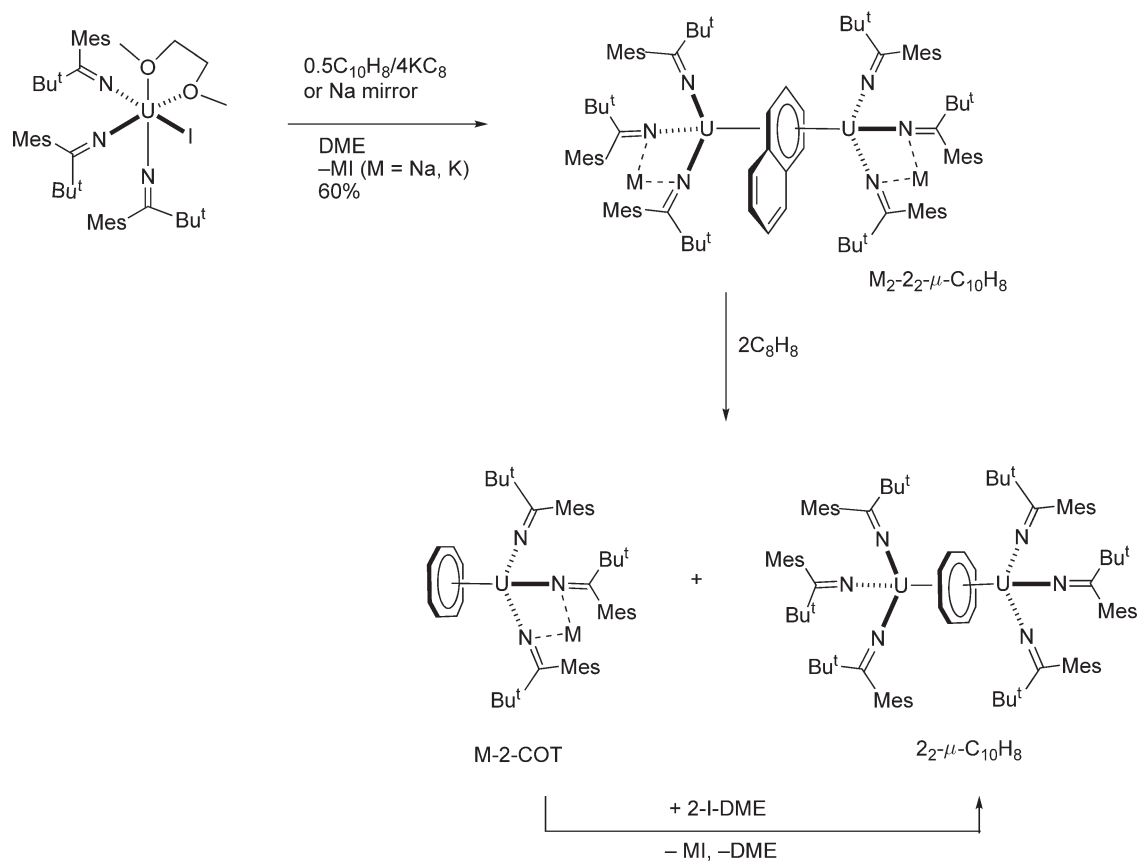
The mixed amide complex  $(COT)U(NEt_2)[N(SiMe_3)_2]$  reacts in THF with  $[NHEt_3][BPh_4]$  under formation of the cationic species  $[(COT)U(THF)_x[N(SiMe_3)_2]]^+$ .<sup>88</sup> A dinuclear cyclooctatetraene uranium complex with a bridging tetraamide ligand has also been synthesized and characterized. The complex was prepared by the transamination reaction of  $(COT)U[N(SiMe_3)_2]_2$  and  $H_2N(CH_2)_3NH(CH_2)_2NH(CH_2)_3NH_2$  (Scheme 80). The X-ray crystal structure reveals the shortest U–U distance of 3.3057(9) Å ever observed in a molecular compound.<sup>159</sup>

Diuranium inverted-sandwich complexes involving naphthalene and cyclooctatetraene have been synthesized with the use of bulky ketimide ancillary ligands (Scheme 81). Reaction of readily available  $UI_3(DME)_2$  with  $KN=C(Bu^t)Mes$  in DME led to the isolation of dark green-brown  $IU(DME)[N=C(Bu^t)Mes]_3$  (=2-I-DME) in 30% yield. In this compound, one DME ligand coordinates to the uranium center in the pocket formed by the mesityl groups. Treatment of  $UI(DME)[N=C(Bu^t)Mes]_3$  with 4 equiv. of  $KC_8$  and 0.5 equiv. of naphthalene in DME allowed the isolation of a naphthalene-bridged compound,  $K_2(\mu-\eta^6:\eta^6-C_{10}H_8)[U\{N=C(Bu^t)Mes\}_3]_2(\mu-\eta^6:\eta^6-C_{10}H_8)$  (=K<sub>2</sub>-2- $\mu$ -C<sub>10</sub>H<sub>8</sub>). The corresponding sodium derivative,  $Na_2[U\{N=C(Bu^t)Mes\}_3]_2(\mu-\eta^6:\eta^6-C_{10}H_8)$  (=Na<sub>2</sub>-2- $\mu$ -C<sub>10</sub>H<sub>8</sub>), was obtained as dark green-brown crystals in 40% yield by reducing 2-I-DME over a sodium mirror in THF in the presence of 0.6 equiv. of naphthalene. Treatment of  $M_2$ -2- $\mu$ -C<sub>10</sub>H<sub>8</sub> ( $M = Na, K$ ) with 2 equiv. of cyclooctatetraene afforded a mixture of two products. The ionic compounds  $K[(COT)U\{N=C(Bu^t)Mes\}_3]$  (=K-2-COT) and  $[Na(Et_2O)][(COT)U\{N=C(Bu^t)Mes\}_3]$  (=Na-2-COT) are insoluble in pentane, facilitating their separation from the neutral inverted-sandwich complex  $[U\{N=C(Bu^t)Mes\}_3]_2(\mu-\eta^8:\eta^8-COT)$  (=2- $\mu$ -COT). Interestingly, the latter compound can also be assembled independently in 90% yield by salt elimination upon reaction of M-2-COT with the iodide 2-I-DME.<sup>160</sup>

The first cationic borohydride and the first dicationic uranium complexes have been synthesized by protonolysis of borohydride precursors. The monocationic compound  $[(COT)U(BH_4)(THF)_2][BPh_4]$  was prepared by treating  $(COT)U(BH_4)_2(THF)$  with 0.87 equiv. of  $[NEt_3H][BPh_4]$  in THF (Scheme 82).<sup>161</sup>



Scheme 80



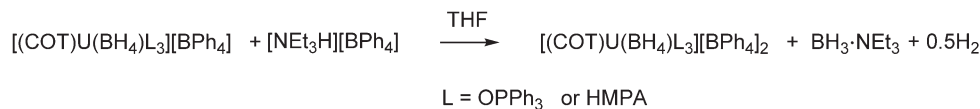
Scheme 81



Scheme 82

The reaction of the monocationic uranium complex and  $[\text{NEt}_3\text{H}][\text{BPh}_4]$  in refluxing THF afforded the dication  $[(\text{COT})\text{U}(\text{THF})_x]^{2+}$ . However, an excess of the ammonium salt was necessary to achieve the complete formation of the complex, which could not be isolated in a pure state from the reaction mixture. Protonation of  $[(\text{COT})\text{U}(\text{BH}_4)\text{L}_3][\text{BPh}_4]$  ( $\text{L} = \text{OPPh}_3$  and HMPA) was much more rapid giving the dications  $[(\text{COT})\text{UL}_3]^{2+}$  (Scheme 83).<sup>161</sup>

The dication adopts a three-legged piano-stool configuration in which the O–U–O angles vary from  $84.0^\circ$  to  $88.2^\circ$  with a mean value of  $87(3)^\circ$ , and average COT–U–O angles of  $127(1)^\circ$ . The uranium atom is  $1.92(2)\text{Å}$  away from the planar cyclooctatetraene ring, and the mean U–C bond distance is  $2.65(3)\text{Å}$ . These values compare well with those determined in the monocationic cyclooctatetraene complexes  $[(\text{COT})\text{U}(\text{NEt}_2)(\text{THF})_3]^+$ .<sup>161</sup>



Scheme 83

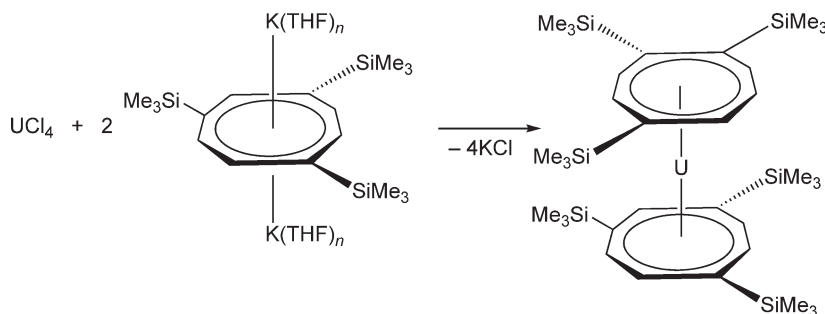
Treatment of  $(\text{COT})\text{U}(\text{BH}_4)_2(\text{THF})$  or  $[(\text{COT})\text{U}(\text{BH}_4)(\text{THF})_2][\text{BPh}_4]$  with Ktmp afforded the mixed cyclooctatetraenyl–phospholyl uranium complex  $(\text{COT})\text{U}(\text{tmp})(\text{BH}_4)(\text{THF})$  as a brown solid in 89% yield. Further reaction with Ktmp with  $(\text{COT})\text{U}(\text{tmp})(\text{BH}_4)(\text{THF})$  gave the ate-type addition derivative  $\text{K}[(\text{COT})\text{U}(\text{tmp})_2(\text{BH}_4)(\text{THF})_x]$ . In the presence of NaOEt,  $(\text{COT})\text{U}(\text{tmp})(\text{BH}_4)(\text{THF})$  was transformed into orange-red  $(\text{COT})\text{U}(\text{tmp})(\text{OEt})$  (69% yield). The cationic compound  $[(\text{COT})\text{U}(\text{tmp})(\text{HMPA})_2][\text{BPh}_4]$  was isolated from the reaction of  $[(\text{COT})\text{U}(\text{HMPA})_3][\text{BPh}_4]$  with Ktmp.<sup>162</sup>

#### 4.02.9.3 Bis(cyclooctatetraenyl) Actinide(IV) Compounds

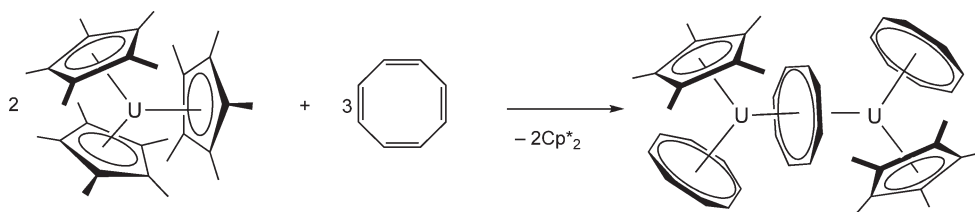
High-resolution Raman spectra for uranocene and thorocene have been measured under liquid nitrogen.<sup>163</sup> 1,1'-Dimesityluranocene has been prepared and investigated by  $^1\text{H}$  NMR spectroscopy. The compound was synthesized by the reaction of  $\text{UCl}_4$  with the potassium salt of the mesitylcyclooctatetraene dianion in THF. The  $^1\text{H}$  NMR spectrum revealed that the mesityl groups are in a locked position with *exo*- and *endo-ortho*-methyl groups. The two mesityl rings were found to be held close to each other, presumably by van der Waals attraction.<sup>164</sup> A uranocene derivative containing the very bulky 1,3,6-tris(trimethylsilyl)cyclooctatetraenyl ligand has been obtained in the form of green/red dichroic crystals by reacting  $\text{UCl}_4$  with 2 equiv. of the dipotassium salt of the ligand (Scheme 84). Bright yellow  $[\text{C}_8\text{H}_5(\text{SiMe}_3)_3\text{-1,3,6}]_2\text{Th}$  was isolated in the same manner in 79% yield.  $\text{NpCl}_4$  reacts with 2 equiv. of  $\text{K}_2[\text{C}_8\text{H}_5(\text{SiMe}_3)_3\text{-1,3,6}](\text{THF})_{1.5}$  to give the red neptunocene complex  $[\text{C}_8\text{H}_5(\text{SiMe}_3)_3\text{-1,3,6}]_2\text{Np}$  in 88% yield after crystallization from pentane. All three polysilylated actinidocenes are easily hydrolyzed but can be sublimed without decomposition at ca. 250–270 °C/ $10^{-3}$  torr.<sup>165,165a</sup>

The electronic ground state of organouranium(V) compounds influenced by different ligands has been investigated by electron paramagnetic resonance (EPR). It was shown that the interactions of 5*f*-orbitals with  $\eta^8\text{-COT}$ ,  $\eta^5\text{-Cp}$ ,  $\eta^5\text{-Cp}^+$ , THF, and  $\text{NR}_2$  ligands are sufficiently small to conserve the ground state quantum number  $J = 5/2$  of the free U(V) ion as a good quantum number for the complex, that the contribution of 5*f*-orbitals to the electronic structure of these compounds is non-bonding, and the metal–ligand bonding should involve mainly uranium 6*d*-orbitals.<sup>166</sup> Large-scale state-average multi-configuration self-consistent field, configuration interaction, averaged coupled-pair functional, and spin–orbit configuration interaction calculations have been carried out for uranocene and thorocene,  $\text{An}(\text{COT})_2$  ( $\text{An} = \text{U}, \text{Th}$ ). It was found that thorocene has a  $^1\text{A}_{1g}(\text{A}_{1g})$  ground state and the single-determinant wave function may be pictured as a Th(IV) compound with 5*f* $^0\pi_{e2u}^4$  configuration. The calculated Th–COT(ring) distance of 2.03 Å was in good agreement with the experimental value of 2.00 Å.<sup>167,168</sup> The geometric structure and electronic properties of the 5*f* $^1$  complex protactinocene  $\text{Pa}(\text{COT})_2$  has been studied using gradient-corrected density functional methods with the inclusion of spin–orbit coupling. The calculated structure of  $\text{Pa}(\text{COT})_2$  with scalar relativistic corrections is intermediate between those of  $\text{Th}(\text{COT})_2$  and  $\text{U}(\text{COT})_2$ . The first 20 vertical ionization energies and the magnetic moment of  $\text{Pa}(\text{COT})_2$  have been predicted based on the spin–orbit calculation. A comparison of the calculated infrared vibrational frequencies and absorption intensities of  $\text{Pa}(\text{COT})_2$  with available experimental data was presented, and the vibrational spectra were assigned.<sup>169</sup>

The synthesis of  $(\mu\text{-COT})[\text{Cp}^*(\text{COT})\text{U}]_2$  from  $\text{Cp}^*_3\text{U}$  and cyclooctatetraene has been achieved. Treatment of  $\text{Cp}^*_3\text{U}$  with COT in a 1 : 1 stoichiometry afforded  $(\text{C}_5\text{Me}_5)_2$  and  $(\mu\text{-COT})[\text{Cp}^*(\text{COT})\text{U}]_2$  (Scheme 85).<sup>90,170,170a</sup>



Scheme 84



Scheme 85

## 4.02.10 Heterobimetallic Compounds

### 4.02.10.1 Metal–Metal Bonded Compounds

The gas-phase reactions of actinide ( $\text{An}^+ = \text{Th}^+, \text{U}^+$ ) cations with iron pentacarbonyl,  $\text{Fe}(\text{CO})_5$ , and with ferrocene,  $\text{Cp}_2\text{Fe}$ , have been studied by Fourier transform ion cyclotron resonance mass spectrometry (FT-ICR/MS). In the case of  $\text{Fe}(\text{CO})_5$ , the observed primary products were of the type  $\text{AnFe}(\text{CO})_x^+$  ( $\text{An} = \text{Th}, \text{U}$ ;  $x = 2$  and  $3$ ), and evidence was obtained for the presence of direct Ln–Fe bonds in these species. With  $\text{Cp}_2\text{Fe}$  the  $\text{An}^+$  cations reacted by metal exchange, yielding the An–bis(cyclopentadienyl) ions  $\text{Cp}_2\text{An}^+$ .<sup>171</sup>

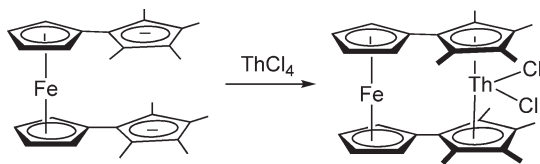
### 4.02.10.2 Heterobimetallic Compounds without Direct Metal–Metal Bonds

The synthesis, structure, and electrochemistry of the first fulvalene actinide complex  $[(\text{Me}_4\text{Fv})_2\text{FeThCl}_2]$  ( $\text{Me}_4\text{Fv} = 1,2,3,4$ -tetramethylfulvalene) was reported in 1995.<sup>172</sup> The compound was obtained by reaction of dilithio[1,1'-bis(tetramethylcyclopentadienyl)ferrocene] with  $\text{ThCl}_4$  in THF (Scheme 86). According to X-ray diffraction studies the complex consists of two tetramethylfulvalene fragments bridging Fe and  $\text{ThCl}_2$  centers. The average Th–C(Cp) and Th–Cl bond lengths are 2.79 and 2.63 Å, respectively. An electrochemical study revealed a quasi-reversible couple at  $-0.15$  V versus an internal standard of ferrocene.<sup>172</sup> More recently, the first urana[1]ferrocenophane complex has been synthesized and characterized. Reaction of  $\text{UCl}_4$  with  $\text{Li}_2\text{fc} \cdot \text{TMEDA}$  ( $\text{fc} = 1,1'$ -ferrocenylene) gave the tris(1,1'-ferrocenylene)uranium complex  $\text{Li}_2[\text{U}(\text{fc})_3(\text{py})_3]$ .<sup>173</sup>

The diphenylphosphinocyclopentadienyl ligand is ideally suited for the construction of early/late transition metal complexes. The heterobimetallic Mo/U complexes  $[(\text{C}_5\text{H}_4\text{PPh}_2)\text{Mo}(\text{CO})_4](\text{C}_5\text{H}_4\text{PPh}_2)\text{UX}$  ( $\text{X} = \text{Cl}, \text{NEt}_2, \text{BH}_4$ ) have been synthesized. Electrochemical measurements showed a significant decrease in the electron density on the uranium atom after coordination to the  $\text{Mo}(\text{CO})_4$  moiety.<sup>174</sup>

Synthesis and reactivity of hydrogen-rich uranium–rhenium compounds have been reported. The tris(cyclopentadienyl)uranium–rhenium hydride complexes  $[(\text{C}_5\text{H}_4\text{R})_3\text{UH}_6\text{Re}(\text{PPh}_3)_2]$  ( $\text{R} = \text{H}, \text{Bu}^t, \text{SiMe}_3$ ) were prepared according to Scheme 87.<sup>175</sup>

The reaction of ring-substituted  $(\text{C}_5\text{H}_4\text{R})_3\text{UCl}$  ( $\text{R} = \text{Bu}^t$  and  $\text{SiMe}_3$ ) with 1 equiv. of  $[\text{K}(\text{THF})_2][\text{ReH}_6(\text{PPh}_3)_2]$  remained incomplete, leading to the equilibrium shown in Scheme 88.<sup>175</sup>

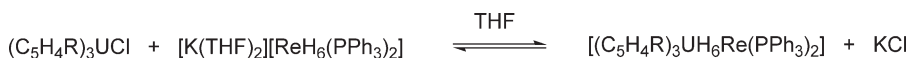


Scheme 86

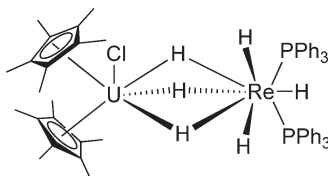


Scheme 87





Scheme 88



Scheme 89

The related reaction of  $\text{Cp}^*_2\text{UCl}(\text{THF})$  and  $[\text{K}(\text{THF})_2][\text{ReH}_6(\text{PPh}_3)_2]$  did not afford the metathesis product  $[\text{Cp}^*_2\text{UH}_6\text{Re}(\text{PPh}_3)_2]$  with elimination of  $\text{KCl}$  but gave the anionic addition compound  $[\text{K}(\text{THF})_2][\text{Cp}^*_2\text{U}(\text{Cl})\text{H}_6\text{Re}(\text{PPh}_3)_2]$ . The borohydride analog  $[\text{K}(\text{THF})_2][\text{Cp}^*_2\text{UB}(\text{H})_4\text{Re}(\text{PPh}_3)_2]$  was prepared similarly. The  $^1\text{H}$  and  $^{31}\text{P}$  NMR spectra revealed that  $[\text{K}(\text{THF})_2][\text{Cp}^*_2\text{CU}(\text{Cl})\text{H}_6\text{Re}(\text{PPh}_3)_2]$  reversibly dissociates in THF into  $\text{Cp}^*_2\text{UCl}(\text{THF})$  and  $[\text{K}(\text{THF})_2][\text{ReH}_6(\text{PPh}_3)_2]$ . Addition of either of these two species caused the equilibrium to be shifted toward the formation of  $[\text{K}(\text{THF})_2][\text{Cp}^*_2\text{U}(\text{Cl})\text{H}_6\text{Re}(\text{PPh}_3)_2]$  (anion shown in Scheme 89).<sup>175</sup>

Reactions of  $\text{Cp}^*_2\text{ThMe}_2$  with the bis(carbollide) complexes  $[\text{NEt}_3\text{H}][\text{Co}(\text{B}_9\text{C}_2\text{H}_{11})_2]$  and  $[\text{NEt}_3\text{H}][\text{Fe}(\text{B}_9\text{C}_2\text{H}_{11})_2]$  in toluene yielded the salt-like species  $[\text{Cp}^*_2\text{ThMe}][\text{Co}(\text{B}_9\text{C}_2\text{H}_{11})_2]$  and  $[\text{Cp}^*_2\text{ThMe}][\text{Fe}(\text{B}_9\text{C}_2\text{H}_{11})_2]$ . A crystal structure determination of the iron derivative revealed tight ion-pairing with three close Th–H–B bridging interactions. The high level of coordinative saturation was taken as an explanation for the chemical inertness of these heterobimetallic salts.<sup>176</sup>

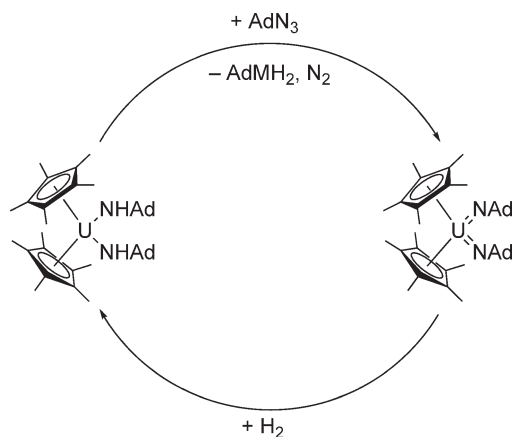
## 4.02.11 Organoactinide Catalysis

Several review articles on special aspects of organoactinide catalysts have been published. Eisen *et al.* gave an account on “Organoactinides—novel catalysts for demanding chemical transformations.”<sup>177</sup> The topic “Organoactinides—new type of catalysts for carbon–silicon bond formation” has also been reviewed by Eisen *et al.*<sup>178</sup> The same authors published a comparative study of the catalytic effect in opening an organoactinide metal coordination sphere (permethylmetallocene vs. *ansa*-metallocene derivatives) using the regioselective dimerization of terminal alkynes and hydrosilylation of alkynes and alkenes with  $\text{PhSiH}_3$  promoted by  $\text{Me}_2\text{Si}(\text{C}_5\text{Me}_4)_2\text{ThBu}^n_2$  as examples.<sup>179</sup>

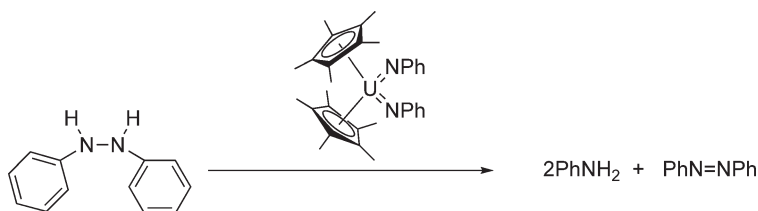
### 4.02.11.1 Organoactinide-catalyzed Hydrogenation Reactions

A thorough investigation of supported organoactinide complexes as heterogeneous catalysts, including a kinetic and mechanistic study of facile arene hydrogenation, has been published. The experiments were carried out with the supported complexes  $\text{Cp}^*\text{Th}(\text{CH}_2\text{Ph})_3/\text{DA}$ ,  $\text{Th}(\text{CH}_2\text{C}_6\text{H}_3\text{Me}_2-1,3,5)_4/\text{DA}$ , and  $\text{Th}(\eta^3\text{-C}_3\text{H}_5)_4/\text{DA}$  (DA = dehydroxylated  $\gamma$ -alumina). In slurry reactions ( $90^\circ\text{C}$ ,  $P_{\text{H}_2} = 180$  psi), the activity for benzene hydrogenation follows the order  $\text{Cp}^*\text{Th}(\text{CH}_2\text{Ph})_3/\text{DA} < \text{Th}(1,3,5\text{-CH}_2\text{C}_6\text{H}_3\text{Me}_2)_4/\text{DA} < \text{Th}(\eta^3\text{-C}_3\text{H}_5)_4/\text{DA}$  with an  $N_t$  value for the tetraallyl derivative of  $\sim 25,000\text{ h}^{-1}\text{ active site}^{-1}$ . This approaches or exceeds most conventional platinum metal catalysts in efficacy for benzene reduction.<sup>23</sup> Structural studies including  $^{13}\text{C}$  CPMAS NMR spectroscopy of the  $^{13}\text{C}_\alpha$ -enriched model adsorbate  $\text{Cp}^*\text{Th}(\text{C}_3\text{H}_7)_2$  chemisorbed on superacidic sulfated zirconia revealed that the adsorbate undergoes a new molecular chemisorptive process: protonolytic M–C  $\sigma$ -bond cleavage at the very strong Brønsted acid sites to yield “cation-like” organometallic electrophiles.<sup>180</sup>

The catalytic reduction of azides and hydrazines involving high-valent organouranium complexes has been investigated.<sup>181</sup>  $\text{Cp}^*_2\text{U}(\text{=NAd})_2$  reacts with hydrogen to give the corresponding reduced bis(amide) complex  $\text{Cp}^*_2\text{U}(\text{NHAd})_2$  (Scheme 90). The reaction proceeded cleanly with a rate of hydrogenation of  $t_{1/2} = 4\text{ h}$ . When  $\text{AdN}_3$  was added to a solution of the bis(amide) complex, the bis(imido) compound  $\text{Cp}^*_2\text{U}(\text{=NAd})_2$  was regenerated. Heating of  $\text{Cp}^*_2\text{U}(\text{NHAd})_2$  to  $55^\circ\text{C}$  in THF with  $\text{AdN}_3$  under 1 atm of hydrogen led to catalytic hydrogenation of  $\text{AdN}_3$  to  $\text{AdNH}_2$ .<sup>181</sup>



Scheme 90



Scheme 91

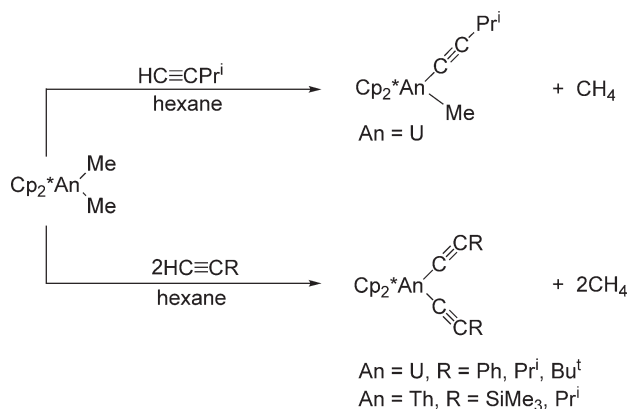
When  $\text{Cp}^*_2\text{U}(=\text{NPh})_2$  was treated with an excess of *N,N'*-diphenylhydrazine in the absence of hydrogen, the substrate was entirely consumed, and aniline and azobenzene were formed in a 2:1 ratio (Scheme 91). The disproportionation indicated that the *N,N'*-diphenylhydrazine acted upon the uranium complexes as both oxidant and reductant.<sup>181</sup>

The cationic metallocene complex  $[\text{Cp}^*_2\text{ThMe}][(\mu\text{-H})(\mu\text{-CHCH}_2\text{Bu}^t)\{\text{B}(\text{C}_6\text{F}_5)_2\}]$  (Scheme 62) has been reported to be a highly active catalyst for 1-hexene hydrogenation.<sup>131</sup>

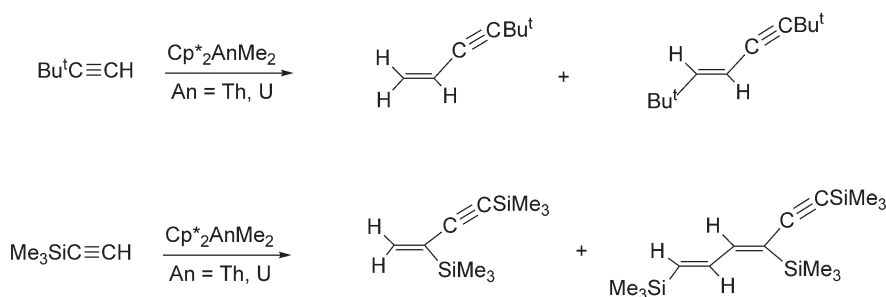
#### 4.02.11.2 Organoactinide-catalyzed Oligomerization Reactions

Organoactinides have been found to catalyze the oligomerization of terminal acetylenes. The  $\text{Cp}^*_2\text{AnMe}_2$  ( $\text{An} = \text{Th}, \text{U}$ ) system has been used for the synthesis of short oligomers.<sup>182</sup> A novel strategy for the catalytic synthesis of short oligomers, dimers and/or trimers, of terminal alkynes has been reported. The method allows control of the extent and, in some cases, the regioselectivity of the catalyzed oligomerization of terminal alkynes promoted by bis(pentamethylcyclopentadienyl)actinide dimethyl complexes. These metallocene precursors are known to promote the simultaneous production of a large number of differently sized oligomers in the presence of terminal alkynes. However, the addition of specific amines ensures the selective synthesis of short oligomers. Catalytic “tailoring” to dimers, or a mixture of dimers and trimers could be achieved by using non-bulky or bulky amines, respectively. Kinetic, spectroscopic, and mechanistic data argue that the turnover-limiting step involves the formation of the mono(amido) thorium acetylide complex with rapid insertion of the alkyne and protonolysis by the amine. In this context, various organoactinides of the type  $\text{Cp}^*_2\text{An}(\text{C}\equiv\text{CR})_2$  ( $\text{An} = \text{Th}, \text{U}$ ) have been synthesized from the corresponding  $\text{Cp}^*_2\text{AnMe}_2$  complexes by addition of an equimolar amount or an excess of the corresponding terminal alkyne (Scheme 92).<sup>183</sup>

Attempts to trap the mono(acetylide) complex  $\text{Cp}^*_2\text{An}(\text{C}\equiv\text{CR})(\text{Me})$  were successful only for the transient species  $\text{Cp}^*_2\text{U}(\text{C}\equiv\text{CPr}^i)(\text{Me})$ . The bis(acetylide) complexes are active catalysts for the linear oligomerization of terminal alkynes  $\text{HC}\equiv\text{CR}$ . The regioselectivity and the extent of oligomerization depend strongly on the alkyne substituent R, whereas the catalytic reactivities are similar for both organoactinides. Oligomerization with less bulky alkyl- and



Scheme 92



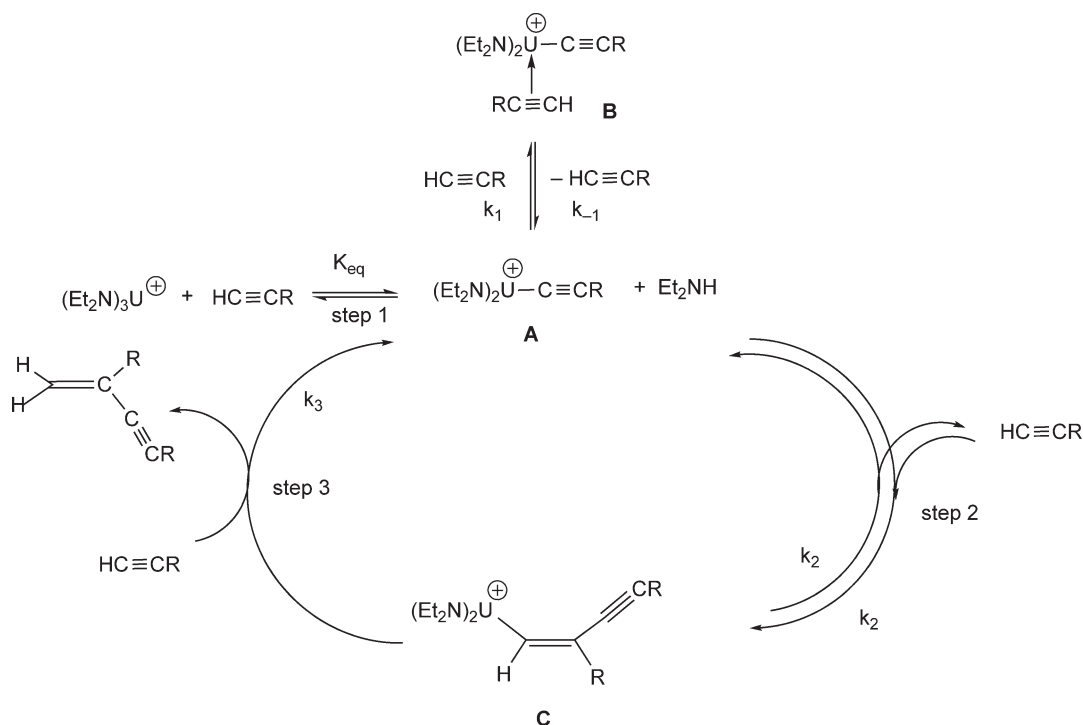
Scheme 93

aryl-substituted alkynes produced a mixture of oligomers. Reaction of  $\text{Cp}^*_2\text{AnMe}_2$  ( $\text{An} = \text{U}, \text{Th}$ ) with excess of *t*-butylacetylene led mainly to the head-to-tail dimer 2,4-di-*t*-butyl-1-butene-3-yne and to traces of the head-to-head dimer (*E*)-1,4-di-*t*-butyl-1-butene-3-yne. The analogous reaction with excess of  $\text{HC}\equiv\text{CSiMe}_3$  yielded small amounts (<5%) of the head-to-tail dimer 2,4-bis(trimethylsilyl)-1-butene-3-yne and large amounts (90–95%) of the head-to-tail-to-head trimer (*E*)-1,4,6-tris(trimethylsilyl)-1,3-hexadiene-5-yne (Scheme 93).<sup>184</sup>

The catalytic activity of the cationic actinide complex  $[(\text{Et}_2\text{N})_3\text{U}][\text{BPh}_4]$  in the dimerization of terminal alkynes has been investigated.<sup>185,186</sup> The regioselectivity in this reaction was mainly toward the geminal dimer, but for bulky alkyne substituents the unexpected *cis*-dimer was also obtained. In this context, the first *f*-element alkyne  $\pi$ -complex  $[(\text{Et}_2\text{N})_2\text{U}(\text{C}\equiv\text{CBu}^t)(\eta^2\text{-HC}\equiv\text{CBu}^t)][\text{BPh}_4]$  has also been characterized. Mechanistic studies showed that the first step in the catalytic cycle is the formation of the acetylide complex  $[(\text{Et}_2\text{N})_2\text{U}(\text{C}\equiv\text{CR})][\text{BPh}_4]$  with the concomitant reversible elimination of  $\text{Et}_2\text{NH}$ , followed by the formation of the alkyne  $\pi$ -complex  $[(\text{Et}_2\text{N})_2\text{U}(\text{C}\equiv\text{CR})(\text{HC}\equiv\text{CR})][\text{BPh}_4]$  (Scheme 94).<sup>186</sup>

#### 4.02.11.3 Organoactinide-catalyzed Polymerization Reactions

The strong Lewis acid tris(perfluorobiphenyl)borane (PBB) has been introduced as catalyst activator in metallocene-based polymerization catalysis. Reactions with thorium metallocene methyls proceeded cleanly to yield cationic complexes. Whereas the reaction of  $\text{Cp}^*_2\text{ThMe}_2$  with  $\text{B}(\text{C}_6\text{F}_5)_3$  yields inseparable mixtures of catalytically inactive products, PBB selectively abstracts a single methyl group to give catalytically active ion pairs.<sup>187</sup> In the course of studying cationic metallocene polymerization catalysts based on tetrakis(pentafluorophenyl)borate and its derivatives, the synthesis and structural characterization of  $[\text{Cp}^*_2\text{ThMe}][\text{B}(\text{C}_6\text{F}_5)_4]$  and its activity in olefin polymerization have been reported.<sup>188</sup> The catalytic activity of  $\text{UCp}^*_3$  in ethylene polymerization has also been tested. It was found that this uranium complex initiates the polymerization and afforded polymer with a high molecular mass.<sup>89,89a</sup> The



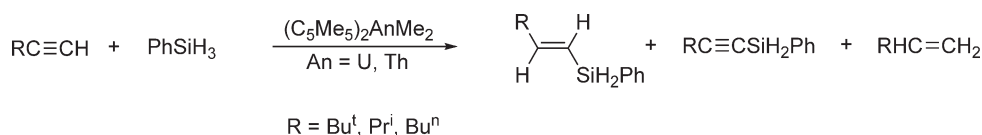
Scheme 94

cationic metallocene complex  $[\text{Cp}^*_2\text{ThMe}][(\mu\text{-H})(\mu\text{-CHCH}_2\text{Bu}^t)\{\text{B}(\text{C}_6\text{F}_5)_2\}]$  has been reported to be a highly active catalyst for ethylene polymerization.<sup>131</sup> The use of actinide metallocene catalysts for the chain growth reaction of  $\alpha$ -olefins on aluminum alkyls has been patented.<sup>189</sup>

#### 4.02.11.4 Organoactinide-catalyzed Hydrosilylation Reactions

Organoactinide complexes of the type  $\text{Cp}^*_2\text{AnMe}_2$  ( $\text{An} = \text{Th}, \text{U}$ ) are efficient catalysts for the hydrosilylation of terminal alkynes.<sup>190</sup> The chemoselectivity and regioselectivity of the reactions were found to be strongly dependent on the nature of the catalyst, the nature of the alkyne, the silane substituents, the ratio between the silane and the alkyne, the solvent, and the reaction temperature. The hydrosilylation reaction of the terminal alkynes with  $\text{PhSiH}_3$  at room temperature produced the *trans*-vinylsilane as the major product along with the silylalkyne and the corresponding alkene (Scheme 95).<sup>190</sup>

At higher temperatures (50–80 °C), besides the products obtained at room temperature, the *cis*-vinylsilane and the double-hydrosilylated alkene, in which the two silicon moieties are connected with the same carbon atom, were obtained. The catalytic hydrosilylation of  $\text{Me}_3\text{SiC}\equiv\text{CH}$  and  $\text{PhSiH}_3$  with  $\text{Cp}^*_2\text{ThMe}_2$  was found to proceed only at higher temperature, although no *cis*-vinylsilane or double-hydrosilylated products were observed. Mechanistic studies on the hydrosilylation of  $\text{Pr}^i\text{C}\equiv\text{CH}$  and  $\text{PhSiH}_3$  in the presence of  $\text{Cp}^*_2\text{ThMe}_2$  showed that the first step in the catalytic cycle is the insertion of an alkyne into a thorium–H bond. The key organoactinide intermediates for the

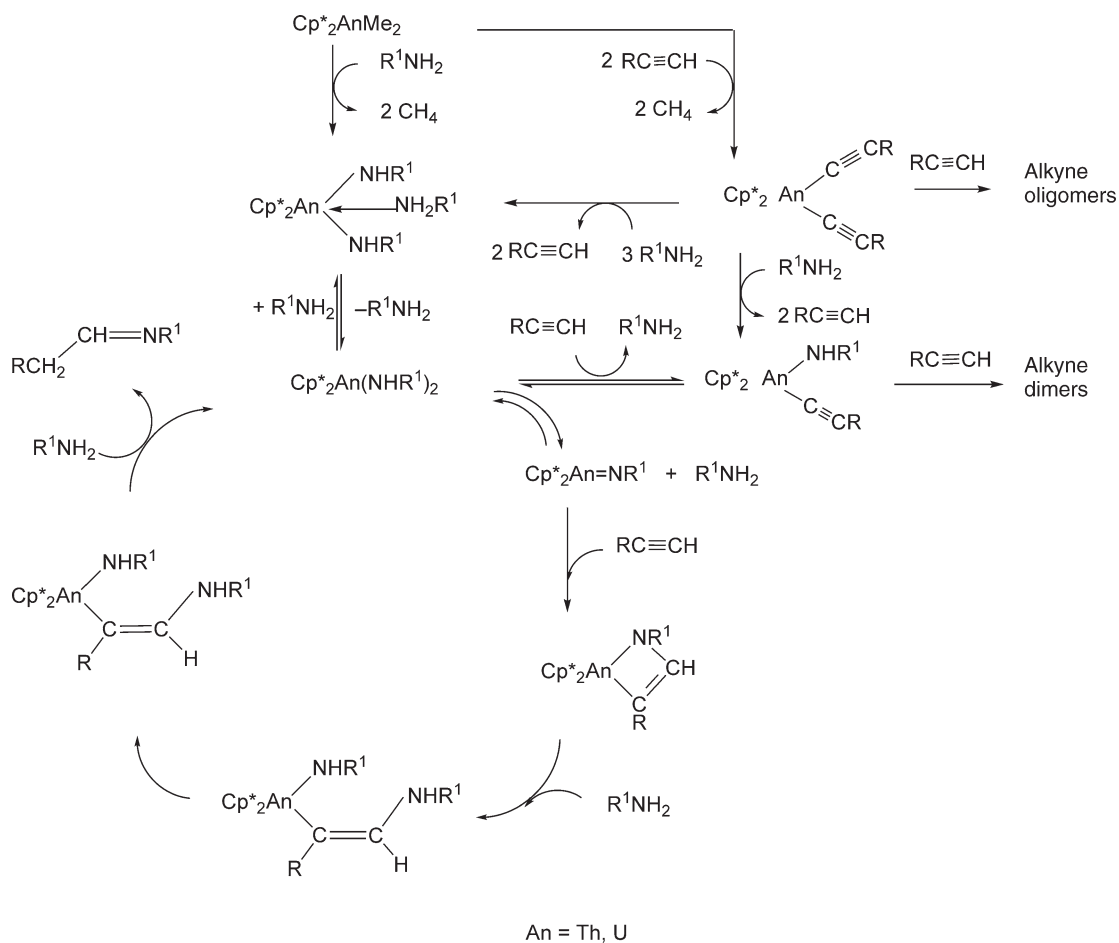


Scheme 95

*cis*-vinylsilane and the double-hydrosilylation products were the complexes  $\text{Cp}^*_2\text{An}(\text{C}\equiv\text{CR})[\text{C}(\text{PhSiH}_2)=\text{CHR}]$  ( $\text{An} = \text{Th}, \text{U}$ ); these complexes were trapped for  $\text{R} = \text{Pr}^i$  and characterized by spectroscopic methods.<sup>190</sup>

#### 4.02.11.5 Organoactinide-catalyzed Hydroamination Reactions

In organoactinide-catalyzed intermolecular hydroamination of terminal alkynes, the regioselectivity of the products can be tuned by the alkyne and metal. Mechanistic studies showed that the rate-limiting step is the formation of an actinide imido complex. For thorium, the imido intermediate  $\text{Cp}^*_2\text{Th}(=\text{NC}_6\text{H}_5)_2(\text{THF})$  has been characterized by standard techniques, including X-ray diffraction.<sup>191</sup> Organoactinide complexes of the type  $\text{Cp}^*_2\text{AnMe}_2$  ( $\text{An} = \text{Th}, \text{U}$ ) have been found to be efficient catalysts for the hydroamination of terminal alkynes with aliphatic primary amines. The chemoselectivity and regioselectivity of the reactions depend strongly on the nature of the catalysts and the nature of the amine and show no major dependence on the nature of the alkyne. The hydroamination reaction of terminal alkynes with aliphatic primary amines catalyzed by organouranium complexes produces the corresponding imines where the amine and the alkyne are regioselectively disposed in a *syn*-regiochemistry, whereas for similar reactions with the organothorium complexes besides the methyl alkylated imine, dimeric and trimeric alkyne oligomers are also produced. The key organoactinide intermediate for the intermolecular hydroamination reaction was found to be the corresponding actinide-imido complex. A plausible scenario is illustrated in [Scheme 96](#).<sup>192</sup>



**Scheme 96**

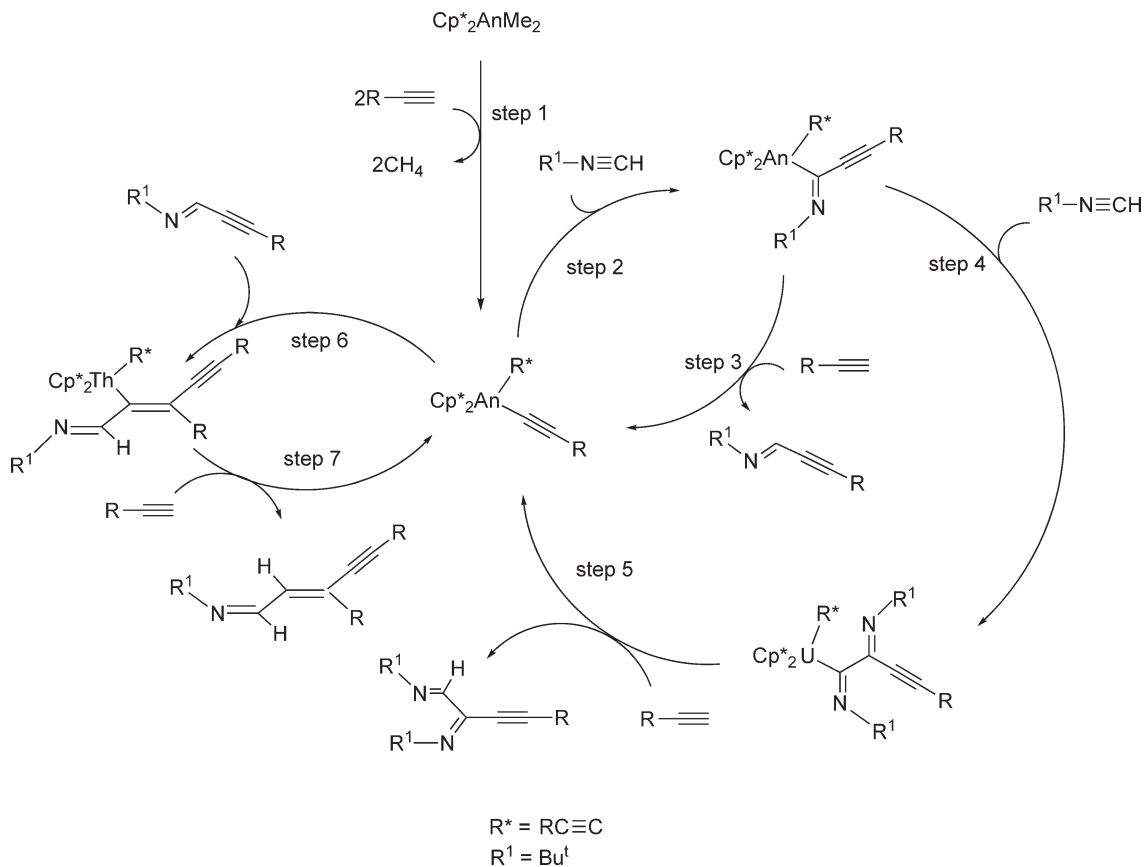
Constrained-geometry complexes of the type  $[\text{M}_2\text{Si}(\text{C}_5\text{Me}_4)(\text{NBu}^i)]\text{An}(\text{NRR}^1)_2$  ( $\text{An} = \text{Th}, \text{U}$ ;  $\text{R} = \text{R}^1 = \text{Me}$ ;  $\text{R} = \text{Me}, \text{R}^1 = \text{Et}$ ;  $\text{R} = \text{R}^1 = \text{Et}$ ) have been reported to be effective precatalysts for intramolecular catalytic hydroamination/cyclization of aminoalkenes and aminoalkynes.<sup>55</sup>

#### 4.02.11.6 Other Organoactinide-catalyzed Reactions

The complex  $[(\text{Et}_2\text{N})_3\text{U}][\text{BPh}_4]$  was investigated as a catalyst in dehydrocoupling reactions of primary amines  $\text{RNH}_2$  with  $\text{PhSiH}_3$  giving the corresponding aminosilanes  $\text{PhSiH}_{3-n}(\text{NHR})_n$  ( $n = 1-3$ ). For the primary silane  $\text{PhSiH}_3$ , the reactivity of  $\text{RNH}_2$  follows the order primary > secondary > tertiary. Similar dehydrocoupling reactions using secondary amines with secondary silanes were found to be less effective. Homodehydrocoupling of the silane was found not to be a competing reaction at room temperature. The hydride  $[(\text{RNH})_2\text{UH}][\text{BPh}_4]$ , which is plausibly formed in the reaction of  $[(\text{RNH})_3\text{U}][\text{BPh}_4]$  with  $\text{PhSiH}_3$  is a likely intermediate in the catalytic cycle.<sup>186</sup>

The actinide complexes Cp<sub>2</sub>AnMe<sub>2</sub> (An = Th, U) have been found to effectively catalyze the coupling reaction of terminal alkynes and *t*-butylnitrile, Bu<sup>t</sup>NC. The catalytic conversion of the isonitrile and alkyne to 1-aza-1,3-enynes was achieved in toluene or benzene at 90–100 °C, while no reaction was observed in the absence of a catalyst. Scheme 97 illustrates a plausible mechanism for the catalytic coupling of Bu<sup>t</sup>NC and terminal alkynes mediated by Cp<sup>\*</sup><sub>2</sub>AnMe<sub>2</sub>.<sup>193</sup>

Selective alkylation of aromatic molecules (benzene, toluene) with  $\alpha$ -chloronorbornene at room temperature to afford the 1:1 addition products *exo*-1-chloro-2-arylnorbornane (aryl = Ph, C<sub>6</sub>H<sub>4</sub>Me-*p*) in good yields has been achieved with the metallocenium ion pair [Cp\*<sub>2</sub>ThMe][B(C<sub>6</sub>F<sub>5</sub>)<sub>4</sub>].<sup>194</sup> The solution structure and aggregation of the catalyst has been studied by NOE and PGSE NMR spectroscopy; this compound exists in toluene solution as simple (inner-sphere-type) ion pair with close cation–anion interactions.<sup>195,196</sup>



### Scheme 97

## References

1. Reynolds, L. T.; Wilkinson, G. J. *Inorg. Nucl. Chem.* **1956**, *2*, 246.
2. Marks, T. J.; Ernst, R. D. In *Comprehensive Organometallic Chemistry I*; Wilkinson, G., Stone, F. G. A., Abel, E. W., Eds.; Pergamon: Oxford, **1982**; pp 173–270.
3. Edelmann, F. T. In *Comprehensive Organometallic Chemistry II*; Abel, E. W., Stone, F. G. A., Wilkinson, G., Eds.; Elsevier: Oxford, **1995**; pp 11–212.
4. Richter, J.; Edelmann, F. T. *Coord. Chem. Rev.* **1996**, *147*, 373.
5. Gun'ko, Yu. K.; Edelmann, F. T. *Coord. Chem. Rev.* **1996**, *156*, 1.
6. Edelmann, F. T.; Gun'ko, Yu. K. *Coord. Chem. Rev.* **1997**, *165*, 163.
7. Edelmann, F. T.; Lorenz, V. *Coord. Chem. Rev.* **2000**, *209*, 99.
8. Hyeon, J.-Y.; Edelmann, F. T. *Coord. Chem. Rev.* **2003**, *241*, 249.
9. Hyeon, J.-Y.; Edelmann, F. T. *Coord. Chem. Rev.* **2003**, *247*, 21.
10. Gottfriedsen, J.; Edelmann, F. T. *Coord. Chem. Rev.* **2005**, *249*, 919.
11. Hyeon, J.-Y.; Gottfriedsen, J.; Edelmann, F. T. *Coord. Chem. Rev.* **2005**, *249*, 2787.
12. Ephritikhine, M. *New J. Chem.* **1992**, *16*, 451.
13. Dormond, A.; Barbier-Baudry, D. *Sci. Synth.* **2003**, *2*, 943.
14. Zhang, G.-F.; Xue, W.-D.; Wang, X.-L.; Zhu, Z.-H.; Wang, H.-Y.; Zou, L.-X.; Sun, Y. *Chin. J. Atom. Mol. Phys.* **2001**, *18*, 372.
15. Andrews, L.; Liang, B.; Li, J.; Bursten, B. E. *J. Am. Chem. Soc.* **2003**, *125*, 3126.
16. Zhou, M.; Andrews, L.; Li, J.; Bursten, B. E. *J. Am. Chem. Soc.* **1999**, *121*, 12188.
17. Li, J.; Bursten, B. E.; Zhou, M.; Andrews, L. *Inorg. Chem.* **2001**, *40*, 5448.
18. Vetere, V.; Maldivi, P.; Adamo, C. *Int. J. Quant. Chem.* **2002**, *91*, 321.
19. Joubert, L.; Maldivi, P. *J. Phys. Chem. A* **2001**, *105*, 9068.
20. Gibson, J. K. *J. Phys. Chem. A* **1998**, *102*, 4501.
21. Gibson, J. K.; Haire, R. G. *Radiochim. Acta* **2001**, *89*, 363.
22. Gibson, J. K.; Haire, R. G. *Radiochim. Acta* **2001**, *89*, 709.
23. Eisen, M. S.; Marks, T. J. *J. Am. Chem. Soc.* **1992**, *114*, 10358.
24. Leonov, M. R.; Il'yushenkov, V. A.; Il'yushenkova, N. V. *Radiokhimiya* **1996**, *38*, 49.
25. Campello, M. P. C.; Calhorda, M. J.; Domingos, A.; Galvao, A.; Leal, J. P.; Matos, A. P.; Santos, I. *J. Organomet. Chem.* **1997**, *538*, 223.
26. Domingos, A.; Marques, N.; Pires de Matos, A.; Santos, I.; Silva, M. *Organometallics* **1994**, *13*, 654.
27. Silva, M.; Marques, N.; de Matos, A. P. *J. Organomet. Chem.* **1995**, *493*, 129.
28. Baudry, D.; Dormond, A.; Hafid, A. *J. Organomet. Chem.* **1995**, *494*, C22.
29. Boaretto, R.; Roussel, P.; Alcock, N. W.; Kingsley, A. J.; Munslow, I. J.; Sanders, C. J.; Scott, P. J. *Organomet. Chem.* **1999**, *591*, 174.
30. Roussel, P.; Boaretto, R.; Kingsley, A. J.; Alcock, N. W.; Scott, P. J. *Chem. Soc., Dalton Trans.* **2002**, 1423.
31. Jantunen, K. C.; Batchelor, R. J.; Leznoff, D. B. *Organometallics* **2004**, *23*, 2186.
32. Nakai, H.; Hu, X.; Zakharov, L. N.; Rheingold, A. L.; Meyer, K. *Inorg. Chem.* **2004**, *43*, 855.
33. Sarsfield, M. J.; Helliwell, M.; Collison, D. *Chem. Commun.* **2002**, 2264.
34. Sarsfield, M. J.; Helliwell, M. *J. Am. Chem. Soc.* **2004**, *126*, 1036.
35. Oldham, W. J., Jr.; Oldham, S. M.; Scott, B. L.; Abney, K. D.; Smith, W. H.; Costa, D. A. *J. Chem. Soc., Chem. Commun.* **2001**, 1348.
36. Carlson, C. N.; Hanusa, T. P.; Brennessel, W. W. *J. Am. Chem. Soc.* **2004**, *126*, 10550.
37. Hitchcock, P. B.; Hu, J.; Lappert, M. F.; Tian, S. *J. Organomet. Chem.* **1997**, *536–537*, 473.
38. Wright, R. J.; Power, P. P.; Scott, B. L.; Kiplinger, J. L. *Organometallics* **2004**, *23*, 4801.
39. Kaltsoyannis, N.; Bursten, B. E. *J. Organomet. Chem.* **1997**, *528*, 19.
40. Hauchard, D.; Cassir, M.; Chivot, J.; Baudry, D.; Ephritikhine, M. *J. Electroanal. Chem.* **1993**, *347*, 399.
41. Lukens, W. W., Jr.; Beshouri, S. M.; Stuart, A. L.; Andersen, R. A. *Organometallics* **1999**, *18*, 1247.
42. Lukens, W. W., Jr.; Allen, P. G.; Bucher, J. J.; Edelstein, N. M.; Hudson, E. A.; Shuh, D. K.; Reich, T.; Andersen, R. A. *Organometallics* **1999**, *18*, 1253.
43. Stults, S.; Andersen, R. A.; Zalkin, A. *J. Organomet. Chem.* **1993**, *462*, 175.
44. Adam, R.; Villiers, C.; Ephritikhine, M.; Lance, M.; Nierlich, M.; Vigner, J. *J. Organomet. Chem.* **1993**, *445*, 99.
45. Parry, J.; Carmona, E.; Coles, S.; Hursthouse, M. *J. Am. Chem. Soc.* **1995**, *117*, 2649.
46. del Mar Conejo, M.; Parry, J. S.; Carmona, E.; Schultz, M.; Brennann, J. G.; Beshouri, S. M.; Andersen, R. A.; Rogers, R. D.; Coles, S.; Hursthouse, M. *Chem. Eur. J.* **1999**, *5*, 3000.
47. Mehdoui, T.; Berthet, J.-C.; Thuery, P.; Ephritikhine, M. *Dalton Trans.* **2004**, 579.
48. Nagao, T.; Igarashi, J. *Physica B* **2003**, *329–333*, 628.
49. Weydert, M.; Brennan, J. G.; Andersen, R. A.; Bergman, R. G. *Organometallics* **1995**, *14*, 3942.
50. Blake, P. C.; Edelstein, N. M.; Hitchcock, P. B.; Kot, W. K.; Lappert, M. F.; Shalimoff, G. V.; Tian, S. *J. Organomet. Chem.* **2001**, *636*, 124.
51. Edelmann, M. A.; Hitchcock, P. B.; Hu, J.; Lappert, M. F. *New J. Chem.* **1995**, *19*, 481.
52. Barnhart, D. M.; Butcher, R. J.; Clark, D. L.; Gordon, J. C.; Watkin, J. G.; Zwick, B. D. *New J. Chem.* **1995**, *19*, 503.
53. Gill, M. S.; Sogoria, V. S. *Indian J. Chem., Sect. A* **1995**, *34A*, 997.
54. Leonov, M. R.; Il'yushenkov, V. A.; Il'yushenkova, N. V. *Zh. Obshch. Khim.* **1996**, *66*, 721.
55. Stubbert, B. D.; Stern, C. L.; Marks, T. J. *Organometallics* **2003**, *22*, 4836.
56. Golden, J. T.; Kazul'kin, D. N.; Scott, B. L.; Voskoboinikov, A. Z.; Burns, C. J. *Organometallics* **2003**, *22*, 3971.
57. Baudry, D.; Dormond, A.; Lesprit, O. *Bull. Soc. Chim. Fr.* **1995**, *132*, 183.
58. Blake, P. C.; Lappert, M. F.; Taylor, R. G.; Atwood, J. L.; Hunter, W. E.; Zhang, H. *J. Chem. Soc., Dalton Trans.* **1995**, 3335.
59. Hughes, R. P.; Lomphey, J. R.; Rheingold, A. L.; Haggerty, B. S.; Yap, G. P. A. *J. Organomet. Chem.* **1996**, *517*, 89.
60. Lukens, W. W., Jr.; Beshouri, S. M.; Bloch, L. L.; Stuart, A. L.; Andersen, R. A. *Organometallics* **1999**, *18*, 1235.
61. Berthet, J. C.; Nierlich, M.; Ephritikhine, M. *Eur. J. Inorg. Chem.* **2002**, 840.
62. Duval, P. B.; Burns, C. J.; Clark, D. L.; Morris, D. E.; Scott, B. L.; Thompson, J. D.; Werkema, E. L.; Jia, L.; Andersen, R. A. *Angew. Chem.* **2001**, *40*, 3462.



- 62a. Duval, P. B.; Burns, C. J.; Clark, D. L.; Morris, D. E.; Scott, B. L.; Thompson, J. D.; Werkema, E. L.; Jia, L.; Andersen, R. A. *Angew. Chem. Int. Ed.* **2001**, *40*, 3357.
63. Cramer, R. E.; Hitt, J.; Chung, T.; Gilje, J. W. *New J. Chem.* **1995**, *19*, 509.
64. Berthet, J. C.; Lance, M.; Nierlich, M.; Ephritikhine, M. *Chem. Commun.* **1998**, 1373.
65. Baudry, D.; Dormond, A.; Hafid, A.; Raillard, C. J. *Organomet. Chem.* **1996**, *511*, 37.
66. Barbier-Baudry, D.; Blaque, O.; Hafid, A.; Nyassi, A.; Sitzmann, H.; Visseaux, M. *Eur. J. Inorg. Chem.* **2000**, 2333.
67. Gulino, A.; Di Bella, S.; Fragalá, I.; Casarin, M.; Seyam, A.; Marks, T. J. *Inorg. Chem.* **1993**, *32*, 3873.
68. Di Bella, S.; Gulino, A.; Lanza, G.; Fragalá, I. L.; Marks, T. J. *J. Phys. Chem.* **1993**, *97*, 11673.
69. Weydert, M.; Andersen, R.; Bergman, R. J. *Am. Chem. Soc.* **1993**, *115*, 8837.
70. Cloke, F. G.; Hawkes, S. A.; Hitchcock, P. B.; Scott, P. *Organometallics* **1994**, *13*, 2895.
71. Berthet, J.-C.; Boisson, C.; Lance, M.; Vigner, J.; Nierlich, M.; Ephritikhine, M. *J. Chem. Soc., Dalton Trans.* **1995**, 3027.
72. Adam, R.; Villiers, C.; Ephritikhine, M. *Tetrahedron Lett.* **1994**, *35*, 573.
73. De Ridder, D. J. A.; Apostolidis, C.; Rebizant, J.; Kanellakopulos, B.; Meier, R. *Acta Crystallogr. Sect. C Cryst. Struct. Commun.* **1996**, *52*, 1436.
74. Berthet, J.-C.; Ephritikhine, M.; Lance, M.; Nierlich, M.; Vigner, J. *J. Organomet. Chem.* **1993**, *460*, 47.
75. Spirlet, M.-R.; Rebizant, J.; Apostolidis, C.; Dornberger, E.; Kanellakopulos, B.; Powietzka, B. *Polyhedron* **1996**, *15*, 1503.
76. Jemine, X.; Goffart, J.; Leverd, P. C.; Ephritikhine, M. *J. Organomet. Chem.* **1994**, *469*, 55.
77. Leverd, P. C.; Ephritikhine, M.; Lance, M.; Vigner, J.; Nierlich, M. *J. Organomet. Chem.* **1996**, *507*, 229.
78. Blake, P. C.; Edelman, M. A.; Hitchcock, P. B.; Hu, J.; Lappert, M. F.; Tian, S.; Müller, G.; Atwood, J. L.; Zhang, H. *J. Organomet. Chem.* **1998**, *551*, 261.
79. Spirlet, M.; Rebizant, J.; Apostolidis, C.; Kanellakopulos, B. *Acta Crystallogr. Sect. C: Cryst. Struct. Commun.* **1993**, *49*, 929.
80. King, W. A.; Marks, T. J. *Inorg. Chim. Acta* **1995**, *229*, 343.
81. Baudry, D.; Dormond, A.; Abdallaoui, I. A. *J. Organomet. Chem.* **1994**, *476*, C15.
82. Maier, R.; Kanellakopulos, B.; Apostolidis, C.; Meyer, D.; Rebizant, J. *J. Alloys Comp.* **1993**, *190*, 269.
83. Leonov, M. R.; Solov'yova, G. V. *Metalloorg. Khim.* **1993**, *6*, 198.
84. Avens, L. R.; Burns, C. J.; Butcher, R. J.; Clark, D. L.; Gordon, J. C.; Schake, A. R.; Scott, B. L.; Watkin, J. G.; Zwick, B. D. *Organometallics* **2000**, *19*, 451.
85. Evans, W. J.; Kozimor, S. A.; Ziller, J. W. *Polyhedron* **2004**, *23*, 2689.
86. Arliguie, T.; Lescop, C.; Ventelon, L.; Leverd, P. C.; Thuery, P.; Nierlich, M.; Ephritikhine, M. *Organometallics* **2001**, *20*, 3698.
87. Evans, W. J.; Kozimor, S. A.; Ziller, J. W.; Kaltsoyannis, N. *J. Am. Chem. Soc.* **2004**, *126*, 14533.
88. Boisson, C.; Berthet, J. C.; Ephritikhine, M.; Lance, M.; Nierlich, M. *J. Organomet. Chem.* **1997**, *533*, 7.
89. Evans, W. J.; Forrestal, K. J.; Ziller, J. W. *Angew. Chem.* **1997**, *109*, 798.
- 89a. Evans, W. J.; Forrestal, K. J.; Ziller, J. W. *Angew. Chem. Int. Ed.* **1997**, *36*, 798.
90. Evans, W. J.; Nyce, G. W.; Forrestal, K. J.; Ziller, J. W. *Organometallics* **2002**, *21*, 1050.
91. Evans, W. J.; Kozimor, S. A.; Ziller, J. W. *J. Am. Chem. Soc.* **2003**, *125*, 14264.
92. Evans, W. J.; Kozimor, S. A.; Nyce, G. W.; Ziller, J. W. *J. Am. Chem. Soc.* **2003**, *125*, 13831.
93. Gibson, J. K.; Haire, R. G. *Organometallics* **2005**, *24*, 119.
94. Clark, D. L.; Gordon, J. C.; Huffman, J. C.; Watkin, J. D.; Zwick, B. D. *New J. Chem.* **1995**, *19*, 495.
95. Barnea, E.; Andrea, T.; Kapon, M.; Eisen, M. S. *J. Am. Chem. Soc.* **2004**, *126*, 5066.
96. Scott, P.; Hitchcock, P. D. *J. Chem. Soc., Dalton Trans.* **1995**, 603.
97. Boisson, C.; Berthet, J.-C.; Lance, M.; Nierlich, M.; Vigner, J.; Ephritikhine, M. *J. Chem. Soc., Chem. Commun.* **1995**, 543.
98. Kiplinger, J. L.; Morris, D. E.; Scott, B. L.; Burns, C. J. *Organometallics* **2002**, *21*, 5978.
99. Morris, D. E.; Da Re, R. E.; Jantunen, K. C.; Castro-Rodriguez, I.; Kiplinger, J. L. *Organometallics* **2004**, *23*, 5142.
100. Rabinovich, D.; Schimke, G. L.; Pennington, W. T.; Nielsen, J. B.; Abney, K. D. *Acta Cryst. C* **1997**, *53*, 1794.
101. Rabinovich, D.; Bott, S. G.; Nielsen, J. B.; Abney, K. D. *Inorg. Chim. Acta* **1998**, *274*, 232.
102. Cramer, R. E.; Ariyaratne, K. A. N. S.; Gilje, J. W. *Z. Anorg. Allg. Chem.* **1995**, *621*, 1856.
103. Ariyaratne, K. A. N. S.; Cramer, R. E.; Jameson, G. B.; Gilje, J. W. *J. Organomet. Chem.* **2004**, *689*, 2029.
104. Danopoulos, A. A.; Hankin, D. M.; Cafferkey, S. M.; Hursthouse, M. B. *J. Chem. Soc., Dalton Trans.* **2000**, 1613.
105. Arney, D.; Burns, C. J. *J. Am. Chem. Soc.* **1993**, *115*, 9840.
106. Radu, N. S.; Engeler, M. P.; Gerlach, C. P.; Tilley, T. D.; Rheingold, A. L. *J. Am. Chem. Soc.* **1995**, *117*, 3621.
107. Ventelon, L.; Lescop, C.; Arliguie, T.; Leverd, P. C.; Lance, M.; Nierlich, M.; Ephritikhine, M. *J. Chem. Soc., Chem. Commun.* **1999**, 659.
108. Lescop, C.; Arliguie, T.; Lance, M.; Nierlich, M.; Ephritikhine, M. *J. Organomet. Chem.* **1999**, *580*, 137.
109. Arliguie, T.; Fourmigué, M.; Ephritikhine, M. *Organometallics* **2000**, *19*, 109.
110. Boisson, C.; Berthet, J.-C.; Lance, M.; Nierlich, M.; Ephritikhine, M. *Chem. Commun.* **1996**, 2129.
111. Boisson, C.; Berthet, J.-C.; Lance, M.; Nierlich, M.; Ephritikhine, M. *J. Organomet. Chem.* **1997**, *548*, 9.
112. Straub, T.; Frank, W.; Reiss, G. J.; Eisen, M. S. *J. Chem. Soc., Dalton Trans.* **1996**, 2541.
113. Peters, R. G.; Scott, B. L.; Burns, C. J. *Acta Cryst. C* **1999**, *55*, 1482.
114. Kiplinger, J. L.; Morris, D. E.; Scott, B. L.; Burns, C. J. *Chem. Commun.* **2002**, 30.
115. Kiplinger, J. L.; Morris, D. E.; Scott, B. L.; Burns, C. J. *Organometallics* **2002**, *21*, 3073.
116. Da Re, R. E.; Jantunen, K. C.; Golden, J. T.; Kiplinger, J. L.; Morris, D. E. *J. Am. Chem. Soc.* **2005**, *127*, 682.
117. Jantunen, K. C.; Burns, C. J.; Castro-Rodriguez, I.; Da Re, R. E.; Golden, J. T.; Morris, D. E.; Scott, B. L.; Taw, F. L.; Kiplinger, J. L. *Organometallics* **2004**, *23*, 4682.
118. Ariyaratne, K. A. N. S.; Cramer, R. E.; Gilje, J. W. *Organometallics* **2002**, *21*, 5799.
119. Arney, D. S. J.; Burns, C. J.; Smith, D. C. *J. Am. Chem. Soc.* **1992**, *114*, 10068.
120. Arney, D. S. J.; Burns, C. J. *J. Am. Chem. Soc.* **1995**, *117*, 9448.
121. Hay, P. J. *Faraday Discuss* **2003**, *124*, 69.
122. Warner, B. P.; Scott, B. L.; Burns, C. J. *Angew. Chem.* **1998**, *119*, 1005.
- 122a. Warner, B. P.; Scott, B. L.; Burns, C. J. *Angew. Chem. Int. Ed.* **1998**, *37*, 959.
123. Peters, R. G.; Warner, B. J.; Scott, B. L.; Burns, C. J. *Organometallics* **1999**, *18*, 2587.
124. Cendrowski-Guillaume, S. M.; Ephritikhine, M. *J. Organomet. Chem.* **1999**, *577*, 161.
125. Arney, D. S. J.; Schnabel, R. C.; Scott, B. C.; Burns, C. J. *J. Am. Chem. Soc.* **1996**, *118*, 6780.



126. Hall, S. W.; Huffmann, J.; Miller, M.; Avens, L.; Burns, C. J.; Arney, D.; England, A.; Sattelberger, A. *Organometallics* **1993**, *12*, 752.
127. Chen, Y. X.; Metz, M. V.; Li, L.; Stern, C. L.; Marks, T. J. *J. Am. Chem. Soc.* **1998**, *120*, 6287.
128. Kiplinger, J. L.; John, K. D.; Morris, D. E.; Scott, B. L.; Burns, C. J. *Organometallics* **2002**, *21*, 4306.
129. Pool, J. A.; Scott, B. L.; Kiplinger, J. L. *J. Am. Chem. Soc.* **2005**, *127*, 1338.
130. England, A. F.; Burns, C. J.; Buchwald, S. L. *Organometallics* **1994**, *13*, 3491.
131. Jia, L.; Yang, X.; Stern, C.; Marks, T. J. *Organometallics* **1994**, *13*, 3755.
132. Grados, P.; Baudry, D.; Ephritikhine, M.; Lance, M.; Nierlich, M.; Vigner, J. *J. Organomet. Chem.* **1994**, *466*, 107.
133. Jemine, W.; Nyce, G. W.; Johnston, M. A.; Ziller, J. W. *J. Am. Chem. Soc.* **2000**, *122*, 12019.
134. Evans, W. J.; Nyce, G. W.; Ziller, J. W. *Organometallics* **2001**, *20*, 5489.
135. Schnabel, R. C.; Scott, B. L.; Smith, W. H.; Burns, C. J. *J. Organomet. Chem.* **1999**, *591*, 14.
136. Cloke, F. G. N.; Hitchcock, P. B. *J. Am. Chem. Soc.* **1997**, *119*, 7899.
137. Cloke, F. G. N.; Green, J. C.; Jardine, C. N. *Organometallics* **1999**, *18*, 1080.
138. Cloke, F. G. N.; Hitchcock, P. B. *J. Am. Chem. Soc.* **2002**, *124*, 9352.
139. Cloke, F. G. N.; Green, J. C.; Kaltsoyannis, N. *Organometallics* **2004**, *23*, 832.
140. Trnka, T. M.; Bonanno, J. B.; Bridgewater, B. M.; Perkin, G. *Organometallics* **2001**, *20*, 3255.
141. Jemine, X.; Guffart, J.; Ephritikhine, M.; Fuger, J. *J. Organomet. Chem.* **1993**, *448*, 95.
142. Korobkov, I.; Gambarotta, S.; Yap, G. P. A. *Angew. Chem.* **2002**, *114*, 3583.
- 142a. Korobkov, I.; Gambarotta, S.; Yap, G. P. A. *Angew. Chem. Int. Ed.* **2002**, *41*, 3433.
143. Rabinovich, D.; Chamberlin, R. M.; Scott, B. L.; Nielsen, J. B.; Abney, K. D. *Inorg. Chem.* **1997**, *36*, 4216.
144. Xie, Z.; Yan, C.; Yang, Q.; Mak, T. C. W. *Angew. Chem.* **1999**, *111*, 1875.
- 144a. Xie, Z.; Yan, C.; Yang, Q.; Mak, T. C. W. *Angew. Chem. Int. Ed.* **1999**, *38*, 1761.
145. Korobkov, I.; Gambarotta, S. *Organometallics* **2004**, *23*, 5379.
146. Li, J.; Bursten, B. E. *J. Am. Chem. Soc.* **1997**, *119*, 9021.
147. Arliguie, T.; Lance, M.; Nierlich, M.; Vigner, J.; Ephritikhine, M. *J. Chem. Soc., Chem. Comm.* **1995**, 184.
148. Arliguie, T.; Lance, M.; Nierlich, M.; Vigner, J.; Ephritikhine, M. *J. Chem. Soc., Chem. Commun.* **1994**, 847.
149. Arliguie, T.; Lance, M.; Nierlich, M.; Ephritikhine, M. *J. Chem. Soc., Dalton Trans.* **1997**, 2501.
150. Cendrowski-Guillaume, S. M.; Le Gland, G.; Lance, M.; Nierlich, M.; Ephritikhine, M. *Comptes Rendus Chimie* **2002**, *5*, 73.
151. Seyferth, D. *Organometallics* **2004**, *23*, 3562.
152. Schake, A.; Avens, L.; Burns, C. J.; Clark, D. L.; Sattelberger, A.; Smith, W. *Organometallics* **1993**, *12*, 1497.
153. Cendrowski-Guillaume, S. M.; Le Gland, G.; Nierlich, M.; Ephritikhine, M. *Eur. J. Inorg. Chem.* **2003**, 1388.
154. Lever, P. C.; Arliguie, T.; Lance, M.; Nierlich, M.; Vigner, J.; Ephritikhine, M. *J. Chem. Soc., Dalton Trans.* **1994**, 501.
155. Arliguie, T.; Thuéry, P.; Fourmigué, M.; Ephritikhine, M. *Organometallics* **2003**, *22*, 3000.
156. Auwer, C. D.; Madic, C.; Berthet, J.-C.; Ephritikhine, M.; Rehr, J. J.; Guillaumont, R. *Radiachim. Acta* **1997**, *76*, 218.
157. Berthet, J.-C.; Ephritikhine, M. *J. Chem. Soc., Chem. Commun.* **1993**, 1566.
158. Boisson, C.; Berthet, J.-C.; Ephritikhine, M.; Lance, M.; Nierlich, M. *J. Organomet. Chem.* **1996**, *522*, 249.
159. Borgne, T. L.; Lance, M.; Nierlich, M.; Ephritikhine, M. *J. Organomet. Chem.* **2000**, *598*, 313.
160. Fedushkin, I. L.; Kurskii, Y. A.; Nevodchikov, V. I.; Bochkarev, M. N.; Mühle, S.; Schumann, H. *Russ. Chem. Bull.* **2002**, *51*, 160.
161. Cendrowski-Guillaume, S. M.; Lance, M.; Nierlich, M.; Ephritikhine, M. *Organometallics* **2000**, *19*, 3257.
162. Cendrowski-Guillaume, S. M.; Nierlich, M.; Ephritikhine, M. *J. Organomet. Chem.* **2002**, *634–644*, 209.
163. Hager, J. S.; Zahardis, J.; Pagni, R. M.; Compton, R. N.; Li, J. *J. Chem. Phys.* **2004**, *120*, 2708.
164. Streitwieser, A.; Lyttle, M. H.; Wang, H.-K.; Boussie, T.; Weinländer, A.; Solar, J. P. *J. Organomet. Chem.* **1995**, *501*, 245.
165. Kilimann, U.; Herbst-Irmer, R.; Stalke, D.; Edelmann, F. T. *Angew. Chem.* **1994**, *106*, 1685.
- 165a. Kilimann, U.; Herbst-Irmer, R.; Stalke, D.; Edelmann, F. T. *Angew. Chem. Int. Ed. Engl.* **1994**, *33*, 1618.
166. Gourier, D.; Caurant, D. *Inorg. Chem.* **1997**, *36*, 5931.
167. Dolg, M.; Fulde, P.; Stoll, H.; Preuss, H.; Chang, A.; Pitzer, R. M. *Chem. Phys.* **1995**, *195*, 71.
168. Liu, W.; Dolg, M.; Fulde, P. *J. Chem. Phys.* **1997**, *107*, 3584.
169. Li, J.; Bursten, B. E. *J. Am. Chem. Soc.* **1998**, *120*, 11456.
170. Evans, W. J.; Nyce, G. W.; Ziller, J. W. *Angew. Chem.* **2000**, *112*, 246.
- 170a. Evans, W. J.; Nyce, G. W.; Ziller, J. W. *Angew. Chem. Int. Ed.* **2000**, *39*, 240.
171. da Conceicao Vieira, M.; Marcalo, J.; de Matos, A. P. *J. Organomet. Chem.* **2001**, *632*, 126.
172. Scott, P.; Hitchcock, P. B. *J. Organomet. Chem.* **1995**, *497*, C1.
173. Bucaille, A.; Borgne, T. L.; Ephritikhine, M.; Daran, J. C. *Organometallics* **2000**, *19*, 4912.
174. Baudry, D.; Dormond, A.; Hafid, A. *New J. Chem.* **1993**, *17*, 465.
175. Cendrowski-Guillaume, S. M.; Ephritikhine, M. *J. Chem. Soc., Dalton Trans.* **1996**, 1487.
176. Yang, X.; King, W.; Sabat, M.; Marks, T. J. *Organometallics* **1993**, *12*, 4254.
177. Dash, A. K.; Gourevich, Y.; Wang, J. Q.; Wang, J.; Kapon, M.; Eisen, M. S. *J. Alloys Compd.* **2002**, *344*, 65.
178. Dash, A. K.; Wang, J. Q.; Wang, J.; Gourevich, I.; Eisen, M. S. *J. Nucl. Sci. Technol.* **2002**, (Suppl. 3), 386.
179. Dash, A. K.; Gourevich, I.; Wang, J. Q.; Wang, J.; Kapon, M.; Eisen, M. S. *Organometallics* **2001**, *20*, 5084.
180. Ahn, H.; Nicholas, C. P.; Marks, T. J. *Organometallics* **2002**, *21*, 1788.
181. Peters, R. G.; Warner, B. P.; Burns, C. J. *J. Am. Chem. Soc.* **1999**, *121*, 5585.
182. Haskell, A.; Wang, J. Q.; Straub, T.; Neyroud, T. G.; Eisen, M. S. *J. Am. Chem. Soc.* **1999**, *121*, 3025.
183. Haskell, A.; Straub, T.; Dash, A. K.; Eisen, M. S. *J. Am. Chem. Soc.* **1999**, *121*, 3014.
184. Straub, T.; Haskell, A.; Eisen, M. S. *J. Am. Chem. Soc.* **1995**, *117*, 6364.
185. Wang, J. Q.; Dash, A. K.; Berthet, J.-C.; Ephritikhine, M.; Eisen, M. S. *Organometallics* **1999**, *18*, 2407.
186. Wang, J. X.; Dash, A. K.; Berthet, J.-C.; Ephritikhine, M.; Eisen, M. S. *J. Organomet. Chem.* **2000**, *610*, 49.
187. Chen, Y.-X.; Stern, C. L.; Yang, S.; Marks, T. J. *J. Am. Chem. Soc.* **1996**, *118*, 12451.
188. Jia, L.; Yang, X.; Stern, C. L.; Marks, T. J. *Organometallics* **1997**, *16*, 842.
189. Samsel, E. G. *Eur. Pat. Appl.* EP 574 854; *US Pat. Appl.* 900 387 (*Chem. Abstr.* **1994**, *121*, 86240).
190. Dash, A. K.; Wang, J. Q.; Eisen, M. S. *Organometallics* **1999**, *18*, 4724.
191. Haskell, A.; Straub, T.; Eisen, M. S. *Organometallics* **1996**, *15*, 3773.

192. Ganesan, M.; Bérubé, C. D.; Gambarotta, S.; Yap, G. P. A. *Organometallics* **2002**, *21*, 1707.
193. Barnea, E.; Andrea, T.; Kapon, M.; Berthet, J.-C.; Ephritikhine, M.; Eisen, M. S. *J. Am. Chem. Soc.* **2004**, *126*, 10860.
194. Dash, A. K.; Jensen, T. R.; Stern, C. L.; Marks, T. J. *J. Am. Chem. Soc.* **2004**, *126*, 12528.
195. Stahl, N. G.; Zuccaccia, C.; Jensen, T. R.; Marks, T. J. *J. Am. Chem. Soc.* **2003**, *125*, 5256.
196. Zuccaccia, C.; Stahl, N. G.; Macchioni, A.; Chen, M.-C.; Roberts, J. A.; Marks, T. J. *J. Am. Chem. Soc.* **2004**, *126*, 1448.

## 4.03

# Complexes of Titanium in Oxidation States 0 to II

---

P J Chirik and M W Bouwkamp, Cornell University, Ithaca, NY, USA

© 2007 Elsevier Ltd. All rights reserved.

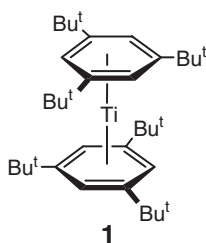
<b>4.03.1 Titanium Arene Complexes</b>	<b>243</b>
<b>4.03.2 Titanium Diene Complexes</b>	<b>246</b>
4.03.2.1 Titanium(0) Diene Complexes	246
4.03.2.2 Titanium(II) Diene Complexes	246
<b>4.03.3 Titanium Carbonyl Complexes</b>	<b>248</b>
<b>4.03.4 Bis(cyclopentadienyl)titanium(II) Complexes</b>	<b>249</b>
4.03.4.1 Bis(cyclopentadienyl)titanium(II) Complexes	249
4.03.4.2 Bis(cyclopentadienyl)titanium(II) Dinitrogen Complexes	250
4.03.4.3 Bis(cyclopentadienyl)titanium(II) Dicarbonyl, Isonitrile, and Phosphine Complexes	250
4.03.4.4 Bis(cyclopentadienyl)titanium(II) Borane Complexes	254
4.03.4.5 Bis( $\omega$ -alkenylcyclopentadienyl)titanium(II) Complexes	254
4.03.4.6 Bis(cyclopentadienyl)titanium(II) Alkyne Complexes	255
4.03.4.7 Bis(cyclopentadienyl)titanium(II) Complexes with Other Unsaturated Hydrocarbons	261
4.03.4.8 Bis(cyclopentadienyl)titanium(II) Diazoalkane Complexes	263
<b>4.03.5 Cyclopentadienyl Cyclohexadienyl Titanium(II) Complexes</b>	<b>264</b>
<b>4.03.6 Bis(pentadienyl)titanium(II) Complexes</b>	<b>265</b>
<b>4.03.7 Bis(phosphacyclopentadienyl)titanium(II) Complexes</b>	<b>265</b>
<b>4.03.8 Bis(trispyrazolylborate)titanium(II) Complexes</b>	<b>266</b>
<b>4.03.9 Porphyrin Titanium(II) Complexes</b>	<b>266</b>
<b>4.03.10 Bis(benzamidinate)titanium(II) Complexes</b>	<b>267</b>
<b>4.03.11 Bis(guanidinate)titanium(II) Complexes</b>	<b>268</b>
<b>4.03.12 Calixarene Titanium(II) Complexes</b>	<b>268</b>
<b>4.03.13 Titanium(II)-Mediated Transformations</b>	<b>269</b>
4.03.13.1 Dinitrogen Functionalization	269
4.03.13.2 Reductive Coupling, Cyclization, Tandem Cyclization Reactions	269
4.03.13.3 Pauson–Khand Reactions	270
4.03.13.4 Cyclotrimerization Reactions	271
4.03.13.5 Nucleophilic Substitution Reactions	273
4.03.13.6 Cyclopropanol Synthesis	274
4.03.13.7 Miscellaneous Organic Transformations	276
<b>References</b>	<b>276</b>

---

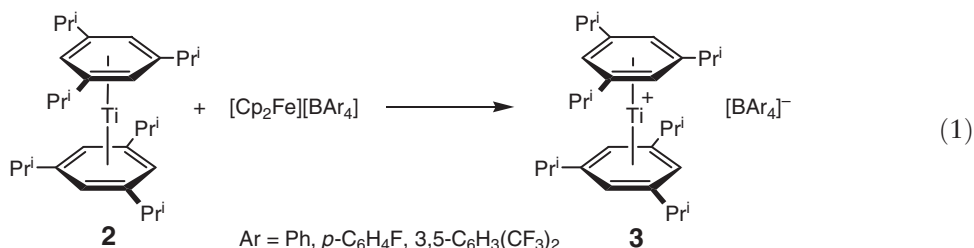
### 4.03.1 Titanium Arene Complexes

Bis(arene)titanium(0) complexes<sup>1</sup> challenge traditional views of early transition metal ligand bonding as electrostatic interactions between a formally high-valent metal center and an anionic ligand are lacking. For the isolable compound,  $\text{Ti}(\eta^6\text{-1,3,5-Bu}^t_3\text{C}_6\text{H}_3)_2$  **1**, the titanium–arene bond dissociation energy has been measured as  $49(1) \text{ kcal mol}^{-1}$  by iodolytic bath calorimetry.<sup>2</sup> Computational studies establish that the metal–arene bonding is dominated by a  $\delta$ -backbonding interaction from admixture of titanium  $d_{xy}$  and  $d_{x^2-y^2}$  orbitals with the appropriate

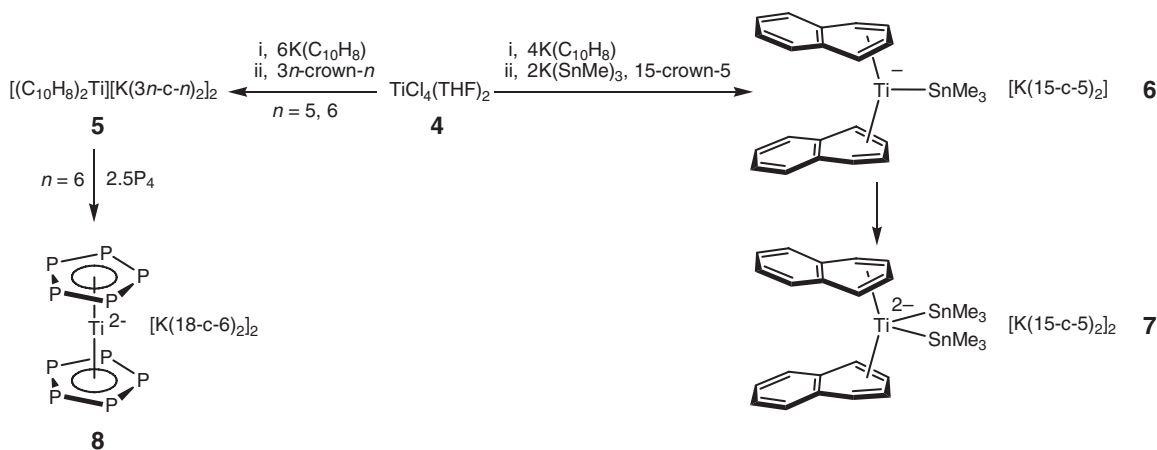
linear combinations of the arene  $\pi$ -system. As expected, this interaction increases down the group 4 triad and is more significant than in the group 6 congeners.



The related sterically hindered bis(arene) sandwich complex,  $\text{Ti}(\eta^6\text{-1,3,5-Pr}_3\text{C}_6\text{H}_3)_2$  **2**, can be oxidized with various ferrocenium salts,  $[\text{Cp}_2\text{Fe}][\text{BAR}_4]$  ( $\text{Ar} = \text{C}_6\text{H}_5$ ,  $p\text{-C}_6\text{H}_4\text{F}$ ,  $3,5\text{-C}_6\text{H}_3(\text{CF}_3)_2$ ), to furnish the first examples of fully characterized titanium(I) species,  $[\text{Ti}(\eta^6\text{-1,3,5-Pr}_3\text{C}_6\text{H}_3)_2][\text{BAR}_4]$  (**3**, Equation (1)).<sup>3</sup> The stability of these compounds in toluene solution is dependent upon the nature of the aryl substituent on the borate anion, where the  $[\text{BPh}_4]^-$  complex decomposes at  $50^\circ\text{C}$  and the  $[\text{B}(p\text{-C}_6\text{H}_4\text{F})_4]^-$  salt in boiling toluene. The  $[\text{B}(3,5\text{-C}_6\text{H}_3(\text{CF}_3)_2)_4]^-$  derivative is the most stable in the series and can even be handled in air for short periods of time. The solid-state structure of  $[\text{Ti}(\eta^6\text{-1,3,5-Pr}_3\text{C}_6\text{H}_3)_2][\text{B}(p\text{-C}_6\text{H}_4\text{F})_4]$  contains planar aryl rings with a ring centroid–metal bond distance of  $1.81\text{ \AA}$ . Both the  $[\text{B}(p\text{-C}_6\text{H}_4\text{F})_4]^-$  and  $[\text{B}(3,5\text{-C}_6\text{H}_3(\text{CF}_3)_2)_4]^-$  salts have magnetic moments consistent with one unpaired electron.



In contrast to neutral bis(naphthalene)titanium,<sup>4</sup> which is a highly reactive and transient species, two electron reduction to the corresponding dianion imparts considerable stability. Reduction of  $\text{TiCl}_4(\text{THF})_2$  **4** with 4 equiv. of  $\text{KC}_{10}\text{H}_8$  followed by addition of 2 equiv. of  $\text{KC}_{10}\text{H}_8$  and treatment with 15-crown-5 (15-c-5), furnishes  $[\text{K}(15\text{-c-5})]_2[\text{Ti}(\text{C}_{10}\text{H}_8)_2]$  (**5**, Scheme 1).<sup>5</sup> If the second addition of  $\text{KC}_{10}\text{H}_8$  is replaced with  $\text{KSnMe}_3$ , the monoanion,  $[\text{Ti}(\text{C}_{10}\text{H}_8)_2\text{SnMe}_3]^-$  **6**, is isolated as its  $[\text{K}(15\text{-c-5})_2]$  salt. Over the course of 2 weeks at  $-20^\circ\text{C}$ , this compound converts to  $[\text{K}(15\text{-c-5})]_2[\text{Ti}(\eta^4\text{-C}_{10}\text{H}_8)_2(\text{SnMe}_3)_2]$  **7** which has been characterized by X-ray diffraction and contains

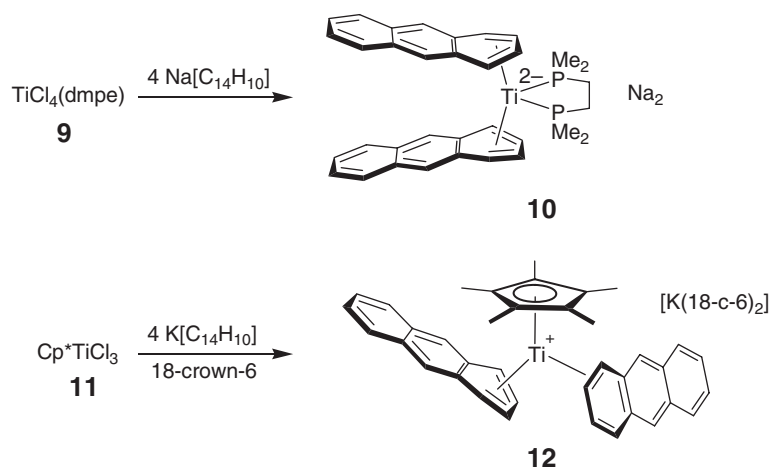


Scheme 1

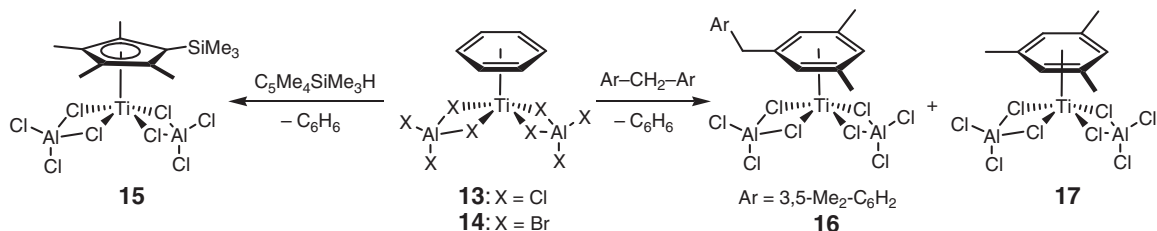
two distinct non-planar  $\eta^4$ -C<sub>10</sub>H<sub>8</sub> rings. *In situ* generated naphthalene compound, [K(18-c-6)]<sub>2</sub>[Ti(C<sub>10</sub>H<sub>8</sub>)<sub>2</sub>] (18-c-6 = 18-crown-6), reacts with white phosphorus to yield the carbon-free titanium sandwich, [(P<sub>5</sub>)<sub>2</sub>Ti]<sup>2-</sup> **8**, with [K(18-c-6)] cations.<sup>6</sup> The compound has a singlet ground state and X-ray analysis has established two parallel P<sub>5</sub><sup>-</sup> ligands with a staggered conformation (Scheme 1). Similar boratabenzene sandwich derivatives have been prepared by addition of acetylene to the boratabenzene carbonyl complex, ( $\eta^6$ -C<sub>5</sub>H<sub>5</sub>-BMe)<sub>2</sub>Ti(CO), to yield a mixture of ( $\eta^6$ -C<sub>5</sub>H<sub>5</sub>-BMe)( $\eta^8$ -C<sub>7</sub>H<sub>7</sub>-BMe)Ti and 1-methyl-boratacyclooctatetraene sandwich.<sup>7</sup>

A reduced anthracene complex has been prepared by reaction of TiCl<sub>4</sub>(dmpe) (dmpe = 1,2-bis(dimethyl)phosphinoethane **9** with Na[C<sub>14</sub>H<sub>10</sub>], furnishing **10** (Scheme 2).<sup>8</sup> The reaction of Cp<sup>+</sup>TiCl<sub>3</sub> **11** with anthracenium anion results in the formation of compound **12** where one arene is  $\eta^2$ -coordinated while the other adopts  $\eta^4$  hapticity. Reaction of the anthracene complexes with CO induces formation of the known carbonyl complexes, Ti(CO)<sub>3</sub>(dmpe)<sup>9</sup> and [Cp<sup>+</sup>Ti(CO)<sub>3</sub>]<sup>-</sup>, respectively.<sup>10</sup>

The formally divalent titanium monoarene complex, ( $\eta^6$ -C<sub>6</sub>H<sub>6</sub>)Ti{( $\mu$ -Cl)<sub>2</sub>AlCl<sub>2</sub>}<sub>2</sub> **13**,<sup>11</sup> has been prepared and serves as useful synthon for a range of other low-valent titanium derivatives. Addition of 1 equiv. of the silylated cyclopentadiene, C<sub>5</sub>HMe<sub>4</sub>(SiMe<sub>3</sub>), with ( $\eta^6$ -C<sub>6</sub>H<sub>6</sub>)Ti{( $\mu$ -Cl)<sub>2</sub>AlCl<sub>2</sub>}<sub>2</sub> affords paramagnetic, (C<sub>5</sub>Me<sub>4</sub>SiMe<sub>3</sub>)Ti{( $\mu$ -Cl)<sub>2</sub>AlCl<sub>2</sub>}<sub>2</sub> (**15**, Scheme 3).<sup>12</sup> When an excess of C<sub>5</sub>HMe<sub>4</sub>SiMe<sub>3</sub> is added, (C<sub>5</sub>Me<sub>4</sub>SiMe<sub>3</sub>)<sub>2</sub>Ti{( $\mu$ -Cl)<sub>2</sub>AlCl<sub>2</sub>}<sub>2</sub> and **15** are obtained as the major and minor products, respectively. Similarly, reaction of dihydro-dicyclopentadienyl with ( $\eta^6$ -C<sub>6</sub>H<sub>6</sub>)Ti{( $\mu$ -Cl)<sub>2</sub>AlCl<sub>2</sub>}<sub>2</sub> affords ( $\eta^5$ -C<sub>10</sub>H<sub>11</sub>)Ti{( $\mu$ -Cl)<sub>2</sub>AlCl<sub>2</sub>}<sub>2</sub>, which has been characterized by X-ray diffraction.<sup>13</sup> In addition to substitution with anionic ligands, ( $\eta^6$ -C<sub>6</sub>H<sub>6</sub>)Ti{( $\mu$ -X)<sub>2</sub>AlX<sub>2</sub>}<sub>2</sub> (X = Cl **13**, Br **14**) also undergoes ligand exchange with various arenes. For example, addition of dimesitylmethane to **13** affords the corresponding arene complex where only one of the two phenyl rings is coordinated to the titanium, **16**, along with the mesityl complex, **17**, arising from Friedel–Crafts-type bond scission under mild conditions (Scheme 3).

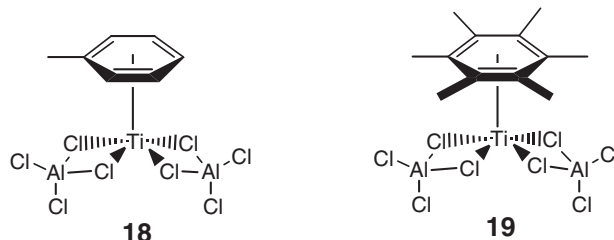


Scheme 2



Scheme 3

The divalent toluene and hexamethylbenzene complexes,  $(\eta^6\text{-C}_6\text{H}_5\text{Me})\text{Ti}\{(\mu\text{-Cl})_2\text{AlCl}_2\}_2$  **18** and  $(\eta^6\text{-C}_6\text{Me}_6)\text{Ti}\{(\mu\text{-Cl})_2\text{AlCl}_2\}_2$  **19**, are active for the syndiospecific polymerization of styrene when activated with methylalumoxane (MAO).<sup>14</sup> While extremely high molecular weight polymers are obtained, the molecular weight distributions are bimodal suggesting the presence of two distinct active species.



Heteroarene complexes,  $(\text{C}_6\text{R}_3\text{H}_2\text{E})_2\text{Ti}$  (E = N, R = Bu<sup>t</sup>; E = P, R = Bu<sup>t</sup>; E = As, R = H, **20**), can be prepared by metal–ligand vapor co-condensation of titanium with the corresponding arene (Scheme 4).<sup>15,16</sup> Distinct <sup>1</sup>H NMR resonances are observed for the aromatic protons at ambient temperature, suggesting restricted arene rotation. Variable-temperature NMR experiments provided barriers of 16 and 17 kcal mol<sup>−1</sup>, respectively, for the ring rotation. Reduction of either compound with potassium metal furnished the titanium(I) salts,  $\text{K}[(\text{C}_6\text{Bu}_3\text{H}_2\text{E})_2\text{Ti}]$  (E = N, P; **21**).

## 4.03.2 Titanium Diene Complexes

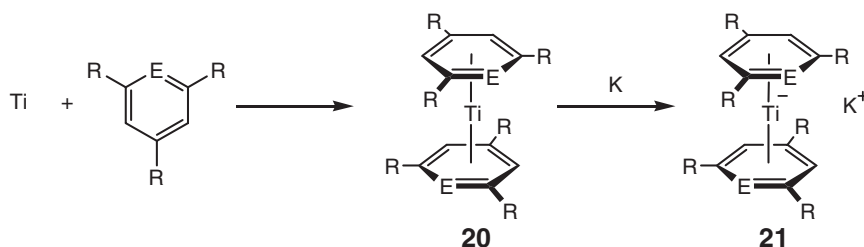
### 4.03.2.1 Titanium(0) Diene Complexes

Examples of both zero and divalent titanium complexes containing diene ligands have been described. Reduction of the titanium(II) dimethyl complex, *trans*-(dmpe)<sub>2</sub>TiMe<sub>2</sub><sup>17</sup> **22**, with AlEt<sub>3</sub> in the presence of 1,3-butadiene furnishes  $(\eta^4\text{-C}_4\text{H}_6)_2\text{Ti}(\text{dmpe})$  **23** (Scheme 5).<sup>18</sup> The molecule can also be prepared by reduction of TiCl<sub>4</sub>(dmpe) **9** with sodium amalgam in the presence of 1,3-butadiene<sup>19</sup> or by salt metathesis with the magnesium butadiene reagent, Mg(C<sub>6</sub>H<sub>4</sub>)(THF)<sub>2</sub>.<sup>20</sup> The solid-state structure of **23** exhibits metrical parameters more consistent with  $\pi^2$ ,  $\eta^4$  diene ligands rather than the  $\sigma^2$ ,  $\pi$  alternative, suggesting the zero-valent canonical form is the most appropriate descriptor.

### 4.03.2.2 Titanium(II) Diene Complexes

The dialkyl complex, **22**, can also be used to prepare divalent titanium diene compounds. Treatment of **22** with either 1,3-butadiene or *trans*, *trans*-1,4-diphenyl-1,3-butadiene at −20 °C yields the mono(diene) dialkyl complexes, (dmpe)TiMe<sub>2</sub>( $\eta^4\text{-C}_4\text{H}_4\text{R}_2$ ) (R = H **24**, Ph **25**).<sup>18</sup> Crystallographic characterization of the diphenyl derivative reveals a distorted octahedral structure with *cis*-methyl groups. The 1,4-diphenyl-1,3-butadiene ligand is  $\eta^4$ -coordinated with an essentially planar carbon skeleton. At longer reaction times at −20 °C, the parent butadiene complex, **24**, reacts with additional butadiene to yield the titanium(IV) complex, **26**. At 25 °C, the starting complex, **22**, is active for the dimerization of 1,3-butadiene to the Diels–Alder dimer, 4-vinylcyclohexene (Scheme 5).<sup>18</sup> The dimethyl complex, *trans*-(dmpe)<sub>2</sub>TiMe<sub>2</sub>, has also been shown to promote the dimerization of ethylene.<sup>21,22</sup>

Diene complexes of the so-called “constrained geometry” monocyclopentadienyl-amido titanium complexes have also been prepared. Interest in these molecules stems from their utility as catalyst precursors in olefin polymerization



Scheme 4



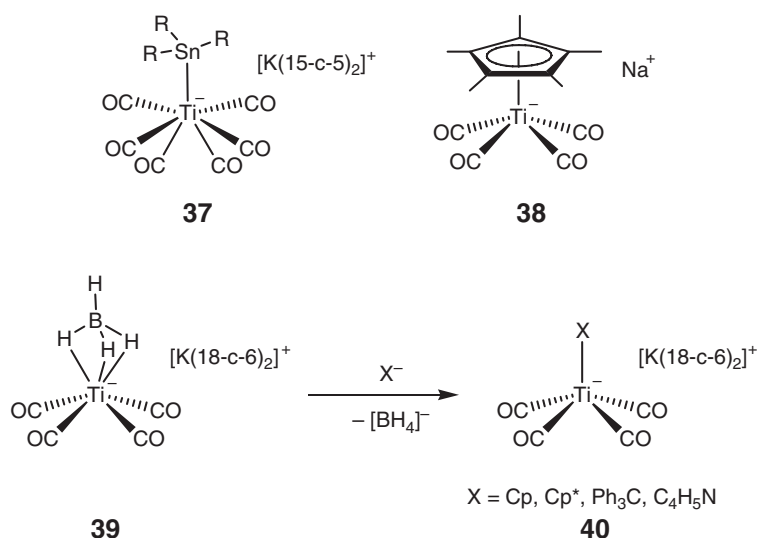
The Bu<sup>t</sup>-substituted complexes furnish solely the “prone” isomer where the cup of the diene is oriented away from the cyclopentadienyl ring.<sup>23</sup> Both the metrical data from the solid-state structure and NMR spectroscopic data support a  $\pi^2, \eta^4$  formalism for the diene ligand, consistent with a divalent titanium center.

Introduction of a phenyl amido substituent affords mixtures of both the prone and supine isomers with the prone being slightly favored (Scheme 6).<sup>23</sup> A combination of two-dimensional NMR experiments has established that in the prone isomers the diene is best described as a  $\pi^2, \eta^4$  diene ligand, consistent with Ti(II). In the supine cases, the spectroscopic data suggest more  $\sigma^2, \pi$  character, indicative of a Ti(IV) metallocycle. When treated with B(C<sub>6</sub>F<sub>5</sub>)<sub>3</sub>, [PhMe<sub>2</sub>NH][B(C<sub>6</sub>F<sub>5</sub>)<sub>4</sub>], or MAO, **29** and **31** are active for the random co-polymerization of ethylene and 1-octene.

Salt metathesis routes have also been used to prepare cyclopentadienyl-amido diene complexes. Treatment of **27** with Mg(butadiene) affords a 5:95 mixture of the prone and supine isomers of  $(\eta^5:\eta^1\text{-C}_5\text{Me}_4\text{SiMe}_2\text{NR})\text{Ti}(\eta^4\text{-CH}_2=\text{CHCH}=\text{CH}_2)$  (**35**, prone; **36**, supine; Scheme 6), respectively.<sup>25</sup> Crystallographic characterization of **36** produced metrical parameters consistent with a  $\pi^2, \eta^4$  butadiene, contrasting the zirconium congener where more  $\sigma^2, \pi$  character is observed.

### 4.03.3 Titanium Carbonyl Complexes

Examples of zero-valent titanium carbonyl complexes have been synthesized. While Ti(CO)<sub>6</sub> is a relatively unstable species, introduction of one anionic R<sub>3</sub>Sn<sup>−</sup> ligand allows isolation of [R<sub>3</sub>SnTi(CO)<sub>6</sub>]<sup>−</sup> (**37**, R = Me, Ph, Cy) derivatives (Scheme 7).<sup>26</sup> The cyclohexyl-substituted compound has been characterized by X-ray diffraction and adopts a capped trigonal prismatic structure in the solid state. Zero-valent tetracarbonyl anions have also been prepared and stabilized by introduction of cyclopentadienyl ligands.<sup>27</sup> While unsolvated  $[(\eta^5\text{-C}_5\text{H}_5)\text{Ti}(\text{CO})_4]^-$  is explosive at room temperature, the complex containing permethylcyclopentadienyl,  $[(\eta^5\text{-C}_5\text{Me}_5)\text{Ti}(\text{CO})_4]^-$  **38**, is thermally robust. More recently, both borohydride and pyrrole anions have been used to stabilize zero-valent titanium carbonyl compounds.<sup>28</sup> Treatment of [K(15-c-5)<sub>2</sub>][Ti(CO)<sub>6</sub>] with BH<sub>3</sub>·THF in THF at −60 °C has furnished [Ti(CO)<sub>4</sub>( $\eta^3\text{-BH}_4$ )]<sup>−</sup> **39**. Solution IR spectra in THF exhibit  $\nu(\text{CO})$  values that are the highest reported for any zero-valent titanium tetracarbonyl complex and suggest that [BH<sub>4</sub>]<sup>−</sup> is the weakest anionic ligand known to stabilize the titanium(0) fragment. Addition of various nucleophiles such as C<sub>5</sub>R<sub>5</sub><sup>−</sup> (R = H, Me), Ph<sub>3</sub>C<sup>−</sup>, and pyrrolyl anion to this compound at 20 °C induces loss of [BH<sub>4</sub>]<sup>−</sup> and formation of the corresponding adducts **40**. In both the cyclopentadienyl and pyrrolyl cases,  $\eta^5$ -coordination of the added nucleophile is observed.



Scheme 7



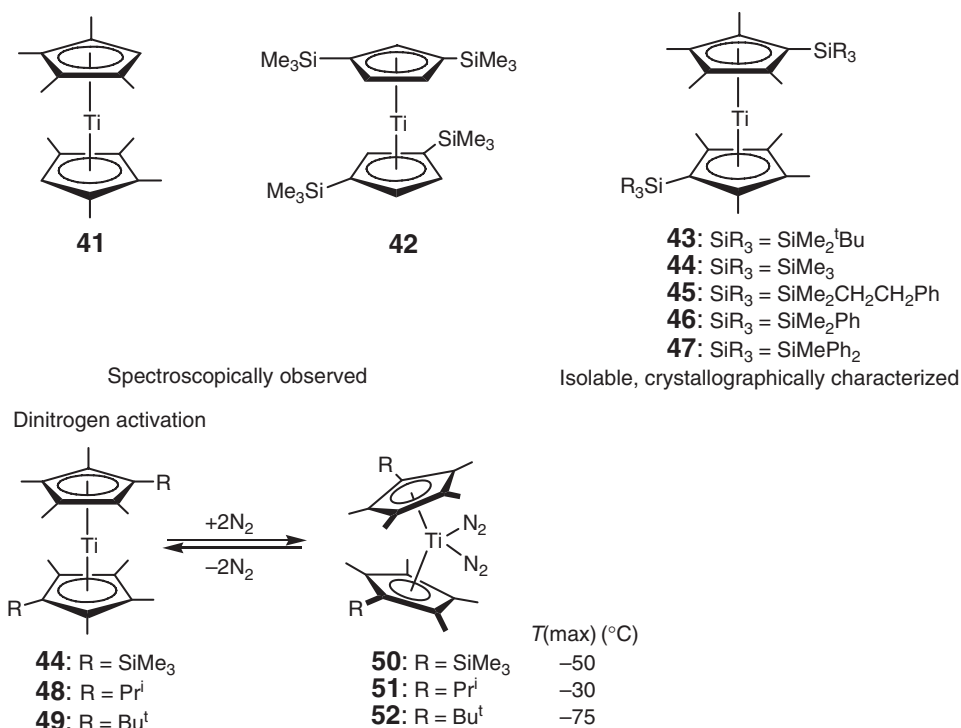
### 4.03.4 Bis(cyclopentadienyl)titanium(II) Complexes

#### 4.03.4.1 Bis(cyclopentadienyl)titanium(II) Complexes

Since the discovery of bis(cyclopentadienyl) metal sandwich complexes with  $(\eta^5\text{-C}_5\text{H}_5)_2\text{Fe}$ ,<sup>29</sup> considerable attention has been devoted to preparing related “titanocenes.”<sup>30</sup> The extreme reactivity of the parent complex,  $(\eta^5\text{-C}_5\text{H}_5)_2\text{Ti}$ , has prevented its isolation or spectroscopic identification.<sup>31</sup> Increasing the steric properties of the cyclopentadienyl ligand affords observable titanium sandwich complexes. Under dynamic vacuum, the dinuclear titanium dinitrogen complex,  $[(\eta^5\text{-C}_5\text{Me}_4\text{H})_2\text{Ti}](\mu_2\text{-}, \eta^1\text{-}, \eta^1\text{-N}_2)$ , loses dinitrogen to afford the spectroscopically observable titanium sandwich,  $(\eta^5\text{-C}_5\text{Me}_4\text{H})_2\text{Ti}$  **41**.<sup>32</sup> A similar approach has been used to observe the silylated titanium sandwich,  $(\eta^5\text{-C}_5\text{H}_3\text{-1,3-SiMe}_3)_2\text{Ti}$  **42** (Scheme 8).<sup>33</sup>

Increasing the size of the cyclopentadienyl substituents has produced the first examples of isolable and crystallographically characterized bis(cyclopentadienyl)titanium sandwiches. Reduction of the sterically encumbered bis(cyclopentadienyl)titanium(III) chloride precursor,  $(\eta^5\text{-C}_5\text{Me}_4\text{SiMe}_2\text{Bu}^t)_2\text{TiCl}$ , with sodium amalgam has produced a red-brown crystalline solid identified as  $(\eta^5\text{-C}_5\text{Me}_4\text{SiMe}_2\text{Bu}^t)_2\text{Ti}$  **43**.<sup>34</sup> The solid-state structure reveals staggered, exactly parallel cyclopentadienyl rings with the sterically demanding  $\text{SiMe}_2\text{Bu}^t$  substituents oriented  $180^\circ$  with respect to each other. As expected for a first row,  $e_g^2$  linear metallocene, a magnetic moment of  $2.4 \mu_B$  is measured, slightly lower than the expected spin-only value for two unpaired electrons.

Loss of a neutral ligand from the coordination sphere of a bent-titanocene derivative has also proved to be an effective strategy for synthesis of the corresponding sandwich complex. Thermolysis of  $(\eta^5\text{-C}_5\text{Me}_4\text{SiMe}_3)_2\text{-Ti}(\eta^2\text{-Me}_3\text{SiC}\equiv\text{CSiMe}_3)$  under dynamic vacuum results in loss of alkyne and formation of the titanocene,  $(\eta^5\text{-C}_5\text{Me}_4\text{SiMe}_3)_2\text{Ti}$  **44**.<sup>35</sup> As with  $(\eta^5\text{-C}_5\text{Me}_4\text{SiMe}_2\text{Bu}^t)_2\text{Ti}$ , the solid-state structure of **44** has exactly parallel cyclopentadienyl rings arising from crystallographically imposed symmetry. Since these initial reports, the number of isolable titanocenes has expanded to include a family of  $(\eta^5\text{-C}_5\text{Me}_4\text{R})_2\text{Ti}$  ( $\text{R} = \text{SiMe}_2\text{CH}_2\text{CH}_2\text{Ph}$ , **45**;  $\text{SiMe}_2\text{Ph}$ , **46**;  $\text{SiMePh}_2$ , **47**) derivatives.<sup>36</sup> As expected for complexes with two unpaired electrons, each compound is EPR silent and exhibits paramagnetically shifted NMR resonances that obey the Curie law from  $0$ – $60^\circ\text{C}$ . In contrast to the two other structurally characterized titanocenes, both  $(\eta^5\text{-C}_5\text{Me}_4\text{SiMe}_2\text{CH}_2\text{CH}_2\text{Ph})_2\text{Ti}$  and  $(\eta^5\text{-C}_5\text{Me}_4\text{SiMePh}_2)_2\text{Ti}$  are nonlinear with centroid–titanium–centroid angles of  $166.0(2)^\circ$  and  $162.2(2)^\circ$ . While the origin of this structural



Scheme 8

difference has not been elucidated, the latter derivatives are thermally robust with melting temperatures above 75 °C. Attempts to prepare related complexes by reduction of the titanocene dichloride complex containing a fluorinated silyl side chain,  $(\eta^5\text{-C}_5\text{Me}_4\text{SiMe}_2\text{CH}_2\text{CH}_2\text{CF}_3)_2\text{TiCl}_2$ , has produced a mixture of a mixed-valent, trinuclear hydride, magnesium complex and a dinuclear titanium–Mg species.<sup>37</sup>

Sterically demanding silyl groups are not required for stability of the titanocenes for peralkylated titanium sandwiches have also been prepared. Reduction of  $(\eta^5\text{-C}_5\text{Me}_4\text{R})_2\text{TiCl}_2$  affords  $(\eta^5\text{-C}_5\text{Me}_4\text{R})_2\text{Ti}$  ( $\text{R} = \text{Pr}^i$  **48**,  $\text{Bu}^t$  **49**), which have been characterized by  $^1\text{H}$  NMR and electronic spectroscopy as well as combustion analysis.<sup>38</sup> At low temperatures, these compounds react with 1 atm of dinitrogen to yield monomeric bis( $\text{N}_2$ ) complexes,  $(\eta^5\text{-C}_5\text{Me}_4\text{R})_2\text{Ti}(\eta^1\text{-N}_2)_2$ .

#### 4.03.4.2 Bis(cyclopentadienyl)titanium(II) Dinitrogen Complexes

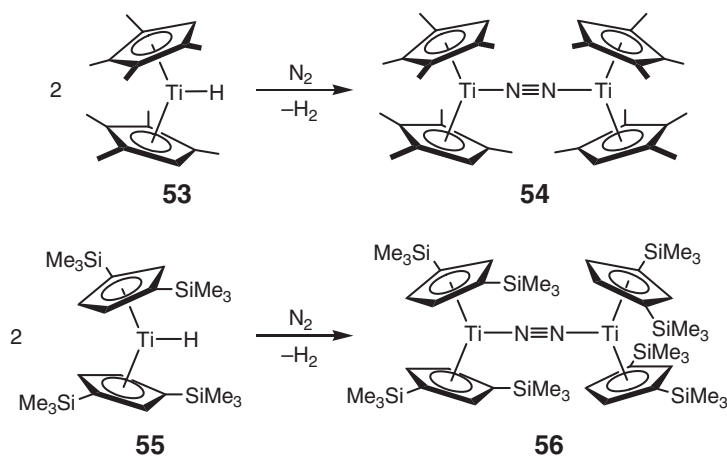
Exposure of the isolated bis(cyclopentadienyl)titanium sandwich complexes, **44**, **48**, and **49**, to 1 atm of dinitrogen at low temperature furnishes the monomeric, bis( $\text{N}_2$ ) compounds,  $(\eta^5\text{-C}_5\text{Me}_4\text{R})_2\text{Ti}(\eta^1\text{-N}_2)_2$  ( $\text{R} = \text{SiMe}_3$  **50**,  $\text{Pr}^i$  **51**,  $\text{Bu}^t$  **52**) (Scheme 8).<sup>38</sup> Dinitrogen coordination is reversible, and repeated cooling and warming cycles allow observation of the bis( $\text{N}_2$ ) compound and the sandwich, respectively. Variable temperature, *in situ* IR spectroscopic experiments have allowed determination of the maximum temperature for  $\text{N}_2$  binding, where smaller cyclopentadienyl substituents favor  $\text{N}_2$ -coordination (Scheme 8). One example,  $(\eta^5\text{-C}_5\text{Me}_4\text{Pr}^i)_2\text{Ti}(\eta^1\text{-N}_2)_2$ , has been characterized by X-ray diffraction and found to be essentially isostructural with more common titanocene dicarbonyl derivatives.

With smaller cyclopentadienyl ligands, dinuclear titanocene dinitrogen complexes are observed. Exposure of the silane complex,  $(\eta^5\text{-C}_5\text{H}_5)_2\text{Ti}(\eta^2\text{-H}_2\text{SiPh}_2)(\text{PMe}_3)$ , to 1 atm of dinitrogen results in displacement of the silane and affords the previously reported dinitrogen compound,  $[(\eta^5\text{-C}_5\text{H}_5)_2\text{Ti}(\text{PMe}_3)]_2(\mu_2\text{-}, \eta^1\text{-}, \eta^1\text{-N}_2)$ .<sup>39,40</sup> Bimetallic reductive elimination of dihydrogen has been used to prepare base-free dinitrogen compounds. Both  $[(\eta^5\text{-C}_5\text{Me}_4\text{H})_2\text{Ti}]_2(\mu_2\text{-}, \eta^1\text{-}, \eta^1\text{-N}_2)$  **54**<sup>32</sup> and  $[(\eta^5\text{-C}_5\text{H}_3\text{-1,3-(SiMe}_3)_2)_2\text{Ti}]_2(\mu_2\text{-}, \eta^1\text{-}, \eta^1\text{-N}_2)$  **56**<sup>33</sup> have been isolated from exposure of the titanocene monohydride to  $\text{N}_2$  (Scheme 9).

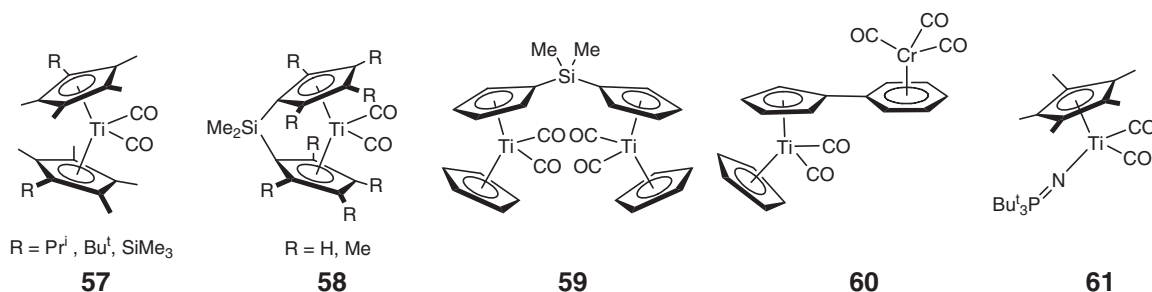
#### 4.03.4.3 Bis(cyclopentadienyl)titanium(II) Dicarbonyl, Isonitrile, and Phosphine Complexes

The synthesis and spectroscopic features of a number of titanocene dicarbonyl derivatives have been reviewed previously.<sup>41</sup> Typically, these complexes are prepared via magnesium reduction of the corresponding dihalide derivative under 1 atm of carbon monoxide. New compounds prepared since COMC(1995) are presented in Scheme 10.<sup>38,42–45</sup> Mixed cyclopentadienyl phosphinimide dicarbonyl compounds such as  $(\eta^5\text{-C}_5\text{Me}_5\text{-}( \text{Bu}^t\text{PN})\text{Ti}(\text{CO})_2$  **61** have also been isolated.<sup>46</sup>

Irradiation of the ligand adducts of the *ansa*-titanocene,  $\text{Me}_2\text{Si}(\eta^5\text{-C}_5\text{H}_4)_2\text{TiL}_2$  (**63**,  $\text{L} = \text{CN-C}_6\text{H}_3\text{Me}_2\text{-2,6}$ ,  $\text{PMe}_2\text{Ph}$ )<sup>42</sup> in the presence of the dicarbonyl compound,  $\text{Me}_2\text{Si}(\eta^5\text{-C}_5\text{H}_4)_2\text{Ti}(\text{CO})_2$ , results in ligand redistribution to yield the  $C_s$  symmetric,  $\text{Me}_2\text{Si}(\eta^5\text{-C}_5\text{H}_4)_2\text{Ti}(\text{CO})\text{L}$  complex. Reduction of the “fly-over” dimer,



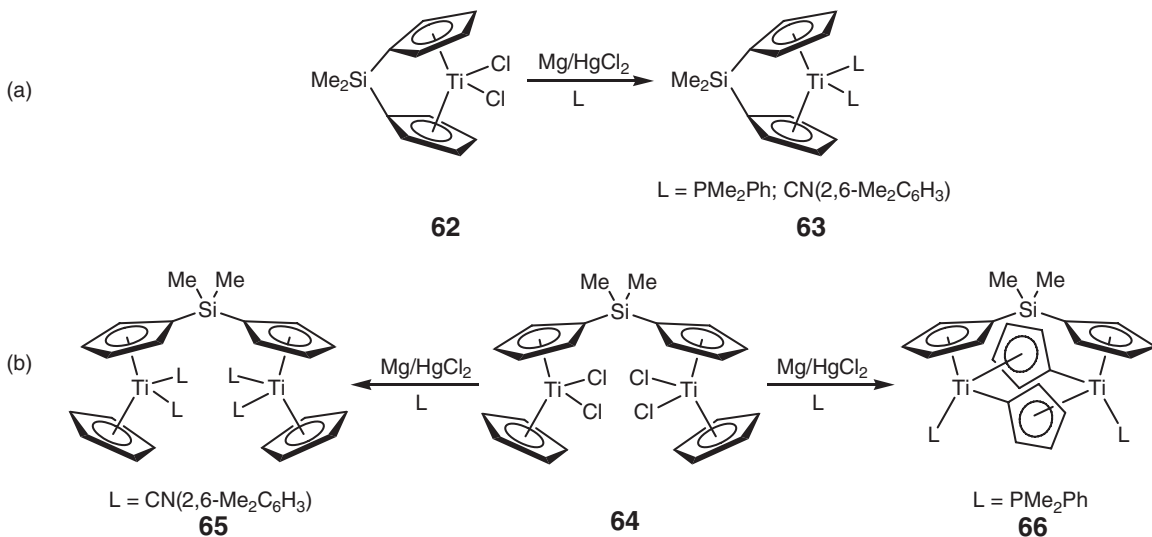
Scheme 9



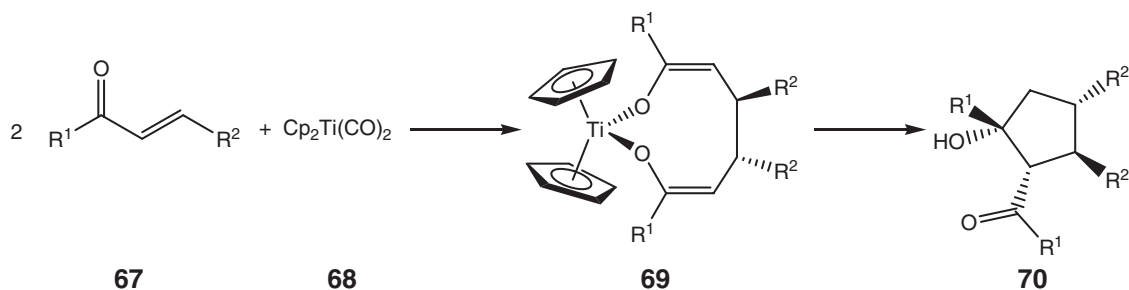
Scheme 10

$[(\eta^5\text{-C}_5\text{H}_5)\text{TiCl}_2]_2\{\mu\text{-Me}_2\text{Si}(\eta^5\text{-C}_5\text{H}_4)_2\}$  **64**, with Na(Hg) or magnesium activated with  $\text{HgCl}_2$  in THF in the presence of  $\text{CN-C}_6\text{H}_3\text{Me}_2\text{-2,6}$  furnishes  $[(\eta^5\text{-C}_5\text{H}_5)\text{Ti}(\text{CNC}_6\text{H}_3\text{Me}_2\text{-2,6})_2]_2\{\mu\text{-Me}_2\text{Si}(\eta^5\text{-C}_5\text{H}_4)_2\}$  **65** (Scheme 11b).<sup>44</sup> Performing a similar reduction in the presence of  $\text{PMe}_2\text{Ph}$  results in activation of a cyclopentadienyl ligand to form the titanium(III) complex,  $[(\text{PMe}_2\text{Ph})\text{Ti}(\mu\text{-}\eta^1\text{-}\eta^5\text{-C}_5\text{H}_4)]_2\{\mu\text{-Me}_2\text{Si}(\eta^5\text{-C}_5\text{H}_4)_2\}$  **66** (Scheme 11b).

Substituted-titanocene dicarbonyl complexes,  $(\eta^5\text{-C}_5\text{R}_n\text{H}_{5-n})_2\text{Ti}(\text{CO})_2$ , have also been used as isolable precursors to highly reactive titanium sandwiches,  $(\eta^5\text{-C}_5\text{R}_n\text{H}_{5-n})_2\text{Ti}$ . For example, reaction of  $\alpha,\beta$ -unsaturated ketones with  $(\eta^5\text{-C}_5\text{H}_5)_2\text{Ti}(\text{CO})_2$  **68** results in reductive coupling of the organic substrate to form  $(\eta^5\text{-C}_5\text{H}_5)_2\text{Ti}(\text{OC}(\text{R}^1)\text{CHCH}(\text{R}^2)\text{CH}(\text{R}^2)\text{CHC}(\text{R}^1)\text{O})$  **69** with liberation of carbon monoxide (Scheme 12).<sup>47,48</sup>



Scheme 11



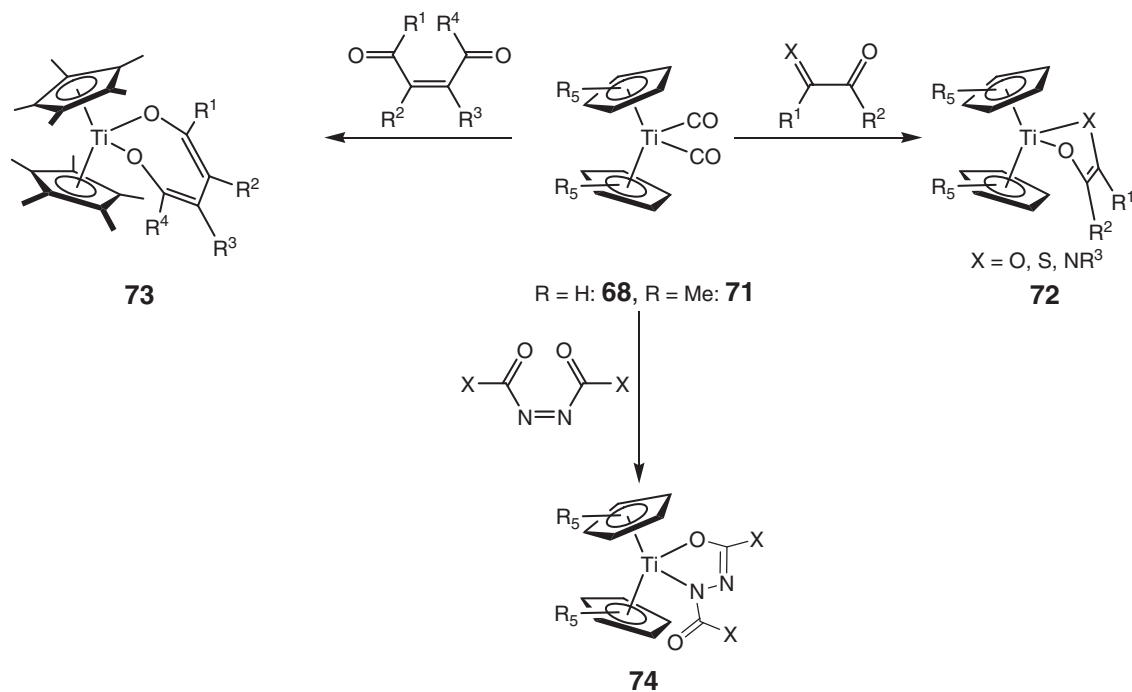
Scheme 12

Acidic hydrolysis afforded the titanocene dichloride and the corresponding 1,3,4-triaryl-2-arylcyclopentadienyl **70** or, in some cases, its dehydrated product.

Formal two-electron reduction of  $\alpha$ -diketones,  $\alpha$ -iminoketones,  $\alpha$ -sulfoxyketones, and 2-butene-diones has been achieved by addition to dicarbonyl complexes,  $(\eta^5\text{-C}_5\text{R}_5)_2\text{Ti}(\text{CO})_2$  ( $\text{R} = \text{H}, \text{Me}$ ), forming the corresponding titanacycles (**72** and **73**, Scheme 13).<sup>49</sup> Analogous reactivity is observed with azodicarboxylic esters **74**.

In analogy to the reaction of  $(\eta^5\text{-C}_5\text{H}_5)_2\text{Ti}(\text{CO})_2$  with elemental sulfur,<sup>50</sup> addition of cyclic organic sulfanes with the dicarbonyl compound results in CO loss concomitant with insertion into the S–S bond (**75–82**, Scheme 14).<sup>51</sup> Likewise, reaction of  $\text{S}_7\text{NR}$  ( $\text{R} = \text{H}, \text{Me}$ ) with  $(\eta^5\text{-C}_5\text{H}_5)_2\text{Ti}(\text{CO})_2$  forms the titanacycles,  $(\eta^5\text{-C}_5\text{H}_5)_2\text{Ti}(\text{S}_2\text{N}(\text{H})\text{S}_5)$  **84** and  $(\eta^5\text{-C}_5\text{H}_5)_2\text{Ti}(\text{S}_3\text{N}(\text{Me})\text{S}_4)$  **83** (Scheme 14).<sup>52</sup> Heating either of these compounds to 115–120 °C furnishes  $(\eta^5\text{-C}_5\text{H}_5)_2\text{TiS}_5$ . The origin of the initial formation of the regioisomers has not been elucidated. Liberation of the heterocycles can be achieved by addition of  $\text{S}_n\text{Cl}_2$  ( $n = 1, 2$ ), producing  $(\eta^5\text{-C}_5\text{H}_5)_2\text{TiCl}_2$  and respectively,  $\text{S}_8\text{NMe}$  and  $\text{S}_9\text{NMe}$ . Both, the parent and the substituted titanocene dicarbonyl complexes,  $(\eta^5\text{-C}_5\text{H}_4\text{R})_2\text{Ti}(\text{CO})_2$  ( $\text{R} = \text{H}, \text{Me}$ ), react with  $\text{RN}(\text{S}_2)_2\text{NR}$  ( $\text{R} = \text{Me}, \text{Oct}$ ) to furnish  $(\eta^5\text{-C}_5\text{H}_4\text{R})_2\text{Ti}(\text{S}_2)_2\text{NR}$  **85**, where the fate of one of the NR groups is unknown.<sup>53</sup>

Treatment of  $(\eta^5\text{-C}_5\text{H}_5)_2\text{Ti}(\text{CO})_2$  **68** with the Lewis acid,  $\text{B}(\text{C}_6\text{F}_5)_3$ , in the presence of *p*-trifluoromethylbenzonitrile results in displacement of the CO ligands to yield  $(\eta^5\text{-C}_5\text{H}_5)_2\text{Ti}(\eta^2\text{-C}, \text{N}(\text{C}_6\text{F}_5)_3\text{BNCC}_6\text{H}_4\text{CF}_3)$  **86** (Scheme 15).<sup>54</sup> The product has been characterized by X-ray diffraction and contains a C–N bond distance of 1.243(3) Å, typical for a C–N double bond. The solid-state structure also establishes an intramolecular interaction with one of the *ortho*-C–F bonds of the borane with a Ti–F distance of 2.453 Å. Hydrolysis of the product or direct reaction of  $(\eta^5\text{-C}_5\text{H}_5)_2\text{Ti}(\text{CO})_2$  with  $(\text{C}_6\text{F}_5)_3\text{B}(\text{OH})_2$  furnishes  $[(\eta^5\text{-C}_5\text{H}_5)_2\text{Ti}][\mu\text{-(OH)B}(\text{C}_6\text{F}_5)_3]$  **87**, which also contains an *ortho*-C–F interaction in the solid state (Ti–F = 2.2841 Å) (Scheme 15). In the absence of water or nitrile,  $(\eta^5\text{-C}_5\text{H}_5)_2\text{Ti}(\text{CO})_2$  undergoes reaction with  $\text{B}(\text{C}_6\text{F}_5)_3$  to yield  $\text{Cp}_2\text{Ti}(\text{CO})(\text{C}(\text{O})\text{B}(\text{C}_6\text{F}_5)_3)$  **88**, which forms an adduct with THF **89** (Scheme 15).<sup>55</sup> The most striking feature of the solid-state structures of these two compounds is the coordination of the  $\eta^2\text{-C}(\text{O})\text{B}(\text{C}_6\text{F}_5)_3$  ligand. In the case of the carbonyl adduct, the oxygen atom of the borane-bound carbonyl is *exo* to the metallocene wedge whereas the *endo* isomer is observed in the case of the THF adduct. IR spectroscopic data, in combination with the metrical parameters, are consistent with a zwitterionic,  $\eta^2$ -acyl complex. The cationic carbonyl complex,  $[(\eta^5\text{-C}_5\text{H}_5)_2\text{Ti}(\text{CO})_2]^+[\text{BPh}_4]^-$  has been obtained via oxidation of  $(\eta^5\text{-C}_5\text{H}_5)_2\text{Ti}(\text{CO})_2$  with  $[(\eta^5\text{-C}_5\text{H}_5)_2\text{Fe}][\text{BPh}_4]$  **90**.<sup>56</sup>



Scheme 13



Monocyclopentadienyltitanium phosphine complexes have also been prepared and reviewed previously.<sup>41</sup> The formally divalent titanium precursor,  $(\eta^5\text{-C}_5\text{H}_5)\text{Ti}(\text{dmpe})_2\text{Cl}$ , serves as a synthon for the corresponding methyl and hydride compounds,  $(\eta^5\text{-C}_5\text{H}_5)\text{Ti}(\text{dmpe})_2\text{R}$  ( $\text{R} = \text{Me}, \text{H}$ ), which are diamagnetic and crystallographically characterized.<sup>57</sup> Addition of ethylene to these compounds results in formation of 1-butene, 3-methyl-1-pentene, and

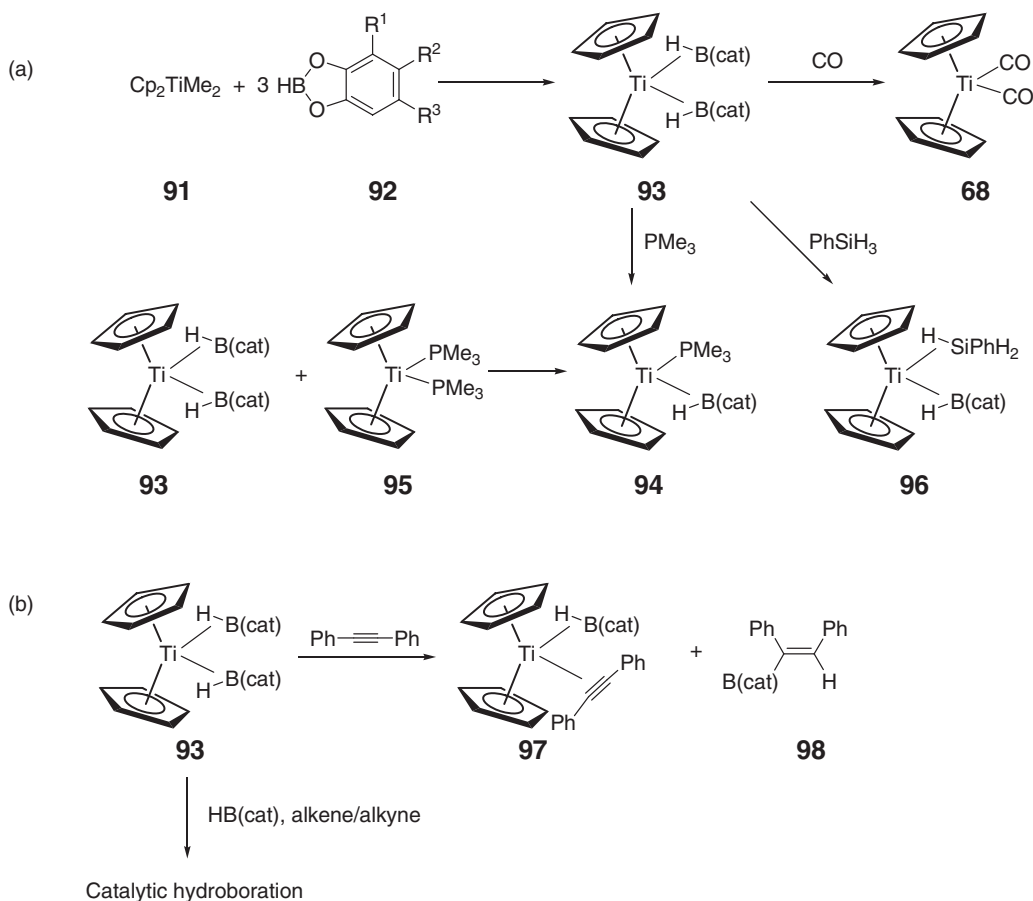
2-ethyl-1-butene in an approximate 70:15:15 ratio. Zero-valent titanium complexes bearing cyclopentadienyl, phosphine, and carbonyl ligands have also been synthesized.<sup>58</sup>

#### 4.03.4.4 Bis(cyclopentadienyl)titanium(II) Borane Complexes

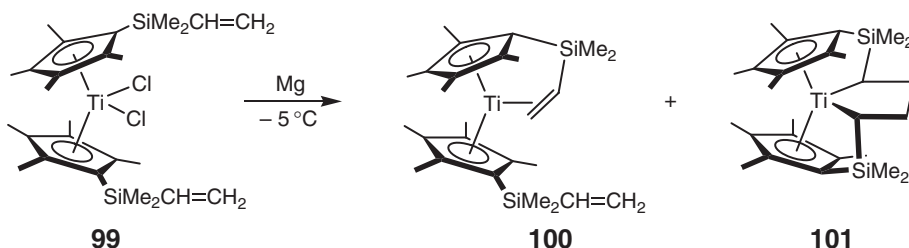
The bis(carbonyl) complex **68** and also the corresponding titanocene dimethyl **91** are active for the hydroboration of alkenes and alkynes.<sup>59</sup> These results have prompted a more systematic study of the interaction of boranes with divalent titanocene derivatives. Addition of 3 equiv. of substituted catechol boranes **92** to **91** results in formation of the corresponding bis(borane)  $\sigma$ -complexes **93** (Scheme 16a).<sup>60,61</sup> The empty orbital on the boron atom facilitates back donation from the titanium center, imparting stability to the compounds. While isolable and crystallographically characterized, the borane ligands are readily displaced by a number of neutral ligands, such as CO **68**, alkynes **97**, silanes **96**, and trimethylphosphine **94**. In case of the alkyne ligand substitution reaction, hydroboration of the unsaturate accompanies ligand substitution **98**. The mixed phosphine–borane adduct, **94**, obtained from the reaction of bis(borane), **93**, with  $\text{PMe}_3$  can alternatively be synthesized by comproportionation of **93** and  $\text{Cp}_2\text{Ti}(\text{PMe}_3)_2$  **95**.<sup>62</sup> The bis(borane) adduct is also found to be active in the hydroboration of olefins and alkynes, resulting in anti-Markovnikov products (Scheme 16b).<sup>63</sup>

#### 4.03.4.5 Bis( $\omega$ -alkenylcyclopentadienyl)titanium(II) Complexes

Reduction of titanocene dihalide complexes bearing alkene-substituted cyclopentadienyl ligands **99** has allowed isolation of formally divalent  $\omega$ -alkenyl complexes at low temperature. Stirring  $(\eta^5\text{-C}_5\text{Me}_4\text{R})_2\text{TiCl}_2$



Scheme 16



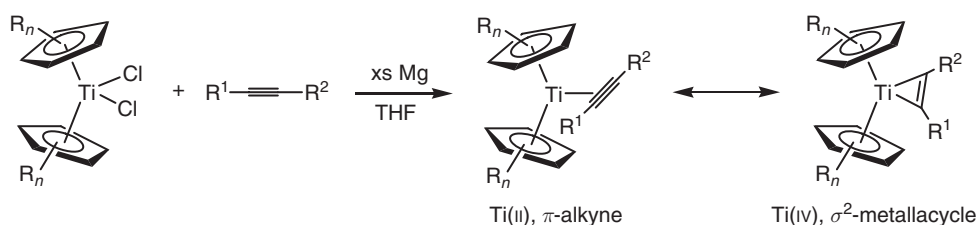
Scheme 17

( $\text{R} = \text{SiMe}_2\text{CH}=\text{CH}_2$ , **99**) with magnesium in THF at  $-5^\circ\text{C}$  yields a 2.3 : 1 mixture of the  $\omega$ -alkenyl compound, **100**, along with the titanacycle, **101** (Scheme 17). Exchange of the free and coordinated alkenyl substituents is slow at room temperature, and line broadening is observed by  $^1\text{H}$  NMR spectroscopy with heating. Interestingly, the ratio of **100** : **101** is unchanged upon standing at room temperature or heating to  $90^\circ\text{C}$  for 6 h.<sup>64</sup> Related complexes with methylene spacers between the cyclopentadienyl ligand and the  $\omega$ -alkene furnish the corresponding titanacyclopentanes upon reduction of the dichloride in the presence of THF.<sup>65</sup>

#### 4.03.4.6 Bis(cyclopentadienyl)titanium(II) Alkyne Complexes

Coordination of a  $\pi$ -acidic alkyne is a common strategy for stabilizing reactive divalent bis(cyclopentadienyl)titanium compounds.<sup>66</sup> Synthesis of  $(\text{C}_5\text{R}_n\text{H}_{5-n})_2\text{Ti}(\eta^2\text{-RC}\equiv\text{CR})$  compounds is typically accomplished by reduction of the corresponding titanocene dichloride compound with magnesium in the presence of the desired alkyne (Scheme 18). A summary of key spectroscopic and metrical data for recently reported titanocene alkyne complexes is presented in Table 1. It is important to note that for the purposes of this review, the alkyne compounds are formally viewed as divalent titanium species containing neutral,  $\pi$ -donor alkyne ligands but, in most cases, the titanium(IV) metallocyclopropene canonical form is the more appropriate descriptor. Typically, the carbon–carbon bond distances of the coordinated alkyne range between 1.286(8) and 1.323(16) Å, significantly elongated with respect to the free acetylene. In addition, both the  $\text{C}\equiv\text{C}$  stretching frequencies,  $\nu_{\text{C}\equiv\text{C}}$ , in the IR spectra ( $1580\text{--}1759\text{ cm}^{-1}$ ) and the  $^{13}\text{C}$  NMR chemical shift,  $\delta(\text{C})$ , of the alkyne carbons ( $116.4\text{--}254.9\text{ ppm}$ ) are consistent with a reduction of the acetylene ligand.

The spectroscopic features of the acetylene ligand are sensitive to subtle changes in metallocene structure. Methylation of the cyclopentadienyl ligands produces a more reduced alkyne ligand, as evidenced from the shifts of the C–C stretches in the IR spectra. This effect has been observed in a series of methylated titanocene complexes,  $(\eta^5\text{-C}_5\text{Me}_n\text{H}_{5-n})_2\text{Ti}(\eta^2\text{-Me}_3\text{SiCCSiMe}_3)$  ( $n=0\text{--}5$ , **102–107**),<sup>78</sup> as well as for the *ansa*-titanocenes,  $(\text{Me}_2\text{Si}(\eta^5\text{-C}_5\text{R}_4)_2)_2\text{Ti}(\eta^2\text{-Me}_3\text{SiCCSiMe}_3)$  ( $\text{R} = \text{H}$  **111**,  $\text{Me}$  **112**)<sup>79,80</sup> In both cases, there is also a trend in the  $^{13}\text{C}$  NMR shifts for the alkyne carbons, where increasing the methylation of the cyclopentadienyl ligands induces a downfield shift, consistent with increased titanacyclopentene character. For the  $(\eta^5\text{-C}_5\text{Me}_n\text{H}_{5-n})_2\text{Ti}(\eta^2\text{-Me}_3\text{SiCCSiMe}_3)$  ( $n=0\text{--}5$ ) series, a linear correlation exists between the  $^{13}\text{C}$  NMR chemical shift and the IR  $\text{C}\equiv\text{C}$  stretch. Comparison of  $(\eta^5\text{-C}_5\text{Me}_4\text{H})_2\text{Ti}(\eta^2\text{-Me}_3\text{SiCCSiMe}_3)$  **106** and  $(\eta^5\text{-C}_5\text{Me}_4\text{SiMe}_3)_2\text{Ti}(\eta^2\text{-Me}_3\text{SiCCSiMe}_3)$  **110**<sup>35</sup> or  $(\eta^5\text{-C}_{10}\text{H}_{11})_2\text{Ti}(\eta^2\text{-Me}_3\text{SiCCSiMe}_3)$  **113** and  $(\eta^5\text{-C}_{10}\text{H}_{10}\text{SiMe}_3)_2\text{Ti}(\eta^2\text{-Me}_3\text{SiCCSiMe}_3)$  **114**<sup>81</sup> demonstrates that as  $\text{SiMe}_3$  groups are



Scheme 18

**Table 1** Selected bond distances, IR and  $^{13}\text{C}$  NMR spectroscopic data

	$\text{Ti}-\text{C}$ (Å)	$\text{C}-\text{C}$ (Å)	$\nu_{\text{C}\equiv\text{C}}$ ( $\text{cm}^{-1}$ )	$\delta(\text{C})$ (ppm)	References
$(\eta^5\text{-C}_5\text{H}_5)_2\text{Ti}(\eta^2\text{-Me}_3\text{SiCCSiMe}_3)$ <b>102</b>			1662 <sup>a</sup> 1687 <sup>b</sup>	244.77 <sup>d</sup>	78, 82
$(\eta^5\text{-C}_5\text{MeH}_4)_2\text{Ti}(\eta^2\text{-Me}_3\text{SiCCSiMe}_3)$ <b>103</b>			1659 <sup>a</sup>	245.28 <sup>d</sup>	78
$(\eta^5\text{-C}_5\text{Me}_2\text{H}_3)_2\text{Ti}(\eta^2\text{-Me}_3\text{SiCCSiMe}_3)$ <b>104</b>			1657 <sup>a</sup>	245.45 <sup>d</sup>	78
$(\eta^5\text{-C}_5\text{Me}_3\text{H}_2)_2\text{Ti}(\eta^2\text{-Me}_3\text{SiCCSiMe}_3)$ <b>105</b>			1627 <sup>a</sup>	246.35 <sup>d</sup>	78
$(\eta^5\text{-C}_5\text{Me}_4\text{H})_2\text{Ti}(\eta^2\text{-Me}_3\text{SiCCSiMe}_3)$ <b>106</b>	2.106(3)	1.303(5)	1609 <sup>a</sup>	248.35 <sup>d</sup>	78
$(\eta^5\text{-C}_5\text{Me}_5)_2\text{Ti}(\eta^2\text{-Me}_3\text{SiCCSiMe}_3)$ <b>107</b>	2.122(3), 2.126(3)	1.309(4)	1598 <sup>a</sup> 1598 <sup>b</sup>	248.51 <sup>d</sup>	67, 82
$(\eta^5\text{-C}_5\text{Me}_4\text{Ph})_2\text{Ti}(\eta^2\text{-Me}_3\text{SiCCSiMe}_3)$ <b>108</b>			1597 <sup>c</sup>	251.0 <sup>d</sup>	68
$(\eta^5\text{-C}_5\text{Me}_4\text{Bn})_2\text{Ti}(\eta^2\text{-Me}_3\text{SiCCSiMe}_3)$ <b>109</b>			1595 <sup>c</sup>	249.1 <sup>d</sup>	100
$(\eta^5\text{-C}_5\text{Me}_4\text{SiMe}_3)_2\text{Ti}(\eta^2\text{-Me}_3\text{SiCCSiMe}_3)$ <b>110</b>	2.125(3), 2.144(3)	1.313(4)	1600 <sup>c</sup>	246.4 <sup>d</sup>	36
$(\text{Me}_2\text{Si}(\eta^5\text{-C}_5\text{H}_4)_2)\text{Ti}(\eta^2\text{-Me}_3\text{SiCCSiMe}_3)$ <b>111</b>			1655 <sup>a</sup> 1683 <sup>b</sup>	248.93 <sup>d</sup>	79, 69
$(\text{Me}_2\text{Si}(\eta^5\text{-C}_5\text{Me}_4)_2)\text{Ti}(\eta^2\text{-Me}_3\text{SiCCSiMe}_3)$ <b>112</b>	2.093(4), 2.105(4)	1.297(5)	1585 <sup>a</sup>	254.86 <sup>d</sup>	70
$(\text{C}_{10}\text{H}_{11})_2\text{Ti}(\eta^2\text{-Me}_3\text{SiCCSiMe}_3)$ <b>113</b>			1628 <sup>c</sup>	247.2 <sup>d</sup>	71
$(\text{C}_{10}\text{H}_{10}\text{SiMe}_3)_2\text{Ti}(\eta^2\text{-Me}_3\text{SiCCSiMe}_3)$ <b>114</b>	2.138(4)	1.286(8)	1610 <sup>c</sup>	238.9 <sup>d</sup>	81
$(\eta^5\text{-C}_5\text{Me}_4\text{H})_2\text{Ti}(\eta^2\text{-Bu}^t\text{CCCHCHBu}^t)$ <b>115</b>	2.068(5), 2.084(4)	1.304(6)	1640 <sup>a</sup>	218.0, 199.4 <sup>d</sup>	100
$(\eta^5\text{-C}_5\text{Me}_5)_2\text{Ti}(\eta^2\text{-Bu}^t\text{CCCHCHBu}^t)$ <b>116</b>			1627 <sup>a</sup>	218.6, 203.9 <sup>d</sup>	100
$(\eta^5\text{-C}_5\text{Me}_4\text{Ph})_2\text{Ti}(\eta^2\text{-Bu}^t\text{CCCHCHBu}^t)$ <b>117</b>			1630 <sup>a</sup>	220.5, 205.4 <sup>d</sup>	100
$(\eta^5\text{-C}_5\text{Me}_4\text{Bn})_2\text{Ti}(\eta^2\text{-Bu}^t\text{CCCHCHBu}^t)$ <b>118</b>			1635 <sup>a</sup>	219.6, 204.7 <sup>d</sup>	100
$(\eta^5\text{-C}_5\text{Me}_4\text{H})_2\text{Ti}(\eta^2\text{-SiMe}_3\text{CCCHCHSiMe}_3)$ <b>119</b>			1645 <sup>a</sup>	231.5, 222.5 <sup>d</sup>	100
$(\eta^5\text{-C}_5\text{Me}_4\text{H})_2\text{Ti}(\eta^2\text{-FcCCCHCHFc})$ <b>120</b>			1630 <sup>a</sup>	210.0, 204.3 <sup>d</sup>	100
$(\eta^5\text{-C}_5\text{Me}_4\text{H})_2\text{Ti}(\eta^2\text{-Bu}^t\text{CCC}(\text{CH}_2)\text{Bu}^t)$ <b>121</b>			1658 <sup>a</sup>	216.1, 208.7 <sup>d</sup>	100
$(\eta^5\text{-C}_5\text{Me}_5)_2\text{Ti}(\eta^2\text{-Bu}^t\text{CCC}(\text{CH}_2)\text{Bu}^t)$ <b>122</b>	2.163(2), 2.102(2)	1.300(3)	1644 <sup>a</sup>	219.4, 205.9 <sup>d</sup>	100
$(\eta^5\text{-C}_5\text{Me}_4\text{Ph})_2\text{Ti}(\eta^2\text{-Bu}^t\text{CCC}(\text{CH}_2)\text{Bu}^t)$ <b>123</b>			1645 <sup>a</sup>	221.2, 209.1 <sup>d</sup>	100
$(\eta^5\text{-C}_5\text{H}_5)_2\text{Ti}(\eta^2\text{-Bu}^t\text{CCSiMe}_3)$ <b>124</b>			1686 <sup>b</sup>	236.4, 205.3 <sup>c</sup>	72
$(\eta^5\text{-C}_5\text{H}_5)_2\text{Ti}(\eta^2\text{-Bu}^n\text{CCSiMe}_3)$ <b>125</b>			1678 <sup>b</sup>	229.7, 204.8 <sup>c</sup>	83
$(\eta^5\text{-C}_5\text{H}_5)_2\text{Ti}(\eta^2\text{-Pr}^n\text{CCSiMe}_3)$ <b>126</b>			1689 <sup>b</sup>	142.5, 217.1 <sup>c</sup>	83
$\text{THf}_2\text{Ti}(\eta^2\text{-Me}_3\text{SiCCSiMe}_3)$ <b>127</b>			1629 <sup>b</sup>	242.3 <sup>d</sup>	69
$\text{THf}_2\text{Ti}(\eta^2\text{-PhCCSiMe}_3)$ <b>128</b>			1652 <sup>b</sup>	220.0 <sup>d</sup>	69
$\text{THf}_2\text{Ti}(\eta^2\text{-PhCCPh})$ <b>129</b>	2.086(4), 2.044(5)	1.287(6)	1671 <sup>b</sup>	196.6 <sup>d</sup>	69
$(\eta^5\text{-C}_5\text{H}_5)_2\text{Ti}(\eta^2\text{-PhCCPh})$ <b>130</b>			1713 <sup>b</sup>	196.5 <sup>d</sup>	73
$(\eta^5\text{-C}_5\text{H}_5)_2\text{Ti}(\eta^2\text{-PhCCSiMe}_3)$ <b>131</b>	2.095(3), 2.118(3)	1.289(4)	1686 <sup>b</sup>	219.63, 212.96 <sup>d</sup>	82
$(\eta^5\text{-C}_5\text{Me}_5)_2\text{Ti}(\eta^2\text{-PhCCSiMe}_3)$ <b>132</b>	2.089(2), 2.139(2)	1.308(3)	1625 <sup>b</sup>	224.9, 213.2 <sup>d</sup>	82
$(\eta^5\text{-C}_5\text{H}_5)_2\text{Ti}(\eta^2\text{-FcCCSiMe}_3)$ <b>133</b>			1685 <sup>c</sup>	208.6, 218.4 <sup>d</sup>	74
$(\eta^5\text{-C}_5\text{Me}_4\text{H})_2\text{Ti}(\eta^2\text{-FcCCSiMe}_3)$ <b>134</b>	2.073(2), 2.115(2)	1.303(3)	1644 <sup>c</sup>	210.9, 217.8 <sup>d</sup>	74
$(\eta^5\text{-C}_5\text{Me}_5)_2\text{Ti}(\eta^2\text{-FcCCSiMe}_3)$ <b>135</b>			1627 <sup>c</sup>	212.6, 218.3 <sup>d</sup>	74
$(\eta^5\text{-C}_5\text{H}_5)_2\text{Ti}(\eta^2\text{-FcCCPh})$ <b>136</b>					74
$(\eta^5\text{-C}_5\text{Me}_4\text{H})_2\text{Ti}(\eta^2\text{-FcCCPh})$ <b>137</b>			1589 <sup>c</sup>	195.7, 199.1 <sup>d</sup>	74
$(\eta^5\text{-C}_5\text{Me}_5)_2\text{Ti}(\eta^2\text{-FcCCPh})$ <b>138</b>	2.088(3), 2.093(3)	1.312(5)	1585 <sup>c</sup>	195.1, 198.5 <sup>d</sup>	74
$(\eta^5\text{-C}_5\text{H}_5)_2\text{Ti}(\eta^2\text{-Bu}^t\text{CCSiMe}_2\text{H}-\kappa\text{H})$ <b>139</b>			1685 <sup>b</sup>	116.4, 216.2 <sup>f</sup> 206.1, 89.4 <sup>g</sup>	75
$(\eta^5\text{-C}_5\text{H}_5)_2\text{Ti}(\eta^2\text{-Me}_3\text{SiCCSiMe}_2\text{H}-\kappa\text{H})$ <b>140</b>			1759 <sup>b</sup>	119.8, 182.3 <sup>h</sup>	75
$(\eta^5\text{-C}_5\text{Me}_5)_2\text{Ti}(\eta^2\text{-Me}_3\text{SnCCSnMe}_3)$ <b>141</b>	2.096(11)	1.323(16)	1580 <sup>a</sup>	244.5 <sup>d</sup>	76
$\text{O}(\text{SiMe}_2(\eta^5\text{-C}_5\text{H}_4)_2)_2\text{Ti}(\eta^2\text{-Me}_3\text{SiCCSiMe}_3)$ <b>142</b>			1687 <sup>b</sup>	242.9 <sup>c</sup>	77

<sup>a</sup>In hexane.<sup>b</sup>In nujol.<sup>c</sup>In KBr.<sup>d</sup>In benzene- $d_6$ .<sup>e</sup>In THF- $d_8$ .<sup>f</sup>In toluene- $d_8$  at 303 K.<sup>g</sup>In toluene- $d_8$  at 193 K.<sup>h</sup>In toluene- $d_8$  at 165 K.

introduced in the alkyne ligand, a red shift is observed by IR spectroscopy but the  $^{13}\text{C}$  NMR shifts move more upfield.

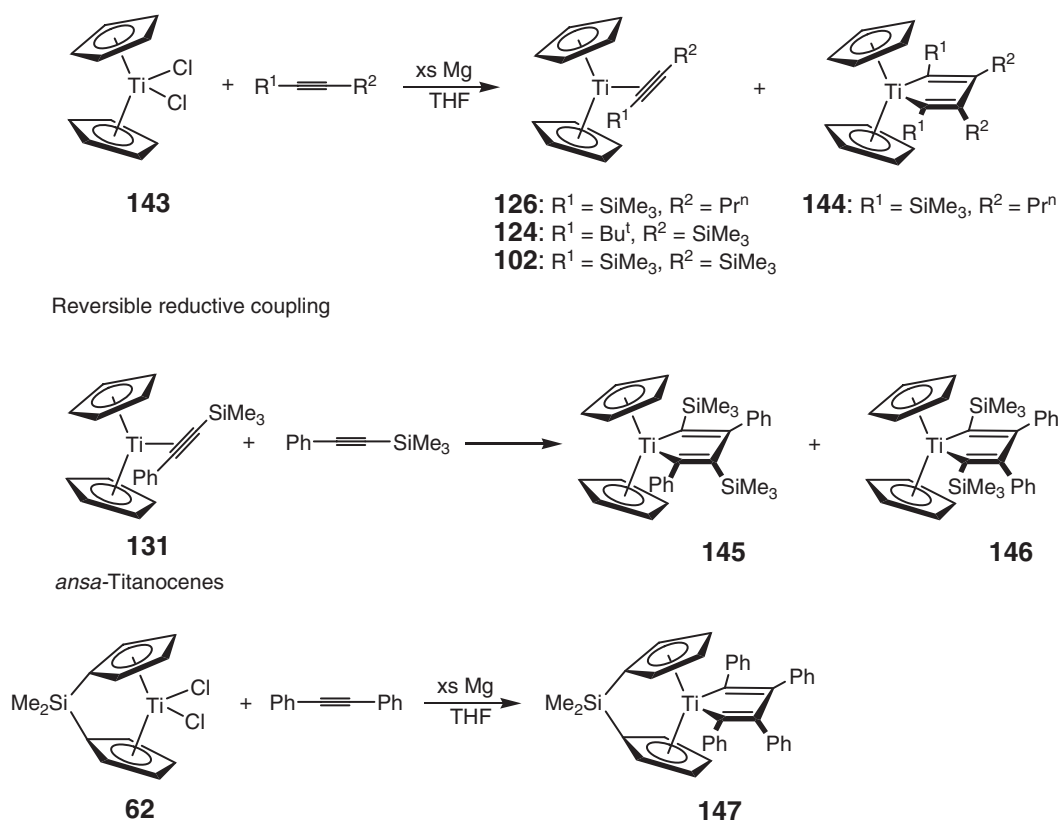
The effects of alkyne substitution on the electronic properties of the titanocene complexes are not as straightforward. In general, it appears that replacing  $\text{SiMe}_3$  substituents with Ph groups increases the backdonation from the titanium to



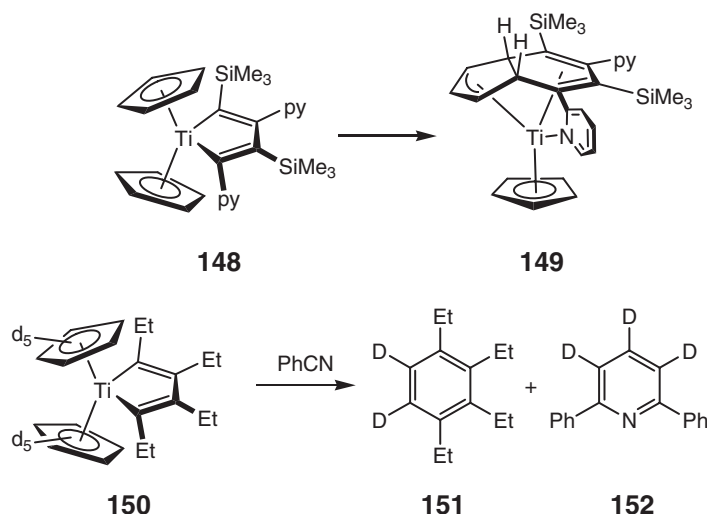
the alkyne, consistent with the electron withdrawing nature of the aromatic rings. This is illustrated by the comparison of the spectroscopic properties of  $(\eta^5\text{-C}_5\text{H}_5)_2\text{Ti}(\eta^2\text{-Me}_3\text{SiCCSiMe}_3)$  **102**,  $(\eta^5\text{-C}_5\text{H}_5)_2\text{Ti}(\eta^2\text{-PhCCSiMe}_3)$  **131**, and  $(\eta^2\text{-C}_5\text{H}_5)_2\text{Ti}(\eta^2\text{-PhCCPh})$  **130**<sup>82</sup> and those of  $(\text{THI})_2\text{Ti}(\eta^2\text{-Me}_3\text{SiCCSiMe}_3)$  **127** (THI = tetrahydroindenyl),  $(\text{THI})_2\text{Ti}(\eta^2\text{-PhCCSiMe}_3)$  **128**, and  $(\text{THI})_2\text{Ti}(\eta^2\text{-PhCCPh})$  **129**.<sup>80</sup> The influence of alkyne sterics on the spectroscopic properties of the compounds has also been examined with  $(\eta^5\text{-C}_5\text{H}_5)_2\text{Ti}(\eta^2\text{-Bu}^t\text{CCSiMe}_3)$  **124**,  $(\eta^5\text{-C}_5\text{H}_5)_2\text{Ti}(\eta^2\text{-Bu}^n\text{CCSiMe}_3)$  **125**, and  $(\eta^5\text{-C}_5\text{H}_5)_2\text{Ti}(\eta^2\text{-Pr}^n\text{CCSiMe}_3)$  **126**,<sup>83</sup> but no clear trend has emerged from the data.

Alkyne steric factors do, however, influence the relative stability and ability to isolate the  $\eta^2$ -adduct. Magnesium reduction of  $(\eta^2\text{-C}_5\text{H}_5)_2\text{TiCl}_2$  in the presence of  $\text{Pr}^n\text{C}\equiv\text{CSiMe}_3$  furnishes a mixture of the  $\eta^2$ -alkyne compound, **126**, and the titanacyclopentadiene, **143**, the result of reductive coupling of 2 equiv. of alkyne (Scheme 19).<sup>83</sup> Reducing the steric bulk of the alkyne by using  $\text{MeC}\equiv\text{CSiMe}_3$  has produced the titanacyclopentadiene as the sole product (Scheme 19). Larger alkynes inhibit reductive coupling, as  $(\eta^5\text{-C}_5\text{H}_5)_2\text{Ti}(\eta^2\text{-Bu}^t\text{CCSiMe}_3)$  **124** and  $(\eta^5\text{-C}_5\text{H}_5)_2\text{Ti}(\eta^2\text{-SiMe}_3\text{CCSiMe}_3)$  **102** are unreactive toward excess alkyne. In contrast,  $(\eta^5\text{-C}_5\text{H}_5)_2\text{Ti}(\eta^2\text{-PhCCSiMe}_3)$  **131** does react with a second equivalent of alkyne to form the metallacycle. Thermolysis of the two regioisomers,  $(\eta^5\text{-C}_5\text{H}_5)_2\text{Ti}(\text{C}(\text{Ph})\text{C}(\text{SiMe}_3)\text{C}(\text{Ph})\text{C}(\text{SiMe}_3))$  **145** and  $(\eta^5\text{-C}_5\text{H}_5)_2\text{Ti}(\text{C}(\text{SiMe}_3)\text{C}(\text{Ph})\text{C}(\text{Ph})\text{C}(\text{SiMe}_3))$  **146**, results in complete conversion to the thermodynamically favored latter isomer, thereby demonstrating the reversibility of the reductive coupling reaction.<sup>83</sup> Magnesium reduction of the *ansa*-titanocene dichloride complex,  $\text{Me}_2\text{Si}(\eta^5\text{-C}_5\text{H}_4)_2\text{TiCl}_2$  **62**, in the presence of 1 equiv. of diphenylacetylene results in reductive coupling to yield, **147** (Scheme 19).<sup>80</sup>

Alkynes bearing donor ligands have also been explored. Addition of  $(\text{C}_5\text{H}_4\text{N})\text{C}\equiv\text{CSiMe}_3$  to the acetylene complex, **102**, initially furnishes a mixture of titanacyclopentadienes. The isomer with pyridine in the  $\alpha$ -position to titanium **148** rearranges to afford the substituted  $\eta^3\text{:}\eta^4$ -indenyl complex, **149** (Scheme 20).<sup>84</sup> A similar reaction is observed upon addition of acetylene to **102**, and in the intramolecular cyclization reaction of dodeca-3,9-diyne.<sup>85,86</sup> The formation of dialkyl-indenyl ligands is suggested to be intermediate in the formation of substituted pyridines **152** and benzenes **151** from reaction of titanacyclopentadiene **150** with nitriles.<sup>87,88</sup>



Scheme 19

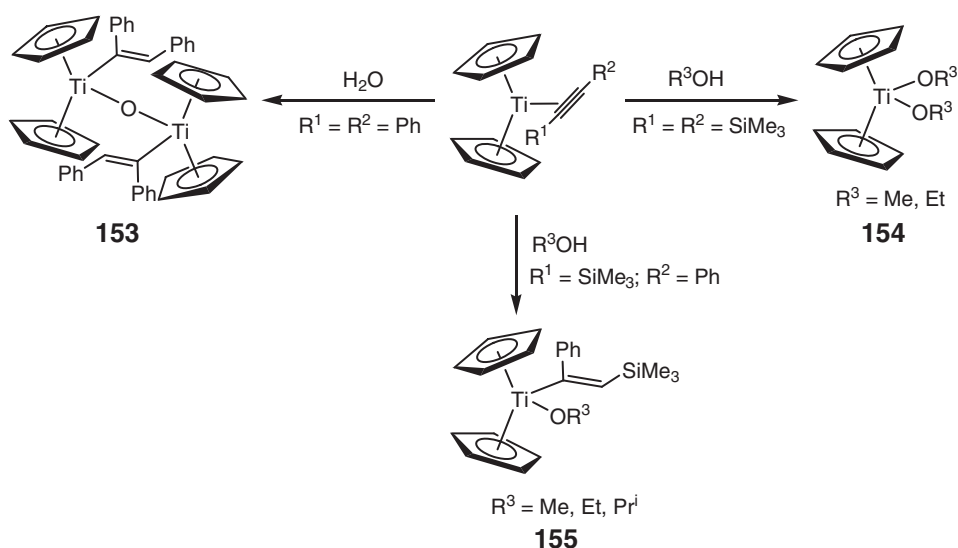


Scheme 20

Titanocene alkyne complexes serve as useful synthons for a range of transformations including acetylene loss to yield “titanocene”-type chemistry or insertion into the titanium–carbon bond. Two recent reviews have been published on the scope of this reactivity with the parent cyclopentadienyl complexes,  $(\eta^5\text{-C}_5\text{H}_5)_2\text{Ti}(\eta^2\text{-RCCR})$ . Reactivity not covered in these reviews is presented here.<sup>66,89</sup>

Hydrolysis of  $(\text{THI})_2\text{Ti}(\eta^2\text{-PhCCPh})$  furnishes the  $\mu$ -oxo dimer,  $[(\text{THI})_2\text{Ti}(\text{C}(\text{Ph})\text{C}(\text{Ph})\text{H})]_2(\mu\text{-O})$ ,<sup>80</sup> similar to previous reports with the parent bis(cyclopentadienyl) complex **153**.<sup>90</sup> While hydrolysis of  $(\eta^5\text{-C}_5\text{H}_5)_2\text{Ti}(\eta^2\text{-Me}_3\text{SiCCSiMe}_3)$  results in loss of the alkyne ligand and yields paramagnetic products, alcoholysis with ROH ( $\text{R} = \text{Me}, \text{Et}$ ) affords the bis(alkoxide) complexes,  $(\eta^5\text{-C}_5\text{H}_5)_2\text{Ti}(\text{OR})_2$  **154**, free alkyne and  $\text{H}_2$  ( $\text{R} = \text{Me}, \text{Et}$ , Scheme 21).<sup>83</sup> For the asymmetric alkyne complex,  $(\eta^5\text{-C}_5\text{H}_5)_2\text{Ti}(\eta^2\text{-PhCCSiMe}_3)$ , regioselective protonation affords  $(\eta^5\text{-C}_5\text{H}_5)_2\text{Ti}(\text{C}(\text{Ph})\text{C}(\text{SiMe}_3)\text{H})(\text{OR})$  **155** ( $\text{R} = \text{Me}, \text{Et}, \text{Pr}^i$ , Scheme 21).

Exposure of the same adduct to  $\text{CO}_2$  yields  $[(\eta^5\text{-C}_5\text{H}_5)_2\text{Ti}]_2(\mu\text{-C}(\text{Ph})\text{C}(\text{SiMe}_3)\text{C}(\text{O})\text{O})$  **156**, analogous to the product reported from  $\text{CO}_2$  addition to  $(\eta^5\text{-C}_5\text{H}_5)_2\text{Ti}(\eta^2\text{-Me}_3\text{CCSiMe}_3)$  and  $(\eta^5\text{-C}_5\text{H}_5)_2\text{Ti}(\eta^2\text{-PhCCPh})$



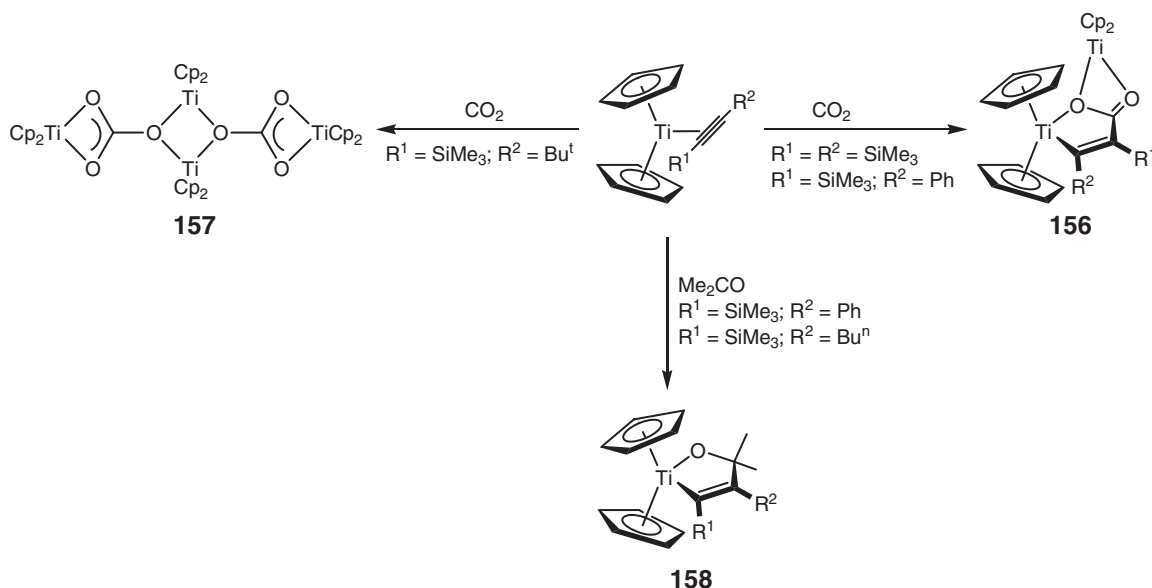
Scheme 21

(Scheme 22).<sup>80</sup> This reaction is also regioselective, affording the product derived from insertion into the titanium–carbon bond. In contrast,  $(\eta^5\text{-C}_5\text{H}_5)_2\text{Ti}(\eta^2\text{-Bu}^t\text{CCSiMe}_3)$  undergoes alkyne loss upon exposure to  $\text{CO}_2$  to furnish the previously reported tetramer,  $[(\eta^5\text{-C}_5\text{H}_5)_2\text{Ti}(\text{CO}_3)]_2$  **157** (Scheme 22).<sup>91</sup> Addition of acetone to  $(\eta^5\text{-C}_5\text{H}_5)_2\text{Ti}(\eta^2\text{-PhCCSiMe}_3)$  or  $(\eta^5\text{-C}_5\text{H}_5)_2\text{Ti}(\eta^2\text{-Bu}^n\text{CCSiMe}_3)$  affords the titanacycles,  $(\eta^5\text{-C}_5\text{H}_5)_2\text{Ti}(\text{C}(\text{SiMe}_3)\text{-C}(\text{R})\text{CMe}_2\text{O})$  **158** ( $\text{R} = \text{Ph}, \text{Bu}^n$ ) (Scheme 22). As demonstrated by the reaction with  $\text{CO}_2$  and alcohols, chemistry at the  $\text{SiMe}_3$  substituted titanium–carbon bond is kinetically favored but the reversibility of acetone insertion affords thermodynamically favored,  $(\eta^5\text{-C}_5\text{H}_5)_2\text{Ti}(\text{C}(\text{SiMe}_3)\text{C}(\text{R})\text{CMe}_2\text{O})$ , in analogy to the reductive coupling of alkynes.

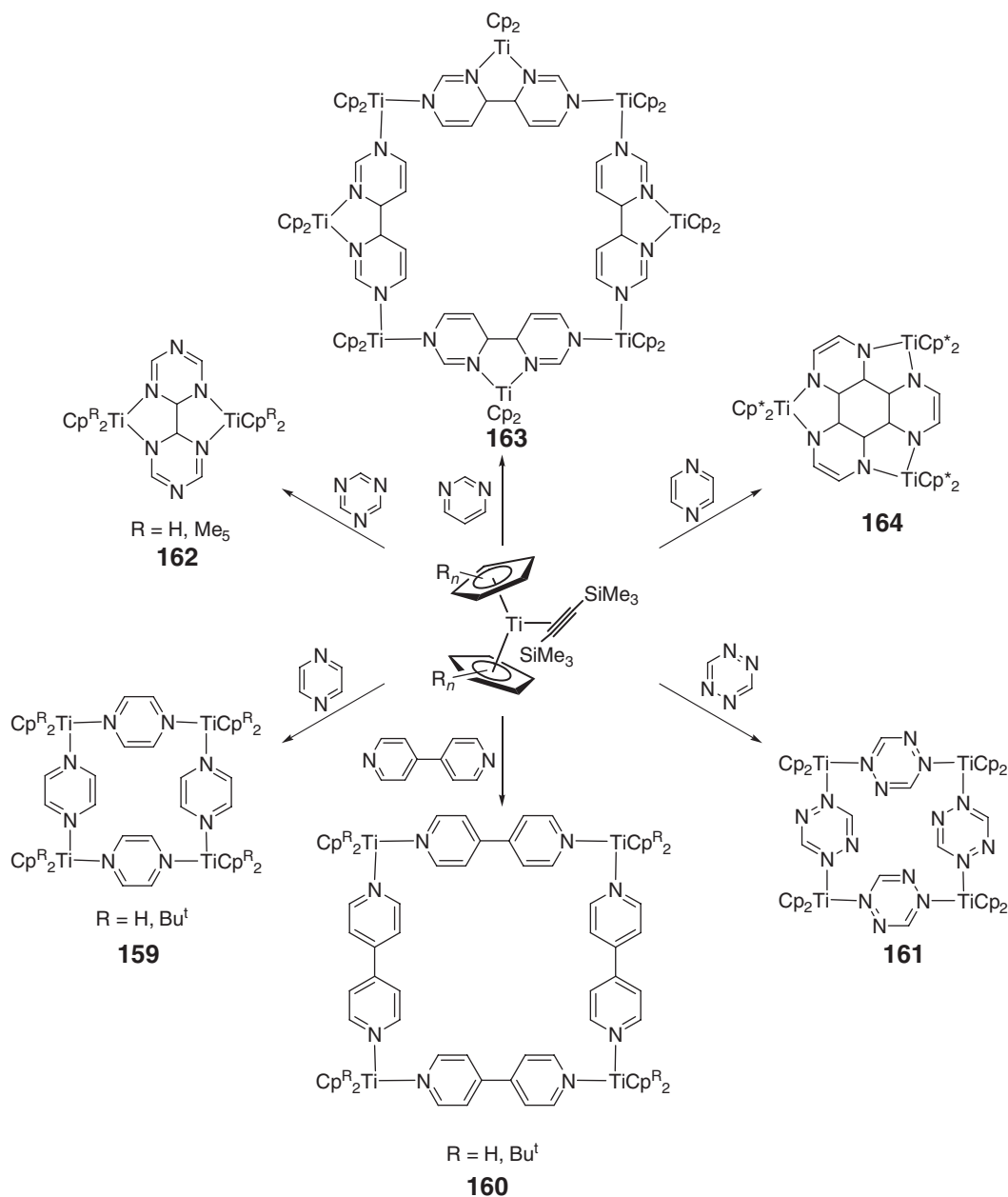
Addition of six-membered nitrogen-based heterocycles to  $(\eta^5\text{-C}_5\text{R}_5)_2\text{Ti}(\eta^2\text{-Me}_3\text{SiCCSiMe}_3)$  ( $\text{R} = \text{H}, \text{Me}$ ) results in a mixture of products including reductive coupling to yield polynuclear titanocene compounds, the ratios of which are dependent on the starting material, the heterocycles and reaction conditions (Scheme 23).<sup>92,93</sup> For example, pyrazine, 4,4-bipyridine, or tetrazine addition to  $(\eta^5\text{-C}_5\text{H}_4\text{R})_2\text{Ti}(\eta^2\text{-Me}_3\text{SiCCSiMe}_3)$  ( $\text{R} = \text{H}, \text{Bu}^t$ ) provides the tetranuclear cluster,  $[(\eta^5\text{-C}_5\text{H}_4\text{R})_2\text{Ti}(\mu_2\text{-C}_4\text{H}_4\text{N}_2)]_4$ ,  $[(\eta^5\text{-C}_5\text{H}_4\text{R})_2\text{Ti}(\mu_2\text{-(C}_5\text{H}_4\text{N)}_2)]_4$ , and  $[(\eta^5\text{-C}_5\text{H}_4\text{R})_2\text{Ti}(\mu_2\text{-C}_2\text{H}_2\text{N}_4)]_4$  respectively, with each *N*-heterocycle bridging two titanium centers **159–161**. Reduction of the heterocycle has not been reported. Reductive coupling is observed upon addition of triazine to  $(\eta^5\text{-C}_5\text{R}_5)_2\text{Ti}(\eta^2\text{-Me}_3\text{SiCCSiMe}_3)$  ( $\text{R} = \text{H}, \text{Me}$ ) and by addition of pyrimidine to  $(\eta^5\text{-C}_5\text{H}_5)_2\text{Ti}(\eta^2\text{-Me}_3\text{SiCCSiMe}_3)$  (**162–164**, Scheme 23). The latter reactions are carried out at higher temperatures.

The reaction of  $(\eta^5\text{-C}_5\text{H}_5)_2\text{Ti}(\eta^2\text{-Me}_3\text{SiCCSiMe}_3)$  **102** and pyridine at ambient temperature induces loss of the acetylene ligand and C–H activation of the heterocycle to furnish the dimeric titanium complex,  $[(\eta^5\text{-C}_5\text{H}_5)_2\text{Ti}]_2(\mu_2\text{-C}_5\text{H}_4\text{N})(\mu_2\text{-H})$  **165** (Scheme 24).<sup>94</sup> At elevated temperatures, this process is accompanied by coupling of cyclopentadienyl ligands to afford the fulvalene complex,  $[(\eta^5\text{-C}_5\text{H}_5)_2\text{Ti}]_2(\mu_2\text{-C}_{10}\text{H}_8)(\mu_2\text{-C}_5\text{H}_4\text{N})(\mu_2\text{-H})$  **166**, and dihydrogen. The analogous reaction with fluorinated pyridines such as *o*-fluoropyridine and pentafluoropyridine results in *ortho*-C–F bond activation to yield similar dimeric titanocene complexes,  $[(\eta^5\text{-C}_5\text{H}_5)_2\text{Ti}]_2(\mu_2\text{-C}_5\text{H}_4\text{N})(\mu_2\text{-F})$  and  $[(\eta^5\text{-C}_5\text{H}_5)_2\text{Ti}]_2(\mu_2\text{-C}_5\text{F}_4\text{N})(\mu_2\text{-F})$ , respectively (**167**, Scheme 24). In the former case, no competing C–H activation has been reported. Similar reactivity is observed with trifluorotriazene, where  $[(\eta^5\text{-C}_5\text{H}_5)_2\text{Ti}]_2(\mu_2\text{-C}_3\text{N}_3\text{F}_2)(\mu_2\text{-F})$  **168** is isolated.

Bidentate *N,N*-heterocycles such as bipyridine induce loss of the alkyne upon reaction with a range of titanocene alkyne complexes,  $(\eta^5\text{-C}_5\text{Me}_n\text{H}_{5-n})_2\text{Ti}(\eta^2\text{-Me}_3\text{SiCCSiMe}_3)$  ( $n = 0, 4, 5$ ), to afford the corresponding bipyridine complexes,  $(\eta^5\text{-C}_5\text{Me}_n\text{H}_{5-n})_2\text{Ti}(\text{bpy})$  **169**.<sup>95</sup> Detailed EPR studies are consistent with a valence tautomeric structure with a titanium(III) center and a bipyridine centered radical (Scheme 25). The analogous reaction with diazofluorene follows a different course. While the alkyne is displaced, the diazofluorene undergoes hydrogen loss to furnish the titanium(III) complexes,  $(\eta^5\text{-C}_5\text{Me}_n\text{H}_{5-n})_2\text{Ti}(\text{diazafluorenyl})$  **170**, and dihydrogen (Scheme 25).<sup>95</sup>

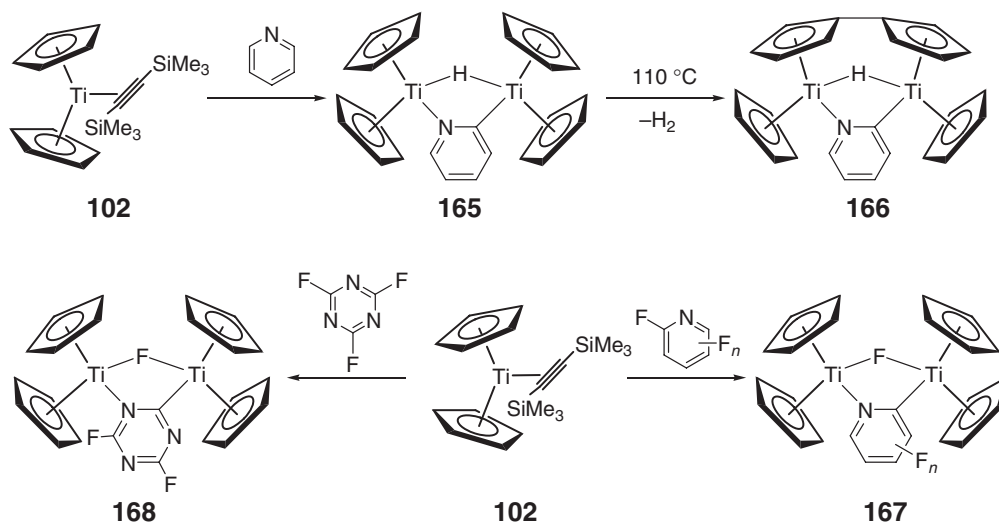


Scheme 22

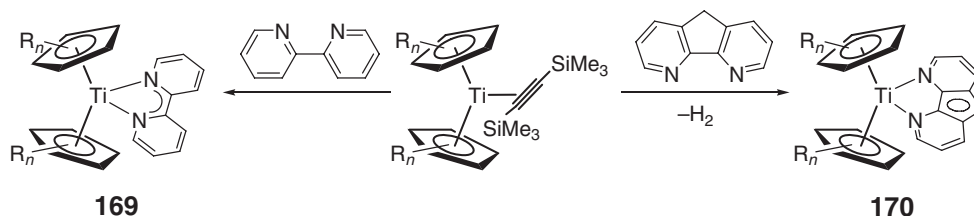


Scheme 23

Titanocene alkyne complexes have also found use in several catalytic applications. A range of well-defined  $\eta^2$ -alkyne compounds is effective for the catalytic hydrosilylation of aldimines and ketimines,<sup>96</sup> dehydrocoupling of hydrosilanes such as  $\text{PhMeSiH}_2$ ,  $\text{Ph}_2\text{SiH}_2$ , and  $\text{PhSiH}_3$ ,<sup>97</sup> ring-opening polymerization of lactams<sup>98</sup> and head-to-head dimerization of 1-alkynes.<sup>99</sup> In contrast to other methylated variants of bis(cyclopentadienyl)titanium- $(\eta^2\text{-Me}_3\text{SiCCSiMe}_3)$ ,  $(\eta^5\text{-C}_5\text{Me}_5)_2\text{Ti}(\eta^2\text{-Me}_3\text{SiCCSiMe}_3)$  catalyzes the head-to-tail dimerization of a series of 1-alkynes. Less congested metallocenes produce a series of trisubstituted benzenes from alkyne cyclotrimerization. The mechanism of the competing pathways has been investigated and several intermediates have been crystallographically characterized.<sup>100</sup> Titanocene alkyne complexes have also been used in the polymerization of acetylene.<sup>101,102</sup>



Scheme 24

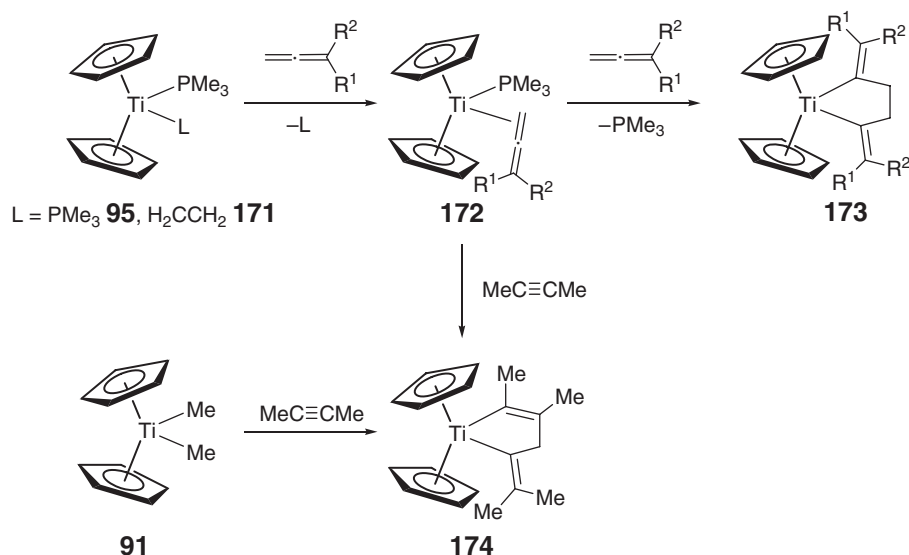


Scheme 25

#### 4.03.4.7 Bis(cyclopentadienyl)titanium(II) Complexes with Other Unsaturated Hydrocarbons

Displacement of the sterically demanding alkyne  $\text{Me}_3\text{SiC}\equiv\text{CSiMe}_3$  from the coordination sphere of the titanocene can be accomplished by addition of substituted butadiynes. Depending on the specific substitution of the diyne, the cyclopentadienyl rings, and the reaction stoichiometry, different products are observed including monomeric  $\eta^4$ -butadiyne adducts, dimeric  $\mu\text{-}\eta^3\text{:}\eta^3$ -butadiyne compounds, dimeric acetylide complexes arising from C–C bond cleavage, as well as dimeric species where two molecules of the butadiyne are reductively coupled. This area has been the subject of a recent review.<sup>103</sup> Coupling of butadiynes has been accomplished by reduction of  $(\eta^5\text{-C}_5\text{Me}_5)_2\text{TiCl}_2$  with magnesium. During these reactions, the  $\eta^5\text{-C}_5\text{Me}_5$  ring becomes annulated to form an eight-membered ring where the triple bond is coordinated to the titanium center.<sup>104</sup> Reductive coupling of butadiynes followed by functionalization of the resulting organotitanium product with hydrogen chloride, bromine, or  $\text{H}_2$  has furnished chiral titanocene derivatives.<sup>105</sup>

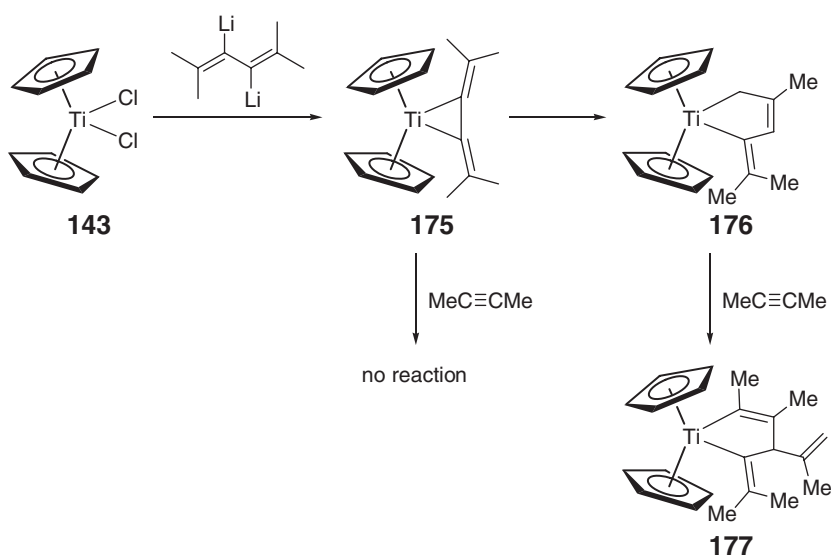
Addition of a series of allenes to the bis(phosphine) complex,  $(\eta^5\text{-C}_5\text{H}_5)_2\text{Ti}(\text{PMe}_3)_2$  **96**, or the mixed olefin phosphine complex,  $(\eta^5\text{-C}_5\text{H}_5)_2\text{Ti}(\text{PMe}_3)(\eta^2\text{-CH}_2\text{CH}_2)$  **171**, results in ligand substitution to yield the corresponding allene complex, **172**, where the allene fragment is coordinated through the least substituted C=C bond (Scheme 26).<sup>106,107</sup> While the parent allene compound decomposes, substituted allenes yield stable compounds that can be isolated in 50–80% yield. Diagnostic  $^{13}\text{C}$  NMR resonances are observed for the titanium-bound carbons in the range of 173–194 ppm, typically observed for other Ti–C( $sp^2$ ) bonds. Crystallographic characterization of **172** reveals a reduced allene ligand with an elongated C–C bond of 1.423(5) Å. Reductive coupling of the allenes can be accomplished by addition of a second equivalent of the hydrocarbon to allene complexes **172** to form  $(\eta^5\text{-C}_5\text{H}_5)_2\text{Ti}(\text{C}=\text{CR}^1\text{R}^2)\text{CH}_2\text{CH}_2\text{C}(\text{=CR}^1\text{R}^2)$  **173** in a regiospecific manner. Coupling with 2-butyne yields



Scheme 26

$(\eta^5\text{-C}_5\text{H}_5)_2\text{Ti}(\text{C}(\text{Me})\text{C}(\text{Me})\text{CH}_2\text{C}(\text{=CMe}_2))$  **174**, which can also be directly prepared from  $(\eta^5\text{-C}_5\text{H}_5)_2\text{TiMe}_2$  **91** with 2-butyne, suggesting that the allene complex,  $(\eta^5\text{-C}_5\text{H}_5)_2\text{Ti}(\eta^2\text{-Me}_2\text{CCCH}_2)$ , may be intermediate in the formation of the final product (Scheme 26).<sup>106</sup>

Preparation of radialene complexes,  $\text{Me}_2\text{C}=\text{C}=\text{C}=\text{CMe}_2$ , has been accomplished by salt metathesis of the titanocene dichloride,  $(\eta^5\text{-C}_5\text{H}_5)_2\text{TiCl}_2$  **143**, with 2,5-dimethyl-3,3-dilithio-hexa-2,4-diene (Scheme 27).<sup>108</sup> The product,  $(\eta^5\text{-C}_5\text{H}_5)_2\text{Ti}(\eta^2\text{-Me}_2\text{CCCCMe}_2)$  **175**, has not been isolated owing to facile rearrangement to the metallacycle,  $(\eta^5\text{-C}_5\text{H}_5)_2\text{Ti}(\text{CC}(\text{Me})\text{C}(\text{H})\text{C}(\text{=CMe}_2))$  **176**. Attempts to couple the radialene with alkynes such as 2-butyne have been unsuccessful. However, reaction of the titanacycle, **176**, with alkynes does form new metallacycles of the general form  $(\eta^5\text{-C}_5\text{H}_5)_2\text{Ti}(\text{C}(\text{R}^1)\text{C}(\text{R}^2))\text{CH}(\text{C}(\text{=CH}_2)\text{Me})\text{C}(\text{=CMe}_2)$  **177**.

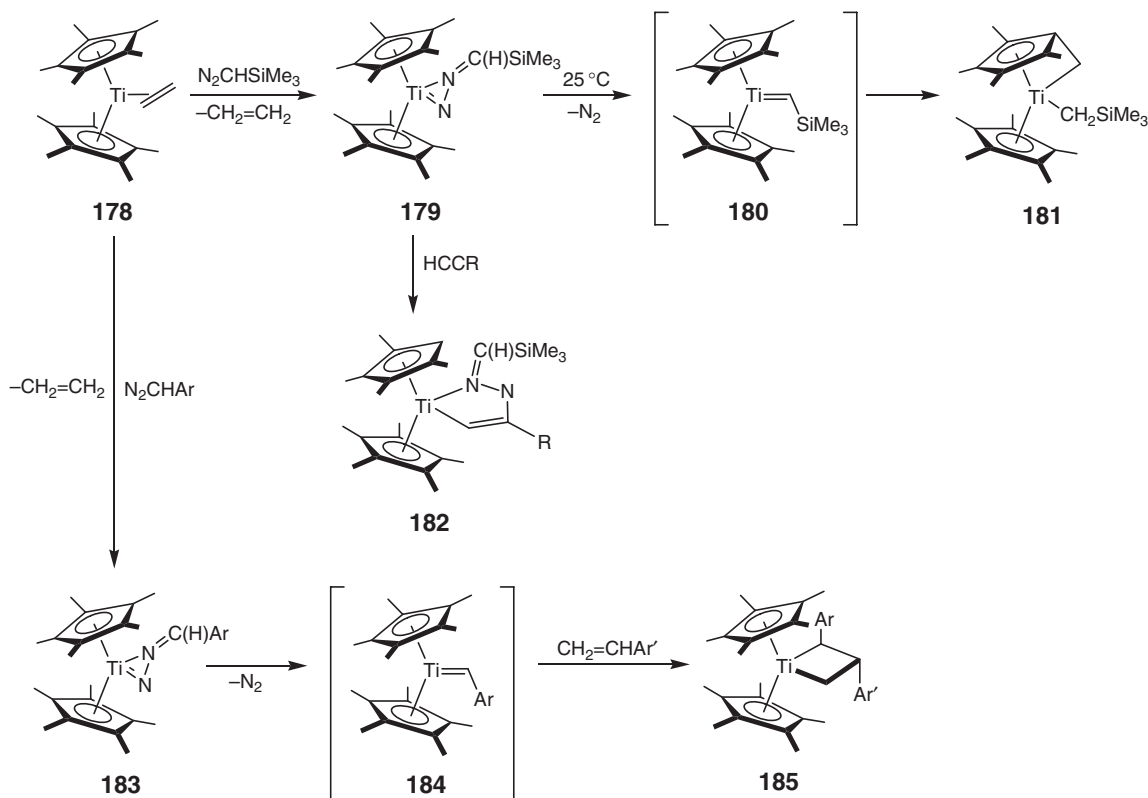


Scheme 27

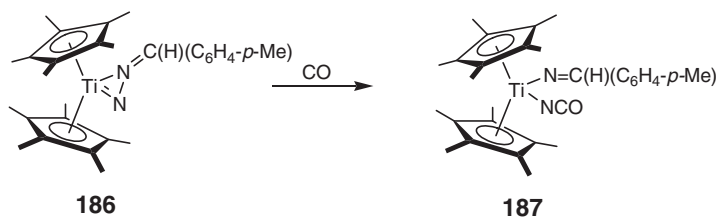
#### 4.03.4.8 Bis(cyclopentadienyl)titanium(II) Diazoalkane Complexes

Titanocene diazoalkane complexes have been synthesized by displacement of weakly bound ligands from the coordination sphere of the metal. Treatment of  $(\eta^5\text{-C}_5\text{Me}_5)_2\text{Ti}(\eta^2\text{-CH}_2=\text{CH}_2)$  **178** with  $\text{Me}_3\text{SiCHN}_2$  results in liberation of 1 equiv. of ethylene and furnishes forest green crystals, identified as  $(\eta^5\text{-C}_5\text{Me}_5)_2\text{Ti}(\eta^2\text{-N}_2\text{CHSiMe}_3)$  (**179**, Scheme 28).<sup>109</sup> In benzene or toluene solution at 25 °C, the diazoalkane complex converts into the alkyl fulvalene complex **181** with a half-life of approximately 12 h. It is believed that this reaction occurs through the transient alkylidene  $(\eta^5\text{-C}_5\text{Me}_5)_2\text{Ti}=\text{CHSiMe}_3$  **180**. Addition of alkynes or allene to the diazoalkane complex produces cycloaddition chemistry where the  $\text{N}_2$  ligand is retained, suggesting significant titanium imido character in the ground state (Scheme 28).<sup>110</sup>

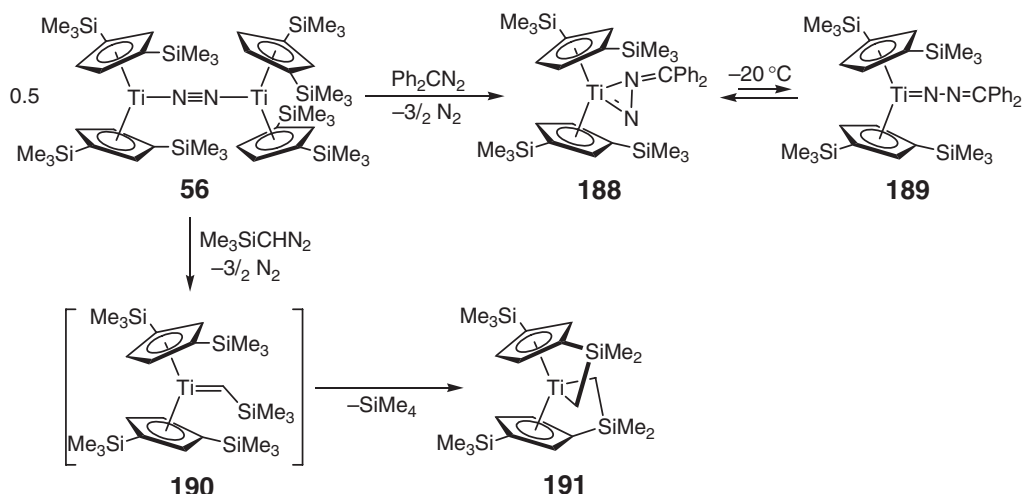
A series of aryl-substituted titanocene diazoalkane complexes,  $(\eta^5\text{-C}_5\text{Me}_5)_2\text{Ti}(\text{N}_2\text{CHAR})$ , has also been synthesized **183**.<sup>111</sup> Dinitrogen loss affords the transient alkylidene complexes **184** that can be trapped with excess styrene to yield the titanacyclobutane complexes,  $(\eta^5\text{-C}_5\text{Me}_5)_2\text{Ti}(\text{CHARCHAR}'\text{CH}_2)$  **185**. Measuring the rate of metallacycle formation as a function of *para*-substituent on the diazoalkane ligand has produced little effect. This observation has



N–N bond cleavage



Scheme 28



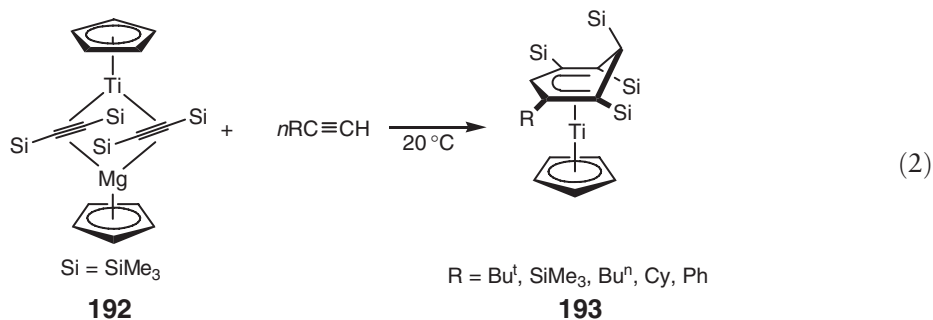
Scheme 29

been rationalized by competing covalent and electrostatic contributions on the reaction rate. Treatment of one of the diazoalkane complexes,  $(\eta^5\text{-C}_5\text{Me}_5)_2\text{Ti}\{\text{N}_2\text{C}(\text{H})\text{C}_6\text{H}_4\text{Me-4}\}$  **186**, with CO induces cleavage of the N–N bond to yield the alkylideneimido isocyanato complex,  $(\eta^5\text{-C}_5\text{Me}_5)_2\text{Ti}(\text{NCO})\text{N}=\text{CHAr}$  **187**.

Diazoalkane complexes of a silylated titanocene have been prepared by displacement of  $\text{N}_2$  from  $[(\eta^5\text{-C}_5\text{H}_3\text{-1,3-(SiMe}_3)_2)_2\text{Ti}]\mu_2\text{-}\eta^1\text{-}\eta^1\text{-N}_2$  **56**.<sup>33</sup> While  $(\eta^5\text{-C}_5\text{H}_3\text{-1,3-(SiMe}_3)_2)_2\text{Ti}_2(\eta^2\text{-N}_2\text{CPh}_2)$  **188** is an isolable compound,  $(\eta^5\text{-C}_5\text{H}_3\text{-1,3-(SiMe}_3)_2)_2\text{Ti}=\text{CHSiMe}_3$  **190** has not been observed directly, converting to the double cyclometallated complex,  $(\eta^5\text{-3-Me}_3\text{SiC}_5\text{H}_3\text{-}\eta^1\text{-1-SiMe}_2\text{CH}_2)_2\text{Ti}$  **191**, at low temperatures (Scheme 29).

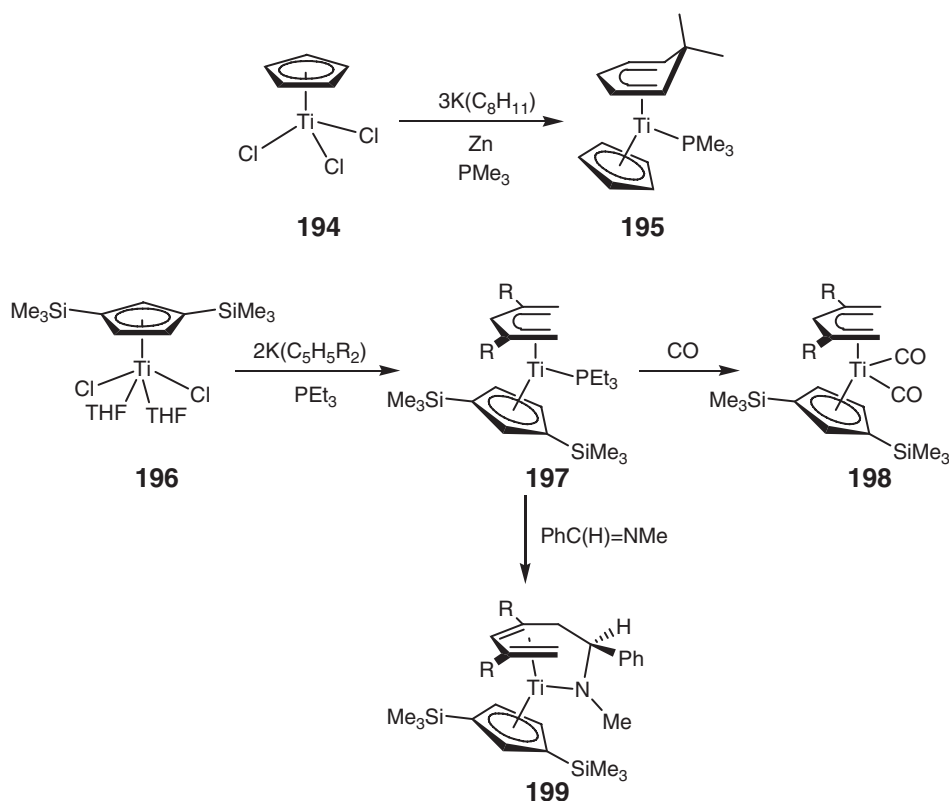
#### 4.03.5 Cyclopentadienyl Cyclohexadienyl Titanium(II) Complexes

Treatment of the titanium–ate” complex,  $(\eta^5\text{-C}_5\text{H}_5)\text{Ti}\{\mu\text{-}\eta^2\text{:}\eta^2\text{-C}_2(\text{SiMe}_3)_2\text{Mg}(\eta^5\text{-C}_5\text{H}_5)\}$  **192**,<sup>112</sup> with excess acetylene furnishes the divalent titanium cyclohexadienyl complex,  $(\eta^5\text{-1,2,4,5,6-pentakis(trimethylsilyl)-cyclohexadienyl})(\eta^5\text{-cyclopentadienyl})\text{titanium}$  **193** (Equation (2)).<sup>113</sup> A series of related compounds prepared from *t*-butylethyne, cyclohexylethyne, 1-hexyne, and phenylethyne have also been synthesized.



Similar cyclopentadienyl cyclohexadienyl complexes, **195**, have been prepared by a straightforward salt-metathesis reaction of  $(\eta^5\text{-C}_5\text{H}_5)\text{TiCl}_3$  **194** with 3 equiv. of  $\text{K}(\text{cyclohexadienyl})$  in the presence of triethylphosphine and zinc.<sup>114</sup> Similarly, reaction of  $(\eta^5\text{-C}_5\text{H}_3\text{-1,3-(SiMe}_3)_2)_2\text{TiCl}_2(\text{THF})_2$  **196** with  $2\text{K}(2,4\text{-C}_5\text{H}_3\text{R}_2)$  and phosphine affords **197** (Scheme 30).<sup>115,116</sup> Complex **197** reacts with CO to yield the dicarbonyl complex, **198**, whereas imines insert into one of the pentadienyl M–C bonds (**199**, Scheme 30).

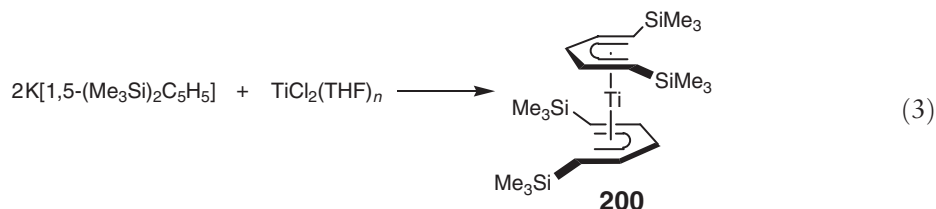




Scheme 30

#### 4.03.6 Bis(pentadienyl)titanium(II) Complexes

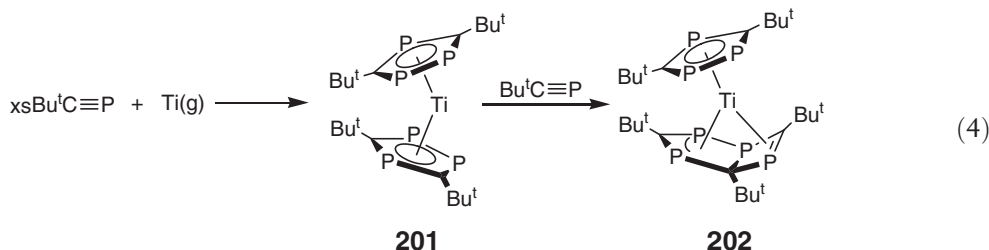
Pentadienyl anions have also been used to stabilize divalent titanium, owing to the ease of introducing sterically demanding groups and their ability to act as better electron acceptors than cyclopentadienyl ligands.<sup>117</sup> Reaction of 2 equiv. of  $\text{K}[1,5-(\text{Me}_3\text{Si})_2\text{C}_5\text{H}_5]$  with titanium dichloride affords a green diamagnetic solid, identified as  $(\eta^5\text{-}1,5-(\text{Me}_3\text{Si})_2\text{C}_5\text{H}_5)_2\text{Ti}$  **200** (Equation (3)).<sup>118</sup> Unlike the methyl-substituted complex,  $(\eta^5\text{-}2,4\text{-C}_7\text{H}_{11})_2\text{Ti}$ , which is a pyrophoric liquid,<sup>119</sup>  $(\eta^5\text{-}1,5-(\text{Me}_3\text{Si})_2\text{C}_5\text{H}_5)_2\text{Ti}$  is only slightly air sensitive and has been characterized by X-ray diffraction. The solid-state structure reveals a “sandwich”-type structure where the two ligands are related by a  $C_2$  axis. The parent bis(pentadienyl)titanium complex,  $(\eta^5\text{-}2,4\text{-C}_7\text{H}_{11})_2\text{Ti}$ , reacts with caged phosphites,  $\text{P}(\text{OCH}_2)_3\text{CR}$  ( $\text{R} = \text{CH}_3, \text{C}_2\text{H}_5$ ), to form the corresponding 16 electron adducts.<sup>120</sup> Competitive binding studies between  $\text{PMe}_3$  and the caged phosphites have led to a revision of the cone angle for the latter species, suggesting that these ligands are not as small as once believed.



#### 4.03.7 Bis(phosphacyclopentadienyl)titanium(II) Complexes

Condensation of titanium vapor with phosphalkyne,  $\text{Bu}^t\text{C}\equiv\text{P}$ , yields the unusual formally 14 electron complex,  $\text{Ti}(\eta^5\text{-P}_3\text{C}_2^t\text{Bu}_2)_2$  **201**, which has been structurally characterized as a monomeric, bent sandwich compound

(Equation (4)).<sup>121</sup> This molecule has also been prepared in solution by reaction of the phosphalkyne with the bis(arene) complex,  $(\eta^6\text{-C}_6\text{H}_5\text{Me})_2\text{Ti}$ , or by salt metathesis of  $\text{TiCl}_4$  with  $n(\text{KP}_3\text{C}_2^t\text{Bu}_2)$  ( $n = 2, 3$ ) in refluxing toluene. The sandwich complex undergoes a [2 + 2]-cycloaddition with  $\text{Bu}^t\text{C}\equiv\text{P}$  to yield  $[\text{Ti}(\eta^5\text{-P}_3\text{C}_2^t\text{Bu}_2)(\eta^3, \eta^2\text{-P}_4\text{C}_3^t\text{Bu}_3)]$  **202**, which has also been characterized by X-ray diffraction.

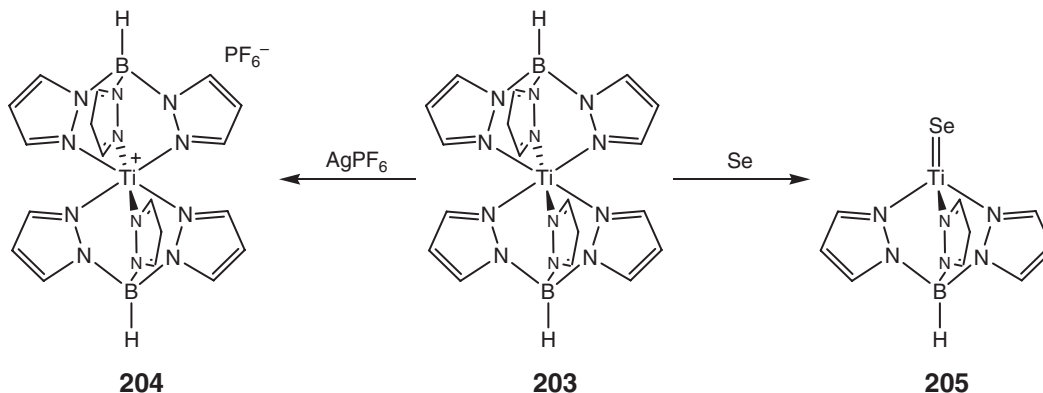


#### 4.03.8 Bis(trispyrazolylborate)titanium(II) Complexes

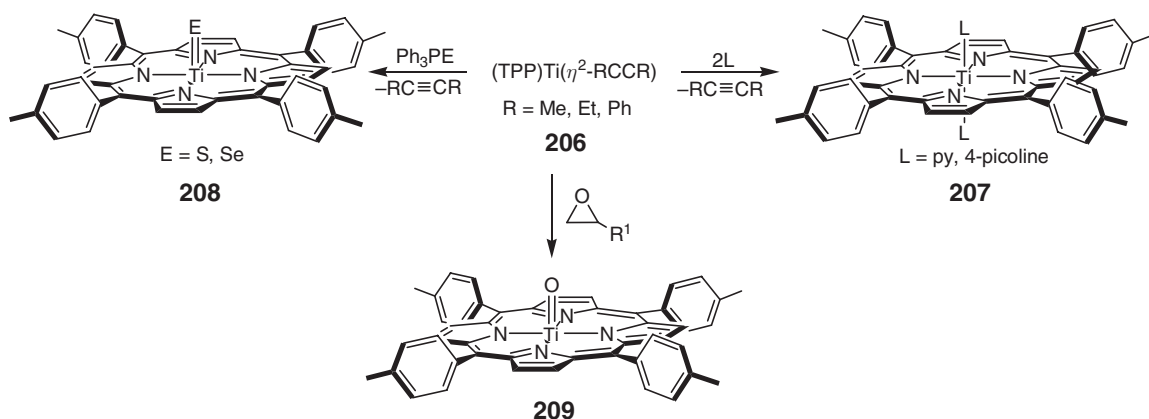
The homoleptic, bis(trispyrazolylborate)titanium(II) complex,  $\text{Tp}_2\text{Ti}$  ( $\text{Tp}$  = trispyrazolylborate; **203**), has been prepared by reaction of 2 equiv. of  $\text{KTp}$  with  $\text{TiCl}_2(\text{TMEDA})$  ( $\text{TMEDA} = N,N,N',N'$ -tetramethylethylenediamine).<sup>122</sup> The dark red, paramagnetic compound has idealized  $D_{3d}$  symmetry in the solid state and is easily oxidized to the corresponding Ti(III) derivative both electrochemically and chemically with  $\text{AgPF}_6$  **204**. Two-electron oxidation to Ti(IV) chalcogenido complexes has been accomplished with pyridine-*N*-oxide as well as with elemental sulfur and selenium (**205**, Scheme 31).

#### 4.03.9 Porphyrin Titanium(II) Complexes

Titanium porphyrin complexes have also proved to be useful platforms for accessing divalent titanium chemistry. Displacement of alkyne from tetratolylporphyrinato complexes,  $(\text{TTP})\text{Ti}(\eta^2\text{-RC}\equiv\text{CR})$  **206** ( $\text{TTP}$  = tetratolylporphyrinato,  $\text{R} = \text{Me}, \text{Et}, \text{Ph}$ ), occurs with simple ligands such as pyridine and 4-picoline to afford the corresponding hexacoordinate bis(ligand) compounds (**207**, Scheme 32).<sup>123</sup> Treatment with di-*p*-tolyldiazomethane furnishes the diazoalkane adduct,  $(\text{TTP})\text{TiNNC}(4\text{-C}_6\text{H}_4\text{CH}_3)_2$ , while atom transfer reactions with  $\text{Ph}_3\text{PE}$  ( $\text{E} = \text{S}, \text{Se}$ ) result in oxidation to form  $(\text{TTP})\text{TiE}$  compounds **208**. Both the hexyne complex,  $(\text{TTP})\text{Ti}(\eta^2\text{-EtC}\equiv\text{CEt})$  and the bis(THF) adduct, *trans*-( $\text{TTP})\text{Ti}(\text{THF})_2$ , undergo chlorine atom abstraction when exposed to vicinal dichloroalkanes or dichloroalkenes to yield the titanium(III) chloride complex,  $(\text{TTP})\text{TiCl}$ .<sup>124</sup> Deoxygenation of epoxides yields the *oxo*-complex,  $(\text{TTP})\text{TiO}$  **209**. The hexyne adduct also reacts with a series of heterocumulenes such as  $\text{Pr}^i\text{N}=\text{C}=\text{NPr}^i$ ,  $\text{Pr}^i\text{NCO}$ , or  $\text{Bu}^t\text{NCO}$  to furnish the imido derivatives,  $(\text{TTP})\text{TiNR}$ .<sup>125</sup> These studies, in combination with phosphine additions and atom transfer reactions with a range of chalcogenido donors, have provided



Scheme 31

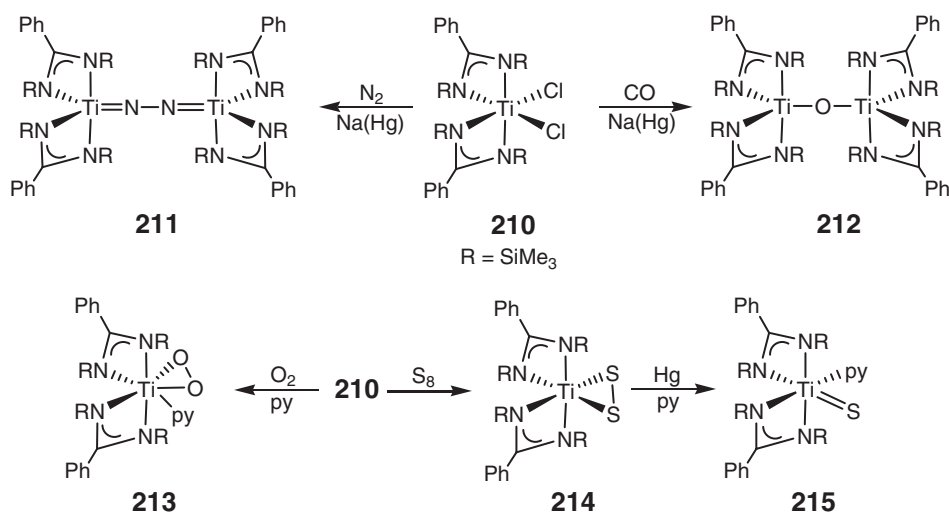


Scheme 32

an estimate of the  $\text{TiE}$  (E = O, S, Se, NR) bond strengths. The hexyne adduct,  $(\text{TTP})\text{Ti}(\eta^2\text{-EtC}\equiv\text{CEt})$ , has also been shown to promote the reductive coupling of carbonyl compounds to yield titanium(IV) diolato complexes.<sup>126</sup>

#### 4.03.10 Bis(benzamidinate)titanium(II) Complexes

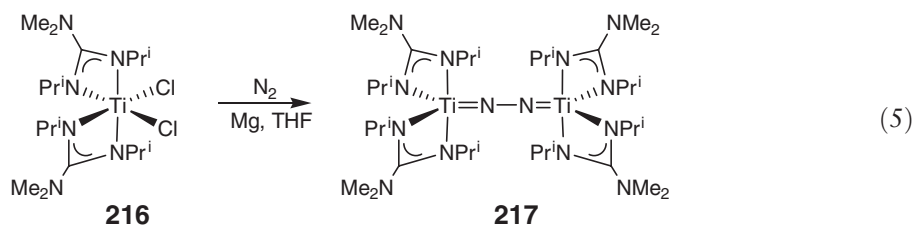
Bis(benzamidinate)titanium complexes have been explored as alternatives to more common cyclopentadienyl and porphyrin derivatives. Reduction of the dichloride complex,  $(\text{PhC}(\text{NSiMe}_3)_2)_2\text{TiCl}_2$  **210**, with 1% Na(Hg) in toluene yields the diamagnetic dinitrogen compound,  $[(\text{PhC}(\text{NSiMe}_3)_2)_2\text{Ti}]_2(\mu_2\text{-}, \eta^1\text{-}, \eta^1\text{-N}_2)$  **211**, as blue-black crystals (Scheme 33).<sup>127</sup> X-ray crystallography establishes an end-on bridging dinitrogen ligand. The short Ti–N bond distances of 1.771(5) and 1.759(5) Å, along with the observed diamagnetism, are more consistent with a  $\text{Ti(IV)}$  rather than  $\text{Ti(II)}$  ground state. While addition of simple ligands such as pyridine and 2,6-dimethylphenyl isocyanide affords the corresponding  $[(\text{PhC}(\text{NSiMe}_3)_2)_2\text{Ti}(\text{L})]_2(\mu_2\text{-}, \eta^1\text{-}, \eta^1\text{-N}_2)$  compounds without  $\text{N}_2$  loss,<sup>128</sup> **211** is unreactive toward  $\text{H}_2$ , CO,  $\text{PMe}_3$ , ethylene, and internal alkynes. Oxidation with excess  $\text{O}_2$  and  $\text{S}_8$  does induce  $\text{N}_2$  dissociation to yield  $(\text{PhC}(\text{NSiMe}_3)_2)_2\text{Ti}(\eta^2\text{-E}_2)$  complexes (**213** and **214**, Scheme 33).<sup>129</sup> The oxygen derivative has been isolated as a pseudo-seven-coordinate adduct with pyridine while the  $\eta^2\text{-S}_2$  compound is converted to the terminal sulfide–pyridine adduct, **215**, upon treatment with mercury in the presence of pyridine.



Scheme 33

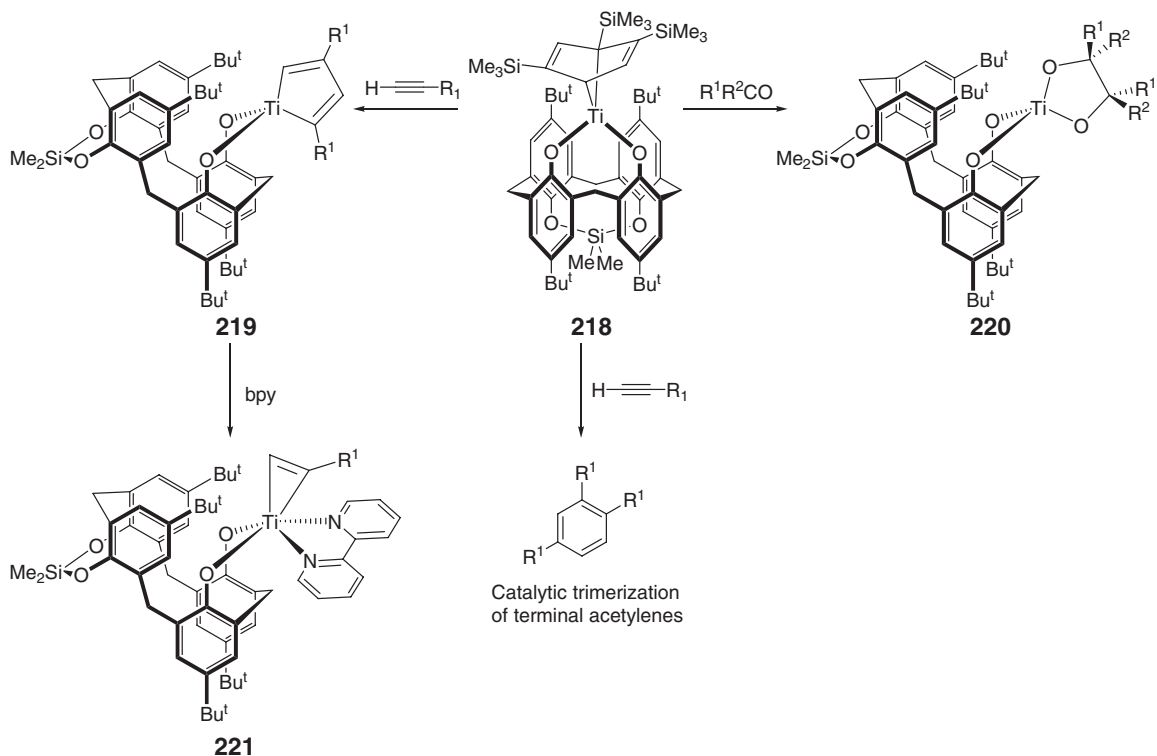
### 4.03.11 Bis(guanidinate)titanium(II) Complexes

Guanidinate ligands are structurally related to amidinates, with incorporation of an amino group on the central carbon of the ligand backbone. Donation from the dialkylamino group lone pair may provide a more electron-rich metal center than the corresponding amidinates. This relationship has been explored with preparation of the bis(guanidinate)titanium dinitrogen complex,  $[(\text{Me}_2\text{N})\text{C}(\text{N}^i\text{Pr}_2)_2\text{Ti}]_2(\mu_2\text{-}\eta^1\text{-}\eta^1\text{-N}_2)$  **217**, by reduction of dichloride precursor, **216**, with magnesium in THF (Equation (5)).<sup>130</sup> As expected for a diamagnetic bridging dinitrogen complex, short Ti–N bond distances of 1.75(1) and 1.72(1) Å are observed, consistent with significant titanium imido character and a Ti(IV) oxidation state. As with the benzamidinate complexes, the dinitrogen compound serves as a synthon for imido, bridging oxo, and sulfido derivatives.



### 4.03.12 Calixarene Titanium(II) Complexes

Introduction of calixarene dianions as ancillary ligands has allowed the synthesis and characterization of numerous low-valent derivatives. The arene complex, (DMSC)/Ti( $\eta^6$ -1,2,4-(Me<sub>3</sub>Si)<sub>3</sub>C<sub>6</sub>H<sub>3</sub>) **218** (DMSC = 1,2-alternate dimethylsilyl-bridged *p*-*tert*-butylcalix[4]arene dianion), promotes the [2 + 2]-cycloaddition of alkynes **219**<sup>131</sup> as well as the coupling of aldehydes and ketones to afford 2,5-dioxatitanacyclopentane or 2-oxatitanacycloheptene compounds (**220**, Scheme 34).<sup>132</sup> Displacement of the arene ligand with bipyridine and alkynes has also been



Scheme 34

observed to form **221**.<sup>133</sup> In each case, the directing ability of the DMSC ligand is important in determining the outcome of the reaction. Recently, a series of modified calixarenes have been prepared and their chemistry with titanium explored. Catalytic cyclotrimerization of terminal and internal alkynes has been observed and has in some cases been attributed to reduced crowding at the titanium center.<sup>134</sup>

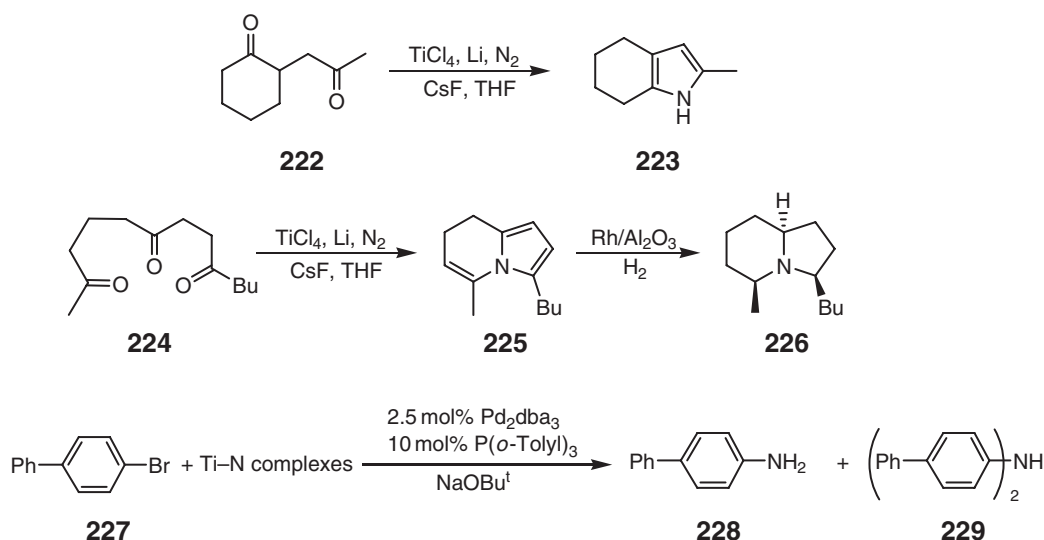
### 4.03.13 Titanium(II)-Mediated Transformations

#### 4.03.13.1 Dinitrogen Functionalization

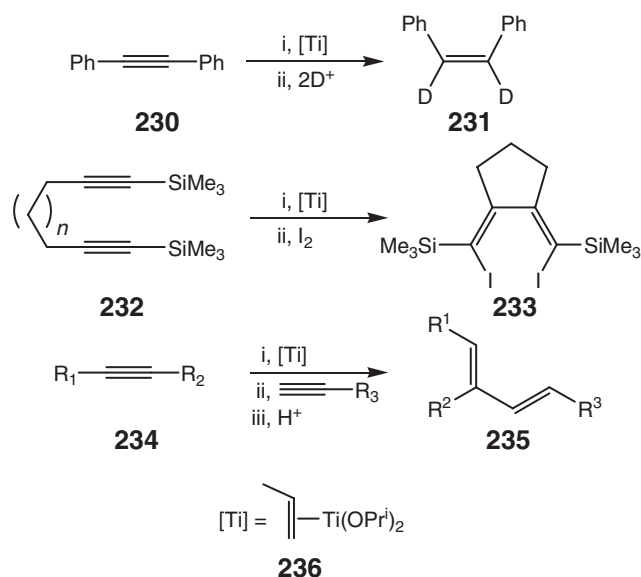
The reducing nature of low-valent titanium compounds makes them well suited for the activation of otherwise inert molecules such as dinitrogen. Reduction of  $\text{TiCl}_4$  or  $\text{Ti}(\text{OPr}^i)_4$  with lithium metal in the presence of  $\text{N}_2$  and  $\text{Me}_3\text{SiCl}$  generates  $\text{N}(\text{SiMe}_3)_3$  which can be used in subsequent transformations.<sup>135</sup> Screening a series of titanium precursors and reducing agents has established that the aforementioned combinations are the most effective.<sup>136</sup> Using this methodology, a series of indole, quinoline, pyrrolizine, and indolizine derivatives have been synthesized from the corresponding diketones (Scheme 35). This approach has also been exploited as a key step in the synthesis of monomarine I **226**.<sup>137</sup> Dry air may also be used as the nitrogen source<sup>136</sup> and has found application in the syntheses of ( $\pm$ )-pumiliotoxin C hydrochloride and ( $\pm$ )-lycopodine.<sup>138</sup> The titanium-promoted nitrogen fixation process can also be coupled to palladium catalysis for the synthesis of anilines<sup>139</sup> and benzamides (Scheme 35).<sup>140</sup>

#### 4.03.13.2 Reductive Coupling, Cyclization, Tandem Cyclization Reactions

*In situ* generated or isolated titanium(II),  $d^2$  complexes have found application in organic synthesis. This area has been the subject of numerous recent reviews and more comprehensive accounts of this chemistry have been published.<sup>141–145</sup> Treatment of suitable titanium(IV) tetrahalide or tetraalkoxide precursors with excess alkyl lithium or Grignard reagents generates a transient divalent titanium species that promotes the reduction of a range of organic substrates. For example, reaction of commercially available  $\text{Ti}(\text{OPr}^i)_4$  with  $\text{Pr}^i\text{MgBr}$  produces a reduced titanium compound, most likely  $(\text{Pr}^i\text{O})_2\text{Ti}(\eta^2\text{-CH}_2\text{=CHMe})$  **236**, that is effective for the regio- and stereoselective reduction of acetylenes to allylic alcohols by treatment with carbonyl compounds (Scheme 36).<sup>146</sup> Using this approach, the hydrolytic reduction of alkynes to *cis*-alkenes, alkenes to alkanes, and azobenzene to diphenylhydrazine has been reported.<sup>147</sup> This method has also been extended to include the stereo- and regiospecific reduction of isolated, conjugated poly-ynes to (*Z*)-dideuterio polyenes using  $\text{D}_2\text{O}$  as the deuterium source and in the preparation of (3*E*, 8*Z*, 11*Z*)-tetradecane-3,8,11-trienyl acetate, the major pheromone of *Scrobiapalpuloidea Absoluta*.<sup>148,149</sup> Interception of the



Scheme 35



Scheme 36

intermediate titanacyclopentadienes with iodine or bromine allows a one-pot synthesis of 1,4-dihalobutadienes from tethered dialkynes.<sup>150</sup> Intermolecular variants of this reaction have also been developed.<sup>151</sup> The rates of reduction of benzonitrile, epoxides, and conjugated olefins can be accelerated by addition of excess  $\text{LiOPr}^i$  and is postulated to form  $\text{Li}_2[\text{Ti}(\text{OPr}^i)_4]$ .<sup>152</sup> Observation of the intermediate titanacycles upon addition of unsaturates to the divalent bis(alkoxide) species has also been reported.<sup>153</sup> Using sterically demanding alkoxide ligands such as  $2,6\text{-Ph}_2\text{C}_6\text{H}_3\text{O}^-$  has allowed crystallographic characterization of several titanacycles.<sup>154</sup> These compounds also allow detailed kinetic and mechanistic investigations into the coupling reactions.

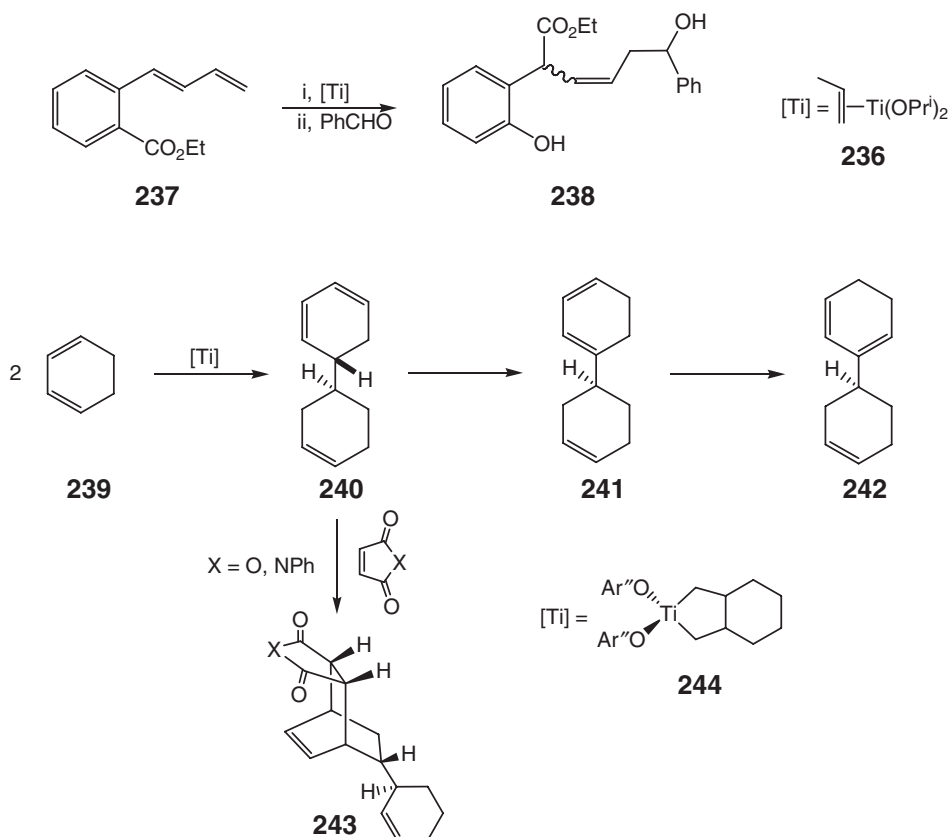
Low-valent titanium alkoxide reagents have also proved to be effective for intra- and intermolecular carbon–carbon bond forming reactions. Intermolecular versions include coupling of homoallylic alcohols,<sup>155–157</sup>  $S_N2'$  reactions involving allylic alcohols<sup>158</sup> and allylic ethers,<sup>159</sup> allenes and alkynes,<sup>160</sup> and olefins.<sup>161,162</sup> Recently, this methodology has been extended to include the coupling of imines to alkynylphosphonates.<sup>163</sup> Numerous intramolecular cyclization reactions have also been described<sup>164–173</sup> and some applied to natural product synthesis (Scheme 37).<sup>174,175</sup>

#### 4.03.13.3 Pauson–Khand Reactions

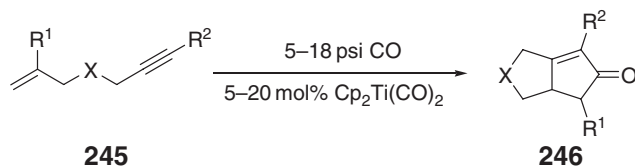
The Pauson–Khand reaction is a powerful tool for the synthesis of cyclopentanones, **246**, from  $\omega$ -alkenylacetylenes, **245**, and carbon monoxide.<sup>176</sup> Enyne cyclization has been catalyzed with nitriles using catalytic  $(\eta^5\text{-C}_5\text{H}_5)_2\text{Ti}(\text{PMe}_3)_2$  **95**<sup>177–179</sup> and other variants have since been discovered where the desired cyclopentenones can be directly prepared from the enyne and CO using  $(\eta^5\text{-C}_5\text{H}_5)_2\text{Ti}(\text{CO})_2$  **68** (Scheme 38).<sup>176,180–184</sup> Addition of  $\text{PMe}_3$  to the latter reaction mixture has proved to be beneficial. Stoichiometric reactions established that the initial step in the catalytic cycle is reductive coupling of the alkyne and the olefin to form the titanacycle. Carbon monoxide insertion followed by reductive elimination generates the observed product.

$\omega$ -Alkenyl-ketones **247** also undergo titanium-promoted Pauson–Khand-type cyclizations to yield **248**. While most heteroatom versions of this reaction are performed using aldehyde substrates, methylketones have also shown to participate in ring closure.<sup>185</sup> When the substrate contains a benzo-linker, catalytic variants have also been developed (Scheme 39).<sup>186</sup>

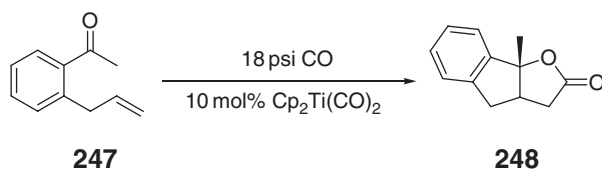
Another variation of the Pauson–Khand is the cyclization of  $\omega$ -alkenyl-aldehydes **249** in the presence of  $\text{HSi}(\text{OEt})_3$  resulting in siloxycyclopentadienes (Scheme 40).<sup>187–189</sup> The observed products, **250**, arise from functionalization of the intermediate titanacycle with silane followed by reductive elimination of product.



Scheme 37



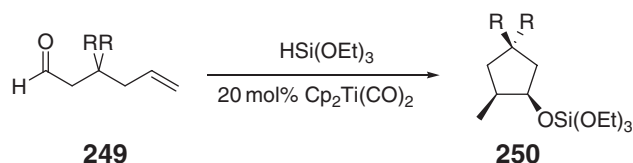
Scheme 38



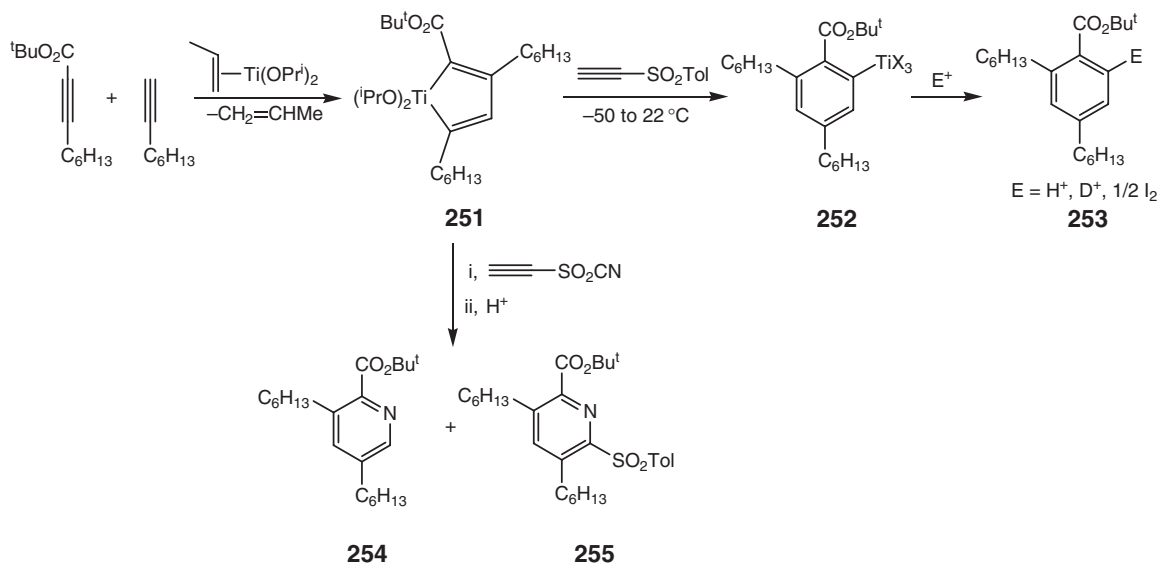
Scheme 39

#### 4.03.13.4 Cyclotrimerization Reactions

Formally divalent, *in situ* generated titanium bis(alkoxide) reagents have also proved to be effective for promoting one-pot, selective Reppe-type<sup>190</sup> cyclotrimerization reactions (Scheme 41). Preparation of dialkoxytitanacyclopentadiene complexes, **251**, proceeds readily from addition of 2 equiv. of alkyne to **236**.<sup>191</sup> Importantly, three different alkynes can be selectively coupled in a highly controlled manner to afford a single organometallic product **252**.



Scheme 40



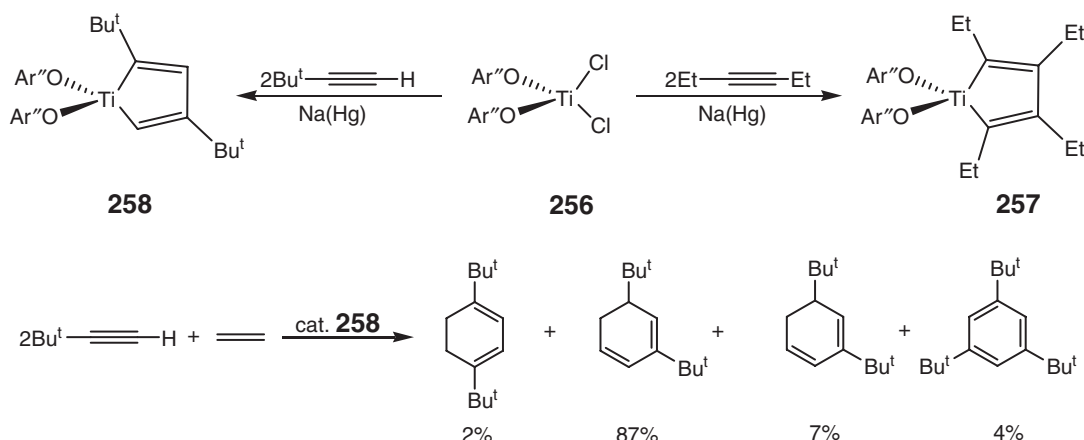
Scheme 41

Subsequent protic workup releases the aromatic compound. The “metalative Reppe” reaction can also be used to prepare iodo-substituted or homologated aromatics by treatment of the titanium aryl compound with iodine or an aldehyde, respectively. This procedure has recently been extended to include pyridine derivatives (**254** and **255**), where the titanacyclopentadiene intermediate can be treated with sulfonylnitriles to afford pyridines after protic workup.<sup>192</sup> As with the alkyne cyclotrimerizations, treatment with the appropriate electrophiles affords iodo- and homologated pyridines.

The use of more sterically demanding alkoxide ligands has allowed isolation of a series of bis(aryloxy) titanium alkyne complexes that are active for cyclotrimerization chemistry. Reduction of  $(\text{Ar}^t\text{O})_2\text{TiCl}_2$  (**256**,  $\text{Ar}^t\text{O}$  = 2,6-diphenylphenoxide) with sodium amalgam in the presence of both terminal and internal alkynes such as 3-hexyne and  $\text{Bu}^t\text{C}\equiv\text{CH}$  furnishes the corresponding titanacyclopentadienes **257** and **258** (Scheme 42).<sup>193,194</sup> Treatment of these isolable and crystallographically characterized complexes with protic sources or iodine gives the corresponding butadiene derivatives. Trisubstituted benzenes can also be prepared with sterically demanding alkynes using **258** as a catalyst.<sup>195</sup> Performing these reactions under 1 atm of ethylene affords the di-*tert*-butylcyclohexa-1,3-dienes with little competing cyclotrimerization.<sup>196</sup> When styrene is used as the olefinic partner, experimental evidence supports a titanaborbornene with an *exo*-phenyl substituent that undergoes a metal-mediated 1,5-shift to yield the observed product.

Cyclotrimerization reactions have also been accomplished with low-valent titanium calixarene compounds by reduction of the dichloride precursor with Mg in the presence of excess alkyne.<sup>131</sup> In these compounds, the arene ligands are significantly folded with a dihedral angle of  $29.7(7)^\circ$ , suggesting significant contribution from the titanium(IV) titanaborbornadiene canonical form. These isolated and crystallographically characterized compounds are efficient catalysts for the regioselective [2 + 2 + 2]-cycloaddition of alkynes. Kinetic studies and the experimentally determined activation parameters are consistent with an associative mechanism for cyclization.



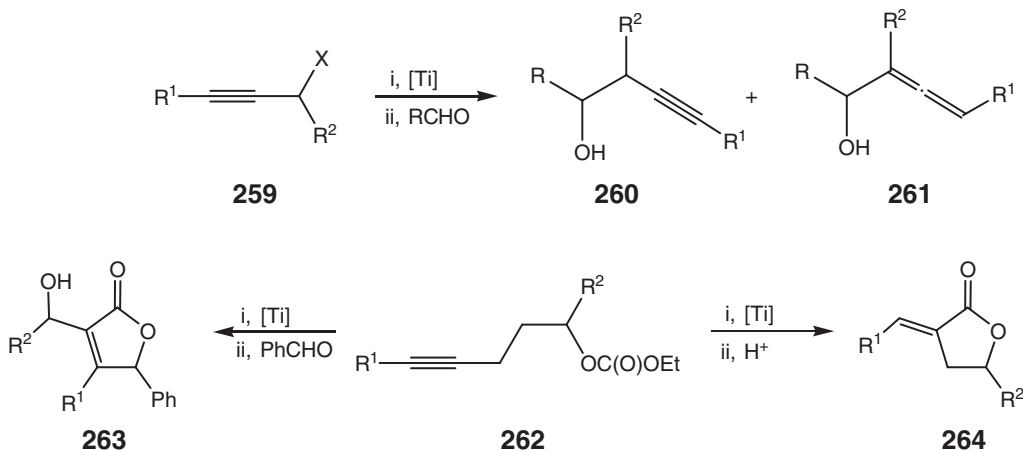


Scheme 42

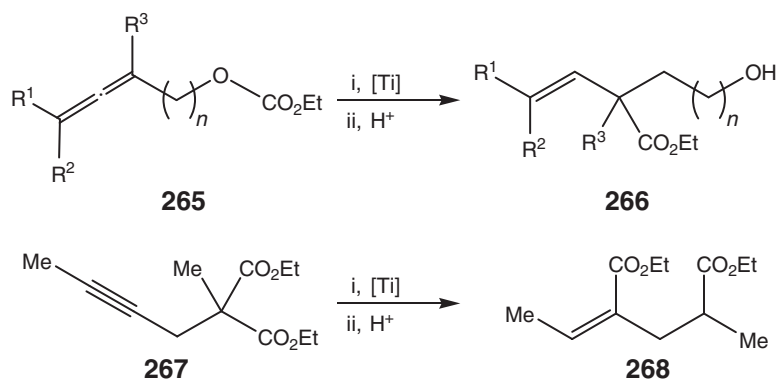
#### 4.03.13.5 Nucleophilic Substitution Reactions

Low-valent titanium alkoxide complexes have proved to be particularly useful in intramolecular nucleophilic acyl substitution (INAS) reactions. Addition of propargyl alcohol derivatives to **236** has been used as an efficient and practical method for the synthesis of allenyltitanium compounds (Scheme 43).<sup>197</sup> Performing the reaction with a homopropargylic carbonate provides access to an allenyltitanium compound with a lactone moiety.<sup>198</sup> This methodology has since been extended to include olefinic carbonates and, through trapping with appropriate electrophiles such as aldehydes and iodine, affords substituted lactones.<sup>199</sup>

Addition of 3,4-alkadienyl carbonates, **265**, to **236** also results in INAS to afford vinyl titanium compounds which react with electrophiles such as  $\text{H}^+$  ( $\text{D}^+$ ) or iodine to yield  $\alpha$ -substituted  $\beta,\gamma$ -unsaturated esters, **266**, in good yields. In general, this method generates products with the (*Z*)-geometry. Moreover, chiral 3,4-alkadienyl carbonates can be stereospecifically converted to optically active  $\alpha$ -substituted  $\beta,\gamma$ -unsaturated esters with exclusively the (*Z*)-geometry (Scheme 44).<sup>200</sup> Treatment of propargylmalonic esters, **267**, with **236** does not result in depropargylation but rather furnishes the olefin ester, **268** (Scheme 44).<sup>201</sup> Likewise, mixtures of diethyl  $\alpha$ -alkyldieneglutarates can be prepared from diethyl methyl(propargyl)malonates. The proposed mechanism for this transformation involves formation of a titanacyclopentene intermediate that undergoes intramolecular carbonyl addition followed by cleavage of the resulting cyclobutane ring through elimination of a titanium enolate. Allenyltitanium compounds have also been synthesized from treatment of carbonates of alka-3,5-diene-1-ols with  $(\text{Pr}^i\text{O})_2\text{Ti}(\eta^2\text{-CH}_2=\text{CHMe})$  which can be regioselectively added to aldehydes.<sup>202</sup>



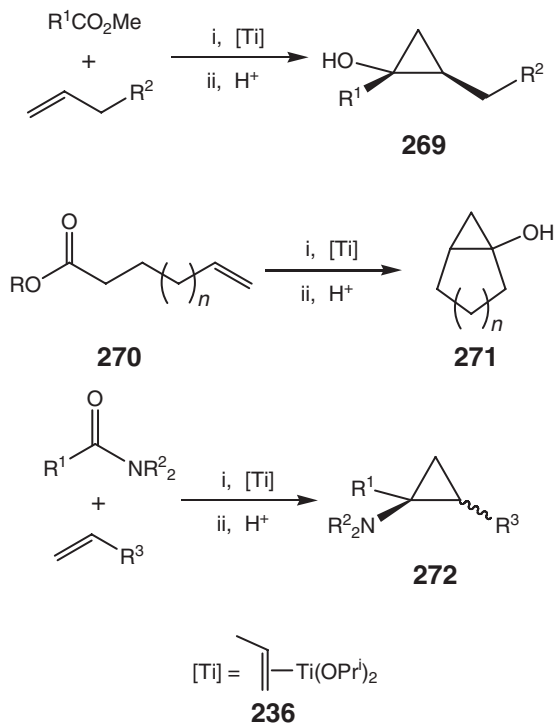
Scheme 43



Scheme 44

#### 4.03.13.6 Cyclopropanol Synthesis

The Kulinkovich hydroxycyclopropanation,<sup>203</sup> whereby a carboxylic ester is treated with excess Grignard reagent in the presence of  $Ti(OPr^i)_4$  to yield *cis*-1,2-dialkylcyclopropan-1-ols, **269**, has emerged as a widely used and studied reaction involving *in situ* generated divalent titanium (Scheme 45). By employing chiral alcohols, enantioselective variants have been reported.<sup>204</sup> One limitation of the original procedure is requirement of an excess of the Grignard reagent and is especially problematic when this reagent is not commercially available. To circumvent this problem, facile olefin exchange of the divalent titanium olefin species **236** has been exploited, allowing efficient inter-<sup>205</sup> and intramolecular<sup>206,207</sup> variants of the reaction to be developed. The scope of this reaction has been extended to include acyl derivatives,<sup>208</sup> homoallylic and bis(homoallylic) esters,<sup>209</sup> ethylene carbonates to form cyclopropanone hemiketals,<sup>210</sup> homoallylic alcohols,<sup>211</sup> and with dialkylformamides to yield *N,N*-dialkylcyclopropylamines.<sup>212,213</sup>

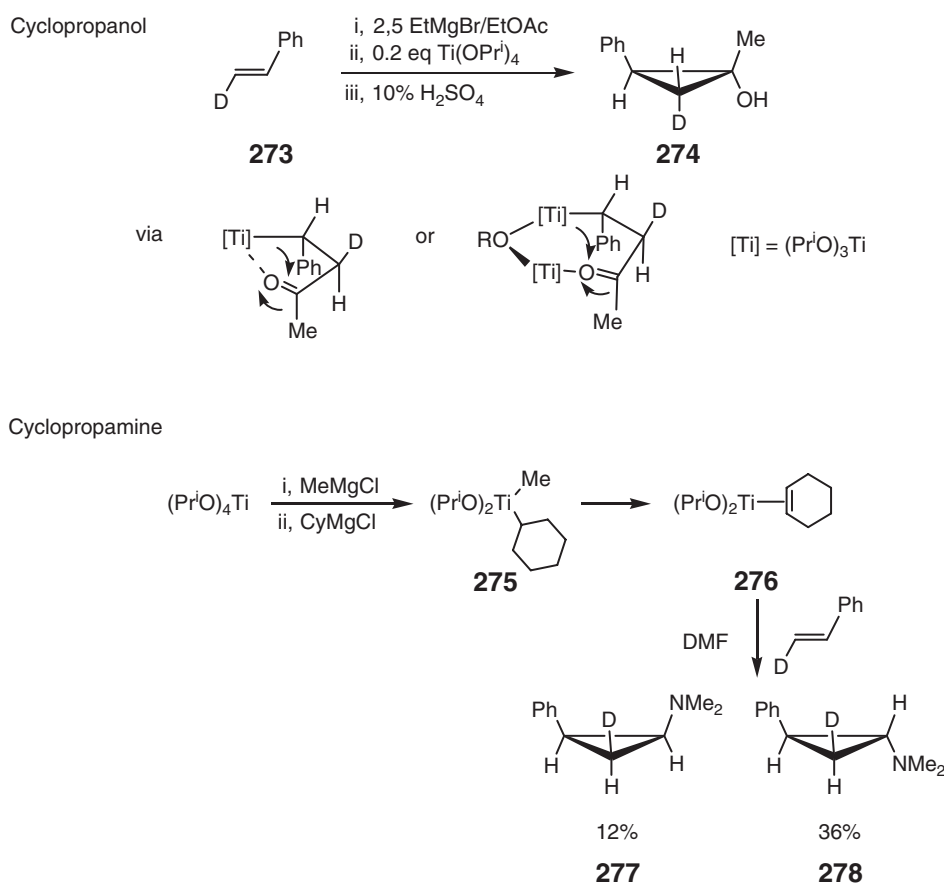


Scheme 45

This method has also been used as a key step in the synthesis of ( $\pm$ )-stigmolone,<sup>214</sup> coupled to an oxyCope rearrangement for the preparation of seven- or eight-membered carbocycles<sup>215</sup> and used as a key step in the synthesis of mitomycin alkaloids.<sup>216</sup> Another variant of the procedure has been developed for the cleavage of allyl ethers to yield alcohols.<sup>217</sup>

While it is generally accepted that an *in situ* generated divalent titanium olefin complex is a key intermediate in hydroxycyclopropanation, several studies have focused on experimentally verifying this assertion. An alternative mechanism involves alkylation and  $\beta$ -hydrogen elimination of the titanium(IV) precursor to yield the corresponding titanium(IV) alkyl hydride olefin complex. To test this possibility, (CD<sub>3</sub>)<sub>2</sub>CHMgBr has been used to generate the reactive titanium species in the hydroxycyclopropanation of styrene with ethyl acetate. Analysis of the resulting cyclopropanol by NMR spectroscopy reveals no incorporation of deuterium, consistent with the divalent titanium olefin intermediate.<sup>218</sup> Performing the *N,N*-bibenzylformamide version of the reaction with dienes and trienes results in olefin exchange reactions and migration of the titanium to yield the most highly substituted alkenylcyclopropylamines.<sup>219</sup>

More detailed isotopic labeling studies have also been performed. Hydroxycyclopropanation of *trans*- $\beta$ -deutero-styrene **273** under Kulinkovich conditions furnishes *cis*-2-phenyl-1-cyclopropanol, **274**, indicating retention of configuration at the carbon bound to titanium and is consistent with frontside attack of the Ti–C bond on a titanium-bound carbonyl.<sup>220</sup> For the related de Meijere cyclopropylamine synthesis, the opposite outcome has been observed where a 3:1 mixture of *N,N*-dimethyl-*N*-(*trans*-3-deutero-*trans*-2-phenylcyclopropyl)amine **278** and *N,N*-dimethyl-*N*-(*cis*-deutero-*cis*-2-phenylcyclopropyl)amine **277** is produced. These products require inversion of configuration at the carbon bound to titanium and are consistent with a W-shaped transition structure for ring closure (Scheme 46).



Scheme 46

### 4.03.13.7 Miscellaneous Organic Transformations

The titanacycle prepared from reduction of  $\text{Ti}(\text{OPr}^i)_4$  with 2 equiv. of  $\text{Pr}^i\text{MgCl}$  in the presence of 1-alkynylphosphonates reacts with addition of Grignard reagents to form vinyl phosphates after aqueous workup.<sup>221</sup> The reactions are proposed to proceed through attack of the excess Grignard reagent on the titanacycle. Using this procedure, a large number of vinyl phosphates have been prepared in good to excellent yield.

Treatment of the thermally stable, formally divalent bis(alkoxide)titanium alkyne complexes,  $(\text{Pr}^i\text{O})_2\text{Ti}(\eta^2\text{-RC}\equiv\text{CR})$  ( $\text{R} = \text{Et}, \text{Pr}, p\text{-Me-C}_6\text{H}_4$ ),<sup>222</sup> with aryl iodides in the presence of  $\text{Ni}(\text{COD})_2$  ( $\text{COD} = 1,5\text{-cyclooctadiene}$ ) affords the corresponding cross-coupled products.<sup>223</sup> Other catalysts such as  $\text{Ni}(\text{acac})_2$  ( $\text{acac} = \text{acetylacetonate}$ ),  $\text{Pd}(\text{OAc})_2$ , and  $\text{Pd}(\text{PPh}_3)_4$  promote the reaction but are significantly less active. As anticipated, aryl iodides undergo cross-coupling more effectively than the corresponding bromides, chlorides, and triflates.

The reader is referred to Chapters 10.03, 11.01, and 11.04 for more information.

## References

- Cloke, F. G. N.; Courtney, K. A. E.; Sameh, A. A.; Swain, A. C. *Polyhedron* **1989**, *8*, 1641.
- King, W. A.; DiBella, S.; Lanza, G.; Khan, K.; Duncalf, D. J.; Cloke, F. G. N.; Fragala, I. L.; Marks, T. J. *J. Am. Chem. Soc.* **1996**, *118*, 627.
- Calderazzo, F.; Ferri, I.; Pampaloni, G.; Englert, U.; Green, M. L. H. *Organometallics* **1997**, *16*, 3100.
- Morand, P. D.; Francis, C. G. *Inorg. Chem.* **1985**, *24*, 56.
- Ellis, J. E.; Blackburn, D. W.; Yuen, P.; Jang, M. *J. Am. Chem. Soc.* **1993**, *115*, 11616.
- Eugenijus, U.; Brennessel, W. W.; Cramer, C. J.; Ellis, J. E.; Schleyer, P. V. R. *Science* **2002**, *295*, 832.
- Fang, X.; Woodmansee, D.; Bu, X.; Bazan, G. C. *Angew. Chem. Int. Ed.* **2003**, *42*, 4510.
- Seaburg, J. K.; Fischer, P. J.; Young, V. G., Jr.; Ellis, J. E. *Angew. Chem. Int. Ed.* **1998**, *37*, 155.
- Domailec, P. J.; Warlow, R. L.; Wreford, S. S. *Organometallics* **1982**, *1*, 935.
- Kelsey, B. A.; Ellis, J. E. *J. Chem. Soc. Chem. Commun.* **1986**, 331.
- Troyanov, S. J. *Organomet. Chem.* **1994**, *475*, 139.
- Horáček, M.; Kupfer, V.; Müller, B.; Thewalt, U.; Mach, K. J. *Organomet. Chem.* **1998**, *552*, 75.
- Mach, K.; Hiller, J.; Thewalt, U.; Sivik, M. R.; Bzowej, E. I.; Paquette, L. A.; Zaegel, F.; Meunier, P.; Gautheron, B. *Organometallics* **1995**, *14*, 2609.
- Kaminsky, W.; Park, Y.-W. *Macromol. Rapid Commun.* **1995**, *16*, 343.
- Arnold, P. L.; Cloke, F. G. N.; Khan, K.; Scott, P. J. *Organomet. Chem.* **1997**, *528*, 77.
- Elschenbroich, C.; Kroker, J.; Nowotny, M.; Behrendt, A.; Metz, B.; Harms, K. *Organometallics* **1999**, *18*, 1495.
- Jensen, J. A.; Wilson, S. R.; Schultz, A. J.; Girolami, G. S. *J. Am. Chem. Soc.* **1987**, *109*, 8094.
- Spencer, M. D.; Wilson, S. R.; Girolami, G. S. *Organometallics* **1997**, *16*, 3055.
- Beatty, R. P.; Datta, S.; Wreford, S. S. *Inorg. Chem.* **1979**, *18*, 3139.
- Wreford, S. S.; Whitney, J. F. *Inorg. Chem.* **1981**, *20*, 3918.
- Spencer, M. D.; Girolami, G. S. *J. Organomet. Chem.* **1994**, *483*, 99.
- Spencer, M. D.; Morse, P. M.; Wilson, S. R.; Girolami, G. S. *J. Am. Chem. Soc.* **1993**, *115*, 2057.
- Devore, D. D.; Timmers, F. J.; Hasha, D. L.; Rosen, R. K.; Marks, T. J.; Deck, P. A.; Stern, C. L. *Organometallics* **1995**, *14*, 3132.
- Abboud, K. A.; Nickias, P. N.; Chen, E. Y. X. *Acta Crystallogr. C* **2001**, *57*, 1408.
- Dahlmann, M.; Schottek, J.; Fröhlich, R.; Kunz, D.; Nissinen, M.; Erker, G.; Fink, G.; Kleinschmidt, R. *J. Chem. Soc., Dalton Trans.* **2000**, 1881.
- Ellis, J. E.; Yuen, P. *Inorg. Chem.* **1993**, *32*, 4998.
- Ellis, J. E.; Frerichs, S. R.; Stein, B. K. *Organometallics* **1993**, *12*, 1048.
- Fischer, P. J.; Young, V. G., Jr.; Ellis, J. E. *Angew. Chem. Int. Ed.* **2000**, *39*, 189.
- Adams, R. D. *J. Organomet. Chem.* **2001**, *637*, 1.
- Fischer, A. K.; Wilkinson, G. J. *Inorg. Nucl. Chem.* **1956**, *2*, 149.
- Brintzinger, H. H.; Bercaw, J. E. *J. Am. Chem. Soc.* **1970**, *92*, 6182.
- De Wolf, J. M.; Blaauw, R.; Meetsma, A.; Teuben, J. H.; Gyepes, R.; Varga, V.; Mach, K.; Veldman, N.; Spek, A. L. *Organometallics* **1996**, *15*, 4977.
- Hanna, T. E.; Keresztes, I.; Lobkovsky, E.; Bernskoetter, W. H.; Chirik, P. J. *Organometallics* **2004**, *23*, 3448.
- Hitchcock, P. B.; Kerton, F. M.; Lawless, G. A. *J. Am. Chem. Soc.* **1998**, *120*, 10264.
- Horáček, M.; Kupfer, V.; Thewalt, U.; Štěpnička, P.; Polášek, M.; Mach, K. *Organometallics* **1999**, *18*, 3572.
- Lukešová, L.; Horáček, M.; Štěpnička, P.; Fejfarová, K.; Gyepes, R.; Císařová, I.; Kubišta, J.; Mach, K. *J. Organomet. Chem.* **2002**, *663*, 134.
- Lukešová, L.; Horáček, M.; Gyepes, R.; Císařová, I.; Štěpnička, P.; Kubišta, J.; Mach, K. *Collect. Czech. Chem. Commun.* **2005**, *70*, 11.
- Hanna, T. E.; Lobkovsky, E.; Chirik, P. J. *J. Am. Chem. Soc.* **2004**, *126*, 14688.
- Spaltenstein, E.; Palma, P.; Kreutzer, K. A.; Willoughby, C. A.; Davis, W. M.; Buchwald, S. L. *J. Am. Chem. Soc.* **1994**, *116*, 10308.
- Berry, D. H.; Procopio, L. J.; Carrol, P. J. *Organometallics* **1988**, *7*, 570.
- Bochmann, M. Titanium Complexes in Oxidation States +2 and +3. In *Comprehensive Organometallic Chemistry II*; Abel, E. W., Stone, F. G. A., Wilkinson, G., Eds.; Elsevier: Oxford, 1995; Vol. 4, Chapter 4, pp 224–230.
- Cuenca, T.; Gómez, R.; Gómez-Sal, P.; Royo, P. *J. Organomet. Chem.* **1993**, *454*, 105.
- Lee, H.; Bonanno, J. B.; Hascall, T.; Cordaro, J.; Hahn, J. M.; Parkin, G. J. *Chem. Soc., Dalton Trans.* **1999**, 1365.
- Cuenca, T.; Padilla, A.; Royo, P.; Parra-Hake, M.; Pellinghelli, M. A.; Tiripicchio, A. *Organometallics* **1995**, *14*, 848.
- Qian, C.; Guo, J.; Sun, J.; Chen, J.; Zheng, P. *Inorg. Chem.* **1997**, *36*, 1286.
- Graham, T. W.; Kickham, J.; Courtenay, S.; Wei, P.; Stephan, D. W. *Organometallics* **2004**, *23*, 3309.

47. Schobert, R.; Maaref, F.; Dürr, S. *Synlett* **1995**, 83.
48. Hampela, F.; Van Eikema Hommes, N.; Hoopsa, S.; Maaref, F.; Schobert, R. *Eur. J. Inorg. Chem.* **1998**, 1253.
49. Dürr, S.; Höhle, U.; Schobert, R. *J. Organomet. Chem.* **1993**, 458, 89.
50. Draganjac, M.; Rauchfuss, T. B. *Angew. Chem.* **1985**, 97, 745.
51. Steudel, R.; Kustos, M.; Münchow, V.; Westphal, U. *Chem. Ber. Recl.* **1997**, 130, 757.
52. Bergemann, K.; Kustos, M.; Krüger, P.; Steudel, R. *Angew. Chem., Int. Ed. Engl.* **1995**, 34, 1330.
53. Steudel, R.; Schumann, O.; Buschmann, J.; Luger, P. *Angew. Chem. Int. Ed.* **1998**, 37, 492.
54. Choukroun, R.; Lorber, C.; Vendier, L. *Eur. J. Inorg. Chem.* **2004**, 317.
55. Choukroun, R.; Lorber, C.; Lepetit, C.; Donnadieu, B. *Organometallics* **2003**, 22, 1995.
56. Calderazzo, F.; Pampaloni, G.; Tripepi, G. *Organometallics* **1997**, 16, 4943.
57. You, Y.; Wilson, S. R.; Girolami, G. S. *Organometallics* **1994**, 13, 4655.
58. Ellis, J. E.; Stein, B. K.; Frerichs, S. R. *J. Am. Chem. Soc.* **1993**, 115, 4066.
59. He, X.; Hartwig, J. F. *J. Am. Chem. Soc.* **1996**, 118, 1696.
60. Hartwig, J. F.; Muhoro, C. N.; He, X. *J. Am. Chem. Soc.* **1996**, 118, 10936.
61. Muhoro, C. N.; He, X.; Hartwig, J. F. *J. Am. Chem. Soc.* **1999**, 121, 5033.
62. Muhoro, C. N.; Hartwig, J. F. *Angew. Chem. Int. Ed.* **1997**, 36, 1510.
63. Hartwig, J. F.; Muhoro, C. N. *Organometallics* **2000**, 19, 30.
64. Lukešová, L.; Štěpnička, P.; Fejfarová, K.; Gyepes, R.; Císařová, I.; Horáček, M.; Kubišta, J.; Mach, K. *Organometallics* **2002**, 21, 2639.
65. Horáček, M.; Štěpnička, P.; Gyepes, R.; Císařová, I.; Tišlerová, I.; Zemánek, J.; Kubišta, J.; Mach, K. *Chem. Eur. J.* **2000**, 6, 2397.
66. Ohff, A.; Pulst, S.; Lefebvre, C.; Peulecke, N.; Arndt, P.; Burlakov, V. V.; Rosenthal, U. *Synlett* **1996**, 111.
67. Varga, V.; Mach, K.; Polášek, M.; Sedmera, P.; Hiller, J.; Thewalt, U.; Troyanov, S. I. *J. Organomet. Chem.* **1996**, 506, 241.
68. Štěpnička, P.; Gyepes, R.; Císařová, I.; Horáček, M.; Kubišta, J.; Mach, K. *Organometallics* **1999**, 18, 4869.
69. Peulecke, N.; Baumann, W.; Kempe, R.; Burlakov, V. V.; Rosenthal, U. *Eur. J. Inorg. Chem.* **1998**, 419.
70. Varga, V.; Hiller, J.; Gyepes, R.; Polášek, M.; Sedmera, P.; Thewalt, U.; Mach, K. *J. Organomet. Chem.* **1997**, 538, 63.
71. Horáček, M.; Štěpnička, S.; Gentil, S.; Fejfarová, K.; Kubišta, J.; Píro, N.; Meunier, P.; Gallou, F.; Paquette, L. A.; Mach, K. *J. Organomet. Chem.* **2002**, 656, 81.
72. Lefebvre, C.; Ohff, A.; Tillack, A.; Baumann, W.; Kempe, R.; Burlakov, V. V.; Rosenthal, U. *J. Organomet. Chem.* **1995**, 501, 179.
73. Burlakov, V. V.; Polyakov, A. V.; Yanovsky, A. I.; Struchkov, Y. T.; Shur, V. B.; Vol'pin, M. E.; Rosenthal, U.; Görls, H. *J. Organomet. Chem.* **1994**, 476, 197.
74. Štěpnička, P.; Gyepes, R.; Císařová, I.; Varga, V.; Polášek, M.; Horáček, M.; Mach, K. *Organometallics* **1999**, 18, 627.
75. Ohff, A.; Kosse, P.; Baumann, W.; Tillack, A.; Kempe, R.; Görls, H.; Burlakov, V. V.; Rosenthal, U. *J. Am. Chem. Soc.* **1995**, 117, 10399.
76. Varga, V.; Mach, K.; Hiller, J.; Thewalt, U.; Sedmera, P.; Polášek, M. *Organometallics* **1995**, 14, 1410.
77. Peulecke, N.; Lefebvre, C.; Ohff, A.; Baumann, W.; Tillack, A.; Kempe, R.; Burlakov, V. V.; Rosenthal, U. *Chem. Ber.* **1996**, 129, 959.
78. Varga, V.; Mach, K.; Polášek, M.; Sedmera, P.; Hiller, J.; Thewalt, U.; Troyanov, S. I. *J. Organomet. Chem.* **1996**, 506, 241.
79. Varga, V.; Hiller, J.; Gyepes, R.; Polášek, M.; Sedmera, P.; Thewalt, U.; Mach, K. *J. Organomet. Chem.* **1997**, 538, 63.
80. Peulecke, N.; Baumann, W.; Kempe, R.; Burlakov, V. V.; Rosenthal, U. *Eur. J. Inorg. Chem.* **1998**, 419.
81. Horáček, M.; Štěpnička, S.; Gentil, S.; Fejfarová, K.; Kubišta, J.; Píro, N.; Meunier, P.; Gallou, F.; Paquette, L. A.; Mach, K. *J. Organomet. Chem.* **2002**, 656, 81.
82. Burlakov, V. V.; Polyakov, A. V.; Yanovsky, A. I.; Struchkov, Y. T.; Shur, V. B.; Vol'pin, M. E.; Rosenthal, U.; Görls, H. *J. Organomet. Chem.* **1994**, 476, 197.
83. Lefebvre, C.; Ohff, A.; Tillack, A.; Baumann, W.; Kempe, R.; Burlakov, V. V.; Rosenthal, U. *J. Organomet. Chem.* **1995**, 501, 179.
84. Rosenthal, U.; Lefebvre, C.; Arndt, P.; Tillack, A.; Baumann, W.; Kempe, R.; Burlakov, V. V. *J. Organomet. Chem.* **1995**, 503, 221.
85. Tillack, A.; Baumann, W.; Ohff, A.; Lefebvre, C.; Spannenberg, A.; Kempe, R.; Rosenthal, U. *J. Organomet. Chem.* **1996**, 520, 187.
86. Thomas, D.; Peulecke, N.; Burlakov, V. V.; Heller, B.; Baumann, W.; Spannenberg, A.; Kempe, R.; Rosenthal, U.; Beckhaus, R. Z. *Anorg. Allg. Chem.* **1998**, 624, 919.
87. Xi, Z.; Sato, K.; Gao, Y.; Lu, J.; Takahashi, T. *J. Am. Chem. Soc.* **2003**, 125, 9570.
88. Kempe, R. *Angew. Chem. Int. Ed.* **2004**, 43, 1463.
89. Rosenthal, U.; Burlakov, V. V.; Arndt, P.; Baumann, W.; Spannenberg, A. *Organometallics* **2003**, 22, 884.
90. Shur, V. B.; Bernadyuk, S. Z.; Burlakov, V. V.; Andrianov, V. G.; Yanovskii, A. I.; Struchkov, Y. T.; Vol'pin, M. E. *J. Organomet. Chem.* **1983**, 243, 157.
91. Fachinetti, G.; Floriani, C.; Chiesi-Villa, A.; Guastini, C. *J. Am. Chem. Soc.* **1979**, 101, 1767.
92. Kraft, S.; Beckhaus, R.; Haase, D.; Saak, W. *Angew. Chem. Int. Ed.* **2004**, 43, 1583.
93. Kraft, S.; Hanuschek, E.; Beckhaus, R.; Haase, D.; Saak, W. *Chem. Eur. J.* **2005**, 11, 969.
94. Piglosiewicz, I. M.; Kraft, S.; Beckhaus, R.; Haase, D.; Saak, W. *Eur. J. Inorg. Chem.* **2005**, 938.
95. Witte, P. T.; Klein, R.; Kooijman, H.; Spek, A. L.; Polášek, M.; Varga, V.; Mach, K. *J. Organomet. Chem.* **1996**, 519, 195.
96. Tillack, A.; Lefebvre, C.; Peulecke, N.; Thomas, D.; Rosenthal, U. *Tetrahedron Lett.* **1997**, 38, 1533.
97. Peulecke, N.; Thomas, D.; Baumann, W.; Fischer, C.; Rosenthal, U. *Tetrahedron Lett.* **1997**, 38, 6655.
98. Arndt, P.; Thomas, D.; Rosenthal, U. *Tetrahedron Lett.* **1997**, 38, 5467.
99. Varga, V.; Petrusová, L.; Čejka, J.; Hanuš, V.; Mach, K. *J. Organomet. Chem.* **1996**, 509, 235.
100. Štěpnička, P.; Gyepes, R.; Císařová, I.; Horáček, M.; Kubišta, J.; Mach, K. *Organometallics* **1999**, 18, 4869.
101. Ohff, A.; Burlakov, V. V.; Rosenthal, U. *J. Mol. Catal. A* **1996**, 108, 119.
102. Beckhaus, R.; Wagner, M.; Burlakov, V. V.; Baumann, W.; Peulecke, N.; Spannenberg, A.; Kempe, R.; Rosenthal, U. *Z. Anorg. Allg. Chem.* **1998**, 624, 129.
103. Rosenthal, U.; Burlakov, V. V.; Arndt, P.; Baumann, W.; Spannenberg, A. *Organometallics* **2005**, 24, 456.
104. Pellny, P.-M.; Kirchbauer, F. G.; Burlakov, V. V.; Baumann, W.; Spannenberg, A.; Rosenthal, U. *Chem. Eur. J.* **2000**, 6, 81.
105. Pellny, P.-M.; Burlakov, V. V.; Baumann, W.; Spannenberg, A.; Horáček, M.; Štěpnička, P.; Mach, K.; Rosenthal, U. *Organometallics* **2000**, 19, 2816.
106. Doxsee, K. M.; Juliette, J. J.; Zientara, K.; Nieckarz, G. *J. Am. Chem. Soc.* **1994**, 116, 2147.
107. Binger, P.; Langhauser, F.; Wedemann, P.; Gabor, B.; Mynott, R.; Krüger, C. *Chem. Ber.* **1994**, 127, 39.
108. Maercker, A.; Groos, A. *Angew. Chem., Int. Ed. Engl.* **1996**, 35, 210.

109. Polse, J. L.; Andersen, R. A.; Bergman, R. G. *J. Am. Chem. Soc.* **1996**, *118*, 8737.
110. Polse, J. L.; Kaplan, A. W.; Andersen, R. A.; Bergman, R. G. *J. Am. Chem. Soc.* **1998**, *120*, 6316.
111. Kaplan, A. W.; Polse, J. L.; Ball, G. E.; Andersen, R. A.; Bergman, R. G. *J. Am. Chem. Soc.* **1998**, *120*, 11649.
112. Varga, V.; Mach, K.; Schmid, G.; Thewalt, U. *J. Organomet. Chem.* **1993**, *454*, C1.
113. Varga, V.; Polášek, M.; Hiller, J.; Thewalt, U.; Sedmera, P.; Mach, K. *Organometallics* **1996**, *15*, 1268.
114. Wilson, A. M.; West, F. G.; Arif, A. M.; Ernst, R. D. *J. Am. Chem. Soc.* **1995**, *117*, 8490.
115. Tomaszewski, R.; Lam, K.-C.; Rheingold, A. L.; Ernst, R. D. *Organometallics* **1999**, *18*, 4174.
116. Hyla-Kryspin, I.; Waldman, T. E.; Meléndez, E.; Trakarnpruk, W.; Arif, A. M.; Ziegler, M. L.; Ernst, R. D.; Gleiter, R. *Organometallics* **1995**, *14*, 5030.
117. Ernst, R. D.; Liu, J.-Z.; Wilson, D. R. *J. Organomet. Chem.* **1983**, *250*, 257.
118. Gedridge, R. W.; Arif, A. M.; Ernst, R. D. *J. Organomet. Chem.* **1995**, *501*, 95.
119. Liu, J.-Z.; Ernst, R. D. *J. Am. Chem. Soc.* **1982**, *104*, 3737.
120. Stahl, L.; Trakarnpruk, W.; Freeman, J. W.; Arif, A. M.; Ernst, R. D. *Inorg. Chem.* **1995**, *34*, 1810.
121. Cloke, F. G. N.; Hanks, J. R.; Hitchcock, P. B.; Nixon, J. F. *Chem. Commun.* **1999**, 1731.
122. Kayal, A.; Kuncheria, J.; Lee, S. C. *Chem. Commun.* **2001**, 2482.
123. Woo, L. K.; Hays, J. A.; Young, V. G.; Day, C. L.; Caron, C.; D'Souza, F.; Kadish, K. M. *Inorg. Chem.* **1993**, *32*, 4186.
124. Wang, X.; Woo, L. K. *J. Org. Chem.* **1998**, *63*, 356.
125. Thorman, J. L.; Young, V. G.; Boyd, P. D. W.; Guzei, I. A.; Woo, L. K. *Inorg. Chem.* **2001**, *40*, 499.
126. Du, G.; Mirafzal, G. A.; Woo, L. K. *Organometallics* **2004**, *23*, 4230.
127. Hagadorn, J. R.; Arnold, J. *J. Am. Chem. Soc.* **1996**, *118*, 893.
128. Hagadorn, J. R.; Arnold, J. *Organometallics* **1998**, *17*, 1355.
129. Hagadorn, J. R.; Arnold, J. *Inorg. Chem.* **1997**, *36*, 2928.
130. Mullins, S. M.; Duncan, A. P.; Bergman, R. G.; Arnold, J. *Inorg. Chem.* **2001**, *40*, 6952.
131. Ozerov, O. V.; Ladipo, F. T.; Patrick, B. O. *J. Am. Chem. Soc.* **2000**, *122*, 6423.
132. Ozerov, O. V.; Parkin, S.; Brock, C. P.; Ladipo, F. T. *Organometallics* **2000**, *19*, 4187.
133. Ozerov, O. V.; Brock, C. P.; Carr, S.; Parkin, S.; Ladipo, F. T. *Organometallics* **2000**, *19*, 5016.
134. Ladipo, F. T.; Sarveswaran, V.; Kingston, J. V.; Huyck, R. A.; Bylikin, S. Y.; Carr, S. D.; Watts, R.; Parkin, S. *J. Organomet. Chem.* **2004**, *689*, 502.
135. Mori, M. *J. Organomet. Chem.* **2004**, *689*, 4210.
136. Mori, M.; Hori, K.; Akashi, M.; Hori, M.; Sato, Y.; Nishida, M. *Angew. Chem. Int. Ed.* **1998**, *37*, 636.
137. Mori, M.; Hori, M.; Sato, Y. *J. Org. Chem.* **1998**, *63*, 4832.
138. Akashi, M.; Sato, Y.; Mori, M. *J. Org. Chem.* **2002**, *66*, 7873.
139. Hori, K.; Mori, M. *J. Am. Chem. Soc.* **1998**, *120*, 7651.
140. Ueda, K.; Sato, Y.; Mori, M. *J. Am. Chem. Soc.* **2000**, *122*, 10722.
141. Geis, O.; Schmalz, H.-G. *Angew. Chem. Int. Ed.* **1998**, *37*, 91.
142. Kulinkovich, O. G.; de Meijere, A. *Chem. Rev.* **2000**, *100*, 2789.
143. Sato, F.; Urabe, H.; Okamoto, S. *Chem. Rev.* **2000**, *100*, 2835.
144. Sato, F.; Urabe, H.; Okamoto, S. *Synlett* **2000**, 753.
145. Eisch, J. J. *J. Organomet. Chem.* **2001**, *617*, 148.
146. Harada, K.; Urabe, H.; Sato, F. *Tetrahedron Lett.* **1995**, *36*, 3203.
147. Eisch, J. J.; Gitua, J. N. *Organometallics* **2003**, *22*, 24.
148. Hungerford, N. L.; Kitching, W. *Chem. Commun.* **1996**, 1697.
149. Hungerford, N. L.; Kitching, W. *J. Chem. Soc., Perkin Trans. 1* **1998**, 1839.
150. Yamaguchi, S.; Jin, R.-Z.; Tamao, K.; Sato, F. *J. Org. Chem.* **1998**, *63*, 10060.
151. Hamada, T.; Suzuki, D.; Urabe, H.; Sato, F. *J. Am. Chem. Soc.* **1999**, *121*, 7342.
152. Eisch, J. J.; Gitua, J. N. *Eur. J. Inorg. Chem.* **2002**, 3091.
153. Eisch, J. J.; Gitua, J. N.; Otieno, P. O.; Shi, X. *J. Organomet. Chem.* **2001**, *624*, 229.
154. Thorn, M. G.; Hill, J. E.; Waratuke, S. A.; Johnson, E. S.; Fanwick, P. E.; Rothwell, I. P. *J. Am. Chem. Soc.* **1997**, *119*, 8630.
155. Isakov, V. E.; Kulinkovich, O. G. *Synlett* **2003**, 967.
156. Nakagawa, T.; Kasatkin, A.; Sato, F. *Tetrahedron Lett.* **1995**, *36*, 3207.
157. Kasatkin, A.; Nakagawa, T.; Okamoto, S.; Sato, F. *J. Am. Chem. Soc.* **1995**, *117*, 3881.
158. Yamashita, K.; Sato, F. *Tetrahedron Lett.* **1996**, *37*, 7275.
159. Kulinkovich, O. G.; Epstein, O. L.; Isakov, V. E.; Khmel'nitskaya, E. A. *Synlett* **2001**, 49.
160. Hideura, D.; Urabe, H.; Sato, F. *Chem. Commun.* **1998**, 271.
161. Waratuke, S. A.; Johnson, E. S.; Thorn, M. G.; Fanwick, P. E.; Rothwell, I. P. *Chem. Commun.* **1996**, 2617.
162. Waratuke, S. A.; Thorn, M. G.; Fanwick, P. E.; Rothwell, A. P.; Rothwell, I. P. *J. Am. Chem. Soc.* **1999**, *121*, 9111.
163. Quntar, A. A. A.; Dembitsky, V. M.; Srebnik, M. *Org. Lett.* **2003**, *5*, 357.
164. Narita, M.; Urabe, H.; Sato, F. *Angew. Chem. Int. Ed.* **2002**, *41*, 3671.
165. Takayama, Y.; Okamoto, S.; Sato, F. *J. Am. Chem. Soc.* **1999**, *121*, 3559.
166. Sato, F.; Urabe, H.; Okamoto, S. *Pure Appl. Chem.* **1999**, *71*, 1511.
167. Urabe, H.; Sato, F. *J. Am. Chem. Soc.* **1999**, *121*, 1245.
168. Urabe, H.; Nakajima, R.; Sato, F. *Org. Lett.* **2000**, *2*, 3481.
169. U. J. S.; Lee, J.; Cha, J. K. *Tetrahedron Lett.* **1997**, *38*, 5233.
170. Urabe, H.; Narita, M.; Sato, F. *Angew. Chem. Int. Ed.* **1999**, *38*, 3516.
171. Urabe, H.; Takeda, T.; Hideura, D.; Sato, F. *J. Am. Chem. Soc.* **1997**, *119*, 11295.
172. Suzuki, K.; Urabe, H.; Sato, F. *J. Am. Chem. Soc.* **1996**, *118*, 8729.
173. Takayama, Y.; Gao, Y.; Sato, F. *Angew. Chem., Int. Ed. Engl.* **1997**, *36*, 851.
174. Campbell, A. D.; Raynham, T. M.; Taylor, R. J. *Chem. Commun.* **1999**, 245.
175. Urabe, H.; Suzuki, K.; Sato, F. *J. Am. Chem. Soc.* **1997**, *119*, 10014.
176. Hicks, F. A.; Kablaoui, N. M.; Buchwald, S. L. *J. Am. Chem. Soc.* **1999**, *121*, 5881.

177. Berk, S. C.; Grossman, R. B.; Buchwald, S. L. *J. Am. Chem. Soc.* **1993**, *115*, 4912.  
178. Hicks, F. A.; Berk, S. C.; Buchwald, S. L. *J. Org. Chem.* **1996**, *61*, 2713.  
179. Berk, S. C.; Grossman, R. B.; Buchwald, S. L. *J. Am. Chem. Soc.* **1994**, *116*, 8593.  
180. Hicks, F. A.; Kablaoui, N. M.; Buchwald, S. L. *J. Am. Chem. Soc.* **1996**, *118*, 9450.  
181. Kablaoui, N. M.; Hicks, F. A.; Buchwald, S. L. *J. Am. Chem. Soc.* **1997**, *119*, 4424.  
182. Hicks, F. A.; Buchwald, S. L. *J. Am. Chem. Soc.* **1999**, *121*, 7026.  
183. Sturla, S. J.; Buchwald, S. L. *J. Org. Chem.* **1999**, *64*, 5547.  
184. Mandal, S. K.; Amin, S. R.; Crowe, W. E. *J. Am. Chem. Soc.* **2001**, *123*, 6457.  
185. Crowe, W. E.; Vu, A. T. *J. Am. Chem. Soc.* **1996**, *118*, 1557.  
186. Kablaoui, N. M.; Hicks, F. A.; Buchwald, S. L. *J. Am. Chem. Soc.* **1996**, *118*, 5818.  
187. Crowe, W. E.; Rachita, M. J. *J. Am. Chem. Soc.* **1995**, *117*, 6787.  
188. Kablaoui, N. M.; Buchwald, S. L. *J. Am. Chem. Soc.* **1996**, *118*, 3182.  
189. Kablaoui, N. M.; Buchwald, S. L. *J. Am. Chem. Soc.* **1995**, *117*, 6785.  
190. Katritzky, A. R.; Rees, C. W., Eds. *Comprehensive Heterocyclic Chemistry*; Pergamon: Oxford, 1984; Vol. 2.  
191. Suzuki, D.; Urabe, H.; Sato, F. *J. Am. Chem. Soc.* **2001**, *123*, 7925.  
192. Suzuki, D.; Tanaka, R.; Urabe, H.; Sato, F. *J. Am. Chem. Soc.* **2002**, *124*, 3518.  
193. Hill, J. E.; Fanwick, P. E.; Rothwell, I. P. *Organometallics* **1990**, *9*, 2211.  
194. Hill, J. E.; Balaich, G.; Fanwick, P. E.; Rothwell, I. P. *Organometallics* **1993**, *12*, 2911.  
195. Johnson, E. S.; Balaich, G. J.; Rothwell, I. P. *J. Am. Chem. Soc.* **1997**, *119*, 7685.  
196. Balaich, G. J.; Rothwell, I. P. *J. Am. Chem. Soc.* **1993**, *115*, 1581.  
197. Nakagawa, T.; Kasatkin, A.; Sato, F. *Tetrahedron Lett.* **1995**, *36*, 3207.  
198. Kasatkin, A.; Okamoto, S.; Sato, F. *Tetrahedron Lett.* **1995**, *36*, 6075.  
199. Okamoto, S.; Kasatkin, A.; Zubaidha, P. K.; Sato, F. *J. Am. Chem. Soc.* **1996**, *118*, 2208.  
200. Yoshida, Y.; Okamoto, S.; Sato, F. *J. Org. Chem.* **1996**, *61*, 7826.  
201. Kasatkin, A.; Yamazaki, T.; Sato, F. *Angew. Chem. Int. Ed.* **1996**, *35*, 1966.  
202. Zubaidha, P. K.; Kasatkin, A.; Sato, F. *J. Chem. Soc., Chem. Commun.* **1996**, 197.  
203. Kulinkovich, O. G.; Sviridov, S. V.; Vasilevskii, D. A.; Pritytskaya, T. S. *Zh. Org. Khim.* **1989**, *25*, 2244 (Engl. Trans. –*J. Org. Chem. USSR* **1990**, 2027).  
204. Corey, E. J.; Rao, S. A.; Noc, M. C. *J. Am. Chem. Soc.* **1994**, *116*, 9345.  
205. Lee, J.; Kim, H.; Cha, J. K. *J. Am. Chem. Soc.* **1996**, *118*, 4198.  
206. Lee, J.; Kang, C. H.; Kim, H.; Cha, J. K. *J. Am. Chem. Soc.* **1996**, *118*, 291.  
207. Kasatkin, A.; Kobayashi, K.; Okamoto, S.; Sato, F. *Tetrahedron Lett.* **1996**, *37*, 1849.  
208. Cho, S. Y.; Lee, J.; Lammi, R. K.; Cha, J. K. *J. Org. Chem.* **1997**, *62*, 8235.  
209. Kasatkin, A.; Sato, F. *Tetrahedron Lett.* **1995**, *36*, 6079.  
210. Lee, J.; Kim, Y. G.; Bae, J. G.; Cha, J. K. *J. Org. Chem.* **1996**, *61*, 4878.  
211. Quan, L. G.; Kim, S.-H.; Lee, J. C.; Cha, J. K. *Angew. Chem. Int. Ed.* **2002**, *41*, 2160.  
212. de Meijere, A.; Williams, C. M.; Kourdioukov, A.; Sviridov, S. V.; Chaplinski, V.; Kordes, M.; Savchenko, A. I.; Stratmann, C.; Noltemeyer, M. *Chem. Eur. J.* **2002**, *8*, 3789.  
213. Chaplinski, V.; de Meijere, A. *Angew. Chem., Int. Ed. Engl.* **1996**, *35*, 413.  
214. Epstein, O. L.; Kulinkovich, O. G. *Tetrahedron Lett.* **2001**, *42*, 3757.  
215. Lee, J.; Kim, H.; Cha, J. K. *J. Am. Chem. Soc.* **1995**, *117*, 9919.  
216. Lee, J.; Ha, J. D.; Cha, J. K. *J. Am. Chem. Soc.* **1997**, *119*, 8127.  
217. Lee, J.; Cha, J. K. *Tetrahedron Lett.* **1996**, *37*, 3663.  
218. Epstein, O. L.; Savchenko, A. I.; Kulinkovich, O. G. *Tetrahedron Lett.* **1999**, *40*, 5935.  
219. Williams, C. M.; Chaplinski, V.; Schreiner, P. R.; de Meijere, A. *Tetrahedron Lett.* **1998**, *39*, 7695.  
220. Casey, C. P.; Strotman, N. A. *J. Am. Chem. Soc.* **2004**, *126*, 1699.  
221. Quntar, A. A. A.; Srebnick, M. *Chem. Commun.* **2003**, 58.  
222. Eisch, J. J.; Gitua, J. N. *Organometallics* **2003**, *22*, 24.  
223. Obora, Y.; Moriya, H.; Tokunaga, M.; Tsuji, Y. *Chem. Commun.* **2003**, 2820.



## 4.04

# Complexes of Titanium in Oxidation State III

---

P Mountford and N Hazari, University of Oxford, Oxford, UK

© 2007 Elsevier Ltd. All rights reserved.

<b>4.04.1 Introduction and Scope</b>	<b>282</b>
<b>4.04.2 Compounds with <math>\eta^1</math>-Ligands</b>	<b>282</b>
4.04.2.1 Homoleptic Compounds	282
4.04.2.2 Compounds with Amide Ligands	283
4.04.2.3 Compounds Supported by Multidentate Anionic Ligands	284
<b>4.04.3 Compounds with <math>\eta^3</math>-Ligands</b>	<b>286</b>
<b>4.04.4 Compounds with Non-Cyclopentadienyl <math>\eta^5</math>-Ligands</b>	<b>287</b>
<b>4.04.5 Monocyclopentadienyl Compounds</b>	<b>288</b>
4.04.5.1 Cationic Compounds	288
4.04.5.2 Compounds with Bridging Hydrides	288
4.04.5.3 Compounds with Fluoride Ligands	289
4.04.5.4 Compounds with Chloride Ligands	290
4.04.5.5 Compounds with Amide Ligands	291
4.04.5.6 Compounds with Thiolate Ligands	291
4.04.5.7 Mixed Metal Compounds	292
4.04.5.8 Polymerization Studies	293
<b>4.04.6 Bis-Cyclopentadienyl Compounds</b>	<b>293</b>
4.04.6.1 Cationic Compounds	293
4.04.6.2 Zwitterionic Compounds	295
4.04.6.3 Compounds with Halide Ligands	296
4.04.6.3.1 Compounds with fluoride ligands	296
4.04.6.3.2 Compounds with chloride ligands	298
4.04.6.3.3 Compounds with iodide ligands	299
4.04.6.4 Compounds with Hydride Ligands	300
4.04.6.5 Compounds with Alkyl Ligands	302
4.04.6.6 Compounds with Allyl and Propargyl Ligands	305
4.04.6.7 Compounds with Ti–N Bonds	308
4.04.6.8 Compounds with Ti–O Bonds	310
4.04.6.9 Compounds with Phosphide, Sulfide, and Telluride Ligands	312
4.04.6.10 Mixed Metal Compounds	314
4.04.6.11 Alkyne Polymerization with Ti(III)	317
<b>4.04.7 Compounds with Carborane Ligands</b>	<b>317</b>
<b>4.04.8 Compounds with <math>\eta^6</math>-Ligands</b>	<b>319</b>
<b>4.04.9 Compounds with <math>\eta^8</math>-Ligands</b>	<b>320</b>
<b>References</b>	<b>320</b>

---



#### 4.04.1 Introduction and Scope

The organometallic chemistry of titanium is dominated by complexes in the +IV oxidation state and in comparison there are relatively few examples of titanium complexes in the +III oxidation state. For information on organotitanium(IV) see Chapter 4.05. However, examples of titanium(III) complexes are more common than examples of titanium complexes in lower oxidation states (for information on organotitanium in oxidation states 0 to II see Chapter 4.03) and titanium(III) chemistry is considerably more advanced than the chemistry of the heavier group 4 metals, zirconium and hafnium in the +III oxidation state. For information on organozirconium(III) and organohafnium(III) see Chapter 4.07.

In this chapter we present a review of organotitanium(III) literature, covering the period from the publication of COMC(1995) up until the middle of 2005. During this period, there have been a number of reports describing the synthesis and properties of new titanium(III) species. The majority of this work has focused on complexes supported by bis-cyclopentadienyl ligand sets, but there has also been progress in developing non-cyclopentadienyl based systems. In addition, significant advances have been made in determining the reactivity and applications of titanium(III) complexes; that research is also summarized in this chapter.

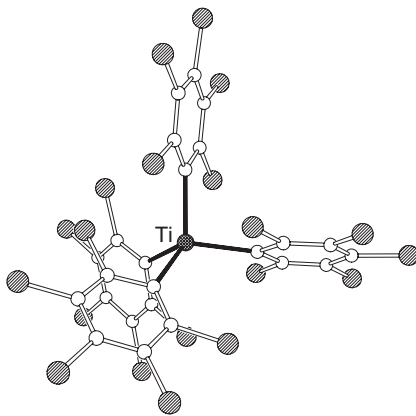
Furthermore, over the past 15 years, it has also been demonstrated that titanium(III) complexes can be used as catalysts in organic transformations. Complexes containing a Ti(III) center have been shown to be active catalysts for the hydrosilylation of lactones, esters, and ketones and have also been used to reduce both aryl and alkyl halides, ketones, aldehydes, aromatic azo compounds, and epoxides. These organic applications of titanium(III) complexes are beyond the scope of this chapter.

#### 4.04.2 Compounds with $\eta^1$ -Ligands

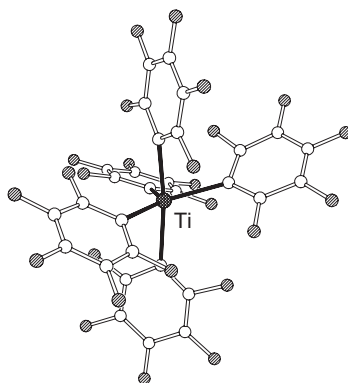
##### 4.04.2.1 Homoleptic Compounds

The anionic homoleptic  $\sigma$ -organotitanium(III) complex  $[\text{Li}(\text{THF})_4][\text{Ti}(\text{C}_6\text{Cl}_5)_4]$  **1** was prepared through the reaction of  $\text{TiCl}_3(\text{THF})_3$  with  $\text{LiC}_6\text{Cl}_5$  in  $\text{Et}_2\text{O}$  at  $-78^\circ\text{C}$ .<sup>1,2</sup> The structure of the related compound  $[\text{Li}(\text{THF})_2(\text{Et}_2\text{O})_2][\text{Ti}(\text{C}_6\text{Cl}_5)_4]$  **1'** (crystallization of **1** in  $\text{CH}_2\text{Cl}_2$ – $\text{Et}_2\text{O}$  mixtures resulted in displacement of two molecules of THF by  $\text{Et}_2\text{O}$ ) was determined by X-ray crystallography and is the only structurally characterized example of a homoleptic four-coordinate alkyl or aryl Ti(III) species (Figure 1). The geometry around Ti in  $[\text{Ti}(\text{C}_6\text{Cl}_5)_4]^-$  is best described as distorted tetrahedral with Ti–C bond lengths of approximately 2.207(5) Å. Controlled chemical oxidation of **1** using  $[\text{N}(4\text{-BrC}_6\text{H}_4)_3][\text{SbCl}_6]$  resulted in the formation of the homoleptic neutral species  $\text{Ti}(\text{C}_6\text{Cl}_5)_4$ .

In contrast, the related reaction between  $\text{TiCl}_3(\text{THF})_3$  and  $\text{LiC}_6\text{F}_5$  did not result in the formation of a homoleptic four-coordinate Ti(III) species. Instead, the five-coordinate dianionic complex  $[\text{NBu}_4]_2[\text{Ti}(\text{C}_6\text{F}_5)_5]$  **2** was isolated.<sup>3</sup> Compound **2** was also obtained from the reaction of the Ti(IV) precursor  $\text{TiCl}_4(\text{Et}_2\text{O})_x$  with  $\text{LiC}_6\text{F}_5$  in the presence of  $[\text{NBu}_4]\text{Br}$  and is the first and only known example of a  $[\text{TiR}_5]^{2-}$  species. The solid-state structure reveals a heavily



**Figure 1** X-ray structure of the  $[\text{Ti}(\text{C}_6\text{Cl}_5)_4]^-$  anion in **1'**.<sup>1</sup> C atoms are represented by open spheres and Cl atoms by shaded spheres.



**Figure 2** X-ray structure of one of the two crystallographically independent  $[\text{Ti}(\text{C}_6\text{F}_5)_5]^{2-}$  anions in **2**.<sup>3</sup> C atoms are represented by open spheres and F atoms by shaded spheres.

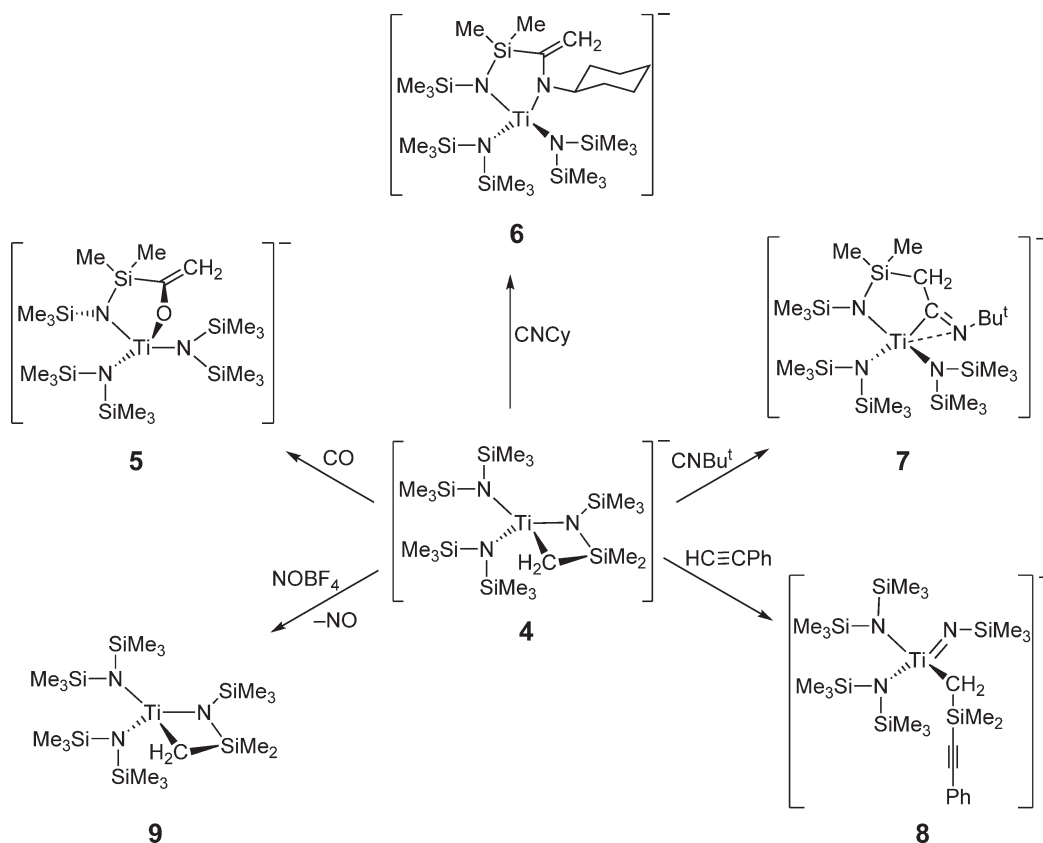
distorted trigonal-bipyramidal arrangement of the  $\text{C}_6\text{F}_5$  ligands around the titanium center (Figure 2). The authors concluded that this large distortion from the ideal trigonal-bipyramidal geometry is probably due to both the Jahn–Teller effect and to steric problems associated with arranging the five  $\text{C}_6\text{F}_5$  around the titanium center. The average Ti–C distance is 2.244(8) Å which is slightly longer than in **1**’.

#### 4.04.2.2 Compounds with Amide Ligands

An initial attempt to form a monomeric Ti(III) alkyl species with amide-supporting ligands was unsuccessful. Gambarotta *et al.* reported that the reaction of  $(\text{Cy}_2\text{N})_2\text{Ti}(\mu\text{-Cl})_2\text{Li}(\text{TMEDA})$  (TMEDA = N,N,N’,N’-tetramethylethylenediamine) with 2 equiv. of MeLi resulted in the formation of the dimeric species  $(\text{Cy}_2\text{N})_2\text{Ti}(\mu\text{-Me})_2\text{Li}(\text{TMEDA})$  with bridging Me ligands.<sup>4</sup> However, Cummins and co-workers subsequently demonstrated that treatment of the “ate” complex  $\{\text{Ar}(\text{R})\text{N}\}_2\text{Ti}(\mu\text{-Cl})_2\text{Li}(\text{TMEDA})$  ( $\text{R} = \text{C}(\text{CD}_3)_2\text{Me}$ ,  $\text{Ar} = 3,5\text{-Me}_2\text{C}_6\text{H}_3$ ) with 1 equiv. of the sterically bulky  $\text{LiCH}(\text{SiMe}_3)_2$  in pentane results in the formation of the monomeric Ti(III) alkyl species  $\{\text{Ar}(\text{R})\text{N}\}_2\text{TiCH}(\text{SiMe}_3)_2$  **3**.<sup>5</sup> Magnetic susceptibility and EPR measurements on **3** were consistent with each molecule possessing one unpaired electron. The compound was crystallographically characterized; the structure showed that one of the aryl amido ligands is coordinated to the metal in an  $\eta^3$ -fashion, involving the nitrogen atom, the aryl *ipso*-carbon and one of the aryl *ortho*-carbons. No evidence was found to suggest an  $\alpha$ -agostic interaction between the  $\text{CH}(\text{SiMe}_3)_2$  ligand and the metal center.

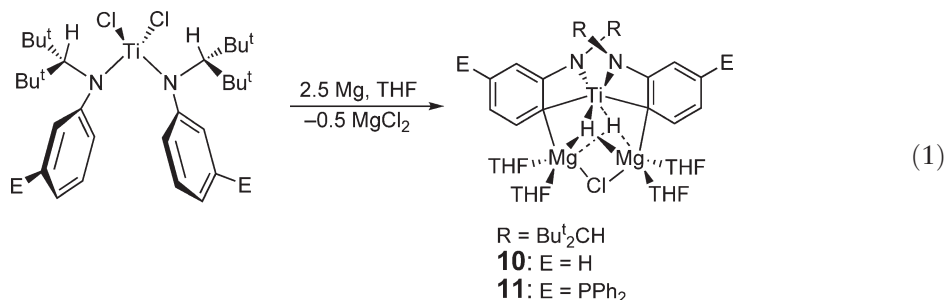
Another alkyl species, the anionic metallacyclic complex  $[\text{Na}(12\text{-crown-4})_2][\{(\text{Me}_3\text{Si})_2\text{N}\}_2\text{TiCH}_2\text{SiMe}_2\text{NSiMe}_3]$  **4** was prepared through the reaction of  $\text{Ti}\{(\text{N}(\text{SiMe}_3)_2)_3\}$  with  $\text{NaN}(\text{SiMe}_3)_2$  in the presence of 2 equiv. of 12-crown-4.<sup>6</sup> The anion in compound **4** is extremely reactive toward a variety of unsaturated substrates (Scheme 1).<sup>7</sup> Reactions with CO and the isonitrile  $\text{CNCy}$  resulted in an initial insertion into the Ti–C bond of **4**, followed by a rearrangement to generate the planar five-membered metallacyclic products  $[\text{Na}(12\text{-crown-4})_2][\{(\text{Me}_3\text{Si})_2\text{N}\}_2\text{Ti-OC}(\text{CH}_2)\text{SiMe}_2\text{NSiMe}_3]$  **5** and  $[\text{Na}(12\text{-crown-4})_2][\{(\text{Me}_3\text{Si})_2\text{N}\}_2\text{TiN}(\text{Cy})\text{C}(\text{CH}_2)\text{SiMe}_2\text{NSiMe}_3]$  **6**, respectively, which contain exocyclic  $\text{C}=\text{CH}_2$  groups. Both **5** and **6** were structurally characterized and have similar structures. In contrast, the reaction of  $\text{CNBu}^t$  with **4** resulted in the formation of the primary insertion product  $[\text{Na}(12\text{-crown-4})_2][\{(\text{Me}_3\text{Si})_2\text{N}\}_2\text{TiC}(\text{NBu}^t)\text{CCH}_2\text{SiMe}_2\text{NSiMe}_3]$  **7** which contains a new Ti(III)–C bond. The reaction between **4** and phenyl acetylene resulted in a redox disproportionation to form the Ti(IV) imido complex  $[\text{Na}(12\text{-crown-4})_2][\{(\text{Me}_3\text{Si})_2\text{N}\}_2\text{Ti}(\text{NSiMe}_3)(\text{CH}_2\text{SiMe}_2\text{C}=\text{CPh})]$  **8** and an uncharacterized Ti(II) species. Complex **8** was structurally characterized; it is clear from the titanium–nitrogen bond lengths that it contains one imido ligand (Ti–N = 1.751(6) Å) and two amido ligands (Ti–N = 2.045(4) and 2.023(4) Å) as well as the Ti–C bond. The neutral Ti(IV) species  $[\{(\text{Me}_3\text{Si})_2\text{N}\}_2\text{TiCH}_2\text{SiMe}_2\text{NSiMe}_3]$  **9** was formed through the oxidation of **4** using  $\text{NOBF}_4$ .

Amide supporting ligands have also been utilized to stabilize a non-cyclopentadienyl supported Ti(III) hydride.<sup>8</sup> Magnesium was used as the reducing agent to convert two related aryl-amido based titanium(IV) dichloride species into the titanium(III)–magnesium hydrides **10** and **11** (Equation 1). These reactions proceed with concomitant intramolecular metallation of the aryl-amido ligand and the structure of **11** was established using X-ray crystallography. Both the arylamido ligands in **11** coordinate to the titanium center in an  $\eta^3$ -fashion. The bonding of the



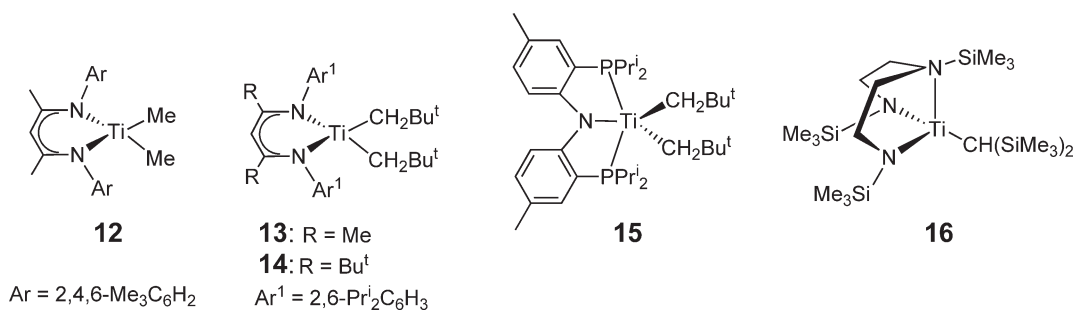
**Scheme 1** Cations in 4–8 have been omitted.

amido ligands is similar to that described for **3**. The *ortho*-carbon atoms which coordinate to the titanium center also coordinate to one magnesium atom each and as a result two Ti( $\mu_2$ -aryl)Mg bonding motifs are formed. The most important structural feature of **11** is the presence of two symmetrical  $\mu_3$ -hydrides which bridge the three metal centers. These bridging hydrides were located in the difference Fourier map, and their presence was also confirmed through EPR experiments and an unambiguous quenching experiment with D<sub>2</sub>O.



#### 4.04.2.3 Compounds Supported by Multidentate Anionic Ligands

A number of Ti(III) alkyl complexes supported by multidentate anionic ligands have been prepared through the alkylation of Ti(III) chloride species. Budzelaar and co-workers reported that the reaction of the mono-( $\beta$ -diketiminato)Ti(III) dichloride, LTiCl<sub>2</sub> (L = ArNC(Me)CHC(Me)NAr; Ar = 2,4,6-Me<sub>3</sub>C<sub>6</sub>H<sub>2</sub>) with MeMgI resulted in the formation of the dimethyl complex LTiMe<sub>2</sub> **12** (Figure 3).<sup>9</sup> Complex **12** is an active catalyst for the



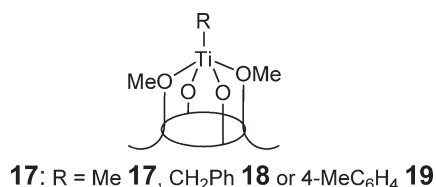
**Figure 3** Ti(III) alkyl complexes supported by multidentate anionic N-donor ligands.

polymerization of  $\alpha$ -olefins when B(C<sub>6</sub>F<sub>5</sub>)<sub>3</sub> is used as a co-catalyst. A similar methodology was used by Mindiola *et al.* to form bis-alkyl species of the type LTi(CH<sub>2</sub>Bu<sup>t</sup>)<sub>2</sub> (L = Ar<sup>1</sup>NC(Me)CHC(Me)NAr<sup>1</sup> = Nacnac **13**; L = Ar<sup>1</sup>NC(Bu<sup>t</sup>)CHC(Bu<sup>t</sup>)NAr<sup>1</sup> = Nacnac<sub>tBu</sub> **14**; L = N{2-P(CHMe<sub>2</sub>)<sub>2</sub>-4-MeC<sub>6</sub>H<sub>3</sub>}<sub>2</sub> **15**; Ar<sup>1</sup> = 2,6-Pr<sup>i</sup><sub>2</sub>C<sub>6</sub>H<sub>3</sub>) through the reaction of the dichloride species LTiCl<sub>2</sub> with LiCH<sub>2</sub>Bu<sup>t</sup> (Figure 3).<sup>10–12</sup> Compounds **13–15** all undergo one electron oxidatively induced  $\alpha$ -abstraction reactions to form stable Ti(IV) alkylidene complexes.

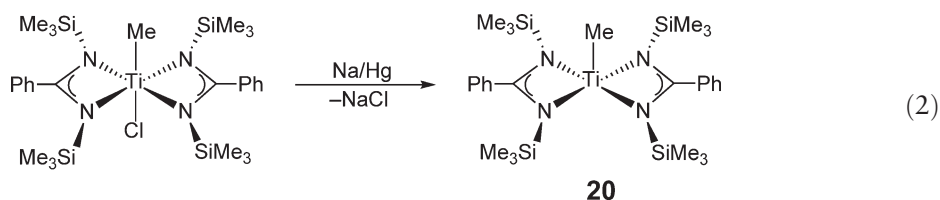
The dimeric diamidoamine-supported Ti(III) chloride (N<sub>2</sub>N)<sub>2</sub>Ti<sub>2</sub>( $\mu$ -Cl)<sub>2</sub> (N<sub>2</sub>N = (Me<sub>3</sub>SiNCH<sub>2</sub>CH<sub>2</sub>)<sub>2</sub>NSiMe<sub>3</sub>) is also a precursor for the synthesis of monomeric alkyls. It reacts cleanly with 2 equiv. of LiCH(SiMe<sub>3</sub>)<sub>2</sub> to form the four-coordinate complex (N<sub>2</sub>N)TiCH(SiMe<sub>3</sub>)<sub>2</sub> **16** (Figure 3).<sup>13</sup> As a result of the geometric constraints imposed by the chelating N<sub>2</sub>N ligand, the geometry of **16** is best described as trigonal-pyramidal rather than tetrahedral. When **16** was reacted with H<sub>2</sub>, a  $\sigma$ -bond metathesis reaction occurred to give the dimeric Ti(III) hydride complex (N<sub>2</sub>N)<sub>2</sub>Ti<sub>2</sub>( $\mu$ -H)<sub>2</sub> and CH<sub>2</sub>(SiMe<sub>3</sub>)<sub>2</sub> as a by-product. Complexes **12–16** were all structurally characterized; the Ti–C bond lengths are comparable, with values ranging from 2.117(3)–2.175(5) Å.

A family of alkyl complexes of the type (Me<sub>2</sub>calix)TiR (Me<sub>2</sub>calix = 1,3-dimethyl ether 4-Bu<sup>t</sup>calix[4]arene, R = Me **17**, CH<sub>2</sub>Ph **18**, 4-MeC<sub>6</sub>H<sub>4</sub> **19**) was prepared from (Me<sub>2</sub>calix)TiCl using either LiR or a Grignard reagent as the alkylating agent (Figure 4).<sup>14</sup> Compound **19** was structurally characterized and the O<sub>4</sub> core of the Me<sub>2</sub>calix displays a tetrahedral distortion. Overall, this results in a trigonal-bipyramidal geometry around the Ti center, with the equatorial plane occupied by the alkyl ligand and two oxygen atoms from the Me<sub>2</sub>calix and the axial plane occupied by the other two oxygen atoms of Me<sub>2</sub>calix. An unusual feature of the solid-state structure of **19** is that each individual molecule hosts inside the Me<sub>2</sub>calix cavity the 4-tolyl ligand of a neighboring molecule; consequently, the structure consists of a head-to-tail chain arrangement of the molecules.

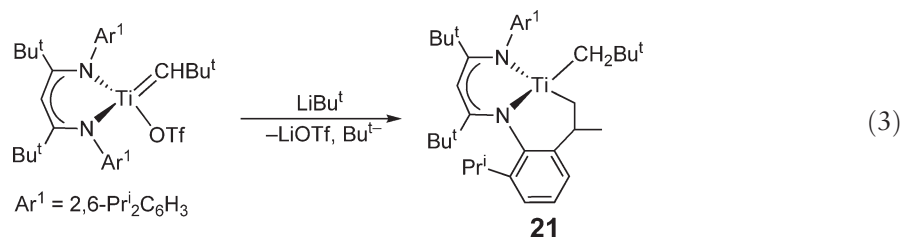
In contrast to the syntheses described above, Hagadorn and Arnold prepared the benzamidinate-supported Ti(III) alkyl species {PhC(NSiMe<sub>3</sub>)<sub>2</sub>}<sub>2</sub>TiMe **20** through the reduction of the Ti(IV) complex {PhC(NSiMe<sub>3</sub>)<sub>2</sub>}<sub>2</sub>TiMeCl with sodium amalgam (Equation (2)).<sup>15</sup> The crystal structure of **20** showed that the geometry of the complex is distorted square pyramidal with the Me ligand in the axial position and the two bidentate benzamidinate ligands around the base. The Ti–C bond length is 2.120(5) Å and there was evidence to suggest an agostic interaction between one of the hydrogen atoms of the methyl ligand and the unsaturated titanium center. A similar reduction of Ti(IV) was utilized in the synthesis of (salen)TiMe(THF) (salen = bis(salicylidene)ethylenediamine) from the chloro methyl complex (salen)TiMeCl.<sup>16</sup>



**Figure 4** Schematic representation of (Me<sub>2</sub>calix)TiR (R = Me **17**, CH<sub>2</sub>Ph **18**, 4-MeC<sub>6</sub>H<sub>4</sub> **19**).

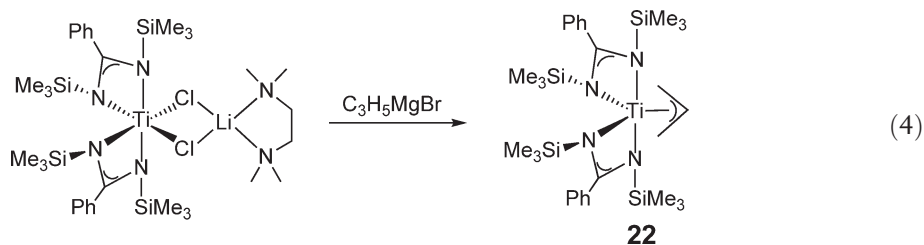


The metallacyclic Ti(III) alkyl complex  $\text{LTi}(\text{CHBu}^t)$  ( $\text{L} = \text{ArNC}(\text{Bu}^t)\text{CHC}(\text{Bu}^t)\text{N}\{2,6\text{-Pr}^i(\text{CH}(\text{CH}_2)(\text{Me}))\text{C}_6\text{H}_3\}$ ) **21** was produced by the one-electron reduction of the Ti(IV) alkylidene complex  $(\text{Nacnac}_{\text{But}})\text{Ti}(\text{CH}_2\text{Bu}^t)(\text{OTf})$  (formed from **14**) with either  $\text{LiBu}^t$  (Equation (3)) or  $\text{KC}_8$ .<sup>17</sup> The first step in this reaction is proposed to be the generation of the transient Ti(III) alkylidene species  $(\text{Nacnac}_{\text{But}})\text{Ti}(\text{CHBu}^t)$  which arises from the loss of either  $\text{LiOTf}$  or  $\text{KOTf}$  and a *tert*-butyl radical from  $(\text{Nacnac}_{\text{But}})\text{Ti}(\text{CH}_2\text{Bu}^t)(\text{OTf})$ . A 1,2-addition of a methyl group from one of the *iso*-propyl groups of the  $\text{Nacnac}_{\text{But}}$  ligand across the  $\text{Ti}=\text{CHBu}^t$  of the transient alkylidene complex then generates the six-membered metallacyclic ring present in **21**. The Ti–C bond lengths are 2.143(2) and 2.173(2) Å, which are in the range typically observed for Ti(III)–alkyl bonds. The related alkylidene complex  $(\text{Nacnac})\text{Ti}(\text{CHBu}^t)(\text{OTf})$  reacts in a similar fashion to  $(\text{Nacnac}_{\text{But}})\text{Ti}(\text{CH}_2\text{Bu}^t)(\text{OTf})$  with  $\text{KC}_8$ . However, as a result of the loss of steric bulk on the ligand the reaction did not proceed cleanly and the metallacyclic product was not isolated.

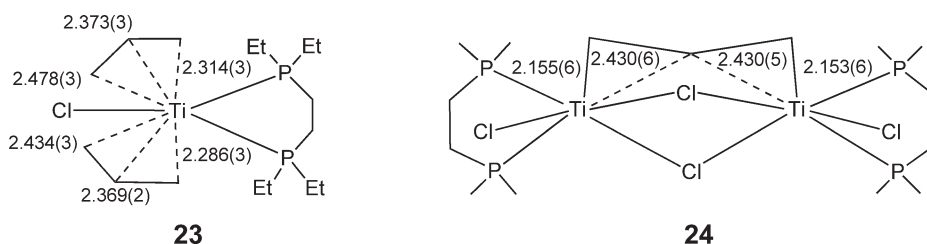


#### 4.04.3 Compounds with $\eta^3$ -Ligands

The reaction of the benzamidinate complex  $\{\text{PhC}(\text{NSiMe}_3)_2\}_2\text{Ti}(\mu\text{-Cl})_2\text{Li}(\text{TMEDA})$  with  $\text{C}_3\text{H}_5\text{MgBr}$  generated the stable Ti(III) allyl  $\{\text{PhC}(\text{NSiMe}_3)_2\}_2\text{Ti}(\eta^3\text{-C}_3\text{H}_5)$  **22** (Equation (4)).<sup>18</sup> The experimental magnetic moment of  $1.63 \mu_{\text{B}}$  is consistent with a  $d^1$  electronic configuration. The bonding of the allyl moiety is asymmetric, and one of the two C–C bond lengths is significantly longer than the other, suggesting different bond orders ( $\text{C}=\text{C} = 1.333(8)$  and  $1.160(7)$  Å). However, the Ti–C bond lengths are comparable, with the shortest distance of  $2.263(4)$  Å being observed between the central carbon of the allyl fragment and the Ti center. The two terminal Ti–C bond distances are  $2.297(4)$  and  $2.368(5)$  Å, respectively. The asymmetry in the allyl ligand is probably due to steric hindrance from the two benzamidinate ligands.



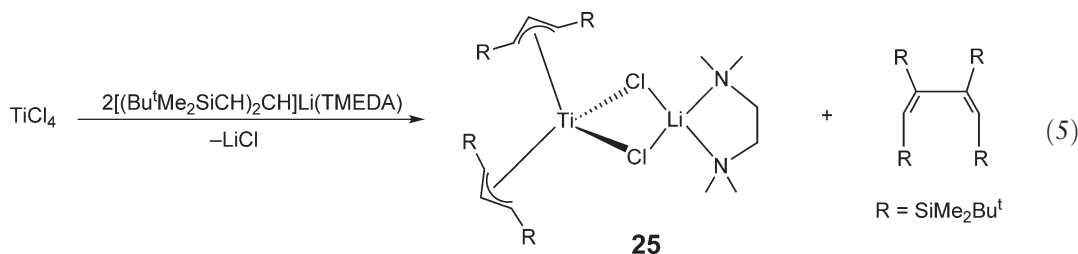
Cotton *et al.* reported that the addition of  $\text{C}_3\text{H}_5\text{MgBr}$  to  $\text{TiCl}_4(\text{depe})$  ( $\text{depe} = 1,2\text{-bis}(\text{diethylphosphino})\text{ethane}$ ) resulted in the clean formation of the bis-allyl Ti(III) species  $\text{TiCl}(\text{depe})(\eta^3\text{-C}_3\text{H}_5)_2$  **23**.<sup>19</sup> The solid-state structure of **23** indicated that the two allyl ligands are unsymmetrically arranged around the Ti center. In each allyl fragment, one terminal allylic carbon is closer to the Ti center than the central carbon, and both these atoms are closer to the metal center than the second terminal allylic carbon (Figure 5). The carbon–carbon distances within the allyl groups are also non-equivalent, presumably as a result of this unsymmetrical bonding.



**Figure 5** Ti–C bond lengths (Å) for the two allyl ligands in  $\text{TiCl}(\text{depe})(\eta^3\text{-C}_3\text{H}_5)$  **23** and  $\text{Ti}_2(\mu\text{-Cl})_2\text{Cl}_2(\text{dmpe})_2(\mu^2\text{-}\eta^3\text{-C}_3\text{H}_5)$  **24**.

Surprisingly, the analogous reaction between  $\text{TiCl}_4(\text{dmpe})$  ( $\text{dmpe} = 1,2\text{-bis}(\text{dimethylphosphino})\text{ethane}$ ) and  $\text{C}_3\text{H}_5\text{MgBr}$  did not result in the formation of a monomeric complex; instead, the binuclear mixed valence species  $\text{Ti}_2(\mu\text{-Cl})_2\text{Cl}_2(\text{dmpe})_2(\mu^2\text{-}\eta^3\text{-C}_3\text{H}_5)$  **24** was generated. This paramagnetic species formally contains one Ti(III) and one Ti(II) center and its EPR spectrum consists of a complex pattern centered at 3428 G. The bridging allyl group is symmetrical, with the central allylic carbon being equidistant from both Ti centers and the two terminal allylic carbons being approximately the same distance away from the Ti center to which they coordinate (Figure 5). The disparity in nuclearity between complexes **23** and **24** may be attributable to the different steric influences of the two phosphine ligands.

As part of an investigation into the polymerization of olefins promoted by Ti(III) and Zr(III) species, Eisen and co-workers prepared the allyl complex  $\{(\text{Bu}^t\text{Me}_2\text{SiCH}_2\text{CH})_2\text{Ti}(\mu\text{-Cl})_2\text{Li}(\text{TMEDA})$  **25** from  $\text{TiCl}_4$  and 2 equiv. of the lithium allyl compound  $[(\text{Bu}^t\text{Me}_2\text{SiCH}_2\text{CH})\text{Li}(\text{TMEDA})$  (Equation (5)).<sup>20</sup> The proposed mechanism for this reaction involves the initial reduction of  $\text{TiCl}_4$  to  $\text{TiCl}_3$  with concomitant formation of  $\text{LiCl}$  and the dimer  $(\text{Bu}^t\text{Me}_2\text{SiCH}=\text{CHCH}(\text{SiMe}_2\text{Bu}^t)\text{CH}(\text{SiMe}_2\text{Bu}^t)\text{CH}=\text{CH}(\text{SiMe}_2\text{Bu}^t))$ . A simple metathesis reaction then occurs between  $\text{TiCl}_3$  and 2 equiv. of  $[(\text{Bu}^t\text{Me}_2\text{SiCH}_2\text{CH})\text{Li}(\text{TMEDA})$  to form **25**. The yield for the reaction is consistent with this mechanism (<50%). The allyl dimer by-product has been fully characterized.

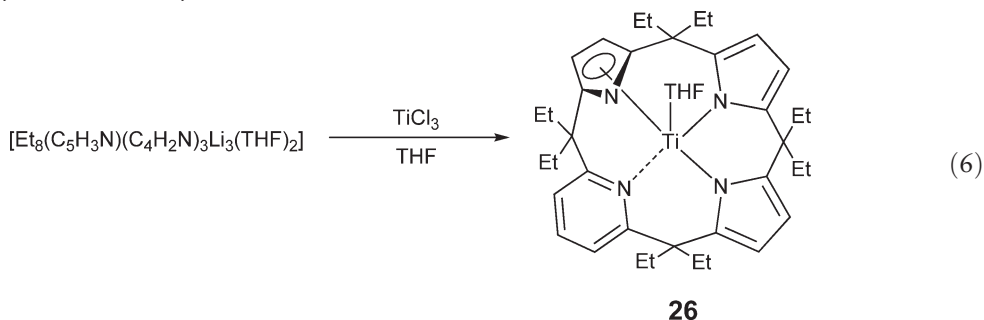


The structure of **25** was confirmed by X-ray crystallography and indicated that both allyl fragments are unsymmetrically bound to the Ti center in a similar fashion to complex **23**. Oxidation of **25** with  $[\text{N}(4\text{-BrC}_6\text{H}_4)_3][\text{SbCl}_6]$  resulted in the formation of the neutral Ti(IV) species  $\{(\text{Bu}^t\text{Me}_2\text{SiCH}_2\text{CH})_2\text{TiCl}_2$ . In the presence of MAO, both this Ti(IV) species and **25** were shown to be active precatalysts for the polymerization of ethylene and propylene. The authors concluded that a cationic Ti(IV) species was the active catalyst for polymerization and that the first step in the polymerization process involved an oxidative coupling reaction between the olefin and **25**, which converted the Ti(III) precatalyst to a Ti(IV) species. The Ti(IV) species then reacted with MAO to generate the active cationic complex.

#### 4.04.4 Compounds with Non-Cyclopentadienyl $\eta^5$ -Ligands

The brown Ti(III) complex **26** containing a *meso*-octaethyl tris(pyrrole)-mono(pyridine) ligand was prepared through the reaction of the lithiated form of the free ligand with  $\text{TiCl}_3$  in the presence of THF (Equation (6)).<sup>21</sup> The effective magnetic moment at 290 K was  $1.79 \mu_B$  indicating that **26** contained a single unpaired electron. The solid-state structure of **26** showed that the tris(pyrrolyl) fragment is bound to the metal center in a highly unusual  $\eta^5\text{:}\eta^1\text{:}\eta^1$ -fashion and that the Ti center is located in a cavity provided by the macrocyclic ligand. In the  $\eta^5$ -coordinated pyrrolyl moiety, the Ti–pyrrolyl (ring centroid) distance is 2.088 Å which is similar to the Ti–Cp (ring centroid) distances

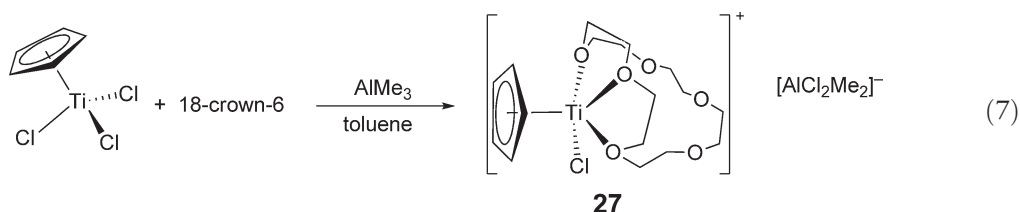
observed in cyclopentadienyl complexes. The elongated Ti–N (pyridine) bond length of 2.415(2) Å suggests that the Ti(III) center may be coordinatively unsaturated.



#### 4.04.5 Monocyclopentadienyl Compounds

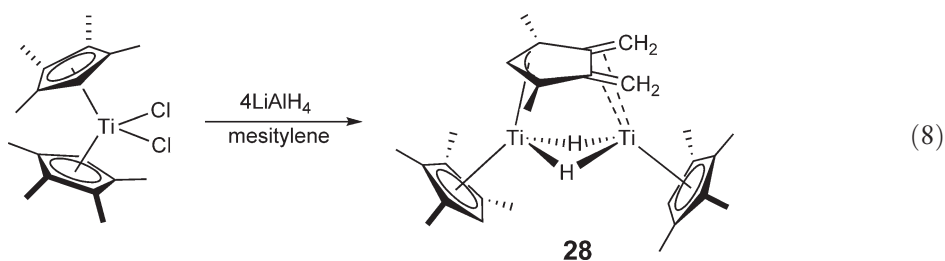
##### 4.04.5.1 Cationic Compounds

The reduction of  $\text{CpTiCl}_3$  ( $\text{Cp} = \eta^5\text{-C}_5\text{H}_5$ ) by  $\text{AlMe}_3$  in the presence of the crown ether 18-crown-6 resulted in the formation of the cationic complex  $[\text{CpTiCl}(\text{18-crown-6})][\text{AlCl}_2\text{Me}_2]$  **27** (Equation (7)).<sup>22</sup> Complex **27** is one of the few examples of a Ti(III) species which contains a coordinated crown ether ligand. The solid-state structure revealed that **27** crystallizes as a series of discrete cations and anions and that there are no contacts of less than 3.5 Å between the ions. The cation is too large for the 18-crown-6 ligand to encapsulate it. Therefore, the crown ether binds to the Ti center in a  $\kappa^3$ -fashion and is highly distorted from its regular geometry. The geometry of the cation is square pyramidal with the Cp ring occupying the apical position.

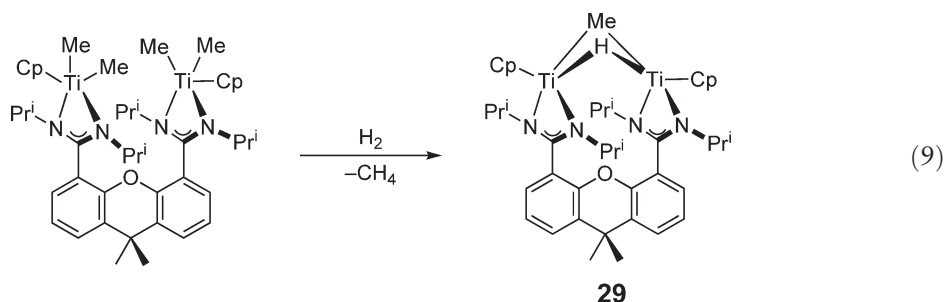


##### 4.04.5.2 Compounds with Bridging Hydrides

The reduction of  $(\eta^5\text{-C}_5\text{HMe}_4)_2\text{TiCl}_2$  with 4 equiv. of  $\text{LiAlH}_4$  in boiling mesitylene generated the novel mixed-valence binuclear Ti(III)/Ti(II) complex **28** which contains two bridging hydride ligands (Equation (8)).<sup>23</sup> Each of the titanium centers is also bound to a  $\text{C}_5\text{HMe}_4$  ring and a bridging organic ligand derived from  $\text{C}_5\text{HMe}_4$ . The structure of **28** was elucidated by X-ray crystallography and it was shown that the Ti(III) center binds to the bridging organic ligand through an  $\eta^3$ -allyl interaction while the Ti(II) center binds to the ligand through two  $\pi$ -bonding interactions with the two exocyclic methylene double bonds. The EPR spectrum at 296 K showed a triplet splitting due to the interaction of the  $d^1$  electron of the Ti(III) center with the two equivalent bridging hydrides.



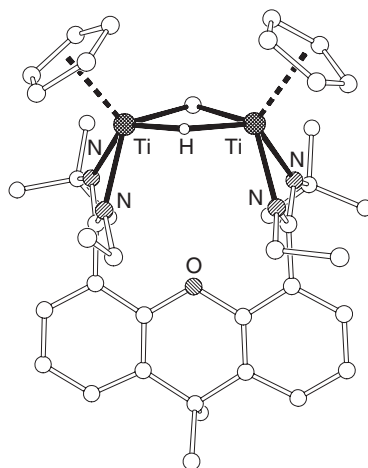
As part of a study into titanium amidinate complexes, Hagadorn and McNevin prepared the dimeric  $[\text{Ti(III)}]_2$  species **29** through the reaction of a  $\text{Ti(IV)}$  alkyl complex with  $\text{H}_2$  (Equation (9)).<sup>24</sup> Complex **29** was characterized by elemental analysis, NMR and IR spectroscopy, and isotopic-labeling studies. The Evans method was used to determine that the magnetic moment of **29** is  $1.14(5) \mu_B$  per dimer. This low value indicated that there is antiferromagnetic coupling between the two  $\text{Ti(III)}$  centers and as a result there was only a slight broadening in the resonances associated with **29** in the  $^1\text{H}$  and  $^{13}\text{C}$  NMR spectra. The structure of **29** was confirmed through NMR-labeling studies performed by  $^2\text{H}$ - and  $^{13}\text{C}$ -labeling of the alkyl groups on the starting material and also by hydrogenating the  $\text{Ti(IV)}$  starting material with  $\text{D}_2$ .



Although **29** was not crystallographically characterized, the crystal structure of a closely related complex, **30**, with an asymmetric amidinate ligand was determined (Figure 6). The Ti centers are both orientated in square-pyramidal geometries with the Cp ligands occupying the axial positions. The amidinate ligands occupy one face of the base of the square pyramid, while the bridging hydride and methyl ligands occupy the other face. The positions of the hydrogen atoms associated with both the bridging alkyl and hydride ligands were located and refined. The two bridging ligands link the metal centers symmetrically. There was no evidence that the  $\text{Ti}-\mu\text{-Me}$  bonds have any agostic character. The relatively short  $\text{Ti}-\text{Ti}$  separation of  $2.9788(6) \text{ \AA}$  indicates that there is probably a weak metal-metal interaction in **30**.

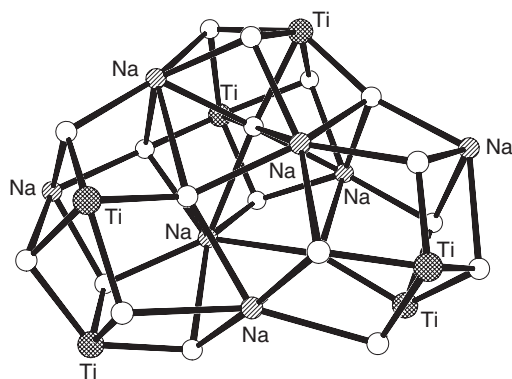
#### 4.04.5.3 Compounds with Fluoride Ligands

Treatment of  $\text{Cp}^*\text{TiF}_3$  ( $\text{Cp}^* = \eta^5\text{-C}_5\text{Me}_5$ ) with 1 equiv. of Na metal in THF resulted in the formation of the cluster compound  $\text{Cp}^*_6\text{Ti}_6\text{Na}_7\text{F}_{19}(\text{THF})_{2.5}$  **31**, which incorporates NaF as a ligand.<sup>25</sup> The solid-state structure of **31** indicated that seven NaF molecules are completely surrounded by six  $\text{Cp}^*\text{TiF}_2$  fragments. The coordination of the NaF molecules which form the central inorganic core is different to that observed in crystalline NaF (Figure 7). Only one of the F atoms is octahedrally coordinated while the others exhibit lower coordination numbers. Interestingly, when the same reduction of  $\text{Cp}^*\text{TiF}_3$  was performed in the presence of dmpe, the larger cluster

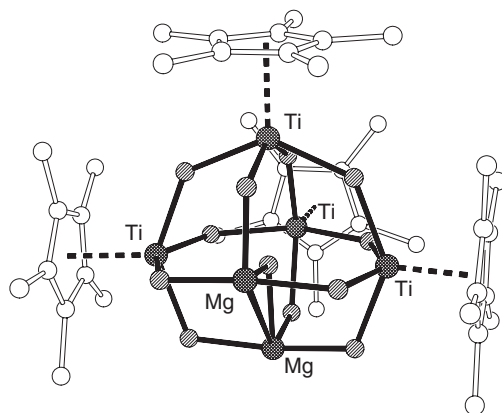


**Figure 6** X-ray structure of **30**.<sup>28</sup> C atoms are represented by open spheres and C-bound H atoms omitted for clarity.





**Figure 7** X-ray structure of the  $\text{Ti}_6\text{Na}_7\text{F}_{19}$  core of **31** with F atoms represented as open spheres.<sup>29</sup>



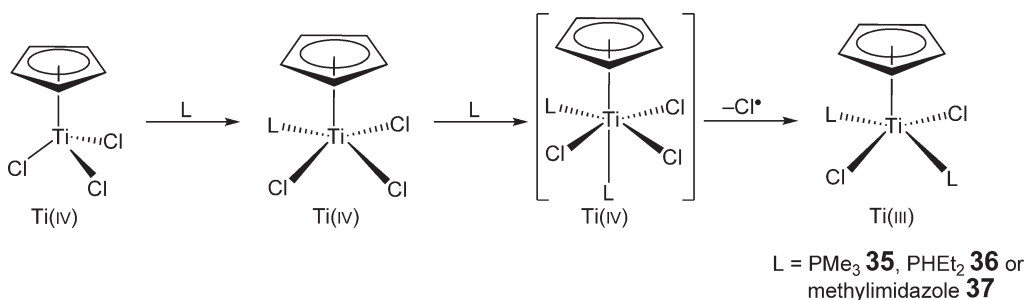
**Figure 8** X-ray structure of **33**.<sup>25</sup> C atoms are represented by open spheres and F atoms by shaded spheres. H atoms and THF molecules are omitted for clarity.

compound  $\text{Cp}^*_{12}\text{Ti}_{14}\text{Na}_{18}\text{F}_{48}(\text{THF})_6$  **32** was obtained.<sup>26</sup> The dmpe was added to the reaction mixture to stabilize the low oxidation state of the titanium and was probably not present in the final product because the fluoride ligand is a preferred donor. Compound **32** consists of a hydrocarbon layer containing 12  $\text{Cp}^*\text{TiF}_2$  units and six sodium-coordinated THF molecules which surrounds an inorganic  $(\text{TiF}_3)_2(\text{NaF})_{18}$  core. The presence of the hydrocarbon layers results in **32** being slightly soluble in hydrocarbon solvents.

Another cluster compound  $\text{Cp}^*_4\text{Ti}_4\text{Mg}_2\text{F}_{12}(\text{THF})_7$  **33**, which contains coordinated  $\text{MgF}_2$  was formed through the reaction of  $\text{Cp}^*\text{TiF}_3$  with 1 equiv. of Mg metal in THF.<sup>25</sup> The structure of **33** was elucidated by X-ray crystallography and indicates that the titanium, magnesium, and fluorine atoms form a cage-like structure (Figure 8). The magnesium atoms are six-coordinate and two of the six sites around the magnesium atoms are occupied by THF molecules. Interestingly, one of these two THF molecules bridges two magnesium atoms which is an unusual coordination mode for THF with alkaline earth metal compounds. When Ca was used as the reducing agent instead of Mg, the cluster compound  $(\text{Cp}^*\text{TiF}_2)_6\text{CaF}_2(\text{THF})$  **34** was generated.<sup>26</sup> The most interesting feature of the solid-state structure of **34** is that it contains two  $\text{Cp}^*_3\text{Ti}_3\text{F}_7(\text{THF})$  fragments linked by a single Ca atom.

#### 4.04.5.4 Compounds with Chloride Ligands

The main products of the reactions of  $\text{CpTiCl}_3$  with  $\text{PMe}_3$  and  $\text{PHET}_2$  were the Ti(IV) complexes  $\text{CpTiCl}_3(\text{PMe}_3)$  and  $\text{CpTiCl}_3(\text{PHET}_2)$ , respectively.<sup>27</sup> However, when these reactions were monitored by EPR spectroscopy, it was established that these were not the only products. Also present in yields of approximately 2% were the reduced Ti(III) species  $\text{CpTiCl}_2\text{L}_2$  ( $\text{L} = \text{PMe}_3$  **35** or  $\text{PHET}_2$  **36**). The EPR spectra of **35** and **36** consisted of triplet resonances due to coupling between the unpaired electron on the Ti center and two equivalent  $^{31}\text{P}$  nuclei. Similarly, when  $\text{CpTiCl}_3$  was



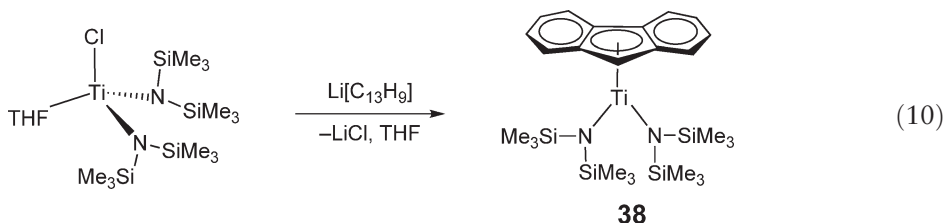
Scheme 2

treated with methylimidazole, a small amount of the Ti(III) complex  $\text{CpTiCl}_2\text{L}_2$  ( $\text{L}$  = methylimidazole **37**) was generated along with the Ti(IV) product  $\text{CpTiCl}_3\text{L}$ . Complex **37** was separated from the Ti(IV) species and isolated in 10% yield. The crystal structure of **37** showed that the geometry around the Ti(III) center is formally square pyramidal with the Cp ligand occupying the axial position. The chloride and methylimidazole ligands are located around the base of the pyramid so that the two chloride ligands are *trans* to each other and the two methylimidazole ligands are also *trans* to each other.

These reactions proceed in the absence of a reducing agent and it was proposed that they follow a free radical reduction mechanism in which the coordination of two equivalents of a strong  $\sigma$ -donor Lewis base causes a radical reductive loss of  $\text{Cl}^\bullet$  from the Ti center (Scheme 2). This mechanism was supported by the observation that no reduced species are observed when the reactions are carried out in the presence of weaker donors such as  $\text{NEt}_3$  or  $\text{PPh}_3$ .

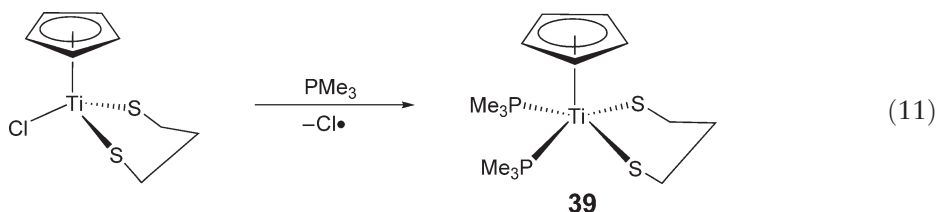
#### 4.04.5.5 Compounds with Amide Ligands

Treatment of  $\{(\text{Me}_3\text{Si})_2\text{N}\}_2\text{TiCl}(\text{THF})$  with fluorenyllithium afforded the amide-supported complex  $(\eta^5\text{-fluorenyl})\text{Ti}\{(\text{N}(\text{SiMe}_3)_2)\}_2$  **38** which contains a coordinated  $\text{C}_5$  ligand as part of the fluorenyl system (Equation (10)).<sup>28</sup> The solid state structure of **38** revealed that there are three crystallographically independent molecules in the unit cell but that these molecules all possess similar bond distances and angles. The Ti–C distances to the carbon atoms of the  $\text{C}_5$  ring are different. The shortest distance was observed between the Ti center and the C–H carbon of the  $\text{C}_5$  ring (values range from 2.325(7)–2.353(7) Å) while the average Ti–C bond lengths of the quaternary carbons range from 2.450(7)–2.528(6) Å. The  $\text{C}_6$  rings of the fluorenyl ligand are tilted out of the plane of the  $\text{C}_5$  ring so that they are further away from the metal center.



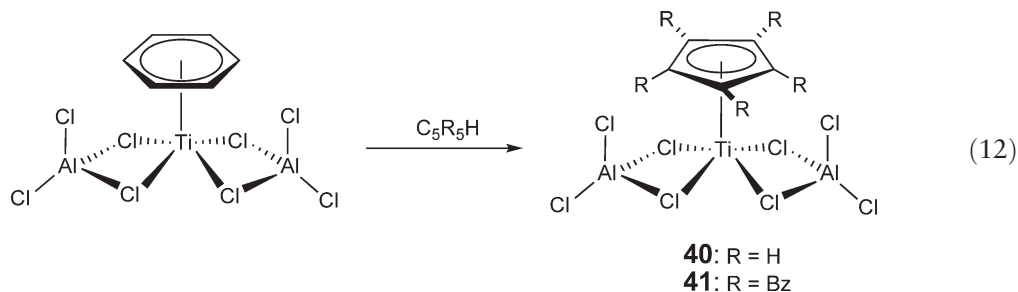
#### 4.04.5.6 Compounds with Thiolate Ligands

The reaction of  $\text{PMe}_3$  with the Ti(IV) thiolate species  $\text{CpTiCl}(\text{SCH}_2\text{CH}_2\text{CH}_2\text{S})$  resulted in the generation of the Ti(III) complex  $\text{CpTi}(\text{SCH}_2\text{CH}_2\text{CH}_2\text{S})(\text{PMe}_3)_2$  **39** (Equation (11)).<sup>27</sup> The mechanism for this reaction is believed to be analogous to that proposed in Scheme 2 with the key step being loss of the chlorine radical. Complex **39** was not isolated and was characterized on the basis of EPR spectroscopy. The EPR spectrum of **39** in THF at room temperature consisted of one triplet resonance due to coupling between the unpaired Ti electron and two equivalent phosphorus nuclei.

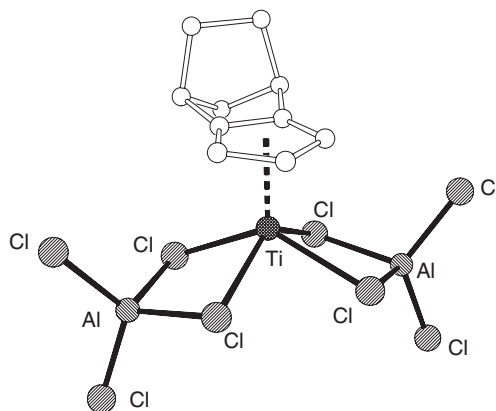


#### 4.04.5.7 Mixed Metal Compounds

Although the synthesis and properties of  $\text{CpTi}\{(\mu\text{-Cl})_2\text{AlCl}_2\}_2$  **40** were first described in 1979,<sup>29</sup> compound **40** has only recently been characterized by X-ray crystallography.<sup>30</sup> Mach *et al.* prepared **40** and the new compound  $(\eta^5\text{-C}_5\text{Bz}_5)\text{Ti}\{(\mu\text{-Cl})_2\text{AlCl}_2\}_2$  **41** ( $\text{Bz} = \text{CH}_2\text{Ph}$ ) through redox reactions between 1 equiv. of the appropriate cyclopentadiene and  $(\eta^6\text{-C}_6\text{H}_6)\text{Ti}\{(\mu\text{-Cl})_2\text{AlCl}_2\}_2$  (Equation (12)). The titanium centers in both **40** and **41** are formally square pyramidal with the four bridging chlorine atoms forming the pyramid base and the Cp or  $\text{C}_5\text{Bz}_5$  ring occupying the axial position. In **41**, all five benzyl groups on the  $\text{C}_5$  ring are directed away from the metal center forming a crown conformation. The geometry around the aluminum centers in both complexes is distorted slightly away from tetrahedral.



Mach *et al.* subsequently demonstrated that the reaction between  $(\eta^6\text{-C}_6\text{H}_6)\text{Ti}\{(\mu\text{-Cl})_2\text{AlCl}_2\}_2$  and isodicyclopentadiene (isodiCpH, tricyclo[5.2.1.0<sup>2,6</sup>]deca-2,5-diene) exclusively formed the *exo*-faced (isodicyclopentadienyl)Ti(III) species  $(\eta^5\text{-C}_{10}\text{H}_{11})\text{Ti}\{(\mu\text{-Cl})_2\text{AlCl}_2\}_2$  **42**.<sup>31</sup> The reaction is believed to be stereoselective because the *exo* face of the Ti(II) starting material is more accessible to the isodiCpH when it replaces the coordinated benzene than the *endo*-face. The room-temperature EPR spectrum of **42** consisted of 11 lines due to interaction between the unpaired electron on the Ti center with two equivalent Al nuclei while the solid-state structure of **42** (Figure 9) is analogous to



**Figure 9** X-ray structure of **42**.<sup>31</sup> C atoms are represented by open spheres and H atoms omitted for clarity.

those described for complexes **40** and **41**. The isodiCp ligand is folded such that the norbornene moiety is tilted away from the bound C<sub>5</sub> plane and further away from the titanium center.

Complexes analogous to **41** containing alkyl groups on the aluminum instead of chlorine atoms have also been prepared. A series of redox reactions between C<sub>5</sub>Bz<sub>5</sub>H and ( $\eta^6$ -C<sub>6</sub>H<sub>6</sub>)Ti{( $\mu$ -Cl)<sub>2</sub>AlCl<sub>2</sub>}<sub>2</sub> in the presence of 0.5, 1.5, or 4.0 equiv. of AlEt<sub>3</sub> resulted in the generation of the paramagnetic complexes ( $\eta^5$ -C<sub>5</sub>Bz<sub>5</sub>)TiAl<sub>2</sub>Cl<sub>8-x</sub>Et<sub>x</sub>, where *x* is equal or close to 1, 2, or 4.<sup>30</sup> These complexes were characterized by EPR and UV spectroscopy and the properties of these species were similar to those observed in other related systems.<sup>32</sup>

#### 4.04.5.8 Polymerization Studies

It is well established that half-sandwich Ti(IV) complexes of the type Cp<sup>R</sup>TiCl<sub>3</sub>, CpTi(OR)<sub>3</sub> (R = Me, Bu, or Ph), and Cp<sup>R</sup>TiR<sub>3</sub> (Cp<sup>R</sup> = Cp or Cp\*, R = Me or Bn) catalyze the polymerization of 1-alkenes, conjugated dienes, styrenes, and ethylene when reacted with a suitable activator (in general a large excess of methylaluminoxane (MAO) is used for chloride and alkoxide complexes, and 1 equiv. of B(C<sub>6</sub>F<sub>5</sub>)<sub>3</sub> or [CPh<sub>3</sub>][B(C<sub>6</sub>F<sub>5</sub>)<sub>4</sub>] is used for alkyl complexes). (For information on olefin polymerization with group IV metal catalysts see: 00065 and for information on organotitanium(IV) see: 00061.) On the basis of a number of *in situ* EPR studies, some researchers have suggested that the active catalysts in these polymerizations are actually Ti(III) species.<sup>33–38</sup> For example, Grassi and co-workers showed that the reaction between Cp\*TiR<sub>3</sub> (R = Me or <sup>13</sup>CH<sub>3</sub>) and equimolar amounts of either B(C<sub>6</sub>F<sub>5</sub>)<sub>3</sub> or [CPh][B(C<sub>6</sub>F<sub>5</sub>)<sub>4</sub>] at room temperature in chlorobenzene resulted in the slow formation of the cationic Ti(III) complexes [Cp\*TiR]<sup>+</sup>.<sup>39,40</sup> These cationic complexes were proposed to arise from the autoreduction of the Ti(IV) cations [Cp\*TiR<sub>2</sub>]<sup>+</sup>. It was subsequently shown that the Ti–R bond in complexes of the type [Cp\*TiR]<sup>+</sup> underwent rapid insertion with styrene, leading Grassi to conclude that Ti(III) species play a vital role in the polymerization of styrene with Cp\*TiR<sub>3</sub>.

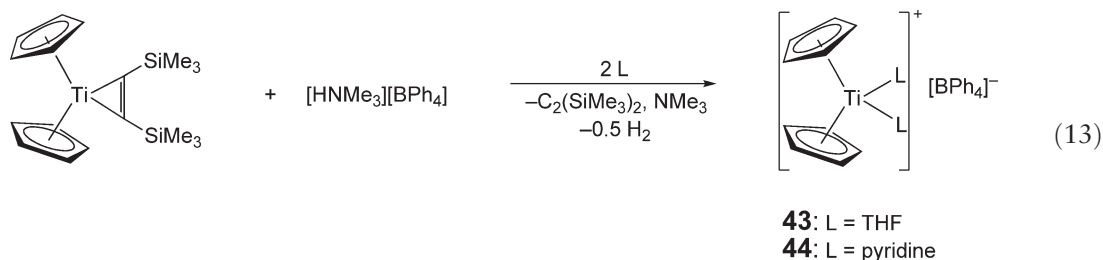
However, there have also been several studies which concluded that Ti(III) species may not be the active species in CpTiCl<sub>3</sub>- or CpTiR<sub>3</sub>-catalyzed polymerizations.<sup>37,41,42</sup> Furthermore, when Baird and co-workers treated Cp\*TiMe<sub>3</sub> with 1 equiv. of B(C<sub>6</sub>F<sub>5</sub>)<sub>3</sub> at room temperature in chlorobenzene (the identical experiment to that performed by Grassi *et al.*), it was found that only 0.01% of the titanium present is in oxidation state +III.<sup>43</sup> This led Baird to disagree with Grassi and suggest that the evidence for Ti(III) species participating as the active catalysts in polymerization using these Ti(IV) systems is ambiguous. At this stage the exact role of Ti(III) species in polymerization using complexes of the type CpTiCl<sub>3</sub> and CpTiR<sub>3</sub> is still unclear.

Several theoretical investigations of polymerization using Ti(III) half-sandwich compounds have been performed to complement the experimental studies. Cavallo and co-workers showed that when the Ti(III) cation [CpTi(CH<sub>2</sub>Ph)]<sup>+</sup> is stabilized by a benzene solvent molecule, the substitution of the benzene by styrene is exothermic by 38 kJ mol<sup>-1</sup>.<sup>44</sup> The calculated barrier for the insertion of styrene into the Ti–CH<sub>2</sub>Ph<sup>+</sup> bond is only 47 kJ mol<sup>-1</sup>, indicating that in theory this mechanism is viable. The product of the insertion reaction is stabilized by an interaction between the aromatic ring of the styrene and the metal center. Although these calculations included solvent effects, no counterions were incorporated into the model system. Therefore, in a related study, Nifant'ev *et al.* examined the effect of the counterion on the addition of styrene to [CpTi(CH<sub>2</sub>Ph)]<sup>+</sup>. They established that the weaker the nucleophilicity of the anion, the higher the exothermicity of the styrene addition to [CpTi(CH<sub>2</sub>Ph)]<sup>+</sup>[A]<sup>-</sup> ([A]<sup>-</sup> = [MeB(C<sub>6</sub>F<sub>5</sub>)<sub>3</sub>]<sup>-</sup> or [B(C<sub>6</sub>F<sub>5</sub>)<sub>4</sub>]<sup>-</sup>).<sup>45</sup>

#### 4.04.6 Bis-Cyclopentadienyl Compounds

##### 4.04.6.1 Cationic Compounds

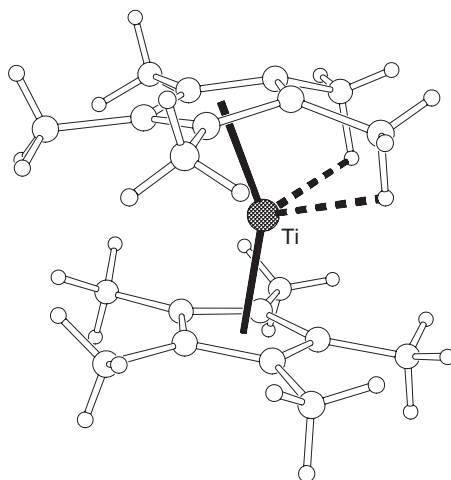
The reaction of the Ti(II) complex Cp<sub>2</sub>Ti{ $\eta^2$ -C<sub>2</sub>(SiMe<sub>3</sub>)<sub>2</sub>} with trimethylammonium tetraphenylborate in the presence of either THF or pyridine led to the one-electron oxidation of the Ti center and the formation of the paramagnetic species [Cp<sub>2</sub>TiL<sub>2</sub>][BPh<sub>4</sub>] (L = THF **43** or pyridine **44**) (Equation (13)).<sup>46</sup> Molecular hydrogen, NMe<sub>3</sub>, and the alkyne C<sub>2</sub>(SiMe<sub>3</sub>)<sub>2</sub> were produced as byproducts. The crystal structure of **44** indicated that the complex adopted a typical bent-metallocene geometry and that the Ti–N bond lengths were typical for a dative bond between a nitrogen lone pair and a Ti center.



Similar ionic compounds of the type  $[\text{Cp}_2\text{TiL}_2][\text{HB}(\text{C}_6\text{F}_5)_3]$  (L =  $\text{Et}_2\text{O}$  **45** or THF **46**) were produced through hydride abstraction reactions between  $\text{Cp}_2\text{Ti}(\mu\text{-H})_2\text{BR}_2$  (R =  $\text{C}_4\text{H}_8$ ,  $\text{C}_5\text{H}_{10}$  or  $\text{C}_8\text{H}_{14}$ ) and  $\text{B}(\text{C}_6\text{F}_5)_3$  when either diethyl ether or THF were used as the solvent.<sup>47</sup> Organic boranes of the type  $\text{HBR}_2$  were produced as the byproducts of these reactions. Dissolution of **45** in THF resulted in replacement of the ether ligands by THF and the formation of **46**. Surprisingly, dissolution of **45** in toluene also resulted in the displacement of  $\text{Et}_2\text{O}$  and the formation of a mixture of  $\text{Cp}_2\text{Ti}(\mu\text{-H})\text{B}(\text{C}_6\text{F}_5)_3(\text{OEt}_2)$  and the 15-electron complex  $\text{Cp}_2\text{Ti}(\mu\text{-H})\text{B}(\text{C}_6\text{F}_5)_3$ . The solid-state structures of **45** and **46** are closely related. The Ti–O distances are 2.231(3) and 2.275(3) Å in **45** and 2.199(1) and 2.223(2) Å in **46**. Compound **46** presumably has shorter Ti–O bond lengths than **45** because THF is a better Lewis base than  $\text{Et}_2\text{O}$ . In both compounds, the geometry around the Ti center is distorted tetrahedral.

Two different synthetic routes were used to synthesize the Ti(III) permethyl titanocene cation  $[\text{Cp}^*_2\text{Ti}][\text{BPh}_4]$  **47**.<sup>48</sup> Treatment of  $\text{Cp}^*_2\text{TiH}$  with  $[\text{Cp}_2\text{Fe}][\text{BPh}_4]$  in toluene generated **47**, ferrocene, and half an equivalent of  $\text{H}_2$ . Alternatively, compound **47** was prepared through the reaction of  $\text{Cp}^*_2\text{TiMe}$  with  $[\text{PhNMe}_2\text{H}][\text{BPh}_4]$  which also resulted in the formation of *N,N*-dimethylaniline and one equivalent of methane as byproducts. The solid-state structure of **47** showed that it contains discrete cations and anions and that there are no direct contacts between the ions. The cation in **47** adopts a bent geometry with one  $\text{Cp}^*$  ring bonded in the usual  $\eta^5$ -fashion and the other  $\text{Cp}^*$  ring bonded so that there are two C–H  $\cdots$  Ti agostic interactions between the methyl substituents on the  $\text{Cp}^*$  ring and the metal (Figure 10). These interactions cause a slippage of the  $\text{Cp}^*$  ring, and as a result, the Ti–C bond lengths to the carbons whose methyl substituents are involved in the agostic bond are shorter than the Ti–C bond lengths to the other carbon atoms of the  $\text{Cp}^*$  ring.

Compound **47** reacted with fluorobenzene to form the fluorobenzene adduct  $[\text{Cp}^*_2\text{Ti}(\eta^1\text{-FC}_6\text{H}_5)][\text{BPh}_4]$  **48**. The solid-state structure of **48** indicated that the fluorobenzene coordinates to the Ti(III) center through the fluorine atom, with a Ti–F bond length of 2.151(2) Å. Interestingly, when **47** was reacted with  $\alpha,\alpha,\alpha$ -trifluorotoluene, the C–F activation products  $\text{Cp}^*_2\text{TiF}_2$  and 1,2-diphenyl-1,1,2,2-tetrafluorotoluene were formed. This indicates that **47** is able to activate benzylic but not aromatic C–F bonds.

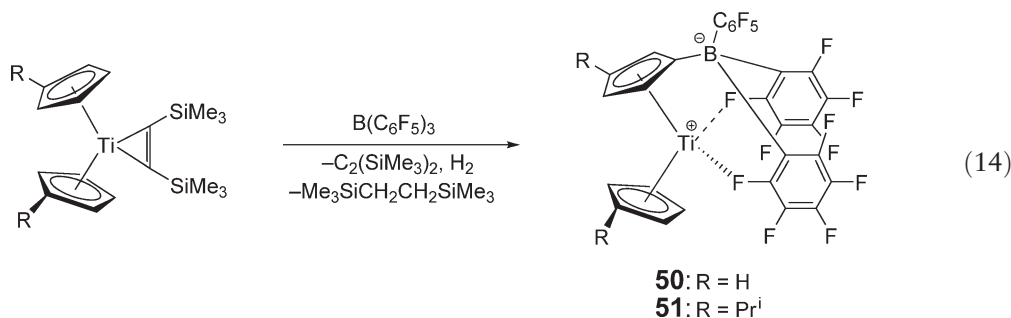


**Figure 10** X-ray structure of the  $[\text{Cp}^*_2\text{Ti}]^+$  cation of **47**.<sup>48</sup> C atoms are represented by large open spheres and H atoms by small open spheres.

Another ion pair,  $[\text{Cp}_2\text{Ti}][\text{HOB}(\text{C}_6\text{F}_5)_3]$  **49**, was prepared through the reaction of  $\text{Cp}_2\text{Ti}(\text{CO})_2$  with the borane hydrate  $\text{H}_2\text{O} \cdot \text{B}(\text{C}_6\text{F}_5)_3$ .<sup>49</sup> However, unlike compound **47**, in the solid state the  $[\text{Cp}_2\text{Ti}]^+$  cation in **49** is not naked; the Ti(III) center is coordinated to an *ortho*-fluorine atom ( $\text{Ti}-\text{F} = 2.2841(17) \text{ \AA}$ ) and to the oxygen atom of the hydroxyborate anion. The Ti–O bond length of  $2.1456(18) \text{ \AA}$  is significantly longer than a typical Ti–O  $\sigma$ -bond, as a result of the hydrogen bond to the oxygen atom. This hydrogen was not located in the Fourier difference map but its presence was unambiguously confirmed through infrared experiments using a deuterium label. The EPR spectrum of **49** in THF consisted of a single line which indicated that there was no interaction between the Ti center and an *ortho*-fluorine atom in solution, and a solvent molecule probably occupies the vacant coordination site.

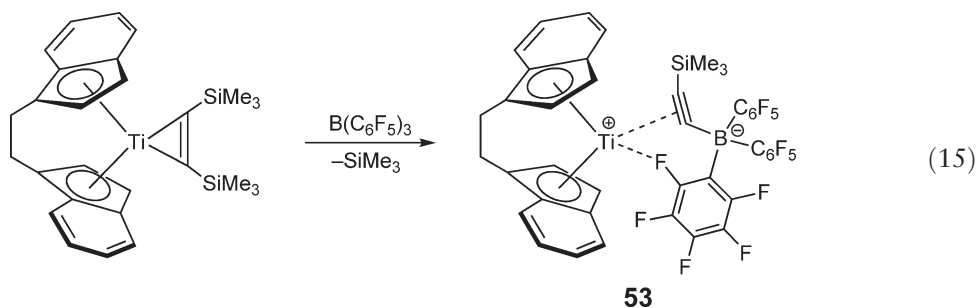
#### 4.04.6.2 Zwitterionic Compounds

The paramagnetic zwitterionic species  $\text{CpTi}\{\eta^5\text{-C}_5\text{H}_4\text{B}(\text{C}_6\text{F}_5)_3\}$  **50** was synthesized through the reaction of  $\text{Cp}_2\text{Ti}\{\eta^2\text{-C}_2(\text{SiMe}_3)_2\}$  with 1 equiv. of  $\text{B}(\text{C}_6\text{F}_5)_3$  in toluene (Equation (14)).<sup>50</sup> This reaction proceeds via an electrophilic substitution of a hydrogen atom on one of the Cp rings by a  $\text{B}(\text{C}_6\text{F}_5)_3$  molecule and half an equivalent of molecular hydrogen was liberated. An analogous reaction occurred between  $(\eta^5\text{-C}_5\text{H}_4\text{Pr}^i)_2\text{Ti}\{\eta^2\text{-C}_2(\text{SiMe}_3)_2\}$  and  $\text{B}(\text{C}_6\text{F}_5)_3$  to form  $(\eta^5\text{-C}_5\text{H}_4\text{Pr}^i)_2\text{Ti}\{\eta^5\text{-1,3-Pr}^i\text{C}_5\text{H}_3\text{B}(\text{C}_6\text{F}_5)_3\}$  **51** in which the 3-hydrogen atom of one of the  $\text{C}_5$  rings is substituted by  $\text{B}(\text{C}_6\text{F}_5)_3$  (Equation (14)).<sup>51</sup> The solid-state structures of **50** and **51** showed that in both complexes there is an interaction between the *ortho*-fluorine atoms of two  $\text{C}_6\text{F}_5$  substituents and the positively charged titanium center. The Ti–F distances are slightly shorter in **50** ( $\text{Ti}-\text{F} = 2.248(2)$  and  $2.223(3) \text{ \AA}$ ) than in **51** ( $\text{Ti}-\text{F} = 2.264(2)$  and  $2.256(2) \text{ \AA}$ ), presumably because of the decrease in the positive charge on the Ti center in **51** as a result of the electron-donating effects of the  $\text{Pr}^i$  groups. The geometry around the Ti centers in **50** and **51** are typical of bent metallocenes, although interestingly the  $\text{C}_5$  rings are eclipsed in **50** and staggered in **51**. The EPR spectrum of **51** showed that in toluene at room temperature there was no interaction between either of the *ortho*-fluorine atoms and the Ti center but at 230 K one *ortho*-fluorine appeared to coordinate. Compound **50** underwent a facile reaction with acetone to give the zwitterionic Ti(III) adduct  $\text{CpTi}\{\eta^5\text{-C}_5\text{H}_4\text{B}(\text{C}_6\text{F}_5)_3\}(\text{Me}_2\text{CO})$ .



A similar type of electrophilic substitution was observed in the reaction between  $\text{Cp}^*\text{Ti}\{\eta^2\text{-C}_2(\text{SiMe}_3)_2\}$  and  $\text{B}(\text{C}_6\text{F}_5)_3$ . In this case, a hydrogen atom from one of the methyl substituents on a single  $\text{Cp}^*$  ring was substituted by a  $\text{B}(\text{C}_6\text{F}_5)_3$  group to give the Ti(III) complex  $\text{Cp}^*\text{Ti}\{\eta^5\text{-C}_5\text{Me}_4\text{CH}_2\text{B}(\text{C}_6\text{F}_5)_3\}$  **52**.<sup>52</sup> The crystal structure of **52** showed that unlike **50** and **51** only one *ortho*-fluorine atom of the  $\text{B}(\text{C}_6\text{F}_5)_3$  group coordinates to the Ti center. The Ti–F bond of  $2.406(3) \text{ \AA}$  is considerably longer than those in **50** and **51**.

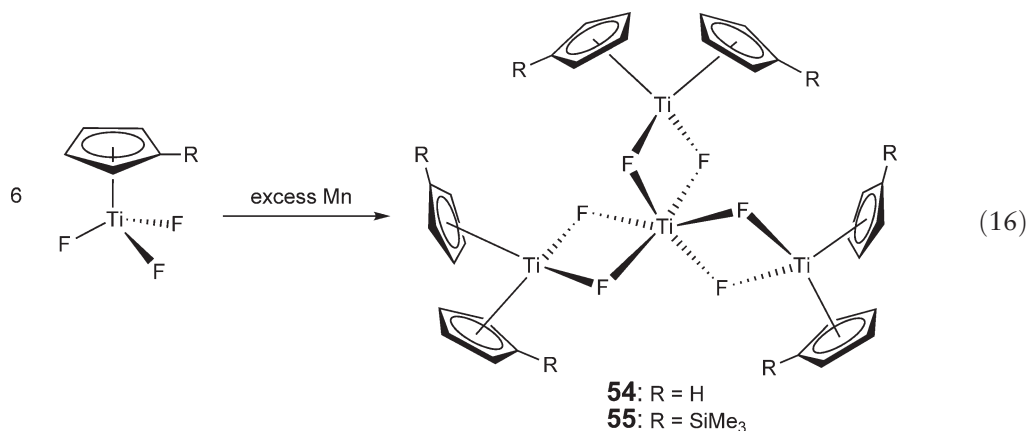
The reaction of the indenyl species  $\text{rac}(\text{BTHIE})\text{Ti}\{\eta^2\text{-C}_2(\text{SiMe}_3)_2\}$  (BTHIE = 1,2-bis(tetrahydroindenyl)ethane) with  $\text{B}(\text{C}_6\text{F}_5)_3$  was different to the reactions described above for Cp complexes.<sup>53</sup> The elimination of  $\text{C}_2(\text{SiMe}_3)_2$  and the electrophilic substitution of a hydrogen atom of the  $\text{C}_5$  ring was not observed. Instead, C–Si bond cleavage was followed by B–C bond formation, to give the zwitterionic Ti(III) complex  $\text{rac}(\text{BTHIE})\text{Ti}\{\eta^2\text{-Me}_3\text{SiC}_2\text{B}(\text{C}_6\text{F}_5)_3\}$  **53** (Equation (15)). The EPR spectrum of **53** in toluene at room temperature contained a large number of lines indicating that the unpaired electron was interacting with one or more fluorine atoms. The solid state structure of **53** confirmed that the Ti center coordinates to one *ortho*-fluorine atom. It also showed that the alkyne ligand is bound weakly to the metal center in an asymmetric fashion with one Ti–C bond significantly shorter than the other ( $\text{Ti}-\text{C}(\text{SiMe}_3) = 1.866(4)$  and  $\text{Ti}-\text{C}(\text{B}(\text{C}_6\text{F}_5)_3) = 1.617(5) \text{ \AA}$ ).



#### 4.04.6.3 Compounds with Halide Ligands

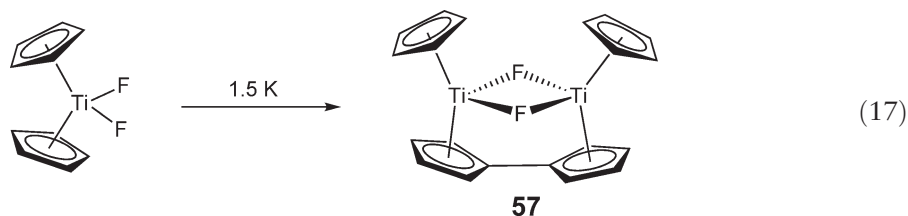
##### 4.04.6.3.1 Compounds with fluoride ligands

A mixture of the Ti(III) complexes  $\{\text{Cp}_2\text{Ti}(\mu\text{-F})_2\}_3\text{Ti}$  **54** and  $\text{Cp}_4\text{Ti}_2(\mu\text{-F})_2$  (this complex is described in COMC (1982))<sup>54</sup> were formed from the reaction of 1 equiv. of  $\text{Cp}_2\text{Ti}(\text{CO})_2$  with  $\text{Cp}_2\text{TiF}_2$ .<sup>55</sup> Complex **54** and the related complex  $\{\text{Cp}^{\text{Si}}_2\text{Ti}(\mu\text{-F})_2\}_3\text{Ti}$  ( $\text{Cp}^{\text{Si}} = \eta^5\text{-C}_5\text{H}_4\text{SiMe}_3$ ) **55** were also prepared through the reduction of  $\text{Cp}^{\text{R}}\text{TiF}_3$  ( $\text{Cp}^{\text{R}} = \text{Cp}$  or  $\text{Cp}^{\text{Si}}$ ) with activated manganese (Equation (16)).<sup>56</sup> These reactions involve the migration of a cyclopentadienyl substituent across metal centers to form a metallocene unit. The structures of **54** and **55** were elucidated by X-ray crystallography and found to be similar. Six bridging fluorine atoms coordinate to the central Ti atom to form a distorted octahedral  $\text{TiF}_6$  moiety. This results in the  $(\text{Cp}^{\text{R}}_2\text{TiF}_2)$  units being arranged in a propeller blade geometry around the central Ti atom.

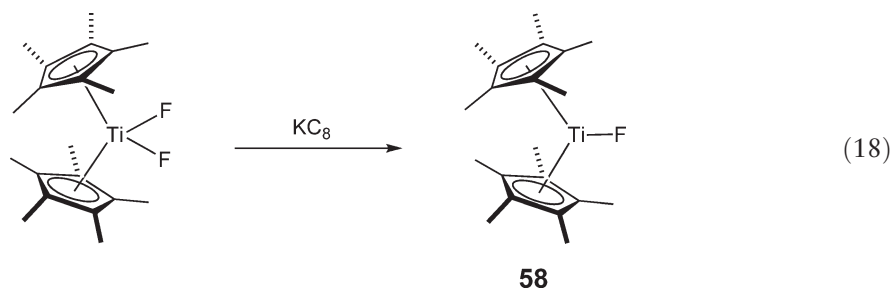


The direct reduction of  $\text{Cp}_2\text{TiF}_2$  and  $\text{Cp}'_2\text{TiF}_2$  ( $\text{Cp}' = \eta^5\text{-C}_5\text{H}_4\text{Me}$ ) with activated aluminum generated the heteronuclear Ti(III) complexes  $\{\text{Cp}_2\text{Ti}(\mu\text{-F})_2\}_3\text{Al}$  **56** and  $\{\text{Cp}'_2\text{Ti}(\mu\text{-F})_2\}_3\text{Al}$ , respectively. These compounds are analogous to **54** and **55**, except that the central Ti(III) $\text{F}_6$  unit has been replaced by Al(III) $\text{F}_6$ . The formation of the strong Al–F bonds is presumably the driving force for these reactions. A similar reaction occurred between gallium metal and  $\text{Cp}_2\text{TiF}_2$  to form  $\{\text{Cp}_2\text{Ti}(\mu\text{-F})_2\}_3\text{Ga}$ , though no reaction was observed when elemental indium was used as the reducing agent.

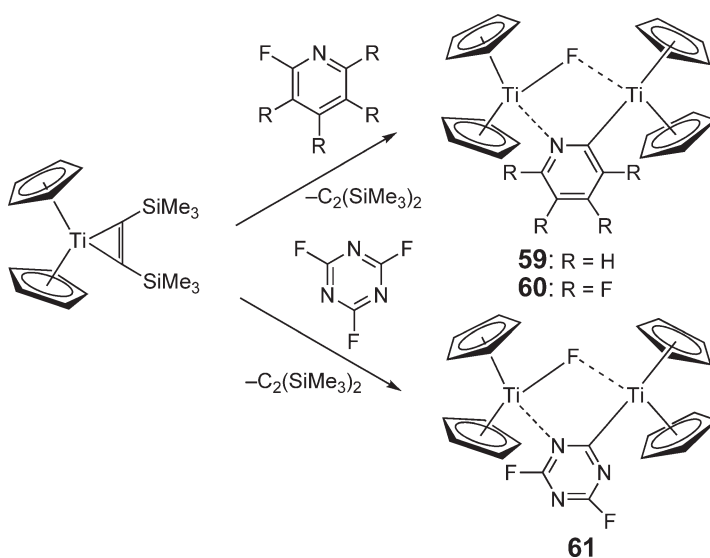
When  $\text{Cp}_2\text{TiF}_2$  was reduced using 1.5 equiv. of potassium, the dimeric Ti(III) fulvalene compound  $\text{Cp}_2\text{Ti}_2(\mu\text{-F})_2(\mu\text{-}\eta^5\text{-C}_{10}\text{H}_8)$  **57** was produced (Equation (17)).<sup>57</sup> This species is an entirely different product to **56** and demonstrates the crucial role that the choice of reducing agent plays in determining the nature of the products of the reduction of  $\text{Cp}_2\text{TiF}_2$ . Compound **57** was also prepared through the reactions of  $\text{Me}_3\text{SnF}$  with binuclear fulvene complexes of the type  $\text{Cp}_2\text{Ti}_2(\mu\text{-X})_2(\mu\text{-}\eta^5\text{-C}_{10}\text{H}_8)$  ( $\text{X} = \text{H}$  or  $\text{Cl}$ ). The structure of **57** was elucidated by X-ray crystallography and the geometry around each Ti center was distorted tetrahedral. The fulvalene ligand is folded so that the two  $\text{C}_5$  rings are not in the same plane (the dihedral angle between the two  $\text{C}_5$  rings is  $15.3(3)^\circ$ ). The average Ti–F bond length is  $2.046 \text{ \AA}$  which is comparable to the Ti–F distance in **54** (in **54**, Ti–F =  $1.975$  and  $2.094 \text{ \AA}$ ).



In contrast to the reactions described above, the reduction of the sterically bulky  $\text{Cp}^*\text{TiF}_2$  with  $\text{KC}_8$  in THF resulted in the formation of the monomeric species  $\text{Cp}^*\text{TiF}$  **58** (Equation (18)).<sup>58</sup> The EPR spectrum of **58** indicated that the complex contained an unpaired electron and hyperfine coupling to one  $^{19}\text{F}$  ( $I = 1/2$ ) nucleus was observed. The solid-state structure of **58** contained two crystallographically independent molecules which are almost identical. The geometry around the Ti center in **58** is similar to that observed in other  $\text{Cp}^*\text{TiX}$  ( $\text{X} = \text{Cl}$ ,  $\text{CH}_2\text{Bu}^t$ , and  $\text{NMePh}$ )<sup>59</sup> complexes. The  $\text{Cp}^*$  rings are staggered and the Ti–F bond lengths in the two independent molecules are 1.845(4) and 1.838(4) Å which are relatively short for Ti–F bonds.



A series of dimeric species with one bridging fluoride ligand were prepared through C–F activation reactions. The reaction of  $\text{Cp}_2\text{Ti}\{\eta^2\text{-C}_2(\text{SiMe}_3)_2\}$  with monofluoropyridine and pentafluoropyridine resulted in the formation of  $\text{Cp}_4\text{Ti}_2(\mu\text{-F})(\mu\text{-}\eta^2\text{-NC}_5\text{H}_4)$  **59** and  $\text{Cp}_4\text{Ti}_2(\mu\text{-F})(\mu\text{-}\eta^2\text{-NC}_5\text{F}_4)$  **60**, respectively (Scheme 3).<sup>60</sup> In these reactions, C–F bond activation occurs at the 2-position of the pyridine ring and a fluorine atom is transferred to the metal center. The formation of **59** is significant because a C–F bond is preferentially activated over a C–H bond. The solid-state structures of **59** and **60** are similar; in both complexes, the bridging fluoride ligand is equidistant to the two Ti



Scheme 3



centers. The pyridyl ring is situated in the same plane as the bridging fluoride, resulting in a co-planar arrangement of the five-membered metallacycle with the pyridyl ring. A similar reaction between  $\text{Cp}_2\text{Ti}\{\eta^2\text{-C}_2(\text{SiMe}_3)_2\}$  and cyanuric fluoride also resulted in C–F activation and the formation of  $\text{Cp}_4\text{Ti}_2(\mu\text{-F})(\mu\text{-}\eta^2\text{-1,3,5-N}_3\text{C}_3\text{F}_2)$  **61** which is closely related to complexes **59** and **60** (Scheme 3).

#### 4.04.6.3.2 Compounds with chloride ligands

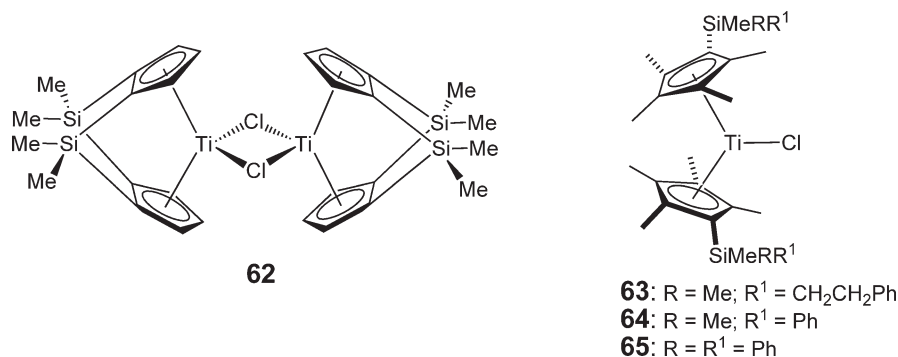
The bis-cyclopentadienyl titanium chloride  $\text{Cp}_2\text{TiCl}$  (mentioned in both COMC (1982) and COMC (1995)) is a chloride-bridged dimer in the solid state and present in both monomeric and dimeric forms in solution.<sup>54,59</sup> When it is used as a catalyst for organic transformations,  $\text{Cp}_2\text{TiCl}$  is often prepared *in situ*. It is generally synthesized either through metathesis reactions between  $\text{TiCl}_3$  and  $\text{TiCp}$  or through the facile reduction of  $\text{Cp}_2\text{TiCl}_2$  with metals such as zinc, aluminum, or manganese. However, the exact nature of the Ti(III) species present in solution is not always clear.

In order to investigate this problem, Daasbjerg and co-workers performed an electrochemical study into the reduction of  $\text{Cp}_2\text{TiX}_2$  (X = Cl, Br, or I) in THF.<sup>61</sup> It was established that in electrochemically reduced solutions of  $\text{Cp}_2\text{TiX}_2$ ,  $[\text{CpTiX}_2]^-$  was the major constituent when X = Cl, but  $\text{Cp}_2\text{TiX}$  and  $\text{Cp}_4\text{Ti}_2(\mu\text{-X})_2$  were the major products when X = Br or I. However, the same researchers subsequently showed that the reduction of  $\text{Cp}_2\text{TiCl}_2$  with zinc, aluminum, or manganese in THF led to a mixture of  $\text{Cp}_2\text{TiCl}$  and  $\text{Cp}_4\text{Ti}_2(\mu\text{-Cl})_2$  and only small quantities of  $[\text{CpTiX}_2]^-$  were present in solution.<sup>62</sup> A related kinetic study showed that the complexes  $\text{Cp}_2\text{TiX}$  and  $\text{Cp}_4\text{Ti}_2(\mu\text{-X})_2$  were the most reactive species with benzyl chloride. Surprisingly, even for X = Cl,  $[\text{CpTiX}_2]^-$  was not very reactive with benzyl chloride. These results suggest that in organic transformations  $\text{Cp}_2\text{TiCl}$  and  $\text{Cp}_4\text{Ti}_2(\mu\text{-Cl})_2$  are responsible for product formation.

A separate EPR study showed that the electrolytic reduction of  $\text{Cp}_2\text{TiX}_2$  (X = Cl or Br) in THF in the presence of  $\text{PMe}_3$  afforded Ti(III) species of the type  $\text{Cp}_2\text{TiX}(\text{PMe}_3)$ .<sup>63</sup> When these reductions were carried out in the presence of more sterically demanding phosphines such as  $\text{PEt}_3$  or  $\text{PPh}_3$ , no coordination was observed. The mechanism of these reactions is thought to involve the initial formation of the reduced dichloride complex  $[\text{Cp}_2\text{TiCl}_2]^-$ . This complex then loses  $\text{Cl}^-$  and forms the transient solvated species  $\text{Cp}_2\text{TiCl}(\text{THF})$ . The coordinated THF molecule is substituted by  $\text{PMe}_3$  to generate  $\text{Cp}_2\text{TiCl}(\text{PMe}_3)$ .

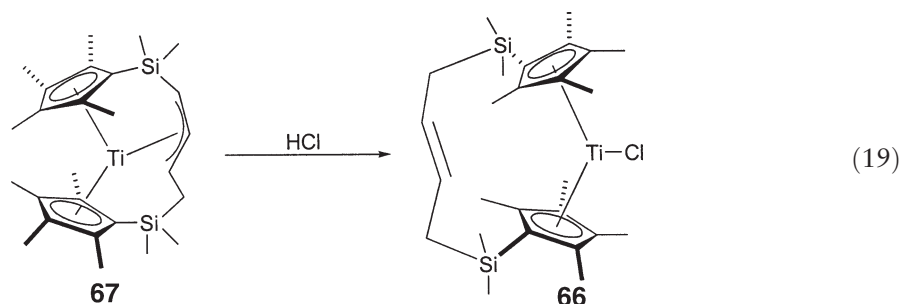
It was noted in COMC (1995) that bis-cyclopentadienyl Ti(III) chlorides with large substituents on the carbon atoms of the  $\text{C}_5$  ring are likely to be monomeric while those with small Cp substituents are likely to be chloride-bridged dimers.<sup>59</sup> Results since the publication of COMC(1995) support this observation. Reduction of the doubly bridged *ansa*-titanocene  $\{(\text{SiMe}_2)_2(\eta^5\text{-C}_5\text{H}_3)_2\}\text{TiCl}_2$  with 1 equiv. of sodium amalgam resulted in the formation of the dimeric species  $\{(\text{SiMe}_2)_2(\eta^5\text{-C}_5\text{H}_3)_2\}_2\text{Ti}_2(\mu\text{-Cl})_2$  **62** (Figure 11).<sup>64</sup> In contrast, the monomeric Ti(III) titanocenes  $(\eta^5\text{-C}_5\text{Me}_4\text{R})_2\text{TiCl}$  (R =  $\text{SiMe}_2\text{CH}_2\text{CH}_2\text{Ph}$  **63**,  $\text{SiMe}_2\text{Ph}$  **64**,  $\text{SiMePh}_2$  **65**) were synthesized when the fully substituted titanocene dichlorides  $(\eta^5\text{-C}_5\text{Me}_4\text{R})_2\text{TiCl}_2$  were reduced with magnesium turnings.<sup>65</sup> Compound **64** was crystallographically characterized. The geometry around the Ti center is pseudo-trigonal planar. The  $\text{C}_5$  rings adopt a staggered configuration with the  $\text{SiMe}_2\text{Ph}$  substituents orientated away from the metal center.

The monomeric titanocene(III) chloride *ansa*- $\{\eta^5, \eta^5\text{-C}_5\text{Me}_4\text{SiMe}_2\text{CH}_2\text{CH}=\text{CHCH}_2\text{SiMe}_2\text{C}_5\text{Me}_4\}\text{TiCl}$  **66**, which is related to **63–65**, was prepared through the reaction of the Ti(III) allyl species **67** (see Section 4.04.6.6, Equation (30)) with HCl (Equation (19)).<sup>66</sup> The formation of the *trans*-double bond in the center of the bridge between the  $\text{C}_5$  ligands in **66** was both stereo- and regio-selective, although products related to the cleavage of Si–C bonds were also formed



**Figure 11** Monomeric and dimeric bis-cyclopentadienyl Ti(III) chloride complexes.

during the reaction. The structure of **66** was elucidated by X-ray crystallography and revealed that the titanocene skeleton is similar to that in  $\text{Cp}^*\text{TiCl}$ . Compound **66** was oxidized by  $\text{AgCl}_2$  to form the Ti(IV) dichloride *ansa*- $\{\eta^5, \eta^5\text{-C}_5\text{Me}_4\text{SiMe}_2\text{CH}_2\text{CH}=\text{CHCH}_2\text{SiMe}_2\text{C}_5\text{Me}_4\}\text{TiCl}_2$ .

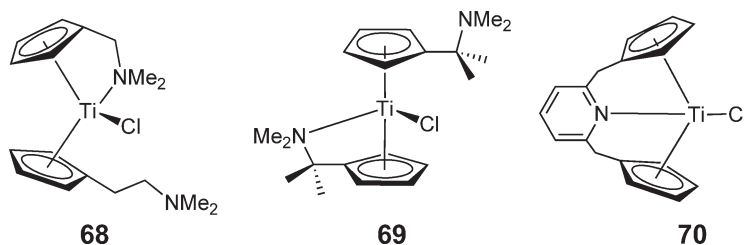


A number of bis-cyclopentadienyl Ti(III) chloride compounds containing amine moieties attached to the cyclopentadienyl rings have been prepared, **68–70** (Figure 12).<sup>67–69</sup> These complexes were made from either  $\text{TiCl}_3$  or  $\text{TiCl}_3(\text{THF})_3$  and the appropriate lithiated ligand. The solid-state structures of both **68** and **69** showed that only one nitrogen arm coordinates to the metal center in these species. The Ti–N bond lengths are 2.428(9) Å in **68** and 2.420(2) Å in **69**.

An unusual reaction occurred between the Ti(IV) precursor  $\text{Cp}_2\text{TiCl}_2$  and 2 equiv. of  $\text{Bu}^t\text{P-P}(\text{Li})\text{-PBu}^t$ .<sup>70</sup> The observed products were the Ti(III) species  $\text{Cp}_2\text{Ti}(\mu\text{-Cl})_2\text{Li}(\text{THF})_2$  **71**,  $\text{Cp}_4\text{Ti}_2(\mu\text{-Cl})_2$  **72**, and the diphosphine  $(\text{Bu}^t\text{P})_2\text{P-P}(\text{PBu}^t)_2$ . A similar reaction between  $\text{Cp}_2\text{TiCl}_2$  and 2 equiv. of  $\text{Bu}^t\text{P-P}(\text{SiMe}_3)\text{Li}$  also resulted in the formation of compounds **71** and **72** and the diphosphine  $(\text{Bu}^t\text{P-PSiMe}_3)_2$ . Both of the diphosphines were unstable and decomposed into a mixture of different species. However, compound **71** was sufficiently stable to be crystallographically characterized. The geometry around the metal center is distorted tetrahedral and the Ti–Cl bond lengths are 2.5527(9) and 2.5339(8) Å. Interestingly, when  $\text{Cp}_2\text{TiCl}_2$  or  $\text{Cp}(\text{Cp}^*)\text{TiCl}_2$  were reacted with  $\text{Bu}^n\text{Li}$  in the presence of  $\text{Bu}^t\text{P-P}(\text{SiMe}_3)_2$ , the products were the Ti(III) fulvalene complexes  $\text{Cp}_2\text{Ti}_2(\mu\text{-Cl})_2(\mu\text{-}\eta^5, \eta^5\text{-C}_{10}\text{H}_8)$  and  $\text{Cp}^*\text{Ti}_2(\mu\text{-Cl})_2(\mu\text{-}\eta^5, \eta^5\text{-C}_{10}\text{H}_8)$ . At this stage, it is unclear what causes this difference in reactivity.

#### 4.04.6.3.3 Compounds with iodide ligands

The preparation of a number of bis-cyclopentadienyl Ti(III) complexes with iodide-supporting ligands is documented in both COMC(1982) and COMC(1995). Recently, Marks *et al.* prepared the complex  $\text{Cp}^{\text{tt}}_2\text{TiI}$  ( $\text{Cp}^{\text{tt}} = \eta^5\text{-1,3-C}_5\text{H}_3\text{Bu}_2$ ) **73** as part of a study into metal–ligand  $\sigma$ -bond enthalpies in group 4 metallocenes.<sup>71</sup> This species was formed from the reaction of  $\text{Cp}^{\text{tt}}_2\text{TiCl}$  with a 10 fold excess of LiI. Simple metathesis reactions between  $\text{Cp}^{\text{tt}}_2\text{TiCl}$  and reagents such as MeLi were unsuccessful due to the bulkiness of the  $\text{Cp}^{\text{tt}}$  ancillary ligand. The solid-state structure of  $\text{Cp}^{\text{tt}}_2\text{TiI}$  was not established but the structures of the related species  $\text{Cp}^{\text{tt}}_2\text{ZrI}$  and  $\text{Cp}^{\text{tt}}_2\text{HfI}$  were determined.<sup>3</sup> The enthalpy of reaction for the addition of  $\text{I}_2$  to  $\text{Cp}^{\text{tt}}_2\text{TiI}$  to form the Ti(IV) species  $\text{Cp}^{\text{tt}}_2\text{TiI}_2$  is 11.7(8) kcal mol<sup>−1</sup> less exothermic than the enthalpy of reaction for the corresponding reaction between  $\text{Cp}^*\text{TiI}$  and  $\text{I}_2$  to form  $\text{Cp}^*\text{TiI}_2$  (Table 1). The relative bond dissociation energies indicate that it requires more energy to remove an iodine ligand from  $\text{Cp}^*\text{TiI}_2$  than from **73**. This difference is attributed to the increased size of  $\text{Cp}^{\text{tt}}$  compared to  $\text{Cp}^*$  which results in a weakening of the Ti–I bond to minimize steric repulsions. Similar experiments established that the bond reaction enthalpies increase down group 4 for the reaction of  $\text{Cp}^{\text{tt}}_2\text{MI}$  with  $1/2 \text{I}_2$  (M = Ti, Zr, or Hf).



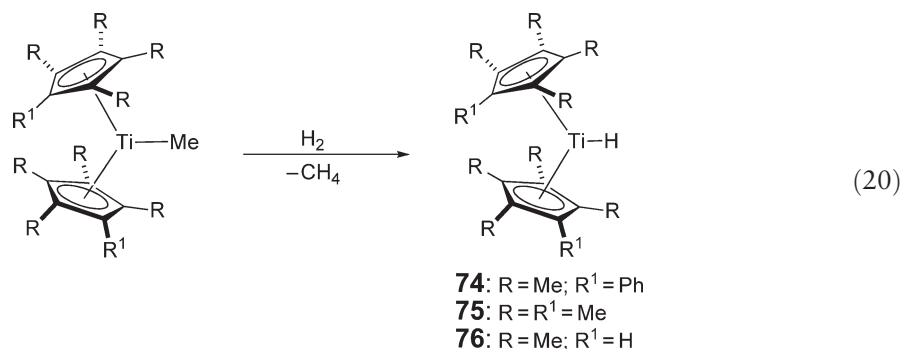
**Figure 12** Amine-supported bis-cyclopentadienyl Ti(III) chloride complexes.

**Table 1** Enthalpies of metallocene iodination (for the reaction  $\text{Cp}^{\text{R}}_2\text{Ml} + 1/2\text{I}_2 \rightarrow \text{Cp}^{\text{R}}_2\text{MlI}_2$  ( $\text{M} = \text{Ti}, \text{Zr}, \text{or Hf}$ ;  $\text{Cp}^{\text{R}} = \text{Cp}^{\text{tt}}$  or  $\text{Cp}^*$ )) and derived metal–ligand bond enthalpies<sup>71</sup>

Compound	$\Delta H_{\text{rxn}}$ (kcal mol <sup>−1</sup> )	$D(L_{\text{M}}\text{M}(\text{I})-\text{I})$ (kcal mol <sup>−1</sup> )
$\text{Cp}^*_2\text{TiI}$	−34.5(6)	40.6(5)
$\text{Cp}^{\text{tt}}_2\text{TiI}$ <b>73</b>	−22.8(5)	52.3(6)
$\text{Cp}^{\text{tt}}_2\text{ZrI}$	−40.2(5)	58.0(5)
$\text{Cp}^{\text{tt}}_2\text{HfI}$	−43.4(4)	61.2(4)

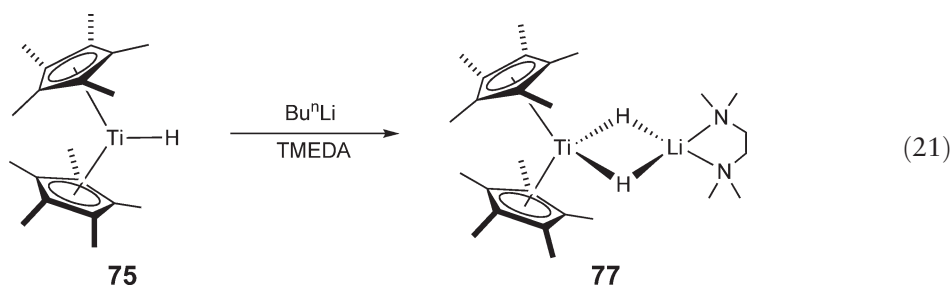
#### 4.04.6.4 Compounds with Hydride Ligands

The monomeric Ti(III) hydride species  $\text{Cp}^{\text{R}}_2\text{TiH}$  ( $\text{Cp}^{\text{R}} = \eta^5\text{-C}_5\text{PhMe}_4$  **74**,  $\text{Cp}^*$  **75**, and  $\eta^5\text{-C}_5\text{HMe}_4$  **76**) were all prepared through reactions between  $\text{H}_2$  and  $\text{Cp}^{\text{R}}_2\text{TiMe}$  (Equation (20)).<sup>72–74</sup> The EPR spectra of all three compounds were consistent with the presence of an unpaired electron and compounds **74** and **75** were crystallographically characterized. The structures of **74** and **75** are closely related and the  $\text{C}_5^{\text{R}}$  rings in both complexes are staggered. The most interesting structural feature of compounds **74** and **75** is the large (ring centroid)–Ti–(ring centroid) angles of 151° in **74** and 150° in **75**. This is evidently a reflection of the small size of the hydride ligand and also minimizes steric strain between the substituents on the back of the  $\text{C}_5$  rings.

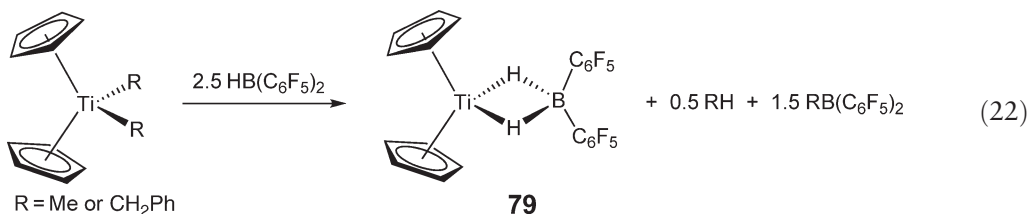


Thermolysis of **75** resulted in the activation of a methyl hydrogen on the  $\text{Cp}^*$  ring and the formation of the fulvene species  $\text{Cp}^*\text{Ti}(\eta^6\text{-C}_5\text{Me}_4\text{CH}_2)$ . Similarly, thermolysis of **74** also led to the activation of a methyl hydrogen on the  $\text{Cp}^*$  ring and gave a mixture of the isomers  $(\eta^5\text{-C}_5\text{PhMe}_4)\text{Ti}(\eta^6\text{-C}_5\text{-1-CH}_2\text{-2-Ph-3,4,5-Me}_3)$  and  $(\eta^5\text{-C}_5\text{PhMe}_4)\text{Ti}(\eta^6\text{-C}_5\text{-1-CH}_2\text{-3-Ph-2,4,5-Me}_2)$ . No activation of the phenyl hydrogens of the  $\text{C}_5\text{PhMe}_4$  ligand was observed. Although **74** and **75** are stable under an atmosphere of dinitrogen, compound **76** reacts with  $\text{N}_2$  to form the dimeric Ti(II) dinitrogen complex  $(\eta^5\text{-C}_5\text{HMe}_4)_2\text{Ti}_2(\mu\text{-N}_2)$ . The unusual reactivity of **76** compared to **74** and **75** is probably due to differences in the electronic properties of the three compounds; the Ti center in **76** is slightly more Lewis acidic than that in either **74** or **75**. Oxidation of compounds **74** and **75** with  $\text{PbCl}_2$  generated the Ti(IV) hydridochlorides  $(\eta^5\text{-C}_5\text{PhMe}_4)_2\text{Ti}(\text{H})\text{Cl}$  and  $\text{Cp}^*_2\text{Ti}(\text{H})\text{Cl}$ , respectively.

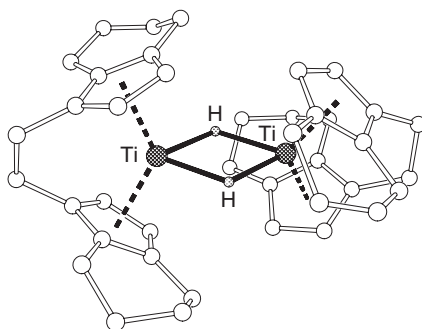
The unusual anionic Ti(III) dihydride  $\text{Cp}^*_2\text{Ti}(\mu\text{-H})_2\text{Li}(\text{TMEDA})$  **77** was prepared through the reaction of  $\text{Bu}^n\text{Li}$  and TMEDA with **75** (Equation (21)).<sup>74</sup> It was also demonstrated that **77** could be prepared through the reaction of  $\{\text{Li}(\text{TMEDA})\}_2\text{C}_{10}\text{H}_8$  with  $\text{Cp}^*_2\text{TiCl}$ . The solid-state structure of **77** indicated that the geometries of both the  $\text{Cp}^*_2\text{Ti}$  and  $\text{Li}(\text{TMEDA})$  units are not unusual. Although the hydride atoms were not located in the difference Fourier map, EPR spectroscopy showed that the trivalent titanium center contained an unpaired electron and was coupled to two equivalent hydrogen nuclei. As a result, **77** was characterized as an anionic dihydride with symmetrically bridging hydrides. It was proposed that **77** is formed by  $\beta$ -hydride elimination from the intermediate  $\text{Cp}^*_2\text{TiH}(\text{Bu}^n)^-$  which is generated from the addition of  $\text{Bu}^n\text{Li}$  to **75**.



As part of a study into metal-catalyzed hydroboration, He and Hartwig isolated the  $\eta^2$ -hydridoborate  $\text{Cp}_2\text{Ti}(\eta^2\text{-H}_2\text{BO}_2\text{C}_6\text{H}_4)$  **78** from the reaction of  $\text{Cp}_2\text{TiMe}_2$  with  $\text{HBO}_2\text{C}_6\text{H}_4$  in the presence of 1-hexene.<sup>75</sup> Compound **78** was characterized primarily on the basis of its EPR spectrum which consisted of a single broad line with no hyperfine coupling. Subsequently, Piers and co-workers synthesized the related compound  $\text{Cp}_2\text{Ti}\{\eta^2\text{-H}_2\text{B}(\text{C}_6\text{F}_5)_2\}$  **79** through the reactions of  $\text{Cp}_2\text{TiR}_2$  ( $\text{R} = \text{Me}$  or  $\text{CH}_2\text{Ph}$ ) with 2.5 equiv. of  $\text{HB}(\text{C}_6\text{F}_5)_2$  (Equation (22)).<sup>76</sup> The byproducts of this reaction were 0.5 equiv. of  $\text{RH}$  and 1.5 equiv. of  $\text{RB}(\text{C}_6\text{F}_5)_2$ . The EPR spectrum of **79** was similar to that of **78** and consisted of a single broad line. Compound **79** was also crystallographically characterized, and although the hydrogen atoms were not refined (they were located in the Fourier difference map), it is clear that the  $[\text{H}_2\text{B}(\text{C}_6\text{F}_5)_2]^-$  ligand was coordinated in an  $\eta^2$ -fashion. The geometry around both the central Ti and B atoms is distorted tetrahedral.



One of the first structurally characterized titanocene(III) hydrides without an additional bridging ligand was the dimeric compound  $\text{rac}(\eta^5, \eta^5\text{-BTHIE})_2\text{Ti}_2(\mu\text{-H})_2$  (BTHIE = 1,2-bis(tetrahydroindenyl)ethane **80**) (Figure 13).<sup>77</sup> Compound **80** was synthesized from the reaction of the Ti(IV) species (BTHIE)/ $\text{TiMe}_2$  with an organosilane in a toluene/hexane solution. The structure of **80** was elucidated by X-ray diffraction which revealed that the unit cell consists of two pairs of the racemic  $R,R$  and  $S,S$  molecules. The hydride bridges are symmetrical and the Ti–H bond length is 1.90(3) Å. There is substantial rotation of the two planes formed by each pair of centroids of the  $\text{C}_5$  rings and Ti with respect to each other. This dihedral angle is normally 0° in complexes of the type  $\text{Cp}_4\text{Ti}_2(\mu\text{-X})_2$  but is 53° in **80**. The EPR spectrum of **80** in frozen toluene consisted of six lines and is typical of a triplet state. The triplet state arises as a result of exchange between the two Ti(III) centers. The distance between the two titanium centers was



**Figure 13** X-ray structure of an  $S,S$  molecule of **80**.<sup>77</sup> C atoms are represented by open spheres and carbon-bound H atoms omitted for clarity.

calculated as 3.39 Å from the dipolar components of the zero-field splitting parameters which is quite close to the experimental value of 3.2288(13) Å.

#### 4.04.6.5 Compounds with Alkyl Ligands

A description of the synthesis of the paramagnetic fulvene complex  $\text{Cp}^*(\eta^1, \eta^5\text{-Fv})\text{Ti}$  **81** (Fv = tetramethylfulvene) is given in COMC (1995).<sup>59</sup> Previously, it has been reported that the fulvene moiety is coordinated to the metal center in a  $\pi\text{-}\eta^6, \sigma\text{-}\eta^1$ -fashion on the basis of magnetic, spectroscopic, and thermochemical data. Recently, Piers and co-workers reported the solid-state structure of **81** (Figure 14) and confirmed that the fulvene ligand binds as a dianionic  $\pi\text{-}\eta^6, \sigma\text{-}\eta^1$ -ligand rather than as a neutral  $\pi\text{-}\eta^6$ -ligand.<sup>78</sup> The distance between the Ti center and the metallated carbon is 2.281(14) Å which is comparable to the Ti–C<sub>alkyl</sub> distance in  $\text{Cp}^*_2\text{TiCH}_2\text{Bu}^+$  (Ti–C = 2.231(5) Å).

The Ti(III) alkyl species **82** and **83** were synthesized through the reaction of  $\text{Cp}_2\text{TiCl}_2$  with bis(2-methoxymethylphenyl)magnesium and bis(2-*N,N*-dimethylaminomethylphenyl)magnesium, respectively (Scheme 4).<sup>79</sup> These reactions proceeded through Ti(IV) intermediates which underwent radical cleavage to give compound **82** or **83** and half an equivalent of the free ligand dimer. The solid-state structure of **82** showed that the geometry around the Ti center is distorted tetrahedral with the oxygen atom of the methoxy group clearly coordinating to the metal center. The Ti–O bond length is 2.200(3) Å which is typical for a dative bond between titanium and oxygen.

An unusual reaction was observed between  $(\eta^5\text{-C}_5\text{Me}_4\text{SiMe}_3)_2\text{TiCl}_2$  and Mg in the presence of bis(trimethylsilyl)acetylene (Equation (23)).<sup>80</sup> The paramagnetic Ti(III) species **84** was formed in 75% yield along with a small amount (10%) of the mixed metal Ti(III) hydride complex **85** (for an alternative synthesis and the crystal structure of **85**, see Section 4.04.6.10). This reaction is interesting because the analogous reactions between  $(\text{C}_5\text{H}_n\text{Me}_{5-n})_2\text{TiCl}_2$  ( $n = 0\text{--}5$ ), Mg, and bis(trimethylsilyl)acetylene give diamagnetic Ti(II) complexes of the type  $(\text{C}_5\text{H}_n\text{Me}_{5-n})_2\text{Ti}\{\eta^2\text{-C}_2(\text{SiMe}_3)_2\}$  in quantitative yields. In this case, the expected product  $(\eta^5\text{-C}_5\text{Me}_4\text{SiMe}_3)_2\text{Ti}\{\eta^2\text{-C}_2(\text{SiMe}_3)_2\}$  was believed to form as an intermediate and then underwent further reaction with Mg to form **84**. The formation of **84** clearly involves the abstraction of a hydrogen atom from an SiMe<sub>3</sub> group on one of the  $\eta^5\text{-C}_5\text{Me}_4\text{SiMe}_3$  rings and the formation of a  $\sigma$ -bond between the Ti center and the dimethylsilylene fragment through a bridging methylene group.

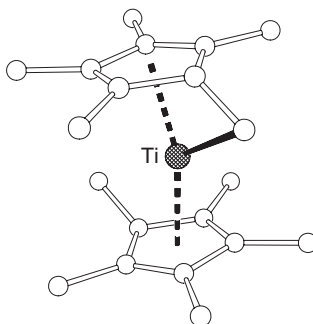
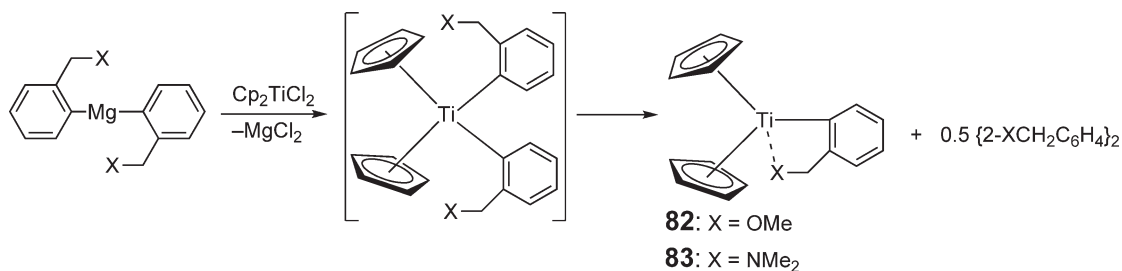
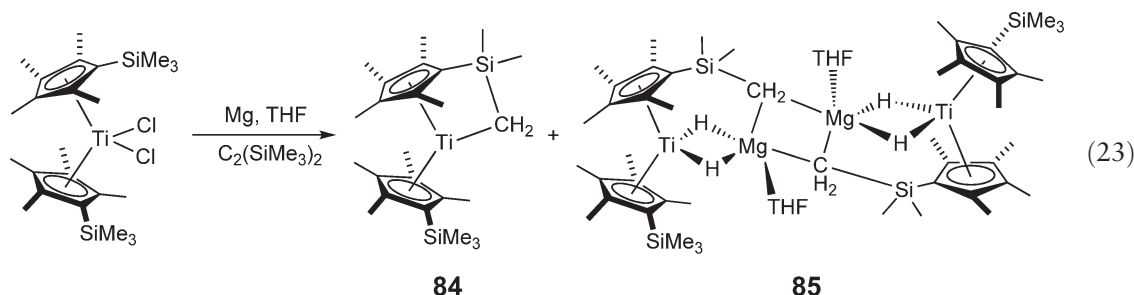


Figure 14 X-ray structure of **81**.<sup>78</sup> C atoms are represented by open spheres and H atoms omitted for clarity.

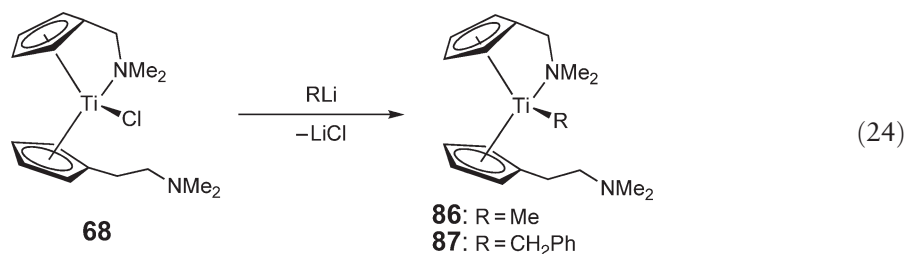


Scheme 4

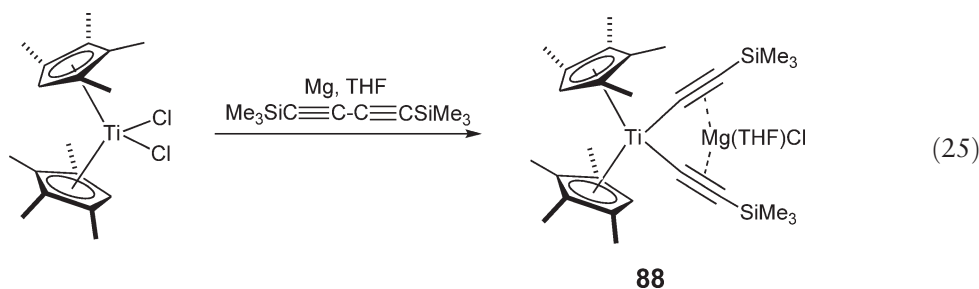
At this stage, it is unclear why compound **85** is also formed during the reaction. Compound **84** was characterized by X-ray crystallography and it was established that the Ti–C  $\sigma$ -bond length is 2.204(5) Å, which is in range generally observed for Ti(III)–alkyl bond lengths.



Instead of using a Ti(IV) starting material, Jutzi and Kleimeier utilised a Ti(III) precursor to synthesize two Ti(III) alkyl species, **86** and **87**, through the alkylation of the Ti(III) monochloride species **68** (Figure 12) with either MeLi or PhCH<sub>2</sub>Li (Equation (24)).<sup>67</sup> The EPR spectra of both these complexes were consistent with the presence of one unpaired electron. Although **86** and **87** were not crystallographically characterized, the authors proposed that only one pendant amine arm from the two C<sub>5</sub> ligands coordinates to the metal center.

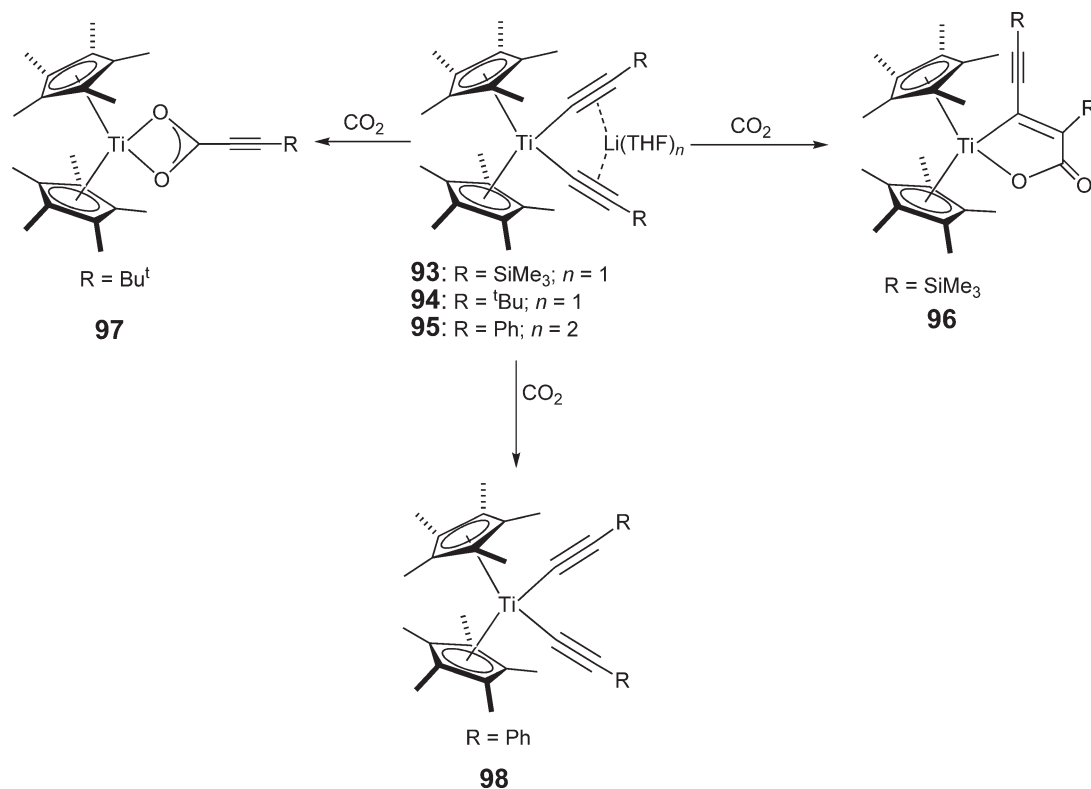


The first titanocene “tweezer” compound  $(\eta^5-C_5HMe_4)_2Ti(\eta^1-C\equiv CSiMe_3)_2Mg(THF)Cl$  **88** was generated through the reduction of  $(\eta^5-C_5HMe_4)_2TiCl_2$  with Mg in the presence of THF and  $Me_3SiC\equiv CC\equiv CSiMe_3$  (Equation (25)).<sup>81</sup> The initial step in the formation of **88** is the reduction of  $(\eta^5-C_5HMe_4)_2TiCl_2$  to the Ti(III) species  $(\eta^5-C_5HMe_4)_2TiCl$  which was detected by EPR spectroscopy. The exact mechanism for the conversion of  $(\eta^5-C_5HMe_4)_2TiCl$  to **88** is unclear but the authors proposed that a transient Ti(II) species is formed which consists of  $MgCl(THF)$  and  $Me_3SiC\equiv CC\equiv CSiMe_3$  coordinated to  $(\eta^5-C_5HMe_4)_2Ti$ . The C–C bond in  $Me_3SiC\equiv CC\equiv CSiMe_3$  then ruptures leading to a rearrangement which results in the formation of **88**. The solid state structure of **88** indicated that the central Ti atom is  $\sigma$ -bonded to two (trimethylsilyl)acetylide groups. The pseudo-tetrahedral Mg atom was located between the acetylide ligands and is  $\pi$ -bonded to the alkyne groups.



After the initial synthesis of **88**, the related alkali metal “tweezer” complexes  $(\eta^5\text{-C}_5\text{HMe}_4)_2\text{Ti}(\eta^1\text{-C}\equiv\text{CSiMe}_3)_2\text{M}$  ( $\text{M} = \text{Li}$  **89**,  $\text{Na}$  **90**,  $\text{K}$  **91**, or  $\text{Cs}$  **92**) were prepared through a redox reaction between the  $\text{Ti(IV)}$  compound  $(\eta^5\text{-C}_5\text{HMe}_4)_2\text{Ti}(\eta^1\text{-C}\equiv\text{CSiMe}_3)_2$  and the appropriate alkali metal.<sup>82</sup> The EPR spectra of **89–92** consisted of a narrow single line with satellites due to coupling to spin-active isotopes of titanium. The approximately equal components of the  $g$ -tensor of rhombic symmetry and the low anisotropy for **89–92** indicated that the unpaired  $d^1$  electron was delocalized over the organic ligands, including the acetylide fragments. Only **92** showed an interaction between the unpaired electron and the alkali metal. Compound **91** was crystallographically characterized and is polymeric in the solid state. The potassium ion is  $\pi$ -bonded to the two acetylide ligands and also weakly  $\eta^5$ -coordinated to a  $\text{C}_5$  ring on an adjoining molecule. The bonding within each individual molecule is similar to that observed in **88**.

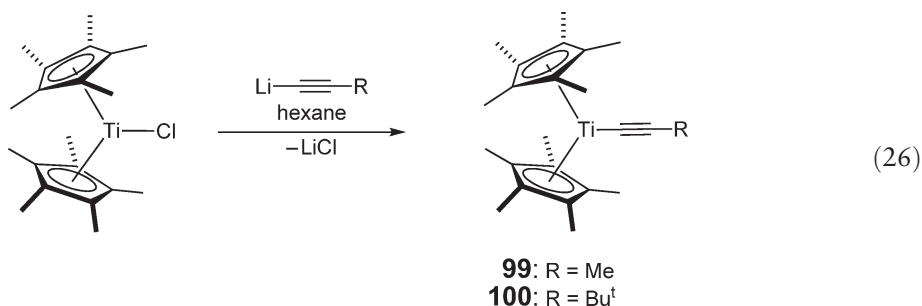
It was also shown that  $\text{Ti(III)}$  tweezer compounds could be prepared through the reaction of lithium acetylides with  $\text{Cp}_2\text{TiCl}$  or  $\text{Cp}^*_2\text{TiCl}$ . Mach *et al.*<sup>82</sup> demonstrated that the reaction of  $(\eta^5\text{-C}_5\text{HMe}_4)_2\text{TiCl}$  with  $\text{LiC}\equiv\text{CC}\equiv\text{CSiMe}_3$  in THF formed the bis-diyndyl species  $(\eta^5\text{-C}_5\text{HMe}_4)_2\text{Ti}(\eta^1\text{-C}\equiv\text{CC}\equiv\text{CSiMe}_3)_2\text{Li}(\text{THF})_2$ . Rosenthal and co-workers subsequently showed that complexes of the type  $\text{Cp}^*_2\text{Ti}(\text{C}\equiv\text{CR})_2\text{Li}(\text{THF})_n$  ( $\text{R} = \text{SiMe}_3$ ,  $n = 1$  **93**;  $\text{R} = \text{Bu}^t$ ,  $n = 1$  **94**;  $\text{R} = \text{Ph}$ ,  $n = 2$  **95**) were formed from the reaction of  $\text{LiC}\equiv\text{CR}$  with  $\text{Cp}^*_2\text{TiCl}$  in THF.<sup>82</sup> Compounds **93–95** all reacted differently with  $\text{CO}_2$  (Scheme 5). The reaction of **93** with  $\text{CO}_2$  generated the  $\text{Ti(IV)}$  titanafuranone **96**. This complex presumably forms as a result of an insertion of  $\text{CO}_2$  into the  $\eta^2$ -butadiyne species  $\text{Cp}^*_2\text{Ti}(\eta^2\text{-Me}_3\text{SiC}\equiv\text{CC}\equiv\text{CSiMe}_3)$  which is generated as a result of a C–C coupling reaction between the two acetylide ligands of **93**. In contrast, the reaction between  $\text{CO}_2$  and **94** yielded the carboxylate species  $\text{Cp}^*_2\text{Ti}(\text{O}_2\text{CC}\equiv\text{CBu}^t)$  **97**. It is proposed that **97** forms as a result of  $\text{CO}_2$  insertion into the  $\text{Ti–C}$  bond of the  $\text{Ti(III)}$  intermediate  $\text{Cp}^*_2\text{Ti}(\text{C}\equiv\text{CBu}^t)$  which is generated by the decooordination of an acetylide ligand from **94**. Surprisingly, the reaction of **95** with  $\text{CO}_2$  led to neither C–C coupling of the acetylide ligands nor insertion of  $\text{CO}_2$ , instead, a simple oxidation of the metal center occurred and the  $\text{Ti(IV)}$  bis-acetylide complex  $\text{Cp}^*_2\text{Ti}(\text{C}\equiv\text{CPh})_2$  **98** was formed.



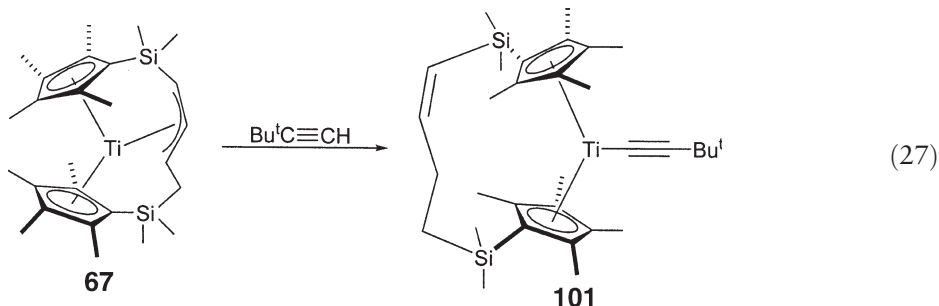
Scheme 5



When  $\text{LiC}\equiv\text{CMe}$  or  $\text{LiC}\equiv\text{CBu}^t$  were reacted with  $\text{Cp}^*_2\text{TiCl}$  in hexane, tweezer-type compounds did not form. Instead, the mono( $\sigma$ -alkynyl) species  $\text{Cp}^*_2\text{Ti}(\text{C}\equiv\text{CMe})$  **99** and  $\text{Cp}^*_2\text{Ti}(\text{C}\equiv\text{CBu}^t)$  **100** were generated (Equation (26)).<sup>83</sup> The coordinated acetylide ligands in these paramagnetic Ti(III) species displayed strong  $\nu(\text{C}\equiv\text{C})$  infrared bands, at  $2080\text{ cm}^{-1}$  in **99** and  $2071\text{ cm}^{-1}$  in **100**. Compound **100** was the first structurally characterized monomeric titanocene(III) monoacetylide and has a typical bent-metalocene structure. The acetylide ligand is clearly bound in an  $\eta^1$ -fashion and the  $\text{Ti}-\text{CCBu}^t$  bond length is  $2.180(6)\text{ \AA}$ . The reaction of **100** with  $\text{CO}_2$  formed the carboxylate species  $\text{Cp}^*_2\text{Ti}(\text{O}_2\text{CC}\equiv\text{CBu}^t)$  **97** which is the same complex that was formed from the reaction of **94** with  $\text{CO}_2$ .



Another Ti(III) mono( $\sigma$ -alkynyl) species, *ansa*- $\{\eta^5, \eta^5\text{-C}_5\text{Me}_4\text{SiMe}_2\text{CH}=\text{CHCH}_2\text{CH}_2\text{SiMe}_2\text{C}_5\text{Me}_4\}\text{Ti}(\text{C}\equiv\text{CBu}^t)$  **101**, was formed through the reaction of *tert*-butylacetylene with the allyl titanocene precursor *ansa*- $\text{Ti}\{\eta^3, \eta^5, \eta^5\text{-C}_5\text{Me}_4\text{SiMe}_2\text{CHCHCHCH}_2\text{SiMe}_2\text{C}_5\text{Me}_4\}$  **67** (Equation (27)).<sup>84</sup> In this reaction, the *tert*-butylacetylene acts as a Brønsted acid and protonates the  $\text{Ti}-\eta^3$ -allyl bond to form a double bond in the *ansa*-bridge. This proton transfer occurs in a stereoselective and regioselective fashion as only the *cis*-product was formed. Interestingly, the double bond was not formed in the center of the *ansa*-bridge but was closer to one  $\text{C}_5$  ring. The EPR spectrum of **101** was consistent with the presence of an unpaired electron and contained one broad line. The solid-state structure of **101** showed that the acetylide group is approximately linear ( $174.05(19)^\circ$ ) and the  $\text{Ti}-\text{C}$  bond length is  $2.108(2)\text{ \AA}$  indicating that the alkyne is bound in an  $\eta^1$ -fashion.

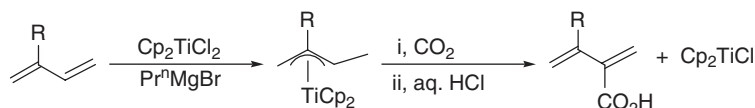


In comparison to the electrolytic reduction of compounds of the type  $\text{Cp}_2\text{TiX}_2$  ( $\text{X} = \text{Cl}, \text{Br}$  or  $\text{I}$ ), the electrolytic reduction of alkyl species of the type  $\text{Cp}_2\text{TiR}_2$  ( $\text{R} = \text{alkyl}$ ) has not been studied in great detail. Samuel and Hénique performed a preliminary study in which they electrolytically reduced  $\text{Cp}_2\text{TiMe}_2$  and  $\text{Ind}_2\text{TiMe}_2$  ( $\text{Ind} = \eta^5\text{-C}_9\text{H}_7$ ) in the presence of phosphines.<sup>63</sup> EPR spectroscopy was used to monitor the reactions *in situ* and determined that at  $230\text{ K}$   $\text{Cp}_2\text{TiMe}_2$  and  $\text{Ind}_2\text{TiMe}_2$  were reduced to the Ti(III) species  $\text{Cp}_2\text{TiMe}(\text{PMe}_3)$  **102** and  $\text{Ind}_2\text{TiMe}(\text{PMe}_3)$  **103**, respectively. It was proposed that these reactions initially generate intermediates of the type  $[\text{Cp}_2\text{TiMe}_2]^-$  and  $[\text{Ind}_2\text{TiMe}_2]^-$ .  $\text{PMe}_3$  then coordinates to these anionic species to form five-coordinate, 19-electron species of the type  $[\text{Cp}_2\text{TiMe}_2(\text{PMe}_3)]^-$  and  $[\text{Ind}_2\text{TiMe}_2(\text{PMe}_3)]^-$  which spontaneously lose a methyl anion to form **102** and **103**. Compound **102** was unstable, and at room temperature it decomposed to form the chelated Ti(III) complex  $\text{Cp}_2\text{TiCH}_2\text{PMe}_2$  and methane.

#### 4.04.6.6 Compounds with Allyl and Propargyl Ligands

In both COMC (1982) and COMC (1995), the syntheses of a variety of different titanocene complexes with allyl-supporting ligands were described.<sup>54,59</sup> In the last 10 years, research into these species has focused on their reactivity.



**Table 2** Reactions of  $\text{Cp}_2\text{Ti}(\eta^3\text{-allyl})$  complexes (**104**  $\text{R} = \text{H}$ ) and (**105**  $\text{R} = \text{Me}$ ) with  $\text{CO}_2$ <sup>85</sup>

Compound	R	Isolated or <i>in situ</i>	Yield of acid (%)	Recovery of $\text{Cp}_2\text{TiCl}_2^a$ (%)
<b>104</b>	H	Isolated	82 <sup>b</sup>	85
<b>104</b>	H	<i>in situ</i>	85 <sup>c</sup>	93
<b>105</b>	Me	Isolated	83 <sup>b</sup>	90
<b>105</b>	Me	<i>in situ</i>	81 <sup>c</sup>	87

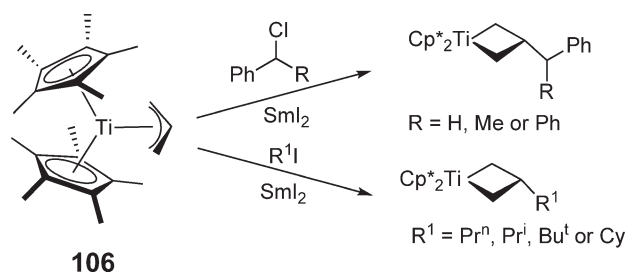
<sup>a</sup>After aerial oxidation of  $\text{Cp}_2\text{TiCl}_2$ .<sup>b</sup>Based on **104** or **105**.<sup>c</sup>Based on diene.

As a part of a comprehensive study into carbon dioxide fixation by bis-cyclopentadienyl Ti(III) allyl complexes, Sato and co-workers<sup>85</sup> prepared a series of substituted allyl complexes through the reduction of  $\text{Cp}_2\text{TiCl}_2$  with at least 2 equiv. of an alkyl Grignard reagent in the presence of diene (a generic description of this reaction is presented in COMC (1982)).<sup>54</sup> By varying the substituents on the diene, a range of different allyl complexes were prepared. A summary of the reactions of  $\text{Cp}_2\text{Ti}(\eta^3\text{-allyl})$  (allyl =  $\text{CH}_2\text{C}(\text{H})\text{CH}(\text{Me})$  **104** or  $\text{CH}_2\text{C}(\text{Me})\text{CH}(\text{Me})$  **105**) with  $\text{CO}_2$  (when **104** and **105** were both prepared *in situ* and isolated) is presented in Table 2.

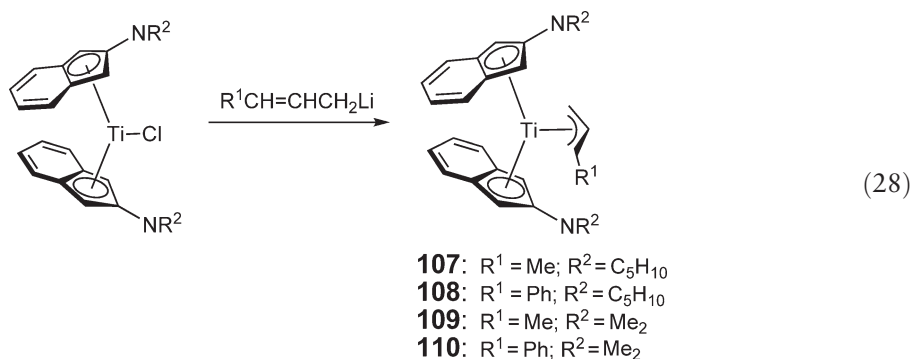
The major advantage of this reaction was that compounds **104** or **105** were generated with high regioselectivity. The new carbon–carbon bond was always formed at the more substituted terminal allylic position of **104** or **105** and as a result after acid workup  $\beta,\gamma$ -unsaturated carboxylic acids were the sole products. From Table 2, it is clear that yields were not significantly affected by whether the complexes were isolated or prepared *in situ*. Sato *et al.* have subsequently demonstrated that this methodology can be used to form carbon–carbon bonds between  $\text{CO}_2$  and a range of different starting dienes.

An interesting radical reaction was observed between  $\text{Cp}^*_2\text{Ti}(\eta^3\text{-C}_3\text{H}_5)$  **106** and several organic radicals. In the presence of the halogen abstraction reagent  $\text{SmI}_2$ , free radical precursors such as alkyl iodides and benzyl chlorides reacted with the Ti(III) allyl species  $\text{Cp}^*_2\text{Ti}(\eta^3\text{-C}_3\text{H}_5)$  **106** to form Ti(IV) titanacyclobutanes (Scheme 6).<sup>86</sup> All of the reactions were regioselective and the radical fragment was always added to the central carbon of the allyl moiety. The authors proposed that the reactions proceeded through direct kinetic attack on the allyl ligand rather than via an initial attack on the metal center followed by rearrangement. Unfortunately, these radical alkylation reactions do not proceed for substituted allyl ligands.

In order to gain further insights into the formation of these titanacyclobutanes, Stryker and co-workers subsequently synthesized the new indenyl Ti(III) allyl complexes (2- $\text{N}(\text{C}_5\text{H}_{10})\text{C}_9\text{H}_6$ ) $_2\text{Ti}(\eta^3\text{-allyl})$  (allyl = 1- $\text{PhC}_3\text{H}_4$  **107** and 1- $\text{MeC}_3\text{H}_4$  **108**) and (2- $\text{NMe}_2\text{C}_9\text{H}_6$ ) $_2\text{Ti}(\eta^3\text{-allyl})$  (allyl = 1- $\text{PhC}_3\text{H}_4$  **109** and 1- $\text{MeC}_3\text{H}_4$  **110**) through the reaction of the appropriate indenyl Ti(III) chloride precursors with either cinnamyl lithium or crotyl magnesium chloride or bromide (Equation (28)).<sup>87,88</sup> The structures of compounds **107**, **109**, and **110** were all elucidated by X-ray diffraction

**Scheme 6**

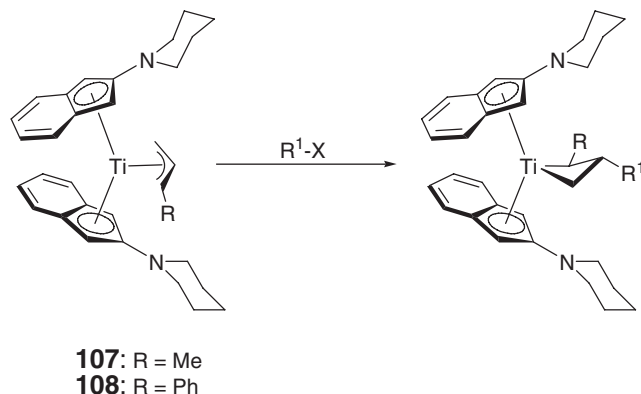
analysis. In all three complexes, the cinnamyl or crotyl ligand is bound to the metal in an  $\eta^3$ -fashion with *syn*-stereochemistry. The terminal carbons of the allyl moiety are pyramidalized and the substituted carbon of the allyl ligand has the longest Ti–C bond length. The solid-state structure of **110** contained two conformers and there was some evidence to suggest that in one of these conformations one of the indenyl rings may have slipped so that it coordinated in an  $\eta^3$ -fashion. In all other cases, the indenyl ligands are clearly  $\eta^5$ -coordinated.



In contrast to **106**, the electron-rich compounds **107–110** (all containing substituted allyl ligands) reacted with free radicals to form titanacyclobutanes. The reactions were all regioselective with alkylation only occurring at the central carbon of the allyl ligand. Thus, *trans*-2,3-disubstituted titanacyclobutanes were formed exclusively. Table 3 summarizes the results of radical alkylation of compounds **107** and **108**.

A new class of titanocene allyl complex incorporating a nitrogen atom in the terminal position of the allyl fragment was developed by Lappert *et al.*<sup>89</sup> The 1-aza-allyltitanocene species  $\text{Cp}_2\text{Ti}\{\eta^3\text{-N(R)C(Bu}^t\text{)C(H)R}\}$  ( $R = \text{SiMe}_3$  **111**) was prepared from the reaction of  $\text{Cp}_2\text{TiCl}$  with 0.5 equiv. of  $\text{Li}_2[\text{N(R)C(Bu}^t\text{)C(H)R}]_2$  (Equation (29)). Interestingly, compound **111** was also obtained from the reaction of the Ti(IV) precursor  $\text{Cp}_2\text{TiCl}_2$  with 1 equiv. of

**Table 3** Reactions of  $\text{Cp}_2\text{Ti}(\eta^3\text{-allyl})$  complexes **107** and **108** with alkyl radical sources<sup>a 87</sup>

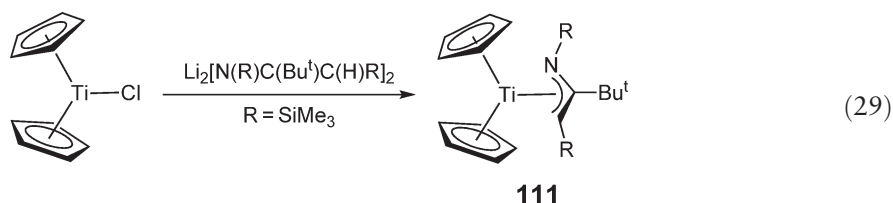


Compound	$R^1$	$X$	Yield (%) <sup>b</sup>
<b>107</b>	$\text{Pr}^i$	I	72
<b>107</b>	Cy	I	80
<b>107</b>	$\text{Bu}^t$	Cl	88
<b>108</b>	$\text{Pr}^i$	I	69
<b>108</b>	Cy	I	70
<b>108</b>	$\text{Bu}^t$	Cl	36

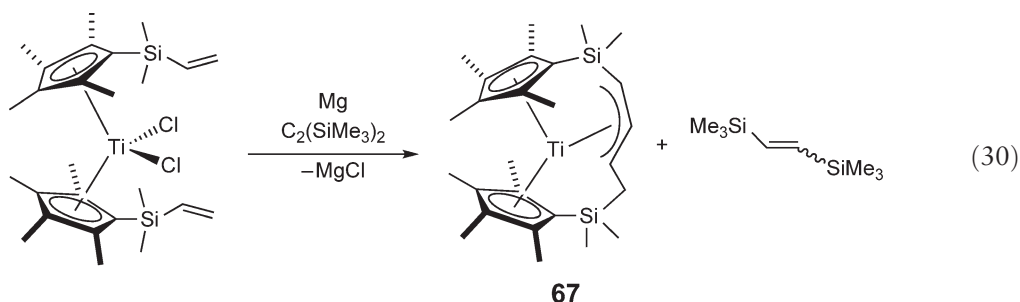
<sup>a</sup>Conditions:  $\text{Sml}_2 \cdot \text{THF}$  (0.1 M in THF), THF,  $-35^\circ\text{C}$  to room temperature, 0.5–3 hours.

<sup>b</sup>Isolated yield.

$\text{Li}_2[\text{N}(\text{R})\text{C}(\text{Bu}^t)\text{C}(\text{H})\text{R}]_2$ . In this reaction, the lithium 1-azaallyl reagent reduces the  $\text{Ti}(\text{IV})$  substrate and is concomitantly oxidized to the organic product  $\{\text{N}(\text{R})\text{C}(\text{Bu}^t)\text{C}(\text{H})\text{R}\}_2$ .



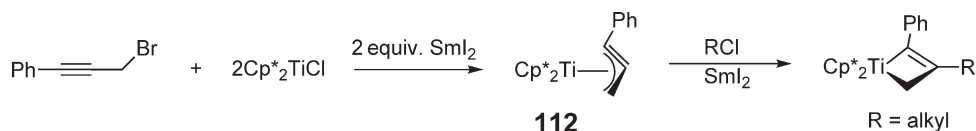
Mach and co-workers demonstrated that the reduction of the titanocene dichloride  $(\eta^5\text{-C}_5\text{Me}_4\text{SiMe}_2\text{CH}=\text{CH}_2)_2\text{TiCl}_2$  with magnesium generates a mixture of the  $\eta^2$ -alkene  $\text{Ti}(\text{II})$  complex  $\text{Ti}(\eta^5\text{-C}_5\text{Me}_4\text{SiMe}_2\text{CH}=\text{CH}_2)(\eta^2, \eta^5\text{-C}_5\text{Me}_4\text{SiMe}_2\text{CH}=\text{CH}_2)$  and the paramagnetic  $\eta^3$ -allyl  $\text{Ti}(\text{III})$  species **67**.<sup>66</sup> Compound **67** forms as a result of proton loss from the ligand and when the reaction was performed in the presence of bis(trimethylsilyl)acetylene as a proton acceptor, **67** was isolated as the sole product (Equation (30)). The bis(trimethylsilyl)acetylene was hydrogenated to a mixture of *E*- and *Z*-1,2-bis(trimethylsilyl)ethene. The solid-state structure of **67** showed that the allyl fragment is bound in an  $\eta^3$ -fashion to the Ti center. The Ti–C bond lengths to the allyl fragment are inequivalent (Ti–C<sub>allyl</sub> = 2.509(9), 2.392(8), and 2.435(8) Å) with the shortest bond length being observed between the Ti center and the central carbon atom of the allyl group. This asymmetry is most probably due to steric effects. The *ansa*-carbon chain is planar and forced the C<sub>5</sub> rings to twist with respect to each other. Compound **67** was oxidized with  $\text{PbCl}_2$  to form the  $\text{Ti}(\text{IV})$   $\eta^1$ -alkenyl product  $\text{TiCl}\{\eta^1, \eta^5, \eta^5\text{-C}_5\text{Me}_4\text{SiMe}_2\text{CHCH}=\text{CHCH}_2\text{SiMe}_2\text{C}_5\text{Me}_4\}$ .



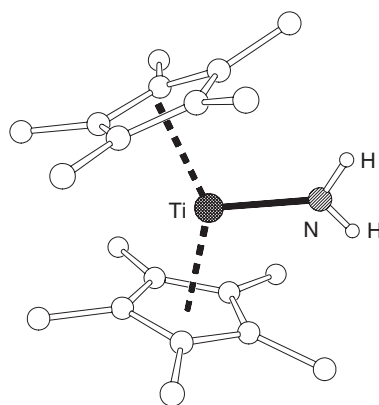
The first  $\text{Ti}(\text{III})$  propargyl complex was prepared by Ogoshi and Stryker in 1998.<sup>90</sup> They showed that the reaction of 1-phenyl-3-bromopropyne with 2 equiv. of  $\text{Cp}^*_2\text{TiCl}$  in the presence of  $\text{SmI}_2$  led to the formation of  $\text{Cp}^*_2\text{Ti}(\eta^3\text{-PhC}_3\text{H}_2)$  **112** (Scheme 7). In contrast, when the same reaction was performed with propargyl bromide, a dimeric  $\text{Ti}(\text{IV})$  titanacyclobutene was formed. Compound **112** underwent regioselective conversion into a titanacyclobutene when it was reacted with an alkyl halide in the presence of  $\text{SmI}_2$  (Scheme 7).

#### 4.04.6.7 Compounds with Ti–N Bonds

In the last 10 years, the solid-state structures of the related titanium(III) amido species  $\text{Cp}^*_2\text{Ti}(\text{NH}_2)$  **113** (Figure 15) and  $\text{Cp}^*_2\text{Ti}(\text{NMeH})$  **114** have been determined.<sup>58,91</sup> The structures are nearly identical, and in both cases the amido ligand adopts the least sterically favorable conformation in order to maximize Ti–N  $\pi$ -bonding. In this conformation



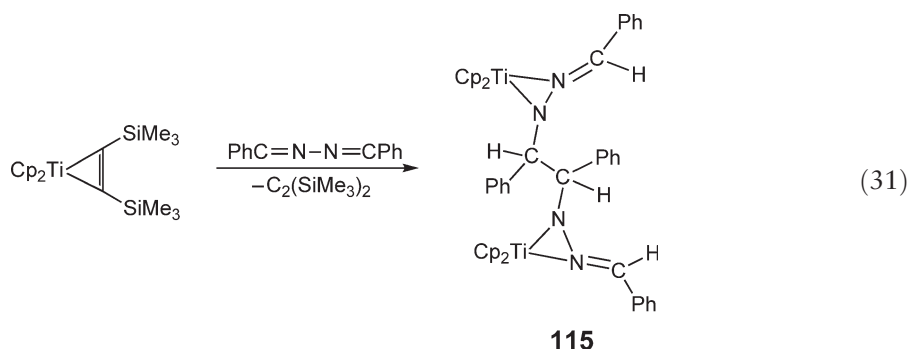
Scheme 7



**Figure 15** X-ray structure of **113**.<sup>91</sup> C atoms are represented by open spheres and carbon-bound H atoms omitted for clarity.

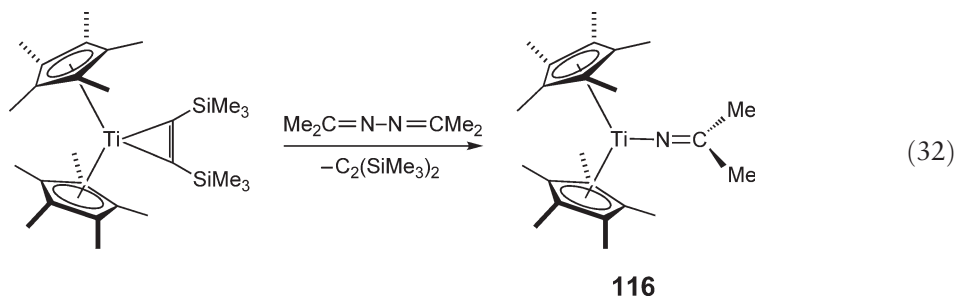
the Ti atom, the two Cp\* ring centroids, and the amido ligand all lie approximately in the same plane. If steric effects dominated, the plane of the amido ligand would be perpendicular to the plane formed by the Ti atom and the Cp\* ring centroids. This conformation is observed in Cp\*<sub>2</sub>Ti(NMePh) which has considerably more steric bulk at the amido nitrogen than either **113** or **114**.<sup>59</sup>

As part of an investigation into the reactions of Cp<sub>2</sub>Ti{η<sup>2</sup>-C<sub>2</sub>(SiMe<sub>3</sub>)<sub>2</sub>} with azines, Ohff *et al.* showed that the dimeric species **115** could be prepared through the reaction of Cp<sub>2</sub>Ti{η<sup>2</sup>-C<sub>2</sub>(SiMe<sub>3</sub>)<sub>2</sub>} with *trans,trans*-benzaldehyde azine (Equation (31)).<sup>92,93</sup> In this reaction a reductive C-C coupling occurs, which converts two azine molecules into a dianionic bridging ligand. The first step in the proposed mechanism for the formation of **115** is believed to be the coordination of a single azine unit to one titanium center through the nitrogen atoms. This species then undergoes a metal-assisted one-electron reduction of the coordinated azine to form the Ti(III) radical complex Cp<sub>2</sub>Ti{N(N=CHPh)C·HPh} which dimerizes to form **115**. In contrast, the reactions of other azines with Cp<sub>2</sub>Ti{η<sup>2</sup>-C<sub>2</sub>(SiMe<sub>3</sub>)<sub>2</sub>} did not result in the formation of complexes analogous to **115** but generated instead either bis(amido) or alkylamido Ti(IV) species. The reaction of **115** with CpCo(C<sub>2</sub>H<sub>4</sub>)<sub>2</sub> resulted in the quantitative formation of the heterobimetallic Ti(IV) complex Cp<sub>2</sub>Ti(μ-N=CHPh)<sub>2</sub>CoCp.

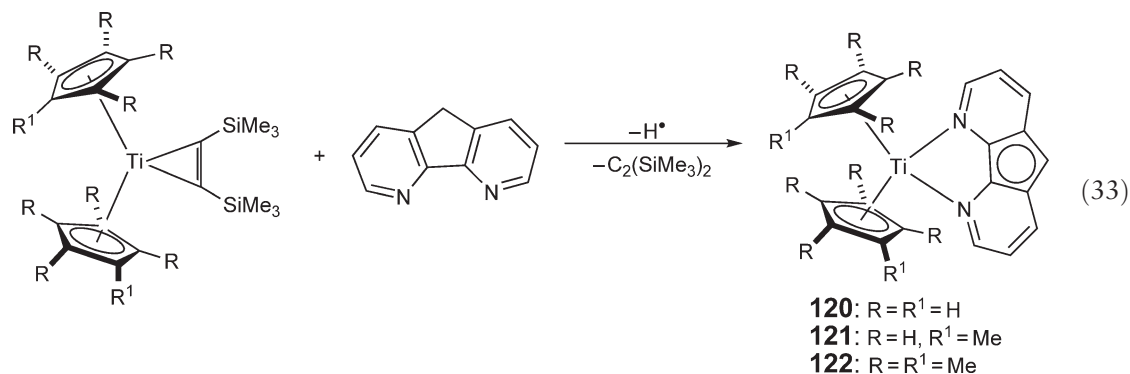


In a closely related study, Mach *et al.* investigated the reactivity of complexes of the type Cp<sup>R</sup><sub>2</sub>Ti{η<sup>2</sup>-C<sub>2</sub>(SiMe<sub>3</sub>)<sub>2</sub>} (Cp<sup>R</sup> = C<sub>5</sub>H<sub>5-n</sub>Me<sub>n</sub>; *n* = 0–5) with the acetone azine Me<sub>2</sub>C=N–N=CMe<sub>2</sub>.<sup>94</sup> A marked difference in reactivity was observed depending on the number of methyl substituents on the C<sub>5</sub> ring. When *n* = 0–4, Ti(IV)-containing products were generated. In contrast, when Cp\*<sub>2</sub>Ti{η<sup>2</sup>-C<sub>2</sub>(SiMe<sub>3</sub>)<sub>2</sub>} was treated with Me<sub>2</sub>C=N–N=N–NCMe<sub>2</sub>, the monomeric Ti(III) ketamide Cp\*<sub>2</sub>Ti(N=CMe<sub>2</sub>) **116** was formed (Equation (32)). There are two possible mechanisms for the formation of **116**. Both involve initial coordination of the azine ligand to the metal center with displacement of the acetylene ligand. This is followed either by loss of an amine radical to form **116** or reaction of the coordinated intermediate with another molecule of Cp\*<sub>2</sub>Ti{η<sup>2</sup>-C<sub>2</sub>(SiMe<sub>3</sub>)<sub>2</sub>} to form a dimeric species which breaks apart to form

two molecules of **116**. The N=C bond length in **116** is 1.240(8) Å and the ketimide ligand is bound in an allene-like mode (Ti=N=C). In order to maximize  $\pi$ -bonding, the plane containing the CMe<sub>2</sub> carbons is perpendicular to that containing the Cp\* ring centroids and Ti.



A family of complexes of the type Cp<sup>R</sup><sub>2</sub>Ti(bpy) (bpy = 2,2'-bipyridine; Cp<sup>R</sup> = Cp **117**,  $\eta^5$ -C<sub>5</sub>HMe<sub>4</sub> **118**, and Cp\* **119**) were prepared through the reactions of Cp<sup>R</sup><sub>2</sub>Ti{ $\eta^2$ -C<sub>2</sub>(SiMe<sub>3</sub>)<sub>2</sub>} with bpy.<sup>95</sup> Although compounds **117–119** could be considered to contain neutral Ti(II) centers, the EPR spectra of these species contained strong evidence for an electronic triplet state, which implies the transfer of one of the valence Ti electrons to the bpy ligand. Hence, compounds **117–119** probably consist of a titanocene Ti(III) center bound to a bipyridine radical anion. The corresponding reactions between Cp<sup>R</sup><sub>2</sub>Ti{ $\eta^2$ -C<sub>2</sub>(SiMe<sub>3</sub>)<sub>2</sub>} and 4,5-diazafluorene (dafH) also resulted in a transfer of a Ti valence electron to the dafH ligand. However, the resulting transient Ti(III) complexes which incorporated the dafH radical anion were unstable and ejected an H radical. The final products of this reaction were the Ti(III) species Cp<sup>R</sup><sub>2</sub>Ti(daf) (Cp<sup>R</sup> = Cp **120**,  $\eta^5$ -C<sub>5</sub>HMe<sub>4</sub> **121**, and Cp\* **122**) which contained the daf anion (Equation (33)). The +III oxidation state of the titanium centers in **120–122** was confirmed by EPR spectroscopy. The EPR spectra of **120–122** in toluene all exhibited a sharp signal in the range  $g = 1.980\text{--}1.982 \mu_B$ , which is consistent with the presence of an unpaired electron.

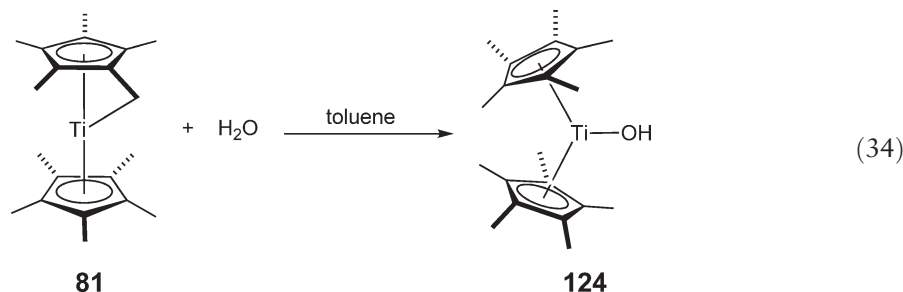


#### 4.04.6.8 Compounds with Ti–O Bonds

It was noted in COMC (1983) that in order to prepare monomeric Ti(III) complexes of the type Cp<sub>2</sub>Ti(OR) (R = alkyl or aryl), the substituent R was required to be sterically bulky or there needed to be some substitution on the cyclopentadienyl ligands.<sup>54</sup> Nagashima *et al.* prepared Cp<sub>2</sub>Ti(OBu<sup>t</sup>) **123** through the reaction of Cp<sub>4</sub>Ti<sub>2</sub>( $\mu$ -Cl)<sub>2</sub> with KOBu<sup>t</sup> in THF.<sup>96</sup> The solid-state structure of **123** revealed that it is structurally similar to both Cp<sub>2</sub>Ti(O-2,6-Bu<sup>t</sup><sub>2</sub>-4-MeC<sub>6</sub>H<sub>2</sub>) and ( $\eta^5$ -C<sub>5</sub>Me<sub>4</sub>H)<sub>2</sub>Ti(OBu<sup>t</sup>); however, its reactivity was quite unusual. Compound **123** reacted with Cp<sub>2</sub>M<sub>2</sub>( $\mu$ -CO)<sub>2</sub>(CO)<sub>4</sub> (M = Mo or W) to form the heterobimetallic Ti(IV) complexes Cp<sub>2</sub>Ti(OBu<sup>t</sup>)( $\mu$ -OC)M(CO)<sub>2</sub>Cp. The reaction with Co<sub>2</sub>(CO)<sub>8</sub> formed the tetrametallic complex Cp<sub>2</sub>Ti(OBu<sup>t</sup>)( $\mu_4$ -OC)Co<sub>3</sub>(CO)<sub>9</sub>.<sup>97</sup> In contrast, photochemical irradiation of a mixture of **123** and Cp<sub>2</sub>Ru<sub>2</sub>( $\mu$ -CO)<sub>2</sub>(CO)<sub>2</sub> resulted in the formation of Cp<sub>2</sub>Ti(OBu<sup>t</sup>)Ru(CO)<sub>2</sub>Cp, which contained a Ti–Ru bond. All of these reactions involve the cleavage of a metal–metal bond in metal carbonyl dimers by a Ti(III) reducing agent.

The reaction of the “tucked in” titanocene Cp\*( $\eta^1, \eta^5$ -Fv)Ti **81** (Fv = tetramethylfulvene) with water in toluene generated Cp\*<sub>2</sub>Ti(OH) **124** (Equation (34)).<sup>98</sup> The EPR spectrum of **124** confirmed the presence of a single

unpaired electron and the solid-state structure of **124** is extremely similar to that of  $\text{Cp}^*_2\text{Ti}(\text{NH}_2)$  **113**. The Ti–O bond length is 1.889(2) Å which indicates that the hydroxide ligand forms a single covalent bond with the metal center. The related hydroxide species *ansa*- $\{\eta^5, \eta^5\text{-C}_5\text{Me}_4\text{SiMe}_2\text{CH}_2\text{CH}=\text{CHCH}_2\text{SiMe}_2\text{C}_5\text{Me}_4\}\text{Ti}(\text{OH})$  **125** was formed through the reaction of *ansa*- $\text{Ti}\{\eta^3, \eta^5, \eta^5\text{-C}_5\text{Me}_4\text{SiMe}_2\text{CHCHCHCH}_2\text{SiMe}_2\text{C}_5\text{Me}_4\}$  **67** with water.<sup>84</sup> The Ti–O bond length in **125** is 1.9153(12) Å which indicates that the insertion of the  $\text{SiC}_4\text{H}_6\text{Si}$  bridge between the  $\text{Cp}^*$  rings weakens the Ti–O bond.



The methoxy analog of **125**, *ansa*- $\{\eta^5, \eta^5\text{-C}_5\text{Me}_4\text{SiMe}_2\text{CH}_2\text{CH}=\text{CHCH}_2\text{SiMe}_2\text{C}_5\text{Me}_4\}\text{Ti}(\text{OMe})$  **126**, was prepared through the reaction of the Ti(III) allyl species **67** with MeOH.<sup>66</sup> Compound **126** is closely related to the chloride species **66**. The Ti–O bond length in **126** was 1.843(2) Å which is considerably shorter than in **125**. The authors suggest that this indicates that the methoxy ligand is a significantly better  $\pi$ -donor than the hydroxyl ligand.

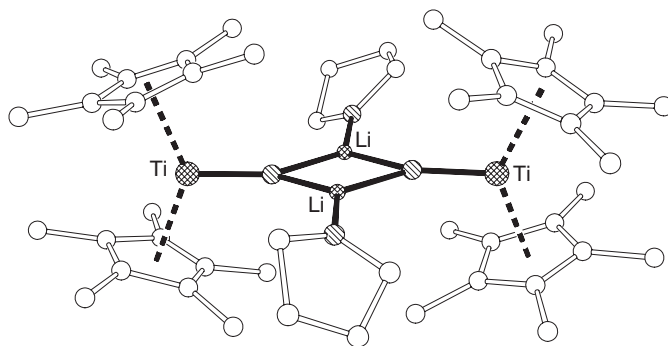
The synthesis and solid state structure of the titanium(III) oxo-bridged species  $\text{Cp}_4\text{Ti}_2(\mu\text{-O})$  **127** are described in COMC (1995).<sup>59</sup> One of the key features of the structure of **127** is that the dihedral angle between the  $\text{Cp}_2\text{Ti}$  fragments is approximately 90°. In contrast to the structure of **127**, the metallocene fragments in the solid-state structure of  $(\eta^5\text{-1,3-C}_5\text{H}_3\text{tBu}_2)_4\text{Ti}_2(\mu\text{-O})$  **128** are related by an inversion center and the Ti–O–Ti linkage is linear.<sup>99</sup> This difference in the structure of the two compounds is presumably related to the large steric bulk of the *tert*-butyl substituents on the  $\text{C}_5$  rings in **128**.

Andersen and Lukens investigated the magnetic properties of **127** and found that it had a triplet ground state as a result of coupling between the two  $d^1$  centers.<sup>100</sup> Variable-temperature magnetic susceptibility experiments found that above 20 K **127** shows intramolecular ferromagnetic coupling and weak intermolecular ferromagnetic coupling. The intramolecular coupling constant was 8.3  $\text{cm}^{-1}$ . Compound **127** is the only example of a bimetallic titanocene in which the Ti(III) centers are ferromagnetically coupled and a density functional theory-based study showed that this was because no antiferromagnetic pathway exists between the two centers.<sup>101</sup> Interestingly, the study also found that as the dihedral angle between the  $\text{Cp}_2\text{Ti}$  fragments is reduced, a through-space interaction develops between the Ti centers which leads to antiferromagnetic coupling when the angle is less than 45°.

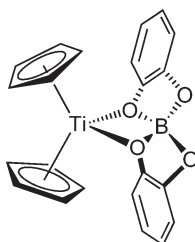
The dimeric alkoxide  $\text{Cp}^*_2\text{Ti}(\mu_3\text{-O})\text{Li}_2(\text{THF})_2(\mu_3\text{-O})/\text{TiCp}^*_2$  **129** was generated through the reaction of water with the dihydride anion  $\text{Cp}^*_2\text{Ti}(\mu\text{-H})_2\text{Li}(\text{TMEDA})$  **77**.<sup>74</sup> The EPR spectrum of **129** consisted of a single line and the magnetic moment was 2.45  $\mu_B$  per dimer or 1.73  $\mu_B$  per titanium. No evidence was found to suggest that there was any coupling between the unpaired electrons on the two titanium centers, and as a result it was proposed that **129** is composed of two anionic  $\text{Cp}^*_2\text{TiO}^-$  moieties which are linked by two Li(THF) fragments. The solid state structure of **129** confirmed that it is dimeric and possessed idealized  $C_{2h}$  symmetry (Figure 16). The atoms of the  $\text{Ti}_2\text{O}_2\text{Li}_2$  core are positioned in the same plane, presumably to avoid steric strain. The  $\text{Cp}^*(\text{centroid})\text{--Ti}$  bond distance ( $\text{Cp}^*(\text{centroid})\text{--Ti} = 2.15$  Å) is slightly longer than normal.

An attempted hydroboration reaction using isoprene, catecholborane, and a catalytic amount of  $\text{Cp}_2\text{TiMe}_2$  resulted in the isolation of the Ti(III) tetraalkoxy complex **130** (Figure 17).<sup>75</sup> The exact mechanism for the formation of **130** is unclear, but the authors proposed that  $\text{Cp}_2\text{Ti}(\eta^2\text{-H}_2\text{BO}_2\text{C}_6\text{H}_4)$  **78** is formed initially and then undergoes a disproportionation reaction to give **130** and  $\text{BH}_4^-$ . The presence of an unpaired electron in **130** was confirmed by EPR spectroscopy and the structure was elucidated by X-ray diffraction. Compound **130** was situated on an inversion center and contains unusually long Ti–O bonds ( $\text{Ti–O} = 2.236(1)$  Å). These distances are slightly longer than those usually observed between Ti and THF and suggest that **130** can also be considered as an ion pair, consisting of  $\text{Cp}_2\text{Ti}^+$  cations and  $\text{O}_2\text{BO}_2\text{C}_6\text{H}_4^-$  anions.

Treatment of the acetylene complexes  $\text{Cp}_2\text{Ti}(\eta^2\text{-C}_2\text{R}_2)$  ( $\text{R} = \text{SiMe}_3$  or Ph) with  $\text{CO}_2$  at room temperature resulted in the formation of the dimeric  $\sigma$ -alkenylcarboxylate complexes **131** and **132** (Equation (35)).<sup>102</sup> The magnetic moment of both complexes was 1.6  $\mu_B$  per titanium atom indicating that they contained trivalent Ti centers. The structure of **132** was elucidated by X-ray diffraction, and the presence of two fused metallacyclic rings was confirmed.

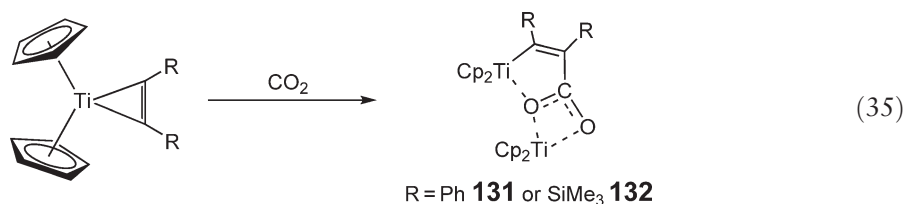


**Figure 16** X-ray structure of **129**.<sup>74</sup> C atoms represented by open spheres and O atoms by shaded spheres. H atoms omitted for clarity.



**Figure 17** Structure of **130**.

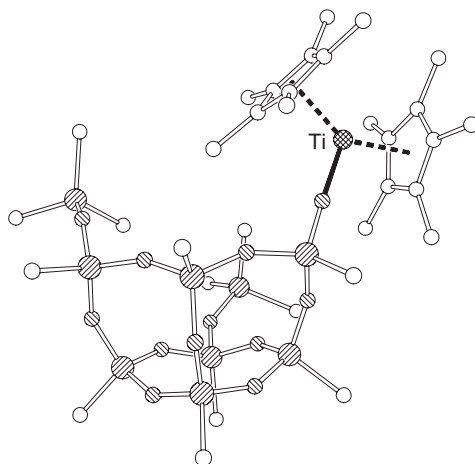
Molecules of **132** contains one three-coordinate oxygen and one two-coordinate oxygen and the Ti–O and O–C bond lengths to the three-coordinate oxygen (Ti–O = 2.258(3) Å, C–O = 1.310(6) Å) are longer than those to the two-coordinate oxygen (Ti–O = 2.178(3) Å, C–O = 1.266(5) Å). Presumably, due to the different coordination environments around the Ti centers, the geometries of the two Cp<sub>2</sub>Ti fragments are not identical. The geometry of one Cp<sub>2</sub>Ti fragment (TiC<sub>3</sub>O) is eclipsed, whereas the geometry of the other fragment (TiOCO) is in between eclipsed and staggered. Both compounds **131** and **132** reacted with oxygen in air to generate Ti(IV) titanafuranone metallacycles of the form Cp<sub>2</sub>Ti{C(R)=C(R)C(O)O}.



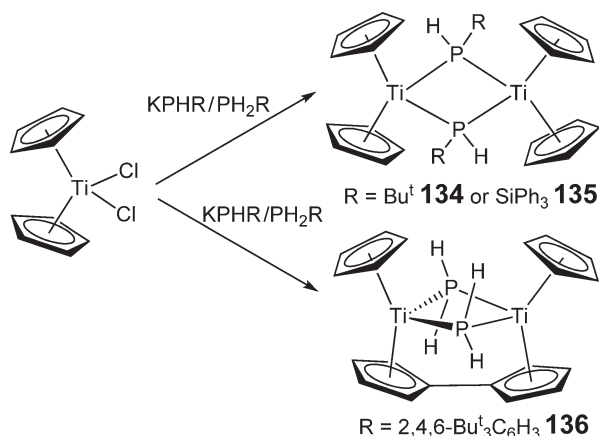
The titanium(III) silsesquioxane complex Cp<sup>\*</sup><sub>2</sub>Ti{Cy<sub>7</sub>Si<sub>7</sub>O<sub>10</sub>(OSiMe<sub>3</sub>)<sub>2</sub>} **133** was prepared through the reaction of Cp<sup>\*</sup>(η<sup>1</sup>,η<sup>5</sup>-Fv)Ti **81** with Cy<sub>7</sub>Si<sub>7</sub>O<sub>9</sub>(OH)(OSiMe<sub>3</sub>)<sub>2</sub>.<sup>103,104</sup> Compound **133** is a model compound for titanium catalysts which are immobilized on silica surfaces. The solid-state structure of **133** showed that the deprotonated silsesquioxane is coordinated to the titanium center as a bulky monodentate ligand (Figure 18). The Ti–O bond length is 1.927(2) Å.

#### 4.04.6.9 Compounds with Phosphide, Sulfide, and Telluride Ligands

The reaction of the primary phosphide KPHBu<sup>t</sup> with Cp<sub>2</sub>TiCl<sub>2</sub> in the presence of the primary phosphine PH<sub>2</sub>Bu<sup>t</sup> resulted in the formation of the dimeric complex Cp<sub>4</sub>Ti<sub>2</sub>(μ-PHBu<sup>t</sup>)<sub>2</sub> **134** (Scheme 8).<sup>105</sup> Similarly, when Cp<sub>2</sub>TiCl<sub>2</sub> was treated with KPH(SiPh<sub>3</sub>) in the presence of PH<sub>2</sub>(SiPh<sub>3</sub>), the anionic complex [Cp<sub>2</sub>Ti{PH(SiPh<sub>3</sub>)<sub>2</sub>}]<sup>−</sup> was detected by EPR spectroscopy, and crystals of the dimeric species Cp<sub>4</sub>Ti<sub>2</sub>{μ-PH(SiPh<sub>3</sub>)<sub>2</sub>}<sub>2</sub> **135** were obtained from



**Figure 18** X-ray structure of **133**.<sup>103</sup> C atoms are represented by open spheres, Si atoms by large-shaded spheres and O by small-shaded spheres. Cyclohexyl ring methylene carbon atoms and all H atoms are omitted for clarity.



**Scheme 8**

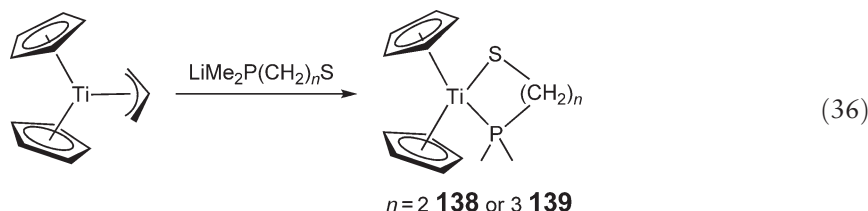
the reaction mixture. In contrast, reaction of  $\text{Cp}_2\text{TiCl}_2$  with the sterically bulky  $\text{KPH}(2,4,6\text{-Bu}^t_3\text{C}_6\text{H}_2)/\text{PH}_2(2,4,6\text{-Bu}^t_3\text{C}_6\text{H}_2)$  led to P–C bond cleavage and the formation of the novel phosphido complex  $\text{Cp}_4\text{Ti}_2(\mu\text{-PH}_2)_2(\mu\text{-}\eta^5\text{-C}_{10}\text{H}_8)$  **136** which contains a bridging fulvalene ligand (Scheme 8).

The Ti(III)  $\mu$ -diphenylphosphide compound  $\text{Cp}_2\text{Ti}_2(\mu\text{-PPh}_2)_2(\mu\text{-}\eta^5\text{-C}_{10}\text{H}_8)$  **137**, which is closely related to **136**, was prepared through the reaction of the Ti(III) fulvalene complex  $\text{Cp}_2\text{Ti}_2(\mu\text{-Cl})_2(\mu\text{-}\eta^5\text{-C}_{10}\text{H}_8)$  with 2 equiv. of  $\text{LiPPh}_2$  in toluene.<sup>106</sup> Reaction of the Ti(IV) species  $\text{Cp}_2\text{Ti}_2\text{Cl}_4(\mu\text{-}\eta^5\text{-C}_{10}\text{H}_8)$  with 4 equiv. of  $\text{LiPPh}_2$  also generated **137**. Compound **137** was characterized by X-ray crystallography. The average Ti–P bond length is 2.644 Å, which is typical for a bridging phosphido ligand. The geometry around the two Ti centers is approximately tetrahedral. The two  $\text{C}_5$  rings in the fulvalene are almost coplanar, with a dihedral angle between the two rings of only 3.0°.

It was proposed that the first step in the mechanism for the formation of compounds **134–136** is the phosphide-driven reduction of the Ti(IV) center in  $\text{Cp}_2\text{TiCl}_2$  to a Ti(II) center with concomitant formation of diphosphines of the type  $\text{P}_2\text{R}_4$ . Oxidative addition of free phosphine to the newly formed Ti(II) center gives a transient species  $\text{Cp}_2\text{TiH}(\text{PRH})$ . This transient species can then either reductively dimerize to give **134** or **135** and  $\text{H}_2$ , or lose  $\text{RH}$  to form the reactive phosphinidene intermediate  $\text{Cp}_2\text{TiPH}$  which can then activate C–H bonds in the cyclopentadienyl ligands to give **136**.



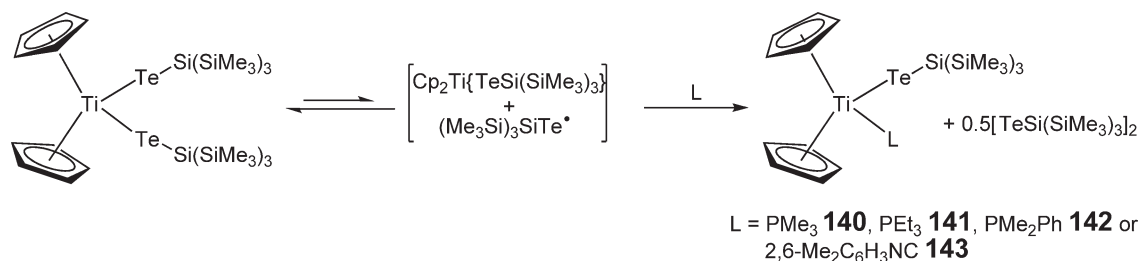
The Ti(III) S,P-complexes  $\text{Cp}_2\text{Ti}\{\text{Me}_2\text{P}(\text{CH}_2)_n\text{S}\}$  ( $n=2$  **138** or  $n=3$  **139**) were formed through the reaction of  $\text{Cp}_2\text{Ti}(\eta^3\text{-C}_3\text{H}_5)$  with 1 equiv. of the appropriate lithiated P–S free ligand (Equation (36)).<sup>107</sup> The EPR spectrum of **138** in THF at room temperature consisted of a doublet (due to coupling to  $^{31}\text{P}$ ,  $I = 1/2$ ) with Ti satellites, while the EPR spectrum of **139** was broad. The solid-state structures of **138** and **139** revealed that both the phosphorus and sulfur atoms of the ligand are coordinated to the Ti(III) center. In **138** a distorted gauche arrangement is observed for the ligand, while the six-membered ring of the ligand in **139** is in a chair conformation. Compound **138** was oxidized to the corresponding Ti(IV) species; the redox potential for the Ti(IV)/Ti(III) couple was determined as  $-1.14$  V against the ferrocenium/ferrocene couple.



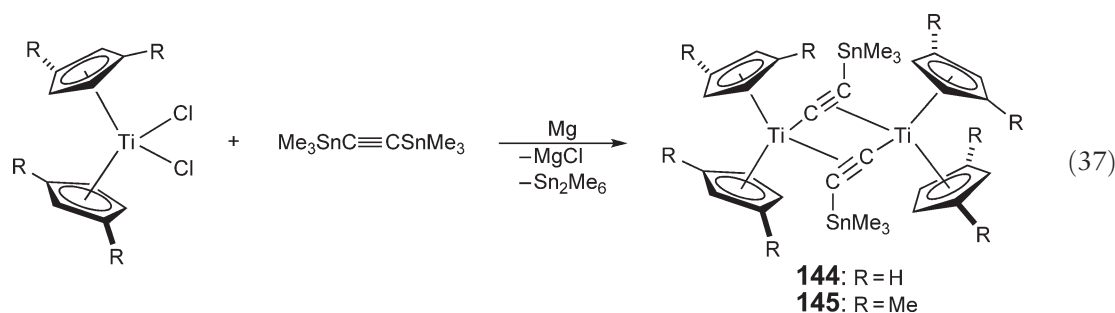
Titanocene tellurolates of the type  $\text{Cp}_2\text{Ti}\{\text{TeSi}(\text{SiMe}_3)_3\}(\text{L})$  ( $\text{L} = \text{PMe}_3$  **140**,  $\text{PEt}_3$  **141**,  $\text{PMe}_2\text{Ph}$  **142**, or  $2,6\text{-Me}_2\text{C}_6\text{H}_3\text{NC}$  **143**) were obtained through the reaction of the Ti(IV) tellurolate  $\text{Cp}_2\text{Ti}\{\text{TeSi}(\text{SiMe}_3)_3\}_2$  with a Lewis base.<sup>108</sup> These complexes presumably form because the Ti(IV) starting material  $\text{Cp}_2\text{Ti}\{\text{TeSi}(\text{SiMe}_3)_3\}_2$  is in equilibrium with a Ti(III) complex and a silyl telluride radical and the Lewis base acts as trap for the Ti(III) species (Scheme 9). Compounds **140–143** were also prepared through the reaction of  $\text{Cp}_2\text{TiCl}$  with  $(\text{THF})_2\text{LiTeSi}(\text{SiMe}_3)_3$  in the presence of the appropriate Lewis base. The EPR spectra and magnetic susceptibility data for compounds **140** and **143** were consistent with the presence of a single unpaired electron. Only **140** was crystallographically characterized. The solid-state structure consists of two similar but crystallographically independent molecules. The geometry around the Ti center is typical for a bent metallocene and the Ti–Te (2.912(3) and 2.879(3) Å) and Ti–P (2.592(5) and 2.589(5) Å) bond distances are similar to those observed in other related species.

#### 4.04.6.10 Mixed Metal Compounds

The diamagnetic dimeric Ti(III) compounds  $(\text{Cp}^R)_4\text{Ti}_2(\mu\text{-}\eta^2, \eta^1\text{-C}\equiv\text{CSnMe}_3)_2$  ( $\text{Cp}^R = \text{Cp}$  **144** or  $\text{C}_5\text{H}_3\text{Me}_2$  **145**) were prepared through the reduction of  $\text{Cp}^R_2\text{TiCl}_2$  with Mg in the presence of bis(trimethylstannyl)acetylene (Equation (37)).<sup>109</sup> The initial step in the proposed mechanism for the formation of **144** and **145** is the reduction of  $\text{Cp}^R_2\text{TiCl}_2$  to the Ti(II) titanocene  $\text{Cp}^R_2\text{Ti}$ . The oxidative addition of bis(trimethylstannyl)acetylene to  $\text{Cp}^R_2\text{Ti}$  is then thought to form an unstable Ti(IV) titanocene which subsequently releases an  $\text{Me}_3\text{Sn}^\cdot$  radical and dimerizes to give either **144** or **145**. The observation of hexamethyldistannane  $\text{Sn}_2\text{Me}_6$  as a byproduct in these reactions supports this mechanism. The solid-state structures of **144** and **145** are similar. The central  $\text{Ti}_2\text{C}_4$  core is approximately planar with the tin atoms lying slightly out of the plane. The strong  $\pi$ -interaction between the Ti atoms and the acetylide results in an elongation in the C–C bond length of the acetylide ( $\text{C–C} = 1.242(7)$  Å) and a partial  $sp^2$  hybridization of the carbon atoms.

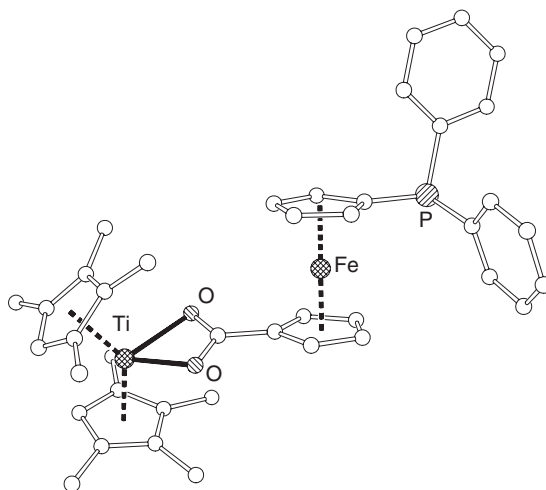


Scheme 9

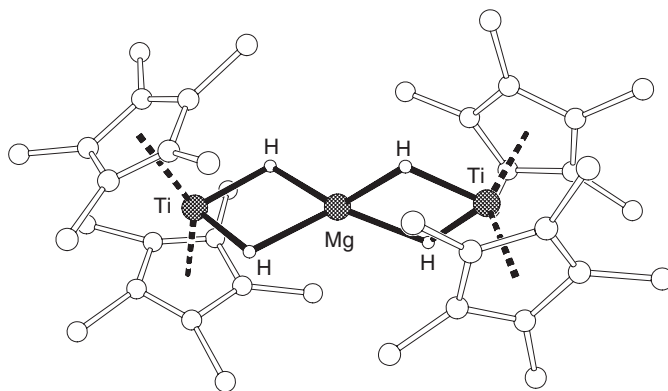


The reaction of 1 equiv. of 1-(diphenylphosphino)ferrocenecarboxylic acid with  $(\eta^5\text{-C}_5\text{HMe}_4)_2\text{Ti}(\eta^2\text{-C}_2(\text{SiMe}_3)_2)$  produced the novel Ti(III)/Fe(II) species **146** (Figure 19).<sup>110</sup> The molecular structure of **146** showed that the C<sub>5</sub> rings of the titanocene moiety are bent and staggered while the C<sub>5</sub> rings of the ferrocene fragment are parallel and adopt a conformation halfway between anticlinal eclipsed and antiperiplanar staggered. The geometry around the titanium is heavily distorted from tetrahedral due to the steric requirements of the C<sub>5</sub> and carboxylate ligands. The carboxylate moiety is bound in an  $\eta^2$ -fashion to the Ti center and the Ti–O bond lengths are almost equivalent (Ti–O = 2.1582(12) and 2.1658(11) Å).

Mach and co-workers prepared the heterobimetallic titanocene hydride complexes  $\{\text{Cp}^{\text{R}}_2\text{Ti}(\mu\text{-H})_2\}_2\text{Mg}$  ( $\text{Cp}^{\text{R}} = \eta^5\text{-C}_5\text{H}_2\text{Me}_3$  **147**,  $\eta^5\text{-C}_5\text{HMe}_4$  **148**, and  $\text{Cp}^*$  **149**) through the reaction of  $\text{Cp}^{\text{R}}_2\text{TiCl}_2$  with dibutylmagnesium, as part of a study into Ti(III) complexes as olefin polymerization catalysts.<sup>111</sup> They had earlier synthesized **149** through the reaction of  $\text{Cp}^*_2\text{TiCl}_2$  with  $\text{Pr}^i\text{MgCl}$  in  $\text{Et}_2\text{O}$ .<sup>112</sup> The yields for the reactions between  $\text{Cp}^{\text{R}}_2\text{TiCl}_2$  and dibutylmagnesium decreased as the number of Me substituents on the C<sub>5</sub> ligands decreased, and no titanocene hydride product was isolated when  $(\eta^5\text{-C}_5\text{H}_3\text{Me}_2)_2\text{TiCl}_2$  was used as the starting material. The complexes were characterized by EPR spectroscopy and X-ray crystallography. The EPR spectra of **147–149** in frozen toluene glass indicated that the complexes were in an electronic triplet state as a result of both Ti centers containing an unpaired electron. The solid-state structures of **147–149** showed that in all three complexes two mutually perpendicular titanocene fragments are attached to one central magnesium atom through bridging hydrides (Figure 20 shows the structure of **149**). The bridging hydrides were located from a Fourier map and were refined anisotropically. Compounds **148** and **149** showed no activity as catalysts for the polymerization of either ethylene or butadiene.

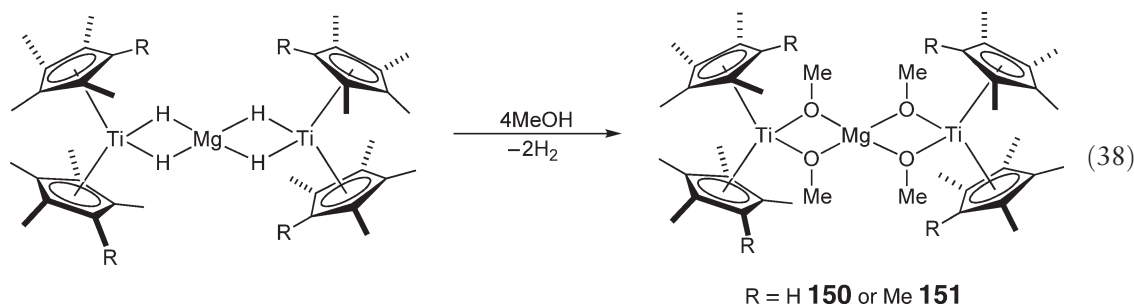


**Figure 19** X-ray structure of **146**.<sup>110</sup> C atoms are represented by open spheres and H atoms omitted for clarity.

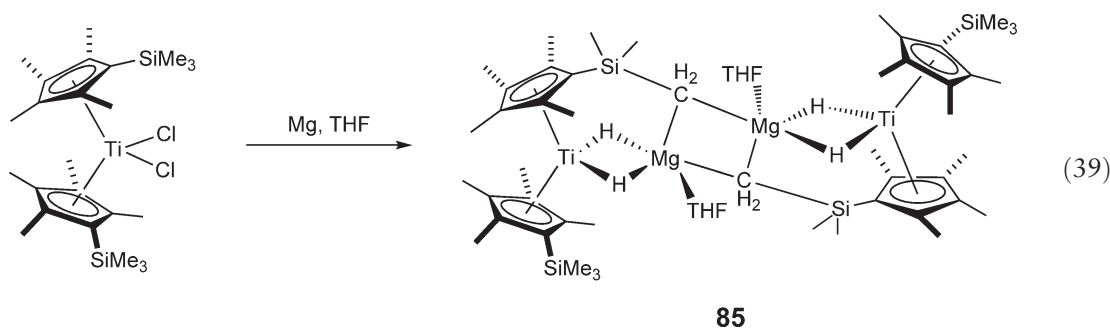


**Figure 20** X-ray structure of **149**.<sup>112</sup> C atoms are represented by open spheres and carbon-bound H atoms omitted for clarity except for hydrides.

The reaction of **148** or **149** with 4 equiv. of methanol resulted in the formation of the trinuclear methoxy-bridged complexes  $(\eta^5\text{-C}_5\text{HMe}_4)_4\text{Ti}_2(\mu\text{-OMe})_4\text{Mg} **150** and  $(\text{Cp}^*)_4\text{Ti}_2(\mu\text{-OMe})_4\text{Mg} **151**, respectively (Equation (38)).<sup>113</sup> In a similar fashion to complexes **148** and **149**, the EPR spectra of **150** and **151** displayed features consistent with the complexes being in an electronic triplet state. The X-ray structure of **150** showed that the molecule contains two non-equivalent octamethyltitanocene units. The geometry around the magnesium atom is distorted tetrahedral. However, unlike **148**, the two octamethyltitanocene fragments are not mutually perpendicular. The dihedral angle between them is  $79.1^\circ$ . The Ti–O bond distances range from 2.094(3) to 2.115(3) Å and are comparable with those observed in other bridged methoxy complexes. Compound **150** reacted with an excess of dibutyl magnesium to give a mixture of **148** and  $(\eta^5\text{-C}_5\text{HMe}_4)_4\text{Ti}_2(\mu\text{-H})_4\text{Mg}_2(\mu\text{-OMe})_2$ .$$



Reduction of  $(\eta^5\text{-C}_5\text{Me}_4\text{SiMe}_3)_2\text{TiCl}_2$  with Mg in THF gave the paramagnetic bridging hydride complex **85** (Equation (39)).<sup>80</sup> When the reaction was monitored by EPR spectroscopy, the transient species  $\text{Cp}^{\text{Si}_2}\text{TiCl}$  was initially observed. However, after 8 h only **85** was present in the spectrum. The main feature of the EPR spectrum of **85** was the triplet splitting due to coupling to 2 equivalent hydrogen nuclei. The solid state structure of the centrosymmetric dimer **85** revealed that the two Ti centers are pseudotetrahedral, while the geometry around the two Mg centers is highly distorted trigonal bipyramidal. Each of the Ti centers is directly linked to an Mg atom through two bridging hydrides and the Ti–H bonds are approximately 0.2 Å shorter than the Mg–H bonds. The Ti centers are also remotely linked to each Mg atom via a bridging methylene group which originated from the  $\text{SiMe}_3$  substituent on the  $\text{C}_5$  ring. The carbon atoms of the two bridging methylene groups are penta-coordinated as they are bound to both Mg atoms as well as to two hydrogen atoms and a silicon atom. The mechanism for this reaction is not clear and the source of the hydrogen atoms used to form the hydride bridges are unknown.

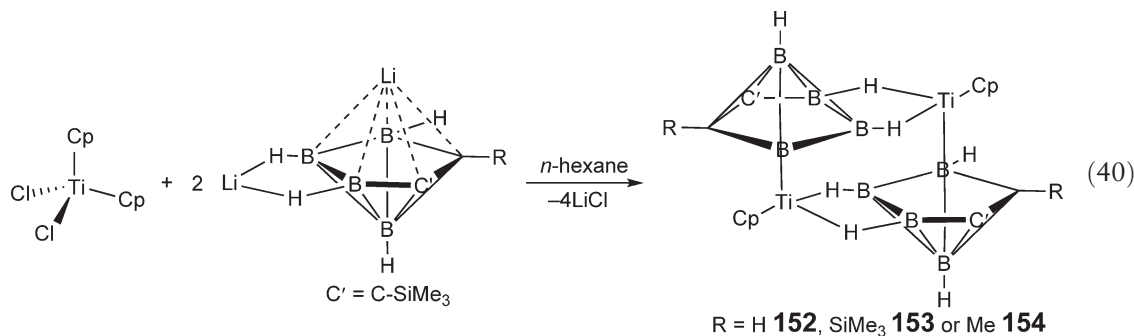


#### 4.04.6.11 Alkyne Polymerization with Ti(III)

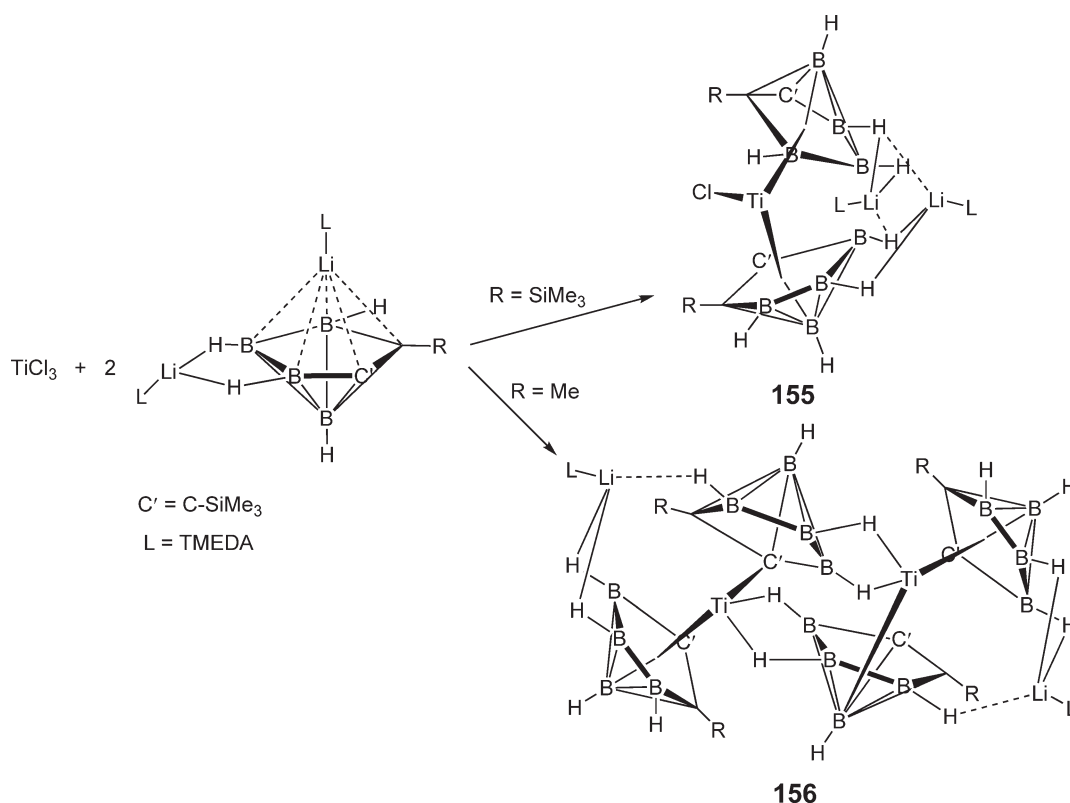
In 1998, Shirakawa and co-workers reported the first titanium complexes which exhibited liquid crystalline behavior.<sup>114</sup> They synthesized one titanocene(IV) complex (PCH506Cp)<sub>2</sub>TiCl<sub>2</sub> which incorporated a liquid crystalline group in the C<sub>5</sub> ligand and two Ti(IV) complexes, Cp<sub>2</sub>Ti(PCH5060)<sub>2</sub> and Cp<sub>2</sub>Ti(PCH5060)Cl in which a liquid crystalline group was coordinated directly to the metal (PCH506 = *p*-(*trans*-4-*n*-pentylcyclohexyl)phenoxyhexyl and PCH5060 = *p*-(*trans*-4-*n*-pentylcyclohexyl)phenoxyhexyloxy). Both (PCH506Cp)<sub>2</sub>TiCl<sub>2</sub> and Cp<sub>2</sub>Ti(PCH5060)<sub>2</sub> were able to catalyze the polymerization of phenylacetylene when AlEt<sub>3</sub> was used as a co-catalyst. An EPR study of the catalyst system formed from the reaction of Cp<sub>2</sub>Ti(PCH5060)<sub>2</sub> with AlEt<sub>3</sub> suggested that the active species for polymerization was a mononuclear Ti(III) species. This species was not isolated and its structure is unknown.

#### 4.04.7 Compounds with Carborane Ligands

The dimeric mixed ligand sandwich titanacarboranes {*commo*-1-Cp-1-Ti-2-R-3-SiMe<sub>3</sub>-2,3-C<sub>2</sub>B<sub>4</sub>H<sub>4</sub>]<sub>2</sub> (R = SiMe<sub>3</sub> **152**, Me **153** or H **154**) were produced from the reactions of Cp<sub>2</sub>TiCl<sub>2</sub> with 2 equiv. of the unsolvated dilithium compounds *closo-exo*-Li-1-Li-2-R-3-(SiMe<sub>3</sub>)-2,3-C<sub>2</sub>B<sub>4</sub>H<sub>4</sub> (Equation (40)).<sup>115,116</sup> Complexes **152–154** all underwent facile oxidation with TiCl<sub>4</sub> in THF to yield the Ti(IV) species 1-Cp-1-Cl-1-THF-1-Ti-2-R-3-SiMe<sub>3</sub>-2,3-C<sub>2</sub>B<sub>4</sub>H<sub>4</sub> (R = SiMe<sub>3</sub>, Me or H). When the TMEDA-solvated dilithiacarborane precursor *closo-exo*-4,5-[(μ-H)<sub>2</sub>Li(TMEDA)]-1-Li(TMEDA)-2,3-(SiMe<sub>3</sub>)<sub>2</sub>-2,3-C<sub>2</sub>B<sub>4</sub>H<sub>4</sub> was treated with TiCl<sub>3</sub> the monomeric Ti(III) sandwich complex {Li(TMEDA)}<sub>2</sub>{1-Cl-1,1'-Ti-(2,3-(SiMe<sub>3</sub>)<sub>2</sub>-2,3-C<sub>2</sub>B<sub>4</sub>H<sub>4</sub>)<sub>2</sub>} **155** was generated (Scheme 10). In contrast, the less sterically bulky precursor *closo-exo*-4,5-[(μ-H)<sub>2</sub>Li(TMEDA)]-1-Li(TMEDA)-2-Me-3-(SiMe<sub>3</sub>)<sub>2</sub>-2,3-C<sub>2</sub>B<sub>4</sub>H<sub>4</sub> reacted with TiCl<sub>3</sub> to form the dimeric species {Li(TMEDA)}<sub>2</sub>{1,1'-Ti-(2-Me-3-SiMe<sub>3</sub>-2,3-C<sub>2</sub>B<sub>4</sub>H<sub>4</sub>)<sub>2</sub>} **156** (Scheme 10).



The solution state EPR spectrum of **155** at room temperature contained a single broad line, while the powder EPR spectrum at 110 K displayed axial signals. In contrast, the paramagnetic complexes **152** and **156** gave

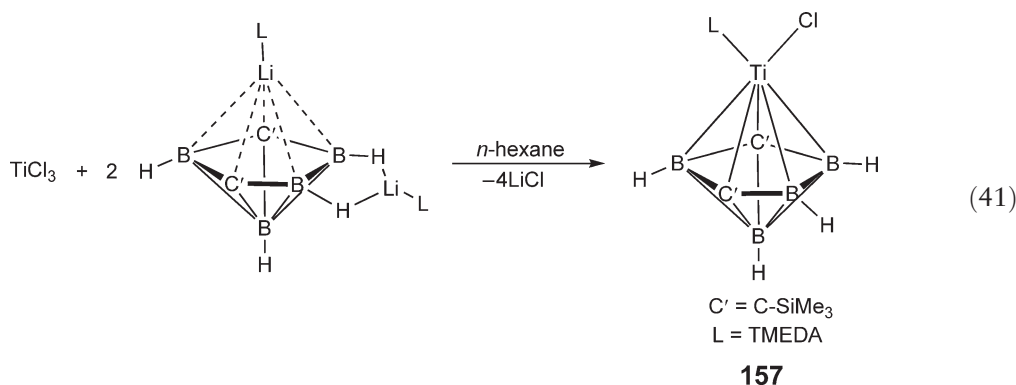


Scheme 10

well-resolved rhombic triplet EPR spectra in glassy frozen toluene solutions at 110 K confirming the presence of two unpaired electrons. The  $g$ -values and ZFS parameters were within the range observed for other dimeric Ti(III) systems. Magnetic susceptibility measurements between 14 and 300 K indicated that the two unpaired  $d$ -electrons in **152** were antiferromagnetically coupled. The magnetic exchange coupling constant was  $-45.8(2) \text{ cm}^{-1}$ , which is significantly lower than that observed in other related Ti(III) systems that contain two unpaired electrons (e.g.,  $J = -268 \text{ cm}^{-1}$  in  $\text{Cp}_4\text{Ti}_2(\mu\text{-OMe})_2$  and  $J = -111 \text{ cm}^{-1}$  in  $\text{Cp}_4\text{Ti}_2(\mu\text{-Cl})_2$ ). This shows that the larger carborane bridge is less effective at facilitating magnetic exchange between the Ti(III) centers than the single atom bridges.

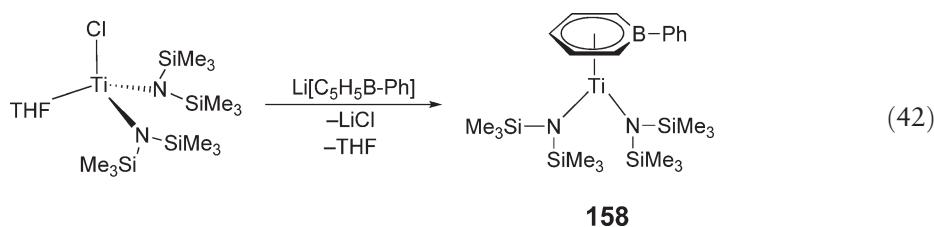
The X-ray structures of **152**, **155**, and **156** indicated that the titanocarboranes all adopt bent sandwich structures with (ring centroid)–Ti–(ring centroid) ranging from  $138.9^\circ$  to  $142.8^\circ$  in **152** and **156** (disorder in the structure of **155** prevented bond lengths and angles from being calculated for this species). This is within the range of values observed in titanocenes. The distances between the Ti centers and the centroids of the Cp and carborane rings in complexes **152** and **156** are similar. The Ti–Cp(ring centroid) distances range from 1.964 to 2.015 Å while the Ti– $\text{C}_2\text{B}_3$  distances range from 2.008 to 2.039 Å. In the structures of **155** and **156**, the  $\text{C}_2\text{B}_3$  rings are oriented so that the carbon atoms of the carborane, rather than the boron atoms, surrounded the open face of the bent sandwich. This indicates that the size of the substituents on the carbon atoms of the carborane has a large influence on whether another ligand can bind to the metal center. Hence, **155** (with two large  $\text{SiMe}_3$  groups on the C-atoms) is monomeric, but **156** (with one  $\text{SiMe}_3$  group and one Me group) is dimeric.

Interestingly, the reaction of  $\text{TiCl}_3$  with *closo-exo*-4,5- $\{(\mu\text{-H})_2\text{Li}(\text{TMEDA})\}$ -1-Li $\{(\text{TMEDA})$ -2,4-( $\text{SiMe}_3$ )<sub>2</sub>-2,4- $\text{C}_2\text{B}_4\text{H}_4\}$  (in this dilithiacarborane precursor the carbon atoms are no longer next to each other) did not produce a complex analogous to **155**. Instead, the monomeric half-sandwich titanacarborane 1-( $\text{TMEDA}$ )-1-Cl-1-Ti-2,4-( $\text{SiMe}_3$ )<sub>2</sub>-2,4- $\text{C}_2\text{B}_4\text{H}_4$  **157** was generated (Equation (41)). Both the solid-state and solution EPR spectra of **155** were consistent with a monomeric  $d^1$ -electron configuration. The solid-state structure of **157** showed that the Ti– $\text{C}_2\text{B}_3$ (centroid) distance in **157** is 1.948 Å, which is comparable to the distances observed in **152**, **155**, and **156**.

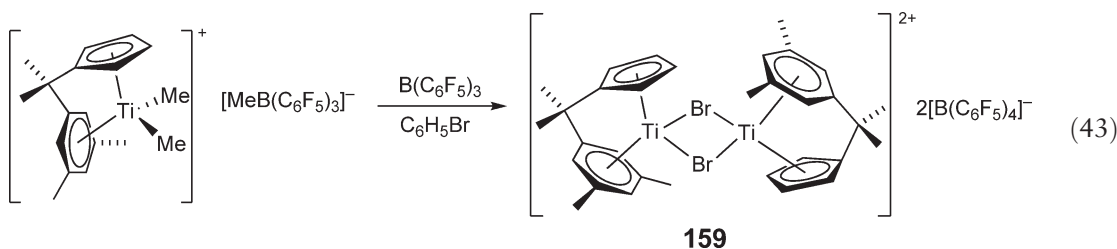


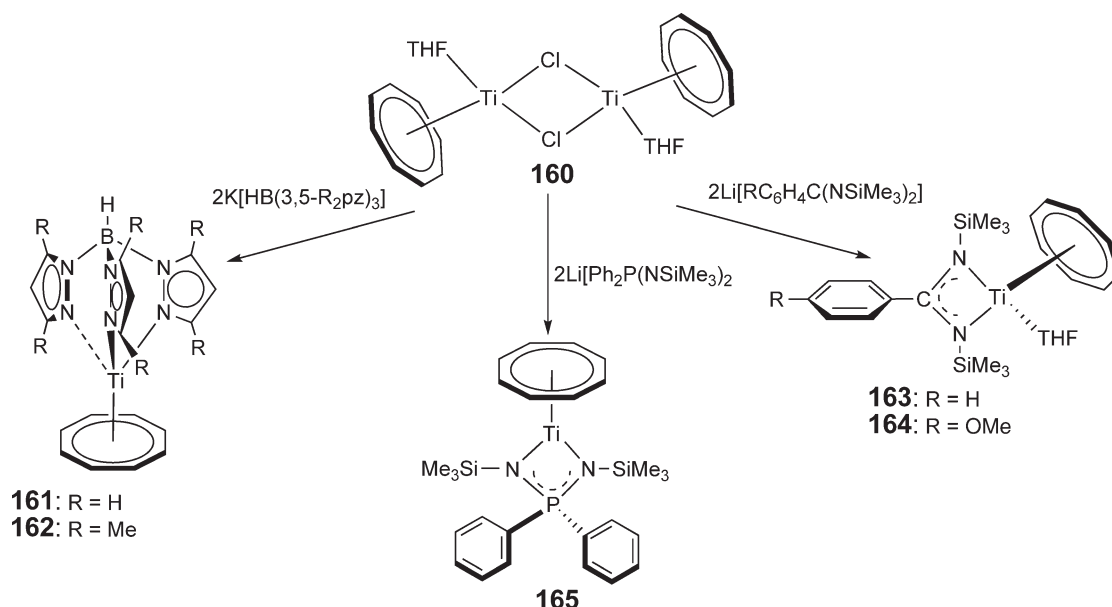
#### 4.04.8 Compounds with $\eta^6$ -Ligands

The Ti(III) complex  $(\text{C}_5\text{H}_5\text{B-Ph})\text{Ti}\{\text{N}(\text{SiMe}_3)_2\}_2$  **158** containing an  $\eta^6$ -coordinated borabenzene ligand was prepared from  $\text{TiCl}\{\text{N}(\text{SiMe}_3)_2\}_2(\text{THF})$  and 1 equiv. of  $\text{Li}[\text{C}_5\text{H}_5\text{B-Ph}]$  (Equation (42)).<sup>28</sup> X-ray crystallography indicated that there are two chemically identical but conformationally distinct molecules of **158** in the asymmetric unit. Compound **158** closely resembles  $(\eta^5\text{-fluorenyl})\text{Ti}\{\text{N}(\text{SiMe}_3)_2\}_2$  **38**, which indicates the close relationship between the borabenzene ligand and cyclopentadienyl type ligands. Both independent molecules of **158** adopt a distorted two-legged piano stool geometry. In one molecule the borabenzene ligand is completely planar, while in the other the boron atom is slightly displaced from the least-squares plane containing the five carbon atoms of the  $\text{C}_5\text{B}$  ring. The authors suggested that this difference was due to packing effects. The phenyl substituent on the boron atom is not co-planar with the  $\text{C}_5\text{B}$  ring but is positioned slightly out of the least-squares plane.



A highly unusual reaction was observed between the ionic Ti(IV) *ansa*-cyclopentadienyl-arene complex  $[(\eta^5, \eta^6\text{-C}_5\text{H}_4\text{CMe}_2\text{Ar})\text{TiMe}_2][\text{MeB}(\text{C}_6\text{F}_5)_3]$  ( $\text{Ar} = 3,5\text{-Me}_2\text{C}_6\text{H}_3$ ),  $\text{B}(\text{C}_6\text{F}_5)_3$  and bromobenzene, which gave the dimeric, dicationic Ti(III) species  $[(\eta^5, \eta^6\text{-C}_5\text{H}_4\text{CMe}_2\text{Ar})_2\text{Ti}_2(\mu\text{-Br})_2][\text{B}(\text{C}_6\text{F}_5)_4]_2$  **159** (Equation (43)).<sup>117</sup> This reaction is unusual in that it involves the reduction of the Ti(IV) center to Ti(III), activation of the C–Br bond in bromobenzene and exchange of the substituents on the boron atom. The yield for the process was 18%. The structure of **159** was elucidated by X-ray crystallography and revealed a centrosymmetric cation. The arene rings are planar but coordinate to the metal in an asymmetric fashion, with Ti–C bond lengths varying from 2.379(3) to 2.713(4) Å. This results in a lengthening of several of the C–C bonds in the arene rings.





Scheme 11

#### 4.04.9 Compounds with $\eta^8$ -Ligands

The dimeric Ti(III) complex  $(\text{COT})_2\text{Ti}_2(\mu\text{-Cl})_2(\text{THF})_2$  ( $\text{COT} = \eta^8\text{-cyclooctatetraenyl}(2-)$ ) **160** was described in COMC (1982).<sup>54</sup> Edelmann *et al.* have subsequently utilized this complex as a precursor to synthesize a variety of monomeric Ti(III) species through metathesis reactions.<sup>118</sup> The reactions of **160** with  $\text{K}[\text{HBpz}_3]$  or  $\text{K}[\text{HB}(3,5\text{-Me}_2\text{pz})_3]$  ( $\text{pz} = \text{pyrazolyl}$ ) generated the half-sandwich Ti(III) species  $(\text{COT})\text{Ti}(\text{HBpz}_3)$  **161** and  $(\text{COT})\text{Ti}(\text{HB}(3,5\text{-Me}_2\text{pz})_3)$  **162**, respectively. The crystal structure of **161** revealed a pseudo-tetrahedral coordination of the ligands around the titanium center. The COT ring is  $\eta^8$ -coordinated and approximately planar. In addition, the organotitanium(III) species  $(\text{COT})\text{Ti}(\text{PhC}(\text{NSiMe}_3)_2)(\text{THF})$  **163**,  $(\text{COT})\text{Ti}(\text{MeOC}_6\text{H}_4\text{C}(\text{NSiMe}_3)_2)(\text{THF})$  **164**, and  $(\text{COT})\text{Ti}(\text{Ph}_2\text{P}(\text{NSiMe}_3)_2)$  **165** were prepared through the reaction of **160** with the appropriate heteroallylic ligands. The reactions of **160** are summarized in Scheme 11.

The reaction between 1 equiv. of the sterically bulky  $\text{COT}''$  ( $\text{COT}'' = 1,4\text{-bis}(\text{trimethylsilyl})\text{cyclooctatetraene}$ ) ligand and  $\text{TiCl}_3(\text{THF})_3$  did not result in the clean formation of an analogous compound to **160**.<sup>119</sup> Instead, a mixture of the Ti(II) species  $(\text{COT}'')_2\text{Ti}$ , the mixed valence Ti(III)/Ti(IV) species  $\{(\text{COT}'')\text{Ti}\}_2(\mu\text{-Cl})_3$  **166** and the asymmetric Ti(III) dimeric species  $\{(\text{COT}'')\text{Ti}(\mu\text{-Cl})_2(\text{THF})\}$  **167** were formed in yields of 15%, 30% and 50%, respectively. X-ray crystallography confirmed that only one of the Ti centers in **167** coordinates to a molecule of THF, although this THF was released when **167** was warmed to  $80^\circ\text{C}$  *in vacuo*. The EPR spectrum of **167** confirmed that the two Ti centers contained unpaired electrons while that of **166** was consistent with a  $\text{COT}''$  Ti(III) species. No unusual line broadening was observed in the EPR spectra of **166** when it was cooled; this suggested that the EPR relaxation time was relatively fast compared to any electron transfer between the two titanium centers.

## References

- Alonso, P. J.; Fornies, J.; Garcia-Monforte, M. A.; Martin, A.; Menjon, B. *Chem. Commun.* **2002**, 728–729.
- Ara, I.; Fornies, J.; Garcia-Monforte, M. A.; Martin, A.; Menjon, B. *Chem. Eur. J.* **2004**, *10*, 4186–4197.
- Alonso, P. J.; Falvello, L. R.; Fornies, J.; Garcia-Monforte, M. A.; Menjon, B. *Angew. Chem., Int. Ed.* **2004**, *43*, 5225–5228.
- Scoles, L.; Minhas, R.; Duchateau, R.; Jubb, J.; Gambarotta, S. *Organometallics* **1994**, *13*, 4978–4983.
- Johnson, A. R.; Davis, W. M.; Cummins, C. C. *Organometallics* **1996**, *15*, 3825–3835.
- Putzer, M. A.; Magull, J.; Goesmann, H.; Neumueller, B.; Dehnicke, K. *Chem. Ber.* **1996**, *129*, 1401–1405.
- Putzer, M. A.; Neumueller, B.; Dehnicke, K. *Z. Anorg. Allg. Chem.* **1998**, *624*, 57–64.
- Mokuolu, Q. F.; Duckmanton, P. A.; Blake, A. J.; Wilson, C.; Love, J. B. *Organometallics* **2003**, *22*, 4387–4389.
- Budzelaar, P. H. M.; Van Oort, A. B.; Orpen, A. G. *Eur. J. Inorg. Chem.* **1998**, 1485–1494.
- Basuli, F.; Bailey, B. C.; Tomaszewski, J.; Huffman, J. C.; Mindiola, D. J. *J. Am. Chem. Soc.* **2003**, *125*, 6052–6053.



11. Basuli, F.; Bailey, B. C.; Watson, L. A.; Tomaszewski, J.; Huffman, J. C.; Mindiola, D. J. *Organometallics* **2005**, *24*, 1886–1906.
12. Bailey, B. C.; Huffman, J. C.; Mindiola, D. J.; Weng, W.; Ozerov, O. V. *Organometallics* **2005**, *24*, 1390–1393.
13. Love, J. B.; Clark, H. C. S.; Cloke, F. G. N.; Green, J. C.; Hitchcock, P. B. *J. Am. Chem. Soc.* **1999**, *121*, 6843–6849.
14. Zanotti-Gerosa, A.; Solari, E.; Giannini, L.; Floriani, C.; Re, N.; Chiesi-Villa, A.; Rizzoli, C. *Inorg. Chim. Acta* **1998**, *270*, 298–311.
15. Hagadorn, J. R.; Arnold, J. *J. Am. Chem. Soc.* **1996**, *118*, 893–894.
16. Coles, S. J.; Hursthouse, M. B.; Kelly, D. G.; Toner, A. J.; Walker, N. M. *J. Organomet. Chem.* **1999**, *580*, 304–312.
17. Basuli, F.; Bailey, B. C.; Huffman, J. C.; Mindiola, D. J. *Organometallics* **2005**, *24*, 3321–3334.
18. Dick, D. G.; Edema, J. J. H.; Duchateau, R.; Gambarotta, S. *Inorg. Chem.* **1993**, *32*, 1959–1962.
19. Cotton, F. A.; Murillo, C. A.; Petrukhina, M. A. *J. Organomet. Chem.* **2000**, *593–594*, 1–6.
20. Ray, B.; Neyroud, T. G.; Kapon, M.; Eichen, Y.; Eisen, M. S. *Organometallics* **2001**, *20*, 3044–3055.
21. Crescenzi, R.; Solari, E.; Floriani, C.; Chiesi-Villa, A.; Rizzoli, C. *Organometallics* **1996**, *15*, 5456–5458.
22. Alvanipour, A.; Atwood, J. L.; Bott, S. G.; Junk, P. C.; Kynast, U. H.; Prinz, H. *J. Chem. Soc., Dalton Trans.* **1998**, 1223–1228.
23. Troyanov, S. I.; Mach, K.; Varga, V. *Organometallics* **1993**, *12*, 3387–3389.
24. Hagadorn, J. R.; McNevin, M. J. *Organometallics* **2003**, *22*, 609–611.
25. Liu, F.-Q.; Kuhn, A.; Herbst-Irmer, R.; Stalke, D.; Roesky, H. W. *Angew. Chem., Int. Ed.* **1994**, *33*, 555–556.
26. Liu, F.-Q.; Stalke, D.; Roesky, H. W. *Angew. Chem., Int. Ed.* **1995**, *34*, 1872–1874.
27. Nadasdi, T. T.; Stephan, D. W. *Inorg. Chem.* **1993**, *32*, 5933–5938.
28. Putzer, M. A.; Lachicotte, R. J.; Bazan, G. C. *Inorg. Chem. Commun.* **1999**, *2*, 319–322.
29. Mach, K.; Antropiusová, H.; Polacek, J. *J. Organomet. Chem.* **1979**, *172*, 325–329.
30. Schmid, G.; Thewalt, U.; Troyanov, S. I.; Mach, K. *J. Organomet. Chem.* **1993**, *453*, 185–191.
31. Mach, K.; Hiller, J.; Thewalt, U.; Sivik, M. R.; Bzowej, E. I.; Paquette, L. A.; Zaegel, F.; Meunier, P.; Gautheron, B. *Organometallics* **1995**, *14*, 2609–2612.
32. Mach, K.; Varga, V.; Antropiusová, H.; Polacek, J. *J. Organomet. Chem.* **1987**, *333*, 205–215.
33. Yim, J.; Chu, K.; Choi, K.; Ihm, S. *Eur. Polym. J.* **1996**, *32*, 1381–1385.
34. Xu, G.; Lin, S. *Macromolecules* **1997**, *30*, 685–693.
35. Po, R.; Cardi, N.; Abis, L. *Polymer* **1998**, *39*, 959–964.
36. Xu, J.; Zhao, J.; Fan, Z.; Feng, L. *Eur. Polym. J.* **1999**, *35*, 127–132.
37. Williams, E. F.; Murray, M. C.; Baird, M. C. *Macromolecules* **2000**, *33*, 261–268.
38. Bonoldi, L.; Abis, L.; Fiocca, L.; Fusco, R.; Longo, L.; Simone, F.; Spera, S. *J. Mol. Catal. A: Chem.* **2004**, *219*, 47–56.
39. Grassi, A.; Zambelli, A.; Laschi, F. *Organometallics* **1996**, *15*, 480–482.
40. Grassi, A.; Saccheo, S.; Zambelli, A.; Laschi, F. *Macromolecules* **1998**, *31*, 5588–5591.
41. Ready, T. E.; Gurge, R.; Chien, J. C. W.; Rausch, M. D. *Organometallics* **1998**, *17*, 5236–5239.
42. Ewart, S. W.; Sarsfield, M. J.; Williams, E. F.; Baird, M. C. *J. Organomet. Chem.* **1999**, *579*, 106–113.
43. Ewart, S. W.; Sarsfield, M. J.; Jeremic, D.; Tremblay, T. L.; Williams, E. F.; Baird, M. C. *Organometallics* **1998**, *17*, 1502–1510.
44. Minieri, G.; Corradini, P.; Zambelli, A.; Guerra, G.; Cavallo, L. *Macromolecules* **2001**, *34*, 2459–2468.
45. Nifant'ev, I. E.; Ustynyuk, L. Y.; Besedin, D. V. *Organometallics* **2003**, *22*, 2619–2629.
46. Ohff, A.; Kempe, R.; Baumann, W.; Rosenthal, U. *J. Organomet. Chem.* **1996**, *520*, 241–244.
47. Plecnik, C. E.; Liu, F. C.; Liu, S. M.; Liu, J. P.; Meyers, E. A.; Shore, S. G. *Organometallics* **2001**, *20*, 3599–3606.
48. Bouwkamp, M. W.; de Wolf, J.; Morales, I. H.; Gercama, J.; Meetsma, A.; Troyanov, S. I.; Hessen, B.; Teuben, J. H. *J. Am. Chem. Soc.* **2002**, *124*, 12956–12957.
49. Choukroun, R.; Lorber, C.; Vendier, L. *Eur. J. Inorg. Chem.* **2004**, 317–321.
50. Burlakov, V. V.; Troyanov, S. I.; Letov, A. V.; Strunkina, L. I.; Minacheva, M. K.; Furin, G. G.; Rosenthal, U.; Shur, V. B. *J. Organomet. Chem.* **2000**, *598*, 243–247.
51. Burlakov, V. V.; Arndt, P.; Baumann, W.; Spannenberg, A.; Rosenthal, U.; Letov, A. V.; Lyssenko, K. A.; Korlyukov, A. A.; Strunkina, L. I.; Minacheva, M. K., *et al.* *Organometallics* **2001**, *20*, 4072–4079.
52. Burlakov, V. V.; Pellny, P. M.; Arndt, P.; Baumann, W.; Spannenberg, A.; Shur, V. B.; Rosenthal, U. *Chem. Commun.* **2000**, 241–242.
53. Arndt, P.; Baumann, W.; Spannenberg, A.; Rosenthal, U.; Burlakov, V. V.; Shur, V. B. *Angew. Chem., Int. Ed.* **2003**, *42*, 1414–1418.
54. Bottrell, M.; Gavens, P. D.; McMeeking, J. In *Comprehensive Organometallic Chemistry I*; Wilkinson, G., Stone, F. G. A., Abel, E. W., Eds.; Pergamon: Oxford, 1982; Vol. 3.
55. Liu, F.-Q.; Gornitzka, H.; Stalke, D.; Roesky, H. W. *Angew. Chem., Int. Ed.* **1993**, *32*, 442–444.
56. Liu, F.-Q.; Kuenzel, A.; Herzog, A.; Roesky, H. W.; Noltemeyer, M.; Fleischer, R.; Stalke, D. *Polyhedron* **1996**, *16*, 61–65.
57. Yu, P.; Murphy, E. F.; Roesky, H. W.; Lubini, P.; Schmidt, H.-G.; Noltemeyer, M. *Organometallics* **1997**, *16*, 313–316.
58. Lukens, W. W., Jr.; Smith, M. R. III; Andersen, R. A. *J. Am. Chem. Soc.* **1996**, *118*, 1719–1728.
59. Bochmann, M. In *Comprehensive Organometallic Chemistry II*; Wilkinson, G., Stone, F. G. A., Abel, E. W., Eds.; Elsevier: Oxford, 1995; Vol. 4.
60. Piglosiewicz, I. M.; Kraft, S.; Beckhaus, R.; Haase, D.; Saak, W. *Eur. J. Inorg. Chem.* **2005**, 938–945.
61. Enemaerke, R. J.; Larsen, J.; Skrydstrup, T.; Daasbjerg, K. *Organometallics* **2004**, *23*, 1866–1874.
62. Enemaerke, R. J.; Larsen, J.; Skrydstrup, T.; Daasbjerg, K. *J. Am. Chem. Soc.* **2004**, *126*, 7853–7864.
63. Samuel, E.; Hénique, J. *J. Organomet. Chem.* **1996**, *512*, 183–187.
64. Cano, A.; Cuenca, T.; Gómez-Sal, P.; Manzanero, A.; Royo, P. *J. Organomet. Chem.* **1996**, *526*, 227–235.
65. Lukešová, L.; Horáček, M.; Štěpnicka, P.; Fejfarová, K.; Gyepes, R.; Čišarová, I.; Kubišta, J.; Mach, K. *J. Organomet. Chem.* **2002**, *663*, 134–144.
66. Lukešová, L.; Štěpnicka, P.; Fejfarová, K.; Gyepes, R.; Čišarová, I.; Horáček, M.; Kupfer, V.; Mach, K. *Organometallics* **2002**, *21*, 2639–2653.
67. Jutzi, P.; Kleimeier, J. *J. Organomet. Chem.* **1995**, *486*, 287–289.
68. Qian, Y.; Guo, R.; Huang, J. *Polyhedron* **1996**, *16*, 195–198.
69. Kotov, V. V.; Frohlich, R.; Kehr, G.; Erker, G. *J. Organomet. Chem.* **2003**, *676*, 1–7.
70. Baum, E.; Matern, E.; Pikies, J.; Robaszkiewicz, A. *Z. Anorg. Allg. Chem.* **2004**, *630*, 1090–1095.
71. King, W. A.; Di Bella, S.; Gulino, A.; Lanza, G.; Fragala, I. L.; Stern, C. L.; Marks, T. J. *J. Am. Chem. Soc.* **1999**, *121*, 355–366.
72. de Wolf, J. M.; Meetsma, A.; Teuben, J. H. *Organometallics* **1995**, *14*, 5466–5468.
73. de Wolf, J. M.; Blaauw, R.; Meetsma, A.; Teuben, J. H.; Gyepes, R.; Varga, V.; Mach, K.; Veldman, N.; Spek, A. L. *Organometallics* **1996**, *15*, 4977–4983.



74. Lukens, W. W., Jr.; Matsunaga, P. T.; Andersen, R. A. *Organometallics* **1998**, *17*, 5240–5247.
75. He, X. M.; Hartwig, J. F. *J. Am. Chem. Soc.* **1996**, *118*, 1696–1702.
76. Chase, P. A.; Piers, W. E.; Parvez, M. *Organometallics* **2000**, *19*, 2040–2042.
77. Xin, S.; Harrod, J. F.; Samuel, E. *J. Am. Chem. Soc.* **1994**, *116*, 11562–11563.
78. Fischer, J. M.; Piers, W. E.; Young, V. G., Jr. *Organometallics* **1996**, *15*, 2410–2412.
79. Goedheijt, M. S.; Nijbacker, T.; Akkerman, O. S.; Bickelhaupt, F.; Veldman, N.; Spek, A. L. *J. Organomet. Chem.* **1997**, *527*, 1–5.
80. Horáček, M.; Hiller, J.; Thewalt, U.; Polášek, M.; Mach, K. *Organometallics* **1997**, *16*, 4185–4191.
81. Troyanov, S. I.; Varga, V.; Mach, K. *Organometallics* **1993**, *12*, 2820–2824.
82. Varga, V.; Mach, K.; Hiller, J.; Thewalt, U. *J. Organomet. Chem.* **1996**, *506*, 109–112.
83. Kirchbauer, F. G.; Pellny, P. M.; Sun, H. S.; Burlakov, V. V.; Arndt, P.; Baumann, W.; Spannenberg, A.; Rosenthal, U. *Organometallics* **2001**, *20*, 5289–5296.
84. Horáček, M.; Cisarová, I.; Lukešová, L.; Kubišta, J.; Mach, K. *Inorg. Chem. Commun.* **2004**, *7*, 713–717.
85. Gao, Y.; Iijima, S.; Urabe, H.; Sato, F. *Inorg. Chim. Acta* **1994**, *222*, 145–153.
86. Casty, G. L.; Stryker, J. M. *J. Am. Chem. Soc.* **1995**, *117*, 7814–7815.
87. Carter, C. A. G.; McDonald, R.; Stryker, J. M. *Organometallics* **1999**, *18*, 820–822.
88. Greidanus, G.; McDonald, R.; Stryker, J. M. *Organometallics* **2001**, *20*, 2492–2504.
89. Hitchcock, P. B.; Lappert, M. F.; Layh, M. Z. *Anorg. Allg. Chem.* **2000**, *626*, 1081–1086.
90. Ogoshi, S.; Stryker, J. M. *J. Am. Chem. Soc.* **1998**, *120*, 3514–3515.
91. Brady, E.; Telford, J. R.; Mitchell, G.; Lukens, W. *Acta Crystallogr., Sect. C: Cryst. Struct. Commun.* **1995**, *C51*, 558–560.
92. Ohff, A.; Zippel, T.; Arndt, P.; Spannenberg, A.; Rosenthal, U. *Organometallics* **1998**, *17*, 1649–1651.
93. Zippel, T.; Arndt, P.; Ohff, A.; Spannenberg, A.; Kempe, R.; Rosenthal, U. *Organometallics* **1998**, *17*, 4429–4437.
94. Rep, M.; Kaagman, J.-W. F.; Elsevier, C. J.; Sedmera, P.; Hiller, J.; Thewalt, U.; Horáček, M.; Mach, K. *J. Organomet. Chem.* **2000**, *597*, 146–156.
95. Witte, P. T.; Klein, R.; Kooijman, H.; Spek, A. L.; Polášek, M.; Varga, V.; Mach, K. *J. Organomet. Chem.* **1996**, *519*, 195–204.
96. Matsubara, K.; Niibayashi, S.; Nagashima, H. *Organometallics* **2003**, *22*, 1376–1382.
97. Niibayashi, S.; Mitsui, K.; Matsubara, K.; Nagashima, H. *Organometallics* **2003**, *22*, 4885–4892.
98. Horáček, M.; Gyepes, R.; Kubišta, J.; Mach, K. *Inorg. Chem. Commun.* **2004**, *7*, 155–159.
99. Sofield, C. D.; Walter, M. D.; Andersen, R. A. *Acta Crystallogr., Sect. E: Struct. Rep. Online* **2004**, *E60*, m1417–m1419.
100. Lukens, W. W., Jr.; Andersen, R. A. *Inorg. Chem.* **1995**, *34*, 3440–3443.
101. Ren, Q.; Chen, Z.; Ren, J.; Wei, H.; Feng, W.; Zhang, L. *J. Phys. Chem. A* **2002**, *106*, 6161–6166.
102. Burlakov, V. V.; Yanovsky, A. I.; Struchkov, Y. T.; Rosenthal, U.; Spannenberg, A.; Kempe, R.; Ellert, O. G.; Shur, V. B. *J. Organomet. Chem.* **1997**, *542*, 105–112.
103. Edelmann, F. T.; Giessmann, S.; Fischer, A. *Chem. Commun.* **2000**, 2153–2154.
104. Edelmann, F. T.; Giessmann, S.; Fischer, A. *J. Organomet. Chem.* **2001**, *620*, 80–89.
105. Ho, J.; Stephan, D. W. *Inorg. Chem.* **1994**, *33*, 4595–4597.
106. Cano, A.; Cuenca, T.; Galakhov, M.; Rodriguez, G. M.; Royo, P.; Cardin, C. J.; Convery, M. A. *J. Organomet. Chem.* **1995**, *493*, 17–25.
107. Matsuzaki, K.; Kawaguchi, H.; Voth, P.; Noda, K.; Itoh, S.; Takagi, H. D.; Kashiwabara, K.; Tatsumi, K. *Inorg. Chem.* **2003**, *42*, 5320–5329.
108. Christou, V.; Wuller, S. P.; Arnold, J. *J. Am. Chem. Soc.* **1993**, *115*, 10545–10552.
109. Varga, V.; Mach, K.; Hiller, J.; Thewalt, U.; Sedmera, P.; Polášek, M. *Organometallics* **1995**, *14*, 1410–1416.
110. Mach, K.; Kubišta, J.; Cisarová, I.; Štepnicka, P. *Acta Crystallogr., Sect. C: Cryst. Struct. Commun.* **2002**, *C58*, m116–m118.
111. Gyepes, R.; Mach, K.; Cisarová, I.; Loub, J.; Hiller, J.; Sindelar, P. *J. Organomet. Chem.* **1995**, *497*, 33–41.
112. Troyanov, S. I.; Varga, V.; Mach, K. *Chem. Commun.* **1993**, 1174–1175.
113. Gyepes, R.; Hiller, J.; Thewalt, U.; Polášek, M.; Sindelar, P.; Mach, K. *J. Organomet. Chem.* **1996**, *516*, 177–185.
114. Piao, G.; Goto, H.; Akagi, K.; Shirakawa, H. *Polymer* **1998**, *39*, 3559–3564.
115. Hosmane, N. S.; Wang, Y.; Zhang, H.; Lu, K.-J.; Maguire, J. A.; Gray, T. G.; Brooks, K. A.; Waldhoer, E.; Kaim, W.; Kremer, R. K. *Organometallics* **1997**, *16*, 1365–1377.
116. Hosmane, N. S.; Wang, Y.; Zhang, H.; Maguire, J. A.; Waldhoer, E.; Kaim, W.; Binder, H.; Kremer, R. K. *Organometallics* **1994**, *13*, 4156–4158.
117. Deckers, P. J. W.; Van der Linden, A. J.; Meetsma, A.; Hessen, B. *Eur. J. Inorg. Chem.* **2000**, 929–932.
118. Kilimann, U.; Noltemeyer, M.; Schaefer, M.; Herbst-Imer, R.; Schmidt, H.-G.; Edelmann, F. T. *J. Organomet. Chem.* **1994**, *469*, C27–C30.
119. Horáček, M.; Kupfer, V.; Thewalt, U.; Polášek, M.; Mach, K. *J. Organomet. Chem.* **1999**, *579*, 126–132.

## 4.05

# Complexes of Titanium in Oxidation State IV

---

T Cuenca, Universidad de Alcalá, Madrid, Spain

© 2007 Elsevier Ltd. All rights reserved.

<b>4.05.1</b>	<b>Introduction</b>	<b>324</b>
<b>4.05.2</b>	<b>Compounds with <math>\eta^1</math>-Ligands without Anionic <math>\pi</math>-Ligands</b>	<b>325</b>
4.05.2.1	Synthesis of Complexes with $\eta^1$ -Ligands	325
4.05.2.1.1	Monoalkyl and related complexes	325
4.05.2.1.2	Dialkyl and related complexes	339
4.05.2.1.3	Trialkyl and related complexes	361
4.05.2.1.4	Tetraalkyl and related complexes	362
4.05.2.1.5	Alkylidene and carbene complexes	364
4.05.2.1.6	Cyanide and isocyanide complexes	367
4.05.2.2	Structures and Properties	368
4.05.2.3	Reactions	369
<b>4.05.3</b>	<b>Mono(Cyclopentadienyl) and Related Compounds</b>	<b>381</b>
4.05.3.1	Mono-Cp Halide Complexes	382
4.05.3.1.1	Synthesis	382
4.05.3.1.2	Structural aspects	398
4.05.3.1.3	Reactions	398
4.05.3.2	Mono-Cp Complexes with Ti–C Bonds	406
4.05.3.2.1	Synthesis	406
4.05.3.2.2	Structural aspects	410
4.05.3.2.3	Reactions	410
4.05.3.3	Mono-Cp Complexes with Ti–N Bonds	413
4.05.3.3.1	Amido complexes	413
4.05.3.3.2	Aza complexes	417
4.05.3.3.3	Imido complexes	419
4.05.3.3.4	Phosphinimido complexes	426
4.05.3.3.5	Amidinato complexes	431
4.05.3.3.6	Complexes with other N-based ligands	434
4.05.3.4	Monocyclopentadienyl–Amido Complexes	437
4.05.3.4.1	Metathesis reactions	438
4.05.3.4.2	Amine elimination	442
4.05.3.4.3	Alkane elimination from homoleptic $\text{TiR}_4$	446
4.05.3.4.4	HCl elimination from $\text{TiCl}_4$ or $\text{TiCp}'\text{Cl}_3$	446
4.05.3.4.5	Dehalosilylation reactions	448
4.05.3.4.6	Miscellaneous	448
4.05.3.5	Mono-Cp Complexes with Ti–O Bonds	465
4.05.3.5.1	Oxo complexes	465
4.05.3.5.2	Alkoxo complexes	473
4.05.3.5.3	Cyclopentadienyl–alkoxo complexes	495
4.05.3.5.4	Complexes with other O-based ligands	500
4.05.3.6	Mono-Cp Complexes with Ti–Chalcogenido Bonds	503
4.05.3.7	Mono-Cp Complexes with Ti–H Bonds	507
<b>4.05.4</b>	<b>Bis(Cyclopentadienyl) and Related Compounds</b>	<b>509</b>
4.05.4.1	Halide Complexes	510
4.05.4.1.1	Synthesis of bis-Cp titanium halides	510

4.05.4.1.2	Properties and structures of bis-Cp titanium halides	530
4.05.4.1.3	Reactions of bis-Cp titanium halides	532
<b>4.05.4.2</b>	<b>Complexes with Ti–C Bonds</b>	<b>542</b>
4.05.4.2.1	Synthesis of bis-Cp titanium hydrocarbyls	542
4.05.4.2.2	Structures and properties of bis-Cp titanium hydrocarbyls	551
4.05.4.2.3	Reactions of bis-Cp titanium hydrocarbyls	551
4.05.4.2.4	Alkylidenes, metallacycles, and related titanium complexes	555
4.05.4.2.5	Ziegler–Natta polymerization	577
<b>4.05.4.3</b>	<b>Complexes with Ti–Sn Bonds</b>	<b>578</b>
<b>4.05.4.4</b>	<b>Complexes with Ti–N Bonds</b>	<b>578</b>
<b>4.05.4.5</b>	<b>Complexes with Schiff Bases and Heterocyclic Compounds</b>	<b>585</b>
<b>4.05.4.6</b>	<b>Complexes with Ti–O Bonds</b>	<b>586</b>
4.05.4.6.1	Titanium oxo, hydroxo, and alkoxo complexes	586
4.05.4.6.2	Complexes with other O-based ligands	594
<b>4.05.4.7</b>	<b>Complexes with Ti–Si Bonds</b>	<b>596</b>
<b>4.05.4.8</b>	<b>Complexes with Ti–Chalcogenide Bonds</b>	<b>596</b>
<b>4.05.4.9</b>	<b>Complexes with Ti–H, and Ti–B Bonds</b>	<b>602</b>
<b>4.05.5</b>	<b><i>ansa</i>-Titanocene Complexes</b>	<b>603</b>
<b>4.05.5.1</b>	<b>Carbon-bridged <i>ansa</i>-titanocene Derivatives</b>	<b>604</b>
4.05.5.1.1	Complexes with one-carbon bridges	604
4.05.5.1.2	Complexes with two-carbon bridges	606
4.05.5.1.3	Complexes with bridges containing more than two carbons	613
<b>4.05.5.2</b>	<b>Silicon-bridged <i>ansa</i>-titanocene Derivatives</b>	<b>616</b>
<b>4.05.5.3</b>	<b><i>ansa</i>-Titanocene Derivatives Bridged by other Heteroatoms</b>	<b>624</b>
<b>4.05.6</b>	<b>Heteropolymetallic Compounds</b>	<b>626</b>
<b>4.05.7</b>	<b>Complexes with Non-cyclopentadienyl <math>\pi</math>-Ligands</b>	<b>646</b>
4.05.7.1	Complexes with $\eta^5$ -Heteroligands	646
4.05.7.2	Complexes with $\eta^6$ -Ligands	652
4.05.7.3	Complexes with $\eta^7$ - and $\eta^8$ -Ligands	653
4.05.7.4	Complexes with More than Two Cyclopentadienyl Ligands	654
<b>4.05.8</b>	<b>Applications of Titanium(IV) Complexes in Synthesis and Catalysis</b>	<b>655</b>
4.05.8.1	Organic Synthesis	655
4.05.8.2	Anti-tumor and Biological Effects	662
<b>References</b>		<b>664</b>

## 4.05.1 Introduction

In the last decade several areas of the organometallic titanium chemistry in the oxidation state IV have been widely developed. Particularly, emphasis on applications in organic reactions and in the polymerization of  $\alpha$ -olefins has contributed to the increasing number of newly synthesized compounds. Organometallic titanium(IV) complexes are generally supported by cyclopentadienyl ligands and many investigations on the chemistry and applications of bis- and mono(cyclopentadienyl) derivatives have been undertaken. The modification of the classical cyclopentadienyl rings has a direct influence on the physical and chemical properties of these substances, with a main focus on stereoselective transformations. Compounds containing a cyclopentadienyl ring connected to a second functionality, both directly bonded to the titanium atom (cyclopentadienyl-amido, cyclopentadienyl-alkoxo, etc.), have received special attention in recent years. Similarly, organometallic titanium(IV) derivatives with non-cyclopentadienyl ligands have become very important because of their role in C–H activation processes and in catalytic reactions. Thus, these compounds have contributed significantly to the progress of synthetic and applied modern chemistry.

This chapter attempts to summarize the literature on this class of complexes from the publication of COMC (1995) to 2004 or early 2005. Synthesis, structure, and chemical properties of organometallic titanium(IV) compounds, which contain different types of Ti–C bonds supported by additional ligands, will be covered. We attempt to highlight the major developments from 1993 and tentatively to reveal new trends in this field over the next few years.

## 4.05.2 Compounds with $\eta^1$ -Ligands without Anionic $\pi$ -Ligands

The most significant advances made in the field of titanium chemistry in recent years concern the synthesis of “well-defined” olefin polymerization catalysts, the vast majority of which contain one or two Cp-like (Cp = cyclopentadienyl) rings. The great success of group 4 Cp derivatives as catalysts for the olefin polymerization has stimulated the interest in the development of related homogeneous catalysts supported by non-Cp ancillary groups. In the last decade group 4 metal complexes that do not have Cp-like ligands bonded to the metal center have become a major research focus. Nevertheless, the chemistry of Ti(IV) metal–carbon  $\sigma$ -bonds in non-Cp ligand environments remains much less explored than that of Cp derivatives. Synthetic procedures to Ti  $\sigma$ -ligand complexes without  $\pi$ -ligands exhibit many difficulties due to the high reactivity and the low thermal stability of the  $\sigma$ -Ti–C bonds. Simple transition metal alkyl complexes may decompose in several ways and the Ti(IV) alkyl and related derivatives are sensitive to air and moisture. For alkyl and related complexes it has been observed that at least one-electron donor ligands such as alkoxo or amido groups must be present in order to stabilize the corresponding organometallic compounds. In an effort to create electron-deficient titanium complexes for catalytic transformations, dialkoxo, diamido, and chelating *O*- and *N*-ligands with bulky substituents are currently being explored and they have been considered as alternatives to the ubiquitous Cp derivatives. Several reviews concerning this subject have appeared.<sup>1,2</sup> The following discussion gives some representative recent examples of these complexes.

### 4.05.2.1 Synthesis of Complexes with $\eta^1$ -Ligands

#### 4.05.2.1.1 Monoalkyl and related complexes

Generally, monoalkyl and monoaryl titanium complexes are prepared by salt metathesis reactions, although other methods of synthesis more sophisticated than this usual procedure are also employed.

TiCl<sub>3</sub>Me has attracted attention because the structure of the methyl group might be affected by Ti···H–C agostic interactions. Its infrared spectrum has been studied.<sup>3</sup> A pure sample of TiCl<sub>3</sub>Me was prepared by treatment of TiCl<sub>4</sub> with 15% molar excess of ZnMe<sub>2</sub>. The photoelectron spectrum of this substance has been measured, and the nature of the Ti–Me bond has been elucidated by variable-energy photoelectron spectroscopy and DFT calculations. The Ti–C bond has significant Ti 3*d* character.<sup>4</sup> All members of the methyl complexes series TiCl<sub>4–*n*</sub>Me<sub>*n*</sub> (*n* = 1–4) have been prepared from MgIme and TiCl<sub>4</sub> or by comproportionation reactions. Combined NMR experimental data and theoretical studies related to these complexes have been reported.<sup>5</sup>

The alkynyltitanium complexes TiCl<sub>3</sub>(C≡CR) (R typically = alkyl groups) are prepared *in situ* by reacting 1-alkynes with TiCl<sub>4</sub> in the presence of Et<sub>3</sub>N. The synthetic potential of these compounds has been illustrated in reactions with a number of electrophiles. In the presence of terminal alkynes, symmetrical 1,3-diynes are formed. The reaction with chlorodiphenylphosphine produces the corresponding alkynyl phosphine, while treatment with triethylphosphite affords tris(phenylethynyl) phosphine by substitution of the three alkoxo groups. The reaction with trimethyl orthoformate gives acetals.<sup>6–9</sup>

The alkyl transfer properties of dialkyl zinc reagents have been studied in the reaction of Zn[CH(SiMe<sub>3</sub>)<sub>2</sub>]<sub>2</sub> with TiCl<sub>4</sub>. The monoalkyl trichloro titanium complex TiCl<sub>3</sub>[CH(SiMe<sub>3</sub>)<sub>2</sub>] was obtained in 83% yield.<sup>10</sup>

##### 4.05.2.1.1.(i) Complexes stabilized by oxygen-ligands

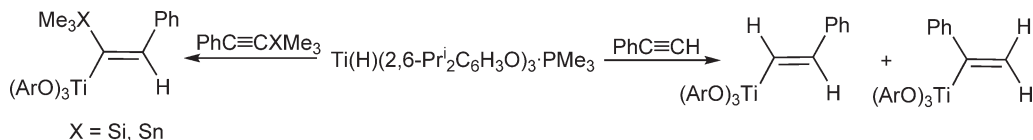
The formation of TiMe(OPr<sup>*i*</sup>)<sub>3</sub> is spectroscopically observed in the reaction of Ti(OPr<sup>*i*</sup>)<sub>4</sub> with ZnMe<sub>2</sub> in C<sub>6</sub>D<sub>6</sub>. This species has been used as a catalyst for the addition of alkyl groups to aldehydes.<sup>11,12</sup> Sequential treatment of TiCl<sub>4</sub>(1,2-DME) with LiMe followed by CF<sub>3</sub>CH<sub>2</sub>OH gives TiCl<sub>2</sub>Me(OCH<sub>2</sub>CF<sub>3</sub>).<sup>13</sup>

The monoalkyl complex TiBu<sup>*t*</sup>(O-2,6-Pr<sup>*i*</sup><sub>2</sub>C<sub>6</sub>H<sub>3</sub>)<sub>3</sub> has been obtained as amber-colored cube-shaped crystals by reacting TiCl(O-2,6-Pr<sup>*i*</sup><sub>2</sub>C<sub>6</sub>H<sub>3</sub>)<sub>3</sub> with LiBu<sup>*t*</sup>. Attempts to convert this alkyl complex into the monohydride Ti(H)(O-2,6-Pr<sup>*i*</sup><sub>2</sub>C<sub>6</sub>H<sub>3</sub>)<sub>3</sub> by thermal transformations have been unsuccessful. Nevertheless, the reactivity of the trialkoxo-hydride complex Ti(H)(O-2,6-Pr<sup>*i*</sup><sub>2</sub>C<sub>6</sub>H<sub>3</sub>)<sub>3</sub>(PMe<sub>3</sub>) has been studied. This compound reacts with phenylacetylene with addition of the Ti–H bond to the C≡C triple bond to give a mixture of two vinyltitanium complexes. Much better

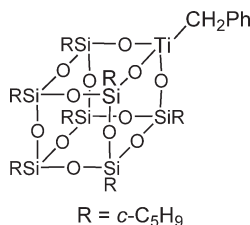
selectivity for the hydrotitanation reaction has been observed with  $\text{Me}_3\text{SiC}\equiv\text{CH}$ , while stereospecificity results by using the alkynes  $\text{Me}_3\text{SiC}\equiv\text{CPh}$  and  $\text{Me}_3\text{SnC}\equiv\text{CPh}$  (Scheme 1).<sup>14</sup>

Reaction of silsesquioxane  $\text{R}_7\text{Si}_7\text{O}_9(\text{OH})_3$  ( $\text{R} = \textit{c}\text{-C}_6\text{H}_{11}$ ,  $\textit{c}\text{-C}_5\text{H}_9$ ) with  $\text{Ti}(\text{CH}_2\text{Ph})_4$  in toluene or diethyl ether occurs with protonolysis to give the monoalkyl derivative  $\text{Ti}(\text{CH}_2\text{Ph})[\text{R}_7\text{Si}_7\text{O}_9(\text{O})_3]$  (Scheme 2).<sup>15–17</sup> Monoalkyl calix[4]arene complexes shown in Scheme 3 have been synthesized. The molecular structure of the phenyl compound has been determined by X-ray diffraction methods.<sup>18</sup>

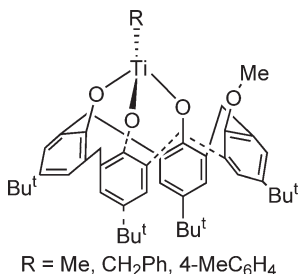
The titanapinacolato complexes  $\text{Ti}(\text{DMSC})(\text{OAr}_2\text{C}-\text{CAr}_2\text{O})$  ( $\text{DMSC} = 1,2\text{-alternate dimethylsilyl-bridged } \textit{p}\text{-tert-butylcalix[4]arene dianion}$ ) react with terminal alkynes with displacement of one of the  $\text{Ar}_2\text{CO}$  units and formation of 3,5-disubstituted 2-oxatitanacyclopent-4-ene derivatives. The reaction is slow at room temperature but proceeds to completion in 3 h at  $80^\circ\text{C}$ . Further reaction with  $\text{Me}_3\text{SiC}\equiv\text{CH}$  proceeds via formal insertion into the  $\text{Ti}-\text{C}$  bond to yield the corresponding 2-oxatitanacycloheptadiene complexes (Scheme 4). The molecular structure of these



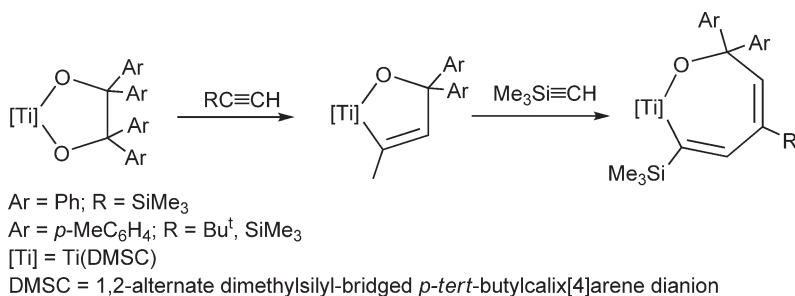
Scheme 1



Scheme 2



Scheme 3



Scheme 4

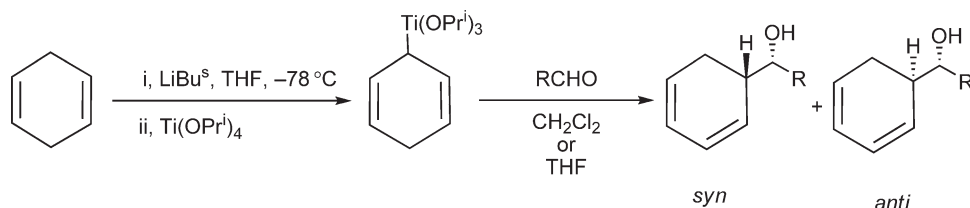
complexes has been determined by X-ray diffraction methods. Mechanistic considerations of these processes are reported.<sup>19</sup>

The  $\eta^1$ -fluorenyl titanium compound  $\text{Ti}(\eta^1\text{-Flu})(\text{OPr}^i)_3$  has been prepared by reaction of  $\text{TiCl}(\text{OPr}^i)_3$  with equimolar amounts of LiFlu. It is obtained as a mixture with the derivative  $\text{Ti}(\eta^5\text{-Flu})(\eta^1\text{-Flu})(\text{OPr}^i)_2$ . The complex has been characterized by X-ray analysis and variable-temperature NMR spectroscopy. In combination with MAO, the compound is a highly efficient initiator for styrene polymerizations, producing highly syndiotactic polymers.<sup>20</sup>

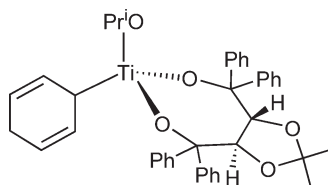
Monoalkynyltitanium derivatives  $\text{TiCl}(\text{C}\equiv\text{CR})(\text{OPr}^i)_2$  are prepared from the *in situ* formation of  $\text{Ti}(\text{II})$  species and subsequent reaction with haloalkynes through an addition– $\beta$ -elimination mechanistic process, showing that this is a powerful method for the synthesis of organometallic compounds. Investigations are carried out in order to rule out the classical oxidative addition of the low-valent titanium species into the carbon–chloro bond. These complexes can further react chemoselectively with a wide range of functionalized electrophiles.<sup>21</sup>

The cyclohexadienyltitanium complex  $\text{Ti}(\text{C}_6\text{H}_7)(\text{OPr}^i)_3$  was prepared from 1,4-cyclohexadiene by lithiation with  $\text{LiBu}^s$  in THF at  $-78^\circ\text{C}$  followed by transmetalation with  $\text{Ti}(\text{OPr}^i)_4$  (Scheme 5). This compound reacts with benzaldehyde to provide the corresponding 1,3-cyclohexadiene derivatives through allylation reactions in excellent yield and high diastereo and enantioselectivity (99%, *syn:anti* = 9:1). The reaction with the monoisopropoxo derivative containing a chiral bis-alkoxo ligand, shown in Scheme 6, provides lower selectivities.<sup>22,23</sup>

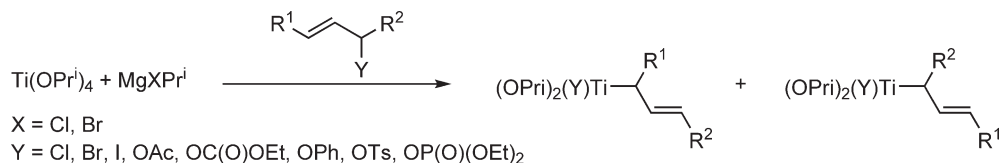
The preparation of allyltitanium compounds including those having functional groups is described by reaction of allylic halides or allylic alcohol derivatives with the system  $\text{Ti}(\text{OPr}^i)_4/\text{MgXPr}^i$  ( $\text{X} = \text{Cl}, \text{Br}$ ) (Scheme 7).<sup>24</sup> Analogous allyltitanium complexes have also been reported by treatment of  $\text{Ti}(\text{II})$  species with allylic alcohol derivatives, which proceeds via an oxidative addition pathway. Their reactions have been studied.<sup>25–27</sup> These compounds are used to promote efficient syntheses of alkylidenecyclopropane and cycloalkane derivatives by regioselective reactions with carbonyl compounds,<sup>28,29</sup> the stereoselective syntheses of optically active substituted piperidines and pyrrolidines from amino acid derivatives,<sup>30</sup> diastereoselective additions to 2,3-*O*-isopropylidenglyceraldehyde,<sup>31</sup> and other asymmetric organic reactions.<sup>32–35</sup>



Scheme 5



Scheme 6



Scheme 7

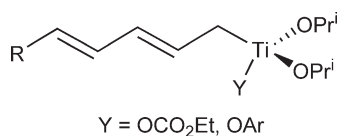
Allenyltitanium systems are formed from propargyl halides or carbonates and a low-valent diisopropoxo- $\eta^2$ -propene Ti(II) species. They are excellent reagents for the synthesis of homopropargyl alcohols by reaction with carbonyl compounds, as examples of carbon–carbon bond-forming processes.<sup>36,37</sup>

Analogous penta-2,4-dienyltitanium complexes (Scheme 8) have been readily prepared from the divalent titanium system  $\text{Ti}(\text{OPr}^i)_4/\text{MgClPr}^i$ , and penta-1,4-dien-3-ol or penta-2,4-dien-1-ol derivatives, such as ethyl carbonates or acetates. These complexes react with aldehydes and ketones with excellent  $\gamma$ -regioselectivity to afford the corresponding penta-1,4-dien-3-yl carbinols in excellent yield.<sup>38</sup> The propargyl titanato derivatives shown in Scheme 9 have been prepared by addition of  $\text{Ti}(\text{OPr}^i)_4$  to a solution of the corresponding organolithium reagent. The action of these organotitanium compounds toward oxazolidines gives  $\beta$ -amino alcohols.<sup>39</sup>

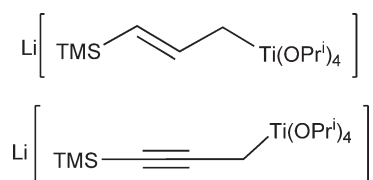
Toluene–ether or toluene–hexane solutions of aryl- and alkyltrialkoxotitanium reagents  $\text{TiR}(\text{OPr}^i)_3$  are prepared by the reactions of the aryl- and alkyl lithium or Grignard reagents with  $\text{TiCl}(\text{OPr}^i)_3$ , followed by careful removal of the salts. These organotitanium compounds react with aldehydes under nucleophilic addition of aryl groups to the (*Si*)-face of the aldehydes with high enantioselectivities (Scheme 10).<sup>40</sup> The allenyl titanium  $\text{Ti}[\text{RC}\equiv\text{CH}(\text{propargyl})](\text{OPr}^i)_3$  is prepared by transmetalation reaction of the corresponding allenyl lithium with  $\text{Ti}(\text{OPr}^i)_4$ .<sup>41</sup> A series of organotitanium compounds (Scheme 11) was obtained by similar reactions. These species are widely applicable in synthetic organic chemistry.<sup>37,42–45</sup>

The chloro Ti complexes with bridging ylide ligands shown in Scheme 12 have been synthesized by treatment of  $\text{TiCl}_2(\text{NMe}_2)_2$  with an excess of the base and nucleophile phosphorus methylide  $(\text{Me}_2\text{N})_3\text{P}=\text{CH}_2$ .<sup>46,47</sup> When Ti–alkoxo complexes are used as the starting materials, this reaction proceeds by a different route. The titanium-substituted ylide species  $\text{TiCl}_2[\text{CH}=\text{P}(\text{NMe}_2\text{N})](\text{OPr}^i)$  and  $\text{TiCl}[\text{CH}=\text{P}(\text{NMe}_2\text{N})](\text{OPr}^i)_2$  are prepared by reaction of  $\text{TiCl}_3(\text{OPr}^i)$ <sup>48</sup> or  $\text{TiCl}_2(\text{OPr}^i)_2$ <sup>49</sup> with  $(\text{Me}_2\text{N})_3\text{P}=\text{CH}_2$  followed by treatment with  $\text{NaSiMe}_3$ . (*E*)-Vinylphosphonium salts are conveniently obtained from the reaction of carbonyl compounds with these ylide compounds. These compounds are good reagents for double olefination reactions, the mechanism of which has been discussed.<sup>50</sup>

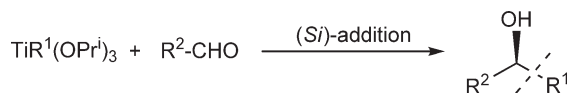
The dimethyl binuclear titanium compounds  $[\text{TiMe}(\mu\text{-OR})(\kappa^3\text{-tbop})]_2$  ( $\text{R} = \text{Me}, \text{Et}$ ) {tbop = 2,2'-thiobis[4-(1,1,3,3-tetramethylbutyl)phenoxo]} are prepared by reaction of the alkoxo complexes  $[\text{Ti}(\text{OR})(\mu\text{-OR})(\kappa^3\text{-tbop})]_2$



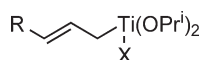
Scheme 8



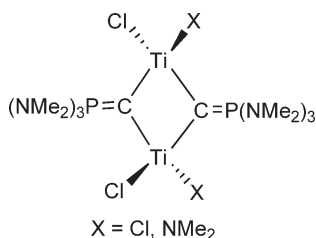
Scheme 9



Scheme 10



Scheme 11



Scheme 12

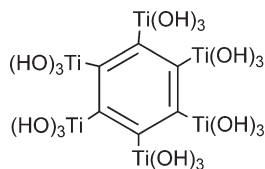
with an excess of  $\text{AlMe}_3$  in toluene. Treatment of the methyl methoxo derivative with an excess of water in toluene results in the hydrolysis of the Ti–Me bonds with evolution of methane and the formation of a tetranuclear  $\mu$ -oxo compound. The alkyl derivatives are supported on  $\text{MgCl}_2$  and activated with aluminum alkyls to give effective catalysts for the polymerization of ethylene.<sup>51</sup>

A DFT calculation has been performed on the oligomerization of the acetylide titanium complex  $(\text{OH})_3\text{Ti}-\text{C}\equiv\text{C}-\text{Ti}(\text{OH})_3$  to the cyclopolyene titanacyclobutadiene  $[\text{Ti}(\text{OH})_3\text{C}]_4$  and titanacyclobenzene  $[\text{Ti}(\text{OH})_3\text{C}]_6$  species (Scheme 13), as simple models of hypothetical molecular metal carbides.<sup>52</sup>

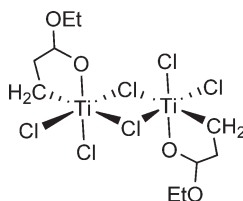
The structure of the well-known homoenolate  $[\text{TiCl}_2(\text{CH}_2\text{CH}_2\text{COOEt})]_2(\mu\text{-Cl})_2$  has been reported; the compound is dimeric both in solution and in the solid state and contains a five-membered metallacycle (Scheme 14).<sup>53</sup>

The reaction of (phenylsulfonyl)trimethylsilylmethane with 2 equiv. of  $\text{LiBu}^n$  in diethyl ether followed by treatment with  $\text{TiCl}(\text{OPr}^i)_3$  affords the lithium titanium sulfone  $\text{Ti}[\text{Me}_3\text{SiCS}(\text{Ph})\text{O}_2\text{Li}](\text{OPr}^i)_3$  (Scheme 15). The molecular structure has been established by X-ray diffraction studies and shows the titanium atom to be bonded to a C( $\alpha$ ) with Ti–C bond lengths in the range of 2.036(7)–2.048 (7) Å.<sup>54</sup>

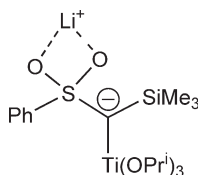
Chiral sulfonimidoyl substituted bis(allyl) and mono(allyl) Ti complexes (Scheme 16) can be generated by the appropriate synthetic methodology. These complexes are effective reagents for the enantio- and diastereoselective



Scheme 13

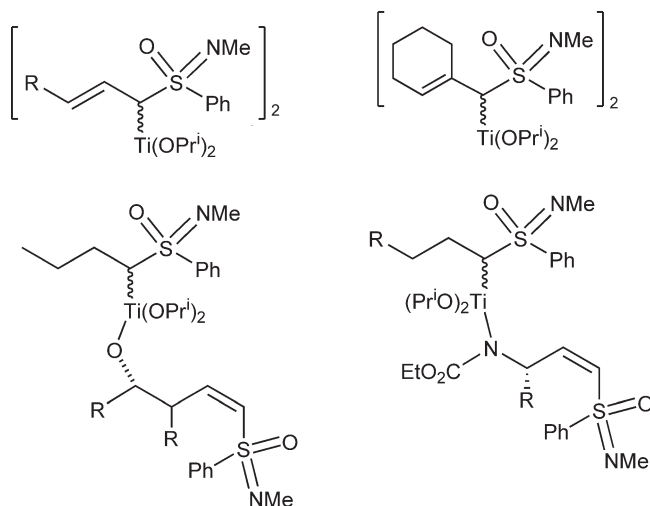


Scheme 14



Scheme 15





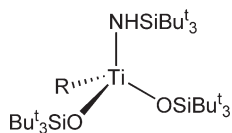
Scheme 16

synthesis of *anti*-configured homopropargylic alcohols by reaction with aldehydes, considered as starting materials for the asymmetric synthesis of amino acids and amino alcohols having three contiguous stereogenic C-atoms.<sup>55–61</sup> Chiral sulfoximino substituted allyl Ti(IV) complexes are used as catalyst for the asymmetric synthesis of 3-substituted unsaturated prolines.<sup>62</sup>

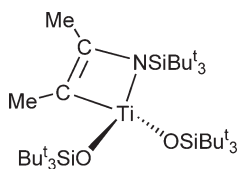
#### 4.05.2.1.1.(ii) Complexes stabilized by oxygen and nitrogen ligands

Monoalkyl amido complexes  $\text{TiR}(\text{silox})_2(\text{Bu}^t_3\text{SiNH})$  ( $\text{R} = \text{Me}, \text{Et}, \text{CH}_2\text{Ph}, \text{CH}=\text{CH}_2, \text{Bu}^c, \text{Bu}^n, \text{Ph}, \text{H}, \text{Pr}^c, \text{Pe}^c, \text{Mes}, n\text{-Hex}, c\text{-Hex}, \eta^3\text{-H}_2\text{CHCH}_2, \eta^3\text{-H}_2\text{CCHCHMe}$ ;  $\text{silox} = \text{Bu}^t_3\text{SiO}$ ) (Scheme 17) are synthesized by metathesis reaction of  $\text{TiCl}(\text{silox})_2(\text{Bu}^t_3\text{SiNH})$  with Grignard or alkyl lithium reagents, by 1,2-RH-addition to  $\text{TiR}(\text{silox})_2(=\text{NSiBu}^t_3\text{Si})$ , or by insertion of alkenes into the titanium–hydride bond of  $\text{TiH}(\text{silox})_2(\text{Bu}^t_3\text{SiNH})$ . The kinetics and thermodynamics of reversible 1,2-RH-elimination from these monoalkyltitanium derivatives have been investigated.<sup>63</sup> The [2 + 2]-cycloaddition product  $\text{Ti}(\text{MeC}=\text{Me})\text{C}-\text{NSiBu}^t_3(\text{OSiBu}^t_3)_2$  (Scheme 18) is irreversibly generated by reaction of  $\text{Ti}(\text{silox})_2(=\text{NSiBu}^t_3\text{Si})$  with  $\text{MeC}\equiv\text{CMe}$ .<sup>64</sup>

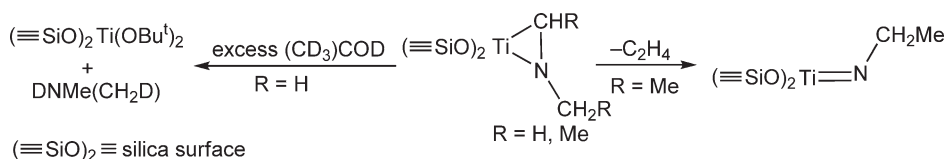
Reaction of hydroxyl silica surface with  $\text{Ti}(\text{NR}_2)_4$  affords yellow grafted bis(amido) titanium(IV) fragments  $(\equiv\text{SiO})_2\text{Ti}(\text{NR}_2)_2$  ( $\text{R} = \text{Me}, \text{Et}$ ), thermal reactions of which proceeds with intramolecular  $\beta$ -H abstraction by a coordinated amido ligand and subsequent liberation of amine to give N-alkylmethylenimino derivatives ( $\text{R} = \text{H}, \text{Me}$ ) (Scheme 19), which exhibit a  $\sigma$ -Ti–C bond. When  $\text{R} = \text{Me}$  the imino complex evolves to a new ethylimido species with formation of  $\text{C}_2\text{H}_4$ . Reaction of  $(\equiv\text{SiO})_2\text{Ti}(\text{CH}_2\text{NMe})$  with *tert*-butyl alcohol- $\text{d}_{10}$  yields the dialkoxo compound  $(\equiv\text{SiO})_2\text{Ti}(\text{OBu}^t)_2$  and dimethylamine  $\text{DNMe}(\text{CH}_2\text{D})$  (Scheme 19).<sup>65</sup>



Scheme 17



Scheme 18



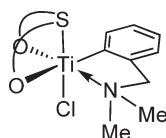
Scheme 19

$\text{TiCl}_2(\text{tbmp})$  containing a sulfide-linked bis(phenoxo) ligand [ $\text{tbmp} = 2,2'$ -thiobis( $6$ - $t$ -Bu-4-methylphenoxo)] reacts with  $\text{Li}(2\text{-NMe}_2\text{CH}_2\text{C}_6\text{H}_4)$  to give the corresponding substituted phenyl derivative (Scheme 20) stabilized by the coordination of the chelating phenyl ligand.<sup>66</sup>

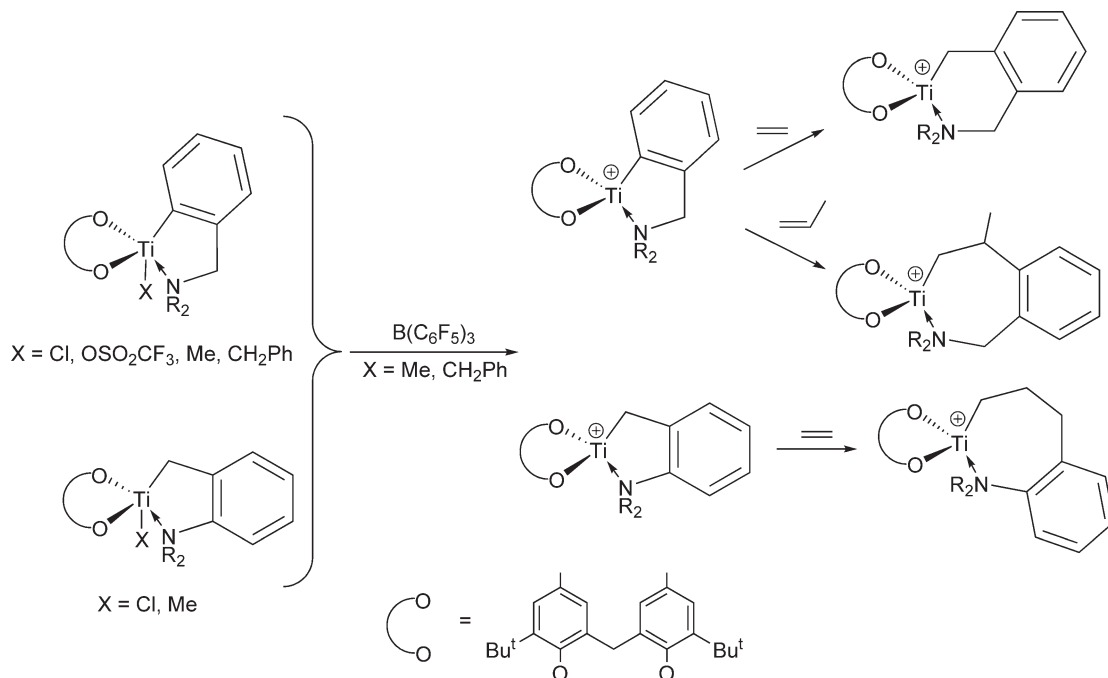
Bis-phenoxo hydrocarbyl five-coordinated titanium complexes (Scheme 21) have been synthesized and spectroscopically characterized. The molecular structure determined by X-ray diffraction shows the metal to have a distorted trigonal-bipyramidal coordination geometry. Cationic four-coordinate derivatives can be generated by reaction of the methyl derivatives with  $\text{B}(\text{C}_6\text{F}_5)_3$ . These cationic species undergo stoichiometric insertions of ethylene and propylene into the Ti–C bond.<sup>67</sup>

Mono- and dimethyl hexacoordinated derivatives containing chelating monoanionic diaminoaryl  $[2,6\text{-C}_6\text{H}_3(\text{CH}_2\text{NMe}_2)_2]^-$  ligands are prepared by treating  $\text{TiCl}_2(\text{OPr}^i)[2,6\text{-C}_6\text{H}_3(\text{CH}_2\text{NMe}_2)_2]$  with 1 or 2 equiv. of  $\text{LiMe}$  in toluene.<sup>68</sup>

The iodo titanium complexes  $\text{Ti}(\text{I})(\text{NRAr}_F)_2(\text{NMe}_2)$  and  $\text{Ti}(\text{I})[\text{O}(2,5\text{-C}_6\text{H}_3\text{Bu}^t_2)](\text{NRAr}_F)(\text{NMe}_2)$  ( $\text{Ar}_F = 2,5\text{-C}_6\text{H}_3\text{FMe}$ ;  $\text{Ar} = 3,5\text{-C}_6\text{H}_3\text{Me}_2$ ,  $2,6\text{-C}_6\text{H}_3\text{Pr}^i_2$ ) containing dimethyl amido protecting groups undergo a selective



Scheme 20



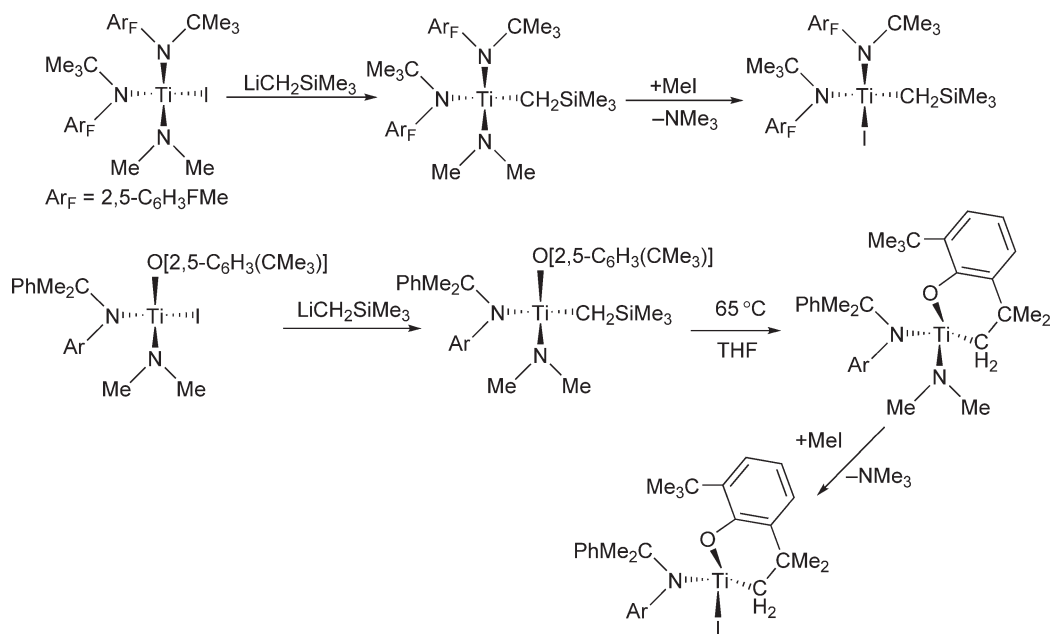
Scheme 21

monoalkylation upon treatment with 1 equiv. of trimethylsilylmethyl lithium to afford the corresponding monoalkyl compounds. The compound with two  $\text{NRAr}_F$  ligands reacts with excess methyl iodide in THF to produce the iodo trimethylsilylmethyl derivative by removal of the dimethyl amido-protecting group. The choice of the solvent is important for the deprotection step; the reaction proceeds relatively rapidly in THF, with moderate rate in diethyl ether, but is extremely slow in hydrocarbons. Thermolysis of the OAr complex gives the expulsion of neopentane, and a cyclometallation reaction is observed. Further treatment with methyl iodide produces the chiral iodo cyclo-metallated complex (Scheme 22).<sup>69</sup>

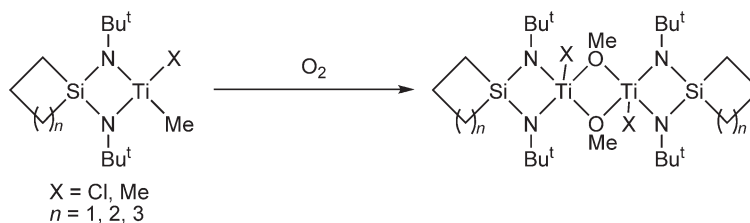
The chloro methyl and the dimethyl diamido complexes  $\text{TiXMe}[(\text{cyclo})\text{Si}(\text{NBu}^t)_2]$  have been prepared. Bulky substituents on the silylene bridge increase the kinetic stability of the spiro-siladiazatitanacycle compound. These complexes react with dioxygen to give the binuclear methoxo-bridge derivatives  $[\text{TiX}\{(\text{cyclo})\text{Si}(\text{NBu}^t)_2\}]_2(\mu\text{-OMe})_2$  through the insertion reaction of  $\text{O}_2$  into the Ti–Me bond (Scheme 23). The molecular structure has been determined by X-ray diffraction.<sup>70–72</sup>

The complexes  $\text{TiXMe}(\text{salen})$  (Scheme 24) are obtained when the dichloro parent compound  $\text{TiCl}_2(\text{salen})$  reacts with  $\text{AlMe}_3$  by further addition of  $\text{OEt}_2$  with additional formation of titanium(III) species (salen = N,N'-bis(salicylidene)ethylenediamine). The reactivity of these compounds has been studied toward magnesium reduction, halide abstraction with  $\text{SbCl}_5$  and  $\text{AgBF}_4$ ,  $\text{SO}_2$  insertion and hydrolysis reactions.<sup>73,74</sup>

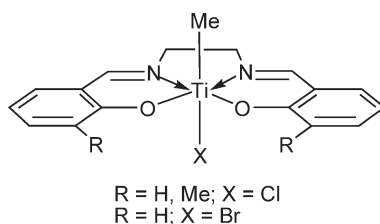
The reaction of  $\text{Ti}(\text{CH}_2\text{Ph})_4$  with the  $C_2$ -symmetric Schiff base ( $\text{H}_2\text{L}$ ), synthesized by condensation of 2,2'-diamino-6,6'-dimethylbiphenyl and 3,5-di-*tert*-butylsalicylaldehyde, leads to the dibenzyl intermediate species  $\text{Ti}(\text{CH}_2\text{Ph})_2\text{L}$ . This rapidly converts into a complex  $\text{Ti}(\text{CH}_2\text{Ph})(\text{LBn})$  (Scheme 25) in which one of the Ti-bound benzyl groups has undergone a highly diastereoselective 1,2-migratory insertion process with one imino group,



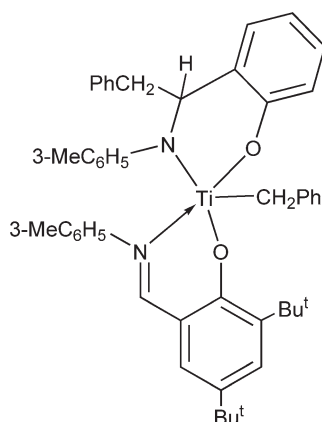
Scheme 22



Scheme 23



Scheme 24



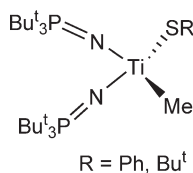
Scheme 25

resulting in a new trianionic ligand bound to the Ti center. The migration of the benzyl group generates a new stereogenic center in the compound, although from  $^1\text{H}$  NMR spectroscopy there is no evidence of more than one diastereoisomer being formed. The molecular structure of this compound, determined by X-ray diffraction, shows that the coordination sphere of the Ti atom is approximately trigonal bipyramidal. Controlled hydrolysis of  $\text{Ti}(\text{CH}_2\text{Ph})(\text{LBn})$  leads to a dimeric  $\mu$ -oxo species in which the amido bond in the starting complex has been protonated to form an amino ligand.<sup>75</sup>

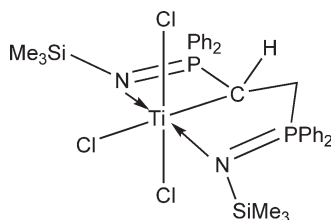
#### 4.05.2.1.1.(iii) Complexes stabilized by nitrogen ligands

The monochloro tris( $\text{Bu}^t_3$ -phosphinimido) titanium complex  $\text{TiCl}(\text{N}=\text{PBu}^t_3)_3$  can be prepared via the reaction of  $\text{TiCl}_2(\text{N}=\text{PBu}^t_3)_2$  with  $\text{LiN}=\text{PBu}^t_3$ . The corresponding alkyl derivatives  $\text{TiR}(\text{N}=\text{PBu}^t_3)_3$  ( $R = \text{Me}, \text{CH}_2\text{Ph}$ ) are accessible by treatment with the appropriate Grignard reagent. Reactivity of these species is described in Section 4.05.2.3.<sup>76</sup> Reactions of the phosphinimido compound  $\text{TiMe}_2(\text{N}=\text{PBu}^t_3)_2$  with 1 equiv. of phenylthiol or *tert*-butylthiol generate the monomethyl species  $\text{TiMe}(\text{SR})(\text{N}=\text{PBu}^t_3)_2$  (Scheme 26). Attempts to effect sulfur insertion into Ti–Me bonds via the reaction of  $\text{TiMe}_2(\text{N}=\text{PBu}^t_3)_2$  with  $\text{S}_8$  were unsuccessful.<sup>77</sup>

$\text{TiCl}_4$  reacts with the bis-phosphinimine  $\text{Me}_3\text{SiN}=\text{P}(\text{Ph})_2\text{CH}_2\text{CH}_2\text{P}(\text{Ph})_2=\text{NSiMe}_3$  to give the titanium complex  $\text{TiCl}_3[\text{Me}_3\text{SiN}=\text{P}(\text{Ph})_2\text{CH}_2\text{CH}_2\text{P}(\text{Ph})_2=\text{NSiMe}_3]$  (Scheme 27) in which one  $\text{CH}_2$  group is metallated with evolution of HCl to give a  $\sigma$ -Ti–C bond. The molecular structure of this complex has been determined by X-ray diffraction.



Scheme 26



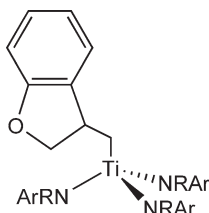
Scheme 27

The bis-trimethylsilylphosphinimino ligand acts as an  $[\text{NCN}]^-$  chelate, and the metal–ligand bonding is best described with a minor contribution of a phosphorus ylide resonance form.<sup>78</sup>

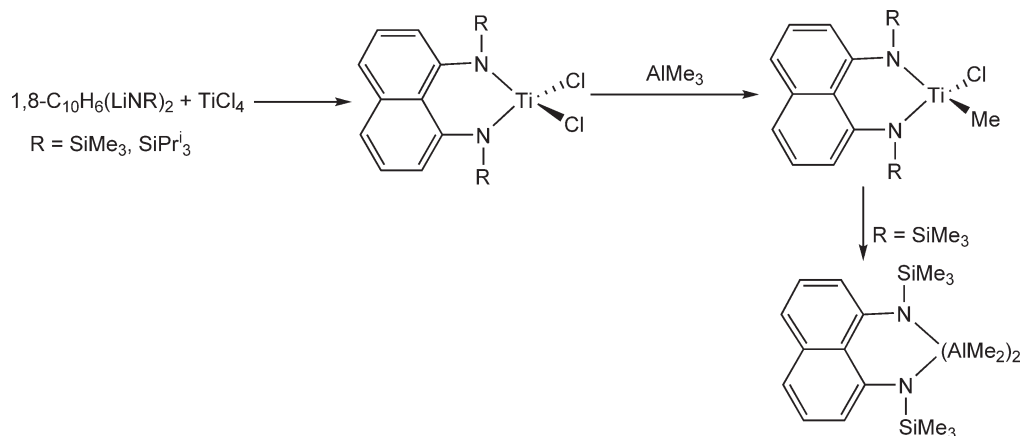
Reaction of the tris-amido titanium(III) compound  $\text{Ti}(\text{NRAr})_3$  ( $\text{R} = \text{Bu}^t$ ,  $\text{Ar} = 3,5\text{-C}_6\text{H}_3\text{Me}_2$ ) with 0.5 equiv. of *o*-bromophenyl allyl ether results in bromine atom abstraction followed by cyclization of the intermediate aryl radical to generate a titanium-bound 3-methylenedihydrobenzofuran product (Scheme 28), which has been spectroscopically characterized in solution.<sup>79</sup>

The reaction of  $1,8\text{-C}_{10}\text{H}_6(\text{LiNR})_2$  with  $\text{TiCl}_4$  produces the diamido dichloro titanium complexes  $\text{TiCl}_2[1,8\text{-C}_{10}\text{H}_6(\text{NR})_2]$ . The compound is scarcely active for ethylene polymerization in the presence of MAO. The crystal structure of the trimethylsilyl derivative has been determined by X-ray diffraction and shows an unusually large  $\text{Cl-Ti-Cl}$  angle ( $120.5^\circ$ ). Complex  $\text{TiCl}_2[1,8\text{-C}_{10}\text{H}_6(\text{NSiMe}_3)_2]$  reacts with  $\text{AlMe}_3$  to give the monomethyl derivative  $\text{TiClMe}[1,8\text{-C}_{10}\text{H}_6(\text{NSiMe}_3)_2]$ , followed by a transmetalation reaction of the amido ligands from titanium to the aluminum center (Scheme 29). By contrast, only monomethylation of  $\text{TiCl}_2[1,8\text{-C}_{10}\text{H}_6(\text{NSiPr}^i)_2]$  occurs at room temperature. Reactions of  $\text{TiCl}_2[1,8\text{-C}_{10}\text{H}_6(\text{NR})_2]$  with a modified MAO have been followed by NMR spectroscopy.<sup>80</sup>

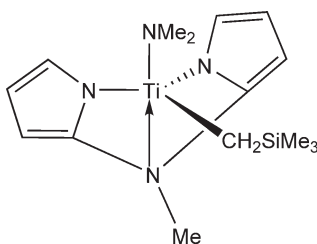
The metathesis reaction of  $\text{Ti}(\text{I})(\text{NMe}_2)_2(\text{dpma})$  ( $\text{dpma} = N,N\text{-dipyrrolyl-}\alpha\text{-methyl-}N\text{-methylamine}$ ) with  $\text{MgCl}(\text{CH}_2\text{SiMe}_3)$  in dioxane/DME affords the Ti–monoalkyl complex  $\text{Ti}(\text{CH}_2\text{SiMe}_3)(\text{NMe}_2)_2(\text{dpma})$  (Scheme 30).



Scheme 28



Scheme 29



Scheme 30

The crystal structure has been determined by X-ray diffraction methods. This compound is obtained as a mixture of two isomers with the alkyl group located in equatorial or axial positions in a pseudo-trigonal-bipyramidal geometry. In the crude reaction product the equatorial complex is present with a slight preference over the axial in a ratio of 1.8:1. Slow conversion between both isomers is observed at room temperature.<sup>81</sup>

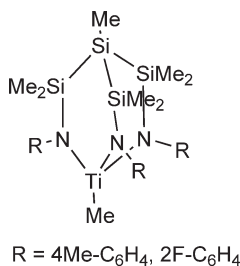
The monomethyl pyrazolato titanium complex  $\text{TiMe}(\text{Bu}^t_2\text{pz})_3$  has been prepared by treatment of the monochloro precursor compound with  $\text{MgClMe}$ .<sup>82</sup>

A methyltitanium complex containing a tripodal amido ligand with a trisilylsilane framework has been prepared by reaction of the titanium chloro precursor with  $\text{LiMe}$  (Scheme 31).<sup>83</sup>

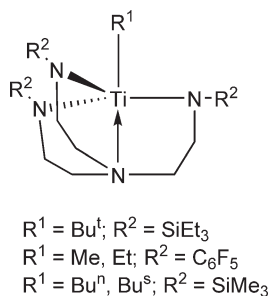
Tridentate trianionic triamido and tetradentate trianionic tris-amido-amino  $[\text{N}(\text{CH}_2\text{CH}_2\text{NR})_3]^{3-}$  ligands have been widely used in the early transition metal chemistry.<sup>84</sup> Monoalkyltitanium complexes  $\text{TiR}^1(\text{L})$  ( $\text{R} = \text{Me}$ ,  $\text{Et}$ ,  $\text{Bu}^n$ ,  $\text{Bu}^s$ ,  $\text{Bu}^t$ ) (Scheme 32) stabilized by a tris-amido-amino ligand of the type  $\text{L} = [(\text{R}^2\text{NCH}_2\text{CH}_2)_3\text{N}]^{3-}$  ( $\text{R}^2 = \text{SiMe}_3$ ,  $\text{SiEt}_3$ ,  $\text{C}_6\text{F}_5$ ) have also been described.<sup>85</sup>

Titanium complexes containing a chelating triamido ligand [*cis,cis*-1,3,5-(3,5- $\text{Bu}^t_2\text{C}_6\text{H}_3\text{N})_3\text{C}_6\text{H}_9$ ]<sup>3-</sup> are reported. The methyl derivative is prepared by reaction of the chloro parent compound with  $\text{MgBrMe}$  in toluene solution. The hydride complex inserts 1-hexene to give the corresponding 1-hexyl derivative which can alternatively be synthesized by treatment of the chloro compound with  $\text{MgBrHex}$  in  $\text{Et}_2\text{O}$  (Scheme 33).<sup>86</sup>

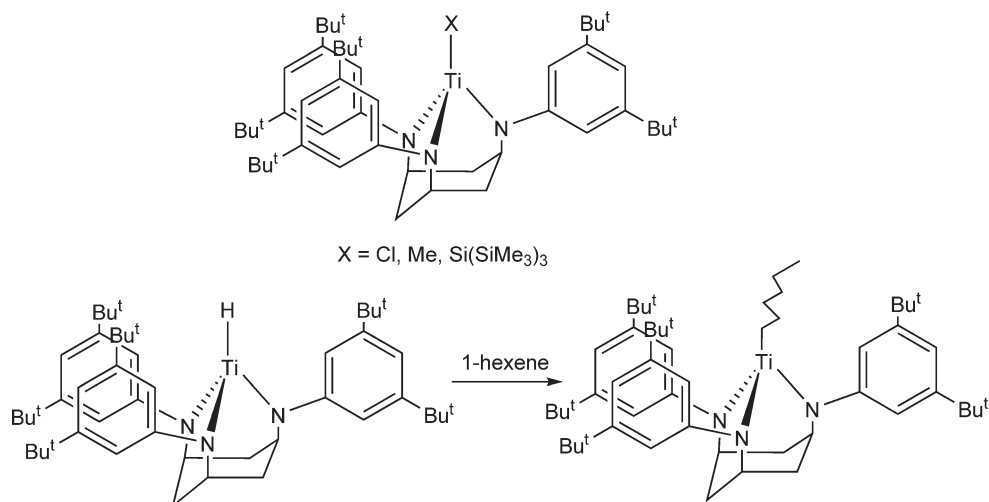
The lithium amidinate  $\text{Li}[\text{Me}_3\text{SiNC}(\text{Ph})\text{N}(\text{CH}_2)_3\text{N}(\text{Me})\text{SiMe}_3] \cdot 2\text{THF}$  containing a pendant methyl(trimethylsilyl)amine functionality reacts with  $\text{TiCl}_4(\text{THF})_2$  to give the amidinato-amido chloro complex  $\text{TiCl}_2[\text{Me}_3\text{SiNC}(\text{Ph})\text{N}(\text{CH}_2)_3\text{NMe}]$  by releasing  $\text{SiClMe}_3$ . The complex has been characterized by X-ray diffraction methods



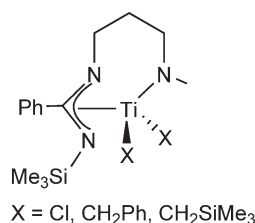
Scheme 31



Scheme 32



Scheme 33



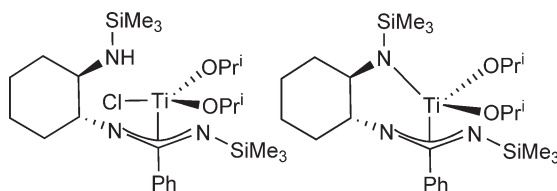
Scheme 34

(Scheme 34). The dichloro compound is converted into the dialkyl derivatives by treatment with  $\text{LiR}$  or  $\text{MgBrR}$  ( $\text{R} = \text{CH}_2\text{Ph}$ ,  $\text{CH}_2\text{SiMe}_3$ ). The dibenzyl complex reacts with  $\text{B}(\text{C}_6\text{F}_5)_3$  in  $\text{C}_6\text{D}_6$  to give a mixture of unidentified products, inactive in the polymerization of ethylene, suggesting that decomposition of the possible generated cationic species is rapid.<sup>87</sup> The analogous amidinato-amido complex supported by the ligand  $\{(1R,2R)\text{-(}-1\text{-[NC(Ph)N(SiMe}_3\text{)]-2-[NSiMe}_3\text{)]-C}_6\text{H}_{10}\}$  has also been reported and its molecular structure determined by X-ray diffraction, showing a new  $\eta^3\text{-}\pi$  and a  $\sigma$ -bond to the titanium atom (Scheme 35).<sup>88</sup>

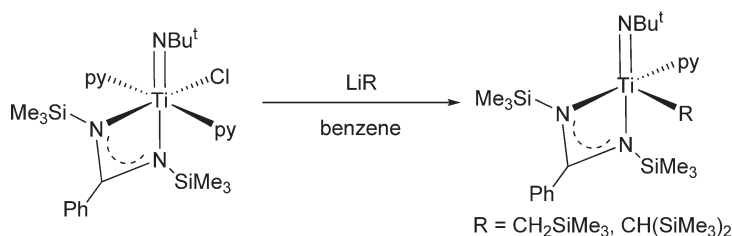
The chloro methyl bis-benzamidinato complex  $\text{TiClMe}[\text{PhC(NSiMe}_3)_2]_2$  has been prepared by treatment of the dichloro precursor  $\text{TiCl}_2[\text{PhC(NSiMe}_3)_2]_2$  with 1 equiv. of  $\text{LiMe}$ .<sup>89</sup>

The chloro imido-amidinato titanium complex  $\text{TiCl(NBu}^t\text{)[PhC(NSiMe}_3)_2\text{](py)}_2$  reacts with  $\text{LiCH}_2\text{SiMe}_3$  or with  $\text{LiCH(SiMe}_3)_2$  in benzene to give rare examples of terminal imido monoalkyltitanium derivatives  $\text{TiR(NBu}^t\text{)[PhC(NSiMe}_3)_2\text{](py)}$  (Scheme 36). The molecular structure of the trimethylsilylmethyl derivative has been determined by X-ray diffraction.<sup>90</sup>

The imido titanium complex supported by a diamido-pyridine framework  $\text{Ti(=NBu}^t\text{)[(2-C}_5\text{H}_4\text{N)C(R)-(CH}_2\text{NSiMe}_3)_2\text{](py)}$  ( $\text{R} = \text{H, Me}$ ) reacts with 2,6-xylyl isocyanide to give the double insertion of the isocyanide into the imido titanium bond and formation of the corresponding four-membered titanacycle with one  $\sigma\text{-Ti-C}$  bond; the

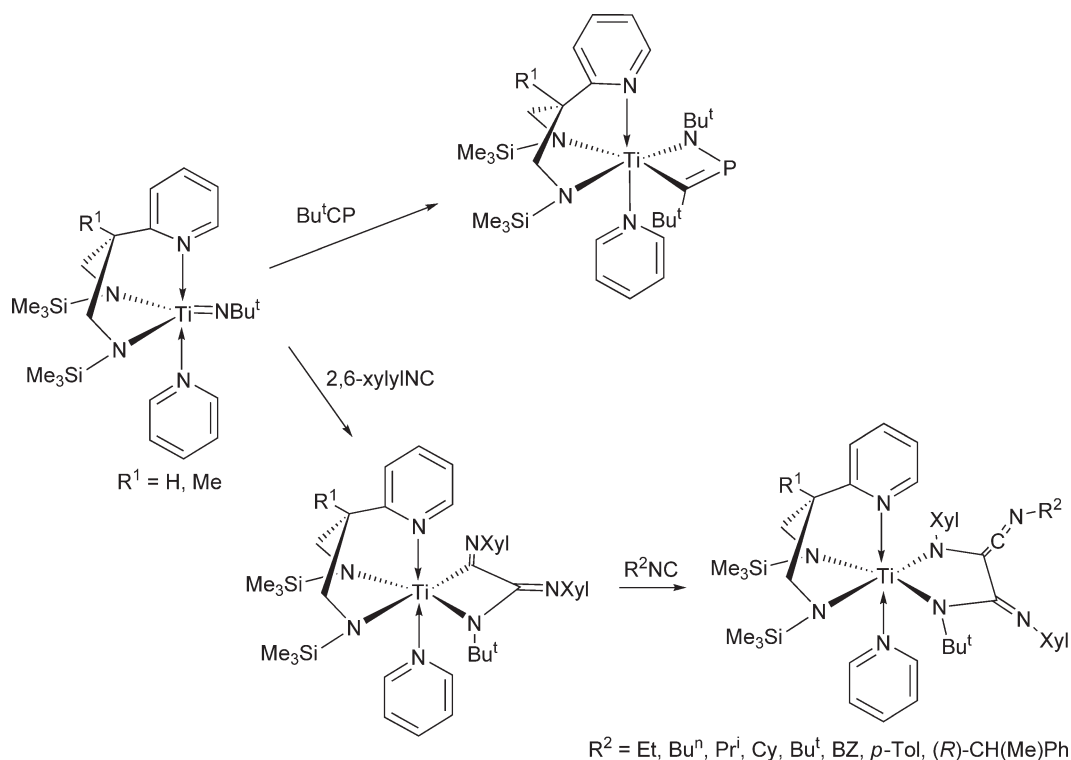


Scheme 35



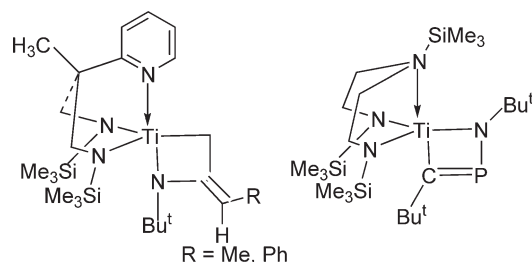
Scheme 36

complex has been characterized by X-ray crystallography. This compound reacts with a whole series of isocyanides to afford iminoketeno complexes. The single crystal X-ray structures of some of these complexes have established the coordination of an imidoyleketeneimino fragment to the metal center (Scheme 37). The reactivity of  $\text{Ti}(=\text{NBu}^t)-[(2-\text{C}_5\text{H}_4\text{N})\text{C}(\text{Me})(\text{CH}_2\text{NSiMe}_3)_2](\text{py})$  toward other types of isocyanide has also been studied to yield diaminodihydropyrimidine coordination derivatives.<sup>91</sup> The imido titanium complex reacts with  $\text{Bu}^t\text{CP}$  to give the azatitanacyclobutene complex  $\text{Ti}(\text{NBu}^t\text{PCBu}^t)[\text{MeC}(2-\text{C}_5\text{H}_4\text{N})(\text{CH}_2\text{NSiMe}_3)_2]$  (Scheme 37) characterized by X-ray diffraction studies. This compound is formed via a  $[2+2]$ -cycloaddition reaction between the phosphalkyne and the imido moieties; it does not react further with an excess of  $\text{Bu}^t\text{CP}$ .<sup>92</sup> Imido titanium complexes stabilized by coordination of diamino-pyridino ligands react with 2-butyne and 1-phenyl-propyne to give unusual transformation to metallacycle four-membered titanaazetidine derivatives via the C–N coupling of the imido group with the respective acetylene. The same reaction products are obtained in  $[2+2]$ -cycloaddition reactions with 1,2-butadiene and phenylallene. The four-membered metallacycle with an exocyclic  $\text{C}=\text{C}$  double bond has been established by X-ray diffraction studies (Scheme 38). A mechanism to explain the observed products from both types of reactions is proposed.<sup>93,94</sup> Reaction of analogous compound with  $\text{P}\equiv\text{CBu}^t$  has been reported to give the cycloaddition product containing a “Ti–N–P=C” four-membered ring (Scheme 38).<sup>95</sup> A review of imido complexes, including titanium derivatives, supported by diamido ligands and their reaction with alkynes, allenes,  $\text{RNCO}$ ,  $\text{RCN}$ , and  $\text{RCP}$  has appeared.<sup>96</sup>

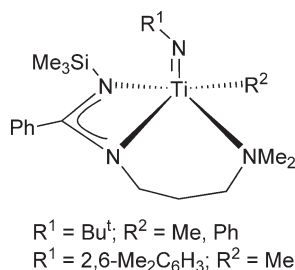


Scheme 37





Scheme 38



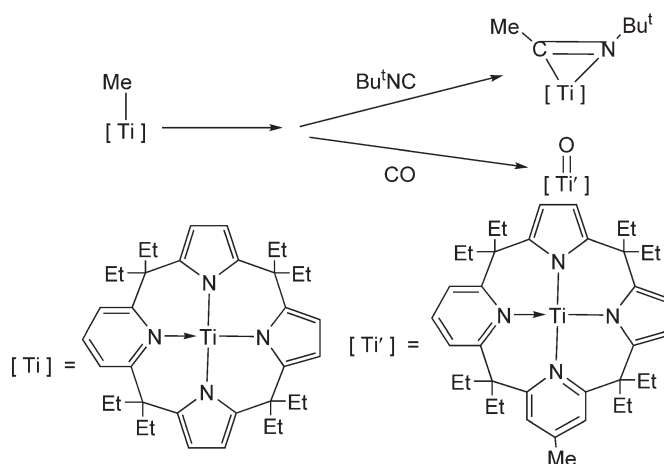
Scheme 39

Monoalkyl-imido Ti complexes supported by the three-carbon pendant arm functionalized *N*-trimethylsilyl benzamidinato ligand Me<sub>3</sub>SiNC(Ph)NCH<sub>2</sub>CH<sub>2</sub>CH<sub>2</sub>NMe<sub>2</sub> have been described (Scheme 39). TiCl(NBu<sup>t</sup>)[Me<sub>3</sub>SiNC(Ph)NCH<sub>2</sub>CH<sub>2</sub>CH<sub>2</sub>NMe<sub>2</sub>] reacts with LiPh to afford the thermally sensitive complex TiPh(NBu<sup>t</sup>)[Me<sub>3</sub>SiNC(Ph)NCH<sub>2</sub>CH<sub>2</sub>CH<sub>2</sub>NMe<sub>2</sub>]. The analogous methyl derivative TiMe(NBu<sup>t</sup>)[Me<sub>3</sub>SiNC(Ph)NCH<sub>2</sub>CH<sub>2</sub>CH<sub>2</sub>NMe<sub>2</sub>] is detected by <sup>1</sup>H NMR spectroscopy in the reaction with LiMe but this compound could not be isolated. Reaction of the arylimido compound TiCl(N-2,6-C<sub>6</sub>H<sub>3</sub>Me<sub>2</sub>)[Me<sub>3</sub>SiNC(Ph)NCH<sub>2</sub>CH<sub>2</sub>CH<sub>2</sub>NMe<sub>2</sub>] with LiMe gives the thermally sensitive TiMe(N-2,6-C<sub>6</sub>H<sub>3</sub>Me<sub>2</sub>)[Me<sub>3</sub>SiNC(Ph)NCH<sub>2</sub>CH<sub>2</sub>CH<sub>2</sub>NMe<sub>2</sub>].<sup>97</sup>

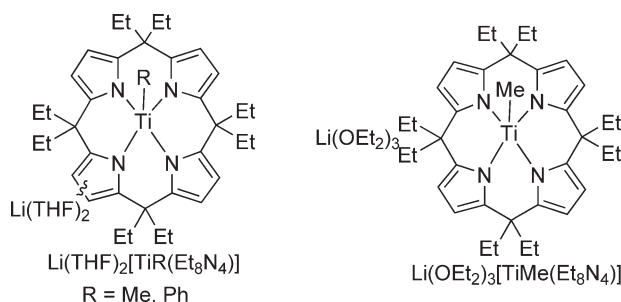
The organometallic methyltitanium macrocycle TiMe[Et<sub>8</sub>(C<sub>5</sub>H<sub>3</sub>N)(C<sub>4</sub>H<sub>2</sub>N)<sub>3</sub>] has been synthesized by alkylation of the chloro precursor TiCl[Et<sub>8</sub>(C<sub>5</sub>H<sub>3</sub>N)(C<sub>4</sub>H<sub>2</sub>N)<sub>3</sub>]Cl. *meso*-Octaethyl tris(pyrrole) mono(pyridine) is lithiated with LiBu<sup>n</sup> and the further reaction with TiCl<sub>4</sub> affords the corresponding chloro tris(pyrrol)-mono(pyridino) titanium derivative which is converted to the methyl complex by treatment with LiMe. The Ti–Me bond undergoes insertion reaction with Bu<sup>t</sup>NC to give the expected η<sup>2</sup>-iminoacyl derivative, while the reaction with CO proceeds with complete cleavage of the C–O bond and the conversion of one pyrrolyl anion to a *p*-methylpyridino ring and a Ti=O unit (Scheme 40).<sup>98,99</sup> Reaction of lithium reagents with the (*meso*-octaethylporphyrinogenato)titanium complex Ti(Et<sub>8</sub>N<sub>4</sub>)(THF)<sub>2</sub> gives the bimetallic Li–Ti compounds Li(THF)<sub>2</sub>[TiR(Et<sub>8</sub>N<sub>4</sub>)] (R=Me, Ph) (Scheme 41). These compounds contain the alkyl or aryl groups bonded to titanium, while the lithium cation remains bonded to the porphyrinogen periphery. The methyl derivative in diethyl ether led to the formation of the lithium salt [Li(OEt<sub>2</sub>)<sub>3</sub>][TiMe(Et<sub>8</sub>N<sub>4</sub>)], without Li···porphyrinogen interactions, which inserts Bu<sup>t</sup>NC to give the corresponding η<sup>2</sup>-iminoacyl derivative, and carbon monoxide to afford a very reactive η<sup>2</sup>-acyl intermediate species which evolves to a monomeric titanyl complex.<sup>100</sup> A binuclear Ti complex containing a Ti=C=C=Ti core supported by a *meso*-octaethylporphyrinogen tetraanion (N<sub>4</sub>Et<sub>8</sub>)<sup>4−</sup> is prepared by reduction of Ti(N<sub>4</sub>Et<sub>8</sub>)·2THF with Li in the presence of ethylene. Two lithium atoms are coordinated to the carbon atoms in the Ti=C=C=Ti core. There is ambiguity about the bonding in this fragment, that is, whether it is best described as Ti=C=C=Ti or alternatively as Ti–C≡C–Ti.<sup>101</sup>

#### 4.05.2.1.1.(iv) Complexes stabilized by phosphorus ligands

The complex TiBr<sub>2</sub>(NMe<sub>2</sub>)<sub>2</sub>[Ph<sub>3</sub>P=CHC(Ph)O], which contains an α-keto-stabilized phosphorus ylide ligand, has been obtained from the reaction of the phosphonium bromide [Ph<sub>3</sub>P=CHC(O)Ph]Br with Ti(NMe<sub>2</sub>)<sub>4</sub>. Its molecular crystal structure has been determined by X-ray diffraction.<sup>102</sup>



Scheme 40



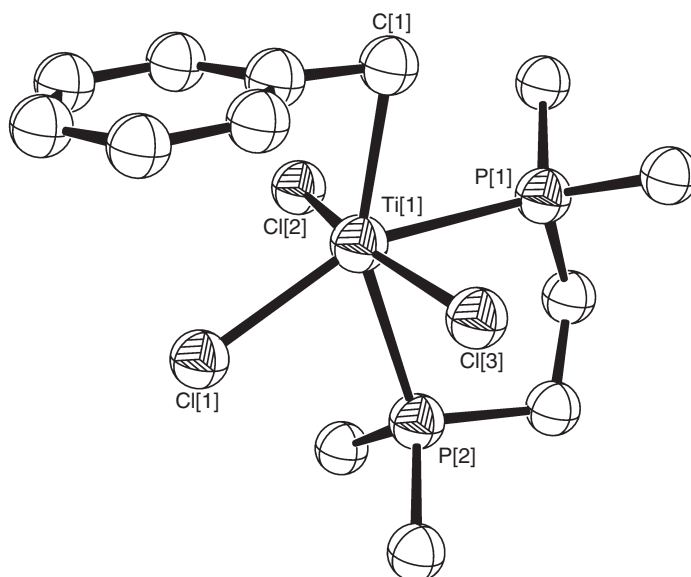
Scheme 41

Treatment of  $\text{TiCl}_4$  with a stoichiometric amount of 1,2-bis(dimethylphosphino)ethane(dmpe) gives  $\text{TiCl}_4(\text{dmpe})$  which can be readily alkylated by 1 or 2 equiv. of  $\text{MgCl}(\text{CH}_2\text{Ph})$  to give the monobenzyl  $\text{TiCl}_3(\text{CH}_2\text{Ph})(\text{dmpe})$  and dibenzyl  $\text{TiCl}_2(\text{CH}_2\text{Ph})_2(\text{dmpe})$  derivatives, respectively. The molecular structures of both alkyl complexes have been determined by X-ray diffraction providing interesting examples of benzyl ligands bending toward the electron-deficient  $\text{Ti}(\text{IV})$  center (Figures 1 and 2).  $\text{Ti}-\text{C}(1)-\text{C}(2)$  angles of  $81.9(2)^\circ$  for the monobenzyl and  $88.9(2)^\circ$  and  $124.9(2)^\circ$  for the dibenzyl derivatives were found.<sup>103</sup>

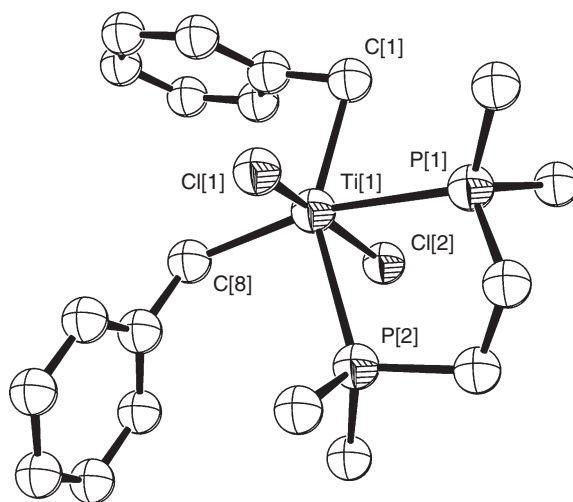
#### 4.05.2.1.2 Dialkyl and related complexes

A significant number of dialkyl titanium complexes, including those containing  $\beta$ -hydrogens as well as alkylidenes, have been reported stabilized by conformationally rigid diamido, imido, or dialkoxo ligands, in the hope that these types of complexes may provide new reagents and catalysts. Complexes containing monodentate amido or alkoxo (A in Scheme 42) or bidentate bis-amido or bis-alkoxo ligands (B in Scheme 42) have recently become the focus of increasing interest and are promising systems in titanium chemistry because of their relationship to the well-known bis-Cp' ( $\text{Cp}'$  = substituted cyclopentadienyl ring) and mono-Cp'-amido analogs (C and D in Scheme 42). One advantage of the neutral or anionic N- or O-donor ligands over  $\text{Cp}^-$  ligands is their easier accessibility, and the resulting metal complexes often exhibit new types of polymerization reactivities.

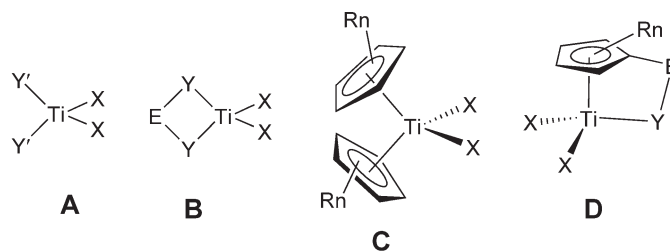
$\text{TiCl}_2\text{Me}_2$  is prepared by reaction of  $\text{TiCl}_4 \cdot 1,2\text{-DME}$  with 2 equiv. of  $\text{LiMe}$  while the sequential treatment of  $\text{TiCl}_4 \cdot 1,2\text{-DME}$  with  $\text{LiMe}$  followed by  $\text{CF}_3\text{CH}_2\text{OH}$  gives  $\text{TiCl}_2\text{Me}(\text{OCH}_2\text{CF}_3)$ . The dimethyl compound is a highly effective reagent for the aminoalkyne cyclization/acyl cyanide sequence.<sup>13</sup> Chiral alkoxo titanium compounds synthesized from  $\text{TiCl}_2\text{Me}_2$  catalyze the enantioselective Diels-Alder reactions of 1,3-cyclohexadiene with N-sulfinylbenzyl carbamate or N-sulfinyl-*p*-toluenesulfonamide.<sup>104</sup>



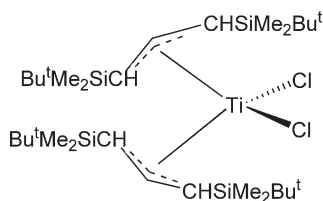
**Figure 1** Molecular structure of complex  $\text{TiCl}_3(\text{CH}_2\text{Ph})\cdot\text{dmpe}$  (reproduced by permission of Elsevier from *J. Organomet. Chem.*, 1999, 573, 78).



**Figure 2** Molecular structure of complex  $\text{TiCl}_2(\text{CH}_2\text{Ph})_2\cdot\text{dmpe}$  (reproduced by permission of Elsevier from *J. Organomet. Chem.*, 1999, 573, 78).



X = anionic ligand  
 CpRn = cyclopentadienyl-type ligand  
 Y = NR, O  
 Y' = amido ( $\text{NR}_2$ ), alkoxo (OR)  
 E = bridging ligand ( $\text{CX}_2$ ,  $\text{SiX}_2$ )



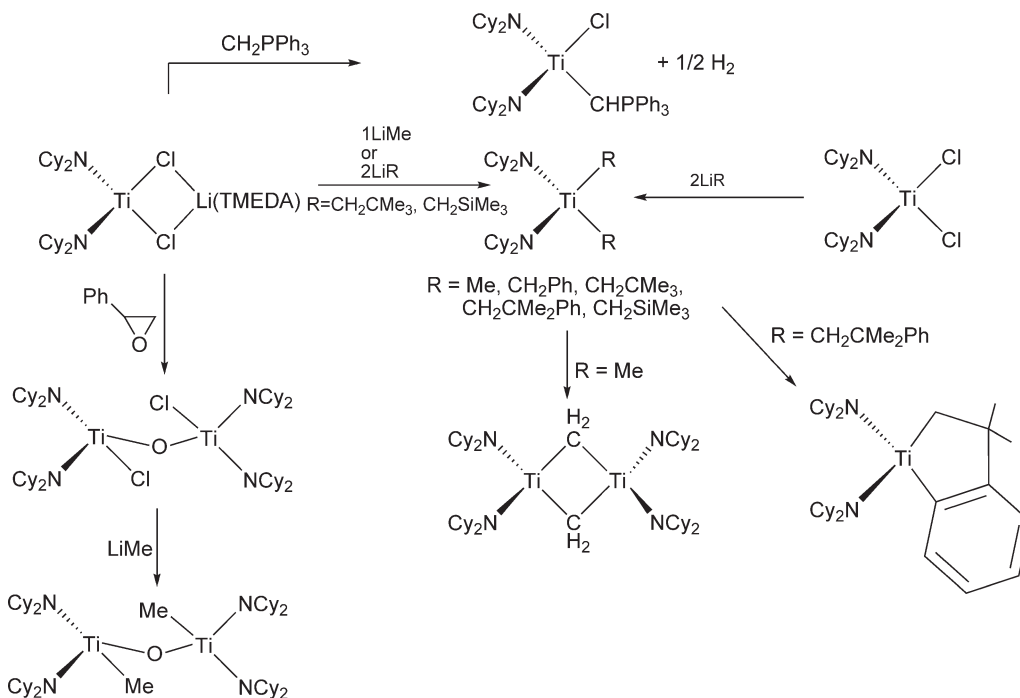
Scheme 43

The bis(allyl) complex  $\text{TiCl}_2[(\text{Bu}^t\text{Me}_2\text{SiCH})_2\text{CH}]_2$  (Scheme 43) is prepared in low yield (11%) by oxidation of the Ti(III) complex  $\text{TiCl}_2[(\text{Bu}^t\text{Me}_2\text{SiCH})_2\text{CH}]_2 \cdot \text{Li}(\text{TMEDA})$  with  $\text{SbCl}_6(4\text{-Br-C}_6\text{H}_4)_3$  in  $\text{CH}_2\text{Cl}_2$  (TMEDA = tetramethylethylenediamine). The allylic moieties interconvert and fluctuate between  $\eta^3$ - and  $\eta^1$ -coordination, causing an alternation between  $C_2$ - and  $C_{2v}$ -symmetries of the complex. The catalytic activity of this complex activated with MAO in the polymerization of propylene and ethylene is studied.<sup>105</sup>

#### 4.05.2.1.2.(i) Complexes stabilized by monodentate amido ligands

Bulky amido groups as ancillary ligands have been used as alternative to the Cp rings for the stabilization of a wide range of alkyltitanium derivatives and group 4 metal diamido dialkyl complexes are receiving special attention as potential catalysts for olefin polymerizations.

A series of tetravalent titanium complexes of the type  $\text{TiR}_2(\text{NCy}_2)_2$  supported by amido ligands have been reported by reactions of trivalent or tetravalent titanium compounds with alkylating reagents under different reaction conditions (Scheme 44). The oxidation of titanium(III) upon reaction with 1 equiv. of methyl lithium is surprising. The reaction of the Ti(III) compound  $[\text{Li}(\text{TMEDA})_2][\text{Ti}(\text{CH}_2\text{Ph})_2\{\text{N}(\text{SiMe}_3)_2\}_2]$  with diphenylfulvene results in the formation of the neutral Ti(IV) complex  $\text{Ti}(\text{CH}_2\text{Ph})_2\{\text{N}(\text{SiMe}_3)_2\}_2$ . All of these complexes display a moderate thermal stability. Alkyl groups lacking  $\beta$ -hydrogens prevent  $\beta$ -H elimination and favor  $\alpha$ -H abstraction during C–H bond metathesis processes. Thermolysis of the methyl derivative  $\text{TiMe}_2(\text{NCy}_2)_2$  in toluene at 60 °C quantitatively and selectively forms the bridging methylene complex  $(\text{NCy}_2)_2\text{Ti}(\mu\text{-CH}_2)_2\text{Ti}(\text{NCy}_2)_2$ . This complex shows resonances at  $\delta$  8.29 in the  $^1\text{H}$  and  $\delta$  224.7 in the  $^{13}\text{C}$  NMR spectra for the bridging methylene groups. The same reaction, although much slower, is



Scheme 44

observed at room temperature. Similar behavior is detected for the neophyl complex  $\text{Ti}(\text{CH}_2\text{CMe}_2\text{Ph})_2(\text{NCy}_2)_2$  which gives the cyclometallated species  $\text{Ti}(\text{CH}_2\text{CMe}_2\text{C}_6\text{H}_4)_2(\text{NCy}_2)_2$ . Similarly,  $[\text{Li}(\text{TMEDA})_2][\text{TiCl}_2(\text{NCy}_2)_2]$  reacts with styrene oxide to the Ti oxo complex  $[\text{TiCl}(\text{NCy}_2)_2]_2(\mu\text{-O})$  which has been alkylated with  $\text{LiMe}$  to give the binuclear methyl derivative  $[\text{TiMe}(\text{NCy}_2)_2]_2(\mu\text{-O})$ .<sup>106,107</sup> The reaction of  $[\text{Li}(\text{TMEDA})_2][\text{TiCl}_2(\text{NCy}_2)_2]$  with the phosphorus ylid  $\text{CH}_2\text{PPh}_3$  gives the tetravalent  $\text{TiCl}(\text{CHPPh}_3)(\text{NCy}_2)_2$  via ylid C–H activation.<sup>108</sup>

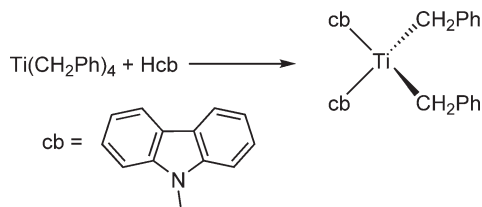
A number of titanium derivatives containing carbazole ligands have been isolated. Reaction of  $\text{Ti}(\text{CH}_2\text{Ph})_4$  with carbazole yields the dibenzyl complex  $\text{Ti}(\text{CH}_2\text{Ph})_2(\text{cb})_2$  (Scheme 45). The reaction of this compound with 2,6-dimethylphenyl isocyanide leads to titanium derivatives containing new carbon–carbon bonds (Section 4.05.2.3).<sup>109,110</sup>

The bis(1-alkynyl) derivatives  $\text{Ti}(\text{C}\equiv\text{CR})_2[(\text{Me}_3\text{Si})_2\text{N}][(\text{CH}_2\text{Me}_2\text{Si})_2\text{N}]$  and  $\text{Ti}(\text{C}\equiv\text{CR})_2[(\text{CH}_2\text{Me}_2\text{Si})_2\text{N}]_2$  are synthesized by reaction of the corresponding dichloro precursors with  $\text{LiC}\equiv\text{CR}$ . The reaction of the bis(1-alkynyl) complexes with trialkylboranes ( $\text{BEt}_3$  or  $\text{BPr}_3$ ) leads almost quantitatively to titana-2,4-cyclopentadienes, in which a diethylboryl group functions as a substituent in 3-position (Scheme 46). It is proposed that these reactions proceed by 1,1-alkylboration.<sup>111</sup>

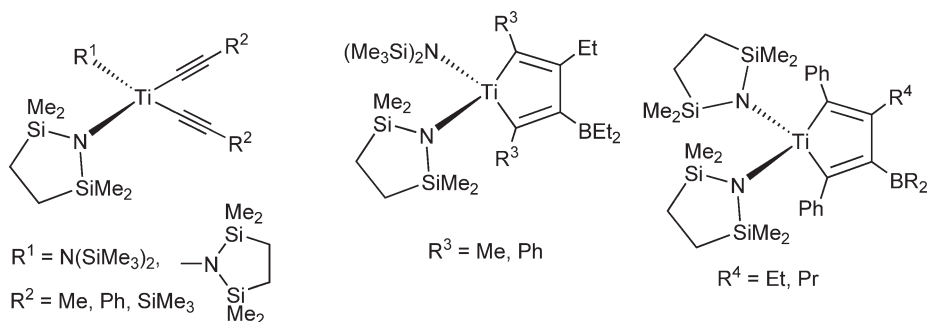
The complex  $\text{TiCl}_2(\text{N}=\text{PBU}^t_3)_2$  is synthesized by reaction of  $\text{TiCl}_3(\text{N}=\text{PBU}^t_3)$  with  $\text{LiN}=\text{PBU}^t_3$ , or alternatively by heating 2 equiv. of the trimethylsilylphosphinimine ( $\text{Bu}^t_3\text{P}=\text{NSiMe}_3$ ) with  $\text{TiCl}_4$  at  $110^\circ\text{C}$  in toluene for 12 h. Alkylation with appropriate Grignard reagents gives the dialkyl derivatives  $\text{TiR}_2(\text{N}=\text{PBU}^t_3)_2$  ( $\text{R} = \text{Me}, \text{CH}_2\text{Ph}, \text{Ph}, \text{allyl}$ ). The reactivity of these species is described in Section 4.05.2.3.<sup>76</sup>

#### 4.05.2.1.2.(ii) Complexes stabilized by chelating diamido and amidinato ligands

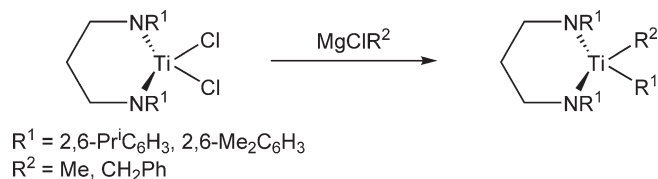
The complexes  $\text{TiCl}_2[\text{RN}(\text{CH}_2)_3\text{NR}]$  ( $\text{R} = 2,6\text{-Pr}^i\text{C}_6\text{H}_3$ ,  $2,6\text{-Me}_2\text{C}_6\text{H}_3$ ) are prepared by reacting the silylated diamines with  $\text{TiCl}_4$  in refluxing xylenes. The dimethyl derivatives  $\text{TiMe}_2[\text{RN}(\text{CH}_2)_3\text{NR}]$  are prepared by alkylation reaction of the dichloro complexes with  $\text{MgBrMe}$ . Analogous benzyl derivatives have been described (Scheme 47).



Scheme 45



Scheme 46



Scheme 47

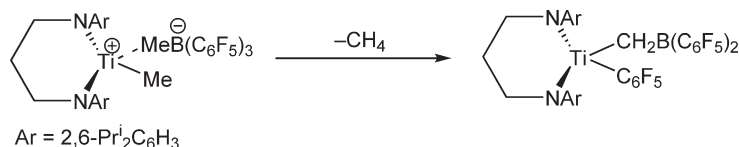
The molecular structure determined by X-ray diffraction shows a distorted tetrahedral geometry around the Ti center. When activated with MAO, these complexes are active for the aspecific polymerization of 1-hexene, generating high molecular weight polymers with narrow molecular weight distributions. The system  $\text{TiMe}_2[\text{ArN}(\text{CH}_2)_2\text{NAr}]/\text{B}(\text{C}_6\text{F}_5)_3$  serves as a living polymerization catalyst of  $\alpha$ -olefins.<sup>112–114</sup> However, in the absence of monomer an inactive compound is formed, representing a formal deactivation of the polymerization system. The dimethyl complexes react with  $\text{B}(\text{C}_6\text{F}_5)_3$  in pentane to give insoluble products characterized as the ionic complexes  $[\text{TiMe}\{\text{ArN}(\text{CH}_2)_2\text{NAr}\}]^+[\text{MeB}(\text{C}_6\text{F}_5)_3]^-$ . For the bulkier compound with  $\text{Ar} = 2,6\text{-Pr}^i_2\text{C}_6\text{H}_3$ , this ionic species is unstable and slowly evolves methane, coupled with  $\text{C}_6\text{F}_5$  transfer from boron to titanium, to give the titanium aryl complex  $\text{Ti}(\text{C}_6\text{F}_5)\text{CH}_2\text{B}(\text{C}_6\text{F}_5)_2\{\text{ArN}(\text{CH}_2)_2\text{NAr}\}$  (Scheme 48) which is inactive as an olefin polymerization catalyst; its molecular structure has been determined by X-ray diffraction.<sup>113,115</sup>

The dimethyl and dibenzyl complexes  $\text{TiR}_2(\text{MABA})$  (Scheme 49) containing the disymmetric diamido ligand ( $\text{MABA} = \text{N},\text{N}'\text{-bis}(\text{trimethylsilyl})\text{amido-benzylamido}$ ) have been prepared by treatment of the chloro precursor compound with the appropriate Grignard reagent. X-ray crystal structures of the benzyl complex show an agostic interaction between the titanium metal center and benzylic protons. This agostic interaction is not suggested in solution, as indicated by NMR spectroscopy. When activated with  $\text{B}(\text{C}_6\text{F}_5)_3$ , the benzyl derivative has moderate catalytic activities for the polymerization of  $\alpha$ -olefins.<sup>116</sup>

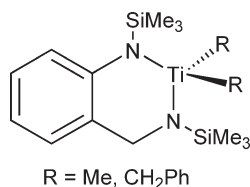
Dialkyltitanium complexes supported by a diamido ligand in which the bridge is an acyclic or cyclic silylene fragment “ $\text{R}_2\text{Si}$ ” have been reported. The presence of the cyclic silylene displays greater steric protection toward the metal center than the acyclic silylene-bridged diamido ligands. Dimethyl and dibenzyl complexes  $\text{TiR}_2[(\text{NBu}^t)_2\text{Si}(\text{cycl})]$  ( $\text{R} = \text{Me}, \text{Bz}$ ) (Scheme 50) are prepared by reaction of the corresponding dichloro precursors with 2 equiv. of  $\text{MgBrR}$  in  $\text{Et}_2\text{O}$  at  $-78^\circ\text{C}$ . Treatment of  $\text{TiCl}_2[(\text{NBu}^t)_2\text{Si}(\text{cycl})]$  with 1 equiv. of  $\text{MgBrMe}$  affords the monomethyl  $\text{TiClMe}[(\text{NBu}^t)_2\text{Si}(\text{cycl})]$  derivative. Subsequent reaction of both methyl complexes with  $\text{O}_2$  proceeds by insertion of the oxygen molecule into the Ti–C bond generating the respective methoxo-bridged titanium dimers  $[\text{Ti}\{(\text{NBu}^t)_2\text{Si}(\text{cycl})\}\text{X}(\mu\text{-OMe})_2]$  ( $\text{X} = \text{Cl}, \text{Me}$ ) (see Scheme 23). Oxygen insertion does not occur with the benzyl derivatives, presumably because the formation of the alkoxo-bridged dimer is hampered by the presence of bulky dibenzyl units (Scheme 50). The molecular structures of these complexes have been determined by X-ray diffraction.<sup>70–72</sup>

The three electron-donating bidentate benzamidinato ligands display attractive properties from a synthetic and reactivity standpoint and they have been used as ancillary groups to stabilize Cp and non-Cp titanium complexes. The  $\text{N},\text{N}'\text{-bis}(\text{trimethylsilyl})\text{benzamidinato}$  ligand has been regarded as a steric equivalent of Cp group. The chloro methyl and dialkyl benzamidinato complexes,  $\text{TiClMe}[\text{PhC}(\text{NSiMe}_3)_2]$  and  $\text{TiR}_2[\text{PhC}(\text{NSiMe}_3)_2]$  (Scheme 51), have been prepared by reaction of the dichloride with the appropriate magnesium reagent. These species are prone to reduction and give products without Ti–C bonds.<sup>117</sup> Analogous titanium complexes have been reported.<sup>118</sup>

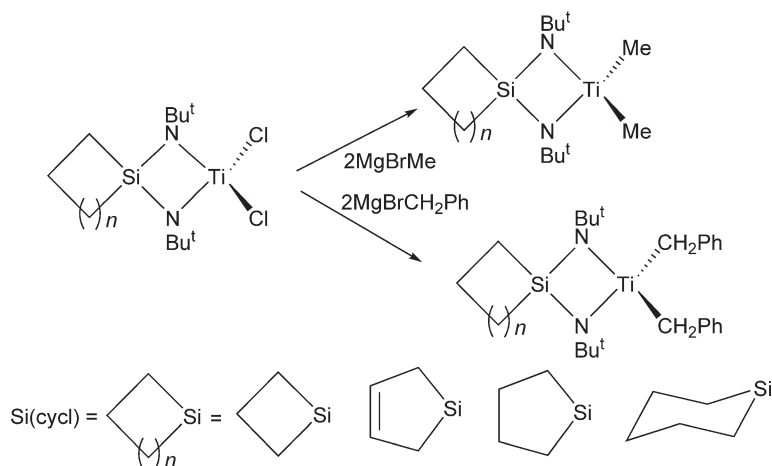
Partial alkylation of the titanium dimer  $[\text{TiCl}_3\{\text{C}_6\text{H}_5\text{C}(\text{NSiMe}_3)_2\}]_2$  with 2 equiv. of  $\text{LiMe}$  gives the chloro methyl binuclear derivative  $[\text{TiMeCl}_2\{\text{C}_6\text{H}_5\text{C}(\text{NSiMe}_3)_2\}]_2$ , while treatment with 6 equiv. of  $\text{LiMe}$  leads to the formation of the mononuclear dimethyl compound  $\text{TiMe}_2[\text{C}_6\text{H}_5\text{C}(\text{NSiMe}_3)_2]$ . The latter is synthesized in better yield by the reaction between  $\text{TiCl}_2[\text{C}_6\text{H}_5\text{C}(\text{NSiMe}_3)_2]$  and  $\text{LiMe}$  (Scheme 52). The  $^1\text{H}$  NMR spectrum of the binuclear



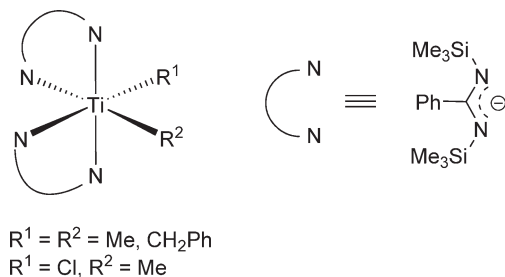
Scheme 48



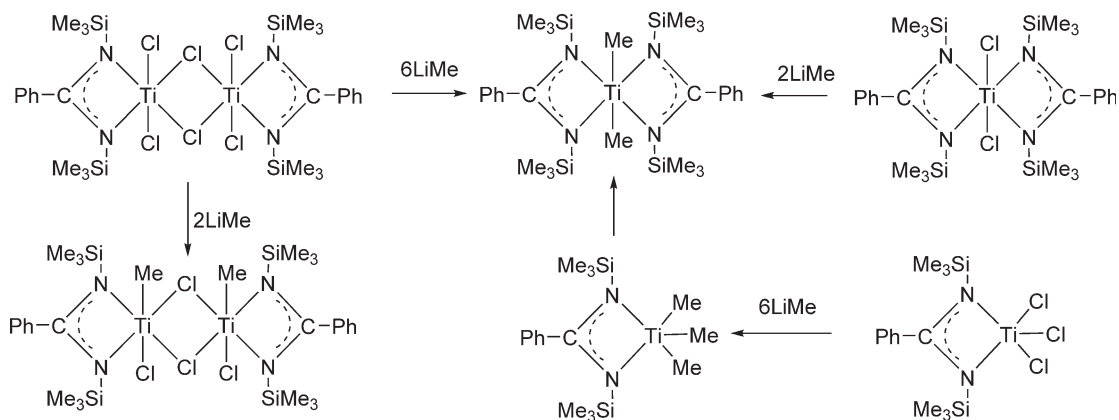
Scheme 49



Scheme 50



Scheme 51

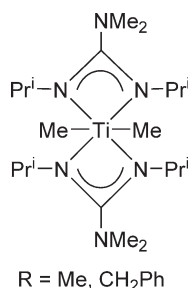


Scheme 52

titanium complex shows a low-field chemical shift at  $\delta$  2.30 for the methyl group attached to titanium. These systems in the presence of MAO as co-catalysts are active as Ziegler–Natta polymerization catalysts.<sup>119</sup>

$\text{TiMe}_4$  reacts with an excess of  $\text{N,N}'$ -bis(trimethylsilyl)-benzamidine to give the corresponding dimethyl bis-benzamidinato complex  $\text{TiMe}_2[\text{PhC}(\text{NSiMe}_3)_2]_2$ . This compound has been characterized by X-ray diffraction.<sup>89</sup>

The isomerization of allylbenzene to *cis*- and *trans*- $\beta$ -methyl styrene has been studied with the benzamidinato complex  $\text{TiMe}_2[p\text{-MeC}_6\text{H}_4\text{C}(\text{NSiMe}_3)_2]$  and the results compared with those obtained with analogous zirconium compounds.<sup>120</sup>



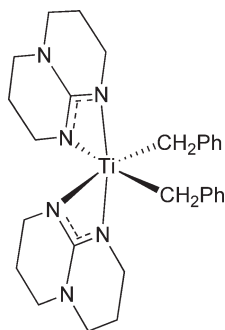
Scheme 53

The dialkyl-guanidinato complexes  $\text{TiR}_2[(\text{Pr}^i\text{N})_2\text{CNMe}_2]_2$  (Scheme 53) have been made by the reaction of the corresponding dichloride with  $\text{LiMe}$  or  $\text{MgCl}(\text{CH}_2\text{Ph})$ . The methyl complex exhibits fluxional behavior in solution according to the NMR spectroscopic studies, while the benzyl complex is stereochemically rigid at room temperature. The reaction of  $\text{TiR}[(\text{Pr}^i\text{N})_2\text{CNMe}_2]$  with 2,6-dimethyl isocyanide affords a new terminal Ti imido complex, an effective catalyst for the hydroamination of alkynes.<sup>121</sup> Titanium dialkyl complexes supported by bicyclic guanidinato ligands have been described. The reaction of 2 equiv. of hppH (1,3,4,6,7,8-hexahydro-2*H*-pyrimido[1,2- $\alpha$ ]pyrimidine) with  $\text{Ti}(\text{CH}_2\text{Ph})_4$  affords the dibenzyl guanidinato complex  $\text{Ti}(\text{CH}_2\text{Ph})_2(\text{hpp})$  (Scheme 54), the molecular structure of which has been determined by X-ray diffraction. NMR spectroscopic study shows that the compound is fluxional in solution. The NMR scale reaction with  $\text{B}(\text{C}_6\text{F}_5)_3$  gives paramagnetic products.<sup>122</sup>

Dialkyltitanium complexes supported by aminotroponiminato ligands have been described. The treatment of  $\text{TiCl}_2(\text{LL})_2$  ( $\text{LL} = \text{N,N}'$ -dimethylaminotroponiminato) with Grignard reagents under different conditions and molar ratios leads to the synthesis of dialkyl or chloro alkyl titanium complexes (Scheme 55). The solid-state structure of some of these complexes have been established by X-ray diffraction. Their reactivity has been widely studied (Section 4.05.2.3).<sup>123–125</sup>

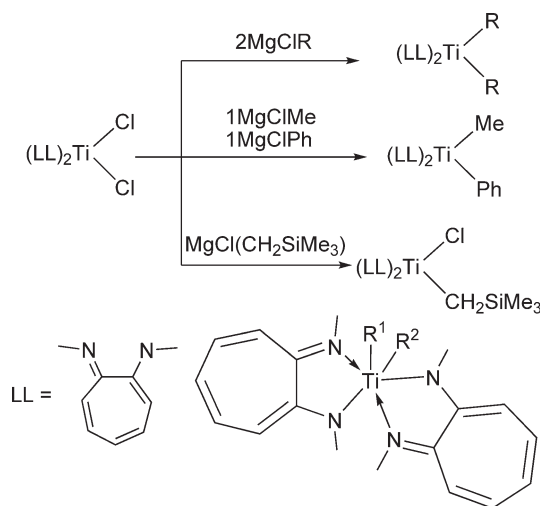
Dialkyl bis(3,5- $\text{Bu}^t_2$ -pyrazolato) titanium complexes  $\text{TiR}_2(\text{Bu}^t_2\text{pz})_2$  (Scheme 56) are prepared by treatment of the dichloro precursor compound with the appropriate alkylating reagent ( $\text{MgClR}$  or  $\text{LiR}$ ). They have been spectroscopically characterized; the molecular structure of the trimethylsilylmethyl derivative is established by X-ray diffraction. Treatment of  $\text{TiMe}_2(\text{Bu}^t_2\text{pz})_2$  with  $\text{Bu}^t$ -amine or isopropyl amine in the presence of pyridine gives imido complexes. The reaction of  $\text{TiMe}_2(\text{Bu}^t_2\text{pz})_2$  with 1,1-dialkylhydrazines was also studied.<sup>82</sup>

The highly air sensitive dialkyl complexes  $\text{TiR}_2[(\text{NBu}^t_2\text{P}(\text{CH}_2)_3\text{PBu}^t_2\text{N})]$  (Scheme 57) are obtained by reaction of the dichloro parent compound with  $\text{LiMe}$  or  $\text{MgCl}(\text{CH}_2\text{Ph})$ . A single crystal X-ray structure analysis has been performed for both alkyl derivatives. The Ti–N (1.807–1.835 Å) and P–N (1.569–1.589 Å) bond distances are compatible with bond orders close to 2.<sup>126</sup> Alkylation of  $\text{TiBr}_2[m\text{-C}_6\text{H}_4(\text{CH}_2\text{PBu}^t\text{=N})_2]$  with precise control of the stoichiometry of  $\text{MgBrMe}$  or  $\text{MgBr}(\text{CH}_2\text{Ph})$  affords the dialkyl complexes  $\text{TiR}_2[m\text{-C}_6\text{H}_4(\text{CH}_2\text{PBu}^t\text{=N})_2]$  (Scheme 58). The molecular structure of the methyl derivative has been determined by X-ray diffraction methods, revealing slightly long Ti–N bond distances (av. 1.818(7) Å). Upon activation with MAO, the methyl complex is a poor catalyst for the polymerization of ethylene.<sup>127</sup> The synthesis of the dimethyl iminophosponamido complexes  $\text{TiMe}_2[\text{Ph}_2\text{P}(\text{NR})_2]_2$  (Scheme 59) has been described by reaction of the dichloro precursor compound with  $\text{LiMe}$  or

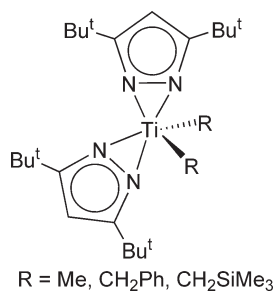


Scheme 54

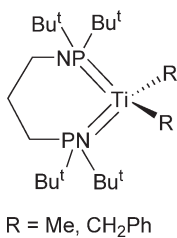




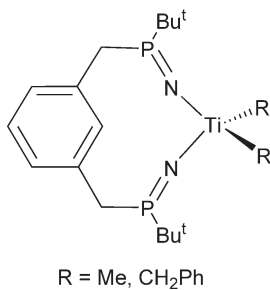
Scheme 55



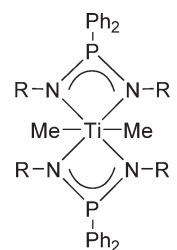
Scheme 56



Scheme 57

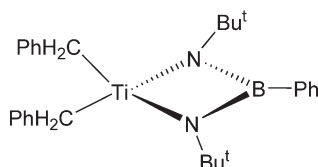


Scheme 58



R = benzyl, *p*-tolyl

Scheme 59

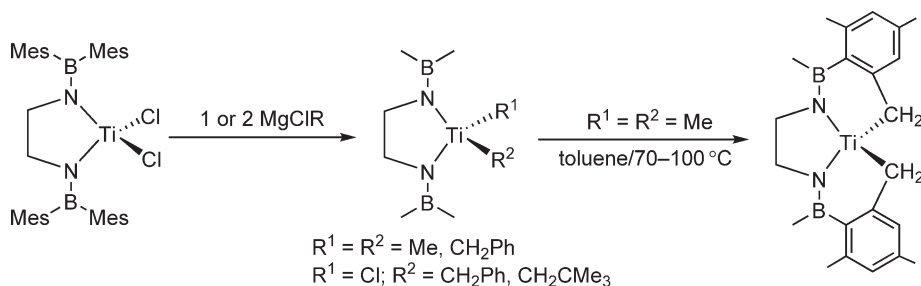


Scheme 60

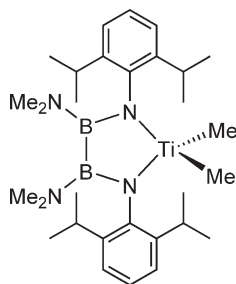
MgBrMe. These complexes, when activated with MAO, are active ethylene polymerization catalysts, providing high molecular weight poly(ethylene) with narrow molecular weight distributions.<sup>128</sup>

The synthesis of the dibenzyl bis(alkylamido)phenylborane complex  $\text{Ti}(\text{CH}_2\text{Ph})_2(\text{Bu}^t\text{N}-\text{BPh}-\text{NBu}^t)$  (Scheme 60) has been described and its molecular structure determined by X-ray diffraction methods.<sup>129</sup>

Titanium compounds containing the new unusual bidentate chelating bis(borylamido) ligand  $[\text{Mes}_2\text{BNCH}_2\text{-CH}_2\text{NBMes}_2]^{2-}$  (Ben) have been made from  $\text{TiCl}_4(\text{THF})_2$  and  $\text{Mg}(\text{Ben})(\text{THF})_2$  to give the dichloro compound  $\text{TiCl}_2(\text{Ben})$ . Complexes  $\text{TiClR}(\text{Ben})$  ( $\text{R} = \text{CH}_2\text{Ph}$ ,  $\text{CH}_2\text{CMe}_3$ ) and  $\text{TiR}_2(\text{Ben})$  ( $\text{R} = \text{Me}$ ,  $\text{CH}_2\text{Ph}$ ) can be prepared by alkylation of  $\text{TiCl}_2(\text{Ben})$  with Grignard reagents in dichloromethane (Scheme 61). An X-ray diffraction study of  $\text{TiCl}(\text{CH}_2\text{Ph})(\text{Ben})$  confirms the proposed ligand conformation and features a highly distorted  $\eta^2$ -benzyl ligand with a  $\text{Ti}-\text{C}_\alpha-\text{C}_{ipso}$  angle of only  $87.0(5)^\circ$ . The dimethyl complex decomposes upon heating by metallation of the mesityl *ortho*-methyl groups.  $\text{TiMe}_2(\text{Ben})$  reacts with  $\text{B}(\text{C}_6\text{F}_5)_3$  to give the cationic Ti species  $[\text{TiMe}(\text{Ben})][\text{MeB}(\text{C}_6\text{F}_5)_3]$ ; its dichloromethane solutions show little polymerization activity toward ethylene as a consequence of strong cation–anion interactions.<sup>130</sup>  $\text{TiCl}_2(\text{CH}_2\text{SiMe}_3)_2$  reacts with lithium salt of the bis(borylamido)ligand  $\text{Li}_2(\text{Cy}_2\text{BNCH}_2\text{-CH}_2\text{NBCy}_2)$  to give the diamido–dialkyl compound  $\text{Ti}(\text{CH}_2\text{SiMe}_3)_2(\text{Cy}_2\text{BNCH}_2\text{-CH}_2\text{NBCy}_2)$  from which the trimethylsilylmethyl ligands can be cleaved off by adding 2 equiv. of  $\text{I}_2$ , resulting in  $\text{TiI}_2(\text{CH}_2\text{SiMe}_3)_2$ . The diiodo complex is converted to new mixed tetraalkyl derivatives  $\text{Ti}(\text{CH}_2\text{SiMe}_3)_2\text{R}_2$  ( $\text{R} = \text{Me}$ ,  $\text{CH}_2\text{CHMe}_2$ ) by treatment with  $\text{MgR}_2$ . These alkyl complexes decompose in solution upon standing overnight.<sup>131</sup> The diamido dimethyl complex  $\text{TiMe}_2[(2,6\text{-diisopropylanilido})\text{-B}(\text{NMe}_2)_2\text{B}(\text{NMe}_2)(2,6\text{-diisopropylanilido})]$  (Scheme 62) has been prepared and tested as pre-catalyst for the olefin polymerization upon activation with MAO and  $\text{B}(\text{C}_6\text{F}_5)_3$  with activities considerably lower than those of Cp-based catalysts. The molecular weights of the polymers produced are activator dependent, and the polydispersities were found to be broader than those observed for Cp-based single-site catalytic systems.<sup>132</sup>



Scheme 61

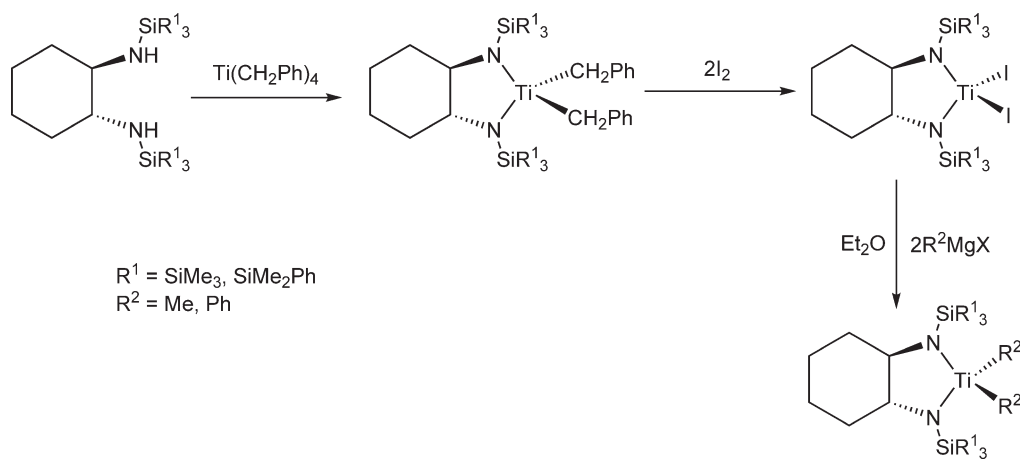


Scheme 62

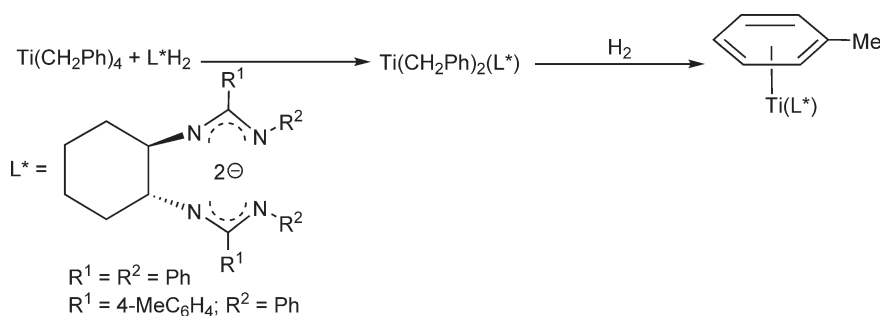
The addition of  $\text{H}_2[\text{Mes}_2\text{N}_2\text{NH}]$  to  $\text{TiCl}_4$  in ether gives a precipitate in which partial attachment of the ligand to the metal center is assumed. Subsequent addition of  $\text{MgIme}$  affords the dimethyl complex  $\text{TiMe}_2[\text{Mes}_2\text{N}_2\text{NH}]$ .<sup>133</sup>

An important contribution in this area of titanium chemistry has been the development of chiral metal complexes incorporating asymmetric bidentate bis-amido ligands. Thus, the complex  $\text{Ti}(\text{CH}_2\text{Ph})_2[(\pm)\text{-trans-1,2-(NSiR}_3)_2\text{-cyclohexane}]$  has been prepared by reaction of the amine precursors with  $\text{Ti}(\text{CH}_2\text{Ph})_4$ . The dibenzyl complex is converted into the di-yodo derivative by treatment with  $\text{I}_2$ . The dimethyl and diphenyl complexes  $\text{TiR}_2[(\pm)\text{-trans-1,2-(NSiR}_3)_2\text{-cyclohexane}]$  ( $\text{R} = \text{Me}, \text{C}_6\text{H}_5$ ) have been synthesized by metathesis reaction of the di-yodo compound with Grignard reagents (Scheme 63). These species are difficult to isolate and handle due to their high solubility. X-ray crystallographic analysis of the dibenzyl derivative has been established indicating small  $\text{N-Ti-N}$  angle [ $91.97(8)^\circ$ ] and large  $\text{C-Ti-C}$  angle [ $117.8(1)^\circ$ ] values.<sup>134</sup>

The reaction of  $\text{L}^*\text{H}_2$  [ $\text{L}^*$  = chiral bis(benzamidinato) ligand] (Scheme 64) with  $\text{Ti}(\text{CH}_2\text{Ph})_4$  in toluene produces the dibenzyl bis(benzamidinato) titanium complex  $\text{Ti}(\text{CH}_2\text{Ph})_2(\text{L}^*)$ , which reacts with  $\text{H}_2$  with initial formation of



Scheme 63



Scheme 64

toluene and a reactive hydrido benzyl species, followed by elimination of the benzyl and hydrido ligands through a C–H coupling process and a  $\sigma$ – $\pi$  rearrangement leading to an isolated  $\eta^6$ -arene complex.<sup>135</sup>

Theoretical studies concerning the ethylene polymerization process by group 4 diamido complexes  $\text{TiMe}_2[\text{RN}(\text{CH}_2)_3\text{NR}]$  by pure quantum mechanical methods (DFT) as well as a combination of molecular mechanics and quantum mechanics (QM/MM) have been reported.<sup>136</sup>

#### 4.05.2.1.2.(iii) Complexes stabilized by tridentate and polydentate N,N-X ligands

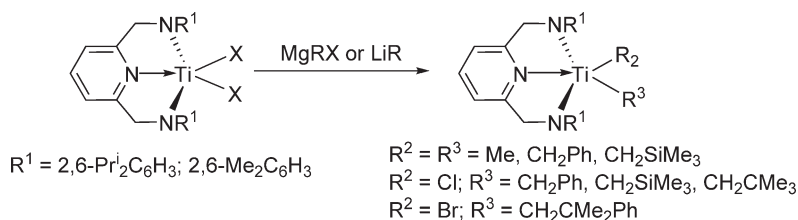
Alkylation of  $\text{TiCl}_2[\text{MeC}(\text{2-C}_5\text{H}_4\text{N})(\text{CH}_2\text{NSiMe}_3)_2]$  with one or two molar equivalents of  $\text{MgClR}$  ( $\text{R} = \text{CH}_2\text{Ph}$ ,  $\text{CH}_2\text{SiMe}_3$ ,  $\text{C}\equiv\text{CSiMe}_3$ ) yields the mono- and dialkyl complexes  $\text{TiClR}[\text{MeC}(\text{2-C}_5\text{H}_4\text{N})(\text{CH}_2\text{NSiMe}_3)_2]$  and  $\text{TiR}_2[\text{MeC}(\text{2-C}_5\text{H}_4\text{N})(\text{CH}_2\text{NSiMe}_3)_2]$ . Depending on the steric demand of the alkyl group, coordination or decoordination of the pyridyl group leads to four- or five-coordinate species. The crystal structure analysis of the pentacoordinate complex  $\text{TiCl}(\text{CH}_2\text{SiMe}_3)[\text{MeC}(\text{2-C}_5\text{H}_4\text{N})(\text{CH}_2\text{NSiMe}_3)_2]$  has been reported.<sup>137</sup>

The reaction of  $\text{TiCl}_2[2,6-(\text{R}^1\text{NCH}_2)_2\text{NC}_5\text{H}_3]$  with various Grignard reagents affords the corresponding dialkyl or halo-alkyl compounds  $\text{TiR}^2\text{R}^3[2,6-(\text{R}^1\text{NCH}_2)_2\text{NC}_5\text{H}_3]$  (Scheme 65). A single crystal X-ray diffraction study of  $\text{TiBr}(\text{CH}_2\text{CMe}_2\text{Ph})[2,6-(\text{R}^1\text{NCH}_2)_2\text{NC}_5\text{H}_3]\cdot\text{C}_6\text{H}_6$  shows a distorted square-pyramid structure with the neophyl group occupying the axial position.<sup>138</sup> Symmetric and asymmetric titanacyclopentadiene titanium complexes (Scheme 66) are synthesized by reduction of the dichloro  $\text{TiCl}_2[2,6-(\text{R}^1\text{NCH}_2)_2\text{NC}_5\text{H}_3]$  with excess 1% Na/Hg amalgam in toluene in the presence of  $>2$  equiv. of an alkyne. Some of these metallacyclic complexes react with an excess of alkyne at  $80^\circ\text{C}$  to give new asymmetric titanacyclopentadiene derivatives. The compound  $\text{Ti}[\text{C}_4\text{H}_2(\text{SiMe}_3)_2][2,6-(\text{R}^1\text{NCH}_2)_2\text{NC}_5\text{H}_3]$  has been characterized by X-ray crystallography. Pyridine–diamido ligand activation is observed in certain cases for these complexes.<sup>139</sup>

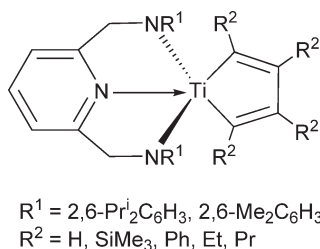
The sterically demanding amino–diamido ligand  $[\text{Me}_3\text{SiN}\{\text{CH}_2\text{CH}_2\text{N}(\text{SiMe}_3)_2\}_2]^{2-}$  ( $\text{L}^{2-}$ ) has been incorporated to the titanium chemistry as an alternative to Cp-based ligands. The treatment of  $\text{TiCl}_2\text{L}$  with  $\text{MgMe}_2$ ,  $\text{LiCH}_2\text{SiMe}_3$ , or  $\text{LiCH}(\text{SiMe}_3)_2$  affords the dialkyl complexes  $\text{TiR}_2\text{L}$  and the monoalkyl derivative  $\text{TiCl}[\text{CH}(\text{SiMe}_3)_2]\text{L}$  (Scheme 67) in which only partial coordination of the amino nitrogen is observed in solution and the solid state. The X-ray crystal structures of dimethyl and the chloro bis(trimethylsilyl)methyl derivatives are described.<sup>140</sup>

Dibenzyl complexes stabilized by tridentate dianionic ligands containing hard and soft pendant donors have been described. Reactions of  $\text{Ti}(\text{CH}_2\text{Ph})_4$  with the corresponding aminophenols give the mononuclear pentacoordinate dibenzyl Ti derivatives (Scheme 68). Activated with MAO, these complexes have been used as catalysts for ethylene polymerization, showing marked activity enhancements for the compounds containing soft donor substituents.<sup>141</sup>

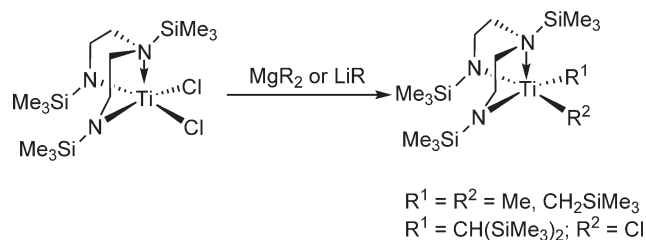
Five-coordinated titanium compounds  $\text{TiX}_2(\text{NON})$  exhibit approximately trigonal-bipyramidal geometries with the two amido ligands in equatorial positions, the two X groups being inequivalent (“twisted *fac*” structure) (Scheme 69).



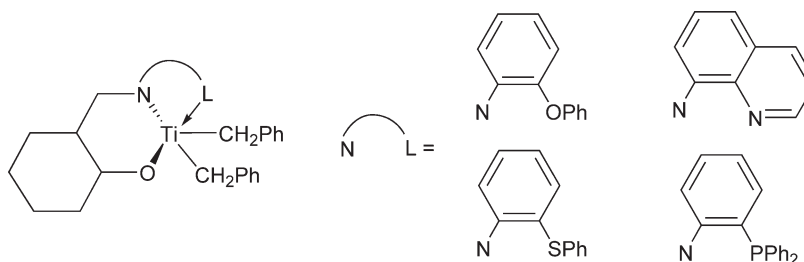
Scheme 65



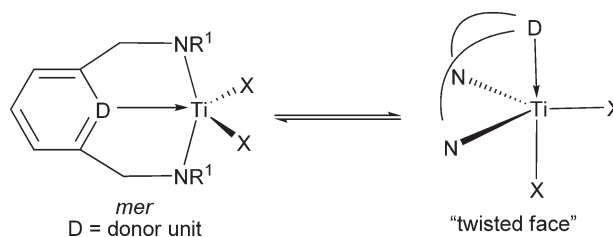
Scheme 66



Scheme 67



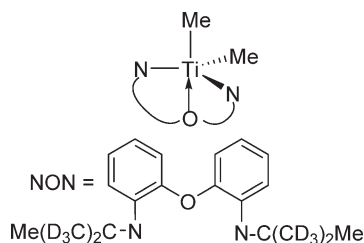
Scheme 68



Scheme 69

Alternatively, a *mer*-structure with the amido atoms in apical positions is also possible. The found "twisted *fac*" structure equilibrates rapidly in solution on the NMR timescale even at low temperature, presumably via the *mer*-structure. For  $\text{Bu}^t$  substituent on the amido nitrogen, the "twisted *fac*" structure is preferred because of the steric interactions between the  $\text{Bu}^t$  and the two equatorial R groups. With the less steric demanding groups  $\text{Pr}^i$  or cyclohexyl as amido substituents, *mer*-structures have been found in the solid state.

Addition of 2 equiv. of  $\text{LiBu}^n$  to the diamine  $\text{H}_2(\text{NON})$  followed by reaction with  $\text{TiCl}_2(\text{NMe}_2)_2$  affords the tetraamido titanium compound  $\text{Ti}(\text{NON})(\text{NMe}_2)_2$ , which can be converted to the new dichloro diamido complex  $\text{TiCl}_2(\text{NON})$  by reaction with  $\text{SiClMe}_3$ . Alkylation of this compound with  $\text{MgClMe}$  gives the dimethyl derivative  $\text{TiMe}_2(\text{NON})$  (Scheme 70). An X-ray diffraction study shows that it has a trigonal-bipyramidal structure. The Ti–O



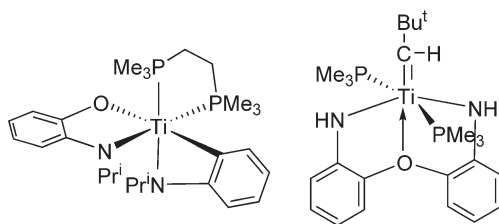
Scheme 70

bond distance (2.402(4) Å) is longer than that expected for a normal Ti–O<sub>donor</sub> bond length (2.15–2.20 Å), although it is much shorter than that found for the Ti–N bond distance in TiMe<sub>2</sub>[(Me<sub>3</sub>SiNCH<sub>2</sub>CH<sub>2</sub>)<sub>2</sub>N(SiMe<sub>3</sub>)],<sup>140</sup> considered essentially uncoordinated.<sup>114,142</sup>

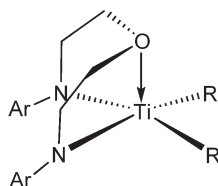
Alkylation of TiCl<sub>2</sub>(R<sup>i</sup>NON) [R<sup>i</sup>NON is the tridentate diamido ligand (R<sup>i</sup>NC<sub>6</sub>H<sub>4</sub>)<sub>2</sub>O<sup>2-</sup>; R<sup>i</sup> = Pr<sup>i</sup>, cyclohexyl] with Grignard reagents gives the corresponding dialkyl derivatives TiR<sub>2</sub>(R<sup>i</sup>NON). These complexes are much more stable than analogous TiCp<sub>2</sub>R<sub>2</sub> derivatives. Their NMR spectroscopic data at room temperature are consistent with C<sub>2v</sub> symmetry. The molecular structure of Ti(CH<sub>2</sub>CHMe<sub>2</sub>)<sub>2</sub>(Pr<sup>i</sup>NON) has been determined by X-ray diffraction and shows a *mer*-configuration. The reaction between Ti(CH<sub>2</sub>CHMe<sub>2</sub>)<sub>2</sub>(Pr<sup>i</sup>NON) and PMe<sub>3</sub> under a nitrogen atmosphere yields a reduced bridging dinitrogen compound, while with Me<sub>2</sub>PCH<sub>2</sub>CH<sub>2</sub>PMe<sub>2</sub>(dmpe) in the absence of dinitrogen Ti(Pr<sup>i</sup>NC<sub>6</sub>H<sub>4</sub>)(Pr<sup>i</sup>NC<sub>6</sub>H<sub>4</sub>O)(dmpe) is obtained (Scheme 71), a pseudo-octahedral species in which one aryl–oxygen bond has been cleaved, through an oxidative addition of an aryl–oxygen bond of the ligand backbone to the titanium atom. Thermal reaction of the analogous neopentyltitanium complex gives an alkylidene species (Scheme 71; Section 4.05.2.1.5). Complexes containing the (Pr<sup>i</sup>NON)<sup>2-</sup> ligand are less crowded than those that contain the (Bu<sup>t</sup>NON)<sup>2-</sup> ligand and titanium derivatives with (Bu<sup>t</sup>NON)<sup>2-</sup> are less stable than complexes with (Pr<sup>i</sup>NON)<sup>2-</sup>.<sup>143</sup> Complexes TiMe<sub>2</sub>[(RN-*o*-C<sub>6</sub>H<sub>4</sub>)<sub>2</sub>O] (R = Bu<sup>t</sup>, SiMe<sub>3</sub>) have been synthesized by reaction of MgClMe with the dichloro precursors. The room-temperature <sup>1</sup>H NMR spectra show one singlet for the titanium methyl groups. The X-ray study for the Bu<sup>t</sup> derivative shows a “twisted *fac*” (Scheme 69) disposition with equatorial amido groups, an axial oxygen donor, and an axial methyl group.<sup>144,145</sup>

The addition of Li<sub>2</sub>[(2,6-R<sub>2</sub>C<sub>6</sub>H<sub>3</sub>NCH<sub>2</sub>CH<sub>2</sub>)<sub>2</sub>O] (R = Me, Et) to TiCl<sub>4</sub>(THF)<sub>2</sub> in diethyl ether leads to the formation of the five-coordinated tridentate-diamido titanium dichloro compounds TiCl<sub>2</sub>[(2,6-R<sub>2</sub>C<sub>6</sub>H<sub>3</sub>NCH<sub>2</sub>CH<sub>2</sub>)<sub>2</sub>O]. Alkylation of these compounds with MgClMe yields the dimethyl titanium complexes TiMe<sub>2</sub>[(2,6-R<sub>2</sub>C<sub>6</sub>H<sub>3</sub>NCH<sub>2</sub>CH<sub>2</sub>)<sub>2</sub>O], while the dibenzyl compound Ti(CH<sub>2</sub>Ph)<sub>2</sub>[(2,6-Me<sub>2</sub>C<sub>6</sub>H<sub>3</sub>NCH<sub>2</sub>CH<sub>2</sub>)<sub>2</sub>O] is obtained, in low yield (15%), via the slow reaction of Ti(CH<sub>2</sub>Ph)<sub>4</sub> with (2,6-Me<sub>2</sub>C<sub>6</sub>H<sub>3</sub>NHCH<sub>2</sub>CH<sub>2</sub>)<sub>2</sub>O (Scheme 72). Activation of the alkyl complexes with [PhNHMe<sub>2</sub>]-[B(C<sub>6</sub>F<sub>5</sub>)<sub>4</sub>] or Ph<sub>3</sub>C[B(C<sub>6</sub>F<sub>5</sub>)<sub>4</sub>] gives very poorly active species for the polymerization of 1-hexene, in contrast to the reactivity observed for other analogous systems. X-ray structure of the benzyl compound shows that both benzyl group are bound in an η<sup>1</sup> fashion.<sup>146,147</sup>

The dibenzyl complex Ti(CH<sub>2</sub>Ph)<sub>2</sub>(Me<sub>2</sub>PMEN) containing the tetradentate diamino–diamido ligand Me<sub>2</sub>PMEN<sup>2-</sup> = N,N′-dimethyl-N,N′-bis[(*S*)-2-methylpyrrolidino]ethylenediamino has been prepared by alkane elimination in the reaction of Ti(CH<sub>2</sub>Ph)<sub>4</sub> with H<sub>2</sub>(Me<sub>2</sub>PMEN) and its molecular structure determined by X-ray diffraction methods (Figure 3). The reaction with 2 equiv. of I<sub>2</sub> in toluene generates the diiodo complex TiI<sub>2</sub>(Me<sub>2</sub>PMEN) which is converted into the dimethyl derivative TiMe<sub>2</sub>(Me<sub>2</sub>PMEN) in the reaction with LiMe in diethyl ether (Scheme 73). An interesting aspect of this report is the stereoselective study about the coordination of

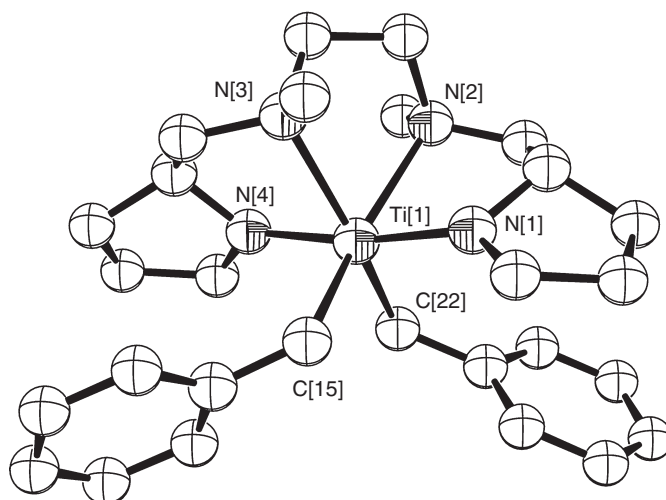


Scheme 71

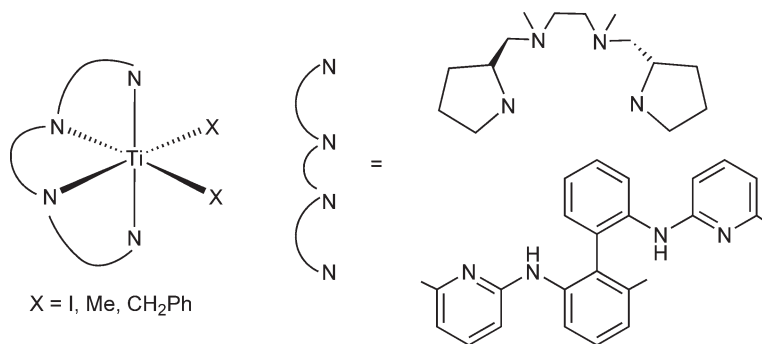


R = Cl, Me, CH<sub>2</sub>Ph  
Ar = 2,6-Me<sub>2</sub>C<sub>6</sub>H<sub>3</sub>; 2,6-Et<sub>2</sub>C<sub>6</sub>H<sub>3</sub>

Scheme 72



**Figure 3** Molecular structure of complex  $\text{Ti}(\text{CH}_2\text{Ph})_2(\text{Me}_2\text{PMEN})$  (reproduced by permission of American Chemical Society from *Organometallics*, **2003**, 22, 4999).



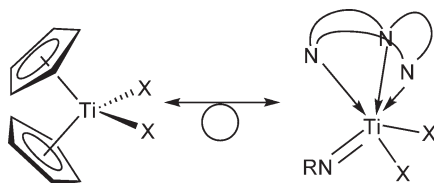
**Scheme 73**

the  $\text{Me}_2\text{PMEN}^{2-}$  ligand to the Ti center. Assuming an ideal octahedral arrangement for the titanium center, 12 isomeric structures are possible, differing in the position (*cis-trans*) of the two alkyl ligands and the configuration of the amido-amino nitrogens. The molecular structure of the benzyl complex exhibits a  $C_2$ -symmetry with a *cis*-disposition of the benzyl ligands and a *trans,cis,S,S* configuration of the pyrrolidino-amino nitrogen atoms. Alkyl abstraction using boron reagents affords cationic alkyl complexes, of which  $[\text{Ti}(\text{CH}_2\text{Ph})(\text{Me}_2\text{PMEN})][\text{B}(\text{C}_6\text{F}_5)_4]$  has been isolated. The ethylene and 1-hexene polymerization behavior when these complexes are activated with  $\text{B}(\text{C}_6\text{F}_5)_3$  or  $\text{Q}[\text{B}(\text{C}_6\text{F}_5)_4]$  ( $\text{Q} = \text{Ph}_3\text{C}$ ,  $\text{HNMe}_2\text{Ph}$ ) are also investigated.<sup>148</sup> Reaction of the chiral 2,2'-biaryl-bridged aminopyridine ligand  $\text{H}_2\text{L}$  (Scheme 73) with  $\text{Ti}(\text{NMe}_2)_4$  affords the complex  $\text{Ti}(\text{NMe}_2)_2\text{L}$ . The dichloro compound  $\text{TiCl}_2\text{L}$  can be synthesized by treatment of  $\text{Ti}(\text{NMe}_2)_2\text{L}$  with  $\text{SiClMe}_3$ , or alternatively by reaction of  $\text{TiCl}_3$  with the potassium salt  $\text{K}_2\text{L}$  followed by oxidation. Alkylation of  $\text{TiCl}_2\text{L}$  gives the dimethyl derivative  $\text{TiMe}_2\text{L}$ . The dibenzyl complex  $\text{Ti}(\text{CH}_2\text{Ph})_2\text{L}$  can be prepared by treatment of  $\text{H}_2\text{L}$  with  $\text{Ti}(\text{CH}_2\text{Ph})_4$  (Scheme 73). These Ti complexes exhibit  $C_2$ -symmetry; the two alkyl groups are retained in mutually *cis*-coordination sites. The chiral biaryl ligand is considered as an alternative to Cp rings.<sup>149</sup>

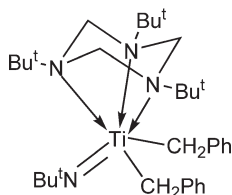
#### 4.05.2.1.2.(iv) Complexes stabilized by imido ligands

Imido titanium complexes of the type  $\text{TiX}_2(=\text{NR})(\text{fac-L}_3)$  ( $\text{L}_3$  = six-electron donor peralkylated triazacyclic ligand) have been considered as isolobal analogs of corresponding bis-Cp derivatives (Scheme 74).

The dibenzyl imido complex  $\text{Ti}(\text{CH}_2\text{Ph})_2(=\text{NBu}^t)(\text{fac-L}_3)$  (Scheme 75) supported by  $\text{L}_3 = 1,3,5\text{-Bu}^t\text{-triazacyclohexane}$  has been synthesized by the reaction of the corresponding dichloro compound with 2 equiv. of  $\text{MgCl}(\text{CH}_2\text{Ph})$



Scheme 74

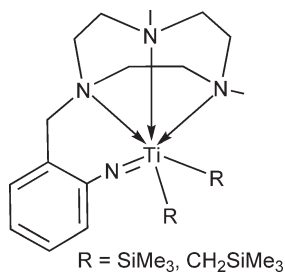


Scheme 75

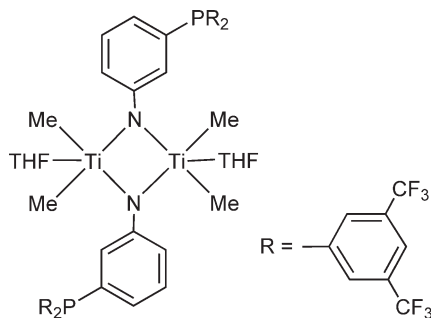
in THF. The molecular structure has been determined by X-ray diffraction. The NMR spectra are temperature dependent and show dynamic behavior in solution.<sup>150</sup>

The dialkyltitanium complexes shown in Scheme 76, supported by a macrocyclic ligand with a chelating imido side functionality, have been synthesized by treatment of the dichloro parent compounds with LiMe or LiCH<sub>2</sub>SiMe<sub>3</sub> in benzene at room temperature. Comparisons between this macrocyclic ligand and *ansa*-bis-Cp and mono-Cp-amido-type ligands are established.<sup>151</sup>

The binuclear tetramethyl complex [TiMe<sub>2</sub>(THF)(μ-NAr)]<sub>2</sub> [Ar = *m*-C<sub>6</sub>H<sub>4</sub>-P(3,5-(CF<sub>3</sub>)<sub>2</sub>C<sub>6</sub>H<sub>3</sub>)<sub>2</sub>] can be prepared by methylation of the chloro parent compound with LiMe in Et<sub>2</sub>O at 0 °C (Scheme 77) and is stabilized by two imido bridges. The molecular structure of this complex has been determined by X-ray diffraction methods and shows that each Ti atom occupies the center of a trigonal bipyramid.<sup>152</sup>



Scheme 76



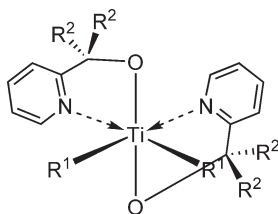
Scheme 77



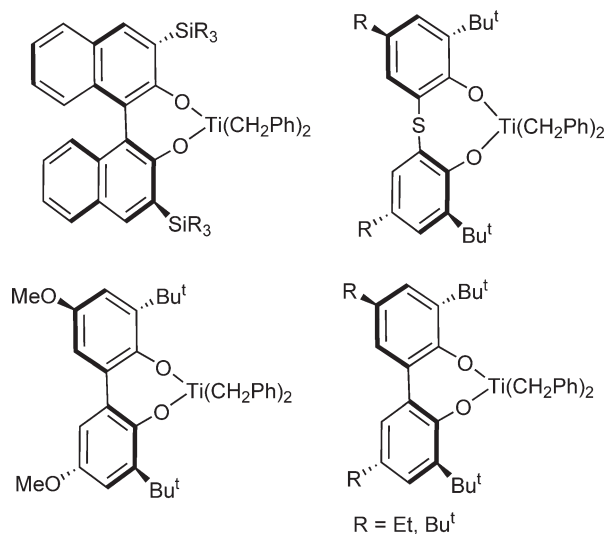
## 4.05.2.1.2.(v) Complexes stabilized by dialkoxo ligands

The synthesis of dialkyl dialkoxo–pyridine complexes  $\text{TiR}^1_2(\text{pyCR}^2_2\text{O})_2$  shown in Scheme 78 has been described.<sup>153</sup>

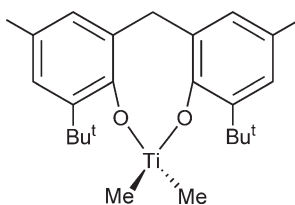
Protonolysis of  $\text{Ti}(\text{CH}_2\text{Ph})_4$  with chelating biphenols and binaphthols at 20 °C yields the sterically hindered chelating alkoxo  $\text{Ti}(\text{CH}_2\text{Ph})_2(\text{O}-\text{O})$  complexes (Scheme 79). This class of systems can be regarded as being analogous to the well-known range of bis-Cp-type titanium complexes. The X-ray crystal structure of  $\text{Ti}(\text{CH}_2\text{Ph})_2[2,2'-(4-\text{OMe},6-\text{tBuC}_6\text{H}_2\text{O})_2]$  is reported.<sup>154</sup> A structural study of the dimethyl bis(phenoxo) titanium complex shown in Scheme 80 has been compared with the analogous bis(isopropoxo) compound.<sup>155</sup> Dialkyltitanium complexes containing the nine-membered metallacyclic ethylene-linked bis(phenoxo) ligand have been synthesized (Scheme 81). The crystal structure of the trimethylsilylmethyl derivative determined by X-ray diffraction shows a  $C_2$ -symmetric conformation. In solution, a fluxional process equivalent to an enantiomerization is detected. Upon activation with MAO, these complexes co-polymerize ethylene and styrene with remarkably high incorporation of styrene.<sup>156</sup> The analogous dimethyl- and dibenzyltitanium compounds stabilized by the 2,2'-ethylenebis(6-isopropylphenoxo) ligand (Scheme 82) have been synthesized by metathetical reaction from the corresponding dichloro derivative by treatment with  $\text{MgClR}$  ( $\text{R} = \text{Me}, \text{CH}_2\text{Ph}$ ). They have been spectroscopically characterized.<sup>157</sup>



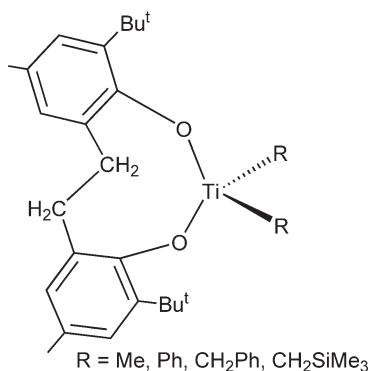
Scheme 78



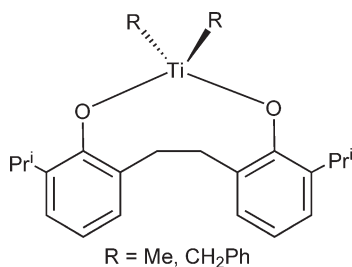
Scheme 79



Scheme 80



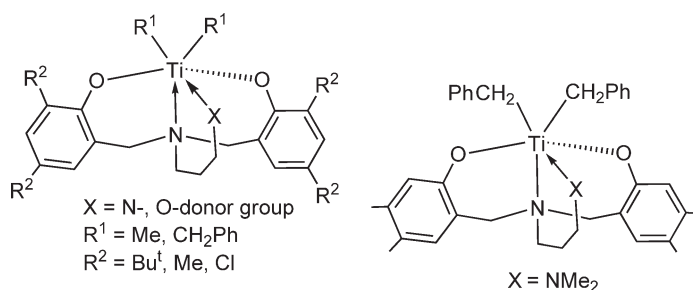
Scheme 81



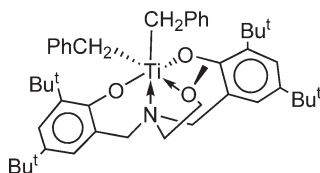
Scheme 82

Dibenzyl and dimethyl Ti complexes supported by amino-bisphenoxo ligands bearing side arm donor groups have been synthesized (Scheme 83). They are prepared by straightforward protonolysis reactions of the ligand precursor with  $\text{TiR}_4$  ( $R = \text{Me, CH}_2\text{Ph}$ ). The molecular structures have been determined by X-ray diffraction. When activated with a suitable Lewis acid, all of these complexes are active catalysts for the polymerization of 1-hexene with living characteristics and the co-polymerization of 1-hexene and 1-octene. The different electronic and steric properties of the side arm donor groups exhibit influence controlling the activity of these catalysts.<sup>158–161</sup>

The dibenzyltitanium complex  $\text{Ti}(\text{CH}_2\text{Ph})_2(\text{ONOO})$  (Scheme 84) containing a dianionic tetradentate bis-phenoxo-amine-ether ligand has been synthesized. Upon activation with  $\text{B}(\text{C}_6\text{F}_5)_3$ , this compound catalyzes the living



Scheme 83



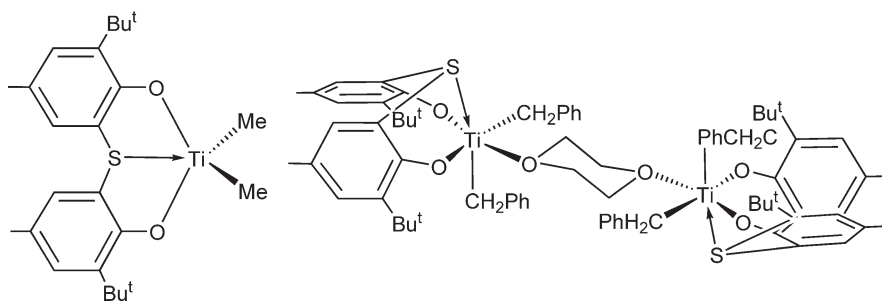
Scheme 84

polymerization of  $\alpha$ -olefins. Living polymerization of 1-hexene is obtained above room temperature to obtain high molecular weight poly(1-hexene). The block co-polymerization of 1-hexene and 1-octene at room temperature is described as well.<sup>162</sup>

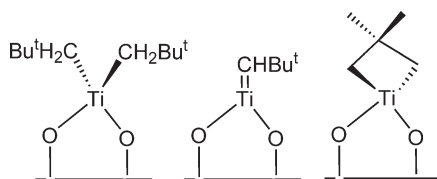
The compound  $\text{TiCl}_2(\text{tbmp}')$  containing the sulfur-linked bis-phenoxo ligand  $\text{tbmp}' = 2,2'$ -thiobis(2- $\text{Bu}^t$ -4-methylphenoxo) is prepared in quantitative yield by treatment of  $\text{TiCl}_4$  with the corresponding bis-phenol. The dichloro compound reacts with  $\text{LiMe}$  to give the thermally robust dimethyl derivative  $\text{TiMe}_2(\text{tbmp}')$  (Scheme 85). The presence of a Ti–S interaction is suggested in this compound from the conformation of the eight-membered chelate bis-phenoxo ring, as deduced by crystallographic studies. The reaction of  $\text{TiCl}_2(\text{tbmp}')$  with benzyl Grignard  $\text{MgBr}(\text{CH}_2\text{Ph})$  in pentane gives the dibenzyl complex  $\text{Ti}(\text{CH}_2\text{Ph})_2(\text{tbmp})$  which is only isolated as a 1,4-dioxane adduct  $[\text{Ti}(\text{CH}_2\text{Ph})_2(\text{tbmp}')]_2(\mu\text{-C}_4\text{H}_8\text{O}_2)$ , the molecular structure of which has been determined by X-ray diffraction methods. X-ray diffraction studies reveal a centrosymmetric 1,4-dioxane-bridged molecule between two fragments containing six-coordinate titanium centers, with the tridentate  $\text{tbmp}'$  ligand in a facial fashion and two  $\eta^1$ -benzyl ligands (Scheme 85).  $\text{TiMe}_2(\text{tbmp}')$  when activated with  $\text{B}(\text{C}_6\text{F}_5)_3$  is active for the polymerization of ethylene.<sup>163</sup>

Silica may be employed as a bidentate ligand to alkyltitanium derivatives. Alkyl and alkylidene complexes having the empirical formula  $\text{Ti}(\text{CH}_2\text{CMe}_3)_2(\equiv\text{SiO}_2)$  and  $\text{Ti}=\text{CHCMe}_3(\equiv\text{SiO}_2)$  incorporating two covalent interactions with oxygen atoms of the silica surface are prepared from the reaction of the corresponding tetra(alkyl) complexes with silica (Scheme 86).<sup>164,165</sup>

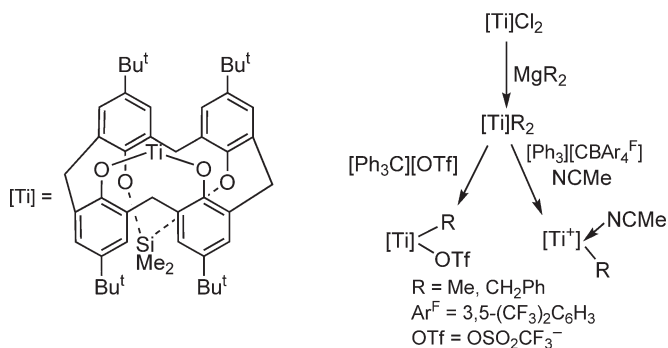
A series of alkyltitanium, titanacyclic, oxatitanacyclic, and  $\eta^6$ -arene derivatives supported by dimethylsilyl-bridged  $p\text{-Bu}^t$ -calix[4]arene ligands have been synthesized, and their reactivity toward organic unsaturated molecules was studied. The calix[4]arene groups act as bis(aryloxo)ligands. These complexes catalyze the  $[2 + 2 + 2]$ -cycloaddition of terminal alkynes  $\text{RC}\equiv\text{CH}$  to give the corresponding substituted benzene with excellent regioselectivity. The reactions of the  $\eta^6$ -arene complexes with aldehydes or ketones proceed with formation of titanacycle and oxatitanacycle derivatives, similarly to the coupling reaction between terminal alkynes and ketones. The direct influence of the calix[4]arene ligand in these reactions is strongly manifested. Structural, kinetic, and mechanistic studies are performed. The bonding nature of the  $\eta^6$ -arene derivatives is discussed. Although the complexes may be conceived as  $\text{Ti}(\text{II})$   $\eta^6$ -arene compounds, they possess significant  $\text{Ti}(\text{IV})$  character and they must be more precisely described as titanaborbornadiene complexes.<sup>166–170</sup> Dialkyltitanium complexes supported by  $p\text{-Bu}^t$ -calix[4]arene ligands have been synthesized by the reaction of the corresponding dichloro derivative with the appropriate dialkylmagnesium compound. The alkyl abstraction with  $\text{Ph}_3\text{C}[\text{BAR}^F_4]$  in the presence of  $\text{MeCN}$  proceeds with formation of the cationic species stabilized in solution by coordination to  $\text{MeCN}$ . Alkyl triflate complexes can be prepared by replacement of one of the alkyl groups by treatment of  $\text{HOTf}$  (Scheme 87). The formulation and structure of these complexes have been confirmed by microanalysis and spectroscopic characterization.<sup>167</sup> These systems are highly regioselective catalysts for the cyclotrimerization of alkynes.<sup>166</sup>



Scheme 85



Scheme 86

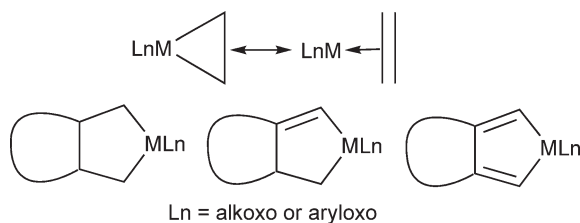


Scheme 87

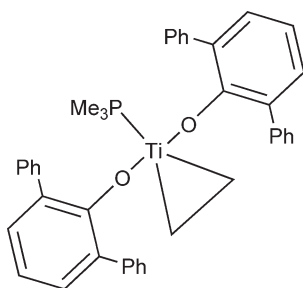
Group 4 metallocycle and metallabicycle systems utilized in organic synthesis are generally supported by Cp ligands. These substances undergo coupling reactions with a variety of electrophile reagents. The reactivities of metal complexes are often considerably affected by the nature of the ligands they have coordinated. The success of Cp-based titanium chemistry has led a number of research groups to develop a parallel chemistry utilizing alternative ligands. In order to test how the reactivity of similar types of metallacyclic derivatives having ligands other than Cp can be modified, extensive studies were conducted replacing the Cp ring with alkoxy ligands on the basis of electronic and steric reasons. Thus, a wide range of new alkoxy titanium metallacycles has been synthesized and their chemical behavior in numerous organic reactions has been studied. Titanium isopropoxide derivatives developed by the Sato group and *ortho*-substituted aryloxy ligation to support organometallic titanium compounds studied by Rothwell (Scheme 88) are important contributions to organometallic titanium chemistry and its application in organic chemistry.

The synthesis, structure, and reactivity of dialkyltitanium derivatives supported by aryloxy ligands have been widely explored by the Rothwell and co-workers.<sup>47</sup> Titanacyclopentadiene complexes can be prepared by reduction of alkoxy titanium derivatives  $TiX_n(OAr)_{2-n}$  in the presence of unsaturated organic molecules (acetylenes and diynes) and participate in a wide range of catalytic and stoichiometric reactions. The synthesis and characterization of dialkyl and metallacyclic compounds  $TiR_2(OAr)_2$  (OAr are 2,6-disubstituted phenoxo ligands;  $R = Me, CH_2Ph$ ), of titanacyclopentane, oxa- and azatitanacyclic as well as titanabicyclic compounds, have been investigated and reported, showing that these types of compounds exhibit significant thermal stability. These compounds can be used as reagents in organic reactions and olefin polymerization catalysis (See Section 4.05.2.3). The ethylene bis-aryloxy trimethylphosphino titanium compound shown in Scheme 89 has been described. The X-ray crystal structure of this compound discloses that the coordination of ethylene causes a substantial increase in the carbon–carbon double bond length from 1.337(2) Å for the free ethylene to 1.425(3) Å and considerable bending of the hydrogen atoms out of the plane of the ethylene molecule. The structure of this complex would appear to be intermediate between the  $\pi$ -ethylene Ti(II) and Ti(IV)–metallacyclopentane resonance structures.<sup>171–173</sup>

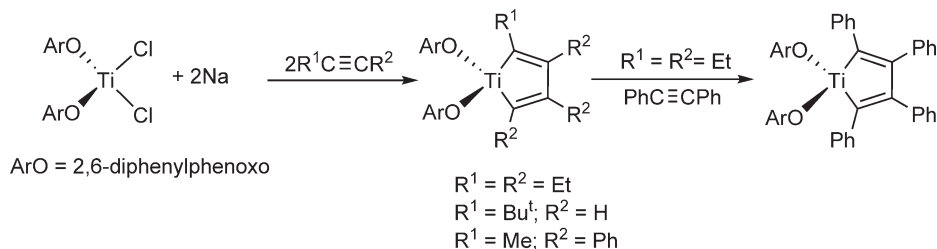
The sodium amalgam reduction of  $TiCl_2(OAr)_2$  (OAr = 2,6-diphenylphenoxo) in hydrocarbon solution in the presence of the alkyne substrates  $EtC\equiv CEt$ ,  $Bu^tC\equiv CH$ , and  $MeC\equiv CPh$  produces the titanacyclopentadiene complexes  $Ti(C_4R_4)(OAr)_2$  (Scheme 90). The use of less bulky substituents on the alkyne substrate in such reactions leads to mixtures of aromatic compounds due to cyclotrimerization reactions. A single crystal X-ray diffraction analysis of the tetraethyl substituted derivative confirms the general structure of these compounds.<sup>174</sup> In similar reactions, the sodium amalgam reduction of  $TiCl_2(OAr)_2$  (OAr = 2,6-diisopropylphenoxo) in the presence of the diynes



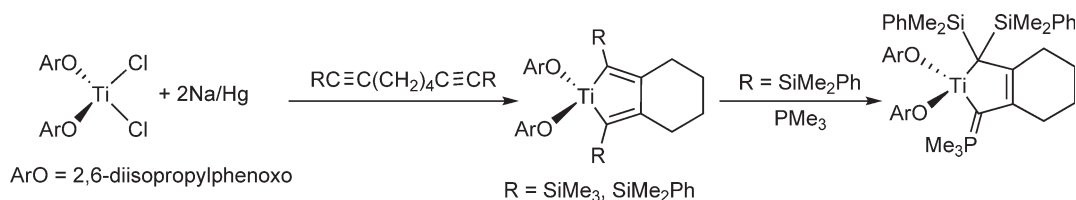
Scheme 88



Scheme 89



Scheme 90

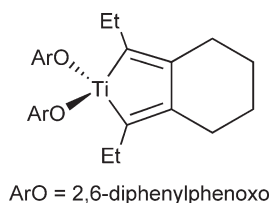


Scheme 91

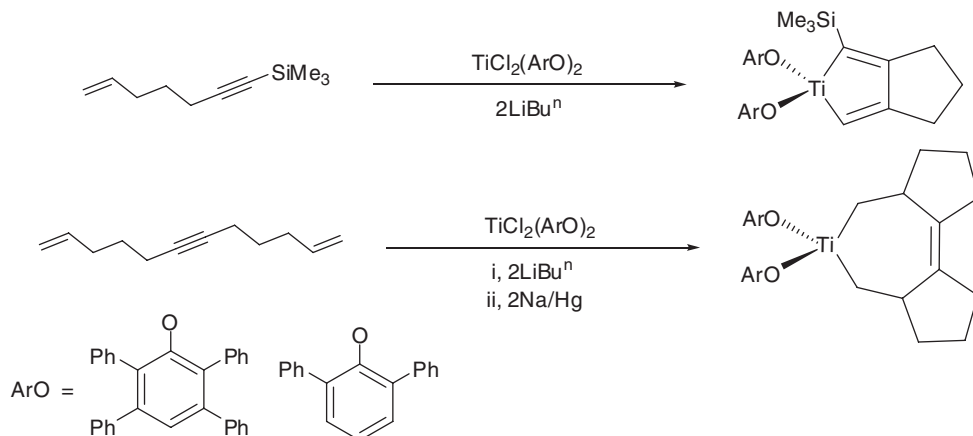
1,8-bis(trimethylsilyl)-1,7-octadiyne or 1,8-bis(dimethylphenylsilyl)-1,7-octadiyne yields the titanacyclopentadiene complexes  $\text{Ti}[\text{C}_2\text{R}_2\text{C}_6\text{H}_8](\text{OAr})_2$  (Scheme 91). Reaction of the dimethylphenylsilyl complex with  $\text{PMe}_3$  results in a ligand-induced rearrangement through migration of a dimethylphenylsilyl substituent from one  $\alpha$ -carbon to the other to form the phosphorus ylid derivative  $\text{Ti}[\text{C}(\text{SiMe}_2\text{Ph})_2\text{C}_6\text{H}_8\text{C}(\text{PMe}_3)](\text{OAr})_2$ . The X-ray structure of this complex has been reported.<sup>175</sup>  $\text{Ti}(\text{CH}_2)_4(\text{OAr})_2$  (OAr = 2,6-diphenylphenoxo) and  $\text{Ti}(\text{CHCMe}=\text{CMeH})(\text{OAr})_2$  (OAr = 2,6-diisopropylphenoxo) are obtained by sodium amalgam reduction of the dichloride complex  $\text{Ti}(\text{OAr})_2\text{Cl}_2$ . Both complexes show similar  $^1\text{H}$  and  $^{13}\text{C}$  NMR spectroscopic properties. The solid-state structure shows a bent titanacyclopentadiene ring which is maintained in solution according to the spectroscopic data indicating that the flipping of the metallacycle ring is slow on the NMR timescale.<sup>176</sup> The titanacyclopentadiene derivatives react with a variety of reagents to give new titanium complexes and they exhibit an extensive stoichiometric as well as catalytic reactivity not demonstrated by their metallocene analogs (Section 4.05.2.3).

Reduction of  $\text{TiCl}_2(\text{OAr})_2$  in the presence of 3,9-dodecadiyne leads to the corresponding titanacyclopentadiene derivative (Scheme 92). This compound catalyzes the reaction of 3,9-dodecadiyne with ethylene to give a mixture of hexalins. In a similar way the titanacyclopentadiene compound  $\text{Ti}(\text{C}_4\text{H}_2\text{Bu}^t)_2(\text{OAr})_2$  catalyzes the reaction of  $\text{BuC}\equiv\text{CH}$  with ethylene or  $\text{PhHC}=\text{CH}_2$  to give *tert*-butyl-substituted benzene derivatives.<sup>177</sup>

The synthesis of bis-aryloxo titanacyclopent-2-ene and titanacyclohept-3-ene (Scheme 93) derivatives has been reported via tricyclization of dienyne. The molecular structure of the titanacyclohept-3-ene has been determined by X-ray diffraction. It is suggested that the formation of the titanacyclohept-3-ene compound proceeds through an insertion of olefin into the Ti–vinyl bond of a titanacyclopent-2-ene intermediate. The metallacycles show interesting reactivity and synthetic usefulness and form novel organic molecules by hydrolysis and thermal catalysis.<sup>178</sup>



Scheme 92



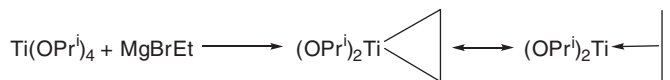
Scheme 93

Titanacyclic derivatives have been prepared by Sato *et al.* by treatment of unsaturated organic molecules and a low-valent titanium species. These compounds have found broad and intensive use in organic synthesis. This procedure is based on the Kulinkovich reaction.  $\text{Ti}(\text{OPr}^i)_4$  reacts with  $\text{MgBrEt}$  to give the titanacyclopentadiene derivative  $\text{Ti}(\text{CH}_2\text{CH}_2)(\text{OPr}^i)_2$  which can act as a  $\text{Ti}(\text{IV})$  1,2-dicarbocation reagent or may exhibit properties of a  $\text{Ti}(\text{II})$  isopropoxo-olefin complex (Scheme 94).<sup>179–181</sup> Methods for the generation of dialkoxo titanacyclopentadienes (dialkoxo-titanium olefin complexes) are surveyed. Alkylation of carboxylic acid derivatives with these reagents is studied.<sup>182</sup> In an investigation of the Kulinkovich cyclopropanol synthesis, a search for the formation of diisopropoxo-titanacyclopentadiene intermediates by warming an ethereal solution of  $\text{TiR}_2(\text{OPr}^i)_2$  ( $\text{R} = \text{Et}, \text{Pr}^i$ ) between  $-78^\circ\text{C}$  and  $+25^\circ\text{C}$  has been studied by chemical trapping with either an ester or nitrile.<sup>183</sup>

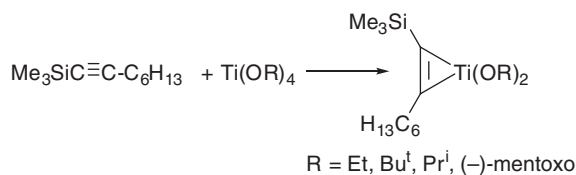
These titanium compounds can be described as an alkene  $\pi$ -complex or a metallacyclopentadiene, which is of practical importance. According to several computational studies, it has been concluded that the alkene titanium complexes are best represented as titanacyclopentadiene derivatives. The synthesis of titanium-alkyne complexes  $\text{Ti}(\text{Me}_3\text{SiC}\equiv\text{CC}_6\text{H}_{13})(\text{OR})_2$  from reaction between 1-(trimethylsilyl)oct-1-yne with achiral or chiral alkoxo titanium compounds  $\text{Ti}(\text{OR})_4$  has been described (Scheme 95).<sup>184</sup> A series of organotitanium compounds (Scheme 96) are obtained by metathesis reactions.<sup>41</sup>

Metallated titanacyclopentadiene derivatives (Scheme 97) can be prepared from the diisopropoxo( $\eta^2$ -propene) titanium compound or from  $\text{TiCp}_2$ (1-butene) and alkynyltitanium species.<sup>185</sup>

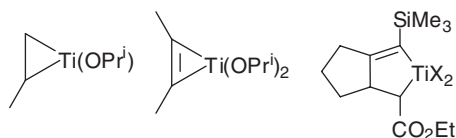
Titanacyclopentadiene complexes (some examples are shown in Scheme 98) can be prepared by reaction of  $\text{Ti}(\text{OPr}^i)_2(\eta^2\text{-propene})$ , which is readily obtained *in situ* from  $\text{Ti}(\text{OPr}^i)_4$  and  $\text{MgClPr}^i$ , with acetylenes and other unsaturated organic molecules. These compounds react with some electrophiles to give intermediates of great



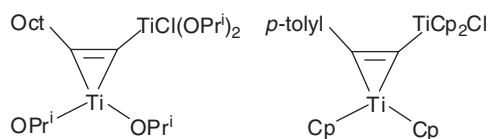
Scheme 94



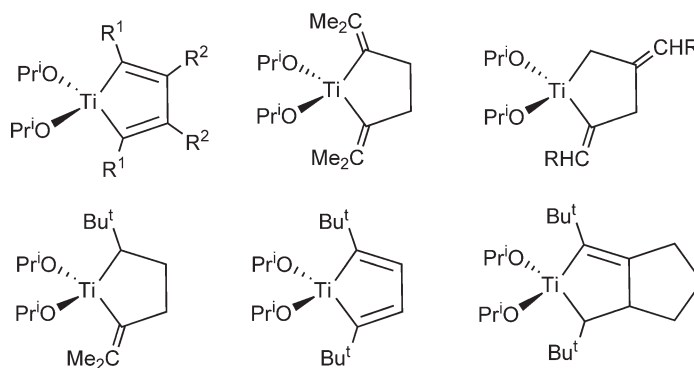
Scheme 95



Scheme 96



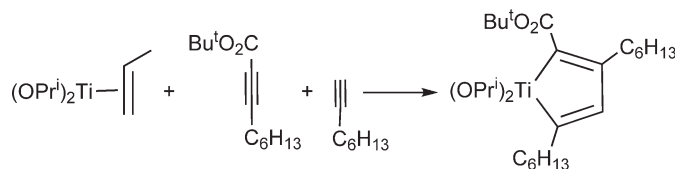
Scheme 97



Scheme 98

utility in organic synthesis and they act as catalysts for the stereoselective synthesis of functionalized conjugated dienes.<sup>24,35,37,186–193</sup>

Ti( $\eta^2$ -propene)(OPr<sup>i</sup>)<sub>2</sub> reacts with the two unsymmetrical acetylenes Bu<sup>t</sup>O<sub>2</sub>C–C≡C–C<sub>6</sub>H<sub>13</sub> and HC≡C–C<sub>6</sub>H<sub>13</sub> to give a dialkoxo–titanacyclopentadiene derivative (Scheme 99) which upon treatment with ethynyl tolyl sulfone produces a new single aryl–titanium compound.<sup>194</sup>



Scheme 99

Enyne titanium complexes are synthesized when enynes are treated with  $\text{Ti}(\text{OPr}^i)_2(\eta^2\text{-propene})$ .<sup>195</sup>  $\omega$ -Vinylimines react with  $\text{Ti}(\text{OPr}^i)_4/\text{MgXPr}^i$  reagents to give the corresponding azatitanacyclopentanes in quantitative yield, which in turn react with  $\text{H}_2\text{O}$ ,  $\text{I}_2$ , and  $\text{O}_2$  to render 2-methyl-, 2-iodomethyl-, 2-hydroxymethyl-1-aminocyclic compounds, respectively. The azatitanacyclopentanes thus generated react with formaldehyde to afford the corresponding 2,3-annulated pyrrolidines in good yield.<sup>196</sup>

#### 4.05.2.1.3 Trialkyl and related complexes

The trialkyltitanium complexes  $\text{TiCl}(\text{CH}_2\text{EMe}_3)_3$  ( $\text{E} = \text{C}, \text{Si}$ ) have been prepared by treatment of the corresponding tetraalkyl derivatives with a solution of dry  $\text{HCl}$  in ether. Attempts to synthesize these compounds by metathesis reaction between  $\text{TiCl}_4$  and  $\text{LiCH}_2\text{EMe}_3$  were unsuccessful because of the tendency of  $\text{Ti}(\text{IV})$  to be reduced by lithium reagents. Nevertheless, the synthesis of the tetraalkyl derivatives  $\text{Ti}(\text{CH}_2\text{EMe}_3)_4$  by reaction of  $\text{TiCl}_4(\text{THF})_2$  with  $\text{LiCH}_2\text{EMe}_3$  has been described (Scheme 100).<sup>197</sup> The synthesis of the alkyl–silyl complexes  $\text{Ti}(\text{CH}_2\text{EMe}_3)_3[\text{Si}(\text{SiMe}_3)_3]$  ( $\text{E} = \text{C}, \text{Si}$ ) (Scheme 100) by reaction of  $\text{TiCl}(\text{CH}_2\text{EMe}_3)_3$  with  $\text{LiSi}(\text{SiMe}_3)_3(\text{THF})_3$  has been reported. The two compounds were characterized by X-ray diffraction, showing the three alkyl and the silyl ligands in a pseudo-tetrahedral disposition around the titanium atom.<sup>198</sup>

The mononuclear benzamidinato derivative  $\text{TiMe}_3[\text{C}_6\text{H}_5\text{C}(\text{NSiMe}_3)_2]$  is synthesized in good yield by the reaction between  $\text{TiCl}_3[\text{C}_6\text{H}_5\text{C}(\text{NSiMe}_3)_2]$  and  $\text{LiMe}$  (Scheme 52, Section 4.05.2.1.2).<sup>119</sup> The trimethyl pyrazolato titanium complex  $\text{TiMe}_3(\text{Bu}^t_2\text{pz})$  (Scheme 101) is prepared by treatment of the trichloro precursor compound with  $\text{MgClMe}$ .<sup>82</sup>

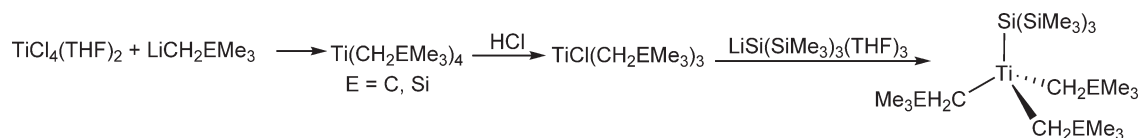
The phosphinimido trichloro titanium complex  $\text{TiCl}_3(\text{N}=\text{P}(\text{Bu}^t)_3)$  can be prepared from the trimethylsilylphosphinimine  $\text{Bu}^t_3\text{P}=\text{NSiMe}_3$  and  $\text{TiCl}_4$ . This compound is converted into the trialkyl complexes  $\text{TiR}_3(\text{N}=\text{P}(\text{Bu}^t)_3)$  ( $\text{R} = \text{Me}, \text{CH}_2\text{Ph}$ ) by reaction with  $\text{MgBrR}$ . Reactivity of these species is described in Section 4.05.2.3.<sup>76</sup>

Studies of silyl trialkyl complexes  $\text{Ti}(\text{CH}_2\text{R}^1)_3\text{SiR}^2_3$  have been reviewed and summarized.<sup>199</sup>

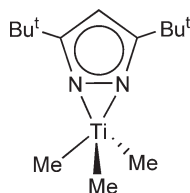
Metallation of 2-(2'-phenol)-6-arylpyridine by reaction with  $\text{Ti}(\text{CH}_2\text{Ph})_4$  is observed to yield toluene and the cyclometallated Ti complex shown in Scheme 102, characterized by NMR spectroscopy.<sup>200</sup>

The  $\eta^1$ -hydroxylamido tribenzyl complex  $\text{Ti}(\text{CH}_2\text{Ph})_3(\text{TEMPO})$  ( $\text{TEMPO} = 2,2,6,6\text{-tetramethyl-1-piperidiny-1-N-oxide}$ ) (Scheme 103) has been made by treatment of  $\text{TiCl}_3(\text{TEMPO})$  with  $\text{MgCl}(\text{CH}_2\text{Ph})$  in ether followed by extraction with pentane. Reaction with  $\text{B}(\text{C}_6\text{F}_5)_3$  proceeds with liberation of toluene and formation of a zwitterionic compound resulting from abstraction of a benzyl ligand and cyclometallation of one methyl group of TEMPO; NMR spectroscopic data indicate that the resulting  $[\text{PhCH}_2\text{B}(\text{C}_6\text{F}_5)_3]^-$  counterion is  $\eta^6$ -bound. Protonolysis of  $\text{Ti}(\text{CH}_2\text{Ph})_4$  with  $\text{R}_2\text{NOH}$  ( $\text{R} = \text{CH}_2\text{Ph}, \text{Et}$ ) yields  $\text{Ti}(\text{CH}_2\text{Ph})_3(\text{ONR}_2)$  (Scheme 103); the molecular structure of the tribenzyl compound has been determined by X-ray diffraction. Reaction of  $\text{Ti}(\text{CH}_2\text{Ph})_3(\text{ONEt}_2)$  with  $\text{B}(\text{C}_6\text{F}_5)_3$  affords an ionic species which was not fully characterized.<sup>201</sup>

The chloro aryltitanium complex  $\text{TiCl}_2(\text{CNN})(\text{OPr}^i)$  ( $\text{CNN} = \text{monoanionic tridentate bisamino-aryl substituted } \text{C}_6\text{H}_4\text{-CH}_2\text{N}(\text{Me})\text{CH}_2\text{CH}_2\text{NMe}_2$ ) has been synthesized as a mixture of two isomers by reaction of the corresponding aryllithium salt with  $\text{TiCl}_3(\text{OPr}^i)$ . The molecular structure of one of the isomers has been determined by X-ray diffraction. The chloro complex reacts with  $\text{LiMe}$  to give the dimethyl aryl compound  $\text{TiMe}_2(\text{CNN})(\text{OPr}^i)$  containing two  $\text{Ti-Me}$  and one  $\text{Ti-aryl}$  bonds, for which in solution an association–dissociation process involving the

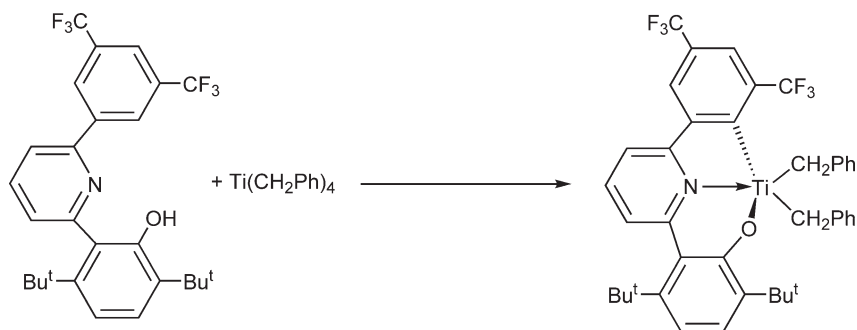


Scheme 100

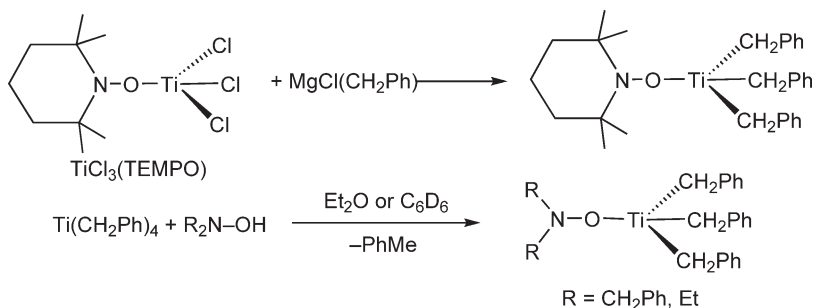


Scheme 101

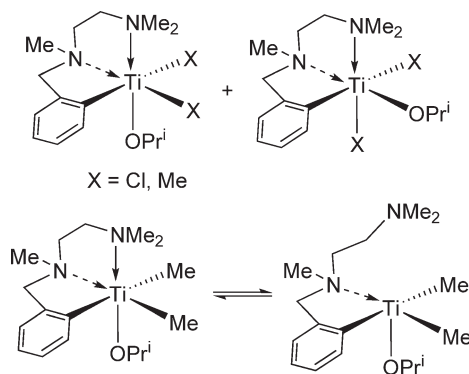




Scheme 102



Scheme 103



Scheme 104

Ti–NMe<sub>2</sub> bond has been proposed (Scheme 104). Preliminary studies indicate these complexes are active in  $\alpha$ -olefin polymerizations.<sup>202</sup>

The Si–OH functions of silsesquioxanes react with tetrabenzyltitanium to give alkyl silsesquioxane titanium derivatives, which are efficient catalysts for the epoxidation of alkenes under mild conditions.<sup>203</sup>

#### 4.05.2.1.4 Tetraalkyl and related complexes

The adduct  $\text{TiMe}_4(\text{THF})_2$  has been isolated. This compound dissociates partially in *n*-pentane to form  $\text{TiMe}_4(\text{THF})$ . The molecular structure of the latter has been determined by X-ray diffraction and shows the titanium atom in a trigonal-bipyramidal geometry, with the THF molecule in axial position.<sup>204</sup> The adduct  $\text{TiMe}_4(\text{Me}_2\text{PCH}_2\text{CH}_2\text{PMe}_2)$  has been synthesized by addition of diphosphine to a solution  $\text{TiMe}_4$  in diethyl ether; its X-ray crystal structure has been determined.<sup>205</sup>

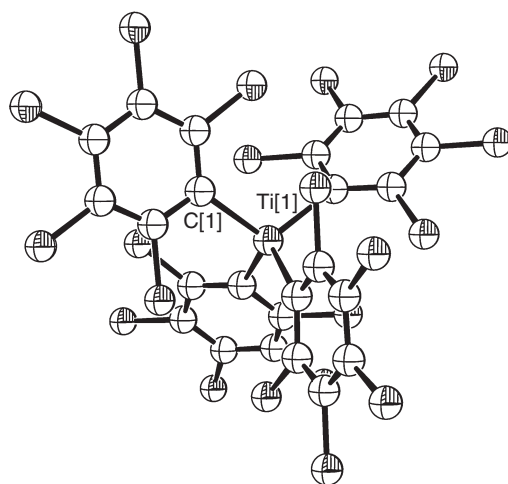
The synthesis and structural information on methyltitanium complexes with different degrees of methylation of  $\text{TiMe}_4$ ,  $\text{TiMe}_3\text{Cl}$ ,  $\text{TiMe}_2\text{Cl}_2$ ,  $\text{TiMeCl}_3$ ,  $[\text{TiMe}_5]^-$ , and  $[\text{Ti}_2\text{Me}_9]^-$  have been reported. All the structures determined

show the methyl and methyl chloro titanium derivatives as having coordination numbers of 5 and 6 around the titanium atom through intermolecular interaction. Only  $\text{TiMe}_4$  would be tetrahedral if it could be obtained free of solvent. Intramolecular interactions are expected only for  $[\text{Ti}_2\text{Me}_9]^-$  anions.<sup>206</sup>

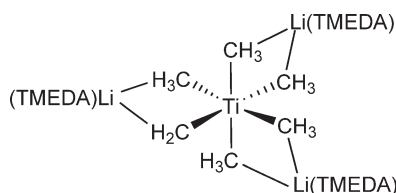
The controlled chemical oxidation of the Ti(III) aryl compound  $[\text{Li}(\text{THF})_4][\text{Ti}(\text{C}_6\text{Cl}_5)_4]$  with  $[\text{N}(4\text{-Br-C}_6\text{H}_4)_4][\text{SbCl}_6]$  in  $\text{CH}_2\text{Cl}_2$  at  $0^\circ\text{C}$  gives the homoleptic Ti(IV) neutral species  $\text{Ti}(\text{C}_6\text{Cl}_5)_4$ , the molecular structure of which has been determined by X-ray diffraction (Figure 4).<sup>207</sup>

The series of neopentyl complexes  $\text{TiNp}_x\text{Cl}_{4-x}$  ( $x = 1, 2, 3$ ) have been prepared by comproportionation reaction between the titanium homoleptic neopentyl complex  $\text{TiNp}_4$  and  $\text{TiCl}_4$ . These complexes are moisture- and light-sensitive. The stability of the complexes at room temperature has been estimated. The neopentyl chloro complexes, and the isotopically labeled species  $\text{TiNp}^d_x\text{Cl}_{4-x}$  [ $\text{Np}^d = \text{CH}(\text{D})\text{CMe}_3$ ] have been spectroscopically characterized; the  $^1\text{H}$  NMR resonance of the  $\text{CH}_2$  protons displays an increasing shift to high frequency in the series  $\text{TiNp}_4$ ,  $\text{TiNp}_3\text{Cl}$ ,  $\text{TiNp}_2\text{Cl}_2$ ,  $\text{TiNpCl}_3$ .<sup>208</sup> The reaction pathways for the thermolysis of tetraneopentyltitanium in solution at  $80^\circ\text{C}$  and the mechanism responsible for its conversion to titanium carbide have been elucidated. Mechanistic studies on the thermolysis of  $\text{TiNp}_4$  under CVD (chemical vapor deposition) and UHV (ultra high vacuum) conditions have been carried out.<sup>209,210</sup>

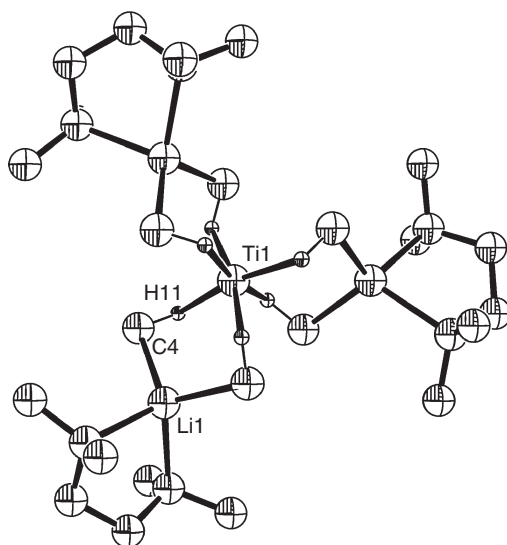
The diamagnetic heterobinuclear complex  $[\text{Ti}(\mu\text{-CH}_3)_5(\mu\text{-CH}_2)][\text{Li}(\text{TMEDA})]_3$  (Scheme 105) is prepared when the toluene solution obtained from the reaction of  $\text{TiCl}_3(\text{THF})_3$  with an excess of  $\text{Li}[\text{N}(\text{SiMe}_3)]$  is thermolyzed, followed by treatment with a mixture of  $\text{CH}_2\text{Cl}_2$  and TMEDA and subsequent recrystallization from hexane. The mechanism and rationalization for the formation of this complex is difficult. The generation of the methyl and the methylene groups from a silazanide intermediate is proposed, although  $\text{CH}_2\text{Cl}_2$  probably also acts as a source of both methyl and methylene ligands. The treatment of the reaction mixture with  $\text{CH}_2\text{Cl}_2$  is a necessary step for the successful isolation of the complex. The compound is stable at room temperature in both the solid state and solution but does react violently with moisture and air. Its molecular structure has been elucidated by X-ray diffraction. In order to account for the observed diamagnetism, one methylene group disordered over the six C atom positions around the Ti center must be proposed, resulting in an unusual and highly fluxional titanium organometallic compound (Figure 5). The structure bonding and the spectroscopic features of this compound are unique. The Ti–C bond



**Figure 4** Molecular structure of complex  $\text{Ti}(\text{C}_6\text{Cl}_5)_4 \cdot 2\text{CH}_2\text{Cl}_2$  (reproduced by permission of Wiley-VCH from *Chem. Eur. J.* 2004, 10, 4186).



**Scheme 105**



**Figure 5** Molecular structure of complex  $[\text{Ti}(\mu\text{-CH}_3)_5(\mu\text{-CH}_2)][\text{Li}(\text{TMEDA})]_3$  (reproduced by permission of Wiley-VCH from *Angew. Chem., Int. Ed. Eng.*, **1995**, 24, 2264).

distances are remarkably long and outside the bonding range, while short Ti–H distances are observed. Therefore, the connection between Ti and the six C atoms appears to have been realized through six hydrogen bonds.<sup>211</sup>

#### 4.05.2.1.5 Alkylidene and carbene complexes

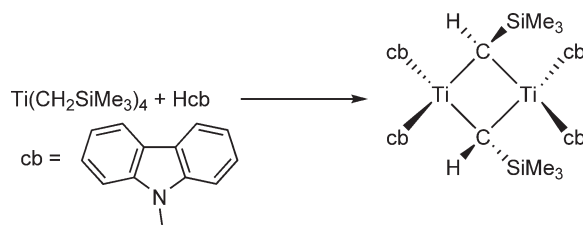
Carbenoid titanium species are proposed to be formed in the reaction of  $\text{Bu}^t\text{CO}$  with low-valent titanium complexes.<sup>212</sup> There is evidence that the reaction of laser-ablated Ti atoms with MeF in argon condensing at 7 K leads to the formation of  $\text{TiFMe}$ , which undergoes a reversible photochemical rearrangement to the methyldene  $\text{Ti}(=\text{CH}_2)\text{FH}$ . The structure of this substance reveals an agostic hydrogen interaction. The formation of  $\text{TiMe}_2\text{F}_2$  also is observed.<sup>213,214</sup>

Thermolysis of the dimethyl derivative  $\text{TiMe}_2(\text{NCy}_2)_2$  in toluene at 60 °C quantitatively and selectively forms the bridging methylene complex  $(\text{NCy}_2)_2\text{Ti}(\text{CH}_2)_2\text{Ti}(\text{NCy}_2)_2$  (Scheme 44, Section 4.05.2.1.2). This complex shows resonances at  $\delta$  8.29 in the  $^1\text{H}$  and  $\delta$  224.7 in the  $^{13}\text{C}$  NMR spectra for the bridging methylene groups.<sup>107</sup>

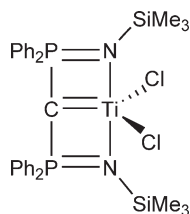
The neopentylidene complex  $\text{Ti}(\text{CHBu}^t)(\text{Pr}^i\text{NON})(\text{PMe}_3)_2$  (Scheme 71, Section 4.05.2.1.2) is isolated after heating a toluene solution of  $\text{Ti}(\text{CH}_2\text{Bu}^t)(\text{Pr}^i\text{NON})$  in the presence of an excess of  $\text{PMe}_3$ . The molecular structure reveals the presence of a distorted alkylidene ligand with a linear neopentylidene disposition and a short Ti–C bond distance (1.884(4) Å), indicating a significant  $\text{CH}_\alpha$  agostic interaction. The  $^{13}\text{C}$  NMR spectrum shows a resonance at  $\delta$  229 for the neopentylidene  $\text{C}_\alpha$  atom, while the alkylidene proton appears in the  $^1\text{H}$  NMR spectrum at  $\delta$  3, remarkably upfield shifted with respect to other alkylidene complexes, characteristic of an alkylidene with a significant agostic interaction.<sup>143</sup>

Titanium derivatives containing carbazole (cb) ligands have been isolated and studied. Reaction of  $\text{Ti}(\text{CH}_2\text{SiMe}_3)_4$  with carbazole yields the alkylidene-bridged dimer  $[\text{Ti}(\mu\text{-CHSiMe}_3)(\text{cb})_2]_2$  (Scheme 106). A singlet at  $\delta$  14.75 is observed in the  $^1\text{H}$  NMR spectrum of the alkylidene complex. The reaction of this compound with 2,6-dimethylphenyl isocyanide leads to titanium derivatives containing new carbon-carbon bonds (Section 4.05.2.3).<sup>109,110</sup>

The titanium carbene complex  $\text{TiCl}_2[\text{C}(\text{Ph}_2\text{P}=\text{NSiMe}_3)_2]$  has been synthesized by metathetical reaction of the dilithium bis(phosphoranimine) salt with  $\text{TiCl}_4$  (Scheme 107).<sup>215</sup> In this bis(iminodiphenylphosphorano)methylene



**Scheme 106**

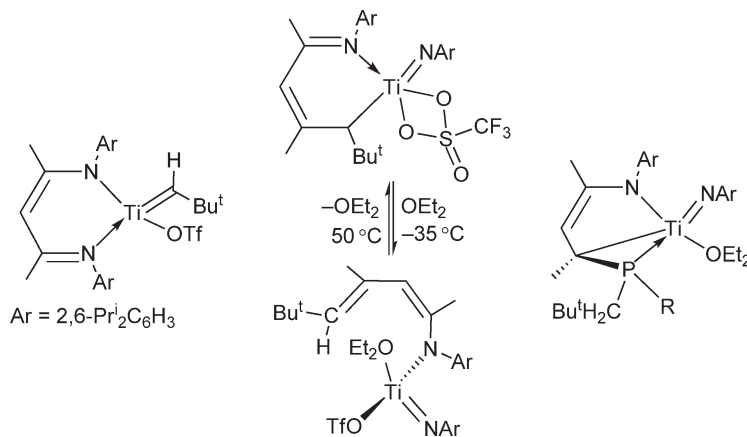


Scheme 107

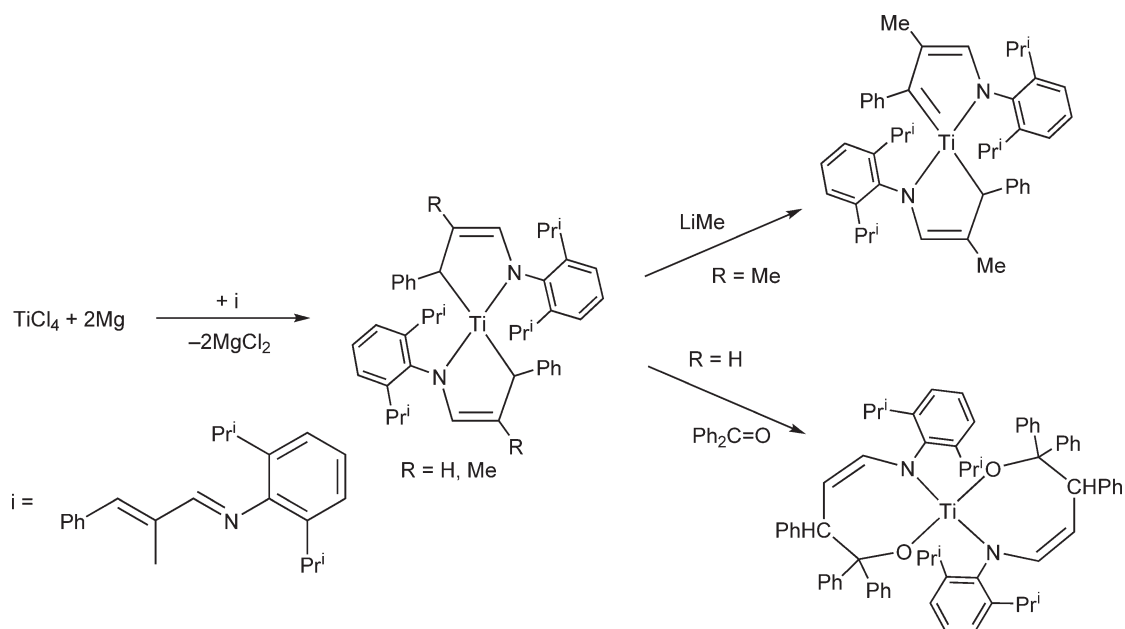
complex, the carbenoid carbon atom is stabilized by the heteroatoms.<sup>216</sup> The carbene  $^{13}\text{C}$  NMR resonance appears at  $\delta$  191.0, downfield shifted with respect to the resonances observed for ylide titanium complexes, but upfield shifted relative to carbene titanium complexes. The molecular structure has been determined by X-ray diffraction showing a relatively short Ti–C bond distance of 2.008(4) Å, suggesting a Ti=C double bond. Preliminary activity studies indicate susceptibility to electrophilic attack at this carbene C-atom, similar to the reactivity of high oxidation state group 5 alkylidene complexes.<sup>215</sup>

Treatment of the amido-imino Ti(III) complex  $\text{TiCl}_2(\text{BDI})\cdot\text{THF}$  [ $\text{BDI} = \text{ArNC}(\text{Me})\text{CHC}(\text{Me})\text{NAr}$ ] with 2 equiv. of  $\text{LiCH}_2\text{Bu}^t$  affords the dialkyl derivative  $\text{Ti}(\text{CH}_2\text{Bu}^t)_2(\text{BDI})$ . A cyclic voltammogram of a solution of the dialkyl compound shows one irreversible oxidation wave at  $-0.90\text{ V}$  (referenced vs.  $\text{FeCp}_2/\text{FeCp}_2^+$ ) for Ti(IV)/Ti(III) couple. Treatment of a pentane solution of the dineopentyl complex with  $\text{AgOTf}$  affords the alkylidene Ti(IV) complex  $\text{Ti}(\text{=CHBu}^t)(\text{OTf})(\text{BDI})$  (Scheme 108) through an oxidatively induced  $\alpha$ -hydrogen abstraction process. A  $\text{C}_\alpha$ -resonance at  $\delta$  271 with  $J_{\text{CH}}$  coupling constant of 95 Hz and a  $\text{CH}_\alpha$  resonance located at  $\delta$  5.23 are spectroscopically observed in the  $^{13}\text{C}$  and  $^1\text{H}$  NMR spectra, respectively. The molecular structure of the alkylidene complex has been determined by X-ray diffraction studies, showing a short Ti=C bond length of 1.830(3) Å. The alkylidene complex exhibits “Wittig-type” reactivity when treated with benzophenone. In solution it decomposes gradually to give a new imido triflate complex supported by a chelating imino-alkyl ligand,  $\text{Ti}(\text{=NAr})(\eta^2\text{-OTf})[\text{ArNC}(\text{Me})\text{CH}=\text{C}(\text{Me})\text{CHBu}^t]$ , formed by a Wittig-type reaction between the neopentylidene and the imino functionality of the BDI ligand. By addition of Lewis bases, such as  $\text{OEt}_2$ , the chelating imino-alkyl ligand exhibits a resonance indicative on an amido-diene behavior (Scheme 108). The nucleophilic and four-coordinated Ti alkylidene complex reacts with  $\text{LiPHR}$  to give low-coordinate and terminal phosphinidene derivatives (Scheme 108).<sup>217,218</sup>

1-Aza-1,3-diene titanium complexes can be prepared by addition of 2 equiv. of Mg turnings to a solution of  $\text{TiCl}_4$  and 2 equiv. of the corresponding 1-aza-1,3-diene at low temperature, followed by warming to room temperature (Scheme 109). The bonding situation in these compounds is best described as a 1-titana-2-azacyclopent-3-ene complexes rather than an  $\eta^4$ -1-aza-1,3-diene disposition. The derivative where  $\text{R} = \text{H}$  reacts with 2 equiv. of benzophenone with addition of the two molecules and formation of two C–C bonds between the heterodiene termini and the carbonyl carbon atoms as well as two strong Ti–O linkages. When 1 equiv. of  $\text{LiMe}$  is added to a solution containing the  $\text{R} = \text{Me}$  derivative, a novel metallacyclic alkylidene compound is formed, with elimination of methane, as a result of the expected facile C–H bond cleavage process. The molecular structures of these complexes have been determined by X-ray diffraction.<sup>219,220</sup>



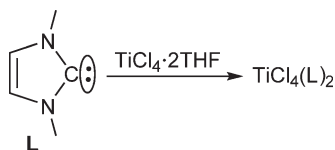
Scheme 108



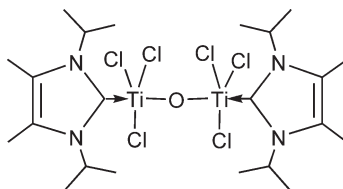
Scheme 109

*N*-heterocyclic “Arduengo-carbenes” (NHCs) are ligands with powerful  $\sigma$ -donor but almost negligible  $\pi$ -acceptor properties and have found a wide range of applications in organic chemistry and catalysis. These carbene ligands are generally stabilized by metals in low oxidation states, but they also coordinate to high oxidation state metals. A few examples of titanium NHC derivatives have been published. The cyclocarbene 1,3-dimethylimidazolin-2-ylidene (**L**) is an interesting nucleophilic ligand capable of generating  $\text{Ti}(\text{IV})$  carbene complexes; for example, treatment with  $\text{TiCl}_4(\text{THF})_2$  gives  $\text{TiCl}_4(\text{L})_2$  (Scheme 110).<sup>221</sup> The optical properties and the absorption spectrum of this compound have been studied. The compound is not luminescent and shows a ligand-to-metal charge transfer absorption at 450 nm.<sup>222</sup> Stable  $\text{Ti}$  NHC complexes have also been reported by the reaction of imidazol-2-ylidenes with  $\text{TiCl}_4$ . The structure of one  $\mu\text{-oxo}$   $\text{Ti}(\text{IV})$  with the 1,3-diisopropyl-4,5-dimethylimidazol-2-ylidene ligand *trans* to the bridging oxygen group has been published (Scheme 111).<sup>223</sup>

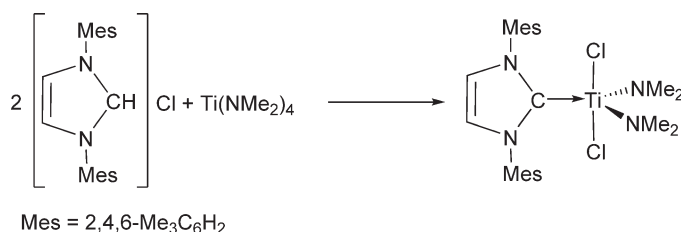
The reaction of 1,3-dimesitylimidazolium chloride with  $\text{Ti}(\text{NMe}_2)_4$  results in the mixed ligand complex  $\text{TiCl}_2(\text{NMe}_2)_2(\text{carbene})$  (carbene = 1,3-dimesitylimidazol-2-ylidene) (Scheme 112), the molecular structure of which has been determined by X-ray diffraction. The environment around the  $\text{Ti}$  atom is a distorted trigonal bipyramid with the two chloride ligands located in the apical positions. The structure shows short intramolecular  $\text{Cl}-\text{C}(\text{carbene})$  contacts.<sup>224</sup>



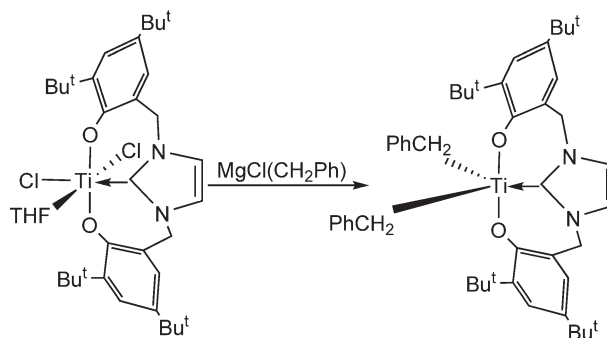
Scheme 110



Scheme 111



Scheme 112



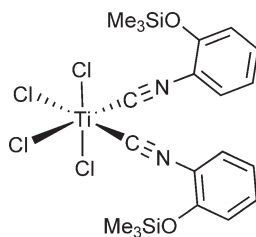
Scheme 113

Dichloro- and dibenzyltitanium complexes containing Arduengo-carbene ligands supported by an imidazolium-linked bis(phenoxo) fragment have been reported (Scheme 113). TiCl<sub>4</sub>(THF)<sub>2</sub> reacts with the sodium salt of 1,3-bis(4,6-di-*tert*-butyl-2-hydroxybenzyl)imidazolium ligand to give the corresponding dichloro carbene derivative which is converted into the dibenzyl complex by reaction with MgCl(CH<sub>2</sub>Ph). The molecular structures of both compounds have been determined by X-ray diffraction. The <sup>13</sup>C NMR spectra show the carbene signals at  $\delta$  164 and 188, respectively. Dynamic behavior in solution is observed. These complexes have been studied as pre-catalyst for ethylene polymerization.<sup>225</sup>

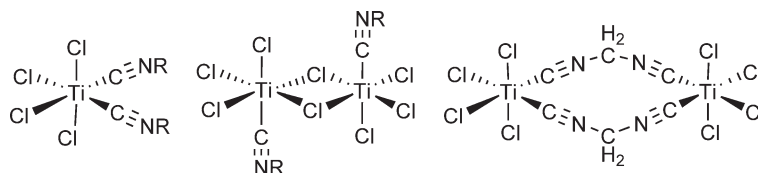
#### 4.05.2.1.6 Cyanide and isocyanide complexes

Reaction of Me<sub>3</sub>SiCN with TiCl<sub>4</sub> occurs readily at room temperature, with initial formation of monoadducts, followed by substitution of chloride ligands by cyanide under more forcing conditions. By choosing appropriate reaction conditions, it has been possible to isolate a series of products of composition, TiCl<sub>4-n</sub>(CN)<sub>*n*</sub>·Me<sub>3</sub>SiCN (*n* = 0–3), for which, dimeric (*n* = 0, 1) or polymeric (*n* = 2, 3) structures containing approximately octahedrally coordinated titanium atoms are proposed. The adducts TiCl<sub>2</sub>(CN)<sub>2</sub>·1.5CH<sub>3</sub>CN and TiCl<sub>2</sub>(CN)<sub>2</sub>·0.5CH<sub>3</sub>CN have been produced from ligand exchange reactions with acetonitrile. The titanium(IV) bromide and iodide systems are also studied.<sup>226</sup>

Addition of TiCl<sub>4</sub> to a solution of trimethylsiloxyphenylisocyanide in *n*-hexane yields the air sensitive octahedral diisocyanide complex TiCl<sub>4</sub>(CNR)<sub>2</sub> (Scheme 114). This complex crystallizes with one molecule of *n*-hexane. Its molecular structure has been determined by X-ray crystallography.<sup>227</sup> The formations of isocyanide titanium complexes are studied as species related with the Passerini reaction assisted by TiCl<sub>4</sub>. Three classes of compounds were identified and exemplified by isolated complexes (Scheme 115).<sup>228</sup>



Scheme 114



Scheme 115

The asymmetric catalytic cyanosilylation of aldehydes<sup>229</sup> and the alkylation of aldehydes with  $\text{ZnEt}_2$ <sup>230</sup> using the chiral cyano binaphthol complex  $\text{Ti}(\text{CN})_2(\text{R})\text{-BINOL}$  have been developed.

#### 4.05.2.2 Structures and Properties

The molecular structure of the ethyl trichloro complex  $\text{TiCl}_3(\text{CH}_2\text{CH}_3)(\text{dmpe})$  has been redetermined by X-ray crystallography at low temperature, with results that are more precise but not significantly different from those previously reported. The extremely bent  $\text{Ti}-\text{C}-\text{C}$  chain as evidence for strong  $\beta$ -agostic interaction was confirmed. Preliminary results on the decomposition reaction of this complex suggest a radical process, rather than  $\beta$ -H transfer with ethylene elimination.<sup>231</sup>

The IR spectra of  $\text{TiCl}_2\text{Me}_2$ ,  $\text{TiCl}_2(\text{CD}_3)_2$ ,  $\text{TiCl}_2(\text{CH}_2\text{D})_2$ , and  $\text{TiCl}_2(\text{CHD}_2)_2$  have been studied in the gas and matrix phases.<sup>3</sup> The structure of  $\text{TiCl}_2\text{Me}_2$  has been determined by NMR and IR spectroscopy, and in the gas phase by electron diffraction.<sup>232</sup> The relationship between  $\pi$ -bonding, electronegativity, and bond angles has been determined.<sup>233</sup> Computational studies concerning the bonding and structure of  $\text{TiCl}_2\text{Me}_2$  have appeared.<sup>232,234</sup>

The  $^1\text{H}$ ,  $^{13}\text{C}$ , and  $^{47,49}\text{Ti}$  NMR spectra of a series of methyl complexes  $\text{TiCl}_{4-n}\text{Me}_n$  have been studied. Experimental and theoretical investigations are reported. A strong deshielding of the Ti chemical shifts is observed as the chloro ligands of  $\text{TiCl}_4$  are successively replaced by methyl groups. The  $^1\text{H}$  and  $^{13}\text{C}$  resonances move in the opposite direction, these signals being shielded as Cl is replaced by Me. The measured values are compared with the data of the main group equivalent compounds  $\text{ECl}_{4-n}\text{Me}_n$  ( $\text{E} = \text{C}, \text{Si}, \text{Sn}, \text{Pb}$ ). The  $\text{Ti}-\text{CH}_3$  and  $\text{Ti}-\text{Cl}$  bonds are essentially  $sd^3$  hybridized with negligible  $\pi$ -contribution at Ti.<sup>5</sup>

The structure of the intermediate of the reaction of  $\text{TiMe}_2(\text{OPr}^i)_2$  with 3-(1-nitro-2-oxocyclohexyl)propanal and its conformation have been investigated by NMR spectroscopy.<sup>235</sup>

Topological analysis of the experimental and theoretical electron densities in  $\text{TiCl}_3\text{Et}(\text{dmpe})$  ( $\text{dmpe} = \text{Me}_2\text{PCH}_2\text{CH}_2\text{PMe}_2$ ) suggests the presence of a bond critical point between titanium and the  $\beta$ -agostic hydrogen atom.<sup>236</sup>

The optimized geometries and relative stabilities for the octahedral complexes formed by  $\text{TiCl}_4$  and  $\text{TiCl}_3\text{Me}$  with various bidentate ligands and  $\alpha$ -alkoxy aldehydes have been studied theoretically using effective core potentials and model potentials at the Hartree–Fock and MP2 levels of theory. The calculated binding energies for the complex formation indicate that the donor strengths of the Lewis bases increase in the order  $\text{NH}_2 > \text{OH} > \text{OC}$ . The calculated values are in satisfactory agreement with the experimental results. A higher stability for the octahedral isomers containing an equatorial methyl group is predicted, caused by a higher deformation of the “ $\text{TiCl}_3\text{Me}$ ” fragment in the isomers with the methyl group being axial, which yields a lower net stabilization. The calculations indicate that the rearrangement between the isomeric octahedral  $\text{TiCl}_3\text{MeL}_2$  complexes occurs via a dissociation–association mechanism with pentacoordinated intermediates in which a donor–acceptor bond is broken. The barrier for the methyl shift from titanium to the carbonyl group of the complexed aldehyde is calculated to be ca.  $19 \text{ kcal mol}^{-1}$  at the MP2 level of theory. The calculations also give a possible explanation for the different mechanism of the analogous reaction of  $\text{TiCl}_3\text{Me}$  with  $\alpha$ -alkoxy ketones.<sup>237,238,239</sup>

Different methods of computation have been performed for comprehensive investigations on the thermal effects and vibrational corrections to transition metal NMR chemical shifts. Studies related to  $\text{TiCl}_x\text{Me}_{4-x}$  ( $x = 0\text{--}3$ ) are included.<sup>240</sup>

Theoretical studies on the decomposition mechanism of tetraalkyltitanium complexes have been reported. Quantum mechanics *ab initio* calculations have been carried out for the unimolecular and bimolecular methane elimination from  $\text{TiMe}_4$ , methane elimination from  $\text{TiMe}_3\text{Pr}^n$  through  $\gamma$ -hydrogen abstraction, and neopentane elimination from  $\text{TiNp}_4$  through  $\alpha$ -hydrogen and  $\gamma$ -hydrogen abstraction. For titanium alkyl complexes, there is an intrinsic preference for  $\alpha$ -hydrogen abstraction over  $\gamma$ -hydrogen abstraction. The first step in the decomposition of

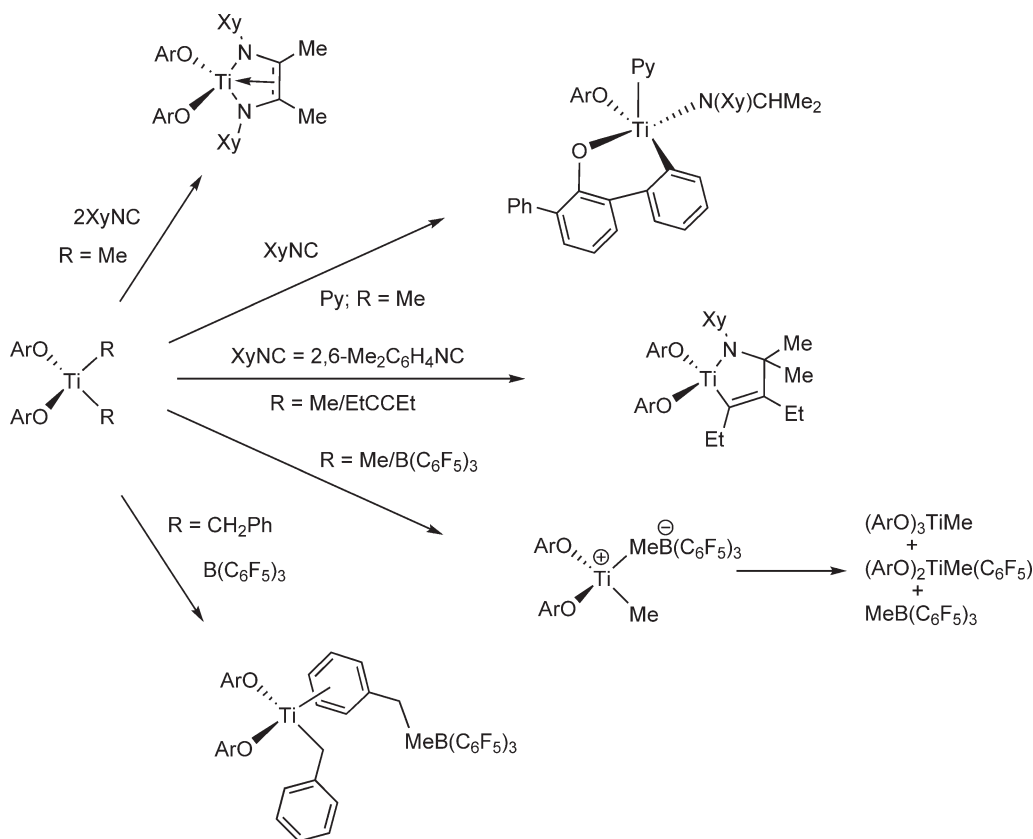
TiMe<sub>4</sub> is bimolecular methane elimination through intermolecular hydrogen abstraction. For the TiMe<sub>4</sub> complex, an intermolecular (bimolecular mechanism)  $\alpha$ -hydrogen abstraction has much lower activation energy than the intramolecular (unimolecular mechanism)  $\alpha$ -hydrogen abstraction. Nevertheless, for steric reasons, the unimolecular mechanism ( $\alpha$ -hydrogen abstraction) has a much lower value for TiNp<sub>4</sub> than that of TiMe<sub>4</sub>.<sup>241,242</sup> These data are in agreement with experimental data.<sup>209</sup>

Studies to determine absolute bond enthalpies  $D(\text{Ti-R})$  in TiR(Bu<sup>t</sup><sub>3</sub>SiNH)(silox)<sub>2</sub> (R = alkyl group) from relative bond strength measurements have been performed.<sup>243</sup>

#### 4.05.2.3 Reactions

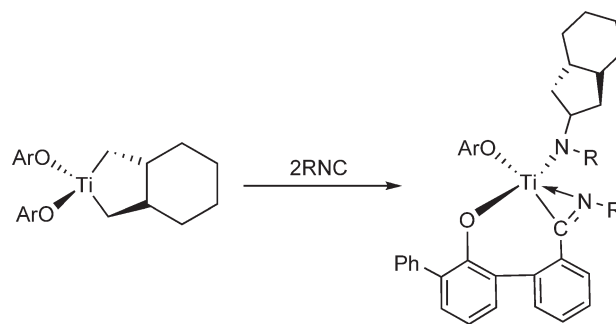
Rothwell's aryloxo complexes TiR<sub>2</sub>(OAr)<sub>2</sub> (OAr = 2,6-disubstituted phenoxo ligand; R = Me or CH<sub>2</sub>Ph; R<sub>2</sub> = metallacycle) can be used as reagents in organic reactions and olefin polymerization catalysis. Some examples are described. The reactivity of dialkyl complexes toward organic isocyanides has been examined. A series of mono and double insertions, C-H bond activation, coupling of alkyne olefins with imine intermediates, cyclometallation and fusion between five- and six-membered carbon ring reactions can be observed. The dibenzyl complexes react with the Lewis acid B(C<sub>6</sub>F<sub>5</sub>)<sub>3</sub> to generate stable zwitterionic species, in which structural studies show that the boron anion is  $\pi$ -bound to the metal center through the original benzyl phenyl ring. In contrast to this behavior, the dimethyl complexes react with B(C<sub>6</sub>F<sub>5</sub>)<sub>3</sub> to produce unstable cationic methyl intermediates (Scheme 116). Metallacyclic derivatives exhibit an extensive reactivity with a variety of reagents to give new titanium complexes. Reactions with isocyanides have been extensively described (Scheme 117).<sup>171-173</sup>

Reactions with Bu<sup>t</sup>NC lead to new organometallic compounds containing an  $\eta^2$ -C,N-bound cyclopentadiene imine, which was structurally characterized as a pyridine adduct (Scheme 118). Reactions with benzonitrile lead to the elimination of 1 equiv. of the corresponding pyridine and formation of the dimeric titanium derivative (ArO)<sub>2</sub>Ti( $\mu$ -PhCN)<sub>2</sub>Ti(OAr)<sub>2</sub> containing two bridging benzonitrile ligands. The compound has been structurally characterized

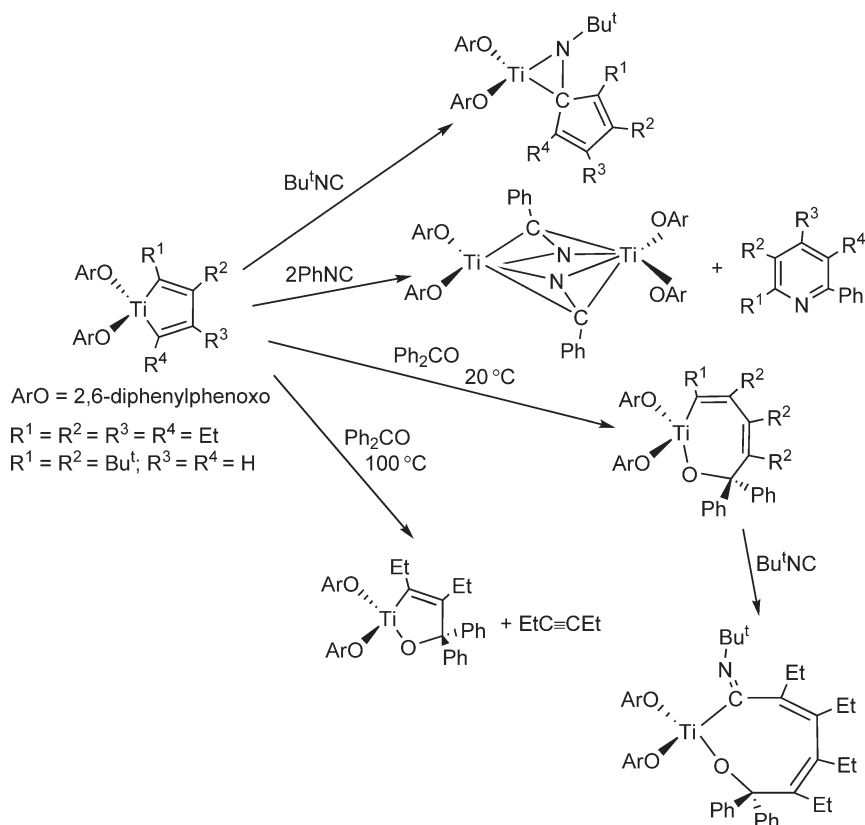


Scheme 116





Scheme 117



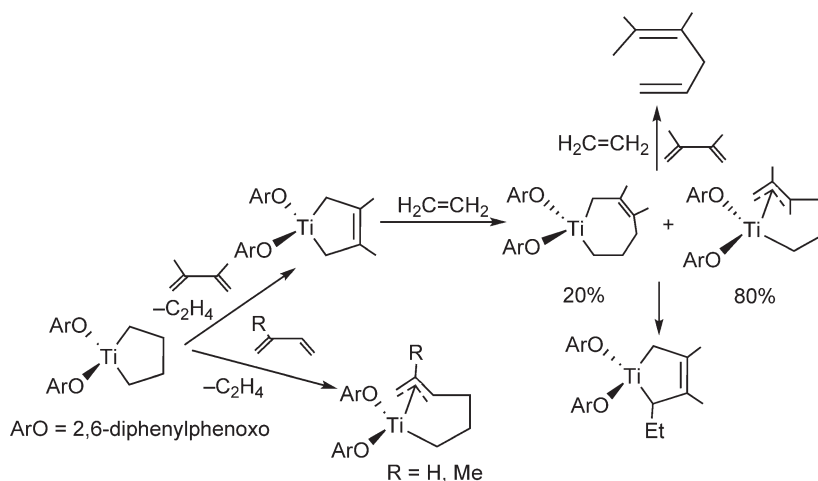
Scheme 118

(Scheme 118) and shows the bridging PhCN unit to be highly reduced and strongly bound to the titanium metal centers. Reactions with acetonitrile produce the corresponding pyridine products and unidentified titanium compounds. The reactions with  $\text{Ph}_2\text{CO}$  at  $20^\circ\text{C}$  proceed with ring expansion to form 2-oxatitanacyclohepta-4-6-diene derivatives; the ketone inserts into the side of the titanacyclopentadiene ring containing the less bulky substituent and gives a single regioisomer product, while the same reaction with  $\text{Ph}_2\text{CO}$  at  $100^\circ\text{C}$  gives the 2-oxatitanacyclopent-4-ene complex (Scheme 118). Further reaction of the 2-oxatitanacyclohepta-4-6-diene complex with  $\text{Bu}^t\text{NC}$  yielded the corresponding  $\eta^2$ -iminoacyl derivative (Scheme 118). The molecular structures of some of these titanium complexes have been determined by X-ray diffraction methods.<sup>174</sup>

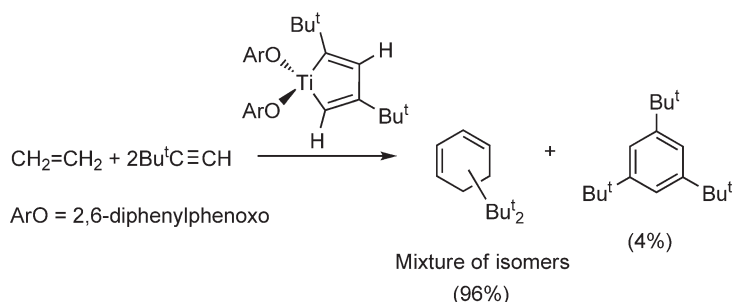
Titanacycle compounds supported by aryloxo ligands catalyze cross-coupling and oligomerization reactions involving 1,3-cyclohexadiene, 1,3-cyclooctadiene, and  $\alpha$ -olefins. Mechanistic aspects are reported.<sup>244</sup> The regio- and the

stereochemistry catalytic reactivity of the titanacyclopentane complex  $\text{Ti}(\text{CH}_2)_4(\text{OAr})_2$  ( $\text{OAr}$  = 2,6-diphenylphenoxo) has been widely studied. This compound catalyzes the selective cross-coupling of 2,3-dimethylbutadiene and isoprene with  $\alpha$ -olefins. The reactions with butadiene or isoprene afford the  $\pi$ -allyl complexes  $\text{Ti}(\text{OAr})_2(\text{CH}_2\text{CR}=\text{CHCH}_2\text{CH}_2\text{CH}_2)$  ( $\text{R} = \text{H}, \text{Me}$ ). In contrast, the reaction with 2,3-dimethylbutadiene forms the titanacyclopent-3-ene complex  $\text{Ti}(\text{OAr})_2(\text{CHCMe}=\text{CHMe})$  and free ethylene.  $\text{Ti}(\text{OAr})_2(\text{CHCMe}=\text{CHMe})$  reacts with ethylene to produce a mixture of *cis*- and *trans*-titanacyclohept-3-ene complex  $\text{Ti}(\text{OAr})_2(\text{CH}_2\text{CMe}=\text{CMeCH}_2\text{CH}_2\text{CH}_2)$ . In the absence of ethylene or 2,3-dimethylbutadiene, this isomeric mixture slowly converts to the titanacyclopent-3-ene complex  $\text{Ti}(\text{OAr})_2(\text{CH}_2\text{CMe}=\text{CMeCH}_2\text{CH}_2)$ . In the presence of an excess of 2,3-dimethylbutadiene and 1 atm of ethylene at 70 °C, the titanacyclopent-3-ene complex produces catalytically the cross-coupled product 4,5-dimethylhexa-1,4-diene with a turnover rate of ca.  $8 \text{ Ti}^{-1} \text{ h}^{-1}$  (Scheme 119). Similar cross-coupling reactions of 2,3-dimethylbutadiene with  $\alpha$ -olefins ( $\text{CH}_2=\text{CHR}$ ,  $\text{R} = \text{Me}, \text{Et}, \text{Ph}, ^t\text{Bu}, \text{SiMe}_3$ ) to produce mixtures of substituted acyclic 1,4-diene products catalyzed by these titanacyclopentadiene complexes are also reported. The scope of these cross-coupling reactions has been extended to the complexes  $\text{Ti}(\text{OAr})_2(\text{CHCMe}=\text{CMeCH})$ ,  $\text{Ti}(\text{OAr})_2\{\text{C}_2(\text{SiMe}_3)_2\text{C}_6\text{H}_8\}$ <sup>175</sup> ( $\text{OAr}$  = 2,6-disopropylphenoxo), and  $\text{Ti}(\text{OAr})_2(\text{C}_4\text{Et}_4)$  ( $\text{OAr}$  = 2,6-diphenylphenoxo). Kinetic studies and mechanistic considerations of the cross-coupling reaction have been carried out.<sup>176</sup>

These complexes act as catalysts for the cyclization of 1,7-octadiene and the dimerization of styrene.<sup>173</sup> The titanacyclopentadiene complexes  $\text{Ti}(\text{C}_4\text{R}_4)(\text{OAr})_2$  catalyze the [2 + 2 + 2]-cycloaddition reactions through a cross-coupling process of two alkyne units with 1 equiv. of olefin for the regio- and stereoselective synthesis of 1,3-cyclohexadiene. As an example, Scheme 120 shows the reaction of the 2,4-di-*tert*-butyltitanacyclopentadiene complex with ethylene in the presence of an excess of  $\text{Bu}^t\text{C}\equiv\text{CH}$  to give a mixture of 1,3-cyclohexadiene isomers along with small amounts of 1,3,5-tri-*tert*-butylbenzene.<sup>245</sup> The same catalytic system produces the cyclotrimerization of  $\text{Bu}^t\text{C}\equiv\text{CH}$  into 1,3,5-tri-*tert*-butylbenzene,<sup>176</sup> while in the presence of one or more equivalents of  $\text{LiC}\equiv\text{CBu}^t$  the



Scheme 119



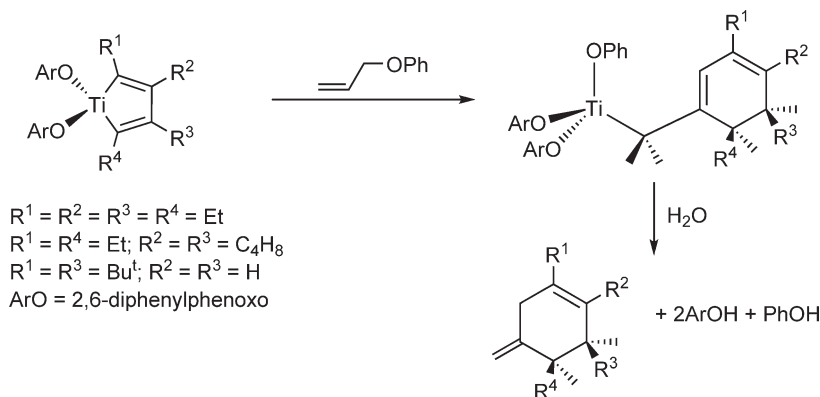
Scheme 120

catalytic formation of 1,3,6-tri-*tert*-butylfulvele along with small amounts of other organic products is observed.<sup>246</sup> Titanacyclopentadiene or titanacyclopentane complexes are isolated as intermediates. A combination of NMR spectroscopy, photochemistry, and molecular mechanics calculations has been applied to determine the stereochemistry of the reaction.

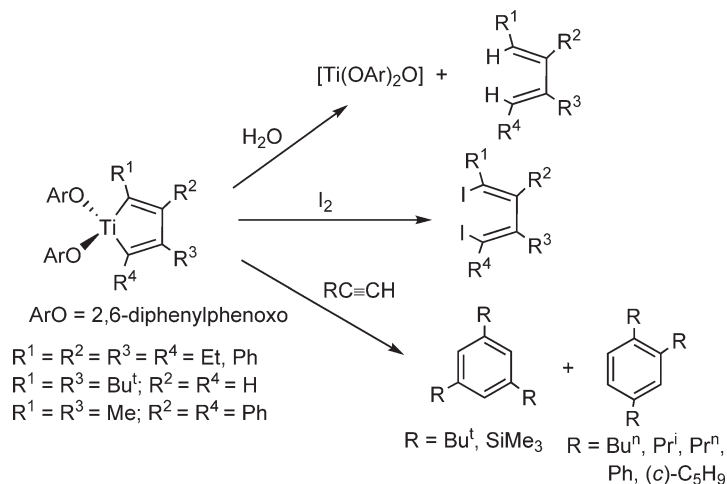
Titanacyclopentadiene complexes  $\text{Ti}(\text{C}_4\text{R}_4)(\text{ArO})_2$  also react slowly with allyl phenyl ether to produce new organometallic products formulated as allyl-trisphenoxo titanium complexes on the basis of their spectroscopic properties. Hydrolysis of these compounds leads to the formation of single regioisomers of substituted methylenecyclohex-3-ene along with 2 equiv. of 2,6-diphenylphenol and 1 equiv. of phenol. A mechanistic discussion suggests the reaction sequence involves initial  $[2 + 2 + 2]$ -cycloaddition followed by cleavage of a phenyl ether bond (Scheme 121).<sup>247</sup>

The metallacyclic compounds react with protic reagents to yield the corresponding substituted 1,3-butadienes and the iodination reactions give the 1,4-diiodo 1,3-butadiene derivatives (Scheme 122). Reactions with different unsaturated organic molecules have also been investigated. They catalyze the cyclotrimerization of a range of alkynes. Terminal alkynes with small substituents produce the 1,2,4-trisubstituted benzene, preferentially, in an exothermic reaction. The more bulky substrates  $\text{Bu}^t\text{C}\equiv\text{CH}$  and  $\text{Me}_3\text{SiC}\equiv\text{CH}$  react more slowly and only the symmetrical 1,3,5-isomer is produced (Scheme 122).<sup>174</sup>

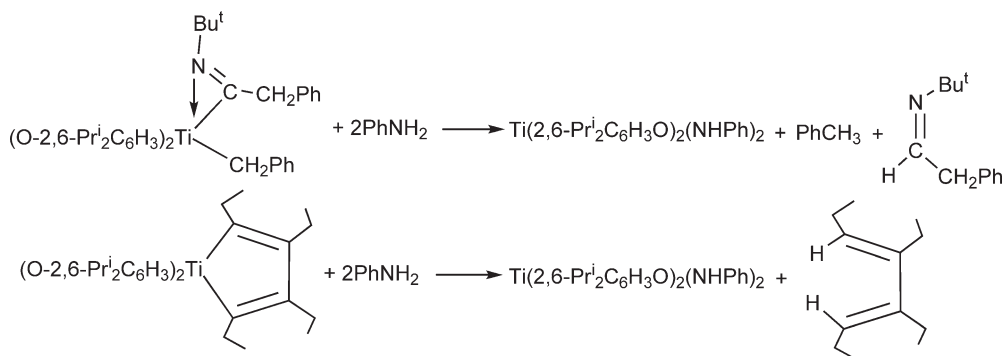
The known<sup>47</sup> organometallic compounds  $\text{Ti}(\text{CH}_2\text{Ph})(\text{O}-2,6-\text{Pr}^i_2\text{C}_6\text{H}_3)_2(\eta^2-\text{Bu}^t\text{N}-\text{CCH}_2\text{Ph})$  and  $\text{Ti}(\text{C}_4\text{Et}_4)(\text{O}-2,6-\text{Pr}^i_2\text{C}_6\text{H}_3)_2$  react with 2 equiv. of aniline in hydrocarbon solvents to produce the bis-amido complex  $\text{Ti}(\text{O}-2,6-\text{Pr}^i_2\text{C}_6\text{H}_3)_2(\text{NHPh})_2$  with formation of the corresponding alkane (Scheme 123).<sup>248</sup>



Scheme 121



Scheme 122

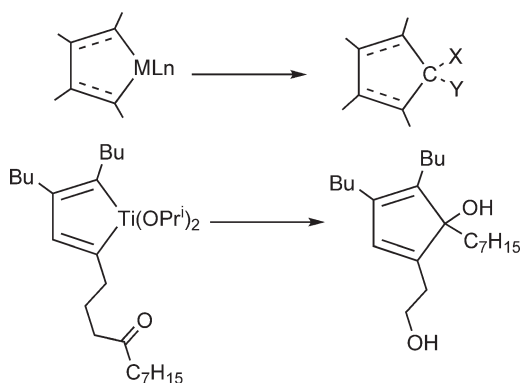


Scheme 123

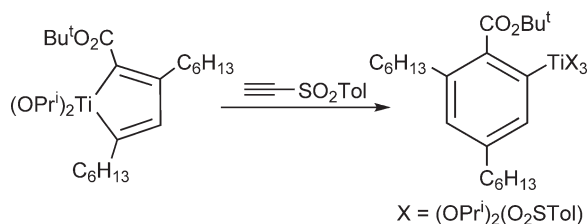
Titanacyclopentadiene complexes synthesized by Sato's procedure react with some electrophiles to give intermediates of great utility in organic synthesis and they act as catalysts for carbon–carbon bond formation and the stereoselective synthesis of functionalized conjugated dienes.<sup>24,35,37,186–193</sup> The chemistry of the system  $\text{Ti}(\text{OPr}^i)_2(\eta^2\text{-propene})$  and related systems has been reviewed, including organic synthesis processes, representative applications to asymmetric synthesis and to natural product synthesis.<sup>249</sup> The reaction involving the generation of alkene or alkyne–titanium complexes through the coordination of the carbon–carbon multiple bond to a titanium center to give organometallic complexes and their use as a source for carbanionic reagents, directly or after conversion to new organotitanium species, for synthetic applications in organic reactions has also been reviewed.<sup>250,251</sup> Bis-alkoxo–titanacyclopropanes and –propenes (Kulinkovich reagents) are versatile reagents for carbon–carbon bond formation and this reaction has been studied.<sup>252</sup>  $\text{Ti}(\text{OPr}^i)_2(\eta^2\text{-propene})$  reacts with olefins and acetylenes in an inter- or intramolecular manner to give mono- or bicyclic dialkoxo titanacycles. Formation of several kinds of the titanacycles and their synthetic applications in organic reactions such as: (i) olefin–olefin cyclizations, (ii) olefin–acetylene cyclizations, (iii) acetylene–acetylene cyclizations, (iv) cyclizations of allenes, (v) cyclizations of unsaturated esters, and (vi) generation of a low-valent alkoxytitanacycle have been studied. The advantageous features of these new titanacycles over bis-Cp metallacycles of group 4 metals in organic synthesis have been highlighted.<sup>253</sup>

The titanacyclopentadiene derivatives are converted into cyclopentadienols (Scheme 124) as an example for organic transformations of metallacyclic complexes into carbocyclic substances.<sup>254</sup>

The selective cyclotrimerization of three different, unsymmetrical acetylenes to give a single aromatic compound is an important organic reaction. This process can be catalyzed by organometallic transition metal compounds. Thus,  $\text{Ti}(\eta^2\text{-propene})(\text{OPr}^i)_2$  reacts with the two unsymmetrical acetylenes  $\text{Bu}^t\text{O}_2\text{C}-\text{C}\equiv\text{C}-\text{C}_6\text{H}_{13}$  and  $\text{HC}\equiv\text{C}-\text{C}_6\text{H}_{13}$  to give a dialkoxo–titanacyclopentadiene derivative which upon treatment with ethynyl tolyl sulfone produces a new single aryl–titanium compound (Scheme 125). The aryl ligand results from a cyclotrimerization process of acetylenes. Other different monoaryl–titanium complexes can be prepared by this metal-assisted Reppe reaction. Mechanistic studies are reported.<sup>194</sup>



Scheme 124

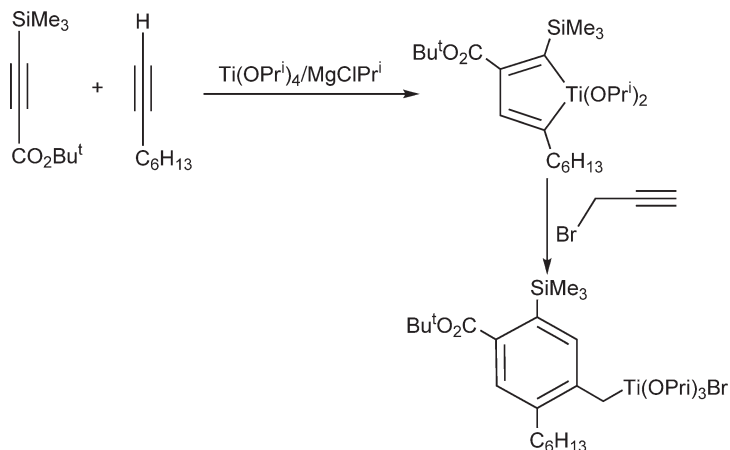


Scheme 125

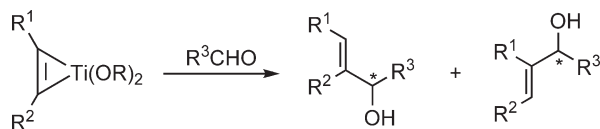
Benzyltitanium compounds have been also obtained by using this Reppe-type transformation. The synthesis of benzyltitanium derivatives, which may have a functional group such as ester or amide, from three acetylenes has been reported. One example is shown in [Scheme 126](#). Titanacyclopentadiene is first formed in the reaction of two different unsymmetrical acetylenes and the titanium system  $\text{Ti}(\text{OPr}^i)_4/2\text{MgClPr}^i$ , according to the Sato procedure. Propargyl bromide is then added as the third acetylene to give a single benzyltitanium compound.<sup>255</sup> An analogous system has been employed for the efficient and practical synthesis of optically active indan-2-ols starting from readily accessible optically active 4-siloxy-1,6-alkadiynes and ethynyl-*p*-tolyl sulfone.<sup>256</sup> The synthesis of metallated pyridines has been similarly reported.<sup>257</sup>

Enyne titanium complexes are synthesized when enynes are treated with  $\text{Ti}(\text{OPr}^i)_2(\eta^2\text{-propene})$ . These species add aldehydes, ketones, and chiral imines to generate multiple stereogenic centers in an acyclic system. Numerous methods for the stereoselective construction of two stereogenic centers are known, although those for more than three in one asymmetric procedure are less common.<sup>195</sup>

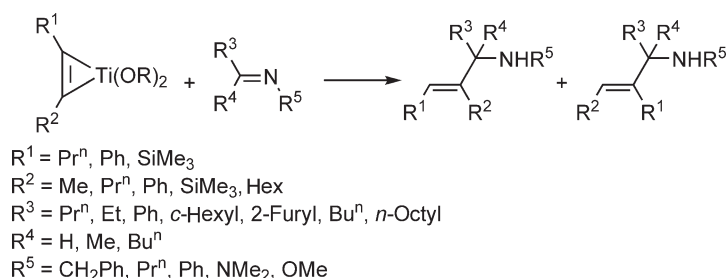
Titanium-alkyne complexes  $\text{Ti}(\text{Me}_3\text{SiC}\equiv\text{CC}_6\text{H}_{13})(\text{OR})_2$ , as well as the chiral complex derived from chloro-tris[(-)-mentho]titanium/ $2\text{MgClPr}^i$  and alkynes, react with carbonyl compounds to afford optically active allylic alcohols in up to 38% ee ([Scheme 127](#)).<sup>184</sup> Introduction of two different electrophiles at each of the acetylenic terminal carbon atoms was possible in a regio- and stereoselective manner.<sup>45</sup> Similarly, the titanacyclopentene compounds react with imines, metalloimines, or hydrazones under mild conditions to afford allylic amines or their derivatives in good to excellent yields ([Scheme 128](#)).<sup>258</sup>



Scheme 126



Scheme 127



Scheme 128

Numerous other organic reactions have been studied by using such metal-assisted systems based on Sato's compounds.<sup>259</sup> Some examples can be mentioned. These systems react with  $\delta$ - and  $\gamma$ -functionalized monosubstituted alkynes to induce an intramolecular cyclization with formation of four- and five-membered cycloalkanols<sup>260</sup> or the hydrotitanation of 1-silyl or 1-stannyl-1-alkynes.<sup>261</sup> A chiral acetylenic ester titanium compound<sup>186</sup> has been used as reagent for the asymmetric and stereoselective synthesis of allyl alcohols.<sup>262</sup> These systems catalyze the practical preparation of optically active *syn*-1-vinyl-2-amino alcohol derivatives<sup>263</sup> and the asymmetric intramolecular cyclization of 2,7- and 2,8-enynyl chiral acetals.<sup>264</sup> In the framework of a plausible cyclization mechanism, several conformational features which can regulate the stereoinduction have been suggested, and they promote the cyclization of a variety of chiral 6-hepten-1-yne to titanabicyclopentenes with excellent yields and degrees of *exo*-stereoselectivity, depending on the substrate's steric requirements.<sup>265</sup> Silylethylene titanium alkoxo derivatives serve as versatile reagents for silylethylation of unsaturated compounds.<sup>266</sup> The use of propargyl alcohol derivatives to synthesize propargylstannanes catalyzed by allenyltitanium derivatives,<sup>267</sup> the synthesis of chiral alkynes by hydrogenolysis and halogenolysis of optically active allenyltitanium compounds with optically active propargyl alcohol derivatives,<sup>268</sup> the conversion of 1-alken-3-yl carbonates to 1-alkenes and 3-chloro-1-alkenes,<sup>269</sup> or reactions with propargyl carbonates or phosphates and dialkyl azodicarboxylates to give  $\alpha$ -hydrazinoalkynes have also been described.<sup>270</sup> The synthesis of exocyclic bis-allenes and cyclobutene derivatives by intramolecular cyclization of tethered propargyl alcohol compounds,<sup>271</sup> the synthesis of 2-substituted and 2,3-disubstituted furans from 2-alkynyl tetramethylethylene acetals and aldehydes,<sup>272</sup> and general synthetic methods for preparation of optically active propargyl- and allylstannanes have been published.<sup>273</sup> The synthesis and preparation of stereo-defined enynes and dienyynes, useful intermediates and important structural constituents in organic synthesis, natural products chemistry and materials science,<sup>274</sup> and the cyclization of enynes having vinylic sulfide, sulfone, or sulfoxide groups catalyzed by titanacycle compounds<sup>275</sup> have been reported. The cross-coupling reaction of  $\text{Ti}(\text{R}^1\text{C}_2\text{R}^2)(\text{OPr}^i)_2$  with aryl iodides in the presence of catalytic amounts of nickel complexes,<sup>276</sup> and the cyclization of enynes with formation of stereodefined bicyclooctenes have been developed.<sup>277</sup> Bis-alkoxo titanacycle derivatives have been used as reagents for the synthesis of vinyl phosphonate and 1,4-bisallylphosphonate compounds.<sup>278–280</sup> Functionalized conjugated diene–titanium alkoxo complexes have been applied to react with aldehydes and other organic molecules with a high regio- and stereoselectivity in the C–C bond formation process.<sup>281</sup> Alkenyloxazoline–titanium complexes formed from Sato's reagent have proved to be versatile templates for diastereoselective and asymmetric coupling reactions.<sup>282</sup> The intermolecular reaction of alkynes with allyl or propargyl compounds mediated by Sato's system, followed by trapping of the resulting vinyltitanium compounds with an electrophile such as  $\text{H}_2\text{O}$ ,  $\text{I}_2$ , or an aldehyde, gives a variety of 1,4-alkadienes or 1,2,4-alkatrienes.<sup>283</sup> 3-Alkoxy-2-propyn-1-yl carbonates react with the Sato system to afford titanated alkoxyallene derivatives which, in turn, react with aldehydes regiospecifically to provide the corresponding  $\gamma$ -addition products in good to excellent yields, thus affording a convenient method for synthesizing  $\gamma$ -hydroxy esters and/or  $\gamma$ -butyrolactones.<sup>284</sup>

Enantio-enriched axially chiral allenyltitanium compounds have been synthesized from optically active propargyl alcohol derivatives by the reaction with a divalent titanium reagent,  $\text{Ti}(\text{OPr}^i)_4/2\text{MgXPr}^i$ , and their reactions with a variety of electrophiles have been studied.<sup>285</sup>

Dialkoxotitanacyclopropane derivatives  $\text{Ti}(\text{CH}_2\text{CR})(\text{OPr}^i)_2$  react with esters to afford cycopropanols via a Kulinkovich hydroxycyclopropanation reaction, an efficient, fast, exothermic, and irreversible organic synthetic method. A detailed mechanism for this process has been explored with density functional theory calculations.<sup>286</sup>

$\text{TiCl}_3\text{Me}$  generated by mixing  $\text{TiCl}_4$  and  $\text{ZnMe}_2$  in a molar ratio 2:1 and the system  $\text{TiMe}_2\text{Cl}_2/\text{ZnMe}_2$  are examples where organotitanium reagents induce alkylative *endo*-cleavage of carbohydrates.<sup>287</sup>

$\text{TiMe}(\text{OPr}^i)_3$  has been used as starting material to generate titanium cyclopropane derivatives, active species that promote the cyclopropanation of *N,N*-dibenzylformamide with formation of cyclopropylamines.<sup>288,289</sup>  $\text{TiMe}(\text{OPr}^i)_3$  reacts with dialkylcarboxamides in the presence of 1.1 equiv. of a Grignard reagent to give cyclopropylamine in better yields than that previously obtained with 2 equiv. of Grignard reagent and 1 equiv. of  $\text{Ti}(\text{OPr}^i)_4$ .<sup>290</sup> Dibenzylformamide is treated with cyclohexylmagnesium bromide in the presence of  $\text{TiMe}(\text{OPr}^i)_3$  and a variety of cyclic and acyclic alkenes and alkadienes to give new mono- and disubstituted as well as bicyclic dialkylcyclopropylamines in yields ranging from 18 to 90%.<sup>291</sup>

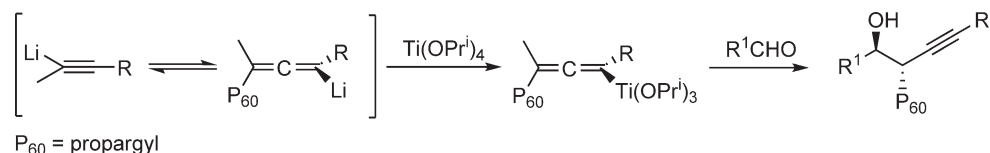
The monoalkyl complexes  $\text{TiR}(\text{OPr}^i)_3$  ( $\text{R} = \text{Me}, \text{Ph}$ ) give cross-coupling reaction products with aryl triflates and halides, in the presence of catalytic amount of palladium compounds.<sup>292</sup> Titanate compounds  $\text{M}[\text{TiR}(\text{OPr}^i)_4]$  produce analogous reactions.<sup>293</sup>

Aryl triisopropoxo titanium derivatives  $\text{TiAr}(\text{OPr}^i)_3$  ( $\text{Ar} = \text{Ph}, 4\text{-FC}_6\text{H}_4, 4\text{-MeOC}_6\text{H}_4, 2\text{-MeC}_6\text{H}_4$ ) have been used as arylating reagents for the rhodium-catalyzed asymmetric 1,4-addition processes for the synthesis of enantiomerically enriched organic products.<sup>294</sup>  $\text{TiMe}(\text{O}^i\text{Bu})_3$  reacts with  $[\text{Rh}(\text{COD})(\mu_2\text{-OH})_2]$  at low temperature to give the alkylation of the  $\text{Rh}(\text{I})$  complex, while the protonolysis reaction yields the oxo-bridged complex  $[\text{Rh}(\text{COD})(\mu_2\text{-OH})(\mu_3\text{-O})_2]_2[\text{Ti}(\text{O}^i\text{Bu})_3]$ , the molecular structure of which has been determined by X-ray diffraction. The properties of this titanium–rhodium complex as a catalyst precursor in heterogeneously catalyzed hydrogenation reactions have been discussed.<sup>295</sup>

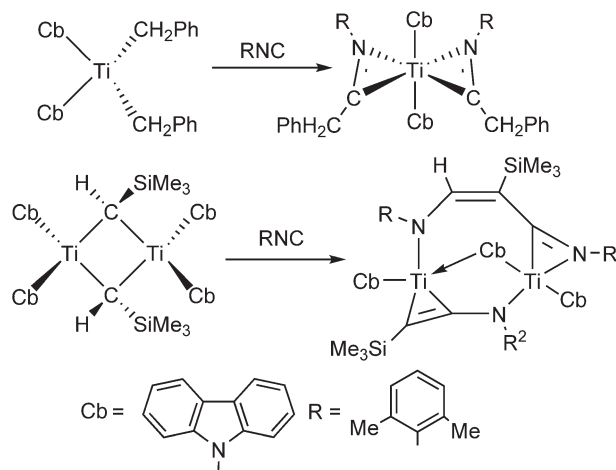
The application of the reaction of the allenyltitanium  $\text{Ti}[\text{RC}\equiv\text{CH}(\text{propargyl})](\text{OPr}^i)_3$  to generate acetylenic diol systems has been studied. (Scheme 129).<sup>41</sup>

Titanium acetylides react with 3-benzyl-tetrahydro-1,3-oxazines and 1,3-oxazolidines to give the corresponding  $\beta$ -aminoacetylenes in modest to good yield.<sup>296</sup> Vinyl  $\text{Ti}(\text{IV})$  species prepared by the alkylation of vinylcarbene complexes with  $\text{Bu}^t\text{Cl}$  react with aldehydes to give allylic alcohols. Reaction with terminal alkynes produces conjugated dienes, in which a vinyl group regioselectively bonds to the unsubstituted side of carbon–carbon triple bond.<sup>297</sup>

The reactions of  $\text{Ti}(\text{CH}_2\text{Ph})_2(\text{cb})_2$  and  $(\text{cb})_2\text{Ti}(\mu\text{-CHSiMe}_3)_2\text{Ti}(\text{cb})_2$  ( $\text{cb} = \text{carbazole}$ ) with 2,6-dimethylphenyl isocyanide lead to titanium derivatives containing new carbon–carbon bonds (Scheme 130). The molecular structures of the insertion products have been determined by X-ray diffraction.<sup>109</sup> Reaction of  $\text{Ti}(\text{CH}_2\text{Ph})_2(\text{cb})_2$  with 2,6-dimethylphenyl isocyanide ( $\text{xylNC}$ ) gives the double insertion product bis(iminoacyl) derivative. The iminoacyl



Scheme 129

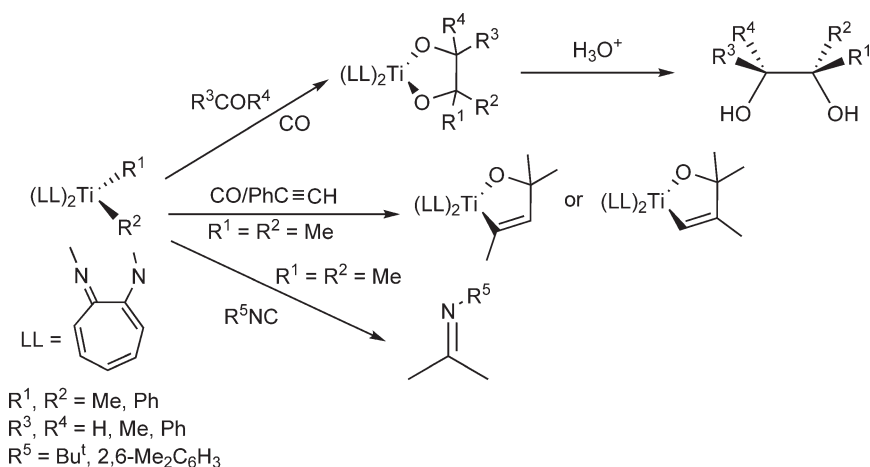


Scheme 130

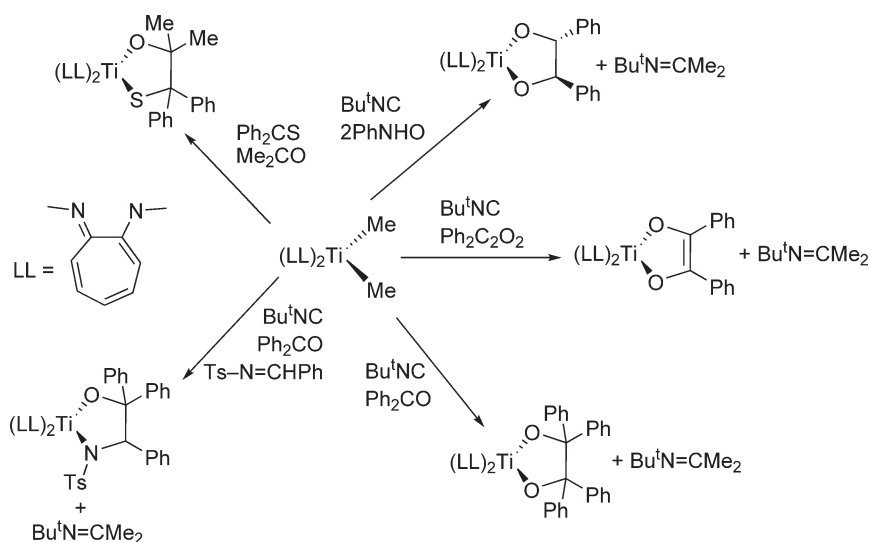
carbon shows a chemical shift at  $\delta$  246.9 in the  $^{13}\text{C}$  NMR spectrum, indicative of an  $\eta^2\text{-C,N}$  binding. Treatment of the binuclear titanium alkylidene-bridged compound  $(\text{cb})_2\text{Ti}(\mu\text{-CHSiMe}_3)_2\text{Ti}(\text{cb})_2$  with 2,6-dimethylphenyl isocyanide gives a new derivative, molecular structure of which has been only elucidated by the solid-state structure, showing a binuclear disposition, containing a total of 3 equiv. of isocyanide within two distinct bridging units. Two terminal and one non-symmetrically bridged carbazole ligands are also present (Scheme 130).<sup>110</sup>

The reactivity of the dialkyl complexes  $\text{TiR}_2(\text{LL})_2$  ( $\text{LL} = \text{N,N}'\text{-dimethylaminotroponiminato}$ ) has been widely studied. Reactions with CO and aldehydes or ketones afford unsymmetrical diolato complexes that convert to the corresponding vicinal diols after hydrolysis. CO and acetylene react to form the oxametallacyclopentene complex. Treatment with RNC yields the free imine and low-valent titanium species (Scheme 131). In the reaction with  $\text{Bu}^t\text{NC}$ , free  $\text{Bu}^t\text{N}=\text{CMe}_2$  is formed and the addition of benzaldehyde or benzyl reagents affords titanium diolato or enediolato complexes. Thiolato-alkoxo or amido-alkoxo titanium complexes can also be similarly prepared (Scheme 132).<sup>123–125</sup>

Dialkyltitanium(IV) derivatives  $\text{TiR}_2\text{X}_2$  ( $\text{R} = \text{Bu}^n, \text{Bu}^t, \text{Pr}^i$ , etc.;  $\text{X} = \text{halo}$  or alkoxo ligands) in THF at  $-78^\circ\text{C}$  react with unsaturated organic substrates such as olefins, acetylenes, azoarenes, aldehydes, ketones, and imines to undergo epimetallation transfer processes in high yield and to generate titanacyclopropane and titanacyclopentene



Scheme 131



Scheme 132



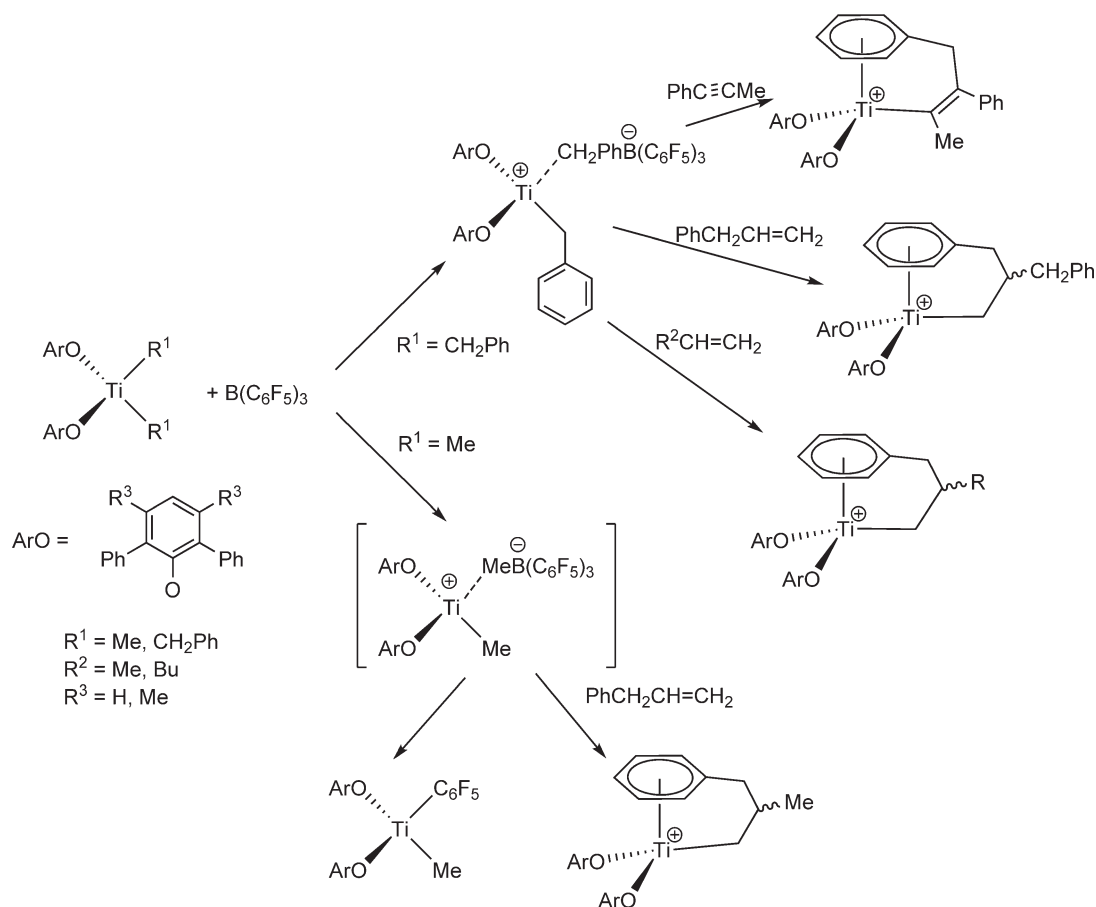
intermediates. These are transformed into useful, metal-free derivatives by protonolysis/deuteriolysis, oxidation or unsaturated monomer insertion into the Ti–C bond. Analogous epimetallation reactions conducted in hydrocarbons lead to stereoselective polymerization of 1-alkenes and the cyclotrimerization of acetylenes.<sup>298,299</sup>

Ti(CH<sub>2</sub>Ph)<sub>4</sub> reacts with N-2-fluorenyl(salicylideneimine) to afford a crystallographically characterized titanium(IV) complex containing two conventional bidentate Schiff base and two O-bound ligands in which the imine function has been reduced by the addition of benzyl and hydrogen moieties.<sup>300</sup> The reaction between TiNp<sub>4</sub> (Np = neopentyl) and isolated hydroxyl groups at the surface of silica that was partially dehydroxylated at 753 K leads to the formation of isolated surface tris(neopentyl) complexes. A mild hydrolysis at 298 K or a calcination at 673 K of the silica-bound TiNp<sub>3</sub> complexes lead to surface species that are catalytically active for the epoxidation of cyclohexene by organic hydroperoxides or aqueous hydrogen peroxide. The activity is compared with the analogous zirconium system.<sup>301,302</sup>

The use of mono-Cp, Cp-amido, diamido, amino-bis(phenolato), bis(phenoxo-imino) and bis(indolideimino) alkyltitanium derivatives as catalysts for the living insertion polymerization of  $\alpha$ -olefins has been widely reviewed.<sup>303</sup>

The interactions of TiCl<sub>3</sub>Me with chloromethyl aluminum derivatives as components of a catalytic system for polymerization of ethylene, in toluene and toluene-*d*<sub>8</sub>, have been studied. High yields of methane formation are observed in a complex equilibrium between the components of the catalytic system, suggesting that Ti–Me and Al–Me bonds are involved in the formation of methane.<sup>304</sup>

Treatment of the dibenzyl compounds Ti(CH<sub>2</sub>Ph)<sub>2</sub>(OAr)<sub>2</sub> with B(C<sub>6</sub>F<sub>5</sub>)<sub>3</sub> gives the corresponding zwitterionic species [Ti(CH<sub>2</sub>Ph)(OAr)<sub>2</sub>]<sup>+</sup>[CH<sub>2</sub>PhB(C<sub>6</sub>F<sub>5</sub>)<sub>3</sub>]<sup>−</sup> which react with phenylpropyne, allylbenzene, propene, or 1-hexene to give the product of the insertion of 1 equiv. of substrate into the Ti–benzyl bond. Reaction of the dimethyl compounds TiMe<sub>2</sub>(OAr)<sub>2</sub> with B(C<sub>6</sub>F<sub>5</sub>)<sub>3</sub> gives unstable species, which polymerize ethylene and propylene (Scheme 133). Within 1 h at room temperature these species convert to TiMe(C<sub>6</sub>F<sub>5</sub>)(OAr)<sub>2</sub> and in the presence of allylbenzene the addition product is obtained.<sup>305</sup>



Scheme 133

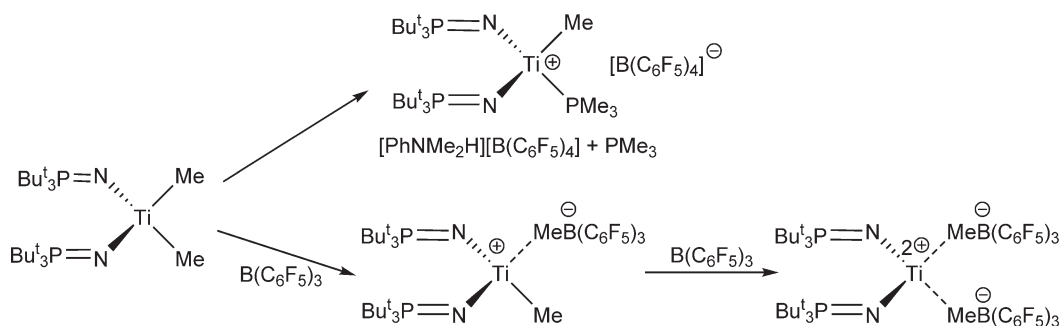
The influence of the ligand environment on the catalytic activity of  $\text{Ti}(\text{CH}_2\text{Ph})_2(\text{O}-\text{O})$  complexes, synthesized with varying steric requirements (Section 4.05.2.1.2; Scheme 79), toward unsaturated hydrocarbons has been studied. In the presence of MAO as co-catalyst they are active for the oligomerization or polymerization of  $\alpha$ -olefins, the polymerization of butadiene, and the catalytic cyclotrimerization of terminal acetylenes. For the polymerization of ethylene, activities of up to  $4.7 \times 10^6 \text{ g PE mol}^{-1} \text{ catalyst h}^{-1}$  have been achieved, yielding polymers with high molecular weights with very broad polydispersities. In contrast, these compounds polymerize 1-hexene with a narrow molecular weight distribution. They are active for the polymerization of butadiene with the sterically more demanding binaphthol inducing selective 1,4-insertions. They also are active for catalytic cyclotrimerization of terminal acetylenes to 1,2,4- and 1,3,5-trisubstituted benzenes. This ratio of benzenes is dependent on the steric bulk of the ancillary binaphthol ligands.<sup>154</sup>

Equimolar amounts of the titanium dimethyl complexes  $\text{TiMe}_2[\text{RN}(\text{CH}_2)_3\text{NR}]$  ( $\text{R} = 2,6\text{-Pr}^i\text{C}_6\text{H}_3$ ,  $2,6\text{-Me}_2\text{C}_6\text{H}_3$ ) containing chelating diamido ligands and  $\text{B}(\text{C}_6\text{F}_5)_3$  catalyze the living aspecific polymerization of  $\alpha$ -olefins at room temperature. The catalytic systems generate high molecular weight polymers with remarkably narrow molecular weight distributions. A noticeable increase in activity and hence molecular weight is observed for polymerizations performed in the presence of  $\text{CH}_2\text{Cl}_2$ .<sup>114</sup> The deactivation mechanism induced by  $[\text{MeB}(\text{C}_6\text{F}_5)_3]^-$  in the  $\text{TiMe}_2[\text{ArN}(\text{CH}_2)_3\text{NAr}]/\text{B}(\text{C}_6\text{F}_5)_3$  catalytic system is studied.  $\text{TiMe}_2[\text{ArN}(\text{CH}_2)_3\text{NAr}]$  reacts with  $\text{B}(\text{C}_6\text{F}_5)_3$  to give the titanium cationic species  $[\text{TiMe}[\text{ArN}(\text{CH}_2)_3\text{NAr}]]^+[\text{MeB}(\text{C}_6\text{F}_5)_3]^-$ , which is an active catalyst for the living polymerization of 1-hexene. Pentane suspensions of this ionic compound evolve methane to afford  $[\text{Ti}(\text{CH}_2\text{B}(\text{C}_6\text{F}_5)_2)(\text{C}_6\text{F}_5)[\text{ArN}(\text{CH}_2)_3\text{NAr}]]$ , which is inactive for the polymerization of  $\alpha$ -olefins. Both complexes have been characterized by X-ray diffraction.<sup>115</sup>

The dimethyl phosphinimido complex  $\text{TiMe}_2(\text{NPBu}^t_3)_2$  affords a remarkably active catalyst for the polymerization of ethylene upon activation with 1 equiv. of  $\text{Ph}_3\text{C}[\text{B}(\text{C}_6\text{F}_5)_4]$  or  $\text{B}(\text{C}_6\text{F}_5)_3$ . The stoichiometric reaction of  $\text{TiMe}_2(\text{NPBu}^t_3)_2$  with  $\text{B}(\text{C}_6\text{F}_5)_3$  generates the zwitterion  $(\text{Bu}^t_3\text{P}=\text{N})_2\text{MeTi}(\mu\text{-Me})\text{B}(\text{C}_6\text{F}_5)_3$  which is an active species. Rather unexpectedly, in the generation of this species the order of addition of the reagents has a dramatic effect on the catalytic activity: adding  $\text{TiMe}_2(\text{Bu}^t_3\text{P}=\text{N})_2$  to a solution of  $\text{B}(\text{C}_6\text{F}_5)_3$  under an ethylene atmosphere produces low activity, while adding the reagents in reverse order gives a highly active system. The reason is that an excess of  $\text{B}(\text{C}_6\text{F}_5)_3$  poisons the catalyst by attacking both methyl groups, to give the bis-zwitterionic species  $(\text{Bu}^t_3\text{PN})_2\text{Ti}[\mu\text{-MeB}(\text{C}_6\text{F}_5)_3]_2$  which has been characterized by NMR spectroscopy and X-ray diffraction. The reaction of  $\text{TiMe}_2(\text{NPBu}^t_3)_2$  with  $[\text{PhNMe}_2\text{H}][\text{B}(\text{C}_6\text{F}_5)_4]$  in the presence of  $\text{PMe}_3$  leads to the phosphine adduct  $[\text{TiMe}(\text{NPBu}^t_3)_2(\text{PMe}_3)][\text{B}(\text{C}_6\text{F}_5)_4]$  (Scheme 134).<sup>76,306,307</sup>

The reaction of  $\text{TiMe}_2(\text{NPBu}^t_3)_2$  with  $\text{AlMe}_3$  has also been examined in detail. Synthetic, structural, and kinetic studies reveal that the phosphinimido ligand exhibits metathesis reaction followed by sequential C–H bond activation affording  $\text{TiAl}_2$  carbide dimer species. This process is in competition with direct C–H bond activation in  $\text{TiMe}_2(\text{NPBu}^t_3)_2$ . The implications of these findings for both olefin polymerization catalysis and C–H bond activation is discussed.<sup>308</sup>

A chelating diamido dimethyltitanium complex activated by dried modified MAO (MMAO) catalyzes the living polymerization of propylene at  $0^\circ\text{C}$  to give a statistically atactic polymer. The heterogenization of the living systems was attempted by supporting MAO, MMAO, and dried MMAO on  $\text{SiO}_2$  as solid activators.<sup>309</sup> Analogous dimethyltitanium complexes in the presence of MMAO from which free  $\text{AlMe}_3$  and  $\text{AlBu}^i_3$  have been reduced to ca. 0.1 mol% have been supported on metal oxides, such as anhydrous silica gel, alumina, or magnesia, for propylene polymerizations.<sup>310</sup> The catalytic properties of systems based on trichloro monoalkyltitanium complexes and chloro



Scheme 134

dialkylaluminum derivatives have been studied during the polymerization of propylene in the presence of graphite. The conditions of the formation of isotactic polypropylene in these systems are determined. ESR spectroscopic data led to the conclusion that titanium is not reduced in the presence of graphite, and the polymerization of propylene occurs on a derivative of titanium(IV).<sup>311</sup>

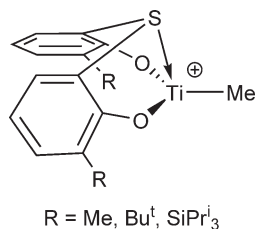
The kinetics of the polymerization of indene in  $\text{CH}_2\text{Cl}_2$  solution, initiated with cumyl methyl ether and cumyl chloride, in the presence of  $\text{TiCl}_3\text{Bu}$ , at variable temperatures (0 to  $-62^\circ\text{C}$ ), have been investigated by adiabatic calorimetry under vacuum. The results may be explained by a propagation involving ionic active centers, as in conventional carbocationic polymerization.<sup>312</sup>

$\text{TiCl}_2\text{Me}_2$  has been studied as an active catalyst for metathesis polymerization reactions.<sup>313</sup> Chloro methyltitanium derivatives  $\text{TiCl}_{4-n}\text{Me}_n$ , ( $n=1-4$ ) are highly active catalysts for the ring-opening metathesis polymerization of dicyclopentadiene.  $\text{TiCl}_2\text{Me}_2$  is the most active, far more active than  $\text{Cp}_2\text{TiMe}_2$ .<sup>313</sup>

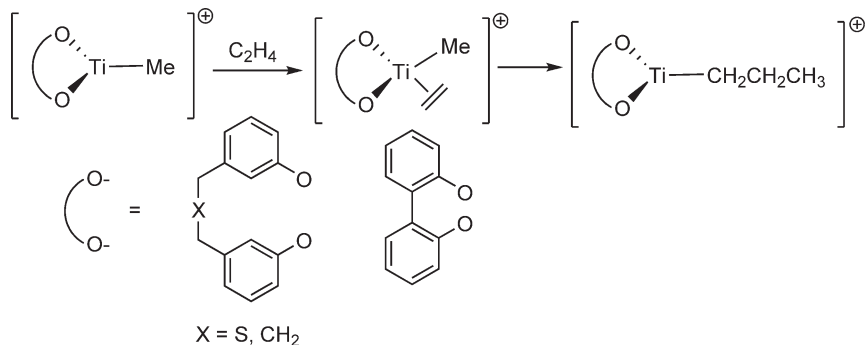
The insertion of ethylene into the titanium–methyl bond in the neutral bimetallic compound  $\text{H}_2\text{Al}(\mu\text{-Cl})_2\text{TiCl}_2\text{Me}$  has been studied using analytic gradient in the geometry optimizations and reaction pathway calculations. The two bridging chloro ligands are found to be important for the migratory insertion and, at the transition state of the olefin insertion step, they are positioned *trans* to the polymer and the ethylene molecule.<sup>314</sup> In a similar study, the insertion process of ethylene in the titanium–carbon bond of the cation  $\text{TiCl}_2\text{Me}^+$  and the same bimetallic species  $\text{H}_2\text{Al}(\mu\text{-Cl})_2\text{TiCl}_2\text{Me}$  has been investigated using DFT (B3LYP) computational calculations. The results suggest that under the conditions used in real polymerization processes both reaction channels (bimetallic complex and separated ion pair) are simultaneously available and that their relative importance and the resulting reaction rate are determined by the solvent polarity.<sup>315</sup>

The effect of structural changes of chloro methyltitanium complexes on regioselectivity in propylene insertion into the methyl–Ti bond was studied by applying paired interacting orbitals (PIO).<sup>316</sup> The effect of *ortho*-substituents (Me,  $\text{Bu}^t$ , and  $\text{SiPr}^i_3$ ) of phenoxo groups in cationic thio-bisphenoxo–methyltitanium catalysts (Scheme 135) on their ethylene polymerization activity has been analyzed by applying *ab initio* molecular orbital theory and DFT.<sup>317</sup>

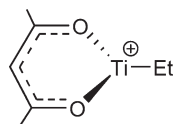
Density functional calculations on the chain initiation reaction shown in Scheme 136 for the ethylene polymerization catalyzed by bis-alkoxo titanium complexes have been studied. Activation barriers of  $6.4 \text{ kcal mol}^{-1}$  are found for the titanium sulfur-bridged catalysts with higher insertion barriers of  $10\text{--}15 \text{ kcal mol}^{-1}$  for the  $\text{CH}_2$ -bridged catalysts. For the S-bridged systems, there is a strong interaction between the metal and the sulfur bridge leading to a less stabilized  $\pi$ -complex and a lower activation energy.<sup>318</sup>



Scheme 135



Scheme 136



Scheme 137

In search of more active new catalysts, density functional theory has been used to predict ethylene insertion barriers for a variety of Ti-chelating bridged complexes of the type  $[YR^1XR^1Y]TiMe^+$  ( $X, Y = O, S, Se, Te$ ;  $R^1 = C_6H_4, C_2H_2, C_2H_4$  with and without substituents). Electron-donating ligands decrease the insertion barriers. Different electronic and steric factors have been considered.<sup>319</sup>

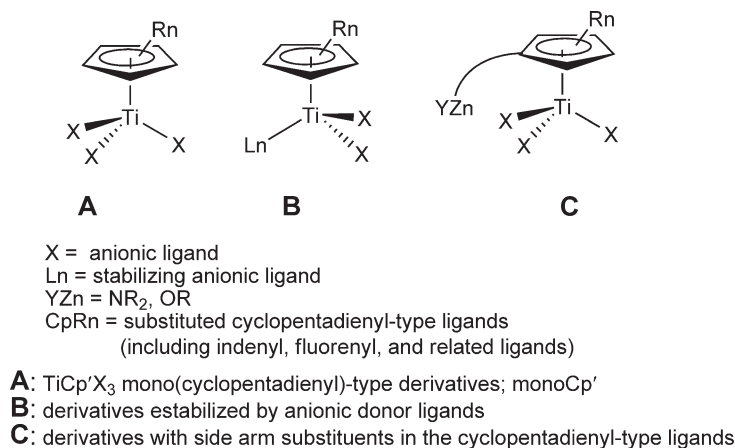
Theoretical calculations at DFT level for ethylene insertion into Ti–Me bonds of cationic alkylamidinato complexes  $[TiMe(R^1NCRNR^1)_2]^+$  ( $R = H, Ph$ ;  $R^1 = H, SiMe_3$ ) have been performed,<sup>320</sup> as have calculations for a bis( $\beta$ -diketonato)titanium model system (Scheme 137) in the presence of ethylene. Special attention is paid to the possible occurrence of agostic alkyl complexes and to the mechanism of ethylene uptake, chain propagation, and termination.<sup>321</sup>

Theoretical study by DFT calculations for the insertion process of ethylene into the titanium–carbon chain for contact ion pair systems of the type  $[L_1L_2TiCH_3(\mu-CH_3)B(C_6F_5)_3]$ , where  $L_1$  and  $L_2$  are Cp,  $NPH_3$ , and other ligands, has been performed.<sup>322</sup>

#### 4.05.3 Mono(Cyclopentadienyl) and Related Compounds

Cyclopentadienyl ( $Cp = C_5H_5$ ) continues to be among the most important ligand in organometallic chemistry because of the formation of a wide range of stable metal complexes, the steric and electronic properties of which can be easily tailored by varying the ring substituents. Mono(cyclopentadienyl) (mono-Cp) derivatives constitute an important class of titanium complexes which are specially active for polymerization of styrene. This kind of catalytic systems can be influenced in their properties by the modification of the Cp substituents in a manner similar to that observed for the metallocene-based propylene polymerization catalysts. It has been shown that Cp systems bearing annelated rings are very active catalysts which keep their productivity and syndiotacticity even at elevated temperatures. Strategies for the developments of new  $Cp'$  titanium derivatives ( $Cp'$  = substituted cyclopentadienyl ligand) as catalysts for the homogeneous olefin polymerization processes have resulted in the synthesis and exploration of a large variety of compounds. Scheme 138 shows representative examples.

The chemistry of substituted mono- and bis-Cp and indenyl trihalo and dihalo  $Ti(IV)$  complexes has been widely and elegantly reviewed. Mono-, bis-Cp, mixed Cp/indenyl and *ansa*-metallocene compounds are covered. Structural aspects affecting catalytic activity and intramolecular coordination of the functionalized ring to the central metal are



Scheme 138

discussed. The application of these complexes as catalysts for the homo- and co-polymerization, isomerization and hydrogenation of olefins, and the metathesis polymerization of cyclic monomers are considered.<sup>323</sup>

### 4.05.3.1 Mono-Cp Halide Complexes

#### 4.05.3.1.1 Synthesis

Mono-Cp compounds with halide ligands continue to be widely used as the starting materials in organometallic transition metal chemistry. The replacement of the  $C_5H_5$  group by substituted Cp ligands results in significant electronic and steric changes affecting the stability and reactivity of the halo derivatives of the group 4 metals. Cyclopentadienyl complexes bearing modifications at the Cp ring have been of great interest due to their capacity to act as coordination polymerization catalysts or catalyst precursors. Thus, a number of substituted Cp titanium derivatives have been prepared using different synthetic reactions. The synthetic methods most frequently mentioned in this work are listed and summarized below:

(i) *Salt metathesis* (Scheme 139).  $LiCp'$  and  $TiCl_4$  often lead to mixtures of the bis(cyclopentadienyl) (bis-Cp') dichloro titanium and the mono-Cp trichloro titanium compounds. In some instances, these reactions can nevertheless be used successfully for the synthesis of ring-substituted mono-Cp' titanium trichlorides.

(ii) *Dehalometallation*. Electrophilic substitution of silylated cyclopentadienes is a well-known and clean preparative method for mono-Cp' complexes of group 4 metals. Silyl cyclopentadienes have been used as mild transfer reagents to synthesize mono-Cp' titanium derivatives following the general dehalodesilylation reaction shown in Scheme 140. Similar reactions using Cp-substituted tin compounds are also well established for this class of derivatives.

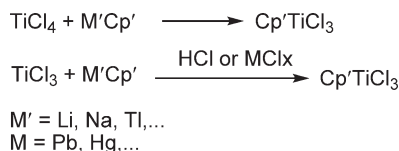
(iii) *Replacement of chloride by reaction with cyclopentadiene* (Scheme 141).

(iv) *Protonolysis of metal amides with cyclopentadiene derivatives* (Scheme 142).

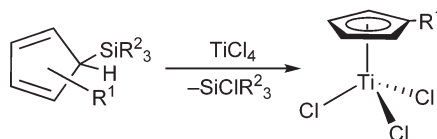
(v) *Ligand redistribution* (Scheme 143).

(vi) *Replacement of alkoxo ligands* An alternative route to ring-substituted Cp' titanium complexes is based on the reaction of Ti-alkoxo derivatives with suitable chlorinating agents ( $HCl$ ,  $CH_3C(O)Cl$ , ...).

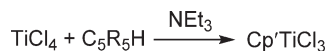
(vii) *Interchange of halide ligands* Replacement of halide ligands is exemplified by the use of  $Me_3SnF$  as a fluorinating agent.



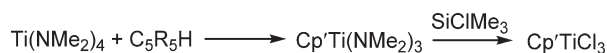
Scheme 139



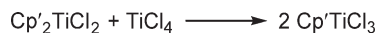
Scheme 140



Scheme 141



Scheme 142



Scheme 143

The following review is organized according to the nature of the Cp substituents.

#### 4.05.3.1.1.(i) Complexes with alkyl- and alkenyl-substituted Cp ligands

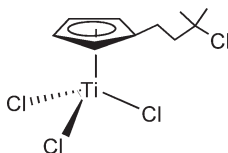
$(\text{C}_5\text{H}_4\text{CH}_2\text{CH}_2\text{CMe}_2\text{Cl})\text{TiCl}_3$  (Scheme 144) has been prepared by reaction of  $\text{TiCl}_4$  with  $\text{Me}_3\text{SiC}_5\text{H}_4\text{CH}_2\text{CH}_2\text{CMe}_2\text{Cl}$  with elimination of  $\text{SiClMe}_3$ .<sup>324</sup>

The trityl Cp compound  $(\text{C}_5\text{H}_4\text{CPh}_3)\text{TiCl}_3$  is obtained by different synthetic methods, that is, reaction of  $\text{TiCl}_4$  with  $\text{Me}_3\text{Si}(\text{C}_5\text{H}_4\text{CPh}_3)$ ,  $\text{Me}_3\text{Sn}(\text{C}_5\text{H}_4\text{CPh}_3)$ , or  $\text{Na}[\text{C}_5\text{H}_4\text{CPh}_3]$ . The molecular structure has been determined by X-ray diffraction. There is a Cl–Ph agostic interaction in the structure. The compound reacts with  $\text{Me}_3\text{SnCp}$  to give the mixed bis-Cp complex  $\text{Cp}(\text{C}_5\text{H}_4\text{CPh}_3)\text{TiCl}_2$  in poor yield.<sup>325</sup>  $\text{TiCl}_4$  reacts with  $\text{Me}_3\text{SiC}_5\text{H}_4\text{CMe}_2\text{C}_{13}\text{H}_9$  to give  $[\text{C}_5\text{H}_4(\text{CMe}_2)\text{C}_{13}\text{H}_9]\text{TiCl}_3$  (Scheme 145), which is readily hydrolyzed in wet acetone to give  $\{[\text{C}_5\text{H}_4(\text{CMe}_2)\text{C}_{13}\text{H}_9]\text{TiCl}_2\}_2(\mu\text{-O})$  (Scheme 329, Section 4.05.3.5.1).<sup>326</sup>

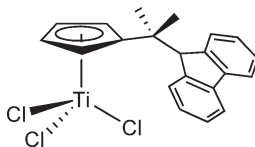
Mono-Cp titanium complexes  $(\text{C}_5\text{H}_4\text{R})\text{TiCl}_3$  (Scheme 146) with pendant phenyl substituents in the Cp ring have been synthesized.<sup>327,328</sup> The benzyl–Cp complex  $(\text{C}_5\text{H}_4\text{CH}_2\text{Ph})\text{TiCl}_3$  has been synthesized by reaction of  $\text{BrCH}_2\text{Ph}$ ,  $\text{LiCp}$ , and  $\text{TiCl}_4$ . In combination with MAO it has been used as a catalytic system for the syndiospecific polymerization of styrene.<sup>329</sup> The reaction of  $\text{Me}_3\text{SiC}_5\text{H}_4\text{C}_6\text{F}_5$  with  $\text{TiCl}_4$  affords  $(\text{C}_5\text{H}_4\text{C}_6\text{F}_5)\text{TiCl}_3$  and its ability to polymerize styrene in the presence of MAO as co-catalyst has been studied in order to measure the effect of the presence of an electron-withdrawing pentafluorophenyl substituent in the Cp rings on the polymerization activity.<sup>330</sup>

The complexes  $(\text{C}_5\text{H}_4\text{CMe}_2\text{R})\text{TiCl}_3$  ( $\text{R} = \text{Ph}$ , 1,3-dimethylphenyl, Me), in the presence of MAO, are effective catalysts for the polymerization of ethylene and they are transformed in catalysts for the ethylene trimerization, producing 1-hexene, depending on the substituent R nature. The hemilabile behavior of the pendant Cp substituent seems to be the responsible for this catalytic performance.<sup>331</sup> A mono-Cp trichloro complex containing a phenylethyl–Cp ligand has also been prepared (Scheme 160; Section 4.05.3.1.1 (iii)).<sup>332</sup>

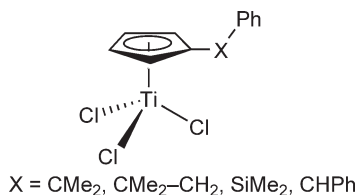
The synthesis of a range of mono-Cp'–arene trichloro titanium complexes (Scheme 147) has been described. An evaluation of the effect of variations on the pendant arene group, the bridge between the Cp and the arene group and



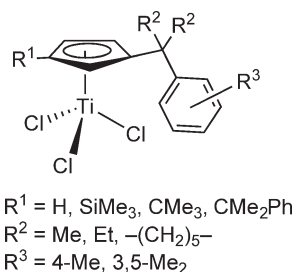
Scheme 144



Scheme 145



Scheme 146



Scheme 147

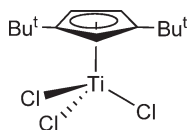
the substituents on the Cp ring on the performance in the ethylene trimerization reaction was studied. It is shown that ligand variations can have a substantial effect on the activity and selectivity of this process. A catalytic cycle for the ethylene trimerization reaction is proposed.<sup>333</sup> Analogous substituted Cp and indenyltitanium trichloro complexes bearing a phenyl or substituted phenyl group bonded to the Cp-type ligand through an isopropylidene bridge have been synthesized and utilized in the polymerization of propene and styrene.<sup>334</sup> The chemistry of mono-Cp titanium complexes with pendant arene groups on the cyclopentadienyl ligand has been reviewed, with an emphasis on cationic titanium dialkyl derivatives and their performance in catalytic olefin conversion.<sup>335</sup>

Reaction of  $1,3\text{-Bu}^t_2\text{-C}_5\text{H}_3\text{SiMe}_3$  with  $\text{TiCl}_4$  in toluene or hexane at room temperature affords the titanium derivative  $(1,3\text{-Bu}^t_2\text{-C}_5\text{H}_3)\text{TiCl}_3$  (Scheme 148).<sup>336,337</sup>

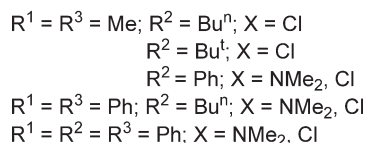
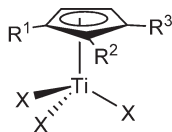
A series of mono-Cp' trichloro titanium complexes (Scheme 149) with 1,2,3-trialkyl-substituted Cp ligands have been synthesized by reaction of the trimethylsilylcyclopentadiene with  $\text{TiCl}_4$  or by treatment of the cyclopentadiene with  $\text{Ti}(\text{NMe}_2)_4$  followed by reaction with  $\text{SiClMe}_3$ . The molecular structure of  $(\text{C}_5\text{H}_2\text{Me}_2\text{Ph})\text{TiCl}_3$  has been determined by X-ray diffraction. The complexes have been tested, in the presence of MAO, as catalysts for the polymerization of styrene.<sup>338</sup>  $(\text{C}_5\text{H}_2\text{Bu}^t_3)\text{TiCl}_3$  is prepared from the lithium salt of the easily available 1,3,5-tri-*tert*-butylcyclopentadiene.<sup>339</sup>

$\text{TiCl}_4$  reacts with  $\text{Me}_2\text{Si}(\text{CH}_2\text{CH}=\text{CHCH}=\text{CH}_2)(\text{C}_5\text{Me}_4\text{H})$  to afford the tetramethyl-Cp complex  $(\text{C}_5\text{Me}_4\text{H})\text{TiCl}_3$ , the molecular structure of which has been determined by X-ray diffraction.<sup>340</sup>

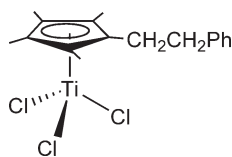
Pentaalkyl Cp-substituted derivatives have also been described.  $(\text{C}_5\text{Me}_4\text{Ph})\text{TiCl}_3$  has been prepared by the reaction of the trimethylsilylcyclopentadiene  $\text{Me}_3\text{Si}(\text{C}_5\text{Me}_4\text{Ph})$  with  $\text{TiCl}_4$ . It can be handled in the air in solid state but it is less stable in solution where different oxochloro complexes are formed.<sup>341</sup> The reaction of  $\text{Me}_3\text{Si}(\text{C}_5\text{Me}_4\text{CH}_2\text{CH}_2\text{Ph})$  with  $\text{TiCl}_4$  has been used to synthesize the trichloro complex  $(\text{C}_5\text{Me}_4\text{CH}_2\text{CH}_2\text{Ph})\text{TiCl}_3$  (Scheme 150), which is further



Scheme 148



Scheme 149



Scheme 150

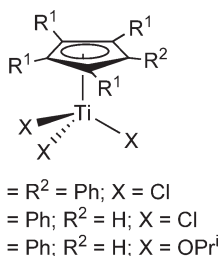
converted into the trimethyl derivative  $(C_5Me_4CH_2CH_2Ph)TiMe_3$ . The latter hydrolyzes readily to  $[(C_5Me_4CH_2CH_2Ph)TiMe_2]_2(\mu-O)$  upon recrystallization in wet pentane. The molecular structure of the trichloro complex was confirmed by X-ray diffraction. Activated with MAO, these compounds catalyze the polymerization of styrene.<sup>342</sup>

$(C_5Ph_5)Ti(OPr^i)_3$  reacts with HCl in toluene at reflux with replacement of the alkoxo ligands to generate the trichloro complex  $(C_5Ph_5)TiCl_3$ . However, the same reaction from  $(C_5HPh_4)Ti(OPr^i)_3$  in pentane resulted only in the cleavage of two isopropoxo ligands to give the dichloro derivative  $(C_5HPh_4)TiCl_2(OPr^i)$  from which the trichloro compound can be obtained by complete chlorination using thionyl chloride (Scheme 151).<sup>343</sup>

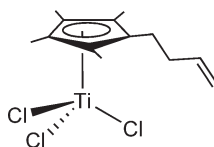
The preparation of  $(C_5Me_5)TiCl_3$ , its reaction with various nucleophiles, the reduction with sodium, magnesium, and calcium to yield new organometallic clusters containing molecular solids and the use as catalysts in the polymerization of olefins are reported.<sup>344</sup>

A variety of functional groups have been used as side-chain modifications to the Cp ring, including  $\omega$ -alkenyl substituents.  $(C_5H_4CH_2CH=CH_2)TiCl_3$ ,  $(C_5H_4CH_2CH_2CH=CH_2)TiCl_3$ ,  $(C_5H_4CH_2CH_2CH_3)TiCl_3$ , and  $(C_5H_4CH_2CH_2CH_2CH_3)TiCl_3$  have been synthesized and characterized. The influence of the alkyl and alkenyl substituent groups on the catalyst activities in the syndiotactic polymerization of styrene has been investigated.<sup>345</sup>  $(C_5Me_4CH_2CH_2CH=CH_2)TiCl_3$  (Scheme 152) and  $(C_5Me_4CH_2CH_2CH=CH_2)TiCl(NBu^i)(4-NC_5H_4Bu^i)$  have been prepared by treatment of  $Li(C_5Me_4CH_2CH_2CH=CH_2)$  with  $TiCl_3(THF)_3$  followed by HCl or  $TiCl_2(NBu^i)(4-NC_5H_4Bu^i)_2$ , respectively.<sup>346</sup>  $TiCl_4$  reacts with  $Me_3Si(C_5Me_4CH_2CH_2CH=CH_2)$  to give the mono-Cp'  $(C_5Me_4CH_2CH_2CH=CH_2)TiCl_3$  which was used to synthesize the mixed bis-Cp' compound  $Cp(C_5Me_4CH_2CH_2CH=CH_2)TiCl_2$ .<sup>347</sup> The complexes  $(C_5Me_4R)TiCl_3$  [ $R = CH(Me)CH=CH_2$ ,  $(CH_2)_2CH=CH_2$ ,  $(CH_2)_3CH=CH_2$ ] have been synthesized, in which the pendant double bonds do not exhibit any interaction with the titanium atom. These complexes are active for the syndiotactic polymerization of styrene in the presence of MAO.<sup>348</sup>

Different ways to carry out conversions of functional groups attached at the Cp rings coordinated at the sensitive group 4 metal derivatives leading to organometallic systems otherwise intact have been reviewed.<sup>349</sup>  $(C_5H_4-allyl)TiCl_3$  is prepared by reaction of  $TiCl_4$  with  $Me_3Si(C_5H_4-allyl)$ . Treatment of the trichloro compound with the metathesis catalyst  $Cl_2(PCy_3)_2Ru=CHPh$  (3 mol%) affords the dititanium compound  $Cl_3Ti(C_5H_4-CH_2CH=CHCH_2-C_5H_4)TiCl_3$  as a mixture of *cis*- and *trans*-isomers (Scheme 153). Similarly, treatment with a

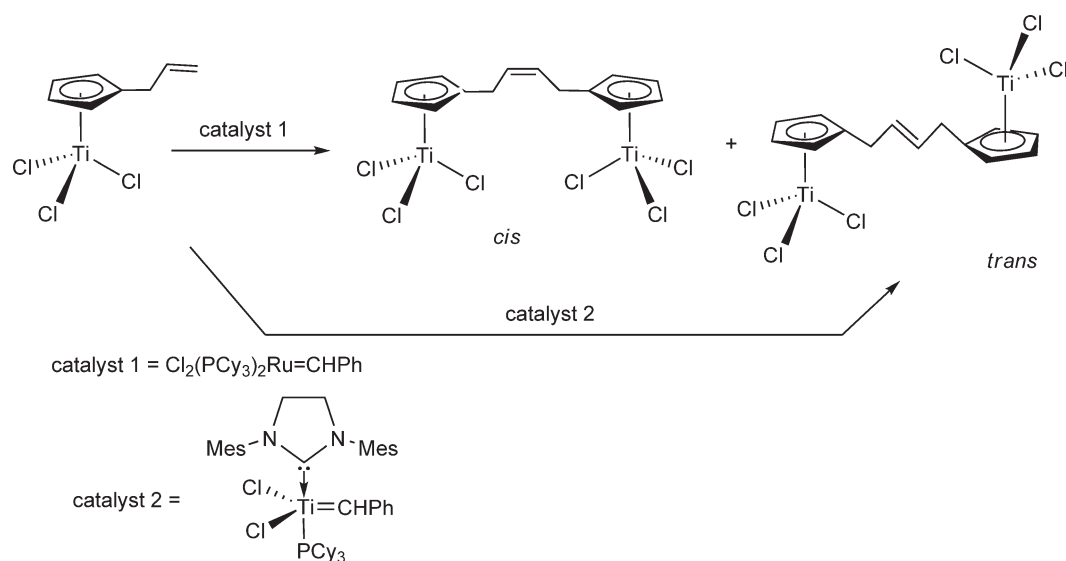


Scheme 151



Scheme 152

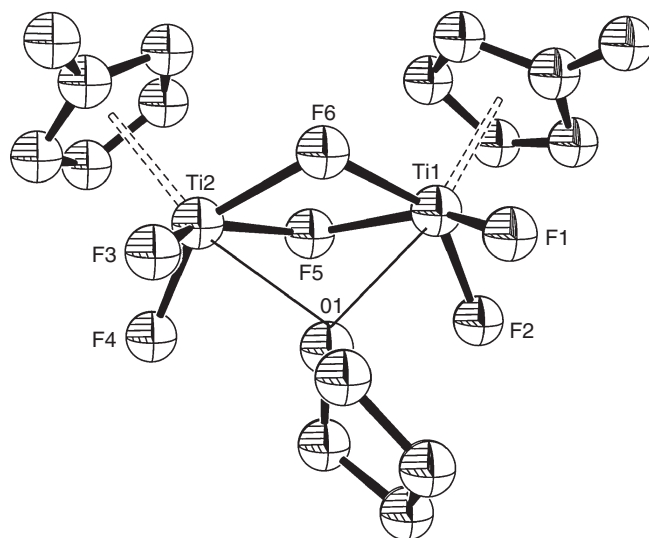




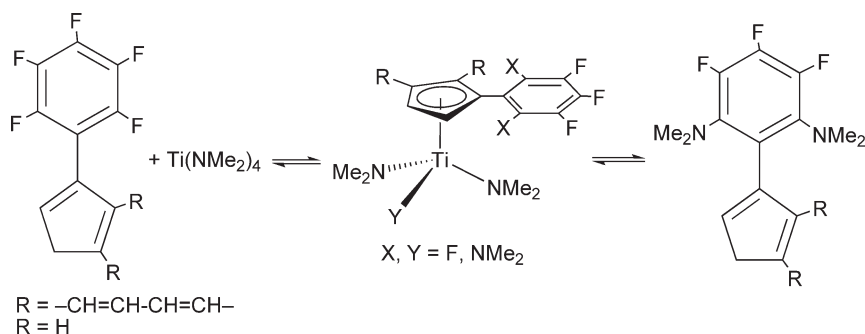
Scheme 153

“second-generation” metathesis catalyst gives the pure *trans*-isomer. Both Ti complexes have been spectroscopically characterized and the molecular structure of the *trans*-isomer has been determined by X-ray diffraction.<sup>350</sup>

Replacement of halide also is a well-developed method for the synthesis of mono-Cp' fluorides. Me<sub>3</sub>SnF is used as a fluorinating agent in the reaction with TiCl<sub>3</sub>Cp' to give the trifluoro complexes Cp'TiF<sub>3</sub> (Cp' = Cp, Cp\*, C<sub>5</sub>Me<sub>4</sub>Et, C<sub>5</sub>H<sub>4</sub>Me) in good yields. Treatment of [Cp\*TiClO]<sub>3</sub> with Me<sub>3</sub>SnF leads to ring expansion to form the eight-membered cyclic compound [Cp\*TiFO]<sub>4</sub>. The structure of (C<sub>5</sub>H<sub>4</sub>Me)TiF<sub>3</sub> consists of a dimer with two fluoride bridges and one THF molecule coordinated through the oxygen to both Ti atoms (Figure 6).<sup>351</sup> The synthesis of the trifluoro complex (C<sub>5</sub>Me<sub>4</sub>Pr<sup>n</sup>)TiF<sub>3</sub> has been described by metathesis reaction of the corresponding trichloro compound with 3 equiv. of Me<sub>3</sub>SnF and its molecular structure determined by X-ray diffraction. Different behavior is observed in this reaction with the analogous zirconium and hafnium derivatives.<sup>352,353</sup> Indenyl complexes have been similarly synthesized and used as catalyst precursors for the syndiospecific polymerization of styrene.<sup>354</sup> The trifluoro complexes Cp'TiF<sub>3</sub> (Cp' = Cp\*, C<sub>5</sub>Me<sub>4</sub>Et) are also obtained by reaction of the corresponding Cp'TiCl<sub>3</sub> with AsF<sub>3</sub>. The reactions of Cp\*TiF<sub>3</sub> with lithium 1,3-diketonate or lithium benzamidinate are studied to give hexacoordinate or



**Figure 6** Molecular structure of complex [(C<sub>5</sub>H<sub>4</sub>Me)TiF<sub>3</sub>]<sub>2</sub>·THF (reproduced by permission of American Chemical Society from *Organometallics*, 1994, 13, 1251).



Scheme 154

pentacoordinate derivatives. The treatment of  $\text{Cp}^*\text{TiF}_3$  with  $\text{Ph}_3\text{PNSiMe}_3$  or  $\text{C}_2\text{H}_2(\text{Ph}_2\text{PNSiMe}_3)_2$  affords  $\text{Cp}^*\text{TiF}_2(\text{Ph}_3\text{PN})$  and  $\text{Cp}^*\text{TiF}_2[\text{C}_2\text{H}_2(\text{Ph}_2\text{PN})_2]$ , respectively. The molecular structures of these compounds have been determined by X-ray diffraction.<sup>355</sup>

The difluoro methoxo compounds  $\text{Cp}'\text{TiF}_2(\text{OMe})$  ( $\text{Cp}' = \text{C}_5\text{H}_4\text{R}$ ;  $\text{R} = \text{H}, \text{Me}, \text{Pr}^i, \text{SiMe}_3, \text{allyl}, \text{CH}_2\text{Ph}$ ) can be obtained by the reaction of the corresponding trimethoxo complexes with the fluorinating agent  $\text{BF}_3 \cdot \text{OMe}_2$ . In the presence of MAO, these compounds were studied as catalysts for the polymerization of styrene.<sup>356</sup>

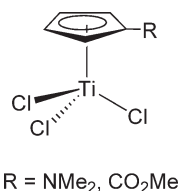
$\text{Ti}(\text{NMe}_2)_4$  reacts with 3-(pentafluorophenyl)indene and pentafluorophenylcyclopentadiene via intramolecular nucleophilic substitution of the *ortho*-C-F groups by  $\text{Ti}-\text{NMe}_2$  fragments to afford aminated arylindenes and arylcyclopentadienes. NMR-scale experiments demonstrate the formation of intermediate fluoro- mono-Cp and monoindenyltitanium complexes (Scheme 154).<sup>357</sup>

#### 4.05.3.1.1.(ii) Complexes with oxygen-based Cp substituents

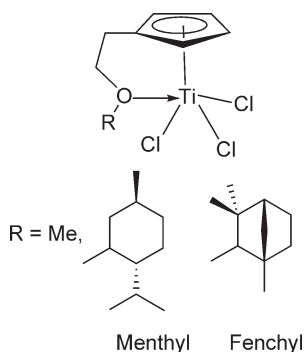
$(\text{C}_5\text{H}_4\text{OSiMe}_2\text{Bu}^t)\text{TiCl}_3$  is prepared by the reaction of  $\text{C}_5\text{H}_4(\text{SiMe}_3)(\text{OSiMe}_2\text{Bu}^t)$  with  $\text{TiCl}_4$ .<sup>358</sup>

The reaction between carbomethoxytrimethylsilylcyclopentadiene and  $\text{TiCl}_4$  in pentane solution affords the mono-Cp complex  $(\text{C}_5\text{H}_4\text{CO}_2\text{Me})\text{TiCl}_3$  (Scheme 155).<sup>343</sup>

Recent years have seen a growing interest in the study of mono-Cp' titanium complexes bearing a neutral pendant substituent with a terminal donor group. Complexes with  $\eta^5:\eta^1$ -ancillary ligands consisting of a Cp' ring covalently linked to an anionic amido or alkoxo moiety are known. The introduction of chelating side chains on the Cp ring bearing neutral O- or N-functionalities has been one strategy to control the high reactivity exhibited by mono-Cp titanium derivatives. This kind of complexes are easily prepared by dehalodesilylation. Intramolecular coordination of the side chain should reduce the Lewis acidity of the metal center and enhance its stability.<sup>362</sup> The compounds  $(\text{C}_5\text{H}_4\text{CH}_2\text{CH}_2\text{OR})\text{TiCl}_3$  ( $\text{R} = \text{Me}, \text{menthyl}, \text{fenchyl}$ ) (Scheme 156) have been synthesized from the reaction of  $\text{Me}_3\text{Si}[\text{C}_5\text{H}_4(\text{CH}_2\text{CH}_2\text{OR})]$  with  $\text{TiCl}_4$  in  $\text{CH}_2\text{Cl}_2$ . The intramolecular coordination of the ether moiety in these compounds is reversible. NMR data for the methyl complex in  $\text{CD}_2\text{Cl}_2$  at room temperature suggest an equilibrium with about 30% of a conformation in which the ether handle is coordinated. For the menthyl and fenchyl derivatives there seems to be no coordination.<sup>363</sup> The similar trichloro alkoxo-alkyl-Cp substituted titanium complexes,  $[\text{C}_5\text{H}_4\text{CH}(\text{Me})\text{CH}_2\text{OMe}]\text{TiCl}_3$ ,  $[\text{C}_5\text{H}_4\text{CH}_2\text{CH}(\text{Me})\text{OMe}]\text{TiCl}_3$ , and  $(\text{C}_5\text{H}_4\text{CH}_2\text{CH}_2\text{CH}_2\text{OMe})\text{TiCl}_3$  have been synthesized. The crystal structure of  $(\text{C}_5\text{H}_4\text{CH}_2\text{CH}_2\text{CH}_2\text{OMe})\text{TiCl}_3$  shows that there is an intramolecular coordination between the ether-oxygen atom and titanium, with an average Ti-O bond length of 2.24 Å. Due to steric limitation around the coordination sphere of titanium, the oxygen atoms in the side chains of the other complexes do not coordinate with the central metal.<sup>364</sup> The analogous tetramethyl-Cp complex  $[\text{C}_5\text{Me}_4\text{CH}_2\text{CH}_2\text{OMe}]\text{TiCl}_3$  has



Scheme 155



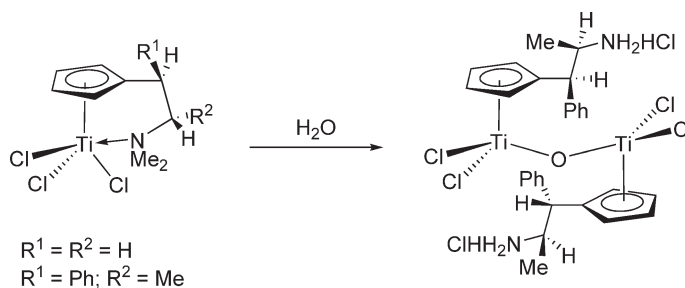
Scheme 156

been described and its molecular structure determined by X-ray diffraction methods. The dynamic behavior in solution has been studied by variable-temperature NMR spectroscopy.<sup>365</sup>  $(C_5H_4CH_2CH_2OMe)TiCl_3$  reacts with  $BBr_3$  to give a compound containing a bromoethyl substituent,  $(C_5H_4CH_2CH_2Br)TiBr_3$ . Hydrolysis of this complex in the presence of  $NBu^t_3$  affords the cyclic  $[(C_5H_4CH_2CH_2Br)TiBr(\mu-O)]_4$ , the molecular structure of which has been determined by X-ray diffraction.<sup>366</sup>

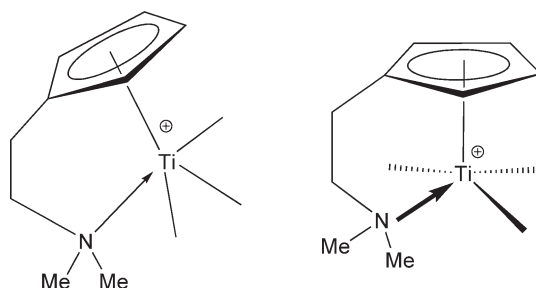
#### 4.05.3.1.1.(iii) Complexes with nitrogen-based Cp substituents

The addition of  $Li(C_5H_4NMe_2)$  to a pentane solution of  $TiCl_4$  produces the amino-Cp substituted compound  $(C_5H_4NMe_2)TiCl_3$  (Scheme 155).<sup>343</sup>

The introduction of aminoethyl side chains into the Cp ring in titanium derivatives leads to interesting changes in structure and reactivity in comparison to the non-substituted Cp complexes. Aminoethyl-functionalized mono-Cp' titanium complexes have been reviewed.<sup>367</sup>  $(C_5H_4CHR^1CHR^2NMe_2)TiCl_3$  ( $R^1 = R^2 = H$ ;  $R^1 = Ph$ ,  $R^2 = Me$ ) have been prepared by treatment of  $TiCl_4$  with the corresponding silylcyclopentadiene by dehalosilylation. These compounds are extremely air sensitive, even more so than the unsubstituted  $TiCl_3Cp$ , and they are readily hydrolyzed to oxo derivatives  $[(C_5H_4CHR^1CHR^2NMe_2 \cdot HCl)TiCl_2]_2(\mu-O)$  (Scheme 157). The spectroscopic data for the trichloro compounds indicate intramolecular and fluxional coordination of the amine side arm.<sup>368,369</sup> By contrast, in  $(C_5H_4CH_2CH_2NMe_2)Ti(NMe_2)_3$ , obtained by reaction of  $Ti(NMe_2)_4$  with  $C_5H_5CH_2CH_2NMe_2$  in toluene, the pendant amino group is not coordinated to the metal.<sup>370,371</sup> The similarly substituted compound  $(C_5Me_4CH_2CH_2NMe_2)TiCl_3$  has also been reported. The catalytic activities and selectivities for styrene, ethylene, and propylene polymerization have been compared with the reference compounds  $CpTiCl_3$  and  $Cp^*TiCl_3$ . This kind of complexes exhibit relatively low activity as a styrene polymerization catalyst but are remarkably active for both ethylene and propylene polymerizations. It is proposed that the active species has a pseudo-titanocene structure (Scheme 158) by the coordination of the nitrogen, which makes it active for ethylene polymerization but unfavorable for styrene polymerization because the strongly coordinated  $NMe_2$  fragment destabilizes the multi-hapto complexation of styrene.<sup>372</sup> The complex  $(C_5H_4CH_2CH_2NMe_2)TiCl_3$  activated with MAO catalyzes the polymerizations of ethylene, propylene, ethylidene norbornene, vinylcyclohexene, and 1,4-hexadiene. The dependence of homopolymerization activity on olefin concentration and comparison with analogous zirconium systems have been studied.<sup>373</sup>



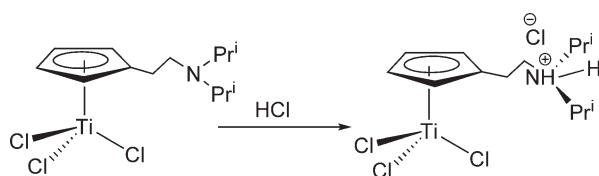
Scheme 157



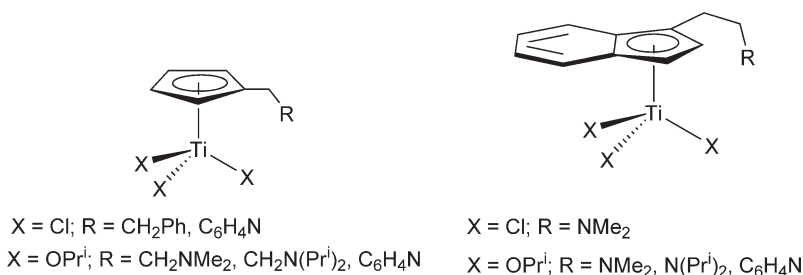
Scheme 158

The synthesis of titanium complexes with the donor-functionalized 2-(N,N-diisopropylaminoethyl)Cp ligand has been described. The reaction of  $\text{TiCl}_4$  with  $\text{Li}(\text{C}_5\text{H}_4\text{CH}_2\text{CH}_2\text{NPr}_2)$  gives  $(\text{C}_5\text{H}_4\text{CH}_2\text{CH}_2\text{NPr}_2)\text{TiCl}_3$  as a highly moisture sensitive substance which easily forms a coordination polymer. This complex reacts with 1 equiv. of HCl under protonation of the amino group to give the monomeric hydrochloride  $[(\text{C}_5\text{H}_4\text{CH}_2\text{CH}_2\text{N}^+\text{HPr}_2)\text{TiCl}_3]\text{Cl}$  (Scheme 159), which shows excellent solubility in polar solvents.<sup>374</sup> A series of aminoalkyl-substituted mono-Cp trichloro, triisopropoxo, and mono(indenyl) triisopropoxo titanium complexes that contain pyridyl (2-picoly), diisopropylaminoethyl, dimethylaminoethyl, and phenylethyl pendant ligands have been prepared (Scheme 160). The utility of these complexes for the polymerization of ethylene, propylene, and styrene has been investigated.<sup>332</sup>

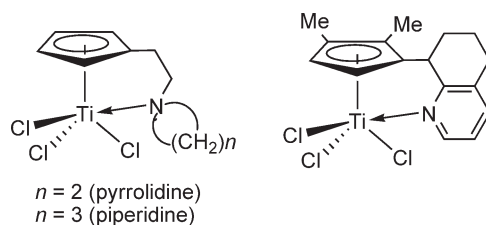
The titanium(IV) mono-Cp complex with linked pyrrolidine(N) and piperidine(N) functions as pendant substituents with an intramolecular nitrogen donor (Scheme 161) have been prepared by reaction of the silylated cyclopentadiene



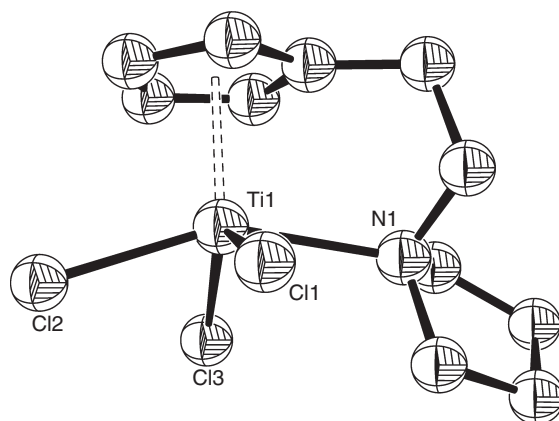
Scheme 159



Scheme 160



Scheme 161



**Figure 7** Molecular structure of complex  $[\text{C}_5\text{H}_4\text{CH}_2\text{CH}_2\text{N}(\text{CH}_2)_4]\text{TiCl}_3$  (reproduced by permission of Elsevier from *J. Organomet. Chem.*, **1995**, 486, 291).

ligand precursor with  $\text{TiCl}_4$ . The structure of the pyrrolidine derivative was established by X-ray diffraction (Figure 7).<sup>375</sup> The 8-quinolylcyclopentadienyl titanium derivative with a chelating side chain has been reported.<sup>376</sup> The synthesis of the chiral trichloro titanium complex shown in Scheme 161 has been described; its molecular structure determined by X-ray crystallography confirms the coordination of the quinolyl nitrogen atom to the titanium center.<sup>377</sup>

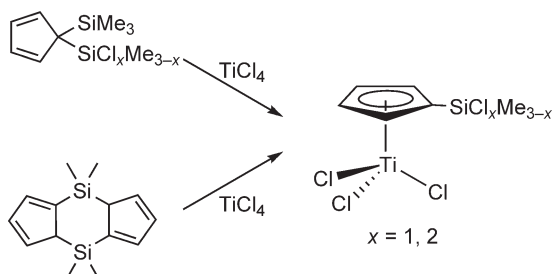
#### 4.05.3.1.1.(iv) Silanyl-Cp and stannyl-Cp substituents

The synthesis and reactivity of transition metal complexes, including titanium derivatives with functionalized silyl-substituted Cp and related ligands, have been reviewed.<sup>378</sup>

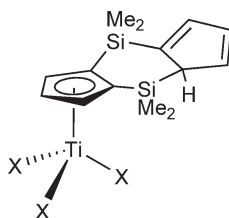
Reactions of  $(\text{SiMe}_3)(\text{SiClMe}_2)\text{C}_5\text{H}_4$  or  $(\text{SiMe}_2\text{C}_5\text{H}_4)_2$  with  $\text{TiCl}_4$  lead to the chlorodimethyl-Cp complex  $[\text{C}_5\text{H}_4(\text{SiClMe}_2)]\text{TiCl}_3$  (Scheme 162) with selective elimination of  $\text{SiClMe}_3$ .<sup>379,380</sup> In a similar reaction, the analogous tetramethyl-Cp derivative  $[\text{C}_5\text{Me}_4(\text{SiClMe}_2)]\text{TiCl}_3$  has been obtained.<sup>381</sup> Similarly, the chlorosilyl-Cp complexes  $(\text{C}_5\text{Me}_4\text{SiXClMe})\text{TiCl}_3$  ( $\text{X} = \text{H}, \text{Cl}$ ) are prepared by reaction of  $\text{TiCl}_4$  with the trimethylsilyl derivatives of the corresponding cyclopentadienes with selective elimination of  $\text{SiClMe}_3$  (Scheme 162). Formation of small amounts of the unsubstituted  $(\text{C}_5\text{Me}_4\text{H})\text{TiCl}_3$  is observed in all these reactions. The mechanism for the formation of this byproduct has been studied. The molecular structure of  $(\text{C}_5\text{Me}_4\text{SiHClMe})\text{TiCl}_3$  has been determined by X-ray diffraction methods.<sup>382,383</sup> These compounds possess two types of metal-halogen bonds, Ti-Cl and Si-Cl, which show different reactivities toward nucleophiles to afford oxo, alkyl, and amido derivatives which react further to give complexes with Ti-C, Ti-N, and Ti-O bonds (see Section 4.05.3.1.3.(i)).

The Cp titanium fluorides  $[1,3\text{-C}_5\text{H}_3(\text{SiMe}_3)\text{R}]\text{TiF}_3$  ( $\text{R} = \text{H}, \text{Me}, \text{SiMe}_3$ ) have been prepared by the reaction of the corresponding chloro titanium compounds with  $\text{SnMe}_3\text{F}$  as fluorinating agent. The reactions are strongly solvent dependent.<sup>384</sup>

The mono-Cp' titanium complex  $[\text{C}_5\text{H}_3(\text{SiMe}_2)_2\text{C}_5\text{H}_4]\text{TiCl}_3$  (Scheme 163) containing the doubly bridged bis(dimethylsilanodiy)l-cyclopentadiene-(cyclopentadienyl) ligand has been prepared in high yields by the reaction of the monolithium salt  $\text{Li}[\text{C}_5\text{H}_3(\text{SiMe}_2)_2\text{C}_5\text{H}_4]$  with  $\text{TiCl}_4$ . The catalytic activity of this compound for ethylene polymerization has been studied using MAO as co-catalyst.<sup>385</sup>

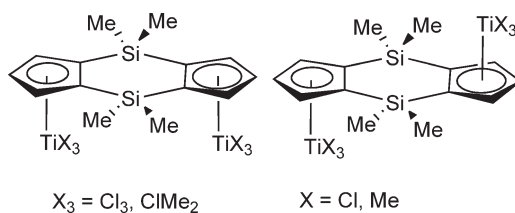


**Scheme 162**

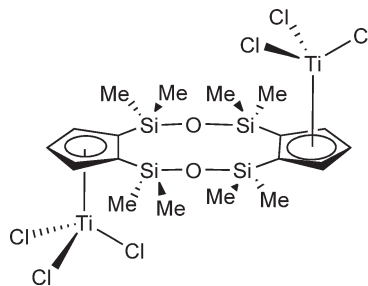


Scheme 163

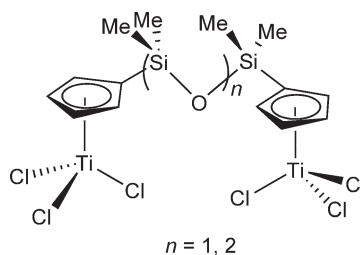
The reaction of  $\text{TiCl}_4$  with  $\text{Li}_2[(\text{C}_5\text{H}_3)_2(\text{SiMe}_2)_2]$  in toluene at room temperature affords a mixture of *cis*- and *trans*- $[(\text{C}_5\text{H}_3)_2(\text{SiMe}_2)_2](\text{TiCl}_3)_2$  in a molar ratio of 1 : 2 after recrystallization (Scheme 164).<sup>386</sup> The molecular structures of the binuclear complexes  $(\text{C}_5\text{H}_4\text{-XMe}_2\text{-C}_5\text{H}_4)(\text{TiCl}_3)_2$  ( $\text{X} = \text{C}, \text{Si}$ ) have been determined by X-ray diffraction.<sup>387</sup>  $\text{TiCl}_4$  reacts with 2 equiv. of doubly disiloxane-bridged distannylated bis(cyclopentadiene)  $(\text{C}_5\text{H}_3\text{SnMe}_3)_2(\mu, \mu\text{-}(\text{Me}_2\text{SiOSiMe}_2)_2)$  to give the doubly bridged binuclear trichloro titanium complex  $[(\text{C}_5\text{H}_3)_2(\mu\text{-Me}_2\text{SiOSiMe}_2)_2](\text{TiCl}_3)_2$  (Scheme 165).<sup>388</sup> Analogous polysiloxane-bridged binuclear complexes have been synthesized by the reaction of the corresponding thallium salts with  $\text{TiCl}_4$  (Scheme 166).<sup>389</sup>



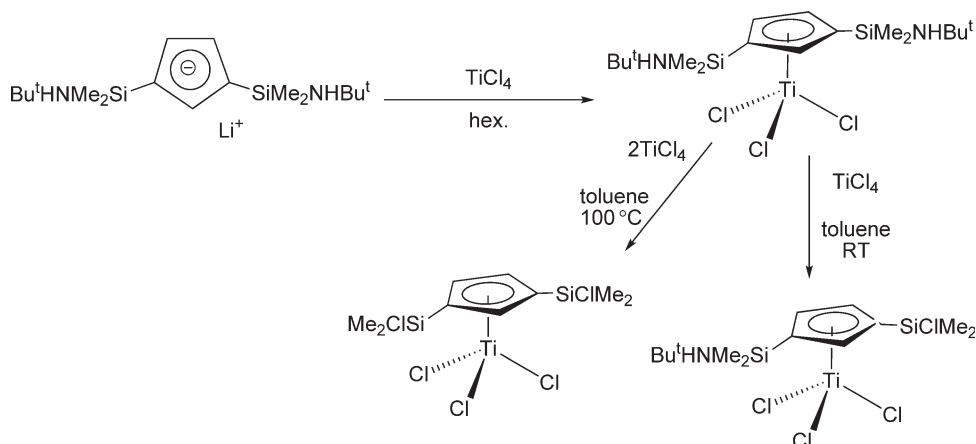
Scheme 164



Scheme 165



Scheme 166



Scheme 167

The monolithium salt  $\text{Li}[\text{1,3-C}_5\text{H}_3(\text{SiMe}_2\text{NHBu}^t)_2]$  reacts with  $\text{TiCl}_4$  in hexane in a straightforward manner to give the bis(dimethylsilylamino) mono-Cp compound  $[\text{1,3-C}_5\text{H}_3(\text{SiMe}_2\text{NHBu}^t)_2]\text{TiCl}_3$ , the molecular structure of which has been determined by X-ray diffraction. This compound reacts with  $\text{TiCl}_4$  to produce partial conversion of one or both  $\text{Si-NHBu}^t$  functions into  $\text{Si-Cl}$  groups. Quantitative transformation is observed when the treatment is carried out with 2 equiv. of  $\text{TiCl}_4$  in toluene at  $100^\circ\text{C}$ , to afford  $[\text{1,3-C}_5\text{H}_3(\text{SiClMe}_2)_2]\text{TiCl}_3$  (Scheme 167). By contrast, the deamination in the presence of  $\text{NEt}_3$  or under thermal conditions affords *ansa*-derivatives.<sup>390</sup>

Reaction of  $1,1\text{-C}_5\text{H}_4(\text{SiMe}_2\text{CH}_2\text{CH}=\text{CH}_2)_2$  with  $\text{TiCl}_4$  affords the allylsilyl-Cp complex  $(\text{C}_5\text{H}_4\text{SiMe}_2\text{CH}_2\text{CH}=\text{CH}_2)\text{TiCl}_3$ .<sup>391</sup>

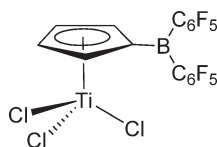
$(\text{C}_5\text{H}_4\text{SiMe}_2\text{CH}_2\text{CH}_2\text{C}_8\text{F}_{17})\text{TiCl}_3$  is prepared by the reaction of the cyclopentadiene precursor  $\text{Me}_3\text{Sn}[\text{C}_5\text{H}_4(\text{SiMe}_2\text{CH}_2\text{CH}_2\text{C}_8\text{F}_{17})]$  with  $\text{TiCl}_4$  with the exclusive removal of  $\text{SnMe}_4$ . Nevertheless, in the reaction of  $\text{Me}_3\text{Si}[(\text{C}_5\text{H}_4)(\text{SiMe}_2\text{CH}_2\text{CH}_2\text{C}_8\text{F}_{17})]$  with  $\text{TiCl}_4$  a mixture of  $(\text{C}_5\text{H}_4\text{SiMe}_2\text{CH}_2\text{CH}_2\text{C}_8\text{F}_{17})\text{TiCl}_3$  and  $(\text{C}_5\text{H}_4\text{SiMe}_3)\text{TiCl}_3$  is obtained.<sup>392</sup>

The compound  $(\text{C}_5\text{H}_4\text{SnMe}_3)\text{TiCl}_3$  with a Cp ligand bearing a stannyl moiety has been structurally characterized.<sup>393</sup>

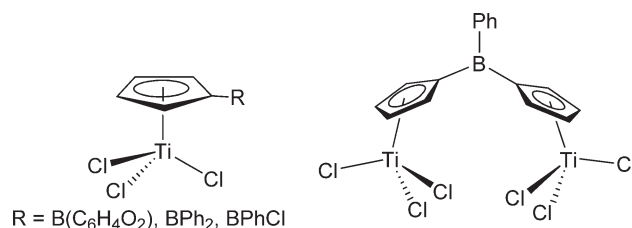
#### 4.05.3.1.1.(v) Complexes with boryl-Cp ligands

Mono-Cp group 4 derivatives containing pendant boryl and borate groups on the Cp ring have been reviewed.<sup>394</sup>

Dehalosilylation of  $\text{Me}_3\text{Si}[\text{C}_5\text{H}_4\text{B}(\text{C}_6\text{F}_5)_2]$  with  $\text{TiCl}_4$  proceeds smoothly to give the highly soluble compound  $[\text{C}_5\text{H}_4\text{B}(\text{C}_6\text{F}_5)_2]\text{TiCl}_3$  (Scheme 168); its structure has been determined by X-ray diffraction. When this compound is treated with 5 equiv. of  $\text{AlEt}_3$  a “self-activating” ethylene polymerization catalyst is obtained.<sup>395</sup> A similar synthetic procedure has been used to prepare a series of related catecholboryl- and phenylboryl-substituted trichloro titanium complexes.<sup>396</sup> Mononuclear borylcyclopentadienyl complexes  $(\text{C}_5\text{H}_4\text{R}^B)\text{TiCl}_3$  [ $\text{R}^B = \text{B}(\text{C}_6\text{H}_4\text{O}_2)$ ,  $\text{BPh}_2$ ,  $\text{BClPh}$ ] and the binuclear compound  $[(\text{C}_5\text{H}_4)_2\text{BPh}](\text{TiCl}_3)_2$  have been prepared by a dehalodesilylation reaction between boryltrimethylsilylcyclopentadiene and  $\text{TiCl}_4$  (Scheme 169). The crystal structure of the binuclear complex has been determined by X-ray diffraction methods. In an NMR study, no correlation was found between the  $^1\text{H}$  and  $^{13}\text{C}$  NMR chemical shifts of the Cp ring and the Lewis acidity of the attached boryl group. Preliminary investigations into the reactivity of these boryl-Cp complexes reveal that they are unstable toward a variety of alkylating reagents, including alkylolithium.<sup>396</sup>



Scheme 168



Scheme 169

## 4.05.3.1.1.(vi) Complexes with phosphorus- and sulfur-substituted Cp ligands

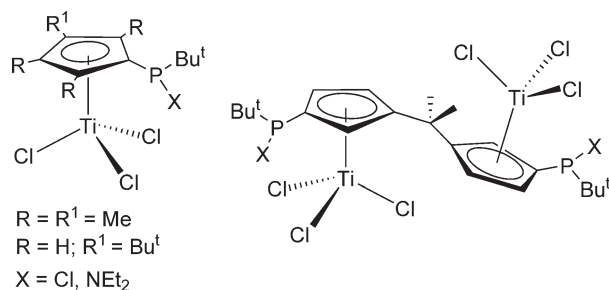
The phosphino-Cp complex  $(C_5H_4PPh_2)TiCl_3$  has been synthesized by treatment of  $TiCl_4$  with the trimethylsilyl-cyclopentadiene derivative  $Me_3Si(C_5H_4PPh_2)$ , while  $[C_5H_4P(=S)Ph_2]TiCl_3$  is prepared by reaction of the lithium and thallium derivatives  $M[C_5H_4P(=S)Ph_2]$  ( $M = Li, Tl$ ) with  $TiCl_4$ . Alternatively,  $[C_5H_4P(=S)Ph_2]TiCl_3$  can be synthesized by ligand redistribution between  $[C_5H_4P(=S)Ph_2]_2TiCl_2$  and  $TiCl_4$ . The molecular structure of  $(C_5H_4PPh_2)TiCl_3$  has been determined by X-ray diffraction.<sup>397</sup>

The tetramethyl-Cp complex  $(C_5Me_4CH_2CH_2PPh_2)TiCl_3$  has been prepared from the reaction of the trimethylsilyl-substituted cyclopentadiene with  $TiCl_4$  and its molecular structure determined by X-ray diffraction methods. The dynamic behavior in solution has been studied by variable-temperature NMR spectroscopy.<sup>365</sup>

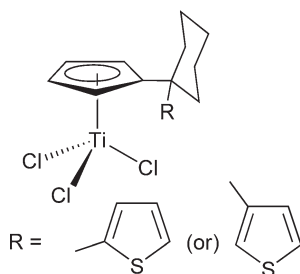
Chloro and alkyl(amino)phosphinyl-substituted Cp complexes have been prepared (Scheme 170). The compounds  $(C_5Me_4PBu^tNEt_2)TiCl_3$  and  $[C_5H_3(Bu^t)PBu^tNEt_2]TiCl_3$  have been synthesized by reaction of  $TiCl_4$  with  $Me_3Sn(C_5Me_4PBu^tNEt_2)$  or  $Me_3Sn[C_5H_3(Bu^t)PBu^tNEt_2]$ , respectively.  $[C_5H_3(Bu^t)PClBu^t]TiCl_3$  is obtained by treatment of the corresponding cyclopentadiene with  $TiCl_4$  in the presence of  $NEt_3$ . In a similar way, the homobimetallic  $[(C_5H_3PBu^tNEt_2)_2CMe_2](TiCl_3)_2$  is prepared. The molecular structure of  $(C_5Me_4PBu^tNEt_2)TiCl_3$  has been determined by X-ray diffraction. Activated with MAO, these complexes show moderate activity in the polymerization of ethylene.<sup>398</sup>

The mono-Cp complex  $(C_5H_4CMe_2PHBu^t)TiCl_3$  has been prepared by the reaction of  $Me_3Si[C_5H_4CMe_2PHBu^t]$  with  $TiCl_4$  in toluene. It has been studied in the catalytic polymerization of ethylene and propylene with activation by MAO as co-catalyst.<sup>399</sup>

Mono-Cp' derivatives with pendant thienyl groups on the Cp ring have been reported (Scheme 171). When activated with MAO, these complexes trimerize ethylene to 1-hexene with considerable activity and high selectivity.



Scheme 170



Scheme 171



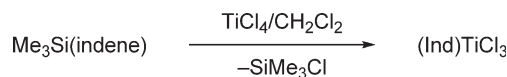
The coordination of the sulfur atom to the Ti center is proposed to be responsible for the selectivity of this reaction.<sup>400</sup>

#### 4.05.3.1.1.(vii) Monoindenyl (Ind), monofluorenyl (Flu), and related complexes

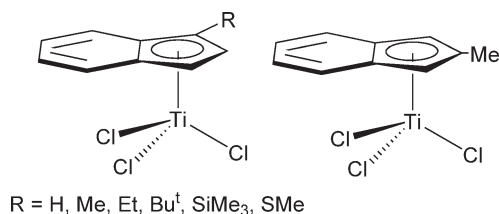
It has been established that the replacement of Cp with an indenyl or fluorenyl ligand has important effects on the catalytic properties of these type of complexes. Monoindenyl and monofluorenyl titanium complexes can generally be prepared by employing dehalosilylation (or analogous dehalostannylation) (Scheme 172), and several such complexes have been described.

(Ind)TiCl<sub>3</sub> has been synthesized, in 97% yield, from the reaction of TiCl<sub>4</sub> and 1-trimethylsilylindene. Its X-ray structure has been determined. This compound has been demonstrated to have unusually high activity and syndio-selectivity in styrene polymerization.<sup>401</sup> The monoindenyl compound, (Ind)TiBr<sub>3</sub>, has been prepared from the interaction of TiBr<sub>4</sub> and Bu<sub>3</sub>Sn(Ind). It, too, was structurally characterized.<sup>402</sup>

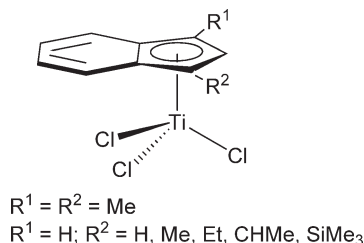
Thermal stability, catalytic activity, and stereospecificity can be modified by controlling the electron-donating/releasing and steric characteristics of the ring substituents. In order to investigate these effects, a variety of 1- and 2-substituted indenyltitanium derivatives (Ind')TiCl<sub>3</sub> (Scheme 173) have been synthesized in excellent yield from reactions of the corresponding trimethylsilylindene derivatives with TiCl<sub>4</sub> and evaluated as styrene polymerization catalysts in toluene solution when activated by MAO. The substituent effect on the polymerization activity has been studied. The syndiospecificities of the titanium complexes were generally very good (65–98%).<sup>403</sup> (Ind')TiCl<sub>3</sub> compounds with the substituted indenyl ligands including 1,3-dimethyl, 1-methyl, 1-ethyl, 1-isopropyl, and 1-(trimethylsilyl)indenyl rings have been synthesized (Scheme 174) and characterized by spectroscopic methods and their catalytic behavior for the polymerization of styrene has been studied. In the presence of MAO, they produce pure syndiotactic polystyrene. The catalytic activity is enhanced by less bulky and better electron-releasing substituents on the indenyl ligand and it is compared with those obtained for (Ind)TiCl<sub>3</sub>/MAO system.<sup>404</sup> Several unsubstituted and substituted monoindenyl titanium complexes have been synthesized (Scheme 175). All of these complexes have been studied as styrene polymerization catalysts in toluene solution when activated with MAO. In general, catalytic activities decrease with each additional methyl substituent. Syndiospecificities are very high.<sup>405</sup> Indenyl trichloro titanium complexes with  $\omega$ -alkenyl functions on the indenyl ring have been synthesized and



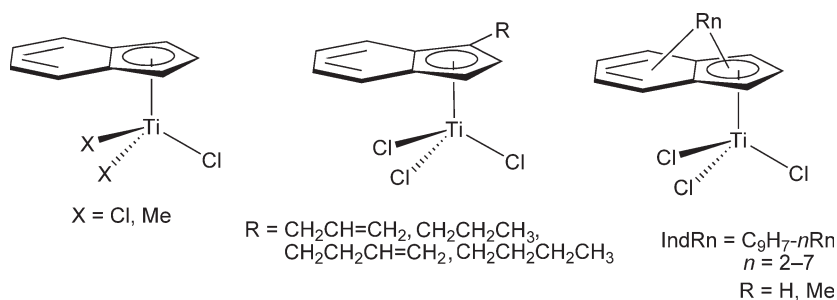
Scheme 172



Scheme 173



Scheme 174

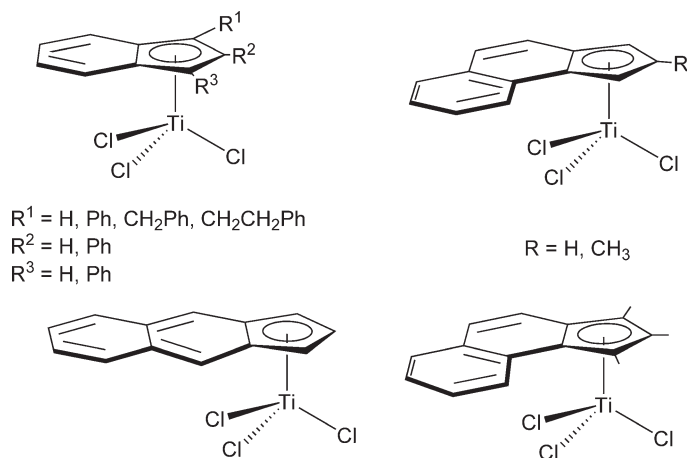


Scheme 175

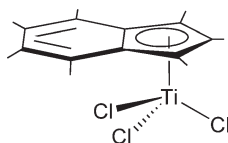
characterized. After activation with MAO these complexes were used as homogeneous and heterogeneous catalysts for the homopolymerization of ethylene and propylene and the co-polymerization of ethylene and 1,7-octadiene.<sup>406</sup>

Trichloro titanium compounds having phenyl groups as ring substituents and benz[*e*]indenyl ligands have been obtained by the reaction of the substituted trimethylsilylindene with  $\text{TiCl}_4$  in  $\text{CH}_2\text{Cl}_2$  solution (Scheme 176). Their catalytic activity for the syndiospecific polymerization of styrene when activated by MAO is compared with  $(\text{Ind})\text{TiCl}_3$ . Phenyl substitution increases polymerization activity in the order  $1,3\text{-Ph}_2\text{Ind} < 2\text{-PhInd} < 1\text{-PhInd}$ . These catalyst precursors are stable in solution toward air and moisture up to 48 h and are indefinitely stable in the solid state.<sup>407</sup> Addition of 1-(trimethylsilyl)heptamethylindene  $\text{Me}_3\text{Si}(\text{C}_9\text{Me}_7)$  to a suspension of  $\text{TiCl}_4$  in THF gives the mono(Ind) complex  $(\text{C}_9\text{Me}_7)\text{TiCl}_3$  in good yield (Scheme 177). The complex was characterized by X-ray diffraction; the  $\text{Ti}-\text{C}_{\text{ring}}$  distances range from 2.352(4) to 2.400(4) Å, with a mean value of 2.370(5) Å consistent with symmetrical bonding of the indenyl ligand to the metal center. The  $\text{Ti}$ -ring centroid distance is 2.036(4) Å.<sup>408</sup>

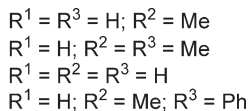
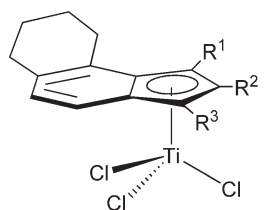
A series of 1- and 2-aryl substituted trichloro indenyltitanium complexes  $(\text{ArInd})\text{TiCl}_3$  ( $\text{Ar} = \text{Ph}, \alpha\text{-Naph}, \beta\text{-Naph}$ ) have been synthesized and tested as catalyst precursors for the syndiospecific polymerization of styrene with MAO as a co-catalyst.<sup>409</sup>



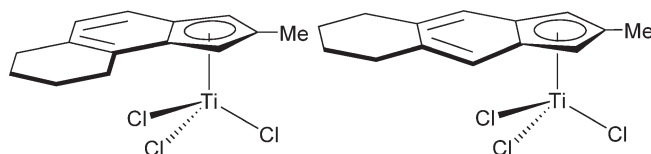
Scheme 176



Scheme 177



Scheme 178



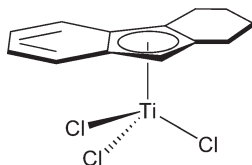
Scheme 179

Several 2-methyl substituted monoindenyltitanium complexes derived from the tetrahydrobenz[*e*]indenyl and its derivatives (Scheme 178) have been synthesized by dehalosilylation. These complexes have been studied, in the presence of MAO, as catalysts for the syndiospecific polymerization of styrene. The influence of the ligand pattern on catalyst activity and polymer properties has been studied. The oxidation state of the active species and the polymerization kinetics are investigated in order to provide more detailed information on polymerization behavior of the active species.<sup>410</sup> The analogous titanium complexes shown in Scheme 179 containing the tetrahydro-2-methylbenz[*e*]indenyl and tetrahydro-2-methylbenz[*f*]indenyl ligands have been synthesized from the corresponding trimethylsilylindene derivative by reaction with  $\text{TiCl}_4$ . When activated with either MAO or  $\text{Ph}_3\text{C}[\text{B}(\text{C}_6\text{F}_5)_4]$ , these complexes catalyze the polymerization of ethylene and propylene.<sup>411</sup>

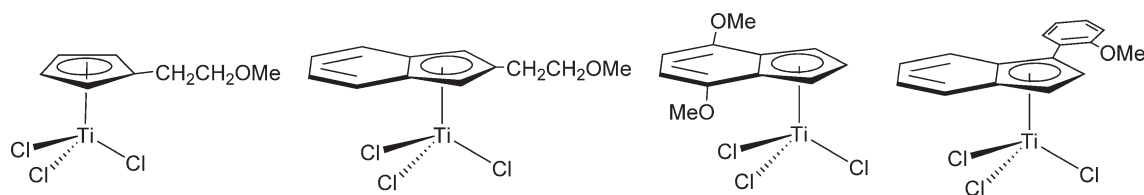
The tetrahydrofluorenyl trichloro titanium compound (Scheme 180) has been prepared by using the dehalosilylation procedure and has been evaluated as a catalyst for styrene polymerization in the presence of MAO as co-catalyst. Syndiotactic polystyrene is obtained with similar characteristics to those reported for other substituted indenyl trichloro titanium derivatives.<sup>403,412</sup>

Several methoxy-substituted Cp and indenyltitanium complexes have been synthesized by dehalosilylation (Scheme 181). Their reactivity as pre-catalysts has been studied in order to investigate the influence of the methoxy substituent on the polymerization behavior. The complexes, when activated with MAO, show only low activity for ethylene, styrene, and propylene polymerization. Oxygen–aluminum coordination between the methoxy group and MAO could be the deactivating factor.<sup>413</sup> The siloxo-substituted Cp and Ind complexes  $(\text{C}_5\text{Me}_4\text{OSiMe}_3)\text{TiCl}_3$  and  $(\text{C}_9\text{H}_6\text{OSiMe}_3)\text{TiCl}_3$  (Scheme 182) have been synthesized and characterized; in the presence of MAO as a co-catalyst they show only low activity for styrene polymerization.<sup>414</sup>

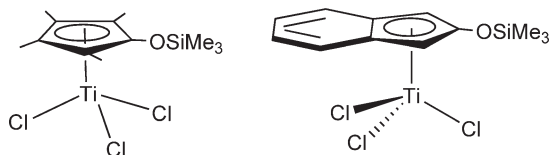
$\text{TiCl}_4$  reacts with  $\beta$ -substituted trimethyltinfluorenes in hexane at  $-40^\circ\text{C}$  to give unstable trichloro fluorenyl  $\text{Ti}(\text{IV})$  complexes, which undergo thermal radical decomposition with quantitative formation of  $\text{TiCl}_4$  and the corresponding bifluorene derivative.<sup>415</sup>



Scheme 180



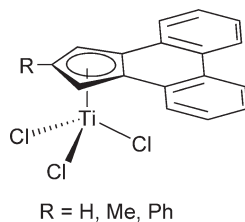
Scheme 181



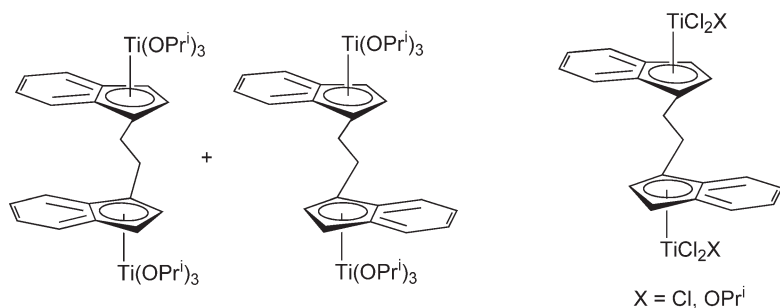
Scheme 182

Trichloro cyclopenta[1]phenanthrene titanium complexes (Scheme 183) have been synthesized. The crystal structure of the 2-methyl-substituted derivative has been determined by X-ray diffraction. In the presence of MAO, these complexes are highly active pre-catalysts for the syndiotactic polymerization of styrene. The 2-phenyl-substituted complex exhibits especially high catalytic activity.<sup>416</sup>

Binuclear monoindenyltitanium(IV) complexes have been synthesized by reaction of the trialkoxo titanium compound  $\text{TiCl}(\text{OPr}^i)_3$  with the lithium salt of the bis-indene reagent.  $[(1,2\text{-CH}_2\text{-1-Ind})\text{Ti}(\text{OPr}^i)_3]_2$  is obtained as a 1 : 1 *rac*- and *meso*-mixture. This complex reacts with  $\text{CH}_3\text{C}(\text{O})\text{Cl}$  in  $\text{CH}_2\text{Cl}_2$  ethyl ether to form  $[(1,2\text{-CH}_2\text{-1-Ind})\text{TiCl}_3]_2$  and in ethyl ether to form  $[(1,2\text{-CH}_2\text{-1-Ind})\text{TiCl}_2(\text{OPr}^i)]_2$  (Scheme 184), which in the presence of MAO are highly syndiospecific catalyst precursors for the polymerization of styrene, although their activities were one order of magnitude lower than for the reference mononuclear compound  $(\text{Ind})\text{TiCl}_3$ .<sup>417</sup>



Scheme 183



$\text{X} = \text{Cl}, \text{OPr}^i$

Scheme 184

#### 4.05.3.1.2 Structural aspects

Structural characterization of several mono-Cp' titanium complexes has been reported. The molecular structures of Cp\*TiCl<sub>3</sub>,<sup>418</sup> (C<sub>5</sub>HMe<sub>4</sub>)TiCl<sub>3</sub>,<sup>418</sup> and (1,2,3-Me<sub>3</sub>C<sub>5</sub>H<sub>2</sub>)TiCl<sub>3</sub><sup>419</sup> have been determined by X-ray diffraction methods. The molecular structures of dichloro (3-Me-2-*p*-tolylsulfonamidobutyl)-Cp, (C<sub>17</sub>H<sub>21</sub>NO<sub>2</sub>S)TiCl<sub>2</sub><sup>420</sup> and dichloro (*p*-tolylsulfonamido prop-1-yl)-Cp (C<sub>15</sub>H<sub>17</sub>NO<sub>2</sub>S)TiCl<sub>2</sub><sup>421</sup> compounds have been determined by X-ray diffraction, showing a five-coordinate geometry for the Ti atom.

Titanium NMR spectroscopic data for a series of mono-Cp' trichloro titanium complexes bearing a Cp ligand substituted with Bu<sup>t</sup> and/or SiMe<sub>3</sub> groups have been collected. Chemical shift values suggest a weak electron-donating effect of the SiMe<sub>3</sub> group, whereas the line widths reflect the symmetry of the five-membered ring's substitution pattern.<sup>422</sup>

The FT-IR spectra of CpTiCl<sub>3</sub> in CCl<sub>4</sub> solutions have been presented at the first and second overtone region.<sup>423</sup>

Substituent effects in mono-Cp and mono-Ind derivatives, including (Ind)TiCl<sub>3</sub>, (1-RC<sub>9</sub>H<sub>6</sub>)TiCl<sub>3</sub> (R = Me, SiMe<sub>3</sub>), (2-SiMe<sub>3</sub>C<sub>9</sub>H<sub>6</sub>)TiCl<sub>3</sub>, (4-MeC<sub>9</sub>H<sub>6</sub>)TiCl<sub>3</sub>, (1,3-Me<sub>2</sub>C<sub>9</sub>H<sub>5</sub>)TiCl<sub>3</sub>, (4,7-Me<sub>2</sub>C<sub>9</sub>H<sub>5</sub>)TiCl<sub>3</sub>, (1-SiMe<sub>3</sub>,4,7-Me<sub>2</sub>C<sub>9</sub>H<sub>4</sub>)TiCl<sub>3</sub>, (1,3,4,7-Me<sub>4</sub>C<sub>9</sub>H<sub>3</sub>)TiCl<sub>3</sub>, [5,6-(CH<sub>2</sub>)<sub>3</sub>C<sub>9</sub>H<sub>6</sub>]TiCl<sub>3</sub>, and [3,4-(CH<sub>2</sub>)<sub>3</sub>C<sub>9</sub>H<sub>6</sub>]TiCl<sub>3</sub> have been studied with cyclic voltammetry and UV-VIS spectroscopy.<sup>424</sup>

The photoreactivity of CpTiCl<sub>3</sub> initiated by ligand-to-metal charge transfer excitation has been studied.<sup>425</sup>

Non-local density functional theory (DFT) calculations for CpTiCl<sub>3</sub> have been performed in order to detail analysis of the metal-Cp bond strength in comparison with the isolobal phosphoraneiminato ligand.<sup>426</sup>

#### 4.05.3.1.3 Reactions

Hydrolysis, redox, metathetical, and halide abstraction reactions are covered here. Some of these reactions lead to specific complexes with Ti-O, Ti-N, and Ti-C bonds which are described in subsequent sections. Comments on the applications of the mono-Cp' trihalo titanium complexes as olefin polymerization pre-catalysts have been mentioned in Section 4.05.3.1.1 and some recent advances in this field are also considered here. (See Chapter 4.09 of this work.)

Coordination complexes of Cp'TiCl<sub>3</sub> with N<sub>2</sub>S<sub>2</sub> and S<sub>2</sub>O<sub>2</sub> ligands derived from *o*-aminobenzenethiol have been synthesized.<sup>427</sup>

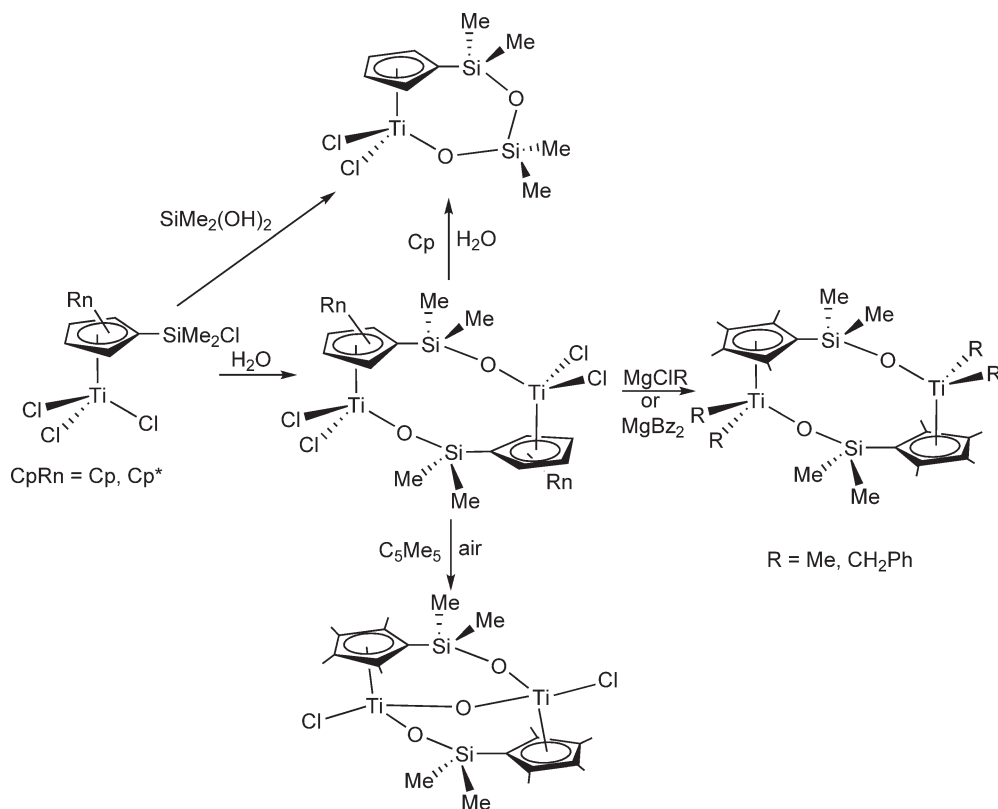
##### 4.05.3.1.3.(i) Hydrolysis reactions

The hydrolysis of mono-Cp titanium(IV) trihalides affords a variety of aggregated titanoxanes. The reaction of Cp\*TiF<sub>3</sub> with O(SnBu<sub>3</sub>)<sub>2</sub> in a molar ratio 1 : 1 gives the eight-membered ring compound [Cp\*TiF(O)]<sub>4</sub>. Its molecular structure shows an almost-planar eight-membered ring. This is the first reported example of a group 4 metal organometallic oxo fluoro derivative.<sup>428</sup> [Cp\*TiF(O)]<sub>4</sub> can alternatively be obtained by ring expansion under treatment of [Cp\*TiClO]<sub>3</sub> with Me<sub>3</sub>SnF.<sup>351</sup>

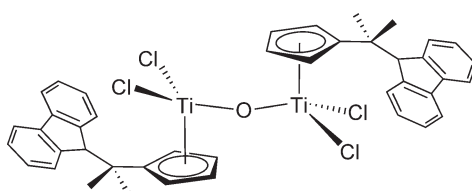
The compounds [C<sub>5</sub>R<sub>4</sub>(SiMe<sub>2</sub>Cl)]TiCl<sub>3</sub> (R = H, Me) possess two types of metal-halogen bonds, Ti-Cl and Si-Cl, showing different chemical behavior toward several nucleophiles to afford oxo, alkyl, and amido derivatives and the wide reactivity of these species has been studied. Reaction with 1 equiv. of water proceeds with elimination of HCl, resulting in the formation of the binuclear titanium methylsiloxo derivative [(C<sub>5</sub>R<sub>4</sub>(SiMe<sub>2</sub>O-)TiCl<sub>2</sub>)<sub>2</sub>] in quantitative yield, which shows the oxygen atom bridging the silicon and the Ti atoms forming an eight-membered ring. The product of a further hydrolysis is strongly dependent on the steric requirements of the Cp ring. Further addition of 1 equiv. of water to the Cp complex gives the mononuclear compound (C<sub>5</sub>H<sub>4</sub>-SiMe<sub>2</sub>O-SiMe<sub>2</sub>O-)TiCl<sub>2</sub>, alternatively obtained by treatment of [C<sub>5</sub>H<sub>4</sub>(SiMe<sub>2</sub>Cl)]TiCl<sub>3</sub> with SiMe<sub>2</sub>(OH)<sub>2</sub>. When a toluene solution of the Cp\* derivative is refluxed in the air over a long period, hydrolysis of one Ti-Cl bond per metal atom results in the formation a "Ti-O-Ti" bridge, maintaining the binuclear system (Scheme 185). [(C<sub>5</sub>R<sub>4</sub>SiMe<sub>2</sub>O-)TiCl<sub>2</sub>]<sub>2</sub> (R = H, Me) can be alkylated by reaction with MgClR (R = Me, CH<sub>2</sub>Ph) or Bz(CH<sub>2</sub>Ph)<sub>2</sub> to give the corresponding alkyl derivatives.<sup>380,381</sup> Hydrolysis of the trichloro and tribenzyl complexes (C<sub>5</sub>H<sub>4</sub>SiMeCl<sub>2</sub>)TiX<sub>3</sub> leads to the  $\mu$ -oxo dititanium compounds [(C<sub>5</sub>H<sub>4</sub>SiMeCl-O)TiX<sub>2</sub>]<sub>2</sub> (X = Cl, CH<sub>2</sub>Ph) (Scheme 192; Section 4.05.3.1.3.(iii)).<sup>382</sup>

[C<sub>5</sub>H<sub>4</sub>(CMe<sub>2</sub>)C<sub>13</sub>H<sub>9</sub>]TiCl<sub>3</sub> is readily hydrolyzed in wet acetone to give {[C<sub>5</sub>H<sub>4</sub>(CMe<sub>2</sub>)C<sub>13</sub>H<sub>9</sub>]TiCl<sub>2</sub>]<sub>2</sub>( $\mu$ -O) (Scheme 186).<sup>326</sup>

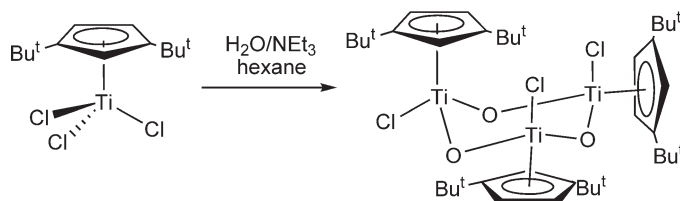
Addition of a stoichiometric amount of water in the presence of NEt<sub>3</sub> to a toluene solution of (1,3-Bu<sup>t</sup><sub>2</sub>-C<sub>5</sub>H<sub>3</sub>)TiCl<sub>3</sub> affords the oxo trimer compound [(1,3-Bu<sup>t</sup><sub>2</sub>-C<sub>5</sub>H<sub>3</sub>)TiCl( $\mu$ -O)]<sub>3</sub> (Scheme 187), the molecular structure of which has been determined by X-ray diffraction methods.<sup>337</sup>



Scheme 185



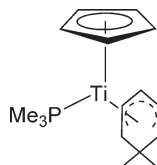
Scheme 186



Scheme 187

#### 4.05.3.1.3.(ii) Reduction reactions of mono-Cp complexes

Low-valent group 4 metal derivatives might be prepared from mono-Cp' titanium(IV) derivatives by mild reductive conditions. The tetracarbonyltitanates(0)  $[\text{Cp}'\text{Ti}(\text{CO})_4]^-$  ( $\text{Cp}' = \text{Cp}, \text{Cp}^*$ ) are prepared as  $\text{Et}_4\text{N}^+$  salts in 40–50% yield by reduction of  $\text{Cp}''\text{TiCl}_3$  with alkali metal naphthalenides at low temperature, followed by carbonylation at atmospheric pressure. Increased yields of up to 70% have been obtained when reduction is done in the presence of excess  $\text{C}_{10}\text{H}_8$ .<sup>429</sup> The reduction of  $\text{CpTiCl}_3$  with zinc and subsequent treatment with 3 equiv. of potassium



Scheme 188

dimethylcyclohexadienide anion in the presence of trimethylphosphine gives the acyclic  $\eta^5$ -cyclohexadienyl complex shown in Scheme 188, which has been studied as a catalyst for coupling reactions with aldehydes and ketones.<sup>430</sup> The reaction of  $\text{CpTiCl}_3$  with  $\text{AlMe}_3$  in the presence of 18-crown-6 resulted in the formation of the titanium(III) complex  $[\text{CpTiCl}(18\text{-crown-6})][\text{AlCl}_2\text{Me}_2]$ . The structure of this compound reveals a cation with a five-coordinate Ti where the centroid of the Cp ring occupies the apex of a square pyramid.<sup>431</sup> Reduction of  $\text{Cp}^*\text{TiCl}_3$  by 4 equiv. of  $\text{KC}_{14}\text{H}_{10}$  in THF at  $-55$  to  $-65^\circ\text{C}$  gives the reduced bis(anthracene) titanium species  $[\text{Cp}^*\text{Ti}(\eta^4\text{-C}_{14}\text{H}_{10})(\eta^2\text{-C}_{14}\text{H}_{10})]^-$ .<sup>432</sup>

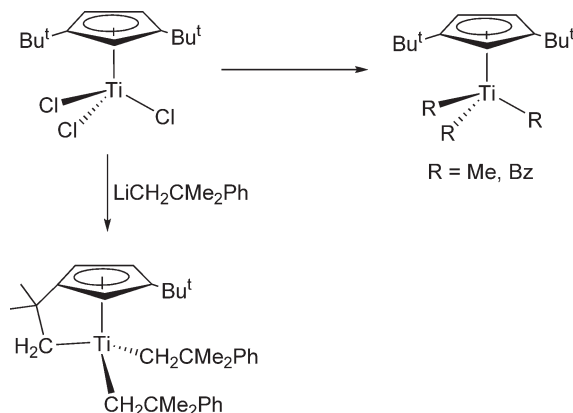
Reactions of  $\text{Cp}^*\text{TiF}_3$  with alkali metals and their fluorides lead to a variety of reduced titanium alkali metal clusters containing Ti–F bonds.<sup>433–435</sup>  $(\text{C}_5\text{H}_4\text{SiMe}_3)\text{TiF}_3$  has been reduced with Zn and Mn to give tetranuclear Ti(III) clusters, which are converted to  $(\text{C}_5\text{H}_4\text{SiMe}_3)_2\text{TiF}_2$  by oxidative fluorination with  $\text{AgF}$ .<sup>352</sup>

#### 4.05.3.1.3.(iii) Metathesis reactions of mono-Cp complexes

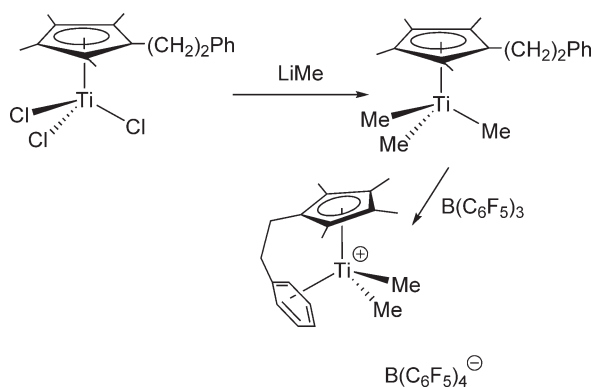
Treatment of  $(1,3\text{-Bu}^t\text{-C}_5\text{H}_3)\text{TiCl}_3$  with the appropriate alkylating reagents in hexane gives the trialkyltitanium complexes  $(1,3\text{-Bu}^t\text{-C}_5\text{H}_3)\text{TiR}_3$  ( $\text{R} = \text{CH}_3, \text{CH}_2\text{Ph}$ ). However, the expected trineophyl compound could not be obtained by reaction with 3 equiv. of  $\text{LiCH}_2\text{CMe}_2\text{Ph}$ ; instead, the ring methyl-metallated complex  $(1\text{-Bu}^t\text{-3-CMe}_2\text{CH}_2\text{C}_5\text{H}_3)\text{Ti}(\text{CH}_2\text{CMe}_2\text{Ph})_2$  was isolated in 90% yield (Scheme 189).<sup>336</sup> The reaction of  $(1,3\text{-Bu}^t\text{-C}_5\text{H}_3)\text{TiCl}_3$  with 2 equiv. of  $\text{LiMe}$  affords the chloro dimethyl derivative  $(1,3\text{-Bu}^t\text{-C}_5\text{H}_3)\text{TiClMe}_2$ .<sup>337</sup>

The trichloro complex  $(\text{C}_5\text{Me}_4\text{CH}_2\text{CH}_2\text{Ph})\text{TiCl}_3$  is converted into the trimethyl derivative  $(\text{C}_5\text{Me}_4\text{CH}_2\text{CH}_2\text{Ph})\text{TiMe}_3$ , which upon recrystallization in wet pentane readily hydrolyzes to  $[(\text{C}_5\text{Me}_4\text{CH}_2\text{CH}_2\text{Ph})\text{TiMe}_2]_2(\mu\text{-O})$ . The methyl compound reacts with 1 equiv. of  $\text{Ph}_3\text{C}[\text{B}(\text{C}_6\text{F}_5)_4]$  to give almost quantitatively the ion pair  $[(\text{C}_5\text{Me}_4\text{CH}_2\text{CH}_2\text{Ph})\text{TiMe}_2]^+[\text{B}(\text{C}_6\text{F}_5)_4]^-$  (Scheme 190), which is thermally unstable in solution and very moisture sensitive. The structural data for the cation indicate intramolecular coordination of the phenyl group to Ti. The catalytic performance for styrene polymerization of these systems has been studied. The polymerization results suggest for the active species an equilibrium between two states, one with and one without intramolecular phenyl coordination, consistent with postulated multihapto coordination of styrene involving both the vinylic double bond and the aromatic ring to the metal center during the catalytic process.<sup>342</sup>

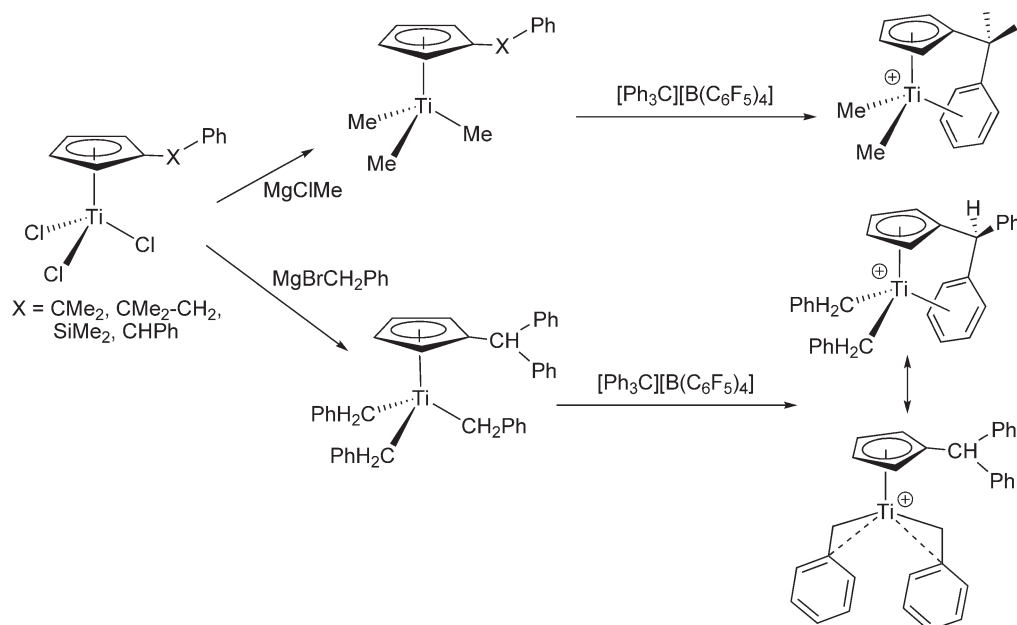
Alkylation of the mono-Cp' trichloro titanium complexes  $(\text{C}_5\text{H}_4\text{R})\text{TiCl}_3$  (Scheme 191) containing pendant phenyl substituents in the Cp ring readily affords the corresponding methyl and benzyl derivatives. Treatment of the trialkyl complexes with  $\text{Ph}_3\text{C}[\text{B}(\text{C}_6\text{F}_5)_4]$  in  $\text{CH}_2\text{Cl}_2$  at low temperatures generates cationic complexes stabilized by  $\pi$ -coordination to the phenyl ring to give *ansa*-arene complexes with one- and two-carbon linkages. The structures



Scheme 189



Scheme 190



Scheme 191

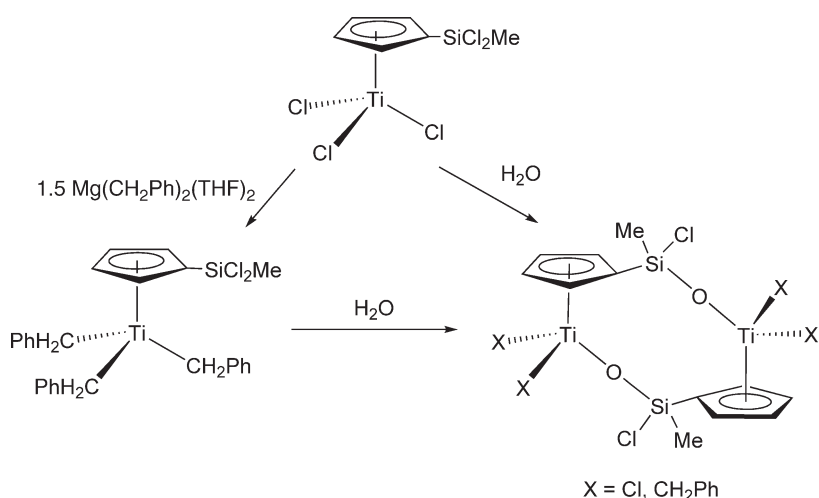
of some of these compounds have been determined by X-ray diffraction. These complexes catalyze the polymerization of propylene.<sup>327,328</sup>

Alkylation of the trichloro titanium derivative  $(\text{C}_5\text{H}_4\text{SiMeCl}_2)/\text{TiCl}_3$  with 1.5 equiv. of  $\text{Mg}(\text{CH}_2\text{C}_6\text{H}_5)_2(\text{THF})_2$  leads to the tribenzyl derivative  $(\text{C}_5\text{H}_4\text{SiMeCl}_2)/\text{Ti}(\text{CH}_2\text{C}_6\text{H}_5)_3$  (Scheme 192).<sup>382</sup> Reaction of the mononuclear  $(\text{C}_5\text{Me}_4\text{SiMe}_2\text{Cl})/\text{TiCl}_3$  with an alkylating reagent renders peralkylated  $(\text{C}_5\text{Me}_4\text{SiMe}_2\text{R})\text{TiR}_3$  ( $\text{R} = \text{Me}, \text{CH}_2\text{Ph}$ ) or partially alkylated  $(\text{C}_5\text{Me}_4\text{SiMe}_2\text{CH}_2\text{SiMe}_3)/\text{TiCl}(\text{CH}_2\text{SiMe}_3)_2$  compounds, depending on the size of the alkyl ligand (Scheme 193).<sup>381</sup>

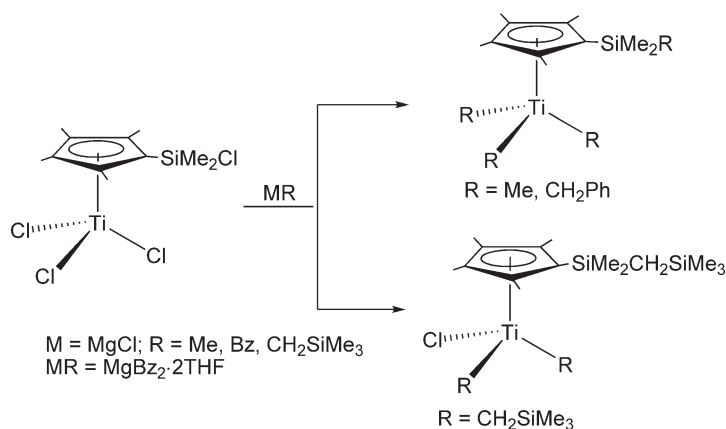
Organometallic fluoro complexes are of special interest since the M–F bonds play a key role in the cleavage, formation, and activation of C–F bonds.<sup>436</sup> The reactivity of the trifluoro complex  $\text{Cp}^*\text{TiF}_3$  toward  $\text{AlR}_3$  ( $\text{R} = \text{Me}, \text{Et}$ ) in comparison with the same reaction carried out with  $\text{Cp}^*\text{TiCl}_3$  has been studied. The methylation of  $\text{Cp}^*\text{TiX}_3$  with an excess of  $\text{AlMe}_3$  is not possible and under thermal conditions these reactions give reduced titanium species. The reduction of  $\text{Ti}(\text{IV})$  to  $\text{Ti}(\text{III})$  is observed when  $\text{Cp}'_2\text{TiF}_2$  ( $\text{Cp}' = \text{Cp}, \text{Cp}^*, \text{C}_5\text{HMe}_4$ ) and  $\text{Cp}^*\text{TiF}_3$  are treated with  $\text{AlEt}_3$ .<sup>437</sup>

The use of argon matrices for trapping molecular  $\text{ZnF}_2$  and  $\text{ZnFMe}$  has also been described.  $\text{ZnF}_2$  does not react directly with organofluoro titanium derivatives due to its high lattice energy and insolubility in organic solvents.





Scheme 192



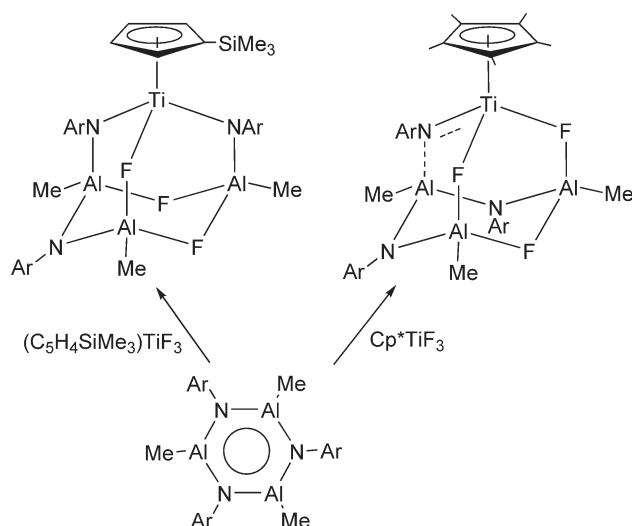
Scheme 193

However,  $\text{ZnF}_2$  prepared *in situ* from  $\text{ZnMe}_2$  and  $\text{SnFMe}_3$  is trapped by  $\text{Cp}^*\text{TiF}_3$  to form  $[\text{Cp}^*\text{TiF}_3]_8(\text{ZnF}_2)_2$  which reacts with  $\text{ZnMe}_2$  to give  $[\text{Cp}^*\text{TiF}_3]_4(\text{ZnFMe})_2$ .<sup>438</sup> Reaction of  $\text{Cp}'\text{TiF}_3$  ( $\text{Cp}' = \text{Cp}^*, \text{C}_5\text{H}_4\text{SiMe}_3$ ) with the trimeric imidoalane  $[\text{AlMe}(\text{NAr})]_3$  gives adamantane-like titanium complexes. The crystal structure of the trimethylsilyl-Cp derivative has been determined. The pentamethyl-Cp derivative in the presence of donor solvents gives a terminal Ti imido compound via cleavage of an aluminum–nitrogen bond, which has been characterized by IR and NMR spectroscopy and X-ray diffraction (Scheme 194).<sup>439</sup>

Lithium fluoride, prepared *in situ* from lithium chloride and trimethyltin fluoride, is trapped by  $\text{Cp}^*\text{TiF}_3(\text{C}_5\text{Me}_5)$  to yield  $[\text{Cp}^*\text{TiF}_3]_4(\text{LiF})$ , the molecular structure of which has been determined by X-ray crystallography and shows two  $[(\text{C}_5\text{Me}_5)_2\text{Ti}_2\text{F}_6]$  units connected by a lithium atom and a bridging fluoro ligand. This compound exhibits, in solution, a dissociation process, studied by variable-temperature  $^{19}\text{F}$  NMR spectroscopy, to yield  $\text{Li}[\text{Cp}^*_2\text{Ti}_2\text{F}_7]$  and  $[\text{Cp}^*\text{TiF}_3]_2$ , accompanied by a cleavage of Ti–F–Ti bonds.<sup>435</sup>

#### 4.05.3.1.3.(iv) Cationic species; polymerization and olefin hydrogenation

Mono- $\text{Cp}'$  titanium derivatives show reactivity as catalyst precursors for olefin polymerizations, particularly for the polymerization of styrene and functionalized monomers. A review highlighting the developments in the design and applications of non-metallocene complexes, including mono-Cp derivatives, as catalyst systems for  $\alpha$ -olefin polymerization has appeared.<sup>440</sup> Titanium complexes bearing Cp in addition to chloro ligands and activated by aluminum



Scheme 194

alkyls ( $AlR_3$ ) or MAO have been tested as ethylene polymerization catalysts.<sup>441</sup> The polymerization of propylene with  $C_5$ -symmetric mono-Cp titanium derivatives at low temperature has been reported.<sup>442</sup> For olefin polymerizations with group 4 metal catalysts, see also Chapter 4.09.

$Cp^*TiCl_3/MAO$  is one of the most effective catalytic system, for producing syndiotactic polystyrene.<sup>401,443</sup> The influence of the type of solvent on the styrene polymerization behavior with  $CpTiCl_3/MAO$  as catalyst at 25 °C has been investigated.<sup>444</sup> The effect of polymerization conditions on styrene polymerizations with  $Cp''TiCl_3$  ( $Cp' = Cp, Cp^*, Ind$ ) and MMAO as co-catalyst have been examined.<sup>445</sup> UV-VIS spectroscopy has been employed to identify the active species in syndiospecific styrene polymerizations in hydrocarbon using homogeneous  $CpTiCl_3$  catalysts in the presence of MAO.<sup>446</sup> The effect of aluminum alkyls on the synthesis of syndiotactic polystyrene with  $CpTiCl_3/MAO$  has been studied.<sup>447</sup> The syndiospecific polymerization of substituted styrenes has been carried out using  $CpTiCl_3/MAO$ <sup>448,449</sup> and  $Cp^*TiCl_3/MAO$ .<sup>450</sup>

The polymerization of 1,3-butadiene with  $CpTiCl_3$  catalysts gives polybutadiene with about 81% *cis*, 18% 1,2, and 1% *trans* units.<sup>451</sup>  $Cp^*TiCl_3$  in the presence of MAO is similarly active.<sup>452</sup> The  $CpTiCl_3/MAO$  system has been used for homopolymerization of 4-vinylpyridine.<sup>453</sup> Compounds  $Cp''TiCl_3$  ( $Cp' = Cp, Cp^*$ ) activated with a large excess of MAO have been found to catalyze the polymerization of a number of conjugated dienes.<sup>454</sup>

The activity of titanium mono- $Cp'$  fluorides for the syndiospecific polymerization of styrene is about 50 times higher than that of the corresponding chloro compounds and gives polymers with significantly higher molecular weights. Alkyl substitution on the Cp ligand can increase the activity.<sup>455–458</sup>  $CpTiF_3$  is a highly active pre-catalyst for the homo- and co-polymerization of styrene and alkylstyrenes. Syndiotactic co-polymers with *p*-methylstyrene, *p*- $Bu^t$ -styrene and  $\alpha$ -methylstyrene can be obtained.<sup>459</sup> Mono-Cp trifluoro titanium complexes have also been used to polymerize butadiene, isoprene, and 1,3-pentadiene.<sup>460</sup>

The co-polymerization of styrene and ethylene in the presence of  $CpTiCl_3/MAO$  has been studied.<sup>461</sup> Conventional Ziegler–Natta catalysts are not very effective in ethylene/ $\alpha$ -olefin co-polymerizations and give inhomogeneous polymers with respect to the styrene incorporation and molecular mass distribution. The styrene content of such polymers is generally less than 1 mol%. Some contradictory results have been reported concerning the ability of the  $CpTiCl_3/MAO$  system to co-polymerize ethylene with styrene.<sup>462,463</sup> The complexes  $Cp''TiCl_3$  ( $Cp' = Cp, Cp^*, C_9H_7$ ) when activated with MAO are active catalysts for the co-polymerization of styrene with 4- $Bu^t$ -dimethylsilyloxystyrene. The ligand effect in the activity of these systems has been studied by UV–VIS spectroscopy.<sup>464</sup> The co-polymerization of styrene with 1,3-butadiene or isoprene has been carried out with  $Cp''TiCl_3$  catalysts ( $Cp' = Cp, Cp^*, Ind$ ) with MAO as co-catalyst.<sup>465</sup>  $CpTiCl_3$  activated with MMAO has been used to prepare *cis*-polybutadiene-block-*syn*-polystyrene co-polymers with long crystalline syndiotactic polystyrene segments bonded to high *cis*-1,4-polybutadiene.<sup>466</sup> Synthesis and properties of syndiotactic graft co-polymer of styrene with polyisoprene macromonomer obtained with  $CpTiCl_3/MAO$  are reported.<sup>467</sup> A novel graft-like co-polymer of syndiotactic polystyrene with polybutadiene is synthesized by polymerization of styrene in a toluene solution of polybutadiene using

the  $\text{CpTiCl}_3/\text{MAO}$  catalytic system.<sup>468</sup> The homo- and co-polymerization of styrene with *p*-methylstyrene, *m*-methylstyrene, 2,4-dimethylstyrene, 2,5-dimethylstyrene, and 2,4,6-trimethylstyrene using  $\text{Cp}^*\text{TiCl}_3/\text{MAO}$  have been studied.<sup>469</sup> The ethylene–styrene co-polymerization with  $\text{CpTiX}_3$  ( $\text{X}=\text{Cl}$  or an alkyl group) has been the subject of a theoretical study.<sup>470</sup>

The mixture of  $\text{CpTiCl}_3$ ,  $\text{ZnPh}_2$ , and MAO has been used to initiate the polymerization of styrene and its co-polymerization with 1-hexadecene and with *p*-*tert*-butylstyrene.<sup>471</sup>  $(\text{Ind})\text{TiCl}_3$  combined with  $\text{ZnPh}_2$  as additive and MAO has been used for the co-polymerization of styrene with 1-alkenes (1-hexene, 1-decene, 1-hexadecene).<sup>472</sup> Similarly,  $\text{CpTiCl}_3$  has been used for the co-polymerization of styrene and *p*-*tert*-butylstyrene.<sup>473</sup> The syndiotactic polymerization of styrene with  $\text{Cp}^*\text{TiCl}_3$  and octahydrofluorenyl trimethoxo titanium complexes in the presence of phenylsilane has been investigated.<sup>474</sup>

Mono-Cp titanium derivatives supported on  $\text{MgCl}_2/\text{AlR}_n(\text{OEt})_{3-n}$  and activated with MAO or borate activators have been used as catalysts for the polymerization of  $\alpha$ -olefins.<sup>475</sup> Powdery syndiotactic polystyrene has been synthesized in a bulk process with the homogeneous system  $\text{Cp}^*\text{TiCl}_3/\text{MAO}/\text{AlBu}_3$ .<sup>476</sup> Studies concerning the initiation step for polymerization of 4-Me-1,3-pentadiene in the presence of  $\text{CpTiCl}_3/\text{MAO}$  and  $\text{Al}(\text{CH}_3)_3$  have been reported.<sup>477</sup> Polymerizations of ethylene and propylene conducted with catalysts based on  $\text{CpTiCl}_3$  modified by trimethylsilanol have been investigated, and a plausible mechanism for the polymerization on the basis of the results has been reported.<sup>478</sup> The reaction of  $\text{Cp}''\text{TiCl}_3$  [ $\text{Cp}'=\text{Cp}$ ,  $\text{Cp}^*$ ,  $\text{C}_5\text{H}_4\text{SiMe}_3$ ,  $\text{C}_5\text{H}_3(\text{SiMe}_3)_2$ ] with poly(styrene-*r*-4-hydroxystyrene) affords immobilized aryloxo–Cp complexes, which have low solubility in toluene, indicative of chemical cross-linking. On MAO activation, these supported compounds have been used for ethylene homopolymerizations to give polyethylene having exclusively butyl short chain branches (SCBs). The formation of SCBs has been found to depend on the Cp substituents.<sup>479</sup> The syndiotactic polymerization of styrene in the presence of heterogenized catalysts  $\text{CpTiCl}_3/\text{Al}_2\text{O}_3\text{--SiO}_2/\text{MAO}$  shows that the yield and selectivity of this reaction depend on the support composition.<sup>480</sup>  $\text{CpTiCl}_3$  supported on a poly(4-vinylpyridine)/silica (PVP/ $\text{SiO}_2$ ) organic–inorganic nanoscale hybrid and used for styrene polymerization gives polymers with a bimodal molecular weight distribution.<sup>481</sup> Substituted Cp titanium complexes anchored on polysiloxanes prepared by a sol–gel procedure have been used in catalyst heterogenization for the hydrogenation of olefinic double bonds. Polysiloxane-anchored cyclopentadienyl- and pentamethylcyclopentadienyl-titanium complexes have been obtained by deprotonation of a polysiloxane  $\text{C}_5\text{HMe}_4\text{CH}_2\text{Si}(\text{OCH}_2\text{CH}_3)_3$  with  $\text{Li}^n\text{Bu}$  followed by reaction with  $\text{CpTiCl}_3$  and  $\text{Cp}^*\text{TiCl}_3$  and their structures examined by solid-state NMR and X-ray photoelectron spectroscopy. The anchored complexes were catalytically active in the hydrogenation of 1-octene.<sup>482</sup>  $\text{MgCl}_2$ -supported complexes  $\text{Cp}'\text{TiCl}_3$  ( $\text{Cp}'=\text{Cp}$ ,  $\text{Cp}^*$ , Ind,  $\text{C}_9\text{Me}_7$ ) have been prepared and applied to propylene polymerization using  $\text{AlBu}_3$  as co-catalyst.<sup>483</sup> A hybrid catalyst prepared from the use of a fourth-generation Ziegler–Natta catalyst, an  $\text{MgCl}_2$ -supported  $\text{TiCl}_4$  and  $\text{CpTiCl}_3$ , has been used for ethylene/1-butene co-polymerization.<sup>484</sup>

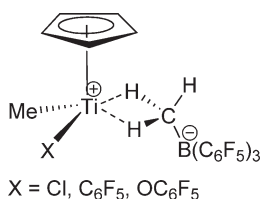
The catalytic system  $(\text{C}_5\text{H}_4\text{CPh}_3)\text{TiCl}_3$ , when activated with MAO, shows activity for stereospecific polymerizations of styrene and 1,3-butadiene.<sup>485</sup>

Synthesis and mechanism of formation of syndiotactic polystyrene using  $\text{Bu}^t$ -substituted cyclopentadienyltitanium complexes have been investigated. Mixtures of  $(\text{C}_5\text{H}_4\text{Bu}^t)\text{TiCl}_3$  and MAO are active for the polymerization of styrene, resulting in essentially 100% syndiotactic polystyrene of narrow polydispersity (ca. 2.0–2.2). MALDI-TOF-MS data show that sPS (syndiotactic polystyrene) samples contain both methyl and ethyl end groups, indicating that the major mechanism of chain termination is via  $\beta$ -hydrogen transfer and that the resulting  $[\text{Ti–H}]^+$  species initiates further chain growth. The polymer molecular weight is dependent on the temperature of polymerization. Experimental data indicate that the number of active titanium centers remains constant during this time. Increasing the quantity of styrene results in an identical percentage conversion.<sup>486,487</sup>

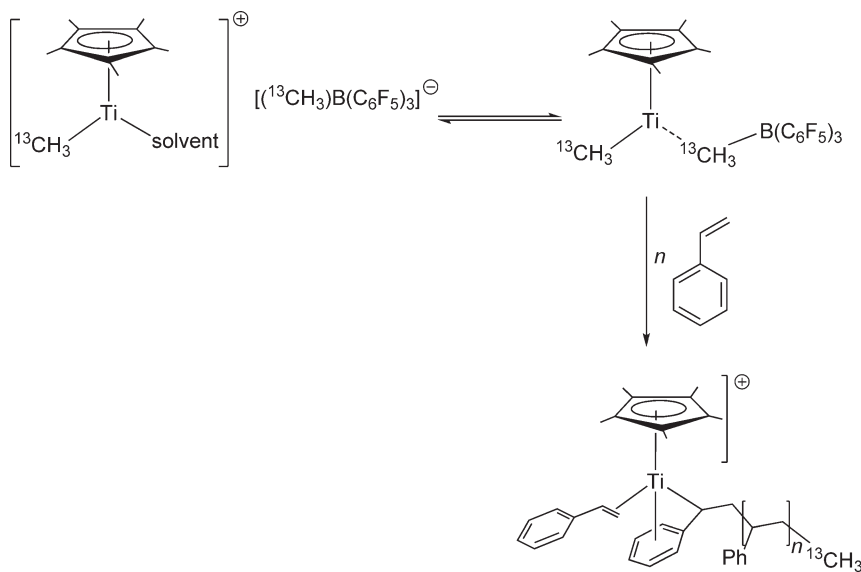
Complexes with pendant ether groups such as  $(\text{C}_5\text{H}_4\text{CH}_2\text{CH}_2\text{OMe})\text{TiCl}_3$ ,  $[\text{C}_5\text{H}_4\text{CH}_2\text{CH}(\text{Me})\text{OMe}]\text{TiCl}_3$ , and tetrahydrofurfuryl–Cp trichloro titanium complexes activated by MAO have been found to trimerize ethylene with high selectivity and moderate activity.<sup>488</sup> The silyl-substituted complexes  $(\text{C}_5\text{H}_4\text{SiMe}_2\text{X})\text{TiCl}_3$  ( $\text{X}=\text{Cl}$ , Me,  $\text{PhOMe}$ ) have been tested as catalyst precursors for the syndiospecific polymerization of styrene.<sup>489</sup>

The syndiotactic polymerization of styrene with *exo*-(isodiCp) $\text{TiCl}_3/\text{MAO}$  has been studied.<sup>490</sup>

Cationic titanium species have received major interest in recent years due to their role as active species in the Ziegler–Natta catalyzed olefin polymerizations. Synthetic methods for such cationic titanium species generally include halide or alkyl abstraction using different kinds of reagents. Thus, the compounds  $\text{Cp}^*\text{TiMe}_2\text{X}$  ( $\text{X}=\text{Cl}$ ,  $\text{C}_6\text{F}_5$ ,  $\text{OC}_6\text{F}_5$ ) react with  $\text{B}(\text{C}_6\text{F}_5)_3$  to form the thermally unstable chiral zwitterions  $\text{Cp}^*\text{TiMeX}(\mu\text{-Me})\text{B}(\text{C}_6\text{F}_5)_3$  (Scheme 195). These compounds exhibit good activities for the polymerization of ethylene to high molecular weight polyethylene. Despite their chirality, propylene polymerization is not stereospecific and gives atactic, elastomeric polypropylene. The microstructure of the resulting polypropylene has been analyzed. An EPR study of the  $\text{Cp}^*\text{TiMe}_3/\text{B}(\text{C}_6\text{F}_5)_3$  system in toluene indicates that <0.01% of the titanium is present as  $\text{Ti(III)}$  during the



Scheme 195



Scheme 196

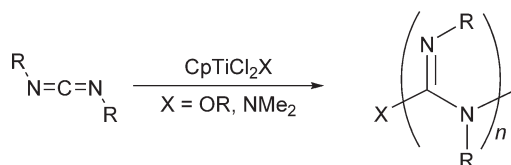
polymerization process, suggesting that a contribution to catalysis by titanium(III) species is unlikely.<sup>491</sup> At temperatures above 0°C, syndiotactic polystyrene is formed via a coordination-type Ziegler–Natta mechanism with a 15-electron Ti(III) species as the active center (Scheme 196).<sup>492</sup> Similar suggestions have been made for a series of Cp''TiR<sub>3</sub>/MAO (R = Cl, alkyl) catalysts for the syndiospecific polymerization of styrene.<sup>493,494</sup>

Mono-Cp' dichloro monoalkyl, monoamido, or monoalkoxo complexes Cp'TiCl<sub>2</sub>X (X = OCH<sub>2</sub>CF<sub>3</sub>, NMe<sub>2</sub>, Me) have been studied as pre-catalysts for the polymerization of functionalized isocyanates in the presence of donor solvents and activated and strained olefins, in some cases resulting in living polymerization. Titanium–alkoxo, titanium–amido, and titanium–alkyl bonds were all found to be active in initiating the insertion of isocyanate monomers. An advantageous consequence of the lower Lewis acidity of the cyclopentadienyl derivatives Cp'TiCl<sub>2</sub>X relative to the non-Cp TiCl<sub>3</sub>(OCH<sub>2</sub>CF<sub>3</sub>) is that the polymerization of highly functionalized monomers is possible. The activity of the catalysts decreased with increasing steric bulk about the metal center and increasing electron donation to the metal center from the ligands. Kinetic and mechanistic investigations are also reported. The use of mono-Cp' trichloro titanium derivatives also provides a general route through which a wide variety of end groups may be incorporated into the polyisocyanate chain.<sup>495,496</sup>

Cp'TiCl<sub>2</sub>X (X = NMe<sub>2</sub>, OEt) have been found to initiate the living polymerization of carbodiimides with reduced activity. The reactivity is largely determined by the steric demands of the monomer. Larger substituents inhibit or prevent the polymerization reaction. The mechanism for this polymerization has been shown to involve initiation by insertion of the monomer into the Ti–X bond to form an intermediate amidinate complex (Scheme 197).<sup>497</sup>

#### 4.05.3.1.3.(v) Halide abstraction

The hexachloroantimonate(v) salts of [Cp'TiCl<sub>2</sub>L<sub>3</sub>]<sup>+</sup>, [Cp'TiClL<sub>4</sub>]<sup>2+</sup>, and [Cp'TiL<sub>5</sub>]<sup>3+</sup> (L = NCMe) are prepared by treatment of Cp'TiCl<sub>3</sub> with SbCl<sub>5</sub> as chloro abstractor in acetonitrile. These products, obtained as the acetonitrile adducts, have been characterized by analytical and <sup>1</sup>H NMR and IR spectroscopy data and in the case of



Scheme 197

$[CpTi(NCMe)_5]^{3+}$  by a crystal structure determination. A significant *trans*-influence of the cyclopentadienyl ligand affects Ti–N bond lengths in the complex. Proton NMR studies indicate the presence of intermediate halo-bridged species in solution during successive halide abstractions  $1 \rightarrow 2 \rightarrow 3$ .<sup>498</sup>

#### 4.05.3.2 Mono-Cp Complexes with Ti–C Bonds

##### 4.05.3.2.1 Synthesis

Examples of mono-Cp' alkyltitanium derivatives can also be found in Section 4.05.3.1.3.(iii), derived by halide metathesis from the corresponding chloro complexes.

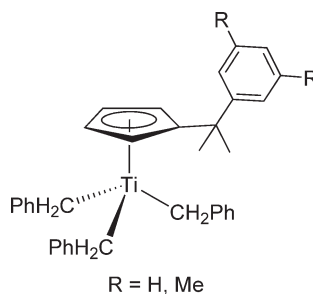
The monomethyl complexes  $(Ind)TiX_2Me$  ( $X = Cl, Br$ ) are efficiently prepared from the corresponding trihalides with  $AlMe_3$ . Their molecular structures have been determined by X-ray diffraction.<sup>402</sup> The tribenzyl compound  $(C_5H_4PPh_3)TiBz_3$  is obtained by alkylation of  $(C_5H_4PPh_3)TiCl_3$  with  $MgBz_2 \cdot 2THF$ .<sup>397</sup> The tribenzyl complexes with Cp–arene ligands  $(C_5H_4CMe_2Ar)Ti(CH_2Ph)_3$  (Scheme 198) react with  $B(C_6F_5)_3$  or  $Ph_3C[B(C_6F_5)_4]$  to give the corresponding cationic species. The thermal decomposition of the neutral and cationic complexes has been studied. Decomposition of both the neutral and cationic derivatives leads to *ortho*-metallation of the pendant arene group, although via different pathways. The cationic species undergo direct  $\sigma$ -bond metathesis, while the neutral compounds initiate the process by  $\alpha$ -abstraction followed by subsequent addition of the arene *o*-CH bond to the alkylidene intermediate.<sup>499</sup>

The  $\eta^5$ -fluorenyl- $\eta^1$ -fluorenyltitanium compound  $(\eta^5\text{-Flu})Ti(\eta^1\text{-Flu})(OPr^i)_2$  has been obtained as a byproduct in the synthesis of  $Ti(\eta^1\text{-Flu})(OPr^i)_3$  by reaction of  $TiCl(OPr^i)_3$  with equimolar amounts of  $LiFlu$ .<sup>500</sup>

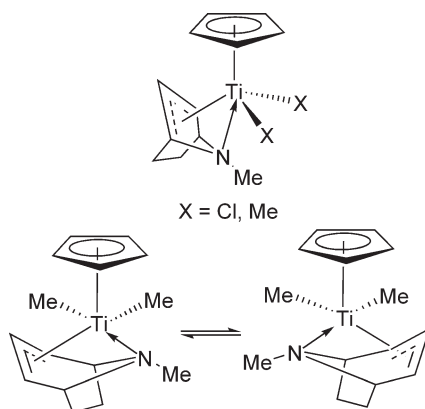
The mixed Cp/Trop (Trop = tropidynyl) complex  $CpTi(Trop)Cl_2$  has been synthesized in 97% yield by reaction of the tropidynyltin reagents with  $CpTiCl_3$ . The dimethyl derivative  $CpTiTropMe_2$  (Scheme 199) can be prepared by treatment with  $LiMe$ . Variable-temperature NMR studies indicate dynamic processes in solution. At room temperature in  $CD_2Cl_2$  the dichloro compound exists as a mixture of two interconverting diastereomers, the major isomer exhibiting apparent  $C_s$ -symmetry and the minor isomer exhibiting  $C_1$ -symmetry. The dimethyl complex exists in solution as a single diastereomer that undergoes interconversion of enantiomers (Scheme 199), giving rise to an average  $C_s$ -symmetric structure according to the NMR spectroscopic studies. The activity of these complexes in ethylene and propylene polymerizations has been evaluated and the nature of the active species investigated.<sup>501</sup>

The synthesis and characterization of the neutral homoenolate  $CpTiCl_2(CH_2CH_2COOEt)$  has been reported (Scheme 200).<sup>53</sup>

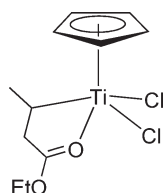
The chiral mono-Cp  $\sigma$ -cyclohexadienyl compound shown in Scheme 201 has been synthesized. The reaction with benzaldehydes proceeds with excellent diastereoselectivity. This reactivity has been used for the synthesis of nephrosteranic acid and chiral lactone compounds.<sup>23</sup>



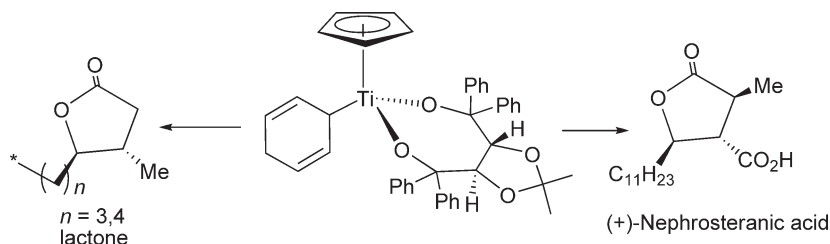
Scheme 198



Scheme 199



Scheme 200

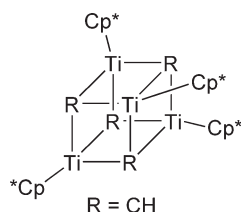


Scheme 201

A series of Ti complexes containing arylaminato ligands  $\text{C}_6\text{H}_4\text{CH}_2\text{R}^-$  ( $\text{R} = \text{dialkylamino}$ ) have been reported. Reaction of  $\text{Cp}^*\text{TiCl}_3$  with 1 equiv. of  $\text{Li}(\text{C}_6\text{H}_4\text{-2-CH}_2\text{R})$  in diethyl ether gives the complexes  $\text{Cp}^*\text{TiCl}_2(\text{C}_6\text{H}_4\text{-2-CH}_2\text{R})$  ( $\text{R} = \text{NMe}_2$ ,  $\text{NEt}_2$ ,  $\text{N}(\text{CH}_2\text{CH}=\text{CH}_2)$ ,  $\text{NC}_4\text{H}_8\text{O}$ ,  $\text{NMeCH}_2\text{Ph}$ ), isolated in good yields. The molecular structures of some of these complexes have been determined by X-ray diffraction methods. The compounds possess distorted square-pyramidal coordination for the Ti atom, with Cp located in the apical position. The coordination of the amino functionality is essential for complex stabilization. These compounds exhibit fluxional behavior in solution, as deduced by NMR spectroscopic studies, involving two consecutive exchange processes, pseudo-rotation reaction, and Ti–N cleavage followed by inversion at the N atom.<sup>504</sup>

The methyldiene cubane  $[\text{Cp}^*\text{Ti}(\mu\text{-CH})_4]$  (Scheme 202) is obtained as a dark brown crystalline solid by thermolysis of  $\text{Cp}^*\text{TiMe}$  in toluene with methane elimination. This transformation was monitored by  $^1\text{H}$  NMR and no intermediates are observed. The signals assignable to the methyldiene groups appear as singlets at  $\delta$  17.75 in the  $^1\text{H}$  NMR and at  $\delta$  490.8 in the  $^{13}\text{C}$  NMR spectra. In order to analyze the interaction between the  $\mu_3$ -ligand and the titanium centers, extended Hückel molecular orbital calculations have been carried out. In contrast, the thermolysis of the trinuclear oxo alkyls  $[\text{Cp}^*\text{Ti}(\mu\text{-O})(\text{CH}_2\text{R})_3]$  ( $\text{R} = \text{H}$ , Me) affords the  $\mu_3$ -alkyldiene derivatives  $[\text{Cp}^*\text{Ti}(\mu\text{-O})]_3(\mu_3\text{-CR})$ .<sup>505–507</sup>

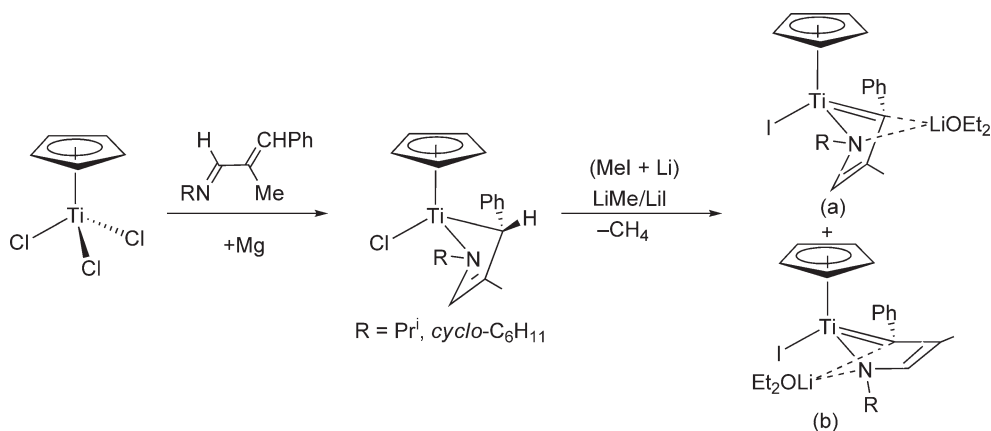
$\text{Cp}^*\text{TiCl}_3$  reacts with Mg in the presence of 1-aza-1,3-dienes to give the corresponding aza-titanacyclopentene derivatives, isolated as air sensitive green-brown crystals. Treatment of these compounds with  $\text{LiMe}$  leads to the



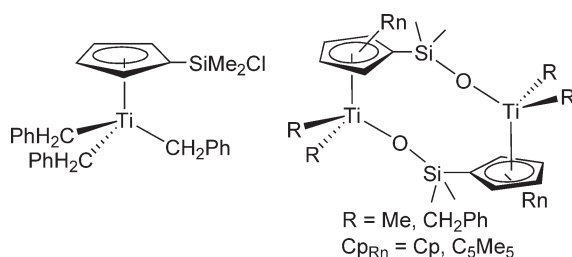
Scheme 202

formation of the methyl derivatives, spectroscopically detected at low temperature in solution and isolated for the cyclohexyl derivative. At room temperature, this reaction proceeds with methane elimination and new metallacyclic titanium–alkylidene complexes are formed. In the  $^{13}\text{C}$  NMR spectra the signals for the metal–heterodiene carbon atoms in these alkylidene derivatives appear at  $\delta$  244.69 and 244.62. An important role in the synthesis of these alkylidene titanium complexes is played by lithium iodide generated in the preparation of  $\text{LiMe}$  and present in the reaction mixture (Scheme 203). The molecular structures of these complexes have been determined by X-ray diffraction. The  $\text{Ti}-\text{C}_{\text{alkylidene}}$  bond lengths are 1.958(3) Å for the isomer (a) and 1.973(4) Å for the isomer (b), shorter than the  $\text{Ti}-\text{C}$  single bond distances, corresponding to a  $\text{Ti}=\text{C}$  double bond.<sup>508</sup> (More examples of aza–titanacycle derivatives are given in Section 4.05.3.3.2).

The complex  $(\text{C}_5\text{H}_4\text{SiMe}_2\text{Cl})\text{TiCl}_3$  has two types of metal–chloro bonds,  $\text{Ti}-\text{Cl}$  and  $\text{Si}-\text{Cl}$ . As discussed in Section 4.05.3.1.3, both bonds are simultaneously involved in reactions with protic reagents such as water. However, reactions with Grignard reagents take place selectively at the  $\text{Ti}-\text{Cl}$  bond to give alkyltitanium derivatives. Reaction with  $\text{Mg}(\text{CH}_2\text{C}_6\text{H}_5)_2(\text{THF})_2$  leads to the tribenzyl derivative  $(\text{C}_5\text{H}_4\text{SiMe}_2\text{Cl})\text{Ti}(\text{CH}_2\text{C}_6\text{H}_5)_3$ . The same reaction with  $\text{MgClMe}$  leads to a yellow oil that spontaneously decomposes with evolution of methane to give a dark paramagnetic unidentified residue. Alkylation of the dimeric oxo derivative  $[(\text{C}_5\text{R}^1\text{SiMe}_2\text{O}-)\text{TiCl}_2]_2$  ( $\text{R}^1 = \text{H}, \text{Me}$ ) with  $\text{MgClMe}$  or  $\text{Mg}(\text{CH}_2\text{C}_6\text{H}_5)_2(\text{THF})_2$  allows the isolation of the oxoalkyl complexes  $[(\text{C}_5\text{H}_4\text{SiMe}_2\text{O}-)\text{TiR}^2]_2$



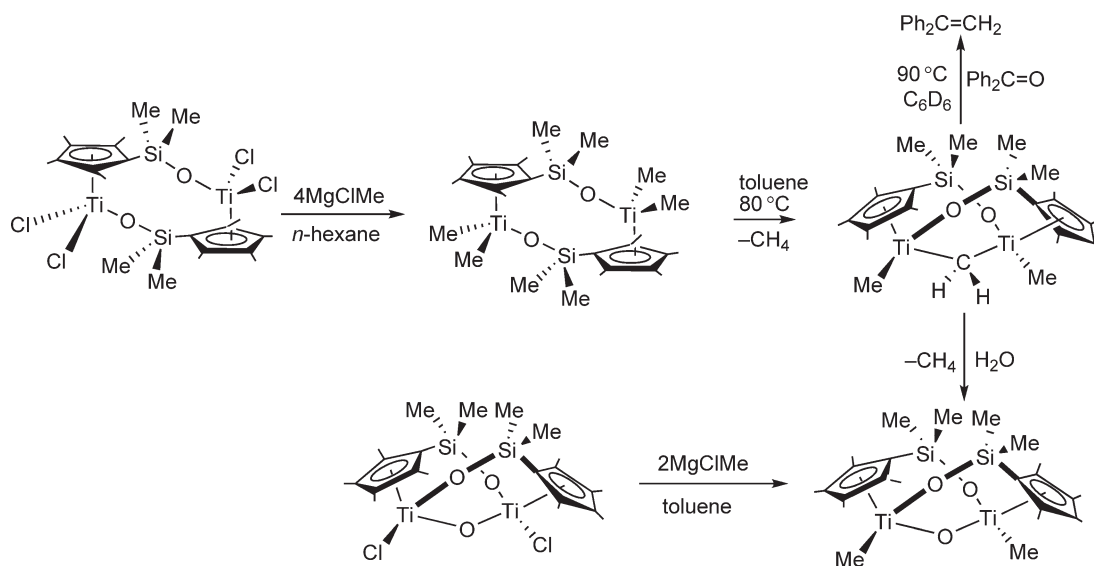
Scheme 203



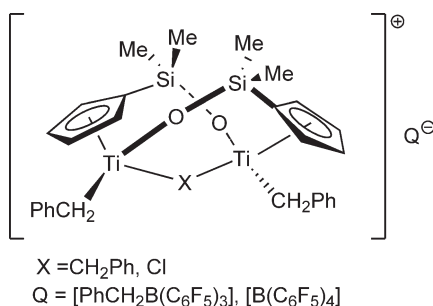
Scheme 204

( $R^2 = \text{Me}, \text{CH}_2\text{C}_6\text{H}_5$ ) (Scheme 204).<sup>380,381</sup> Methylation of the chlorosilyl-Cp' complexes  $(\text{C}_5\text{Me}_4\text{SiMeXCl})\text{TiCl}_3$  ( $X = \text{H}, \text{Cl}$ ) and  $(\text{C}_5\text{Me}_4\text{SiMe}_3)\text{TiCl}_3$  with  $\text{MgClMe}$  under appropriate conditions affords the corresponding trimethyl complexes. Attempts to isolate partially methylated complexes by reactions with variable molar ratios of  $\text{MgClMe}$  are performed.<sup>383</sup>

$[(\mu, \eta^5\text{-C}_5\text{Me}_4\text{SiMe}_2\text{-O})\text{TiCl}_2]_2$  reacts with stoichiometric amount of  $\text{MgClMe}$  to give the tetramethyl derivative  $[(\mu, \eta^5\text{-C}_5\text{Me}_4\text{SiMe}_2\text{-O})\text{TiMe}_2]_2$ , thermolysis of which affords the methylene-bridged titanium compound  $[(\mu, \eta^5\text{-C}_5\text{Me}_4\text{SiMe}_2\text{-O})\text{TiMe}]_2(\mu\text{-CH}_2)$ , accompanied by the evolution of methane. Reaction of the  $\mu$ -methylene compound with water affords the isostructural  $\mu$ -oxo complex  $[(\mu, \eta^5\text{-C}_5\text{Me}_4\text{SiMe}_2\text{-O})\text{TiMe}]_2(\mu\text{-O})$ , which can be alternatively obtained by methylation of the chloro compound  $[(\mu, \eta^5\text{-C}_5\text{Me}_4\text{SiMe}_2\text{-O})\text{TiCl}]_2(\mu\text{-O})$ , while the reaction with benzophenone follows the typical "Wittig-type" reactions studied in organic chemistry (Scheme 205). The molecular structure of the  $\mu\text{-CH}_2$  complex has been determined by X-ray diffraction methods.<sup>509</sup>  $[(\mu, \eta^5\text{-C}_5\text{H}_4\text{SiMe}_2\text{-O})\text{TiCl}_2]_2$  can be alkylated by reaction with  $\text{MgClMe}$  or  $\text{Mg}(\text{CH}_2\text{Ph})_2 \cdot 2\text{THF}$  to give the tetraalkyl derivatives.<sup>380</sup> Treatment of  $[(\mu, \eta^5\text{-C}_5\text{H}_4\text{SiMe}_2\text{-O})\text{Ti}(\text{CH}_2\text{Ph})_2]_2$  with the Lewis acids  $\text{B}(\text{C}_6\text{F}_5)_3$  or  $(\text{Ph}_3\text{C})[\text{B}(\text{C}_6\text{F}_5)_4]$  in toluene at room temperature affords the thermally unstable binuclear monocationic compound  $\{[(\mu, \eta^5\text{-C}_5\text{H}_4\text{SiMe}_2\text{-O})\text{Ti}]_2(\text{CH}_2\text{Ph})_3\}^+\text{Q}^-$ . In aromatic solvents it decomposes to give paramagnetic mixed valence species, while in chlorinated solvents it evolves to the  $\mu$ -chloro derivative  $\{[(\mu, \eta^5\text{-C}_5\text{H}_4\text{SiMe}_2\text{-O})(\text{CH}_2\text{Ph})_2\text{Ti}]_2(\mu\text{-Cl})\}^+\text{Q}^-$  (Scheme 206).<sup>510</sup> Alkylation of *cis*- and *trans*- $[(\text{C}_5\text{H}_3)_2(\text{SiMe}_2)_2](\text{TiCl}_3)_2$  with  $\text{MgClMe}$  leads, respectively, to the partially alkylated *cis*- $[(\text{C}_5\text{H}_3)_2(\text{SiMe}_2)_2](\text{TiClMe})_2$  and the totally alkylated *trans*- $[(\text{C}_5\text{H}_3)_2(\text{SiMe}_2)_2](\text{TiMe}_3)_2$  compounds (Scheme 164; Section 4.05.3.1.1.(iv)).<sup>386</sup>



Scheme 205



Scheme 206



#### 4.05.3.2.2 Structural aspects

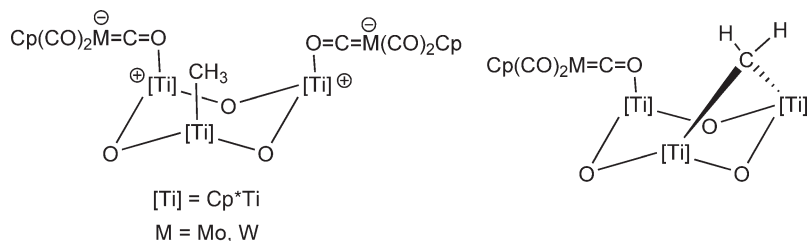
Information on the properties of C–H bonds in alkyl–metal compounds is often obtained by means of NMR spectroscopy, although these spectroscopic data do not lead directly to satisfactory information concerning agostic interactions, CH activation, or hydride-transfer processes. In this sense information on ethylmetal complexes is particularly desirable in view of their importance in this type of processes. This kind of information is better contained by vibrational spectroscopy. The vibrational spectra of various isotopomers of the methyl- and ethyltitanium complexes  $\text{Cp}^*\text{TiCl}_2\text{R}$  ( $\text{R} = \text{CH}_3, \text{CD}_3, \text{CHD}_2, \text{CH}_3\text{CH}_2, \text{CD}_3\text{CH}_2, \text{CH}_3\text{CD}_2, \text{CHD}_2\text{CD}_2$ ) have been described and used to estimate the CH bond lengths, bond strengths, and HCH angles from the resonance-corrected frequency data. A method for the calculation of Fermi resonance shifts on CH and CD stretching modes in methyl groups is elaborated. The results show the methyl group to be markedly asymmetric, with the CH bond *trans* to the Cp ligand being ca. 0.005 Å longer and 15 kJ mol<sup>−1</sup> weaker than those *trans* to the chloro ligand. In the ethyl compounds, the terminal methyl group is similarly asymmetric, again with one weak bond and two stronger bonds. The results of the frequencies for the methylene group appear to point to a direct  $\alpha$ -interaction between at least one of the methylene CH bonds and the titanium atom. A similar effect may also occur in the methyl derivative.<sup>511</sup>

#### 4.05.3.2.3 Reactions

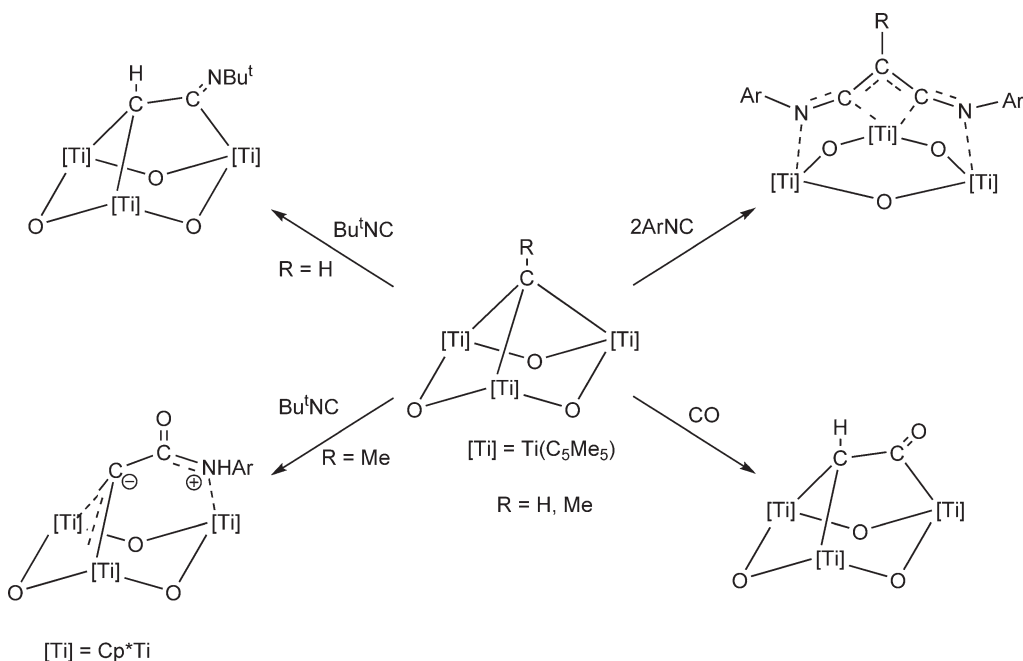
$\mu$ -Methylene titanium/transition metal heterobimetallic complexes have been previously reported.<sup>512</sup> The synthesis of the  $\mu_3$ -alkylidyne compound  $[\text{Cp}^*\text{Ti}(\mu\text{-O})]_3(\mu_3\text{-CH})$  has been described and the reactivity of the  $\text{Ti}_3\text{-}\mu_3\text{-CH}$  fragment studied in reactions with carbonyl hydride transition metal complexes to give a new substance containing the  $(\text{Ti-O-Ti})(\mu_2\text{-CH}_2)$  fragment. Reaction of  $[\text{Cp}^*\text{Ti}(\mu\text{-O})]_3(\mu_3\text{-CH})$  with  $\text{Cp}^*\text{M}(\text{CO})_3\text{H}$  ( $\text{M} = \text{Mo}, \text{W}$ ) leads to the formation of Lewis acid carbonyl adducts  $[\text{Cp}^*_3\text{Ti}_3(\mu\text{-O})_3\text{Me}][(\mu\text{-OC})\text{M}(\text{CO})_2\text{Cp}]_2$ . The formation of the methylene-bridging intermediates  $[\text{Cp}^*_3\text{Ti}_3(\mu\text{-O})_3(\mu\text{-CH}_2)][(\mu\text{-OC})\text{M}(\text{CO})_2\text{Cp}]$  is proposed in this process (Scheme 207). In the <sup>1</sup>H NMR spectra the protons of the CH<sub>2</sub> bridging group appear as an AB spin system at  $\delta$  6.60 and 6.00 with coupling constant values of <sup>2</sup>*J*<sub>HH</sub> = 10 Hz. The <sup>13</sup>C NMR spectrum shows the methylene carbon resonances at  $\delta$  198.<sup>507</sup> The reactivity of the  $\mu_3$ -alkylidyne titanium complex  $[\text{Cp}^*\text{Ti}(\mu\text{-O})]_3(\mu_3\text{-CR})$  ( $\text{R} = \text{H}, \text{Me}$ ) toward isocyanides and CO has been found to give different monoinsertion or diinsertion products depending on the reaction conditions. Some illustrative examples are shown in Scheme 208.<sup>513</sup>

$(\text{C}_5\text{H}_4\text{CMe}_2\text{Ar})\text{TiMe}_3$  ( $\text{Ar} = 3,5\text{-dimethylphenyl}$ ) reacts with  $\text{B}(\text{C}_6\text{F}_5)_3$  to give the ionic compound  $[(\text{C}_5\text{H}_4\text{CMe}_2\text{Ar})\text{-TiMe}_2][\text{MeB}(\text{C}_6\text{F}_5)_3]$  in which the aryl–Cp substituent is coordinated to the titanium center to give an *ansa*-arene complex. The NMR data are consistent with a non-coordinated anion and show substantial intramolecular coordination chemical shifts for the phenyl ring. The presence of an excess of  $\text{B}(\text{C}_6\text{F}_5)_3$  leads to the formation of  $\text{BMe}(\text{C}_6\text{F}_5)_2$  and the titanium species  $[(\text{C}_5\text{H}_4\text{CMe}_2\text{Ar})\text{TiMe}(\text{C}_6\text{F}_5)][\text{MeB}(\text{C}_6\text{F}_5)_3]$ . In the <sup>13</sup>C NMR spectrum of this compound, a triplet at  $\delta$  102.7 with <sup>3</sup>*J*<sub>CF</sub> = 7.3 Hz is observed for the Ti–Me group. In bromobenzene solution these species evolve with formation of the titanium(III) compound  $[(\text{C}_5\text{H}_4\text{CMe}_2\text{Ar})\text{Ti}(\mu\text{-Br})]_2[\text{B}(\text{C}_6\text{F}_5)_4]$ , the molecular structure of which has been determined by X-ray diffraction indicating a highly asymmetric bonding of the Ph ring to the Ti atom. The formation of this complex involves reduction of the titanium center, cleavage of the solvent Br–C bond, and a scrambling of the substituents on the borane/borate species.<sup>328</sup>

Metallocene derivatives are the most extensively studied class of homogeneous catalysts for the polymerization of olefins. Less saturated and less hindered mono-Cp group 4 metal species of the type  $[\text{Cp}'\text{MR}_2]^+$  ( $\text{Cp}'$  denotes Cp or a substituted cyclopentadienyl ring) may also behave as useful catalysts or initiators for olefin polymerization. Catalysts for syndiospecific polymerization of styrene based on mono-Cp titanium derivatives with different substituents on the Cp ligand and with various types of tetraphenylborates have been examined. A good relationship between the



Scheme 207



Scheme 208

electron density of titanium atom and the space for styrene coordination has been found.<sup>514</sup> Mixtures of  $\text{Cp}^*\text{TiMe}_3$  and  $\text{B}(\text{C}_6\text{F}_5)_3$  produce the zwitterion  $\text{Cp}^*\text{TiMe}_2(\mu\text{-Me})\text{B}(\text{C}_6\text{F}_5)_3$  which acts as the source for the 10-electron cationic species  $[\text{Cp}^*\text{TiMe}_2]^+$ . The compound  $\text{Cp}^*\text{TiMe}_2(\mu\text{-Me})\text{B}(\text{C}_6\text{F}_5)_3$  reacts further with  $\text{Cp}^*\text{TiMe}_3$  to give the unstable binuclear methyl-bridged ion pair  $[\text{Cp}^*\text{TiMe}_2(\mu\text{-Me})\text{Ti}(\text{C}_5\text{Me}_5)\text{Me}_2]^+[\text{MeB}(\text{C}_6\text{F}_5)_3]^-$  and spectroscopically characterized coordinated arene species.<sup>515–517</sup>

The  $\text{Cp}^*\text{TiMe}_3/\text{B}(\text{C}_6\text{F}_5)_3$  system is one of the most versatile and potentially useful olefin polymerization initiators known. It has been claimed as a true Ziegler–Natta catalyst<sup>518</sup> for ethylene,<sup>519–522</sup> propylene in the presence and absence of aromatic solvents,<sup>523</sup> styrene (syndiotactic polystyrene) and substituted styrene ( $\alpha$ -methylstyrene to largely syndiotactic polymer),<sup>493,519,521,524,525</sup> 1-hexene,<sup>522,526,527</sup> norbornene and 1,5-hexadiene,<sup>528</sup> and an excellent initiator for polymerization of norbornene via Ziegler and ROMP processes and of 1,5-hexadiene via cyclopolymerization.<sup>519,528</sup>  $\text{Cp}^*\text{TiMe}_3$  in the presence of  $\text{B}(\text{C}_6\text{F}_5)_3$  is a very suitable system for preparing engineering parts made of syndiotactic polystyrene by a reaction injection molding (RIM) process.<sup>529</sup> The system  $\text{Cp}^*\text{Ti}(\text{CH}_2\text{Ph})_3/\text{B}(\text{C}_6\text{F}_5)_3$  has been found to polymerize ethylene and  $\text{Cp}^*\text{Ti}(\text{CH}_2\text{Ph})_3/\text{B}(\text{C}_6\text{F}_5)_3/\text{AlMe}_3$  to polymerize propylene to atactic polymers.<sup>520</sup> The catalytic system  $\text{Cp}^*\text{TiMe}_3/\text{Al}(\text{octyl})_3$  has been used for the polymerization of styrene and 4-methylstyrene.<sup>530</sup>  $\text{Cp}^*\text{Ti}(\text{CH}_2\text{Ph})_3/\text{Ph}_3\text{C}[\text{B}(\text{C}_6\text{F}_5)_4]$  is also a good polymerization catalyst.<sup>531</sup> Control of regiospecificity in propene polymerization with  $\text{SiO}_2$ -supported  $\text{Cp}^*\text{TiMe}_3$  catalysts has been studied.<sup>532</sup>

The catalyst  $\text{Cp}^*\text{Ti}(\text{CH}_2\text{Ph})_3/\text{B}(\text{C}_6\text{F}_5)_3$  co-polymerizes ethylene and styrene and gives poly(ethylene-*co*-styrene) in a mixture of polyethylene and syndiotactic polystyrene.<sup>533</sup> Co-polymerizations of ethylene and styrene<sup>534</sup> and branched polyethylene containing significant amounts of almost exclusively butyl branches have been developed from a simple ethylene feed using this system, and the mechanism of branch formation is discussed.<sup>534–536</sup> The co-polymerization of propene with 7-methyl-1,6-octadiene is catalyzed by  $\text{Cp}^*\text{TiMe}_3/\text{B}(\text{C}_6\text{F}_5)_3$  and gives atactic random co-polymers with unsaturated side chains.<sup>537</sup>

The catalytic systems  $\text{Cp}^*\text{TiMe}_3/\text{MAO}$  and  $\text{Cp}^*\text{TiCl}_3/\text{MAO}$  have been studied using  $^{13}\text{C}$  and  $^1\text{H}$  NMR spectroscopy in toluene and chlorobenzene solutions within the temperature range 253–293 K and at Al/Ti ratios 30–300. It was shown that upon activation of  $\text{Cp}^*\text{TiMe}_3$  mainly the “cation-like” intermediate  $\text{Cp}^*\text{Me}_2\text{Ti}^+-\text{Me}^--\text{Al}(\text{MAO})$  is formed, while three types of titanium(IV) complexes were identified in the chloro system  $\text{Cp}^*\text{TiCl}_3/\text{MAO}$ . They are the methylated complexes  $\text{Ti}(\text{C}_5\text{Me}_5)\text{MeCl}_2$  and  $\text{Cp}^*\text{TiMe}_2\text{Cl}$  and “cation-like” intermediates.<sup>538</sup> The system  $\text{Cp}^*\text{Ti}(\text{CH}_2\text{Ph})_3/\text{MAO}$  has been employed to catalyze propene polymerization at ambient pressure. An atactic high molecular weight polypropylene elastomer is produced.<sup>539</sup> Reaction of  $\text{Cp}^*\text{Ti}(\text{CH}_2\text{SiMe}_3)_3$  with  $\text{B}(\text{C}_6\text{F}_5)_3$  in hydrocarbon solvents affords the ionic complex  $[\text{Cp}^*\text{Ti}(\text{CH}_2\text{SiMe}_3)_2][\text{Me}_3\text{SiCH}_2\text{B}(\text{C}_6\text{F}_5)_3]$  which was used to polymerize

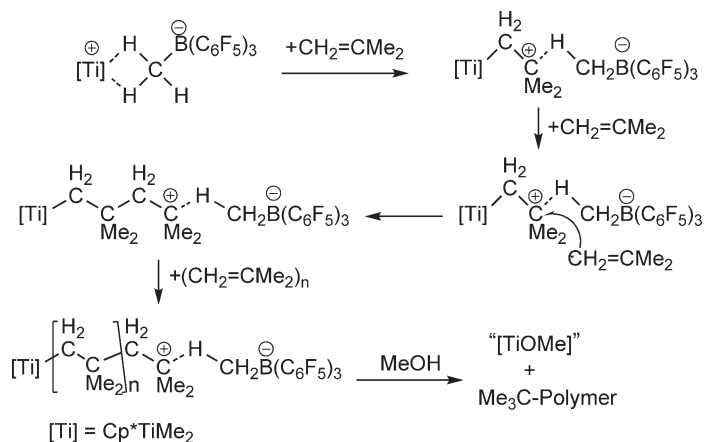
styrene. The role of the Lewis acid co-catalyst and the effect of the counteranion structure on the polymerization process was studied.<sup>540</sup>

Mono-Cp' titanium catalyst systems are also suitable for the polymerization of polar and non-polar olefinic monomers. The reduction of a mixture of Cp\*TiMe<sub>3</sub> and Ph<sub>3</sub>C[B(C<sub>6</sub>F<sub>5</sub>)<sub>4</sub>] with zinc produces a catalyst for the syndiotactic homopolymerization of styrene. The same catalyst mediates the polymerization of methyl methacrylate to poly(methyl methacrylate) (PMMA) with >65% of syndiotacticity. This system is also effective for the co-polymerization of styrene/methyl methacrylate upon optimal conditions. A new polymerization mechanism to explain the characteristics of the polymers is proposed based on sequential conjugate addition steps.<sup>541</sup>

The co-polymerization of isobutylene and isoprene by a cationic mechanism is the basis for the industrially important manufacture of butyl rubber. The cationic species [Cp\*TiMe<sub>2</sub>]<sup>+</sup> generated by reaction of Cp\*TiMe<sub>3</sub> and B(C<sub>6</sub>F<sub>5</sub>)<sub>3</sub> does behave as a very effective cationic initiator in this reaction.<sup>542</sup> The effects of polymerization temperature on the polymer molecular weight and polydispersity of the resulting poly(isobutylene) have been investigated. The suggested mechanism is depicted in Scheme 209.<sup>543</sup> The Cp\*TiMe<sub>3</sub>/B(C<sub>6</sub>F<sub>5</sub>)<sub>3</sub> system is also an excellent carbocationic polymerization initiator for other functionalized monomers.<sup>519,521,544</sup> The neutral borane, B(C<sub>6</sub>F<sub>5</sub>)<sub>3</sub>, is also a carbocationic polymerization initiator, but its efficiency is low; the activity is most probably due to the traces of its hydrate as a proton source.<sup>544</sup> The systems [Cp\*TiMe<sub>2</sub>][B(C<sub>6</sub>F<sub>5</sub>)<sub>4</sub>] and [Cp\*TiMe<sub>2</sub>](*n*-C<sub>18</sub>H<sub>37</sub>E)B(C<sub>6</sub>F<sub>5</sub>)<sub>3</sub> (E = O, S) containing a weakly coordinating counteranion have also been used as carbocationic initiators of isobutene homopolymerizations in the temperature range of -40 to -10 °C<sup>545</sup> and for the co-polymerization of isobutene with isoprene at relatively high temperatures.<sup>546</sup>

It has been proposed that the cationic Ti(III) intermediate [Cp\*TiMe]<sup>+</sup> may be the true active species in the Cp\*TiMe<sub>3</sub>/B(C<sub>6</sub>F<sub>5</sub>)<sub>3</sub> system for the synthesis of syndiotactic polystyrene.<sup>547</sup> There is experimental evidence from EPR investigations on mixtures of Cp\*TiMe<sub>3</sub> and Cp\*Ti(CH<sub>2</sub>Ph)<sub>3</sub> with B(C<sub>6</sub>F<sub>5</sub>)<sub>3</sub> or Ph<sub>3</sub>CB(C<sub>6</sub>F<sub>5</sub>)<sub>4</sub> that the initially formed ionic products, such as Cp\*TiMe<sub>2</sub>(*μ*-Me)B(C<sub>6</sub>F<sub>5</sub>)<sub>3</sub>, rapidly decompose to Ti(III) species (Scheme 196).<sup>548-552</sup> Similar suggestions have been made for the Cp\*Ti(OMe)<sub>3</sub>/MAO and Cp\*<sub>2</sub>Ti(OMe)<sub>2</sub>/MAO systems.<sup>553,554</sup> On the other hand, combined NMR/EPR studies on the catalytic systems Cp\*TiMe<sub>3</sub>/B(C<sub>6</sub>F<sub>5</sub>)<sub>3</sub>, Cp\*TiMe<sub>3</sub>/Ph<sub>3</sub>CB(C<sub>6</sub>F<sub>5</sub>)<sub>4</sub>, and Cp\*TiCl<sub>2.3</sub>/MAO have suggested that the involvement of EPR-active titanium(III) species as catalysts is ambiguous.<sup>555</sup>

Species of the type [Cp\*TiMe(OR)]<sup>+</sup> have been synthesized and shown to be less active than [Cp\*TiMe<sub>2</sub>]<sup>+</sup>.<sup>519</sup> The synthesis, characterization, and solution chemistry of the compounds Cp\*TiMe<sub>2</sub>X (X = C<sub>6</sub>F<sub>5</sub>, OC<sub>6</sub>F<sub>5</sub>) and Cp\*TiMe(OC<sub>6</sub>F<sub>5</sub>)<sub>2</sub> which contain poor  $\pi$ -electron donor ligands have been investigated.<sup>491,556,557</sup> These complexes have been characterized by a variety of techniques, including <sup>47/49</sup>Ti NMR spectroscopy. On reaction with B(C<sub>6</sub>F<sub>5</sub>)<sub>3</sub>, these compounds form Cp\*TiMeX(*μ*-Me)B(C<sub>6</sub>F<sub>5</sub>)<sub>3</sub> and [Cp\*TiMe(OC<sub>6</sub>F<sub>5</sub>)<sub>2</sub>][MeB(C<sub>6</sub>F<sub>5</sub>)<sub>3</sub>] as thermally unstable species. The solution chemistry of these species suggested that bulky substituents at the metal center can result in reduced metal cation-anion interactions in spite of the intrinsic electrophilicity of the metal centers. The reactions of Cp\*TiMe<sub>2</sub>X (X = Me, C<sub>6</sub>F<sub>5</sub>, OC<sub>6</sub>F<sub>5</sub>, Cl) with [Ph<sub>3</sub>C][B(C<sub>6</sub>F<sub>5</sub>)<sub>4</sub>] give thermally unstable dititanium complexes {[Cp\*TiMeX]<sub>2</sub>(*μ*-Me)} [B(C<sub>6</sub>F<sub>5</sub>)<sub>4</sub>]. These compounds behave as sources of the 10-electron cations [Cp\*TiMeX]<sup>+</sup>, which exhibit higher activities as ethylene and propylene polymerization catalysts than the analogous



Scheme 209

$\text{Cp}^*\text{TiMeX}(\mu\text{-Me})\text{B}(\text{C}_6\text{F}_5)_3$  compounds. The effect of substitution of a methyl ligand of  $[\text{Cp}^*\text{TiMe}_2]^+$  by a more electron withdrawing, to give  $[\text{Cp}^*\text{TiR}_2]^+$  ( $\text{R} = \text{C}_6\text{F}_5, \text{OC}_6\text{F}_5, \text{Cl}$ ), in the catalytic activity has been explored.<sup>558</sup>

The mono- $\text{Cp}'$ -arene complexes  $(\text{C}_5\text{H}_3\text{R}\text{-bridge-Ar})\text{TiX}_3$  ( $\text{R} = \text{H}, \text{SiMe}_3, \text{Bu}^t$ ;  $\text{Ar} = \text{Ph}, 4\text{-MeC}_6\text{H}_4; 3,6\text{-Me}_2\text{C}_6\text{H}_3$ ;  $\text{X} = \text{Cl}, \text{Me}$ ) shown in Scheme 147 (Section 4.05.3.1.1.(i)) with a hemilabile ancillary arene ligand are generators of a class of highly active catalysts for the selective trimerization of ethylene to 1-hexene.<sup>331,333</sup> Comprehensive theoretical mechanistic studies for these pre-catalysts, exploring the elementary steps and tentative catalytic cycle, have been reported.<sup>559-562</sup>

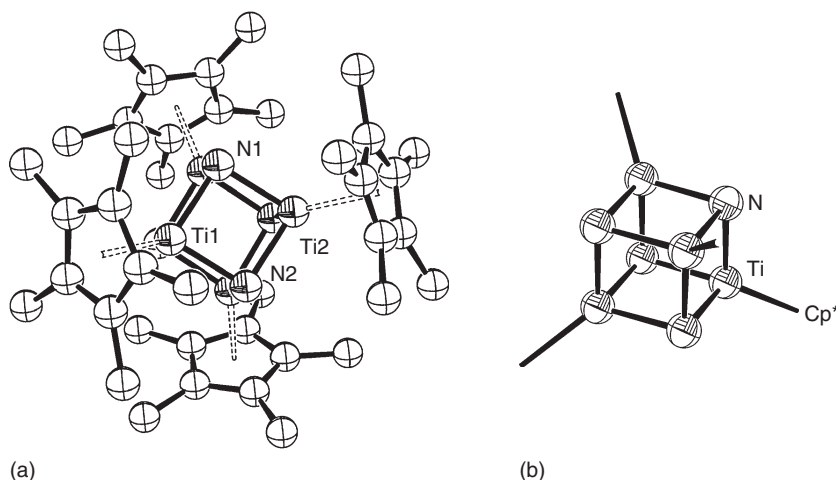
The activity of some mono- $\text{Cp}'$  and  $\text{Cp}$ -amido methyl Ti derivatives in  $\alpha$ -olefin polymerization process has been studied and the effects of the co-catalyst based on perfluoroborate compounds evaluated.<sup>563</sup> A detailed theoretical study of the ethylene trimerization at the cationic *ansa*- $\text{Cp}$ -arene fragment “ $(\text{C}_5\text{H}_4\text{CH}_2\text{C}_6\text{H}_5)\text{Ti}^+$ ” has been reported. The results confirm general features of previous proposals although they differ in other mechanistic details.<sup>561</sup> A DFT study on ethylene trimerization catalyzed by  $(\text{C}_5\text{H}_4\text{CMe}_2\text{C}_6\text{H}_5)\text{TiCl}_3/\text{MAO}$  to selectively give 1-hexene has been performed.<sup>559,562</sup>

### 4.05.3.3 Mono-Cp Complexes with Ti–N Bonds

#### 4.05.3.3.1 Amido complexes

The amido ligand is isoelectronic with the alkyl and alkoxo groups and has the possibility to exhibit N–M  $\pi$ -interactions in order to stabilize the systems they form. Different synthetic reactions are used to prepare mono- $\text{Cp}'$  titanium derivatives containing amido ligands. These compounds are normally synthesized by: (i) the action of the corresponding amide salt on  $\text{Cp}''\text{TiCl}_3$ , (ii) displacement of amine from a homoleptic amido titanium compound by a  $\text{Cp}'$  reagent, (iii) dehalosilylation reactions, and (iv) elimination of alkane by reaction of an alkyltitanium compound with amine.

The mononuclear amido titanium  $\text{Cp}^*\text{TiCl}_{2-n}(\text{NR}_2)_n$  ( $n = 1$ ;  $\text{R} = \text{Me}, \text{SiMe}_3$ ;  $n = 2$ ,  $\text{R} = \text{Me}, \text{Ph}$ ;  $n = 3$ ,  $\text{R} = \text{Me}, \text{Et}$ ), binuclear  $[\text{Cp}^*\text{TiCl}_{2-n}(\text{NR}_2)_n]_2(\mu\text{-O})$  ( $n = 1$ ,  $\text{R} = \text{Me}, \text{Ph}$ ;  $n = 2$ ,  $\text{R} = \text{Me}$ ), and trinuclear  $[\text{Cp}^*\text{TiCl}_{3-n}(\text{NMe}_2)_n]_3(\mu\text{-O})_3$  ( $n = 1, 3$ ) compounds are easily prepared by anion exchange reactions between  $\text{Cp}^*\text{TiCl}_3$  and stoichiometric amounts of the appropriate lithium amide under different reaction conditions. The crystal structure of  $\text{Cp}^*\text{Ti}(\text{NMe}_2)_3$  has been established by X-ray crystallography and is shown to be monomeric with the typical three-legged piano stool structure.<sup>564</sup> The molecular structure of this complex has been studied by gas electron diffraction and DFT calculations on this model compounds have been carried out.<sup>565</sup> The reactivity of these amido complexes has been widely studied. Treatment of  $\text{Cp}^*\text{Ti}(\text{NMe}_2)_3$  with an excess of ammonia in toluene at  $90^\circ\text{C}$  leads to the formation of the nitride cubane complex  $[\text{Cp}^*\text{Ti}(\mu_3\text{-N})]_4$  (Figures 8(a) and 8(b)) with a molecular structure showing a  $\text{Ti}_4\text{N}_4$  core where the titanium and the nitrogen atoms are located on alternating vertices with values of  $90^\circ$  for all the Ti–N–Ti and N–Ti–N angles.<sup>566</sup> Insertion of  $\text{CO}_2$  (approx. 1 atm.) into the metal–nitrogen bond in the complexes



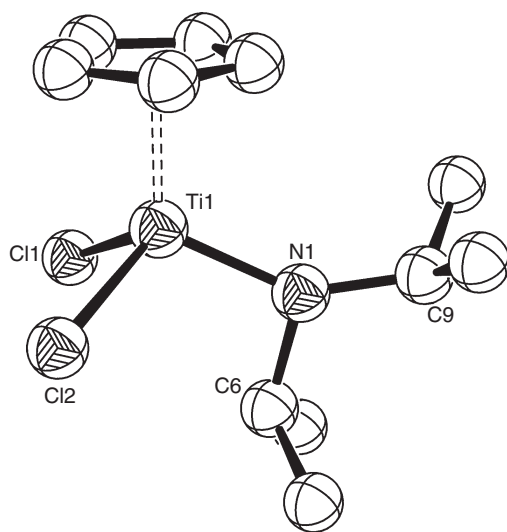
**Figure 8** Two views [(a) from one face; (b)  $\text{Ti}_4\text{N}_4$  core] of molecular structure of complex  $[\text{Cp}^*\text{Ti}]_4(\mu_3\text{-N})_4$  (reproduced by permission of the Royal Society of Chemistry from *J. Chem. Soc., Chem. Commun.*, **1995**, 2185).

$\text{Cp}^*\text{Ti}(\text{NR}_2)_3$  ( $\text{R} = \text{Me}, \text{Et}$ ) gives carbamato products  $\text{Cp}^*\text{Ti}(\text{O}_2\text{CNR}_2)_3$  which on hydrolysis furnish the O-bridged binuclear compound  $[\text{Cp}^*\text{Ti}(\text{O}_2\text{CNR}_2)_2]_2(\text{O})$ . Strong bands around  $1550\text{ cm}^{-1}$  are observed in the IR spectra for the  $\text{O}_2\text{CNR}_2$  moieties.<sup>567</sup> Treatment of  $\text{Cp}^*\text{TiCl}(\text{NR}_2)_2$  ( $\text{R} = \text{Me}, \text{Ph}$ ) with various alkyl- or aryllithium reagents generates the corresponding alkyl(aryl)bis[dialkyl(aryl)amido] derivatives  $\text{Cp}^*\text{TiR}^1(\text{NR}_2)_2$  in high yield ( $\text{R}^1 = \text{CH}_2\text{SiMe}_3, \text{Me}, \text{Ph}$ ).<sup>568</sup>  $\text{Cp}^*\text{Ti}(\text{NMe}_2)_3$  reacts with metal carbonyls,  $\text{M}'(\text{CO})_n$  ( $n = 6, \text{M}' = \text{Cr}, \text{Mo}, \text{W}; n = 5, \text{M}' = \text{Fe}$ ), to give heterobimetallic derivatives through the carbonyl insertion into the Ti–N bond.<sup>569</sup> Thermal decomposition of these amido titanium complexes has been studied to afford different binuclear  $\mu$ -imido titanium derivatives. Reaction above  $145^\circ\text{C}$  in benzene- $d_6$  solution activates the  $\text{Cp}^*$  ligand to give the Cp–amido complex  $(\text{C}_5\text{Me}_4\text{CH}_2\text{CH}_2\text{NMe})\text{TiCl}_2$  which reacts with isocyanide under the insertion into the Ti–N bond.<sup>570</sup>

$\text{Cp}^*\text{TiCl}_3$  reacts with 1 equiv. of  $\text{LiNMe}_2$  to give the monoamido complex  $\text{Cp}^*\text{TiCl}_2(\text{NMe}_2)$  which can be alkylated by reaction with  $\text{LiR}$  ( $\text{R} = \text{Me}, \text{Ph}$ ) or  $\text{Mg}(\text{CH}_2\text{Ph})_2 \cdot 2\text{OEt}_2$  to afford the corresponding bis-alkyl derivatives. The molecular structure of  $\text{Cp}^*\text{Ti}(\text{CH}_2\text{Ph})_2(\text{NMe}_2)$  has been determined by X-ray diffraction methods. Reaction of  $\text{Cp}^*\text{Ti}(\text{CH}_2\text{Ph})_2(\text{NMe}_2)$  with  $\text{B}(\text{C}_6\text{F}_5)_3$  results in the formation of the monobenzyl cationic solvent-separated ion pair  $[\text{Cp}^*\text{Ti}(\text{CH}_2\text{Ph})(\text{NMe}_2)][\text{PhCH}_2\text{B}(\text{C}_6\text{F}_5)_3]$  which decomposes above  $0^\circ\text{C}$  to give unidentified products. An analogous chemical behavior is observed for the dimethyl complex. These systems are efficient catalysts for the polymerization of styrene.<sup>571</sup> The complexes  $\text{Cp}'\text{Ti}(\text{NMe}_2)_3$  ( $\text{Cp}' = \text{Cp}, \text{Cp}^*, \text{Ind}, \text{C}_5\text{H}_4\text{CH}_2\text{CH}_2\text{NMe}_2$ ) have been prepared similarly and their catalytic properties in the polymerization of  $\alpha$ -olefins examined.<sup>572</sup> The structure of the bis(trimethylsilyl)amido complex  $\text{CpTiCl}_2[\text{N}(\text{SiMe}_3)_2]$  has been reported.<sup>573</sup> The tris-amide  $(\text{C}_5\text{H}_4\text{CH}_2\text{CH}_2\text{NPr}^i_2)\text{Ti}(\text{NMe}_2)_3$  is prepared by the reaction of  $\text{C}_5\text{H}_5\text{CH}_2\text{CH}_2\text{NPr}^i_2$  with  $\text{Ti}(\text{NMe}_2)_4$ .<sup>374</sup>

The stoichiometric reaction of  $(\text{C}_5\text{R}_5)\text{TiCl}_3$  ( $\text{R} = \text{H}, \text{Me}$ ) with 1 equiv. of  $\text{LiNPr}^i_2$  in toluene provides a convenient method for the preparation of mono-Cp titanium diisopropyl–amido complexes  $(\text{C}_5\text{R}_5)\text{TiCl}_2(\text{NPr}^i_2)$ . The structures of these two mononuclear, 14-electron complexes have been characterized by X-ray diffraction and show a pseudo-tetrahedral geometry for the titanium center; the Ti–N bond distance is consistent with the presence of a double bond. In the solid state, the Cp derivative is characterized by a  $\beta$ -agostic interaction involving the methine C–H bond of the isopropyl group (Figure 9). The stereoelectronic influence of the replacement of the Cp ring by the bulkier and more  $\pi$ -donating  $\text{Cp}^*$  ring is illustrated by an increase in the  $\text{Cp}(\text{c})\text{--Ti--N}$  angle and the loss of the  $\beta$ -agostic interaction with the  $\text{Pr}^i$  methine C–H moiety.<sup>574</sup>

A series of analogous indenyl dimethylamido complexes has been described. Reactions of the indenyl compound  $(\text{Ind})\text{TiCl}_3$  with 1 equiv. of  $\text{LiNMe}_2$  afford the monoamido  $(\text{Ind})\text{TiCl}_2(\text{NMe}_2)$ . When 2 equiv. of  $\text{LiNMe}_2$  are used, the bis-amide  $(\text{Ind})\text{TiCl}(\text{NMe}_2)_2$  is obtained, while the reaction with 3 equiv. of the lithium amide gives a mixture of  $(\text{Ind})\text{Ti}(\text{NMe}_2)_3$  and  $\text{Ti}(\text{NMe}_2)_4$ . Compound  $(\text{Ind})\text{Ti}(\text{NMe}_2)_3$  can be obtained as a pure compound by treatment of  $\text{Ti}(\text{NMe}_2)_4$  with  $\text{C}_9\text{H}_8$ . The monochloro  $(\text{Ind})\text{TiCl}(\text{NMe}_2)_2$  and dichloro  $(\text{Ind})\text{TiCl}_2(\text{NMe}_2)$  can be alkylated by reaction with the appropriate alkyllithium reagent to give the corresponding mono- $(\text{Ind})\text{TiMe}(\text{NMe}_2)_2$  or dialkyl



**Figure 9** Molecular structure of complex  $\text{CpTiCl}_2(\text{NPr}^i_2)$  (reproduced by permission of Elsevier from *J. Organomet. Chem.*, 1995, 497, 17).

derivatives (Ind)TiR<sub>2</sub>(NMe<sub>2</sub>) (R = Me, CH<sub>2</sub>SiMe<sub>3</sub>, C≡CPh, C≡CSiMe<sub>3</sub>). The solid-state molecular structure of (Ind)TiCl<sub>2</sub>(NMe<sub>2</sub>) has been determined. Chemical studies, <sup>1</sup>H and <sup>13</sup>C NMR data, and DFT theoretical calculations indicate that the indenyl ring remains approximately planar and exhibits an η<sup>5</sup>-coordination mode in all the complexes.<sup>575</sup> (Ind)Ti(NMe<sub>2</sub>)<sub>2</sub>(NHBu<sup>t</sup>) has been identified as an intermediate species in the evolution of (Ind)TiCl(NMe<sub>2</sub>)<sub>2</sub>. Preliminary studies on the catalytic activity of (Ind)TiCl<sub>2</sub>(NMe<sub>2</sub>) in the polymerization of ethylene and propylene are reported.<sup>576</sup>

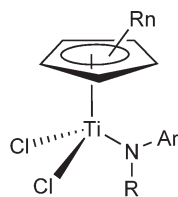
The Cp–anilido Ti(IV) complexes Cp'TiCl<sub>2</sub>(NArR) (Scheme 210) have been prepared in toluene by the reaction of Cp'TiCl<sub>3</sub> with the corresponding lithium anilide, and the molecular structure of (1,3-Me<sub>2</sub>C<sub>5</sub>H<sub>3</sub>)/TiCl<sub>2</sub>[N(2,6-Me<sub>2</sub>C<sub>6</sub>H<sub>3</sub>)(SiMe<sub>3</sub>)] has been determined by X-ray crystallography. These complexes, in the presence of MAO, exhibit high catalytic activities for ethylene polymerization, the molecular weight for the resultant polyethylene depending upon the Cp' ligand used. They show low catalytic activity for propylene polymerization and give atactic polymer with high molecular weight and narrow polydispersity.<sup>577</sup> The mono-Cp anilido complexes Cp'TiCl<sub>2</sub>[N(2,6-Me<sub>2</sub>C<sub>6</sub>H<sub>3</sub>)(SiMe<sub>3</sub>)] (Cp' = Cp, Cp\*, 1,3-Me<sub>2</sub>C<sub>5</sub>H<sub>3</sub>) have been studied in the polymerization of ethylene, propylene, and styrene in the presence of MAO.<sup>578</sup>

The diamido methyltitanium complex shown in Scheme 211 is formed by the addition of a solution of the corresponding tetraaminosilane to Cp\*TiMe<sub>3</sub> in *n*-hexane. Its molecular structure has been determined by X-ray diffraction.<sup>579</sup>

(C<sub>5</sub>H<sub>4</sub>SiMe<sub>2</sub>Cl)TiCl<sub>3</sub> is a very versatile starting material for preparing new mono-Cp' titanium derivatives; for example, the reaction with nitrogen donor reagents leads to a series of alkyl amido, benzamidinato, and mono-Cp–amido derivatives (Scheme 212; see also Scheme 264 in Section 4.05.3.4).<sup>580,581</sup> Treatment of (C<sub>5</sub>H<sub>4</sub>SiMe<sub>2</sub>Cl)TiCl<sub>3</sub> with 1 equiv. of LiN(SiMe<sub>3</sub>)<sub>2</sub> affords the dichloro amido titanium derivative (C<sub>5</sub>H<sub>4</sub>SiMe<sub>2</sub>Cl)TiCl<sub>2</sub>[N(SiMe<sub>3</sub>)<sub>2</sub>], indicating the selectivity of the Ti–Cl bond. In the presence of LiNHBu<sup>t</sup> the Si–Cl and one of the Ti–Cl functions react to give the Cp–amido complex (C<sub>5</sub>H<sub>4</sub>SiMe<sub>2</sub>ClNHBu<sup>t</sup>)TiCl<sub>2</sub>[N(SiMe<sub>3</sub>)<sub>2</sub>] (Scheme 212).<sup>382</sup>

Deprotonation of Ti(NMe<sub>2</sub>)<sub>4</sub> with C<sub>5</sub>H<sub>4</sub>(SiMe<sub>2</sub>NHBu<sup>t</sup>)<sub>2</sub> in toluene gives the mono-Cp derivative [C<sub>5</sub>H<sub>3</sub>(SiMe<sub>2</sub>NHBu<sup>t</sup>)<sub>2</sub>][Ti(NMe<sub>2</sub>)<sub>3</sub>] (Scheme 213). Heating at 50 °C is required to complete the reaction.<sup>582</sup>

Reaction of the ligand precursors (C<sub>5</sub>H<sub>5</sub>)B(NPr<sup>i</sup>)<sub>2</sub>(NHR) (R = Cy, Bu<sup>t</sup>) with Ti(NMe<sub>2</sub>)<sub>4</sub> does not result in the expected bridged compounds, but rather in the mono-Cp tris-amido complexes [(C<sub>5</sub>H<sub>4</sub>)B(NPr<sup>i</sup>)<sub>2</sub>(NHR)]Ti(NMe<sub>2</sub>)<sub>3</sub> (Scheme 214), characterized by NMR and IR spectroscopy.<sup>583</sup> A similar reaction of (C<sub>5</sub>H<sub>5</sub>)<sub>2</sub>BN(SiMe<sub>3</sub>)<sub>2</sub> with Ti(NMe<sub>2</sub>)<sub>4</sub> affords the binuclear mono-Cp tris-amido complex [(η<sup>5</sup>-C<sub>5</sub>H<sub>4</sub>)<sub>2</sub>BN(SiMe<sub>3</sub>)<sub>2</sub>][Ti(NMe<sub>2</sub>)<sub>3</sub>]<sub>2</sub> (Scheme 214).<sup>584</sup>



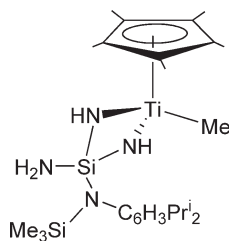
Ar = 2,6-Me<sub>2</sub>C<sub>6</sub>H<sub>3</sub>

CpRn = Cp\*; R = SiMe<sub>3</sub>

CpRn = 1,3-Me<sub>2</sub>C<sub>5</sub>H<sub>3</sub>; R = SiMe<sub>3</sub>

CpRn = Cp; R = SiMe<sub>3</sub>, SiBu<sup>t</sup>Me<sub>2</sub>

Scheme 210

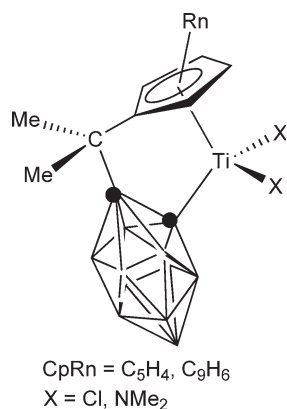


Scheme 211

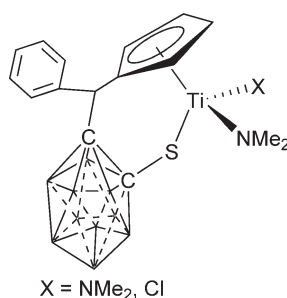


The synthesis and X-ray diffraction study of amido and chloro titanium complexes containing a bidentate bifunctional Cp–carborane constrained-geometry ligand  $[\eta^5\text{-}\sigma\text{-Me}_2\text{C}(\text{C}_5\text{H}_4)(\text{C}_2\text{B}_{10}\text{H}_{10})]\text{Ti}(\text{NMe}_2)_2$  have been reported.<sup>586</sup> Analogous bis-amido titanium complexes containing Cp–carborane and Ind–carborane ligands  $[\eta^5\text{-}\sigma\text{-Me}_2\text{C}(\text{C}_5\text{H}_4)(\text{C}_2\text{B}_{10}\text{H}_{10})]\text{Ti}(\text{NMe}_2)_2$  and  $[\eta^5\text{-}\sigma\text{-Me}_2\text{C}(\text{C}_5\text{H}_4)(\text{C}_2\text{B}_{10}\text{H}_{10})]\text{Ti}(\text{NMe}_2)_2$  and the chloro amido derivative  $[\eta^5\text{-}\sigma\text{-Me}_2\text{C}(\text{C}_5\text{H}_4)(\text{C}_2\text{B}_{10}\text{H}_{10})]\text{TiCl}(\text{NMe}_2)$  (Scheme 215) have been synthesized and characterized. The structures





Scheme 215



Scheme 216

of some of these complexes have been determined by single crystal X-ray diffraction. They exhibit a very high ethylene polymerization activity when they are activated with MAO.<sup>587</sup> The synthesis of the mono-Cp complex [C<sub>5</sub>H<sub>4</sub>CH(Ph)-1,2-C<sub>2</sub>B<sub>10</sub>H<sub>10</sub>-1-S]Ti(NMe<sub>2</sub>)<sub>2</sub> has been described; it undergoes a monohalogenation reaction in the presence of SiClMe<sub>3</sub> or Me<sub>3</sub>HNCl to give the chloro-amido derivative [C<sub>5</sub>H<sub>4</sub>CH(Ph)-1,2-C<sub>2</sub>B<sub>10</sub>H<sub>10</sub>-1-S]TiCl(NMe<sub>2</sub>) (Scheme 216). The molecular structure of the diamido complex has been determined by X-ray diffraction.<sup>588</sup>

The amido complex CpTiCl<sub>2</sub>(NMe<sub>2</sub>) has been studied as an effective catalyst for the living polymerization of isocyanides with acrylate side groups to generate chiral poly(isocyanate)s with lyotropic liquid crystalline structures.<sup>589,590</sup> The heterogeneous ethylene polymerization catalyst formed by supporting (C<sub>5</sub>H<sub>4</sub>SiMe<sub>3</sub>)Ti(NMe<sub>2</sub>)<sub>3</sub> on chemically modified silica surface, and results on ethylene polymerization in the presence of MAO have been described.<sup>591</sup> The complexes CpTi(NR<sub>2</sub>)<sub>3</sub> have been tested in ethene polymerization and the effect of the alkyl-amine groups on their activities has been explored.<sup>592</sup>

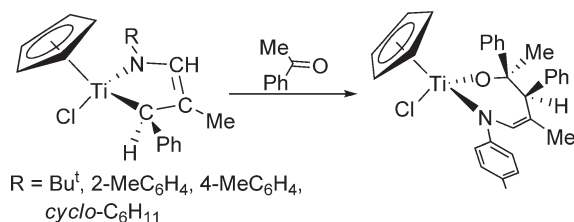
Ceramic thin films containing titanium, vanadium, carbon, oxygen, and nitrogen are obtained on steel substrates at 873 K, under nitrogen and helium gases and at low pressure, by chemical vapor deposition (CVD) from CpTiCl<sub>2</sub>[N(SiMe<sub>3</sub>)<sub>2</sub>] and Cp<sub>2</sub>VMe<sub>2</sub>.<sup>593</sup>

#### 4.05.3.3.2 Aza complexes

More aza titanium derivatives can also be found in Section 4.05.3.2.1 as examples of mono-Cp' complexes containing Ti–C bonds.

Group 4 transition aza–metal–diene complexes have received considerable attention because of their unique M–N and M–C bonding properties and their high reactivity toward a broad range of electrophiles and unsaturated hydrocarbons. Reduction of CpTiCl<sub>3</sub> with magnesium in THF in the presence of the appropriate 1-aza-1,3-diene affords the 1-aza-1,3-diene titanium complexes CpTiCl[N(R)CH=C(Me)CH(Ph)] (Scheme 217). Spectroscopic data indicate that the aza–diene ligands adopt a *cis-supine* conformation; in the case of the Bu<sup>t</sup> derivative a solution equilibrium with the *prone*-disposition is observed. The chemical shifts of the terminal carbon atoms of the aza–diene





Scheme 217

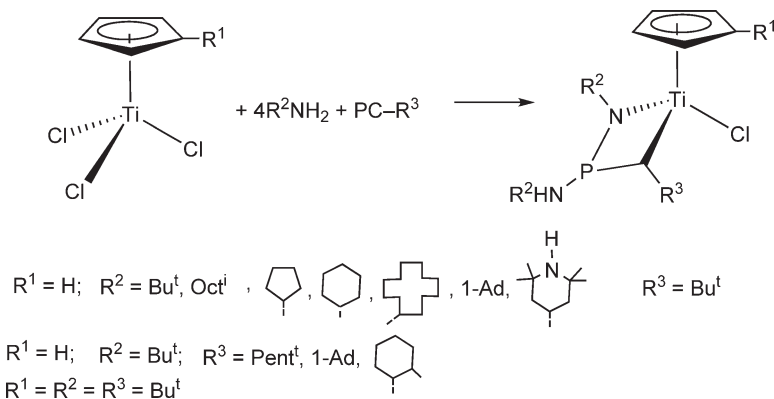
ligands in the  $^{13}\text{C}$  NMR spectra are significantly low-field shifted in comparison with those of alkyltitanium complexes. The  $^1J_{\text{CH}}$  coupling constants of the terminal carbon atoms of these ligands are considerably smaller than is usual for  $sp^2$ -hybridized C and suggest an  $sp^3$  rehybridization of these carbon atoms. The molecular structures of these compounds have been established by X-ray diffraction. They show the  $\eta^4$ - $\pi$  bonding of the aza-diene ligands relative to the  $\sigma^2$ -bonding found for the bis-Cp derivatives. The 4-MeC<sub>6</sub>H<sub>4</sub> derivative reacts with acetophenone to give an azoxatitanacyclic complex.<sup>594</sup>

Addition of 2 equiv. of primary amines RNH<sub>2</sub> to a suspension of Cp'TiCl<sub>3</sub> and phosphoalkynes P≡CR in toluene at room temperature gives azaphosphatitanacyclobutane derivatives (Scheme 218). The mechanism of the formation of these complexes is thought to proceed via Ti-imido intermediates.<sup>595</sup>

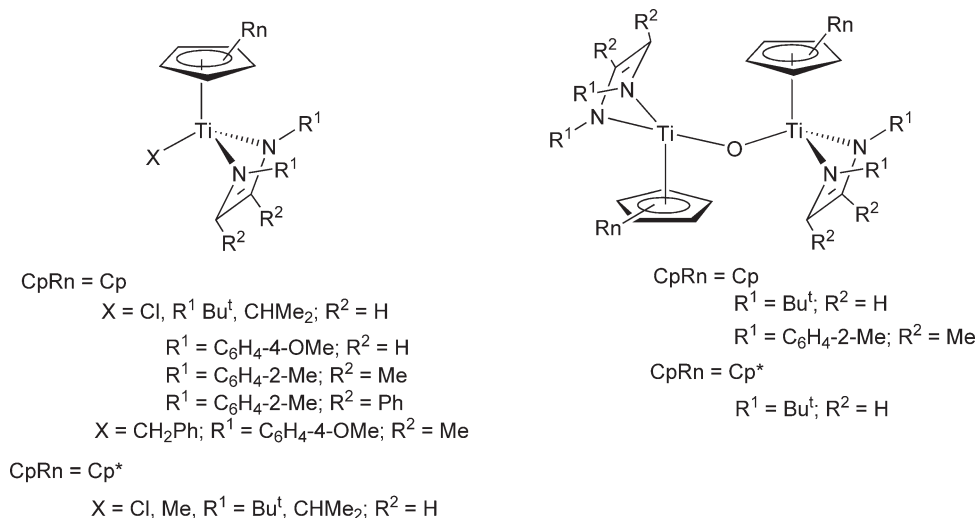
Reaction of Cp'TiCpCl<sub>3</sub> with 1 equiv. of Mg in the presence of 1,4-diaza-1,3-dienes (DAD) affords mononuclear titanium Cp'TiCpCl(DAD) complexes. The DAD ligands prefer the  $\sigma^2$ - $\pi$ -coordination geometry with a *supine*-conformation of the heterodiene. The chloro derivatives can be alkylated by reaction with MgCl(CH<sub>2</sub>Ph) to give monobenzyl compounds. An X-ray study reveals that the alkylation does not change appreciably the DAD bonding parameters in comparison with the starting chloro complexes. Hydrolysis reactions produce binuclear  $\mu$ -oxo derivatives (Scheme 219).<sup>596</sup> The synthesis of (C<sub>5</sub>R<sub>5</sub>)TiCl(DAD) complexes has also been described by the reaction of (C<sub>5</sub>R<sub>5</sub>)TiCl<sub>3</sub> with the dilithium salts of Pr<sup>i</sup><sub>2</sub>- and Bu<sup>t</sup><sub>2</sub>-substituted 1,4-diaza-1,3-butadienes. Alkylation of the chloro derivatives with MgClMe or LiMe gives the methyl complexes (C<sub>5</sub>R<sub>5</sub>)TiMe(DAD). The topomerization process between the *supine*- and *prone*-dispositions in Cp'TiCl(Bu<sup>t</sup><sub>2</sub>-DAD) has been observed in solution by variable-temperature NMR spectroscopy. Hydrolysis of Cp'TiCl(Bu<sup>t</sup><sub>2</sub>-DAD) in pentane solution affords the oxo-bridge derivative [Cp'Ti(Bu<sup>t</sup><sub>2</sub>-DAD)]<sub>2</sub>( $\mu$ -O) (Scheme 219). The molecular structure of TiMe(C<sub>5</sub>Me<sub>5</sub>)(Pr<sup>i</sup>-DAD) has been determined by X-ray crystal diffraction and shows a distorted trigonal-bipyramidal structure.<sup>597</sup>

R(NH<sub>2</sub>)<sub>2</sub>Si-Si(NH<sub>2</sub>)<sub>2</sub>R (R = PhNSiMe<sub>3</sub>) reacts with Cp\*TiMe<sub>3</sub> to give the diaza-disila-titanacyclopentane Ti(C<sub>5</sub>Me<sub>5</sub>)Me[HN(R)(NH<sub>2</sub>)Si-Si(NH<sub>2</sub>)(R)NH], the molecular structure of which is reported.<sup>598</sup>

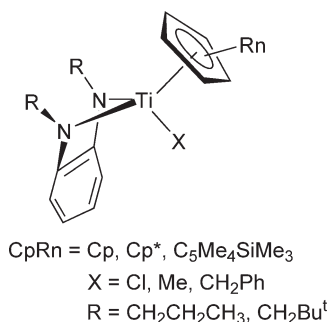
The chelating chloro diamido titanium complexes Cp'TiCl[1,2-C<sub>6</sub>H<sub>4</sub>(NR<sup>1</sup>)<sub>2</sub>] (R<sup>1</sup> = CH<sub>2</sub>CH<sub>2</sub>CH<sub>3</sub>, CH<sub>2</sub>Bu<sup>t</sup>) have been synthesized by treatment of the dilithium salts of the corresponding 1,2-phenyldiamines with Cp'TiCl<sub>3</sub>.<sup>599</sup> The chloro complexes can be alkylated by reaction of MgClR to give the monoalkyl derivatives Cp'TiR<sup>2</sup>[1,2-C<sub>6</sub>H<sub>4</sub>(NR<sup>1</sup>)<sub>2</sub>] (R<sup>2</sup> = Me, CH<sub>2</sub>Ph) (Scheme 220).<sup>600</sup> The molecular structures of these complexes have been determined by X-ray diffraction. The compounds have been further investigated as potential olefin polymerization



Scheme 218



Scheme 219



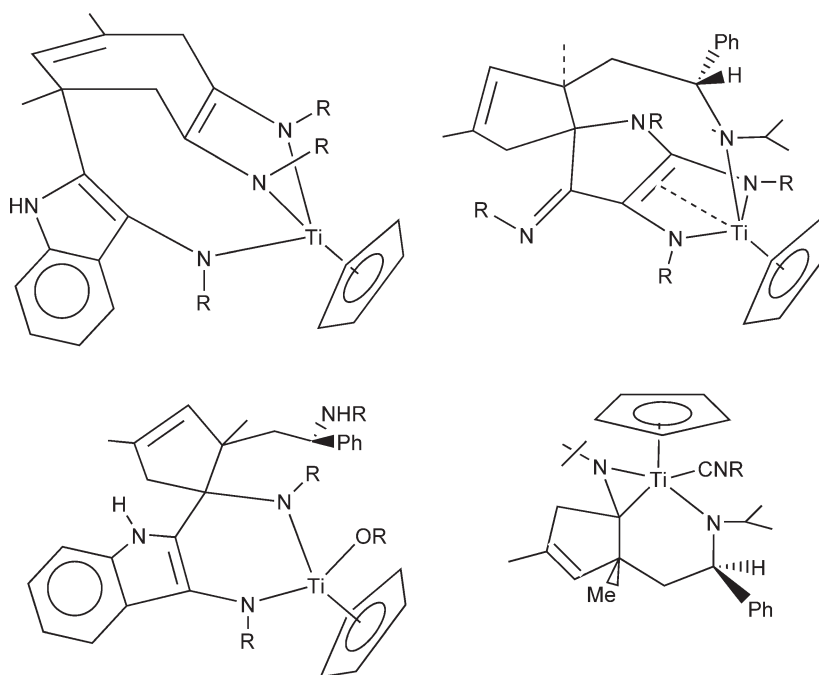
Scheme 220

catalysts; upon addition of MAO, the chloro and alkyl complexes show low activity toward the polymerization of ethylene and styrene. No methylation is observed during the treatment of the chloro compounds with  $\text{AlMe}_3$ . Instead, these reactions give the binuclear aluminum complexes  $\text{Al}_2\text{Me}_4[1,2\text{-C}_6\text{H}_4(\text{NR}^1)_2]$  ( $\text{R}^1 = \text{CH}_2\text{CH}_2\text{CH}_3$ ,  $\text{CH}_2\text{Bu}^t$ ) through transmetalation of the diamido ligand. This reaction suggests ligand transfer to Al as a catalyst deactivation process in olefin polymerization reactions. The methyl derivatives react with solid MAO with the formation of zwitterionic species depending on the nature of the solvent.

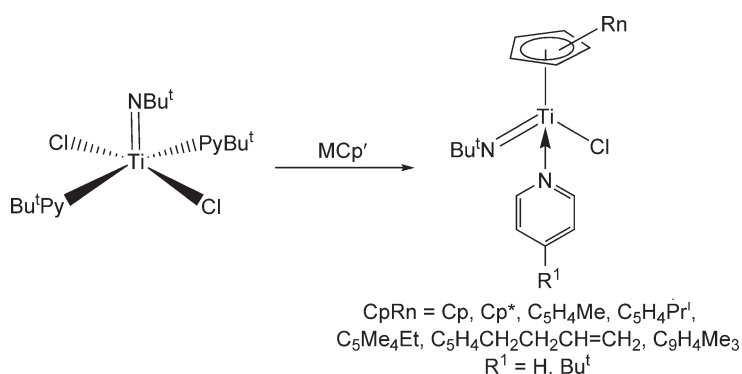
A series of diaza-titanacyclopentene and related complexes (Scheme 221) can be generated by coupling reactions of mono-Cp derivatives with imines, followed by the incorporation of a second substrate, such as ketone or isonitrile. In these reactions a chiral center is generated at the coupled imine carbon atom with potential applications to generate further chiral centers.<sup>601,602</sup>

#### 4.05.3.3.3 Imido complexes

The synthesis, characterization, and chemical behavior of mono- and bis-Cp' imido titanium complexes have been well explored.<sup>603</sup> The chloro imido titanium compounds  $\text{TiCl}_2(\text{NBu}^t)_2\text{L}_2$  (L is a substituted or unsubstituted pyridine ligand) have resulted in useful precursors to prepare mono-Cp' and bis-Cp' imido titanium derivatives. The pyridine adducts  $\text{TiCl}_2(\text{NBu}^t)(\text{NC}_5\text{H}_4\text{R})_n$  ( $\text{R} = \text{H}, \text{Bu}^t$ ) react with  $\text{MCp}'$  ( $\text{M} = \text{Li}, \text{Na}$ ) to afford the mono-Cp derivatives  $\text{Cp}'\text{Ti}(\text{NBu}^t)\text{Cl}(\text{NC}_5\text{H}_4\text{R})$  ( $\text{Cp}' = \text{Cp}, \text{Cp}^*, \text{C}_5\text{H}_4\text{Me}, \text{C}_5\text{H}_4\text{Pr}^i, \text{C}_5\text{Me}_4\text{Et}, \text{C}_5\text{Me}_4\text{CH}_2\text{CH}_2\text{CH}=\text{CH}_2$ ) (Scheme 222). The complex  $\text{CpTiCl}(\text{NBu}^t)(\text{NC}_5\text{H}_5)$  readily loses pyridine under vacuum in the solid state to form the binuclear complex  $[\text{CpTiCl}(\mu\text{-NBu}^t)]_2$ . Variable-temperature NMR spectra show that the coordinated pyridine exchanges with free pyridine via an associative mechanism. The same reaction with  $\text{Li}(\text{C}_9\text{H}_4\text{Me}_3)$  gives the corresponding



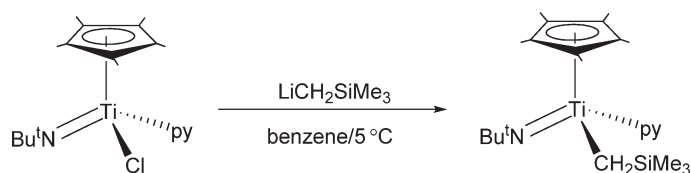
Scheme 221



Scheme 222

indenyl complex  $(\text{C}_9\text{H}_4\text{Me}_3)\text{TiCl}(\text{NBu}^t)(4\text{-NC}_5\text{H}_4\text{Bu}^t)$ .  $(\text{C}_9\text{H}_7)\text{TiCl}(\text{NBu}^t)(\text{NC}_5\text{H}_5)$  has been similarly synthesized. Pyrazolylborate-imido and macrocyclic imido titanium derivatives are also prepared.<sup>604,605</sup>  $\text{Cp}^*\text{TiCl}(\text{NBu}^t)(\text{py})$  reacts with  $\text{LiCH}_2\text{SiMe}_3$  in cold benzene to give a rare example of a terminal imido alkyltitanium derivative  $\text{Cp}^*\text{Ti}(\text{CH}_2\text{SiMe}_3)(\text{NBu}^t)(\text{py})$  (Scheme 223); its molecular structure has been determined by X-ray diffraction.<sup>90</sup>

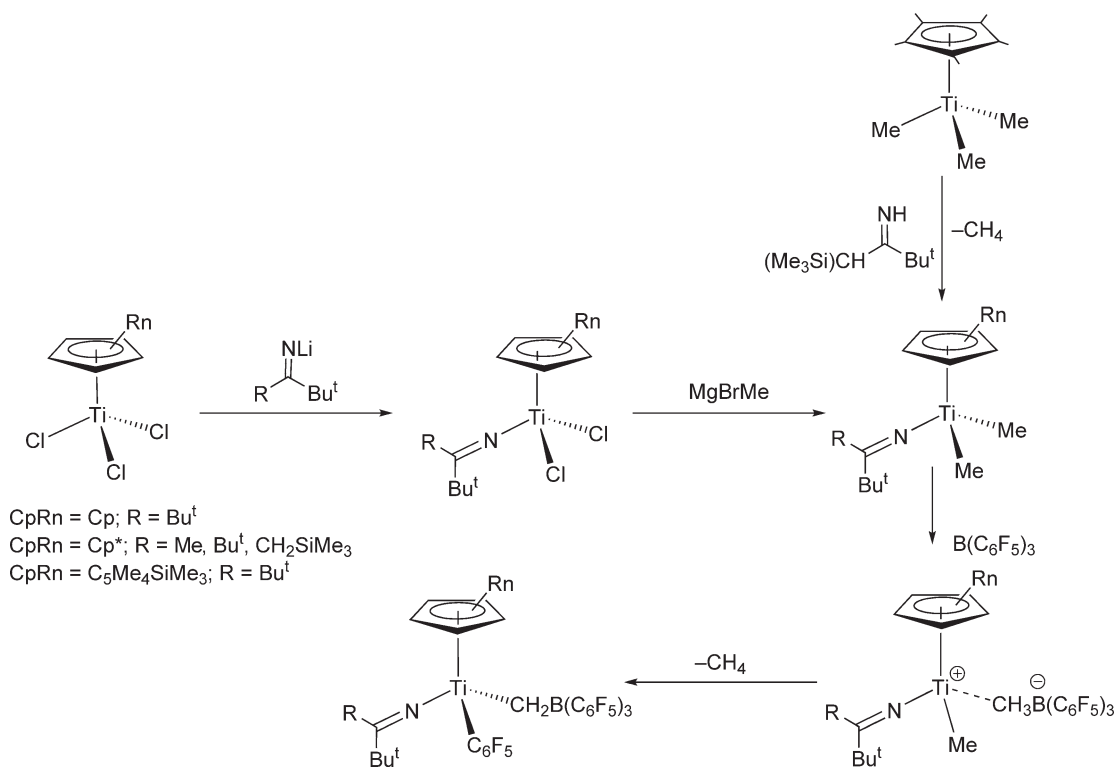
The reaction of  $\text{Cp}^*\text{TiCl}_3$  and  $\text{LiNHBu}^t$  in hexane yields the titanate complex  $\text{Li}[\text{Cp}^*\text{Ti}(=\text{NBu}^t)(\text{NHBu}^t)_2]$ , which exhibits a terminal *tert*-butylimido ligand. The X-ray structural characterization is also described.<sup>606</sup>



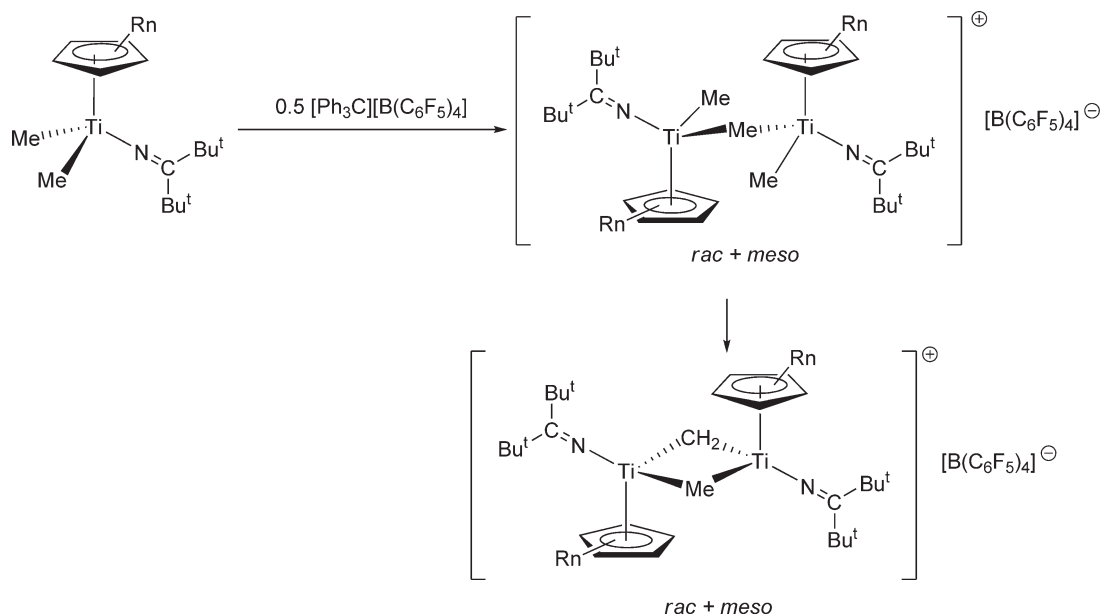
Scheme 223

Reaction of  $\text{TiCl}_3[\text{N}(\text{SiMe}_3)(\text{CH}_2\text{CH}_2\text{py})]$  with  $\text{NaCp}$  affords the Cp-amido-amino complex  $\text{Cp}^*\text{TiCl}_2[\text{N}(\text{SiMe}_3)(\text{CH}_2\text{CH}_2\text{py})]$ , while the related imido derivative  $[\text{Cp}^*\text{TiCl}(\text{NCH}_2\text{CH}_2\text{py})]_n$  is obtained by treatment of  $[\text{TiCl}_2(\text{NCH}_2\text{CH}_2\text{py})]_n$  with  $\text{NaCp}$ .  $\text{Cp}^*\text{TiCl}_3$  reacts with the sodium salt of 2-(N-phenylamino)ethyl-2-pyridine with ligand cleavage to give the previously reported<sup>607</sup> complex  $[\text{Cp}^*\text{TiCl}(\mu\text{-NPh})_2]_2$ .<sup>608</sup>

The dichloro mono-Cp ketimido complexes  $\text{Cp}^*\text{TiCl}_2[\text{N}=\text{C}(\text{R})\text{Bu}^t]$  have been prepared by treatment of  $\text{Cp}^*\text{TiCl}_3$  with  $\text{Li}[\text{N}=\text{C}(\text{R})\text{Bu}^t]$ . These complexes react with  $\text{MgBrMe}$  to give the corresponding dimethyl derivatives  $\text{Cp}^*\text{TiMe}_2[\text{N}=\text{C}(\text{R})\text{Bu}^t]$ . The dimethyl compound  $\text{Cp}^*\text{TiMe}_2[\text{N}=\text{C}(\text{Bu}^t)\text{CH}(\text{SiMe}_3)_2]$  is generated directly from  $\text{Cp}^*\text{TiMe}_3$  and the free ketimine, with elimination of methane. Dynamic  $^1\text{H}$  NMR studies show that in solution the ketimido ligands in these compounds rotate rapidly about Ti–N bond on the NMR timescale.  $\text{B}(\text{C}_6\text{F}_5)_3$  catalyzes the disproportionation process between  $\text{Cp}^*\text{TiCl}_2(\text{N}=\text{CBu}^t_2)$  and  $\text{Cp}^*\text{TiMe}_2(\text{N}=\text{CBu}^t_2)$  to give the chloro methyl complex  $\text{Cp}^*\text{TiClMe}(\text{N}=\text{CBu}^t_2)$  which converts to the mixed dialkyl derivative  $\text{Cp}^*\text{TiMe}(\text{CH}_2\text{SiMe}_3)(\text{N}=\text{CBu}^t_2)$  by reaction with  $\text{MgBrCH}_2\text{SiMe}_3$ . The dimethyl complexes  $\text{Cp}^*\text{TiMe}_2[\text{N}=\text{CBu}^t(\text{R})]$  react with  $\text{B}(\text{C}_6\text{F}_5)_3$  to afford the ion pair  $\{\text{Cp}^*\text{TiMe}[\text{N}=\text{CBu}^t(\text{R})]\}[\text{MeB}(\text{C}_6\text{F}_5)_3]$ . Compound  $\{\text{Cp}^*\text{Ti}(\text{CH}_2\text{SiMe}_3)[\text{N}=\text{C}(\text{R})\text{Bu}^t]\}^+[\text{MeB}(\text{C}_6\text{F}_5)_3]^-$  is obtained similarly. NMR spectra in aromatic solvents suggest an unassociated anion. These ion pairs decompose by loss of methane to produce the neutral compounds  $\{\text{Cp}^*\text{Ti}(\text{C}_6\text{F}_5)[\text{N}=\text{CBu}^t(\text{R})]\}[\text{CH}_2\text{B}(\text{C}_6\text{F}_5)_2]$  (Scheme 224). This reaction represents a catalyst deactivation pathway for these ion pairs in olefin polymerization processes. Kinetic and mechanistic studies for these reactions are reported. The X-ray crystal structure of  $[\text{Cp}^*\text{Ti}(\text{C}_6\text{F}_5)(\text{N}=\text{CBu}^t_2)]_2[\text{CH}_2\text{B}(\text{C}_6\text{F}_5)_2]$  has been determined.<sup>609</sup> The reactions of the dimethyl complexes  $\text{Cp}^*\text{TiMe}_2(\text{N}=\text{CBu}^t_2)$  ( $\text{Cp}^* = \text{Cp}, \text{Cp}^*, \text{C}_5\text{H}_4\text{SiMe}_3$ ) with  $\text{Ph}_3\text{C}[\text{B}(\text{C}_6\text{F}_5)_4]$  lead to the formation of the cationic binuclear methyl-bridged complexes  $\{[\text{Cp}^*\text{TiMe}(\text{N}=\text{CBu}^t_2)]_2(\mu\text{-Me})\}^+$  as mixtures of *rac*- and *meso*-diastereomers. The  $^1J_{\text{CH}}$  coupling of 136(1) Hz for the  $\mu$ -methyl group is in agreement with a trigonal-bipyramidal carbon geometry. In bromobenzene, these cationic complexes cleanly evolve methane at room temperature over the course of a few hours to give the cationic  $\mu$ -methyl  $\mu$ -methylene binuclear species  $\{\text{Cp}^*\text{Ti}(\text{N}=\text{CBu}^t_2)]_2(\mu\text{-Me})(\mu\text{-CH}_2)\}^+$  (Scheme 225) which show  $^1J_{\text{CH}}$  coupling constants of 112 and 121 Hz for the  $\mu$ -methyl and  $\mu$ -methylene groups, respectively, suggesting that the methyl bridge is no longer linear. The compound with the sterically less demanding Cp ligand is



Scheme 224



Scheme 225

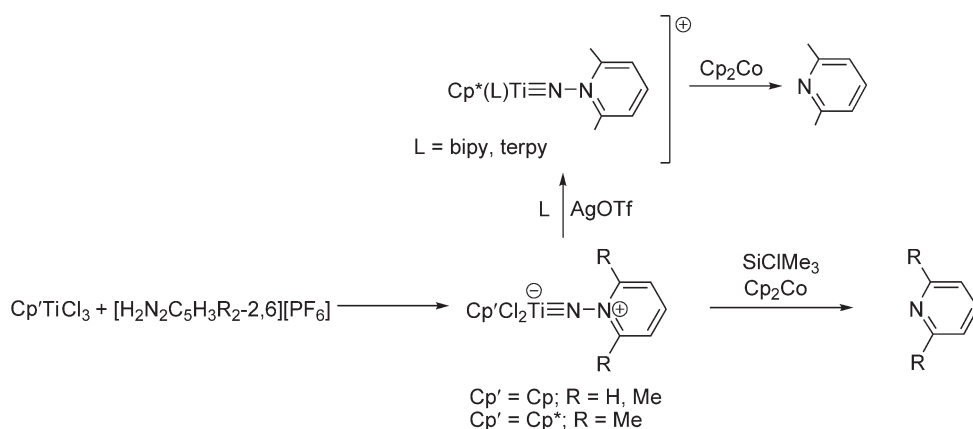
formed as a mixture of *rac/meso* diastereomers, while for the complexes with the bulkier  $\text{Cp}^*$  and  $\text{C}_5\text{Me}_4\text{SiMe}_3$  ligands, the *rac*-isomers are formed exclusively. Dynamic NMR and crossover experiments are carried out in order to study dissociation, intramolecular methyl group exchange, or diastereomer interconversion processes.<sup>610</sup> The ketimido complex  $(\text{Ind})\text{TiCl}_2(\text{NCBu}_2)$  is prepared by metathetical reaction of  $(\text{Ind})\text{TiCl}_3$  with  $\text{LiNCBu}_2$ , and its molecular structure was determined by X-ray diffraction methods. This complex and the analogous previously described Cp derivatives  $\text{Cp}'\text{TiCl}_2(\text{NCBu}_2)$  ( $\text{Cp}' = \text{Cp}, \text{Cp}^*$ ) catalyze the homopolymerization of ethylene and propylene.<sup>611</sup> The effects of Cp substituents in homopolymerizations of ethylene and 1-hexene and for ethylene/1-hexene co-polymerizations using the non-bridged ketimido titanium complexes of the type  $\text{Cp}'\text{TiCl}_2(\text{N}=\text{CBu}_2)$  ( $\text{Cp}' = \text{Cp}, \text{Cp}^*, \text{BuC}_5\text{H}_4, \text{Ind}$ ), in the presence of MAO as co-catalyst, have been studied. The complexes show significant activities for ethylene polymerizations. The higher activity for the 1-hexene polymerizations is found for the unsubstituted Cp derivative and they exhibit high activities for the ethylene/1-hexene co-polymerizations. The compounds also show activities for the syndiospecific styrene polymerizations, although the observed activities are much lower than those with  $\text{Cp}^*\text{TiCl}_3$ .<sup>612,613</sup>

By using the 1-aminopyridinium salt  $[\text{NH}_2\text{NC}_5\text{H}_3\text{R}_{2-2,6}][\text{PF}_6]$  ( $\text{R} = \text{H}, \text{Me}$ ) as starting material, neutral and cationic (1-pyridinio)imido dichloro titanium complexes have been synthesized. Compounds  $\text{Cp}'\text{TiCl}_2(\text{NNC}_5\text{H}_3\text{R}_{2-2,6})$  ( $\text{Cp}' = \text{Cp}, \text{Cp}^*$ ) have been prepared by the reaction of the pyridinium salt with  $\text{Cp}'\text{TiCl}_3$  and their structures determined by X-ray diffraction. These complexes are formally zwitterionic species having an anionic titanium center. The zwitterionic nature may account for the low solubility in aromatic hydrocarbon solvents. Cationic complexes  $[\text{Cp}^*\text{Ti}(\text{NNC}_5\text{H}_3\text{Me}_{2-2,6})(\text{L})][\text{OTf}]$  ( $\text{L} = \text{bipy}, \text{terpy}$ ) can be generated from  $\text{Cp}^*\text{TiCl}_2(\text{NNC}_5\text{H}_3\text{Me}_{2-2,6})$  through reaction with  $\text{AgOTf}$  in the presence of bipy and terpy, respectively ( $\text{terpy} = 2,2':6',2' \text{-terpyridine}$ ). The N–N bond in these complexes could be cleaved by reduction with sodium amalgam or by reaction with cobaltocene or with cobaltocene in the presence of a proton analog like  $\text{Me}_3\text{SiCl}$  (Scheme 226).<sup>614</sup>

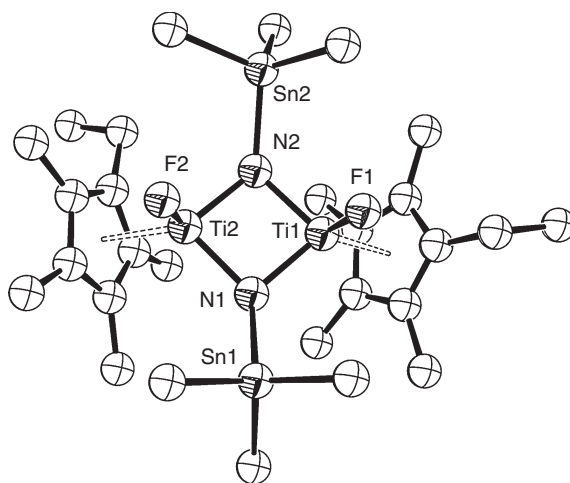
$\text{Me}_3\text{SnF}$  has been used as fluorinating agent in the reaction with chloro titanium derivatives to give the fluoro imido compounds  $[(\text{C}_5\text{H}_4\text{Me})\text{TiF}(\text{NPh})]_2$  and  $[(\text{C}_5\text{H}_4\text{SiMe}_3)\text{TiF}(\text{NBu}^t)]_2$ . The fluoro complexes  $[\text{Cp}'\text{TiF}(\text{N}(\text{SnMe}_3))]_2$  ( $\text{Cp}' = \text{C}_5\text{Me}_4\text{Et}, \text{C}_5\text{H}_4\text{Me}$ ) are obtained in high yield by the reaction of  $\text{N}(\text{SnMe}_3)_3$  with  $\text{Cp}'\text{TiF}_3$ . The structures of these compounds exhibit imido bridge ligands (Figure 10).<sup>615</sup>

The phenylimido-bridged dimer  $[(\text{C}_5\text{H}_4\text{CH}_2\text{CH}_2\text{CH}_2\text{N}(\text{H})\text{CMe}_3)\text{Ti}(\text{NHPh})(\mu\text{-NPh})]_2$  is obtained by reaction of the Cp-amido complex  $(\text{C}_5\text{H}_4\text{CH}_2\text{CH}_2\text{CH}_2\text{NCMe}_3)/(\text{NMe}_2)_2$  with aniline. Its molecular structure has been determined by X-ray diffraction and reveals a slightly asymmetric  $\text{Ti}(\mu\text{-NPh})_2\text{Ti}$  core (Scheme 281, Section 4.05.3.4).<sup>616</sup>

Magnesium amides and imides have provided to be useful as possible transfer agents for  $\text{-NR}_2$  and  $\text{-NR}$  ligands to transition metals. The magnesium imide  $\text{Mg}(\text{NPh})(\text{THF})$  has been reported as a suitable transfer agent for the imido

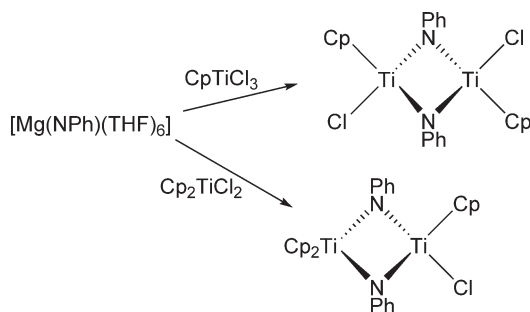


Scheme 226

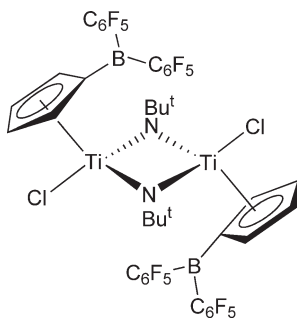


**Figure 10** Molecular structure of complex  $[(\text{C}_5\text{Me}_4\text{Et})\text{TiF}(\text{NSnMe}_3)]_2$  (reproduced by permission of American Chemical Society from *Inorg. Chem.*, **1996**, 35, 741).

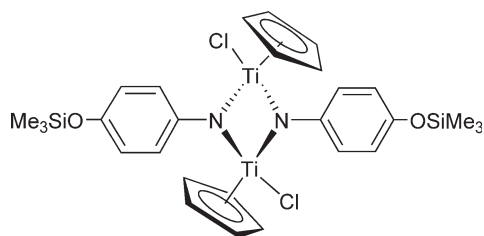
group NPh to titanium and zirconium metals to give the corresponding imido derivatives. The reaction with  $\text{Cp}'\text{TiCl}_3$  affords the imido-bridged complex  $[\text{Cp}'\text{TiCl}(\mu\text{-NPh})]_2$ , while the reaction with  $\text{Cp}_2\text{TiCl}_2$  yields the binuclear complex  $\text{Cp}(\text{Cl})\text{Ti}(\text{NPh})_2\text{TiCp}_2$  containing a mono- and a bis-Cp titanium fragment (Scheme 227). In contrast, the reaction with  $\text{Cp}_2\text{ZrCl}_2$  exclusively leads to the binuclear bis-Cp zirconium compound. The crystal structures of these compounds have been determined by X-ray diffraction.<sup>607</sup>



Scheme 227



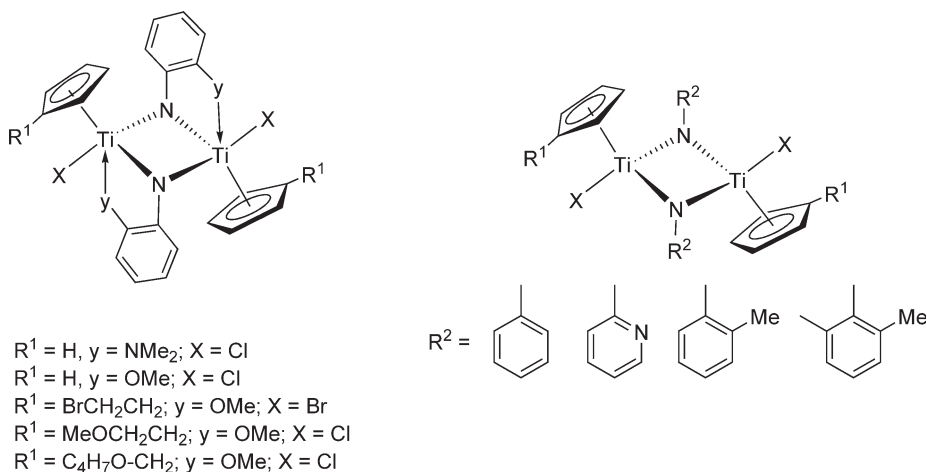
Scheme 228



Scheme 229

Reactions of  $[\text{C}_5\text{H}_4\text{B}(\text{C}_6\text{F}_5)_2]\text{TiCl}_3$  with  $\text{LiHNBu}^t$  afford the  $\mu$ -imido complex  $\{[\text{C}_5\text{H}_4\text{B}(\text{C}_6\text{F}_5)_2]\text{TiCl}\}_2(\mu\text{-NBu}^t)_2$  (Scheme 228).<sup>617</sup>  $\text{CpTiCl}_3$  reacts with the siloxylaniline  $p\text{-Me}_3\text{SiOC}_6\text{H}_4\text{NH}_2$  in the presence of  $\text{NEt}_3$  to give the  $\mu$ -imido compound  $[\text{CpTiCl}(\mu\text{-NC}_6\text{H}_4\text{-}p\text{-OSiMe}_3)]_2$  (Scheme 229).<sup>618</sup>

Titanium  $\mu$ -imido complexes with intramolecular coordination between Ti and O or N atoms located in the imido ligands have been reported (Scheme 230).<sup>619</sup> Reactions of  $(\text{C}_5\text{H}_4\text{R})\text{TiX}_3$  ( $\text{X} = \text{Cl}, \text{Br}$ ) with 1 equiv. of  $\text{LiNH}(2\text{-MeOC}_6\text{H}_4)$  or  $\text{MgN}(2\text{-Me}_2\text{NC}_6\text{H}_4) \cdot \text{THF}$  afford  $\mu$ -imido complexes which include intramolecular titanium–oxygen or titanium–nitrogen coordination. Similar reactions of substituted mono- $\text{Cp}'$  titanium complexes with  $\text{LiNHPh}$ ,  $\text{LiNH}(2\text{-MeC}_6\text{H}_4)$ ,  $\text{MgN}(2,6\text{-Me}_2\text{C}_6\text{H}_3) \cdot \text{THF}$  or  $\text{LiNH}(2\text{-Py})$  in the presence of  $\text{NEt}_3$  lead to the formation of  $\mu$ -imido complexes in which the intramolecular coordination is not present (Scheme 230). The catalytic activity and selectivity for styrene polymerization has been investigated.<sup>618</sup>

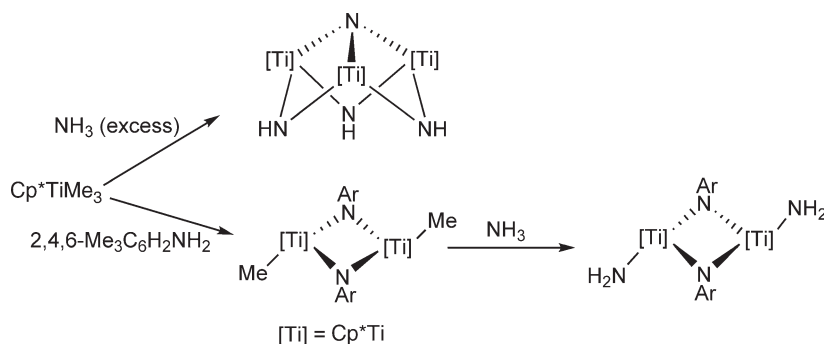


Scheme 230

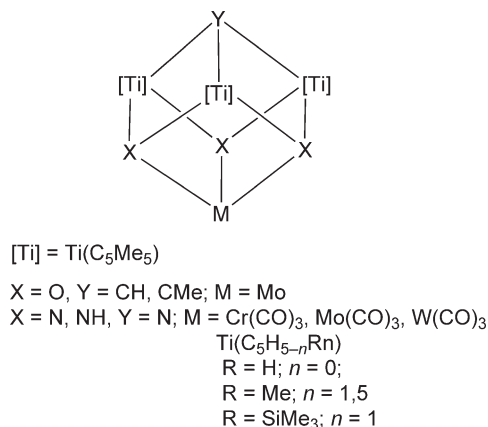
The reaction of  $(C_5H_4Me)TiCl_3$  with the lithium diazoalkane  $Me_3SiCLiN_2$  in THF results in the formation of the imido-bridged binuclear complex  $[(C_5H_4Me)TiCl(\mu-NCSiMe_3)]_2$  with migration of the  $SiMe_3$  group to N. The mechanism for the formation of this complex is not clear; its molecular structure has been determined by X-ray diffraction. The central core of the structure contains a planar four-membered  $Ti_2N_2$  ring with Ti–N bond distances in the range of 1.916–1.878 Å.<sup>620</sup>

The ammonolysis reactions of  $Cp^*TiX_3$  ( $X = Cl, Me$ ) with  $NH_3$  and primary amines have also been studied. Compound  $Cp^*TiMe_3$  reacts with an excess of  $NH_3$  to give the previously reported trinuclear complex  $[Cp^*Ti(\mu-NH)]_3(\mu_3-N)$ <sup>621</sup> as a yellow solid. Treatment of  $Cp^*TiMe_3$  with 2,4,6-trimethylaniline affords the binuclear  $[Cp^*TiMe(\mu-NAr)]_2$  which is converted into the amido compound  $[Cp^*Ti(NH_2)(\mu-NAr)]_2$  by reaction with an excess of  $NH_3$  (Scheme 231). Subsequent reaction of  $[Cp^*Ti(\mu-NH)]_3(\mu_3-N)$  with the amido compound  $(C_5H_{5-n}R_n)Ti(NMe_2)_3$  affords the cubane nitrido complexes  $[(C_5Me_5)_3Ti_4(C_5H_{5-n}R_n)](\mu_3-N)_4$  (Scheme 232) with elimination of dimethylamine. The analogous ammonolysis reaction of  $Cp^*TiCl_3$  with an excess of  $NH_3$  has been performed to produce the binuclear complex  $(C_5Me_5)_3Ti_2Cl_2(NH_3)(\mu-N)$ . All these compounds have been characterized by  $^1H$ ,  $^{13}C$ , and  $^{15}N$  NMR spectroscopy and the molecular structures of some of them have been determined by X-ray diffraction.<sup>622</sup>

The imido–nitrido complex  $[Cp^*Ti(\mu-NH)]_3(\mu_3-N)$  reacts with  $MN(SiMe_3)_2$  ( $M = Li, Na, K$ ) to give the alkali metal derivatives  $\{M(\mu_3-NH)_2(\mu_4-N)[(C_5Me_5)_3Ti_3(\mu_3-N)]\}_2$  and  $M(\mu_3-NH)_5(\mu_3-N)[(C_5Me_5)_3Ti_3(\mu_3-N)]_2$ . The crystal structures indicate an edge-linked double azahetero-metalocubane  $[Li_2Ti_6N_8]$  or corner-shared double-cube  $[MTi_6N_8]$  cubane core (see Scheme 253).<sup>623</sup> Treatment of  $[Cp^*Ti(\mu-NH)]_3(\mu_3-N)$  with 2 equiv. of  $M[N(SiMe_3)_2]$  ( $M = Li, Na, K$ ) gives the alkali metal derivatives  $[M(\mu_3-N)(\mu_3-NH)_2][Cp^*_3Ti_3(\mu_3-N)]$ . Reaction of the lithium derivative with  $MClMe_3$  ( $M = Si, Sn$ ) or  $MCl$  ( $M = In, Tl$ ) shows the ability to transfer the “ $(\mu-NH)_2(\mu_3-N)-Ti_3Cp^*_3(\mu_3-N)$ ” unit to afford  $Cp^*_3Ti_3(\mu-NH)(\mu-NMMe_3)(\mu_3-N)$  and  $M(\mu_3-N)(\mu_3-NH)_2Ti_3Cp^*_3(\mu_3-NMMe_3)(\mu_3-N)$ , respectively, which provides a convenient synthetic route for titanium nitrido derivatives containing silicon,

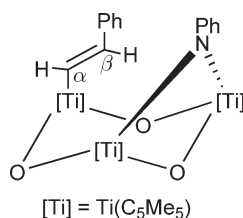


Scheme 231

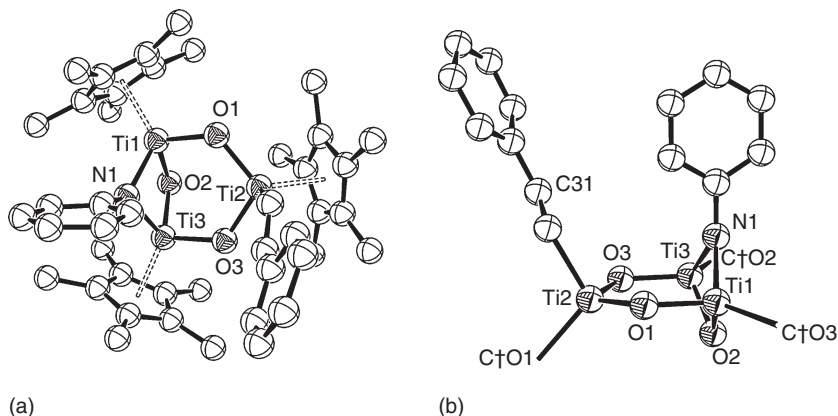


Scheme 232





Scheme 233



**Figure 11** Two views of the molecular structure of complex  $[\text{Cp}^*\text{Ti}(\text{O})_3(\text{CH}=\text{CHPh})(\mu\text{-NPh})]$  (reproduced by permission of the Royal Society of Chemistry from *Chem. Commun.*, **1999**, 1839).

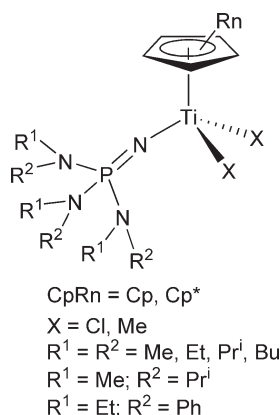
tin, indium, or thallium atoms.<sup>624</sup> Similar complexes exhibiting the single cube  $[\text{MTi}_3\text{N}_4]$  (Scheme 232) or the edge-linked double azahetero-metallocubane  $[\text{Li}_2\text{Ti}_6\text{N}_8]$  have also been described (Section 4.05.3.3.6).<sup>622,625–628</sup> Analogous double cube-type titanium nitrido complexes bearing corner-shared double-cube  $[\text{MTi}_6\text{N}_8]$  structures can be prepared by the reaction of  $[\text{Cp}^*\text{Ti}(\mu\text{-NH})]_3(\mu_3\text{-N})$  with  $\text{Ti}(\text{N}-2,4,6\text{-C}_6\text{H}_2\text{Me}_3)\text{Cl}_2(\text{py})_3$  or  $\text{M}(\text{NMe}_2)_4$  ( $\text{M} = \text{Ti}, \text{Zr}$  and  $\text{Ta}$  and  $\text{Nb}$  compounds).<sup>625,627</sup> The synthesis of this type of complexes incorporating magnesium and barium in the core of single cubane or corner-shared double-cube structure has been similarly described.<sup>629</sup> The formally  $\text{Ti}(\text{III})$  cluster  $\text{Cp}_4\text{Ti}_4(\mu_3\text{-NSnMe}_3)_4$  incorporating a cubane core has been reported.<sup>630</sup>

Photochemical incorporation of *N*-benzylideneaniline ( $\text{PhCH}=\text{NPh}$ ) into the complex  $[\text{Cp}^*\text{Ti}(\text{O})_3(\mu_3\text{-CH})]$  occurs by breaking of the  $\text{C}=\text{N}$  imine bond and formation of a bridging imido and  $\sigma$ -alkenyl groups bonded to the  $\text{Ti}_3\text{O}_3$  core (Scheme 233). The protons of the  $\sigma$ -bonded styryl group appear as an AB spin system in the  $^1\text{H}$  NMR spectrum ( $^3J_{\text{HH}} = 18.3$  Hz) and it is characterized by a doublet of doublets at  $\delta$  190.4 ( $^1J = 126.0$  Hz;  $^2J = 2.5$  Hz.) and a doublet of multiplets at  $\delta$  140.2 ( $^1J = 154.4$  Hz) for the  $\text{C}_\alpha$  and  $\text{C}_\beta$  resonances, respectively, in the  $^{13}\text{C}$  NMR spectrum. The crystal structures of the products have been determined by X-ray diffraction (Figure 11).<sup>631</sup>

The mechanism of hydroamination of allenes, alkynes, and alkenes catalyzed by Cp imido titanium complexes has been studied using high-level DFT model calculations.<sup>632</sup> In an attempt to determine the catalytic species in the hydroamination processes catalyzed by  $\text{Cp}_2\text{TiMe}_2$ ,<sup>633</sup> the reaction of the dimethyl bis-Cp titanium compound with 2,6-dimethylaniline in the presence of pyridine has been studied. The thermolysis of the reaction mixture affords a single Cp amido imido derivative  $\text{Cp}(\text{NHAr})(\text{Py})\text{Ti}=\text{NAr}$ , which undergoes facile ligand exchange with  $\text{Me}_3\text{PO}$  to give  $\text{Cp}(\text{NHAr})(\text{Me}_3\text{PO})\text{Ti}=\text{NAr}$ . Compound  $\text{Cp}(\text{NHAr})(\text{Py})\text{Ti}=\text{NAr}$  catalyzes the hydroamination of allenes at an unusually low temperature. The molecular structure of the pyridine adduct has been determined by X-ray diffraction studies (for more examples on hydroamination of unsaturated organic molecules, see Section 4.05.7).<sup>634</sup>

#### 4.05.3.3.4 Phosphinimido complexes

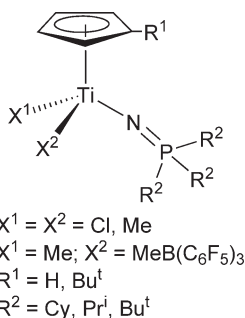
Recent progresses in the development of the titanium–phosphinimido complexes and their application as olefin polymerization pre-catalysts have been reviewed<sup>635–637</sup> and related computational studies have been reported.<sup>638</sup> Based on these theoretical results, the synthesis of a family of pre-catalysts of general formula  $\text{Cp}^*\text{TiX}_2[\text{NP}(\text{NR}_2)_3]$  ( $\text{X} = \text{Cl}, \text{Me}$ ) (Scheme 234) containing the tris(amino)phosphinimido ligand has been described.<sup>638</sup>



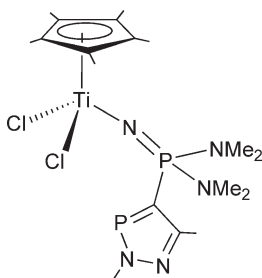
Scheme 234

The synthesis and characterization of a series of mono-Cp phosphinimido dichloro and dialkyl complexes  $\text{Cp}'\text{TiX}_2(\text{NPR}_3)$  ( $\text{Cp}' = \text{Cp}, \text{Cp}^*, \text{C}_5\text{H}_4\text{SiMe}_3, \text{C}_5\text{H}_4\text{Bu}^t, \text{C}_5\text{H}_4\text{Bu}^n, \text{C}_5\text{HPh}_4, \text{indenyl}$ ;  $\text{X} = \text{Cl}, \text{Me}, \text{CH}_2\text{Ph}, \text{CH}_2\text{SiMe}_3, \text{Ph}, 3,5\text{-C}_6\text{H}_3(\text{CF}_3)_2, 2,3,4,5\text{-C}_6\text{HF}_4, \text{OC}_6\text{H}_3\text{-2,6-Pr}_2^i$ ;  $\text{R} =$  a variety of alkyl and aryl groups) (Scheme 235) have been described. Using the strategy, based on the steric and electronic analogy between bulky phosphinimido and Cp ligands, these complexes have been used as precursors for the ethylene polymerization catalysis with several types of activators. Trends and patterns in the structure–activity relationship have been discussed and the implications for catalyst design evaluated. The dimethyl derivatives react with  $\text{B}(\text{C}_6\text{F}_5)_3$  to give the zwitterionic compounds  $\text{Cp}'\text{TiMe}(\text{NPR}_3)(\mu\text{-Me})\text{B}(\text{C}_6\text{F}_5)_3$ . The molecular structure of the  $\text{C}_5\text{H}_5$  derivative has been determined by X-ray diffraction. Cp phosphinimido complexes in the presence of MAO,  $\text{B}(\text{C}_6\text{F}_5)_3$ , or  $\text{Ph}_3\text{C}[\text{B}(\text{C}_6\text{F}_5)_4]$  are active catalysts for ethylene polymerization.<sup>639,640</sup> The compound  $\text{CpTiCl}_2(\text{NPM}_3)$  has been synthesized and characterized by X-ray crystallography. The molecules are monomeric with an almost-linear  $\text{N}=\text{PMe}_3^-$  ligand.<sup>641</sup>

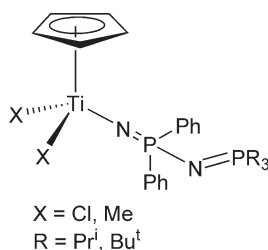
The complex shown in Scheme 236 has been synthesized by reaction of trimethylsilylimino bis(dimethylamino)-phosphorano diazaphosphole with  $\text{Cp}^*\text{TiCl}_3$ .<sup>642</sup> The dichloro and dimethyl phosphinimido complexes



Scheme 235



Scheme 236



Scheme 237

$\text{Cp}^*\text{TiX}_2(\text{NPPH}_2\text{NPR}_3)$  ( $\text{X} = \text{Cl}, \text{Me}$ ;  $\text{R} = \text{Pr}^i, \text{Bu}^t$ ) (Scheme 237) have been synthesized, and the molecular structure of  $\text{Cp}^*\text{TiCl}_2(\text{NPPH}_2\text{NPPr}^i_3)$  was determined by X-ray diffraction. The chloro complexes have been activated with MAO and the dimethyl derivatives with  $\text{B}(\text{C}_6\text{F}_5)_3$  to give active catalysts for the polymerization of ethylene.  $\text{Cp}^*\text{TiMe}_2[\text{NPPH}_2(\text{NPBu}^t_3)]$  reacts with  $\text{B}(\text{C}_6\text{F}_5)_3$  in  $\text{CH}_2\text{Cl}_2$  to give a mixture of products, one of which has been identified as  $[\text{Cp}^*\text{Ti}(\text{NPPH}_2\text{NPBu}^t_3)(\mu\text{-Cl})_2[\text{B}(\text{C}_6\text{F}_5)_4]]_2$ .<sup>643</sup> The synthesis of the complexes  $\text{Cp}'\text{TiX}_2(\text{NPBzR})$  ( $\text{Cp}' = \text{Cp}, \text{Cp}^*$ ;  $\text{R} = \text{Bu}^t, \text{Cy}$ ;  $\text{X} = \text{Cl}, \text{Me}$ ) and  $p\text{-C}_6\text{H}_4[\text{CH}_2(\text{R}_2)\text{PN}^+\text{TiCpX}_2]_2$  has been described. The activity of these species as catalyst precursors in ethylene polymerization activated by MAO or  $\text{Ph}_3\text{C}[\text{B}(\text{C}_6\text{F}_5)_4]$  has been evaluated.<sup>644</sup>

A series of mono- and bis-Cp and indenyltitanium complexes containing  $\eta^5$ - and  $\eta^1$ -Cp or Ind ligands supported by phosphinimido ligands have been described.<sup>645</sup> The compound  $(\eta^5\text{-Cp})\text{TiCl}_2(\text{NPBu}^t_3)$  reacts with  $\text{NaCp}(\text{DME})$  to give  $(\eta^5\text{-Cp})_2\text{Ti}(\text{NPBu}^t_3)\text{Cl}$  or  $(\eta^5\text{-Cp})_2\text{Ti}(\text{NPBu}^t_3)(\eta^1\text{-C}_5\text{H}_5)$ , depending of the stoichiometry. Treatment with LiInd affords  $(\eta^5\text{-Cp})\text{TiCl}(\text{NPBu}^t_3)(\eta^1\text{-Ind})$  or  $(\eta^5\text{-Cp})\text{Ti}(\text{NPBu}^t_3)(\eta^1\text{-Ind})_2$ . The mono-Ind complex  $(\eta^5\text{-C}_9\text{H}_7)\text{Ti}(\text{NPBu}^t_3)\text{Cl}_2$ , synthesized by reaction of  $(\eta^5\text{-C}_9\text{H}_7)\text{TiCl}_3$  with  $\text{Me}_3\text{SiNPBu}^t_3$ , reacts with LiInd to produce  $(\eta^5\text{-C}_9\text{H}_7)\text{TiCl}(\text{NPBu}^t_3)(\eta^1\text{-Ind})$  or  $(\eta^5\text{-C}_9\text{H}_7)\text{Ti}(\text{NPBu}^t_3)(\eta^1\text{-Ind})_2$ .  $(\eta^5\text{-C}_9\text{H}_7)\text{TiCl}_2(\text{NPBu}^t_3)$  is converted to the dimethyl derivative  $(\eta^5\text{-C}_9\text{H}_7)\text{TiMe}_2(\text{NPBu}^t_3)$  by alkylation with methyl Grignard reagents (Scheme 238). X-ray diffraction studies of some of these complexes are reported. Steric crowding appears to be the major factor in determining the binding modes of the Cp and indenyl ligands. The structural data result in a view of the phosphinimido ligand as a sterically demanding, four-electron donor ligand.  $^1\text{H}$  temperature-dependent NMR studies are carried out to infer an  $\eta^5\text{-}\eta^1$  ligand exchange process with an approximate barrier of  $8\text{--}9\text{ kcal mol}^{-1}$ .

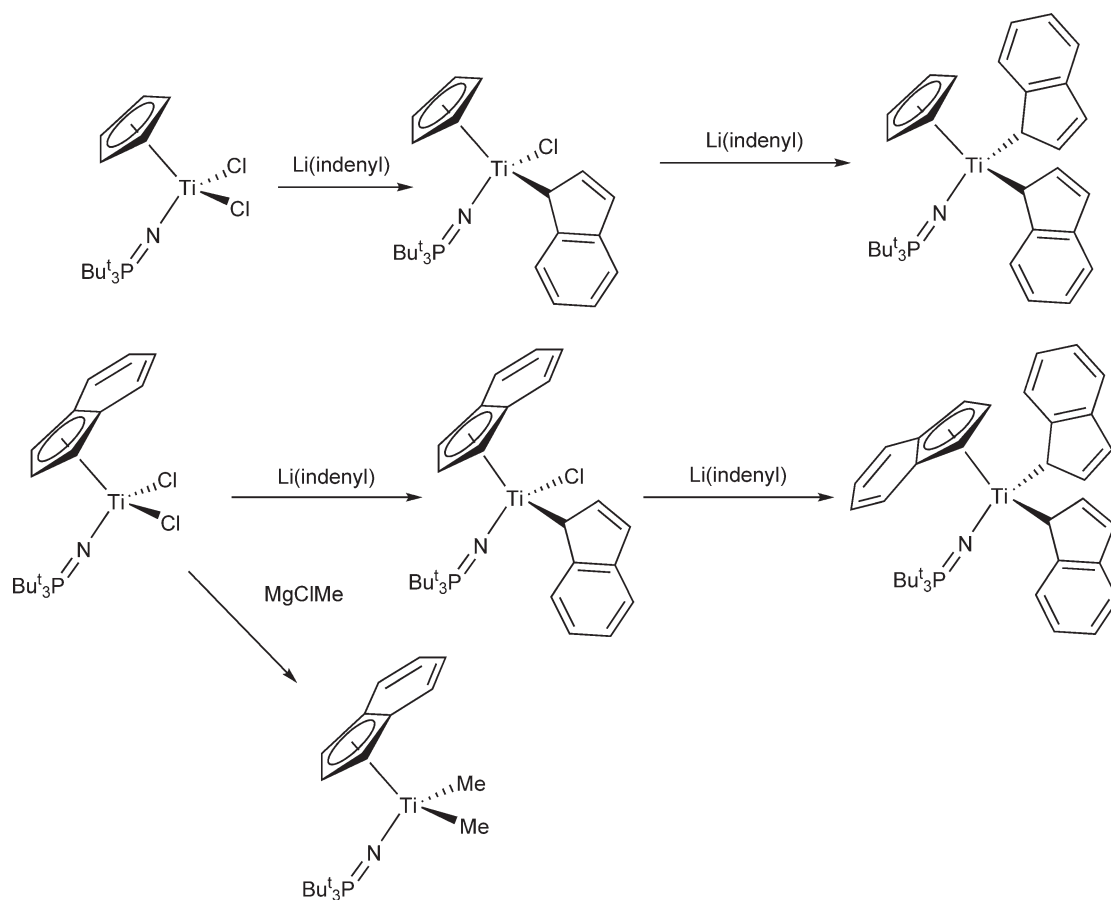
The *cage*-phosphinimido compounds  $\text{Cp}^*\text{TiCl}_2[\text{NPR}(\text{C}_6\text{H}_4\text{O}_3\text{-Me}_4)]$  ( $\text{R} = \text{Ph}, \text{Cy}$ ) can be prepared by reaction of the trimethylsilyl phosphinimine  $\text{Me}_3\text{Si}[\text{NPR}(\text{C}_6\text{H}_4\text{O}_3\text{-Me}_4)]$  with  $\text{Cp}^*\text{TiCl}_3$  in refluxing benzene. These compounds are alkylated by reaction with  $\text{MgBrMe}$  yielding the dimethyl complexes  $\text{Cp}^*\text{TiMe}_2[\text{NPR}(\text{C}_6\text{H}_4\text{O}_3\text{-Me}_4)]$  and their reactions with  $\text{AlMe}_3$  have been investigated (Scheme 239). Opening of the phosphadmantyl *cage* with transfer of a methyl group from the aluminum reagent is observed according to X-ray diffraction structural data. The molecular structure of  $\text{Cp}^*\text{TiMe}_2[\text{NP}(\text{Ph})(\text{C}_6\text{H}_4\text{O}_3\text{-Me}_4)]$  has been determined by X-ray diffraction methods. The dichloro derivatives in the presence of MAO and the dimethyl complexes in the presence of  $\text{Ph}_3\text{C}[\text{B}(\text{C}_6\text{F}_5)_4]$  have been tested as ethylene polymerization catalysts but were found to give only minimal amount of polymer.<sup>646</sup>

The reaction of the bis(iminophosphoranyl)methanes  $\text{CH}_2(\text{R}_2\text{P}=\text{NSiMe}_3)_2$  ( $\text{R} = \text{Me}, \text{Ph}, \text{Cy}$ ) with 2 equiv. of  $\text{Cp}^*\text{TiCl}_3$  gives the binuclear air and moisture sensitive complexes  $[\text{Cp}^*\text{TiCl}_2]_2[\mu\text{-CH}_2(\text{R}_2\text{P}=\text{N})_2]$  (Scheme 240). Some of these were characterized by X-ray diffraction. The monometallated derivatives  $\text{Cp}^*\text{TiCl}_2(\text{N}=\text{PR}_2\text{CH}_2\text{R}_2\text{P}=\text{NSiMe}_3)$  have been observed as intermediates in these reactions as deduced by  $^{31}\text{P}$  NMR spectroscopy but attempts to isolate the pure monosubstituted products have been not successful.<sup>647</sup> The complexes  $\text{Cp}^*\text{TiCl}_2[\text{N}=\text{PPh}_2(\text{Pr}^n)\text{NP}(\text{E})\text{Ph}_2]$  (Scheme 241) are obtained by reaction of  $\text{Cp}^*\text{TiCl}_3$  with the corresponding phosphiniminophosphine or the related oxidized phosphinimines.<sup>648</sup>

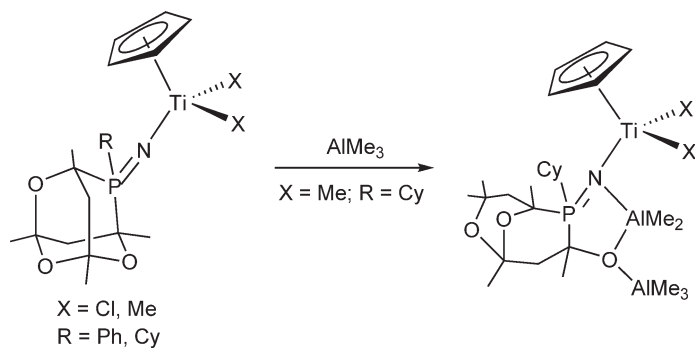
A series of mono-Cp phosphinimido mononuclear and binuclear titanium complexes have been obtained by reactions of  $\text{Cp}^*\text{TiCl}_3$  with trimethylsilyliminophosphines by a dehalosilylation (Scheme 242). The molecular structures of some of these complexes have been determined by X-ray diffraction.<sup>649</sup>

Titanium complexes with the tropidynyl ligand as Cp-equivalent and containing a phosphinimido or ketimido ligand have been described (Scheme 243).<sup>650</sup>

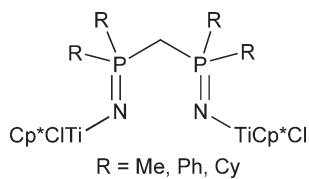
Thiolato titanium complexes have been developed supported by Cp and phosphinimido ligands, in an attempt to compare their chemical behavior with the corresponding bis-Cp derivatives, using the steric and electronic analogy between Cp and imido functionalities. Compounds of the type  $\text{Cp}^*\text{Ti}(\text{N}=\text{PPr}^i_3)(\text{SR}^2)_2$  (Scheme 244) are prepared by reaction of the dichloro complex with the corresponding lithium thiolates  $\text{LiSR}$ , or alternatively by protonolysis of  $\text{Ti-Me}$



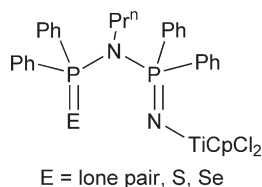
Scheme 238



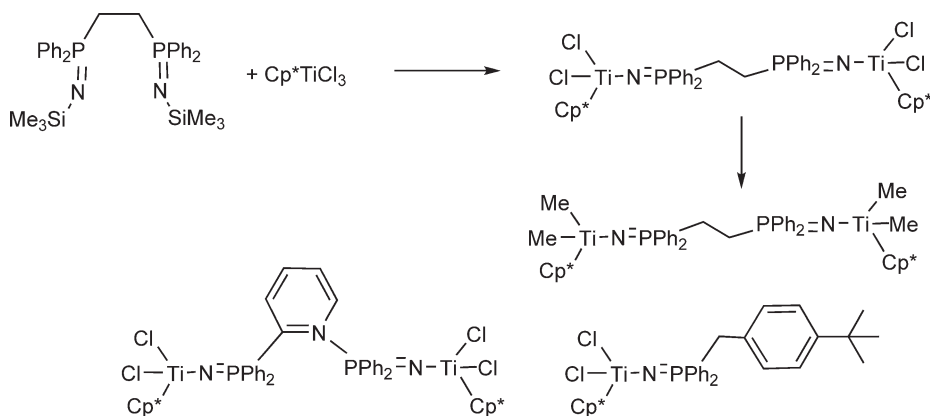
Scheme 239



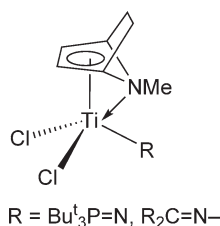
Scheme 240



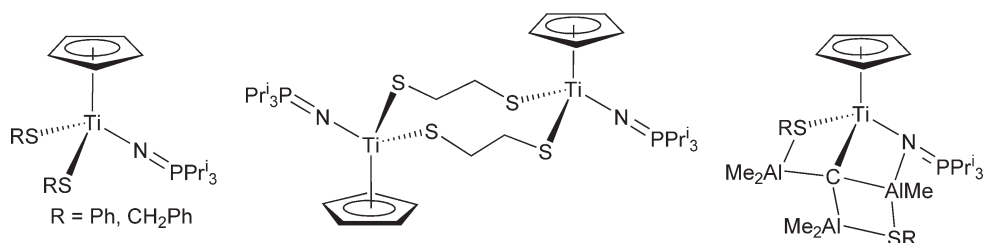
Scheme 241



Scheme 242

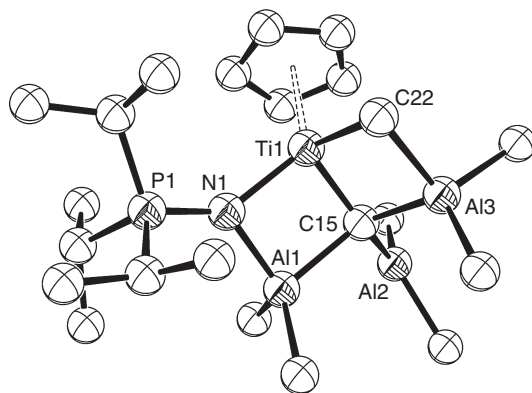


Scheme 243

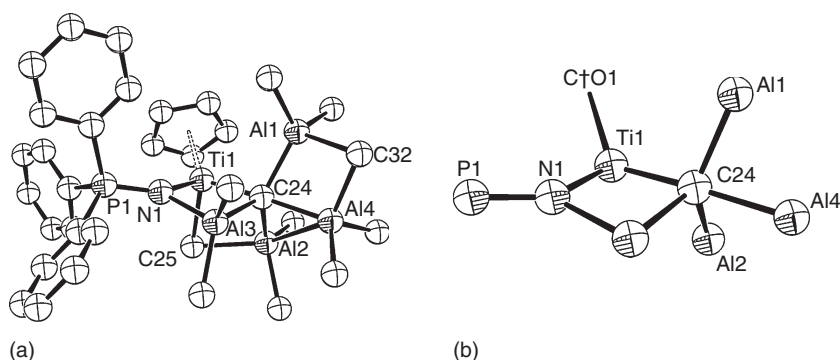


Scheme 244

bonds using the dimethyl complex  $\text{CpTiMe}_2(\text{NPPr}^i_3)$ . The reactions of these thiolate derivatives with excess  $\text{AlMe}_3$  have been found to proceed via initial binding of  $\text{AlMe}_3$  to the thiolate, followed by facile methyl/thiolate ligand exchange and subsequent C–H bond activation. The result is a triple C–H bond activation of a methyl group to give Ti–Al–carbide clusters. On the basis of spectroscopic data and the X-ray structures, the reaction products were identified as  $\text{CpTi}(\mu\text{-SR})(\mu\text{-NPPr}^i_3)(\text{C})(\text{AlMe}_2)_2(\mu\text{-SR})\text{AlMe}$  ( $R = \text{Ph}, \text{CH}_2\text{Ph}$ ) (Scheme 244).<sup>651</sup> More extensive studies have concluded that multiple C–H bond activation to give carbide and methine Ti–Al aggregates is a general feature of phosphinimido titanium pre-catalysts when treated with aluminum methyl activators. The triple C–H activation process also is observed in the reaction of the dimethyl amido complex  $\text{CpTiMe}_2(\text{NPPr}^i_3)$  with 4 equiv. of  $\text{AlMe}_3$ , which produces  $\text{CpTi}(\mu_2\text{-Me})(\mu\text{-NPPr}^i_3)(\mu_4\text{-C})(\mu_2\text{-AlMe}_2)_2(\text{AlMe}_2)$  (Figure 12). The molecular structure of this compound was confirmed by X-ray



**Figure 12** Molecular structure of complex  $\text{CpTi}(\mu_2\text{-Me})(\mu\text{-NPPri}_3)(\mu_4\text{-C})(\mu_2\text{-AlMe}_2)_2(\text{AlMe}_2)$  (reproduced by permission of Wiley-VCH from *Angew. Chem., Int. Ed.*, **2000**, 39, 3263).



**Figure 13** Two views [(a) titanium coordination around; (b) carbide coordination sphere] of the molecular structure of complex  $\text{CpTi}(\mu_2\text{-Me})(\mu\text{-NPPri}_3)(\mu_5\text{-C})(\mu_2\text{-AlMe}_2)_2(\text{AlMe}_2)(\text{AlMe}_3)$  (reproduced by permission of Wiley-VCH from *Angew. Chem., Int. Ed.*, **2000**, 39, 3263).

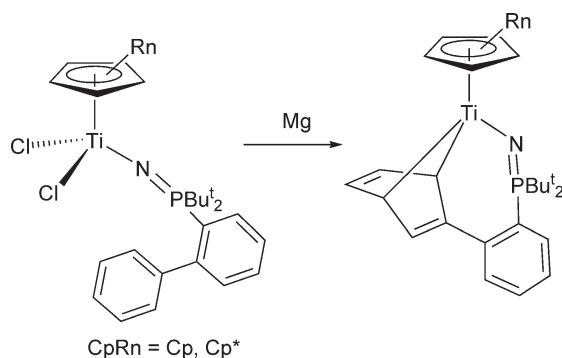
diffraction. The titanium–carbide bond distance [ $1.874(4) \text{ \AA}$ ] is significantly shorter than terminal Ti–Me bond distances. Resonances assignable to the carbide carbon atom are not observed in the  $^{13}\text{C}$  NMR spectrum, probably due to the cumulative effects of the long relaxation time of the quaternary carbon atom, although in the  $^{13}\text{C}$  NMR spectrum of the  $^{13}\text{C}$ -labeled derivative a signal attributed to the carbide carbon atom appears at  $\delta$  304.7. The three-coordinate aluminum in this compound coordinates diethyl ether. Similarly, the reaction of  $\text{CpTiMe}_2(\text{NPr}^i_3)$  with an excess of  $\text{AlMe}_3$  gives the compound  $\text{CpTi}(\mu_2\text{-Me})(\mu\text{-NPPri}_3)(\mu_5\text{-C})(\mu_2\text{-AlMe}_2)_2(\text{AlMe}_2)(\text{AlMe}_3)$ . Crystallographic studies confirm the presence of a five-coordinate carbide carbon atom in the molecular structure of this complex (Figure 13).<sup>652,653,77</sup>

$\text{CpTiCl}_2(\text{NPBu}^t_3)$  is reduced with Mg powder in benzene to give the binuclear Ti(III) complex  $[\text{CpTi}(\text{NPBu}^t_3)(\mu\text{-Cl})_2]_2$ .<sup>654</sup> Reduction of phosphinimido Ti(IV) compounds  $\text{CpTiCl}_2(\text{NPR}_3)$  ( $\text{R} = \text{Me}, \text{Pr}^i, \text{Bu}^t$ ) with Mg affords Ti(III), Ti(II), and Ti(IV) metallacyclic species. Reactions of  $\text{CpTiCl}_2(\text{NPBu}^t_3)$  with Mg in the presence of 2,3-dimethyl-1,3-butadiene, diphenylacetylene, phenylacetylene, bis(trimethylsilyl)acetylene, ethylene, or propylene proceed to give monometallic metallacyclic Ti(IV) complexes. Intramolecular formation of titanacycle complexes has also been achieved upon analogous reduction of  $\text{Cp}''\text{TiCl}_2[\text{NPBu}^t_2(2\text{-C}_6\text{H}_4\text{Ph})]$  ( $\text{Cp}' = \text{Cp}, \text{Cp}^*$ ) to afford products (Scheme 245) containing  $\eta^6$ -interactions between Ti and the pendant arene ring of the biphenyl substituents, suggested by NMR spectroscopic data and the molecular structure. The molecular structures of the metallacyclic derivatives have been determined by X-ray diffraction studies.<sup>655</sup>

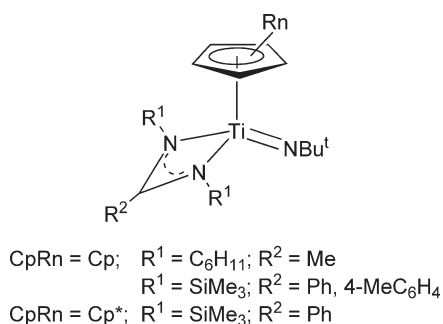
#### 4.05.3.3.5 Amidinato complexes

*N,N'*-amidinato groups act as ligands which in combination with Cp rings provide stable coordination environments for transition metals. These “NCN” ligands act as three-electron donating groups.

The amidinato–imido titanium complexes shown in Scheme 246 have been obtained by salt metathesis methods.<sup>90,656</sup> Complexes containing a  $\text{Cp}^*$  and the *N*-alkylated benzamidinato ligands have been synthesized by treatment



Scheme 245

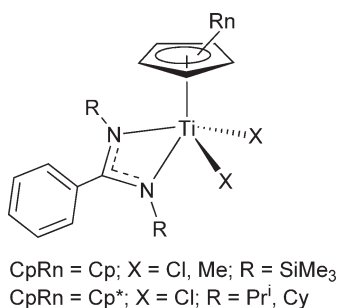


Scheme 246

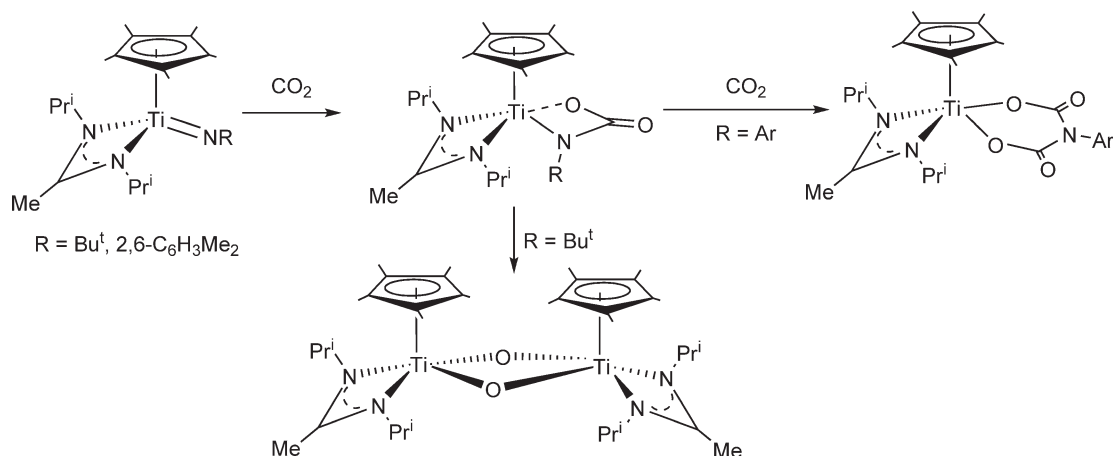
of Cp<sup>\*</sup>TiCl<sub>3</sub> with the lithium benzamidinate (Scheme 247).<sup>657</sup> The compounds (C<sub>5</sub>R<sub>5</sub>)TiCl<sub>2</sub>[(NSiMe<sub>3</sub>)<sub>2</sub>CPh] (R = H, Me) are prepared by reaction of (C<sub>5</sub>R<sub>5</sub>)TiCl<sub>3</sub> and the lithium salt Li[PhC(NSiMe<sub>3</sub>)<sub>2</sub>].<sup>658,659</sup> The dimethyl Cp<sup>\*</sup>TiMe<sub>2</sub>[(NSiMe<sub>3</sub>)<sub>2</sub>CPh] has also been synthesized by reaction of the chloro precursor compound with LiMe in toluene at -80 °C and the crystal structure determined (Scheme 247).<sup>660</sup>

Reaction of the Cp-amidinato imido titanium complexes Cp<sup>\*</sup>Ti[MeC(NPr<sup>i</sup>)<sub>2</sub>](NR) (R = Bu<sup>t</sup>, 2,6-C<sub>6</sub>H<sub>3</sub>Me<sub>2</sub>) with CO<sub>2</sub> proceed via initial cycloaddition reactions to give N-O-carbamato complexes. The Bu<sup>t</sup> derivative does not react with an excess of CO<sub>2</sub> and it undergoes a retrocyclization process with the formation of Bu<sup>t</sup>NCO and the binuclear μ-oxo compound {Cp<sup>\*</sup>Ti[MeC(NPr<sup>i</sup>)<sub>2</sub>]}<sub>2</sub>(μ-O). The aryl derivatives exhibit a double CO<sub>2</sub> insertion process to give Cp<sup>\*</sup>Ti[MeC(NPr<sup>i</sup>)<sub>2</sub>][O(CO)N(Ar)(CO)O] (Scheme 248).<sup>661</sup>

The lithium amidinate Li[Me<sub>3</sub>SiNC(Ph)N(CH<sub>2</sub>)<sub>3</sub>N(Me)SiMe<sub>3</sub>]·2THF containing a pendant methyl(trimethylsilyl)-amine functionality reacts with CpTiCl<sub>3</sub> to give the Cp amidinato amido chloro complex CpTiCl[Me<sub>3</sub>SiNC(Ph)N(CH<sub>2</sub>)<sub>3</sub>NMe], which has been characterized by X-ray diffraction. Further treatment, in C<sub>6</sub>D<sub>6</sub>, of the amidinato-amido



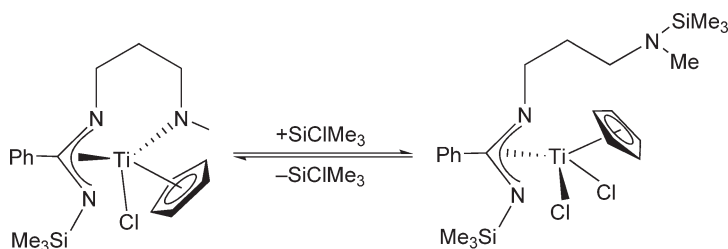
Scheme 247



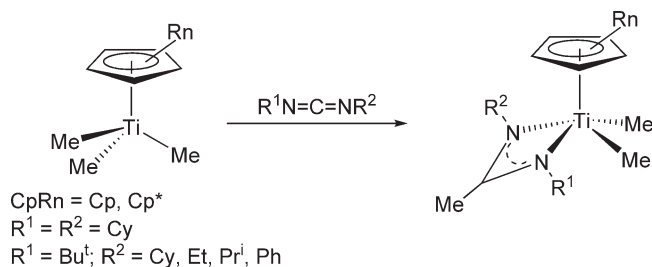
Scheme 248

compound with SiClMe<sub>3</sub> leads to the formation of Cp'TiCl<sub>2</sub>[Me<sub>3</sub>SiNC(Ph)N(CH<sub>2</sub>)<sub>3</sub>N(Me)SiMe<sub>3</sub>] in a reversible reaction (Scheme 249).<sup>87</sup>

Carbodiimides R<sup>1</sup>N=C=NR<sup>2</sup> insert into the Ti–C bond of Cp'TiMe<sub>3</sub> (Cp' = Cp, Cp\*) to give amidinato derivatives (Scheme 250). Similar reactions have been described by using optically pure (*R,R*)- and *meso*-(*R,S*)-1,3-bis(1-phenylethyl)carbodiimides. Chiral titanium complexes are obtained where R<sup>1</sup> is not equal to R<sup>2</sup> with low barriers for the racemization process involving amidinato “ring flipping” that exchanges the magnetic environments of the diastereotopic methyl groups bonded to the titanium center. These complexes exhibit configurational instability and their conformational and stereochemical properties in solution and in the solid state have been suitably studied. Upon activation with MAO these complexes are active for the polymerization of ethylene.<sup>662,663</sup> The binuclear bis(amidinato) complex [Cp'TiMe<sub>2</sub>N(Bu<sup>t</sup>)C(Me)N(CH<sub>2</sub>CH<sub>2</sub>-)]<sub>2</sub> has been prepared by reaction of the α,ω-biscarbodiimide Bu<sup>t</sup>N=C=N(CH<sub>2</sub>)<sub>4</sub>N=C=NBu<sup>t</sup> with 2 equiv. of Cp'TiMe<sub>3</sub>. The compound is obtained as a rapidly equilibrating mixture of *meso*- and *d,l*-stereoisomers in solution. Nevertheless, single crystals of the *rac*-isomer can be isolated by crystallization from pentane at –35 °C and the structure was determined by X-ray diffraction (Scheme 251).<sup>664</sup>

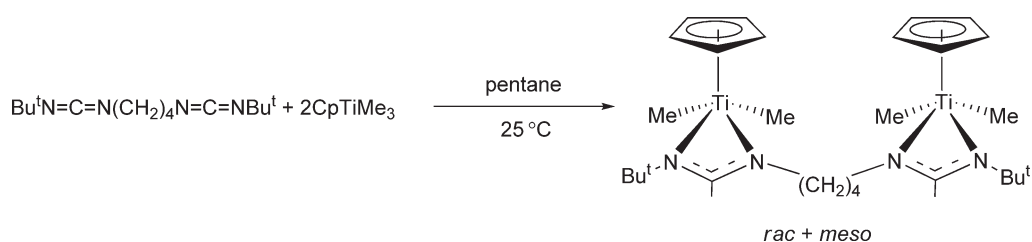


Scheme 249

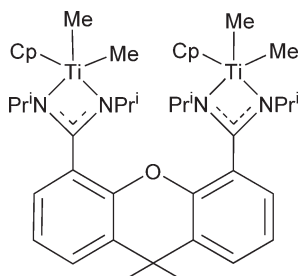


Scheme 250





Scheme 251



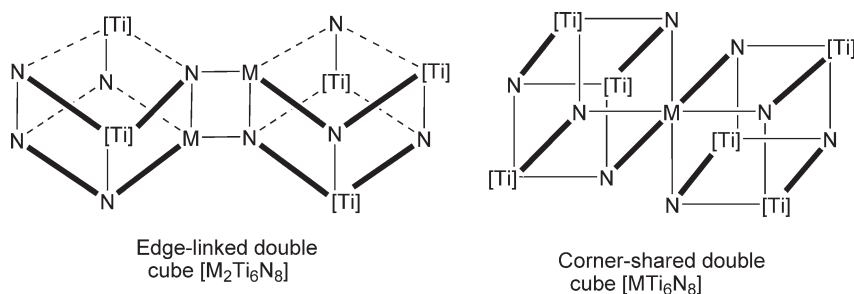
Scheme 252

The binuclear complex  $\text{Cp}_2\text{Ti}_2\text{Me}_4(\text{bis-amidinato})$  shown in Scheme 252 supported by a bridged bis-amidinato ligand based on a 9,9-dimethylxanthene backbone has been synthesized by the reaction in toluene of  $\text{CpTiMe}_3$  with the corresponding bis-amidine molecule. Reaction of this complex with  $\text{H}_2$  affords bis-amidinato  $\mu$ -methyl,  $\mu$ -hydrido Ti(III) derivatives.<sup>665</sup>

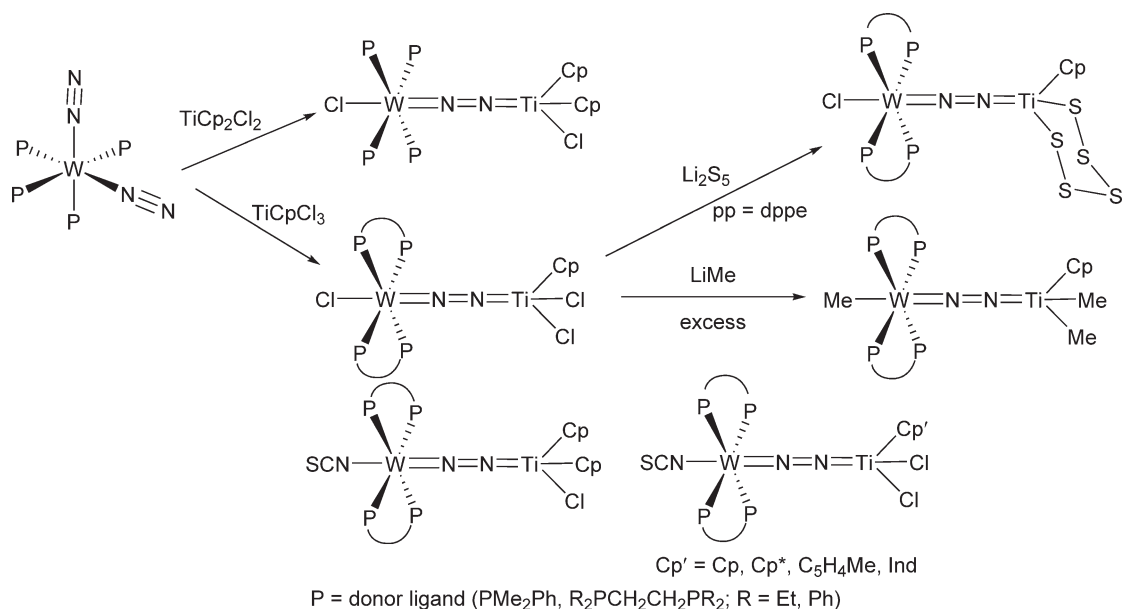
#### 4.05.3.3.6 Complexes with other N-based ligands

Nitrido titanium compounds exhibiting the single cube  $[\text{MTi}_3\text{N}_4]$  (Scheme 232), the edge-linked double azaheterometallobutane  $[\text{Li}_2\text{Ti}_6\text{N}_8]$  cubane or corner-shared double-cube  $[\text{MTi}_6\text{N}_8]$  disposition (Scheme 253) with participation of group 1, 2, and transition metals, have been prepared by reactions of  $\mu$ -imido titanium compounds with the appropriate reagents (see Section 4.05.3.3.3).<sup>622,625–628</sup> DFT calculations have been carried out on the cluster  $[\text{CpTi}(\mu_3\text{-N})_4]$  with the aim of comparing the energies and the electronic structures of the cubane and planar forms. Calculations indicate that the cubane conformation is much more stable than the structure in which the four metals and the four nitrogens are in the same plane.<sup>666</sup>

Heterobimetallc complexes containing a dinitrogen bridge between group 6 and group 4 metals have been reported (Scheme 254). The dinitrogen tungsten compound *cis*- $\text{W}(\text{N}_2)_2(\text{PMe}_2\text{Ph})_4$  reacts with  $\text{Cp}_2\text{TiCl}_2$  or  $\text{Cp}'\text{TiCl}_3$  ( $\text{Cp}' = \text{Cp}, \text{Cp}^*, \text{C}_5\text{H}_4\text{Me}, \text{Ind}$ ) to afford  $\mu$ - $\text{N}_2$  complexes  $\text{Cl}(\text{PMe}_2\text{Ph})_4\text{W}=\text{N}=\text{N}=\text{TiCp}_2\text{Cl}$  and  $\text{Cl}(\text{PMe}_2\text{Ph})_4\text{W}=\text{N}=\text{N}=\text{TiCp}'\text{Cl}_2$ . The coordinated dinitrogen can be considered as a formal  $\text{N}_2^{2-}$  (diazene- $^{2-}$ ) ligand which acts as a four-electron donor to each of the W and Ti atoms. The molecular structure of the mono-Cp



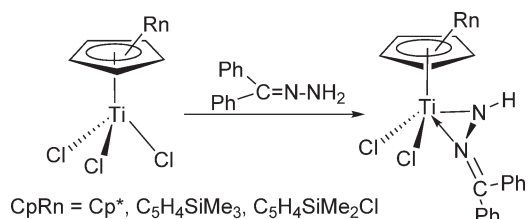
Scheme 253



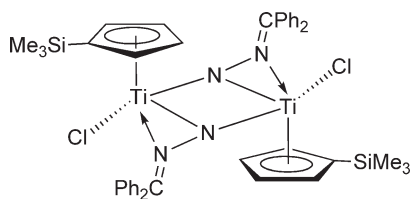
Scheme 254

derivative has been determined by X-ray diffraction methods and shows an almost-linear Ti–N–N–W array with a Ti–N bond distance of 1.792 Å. Cl(PMe<sub>2</sub>Ph)<sub>4</sub>W=N=N=TiCp<sub>2</sub>Cl reacts with 10 molar equiv. of H<sub>2</sub>SO<sub>4</sub> in MeOH at room temperature to give 0.86 mol of NH<sub>3</sub> and 0.08 mol of N<sub>2</sub>H<sub>4</sub> per mol of the heterobimetallic compound. Tungsten dinitrogen complexes with chelating phosphine ligands R<sub>2</sub>PCH<sub>2</sub>CH<sub>2</sub>PR<sub>2</sub> (R = Et, Ph) are unreactive toward Cp<sub>2</sub>TiCl<sub>2</sub>, but they react with Cp'TiCl<sub>3</sub> to give similar complexes, which can be methylated with LiMe. Activated with MMAO these compounds polymerize ethylene and co-polymerize ethylene and 1-hexene. The complex Cp<sub>2</sub>Ti(OTf)<sub>2</sub> is also effective for the synthesis of μ-N<sub>2</sub> W–Ti derivatives. Analogous complexes are formed by reacting (NBu<sup>t</sup>)<sub>4</sub>[W(NCS)(N<sub>2</sub>)(dppe)<sub>2</sub>] with Cp<sub>2</sub>TiCl<sub>2</sub> or Cp'TiCl<sub>3</sub>.<sup>667–669</sup>

Monohydrazonide(I-) compounds Cp'TiCl<sub>2</sub>[N(H)NCPh<sub>2</sub>] [Cp' = Cp\*, C<sub>5</sub>H<sub>4</sub>SiMe<sub>3</sub>, C<sub>5</sub>H<sub>4</sub>SiMe<sub>2</sub>Cl] have been synthesized by treatment of the corresponding mono-Cp trichloro derivatives Cp'TiCl<sub>3</sub> with hydrazone in the presence of 1 equiv. of NEt<sub>3</sub> (Scheme 255). (C<sub>5</sub>H<sub>4</sub>SiMe<sub>3</sub>)TiCl<sub>2</sub>[N(H)NCPh<sub>2</sub>] reacts with NEt<sub>3</sub> in toluene to give the binuclear complex [(C<sub>5</sub>H<sub>4</sub>SiMe<sub>3</sub>)TiCl(μ-NNCPh<sub>2</sub>)<sub>2</sub>] (Scheme 256), the molecular structure of which has been



Scheme 255



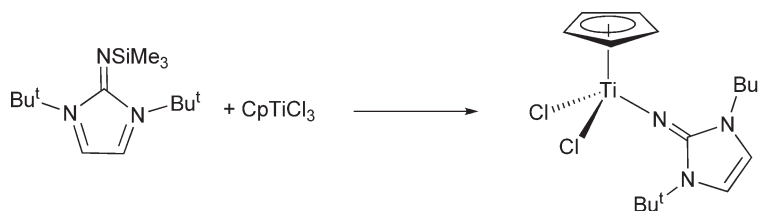
Scheme 256

determined by X-ray diffraction methods and shows two “(C<sub>5</sub>H<sub>4</sub>SiMe<sub>3</sub>)TiCl” units bridged by two hydrazonide(2-) ligands which form a symmetrical Ti<sub>2</sub>(NN)<sub>2</sub> core. These hydrazonide compounds have been activated with MAO and are suitable for olefin polymerizations.<sup>670</sup>

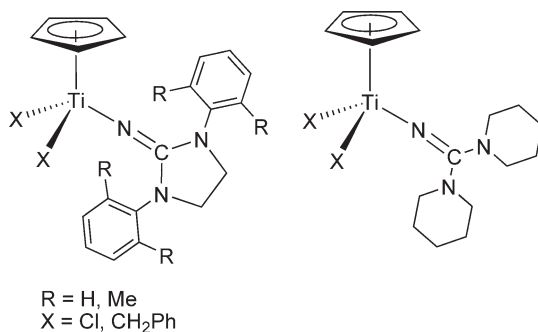
CpTiCl<sub>3</sub> reacts with N-silylated 2-iminoimidazoline in toluene at room temperature overnight to give the corresponding imidazolin-2-iminato derivative (Scheme 257). Its molecular structure has been determined by X-ray diffraction.<sup>671</sup>

The mono-Cp dichloro titanium compounds containing monoanionic iminoamidazolidine ligands CpTiCl<sub>2</sub>[N=C(NR<sub>2</sub>)<sub>2</sub>] (Scheme 258) have been made by the reaction of CpTiCl<sub>3</sub> with the lithium salts of the corresponding ligands. Reactions of the dichloro derivatives with 2 equiv. of benzyl Grignard reagents afford the dibenzyl complexes. The molecular structure of CpTiCl<sub>2</sub>[N=C(NCH<sub>2</sub>)<sub>2</sub>(2,6-Me<sub>2</sub>C<sub>6</sub>H<sub>3</sub>)<sub>2</sub>] as determined by X-ray diffraction shows a short Ti–N distance of 1.792(2) Å, suggesting substantial π-donation to the Ti center. The dibenzyl complex CpTi(CH<sub>2</sub>Ph)<sub>2</sub>[N=C(NCH<sub>2</sub>)<sub>2</sub>(2,6-Me<sub>2</sub>C<sub>6</sub>H<sub>3</sub>)<sub>2</sub>] reacts with B(C<sub>6</sub>F<sub>5</sub>)<sub>3</sub> with smooth abstraction of one benzyl group to give the ionic complex {CpTi(CH<sub>2</sub>Ph)[N=C(NCH<sub>2</sub>)<sub>2</sub>(2,6-Me<sub>2</sub>C<sub>6</sub>H<sub>3</sub>)<sub>2</sub>][PhCH<sub>2</sub>B(C<sub>6</sub>F<sub>5</sub>)<sub>3</sub>], in which the anion is non-coordinated and the cationic metal center is stabilized by an η<sup>2</sup>-bonded benzyl ligand. These complexes are effective catalysts, in the presence of B(C<sub>6</sub>F<sub>5</sub>)<sub>3</sub>, for the homopolymerization of ethylene.<sup>672</sup>

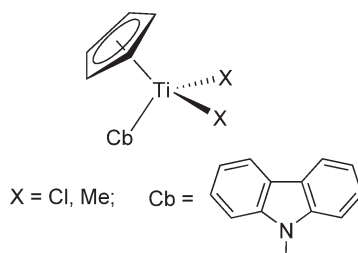
The reaction of CpTiCl<sub>3</sub> with potassium carbazolate (Kcb) leads to the formation of CpTiCl<sub>2</sub>(cb); the structure has been determined by X-ray diffraction. The dichloro complex can be alkylated by reaction with LiMe to give the dimethyl derivative CpTiMe<sub>2</sub>(cb) (Scheme 259).<sup>110</sup>



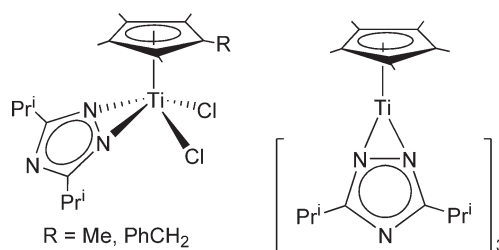
Scheme 257



Scheme 258



Scheme 259



Scheme 260

Titanium complexes containing  $\eta^2$ -1,2,4-triazolato (tz) ligands, bearing bulky isopropyl groups in 3,5 positions, have been synthesized. Reaction of  $(C_5Me_4CH_2Ph)/TiCl_3$  and  $Cp^*TiCl_3$  with 1 or 3 equiv. of the potassium salt of the triazolato ligand affords the mono- or tris-triazolato complexes  $(C_5Me_4R)TiCl_2(tz)$  ( $R = Me, CH_2Ph$ ) and  $Cp^*Ti(tz)_3$  in which the tz ligand is  $\eta^2$ -coordinated (Scheme 260). The analogous  $CpTiCl_2(tz)$  is formed. The compounds have been characterized by NMR spectroscopy, mass spectrometry, elemental analysis, and X-ray crystallography.<sup>673</sup>

The reaction of  $(EBI)H_2$  [ $EBI$  = ethylene-1,2-bis(indenyl)] and titanium amides did not give the expected *ansa*-titanocene products. Even with the azetidine complex,  $Ti(NC_3H_6)_4$  reacts with only a single amine elimination to give the mono(indenyl) derivative  $(C_9H_6CH_2CH_2C_9H_7)/Ti(NC_3H_6)_3$ . By contrast, *ansa*-zirconocene and hafnocene are easily obtained by the amine elimination process. It is likely that increased steric crowding around the smaller Ti disfavors the second amine elimination.<sup>674</sup>

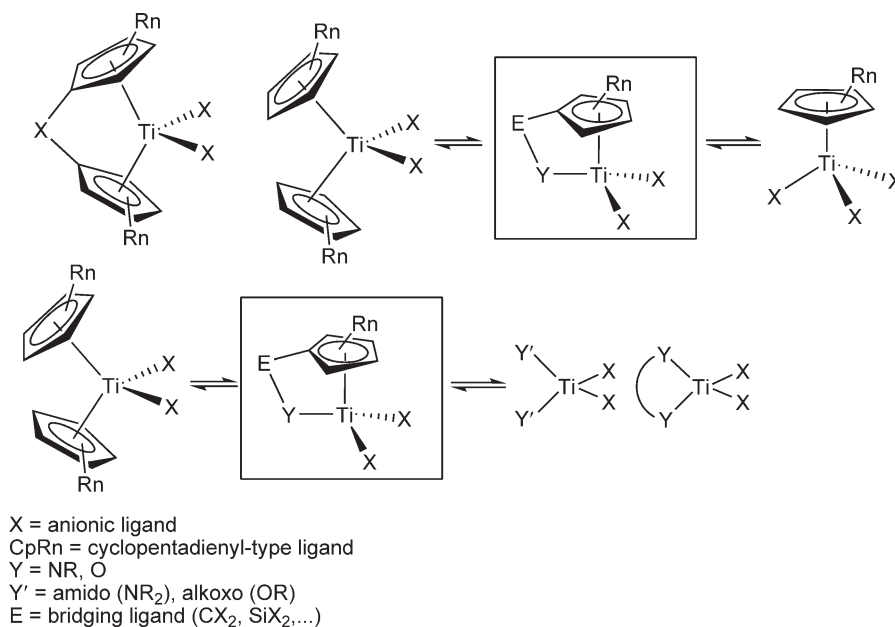
#### 4.05.3.4 Monocyclopentadienyl–Amido Complexes

Recent years have seen a strong interest in Cp complexes of early transition metals with neutral or anionic Lewis base substituents on the Cp ligands. Mono-Cp transition metal complexes are electronically and sterically less constrained around the metal center, and this less crowded ligand sphere leads to potentially higher reactivity toward unsaturated organic molecules. The replacement of the classical bis-Cp ligand set by bidentate systems in which two Cp-type rings (*ansa*-metallocenes) or one Cp and a different anionic functionality are linked by a bridging group has created a range of new derivatives with remarkable variation in chemical properties. A prime example is the combination of Cp ligands with anionic amido or alkoxo moieties. The Cp–amido complexes have a covalently attached N-donor group which electronically stabilizes the metal center, while the bridging group considerably opens the metal coordination sphere compared to conventional bis-Cp complexes.

Mono-Cp amido titanium complexes resemble in many respects the behavior exhibited by bis-Cp and *ansa*-metallocene derivatives (Scheme 261), and they can be regarded as intermediate dispositions between these complexes and the mono-Cp derivatives. This structural analogy explains the similarities in chemical behavior exhibited by these compounds, for example, in polymerization processes. Alternatively, they can be considered as hybrids of bis-Cp and the more electronically unsaturated and more sterically open bis-amido (or bis-alkoxo) compounds (Scheme 261). For the Cp–amido derivatives the Cp(centroid)–Ti–N bite angle is generally smaller than the typical Cp(centroid)–Ti–Cp(centroid) angle in the corresponding bis-Cp complexes. The Cp–amido complexes are distinguished by a sterically accessible active site and more electron-deficient titanium center. Their ability to easily incorporate styrene, particularly in co-polymerization with ethylene, the remarkable stability at high temperatures, and the low propensity to be reduced by MAO have made these compounds particularly attractive catalysts (see also Chapter 4.09).

Bridged Cp–amido titanium complexes are generally referred to as “constrained-geometry” catalysts (CGCs) and continue to attract considerable attention in polymerization catalysis. For example, they are capable of producing polyolefins with long chain branching, with corresponding advantages in polymer processing due to increased melt strength, and of co-polymerizing ethylene with styrene without producing detectable amounts of homopolymer impurities.<sup>675</sup> They promote the efficient co-polymerization of ethylene with 1-alkenes to give new grades of polyethylene. Indenyl–amido titanium complexes are also known.

A monograph including complexes with Cp–amido ligands has recently been published.<sup>676</sup> The role of the group 4 Cp–amido derivatives as catalyst precursors for olefin polymerization has been reviewed.<sup>677</sup> A review highlighting the



Scheme 261

**Table 1** Synthetic methods for the preparation of mono-Cp-amido titanium derivatives

Key	Method
I	Metathesis reaction
II	Amine elimination from homoleptic Ti(NR <sub>2</sub> ) <sub>3</sub>
III	Alkane elimination from homoleptic TiR <sub>4</sub>
IV	HCl elimination from TiCl <sub>4</sub> or TiCp'Cl <sub>3</sub>
V	Dehalosilylation

developments in the design and applications of non-metallocene complexes including Cp-amido derivatives as catalyst systems for  $\alpha$ -olefin polymerization has appeared.<sup>440</sup>

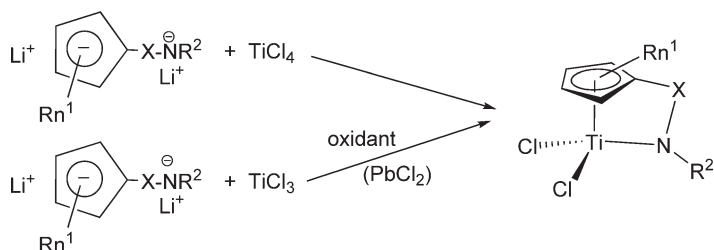
It is well established that the nature of the bridge between the Cp and the amido functionality has a profound effect on the reactivity and electronic properties of these complexes. A variety of linkers have been used. Varying the bridging unit provides a powerful method to alter the structure–reactivity relationship in these complexes. In the majority of cases, SiMe<sub>2</sub>-bridged (Cp–SiMe<sub>2</sub>–NR) ligands have been employed, although several variations of this bridge have been reported. A few examples report an  $sp^2$ -C<sub>1</sub> or  $sp^3$ -C<sub>1</sub> hydrocarbyl linker. Complexes with boron-bridged Cp-amido functionalities have been reviewed.<sup>678</sup>

In view of the commercial potential of these catalysts, efficient synthetic procedures for the synthesis of this type of complexes have been developed.<sup>679–684</sup> They are summarized in Table 1 and illustrated with examples.

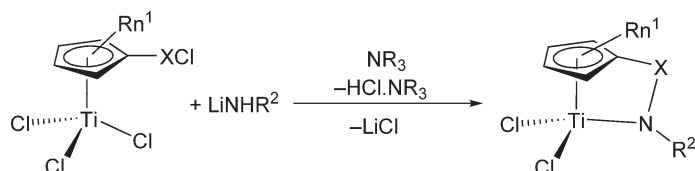
#### 4.05.3.4.1 Metathesis reactions

- Metathetical reaction between the dilithium salt of the Cp-amido dianion with TiCl<sub>4</sub> or TiCl<sub>3</sub> followed by oxidation (Scheme 262).
- Reaction between LiNHR and halide-substituted mono-Cp titanium compounds (Scheme 263).

The complexes (C<sub>5</sub>H<sub>4</sub>SiMe<sub>2</sub>NCH<sub>2</sub>C<sub>6</sub>H<sub>3</sub>X<sub>2-2,5</sub>)/TiCl<sub>2</sub> (X = H, F) containing a Cp-benzylamido ligand have been prepared by treatment of (C<sub>5</sub>H<sub>4</sub>SiMe<sub>2</sub>Cl)TiCl<sub>3</sub> with Li(HNCH<sub>2</sub>C<sub>6</sub>H<sub>3</sub>X<sub>2-2,5</sub>). The tetramethyl-Cp dichloro derivative (C<sub>5</sub>Me<sub>4</sub>SiMe<sub>2</sub>NCH<sub>2</sub>C<sub>6</sub>H<sub>5</sub>)/TiCl<sub>2</sub> is obtained by the reaction of TiCl<sub>3</sub>(THF)<sub>3</sub> with Li<sub>2</sub>(NCH<sub>2</sub>C<sub>6</sub>H<sub>3</sub>X<sub>2-2,5</sub>)



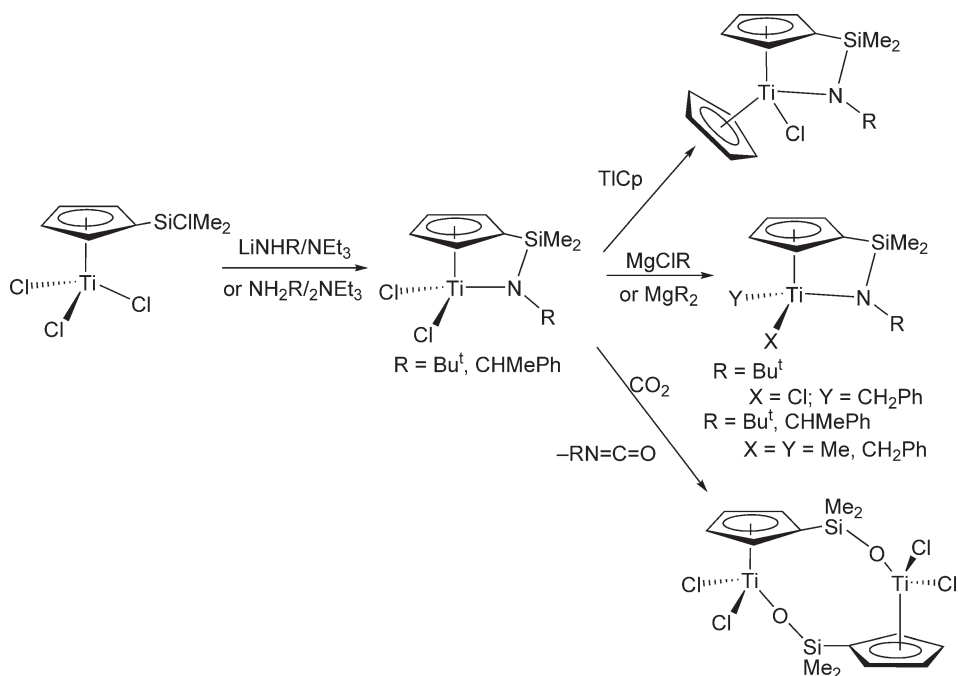
Scheme 262



Scheme 263

followed by an oxidation process. The dichloro complexes can be alkylated to afford the corresponding dialkyl derivatives. The molecular structure of  $(\text{C}_5\text{Me}_4\text{SiMe}_2\text{NCH}_2\text{C}_6\text{H}_5)\text{Ti}(\text{CH}_2\text{Ph})_2$  determined by X-ray diffraction suggests the presence of  $\alpha$ -agostic bonding of one of the benzyl groups to the Ti center.<sup>685</sup>

The compounds  $(\text{C}_5\text{H}_4\text{SiMe}_2\text{NR})\text{TiCl}_2$  ( $\text{R} = \text{Bu}^t$ ,  $\text{CHMePh}$ ) (Scheme 264) are obtained by the reaction of  $(\text{C}_5\text{H}_4\text{SiClMe}_2)\text{TiCl}_3$  with  $\text{LiNHR}$  in the presence of  $\text{NEt}_3$  or alternatively by the treatment of the trichloro complex with  $\text{NH}_2\text{R}$  in the presence of  $\text{NEt}_3$ . Reactivity of this Cp-amido complex with  $\text{TiCp}$ , alkylating reagents, and  $\text{CO}_2$  has been studied to give mixed bis-Cp, alkyl derivatives and one binuclear titanium complex bearing a Ti–O–Si unit with the



Scheme 264

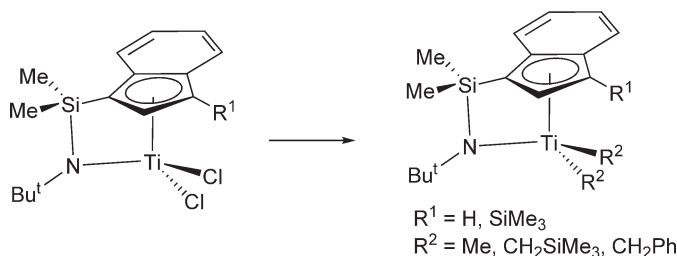
elimination of alkyl isocyanate  $\text{RN}=\text{C}=\text{O}$ .<sup>581</sup> Treatment of  $(\text{C}_5\text{H}_4\text{SiCl}_2\text{Me})\text{TiCl}_3$  with 1 equiv. of  $\text{LiN}(\text{SiMe}_3)_2$  affords the dichloro amido titanium derivative  $(\text{C}_5\text{H}_4\text{SiCl}_2\text{Me})\text{TiCl}_2[\text{N}(\text{SiMe}_3)_2]$  indicating the selectivity of the Ti–Cl bond. In the presence of  $\text{LiNHBu}^t/\text{NEt}_3$ , the Si–Cl and one of the Ti–Cl react to give the Cp-amido complex  $(\text{C}_5\text{H}_4\text{SiClMeNBu}^t)\text{TiCl}_2$  (Scheme 212).<sup>382</sup> Reaction of the tetramethyl-chlorosilyl-Cp complexes  $(\text{C}_5\text{Me}_4\text{SiClXMe})\text{TiCl}_3$  (X = H, Cl) with 2 equiv. of  $\text{LiNHBu}^t$  gives the Cp-amido derivatives  $(\text{C}_5\text{Me}_4\text{SiXMeNBu}^t)\text{TiCl}_2$ , which can be methylated by reaction with  $\text{MgClMe}$ . The “Si–NBu<sup>t</sup>–Ti” bridging group in these complexes reacts with different chlorinated agents. Treatment with  $\text{TiCl}_4$  produces  $(\text{C}_5\text{Me}_4\text{SiClHMeHCl})\text{TiCl}_3$ , while reaction with  $\text{BCl}_3$  gives  $(\text{C}_5\text{Me}_4\text{SiCl}_2\text{Me})\text{TiCl}_3$ .<sup>383</sup>

The limited stability of monoindenyltitanium complexes is improved by the introduction of linked amido-functionality. The compounds  $(\text{C}_9\text{H}_5\text{RSiMe}_2\text{N}^t\text{Bu})\text{TiX}_2$  (R = H,  $\text{SiMe}_3$ ; X = Cl, Me,  $\text{CH}_2\text{SiMe}_3$ ,  $\text{CH}_2\text{Ph}$ ) (Scheme 265) containing the amido-functionalized indenyl ligand have been synthesized by the reaction of the dilithium derivative  $\text{Li}_2(\text{C}_9\text{H}_5\text{RSiMe}_2\text{N}^t\text{Bu})$  with  $\text{TiCl}_3(\text{THF})_3$  followed by oxidation or by the alkylation of the dichloro derivative.<sup>686</sup>

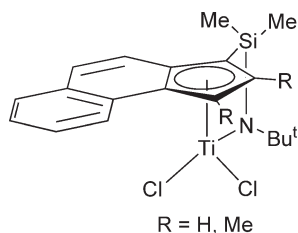
The 2-substituted-benzen[e]indenyl-amido complex  $[(2\text{-R-BenzInd})\text{SiMe}_2\text{NBu}^t]\text{TiCl}_2$  (Scheme 266) has been synthesized by the reaction of  $\text{TiCl}_4(\text{THF})_2$  with the dilithium salt of the indenyl-amido ligand. Activated with MAO, these complexes show ethylene/1-octene co-polymerization activity.<sup>688</sup> The analogous disubstituted benz[e]indenyl-amido complex  $[(2\text{-}3\text{-R}_2\text{BenzInd})\text{SiMe}_2\text{NBu}^t]\text{TiCl}_2$  (Scheme 266) has been synthesized. A series of Cp-, indenyl-, and fluorenyl-amido Ti compounds have been studied as catalyst precursors for the polymerization of 4-methyl-1-pentene and the co-polymerization of ethylene/4-methyl-1-pentene.<sup>689</sup>

Silyl-bridged indenyl *tert*-butylamido complexes in which heterocycles are condensed onto the indenyl ligand have been prepared by this synthetic methodology. Some examples are shown in Scheme 267. The molecular structures have been determined by single crystal X-ray diffraction. These complexes are active, in combination with  $\text{Ph}_3\text{C}[\text{B}(\text{C}_6\text{F}_5)_3]$  or MAO, to produce high molecular weight syndiotactic amorphous polypropylene (*sam*-PP; a polypropylene having a prevailing syndiotactic microstructure with syndiotactic pentad contents *rrrr* up to 40–55% and slowly developing a low level of crystallinity at room temperature). The influence of the ligand substituents on the polymerization activity has been rationalized and the mechanical properties of the polymer have been studied.<sup>690, 691</sup>

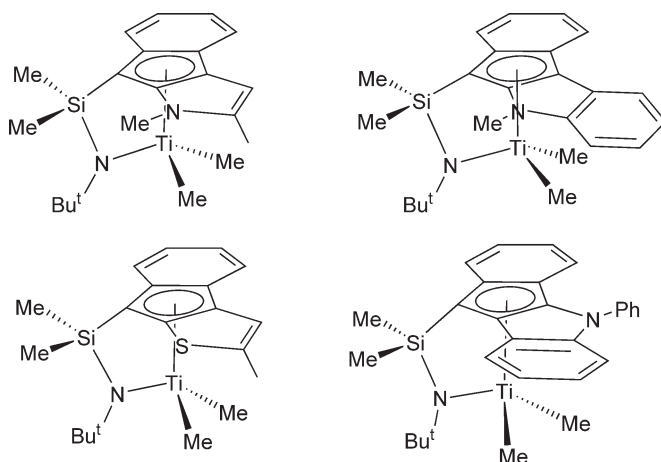
Analogous complexes with fluorenyl ligands have been described.  $(\text{FluSiMe}_2\text{NBu}^t)\text{TiCl}_2$  (Scheme 268) has been prepared by the reaction of  $\text{TiCl}_3(\text{THF})_3$  with the dilithium salt of the fluorenyl-amide compound, followed by  $\text{PbCl}_2$  oxidation. The dimethyl complex is obtained by the reaction of the dichloro compound with  $\text{LiMe}$  in toluene at  $-78^\circ\text{C}$ . When activated with MAO or boron compounds the dimethyl derivative produces syndiorich polypropylene by a chain-end controlled mechanism.<sup>692</sup> More syndiospecific ligands have been designed by introducing *tert*-butyl ring substituents, as in



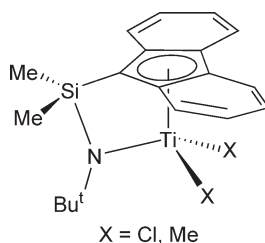
Scheme 265



Scheme 266



Scheme 267

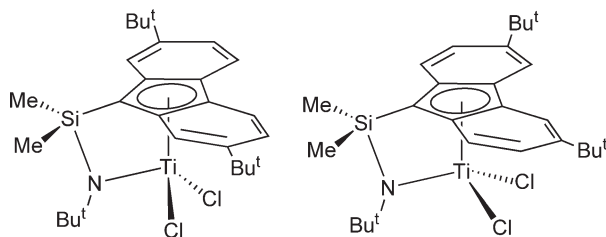


Scheme 268

the complexes  $(2,7\text{-Bu}^t\text{FluSiMe}_2\text{NBu}^t)\text{TiCl}_2$  and  $(3,6\text{-Bu}^t\text{FluSiMe}_2\text{NBu}^t)\text{TiCl}_2$  (Scheme 269). These derivatives, activated with MAO, give high molecular weight syndiotactic polypropylene with high activity, although the polymers exhibited only very limited crystallinity.<sup>693,693a,693b</sup>

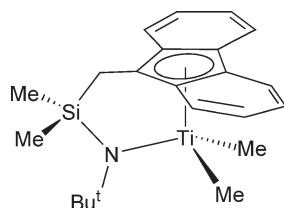
A fluorenyl-amido complex with an expanded bridge,  $[\text{C}_{13}\text{H}_8\text{-CH}_2\text{Si}(\text{Me}_2)\text{NBu}^t]\text{TiCl}_2$  (Scheme 270), has been prepared by reacting the lithium salt of the fluorenyl-amido ligand with  $\text{TiCl}_4$ .<sup>694</sup>

Complexes with two carbon linkers  $[\text{C}_5\text{Me}_4(\text{CH}_2)_2\text{NR}]\text{TiCl}_2$  (Scheme 271) have been obtained by the reaction of the lithium salts of the corresponding tetramethylcyclopentadienyl amide with  $\text{TiCl}_3(\text{THF})_3$  followed by oxidation with  $\text{PbCl}_2$ . In the presence of MAO these complexes have been tested for catalytic propylene homopolymerization. Surprisingly, the catalysts with  $\text{R} = \text{Pr}^i$ ,  $\text{Bu}^t$  are inactive, and only for  $\text{R} = \text{Me}$  the formation of atactic polypropylene was observed. This is in marked contrast with the analogous systems with  $\text{SiMe}_2$  bridge ligands that readily homopolymerize propylene under similar conditions.<sup>695</sup> Studies on olefin polymerization reactions with titanium complexes containing the ligands  $[(\text{C}_5\text{H}_4)(\text{CH}_2)_n\text{NR}]^{2-}$  ( $n = 2, 3$ ;  $\text{R} = \text{Me}, \text{Et}, \text{Pr}^i, \text{Bu}^t$ ) show a clear dependence of polymer molecular weight on the size of the amide substituent, while  $M_w$  increases with decreasing size of  $\text{R}$ .<sup>696</sup>

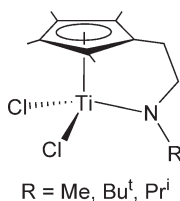


Scheme 269

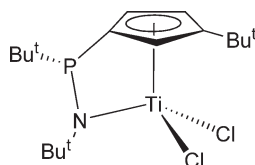




Scheme 270



Scheme 271



Scheme 272

Phosphide-bridged CGC-type complexes are obtained by reacting  $[\text{C}_5\text{H}_3\text{Bu}^t(\text{PClBu}^t)]\text{TiCl}_3$  with  $\text{LiNHBu}^t$  in the presence of  $\text{NEt}_3$  to give  $[\text{C}_5\text{H}_3\text{Bu}^t(\text{PBu}^t\text{NBu}^t)]\text{TiCl}_2$  (Scheme 272) as a mixture of two diastereomers due to *syn*- and *anti*-orientations of the  $\text{Bu}^t$  group at the phosphorus atom. The compound has been spectroscopically characterized and exhibits moderate activity in the polymerization of ethylene when activated with MAO.<sup>398</sup>

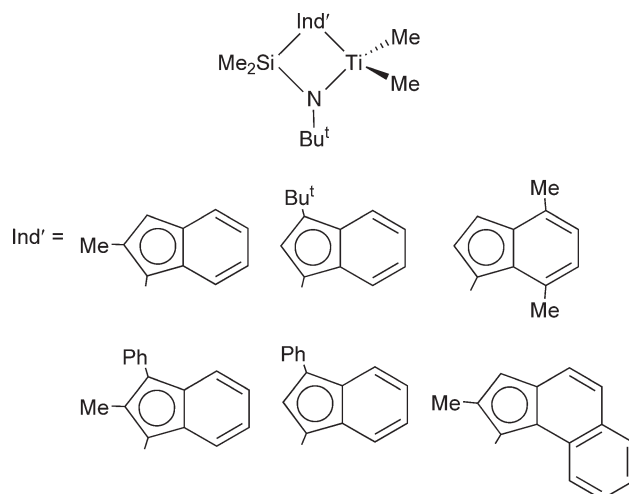
(iii) A new synthetic method has been extended and modified by Resconi for the synthesis of a series of Cp-amido titanium complexes.<sup>697</sup>

The synthesis and spectroscopic characterization of a series of Ind-amido dimethyl complexes (Schemes 273, 274), which differ in the substituents on the indenyl ligand, have been reported. The synthetic method consists of the reaction of the  $\pi$ -ligand with a two fold excess of  $\text{LiMe}$  and treatment with  $\text{TiCl}_4$  (Scheme 500: Section 4.05.4.2.1). These complexes are used as precursors for propylene polymerization catalysts, both in liquid monomer and in solution, in the presence of different co-catalysts (borates and MAO) and under different reaction conditions. All complexes produce amorphous polypropylene. Catalytic activity and polymer molecular weight strongly depend on the substitution pattern.<sup>687</sup> These complexes have been employed, in the presence of MMAO, for the alternating stereospecific co-polymerization of ethylene with cycloolefins (cyclopentene, cycloheptene, and cyclooctene). The chiral indenyl Ti complexes produce exclusively 1,2-enchainment of the cycloolefin to generate highly stereoregular and alternating co-polymers.<sup>698</sup>

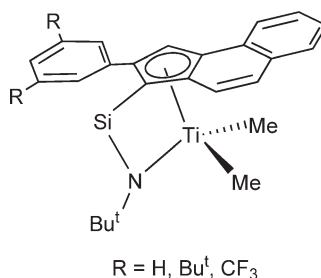
#### 4.05.3.4.2 Amine elimination

Amine elimination using  $\text{M}(\text{NR}_2)_4$  precursors is shown in Scheme 275.<sup>674,699–704</sup>

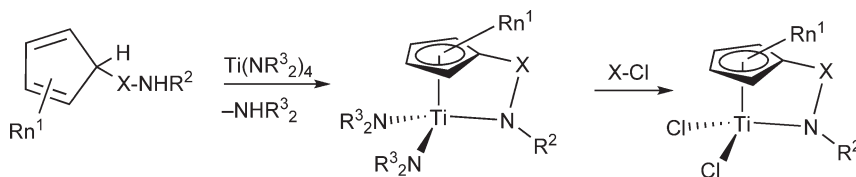
Amine elimination has been applied in the reaction of  $(\text{C}_5\text{H}_5)\text{SiMe}_2\text{NHBu}^t$  with  $\text{Ti}(\text{NMe}_2)_4$  to give  $(\text{C}_5\text{H}_4\text{SiMe}_2\text{NBu}^t)\text{Ti}(\text{NMe}_2)_2$ , which can be converted into the dichloro complex  $(\text{C}_5\text{H}_4\text{SiMe}_2\text{NBu}^t)\text{TiCl}_2$  by reaction with  $(\text{NEt}_3\text{H})\text{Cl}$  or anhydrous  $\text{HCl}$  gas in toluene. The molecular structure of  $(\text{C}_5\text{H}_4\text{SiMe}_2\text{NBu}^t)\text{Ti}(\text{NMe}_2)_2$  has been determined by X-ray crystallography.<sup>705</sup> The complexes  $(\text{Cp}'\text{SiMe}_2\text{NBu}^t)\text{TiCl}_2$  ( $\text{Cp}' = \text{C}_5\text{Me}_4, 2,4\text{-C}_5\text{H}_2\text{Me}_2$ ,



Scheme 273



Scheme 274

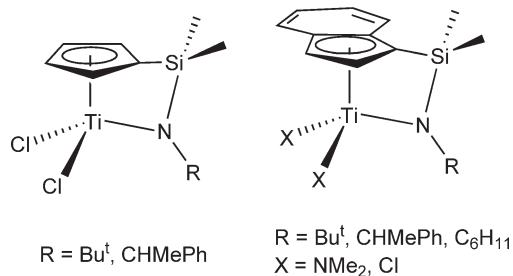


Scheme 275

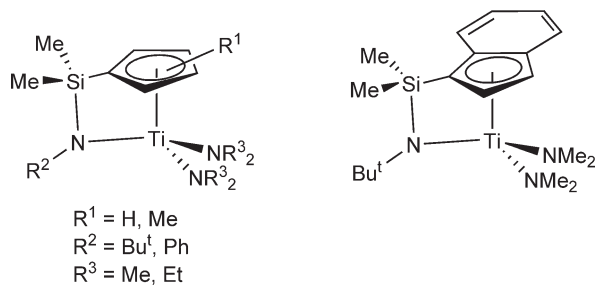
3-Bu<sup>t</sup>C<sub>5</sub>H<sub>3</sub>, C<sub>9</sub>H<sub>6</sub>) have been synthesized either by the standard salt metathesis or the amine elimination procedure. These compounds are used as pre-catalysts for norbornene homopolymerization and ethylene–norbornene co-polymerization. The influence of the catalyst symmetry and structure on the activity, norbornene incorporation, and polymer and co-polymer microstructure has been studied.<sup>706</sup>

The Cp and Ind complexes (Cp'SiMe<sub>2</sub>NR)TiX<sub>2</sub> have been synthesized by the amine elimination or the metathesis route (Scheme 276). Two optically active complexes based on (*S*)(–)( $\alpha$ )methylbenzylamine have been prepared and the molecular structure of (+)(*R*)-[IndSiMe<sub>2</sub>N(CHMePh)]TiCl<sub>2</sub> was determined by X-ray crystallography. In the presence of MAO, the complexes polymerize propylene to high molecular weight atactic polymers with slight syndiotactic enrichment. Catalytic properties are dependent on the nature of the Cp and the amido substituents. Incorporation of a chiral amine into the ligand framework has little effect on stereospecificity.<sup>707,708</sup>

Ti(NEt<sub>2</sub>)<sub>4</sub> and Ti(NMe<sub>2</sub>)<sub>4</sub> react with silyl-substituted cyclopentadienes and indenenes to yield Cp–amido and indenyl–amido complexes of type (CpSiMe<sub>2</sub>NR<sup>1</sup>)Ti(NR<sup>2</sup>)<sub>2</sub>. The complexes have been characterized by <sup>1</sup>H, <sup>13</sup>C, and <sup>29</sup>Si NMR spectroscopy, IR, and mass spectrometry. The capabilities and limitations of the “salt-free” procedure have been discussed (Scheme 277).<sup>700</sup>



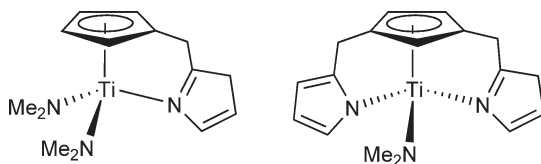
Scheme 276



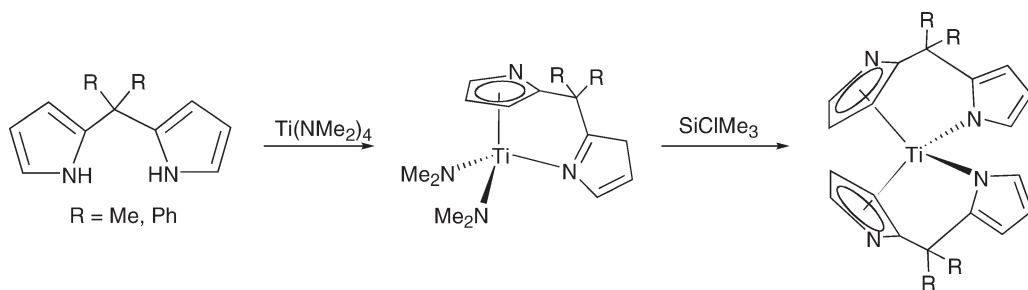
Scheme 277

The *ansa*-Cp-pyrrolyl complex  $[(\text{C}_5\text{H}_4)\text{CH}_2(2\text{-C}_4\text{H}_3\text{N})]\text{Ti}(\text{NMe}_2)_2$  is obtained by the reaction of  $\text{Ti}(\text{NMe}_2)_4$  with  $(\text{C}_5\text{H}_5)\text{CH}_2(2\text{-C}_4\text{H}_3\text{NH})$  via amine elimination, while the treatment with the cyclopentadiene ligand containing two pendant pyrrolyl arms affords  $\{1,3\text{-}[\text{CH}_2(2\text{-C}_4\text{H}_3\text{N})]_2(\text{C}_5\text{H}_3)\}\text{Ti}(\text{NMe}_2)_2$  (Scheme 278). The molecular structures of both pyrrolyl compounds have been determined by single crystal X-ray diffraction.<sup>709</sup>

The transamination reaction between  $\text{Ti}(\text{NMe}_2)_4$  and *meso*-disubstituted dipyrrolylmethanes yields  $[(\eta^5\text{-C}_4\text{H}_3\text{N})(\eta^1\text{-C}_4\text{H}_3\text{N})\text{CR}_2]\text{Ti}(\text{NMe}_2)_2$  ( $R = \text{Me}, \text{Ph}$ ) derivatives (Scheme 279). The structure of compound for  $R = \text{Me}$  has been determined by X-ray diffraction methods. The presence of the nitrogen atom in the pyrrole ring



Scheme 278



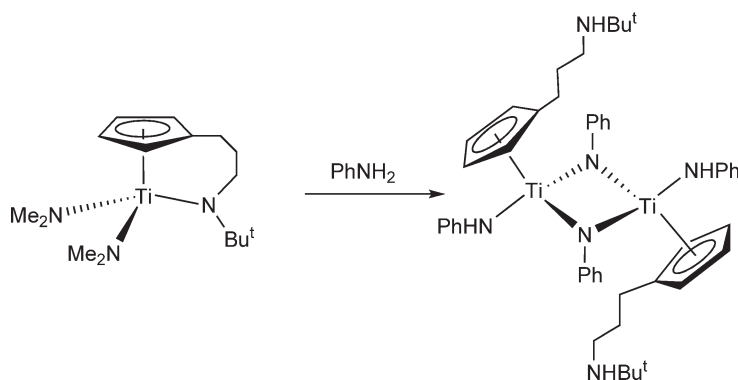
Scheme 279

reduces the symmetry of the  $\pi$ -ligand, so the compounds are obtained as chiral substances. Treatment with  $\text{SiClMe}_3$  affords the bis(pyrrolido) complexes  $[(\eta^5\text{-C}_4\text{H}_3\text{N})(\eta^1\text{-C}_4\text{H}_3\text{N})\text{CR}_2]_2\text{Ti}$ .<sup>710</sup> The synthesis and structure of similar dipyrrolylmethane complexes have been reported. Alkynes are rapidly hydroaminated by primary amines catalyzed by these Ti derivatives.<sup>711</sup> Hydroamination of enynes to generate  $\alpha,\beta$ -unsaturated imines can be produced by these titanium pyrrolyl complexes.<sup>712</sup>

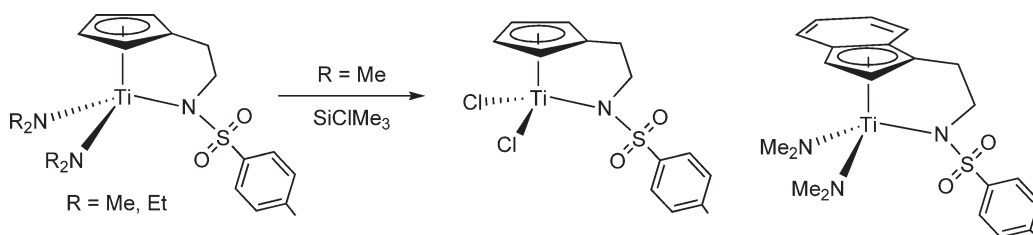
The reaction of  $\text{Ti}(\text{NMe}_2)_4$  with the amine-functionalized cyclopentadiene  $\text{C}_5\text{H}_5\text{CH}_2\text{CH}_2\text{CH}_2\text{NHBu}^t$  gives the Cp-amido complex  $(\text{C}_5\text{H}_4\text{CH}_2\text{CH}_2\text{CH}_2\text{NHBu}^t)\text{Ti}(\text{NMe}_2)_2$  which reacts with aniline to generate the phenylimido-bridged dimer  $[\text{Ti}(\text{C}_5\text{H}_4\text{CH}_2\text{CH}_2\text{CH}_2\text{NHBu}^t)(\text{NPh})(\mu\text{-NPh})]_2$ . The molecular structure reveals a slightly asymmetric  $\text{Ti}(\mu\text{-NPh})_2\text{Ti}$  core (Scheme 280).<sup>616</sup>

Mono-Cp and monoindenyl sulfonamido diamido compounds are also obtained by this synthetic procedure (Scheme 281).  $(\text{C}_5\text{H}_4\text{CH}_2\text{CH}_2\text{NSO}_2\text{C}_6\text{H}_4\text{Me})\text{Ti}(\text{NMe}_2)_2$  reacts with 2 equiv. of  $\text{SiClMe}_3$  to give the dichloro complex, the molecular structure of which has been determined by single crystal X-ray crystallography.<sup>713</sup>

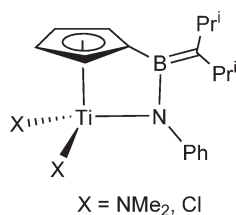
The compound  $[\text{C}_5\text{H}_4\text{B}(\text{NPr}^i)_2\text{NPh}]\text{Ti}(\text{NMe}_2)_2$  containing a boron-bridged cyclopentadienyl-amido ligand has been prepared by amine elimination. Subsequent treatment with  $\text{SiClMe}_3$  gives the corresponding dichloro complex  $[\text{C}_5\text{H}_4\text{B}(\text{NPr}^i)_2\text{NPh}]\text{TiCl}_2$  (Scheme 282). The molecular structure of the  $\text{NMe}_2$  derivative has been established by X-ray diffraction. In the presence of MAO they are effective catalysts for ethylene polymerization.<sup>714</sup>



Scheme 280



Scheme 281



Scheme 282

#### 4.05.3.4.3 Alkane elimination from homoleptic $\text{TiR}_4$

A new strategy to synthesize CGC-type of complexes involves the reaction of the neutral ligand directly with tetraalkyltitanium derivatives with elimination of alkane (Scheme 283).

$(\text{C}_5\text{Me}_4\text{SiMe}_2\text{N}^t\text{Bu})\text{Ti}(\text{CH}_2\text{Ph})_2$  is prepared in 90% yield by the reaction of  $\text{C}_5\text{Me}_4\text{HSiMe}_2\text{N}^t\text{HBu}^t$  with  $\text{Ti}(\text{CH}_2\text{Ph})_4$  in toluene at  $60^\circ\text{C}$  for 12 h in the absence of light. The reaction with  $\text{B}(\text{C}_6\text{F}_5)_3$  or  $\text{Ph}_3\text{C}[\text{B}(\text{C}_6\text{F}_5)_4]^-$  affords C–H activation of a methyl–cyclopentadienyl substituent to give a rare metallated fulvene complex with  $\eta''$ -bonding of the benzyl group to titanium center (Scheme 284). Variable-temperature  $^1\text{H}$  NMR studies of the complex  $\{[\text{C}_5\text{Me}_3(-\text{CH}_2-)\text{SiMe}_2\text{N}^t\text{Bu}^t]\text{Ti}\}^+[\text{CH}_2\text{PhB}(\text{C}_6\text{F}_5)_3]^-$  indicate a phenyl ring facial perturbation process. These complexes are highly active homogeneous catalysts for the ethylene and propylene polymerization.<sup>715</sup>

The bis(amidosilyl)cyclopentadiene  $\text{C}_5\text{H}_4[\text{SiMe}_2(\text{N}^t\text{HBu}^t)]_2$  reacts with  $\text{Ti}(\text{CH}_2\text{Ph})_4$  under selective deprotonation of the more acidic cyclopentadiene proton to give the Cp–monosilylamido derivative  $[\text{C}_5\text{H}_3(\text{SiMe}_2\text{N}^t\text{HBu}^t)-\text{SiMe}_2\text{N}^t\text{Bu}^t]\text{Ti}(\text{CH}_2\text{Ph})_2$  which can be transformed to the Cp–bis-silylamido  $[\text{C}_5\text{H}_3(\text{SiMe}_2\text{N}^t\text{HBu}^t)_2]\text{Ti}(\text{CH}_2\text{Ph})_2$  by refluxing the solution in toluene. Treatment of this complex with  $\text{B}(\text{C}_6\text{F}_5)_3$  gives the cationic complex  $\{\text{Ti}[\text{C}_5\text{H}_3(\text{SiMe}_2\text{N}^t\text{HBu}^t)_2]\}^+[\text{PhCH}_2\text{B}(\text{C}_6\text{F}_5)_3]^-$  (Scheme 285), the molecular structure of which has been determined by X-ray diffraction (Figure 14). The Cp–bis-silylamido ligand acts as a tridentate ligand and shows a strongly constrained geometry. Interaction between the Ti center and a “*meta*-C–H bond” or alternatively by a “*meta*-C atom” of the phenyl ring of the benzylborate anion is observed.<sup>716</sup> DFT calculations for the neutral and cationic species are described and provide an explanation for their remarkable structural features.<sup>582</sup>

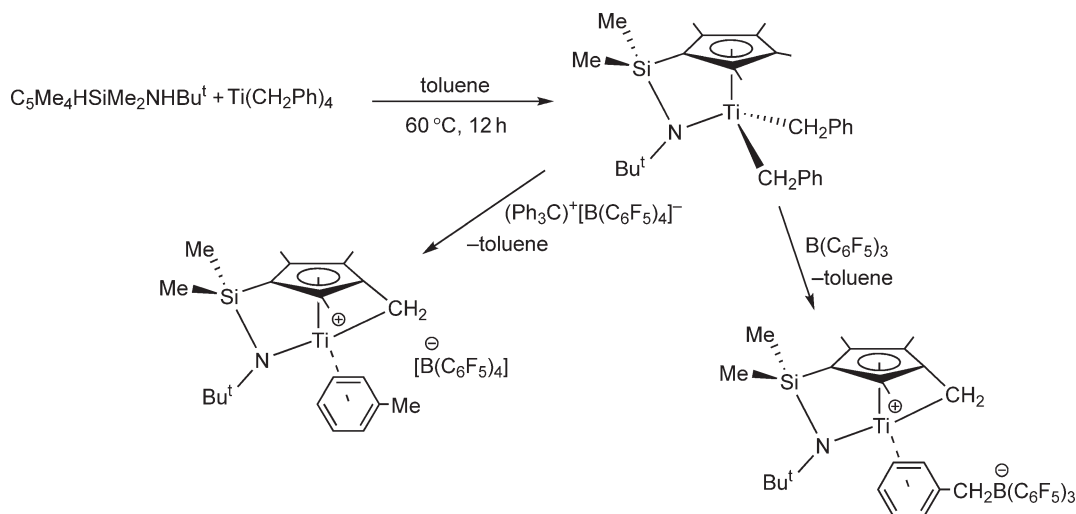
#### 4.05.3.4.4 HCl elimination from $\text{TiCl}_4$ or $\text{TiCp}'\text{Cl}_3$

Reaction of the neutral form of the cyclopentadienyl–amine with  $\text{TiX}_4$  in the presence of a base  $\text{NR}_3$  (generally  $\text{NEt}_3$ ) to trap the generated  $\text{HX}$  is shown in Scheme 286. Alternative treatment of  $\text{Cp}'\text{TiCl}_3$  with  $\text{H}_2\text{NR}$  in the presence of a base is also considered.

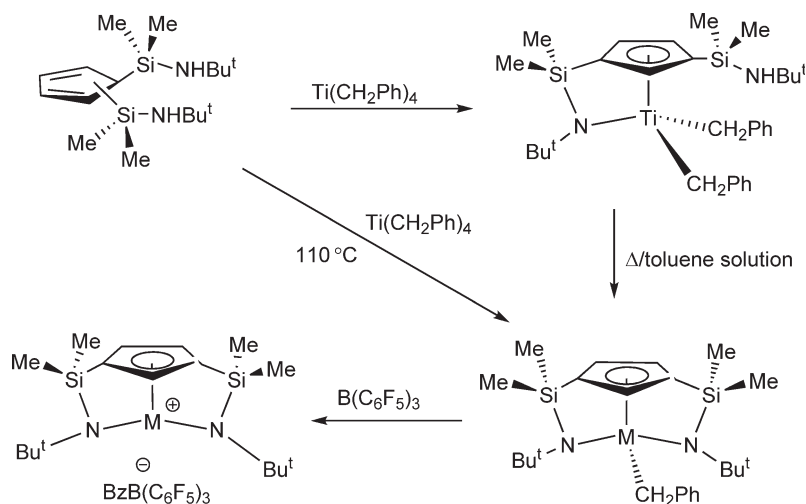
The complexes  $[\text{C}_5\text{H}_4(\text{CH}_2)_n\text{NR}]\text{TiCl}_2$  (Scheme 287) have been made by the reaction of  $\text{C}_5\text{H}_5(\text{CH}_2)_n\text{NHR}$  with  $\text{TiCl}_4$  in the presence of  $\text{NEt}_3$ . In order to assess the structural consequences of a  $\text{C}_2$ - or a  $\text{C}_3$ -backbone, the molecular



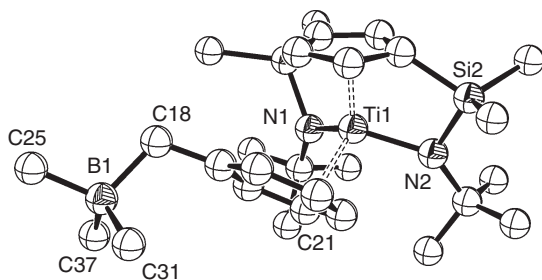
Scheme 283



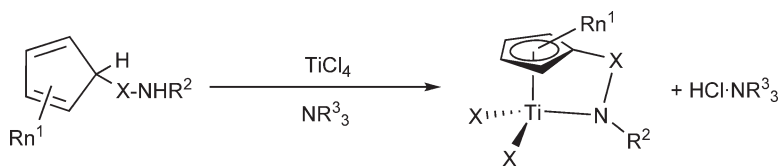
Scheme 284



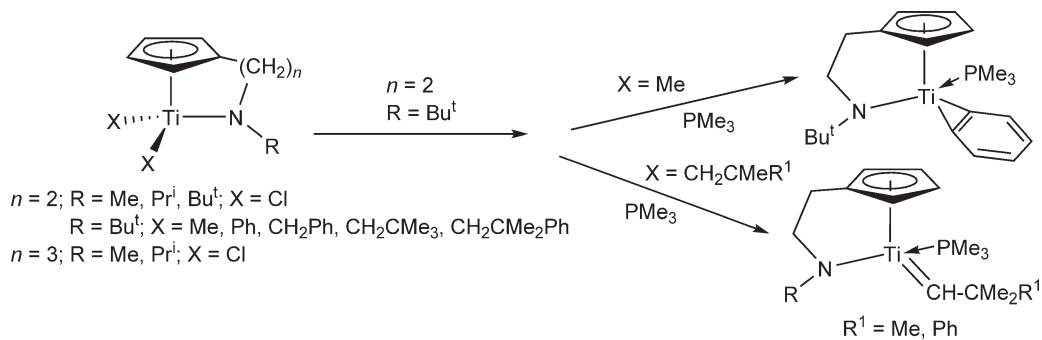
Scheme 285



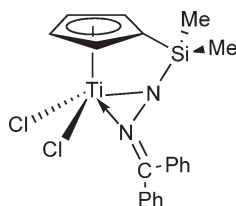
**Figure 14** Molecular structure of complex  $[\text{C}_5\text{H}_3(\text{SiMe}_2\text{NHBu}^t)_2\text{Ti}]^+ [\text{PhCH}_2\text{B}(\text{C}_6\text{F}_5)_3]^-$  (reproduced by permission of Wiley-VCH from *Angew. Chem., Int. Ed. Eng.*, **2001**, 40, 2495).



Scheme 286



Scheme 287



Scheme 288

structures of these complexes have been determined by X-ray diffraction. The shorter C<sub>2</sub>-spacer leaves a much more open ligand aperture. The dichloro complexes are converted to the dialkyl derivatives [C<sub>5</sub>H<sub>4</sub>(CH<sub>2</sub>)<sub>2</sub>NBu<sup>+</sup>]<sup>−</sup>TiR<sub>2</sub> by metathesis with organolithium or Grignard reagents. Thermolysis of the dialkyl complexes in the presence of PMe<sub>3</sub> proceeds with selective C–H activation and alkane elimination through α- or β-H elimination, to give the benzyne, neopentylidene, or neophylidene complexes (Scheme 287). Reaction of the dibenzyl compound [C<sub>5</sub>H<sub>4</sub>(CH<sub>2</sub>)<sub>2</sub>NBu<sup>+</sup>]<sup>−</sup>Ti(CH<sub>2</sub>Ph)<sub>2</sub> with B(C<sub>6</sub>F<sub>5</sub>)<sub>3</sub> gives the {[C<sub>5</sub>H<sub>4</sub>(CH<sub>2</sub>)<sub>2</sub>NBu<sup>+</sup>]<sup>−</sup>Ti(CH<sub>2</sub>Ph)}<sup>+</sup> cation which is an active catalyst for the polymerization of ethylene and propylene.<sup>717</sup>

Compound (C<sub>5</sub>H<sub>4</sub>SiClMe<sub>2</sub>)TiCl<sub>3</sub> reacts, in the presence of 2 equiv. of NEt<sub>3</sub>, with H<sub>2</sub>NN=CPh<sub>2</sub> to afford the hydrazone derivative (C<sub>5</sub>H<sub>4</sub>SiMe<sub>2</sub>NNCPh<sub>2</sub>)TiCl<sub>2</sub> (Scheme 288).<sup>670</sup>

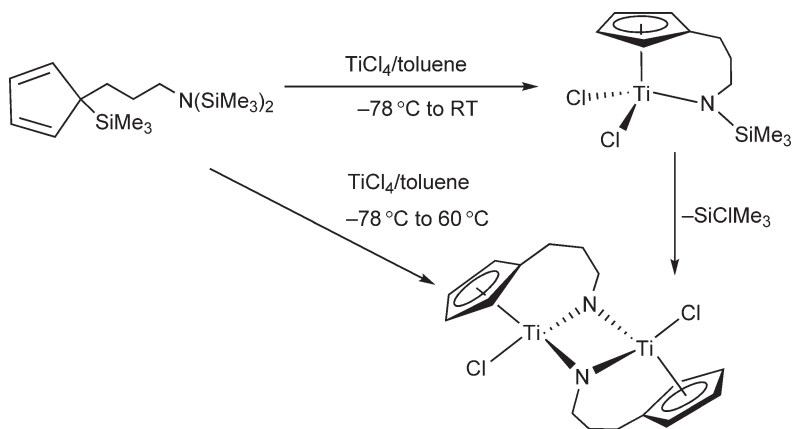
#### 4.05.3.4.5 Dehalosilylation reactions

The mononuclear [C<sub>5</sub>H<sub>4</sub>(CH<sub>2</sub>)<sub>3</sub>N(SiMe<sub>3</sub>)]TiCl<sub>2</sub> and the binuclear {[C<sub>5</sub>H<sub>4</sub>(CH<sub>2</sub>)<sub>3</sub>(μ-N)] TiCl}<sub>2</sub> complexes have been prepared by the reaction of TiCl<sub>4</sub> with C<sub>5</sub>H<sub>4</sub>(SiMe<sub>3</sub>)(CH<sub>2</sub>)<sub>3</sub>N(SiMe<sub>3</sub>)<sub>2</sub> with elimination of 2 or 3 equiv. of SiClMe<sub>3</sub> (Scheme 289). From the mononuclear compound the elimination of SiClMe<sub>3</sub> leads to the formation of the binuclear complex as suggested by NMR spectroscopy.<sup>718,719</sup>

#### 4.05.3.4.6 Miscellaneous

Following these synthetic methods a wide number of mono-Cp'-amido titanium derivatives have been prepared. An overview of examples organized according to the nature of the cyclopentadienyl-type ligand (Cp, Cp', Ind, Flu) and the bridging group (Si, C, B) connecting the Cp-type and the amido functionalities is presented.

Compound (C<sub>5</sub>H<sub>4</sub>SiMe<sub>2</sub>NBu<sup>+</sup>)TiCl<sub>2</sub> has been synthesized and used as pre-catalyst for ethylene polymerization. The activities and the properties of the polymers have been compared to similar zirconium and hafnium derivatives.<sup>720</sup> The consequences of anion–cation interactions on the activity of CGC group 4 metal complexes in olefin polymerizations have been explored for a series of zirconocene derivatives as well as the cationic species [(C<sub>5</sub>Me<sub>4</sub>SiMe<sub>2</sub>NBu<sup>+</sup>)TiMe]<sup>+</sup> with the sterically congested tris(perfluorobiphenyl)fluoroaluminate as the counteranion.<sup>721</sup> The co-polymerization of ethylene and 1-butene by (C<sub>5</sub>Me<sub>4</sub>SiMe<sub>2</sub>NBu<sup>+</sup>)TiCl<sub>2</sub> in the presence of



Scheme 289

$\text{Ph}_3\text{C}[\text{B}(\text{C}_6\text{F}_5)_4]/\text{AlBu}^i_3$  as activator has been studied and a high degree of 1-butene incorporation in the resulting copolymer was found.<sup>722</sup>

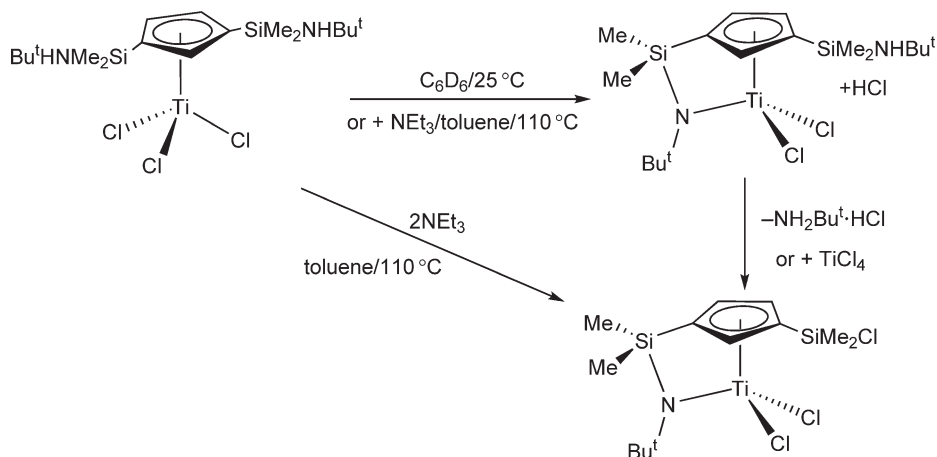
The Cp-amido complexes  $[\text{C}_5\text{H}_3\text{RSiMe}_2\text{N}(2,6\text{-Me}_2\text{C}_6\text{H}_3)]\text{TiX}_2$  ( $\text{R} = \text{H}, \text{Me}, \text{CH}_2\text{Ph}, \text{Bu}^t$ ;  $\text{X} = \text{Cl}, \text{NMe}_2$ ) have been synthesized and the molecular structure of  $[\text{C}_5\text{H}_3\text{SiMe}_2\text{N}(2,6\text{-Me}_2\text{C}_6\text{H}_3)]\text{Ti}(\text{NMe}_2)_2$  has been determined by X-ray diffraction. The complexes polymerize ethylene and propylene in the presence of MAO or  $\text{Ph}_3\text{C}[\text{B}(\text{C}_6\text{F}_5)_4]/\text{AlBu}^i_3$ .<sup>723</sup> The complexes  $(\text{C}_5\text{Me}_3\text{RSiMe}_2\text{NBu}^t)\text{TiCl}_2$  ( $\text{R} = \text{H}, \text{Ph}, 4\text{-fluorophenyl}, 1\text{-methylallyl}$ ) have been synthesized and spectroscopically characterized. The solid-state structure of the 1-methylallyl substituted derivative has been determined.<sup>724</sup>

The compounds  $(\text{C}_5\text{Me}_4\text{SiMe}_2\text{NR})\text{TiCl}_2$  ( $\text{R} = \text{Bu}^t, \text{Ph}, \text{C}_6\text{F}_5, \text{SO}_2\text{Ph}, \text{SO}_2\text{Me}$ ) have been synthesized, characterized by X-ray crystallography, and investigated for styrene and propylene homopolymerizations and ethylene-styrene co-polymerizations in the presence of MAO.<sup>725</sup>

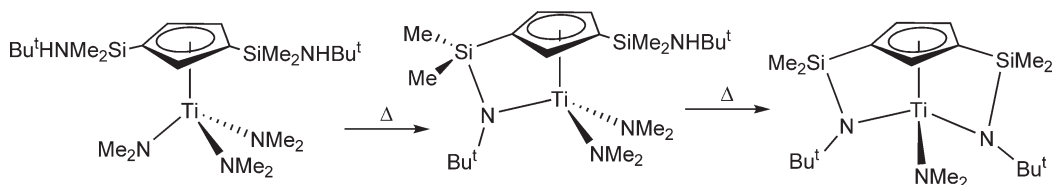
The molecular structure of  $(\text{C}_5\text{Me}_4\text{SiMe}_2\text{NC}_6\text{H}_3\text{Pr}^i_2)\text{TiCl}_2$  has been determined by X-ray diffraction.<sup>726</sup>

Compound  $[\text{C}_5\text{H}_3(\text{SiMe}_2\text{NHBu}^t)_2]\text{TiCl}_3$  (Scheme 167; Section 4.05.3.1.1.(iv)), is thermally not stable. In  $\text{C}_6\text{D}_6$  solution at  $25^\circ\text{C}$ , partial formation of the *ansa*-compound  $[\text{C}_5\text{H}_3(\text{SiMe}_2\text{NBu}^t)(\text{SiMe}_2\text{NHBu}^t)\text{TiCl}_2]$  takes place with elimination of  $\text{HCl}$ , which, under these conditions, protonates the remaining free amino  $\text{Si-NHBu}^t$  group to give the dissymmetric chlorodimethylsilyl-Cp complex  $[\text{C}_5\text{H}_3(\text{SiMe}_2\text{NBu}^t)\text{SiMe}_2\text{Cl}]\text{TiCl}_2$ . Similar products are formed on treatment of  $[\text{C}_5\text{H}_3(\text{SiMe}_2\text{NHBu}^t)_2]\text{TiCl}_3$  with  $\text{NEt}_3$  (Scheme 290). In the presence of  $\text{NEt}_3$ , the ring-closing reaction of the first silyl- $\eta^1$ -amido group is selective, although under these conditions simultaneous deamination of the remaining amidosilane only gives the chlorodimethyl-Cp-amido derivative, such that the formation of the second silyl amido bridge is prevented.<sup>390</sup> When a toluene solution of  $[\text{C}_5\text{H}_3(\text{SiMe}_2\text{NHBu}^t)_2]\text{Ti}(\text{NMe}_2)_3$  is heated at reflux for 5 h, the deprotonation of only one  $\text{SiMe}_2\text{NHBu}^t$  substituent is observed with elimination of  $\text{NHMe}_2$  and formation of the Cp-amido complex  $[\text{C}_5\text{H}_3(\text{SiMe}_2\text{NHBu}^t)\text{SiMe}_2\text{NBu}^t]\text{Ti}(\text{NMe}_2)_2$ . Complete deprotonation of the remaining uncoordinated  $\text{SiMe}_2\text{NHBu}^t$  group by heating the corresponding toluene solutions under reflux gives  $[\text{C}_5\text{H}_3(\text{SiMe}_2\text{NBu}^t)_2]\text{Ti}(\text{NMe}_2)$  (Scheme 291). The bis-Cp-amido derivatives  $\text{Ti}[\text{C}_5\text{H}_3(\text{SiMe}_2\text{NBu}^t)_2]\text{X}$  ( $\text{X} = \text{NMe}_2, \text{CH}_2\text{Ph}$ ) and the mono-*ansa*-compound  $\text{Ti}[\text{C}_5\text{H}_4\{(\text{SiMe}_2\text{NBu}^t)(\text{SiMe}_2\text{NHBu}^t)\}](\text{NMe}_2)_2$  react with  $\text{NEt}_3\cdot\text{HCl}$  to produce protonation products involving the Ti-N and Ti-C bonds (Scheme 292).<sup>390</sup>

The Cp-amido ester enolate complexes  $(\text{C}_5\text{Me}_4\text{SiMe}_2\text{NBu}^t)\text{TiX}[\text{OC}(\text{OPr}^i)=\text{CMe}_2]$  ( $\text{X} = \text{Cl}, \text{Me}$ ) have been synthesized, and the molecular structure of the methyl derivative has been determined by X-ray crystallography.

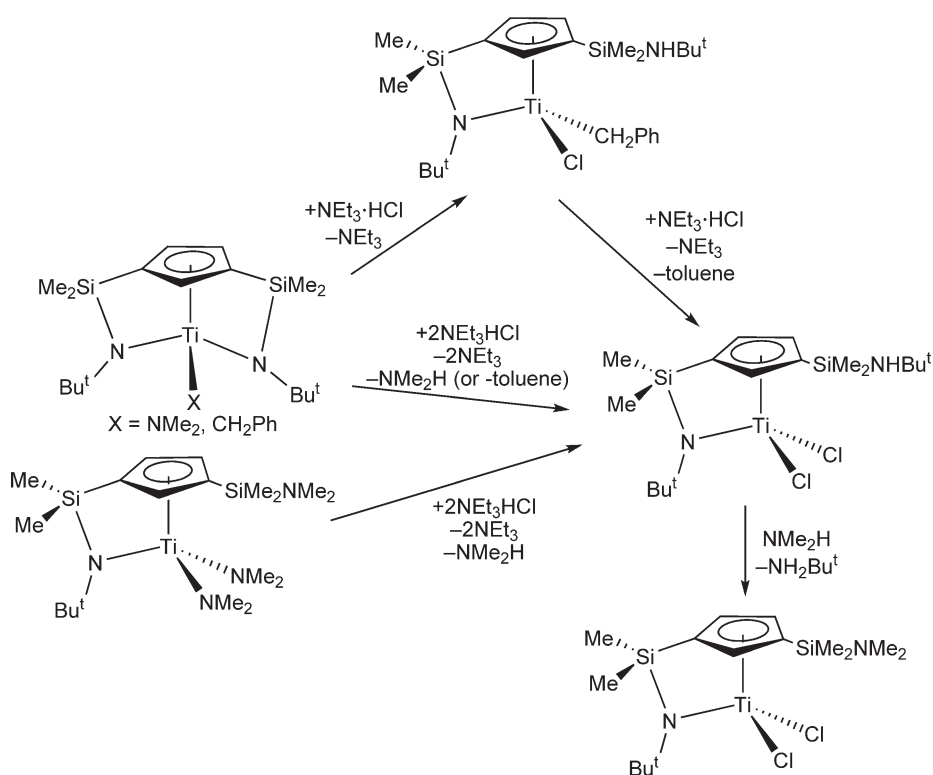


Scheme 290



Scheme 291

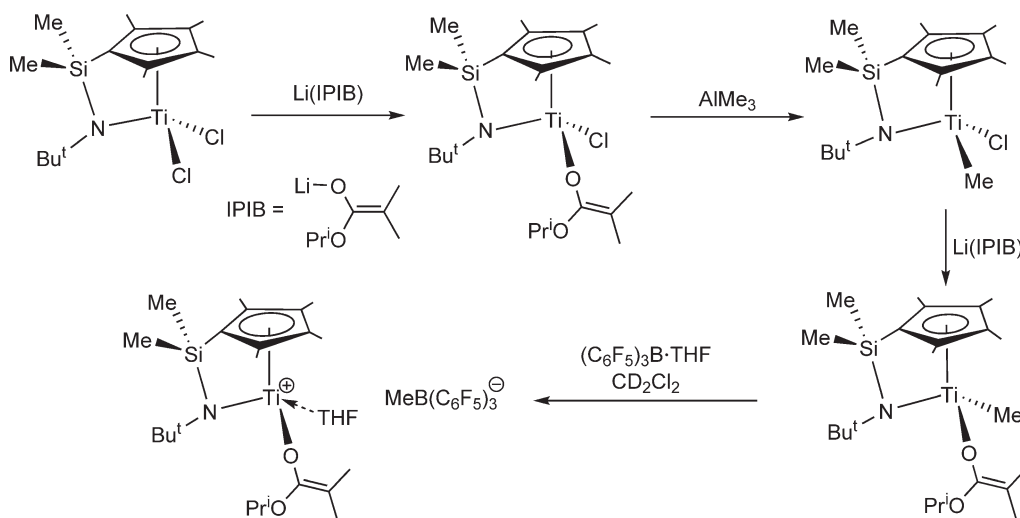




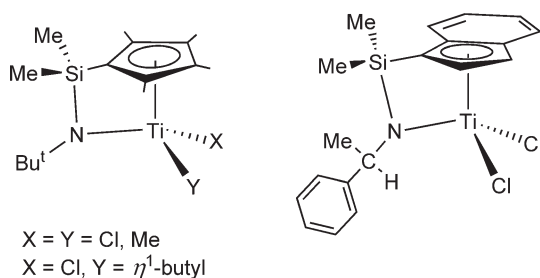
Scheme 292

The reaction of the methyl complex with  $\text{B}(\text{C}_6\text{F}_5)_3 \cdot \text{THF}$  in  $\text{CH}_2\text{Cl}_2$  readily generates the corresponding cationic ester enolate complex (Scheme 293). These compounds have been investigated for living and syndiospecific polymerization of methyl methacrylates. The polymer characteristics obtained with the cationic complex are remarkably similar to those by  $[(\text{C}_5\text{Me}_4\text{SiMe}_2\text{NBu}^t)\text{TiMe}]^+[\text{MeB}(\text{C}_6\text{F}_5)_3]^-$ , suggesting that the same propagating mechanism is operative for both initiators.<sup>727</sup>

$(\text{C}_5\text{Me}_4\text{SiMe}_2\text{NBu}^t)\text{TiCl}_2$  reacts with dibutylmagnesium in THF to form a robust monobutyl monochloro complex  $(\text{C}_5\text{Me}_4\text{SiMe}_2\text{NBu}^t)\text{TiCl}(\text{Bu})$  and with 2 equiv. of  $\text{LiMe}$  to yield the dimethyl complex  $(\text{C}_5\text{Me}_4\text{SiMe}_2\text{NBu}^t)\text{TiMe}_2$ .



Scheme 293



Scheme 294

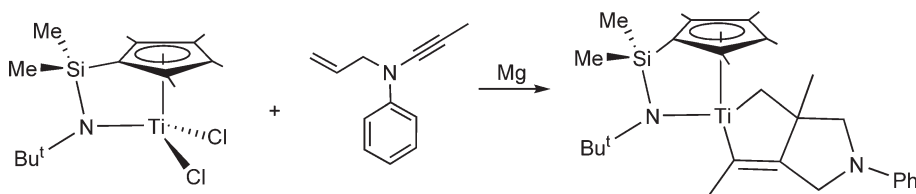
X-ray diffraction studies for the butyl complex indicate an undistorted  $\eta^1$ -butyl ligand with no evidence of  $\alpha$ - or  $\beta$ -agostic interactions. These complexes and the chiral complex  $(\text{C}_9\text{H}_6\text{SiMe}_2\text{N-CHMePh})\text{TiCl}_2$  (Scheme 294), when activated with  $\text{B}(\text{C}_6\text{F}_5)_3$ ,  $\text{Ph}_3\text{C}[\text{B}(\text{C}_6\text{F}_5)_4]$ , or  $\text{AlEt}_3$ , are catalysts for the carboalumination of olefins. Mechanistic studies suggest a reductive coupling step. Further evidence for this is provided by the reaction of  $\text{TiCl}_2(\text{C}_5\text{Me}_4\text{SiMe}_2\text{NBu}^t)$  with magnesium metal and N-allyl-N-2-butyraniline which generates a titanacyclopentene derivative (Scheme 295), molecular structure of which was determined by X-ray diffraction methods.<sup>728</sup>

Cp-amido complexes with conjugated dienes have been described. Reduction of  $(\text{C}_5\text{Me}_4\text{SiMe}_2\text{NR})\text{TiCl}_2$  with  $\text{Li}^n\text{Bu}$  in the presence of 1,3-dienes yields Cp-amido diene titanium complexes. Depending on the identity of R, Ti(II) diene  $\pi$ -complexes or Ti(IV) metallacyclopentene geometries are preferred (Scheme 296). The compounds are highly active olefin polymerization catalysts, with the activity depending also on the nature of the substituent R.<sup>729</sup> The replacement of  $\text{Cp}^*$  by Cp has an important effect on the properties of this type of complexes. The metathetical reaction of  $(\text{C}_5\text{H}_4\text{SiMe}_2\text{NBu}^t)\text{TiCl}_2$  with  $[\text{Mg}(\text{C}_4\text{H}_6)(\text{THF})_2]_n$  proceeds with the formation of  $(\text{C}_5\text{H}_4\text{SiMe}_2\text{NBu}^t)\text{Ti}(\text{C}_4\text{H}_6)$ , characterized by NMR spectroscopy and X-ray diffraction. The results of the spectroscopic and X-ray structural analysis of this Cp derivative are consistent with a Ti(II) diene  $\pi$ -bonding description.<sup>730</sup>

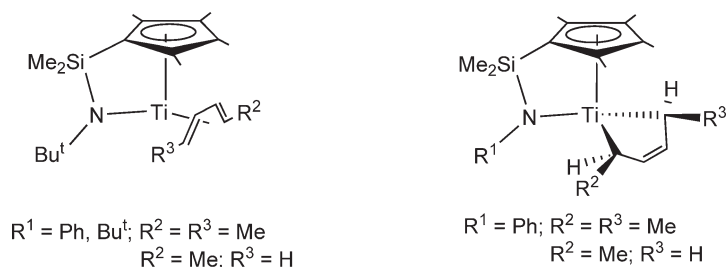
$(\text{C}_5\text{Me}_4\text{SiMe}_2\text{NBu}^t)\text{TiCl}_2$  reacts with “butadienemagnesium” to give the butadiene complex  $(\text{C}_5\text{Me}_4\text{SiMe}_2\text{NBu}^t)\text{-Ti}(\text{cis-}\eta^4\text{-C}_4\text{H}_6)$ , isolated as a 5:95 equilibrium mixture of the *supine*- and *prone*-isomers (Scheme 297).<sup>732</sup>

Reaction of  $(\text{C}_5\text{Me}_4\text{SiMe}_2\text{NBu}^t)\text{TiCl}_2$  with disubstituted 1,3-butadiynes affords five-membered titanacyclocumene complexes, from which the insertion of  $\text{CO}_2$  forms the binuclear titanafuranone complexes (Scheme 298). The molecular structures of these complexes have been determined by X-ray diffraction methods.<sup>733</sup>

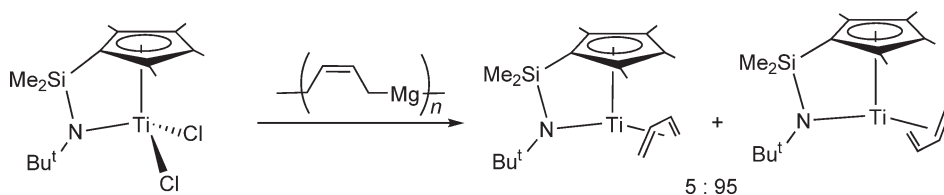
The cationic reactivity of the Cp-amido derivatives has been studied.



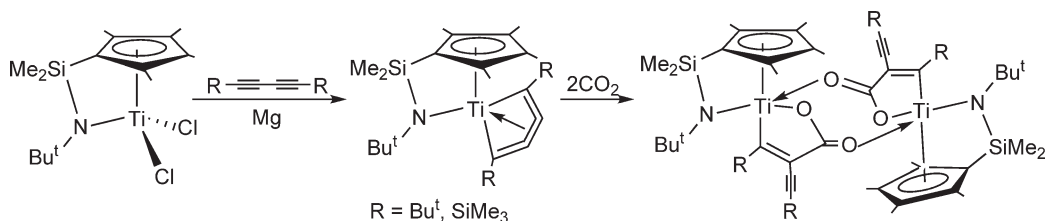
Scheme 295



Scheme 296



Scheme 297

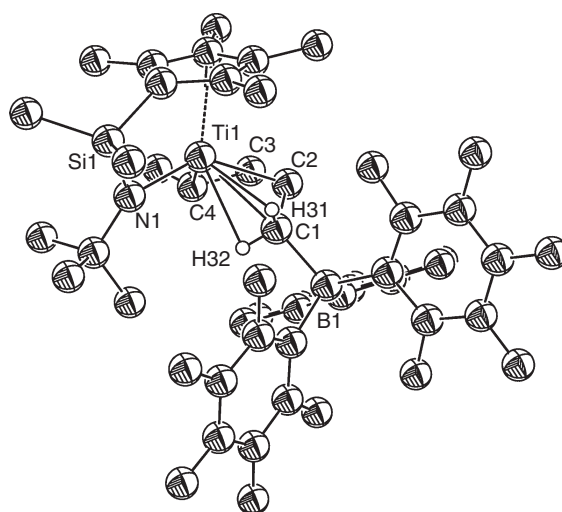


Scheme 298

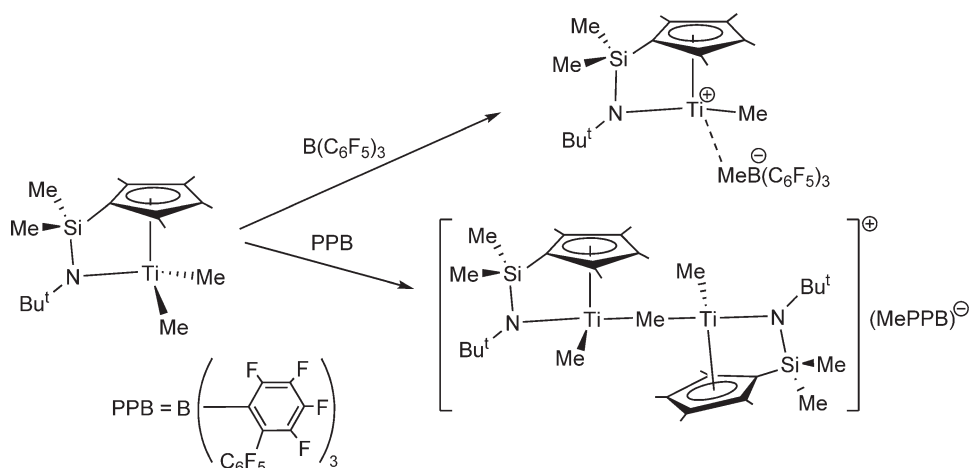
When  $(C_5Me_4SiMe_2N^tBu)Ti(1,3\text{-pentadiene})$  is treated with  $B(C_6F_5)_3$ , an active olefin polymerization catalyst is formed. The reaction of the titanium diene complex with  $B(C_6F_5)_3$  or  $Al(C_6F_5)_3$  in a 1:1 molar ratio in hexane solution at room temperature affords crystalline solids with the empirical composition  $(C_5Me_4SiMe_2N^tBu)Ti(1,3\text{-pentadiene})\cdot M(C_6F_5)_3$  ( $M = B, Al$ ). The X-ray diffraction studies revealed a zwitterionic structure in which the  $M(C_6F_5)_3$  groups are bonded to the terminal  $CH_2$  carbon atoms of the pentadiene ligand. Additional stabilization is provided by two agostic  $Ti\cdots H-C$  interactions (Figure 15).<sup>731</sup>

Cationic benzyltitanium complexes  $[(C_5Me_4SiMe_2NR)Ti(CH_2Ph)]^+$  ( $R = Me, Pr^i, Bu^t$ ) are formed by the reaction of the dibenzyltitanium precursors  $(C_5Me_4SiMe_2NR)Ti(CH_2Ph)_2$  with  $B(C_6F_5)_3$  and  $Ph_3C[B(C_6F_5)_4]$  in bromobenzene. NMR spectroscopic studies suggest that the benzyltitanium cations contain a fluxional  $\eta^2$ -coordinated benzyl ligand. Kinetic analysis shows that the decomposition of the benzyltitanium cations is first order and that the amido substituents in the linked Cp-amido ligand influence the lability of these benzyltitanium cations. The ethylene polymerization activity has been studied.<sup>734</sup>

$Ti(C_5Me_4SiMe_2NBu^t)Me_2$  is synthesized by the reaction of the corresponding dichloro compound with  $LiMe$  at low temperature. The dimethyl complex reacts with  $B(C_6F_5)_3$  to give the mononuclear cationic complex  $[Ti(C_5Me_4SiMe_2NBu^t)Me]^+[MeB(C_6F_5)_3]^-$  with coordination of the anion to the cationic titanium fragment. The



**Figure 15** Molecular structure of complex  $(C_5Me_4SiMe_2N^tBu)Ti(1,3\text{-pentadiene})\cdot B(C_6F_5)_3$  (reproduced by permission of the Royal Society of Chemistry from *Chem. Commun.*, **1999**, 437).



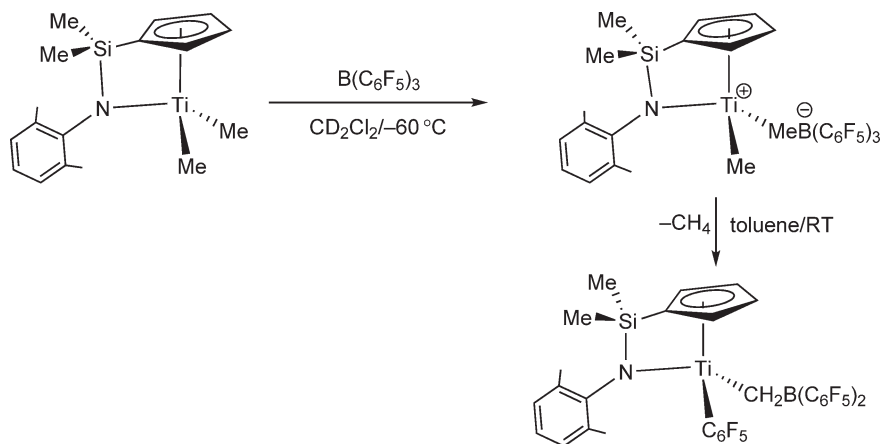
Scheme 299

analytically pure dinuclear cationic species  $[(C_5Me_4SiMe_2NBu^t)MeTi-Me-TiMe(C_5Me_4SiMe_2NBu^t)]^+$  is obtained when the same reaction is carried out with tris(2,2',2''-perfluorobiphenyl)borane (Scheme 299). The formation of the same cationic species is spectroscopically observed in the reaction with  $Ph_3C[B(C_6F_5)_4]$ . These results are explained in terms of the competition of the anionic borate salts and the neutral dimethyl compound for coordination to the highly electrophilic titanium cationic center.<sup>715</sup>

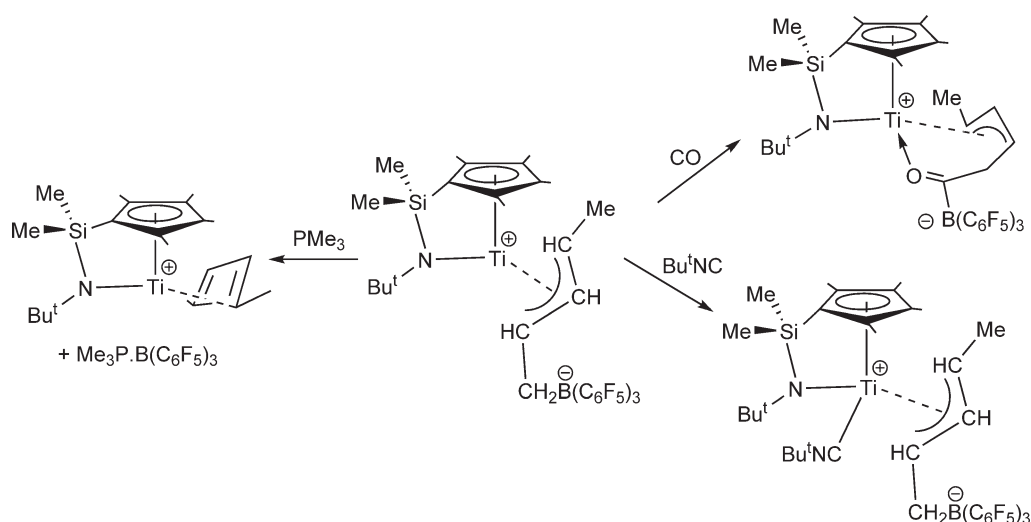
The dimethyl complex  $(C_5H_4SiMe_2NC_6H_3Me_2)TiMe_2$  reacts with  $B(C_6F_5)_3$  in hexane at room temperature to give the ion pair  $[(C_5H_4SiMe_2NC_6H_3Me_2)TiMe][MeB(C_6F_5)_3]$  as a thermally stable bright yellow microcrystalline solid, which in toluene at room temperature slowly evolves methane to give the neutral complex  $(C_5H_4SiMe_2NC_6H_3Me_2)Ti(C_6F_5)(CH_2B(C_6F_5)_2)$  (Scheme 300). The molecular structure of this complex has been determined by X-diffraction.<sup>735</sup>

The zwitterionic complex  $(C_5Me_4SiMe_2NBu^t)Ti[\eta^3-Me-(CH)_3-CH_2B(C_6F_5)_3]$  reacts with CO to give the titanium acylborate complex  $(C_5Me_4SiMe_2NBu^t)Ti[\eta^3-Me-(CH)_3-CH_2(CO)B(C_6F_5)_3]$ , while reaction with  $Bu^tNC$  affords the isocyanide adduct  $(C_5Me_4SiMe_2NBu^t)Ti[\eta^3-Me-(CH)_3-CH_2B(C_6F_5)_3](CNBu^t)$ . The molecular structures of both compounds have been determined by X-ray diffraction studies. Addition of 1 equiv. of  $PMe_3$  to  $(C_5Me_4SiMe_2NBu^t)Ti[\eta^3-Me-(CH)_3-CH_2B(C_6F_5)_3]$  results in the abstraction of  $B(C_6F_5)_3$  with the formation of  $Me_3P-B(C_6F_5)_3$  to give the diene complex  $(C_5Me_4SiMe_2NBu^t)Ti(1,3\text{-pentadiene})$  (Scheme 301).<sup>736</sup>

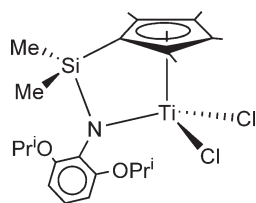
The molecular structure determined by X-ray diffraction methods and molecular mechanics (MM) calculations on  $[C_5Me_4SiMe_2N(2,6\text{-}OPr^i_2C_6H_3)]TiCl_2$  (Scheme 302) have been published. The relationship between structure and catalytic activity based on MM calculations is also discussed.<sup>737</sup>



Scheme 300



Scheme 301

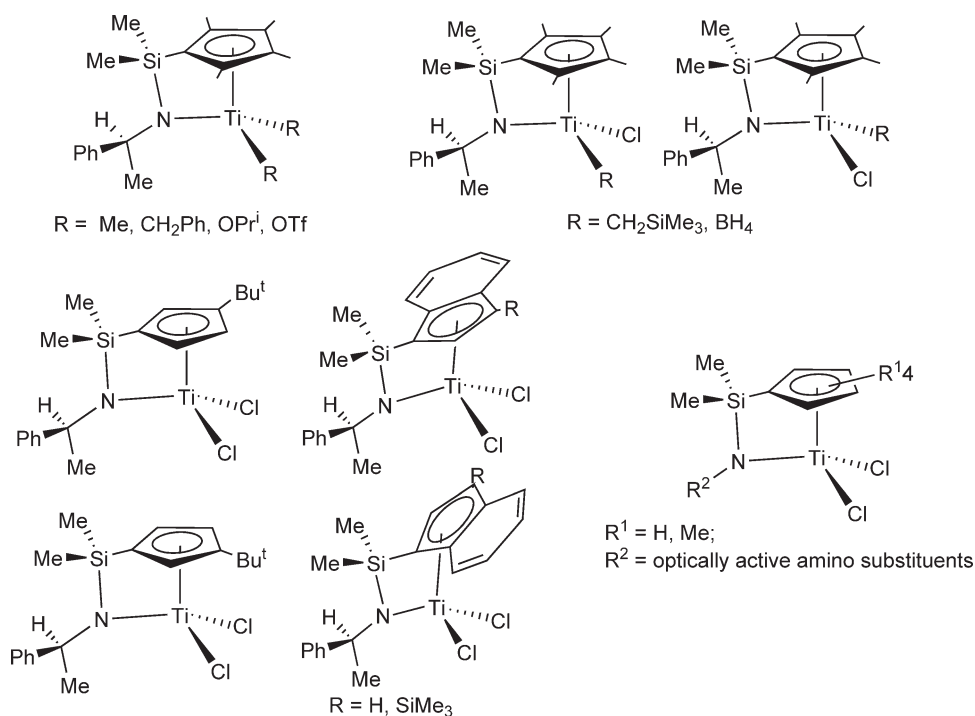


Scheme 302

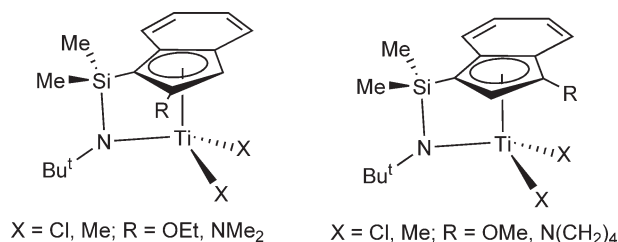
An extensive series of optically active titanium complexes containing a chiral linked Cp-amido ligand has been synthesized. Their catalytic properties for imine hydrogenation have been studied.<sup>738</sup> Optically active titanium complexes  $[\text{C}_5\text{R}_4\text{SiMe}_2\text{NC}_6\text{H}_{10}(\text{OCH}_2\text{Ph})_2]\text{TiCl}_2$  ( $\text{R} = \text{H}, \text{Me}$ ), which contain a Cp ligand linked to the chiral *trans*-2-benzyloxycyclohexylamido group, have been synthesized and characterized in both enantiomerically pure forms. A single crystal X-ray structure analysis of the (–)-(*R,R*)-enantiomer shows a structure in which the benzyloxy group in the amido side chain is not interacting with the titanium center. Upon activation with  $\text{LiBu}^n$ , these complexes hydrogenate acetophenone *N*-benzylimine with low enantioselectivity.<sup>739</sup> Dialkyl compounds (–)-(*S*)-(C<sub>5</sub>Me<sub>4</sub>SiMe<sub>2</sub>NCHMePh)-TiR<sub>2</sub> have been synthesized from the dichloro parent compound without significant racemization at the stereogenic center, while the monosubstituted complexes (–)-(*S*)-(C<sub>5</sub>Me<sub>4</sub>SiMe<sub>2</sub>NCHMePh)TiClR are formed as mixtures of diastereomers. In order to determine the diastereoselectivity during the formation of these derivatives, planar chirality in the Cp ring has been additionally introduced to give a diastereomeric mixture of products. Complexes containing enantiomerically pure amido-substituted ligands have also been synthesized and characterized (Scheme 303).

The synthesis of the Ind-amido titanium complexes  $[(\text{C}_9\text{H}_5\text{R})\text{SiMe}_2\text{NBu}]\text{TiX}_2$  (Scheme 304) with alkoxy and amido substituents at 2- and 3-indenyl position has been reported and the molecular structures of the derivatives for  $\text{R} = \text{NMe}_2$  and  $\text{N}(\text{CH}_2)_4$  have been determined by X-ray diffraction. The methyl derivatives are activated with  $\text{B}(\text{C}_6\text{F}_5)_3$  and studied as catalytic systems for the ethylene/1-octene co-polymerization. A dramatic effect of the indenyl substituent nature on catalyst efficiency and polymer properties is observed.<sup>740</sup>

Ind-amido titanium complexes with  $\omega$ -alkenyl functions in position 2 of the indenyl ring have been synthesized and characterized. After activation with MAO, these complexes were used as homogeneous and heterogeneous catalysts for the homopolymerization of ethylene and propylene and the co-polymerization of ethylene and 1,7-octadiene.<sup>406</sup> A series of alkyl-,  $\omega$ -alkenyl-, and  $\omega$ -phenylalkyl-substituted Cp- and Ind-amido dichloro titanium complexes have been synthesized and characterized. The  $\omega$ -phenylalkyl-substituted complexes react with  $\text{LiBu}$  to give metallacycles via a CH activation reaction on the *ortho*-position of the phenyl group (Scheme 305).<sup>741,742</sup> After activation with MAO, these complexes catalyze ethylene polymerizations. The substituents on the aromatic system influence the polymerization activity of the catalysts and the properties of the polyethylene. The  $\omega$ -alkenyl-substituted catalysts show self-immobilization in ethylene polymerization.



Scheme 303



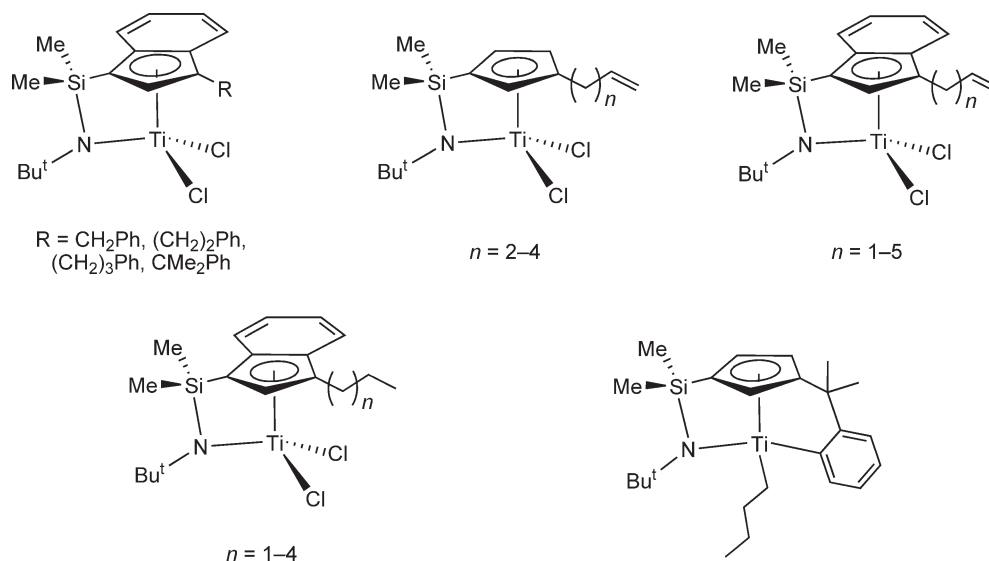
Scheme 304

The Ind-amido complex  $(2\text{-C}_9\text{H}_6\text{SiMe}_2\text{NBu}^t)\text{TiCl}_2$  with the silyl bridge in position 2 on the indenyl ring has been synthesized. Its molecular structure and its use as a single site catalyst in the co-polymerization of ethylene and propylene is reported.<sup>743</sup>

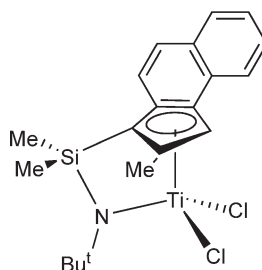
The dichloro methylbenz[e]indenyl compound shown in Scheme 306 has been prepared by reaction of the corresponding lithium indenyl salt with  $\text{TiCl}_3(\text{THF})_3$  followed by oxidation with  $\text{PbCl}_2$ .<sup>744</sup>

The complexes  $[\text{C}_9\text{H}_6(\text{CH}_2)_2\text{NEt}]\text{Ti}(\text{NEt}_2)_2$  and  $[\text{C}_{13}\text{H}_8(\text{CH}_2)_2\text{NEt}]\text{Ti}(\text{NEt}_2)_2$  have been synthesized and characterized by spectroscopy techniques. These compounds activated by MAO are used for homogeneous ethylene polymerizations.<sup>745</sup>

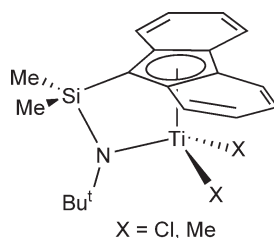
The fluorenyl-amido compounds  $(\text{FluSiMe}_2\text{NBu}^t)\text{TiX}_2$  ( $X = \text{Cl}, \text{Me}$ ) have been prepared (Scheme 307). The dimethyl complex reacts with  $\text{Ph}_3\text{C}[\text{B}(\text{C}_6\text{F}_5)_4]$  to give the ion pair species  $[(\text{C}_{13}\text{H}_8\text{SiMe}_2\text{NBu}^t)\text{TiMe}][\text{B}(\text{C}_6\text{F}_5)_4]$ , a highly active and stereoselective catalyst for the co-polymerization of ethylene with styrene.<sup>746</sup> In the presence of  $\text{B}(\text{C}_6\text{F}_5)_3$ ,  $(\text{FluSiMe}_2\text{NBu}^t)\text{TiMe}_2$  promotes the living polymerization of propylene at  $-50^\circ\text{C}$  in a highly regiospecific manner, while the catalytic system is deactivated even at  $0^\circ\text{C}$ . The system  $\text{TiMe}_2(\text{FluSiMe}_2\text{NBu}^t)/\text{MAO}$  produces low molecular weight polypropylene with terminal  $\text{Al-C}$  bonds at  $40^\circ\text{C}$  since  $\text{AlMe}_3$  in MAO acts as an effective chain-transfer agent.<sup>692</sup> The heterogenization of the living systems has been attempted by supporting MAO, MMAO, and dried MMAO on  $\text{SiO}_2$ .<sup>309</sup> Living polymerization of propylene is seen with the precursor  $(\text{FluSiMe}_2\text{NBu}^t)\text{TiMe}_2$  when dried MAO free from  $\text{AlMe}_3$  is used as co-catalyst at  $0^\circ\text{C}$ , to give high molecular weight polymer without deactivation of the catalytic system.<sup>747</sup> Living polymerization of 1-hexene is also observed with this fluorenyl-amido titanium system.<sup>748</sup>



Scheme 305



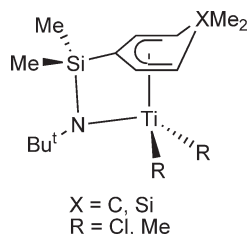
Scheme 306



Scheme 307

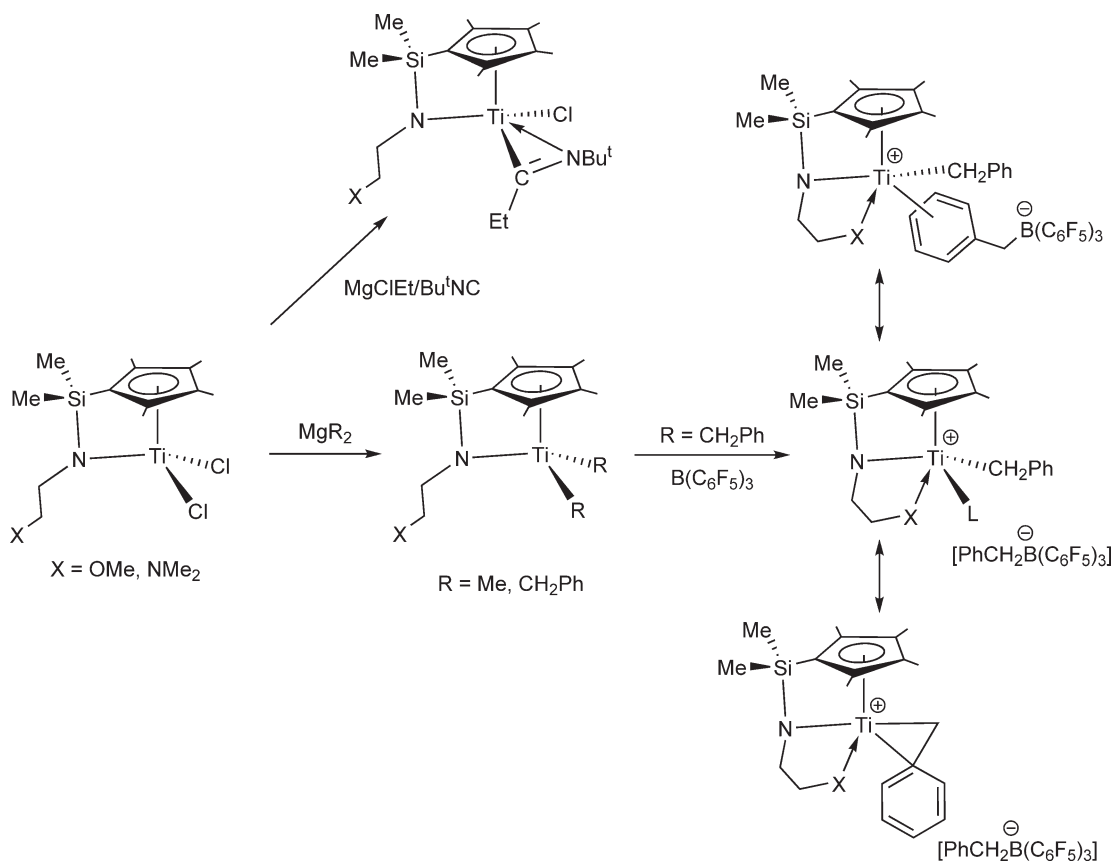
“Open” dieny l ligands can be used as a viable replacement for the Cp ring in complexes containing a pendant amido group to give pentadienyl–amido derivatives. The novel constrained-geometry complexes [C<sub>5</sub>H<sub>4</sub>XMe<sub>2</sub>–SiMe<sub>2</sub>–NBu<sup>t</sup>][TiR<sub>2</sub>] (Scheme 308) based on dimethylcyclohexadienyl and dimethylsilacyclohexadienyl ligands have been prepared, spectroscopically characterized, and the molecular structure determined by single crystal X-ray diffraction. Cyclohexadienyl fragments have been found to be η<sup>5</sup>-coordinated with substantial coordination slippage. The reduction potentials of these complexes have been determined by cyclic voltammetry measurements; the results indicate that the electron-donating ability of the cyclohexadienyl ring is nearly identical to that of the tetramethylcyclopentadienyl ligand.<sup>749</sup>

Titanium complexes containing tridentate Cp–amido ligands with an additional pendant neutral coordination site have been synthesized. Such tridentate Cp–amido ligands provide an electron count identical to that of two Cp



Scheme 308

ligands, and the pendant donor arm can protect the metal center, for example, in cationic species. Generally, fluxional coordination on the NMR timescale has been observed for these systems, and the activity in olefin polymerization processes is decreased. O-, N-, S-, and P-donor arms have been used. The dichloro complexes  $[\text{C}_5\text{R}_4\text{SiMe}_2\text{NCH}_2\text{CH}_2\text{X}]\text{TiCl}_2$  ( $\text{R} = \text{H}, \text{Me}$ ) ( $\text{X} = \text{OMe}, \text{NMe}_2$ ) are made from  $[\text{C}_5\text{R}_4\text{SiMe}_2\text{Cl}]\text{TiCl}_3$  and lithium amides  $\text{Li}(\text{NHCH}_2\text{CH}_2\text{X})$ . NMR spectroscopic studies suggest the presence of an equilibrium between the tri- and bidentate bonding mode of the Cp-amido ligand. A single crystal X-ray structural analysis of the methoxo derivative reveals that the alkoxo function is not intramolecularly coordinated in the solid state. The halo complexes can be alkylated with Grignard or dialkylmagnesium reagents to give the corresponding dialkyltitanium derivatives as stable substances. It appears that the additional donor group X on the amido substituent has no direct influence on the stability of these complexes. The addition of  $\text{Bu}^t\text{NC}$  to the reaction mixture of  $[\text{C}_5\text{Me}_4\text{SiMe}_2\text{NCH}_2\text{CH}_2\text{X}]\text{TiCl}_2$  and  $\text{MgClEt}$  leads to the chiral imino-acyl compound  $[\text{C}_5\text{Me}_4\text{SiMe}_2\text{NCH}_2\text{CH}_2\text{X}]\text{TiCl}(\text{EtC}=\text{NBu}^t)$ . When the dibenzyl derivative is reacted with  $\text{B}(\text{C}_6\text{F}_5)_3$  in bromobenzene at room temperature, clean formation of the Ti-benzyl cation is observed (Scheme 309).  $^{19}\text{F}$  NMR spectroscopic data ( $\Delta\delta_{\text{m-p}}$  chemical shifts) indicate free  $[\text{PhCH}_2\text{B}(\text{C}_6\text{F}_5)_3]^-$  anions.



Scheme 309



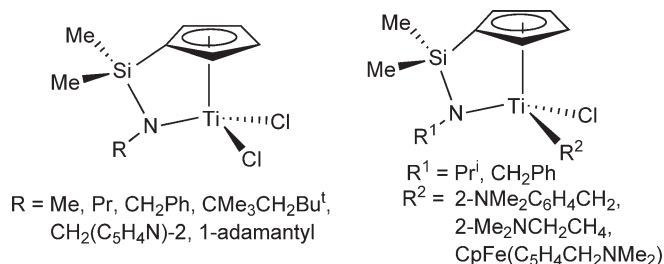
The polymerization of ethylene and 1-hexene has been studied.<sup>750,751</sup> The reaction of  $[\text{C}_5\text{H}_4\text{SiMe}_2\text{NCH}_2\text{CH}_2\text{NMe}_2]\text{Ti}(\text{CH}_2\text{Ph})_2$  with  $\text{B}(\text{C}_6\text{F}_5)_3$  has been investigated in order to understand the nature of the cationic 12-electron species  $[(\text{C}_5\text{H}_4\text{SiMe}_2\text{NCH}_2\text{CH}_2\text{NMe}_2)\text{Ti}(\text{CH}_2\text{Ph})]^+$  and its behavior in the  $\alpha$ -olefin polymerizations.<sup>752</sup>

Cp-amido titanium complexes containing different amido substituents including amino functionalities (Scheme 310) have been prepared by the appropriate synthetic route and spectroscopically and structurally characterized. In some cases, intramolecular coordination of the amino–nitrogen atom is observed according to the X-ray diffraction data. These complexes when activated with MAO are catalytically active for ethylene polymerization.<sup>753</sup>

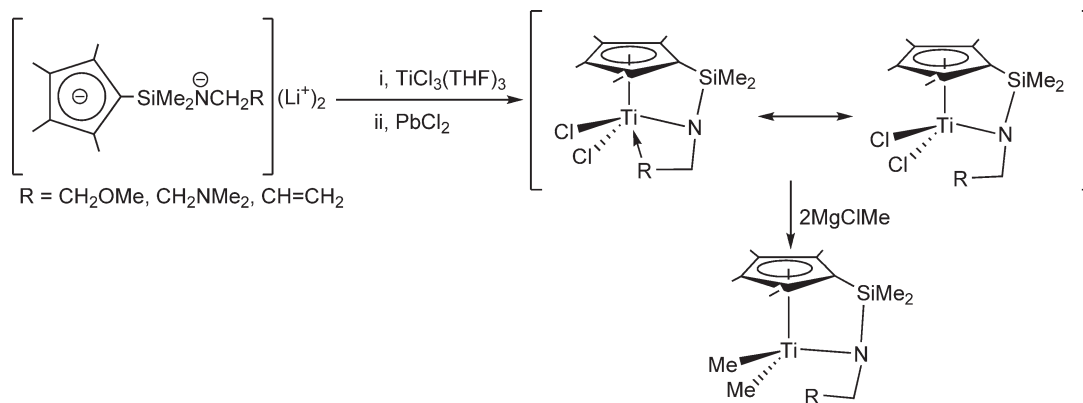
The titanium complexes  $(\text{C}_5\text{Me}_4\text{SiMe}_2\text{NCH}_2\text{R})\text{TiCl}_2$  ( $\text{R} = \text{CH}_2\text{OMe}$ ,  $\text{CH}_2\text{NMe}_2$ ,  $\text{CH}=\text{CH}_2$ ) are obtained, in good yields, by the reaction of the corresponding Cp lithium salts with  $\text{TiCl}_3(\text{THF})_3$  in THF followed by oxidation with  $\text{PbCl}_2$ . On the basis of variable-temperature NMR data, a fluxional behavior between free and coordinated donor side chain is proposed. The synthesis of the titanium complex with the pendant  $\text{C}=\text{C}$  unit has been developed in an attempt to coordinate the allyl substituent to the titanium atom, although there is no evidence for  $\text{C}=\text{C}$  coordination of the allyl group. The chloro compounds are converted to the dimethyl derivatives (Scheme 311) by reaction with  $\text{MgClMe}$ ; NOE experiments indicate that in this case there is no coordination of the pendant side chain.<sup>754</sup>

Reaction of  $(\text{C}_5\text{H}_4\text{SiMe}_2\text{Cl})\text{TiCl}_3$  with diamines provides a very convenient synthetic strategy for the preparation of different types of Cp-amido titanium derivatives (Scheme 312). The influence of several factors on the final products in these reactions, including the nature of the substituents groups in the amine nitrogen atom, the size of the amine carbon chain, and the reaction stoichiometry, has been studied.  $[\text{C}_5\text{H}_4\text{SiMe}_2\text{N}(\text{Me})\text{CH}_2\text{CH}_2\text{N}(\text{Me})]\text{TiCl}_2$  reacts with  $\text{MgClR}$  ( $\text{R} = \text{Me}$ ,  $\text{CH}_2\text{Ph}$ ) or  $\text{LiNMe}_2$  to give the corresponding dialkyl or diamido derivatives. The compounds exhibit different type of fluxional behavior in solution, the kinetic parameters of which have been determined. The molecular structures of  $[\eta^5\text{-C}_5\text{H}_4\text{SiMe}_2\text{N}(\text{Me})\text{CH}_2\text{CH}_2\text{-}\eta\text{-N}(\text{Me})]\text{TiCl}_2$  and  $[[\eta^5\text{-C}_5\text{H}_4\text{SiMe}_2\text{-}\eta\text{-N-CH}_2\text{CH}_2\text{-}\eta\text{-NH}(\text{CHMe}_2)]\text{TiCl}_2$  have been determined by X-ray diffraction.<sup>755,756</sup>

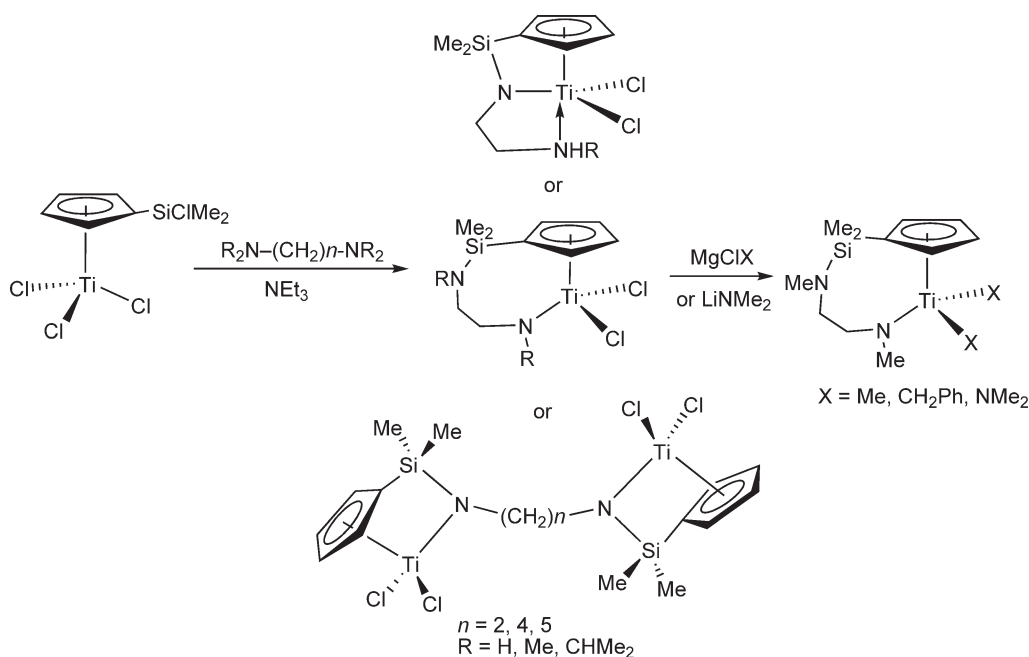
The hydrazido unit can be used as a Cp side arm donor substituent instead of the amido functionality and to stabilize cationic catalytic species. The synthesis and characterization of amido, chloro, and methyl Cp-hydrazido titanium complexes  $(\text{C}_5\text{Me}_4\text{SiMe}_2\text{NNMe}_2)\text{TiR}_2$  ( $\text{R} = \text{NMe}_2$ ,  $\text{Cl}$ ,  $\text{Me}$ ) (Scheme 313) have been made by general



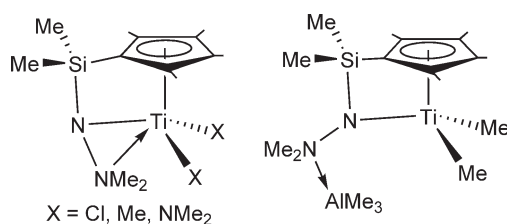
**Scheme 310**



**Scheme 311**



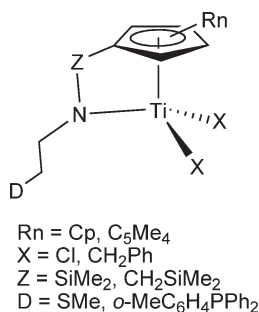
Scheme 312



Scheme 313

synthetic procedures. Spectroscopic evidence for the  $\eta^2$ -coordination of the hydrazido moiety has been obtained for the chloro and methyl derivatives. In the case of the dimethyl complex, in the presence of  $\text{AlMe}_3$ , the hydrazido- $\text{NMe}_2$  moiety is apparently coordinated to aluminum. The reaction with  $\text{H}_2\text{O}$  produces a tetrameric organotitanoxane compound with an adamantane-like cage structure (Scheme 343; Section 4.05.3.5.1). The structures of these compounds have been confirmed by X-ray crystallography.<sup>757,758</sup>

The complexes  $(\text{C}_5\text{R}_4\text{-Z-NCH}_2\text{CH}_2\text{D})\text{TiR}_2$  (Scheme 314) containing Cp-amido ligand with thioether or phosphine side arms are prepared by general synthetic procedures. The molecular structure of  $(\text{C}_5\text{R}_4\text{SiMe}_2\text{NCH}_2\text{CH}_2\text{SMe})\text{TiCl}_2$



Scheme 314

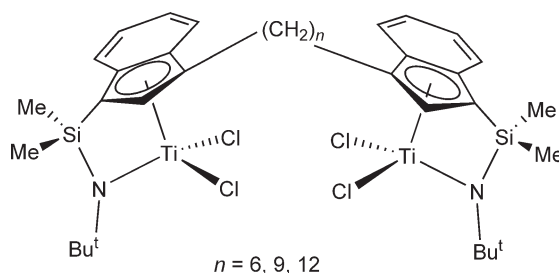
has been confirmed by X-ray diffraction; there is no intramolecular interaction between sulfur and titanium, in contrast to the analogous zirconium derivative. On the other hand, NMR spectroscopic data for the phosphino-functionalized compound suggest metal–phosphine bonding. Reaction between the dibenzyl complex  $(C_5R_4SiMe_2NCH_2CH_2SMe)Ti(CH_2Ph)_2$  and  $B(C_6F_5)_3$  in  $C_6D_5Br$  affords cleanly the solvent-separated ion pairs. Mixtures of the dichloro complex  $(C_5R_4SiMe_2NCH_2CH_2SMe)TiCl_2$  and MAO catalyze the polymerization of ethylene with moderate activities.<sup>759</sup>

Binuclear Ti complexes supported by Cp–amido ligands have been synthesized as new catalysts for  $\alpha$ -olefin polymerizations. The properties of these complexes could be of interest since they can serve as models for catalysts where two linked active sites exhibit cooperative behavior. Their reactivity may therefore differ significantly from that of mononuclear analogs.

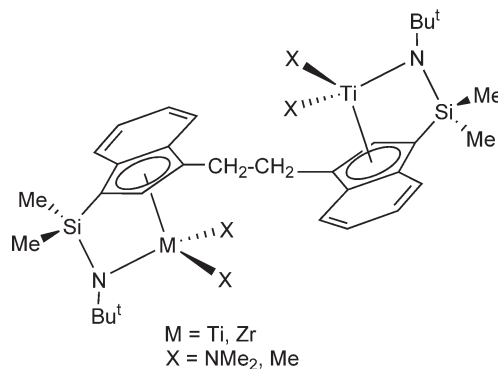
The binuclear complexes linked via the amido function, of the type  $[(C_5H_4SiMe_2N)TiCl]_2(\mu-(CH_2)_n)$  ( $n = 2, 4, 5$ ), can be obtained by the reaction of  $(C_5H_4SiMe_2Cl)TiCl_3$  with 0.5 equiv. of  $H_2N-(CH_2)_n-NH_2$  in the presence of  $NEt_3$  (Scheme 312).<sup>755,756</sup> Another strategy is to link two titanium fragments via the Cp ligands, as in  $[(C_9H_5SiMe_2NBu^t)TiCl]_2(\mu-(CH_2)_n)$  (Scheme 315), which has been prepared by treating 2 equiv. of  $TiCl_3(THF)_3$  with the corresponding tetralithium salts of the ligand followed by oxidation by  $AgCl$ . In the presence of MAO, they are active catalysts for the co-polymerization of ethylene and styrene. The styrene content in the co-polymers formed by the binuclear catalysts is higher than that in the co-polymer formed by the analogous mononuclear derivative.<sup>760</sup> Similar binuclear Ti compounds have been used as precursors for the polymerization of ethylene, propylene, and styrene.<sup>761</sup>

The synthesis of homo- (Ti–Ti) and heterobinuclear (Ti–Zr) complexes linked by 1,2- $C_2H_4$  linker groups as shown in Scheme 316 has been reported. The molecular structures of the dimethylamido derivatives have been determined by X-ray diffraction methods. In the presence of binuclear borate activators, the methyl complexes produce long-chain branched polyethylene and polystyrene in homopolymerization reactions and ethylene–styrene co-polymers. The polymerization behavior differs from that obtained with the mononuclear compound  $(3\text{-ethylindenyl}SiMe_2NBu^t)TiMe_2$  (Scheme 317).<sup>762–764</sup>

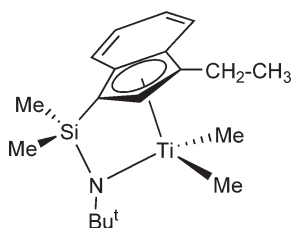
Cp/amido titanium complexes with  $sp^3-C^1$ -bridges,  $(C_5H_2Me_2-CHR-NBu^t)TiX_2$  ( $X = NMe_2, Cl$ ) (Scheme 318), are synthesized using fulvenes with substituents in 1-, 4-, and 6-positions. The compounds  $C_5H_3Me_2-CHR-NHBu^t$



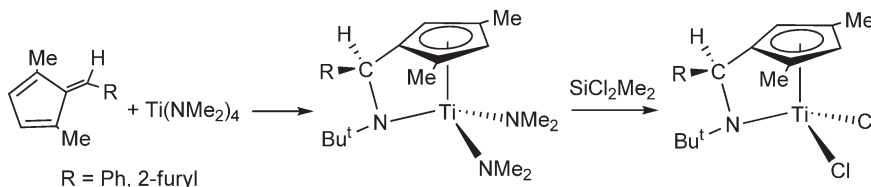
Scheme 315



Scheme 316



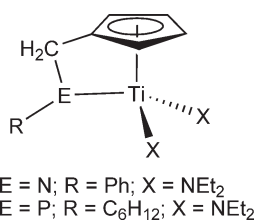
Scheme 317



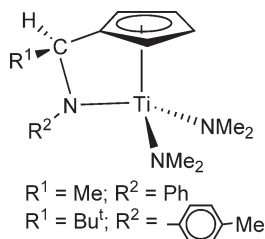
Scheme 318

( $R = \text{Ph, 2-furyl}$ ) react with  $\text{Ti}(\text{NMe}_2)_4$  to afford the bis(dimethylamido) complexes, which can be transformed to the dichloro derivatives by treatment with  $\text{SiCl}_2\text{Me}_2$ . The solid-state structures of  $(\text{C}_5\text{H}_2\text{Me}_2\text{-CHR-NBu}^t)\text{TiCl}_2$  have been determined by X-ray crystallography. The complexes are active toward the polymerization of ethylene when activated with MAO.<sup>765</sup>

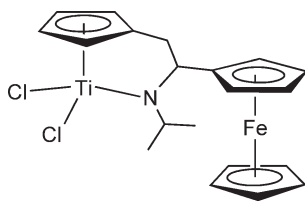
The complex  $(\text{C}_5\text{H}_4\text{CH}_2\text{NEt})\text{Ti}(\text{NEt}_2)_2$  has been synthesized and characterized by IR spectroscopy. When activated with MAO, this compound is active for homogeneous ethylene polymerization and ethylene/propene copolymerization.<sup>766</sup> The analogous  $\text{CH}_2$ -bridged Cp-amido and Cp-phosphido compounds  $(\text{C}_5\text{H}_4\text{CH}_2\text{ER})\text{Ti}(\text{NEt}_2)_2$  (Scheme 319) have been prepared and the molecular structures determined by X-ray diffraction methods. These complexes are active homogeneous ethylene polymerization catalysts when treated with excess MAO. The polymerization activity depends on the NR/PR substituents and is comparable to the analogous silicon-bridged catalysts.<sup>767</sup> The compounds  $[(\text{C}_5\text{H}_4\text{CHR}^1\text{NR}^2)]\text{Ti}(\text{NMe}_2)_2$  ( $R^1 = \text{Me}$ ,  $R^2 = \text{Ph}$ ;  $R^1 = \text{Bu}^t$ ,  $R^2 = p\text{-tolyl}$ ) (Scheme 320) have been synthesized. The X-ray crystal structures of these complexes and their reactivity in olefin polymerizations has been compared with other similar systems from the literature. Structural data indicate that these complexes



Scheme 319



Scheme 320



Scheme 321

exhibit  $\text{Cp}_{\text{centroid}}\text{--Ti--N}$  angles that are by ca.  $10^\circ$  smaller and that their coordination gap aperture is correspondingly larger than in their respective  $\text{Me}_2\text{Si}$ -bridged analogs.<sup>768</sup>

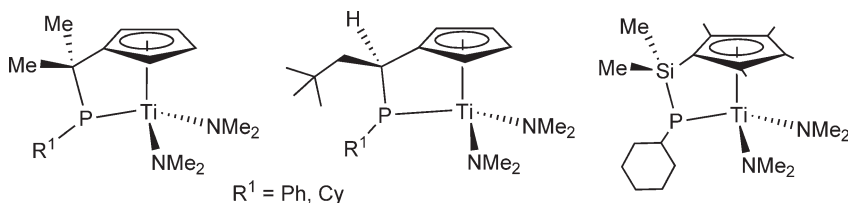
The synthesis and characterization of the ferrocenyl-substituted cyclopentadienyl-amido titanium complex shown in Scheme 321 has been reported.<sup>769</sup>

Transmetallation of  $\text{Li}_2[(\text{C}_4\text{H}_4)\text{CR}^2\text{R}^3\text{PR}^1]$  with  $\text{TiCl}_2(\text{NMe}_2)_2$  affords the  $\text{CR}_2$ -bridged phosphido derivatives  $[(\text{C}_4\text{H}_4)\text{CR}^2\text{R}^3\text{PR}^1]\text{Ti}(\text{NMe}_2)_2$  (Scheme 322).<sup>770</sup> The Cp-phosphido titanium complex  $[(\text{C}_5\text{Me}_4)\text{--SiMe}_2\text{--PCy}]\text{Ti}(\text{NMe}_2)_2$  (Scheme 322) has been synthesized by the same procedure. The molecular structures show a distorted “constrained-geometry” disposition due to the presence of a chiral, non-planar coordination geometry at the phosphorus atom. The inversion barrier at phosphorus is low. Upon activation with an excess of MAO, these complexes are active catalysts for ethylene/1-octene co-polymerizations.<sup>771</sup>

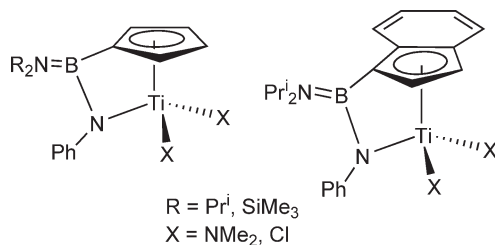
The metathesis reaction of  $[\text{C}_5\text{H}_3(\text{Bu}^t\text{PClBu}^t)]\text{TiCl}_3$  with  $\text{LiNHBu}^t$  in the presence of  $\text{NEt}_3$  affords the Cp-phosphinimido compound  $[\text{C}_5\text{H}_3(\text{Bu}^t)(\text{PBU}^t\text{NBU}^t)]\text{TiCl}_2$  (Scheme 272) obtained as a mixture of *syn*- and *anti*-diastereomers with respect to the orientation of the  $\text{Bu}^t$  groups at the phosphorus atom and the Cp ligand.<sup>398</sup>

Boron-bridged Cp-amido group 4 derivatives have been reviewed.<sup>394</sup> Boron-bridged Cp-amido derivatives are prepared in good yields by amine elimination reaction from  $\text{Ti}(\text{NMe}_2)_4$  (Schemes 282 and 323). The analogous indenyl-amido complex  $[\text{C}_9\text{H}_6\text{B}(\text{NPr}_2)_2\text{NPh}]\text{Ti}(\text{NMe}_2)_2$  has been synthesized. Subsequent deamination-chlorination with excess  $\text{SiClMe}_3$  yields the corresponding dichloro compound (Scheme 323). The molecular structures of  $[\text{C}_5\text{H}_4\text{B}(\text{NR}_2)_2\text{NPh}]\text{TiCl}_2$  ( $\text{R} = \text{Pr}^i$ ,  $\text{SiMe}_3$ ) and  $[\text{C}_9\text{H}_6\text{B}(\text{NPr}_2)_2\text{NPh}]\text{Ti}(\text{NMe}_2)_2$  have been determined by X-ray diffraction.<sup>583</sup>

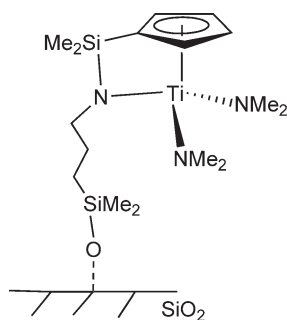
Heterogeneous mono-Cp-amido titanium complexes have been prepared by the immobilization of the titanium derivatives on different supports. These are of interest as catalysts for the polymerization of ethylene, propylene, and styrene. A heterogeneous Cp-amido catalyst has been prepared by anchoring  $[(\text{C}_5\text{H}_4)\text{SiMe}_2(\text{N}(\text{CH}_2)_3\text{SiMe}_2\text{--O--SiO}_2)]\text{Ti}(\text{NMe}_2)_2$  (Scheme 324) to a bifunctional ligand surface on  $\text{SiO}_2$ . The material was fully characterized by  $^1\text{H}$ ,  $^{13}\text{C}$ , and  $^{29}\text{Si}$  solid-state NMR and FTIR spectroscopy. The activity in the polymerization of ethylene, in the presence of MAO as co-catalyst, was however very low.<sup>772</sup>



Scheme 322



Scheme 323



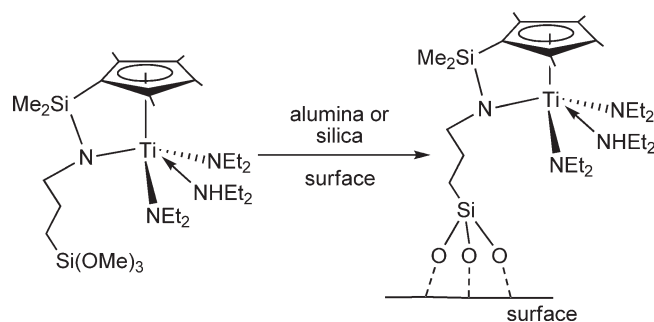
### Scheme 324

Reactions of  $\text{C}_5\text{Me}_4\text{HSiMe}_2\text{NH}(\text{CH}_2)_3\text{Si}(\text{OMe})_3$  with  $\text{Ti}(\text{NEt}_2)_4$  afford the complex  $[\text{C}_5\text{Me}_4\text{SiMe}_2\text{N}(\text{CH}_2)_3\text{Si}(\text{OMe})_3]\text{Ti}(\text{NEt}_2)_2\cdot\text{NEt}_2\text{H}$ . This complex has been anchored to either silica or alumina (Scheme 325) and the  $\alpha$ -olefin polymerization activities of the unsupported and supported complexes have been measured. Catalytic activity is dependent on MAO and titanium concentration. Polymerization of propylene produces high molecular weight atactic polymers with elastomeric properties. The heterogeneous system gives higher molecular weights.<sup>773</sup>

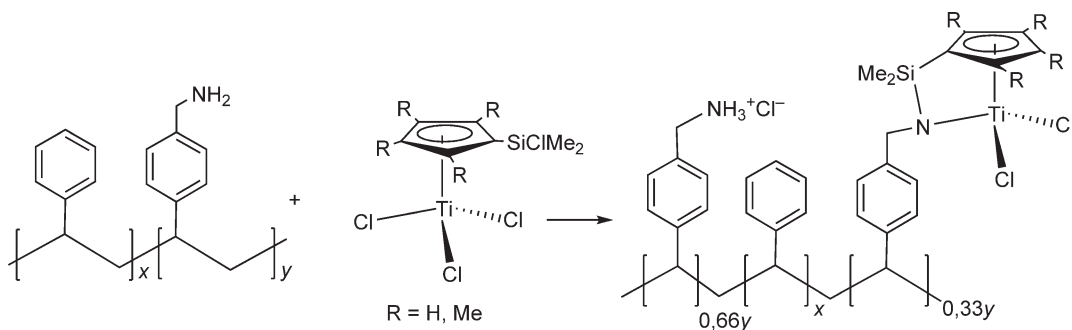
Reaction of  $\text{C}_5\text{Me}_4(\text{SiMe}_3)(\text{SiMe}_2\text{Cl})$  with  $\text{TiCl}_4$  results in the exclusive formation of  $(\text{C}_5\text{Me}_4\text{SiMe}_2\text{Cl})\text{TiCl}_3$ , which is supported on (aminomethyl)polystyrene leading to the assembly of the Cp-amido compounds (Scheme 326). The supported complexes have been spectroscopically characterized and tested, in the presence of MAO, as catalysts for the polymerization of ethylene and ethylene/1-octene co-polymerizations.<sup>774</sup>

Studies on  $\alpha$ -olefin polymerization with Cp-amido titanium complexes have been performed.

(C<sub>5</sub>Me<sub>3</sub>RSiMe<sub>2</sub>NBu<sup>t</sup>)TiCl<sub>2</sub> (R = alkyl or aryl substituents) complexes in combination with MAO have been found to be highly efficient catalysts toward ethylene polymerization. The compounds with aromatic R groups display higher activity than those with aliphatic ones.<sup>775</sup> Polymerization of propylene with (C<sub>5</sub>Me<sub>3</sub>RSiMe<sub>2</sub>NBu<sup>t</sup>)TiCl<sub>2</sub> (R = H, Me, Ph, 4-fluorophenyl, but-2-en-2-yl, butyl) activated with an excess of MAO reveals a moderate effect



### Scheme 325



Scheme 326

of the substituent R on the catalytic activity and the molecular weight of polypropylene.<sup>776</sup> Polymerization of propylene with  $(C_5Me_4SiMe_2NBu^t)TiMe_2$  activated with various co-catalysts has been described.<sup>777</sup> Cp-amido titanium complexes have been used to polymerize butadiene, isoprene, and 1,3-pentadiene.<sup>460</sup> Dimethylsilylbis(2-methyl-4-phenyl-1-indenyl) $TiCl_2$  in combination with MAO produces isotactic polypropylene more stereoregular than that obtained with traditional heterogeneous catalysts.<sup>778</sup>

The co-polymerization of ethylene with styrene using  $(C_5Me_4SiMe_2NR)TiCl_2$  ( $R = Bu^t$ , cyclohexyl) in the presence of MAO<sup>779</sup> and complexes of the general formula  $(Cp'SiMe_2NR)TiCl_2$  ( $Cp' = C_5Me_4$ , 1-Ind, 3-SiMe<sub>3</sub>Ind;  $R = Bu^t$ ,  $CH_2Ph$ )<sup>780</sup> has been studied. Ethylene/propylene co-polymerization has been performed in solution with the single center catalyst system based on a Cp-amido complex  $(C_5Me_4SiMe_2NBu^t)TiCl_2/MAO$ .<sup>781</sup> Co-polymerization of ethylene and 2-vinylnaphthalene,<sup>782</sup> ethylene/1-octene<sup>783</sup> and ethylene/1-butene,<sup>783</sup> ethylene/1-hexene,<sup>784</sup> ethylene/1-eicosene,<sup>785</sup> and the co-polymerization of ethylene with poly(propylene) macromonomer (PPM)<sup>786</sup> have been investigated with this catalytic system. Compound  $(C_5Me_4SiMe_2NBu^t)TiCl_2$  has been used as a pre-catalyst for the synthesis of poly(propylene- $\gamma$ -styrene) obtained by the combination with the atom-transfer radical polymerization (ATRP) process.<sup>787</sup>  $(C_5Me_4SiMe_2NBu^t)TiCl_2$  when activated with MAO has been used to synthesize poly(ethylene-co-norbornene).<sup>788</sup>

The ethylene/styrene co-polymerization with the Cp-amido-type complex *exo*-(isodiCpSiMe<sub>2</sub>NBu<sup>t</sup>) $TiCl_2/MAO$  has been studied.<sup>490</sup>

The catalytic activity of the system  $(C_5Me_4SiMe_2NBu^t)TiMe_2/Ph_3C[B(C_6F_5)_4]$  in the co-polymerization of ethylene and styrene has been examined.<sup>789</sup> The Cp-amido complex dimethylsilyltetramethylCp-cyclododecylamido dimethyl Ti(IV), when activated with different co-catalysts, such as dimethylanilinium tetrakis(pentafluorophenyl)borate,  $Ph_3C[B(C_6F_5)_4]$  or MAO, co-polymerizes ethylene with isobutylene to give alternating co-polymers.<sup>790</sup>

Effects of the co-catalyst for ethylene homopolymerization as well as for ethylene/styrene co-polymerization using the Ind-amido complexes  $(IndSiMe_2NR)TiX_2$  ( $R = Bu^t$ , cyclohexyl;  $X = Cl$ , Me) have been explored.<sup>791</sup> The fluorenyl-amido complex  $(FluSiMe_2NBu^t)TiMe_2$  activated with  $B(C_6F_5)_3$  has been used for the living polymerization of 1-octene, 1-butene, and 1-hexene.<sup>792</sup> Polymerization of propylene has been conducted at 0 °C in heptane using  $(FluSiMe_2NBu^t)TiMe_2$  activated with MAO and MMAO.<sup>793</sup> The ethylene polymerization with  $(C_5Me_4SiMe_2NR)TiX_2$  ( $R = Me$ ,  $Pr^i$ ,  $Bu^n$ ;  $X = Cl$ , Me, Bz) over borate-modified silica supports has been studied.<sup>794</sup>  $(C_5Me_4SiMe_2NR)TiCl_2$  ( $R = Me$ ,  $Bu^t$ ) supported on pyridyl-ethylsilane-modified silica and homogeneous dibromo nickel catalyst having a pyridyl-2,6-diisopropylphenylimine ligand in the presence of MMAO has been investigated for the synthesis of branched polyethylenes.<sup>795</sup>  $(C_5Me_4SiMe_2NBu^t)TiX_2$  ( $X = Cl$ , Me,  $CH_2Ph$ ) when activated with  $[Ph_3C[NC_5H_5]][B(C_6F_5)_4]$  and silica-supported tritylpyridinium tetrakis(pentafluorophenyl)borate has been used for the ethylene polymerization. The catalytic species have been studied using NMR spectroscopy.<sup>796</sup>

Homogeneous "tandem catalysts" based on mixtures of  $Cp_2ZrCl_2$  and  $(C_5Me_4SiMe_2NC_{12}H_{23})TiCl_2$  activated with MAO give branch-block ethylene/butene co-polymers. While the zirconium compound produces vinyl-terminated macromonomers, the titanium catalyst incorporates the vinyl functionality into ethylene/butene co-polymer backbones, producing branch-block compositions. These polymers show good thermoplastic elastomeric properties.<sup>797</sup> The system  $(3-Et-Ind-SiMe_2NBu^t)ZrMe_2 + (C_5Me_4SiMe_2NBu^t)TiCl_2$  has been used as a mixed metal catalyst. The catalyst shows an interesting cooperativity effect between two single site centers and increases the efficiency of homogeneous heterobimetallic catalysts for the production of LLDPE (linear low density polyethylene).<sup>798</sup> The "tandem catalytic system" formed by a mixture of  $[(C_5Me_4SiMe_2NBu^t)TiMe][MeB(C_6F_5)_3]$  and a nickel complex has been used for the preparation of LLDPE. In this system, the nickel catalyst dimerizes or oligomerizes ethylene to  $\alpha$ -olefins while the titanium complex incorporates these into the growing polyethylene chain.<sup>799</sup>

The cationic methyl complex  $[(C_5Me_4SiMe_2NBu^t)TiMe]^+[MeB(C_6F_5)_3]^-$  is also active for the polymerization of methyl methacrylate and gives syndiotactic poly(methyl methacrylate) at room temperature.<sup>727,800</sup>

DFT calculations combined with molecular mechanics methods have been used to study the first ( $R = Me$ ) and the second ( $R = propyl$ ) insertion of the ethylene monomer into the Ti-R bond of  $(CpSiMe_2NBu^t)(R)Ti(\mu-Me)B(C_6F_5)_3$ . The influence of the counterion and the solvent effects on the energetic profile of the polymerization have been evaluated.<sup>801,802</sup> Theoretical investigations have also been directed at mechanistic aspects of olefin polymerizations catalyzed by mono-Cp titanium complexes.<sup>803-805</sup> The chain propagation mechanism,<sup>806</sup> the chain termination and the long-chain branching processes for the olefin polymerization catalyzed by Cp-amido titanium complexes have been comprehensively surveyed using static and dynamic DFT.<sup>807</sup> The chain propagation mechanism in the olefin polymerization process catalyzed by cationic Cp-amido derivatives with simplified ligands,  $[(C_5H_4-SiH_2-NH)MMe]^+$  ( $M = Ti$ , Zr, Hf), and the titanium(III) derivative  $(C_5H_4-SiH_2-NH)TiMe$  has been studied by DFT and molecular mechanics calculations. One of the objectives of the study was to compare the insertion process involving the cationic Ti(IV) species with its neutral Ti(III) counterpart. The insertion process for both oxidation states

was found to be quite feasible, with both the Ti(IV) and Ti(III) complexes possessing modest insertion energy barriers. The insertion process for the Ti(IV), Zr(IV), and Hf(IV) has been compared, and it was found that the insertion barriers increased in the order  $\text{Ti} < \text{Zr} \approx \text{Hf}$ .<sup>808</sup> Theoretical calculations at *ab initio* quantum chemical level concerning the energetic, structural, and dynamic aspects of ethylene polymerization catalyzed by Cp-amido Ti complexes have been reported.<sup>693</sup>

#### 4.05.3.5 Mono-Cp Complexes with Ti–O Bonds

Structurally characterized organometallic hydroxo complexes of transition metals including mono- and bis-Cp titanium derivatives have been reviewed.<sup>809</sup>

##### 4.05.3.5.1 Oxo complexes

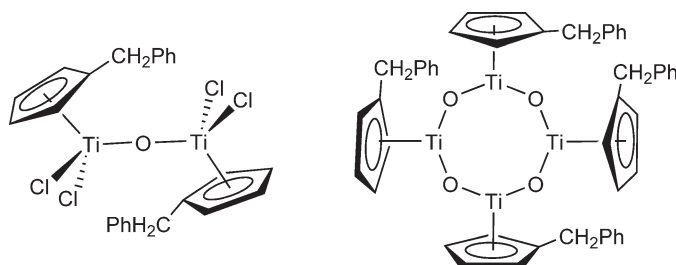
The hydrolysis reactions of mono-Cp derivatives  $\text{Cp}'\text{TiCl}_3$  ( $\text{Cp}'$  = different types of cyclopentadienyl ligands) lead to organotitanoxane complexes.<sup>810</sup> Under controlled conditions,  $\text{Cp}^*\text{TiMe}_3$  is hydrolyzed in toluene at room temperature to give the oxo-bridged binuclear compound  $[\text{Cp}^*\text{TiMe}_2]_2(\mu\text{-O})$  with evolution of methane. Reaction of  $\text{Cp}^*\text{TiCl}_3$  with water in the presence of  $\text{NEt}_3$  affords  $[\text{Cp}^*\text{Ti}_4\text{Cl}_2](\mu\text{-O})_5$ , which reacts with  $\text{SnFMe}_3$  to give  $[\text{Cp}^*\text{Ti}_4\text{F}_2](\mu\text{-O})_5$  and with  $\text{AlMe}_3$  is converted to the methyl derivative  $[\text{Cp}^*\text{Ti}_4\text{Me}_2](\mu\text{-O})_5$ . The crystal structures of  $[\text{Cp}^*\text{TiMe}_2]_2(\mu\text{-O})$  and  $[\text{Cp}^*\text{Ti}_4\text{Me}_2](\mu\text{-O})_5$  are described.<sup>811</sup> The synthesis of organotitanoxane complexes  $[\text{Cp}^*\text{Ti}_4\text{R}_2](\mu\text{-O})_5$  ( $\text{R} = \text{Me}, \text{Et}, \text{Ph}$ ) have been reported, although crystallographic data were poor.<sup>812</sup> Alkylation reactions of  $[\text{Cp}^*\text{TiFO}]_4$  and  $[(\text{C}_5\text{Me}_4\text{Et})\text{TiFO}]_4$  with  $\text{AlMe}_3$  proceed with activation of the Ti–F bonds.<sup>813</sup>

In the synthesis of benzyl-substituted Cp titanium complexes, oxo derivatives of the types shown in Scheme 327 are obtained when wet solvents are used.<sup>814</sup>

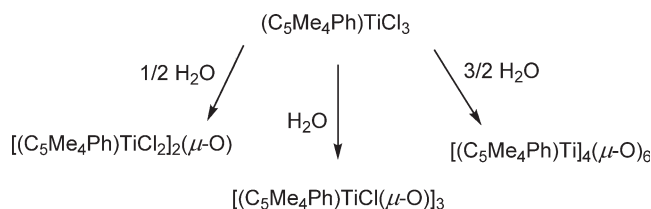
The oxochloro complexes  $[(\text{C}_5\text{Me}_4\text{Ph})\text{TiCl}_2]_2(\mu\text{-O})$ ,  $[(\text{C}_5\text{Me}_4\text{Ph})\text{TiCl}(\mu\text{-O})]_3$ , and  $[(\text{C}_5\text{Me}_4\text{Ph})\text{Ti}]_4(\mu\text{-O})_6$  have been prepared when  $(\text{C}_5\text{Me}_4\text{Ph})\text{TiCl}_3$  is hydrolyzed in toluene solution using different amounts of water (Scheme 328). The crystal structures of  $[(\text{C}_5\text{Me}_4\text{Ph})\text{TiCl}_2]_2(\mu\text{-O})$  and  $[(\text{C}_5\text{Me}_4\text{Ph})\text{Ti}]_4(\mu\text{-O})_6$  have been determined by X-ray diffraction.<sup>341</sup>

The trichloro compound  $(\text{C}_5\text{H}_4\text{CMe}_2\text{C}_{13}\text{H}_9)\text{TiCl}_3$  (Section 4.05.3.1.1) is readily hydrolyzed in wet acetone to give the  $\mu$ -oxo complex  $[(\text{C}_5\text{H}_4\text{CMe}_2\text{C}_{13}\text{H}_9)\text{TiCl}_2]_2(\mu\text{-O})$  (Scheme 329).<sup>326</sup>

The binuclear  $\mu$ -oxo compound (Scheme 330) has been prepared and is readily isolated by chromatography. Subsequent treatment with  $\text{SiXMe}_3$  ( $\text{X} = \text{Cl}, \text{I}, \text{OTf}$ ) followed by transmetalation and desymmetrization reaction with the lithium salt of cyclohexadiene affords an excellent reagent for the transfer of cyclohexadienyl groups to various aldehydes.<sup>503</sup>

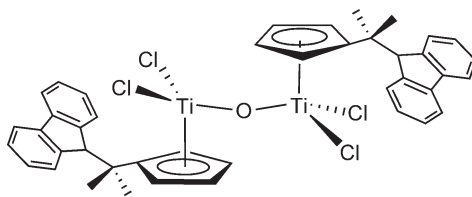


Scheme 327

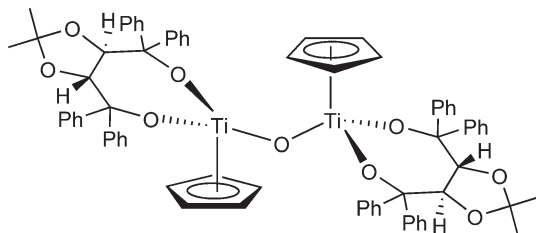


Scheme 328





Scheme 329



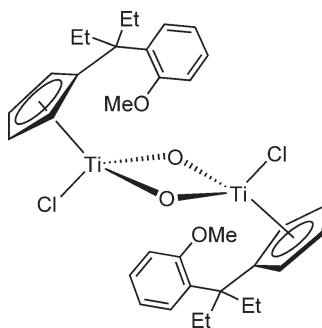
Scheme 330

The synthesis of a binuclear oxo-bridged titanium compound (Scheme 331) with potentially hemilabile methoxy-aryl-substituted Cp ligands has been described.<sup>815</sup>

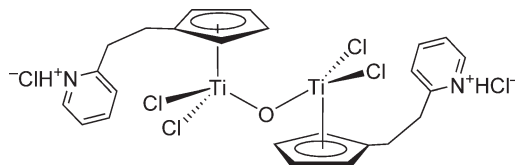
The  $\mu$ -oxo complex shown in Scheme 332 containing a pendant 2-pyridinium side arm has been isolated by hydrolysis of the corresponding titanium trichloride.<sup>332</sup>

Treatment of the trinuclear compound  $[\text{Cp}^*\text{TiCl}(\mu\text{-O})]_3$  with 3 equiv. of allylmagnesium chloride in toluene at low temperature leads to the preparation of new oxo-allyl trinuclear titanium complexes (Scheme 333). When the same reactions are carried out in THF, conversion of the allyl ligand into the 2-allyl-1,3-propanediyl group bridging two titanium atoms is observed through migration of one allyl group to the  $\beta$ -carbon of the adjacent allyl ligand. The crotyl complex  $[\text{Cp}^*\text{Ti}(\mu\text{-O})(\text{CH}_2\text{CH}=\text{CHMe})]_3$  has also been synthesized and characterized by X-ray diffraction.<sup>816</sup>

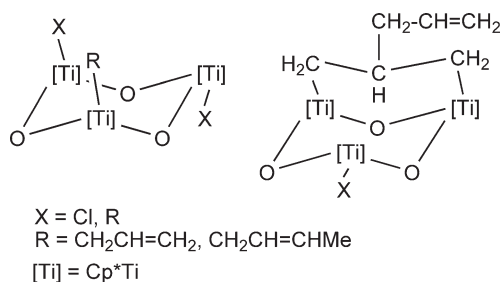
The oxo trimer  $[\text{Cp}^*\text{TiCl}(\mu\text{-O})]_3$  can be alkylated (partially or totally) by reaction with the appropriate stoichiometry of the organolithium LiR or Grignard reagents to afford  $[\text{Cp}^*\text{Ti}(\mu\text{-O})]_3\text{ClR}_2$  (R = Me, Et, Ph) or  $[\text{Cp}^*\text{TiR}(\mu\text{-O})]_3$  (R = Me, Ph, *p*-MeC<sub>6</sub>H<sub>4</sub>, C $\equiv$ Ph, Et, Pr, CH<sub>2</sub>Ph, C $\equiv$ CH). The thermal decomposition of  $[\text{Cp}^*\text{TiEt}(\mu\text{-O})]_3$  at



Scheme 331

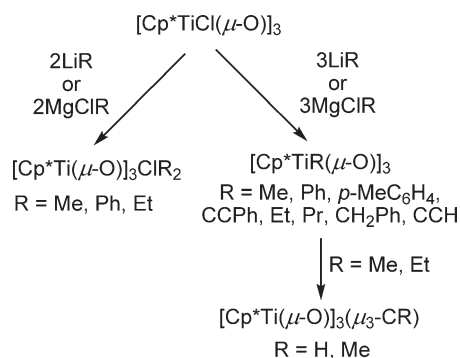


Scheme 332

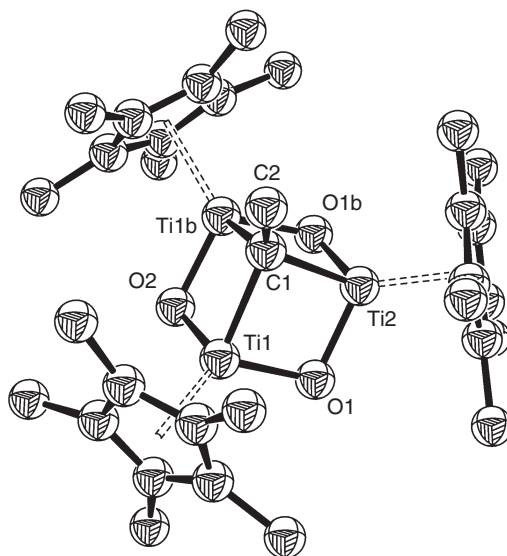


Scheme 333

temperatures in the range of 195–200 °C leads to the preparation of the first example of a  $d^0$ -( $\mu_3$ -alkylidyne) complex  $[\text{Cp}^*\text{Ti}(\text{O})]_3(\mu_3\text{-CMe})$  (Scheme 334), the molecular structure of which has been determined by X-ray diffraction (Figure 16). The three titanium atoms are located in an almost-perfect equilateral triangle capped by the ethylidyne ligand, with short non-bonding  $\text{Ti} \cdots \text{Ti}$  contacts (average value 2.82 Å). The  $^{13}\text{C}$  NMR spectrum of the alkylidyne compound shows a low-field shifted quartet at  $\delta$  401.7 ( $^2J_{\text{CH}} = 6.4$  Hz.) for the  $\text{C}_\alpha$  of the ethylidyne ligand.<sup>505</sup> The  $\mu_3$ -methylidyne compound  $[\text{Cp}^*\text{Ti}(\text{O})]_3(\mu_3\text{-CH})$  is obtained by thermolysis of  $[\text{Cp}^*\text{TiMe}(\text{O})]_3$  under analogous



Scheme 334



**Figure 16** Molecular structure of complex  $[\text{Cp}^*\text{Ti}(\text{O})]_3(\mu_3\text{-CMe})$  (reproduced by permission of American Chemical Society from *Organometallics*, 1994, 13, 2159).

conditions. The  $^1\text{H}$  NMR spectrum shows the signal for the CH group at  $\delta$  12.59, while in the  $^{13}\text{C}$  NMR spectrum the resonance appears at  $\delta$  393.8.<sup>507</sup>

Studies concerning the behavior of the alkylidyne groups supported by the trinuclear  $[\text{Cp}^*\text{Ti}(\text{O})]_3$  unit as a molecular model for the interactions of hydrocarbons with metal–oxide surfaces have revealed unprecedented chemical reactivity. Firstly, reactions where the  $\text{Ti}_3\text{O}_3$  core is maintained without participation in the processes have been observed.

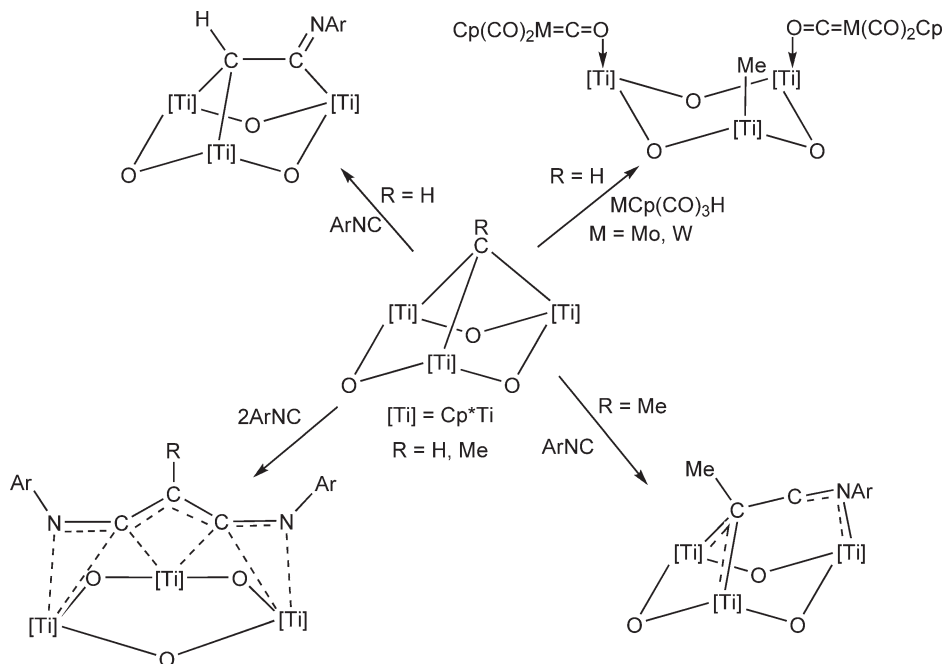
Carbonyl hydride transition metal compounds transform the methylidyne group into an Me ligand with the formation of Lewis acid carbonyl adducts.<sup>507</sup> CO and isocyanides react with the alkylidyne compounds to give products of single or double insertion into the  $\mu_3$ -carbon–titanium bond (Scheme 335).<sup>513</sup> Thermal and/or photochemical reactions of the ethylidyne complex with ketones take place with the insertion of the ketone carbonyl group into an intermediate “Ti–H” species with the formation of alkoxo–vinylidene derivatives.<sup>817</sup> The photochemical incorporation of N-benzylidene(phenyl)amine into  $[\text{Cp}^*\text{Ti}(\mu\text{-O})]_3(\mu_3\text{-CH})$  has been shown to give alkylidyne/imine metathesis reactions.  $\text{PhCH}=\text{NPh}$  reacts with the trinuclear titanium complex with breaking of the  $\text{C}=\text{N}$  imine bond and formation of the  $\mu$ -imido  $\sigma$ -alkenyl complex. The  $^{13}\text{C}$  NMR spectrum shows a doublet of doublets at  $\delta$  190.4 ( $^1J = 126.0$ ,  $^2J = 2.5$  Hz) and a doublet of multiplets at  $\delta$  140.2 ( $^1J = 154.5$ ) corresponding to  $\text{C}_\alpha$ - and  $\text{C}_\beta$ -resonances, respectively. The crystal structure of this complex has been determined by X-ray diffraction.<sup>631</sup> Treatment of amines, diamines, and  $\text{Ph}_2\text{C}=\text{NH}$  as hydrogen-donor reagents with the alkylidyne titanium complexes produces the partial hydrogenation of the alkylidyne moiety with the formation of new oxo derivatives (Scheme 336).<sup>818</sup>

In a second class of reactions, the  $\text{Ti}_3\text{O}_3$  core acts as a neutral macrocyclic tridentate six-electron donor ligand, in some cases without implicating the alkylidyne group. Thus, the reaction of  $[\text{Cp}^*\text{Ti}(\text{O})]_3(\mu_3\text{-CR})$  ( $\text{R} = \text{H}, \text{Me}$ ) with transition metal carbonyl complexes provides an effective route to heterometallacubane derivatives  $\text{Cp}^*_3\text{Ti}_3(\mu_3\text{-CR})(\mu_3\text{-O})\text{M}(\text{CO})_n$ .<sup>626</sup> Treatment of the methylidyne complex with alkali and alkaline earth metal alkyls and amides involves deprotonation of the methylidyne ligand to form heterometallacubane species where the alkali metal is incorporated at the free vertex of an incomplete cubic  $\text{Ti}_3\text{O}_3\text{C}$  core (Scheme 337).<sup>819,820</sup>

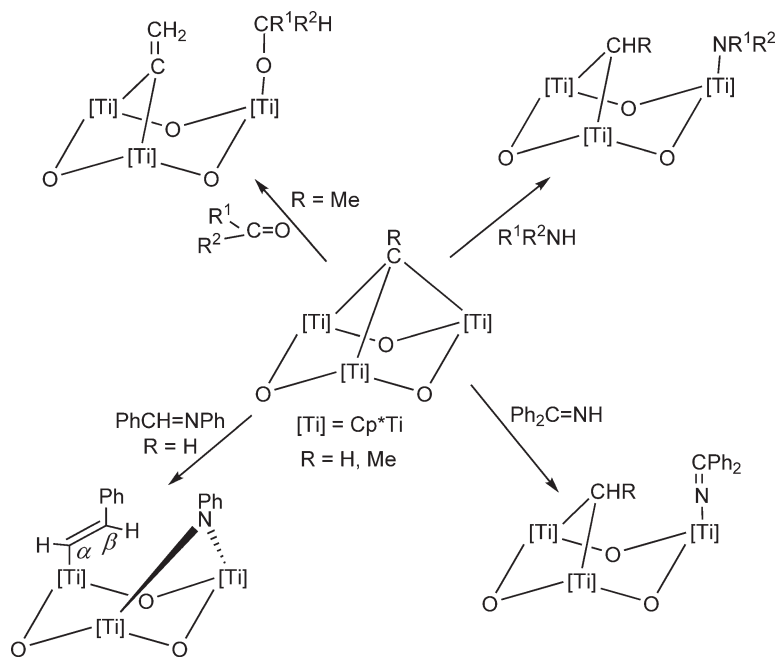
The reaction of  $[\text{Cp}^*\text{TiCl}(\mu\text{-O})]_3$  with anhydrous silver salts of a variety of oxyanions ( $\text{SO}_4^{2-}$ ,  $\text{CrO}_4^{2-}$ ,  $\text{NO}_3^-$ , and  $\text{ReO}_4^-$ ) in organic solvents leads to the isolation of a series of heterobimetallic compounds (Section 4.05.6).<sup>821</sup>

$(\text{C}_5\text{H}_4\text{SiMe}_2\text{Cl})\text{TiCl}_3$  reacts with  $\text{LiOH}$  to afford the oxo-bridged compound  $[(\text{C}_5\text{H}_4\text{SiMe}_2\text{Cl})\text{TiCl}_2]_2(\mu\text{-O})$  (Scheme 338).<sup>822</sup>

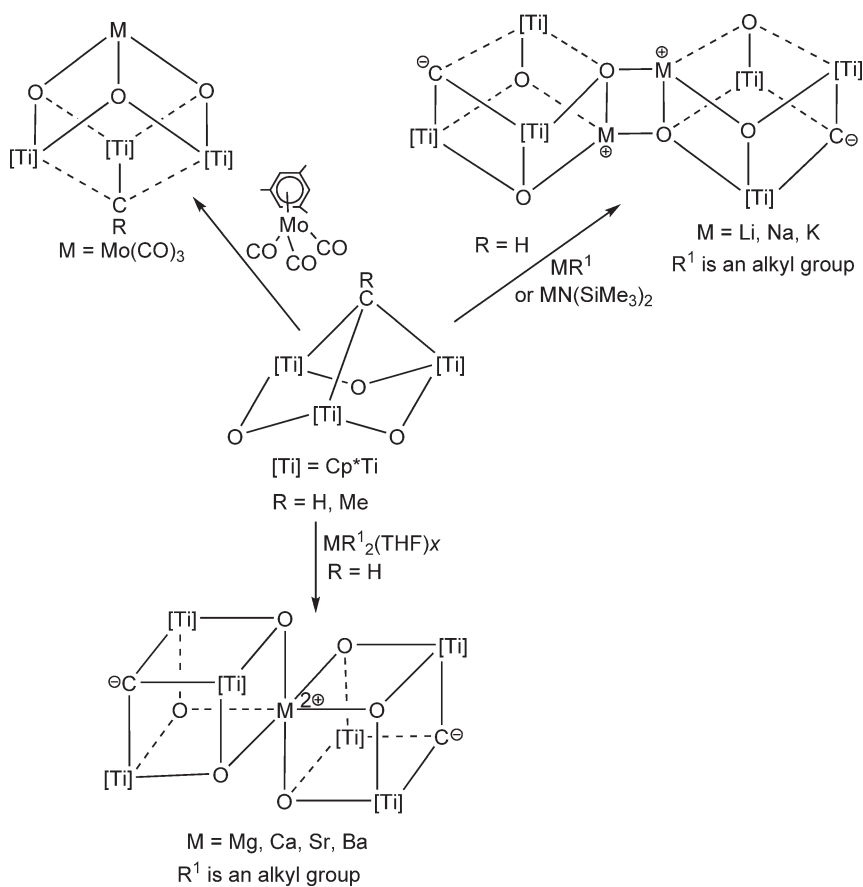
The reaction of  $\text{TiCl}_4$  with  $\text{Li}_2[(\text{C}_5\text{H}_3)_2(\text{SiMe}_2)_2]$  in toluene at room temperature affords a mixture of *cis*- and *trans*- $[(\text{C}_5\text{H}_3)_2(\text{SiMe}_2)_2](\text{TiCl}_3)_2$  in a molar ratio of 1:2 after recrystallization (Scheme 164; Section 4.05.3.1.1.(iv)).



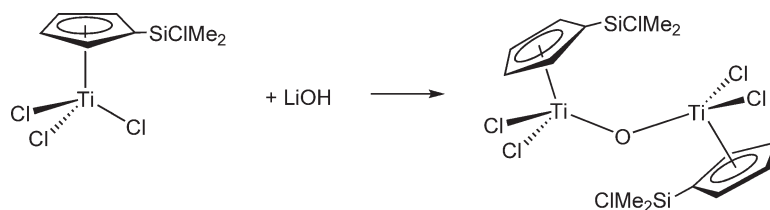
Scheme 335



Scheme 336



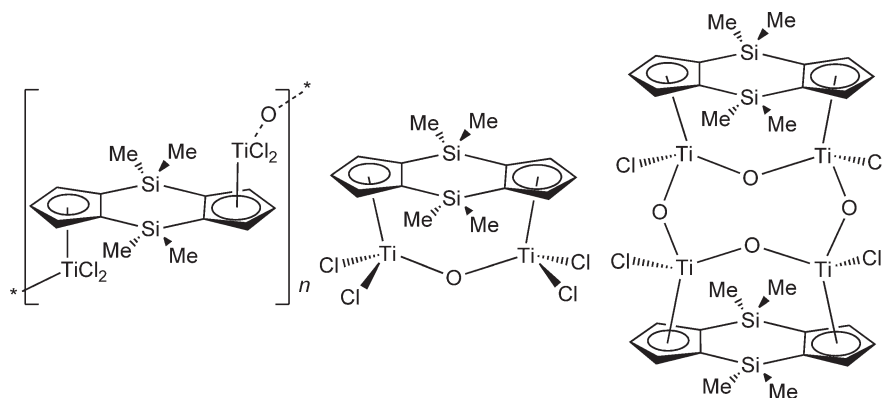
Scheme 337



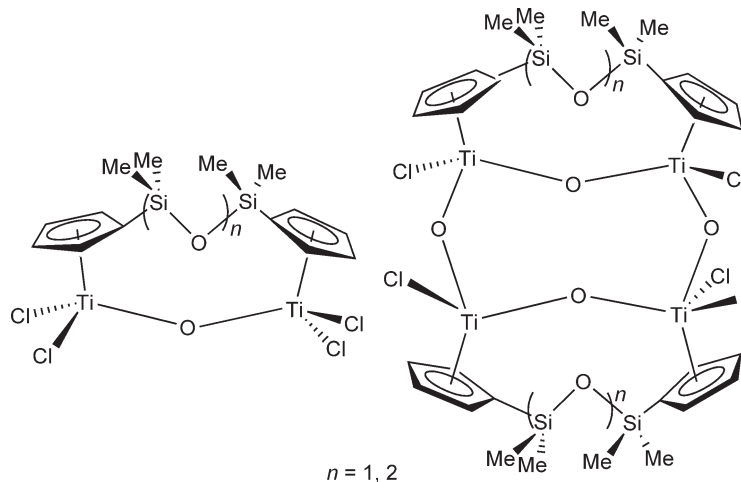
Scheme 338

The complex  $trans-[(C_5H_5)_2(SiMe_2)_2](TiCl_3)_2$  is hydrolyzed immediately by the addition of water to THF solutions to give  $trans-[(C_5H_5)_2(SiMe_2)_2](TiCl_2)_2(\mu-O)$  which is insoluble in all organic solvents, whereas hydrolysis of  $cis-[(C_5H_5)_2(SiMe_2)_2](TiCl_3)_2$  under different conditions led to the binuclear  $\mu$ -oxo complex  $cis-[(C_5H_5)_2(SiMe_2)_2](TiCl_2)_2(\mu-O)$  and two stereoisomers of the tetranuclear oxo complex  $\{[(C_5H_5)_2(SiMe_2)_2](TiCl_2)_2(\mu-O)\}_2(\mu-O)_2$  (Scheme 339). The molecular structure of one of the tetranuclear stereoisomers has been determined by X-ray diffraction.<sup>386</sup> Related polysiloxane-bridged binuclear complexes have been synthesized (Scheme 340).<sup>389</sup>

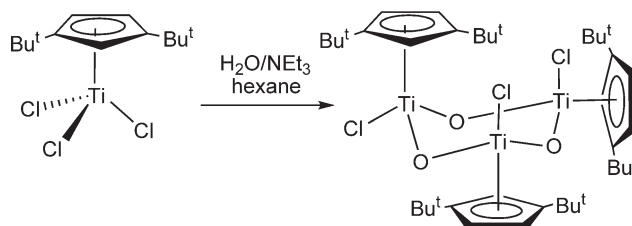
Addition of a stoichiometric amount of water in the presence of  $NEt_3$  to a toluene solution of  $(1,3-Bu^t_2-C_5H_3)TiCl_3$  affords the oxo trimer compound  $[(1,3-Bu^t_2-C_5H_3)TiCl(\mu-O)]_3$  (Scheme 341). The molecular structure has been determined.<sup>337</sup>



Scheme 339



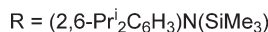
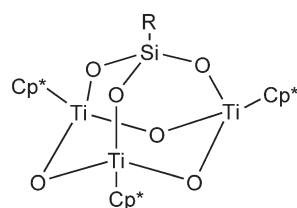
Scheme 340



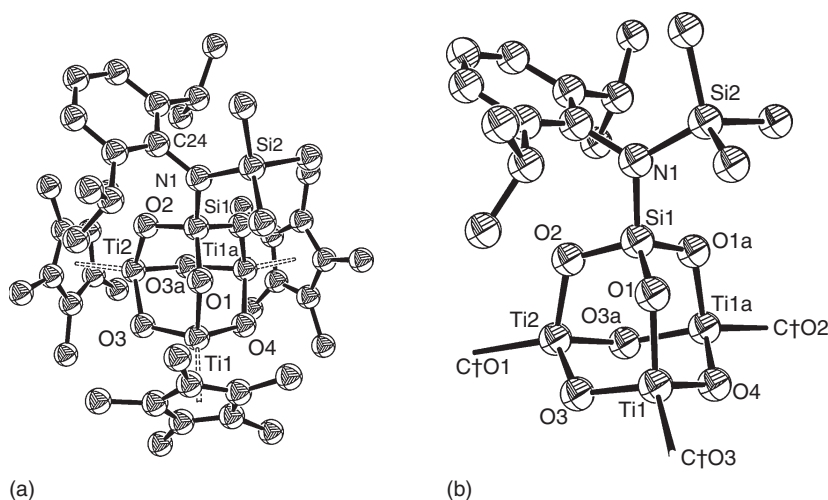
Scheme 341

The reaction of the arylaminosilanetriol  $[(2,6\text{-Pr}_2\text{C}_6\text{H}_3)\text{NSiMe}_3]\text{Si}(\text{OH})_3$  with  $\text{Cp}^*\text{TiCl}_3$  in the presence of  $\text{NEt}_3$  affords a titanasilicate which is free of Cp and chloro ligands. However, the reaction of the cyclic organometallic complex  $[\text{Cp}^*\text{TiMe}(\mu\text{-O})]_3$  with the same silanetriol gives a compound with an adamantanoid cage structure with two different metal atoms (Ti and Si) in the bridgehead positions (Scheme 342) (Figure 17).<sup>323</sup> The structurally related tetrameric organotitanoxane shown in Scheme 343 has been prepared by hydrolysis of hydrazido titanium complexes.<sup>757,758</sup>

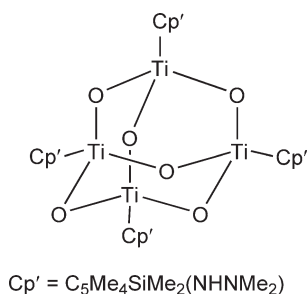
Synthetic methodology involving the reductive coupling of oxo chloro titanium(IV) complexes has been reported as a new strategy to prepare polyoxo aggregates of this metal. Reduction of the Cp-substituted oxo chloro complexes  $[(\text{C}_5\text{H}_4\text{R})\text{TiCl}(\mu_2\text{-O})]_4$  and  $[(\text{C}_5\text{H}_4\text{R})\text{TiCl}_2(\mu_2\text{-O})]_2$  ( $\text{R} = \text{H}, \text{Me}, \text{SiMe}_3$ ) with a variety of reducing agents in THF leads, depending on the reducing agents, to the hexanuclear titanoxanes  $[(\text{C}_5\text{H}_4\text{R})_6\text{Ti}_6\text{Cl}_{8-n}\text{O}_n]$  ( $n = 4, 6, 8$ ) (Scheme 344). Structural and theoretical studies are also reported. All the complexes contain an octahedron of titanium atoms faced by triply bridging oxygen and chloro ligands in the reported ratio. Molecular orbital calculations indicate that a band of 12 non-bonding orbitals may accommodate the electrons in excess of those needed for the existence of the  $\text{Ti}_6$  skeleton and so the systems can be used in their intact form for storing and releasing electrons.<sup>824</sup>



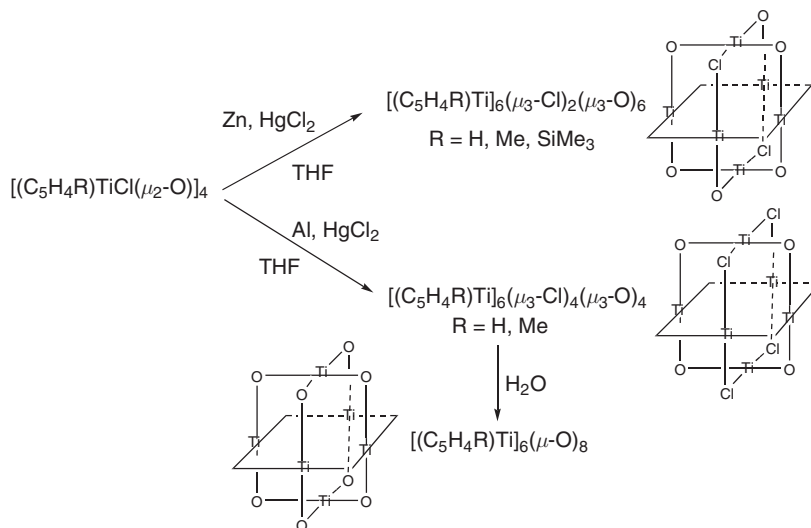
Scheme 342



**Figure 17** Two views of the molecular structure of complex  $[\text{Cp}^*\text{Ti}(\mu\text{-O})]_3(\mu_3\text{-O}_3\text{SiR})$  [ $\text{R} = 2,6\text{-Pr}_2\text{C}_6\text{H}_3\text{NSiMe}_3$ ] [(b):  $\text{Ti}_3\text{O}_6\text{Si}$  core] (reproduced by permission of Wiley-VCH from *Angew. Chem., Int. Ed. Eng.*, **1997**, 36, 1001).



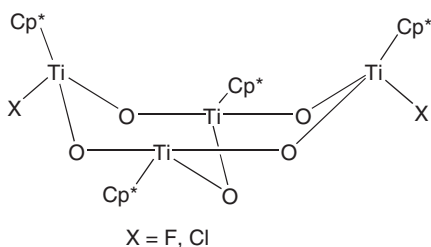
Scheme 343



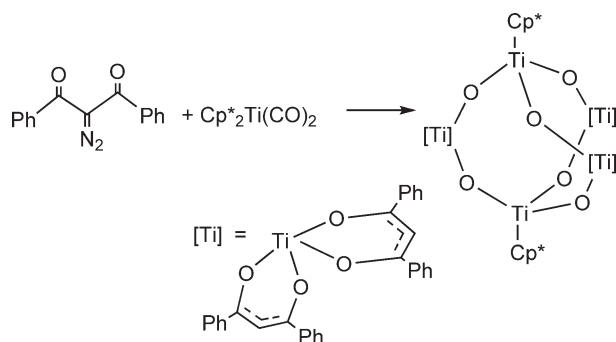
Scheme 344

The molecular structure of  $(\text{CpTi})_8(\mu\text{-O})_{12}$  has been determined by X-ray diffraction methods.<sup>825</sup>

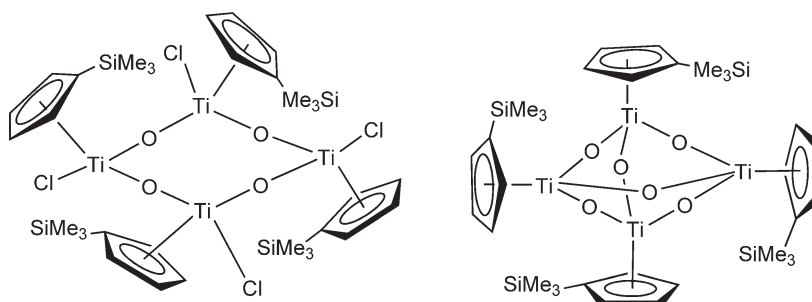
Organotitanoxano chloro complexes can be easily fluorinated by  $\text{Me}_3\text{SnF}$  via a four-membered ring  $[\text{Ti}]-(\mu\text{-F})-(\mu\text{-Cl})-[\text{Sn}]$  intermediate. Treatment of  $[\text{Cp}^*\text{TiClO}]_3$  with  $\text{Me}_3\text{SnF}$  leads to ring expansion to form the eight-membered cyclic compound  $[\text{Cp}^*\text{Ti}(\mu\text{-O})\text{F}]_4$ .<sup>351</sup> The fluoro titanoxane  $\text{Cp}^*_4\text{Ti}_4\text{O}_5\text{F}_2$  has been synthesized from  $\text{Cp}^*_4\text{Ti}_4\text{O}_5\text{Cl}_2$  and  $\text{Me}_3\text{SnF}$ . The molecular structures of both, the chloro and fluoro complexes as established by X-ray diffraction, exhibit a “butterfly” disposition (Scheme 345). Organotitanoxano fluoro complexes can be also converted to the corresponding chloro derivatives and even further to the oxygen-free chloro titanium derivatives by reaction with an excess of  $\text{Me}_3\text{SnCl}$ .  $\text{Cp}^*_4\text{Ti}_4\text{O}_5\text{F}_2$  and  $[\text{Cp}^*\text{Ti}(\mu\text{-O})\text{F}]_4$  react with  $\text{AlR}_3$  to give the corresponding alkylaluminum adducts with different stoichiometries. These adducts further yield alkylated compounds. The crystal structures of the complexes generated in these reactions have been determined by X-ray diffraction.<sup>826</sup>



Scheme 345



Scheme 346



Scheme 347

The structure of the cyclic tetranuclear iodo ( $\mu$ -oxo) complex  $[(\text{C}_5\text{H}_4\text{Me})\text{TiIO}]_4$  has been determined by X-ray diffraction. The central eight-membered ( $\text{Ti}-\text{O}$ ) $_4$  ring deviates appreciably from planarity, with the Cp and iodo ligands located alternately above and below the ring.<sup>827</sup>

$\text{Cp}^*_2\text{Ti}(\text{CO})_2$  reacts with the acyclic phenyl-substituted 2-diazo-2,3-diketone to give a heteroleptic, trigonal-bipyramidal oxygen-bridged  $\text{Ti}_5\text{O}_6$  cluster containing six unsymmetric six-membered titanadioxacyclic ligands (Scheme 346). The molecular structure of the cluster has been determined by X-ray diffraction.<sup>828</sup>

The electrochemical behavior, in non-aqueous solvents, of some mono- and bis-Cp' oxo homo- and heteropoly-nuclear titanium derivatives containing oxo bridges between different metals has been investigated (Scheme 347). Cyclic voltammetry, square wave voltammetry, and polarography have been used to determine and compare the redox properties of these compounds.<sup>829</sup>

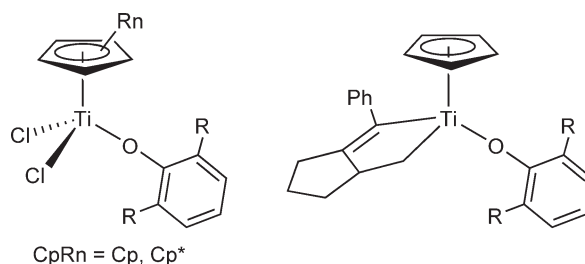
The molecular and electronic structures of  $(\text{CpM})_4(\mu_2-\text{E})_6$  and  $(\text{CpM})_4(\mu_2-\text{E})_3(\mu_3-\text{E})_3$  ( $\text{E} = \text{O}, \text{Se}$ ) for titanium as well as group 5 and 6 transition metals have been compared using extended Hückel molecular orbital calculations. The conclusions indicate that the  $\text{M}_4(\mu_2-\text{O})_3(\mu_3-\text{O})_3$  structure cannot exist unless the  $\text{M}_4$ -tetrahedron is severely distorted by lengthening of the  $\text{M}(\text{apical})-\text{M}(\text{basal})$  distance. The  $\text{M}_4(\mu_2-\text{Se})_3(\mu_3-\text{Se})_3$  structure can exist with a small distortion. The  $\text{M}_4(\mu_2-\text{E})_6$  structure is preferred over  $\text{M}_4(\mu_2-\text{E})_3(\mu_3-\text{E})_3$  when  $\text{M}-\text{E}$  multiple bonding is important, that is, when  $\text{E} = \text{O}$ . There is little  $\text{M}-\text{M}$  interaction in any of the cluster orbitals.<sup>830</sup>

#### 4.05.3.5.2 Alkoxo complexes

Organotitanium alkoxides are a subject of continuing interest with respect to structure and reactivity. Several monoalkoxo complexes  $\text{CpTiCl}_2(\text{OR})$  ( $\text{R} = \text{alkyl, aryl}$ ) have been prepared by different synthetic procedures. Pure final products can be isolated if the R groups are bulky. Particularly good yields are obtained for phenoxo complexes with 2,6-diisopropyl substituents. Electrochemical studies of the complexes in dry THF have been carried out.<sup>831</sup>

The synthesis and characterization of a family of mono-Cp dichloro complexes with disubstituted aryloxo ligands has been reported, and their molecular structures provide some means of quantifying the number of electrons donated to the metal center by an aryloxo ligand. These complexes can be reduced by Grignard reagents or  $\text{LiBu}^n$  in the presence of enynes. The formation of metallacyclic derivatives (Scheme 348) was observed for the Cp but not for the  $\text{Cp}^*$  complexes, as deduced by NMR spectroscopy. The complexes have been investigated as catalysts



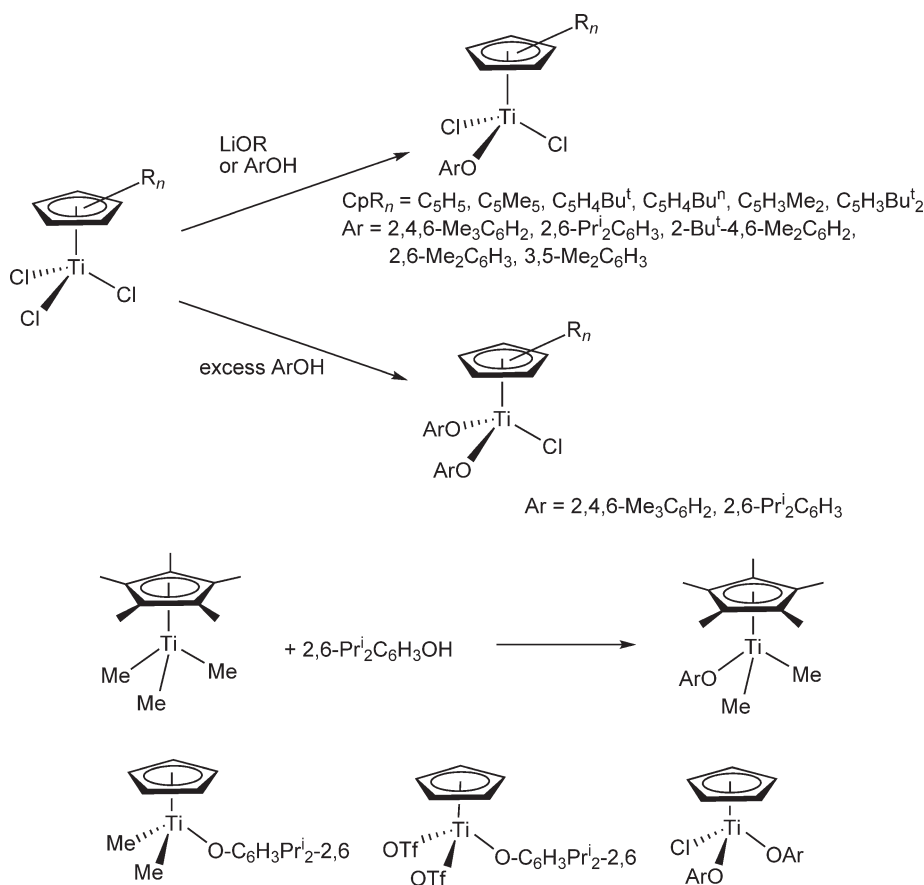


Scheme 348

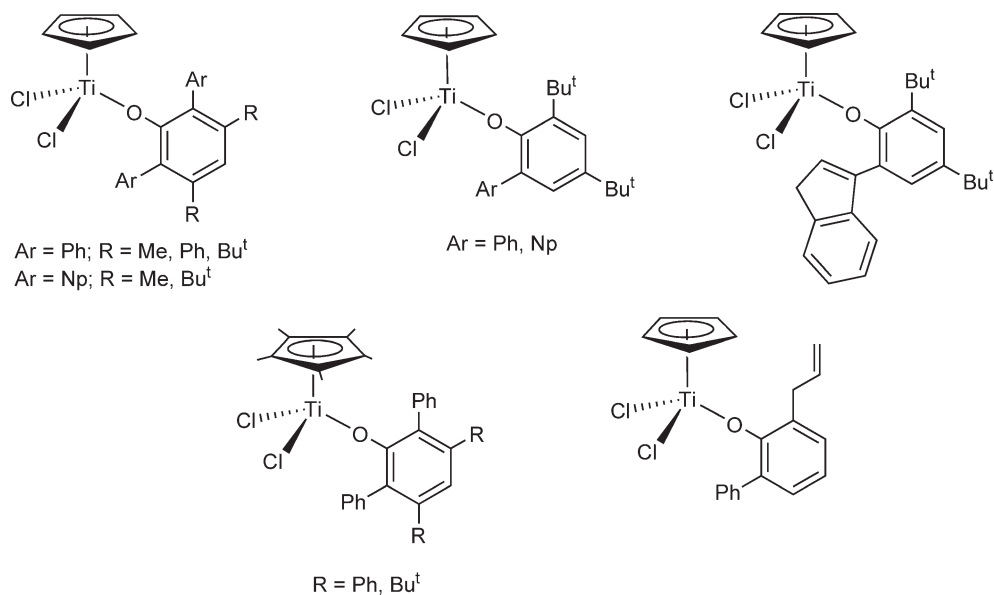
for the Pauson–Khand reaction; their chemical behavior is analogous to bis-Cp Ti derivatives.<sup>832–835</sup> The efficiency of the carbonylation and cyclization reactions depends upon the substitution of the aryloxy ligand.<sup>836</sup>

Several series of mono-aryloxy and bis-aryloxy titanium derivatives have been prepared by the routes outlined in Scheme 349. Activated by MAO the compounds are used as efficient catalysts for the syndiospecific polymerization of styrene and the co-polymerization of ethylene and styrene. The molecular structures of some of these compounds have been determined by X-ray diffraction. The Ti–O–C bond angle in the structure of  $\text{Cp}^*\text{TiCl}_2(\text{O}-2,6\text{-Pr}_2\text{C}_6\text{H}_3)$  differs significantly from those that are observed for the other structures. The effect of the substituents, both on the Cp ring and the alkoxo group, plays an essential role for the catalytic activity and the properties of the polymer obtained.<sup>578,779,837–847</sup>

Scheme 350 shows the structures of a number of mono-Cp titanium complexes with more elaborately substituted aryloxy ligands. The compounds are formed by the reaction of  $\text{Cp}^*\text{TiCl}_3$  with 1 equiv. of the substituted phenol in the presence of an excess of pyridine or by treatment of the lithium phenoxide with  $\text{Cp}^*\text{TiCl}_3$ ; some of them have been



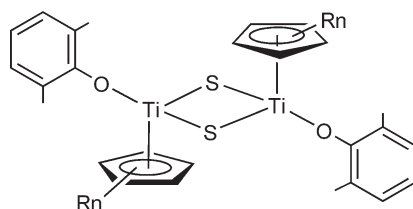
Scheme 349



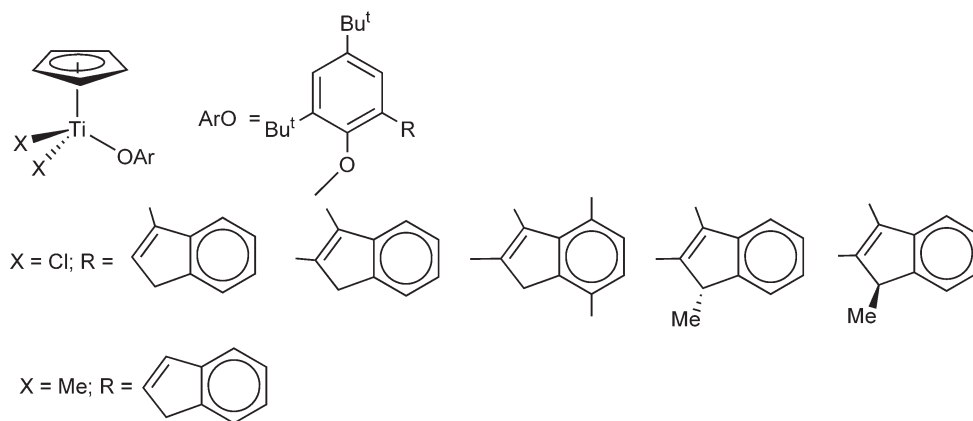
Scheme 350

characterized by X-ray diffraction. Reduction with Na/Hg gives binuclear Ti(III) species with a  $\text{Ti}(\mu\text{-Cl})_2\text{Ti}$  core.<sup>848</sup> Analogous chloro and sulfido aryloxo titanium derivatives have also been reported (Scheme 351).<sup>849</sup>

The 2-(indenyl)-phenoxo ligand exhibits different coordination modes to Ti center. Mono-Cp monoalkoxo dichloro and dimethyltitanium derivatives containing 4,6-di-*t*-butylphenoxo-indenyl ligands have been synthesized (Scheme 352). Reactions of the corresponding phenols with  $\text{CpTiCl}_3$  in the presence of pyridine generates the



Scheme 351

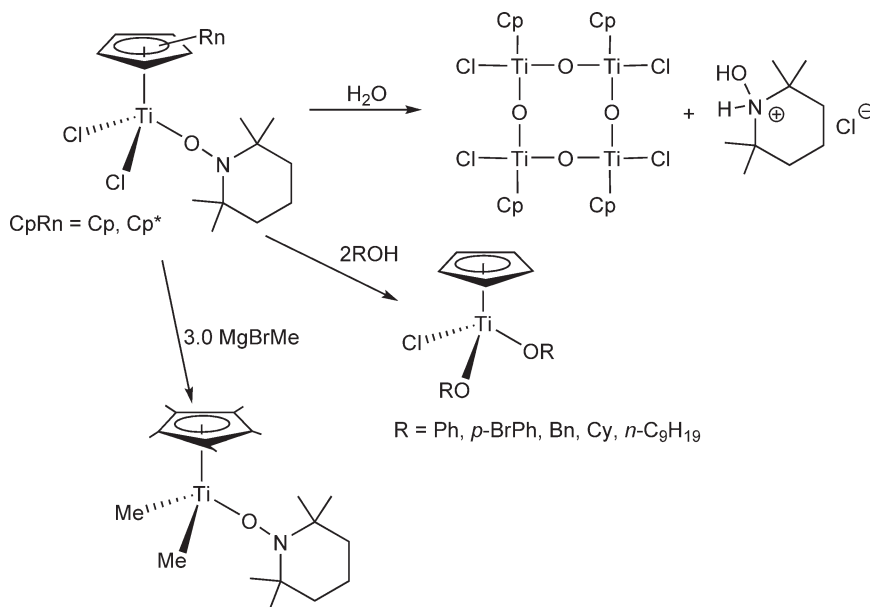


Scheme 352

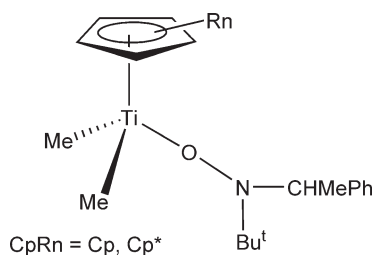
monoaryloxo derivatives with no evidence of the deprotonation of the indenyl ring. They exist in solution and the solid state as diastereoisomers. The attempted deprotonation of the indenyl ring by treatment with  $\text{LiBu}^n$  does not lead to indenyl coordination but instead gives a  $\text{Ti(III)}$  binuclear compound. The compound 2-(inden-3-yl)-4,6-di-*tert*-butylphenol reacts with  $\text{CpTiCl}_3$  in the presence of pyridine to give the complex  $\text{CpTiCl}_2[\text{OC}_6\text{H}_2\text{-4,6-Bu}^t_2\text{-Ind-2}]$ , which is converted into the dimethyl derivative  $\text{CpTiMe}_2[\text{OC}_6\text{H}_2\text{Bu}^t_2\text{-4,6-Ind-2}]$  by reaction with 2 equiv. of  $\text{LiMe}$ ; surprisingly, deprotonation of the indenyl ligand is not observed. The molecular structure of the dichloro complex has been determined by X-ray diffraction. Variable-temperature NMR studies in toluene- $d_8$  allow the barrier to inden-3-yl rotation (enantiomer interconversion) to be estimated at  $\sim 13.5 \text{ kcal mol}^{-1}$  (at room temperature). The unsubstituted 2-(inden-3-yl)-4,6-di-*tert*-butylphenol and the substituted 2-(2,3- $\text{Me}_2$ -inden-3-yl)-4,6-di-*tert*-butylphenol react with  $\text{Ti}(\text{NMe}_2)_4$  to give a mixture of the *p-R* and *p-S* indenyl-alkoxo bis-amido Ti complexes via activation of the phenolic OH and indenyl CH bonds. This mixture can be resolved using binaphthol to give the corresponding *p-R,S* and *p-S,S* binaphtholato complexes.<sup>850-852</sup>

The monoalkoxo complexes  $\text{CpTiCl}_2(\text{OR})(\text{R} = \text{methoxyethyl, methoxypropyl, methoxy-isopropyl, } o\text{-methoxyphenyl, tetrahydrofurfuryl})$  have been synthesized, characterized and, when activated with MAO, tested as catalyst precursors for the syndiospecific polymerization of styrene.<sup>853,854</sup>

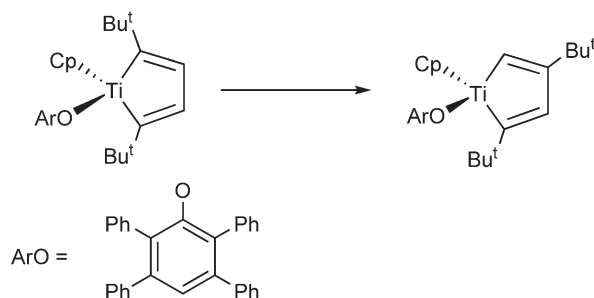
The  $\eta^1$ -hydroxylamido complexes  $\text{Cp}'_2\text{TiCl}(\text{TEMPO})$  and  $\text{Cp}'\text{TiCl}_2(\text{TEMPO})$  ( $\text{Cp}' = \text{Cp, Cp}^*$ ) are formed by trapping the corresponding  $\text{Ti(III)}$  intermediate with the stable nitroxyl radical TEMPO, which is the oxidized form of a hydroxylamine. The reaction of  $\text{Cp}^*\text{TiCl}_2(\text{TEMPO})$  with  $\text{MgBrMe}$  gives the corresponding dimethyl compound (Scheme 353). The preparation of related complexes  $\text{Cp}''\text{TiMe}_2[\text{ON}(\text{NBu}^t)(\text{CHMePh})]$  ( $\text{Cp}' = \text{Cp, Cp}^*$ ) has also been reported (Scheme 354). The molecular structures of  $\text{Cp}''\text{TiCl}_2(\text{TEMPO})$  have been determined by X-ray diffraction methods. When activated with 2,6-diisopropyl-N,N-dimethylanilinium tetrakis(pentafluorophenyl)borate



Scheme 353



Scheme 354



Scheme 355

(<sup>i</sup>PrAFPB), these alkyl derivatives efficiently co-polymerize ethylene and 1-hexene to provide co-polymers with higher 1-hexene contents in higher productivities than the related  $\text{Cp}^*\text{Ti}(\text{CH}_2\text{Ph})_3$ -based catalysts under identical conditions.<sup>855–857</sup> The hydrolysis of  $\text{Cp}^*\text{TiCl}_2(\text{TEMPO})$  is instantaneous in the presence of traces of water and gives  $[\text{Cp}^*\text{TiClO}]_4$  and the protonated hydroxylamine (Scheme 353). Treatment of  $\text{Cp}^*\text{TiCl}_2(\text{TEMPO})$  with 2 equiv. of ROH gives the dialkoxo compound  $\text{Cp}^*\text{TiCl}(\text{OR})_2$  and the TEMPOH·HCl salt.<sup>858</sup>

The tetraphenylphenolate  $\text{Cp}^*\text{TiCl}_2(\text{OC}_6\text{HPh}_4\text{-2,3,5,6})$  is obtained in high yield by addition of 1 equiv. of the parent phenol to a mixture of  $\text{Cp}^*\text{TiCl}_3$  and pyridine. The reduction of this compound with sodium amalgam (2Na per Ti) in the presence of excess of  $\text{HC}\equiv\text{CBu}^t$  leads to the formation of the titanacyclopentadiene  $\text{Cp}^*\text{Ti}(\text{ArO})(\text{C}_4\text{H}_2\text{-Bu}^t\text{-2,5})$  (Scheme 355). The structure of the product was confirmed by an X-ray diffraction. When a  $\text{C}_6\text{D}_6$  solution of this compound is heated at 100 °C in a sealed tube, the formation of the 2,4-isomer  $\text{Cp}^*\text{Ti}(\text{ArO})(\text{C}_4\text{H}_2\text{-Bu}^t\text{-2,4})$  is spectroscopically detected. An attempt was made to rationalize the regiochemistry of the kinetic titanacyclopentadiene product in terms of steric factors within the intermediate bis(alkyne) complex.<sup>860</sup>

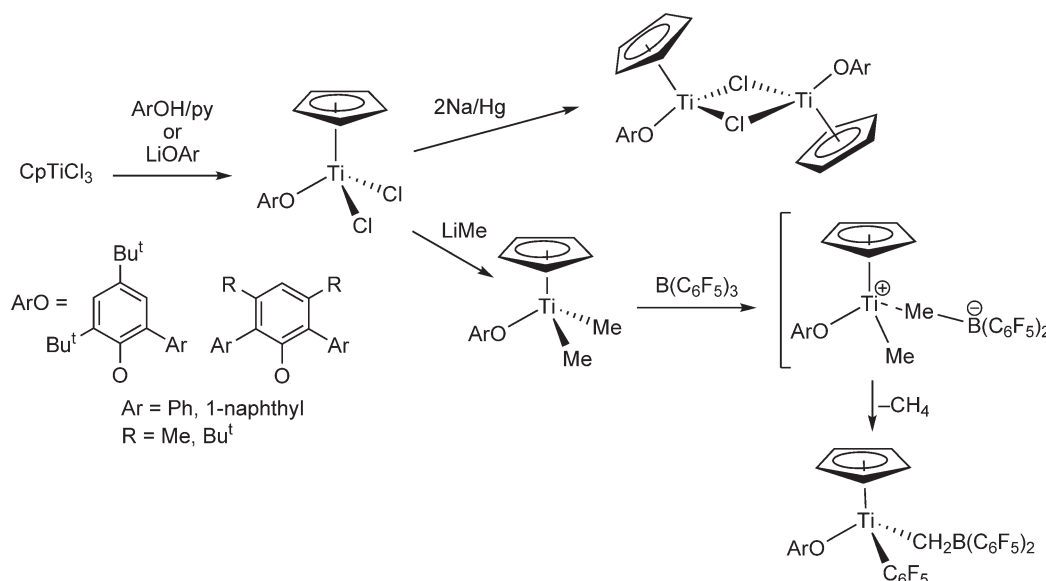
$\text{Cp}^*\text{TiCl}_2(\text{OR})$  ( $\text{Cp}^* = \text{Cp}$ ,  $\text{C}_5\text{H}_4\text{CHMe}_2$ ,  $\text{C}_5\text{H}_4\text{CH}_2\text{CH}_2\text{OMe}$ ; R = menthyl, fenchyl) have been synthesized, characterized, and tested as catalyst precursors for the syndiospecific polymerization of styrene.<sup>859</sup>

Chiral alkoxo derivatives  $\text{Cp}^*\text{TiCl}_2(\text{OR})$  have been synthesized from the reaction of  $\text{Cp}^*\text{TiCl}_3$  with 1 equiv. of ROH (ROH = adamantanol, 1*R*,2*S*,5*R*-(–)-menthol, 1*S*-endo-(–)-borneol, *cis*-1,3-(–)-benzylideneglycerol, 1,2:3,4-di-*O*-isopropylidene- $\alpha$ -D-galactopyranose) in the presence of  $\text{NEt}_3$ . The molecular structures of these complexes have been determined.<sup>861</sup> Reactions of  $\text{Cp}^*\text{TiCl}_3$  with chiral and achiral phenols in the presence of pyridine or of the corresponding lithium alkoxide salts in the appropriate molar ratio give the monoalkoxo titanium derivatives  $\text{Cp}^*\text{TiCl}_2(\text{OAr})$ . Reduction with sodium amalgam leads to titanium(III) containing a  $\text{Ti}(\mu\text{-Cl})_2\text{Ti}$  core. Treatment of these chloro aryloxo complexes with  $\text{LiMe}$  leads to the dimethyl compounds  $\text{Cp}^*\text{TiMe}_2(\text{OAr})$  as yellow solids. Addition of  $\text{B}(\text{C}_6\text{F}_5)_3$  to benzene or toluene solutions of the dimethyl derivatives generates the corresponding cationic methyl species  $[\text{Cp}^*\text{TiMe}(\text{OAr})][\text{MeB}(\text{C}_6\text{F}_5)_3]$  which deactivates via methane elimination to form  $\text{Cp}^*\text{Ti}(\text{C}_6\text{F}_5)(\text{OAr})\text{-CH}_2\text{B}(\text{C}_6\text{F}_5)_2$  (Scheme 356). The crystal structures of some of these complexes have been determined.<sup>862,863</sup>

$\text{Cp}^*\text{TiCl}_2\text{Me}$  reacts with MOR (M = Li, Na; R =  $\text{CH}_2\text{CH}=\text{CMe}_2$ ) to give  $\text{Cp}^*\text{TiClMe}(\text{OR})$  as a yellow liquid.<sup>864</sup> Monoalkoxo complexes  $\text{Cp}^*\text{TiCl}_2(\text{OR})$  (R = cyclohexyl,  $\text{CH}_2\text{CHMe}_2$ ,  $\text{CHEt}_2$ ,  $\text{CH}_2\text{Ph}$ ) have been prepared by the reaction of  $\text{Cp}^*\text{TiCl}_3$  with the appropriate alcohol.<sup>865</sup>

Formation of neutral and cationic methyl derivatives of titanium containing one Cp and one disubstituted aryloxo ligands have been reported.  $\text{Cp}^*\text{TiMe}_2(\text{OAr})$  can be prepared by the reaction of  $\text{Cp}^*\text{TiCl}_2(\text{OAr})$  with 2 equiv. of  $\text{LiMe}$  or by the addition of parent phenol ( $\text{HOAr}$ ) to a cold ether solution of  $\text{Cp}^*\text{TiMe}_3$ . The compounds are stable, except for those containing less bulky *o*-methyl substituted phenoxo ligands. In the case of 2,6-dimethyl-phenoxo derivatives, slow decomposition is observed to produce mixtures of bis(aryloxo) monomethyl complexes and  $\text{Cp}^*\text{TiMe}_3$ . The dimethyl compounds react with  $\text{B}(\text{C}_6\text{F}_5)_3$  to generate cationic methyl species, which readily eliminate methane at room temperature to afford compounds of the type  $\text{Cp}^*\text{Ti}(\text{OAr})(\text{C}_6\text{F}_5)\text{CH}_2\text{B}(\text{C}_6\text{F}_5)_2$ . X-ray crystal structures have been obtained for the dimethyl compounds. The decomposition kinetics of the cationic methyl compounds have been measured.<sup>866</sup>

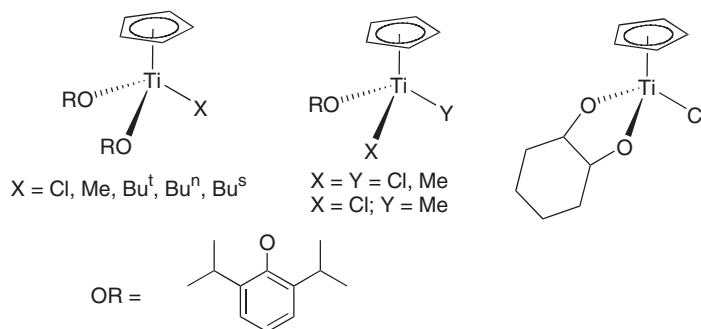
The structural analysis of  $\text{Cp}^*\text{TiMe}_2(\text{O-2,6-Pr}^i\text{C}_6\text{H}_3)$  and  $\text{Cp}^*\text{TiMe}(\text{OTf})(\text{O-2,6-Pr}^i\text{C}_6\text{H}_3)$  has been described and the effect of the organoboron compounds as co-catalysts in 1-hexene polymerizations has been studied.<sup>867</sup> The molecular structures of  $\text{Cp}^*\text{TiCl}_2(\text{OCy})$ ,<sup>865</sup>  $\text{Cp}^*\text{TiCl}_2(\text{OPr}^i)$ ,<sup>868</sup> and  $\text{Cp}^*\text{TiCl}_2[\text{O-1-(4-methoxy-phenyl)cyclohexyl}]$ <sup>869</sup> have been determined.



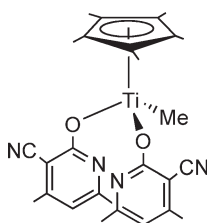
Scheme 356

The mono- and bis-aryloxo complexes  $\text{CpTiXY(OC}_6\text{H}_3\text{Pr}^i_2)$  and  $\text{CpTiX(OC}_6\text{H}_3\text{Pr}^i_2)_2$  ( $\text{X} = \text{Cl, Me}$ ) (Scheme 357) have been prepared and characterized. The chloro compounds in the presence of MAO act as catalysts for ethylene polymerizations. The inclusion of the second aryloxo ligand enhances the activity of the catalysts. The reaction of  $\text{CpTiCl}_2(\text{OC}_6\text{H}_3\text{Pr}^i_2)$  with  $\text{AlMe}_3$  gives the chloro methyl complex  $\text{CpTiClMe(OC}_6\text{H}_3\text{Pr}^i_2)$ , while an excess of  $\text{AlMe}_3$  affords  $\text{CpTiMe}_2(\text{OC}_6\text{H}_3\text{Pr}^i_2)$  and the transmetalation product  $\text{AlMe}_2(\text{OC}_6\text{H}_3\text{Pr}^i_2)$ . In contrast, the catecholate complex  $\text{CpTi(O}_2\text{C}_6\text{H}_4)\text{Cl}$  reacts with  $\text{AlMe}_3$  to give the paramagnetic species  $\text{CpTi(O}_2\text{C}_6\text{H}_4)\text{AlClMe}_2$ .<sup>870</sup>

The oxo-pyridine Ti(IV) complex shown in Scheme 358 has been prepared by the reaction of  $\text{Cp}^*\text{TiMe}_3$  with 2 equiv. of 3-cyano-2-hydroxy-4,6-dimethylpyridine.<sup>871</sup>



Scheme 357



Scheme 358

The compounds  $\text{Cp}'\text{TiCl}_3$  ( $\text{Cp}' = \text{C}_5\text{H}_4\text{R}$ ;  $\text{R} = \text{H, Me, Pr}^i, \text{SiMe}_3, \text{allyl, CH}_2\text{Ph}$ ) react with  $\text{MeOH}$  in the presence of  $\text{NEt}_3$  to give the trimethoxy derivatives  $\text{TiCp}'(\text{OMe})_3$ , from which the difluoro methoxy compounds  $\text{Cp}'\text{TiF}_2(\text{OMe})$  can be obtained by reaction with  $\text{BF}_3 \cdot \text{OMe}_2$ . In the presence of MAO, these compounds catalyze the polymerization of styrene.<sup>356</sup> The allyloxide  $\text{Cp}^*\text{Ti}(\text{OCH}_2\text{CH}=\text{CH}_2)_3$  has been prepared and employed to polymerize propylene in the presence of MAO.<sup>872</sup>  $\text{Cp}^*\text{Ti}(\text{OMe})_3$  and  $\text{Cp}^*\text{Ti}(\text{OCH}_2\text{CH}=\text{CH}_2)_3$ , activated with MAO, also catalyze the syndiospecific polymerization of styrene.<sup>873</sup>

$\text{Cp}^*\text{Ti}(\text{OC}_6\text{F}_5)_3$  is formed, as an orange crystalline solid, by reaction of  $\text{Cp}^*\text{TiCl}_2\text{Me}$  with an excess of  $\text{C}_6\text{F}_5\text{OH}$ . Lower molar ratios of phenol are used and intractable product mixtures are obtained.<sup>864</sup>

The isopropoxide derivatives  $(\text{C}_5\text{R}_4\text{R}')\text{Ti}(\text{OPr}^i)_3$  ( $\text{R}^i = \text{H, R} = \text{Me, Ph}$ ;  $\text{R}^i = \text{PPh}_2, \text{R} = \text{Me}$ ;  $\text{R}^i = \text{SiMe}_3, \text{R} = \text{Me}$ ) are obtained in high yields from  $\text{TiCl}(\text{OPr}^i)_3$  and the corresponding substituted Cp lithium or potassium salts. Their catalytic activities for syndiospecific styrene polymerization have been compared with the reference compound  $\text{CpTi}(\text{OPr}^i)_3$ . The complex  $(\text{C}_5\text{HMe}_4)\text{Ti}(\text{OPr}^i)_3$  shows the highest activity and produces polystyrene with the highest syndiotacticity and molecular weight.<sup>525</sup>

$\text{Cp}^*\text{Ti}(\text{OCH}_2\text{CH}=\text{CH}_2)_3$  has been synthesized and employed, in the presence of MMAO, in the study on ethylene-propylene co-polymerizations.<sup>359–361</sup>

The tricinnamyloxo complex  $\text{Cp}^*\text{Ti}(\text{OCH}_2\text{CH}=\text{CHPh})_3$  has been prepared and used for the polymerization of 1-butene in the presence of MAO.<sup>874</sup>

The reaction between equimolar amounts of  $\text{Na}(\text{C}_5\text{Ph}_5)$  or  $\text{Li}(\text{C}_5\text{H}_4\text{PPh}_2)$  with  $\text{TiCl}(\text{OPr}^i)_3$  has produced the corresponding Cp derivatives  $(\text{C}_5\text{Ph}_5)\text{Ti}(\text{OPr}^i)_3$  and  $(\text{C}_5\text{H}_4\text{PPh}_2)\text{Ti}(\text{OPr}^i)_3$ , while the tetraphenyl-Cp compound  $(\text{C}_5\text{HPh}_4)\text{Ti}(\text{OPr}^i)\text{Cl}_2$  is formed from the reaction of  $(\text{C}_5\text{HPh}_4)\text{Ti}(\text{OPr}^i)_3$  with  $\text{HCl}$  in pentane at reflux for 1.5 h.<sup>343</sup>

The reaction of the amido complex  $(\text{C}_5\text{H}_4\text{CH}_2\text{CH}_2\text{NPr}^i_2)\text{Ti}(\text{NMe}_2)_3$  with 3 equiv. of isopropanol affords the trialkoxo compound  $(\text{C}_5\text{H}_4\text{CH}_2\text{CH}_2\text{NPr}^i_2)\text{Ti}(\text{OPr}^i)_3$ .<sup>374</sup> A series of aminoalkyl-substituted mono-Cp trichloro, triisopropoxo, and mono(indenyl) triisopropoxo titanium complexes that contain pyridyl (2-picoly), diisopropylaminoethyl and dimethylaminoethyl, and phenylethyl pendant arms have been prepared (Scheme 159; Section 4.05.3.1.1.(iii)). The utility of these complexes for the polymerization of ethylene, propylene, and styrene has been investigated.<sup>332</sup>

The trialkoxo complexes  $\text{CpTi}(\text{OR})_3$  ( $\text{OR} = \text{furfuryloxy, tetrahydrofurfuryloxy, and tribenzyloxy}$ ) have been synthesized and tested as pre-catalysts for the polymerization of styrene.<sup>875</sup>

$\text{Cp}^*\text{TiX}(\text{OTf})_2$  ( $\text{X} = \text{Me, OMe, OC}_6\text{H}_2\text{Me}_3\text{-2,4,6}$ ) and  $\text{Cp}^*\text{Ti}(\text{O-C}_6\text{H}_4)(\text{OTf})$  have been synthesized via metathesis of the corresponding chloro complexes with silver triflate.  $\text{Cp}^*\text{Ti}(\text{OH})(\text{OTf})_2$  is prepared by controlled hydrolysis of  $\text{Cp}^*\text{TiMe}(\text{OTf})_2$ . The solid-state structures of these complexes have been determined by X-ray diffraction. Polymerization of styrene at  $50^\circ\text{C}$  with these complexes, in the absence of activator, is described, indicating very low activity. In the presence of MAO, all of the complexes show high activity for the synthesis of syndiotactic polystyrene.<sup>876</sup> Reaction of  $\text{Cp}^*\text{TiMe}(\text{OTf})(\text{OAr})$  ( $\text{OAr} = \text{O-2,6-Pr}^i_2\text{C}_6\text{H}_3$ ) with 5-hexen-1-ol in *n*-hexane gives  $\text{Cp}^*\text{Ti}[\text{OCH}_2(\text{CH}_2)_n\text{CH}=\text{CH}_2](\text{OTf})(\text{OAr})$  ( $n = 1, 3$ ). The molecular structure for  $n = 3$  has been determined by X-ray crystallography. Reaction of  $\text{Cp}^*\text{TiMe}_2(\text{OAr})$  with both 5-hexen-1-ol and 3-buten-1-ol yields  $\text{Cp}^*\text{TiMe}[\text{OCH}_2(\text{CH}_2)_n\text{CH}=\text{CH}_2](\text{OAr})$  ( $n = 1, 3$ ), which were spectroscopically characterized, although attempts to isolate these complexes were not successful.<sup>877</sup>

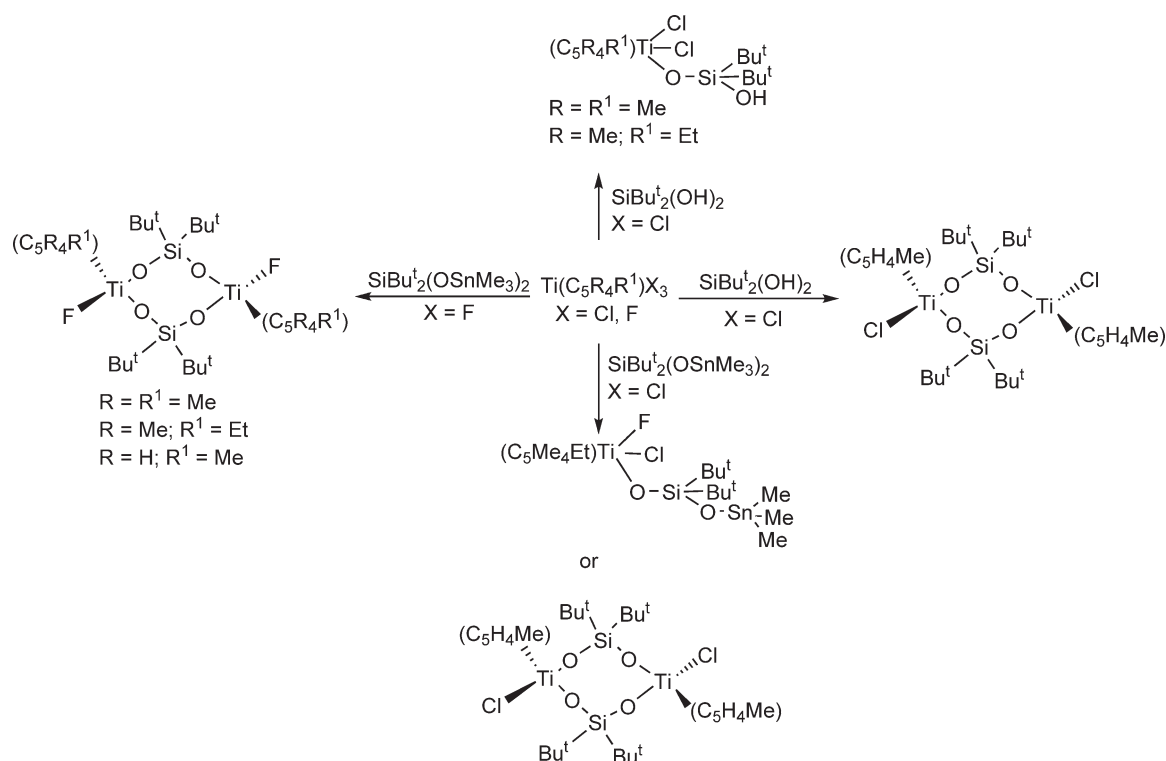
The synthesis and characterization of the indenyl species  $(1\text{-MeInd})\text{TiCl}_2(\text{OR})$  ( $\text{R} = \text{Me, Et, Pr}^i, \text{Bu}^t, \text{cyclo-C}_6\text{H}_{11}$ ) have been reported. They have been applied as catalysts for the syndiotactic polymerization of styrene.<sup>878</sup> Binuclear mono-Ind titanium(IV) complexes have been synthesized by reaction of  $\text{TiCl}(\text{OPr}^i)_3$  with the lithium salt of the bis-indene reagent.  $[(\text{-CH}_2\text{-1-Ind})\text{Ti}(\text{OPr}^i)_3]_2$  is obtained as a 1:1 *rac*- and *meso*-mixture (Scheme 184; Section 4.05.3.1.1.(vii)).<sup>417</sup>

The indenyl complex  $(\text{Ind})\text{TiCl}_2(\text{OMe})$  has been prepared from  $(\text{Ind})\text{TiCl}_3$  and lithium methoxide and the crystal structure determined by X-ray diffraction. The structure shows a  $C_s$ -symmetric piano stool conformation with a strongly  $\pi$ -donating methoxy group *trans* to the indenyl ring. The compound catalyzes the ring-opening polymerization of  $\epsilon$ -caprolactone with significantly more efficiency than analogous cyclopentadienyl derivatives.<sup>879</sup>

The alkoxo complexes  $(\text{Ind})\text{TiCl}_2(\text{OR})$  ( $\text{R} = \text{Me, Et, Pr}^i, \text{cyclohexyl}$ ) have been prepared and evaluated as catalysts for the syndiospecific polymerization of styrene when activated with MAO.<sup>880</sup>

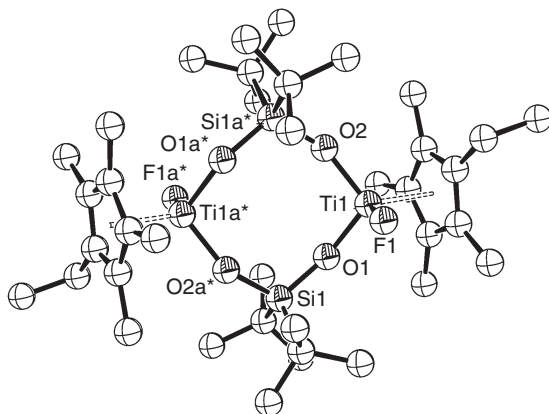
The fluorenyltitanium compound  $(\eta^5\text{-Flu})\text{Ti}(\eta^1\text{-Flu})(\text{OPr}^i)_2$  has been prepared by the reaction of  $\text{TiCl}(\text{OPr}^i)_3$  with equimolar amounts of  $\text{LiFlu}$ . It is obtained as a mixture with the derivative  $\text{Ti}(\eta^1\text{-Flu})(\text{OPr}^i)_3$ . The complex has been characterized by X-ray analysis and temperature-dependent NMR spectroscopy. In combination with MAO, the compound is a highly efficient catalyst for styrene polymerization and produces highly syndiotactic polymers.<sup>20</sup>

Mono-Cp titanium trihalides react with  $\text{SiBu}^t_2(\text{OH})_2$  or  $\text{SiBu}^t_2(\text{OSnMe}_3)_2$  to give cyclic and acyclic halo titanium siloxanes with structures depending on the substituents on the Cp and on the nature of the halide ligands. The



Scheme 359

fluoro complexes are cyclic, while acyclic chloro derivatives are accessible when using bulky Cp ligands. Treatment of  $(C_5R_4R^1)TiCl_3$  ( $R = R^1 = Me$ ;  $R = Me, R^1 = Et$ ) with  $SiBu_2(OH)_2$  affords the acyclic titanium siloxane complexes  $(C_5R_4R^1)TiCl_2(OSiBu_2O)(OH)$ . Compound  $(C_5H_4Me)TiCl_3$  gives the titanium siloxane product  $[(C_5H_4Me)TiCl(OSiB_2O)]_2$  containing an eight-membered  $TiOSiOTiOSiO$  ring. Compounds  $(C_5R_4R^1)TiF_3$  ( $R = R^1 = Me$ ;  $R = Me, R^1 = Et$ ;  $R = H, R^1 = Me$ ) react with  $SiBu_2(OSnMe_3)_2$  leading to the analogous fluoro derivative  $[(C_5R_4R^1)TiF(OSiBu_2O)]_2$ . By contrast, the reactions of  $(C_5R_4R^1)TiCl_3$  with  $SiBu_2(OSnMe_3)_2$  yield  $(C_5R_4R^1)TiCl_2(OSiBu_2OSnMe_3)$  ( $R = Me, R^1 = Et$ ) or  $[(C_5H_4Me)TiCl(OSiBu_2O)]_2$  ( $R = H, R^1 = Me$ ) (Scheme 359). The crystal structures of two cyclic titanium derivatives  $[(C_5Me_4Et)TiF(OSiBu_2O)]_2$  and  $[(C_5H_4Me)TiF(OSiBu_2O)]_2$  have been determined (Figure 18).<sup>881</sup>



**Figure 18** Molecular structure of complex  $[(C_5Me_4Et)TiF(OSiBu_2O)]_2$  (reproduced by permission of the Royal Society of Chemistry from *J. Chem. Soc., Dalton Trans.*, **1995**, 2453).

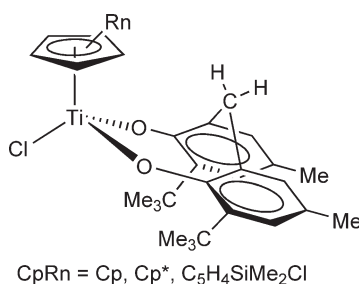
Polydentate alkoxo ligands exhibit high negative charge, suitable to stabilize high oxidation states of electropositive metals. Rigidity and chelating properties may also prevent secondary reactions. Examples are dialkoxo complexes shown in [Scheme 360](#), synthesized from the corresponding titanium trichlorides with the lithium salt of the diol. The molecular structures of the Cp and Cp\* compounds have been determined by X-ray crystallography. DFT calculations are performed in order to elucidate the energies and geometries for these compounds. Upon addition of MAO, the bisphenoxo complexes are active in the polymerization of  $\alpha$ -olefins.<sup>882</sup>

Titanium complexes with chelating alkoxo ligands Cp\*Ti(O<sub>2</sub>Bz)(OBzOH) and Cp\*Ti(Me)(OCH<sub>2</sub>)<sub>2</sub>py have been synthesized by the reaction of Cp\*TiMe<sub>3</sub> with 2-hydroxybenzyl alcohol (HO)<sub>2</sub>Bz and 2,6-pyridinedimethanol (HOCH<sub>2</sub>)<sub>2</sub>py, respectively.<sup>883</sup>

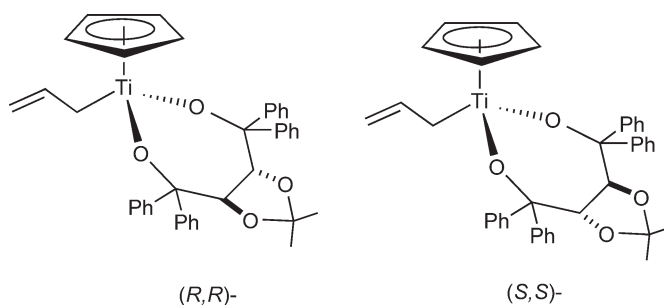
Chiral diolato titanium allyls ([Scheme 361](#)) have been used in the synthesis of (+)-sedamine in an 11 step procedure in which the allyltitanation reaction is the key step.<sup>884</sup> The analogous chiral crotyltitanium compound ([Scheme 362](#)) directs the nucleophilic addition to the *Si*-face of aldehydes to give a mixture of diastereomeric homoallylic alcohols.<sup>885,886</sup>

Examples of chiral Cp titanium complexes containing dialkoxo ligands, including fluoro derivatives, are shown in [Scheme 363](#). The fluoro ligands might add catalytic properties to the compounds.<sup>887</sup>

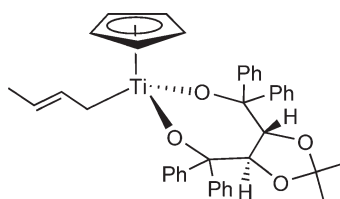
The binuclear titanium complex shown in [Scheme 364](#), supported by chiral diolato ligands, has been prepared as yellow crystals by the reaction of Cp\*TiCl<sub>3</sub> with the corresponding diol in the presence of NEt<sub>3</sub> in toluene at room temperature and its molecular structure determined by X-ray diffraction.<sup>888</sup>



**Scheme 360**

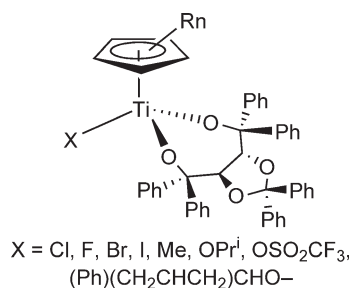


**Scheme 361**

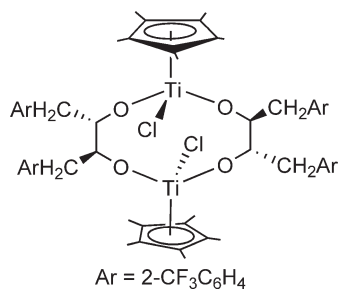


**Scheme 362**



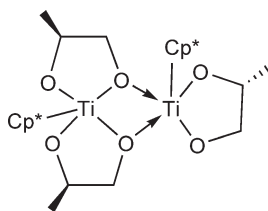


Scheme 363

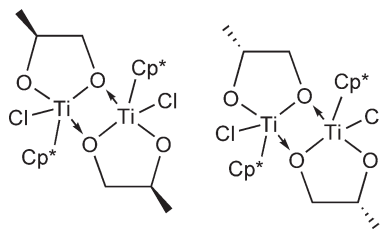


Scheme 364

Complex [Cp<sup>\*</sup>Ti]<sub>2</sub>(1,2-propanediolato)<sub>3</sub> (Scheme 365) has been prepared by treatment of Cp<sup>\*</sup>TiMe<sub>3</sub> with 1,2-propanediol with liberation of methane. The X-ray crystal structure shows an unsymmetrical bridge between a formally anionic Cp<sup>\*</sup>Ti(1,2-propanediolato)<sub>2</sub> and a cationic Cp<sup>\*</sup>Ti(1,2-propanediolato) subunit. Reaction of Cp<sup>\*</sup>TiCl<sub>3</sub> with 1,2-propanediol in the presence of an excess of pyridine affords the binuclear compound [Cp<sup>\*</sup>TiCl(1,2-propanediolato)]<sub>2</sub>, characterized by X-ray diffraction (Scheme 366). Under the reaction conditions, this compound is apparently not completely stable and after prolonged period of time it evolves to a new trinuclear species containing two “Cp<sup>\*</sup>TiCl(1,2-propanediolato)” subunits connected by a bridging “Ti(1,2-propanediolato)<sub>2</sub>” fragment as deduced by crystallographic characterization. The chloro complex [Cp<sup>\*</sup>TiCl(1,2-propanediolato)]<sub>2</sub> gives an active catalyst for the syndiotactic polymerization of styrene upon treatment with excess MAO in toluene solution.<sup>889</sup>



Scheme 365



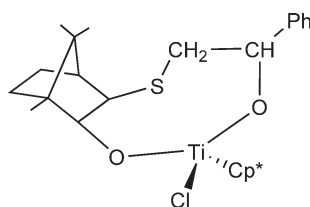
Scheme 366

The chelating diolato compound  $\text{Cp}^*\text{Ti}(\text{O}_2\text{C}_{18}\text{H}_{24}\text{S})\text{Cl}$  (Scheme 367) has been synthesized by treatment of the corresponding diol with  $\text{Cp}^*\text{TiCl}_3$  in the presence of  $\text{NEt}_3$ . Its molecular structure has been determined by X-ray diffraction methods.<sup>890</sup>

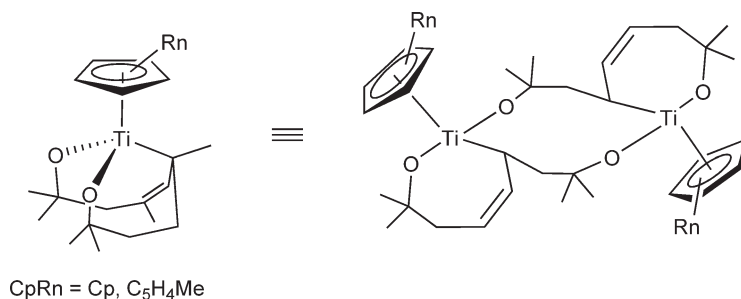
Low-valent titanium pentadienyl complexes are known and reactions of these compounds with unsaturated organic molecules have been explored.<sup>430</sup> The pentadienyl titanium(II) complexes  $\text{Cp}'\text{Ti}(\text{C}_5\text{H}_7)(\text{PMe}_3)$  ( $\text{Cp}' = \text{Cp}, \text{C}_5\text{H}_4\text{Me}$ ) react with acetone under coupling of the ketone and the pentadienyl ligand to give the diolates shown in Scheme 368. Crystallographic studies confirm the  $\eta^1$ -allyl mode,  $\text{Cp}'\text{Ti}(\sigma\text{-allyl})(\text{OR})_2$ , in the isolated dimer. The analogous compound  $\text{Cp}'\text{Ti}(2,4\text{-C}_7\text{H}_{11})(\text{C}_3\text{H}_6\text{O})_2$  is monomeric.<sup>343</sup>

Complexes  $\text{Cp}'\text{Ti}(\text{O}_3\text{C}_6\text{H}_9)$  containing the *cis*-1,3,5-cyclohexanetrialkoxo ligand have been synthesized by the reaction of the corresponding trichloro compound with *cis*-1,3,5-cyclohexanetriol in the presence of 3 equiv. of triethylamine (Scheme 369). Structure determination reveals the adamantane-like cage structure to be slightly distorted. The complexes are stable to dry air and show kinetic stability to alcohol exchange with 3 molar equiv. of ethanol. A very large excess of ethanol, or the more acidic phenol, overcomes this kinetic barrier and displaces the triol.<sup>891,892</sup>

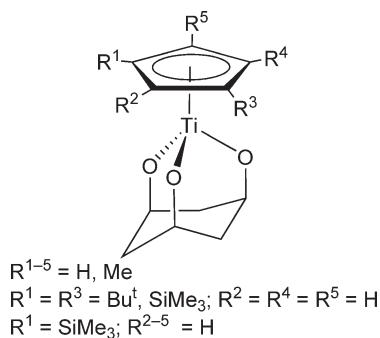
$\text{Cp}^*\text{Ti}(\text{O}-2,6\text{-Me}_2\text{C}_6\text{H}_3)\text{Cl}_2$  reacts with dilithium salt  $(\text{LiOSiPh}_2)_2\text{O}$  to give the titanatrisiloxane ring compound  $\text{Cp}^*\text{TiCl}(\text{OSiPh}_2\text{OSiPh}_2\text{OSiPh}_2\text{O})$  (Scheme 370). The molecular structure reveals an unusual butterfly-like conformation for the central eight-membered  $\text{TiSi}_3\text{O}_4$  ring. This is a product of siloxane chain expansion, presumably the



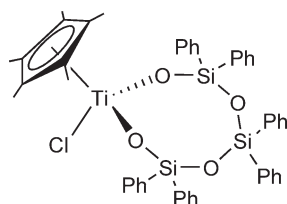
Scheme 367



Scheme 368



Scheme 369

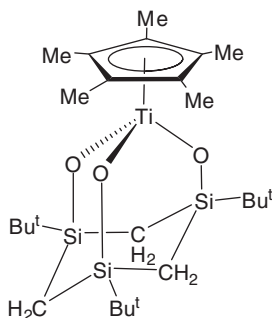


Scheme 370

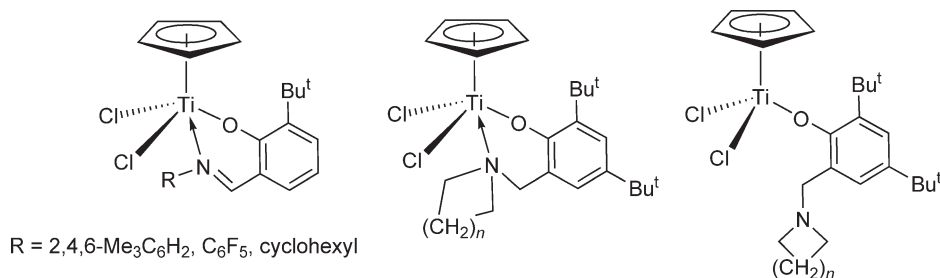
consequence of ring strain in the titanadisi-oxane system.<sup>893</sup>  $\text{Cp}^*\text{TiCl}_3$  reacts with *cis-cis*-[ $\text{Bu}^t\text{Si}(\text{OH})\text{--CH}_2$ ]<sub>3</sub> in hexane solution in the presence of  $\text{NEt}_3$  to give the 2,8,9-trioxa-3,5,7-trisila-1-titanaadamantane derivative (Scheme 371), the molecular structure of which has been determined by X-ray diffraction.<sup>894</sup>

The salicylaldiminato ligand (better known as phenoxo-imine) has been widely used in titanium chemistry. The compounds  $\text{CpTiCl}_2[\text{OC}_6\text{H}_3\text{--}2\text{--Bu}^t\text{--}6\text{--}(\text{HC}=\text{NR})]$  and the phenoxo-amines  $\text{CpTiCl}_2[\text{OC}_6\text{H}_2\text{--}2,4\text{--Bu}^t\text{--}6\text{--NRMe}]$  (Scheme 372) are prepared by reacting  $\text{CpTiCl}_3$  with 1 equiv. of the corresponding lithium phenoxides. The molecular structures of some of these complexes have been determined by X-ray diffraction methods. The phenoxo-imine derivatives exhibit a distorted square-pyramidal geometry for the Ti atom, with the Cp located in the apical position and an *N,O*-chelating phenoxo ligand. The coordination of phenoxo-amine ligands may be bidentate or monodentate and the bonding of these groups to the Ti center is discussed. When activated with MAO, the compounds are moderately active in ethylene and 1-hexene homopolymerizations and ethylene/1-hexene co-polymerizations. Polyethylene with a multimodal molecular weight distribution is obtained, consistent with multiple active sites.<sup>895</sup> Analogous mono-Cp phenoxo-imine complexes without bulky *ortho*-substituents have been reported and their polymerization activities studied.<sup>896</sup>

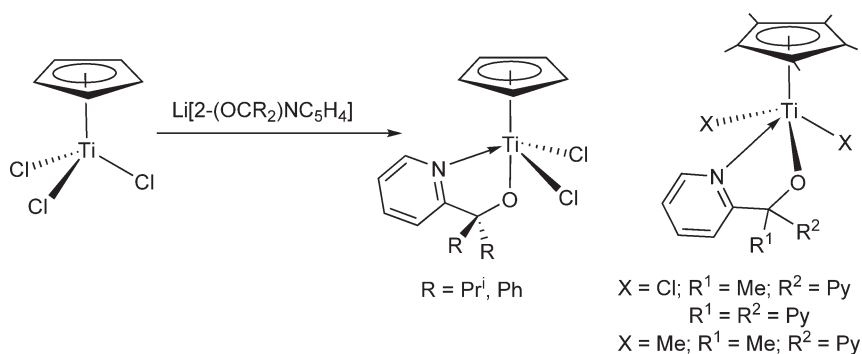
$\text{CpTiCl}_3$  reacts with  $\text{Li}[2\text{--}(\text{OCR}_2)\text{NC}_5\text{H}_4]$  to give the mono-Cp pyridylalkoxo complex  $\text{CpTiCl}_2[2\text{--}(\text{OCR}_2)\text{NC}_5\text{H}_4]$  (Scheme 373). The molecular structure of the  $\text{Pr}^I$  derivative has been determined by single crystal X-ray analysis and reveals that the Cp ligand is asymmetrically bonded and the pyridylalkoxo is a bidentate ligand. The Ti–C(ring) bond distances differ significantly ( $\Delta\text{Ti--C} = 0.0672 \text{ \AA}$ ). In the presence of MAO, toluene solutions of these complexes catalyze the polymerization of ethylene generating high molecular weight polymers with narrow molecular weight



Scheme 371



Scheme 372

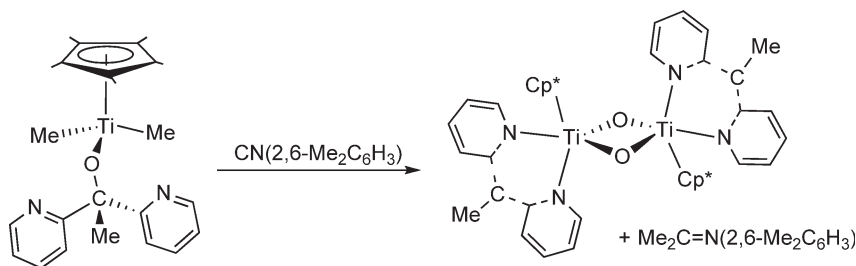


Scheme 373

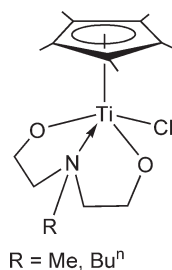
distributions.<sup>897</sup>  $\text{Cp}^*\text{TiMe}_3$  reacts with the alcohol  $\text{HOCPy}_3$  to give the monoalkoxo derivative  $\text{Cp}^*\text{TiMe}_2(\text{OCPy}_3)$ . Treatment of  $\text{Cp}^*\text{TiMe}_3$  with the ketone  $\text{Py}_2\text{CO}$  affords the analogous monoalkoxo derivative  $\text{Cp}^*\text{TiMe}_2(\text{OCMePy}_2)$  through the insertion of the ketone into the titanium–methyl bond. The dichloro complexes  $\text{Cp}^*\text{TiCl}_2(\text{OCRPy}_2)$  ( $\text{R} = \text{Me}, \text{Py}$ ) can be obtained by the reaction of  $\text{Cp}^*\text{TiCl}_3$  with  $\text{LiOCRPy}_2$ . The molecular structure, determined by X-ray diffraction methods, indicates that the pyridylalkoxo ligand is coordinated through the oxygen atom and one of the nitrogen atoms of the pyridyl groups (Scheme 373).<sup>898</sup> The bis(2-pyridyl)carbyl titanium(IV) complex  $[\text{Cp}^*\text{Ti}(\text{CMePy}_2)(\mu\text{-O})_2]$  is obtained by the reaction of  $\text{Cp}^*\text{TiMe}_2(\text{OCMePy}_2)$  with 1 equiv. of 2,6-dimethylphenylisocyanide (Scheme 374), and characterized by NMR spectroscopy and X-ray diffraction studies. The formation of the  $\mu$ -oxo complex involves the C–O bond cleavage of the alkoxo ligand with abstraction of oxygen by the titanium center.<sup>899</sup>

The synthesis of  $\text{Cp}^*\text{TiCl}_2(\text{ON})$  containing the 8-hydroxy-quinoline<sup>900</sup> and  $\text{Cp}^*\text{TiCl}(\text{OO})$  containing bisphenoxo<sup>901</sup> ligands is described. They are active for ethylene polymerization in the presence of MAO as co-catalyst.

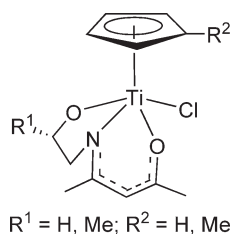
$\text{Cp}^*\text{TiCl}_3$  reacts with N-alkyl-N,N-diethanolamine, in the presence of  $\text{NEt}_3$ , to give the chloro dialkoxo amino complexes  $\text{Cp}^*\text{TiCl}[(\text{OCH}_2\text{CH}_2)_2\text{NR}]$  ( $\text{R} = \text{Me}, \text{Bu}^n$ ) (Scheme 375) as slightly air sensitive and thermally unstable compounds. In the presence of MMAO, these complexes show moderate activities in ethylene polymerization and fairly good activities in syndiotactic styrene polymerization.<sup>902</sup>



Scheme 374



Scheme 375

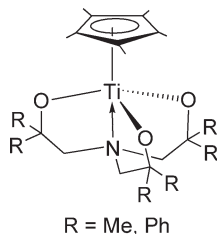


Scheme 376

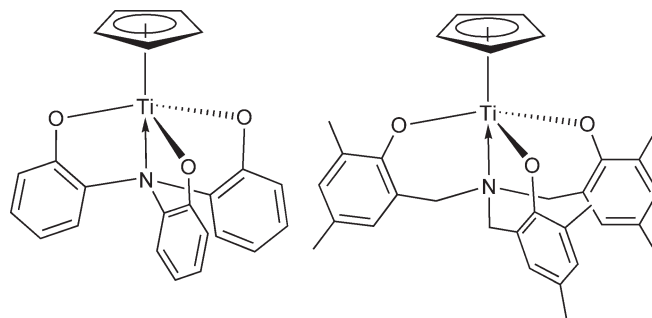
N-hydroxyalkyl-functionalized ketimines have been used as ligand precursors for mono-Cp titanium chemistry. The addition of a THF solution of the  $\beta$ -ketimines  $\text{MeC(O)CH}_2\text{C(Me)NCH}_2\text{CH(R)OH}$  to a THF solution of  $\text{Cp}^*\text{TiCl}_3$  in the presence of  $\text{NEt}_3$  leads to the formation of  $\text{TiCp}^*\text{Cl[MeC(O)CHC(Me)NCH}_2\text{CH(R)O]}$  ( $\text{Cp}^* = \text{Cp, C}_5\text{H}_4\text{Me}$ ) (Scheme 376), characterized by NMR spectroscopy and X-ray diffraction. These complexes adopt a square-pyramidal coordination geometry with the Cp occupying the apical site with the tridentate ketiminato and the chloro ligands occupying basal positions. Upon standing in THF solutions containing  $\text{NEt}_3\text{HCl}$ , the Ti–Cp bond is protolyzed.<sup>906</sup>

A series of titanatrene derivatives has been synthesized by reaction of  $\text{Cp}^*\text{TiCl}_3$  with the appropriate triethanolamine in the presence of  $\text{NEt}_3$  (Scheme 377). The X-ray structures show that the complexes are monomeric with the Cp ligand *trans* to N. In the presence of MMAO, they show very high catalytic activity for the syndiotactic polymerization of styrene.<sup>907,908</sup> The complex  $\text{Cp}^*\text{Ti[(OCH}_2\text{CH}_2)_3\text{N]}$  contains a tetradentate triethoxo–amine ligand, a “titanatrene” structure.<sup>903–905</sup>

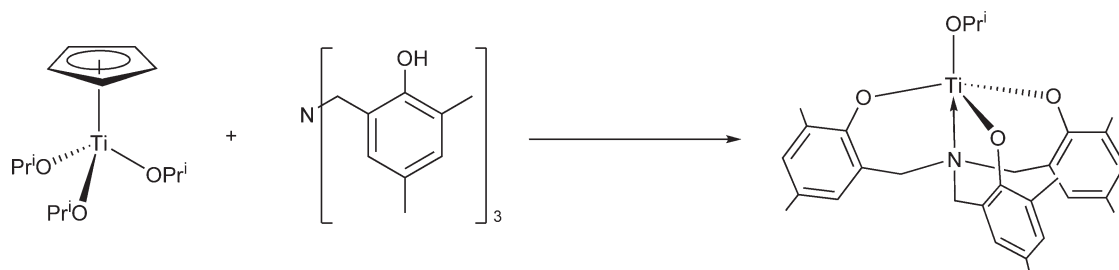
The synthesis of mono-Cp triphenoxo titanium complexes with the chelating tris(2-hydroxyphenyl)amine and tris(2-hydroxy-3,5-dimethylbenzyl)amine has been reported (Scheme 378). Electrochemical experiments provide useful information on the reduction potentials of the compounds, from which it is clear that tris(2-hydroxy-3,5-dimethylbenzyl)amine is a stronger donor than tris(2-hydroxyphenyl)amine. The chelate ring size is also important: while the reduction of complex containing tris(2-hydroxyphenyl)amine is largely reversible, the reduction of the tris(hydroxybenzyl)amine derivative is irreversible. In the presence of MAO these compounds show high activity and appreciable selectivity for the preparation of syndiotactic polystyrene.<sup>909</sup>



Scheme 377



Scheme 378



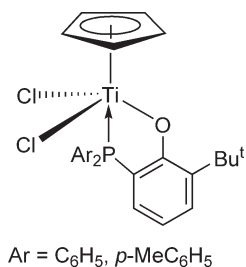
Scheme 379

$\text{Ti}(\text{OPr}^i)_4$  reacts with  $\text{NaCp}$  to afford  $\text{CpCp}(\text{OPr}^i)_3$ . The addition of tris(2-hydroxy-3,5-dimethylbenzyl)amine to this compound results in the displacement of the  $\eta^5\text{-Cp}$  ligand to give the corresponding tetraalkoxo derivative (Scheme 379). A value of  $335 \text{ kJ mol}^{-1}$  has been calculated for the  $\text{Cp-Ti}$  bond dissociation energy. This compound has catalytic activity in the bulk and solution polymerization of lactide.<sup>910</sup>

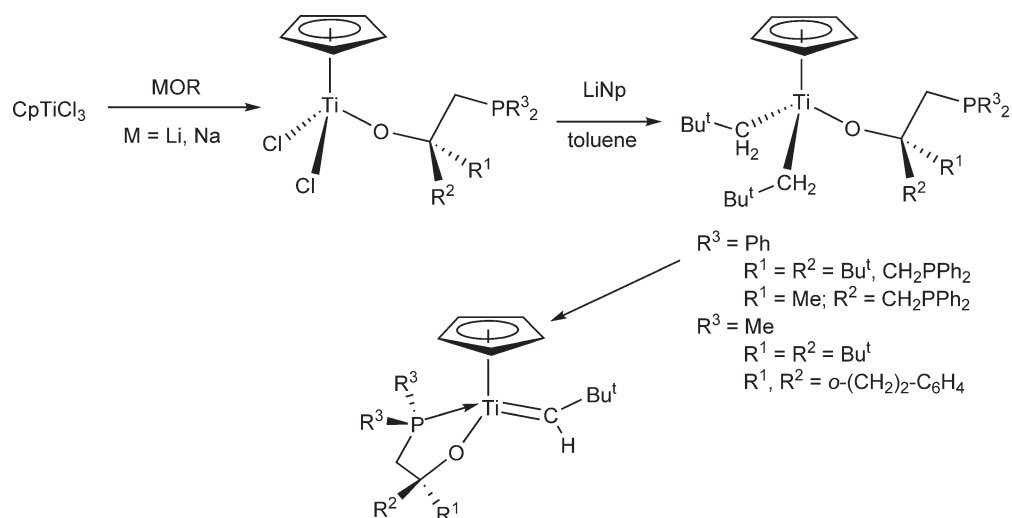
The titanium complexes bearing *o*-phosphinophenoxo ligands shown in Scheme 380 are prepared by metallation of the corresponding phenol followed by reaction with  $\text{Cp}^*\text{TiCl}_3$ . The complexes were found to be fluxional by  $^1\text{H}$  NMR analysis at low temperature. The X-ray structure shows that in the solid state the molecule is chiral at the metal center. These complexes are effective catalysts for olefin hydrogenation and imine hydrosilylation.<sup>911</sup>

Mono- $\text{Cp}$  neopentylidene complexes stabilized by bulky phosphinoalkoxo ancillary ligands are readily accessible via the corresponding dineopentyl complexes (Scheme 381). The formation of these species is assisted by the bulky  $\text{P-O}$  chelate. The parent chloro complexes can be obtained by the reaction of  $\text{Cp}^*\text{TiCl}_3$  and the lithium or sodium alkoxide. The chloro ligands can be replaced with neopentyl groups in a stepwise process to give the dineopentyl derivatives. With less bulky phosphinoalkoxy ligands a mixture of products is obtained where transmetallation reactions are observed in which the alkoxo ligand is removed from the titanium atom. Warming the dineopentyl complexes gives the alkylidene derivatives and neopentane. The phenyl-phosphino alkoxo complexes are not isolated in a pure state because the alkylidene unit reacts with the phenyl groups of the phosphine moiety in a reversible cyclometallation process (Scheme 382). The X-ray crystal structure of the cyclometallated compound has been determined. The distance for the  $\text{Ti-C}_{\text{aryl}}$  is  $2.149(4) \text{ \AA}$  and the  $\text{Ti-C}_{\text{neopentyl}}$  is  $2.120(4) \text{ \AA}$ . The  $\text{Ti-H}$  distance and the  $\text{Ti-C-H}$  angle values for the neopentyl ligand indicate the possibility of a weak  $\alpha$ -agostic interaction.<sup>912</sup> In order to avoid the *ortho*-metallation reaction, the ligand structure was modified by replacing the phenyl rings with methyl groups. This allowed the isolation of well-defined neopentylidene species suitable for structural characterization and reactivity studies. These alkylidene derivatives react with  $\alpha$ -olefins to form metallocycles, and with  $\text{CO}$  to form ketene complexes. An olefin metathesis reaction takes place on treatment with ethylene, although in low yield (Scheme 382). The structure of the alkylidene oxo-phosphino complex  $\text{Cp}^*\text{Ti}(\text{=CHBu}^t)(\text{PMe}_2\text{CH}_2\text{C}(\text{O})\text{-CMe}_2\text{-}o\text{-C}_6\text{H}_4\text{CMe}_2)$  has been determined by X-ray analysis. The  $\text{Ti}=\text{C}$  double bond distance is  $1.911(3) \text{ \AA}$  and the structure shows a  $\text{Ti}\cdots\text{H}$   $\alpha$ -agostic distortion of the alkylidene ligand with the  $\text{Ti-H}$  distance of  $2.05(5) \text{ \AA}$ . The alkylidene hydrogen resonance appears at  $\delta 12$  in the  $^1\text{H}$  NMR spectrum and the alkylidene carbon resonance is found at  $\delta 280$  in the  $^{13}\text{C}$  NMR spectrum, both signals as a doublet due to coupling to phosphorus (Figure 19).<sup>913</sup>

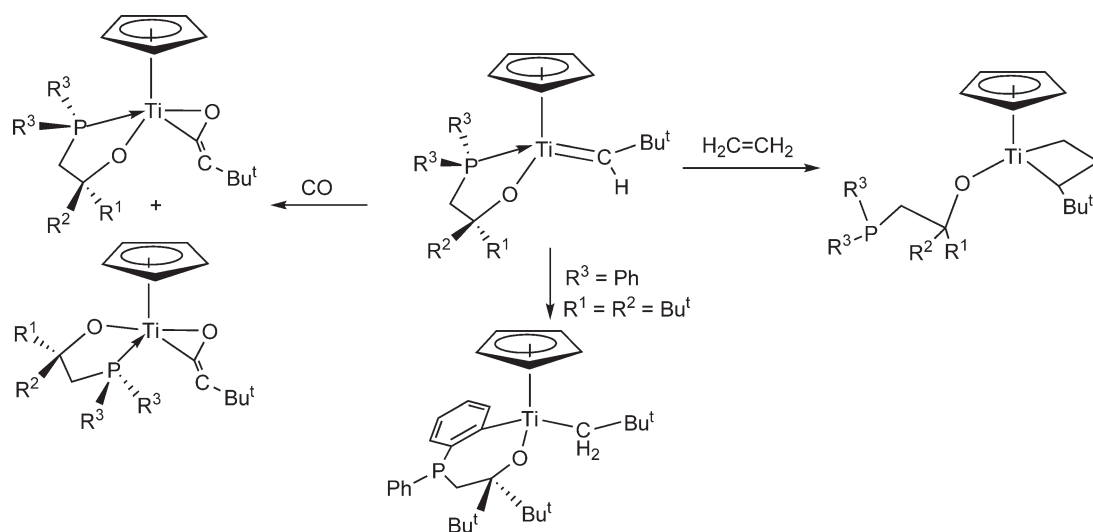
Mono- $\text{Cp}$  chloro titanium complexes containing a sulfide-bridged chelating bis(aryloxo) ligand have been synthesized and characterized (Scheme 383). The complex  $\text{Ti}(\text{tbp})\text{Cl}_2$  reacts with  $\text{LiCp}'$  ( $\text{Cp}' = \text{Cp}, \text{Cp}^*, \text{C}_5\text{H}_4\text{SiMe}_3$ ) to



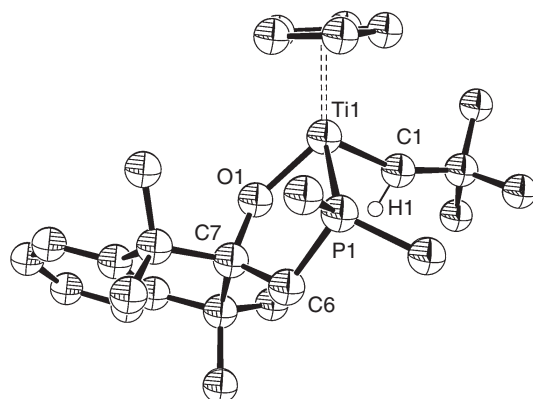
Scheme 380



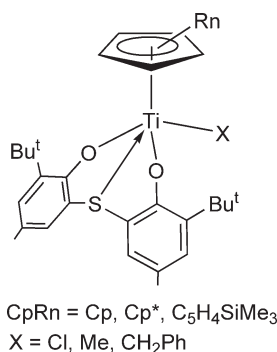
Scheme 381



Scheme 382



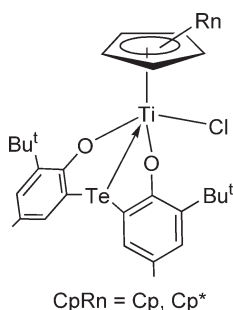
**Figure 19** Molecular structure of complex  $\text{CpTi}(\text{CHBu}^t)(\text{PMe}_2\text{-CH}_2\text{C(O)-CMe}_2\text{-}o\text{-C}_6\text{H}_4\text{CMe}_2)$  (reproduced by permission of American Chemical Society from *Organometallics*, **1995**, 14, 1278).



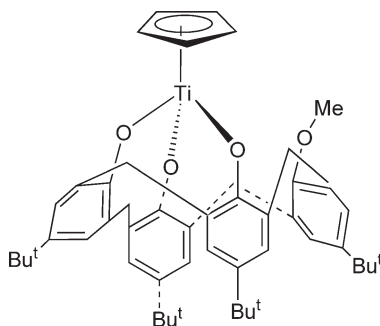
Scheme 383

give the corresponding mono-Cp chloro titanium derivatives  $\text{Cp}'\text{TiCl}[2,2'\text{-S}(\text{OC}_6\text{H}_2\text{-4-Me-6-Bu}^t)_2]$ .<sup>66</sup> Alkylation of the chloro complexes gives the methyl and benzyl derivatives  $\text{Cp}'\text{TiR}[2,2'\text{-S}(\text{OC}_6\text{H}_2\text{-4-Me-6-Bu}^t)_2]$ . The crystal structure of the chloro complex has been determined by X-ray diffraction and shows a monomeric four-legged piano stool structure with the sulfur and chloro ligands in *trans*-positions. A long titanium–sulfur bond length of 2.907(1) Å is observed.<sup>914</sup> These complexes have been used as pre-catalysts for polymerization of ethylene and to prepare syndiotactic polystyrene. They can also polymerize dienes and co-polymerize ethylene with styrene.<sup>915,916</sup> The analogous tellurium complexes  $\text{Cp}'\text{TiCl}[2,2'\text{-Te}(\text{4-Me-6-Bu}^t\text{-C}_6\text{H}_2\text{O})_2]$  ( $\text{Cp}' = \text{Cp}, \text{Cp}^*$ ) have been prepared by the reaction of the dialkoxo dilithium salt with the corresponding  $\text{Cp}'\text{TiCl}_3$ . The X-ray structure of  $\text{Cp}^*\text{TiCl}[2,2'\text{-Te}(\text{4-Me-6-Bu}^t\text{-C}_6\text{H}_2\text{O})_2]$  shows that Te atom is coordinated to Ti (Scheme 384).<sup>917</sup> The mono-Cp complexes containing the tellurium-bridged bis(aryloxo) ligand show 20–50 times higher activities than the similar methylene-bridged ligands. The coordination of tellurium is proposed to be responsible for this activity. These compounds have been studied as catalyst precursors for the polymerization of polar monomers (cyclic esters).<sup>918</sup>

The mono-Cp calix[4]arene complex shown in Scheme 385 has been synthesized by the reaction of the parent chloro compound with NaCp; the molecular structure has been determined by X-ray diffraction methods.<sup>919</sup>

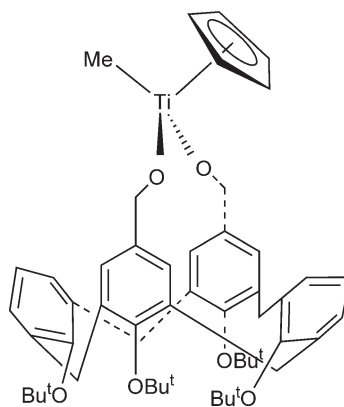


Scheme 384



Scheme 385





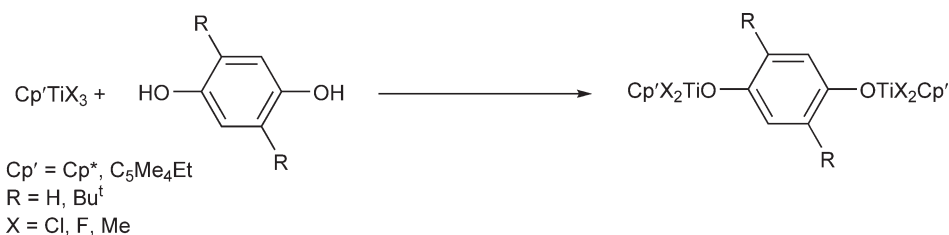
Scheme 386

The reaction of 5,17-bis(hydroxymethyl)-tetra-*n*-butoxycalix[4]arene  $[(\text{HOCH}_2)_2\text{-Bu}^n_4\text{Clx}]$  (Clx = calix[4]arene) with  $\text{Cp}^*\text{TiMe}_3$  affords the derivative  $\text{Cp}^*\text{TiMe}[(\text{OCH}_2)_2\text{-Bu}^n_4\text{Clx}]$  (Scheme 386) in quantitative yield; it was characterized by ESI-MS and NMR methods.<sup>920</sup> Reaction of *p*- $\text{Bu}^t$ -calix[6]arene with 2 equiv. of potassium metal in methanol followed by treatment with  $\text{Cp}_2\text{TiCl}_2$  affords a mononuclear mono-Cp Ti(IV) complex. The same reaction with 4 equiv. of potassium metal gives a binuclear compound. Both compounds have the same inverted double cone conformation with Cp in one of the cavities.<sup>921</sup> Lithiation of *p*- $\text{Bu}^t$ -calix[6]arene followed by reaction with  $\text{Cp}_2\text{TiCl}_2$  produces a tetranuclear mono-Cp Ti(IV) complex where a single calix[4]arene in a cone conformation provides O-phenoxo coordination to four titanium atoms, with additional  $\mu$ -oxo bridging between titanium centers in an eight-membered ring.<sup>922</sup>

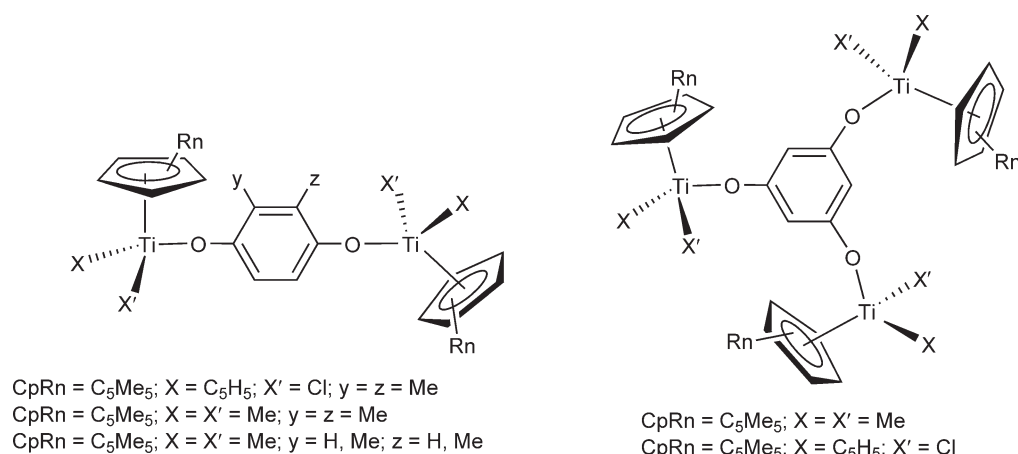
Compounds structurally characterized as  $\text{Cp}'\text{X}_2\text{Ti-OC}_6\text{H}_4\text{-}^t\text{Bu}_n\text{O-TiX}_2\text{Cp}'$  shown in Scheme 387 have been synthesized by the reaction of  $\text{Cp}'\text{TiCl}_3$  with hydroquinones. Such compounds are also formed upon treatment of titanium(III) precursors with benzoquinone.<sup>923</sup> The mono-Cp bi- and trimetallic complexes  $[\text{Cp}^*\text{TiX}_2]_2[\mu\text{-1,4-O}(\text{C}_6\text{H}_2\text{YZ})\text{O}]$  and  $[\text{Cp}^*\text{TiX}_2]_3[(\mu_3\text{-1,3,5-C}_6\text{H}_3\text{O}_3)]$  (Scheme 388) have been synthesized by different synthetic methods. The structure of  $[\text{Cp}^*\text{TiMe}_2]_2[\mu\text{-1,4-O}(\text{C}_6\text{H}_2\text{Me}_2)\text{O}]$  has been determined by X-ray diffraction.<sup>924</sup>

Analogous Cp derivatives have been described. The mononuclear aryloxo derivatives  $\text{Cp}'\text{TiCl}_2[\text{OC}_6\text{H}_3(\text{OMe})(\text{C}_3\text{H}_5)]$  are synthesized by the reaction of  $\text{Cp}'\text{TiCl}_3$  with the corresponding alcohol or alkoxo lithium salt (Scheme 388). Cyclic voltammetric studies for these complexes have been described. The dinuclear complexes show two irreversible overlapped reduction waves, while the mononuclear derivatives exhibit a reversible wave. The reduction peaks are broad and poorly defined at potentials between  $-1.34$  and  $1.68$  V, indicating that the titanium center in the mononuclear complexes is slightly more electron rich than in the homodinuclear compounds.<sup>925</sup> Hydrosilylation of 4-allyl-2-methoxyphenol (eugenol) with silane dendrimers followed by reaction with  $\text{Cp}'\text{TiCl}_3$  provides an effective route for the attachment of Cp titanium complexes to the dendritic periphery (Scheme 389).<sup>926</sup>

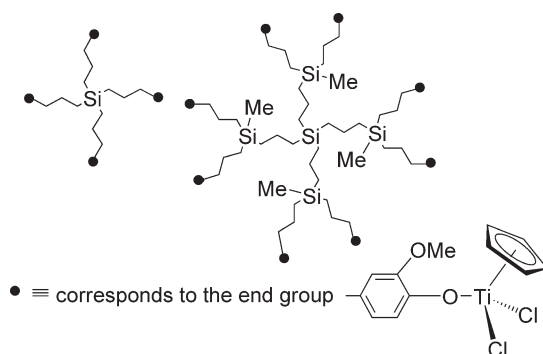
Reactions of  $\text{Cp}'\text{TiCl}_2\text{Me}$  or  $\text{Cp}'\text{TiMe}_3$  with dendrimers of first, second, or fourth generations afford the corresponding organometallic titanium-decorated dendrimers (Scheme 390). The dendritic framework remains chemically inert and spectroscopically unchanged by the modifications in the periphery, while the organometallic unit shows spectroscopic and chemical properties similar to the mononuclear counterparts.<sup>927</sup>



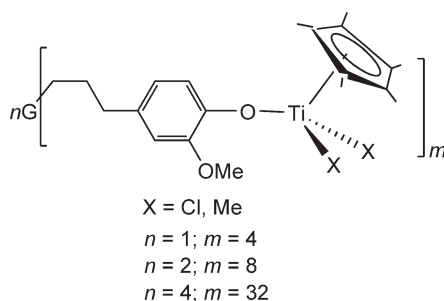
Scheme 387



Scheme 388



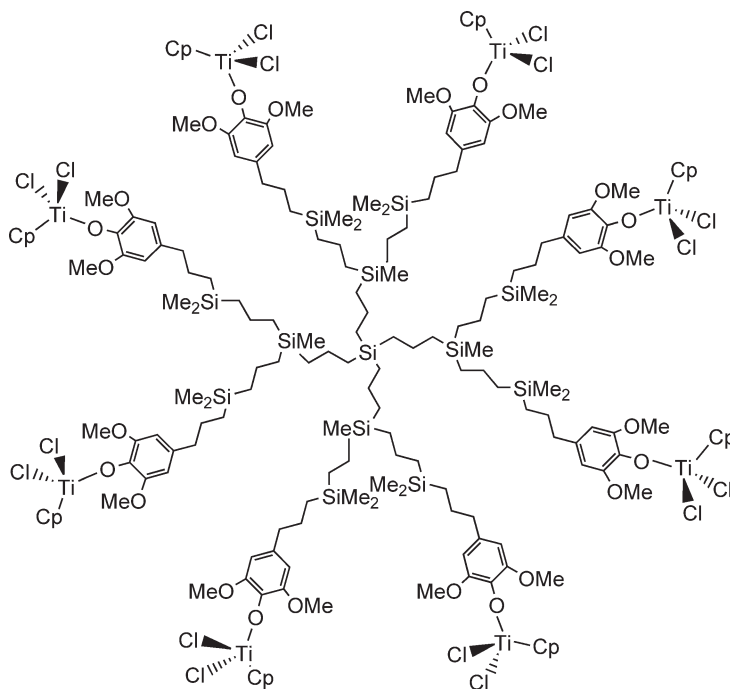
Scheme 389



Scheme 390

The synthesis of carbosilane dendrimers containing peripheral “ $\text{CpTiCl}_2$ ” units has been reported. Treatment of  $\text{CpTiCl}_3$  with 4-allyl-2,6-dimethoxyphenol gives the corresponding aryloxo complex  $\text{CpTi}(\text{OR})\text{Cl}_2$ . Hydrosilylation of the allyl group of 4-allyl-2-methoxyphenol or 4-allyl-2,6-dimethoxyphenol with  $\text{SiHET}_3$  and subsequent reaction with  $\text{CpTiCl}_3$  leads to the analogous mononuclear alkoxo compounds. This synthetic procedure has been used as a model for the preparation of new peripheral carbosilane metallodendrimers (Scheme 391).<sup>928</sup>

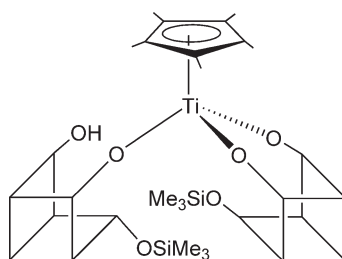
Titanium catalysts immobilized on silica have been modeled using siloxane compounds. Corner capping of the silsesquioxane framework gives the tetrameric derivative  $(\text{C}_5\text{H}_4\text{Me})_4\text{Ti}_4[(\text{SiBu}^t)_4\text{O}_{12}]$ .<sup>929</sup>  $\text{Cp}_2\text{TiCl}_2$  reacts with the incompletely condensed silsesquioxane  $\text{Cy}_7\text{Si}_7\text{O}_9(\text{OH})_2(\text{OSiMe}_3)$  to give the binuclear  $\mu$ -oxo derivative



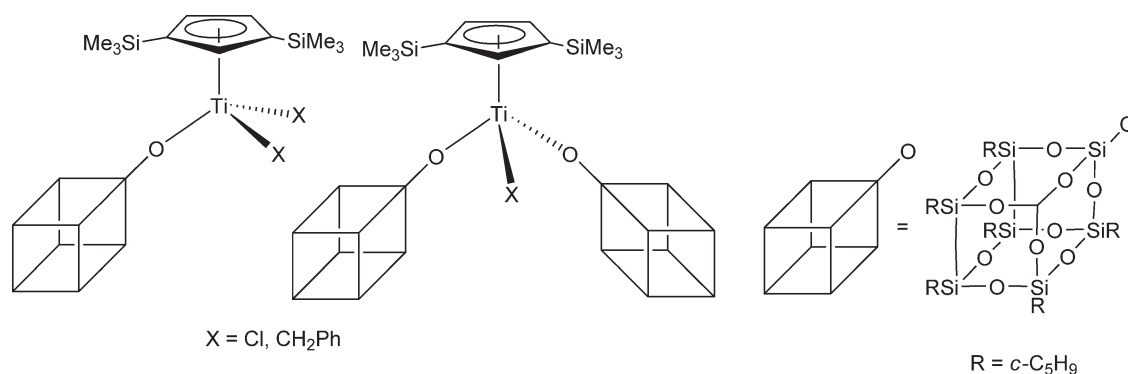
Scheme 391

$[\text{Cp}^*\text{Ti}(\text{C}_7\text{Si}_7\text{O}_{11})(\text{OSiMe}_3)]_2(\mu\text{-O})$ , while the same reaction using  $\text{Cp}^*_2\text{TiCl}_2$  affords the trinuclear compound  $\text{Cp}^*_2\text{Ti}_3\text{O}_3[(\text{C}_7\text{Si}_7\text{O}_{11})(\text{OSiMe}_3)]_2$ . The molecular structures of these titanium silsesquioxane derivatives have been determined by X-ray diffraction.<sup>930</sup> The monosilylated silsesquioxane  $\text{C}_7\text{Si}_7\text{O}_9(\text{OH})_2(\text{OSiMe}_3)$  reacts with the fulvene titanium(III) complex  $\text{Cp}^*\text{Ti}(\text{C}_5\text{Me}_4\text{CH}_2)$  to give a mono-Cp silsesquioxane titanium(IV) compound  $\text{Cp}^*\text{Ti}[\text{C}_7\text{Si}_7\text{O}_9(\text{O})_2(\text{OSiMe}_3)][\text{C}_7\text{Si}_7\text{O}_9(\text{O})(\text{OH})(\text{OSiMe}_3)]$  (Scheme 392). The X-ray diffraction analysis reveals the presence of two silsesquioxane molecules bonded in different ways to the titanium center. This compound can be considered as a molecular model for a Ti olefin polymerization catalyst immobilized on a silica surface. In these reactions, cyclopentadiene is eliminated, involving a  $\text{Ti-Cp}^*$  bond cleavage.<sup>931</sup>

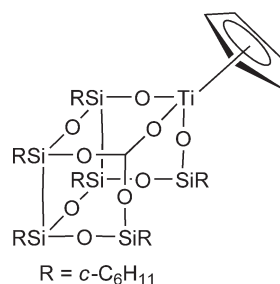
Reactions of  $[1,3\text{-C}_5\text{H}_3(\text{SiMe}_3)_2]\text{TiCl}_3$  with the lithium or thallium salts  $\text{M}[(\text{-C}_5\text{H}_9)_7\text{Si}_8\text{O}_{13}]$  or  $\text{TiOSiPh}_3$  give either the dichloro or the monochloro derivatives  $[\text{C}_5\text{H}_3(\text{SiMe}_3)_2]\text{TiCl}_2(\text{OR})$  and  $[\text{C}_5\text{H}_3(\text{SiMe}_3)_2]\text{TiCl}(\text{OR})_2$  [ $\text{OR} = (\text{-C}_5\text{H}_9)_7\text{Si}_8\text{O}_{13}$ ,  $\text{OSiPh}_3$ ]. The protonolysis of  $[\text{C}_5\text{H}_3(\text{SiMe}_3)_2]\text{TiR}_3$  ( $\text{R} = \text{Me}$ ,  $\text{CH}_2\text{Ph}$ ) with the silanol  $(\text{-C}_5\text{H}_9)_7\text{Si}_8\text{O}_{12}(\text{OH})$  or  $\text{HOSiPh}_3$  yields the corresponding monoalkyl or bis-alkyl silsesquioxane and siloxide derivatives (Scheme 393). When activated with MAO or  $\text{B}(\text{C}_6\text{F}_5)_3$  these complexes are active catalysts for the polymerization of ethylene.<sup>17,932–934</sup> The silsesquioxo titanium derivative  $\text{TiCp}[\text{O}_{12}\text{Si}_7(\text{-C}_6\text{H}_{11})]$  (Scheme 394)<sup>203</sup> is an active and robust homogeneous catalyst for alkene epoxidation; its immobilization into an MCM-41 mesoporous silicate has been reported.<sup>935</sup>



Scheme 392



Scheme 393



Scheme 394

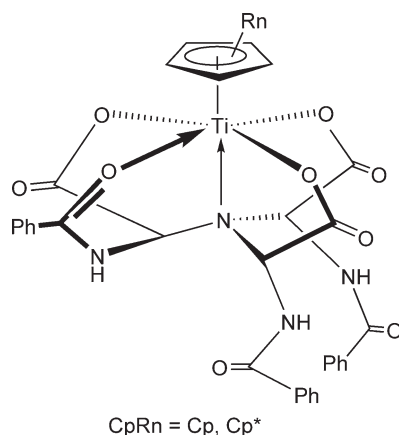
Metallation of incompletely condensed silsesquioxanes of the type  $\text{R}_7\text{Si}_7\text{O}_9[\text{O}(\text{SiR}^1\text{O}_2)_n]\text{OH}$  ( $R = n\text{-C}_5\text{H}_9, n\text{-C}_6\text{H}_{11}$ ;  $R^1 = \text{Me}, \text{Ph}$ ;  $n = 1\text{--}4$ ) with  $[\text{1,3-C}_5\text{H}_3(\text{SiMe}_3)_2]\text{Ti}(\text{CH}_2\text{Ph})_3$  in 1 : 1 molar ratio affords the corresponding monomeric dibenzyl titanasilsesquioxane derivatives, isolated as viscous oils after evaporation of the hydrocarbon solvents. Attempts to force the reaction with a second equivalent of silsesquioxane failed. The catalytic activities of the cationic complexes formed by treatment of the neutral benzyl complex with  $\text{B}(\text{C}_6\text{F}_5)_3$  or  $\text{Ph}_3\text{C}[\text{B}(\text{C}_6\text{F}_5)_4]$  have been tested in 1-hexene polymerization in order to study the effect of the siloxane functionalities in the proximity of the active site on the highly Lewis-acidic titanium center. Comparison of the catalytic activity with analogous titanium systems based on the closed  $\text{R}_7\text{Si}_8\text{O}_{12}(\text{OH})$  silanol leads to the conclusion that the presence of a neighboring siloxane ring causes considerable retardation of the polymerization process but improves the stability of the catalyst.<sup>936</sup>

The vinyl silsesquioxane trisilanol  $(\text{H}_2\text{C}=\text{CH})(n\text{-C}_6\text{H}_{11})_6\text{-Si}_7\text{O}_9(\text{OH})_3$  reacts with  $\text{Cp}^*\text{TiCl}_3$  to give the compound  $\text{Cp}^*\text{Ti}[(\text{H}_2\text{C}=\text{CH})(n\text{-C}_6\text{H}_{11})_6\text{-Si}_7\text{O}_9]$ , characterized by  $^{13}\text{C}$  NMR spectroscopy, which can be immobilized over methylhydrosiloxane–dimethylsiloxane co-polymers to form organosiliceous materials. The catalytic activity of these materials in the epoxidation of cyclooctene has been studied.<sup>937</sup>

Mono-Cp titanium binuclear complexes with trisiloxane bridges have been synthesized. In the presence of MMAO, these complexes initiate the polymerizations of ethylene and styrene.<sup>938</sup>

Macrocyclic mono-Cp titanium(IV) complexes with peptide-derived ligands coordinated to the titanium atom have been described by the reaction of the pseudo-nonapeptide with 3 equiv. of NaOMe in  $\text{CH}_2\text{Cl}_2$  and subsequent reaction with  $\text{Cp}'\text{TiCl}_3$  ( $\text{Cp}' = \text{Cp}, \text{Cp}^*$ ) (Scheme 395). The molecular structure of the  $\text{Cp}^*$  derivative has been determined by X-ray diffraction and shows a distorted pseudo-octahedral titanium environment.<sup>939</sup>

Mono-Cp alkoxo Ti derivatives have been extensively used in olefin polymerizations and co-polymerizations. Ligand modifications of the Cp fragment in this type of complexes give efficient catalysts for ethylene and syndiospecific styrene polymerizations.<sup>480,940–943</sup> Mono-Cp titanium complexes containing phenoxo ligands having different electron donor properties  $\text{Cp}^*\text{TiCl}_2(\text{OC}_6\text{H}_4\text{X}-p)$  ( $X = \text{H}, \text{Cl}, \text{Bu}^t, \text{OMe}, \text{NO}_2$ ) have been studied as catalytic systems for styrene polymerizations in the presence of MAO. These catalysts have been investigated by polarography and EPR studies to evaluate their Ti(III) content.<sup>941</sup>



Scheme 395

Styrene polymerizations with  $\text{Cp}^*\text{TiCl}_2(\text{OPr}^i)/\text{MAO}$ <sup>944</sup> and  $\text{Cp}^*\text{TiCl}_2(\text{OR})/\text{MAO}$ ,  $\text{BF}_3 \cdot \text{OEt}_2$  ( $\text{R} = \text{cyclohexyl}$ ,  $\text{CH}_2\text{Ph}$ ,  $p\text{-Bu}^t\text{C}_6\text{H}_4$ ,  $\text{Bu}^n$ ,  $\text{Bu}^i$ ,  $\text{CH}_2\text{CH}=\text{CH}_2$ ) have been described.<sup>859,945,946</sup> The syndiospecific polymerization of styrene catalyzed by dialkoxo complexes  $\text{Cp}^*\text{TiCl}_2(\text{OR})$  has been studied.<sup>854,947</sup>

The co-polymerization of ethylene with styrene using  $(\text{C}_5\text{H}_5\text{Me}_2)/\text{TiCl}_2(\text{O}-2,6\text{-Pr}^i_2\text{C}_6\text{H}_3)$  in the presence of MAO has been explored.<sup>779</sup> The co-polymerization of ethylene with 1-hexene by  $\text{Cp}^*\text{TiX}_2(\text{O}-2,6\text{-Pr}^i_2\text{C}_6\text{H}_3)$  ( $\text{Cp}^* = \text{Cp}$ ,  $\text{Cp}^*$ ,  $1,3\text{-Bu}^t_2\text{C}_5\text{H}_3$ ,  $\text{C}_5\text{H}_4\text{Bu}^t$ ,  $1,3\text{-Me}_2\text{C}_5\text{H}_3$ ) and  $\text{Cp}^*\text{TiX}_2(\text{O}-2,6\text{-Me}_2\text{C}_6\text{H}_3)$  ( $\text{Cp}^* = \text{Cp}^*$ ,  $1,3\text{-Bu}^t_2\text{C}_5\text{H}_3$ ), in the presence of MAO as co-catalyst, has been studied.<sup>846</sup>  $\text{Cp}^*\text{TiX}_2(\text{O}-2,6\text{-Pr}^i_2\text{C}_6\text{H}_3)$  ( $\text{X} = \text{Cl}$ ,  $\text{Me}$ ) exhibit high catalytic activity for 1-hexene polymerization in the presence of MAO and borate salts.<sup>948,949</sup>

Syndiotactic polystyrene has been prepared using catalyst systems containing  $\text{Cp}^*\text{TiR}(\text{OTf})_2/\text{MAO}$  ( $\text{R} = \text{Me}$ ,  $\text{OMe}$ ,  $\text{O}-2,4,6\text{-Me}_3\text{C}_6\text{H}_2$ ;  $\text{OTf}$ ) and  $[\text{Cp}^*\text{Ti}(\mu\text{-OH})(\mu\text{-OTf})(\text{OTf})_2]/\text{MAO}$ .<sup>950</sup>

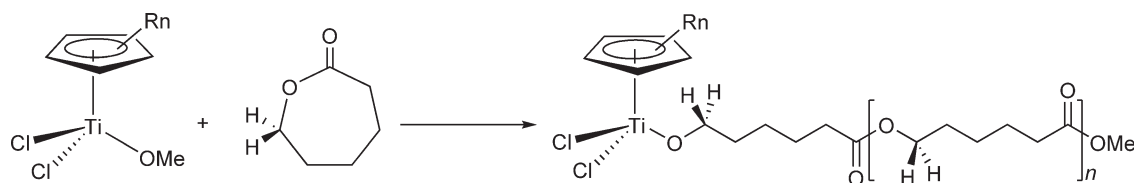
Atactic polypropylene has been synthesized with homogeneous catalytic systems based on mono-Cp trialkoxo titanium complexes activated by MAO.<sup>951</sup> Syndiotactic polystyrene has been synthesized with different mono-Cp trialkoxo titanium derivatives activated by MAO and  $\text{AlMe}_3$ , and the catalytic efficiency has been compared with bis- $\text{Cp}'$  titanium catalysts.<sup>952</sup> The titanium ligands affect both catalytic activity and stereoregularity of the polypropylene obtained. For the  $\text{Cp}^*\text{Ti}(\text{OPr}^n)_3/\text{MAO}$  system, factors influencing the propylene polymerization, such as temperature,  $\text{Al}/\text{Ti}$  molar ratio, and monomer pressure, have been studied.

Substituted styrenes with linear alkyl substituents ( $\text{C}_6$  to  $\text{C}_{12}$ ) at the *para*-position on the phenyl ring have been polymerized using  $\text{Cp}^*\text{Ti}(\text{OMe})_3/\text{MAO}$  as catalyst,<sup>953</sup> and the kinetics of the syndiospecific slurry polymerization of styrene in heptane with this catalyst has been investigated.<sup>954</sup>

The syndiospecific polymerization of styrene has been investigated with the compound  $[\text{Cp}^*\text{Ti}(\text{OCOCF}_3)_2]_2(\mu\text{-O})$  and the  $\eta^5$ -octahydrofluorenyl (*ohf*) titanium trialkoxo derivatives (*ohf*) $\text{Ti}(\text{OR})_3$  ( $\text{R} = \text{Me}$ ,  $\text{COC}_6\text{F}_5$ ,  $\text{COCF}_3$ ) and (*ohf*) $\text{Ti}(\text{OMe})_2(\text{OCOCF}_3)$  in the presence of relatively low amounts of MAO and  $\text{AlBu}^i_3$ , and the results compared to  $\text{Cp}^*\text{TiCl}_3$  and  $\text{Cp}^*\text{Ti}(\text{OMe})_3$ .<sup>457</sup> Highly syndiotactic polystyrene is prepared using catalytic systems containing  $\text{Cp}^*\text{TiMe}(\text{OTf})_2$ ,  $\text{Cp}^*\text{Ti}(\text{OMe})(\text{OTf})_2$ ,  $\text{Cp}^*\text{Ti}(\text{O}-2,4,6\text{-Me}_3\text{C}_6\text{H}_2)(\text{OTf})_2$ , or  $[\text{Cp}^*\text{Ti}(\text{OTf})(\mu\text{-OH})(\mu\text{-OTf})_2]$ .<sup>955</sup>

The trialkoxo compound  $\text{Cp}^*\text{Ti}(\text{OBz})_3$  is activated with several kinds of MMAO, containing different amounts of residual  $\text{AlMe}_3$ , to produce catalysts for the synthesis of branched polyethylene. The influence of the residual  $\text{AlMe}_3$  content in MMAO on the formation of the active species is studied. Reduction of  $\text{Ti}(\text{IV})$  to give more favorable  $\text{Ti}(\text{III})$  and  $\text{Ti}(\text{II})$  active species for the ethylene polymerization is suggested. The branch length is mainly controlled by the polymerization temperature, and its distribution is mainly dependent on the catalyst structure.<sup>956–958</sup> The syndiospecific polymerization of styrene, the atactic polymerization of propene,<sup>942,959,960</sup> the stereoregular polymerizations of 1-butene<sup>961</sup> and norbornene,<sup>962</sup> and the co-polymerizations of styrene/ethylene and styrene/1-butene<sup>963–966</sup> have also been described using this catalytic system.  $\text{Cp}^*\text{Ti}(\text{OBz})_3/\text{MMAO}$  catalyzes the sequential block co-polymerization of styrene and ethylene,<sup>967</sup> while  $\text{Cp}^*\text{TiX}_3$  ( $\text{X} = \text{BzO}$ ,  $p\text{-MeO}-\text{H}_5\text{C}_6\text{O}$ ) in the presence of MAO catalyzes the polymerization of butadienes.<sup>452</sup>

The allyloxo complex  $\text{Cp}^*\text{Ti}(\text{OCH}_2\text{-CH}=\text{CH}_2)_3$  has been used as a catalyst precursor for the synthesis of polybutene-1 in the presence of MAO as co-catalyst.<sup>968</sup> Mono-Cp trialkoxo complexes with different sterically demanding substituents have been used as pre-catalysts for the preparation of syndiotactic polystyrene in water.<sup>969</sup>



Scheme 396

Mono-Cp monoalkoxo titanium derivatives in the absence of MAO have been used as structurally well-defined mononuclear initiators for the ring-opening polymerization of four-, six-, and seven-membered lactones.<sup>970</sup> The ring-opening polymerization of  $\epsilon$ -caprolactone with living characteristics is initiated by  $\text{CpTiCl}_2(\text{OCH}_3)$  in toluene solution or in bulk at  $110^\circ\text{C}$  over a period of several hours. The substitution pattern of the Cp ligand exerts a significant effect on the ring-opening process. When a series of substituted complexes  $(\text{C}_5\text{H}_{5-n}\text{R}_n)/\text{TiCl}_2(\text{OCH}_3)$  were examined for this ring-opening reaction, both the  $\text{SiMe}_3$  and  $\text{Bu}^t$  substituents were found to enhance the reactivity (Scheme 396).<sup>971</sup>

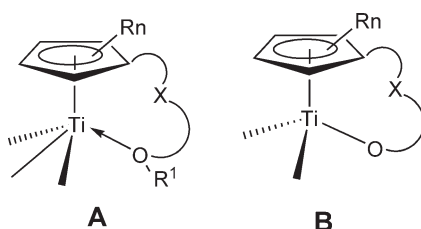
Stereoselective aldol reactions of menthyl acetate enolates, and allylations with benzaldehyde mediated by mono-Cp monochloro bis-alkoxo chiral titanium complexes have been reported.<sup>972</sup>

Allyltitanium compounds and Ti enolates derived from mono-Cp chloro titanium complexes with two chiral alkoxo ligands add to aldehydes with high enantioface discrimination.<sup>973</sup>

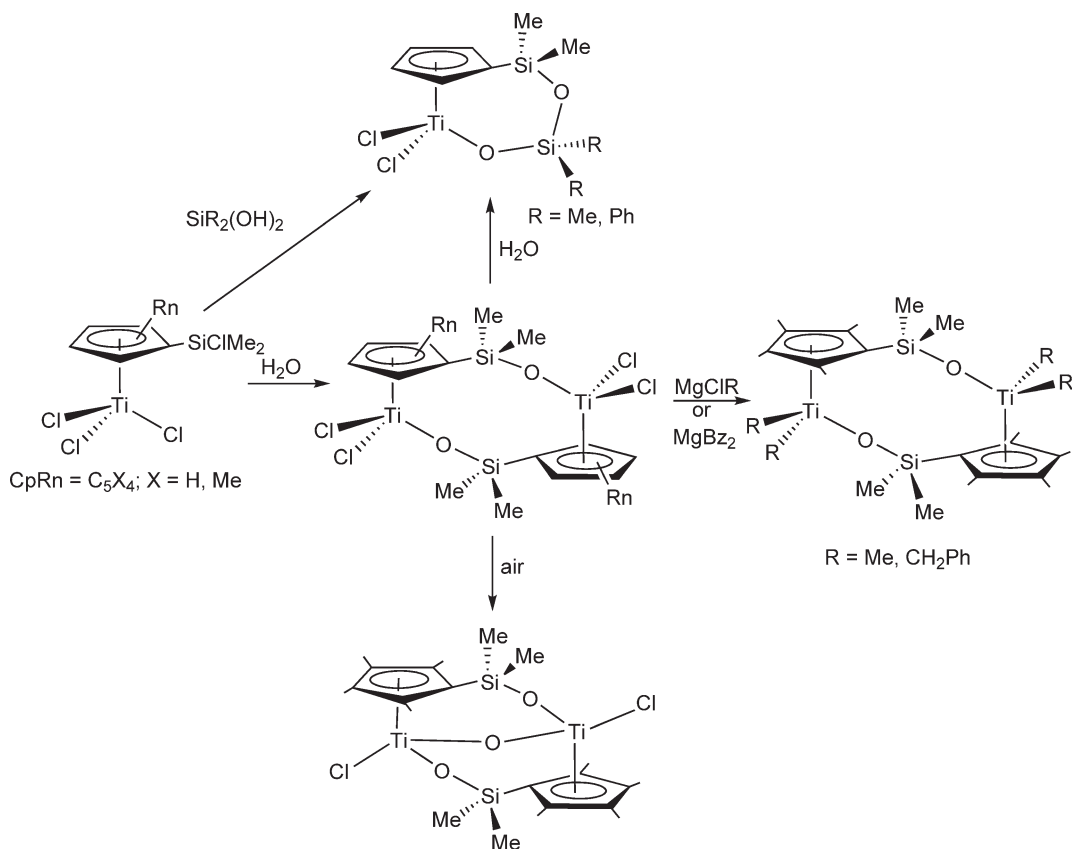
#### 4.05.3.5.3 Cyclopentadienyl-alkoxo complexes

Cp-alkoxo ligands can generally be classified as two principal types: functionalized ligands containing a neutral O-donor group forming a hemilabile ligand (**A** in Scheme 397), or ligands with an anionic O donor (**B** in Scheme 397) giving Cp-alkoxo chelate complexes reminiscent to Cp-amido compounds. Cp-alkoxo derivatives can be prepared by different synthetic routes; their chemistry is much less developed than that of Cp-amido compounds.

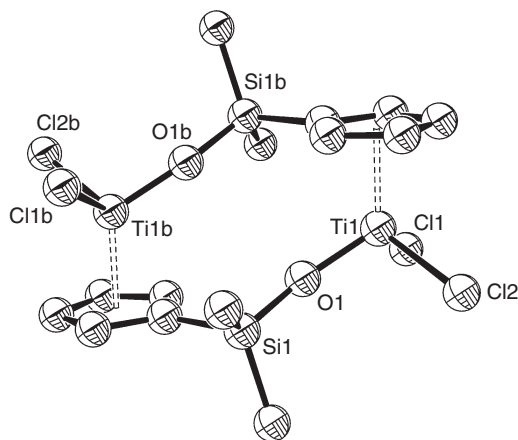
The reaction of  $(\text{C}_5\text{X}_4\text{SiClMe}_2)\text{TiCl}_3$  ( $\text{X} = \text{H}, \text{Me}$ ) with 1 equiv. of water in toluene takes place with elimination of HCl, resulting in the formation of the binuclear titanium methylsiloxane derivative  $[(\text{C}_5\text{X}_4\text{SiMe}_2\text{O})\text{TiCl}_2]_2$  (Scheme 398) in quantitative yield. The molecular structure of the “ $\text{C}_5\text{H}_4$ ” derivative has been determined by X-ray diffraction. This compound is the analog of the Cp-amido complex  $(\text{C}_5\text{H}_4\text{SiMe}_2\text{NR})\text{TiCl}_2$  with the important difference that the oxo complex is not monomeric but dimeric; two “ $(\text{C}_5\text{H}_4\text{SiMe}_2)\text{TiCl}_2$ ” fragments are connected by two oxygen bridges (Figure 20). The compound  $[(\text{C}_5\text{H}_4\text{SiMe}_2\text{O})\text{TiCl}_2]_2$  is also obtained by treatment of  $(\text{C}_5\text{H}_4\text{SiMe}_2\text{NBu}^t)\text{TiCl}_2$  with  $\text{CO}_2$  (Scheme 264; Section 4.05.3.4). The binuclear compound reacts with 1 equiv. of water to afford the mononuclear compound  $(\text{C}_5\text{H}_4\text{SiMe}_2\text{OSiMe}_2\text{O})\text{TiCl}_2$ , which is obtained with higher yield by the direct reaction of  $(\text{C}_5\text{H}_4\text{SiClMe}_2)\text{TiCl}_3$  with  $\text{SiMe}_2(\text{OH})_2$ .<sup>380,581</sup> The analogous complex  $(\text{C}_5\text{H}_4\text{SiMe}_2\text{OSiPh}_2\text{O})\text{TiCl}_2$  is obtained by treatment of  $(\text{C}_5\text{H}_4\text{SiClMe}_2)\text{TiCl}_3$  with  $\text{SiPh}_2(\text{OH})_2$ .<sup>822</sup> Reaction of  $[(\text{C}_5\text{H}_4\text{SiMe}_2\text{O})\text{TiCl}_2]_2$  with alkylating reagents and further treatment with Lewis acids  $\text{B}(\text{C}_6\text{F}_5)_3$  or  $\text{Ph}_3\text{C}[\text{B}(\text{C}_6\text{F}_5)_4]$  gives monocationic species (Section 4.05.3.2.1).<sup>510</sup> The tetramethyl-Cp compound can be alkylated with the appropriate alkylating reagent to give  $[(\text{C}_5\text{Me}_4\text{SiMe}_2\text{O})\text{TiR}_2]_2$  ( $\text{R} = \text{Me}, \text{CH}_2\text{Ph}$ ),<sup>381</sup> from which  $\mu$ -oxo and  $\mu$ - $\text{CH}_2$  derivatives have been obtained (Scheme 205; Section 4.05.3.2.1).<sup>509</sup> Hydrolysis of the trichloro and tribenzyl complexes  $(\text{C}_5\text{H}_4\text{SiMeCl}_2)\text{TiX}_3$  leads to the  $\mu$ -oxo dititanium compounds  $[(\text{C}_5\text{H}_4\text{SiMeClO})\text{TiX}_2]$  ( $\text{X} = \text{Cl}, \text{CH}_2\text{Ph}$ ) (Scheme 192; Section 4.05.3.1.3.(iii)).<sup>382</sup>



Scheme 397



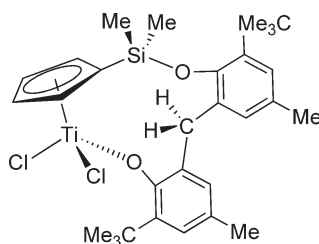
Scheme 398



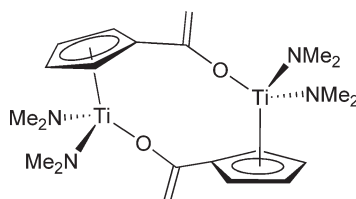
**Figure 20** Molecular structure of complex  $[(\text{C}_5\text{H}_4\text{SiMe}_2\text{O})\text{TiCl}_2]_2$  (reproduced by permission of American Chemical Society from *Organometallics*, **1995**, 14, 177).

$(\text{C}_5\text{H}_4\text{SiClMe}_2)\text{TiCl}_3$  reacts with 2,2'-methylene-bis(4-methyl-6-*t*-butyl-phenol) in the presence of 2 equiv. of  $\text{NE}_3$  to give the Cp-aryloxo compound shown in Scheme 399, involving the reactions of the Si-Cl and one of the Ti-Cl bonds. Its molecular structure has been determined by X-ray diffraction.<sup>882</sup>

A binuclear titanium complex  $\{[\text{Cp}-\text{C}(=\text{CH}_2)-\text{O}]\text{Ti}(\text{NMe}_2)_2\}_2$  (Scheme 400) containing an  $sp^2$ -C<sub>1</sub> linker between the Cp ligand and the oxygen atom of a formally bridging Cp-C-O framework has been synthesized by transmetalation reaction of  $\text{M}_2[\text{CpC}(=\text{CH}_2)\text{O}]$  ( $\text{M} = \text{Li, Na}$ ) with  $\text{TiCl}_2(\text{NMe}_2)_2$ .<sup>974</sup>



Scheme 399

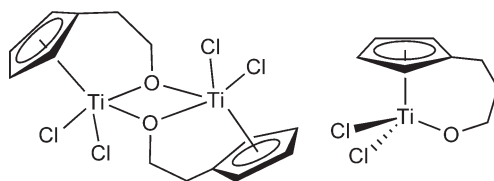


Scheme 400

A convenient route for the preparation of Cp-alkoxo titanium complexes is the dehalosilylation reaction of the trimethylsilylcyclopentadiene siloxy ethers  $\text{Me}_3\text{SiC}_5\text{H}_4(\text{CH}_2)_n\text{OSiMe}_3$  with  $\text{TiCl}_4$  to give  $[\text{C}_5\text{H}_4(\text{CH}_2)_n\text{O}]\text{TiCl}_2$  ( $R = \text{H}, \text{Me}; n = 2, 3$ ). The compound with  $n = 2$  is a dimer, while  $n = 3$  gives a monomeric structure in solid state (Scheme 401).<sup>975</sup> The analogous tetramethyl-Cp complex  $[\text{C}_5\text{Me}_4(\text{CH}_2)_3\text{O}]\text{TiCl}_2$  is similarly made and reacts with alkyllithium or Grignard reagents to afford the dialkyls  $[\text{C}_5\text{Me}_4(\text{CH}_2)_3\text{O}]\text{TiR}_2$  as crystalline solids. The treatment of the dibenzyl complex with  $\text{B}(\text{C}_6\text{F}_5)_3$  in bromobenzene solvent gives deep red solutions of the ionic compound  $[(\text{C}_5\text{Me}_4(\text{CH}_2)_3\text{O})\text{Ti}(\text{CH}_2\text{Ph})]^+[\text{PhCH}_2\text{B}(\text{C}_6\text{F}_5)_3]^-$ , identified by NMR spectroscopy. The bis(trimethylsilylmethyl) complex also reacts with  $\text{B}(\text{C}_6\text{F}_5)_3$  in bromobenzene solvent to give an ionic complex formed when one Me group is removed from one of the  $\text{CH}_2\text{SiMe}_3$  ligands to give a silyl-alkoxo ligand coordinated to the titanium atom. The presence of THF as Lewis base induces an intramolecular nucleophilic attack of the  $\text{CH}_2\text{SiMe}_3$  group on the silicon atom of the silyl-alkoxo ligand (Scheme 402). Nucleophilic attack to the Si atom in the “Ti–O–Si–C” unit is also observed in the reaction with anhydrous HCl. The bis(neopentyl) complex does not react with  $\text{B}(\text{C}_6\text{F}_5)_3$  due to the steric bulk of the alkyl groups.<sup>976</sup> Similar titanium complexes with bidentate Cp-alkoxo ligands have been synthesized (Scheme 403) and used as catalysts for the hydrosilylation of acetophenone, the hydrogenation of 2-phenylpyrrolidone and 2-phenylbutene, and the polymerization of styrene.<sup>324</sup>

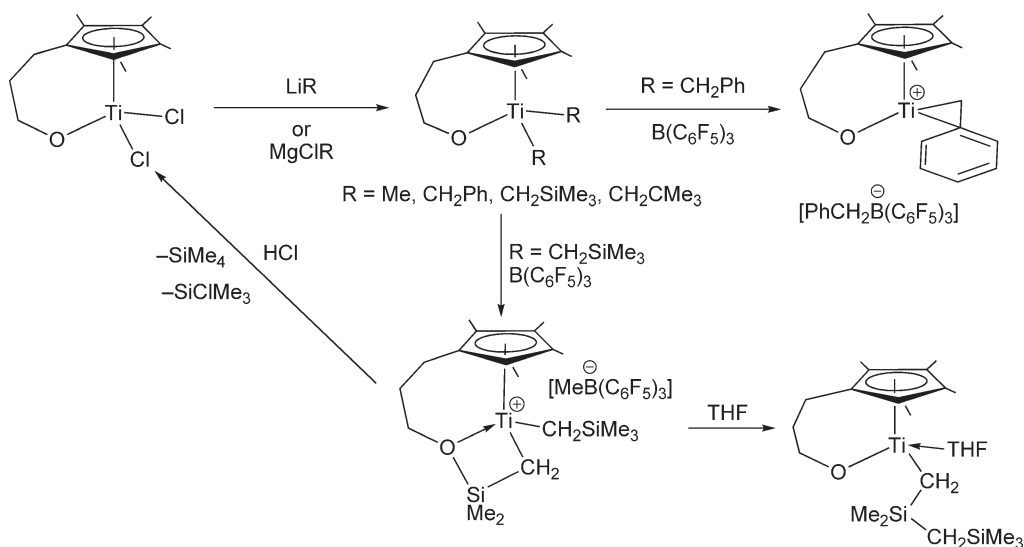
At elevated temperatures, the complex  $(\text{C}_5\text{Me}_4\text{CH}_2\text{CH}_2\text{OMe})\text{TiCl}_3$  undergoes a conversion into  $(\text{C}_5\text{Me}_4\text{CH}_2\text{CH}_2\text{O})\text{TiCl}_2$  with the elimination of MeCl (Scheme 404).<sup>365</sup>

$(\text{C}_5\text{H}_4\text{CMe}_2\text{-2-C}_6\text{H}_4\text{O})\text{TiCl}_2$  (Scheme 405) can be prepared in different ways. Thermolysis of  $(\text{C}_5\text{H}_4\text{CMe}_2\text{-2-C}_6\text{H}_4\text{OMe})\text{TiCl}_3$  affords the dichloro compound by the elimination of MeCl. The properties of  $(\text{C}_5\text{H}_4\text{CMe}_2\text{-2-C}_6\text{H}_4\text{O})\text{TiCl}_2$  in the presence of MAO or the co-catalyst system  $\text{AlBu}_3/[\text{Me}_2\text{PhNH}]^+[\text{B}(\text{C}_6\text{F}_5)_4]^-$  as catalyst for the polymerization of ethylene at high pressures (150 MPa) and high temperatures (210 °C) have been investigated. The higher activities are obtained with the Ti/MAO catalyst system, with the polymerization results being comparable

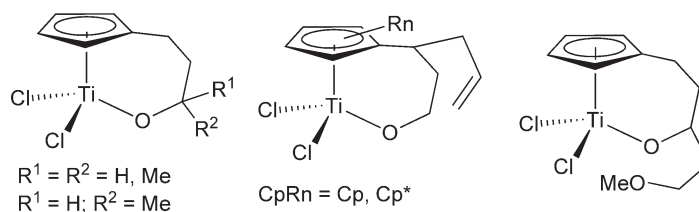


Scheme 401

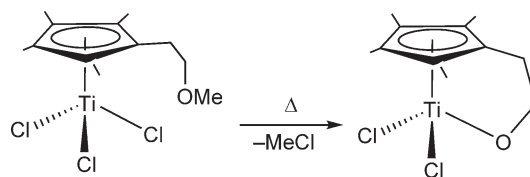




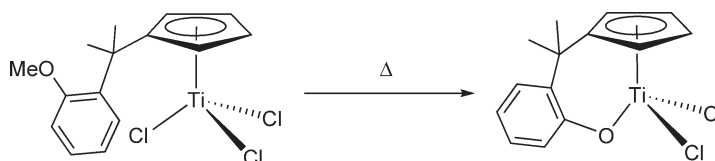
Scheme 402



Scheme 403



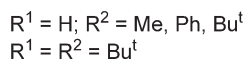
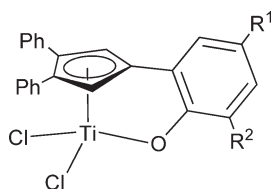
Scheme 404



Scheme 405

with that obtained with the catalytic system  $\text{Me}_2\text{Si(IndH}_4)_2\text{ZrCl}_2$ . The ethylene/1-hexene co-polymerization productivity has also been studied.<sup>977,978</sup>

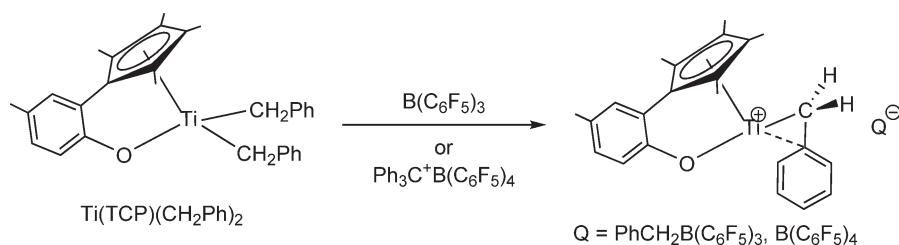
The Cp-phenoxo dichloro complexes shown in Scheme 406 have been prepared by the reaction of  $\text{TiCl}_4$  with the dilithio salt of the corresponding Cp-phenoxide ligands. Alternatively, the treatment of the cyclopentadienylphenols with  $\text{TiCl}_4$  in 1 : 1 molar ratio forms the coordination intermediates which are converted into the final products by



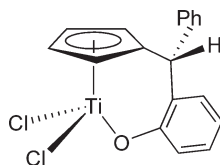
Scheme 406

reaction with  $LiBu^n$ . The introduction of bulky substituents on the Cp and the phenoxo groups prevent the formation of multinuclear species and bis-Cp derivatives. Attempts to synthesize these complexes through amine elimination, alkane elimination, or dehalosilylation processes have been unsuccessful. The yields of the reactions have been moderate and depend on the nature of the substituents. These complexes are relatively stable to air and moisture and they also show good thermal stability. The crystal structures of the complexes have been determined by X-ray diffraction. When activated with  $AlBu^i_3$  and  $Ph_3C[B(C_6F_5)_4]$ , they exhibit reasonable catalytic activity for ethylene polymerization, producing polyethylenes with moderate molecular weights and melt transition temperatures. They also show good catalytic activity for co-polymerization of ethylene with 1-hexene.<sup>979,980</sup> The synthesis of a similar tetramethyl-Cp derivative has been described from  $Ti(CH_2Ph)_4$ ; its reaction with  $Ph_3C[B(C_6F_5)_4]$  gives the corresponding cationic monobenzyl species.  $Ti(CH_2Ph)_4$  reacts with  $(TCP)H_2$  to give the dibenzyl Cp-phenoxo compound  $(TCP)Ti(CH_2Ph)_2$ , the molecular structure of which has been determined by X-ray diffraction ( $(TCP)H_2 = 2$ -tetramethylcyclopentadienyl)-4-methylphenol). NMR spectroscopy indicates that in solution at room temperature the two benzyl groups are magnetically equivalent, while in the solid state one benzyl group is coordinated in a normal  $\eta^1$ - and the other in an  $\eta^2$ -mode. The compound reacts at low temperature on the NMR scale with  $B(C_6F_5)_3$  or  $Ph_3C[B(C_6F_5)_4]$  with the formation of the corresponding cationic complexes  $[(TCP)Ti(CH_2Ph)]^+Q^-$  [ $Q = PhCH_2B(C_6F_5)_3$  or  $B(C_6F_5)_4$ ] (Scheme 407). Upon activation with  $Ph_3C[B(C_6F_5)_4]$  the system is highly active for ethylene, propylene, and styrene polymerization.<sup>981</sup> The molecular structure of the dichloro Cp-phenyl-methyl phenoxo compound,  $Ti(C_{18}H_{14}O)Cl_2$  with a chiral C atom, has been determined by X-ray diffraction methods (Scheme 408).<sup>982</sup>

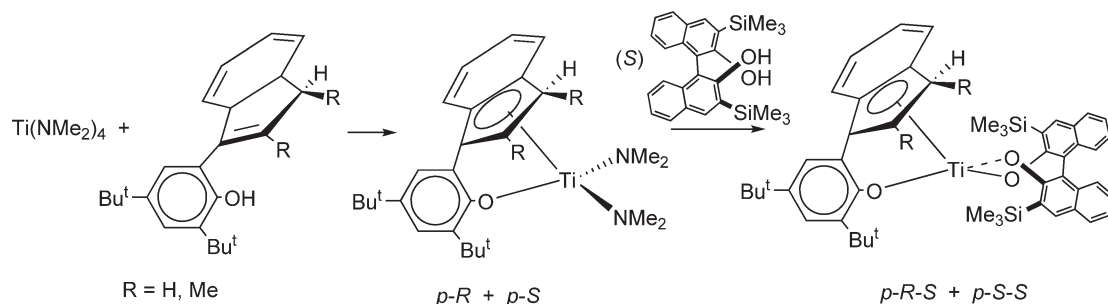
Substituted 2-(indenyl)-phenols react with  $Ti(NMe_2)_4$  to give the 2-(indenyl)-phenoxo diamido titanium derivatives (Scheme 409), obtained as a mixture of (*p*-*R*) and (*p*-*S*) enantiomers within the unit cell due to the planar



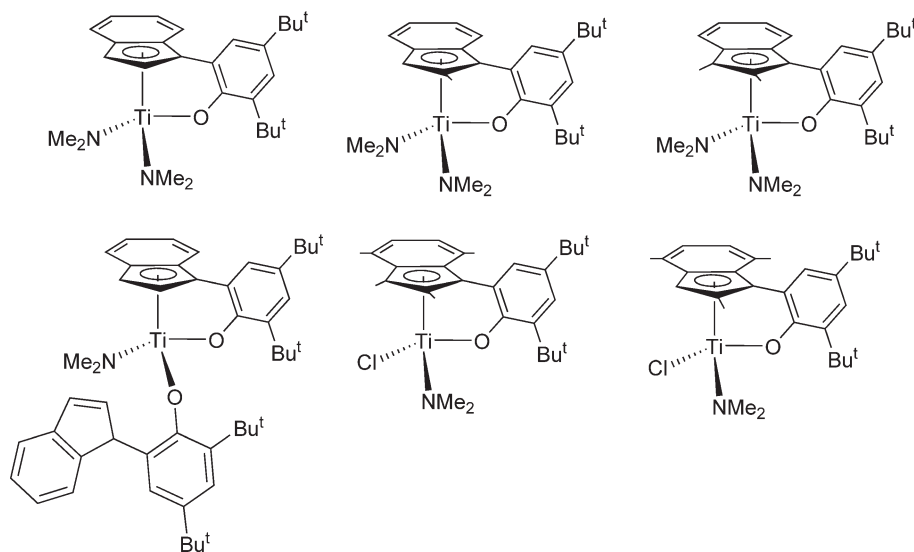
Scheme 407



Scheme 408



Scheme 409



Scheme 410

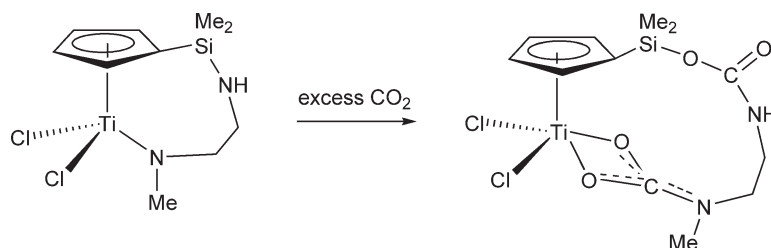
chirality generated by the indenyl coordination. Resolution to give a mixture of two diastereoisomers ( $p\text{-R,S}$ ) and ( $p\text{-S,S}$ ) is possible by a reaction with  $(S)$ -3,3'-bis(trimethylsilyl)-1,1'-binaphthol. Recrystallization gives the pure ( $p\text{-S,S}$ ) form, the molecular structure of which has been determined by X-ray diffraction.<sup>851</sup> Similar products are obtained from the reaction of  $\text{Ti}(\text{NMe}_2)_4$  with 2-(inden-3-yl)-4,6-di-*tert*-butylphenol and its 2-methyl, 1,2-dimethyl, and 2,4,7-trimethyl substituted derivatives (Scheme 410). Treatment of  $\text{TiCl}_2(\text{NMe}_2)_2$  with the 1,2,4,7-tetramethyl substituted compound affords the analogous chloro amido titanium complex (Scheme 410). The metal coordination of this series of compounds is best described as pseudo-tetrahedral, with the indenyl ring occupying one site of a three-legged piano stool geometry.<sup>984</sup>

Indenyl-alkoxo derivatives have been employed to catalyze the syndiospecific polymerization of styrene.<sup>985</sup> *Ab initio* investigations of the synthesis of the tetramethyl-Cp-propoxo dichloro titanium complex  $\text{Ti}[\text{C}_5\text{Me}_4(\text{CH}_2)_3\text{O}]\text{Cl}_2$  from  $\text{Ti}[\text{C}_5\text{Me}_4(\text{CH}_2)_3\text{OMe}]\text{Cl}_3$  have been reported.<sup>986</sup>

#### 4.05.3.5.4 Complexes with other O-based ligands

$\text{CpTiCl}_2(\text{dbm})$  ( $\text{dbm} = \beta$ -diketonate ligands) and  $\text{CpTiCl}(\text{dbm})_2$ <sup>987</sup> and the supported catalysts  $\text{CpTi}(\text{dbm})\text{Cl}_2/\text{MgCl}_2$ <sup>988</sup> and  $\text{CpTi}(\text{dbm})\text{Cl}_2/\text{MgCl}_2\text{-SiO}_2$ <sup>989</sup> have been synthesized and used, in the presence of MAO, for the ethylene polymerization and the preparation of syndiotactic polystyrene.

$[\text{C}_5\text{H}_4\text{SiMe}_2\text{N}(\text{Me})\text{CH}_2\text{CH}_2\text{N}(\text{Me})]\text{TiCl}_2$  reacts with an excess of  $\text{CO}_2$  in  $\text{CHCl}_3$  to give the dicarbamate derivative  $[\text{C}_5\text{H}_4\text{SiMe}_2\text{OC}(\text{O})\text{N}(\text{Me})\text{CH}_2\text{CH}_2\text{N}(\text{Me})\text{-}\eta^2\text{-CO}_2]\text{TiCl}_2$  (Scheme 411) through the double insertion of  $\text{CO}_2$  into the Si-N and Ti-N bonds. The carbamate groups are bound in  $\eta^2\text{-Ti}$  and  $\eta^1\text{-Si}$  fashion. Thermal decomposition



Scheme 411

of this complex affords the  $\mu$ -oxo titanium derivative  $[(C_5H_4SiMe_2O)_2TiCl_2]$  with elimination of  $CO_2$  and 1,3-dimethyl-2-imidazolidinone.<sup>755</sup>

Phosphinato and related titanium complexes containing a fluoro ligand have been synthesized by the reaction of  $Cp^*TiF_3$  with trimethylsilyl esters of sulfonic, phosphinic, and carboxylic acids. The molecular structures of the corresponding binuclear sulphonato, phosphinato, and carboxylato complexes have been determined by single crystal X-ray diffraction (Scheme 412). In these complexes, each titanium atom is bonded to a terminal fluoro ligand, and the two titanium atoms are connected by two bridging fluoro as well as two bridging sulphonato, phosphinato, or carboxylato groups, respectively.<sup>990</sup> The reactions of  $Cp^*TiF_3$  with  $Me_3SiOPOPh_2$ ,  $Me_3SiOSO_2-p-C_6H_4Me$ , and  $Al(OMe)_3$  lead to the formation of the dimers  $[Cp^*TiF(\mu-F)(\mu-OPOPh)_2]$ ,  $[Cp^*TiF(\mu-F)(\mu-OSO_2-p-C_6H_4Me)_2]$ , and  $[Cp^*TiF(\mu-F)(\mu-OMe)_2]$ , respectively, in good yields.  $Cp^*TiF_3$  reacts with  $Al(OH)_3$  to afford the known tetramer  $[Cp^*TiF(\mu-O)_4]$ .<sup>991</sup> The reaction of  $Ph_2P(O)(OSiMe_3)$  with  $CpTiCl_3$  in  $CH_2Cl_2$  yields the binuclear complex  $CpTiCl_2(\mu-Ph_2PO_2)_2$  containing bridging phosphinato ligands.<sup>992</sup>

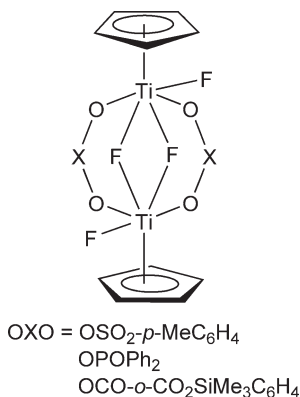
Reactions of  $Cp^*TiMe_3$  with butylphosphonic acids  $RP(O)(OH)_2$  ( $R = Me, Ph$ ) yield the air stable phosphonato titanium compounds which are readily soluble in organic solvents (Scheme 413). An analogous product is obtained in the reaction between  $Cp^*TiCl_3$  and methylphosphonic acid. These titanophosphonato derivatives mentioned are examples of organic, soluble molecular transition metal phosphonato cages.<sup>993</sup>

The synthesis of the fragment “ $Cp^*Ti$ ” supported on a mesoporous aluminophosphate has been described; the coordination mode of the  $Cp^*Ti(IV)$  fragment is as depicted in Scheme 414.<sup>994</sup>

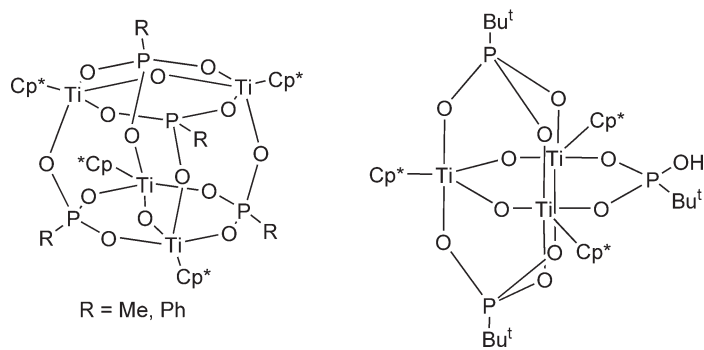
The titanium carboxylates  $[Cp^*Ti(OCOR)_2]_2$  ( $R = H, Ph$ ) are obtained when “titanocene”  $(Cp^*TiH)_2(C_{10}H_8)$  reacts with carboxylic acids; the three bridge groups are replaced by four carboxylato bridges (Scheme 415). The structure of the resulting formiato complex has been determined by X-ray crystallography.<sup>995</sup>

Treatment of the Schiff base tin(II) species  $Sn(salen)$  ( $salen = N,N'$ -bis(salicylidene)ethylenediamine) with a solution of  $Cp_2TiCl_2$  in  $CH_2Cl_2$  affords the mono-Cp complex  $CpTiCl(salen)$  (Scheme 416), accompanied by  $SnCpCl$ .<sup>996</sup>

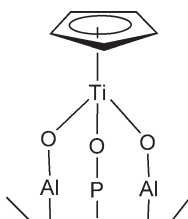
The reactions of  $Cp^*TiCl_3$  with 4-amino-3-mercapto-6-methyl-5-oxo-1,2,4-triazine and its Schiff bases (derived from benzaldehyde, 2-chlorobenzaldehyde, anisaldehyde, salicylaldehyde, 2-hydroxynaphthaldehyde, and 2-hydroxyacetophenone) have been studied in THF and  $CH_2Cl_2$  in the absence and presence of amine in different molar ratios.<sup>997</sup>



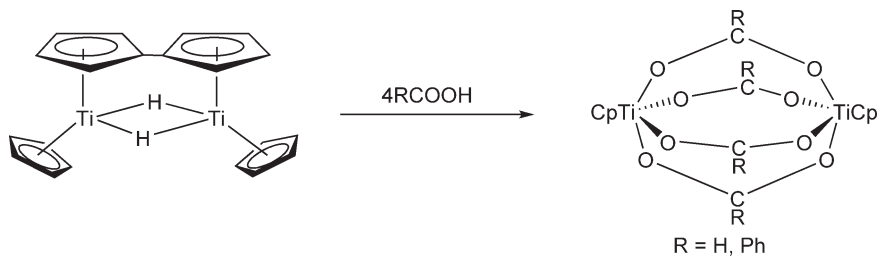
Scheme 412



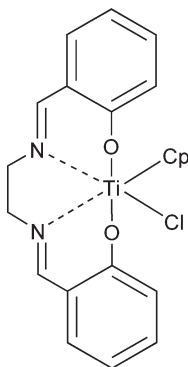
Scheme 413



Scheme 414



Scheme 415



Scheme 416

$\text{CpTiCl}_3$  reacts with 5-chloro-8-hydroxyquinoline (oxH) in acetonitrile to give the 8-hydroxyquinolinato complex  $\text{CpTiCl(ox)}_2$ . Its molecular structure has been determined by X-ray diffraction which shows a *cis*-N and the *trans*-O configuration.<sup>998</sup>

The molecular structures of Cp and Ind titanium complexes containing *p*-tolylsulfonamido ring substituents have been reported. Coordination of Ti atom to the N and O atoms of the *p*-tolylsulfonamido ligand is observed.<sup>999–1002</sup>

#### 4.05.3.6 Mono-Cp Complexes with Ti–Chalcogenido Bonds

The chemistry of early transition metal complexes containing a chalcogenido–metal bond is an area of continuing interest because of their unusual electronic structures and properties, and the relevance of such compounds as models for several important industrial catalytic processes. A variety of titanium complexes containing Ti–S bonds are known and this chemistry has been reviewed.<sup>1003,1004</sup>

Mono-Cp alkoxo and aryloxo titanium thiolates and sulfides have been widely reported. These complexes show an interesting reactivity, including C–H and C–S bond activation and reduction of Ti(IV) to Ti(III). The incorporation of bulky aryloxo ligands in the coordination environment of the titanium center limits some of this reactivity and alters the chemistry of the compounds considerably. The implications of the electronic and steric effects of these ancillary ligands have been considered.<sup>1005–1008</sup>

The deprotonation reaction of  $\text{Cp}_2\text{Ti(SH)}_2$  with NaH in THF proceeds unexpectedly with the elimination of CpH to give the anionic sulfide-bridged titanium(IV) dimer,  $\text{Na}_2[\text{CpTi}(\mu\text{-S})(\text{S})_2]$ . The molecular structure of this compound has been determined by X-ray diffraction and shows a terminal sulfido ligand with a short Ti–S bond distance of ca. 2.2 Å, indicating nearly double bond character (Scheme 417). It adopts a *syn*-Ti=S configuration and is stabilized by interactions with THF-solvated sodium cations.<sup>1009</sup>

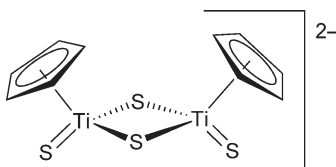
The sulfide clusters  $(\text{CpTi})_4(\mu_3\text{-S})_3(\mu_2\text{-S})(\mu_2\text{-SEt})_2$  and  $(\text{CpTi})_6(\mu_3\text{-S})_3(\mu_3\text{-O})_4$  are prepared by C–S bond cleavage when mixtures of  $\text{CpTiCl}_2\text{Me}$ , thiol, and base are thermolyzed at 80 °C. Both compounds have been crystallographically characterized.<sup>1010</sup>

Mono-Cp dichloro complexes with substituted aryl sulfido ligands  $\text{CpTiCl}_2(\text{SAr})$  ( $\text{SAr} = \text{SC}_6\text{H}_4\text{Me-4}$ ;  $\text{SC}_6\text{H}_2\text{Me}_3\text{-2,4,6}$ ;  $\text{SC}_6\text{H}_2\text{Pr}^i\text{-2,4,6}$ ;  $\text{SC}_6\text{H}_2\text{Ph}_3\text{-2,4,6}$ ) have been synthesized by the reaction of  $\text{CpTiCl}_3$  with 1 equiv. of the lithium salt of the corresponding aryl sulfides in benzene. X-ray diffraction studies show that each metal center possesses a pseudo-tetrahedral geometry. These compounds undergo one-electron reduction to produce sulfur-bridged dimers of the type  $[\text{CpTiCl}(\mu\text{-SAr})]_2$  ( $\text{SAr} = \text{SC}_6\text{H}_2\text{Me}_3\text{-2,4,6}$ ;  $\text{SC}_6\text{H}_2\text{Pr}^i\text{-2,4,6}$ ).<sup>1011</sup>

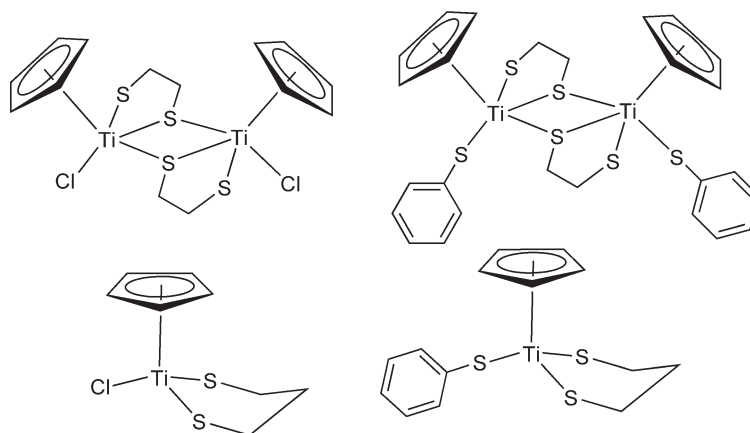
The reaction of  $\text{CpTiCl}_3$  with 1 equiv. of  $\text{Li}[\text{Me}_2\text{P}(\text{CH}_2)_3\text{S}]$  gives the monothiolato compound  $\text{CpTiCl}_2[\text{S}(\text{CH}_2)_3\text{PMe}_2]$ , while treatment of  $\text{Cp}^*\text{TiCl}_3$  with 3 equiv. of  $\text{Li}[\text{Me}_2\text{P}(\text{CH}_2)_3\text{S}]$  affords  $\text{Cp}^*\text{Ti}[\text{S}(\text{CH}_2)_3\text{PMe}_2]_3$ . The molecular structures of both compounds have been determined by X-ray diffraction. Complex  $\text{CpTiCl}_2[\text{S}(\text{CH}_2)_3\text{PMe}_2]$  has the thiolato ligand coordinated to Ti through P and S. In complex  $\text{Cp}^*\text{Ti}[\text{S}(\text{CH}_2)_3\text{PMe}_2]_3$ , one of the three thiolato ligands coordinates to Ti center as an S, P chelate, while the two other thiolate ligands are only S-bound.<sup>1012</sup>

Ethane- and propane-1,2-dithiolato Cp titanium derivatives have been reported. They are reduced by boron and tin hydrides.<sup>1013,1014</sup> Mono-Cp titanium(IV) sulfido complexes have been made by treatment of  $\text{CpTiCl}_3$  with dithiols in the presence of donor ligands such as imidazole or  $\text{PMe}_3$  under different reaction conditions (Scheme 418).<sup>1015</sup> The structures of the compounds have been reported. Electrochemical studies suggest that these compounds are formed through a radical mechanism.<sup>1016</sup>

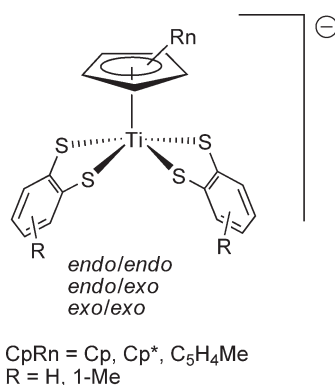
The anionic bis(1,2-arenedithiolato) titanium derivatives  $[\text{Cp}'\text{Ti}(\text{S}_2\text{C}_6\text{H}_3\text{R})_2]^-$  ( $\text{Cp}' = \text{Cp}$ ,  $\text{Cp}^*$ ,  $\text{C}_5\text{H}_4\text{Me}$ ) (Scheme 419) have been prepared as the thallium(I) salts by the reaction of  $\text{Cp}'\text{TiCl}_3$  and thallium dithiolate in THF. The molecular structures of the complexes have been determined by X-ray diffraction.<sup>1017</sup> Thallium(I) derivatives of



Scheme 417



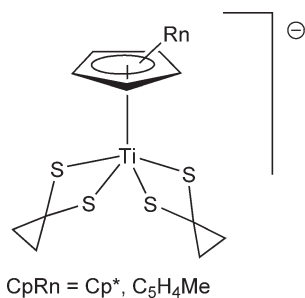
Scheme 418



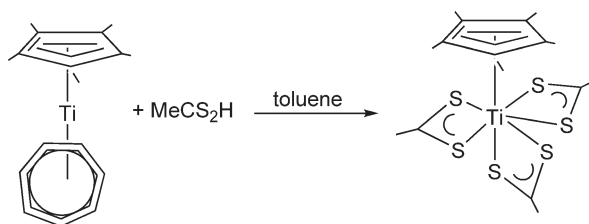
Scheme 419

mono-Cp bis(1,2-ethanedithiolato)titanium,  $\text{Ti}[\text{Cp}''\text{Ti}(1,2\text{-S}_2\text{C}_2\text{H}_4)_2]$  (Scheme 420), have been isolated in good yields from reactions of  $\text{Cp}''\text{TiCl}_3$  with the thallium salts of the ethane-1,2-dithiol. Conformational changes of the chelating dithiolato ligands have been monitored by variable-temperature  $^1\text{H}$  NMR spectroscopy. The synthesis of the aryl monothiolate  $\text{CpTi}(\text{SC}_6\text{H}_5)_3$  is also described and its structure determined by X-ray diffraction. Two of the three phenyl rings are overlapping and are approximately parallel and may indicate some  $\pi$ -interaction between them.<sup>1018</sup>

A new and facile synthetic method to prepare complexes with Ti–S bonds is based on the oxidation of the low-valent titanium sandwich complex  $\text{CpTi}(\text{C}_7\text{H}_7)$  with dithiocarboxylic acid to give the Ti(IV) dithioacetate  $\text{CpTi}(\text{S}_2\text{CMe})_3$  (Scheme 421). The compound has been fully characterized including X-ray crystallography. It consists of discrete seven-coordinate molecules with a slightly distorted pentagonal-bipyramidal coordination



Scheme 420



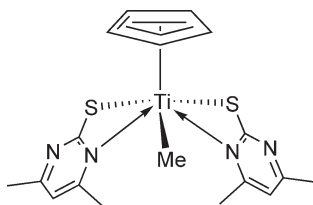
Scheme 421

geometry of the titanium atom. The average equatorial Ti–S distance of 2.619 Å is appreciably longer than the axial Ti–S distance, 2.545(3) Å.<sup>1019</sup>

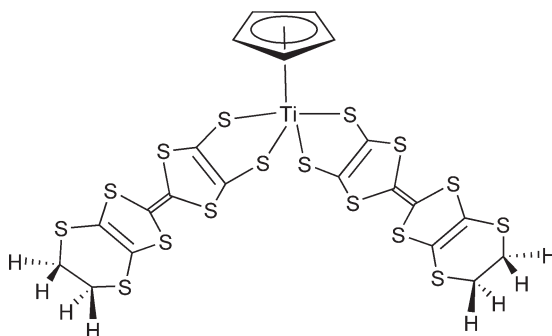
The heterocyclic dithiolate  $\text{Cp}^*\text{TiMe}(\text{SR})_2$  (Scheme 422) is accessible from  $\text{Cp}^*\text{TiMe}_3$  and 4,6-dimethyl-2-mercaptopyrimidine in a 1 : 2 molar ratio. Fluxional behavior is observed in solution.<sup>1020</sup>

Reactions of  $\text{Cp}'\text{TiCl}_3$  ( $\text{Cp}' = \text{Cp}, \text{Cp}^*$ ) with  $(\text{NMe}_4)_2\text{C}_8\text{H}_4\text{S}_8$  give the complexes  $(\text{NMe}_4)[\text{TiCp}'(\text{C}_8\text{H}_4\text{S}_8)_2]$  [ $\text{C}_8\text{H}_4\text{S}_8^{2-} = \{(4,5\text{-ethylenedithio})\text{-}1,3\text{-dithiole-}2\text{-ylidene}\}\text{-}1,3\text{-dithiole-}4,5\text{-dithiolate}$ ] (Scheme 423). Crystal structure, molecular geometries, electrochemical and spectroscopic properties, and electrical conductivities are reported. This compound exhibits low oxidation potentials for  $\text{C}_8\text{H}_4\text{S}_8$  ligand oxidation and is oxidized by iodine or 7,7,8,8-tetracyano-*p*-quinodimethane.<sup>1021,1022</sup>

A facile and convenient route to mono-Cp thio-titana-cyclopropane derivatives has been reported and the reactivity of these thio metallacycles toward protonic and unsaturated organic reagents and  $\text{PMe}_3$  has been described. Some representative reactions are summarized in Scheme 424. The thio-metallacyclic complexes  $[(\text{C}_5\text{H}_4\text{R})\text{Ti}(\text{SCHCH}_2\text{CH}_2\text{S})_2]$  ( $\text{R} = \text{H}, \text{Me}$ ) are readily prepared from the reaction of  $(\text{C}_5\text{H}_4\text{R})\text{TiCl}(\text{SCH}_2\text{CH}_2\text{CH}_2\text{S})$  with  $\text{LiMe}$ ,  $\text{AlMe}_3$ , or  $\text{LiBu}^t$ . Reaction with  $\text{PMe}_3$  leads to the cleavage of these dimers. The Cp compound undergoes facile acidolysis with  $\text{HCl}$ , acetic acid,  $\text{PhSH}$ , and propanedithio. It reacts with benzophenone under insertion into the Ti–C bond to give  $\text{CpTi}[\text{SCH}(\text{OCPh}_2)\text{CH}_2\text{CH}_2\text{S}]$ , while reactions with cyclohexanone, 2-methylcyclohexanone, menthone, and nopinone give addition products with varying degrees of diastereoselectivity. As an example, the treatment with cyclohexanone produces a binuclear compound  $[\text{CpTi}\{\text{SCH}(\text{C}_6\text{H}_{10}\text{O})\text{CH}_2\text{CH}_2\text{S}\}]_2$ , which has been characterized by X-ray diffraction (Figure 21). The Ti atom environment is described as a “four-legged piano stool” geometry, showing the presence of two tridentate  $\text{S}_2\text{O}$  ligands with two thiolate sulfur atoms bridging the two Ti atoms. Reactions with a series of imines are

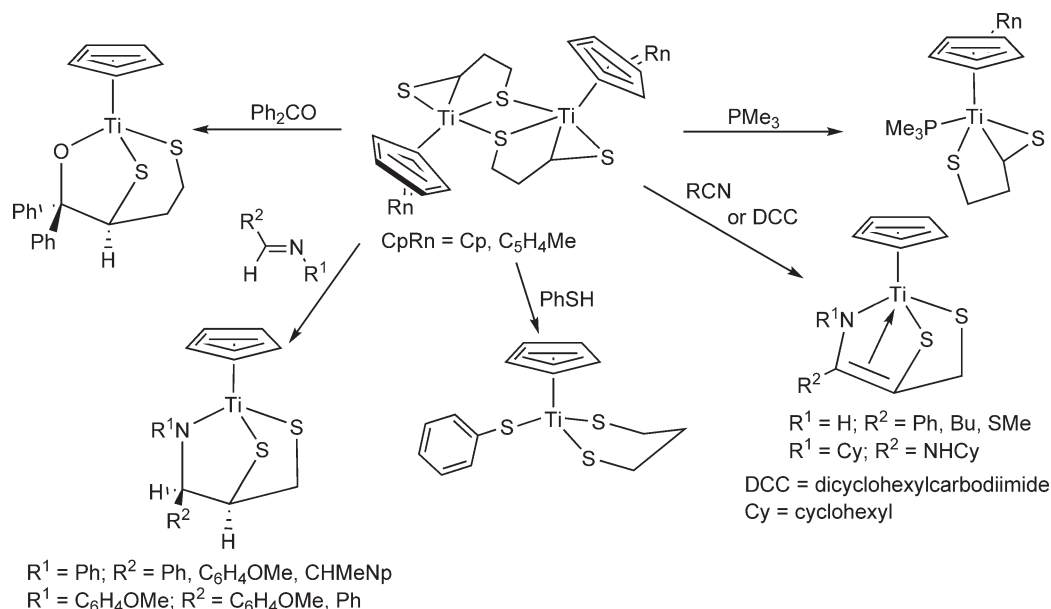


Scheme 422

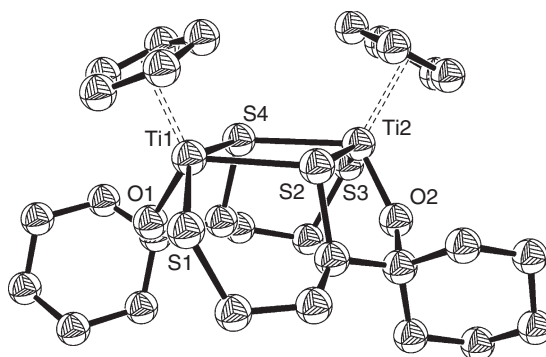


Scheme 423





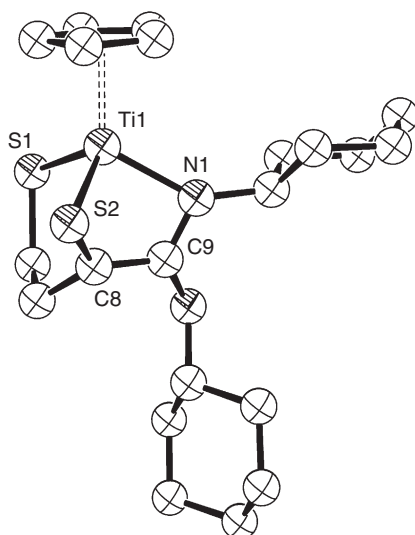
Scheme 424



**Figure 21** Molecular structure of complex  $\{\text{CpTi}[\text{SCH}(\text{C}_6\text{H}_{10}\text{O})\text{CH}_2\text{CH}_2\text{S}]\}_2$  (reproduced by permission of American Chemical Society from *Organometallics*, **1996**, 15, 2320).

also described, where the diastereoselectivity observed is a function of the steric demands of the imine substituents. Reactions with nitriles, methyl isocyanate, dicyclohexylcarbodiimide (DCC), and phenyl thioisocyanate result in insertion of the substrate and subsequent enolization. Crystallographic characterization of a number of these reaction products is reported. The reaction with DCC proceeds with a C to N exocyclic N atom migration to give an exocyclic amino group and the crystal structure of the final product  $\text{CpTi}\{\text{SC}=[\text{C}(\text{NHCy})(\text{NCy})]\text{CH}_2\text{CH}_2\text{S}\}$  is shown in Figure 22. Kinetic studies for the reactions with benzophenone and cyclohexanone have been performed and the nature of the products, reaction mechanisms, and reactivity of strained thiatitanacyclopropane rings are discussed in the light of EHMO calculations.<sup>1023,1024</sup>

Thiolato titanium phosphinimido complexes have been synthesized in an attempt to compare their chemical behavior with that of the corresponding bis-Cp derivatives, using the steric and electronic analogy between Cp and phosphinimido ligands. The thiolates  $\text{CpTi}(\text{N}=\text{PP}^i)(\text{SR})_2$  ( $\text{R} = \text{Ph}, \text{CH}_2\text{Ph}$ ) are prepared by the reaction of the dichloro complex with the corresponding lithium thiolates  $\text{LiSR}$ . These complexes react with  $\text{AlMe}_3$  with triple C–H bond activation of a methyl group to give Ti–Al–carbide clusters. On the basis of spectroscopic data and the X-ray structure, the resulting compounds of these reactions can be formulated as  $\text{CpTi}(\mu\text{-SR})(\mu\text{-NPP}^i_3)(\mu_4\text{-C})(\text{AlMe}_2)_2(\mu\text{-SR})\text{AlMe}$ .<sup>651</sup> The phosphinimido titanium complexes are used as pre-catalysts in a wide range of polymerization of olefins, and their interaction with Al alkyl activators is therefore of obvious interest. The studies suggest that



**Figure 22** Molecular structure of complex  $\{\text{CpTi}[\text{SC}=\text{C}(\text{NHCy})(\text{NCy})]\text{CH}_2\text{CH}_2\text{S}\}$  (reproduced by permission of American Chemical Society from *Organometallics*, **1996**, 15, 2320).

generally multiple C–H bond activation processes in these systems are facile and convert the active catalyst to carbide and methine Ti–Al aggregates.

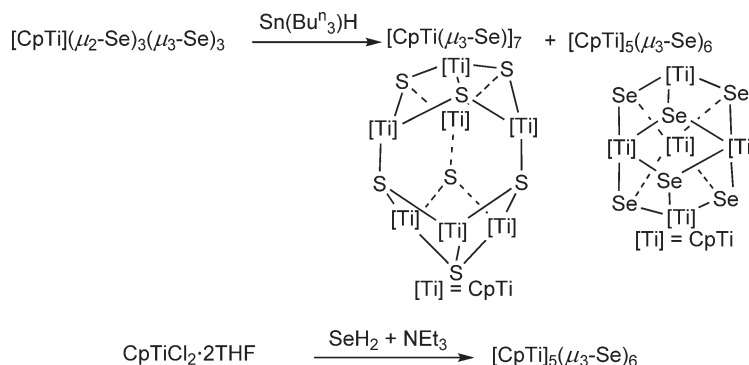
The reduction of  $(\text{CpTi})_4(\mu_2\text{-Se})_3(\mu_3\text{-Se})_3$  with  $\text{Bu}^n_3\text{SnH}$  results in a mixture of  $[\text{CpTi}(\mu_3\text{-Se})_7]$  and  $(\text{CpTi})_5(\mu_3\text{-Se})_6$ . The latter is also produced in the oxidation of the Ti(III) complex  $\text{CpTiCl}_2(\text{THF})_2$  with  $\text{SeH}_2$  in THF in the presence of  $\text{NEt}_3$  (Scheme 425). The hexaselenide cluster was identified by NMR and EPR spectroscopy, mass spectrometry, and X-ray diffraction. It is paramagnetic with one unpaired electron. The structure (Figure 23) shows a trigonal-bipyramidal arrangement of Ti atoms [average  $\text{Ti}(\text{ap})\text{--Ti}(\text{eq})$  3.215(2) Å, average  $\text{Ti}(\text{eq})\text{--Ti}(\text{eq})$  3.374(3) Å]. The structure of  $[\text{CpTi}(\mu_3\text{-Se})_7]$ , based on spectroscopic data, consists of two interpenetrating monocapped octahedra, one of titanium and one of selenium atoms.<sup>1025</sup>

The crystal structure of  $(\text{CpTi})_6(\mu_3\text{-Te})_6(\mu_3\text{-O})_2$  has been described.<sup>1026</sup>

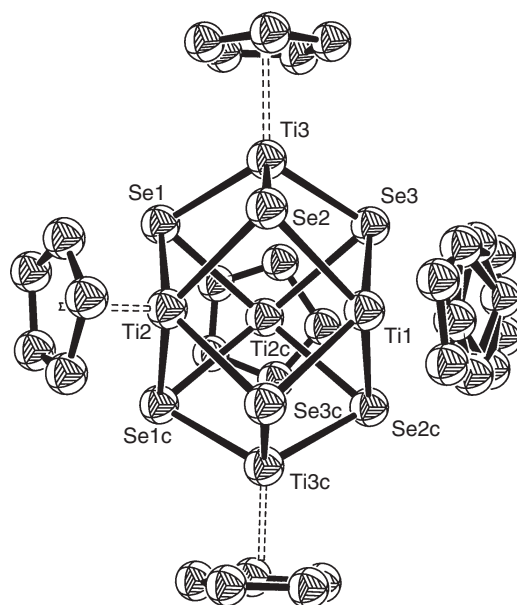
#### 4.05.3.7 Mono-Cp Complexes with Ti–H Bonds

Mono-Cp and bis-Cp titanium hydrido derivatives have been reviewed.<sup>1027</sup> The Cp-amido species  $(\text{C}_5\text{Me}_4\text{SiMe}_2\text{NCHMePh})\text{TiCl}(\mu\text{-H}_3\text{BH})$  has been described.<sup>738</sup>

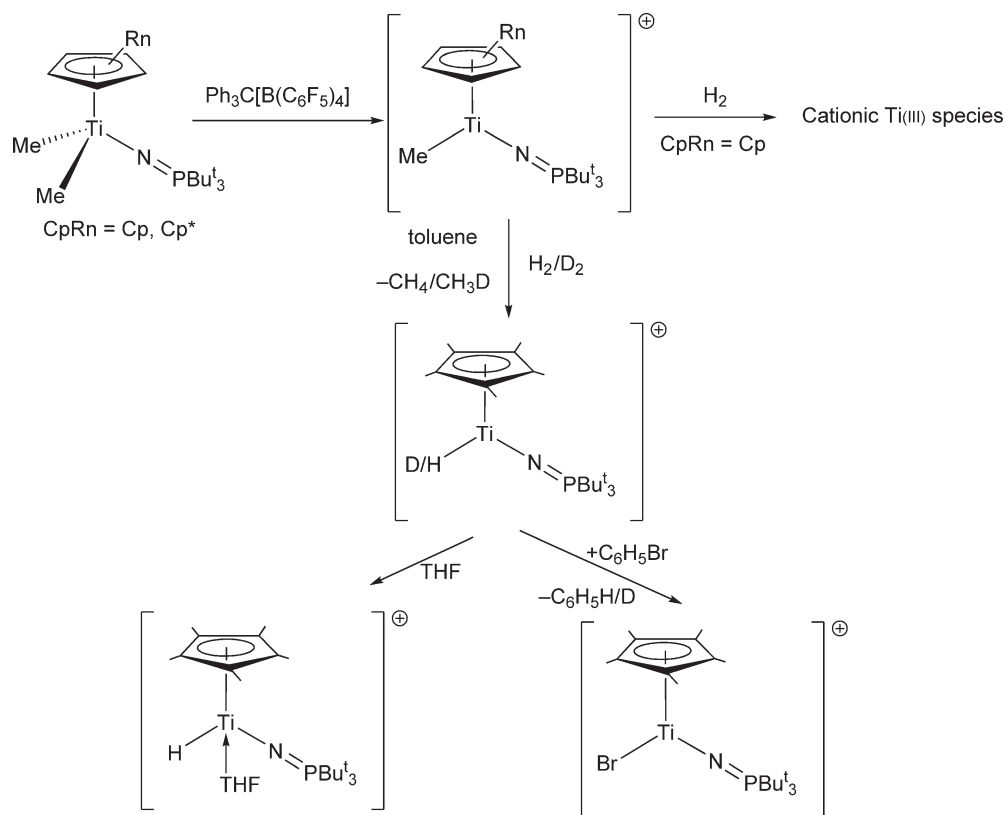
Treatment of the mono-Cp phosphinimido complex  $\text{CpTiMe}_2(\text{NPBu}^t_3)$  with  $\text{B}(\text{C}_6\text{F}_5)_3$  affords cationic species which react with  $\text{H}_2$  with slow conversion of the anionic fragment  $[\text{MeB}(\text{C}_6\text{F}_5)_3]^-$  to  $[\text{HB}(\text{C}_6\text{F}_5)_3]^-$ .<sup>640</sup> Analogous reactions of  $\text{Cp}'\text{TiMe}_2(\text{NPBu}^t_3)$  ( $\text{Cp}' = \text{Cp}, \text{Cp}^*$ ) with  $\text{Ph}_3\text{C}[\text{B}(\text{C}_6\text{F}_5)_4]$  have been described to give the corresponding monomethyl cationic derivatives (Scheme 426). The  $[\text{Cp}'\text{TiMe}(\text{NPBu}^t_3)]^+$  cation reacts with  $\text{H}_2$  to give Ti(III)



**Scheme 425**



**Figure 23** Molecular structure of complex  $(\text{CpTi})_5(\mu_3\text{-Se})_6$  (reproduced by permission of American Chemical Society from *Organometallics*, **1996**, 15, 809).



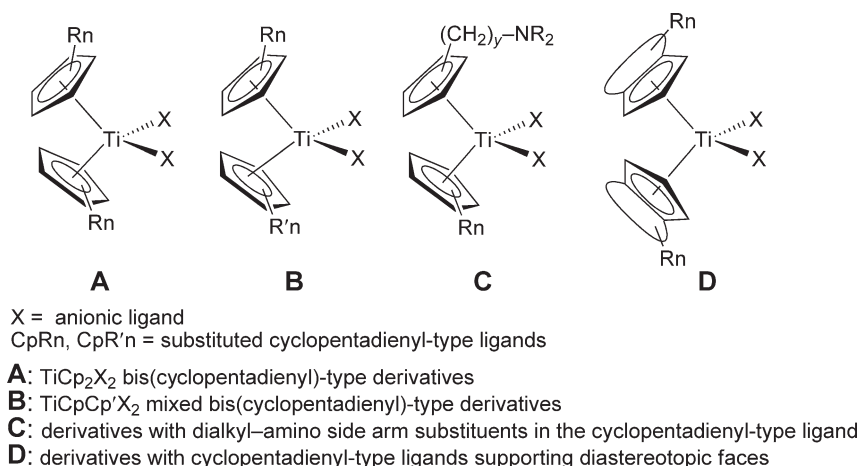
**Scheme 426**

compounds. On the other hand, the more hindered  $[\text{Cp}^*\text{TiMe}(\text{NPBu}_3)]^+$  cation reacts with  $\text{H}_2$  to give the expected cationic hydrido complex which can be stabilized by the addition of a slight excess of THF to a toluene solution of this compound. The molecular structure of the THF adduct has been determined by X-ray diffraction. When dissolved in bromobenzene, the base-free species is converted into the cationic bromo derivative.<sup>1028</sup>

#### 4.05.4 Bis(Cyclopentadienyl) and Related Compounds

The chemistry of the group 4 bis(cyclopentadienyl)-type (bis-Cp) derivatives, including indenyl and fluorenyl complexes, has made dramatic progress since the first simple unsubstituted Cp and Ind complexes were reported in the 1950s and 1960s. The discovery of olefin polymerization activity when activated with a co-catalyst, their ability to activate small molecules, and the special stability of Cp ligands have contributed to the rise of interest in group 4 metallocene derivatives. The Cp group remains the most important ligand in transition metal organometallic chemistry; Cp and Ind ligands can stabilize metals in low and high oxidation states, while the possibility of changes in hapticity provides adaptability to changes in electronic and steric requirements of the central metal. The substitution pattern of Cp ligand can of course be varied widely. The synthesis of new substituted ligands (unbridged or bridged) and different synthetic methodologies to metallate these ligands has produced an increasing variety of new bis-Cp-type derivatives. This strategy can bring about significant changes in the chemical reactivity and structural behavior of the metal complex. The main developments in the last years have been the synthesis of *ansa*-metallocenes as effective catalysts for the stereoregular polymerization of 1-alkenes and the use of chiral bis-Cp titanium catalysts in organic reactions. New types of bicyclo alkyl-fused ring derivatives have been reported. The synthesis and stabilization of fluorenyl (Flu) titanium complexes remains problematic; apparently, the Flu ligand is substantially more weakly bound to the titanium than Cp or Ind ligands and in the presence of strong donor ligands has a propensity for irreversible “ring-slippage” reactions. Different types of these compounds (Scheme 427) are represented with examples.

A number of monographs on Cp and chiral Cp titanium compounds have been published.<sup>1029–1031</sup> The chemistry of substituted mono- and bis-Cp and Ind Ti (iv) halide complexes has been widely and elegantly reviewed, including mixed Cp/Ind and *ansa*-metallocene compounds, structural aspects affecting the catalytic activity, and intramolecular coordination of the functionalized ring to the central metal. The applications of these complexes as catalysts for the homo- and co-polymerization, isomerization and hydrogenation of olefins, and metathesis polymerization of cyclic monomers are considered.<sup>323</sup> In recent years, an increasing number of bis-Cp titanium complexes with electronically modified Cp ligands have been reported with, in some cases, considerably altered catalytic properties. Bis(indenyl) complexes of titanium that contain nitrogen, oxygen, and sulfur atoms directly bonded to the five- or six-membered rings of the Ind ligand framework have been reviewed. Their synthesis, characterization, and applications are covered; catalytic performance is briefly mentioned, with emphasis on olefin polymerization.<sup>1032</sup>



Scheme 427

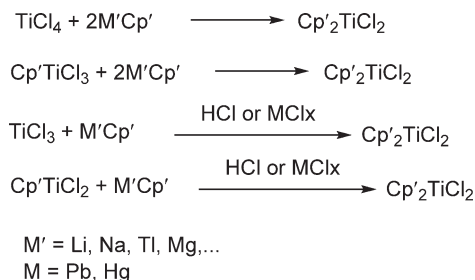
#### 4.05.4.1 Halide Complexes

##### 4.05.4.1.1 Synthesis of bis-Cp titanium halides

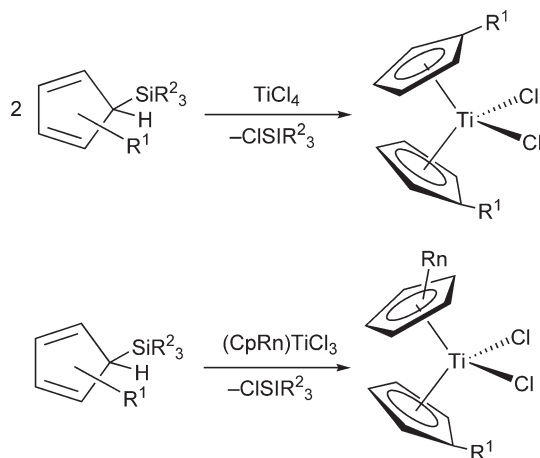
Replacement of the hydrogen atoms on Cp by substituted groups results (Cp') in major changes in both chemical and physical properties of the metal complexes. Bis-Cp' dihalo titanium complexes have been investigated intensively. They have been prepared by using different synthetic reactions. Those more frequently mentioned in this chapter are listed and summarized:

- (i) *Salt metathesis* Metathesis by reaction of the substituted cyclopentadiene salt (Li, Na, Tl, Mg, ...) with  $\text{TiCl}_4$ ,  $\text{Cp}'\text{TiCl}_3$ , or alternatively with  $\text{TiCl}_3$  or  $\text{Cp}'\text{TiCl}_2$  followed by treatment with an oxidant reagent (Scheme 428).
- (ii) *Dehalometalation* The same method based on electrophilic substitution in silylated cyclopentadienes (or analogous tin compounds) described for the preparation of mono-Cp' derivatives can be applied to the synthesis of bis-Cp complexes (Scheme 429).
- (iii) *Interchange of halide ligands* Replacement of halo ligands is a well-developed method to the synthesis of this type of compounds.  $\text{Me}_3\text{SnF}$  is generally used as a fluorinating agent.
- (iv) *Oxidative process* (Scheme 430) This methodology has been applied to study the reactivity of a series of bis( $\omega$ -alkenyl)- and  $\omega$ -alkenyl-dimethylsilyl-Cp substituted dichloro titanium complexes in reactions with Mg, to give reduced titanium species, from which new bis-Cp' and *ansa*- dichloro derivatives can be obtained by treatment with an oxidant agent (Section 4.05.4.1.3(i)).<sup>1033–1035</sup>
- (v) *Halogenation of Ti–C bonds* (Scheme 431)

The following sections are organized according to the nature of the Cp ring substituents.



Scheme 428



Scheme 429



Scheme 430



Scheme 431

4.05.4.1.1.(i) Bis-Cp<sub>2</sub> and mixed CpCp' derivatives

## 4.05.4.1.1.(i).(a) Alkyl- and alkenyl-substituted Cp

The mixed-ring titanium compound Cp(Ind)TiCl<sub>2</sub> is prepared by the reaction of LiInd with CpTiCl<sub>3</sub> and shows high catalytic activity as homogeneous ethylene polymerization catalyst in combination with MAO as co-catalyst.<sup>1036</sup>

The complexes (C<sub>5</sub>H<sub>4</sub>R)<sub>2</sub>TiCl<sub>2</sub> (R = H, Me, C<sub>6</sub>H<sub>11</sub>) have been synthesized and their activity for the hydrogenation of polystyrene–poly-1-butene–polystyrene co-polymer studied.<sup>1037</sup>

Cp(1,2-C<sub>5</sub>H<sub>3</sub>Me<sub>2</sub>)TiCl<sub>2</sub> and (1,2-C<sub>5</sub>H<sub>3</sub>Me<sub>2</sub>)<sub>2</sub>TiCl<sub>2</sub> have been synthesized by the reaction of Li(1,2-C<sub>5</sub>H<sub>3</sub>Me<sub>2</sub>) with CpTiCl<sub>3</sub> or TiCl<sub>3</sub>/HCl, respectively. NMR spectroscopic characterization and the molecular structure of (1,2-C<sub>5</sub>H<sub>3</sub>Me<sub>2</sub>)<sub>2</sub>TiCl<sub>2</sub> are reported.<sup>1038</sup>

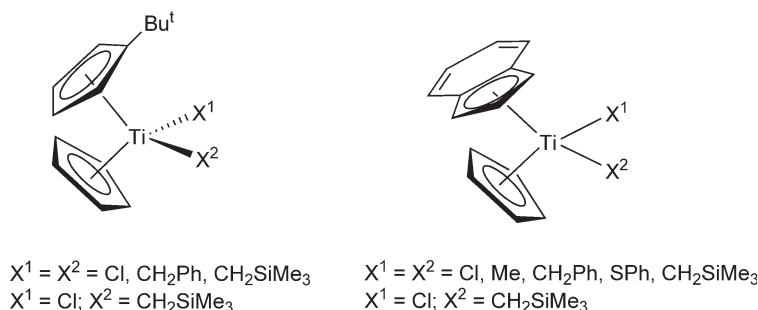
The reaction of (Me<sub>3</sub>Sn)C<sub>5</sub>H<sub>4</sub>(C<sub>6</sub>F<sub>5</sub>) with TiCl<sub>4</sub> affords [C<sub>5</sub>H<sub>4</sub>(C<sub>6</sub>F<sub>5</sub>)<sub>2</sub>]<sub>2</sub>TiCl<sub>2</sub> and its ability to polymerize ethylene in the presence of MAO as co-catalyst has been studied in order to measure the effect of the presence of an electron-withdrawing pentafluorophenyl substituent in the Cp rings on the polymerization activity.<sup>330</sup>

The synthesis of (C<sub>5</sub>Me<sub>4</sub>Ph)<sub>2</sub>TiCl<sub>2</sub> has been described and its molecular structure determined by X-ray diffraction methods.<sup>1039</sup>

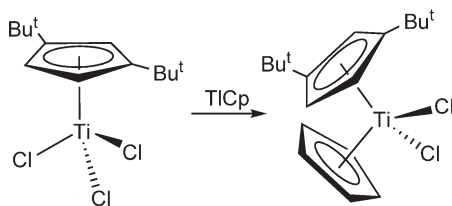
The trityl–Cp compound (C<sub>5</sub>H<sub>4</sub>CPh<sub>3</sub>)TiCl<sub>3</sub> reacts with Me<sub>3</sub>SnC<sub>5</sub>H<sub>5</sub> to give the mixed ligand complex Cp(C<sub>5</sub>H<sub>4</sub>CPh<sub>3</sub>)TiCl<sub>2</sub> with low yield.<sup>325</sup>

Complexes (C<sub>5</sub>H<sub>4</sub>Bu<sup>t</sup>)<sub>2</sub>TiCl<sub>2</sub> and (C<sub>5</sub>H<sub>3</sub>Bu<sup>t</sup>)<sub>2</sub>TiCl<sub>2</sub> have been prepared by the reaction of the corresponding lithium salt with TiCl<sub>4</sub>. In the presence of MAO they are active for ethylene polymerization.<sup>1040</sup> (1,3-Bu<sup>t</sup><sub>2</sub>-C<sub>5</sub>H<sub>3</sub>)<sub>2</sub>TiI<sub>2</sub> has been prepared from (1,3-Bu<sup>t</sup><sub>2</sub>-C<sub>5</sub>H<sub>3</sub>)<sub>2</sub>TiI by oxidation with I<sub>2</sub>.<sup>1041</sup> The mono-Cp and mono-Ind complexes (C<sub>5</sub>H<sub>4</sub>Bu<sup>t</sup>)TiCl<sub>3</sub> and (C<sub>9</sub>H<sub>7</sub>)TiCl<sub>3</sub> react with LiCp or SnCpBu<sup>t</sup>, respectively, to give the mixed ring compounds Cp(C<sub>5</sub>H<sub>4</sub>Bu<sup>t</sup>)TiCl<sub>2</sub> and Cp(C<sub>9</sub>H<sub>7</sub>)TiCl<sub>2</sub>. These have been used to prepare a range of mono- and disubstituted titanium(IV) alkyl and benzenethiolate complexes. The structures of these compounds have been established by X-ray diffraction and NMR and nuclear Overhauser effect experiments (Scheme 432).<sup>1042</sup>

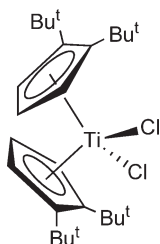
The mixed bis-Cp compound Cp(1,3-Bu<sup>t</sup><sub>2</sub>-C<sub>5</sub>H<sub>3</sub>)TiCl<sub>2</sub> is obtained by treatment of (1,3-Bu<sup>t</sup><sub>2</sub>-C<sub>5</sub>H<sub>3</sub>)TiCl<sub>3</sub> with TiCp (Scheme 433).<sup>337</sup> The similar mixed bis-Cp compound (Bu<sup>t</sup>C<sub>5</sub>H<sub>4</sub>)(1,3-Bu<sup>t</sup><sub>2</sub>-C<sub>5</sub>H<sub>3</sub>)TiCl<sub>2</sub> has been prepared by the reaction of (1,3-Bu<sup>t</sup><sub>2</sub>-C<sub>5</sub>H<sub>3</sub>)TiCl<sub>3</sub> with Li(Bu<sup>t</sup>C<sub>5</sub>H<sub>4</sub>) and its reactivity toward ammonium thiocyanate studied (Scheme 624; Section 5.4.8).<sup>1043</sup> The 1,2-di-Bu<sup>t</sup>-Cp anion has been used to prepare (1,2-Bu<sup>t</sup><sub>2</sub>-C<sub>5</sub>H<sub>3</sub>)<sub>2</sub>TiCl<sub>2</sub> (Scheme 434). According to its X-ray structure the 1,2-di-Bu<sup>t</sup>-Cp ligands are arranged with all four Bu<sup>t</sup> groups in the open part of the wedge between the two tilted Cp rings, but the steric interactions between the substituents result in a conformationally dictated C<sub>2</sub>-symmetric molecule. NMR spectra suggest a facile dynamic process involving exchange between Bu<sup>t</sup> sites.<sup>1044</sup>



Scheme 432



Scheme 433



Scheme 434

Bulky Cp transition metal complexes have attracted much attention. The reaction of the titanium(III) complex  $\text{CpTiCl}_2$  with  $\text{K}(\text{C}_5\text{Bz}_5)$  affords  $\text{Cp}(\text{C}_5\text{Bz}_5)\text{TiCl}$  from which the dichloro bis-Cp compound  $\text{Cp}(\text{C}_5\text{Bz}_5)_2\text{TiCl}_2$  could be prepared by oxidation with  $\text{AgCl}$ . The X-ray study reveals that in the molecular structure only one of the Bz substituents is inclined toward the Ti atom.<sup>1045</sup>

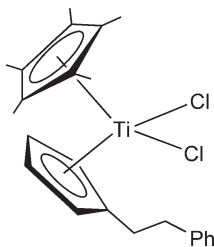
The reaction of  $\text{Ti}(\text{C}_5\text{H}_4\text{CH}_2\text{CH}_2\text{Ph})$  with  $\text{Cp}^*\text{TiCl}_3$  affords the mixed bis-Cp complex  $\text{Cp}^*(\text{C}_5\text{H}_4\text{CH}_2\text{CH}_2\text{Ph})\text{TiCl}_2$  (Scheme 435).<sup>332</sup>

Compound  $(\text{C}_5\text{H}_2-2,3-\text{Me}_2-1,4-\text{Ph}_2)_2\text{TiCl}_2$  has been prepared by the reaction of the lithium salt of 2,3-dimethyl-1,4-diphenylcyclopentadiene with  $\text{TiCl}_3(\text{THF})_3$  after oxidation with  $\text{CCl}_4$  and recrystallization from a toluene/hexane mixture. The crystal structure has been determined by X-ray crystallography. In the presence of MAO, this compound is inactive for the polymerization of ethylene.<sup>1046</sup>

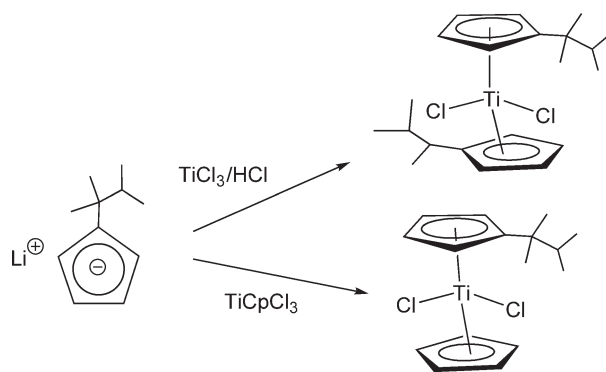
The synthesis of a series of 1-methyl-3-aryl-Cp-substituted dichloro bis-Cp titanium complexes and their structural characterization have been reported.<sup>1047</sup>

The  $C_2$ -symmetric complex  $(\text{C}_5\text{H}_4\text{CMe}_2\text{CHMe}_2)_2\text{TiCl}_2$  has been synthesized by the reaction of 2 equiv of  $\text{Li}[\text{C}_5\text{H}_4\text{CMe}_2\text{CHMe}_2]$  and  $\text{TiCl}_3(\text{THF})_3$  followed by oxidation with  $\text{HCl}$ . The reaction of the lithium salt with  $\text{CpTiCl}_3$  affords the mixed bis-Cp compound  $\text{Cp}(\text{C}_5\text{H}_4\text{CMe}_2\text{CHMe}_2)\text{TiCl}_2$  (Scheme 436). NMR spectroscopic studies in solution are carried out in order to interpret the observed NOE signals involving the distal protons of the substituted Cp ligands. The molecular structure of  $(\text{C}_5\text{H}_4\text{CMe}_2\text{CHMe}_2)_2\text{TiCl}_2$  has been determined by X-ray diffraction. These compounds have been used as catalytic precursors for the dehydropolymerization of silanes to polysilanes.<sup>1048</sup>

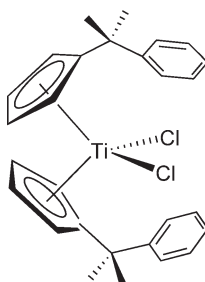
The synthesis and the activity of the 1-phenyl-1-methylethyl-Cp titanium dichloride shown in Scheme 437 as a pre-catalyst for ethylene polymerization has been studied.<sup>1049</sup> Reaction of  $\text{TiCl}_4$  with  $\text{Li}[\text{Me}_2\text{C}(\text{C}_5\text{H}_4)(\text{C}_{13}\text{H}_9)]$



Scheme 435



Scheme 436

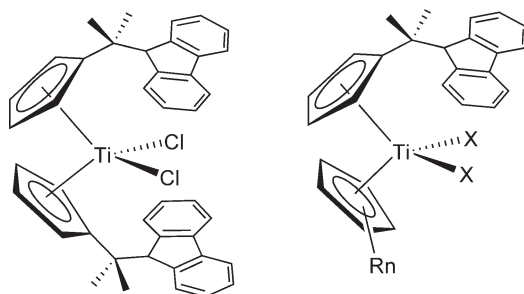


Scheme 437

affords the bis-Cp' derivative  $[\text{Me}_2\text{C}(\text{C}_5\text{H}_4)(\text{C}_{13}\text{H}_9)]_2\text{TiCl}_2$ , while treatment of  $\text{Cp}''\text{TiCl}_3$  ( $\text{Cp}' = \text{Cp}$ ,  $\text{Cp}''$ ) with  $\text{Ti}[\text{Me}_2\text{C}(\text{C}_5\text{H}_4)(\text{C}_{13}\text{H}_9)]$  gives the “mixed ring” complex  $\text{Cp}'[\text{Me}_2\text{C}(\text{C}_5\text{H}_4)(\text{C}_{13}\text{H}_9)]\text{TiCl}_2$ . The molecular structure of  $[\text{Me}_2\text{C}(\text{C}_5\text{H}_4)(\text{C}_{13}\text{H}_9)]_2\text{TiCl}_2$  as determined by X-ray diffraction shows that the Cp ring is  $\eta^5$ -bound, whereas the Flu ring is not coordinated to the metal center (Scheme 438).<sup>326</sup>

The formation of biphenyl-substituted bis-Cp titanium complexes (Scheme 439) has been detected during the synthesis of *ansa*-biphenyl-bridged bis-Cp derivatives.<sup>1050</sup> The synthesis of the bis(tetrahydroindenyl) dichloride  $(\text{C}_9\text{H}_{10})\text{TiCl}_2$ <sup>1051</sup> and of  $[\text{C}_5\text{H}_3(1,2\text{-CH}_2\text{-})_n]_2\text{TiCl}_2$  ( $n = 4\text{--}6$ ) (Scheme 440)<sup>1052</sup> have been reported.

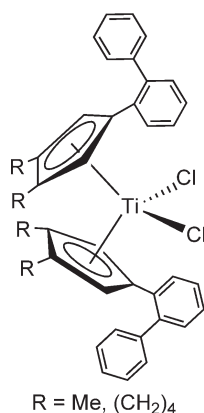
The synthesis of the mononuclear compound  $\text{Cp}[(\text{C}_5\text{H}_4)\text{CH}_2(\text{C}_5\text{H}_5)]\text{TiCl}_2$  is described by the reaction of  $\text{Na}[(\text{C}_5\text{H}_4)\text{CH}_2(\text{C}_5\text{H}_5)]$  with  $\text{CpTiCl}_3$ . Reduction with Mg/Hg in the presence of CO yields the Ti(II) complex  $\text{Cp}[(\text{C}_5\text{H}_4)\text{CH}_2(\text{C}_5\text{H}_5)]\text{Ti}(\text{CO})_2$ .<sup>1053</sup>



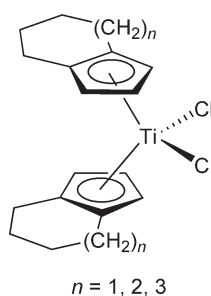
$\text{CpRn} = \text{Cp}$ ;  $\text{X} = \text{Cl}$   
 $\text{CpRn} = \text{Cp}''$ ;  $\text{X} = \text{Cl}, \text{Me}$

Scheme 438





Scheme 439

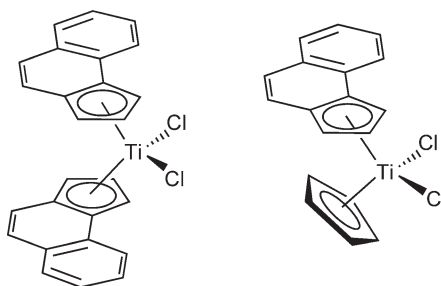


Scheme 440

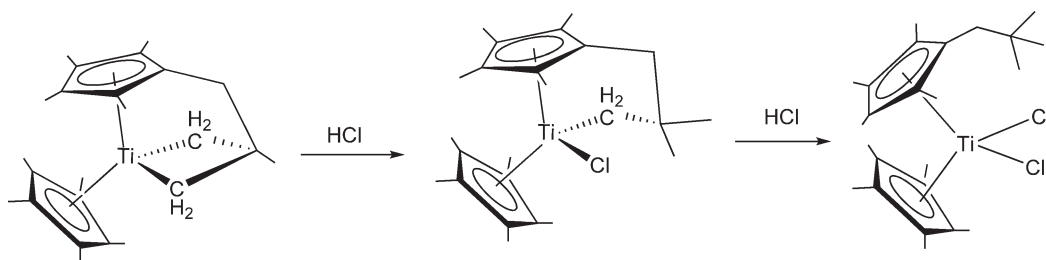
The unbridged bis(2-methylbenz[*e*]indenyl) and the mixed ring Cp 2-methylbenz[*e*]indenyltitanium complexes have been synthesized and evaluated as catalyst precursors for the polymerization of ethylene and propylene (Scheme 441). They exhibit low activity for the olefin polymerization when activated with either MAO or trityl borate.<sup>1054</sup>

The preparation of fluorinated organometallic compounds of early transition metals encounters serious difficulties associated with the electrophilic nature of the metal centers resulting in the reduced stability of the complexes and a propensity for fluoride transfer to the metal. The last decade has seen the development of this area and fluoroorganometallic titanium derivatives have been reported. A review summarizes the use of  $\text{AsF}_3$  and  $\text{Me}_3\text{SnF}$  as fluorinating agents in the synthesis of Cp derivatives of Ti and other group 4, 5, and 6 metals.<sup>1055</sup> The synthesis of Cp titanium fluorides  $(\text{C}_5\text{H}_4\text{R})_2\text{TiF}_2$  ( $R = \text{H}, \text{Me}, \text{SiMe}_3$ ) is possible by halide exchange with  $\text{Me}_3\text{SnF}$ . The reaction is sensitive to the solvent used.<sup>384</sup>

The two Ti–C bonds in  $\text{Cp}^*\text{Ti}[\eta^5:\eta^2\text{-C}_5\text{Me}_4\text{CH}_2\text{CMe}(\text{CH}_2)_2]$  (see Section 4.05.4.2.4, Metallacyclic compounds) are cleaved by 2 equiv. of HCl to give the dichloro compound  $\text{Cp}^*(\text{C}_5\text{Me}_4\text{CH}_2\text{Bu}^t)\text{TiCl}_2$  (Scheme 442).<sup>1056</sup>



Scheme 441



Scheme 442

Bis-Cp titanium derivatives containing liquid-crystalline (LC) groups as substituents in the Cp ligand  $(\text{C}_5\text{H}_4\text{PCH5060})_2\text{TiCl}_2$  or coordinated to the titanium atoms  $\text{Cp}_2\text{Ti}(\text{PCH5060})_2$  and  $\text{Cp}_2\text{TiCl}(\text{PCH5060})$  have been synthesized ( $\text{PCH5060} = p\text{-(trans-4-}n\text{-pentylcyclohexyl)phenoxyhexyloxy}$ ). Polarizing optical microscope observations and differential scanning calorimetry measurements indicate that these complexes exhibit LC behavior. They can polymerize phenylacetylene to give poly(phenylacetylene) with the aid of  $\text{AlEt}_3$  as co-catalyst.<sup>1057,1058</sup>

#### 4.05.4.1.1.(i).(b) Cp complexes with oxygen substituents

The siloxy-substituted complexes  $(\text{C}_5\text{H}_4\text{OSiR}_3)_2\text{TiCl}_2$  and  $\text{Cp}'(\text{C}_5\text{H}_4\text{OSiR}_3)\text{TiCl}_2$  ( $\text{Cp}' = \text{Cp}, \text{Cp}^*$ ) (Scheme 443) are prepared by deprotonation of the corresponding trialkyl-siloxy-cyclopentadiene with  $\text{LiBu}^n$ , followed by treatment with  $\text{TiCl}_4$  or  $\text{Cp}'\text{TiCl}_3$ . All attempts to obtain  $\text{Cp}^*(\text{C}_5\text{H}_4\text{OSiEt}_3)\text{TiCl}_2$  give mixtures of this complex with  $\text{Cp}^*(\text{C}_5\text{H}_4\text{OH})\text{TiCl}_2$  (Scheme 443).<sup>358</sup>

The bis-Cp'  $[\text{C}_5\text{H}_4(\text{CH}_2)_3\text{OMe}]_2\text{TiCl}_2$  and the mixed ligand compounds  $\text{Cp}[\text{C}_5\text{H}_4(\text{CH}_2)_3\text{OMe}]\text{TiCl}_2$  and  $[\text{C}_5\text{H}_4(\text{CH}_2)_3\text{OMe}][\text{C}_5\text{H}_4(\text{CH}_2)_2\text{OMe}]\text{TiCl}_2$  can be obtained by reaction of  $\text{K}[\text{C}_5\text{H}_4(\text{CH}_2)_3\text{OMe}]$  with  $\text{TiCl}_4$ ,  $\text{CpTiCl}_3$  or  $[\text{C}_5\text{H}_4(\text{CH}_2)_2\text{OMe}]\text{TiCl}_3$ , respectively.<sup>1059</sup> The chloro alkoxo-alkyl-Cp-substituted titanium complexes  $(\text{C}_5\text{H}_4\text{CH}_2\text{CH}_2\text{OMe})_2\text{TiCl}_2$  and  $\text{Cp}(\text{C}_5\text{H}_4\text{CH}_2\text{CH}_2\text{OMe})\text{TiCl}_2$  react with  $\text{BBr}_3$  to give titanium compounds containing Cp ligands with bromoethyl substituents,  $(\text{C}_5\text{H}_4\text{CH}_2\text{CH}_2\text{Br})_2\text{TiBr}_2$  and  $\text{Cp}(\text{C}_5\text{H}_4\text{CH}_2\text{CH}_2\text{Br})\text{TiBr}_2$ , respectively.<sup>366</sup>

Benzyl-substituted and MeO-containing benzyl-substituted Cp titanium complexes of the type shown in Scheme 444 have been prepared according to general synthetic routes. In the preparation of *o*-MeO-benzyl derivatives, cyclization of the ligand with elimination of  $\text{MeCl}$  to give titanoxacycle complexes is observed when ethyl or larger groups are present in the benzyl fragment. Crystal structures of some of these complexes are reported.<sup>814</sup>

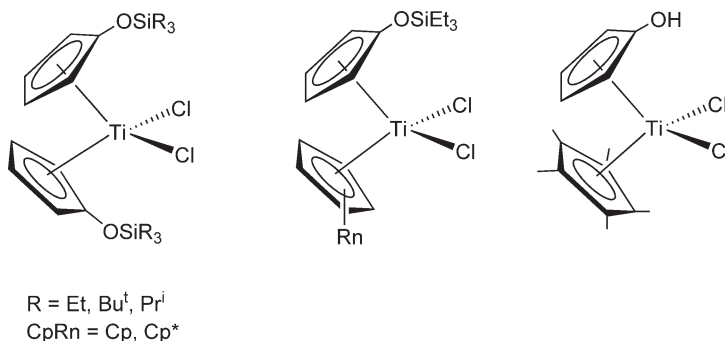
The mixed complex  $\text{CpCp}'\text{TiCl}_2$  (Scheme 445) containing one carbohydrate-substituted Cp ring has been synthesized by reaction of the thallium salt of the carbohydrate-derived Cp ligand with  $\text{CpTiCl}_3$  in THF.<sup>1060</sup>

Mixed ligand titanocenes may be supported using covalent spacers attached to a resin via a stable C–C bond (Scheme 446). The titanium content of this heterogenized system has been determined using inductively coupled plasma-atomic emission spectroscopy.<sup>1061</sup>

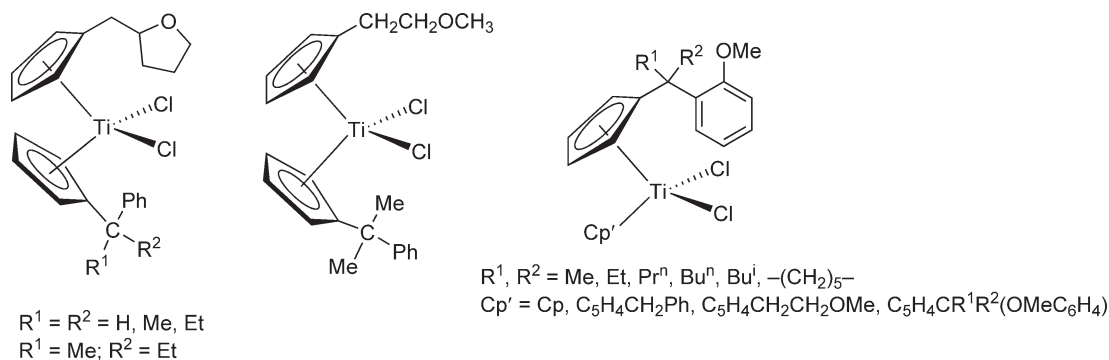
#### 4.05.4.1.1.(i).(c) Bis-Cp complexes with nitrogen-based Cp substituents

More examples in Section 4.05.4.1.1.(ii)

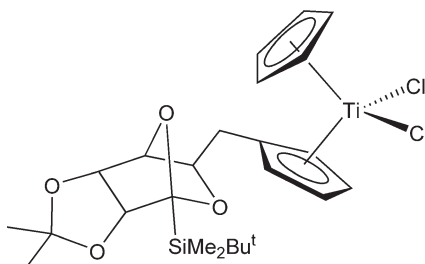
Pyrrolyl ligand and analogous N-heterocycles are isoelectronic with the Cp ring. Titanium complexes with this type of ligands have been described (Section 4.05.7).



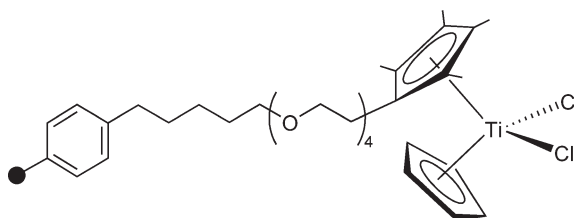
Scheme 443



Scheme 444



Scheme 445



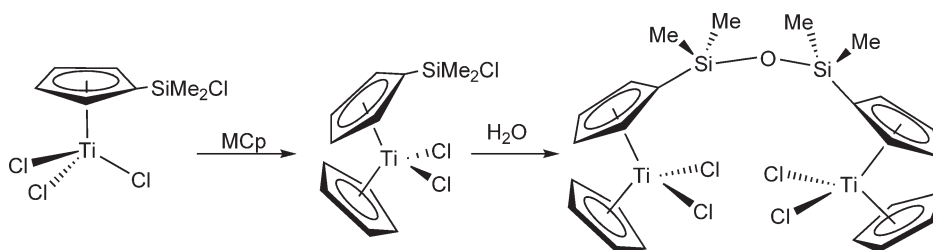
Scheme 446

#### 4.05.4.1.1.(i).(d) Bis-Cp complexes with silanyl and stannyl Cp substituents

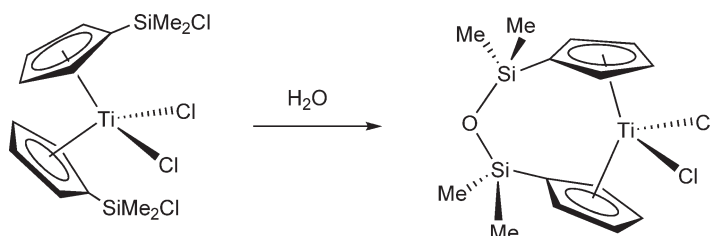
The synthesis and reactivity of transition metal complexes, including titanium derivatives with functionalized silyl-substituted Cp and related ligands, have been reviewed.<sup>378</sup>

$(\text{C}_5\text{H}_4\text{SiMe}_3)_2\text{TiCl}_2$  has been synthesized and its molecular structures determined by X-ray diffraction methods. The steric congestion between the two chloro ligands and two trimethylsilyl groups results in a nearly eclipsed conformation of the rings. The electronic effect of the  $\text{SiMe}_3$  group upon various properties has been studied.<sup>1062</sup> The molecular structure of  $(\text{C}_5\text{H}_4\text{SiMe}_3)_2\text{TiI}_2$  has been determined by X-ray diffraction.<sup>1063</sup>

Addition of 2 equiv. of  $\text{C}_5\text{H}_5(\text{SiClMe}_2)$  to a solution of  $\text{TiCl}_4$  in toluene under reflux and in the presence of 2 equiv. of  $\text{NEt}_3$  affords  $(\text{C}_5\text{H}_4\text{SiClMe}_2)_2\text{TiCl}_2$ . The reaction of the trichloride  $(\text{C}_5\text{H}_4\text{SiClMe}_2)\text{TiCl}_3$  with  $\text{MCp}'$  ( $\text{M} = \text{Na, K, Ti}$ ) gives the mixed bis-Cp complexes  $\text{Cp}'(\text{C}_5\text{H}_4\text{SiClMe}_2)\text{TiCl}_2$  ( $\text{Cp}' = \text{Cp, Cp}^*, 1,3\text{-Bu}^t_2\text{C}_5\text{H}_3$ ) (Scheme 447).<sup>379,822,1064</sup>  $\text{Cp}(\text{C}_5\text{H}_4\text{SiClMe}_2)\text{TiCl}_2$  reacts with  $\text{H}_2\text{O}$  to give the siloxane-bridged compound  $(\text{TiCpCl}_2)_2\text{---}[\text{C}_5\text{H}_4\text{Si}(\text{Me}_2)\text{---O---Si}(\text{Me}_2)\text{C}_5\text{H}_4]\text{Cl}_2$  (Scheme 447).<sup>822</sup> Similarly, the hydrolysis of  $(\text{C}_5\text{H}_4\text{SiClMe}_2)_2\text{TiCl}_2$  affords the mononuclear compound  $[(\text{C}_5\text{H}_4\text{SiMe}_2)_2(\mu\text{-O})]\text{TiCl}_2$  (Scheme 448). The Si-Cl bond of the mixed bis-Cp complex  $(1,3\text{-Bu}^t_2\text{C}_5\text{H}_3)(\text{C}_5\text{H}_4\text{SiClMe}_2)\text{TiCl}_2$  reacts selectively with 1 equiv. of  $\text{LiNHBu}^t$  in toluene at  $50\text{--}60^\circ\text{C}$  to give the amido-Cp-substituted compound  $(1,3\text{-Bu}^t_2\text{C}_5\text{H}_3)(\text{C}_5\text{H}_4\text{SiMe}_2\text{NHBu}^t)\text{TiCl}_2$ , while the same reaction with 2 equiv. of the lithium amide gives the Cp-amido compound  $(1,3\text{-Bu}^t_2\text{C}_5\text{H}_3)(\text{C}_5\text{H}_4\text{SiMe}_2\text{NBu}^t)\text{TiCl}$  by reaction of the Si-Cl and one of the Ti-Cl bonds.<sup>1064</sup> Analogous  $\text{Cp}(\text{C}_5\text{H}_4\text{SiMe}_2\text{Bu}^t)\text{TiCl}_2$  has been prepared by treatment of  $\text{CpTiCl}_3$  with



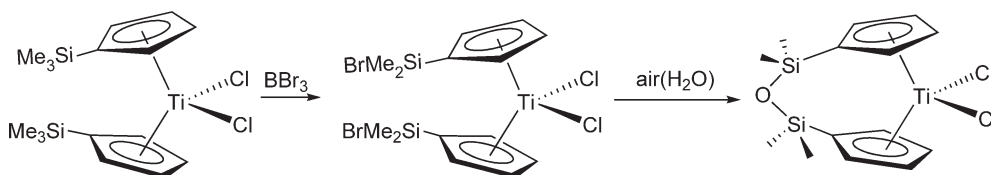
Scheme 447



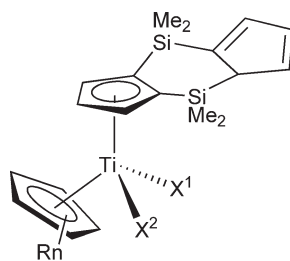
Scheme 448

$\text{Ti}(\text{C}_5\text{H}_4\text{SiMe}_2\text{Bu}^t)$ .<sup>1065</sup>  $(\text{C}_5\text{H}_4\text{SiBrMe}_2)_2\text{TiCl}_2$  is obtained by boron–silicon exchange in the reaction of  $(\text{C}_5\text{H}_4\text{SiMe}_3)_2\text{TiCl}_2$  with  $\text{BBr}_3$ . Hydrolysis of  $(\text{C}_5\text{H}_4\text{SiBrMe}_2)_2\text{TiCl}_2$  with water in THF affords the *ansa*-titanocene having a disiloxane bridging group (Scheme 449).<sup>1066</sup>

The mixed bis-Cp dichloride  $\text{Cp}'[\text{C}_5\text{H}_3(\text{SiMe}_2)_2\text{C}_5\text{H}_4]\text{TiCl}_2$  ( $\text{Cp}' = \text{Cp}, \text{Cp}^*$ ) has been prepared in high yields by the reaction of the monolithium salt  $\text{Li}[\text{C}_5\text{H}_3(\text{SiMe}_2)_2\text{C}_5\text{H}_4]$  with  $\text{Cp}''\text{TiCl}_3$ . The chloro complexes react with alkylating agents to give chloroalkyl or dialkyl derivatives (Scheme 450). The catalytic activity of some of these compounds for ethylene polymerization has been studied using MAO as co-catalyst.<sup>385</sup> Bis-Cp complexes bearing the  $\text{SiMe}_3$  or  $\text{SiMe}_2\text{H}$  substituted doubly bridged Cp system (Scheme 451) have been synthesized by the reaction of

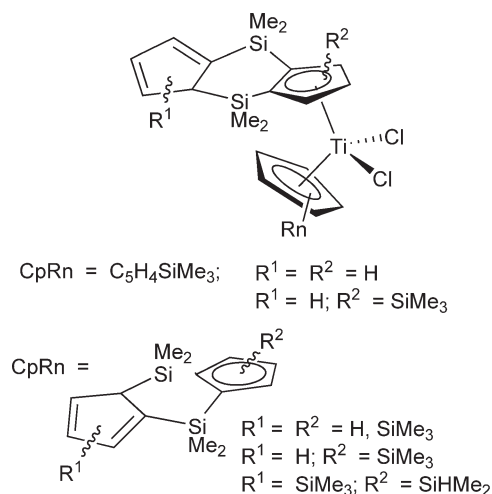


Scheme 449



$\text{CpRn} = \text{Cp}, \text{Cp}^*$   
 $\text{X}^1 = \text{X}^2 = \text{Cl}, \text{Me}$   
 $\text{X}^1 = \text{Cl}; \text{X}^2 = \text{Me}, \text{Et}$

Scheme 450



Scheme 451

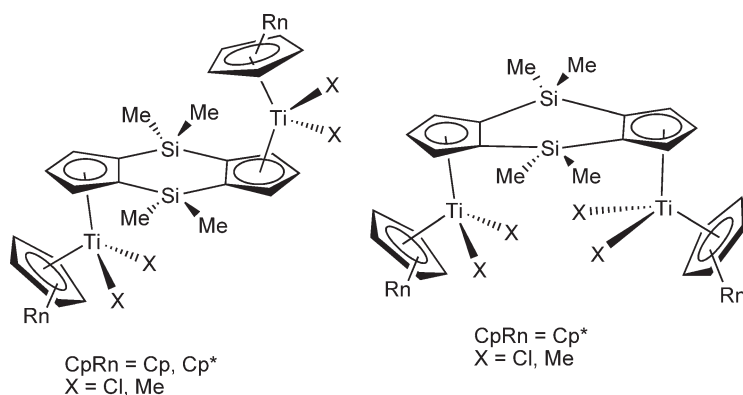
$\text{TiCl}_4$  or  $(\text{C}_5\text{H}_4\text{SiMe}_3)\text{TiCl}_3$  with the corresponding lithium  $\text{Cp}'$  reagent. The catalytic activity in ethylene and propylene homopolymerizations and ethylene/propylene co-polymerizations has been studied.<sup>1067</sup> Reaction of  $\text{Li}[(\text{C}_5\text{H}_3)_2(\text{SiMe}_2)_2]$  with  $\text{Cp}^*\text{TiCl}_3$  affords the bimetallic complexes *trans*- and *cis*- $[\text{Cp}^*\text{TiCl}_2]_2[\mu-(\text{C}_5\text{H}_3)_2(\text{SiMe}_2)_2]$ . The *trans*-form precipitates from the reaction medium and thus could be separated from the *cis*-isomer. Reaction with  $\text{CpTiCl}_3$  produces only the *trans*-isomer  $(\text{CpTiCl}_2)_2[\mu-(\text{C}_5\text{H}_3)_2(\text{SiMe}_2)_2]$ . Reactions with 4 equiv. of  $\text{LiMe}$  give the corresponding tetramethyl derivatives (Scheme 452).<sup>1068</sup>

$\text{Cp}[\text{C}_5\text{H}_4\text{Si}(\text{Me}_2)\text{CH}=\text{CH}_2]\text{TiCl}_2$  and  $\text{Me}_2\text{Si}[\text{OCH}_2\text{CH}_2\text{CH}_2\text{SiMe}_2\text{CH}_2\text{CH}_2\text{SiMe}_2-\text{C}_5\text{H}_4-\text{TiCpCl}_2]_2$  (Scheme 453) and have been used as heterogeneous catalysts on clay minerals for ethylene polymerization.<sup>1069</sup>

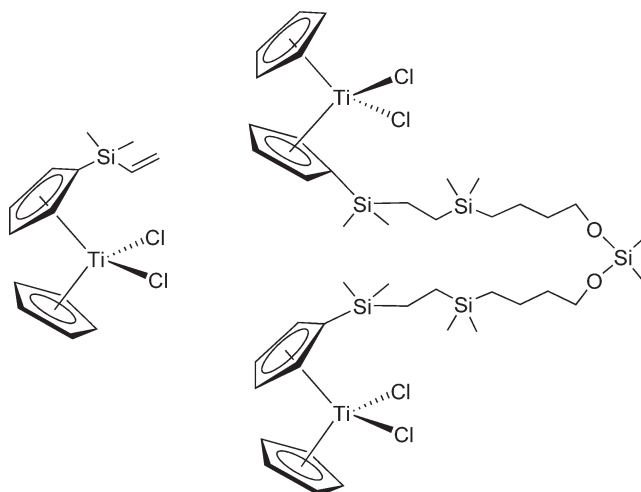
The mixed bis-Cp complexes  $\text{Cp}'(\text{C}_5\text{H}_4\text{SiMe}_2\text{CH}_2\text{CH}=\text{CH}_2)\text{TiCl}_2$  ( $\text{Cp}' = \text{Cp}, \text{Cp}^*, \text{C}_5\text{H}_4\text{SiMe}_2\text{CH}_2\text{CH}=\text{CH}_2$ ) have been prepared. The molecular structure of the  $\text{Cp}^*$  derivative has been determined by X-ray diffraction.<sup>391</sup>

Halogen exchange of Ti chlorides with  $\text{Me}_3\text{SnF}$  gives the Cp titanium fluorides  $[\text{1,3-C}_5\text{H}_3(\text{SiMe}_3)\text{R}]_n\text{TiF}_m$  ( $\text{R} = \text{H}, \text{Me}, \text{SiMe}_3; n = m = 2$ ).<sup>384</sup> Mixed bis-Cp complexes containing Cp rings with polyfluorinated substituents have been synthesized.  $(\text{C}_5\text{H}_4\text{SiMe}_3)(\text{C}_5\text{H}_4\text{SiMe}_2\text{CH}_2\text{CH}_2\text{C}_8\text{F}_{17})\text{TiCl}_2$  and  $(\text{C}_5\text{H}_4\text{SiMe}_3)[\text{C}_5\text{H}_3(\text{SiMe}_2\text{CH}_2\text{CH}_2\text{C}_8\text{F}_{17})_2]\text{TiCl}_2$  are prepared by treatment of the fluorinated lithium cyclopentadienide with  $(\text{C}_5\text{H}_4\text{SiMe}_3)\text{TiCl}_3$ . The analogous reaction with  $\text{TiCl}_3(\text{THF})_3$  followed by oxidation with  $\text{PbCl}_2$  affords the bis-Cp complex  $(\text{C}_5\text{H}_4\text{SiMe}_2\text{CH}_2\text{CH}_2-\text{C}_8\text{F}_{17})_2\text{TiCl}_2$ , the molecular structure of which has been determined by X-ray diffraction.<sup>392</sup>

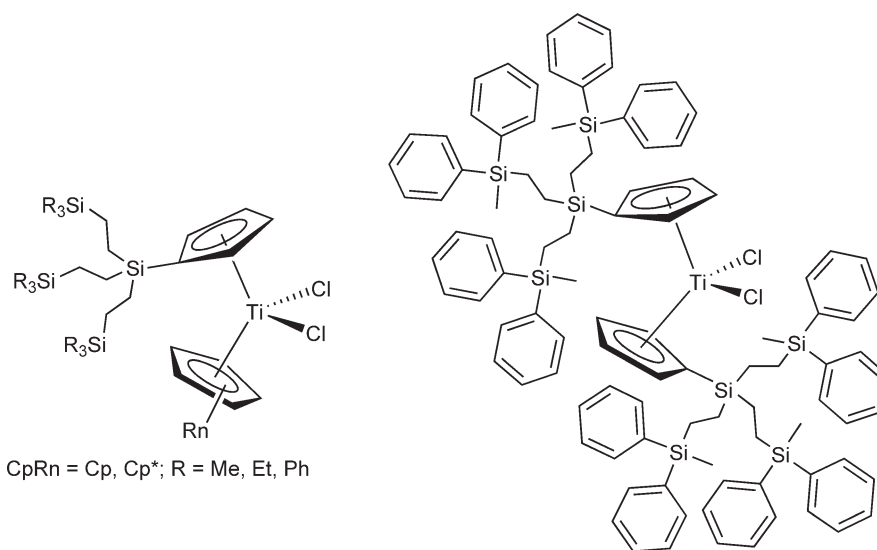
A series of bis-Cp Ti derivatives where the Cp ring is attached to a dendrimeric unit have been obtained by reaction of the potassium salt of dendritic cyclopentadienides with  $\text{CpTiCl}_3$  or  $\text{TiCl}_4$  (Scheme 454). Cyclic voltammograms and catalytic behavior of these complexes in ethylene polymerization, using MAO as a co-catalyst, have been studied and compared to that of related non-dendritic complexes.<sup>1070</sup>



Scheme 452



### Scheme 453



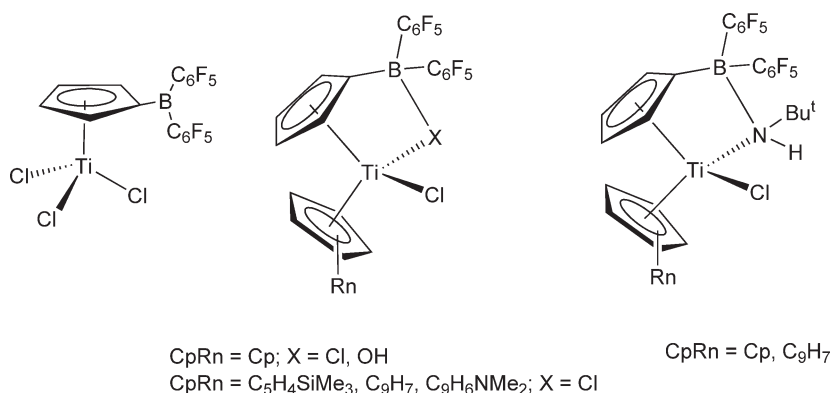
### Scheme 454

Complexes containing the Ti–Sn bond have been isolated by the oxidation–elimination reaction between  $\text{Cp}_2\text{Ti}(\text{CO})_2$  and aryltin halides. Free radicals are proposed as intermediates.<sup>1071</sup>

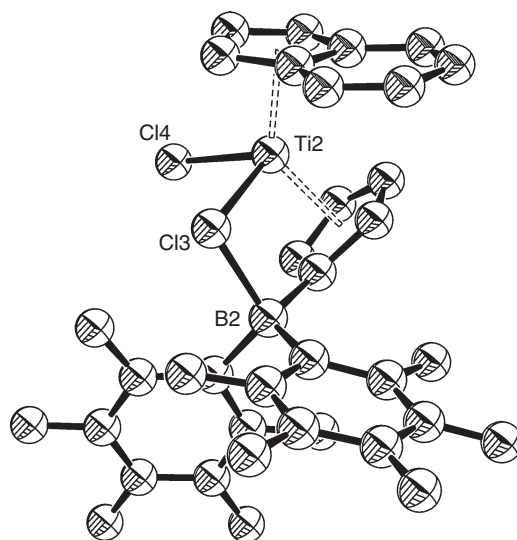
#### 4.05.4.1.1.(i).(e) Bis-Cp complexes with boryl substituents

Boryl-Cp' and bis-Cp group 4 derivatives containing pendant boron substituents on the Cp ring have been reviewed.<sup>394</sup>

Titanium complexes with Cp' ligands bearing Lewis-acidic bis(pentafluorophenyl)boryl substituents have been found to activate chloro ligands, depending on the substituted Cp'–Ti–Cl angle.<sup>1072</sup> The trichloro complex [C<sub>5</sub>H<sub>4</sub>B(C<sub>6</sub>F<sub>5</sub>)<sub>2</sub>]<sub>2</sub>TiCl<sub>3</sub><sup>395</sup> reacts with LiCp' to give the mixed bis-Cp' derivatives Cp'[C<sub>5</sub>H<sub>4</sub>B(C<sub>6</sub>F<sub>5</sub>)<sub>2</sub>(μ-Cl)]TiCl (Scheme 455), from which Cp[C<sub>5</sub>H<sub>4</sub>B(C<sub>6</sub>F<sub>5</sub>)<sub>2</sub>(μ-OH)]TiCl is obtained under hydrolysis conditions. In these complexes, the B–Cl or B–OH moieties form bridges to the titanium center and exhibit relatively short B–Cl (B–O) and elongated Ti–Cl (Ti–O) bonds (Figure 24). The compounds are fluxional in solution, with the B(C<sub>6</sub>F<sub>5</sub>)<sub>2</sub> fragment switching rapidly between the two chloro ligands. Reaction of Cp[C<sub>5</sub>H<sub>4</sub>B(C<sub>6</sub>F<sub>5</sub>)<sub>2</sub>]<sub>2</sub>TiCl<sub>2</sub> with LiNHBU<sup>t</sup> or NaNH<sub>2</sub> gives the corresponding aminoborates Cp[C<sub>5</sub>H<sub>4</sub>B(C<sub>6</sub>F<sub>5</sub>)<sub>2</sub>(μ-NHR)]TiCl. C–F...H–N hydrogen bonding to one of the



Scheme 455



**Figure 24** Molecular structure of complex  $(\text{Ind})[\text{C}_5\text{H}_4\text{B}(\text{C}_6\text{F}_5)_2]\text{TiCl}_2$  (reproduced by permission of American Chemical Society from *Organometallics*, **2000**, *19*, 1599).

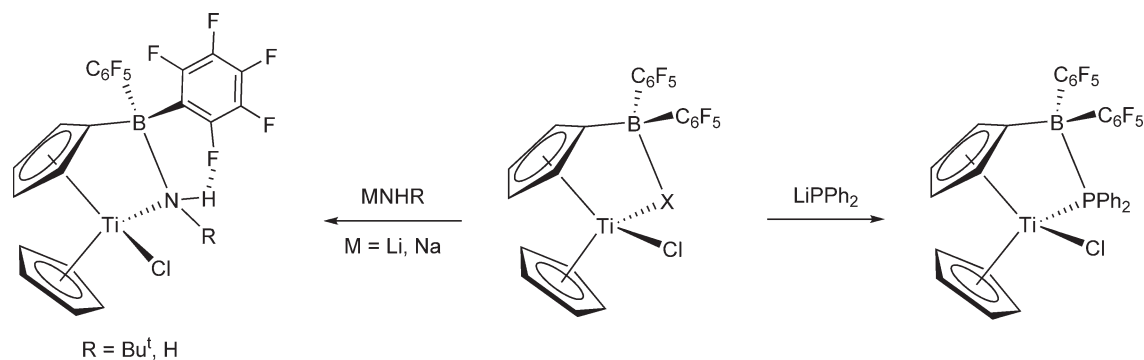
*ortho*-F atoms of a  $\text{C}_6\text{F}_5$  ring has been observed that is strong enough to persist in solution at room temperature. The molecular structures of some of these compounds have been determined by X-ray diffraction, and a reinvestigation of the crystal structure of  $[\text{C}_5\text{H}_4\text{B}(\text{C}_6\text{F}_5)_2]\text{TiCl}_3$  has been carried out. An analogous reaction with  $\text{LiPPh}_2$  gives  $\text{Cp}[\text{C}_5\text{H}_4\text{B}(\text{C}_6\text{F}_5)_2(\text{PPh}_2)]\text{TiCl}$  (Scheme 456).<sup>617,1073</sup>

Thermally stable complexes  $\text{Cp}^*(\text{C}_5\text{H}_4\text{CMe}_2\text{CB}_{10}\text{H}_{10}\text{CR})\text{TiCl}_2$  ( $\text{R} = \text{H}, \text{Me}$ ) and  $\text{Cp}^*(\text{C}_5\text{H}_4\text{CMe}_2\text{CB}_{10}\text{H}_{10}\text{C})\text{TiCl}$  (Scheme 457) have been prepared via metathesis reactions of  $\text{Cp}^*\text{TiCl}_3$  with monolithium or dilithium salts of the *o*-carborano ligand, respectively. A single crystal X-ray diffraction study has been carried out. In the presence of MMAO, they are active polymerization catalysts and produce high density polyethylene.<sup>1074</sup>

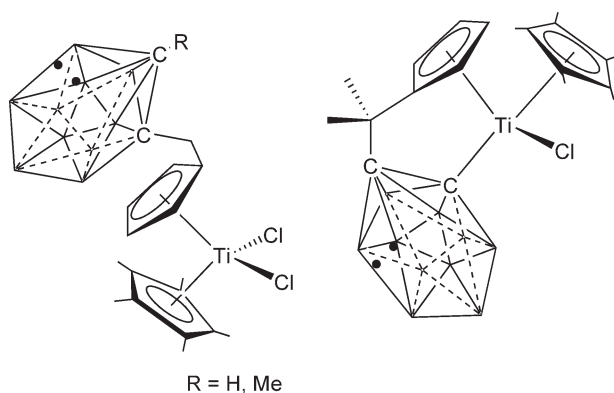
#### 4.05.4.1.1.(i).(f) Cp ligands with P and S substituents

$\text{CpTiCl}_3$  reacts with  $\text{Li}[\text{C}_5\text{Me}_3(\text{PPh}_2)_2]$  to give the mixed bis-Cp complex  $\text{Cp}[\text{C}_5\text{Me}_3(\text{PPh}_2)_2]\text{TiCl}_2$ , which is used as a metalloligand to prepare heterobimetallic Ti-late transition metal complexes (Scheme 705; Section 4.05.6).<sup>1075</sup>

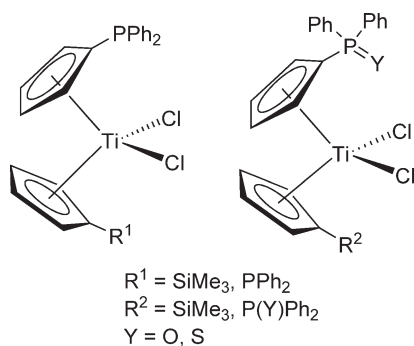
Substituted mixed bis-Cp' dichloro titanium complexes containing diphenyloxo- or diphenylthiophosphoryl-Cp ligands are obtained by oxidation reaction of the corresponding diphenylphosphino-Cp derivatives with  $\text{S}_8$  or  $\text{H}_2\text{O}_2$  (Scheme 458).<sup>1076</sup> The reaction of  $\text{TiCl}_4$  with 2 equiv. of  $\text{M}[\text{C}_5\text{H}_4\text{P}(=\text{S})\text{Ph}_2]$  ( $\text{M} = \text{Li}, \text{Ti}$ ) affords  $[\text{C}_5\text{H}_4\text{P}(=\text{S})\text{Ph}_2]_2\text{TiCl}_2$ . The mixed bis-Cp complex  $\text{Cp}[\text{C}_5\text{H}_4\text{P}(=\text{S})\text{Ph}_2]\text{TiCl}_2$  is obtained by treatment of  $\text{Ti}[\text{C}_5\text{H}_4\text{P}(=\text{S})\text{Ph}_2]$  with  $\text{CpTiCl}_3$ .<sup>397</sup>



Scheme 456



Scheme 457



Scheme 458

The sodium salt  $\text{Na}(\text{C}_5\text{Me}_4\text{SPr}^n)$  reacts with  $\text{TiCl}_3(\text{THF})_3$  followed by treatment with  $\text{CCl}_4$  to give the bis-Cp complex  $(\text{C}_5\text{Me}_4\text{SPr}^n)_2\text{TiCl}_2$ . The introduction of the propylthio group on the Cp ring increases the reduction potential by about 150 mV with respect to the value found for  $(\text{C}_5\text{Me}_4\text{H})_2\text{TiCl}_2$ . The crystal structure of this complex has been determined by X-ray diffraction.<sup>1077</sup> The synthesis and the molecular structure of  $(\text{C}_5\text{H}_4\text{SPr}^n)_2\text{TiCl}_2$  have been reported.<sup>1078</sup>



## 4.05.4.1.1.(f),(g) Binuclear complexes

For more examples of this type of complexes, see Section 4.05.6. The synthesis of homobinuclear and heterobinuclear bis-Cp titanium complexes is reviewed. The research about their activity on polymerization of  $\alpha$ -olefins is summarized. The mechanism about binuclear metallocene catalyst is also discussed in this chapter.<sup>1079</sup>

The fulvalene compound  $[\text{CpTiCl}_2]_2(\text{C}_{10}\text{H}_8)$  is prepared by treatment of the hydrido titanium(III) compound  $[\text{CpTi}(\mu\text{-H})]_2(\text{C}_{10}\text{H}_8)$  with  $\text{Cl}_2$  in  $\text{CH}_2\text{Cl}_2$  solution. The alkylation and hydrolysis reactions of this compound have been studied to give the tetraalkyl  $[\text{CpTiR}_2]_2(\text{C}_{10}\text{H}_8)$  and the  $\mu$ -oxo  $[\text{CpTiCl}]_2(\mu\text{-O})(\text{C}_{10}\text{H}_8)$  derivatives (Scheme 459), the molecular structure of which has been determined by X-ray diffraction. A small Ti–O–Ti angle ( $159.4^\circ$ ) with significant deviation from linearity is observed.<sup>1080</sup>

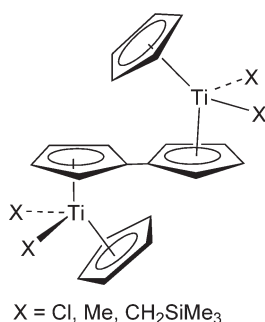
The reaction of  $\text{Li}[(\text{C}_5\text{H}_4)_2\text{CH}_2]$  with  $\text{CpTiCl}_3$  gives the binuclear complex  $(\text{CpTiCl}_2)_2[(\text{C}_5\text{H}_4)_2\text{CH}_2]$ , which on treatment with  $\text{Mg/Hg}$  is reduced to the corresponding Ti(III)–Ti(III) derivative  $(\text{CpTiCl})_2[(\text{C}_5\text{H}_4)_2\text{CH}_2]$ ; it is converted to the  $\mu$ -oxo compound  $(\text{CpTiCl})_2[(\text{C}_5\text{H}_4)_2\text{CH}_2](\mu\text{-O})$  when exposed to air.<sup>1053</sup>

The synthesis of an *ansa*-disymmetric alkylidene bridged binuclear titanium complex (Scheme 654; Section 4.05.5) has been described and its use in ethylene polymerization in the presence of MAO was investigated.<sup>1081</sup>

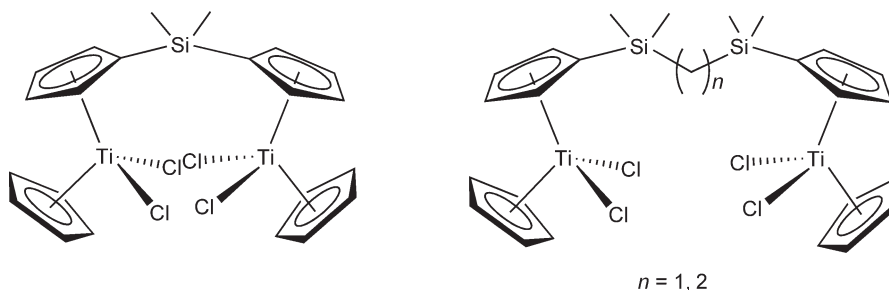
Monobridged bimetallic titanium complexes of the formula  $(\text{CpTiCl}_2)[\mu\text{-X}(\text{C}_5\text{H}_4)_2]$  shown in Scheme 460 have been synthesized and characterized. These complexes have been tested as catalysts for the dehydrocoupling of  $\text{SiPhH}_3$  to produce mixtures of linear and cyclic polyphenylsilanes.<sup>1082</sup> Analogous complexes  $\text{Cl}_2\text{Cp}'\text{Ti}(\text{C}_5\text{H}_4\text{-SiMe}_2\text{SiMe}_2\text{-C}_5\text{H}_4)\text{TiCp}'\text{Cl}_2$  ( $\text{Cp}' = \text{C}_5\text{H}_4\text{Bu}^t$ ,  $\text{C}_9\text{H}_6$ ) have been synthesized by reaction of the lithium salt of the tetramethyldisilane-bridged cyclopentadiene with  $\text{TiCl}_4(\text{THF})_2$ . The molecular structure of the  $\text{C}_5\text{H}_4\text{Bu}^t$  compound has been determined by X-ray diffraction methods. These complexes are used for the catalytic polymerization of ethylene after the activation with MAO.<sup>1083</sup> The synthesis of the bridged binuclear compounds  $\text{X}_2\text{Ti}(\text{C}_5\text{H}_4)_2(\text{Me})\text{Si-Si}(\text{Me})(\text{C}_5\text{H}_4)_2\text{TiX}_2$  ( $\text{X} = \text{Cl}$ ,  $\text{Me}$ ) has been reported and the molecular structure of the chloride derivative determined by X-ray diffraction.<sup>1084</sup>

$(\text{C}_5\text{H}_4\text{SiMe}_3)\text{TiCl}_3$  reacts with the lithium salt  $\text{Li}_2[(\text{C}_5\text{H}_3)_2(\text{SiMe}_2)_2]$  to afford a binuclear titanium compound with the doubly bridged Cp system connecting the two Ti atoms (Scheme 461). Its catalytic activity in ethylene polymerization has been studied.<sup>1067</sup>

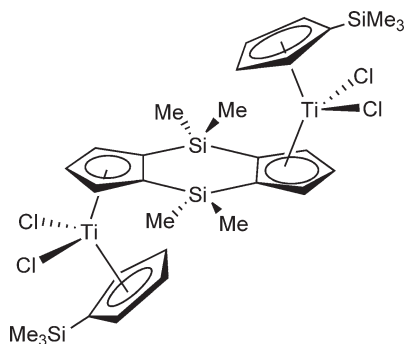
The amino-silyl-Cp-substituted compound  $(\text{C}_5\text{Me}_4\text{SiMe}_2\text{NMe}_2)_2\text{TiCl}_2$  undergoes hydrolytic cleavage of the Si–N bonds to give dimethylamine and the doubly siloxane-bridged binuclear complex  $\text{Cl}_2\text{Ti}(\text{C}_5\text{Me}_4\text{-SiMe}_2\text{-O-SiMe}_2\text{-C}_5\text{Me}_4)_2\text{TiCl}_2$ .<sup>1085</sup>



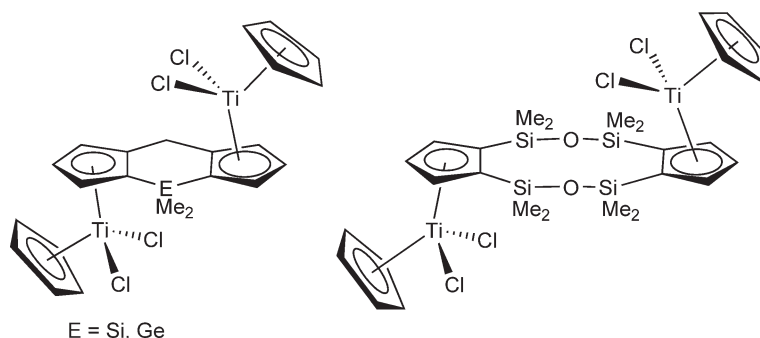
Scheme 459



Scheme 460



Scheme 461



Scheme 462

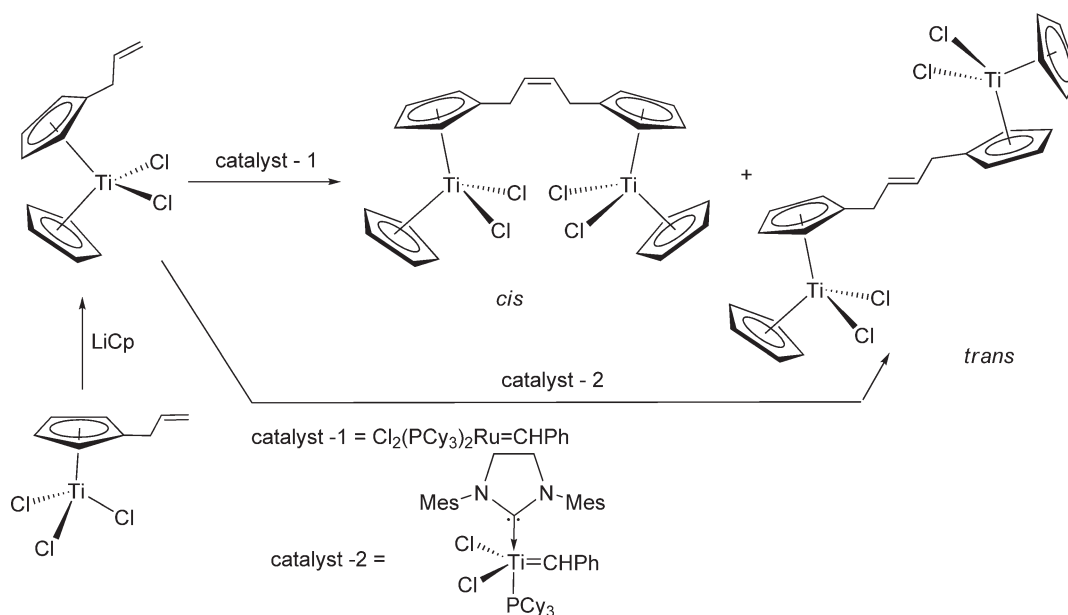
Binuclear mixed bis-Cp titanium complexes (Scheme 462) in which both metal atoms are connected by a doubly bridged bis-Cp' ligand (see also Scheme 452) have been synthesized by the reaction of  $\text{CpTiCl}_3$  with the corresponding lithium salts of the bridged Cp groups. Their catalytic properties for ethylene polymerization in the presence of MAO have been studied.<sup>1086</sup> The tetramethyldisiloxanediyl-bridged binuclear complexes  $\text{Cl}_2\text{CpTi}(\text{C}_5\text{R}_4\text{-SiMe}_2\text{-O-SiMe}_2\text{-C}_5\text{R}_4)\text{TiCpCl}_2$  ( $\text{R} = \text{H}, \text{SiMe}_3$ ) have been synthesized by the reaction of the dilithium salts  $\text{Li}_2[\text{C}_5\text{R}_4\text{-SiMe}_2\text{-O-SiMe}_2\text{-C}_5\text{R}_4]$  with  $\text{CpTiCl}_3$ . Their catalytic behavior for the polymerization of ethylene under different conditions has been investigated and compared with  $\text{Cp}_2\text{TiCl}_2$ . The  $\text{SiMe}_3\text{-Cp}$ -substituted derivative exhibits an unexpected temperature dependence for ethylene polymerization.<sup>1087</sup> The molecular structures of the siloxo-bridged complexes  $[(\text{C}_5\text{R}_5)\text{TiCl}_2]_2(\mu\text{-C}_5\text{H}_4\text{SiMe}_2\text{-O-SiMe}_2\text{C}_5\text{H}_4)$  ( $\text{R} = \text{H}, \text{Me}$ ) have been determined by X-ray diffraction.<sup>1088</sup>

$\text{Cp}(\text{C}_5\text{H}_4\text{-allyl})\text{TiCl}_2$  is prepared by the reaction of  $(\text{C}_5\text{H}_4\text{-allyl})\text{TiCl}_3$  with  $\text{LiCp}$ . Treatment of  $\text{Cp}(\text{C}_5\text{H}_4\text{-allyl})\text{TiCl}_2$  with the metathesis catalyst Ru-carbene complex  $\text{Cl}_2(\text{PCy}_3)_2\text{Ru}=\text{CHPh}$  (3 mol.%) affords the dititanium compound  $\text{Cl}_2\text{CpTi}(\text{C}_5\text{H}_4)\text{-CH}_2\text{CH}=\text{CHCH}_2\text{-(C}_5\text{H}_4)\text{TiCpCl}_2$ , obtained as a mixture of *cis*- and *trans*-isomers (Scheme 463). Similarly, treatment with a "second-generation" metathesis catalyst gives the pure *trans*-isomer. Both complexes have been spectroscopically characterized.<sup>350</sup>

#### 4.05.4.1.1.(ii) Cp ligands with functionalized side arms

Some complexes described in Section 4.05.4.1.1.(i) could also be mentioned in this section.

Among the Cp' ligands, those with an additional donor function in the side chain have received increasing interest in the chemistry of Ti(IV). A Cp ligand with a side-chain functionality (amino, amido, ether, etc.,) may act as a bidentate ligand. Under certain conditions, this type of ligands can reversibly coordinate to the metal center, temporarily blocking vacant coordination sites, and important reactivity effects can derive from this behavior. This could potentially stabilize electron-deficient metal centers by intramolecular coordination, thus providing a means of isolating and characterizing highly reactive intermediates and products. Heterobimetallic complexes synthesized with these functionalized ligands may have improved catalytic properties. Anchoring of a Cp complex onto a solid support through functional side arms is also feasible. Recently, interest in amino-functionalized mono-Cp and bis-Cp titanium

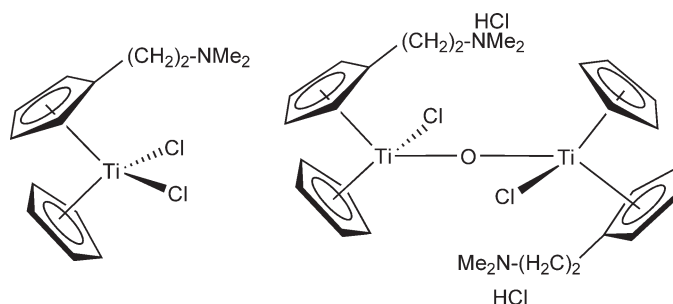


Scheme 463

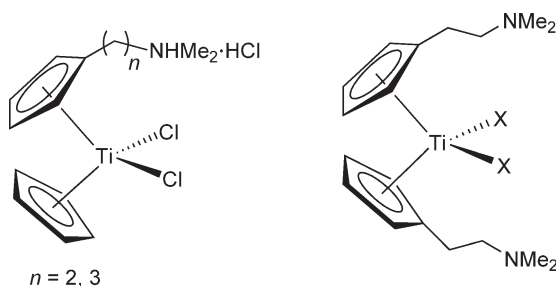
compounds has increased because of their potential as selective olefin polymerization catalyst precursors. It has been shown that quaternization of the pendant amino group results in water-soluble species. These systems have also proved useful as potentially biologically active species with anti-tumor properties.

Reaction of  $\text{Li}[\text{C}_5\text{H}_4\text{CMe}_2\text{NMe}_2]$  with  $\text{TiCl}_4(\text{THF})_2$  affords the bis-Cp compound  $(\text{C}_5\text{H}_4\text{CMe}_2\text{NMe}_2)_2\text{TiCl}_2$ , in which both Cp rings contain a dimethylaminomethyl substituent. The molecular structure has been determined by X-ray diffraction.<sup>1089</sup>

The introduction of aminoethyl side chain into Cp titanium derivatives leads to interesting changes in structure and reactivity in comparison to the non-substituted Cp complexes, and aminoethyl-functionalized bis-Cp titanium complexes have been reviewed.<sup>367</sup> The (N,N-dimethylaminoethyl)Cp ligand has been used to synthesize mono- and bis-Cp titanium complexes following classical procedures. The coordination behavior of the dimethylamino function has been studied on the basis of  $^1\text{H}$  NMR spectroscopy and X-ray crystal structure information.<sup>371</sup> The mixed ring dichloro titanium compound  $\text{Cp}[\text{C}_5\text{H}_4(\text{CH}_2)_2\text{NMe}_2]\text{TiCl}_2$  (Scheme 464) is prepared by ligand metathesis of the corresponding  $[\text{C}_5\text{H}_4(\text{CH}_2)_2\text{NMe}_2]\text{TiCl}_3$  with  $\text{TiCp}$ . The dichloro complex is exceedingly moisture sensitive and in  $\text{CH}_2\text{Cl}_2$  rapidly gives the hydrolysis product  $[\text{CpTi}(\text{Cl})\text{C}_5\text{H}_4(\text{CH}_2)_2\text{NMe}_2\cdot\text{HCl}]_2(\text{O})$  (see Scheme 589; Section 4.05.4.6.1).<sup>372</sup> The synthesis of such  $d^0$ -metal complexes turned out to be difficult because intramolecular coordination of the pendant amine and the presence of intermolecular coordination led to oligomeric and polymeric species that were difficult to characterize.<sup>370</sup>



Scheme 464



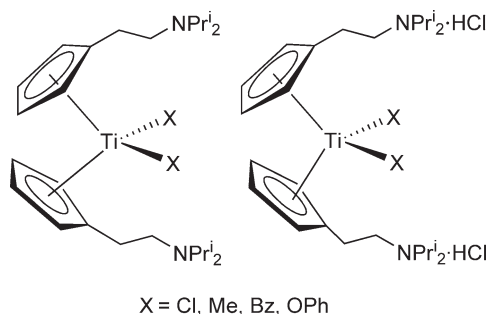
Scheme 465

The synthesis of  $\text{Cp}[\text{C}_5\text{H}_4(\text{CH}_2)_n\text{NMe}_2]\text{TiCl}_2$  ( $n = 2, 3$ ) has been described by the reaction of  $\text{CpTiCl}_3$  with  $\text{Me}_3\text{SiC}_5\text{H}_4(\text{CH}_2)_n\text{NMe}_2$ .<sup>1090</sup> A straightforward synthetic way for the preparation of these complexes has been reported by treatment of  $\text{CpTiCl}_3$  with the lithium salt of the aminoethyl substituted Cp ligand. These complexes are obtained as air and moisture-sensitive substances. They react with HCl dissolved in methanol to give the ammonium salts  $\text{Cp}[\text{C}_5\text{H}_4(\text{CH}_2)_n\text{NHMe}_2\cdot\text{HCl}]\text{TiCl}_2$  (Scheme 465). The molecular structure has been determined by X-ray diffraction for the compound with  $n = 3$ .<sup>1091</sup> Reaction of  $\text{Li}[\text{C}_5\text{H}_4\text{CH}_2\text{CH}_2\text{NMe}_2]$  with  $\text{TiCl}_4$  gives  $(\text{C}_5\text{H}_4\text{CH}_2\text{CH}_2\text{NMe}_2)_2\text{TiCl}_2$  (Scheme 465).<sup>1092</sup>

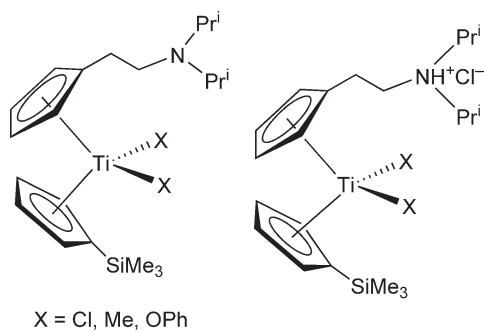
$\text{Cp}'(\text{C}_5\text{Me}_4\text{CH}_2\text{CH}_2\text{NMe}_2)\text{TiCl}_2$  ( $\text{Cp}' = \text{Cp}, \text{Cp}^*$ ) are obtained by oxidation of the  $\text{Ti(III)}$  compounds  $\text{Cp}'(\text{C}_5\text{Me}_4\text{CH}_2\text{CH}_2\text{NMe}_2)\text{TiCl}$  with  $\text{PbCl}_2$ . The molecular structure of the  $\text{Cp}^*$  derivative has been determined by X-ray diffraction, which reveals a non-coordinated  $\text{NMe}_2$  group. The dichloro compounds have been converted to a series of dialkyl, vinyl, titanacyclobutane, and fulvene complexes by the appropriate reactions (Scheme 531; Section 4.05.4.2.4).<sup>1093</sup>

The bis-Cp dichloro complexes with (diisopropylamino)ethyl-functionalized Cp rings have been synthesized by metathesis reaction between the lithium salt of the Cp ring and  $\text{TiCl}_4$ . Dialkyl and diphenoxo titanium complexes are also prepared (Scheme 466). The chloro complexes are pre-catalysts in the polymerization of ethylene.<sup>1094</sup>

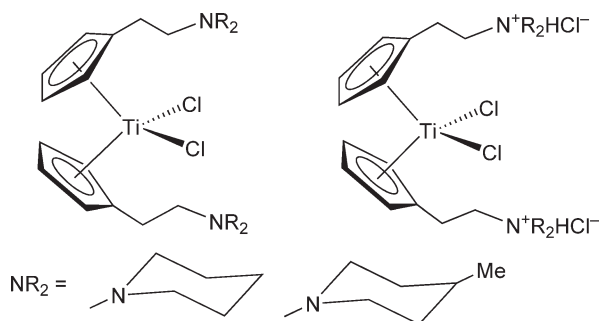
The mixed ligand titanocene  $(\text{C}_5\text{H}_4\text{SiMe}_3)(\text{C}_5\text{H}_4\text{CH}_2\text{CH}_2\text{NPr}_2)\text{TiCl}_2$  has been prepared by the reaction of  $\text{Li}[\text{C}_5\text{H}_4\text{CH}_2\text{CH}_2\text{NPr}_2]$  with  $(\text{C}_5\text{H}_4\text{SiMe}_3)\text{TiCl}_3$ . Reaction of this chloro compound with  $\text{LiMe}$  or  $\text{LiOPh}$  affords the dimethyl and diphenoxo derivatives. The dichloro complex reacts with 1 equiv. of HCl with protonation of the amino group to give the corresponding air- and water-stable dichloro-hydrochloride complex (Scheme 467). These compounds are precursors for  $\alpha$ -olefin polymerization catalysts.<sup>367,1095</sup> Analogous water-soluble and stable protected nitrogen-functionalized bis-Cp dichloro complexes have been synthesized by direct reaction of the sodium salts of the amino-substituted cyclopentadienes with  $\text{TiCl}_4$ . The corresponding dihydrochloride bis-Cp salts (Scheme 468) can be prepared by direct treatment of the amino-substituted cyclopentadienes with  $\text{TiCl}_4$ , or alternatively from the reaction of the dichloro compounds with HCl. One of these hydrochloride salts reacts with 4 equiv. of  $\text{LiMe}$  to afford the neutral dimethyl complex (Scheme 469).<sup>1096</sup> Complexes containing one ionic arm have also been made and their molecular structures determined by X-ray diffraction (Scheme 470).<sup>1097</sup> These compounds exhibit significant cytotoxicity against a number of different human tumor cell lines including a defined Cisplatin-resistant cell line. A similar series of water-soluble bis-Cp dichloro titanium derivatives containing alkylammonium groups pendant to



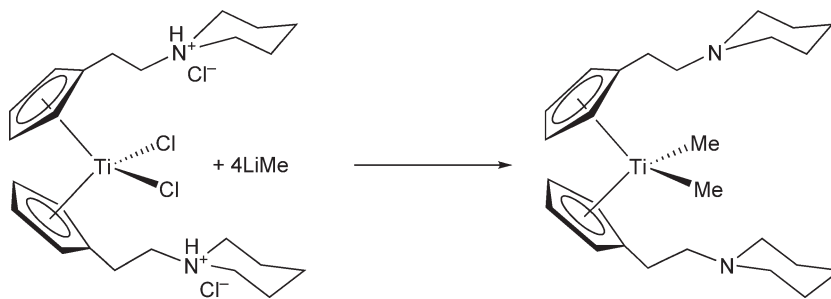
Scheme 466



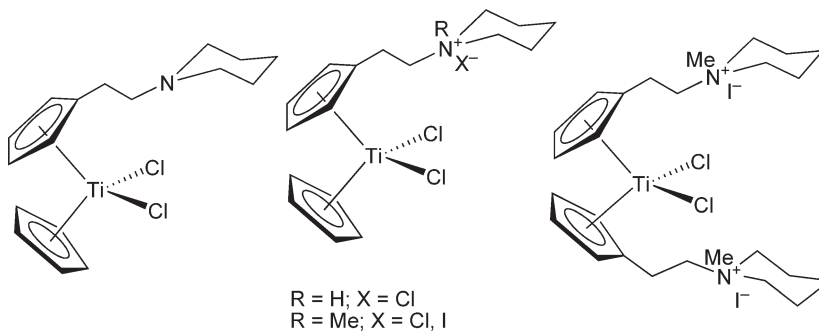
Scheme 467



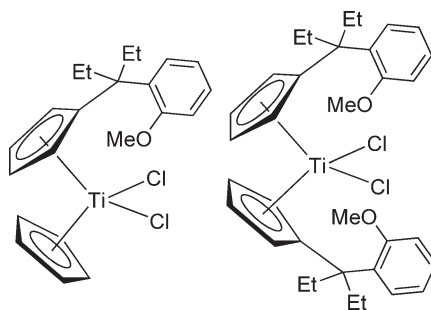
Scheme 468



Scheme 469



Scheme 470



Scheme 471

one (monocationic complexes) or both (dicationic complexes) Cp rings, supporting piperidinyl and 2-aminoethyl or 3-aminopropyl groups, has been synthesized and characterized. The *in vitro* cytotoxicity of these potential anticancer drugs has been studied (see Section 4.05.7).<sup>1098</sup>

Reactions of the substituted lithium cyclopentadienide reagents  $\text{Li}(\text{C}_5\text{H}_4\text{--CMe}_2\text{CH}_2\text{CH}_2\text{CONR}_2)$  with  $\text{Cp}^*\text{TiCl}_3$  gave the mixed bis-Cp complexes  $\text{Cp}(\text{C}_5\text{H}_4\text{--CMe}_2\text{CH}_2\text{CH}_2\text{CONR}_2)\text{TiCl}_2$  ( $\text{NR}_2 = \text{NMe}_2, \text{NEt}_2, \text{pyrrolidino}$ ). Treatment of  $\text{Cp}[(\text{C}_5\text{H}_4\text{--CMe}_2\text{CH}_2\text{CH}_2\text{CONMe}_2)\text{TiCl}_2]$  with  $(\text{Et}_3\text{O})^+(\text{BF}_4)^-$  results in chloro abstraction with the formation of the corresponding cationic complex stabilized with the  $\text{BF}_4^-$  anion, in which the carboxamido oxygen atom intramolecularly coordinates to titanium center. The molecular structure of the cationic compound has been determined by X-ray diffraction.<sup>1099</sup>

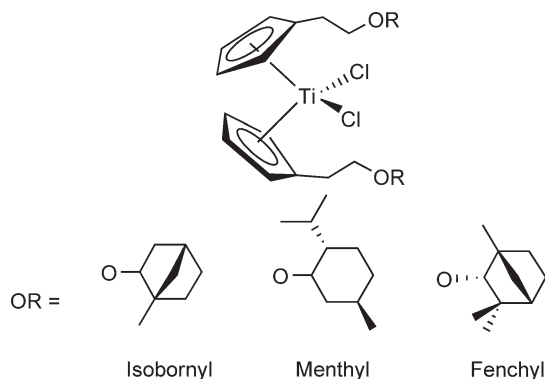
Phosphine-substituted complexes  $[\text{C}_5\text{H}_4(\text{CH}_2)_n\text{PPh}_2]_2\text{TiCl}_2$  ( $n = 1, 2$ ) (Scheme 702; Section 4.05.6) have been synthesized by the reaction of the potassium salt  $\text{K}[\text{C}_5\text{H}_4(\text{CH}_2)_n\text{PPh}_2]$  with  $\text{TiCl}_3$  followed by oxidation with  $\text{HCl}$ .<sup>1100</sup>

$\text{Cp}^*\text{TiCl}_3$  reacts with lithium[3-(*o*-methoxy-phenyl)pentyl]cyclopentadienide to give the bis-Cp' complex where the Cp ligands support methoxo functionalities (Scheme 471).<sup>815</sup>

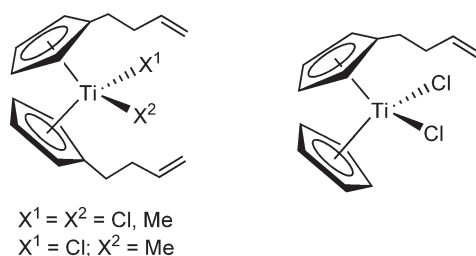
Substituted bis-Cp dichloro complexes with a chiral alkoxo unit linked to the Cp ring by an ethylene spacer group have been prepared by conventional salt metathesis reactions (Scheme 472). The analogous achiral methoxo derivative has also been made.<sup>1101</sup>

A series of titanium complexes containing the 1-(3-butenyl)-2,3,4,5-tetramethyl-Cp ligand  $\text{C}_5\text{Me}_4\text{CH}_2\text{CH}_2\text{CH}=\text{CH}_2$  have been synthesized and characterized.  $(\text{C}_5\text{Me}_4\text{CH}_2\text{CH}_2\text{CH}=\text{CH}_2)_2\text{TiCl}_2$  is prepared by the reaction of the cyclopentadiene lithium salt with  $\text{TiCl}_3$  in dimethoxyethane, followed by oxidation using  $\text{PbCl}_2$ ; it can be alkylated with  $\text{LiMe}$ .  $\text{TiCl}_4$  reacts with  $\text{Me}_3\text{SiC}_5\text{Me}_4\text{CH}_2\text{CH}_2\text{CH}=\text{CH}_2$  to give  $(\text{C}_5\text{Me}_4\text{CH}_2\text{CH}_2\text{CH}=\text{CH}_2)\text{TiCl}_3$ , which was used to synthesize the mixed bis-Cp compound  $\text{Cp}(\text{C}_5\text{Me}_4\text{CH}_2\text{CH}_2\text{CH}=\text{CH}_2)\text{TiCl}_2$  (Scheme 473).<sup>347</sup> The synthesis of  $\text{Cp}'(\text{C}_5\text{H}_4\text{CR}_2\text{CH}_2\text{CH}=\text{CH}_2)\text{TiCl}_2$  ( $\text{Cp}' = \text{Cp}, \text{C}_5\text{H}_4\text{CR}_2\text{CH}_2\text{CH}=\text{CH}_2$ ) has been described.<sup>1102</sup>

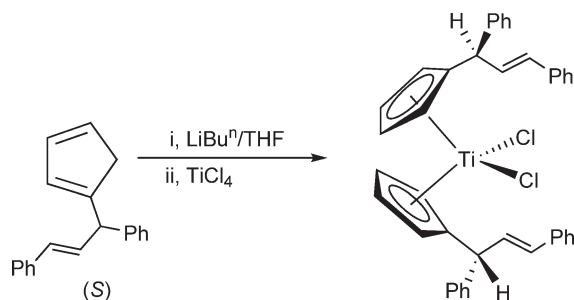
The lithium cyclopentadienide generated by treatment of (*S*)-allylated cyclopentadiene (98% ee) with  $\text{LiBu}^n$  in THF is allowed to react with  $\text{TiCl}_4$  to give the corresponding bis-Cp' derivative containing allylic side chains on both Cp rings (Scheme 474).<sup>1103</sup>



Scheme 472



Scheme 473



Scheme 474

#### 4.05.4.1.1.(iii) Chiral complexes

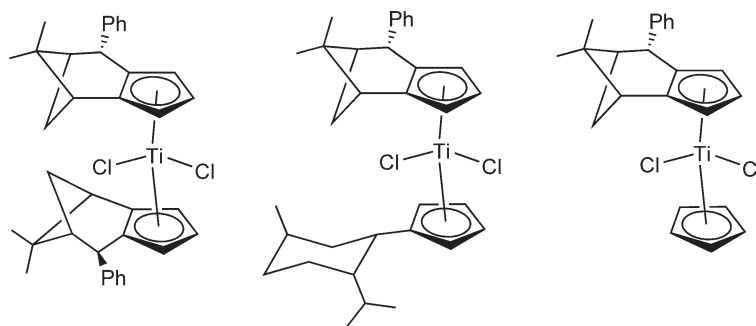
A class of chiral titanium complexes is obtained when the metal atom is the sole center of chirality. These substances are usually described as “chiral-at-metal” complexes and the chirality is based on the stereogenic titanium atom with four different ligands. The synthesis of racemic “chiral-at-metal” titanium complexes has been reported. Methods for the preparation of such racemic titanium compounds imply: (i) nucleophilic displacement of one of the chloro ligands from mixed ring bis-Cp' dichloro derivatives using a Grignard, alkali metal, or related reagents; (ii) the reaction of a prochiral dialkyl or dithiophenolato bis-Cp' complex with 1 equiv. of a chloride source (lithium chloride); (iii) the third synthetically approach is the useful ligand distribution reaction between dichloro CpCp'TiCl<sub>2</sub> and dialkyl or bis(thiophenolato) complexes CpCp'TiX<sub>2</sub>.<sup>1104</sup> The preparation of racemic “chiral-at-metal” titanium complexes by transmetallation reactions using boron reagents has also been reported. Enantiomerically enriched products cannot be isolated through this method due to the formation of complexes between the titanium products and the borane byproducts.<sup>1105</sup>

Considerable attention has been given in recent years to the complexation of Cp ligands with chiral substituents to give enantiomers or diastereomers. This strategy can provide optically bis-Cp-type complexes which are of interest because of their ability to effect asymmetric homogeneous organic reactions. Thus, the synthesis of a variety of non-bridged optically active *C*<sub>2</sub>- and *C*<sub>1</sub>-symmetric bis-Cp titanium and zirconium complexes containing either identical or different ligands derived from fusing cyclopentadiene rings is reported. A pertinent review has appeared.<sup>1030</sup>

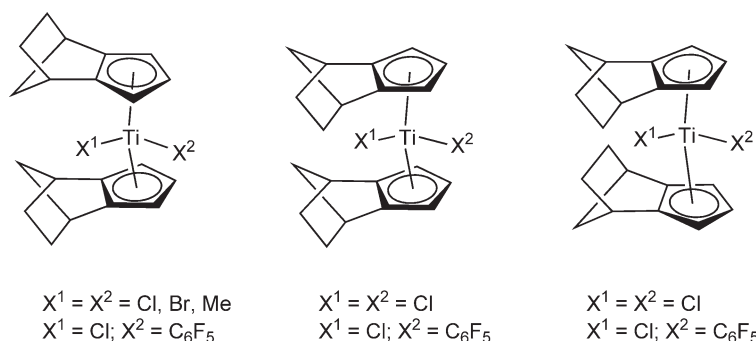
Some examples for complexes of this type are shown in Scheme 475. They show catalytic ability to effect the asymmetric hydrogenation of 2-phenyl-1-butene and 2-( $\alpha$ -naphthyl)-1-butene with variable enantioselectivity depending on the characteristics of the particular ligand system.<sup>1106</sup>

A mixture of *endo,exo*-, *endo,endo*-, and *exo,exo*-(isodiCp)<sub>2</sub>TiCl<sub>2</sub> in different molar ratios can be obtained by using Li(isodiCp), depending on the temperature of the reaction.<sup>1107</sup> The activity of these complexes in olefin polymerization has been studied. The diastereomeric complexes (isodiCp)<sub>2</sub>TiCl<sub>2</sub> (Scheme 476) have been prepared in stereocontrolled reactions. They react with LiC<sub>6</sub>F<sub>5</sub> to give the air stable, crystalline (isodiCp)<sub>2</sub>TiCl(C<sub>6</sub>F<sub>5</sub>) triad, whose members are readily distinguished by their NMR spectra. An X-ray crystallographic analysis of the three diastereomers has been performed. The *exo,exo* isomer reacts with boron BBr<sub>3</sub> or LiMe to give the dibromo and dimethyl derivatives, respectively, which show reasonable stability. In contrast, the *endo,endo* and *endo,exo* dichloro complexes do not lead to stable products under analogous conditions.<sup>1108</sup>

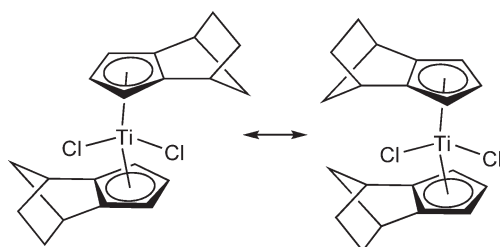
The synthesis and conformational characterization of the *exo,exo*-bis(isodiCp) dichloro titanium compound shown in Scheme 477 has been described. Dynamic NMR spectroscopy suggests a chiral *C*<sub>2</sub>-symmetric structure in solution



Scheme 475



Scheme 476



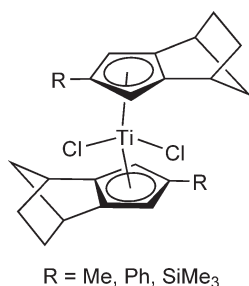
Scheme 477

that is characterized by a bis-lateral:anti orientation of the annulated bicyclo[2.2.1]heptene moieties at the bent-metalocene wedge, with an activation energy for the conformational inversion of  $9.8 \text{ kcal mol}^{-1}$ . This complex, in the presence of MAO, is a moderately active homogeneous Ziegler catalyst for olefin polymerization. The analogous zirconium complex has also been described.<sup>1109</sup> The *exo,exo*-bis(isodiCp) titanium dichlorides containing different Cp substituents have been prepared by the metathesis reaction between the corresponding lithium isodicyclopentadienide reagent with  $\text{TiCl}_4$  in THF (Scheme 478). The compounds have been characterized by solution NMR measurements, which also permit the calculation of rotational barriers. The molecular structure of *exo,exo*-bis-(3-diphenylphosphinoisodicyclopentadienyl)titanium has been determined by X-ray crystallography. Upon activation with MAO the complexes are poor catalysts for the polymerization of propene.<sup>1110</sup>

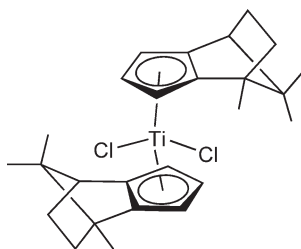
The reduction of *exo,exo*-(isodiCp)<sub>2</sub>TiCl<sub>2</sub> with magnesium or LiBu affords the corresponding monochloro Ti(III) derivative, while the reduction with an excess of magnesium in the presence of bis(trimethylsilyl)ethylene (btmsc) gives the Ti(II)-alkyne complex.<sup>1111</sup>

The bis-Cp' dichloro titanium complex with the camphor-substituted Cp ring (Scheme 479) is prepared from the corresponding cyclopentadiene compound by reaction with LiBu<sup>n</sup>, metallating with  $\text{TiCl}_3$  followed by oxidation with HCl/air. From the initially formed 9:1 mixture of *C*<sub>2</sub>- and *C*<sub>1</sub>-symmetric bis-Cp derivatives, the pure *C*<sub>2</sub>-diastereomer





Scheme 478



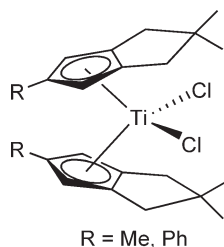
Scheme 479

could be isolated by recrystallization with hexanes.<sup>1112</sup> The bis(tetrahydropentalenyl) compound shown in [Scheme 480](#) has been synthesized from the lithium salt of the appropriate cyclopentadiene with TiCl<sub>3</sub> followed by oxidation with HCl.<sup>1113</sup>

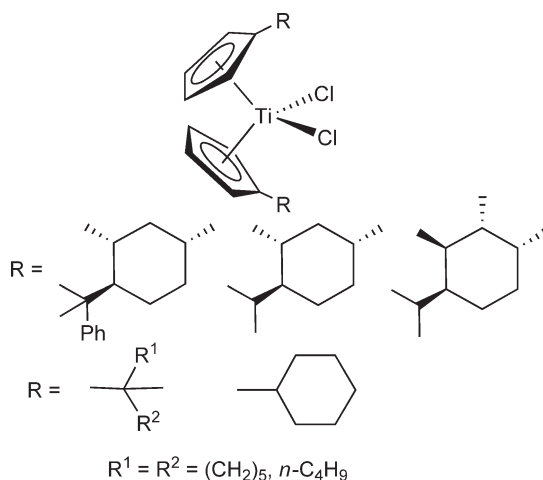
Enantiomerically pure bis-Cp derivatives with chiral Cp ligands have been used with success in the catalytic enantioselective opening of *meso*-epoxides via electron transfer (see [Section 4.05.8](#)). The structural features are of relevance for the understanding of activity and selectivity of these complexes in diastereoselective reactions and for the design of novel catalysts. A comparison of the structure of three of these bis-Cp Ti derivatives ([Scheme 481](#)) in the solid state and in solution determined by X-ray crystallography and NMR methods indicated that the structures in the crystal and in solution are the same, and that applications of these complexes in catalysis can be discussed on the basis of crystallographic data.<sup>1114</sup> In a similar study, the 1-methylcyclohexyl-Cp, 1-butyl-1-methylbutyl-Cp, and cyclohexyl-Cp titanocene dichlorides ([Scheme 481](#)) have been prepared and their molecular structures compared. The use of these three compounds in radical addition reactions has been studied.<sup>1115</sup>

#### 4.05.4.1.2 Properties and structures of bis-Cp titanium halides

The crystal structures of a series of previously published bis-Cp-type titanium compounds have been reported. The molecular structure of Cp<sub>2</sub>TiBr<sub>2</sub> has been determined by X-ray diffraction. The compound appears to be isostructural with the corresponding chloro derivative.<sup>1116,1117</sup> The crystal and molecular structure of (C<sub>5</sub>HMe<sub>4</sub>)<sub>2</sub>TiCl<sub>2</sub> has been compared to that of permethylated Cp<sup>\*</sup><sub>2</sub>TiCl<sub>2</sub> analog. A significant shift of the Ti atom from the symmetrical position



Scheme 480



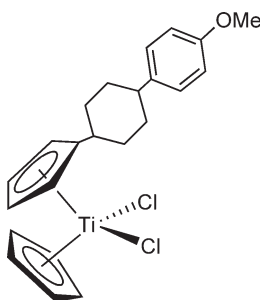
Scheme 481

inside the dihedral angle of the Cp' rings has been found in the  $C_5HMe_4$  compound. In the Cp\* derivative all the Ti–C(ring) distances have approximately the same value, while in the  $C_5HMe_4$  complex these distances differ by 0.1 Å, those to the internal carbon atoms being shortest. The CE–Ti–CE angle (CE = Cp ring centroid) increases with the number of Me substituents.<sup>1118</sup> The structure of the mixed valence chloro carbonato complex  $(C_5Me_5)_2(Cl)Ti(CO_3)Ti(C_5Me_5)_2$  has been established by X-ray diffraction. In spite of the fact that this complex contains both Ti(IV) and Ti(III) atoms within the same molecule, the geometric parameters of the different oxidation state environments are similar.<sup>1119</sup>  $(C_5H_4SiMe_3)[C_5H_3(SiMe_3)_2]TiF_2$  has been crystallographically and spectroscopically characterized.<sup>1120</sup> The molecular structure of  $(1,2,4-C_5H_2Me_3)_2TiCl_2$  has been determined by X-ray diffraction.<sup>1121</sup> The structure of a mixed bis-Cp' titanium complex with a Cp and the 2-propenyl–Cp ligand,  $Cp(C_8H_9)TiCl_2$ , has been reported.<sup>1122</sup> The molecular structure of the methoxy–phenyl–cyclohexyl-substituted compound shown in Scheme 482 has been determined.<sup>869</sup>

The  $^1H$ – $^1H$  TOCSY and  $^1H$ – $^1H$  NOESY NMR studies of a series of substituted Ind titanium complexes using nuclear Overhauser effects have been used to investigate structural features of these derivatives.<sup>1123</sup>

Rate laws and kinetic parameters for substitution reactions at complexes  $Cp_2TiX_2$  in acetonitrile solution at 298.2 K have been reported (X = halide or alkoxide). Reactivities are discussed in terms of the nature of the leaving group, the entering group, and the non-leaving Cp ligand. A volume of activation of  $-15\text{ cm}^3\text{ mol}^{-1}$  has been determined for the reaction with thiocyanate.<sup>1124</sup>

A group of bicycloalkyl–bis-Cp-substituted and 1,2-disubstituted titanium dichlorides have been examined by X-ray photoelectron spectroscopy in order to gauge if the rather large steric requirements of these ligands exert greater or lesser impact on the binding energy of the titanium center relative to the electronic effect of alkyl substitution. The structural information and associated Fenske–Hall calculations reveal an important ring slippage. The inductive contributions of substituents directly bonded to the Cp rings dominate over the steric contributions of the space-demanding ligands in controlling the electronic changes at the core titanium atom.<sup>1038</sup>



Scheme 482

The electrochemical properties of  $\text{Cp}'_2\text{TiCl}_2$  ( $\text{Cp}' = \text{Cp}, \text{Cp}^*, \text{C}_5\text{H}_4\text{Me}, \text{C}_5\text{H}_4\text{Cl}, \text{C}_5\text{H}_4\text{CO}_2\text{Me}$ ) in THF solution have been examined. These compounds undergo two reduction steps. The steric bulk of the pentamethyl and the possibility of chelation in the carbomethoxy derivative influence the electrochemical behavior. The standard potentials decrease to more negative values in the order:  $\text{C}_5\text{H}_4\text{CO}_2\text{Me} > \text{C}_5\text{H}_4\text{Cl} > \text{Cp} > \text{C}_5\text{H}_4\text{Me} > \text{Cp}^*$ .<sup>1125</sup> The first reduction step of  $(\text{C}_5\text{Me}_4\text{SPr}^i)_2\text{TiCl}_2$  in THF solution has been investigated by cyclic voltammetry.<sup>1126</sup>

The electrochemical oxidation of bis-Cp-type titanocene dichlorides gives cationic species which have been characterized by spectroscopic and spectroelectrochemical methods.<sup>1127</sup> A detailed electrochemical study of the reduction of  $\text{Cp}_2\text{TiCl}_2$  in THF containing trimethylphosphine is reported. It has been demonstrated that both  $\text{Cp}_2\text{TiCl}(\text{PMe}_3)$  and  $\text{Cp}_2\text{Ti}(\text{PMe}_3)_2$  can be prepared electrochemically. The successive replacement of  $\text{Cl}^-$  by  $\text{PMe}_3$  in the series:  $\text{Cp}_2\text{TiCl}_2$ ,  $[\text{Cp}_2\text{TiCl}(\text{PMe}_3)]^-$ , and  $[\text{Cp}_2\text{Ti}(\text{PMe}_3)_2]^{2-}$  makes the reduction of Ti(IV) to Ti(III) easier by 300–400 mV.<sup>1128</sup> Cyclic voltammetry has been used to study electronic and steric effects of methyl substituents in a complete series of methyl-substituted bis-Cp' dichloro titanium complexes  $(\text{C}_5\text{H}_{5-n}\text{Me}_n)_2\text{TiCl}_2$ ,  $(\text{C}_5\text{Me}_4\text{SiMe}_3)_2\text{TiCl}_2$ ,  $(\text{C}_5\text{Me}_4\text{Ph})_2\text{TiCl}_2$ ,  $(\text{C}_5\text{Me}_4\text{p-C}_6\text{H}_4\text{F})_2\text{TiCl}_2$ ,  $(\text{C}_5\text{Me}_4\text{CH}_2\text{Ph})_2\text{TiCl}_2$ , and the *ansa*-compound  $\text{Me}_2\text{Si}(\text{C}_5\text{H}_4)_2\text{TiCl}_2$ . The standard potential of the first electron uptake generally shifts to more negative values proportionally to the number of methyl groups on the Cp ring, with an increment of 0.093 V per methyl group. These positive shifts can be explained by a steric strain between the Cp ligands which lowers the dihedral angle between Cp ring planes and thus decreases energies of bent-titanocene  $1a_1$  and  $b_2$  LUMOs. This conclusion is corroborated by the voltammetry of the *ansa*-compound.<sup>1129</sup>

Tandem mass spectrometric techniques have been used for the characterization of gas-phase neutral and ionic bis-Cp species.<sup>1130</sup>

Systematic electronic luminescence spectroscopy studies to probe the low-lying excited states of a series of Cp–Ti(IV) derivatives have been reported.  $\text{Cp}'_2\text{TiX}_2$  and  $\text{Cp}''\text{TiX}_3$  ( $\text{X} = \text{halogen}$ ) exhibit an intense, long-lived charge-transfer phosphorescence at 77 K arising from the radiative decay of a  $\text{Cp} \rightarrow \text{Ti}$  charge-transfer triplet excited state. The phosphorescence band can be shifted systematically by varying X or by replacing Cp with  $\text{Cp}^*$ . Trends in the phosphorescence spectra follow closely related trends previously noted in the electronic absorption spectra, photoelectron spectra, and photochemical behavior of these complexes. It is proposed that the presence or absence of charge-transfer phosphorescence can be used as a diagnostic tool to determine the relative energy ordering of the valence  $\text{Cp}'$  and X orbitals in Ti(IV) compounds.<sup>1131</sup>

Thermal effects and vibrational corrections to transition metal NMR chemical shifts have been the subject of comprehensive investigations using different computational methods, including studies on  $\text{Cp}_2\text{TiX}_2$  ( $\text{X} = \text{Cl}, \text{F}$ ).<sup>240</sup>

According to elemental analysis, cyclic voltammetry, EPR, IR, and UV–VIS spectroelectrochemistry, the reactions of  $\text{TiCp}'_2(\text{CO})_2$  with TCNE or TCNQ lead to the formation of the Ti(IV) species  $\text{TiCp}'_2(\text{CO})_2(\text{TCNX})$  ( $\text{Cp}' = \text{Cp}, \text{Cp}^*$ ) containing the pseudohalide  $\text{TCNX}^{2-}$  anions ( $\text{TCNX} = \text{TCNE}$  and  $\text{TCNQ}$ ).<sup>1132</sup>

#### 4.05.4.1.3 Reactions of bis-Cp titanium halides

Redox and metathetical reactions are covered in this section. Some of these reactions lead to specific complexes with Ti–O, Ti–N, and Ti–C bonds which could be alternatively collected in subsequent sections. Comments on the applications of the bis-Cp' dihalo titanium complexes as olefin polymerization pre-catalysts and reagents in organic reactions are mentioned.

A review on the most important synthetic methods and chemical transformations of bis-Cp titanium derivatives containing a Ti–C  $\sigma$ -bond has appeared.<sup>1133</sup>

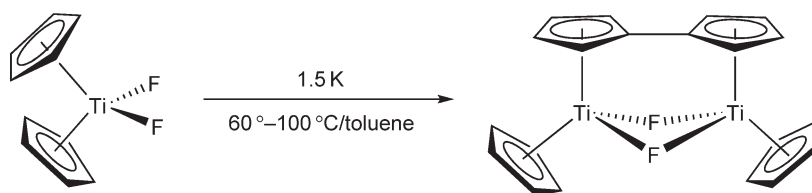
The intramolecular coordination chemistry of substituted bis-Cp' titanium complexes, dealing with the syntheses, reactions, structures, and some applications in homogeneous and catalytic reactions, has been summarized.<sup>1134</sup>

##### 4.05.4.1.3.(i) Reductions of bis-Cp titanium halides

The reduction of a series of Cp titanium derivatives with different reducing agents have been studied. Reduction of bis-Cp titanium dichlorides with electropositive metals in the presence of  $\pi$ - or lone pair electron donor ligands is a general reaction of titanium(IV) complexes and gives thermally stable low-valent titanium derivatives. In the absence of donor ligands, C–H bond activation processes of the Cp ligands can be observed, with the formation of binuclear compounds containing bridging Cp ligands.

The use of  $\text{Cp}_2\text{TiCl}_2$  as a colorimetric indicator for inert atmosphere techniques through the synthesis of the titanium(III) complex  $[\text{Cp}_2\text{Ti}(\text{NCMe})_2]^+$  has been described.<sup>1135</sup>

The reduction of  $\text{Cp}_2\text{TiF}_2$  and  $(\text{C}_5\text{H}_4\text{Me})_2\text{TiF}_2$  with sodium amalgam affords the titanium(III) derivatives  $(\text{Cp}_2\text{TiF})_2$  and  $[(\text{C}_5\text{H}_4\text{Me})_2\text{TiF}]_2$ , respectively, which can alternatively be prepared by fluorination of  $(\text{Cp}_2\text{TiCl})_2$



Scheme 483

and  $[(\text{C}_5\text{H}_4\text{Me})_2\text{TiCl}]_2$  with  $\text{Me}_3\text{SnF}$ .<sup>351</sup>  $\text{Cp}_2\text{TiF}_2$  is reduced with 1.5 equiv. of potassium in toluene at 60–100 °C to give the titanium(III)  $\eta^5\text{-}\eta^5$ -fulvalene complex  $[\text{CpTi}(\mu\text{-F})](\text{C}_{10}\text{H}_8)$  (Scheme 483).<sup>1136</sup>

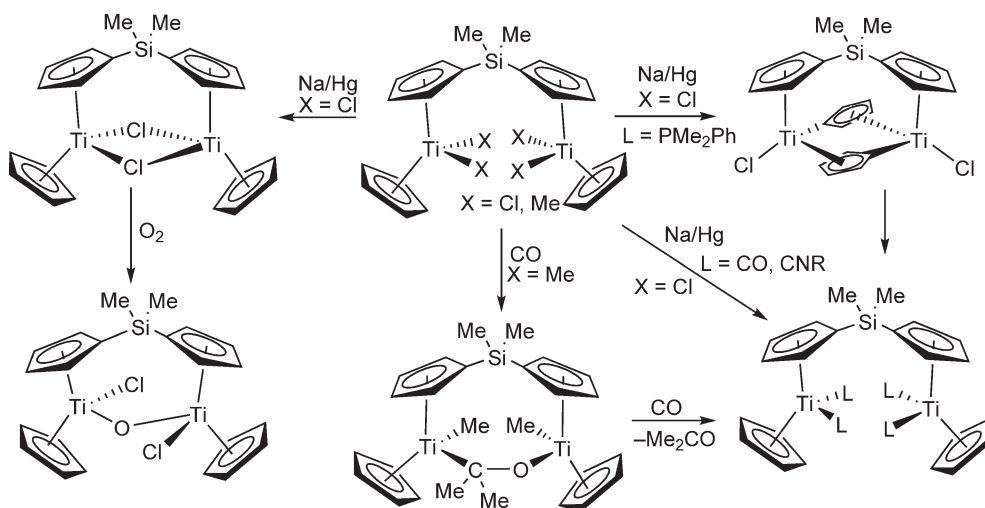
The reactions of  $\text{Cp}'_2\text{TiCl}_2$  ( $\text{Cp}' = \text{Cp}, \text{Cp}^*$ ) with lithium phosphides afford Ti(III) species.<sup>1137</sup> The binuclear tetrachloro fulvalene compound  $[\text{CpTiCl}_2]_2(\mu\text{-C}_{10}\text{H}_8)$  reacts with 2 equiv. of  $\text{LiPPh}_2$  to give the Ti(III) derivative  $[\text{CpTi}(\mu\text{-Cl})]_2(\mu\text{-C}_{10}\text{H}_8)$  with elimination of  $\text{Ph}_2\text{P-PPh}_2$ , while the treatment with 4 equiv. of  $\text{LiPPh}_2$  affords the phosphido-bridged Ti(III) compound  $[\text{CpTi}(\mu\text{-PPh}_2)]_2(\mu\text{-C}_{10}\text{H}_8)$ .<sup>1138</sup>

The binuclear chlorotitanium(III) derivative  $[\text{CpTi}(\mu\text{-Cl})]_2[\mu\text{-Me}_2\text{Si}(\text{C}_5\text{H}_4)_2]$  has been synthesized by reduction of the titanium(IV) derivative  $[\text{CpTiCl}_2]_2[\mu\text{-Me}_2\text{Si}(\text{C}_5\text{H}_4)_2]$  with sodium amalgam. Reduction in the presence of the appropriate donor ligand gives the titanium(II) adducts  $[\text{CpTi}(\text{L})_2]_2[\mu\text{-Me}_2\text{Si}(\text{C}_5\text{H}_4)_2]$  ( $\text{L} = \text{CO}, \text{CNC}_6\text{H}_3\text{Me}_2\text{-2,6}$ ), while similar reduction in the presence of  $\text{PMe}_2\text{Ph}$  resulted in the loss of hydrogen and activation of C–H ring bonds with the formation of a diamagnetic Ti(III) complex with two  $\eta^1\text{-}\eta^5\text{-C}_5\text{H}_4$  bridging groups. The dicarbonyl derivative  $[\text{CpTi}(\text{CO})_2]_2[\mu\text{-Me}_2\text{Si}(\text{C}_5\text{H}_4)_2]$  is also obtained by the reaction of the dimethyl derivative  $[\text{CpTiMe}_2]_2[\mu\text{-Me}_2\text{Si}(\text{C}_5\text{H}_4)_2]$  with CO. An acetone-coordinated titanium compound has been identified as an intermediate in this reaction (Scheme 484).<sup>1139</sup>

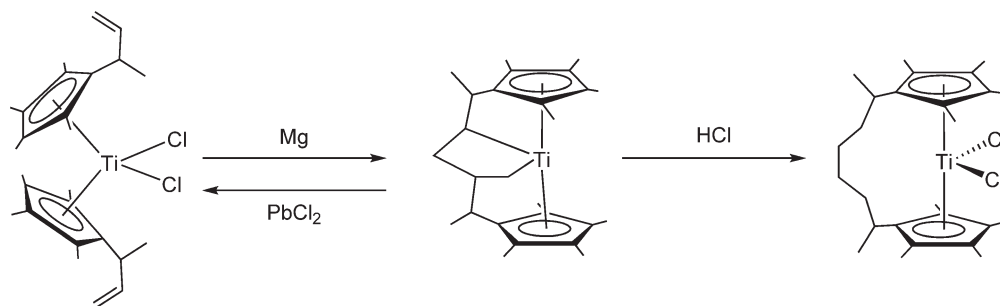
The reduction of  $\text{Cp}_2\text{TiCl}_2$  with allyllithium generates alkylidene species as intermediate species in the preparation of vinylcyclopropanes (see Section 4.05.4.2.4; alkylidene compounds).<sup>1140</sup>

The reaction of  $\text{Cp}_2\text{TiCl}_2$  with an excess of  $\text{Li}[\text{BH}_3\text{Me}]$  has been described to give the Ti(III) borohydride  $\text{Cp}_2\text{Ti}(\mu\text{-H})_2\text{BHMMe}$ .<sup>1141</sup>

Magnesium metal reduces bis-Cp titanium complexes under different conditions. The bis( $\omega$ -alkenyl)-substituted tetramethyl-Cp titanium complexes  $(\text{C}_5\text{Me}_4\text{R})_2\text{TiCl}_2$  [ $\text{R} = \text{CH}(\text{Me})\text{CH}=\text{CH}_2, (\text{CH}_2)_2\text{CH}=\text{CH}_2, (\text{CH}_2)_3\text{CH}=\text{CH}_2$ ] can be reduced by Mg in THF to give bis-Cp' titanacyclopentanes as a result of the oxidative coupling of the double bonds across a titanocene intermediate. The titanacyclopentanes react with  $\text{PbCl}_2$  to recover the dichloro starting materials. In the case of the  $(\text{CH}_2)_3\text{CH}=\text{CH}_2$  derivative, a carbon–carbon double bond isomerization is observed. The titanacycles can be opened with HCl to give *ansa*-bis-Cp dichlorides with the bridging aliphatic chain containing five or eight carbon atoms; one example of this chemical behavior is represented in Scheme 485. The acidolysis

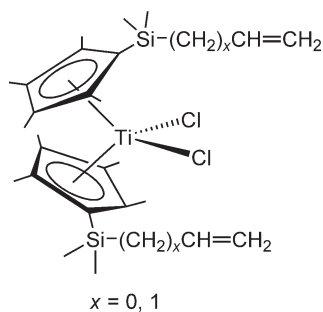


Scheme 484

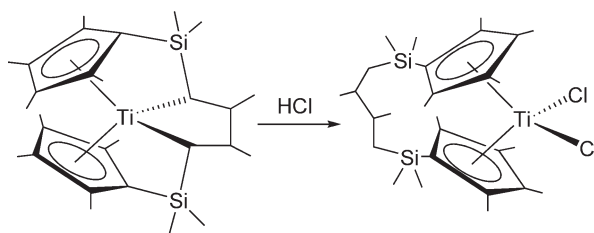


Scheme 485

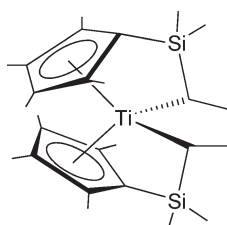
reaction of these complexes has been studied. The molecular structures of the compounds have been determined by X-ray diffraction.<sup>1033</sup> Similar complexes bearing  $\omega$ -alkenyl–dimethylsilyl–Cp substituted ligands have been synthesized (Scheme 486). The reduction of these complexes produces highly reactive Ti(II) intermediates, which immediately undergo intramolecular reactions with the pendant double bonds in a way dependent on the length of the alkenyl chain. A titanacyclopentane can be obtained which is opened by treatment with HCl to give an *ansa*-titanocene dichloro derivative with a six-membered saturated bridging chain (Scheme 487). The analogous titanacyclopentane shown in Scheme 488 can also be obtained as a mixture with an  $\eta^2$ -alkene Ti(II) derivative. Analogous reactions afford different alkenyl or *ansa*-titanocene dichloro complexes (Scheme 489). These compounds have been



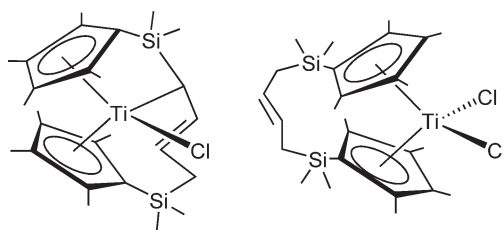
Scheme 486



Scheme 487



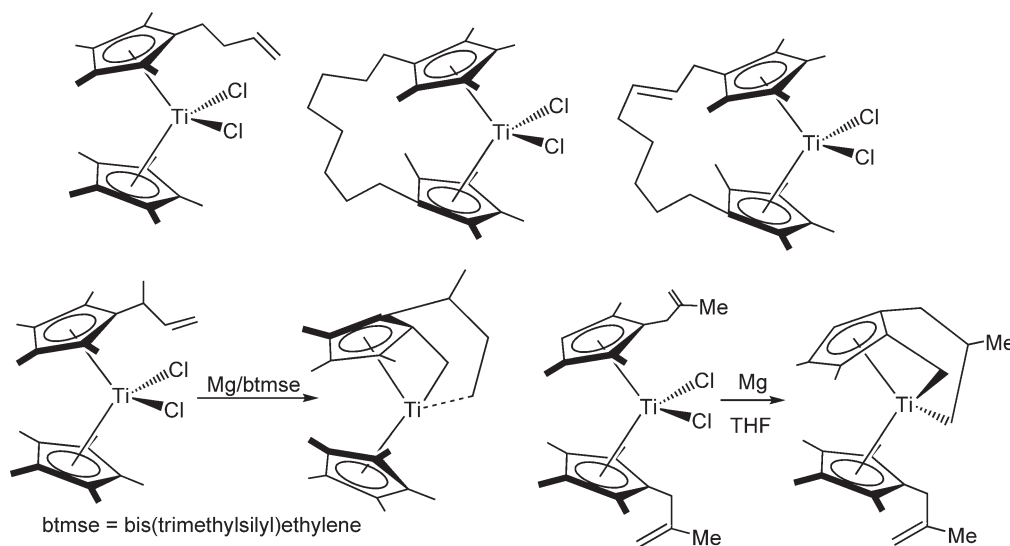
Scheme 488



Scheme 489

characterized by X-ray crystallography.<sup>1034</sup> The syntheses of tetramethyl-Cp complexes having a pendant double bond and of *ansa*-titanocene dichlorides (Scheme 490) by the appropriate synthetic method have been reported. Reduction with magnesium in THF in the presence of btmse affords different products depending on the nature of the alkenyl chain. Ti(II) complexes with coordinated double bonds are generally obtained. The reaction with  $\text{Cp}^*[\text{C}_5\text{Me}_4\text{CH}(\text{Me})\text{CH}=\text{CH}_2]\text{TiCl}_2$  affords a Ti(IV) derivative with two new Ti–C bonds,  $\text{Cp}^*\text{Ti}\{\text{C}_5\text{Me}_3(\text{CH}_2)[\text{CH}(\text{Me})\text{CH}_2\text{CH}_2]\}$  (Scheme 490). The formation of this complex from the respective bis-Cp derivative requires formally an activation (oxidative addition) of one C–H bond of the methyl group adjacent to the unsaturated chain followed by a hydrogen shift (hydrometallation). The structure has been determined by X-ray crystallography.<sup>1035</sup> The reduction of  $[\text{C}_5\text{Me}_4(\text{CH}_2\text{CMe}=\text{CH}_2)]_2\text{TiCl}_2$  with Mg in THF takes place with intramolecular cycloaddition to yield the diamagnetic Ti(IV) Cp-ring-tethered titanacyclopentane derivative shown in Scheme 490. The molecular structure of this compound has been determined by X-ray diffraction.<sup>1142</sup>

$\text{Cp}_2\text{TiCl}_2$  is reduced with Mg powder activated by 1,2-dibromoethane and the species thus formed react with allyl propargyl ethers to afford 3-methylenetetrahydrofurans in good yields. It is noteworthy that the titanium- and zirconium-mediated cyclizations proceed with inverse stereoselectivity.<sup>1143</sup> The reaction of  $(\text{C}_5\text{HMe}_4)_2\text{TiCl}_2$  with Mg in THF in the presence of  $\text{Me}_3\text{SiC}\equiv\text{C}-\text{C}\equiv\text{CSiMe}_3$  affords the bimetallic Ti(III)–Mg tweezer complex  $[(\text{C}_5\text{HMe}_4)_2\text{Ti}(\text{C}\equiv\text{CSiMe}_3)_2][\text{Mg}(\text{THF})\text{Cl}]$  which has been characterized by X-ray diffraction.<sup>1144</sup> The same reduction process in the presence of  $\text{Bu}^t\text{C}\equiv\text{CH}$  induces the dimerization of the *tert*-butylacetylene with the formation of a Ti(III)–Mg hydride species.<sup>1145</sup> The reduction of  $(\text{C}_5\text{Me}_4\text{SiMe}_3)_2\text{TiCl}_2$  with excess Mg in THF in the presence or absence of acetylene yields paramagnetic titanium(III) compounds in which one  $\text{SiMe}_3$  group has been activated by hydrogen abstraction.<sup>1146</sup> The reduction of  $(\text{C}_5\text{H}_{5-n}\text{Me}_n)_2\text{TiCl}_2$  ( $n = 0, 2-5$ ) with Mg in THF and in the presence of the stannyl acetylene  $\text{C}_2(\text{SnMe}_3)_2$  affords monomeric Ti(II) and diamagnetic dimeric Ti(III) compounds, which have been isolated and characterized by X-ray structure analyses. The molecular structures of all the compounds are very similar to those of analogous trimethylsilyl-substituted compounds.<sup>1147</sup>



Scheme 490

The reduction of  $\text{Cp}_2\text{TiCl}_2$  with Mg in the presence of  $\text{P}(\text{OEt})_3$  affords the titanium(II) complex  $\text{Cp}_2\text{Ti}[\text{P}(\text{OEt})_3]_2$  which was used as a catalyst for the carbonyl olefination of thioacetals through a titanium–alkylidene intermediate (see Section 4.05.4.2.4; alkylidene complexes).<sup>1148</sup>

Reduction of  $\text{Cp}_2\text{TiCl}_2$  with Mg in the presence of propargyl acetates gives allenyl Ti intermediates which react with nucleophilic reagents such as aldehydes, ketones, acetonitrile, and allyl bromide to give carbon–carbon bond-forming products in moderate yields.<sup>1149</sup>

The reduction of  $(\text{C}_5\text{Me}_4\text{Ph})_2\text{TiCl}_2$  with Mg in THF affords a mixture of mononuclear and binuclear paramagnetic and diamagnetic substances.<sup>1150</sup>

Reduction of the peralkyl silyl–Cp' compounds  $(\text{C}_5\text{Me}_4\text{R})_2\text{TiCl}_2$  ( $\text{R} = \text{SiMe}_2\text{CH}_2\text{CH}_2\text{Ph}$ ,  $\text{SiMe}_2\text{Ph}$ ,  $\text{SiMePh}_2$ ) with Mg in THF proceeds via monochloro Ti(III) intermediates to finally afford stable monomeric titanocenes  $\text{Ti}(\text{C}_5\text{Me}_4\text{R})_2$ .<sup>1151</sup>

Reduction of  $\text{Cp}'_2\text{TiCl}_2$  with the Grignard reagent  $\text{MgXPr}^i$  affords the crystalline complexes  $[\text{Cp}'_2\text{Ti}(\mu\text{-H})_2\text{Mg}(\text{OEt}_2)(\mu\text{-X})]_2$  ( $\text{Cp}' = \text{Cp}$ ,  $\text{C}_5\text{HMe}_4$ ,  $\text{C}_5\text{H}_2\text{Me}_3$ ;  $\text{X} = \text{Cl}$ ,  $\text{Br}$ ). The crystal structures of the tetramethyl–Cp derivatives have been determined by X-ray diffraction.<sup>1152</sup> Reduction of  $\text{Cp}_2\text{TiCl}_2$  sequentially with  $\text{Et}_2\text{O}$  solutions of  $\text{Pr}^i\text{MgCl}$  and with  $\text{PhMgBr}$  in dry degassed toluene at room temperature affords the titanium(III) derivative  $\text{Cp}_2\text{TiPh}$ , an active species for the reductive radical cyclization of cyanoketones and keto esters.<sup>1153</sup>  $\text{Cp}_2\text{TiCl}_2$  is reduced by treatment with bis(2-methoxymethylphenyl) magnesium or bis(2-N,N-dimethylaminomethylphenyl)–magnesium to give the titanium(III) compounds  $\text{Cp}_2\text{Ti}(2\text{-RCH}_2\text{C}_6\text{H}_4)$  ( $\text{R} = \text{OMe}$ ,  $\text{NMe}_2$ ) and elimination of biphenyl. The formation of the intermediate titanium(IV) compound  $\text{Cp}_2\text{Ti}(2\text{-RCH}_2\text{C}_6\text{H}_4)_2$  is proposed.<sup>1154</sup>

The system  $\text{Cp}'_2\text{TiCl}_2/\text{MgClPr}^i/\text{Et}_2\text{O}$  ( $\text{Cp}' = \text{Cp}$ ,  $\text{Cp}^*$ ) affords low-valent Ti–hydride–Mg compounds by reduction processes.<sup>1155,1156</sup> The mixture  $(\text{C}_5\text{H}_{5-n}\text{Me}_n)_2\text{TiCl}_2/\text{MgClPr}^i/\text{Et}_2\text{O}$  ( $n = 0\text{--}5$ ) provides excellent catalyst systems for the head-to-tail dimerization of terminal acetylenes. The catalytic activity and the selectivity have been analyzed depending on the number of the Me substituents on the Cp ring. ESR investigations suggest the formation of Ti(III) species as intermediates.<sup>1157</sup> The  $\text{Cp}_2\text{TiCl}_2/\text{MgClPr}^i/\text{THF}$  system catalyzes the dimerization of  $\text{Bu}^t\text{-acetylene}$  exclusively to 2,4- $\text{Bu}^t\text{-1-buten-3-yne}$ .<sup>1150</sup>

$\text{Cp}_2\text{TiCl}_2$  is reduced by Grignard reagents in the presence of dienes to give  $\text{Cp}_2\text{Ti}(\eta^3\text{-allyl})$  complexes. These compounds react with  $\text{CO}_2$  in highly regioselective manner to give carboxylate derivatives, which, after hydrolytic workup, afford unsaturated carboxylic acids.<sup>1158</sup>

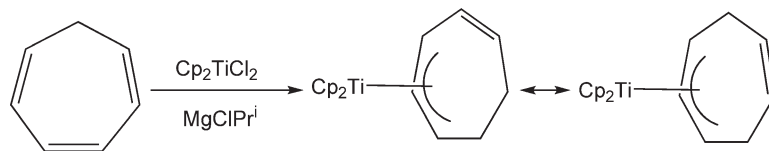
$\text{Cp}_2\text{TiCl}_2$  reacts with  $\text{MgClPr}^i$  in the presence of cycloheptatriene to give  $\eta^3\text{-cycloheptadienyltitanium}$  isomers (Scheme 491), which undergo *in situ* addition to aldehydes to produce a mixture of 1,3- and 1,4-cycloheptadienyl alkyl (aryl) carbinols. The reaction opens a simple way to functionalized 1,4-cycloheptadienes, some of which are closely related to biologically active compounds.<sup>1159</sup>

$\text{Cp}_2\text{TiCl}_2$  is reduced by Zn to generate the Ti(III) compound  $\text{Cp}_2\text{TiCl}$ , used as electron-transfer catalyst for the synthesis of cyclopropanes and cyclobutanes with epoxides as radical precursors.<sup>1160</sup> This system is suited for the reduction of ketones to secondary alcohols.<sup>1161</sup>

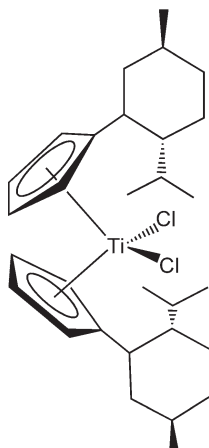
Reduction of  $\text{Cp}_2\text{TiCl}_2$  by zinc produces an active species for the radical cyclization reactions of substituted  $\alpha$ -(prop-2-ynoxy) epoxides.<sup>1162</sup>  $\text{Cp}_2\text{TiCl}_2$  is reduced with powdered zinc in THF to produce  $\text{Cp}_2\text{TiCl}$  *in situ*, Nugent's reagent, an efficient catalytic agent for organic reactions.<sup>1163,1164</sup>

$\text{Cp}_2\text{TiCl}_2$  has been reduced in the presence of  $\text{Me}_3\text{SiCl}$ , zinc powder, and imidazole to give a catalytic system for the reductive radical cyclization of ketonitriles to produce 2-amino-3-cyano-2-cyclopenten-1-ols in moderate yields with high *trans*-selectivity.<sup>1165</sup>

The reaction of  $\text{Cp}_2\text{TiF}_2$  with  $\text{AlEt}_3$  in 1:1 molar ratio has been reported to give  $[\text{Cp}_2\text{Ti}(\mu\text{-F})_2\text{AlEt}_2]_2$ . When an excess of  $\text{AlEt}_3$  is used, the compound  $[\text{Cp}(\text{C}_5\text{H}_4)\text{Ti}(\mu\text{-H})\text{AlEt}_2]_2$  is formed.<sup>1166</sup>  $\text{Cp}_2\text{TiCl}_2$  reacts with  $\text{LiAlH}_4$  to give reduced bis-Cp titanium hydrido aluminum derivatives which have been characterized by X-ray diffraction studies.<sup>1167</sup> The binuclear compound  $[(\text{C}_5\text{HMe}_4)\text{Ti}(\text{H})]_2[\mu\text{-C}_5\text{H}(\text{CH}_3)_2(\text{CH}_2)_2]$  is obtained by the reduction of  $(\text{C}_5\text{HMe}_4)_2\text{TiCl}_2$  with  $\text{LiAlH}_4$  in boiling mesitylene. Its X-ray crystal structure has been determined.<sup>1168</sup>



Scheme 491



Scheme 492

The system  $\text{Cp}_2\text{TiCl}_2/\text{AlClBu}^i_2$  is an efficient reagent for hydroalumination of disubstituted acetylenes in a regio- and stereoselective method for the synthesis of *E*-alkenylchloralanes.<sup>1169</sup> The reduction carbonylation of  $\text{Cp}_2\text{TiCl}_2$  at room temperature by chloroaluminate molten salts or ionic liquids has been reported.<sup>1170</sup>

$\text{Cp}_2\text{TiCl}_2$  can be reduced by reaction with organohydroborate salts to give Ti(III) species  $\text{Cp}_2\text{Ti}(\mu\text{-H})_2\text{BR}_2$  having a four-membered  $\text{Ti}(\mu\text{-H})_2\text{B}$  ring.  $\text{Cp}_2\text{TiCl}_2$  reacts with 2 equiv. of  $[\text{Li}(\text{OEt}_2)][\text{B}(\text{C}_6\text{F}_5)_2\text{H}_2]$  with  $\text{Cp}_2\text{TiCl}_2$  in benzene to give the violet Ti(III) compound  $\text{Cp}_2\text{Ti}(\mu\text{-H})_2\text{B}(\text{C}_6\text{F}_5)_2$  with elimination of  $\text{H}_2$ , indicating that the reduction of Ti(IV) is produced by the tetrahydroborate anion, in a similar manner to  $\text{Li}[\text{BH}_4]$ .<sup>1171,1172</sup> The hydride ion abstraction from these compounds has been studied in coordinating and non-coordinating solvents,<sup>1173</sup> and neutron diffraction studies have been performed.<sup>1174</sup>

Reduction of  $\text{Cp}_2\text{TiCl}_2$  with metallic manganese generates Ti(III) catalysts for the addition of allyl bromide to carbonyl compounds. This method can be used for asymmetric reactions if Brintzinger's compound *rac*-(ebthi) $_2\text{TiCl}_2$  or the previously synthesized chiral derivative<sup>1175</sup> shown in Scheme 492 are used. When chiral bis-Cp complexes are employed, acceptable yields of optically active products are obtained.<sup>1176</sup>

Reduction of  $\text{Cp}_2\text{TiF}_2$  with gallium leads to the formation of  $\text{Ga}_3[\text{Cp}_2\text{TiF}_2]$ .<sup>352</sup>

Electrochemical reduction of  $\text{Cp}_2\text{TiX}_2$  ( $\text{X} = \text{Cl}, \text{Br}, \text{I}$ ) is a convenient route to generate Ti(III) species without the need of chemical reducing agents. Details on the reduction mechanism are described on the basis of cyclic voltammetric and kinetic parameters, in order to elucidate the nature of the different species present in solution. Quantitative information from the recorded voltammograms is extracted. Kinetic investigations of the reactions between electrochemically reduced solutions of  $\text{Cp}_2\text{TiX}_2$  and benzyl chloride show that the reactive species are  $\text{Cp}_2\text{TiX}$  and  $(\text{Cp}_2\text{TiX})_2$ , with almost no contribution from  $[\text{Cp}_2\text{TiX}_2]^-$ , even in the case of  $\text{X} = \text{Cl}$ .<sup>1177</sup>

A comparative study by EPR has been made on the electrolytic reduction of  $\text{Cp}_2\text{TiX}_2$  ( $\text{X} = \text{Cl}, \text{Br}, \text{Me}$ ) and  $\text{Ind}_2\text{TiMe}_2$  in the presence of phosphines. Monohalo and monomethyl phosphine complexes,  $\text{Cp}_2\text{TiCl}(\text{PMe}_3)$  and  $\text{Cp}'_2\text{TiMe}(\text{PMe}_3)$  ( $\text{Cp}' = \text{Cp}, \text{Ind}$ ), have been characterized as the reduction products.<sup>1178</sup> The electrochemical reduction of  $\text{Cp}_2\text{TiCl}_2$  has been studied. It has been established that the reduction process with either Mn or Zn leads to the same redox-active intermediate, the Ti(III) species  $\text{Cp}_2\text{TiCl}$ , which is in equilibrium with its dimer.<sup>1179</sup>

$\text{Cp}_2\text{TiCl}_2$  and other substituted bis-Cp titanium derivatives, including enantiomerically pure chiral complexes, have been used as excellent catalysts for the reductive ring opening of epoxides. This process involves Ti(III) species and subsequent radical reactions.<sup>1175,1180–1184</sup>

The reduction of  $\text{Cp}_2\text{TiCl}_2$ ,  $\text{CpTiCl}_3$ , or  $\text{Cp}_2\text{TiClEt}$  under different conditions in the presence of the TEMPO radical leads to Ti–TEMPO complexes.<sup>855,856,1185</sup>

#### 4.05.4.1.3.(ii) Ligand metathesis reactions of titanocene dihalides

$\text{Cp}_2\text{TiCl}_2$  reacts with 2 equiv. of  $\text{Me}_3\text{SiCH}(\text{MgBr})_2$  to give a complicated reaction mixture from which no pure compounds could be isolated.<sup>1186</sup> The reaction of  $\text{Cp}_2\text{TiCl}_2$  with lithium *tert*-butoxytitanate compounds in different ratios gives trinuclear titanium complexes.<sup>1187</sup>



$\text{Cp}_2\text{TiCl}_2$  reacts with  $\text{HCl(g)}$  in the presence of 18-crown-6 with loss of both Cp ligands to form the hydronium salt  $[\text{H}_3\text{O(18-crown-6)}][\text{TiCl}_5(\text{H}_2\text{O})]$ . The crystal structure shows that the  $\text{H}_3\text{O}^+$  ion resides within the crown ether and has a pyramidal structure.<sup>431</sup>

The Ti–Cp bond is cleaved by the reaction of  $\text{Cp}_2\text{TiCl}_2$  with the lithium salt of Schiff bases to give racemic titanium Schiff base complexes.<sup>1188</sup> Reactions of  $\text{Cp}_2\text{TiCl}_2$  in aqueous solutions or two-phase systems have been developed for the preparation of bisCp diphenoxo and salicylato titanium complexes.<sup>1189,1190</sup> A series of bis-Cp salicylato titanium complexes have been prepared.<sup>1191–1193</sup> The reactions of  $\text{Cp}_2\text{TiCl}_2$  with hydrazones ( $\text{H}_2\text{L}$ ) derived from isatin and aromatic acid hydrazides (benzoic, 4-chlorobenzoic, 4-nitrobenzoic, 4-methoxybenzoic, picolinic, nicotinic, and isonicotinic) have been found to give complexes of the type  $\text{Cp}_2\text{Ti(L)}$ . Tentative structural conclusions are drawn for the reaction products based upon elemental analyses, electrical conductance, magnetic moments, and spectroscopic (UV–VIS, IR,  $^1\text{H}$  NMR, and  $^{13}\text{C}$  NMR) data.<sup>1194</sup> Coordination complexes of  $\text{Cp}_2\text{TiCl}_2$  with  $\text{N}_2\text{S}_2$  and  $\text{S}_2\text{O}_2$  ligands derived from *o*-aminobenzenethiol exhibiting distorted trigonal-bipyramidal geometry have been synthesized.<sup>1195</sup>

The dynamic stereochemistry of substitution reactions from pairs of racemic diastereomeric pseudohalogen, thiocyanate, and isocyanate bis-Cp' complexes has been reinvestigated. The studied complexes  $\text{Cp}(1\text{-Me-2-Pr}^i\text{C}_5\text{H}_3)\text{Ti(X)R}$  ( $\text{X} = \text{NCO, NCS, Cl}$ ;  $\text{R} = \text{OAr, Br, SC}_6\text{H}_5$ ) have a central chirality at the metal atom and a planar chirality at the substituted Cp ring. The metathesis reactions occur with retention or inversion of the configuration at the titanium atom, depending on the reaction conditions and the nature of the X substituent. The results are supported by the crystallographic studies.<sup>1196</sup>

$\text{Cp}_2\text{TiCl}_2$  is used as a precursor for TiC coatings deposited on steel substrate by chemical vapor deposition.<sup>1197</sup>

$\text{Cp}_2\text{TiCl}_2$  reacts with  $\text{Fe}[\text{C}(\text{NMe}_2)_3](\text{CO})_4[\text{C}(\text{O})\text{NMe}_2]$  with the formation of  $[\text{C}(\text{NMe}_2)_3](\text{FeCl}_4)$ .<sup>1198</sup>

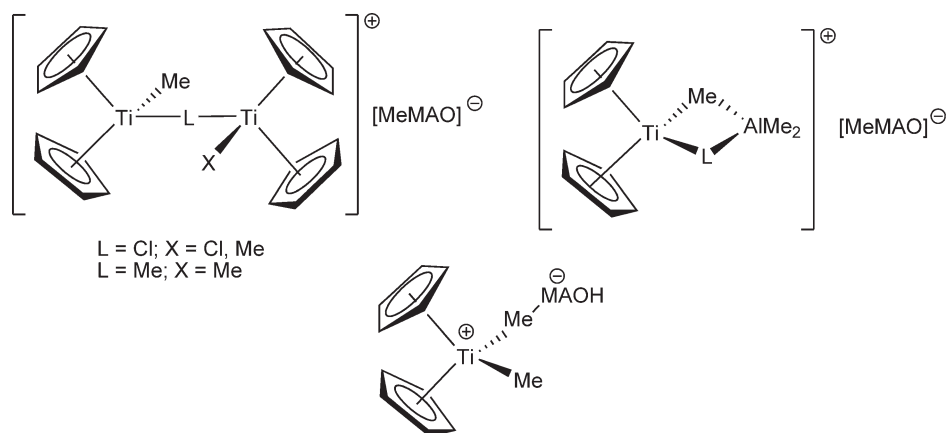
#### 4.05.4.1.3.(iii) Olefin polymerization

This section summarizes simple aspects related to the polymerization of  $\alpha$ -olefins catalyzed by bis-Cp' dichloro titanium complexes. Cp'–titanium derivatives as catalysts for the polymerization of  $\alpha$ -olefins remain very important for the production of commercial polymers; significant effort continues to be devoted to the discovery of new Cp complexes to obtain greater control over polymer properties.<sup>1199</sup> Chapter 4.09 provides a more comprehensive review of the catalytic applications of titanium complexes in the  $\alpha$ -olefin polymerizations. Since the discovery of the stereospecific polymerization of propylene by G. Natta in 1954, there have been rapid advances in the design of new generation olefin polymerization catalysts and polyolefin products worldwide. The major events that have occurred in the area of Ziegler–Natta catalysis, illustrating the contributions of organometallic chemistry in the exciting story of the evolution of well-defined, “single-site” metallocene catalysts and the developments in mechanistic understanding of polymerization processes, have been highlighted<sup>1200</sup> and advances in the chemistry of bis-Cp' titanium complexes as catalysts for the production of industrial polymers have been reviewed.<sup>1201</sup> Ethylene polymerization catalysts based on titanium complexes with a ligand environment involving alkyl, Cp', or Ind groups show distinctive polymerization characteristics.<sup>1202</sup> Titanium complexes bearing Cp' ligands have been tested in ethylene polymerizations after activation with aluminum alkyls ( $\text{AlR}_3$ ) or MAO.<sup>441</sup> Bis-Cp' titanium complexes as precursors for  $\alpha$ -olefin polymerizations have been reviewed.<sup>1203,1204</sup> Living-like polymerization of propylene with mixed bis-Cp titanium catalyst systems has been reported.<sup>1205</sup>

The effects of polymerization conditions on the molecular weight distribution of polyethylene synthesized with  $\text{Cp}_2\text{TiCl}_2/\text{MAO}$  catalysts have been studied in comparison with analogous zirconium and hafnium complexes.<sup>1206,1207</sup>

The catalytic systems  $\text{Cp}_2\text{TiMe}_2/\text{MAO}$  and  $\text{Cp}_2\text{TiClMe}/\text{MAO}$  for ethylene polymerizations and norbornene oligomerizations have been spectroscopically studied and sharp  $^{13}\text{C}$  NMR resonances have been tentatively assigned to ion pair species  $[\text{Cp}_2\text{TiMe}]^+[\text{X-MAO}]^-$  ( $\text{X} = \text{Cl, Me}$ ).<sup>1208–1210</sup> For the catalytic system  $\text{Cp}_2\text{TiCl}_2/\text{MAO}$ , several products have been identified by NMR spectroscopy. The activation of  $\text{Cp}_2\text{TiCl}_2$  with MAO leads to the formation of the intermediates shown in Scheme 493. The concentration of these species in the mixture depends on the Al:Ti ratios. In contrast, the system  $(\text{C}_5\text{Me}_4\text{SiMe}_2\text{NBu}^i)\text{TiCl}_2/\text{MAO}$  gives only zwitterion-like but no heterobinuclear species.<sup>1211</sup>

The species formed between  $\text{AlCl}_3$  and either  $\text{Cp}_2\text{TiCl}_2$  or  $\text{Cp}_2\text{Ti}(\text{CH}_2\text{SiMe}_3)\text{Cl}$  in chloroalkane solution have been studied by means of multinuclear NMR spectroscopy in order to establish the influence of the contact and solvent-separated ion pairs on the activity for ethylene polymerization. The species involved in the equilibria, the changes as a function of temperature, concentration, the ratio of reagents, and the nature of the solvent were



Scheme 493

evaluated. It has been concluded that the solvent-separated ion pair is the most active catalyst and that the arene-solvated species (when the polymerization is conducted in arene solution) is the least active catalyst.<sup>1212,1213</sup>

The system  $\text{Cp}_2\text{TiCl}_2/\text{MAO}$  is suggested to be less active than  $\text{CpTiCl}_3/\text{MAO}$  and  $\text{Cp}_2\text{TiCl}/\text{MAO}$  in the polymerization of 1,3-butadiene, 4-methyl-1,3-pentadiene, and styrene to give predominantly *cis*-1,4-polybutadiene, 1,2-syndiotactic poly(4-methyl-1,3-pentadiene), and syndiotactic polystyrene.<sup>1214</sup>

The role of  $[\text{Cp}_2\text{TiX}]^+$  ions ( $X = \text{Cl, Me}$ ) in coordination polymerization of olefins has been studied by means of electro dialysis, mass spectrometric, and quantum chemical investigations.<sup>1215</sup>

The olefin polymerization catalyst based on  $\text{Cp}_2\text{TiCl}^{13}\text{CH}_3/\text{B}(\text{C}_6\text{F}_5)_3$  has been studied by varying solvent polarity and catalyst concentration. Reaction equilibria and polymerization with carbon-13 enriched ethylene have been studied by  $^{13}\text{C}$  NMR spectroscopy.<sup>1216</sup>

The ethylene polymerization activity of the system  $\text{Cp}_2\text{TiClMe}/\text{AlClMe}_2$  has been investigated and compared with Ti(III) and Ti(II) systems.<sup>1217</sup>

The systems  $(\text{C}_5\text{Me}_4\text{SiMe}_2\text{NBu}^t)\text{TiCl}_2$  and  $\text{Cp}_2\text{TiCl}_2$  using MAO as co-catalyst co-polymerize ethylene and poly(propylene) macromonomer (PPM).<sup>786</sup>

The ethylene polymerization characteristics of the complexes  $(\text{CpR}^1)(\text{CpR}^2)\text{TiCl}_2$  ( $\text{R}^1 = \text{R}^2 = \text{H, Me, Et, Pr}^i, \text{Bu}^t, \text{SiMe}_3, \text{CMe}_2\text{Ph, CO}_2\text{Me}$ ;  $\text{R}^1 = \text{H, R}^2 = \text{Me, Bu}^t, \text{SiMe}_3, \text{CMe}_2\text{Ph, CO}_2\text{Me}$ ) in the presence of  $\text{Al}_2\text{Et}_3\text{Cl}_3$  as co-catalyst have been compared. Crystallographic data for  $(\text{CpR})_2\text{TiCl}_2$  complexes indicate that the Cl–Ti–Cl angle decreases as the size of R increases. The steric effect dominates the order of observed activities.<sup>1218</sup> The catalytic activity of new substituted dichloro bis- $\text{Cp}'$  titanium complexes has been primarily evaluated. The role of organo Lewis acids as co-catalysts was examined.<sup>1219</sup>

The polymerization of alkenes by bis- $\text{Cp}'$  titanium derivatives activated with pentafluorophenoxy alumoxane, an oligomeric compound containing  $-\text{Al}(\text{OC}_6\text{F}_5)-\text{O}-$  units, has been reported.<sup>1220</sup>

The polymerization of styrene using the combined system  $\text{ZnPh}_2/(\text{C}_5\text{H}_4\text{Bu}^n)_2\text{TiCl}_2/\text{MAO}$  in toluene at  $60^\circ\text{C}$  produces highly syndiotactic polystyrene.<sup>1221</sup> The homogeneous catalyst system  $\text{Cp}_2\text{TiCl}_2/\text{AlEt}_3 + \text{SiClR}_3$  ( $\text{R} = \text{Me, Ph}$ ) polymerizes ethylene in toluene.<sup>1222</sup>

$\text{Cp}'_2\text{TiCl}_2$  ( $\text{Cp}' = \text{Cp, C}_5\text{H}_4\text{Bu}^n$ ) combined with diphenylzinc additive initiator systems, including  $\text{ZnPh}_2$  and MAO, have been used for the co-polymerization of styrene with 1-alkenes (1-hexene, 1-decene, and 1-hexadecene)<sup>472</sup> and the co-polymerization of styrene and *p*-*tert*-butylstyrene.<sup>473</sup>

Diphenylacetylene has been polymerized by  $\text{Cp}_2\text{TiCl}_2$  with irradiation of light.<sup>1223</sup>

$\text{Cp}_2\text{TiCl}_2$  has been assessed as additive that controls polymer chain growth in the polymerization of methyl methacrylate.<sup>1224</sup> Methyl methacrylate is easily polymerized in the photopolymerization with  $\text{Cp}_2\text{TiCl}_2$  in a water-methanol mixture under irradiation of a 15 W fluorescent room lamp. The polymerization proceeded heterogeneously.<sup>1225</sup> This process in the presence of 2,2'-bipyridyl, 1,10-phenanthroline, or sparteine as the chelating reagent has been studied.<sup>1226</sup> Similar studies on the polymerization of methacrylate monomers such as methyl methacrylate, ethyl methacrylate, phenyl methacrylate, and benzyl methacrylate at  $40^\circ\text{C}$  have also been performed.<sup>1227</sup> The results of co-polymerization of methyl methacrylate and acrylonitrile indicate that this process proceeds through a radical mechanism.<sup>1228</sup> The mechanism of the controlled radical polymerization of styrene and methyl methacrylate in the

presence of  $\text{Cp}_2\text{TiCl}_2$  has been studied using quantum chemical calculations and electron spin resonance spectroscopy.<sup>1229</sup>

Titanocene fluorides, when activated with MAO, have been found to exhibit high catalytic activity for the polymerization of olefins, especially for styrene to produce syndiotactic polymer. Generally, the activity of the fluoro complexes is about 30 times higher than that of the chloro analogs.<sup>456,455</sup>

$\text{MgCl}_2$ -supported  $\text{Cp}_2\text{TiCl}_2$  was studied as a catalyst for the ethylene polymerization in the presence of trialkylaluminum. Stabilization of the active species, the cation-like complex  $\text{Cp}_2\text{TiR}^+$ , by absorption on  $\text{MgCl}_2$  is proposed.<sup>1230</sup>

Bis-Cp titanium derivatives supported on  $\text{MgCl}_2/\text{AlR}_n(\text{OEt})_{3-n}$ , activated with MAO or borate activators, have been used as catalytic systems for the polymerization of  $\alpha$ -olefins.<sup>475</sup> Supports of type  $\text{MgCl}_2/\text{AlR}_n(\text{OEt})_{3-n}$  have been shown to be effective for the immobilization and activation of  $\text{Cp}_2\text{TiCl}_2$  and other single-site olefin polymerization catalysts without the use of MAO or a borate activator. Polyethylene with a spherical particle morphology and narrow molecular weight distribution has been obtained.<sup>1231</sup>

The catalytic system  $\text{Cp}_2\text{TiCl}_2/\text{MgClPr}^i$  polymerizes isoprene to a mixture of dimers and higher oligomers. The substituent effects of a series of alkyl ring-substituted complexes  $\text{Cp}'_2\text{TiCl}_2$  on the catalytic activity have been investigated. A mechanism of the reaction has been proposed.<sup>1232</sup>

$\text{Cp}_2\text{TiCl}_2$  has been supported over magnesium chloride using the soluble tetrahydrofuran complex of magnesium chloride. The supported catalyst polymerized ethylene with high activities in the presence of MAO.<sup>1233</sup> Conventional Ziegler–Natta catalysts based on  $\text{TiCl}_4$  supported on  $\text{MgCl}_2$  have been modified by replacing the chloro ligands by Cp and substituted Cp rings.<sup>1234</sup>

Silica-supported  $\text{MgCl}_2/\text{Cp}_2\text{TiCl}_2$  catalysts ( $\text{M} = \text{Ti}$  or  $\text{Zr}$ ) have been prepared by depositing a homogeneous solution of  $\text{Cp}_2\text{TiCl}_2$  and anhydrous  $\text{MgCl}_2$  in THF onto high surface area silica ( $\text{SiO}_2$ ). They show higher polymerization activities than comparable  $\text{Cp}_2\text{TiCl}_2$  catalysts supported on either  $\text{SiO}_2$  or  $\text{MgCl}_2$  alone.<sup>1235</sup>

Gel-type poly(styrene-*co*-divinylbenzene) beads have been used as a carrier to encapsulate bis-Cp titanium catalysts through a simple swelling–shrinking procedure. These catalytic species are homogeneously distributed in the PS bead particle and exhibit high and stable ethylene polymerization and ethylene/1-hexene co-polymerization activity.<sup>1236</sup>

The thermodynamics of the reaction of the ethylene molecule with the  $\text{Cp}_2\text{TiClMe}/\text{AlClMe}_2$  system, as a model for olefin polymerization with homogeneous Ziegler–Natta catalysts, has been investigated using DFT calculations.<sup>1237</sup>

A mathematical model, including the main morphological features of the polymerization process, has been developed to study supported bis-Cp titanium derivatives as catalysts for olefins polymerization.<sup>1238</sup>

A series of mixed bis-Cp' dichloro Ti derivatives, previously synthesized by conventional methods,<sup>1090,1219,1239–1241</sup> have been used as catalysts for the ring-opening metathesis polymerization of norbornene<sup>1242</sup> and dicyclopentadiene.<sup>1243</sup> The catalytic system  $\text{Cp}_2\text{TiCl}_2/\text{MgXR}$  has been employed similarly.<sup>1244</sup>

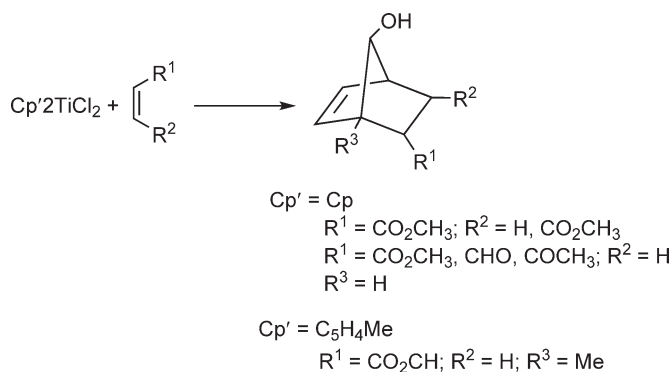
#### 4.05.4.1.3.(iv) Organic reactions

The extensive use of Cp'–titanium complexes in the development of organic synthetic methodology is beyond the scope of this chapter. We include here some examples of the various reaction types in which titanium(IV) derivatives are used as reagents in organic synthesis, although no attempt has been made to cover this subject comprehensively. Section 4.05.8 covers additionally an overview of the applications of titanium complexes in stoichiometric and catalytic organic reactions.

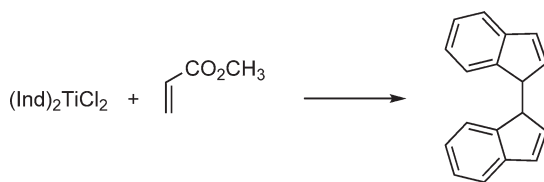
The use of bis-Cp' titanium complexes as catalytic systems for reductive transformations via one-electron transfer in organic reaction has been reviewed.<sup>1245</sup>

The reactions of  $\text{Cp}_2\text{TiCl}_2$  with electron-deficient olefins offer a facile route to diastereomerically pure substituted 7-hydroxynorbornenes (Scheme 494) which are otherwise difficult to prepare. The reaction also exhibits mild regioselectivity. The effects of solvents, added reagents, and alkene structure upon the reaction has been studied. The reaction is an example of a metal-assisted oxidative [4 + 2]-cycloaddition of alkenes with Cp ligands. By contrast,  $(\text{Ind})_2\text{TiCl}_2$  reacts with methylacrylate to give a product of net reductive coupling of indenyl ligands instead of the cycloaddition product (Scheme 495).<sup>1246</sup>

The preparation of allylsilanes from allyl ethers and chlorosilanes is catalyzed by  $\text{Cp}_2\text{TiCl}_2$ .<sup>1247</sup> The process involves reaction of  $\text{Cp}_2\text{TiCl}_2$  with  $\text{Bu}^n\text{MgCl}$  to generate  $\text{Cp}_2\text{TiBu}^n_2$  which readily decomposes to Ti(II) complexes with subsequent reaction of allyl ether to afford bis-Cp allyl derivatives and further transmetallation with  $\text{Bu}^n\text{MgCl}$ .<sup>24,1248</sup>



Scheme 494



Scheme 495

The reduction–deoxygenation coupling of aromatic amides in the presence of stoichiometric amount of organosilanes is catalyzed by  $\text{Cp}_2\text{TiX}_2$  ( $\text{X} = \text{F}, \text{Me}$ ).<sup>1249–1251</sup>

$\text{Cp}_2\text{TiCl}_2$  combined with various reducing agents, including  $\text{LiBu}^n$ ,  $\text{LiPh}$ , and  $\text{AlEt}_3$  has been evaluated for the hydrogenation of polystyrene– $\beta$ -polybutadiene– $\beta$ -polystyrene block co-polymers.<sup>1252</sup> The addition reaction of bromodifluoroacetate with electron-deficient *gem*-dicyanoalkenes is promoted smoothly by the  $\text{Cp}_2\text{TiCl}_2/\text{Zn}$  system and gives the corresponding  $\alpha,\alpha$ -difluoroesters as the addition–reduction products.<sup>1253</sup> Reductive debromination of *vic*-dibromides to alkenes with the  $\text{Cp}_2\text{TiCl}_2/\text{indium}$  system has been studied.<sup>1254</sup> The mechanism of hydromagnesiation reaction of alkynes with an alkyl Grignard reagent catalyzed by  $\text{Cp}_2\text{TiCl}_2$  has been elucidated. It is suggested that the regiochemistry of the reaction is controlled by the transmetallation step from titanium to magnesium.<sup>1255</sup>

A catalytic cycle has been developed for the conversion of glycosyl halides to their corresponding glycals using  $\text{Cp}_2\text{TiCl}_2$  with only 30% of the *in situ* generated single electron reducing agent in contrast to the 2 equiv. normally employed.<sup>1256</sup>

Diverse methods and a variety of reagents have been developed for the dehalogenation reaction of organic halides. Catalytic dechlorination of aromatic chlorides has been efficiently performed using Grignard reagents in the presence of catalytic amount of  $\text{Cp}_2\text{TiCl}_2$ .<sup>1257</sup>  $\text{Cp}_2\text{TiF}_2$  catalyzes the defluorination of perfluorocarbons.<sup>1258</sup>

The mixture of  $\text{Cp}_2\text{TiCl}_2$  and a hydride reagent catalyzes the dehalogenation of monohalopyridines at room temperature to give pyridine.<sup>1259</sup>

$\text{Cp}_2\text{TiCl}_2$  exhibits antiselectivity when used as additive in stereoselective aldol reactions of (*S*)-(–)-2-(pyrrolidin-2-yl)propan-2-ol with benzaldehyde.<sup>1260</sup>  $\text{Cp}_2\text{TiCl}_2$  catalyzes the reduction of imines to amines. These reactions employ  $\text{Bu}^n\text{MgCl}$  as the stoichiometric reducing agent.<sup>1261</sup> Titanium compounds catalyze the reduction of imines and carbonyl-containing compounds. Highly enantioselective imine hydrosilylation using the (*S,S*)-etbhi difluoro titanium complex has been reported. The procedure converts imines to amines under mild conditions. The catalysis activation proceeds through conversion of a Ti–F to a Ti–H bond.<sup>1262</sup>

The system  $\text{Cp}_2\text{TiX}_2/t$ -butyl hydroperoxide (TBHP) ( $\text{X} = \text{Cl}, \text{OTf}$ ) catalyzes the oxidation of sulfides to sulf-oxides. In the presence of (+)-(*R*)-BINOL, as chiral ligand and activated with 4 Å molecular sieves, an asymmetric reaction is observed.<sup>1263</sup>

The addition of a catalytic amount of  $\text{Cp}_2\text{TiCl}_2$  dramatically increases the yield of the hydroacylated ketone formed in the hydroacylation of 1-alkenes with heteroaromatic aldehydes by using Wilkinson's complex and 2-amino-3-picoline as co-catalysts.<sup>1264</sup>  $\text{Cp}_2\text{TiCl}_2$  catalyzes the reduction of aryl halides by sodium borohydride. The reaction scope and mechanism are solvent dependent.<sup>1265</sup>

$\text{Cp}_2\text{TiCl}_2$ ,  $\text{Cp}^*\text{TiCl}_2(\text{OMe})$ , and  $\text{Cp}^*\text{TiCl}_2(\text{NMe}_2)$  catalyze the cycloisomerization of 1,6-dienes in the presence of a catalytic amount of  $\text{Bu}^n\text{MgBr}$ , providing the corresponding 2-methyl-1-methylenecyclopentanes with high efficiency. In contrast, catalysis using the more sterically encumbered *ansa*-*etbhi* dichloro titanium compound leads to the predominant formation of methylenecyclohexanes.<sup>1266</sup>  $\text{Cp}_2\text{TiCl}_2$  has been used as a catalyst in the presence of  $\text{Bu}^n\text{MgCl}$  for the double silylation of 1,3-butadienes with chlorosilanes to give 1,4-disilylated 2-butenes in good yields. Similar reactions with aryl-substituted alkenes proceed with the formation of 1,2-disilylated products.<sup>1267</sup>

A practical titanium-catalyzed synthesis of bicyclic cyclopentenones and allylic amines is described. The process converts enyne substrates to iminocyclopentenones using 10 mol% of the air- and moisture-stable pre-catalyst  $\text{Cp}_2\text{TiCl}_2$  in the presence of  $\text{LiBu}^n$  and triethylsilyl cyanide.<sup>1268</sup>

The chloromethylation reaction of bis- $\text{Cp}^*$  dichloro titanium complexes in the presence of polyformaldehyde and dry hydrogen chloride has been reported.<sup>1269</sup>

Mixtures of  $\text{Cp}_2\text{TiCl}_2$  or  $\text{Cp}_2\text{TiClMe}$  with  $\text{AlMe}_3$  or  $\text{AlClMe}_2$  promote the carbometallation reaction of diphenyl acetylene and other alkynes with methylalanes. Mechanistic aspects have been discussed, the process is apparently multimechanistic. With 1:1 mixtures of  $\text{Ti}/\text{Al}$ , the reaction proceeds exclusively via methyltitanation to give a 98% stereoisomerically pure (*E*)-1,2-diphenyl-1-propenyl bis- $\text{Cp}$  chloro titanium compound which is converted in the methyltitanium derivative by reaction with  $\text{LiMe}$ . In cases where a 2:1 mixture of  $\text{AlMe}_3$  and  $\text{Cp}_2\text{TiCl}_2$  is used, the course of reaction varies and is very much dependent on several reaction parameters. The formation of the Tebbe reagent or fast methyltitanation is observed before the formation of the Tebbe reagent, depending on the reaction conditions. The reaction of 5-decyne with a 1:1 mixture of  $\text{AlMe}_3$  and  $\text{Cp}_2\text{TiCl}_2$  provides 6-methyl-4,5-decadiene in 92% yield, while the corresponding reaction of 1-octyne gives, after protonolysis, 2-methyl-1-octene only in 25% yield along with at least three unidentified but apparently dimeric products.<sup>1270</sup>

The reducing species involved in  $\text{Cp}_2\text{TiCl}_2/\text{Mn}$  and  $\text{Cp}_2\text{TiCl}_2/\text{Zn}$  promoted pinacol coupling reactions have been studied using a combination of kinetics, voltammetry, and product analysis.<sup>1179</sup>

The system  $\text{Cp}_2\text{TiCl}_2/\text{In}$  is active for the reduction of aromatic nitro compounds to aromatic amines,<sup>1271</sup> for the deoxygenation of amine-N-oxides,<sup>1272</sup> and the reduction of sulfoxides.<sup>1273</sup>

## 4.05.4.2 Complexes with Ti–C Bonds

### 4.05.4.2.1 Synthesis of bis- $\text{Cp}$ titanium hydrocarbyls

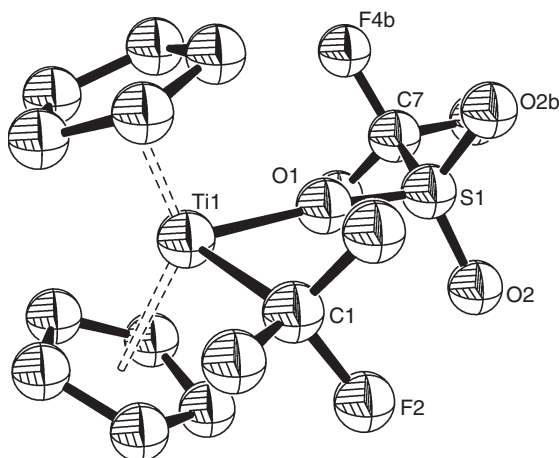
Bis- $\text{Cp}^*$  titanium complexes with Ti–C bonds (alkyl, aryl, benzyl, alkenyl, alkynyl, ...) are generally accessible by metathetical ligand exchange reaction between the dihalo precursor with the appropriate organolithium or organomagnesium derivatives. The reducing nature of the  $\text{LiR}$ ,  $\text{MgXR}$ , or  $\text{MgR}_2$  reagents can become a problem for the synthesis of these titanium derivatives. Alternative methodologies for the preparation of  $\sigma$ -Ti–C bonds have proved advantageous because of higher yields and greater selectivities.

The perfluoromethyl compound  $\text{Cp}_2\text{TiF}(\text{CF}_3)$  is prepared by the addition of  $\text{Me}_3\text{SiCF}_3$  and  $\text{CsF}$  to a suspension of  $\text{Cp}_2\text{TiF}_2$  in THF. The compound is unaffected by brief exposure to air but is thermally sensitive. The Ti– $\text{CF}_3$  bond is remarkably robust and this compound does not react with nucleophiles, although treatment with  $\text{B}(\text{C}_6\text{F}_5)_3$  results in the immediate formation of intractable products. On reaction with  $\text{Me}_3\text{Si}(\text{OTf})$ , the complex is converted to  $\text{Cp}_2\text{Ti}(\text{CF}_3)(\text{OTf})$ , which in the presence of pyridine gives the adduct  $\text{Cp}_2\text{Ti}(\text{CF}_3)(\text{OTf})(\text{py})$ . The molecular structures of these complexes have been determined by X-ray diffraction (Figure 25).<sup>1274</sup>

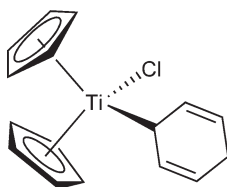
The titanocene aryls  $(\text{C}_5\text{H}_4\text{R})_2\text{TiAr}_2$  ( $\text{R} = \text{H}$ ,  $\text{Ar} = \text{C}_6\text{H}_5$ , *p*- $\text{MeC}_6\text{H}_4$ , *m*- $\text{MeC}_6\text{H}_4$ ;  $\text{R} = \text{Me}$ ,  $\text{Ar} = \text{C}_6\text{H}_5$ , *p*- $\text{MeC}_6\text{H}_4$ ;  $\text{R} = \text{C}_6\text{H}_{11}$ ,  $\text{Ar} = \text{C}_6\text{H}_5$ , *p*- $\text{MeC}_6\text{H}_4$ ) have been synthesized and tested as catalysts for the hydrogenation of styrene-1-butene-styrene terpolymers.<sup>1037</sup> The bis- $\text{Cp}$  cyclohexadienyl compound (Scheme 496) has been prepared and applied to transfer the cyclohexadienyl group to various aldehydes.<sup>23</sup>

$\text{Cp}'_2\text{Ti}(\text{CH}_2\text{CMe}_3)_2$  ( $\text{Cp}' = \text{Cp}$ ,  $\text{C}_5\text{H}_4\text{Me}$ ) can be prepared as the product of the reaction between  $\text{Cp}'_2\text{TiCl}_2$  and  $\text{Mg}(\text{CH}_2\text{CMe}_3)_2 \cdot \text{dioxane}$  or  $\text{LiCH}_2\text{CMe}_3$  in diethyl ether at low temperature. These compounds can be stored cold and they decompose at room temperature via  $\alpha$ -H abstraction to give neopentane and thermally stable alkylidene titanium complexes (Scheme 524; Section 4.05.4.2.4).<sup>1275</sup>

The complexes  $\text{Cp}(\text{C}_5\text{H}_4\text{Bu}^t)\text{TiCl}_2$  and  $\text{Cp}(\text{C}_9\text{H}_7)\text{TiCl}_2$  have been used to prepare a range of mono- and disubstituted titanium(IV) alkyl derivatives (Scheme 432; Section 4.05.4.1.1.(i).(a)).<sup>1042</sup> Treatment of  $\text{Cp}(1,3\text{-Bu}^t_2\text{C}_5\text{H}_3)\text{TiCl}_2$  with  $\text{AlMe}_3$  permits the monoalkylation to give  $\text{Cp}(1,3\text{-Bu}^t_2\text{C}_5\text{H}_3)\text{TiClMe}$ , while the reaction with 2 equiv. of  $\text{LiMe}$  affords the dimethyl derivative  $\text{Cp}(1,3\text{-Bu}^t_2\text{C}_5\text{H}_3)\text{TiMe}_2$ . When  $\text{MgBz}_2 \cdot 2\text{THF}$  or  $\text{LiCH}_2\text{CMe}_2\text{Ph}$  were used as alkylating agents, the corresponding dialkyl complexes were not obtained; instead, the formation of toluene or *tert*-butyl benzene was observed and the ring-metallated complexes



**Figure 25** Molecular structure of complex  $\text{Cp}_2\text{Ti}(\text{CF}_3)(\text{OTf})$  (reproduced by permission of American Chemical Society from *J. Am. Chem. Soc.*, **2003**, 125, 14712).

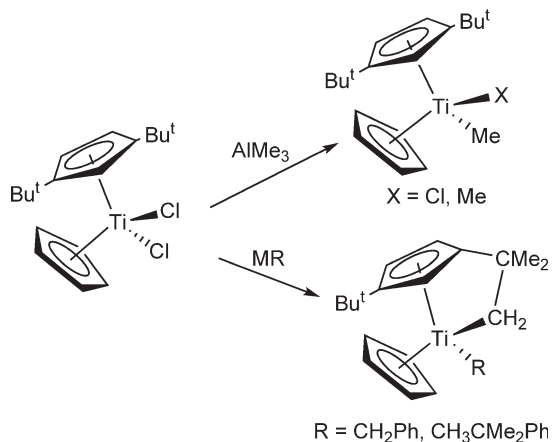


**Scheme 496**

$\text{Cp}(1\text{-Bu}^t\text{-3-CH}_2\text{CMe}_2\text{C}_5\text{H}_3)\text{TiR}$  were isolated as the result of intramolecular activation of one of the *tert*-butyl-substituted rings and the elimination of the hydrocarbon (Scheme 497).<sup>337</sup>

The “mixed ring” dimethyl compound  $\text{Cp}^*[\text{C}_5\text{H}_4(\text{CMe}_2)(\text{C}_{13}\text{H}_9)]\text{TiMe}_2$  is obtained by alkylation of the dichloro compound  $\text{Cp}^*[\text{C}_5\text{H}_4(\text{CMe}_2)(\text{C}_{13}\text{H}_9)]\text{TiCl}_2$  with  $\text{LiMe}$  (Scheme 438; Section 5.4.1.1.a).<sup>326</sup>

$\text{Cp}_2\text{TiCl}_2$  reacts with  $(\text{OPr}^i)_3\text{SiCH}_2\text{MgCl}$  to give the stable mono- or bis-alkyl derivatives  $\text{Cp}_2\text{TiCl}[\text{CH}_2\text{Si}(\text{OPr}^i)_3]$  or  $\text{Cp}_2\text{Ti}[\text{CH}_2\text{Si}(\text{OPr}^i)_3]_2$ , the molecular structures of which have been determined by X-ray diffraction. Treatment of  $\text{Cp}_2\text{TiCl}[\text{CH}_2\text{Si}(\text{OPr}^i)_3]$  with  $[\text{Cu}(\text{CH}_3\text{CN})_4]\text{PF}_6$  affords  $\text{Cp}_2\text{TiF}_2$ , while the reaction with  $\text{NaCo}(\text{CO})_4$  proceeds to give the  $\mu$ -oxo compound  $\text{Cp}_2[\text{CH}_2\text{Si}(\text{OPr}^i)_3]\text{Ti-O-TiCp}_2\text{Cl}$ .<sup>1276</sup>



**Scheme 497**

$\text{Cp}(\text{C}_5\text{H}_4\text{SiMe}_2\text{Bu}^i)\text{Ti}(\text{CH}_2\text{Ph})_2$  has been prepared by the alkylation of  $\text{Cp}(\text{C}_5\text{H}_4\text{SiMe}_2\text{Bu}^i)\text{TiCl}_2$  with  $\text{BzMgCl}$ .<sup>1065</sup>

Alkylation of the mixed bis-Cp complex  $\text{Cp}(\text{C}_5\text{H}_4\text{SiMe}_2\text{CH}_2\text{CH}=\text{CH}_2)\text{TiCl}_2$  with  $\text{MeMgCl}$  affords the chloro monomethyl derivative  $\text{Cp}(\text{C}_5\text{H}_4\text{SiMe}_2\text{CH}_2\text{CH}=\text{CH}_2)\text{TiClMe}$ , while treatment with 2 equiv. of  $\text{LiMe}$  or  $\text{BzMgCl}$  gives the dialkyl compounds  $\text{Cp}(\text{C}_5\text{H}_4\text{SiMe}_2\text{CH}_2\text{CH}=\text{CH}_2)\text{TiR}_2$  ( $\text{R} = \text{Me}, \text{CH}_2\text{Ph}$ ).<sup>391</sup>

$(\text{C}_5\text{Me}_4\text{CH}_2\text{CH}_2\text{CH}=\text{CH}_2)_2\text{TiCl}_2$  (Scheme 473; Section 4.05.4.1.1.(ii)) is converted into the corresponding dimethyl derivative, the molecular structure of which has been confirmed by an X-ray analysis. The reaction of the dimethyl complex with  $\text{B}(\text{C}_6\text{F}_5)_3$  was monitored by NMR spectroscopy; however, no tractable products could be isolated.<sup>347</sup>

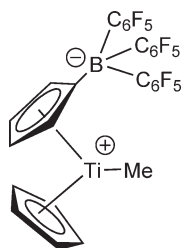
$(\text{C}_5\text{H}_5\text{CH}_2\text{CH}_2\text{NPr}^i)_2\text{TiR}_2$  ( $\text{R} = \text{Me}, \text{Bz}$ ) are obtained by treatment of the dichloro complexes (Scheme 466; Section 4.05.4.1.1.(ii)) with  $\text{LiMe}$  or  $\text{BzMgBr}$  in diethyl ether. The methyl complex is highly moisture sensitive, while the benzyl derivative is stable toward air at room temperature for a short period of time. They catalyze the dehydrogenative coupling of phenylsilane to oligosilanes in excellent yields.<sup>1094</sup>

The synthesis of the borate-substituted Cp complex  $\text{Cp}[\text{C}_5\text{H}_4\text{B}(\text{C}_6\text{F}_5)_3]\text{TiMe}$  has been reported. This complex has been studied as “single-component” zwitterionic catalyst for olefin polymerization and shows a very weakly coordinating boron substituent (Scheme 498).<sup>1277</sup>

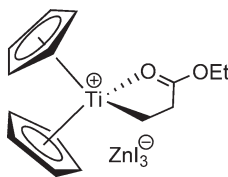
The synthesis and characterization of the neutral homoenolate mono-Cp  $\text{CpTiCl}_2(\text{CH}_2\text{CH}_2\text{COOEt})$  and cationic bis-Cp titanium  $[\text{Cp}_2\text{TiCH}_2\text{CH}_2\text{COOEt}]^+\text{ZnI}_3^-$  derivatives have been reported. The molecular structure of the cationic complex shows ester coordination to give a five-membered metallacycle (Scheme 499).<sup>53</sup>

The chloro fulvalene compound  $(\text{TiCpCl}_2)_2(\mu\text{-C}_{10}\text{H}_8)$  is alkylated to give tetraalkyl derivatives (Scheme 459; Section 4.05.4.1.1.(i).(g)).<sup>1080</sup> The binuclear fulvalene-bridged compound  $(\text{CpTiPh}_2)_2(\mu\text{-C}_{10}\text{H}_8)$  was obtained; its X-ray structure shows the Ti atoms in a *trans*-arrangement with respect to the fulvalene group.<sup>1278</sup>

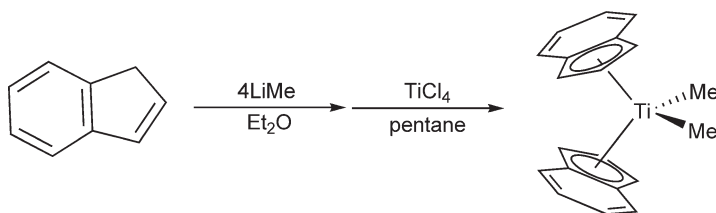
The reaction of indene with twofold excess of  $\text{LiMe}$  in  $\text{Et}_2\text{O}$  generates the ligand anion without detectable side-reactions. Subsequent reaction with  $\text{TiCl}_4$  in pentane gives the bis-indenyldimethyltitanium complex directly (Scheme 500).<sup>1279</sup>



Scheme 498



Scheme 499



Scheme 500



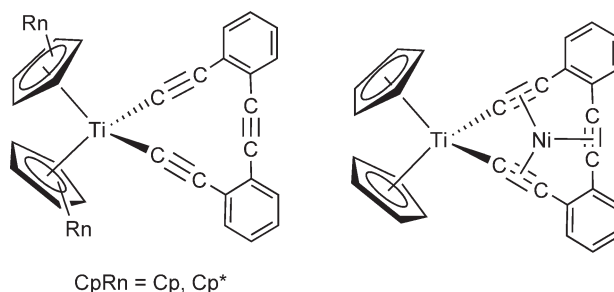
The chemistry of bis(alkynyl) metal complexes, including the titanium derivatives, focusing on the synthesis, chemical behavior, structure, and bonding of different type of mononuclear and heterometallic molecules has been discussed in a review.<sup>1280</sup> A review focusing the preparation and the reactivity of compounds of the type  $\text{Cp}'_2\text{Ti}(\sigma\text{-C}\equiv\text{CR})_2$  ( $\text{Cp}' = \text{Cp}, \text{Cp}^*$ ) has appeared which summarizes special aspects of C–C coupling and cleavage processes in organic reactions.<sup>1281</sup>

The diacetylide complexes  $\text{Cp}'_2\text{Ti}(\text{C}\equiv\text{CSiMe}_3)_2$  ( $\text{Cp}' = \text{Cp}^*$ ,<sup>1281</sup>  $\text{C}_5\text{HMe}_4$ ,<sup>1282</sup> and  $\text{C}_5\text{H}_4\text{CH}_2\text{CH}_2\text{NMe}_2$ <sup>1092</sup>) are synthesized by treatment of  $\text{LiC}\equiv\text{CSiMe}_3$  with  $\text{Cp}'_2\text{TiCl}_2$ . Similarly,  $\text{Cp}^*_2\text{Ti}(\text{C}\equiv\text{CBu}^t)_2$  has been described.<sup>1283</sup> The titanium(III) “ate” complex  $\text{Cp}^*_2\text{Ti}(\text{C}\equiv\text{CPh})_2\text{Li}(\text{THF})_2$  reacts under an atmosphere of  $\text{CO}_2$  to give the bis(acetylide) derivative  $\text{Cp}^*_2\text{Ti}(\text{C}\equiv\text{CPh})_2$  with 35% yield.<sup>1284</sup> The synthesis and characterization of a family of  $\sigma$ -acetylide derivatives  $\text{Cp}_2\text{Ti}(\text{CH}_2\text{SiMe}_3)(\text{C}\equiv\text{CR})$  [ $\text{R} = \text{SiMe}_3$ ,  $(\eta^5\text{-C}_5\text{H}_4)\text{FeCp}$ ,  $\text{C}_6\text{H}_3(\text{CH}_2\text{NMe}_2)\text{-3,5}$ ,  $\text{C}_6\text{H}_4\text{-I-4}(\text{CH}_2\text{NMe}_2)\text{-3,5}$ ,  $\text{C}_6\text{H}_4\text{CN-4}$ ,  $\text{C}_5\text{H}_4\text{N-4}$ ,  $\text{C}_6\text{H}_4\text{-C}\equiv\text{C-TiCp}_2(\text{CH}_2\text{SiMe}_3)$ ] have been described. These monoalkynyl derivatives react with Cu(I) salts suggesting the coordination of the  $\text{C}\equiv\text{C}$  unit to Cu(I), but the resulting intermediates are prone to rapid ligand exchange. The electrochemical behavior, the redox stability, and reactions with late transition metal complexes (Ru, Pt) to afford heterobimetallic compounds are reported.<sup>1285</sup>

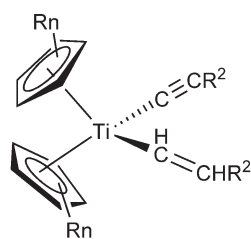
Cyclic acetylide titanium complexes containing the *o*-bis(ethynyl)tolane ligand have been synthesized, characterized, and used to prepare a heterobimetallic derivative with an Ni atom coordinated to three alkyne functionalities (Scheme 501).<sup>1286</sup>

The substituted bis- $\text{Cp}'$  alkynyl–alkenyl  $(\text{C}_5\text{Me}_4\text{R}^1)_2\text{Ti}(\text{C}\equiv\text{CR}^2)(\text{CH}=\text{CHR}^2)$  (Scheme 502) have been synthesized by reaction of the bis(trimethylsilyl)ethyne complex  $(\text{C}_5\text{Me}_4\text{R}^1)_2\text{Ti}(\text{Me}_3\text{SiC}_2\text{SiMe}_3)$  with 1-alkynes; the crystal structures have been determined by X-ray diffraction. Photolysis of these complexes involves dimerization processes with coupling of the two  $\sigma$ -ligands to give complexes with 1,4-disubstituted but-1-en-3-yne.<sup>1287</sup>

Reaction of  $\text{CpCp}^*\text{TiCl}_2$  with 2 equiv. of  $\text{LiCH}=\text{CH}_2$  enables the isolation of a titanium(IV)–divinyl complex  $\text{CpCp}^*\text{Ti}(\text{CH}=\text{CH}_2)_2$ , while the reaction with the lithium reagent in a molar ratio of 1:1 affords the chloro vinyl complex  $\text{CpCp}^*\text{TiCl}(\text{CH}=\text{CH}_2)$  which is converted into the methyl derivative  $\text{Cp}(\text{C}_5\text{Me}_5)\text{TiMe}(\text{CH}=\text{CH}_2)$  through further alkylation with LiMe. Quantitative isomerization of  $\text{CpCp}^*\text{Ti}(\text{CH}=\text{CH}_2)_2$  to the methylenemetallacyclobutane  $\text{CpCp}^*\text{Ti}[\text{C}(\text{CH}_2)\text{CH}_2\text{CH}_2]$  occurs as a consequence of characteristic  $\alpha$ -H transfer (Scheme 503).<sup>1288</sup> Complexes  $\text{Cp}^*_2\text{TiX}(\text{CH}=\text{CH}_2)$  ( $\text{X} = \text{F}, \text{Cl}, \text{Br}$ ) can be formed directly by the reaction of the corresponding  $\text{Cp}^*_2\text{TiX}_2$  complexes and vinyl lithium or by anion exchange (Scheme 504).



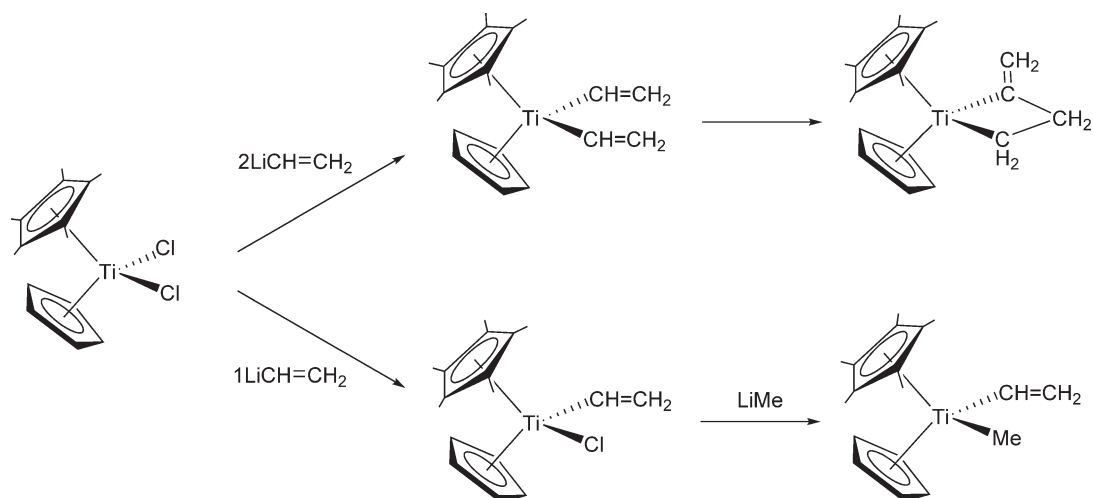
Scheme 501



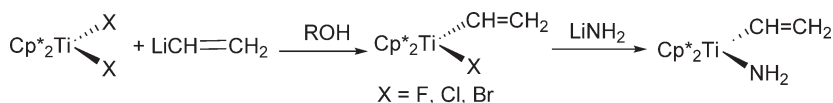
$\text{CpRn} = \text{C}_5\text{Me}_4\text{R}^1$ ,  $\text{R}^1 = \text{H}, \text{Me}, \text{Ph}, \text{Bz}$   
 $\text{R}^2 = \text{Bu}^t, \text{SiMe}_3, \text{ferrocenyl}$

Scheme 502





Scheme 503

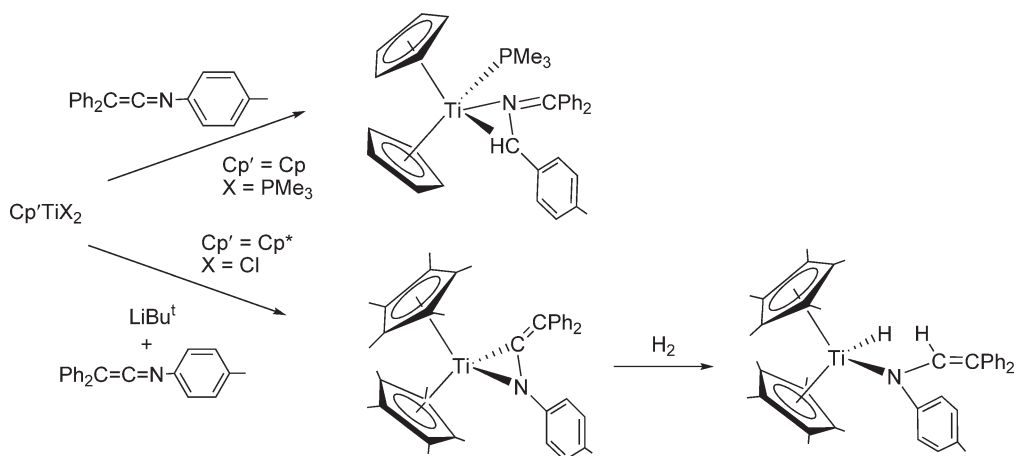


Scheme 504

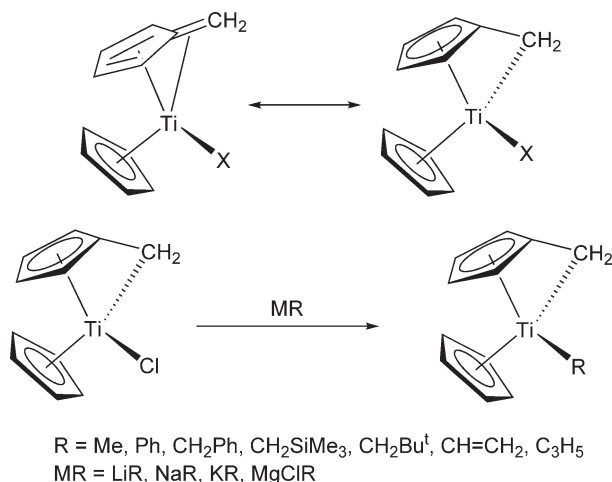
The synthesis and the molecular structure of the fluoro vinyltitanocene  $\text{Cp}^*_2\text{TiF}(\text{CH=CH}_2)$  have been described.<sup>1289</sup> The reaction of perfluorovinyl lithium with  $\text{Cp}_2\text{TiX}_2$  ( $\text{X} = \text{Cl}, \text{F}$ ) affords the chloro and fluoro derivatives  $\text{Cp}_2\text{TiX}(\text{CF=CF}_2)$ . When slightly more than 2 equiv. of the lithium salt is used, the complex  $\text{Cp}_2\text{Ti}(\text{CF=CF}_2)_2$  is obtained. The titanium–carbon bond distances of the perfluorovinyl group have been determined by Ti K-edge EXAFS studies.  $\text{Cp}_2\text{TiX}_2$  ( $\text{X} = \text{Cl}, \text{F}$ ) react at low temperature with  $\text{Li}(\text{ClC=CF}_2)$  to give the 1-chloro-2,2-difluorovinyl complexes  $\text{Cp}_2\text{TiX}_n(\text{ClC=CF}_2)_{2-n}$  ( $n = 0, 1$ ). The complexes have been characterized by NMR spectroscopy and in the case of  $\text{Cp}_2\text{TiCl}(\text{ClC=CF}_2)$  by single crystal X-ray diffraction. The magnitude of the  $^{19}\text{F}$ – $^{19}\text{F}$  coupling constants (45–60 Hz) is consistent with a *geminal*-disposition. These complexes are prone to decompose in the solution with complete loss of the fluorovinyl group and formation of intractable byproducts. This process has been studied in a range of hydrocarbon and non-hydrocarbon solvents. In order to develop more stable systems, the ancillary ligands have been modified. The stabilities of  $\text{Cp}^*_2\text{TiF}_n(\text{FC=CF}_2)_{2-n}$  ( $n = 0, 1$ ) and  $\text{Cp}^*_2\text{TiMe}(\text{ClC=CF}_2)$  have been investigated; in the case of  $\text{Cp}^*_2\text{TiMe}(\text{ClC=CF}_2)$  this has led to the spectroscopic characterization of the  $\pi$ -complex  $\text{Cp}^*_2\text{TiMe}(\eta^2\text{-ClHC=CF}_2)$  as an intermediate in the solution-phase decomposition pathway.<sup>1290,1291</sup>

The synthesis, structural characterization, and reactivity of ketenimine titanium complexes are described.  $\text{Cp}_2\text{Ti}(\text{PMe}_3)_2$  react with *N*-(*p*-tolyl)diphenylketenimine to give  $\text{Cp}_2\text{Ti}(\eta^2\text{-CN-Ph}_2\text{C=C=NPh})(\text{PMe}_3)$ , while the pentamethyl Cp-substituted derivative  $\text{Cp}^*_2\text{Ti}(\eta^2\text{-CN-Ph}_2\text{C=C=NPh})$  is prepared by the reaction of  $\text{Cp}^*_2\text{TiCl}_2$  with  $\text{LiBu}^t$  and subsequent treatment of the “ $\text{Cp}^*_2\text{Ti}$ ” species generated *in situ* with *N*-(*p*-tolyl)diphenylketenimine. The X-ray diffraction studies confirm the  $\eta^2\text{-CN}$  coordination of the ketenimine ligand. Coupling reactions are observed in the presence of 2 equiv. of ketenimine.  $\text{Cp}^*_2\text{Ti}(\eta^2\text{-CN-Ph}_2\text{C=C=NPh})$  reacts with dihydrogen to give a hydride enamidato complex (Scheme 505).<sup>1292</sup>

The reactivity of titanium tetramethylfulvene complexes can be best explained in terms of  $\eta^5\text{-Cp}$ –alkyl bonding of the fulvene ligand, although spectroscopic and structural data point to a significant contribution of an  $\eta^4\text{-diene-}\eta^2\text{-olefin}$  resonance form.  $\text{Cp}^*(\text{Fv})\text{TiCl}$  ( $\text{Fv} = \text{C}_5\text{Me}_4\text{CH}_2$ ) reacts with alkali metal alkyls or Grignard reagents to give the alkyl derivatives  $\text{Cp}^*(\text{Fv})\text{TiR}$ , while the reaction with  $\text{LiEt}$  yields the ethylene adduct  $\text{Cp}^*_2\text{Ti}(\eta^2\text{-C}_2\text{H}_4)$  (Scheme 506). The thermolysis of the fulvene complexes  $\text{Cp}(\text{Fv})\text{TiR}$  has been studied. The decomposition pathways show a remarkable dependence on the nature of the R group.<sup>1293</sup>



Scheme 505

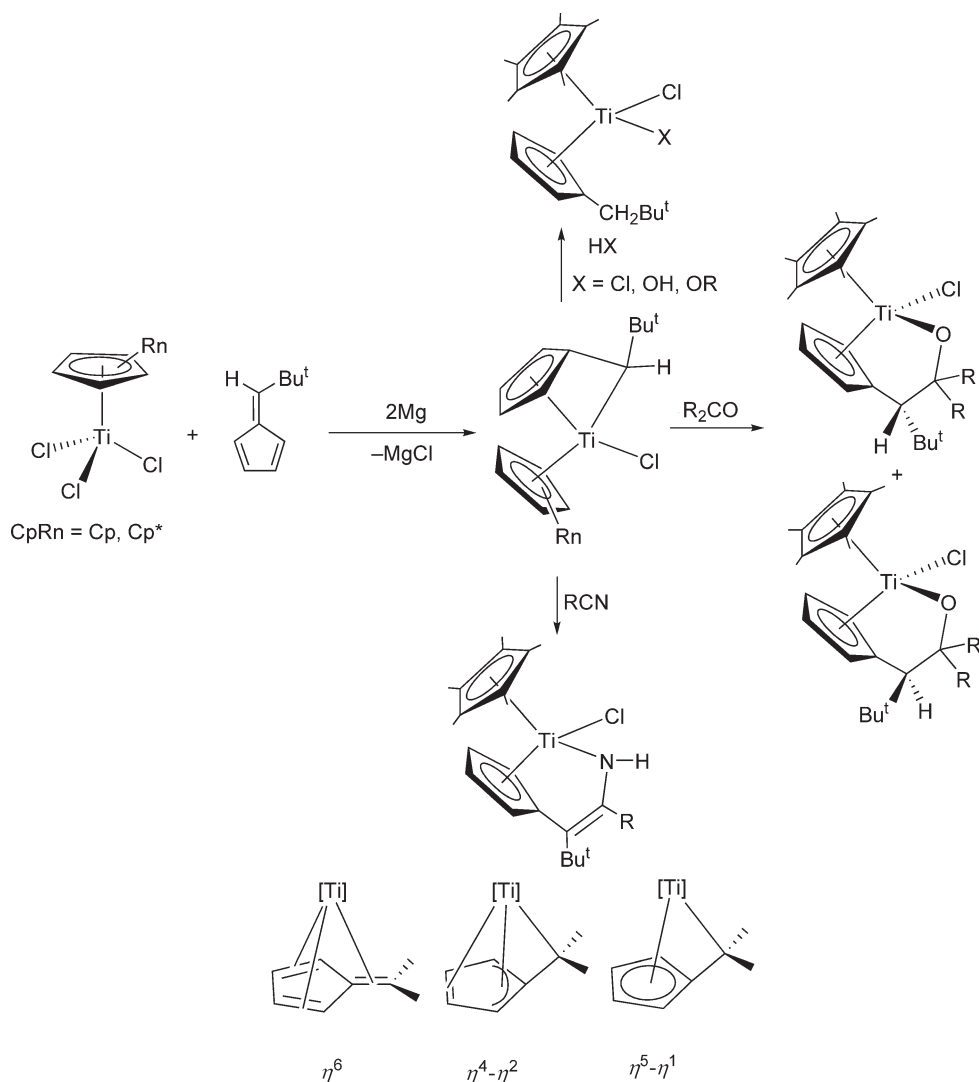


Scheme 506

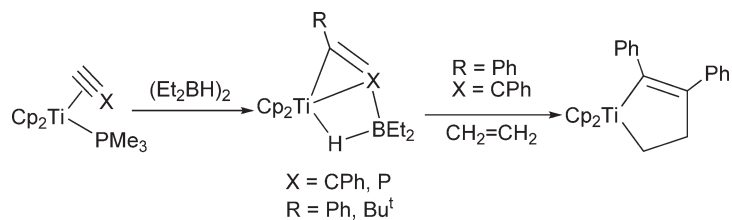
Several  $\sigma$ -C titanocene compounds can be prepared by Mg reduction of dihalo complexes containing  $\omega$ -alkenyl- and  $\omega$ -alkenyl-dimethylsilyl-Cp substituents (Section 4.05.4.1.3.(ii)).

Reactions of  $\text{Cp}'\text{TiCl}_3$  ( $\text{Cp}' = \text{Cp}, \text{Cp}^*$ ) with Mg in the presence of 6-*tert*-butylfulvene afford the corresponding fulvene titanium complexes (Scheme 507), the structures of which have been confirmed by X-ray diffraction. The coordinated fulvene can be considered as an  $\eta^6$ -olefinic ligand ( $\text{Ti}^{\text{III}}$  complex) or an  $\eta^4$ : $\eta^2$ - or  $\eta^5$ : $\eta^1$ -dianionic ligand ( $\text{Ti}^{\text{IV}}$  complex). The exocyclic carbon atom of the fulvene ligand coordinated to titanium exhibits strong nucleophilic character. These compounds react with simple electrophiles to give substituted mixed bis-Cp derivatives. Insertion reactions with ketones and nitriles have been studied. With ketones,  $\pi$ -face differentiation and “frontside” or “backside” attack can be observed to give the possible diastereomers, while with isonitriles imine–enamine rearrangement takes place (see Section 4.05.4.2.3).<sup>1294</sup>

Bimetallic complexes containing planar tetracoordinate carbon atoms bridging a group 4 transition metal and a main group element are of current interest due to their unusual bonding and reactivity pathways.<sup>1295</sup> Binuclear titanium–boron complexes with planar tetracoordinate carbon or a planar tricoordinate phosphorus atoms are obtained by the reaction of tolane or phosphoalkyne titanium complexes with tetraethyldiborane (Scheme 508). The X-ray structure investigations conclusively show the planar geometry of the five-membered skeleton containing the two olefinic carbon atoms. The  $^{31}\text{P}$  NMR spectroscopic data for the phosphorus compound clearly indicate the planar-coordinated phosphorus atom. The compounds are thermally stable and they are highly reactive toward unsaturated substrates.<sup>1296</sup>

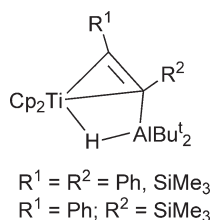


Scheme 507

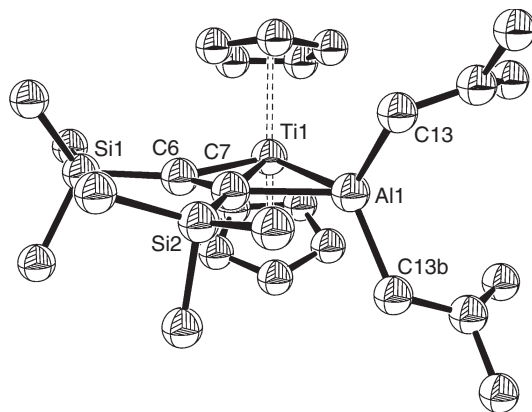


Scheme 508

The reactivity of these complexes has been studied (Section 4.05.4.2.3). Similarly, the reaction of bis-Cp-alkyne and alkene Ti complexes with aluminum or boron organic compounds has been intensively investigated to give bimetallic systems containing planar tetracoordinate carbon atom bridging between Ti and Al or B atoms (Scheme 509). Under certain conditions, these complexes regenerate the starting compounds. The crystal structures exhibit planar, bicyclic five-membered ring system consisting of the Ti atom, the hydridic hydrogen, Al (or B),  $\text{C}_\beta$ , and  $\text{C}_\alpha$  (Figure 26). These compounds have been tested as initiators in the ring-opening polymerization of lactones.<sup>1297,1298</sup>



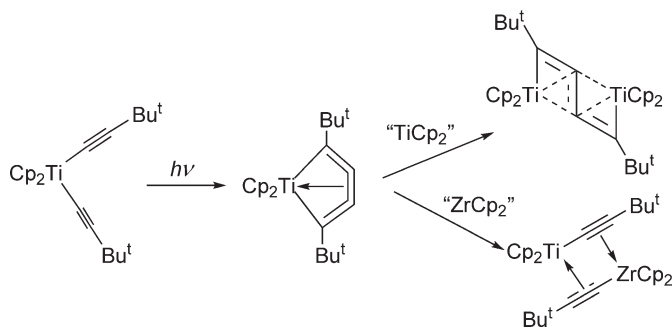
Scheme 509



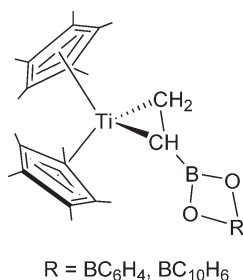
**Figure 26** Molecular structure of complex  $Cp_2Ti(\mu-\eta^1-\eta^2-Me_3SiC\equiv CSiMe_3)(\mu-H)(AlBu_2)$  (reproduced by permission of Wiley-VCH from *Eur. J. Inorg. Chem.* **2001**, 2885).

Irradiation of  $Cp_2Ti(C\equiv CBu^t)_2$  affords the five-membered titanacyclocumulene  $Cp_2Ti(\eta^4-1,2,3,4-Bu^tC_4Bu^t)$ ; further reactions with “ $TiCp_2$ ” or with “ $ZrCp_2$ ” give the bridging 1,3-butadiene ( $TiCp_2$ )<sub>2</sub>[ $\mu-\eta(1-3),\eta(2-4)-trans-trans-Bu^tC_2-C_2Bu^t$ ] or  $TiCp_2(\mu-\eta^1-\eta^2-C\equiv CBu^t)ZrCp_2(\mu-\eta^1-\eta^2-C\equiv CBu^t)$ , respectively (Scheme 510).<sup>1299,1300</sup> The nature of the complex formed between the unit “ $TiCp_2$ ” and disubstituted butadiyne  $R^1C\equiv C-C\equiv CR^2$  ligands depends strongly on the nature of the  $R^1$  and  $R^2$  substituents. For  $R^1 = R^2 = SiMe_3$ , the binuclear  $Ti(III)$  complex  $[Cp_2Ti(C\equiv CSiMe_3)]_2$  is formed. For other symmetrically or unsymmetrically substituted butadiynes ( $R^1 = R^2 = Ph, Bu^t$ ;  $R^1 = SiMe_3, R^2 = Ph, Bu^t$ ), binuclear complexes are obtained with a  $\mu-\eta(1-3),\eta(2-4)-trans-trans$ -butadiene unit (“zigzag butadiyne”) between the two titanium centers. These 1,3-diyne ligands bridging two metals exhibit planar coordination geometry at the tetravalent carbon atoms (Scheme 563; see Section 4.05.4.2.4; metallacycle compounds).<sup>1301,1302</sup>

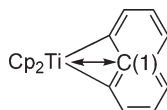
The complex shown in Scheme 511 is formed by the reaction of  $Cp^*_2Ti(CH_2=CH_2)$  with the corresponding borane in appropriate conditions. These complexes are intermediates in the dehydrogenative borylation of ethylene through the selective conversion of a titanium–olefin bond to vinyl borate esters.<sup>1303</sup>



Scheme 510



Scheme 511

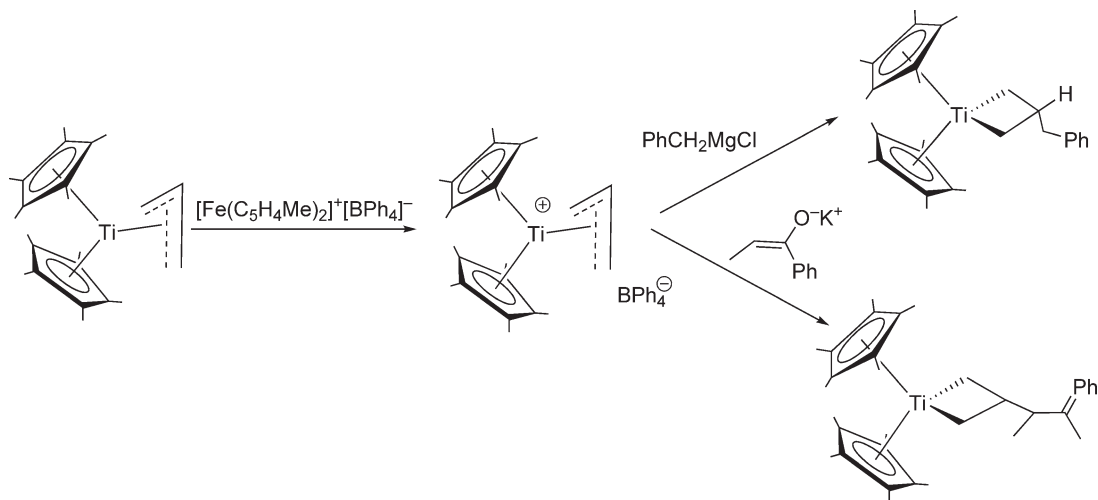


Scheme 512

The compound shown in Scheme 512 has been reported. The Ti–C(1) distance of 2.442(7) Å is shorter than the sum of the van der Waals radii and it is unclear whether an electronic interaction is present but a bonding interaction is excluded on the basis of orbital symmetry considerations.<sup>1304</sup>

The unsaturated cationic titanium allyl compound  $[\text{Cp}^*_2\text{Ti}(\text{allyl})]^+\text{BPh}_4^-$  is prepared by oxidation of the titanium(III) allyl complex  $\text{Cp}^*_2\text{Ti}(\text{allyl})$  with a ferrocenium cation. Nucleophilic addition to the cationic unit proceeds regioselectively to the central allylic position. Reaction with benzyl Grignard or the enolate of propiophenone affords the corresponding titanacyclobutane complexes (Scheme 513).<sup>1305</sup>

The bis-Cp dicarbonyl dication  $[\text{Cp}_2\text{Ti}(\text{CO})_2](\text{BPh}_4)_2$  has been obtained in toluene under carbon monoxide by double protonation of  $\text{TiCp}_4$  with  $[\text{NH}(\text{Bu}^n)_3]\text{BPh}_4$  or by two-electron oxidation of  $\text{Cp}_2\text{Ti}(\text{CO})_2$  with  $[\text{FeCp}_2]\text{BPh}_4$ . This compound is thermally stable and does not lose CO at room temperature even under high vacuum. Its IR spectrum exhibits two strong carbonyl absorptions at 2119 and 2099  $\text{cm}^{-1}$ . The reactivity of this dicarbonyl derivative has been examined. Carbon monoxide is readily lost in the presence of chloride ions to give  $\text{Cp}_2\text{TiCl}_2$ . Replacement of CO with  $\text{NH}(\text{Et})_2$  and dmpe is also observed to give  $[\text{TiCp}_2\text{L}_2](\text{BPh}_4)_2$  ( $\text{L} = \text{NH}(\text{Et})_2$ , dmpe). The complex is reduced with  $\text{CoCp}_2$ , with the formation of  $\text{Cp}_2\text{Ti}(\text{CO})_2$ .<sup>1306</sup>



Scheme 513

#### 4.05.4.2.2 Structures and properties of bis-Cp titanium hydrocarbyls

The molecular structures of  $\text{Cp}_2\text{TiCl}(\text{C}_6\text{F}_5)$ <sup>1307</sup> and  $\text{Cp}_2\text{TiMe}_2$ <sup>1308</sup> have been determined by X-ray diffraction. The dimethyl compound is isostructural with the analogous zirconium and hafnium complexes. The molecular structure of bis-Cp 2,2'-biphenyl titanium, determined by X-ray diffraction methods, has been reported.<sup>1309</sup>

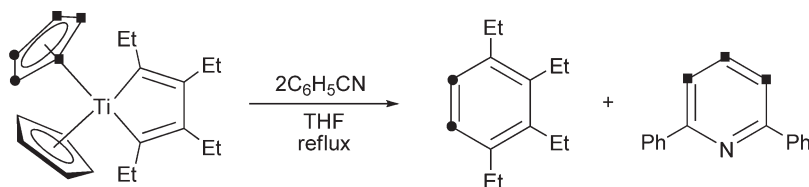
The coordination of 1,3-diynes as bridging ligands between two bis-Cp units is in many cases associated with the cleavage of their central C–C single bond. Dynamic NMR studies on binuclear bis-Cp Ti complexes bridged by  $\text{Me}_3\text{Si}-\text{C}\equiv\text{C}-\text{C}\equiv\text{C}-\text{CMe}_3$  have been performed in order to understand the C–C single bond metathesis reaction. The existence of an equilibrium is suggested between the binuclear complex and an isomer formed by cleavage of the central C–C bond and exhibiting two bridging  $\sigma$ -alkynyl ligands, that may interchange the disposition between the titanium atoms.<sup>1310</sup>

Reaction enthalpies of bis-Cp derivatives  $\text{Cp}'_2\text{TiMe}_2$  ( $\text{Cp}' = \text{Cp}, \text{Cp}^*, \text{C}_5\text{H}_3\text{Me}_2$ ) and the Cp-amido complex  $(\text{C}_5\text{Me}_4\text{SiMe}_2\text{NBu}^t)\text{TiMe}_2$  with the strong Lewis acid  $\text{B}(\text{C}_6\text{F}_5)_3$  have been measured using batch titration calorimetry in toluene. Methide abstraction to form the corresponding  $[\text{Cp}'_2\text{TiMe}]^+[\text{MeB}(\text{C}_6\text{F}_5)_3]^-$  contact ion pairs is exothermic, with the exothermicity increasing as Cp–methyl substitution increases.<sup>1311</sup>

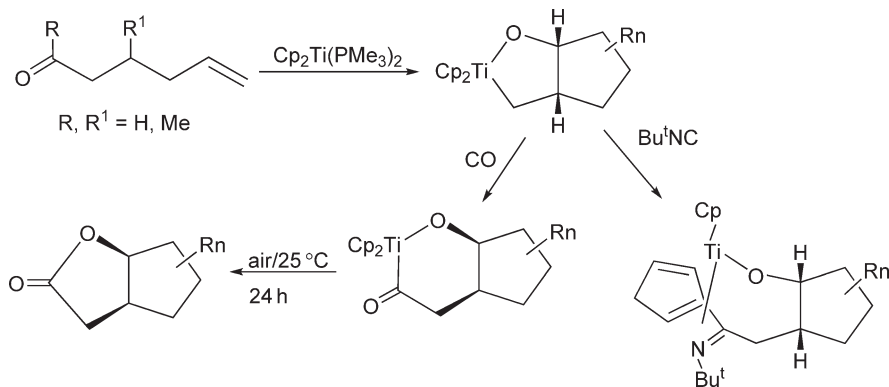
#### 4.05.4.2.3 Reactions of bis-Cp titanium hydrocarbyls

A reason for the extensive use of the Cp ligands in organometallic chemistry is the great stability of the  $\eta^5$ -Cp bonding mode. In most organometallic reactions of Cp titanium derivatives, the  $\eta^5$ -Cp rings are spectator ligands. Nevertheless, some reactions have been found in which the  $\text{Ti}-\eta^5\text{-Cp}$  fragment can be remarkably reactive, and activation and functionalization of Cp ligands bonded to Ti centers have been observed. An overview of the reactivity of the Cp ligands in titanium derivatives for new arene synthesis reactions has been reported.<sup>1312</sup> The  $\eta^5$ -Cp ligand participates unexpectedly in the pinacol coupling of ketones with the  $\text{Ti}(\text{II})$  compound  $\text{Cp}_2\text{Ti}(\text{PMe}_2)_2$ , with fulvene formation.<sup>1313</sup>  $\text{Cp}_2\text{TiBu}^n_2$  reacts with 2 equiv. of 3-hexyne to give a titanacyclopentadiene derivative, which reacts with 2 equiv. of benzonitrile to afford substituted benzene and pyridine compounds. This novel arene synthesis proceeds through an unprecedented double C–C bond cleavage of one of the two Cp ligands in the titanacyclopentadiene complex with transformation of the resulting two pieces, such that a two-carbon unit and a three-carbon unit are incorporated into a benzene and a pyridine product, respectively (Scheme 514). Direct evidence for the Cp bond cleavage has been unambiguously provided using isotopically labeled compounds. A bimolecular reaction pathway has been excluded by the experimental results.<sup>1314</sup>

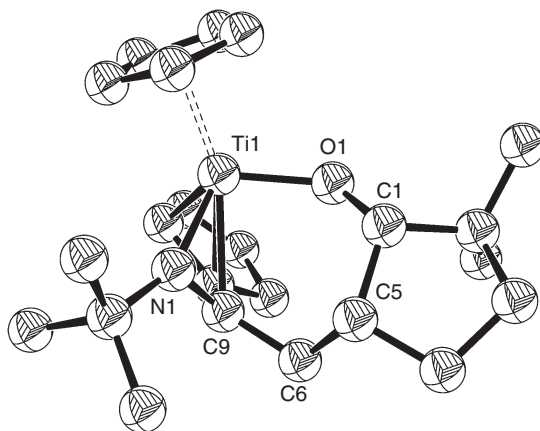
$\eta^5$ -Cp ligands can participate in C–C bond formations that completely remove the Cp ring from the metal.<sup>1315</sup> For example, titanacyclic derivatives (Scheme 515) can be prepared by reacting  $\text{Cp}_2\text{Ti}(\text{PMe}_3)_2$  with  $\delta,\varepsilon$ -unsaturated



Scheme 514



Scheme 515



**Figure 27** Molecular structure of complex  $\text{CpTi}[\text{C}_5\text{H}_5\text{-C(=NBU)-CH}_2\text{-(C}_5\text{H}_6\text{Me}_2\text{)-O}]$  (reproduced by permission of American Chemical Society from *J. Am. Chem. Soc.*, **1996**, 118, 5508).

carbonyl compounds. Upon treatment of these complexes with CO, carbonylated metallacycles are formed via insertion of CO into the Ti–C bond. Reductive elimination of  $\gamma$ -butyrolactones occurs from these carbonylated metallacycle derivatives induced thermally or oxidatively upon treatment with a suitable Lewis acid.<sup>1316</sup> Replacing CO with the isoelectronic  $\text{Bu}^t\text{NC}$  isonitrile ligand, a similar reaction proceeds but leads to a new complex where one of the  $\eta^5$ -Cp ligand is converted to an  $\eta^4$ -azadiene ligand, formed from the coupling of the incoming  $\text{Bu}^t\text{NC}$  ligand to both the metallacycle ring and one of the Cp ligands (Scheme 515). The molecular structure of this complex has been confirmed by X-ray diffraction (Figure 27). The short Ti–N bond distance [1.886(5) Å] and the planar nitrogen geometry suggest significant  $p_\pi$ – $d_\pi$  Ti–N interaction. Acid-mediated hydrolysis, air oxidation, and acetone insertion reactions have been studied.<sup>1315</sup>

More examples demonstrating that  $\eta^5$ -Cp ligand are not always benign spectators are described in Schemes 564 and 565 (Section 4.05.4.2.4.(ii)).

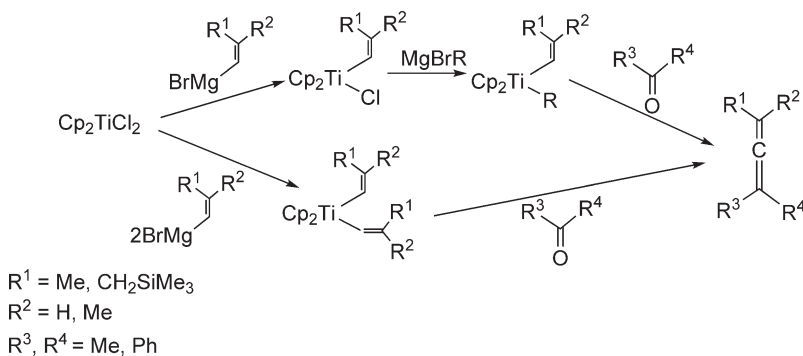
An overview of the applications of bis-Cp' titanium derivatives in catalytic reactions of Si–H bonds has appeared.<sup>1317</sup>

$\text{Cp}_2\text{TiMe}_2$  has been described as a useful reagent for C–C and C–N bond formation.<sup>633</sup> Organosilanes react with  $\text{Cp}_2\text{TiMe}_2$  to give the reduced titanium species  $\text{Cp}_2\text{Ti}(\mu\text{-SiR}_2\text{H})(\mu\text{-H})\text{TiCp}_2$ ,  $[\text{Cp}_2\text{Ti}(\mu\text{-SiR}_2\text{H})_2]$ , and  $[\text{Cp}_2\text{TiH}]_2(\mu\text{-H})$  ( $\text{R} = \text{H, Me, Bu}^n$ ).<sup>1318</sup> The reduction of  $(\text{C}_5\text{HMe}_4)_2\text{Ti}(\text{C}\equiv\text{CSiMe}_3)_2$  with alkali metals in toluene affords the titanocene(III) diacetylide  $\text{M}^+ [\text{Ti}(\text{C}_5\text{HMe}_4)_2(\text{C}\equiv\text{CSiMe}_3)_2]^-$ .<sup>1282,1319,1320</sup> The reactions of  $\text{Cp}_2\text{TiR}_2$  ( $\text{R} = \text{Me, CH}_2\text{Ph}$ ) with 2.5 equiv. of  $\text{HB}(\text{C}_6\text{F}_5)_2$  proceed to give the Ti(III) complex  $\text{Cp}_2\text{Ti}[\eta^2\text{-H}_2\text{B}(\text{C}_6\text{F}_5)_2]$ , which has been fully characterized. A plausible explanation for these observations, which contrast with other reactions of boranes with group 4 metallocenes, is presented. It involves an exchange of alkyl and hydride between titanium and borane, followed by reductive elimination of RH forming “ $\text{Cp}_2\text{Ti}$ .” Comproportionation with  $\text{Cp}_2\text{TiR}_2$  affords the Ti(III) derivative  $\text{Cp}_2\text{TiR}$ , which reacts with 2 equiv. of  $\text{HB}(\text{C}_6\text{F}_5)_2$  to give the complex  $\text{Cp}_2\text{Ti}[\eta^2\text{-H}_2\text{B}(\text{C}_6\text{F}_5)_2]$  and  $\text{RB}(\text{C}_6\text{F}_5)_2$ .<sup>1321</sup>

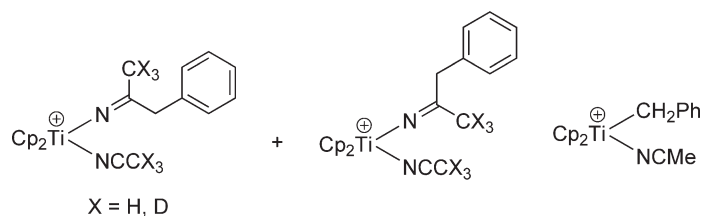
$\text{Cp}_2\text{TiCl}_2$  or  $\text{Cp}_2\text{TiClR}$  react with the appropriate amount of alkenylmagnesium bromide to give alkenyl and dialkenyl bis-Cp titanium derivatives. These substances are too unstable for normal isolation; nevertheless, they can be reacted with carbonyl compounds *in situ* at 0 °C to give the corresponding allenes (Scheme 516).<sup>1322</sup>

The isomerization process of the fulvene titanium allyl complex  $\text{Cp}^*(\text{Fv})\text{Ti}(\eta^3\text{-C}_3\text{H}_5)$ <sup>1293</sup> ( $\text{Fv} = \text{C}_5\text{Me}_4\text{CH}_2$ ) (Scheme 506; Section 4.05.4.2.1) to the 1-propenyl  $\text{Cp}^*\text{FvTi}(\eta^1\text{-CH=CHMe})$  has been investigated. Mechanistic, kinetic, and thermodynamic aspects suggest that the reaction proceeds via reversible first-order steps with the participation of four intermediates.<sup>1323</sup>

The reaction of  $\text{Cp}_2\text{Ti}(\text{CH}_2\text{Ph})_2$  with  $\text{AgBPh}_4$  in acetonitrile entails initial generation of the reactive cationic monobenzyl species  $[\text{Cp}_2\text{Ti}(\text{CH}_2\text{Ph})(\text{NCCH}_3)]^+$ , followed by a competitive process: it can react either by nitrile insertion to give the azomethine titanium(IV) compound  $[\text{TiCp}_2\{\text{N}=\text{C}(\text{CH}_3)\text{CH}_2\text{Ph}\}(\text{NCCH}_3)]^+$ , isolated as a mixture of 2/1 ratio of diastereoisomers (Scheme 517), or by Ti–benzyl bond homolysis, which yields the known paramagnetic cationic Ti(III) complex  $[\text{TiCp}_2(\text{NCCH}_3)_2]^+$ . Dibenzyl is also obtained in the reaction mixture. Similar behavior is observed in the reaction of  $\text{Cp}_2\text{Ti}(\text{CH}_2\text{Ph})_2$  with either  $\text{Fe}(\text{C}_5\text{H}_4\text{Me})_2^+$ ,  $\text{HNMe}_3^+$  or  $\text{NaBPh}_4$  in THF, which yield the cationic Ti(III) complex  $[\text{TiCp}_2(\text{THF})_2]^+$ . The analogous metastable, base-free ion pair  $[\text{Cp}_2\text{Ti}(\text{CH}_2\text{Ph})][\text{CB}_{11}\text{H}_{12}]$ , observed spectroscopically, reacts with  $\text{CD}_3\text{CN}$  to form  $[\text{TiCp}_2\{\text{N}=\text{C}(\text{CD}_3)\text{CH}_2\text{Ph}\}(\text{NCCD}_3)]^+$  as the  $\text{CB}_{11}\text{H}_{12}^-$  salts.



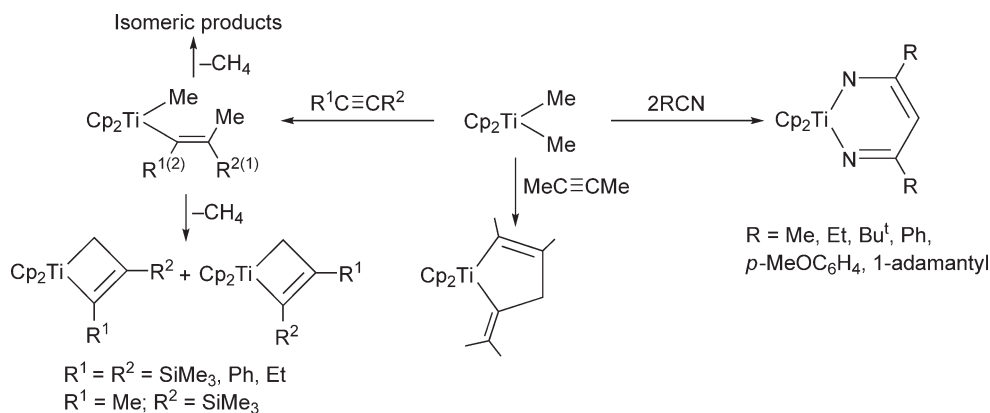
Scheme 516



Scheme 517

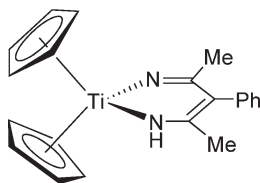
The chemistry of these reactive  $[\text{Cp}_2\text{TiCH}_2\text{Ph}(\text{L})]^+$  species has been contrasted with that of related group 4 metal complexes with the zirconium derivative being more resistant to  $\text{CH}_3\text{CN}$  insertion.<sup>1324</sup>

$\text{Cp}_2\text{TiMe}_2$  reacts with alkynes to afford the vinyl complexes resulting from insertion of the alkyne into one of the Ti–Me bonds. Thermolysis of these vinyl complexes results, generally, in extrusion of methane and formation of the titanacyclobutene (Scheme 518). The intermediate vinyl complex can undergo alternative methane elimination in which titanacyclobutene is disfavored and the formation of isomeric products can be then observed. Thus, the formation of the titanacyclopentene (Scheme 518) is observed when  $\text{Cp}_2\text{TiMe}_2$  reacts with 2-butyne under certain reaction conditions. Synthetic, mechanistic, and kinetic studies are reported. Two equivalents of nitriles react with  $\text{Cp}_2\text{TiMe}_2$  to afford not azatitanacyclobutenes but rather diazatitanacyclohexadienes (Scheme 518). The formation of a titanacyclopropane (allene complex) intermediate species has been proposed (for analogous results, see Section 4.05.4.3.4, Scheme 547).<sup>1325,1326</sup>



Scheme 518



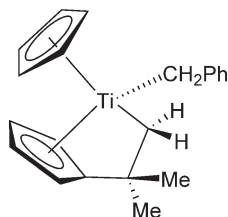


Scheme 519

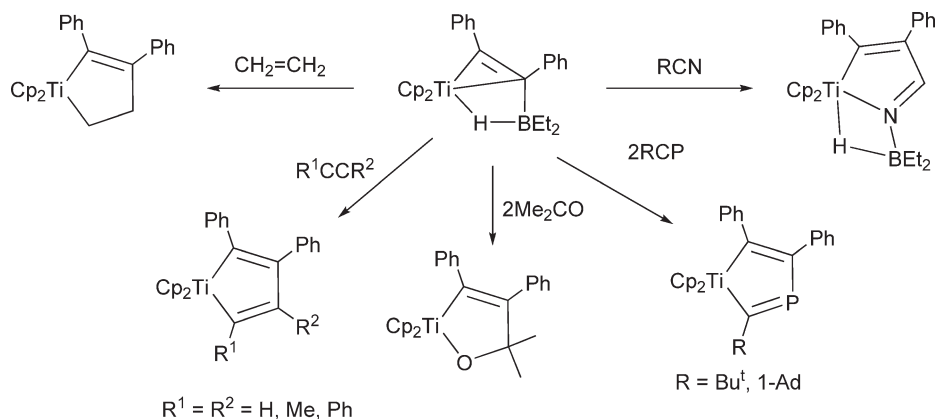
$\text{Cp}_2\text{Ti}(\text{CH}_2\text{Ph})_2$  is thermolyzed in the presence of acetonitrile to give the double insertion product (Scheme 519). The reaction with cyclododecanone leads to olefination. The major product in the thermolysis of  $\text{Cp}(\text{C}_5\text{H}_4\text{Bu}^t)\text{Ti}(\text{CH}_2\text{Ph})_2$  in toluene is the metallacycle shown in Scheme 520, which results from the C–H activation of one methyl ligand of the  $\text{Bu}^t$  group and elimination of toluene.<sup>1327</sup>

The diastereomerically pure complex  $\text{Cp}^*[\text{C}_5\text{H}_4\text{C}(\text{H})\text{Bu}^t]\text{TiCl}^{311}$  reacts with various carbonyl compounds (ketones, aldehydes, and esters) to give  $\sigma, \pi$ -chelate complexes with Cp-alkoxo ligands through insertion of the carbonyl group into the “Ti–C(H)Bu<sup>t</sup>” bond (Scheme 507; Section 4.05.4.2.1). The final products were spectroscopically and structurally characterized by NMR and X-ray diffraction. This procedure provides a convenient access to complexes where new chiral centers are formed directly in the coordination sphere of the Ti atom in a well-defined manner. Reactions with benzophenone, acetone, and formaldehyde were studied. Mixtures of diastereoisomers are obtained (Scheme 507; Section 4.05.4.2.1). The diastereoisomer ratio can be influenced by electronic and steric effects. Insertion of activating (electron-donating) or deactivating (electron-accepting) substituents in *para*-position at the phenyl rings of the benzophenone permits the evaluation of electronic effects on the reaction. Studies concerning the diastereoselectivity of the insertion reaction, mechanistic reflections, and rearrangement of diastereoisomers are included.<sup>1328–1330</sup>

Reactions of the *anti*-van’t Hoff/le Bel titanium complex  $\text{Cp}_2\text{Ti}(\text{PhC})_2(\text{HBEt}_2)$  with ethylene, acetylenes, phosphacetylenes, acetone, and nitriles give metallacycle or bimetallic compounds (Scheme 521). In some cases, hydroboration of the C–C or C–heteroatom multiple bond in the substrates is observed.<sup>1331</sup>  $(\text{C}_5\text{Me}_5)_2\text{Ti}[\eta^2\text{-CH}_2\text{=CHB}(\text{Cat})]^{1303}$



Scheme 520



Scheme 521

(Scheme 511; Section 4.05.4.2.1) is thought to promote boron–carbon bond formation through a mechanism proceeding by ring-opening  $\sigma$ -bond metathesis and  $\beta$ -hydrogen elimination and accounts for retention of the C=C bond.<sup>1332</sup>

The reactivity of  $[\text{Cp}_2\text{TiMe}]^+\text{B}(\text{C}_6\text{F}_5)_4^-$  toward tripeptides to give cationic bis-Cp peptide Ti derivatives and their chemical behavior has been studied. In these compounds, the strongly electrophilic  $[\text{Cp}_2\text{TiMe}]^+$  cation is coordinated to a single carboxamide carbonyl oxygen atom. In some cases, the migration of the  $[\text{Cp}_2\text{TiMe}]^+$  group along the peptide chain was observed. The selective formation of these series of (peptide)–bis-Cp cation complexes has been spectroscopically analyzed by means of their very characteristic  $^1\text{H}$  and  $^{13}\text{C}$  NMR spectra.<sup>1333</sup>

The migratory insertion of CO into the Ti–Me bond in  $\text{Cp}_2\text{TiMe}_2$  has been investigated by both static and dynamic density functional theory calculations. CO coordination prior to insertion has been analyzed considering both “lateral” and “central” approaches, and the two pathways were found to be kinetically equivalent. The O–“outside”  $\eta^2$ -bound acyl complex is more stable than the O–“inside” isomer by  $4.0 \text{ kcal mol}^{-1}$ , with an isomerization energy barrier of  $9.6 \text{ kcal mol}^{-1}$ .<sup>1334</sup>

The polymerization of 1,2-diphenylsilane catalyzed by  $\text{Cp}_2\text{TiMe}_2$  has been revisited in detail to extend the interpretation of  $^{29}\text{Si}$  NMR spectroscopy data of the polymers. In the same report, the use of (*S,S*)-(ebthi)Ti binaphtholate as dehydrocoupling catalyst for the production of cyclopolysilanes is described.<sup>1335</sup>

The complexes  $\text{Cp}'_2\text{Ti}(\text{Me}_3\text{SiC}_2\text{SiMe}_3)_2$  have been used as catalysts for the ring-opening polymerization of  $\varepsilon$ -caprolactones.<sup>1336</sup>

Dehydrocoupling of hydrosilanes is one of the alternative synthetic routes to polysilanes.  $\text{Cp}_2\text{TiMe}_2$  and the *ansa*-titanium compound *rac*-(ebthi)TiMe<sub>2</sub> catalyze the reactions of silanes with allylic and homoallylic alcohols. Different products are obtained depending on the catalyst type, concentration, and the substituents on the silicon atom.<sup>1337</sup> The reactions of symmetrical and unsymmetrical disilanes with catalytic quantities of  $\text{Cp}_2\text{TiCl}_2/\text{Bu}^n\text{Li}$  and *cis*-cyclooctene have been studied. Analysis of the product distribution in these reactions indicate that both Si–Si bond cleavage and Si–H dehydrocoupling of the starting disilane occur. Some possible reaction pathways and the rationalization of the product distributions and apparent isomer preferences through both  $\sigma$ -bond metathesis steps and metal silylene intermediates are discussed.<sup>1338</sup>

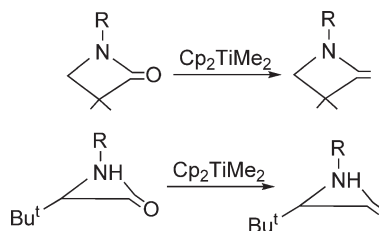
$\text{Cp}_2\text{TiMe}_2$  is a suitable reagent for the methylenation of heteroatom-substituted carbonyl compounds in the reactions with  $\alpha$ - and  $\beta$ -lactams (Scheme 522). It reacts with 1-aryl-2-azetidinones with the formation of methylene azetidine compounds. Analogous reactions with aziridinines afford methylene aziridine compounds.<sup>1339</sup>

The reaction of  $[\text{Rh}(\mu\text{-OH})(\text{COD-1,5})_2]$  with  $\text{Cp}_2\text{TiMe}_2$  proceeds with methane elimination to give  $\text{TiO}_2$  and the Cp rhodium derivative  $\text{CpRh}(\text{COD-1,5})$ .<sup>295</sup>

#### 4.05.4.2.4 Alkylidenes, metallacycles, and related titanium complexes

##### 4.05.4.2.4.(i) Alkylidenes

Alkylidene–metal complexes play a key role in several important reactions such as transition metal-catalyzed olefin and alkyne polymerization, olefin metathesis or olefination of carbonyl compounds. C–C coupling reactions mediated by these transition metal complexes form also a major area of chemical research. Carbene–carbene coupling reactions involving polarized transition metal carbon double bonds open new routes to C–C bond formation. The last decade has seen a great deal of interest in model studies with defined and isolable alkylidene titanium derivatives. Although alkylidene titanium species have been generally proposed as intermediates in a variety of reactions with unsaturated organic molecules (olefins, alkynes, ketones, ...) or solvent C–H bonds, stable alkylidene titanium complexes are known and the preparative and catalytic applications of the Ti=C unit has been extended to give different types of stable cycloaddition products, allowing investigations of structure and reactivity patterns. Comprehensive reviews



Scheme 522

have appeared.<sup>1340,1341</sup> Annual surveys of the chemistry of the transition metal–carbon double and triple bonds have appeared.<sup>1342–1348</sup> The synthesis and reactivity of titanoxo units as fragments of transition metal Fischer carbene complexes have been reviewed.<sup>1349</sup> Titanium and related early transition metal carbenoid as reagents for applications in organic synthesis is the focus of a recent review.<sup>1350,1351</sup> The formation, structure types, reactivity, and selected applications of carbene complexes of titanium and the rest of group 4 elements have been reviewed.<sup>1352</sup>

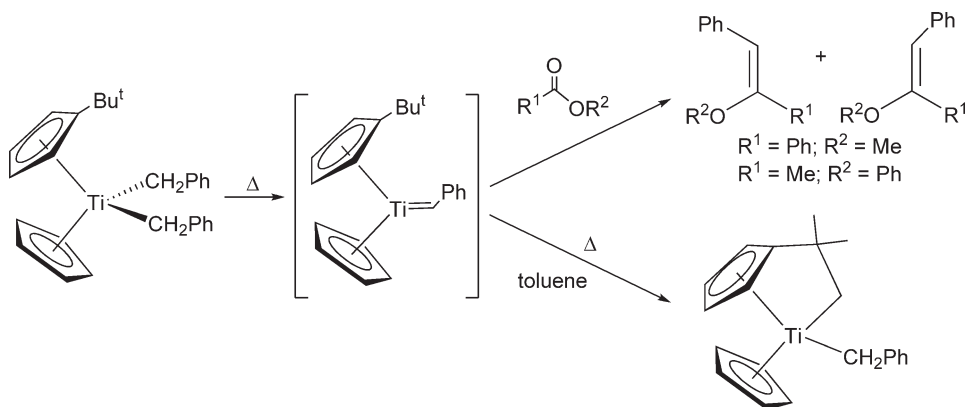
Cp alkylidene titanium complexes have been generally generated by decomposing dialkyl and related titanium derivatives or from treatment of thioacetals with  $\text{Ti(II)}$  compounds. Thermolyzing diazoalkane complexes permits the synthesis of non-Cp alkylidene titanium derivatives (see Section 4.05.2).

$\text{Cp}_2\text{Ti}(\text{CH}_2\text{Ph})_2$  is thermolyzed in the presence of acetonitrile<sup>1327</sup> (Schemes 519 and 520; Section 4.05.4.2.3) and carbonyl compounds. Decomposition of the dibenzyl complex  $\text{Cp}(\text{C}_5\text{H}_4\text{Bu}^t)\text{Ti}(\text{CH}_2\text{Ph})_2$  in the presence of carbonyl compounds affords carbonyl olefination products via titanium carbene intermediate species. This reaction proceeds with higher stereoselectivity than the complex featuring unsubstituted Cp ligands. Decomposition of the dibenzyl complex in the absence of carbonyl compounds leads to the C–H insertion product (Scheme 523).

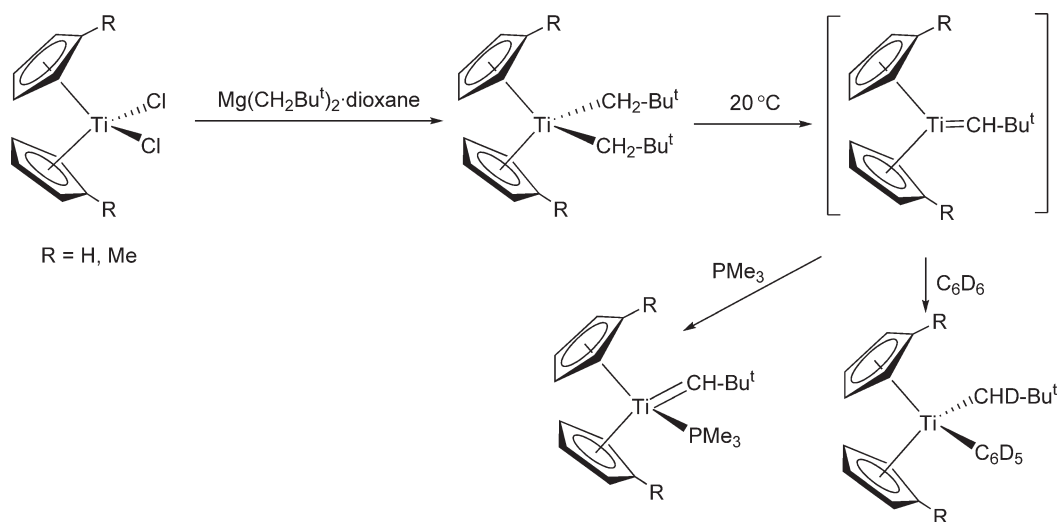
The formation of the thermally stable alkylidene titanium complex  $\text{Cp}'_2\text{Ti}(\text{CHCMe}_3)\text{PMe}_3$  ( $\text{Cp}' = \text{Cp}, \text{C}_5\text{H}_4\text{Me}$ ) has been mentioned.<sup>1275</sup> Bis-Cp bis(neopentyl) titanium complexes form attractive precursors of unsaturated alkylidene derivatives that are able to effect inter- or intramolecular C–H activation. The synthesis and spectroscopic characterization of the bis(neopentyl) complexes  $(\text{C}_5\text{H}_4\text{R})_2\text{Ti}(\text{CH}_2\text{Bu}^t)_2$  ( $\text{R} = \text{H}, \text{Me}$ ) are described. These compounds decompose in solution at ambient temperature through  $\alpha$ -H abstraction to give bis-Cp neopentylidene intermediates under mild conditions, that can be trapped with  $\text{PMe}_3$  to yield the alkylidene complexes  $(\text{C}_5\text{H}_4\text{R})_2\text{Ti}(\text{CHBu}^t)(\text{PMe}_3)$ . Resonances at  $\delta$  12.32 and 312.9 are observed in the  $^1\text{H}$  and  $^{13}\text{C}$  NMR spectra for the proton and carbon atom of the  $\text{Ti}=\text{CH}$  group. In the absence of phosphine, intermolecular activation of C–H bonds of hydrocarbon solvents (benzene, *p*-xylene) to the  $\text{Ti}=\text{C}$  double bond produces  $(\text{C}_5\text{H}_4\text{R})_2\text{Ti}(\text{CH}_2\text{Bu}^t)\text{R}$ . Competition between ring expansion and C–H addition has been observed in aromatic solvents in the presence of THF.  $\text{Cp}_2\text{Ti}(\text{CH}_2\text{CMe}_3)_2$  in  $\text{C}_6\text{D}_6$  evolves to the phenyl complex  $\text{TiCp}_2(\text{CHDCMe}_3)(\text{C}_6\text{D}_5)$ , while its reaction with deuterated *p*-xylene produces  $\text{Cp}_2\text{Ti}(\text{CHDCMe}_3)(\text{CD}_2\text{C}_6\text{D}_4\text{CD}_3\text{-}p)$ . (Scheme 524).<sup>1275</sup>

The transformation of vinyltitanium complexes to vinylidene intermediates under mild conditions has significantly improved the access to short-lived carbene complexes of titanium. The generation of the vinylidene species “ $\text{Cp}'_2\text{Ti}=\text{C}=\text{CH}_2$ ” has opened new aspects in the chemistry of titanium–carbene complexes and it exhibits a wide variety of reactions with unsaturated molecules, leading to derivatives of high thermal stability. It reacts with unsaturated molecules to give many stable [2 + 2]-cycloaddition products of a various types. Aspects of the chemistry of these titanium–carbenoid complexes have been reviewed.<sup>1029,1353–1355</sup> The observed regioselectivity for all these reactions can be explained by the polarities of the unsaturated compounds used in the cycloaddition reactions toward the polarized  $\text{Ti}^{\delta+}-\text{C}^{\delta-}$  double bond in the metal vinylidene. Large differences in the partial charges of the unsaturated molecules (isocyanates, nitriles, alkynes) lead to stereochemically pure compounds with the more negative unit being bonded to titanium, while using reagents with small differences in the charge separation gives regioisomers.

Liberation of ethylene from the titanium cyclobutane complex  $\text{Cp}^*_2\text{Ti}[\text{C}(\text{=CH}_2)\text{CH}_2\text{CH}_2]$  generates the corresponding titana–allene species,  $\text{Cp}^*_2\text{Ti}=\text{C}=\text{CH}_2$  which, surprisingly, behaves differently in trapping reactions with



Scheme 523

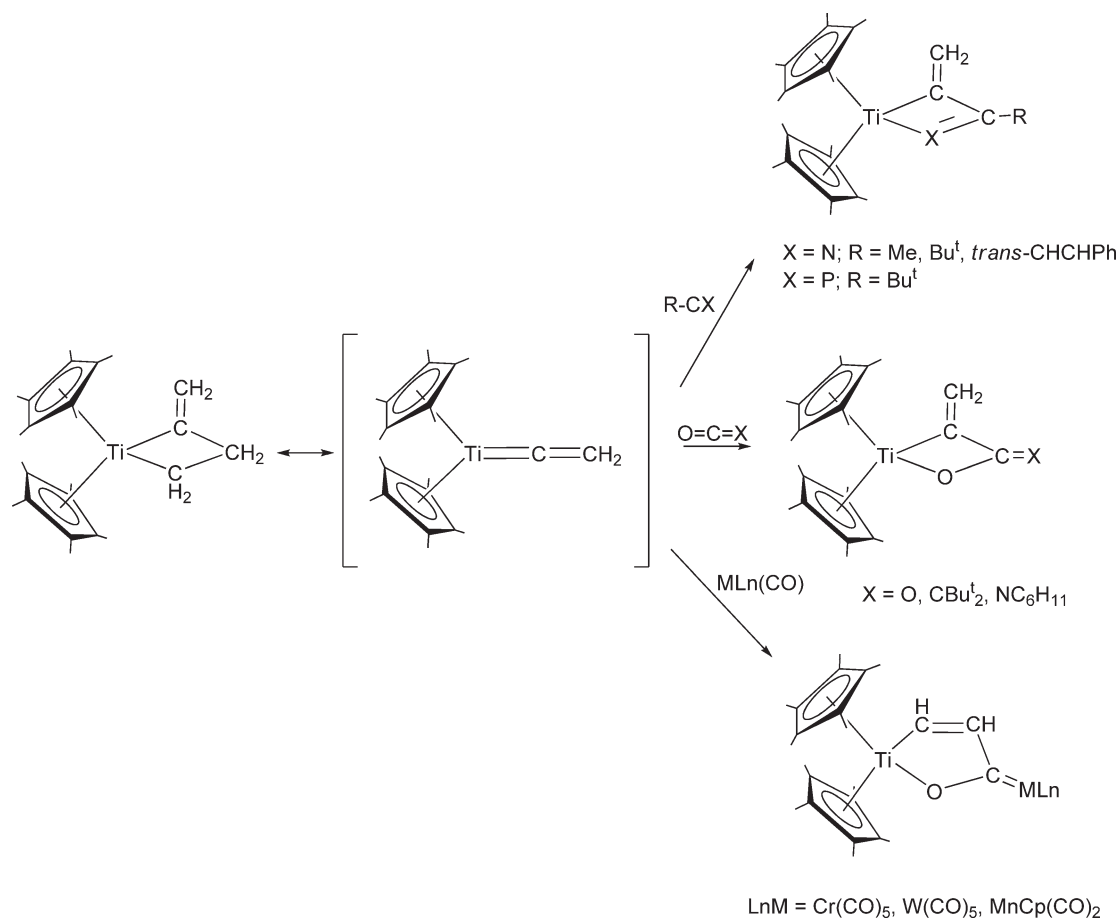


Scheme 524

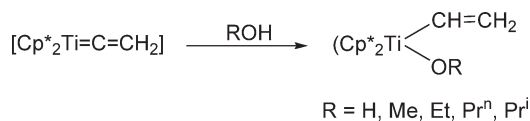
various compounds. Some examples are selected here. In the presence of carbon dioxide, ketenes, and isocyanates the four-membered titanacycles  $\text{Cp}^*_2\text{Ti}[\text{C}(\text{=CH}_2)\text{C}(\text{=X})\text{O}]$  ( $\text{X}=\text{O}$ ,  $\text{CR}_2$ ,  $\text{NR}$ ) are formed. With metal carbonyls  $\text{ML}_n(\text{CO})$ , the products are the corresponding Fischer carbene complexes which have a planar metallacyclopentene unit.<sup>1356</sup> Similar reaction with nitriles or phosphacetylenes permits the synthesis of 1-aza-2-titanacyclobut-4-ene and 1-phospha-2-titanacyclobut-4-ene, the molecular structure of which has been determined (Scheme 525).<sup>1357</sup> The reactions with proton-donating substrates ( $\text{ROH}$ ,  $\text{H}_2\text{O}$ ) yield vinyltitanium derivatives  $\text{Cp}^*_2\text{Ti}(\text{CH}=\text{CH}_2)(\text{OR})$  (Scheme 526). The titana-allene compound  $\text{Cp}^*_2\text{Ti}=\text{C}=\text{CH}_2$  reacts with acetylenes to form methylenetitanacyclobutenes and vinyltitanium acetylide derivatives. The reaction with symmetrical alkynes gives metallacyclobutenes  $\text{Cp}^*_2\text{Ti}(\text{CR}=\text{C}(\text{R})=\text{CH}_2)$  by a  $[2+2]$ -cycloaddition process. When unsymmetrical alkynes are used, different regioisomers can be isolated (Scheme 527). Vinyl acetylides can also be obtained. The structures of some of these compounds have been determined by X-ray diffraction. The pseudo-tetrahedral molecules contain planar cyclobutene rings.<sup>1358</sup> Reactions with 1,3-diynes  $\text{RC}\equiv\text{C}-\text{C}\equiv\text{CR}$  ( $\text{R}=\text{Me}$ ,  $\text{Ph}$ ,  $\text{SiMe}_3$ ,  $\text{CMe}_3$ ) give metallacyclobutenes with the exclusive formation of one regioisomer exhibiting the  $\text{C}=\text{CR}$  substituent in the  $\alpha$ -position of the metallacycle.<sup>1359</sup> The reactions of  $\text{Cp}^*_2\text{Ti}=\text{C}=\text{CH}_2$  with a variety of enolizable ketones and diphenylketene<sup>1360</sup> yield vinyltitanium enolates under regio- and stereoselective control in excellent yield (Scheme 528). A single crystal diffraction study shows an O-bonded monomeric enolate with a short  $\text{Ti}-\text{O}$  distance. These complexes do not exhibit typical enolate reactivity.<sup>1361</sup> Coupling of this species with imines affords alkenyl titanium-imine complexes,<sup>1362</sup> while attempts to trap the titanium-vinylidene intermediate as titanacyclobutenes via coupling with alkynes failed.<sup>1363</sup>  $\text{Cp}^*_2\text{Ti}=\text{C}=\text{CH}_2$  reacts with 1 equiv. of carbodiimide  $\text{RN}=\text{C}=\text{NR}$  ( $\text{R}=\text{p-MeC}_6\text{H}_5$ ,  $\text{C}_6\text{H}_{11}$ ) or N-benzylidene  $\text{PhN}=\text{C}(\text{Ph})\text{H}$  to give azatitanacyclobutane derivatives  $\text{Cp}^*_2\text{Ti}[\text{RN}-\text{C}(\text{=NR})-\text{C}=\text{CH}_2]$  and  $\text{Cp}^*_2\text{Ti}[\text{PhN}-\text{C}(\text{Ph})(\text{H})-\text{C}=\text{CH}_2]$ , respectively, as  $\text{N}=\text{C}$ -cycloaddition products. These azatitanacyclobutenes are unreactive toward typical ring enlargements, as observed for other similar four-membered titanacycles. The molecular structure of  $\text{Cp}^*_2\text{Ti}[\text{RN}-\text{C}(\text{=NR})-\text{C}=\text{CH}_2]$  ( $\text{R}=\text{p-MeC}_6\text{H}_5$ ) has been determined by X-ray diffraction.<sup>1364</sup>

The titanacycle derivatives obtained in these reactions are isolable products and can therefore serve as substrates to investigate subsequent reactions.<sup>1365–1368</sup> In order to gain a more detailed knowledge of the electronic properties of these complexes and to explain the structure–reactivity relationships, restricted Hartree–Fock *ab initio* calculations have been carried out.<sup>1369</sup>

Titanathietane complexes are obtained as brown crystals of high thermal stability when the vinylidene intermediate species reacts with isothiocyanates  $\text{RNCS}$  by a  $[2+2]$ -cycloaddition process (Scheme 529). Complexes with the sulfur atom in  $\alpha$ -position bonded to titanium are formed exclusively. The structure for the cyclohexyl derivative has been confirmed by X-ray diffraction. Heating of these titanathietane complexes in the presence of pyridine at  $80^\circ\text{C}$  for 20 min results in isomerization, with the formation of a new titanacyclobutane compound (Scheme 529). The regioselectivity of these reactions was discussed on the basis of Hartree–Fock *ab initio* calculations.<sup>1365</sup>



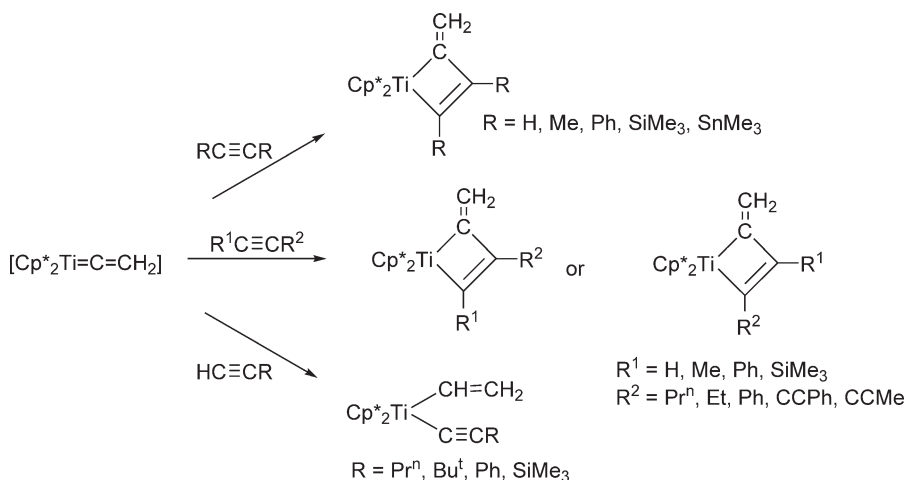
Scheme 525



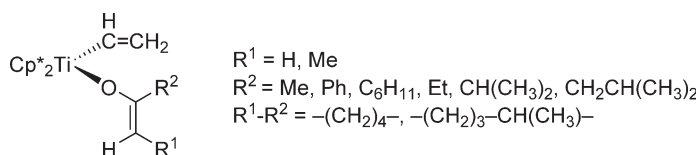
Scheme 526

Heterobinuclear complexes are formed by the reactions of the  $\alpha$ -C-nucleophilic vinylidene complex  $\text{Cp}^*_2\text{Ti}=\text{C}=\text{CH}_2$  with middle or late transition metal compounds. The reaction with the electrophilic methoxy carbene  $(\text{CO})_5\text{Cr}=\text{C}(\text{OMe})\text{Me}$  yields binuclear compounds, isolated as red crystals and formed in an unusual metal-centered C-C coupling reaction. Further isomerization of the exocyclic double bond is observed. When the aminocarbene complex  $(\text{CO})_5\text{Cr}=\text{C}(\text{NHPr}^i)\text{Me}$ , which is less electrophilic than alkoxy-carbenes, is used, a different type of reaction occurs and a binuclear dititanacyclobutene complex is formed (Scheme 530). A single crystal X-ray structural analysis of this compound confirms the proposed constitution.<sup>1370,1371</sup> The reactions with group 12 complexes proceed to give heterobinuclear  $\mu$ -vinylidene compounds (Scheme 530).<sup>1372,1373</sup> The molecular structure of the titanium-gold compound has been determined by X-ray diffraction analysis, which reveals a titanium-gold bond asymmetrically bridged by a vinylidene ligand. A semibridging bonding mode for the  $\text{C}=\text{CH}_2$  group in these complexes is indicated by NMR spectroscopic and X-ray diffraction data.<sup>1374</sup>

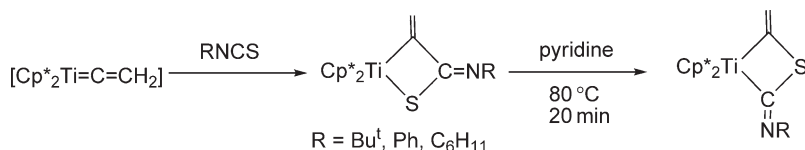
The stabilization of  $\text{Cp}^*_2\text{Ti}=\text{C}=\text{CH}_2$  by donor ligands or donor-functionalized Cp groups has not been successful.  $\text{Cp}(\text{C}_5\text{Me}_4\text{CH}_2\text{CH}_2\text{NMe}_2)\text{TiCl}_2$  and  $\text{Cp}^*(\text{C}_5\text{Me}_4\text{CH}_2\text{CH}_2\text{NMe}_2)\text{TiCl}_2$  are obtained by oxidation of the Ti(III) compounds  $\text{Cp}(\text{C}_5\text{Me}_4\text{CH}_2\text{CH}_2\text{NMe}_2)\text{TiCl}$  and  $\text{Cp}^*(\text{C}_5\text{Me}_4\text{CH}_2\text{CH}_2\text{NMe}_2)\text{TiCl}$  with  $\text{PbCl}_2$ . The molecular structures



Scheme 527



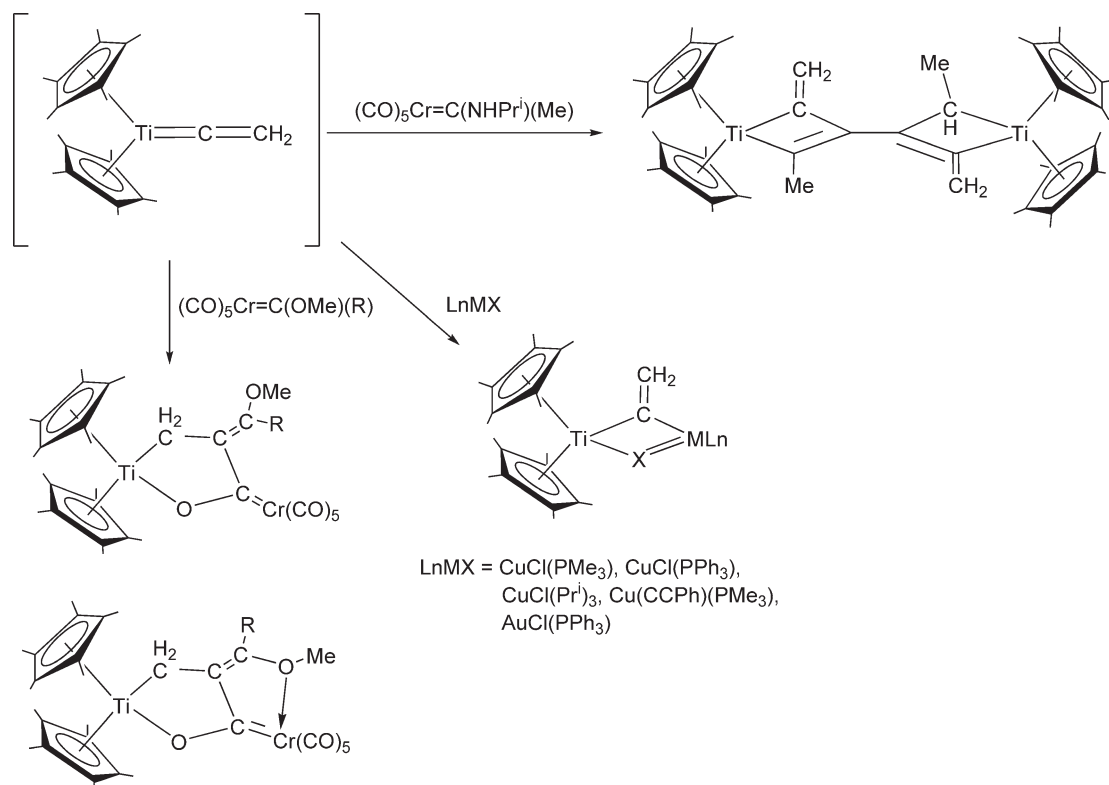
Scheme 528



Scheme 529

of  $Cp^*(C_5Me_4CH_2CH_2NMe_2)TiCl_2$  have been determined by X-ray diffraction, which reveals non-coordination of the  $NMe_2$  group. The dichloro compounds are converted to a series of dialkyl, vinyl, titanacyclobutane, and fulvene complexes by the appropriate reactions (Scheme 531). The vinylidene species " $Cp^*(C_5Me_4CH_2CH_2NMe_2)Ti=C=CH_2$ " reacts very similarly to the analogous  $Cp^*_2Ti=C=CH_2$ . The introduction of an  $NMe_2$ -functionalized side chain does not seem to be effective enough for stabilization for the short-lived titanium-alkylidene species.<sup>1093</sup>

A practical method for the preparation of alkylidene titanium derivatives has recently been developed.  $Cp_2Ti[P(OEt)_3]_2$ , freshly prepared by the reduction of  $TiCp_2Cl_2$  with Mg in the presence of triethyl phosphite and 4 Å molecular sieves, reacts with thioacetals and other sulfur compounds to give titanium alkylidenes (with or without hydrogen atoms in  $\beta$ -position to the metal atom). This method seems ideal for making functionalized alkylidene titanium compounds. These reactions proceed with the formation of titanium carbene and titanacyclobutane intermediates and promote the transformation of unsaturated thioacetals, thiol esters, and generally the sulfur compound to organic substances.<sup>1148,1375–1379</sup> Their applications to organic synthesis including some guiding concepts have been reviewed.<sup>1380</sup> Titanium alkylidenes obtained from dithioacetals are reagents for carbonyl olefinations. Highlights for this process have been reported.<sup>1381</sup> This methodology can be used for the synthesis of  $\omega$ -hydroxy ketones by the carbonyl olefination of  $\omega,\omega$ -bis(phenylthio)alkyl alkanoates<sup>1382</sup> or the synthesis of allylsilanes by reaction from 2,4-bis(phenylthio)but-3-enylsilanes<sup>1383</sup> and the preparation of ketones from thioacetals and alkyl nitriles.<sup>1384</sup> The generation of titanium carbene species by desulfurization of thioacetals having a carbon–carbon

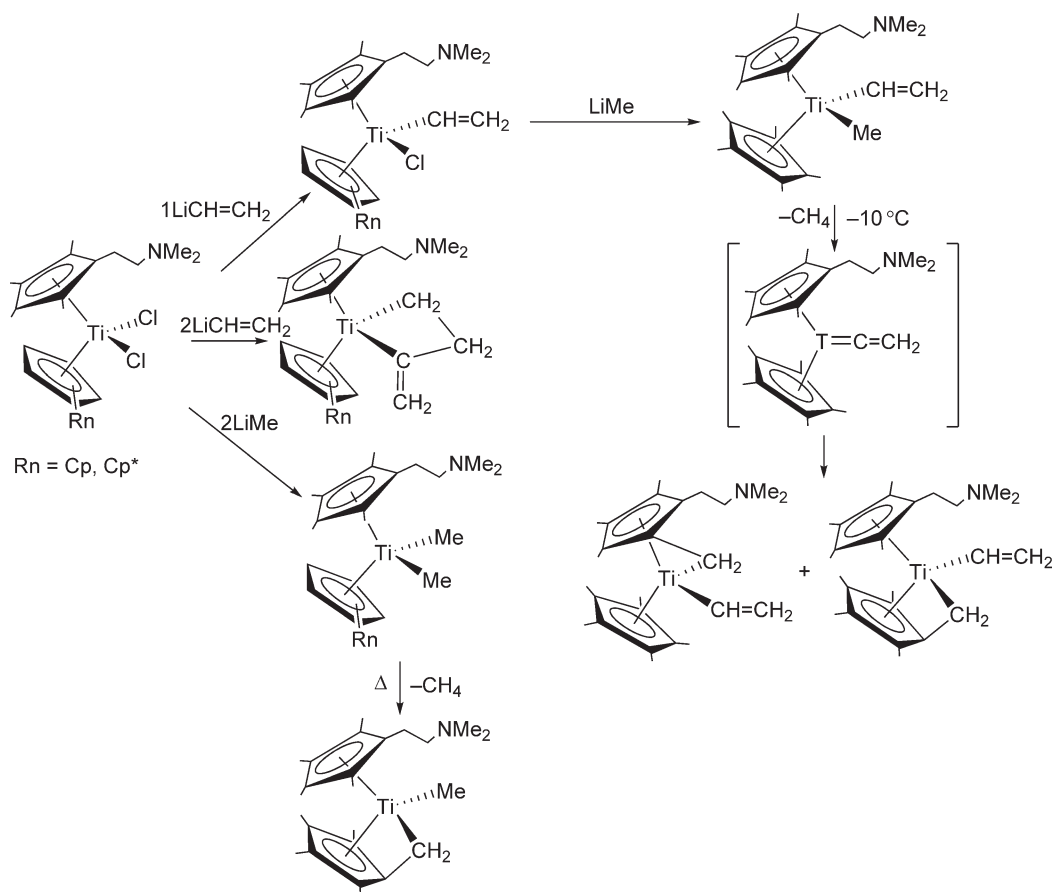


Scheme 530

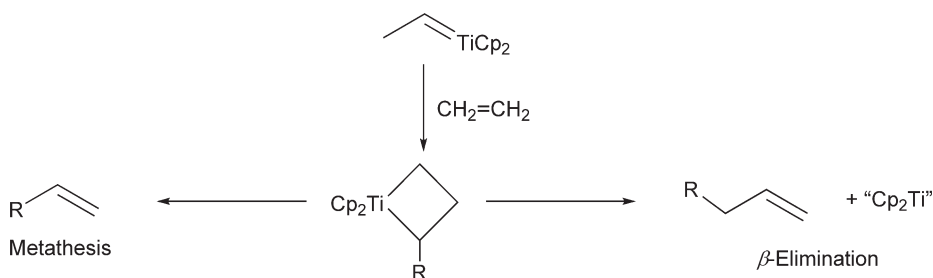
double bond has also been used for the cyclization reactions to give cycloalkenes in good yield.<sup>1385</sup> Similarly, polymer-supported esters are smoothly converted into enol ethers using a bis-Cp alkylidene prepared by treatment of 2-Bu<sup>t</sup>-dimethylsilyloxybenzaldehyde diphenyldithioacetal with the low-valent titanium species Cp<sub>2</sub>Ti[P(OEt)<sub>2</sub>]<sub>2</sub>.<sup>1386</sup> Alkylidene titanium derivatives or their equivalents easily formed by this procedure react with organic molecules having other C–O<sup>1387–1389</sup> and C–C multiple bonds, alkenes<sup>1140</sup> or alkynes,<sup>1390</sup> and trialkyl(allyl)silanes.<sup>1391</sup> These compounds react with ethylene with selective transformation to two types of terminal olefins, one with one-carbon homologation and the other one with two-carbon homologation, depending on the Ti species employed to generate the alkylidene titanium compound. The reaction proceeds with the formation of titanacyclobutane intermediates which evolve with the elimination of Cp<sub>2</sub>Ti=CH<sub>2</sub> by a metathesis pathway, or alternatively by β-elimination and formation of Ti(II) derivatives (Scheme 532).<sup>1392</sup> These alkylidene titanium derivatives react with group 14 hydrides to afford silanes, germanes, and stannanes.<sup>1393</sup> They have been used for the formation of cyclic amines,<sup>1394</sup> the transformation of ketones into 1-chloro and α,1-dichloro-1-alkenes,<sup>1395</sup> preparation of enol ethers by carbonyl olefination,<sup>1396</sup> and the formation of pyrrolidines by intramolecular reaction of thio-propyl anilides.<sup>1397</sup>

The method has been used to develop benzylidene Ti(IV) complexes that catalyze the synthesis of benzofuranes and indoles in high purity using a chameleon path approach. A range of functional groups are tolerated within the benzylidene Ti(IV) reagents.<sup>1398</sup> Thio-functionalized benzylidene titanium complexes generated by this process are used for the synthesis of 2-substituted benzo[*b*]thiophenes<sup>1399</sup> and other synthetic organic reactions.<sup>1400–1402</sup> A selected few of quinolines have been prepared by using alkylidene titanium compounds, which are synthesized by using this method.<sup>1403</sup>

The addition of aryldiazoalkanes to Cp<sup>\*</sup><sub>2</sub>Ti(C<sub>2</sub>H<sub>4</sub>) affords η<sup>2</sup>-N<sub>2</sub>-aryldiazoalkane titanium complexes that undergo facile N<sub>2</sub>-loss at room temperature or can be more thermally stable depending on the nature of the diazoalkene substituent. Different reactivity pathways of these diazoalkane complexes have been studied. They unusually release dinitrogen thermally to give transient carbene complexes which may be trapped with styrene to form the titanacyclobutane complexes (C<sub>5</sub>Me<sub>5</sub>)<sub>2</sub>Ti(ChArCHPhCH<sub>2</sub>). A variety of reactions have been reported involving the



Scheme 531



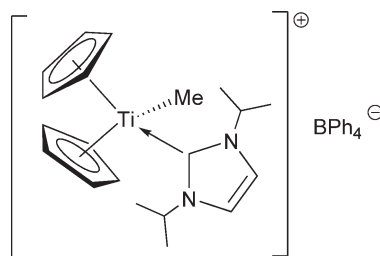
Scheme 532

retention of N<sub>2</sub> (Scheme 580; Section 4.05.4.4).<sup>1404–1406</sup> Analogous reactions of Cp<sub>2</sub>Ti(C<sub>2</sub>H<sub>4</sub>) with N<sub>2</sub>Ph have been described to give compounds with Ti–N bonds (Scheme 573; Section 4.05.4.4).<sup>1407</sup>

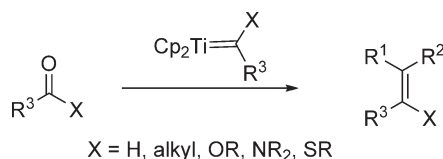
The cationic titanium species [Cp<sub>2</sub>TiMe]<sup>+</sup> can be stabilized by coordination of neutral Arduengo carbene ligands with strong bonds between the Ti and the carbon atoms. The observed conformational orientation of the carbene ligand indicates its strong σ-donor character, confirmed by the results of the theoretical calculations (Scheme 533).<sup>1408</sup>

Complexes Cp<sub>2</sub>TiMe<sub>2</sub>, Cp<sub>2</sub>TiClMe, CpTiMe<sub>3</sub>, and Cp<sub>2</sub>Ti(CH<sub>2</sub>CMe<sub>3</sub>)<sub>2</sub> catalyze the ROMP of norbornene. The initiation of this process by thermally generated alkylidene titanium species and subsequent formation of titanacyclobutane complexes is proposed. The presence of THF as the solvent can inhibit the ROMP activity.<sup>1409</sup> Developments of practical methods to carry out olefination reactions of aldehydes, ketones, and





Scheme 533



Scheme 534

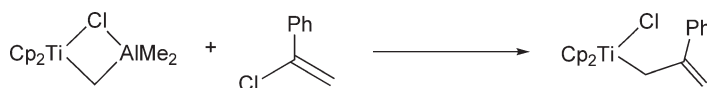
heteroatom-substituted carbonyl compounds catalyzed by bis-Cp alkylidene titanium species  $\text{Cp}_2\text{Ti}=\text{CR}^1\text{R}^2$  have been reported (Scheme 534).<sup>1410–1414</sup>

The titanium methylene species  $\text{Cp}_2\text{Ti}=\text{CH}_2$  can be generated from the Tebbe reagent<sup>512</sup> or from dialkyltitanium derivatives.<sup>1415</sup>  $\text{Cp}_2\text{Ti}=\text{CH}_2$  has been used as a useful synthetic tool for the Wittig-like methylenation of carbonyl compounds and several different mechanisms have been proposed for ester olefinations. Mechanistic studies for the olefination of these reagents using  $\text{Cp}_2\text{TiMe}_2$  suggest that the reaction proceeds via the titanium carbene  $\text{Cp}_2\text{Ti}=\text{CH}_2$ . These findings are inconsistent with the methyl addition mechanism proposed in the literature.<sup>1044</sup> The reaction of the Tebbe compound with carbonyl substrates such as aldehydes, ketones, esters, and amides into alkenes has been studied theoretically. An extended Hückel approach was used to obtain a qualitative picture of the molecular orbital interactions leading to the expected titanaoxetane intermediate.<sup>1416</sup> A new strategy based on the olefin metathesis reaction for the generation of cyclic enol ethers directly from olefin ethers using the Tebbe reagent has been reported.<sup>1417</sup> The deoxygenation of sulfoxides, N-oxides, and selenoxides is catalyzed by  $\text{Cp}_2\text{Ti}=\text{CH}_2$ , generated either from the Tebbe  $\text{Cp}_2\text{Ti}(\mu\text{-CH}_2)(\mu\text{-Cl})\text{AlMe}_2$  or Petasis  $\text{Cp}_2\text{TiMe}_2$  reagents.<sup>1418</sup> The titanium carbene species  $\text{Cp}_2\text{Ti}=\text{CH}_2$  generated either from Tebbe's complex  $\text{Cp}_2\text{Ti}(\mu\text{-CH}_2)(\mu\text{-Cl})\text{AlMe}_2$  or Grubbs' bis-Cp titanacyclobutane compound catalyzes the conversion of *meso*-alkenes to chiral alkenes through ring-opening/ring-closing olefin metathesis with the formation of 7-*anti*-(3-methyl-3-butenyl)norbornene. Attempts to form a chiral Tebbe-type complex from binaphthyl-bridged *ansa*-bis(indenyl) titanium derivatives were unsuccessful (cf. Scheme 660; Section 4.05.5).<sup>1419</sup> A tandem metathesis carbonyl olefination sequence for organic alkene esters using the Tebbe reagent has been reported. The final product features the ring systems present in ciguatoxin.<sup>1420</sup> Organic methylene-transfer reactions with the Tebbe reagent have been studied.<sup>1421</sup>

The formation of allyltitanium complexes via the reaction of alkenyl chlorides with the Tebbe reagent has been reported (Scheme 535), through a mechanism involving a [2 + 2]-cycloaddition followed by  $\beta$ -elimination of chloride.<sup>1422,1423</sup>

The carbonyl olefination using a reagent formed from  $\text{CH}_2(\text{ZnI})_2$  and  $\text{TiCl}_2$  is thought to involve addition to a titanium carbene complex.<sup>1424</sup>

The activation barriers and reaction energies for the [2 + 2]-cycloaddition of bis-Cp vinylidene titanium complexes with different reagents with double and triple bonds have been theoretically investigated.<sup>1425</sup>



Scheme 535

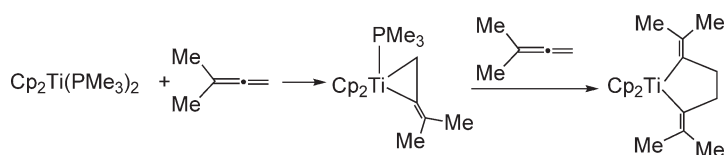
## 4.05.4.2.4.(ii) Metallacycles

$\text{Cp}_2\text{Ti}(\text{PMe}_3)_2$  reacts with 3-methyl-1,2-butadiene to give the allene complex  $\text{Cp}_2\text{Ti}(\text{CH}_2\text{CCMe}_2)\text{PMe}_3$  which incorporate a second molecule of the allene to produce the resulting coupling compound (Scheme 536).<sup>1326</sup> The reaction of  $\text{Cp}^*_2\text{Ti}(\text{PMe}_3)_2$  with an excess of methylenecyclopropane at  $0^\circ\text{C}$  leads regioselectively to the titanacyclopentane derivative shown in Scheme 537.<sup>1426</sup> The titanacycle complex shown in Scheme 538 was isolated as an air sensitive solid and is considered to be the intermediate in enyne cyclization reactions.<sup>1427,1428</sup>

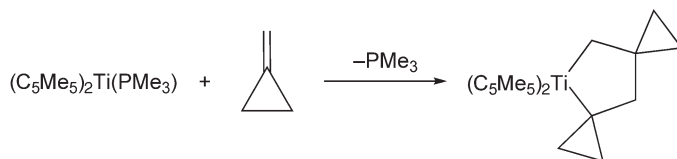
The highly regioselective addition of organic free radicals to an odd-electron  $\eta^3$ -allyl complex (Scheme 539) has been used as a general route to convert  $\text{Ti}(\text{III})$ -allyl derivatives into a series of titanacycle complexes.  $\text{Cp}^*_2\text{Ti}(\eta^3\text{-C}_3\text{H}_5)$  reacts with different free radicals with addition exclusively at the central carbon of the allyl ligand providing a very convenient entry into titanacyclobutane derivatives.<sup>1429</sup> The  $\text{Ti}(\text{III})$  propargyl system results in a more appropriate radical trap reagent. Titanacyclobutene derivatives are easily obtained in the attempts to synthesize propargyl  $\text{Ti}(\text{III})$  complexes by a regioselective addition of organic free radicals or by dimerization processes. Mechanistic studies concerning these reactions have been reported.<sup>1430</sup> The regioselective radical alkylation is favored by increasing the electron density at the metal center by using more electron-rich ancillary ligands. Strongly donating dialkyl-amino-substituted Cp ligands promote the selective central carbon alkylation at substituted allyl ligands by enhancing a one-electron  $d_{3d1}-\pi^*$  donation. Thus, bis(piperidinoindenyl) titanium(III) 1-phenylallyl and the analogous 1-methylallyl derivatives undergo central allyl carbon radical alkylation by reaction with 2-iodopropane, iodocyclohexane, or  $\text{Bu}^t\text{Cl}$  to give 2,3-disubstituted titanacyclobutane complexes which have been spectroscopically characterized (Scheme 540).<sup>1431</sup> The sterically less demanding but similarly electron-rich bis(2-N,N-dimethylaminoindenyl) $\text{Ti}(\text{III})$  template results in an analogous compatible system with an extended range of radical alkylations increasing the thermal stability of the resulting  $\alpha$ -methyl substituted titanacyclobutane complexes (Scheme 541).<sup>1432</sup>

Titanacyclopentene and titanacyclopentadiene compounds are obtained by the reaction of  $\text{Cp}_2\text{TiCl}_2$  with 3,4-dithio-2,5-dimethyl-2,4-hexadiene, depending on the reaction conditions (Scheme 542). The titanacyclopentene complexes react with 2-butyne and 1-hexyne to give insertion reaction products.<sup>1433</sup>

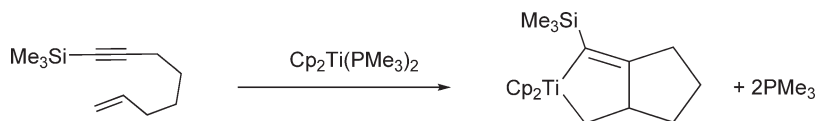
Titanacycle derivatives (Scheme 543) are obtained predominantly as one isomer of the probably expected products, as a result of the reaction between a titanium aryne intermediate, generated in the pyrolysis of bis-Cp diaryl complexes with diphenylacetylene. The reaction with  $\text{Cr}(\text{CO})_3(\text{CH}_3\text{CN})_3$  affords a heterobinuclear  $\text{Ti}$ -arene-Cr



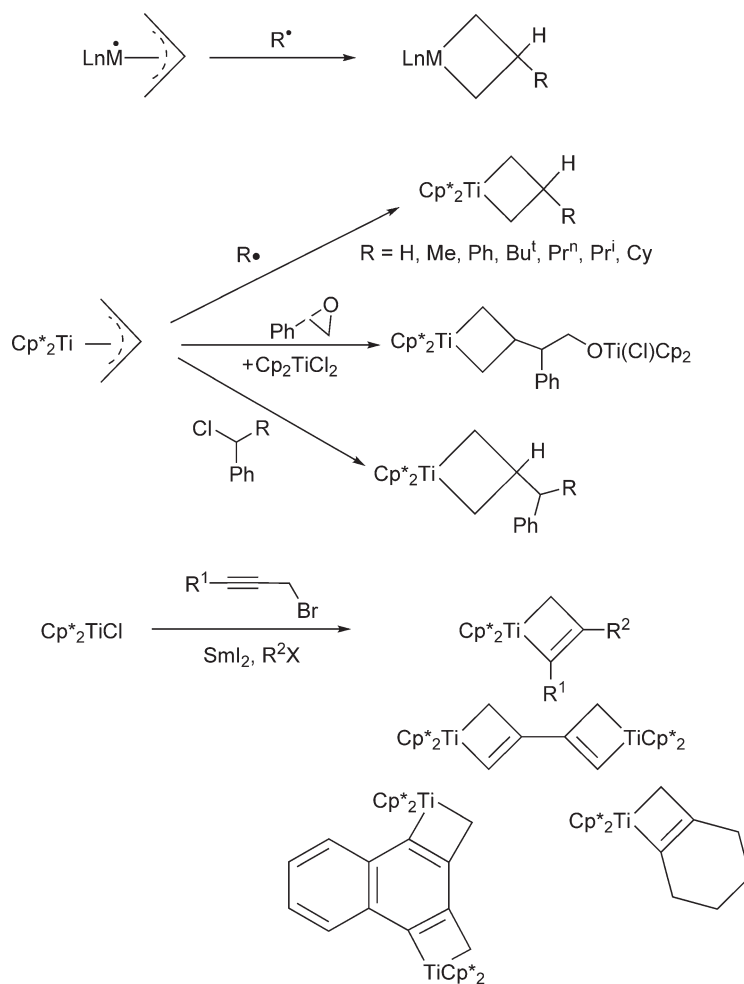
Scheme 536



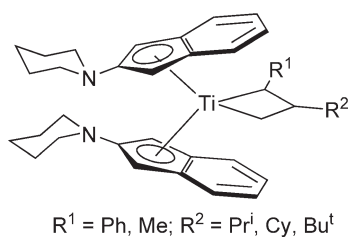
Scheme 537



Scheme 538



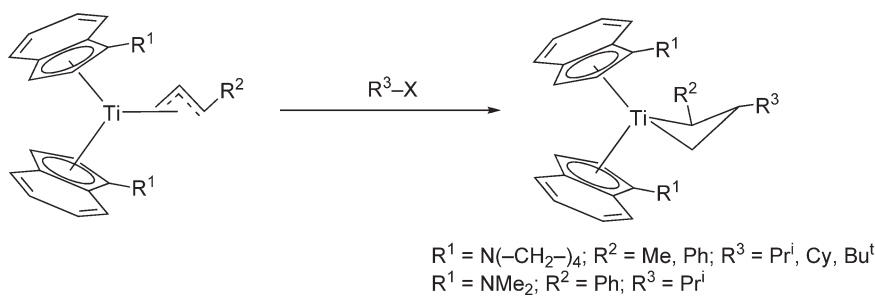
Scheme 539



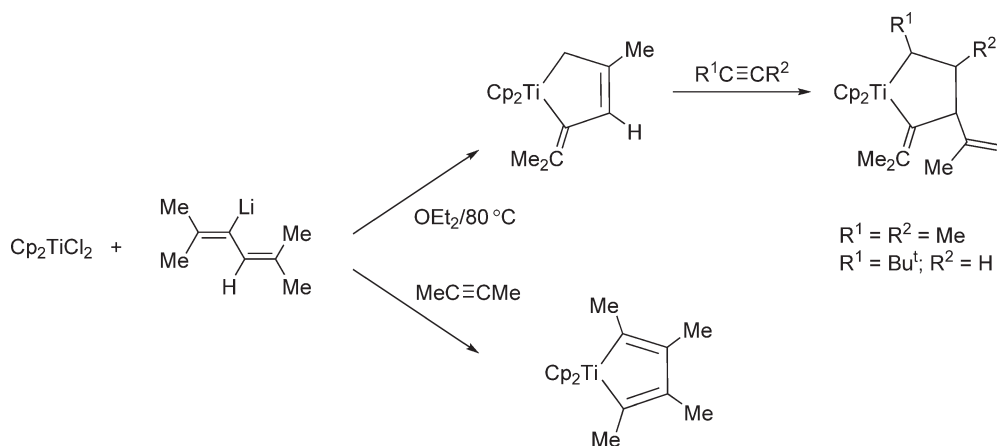
Scheme 540

derivative, the crystal structure of which has been determined.<sup>1434</sup> Titanaindanes can easily be prepared by the reaction of  $\eta^2$ -aryne-titanocene intermediates with ethylene.  $(\text{C}_5\text{H}_4\text{Me})_2\text{TiPh}_2$  thermally induces benzene elimination to give the benzyne-titanocene which reacts with ethylene to give the titanaindane complex. An X-ray diffraction study has shown that the indane complex adopts a bent-metallocene conformation, which has one Cp-bound methyl group in a lateral position and the other oriented toward the narrow backside of the metallocene wedge (Scheme 544).<sup>1435</sup>

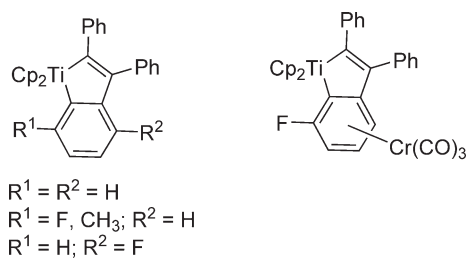
Bis-Cp titanacyclopent-3-yne complexes have been synthesized and structurally characterized (Scheme 545). Short Ti-C bonds emphasize the ring strain of the five-membered cyclic alkyne structure.<sup>1436</sup>



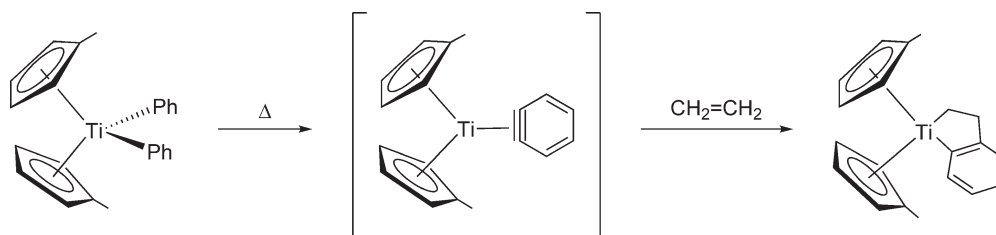
Scheme 541



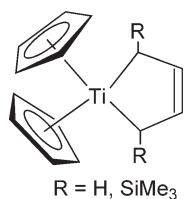
Scheme 542



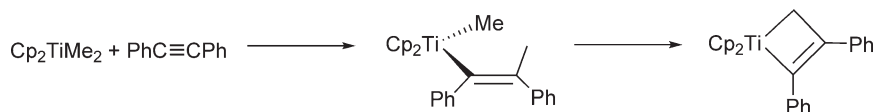
Scheme 543



Scheme 544



Scheme 545

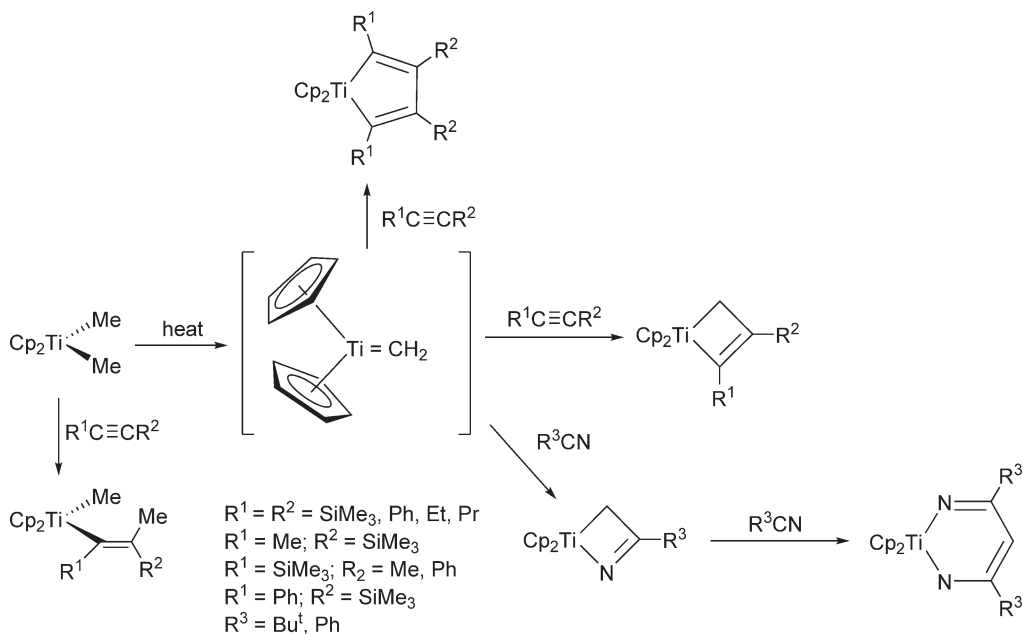


Scheme 546

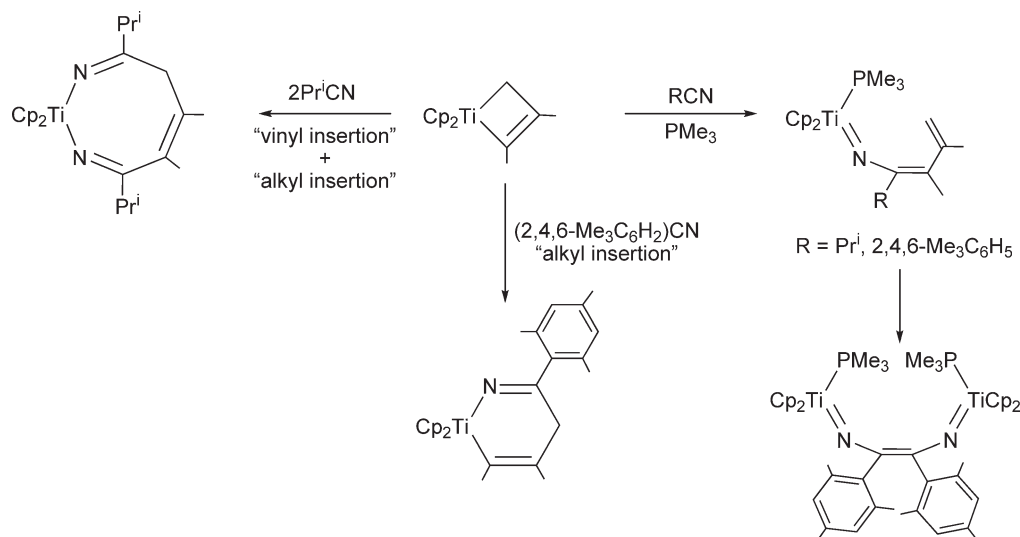
Carbometallation of alkynes by  $\text{Cp}_2\text{TiMe}_2$  affords vinyl complexes which serve as intermediates for the formation of titanacyclobutenes (Scheme 546). Alkyne insertion to form the vinyl species followed by oxidative addition into the  $\gamma\text{-C-H}$  bond and reductive elimination of methane is proposed.<sup>1437</sup>

The reaction of  $\text{Cp}_2\text{TiMe}_2$  with alkynes under thermal conditions affords titanacyclobutene complexes. Variable amounts of titanium vinyl derivatives are observed through a competitive migratory insertion process, in some cases, the portion of this increases as the temperature is lowered. The reaction with unsymmetrical alkynes produces mixed regioselectivities. Analogous reactions with nitriles form 1,3-diaza-2-titana-1,4-cyclohexadiene complexes (Scheme 547). The titanacyclic derivatives react with aldehydes, ketones, phosphorus dichlorides, and nitriles to give various titanium-free products (the same chemical behavior has been studied separately<sup>1325,1326</sup>).<sup>1438</sup>

Reactions of bis-Cp titanacyclobutene with nitriles in the presence of  $\text{PMe}_3$  as a trapping reagent have provided access to crystalline titanocene imido complexes, for which structural details and metrical parameters are reported. When these reactions are performed in the absence of  $\text{PMe}_3$ , azatitanacyclohexadienes or diazatitanacyclooctadienes are obtained as a consequence of alkyl or vinyl insertions (Scheme 548).<sup>1439</sup>



Scheme 547



Scheme 548

The titanacycle derivative  $\text{Cp}^*_2\text{Ti}[\text{C}(\text{=CH}_2)\text{CH}_2\text{CH}_2]$  reacts with isonitriles or diphenylketones at room temperature to give five- and six-membered metallacycle derivatives  $\text{Cp}^*_2\text{Ti}[\text{C}(\text{=CH}_2)\text{CH}_2\text{CH}_2\text{C}(\text{=NR})]$  and  $\text{Cp}^*_2\text{Ti}[\text{C}(\text{=CH}_2)\text{CH}_2\text{CH}_2\text{C}(\text{=CPh}_2)\text{O}]$ , the structures of which have been determined by X-ray diffraction. The unsaturated molecules  $\text{Ph}_2\text{C}=\text{C}=\text{O}$ ,  $\text{CO}_2$ , or isocyanates are not inserted.<sup>1366</sup>

Low temperature activation of  $\text{Cp}^*_2\text{Ti}[\eta^1\text{-}\eta^1\text{-CH}_2\text{CH}(\text{CH}_2\text{CH}=\text{CH}_2)\text{CH}_2]$  with  $[\text{HNMePh}_2][\text{B}(\text{C}_6\text{F}_5)_4]$  leads to the formation of  $\text{Cp}^*_2\text{Ti}[\eta^1\text{-}\eta^2\text{-CH}_2\text{CH}(\text{CH}_3)\text{CH}_2\text{CH}=\text{CH}_2][\text{B}(\text{C}_6\text{F}_5)_4]$ , which undergoes rapid quantitative  $\pi$ -allyl elimination at temperatures as low as  $-140^\circ\text{C}$  to give the cationic titanium allyl complex  $[\text{Cp}^*_2\text{Ti}(\eta^3\text{-CH}_2\text{CHCH}_2)][\text{B}(\text{C}_6\text{F}_5)_4]$ . This ion pair exhibits a static structure at low temperatures, but on warming interconversion of  $\eta^3$ - to  $\eta^1$ -bonding modes can be observed. Reaction with  $\text{B}(\text{C}_6\text{F}_5)_3$  results in  $\beta$ -allyl elimination with the formation of  $[\text{Cp}^*_2\text{Ti}(\eta^3\text{-CH}_2\text{CHCH}_2)][\text{CH}_2=\text{CHCH}_2\text{B}(\text{C}_6\text{F}_5)_3]$ .<sup>1440</sup>

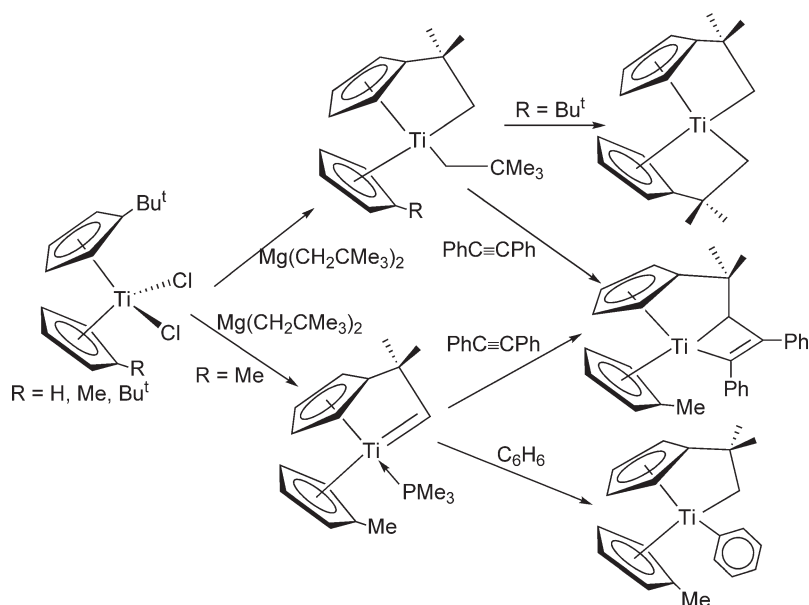
Bis-Cp neopentyl complexes with one cyclometallated *tert*-butyl-Cp group,  $(\text{C}_5\text{H}_4\text{CMe}_2\text{CH}_2)(\text{C}_5\text{H}_4\text{R})\text{Ti}(\text{CHBu}^t)$  ( $\text{R} = \text{H}, \text{Me}, \text{Bu}^t$ ), are obtained from the corresponding bis-Cp dichloro titanium derivatives and  $\text{Mg}(\text{CH}_2\text{CBu}^t)_2$ . These compounds lose neopentane by  $\alpha$ -H abstraction from the cyclometallated ligand to generate alkylidene species in which the alkylidene moiety is connected to one of the cyclopentadienyl ligands. These species exhibit a wide range of reactivity toward benzene-*d*<sub>6</sub> and unsaturated substrates (alkynes, ethene, benzonitrile), initiated by cycloaddition to the  $\text{Ti}=\text{C}$  bond (Scheme 549).<sup>1441</sup>

The oxidative methodology has been applied to study the reactivity of a series of bis( $\omega$ -alkenyl)- and  $\omega$ -alkenyl-dimethylsilyl-Cp-substituted dichloro titanium complexes in reductive reactions with Mg to give a series of titanacycle derivatives (Section 4.05.4.1.3.(i)).<sup>1033–1035,1142</sup> The complex  $\text{Cp}^*\text{Ti}[\eta^5\text{-}\eta^2\text{-C}_5\text{Me}_4\text{CH}_2\text{CMe}(\text{CH}_2)_2]$ , in which a four-membered titanacycle is tethered to a tetramethyl-Cp ligand by a methylene bridge, is obtained by reaction of the fulvene complex  $\text{Cp}^*\text{Ti}(\text{C}_5\text{Me}_4\text{CH}_2)\text{Cl}$  with  $\text{MgBr}(2\text{-methylallyl})$ . Thermolysis gives a new fulvene compound (Scheme 550).<sup>1056</sup>

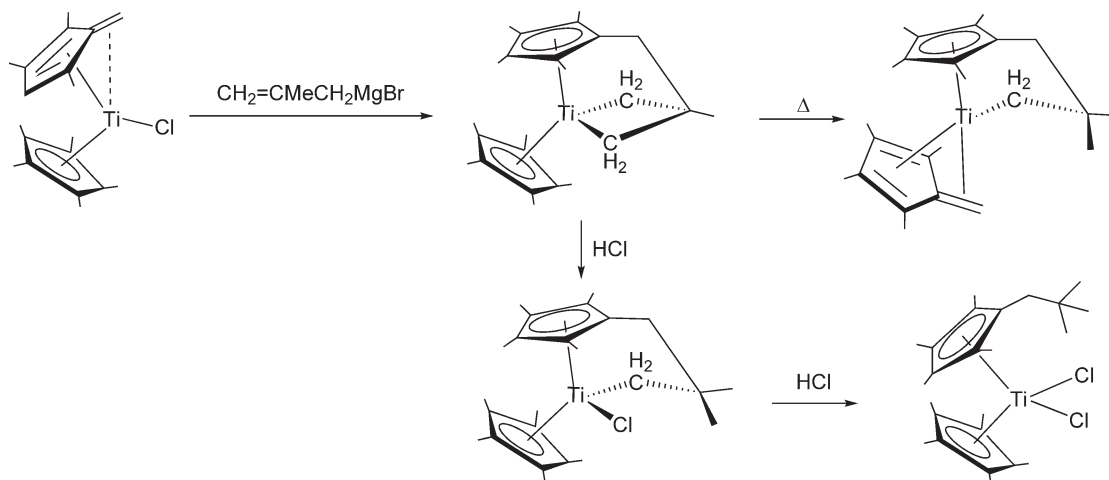
The reaction of 6,6-diphenylfulvene with Ti atoms to give the “tuck-in” bis-Cp derivative ( $\Delta H = -136.8 \text{ kcal mol}^{-1}$ ) and the reaction of 6-diphenylfulvene with  $\text{TiCl}_2$  to afford the *trans*-[(1,2-diphenyl-1,2-dicyclopentadienyl)ethanediy] dichloro Ti(IV) *ansa*-compound ( $\Delta H = -114.4 \text{ kcal mol}^{-1}$ ) (Scheme 551) have been studied and the corresponding reaction enthalpies have been calculated.<sup>1442</sup>

The reaction of  $[\text{C}_5\text{H}_3(\text{SiMe}_3)_2]_2\text{Ti}-\text{N}_2-\text{Ti}[\text{C}_5\text{H}_3(\text{SiMe}_3)_2]_2$  with the diazoalkane  $\text{Me}_3\text{SiCHN}_2$  leads to the isolation of a double cyclometallated bis-Cp complex, arising from facile intramolecular C–H activation of the Cp substituent by a transient titanocene alkylidene (Scheme 552), while treatment with the diazoalkane  $\text{Ph}_2\text{CN}_2$  affords the corresponding diazoalkane compound.<sup>1443</sup>

The reactivity of the four-membered ring heterocyclic molecule  $\text{Cp}_2\text{Ti}(\text{CH}_2\text{SiMe}_2\text{NSiMe}_3)$  as a single-source precursor to titanium-based ceramic thin films has been studied under atmospheres of nitrogen, argon, and helium.<sup>1444</sup>



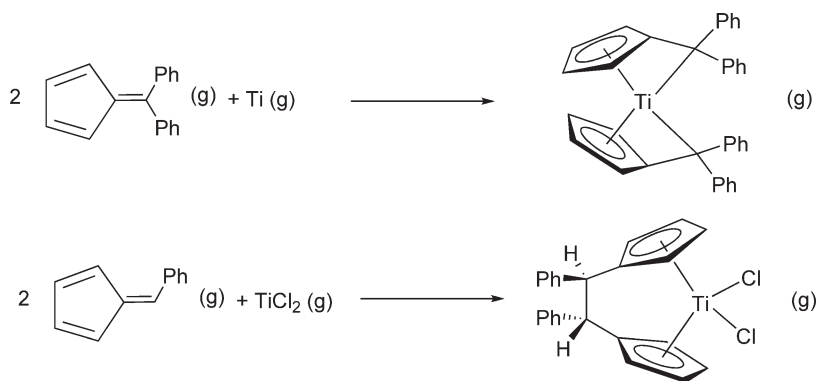
Scheme 549



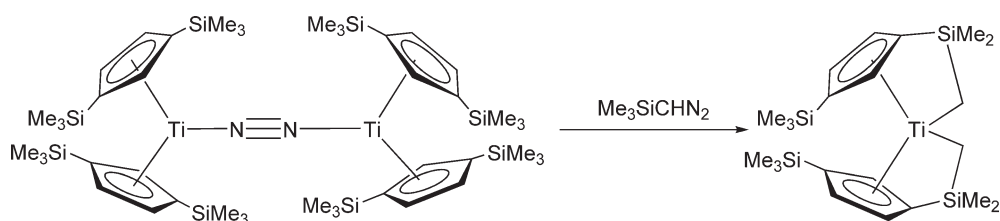
Scheme 550

A series of titanacycles have been studied by *ab initio* calculations. The energy differences between the presumably four-membered titanacycles derived from formal  $[2+2]$ -cycloadditions and  $[\text{Cl}_2\text{Ti}=\text{CH}_2]$  and  $[\text{Cl}_2\text{Ti}=\text{C}=\text{CH}_2]$  intermediate have been calculated and compared with systems where the chloro ligands are replaced by Cp rings. Titanacycles with exocyclic methylene groups or without exocyclic methylene groups can be formed. The exocyclic methylene groups in the  $\alpha$ -position of the titanacycle generated from  $[\text{Cl}_2\text{Ti}=\text{C}=\text{CH}_2]$  exhibit higher stability compared with the products formed from  $[\text{Cl}_2\text{Ti}=\text{CH}_2]$ .<sup>1369</sup> A DFT study of olefin metathesis in the titanacyclobutane system  $\text{Cp}_2\text{Ti}(\text{C}_3\text{H}_4\text{R}^1\text{R}^2)$ , in which the alkyl substituents  $\text{R}^1$  and  $\text{R}^2$  are at the  $\beta$ -position of the metallacyclobutane ring, has provided an estimate of the relative stabilities of the metallacyclobutanes and reaction barriers for the olefin insertions; these data have been compared with experimental findings. The role of this titanium system as a ROMP catalyst has also been discussed.<sup>1445</sup>

A method enabled for the easy access to titanacycle complexes has been widely developed. Combinations of  $\text{Cp}_2\text{TiCl}_2/2\text{MgBrEt}$  and  $\text{Cp}_2\text{TiCl}_2/2\text{LiBu}^n$  are effective reagents for the intermolecular coupling of ethylene with



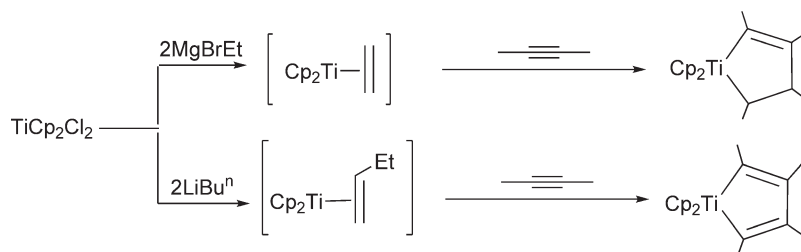
Scheme 551



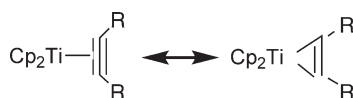
Scheme 552

alkynes to give monocyclic titanacyclopentene derivatives and for intermolecular coupling of two alkynes to give titanacyclopentadienes (Scheme 553).<sup>1446</sup>

Bis-Cp' acetylene complexes containing no additional stabilizing ligands are known which have structures close to that of titanacyclopentene and can be formally considered intermediate between oxidation states IV or II (Scheme 554). These two alternatives can be distinguished by their structural parameters and the reactivity behavior. In the reaction toward unsaturated molecules, insertion into the Ti–C bond of the titanacyclopentene, displacement of the acetylene, and the formation of low-valent titanium complexes or alternative pathways can be observed. The general procedure for the synthesis of these complexes is the reaction of Cp<sub>2</sub>TiCl<sub>2</sub> with a reducing agent in the presence of the acetylene.<sup>1447</sup> Their chemical properties have been investigated.

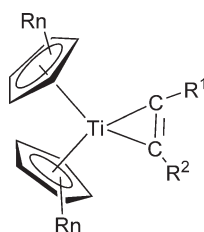


Scheme 553



Scheme 554





CpRn = Cp, Cp\*

R<sup>1</sup> = R<sup>2</sup> = Ph, SiMe<sub>3</sub>

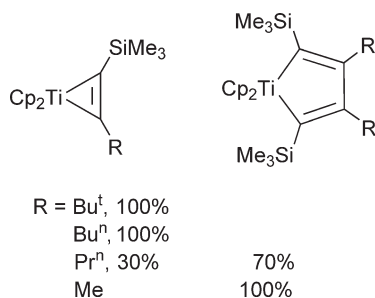
R<sup>1</sup> = Ph; R<sup>2</sup> = SiMe<sub>3</sub>

**Scheme 555**

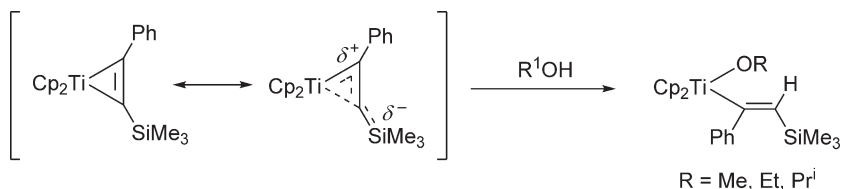
The X-ray crystal structure of Cp<sup>\*</sup><sub>2</sub>Ti(CH<sub>2</sub>CH<sub>2</sub>) shows that the C–C bond of the coordinated ethylene is substantially increased compared to that of free ethylene, from 1.337(2) Å to 1.438(5) Å. There is also considerable bending of the hydrogen atoms out of the plane of the ethylene molecule. This complex has therefore significant Ti(IV)–metallacyclopropane character.<sup>173</sup>

Bis-Cp' acetylene complexes Cp'<sub>2</sub>Ti(R<sup>1</sup>C<sub>2</sub>R<sup>2</sup>) (Cp' = Cp, Cp\*; R<sup>1</sup> = R<sup>2</sup> = Ph, SiMe<sub>3</sub>; R<sup>1</sup> = Ph, R<sup>2</sup> = SiMe<sub>3</sub>) without additional ligands have been prepared by the reaction of Cp'<sub>2</sub>TiCl<sub>2</sub> with equimolar amounts of Mg and the appropriate acetylene R<sup>1</sup>C<sub>2</sub>R<sup>2</sup> in THF (Scheme 555). The structures of some of these complexes have been confirmed by X-ray diffraction. One of the most important features is that the coordinated carbon–carbon bond is in all cases considerably longer than a normal triple carbon–carbon bond. Although they have similar structures, they differ in their reactivity depending on the nature of the acetylene substituents. Cp<sub>2</sub>Ti(Me<sub>3</sub>SiC<sub>2</sub>SiMe<sub>3</sub>) is considered as an excellent titanocene “TiCp<sub>2</sub>” fragment precursor. The synthesis, structure, and chemistry of Cp<sub>2</sub>Ti(Me<sub>3</sub>SiC<sub>2</sub>SiMe<sub>3</sub>) has been reviewed.<sup>1448,1449</sup> The preparation of a whole series of the (C<sub>5</sub>H<sub>5–n</sub>Me<sub>n</sub>)<sub>2</sub>Ti[Me<sub>3</sub>SiC<sub>2</sub>SiMe<sub>3</sub>] (*n* = 0–5) has been reported by the reduction of the corresponding bis-Cp' titanium dichlorides with Mg in THF in the presence of bis(trimethylsilyl)acetylene. Their spectroscopic characteristics, products of their thermal decomposition, and crystal structures are also reported. The coordinated acetylene ligand has the C–C bond length close to that of a double bond with substantial contribution of *sp*<sup>2</sup> hybridization, reflected in a large bending of SiMe<sub>3</sub> groups from the linear geometry. The Me substituents have an important influence on the reactivity of these compounds.<sup>1450</sup> Different titanacycles can be obtained in the reaction of Cp<sub>2</sub>TiCl<sub>2</sub> with magnesium and alkynylsilanes RC≡CSiMe<sub>3</sub>. Depending on the silyl substituents, this reaction gives titanacycloprenes, titanacyclopentadienes or, in a competition reaction, both types of complexes (Scheme 556). The compound Cp<sub>2</sub>Ti(Bu<sup>t</sup>C<sub>2</sub>SiMe<sub>3</sub>) has been characterized by X-ray crystal structure analysis. Structural and spectroscopic data were compared to investigate the influence of different alkyl, aryl, or trimethylsilyl (Bu<sup>t</sup>, Ph, SiMe<sub>3</sub>) substituents on alkyne complexation. The chemo- and regioselectivities of the obtained alkyne complexes were studied in reactions with alkynes, alcohols, carbon dioxide, and acetone. The kinetic products tend to be those with β-SiMe<sub>3</sub> substituents; these rearrange in some case to the thermodynamically more stable α-SiMe<sub>3</sub> substituted products (Scheme 557).<sup>1451</sup>

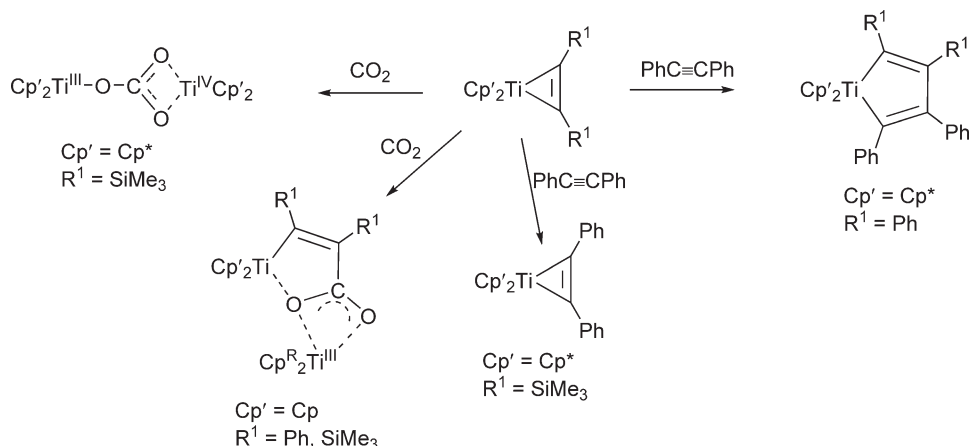
The reactivity of these species has been widely studied. Oxidative additions with unsaturated organic molecules afford an important number of titanacycle derivatives. Some of these reactions are summarized below.



**Scheme 556**

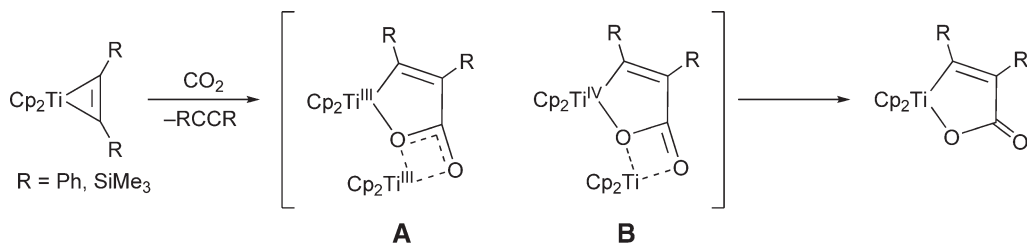


Scheme 557

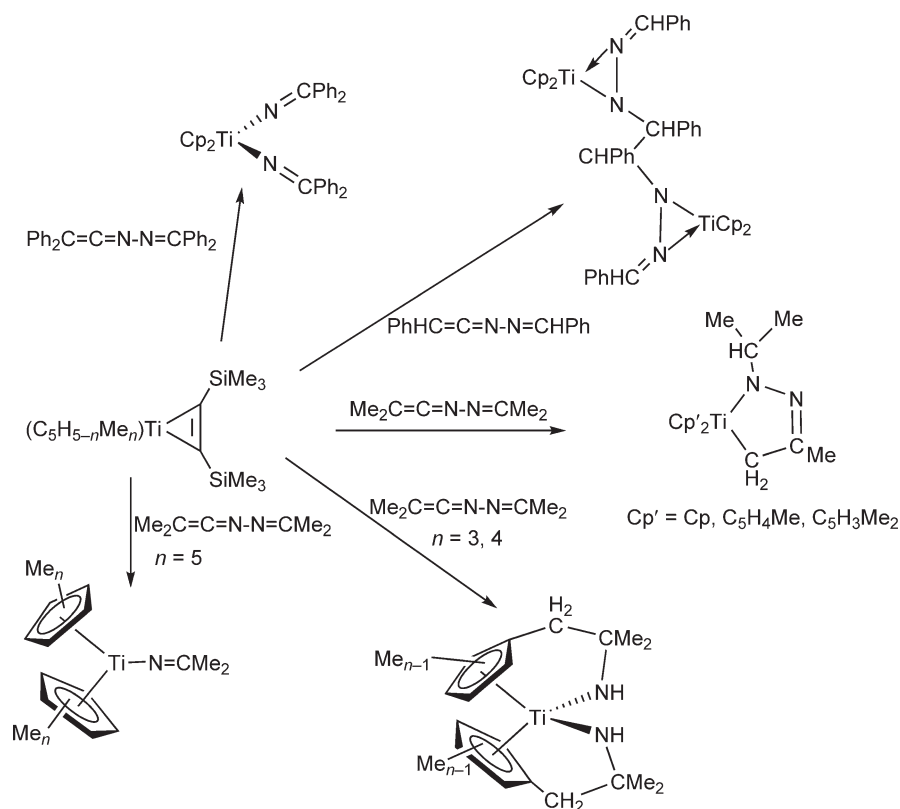


Scheme 558

Reactions with  $\text{CO}_2$  and acetylenes are shown in Scheme 558. The chemoselectivity of these reactions and the structures of the products depend strongly on the nature of the Cp and the alkyne substituents.<sup>1452,1453</sup> Reactions of the Cp derivative with  $\text{CO}_2$  in aliphatic hydrocarbon solutions at room temperature give binuclear titanium(III)  $\sigma$ -alkenylcarboxylate complexes and free acetylene. The structure of the  $\text{SiMe}_3$  derivative has been elucidated by X-ray diffraction and shows the presence of two fused chelate cycles and a tricoordinated oxygen atom. Reactions of these species with oxygen release one “ $\text{TiCp}_2$ ” unit with the formation of titanafuranone metallacycles. To understand this behavior, the resonance form B (Scheme 559) must have certain contribution to the electronic structure of the alkenylcarboxylate complexes. For the pentamethyl-Cp derivative, the alkyne is not coupled and a carbonate bridge complex is obtained (Scheme 558). X-ray diffraction studies of the phenyl titanofuranone derivative have been carried out.<sup>1454</sup> The complex (*meso*-ebthi) $\text{Ti}(\eta^2\text{-PhC}\equiv\text{CSiMe}_3)$  reacts with  $\text{CO}_2$  with the insertion into the Ti-CPh bond with atypical regioselectivity to yield the  $\alpha$ -silyl-substituted *meso*-(ebthi)titanafuranone derivative. In the analogous reactions of the complexes  $\text{L}_2\text{Ti}(\eta^2\text{-PhC}\equiv\text{CSiMe}_3)$  with  $\text{CO}_2$  [ $\text{L}_2 = (\text{thi})_2$ , (*rac*-ebthi) and  $\text{Cp}^*_2$ ], typical regioselectivity, that is, insertion into the M-CSi bond of the titanacyclopentene, is observed, yielding the  $\beta$ -silyl-substituted titanafuranones. These results show that insertion of  $\text{CO}_2$  into the M-C bond of the titanacyclopentene structure of the alkyne titanium complexes is governed by the substitution pattern of the alkyne and the steric environment around the metal center.<sup>1455</sup> The titanacyclopentadiene complex  $\text{Me}_2\text{Si}(\text{C}_5\text{H}_4)_2\text{Ti}(\text{C}_4\text{Ph}_4)$  is obtained by reacting  $\text{Me}_2\text{Si}(\text{C}_5\text{H}_4)_2\text{Ti}(\eta^2\text{-PhC}\equiv\text{CPh})$  with  $\text{PhC}\equiv\text{CPh}$ , while  $(\text{thi})_2\text{Ti}(\eta^2\text{-PhC}\equiv\text{CPh})$  is hydrolyzed to the



Scheme 559

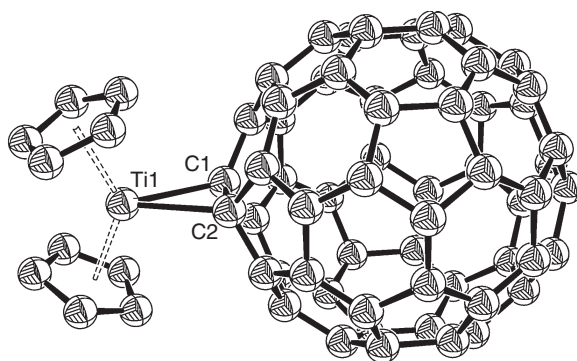


Scheme 560

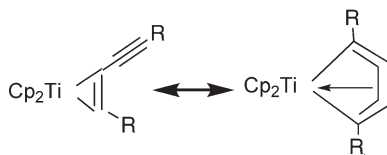
$\mu$ -oxo complex  $[(\eta^5-Cp)_2Ti(PhC=CHPh)]_2(\mu-O)$ .<sup>1453</sup> The reactions of  $Cp'_2Ti(Me_3SiC\equiv SiMe_3)$  ( $Cp' = Cp, Cp^*$ ) with  $H_2O$  and  $CO_2$  have been compared to understand the influence of the  $Cp'$  ligands on the reaction pathways and the obtained products. The permethyltitanocene complex hydrolyzes to the dihydroxy complex  $Cp'_2Ti(OH)_2$ , whereas the  $\mu$ -oxo derivative  $Cp_2TiOTiCp_2$  is obtained in the reaction of the corresponding bis-Cp derivative with water.<sup>1456</sup>

Reactions of  $(C_5H_{5-n}Me_n)_2Ti(\eta^2-Me_3SiC\equiv SiMe_3)$  ( $n = 0-5$ ) with azines  $R^1R_2C-N-N-C R^1R^2$  ( $R^1, R^2 = H, Me, Ph$ ) give different final products depending on the number of Me substituents at the  $Cp'$  ligands and the nature of the azine substituents (Scheme 560).<sup>1457</sup>

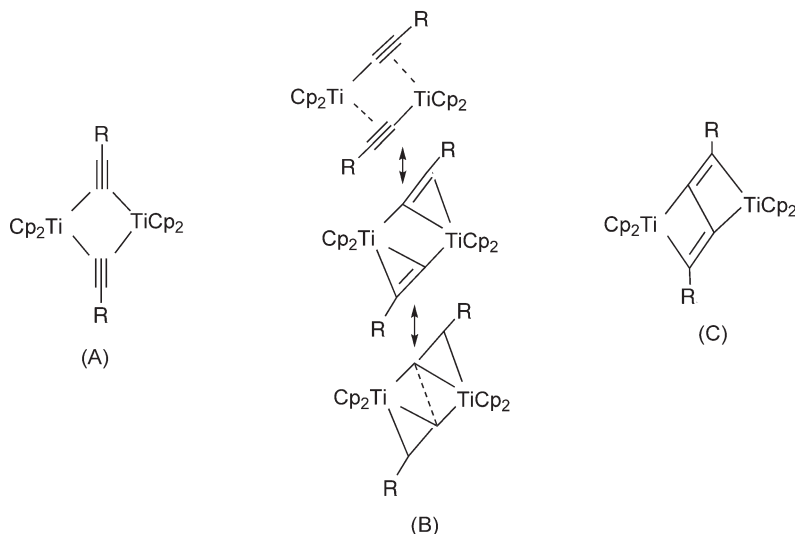
$Cp_2Ti(\eta^2-Me_3SiC\equiv SiMe_3)$  reacts with an equimolar amount of fullerene-60 at room temperature under argon to give  $Cp_2Ti(\eta^2-C_{60})$ . The molecular structure determined by X-ray diffraction (Figure 28) shows a significant elongation of the fullerene C(1)–C(2) bond coordinated to titanium, akin to a titanacyclopropane structure.<sup>1458</sup>



**Figure 28** Molecular structure of complex  $Cp_2Ti(\eta^2-C_{60}) \cdot MeC_6H_5$  (reproduced by permission of Wiley-VCH from *Eur. J. Inorg. Chem.* **1999**, 1855).



Scheme 561



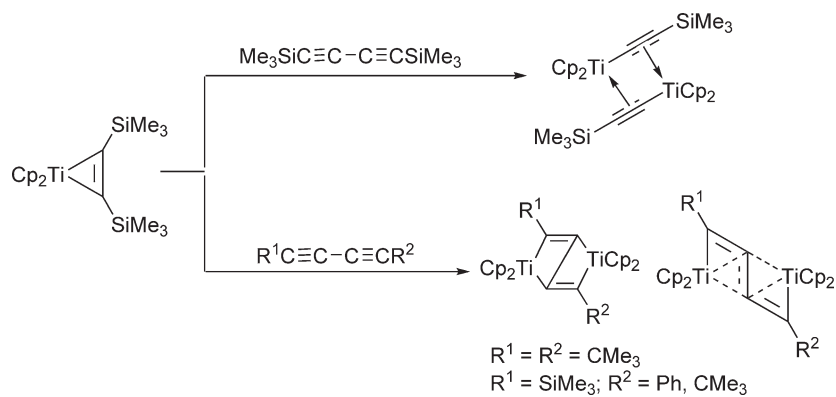
Scheme 562

Many recent investigations in this field of chemistry have been directed toward the synthesis and study of diyne titanium complexes. The “ $\text{TiCp}_2$ ” precursor compound  $\text{Cp}_2\text{Ti}(\text{Me}_3\text{SiC}_2\text{SiMe}_3)$  reacts with 1,4-disubstituted 1,3-butadiynes to give five-membered titanacyclocumulenes, the structures and stability of which depend strongly on the diyne substituents. Mononuclear or binuclear homobimetallic derivatives can be formed. For the mononuclear complexes, an equilibrium between the cyclocumulene and an alkyne structure is possible (Scheme 561). Binuclear complexes may exhibit different structural types (Scheme 562).

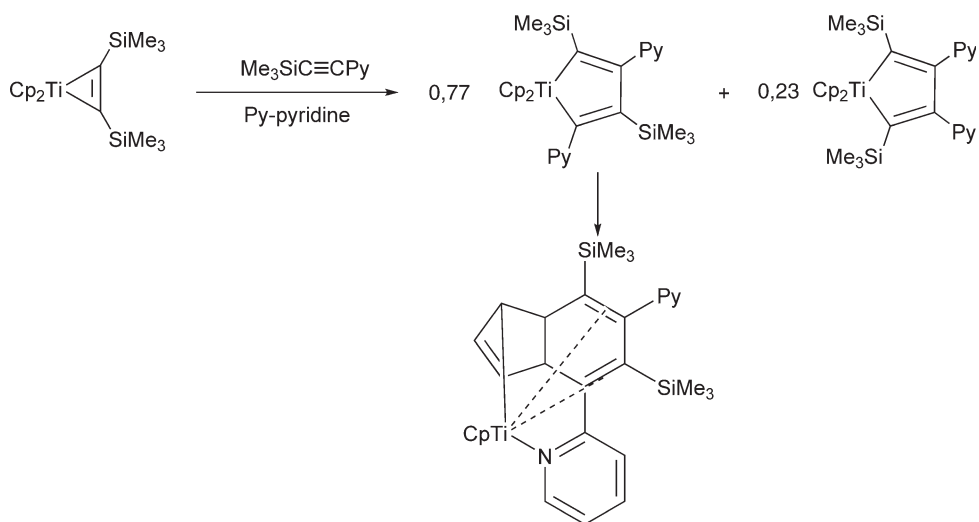
With  $\text{R} = \text{SiMe}_3$ , C–C bond cleavage is favored by the instability of the cyclocumulene formed. With  $\text{R} = \text{Bu}^t$ , a stable complex is obtained that is unreactive toward CO,  $\text{H}_2\text{O}$ , or acetone. With  $\text{R} = \text{Ph}$ , the titanacyclocumulene is stable in the solid state but in solution the compound can react as a cumulene as an alkyne or simultaneously as both.<sup>1459–1461</sup> Theoretical studies concerning the factors that control the structural features of these substances have been reported.<sup>1462,1463</sup> “Zigzag butadiyne” binuclear bis-Cp titanium complexes are obtained by reaction with disubstituted butadiynes, though the structures depend strongly on the nature of the substituents. For  $\text{SiMe}_3$  substituents, the starting butadiyne is cleaved by titanocene to yield the binuclear complex  $[\text{Cp}_2\text{Ti}(\text{C}\equiv\text{CSiMe}_3)]_2$ , while for other symmetrically substituted or unsymmetrically substituted butadiynes the reaction proceeds to binuclear complexes with a central 1,4-disubstituted *trans,trans*-butadiene bridging unit between the two titanium centers (Scheme 563).<sup>1301</sup>

The reactivity with alkynylsilanes  $\text{RC}\equiv\text{CSiMe}_2\text{H}$  has been studied, including the dynamic behavior in solution and the characterization of the Si–H–Ti interactions in relationship to catalytic reactions.<sup>1459,1464–1466</sup>

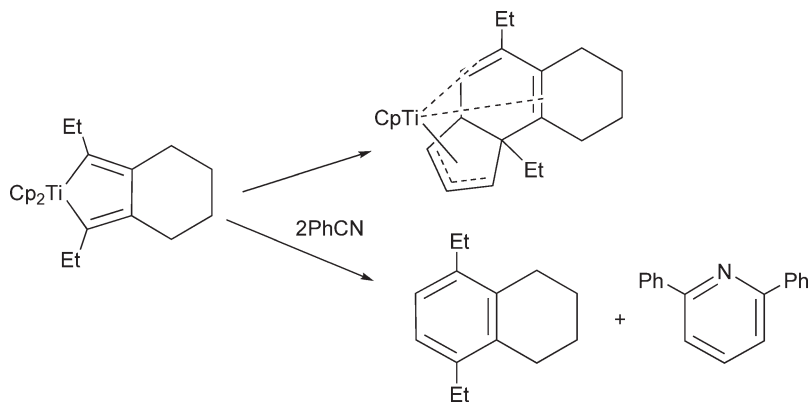
The reaction of  $\text{Cp}_2\text{Ti}(\text{Me}_3\text{SiC}_2\text{SiMe}_3)$  with  $\text{Me}_3\text{SiC}\equiv\text{Cpy}$  ( $\text{py} = \text{pyridine}$ ) gives an asymmetric titanacyclopentene which undergoes an intramolecular reaction of the titanacyclopentadienyl unit with one of the two Cp ligands, leading unexpectedly to a dihydroindenyl complex (Scheme 564). Dihydroindenyl Ti complexes are unstable and this reaction can be regarded as the first step in an arene formation process.<sup>1467,1468</sup> The titanacyclic compound shown in Scheme 565 rearranges at room temperature to a titanacyclopentadiene derivative via intramolecular cyclization;<sup>1469</sup> in the presence of benzonitrile, tetrahydronaphthalene and diphenylpyridine are formed.<sup>1314</sup> These results illustrate a mode of reactivity for bis-Cp Ti derivatives and demonstrate that  $\eta^5\text{-Cp}$  ligands are not always the benign spectators they are often assumed to be (see Section 4.05.4.2.3).



Scheme 563



Scheme 564



Scheme 565

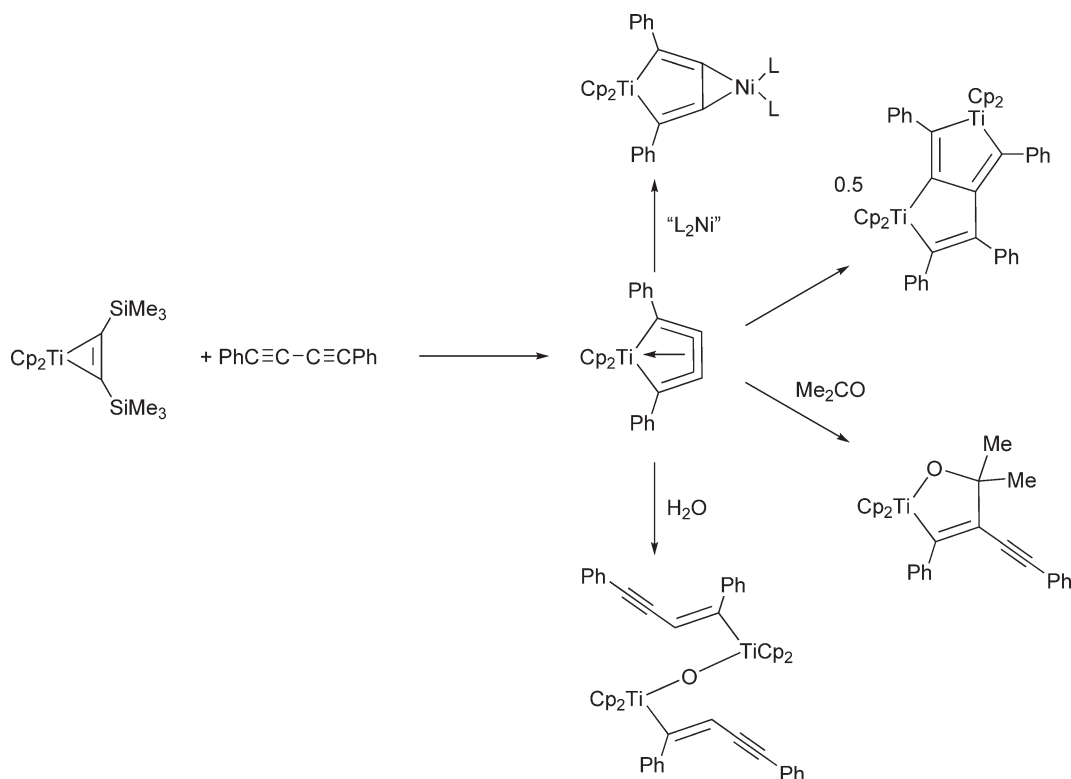
Conjugated and non-conjugated diynes have been demonstrated to react with titanocene to give different type of products. The complex  $\text{Cp}_2\text{Ti}(\eta^2\text{-Me}_3\text{SiC}_2\text{SiMe}_3)$ , used as titanocene source, reacts with butadiynes to afford five-membered titanacyclocumulene derivatives  $\text{Cp}_2\text{Ti}(\eta^4\text{-1,2,3,4-RC}_4\text{R})$ . According to the X-ray structures, these complexes contain a planar ring system with three C–C double bonds, with the central bond coordinated to titanium. Some reactions of this type of complex have been investigated. The reaction with an equimolar amount of  $\text{PhC}\equiv\text{C-C}\equiv\text{CPh}$  in hexane gives the unstable phenyl-substituted five-membered titanacyclocumulene which is stabilized by dimerization. The cumulene reacts with  $\text{Ni}(0)$  complexes to give the corresponding heterobimetallic complexes, which react with acetone to form titanahydrofuran derivatives, while in the presence of water hydrolysis takes place (Scheme 566). The crystal structures of these reaction products have been determined.<sup>1470,1471</sup> Examples of dimerization of titanacyclocumulene derivatives have also been in the reactions with  $\text{RC}\equiv\text{C-C}\equiv\text{CR}^1$ , where bimetallic complexes can be formed with or without cleavage of the internal C–C bonds.<sup>1472</sup>

These titanium systems mediate the metathesis of C–C bonds and recombination processes with disubstituted butadiynes.<sup>1461</sup> Intramolecular cyclization of terminal disubstituted  $\alpha,\omega$ -diynes with successive unusual Cp cleavage and new intramolecular C–C coupling processes have been observed in the reaction with the terminal disubstituted diynes  $\text{RC}\equiv\text{C}-(\text{CH}_2)_n\text{-C}\equiv\text{CR}$  (Scheme 567). The stability of the resulting products is determined by the spacer length ( $n = 2, 4, 5, 6$ ). An increase in spacer length ( $n > 4$ ) provides undefined secondary and decomposition products. The X-ray structures of the some of the resulting products have been reported.<sup>1469</sup>

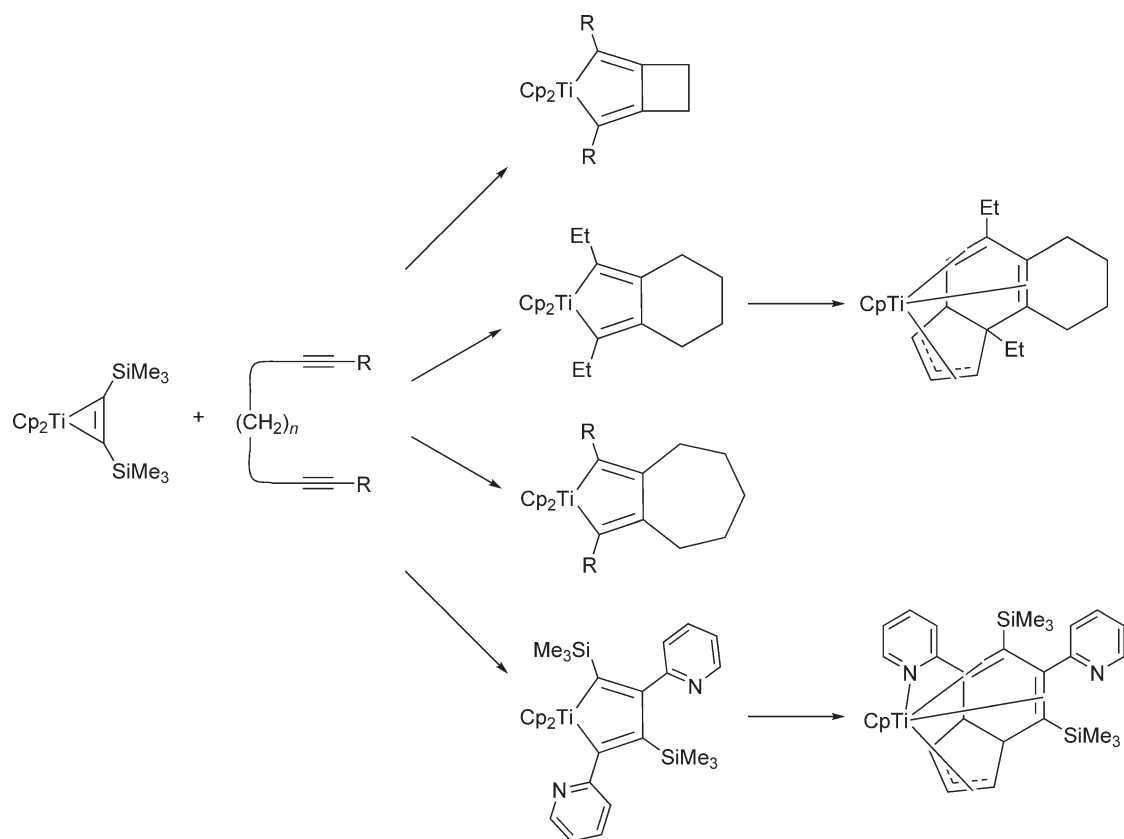
$\text{Cp}_2\text{Ti}(\eta^2\text{-Me}_3\text{SiC}_2\text{SiMe}_3)$  reacts with 1,4-diazadienes  $\text{RN}=\text{CHCH}=\text{NR}$  to afford 1-titana-2,5-diazacyclopent-3-ene complexes, while in the analogous reaction with differently substituted azines  $\text{R}_2\text{C}=\text{NN}=\text{CR}_2$  the products depend strongly on the substituents R. With  $\text{R} = \text{Me}$ , a substitution of the alkyne by the azine and a subsequent CH activation to the 1-titana-2,3-diazacyclopent-3-ene species is observed (Scheme 581; Section 4.05.4.4).<sup>1473,1474</sup>

$\text{Cp}_2\text{Ti}(\text{Me}_3\text{SiC}_2\text{SiMe}_3)$  has been used as a reagent for the amination of chloroalkynes but leads only to low yields of indoles.<sup>1475</sup>

Remarkable differences in behavior are found when the analogous permethyl derivatives are studied. The increased steric bulk, solubility, and electron-donor characteristics produce different spectroscopic and reactivity properties. Reduction of  $\text{Cp}^*_2\text{TiCl}_2$  with Mg in the presence of disubstituted 1,3-butadiynes leads to different final



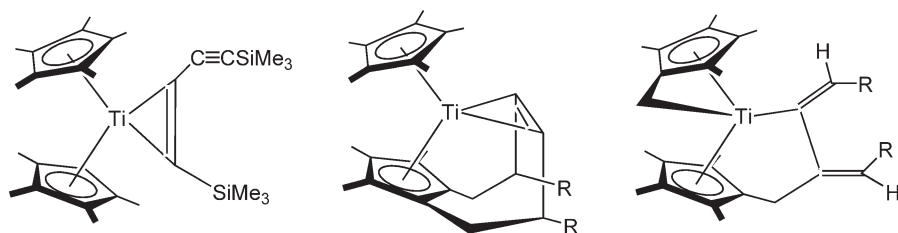
Scheme 566



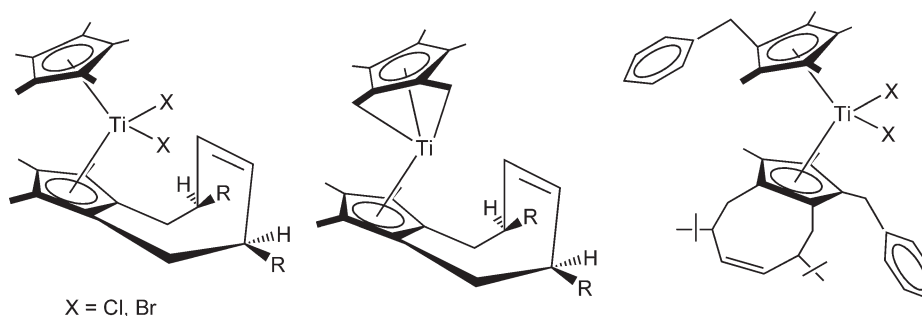
Scheme 567

products depending strongly on the diyne substituents. With  $\text{SiMe}_3$  substituents, titanacyclopentadiene derivatives are obtained. The reactions with other  $\text{R}^1\text{C}\equiv\text{C}-\text{C}\equiv\text{CR}^2$  proceed via C-H activations and are suitable for the synthesis of different C-C coupling products of the diyne and the pentamethyl-Cp ring. For *tert*-butyl substituted diynes, the coupling of the butadiyne with two methyl groups of one  $\text{Cp}^*$  ligand is observed, resulting in one pentamethyl-Cp ligand being annellated to an eight-membered ring with a C-C triple bond coordinated to the titanium center. When Me or Ph substituted diynes are used, a different activation process is observed to give a fulvene as well as a butadienyl-substituted ligand (Scheme 568). These complexes react with  $\text{CO}_2$  with insertion processes to give titanafuranone derivatives. Thermolysis reactions have also been studied.<sup>1283,1476–1479</sup> In these systems, the  $\text{Cp}^*$  ligand participates in a large number of coupling reactions. Thermally induced replacement of coordinated alkynes or functionalizations with simple reagents ( $\text{H}_2$ , HCl, HBr) allows the preparation of other coupling products shown in Scheme 569.<sup>1450,1452,1480</sup>

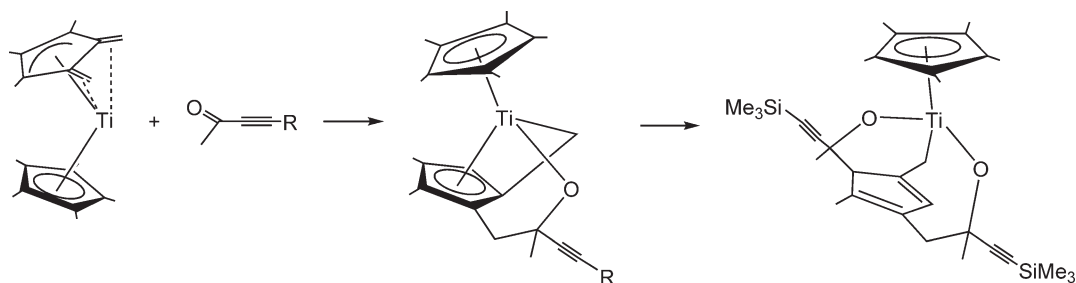
The permethylated cyclopentadienyl  $\eta^3:\eta^4$ -allyldiene  $\text{Ti}(\text{II})$  complex  $\text{Cp}^*_2\text{Ti}[\text{C}_5\text{Me}_3(\text{CH}_2)_2]$  reacts with alkynyl-ketones  $\text{RC}\equiv\text{CC}(\text{O})\text{Me}$  ( $\text{R} = \text{SiMe}_3$ , ferrocenyl) to give the expected products of the  $\text{C}=\text{O}$  group insertion into one



Scheme 568



Scheme 569



Scheme 570

Ti-CH<sub>2</sub> bond. The SiMe<sub>3</sub> derivative could not be isolated in pure form due to its high solubility and the product of a formally [1 + 2]-addition was isolated (Scheme 570). The molecular structures have been determined by single crystal X-ray diffraction.<sup>1481</sup>

#### 4.05.4.2.5 Ziegler–Natta polymerization

One of the most remarkable aspect on the bis-Cp' titanium derivative chemistry has been the production of new and unprecedented variety of polyolefins. The use of this type of complexes as Ziegler–Natta pre-catalysts for the olefin polymerization has opened new possibilities to produce polyolefins with different properties, and significant effort has been devoted to the design of new bis-Cp' catalyst structures. This section summarizes simple aspects related to the polymerization of  $\alpha$ -olefins catalyzed by bis-Cp' titanium complexes containing a  $\sigma$ -Ti-C bond. A more comprehensive review of the catalytic applications of titanium complexes in the  $\alpha$ -olefin polymerization processes is covered in Chapter 4.09.

Numerous investigations into the use of group 4 organometallic complexes as pre-catalysts for the polymerization of olefins have been reviewed.<sup>453,1482–1490</sup> A *Chemical Reviews* special issue provides comprehensive coverage of olefin polymerizations including titanium catalysts.<sup>1491</sup> Cationic alkyl derivatives of group 4 metallocenes of the type [Cp'<sub>2</sub>MR]<sup>+</sup> have been recognized as the catalytically active species in metallocene-based olefin polymerization catalysis,<sup>1492</sup> and the chemistry of these highly electrophilic cationic  $d^0$ -complexes in polymerization catalysis has been reviewed.<sup>1493</sup> Another review concentrates on stereospecific olefin polymerization using chiral bis-Cp' catalysts.<sup>1494</sup> Developments in the search of new olefin polymerization catalysts beyond metallocenes have been summarized.<sup>1495</sup> Studies on  $\alpha$ - and  $\beta$ -deuterium isotope effects in the MgX<sub>2</sub>- and MAO-promoted intramolecular olefin insertion of Cp<sub>2</sub>TiRCl have been reported. Cyclization systems as models for  $\alpha$ -olefin polymerization have been examined and the dependence of chain-end control upon the Lewis acid co-catalyst in the polymerization system has been considered. Comparison of cyclization rates reveals deuterium isotope effects for the  $\alpha$ - and  $\beta$ -sites of a propagating poly  $\alpha$ -olefin chain model. The polymerization of 1-pentene and 1-hexene is studied. There is evidence for  $\alpha$ -hydrogen participation in the rate-determining step of intramolecular olefin insertion into a titanium–carbon bond. Slight  $\beta$ -hydrogen participation has also been detected.<sup>1496</sup>

Cp<sub>2</sub>TiMe<sub>2</sub> is activated by various borate salts to give catalytic systems for the polymerization of ethylene, propylene, and styrene. A conventional Ziegler–Natta coordination polymerization mechanism is proposed for ethylene and propylene polymerization, while a carbocationic polymerization mechanism has been suggested for styrene.<sup>1497</sup>



Reactions of  $\text{Cp}_2\text{TiClMe}$ ,  $\text{Cp}_2\text{TiMe}_2$ ,<sup>1208,1209,1498</sup> and  $\text{Cp}_2\text{TiCl}_2$ <sup>1211</sup> with  $\text{AlMe}_3$  and/or MAO have been monitored by  $^1\text{H}$  and  $^{13}\text{C}$  NMR spectroscopy in order to study the formation and the nature of Ti/Al adducts that play a role in the olefin polymerization processes catalyzed by these complexes. A wide range of temperatures and Al/Ti ratios have been used. From the results, it is possible to deduce that in reactions with  $\text{Cp}_2\text{TiClMe}$  and  $\text{Cp}_2\text{TiCl}_2$ , MAO is a better alkylating agent and it has a greater capacity for producing and stabilizing cation-like species.

The complex  $\text{Cp}_2\text{TiCl}(\text{C}\equiv\text{CSiMe}_3)$  supported on clay minerals has been used as heterogeneous catalyst for ethylene polymerization.<sup>1069</sup> The heterogenization of homogeneous bis- $\text{Cp}'$  catalysts for olefin polymerization in order to support these systems for industrial applications has been studied.<sup>1499</sup>

Mechanistic studies of Ziegler–Natta olefin polymerization have been carried out in order to examine the role of Lewis acid co-catalysts and competitive intramolecular Ti–C versus the Al–C alkene insertion reactions.<sup>1500</sup> A DFT study has been conducted on the methide abstraction by  $\text{B}(\text{C}_6\text{F}_5)_3$  from mono- $\text{Cp}$ , mono- $\text{Cp}$ –amido, and bis- $\text{Cp}$  group 4 metal complexes. Reactions of the contact ion pair with ethylene and the solvent have also been investigated.<sup>1501</sup> The reactions of methane and dihydrogen molecules with the highly Lewis acid cations  $[\text{TiCp}_2\text{Me}]^+$  and  $[\text{TiCp}_2\text{H}]^+$  have been investigated by DFT calculations. These gradient-corrected density functional methods give insight into the mechanism of H/D exchange in methane in the presence of Ziegler–Natta-type catalysts observed experimentally. It is shown that organometallic cationic complexes of Ti(IV) may prove to be promising systems for C–H and H–H bond activation under mild conditions.<sup>1502</sup>

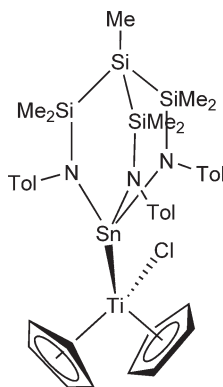
DFT calculations have been performed to investigate the thermodynamics of formation of olefin-separated ion pairs between  $\text{Cp}_2\text{TiMe}_2$  and MAO in the polymerization of olefins.<sup>1503</sup> A DFT study for C–H bonds in the reaction of  $[\text{Cp}_2\text{TiMe}]^+$  with  $\text{RH}$  ( $\text{R} = \text{Me}, \text{Et}, \text{Pr}, \text{Pr}^i$ ) has been carried out.<sup>1504</sup> The potential energy surfaces for reactions of ethylene with  $[\text{Cp}_2\text{TiR}]^+$ ,  $\text{Cp}_2\text{TiClR}$ , and  $\text{Cp}_2\text{TiClR}\cdot\text{AlH}_2\text{Cl}$  ( $\text{R} = \text{H}, \text{Me}$ ) have been calculated by *ab initio* molecular orbital methods.<sup>1505</sup> The insertion process of the ethylene into the titanium–carbon chain for contact ion pair systems of the type  $[\text{L}_1\text{L}_2\text{TiCH}_3-(\mu\text{-CH}_3)\text{-B}(\text{C}_6\text{F}_5)_3]$ , where  $\text{L}_1$  and  $\text{L}_2$  are  $\text{Cp}$ ,  $\text{NPH}_3$ , and other ligands, has been examined using DFT methods.<sup>1506</sup>

#### 4.05.4.3 Complexes with Ti–Sn Bonds

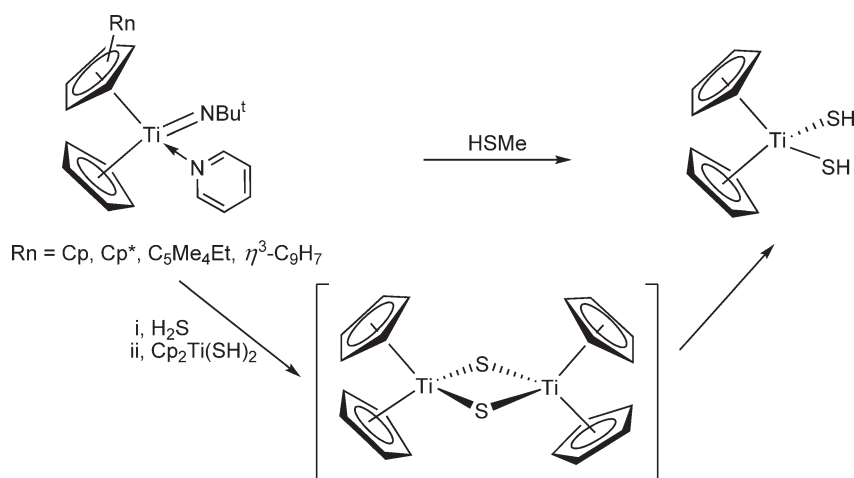
Reaction of  $\text{Cp}_2\text{TiCl}_2$  with  $\text{Li}(\text{OEt}_2)\text{Sn}\{\text{MeSi}[\text{SiMe}_2\text{N}(4\text{-CH}_3\text{C}_6\text{H}_4)]_3\}$  gives the nucleophilic substitution of one of the chloro ligand to afford the compound  $\text{Cp}_2\text{TiCl}[\text{Sn}\{\text{MeSi}(\text{SiMe}_2\text{NC}_6\text{H}_4\text{Me-4})_3\}]$  showing a Ti–Sn bond (Scheme 571), which has been characterized by elemental analysis and NMR spectroscopy.<sup>1507</sup>

#### 4.05.4.4 Complexes with Ti–N Bonds

Quantum chemical calculations and IR spectroscopic studies have been performed on the complex  $\text{Cp}_2\text{Ti}(\text{NCS})_2$  to investigate the ligand-to-metal charge transfer excited states.<sup>1508</sup> The complexes  $(\text{C}_5\text{H}_4\text{R})_2\text{Ti}(\text{NCSe})_2$  ( $\text{R} = \text{Me}, \text{SiMe}_3, \text{SiEt}_3$ ) have been prepared from  $(\text{C}_5\text{H}_4\text{R})_2\text{TiCl}_2$  with  $\text{KSeCN}$  in acetone. An X-ray analysis confirms the results of IR studies that these complexes contain N-bonded selenocyanato ligands.<sup>1509</sup>



Scheme 571



Scheme 572

The molecular structure of  $[\text{Ti}_2\text{Cp}_4(\text{N}_3)_2](\mu\text{-O})$  has been determined by X-ray diffraction, showing a binuclear complex with two bis-Cp azido fragments connected through the oxygen bridge.<sup>1510</sup>

Titanium amido and imido complexes are of increasing interest as reagents in organic transformations and catalysis.<sup>1511</sup> For ease of representation, the terminal titanium–imido or titanium–oxo linkages are generally drawn as “Ti=X” (X=NR, O). Nevertheless, the formal metal–ligand multiple bonds in these complexes are better described as  $\sigma^2\text{-}\pi^4$  triple bonds.

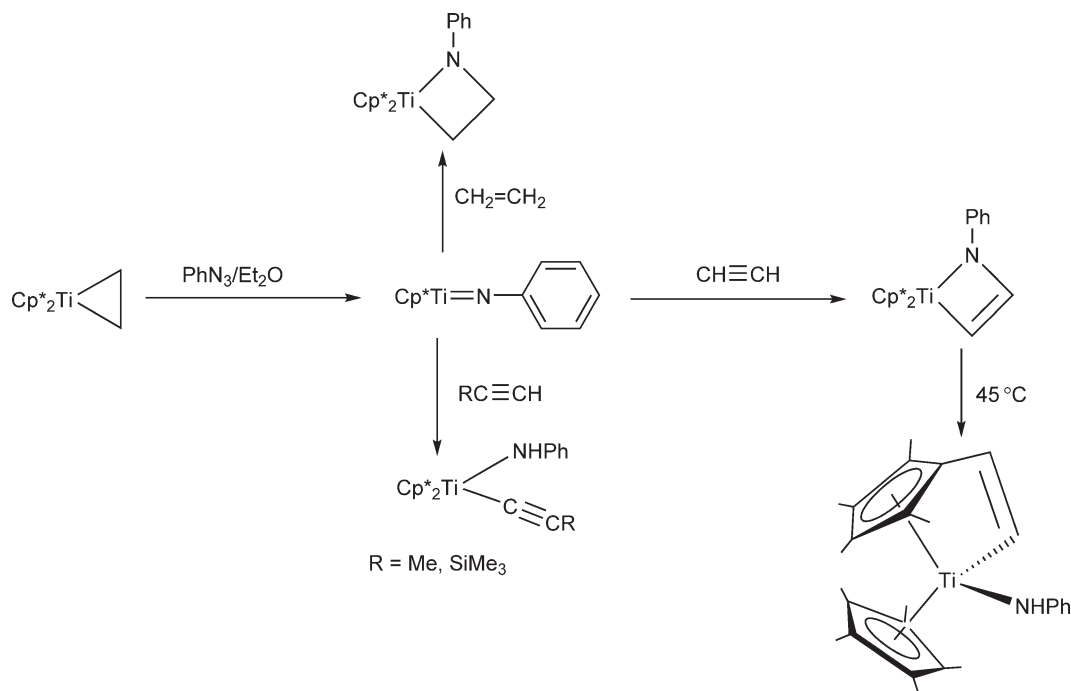
The bis-Cp amido ketiminato complex  $\text{Cp}_2\text{Ti}(\text{NHCHPh}_2)(\text{N}=\text{CPh}_2)$  can be prepared by the reaction of  $\text{Cp}_2\text{Ti}(\text{Me}_3\text{SiC}_2\text{SiMe}_3)_2$  with 2 equiv. of  $\text{HN}=\text{CPh}_2$  in *n*-hexane at room temperature.<sup>1512</sup>

The synthesis, characterization, and chemical behavior of mono- and bis-Cp' imido titanium complexes have been well explored.<sup>603</sup> The reactions of  $(\text{C}_5\text{Me}_4\text{R})\text{Ti}(\text{NBu}^t)\text{Cl}(\text{NC}_5\text{H}_5)$  (R=Me, Et) with NaCp give the mixed Cp complexes  $\text{Cp}(\text{C}_5\text{Me}_4\text{R})\text{Ti}(\text{NBu}^t)(\text{NC}_5\text{H}_5)$ , which show fluxional behavior and exhibit reversible pyridine dissociation at higher temperatures and restricted rotation about the Ti–N (pyridine) bond at lower temperatures.  $\text{CpTi}(\text{NBu}^t)\text{Cl}(\text{NC}_5\text{H}_5)$  reacts with  $\text{Li}[\text{C}_9\text{H}_7]$  with the formation of the mixed  $\eta^5\text{-Cp } \eta^3\text{-indenyl}$  derivative  $\text{Cp}(\text{C}_9\text{H}_7)\text{Ti}(\text{NBu}^t)(\text{NC}_5\text{H}_5)$  (Scheme 572). The trihapto coordination of the indenyl ligand in this complex is consistent with strong  $\pi$ -donor characteristics of the imido ligand.<sup>605</sup>  $(\text{C}_9\text{H}_7)\text{TiCl}(\text{NBu}^t)(\text{NC}_5\text{H}_5)$  and  $\text{Cp}_2\text{Ti}(\text{NBu}^t)(\text{NC}_5\text{H}_5)$  have been similarly synthesized.<sup>604</sup> The reaction of  $\text{Cp}_2\text{Ti}(\text{NBu}^t)(\text{NC}_5\text{H}_5)$  with an excess of  $\text{SH}_2$  or  $\text{MeSH}$  gives  $\text{Cp}_2\text{Ti}(\text{SX})_2$  (X=H, Me).<sup>1513</sup> The labile bis( $\mu$ -sulfido) complex  $(\text{Cp}_2\text{Ti})_2(\mu\text{-S})_2$ , identified as an intermediate in the reaction of  $\text{Cp}_2\text{Ti}(\text{NBu}^t)(\text{NC}_5\text{H}_5)$  with  $\text{SH}_2$ , is obtained by the reaction of  $\text{Cp}_2\text{Ti}(\text{SH})_2$  with  $\text{Cp}_2\text{Ti}(\text{NBu}^t)(\text{NC}_5\text{H}_5)$  (Scheme 572).

The base-free titanium imido compound  $\text{Cp}^*_2\text{Ti}=\text{NPh}$  can be prepared by the reaction of  $\text{Cp}^*_2\text{Ti}(\text{C}_2\text{H}_4)$  with  $\text{PhN}_3$ . This complex reacts with ethylene or acetylene to give the azatitanacyclobutane  $\text{Cp}^*_2\text{Ti}(\text{CH}_2\text{CH}_2\text{NPh})$  or the azatitanacyclobutene  $(\text{C}_5\text{Me}_5)_2\text{Ti}(\text{CH}=\text{CHNPh})$ . In the case of ethylene, the cycloaddition is reversible.  $\text{Cp}^*_2\text{Ti}=\text{NPh}$  reacts with terminal alkynes with activation of the C–H bond to give amido–acetylide complexes. The ring-activated complex  $\text{Cp}^*\text{Ti}(\text{C}_5\text{Me}_4\text{CH}_2\text{CH}=\text{CH})(\text{NHPh})$  is obtained under thermolysis of  $\text{Cp}^*_2\text{Ti}(\text{CH}=\text{CHNPh})$  (Scheme 573).<sup>1407</sup>

The end-on bound dinitrogen complex  $[\text{C}_5\text{H}_3(\text{SiMe}_3)_2]_2\text{Ti}-\text{N}_2-\text{Ti}[\text{C}_5\text{H}_3(\text{SiMe}_3)_2]_2$  reacts with organic azides to give monomeric, base-free bis-Cp imido complexes, with displacement of the dinitrogen molecule. They are unreactive toward C–H bonds, but the Ti–N linkage is readily hydrogenated and participates in group transfer reactions with unsaturated organic molecules such as carbon monoxide and benzophenone (Scheme 574). Reaction of  $[\text{C}_5\text{H}_3(\text{SiMe}_3)_2]_2\text{Ti}-\text{N}_2-\text{Ti}[\text{C}_5\text{H}_3(\text{SiMe}_3)_2]_2$  with the diazoalkane  $\text{Me}_3\text{SiCHN}_2$  leads to the isolation of a double cyclometallated bis-Cp complex (Scheme 552; Section 4.05.4.2.4.(ii)), while treatment with the diazoalkane  $\text{Ph}_2\text{CN}_2$  affords the corresponding diazoalkane compound.<sup>1443</sup>

The binuclear complex  $\text{Cp}(\text{Cl})\text{Ti}(\text{NPh})_2\text{TiCp}_2$  containing mono- and bis-Cp titanium fragments connected through an imido bridge unit is synthesized by the reaction of the magnesium imide reagent  $\text{Mg}(\text{NPh})(\text{THF})$  with  $\text{Cp}_2\text{TiCl}_2$ . In contrast, the reaction with  $\text{Cp}_2\text{ZrCl}_2$  exclusively leads to the binuclear compound containing dicyclopentadienyl zirconium fragments (see Section 4.05.3.3.3).<sup>607</sup>



Scheme 573

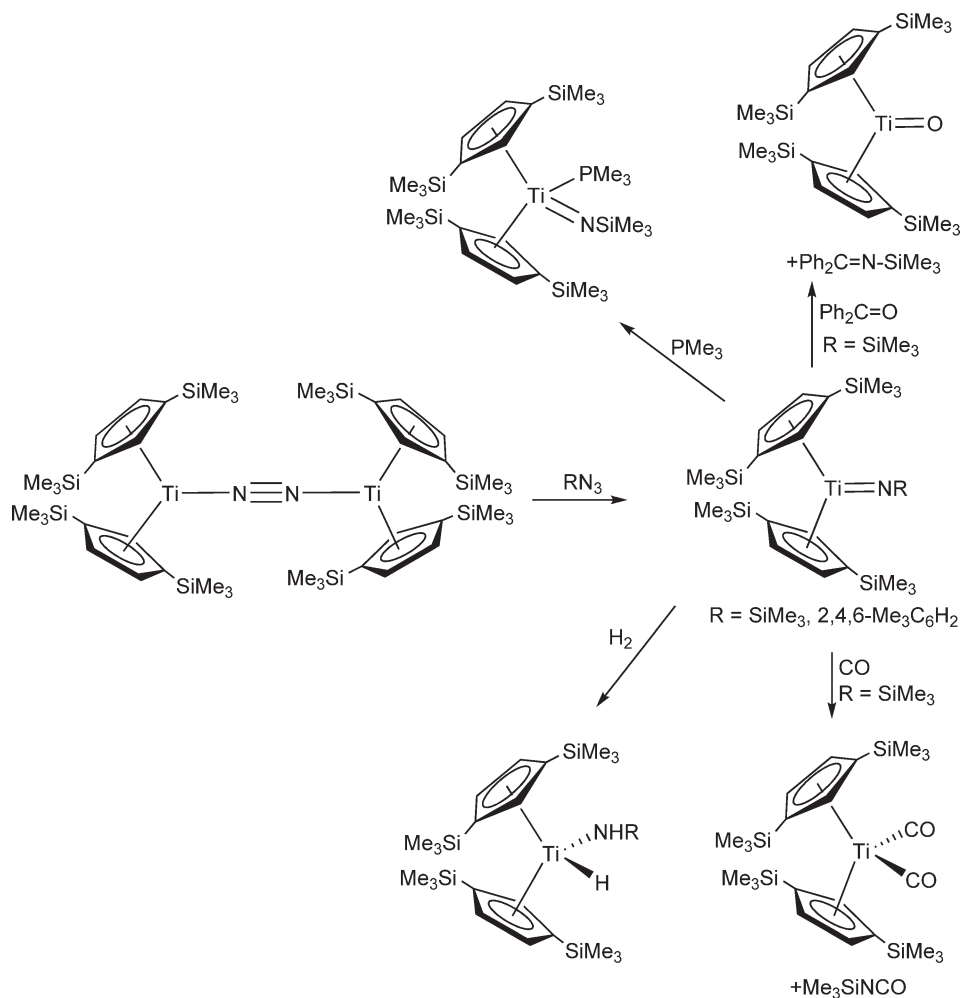
The metallaallene  $\text{Cp}^*_2\text{Ti}=\text{C}=\text{CH}_2$  generated by liberation of ethylene from the titanium cyclobutane  $\text{Cp}^*_2\text{Ti}[\text{C}(\text{=CH}_2)\text{CH}_2\text{CH}_2]$  (see Section 4.05.4.2.4.(i)) reacts with an excess of nitrile at high temperatures under insertion of two molecules to give  $\text{Cp}^*_2\text{Ti}[(\text{NCR})_2\text{C}=\text{CH}_2]$  (Scheme 575).<sup>1357</sup>

Group 4 transition metal–diene complexes possess unique M–C bonding properties and show high reactivity toward a broad range of electrophiles and unsaturated hydrocarbons. The 1-aza-1,3-diene bis-Cp complexes  $\text{Cp}_2\text{Ti}[\text{N}(\text{R}^1)\text{CH}=\text{C}(\text{R}^2)\text{CH}(\text{Ph})]$  (Scheme 576) have been prepared by addition of magnesium turnings to an equimolar mixture of  $\text{Cp}_2\text{TiCl}_2$  and the appropriate 1-aza-1,3-diene. The  $^1J_{\text{CH}}$  coupling constants of the terminal carbon atoms of the coordinated aza–diene ligands are considerably smaller than the usual values found for  $sp^2$ -hybridized carbon atoms and suggest  $sp^3$ -C atoms. The molecular structures of these compounds have been established by X-ray diffraction and show no interaction between the titanium atom and the unsaturated C–C bond of the ligand.<sup>594</sup> Reaction of  $\text{Cp}_2\text{TiCl}_2$  with 1 equiv. of Mg in the presence of 1,4-diaza-1,3-dienes (DAD) affords mononuclear titanium  $\text{Cp}_2\text{Ti}(\text{DAD})$  complexes (Scheme 577). Temperature-dependent NMR studies are carried out to estimate the energy barrier of the thermal-induced inversion of the folded diazametallacyclopentene rings and to identify rotameric isomers. Accordingly, mixtures of *meso*- and *rac*-rotamers are found.<sup>596</sup>

A series of mono- and bis-Cp and Ind titanium complexes containing  $\eta^5$ - and  $\eta^1$ -Cp or Ind ligands supported by phosphiniminato ligands have been described. The compound  $\text{CpTi}(\text{NPBu}^t_3)_2\text{Cl}_2$  reacts with  $\text{NaCp}(\text{DME})$  to give  $(\eta^5\text{-Cp})_2\text{Ti}(\text{NPBu}^t_3)\text{Cl}$  or  $(\eta^5\text{-Cp})_2\text{Ti}(\text{NPBu}^t_3)(\eta^1\text{-C}_5\text{H}_5)$ , depending on the stoichiometry (Scheme 578).<sup>645</sup>

The mixed bis-Cp' titanium compound  $\text{CpCp}^*\text{TiCl}_2$  reacts with 1 or 2 equiv. of  $\text{LiN}(\text{H})\text{NCPh}_2$ , in toluene at 78 °C, to give the hydrazonide(1-) derivatives  $\text{CpCp}^*\text{TiCl}[\text{N}(\text{H})\text{NCPh}_2]$  and  $\text{CpCp}^*\text{Ti}[\text{N}(\text{H})\text{NCPh}_2]_2$ , respectively, in high yield (Scheme 579). These hydrazonide compounds have been activated with MAO and are active in olefin polymerizations.<sup>670</sup>

The addition of aryldiazoalkanes to  $\text{Cp}^*_2\text{Ti}(\text{C}_2\text{H}_4)$  affords  $\eta^2$ - $\text{N}_2$ -aryldiazoalkane titanium complexes that undergo facile  $\text{N}_2$ -loss at room temperature or can be more thermally stable, depending on the nature of the diazoalkene substituent. Different reactivity pathways of these diazoalkane complexes have been studied. They unusually release dinitrogen thermally to give transient carbene complexes which may be trapped with styrene to form the titana-cyclobutane complexes  $\text{Cp}^*_2\text{Ti}(\text{CHArCHPhCH}_2)$ . A variety of reactions have been reported involving the retention of  $\text{N}_2$ . Reaction with  $\text{Bu}^t\text{NC}$  results in a coordination change of the diazoalkane fragment from  $\eta^2$  to  $\eta^1$  to give  $\text{Cp}^*_2\text{Ti}(\eta^1\text{-N}_2\text{CHPh})(\text{Bu}^t\text{NC})$ . Trineopentylaluminum coordinates to the terminal nitrogen atom on the diazoalkane fragment to form  $\text{Cp}^*_2\text{Ti}[\text{N}(\text{AlNp}_3)\text{N}(\text{C}(\text{H})\text{C}_6\text{H}_4\text{Me})]$ , as determined by X-ray crystallography. They undergo N–N

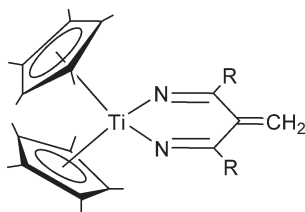


Scheme 574

bond cleavage when treated with CO to form an alkylideneimido isocyanato complex and silanes add across the Ti–N bond to give the (*E*)-isomers as the kinetic product and the (*Z*)-isomers as the thermodynamic product (Scheme 580). Kinetic and mechanistic studies of these reactions have been carried out. The regiochemistry of the reactions is determined by a combination of NMR techniques. The reactivity pattern of these compounds is analogous to that exhibited by complexes containing Ti=X multiple bonds suggesting that the bonding in these diazoalkane titanium complexes can be described as intermediate between an imido and an olefin adduct.<sup>1404–1406</sup>

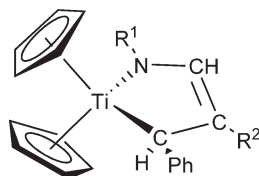
The reaction of  $\text{Cp}_2\text{Ti}(\eta^2\text{-Me}_3\text{SiC}_2\text{SiMe}_3)$  with 1,4-diazadienes  $\text{RN=CHCH=NR}$  affords 1-titana-2,5-diazacyclopent-3-ene complexes, while in the analogous reactions with differently substituted azines  $\text{R}_2\text{C=NN=CR}_2$  the products depend strongly on the substituents R. With R = Me, a substitution of the alkyne by the azine and a subsequent CH activation to the 1-titana-2,3-diazacyclopent-3-ene species is observed. When R = Ph, a paramagnetic binuclear Ti(III) complex is obtained from which the central C–C bond can be cleaved in a reaction with  $\text{CpCo}(\text{C}_2\text{H}_4)_2$ , followed by activation of the N–N bond of the azine and formation of the heterobimetallic complex  $\text{Cp}_2\text{Ti}(\mu\text{-N=CHPh})_2\text{CoCp}$ . If R = Ph, the central N–N single bond of the azine is cleaved and the bis(imido) complex  $\text{Cp}_2\text{Ti}(\text{N=CPh}_2)_2$  is isolated (Scheme 581).<sup>1473,1474</sup>

Reactions of  $\text{Cp}'_2\text{Ti}(\text{Me}_3\text{SiC}_2\text{SiMe}_3)$  ( $\text{Cp}' = \text{Cp}, \text{Cp}^*$ ) with triazine afford binuclear chelate complexes. Reactions with pyrazine display varied behavior and trinuclear and tetranuclear complexes are formed. The reaction with pyrimidine gives octanuclear complexes. C–C coupling reactions are observed in these reactions. Some molecular structures of these products have been determined by X-ray diffraction (Scheme 582).<sup>1514</sup>



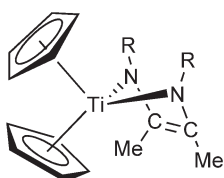
$R = \text{Bu}^t, \text{CHCHPh}$

Scheme 575



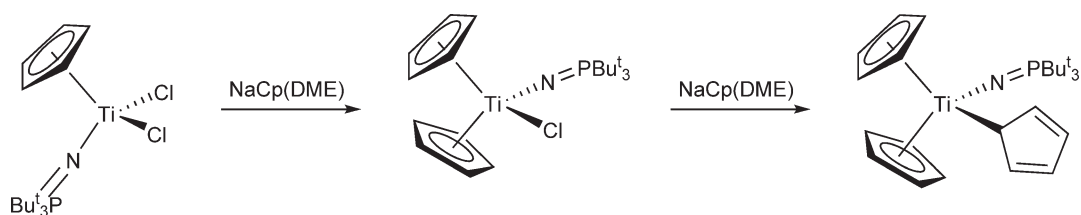
$R^1 = \text{Bu}^t, 4\text{-MeC}_6\text{H}_4; R^2 = \text{H}$   
 $R^1 = \text{cyclo-C}_6\text{H}_{11}; R^2 = \text{Me}$

Scheme 576

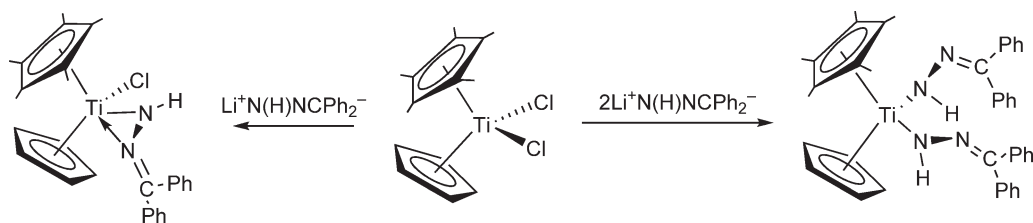


$R = \text{C}_6\text{H}_4\text{-2-Me}, \text{C}_6\text{H}_4\text{-4-Me}, \text{C}_6\text{H}_4\text{-4-OMe}, 1\text{-C}_{10}\text{H}_7$

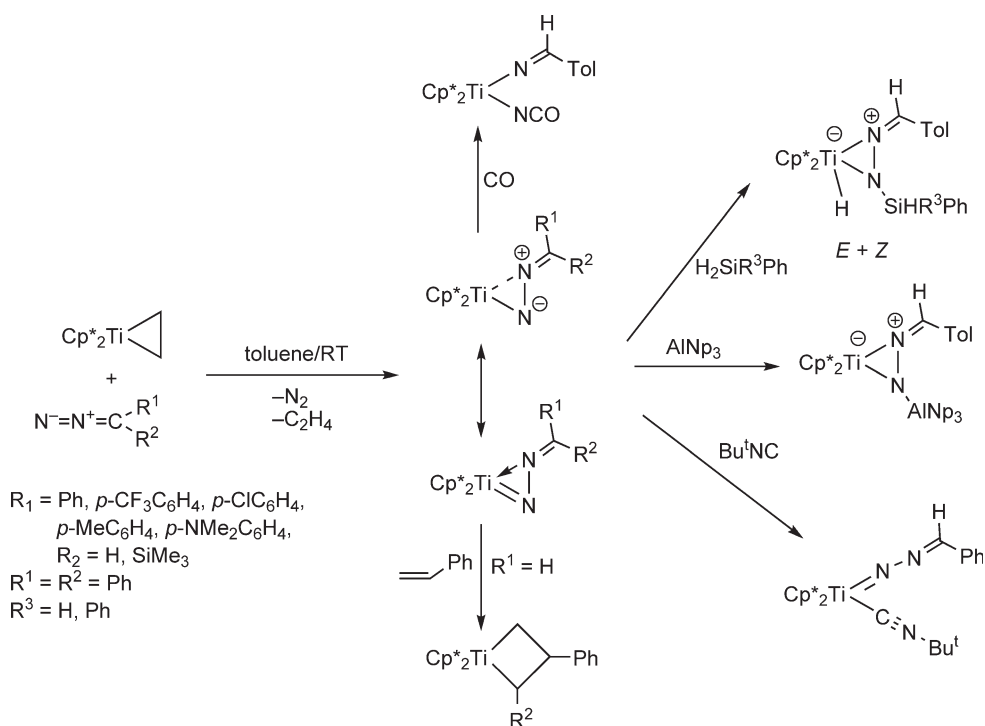
Scheme 577



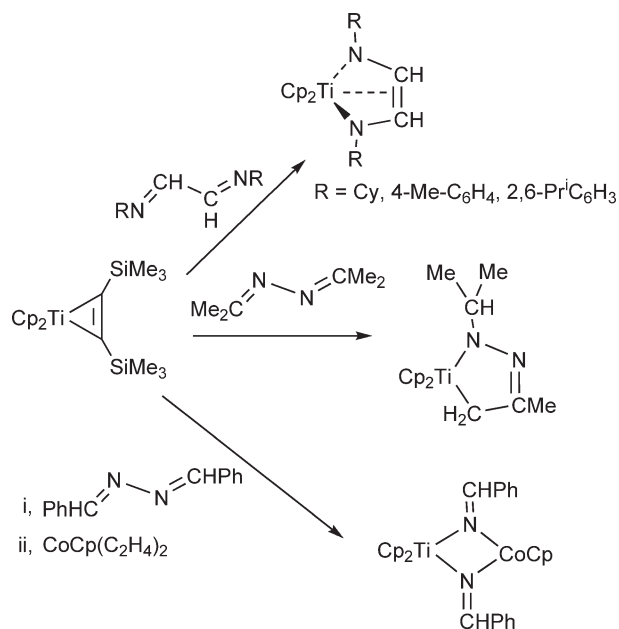
Scheme 578



Scheme 579

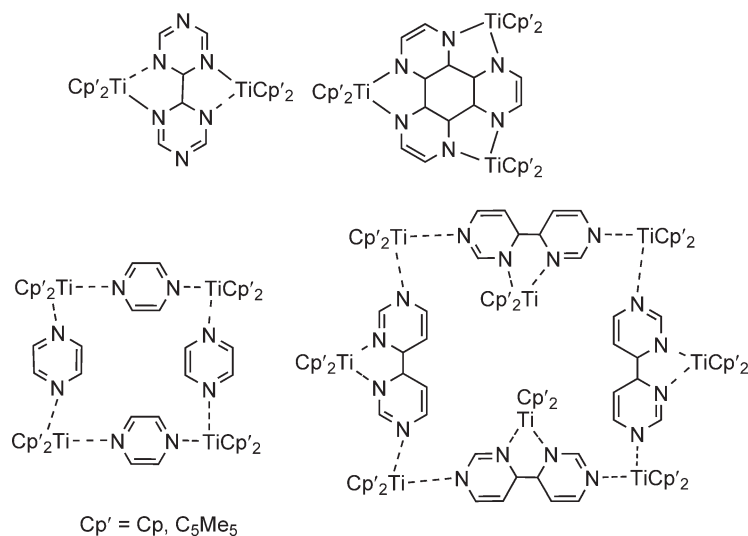


Scheme 580

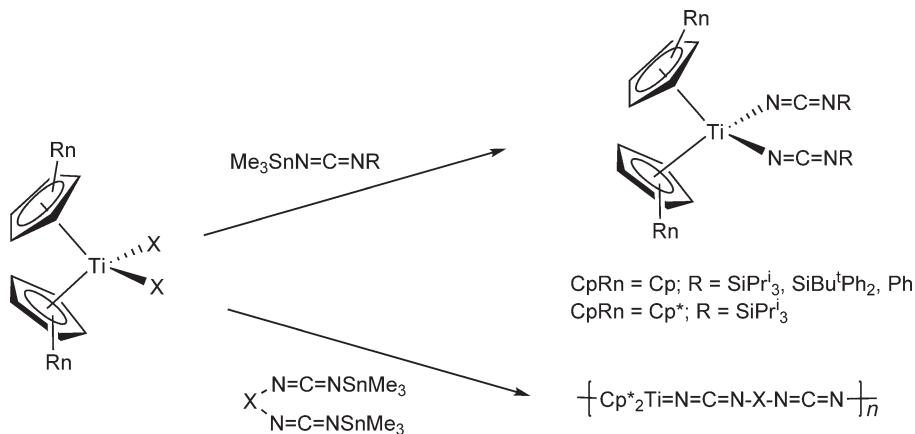


Scheme 581

Transmetallation reactions between  $\text{Me}_3\text{Sn}-\text{N}=\text{C}=\text{N}-\text{R}^1$  and  $\text{Cp}'_2\text{TiCl}_2$  ( $\text{Cp}' = \text{Cp}, \text{Cp}^*$ ) have been used to synthesize the bis(carbodiimido) titanium complexes  $\text{Cp}'_2\text{Ti}(\text{N}=\text{C}=\text{N}-\text{R}^1)_2$  in moderate to high yields, with selective reaction at the Sn-N bond. The structure of  $\text{Cp}_2\text{Ti}(\text{N}=\text{C}=\text{N}-\text{Ph})_2$  has been determined by X-ray crystallography. Treatment of  $\text{Cp}^*_2\text{TiCl}_2$  with  $\text{Me}_3\text{Sn}-\text{N}=\text{C}=\text{N}-\text{X}-\text{N}=\text{C}=\text{N}-\text{SnMe}_3$  produces oligomeric complexes (Scheme 583).<sup>1515</sup>

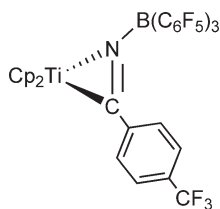


Scheme 582

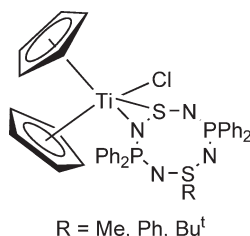


### Scheme 583

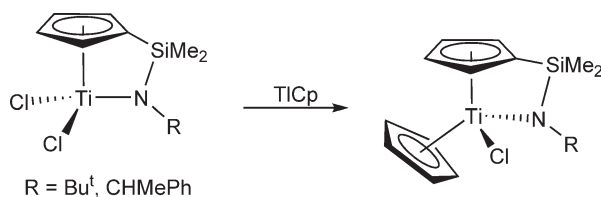
The synthesis of the titana–azirine complex  $\text{Cp}_2\text{Ti}[\eta^2\text{-C}_3\text{N-F}_3\text{CC}_6\text{H}_4\text{CN}\cdot\text{B}(\text{C}_6\text{F}_5)_3]$  (Scheme 584) by reaction of  $\text{Cp}_2\text{Ti}(\text{CO})_2$  with the borane adducts  $\text{CF}_3\text{C}_6\text{H}_4\text{CN}\cdot\text{B}(\text{C}_6\text{F}_5)_3$  has been described and its molecular structure has been determined by X-ray diffraction methods. The C–N nitrile bond is attached to Ti atom through two  $\sigma$ -type Ti–C and Ti–N bonds of 2.075(2) and 2.0940(18) Å, respectively. The C–N bond distance is typical of a C–N double bond. This result confirms the role of the borane reagent in activating a nitrile bond.<sup>1516</sup>



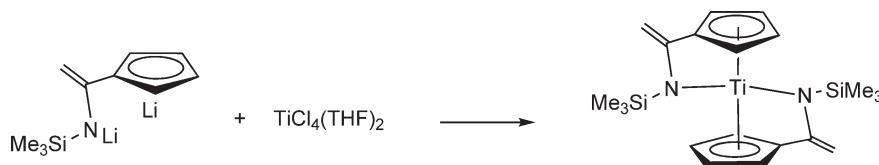
### Scheme 584



Scheme 585



Scheme 586



Scheme 587

The reaction of  $\text{Cp}_2\text{TiCl}_2$  with  $[\text{Li}(\text{Ph}_4\text{P}_2\text{N}_4\text{S}_2\text{R})/\text{THF}]_2$  ( $R = \text{Me, Ph, Bu}^t$ ) in deoxygenated THF produces complexes of the type  $\text{Cp}_2\text{TiCl}(\text{Ph}_4\text{P}_2\text{N}_4\text{S}_2\text{R})$  in which the heterocyclic ligand is  $\eta^2$ -N,S-bonded to the metal (Scheme 585).<sup>1517</sup>

The Si–Cl bond of the mixed bis-Cp complex  $(1,3\text{-Bu}^t_2\text{C}_5\text{H}_3)(\text{C}_5\text{H}_5\text{SiClMe}_2)/\text{TiCl}_2$  reacts selectively with 1 equiv. of  $\text{LiNHBU}^t$  in toluene at  $50\text{--}60^\circ\text{C}$  to give the amidosilyl–Cp substituted compound  $(1,3\text{-Bu}^t_2\text{C}_5\text{H}_3)(\text{C}_5\text{H}_5\text{SiMe}_2\text{NH}^t\text{Bu})\text{TiCl}_2$ , while the same reaction with 2 equiv. of the lithium amide gives the Cp/Cp–amido derivative  $(1,3\text{-Bu}^t_2\text{C}_5\text{H}_3)(\text{C}_5\text{H}_5\text{SiMe}_2\text{NBu})\text{TiCl}$  by reaction of the Si–Cl and one of the Ti–Cl bonds.<sup>1518</sup> Reaction of  $(\text{C}_5\text{H}_4\text{SiMe}_2\text{NR})\text{TiCl}_2$  ( $R = \text{Bu}^t, \text{CHMePh}$ ) with  $\text{TICp}$  affords the Cp/Cp–amido complexes  $\text{Cp}(\text{C}_5\text{H}_4\text{SiMe}_2\text{NR})\text{TiCl}$  (Scheme 586).<sup>581</sup>

The *spiro* bis-Cp–amido complex  $\text{Ti}[\text{C}_5\text{H}_4\text{C}(\text{=CH}_2)\text{N}(\text{SiMe}_3)]_2$  (Scheme 587) has been isolated in 81% yield by treatment of lithium [1-(lithio-N-trimethylsilylamido)ethenyl]cyclopentadienide with  $\text{TiCl}_4(\text{THF})_2$ .<sup>983</sup>

The molecular structure of the bis-Cp N,N-bis(cyclohexyl)-diazabuta-1,3-diene titanium complex has been determined by X-ray diffraction.<sup>1519</sup>

#### 4.05.4.5 Complexes with Schiff Bases and Heterocyclic Compounds

$\text{Cp}_2\text{TiCl}_2$  reacts with Schiff bases (SBH) to give a series of complexes  $\text{Cp}_2\text{TiCl}(\text{SB})$ , where  $\text{SB}^-$  is the anion of the Schiff base. Bis-Cp titanium complexes stabilized by the coordination of Schiff bases derived from 2-hydroxynaphthalene-1-carbaldehyde and 4-substituted anisidines or aniline,<sup>1520</sup> salicylidene-*o*-phenylenediamine, salicylidene-*p*-phenylenediamine, 2-hydroxynaphthalene-1-carbaldehyde-*o*-phenylenediamine, 2-hydroxynaphthalene-1-carbaldehyde-*p*-phenylenediamine,<sup>1521</sup> and 1,4-dihydrazinophthalazine<sup>1522</sup> have been reported. The resulting complexes have been characterized on the basis of their elemental analysis and IR, NMR, and electronic spectral studies. The chelate complexes  $\text{Cp}_2\text{Ti}(\text{SB})_2$ , where SB is salicylidene-4-methylaniline, have been synthesized and the course of thermal degradation of the compound studied by thermogravimetric (TG) and differential thermal analysis (DTA).<sup>1523</sup>  $\text{Cp}_2\text{TiCl}_2$  reacts with the Schiff bases derived from the condensation of salicylaldehyde with *o*-aminophenol or *o*-aminothiophenol in a non-aqueous medium to give ionic complexes of the type  $[\text{TiCp}_2\text{L}_2]\text{Cl}_2$



( $\text{L}$  = salicylidene-*o*-aminophenol, salicylidene-*o*-aminothiophenol). The complexes have been assigned square-pyramidal geometries.<sup>1524</sup>

The reactions of  $\text{Cp}_2\text{TiCl}_2$  with 4-amino-3-mercapto-6-methyl-5-oxo-1,2,4-triazine and its Schiff bases (derived from benzaldehyde, 2-chlorobenzaldehyde, anisaldehyde, salicylaldehyde, 2-hydroxynaphthaldehyde and 2-hydroxyacetophenone) have been studied in THF and  $\text{CH}_2\text{Cl}_2$  in the absence and presence of amine in different molar ratios.<sup>997</sup>

The reactions of  $\text{Cp}_2\text{TiCl}_2$  with a class of organometallic thiosemicarbazones (LH), derived by condensing acetylferrocene with substituted thiosemicarbazides or with Schiff bases (L), derived by the condensation of acetylferrocene with ethylenediamine, *o*-phenylenediamine, 4-methyl-*o*-phenylenediamine, 1,8-diaminonaphthalene, and 2,6-diaminopyridine, have been studied to give a type of bimetallic products  $\text{Cp}_2\text{TiClFe(L)}$ . Attempts have been made to establish a correlation between biological activity and the structures of the products.<sup>1525,1526</sup>

The Ti–Cp bond is cleaved by reaction of  $\text{Cp}_2\text{TiCl}_2$  with the lithium salt of Schiff base to give racemic complexes of titanium.<sup>1188</sup>

#### 4.05.4.6 Complexes with Ti–O Bonds

##### 4.05.4.6.1 Titanium oxo, hydroxo, and alkoxo complexes

The synthesis and reactivity of titanoxo units as fragments of transition metal Fischer carbene complexes have been reviewed.<sup>1349</sup> Other reviews have appeared covering structurally characterized organometallic hydroxo complexes of transition metals including mono- and bis-Cp titanium derivatives.<sup>809</sup>

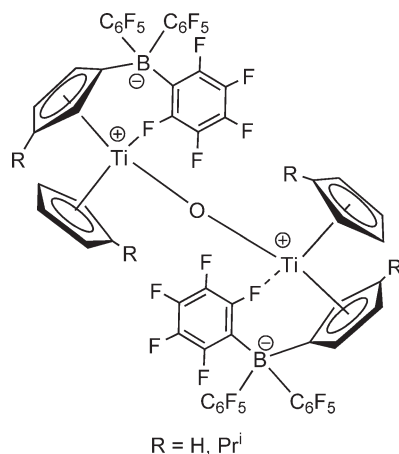
Addition of nitrous oxide to  $\text{Cp}^*_2\text{Ti}(\text{C}_2\text{H}_4)$  in a solution of 1:10 THF/pyridine results in the formation of a crystalline solid characterized as  $\text{Cp}^*_2\text{Ti}(=\text{O})(\text{py})$ . The  $\nu(\text{Ti}=\text{O})$  stretching frequency is observed at  $852\text{ cm}^{-1}$  in the IR spectrum. The molecular structure of the 4-phenylpyridine analog has been determined by X-ray diffraction and shows a Ti–O bond distance of  $1.665(3)\text{ \AA}$ .<sup>1527</sup>

Other structurally characterized oxo complexes are the Ti(IV)–Ti(III) titanate  $\text{Li}[\text{Cp}^*_2\text{Ti}(\text{C}\equiv\text{CSiMe}_3)_2\text{Ti}(\text{C}_5\text{Me}_5)_2\text{O}]$ <sup>1528</sup> and the binuclear azide complex  $[\text{Ti}_2\text{Cp}_4(\text{N}_3)_2](\mu\text{-O})$ .<sup>1510</sup> The oxygen-bridged selenocyanate  $[(\text{C}_5\text{H}_4\text{Me})_2\text{Ti}(\text{NCSe})_2](\mu\text{-O})$  is formed by air oxidation of  $(\text{C}_5\text{H}_4\text{Me})_2\text{Ti}(\text{NCSe})_2$ .<sup>1509</sup>

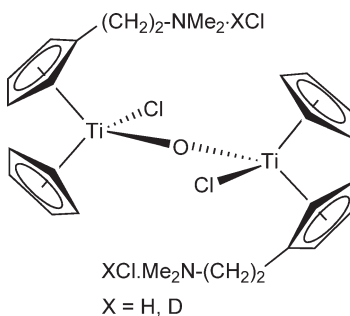
The reaction of  $\text{Cp}_2\text{TiCl}_2$  with KCN in a methanol/chloroform mixture gives  $\text{Cp}_2\text{Ti}(\text{CN})(\text{OCH}_3)$ . When the same reaction is carried out in wet methanol, the oxo-bridged cyano complex  $[\text{Cp}_2\text{Ti}(\text{CN})]_2(\mu\text{-O})$  is obtained. The structures of both compounds have been determined by X-ray crystallography.<sup>1529</sup> Analogous reactions have been described from  $\text{Cp}'_2\text{TiCl}_2$  ( $\text{Cp}' = \text{Cp}, \text{C}_5\text{H}_4\text{Me}$ ) in boiling methanol.<sup>1530</sup>

The binuclear titanium complex  $\text{Cp}_2\text{TiCl}(\mu\text{-O})\text{TiCl}(\text{acac})_2$  is formed by the reaction of  $\text{Cp}_2\text{TiCl}_2$  with 2 equiv. of 2,4-pentanedione in the presence of  $\text{NEt}_3$  in  $\text{CH}_3\text{CN}$  at room temperature. Its molecular structure has been determined by X-ray diffraction. On activation with  $\text{LiBu}^n$ , the compound catalyzes the reaction of phenylsilane with aldehydes to give O-silylation products.<sup>1531</sup>

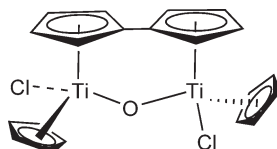
The air oxidation of the zwitterionic Ti(III) complexes  $\text{Cp}^i\text{Ti}[\text{C}_5\text{H}_4\text{B}(\text{C}_6\text{F}_5)_3]$  and  $(\text{C}_5\text{H}_4\text{Pr}^i)\text{Ti}[\text{1,3-C}_5\text{H}_3\text{Pr}^i\text{B}(\text{C}_6\text{F}_5)_3]$  affords the zwitterionic  $\mu\text{-oxo}$  Ti(IV) binuclear derivatives  $[\text{Cp}^i\text{Ti}[\text{C}_5\text{H}_4\text{B}(\text{C}_6\text{F}_5)_3]]_2(\mu\text{-O})$  and  $[(\text{C}_5\text{H}_4\text{Pr}^i)\text{Ti}[\text{1,3-C}_5\text{H}_3\text{Pr}^i\text{B}(\text{C}_6\text{F}_5)_3]]_2(\mu\text{-O})$  (Scheme 588).<sup>1532,1533</sup>



Scheme 588



Scheme 589



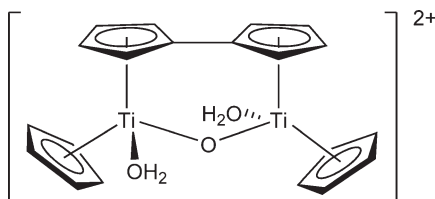
Scheme 590

The dichloro complex  $\text{Cp}[\text{C}_5\text{H}_4(\text{CH}_2)_2\text{NMe}_2]\text{TiCl}_2$  is exceedingly moisture sensitive and the hydrolysis product  $\{\text{Cp}[\text{C}_5\text{H}_4(\text{CH}_2)_2\text{NMe}_2\cdot\text{XCl}]\text{TiCl}\}_2(\text{O})$  ( $\text{X} = \text{H}, \text{D}$ ) is rapidly obtained (Scheme 589).<sup>372</sup> Hydrolysis of the fulvalene compound  $[\text{Cp}'\text{TiCl}_2]_2(\mu\text{-C}_{10}\text{H}_8)$  gives the  $\mu$ -oxo derivative  $[\text{Cp}'\text{TiCl}]_2(\mu\text{-C}_{10}\text{H}_8)(\mu\text{-O})$  (Scheme 590), the molecular structure of which has been determined by X-ray diffraction. A smaller  $\text{Ti}\text{--O}\text{--Ti}$  angle ( $159.4^\circ$ ) with significant deviation from linearity is observed.<sup>1080</sup>

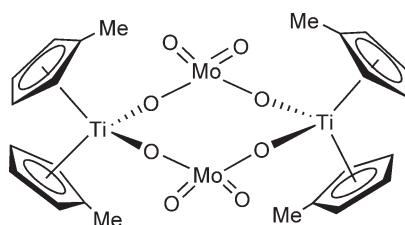
The ionic fulvalene titanium complex  $[\{\text{Cp}'\text{Ti}(\text{H}_2\text{O})\}_2(\mu\text{-C}_{10}\text{H}_8)(\mu\text{-O})]^{2+}[\text{OTf}^-]_2\cdot 1/2\text{THF}$  (Scheme 591) can be prepared as an air stable compound by the reaction of binuclear  $[\text{Cp}'\text{Ti}(\mu\text{-H})]_2(\mu\text{-C}_{10}\text{H}_8)$  with trifluoromethanesulphonic acid in the presence of small amounts of water. A reaction intermediate is  $[\text{TiCp}(\text{OTf})_2]_2(\mu\text{-C}_{10}\text{H}_8)$ . The molecular structure of the  $\mu$ -oxo aquo fulvalene complex has been confirmed by X-ray crystallography.<sup>1534</sup>

The binuclear complex  $(\text{Cp}'\text{TiCl})_2[(\text{C}_5\text{H}_4)_2\text{CH}_2]$  is converted to the  $\mu$ -oxo compound  $(\text{Cp}'\text{TiCl})_2[(\text{C}_5\text{H}_4)_2\text{CH}_2](\mu\text{-O})$  when exposed to air.<sup>1053</sup>

The electrochemical behavior, in non-aqueous solvents, of some mono- and bis- $\text{Cp}'$  oxo homo- and heteropolynuclear titanium derivatives containing oxo bridges between different metals is described (Scheme 592). Cyclic voltammetry, square wave voltammetry, and polarographic studies have been used to elucidate and compare the redox properties of these compounds.<sup>829</sup>



Scheme 591



Scheme 592

$\text{Cp}_2\text{TiCl}_2$  reacts with  $\text{NaOOBu}^t$  in THF at  $-20^\circ\text{C}$  to give the alkylperoxo Ti(IV) complex  $\text{Cp}_2\text{TiCl}(\text{OOBu}^t)$ , characterized by elemental analysis, NMR spectroscopy, mass spectrometry, and X-ray diffraction. The *tert*-butyl peroxy ligand is bound through only one oxygen. Mechanistic studies of its decomposition implicate O–O bond homolysis without change in the metal oxidation state.<sup>1535</sup>

Cp compounds of the group 4 elements containing achiral or chiral alkoxo or phenoxo ligands are attracting increasing attention as prominent catalytic reagents in organic reactions.

The molecular structure of  $\text{Cp}_2\text{TiCl}(\text{OMe})$  determined by X-ray diffraction has been published. The Ti–O–C bond angle of  $141.4(3)^\circ$  is significantly greater than the corresponding angle in the ethoxo complex analog, resulting in a shortened Ti–O bond and indicating greater  $\pi$ -character bond.<sup>1536</sup>

The synthesis of the complex  $\text{Cp}_2\text{Ti}(\text{OC}_6\text{H}_3\text{Pr}^i)_2\text{Cl}$  has been described. In combination with MAO, this compound effects the polymerization of ethylene.<sup>870</sup>

The reaction of  $\text{Cp}_2\text{TiCl}(\text{X})$  ( $\text{X} = \text{Cl}, \text{Me}$ ) with 2-methoxybenzyl alcohol in the presence of  $\text{NEt}_3$  under refluxing benzene gives the bis-Cp monoalkoxo derivatives  $\text{Cp}_2\text{Ti}(\text{X})(o\text{-OCH}_2\text{C}_6\text{H}_4\text{OMe})$  ( $\text{X} = \text{Cl}, \text{Me}$ ) (Scheme 593).<sup>890</sup>

Reaction of  $\text{Cp}_2\text{TiCl}_2$  with  $\text{Ph}_3\text{SiOH}$  in the presence of pyridine gives the  $\text{Cp}_2\text{TiCl}(\text{OSiPh}_3)$  compound, characterized by IR spectroscopy and X-ray crystallography.<sup>1537</sup>  $(\text{C}_5\text{H}_4\text{Me})_2\text{TiCl}_2$  reacts with  $\text{Bu}^t_2\text{Si}(\text{OH})_2$  in the presence of  $\text{NEt}_3$  resulting in the silanoxo complex  $(\text{C}_5\text{H}_4\text{Me})_2\text{TiCl}(\text{OSiBu}^t_2\text{OH})$ .<sup>881</sup> Reaction of the organic soluble  $\text{RSi}(\text{OH})_3$  [ $\text{R} = \text{N}(2,6\text{-Pr}^i_2\text{C}_6\text{H}_3)(\text{SiMe}_3)$ ] with  $\text{Cp}_2\text{TiCl}_2$  in dimethoxyethane as the solvent leads to the formation of  $\text{Cp}_2\text{TiCl}[\text{OSiR}(\text{OH})_2]$ , the molecular structure of which has been determined.<sup>1538</sup>

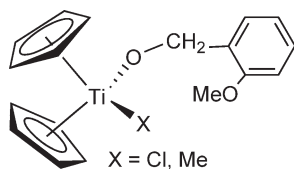
The condensation reaction of  $\text{CpFe}(\text{CO})_2(\text{CH}_2\text{SiMe}_2\text{OH})$  with  $\text{Cp}_2\text{TiCl}_2$  in toluene in the presence of  $\text{NEt}_3$  affords the heterosiloxane  $\text{Cp}(\text{CO})_2\text{Fe}-\text{CH}_2\text{SiMe}_2\text{O}-\text{TiCp}_2\text{Cl}$  (Scheme 594). The second Ti–Cl does not become involved in this reaction, in contrast to the behavior observed for the analogous zirconium derivatives.<sup>1539</sup> This difference in the reactivity between the analogous Ti and Zr derivatives has also been observed in the synthesis of siloxy–metal derivatives  $[\text{C}_5\text{H}_3(\text{SiMe}_3)_2]\text{TiCl}_3$  with hydroxysilsesquixane and terphenylsilanol.<sup>932</sup>

$\text{Cp}_2\text{Ti}(\text{OC}_6\text{H}_4\text{PPh}_2)_2$  is obtained when  $\text{Cp}_2\text{TiCl}_2$  reacts with the 2-(diphenyl-phosphino)phenol  $\text{HO}(\text{C}_6\text{H}_4)\text{PPh}_2$  in the presence of imidazole.<sup>1540</sup> The titanium and zirconium phenoxo complexes  $\text{Cp}_2\text{M}(\text{OAr})_2$  ( $\text{Ar} = \text{C}_6\text{H}_5$ , *p*- $\text{MeOC}_6\text{H}_4$ , *p*- $\text{MeC}_6\text{H}_4$ , *p*- $\text{ClC}_6\text{H}_4$ , *p*- $\text{CNC}_6\text{H}_4$ ) are shown to be stable and tunable precursors of dehydrocoupling silane catalysts.<sup>1541</sup>  $(\text{C}_5\text{H}_5\text{CH}_2\text{CH}_2\text{NPr}^i)_2\text{Ti}(\text{OPh})_2$  (Scheme 466; Section 4.05.4.1.1.(ii)) is obtained as an air stable yellow solid when the corresponding dichloro derivative reacts with 2 equiv. of lithium phenoxide. The dialkoxo compound catalyzes the dehydrogenative coupling of phenylsilane to oligosilanes in excellent yields.<sup>1094</sup>

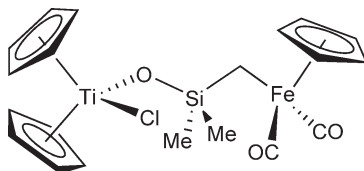
The complex  $(\text{C}_5\text{Me}_4\text{CH}_2\text{CH}_2\text{CH}=\text{CH}_2)\text{TiCl}_3$  has been used to synthesize the mixed bis-Cp compound  $\text{Cp}(\text{C}_5\text{Me}_4\text{CH}_2\text{CH}_2\text{CH}=\text{CH}_2)\text{TiCl}_2$  which is further converted into  $\text{Cp}(\text{C}_5\text{Me}_4\text{CH}_2\text{CH}_2\text{CH}=\text{CH}_2)\text{Ti}(\text{OTf})_2$ .<sup>347</sup>

Bis-Cp complexes with a chelating bis-phenoxo ligand,  $\text{Cp}^*_2\text{Ti}[(\text{OC}_6\text{H}_2\text{-4-Me-6-Bu}^t)_2\text{X}]$  ( $\text{X} = \text{CH}_2, \text{CH}_2\text{CH}_2, \text{S}, \text{O}$ ) have been studied as pre-catalyst for the polymerization of styrene in the presence of MAO.<sup>916</sup>

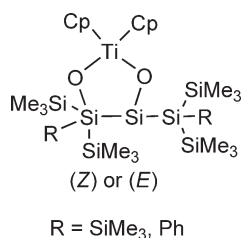
Cyclic bis-alkoxo complexes of the type  $\text{Cp}_2\text{Ti}(\text{O}-\text{O})$  have been synthesized by reacting  $\text{Cp}_2\text{TiCl}_2$  with  $\text{HO}-\text{OH}$  in the presence of sodium amide ( $\text{HO}-\text{OH}$  = substituted and unsubstituted dibasic phenols, biphenols, and binaphthols).<sup>1542</sup>



Scheme 593



Scheme 594



Scheme 595

(Z)- and (E)-isomers of complexes containing 2,5-dioxa-3,4-disilatitanacyclopentane five-membered rings (Scheme 595) can be prepared in high yields by reacting  $\text{Cp}_2\text{TiCl}_2$  with the appropriate diastereomerically pure diol. The crystal structures have been determined by X-ray diffraction.<sup>1543</sup>

Bis-Cp titanium binuclear complexes with trisiloxane bridges are synthesized. These complexes, in the presence of MMAO, initiate the polymerization of ethylene and styrene.<sup>938</sup>

$\text{Cp}_2\text{Ti}(\text{CO})_2$  reacts with 2 equiv. of  $\alpha,\beta$ -unsaturated ketones to yield the nine-membered titana-2,9-dioxacyclonona-3,7-dienes, which can be used for the selective synthesis of substituted cyclopentanols, diketones, or cyclopentenones. X-ray crystal structures and *ab initio* calculations have been reported.<sup>1544</sup>

Bis-Cp complexes containing silsesquioxane ligands with alkenylsilyl and trimethylsilyl substituted groups coordinated to the Ti atom have been synthesized by reaction of the silsesquioxane disilanol with  $\text{Cp}_2\text{TiCl}_2$ . Silsesquioxane groups bearing alkenylsilyl groups can be easily converted to derivatives with ethoxysilyl groups by the hydrosilylative reaction. The preliminary examination of the catalytic activity of these silsesquioxane derivatives toward the epoxidation of cyclohexene by *tert*-butyl hydroperoxide reveals a modest catalytic activity. The presence of alkenylsilyl groups has been found to accelerate the reactions.<sup>1545</sup>

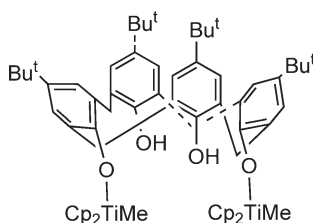
Reaction of  $\text{Cp}_2\text{TiCl}_2$  with premodified silica gel surfaces has been studied. The silica gel surface was pretreated to selectively eliminate non-hydrogen-bonded silanols, hydrogen-bonded silanols, or both before reaction. It has been found that the titanium compound reacts predominantly with the non-hydrogen-bonded silanols.<sup>1546</sup>

Reactions of Cp titanium complexes with calix[4]arene have been described.  $\text{Cp}_2\text{TiCl}_2$  reacts with alkali metal dianions formed by deprotonation of *p*-Bu<sup>t</sup>-calix[4]arene with the cleavage of one Cp ligand per titanium center to give a monocalixarene tetranuclear complex.<sup>922</sup> *p*-Bu<sup>t</sup>-calix[4]arene reacts with 1 or 2 equiv. of  $\text{Cp}_2\text{TiCl}_2$  with cleavage with both chloro and one Cp ligands.<sup>921</sup> A cleaner reaction is observed in the treatment of *p*-Bu<sup>t</sup>-calix[4]arene with the dimethyl complex  $\text{Cp}_2\text{TiMe}_2$ . Reaction of *p*-Bu<sup>t</sup>-calix[4]arene with 2 equiv. of  $\text{Cp}_2\text{TiMe}_2$  results in the 1,3-dimetallation of the calixarene in the cone conformation high yield by the selective cleavage of one Ti–Me group to give the binuclear titanium complex shown in Scheme 596.<sup>1547</sup>

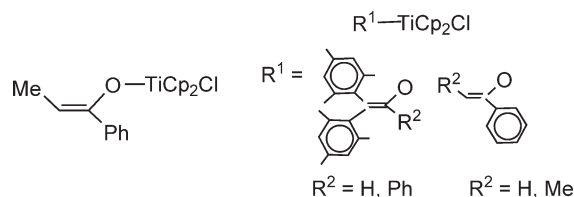
Titanium enolato complexes have been used as important synthetic carbon nucleophiles in stereoselective organic reactions. However, synthetic, structural, and characterization aspects of this type of complexes are rather scarce, because they are generally used *in situ* rather than in isolated form.

The bis-enolato  $\text{Cp}_2\text{Ti}[\text{OC}(\text{Ph})=\text{CHPh}]_2$  has been synthesized by reaction of  $\text{Cp}_2\text{TiCl}_2$  with the Li salt of the phosphinoenolate ligand. The complex reacts with platinum complexes to afford heterobimetallic derivatives.<sup>1548</sup>

The nucleophilic bis(enolato) complex  $\text{Cp}_2\text{Ti}(\text{OCMe}=\text{CH}_2)_2$  adds one or two molar equiv of the organometallic Lewis acid  $\text{B}(\text{C}_6\text{F}_5)_3$  to form the zwitterionic addition products  $\text{Cp}_2\text{Ti}(\text{OCMe}=\text{CH}_2)[\text{OCMe}=\text{CH}_2\text{B}(\text{C}_6\text{F}_5)_3]$  and  $\text{Cp}_2\text{Ti}[\text{OCMe}=\text{CH}_2\text{B}(\text{C}_6\text{F}_5)_3]_2$ , respectively. The molecular structure of the bis-adduct has been determined by



Scheme 596



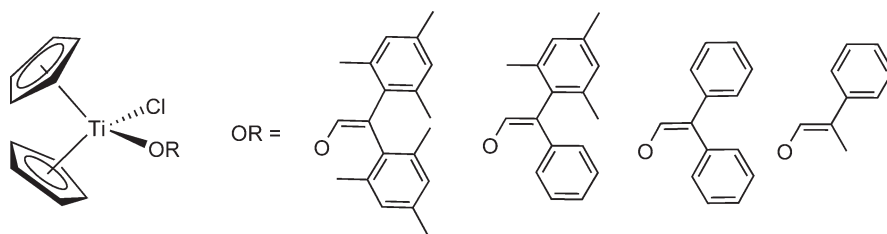
Scheme 597

X-ray diffraction. The bis(enolato) complex  $\text{Cp}_2\text{Ti}(\text{OCMe}=\text{CH}_2)_2$  in the presence of  $\text{B}(\text{C}_6\text{F}_5)_3$  serves as an initiator for the polymerization reaction of methyl vinyl ketone.<sup>1549</sup>

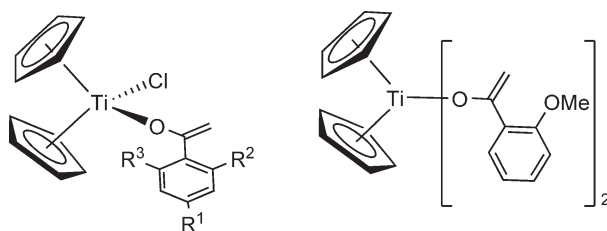
The titanium enolato complexes shown in Scheme 597 have been used to form intramolecular carbon–carbon bonds through diastereoselective enolate coupling reactions.<sup>1550</sup>

The formation of titanium enolato radical cations in solution and their reactions with  $\pi$ -nucleophiles to give direct carbon–carbon bond formation have been investigated. The stable bis-Cp chloro titanium enolato compounds shown in Scheme 598 have been synthesized in analytically pure form from the corresponding enol or carbonyl precursor by quantitative deprotonation with sodium hydride followed by reaction with  $\text{Cp}_2\text{TiCl}_2$  in THF at room temperature.<sup>1551–1553</sup> The structure and reactivity of these complexes and their radical cations have been studied from both a preparative and mechanistic point of view. Special attention is given to the M–O bond cleavage and the C–C coupling at the stage of the radical cations. The results have provided a novel selective oxidative coupling method for enolates and phenolates through an intramolecular variant.<sup>1554</sup>

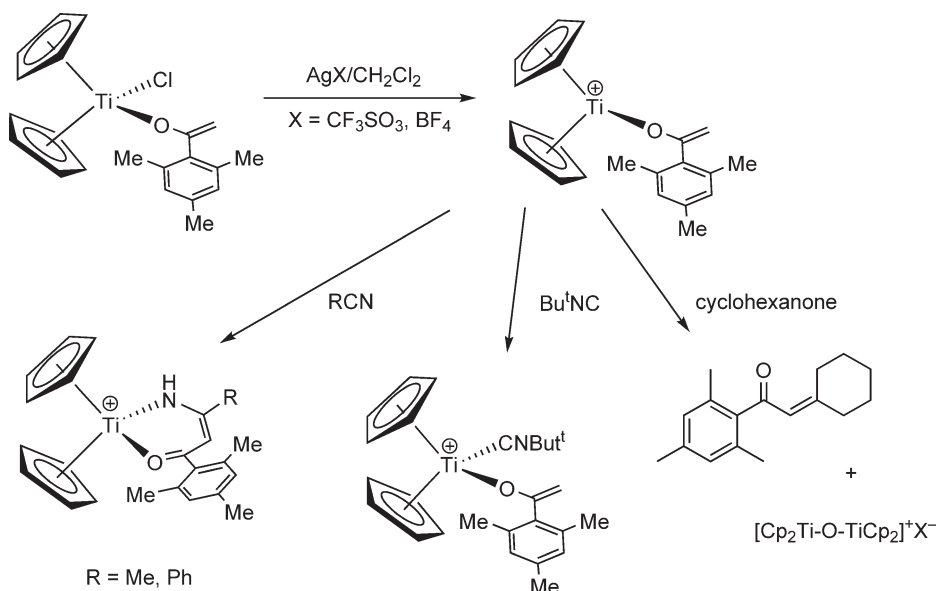
The use of 2-methoxy- or 2,4,6-trimethyl-acetophenone as the source of enolato ligands allows the synthesis of the titanium enolato compounds  $\text{Cp}_2\text{TiCl}[\text{OC}(\text{CH}_2)\text{C}_6\text{H}_2\text{R}_{3-2,4,6}]$  (Scheme 599) by reaction of  $\text{Cp}_2\text{TiCl}_2$  with the corresponding potassium enolate salts in molar ratio 1:1. The use of 2 equiv. of potassium enolate permits the formation of the bis-enolato  $\text{Cp}_2\text{Ti}[\text{OC}(\text{CH}_2)\text{C}_6\text{H}_4\text{OMe-2}]_2$  (Scheme 599).  $\text{Cp}_2\text{TiCl}[\text{OC}(\text{CH}_2)\text{C}_6\text{H}_2\text{Me}_{3-2,4,6}]$  is ionized with  $\text{AgO}_3\text{SCF}_3$  or  $\text{AgBF}_4$ , which increases the metal acidity. The cationic form readily reacts with cyclohexanone to give  $[2,4,6\text{-Me}_3\text{C}_6\text{H}_2\text{C}(\text{O})\text{-CH}=\text{C}_6\text{H}_{10}]$  and titanium oxo species. Reaction with  $\text{Bu}^t\text{NC}$  forms the adduct, while the reactions with acetonitrile and benzonitrile, where the binding of the nitrile prompts attack by the nucleophilic enolato on the nitrile, gives the  $\beta$ -keto enamine derivatives N,O-bonded to the  $[\text{Cp}_2\text{Ti}]^{2+}$  fragment (Scheme 600). The structures of some of these keto enamine derivatives have been determined by X-ray diffraction.<sup>1555</sup>



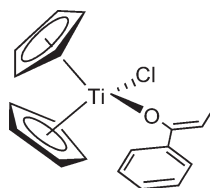
Scheme 598



Scheme 599



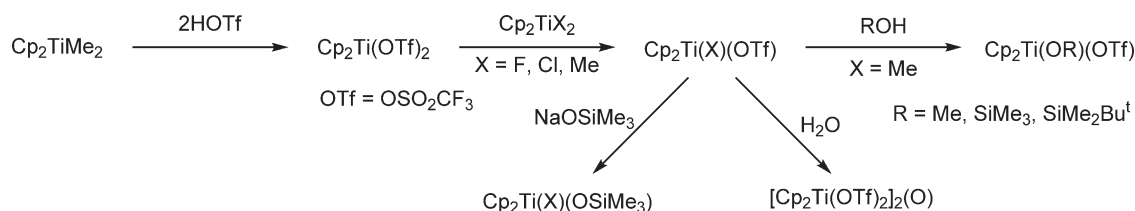
Scheme 600



Scheme 601

The oxidation of titanium enolato complexes, derived from a transmetalation reaction of the corresponding lithium enolates with  $\text{Cp}_2\text{TiCl}_2$ , by dimethyldioxirane has been investigated as a general, convenient, effective, and chemo- and diastereoselective synthesis of  $\alpha$ -hydroxy carbonyl compounds. The Cp derivative shown in [Scheme 601](#) results in much higher diastereoselectivities than other enolato complexes studied.<sup>1556</sup>

The synthesis and reactivity of bis-Cp' titanium triflates (OTf) have been described. Triflate can be used as a substitute for chloro ligands in metathesis reactions. The bis-triflate  $\text{Cp}_2\text{Ti}(\text{OTf})_2$  is easily accessible from  $\text{Cp}_2\text{TiMe}_2$  and HOTf. Comproportionation reactions between  $\text{Cp}_2\text{Ti}(\text{OTf})_2$  and  $\text{Cp}_2\text{TiX}_2$  ( $\text{X} = \text{F}, \text{Cl}, \text{Me}$ ) give the mixed ligand complexes  $\text{Cp}_2\text{Ti}(\text{X})(\text{OTf})$ . The compounds  $\text{Cp}_2\text{TiMe}(\text{OTf})$  and  $\text{Cp}_2\text{Ti}(\text{OSiMe}_3)(\text{OTf})$  react with  $\text{H}_2\text{O}$  to give the oxo-bridged dimer  $[\text{Cp}_2\text{Ti}(\text{OTf})_2]_2(\mu\text{-O})$ , while  $\text{NaOSiMe}_3$  reacts in general with monotriflate compounds with substitution of triflate ([Scheme 602](#)).<sup>1557</sup> The compound  $\text{Cp}^*_2\text{TiCl}(\text{OTf})$  has been isolated and characterized by X-ray diffraction during attempts to construct Ti-vinyl cations  $[\text{Cp}^*_2\text{Ti}(\text{CH}=\text{CH}_2)]^+$  from  $\text{Cp}^*_2\text{Ti}[\text{C}(\text{CH}_2)=\text{CH}_2\text{CH}_2]$  in the reaction with  $\text{CF}_3\text{SO}_3\text{H}$ .<sup>1289</sup>  $\text{Cp}_2\text{Ti}(\text{OTf})_2$  and related chiral titanium complexes have been used as Lewis acid catalysts for organic reactions.<sup>1558</sup>



Scheme 602

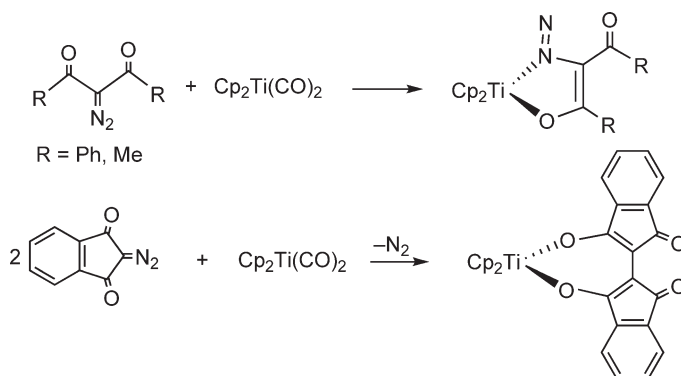
The complex  $\text{Cp}_2\text{Ti}(\text{OTf})_2$  induces [3 + 2]-nitron-olefin cycloaddition reactions by a concerted process. The reaction proceeds via the intermediate  $[\text{Cp}_2\text{Ti}(\text{nitron})_2]^{2+}$ . The crystal structure of one of these adducts is reported. Asymmetric induction has been observed when the chiral *ansa*-compound (*S,S*-cyclacene)/ $\text{Ti}(\text{OTf})_2$  (Scheme 655; Section 4.05.5) is used as catalytic species.<sup>1559</sup>

The complex  $[\text{Cp}^*_2\text{Ti}(\text{H}_2\text{O})_2](\text{CF}_3\text{SO}_3)_2$  is an efficient catalyst for the Diels–Alder reaction even when water is present, while  $\text{Cp}_2\text{Ti}(\text{CF}_3\text{SO}_3)_2$  is an efficient catalyst for the Diels–Alder and Mukaiyama reactions<sup>1560</sup> as well as for a variety of reactions between allylic silanes and orthoesters, acetals, ketals, aldehydes, and ketones for the Sakurai reaction.<sup>1561</sup>

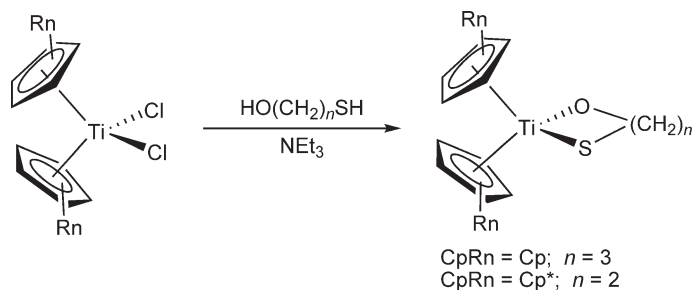
$\text{Cp}_2\text{Ti}(\text{CO})_2$  reacts with acyclic aliphatic or aromatic 2-diazo-2,3-diketones with evolution of 2 equiv. of CO and formation of O,N-chelating complexes. The same reaction with bicyclic 2-diazoindane-1,3-dione proceeds with elimination of  $\text{N}_2$  to give the seven-membered 1-titana-2,O-heterocyclic complex (Scheme 603).<sup>828</sup>

Dichloro substituted bis-Cp' titanium compounds react with  $\text{HO}(\text{CH}_2)_n\text{SH}$  in the presence of  $\text{NEt}_3$  to give the monomeric chelate complex  $\text{Cp}'_2\text{Ti}[\text{O}(\text{CH}_2)_n\text{S}]$  (Scheme 604). A slightly different behavior is observed for the analogous reaction with zirconium.<sup>1562,1563</sup>

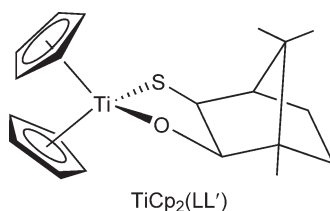
A bis-Cp compound with a chiral heterodifunctional ligand derived from (+)-camphor (Scheme 605) containing oxygen and sulfur donor atoms has been prepared by the reaction of  $\text{Cp}_2\text{TiCl}_2$  with the corresponding diprotonated



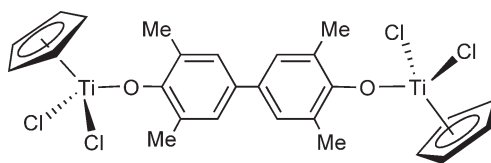
Scheme 603



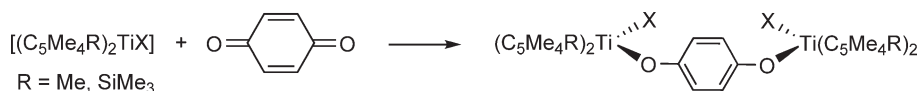
Scheme 604



Scheme 605



Scheme 606



Scheme 607

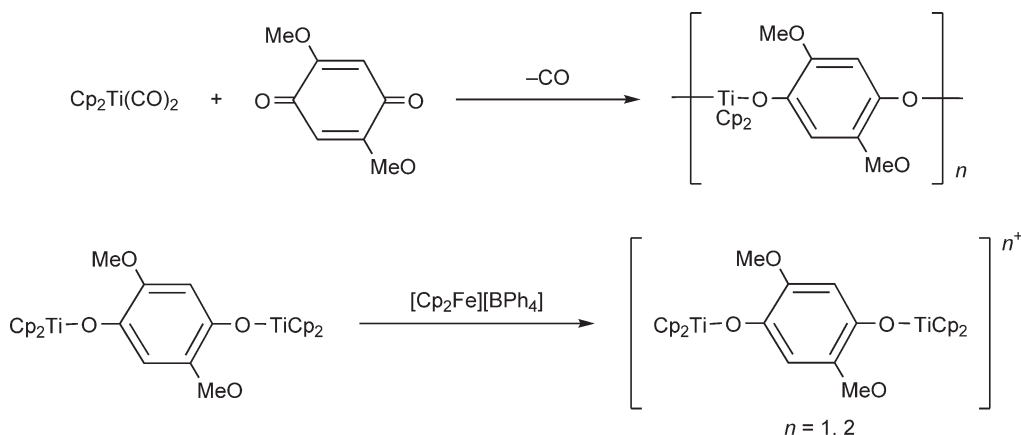
molecule in the presence of triethylamine. This complex decomposes either in the solid state or in solution to give a mixture of several unidentified products.<sup>1564</sup>

Cp<sub>2</sub>TiCl<sub>2</sub> reacts with the 4,4'-biphenol Me<sub>4</sub>BIPOH<sub>2</sub> bearing methyl substituents in the 3,3',5,5'-positions to give the binuclear complex (Cp<sub>2</sub>TiCl)<sub>2</sub>(Me<sub>4</sub>BIPO) (Scheme 606).<sup>1565</sup> Compounds structurally characterized as Cp'<sub>2</sub>XTi-OC<sub>6</sub>H<sub>4-n</sub><sup>t</sup>Bu<sub>n</sub>O-TiXCp'<sub>2</sub> shown in Scheme 607 have been synthesized by the reaction of Cp'<sub>2</sub>TiCl<sub>2</sub> with hydroquinones. Such compounds are also formed upon treatment of titanium(III) precursors with benzoquinone. The structure of [Cp'<sub>2</sub>TiCl]<sub>2</sub>(μ-OC<sub>6</sub>H<sub>4</sub>O) has been solved by X-ray diffraction.<sup>923</sup> The bimetallic and trimetallic complexes [Cp'<sub>2</sub>TiX]<sub>2</sub>(μ-1,4-O<sub>2</sub>(C<sub>6</sub>H<sub>2</sub>Me)) and [Cp'<sub>2</sub>TiX]<sub>3</sub>(μ<sub>3</sub>-1,3,5-C<sub>6</sub>H<sub>3</sub>O<sub>3</sub>) have been synthesized (Scheme 388; Section 4.05.3.5.2). In these complexes the Ti atom is linked to a benzene core through oxo groups.<sup>924</sup>

The 2,5-dimethoxy-1,4-benzoquinone undergoes two-electron reduction in the reaction with Cp<sub>2</sub>Ti(CO)<sub>2</sub> at 60–70 °C to give the alkoxo complex [Cp<sub>2</sub>Ti(C<sub>8</sub>H<sub>8</sub>O<sub>3</sub>)]<sub>n</sub>. The bimetallic Ti(III) complex (Cp<sub>2</sub>Ti)<sub>2</sub>{O<sub>2</sub>C<sub>6</sub>H<sub>2</sub>(OMe)<sub>2</sub>} undergoes one- or two-electron oxidations to afford cationic complexes of the general formula [(Cp<sub>2</sub>Ti)<sub>2</sub>(C<sub>8</sub>H<sub>8</sub>O<sub>4</sub>)]<sup>n+</sup> (n = 1, 2) isolated as the tetraphenylborate salts (Scheme 608).<sup>1566</sup>

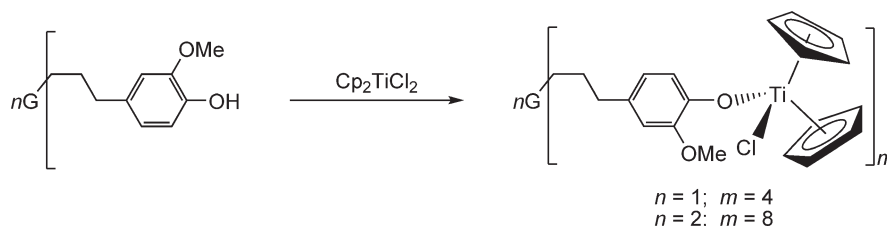
Reactions of Cp<sub>2</sub>TiCl<sub>2</sub> with dendrimers of first, second, or fourth generations afford the corresponding organometallic titanium dendrimers (Scheme 609). The dendritic framework remains chemically inert and spectroscopically insensitive to changes in the periphery, while the organometallic units show spectroscopic and chemical properties similar to the mononuclear counterparts.<sup>927</sup>

Bis-Cp' complexes containing chelating Cp-alkoxo rings have been described. Benzyl-substituted and MeO-containing benzyl-substituted Cp titanium complexes of the type shown in Scheme 444, Section 4.05.4.1.1.(i).(b) have been prepared. The *o*-MeO-benzyl-substituted derivatives cyclized with the elimination of MeCl to give titanoxacyclic complexes when ethyl or larger groups are present on the benzyl fragment. Titanoxacyclic complexes can be formed from bis-Cp' dihalide derivatives containing methoxy-phenyl-substituted

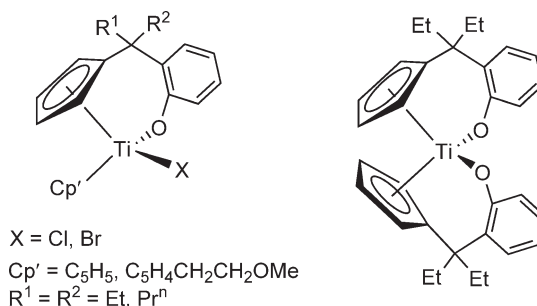


Scheme 608

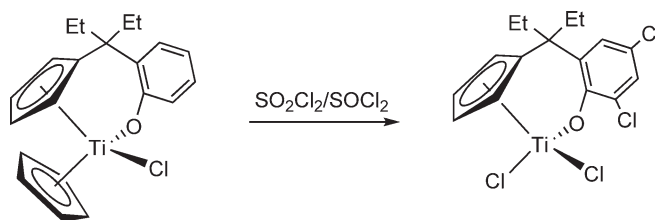




Scheme 609



Scheme 610



Scheme 611

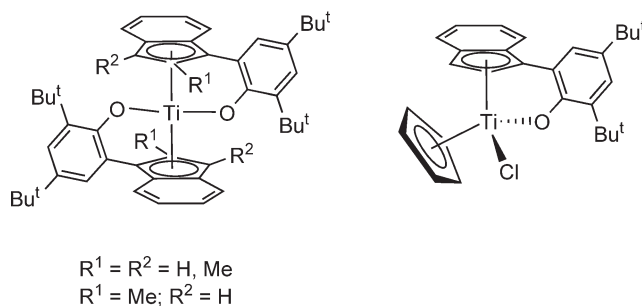
$\text{Cp}$  ligands via multiple bond cleavage of  $\text{Me-O}$  and  $\text{Ti-halide}$  bonds (Scheme 610). The reaction is promoted by  $\text{LiBr}$ <sup>1567</sup> or  $\text{BBR}_3$ . The crystal structures of some of these complexes and of related benzyl-substituted  $\text{Cp}$  complexes have been reported. Mechanistic studies suggest a two-step mechanism; the first step involves halogen  $\text{Cl-Br}$  interchange and the second step an intramolecular elimination.<sup>814,815,1568</sup> Chlorination of these complexes by  $\text{SO}_2\text{Cl}_2/\text{SOCl}_2$  has been studied (Scheme 611). The chlorination of the unsubstituted  $\text{Cp}$  derivative with  $\text{SO}_2\text{Cl}_2$  is carried out more easily than substituted  $\text{Cp}$  complexes, with replacement of the  $\text{Cp}$  group by a chloro ligand and chlorination of the benzene ring.<sup>1569</sup>

The reactions of 2 equiv. of 2-(inden-3-yl)-4,6-di-*tert*-butylphenol and its methyl-indenyl analogs with  $\text{Ti}(\text{NMe}_2)_4$  proceed with deprotonation at both the phenolic  $\text{OH}$  and the indenyl ring, leading to the elimination of dialkylamine and the introduction of two chelating indenyl-phenoxo ligands. Metathetical exchange of the dilithium salt of the indenyl phenol with  $\text{TiCl}_4$  affords the same products (Scheme 612). The combination of the three chiral elements (two planar chiral indenyl rings and an axially chiral metal center) generates distinct diastereoisomers, according to spectroscopic evidence. Two forms have been structurally characterized.<sup>984</sup> The analogous mono- $\text{Cp}$  indenyl-phenoxo chloro compound can be prepared by treatment of  $\text{CpTiCl}_3$  with the dilithium salt of the indenyl phenol (Scheme 612).<sup>852</sup>

#### 4.05.4.6.2 Complexes with other O-based ligands

The coordination chemistry of  $\text{Cp}$  titanium carboxylates and related complexes has been reviewed. The synthetic methods, structural characteristics, coordination modes, and reactivities are covered.<sup>1570</sup>

$\text{Cp}_2\text{TiCl}_2$  reacts with sodium acetyl salicylate or sodium salicylate in dry benzene to give bis- $\text{Cp}$  diaspirin and disalicylate titanium(IV) complexes.<sup>1571</sup> The molecular structure of  $\text{Cp}_2\text{Ti}(\text{sal})$  containing the dianionic salicylato



Scheme 612

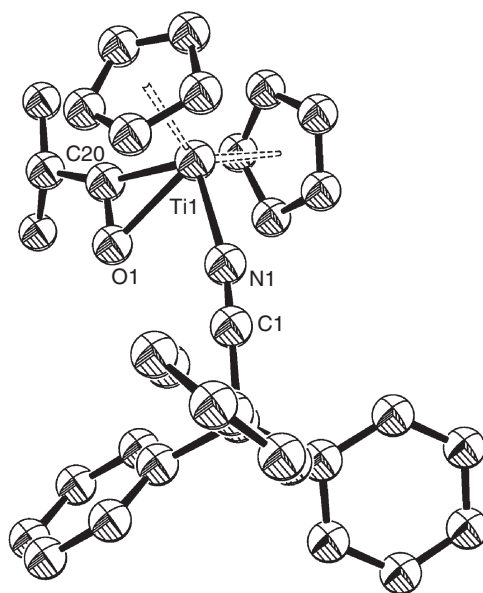
ligand  $\text{sal} = \text{O}_2\text{CC}_6\text{H}_4\text{O}^{2-}$  has been re-examined. The X-ray structure determination confirmed the chelating nature of the salicylato ligand which is bonded to the metal through the phenolic and one of the carboxylato oxygen atoms. New 3,5- $\text{Bu}^t$ -salicylato analog complexes have been prepared and characterized.<sup>1572</sup>

Reactions of  $\text{Cp}_2\text{TiCl}_2$  in aqueous solutions or two-phase systems have been developed for the preparation of bis-Cp diphenoxo and salicylato titanium complexes.<sup>1189,1190</sup> Different bis-Cp salicylato titanium complexes have been prepared in a  $\text{H}_2\text{O}/\text{CHCl}_3$  mixture in a two-phase reaction. Mechanistic studies have been carried out to conclude that the interfacial reaction seems to be similar to the mechanism in an ion reaction.<sup>1191–1193</sup>

An interfacial method for the synthesis of bis-Cp titanium complexes with bulky substituted benzoic acids has been reported.<sup>1573</sup>  $\text{Cp}_2\text{TiCl}_2$  and  $\text{Cp}_2\text{TiPh}_2$  react with molecular carboxylic acids and co-polymers bearing carboxylic acid groups to give linear, soluble co-polymers containing titanium, which are of interest for use in targets for inertial-confinement fusion (ICF) experiments; these complexes are useful as spectroscopic probe for studying the nuclear fusion process.<sup>1574</sup>

The molecular structure of the bis-formato compound  $\text{Cp}_2\text{Ti}(\text{HCO}_2)_2$  has been determined; the Ti–O–C bond angles are larger and the Ti–O bond lengths are longer than those in related alkoxides.<sup>1575</sup>

The synthesis and X-ray crystal structure determination of the cationic acyl complex  $\text{Cp}_2\text{Ti}(\eta^2\text{-COPr}^i\text{-[NC-B(C}_6\text{H}_5)_3])$  has been described. In the  $^{13}\text{C}$  NMR spectrum, the acyl carbon exhibits an unusual highly deshielded chemical shift of  $\delta$  340.4, consistent with carbenoid character. The complex is pentacoordinated and zwitterionic, with the nitrogen atom of the  $[\text{NC-B(C}_6\text{H}_5)_3]^-$  anion bound to titanium. (Figure 29).<sup>1576</sup>



**Figure 29** Molecular structure of complex  $\text{Cp}_2\text{Ti}(\eta^2\text{-COPr}^i\text{-[NC-B(C}_6\text{H}_5)_3])$  (reproduced by permission of Elsevier from *J. Organomet. Chem.*, 1996, 516, 11).

A series of salts  $[\text{Cp}_2\text{TiL}]^+\text{X}^-$  ( $\text{X}^- = \text{Cl}^-, \text{I}^-, \text{Br}^-, \text{ClO}_4^-, \text{ZnCl}_3^-, \text{CdCl}_4^{2-}, \text{HgCl}_3^-, \text{FeCl}_4^-$ ) where HL = 2,3-dihydroxypyridine and 2-amino-3-hydroxypyridine have been synthesized and characterized.<sup>1577</sup> These complexes react with dithiocarbamates resulting in the isolation of ionic dithiocarbamate salts.<sup>1578</sup> The behavior of xanthate salts of bis-Cp Ti(IV) 2,3-dihydroxypyridine and 2-amino-3-hydroxypyridine chelate derivatives has been studied by polarography.<sup>1579</sup>

Bis-Cp titanium amino acid complexes have been synthesized in an aqueous medium by the reaction of  $\text{Cp}_2\text{TiCl}_2$  with the sodium or potassium salts of the corresponding amino acids, or in non-aqueous media by the reaction of  $\text{Cp}_2\text{TiCl}_2$  with the amino acids in the presence of  $\text{NEt}_3$ . It has been found that in an aqueous medium the reaction is faster, and the product yields are higher.<sup>1580</sup>

Reactions of silver(I) or sodium cyanoacetates with  $\text{Cp}_2\text{TiCl}_2$  afford the bis(cyanoacetato) complex  $\text{Cp}_2\text{Ti}(\text{O}_2\text{CCH}_2\text{CN})_2$ . The molecular structure shows O-unidentate carboxylate groups; the cyano–nitrogen atom is not bonded to the metal. This compound can alternatively be prepared from  $\text{Cp}_2\text{TiMe}_2$  and cyanoacetic acid.<sup>1581</sup>

$\text{Cp}_2\text{TiMe}_2$  reacts selectively with a variety of dialkyltartrates with protonolytic cleavage of one of its Ti–Me bonds to form the respective binuclear  $[\text{Cp}_2\text{TiMe}]_2(\mu\text{-tartrato})$  complexes. The complexes were characterized by X-ray crystal structure analyses. A comparison of the characteristic structural parameters are indicative of an increased metal–oxygen  $\pi$ -interaction in the order  $\text{Ti} < \text{Hf} < \text{Zr}$ , which may explain the different chemical behavior observed in this series of compounds.<sup>1582</sup>

A series of titanium chelate complexes with biologically active monofunctional bidentate semicarbazones having O,N donors have been prepared by reacting  $\text{Cp}_2\text{TiCl}_2$  with the appropriate ligand in 1:1 and 1:2 stoichiometries. The ligands were prepared by condensing heterocyclic ketones and semicarbazide hydrochlorides in presence of NaOAc.<sup>1583</sup>

The reactions of  $\text{Cp}_2\text{TiCl}_2$  with 2,6-diacetylpyridine-bis(S-alkylisothiosemicarbazones) give bis-Cp complexes with isothiosemicarbazone ligands coordinated to the titanium atom which contain terminal free amino groups. Reactions of these derivatives with  $\beta$ -diketones have been carried out to afford cyclic complexes.<sup>1584</sup>

The molecular structure of the ionic complexes  $[\text{Cp}_2\text{Ti}(\text{L-Met})_2]\text{Cl}_2$ <sup>1585</sup> and  $[(\text{C}_5\text{H}_4\text{Me})_2\text{Ti}(\text{N-Me-gly})]_2\text{Cl}_2$  have been determined by X-ray diffraction.<sup>988</sup>

Coordination of the “ $\text{Cp}_2\text{Ti}$ ” fragment to a mesoporous aluminophosphate (Scheme 613) has been described and the bonding of the Ti(IV) centers has been studied.<sup>994</sup>

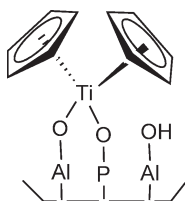
#### 4.05.4.7 Complexes with Ti–Si Bonds

$\text{Cp}_2\text{Ti}(\text{PMe}_3)_2$  reacts with  $\text{SiH}_2\text{Ph}_2$  to give  $\text{Cp}_2\text{Ti}(\text{SiH}_2\text{Ph}_2)(\text{PMe}_3)_2$ . The molecular structure shows short Ti–Si and long Si–H distances which, together with the low Si–H NMR coupling constants, indicate that this compound is best described as a titanium(IV) silyl hydride than a titanium(II) silane complex.<sup>1586</sup> The closely analogous compound  $\text{Cp}_2\text{Ti}(\text{SiH}_3\text{Ph})(\text{PMe}_3)_2$  has been made from  $\text{Cp}_2\text{Ti}(\text{PMe}_3)_2$  and  $\text{SiH}_3\text{Ph}$ .<sup>1587</sup>

The bis-Cp derivatives  $\text{Cp}_2\text{Ti}(\text{HSiR}_3)(\text{PMe}_3)$  ( $\text{SiR}_3 = \text{SiCl}_3, \text{SiMeCl}_2, \text{SiPh}_2\text{Cl}, \text{SiMePhCl}$ ) have been prepared by the addition of  $\text{SiHR}_3$  to  $\text{Cp}_2\text{Ti}(\text{PMe}_3)_2$ . Spectroscopic and structural features, supported by DFT theoretical calculations, establish that these compounds are  $\sigma$ -silane complexes. They exhibit silicon–hydride coupling constants  $J(\text{Si–H})$  in the range of 22–40 Hz. The  $\text{Cp}_2\text{Ti}(\text{PMe}_3)$  fragment seems to be unique in supporting this type of compounds.<sup>1588</sup>

#### 4.05.4.8 Complexes with Ti–Chalcogenide Bonds

The chemistry of organometallic Ti(IV) chalcogenides and hydrochalcogenides has attracted interest due to their nature of bonding and conformational aspects, their potential applications for the synthesis of organic molecules



Scheme 613

containing heteroatoms, or their anti-tumor activity. Of special interest is the synthesis of disulfido and diselenido titanium derivatives with potential applications in the formation of heterobimetallic complexes in order to probe mutual electronic and chemical effects between the metal centers held in close proximity. Hydrosulfido complexes are potentially valuable for the understanding of metal–sulfide-based hydrogenation and hydrodesulfuration processes.

The synthesis and conformational analysis of  $\text{Cp}_2\text{TiS}_5$  by variable-temperature  $^1\text{H}$  NMR spectroscopy has been reported as an experiment for an integrated advanced laboratory course.<sup>1589</sup> The crystal and molecular structure of  $(\text{C}_5\text{H}_4\text{Me})_2\text{TiS}_5$  has been determined by X-ray diffraction.<sup>1590</sup>

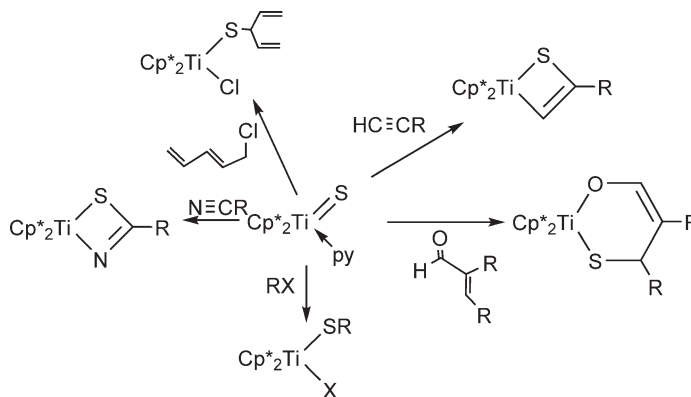
The electronic spectrum of  $\text{Cp}_2\text{TiS}_5$  shows a long-wavelength absorption at  $\lambda_{\text{max}} = 492\text{ nm}$  which has been assigned to the lowest-energy ligand-to-metal charge transfer (LMCT) transition. The photolysis of this complex in  $\text{CH}_2\text{Cl}_2$  leads to the formation of  $\text{Cp}_2\text{TiCl}_2$  and elemental sulfur.<sup>1591</sup>

The synthesis of monomeric Cp sulfido and disulfido titanium complexes has been described. Their reaction with  $\text{H}_2$  constitutes one of the first examples of  $\text{H}_2$ -activation by a terminal Ti–S bond.

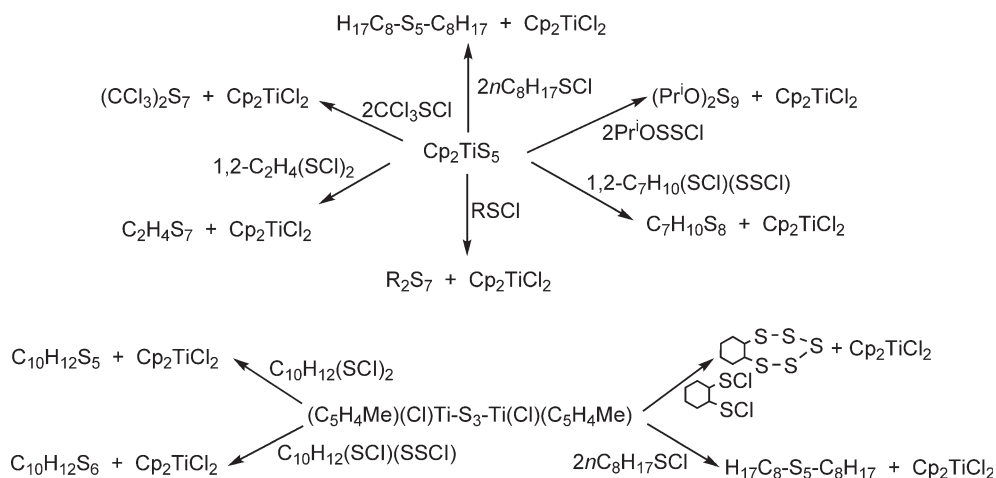
$\text{Cp}^*_2\text{Ti}(\text{CH}_2\text{CH}_2)$  reacts with  $\text{S}_8$  in toluene/pyridine to give  $\text{Cp}^*_2\text{Ti}(=\text{S})(\text{py})$ , the structure of which has been determined. Reaction of this complex with  $\text{H}_2$  affords the hydride hydrosulfido compound  $\text{Cp}^*_2\text{Ti}(\text{SH})(\text{H})$ .  $^1\text{H}$  NMR spectroscopy indicates that intramolecular hydride exchange between the hydrosulfido and hydride ligands occurs in solution. Addition of 1 equiv. of elemental sulfur to  $\text{Cp}^*_2\text{Ti}(=\text{S})(\text{py})$  gives  $\text{Cp}^*_2\text{Ti}(\eta^2\text{-S}_2)$ . The acetylene insertion into the Ti–S bond of  $\text{Cp}^*_2\text{Ti}(\eta^2\text{-S}_2)$  produces a vinyl disulfido complex.<sup>1592</sup>  $\text{Cp}^*_2\text{Ti}(=\text{S})(\text{py})$  is also prepared by the reaction of  $\text{Cp}^*_2\text{Ti}(\text{S}_2)$  with pyridine. The reactivity of  $\text{Cp}^*_2\text{Ti}(=\text{S})(\text{py})$  with various silanes leads to  $\text{Cp}^*_2\text{Ti}(\text{H})\text{SSiMe}_3$ ,  $\text{Cp}^*_2\text{Ti}(\text{H})\text{SSiHEt}_2$ , or  $\text{Cp}^*_2\text{Ti}(\text{H})\text{SSiHMe}_2$ . Reaction of  $\text{Cp}^*_2\text{Ti}(\text{S}_2)$  with phosphines in the presence of  $\text{H}_2$  gives  $\text{Cp}^*_2\text{Ti}(\text{H})\text{SH}$  and the corresponding phosphine sulfide, while on treatment with  $\text{H}_2$  the compound  $\text{Cp}^*_2\text{Ti}(\text{SH})_2$  is obtained. These reactions provide models for a possible mechanism of  $\text{H}_2$  activation in metal–sulfido hydrodesulfurization catalysts.<sup>1593</sup> Complexes containing the  $\text{Cp}^*_2\text{Ti}=\text{S}$  unit undergo a wide range of reversible cycloaddition reactions. The nucleophilicity of  $\text{Cp}^*_2\text{Ti}(=\text{S})(\text{py})$  has been found to lead to regioselective  $\text{S}_{\text{N}}2'$  substitution reactions with allyl chlorides. The treatment with terminal alkynes  $\text{HC}\equiv\text{CR}$  gives thiametallacyclobutenes  $\text{Cp}^*_2\text{Ti}[\text{SC}(\text{R})=\text{CH}]$ . The terminal sulfido complex reacts with alkyl halides  $\text{RX}$  to give  $\text{Cp}^*_2\text{Ti}(\text{X})\text{SR}$ , derived from the formal 1,2-addition across the titanium–sulfur bond. Treatment with allyl halides results in the formation of  $\text{Cp}^*_2\text{Ti}(\text{X})(\text{SCH}_2\text{CHCH}_2)$ . Kinetic studies have been carried out. The reactions with allyl tosylate show that substitution of the tosylate functionality proceeds via an  $\text{S}_{\text{N}}2$  pathway. Heterocycles are formed from the reactions with  $\alpha,\beta$ -unsaturated aldehydes (Scheme 614).<sup>1594</sup>

The reactions of mono- or polynuclear sulfido titanium complexes with organic or inorganic S–Cl compounds can be used to synthesize homocycles, heterocycles, or linear organic polysulfides (Scheme 615).<sup>1595–1598</sup> Reactions of  $\text{Cp}_2\text{TiS}_5$  with organic sulfonyl chloride or related SCl compounds lead to the formation of chain-like polysulfanes with up to 9 sulfur atoms, or to cyclic polysulfanes with up to 11 sulfur atoms.<sup>1595,1599,1600</sup> The polysulfido complex  $(\text{C}_5\text{H}_4\text{Me})_2(\text{Cl})\text{Ti}-\text{S}_3-\text{Ti}(\text{Cl})(\text{C}_5\text{H}_4\text{Me})_2$ <sup>1601,1602</sup> acts as an  $\text{S}_3$  group transfer reagent in the reactions with sulfonyl chlorides to generate chain-like and cyclic organic polysulfanes.<sup>1603</sup>

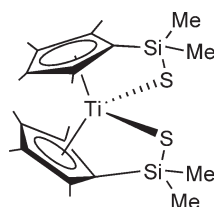
The addition of an excess of gaseous  $\text{H}_2\text{S}$  to a toluene solution of  $(\text{C}_5\text{Me}_4\text{SiMe}_2\text{NMe}_2)_2\text{TiCl}_2$  affords the sulfido-tethered bis-Cp compound  $(\text{C}_5\text{Me}_4\text{SiMe}_2\text{S})_2\text{Ti}$  (Scheme 616) by cleavage of both Si–N and Ti–Cl bonds.



Scheme 614



Scheme 615

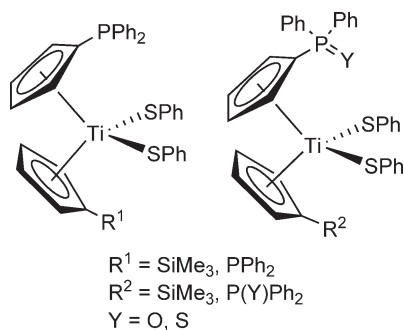


Scheme 616

$[\text{NH}_2\text{Me}_2]\text{Cl}$  is formed as the byproduct. The crystal structure of the compound has been determined by single crystal X-ray diffraction. The S–Ti–S angle indicates that the bridged structure does not impose steric strain.<sup>1604</sup>

The synthesis of the benzenethiolato complex  $\text{Cp}(\text{C}_5\text{H}_4\text{Bu}^t)\text{Ti}(\text{SPh})_2$  has been described (Scheme 432; Section 4.05.4.1.1.(i).(a)).<sup>1042</sup> The thiolates  $(\text{C}_5\text{H}_4\text{SiMe}_3)_2\text{Ti}(\text{SR})_2$  ( $\text{R} = \text{C}_6\text{F}_5$ ,  $\text{C}_6\text{H}_5$ ,  $\text{CH}_2\text{C}_6\text{H}_5$ ,  $\text{C}_2\text{H}_5$ ) and  $(\text{C}_5\text{H}_4\text{SiMe}_3)_2\text{TiCl}(\text{SC}_6\text{H}_{11})$  have been synthesized by the reaction of  $(\text{C}_5\text{H}_4\text{SiMe}_3)_2\text{TiCl}_2$  with the appropriate thiol in the presence of  $\text{NEt}_3$ . The crystal structure of  $(\text{C}_5\text{H}_4\text{SiMe}_3)_2\text{Ti}(\text{SC}_6\text{F}_5)_2$  has been determined by X-ray diffraction.<sup>1605</sup> Substituted mixed bis-Cp' dithiolato titanium complexes containing diphenyloxo- or diphenylthiophosphoryl–Cp ligands are obtained by oxidation of diphenylphosphino–Cp derivatives with  $\text{S}_8$  or  $\text{H}_2\text{O}_2$  (Scheme 617).<sup>1076</sup>

The syntheses of bis-Cp 2,3-quinoxaline–dithiolato titanium(IV) and bis-Cp' 1,2-ethenedithiolato titanium derivatives have been described ( $\text{Cp}' = \text{C}_5\text{H}_3\text{PhMe}$ ). The redox properties of these compounds in neutral solutions have been studied. All the compounds exhibit a reversible one-electron reduction process, the potential of which is



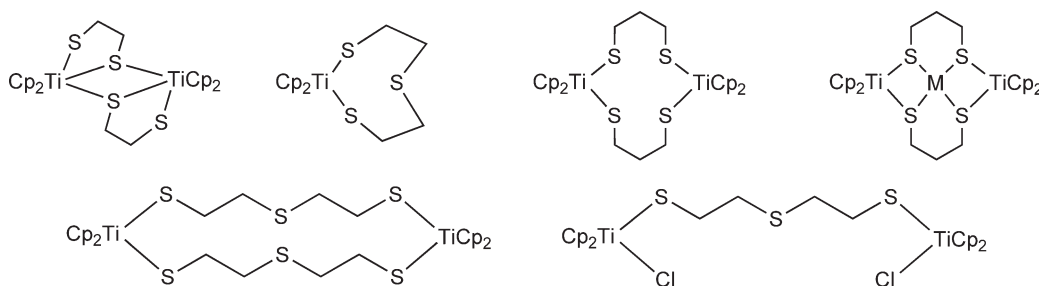
Scheme 617

dependent on the nature of the dithiolato ligand. A second reduction process is observed in the 2,3-quinoxaline derivatives.<sup>1606</sup>  $\text{Cp}^*_2\text{Ti}(\text{dithiolato})$  complexes are prepared by reacting  $\text{Cp}^*_2\text{TiCl}_2$  with the dithiolato ligands  $\text{dmit}^{2-}$  or  $\text{dddt}^{2-}$  ( $\text{dmit}^{2-} = 1,3\text{-dithiole-2-thione-4,5-dithiolato}$ ;  $\text{dddt}^{2-} = 5,6\text{-dihydro-1,4-dithiine-2,3-dithiolato}$ ). The molecular structure of  $\text{Cp}^*_2\text{Ti}(\text{dmit})$  has been determined by X-ray diffraction and shows the  $\text{TiS}_2\text{C}_2$  plane folded along the S–S axis by  $38^\circ$ . Cyclic voltammetry shows a reversible reduction wave for the  $\text{Ti(IV)}\text{--Ti(III)}$  process, while an irreversible ligand-centered process is observed for the oxidation reaction. The dynamic behavior of the folded ligand has been characterized by variable-temperature  $^1\text{H}$  NMR studies. Extended Hückel calculations explain the geometry of the complexes and indicate that the steric constraint of the  $\text{Cp}^*$  rings prevails over the Ti–dithiolene interactions.<sup>1607,1608</sup>

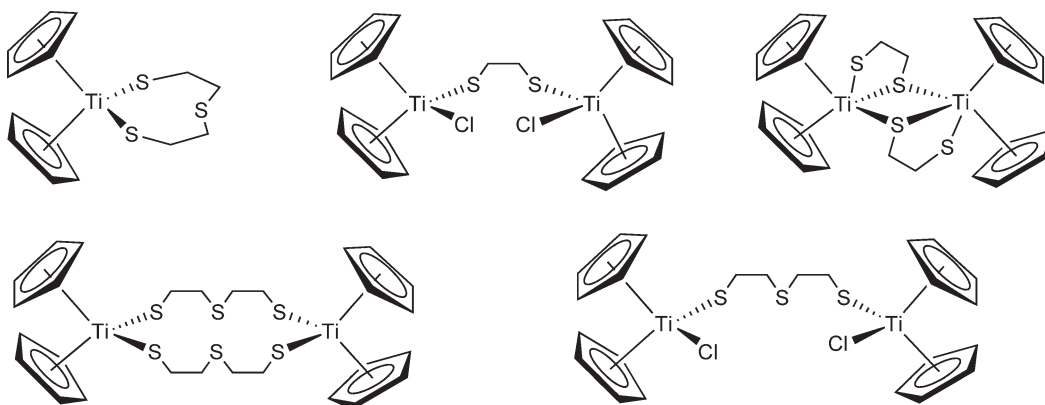
Several macrocyclic bis-Cp sulfido complexes have been prepared by treatment of  $\text{Cp}_2\text{TiCl}_2$  with dithiols in the presence of donor ligands such as imidazole or  $\text{PMe}_3$  under different reaction conditions. Some representative examples are shown in Schemes 618 and 619. Such compounds can act as metalloligands for late transition metals, although the Ti–S bonds are susceptible to cleavage in these reactions, leading to redistribution processes to give thermodynamically more stable species, or to thiolato ligand-transfer reactions.<sup>1015</sup> The reactivity, structural and electrochemical behavior of these compounds suggest that a radical mechanism is operative in the formation of the complexes.<sup>1016</sup>

Reactions of  $\text{Cp}'_2\text{TiCl}_2$  ( $\text{Cp}' = \text{Cp}, \text{Cp}^*$ ) with  $\text{Li}_2\text{C}_8\text{H}_4\text{S}_8$  (see Scheme 423; Section 4.05.3.6) give the complexes  $\text{Cp}'_2\text{Ti}(\text{C}_8\text{H}_4\text{S}_8)$ . Crystal structure, molecular geometries, electrochemical and spectroscopic properties, and electrical conductivities are studied.<sup>1021</sup> Electrochemical properties and the electrical conductivities are discussed on the basis on their electronic states and molecular interactions among the complex moieties in the solid state. These species show high electric conductivities. The effects of one-electron oxidation on the molecular structure and the atomic spin densities of the oxidized species have been rationalized with theoretical calculations.<sup>1609</sup>

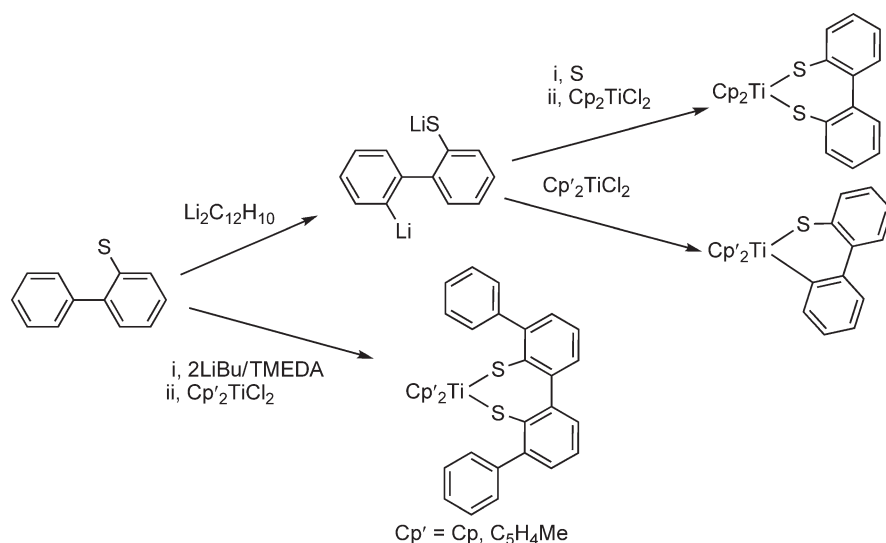
Dibenzothiophene is metallated by reaction with  $\text{Li}_2\text{C}_{12}\text{H}_{10}$ . Treatment of the resulting salt  $2,2'\text{-Li}(\text{LiS})\text{C}_{12}\text{H}_8$  with  $\text{Cp}'_2\text{TiCl}_2$  affords  $\text{Cp}'_2\text{Ti}(\text{SC}_{12}\text{H}_8)$ . The molecular structure of  $(\text{C}_5\text{H}_4\text{Me})_2\text{Ti}(\text{SC}_{12}\text{H}_8)$  has been determined. When dibenzothiophene is treated with  $\text{LiBu}^n$  in the presence of TMEDA and reacted with  $\text{Cp}'_2\text{TiCl}_2$ , the



Scheme 618



Scheme 619



Scheme 620

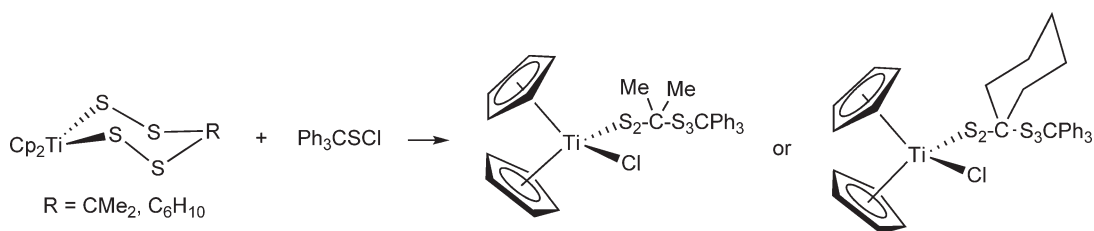
complexes  $\text{Cp}'_2\text{Ti}(\text{S}_2\text{C}_{24}\text{H}_{16})$  are formed. The synthesis of  $\text{Cp}_2\text{Ti}(\text{S}_2\text{C}_{12}\text{H}_8)$  is achieved by the reaction of 2,2'-Li(LiS) $\text{C}_{12}\text{H}_8$  with 1 equiv. of sulfur followed by treatment with  $\text{Cp}_2\text{TiCl}_2$  (Scheme 620).<sup>1610</sup>

$\text{Cp}_2\text{TiCl}_2(\text{S}_2\text{RS}_3\text{CPh}_3)$  ( $\text{R} = \text{CMe}_2, \text{C}_6\text{H}_{10}$ ) have been prepared by the reaction of the six-membered metallacycle  $\text{Cp}_2\text{Ti}(\text{S}_4\text{R})$  with the sulfenyl chloride  $\text{Ph}_3\text{CSCl}$  (Scheme 621). These complexes are treated with sulfenyl chlorides ( $\text{RSCl}$  or  $\text{RSSCl}$ ) or with  $\text{SO}_2\text{Cl}_2$ ,  $\text{SCl}_2$ , or  $\text{S}_2\text{Cl}_2$  to obtain thiaalkanes and other sulfur-rich species, as well as  $\text{Cp}_2\text{TiCl}_2$ .<sup>1611</sup>

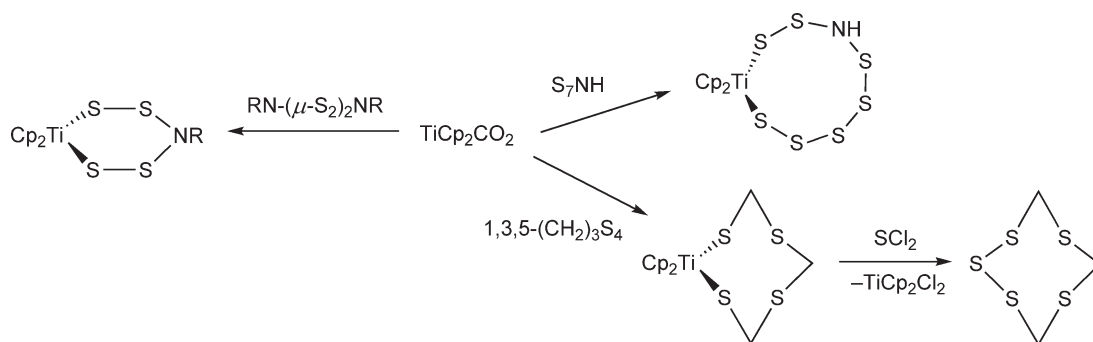
$\text{Cp}_2\text{Ti}(\text{C}_8\text{H}_4\text{S}_8)$  exhibits low oxidation potentials for the  $\text{C}_8\text{H}_4\text{S}_8$  ligand and is oxidized by iodine or 7,7,8,8-tetracyano-*p*-quinodimethane.<sup>1022</sup>

$\text{S}_7\text{NH}$  and  $\text{S}_7\text{NMe}$  have been used as novel chelating ligands in bis-Cp titanium complexes.  $\text{Cp}_2\text{Ti}(\text{S}_7\text{NR})$  ( $\text{R} = \text{H}, \text{Me}$ ) have been synthesized by the reaction of  $\text{Cp}_2\text{Ti}(\text{CO})_2$  with  $\text{S}_7\text{NH}$  or  $\text{S}_7\text{NMe}$  in hexanes and studied as suitable ligand-transfer reagents.<sup>1612</sup> Similarly,  $\text{Cp}_2\text{Ti}(\text{CO})_2$  reacts with the S–S bond of a series of homo- and heterocycles containing sulfur atoms with insertion of the bis-Cp titanium fragment and liberation of two molecules of CO (Scheme 622). These complexes allow the preparation of different sulfinimide heterocycles.<sup>1612–1615</sup>

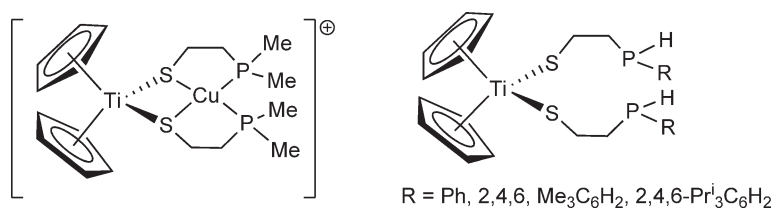
$\text{Cp}_2\text{TiCl}_2$  reacts with the lithium salt of the hybrid P–S anions  $\text{Me}_2\text{P}(\text{CH}_2)_n\text{S}^-$  ( $n = 2$ , dmpet;  $n = 3$ , dmppt) to give the neutral complexes  $\text{Cp}_2\text{Ti}[\text{S}(\text{CH}_2)_n\text{PMe}_2]_2$ , with monodentate S-coordinated thiolato ligands, and the cationic compounds  $[\text{Cp}_2\text{TiS}(\text{CH}_2)_n\text{PMe}_2]\text{BPh}_4$  bearing chelating S,P-ligands. The structures of these complexes have been confirmed by X-ray diffraction, and electrochemical studies have been performed. The compounds are precursors for heterobimetallic complexes; for example,  $[\text{Cp}_2\text{Ti}(\text{dmpet})_2\text{Cu}]\text{PF}_6$  has been isolated from the reaction with  $[\text{Cu}(\text{CH}_3\text{CN})_4]\text{PF}_6$  (Scheme 623). The Ti–Cu distance is 2.95(1) Å.<sup>1012</sup> Diastereomeric mixtures (ratio ca. 1:1) of *rac*- and *meso*- $\text{Cp}_2\text{Ti}(\text{SCH}_2\text{CH}_2\text{PHR})_2$  (Scheme 623) are obtained by the reaction of  $\text{Cp}_2\text{TiCl}_2$  with  $\text{RHPCH}_2\text{CH}_2\text{SH}$  in the presence of  $\text{NEt}_3$ . Reactions of these compounds with  $[\text{Cu}(\text{CH}_3\text{CN})_4]\text{BF}_4$  afford heterobimetallic Ti–Cu derivatives.<sup>1616</sup>



Scheme 621



Scheme 622



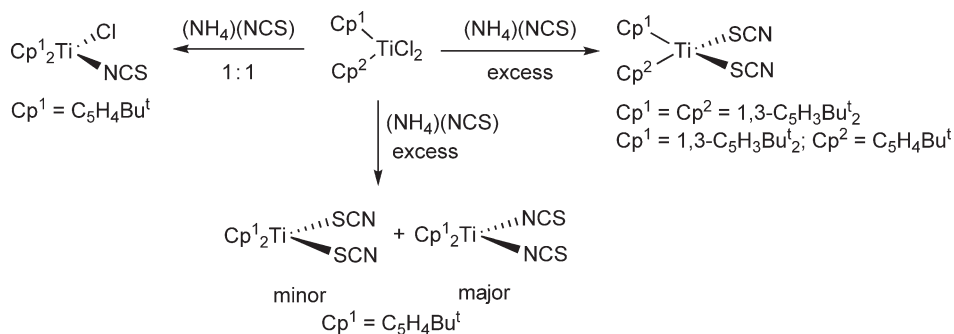
Scheme 623

Homobimetallic Ti complexes with the tetrathiafulvalene tetrathiolato ligand ( $S_2T'TFS_2$ ) have been reported. The synthesis of the complexes  $Cp'_2TiS_2T'TFS_2TiCp'_2$  ( $Cp' = Cp, Cp^*$ ) has been described. These compounds form charge-transfer complexes with TCNQ (7,7,8,8-tetracyano-*p*-quinodimethane).<sup>1617</sup>

The bis-Cp titanium bis(*t*-butanethiolato) and bis(ethanethiolato) complexes have been used as a single-source precursors for the preparation of thin films of titanium sulfides by metal-organic chemical vapour deposition (MOCVD). The crystal and molecular structures of the precursor complexes have been determined for comparison with homologous complexes of the general formula  $Cp_2Ti(SR)_2$ .<sup>1618</sup>

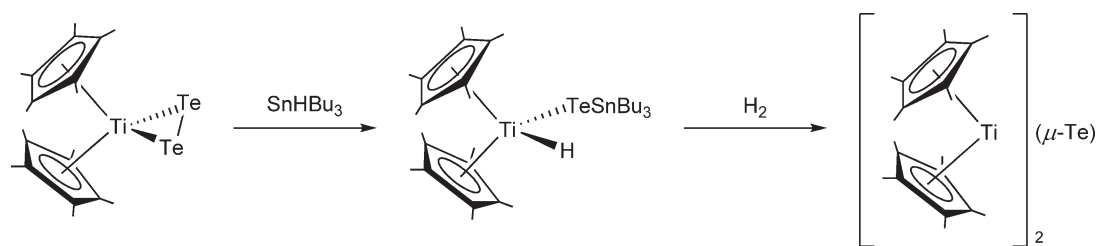
Titanocene dichlorides with substituted Cp ligands react with ammonium thiocyanate to afford S- or N-bonded thiocyanato complexes depending on the reaction conditions and the nature of the ring substituted (Scheme 624). The crystal structure of  $(C_5H_4Bu^t)_2Ti(NCS)_2$  has been determined.<sup>1043</sup>

Attempts to synthesize Cp titanium complexes with a terminal  $Ti=Te$  moiety have met with difficulties. One of the principal factors for this is the particularly weak  $Ti=Te$  interaction.  $Ti=E$  bond energies for  $Cp_2Ti=O$  ( $152.6 \text{ kJ mol}^{-1}$ ) and  $Cp_2Ti=Te$  ( $130.3 \text{ kJ mol}^{-1}$ ) have been calculated. The hydrido titanium(III) complex  $Cp^*_2TiH$  reacts with elemental selenium or tellurium to give mono- and diselenido and tellurido complexes. The possible involvement of monomeric terminal chalcogenides  $Cp^*_2Ti(E)$  ( $E = O, S, Se, Te$ ) in these reactions has been probed experimentally and computationally by means of DFT calculations.

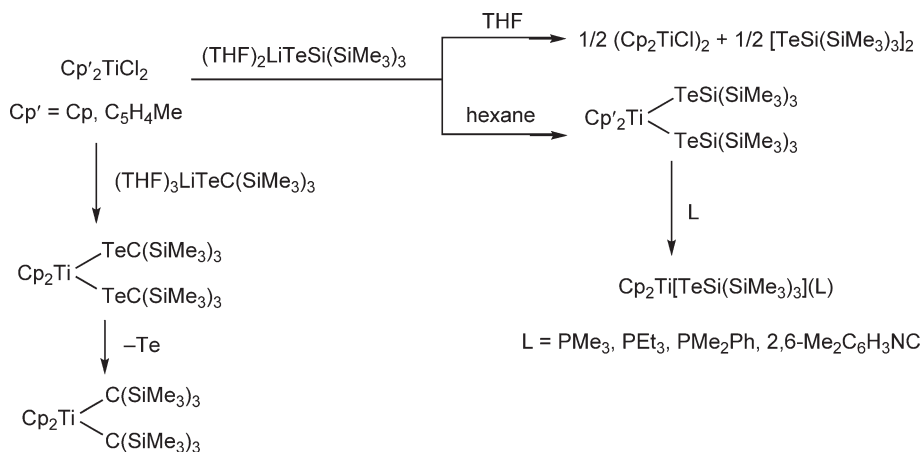


Scheme 624





Scheme 625



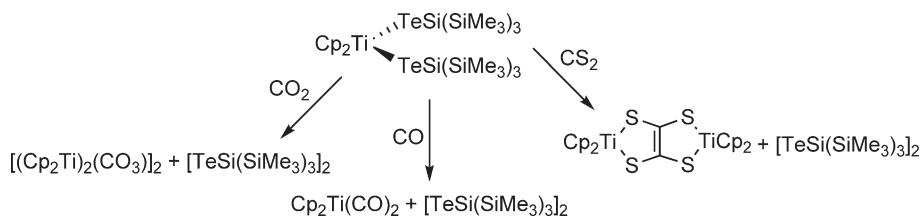
Scheme 626

Several unsuccessful attempts to generate and trap  $\text{Cp}^*_2\text{Ti}(\text{Te})$  are described, suggesting that these species have a very weak Ti–Te bond and a readily accessible triplet excited state, rendering complexes difficult to trap with Lewis bases, in contrast to other zirconium and hafnium terminal chalcogenido complexes.<sup>1619</sup> The synthesis of a compound containing a multiply bonded  $\text{Ti}=\text{Te}$  moiety stabilized by macrocyclic ligands has been reported.<sup>1620</sup> Attempts to synthesize terminal titanium tellurido complexes have only led to the bridging telluride  $(\text{Cp}^*_2\text{Ti})_2(\mu\text{-Te})$  and the ditelluride  $\text{Cp}^*_2\text{Ti}(\eta^2\text{-Te}_2)$ .<sup>1621</sup>  $\text{Cp}^*_2\text{Ti}(\eta^2\text{-Te}_2)$  reacts with  $\text{HSnBu}_3$  to eliminate  $\text{Te}(\text{SnBu}_3)_2$ , producing an unstable Ti(IV) species formulated as a stannyltelluroloato hydrido compound  $\text{Cp}^*_2\text{Ti}(\text{TeSnBu}_3)(\text{H})$  (Scheme 625). Solutions of this complex lose  $\text{H}_2$  at a moderate rate to give the paramagnetic compound  $(\text{Cp}^*_2\text{Ti})_2(\mu\text{-Te})$ . These derivatives have been studied as intermediates in the catalytic cycle of the heterodehydrocoupling process of tributylstannane and tellurium.<sup>1622</sup>

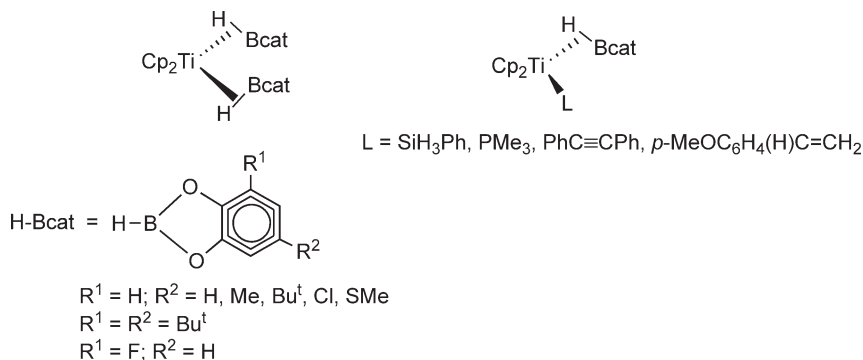
The silyltelluroloato titanium compounds  $\text{Cp}'_2\text{Ti}[\text{TeSi}(\text{SiMe}_3)_3]_2$  ( $\text{Cp}' = \text{Cp}, \text{C}_5\text{H}_4\text{Me}$ ) are synthesized by treatment of the corresponding titanocene dichlorides with 2 equiv. of  $(\text{THF})_2\text{LiTeSi}(\text{SiMe}_3)_3$  in hexane. The same reaction performed in THF results in quantitative reduction to Ti(III) species. The X-ray structures of the methyl–Cp derivative have been determined; the data have been compared with similar zirconium complexes. By contrast, treatment of  $\text{Cp}_2\text{TiCl}_2$  with the alkyl telluroloato reagent  $(\text{THF})_3\text{-LiTeC}(\text{SiMe}_3)_3$  leads to the alkyl complex  $\text{Cp}_2\text{Ti}[\text{C}(\text{SiMe}_3)_3]_2$  through the unstable intermediate  $\text{Cp}_2\text{Ti}[\text{TeC}(\text{SiMe}_3)_3]_2$  which extrudes elemental tellurium between  $-60$  and  $-20^\circ\text{C}$ . Addition of Lewis bases to  $\text{Cp}_2\text{Ti}[\text{TeSi}(\text{SiMe}_3)_3]_2$  results in the formation of Ti(III) derivatives  $\text{Cp}_2\text{Ti}[\text{TeSi}(\text{SiMe}_3)_3]_2(\text{L})$  (Scheme 626). The reactions of  $\text{Cp}_2\text{Ti}[\text{TeSi}(\text{SiMe}_3)_3]_2$  with  $\text{CO}$ ,  $\text{CO}_2$ , and  $\text{CS}_2$  have been described (Scheme 627).<sup>1623</sup>

#### 4.05.4.9 Complexes with Ti–H, and Ti–B Bonds

Mono- $\text{Cp}'$  and bis- $\text{Cp}'$  titanium hydrido derivatives have been reviewed.<sup>1027</sup> The hydrido alkoxo complex  $\text{Cp}^*_2\text{Ti}(\text{H})(\text{OMe})$  is obtained by oxidative addition of  $\text{CH}_3\text{OH}$  to  $\text{Cp}^*_2\text{Ti}$ , generated from  $\text{Cp}^*_2\text{Ti}(\text{Me}_3\text{SiC}\equiv\text{CSiMe}_3)$ .<sup>1363</sup>



Scheme 627



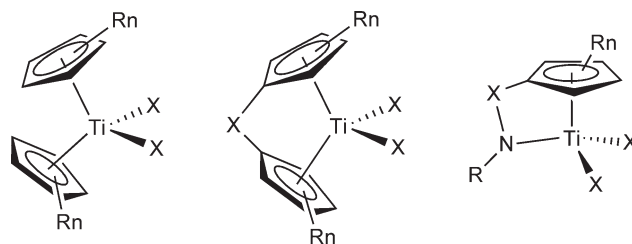
Scheme 628

$\text{Cp}_2\text{TiCl}_2/\text{NaBH}_4$  mixtures have been studied as a convenient system for the hydroboration of alkenes. Mechanistic studies for these reactions are reported. These processes provide different regioselectivities and are catalyzed by the isolated  $\text{Cp}_2\text{Ti}(\mu\text{-H})_2\text{BH}_2$  species. Lithium borohydride appears to be involved in the formation of the true catalytically active complex. Extensive  $^{11}\text{B}$  NMR experiments indicated that the predominant products in the hydroboration reaction of  $\text{Ph-CH=CH}_2$  are a regiomeric mixture of tetraalkylborates, with minor amounts of trialkylborohydrides.<sup>1624,1625</sup>

Early transition metal complexes have been found to catalyze olefin and acetylene hydroboration reactions with monoboranes such as catecholborane or pinacolborane. They are efficient catalysts for the hydroboration of alkenes.  $\text{Cp}_2\text{TiMe}_2$  reacts with 3–5 equiv. of substituted catecholboranes with elimination of  $\text{CH}_4$  to form the Ti–bis(borane) complexes  $\text{Cp}_2\text{Ti}(\text{HBcat})_2$  in high yields, from which  $\text{Cp}_2\text{Ti}(\text{HBcat})(\text{L})$  derivatives can be prepared (Scheme 628). The compound  $\text{Cp}_2\text{Ti}(\text{HBcat})_2$  can be described as a Ti(IV) complex of the dianion  $\text{H}_2\text{B}_2\text{cat}_2^{2-}$ , which is analogous to  $\text{B}_2\text{H}_6^{2-}$ . Alternatively, these complexes can be described as Ti(II) derivatives containing neutral coordinated boranes. Structural and spectroscopic data and theoretical calculations indicate Ti(II) rather Ti(IV). The reactivity of these complexes has been studied and it is dominated by borane displacement and additions to C–C and C–N multiple bonds and Si–H bonds. They are efficient catalysts for the hydroboration of alkenes.<sup>1626–1629</sup> A detailed mechanistic analysis of the hydroboration process of vinylarenes catalyzed by the substituted bis(borane) titanium complex  $\text{Cp}_2\text{Ti}(\text{HBcat})_2$  is reported.<sup>1630</sup> Theoretical calculations on the proposed reaction mechanism for this process have been reported.<sup>1631</sup> The silane compound has been later suggested to be a silylborato complex on the basis of theoretical studies.<sup>1632</sup> The geometries of  $\sigma\text{-H-BR}_2$  titanium complexes  $\text{Cp}_2\text{Ti}(\text{HBcat})_2$  (cat =  $\text{O}_2\text{C}_6\text{H}_4$ ) have been theoretically optimized by semiempirical PM3 (tm) methods.<sup>1633</sup>

#### 4.05.5 *ansa*-Titanocene Complexes

*ansa*-Metallocene complexes are bis- $\text{Cp}'$  or related derivatives where the two rings are connected by a bridge (*ansa* = Latin “handle”). The introduction of a linkage between the two  $\text{Cp}'$  rings prevents mutual Cp ligand rotation and imposes rigidity and symmetry on the ligand framework. This complex design strategy has received wide attention in the chemistry of group 4 metals due to its particular success in stereoselective catalysis. More recently, a new family of substances has been developed from *ansa*-metallocene complexes by exchanging one  $\text{Cp}'$  ring by an amido moiety, to give Cp–amido derivatives (Section 4.05.3.4). Both type of complexes give some of the most active



Scheme 629

and selective olefin polymerization catalysts based on group 4 transition metals. Scheme 629 shows structural comparisons between this type of compounds.

The chemistry of *ansa*-metallocene compounds has been the subject of several reviews. Structural aspects affecting the catalytic activity and the application of these complexes as catalysts for the homo- and co-polymerization of olefins have been considered.<sup>323</sup> The evolution of the *ansa*-bridge complexes in terms of the various synthetic approaches used to construct the bridged ligand framework, the variety of bridges introduced, and the effect of the bridge on the structure and reactivity of *ansa*-titanocene and other transition metal complexes as compared with their unbridged counterparts has been reviewed.<sup>1634</sup>

Numerous titanium complexes possessing bis-Cp', bis-Ind, or bis-Flu systems connected by carbon-, silicon-, germanium-, phosphorus-, or boron-based bridging groups have been reported. The synthesis of Ti(IV) *ansa*-complexes starting from TiCl<sub>4</sub> and alkali metal or magnesium salts of bridged cyclopentadienides is complicated by side-reactions such as reduction to Ti(III) species. Usually, the desired complexes are produced only in low yields. Alternatively, synthesis of this kind of complexes can be generally achieved by transmetallation reaction by using silyl- or stannyl-cyclopentadiene reagents, reaction of TiCl<sub>4</sub> with cyclopentadiene in the presence of NEt<sub>3</sub>, treatment of Ti(III) chloride with lithium cyclopentadienyls followed by oxidation, reduction of fulvalene with TiCl<sub>2</sub>, or reaction of Cp-amido complexes with LiInd.

#### 4.05.5.1 Carbon-bridged *ansa*-titanocene Derivatives

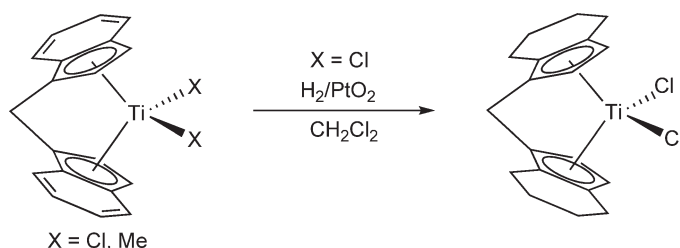
The use of chiral catalysts leads to asymmetric induction in C–C and C–H bond-forming processes. Complexes with chiral and achiral bridges have been prepared, as racemic mixtures or, when required, in enantiomerically pure forms.

An overview of the synthetic methodologies for the preparation of ligands and their incorporation into chiral titanium derivatives has been reported.<sup>1030</sup> The asymmetric thermal transformation of binaphthol complexes has been described as a convenient method for the high yield synthesis of enantiopure *ansa*-titanium and zirconium complexes.<sup>1635</sup> Enantiomeric resolution of *ansa*-metallocene racemates yields no more than 50% of a particular enantiomer. However, the synthesis of a biphenyl-bridged bis-Cp' titanium complex to give enantiopure isomers through BINOL-induced asymmetric transformation has been reported.<sup>1635</sup> This species is an efficient asymmetric catalyst for imine hydrogenation.<sup>1636</sup> Chiral *ansa*-titanocene complexes have become useful catalysts for asymmetric organic reaction.<sup>1637,1638</sup>

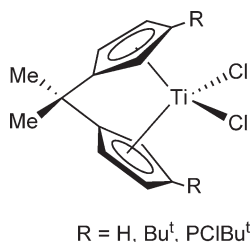
##### 4.05.5.1.1 Complexes with one-carbon bridges

*ansa*-Titanocenes with one carbon atom unit bridging the two Cp ligands are rare due to the difficulties in the synthesis of such ligands, although a few examples have been reported. The incorporation of an R<sub>2</sub>C bridge into the *ansa*-ligand leads to significant steric and electronic effects compared with unbridged or R<sub>2</sub>Si-bridged bis-Cp' analogs.

The study of methylene-bridged *ansa*-titanium complexes has received less attention than the similar ethylene-bridged bis-Ind derivatives, in part due to the difficulties for the preparation of the methylene bis-Ind ligands. Deprotonation of bis(1-indenyl)methane with 2 equiv. of LiBu<sup>n</sup> followed by reaction with TiCl<sub>4</sub>(THF)<sub>2</sub> affords the *ansa-rac*-methylenebis(1-Ind) dichloro titanium complex, though it was not isolated in analytically pure form. The *ansa-rac*-methylenebis(4,5,6,7-tetrahydro-1-Ind) titanium dichloride was obtained by hydrogenation of the bis-Ind precursor (Scheme 630). Its molecular structure reveals an acute angle of 98.9(2)° at the methylene bridge carbon atom.<sup>1639</sup> However, the methylene-bis-Ind dichloride *rac*-(CH<sub>2</sub>Ind<sub>2</sub>)TiCl<sub>2</sub> has been prepared in an analytically pure form, in low yield (16%), according to the same reaction, by treatment of TiCl<sub>4</sub>(THF)<sub>2</sub> with dilithium salt of



Scheme 630

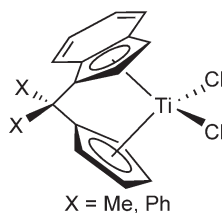


Scheme 631

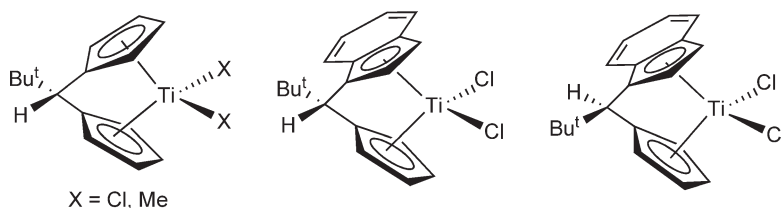
bis(Ind)methane in THF or alternatively by the reaction (with 38% yield) of  $\text{TiCl}_4$  with bis[3-(SnBu<sub>3</sub>)Ind]methane. Treatment of the dichloro compound with 2 equiv. of LiMe in diethyl ether gives the corresponding dimethyl complex *rac*-(CH<sub>2</sub>Ind)<sub>2</sub>TiMe<sub>2</sub> (Scheme 630), which has been isolated in 64% yield, and characterized by X-ray crystal structure analysis.<sup>1640</sup>

The formation of  $\text{Me}_2\text{C}(\text{C}_5\text{H}_4)_2\text{TiCl}_2$  (Scheme 631) is observed by slow decomposition of the highly air sensitive Ti(III) species  $(\text{C}_5\text{H}_4\text{CMe}_2\text{PHR})_2\text{TiCl}$  with the generation of  $(\text{PR})_n$  and  $\text{PH}_2\text{R}$  ( $\text{R} = \text{Ph, Bu}^t$ ).<sup>1641</sup> The X-ray crystal structure of this *ansa*-titanium complex had been previously described. Comparison of the structure of the molecule with analogous characterized systems is made; in particular, the Cp(centroid)–M–Cp(centroid) angle, the position of the metal relative to the Cp rings, and the uniformity of the C–C bond lengths in the Cp rings are discussed.<sup>1642</sup> The complex  $\text{Me}_2\text{C}(3\text{-C}_5\text{H}_3\text{Bu}^t)_2\text{TiCl}_2$  has been synthesized by metathesis reaction of the dilithium–cyclopentadienyl salt with  $\text{TiCl}_3$  followed by treatment with HCl and is obtained as a mixture of the *anti/syn* isomers in 1 : 1 molar ratio (Scheme 631).<sup>1643</sup> The *ansa*-compound  $\text{Me}_2\text{C}(\text{C}_5\text{H}_3\text{PClBu}^t)_2\text{TiCl}_2$  (Scheme 631) has been prepared by the reaction of  $\text{TiCl}_4$  with the *ansa*-cyclopentadiene  $\text{Me}_2\text{C}(\text{C}_5\text{H}_4\text{PClBu}^t)_2$  in the presence of  $\text{NEt}_3$  and elimination of the ammonium salt.<sup>398</sup>

The synthesis of the propylidene-bridged mixed Cp–indenyl compound  $\text{Me}_2\text{C}(\text{Cp})(\text{Ind})\text{TiCl}_2$  (Scheme 632) has been described. This complex and its zirconium analog polymerize propylene to give high molecular weight polymers with low stereoregularity. Depending on the polymerization conditions, they produce elastomeric PP. Studies concerning the influence of catalyst structure and the polymerization conditions on the polymer properties<sup>702</sup> and the propagation models on the polymerization processes have been carried out.<sup>701</sup> The structure of this compound has been determined by X-ray analysis.<sup>1644</sup> The synthesis of the analogous  $\text{Ph}_2\text{C}$ -bridged complex  $\text{Ph}_2\text{C}(\text{Cp})(\text{Ind})\text{TiCl}_2$  (Scheme 632) has also been described. In the presence of MAO, it is a catalyst for the formation of isotactic polypropylene and syndiotactic polystyrene.<sup>1645</sup>



Scheme 632



Scheme 633

The unsymmetrical *ansa*-compound  $\text{Me}_2\text{C}(\text{3-C}_5\text{H}_3\text{Bu}^t)(\text{3-C}_9\text{H}_5\text{Bu}^t)\text{TiCl}_2$  has been synthesized and the isomers separated by repeated recrystallizations.<sup>1646</sup>

Reaction of the lithium salt of Cp–Ind ligands with  $\text{TiCl}_4$  produces the new chiral *ansa*-titanocenes containing an asymmetric  $\text{CHBu}^t$  bridge. The chloro ligands can be easily replaced by methyl groups. Analogous chiral mixed Cp–indenyl derivatives have been described. (Scheme 633).<sup>1647</sup>

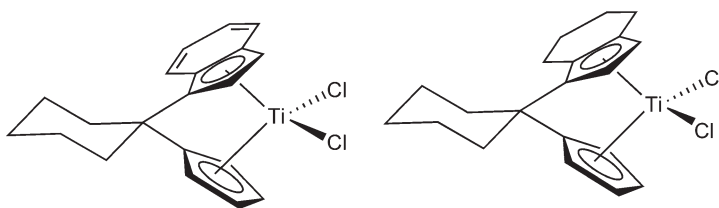
An analogous *ansa*-titanium complex containing a Cp–indenyl bridging ligand (Scheme 634) prepared from indene and pentamethylene fulvene has also been published. The catalytic hydrogenation of this complex affords the corresponding Cp–tetrahydroindenyl derivative, for which the X-ray structure indicates a significant strain in the molecule. The rates of the catalytic hydrogenation of 2-phenylpyrroline by these two complexes are apparently affected by difference in electron density at the metal center.<sup>1648</sup>

The lithium salt of [4-cyclopentadienylidene-4,7,7-trimethyl-4,5,6,7-tetrahydroindenyl] reacts with  $\text{TiCl}_4$  to give the *ansa*-compound shown in Scheme 635. Its reaction with  $\text{LiMe}$  yields the corresponding dimethyl derivative. These  $\text{C}_1$ -bridged *ansa*-titanocenes are unusually rigid. Both complexes have been characterized by X-ray diffraction and employed as homogeneous Ziegler–Natta catalysts for propylene polymerizations to form low molecular weight products.<sup>1649</sup>

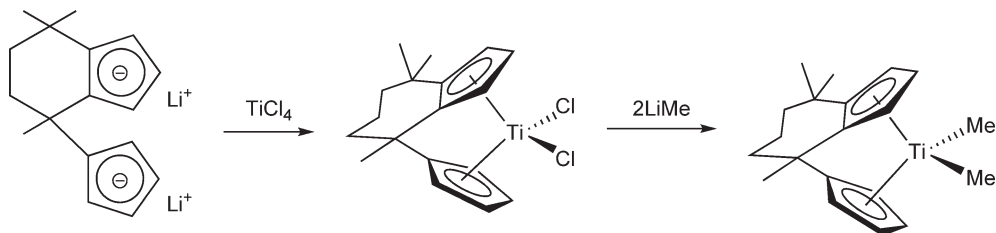
The *racemo*-pair of a new *ansa*-titanium complex (Scheme 636) is obtained by the reaction of the lithium salt of the corresponding substituted cyclopentadienyl organic molecule with  $\text{TiCl}_3$  in diethyl ether/toluene followed by oxidation with  $\text{HCl}$ . One of the *racemo*-forms was isolated as a pure substance and its structure determined by X-ray diffraction.<sup>1650</sup>

#### 4.05.5.1.2 Complexes with two-carbon bridges

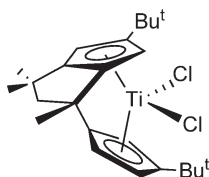
Novel synthetic approaches to chiral ethylene-bridged *ansa*-complexes possessing stereogenic centers on the bridging carbon chain (Scheme 637) have been described through the synthesis of 1,2-bis(Cp)ethane from 1,4-disulfones using



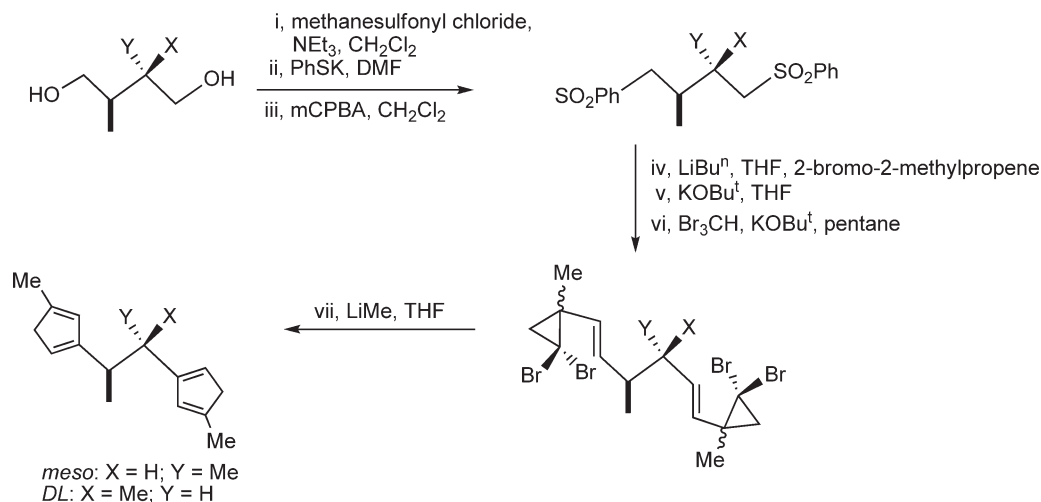
Scheme 634



Scheme 635



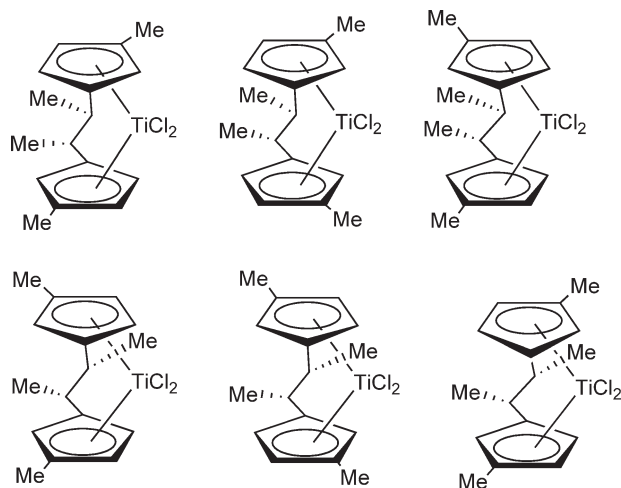
Scheme 636



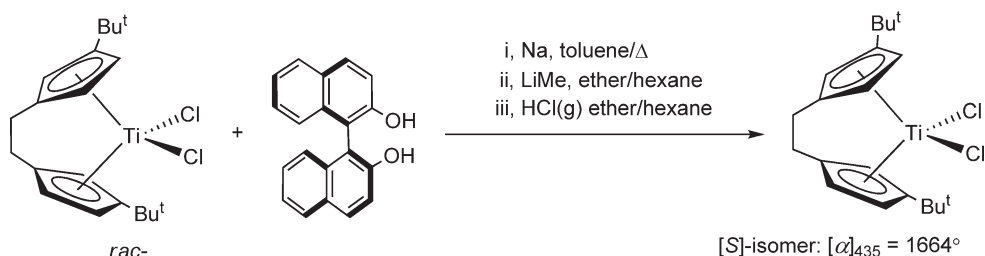
Scheme 637

a bis-cycloalkylation–bis elimination strategy. The dilithium salt derived from the bis-cyclopentadiene was treated with  $\text{TiCl}_3(\text{THF})_3$  to afford the dichloro ethylene bridge *ansa*-titanium derivative after oxidation with HCl. The influence of tether substitution on the diastereoselection in the *ansa*-complex formation has been examined (Scheme 638).<sup>1651,1652</sup>

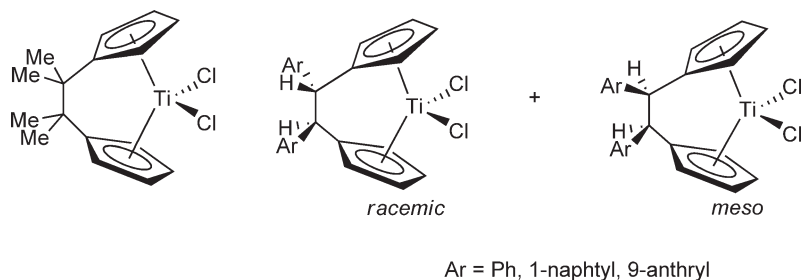
[*S*]-1,2-ethylene-bis(3- $\text{C}_5\text{H}_3\text{Bu}^t$ ) titanium dichloride can be obtained in high optical purity through kinetic resolution of the parent racemate using [*S*]-binaphthol (Scheme 639). The structure of the corresponding titanium



Scheme 638



Scheme 639



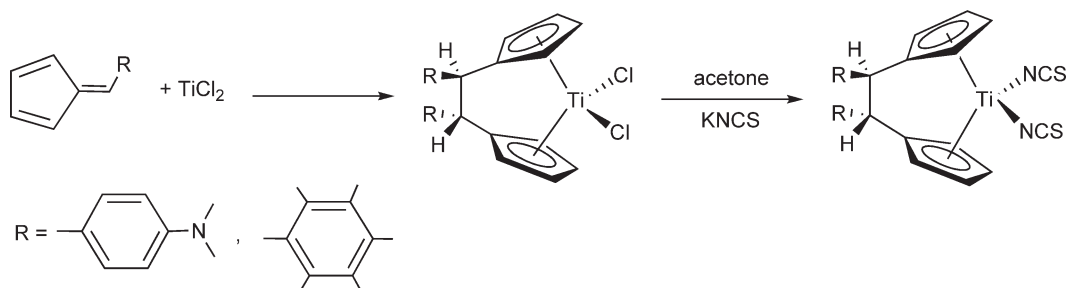
Scheme 640

binaphtholate formed in the first step of the reaction has been characterized by X-ray crystallography. (1-Methylallyl)-1,2-ethylene bis(3-CpBu<sup>t</sup>) titanium is formed *in situ* by reduction of the enantiomerically pure titanium dichloride; the Ti(III) allyl reacts with aldehydes to provide β-methyl homoallylic alcohols with variable diastereo- and enantioselectivity. The stereoselectivity of the reaction depends on the steric bulk of the aldehyde, and the results have been rationalized by molecular modeling studies.<sup>1653</sup>

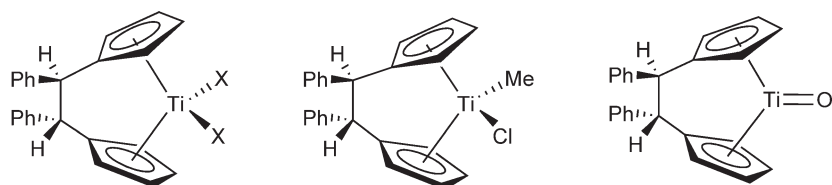
The reductive coupling of fulvenes is a convenient method and a novel and versatile route for the preparation of *ansa*-bis-Cp' titanium complexes with ethylene bridges. The *ansa*-bis-Cp complexes shown in Scheme 640 have been prepared by reduction of the appropriate fulvene reagent with TiCl<sub>2</sub>. The complexes in combination with MAO are highly active in ethylene polymerization and give linear, high density polymers.<sup>1654</sup>

Reductive coupling of fulvenes with TiCl<sub>2</sub> affords the N,N-dimethylaminophenyl and pentamethylphenyl substituted complexes shown in Scheme 641. The determined *cis:trans* ratios at the bridge were 60:40 and 93:7, respectively. The corresponding dithiocyanato complexes are synthesized by the reaction with KNCS in acetone under reflux. The *in vitro* cytotoxicity of these complexes has been determined.<sup>1655</sup>

The previously isolated<sup>1654</sup> *ansa-trans*-(1,2-diphenyl-1,2-dicyclopentadienyl)ethanediyl titanium dichloride has been prepared by a new route, involving the reductive dimerization of 6-phenylfulvene with activated calcium powder followed by treatment with TiCl<sub>3</sub>/AlCl<sub>3</sub> (1:3) and oxidation in air. This complex has been used to synthesize a variety of other *ansa*-derivatives through ligand replacement (Scheme 642). The reaction of 6,6-diphenylfulvene



Scheme 641



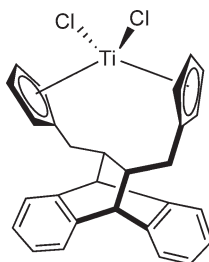
X = Cl, Me, NCS, NCO, OPh

Scheme 642

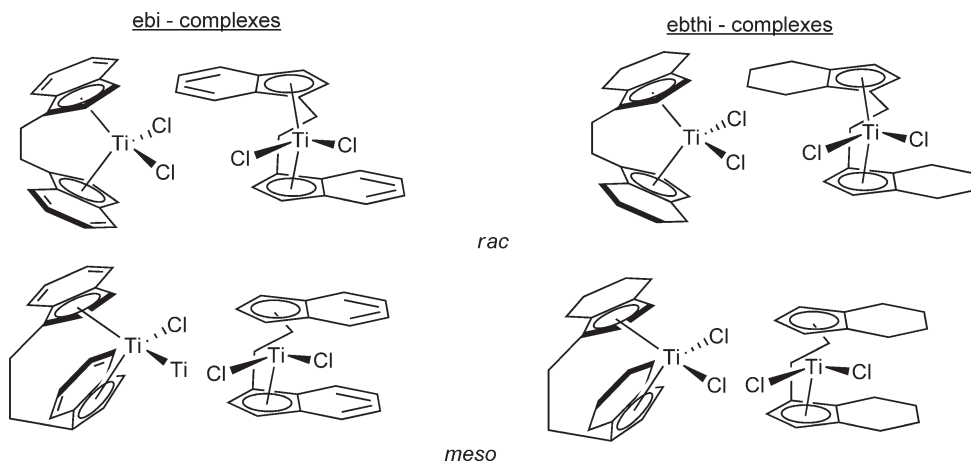
with Ti atoms to give the “tucked-in” bis-Cp derivative and the reaction of 6-diphenylfulvene with  $\text{TiCl}_2$  to afford the *trans*–[(1,2-diphenyl-1,2-dicyclopentadienyl)ethanediyl] dichloro Ti(IV) *ansa*-compound (Scheme 551; Section 4.05.4.3.4) have been studied and the corresponding reaction enthalpy calculated.<sup>1656</sup>

The chiral complex shown in Scheme 643, *ansa-trans*–(11*R*,12*R*)–bis-Cp dibenzobicyclo[2.2.2]octano titanium dichloride, which contains two Cp groups bridged by a chiral  $\text{C}_4$ -connector, has been prepared from the dilithium salt of *trans*–(11*R*,12*R*)–bis–(cyclopentadienyl–methyl)–9,10-dihydro-9,10-ethanoanthracene by reaction with  $\text{TiCl}_4$ .<sup>1657</sup>

The majority of the chiral titanium complexes are due to the presence of one or more centers of chirality in one or more of the ligands. A further group of complexes are chiral due to conformational restrictions, notably the so-called “ebi” and “ebthi” metallocenes. The developments of the chiral ethylene bis(indenyl) (ebi) and ethylene bis(tetrahydroindenyl) (ebthi) titanium derivatives (Scheme 644) in enantioselective organic reactions have been highlighted. An efficient synthesis of the dichloro bis(tetrahydroindenyl) titanium complex through a new strategy in the design of the ring ligand has been reported, using the commercially available THF adduct of  $\text{TiCl}_4$  at  $-20^\circ\text{C}$ .<sup>1051</sup> The use of  $\text{TiCl}_4$  adducts with sterically bulky ethers induces high diastereoselectivity in the synthesis of this type of



Scheme 643



Scheme 644



complexes. Likewise,  $\text{TiCl}_4$  adducts with 2,5-dimethyltetrahydrofuran or hydrobenzoin dimethyl ether have been tested to give a highly diastereoselective synthesis of dichloro *d,l*-ebthi titanium compounds. A diastereo- and enantioselective route to this compound has been described using  $\text{TiCl}_3$  complexes with tropos (chirally flexible) biphenol and atropos (chirally rigid) binaphthol ethers.<sup>1658</sup> The chemistry of the chiral ebthi titanium and zirconium complexes has been reviewed with regard to the general procedures for the synthesis and resolution of racemic complexes, especially in relation to their utility in catalytic and enantioselective C–C and C–H bond formations.<sup>1638</sup> An improved procedure for the resolution of *rac*-ebthi titanium derivatives has been developed. This method avoids the necessity of chromatographic purification which limits the scale up of previously published resolution procedures.<sup>1659</sup> The *ansa*-ebi titanium complexes that contain nitrogen, oxygen, and sulfur atoms directly bonded to the five- or six-membered rings of the Ind ligand framework have been reviewed.<sup>1032</sup>

The molecular structure of  $(\text{ebi})\text{TiCl}_2$  has been determined by X-ray diffraction.<sup>1660</sup> *S,S*-(ebthi) $\text{TiX}_2$  derivatives have been used to effect the catalytic hydrosilylation of a wide variety of dialkyl ketones.<sup>1661</sup>

For the enantioselective hydrosilylation of imines,  $(\text{ebthi})\text{TiF}_2$  acts as a catalyst. This reaction has been applied to the synthesis of an active compound for the treatment of hyperparathyroidism.<sup>1662</sup>  $(\text{Ebhti})\text{TiF}_2$  with polymethylhydrosiloxane (PMHS) as the stoichiometric reducing agent has been used as a catalyst for the asymmetric reduction of *N*-aryl imines to yield chiral amines with enantiomeric excesses above 90%.<sup>1663</sup> The reductive carbonylation of *(S,S)*-ebthi) $\text{TiMe}_2$  affords *(S,S)*-ebthi) $\text{Ti}(\text{CO})_2$  which can also be synthesized by reduction of *(S,S)*-ebthi) $\text{TiCl}_2$  with Mg in the presence of CO. The dicarbonyl compound is an active catalyst to convert 1,6-enynes to the corresponding cyclopentenones with excellent enantioselectivity.<sup>834</sup>

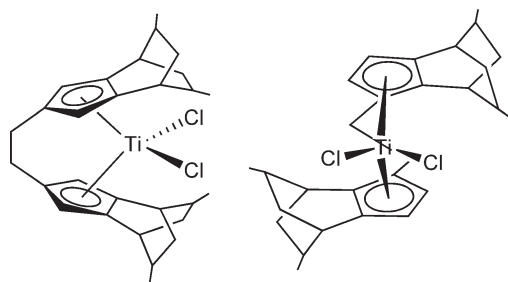
The complex *(S,S)*-(ebthi) $\text{TiCl}(\text{OMe})$  has been synthesized from the corresponding titanium dichloride. This compound catalyzes the asymmetric aldol reaction of enol trichloroacetate of cyclohexanone with aromatic aldehydes with the result that the optically active *syn*-aldol adduct is obtained with up to 91% ee.<sup>1664</sup>

The chiral triflate complex  $(\text{ebthi})\text{Ti}(\text{OTf})_2$  has been synthesized by the reaction of the parent dichloride with  $\text{AgOTf}$  and used to catalyze the Diels–Alder reaction of cyclopentadiene with oxazolidinone-derived dienophiles. The level of asymmetric induction is dramatically affected by solvent polarity and this behavior can be partially explained with reference to the results of variable-temperature NMR studies.<sup>1665</sup>

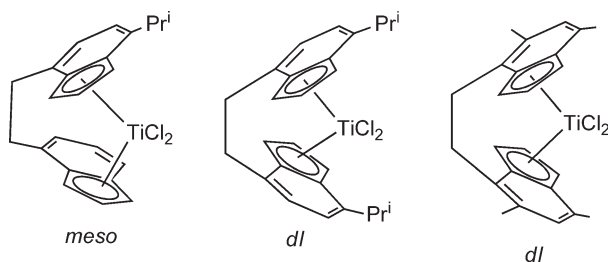
Dehydrocoupling of hydrosilanes is one of the alternative synthetic routes to polysilanes. The  $\text{Cp}_2\text{TiMe}_2$ -mediated polymerization of 1,2-diphenylsilane reaction has been re-examined in detail, including  $^{29}\text{Si}$  NMR spectroscopy to establish the polymer characteristics. In the same report, the use of the *(S,S)*-ebthi titanium binaphtholate as catalyst for the production of cyclopolysilanes in dehydrocoupling reactions is described.<sup>1335</sup> *rac*-(Ebthi) $\text{TiMe}_2$  catalyzes the reactions of silanes with allylic and homoallylic alcohols. Distribution of different products depending on the catalyst type, concentration, and the substituents on the silicon atom are obtained.<sup>1337</sup> The hydrosilylation of prochiral ketones using catalysts prepared by alkylation of  $(\text{ebthi})\text{Ti}$  1,1'-binaphth-2,2'-diolate with  $\text{LiMe}$  and  $\text{LiBu}^n$  using  $\text{SiH}(\text{OEt})_3$ ,  $\text{SiHMe}(\text{OEt})_2$ ,  $(\text{SiHMeO})_4$ ,  $\text{Me}_3\text{SiO}[\text{MeSi}(\text{H})\text{O}]_n\text{SiMe}_3$ , and  $\text{SiH}_3\text{Me}$  as the hydrosilanes has been described.<sup>1666</sup>

The synthesis, structural determination, and reactivity of  $C_2$ -symmetric ethylene-bridged *ansa*-bis(DiMeBCOCp) titanium compounds has been investigated (Scheme 645). The complexes have been characterized by X-ray crystallography and applied as catalysts for the enantioselective isomerization of alkenes, though they prove to be less enantioselective than the known chiral *ansa*-bis-Ind titanium catalyst.<sup>1667</sup>

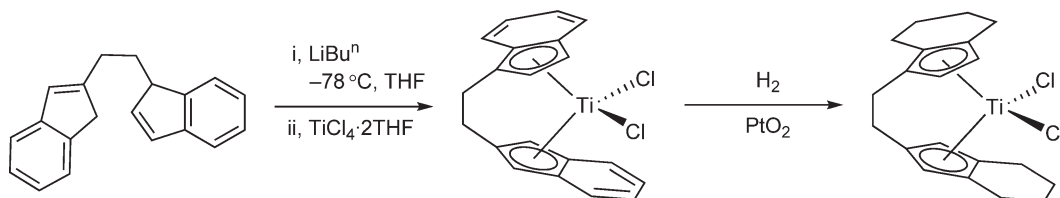
*ansa*-Bis(indenyl) titanium complexes connected via ethylene bridges in the C7 and C7' positions on the indenyl six rings have been made by reaction of  $\text{TiCl}_3$  with the lithium salt of the corresponding ethylene-bis(indenyl) reagent followed by oxidation with HCl. These complexes have a comparatively open structure (Scheme 646).<sup>1668</sup>



Scheme 645



Scheme 646

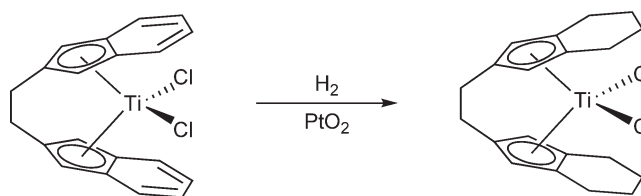


Scheme 647

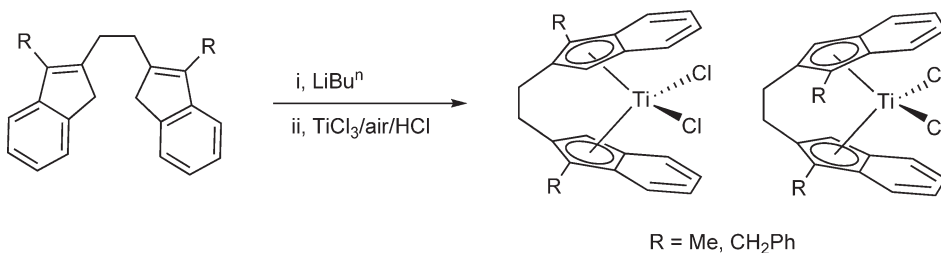
Several complexes with ethylene bridges in 2-positions have been described. Metallation of 1-(2-Ind)-2-(3-Ind)-ethane with  $\text{LiBu}^n$  and subsequent treatment with  $\text{TiCl}_4(\text{THF})_2$  affords the corresponding *ansa*-complex shown in Scheme 647, which can be hydrogenated with Adam's catalyst under ambient conditions to give the more robust bis(tetrahydroindenyl) derivative.<sup>1669</sup>

The hydrogenation of [ethylenebis(2-indenyl)] titanium dichloride with  $\text{PtO}_2$  has also been described (Scheme 648).<sup>1670</sup>

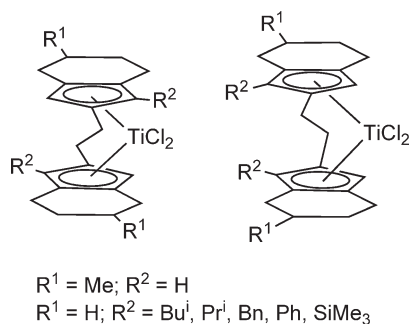
Ethylene-bridged bis(indenyl) titanium complexes in which the Ind ligands are attached at the 2-position and containing alkyl substituents in 1-position have been obtained as a mixtures of *meso*- and *racemo*-isomers (Scheme 649). The assignment of the stereochemistry for these compounds has been established on the basis of spectroscopic data and crystal structure determinations. These compounds act as catalysts for the epoxidation of unfunctionalized alkenes. The catalytic activity of this new class of complexes in epoxidation reactions was in some cases found to exceed that of known bis-Cp' titanium complexes.<sup>1670</sup>



Scheme 648



Scheme 649

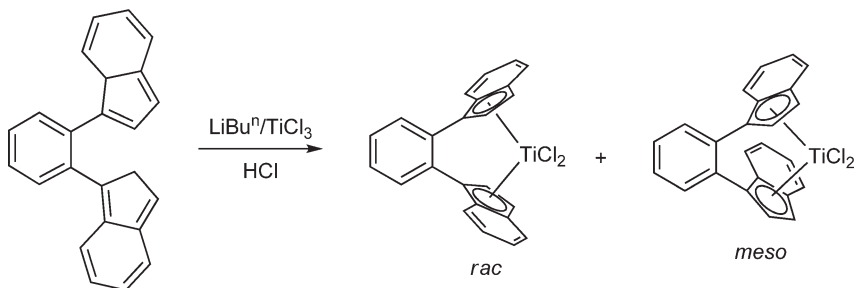


Scheme 650

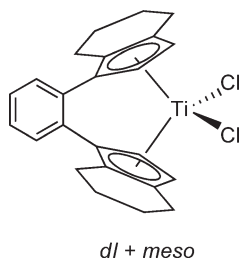
Titanium complexes derived from ethylene-bridged 2-indenyl ligands (Scheme 650) have been prepared by reductive dehydroxy coupling of 2-(hydroxymethyl)indenes with low-valent titanium compounds. Alkyl substitution of the indene ring at C(3) improves the regioselectivity of the reductive coupling.<sup>1671</sup>

Deprotonation of 1,2-bis(1-indenyl)benzene with  $\text{LiBu}^n$  provides a red solution of the corresponding dianion which has been treated with  $\text{TiCl}_3$  followed by oxidation with  $\text{HCl}$  to form a 1 : 1 mixture of the *rac*- and *meso*-isomers of the corresponding titanocenes (Scheme 651).<sup>1672</sup> The phenyl-bridged bis(tetrahydroindenyl) titanium complex shown in Scheme 652 has been synthesized by deprotonation of the parent bis(indene) with  $\text{LiBu}^n$  followed by treatment with  $\text{TiCl}_3$  and air oxidation in the presence of  $\text{HCl}$ . The complex is obtained as a 4 : 1 mixture of *rac*- and *meso*-isomers. Crystallization from hot toluene results in the isolation of the *dl*-isomer in high yield. Its molecular structure shows a very obtuse angle between the Ind ligands.<sup>1673</sup>

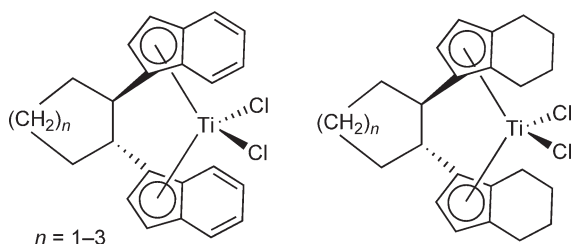
The *trans*-1,2-cycloalkylene-bridged bis-Ind titanium complexes with bridging hydrocarbyl moieties and their corresponding bis(tetrahydroindenyl) derivatives (Scheme 653) have been prepared as a mixture of diastereoisomers. Chromatographic separation and recrystallization give the pure *ansa*-bis(tetrahydroindenyl) complexes with bridging cyclopentylene, cyclohexylene, and cycloheptylene moieties. Activation with MAO gives active homogeneous Ziegler catalysts for the polymerization of propylene. The *meso*-like diastereoisomers are practically inactive compared to the *rac*-like systems.<sup>1674</sup>



Scheme 651



Scheme 652



Scheme 653

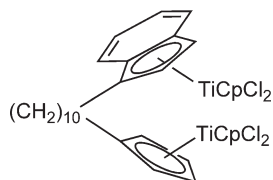
#### 4.05.5.1.3 Complexes with bridges containing more than two carbons

Binuclear complexes containing *ansa*-bisCp' groups as bridging ligands have been described (see Section 4.05.4.1.1.(i).(g)). The alkylidene-bridged binuclear *ansa*-titanocene shown in Scheme 654 polymerizes ethylene in the presence of MAO.<sup>1081</sup> The binuclear compound  $[\text{CH}_2(\text{C}_5\text{H}_4)_2](\text{TiCl}_3)_2$  is obtained by the treatment of  $[\text{CH}_2(\text{C}_5\text{H}_4)_2]_2(\text{TiCl}_2)$  with  $\text{TiCl}_4$ . Reaction with  $\text{Na}[(\text{C}_5\text{H}_4)_2\text{CH}_2]$  affords the doubly bridged complex  $[\text{CH}_2(\text{C}_5\text{H}_4)_2]_2(\text{TiCl}_2)_2$  which is reduced with  $\text{Mg}/\text{Hg}$  to  $[\text{CH}_2(\text{C}_5\text{H}_4)_2]_2(\text{TiCl})_2$ , and further oxidized to  $[\text{CH}_2(\text{C}_5\text{H}_4)_2]_2(\text{TiCl})_2(\mu\text{-O})$ .<sup>1053</sup>

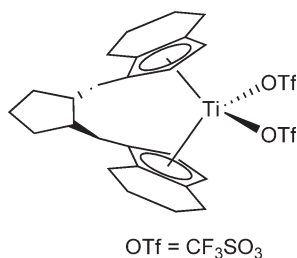
The chiral *ansa*-complex  $\text{Ti}(\text{S,S-cyclacene})(\text{OTf})_2$  (Scheme 655) catalyzes asymmetric [3 + 2]-nitron-olefin cycloaddition reactions.<sup>1559</sup>

One successful approach for the selective formation of conformationally well-defined  $C_2$ -symmetric *ansa*-metallocenes has been the use of bis-aryl or binaphthyl bridges to link Cp or Ind ligands. Another approach has been to use doubly bridged bis-Cp ligands. A third methodology implies the application of the Nazarov cyclization for the preparation of rigid doubly bridged bis-indene compounds which lead to  $C_2$ -symmetric *ansa*-metallocenes.

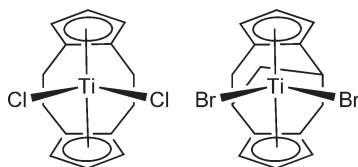
The bis-Cp titanium compound  $(\text{C}_2\text{H}_4)_2(\text{C}_5\text{H}_3)_2\text{TiCl}_2$  (Scheme 656) containing two ethanediyl bridges between the Cp rings is obtained by the reaction of the dilithium salt with  $\text{TiCl}_3(\text{THF})_3$  after appropriate workup. Its molecular



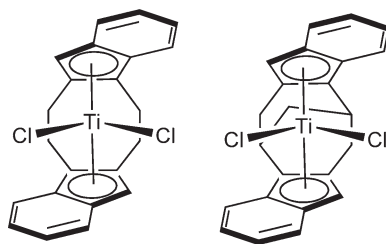
Scheme 654



Scheme 655



Scheme 656



Scheme 657

structure has been determined by X-ray diffraction.<sup>1675</sup> By using the Nazarov cyclization method, the compounds shown in Scheme 657 have been prepared.<sup>1676</sup> Analogous Cp derivatives (Scheme 656) are also known.<sup>1677</sup>

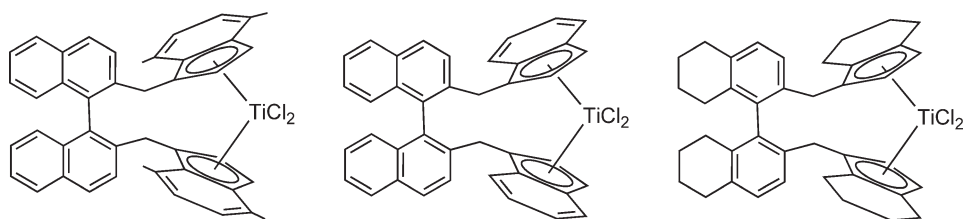
New hydrogenated tetrahydroindenyl and substituted Ind *ansa*-titanocene complexes have been synthesized in an effort to modify the steric environment around the titanium atom in complexes containing chiral bridges connecting two binaphthyl substituted Ind ligands (Scheme 658). The molecular structure of some of these complexes has been determined by X-ray crystallography.  $C_1$ -symmetry is observed in the solid state, although in solution at room temperature the NMR spectra indicate  $C_2$ -symmetry.<sup>1678</sup>

Details for the preparation of a range of bis-aryl and binaphthyl 2-position bridged bis-Ind compounds and the formation of *ansa*-titanium derivatives via metallation reactions have been reported (Scheme 659).<sup>1113,1679</sup> Reaction of the dilithium anions of the appropriate indene compounds with  $TiCl_3$  followed by oxidation with HCl gives the corresponding bis-Ind complexes in good yields. The bis-aryl bridged bis-Ind ligands give only a single chiral isomer of the complexes, the bis-aryl link determining the chirality of the complex, and the indenyl ligands projecting their  $C_2$ -chirality directly to the site of reaction. X-ray diffraction confirms the expected structures. The *in situ* prepared bis(2-Ind) complexes are readily reduced with  $H_2$  and Adam's catalyst to the tetrahydroindenyl complexes.<sup>1679</sup>

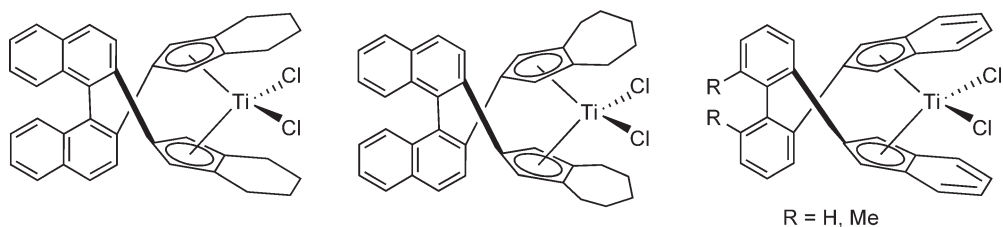
Attempts to form a chiral Tebbe-type complex from *ansa*-bis(binaphthyl) dichloro or dimethyl titanium derivatives have been unsuccessful (Scheme 660).<sup>1419</sup>

Biphenyl-bridged bis-Cp' titanocene dichloride and dimethyl complexes have been synthesized, and the kinetic resolution of the racemic final mixture of the products has been carried out. A mixture of diastereomers is obtained by treatment of the dimethyl compound with *O*-acetyl-mandelic acid, while enantiomerically pure products result in the reaction of the dichloro derivative with (*R*)-binaphthol and 1 equiv. of  $LiBu^n$  (Scheme 661).<sup>1050</sup>

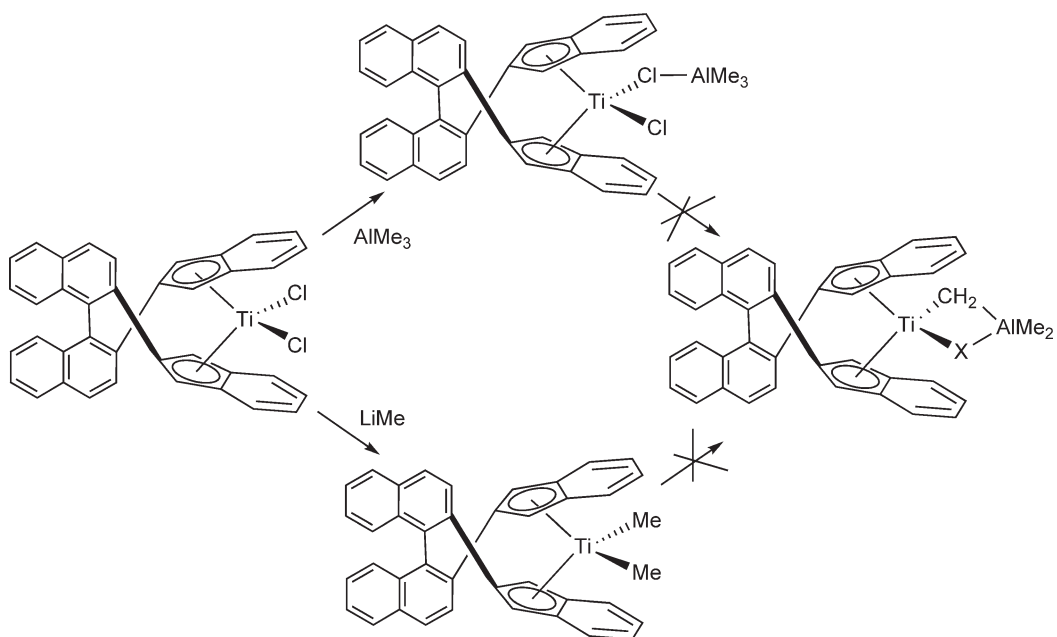
The  $C_2$ -symmetric complex ethylene bis(tetrahydroindenyl) titanium 1,1'-binaphth-2,2'-dithiolate has been used to catalyze the asymmetric hydrogenation of unfunctionalized trisubstituted olefins.<sup>1680</sup> The kinetic resolution of racemic disubstituted 1-pyrrolidines via asymmetric reduction has been described.<sup>1681</sup>



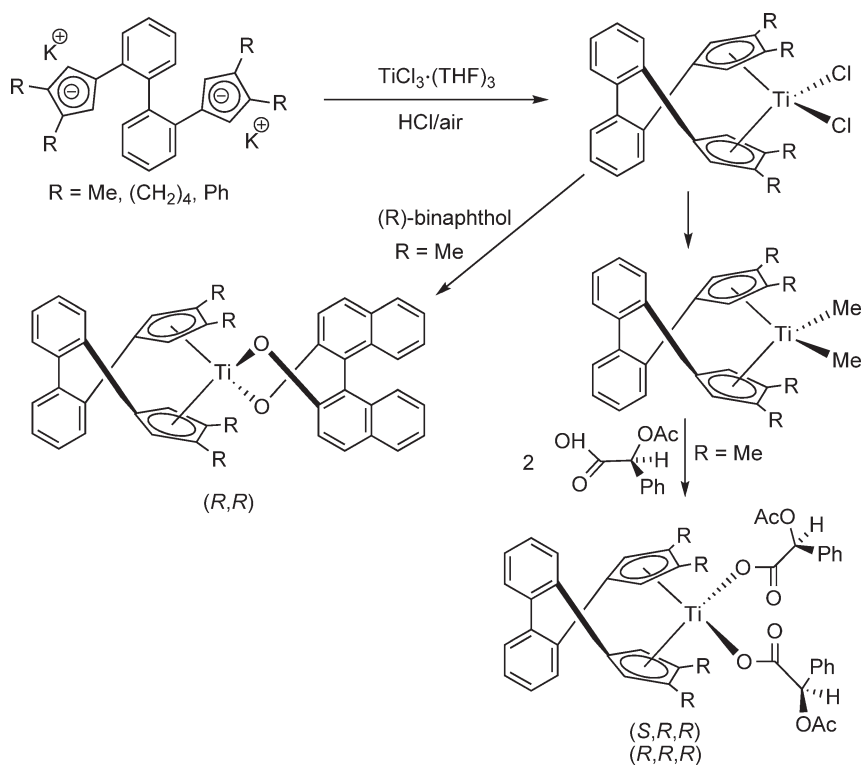
Scheme 658



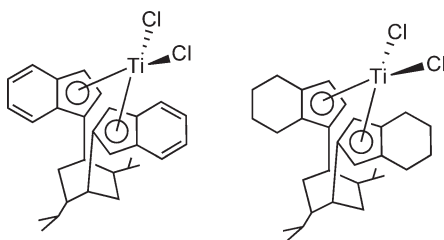
Scheme 659



Scheme 660



Scheme 661



Scheme 662

Full details for the preparation of dichloro *ansa*-bis-Ind and *ansa*-bis(tetrahydroindenyl) titanium derivatives with the 2,5-diisopropylcyclohexane bridging group (Scheme 662) have been reported along with their X-ray structures. The compounds were used to catalyze the enantioselective pinacol coupling of benzaldehyde.<sup>1682</sup>

The complex *syn*-[2,2-bis(3-isopropyl-cyclopentadienyl)propane] titanium dichloride (C<sub>19</sub>H<sub>26</sub>)TiCl<sub>2</sub> shows a short-bridged *ansa*-metallocene arrangement. It has been used as a pre-catalyst in polymerization processes. Its molecular structure was studied by X-ray diffraction; the most important structural feature is the distortion in the angles caused by the short bridge.<sup>1683</sup>

Studies on dichloro *ansa*-Cp titanium compounds as catalytic systems, in the presence of MAO for the polymerization of ethylene and propylene, have been described.<sup>1684</sup>

The *ansa*-linked macrocycle imido titanium complexes have been described. They are isolobal analogs of *ansa*-linked bis-Cp complexes and relatives of Cp-amido olefin polymerization catalysts.<sup>1685</sup>

The *ansa*-titanium complexes containing tetramethyl-Cp ligands bridged by five- or eight-membered aliphatic chains can be reduced with magnesium to afford a series of monochloro Ti(III) derivatives which have been characterized by spectroscopic methods (see Section 4.05.4.1.3.(i)).<sup>1033–1035,1142,1151,1686</sup>

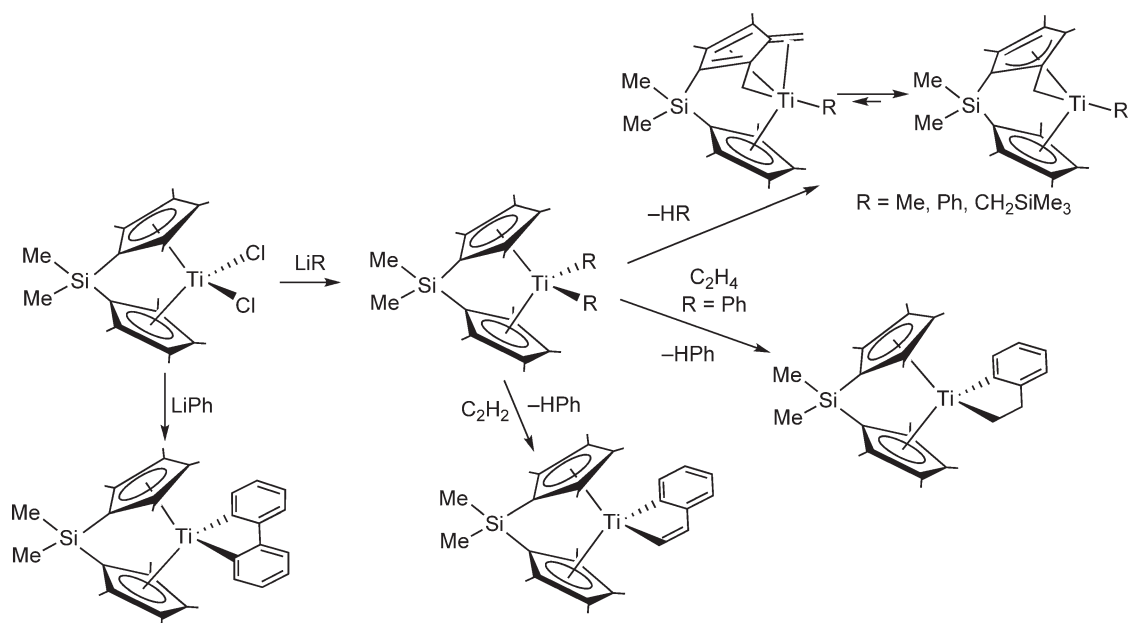
#### 4.05.5.2 Silicon-bridged *ansa*-titanocene Derivatives

The reaction of Me<sub>2</sub>Si(C<sub>5</sub>H<sub>4</sub>)<sub>2</sub>TiCl<sub>2</sub> with LiCH<sub>2</sub>PPh<sub>2</sub>·TMEDA affords the dialkyl derivative Me<sub>2</sub>Si(C<sub>5</sub>H<sub>4</sub>)<sub>2</sub>Ti(CH<sub>2</sub>PPh<sub>2</sub>)<sub>2</sub>, which was used as a catalyst for the hydrogenation of olefins.<sup>1687</sup> Me<sub>2</sub>Si(C<sub>5</sub>H<sub>4</sub>)<sub>2</sub>TiCl<sub>2</sub> is reduced with HgCl<sub>2</sub>-activated Mg in THF in the presence of ligands L to give titanium(II) adducts Me<sub>2</sub>Si(C<sub>5</sub>H<sub>4</sub>)<sub>2</sub>TiL<sub>2</sub> [L = CO, PMe<sub>2</sub>Ph, CNC<sub>6</sub>H<sub>3</sub>Me<sub>2</sub>-2,6].<sup>1688</sup>

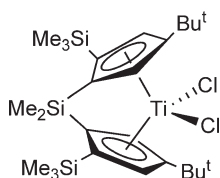
The *ansa*-titanium derivatives Me<sub>2</sub>Si(C<sub>5</sub>H<sub>4</sub>)<sub>2</sub>TiR<sub>2</sub> (R = Me, Ph) react with LiR (R = Me, Ph) to give titanium(III) derivatives.<sup>1689</sup>

The *ansa*-bis-Cp derivatives MeRSi(C<sub>5</sub>H<sub>4</sub>)<sub>2</sub>TiCl<sub>2</sub>, MeRSi(C<sub>5</sub>H<sub>4</sub>)(C<sub>5</sub>Me<sub>4</sub>)TiCl<sub>2</sub>, and MeRSi(C<sub>5</sub>Me<sub>4</sub>)<sub>2</sub>TiCl<sub>2</sub>, containing vinyl and allyl substituents (CH=CH<sub>2</sub>, CH<sub>2</sub>CH=CH<sub>2</sub>) bonded to the bridging silicon atom, have been synthesized by the reaction of the lithium salt of the *ansa*-Cp derivative with TiCl<sub>4</sub>. The reactivity of some of these complexes has been tested in hydrogenation and hydroboration processes.<sup>1690</sup>

Several permethylated *ansa*-titanocene complexes containing silicon-based bridging groups have been synthesized and structurally characterized by X-ray diffraction. The compound Me<sub>2</sub>Si(C<sub>5</sub>Me<sub>4</sub>)<sub>2</sub>TiCl<sub>2</sub> (Scheme 663) has been obtained in low yield by the reaction of TiCl<sub>4</sub> with the lithium salt of the corresponding Cp dianion. The formation of polytitanium complex byproducts and oxidation processes of the Cp anion by TiCl<sub>4</sub> are thought to be responsible for the low yield of *ansa*-product. Reduction of this complex with LiBu<sup>n</sup> or with Mg in the presence of acetylenes produces low-valent *ansa*-titanium derivatives. The molecular structures, steric and electronic properties of the bis-Cp' and the *ansa*-titanium derivatives have been compared.<sup>1691</sup> The reactions with the appropriate lithium alkyl reagents give the corresponding dialkyl or diamido derivatives Me<sub>2</sub>Si(C<sub>5</sub>Me<sub>4</sub>)<sub>2</sub>TiR<sub>2</sub>. Interestingly, the reaction with an excess of LiPh results in C–C coupling and the formation of the biphenyl-2,2'-diyl complex. The dialkyl complexes are used as precursors to prepare other derivatives via reaction of the Ti–C bonds. In the absence of a substrate, the dialkyl complexes eliminate alkane HR to give the corresponding fulvene derivatives. The titanium–fulvene interaction in these complexes may be considered to have similar character to that of a metal–trialkylidene-methane disposition (see Scheme 663). Elimination of benzene from Me<sub>2</sub>Si(C<sub>5</sub>Me<sub>4</sub>)<sub>2</sub>TiPh<sub>2</sub> presumably evolves through formation of a benzyne intermediate, which can be trapped by reaction with C<sub>2</sub>H<sub>4</sub> or C<sub>2</sub>H<sub>2</sub> (Scheme 663). The molecular structures of majority of the synthesized complexes have been determined by X-ray diffraction and the crystallographic data are compared with the analogous non-bridged dichloro titanium compounds.<sup>1692</sup>



Scheme 663



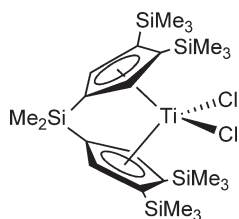
Scheme 664

The complexes  $\text{Me}_2\text{E}(\text{C}_5\text{H}_4)(\text{C}_5\text{Me}_4)\text{TiCl}_2$  ( $\text{E} = \text{Si}, \text{Ge}$ ) have been prepared by the reaction of the corresponding lithium salt of the *ansa*-cyclopentadiene with  $\text{TiCl}_4(\text{THF})_2$  and the molecular structure of the silyl derivative has been determined by X-ray diffraction. In combination with MAO, the silyl derivative catalyzes the polymerization of ethylene.<sup>1693</sup>

$\text{TiCl}_3(\text{THF})_3$  reacts with  $\text{K}_2\text{Bp}$  followed by air oxidation in the presence of  $\text{HCl}$  to give *rac*- $\text{TiBpCl}_2$  (Scheme 664). The compound was isolated as a dark-green solid and its molecular structure determined by X-ray diffraction. Intramolecular steric repulsions are important in this structure.<sup>1694</sup>

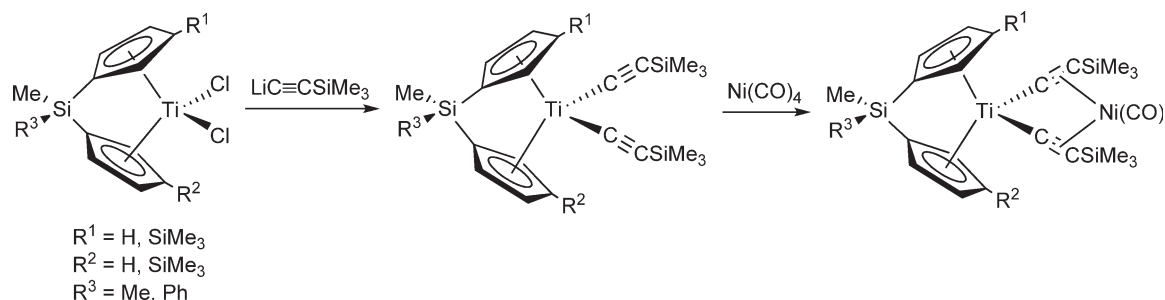
The synthesis of  $\text{Me}_2\text{Si}\{\text{C}_5\text{H}_2(\text{SiMe}_3)_2\}_2\text{TiCl}_2$  (Scheme 665) has been reported by the reaction of the potassium salt of the bis-Cp anion with  $\text{TiCl}_4(\text{THF})_2$ , the X-ray crystal structure of which has been determined. The complex has been tested for ethylene polymerization in the presence of MAO.<sup>1695</sup>

The molecular structure of  $\text{Me}_2\text{Si}(\text{C}_5\text{H}_4)_2\text{Ti}(\text{S})_5$  has been determined by X-ray diffraction methods.<sup>1696</sup>  $\text{Me}_2\text{Si}(\text{C}_5\text{H}_4)_2\text{TiCl}_2$  reacts with a solution of  $\text{Li}_2\text{Se}_5$ , prepared *in situ*, to give the *ansa*-titana-cyclohexaselenano

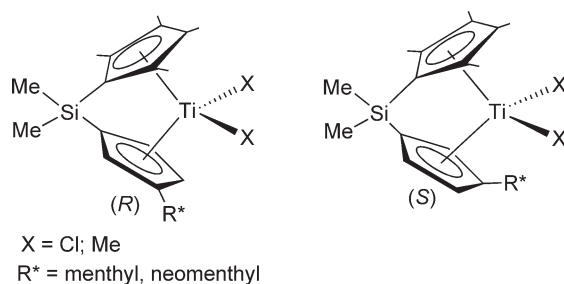


Scheme 665





Scheme 666

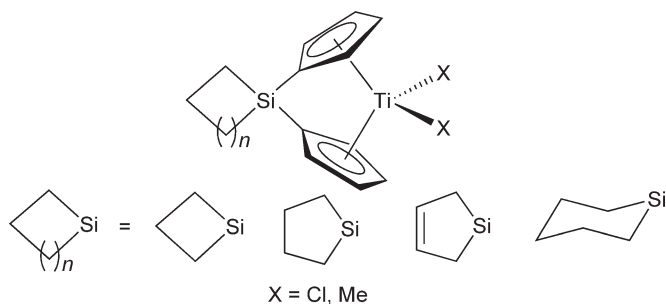


Scheme 667

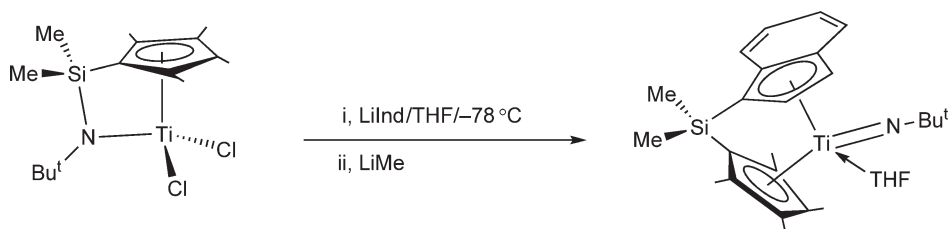
compound  $\text{Me}_2\text{Si}(\text{C}_5\text{H}_4)_2\text{TiSe}_5$ . Its molecular structure consists of discrete molecules with the  $\text{TiSe}_5$  ring in the chair conformation and it is very similar to that found for the sulfur analog  $\text{Me}_2\text{Si}(\text{C}_5\text{H}_4)_2\text{Ti}(\text{S})_5$ .<sup>1697</sup>

The bis(alkynyl) derivatives  $\text{MeR}^3\text{Si}(\text{C}_5\text{H}_3\text{R}^1)(\text{C}_5\text{H}_3\text{R}^2)\text{Ti}(\text{C}\equiv\text{CSiMe}_3)_2$  (Scheme 666) are obtained by the reaction of the parent dichlorides with 2 equiv. of  $\text{LiC}\equiv\text{CSiMe}_3$ . These compounds react with  $\text{Ni}(\text{CO})_4$  to afford  $\{\text{MeR}^3\text{Si}(\text{C}_5\text{H}_3\text{R}^1)(\text{C}_5\text{H}_3\text{R}^2)\text{Ti}(\text{C}\equiv\text{CSiMe}_3)_2\}\text{Ni}(\text{CO})$  containing a low-valent nickel–monocarbonyl fragment stabilized by the chelating effect of both alkynyl ligands. The properties of the  $\text{MeR}^3\text{Si}$ -bridged titanocenes in comparison to the appropriate unbridged species have been discussed. Both type of complexes exhibit similar spectroscopic data. The unbridged  $\text{Ti-Ni}$  derivatives are stable in the solid state as well as in solution, while the analogous silyl-bridged complexes decompose in solution.<sup>1698</sup>

The chiral *ansa*-bis- $\text{Cp}'$  complexes  $\text{Me}_2\text{Si}(\text{C}_5\text{Me}_4)(\text{C}_5\text{H}_3\text{-3-R}^*)\text{TiCl}_2$  ( $\text{R}^* = \text{menthyl, neomenthyl}$ ) (Scheme 667) are synthesized as a mixture of diastereoisomers, which differ only by which face of the asymmetrically substituted  $\text{Cp}$  ring is bonded to titanium. In addition to the chiral substituents, these 1,3-substituted derivatives exhibit planar chirality. Optically pure diastereomers are obtained by crystallization or isomerization using UV irradiation. In the case of the menthyl compounds, both diastereoisomers have been isolated and their absolute configurations determined by X-ray crystallography. The neomenthyl derivatives are obtained as a 1.4:1 mixture of diastereoisomers. The optically pure  $\text{Me}_2\text{Si}(\text{C}_5\text{Me}_4)(\text{C}_5\text{H}_3\text{-3-menthyl})\text{TiCl}_2$  can be converted into the corresponding dimethyl derivative. Both  $\text{Me}_2\text{Si}(\text{C}_5\text{Me}_4)(\text{C}_5\text{H}_3\text{-3-menthyl})\text{TiCl}_2$  diastereoisomers catalyze the hydrosilylation of ketones, for which the (*R*)-isomer is the more stereoselective catalyst.<sup>1699</sup> The catalytic properties of these compounds, which have different faces of the asymmetric  $\text{Cp}$  ring coordinated to the  $\text{Ti}$  center, in particular their ability to catalyze the hydrosilylation of ketones and the hydrogenation of alkenes, have been studied, after activation with  $\text{LiBu}^n$ . Inspection of the crystal structures of both diastereoisomers allows the difference in stereoselectivity to be rationalized. Highest *ee*'s and rates of hydrosilylation were observed with aryl ketones containing electron-donating groups in the ring.<sup>1700</sup> Propylene polymerizations with *rac*- $\text{Me}_2\text{Si}(\text{C}_5\text{H}_3\text{Me})_2\text{MCl}_2$  ( $\text{M} = \text{Ti, Zr, Hf}$ ) in combination with MAO have been carried out to study the effect of the metal species on catalytic activity, stereoregularity, regioregularity, and molecular weight of poly(propylene). The titanium catalyst shows the lowest activity among the three catalysts. The stereospecificity of the titanium based catalyst is very high and the portion of the *mmmm* pentads is roughly as high as for the zirconium and hafnium analog. On the other hand, the regiospecificity of the titanium-based catalyst is low and only a 1,3-regioirregular structure was observed.<sup>1701</sup>



Scheme 668

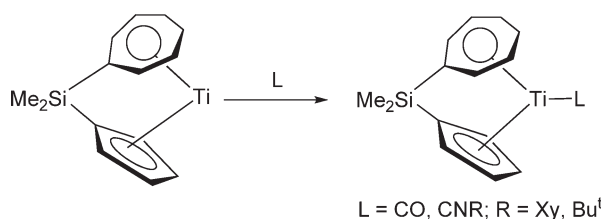


Scheme 669

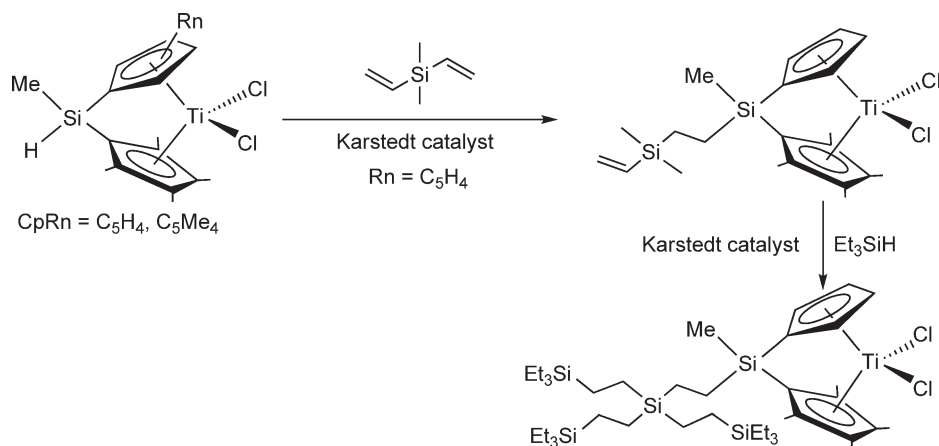
A series of silacycloalkyl-bridged *ansa*-titanium derivatives have been synthesized (Scheme 668). The compounds  $(\text{cyclo})\text{SiCp}_2\text{TiCl}_2$  have been prepared by the reaction of  $\text{TiCl}_4$  with the dilithium salt of the bridged bis-Cp reagent in diethyl ether. Methylation of diethyl ether solutions of the dichloride derivatives with  $\text{MgBrMe}$  affords the corresponding dimethyl complexes. The catalytic activity for ethylene polymerization has been studied, and DFT calculations establish that the size of the bridge ring influences the catalytic activity, that is, the silacyclohexyl complex shows higher activity than the conformationally less stable silacyclobutyl- and pentyl-bridged complexes. The catalytic activity is enhanced by silacycloalkyl bridges as a consequence of their increased conformational stability.<sup>1702</sup>

An unprecedented route to an imido *ansa*-titanium complex (Scheme 669) containing a dimethylsilyl-bridged  $\eta^5$ -tetramethyl-Cp- $\eta^5$ -Ind ligand and a near-linear terminal imido group has been reported by the reaction of  $[(\text{C}_5\text{Me}_4)\text{SiMe}_2\text{NBu}^t]\text{TiCl}_2$  with LiInd in THF at  $-78^{\circ}\text{C}$ , followed by direct addition of LiMe. The molecular structure has been determined by X-ray diffraction. This compound is an effective initiator for the syndiospecific polymerization of MMA. The polymerization activity is substantially enhanced by activation with the strong Lewis acid  $\text{Al}(\text{C}_6\text{F}_5)_3$ .<sup>1703–1705</sup>

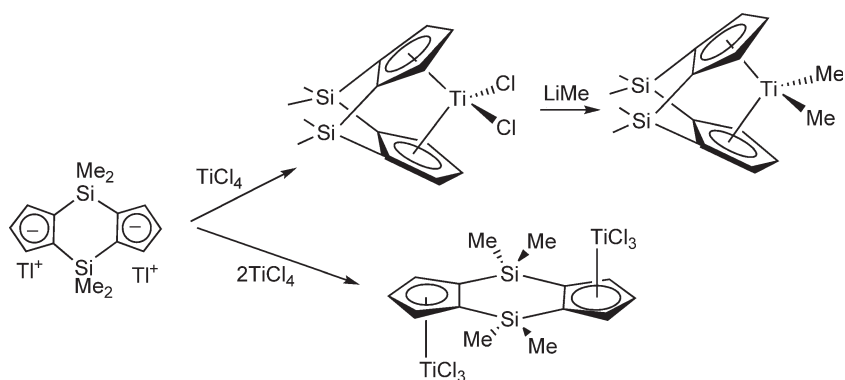
The complex shown in Scheme 670 appears to be the first example of an *ansa*-cycloheptatrienyl-Cp titanium complex. Its reactivity toward  $\sigma$ -donor and  $\pi$ -acceptor ligands demonstrates that this complex does not behave like a low-valent titanium compound but rather bears a closer resemblance to a Lewis-acidic  $\text{Ti}(\text{IV})$  complex. Based on theoretical calculations, this behavior can be attributed to a strong and appreciably covalent Ti-cycloheptatrienyl interaction, which leads to highly stabilized frontier orbitals and consequently to a diminishing  $\pi$ -electron donor ability.<sup>1706</sup>



Scheme 670



Scheme 671



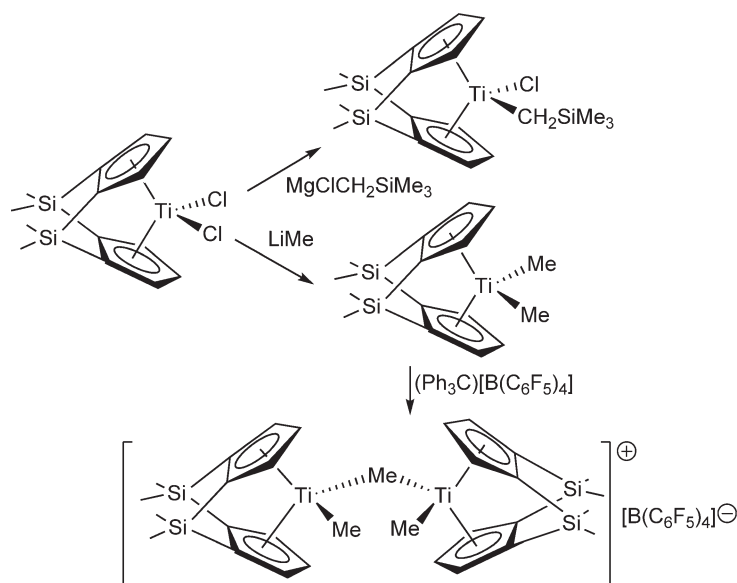
Scheme 672

The *ansa*-compounds MeHSi(C<sub>5</sub>R<sub>4</sub>)(C<sub>5</sub>Me<sub>4</sub>)TiCl<sub>2</sub> (R = H, Me) can be synthesized by the reaction of TiCl<sub>4</sub> with the lithium salt of the *ansa*-Cp ligand precursors. Hydrosilylation with Si(CH=CH<sub>2</sub>)<sub>4</sub> or Me<sub>2</sub>Si(CH=CH<sub>2</sub>)<sub>2</sub> in the presence of Karstedt catalyst affords new derivatives formed by the reaction of only one of the double bonds of the silane substrate. Further hydrosilylations of the vinyl groups are possible in the presence of Et<sub>3</sub>SiH (Scheme 671).<sup>1707</sup>

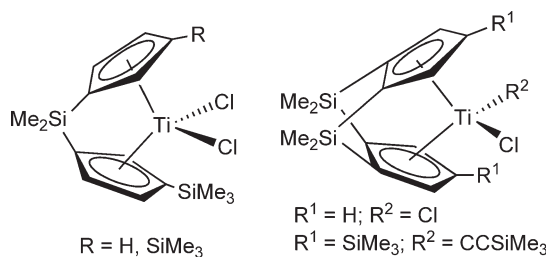
Doubly bridged *ansa*-titanium complexes are considered as a new class of stereorigid catalysts for stereospecific  $\alpha$ -olefin polymerization. Doubly silyl bridged *ansa*-complexes are considerably more strained than their singly bridged analogs.

The reaction of Ti<sub>2</sub>[(C<sub>5</sub>H<sub>3</sub>)<sub>2</sub>(SiMe<sub>2</sub>)<sub>2</sub>] with 1 equiv. of TiCl<sub>4</sub> leads to (Me<sub>2</sub>Si)<sub>2</sub>(C<sub>5</sub>H<sub>3</sub>)<sub>2</sub>TiCl<sub>2</sub> which can be methylated with LiMe or MgClMe to give the corresponding dimethyl derivative. When the same reaction is performed with 2 equiv. of TiCl<sub>4</sub> at room temperature, the mono-Cp product (TiCl<sub>3</sub>)<sub>2</sub>[ $\mu$ -(C<sub>5</sub>H<sub>3</sub>)<sub>2</sub>(SiMe<sub>2</sub>)<sub>2</sub>] is obtained. The molecular structures of these compounds have been determined by X-ray diffraction. (TiCl<sub>3</sub>)<sub>2</sub>[ $\mu$ -(C<sub>5</sub>H<sub>3</sub>)<sub>2</sub>(SiMe<sub>2</sub>)<sub>2</sub>] is a binuclear complex with the metals in *trans*-position relative to the ligand plane (Scheme 672).<sup>1708</sup> (Me<sub>2</sub>Si)<sub>2</sub>(C<sub>5</sub>H<sub>3</sub>)<sub>2</sub>TiCl<sub>2</sub> is reduced with LiBHET<sub>3</sub> to give unidentified Ti(III) species,<sup>1709</sup> while the reaction with ClMgCH<sub>2</sub>SiMe<sub>3</sub> gives the chloro alkyl derivative (Me<sub>2</sub>Si)<sub>2</sub>(C<sub>5</sub>H<sub>3</sub>)<sub>2</sub>TiCl(CH<sub>2</sub>SiMe<sub>3</sub>) and treatment with LiMe affords the dimethyl complex (Me<sub>2</sub>Si)<sub>2</sub>(C<sub>5</sub>H<sub>3</sub>)<sub>2</sub>TiMe<sub>2</sub>. The cationic titanium species [(Me<sub>2</sub>Si)<sub>2</sub>(C<sub>5</sub>H<sub>3</sub>)<sub>2</sub>TiMe]<sup>+</sup> is obtained by the reaction of the dimethyl compound with [Ph<sub>3</sub>C][B(C<sub>6</sub>F<sub>5</sub>)<sub>4</sub>] at -78 °C, as demonstrated by NMR spectroscopy (Scheme 673). Titanium(III) species are obtained by reduction of the dichloro complex with 1 equiv. of sodium amalgam.<sup>1710</sup>

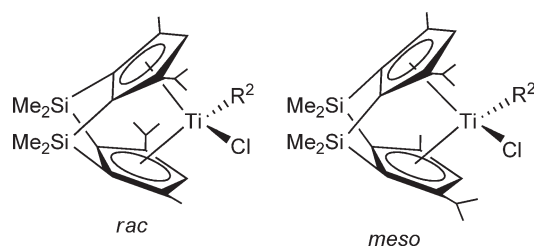
The synthesis of *ansa*- and doubly dimethylsilyl-bridged titanocenes supporting trimethylsilyl-substituted Cp rings have been described (Scheme 674). Polymerization of ethylene and propylene with these catalysts in the presence of MAO has been studied.<sup>1711</sup>



Scheme 673

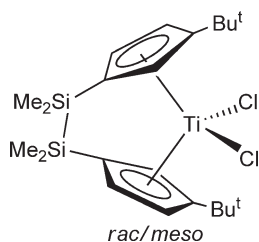


Scheme 674

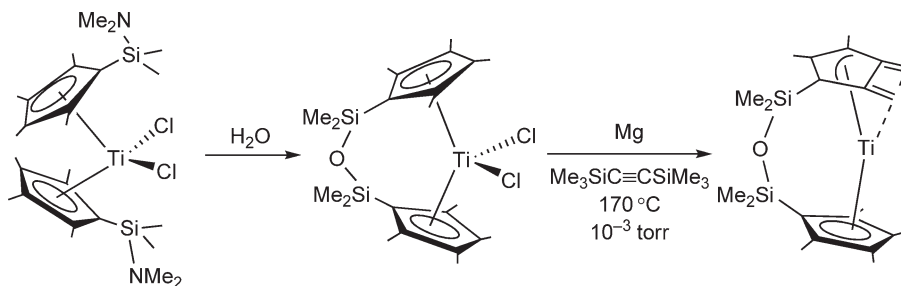


Scheme 675

A 1:1 *rac:meso* mixture of the doubly  $\text{SiMe}_2$ -bridged complex  $\text{Me}_2\text{Si}(\text{C}_5\text{H}-3\text{-Pr}^i-5\text{-Me})\text{TiCl}_2$  (Scheme 675) has been obtained, surprisingly, by treatment of the lithium salt of the *rac*-Cp reagent with  $\text{TiCl}_3(\text{THF})_3$  followed by oxidation with  $\text{PbCl}_2$ . The racemic component is obtained by recrystallization from toluene and its crystal structure has been determined by X-ray diffraction. The *rac-meso* interchange occurs in benzene solution just above room temperature, affording an approximately 1:1 mixture of *rac:meso* components. The thermodynamic parameters have been calculated.<sup>1712</sup> In the presence of MAO,  $(\text{Me}_2\text{Si})_2(\text{C}_5\text{H}_2\text{Pr}^i-4)(\text{C}_5\text{HPr}^i-2-3,5)\text{TiCl}_2$  as catalyst produces atactic polypropylene.<sup>1712</sup>



Scheme 676



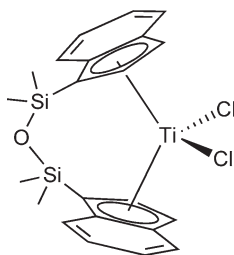
Scheme 677

The disilyl-bridged complexes  $(C_5R_4-SiMe_2-SiMe_2-C_5R_4)TiCl_2$  ( $R=H, Me$ ) have been synthesized.<sup>1713,1714</sup> The complex  $Me_4Si_2(C_5H_3Bu^t-3)_2TiCl_2$  (Scheme 676) has been obtained by the reaction of  $TiCl_4(THF)_2$  with  $Li_2[Me_4Si_2(C_5H_3Bu^t-3)_2]$  as a mixture of *rac*- and *meso*-isomers in about 2:3 molar ratio. Fractional crystallization from  $CH_2Cl_2$ /hexane allows the separation of both isomers. The molecular structure of the *meso*-isomer has been determined. In the presence of MAO, this complex has been employed as ethylene polymerization catalyst, with low activities.<sup>1715</sup> The analogous complexes  $Me_4Si_2(C_5H_3Me-3)_2TiCl_2$ ,  $Me_4Si_2(C_5H_3R-3)(C_5H_4)TiCl_2$  ( $R=Me, Bu^t$ ), and  $Me_4Si_2(1-C_9H_7)_2TiCl_2$  ( $x=6, 10$ ) have been synthesized and used for the polymerization of ethylene after activation with MAO.<sup>1716,1717</sup>

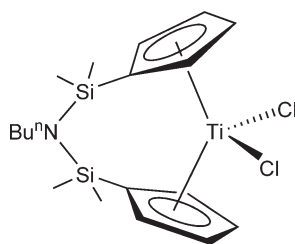
$(C_5H_4SiClMe_2)_2TiCl_2$  reacts with stoichiometric amount of water with selective hydrolysis of the Si-Cl bond to give the previously reported compound  $[Me_2SiOSiMe_2(C_5H_4)_2]TiCl_2$  (Scheme 448; Section 4.05.4.1.1.(i).(d)).<sup>1064</sup>  $(C_5H_4SiBrMe_2)_2TiCl_2$  is obtained by boron-silicon exchange reaction in the reaction of  $(C_5H_4SiMe_3)_2TiCl_2$  with  $BBr_3$ . Hydrolysis of  $(C_5H_4SiBrMe_2)_2TiCl_2$  with water in THF affords the *ansa*-titanocene with a bridging disiloxane group (Scheme 449; Section 4.05.4.1.1.(i).(d)).<sup>1066</sup>

The hydrolysis of Si-N bonds in the amido-silyl Cp substituted compound  $(C_5Me_4SiMe_2NMe_2)_2TiCl_2$  affords the *ansa*-derivative with a tetramethyldisiloxane bridge  $[(C_5Me_4-SiMe_2)_2(\mu-O)]TiCl_2$ .<sup>1085</sup> The reduction of this complex with magnesium in the presence of bis(trimethylsilyl)acetylene affords the *ansa*-Ti(II) alkyne derivative. Its thermal decomposition in vacuum gives an asymmetric, allyldiene complex (Scheme 677).<sup>1718</sup>

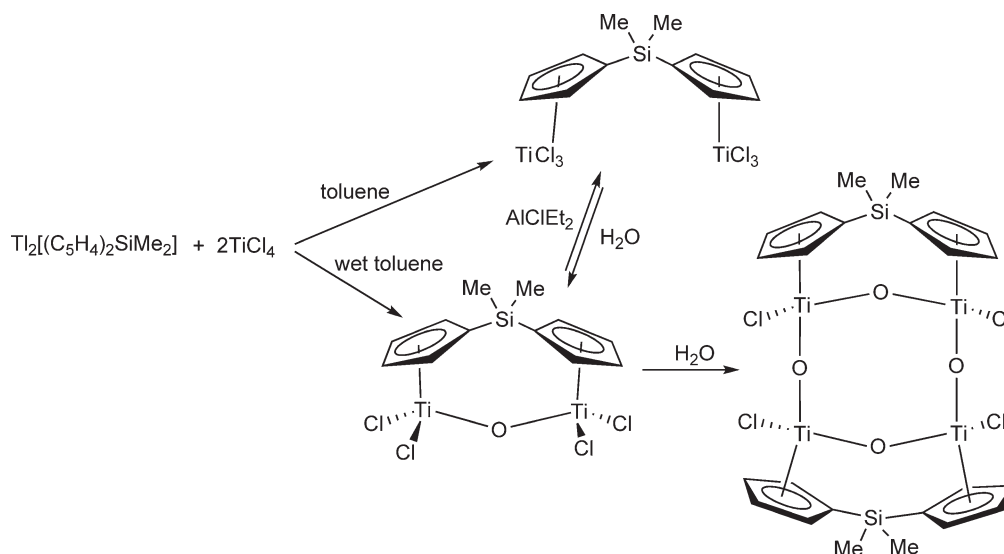
The siloxane-bridged bis(indenyl) complex shown in Scheme 678 has been synthesized from the corresponding lithium salt of 1,1,3,3-tetramethyl-1,3-bis(indenyl)disiloxane and  $TiCl_4$ . This compound polymerizes ethylene only



Scheme 678



Scheme 679



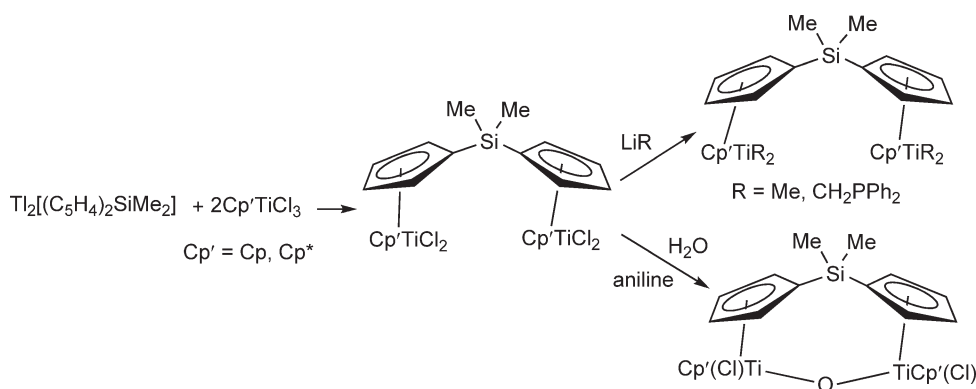
Scheme 680

when activated with MAO but not with  $[\text{Ph}_3\text{C}]^+[\text{B}(\text{C}_6\text{F}_5)_4]^-/\text{TIBA}$  and does not polymerize propylene with either co-catalyst. Electron donation from the oxygen atom of the siloxane bridge to the metal center is proposed in the intermediate species formed in the polymerization process.<sup>1719</sup> The compound is converted to the corresponding tetrahydroindenyl by hydrogenation over  $\text{PtO}_2$ .<sup>1720</sup>

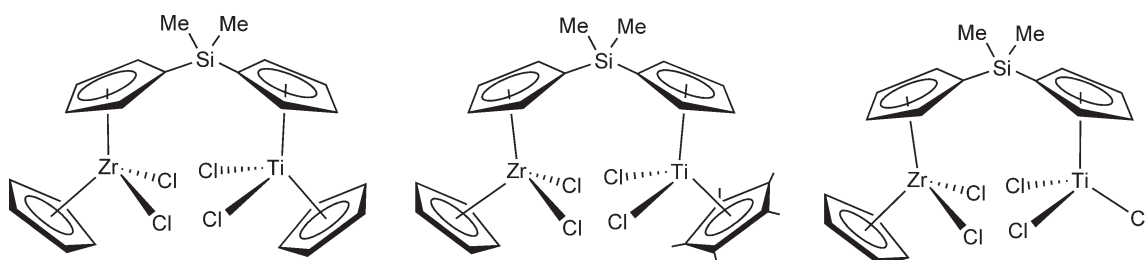
$[\text{C}_5\text{H}_4\text{-SiMe}_2(\text{Bu}^n)\text{SiMe}_2\text{-C}_5\text{H}_4]\text{TiCl}_2$  has been prepared (Scheme 679). In combination with MAO it is a highly active olefin polymerization catalyst.<sup>1721</sup>

The *ansa*-bridged homobinuclear titanium and heterobinuclear titanium–zirconium complexes have been reported. For more examples of this type of complexes, see Sections 4.05.4.1.1.(i),(g) and 4.05.4.1.3.(i)

The reaction of  $\text{Ti}_2[(\text{C}_5\text{H}_4)_2\text{SiMe}_2]$  with 2 equiv. of  $\text{TiCl}_4$  produces the binuclear compound  $[\mu-(\text{C}_5\text{H}_4)_2\text{SiMe}_2](\text{TiCl}_3)_2$ . Controlled hydrolysis of this complex gives the binuclear  $\mu$ -oxo compound  $[\mu-(\text{C}_5\text{H}_4)_2\text{SiMe}_2](\text{TiCl}_2)_2(\mu\text{-O})$ , which reacts with  $\text{AlCl}_2\text{Et}$  to regenerate quantitatively the complex  $[\mu-(\text{C}_5\text{H}_4)_2\text{SiMe}_2](\text{TiCl}_3)_2$ . The tetranuclear  $\mu$ -oxo compound  $[\{\mu-(\text{C}_5\text{H}_4)_2\text{SiMe}_2\}(\text{TiCl}_2)_2(\mu\text{-O})]_2(\mu\text{-O})_2$  is obtained when  $[\mu-(\text{C}_5\text{H}_4)_2\text{SiMe}_2](\text{TiCl}_3)_2$  or  $[\mu-(\text{C}_5\text{H}_4)_2\text{SiMe}_2](\text{TiCl}_2)_2(\mu\text{-O})$  are treated with water in acetonitrile (Scheme 680). The crystal structure of the tetranuclear compound has been determined by X-ray diffraction and shows a non-planar  $\text{Ti}_4\text{O}_4$  core, not previously reported for other similar  $\text{Ti}_4\text{O}_x$  systems.<sup>1722</sup> Reaction of  $\text{Ti}_2[(\text{C}_5\text{H}_4)_2\text{SiMe}_2]$  with 2 equiv. of  $\text{Cp}^*\text{TiCl}_3$  ( $\text{Cp}^* = \text{Cp}$ ,  $\text{Cp}^*$ ) produces the binuclear bis- $\text{Cp}^*$ -type compound  $(\text{Cp}^*\text{TiCl}_2)_2[\mu-(\text{C}_5\text{H}_4)_2\text{SiMe}_2]$  which can be alkylated with  $\text{LiR}$  ( $\text{R} = \text{Me}$ ,  $\text{CH}_2\text{PPh}_2\cdot\text{TMEDA}$ ) to afford the corresponding dialkyl derivatives. Treatment of  $(\text{Cp}^*\text{TiCl}_2)_2[\mu-(\text{C}_5\text{H}_4)_2\text{SiMe}_2]$  with  $\text{H}_2\text{O}$  gives the  $\mu$ -oxo complex  $[(\text{Cp}^*\text{TiCl}_2)_2[\mu-(\text{C}_5\text{H}_4)_2\text{SiMe}_2]](\mu\text{-O})$  (Scheme 681). The molecular structures of  $[\text{Cp}^*\text{TiCl}_2]_2[\mu-(\text{C}_5\text{H}_4)_2\text{SiMe}_2]$  and the  $\mu$ -oxo complexes have been determined by single crystal X-ray diffraction.<sup>1723</sup> The compounds  $[\text{Cp}^*\text{TiX}_2]_2[\mu-(\text{C}_5\text{H}_4)_2\text{SiMe}_2]$  ( $\text{X} = \text{Cl}$ ,  $\text{CH}_2\text{PPh}_2$ ) have been used as catalysts for the hydrogenation of olefins.<sup>1687</sup>



Scheme 681



Scheme 682

The compounds  $(\text{CpZrCl}_2)\{\mu-(\text{C}_5\text{H}_4)_2\text{SiMe}_2\}(\text{CpTiCl}_2)$ ,  $(\text{CpZrCl}_2)\{\mu-(\text{C}_5\text{H}_4)_2\text{SiMe}_2\}[(\text{C}_5\text{Me}_5)\text{TiCl}_2]$ , and  $(\text{CpZrCl}_2)\{\mu-(\text{C}_5\text{H}_4)_2\text{SiMe}_2\}(\text{TiCl}_3)$  have been synthesized (Scheme 682). When activated with MAO, they are catalysts for the polymerization of ethylene and propylene.<sup>1724,1725</sup>

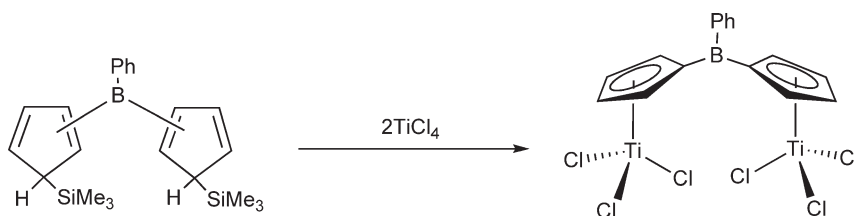
A combined *ab initio* molecular orbital study on the isotacticity control in propylene polymerizations with *ansa*-silylene-bridged group 4  $C_2$ -symmetric and asymmetric metallocene catalysts has been reported. The objective was to study the mechanism of isotactic stereoregulation at the insertion transition state and to provide a qualitative measure of the factors controlling the stereoregulation in propylene polymerization. To attain good stereoregulation, the substituents at the 2- and 4-positions of the Ind-based metallocene are very important. Among group 4 bis-Ind and bis(tetrahydroindenyl) complexes, titanium derivatives in general have a substantially better capability of producing an isotactic sequence than zirconium and hafnium analogs, due to the smaller atomic size of the central metal.<sup>1726</sup> The mechanism of the insertion polymerization of styrene with *ansa*-Ti derivatives has been investigated by the density functional theory.<sup>1727</sup>

#### 4.05.5.3 *ansa*-Titanocene Derivatives Bridged by other Heteroatoms

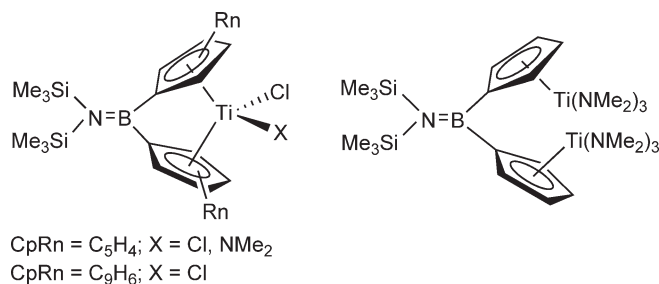
The synthesis of the germyl-bridged complex  $\text{Me}_2\text{Ge}(\text{C}_5\text{H}_4)(\text{C}_5\text{Me}_4)\text{TiCl}_2$  has been described.<sup>1693</sup> The symmetric and asymmetric *ansa*-complexes containing germanium-bridged ligands  $\text{Me}_2\text{Ge}(\text{C}_5\text{Me}_4)(\text{C}_5\text{R}_4)\text{TiCl}_2$  ( $\text{R}_4 = \text{Me}_4, \text{H}_4, \text{H}_3\text{Me}$ ) have been prepared by the reaction of  $\text{TiCl}_4$  with the corresponding lithium reagent. Preliminary results on the catalytic activity of these complexes in the polymerization of ethylene and propylene have been reported.<sup>1728</sup>

The *ansa*-bridged group 4 titanium derivatives containing boron bridges have been reviewed.<sup>394,678,1729</sup> The synthesis of the PhB-bridged homobimetallic titanium compound (Scheme 683) has been described using the dehalosilylation method.<sup>1729</sup>

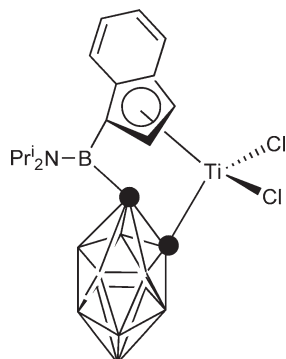
Bis-Cp and bis-Ind titanium complexes where both rings are connected by a boron bridge (Scheme 684) have been synthesized and characterized in solution by multinuclear NMR spectroscopy. The molecular structure of  $(\text{Me}_3\text{Si})_2\text{N}=\text{B}(\text{C}_5\text{H}_4)_2\text{TiCl}_2$  has been determined by X-ray diffraction.<sup>584,1730</sup>



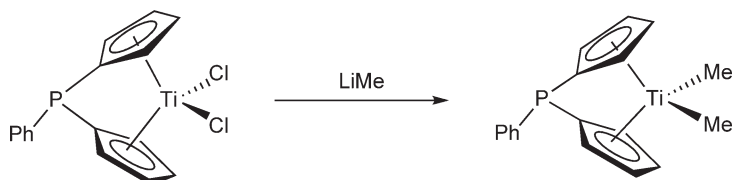
Scheme 683



Scheme 684



Scheme 685



Scheme 686

The salt metathesis reaction between  $\text{TiCl}_4(\text{THF})_2$  and  $\text{Li}_2[(\text{Pr}^i_2\text{NB})(\text{C}_9\text{H}_6)(\text{C}_2\text{B}_{10}\text{H}_{10})](\text{Et}_2\text{O})_2$  gives  $(\text{Pr}^i_2\text{NB})(\text{C}_9\text{H}_6)(\text{C}_2\text{B}_{10}\text{H}_{10})/\text{TiCl}_2$  (Scheme 685), which can also be prepared from the reaction of the lithium salt with 1 equiv. of  $\text{TiCl}_3(\text{THF})_3$ , followed by addition of 0.5 equiv. of  $\text{PbCl}_2$  in THF. This compound exhibits a moderate activity in the ethylene polymerization upon activation with MAO.<sup>1731</sup>

The phosphorus-bridged complex  $\text{PhP}(\text{C}_5\text{Me}_4)_2\text{TiCl}_2$  has been synthesized from  $\text{TiCl}_4(\text{THF})_2$  and  $\text{Li}_2[(\text{C}_5\text{Me}_4)_2\text{PPh}]$ . The dimethyl derivative  $\text{PhP}(\text{C}_5\text{Me}_4)_2\text{TiMe}_2$  can be prepared by subsequent treatment with  $\text{LiMe}$  (Scheme 686). The  $\text{PhP}$  bridge is oxidized to  $\text{PhP}(=\text{E})$  ( $\text{E} = \text{O}, \text{S}, \text{Se}$ ) upon reaction of the complexes with  $\text{O}_2$ ,  $\text{S}_m$ , or  $\text{Se}_m$ .<sup>1732</sup>



#### 4.05.6 Heteropolymetallic Compounds

The synthesis and study of early–late heteropolynuclear transition metal compounds is an active subject of interest in organometallic chemistry. The presence of two metal atoms, an electron-deficient and an electron-rich transition metal, in close proximity to one another could result in cooperative reactions with substrate molecules. Special attention has focused on titanium–transition metal complexes because of their ability to promote the activation of polar organic molecules, potential applications in homogeneous catalytic processes, and their relationship with strong metal–support interactions in some heterogeneous catalytic systems. A variety of compound types with different combinations of titanium and late transition metals are now known. Many of these compounds contain Cp and appropriate functionalized bridging ligands (phosphine, phosphido, thiolato, C-substituted rings, ...). A review covering work published from January 1988 to December 1997 on the structure and reactivity of early–late heterobimetallic complexes has appeared.<sup>1733</sup> Complexes with unbridged metal–metal bonds and containing different type of bridging ligands are covered.<sup>1733</sup> The properties of highly polar metal–metal bonds in early–late heterobimetallic complexes have also been highlighted.<sup>1734</sup>

Heterobinuclear complexes are formed by reactions of the vinylidene complex  $\text{Cp}^*\text{Ti}=\text{C}=\text{CH}_2$  with late transition metal compounds (see Section 4.05.4.2.4; Alkylidene complexes).

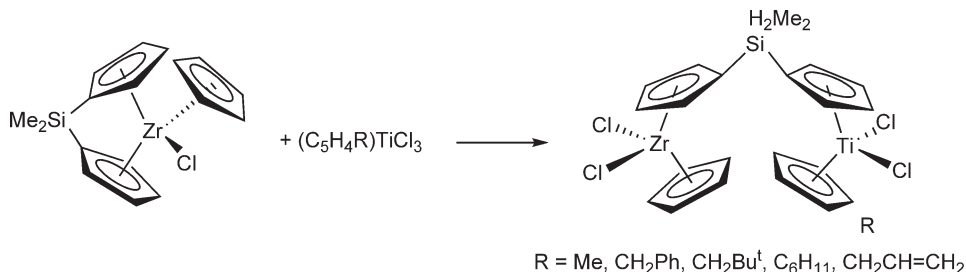
The use of heterobifunctional ligands is a very convenient method to link two different transition metals. Heterobimetallic Ti–Zr complexes (Scheme 687) have been prepared by the reaction of  $\text{Cp}[(\text{C}_5\text{H}_4)_2\text{SiMe}_2]\text{ZrCl}$  with  $(\text{C}_5\text{H}_4\text{R})\text{TiCl}_3$  in toluene under reflux. In the presence of MAO, these complexes are highly active catalysts for the polymerization of ethylene.<sup>1735</sup>

The diisothiocyanato compound  $\text{Cp}_2\text{Ti}(\text{NCS})_2$  reacts with  $\text{MCl}_2$  [ $\text{M} = \text{Cu}, \text{Pd}, \text{Pt}, \text{CuCl}(\text{PPh}_3)_3, \text{RuCl}_2(\text{PPh}_3)_3, \text{RuCl}_2(\text{DMSO})_4$ ] to give heterobimetallic complexes of stoichiometry  $\text{Cp}_2\text{Ti}(\mu\text{-NCS})_2\text{MCl}_2$  ( $\text{M} = \text{Cu}, \text{Pd}$  or  $\text{Pt}$ ) and  $\text{Cp}_2\text{Ti}(\mu\text{-NCS})_2\text{M}$  [ $\text{M} = \text{CuCl}(\text{PPh}_3)_2, \text{RuCl}_2(\text{PPh}_3)_2, \text{RuCl}_2(\text{DMSO})_2$ ]. These compounds have been characterized by physicochemical and spectroscopic methods.<sup>1736</sup>

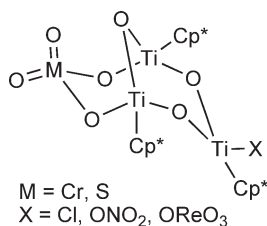
Reaction of  $[\text{Cp}^*\text{Ti}(\mu\text{-NH})_3(\mu_3\text{-N})]$  with  $[\text{MCl}(\text{cod})]_2$  ( $\text{M} = \text{Rh}, \text{Ir}$ ;  $\text{cod} = 1,5\text{-cyclooctadiene}$ ) affords the ionic complexes  $[(\text{cod})\text{M}(\mu_3\text{-NH})_3\text{Ti}_3\text{Cp}^*_3(\mu_3\text{-N})]\text{Cl}$ . Treatment of these complexes with  $\text{AgBPh}_4$  leads to anion metathesis and formation of the analogous tetraphenyl–borate derivatives. The lithium derivative  $[\text{Li}(\mu_3\text{-NH})_2(\mu_3\text{-N})\text{Ti}_3\text{Cp}^*_3(\mu_3\text{-N})_2\cdot\text{C}_7\text{H}_8]$  reacts with  $[\text{MCl}(\text{cod})]_2$  and  $[\text{RhCl}(\text{C}_2\text{H}_4)_2]_2$  to give the neutral complexes  $[(\text{cod})\text{M}(\mu_3\text{-NH})_2(\mu_3\text{-N})\text{Ti}_3\text{Cp}^*_3(\mu_3\text{-N})]$  and  $[\text{Rh}(\text{C}_2\text{H}_4)_2(\mu_3\text{-NH})_2(\mu_3\text{-N})\text{Ti}_3\text{Cp}^*_3(\mu_3\text{-N})]$ . X-ray crystal diffraction studies reveal a cube-type core for these compounds. DFT calculations have been carried out on the ionic and neutral azaheterometallobutane complexes to understand their electronic structures.<sup>628</sup>

$\text{Cp}_2\text{TiCl}_2$  reacts with 2 equiv. of  $\text{Na}[(\text{C}_5\text{H}_4\text{Me})\text{Mn}(\text{CO})_2(\text{CN})]$  to give  $\text{Cp}_2\text{Ti}[(\mu\text{-CN})\text{Mn}(\text{C}_5\text{H}_4\text{Me})(\text{CO})_2]_2$  as deep blue crystals. Similarly  $\text{TiCl}_4$ ,  $\text{CpTiCl}_3$ , and  $[\text{Cp}_2\text{TiCl}]_2(\text{O})$  also react with  $\text{Na}[(\text{C}_5\text{H}_4\text{Me})\text{Mn}(\text{CO})_2(\text{CN})]$  to afford analogous titanium–manganese heterobimetallic complexes.<sup>1737</sup> The metal carbonylate  $\text{Na}[\text{CpFeCO}_2]$  reacts with  $\text{Cp}_2\text{TiCl}_2$  at room temperature to yield the iron–titanium bonded compound  $\text{Cp}_2\text{Ti}[\text{CpFeCO}_2]_2$ , characterized by IR and mass spectra and elemental analyses.<sup>1738</sup>  $\text{Cp}_2\text{Ti}[\text{Co}(\text{CO})_4]_2$  has been prepared by alkane elimination of  $\text{Cp}_2\text{TiMe}_2$  with  $\text{HCo}(\text{CO})_4$  or alternatively by salt elimination from  $\text{Cp}_2\text{TiCl}_2$  with  $\text{Na}[\text{Co}(\text{CO})_4]$ .<sup>1739</sup>

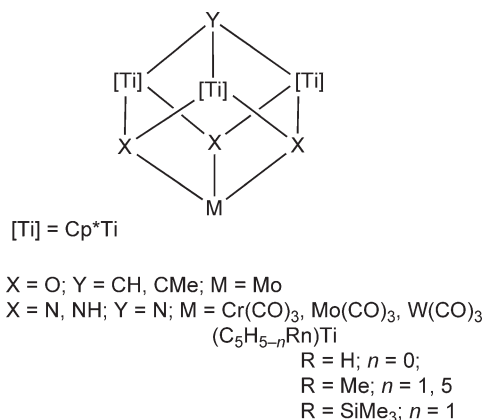
The chemistry of organo heterometallic oxo complexes has become a subject of great interest, since these compounds have been regarded as models for heterogeneous catalysts and metal–support interactions, for applications in metal-catalyzed oxo-transfer reactions and the use of such compounds as precursor to mono- and multi-component oxides. The oxophilic character of group 4 metals favors reaction with oxygen ligands. The synthesis of the complex  $(\text{Cp}_2\text{TiCl})[\text{Mo}(\text{C}_5\text{Me}_5)(\text{O})_2](\mu\text{-O})$  has been reported.<sup>1740</sup> A theoretical study on the simple anion  $[\text{CpTi}(\text{Mo}_5\text{O}_{18})]^{3-}$  based on extended Hückel calculations has been described. The frontier orbitals of the trianion



Scheme 687



Scheme 688



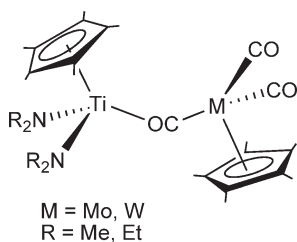
Scheme 689

have been examined in order to rationalize its reactivity toward electrophilic and nucleophilic reagents. Supposing that the reactions might be orbitally controlled, attack by electrophiles should take place at the Cp ligand, the titanium atom or two of the oxygens adjacent to this metal, which determine the HOMO of the molecule. The nature of the LUMO suggests nucleophilic attack at one of the equatorial molybdenum atoms.<sup>1741</sup>

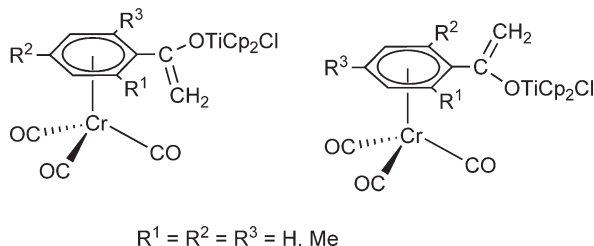
The reaction of  $[\text{Cp}^*\text{Ti}(\mu\text{-O})]_3$  with anhydrous silver salts  $\text{AgX}$  in organic solvents leads to precipitation of silver chloride and formation of chromate, sulfate, perhenate, and nitrate titanium derivatives (Scheme 688). The molecular structures of some of these compounds have been determined by X-ray diffraction.<sup>821</sup> The trinuclear bridging alkylidyne complexes  $[\text{Cp}^*\text{Ti}(\mu\text{-O})]_3(\mu_3\text{-CR})$  ( $R = \text{H, Me}$ ) and the isoelectronic imide  $[\text{Cp}^*\text{Ti}(\mu\text{-NH})]_3(\mu_3\text{-N})$  exhibit a very rich chemistry. Carbonyl hydrides and unsaturated molecules such as CO, RNC, and ketones can be incorporated in the  $\text{Ti}_3\text{O}_3$  core with direct participation of the alkylidyne unit (see Section 4.05.3.5.1).<sup>817</sup> These complexes can also act as tridentate six-electron donor ligands. They react with  $\text{M(CO)}_3\text{L}$  ( $L = \text{Me}_3\text{C}_6\text{H}_3, \text{CO}$ ;  $M = \text{Cr, Mo, W}$ ) to give heterometallic cubane derivatives  $[\text{Cp}^*\text{Ti}(\mu\text{-X})]_3(\mu_3\text{-Y})[\text{M(CO)}_3]$  (Scheme 689) which maintain unaltered alkylidyne or nitrido ligands. They have been characterized by NMR spectroscopy; the molecular structure of  $[\text{Cp}^*\text{Ti}(\mu\text{-O})]_3(\mu_3\text{-CMe})[\text{Mo(CO)}_3]$  has been determined by X-ray diffraction. For the alkylidyne compounds, downfield-shifted signals for the CR groups are observed in the  $^{13}\text{C}$  NMR spectra ( $\delta$  410–435). To understand the electronic structures of these heterocubane complexes, theoretical density functional studies have been applied.<sup>626</sup>

Extended studies modeling rhodium complexes supported on titania–silica fragments containing Cp–Ti bonds have been reported. Complexes such as  $\text{Cp}^*\text{Ti}(\mu_3\text{-O})[\text{Rh}(\text{cod})]$ ,<sup>1742</sup>  $[\text{Cp}^*\text{TiMe}(\text{O}_2\text{SiPh}_2)]_2$ ,<sup>1743</sup> and  $[\text{Cp}^*\text{Ti}]_2(\text{O}_2\text{SiPh}_2)_3$ <sup>1743</sup> are regarded as model, for titania–silica systems. The reaction of  $[\text{Cp}^*\text{TiMe}(\text{O}_2\text{SiPh}_2)]_2$  with  $[\text{Rh}(\mu\text{-OH})(\text{cod})]_2$  gives  $[\text{Cp}^*\text{TiMe}(\text{O}_2\text{SiPh}_2)]_2$  with elimination of methane.<sup>1743</sup>

$\text{Cp}^*\text{Ti}(\text{O}_2\text{Bz})(\text{OBzOH})$  reacts with  $[\text{M}(\mu\text{-OH})(\text{cod})]_2$  ( $M = \text{Rh, Ir}$ ) to give the heterobimetallic complexes  $\text{Cp}^*\text{Ti}(\text{O}_2\text{Bz})_2\text{M}(\text{cod})$ . Carbon monoxide readily replaces the cod ligand in the rhodium compound to give the dicarbonyl derivative  $\text{Cp}^*\text{Ti}(\text{O}_2\text{Bz})_2\text{Rh}(\text{CO})_2$ . The reactions of the monomethyl compound  $\text{Cp}^*\text{Ti}(\text{Me})(\text{OCH}_2)_2\text{py}$  with  $[\text{M}(\mu\text{-OH})(\text{cod})]_2$  afford  $\text{Cp}^*\text{Ti}(\text{OCH}_2)_2\text{py}(\mu\text{-O})\text{M}(\text{cod})$  by protonolysis of the Ti–Me bond. The molecular structures of some of these complexes have been established by single crystal X-ray diffraction.<sup>883</sup>



Scheme 690



Scheme 691

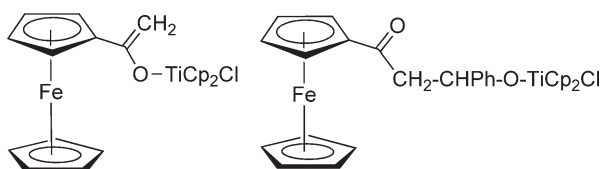
The heterobimetallic derivatives  $\text{Cp}^*(\text{R}_2\text{N})_2\text{Ti}(\text{OC})\text{M}(\text{CO})_2\text{Cp}$  ( $\text{R} = \text{Me, Et}$ ;  $\text{M} = \text{Mo, W}$ ) (Scheme 690) are synthesized by the reaction of  $\text{Cp}^*\text{Ti}(\text{NR}_2)_3$  with  $\text{MCp}(\text{CO})_3\text{H}$  where the two metals are bridged by a carbonyl group, as deduced by IR and  $^{13}\text{C}$  NMR spectroscopic data.<sup>1744</sup>

The formation of the heterobimetallic compounds  $\text{Cp}_2\text{Ti}(\text{OBu}^t)(\mu\text{-OC})\text{MCp}(\text{CO})_2$  ( $\text{M} = \text{Mo, W}$ ) is described by reductive cleavage of the metal–metal bond in the reaction of  $[\text{MCp}(\text{CO})_3]_2$  with the Ti(III) alkoxo derivative  $\text{Cp}_2\text{TiOBu}^t$ . The reaction is accompanied by oxidation of Ti(III) to Ti(IV) to give the final products bearing the carbonyl bridge. The heterobimetallic complexes are diamagnetic and they have been characterized by NMR spectroscopy and the molecular structure of the Mo compound.<sup>1745</sup> This strategy has also been used to synthesize heterobimetallic Ti–Co complexes formed by reductive cleavage of a Co–Co bond in  $\text{Co}_2(\text{CO})_8$  by reaction with  $\text{Cp}'_2\text{TiOBu}^t$  ( $\text{Cp}' = \text{Cp, Cp}^*$ ).<sup>1746</sup>

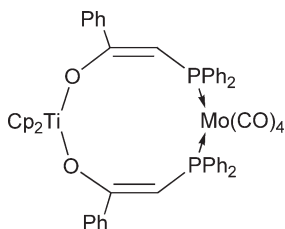
$\text{Cp}^*\text{Ti}(\text{NMe}_2)_3$  reacts with metal carbonyls,  $\text{M}(\text{CO})_n$  ( $n = 6$ ,  $\text{M} = \text{Cr, Mo, W}$ ;  $n = 5$ ,  $\text{M} = \text{Fe}$ ) to give heterobimetallic derivatives through the carbonyl insertion reaction into the Ti–N bond. When the group 6 metal complexes are heated at  $80^\circ\text{C}$  in toluene for several days, CO evolution is detected and  $\text{Cp}^*\text{Ti}(\mu\text{-NMe}_2)_2[\text{O}(\text{NMe}_2)\text{C}]\text{M}(\text{CO})_n$  are obtained. The same reaction with the iron compound evolves with double insertion of CO and formation of two carbene groups, without evolution of CO. The molecular structure has been determined by an X-ray diffraction and shows the oxygen atom bound to the oxophilic titanium atom, while the carbon forms a Fischer carbene-like complex.<sup>569</sup>

Heterobimetallic enolato derivatives  $(\text{CO})_3\text{Cr}[\eta^6\text{-}2,4,6\text{-R}^1\text{R}^2\text{R}^3\text{C}_6\text{H}_2\text{-C}(\text{CH}_2)\text{O}]\text{TiCp}_2\text{Cl}$  have been made by the deprotonation reaction of  $\text{Cr}(\text{CO})_3(\eta^6\text{-}2,4,6\text{-R}^1\text{R}^2\text{R}^3\text{C}_6\text{H}_2\text{-COMe})$  followed by treatment with  $\text{Cp}_2\text{TiCl}_2$ . In all these complexes, the enolate functionality is O-bound to titanium. The methyl-substituted arene complex has been isolated as an 85:15 diastereomer mixture, with a significant diastereoselection for the most hindered form (Scheme 691). The two diastereoisomers cannot be interconverted thermally because of the very high barrier of free rotation around the phenyl–C(enolate) bond.<sup>1747</sup> The titanium enolate  $\text{CpFeCp}[\text{C}(\text{CH}_2)\text{O}]\text{TiCp}_2\text{Cl}$  has been isolated in good yield as crystalline solid by the reaction of the potassium iron enolate with  $\text{Cp}_2\text{TiCl}_2$ . It has been characterized by  $^1\text{H}$  and  $^{13}\text{C}$  NMR spectroscopy. The aldol reaction with benzaldehyde leads to the corresponding metal aldol derivative  $\text{CpFeCp}[\text{C}(\text{O})\text{CH}_2\text{CHPh}]\text{OTiCp}_2\text{Cl}$  (Scheme 692).<sup>1748</sup>

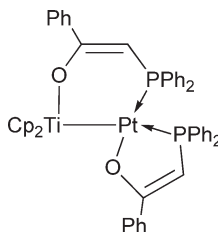
The bis-enolato compound  $\text{Cp}_2\text{Ti}[\text{OC}(\text{Ph})=\text{CHPPh}_2]_2$  reacts with  $\text{Mo}(\text{CO})_4(\text{norbornadiene})$  to give the Ti–Mo bimetallic complex  $\text{Cp}_2\text{Ti}[\text{OC}(\text{Ph})=\text{CHPPh}_2]_2\text{Mo}(\text{CO})_4$  containing bridging enolate ligands (Scheme 693). The reaction with  $\text{Pt}(\text{C}_2\text{H}_4)(\text{PPh}_3)_2$  proceeds with partial enolate ligand transfer to give  $\text{Cp}_2\text{Ti}[\text{OC}(\text{Ph})=\text{CHPPh}_2](\text{PtOC}(\text{Ph})=\text{CHPPh}_2)$  (Scheme 694) in which one phosphinoenolate acts as bridging ligand spanning a Ti–Pt bond, while the other chelates the Pt center. The molecular structure of this complex has been



Scheme 692



Scheme 693

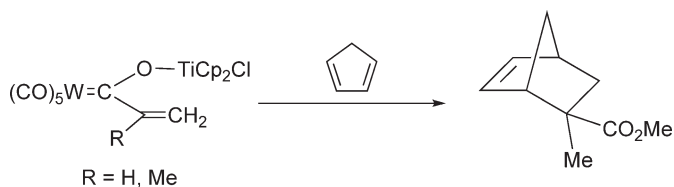


Scheme 694

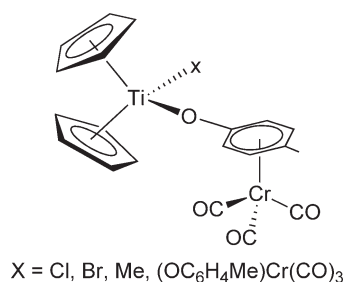
determined by X-ray diffraction and shows a Ti–Pt bond distance of 2.721(2) Å. The  $^{31}\text{P}$  NMR spectra exhibit a low-field resonance at  $\delta -56.1$  with a very reduced  $J_{\text{PtP}}$  coupling constant of 1053 Hz. Theoretical calculations suggest a quasi Ti(III)–Pt(I) covalent bond.<sup>1548</sup>

The vinyl and 2-propenyl complexes  $(\text{CO})_5\text{W}[\text{C}(\text{CR}=\text{CH}_2)](\text{OTiCp}_2\text{Cl})$  ( $\text{R} = \text{H}, \text{Me}$ ) are prepared by metallation of the acyl complexes  $[(\text{CO})_5\text{WC}(\text{O})(\text{CR}=\text{CH}_2)]^-$  with  $\text{Cp}_2\text{TiCl}_2$ . These complexes undergo reaction with cyclopentadiene to give predominantly the *exo*-Diels–Alder adduct in high yield (Scheme 695). X-ray crystal structures and molecular mechanics calculations suggest that the reaction may be controlled by steric factors.<sup>1749</sup>

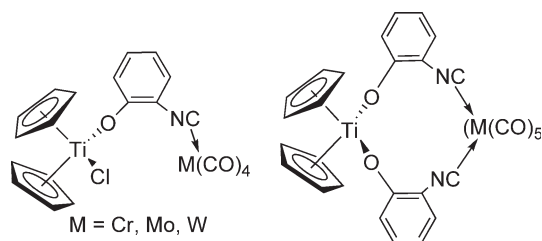
$\text{Cp}_2\text{TiXMe}$  ( $\text{X} = \text{Cl}, \text{Br}, \text{Me}$ ) react with  $\text{Cr}(\text{C}_6\text{H}_5\text{CO}_2\text{H})(\text{CO})_3$  with evolution of methane and formation of  $\text{Cp}_2\text{TiX}[(\mu\text{-O}_2\text{CC}_6\text{H}_5)\text{Cr}(\text{CO})_3]$ , which could not be isolated in pure form. Nevertheless, the reaction of  $\text{Cp}_2\text{TiMe}_2$  with the arene chromium complex yields  $\text{Cp}_2\text{Ti}[(\mu\text{-O}_2\text{CC}_6\text{H}_5)\text{Cr}(\text{CO})_3]_2$ , isolated as a solid that is stable in air for several days. IR spectra of the complexes show that the carboxylate groups coordinate to Ti in monodentate fashion.<sup>1750</sup> Similar reactions of  $\text{Cp}_2\text{TiMeX}$  ( $\text{X} = \text{Cl}, \text{Br}, \text{Me}$ ) with  $\text{Cr}(\text{HOC}_6\text{H}_4\text{Me})(\text{CO})_3$  form  $\text{Cp}_2\text{TiX}[(\mu\text{-OC}_6\text{H}_4\text{Me})\text{Cr}(\text{CO})_3]$ , and the reaction of  $\text{Cp}_2\text{TiMe}_2$  with the arene chromium complex yields  $\text{Cp}_2\text{Ti}[(\mu\text{-OC}_6\text{H}_4\text{Me})\text{Cr}(\text{CO})_3]_2$  (Scheme 696).<sup>1751</sup> The X-ray structure confirms the coordination mode of the carboxylate groups.



Scheme 695



Scheme 696



Scheme 697

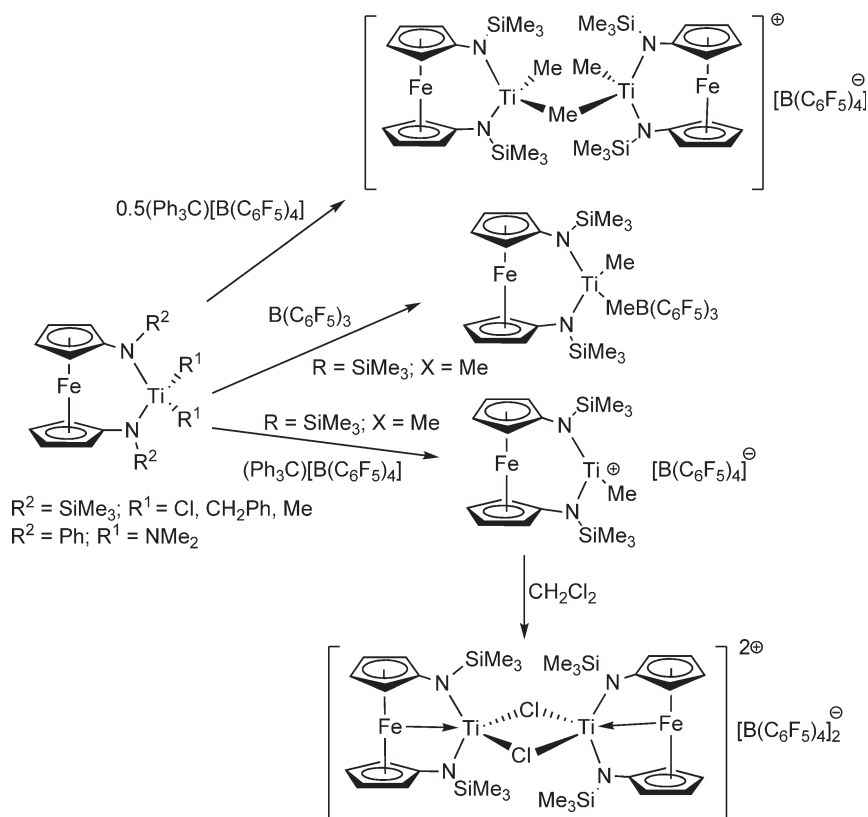
The synthesis of the Ti-group 6 heterobimetallic compounds  $\text{Cp}_2\text{ClTi}[\text{O}(o\text{-C}_6\text{H}_4)\text{NC}]\text{M}(\text{CO})_5$  and  $\text{Cp}_2\text{Ti}[\text{O}(o\text{-C}_6\text{H}_4)\text{NC}]_2\text{M}(\text{CO})_4$  ( $M = \text{Cr, Mo, W}$ ) has been described and the molecular structures of the products reported. The “bis-Cp–Ti” framework may act as either a mono- or bidentate ligand in which the titanium is O-bonded and the group 6 metal isocyanide coordinated (Scheme 697).<sup>1752</sup>

Heterobimetallic Ti–Pt complexes containing hydroxypyridine ligands bridging the “ $\text{Cp}_2\text{TiCl}$ ” and “ $\text{PtCl}_2(\text{DMSO})$ ” fragments have been reported and their properties as potential anticancer drugs studied.<sup>1753</sup>

A wide variety of heterobimetallic compounds containing a “ $\text{Cp}_2\text{Ti}$ ” unit linked to Pd, Pt, Cu, Ag, or Au centers using carboxylate with additional N-donor functionalities bridging units have been synthesized and characterized. Cationic tetranuclear  $\text{Ti}_2\text{Pt}_2$  complexes with isonicotinato bridging groups<sup>1754</sup> and non-ionic binuclear macrocyclic Ti–Pd, Ti–Pt or Ti–Au, or trinuclear acyclic  $\text{TiCu}_2$  or  $\text{TiAu}_2$  derivatives containing nicotinato, thiophenoxyacetato, and diphenylphosphinoacetato bridging groups have been prepared.<sup>1755</sup> The molecular structures of some of these compounds have been determined by X-ray diffraction.

The 1,1'-diamino ferrocenes ( $\text{C}_5\text{H}_4\text{NHR}^1$ )<sub>2</sub>Fe ( $\text{R}^1 = \text{SiMe}_3, \text{Ph}$ ) react with  $\text{TiR}^2_4$  ( $\text{R}^2 = \text{CH}_2\text{Ph, NMe}_2$ ) through aminolysis to give the derivatives  $\text{TiR}^2_2[\text{Fe}(\text{C}_5\text{H}_4\text{NR}^1)_2]$ , where the ferrocene diamido fragment acts as a chelate ligand. The dichloride complex  $\text{TiCl}_2[\text{Fe}(\text{C}_5\text{H}_4\text{NR})_2]$  is obtained by treatment of lithium or magnesium salt of the ferrocene diamide with  $\text{TiCl}_4(\text{THF})_2$ . The compound  $\text{TiMe}_2[\text{Fe}(\text{NSiMe}_3)_2]$  has been synthesized by alkylation of the dichloride complex with  $\text{LiMe}$  in  $\text{Et}_2\text{O}$  and characterized by X-ray diffraction. The long Fe–Ti distance of 3.32 Å precludes any significant direct metal–metal interaction.<sup>1756</sup> The dimethyl derivative  $\text{TiMe}_2[\text{Fe}(\text{C}_5\text{H}_4\text{NSiMe}_3)_2]$  reacts with 1 equiv. of  $\text{B}(\text{C}_6\text{F}_5)_3$  or  $\text{Ph}_3\text{C}[\text{B}(\text{C}_6\text{F}_5)_4]$  with abstraction of one of the methyl groups to give the corresponding Ti cationic species  $[\text{TiMe}[\text{Fe}(\text{NSiMe}_3)_2]]^+\text{Q}^-$  [ $\text{Q}^- = \text{MeB}(\text{C}_6\text{F}_5)_3, \text{B}(\text{C}_6\text{F}_5)_4$ ] stabilized by direct Ti–Fe interactions. Treatment of the dimethyl derivative with 0.5 equiv. of  $\text{Ph}_3\text{C}[\text{B}(\text{C}_6\text{F}_5)_4]$  affords the binuclear cationic compound  $[\{\text{TiMe}[\text{Fe}(\text{NSiMe}_3)_2]\}_2(\mu\text{-Me})]^+[\text{B}(\text{C}_6\text{F}_5)_4]^-$  (Scheme 698). The molecular structure shows a Ti–Fe distance of 3.07 Å, some 0.25 Å shorter than in the neutral dimethyl complex, indicating a weak Fe–Ti donor bond in order to stabilize the cationic center. Interaction between the borate methyl group with Ti is also observed. These cationic species are active in the polymerization of 1-hexene and produce short-chain oligomers of 5 to 6 monomer units.  $[\text{Ti}^+\text{Me}[\text{Fe}(\text{NSiMe}_3)_2]][\text{B}(\text{C}_6\text{F}_5)_4]^-$  is unstable in  $\text{CD}_2\text{Cl}_2$  with the formation of the chloro derivative  $[\text{TiCl}[\text{Fe}(\text{NSiMe}_3)_2]]_2[\text{B}(\text{C}_6\text{F}_5)_4]_2$ , which exhibits a short Ti–Fe distance of 2.49 Å, ascribed to the formation of a dative bond from Fe to Ti (Scheme 698).<sup>1757,1758</sup>

The N,N-dimethylamino-substituted ferrocenyl group  $\text{FeCp}[\text{C}_5\text{H}_3(\text{CH}_2)_n\text{NR}_2]^-$  ( $\text{L}^-$ ) has been used as a ligand to produce heterobimetallic complexes.  $\text{Cp}_2\text{TiCl}_2$  reacts with  $\text{LiFeCp}[\text{C}_5\text{H}_3(\text{CH}_2)_n\text{NMe}_2]$  to give

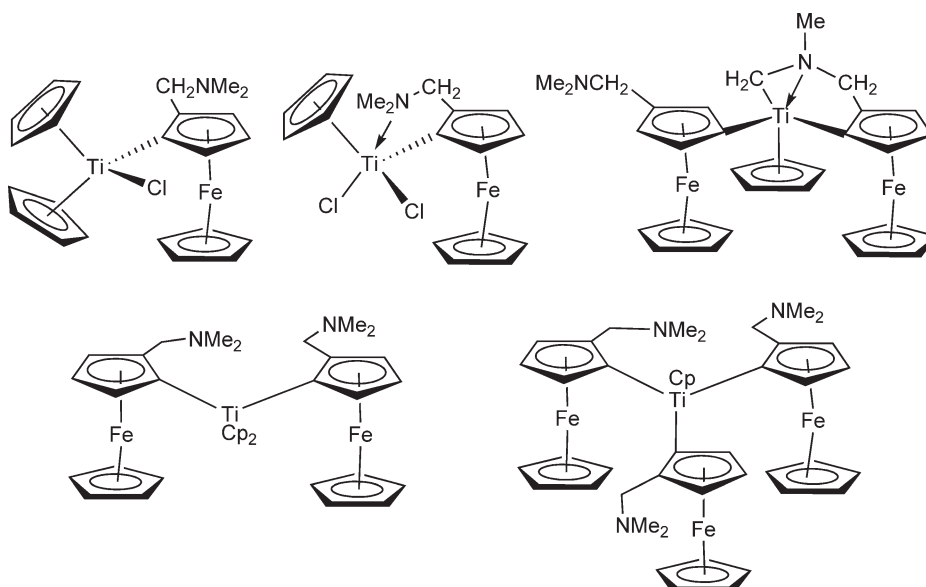


Scheme 698

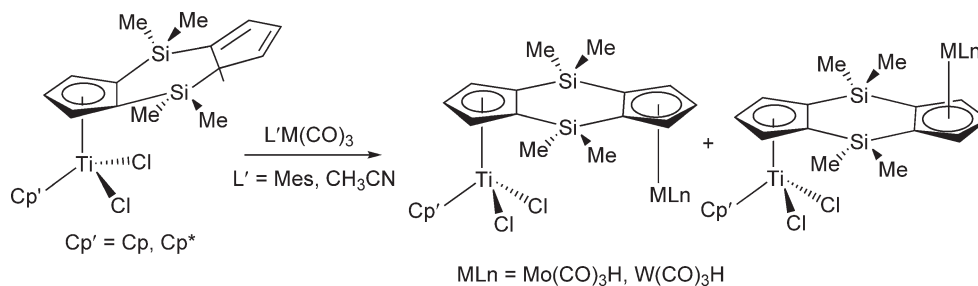
$\text{Cp}_2\text{TiCl}_2[\text{FeCp}[\text{C}_5\text{H}_3(\text{CH}_2)_n\text{NMe}_2]]$  ( $n = 1, 2$ ). The presence of two Cp rings coordinated to titanium forces the ligand to be monodentate, while in the mono-Cp titanium complex  $\text{CpCl}_2\text{Ti}-(\text{C}_5\text{H}_3\text{CH}_2\text{NMe}_2)-\text{FeCp}$  the ligand exhibits chelating behavior. Similar  $\text{Cp}_2\text{TiL}_2$ ,  $\text{CpTiClL}_2$ , and  $\text{CpTiL}_3$  complexes are obtained. Elimination of HL and related metallation occurs in the unstable complex  $\text{CpTiL}_3$  to give a novel ligand reaction with the formation of the compound  $\text{CpTi}-(\text{C}_5\text{H}_3\text{CH}_2\text{NMe}_2-\text{FeCp})[(\text{C}_5\text{H}_3\text{CH}_2\text{NMe}_2\text{CH}_2)-\text{FeCp}]$  (Scheme 699). The complexes were characterized by NMR spectroscopy and crystal structure analysis.<sup>1759–1761</sup> Analogous ferrocenyl–titanium compounds have been synthesized and investigated.<sup>1762</sup>

$\text{Cp}_2\text{TiCl}_2$  reacts with bis(hydrazones) derived from 1,1'-diacetylferrocene in THF in the presence of a base to give complexes of the type  $(\text{Cp}_2\text{TiCl}_2)\text{L}$  [ $\text{LH}_2 = \text{ferrocenyl bis(hydrazones)}$ ].<sup>1763</sup> Reaction of thiosemicarbazones, derived by the condensation of acetylferrocene and different thiosemicarbazides (phenyl thiosemicarbazide, 4-chlorophenyl thiosemicarbazide, 4-nitrophenyl thiosemicarbazide, 2-methylphenyl thiosemicarbazide, 4-methylphenylthiosemicarbazide), with  $\text{CpTiCl}_3$  has been studied in anhydrous tetrahydrofuran in the presence of amine to give acetylferrocenyl thiosemicarbazone titanium derivatives. Tentative structural conclusions are drawn for the reaction products based upon elemental analyses, electrical conductance, magnetic moment, and spectroscopic (electronic, infrared, and  $^1\text{H}$  NMR) data.<sup>1764</sup> The reactions of  $\text{CpTiCl}_3$  with ligands (LH) derived from 3-phenyl/substituted phenyl-4-amino-5-mercapto-1,2,4-triazole and acetylferrocene, with hydrazones, derived by the condensation of acetylferrocene with different aromatic acid hydrazides or with Schiff bases (L), derived by the condensation of acetylferrocene with ethylenediamine, *o*-phenylenediamine, 4-methyl-*o*-phenylenediamine, 1,8-diaminonaphthalene, and 2,6-diaminopyridine give complexes  $\text{CpTiCl}_2\text{Fe}(\text{L})$ . Tentative structural conclusions are drawn for these complexes based upon elemental analysis, electronic conductance, magnetic moment, and spectroscopic (electronic, IR,  $^1\text{H}$  and  $^{13}\text{C}$  NMR) data.<sup>1526,1765,1766</sup> The synthesis and spectroscopic studies of mono- and bis-Cp titanium derivatives with S-alkyl- $\beta$ -N-(acetylferrocenyl) methylene dithiocarbazates have been described.<sup>1767</sup>

$\text{CpTiCl}_3$  reacts with sodium salts of ferrocenylcarboxylates to afford biferrocenylcarboxylato derivatives of mono-Cp chloro titanium(IV) which show monodentate carboxylate bonding.<sup>1768,1769</sup>



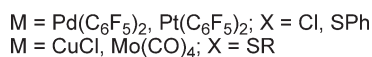
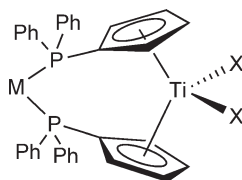
Scheme 699



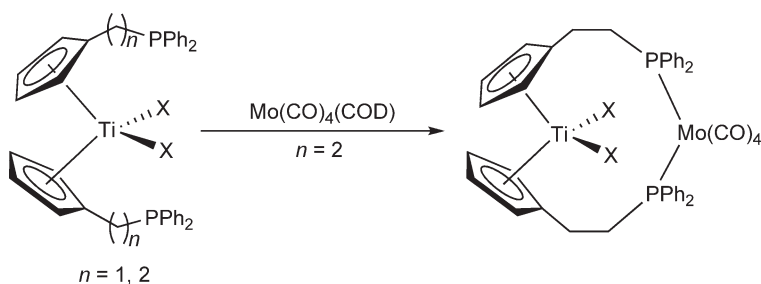
Scheme 700

$\text{Cp}'\text{TiCl}_2[(\eta^5\text{-C}_5\text{H}_3)(\text{SiMe}_2)_2(\text{C}_5\text{H}_4)]$  ( $\text{Cp}' = \text{Cp}, \text{Cp}^*$ ) reacts with  $\text{M}(\text{CO})_3(\text{MeCN})_3$  ( $\text{M} = \text{Mo}, \text{W}$ ) or  $\text{Mo}(\text{CO})_3(\text{mesitylene})$  to give the heterobinuclear compounds  $\text{Cp}'\text{TiCl}_2\{\mu\text{-}[(\eta^5\text{-C}_5\text{H}_3)(\text{SiMe}_2)_2(\text{C}_5\text{H}_4)]\}\text{MH}(\text{CO})_3$  (Scheme 700) isolated as single *cis*- and *trans*-isomers or as mixtures of both depending on the starting complex and the reaction conditions. The molar ratio of the two resulting isomers is controlled by thermodynamic and kinetic factors which prevent the application of stereoselective methods for some of the products. The molecular structure of the tungsten compound has been studied by X-ray diffraction methods.<sup>1770</sup>

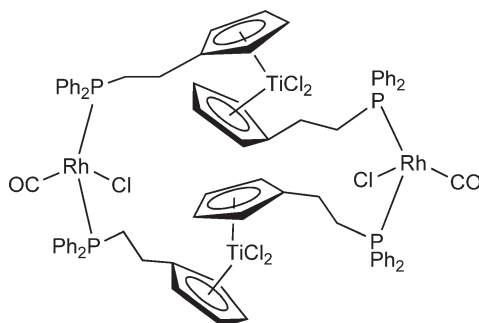
Phosphine-substituted Cp rings are considered as suitable functional ligands to synthesize heterobimetallic titanium-late transition metal complexes.  $(\text{C}_5\text{H}_4\text{PPh}_2)\text{TiX}_2$  ( $\text{X} = \text{Cl}, \text{SPh}$ ) react with *cis*- $\text{M}(\text{C}_6\text{F}_5)_2(\text{THF})_2$  to give the heterobimetallic compounds  $(\text{C}_5\text{H}_4\text{PPh}_2)\text{TiX}_2\text{-M}(\text{C}_6\text{F}_5)_2$  (Scheme 701), characterized by  $^1\text{H}$ ,  $^{31}\text{P}$ , and  $^{19}\text{F}$  NMR



Scheme 701



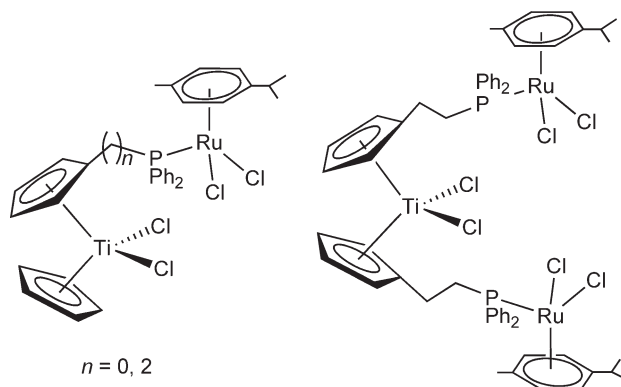
Scheme 702



Scheme 703

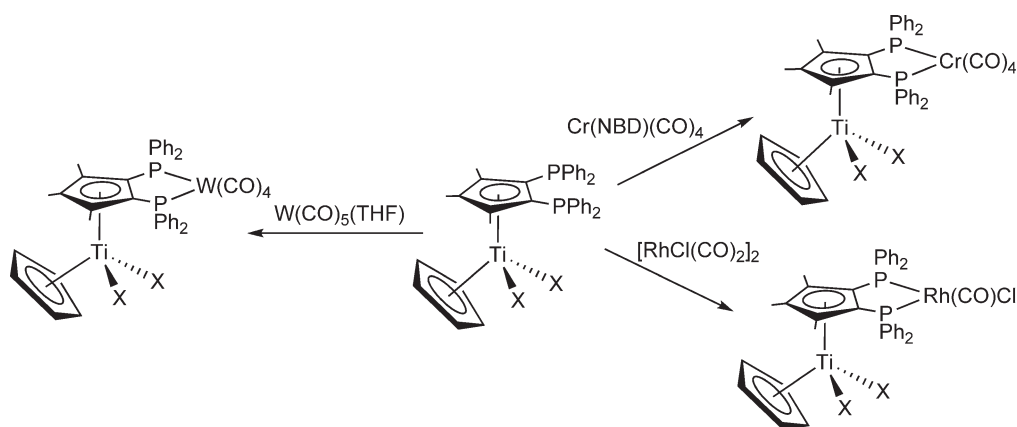
spectroscopies and FAB mass spectrometry.<sup>1771</sup> Analogous Ti–Cu and Ti–Mo have been described (Scheme 701).<sup>1772</sup> The complexes  $[\text{C}_5\text{H}_4(\text{CH}_2)_n\text{PPh}_2]_2\text{TiCl}_2$  ( $n = 1, 2$ ) react with middle or late metal compounds to give binuclear or tetranuclear heterobimetallic complexes with the Cp–phosphinoalkyl ligands bridging the heteroatoms.  $[\text{C}_5\text{H}_4(\text{CH}_2)_n\text{PPh}_2]_2\text{TiCl}_2$  can act as a bidentate ligand with group 6 metals<sup>1100</sup> (Scheme 702) or as bridging ligand with group 8 and 10 metals (Scheme 703).<sup>1773</sup> The reactions of titanium complexes  $\text{CpTiCl}_2[\text{C}_5\text{H}_4(\text{CH}_2)_n\text{PPh}_2]$  ( $n = 0, 2$ ) and  $[\text{C}_5\text{H}_4(\text{CH}_2)_n\text{PPh}_2]_2\text{TiCl}_2$  with  $[\text{Ru}(p\text{-cumene})\text{Cl}_2]_2$  give the heterobimetallic or trimetallic derivatives (Scheme 704). The molecular structure of the bimetallic compounds has been determined by X-ray diffraction.<sup>1774</sup>

$\text{CpTiCl}_2[\text{C}_5\text{Me}_3(\text{PPh}_2)_2]$  has been used as a metalloligand to prepare heterobimetallic Ti–late transition metal complexes (Scheme 705) through the bridging 1,2-bis(diphenylphosphanyl)trimethylcyclopentadienyl chelate fragment.<sup>1075</sup>

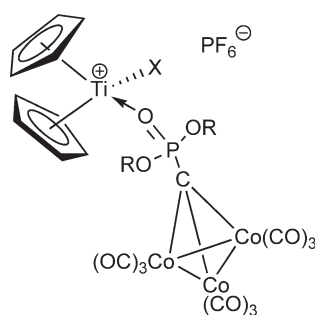


Scheme 704





Scheme 705



Scheme 706

Ligands bearing phosphonato functionalities are useful in coordination chemistry. Early–late heterobimetallic complexes can be prepared with the presence of functionalized bridging ligands bearing P=O unit. The compound shown in Scheme 706 has been prepared.<sup>1775</sup>

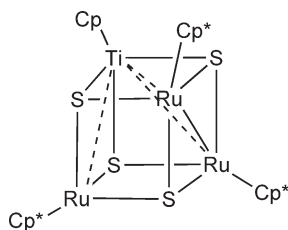
Thiolato and S-based ligands have often been also used to bridge two metals with the formation of heterobimetallic complexes. The synthesis and reactivity of cubane-type sulfido clusters containing titanium–late transition metals have been reviewed.<sup>1776,1777</sup>

The controlled synthesis of Ti- $d^8$  early–late heteropolynuclear diolefin and carbonyl clusters has been reported. The synthetic approach was based on deprotonation reactions involving  $\text{Cp}_2\text{Ti}(\text{SH})_2$  and appropriate rhodium and iridium diolefin and carbonyl compounds. The catalytic activity of some representative Ti–Rh compounds toward alkene hydroformylation has been explored.<sup>1778</sup>

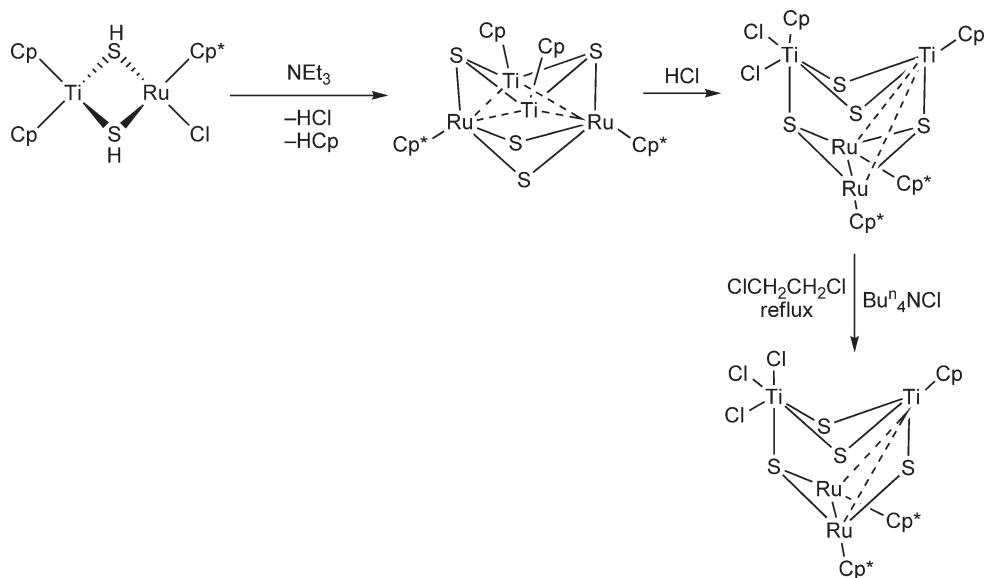
Sulfido-bridged titanium–iridium heterobimetallic complexes have been described. Compound  $\text{CpClTi}(\mu\text{-S})_2\text{Ir}(\text{C}_5\text{Me}_5)\text{PMe}_3$  has been synthesized by the reaction of  $\text{CpTiCl}_3$  with  $\text{Ir}(\text{C}_5\text{Me}_5)(\text{SH})_2\text{PMe}_3$ . X-ray diffraction studies indicate a short Ti–Ir distance of 2.989(2) Å and acute mean Ti–S–Ir angles of 80.0°, suggesting the presence of an interaction between both metals, probably a dative bond from the  $d^6$ -Ir to  $d^0$ -Ti center.<sup>1779</sup>

The synthesis of the cubane-type sulfido cluster  $(\text{TiCp})[\text{Ru}(\text{C}_5\text{Me}_5)]_3(\mu_3\text{-S})_4$  (Scheme 707) is described by crossed condensation of the two hydrosulfido-bridged binuclear complexes  $(\text{TiCp}_2)(\mu\text{-SH})_2[\text{Ru}(\text{C}_5\text{Me}_5)\text{Cl}]$  and  $[\text{Ru}(\text{C}_5\text{Me}_5)\text{Cl}]_2(\mu\text{-SH})_2$ .<sup>1780</sup>

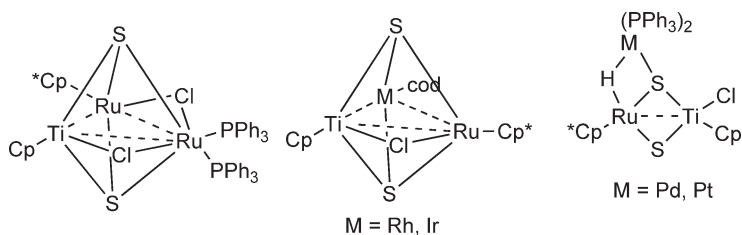
A series of heterobinuclear Ti/Ru complexes are obtained from the initial treatment of  $\text{Cp}_2\text{Ti}(\text{SH})_2$  with  $[\text{Cp}^*\text{RuCl}]_2$  and subsequent reactions with excess of triethylamine,  $[\text{Cp}_2\text{Fe}][\text{PF}_6]$ , excess of HCl, and boiling 1,2-dichloroethane. Some cubane-type sulfido clusters are obtained. X-ray diffraction studies and extended Hückel molecular orbital calculations are carried out suggesting the existence of  $\text{Ru} \rightarrow \text{Ti}$  dative bonds and weak Ti–Ti interactions. Substitution of one of the Cp rings by a chloro ligand in boiling 1,2-dichloroethane is also observed (Scheme 708).<sup>1781</sup>



Scheme 707



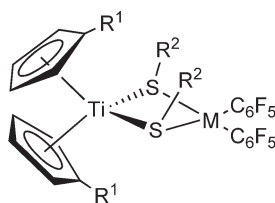
Scheme 708



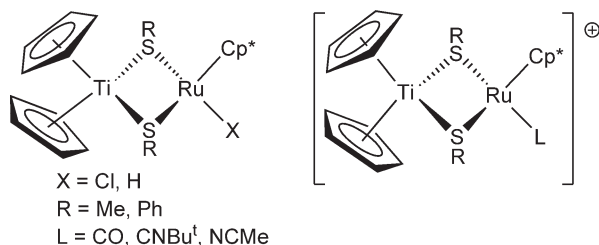
Scheme 709

The hydrosulfido-bridged Ti–Ru heterobimetallic complex  $\text{Cp}_2\text{Ti}(\mu_2\text{-SH})_2\text{RuCp}^*\text{Cl}$ <sup>1781,1782</sup> reacts with  $\text{RuCl}_2(\text{PPh}_3)_3$  or  $[\text{M}(\text{cod})\text{Cl}]_2$  ( $\text{M} = \text{Rh}, \text{Ir}$ ) in the presence of an excess of  $\text{NEt}_3$  to give “TiRu<sub>2</sub>” and “TiRuM” mixed metal sulfido clusters. The reactions with  $\text{M}(\text{PPh}_3)_4$  ( $\text{M} = \text{Pd}, \text{Pt}$ ) afford the “TiRuM” trinuclear clusters with an unprecedented  $\text{M}_3(\mu_3\text{-S})(\mu_2\text{-S})$  core (Scheme 709). The structures of these triangular clusters have been determined by X-ray diffraction.<sup>1783</sup>

Reaction of the bis(hydrosulfido) complex  $\text{Cp}^*\text{Rh}(\text{SH})_2(\text{PMe}_3)$  with  $\text{Cp}^*\text{TiCl}_3$  in the presence of  $\text{NEt}_3$  leads to the formation of the sulfido-bridged titanium–rhodium complex  $\text{CpClTi}(\mu_2\text{-S})_2\text{RhCp}^*(\text{PMe}_3)$ , the molecular structure of which has been determined by X-ray diffraction studies.<sup>1784</sup>



Scheme 710

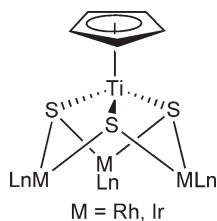


Scheme 711

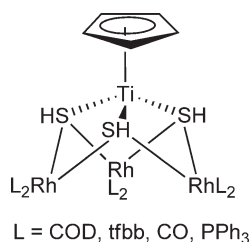
A series of Ti–Pt and Ti–Pd heterobinuclear compounds with double thiolato bridges have been reported. *cis*- $\text{M}(\text{C}_6\text{F}_5)_2(\text{THF})_2$  ( $M = \text{Pd, Pt}$ ) react with the bis-Cp thiolato complexes  $\text{Cp}'_2\text{Ti}(\text{SR})_2$  ( $\text{Cp}' = \text{Cp, C}_5\text{H}_4\text{SiMe}_3$ ) to give the binuclear air sensitive complexes  $\text{Cp}'_2\text{Ti}(\mu\text{-SR})_2\text{M}(\text{C}_6\text{F}_5)_2$  in which the thiolato Ti(IV) fragment is acting as a metalloligand toward the  $\text{M}(\text{C}_6\text{F}_5)_2$  unit. The crystal structure of the Pd complex has been established by single crystal X-ray crystallography (Scheme 710).<sup>1785</sup> Reaction of  $\text{Cp}_2\text{Ti}(\text{EAr})_2$  ( $\text{E} = \text{Se, Te}$ ;  $\text{Ar} = \text{Ph, 4-MeC}_6\text{H}_4, 4\text{-OMeC}_6\text{H}_4, 4\text{-OEtC}_6\text{H}_4$ ) with  $(\text{dppe})\text{M}(\text{ClO}_4)_2$  and  $\text{MCl}_2(\text{PhCN})_2$  ( $M = \text{Ni, Pd, Pt}$ ) yields heterobimetallic complexes of the type  $\text{Cp}_2\text{Ti}(\mu\text{-EAr})_2\text{ML}_n$ .<sup>1786</sup>

The complexes  $\text{Cp}_2\text{Ti}(\text{SR})_2$  ( $R = \text{Ph or Me}$ ) react with  $\text{Cp}^*\text{RuCl}(\text{cod})$  to give the Ti–Ru compounds  $\text{Cp}_2\text{Ti}(\mu\text{-SR})_2\text{RuCp}^*\text{Cl}$ . X-ray analysis of the phenyl compound indicates that two phenyl groups on the sulfur atoms are in *syn*-conformation. These complexes react with  $\text{KBH}(\text{Bu}^s)_3$  to afford hydride complexes  $\text{Cp}_2\text{Ti}(\mu\text{-SR})_2\text{RuCp}^*(\text{H})$ , and with  $\text{Ag}^+$  in the presence of donor ligands L to afford  $[\text{Cp}_2\text{Ti}(\mu\text{-SR})_2\text{RuCp}^*(\text{L})]^+$  (Scheme 711). The molecular structures of some of these cationic complexes have been determined.<sup>1787,1788</sup> Bis-Cp bis-thiolato titanium complexes  $\text{Cp}_2\text{Ti}(\text{SR})_2$  ( $R = \text{Et, Pr}^i, p\text{-MeC}_6\text{H}_4, \text{Ph}$ ) and  $\text{Cp}_2\text{Ti}(\text{S-S})$  ( $\text{S-S} = \text{S}_2\text{C}_6\text{H}_4, \text{S}_2\text{C}_2\text{H}_4$ ) react with  $\text{PtCl}_2(\text{cod})$  in THF or  $\text{CH}_2\text{Cl}_2$  with thiolato transfer from titanium to platinum and formation of  $\text{Cp}_2\text{TiCl}_2$ . The reactions of  $\text{Cp}_2\text{Ti}(\text{SR})_2$  ( $R = p\text{-MeC}_6\text{H}_4, \text{Ph}$ ) with  $\text{PtCl}_2(\text{cod})$  in toluene give heterobimetallic complexes which release  $\text{Cp}_2\text{TiCl}_2$  on dissolution in THF or  $\text{CH}_2\text{Cl}_2$ .<sup>1789</sup>

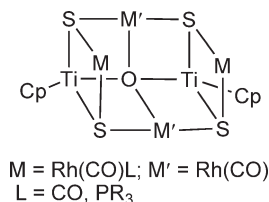
The anion  $[(\text{CpTiS})_2(\mu\text{-S})]^{2-}$  obtained by monodeprotonation of  $\text{Cp}_2\text{Ti}(\text{SH})_2$  with  $\text{LiBu}^t$  in THF reacts with complexes  $[\text{M}(\mu\text{-Cl})(\text{diolfin})]_2$  ( $M = \text{Rh, Ir}$ ) to give the tetranuclear derivatives  $\text{CpTi}(\mu_3\text{-S})_3\text{M}_3(\text{diolfin})_3$ . Carbonylation reactions and further treatment with P-donor ligands afford Rh- and Ir-substituted complexes  $\text{CpTi}(\mu_3\text{-S})_3\text{M}_3\text{L}_x$  (Scheme 712). Spectroscopic data indicate fluxional behaviour in solution. Structural studies and



Scheme 712



Scheme 713

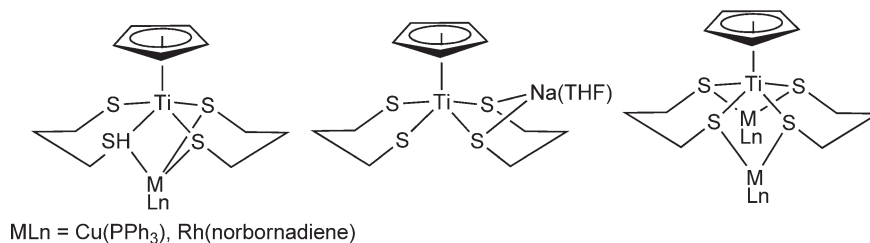


Scheme 714

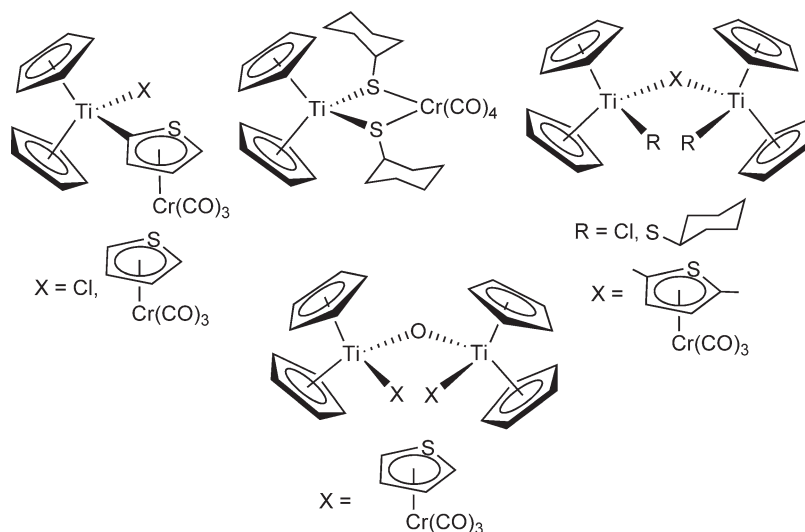
general comments on bonding considerations are reported.<sup>1790</sup> These complexes show catalytic activity in hydroformylation of olefins.<sup>1791</sup> The binuclear thiotitanato complex  $[(\text{CpTiS})_2(\mu\text{-S})_2]^{2-}$  serves as a useful precursor to early-late heterobimetallic cubane-type sulfido clusters containing titanium. Reactions with  $[\text{Cp}^*\text{Ru}(\mu_3\text{-Cl})_4]$ ,  $[\text{M}(\text{cod})(\mu\text{-Cl})_2]$  (M = Rh, Ir), and  $[\text{Cu}(\mu_3\text{-Cl})(\text{PPh}_3)_4]$  afford the Ti-late cubane-type derivatives  $(\text{CpTi})_2[\text{Cp}^*\text{Ru}]_2(\mu_3\text{-S})_4$ ,  $(\text{CpTi})_2[\text{M}(\text{cod})]_2(\mu_3\text{-S})_4$ , and  $(\text{CpTi})_2[\text{Cu}(\text{PPh}_3)]_2(\mu_3\text{-S})_4$ , the molecular structures of which have been determined by X-ray diffraction.<sup>1792</sup>

Reaction of  $\text{Cp}_2\text{Ti}(\text{SH})_2$  with  $[\text{Rh}(\mu\text{-OMe})(\text{cod})]_2$  under strict anhydrous conditions gives the tetranuclear compound  $\text{CpTi}(\mu\text{-S})_3[\text{Rh}(\text{cod})]_3$ , obtained as a yellow solid.<sup>1793</sup> The analogous heterotetranuclear complex  $\text{CpTi}(\mu_3\text{-S})_3[\text{Rh}(\text{tfbb})]_3$  has been prepared in moderate yield by reacting  $\text{Cp}_2\text{Ti}(\text{SH})_2$  with  $[\text{Rh}(\mu\text{-MeO})(\text{tfbb})]_2$  in toluene at room temperature, and its structure has been determined by X-ray diffraction (tfbb = tetrafluorobenzobarrelene). Replacement reactions of the diolefin ligands by CO and  $\text{PPh}_3$  occur with retention of the structure and nuclearity giving  $\text{CpTi}(\mu_3\text{-S})_3(\text{RhL}_2)_3$ , which shows the remarkable stability of the incomplete cubane framework formed by the early and late transition metals bridged by sulphido ligands (Scheme 713). These molecules could be considered as molecular models for the deactivation of commercial metal sulfido catalysts.<sup>1794</sup> The oxosulfido complex  $[\text{CpTi}]_2(\mu_4\text{-O})(\mu_3\text{-S})_4[\text{Rh}_4(\text{CO})_6]$  is obtained by carbonylation of the precursor Ti/Rh mixture in the presence of traces of water. This complex reacts with a variety of P-donor ligands with replacement of carbon monoxide (Scheme 714). The molecular structures of these complexes have been determined by X-ray diffraction and show an unexpected incomplete cubane structure lacking one vertex.<sup>1795</sup>

Cu(I) and Rh(I) derivatives of the anion  $[\text{CpTi}\{\text{S}(\text{CH}_2)_n\text{S}\}_2]^-$  are synthesized by using the sodium salts as precursor reagent. Oligomeric  $[\text{TiCp}\{\text{S}(\text{CH}_2)_n\text{S}\}_2\text{M}]_x$  or heterobimetallic complexes  $[\text{TiCp}\{\text{S}(\text{CH}_2)_n\text{S}\}_2(\text{MLn})]$  are formed (Scheme 715).<sup>1795</sup>



Scheme 715



Scheme 716

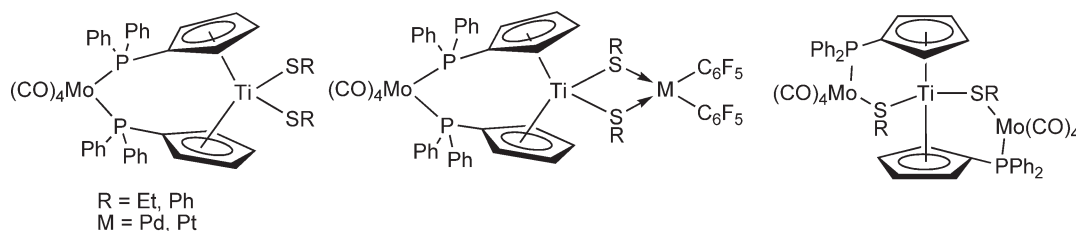
A series of Ti complexes of  $\pi$ -coordinated thiophene derivatives have been reported. Some of these compounds are shown in Scheme 716.  $\pi$ -Coordinated carbonylchromium complexes of thiophene and benzothiophene are readily lithiated with  $\text{LiBu}^n$  and react with  $\text{Cp}_2\text{TiCl}_2$  to afford heterobinuclear Ti–Cr complexes.<sup>1796</sup>

The copper compound  $\text{Cu}[\text{S}(\text{SiMe}_2)_2](\text{PET}_3)_3$  reacts with  $\text{CpTiCl}_3$  in toluene at  $-50^\circ\text{C}$  to give the octanuclear heterobimetallic sulfido cluster complex  $\text{Cp}_2\text{Ti}_2\text{Cu}_6\text{S}_6(\text{PET}_3)_6$ , characterized by X-ray diffraction. In the molecular structure, the centrosymmetric octanuclear core is a distorted  $\text{Ti}_2\text{Cu}_6$  cube with  $\mu_4\text{-S}^{2-}$  ligands occupying positions above the center of each of the six faces. The average Cu–Ti distance of 2.869 Å suggests the existence of a dative bond between the  $d^{10}$ -Cu atom and the  $d^0$ -Ti atom.<sup>1797</sup>

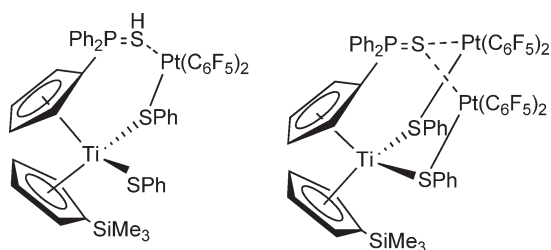
The fragment  $\text{CpTi}(\text{acac})\text{S}_2$  is considered as an S-donor metalloligand that supports the binuclear moiety  $\text{Ir}_2(\text{CO})_4$  in the complex  $\text{CpTi}(\text{acac})(\mu_3\text{-S})_2[\text{Ir}(\text{CO})_2]_2$ , which is obtained upon carbonylation of  $\text{CpTi}(\text{acac})(\mu_3\text{-S})_2[\text{Ir}(\text{diolefin})_2]_2$ . In this  $\text{TiIr}_2$  system the titanium fragment, as a metalloligand, exerts important steric and electronic influences on the reactivity of the Ir metal toward electrophiles. Thus, the reactivity of this complex with iodine, alkyl iodides, and activated acetylenes has been studied.<sup>1798</sup>

The synthesis of various heteropolynuclear compounds by using  $(\text{C}_5\text{H}_4\text{PPh}_2)_2\text{Ti}(\text{SR})_2$  ( $\text{R} = \text{Et}$  or  $\text{Ph}$ ) as metalloligands to transition metal complexes has been described, combining the Cp–phosphine and the thiolato bridging ligands. The synthetic procedure involves replacement of neutral ligands by the Cp–diphenylphosphine coordinated to the titanium atom. The ability of the S atoms in the thiolato ligands to act as Lewis bases leads to a further increase in nuclearity. Thus, complexes of the type shown in Scheme 717 are known.<sup>1799</sup> Similar Ti–Pt and Ti–Pt<sub>2</sub> complexes (Scheme 718) have been synthesized by the reaction of  $[\text{C}_5\text{H}_4\text{P}(=\text{S})\text{Ph}_2](\text{C}_5\text{H}_4\text{SiMe}_3)\text{Ti}(\text{SPh})_2$  with *cis*- $\text{Pt}(\text{C}_6\text{F}_5)_2(\text{THF})_2$ .<sup>1800</sup>

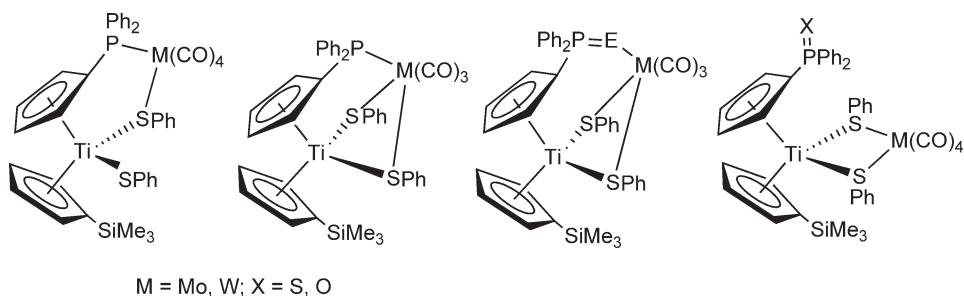
Heterobinuclear thiolato complexes containing a mixed monosubstituted Cp–Ti(IV) fragment  $(\text{C}_5\text{H}_4\text{R})\text{-}(\text{C}_5\text{H}_4\text{SiMe}_3)\text{Ti}(\text{SPh})_2$  ( $\text{R} = \text{PPh}_2$ ,  $\text{Ph}_2\text{P}=\text{O}$ ,  $\text{Ph}_2\text{P}=\text{S}$ ) and group 6 and late transition metals have been reported in which the two thiolato groups and one of the substituted Cp rings act as bridging ligands. The crystal structures of



Scheme 717



Scheme 718

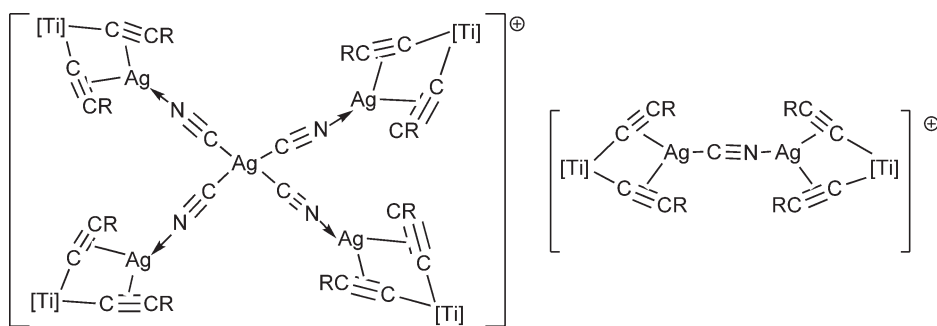


Scheme 719

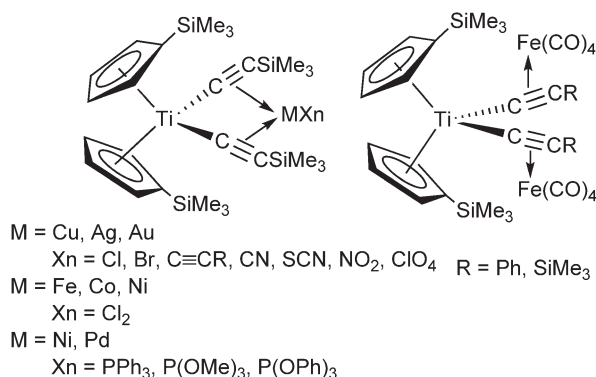
these complexes confirm that the titanium precursor acts in some cases as a tridentate metalloligand (Scheme 719).<sup>1801,1802</sup>

Bis( $\sigma$ -alkynyl) compounds can be used for the preparation of homo- and heteropolynuclear complexes of the type  $L_nM^1(\mu-C\equiv CR^1)(\mu-C\equiv CR^2)M^2L_m$  containing bridging  $\sigma$ - $\pi$ -alkynyl groups between metal centers, in which the bonding of the  $\mu-C\equiv CR$  ligand can be widely varied depending on different metals, ligands, and substituents. The synthesis and chemical behavior of a series of heterobimetallic Ti-late transition metal complexes (groups 8, 10, and/or 11) have been discussed. The titanium and the late metals are linked by carbon-rich  $\pi$ -conjugated organic units, mainly  $\sigma$ - and  $\pi$ -bonded alkynyls, and these species are well suited for studying electronic communications between the corresponding metal centers. The structural aspects and electrochemical properties of the complexes have been reported.<sup>1803</sup>

Complexes  $(C_5H_4SiMe_3)_2Ti(C\equiv CR)_2$  have been used as a bidentate chelating organometallic ligand (organometallic  $\pi$ -tweezer) to stabilize monomeric  $MX_n$  units ( $M$  = transition metals). Complexes  $[(C_5H_4SiMe_3)_2Ti(C\equiv CR^1)_2]MR^2$  ( $R^1$  =  $SiMe_3$ , Ph, Bu<sup>t</sup>;  $R^2$  = organic or inorganic ligand;  $M$  = late transition metal) have been prepared.<sup>1804,1805,1373,1372,1806–1812,1302</sup> The compounds  $[(C_5H_4SiMe_3)_2Ti(C\equiv CPh)_2]HgX_2$  [ $X_2$  = (CN)<sub>2</sub>, (CF<sub>3</sub>)<sub>2</sub>(Ph)] have been prepared by the reaction of  $(C_5H_4SiMe_3)_2Ti(C\equiv CPh)_2$  with  $HgX_2$ .<sup>1805</sup> The reactions of  $(C_5H_4SiMe_3)_2Ti(C\equiv CSiMe_3)_2$  with the silver salts AgCN yield the compounds  $(C_5H_4SiMe_3)_2Ti(C\equiv CSiMe_3)_2\cdot AgCN$  (Scheme 720). The crystal structures have been determined.<sup>1813,1814</sup> The fragment  $(C_5H_4SiMe_3)_2Ti(C\equiv CR)_2$  ( $R$  = Ph,  $SiMe_3$ ) stabilizes Ag(I) complexes to produce the nonametallic Ag<sub>5</sub>Ti<sub>4</sub> molecule based on the  $[Ag(C\equiv N)_4]^{3-}$  core, which decompose in solution to give a new tetranuclear Ti<sub>2</sub>Ag<sub>2</sub> complex (Scheme 720). The molecular structure of the tetranuclear compound has been determined by X-ray diffraction.<sup>1815</sup> Similar complexes with  $MCl_2$  ( $M$  = Fe, Co, Ni) and  $MX$  ( $M$  = Cu, Au) fragments have been reported (Scheme 720).<sup>1280,1816–1820</sup> Different chemical behavior is observed and discussed in the reactions of  $(C_5H_4SiMe_3)_2Ti(C\equiv CR^1)(C\equiv CR^2)$  with  $AuCl_3L$  and  $AuClL$  depending on the nature of  $L$  and the alkyne substituent. Reaction of  $(C_5H_4SiMe_3)_2Ti(C\equiv CSiMe_3)_2$  with  $AuCl_3(py)$  produces  $(C_5H_4SiMe_3)_2TiCl_2$ ,  $Me_3SiC\equiv C-C\equiv CSiMe_3$ , and Au(0). The reaction with the Au(I) compound  $AuCl(PPh_3)$  gives  $(C_5H_4SiMe_3)_2TiCl_2$  and  $Au(C\equiv CSiMe_3)(PPh_3)$ , while in the reaction with  $AuCl(SMe_2)$  a mixture of  $(C_5H_4SiMe_3)_2TiCl_2$  and the heterobimetallic compound  $(C_5H_4SiMe_3)_2Ti(C\equiv CSiMe_3)_2AuC\equiv CSiMe_3$  is formed. Compounds of the type  $[(C_5H_4SiMe_3)_2Ti(C\equiv CR^1)(C\equiv CR^2)]AuC\equiv CR$  can be synthesized in much better yields by the reaction of  $(C_5H_4SiMe_3)_2Ti(C\equiv CR^1)(C\equiv CR^2)$  with  $Au(C\equiv CR)(SMe_2)$ . The thermolysis of these Au(I) complexes eliminates the bis-Cp' bis(alkynyl) titanium fragment, the coupling products  $R^3-R^3$  and gold films. The X-ray structure analyses of

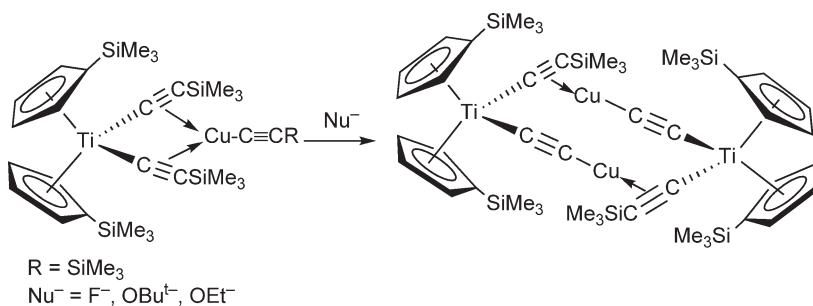


[Ti] =  $(C_5H_4SiMe_3)_2Ti$   
 R = SiMe<sub>3</sub>, Ph



Scheme 720

some of these compounds are reported. Theoretical calculations on the nature of the Au–C bond have been carried out.<sup>1821</sup> Cu(I)-stabilized complexes with the organometallic  $\pi$ -tweezer  $Cp'_2Ti(C\equiv CSiMe_3)_2$  have also been described.<sup>1822</sup>  $LiC\equiv CR$  (R = SiMe<sub>3</sub>, Bu<sup>t</sup>, Ph) react with  $[(C_5H_4SiMe_3)_2Ti(C\equiv CSiMe_3)_2]CuCl$  to give the alkynylcopper(I) complexes  $[(C_5H_4SiMe_3)_2Ti(C\equiv CSiMe_3)_2]Cu(C\equiv CR)$ , independently prepared from  $(C_5H_4SiMe_3)_2Ti(C\equiv CSiMe_3)_2$  and  $1/n [CuC\equiv CR]_n$ . The complex with R = SiMe<sub>3</sub> reacts with nucleophiles (OBu<sup>t</sup>–, OEt–, F–) with the formation of the remarkably stable bimetallic acetylide complex  $[(C_5H_4SiMe_3)_2Ti(C\equiv CSiMe_3)(CuC\equiv C)]_2$ , the molecular structure of which has been determined (Scheme 721).<sup>1809</sup> Intramolecular addition of a Cu–C bond across the alkyne triple bond of  $[(C_5H_4SiMe_3)_2Ti(C\equiv CSiMe_3)_2]CuR$  gives the bis-alkenyl complex  $(C_5H_4SiMe_3)_2Ti(C\equiv CSiMe_3)[\mu-C=C(SiMe_3)(R)]Cu$ .<sup>1823</sup> The chemistry of complexes of the type  $[Cp_2Ti(C\equiv CR^1)_2]CuR$  toward different organic substrates has been explored, such as acyl chlorides and anhydrides to give C–C bond-forming processes.<sup>1824</sup> The trinuclear  $(C_5H_4SiMe_3)_2Ti(C\equiv CR)_2[Fe(CO)_4]_2$  can also be isolated (Scheme 720).<sup>1825</sup> Low-valent nickel carbonyl compounds stabilized by coordination to  $Cp'_2Ti(C\equiv CSiMe_3)_2$  have



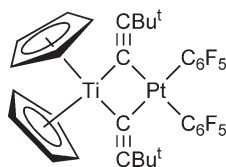
Scheme 721

been synthesized and their reactions with  $\text{P(OR)}_3$  affecting the Ni–CO fragment are described.<sup>1826</sup>  $(\text{C}_5\text{H}_4\text{SiMe}_3)_2\text{Ti}(\text{C}\equiv\text{CPh})_2$  reacts with equimolar amounts of  $\text{CuBr}$ ,  $\text{Ni(PPh}_3)_3$ , or  $\text{Pd(PPh}_3)_4$  with the formation of the heterobimetallic complexes of general type  $(\text{C}_5\text{H}_4\text{SiMe}_3)_2\text{Ti}(\text{C}\equiv\text{CPh})_2\cdot\text{ML}_n$  [ $\text{ML}_n = \text{CuBr}$ ,  $\text{Ni(PPh}_3)_3$ ,  $\text{Pd(PPh}_3)_4$ ], in which the respective transition metal atoms are linked by  $\sigma$ - $\pi$ -bound alkynyl ligands. The solid-state structures of  $(\text{C}_5\text{H}_4\text{SiMe}_3)_2\text{Ti}(\text{C}\equiv\text{CPh})_2$  and the palladium complex are reported.<sup>1827</sup> The synthesis of a series of mixed Ti–late metal complexes of the general type  $[(\text{C}_5\text{H}_4\text{SiMe}_3)_2\text{Ti}(\text{C}\equiv\text{CSiMe}_3)_2]\text{ML}$  ( $\text{M} = \text{Ni}$ ,  $\text{Pd}$ ;  $\text{L} = \text{PPh}_3$ ,  $\text{P(OMe)}_3$ ,  $\text{P(OPh)}_3$ ) (Scheme 720) has been reported with  $\eta^2$ -coordination of the  $\text{C}\equiv\text{C}$  bond to Ni or Pd. Cyclic voltammetric studies reveal the electron-donating character of the coordinated  $\text{M(0)}$  centers, which is demonstrated by the shift of the  $\text{Ti(IV)/Ti(III)}$  reduction to a more negative potential. This reductive process also exhibits a dependence on the  $\pi$ -acidity of the respective Lewis base ligand. The molecular structure of  $[(\text{C}_5\text{H}_4\text{SiMe}_3)_2\text{Ti}(\text{C}\equiv\text{CSiMe}_3)_2]\text{Pd(PPh}_3)_2$  has been determined by X-ray diffraction.<sup>1828</sup>

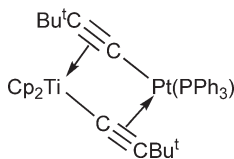
The reaction between  $\text{Cp}_2\text{Ti}(\text{C}\equiv\text{CBu}^t)_2$  and *cis*- $\text{Pt}(\text{C}_6\text{F}_5)_2(\text{THF})_2$  gives the Ti–Pt complex  $\text{Cp}_2\text{Ti}(\mu\text{-C}\equiv\text{CBu}^t)_2\text{Pt}(\text{C}_6\text{F}_5)_2$  which has been shown by X-ray crystallography to contain two asymmetric  $\mu_2$ - $\eta^1$ -alkynyl ligands bridging both metal centers (Scheme 722).<sup>1829</sup> The reaction with  $\text{Pt}(\text{C}_2\text{H}_4)(\text{PPh}_3)_2$  in THF affords the asymmetrically bridged heterometallic complex  $\text{Cp}_2\text{Ti}(\text{C}\equiv\text{CBu}^t)\text{Pt(PPh}_3)_2$ , obtained as moderately air stable red crystals, that can formally be considered as a binuclear  $\text{Ti(III)}\text{--Pt(I)}$  compound (Scheme 723). The electronic effects and/or steric demands of the alkynyl substituents affect the bonding features of this type of complexes.<sup>1830</sup>

$(\text{C}_5\text{H}_4\text{CH}_2\text{CH}_2\text{NMe}_2)_2\text{TiCl}_2$  reacts with 2 equiv. of  $\text{LiC}\equiv\text{CSiMe}_3$  to afford the bis(alkynyl) titanocene  $(\text{C}_5\text{H}_4\text{CH}_2\text{CH}_2\text{NMe}_2)_2\text{Ti}(\text{C}\equiv\text{CSiMe}_3)_2$ . The reaction of this compound with oligomeric or polymeric copper(I) or silver(I) compounds affords the heterobimetallic titanium–copper or titanium–silver complexes  $(\text{C}_5\text{H}_4\text{CH}_2\text{CH}_2\text{NMe}_2)_2\text{Ti}(\text{C}\equiv\text{CSiMe}_3)_2\cdot\text{MX}$  (Scheme 724). The solid-state structures of two of these compounds have been reported.<sup>1092</sup>

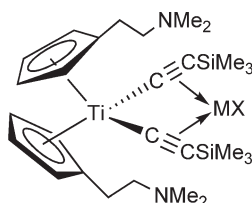
The reaction of  $(\text{C}_5\text{H}_4\text{SiMe}_3)_2\text{TiCl}_2$  with  $\text{LiC}\equiv\text{C--C}\equiv\text{CR}$  ( $\text{R} = \text{Et}$ ,  $\text{SiMe}_3$ ) and  $\text{LiC}\equiv\text{C--SiMe}_2\text{--C}\equiv\text{CSiMe}_3$  produces  $(\text{C}_5\text{H}_4\text{SiMe}_3)_2\text{Ti}(\text{C}\equiv\text{C--C}\equiv\text{CR})_2$  and  $(\text{C}_5\text{H}_4\text{SiMe}_3)_2\text{Ti}(\text{C}\equiv\text{C--SiMe}_2\text{--C}\equiv\text{CSiMe}_3)_2$  in high yield. These compounds react with  $\text{Ni(CO)}_4$  to afford the heterobimetallic titanium–nickel complexes  $(\text{C}_5\text{H}_4\text{SiMe}_3)_2\text{Ti}(\text{C}\equiv\text{C--C}\equiv\text{CR})_2\cdot\text{Ni(CO)}$  and  $(\text{C}_5\text{H}_4\text{SiMe}_3)_2\text{Ti}(\text{C}\equiv\text{C--SiMe}_2\text{--C}\equiv\text{CSiMe}_3)_2\cdot\text{Ni(CO)}$ . Reactions with  $\text{Co}_2(\text{CO})_8$ ,



Scheme 722



Scheme 723

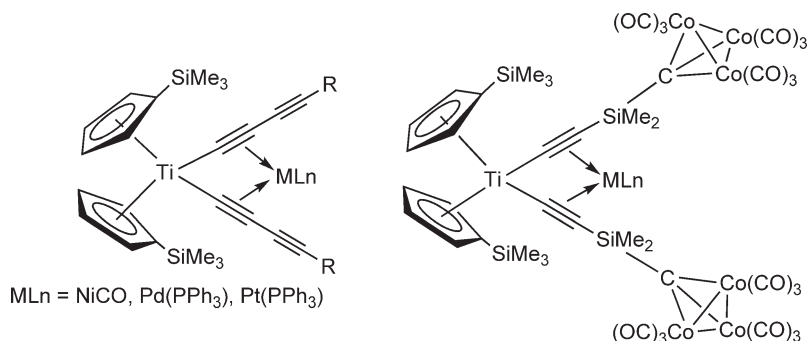


Scheme 724

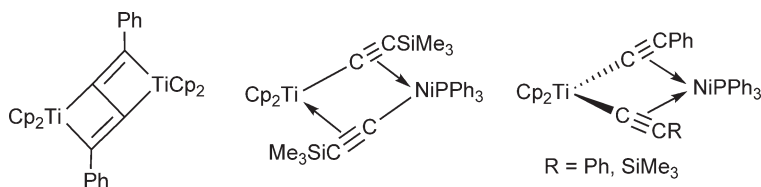


$\text{Pd}(\text{PPh}_3)_4$ , or  $\text{Pt}(\text{PPh}_3)_2(\text{H}_2\text{C}=\text{CH}_2)$  give different heterobimetallic or polymetallic complexes in which the inner or outer  $\text{C}\equiv\text{C}$  triple bonds are coordinated to the late transition metal. Some illustrative examples are shown in [Scheme 725](#). Some X-ray structures are reported.<sup>1831</sup> Analogous heterobimetallic complexes with late transition metal (Cu, Ru, Pt) can be prepared by the reaction of the monoalkynyltitanium compounds  $\text{Cp}_2\text{Ti}(\text{CH}_2\text{SiMe}_3)(\text{C}\equiv\text{CR})$  with the appropriate late transition metal salt.<sup>1285</sup>

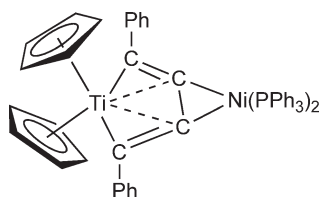
The titanocene ("Cp<sub>2</sub>Ti") generator  $\text{Cp}_2\text{Ti}(\text{Me}_3\text{SiC}\equiv\text{CSiMe}_3)$  reacts with the unsymmetrically substituted butadiyne  $\text{PhC}\equiv\text{CC}\equiv\text{CSiMe}_3$  to give a product with a bridging tetrahydro-(1-3- $\eta$ ):(2-4- $\eta$ )-*trans,trans*-butadiene unit (zigzag butadiene) between two titanium centers ([Scheme 726](#)); the cleavage of the central C–C single bond of the butadiyne is not observed.<sup>1832</sup> By contrast,  $\text{Cp}_2\text{Ti}(\text{Me}_3\text{SiC}\equiv\text{CSiMe}_3)$  reacts with  $\text{Ni}(\text{PPh}_3)_2(\text{Me}_3\text{SiC}\equiv\text{C}-\text{C}\equiv\text{CSiMe}_3)$  with C–C cleavage to give the heterobimetallic acetylide compound  $\text{Cp}_2\text{Ti}(\mu-\text{C}\equiv\text{CSiMe}_3)\text{-Ni}(\text{PPh}_3)(\mu-\text{C}\equiv\text{CSiMe}_3)$  ([Scheme 726](#)), characterized by IR and NMR spectroscopy, and X-ray crystallography. Two  $\sigma,\pi$ -bridging acetylide units are  $\sigma$ -bonded to each of the two metals and  $\pi$ -bonded to the second metal. The compound is highly fluxional in solution at room temperature. The NMR study shows that at 190 K an equilibrium exists between one isomer with two non-equivalent and another isomer with two equivalent acetylide units. The same reaction with the complexes  $\text{Ni}(\text{PPh}_3)_2(\text{PhC}\equiv\text{C}-\text{C}\equiv\text{CR})$  ( $\text{R}=\text{Ph}$ ,  $\text{SiMe}_3$ ) yields  $\text{Cp}_2\text{Ti}(\text{C}\equiv\text{CR})\text{-(C}\equiv\text{CPh)Ni}(\text{PPh}_3)$  where both acetylide units are  $\sigma$ -bonded to the titanium atom and  $\pi$ -bonded to the nickel atom, giving a tweezer-like structure. In the heterobinuclear compound  $\text{Cp}_2\text{Ti}(\text{PhC}\equiv\text{CC}=\text{CPh})_2\text{Ni}(\text{PPh}_3)_2$ , the nickel fragment is coordinated to two ring carbon atoms of a titanacyclocumulene resulting in a structure with a pair of planar tetracoordinate carbon atoms ([Scheme 727](#)).<sup>1832</sup> These results conclude that nickel(0) complexes containing five-membered titanacyclocumulenes can be considered as intermediates in the cleavage of C–C bonds of



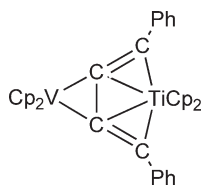
Scheme 725



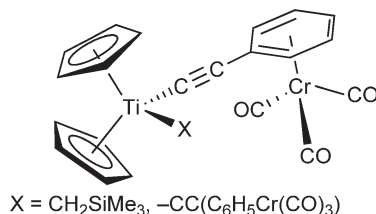
Scheme 726



Scheme 727



Scheme 728



Scheme 729

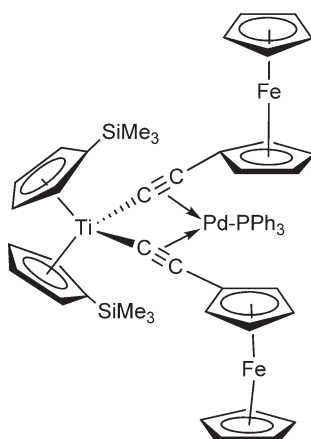
disubstituted butadiynes, showing different ways of reactivity depending on the butadiyne substituents and the stoichiometry of the reactions.<sup>1299</sup> Analogous central C–C single bond activation in disubstituted butadiynes has been observed accompanied by P–C bond activation in  $\text{PPh}_3$ , with coupling of the resulting fragments to give the complexes  $\text{Cp}_2\text{Ti}(\mu\text{-}\sigma,\eta^2\text{-C}\equiv\text{CPh})(\mu\text{-}\sigma,\eta^2\text{-C}\equiv\text{CSiMe}_3)(\text{NiPPh}_3)$  and the phosphido-bridged  $\sigma\text{-}\pi$ -acetylide complex  $\text{Cp}_2\text{Ti}(\mu\text{-}\sigma,\eta^2\text{-C}\equiv\text{CPh})(\mu\text{-PPh}_2)(\text{NiPPh}_3)$ .<sup>1833</sup> The Ti–V organometallic butadiyne-bridged compound  $\text{Cp}_2\text{Ti}(\mu\text{-}\eta^2\text{-}\eta^4\text{-PhC}_4\text{Ph})\text{VCp}_2$  has been synthesized by the reaction of  $\text{Cp}_2\text{Ti}(\text{C}\equiv\text{CPh})_2$  with  $\text{VCp}_2$  in toluene at room temperature. The molecular structure determined by X-ray diffraction shows that the two internal carbon atoms of the butadiyne skeleton are planar and tetracoordinated (Scheme 728).<sup>1834–1836</sup>

Bi- and trimetallic Ti(IV)–Cr(0) complexes  $\text{Cp}_2(\text{CH}_2\text{SiMe}_3)\text{Ti}\text{-C}\equiv\text{C}(\eta^6\text{-C}_6\text{H}_5)\text{Cr}(\text{CO})_3$  and  $\text{Cp}_2\text{Ti}[\text{C}\equiv\text{C}(\eta^6\text{-C}_6\text{H}_5)\text{Cr}(\text{CO})_3]_2$  (Scheme 729) have been prepared as highly unstable compounds by reacting  $\text{Li}[\text{C}\equiv\text{C}(\eta^6\text{-C}_6\text{H}_5)\text{Cr}(\text{CO})_3]$  with  $\text{Cp}_2\text{TiCl}(\text{CH}_2\text{SiMe}_3)$  and  $\text{Cp}_2\text{TiCl}_2$ , respectively. The chemical and electrochemical properties of these complexes have been studied and compared to related ferrocenyl derivatives. The cyclic voltammogram of the trinuclear compound shows a quasi-reversible reduction wave at  $E = -1.60\text{ V}$  ( $\Delta E = 100\text{ mV}$ ), assigned to the Ti(IV)/Ti(III) redox couple. The Ti(IV)/Ti(III) redox potential is shifted to a more positive value in comparison to the non-coordinated tweezer molecule  $\text{Cp}_2\text{Ti}(\text{C}\equiv\text{CPh})_2$ , indicating an easier reduction process of the titanium atom. This can be explained by the electron-withdrawing effect of the  $(\eta^6\text{-benzene})\text{Cr}(\text{CO})_3$  unit.<sup>1837</sup> The analogous compound  $\text{Cp}_2\text{Ti}(\text{C}\equiv\text{CFc})_2$  ( $\text{Fc} = \eta^5\text{-C}_5\text{H}_4\text{FeCp}$ ) has been synthesized and structurally characterized by X-ray diffraction. The cyclic voltammogram shows one reversible reduction wave at  $E = -1.28\text{ V}$  ( $\Delta E = 73\text{ mV}$ ). The complex reacts with  $\text{Ni}(\text{CO})_4$  to give the tetrametallic derivative  $\text{Cp}_2\text{Ti}(\text{C}\equiv\text{CFc})_2\cdot\text{Ni}(\text{CO})$ .<sup>1838</sup> The complex  $(\text{C}_5\text{H}_4\text{SiMe}_3)_2\text{Ti}(\text{C}\equiv\text{CFc})_2$  reacts with  $\text{Pd}(\text{PPh}_3)_2$  to generate  $(\text{C}_5\text{H}_4\text{SiMe}_3)_2\text{Ti}(\text{C}\equiv\text{CFc})_2\cdot\text{Pd}(\text{PPh}_3)$  (Scheme 730). The cyclic voltammogram of this compound shows an irreversible Ti(IV)/Ti(III) reduction wave at  $E = -2.72\text{ V}$ , in contrast to the reversible reduction wave at  $E = 1.99$  ( $\Delta E = 120\text{ mV}$ ) observed for  $(\text{C}_5\text{H}_4\text{SiMe}_3)_2\text{Ti}(\text{C}\equiv\text{CFc})_2$ .<sup>1839</sup>

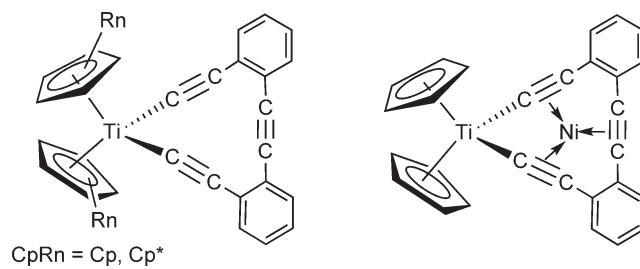
A heterobimetallic Ti–Ni complex has been synthesized and characterized where the Ni atom is coordinated to three alkyne functionalities of a bis-Cp acetylide titanium fragment containing the *o*-bis(ethynyl)tolane ligand (Scheme 731).<sup>1286</sup>

Thioalkyne titanium derivatives with functionalized Cp rings  $(\text{C}_5\text{H}_4\text{R}^1)(\text{C}_5\text{H}_4\text{R}^2)\text{Ti}(\text{SC}\equiv\text{CR})_2$  ( $\text{R} = \text{Ph}, \text{Bu}^t$ ,  $\text{R}^1 = \text{R}^2 = \text{SiMe}_3$ ;  $\text{R} = \text{Bu}^t$ ,  $\text{R}^1 = \text{SiMe}_3$ ,  $\text{R}^2 = \text{PPh}_2$ ;  $\text{R} = \text{Bu}^t$ ,  $\text{R}^1 = \text{R}^2 = \text{PPh}_2$ ) have been prepared and used as precursors for the synthesis of heterobinuclear Ti–M ( $\text{M} = \text{Mo}, \text{Pd}, \text{Pt}$ ) complexes with different coordination modes (Scheme 732). The crystal structures of some of these complexes have been reported.<sup>1840</sup>

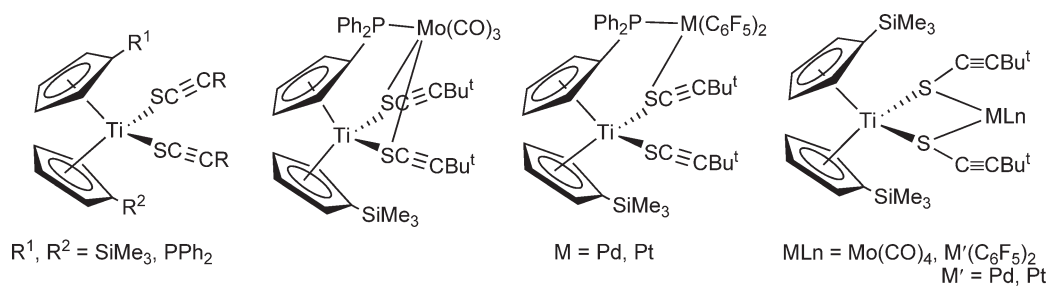
Mononuclear bis(alkyne) derivatives of functionalized bis-Cp derivatives  $(\text{C}_5\text{H}_4\text{R})_2\text{Ti}(\text{C}\equiv\text{CBu}^t)_2$  ( $\text{R} = \text{PPh}_2$ ,  $\text{Ph}_2\text{P}=\text{O}$ ,  $\text{Ph}_2\text{P}=\text{S}$ ) have been isolated by the reaction of  $\text{Ti}(\text{C}_5\text{H}_4\text{R})_2\text{Cl}_2$  with  $\text{LiC}\equiv\text{CBu}^t$  in diethyl ether. These compounds react with  $(\text{CuCl})_n$  or  $\text{Mo}(\text{CO})_4\text{L}_2$  to give heterobimetallic and heterotrimetallic complexes (Scheme 733) through the coordination of the acetylide and the Cp' ligands.<sup>1772</sup>



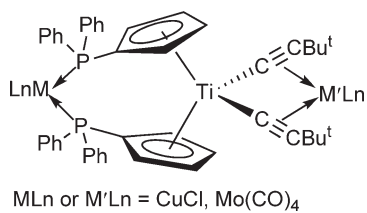
Scheme 730



Scheme 731



Scheme 732



Scheme 733

Alkylideneamido (imido) groups are suitable bridging ligands for early–late heterobimetallic complexes because they show high basicity and coordinate to both early and late transition metals. There are a few examples of heterobimetallic titanium compounds with bridging imido ligands. The heterobimetallic Ti–Co compound  $\text{Cp}_2\text{Ti}(\mu\text{-N}=\text{CPh}_2)_2\text{CoCp}$  has been described.<sup>1841,1842</sup>

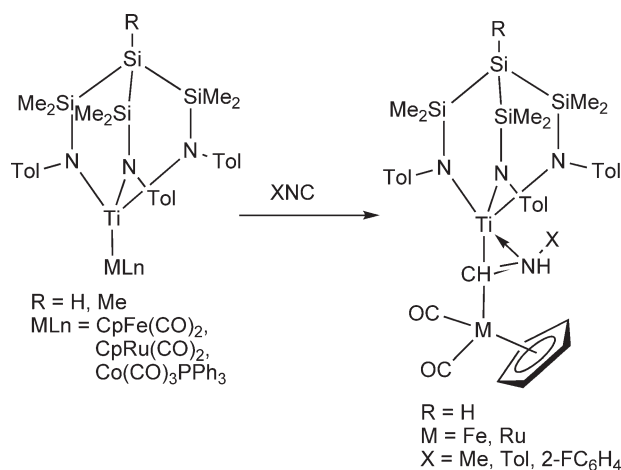
The trinuclear compound  $(\text{NMe}_3\text{Cet})_6[\text{Cp}_2\text{Ti}(\mu\text{-NC-Ru}(\text{CN})_5)_2]$  has been prepared. In  $\text{CHCl}_3$  solution, it shows an intense long-wavelength absorption at  $\lambda_{\text{max}} = 630 \text{ nm}$  which has been assigned to an a  $\text{Ru(II)} \rightarrow \text{Ti(IV)}$  metal-to-metal charge transfer (MMCT) transition.<sup>1843</sup>

Titanium–transition metal complexes containing unbridged metal–metal bonds are rare. Stabilization of such complexes can be achieved by alkoxo or amido ancillary ligands coordinated to titanium. Binuclear complexes in which the two metal atoms are directly bonded to one another may display special cooperative reactivity between the two electronically very different reactive sites. Thus, the electropositive early transition metal may react with more Lewis-basic reagents while the nucleophilic late transition metal fragment will attack the more acidic reagents. The complexes  $\text{MeSi}[\text{SiMe}_2\text{N}(p\text{-tolyl})]_3\text{Ti-M}(\text{CO})_2\text{Cp}$  ( $\text{M} = \text{Fe, Ru}$ ) containing metal–metal bonded “early–late heterobimetallic” units have been synthesized and isolated as thermally stable compounds in the solid state and in solution. The presence of unsupported metal–metal bonds was confirmed by X-ray crystal structure determinations. These complexes react with isocyanides to give metalla–iminoacyl complexes. Thus, the reaction of the Ti–Fe and Ti–Ru bonds in  $\{\text{MeSi}[\text{SiMe}_2\text{N}(4\text{-CH}_3\text{C}_6\text{H}_4)]_3\text{Ti-MCp}(\text{CO})_2\}$  with 1 equiv. of  $\text{MeN}\equiv\text{C}$  takes place with insertion of the isocyanide into the polar metal–metal bond to give  $\{\text{MeSi}[\text{SiMe}_2\text{N}(4\text{-CH}_3\text{C}_6\text{H}_4)]_3\text{Ti}(\eta^2\text{-C}=\text{NMe})\text{MCp}(\text{CO})_2\}$  (Scheme 734). This behavior can be viewed as an example of the  $\alpha$ -addition reaction of an electrophilic and a nucleophilic metal center to the carbon atom of an isocyanide molecule. The  $^{13}\text{C}$  NMR resonances of iminoacyl groups are observed at remarkably low field ( $\delta$  267.8–303.8).<sup>1844,1845</sup> Unbridged bimetallic complexes containing Ti–Fe, Ti–Ru, and Ti–Co bonds stable in solution have also been reported. They are chemically fairly robust toward attack by weak nucleophiles at ambient temperature.<sup>1846</sup>

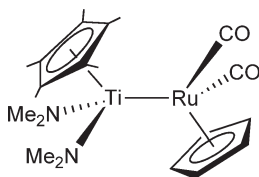
The reaction of the Ti(III) alkoxo derivative  $\text{Cp}_2\text{TiOBU}^t$  with  $[\text{RuCp}(\text{CO})_2]_2$  does not occur thermally, but is accomplished under photoirradiation to afford  $\text{Cp}_2(\text{OBU}^t)\text{Ti-RuCp}(\text{CO})_2$  in which a direct metal–metal Ti–Ru bond is proposed. The Ti–Ru compound thermally undergoes fragmentation to regenerate the starting materials. The formation of this Ti–Ru complex is formally considered as the metal–metal bond cleavage of a metal carbonyl dimer by a Ti(III) reducing reagent. Possible reaction mechanisms have been discussed.<sup>1745</sup>

The X-ray structural investigation of an unbridged Ti–Co bond in  $(\text{RO})_3\text{Ti-Co}(\text{CO})_3(\text{L})$  ( $\text{R} = \text{Bu}^t, \text{Pr}^i, \text{CH}(\text{CF}_3)_2, \text{Ph}$ ;  $\text{L} = \text{CO}, \text{PPh}_3$ ) has been reported. The presence of alkoxo ligands provides thermal stability to these complexes.<sup>1847</sup>

The reaction of  $\text{Cp}^*\text{Ti}(\text{NMe}_2)_3$  with  $\text{RuCp}(\text{CO})_2\text{H}$  gives  $\text{Cp}^*(\text{NMe}_2)_2\text{Ti-Ru}(\text{CO})_2\text{Cp}$  in which a metal–metal bond between the titanium and ruthenium atoms is proposed (Scheme 735).<sup>1744</sup>



Scheme 734



Scheme 735

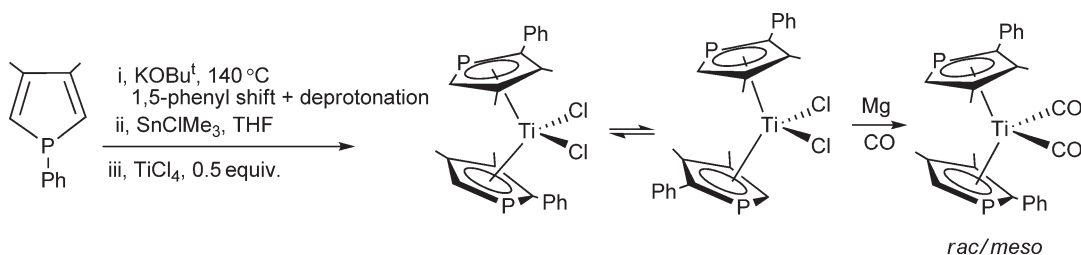
## 4.05.7 Complexes with Non-cyclopentadienyl $\pi$ -Ligands

### 4.05.7.1 Complexes with $\eta^5$ -Heteroligands

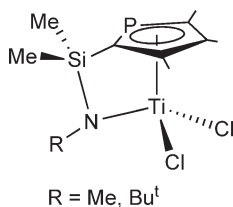
This section describes complexes with heterocyclic  $\pi$ -ligands, notably those containing N, P, and carboranyl rings. Phospholyl anions ( $C_4R_4P^-$ ) are analogs of the Cp anions ( $C_5R_5^-$ ). A modified methodology for the synthesis of the chiral phospha–titanium complex bis(3,4-dimethyl-2-phenylphospholyl)titanium dichloride (Scheme 736) has been reported, including its X-ray crystal structure. The activation parameters for the *rac/meso* isomerization are relevant to the applications of this type of compounds for stereoselective catalysis. The reduction of  $(C_4Me_4P)_2TiCl_2$  with Mg in the presence of CO affords the Ti(II) derivative  $(C_4Me_4P)_2Ti(CO)_2$ .<sup>1848</sup> A similar reaction with  $(C_4HMe_2PhP)_2TiCl_2$  leads to the chiral dicarbonyl compound  $(C_4HMe_2PhP)_2Ti(CO)_2$  (Scheme 736) for which the *rac/meso* isomerization process has been studied. The mechanism of the isomerization depends on the different oxidation states of the Ti atom.<sup>1849</sup>

The bridged phospholyl–amido complexes shown in Scheme 737 have been synthesized. The compound is structurally similar to the well-known “constrained-geometry” Cp–amido compound  $(C_5Me_4SiMe_2NBu^t)TiCl_2$ , and preliminary ethylene polymerization data for the phospholyl complexes show indeed comparable catalyst activities.<sup>1850</sup>

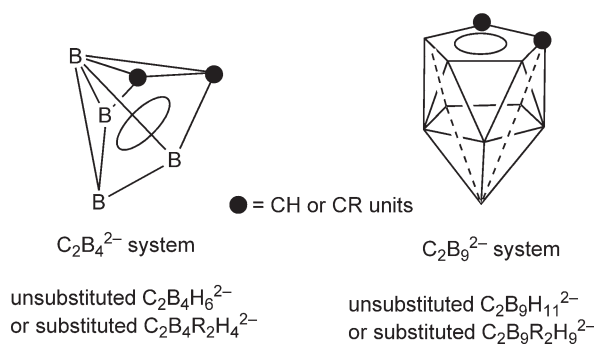
Boron-containing ligands can replace  $\eta^5$ -Cp rings in transition metal chemistry. They exhibit substantially different steric and electronic properties. Borollide ligands can formally be derived by the replacement of CH units of carbocyclic ligands by  $BH^-$ . Titanium derivatives of the  $C_2B_4^{2-}$  system have been synthesized and structurally characterized, in which the Ti atom is  $\eta^5$ -bound to the  $C_2B_3$  five-membered face (Scheme 738). The reaction chemistry of these complexes is, however, very limited, due to the hindrance of the carboranyl ligand and the low stability of the corresponding alkyl derivatives. Metallocarboranyl titanium derivatives of the  $C_2B_9^{2-}$  system are also known (Scheme 738). Their alkyl compounds are more stable and they exhibit a richer reaction chemistry.



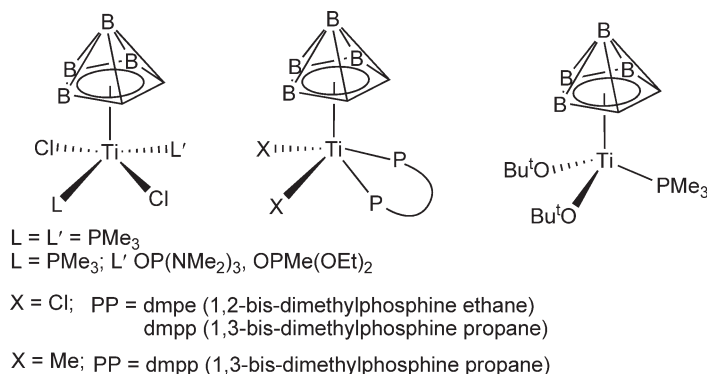
Scheme 736



Scheme 737



Scheme 738

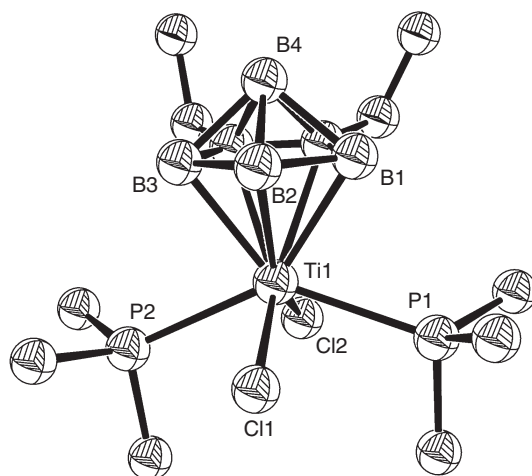


Scheme 739

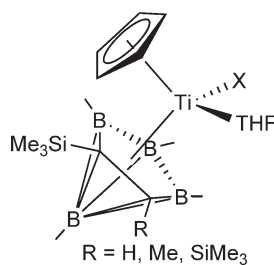
$TiCl_4(PMe_3)_2$  reacts with  $Li_2(Et_2C_2B_4H_4)$  with the formation of the *closo*-titanacarborane complex  $(Et_2C_2B_4H_4)TiCl_2(PMe_3)_2$ . The X-ray analysis reveals a square-pyramidal structure with *trans*-phosphine ligands. The  $PMe_3$  ligands can be exchanged by monodentate phosphine oxide but only one  $PMe_3$  is replaced, while  $(Et_2C_2B_4H_4)TiCl_2(PMe_3)_2$  reacts with *dmpe* or *dmpp* to give  $(Et_2C_2B_4H_4)TiCl_2(LL)$  ( $LL = dmpe, dmpp$ ) with *cis*-coordination in a square-pyramidal structure. The reaction of  $(Et_2C_2B_4H_4)TiCl_2(PMe_3)_2$  with  $KOBu^t$  affords  $(Et_2C_2B_4H_4)Ti(OBu^t)_2(PMe_3)$  with displacement of both chlorides and loss of one phosphine ligand.  $(Et_2C_2B_4H_4)TiCl_2(dmpp)$  can be alkylated with  $LiMe$  to give the dimethyl complex  $(Et_2C_2B_4H_4)TiMe_2(dmpp)$  (Scheme 739). Some of these compounds have been structurally characterized by X-ray crystallography (Figure 30). In the presence of MAO, they are catalyst precursors for the polymerization of ethylene, although the choice of phosphine ligand has a dramatic effect on catalyst activity. Several different catalyst species are probably active in these reaction mixtures, giving rise to polyethylene products of broad polydispersity.<sup>1851</sup>

The synthesis of a mixed Ti(IV) complex based on Cp and the small carborane ligand  $C_2B_4^{2-}$  has been reported. The compounds  $Cp[2,3-R_2-2,3-C_2B_4H_4]TiCl$  are prepared by reduction of  $Cp_2TiCl_2$  with *closo-exo*-Li-1-Li[2,3- $R_2$ -2,3- $C_2B_4H_4$ ] and subsequent chemical oxidation with anhydrous  $TiCl_4$  in THF (Scheme 740). The crystal structure shows a distorted tetrahedral environment about the metal center similar to those of bis-Cp' titanium derivatives (Figure 31).<sup>1852,1853</sup>

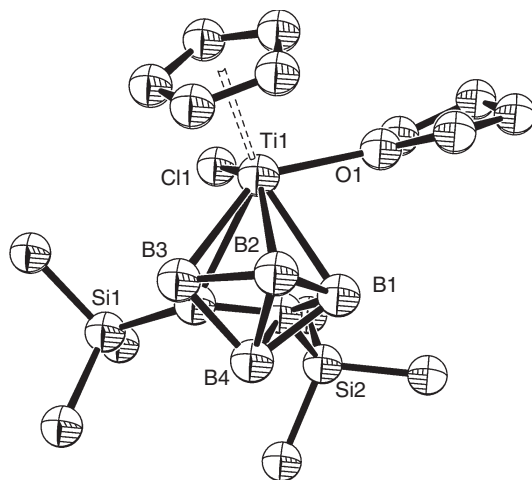
The synthesis of  $d^0$ -mixed bis-Cp'-type titanium complexes containing Cp' and the  $C_2B_9^{2-}$  carborane ligands has been reported.<sup>1851,1854</sup> The complex  $Cp^*(\eta^5-C_2B_9H_{11})TiMe$  has been prepared by the reaction of  $Cp^*TiMe_3$  with  $C_2B_9H_{13}$ . The titanacarborane complex is obtained as a thermally sensitive product and has been characterized by NMR spectroscopy. This carborane compound undergoes intramolecular C-H activation by decomposition at 23 °C to give the fulvene complex  $Ti(C_5Me_4CH_2)(\eta^5-C_2B_9H_{11})$ , and forms adducts with Lewis bases and inserts 2-butyne, acetonitrile, and CO to yield bent-titanocene-like derivatives (Scheme 741). X-ray diffraction analysis of some of these complexes have been carried out.<sup>1855,1856</sup> The molecular structures of the dicarbollide complex  $Cp^*(\eta^5-C_2B_9H_{11})TiMe$  and the dicarbollide fulvene complex  $Ti(C_5Me_4CH_2)(\eta^5-C_2B_9H_{11})$ , obtained from  $Cp^*(\eta^5-C_2B_9H_{11})TiMe$  by methane elimination, have been determined by X-ray diffraction.<sup>1857</sup>



**Figure 30** Molecular structure of complex  $(\text{Et}_2\text{C}_2\text{B}_4\text{H}_4)\text{TiCl}_2(\text{PMe}_3)_2$  (reproduced by permission of American Chemical Society from *J. Am. Chem. Soc.* **2000**, 122, 10573).

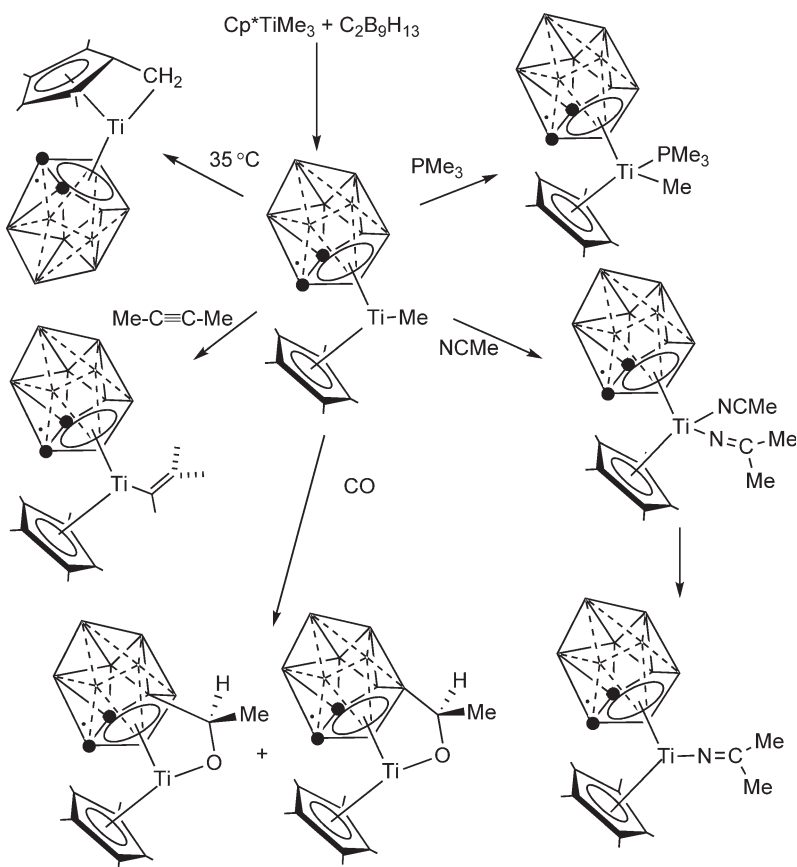


**Scheme 740**

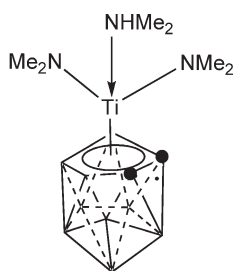


**Figure 31** Molecular structure of complex  $\text{Cp}[2,3-(\text{SiMe}_3)_2-2,3-\text{C}_2\text{B}_4\text{H}_4]\text{TiCl}\cdot\text{THF}$  (reproduced by permission of American Chemical Society from *Organometallics* **1994**, 13, 4156).

The treatment of  $\text{Pr}_2\text{NB}(\text{C}_9\text{H}_7)(\text{C}_2\text{B}_{10}\text{H}_{11})$  with  $\text{Ti}(\text{NMe}_2)_4$  leads to the isolation of  $(\eta^5\text{-C}_2\text{B}_9\text{H}_{11})\text{-Ti}(\text{NMe}_2)_2(\text{NHMe}_2)$  (Scheme 742) by a process involving the attack of  $\text{NMe}_2^-$  in  $\text{Ti}(\text{NMe}_2)_4$  to the bridging B atom and the cage B atom. The molecular structure of this complex has been determined.<sup>1731,1854</sup> The analogous ethyl-amido monodicarbollide titanium compound  $(\eta^5\text{-C}_2\text{B}_9\text{H}_{11})\text{Ti}(\text{NEt}_2)_2(\text{NHEt}_2)$ , when activated with MAO,



Scheme 741



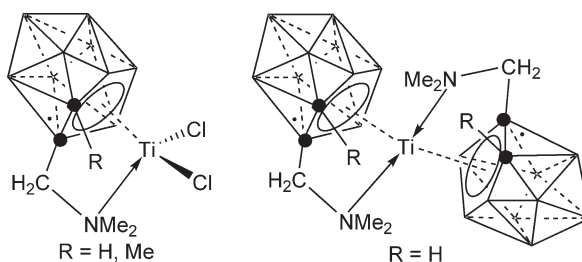
Scheme 742

polymerizes ethylene with good activity and styrene to produce syndiotactic polystyrene with very low activity. Attempts to co-polymerize ethylene with styrene afforded mixtures of the two homopolymers.<sup>1858</sup>

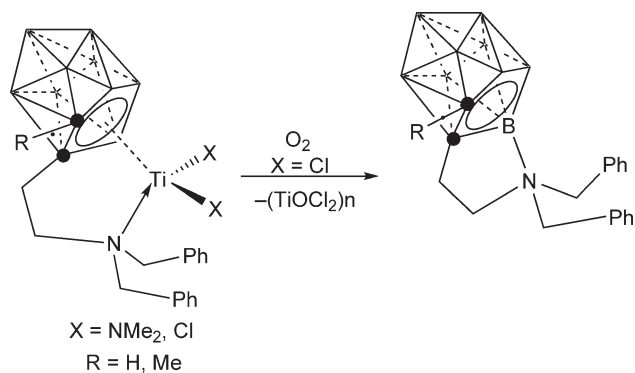
The compound  $(\eta^5\text{-}\eta^1\text{-RC}_2\text{B}_9\text{H}_9\text{CH}_2\text{NMe}_2)\text{TiCl}_2$  ( $\text{R} = \text{H}, \text{Me}$ ), containing the dimethylamino dicarbollyl ligand analogous to the mono-Cp amido titanium complexes, has been synthesized and characterized by  $^{11}\text{B}$ ,  $^{13}\text{C}$ , and  $^1\text{H}$  NMR spectroscopy. In the presence of MMAO, this complex exhibits moderate catalytic activity for ethylene polymerization and produces high molecular weight polymers. The bis(dicarbollyl) complex  $\text{Ti}(\eta^5\text{-}\eta^1\text{-C}_2\text{B}_9\text{H}_{10}\text{-CH}_2\text{NMe}_2)_2$  has also been prepared (Scheme 743).<sup>1859</sup>

Dibenzylamino-ethyl dicarbollide titanium compounds have been described.  $[(\eta^5\text{-RC}_2\text{B}_9\text{H}_9)(\text{CH}_2)_2\text{-}(\eta^1\text{-NBz}_2)]\text{Ti}(\text{NMe}_2)_2$  ( $\text{R} = \text{H}, \text{Me}$ ) are synthesized by treatment of the *nido*-carborane with  $\text{Ti}(\text{NMe}_2)_4$ . The diamido

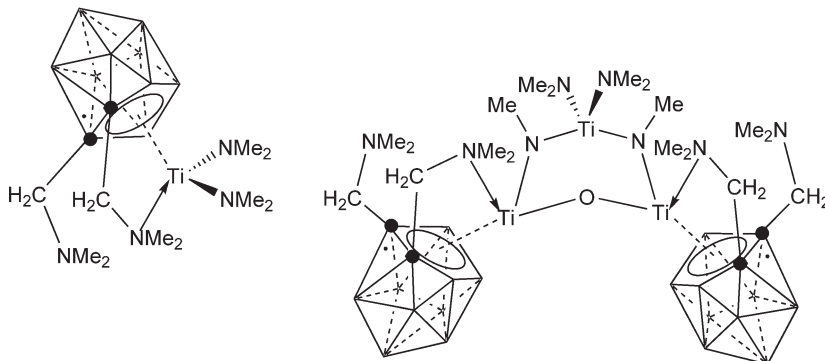




### Scheme 743



Scheme 744

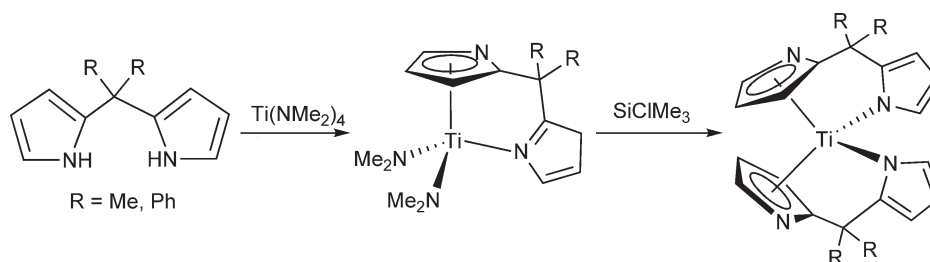


### Scheme 745

complexes react with  $\text{Me}_3\text{SiCl}$  to yield the dichloro compounds  $[(\eta^5\text{-RC}_2\text{B}_9\text{H}_9)(\text{CH}_2)_2(\eta^1\text{-NBz}_2)]\text{TiCl}_2$ , which exhibit unusual B,N-cyclization when reacted with  $\text{O}_2$ , leading to the production of exocyclic dicarbollides (Scheme 744).<sup>1860</sup>

The mono- and trimetallic titanium complexes shown in [Scheme 745](#) contain the multidentate dicarbollide ligand *nido*-7,8-(Me<sub>2</sub>NCH<sub>2</sub>)<sub>2</sub>-7,8-C<sub>2</sub>B<sub>9</sub>H<sub>9</sub> coordinated to the Ti center in a similar fashion to a Cp-amido ligand; the compounds have been structurally characterized.<sup>1861</sup>

Pyrrolyl ligands  $\eta^5$ -coordinated to titanium give less stable compounds than the isoelectronic Cp group, and  $\eta^5$ -pyrrolyltitanium derivatives are relatively rare.

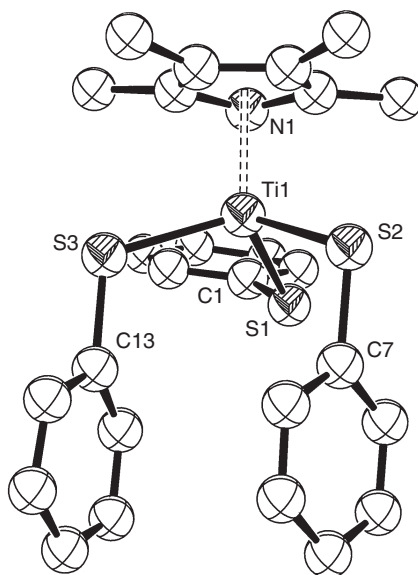


Scheme 746

The transamination reaction between  $\text{Ti}(\text{NMe}_2)_4$  and *meso*-disubstituted dipyrrolylmethanes yields  $[\text{R}_2\text{C}-(\eta^5\text{-C}_4\text{H}_3\text{N})(\eta^1\text{-C}_4\text{H}_3\text{N})]\text{Ti}(\text{NMe}_2)_2$  (R = Me, Ph) derivatives (Scheme 746). The structure of the compound with R = Me has been determined by X-ray diffraction. The presence of the nitrogen atom in the pyrrole ring reduces the symmetry of the  $\pi$ -ligand, so the compounds are obtained as chiral substances. Treatment with  $\text{Me}_3\text{SiCl}$  affords the bis(pyrrolido) complexes  $[(\eta^5\text{-C}_4\text{H}_3\text{N})(\eta^1\text{-C}_4\text{H}_3\text{N})\text{CR}_2]_2\text{Ti}$ .<sup>710</sup> The synthesis and structure of similar dipyrrolylmethane complexes have been reported. Alkynes are rapidly hydroaminated by primary amines catalyzed by these Ti derivatives.<sup>711</sup> Hydroamination of enynes to generate  $\alpha,\beta$ -unsaturated imines can be produced by these titanium pyrrolyl complexes.<sup>712</sup>

$\text{Cp}^*\text{TiCl}_3$  reacts with the lithium salt of 2,3,4,5-tetramethylpyrrole to give the mixed ring complex  $\text{Cp}^*(\eta^5\text{-NC}_4\text{Me}_4)\text{TiCl}_2$  as a red crystalline compound which is extremely sensitive to moisture. Its crystal structure shows a distorted pseudo-tetrahedral geometry with an  $\eta^5$ -coordinated pyrrolyl ligand. The complexes  $(\eta^5\text{-NC}_4\text{Me}_4)_2\text{TiCl}_2$ ,  $(\eta^5\text{-NC}_4\text{Me}_4)\text{TiX}_3$  (X = Cl, SPh), and  $(\eta^5\text{-NC}_4\text{Me}_4)\text{TiCl}_2(\text{SPh})$  have also been synthesized and their molecular structures determined by X-ray diffraction. Figure 32 shows the structure of  $(\eta^5\text{-NC}_4\text{Me}_4)\text{Ti}(\text{SPh})_3$ .<sup>1862</sup>  $(\text{NC}_4\text{Me}_4)\text{TiCl}_3$  reacts with LiMe in toluene at low temperature to afford the monomethyl derivative  $(\text{NC}_4\text{Me}_4)\text{TiCl}_2\text{Me}$ , while the tribenzyl compound  $(\text{NC}_4\text{Me}_4)\text{Ti}(\text{CH}_2\text{Ph})_3$  only is obtained by reacting  $\text{Ti}(\text{CH}_2\text{Ph})_4$  with  $\text{HNC}_4\text{Me}_4$ . Based upon the X-ray structure and theoretical *ab initio* calculations, an agostic interaction has been postulated for  $(\text{NC}_4\text{Me}_4)\text{TiCl}_2\text{Me}$ .<sup>1863</sup>

The complexes  $\text{CpNpTiCl}_2$  (Np is an azole ligand analogous to Cp: Pyr, Id, Ai, Bi) have been synthesized and studied as catalysts in the presence of MAO for ethylene polymerization.<sup>1864</sup>



**Figure 32** Molecular structure of complex  $(\eta^5\text{-NC}_4\text{Me}_4)\text{Ti}(\text{SPh})_3$  (reproduced by permission of the Royal Society of Chemistry from *J. Chem. Soc., Dalton Trans.*, **1997**, 1055).

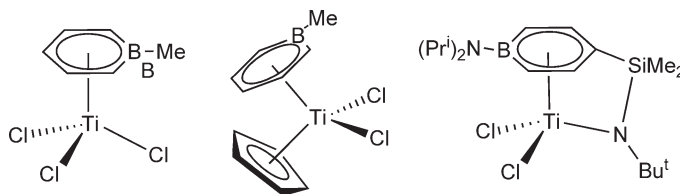
### 4.05.7.2 Complexes with $\eta^6$ -Ligands

Monoanionic boratabenzene ligands can formally be derived from benzene by replacement of CH by  $BR^-$ . Boratabenzene ligands are less basic and less nucleophilic than  $Cp'$  rings, but replacement of  $Cp'$  by boratabenzene ligands in titanium chemistry has been studied.

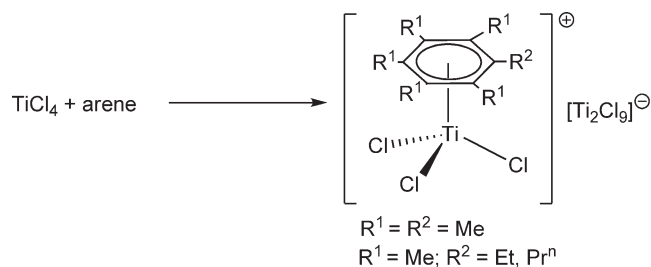
Boratabenzene complexes  $(C_6H_5BMe)TiCl_3$  and  $Cp(C_6H_5BMe)TiCl_2$  without stabilizing substituents at the boron atom have been prepared by transmetallation reactions with  $TiCl_4$  or  $CpTiCl_3$  and  $C_6H_5BMe(XMe_3)$  ( $X = Si, Sn$ ). The molecular structures have been determined by X-ray diffraction. The redox potential is shifted to more anodic values in comparison with the  $Cp$  analogs, by increasing the transfer of electron density from the boratabenzene ligand to the metal center (Scheme 747).<sup>1865</sup> The synthesis and spectroscopic characterization of a boratabenzene titanium complex analogous to  $Cp$ -amido derivatives has also been described.<sup>1866</sup>

Arene complexes of group 4 transition metals remain poorly studied in comparison with derivatives of many other transition elements.  $\eta^6$ -Arene complexes of  $d^0$ -tetravalent Ti, Zr, and Hf are extremely rare. The investigation of titanium(IV) hexaalkyl-arene complexes gives insight into the stability of high-valent metal arene complexes. In contrast to low-valent transition metal arene derivatives, these complexes are in equilibrium with the free arenes. The stability of the complexes depends strongly on both the donor ability of the arene and on their solubility. For complexes of Ti(IV), the coordination of the arene ligand to the metal atom involves the substitution of an electro-negative ligand for the neutral arene molecule with the formation of cationic complexes or zwitterionic species. Remarkable differences between Ti and Zr and Hf are generally observed. The arene ligand is weakly bonded and can easily be replaced by other donor ligands. This type of complex exhibits catalytic activity in olefin polymerization and other organic reactions. The synthetic methods and main structural types of arene complexes of Ti and Zr in different oxidation states have been reviewed. In general, the stability of arene complexes increases with increasing alkyl substitution, that is increasing donor strength, and from the iodo to the chloro derivatives, the M-C distances being independent of X within the known structural types. Differences between the structural chemistry of Ti and Zr arene complexes are determined by the different sizes of the metal centers. Generally 16- and 18-electron complexes are most stable.<sup>1867</sup>

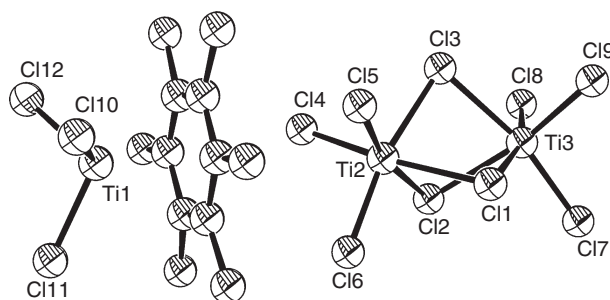
The reaction of  $TiCl_4$  with  $C_6Me_6$  in  $CH_2Cl_2$  or 1,2- $C_6H_4Cl_2$  led to a  $d^0$ -arene complex  $[(C_6Me_6)TiCl_3]^+[Ti_2Cl_9]^-$  which has been structurally characterized by X-ray diffraction (Scheme 748; Figure 33). The molecular structure has a three-legged piano stool geometry. The  $^1H$  NMR spectrum of the reaction mixture indicates the presence of a charge transfer intermediate. The compound is highly stable and promotes the stoichiometric cyclotrimerization of but-2-yne. Theoretical calculations explain the high stability of the titanium(IV) derivatives, as well as the weaker arene-metal interaction in the titanium(III) derivatives. Also, a strong positive charge was found on the benzene hydrogens, consistent with an electrophilic activation of the benzene ring.<sup>1868</sup> Ethylpentamethylbenzene and propylpentamethylbenzene react with an excess of  $TiCl_4$  to give the analogous ionic arene Ti(IV) complexes (Scheme 748).<sup>1869</sup>



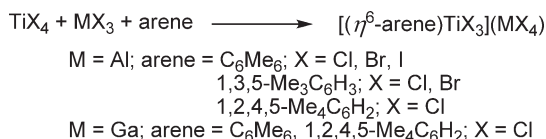
Scheme 747



Scheme 748



**Figure 33** Molecular structure of complex  $[(\text{C}_6\text{Me}_6)\text{TiCl}_3]^+[\text{Ti}_2\text{Cl}_9]^-$  (reproduced by permission of American Chemical Society from *Inorg. Chem.*, **1994**, 33, 2018).



**Scheme 749**

$\text{AlX}_3$  also may behave as a dehalogenating agent in the reaction with  $\text{TiCl}_4$ , thus leaving free coordination sites available for subsequent titanium–arene bond formation. Halide abstraction by  $\text{AlX}_3$  from  $\text{TiX}_4$  is consistent with the higher Al–Cl bond strength with respect to the Ti–Cl bond strength.  $\text{AlX}_3$  reacts with  $\text{TiX}_4$  in the presence of arenes to give ionic  $[(\eta^6\text{-arene})\text{TiX}_3]^+[\text{AlX}_4]^-$  (arene =  $\text{C}_6\text{Me}_6$ ,  $\text{X} = \text{Cl, Br, I}$ ) derivatives (Scheme 749). The structure of  $[(\text{C}_6\text{Me}_6)\text{TiCl}_3][\text{AlCl}_4]$  has been determined by X-ray diffraction. Formation of complexes with less methyl-substituted arene ligands has been established by  $^{13}\text{C}$  NMR spectroscopy.<sup>1870</sup> Analogous  $[(\eta^6\text{-arene})\text{TiX}_3][\text{AlX}_4]$  (arene = 1,3,5- $\text{Me}_3\text{C}_6\text{H}_3$ ,  $\text{X} = \text{Cl, Br}$ ; arene = 1,2,4,5- $\text{Me}_4\text{C}_6\text{H}_2$ ,  $\text{X} = \text{Cl}$ ) have been synthesized. Arene displacement from  $[(\eta^6\text{-arene})\text{TiX}_3][\text{AlX}_4]$  occurs with THF or  $\text{TiCp}$  to afford  $\text{TiCl}_4(\text{THF})_2$  or  $\text{CpTiCl}_3$ , respectively. The titanium(IV) arene complexes efficiently promote the hydrogen–deuterium exchange of the ring protons between  $\text{C}_6\text{D}_6$  and the arene ligand.<sup>1871</sup> A high-valent hexaethylbenzene Ti complex is formed in the reaction of hexaethylbenzene with  $\text{TiCl}_4$  when  $\text{AlCl}_3$  is used.<sup>1872</sup>

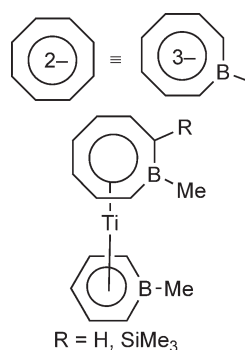
The Ga–Cl bond strength is lower than Al–Cl. Nevertheless,  $\text{GaCl}_3$  could still act as a halide abstractor from  $\text{TiCl}_4$  if sufficient stability is gained by forming a new bond to the aromatic hydrocarbon. Tetrachlorogallates of titanium(IV) of general formula  $[(\eta^6\text{-arene})\text{TiCl}_3][\text{GaCl}_4]$  (Scheme 749) have also been obtained by the reaction of  $\text{TiCl}_4$  with the appropriate arene in the presence of  $\text{GaCl}_3$  in toluene.<sup>1870</sup>

The reaction of a hexane/toluene solution of  $\text{Cp}^*\text{TiMe}_3$  with  $\text{B}(\text{C}_6\text{F}_5)_3$  affords predominantly the yellow compound  $\text{Cp}^*\text{Me}_2\text{Ti}(\mu\text{-Me})\text{B}(\text{C}_6\text{F}_5)_3$ . The addition of toluene to a  $\text{CD}_2\text{Cl}_2$  solution of this complex results in only partial conversion to toluene–adduct complex  $[\text{Cp}^*\text{TiMe}_2(\eta^1\text{-PhMe})][\text{BMe}(\text{C}_6\text{F}_5)_3]$  identified by its  $^1\text{H}$  NMR resonances. A different behavior is observed for Zr and Hf which form stable arene complexes.<sup>516</sup>

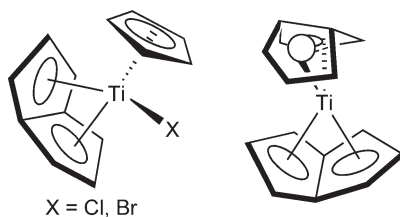
#### 4.05.7.3 Complexes with $\eta^7$ - and $\eta^8$ -Ligands

The synthesis and structural characterization of the first example of an *ansa*-cycloheptatrienyl–Cp titanium complex (Scheme 670; Section 4.05.5) has been reported. Its reactivity toward  $\sigma$ -donors/ $\pi$ -acceptor ligands demonstrates that this complex does not behave like a low-valent titanium compound but rather bears a closer resemblance to Lewis-acidic Ti(IV) complexes. Based on theoretical calculations, this behavior can be attributed to a strong and appreciably covalent Ti–cycloheptatrienyl interaction which leads to highly stabilized frontier orbitals and consequently to a diminishing  $\pi$ -electron release ability.<sup>1706</sup>

The boratacyclooctatetraenyl trianion ( $\text{BCOT}^{3-}$ ) is a versatile ligand for transition metals. The boratacyclooctatetraenyl Ti(IV) complexes  $\text{Ti}(\text{C}_5\text{H}_5\text{B-Me})(2\text{-R-C}_7\text{H}_6\text{B-Me})$  ( $\text{R} = \text{H, SiMe}_3$ ) (Scheme 750) can be obtained from the boratabenzene Ti(II) complex  $\text{Ti}(\text{C}_5\text{H}_5\text{B-Me})_2(\text{CO})$  by oxidative coordination of acetylenes upon insertion of the acetylene molecule into the B–C bond of the boratabenzene ring. The molecular structures of both complexes have been determined by X-ray diffraction.<sup>1873</sup>



Scheme 750



Scheme 751

Studies on  $\text{Ti}(\text{C}_8\text{H}_6)_2$  complexes containing the  $\text{C}_8\text{H}_6^{2-}$  ligands and the relationship between the molecular orbitals in  $\text{C}_8\text{H}_6^{2-}$ ,  $\text{C}_8\text{H}_8^{2-}$ , and  $\text{Cp}^-$  have been reported. It was shown that the  $d_z^2$  orbital of the titanium metal atom is of suitable symmetry for  $\pi$ -bonding in these complexes, unlike in the  $\text{Ti}(\text{C}_8\text{H}_8)_2$  complexes derived from cyclooctatetraene.<sup>1874</sup>

$\text{TiCl}_4(\text{THF})_2$  reacts with 2 equiv. of  $\text{Li}_2[\text{C}_8\text{H}_6(\text{SiMe}_3)_2]$  in THF to afford the 1,4-bis(trimethylsilyl) cyclooctatetraenyl titanium derivative  $\text{Ti}[\text{C}_8\text{H}_6(\text{SiMe}_3)_2]_2$ . X-ray studies show that the compound adopts a structure in which one ring is bound in an  $\eta^8$ -fashion, while the other adopts an intermediate disposition between the  $\eta^3$ -structure found for the analogous Zr complex and the  $\eta^4$ -structure found in  $[\text{Ti}(\text{C}_8\text{H}_8)_2]$ . This unusual bonding situation has been studied using extended Hückel molecular orbital calculations and photoelectron spectroscopy. Variable-temperature solution NMR studies on  $\text{M}[\text{C}_8\text{H}_6(\text{SiMe}_3)_2]_2$  show that the two rings become equivalent on the NMR timescale above 328 K.<sup>1875</sup>

The titanium(0) bis(arene) complex  $\text{Ti}(\eta^6\text{-toluene})_2$  reacts with 9,10-phenanthrenequinone with release of the arene ligands and formation of a diamagnetic brown compound  $\text{Ti}(\text{C}_{14}\text{H}_8\text{O}_2)_3$ , best formulated as a binuclear titanium(IV) derivative containing both 9,10-phenanthrenesemiquinone (PSQ) and 9,10-phenanthrenediolato (PDA) ligands, suggesting the presence of two quinone ligands with differing formal charges, namely  $-1$  and  $-2$ . The diamagnetism of the complex can be explained by an intramolecular spin coupling mechanism between the two semiquinone ligands.<sup>1876</sup>

The dilithiumpentalenediide salt  $\text{Li}_2(\text{C}_8\text{H}_6)$  reacts with  $\text{CpTiCl}_2$  to give the paramagnetic  $d^1$ -complex  $\text{CpTi}(\text{C}_8\text{H}_6)$  which is converted to the Ti(IV) compound  $\text{CpTi}(\text{C}_8\text{H}_6)\text{X}$  ( $X = \text{Cl}, \text{Br}$ ) by further treatment with  $\text{C}_2\text{H}_4\text{X}_2$ . The molecular structure of the paramagnetic compound has been determined by X-ray diffraction. The pentalene function acts as an eight-electron ligand and shows a strong folding of the bicyclic ligand toward the titanium atom. The bis(pentalene) titanium  $\text{Ti}(\text{C}_8\text{H}_6)_2$  can be prepared by the reaction of  $\text{CpTi}(\text{C}_8\text{H}_6)\text{X}$  with  $\text{Li}_2(\text{C}_8\text{H}_6)$  in THF with elimination of  $\text{LiX}$  and  $\text{LiCp}$  (Scheme 751).  $\text{Ti}(\text{C}_8\text{H}_5\text{Me})_2$  is similarly synthesized. These bis(pentalene) titanium complexes have to be classified as diamagnetic 20-electron complexes.<sup>1877</sup> The electronic structure of these pentalene complexes has been calculated based on photoelectron spectroscopic studies.<sup>1878</sup>

#### 4.05.7.4 Complexes with More than Two Cyclopentadienyl Ligands

Variable-temperature 1D and 2D CP/MAS NMR spectra of  $\text{Cp}_2\text{Ti}(\eta^1\text{-C}_5\text{H}_5)_2$  have been reported. The compound is fluxional. The rearrangement mechanism of the  $\eta^1$ -Cp rings in this complex proceeds via a single sigmatropic process.<sup>1879</sup>

A survey of the  $\text{MCp}_4$  ( $\text{M} = \text{Ti}, \text{Zr}, \text{Hf}$ ) chemistry including a re-examination of synthetic procedures, characterization, and reactivity aspects has been reported.<sup>1880</sup>

## 4.05.8 Applications of Titanium(IV) Complexes in Synthesis and Catalysis

### 4.05.8.1 Organic Synthesis

Titanium complexes have been extensively employed in the development of organic synthetic methodology, although this subject is beyond the scope of this chapter. No attempts were made to cover this aspect comprehensively in this chapter. The following discussion reports some representative examples of these various type of reactions. Overviews of organotitanium in organic reactions have been reported.<sup>1881–1884</sup> A review focusing on the use of Cp titanium derivatives for the reactions in organic synthesis has appeared.<sup>1885</sup> Some reference works and reviews concerning metallocene catalyst for olefin polymerization<sup>1886</sup> and chiral metallocenes in synthesis<sup>1887</sup> have appeared. The reaction involving the generation of alkene or alkyne–titanium complexes through the coordination of carbon–carbon multiple bonds to titanium to give organometallic complexes and their use as a source of carbanionic reagents, directly or after conversion to new organotitanium species, for synthetic applications in organic reactions has been reviewed.<sup>250</sup> The use of dicarbanionic Ti species derived from organometallic compounds as reagents in organic synthesis<sup>180</sup> and the organic synthetic utility of carbotitanation reaction of alkynes<sup>1888</sup> have been reviewed, as has been the stereochemistry of the cyclopropane formation catalyzed by organometallic titanium species.<sup>1889</sup> Synthetic applications of alkyl- and alkenyltitanium derivatives in the preparation of cyclopropylamines<sup>1890</sup> and cyclopropanols<sup>179</sup> have been reviewed.

$\text{TiMe}(\text{OPr}^i)_3$  has been used as a reagent for the aminocyclopropanation of 1-ethenylcycloalkanes with  $\text{N,N}$ -dibenzyl and  $\text{N,N}$ -dimethylformamide to give bicyclo alkanes.<sup>1891</sup> The enantioselective addition of alkyl groups to aldehydes and ketones using  $\text{TiMe}(\text{OPr}^i)_3$ <sup>12</sup> and the analogous phenylacetylide titanium derivative have been described.<sup>1892</sup>  $\text{TiMe}(\text{OPr}^i)_3$ , prepared by the reaction of  $\text{LiMe}$  with  $\text{TiCl}(\text{OPr}^i)_3$ , has been used as a reagent for the synthesis of cyclopropane-annulated azaoligoheterocycles by intramolecular reductive cyclopropanation of cyclic amino acid amides.<sup>1893</sup> The dimethyl derivative  $\text{TiMe}_2(\text{OPr}^i)_2$  converts  $\text{N,N}$ -dialkylcarboxamides selectively into cyclopropylamines.<sup>1894</sup>

An efficient isomerization of aliphatic and cyclic olefins is achieved using well-defined bis-Cp alkyne titanium complexes as catalysts. These complexes isomerize 1-alkenes to internal alkenes under mild conditions. The titanium complex can be recovered quantitatively. Cyclic olefins, for example, cyclohexadienes, also undergo isomerization, but with a competing intermolecular hydrogen-transfer reaction, much more favored for Zr than for Ti complexes.<sup>1895</sup>

The systems  $\text{Cp}'_2\text{TiX}_2/\text{LiBu}^n$  ( $\text{Cp}'$  are substituted Cp rings and X are halo and alkoxo ligands) have been studied as catalysts for the hydrogenation of olefins. The effects of Cp ring substituents and various operating factors including the amount of catalyst, the solvents, and air- and water-free conditions on the catalytic activity, and the stability of the catalytic system have been investigated.<sup>1896</sup>

$\text{Cp}_2\text{TiCl}_2$  is an efficient catalyst for the diastereoselective monooxidation of 2-substituted 1,3-dithianes and 1,3-dithiolanes by *tert*-butyl hydroperoxide.<sup>1897</sup>

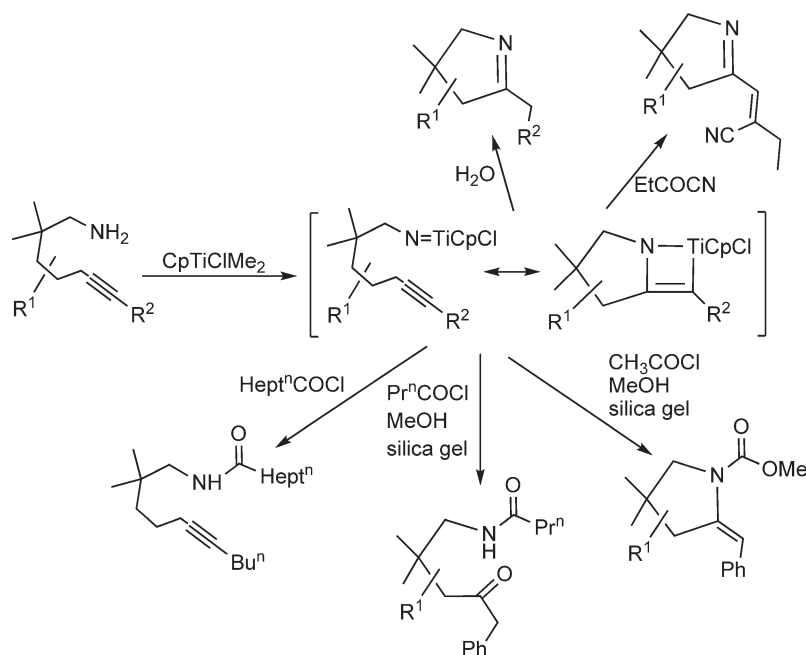
A series of bis-Cp, mono-Cp, Cp–benzamidinato, Cp–aryloxo, and Cp–amido Ti complexes have been used as catalysts for the hydroboration of 1-hexene in the presence of catecholborane reagents.<sup>1898</sup>

A method for silylation of allyl ethers with chlorosilanes has been developed based on  $\text{Cp}_2\text{TiCl}_2$  as catalyst.<sup>1247</sup>

The cyclodehydration of diols to cyclic ethers has been carried out in the presence of  $\text{Cp}_x\text{TiCl}_{4-x}$  ( $x = 0–2$ ) as catalyst.<sup>1899</sup>

Treatment of  $\text{CpTiCl}_3$  with  $\text{LiMe}$  provides solutions of  $\text{CpTiClMe}_2$ , which are used to react with alkynylamines in the dark with immediate evolution of methane and formation of azatitanetene derivatives through intermediate species containing titanium–imido bonds, “ $\text{R–N}=\text{TiCpCl}$ .” Protonolysis of these derivatives gives 2-H pyrroles in good yields. The reaction with acyl cyanamides gives rise to products derived from formal cyanoalkylidenation, while treatment with chloroformate or butanoyl chloride followed by methanolysis in the presence of silica gel gives enamide or ketoamide and acylation with octanoyl chloride provides alkynylamide. These reactions are examples of intramolecular imidotitanium–alkyne [2 + 2]-cycloaddition–azatitanetene acylation processes which represent a general and highly efficient sequence for the synthesis of pyrrolidine derivatives (Scheme 752).<sup>1900,1901</sup>

A new method for the regioselective carbosilylation of unsaturated carbon–carbon bonds in alkenes and dienes has been developed using  $\text{Cp}_2\text{TiCl}_2$  as catalyst. The reaction proceeds efficiently at 0 °C in THF in the presence of Grignard reagents. A plausible pathway of the catalytic cycle is reported.<sup>1248</sup>



Scheme 752

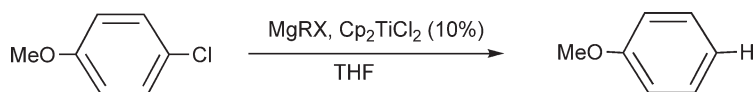
The hydrogenation of 1-hexene is catalyzed by bis- $Cp'$  titanium derivatives with various substituted groups on the  $Cp$  ring in combination with “nano-sized” sodium hydride. When the steric hindrance of the substituted  $Cp$  group is relatively small, the complex gives high initial catalytic activity but poor stability, whereas when the steric hindrance is large the complex is initially less active but more stable. The combination of bis- $Cp'$  titanium derivatives with commercial sodium hydride which was synthesized at high temperatures did not display any catalytic activity for the hydrogenation of 1-hexene.<sup>1902</sup>

$Cp_2TiCl_2$  catalyzes the cyclization of epoxides on olefins and alkynes to give carbocyclic products. This is an efficient method for the construction of tetrahydrofurans and carbocyclic five-membered rings that should be of interest for the synthesis of biologically active molecules. Transition state models based on titanium alkoxo complexes for the formation of the possible diastereoisomers have been proposed.<sup>1903</sup>  $Cp_2TiCl_2$  has been used as a reagent for the formation of vinylcyclopropanols from silylketene, showing that it is clearly not a good titanium source for this reaction.<sup>1904</sup> Complexes  $Cp_2TiX_2$  ( $X = F, Me$ ) have been used, in the presence of a stoichiometric amount of an organosilane reagent, as effective catalysts for the reduction–deoxygenation coupling of amides to form vicinal diamines, substances present in natural products and with many applications in medical chemistry and organic reactions.<sup>1249</sup>

The use of THF solvent has been found to dramatically improve the reactivity of  $Cp_2TiCl_2$ -catalyzed dehalogenation reaction of aromatic chlorides performed with alkyl Grignard reagents (Scheme 753).<sup>1257</sup> (*R,R*)-(cbthi)Ti binaphtholate catalyzes the dehalogenation of alkyl halides in the presence of a stoichiometric amount of a magnesium alkyl reducing agent. No detectable difference in the rate of reduction between the two enantiomers of the alkyl halide has been observed.<sup>1905</sup>

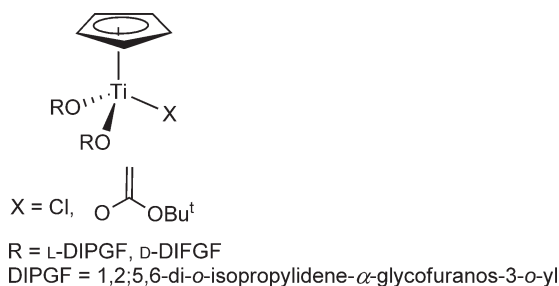
A catalytic cycle has been developed for the conversion of glycosyl halides to their corresponding glycals using  $Cp_2TiCl_2$ . A mechanistic proposal for the catalytic cycle is reported.<sup>1256</sup>

$Cp$  titanium derivatives have been investigated as catalytic systems for the ring opening of oxabicycles. The titanium complexes  $Cp_2TiCl_2$ ,  $(C_5Me_4SiMe_2NBu^t)TiCl_2$ , and  $[C_9H_7SiMe_2NC(Me)(H)Ph]TiCl_2$  catalyze the enantioselective nucleophilic ring-opening reaction of oxanorbornenes and oxabicyclo[3.2.1]octanes.<sup>1906</sup>



Scheme 753





Scheme 754

The asymmetric sulfoxidation of prochiral sulfides by Cp-based catalytic system including those containing alkoxo chiral ligands has been studied.<sup>1897</sup> Investigations have been carried out on the oxidation of sulfides to sulfoxides catalyzed by  $\text{Cp}_2\text{TiX}_2$  ( $X = \text{Cl}, \text{OTf}$ )/*t*-butyl hydroperoxide.<sup>1263</sup>  $\text{Cp}_2\text{TiCl}_2$  and (ebthi) $\text{TiCl}_2$  have been used as catalysts for the oxidation with  $\text{Bu}^t$ -hydroperoxide of racemic  $\beta$ -hydroxysulfides having a stereogenic carbon center in  $\alpha$ - or  $\beta$ -position with respect to the sulfur atom.  $\beta$ -Hydroxysulfides are oxidized in high yields to the corresponding sulfoxides.<sup>1907</sup>

The use of various catalysts in the asymmetric addition of HCN (or an equivalent reagent) to achiral aldehydes and ketones, giving optically active cyanohydrins has been discussed. The catalysts include enzymes, chiral polymers, boron, and chiral titanium complexes.<sup>1908</sup>

Alkoxo complexes  $\text{CpTiX}(\text{OR})_2$  (Scheme 754) have been used as catalysts for organic aldol condensation reactions in the synthesis of stereogenic centers.<sup>1909</sup>

$\text{Cp}_2\text{Ti}(\text{p-ClC}_6\text{H}_4\text{O})_2$  reacts with polymethyl hydroxiloxane to give an active center for the reduction of lactones to lactols.<sup>1910</sup>

$\eta^1$ -Allylmetal complexes are useful reagents for stereochemical reactions with aldehydes. Many ally-metal complexes undergo a rapid haptotropic rearrangement. The stereochemical outcome of these reactions depends on whether the haptotropic rearrangement is faster or slower than the reaction with the aldehyde. Studies to get information about the haptotropic rearrangement of cyclohexenyl-titanium triisopropoxide, and titanium tetraisopropoxide in comparison with the addition to aldehydes have been performed.<sup>1911</sup> Enantiopure mono-Cp dialkoxo allyltitanium complexes containing (*R,R*)- or (*S,S*)-tartrate ligands produce the selective allyltitanation of  $\alpha,\beta$ -acetylenic aldehydes for the synthesis of propargyl alcohols.<sup>1912</sup> Analogous enantioselective allyltitanation of protected  $\alpha$ -hydroxy aldehydes has been studied for the synthesis of 1,2-, 1,3-, and 1,5-diols.<sup>1913</sup>

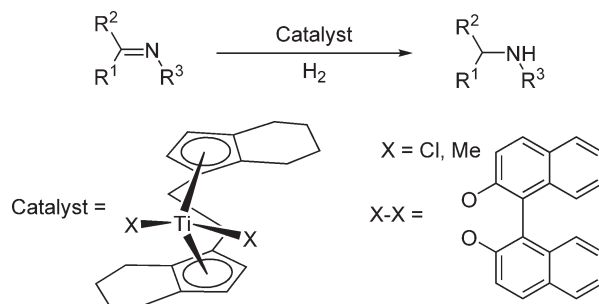
The synthesis of dihydrofurans with an additional ester moiety and one or two quaternary centers are prepared from titanium enolates formed by reactions of 3,4-dienoates with  $\text{Cp}_2\text{TiCl}_2$ .<sup>1914</sup> Titanium enolate derivatives  $\text{TiCl}_3[\text{CH}_2\text{CH}_2\text{C}(=\text{O})\text{OEt}]$  and the Tebbe reagent compound have been applied in the synthesis of pumilio-toxin.<sup>1915</sup> Chiral allyl and mono-Cp chloro enolato titanium compounds add with high enantioface discrimination to aldehyde.<sup>973</sup>

A highly flexible catalytic one-pot procedure for the synthesis of indoles employing *ortho*-chloro-substituted 1-phenyl-2-alkyl-alkynes or phenyl(aminoalkyl)alkynes as starting materials through a reaction catalyzed by  $\text{Cp}_2\text{TiMe}_2$  has been reported.<sup>1916</sup>

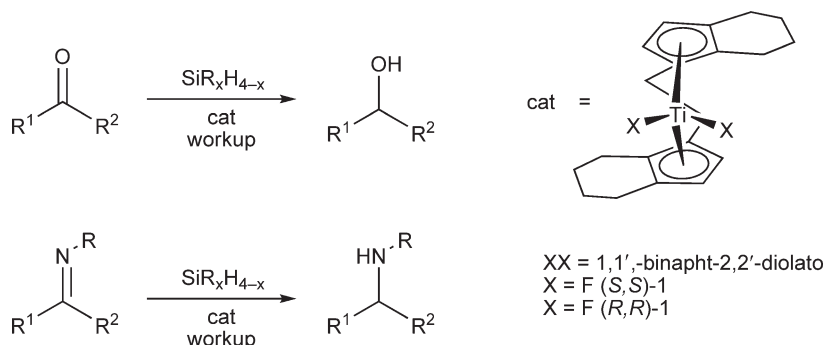
Titanacyclopropane derivatives have been used as efficient reagents for a series of organic reactions. The synthesis of 1-(1-alkenyl)cyclopropanols,<sup>1917</sup> (2)-2-alkyl-1-ethenylcyclopropanols,<sup>1918</sup> and the diastereoselective formation of (*Z*)-1-(1-alkenyl)-2-substituted-cyclopropyl esters<sup>1919</sup> have been reported. A variety of cyclobutenedione derivatives, including squaric esters, react with  $\text{Cp}_2\text{TiMe}_2$  to afford the corresponding methylenation products. With certain mixed-substituted substrates the reaction proceeds preferably at a ketonic carbonyl rather than a vinylogous ester.<sup>1411</sup>

Bis-Cp' titanium complexes catalyze the reduction of imines and carbonyl compounds. Kinetic and mechanistic investigations of the catalytic asymmetric hydrogenation of imines catalyzed by chiral *ansa*-ebthi titanium complexes have been reported.<sup>1920</sup> The asymmetric titanocene-catalyzed hydrogenation of cyclic and acyclic imines has been studied in detail (Scheme 755). Kinetic studies are consistent with a mechanism involving a fast insertion of the imine into a titanium hydride bond to form a titanium amide intermediate, followed by slow reaction of the amide complex with hydrogen to produce the amine and to regenerate the titanium hydride. A stereochemical model based on steric and electronic considerations has been proposed to account for the observed selectivity. This model can aid in predicting the absolute configurations of the amines formed in this process.<sup>1920</sup>





Scheme 755

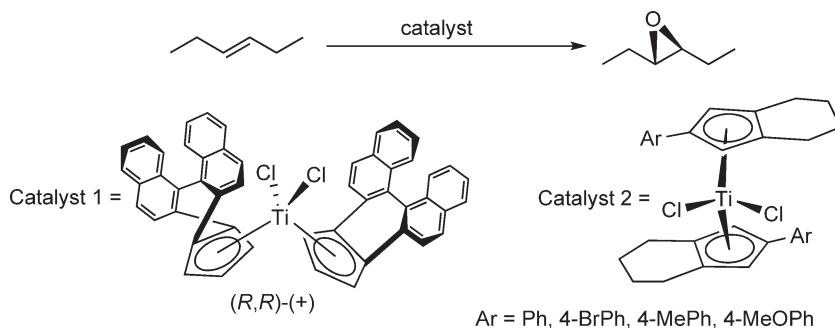


Scheme 756

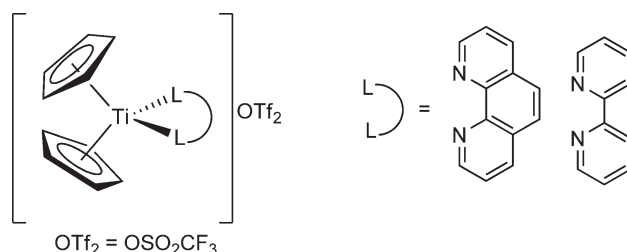
$\text{Cp}_2\text{TiCl}_2$  catalyzes the hydroalumination of  $\alpha$ -olefins in the presence of  $\text{AlEt}_3$ .<sup>1921</sup> The hydrozincation of conjugated dienes or alkynes is catalyzed by  $\text{Cp}_2\text{TiCl}_2$  in the presence of a zinc-hydride species generated by the reaction of  $\text{ZnI}_2$  and  $\text{LiH}$ .<sup>1922,1923</sup> The diastereoselective addition of  $\text{ZnBu}_2$  to aldehydes in the presence of  $\text{Cp}_2\text{TiCl}_2$  has been studied.<sup>1924</sup>

Hydrosilylation of unsaturated organic molecules is an attractive organic reaction. Asymmetric hydrosilylation of prochiral ketones or imines provides effective routes to optically active secondary alcohols or chiral amines (Scheme 756). These asymmetric processes can be catalyzed by titanium derivatives. The (S,S)-ebthi difluoro titanium complex has been synthesized from the corresponding chloro compound.<sup>1659</sup> This compound results in a very active system for the highly enantioselective hydrosilylation of acyclic and cyclic imines<sup>1262,1925</sup> and asymmetric hydrosilylation reactions of ketones including aromatic ketones.<sup>1661,1666,1926–1929</sup> An analogous 1,1'-binaphth-2,2'-diolato complex catalyzes the enantioselective hydrosilylation of ketones.<sup>1927</sup>

The dichloro bis(binaphthyl-Cp) titanium compound (catalyst 1 in Scheme 757) has shown excellent ability to catalyze the asymmetric epoxidation of unfuctionalized alkenes with virtually the same selectivity as previously



Scheme 757



Scheme 758

reported for bridged chiral bis-Ind titanium complexes. The catalytic activity of this complex has been compared to similar Nb complexes.<sup>1930</sup> Dichloro bis(2-aryl-4,5,6,7-tetrahydroindenyl) titanium derivatives (catalyst 2 in Scheme 757) have been synthesized with the Ind ligands containing sterically similar but electronically different phenyl substituents. These complexes can promote the catalytic epoxidation of *trans*-3-hexene in the presence of Bu<sup>t</sup>-hydroperoxide. The electronic nature of the Ind ligands exerts a significant influence on the catalytic activity.<sup>1931</sup>

The titanium compounds CpTiCl<sub>3</sub>, Cp<sub>2</sub>TiCl<sub>2</sub>, and CH<sub>2</sub>(C<sub>5</sub>H<sub>4</sub>)<sub>2</sub>TiCl<sub>2</sub> have been used as catalysts for the diastereoselective epoxidation of allylic alcohols.<sup>1932</sup> [TiCp<sub>2</sub>(LL)]<sup>2+</sup> (LL = 1,10-phenanthroline, 2,2'-bipyridine) (Scheme 758) have been studied in order to determine the importance of the ancillary chelated ligands versus the metal center for the membrane-permeabilizing action and their effects on lipid epoxidation reactions.<sup>1933</sup>

The influence of the steric congestion on the catalytic performance of Ti(IV) active centers in the epoxidation of alkenes has been probed using a range of soluble-based silesquioxane species.<sup>1934</sup> Bis-homoallylic alcohols are diastereoselectively converted, in good yields, into tetrahydrofuranols and tetrahydropyrans, catalyzed by mono-Cp and bis-Cp Ti derivatives in the presence of Bu<sup>t</sup>-hydroperoxide activated with 4 Å molecular sieves.<sup>1935</sup>

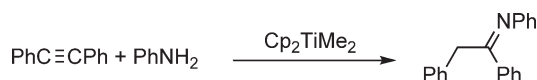
Various methods for anchoring Cp titanium derivatives onto organic or inorganic supports have been developed. Heterogeneous epoxidation catalysts have been prepared by the co-polycondensation of Cp<sub>2</sub>TiCl<sub>2</sub> and (CpTiCl<sub>2</sub>)<sub>2</sub>O with tetraethoxysilane by a modified sol-gel procedure, and the use in epoxidations of non-activated olefins have been described.<sup>1936</sup>

Ti/silica catalysts have been prepared by grafting Cp<sub>2</sub>TiCl<sub>2</sub> on hydrophilic amorphous silica with different Ti contents under mild conditions, active for the epoxidation of cyclohexene.<sup>1937</sup> Titanium catalysts prepared by grafting Cp<sub>2</sub>TiCl<sub>2</sub> on SiO<sub>2</sub> are active for the diastereoselective epoxidation of hydroxy-containing unsaturated terpenes.<sup>1938</sup>

Detailed spectroscopic and computational studies conclude that CpTi-(O-Si≡)<sub>3</sub> is more likely to be formed than Cp<sub>2</sub>Ti-(O-Si≡)<sub>2</sub> bis-Cp systems.<sup>1939</sup> Grafted products are prepared by treatment of an excess of the *ansa*-titanium compound Me<sub>2</sub>Si(C<sub>5</sub>H<sub>4</sub>)<sub>2</sub>TiCl<sub>2</sub> with surfactant-templated aluminosilicates. The materials have been characterized by elemental analysis and solid analytical techniques and are good catalysts for the epoxidation of cyclooctene.<sup>1940</sup> Materials containing highly accessible and well-ordered titanium sites prepared by grafting Cp<sub>2</sub>TiCl<sub>2</sub> on the surface of the pure silica ITQ-2 material have been prepared and used as excellent catalysts for epoxidation of olefins, yielding high conversions and selectivities to the desired epoxides.<sup>1941</sup> Intercalation of Cp<sub>2</sub>TiCl<sub>2</sub> into the pores of a zeolite-type framework by diffusing a solution of this compound in chloroform into the mesopores followed by treatment with NEt<sub>3</sub> to activate the Si-OH groups of the silica has been developed. After calcinations at 550 °C, the removal of the Cp is observed to give a system which catalyzes the epoxidation of cyclohexene in the presence of alkyl hydroperoxides. The catalyst is rapidly deactivated, although it can be regenerated by calcinations at 550 °C without structural modification or loss of catalytic activity.<sup>1942-1944</sup>

The hydroamination reaction, that is, the direct addition of an N-H bond across a C-C multiple bond, is a highly economical method for synthesizing substituted amines. Cp and Ind titanium complexes are very efficient catalysts for the hydroamination of alkynes. Employing appropriate catalysts, the hydroamination of alkynes can be achieved both intra- and intermolecularly, which offers high synthetic flexibility. The Ti-catalyzed hydroamination of alkynes is a highly flexible synthetic approach to a wide range of biologically interesting classes of compounds. Developments of the Ti-catalyzed intermolecular hydroamination of alkynes have been reviewed.<sup>1945</sup> A microreview dealing with group IV-catalyzed hydroamination reactions of alkynes and allenes and covering the literature before August 2002 has appeared.<sup>1946</sup> The applications of Cp derivatives of Ti as hydroamination catalysts have been reviewed.<sup>1947</sup>

The intermolecular hydroamination of alkynes can be catalyzed by Cp<sub>2</sub>TiMe<sub>2</sub> (Scheme 759). It is assumed that metal imido intermediates are formed.<sup>1948,1949</sup> Cp<sub>2</sub>TiMe<sub>2</sub> is an efficient catalyst for the hydroamination of



Scheme 759

alkyl(aryl)alkyne compounds, which takes place regioselectively in the 2-position, to give  $\alpha$ -arylketimine derivatives.<sup>1950</sup> The intramolecular hydroamination of alkynes and allenes catalyzed by  $\text{Cp}_2\text{TiMe}_2$  and  $\text{CpTi(=NAr)(NHAr)(py)}$  has been studied.<sup>1951</sup>  $\text{Cp}_2\text{TiMe}_2$  is a very active catalyst for the coupling of alkynes with arylamines and sterically hindered *tert*-alkyl and *sec*-alkylamines. Hydroamination reactions employing sterically less hindered amines, such as benzylamines or *n*-hexylamine, are very slow and proceed in poor yields. Mechanistic and kinetic investigations have been reported.<sup>1952</sup> Similar processes of intermolecular hydroamination of alkynes<sup>1953–1957</sup> and hydroamination/cyclization of aminoalkynes catalyzed by  $\text{Cp}_2\text{TiMe}_2$  have been studied. A series of bis-Cp' dimethyl complexes,  $\text{Cp}'_2\text{TiMe}_2$  ( $\text{Cp}' = \text{Cp}, \text{Cp}^*, \text{C}_5\text{H}_4\text{R}, \text{R} = \text{Me}, \text{Et}, \text{Pr}^i, \text{Bu}^t$ ),  $(\text{Ind})_2\text{TiMe}_2$ , Cp-amido compounds  $(\text{C}_5\text{H}_4\text{SiMe}_2\text{NR})\text{Ti}(\text{NMe}_2)_2$  ( $\text{R} = \text{Bu}^t, \text{Ph}$ ), the mono-Cp derivative  $\text{CpTiMe}_2(\text{N}=\text{PPh}_3)$ , and imido complexes  $\text{Cp}_2\text{Ti(=NBU}^t)(\text{py})$  and  $\text{CpTiCl(=NBU}^t)(\text{py})$  have been tested and compared as reagents for the intermolecular hydroamination of alkynes. Two reactions have been studied, the treatment of diarylalkynes and dialkylalkynes with arylamines. The bis-Ind complex  $(\text{C}_9\text{H}_7)_2\text{TiMe}_2$ <sup>1279</sup> has been found to be a highly active catalyst for the intermolecular hydroamination of alkynes. The reactions of primary aryl-, *tert*-alkyl-, *sec*-alkyl, and *n*-alkylamines with internal and terminal alkynes have been studied.<sup>1958</sup>  $\text{Cp}_2\text{TiMe}_2$  as a catalyst for the intramolecular hydroamination of aminoalkynes and aminoallenes has been reported.<sup>1959</sup>

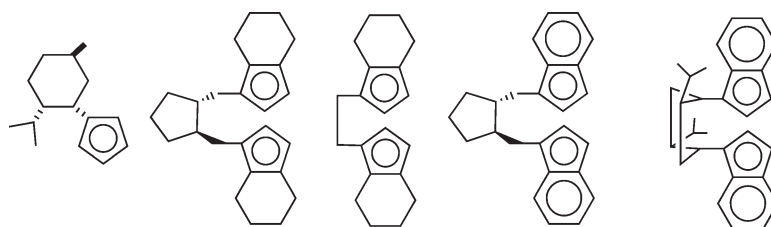
Hydroamination of internal alkynes (diphenylacetylene and 1-phenylpropyne) with aniline or *tert*-butylamine proceeds to give the corresponding *anti*-Markonikov functionalized imines with high yields in the presence of the bis-Cp titanacyclopentene complexes  $\text{Cp}_2\text{Ti}(\eta^2\text{-Me}_3\text{SiC}\equiv\text{CR})$  ( $\text{R} = \text{SiMe}_3, \text{Ph}$ ).<sup>1960</sup> Hydroamination reactions of aliphatic alkynes with aliphatic, benzylic, and aromatic amines, and of terminal alkynes and hydrazines have been studied using the complexes  $\text{Cp}'_2\text{Ti}(\text{Me}_3\text{SiC}\equiv\text{CSiMe}_3)$  ( $\text{Cp}' = \text{Cp}, \text{Cp}^*, \text{C}_5\text{H}_4\text{Et}$ ). Mechanism and theoretical calculations of the  $\text{CpTi(=NR)(NHR)}$  ( $\text{R} = 4\text{-C}_6\text{H}_4\text{X}; \text{X} = \text{H}, \text{F}, \text{Cl}, \text{Me}, 2,6\text{-Me}_2\text{C}_6\text{H}_3$ ) catalyzed hydroamination of terminal alkynes with different substituted anilines and *tert*-butylamine have been included.<sup>1961,1962</sup>

The syntheses and structures of similar dipyrrolylmethane complexes have been reported. Alkynes are rapidly hydroaminated by primary amines catalyzed by these Ti derivatives.<sup>711</sup> Hydroamination of enynes to generate  $\alpha, \beta$ -unsaturated imines can be produced using titanium pyrrolyl complexes.<sup>712</sup>

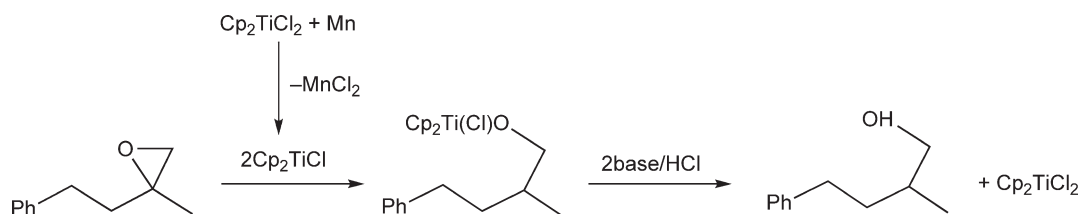
$\text{Cp}_2\text{TiCl}_2$  can be reduced with different reducing agents to afford low-valent Ti species which have been extensively used as mild and useful reagents to promote carbon–carbon bond formations.<sup>1963</sup> Titanium compounds have been studied as catalysts for radical reactions.<sup>1964</sup>

A series of chiral bis-Cp' titanium complexes based on the ligands shown in Scheme 760 react with  $\text{Pr}^i\text{MgCl}$  and 2-alkylbutadiene to generate bis-Cp' allyl Ti(III) derivatives which upon treatment with carbon dioxide or  $\text{RCHO}$  ( $\text{R} = \text{Ph}, \text{Et}, \text{Pr}^i, \text{Bu}^t$ ) give the corresponding optically active  $\beta, \gamma$ -unsaturated carboxylic acids or threo-homoallyl alcohols with high enantiomeric purities of up to 96%.<sup>1965</sup>

Polymer-supported titanium catalysts can be regenerated. A series of polymer-supported  $\text{CpCp}'\text{TiCl}_2$  ( $\text{Cp}' = \text{polymer substituted Cp rings}$ ) has been reduced by  $\text{Pr}^i\text{MgBr}$  *in situ*, and used as catalysts for the hydrogenation of styrene, the isomerization of 1,5-cyclooctadiene and 1,5-hexadiene, and the reduction of carbonyl compounds. In some cases, the introduction of a polymer ligand on the Cp ring restricts the aggregation of active sites and the formation of inactive dimeric titanium species, and results in an activity increase.<sup>1240</sup>



Scheme 760



Scheme 761

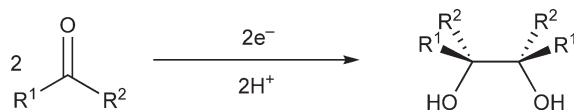
$\text{Cp}_2\text{TiCl}_2$  is reduced to give a catalyst for the cascade cyclization of epoxypolyenes.<sup>1966</sup>  $\text{Cp}_2\text{TiCl}_2$  reduced by manganese metal in THF at room temperature mediates intramolecular vinylations by radical cyclization and  $\beta$ -elimination of phosphine oxides.<sup>1967</sup> Catalytic amounts of  $\text{Cp}_2\text{TiCl}_2$  in the presence of Mn and  $\text{Me}_3\text{SiCl}$  cyclize olefinic iodoethers in moderate yields, with the formation of tetrahydrofurans. Stoichiometric amounts of  $\text{Cp}_2\text{TiCl}_2$  lead to higher yields. With the catalytic system  $\text{Cp}_2\text{TiCl}_2/\text{Zn}/\text{Me}_3\text{SiCl}$ , the desired cyclization product is not obtained, and only the corresponding  $\beta$ -elimination product is isolated.<sup>1968</sup>

$\text{Cp}_2\text{TiCl}_2$  catalyzes the highly regioselective reduction opening reactions of epoxides.<sup>1969</sup> A key step in the catalytic cycle is the formation of  $\beta$ -titanoxo radicals via single-electron transfer and protonation of titanium–oxygen and titanium–carbon bonds (Scheme 761). This method combines the advantages of radical reactions, high functional group tolerance, and stability of radicals under protic conditions, with the ability of organometallic complexes to determine the course of transformations in reagent-controlled reactions.<sup>1970–1973</sup> The *in situ* reduction of  $\text{Cp}_2\text{TiCl}_2$  with Mn results in a very convenient method to generate low-valent Ti(III) complex  $\text{Cp}_2\text{TiCl}$ .<sup>1974–1979</sup> The 5-*exo*-cyclizations of epoxides<sup>1903,1980</sup> and the opening of *meso*-epoxides<sup>1981,1982</sup> catalyzed by  $\text{Cp}_2\text{TiCl}_2$  have been reported. The synthesis of tri- and tetrasubstituted olefins by cyclization radical addition reactions catalyzed by alkoxo organometallic titanium derivatives has been described.<sup>1983</sup>

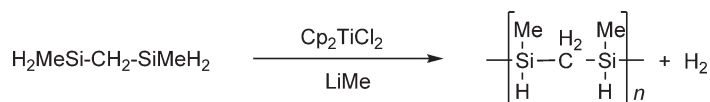
Allylation of aldehydes<sup>1984</sup> and stereoselective synthesis of furans<sup>1162,1985</sup> catalyzed by the systems  $\text{Cp}_2\text{TiCl}_2/\text{Zn}$  have been described. Radical cyclization reaction of epoxides using  $\text{Cp}_2\text{TiCl}_2/\text{Zn}$  has attracted much attention leading to the synthesis of a number of naturally occurring compounds and related products.<sup>1980,1986</sup>  $\text{Cp}_2\text{TiCl}_2$  plays an important role in the catalytic cycle leading to exocyclic alkenes.<sup>1987</sup> The selective reduction of ketones to secondary alcohols is achieved in aqueous media catalyzed by the system  $\text{Cp}_2\text{TiCl}_2/\text{Zn}$ . The role played by the Ti compound is essential. Thus, when acetophenone was treated under the same conditions but excluding titanium, the starting ketone was recovered unchanged. When  $\text{Cp}_2\text{TiCl}_2$  is added, 1-phenylethanol is obtained in 71% yield.<sup>1161</sup>  $\text{Cp}_2\text{TiCl}_2/\text{Zn}$  and  $\text{Cp}_2\text{TiCl}_2/\text{Al}$  mediate reductive cyclizations of organic halides under photoirradiation conditions.<sup>1988</sup> The catalytic system  $\text{Cp}_2\text{TiCl}_2/\text{Zn}/\text{Me}_3\text{SiCl}$  works well for the diastereoselective cyclization of ketonitriles.<sup>1165</sup>

Diastereoselectivities of up to 98.5:1.5 for carbonyl reductions by using catalytic amounts of racemic (ebthi)TiCl<sub>2</sub> compound *in situ* reduction with zinc have been obtained. A disadvantage of this methodology is the fact that only aromatic and  $\alpha,\beta$ -unsaturated aldehydes can be coupled while aliphatic aldehydes do not react under these conditions.<sup>1989,1990</sup>

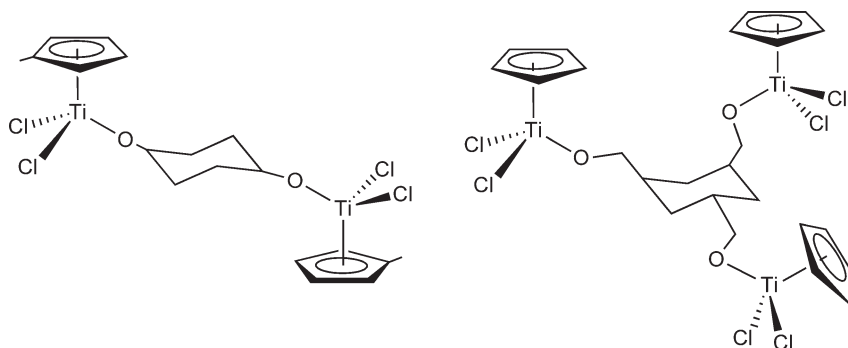
The pinacol coupling reaction is an effective method for generating carbon–carbon bonds to give molecules with 1,2-difunctionalities (Scheme 762). A series of titanium bis-Cp' derivatives have been tested as pre-catalysts for the coupling of aliphatic aldehydes. The effects of catalyst structural variation on the activity and selectivity of bis-Cp' titanium-catalyzed pinacol coupling of cyclohexane carboxaldehyde by M/Me<sub>3</sub>SiCl (M = Mn, Zn) have been evaluated.<sup>1991–1993</sup> The reduction of  $\text{Cp}_2\text{TiCl}_2$  with  $\text{Pr}^i\text{MgCl}$  followed by treatment with  $\text{PhMgBr}$  affords  $\text{Cp}_2\text{TiPh}$ , an active species for the diastereoselective inter- and intramolecular pinacol coupling of aldehydes. The same catalytic species is formed by reducing  $\text{Cp}_2\text{TiClPh}$  with Zn powder.<sup>1994</sup>



Scheme 762



Scheme 763



Scheme 764

A series of reduced systems based on bis-Cp titanium complexes have been used for stereoselective pinacolization reactions. (Propargyl aldehyde) $\text{Co}_2(\text{CO})_6$  complexes undergo pinacol coupling reactions with several pinacolization reagents including  $\text{Cp}_2\text{TiCl}_2/\text{Bu}^{\text{sec}}\text{MgCl}$ ,  $\text{Cp}_2\text{TiCl}_2/\text{Mn}/\text{Me}_3\text{SiCl}$ ,<sup>1993</sup> and  $\text{Cp}_2\text{TiCl}_2/\text{SmI}_2$  exclusively giving *syn*-(*dl*)-diacetylenic diol complexes.<sup>1995</sup> Pinacol coupling of aromatic aldehydes catalyzed by  $\text{Cp}_2\text{TiCl}_2/\text{Zn}$ -based systems<sup>1990,1996</sup> and performed under buffered protic conditions<sup>1989,1997,1998</sup> have been reported.

The reduction of  $\text{Cp}_2\text{TiCl}_2$  with samarium gives Ti(III) active species for the reduction of sulfoxides.<sup>1999</sup>

The titanium complexes  $\text{Cp}_2\text{Ti}(\text{OAr})_2$  (Ar = Ph, *p*- $\text{MeOC}_6\text{H}_4$ , *p*- $\text{MeC}_6\text{H}_4$ , *p*- $\text{ClC}_6\text{H}_4$ , *p*- $\text{CNC}_6\text{H}_4$ ) are stable precursors of dehydrocoupling catalysts. They polymerize primary silanes at 50 °C or below.<sup>1541</sup> Polycondensation of 2,4-disilapentane in the presence of  $\text{Cp}_2\text{TiCl}_2/\text{LiMe}$  catalysts affords polysilicarbosilane polymers possessing Si-CH<sub>2</sub>-Si units in their chain (Scheme 763). These substances are potential silicon carbide ceramic precursors.<sup>2000</sup>

Ti-alkoxo, Ti-amido and Ti-alkyl bonds have been found to be active in initiating the insertion of isocyanate monomers to give different type of polyisocyanate molecules.  $\text{Cp}'\text{TiCl}_2\text{X}$  ( $\text{Cp}' = \text{Cp}$ , X =  $\text{OCH}_2\text{CF}_3$ ,  $\text{NMe}_2$ , Me;  $\text{Cp}' = \text{Cp}^*$ , X =  $\text{OCH}_2\text{CF}_3$ ) are very useful catalysts for the polymerization of isocyanates. They polymerize monomers possessing a very high degree of functionality. These polymerizations are also tolerant toward the addition of Lewis bases. A mechanism for this type of polymerization has been suggested.<sup>496,495</sup> Bifunctional<sup>1917</sup> and trifunctional initiators have also been investigated (Scheme 764). They produce polyblock polymers and co-polymers and well-defined three-arm polyisocyanates.<sup>2001</sup>

Bis-Cp acetylido titanium complexes have drawn considerable attention in regard to their third-order non-linear optical properties.<sup>2002</sup>

#### 4.05.8.2 Anti-tumor and Biological Effects

There has been increasing interest in the coordination behavior of Cp titanium derivatives toward simple species that possess oxygen and/or nitrogen donor functions of biological molecules, and in recent years titanium complexes containing biologically important ligands synthesized under physiological conditions have been reported. Many of these complexes exhibit anti-tumor activity against numerous experimental tumors. Titanium complexes in cancer treatment have been reviewed.<sup>2003</sup> The complexes  $\text{Cp}_2\text{TiX}_2$  (X = halo ligand) are a class of small, hydrophobic organometallic anticancer agents that exhibit anti-tumour properties against numerous cell lines.  $\text{Cp}_2\text{TiCl}_2$  has been the most widely studied metallocene and has proved to be one of the more effective species.<sup>2004–2006</sup> There is current medicinal interest in the pronounced anti-tumor properties and low toxic side-effects of some Ti(IV) complexes.<sup>2007–2009</sup>  $\text{Cp}_2\text{TiCl}_2$  has been tested against the human testicular cancer cell lines Tera-2 and Ntera-2 using both 3-(4,5-dimethylthiazol-2-yl)-2,5-diphenyltetrazolium bromide assays and apoptosis assays.<sup>2010</sup> The ability of  $\text{Cp}_2\text{TiCl}_2$  and

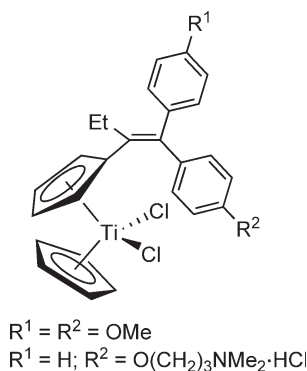
the biologically inactive derivative  $(C_5H_4Me)_2TiCl_2$  to inhibit the relaxation of supercoiled plasmid DNA pBR322 by human topoisomerase II has been studied by gel electrophoresis.<sup>2011</sup> The formation of  $Cp_2TiCl_2$ -DNA complexes has been implicated in the mechanism of anti-tumour properties. These properties have been reviewed.<sup>2012</sup> A limited problem in this development is the low stability of Cp titanium complexes in aqueous solutions and only non-aqueous solutions have usually been studied. Some authors claim that not the titanium complexes themselves but the cyclopentadiene formed during the decomposition of the titanium derivatives is the anti-tumor-active species.

$Cp_2TiCl_2$  reacts with  $\alpha$ -amino acids (aa = amino acid) in water-like solvents (MeOH, not necessary anhydrous) to give the bioinorganic titanium(IV) amino acid complexes  $[Cp_2Ti(aa)_2]^{2+}Cl_2$  (aa: glycine, L-alanine, 2-methylalanine). The complexes are stable solids at room temperature and are not sensitive toward air and moisture. The structure of the 2-methylalanine derivative has been determined by X-ray diffraction.<sup>2013,2014</sup> The behavior of these substances in aqueous media has been reported. The hydrolysis of  $Cp'_2TiX_2$  ( $Cp' = Cp, C_5H_4Me; X = Cl, glycinate$ ) in aqueous solutions at pH = 2–8 has been studied by NMR spectroscopy. Complex pH-dependent equilibria involve a series of soluble ionic species. In the presence of nucleotides, titanium complexes are formed which are hydrolytically stable and exhibit anti-tumor activity.<sup>2015</sup> The synthesis of analogous ionic titanium compounds has been described in order to prepare titanium model complexes containing biologically important ligands. The complexes  $[Cp_2Ti(aa)_2]Cl_2$  (aa = DL-phenylalanine, DL-4-fluorophenylalanine) react with  $AgAsF_6$  with the formation of  $[Cp_2Ti(aa)_2][AsF_6]_2$ , which have been characterized by chemical analyses and NMR ( $^1H, ^{14}N, ^{19}F$ ), infrared, and Raman spectroscopy. The antimicrobial behavior (against *E. coli*) of all complexes has been determined in comparison with the free amino acids. These compounds are of great interest as models involving titanium complexes with  $\alpha$ -amino acids.<sup>2016</sup>

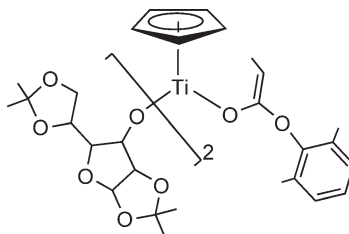
Compounds containing amino-functionalized mono-Cp and bis-Cp ligands can be quaternized on the pendant amino group to result in water-soluble species (Schemes 467–470; Section 4.05.4.1.1.(ii)), which exhibit significant cytotoxicity against a number of different human tumor cell lines including a defined cisplatin-resistant cell line.<sup>1097,1096</sup> A series of water-soluble bis-Cp dichloro titanium derivatives containing alkylammonium groups pendant to one Cp ring (monocationic complexes) or both Cp rings (dicationic complexes) has been synthesized and characterized. The *in vitro* cytotoxicities of these complexes of potential anticancer drugs have been assessed against human lung cancer (H209, A549, H209/CP) and ovarian cancer (A2780, A2780/CP) cell lines, and the results are compared with the cytotoxicities of both *cis*- $PtCl_2(NH_3)_2$  and  $Cp_2TiCl_2$ . Dicationic complexes generally exhibit greater potency than the corresponding monocationic analogs, and derivatives containing protonated piperidinyl rings exhibit greater potency than the compounds containing protonated 2-aminoethyl or 3-aminopropyl groups.<sup>1098</sup>

$Cp_2TiCl_2$  undergoes rapid and complete hydrolysis in the presence of biological molecules to form species which exhibit anticancer, antibacterial, antiviral, anti-inflammatory, and insecticidal properties.<sup>2017–2019</sup> The interactions of  $Cp_2TiCl_2$ , as an anticancer drug, with *N,N'*-ethylenebis(*o*-hydroxyphenylglycine) and adenosine triphosphate have been studied by  $^1H$  and  $^{31}P$  NMR spectroscopy in order to investigate the pH-dependent competitive effects between these bindings.<sup>2017</sup>

The bis-Cp titanium molecules shown in Scheme 765 have been synthesized and used as potential antiestrogenic vectors to the estradiol receptor and a recognized cytotoxic molecule. They also proved to be particularly easy to exchange with Re in order to prepare organometallic radiopharmaceutical compounds with antiestrogenic properties.<sup>2020</sup> These processes have been used as a source for  $Re(CO)_3$  through thermal ligand-transfer reaction between Cp titanium complexes and  $Re_2(CO)_{10}$ .<sup>2021</sup>



Scheme 765



Scheme 766

The potential use of  $\text{Cp}_2\text{TiCl}_2$  in the treatment of neoplasia has been reported.<sup>2022</sup> The reaction of  $\text{Cp}_2\text{TiCl}_2$  with phosphorus- and sulfur-based  $\beta$ -amino acid analogs under atmospheric conditions has also been described.<sup>2023</sup> The reactions of  $\text{Cp}_2\text{TiCl}_2$  with organometallic acetylferrocene thiosemicarbazones to give bimetallic products have been reported. Physicochemical and spectral studies have been carried out in order to establish a correlation between the biological activity and the structures of the compounds.<sup>1525</sup>

A series of organotitanium(IV) chelate derivatives with biologically active monofunctional bidentate semicarbazones having the O,N-donor systems have been prepared by reacting 1:1 and 1:2 stoichiometric proportions of  $\text{Cp}_2\text{TiCl}_2$  with the appropriate ligand, prepared by condensing heterocyclic ketones and semicarbazide hydrochlorides in the presence of NaOAc. Trigonal-bipyramidal and octahedral structures have been suggested for the 1:1 and 1:2 (M:L) complexes on the basis of spectroscopic analyses.<sup>1583,2024,2025</sup>

The cytotoxic properties of the *ansa*-derivatives dichloro [1,2-di(cyclopentadienyl)-1,2-di(*p*-N,N-dimethylamino-phenyl)ethanediyl] titanium and dichloro [1,2-di(cyclopentadienyl)-1,2-bis(pentamethylphenyl)ethanediyl] titanium (Scheme 641: Section 4.05.5) have been studied. These compounds have been tested for their activity on biological behavior. The pentamethylphenyl substitute does not show a cytotoxic effect, but when *p*-N,N-dimethylaminophenyl was tested against pig kidney carcinoma cells (LLC-PK) or human ovarian carcinoma cells (A2780/cp70), high inhibitory concentrations are observed. The cytotoxicity of this compound is therefore very promising, since it shows significant higher activity compared to  $\text{Cp}_2\text{TiCl}_2$ .<sup>1655</sup>

Duthaler's chiral propionic enolate titanium compound (Duthaler's reagent; Scheme 766) has been used to introduce stereochemistry in the asymmetric synthesis of a protein phosphatase inhibitor tautomycin.<sup>2026</sup>

## Acknowledgments

The author gratefully acknowledges Dr. Alfredo Sebastián for his collaboration, help, and excellent work on the design of the schemes and figures included in this chapter.

## References

1. Kempe, R. *Angew. Chem., Int. Ed.* **2000**, *39*, 468–493.
2. Gade, L. H. *Chem. Commun.* **2000**, 173–181.
3. McGrady, G. S.; Downs, A. J.; Bednall, N. C.; McKean, D. C.; Thiel, W.; Jonas, V.; Frenking, G.; Scherer, W. *J. Phys. Chem. A* **1997**, *101*, 1951–1968.
4. Field, C. N.; Green, J. C.; Kaltsoyannis, N.; McGrady, G. S.; Moody, A. N.; Siggel, M.; DeSimone, M. *J. Chem. Soc., Dalton Trans.* **1997**, 213–219.
5. Berger, S.; Bock, W.; Frenking, G.; Jonas, V.; Muller, F. *J. Am. Chem. Soc.* **1995**, *117*, 3820–3829.
6. Bharathi, P.; Periasamy, M. *Organometallics* **2000**, *19*, 5511–5513.
7. Periasamy, M.; Reddy, M. R.; Kanth, J. V. B. *Tetrahedron Lett.* **1996**, *37*, 4767–4770.
8. Periasamy, M.; Srinivas, G.; Bharathi, P. *J. Org. Chem.* **1999**, *64*, 4204–4205.
9. Periasamy, M.; Srinivas, G.; Karunakar, G. V.; Bharathi, P. *Tetrahedron Lett.* **1999**, *40*, 7577–7580.
10. Schormann, M.; Varkey, S. P.; Roesky, H. W.; Noltemeyer, M. *J. Organomet. Chem.* **2001**, *621*, 310–316.
11. Wu, K. H.; Gau, H. M. *Organometallics* **2004**, *23*, 580–588.
12. Balsells, J.; Davis, T. J.; Carroll, P.; Walsh, P. J. *J. Am. Chem. Soc.* **2002**, *124*, 10336–10348.
13. Duncan, D.; Livinghouse, T. *Organometallics* **1999**, *18*, 4421–4428.
14. Noth, H.; Schmidt, M. *Organometallics* **1995**, *14*, 4601–4610.
15. Crocker, M.; Herold, R. H. M.; Orpen, A. G. *Chem. Commun.* **1997**, 2411–2412.
16. Crocker, M.; Herold, R. H. M.; Orpen, A. G.; Overgaag, M. T. A. *J. Chem. Soc., Dalton Trans.* **1999**, 3791–3804.



17. Duchateau, R.; Abbenhuis, H. C. L.; van Santen, R. A.; Meetsma, A.; Thiele, S. K. H.; van Tol, M. F. H. *Organometallics* **1998**, *17*, 5663–5673.
18. Zanotti-Gerosa, A.; Solari, E.; Giannini, L.; Floriani, C.; Re, N.; Chiesi-Villa, A.; Rizzoli, C. *Inorg. Chim. Acta* **1998**, *270*, 298–311.
19. Kingston, J. V.; Ozerov, O. V.; Parkin, S.; Brock, C. P.; Ladipo, F. T. *J. Am. Chem. Soc.* **2002**, *124*, 12217–12224.
20. Knjazhanski, S. Y.; Cadenas, G.; García, M.; Pérez, C. M.; Nifant'ev, I. E.; Kashulin, I. A.; Ivchenko, P. V.; Lyssenko, K. A. *Organometallics* **2002**, *21*, 3094–3099.
21. Liard, A.; Kaftanov, J.; Chechik, H.; Farhat, S.; Morlender-Vais, N.; Averbuj, C.; Marek, I. *J. Organomet. Chem.* **2001**, *624*, 26–33.
22. Schleh, F.; Studer, A. *Angew. Chem., Int. Ed.* **2004**, *43*, 313–315.
23. Schleh, F.; Vogler, T.; Harms, K.; Studer, A. *Chem. Eur. J.* **2004**, *10*, 4171–4185.
24. Kasatkin, A.; Nakagawa, T.; Okamoto, S.; Sato, F. *J. Am. Chem. Soc.* **1995**, *117*, 3881–3882.
25. Xin, T.; Okamoto, S.; Sato, F. *Tetrahedron Lett.* **1998**, *39*, 6927–6930.
26. Teng, X.; Takayama, Y.; Okamoto, S.; Sato, F. *J. Am. Chem. Soc.* **1999**, *121*, 11916–11917.
27. Teng, X.; Kasatkin, A.; Kawanaka, Y.; Okamoto, S.; Sato, F. *Tetrahedron Lett.* **1997**, *38*, 8977–8980.
28. Kasatkin, A.; Sato, F. *Angew. Chem., Int. Ed. Engl.* **1996**, *35*, 2848–2849.
29. Takayama, Y.; Gao, Y.; Sato, F. *Angew. Chem., Int. Ed. Engl.* **1997**, *36*, 851–853.
30. Takayama, Y.; Okamoto, S.; Sato, F. *Tetrahedron Lett.* **1997**, *38*, 8351–8354.
31. Yamashita, K.; Urabe, H.; Sato, F. *Tetrahedron Lett.* **1997**, *38*, 4619–4622.
32. Urabe, H.; Takeda, T.; Hideura, D.; Sato, F. *J. Am. Chem. Soc.* **1997**, *119*, 11295–11305.
33. Hikichi, S.; Gao, Y.; Sato, F. *Tetrahedron Lett.* **1997**, *38*, 2867–2870.
34. Mizojiri, R.; Urabe, H.; Sato, F. *Tetrahedron Lett.* **1999**, *40*, 2557–2560.
35. Yamaguchi, S.; Jin, R. Z.; Tamao, K.; Sato, F. *J. Org. Chem.* **1998**, *63*, 10060–10062.
36. Okamoto, S.; An, D. K.; Sato, F. *Tetrahedron Lett.* **1998**, *39*, 4551–4554.
37. Nakagawa, T.; Kasatkin, A.; Sato, F. *Tetrahedron Lett.* **1995**, *36*, 3207–3210.
38. Okamoto, S.; Sato, F. *J. Organomet. Chem.* **2001**, *624*, 151–156.
39. Agami, C.; Comesse, S.; Kadouri-Puchot, C. *J. Org. Chem.* **2002**, *67*, 1496–1500.
40. Weber, B.; Seebach, D. *Tetrahedron* **1994**, *50*, 7473–7484.
41. Anies, C.; Lallemand, J. Y.; Pancrazi, A. *Tetrahedron Lett.* **1996**, *37*, 5519–5522.
42. Gao, Y. A.; Sato, F. *J. Org. Chem.* **1995**, *60*, 8136–8137.
43. Okamoto, S.; Kasatkin, A.; Zubaidha, P. K.; Sato, F. *J. Am. Chem. Soc.* **1996**, *118*, 2208–2216.
44. Suzuki, K.; Urabe, H.; Sato, F. *J. Am. Chem. Soc.* **1996**, *118*, 8729–8730.
45. Harada, K.; Urabe, H.; Sato, F. *Tetrahedron Lett.* **1995**, *36*, 3203–3206.
46. Hughes, K. A.; Dopico, P. G.; Sabat, M.; Finn, M. G. *Angew. Chem., Int. Ed. Engl.* **1993**, *32*, 554–555.
47. Bochmann, M. In *Comprehensive Organometallic Chemistry II*; Abel, E. W., Stone, F. G. A., Wilkinson, G., Eds.; Elsevier: Oxford, 1995; Vol. 4, p 280.
48. Reynolds, K. A.; Dopico, P. G.; Sundermann, M. J.; Hughes, K. A.; Finn, M. G. *J. Org. Chem.* **1993**, *58*, 1298–1299.
49. Reynolds, K. A.; Dopico, P. G.; Brody, M. S.; Finn, M. G. *J. Org. Chem.* **1997**, *62*, 2564–2573.
50. Reynolds, K. A.; Finn, M. G. *J. Org. Chem.* **1997**, *62*, 2574–2593.
51. Janas, Z.; Jerzykiewicz, L. B.; Przybylak, K.; Sobota, P.; Szczegot, K. *Eur. J. Inorg. Chem.* **2004**, 1639–1645.
52. Belanzoni, P.; Sgamellotti, A.; Re, N.; Floriani, C. *Inorg. Chem.* **2000**, *39*, 1147–1151.
53. Cozzi, P. G.; Carofiglio, T.; Floriani, C.; Chiesivilla, A.; Rizzoli, C. *Organometallics* **1993**, *12*, 2845–2848.
54. Muller, J. F. K.; Neuburger, M.; Weber, H. P. *J. Am. Chem. Soc.* **1999**, *121*, 12212–12213.
55. Reddy, L. R.; Gais, H. J.; Woo, C. W.; Raabe, G. *J. Am. Chem. Soc.* **2002**, *124*, 10427–10434.
56. Schleusner, M.; Gais, H. J.; Koep, S.; Raabe, G. *J. Am. Chem. Soc.* **2002**, *124*, 7789–7800.
57. Reggelin, M.; Zur, C. *Synthesis* **2000**, 1–64.
58. Reggelin, M.; Weinberger, H. *Angew. Chem., Int. Ed. Engl.* **1994**, *33*, 444–446.
59. Hainz, R.; Gais, H. J.; Raabe, G. *Tetrahedron: Asymmetry* **1996**, *7*, 2505–2508.
60. Gais, H. J.; Hainz, R.; Muller, H.; Bruns, P. R.; Giesen, N.; Raabe, G.; Runsink, J.; Nienstedt, S.; Decker, J.; Schleusner, M., *et al.* *Eur. J. Org. Chem.* **2000**, 3973–4009.
61. Gais, H. J.; Muller, H.; Decker, J.; Hainz, R. *Tetrahedron Lett.* **1995**, *36*, 7433–7436.
62. Tiwari, S. K.; Schneider, A.; Koep, S.; Gais, H. J. *Tetrahedron Lett.* **2004**, *45*, 8343–8346.
63. Bennett, J. L.; Wolczanski, P. T. *J. Am. Chem. Soc.* **1997**, *119*, 10696–10719.
64. Bennett, J. L.; Wolczanski, P. T. *J. Am. Chem. Soc.* **1994**, *116*, 2179–2180.
65. Beaudoin, M.; Scott, S. L. *Organometallics* **2001**, *20*, 237–239.
66. Fokken, S.; Spaniol, T. P.; Kang, H. C.; Massa, W.; Okuda, J. *Organometallics* **1996**, *15*, 5069–5072.
67. Gielens, E.; Dijkstra, T. W.; Berno, P.; Meetsma, A.; Hessen, B.; Teuben, J. H. *J. Organomet. Chem.* **1999**, *591*, 88–95.
68. Donkersvoort, J. G.; Jastrzebski, J.; Deelman, B. J.; Kooijman, H.; Veldman, N.; Spek, A. L.; van Koten, G. *Organometallics* **1997**, *16*, 4174–4184.
69. Johnson, A. R.; Davis, W. M.; Cummins, C. C. *Organometallics* **1996**, *15*, 3825–3835.
70. Kim, S. J.; Jung, I. N.; Yoo, B. R.; Kim, S. H.; Ko, J. J.; Byun, D. J.; Kang, S. O. *Organometallics* **2001**, *20*, 2136–2144.
71. Kim, S. J.; Jung, I. N.; Yoo, B. R.; Cho, S.; Ko, J.; Kim, S. H.; Kang, S. O. *Organometallics* **2001**, *20*, 1501–1503.
72. Kim, S. J.; Choi, D. W.; Lee, Y. J.; Chae, B. H.; Ko, J. J.; Kang, S. O. *Organometallics* **2004**, *23*, 559–567.
73. Kelly, D. G.; Toner, A. J.; Walker, N. M.; Coles, S. J.; Hursthouse, M. B. *Polyhedron* **1996**, *15*, 4307–4310.
74. Coles, S. J.; Hursthouse, M. B.; Kelly, D. G.; Toner, A. J.; Walker, N. M. *J. Organomet. Chem.* **1999**, *580*, 304–312.
75. Woodman, P. R.; Alcock, N. W.; Munslow, I. J.; Sanders, C. J.; Scott, P. J. *Chem. Soc., Dalton Trans.* **2000**, 3340–3346.
76. Stephan, D. W.; Guerin, F.; Spence, R. E. V.; Koch, L.; Gao, X. L.; Brown, S. J.; Swabey, J. W.; Wang, Q. Y.; Xu, W.; Zoricak, P., *et al.* *Organometallics* **1999**, *18*, 2046–2048.
77. Ong, C.; Kickham, J.; Clemens, S.; Guerin, F.; Stephan, D. W. *Organometallics* **2002**, *21*, 1646–1653.
78. Sarsfield, M. J.; Thornton-Pett, M.; Bochmann, M. *J. Chem. Soc., Dalton Trans.* **1999**, 3329–3330.
79. Agapie, T.; Diaconescu, P. L.; Mindiola, D. J.; Cummins, C. C. *Organometallics* **2002**, *21*, 1329–1340.
80. Lee, C. H.; La, Y. H.; Park, S. J.; Park, J. W. *Organometallics* **1998**, *17*, 3648–3655.



81. Li, Y. H.; Turnas, A.; Giszewski, J. T.; Odom, A. L. *Inorg. Chem.* **2002**, *41*, 6298–6306.
82. Yelamos, C.; Heeg, M. J.; Winter, C. H. *Organometallics* **1999**, *18*, 1168–1176.
83. Findeis, B.; Schubart, M.; Gade, L. H.; Moller, F.; Scowen, I.; McPartlin, M. *J. Chem. Soc., Dalton Trans.* **1996**, 125–132.
84. Schrock, R. R. *Acc. Chem. Res.* **1997**, *30*, 9–16.
85. Schrock, R. R.; Cummins, C. C.; Wilhelm, T.; Lin, S.; Reid, S. M.; Kol, M.; Davis, W. M. *Organometallics* **1996**, *15*, 1470–1476.
86. Turculet, L.; Tilley, T. D. *Organometallics* **2004**, *23*, 1542–1553.
87. van Meerendonk, W. J.; Schroder, K.; Brussee, E. A. C.; Meetsma, A.; Hessen, B.; Teuben, J. H. *Eur. J. Inorg. Chem.* **2003**, 427–432.
88. Li, J. F.; Huang, S. P.; Weng, L. H.; Liu, D. S. *Eur. J. Inorg. Chem.* **2003**, 810–813.
89. Thiele, K. H.; Windisch, H.; Edelmann, F. T.; Kilimann, U.; Noltemeyer, M. *Z. Anorg. Allg. Chem.* **1996**, *622*, 713–716.
90. Stewart, P. J.; Blake, A. J.; Mountford, P. *Organometallics* **1998**, *17*, 3271–3281.
91. Bashall, A.; Collier, P. E.; Gade, L. H.; McPartlin, M.; Mountford, P.; Pugh, S. M.; Radojevic, S.; Schubart, M.; Scowen, I. J.; Trosch, D. J. M. *Organometallics* **2000**, *19*, 4784–4794.
92. Pugh, S. M.; Trosch, D. J. M.; Wilson, D. J.; Bashall, A.; Cloke, F. G. N.; Gade, L. H.; Hitchcock, P. B.; McPartlin, M.; Nixon, J. F.; Mountford, P. *Organometallics* **2000**, *19*, 3205–3210.
93. Trösch, D. J. M.; Collier, P. E.; Bashall, A.; Gade, L. H.; McPartlin, M.; Mountford, P.; Radojevic, S. *Organometallics* **2001**, *20*, 3308–3313.
94. Bashall, A.; Collier, P. E.; Gade, L. H.; McPartlin, M.; Mountford, P.; Trösch, D. J. M. *Chem. Commun.* **1998**, 2555–2556.
95. Cloke, F. G. N.; Hitchcock, P. B.; Nixon, J. F.; Wilson, D. J.; Mountford, P. *Chem. Commun.* **1999**, 661–662.
96. Gade, L. H.; Mountford, P. *Coord. Chem. Rev.* **2001**, *216*, 65–97.
97. Croft, A. C. R.; Boyd, C. L.; Cowley, A. R.; Mountford, P. *J. Organomet. Chem.* **2003**, *683*, 120–130.
98. Crescenzi, R.; Solari, E.; Floriani, C.; Chiesi-Villa, A.; Rizzoli, C. *Organometallics* **1996**, *15*, 5456–5458.
99. Crescenzi, R.; Solari, E.; Floriani, C.; Re, N.; Chiesi-Villa, A.; Rizzoli, C. *Organometallics* **1999**, *18*, 606–618.
100. de Angelis, S.; Solari, E.; Floriani, C.; Chiesi-Villa, A.; Rizzoli, C. *Organometallics* **1995**, *14*, 4505–4512.
101. de Angelis, S.; Solari, E.; Floriani, C.; Chiesi-Villa, A.; Rizzoli, C. *Angew. Chem., Int. Ed. Engl.* **1995**, *34*, 1092–1094.
102. Spannenberg, A.; Baumann, W.; Rosenthal, U. *Appl. Organomet. Chem.* **2000**, *14*, 611–615.
103. Cotton, F. A.; Murillo, C. A.; Petrukhina, M. A. *J. Organomet. Chem.* **1999**, *573*, 78–86.
104. Bayer, A.; Gautun, O. R. *Tetrahedron Lett.* **2000**, *41*, 3743–3746.
105. Ray, B.; Neyroud, T. G.; Kapon, M.; Eichen, Y.; Eisen, M. S. *Organometallics* **2001**, *20*, 3044–3055.
106. Minhas, R. K.; Scoles, L.; Wong, S.; Gambarotta, S. *Organometallics* **1996**, *15*, 1113–1121.
107. Scoles, L.; Minhas, R.; Duchateau, R.; Jubb, J.; Gambarotta, S. *Organometallics* **1994**, *13*, 4978–4983.
108. Berno, P.; Gambarotta, S.; Kotila, S.; Erker, G. *Chem. Commun.* **1996**, 779–780.
109. Riley, P. N.; Fanwick, P. E.; Rothwell, I. P. *Chem. Commun.* **1997**, 1109–1110.
110. Riley, P. N.; Fanwick, P. E.; Rothwell, I. P. *J. Chem. Soc., Dalton Trans.* **2001**, 181–186.
111. Wrackmeyer, B.; Pedall, A.; Weidinger, J. *J. Organomet. Chem.* **2002**, *649*, 225–231.
112. Scollard, J. D.; McConville, D. H.; Vittal, J. J.; Payne, N. C. *J. Mol. Catal. A: Chem.* **1998**, *128*, 201–214.
113. Scollard, J. D.; McConville, D. H.; Payne, N. C.; Vittal, J. J. *Macromolecules* **1996**, *29*, 5241–5243.
114. Scollard, J. D.; McConville, D. H. *J. Am. Chem. Soc.* **1996**, *118*, 10008–10009.
115. Scollard, J. D.; McConville, D. H.; Rettig, S. J. *Organometallics* **1997**, *16*, 1810–1812.
116. Jeon, Y. M.; Heo, J.; Lee, W. M.; Chang, T. H.; Kim, K. *Organometallics* **1999**, *18*, 4107–4113.
117. Hagadorn, J. R.; Arnold, J. *Organometallics* **1998**, *17*, 1355–1368.
118. Littke, A.; Sleiman, N.; Bensimon, C.; Richeson, D. S.; Yap, G. P. A.; Brown, S. J. *Organometallics* **1998**, *17*, 446–451.
119. Flores, J. C.; Chien, J. C. W.; Rausch, M. D. *Organometallics* **1995**, *14*, 1827–1833.
120. Averbuj, C.; Eisen, M. S. *J. Am. Chem. Soc.* **1999**, *121*, 8755–8759.
121. Ong, T. G.; Yap, G. P. A.; Richeson, D. S. *Organometallics* **2002**, *21*, 2839–2841.
122. Coles, M. P.; Hitchcock, P. B. *Organometallics* **2003**, *22*, 5201–5211.
123. Steinhuebel, D. P.; Lippard, S. J. *Organometallics* **1999**, *18*, 3959–3961.
124. Steinhuebel, D. P.; Lippard, S. J. *Organometallics* **1999**, *18*, 109–111.
125. Steinhuebel, D. P.; Lippard, S. J. *J. Am. Chem. Soc.* **1999**, *121*, 11762–11772.
126. Siemeling, U.; Kolling, L.; Stammer, A.; Stammer, H. G. *J. Chem. Soc., Dalton Trans.* **2002**, 3277–3279.
127. Hollink, E.; Stewart, J. C.; Wei, P. R.; Stephan, D. W. *Dalton Trans.* **2003**, 3968–3974.
128. Vollmerhaus, R.; Shao, P. C.; Taylor, N. J.; Collins, S. *Organometallics* **1999**, *18*, 2731–2733.
129. Manke, D. R.; Nocera, D. G. *Inorg. Chim. Acta* **2003**, *345*, 235–240.
130. Warren, T. H.; Schrock, R. R.; Davis, W. M. *Organometallics* **1996**, *15*, 562–569.
131. Warren, T. H.; Schrock, R. R.; Davis, W. M. *Organometallics* **1998**, *17*, 308–321.
132. Patton, J. T.; Feng, S. G. G.; Abboud, K. A. *Organometallics* **2001**, *20*, 3399–3405.
133. Liang, L. C.; Schrock, R. R.; Davis, W. M.; McConville, D. H. *J. Am. Chem. Soc.* **1999**, *121*, 5797–5798.
134. Tsuie, B.; Swenson, D. C.; Jordan, R. F.; Petersen, J. L. *Organometallics* **1997**, *16*, 1392–1400.
135. Hagadorn, J. R.; Arnold, J. *Angew. Chem., Int. Ed.* **1998**, *37*, 1729–1731.
136. Deng, L. Q.; Ziegler, T.; Woo, T. K.; Margl, P.; Fan, L. Y. *Organometallics* **1998**, *17*, 3240–3253.
137. Friedrich, S.; Schubart, M.; Gade, L. H.; Scowen, I. J.; Edwards, A. J.; McPartlin, M. *Chem. Ber. Recl.* **1997**, *130*, 1751–1759.
138. Guerin, F.; McConville, D. H.; Payne, N. C. *Organometallics* **1996**, *15*, 5085–5089.
139. Guerin, F.; McConville, D. H.; Vittal, J. J. *Organometallics* **1997**, *16*, 1491–1496.
140. Clark, H. C. S.; Cloke, G. N.; Hitchcock, P. B.; Love, J. B.; Wainwright, A. P. *J. Organomet. Chem.* **1995**, *501*, 333–340.
141. Oakes, D. C. H.; Kimberley, B. S.; Gibson, V. C.; Jones, D. J.; White, A. J. P.; Williams, D. J. *Chem. Commun.* **2004**, 2174–2175.
142. Baumann, R.; Davis, W. M.; Schrock, R. R. *J. Am. Chem. Soc.* **1997**, *119*, 3830–3831.
143. Baumann, R.; Stumpf, R.; Davis, W. M.; Liang, L. C.; Schrock, R. R. *J. Am. Chem. Soc.* **1999**, *121*, 7822–7836.
144. Schrock, R. R.; Baumann, R.; Reid, S. M.; Goodman, J. T.; Stumpf, R.; Davis, W. M. *Organometallics* **1999**, *18*, 3649–3670.
145. Schrock, R. R.; Liang, L. C.; Baumann, R.; Davis, W. M. *J. Organomet. Chem.* **1999**, *591*, 163–173.
146. Schrock, R. R.; Schattenmann, F.; Aizenberg, M.; Davis, W. M. *Chem. Commun.* **1998**, 199–200.
147. Aizenberg, M.; Turculet, L.; Davis, W. M.; Schattenmann, F.; Schrock, R. R. *Organometallics* **1998**, *17*, 4795–4812.
148. Carpentier, J. F.; Martin, A.; Swenson, D. C.; Jordan, R. F. *Organometallics* **2003**, *22*, 4999–5010.

149. Westmoreland, I.; Munslow, I. J.; O'Shaughnessy, P. N.; Scott, P. *Organometallics* **2003**, *22*, 2972–2976.
150. Wilson, P. J.; Blake, A. J.; Mountford, P.; Schroder, M. *J. Organomet. Chem.* **2000**, *600*, 71–83.
151. Male, N. A. H.; Skinner, M. E. G.; Bylikin, S. Y.; Wilson, P. J.; Mountford, P.; Schroder, M. *Inorg. Chem.* **2000**, *39*, 5483–5491.
152. Said, M.; Hughes, D. L.; Bochmann, M. *Dalton Trans.* **2004**, 359–360.
153. Kim, I.; Nishihara, Y.; Jordan, R. F.; Rogers, R. D.; Rheingold, A. L.; Yap, G. P. A. *Organometallics* **1997**, *16*, 3314–3323.
154. Vanderlinden, A.; Schaverien, C. J.; Meijboom, N.; Ganter, C.; Orpen, A. G. *J. Am. Chem. Soc.* **1995**, *117*, 3008–3021.
155. Porri, L.; Ripa, A.; Colombo, P.; Miano, E.; Capelli, S.; Meille, S. V. *J. Organomet. Chem.* **1996**, *514*, 213–217.
156. Fokken, S.; Spaniol, T. P.; Okuda, J.; Sernetz, F. G.; Mulhaupt, R. *Organometallics* **1997**, *16*, 4240–4242.
157. Anthis, J. W.; Filippov, I.; Wigley, D. E. *Inorg. Chem.* **2004**, *43*, 716–724.
158. Groysman, S.; Goldberg, I.; Kol, M.; Genizi, E.; Goldschmidt, Z. *Organometallics* **2003**, *22*, 3013–3015.
159. Tshuva, E. Y.; Goldberg, I.; Kol, M.; Goldschmidt, Z. *Inorg. Chem. Commun.* **2000**, *3*, 611–614.
160. Groysman, S.; Goldberg, I.; Kol, M.; Genizi, E.; Goldschmidt, Z. *Inorg. Chim. Acta* **2003**, *345*, 137–144.
161. Groysman, S.; Tshuva, E. Y.; Golderg, I.; Kol, M.; Goldschmidt, Z.; Shuster, M. *Organometallics* **2004**, *23*, 5291–5299.
162. Tshuva, E. Y.; Goldberg, I.; Kol, M.; Goldschmidt, Z. *Chem. Commun.* **2001**, 2120–2121.
163. Fokken, S.; Reichwald, F.; Spaniol, T. P.; Okuda, J. *J. Organomet. Chem.* **2002**, *663*, 158–163.
164. Beaudoin, M. C.; Womiloju, O.; Fu, A. Q.; Ajjou, J. A. N.; Rice, G. L.; Scott, S. L. *J. Mol. Catal. A: Chem.* **2002**, *190*, 159–169.
165. Alladin, T.; Beaudoin, M. C.; Scott, S. L. *Inorg. Chim. Acta* **2003**, *345*, 292–298.
166. Ozerov, O. V.; Ladipo, F. T.; Patrick, B. O. *J. Am. Chem. Soc.* **1999**, *121*, 7941–7942.
167. Ozerov, O. V.; Rath, N. P.; Ladipo, F. T. *J. Organomet. Chem.* **1999**, *586*, 223–233.
168. Ozerov, O. V.; Brock, C. P.; Carr, S. D.; Ladipo, F. T. *Organometallics* **2000**, *19*, 5016–5025.
169. Ozerov, O. V.; Parkin, S.; Brock, C. P.; Ladipo, F. T. *Organometallics* **2000**, *19*, 4187–4190.
170. Ozerov, O. V.; Patrick, B. O.; Ladipo, F. T. *J. Am. Chem. Soc.* **2000**, *122*, 6423–6431.
171. Thorn, M. G.; Etheridge, Z. C.; Fanwick, P. E.; Rothwell, I. P. *J. Organomet. Chem.* **1999**, *591*, 148–162.
172. Thorn, M. G.; Fanwick, P. E.; Rothwell, I. P. *Organometallics* **1999**, *18*, 4442–4447.
173. Thorn, M. G.; Hill, J. E.; Waratuke, S. A.; Johnson, E. S.; Fanwick, P. E.; Rothwell, I. P. *J. Am. Chem. Soc.* **1997**, *119*, 8630–8641.
174. Hill, J. E.; Balaich, G.; Fanwick, P. E.; Rothwell, I. P. *Organometallics* **1993**, *12*, 2911–2924.
175. Balaich, G. J.; Fanwick, P. E.; Rothwell, I. P. *Organometallics* **1994**, *13*, 4117–4118.
176. Balaich, G. J.; Hill, J. E.; Waratuke, S. A.; Fanwick, P. E.; Rothwell, I. P. *Organometallics* **1995**, *14*, 656–665.
177. Balaich, G. J.; Rothwell, I. P. *J. Am. Chem. Soc.* **1993**, *115*, 1581–1583.
178. Himes, R. A.; Fanwick, P. E.; Rothwell, I. P. *Chem. Commun.* **2003**, 18–19.
179. Kulinkovich, O. G. *Chem. Rev.* **2003**, *103*, 2597–2632.
180. Kulinkovich, O. G.; de Meijere, A. *Chem. Rev.* **2000**, *100*, 2789–2834.
181. Kulinkovich, O. G. *Pure Appl. Chem.* **2000**, *72*, 1715–1719.
182. Kulinkovich, O. G. *Russ. Chem. Bull.* **2004**, *53*, 1065–1086.
183. Eisch, J. J.; Adeosun, A. A.; Gitua, J. N. *Eur. J. Org. Chem.* **2003**, 4721–4727.
184. Takayanagi, Y.; Yamashita, K.; Yoshida, Y.; Sato, F. *Chem. Commun.* **1996**, 1725–1726.
185. Averbuj, C.; Kaftanov, J.; Marek, I. *Synlett* **1999**, 1939–1941.
186. Hamada, T.; Suzuki, D.; Urabe, H.; Sato, F. *J. Am. Chem. Soc.* **1999**, *121*, 7342–7344.
187. Urabe, H.; Sato, F. *J. Am. Chem. Soc.* **1999**, *121*, 1245–1255.
188. Urabe, H.; Sato, F. *J. Org. Chem.* **1996**, *61*, 6756–6757.
189. Urabe, H.; Hata, T.; Sato, F. *Tetrahedron Lett.* **1995**, *36*, 4261–4264.
190. Hideura, D.; Urabe, H.; Sato, F. *Chem. Commun.* **1998**, 271–272.
191. Urabe, H.; Takeda, T.; Sato, F. *Tetrahedron Lett.* **1996**, *37*, 1253–1256.
192. Urabe, H.; Suzuki, K.; Sato, F. *J. Am. Chem. Soc.* **1997**, *119*, 10014–10027.
193. Block, E.; Birringer, M.; He, C. H. *Angew. Chem., Int. Ed.* **1999**, *38*, 1604–1607.
194. Suzuki, D.; Urabe, H.; Sato, F. *J. Am. Chem. Soc.* **2001**, *123*, 7925–7926.
195. Hamada, T.; Mizojiri, R.; Urabe, H.; Sato, F. *J. Am. Chem. Soc.* **2000**, *122*, 7138–7139.
196. Uchikawa, W.; Matsuno, C.; Okamoto, S. *Tetrahedron Lett.* **2004**, *45*, 9037–9040.
197. McAlexander, L. H.; Li, L. T.; Yang, Y. H.; Pollitte, J. L.; Xue, Z. L. *Inorg. Chem.* **1998**, *37*, 1423–1426.
198. McAlexander, L. H.; Hung, M. L.; Li, L. T.; Diminnie, J. B.; Xue, Z. L.; Yap, G. P. A.; Rheingold, A. L. *Organometallics* **1996**, *15*, 5231–5235.
199. Chen, T. N.; Xue, Z. L. *Chin. J. Inorg. Chem.* **1999**, *15*, 413–422.
200. Kui, S. C. F.; Zhu, N. Y.; Chan, M. C. W. *Angew. Chem., Int. Ed.* **2003**, *42*, 1628–1632.
201. Mahanthappa, M. K.; Cole, A. P.; Waymouth, R. M. *Organometallics* **2004**, *23*, 1405–1410.
202. Donkervoort, J. G.; Kronenburg, C. M. P.; Deelman, B. J.; Jastrzebski, J.; Veldman, N.; Spek, A. L.; van Koten, G. *J. Organomet. Chem.* **1997**, *547*, 349–355.
203. Abbenhuis, H. C. L.; Krijnen, S.; van Santen, R. A. *Chem. Commun.* **1997**, 331–332.
204. Windisch, H.; Thiele, K. H.; Kociokkohn, G.; Schumann, H. *Z. Anorg. Allg. Chem.* **1995**, *621*, 861–864.
205. Thiele, K. H.; Windisch, H.; Schumann, H.; Kociokkohn, G. *Z. Anorg. Allg. Chem.* **1994**, *620*, 523–526.
206. Kleinhenz, S.; Seppelt, K. *Chem. Eur. J.* **1999**, *5*, 3573–3580.
207. Ara, I.; Fornies, J.; Garcia-Monforte, M. A.; Martín, A.; Menjón, B. *Chem. Eur. J.* **2004**, *10*, 4186–4197.
208. Hughes, A. K.; Kingsley, A. J. *J. Organomet. Chem.* **1997**, *539*, 109–114.
209. Cheon, J.; Rogers, D. M.; Girolami, G. S. *J. Am. Chem. Soc.* **1997**, *119*, 6804–6813.
210. Cheon, J.; Dubois, L. H.; Girolami, G. S. *J. Am. Chem. Soc.* **1997**, *119*, 6814–6820.
211. Berno, P.; Jenkins, H.; Gambarotta, S.; Blixt, J.; Facey, G. A.; Detellier, C. *Angew. Chem., Int. Ed. Engl.* **1995**, *34*, 2264–2266.
212. Villiers, C.; Vandaïs, A.; Ephritikhine, M. *J. Organomet. Chem.* **2001**, *617*, 744–747.
213. Cho, H. G.; Andrews, L. *Inorg. Chem.* **2004**, *43*, 5253–5257.
214. Cho, H. G.; Andrews, L. *J. Phys. Chem. A* **2004**, *108*, 6294–6301.
215. Cavell, R. G.; Babu, R. P. K.; Kasani, A.; McDonald, R. *J. Am. Chem. Soc.* **1999**, *121*, 5805–5806.
216. Cavell, R. G.; Babu, R. P. K.; Aparna, K. *J. Organomet. Chem.* **2001**, *617*, 158–169.
217. Basuli, F.; Bailey, B. C.; Tomaszewski, J.; Huffman, J. C.; Mindiola, D. J. *J. Am. Chem. Soc.* **2003**, *125*, 6052–6053.

218. Basuli, F.; Tomaszewski, J.; Huffman, J. C.; Mindiola, D. J. *J. Am. Chem. Soc.* **2003**, *125*, 10170–10171.
219. Scholz, J.; Kahlert, S.; Gørls, H. *Organometallics* **2004**, *23*, 1594–1603.
220. Scholz, J.; Gørls, H. *Organometallics* **2004**, *23*, 320–322.
221. Herrmann, W. A.; Ofele, K.; Elison, M.; Kuhn, F. E.; Roesky, P. W. *J. Organomet. Chem.* **1994**, *480*, C7–C9.
222. Kunkely, H.; Vogler, A. *J. Organomet. Chem.* **2003**, *684*, 113–116.
223. Kuhn, N.; Kratz, T.; Blaser, D.; Boese, R. *Inorg. Chim. Acta* **1995**, *238*, 179–181.
224. Shukla, P.; Johnson, J. A.; Vidovic, D.; Cowley, A. H.; Abernethy, C. D. *Chem. Commun.* **2004**, 360–361.
225. Aihara, H.; Matsuo, T.; Kawaguchi, H. *Chem. Commun.* **2003**, 2204–2205.
226. Westwood, A.; Nicholls, D. *Inorg. Chim. Acta* **1996**, *244*, 259–264.
227. Hahn, F. E.; Lugger, T. *J. Organomet. Chem.* **1995**, *501*, 341–346.
228. Carofiglio, T.; Cozzi, P. G.; Floriani, C.; Chiesivilla, A.; Rizzoli, C. *Organometallics* **1993**, *12*, 2726–2736.
229. Mori, M.; Imma, H.; Nakai, T. *Tetrahedron Lett.* **1997**, *38*, 6229–6232.
230. Mori, M.; Nakai, T. *Tetrahedron Lett.* **1997**, *38*, 6233–6236.
231. Cotton, F. A.; Petrukhina, M. A. *Inorg. Chem. Commun.* **1998**, *1*, 195–196.
232. McGrady, G. S.; Downs, A. J.; McKean, D. C.; Haaland, A.; Scherer, W.; Verne, H. P.; Volden, H. V. *Inorg. Chem.* **1996**, *35*, 4713–4718.
233. Kaupp, M. *Chem. Eur. J.* **1999**, *5*, 3631–3643.
234. Jonas, V.; Boehme, C.; Frenking, G. *Inorg. Chem.* **1996**, *35*, 2097–2099.
235. Hollenstein, S.; Hesse, M. *Helv. Chim. Acta* **1996**, *79*, 827–836.
236. Scherer, W.; Hieringer, W.; Spiegler, M.; Sirsch, P.; McGrady, G. S.; Downs, A. J.; Haaland, A.; Pedersen, B. *Chem. Commun.* **1998**, 2471–2472.
237. Jonas, V.; Frenking, G.; Reetz, M. T. *Organometallics* **1993**, *12*, 2111–2120.
238. Jonas, V.; Frenking, G.; Reetz, M. T. *Organometallics* **1995**, *14*, 5316–5324.
239. Reetz, M. T.; Raguse, B.; Seitz, T. *Tetrahedron* **1993**, *49*, 8561–8568.
240. Grigoleit, S.; Buhl, M. *Chem. Eur. J.* **2004**, *10*, 5541–5552.
241. Wu, Y. D.; Peng, Z. H.; Xue, Z. L. *J. Am. Chem. Soc.* **1996**, *118*, 9772–9777.
242. Wu, Y. D.; Peng, Z. H.; Chan, K. W. K.; Liu, X. Z.; Tuinman, A. A.; Xue, Z. L. *Organometallics* **1999**, *18*, 2081–2090.
243. Bennett, J. L.; Vaid, T. P.; Wolczanski, P. T. *Inorg. Chim. Acta* **1998**, *270*, 414–423.
244. Waratuke, S. A.; Thorn, M. G.; Fanwick, P. E.; Rothwell, A. P.; Rothwell, I. P. *J. Am. Chem. Soc.* **1999**, *121*, 9111–9119.
245. Johnson, E. S.; Balaich, G. J.; Rothwell, I. P. *J. Am. Chem. Soc.* **1997**, *119*, 7685–7693.
246. Johnson, E. S.; Balaich, G. J.; Fanwick, P. E.; Rothwell, I. P. *J. Am. Chem. Soc.* **1997**, *119*, 11086–11087.
247. Balaich, G. J.; Rothwell, I. P. *Tetrahedron* **1995**, *51*, 4463–4470.
248. Zambrano, C. H.; Profilet, R. D.; Hill, J. E.; Fanwick, P. E.; Rothwell, I. P. *Polyhedron* **1993**, *12*, 689–708.
249. Sato, F.; Urabe, H.; Okamoto, S. *Synlett* **2000**, 753–775.
250. Sato, F.; Urabe, H.; Okamoto, S. *Chem. Rev.* **2000**, *100*, 2835–2886.
251. Sato, K.; Okamoto, S. *Adv. Synth. Catal.* **2001**, *343*, 759–784.
252. Breit, B. *J. Prakt. Chem., Chem. Ztg.* **2000**, *342*, 211–214.
253. Urabe, H. *J. Synth. Org. Chem. Jpn.* **1999**, *57*, 492–502.
254. Urabe, H.; Narita, M.; Sato, F. *Angew. Chem., Int. Ed.* **1999**, *38*, 3516–3518.
255. Tanaka, R.; Nakano, Y.; Suzuki, D.; Urabe, H.; Sato, F. *J. Am. Chem. Soc.* **2002**, *124*, 9682–9683.
256. Hanazawa, T.; Sasaki, K.; Takayama, Y.; Sato, F. *J. Org. Chem.* **2003**, *68*, 4980–4983.
257. Suzuki, D.; Tanaka, R.; Urabe, H.; Sato, F. *J. Am. Chem. Soc.* **2002**, *124*, 3518–3519.
258. Gao, Y.; Harada, K.; Sato, F. *Tetrahedron Lett.* **1995**, *36*, 5913–5916.
259. Sato, F.; Urabe, H. In *Titanium and Zirconium in Organic Synthesis*; Marek, I., Ed.; Wiley-VCH: Weinheim, 2002; pp 319–354.
260. Morlender-Vais, N.; Solodovnikova, N.; Marek, I. *Chem. Commun.* **2000**, 1849–1850.
261. Urabe, H.; Hamada, T.; Sato, F. *J. Am. Chem. Soc.* **1999**, *121*, 2931–2932.
262. Suzuki, D.; Urabe, H.; Sato, F. *Angew. Chem., Int. Ed.* **2000**, *39*, 3290–3292.
263. Okamoto, S.; Fukuhara, K.; Sato, F. *Tetrahedron Lett.* **2000**, *41*, 5561–5565.
264. Takayama, Y.; Okamoto, S.; Sato, F. *J. Am. Chem. Soc.* **1999**, *121*, 3559–3560.
265. Banti, D.; Cicogna, F.; Di Bari, L.; Caporusso, A. M. *Tetrahedron Lett.* **2000**, *41*, 7773–7777.
266. Mizojiri, R.; Urabe, H.; Sato, F. *J. Org. Chem.* **2000**, *65*, 6217–6222.
267. An, D. K.; Okamoto, S.; Sato, F. *Tetrahedron Lett.* **1998**, *39*, 4861–4864.
268. An, D. K.; Okamoto, S.; Sato, F. *Tetrahedron Lett.* **1998**, *39*, 4555–4558.
269. Matsuda, S.; An, D. K.; Okamoto, S.; Sato, F. *Tetrahedron Lett.* **1998**, *39*, 7513–7516.
270. An, D. K.; Hirakawa, K.; Okamoto, S.; Sato, F. *Tetrahedron Lett.* **1999**, *40*, 3737–3740.
271. Delas, C.; Urabe, H.; Sato, F. *Tetrahedron Lett.* **2001**, *42*, 4147–4150.
272. Teng, X.; Wada, T.; Okamoto, S.; Sato, F. *Tetrahedron Lett.* **2001**, *42*, 5501–5503.
273. Okamoto, S.; Matsuda, S.; An, D. K.; Sato, F. *Tetrahedron Lett.* **2001**, *42*, 6323–6326.
274. Delas, C.; Urabe, H.; Sato, F. *Chem. Commun.* **2002**, 272–273.
275. Narita, M.; Urabe, H.; Sato, F. *Angew. Chem., Int. Ed.* **2002**, *41*, 3671–3674.
276. Obora, Y.; Moriya, H.; Tokunaga, M.; Tsuji, Y. *Chem. Commun.* **2003**, 2820–2821.
277. Urabe, H.; Suzuki, D.; Sasaki, M.; Sato, F. *J. Am. Chem. Soc.* **2003**, *125*, 4036–4037.
278. Quntar, A. A.; Baum, O.; Shibli, A.; Dembitsky, V. M.; Srebnik, M. *Angew. Chem., Int. Ed. Engl.* **2003**, *42*, 4777–4779.
279. Quntar, A. A.; Srebnik, M. *Chem. Commun.* **2003**, 58–59.
280. Al Quntar, A. A.; Dembitsky, V. M.; Srebnik, M. *Org. Lett.* **2003**, *5*, 357–359.
281. Urabe, H.; Mitsui, K.; Ohta, S.; Sato, F. *J. Am. Chem. Soc.* **2003**, *125*, 6074–6075.
282. Mitsui, K.; Sato, T.; Urabe, H.; Sato, F. *Angew. Chem., Int. Ed.* **2004**, *43*, 490–492.
283. Okamoto, S.; Takayama, Y.; Gao, Y.; Sato, F. *Synthesis* **2000**, 975–979.
284. Hanazawa, T.; Okamoto, S.; Sato, F. *Org. Lett.* **2000**, *2*, 2369–2371.
285. Okamoto, S. *J. Synth. Org. Chem. Jpn.* **2001**, *59*, 1204–1211.
286. Wu, Y. D.; Yu, Z. X. *J. Am. Chem. Soc.* **2001**, *123*, 5777–5786.

287. Olsson, R.; Rundstrom, P.; Persson, B.; Frejd, T. *Carbohydr. Res.* **1998**, *307*, 13–18.
288. Williams, C. M.; Chaplinski, V.; Schreiner, P. R.; de Meijere, A. *Tetrahedron Lett.* **1998**, *39*, 7695–7698.
289. Chaplinski, V.; de Meijere, A. *Angew. Chem., Int. Ed. Engl.* **1996**, *35*, 413–414.
290. Chaplinski, V.; Winsel, H.; Kordes, M.; de Meijere, A. *Synlett* **1997**, 111–114.
291. de Meijere, A.; Williams, C. M.; Kourdioukov, A.; Sviridov, S. V.; Chaplinski, V.; Kordes, M.; Savchenko, A. I.; Stratmann, C.; Noltemeyer, M. *Chem. Eur. J.* **2002**, *8*, 3789–3801.
292. Han, J. W.; Tokunaga, N.; Hayashi, T. *Synlett* **2002**, 871–874.
293. Flemming, S.; Kabbara, J.; Nickisch, K.; Neh, H.; Westermann, J. *Tetrahedron Lett.* **1994**, *35*, 6075–6078.
294. Hayashi, T.; Tokunaga, N.; Yoshida, K.; Han, J. W. *J. Am. Chem. Soc.* **2002**, *124*, 12102–12103.
295. Selent, D.; Pickardt, J.; Claus, P. *J. Organomet. Chem.* **1994**, *468*, 131–138.
296. Wu, M. J.; Yan, D. S.; Tsai, H. W.; Chen, S. H. *Tetrahedron Lett.* **1994**, *35*, 5003–5004.
297. Takeda, T.; Saeki, N.; Takagi, Y.; Fujiwara, T. *Chem. Lett.* **2000**, 1198–1199.
298. Eisch, J. J.; Gitua, J. N. *Organometallics* **2003**, *22*, 24–26.
299. Eisch, J. J.; Gitua, J. N. *Organometallics* **2003**, *22*, 4172–4174.
300. Coles, S. J.; Hursthouse, M. B.; Kelly, D. G.; Toner, A. J.; Walker, N. M. *Can. J. Chem., Rev. Can. Chim.* **1999**, *77*, 2095–2098.
301. Holmes, S. A.; Quignard, F.; Choplin, A.; Teissier, R.; Kervennal, J. J. *Catal.* **1998**, *176*, 173–181.
302. Holmes, S. A.; Quignard, F.; Choplin, A.; Teissier, R.; Kervennal, J. J. *Catal.* **1998**, *176*, 182–191.
303. Coates, G. W.; Hustad, P. D.; Reinartz, S. *Angew. Chem., Int. Ed.* **2002**, *41*, 2236–2257.
304. Khrushch, N. E.; Dyachkovskii, F. S. *Kinet. Catal.* **1994**, *35*, 213–217.
305. Thorn, M. G.; Etheridge, Z. C.; Fanwick, P. E.; Rothwell, I. P. *Organometallics* **1998**, *17*, 3636–3638.
306. Guerin, F.; Stewart, J. C.; Beddie, C.; Stephan, D. W. *Organometallics* **2000**, *19*, 2994–3000.
307. Guerin, F.; Stephan, D. W. *Angew. Chem., Int. Ed.* **2000**, *39*, 1298–1300.
308. Kickham, J. E.; Guerin, F.; Stephan, D. W. *J. Am. Chem. Soc.* **2002**, *124*, 11486–11494.
309. Shiono, T. *Catal. Surv. Asia* **2003**, *7*, 47–62.
310. Hagimoto, H.; Shiono, T.; Ikeda, T. *Macromol. Chem. Phys.* **2004**, *205*, 19–26.
311. Nedorezova, P. M.; Adrov, O. I.; Guzman, I. S.; Dyachkovsky, F. S. *Vysokomol. Soedin.* **1993**, *35*, A385–A387.
312. Thomas, L.; Polton, A.; Tardi, M.; Sigwalt, P. *Macromolecules* **1995**, *28*, 2105–2111.
313. Liu, J. F.; Zhang, D. F.; Huang, J. L.; Qian, Y. L.; Chan, A. S. C. *J. Polym. Sci. Pol. Chem.* **2000**, *38*, 1639–1643.
314. Jensen, V. R.; Borge, K. J.; Ystenes, M. J. *Am. Chem. Soc.* **1995**, *117*, 4109–4117.
315. Bernardi, F.; Bottoni, A.; Miscione, G. P. *Organometallics* **1998**, *17*, 16–24.
316. Shiga, A.; Kawamura-Kuribayashi, H.; Sasaki, T. *J. Mol. Catal.* **1993**, *79*, 95–115.
317. Kawamura-Kuribayashi, H.; Miyatake, T. *J. Organomet. Chem.* **2003**, *674*, 73–85.
318. Froese, R. D. J.; Musaev, D. G.; Matsubara, T.; Morokuma, K. *J. Am. Chem. Soc.* **1997**, *119*, 7190–7196.
319. Froese, R. D. J.; Musaev, D. G.; Morokuma, K. *Organometallics* **1999**, *18*, 373–379.
320. Ramos, J.; Cruz, V.; Muñoz-Escalona, A.; Martínez-Salazar, J. *Polymer* **2001**, *42*, 7275–7284.
321. Bühl, M.; Mauschick, F. T. *J. Organomet. Chem.* **2002**, *648*, 126–133.
322. Vanka, K.; Xu, Z. T.; Ziegler, T. *Isr. J. Chem.* **2002**, *42*, 403–415.
323. Qian, Y. L.; Huang, J. L.; Bala, M. D.; Lian, B.; Zhang, H. *Chem. Rev.* **2003**, *103*, 2633–2690.
324. Christie, S. D. R.; Man, K. W.; Whitby, R. J.; Slawin, A. M. Z. *Organometallics* **1999**, *18*, 348–359.
325. Rufanov, K. A.; Churakov, A. V.; Kazennova, N. B.; Brusova, G. P.; Lemenovskii, D. A.; Kuzmina, L. G. *J. Organomet. Chem.* **1995**, *498*, 37–39.
326. Dorado, I.; Flores, J. C.; Galakhov, M.; Gómez-Sal, P.; Martín, A.; Royo, P. J. *Organomet. Chem.* **1998**, *563*, 7–14.
327. Sassmannshausen, J.; Powell, A. K.; Anson, C. E.; Wocadlo, S.; Bochmann, M. J. *Organomet. Chem.* **1999**, *592*, 84–94.
328. Deckers, P. J. W.; van der Linden, A. J.; Meetsma, A.; Hessen, B. *Eur. J. Inorg. Chem.* **2000**, 929–932.
329. Schwecke, C.; Kaminsky, W. *J. Polym. Sci., Pol. Chem.* **2001**, *39*, 2805–2812.
330. Maldanis, R. J.; Chien, J. C. W.; Rausch, M. D. *J. Organomet. Chem.* **2000**, *599*, 107–111.
331. Deckers, P. J. W.; Hessen, B.; Teuben, J. H. *Angew. Chem., Int. Ed. Engl.* **2001**, *40*, 2516–2519.
332. Blais, M. S.; Chien, J. C. W.; Rausch, M. D. *Organometallics* **1998**, *17*, 3775–3783.
333. Deckers, P. J. W.; Hessen, B.; Teuben, J. H. *Organometallics* **2002**, *21*, 5122–5135.
334. Longo, P.; Amendola, A. G.; Fortunato, E.; Boccia, A. C.; Zambelli, A. *Macromol. Rapid Commun.* **2001**, *22*, 339–344.
335. Hessen, B. *J. Mol. Catal. A: Chem.* **2004**, *213*, 129–135.
336. Amor, J. I.; Cuenca, T.; Galakhov, M.; Royo, P. J. *Organomet. Chem.* **1995**, *497*, 127–131.
337. Amor, J. I.; Cuenca, T.; Galakhov, M.; Gómez-Sal, P.; Manzanero, A.; Royo, P. J. *Organomet. Chem.* **1997**, *535*, 155–168.
338. Lee, B. Y.; Han, J. W.; Heo, H. M.; Lee, I. S.; Chung, Y. K. *J. Organomet. Chem.* **2001**, *627*, 233–238.
339. Sitzmann, H.; Zhou, P.; Wolmershauser, G. *Chem. Ber.* **1994**, *127*, 3–9.
340. Evans, W. J.; Giarikos, D. G.; Ziller, J. W. *J. Organomet. Chem.* **2003**, *688*, 200–205.
341. Bjorgvinsson, M.; Halldorsson, S.; Arnason, I.; Magull, J.; Fenske, D. *J. Organomet. Chem.* **1997**, *544*, 207–215.
342. Flores, J. C.; Wood, J. S.; Chien, J. C. W.; Rausch, M. D. *Organometallics* **1996**, *15*, 4944–4950.
343. Barry, S.; Kucht, A.; Kucht, H.; Rausch, M. D. *J. Organomet. Chem.* **1995**, *489*, 195–199.
344. Roesky, H. W.; Herzog, A.; Liu, F. Q. *J. Fluorine Chem.* **1995**, *72*, 183–185.
345. Qian, X. M.; Huang, J. L.; Qian, Y. L.; Wang, C. *Appl. Organomet. Chem.* **2003**, *17*, 277–281.
346. Butakoff, K. A.; Lemenovskii, D. A.; Mountford, P.; Kuzmina, L. G.; Churakov, A. V. *Polyhedron* **1996**, *15*, 489–499.
347. Okuda, J.; Duplooy, K. E.; Toscano, P. J. *J. Organomet. Chem.* **1995**, *495*, 195–202.
348. Zemanek, J.; Frohlichova, L.; Sindelar, P.; Stepnicka, P.; Cisarova, I.; Varga, V.; Horacek, M.; Mach, K. *Collect. Czech. Chem. Commun.* **2001**, *66*, 1359–1374.
349. Erker, G.; Kehr, G.; Frohlich, R. *J. Organomet. Chem.* **2004**, *689*, 1402–1412.
350. Sierra, J. C.; Huerlander, D.; Hill, M.; Kehr, G.; Erker, G.; Frohlich, R. *Chem. Eur. J.* **2003**, *9*, 3618–3622.
351. Herzog, A.; Liu, F. Q.; Roesky, H. W.; Demsar, A.; Keller, K.; Noltemeyer, M.; Pauer, F. *Organometallics* **1994**, *13*, 1251–1256.
352. Liu, F. Q.; Kunzel, A.; Herzog, A.; Roesky, H. W.; Noltemeyer, M.; Fleischer, R.; Stalke, D. *Polyhedron* **1997**, *16*, 61–65.
353. Kunzel, A.; Parisini, E.; Roesky, H. W.; Sheldrick, G. M. *J. Organomet. Chem.* **1997**, *536*, 177–180.



354. Xu, G. X.; Ruckenstein, E. *J. Polym. Sci., Pol. Chem.* **1999**, *37*, 2481–2488.
355. Sotoodeh, M.; Leichtweis, I.; Roesky, H. W.; Noltemeyer, M.; Schmidt, H. G. *Chem. Ber. Recl.* **1993**, *126*, 913–919.
356. Qian, X. M.; Huang, J. L.; Qian, Y. L. *J. Organomet. Chem.* **2004**, *689*, 1503–1510.
357. Deck, P. A.; Konate, M. M.; Kelly, B. V.; Slebodnick, C. *Organometallics* **2004**, *23*, 1089–1097.
358. Plenio, H.; Warnecke, A. *J. Organomet. Chem.* **1997**, *544*, 133–137.
359. Xie, M. R.; Wu, Q.; Lin, S. G. *Acta Polym. Sin.* **2000**, 774–778.
360. Xie, M. R.; Wu, Q.; Lin, S. G. *Acta Polym. Sin.* **2000**, 779–782.
361. Xie, M. R.; Wu, Q.; Lin, S. G. *Acta Polym. Sin.* **2000**, 783–787.
362. Okuda, J. *Comm. Inorg. Chem.* **1994**, *16*, 185–205.
363. van der Zeijden, A. A. H.; Mattheis, C.; Fröhlich, R. *Organometallics* **1997**, *16*, 2651–2658.
364. Huang, J. L.; Zhang, Y. H.; Huang, Q. L.; Qian, Y. L. *Inorg. Chem. Commun.* **1999**, *2*, 104–106.
365. Krut'ko, D. P.; Borzov, M. V.; Veksler, E. N.; Churakov, A. V.; Mach, K. *Polyhedron* **2003**, *22*, 2885–2894.
366. Li, Z.; Huang, J. L.; Qian, Y. L.; Chan, A. S. C.; Leung, K. S. Y.; Wong, W. T. *Inorg. Chem. Commun.* **1999**, *2*, 396–398.
367. Jutzi, P.; Redeker, T. *Eur. J. Inorg. Chem.* **1998**, 663–674.
368. Flores, J. C.; Chien, J. C. W.; Rausch, M. D. *Organometallics* **1994**, *13*, 4140–4142.
369. van der Zeijden, A. A. H. *J. Organomet. Chem.* **1996**, *518*, 147–153.
370. Jutzi, P.; Siemeling, U. *J. Organomet. Chem.* **1995**, *500*, 175–185.
371. Jutzi, P.; Kleimeier, J. *J. Organomet. Chem.* **1995**, *486*, 287–289.
372. Flores, J. C.; Chien, J. C. W.; Rausch, M. D. *Macromolecules* **1996**, *29*, 8030–8035.
373. Chien, J. C. W.; Yu, Z. T.; Marques, M. M.; Flores, J. C.; Rausch, M. D. *J. Polym. Sci., Pol. Chem.* **1998**, *36*, 319–328.
374. Jutzi, P.; Redeker, T.; Neumann, B.; Stämmler, H. G. *J. Organomet. Chem.* **1997**, *533*, 237–245.
375. Herrmann, W. A.; Morawietz, M. J. A.; Priemeier, T.; Mashima, K. *J. Organomet. Chem.* **1995**, *486*, 291–295.
376. Enders, M.; Rudolph, R.; Pritzkow, H. *Chem. Ber.* **1996**, *129*, 459–463.
377. Enders, M.; Rudolph, R.; Pritzkow, H. *J. Organomet. Chem.* **1997**, *549*, 251–256.
378. Cuenca, T.; Royo, P. *Coord. Chem. Rev.* **1999**, *195*, 447–498.
379. Churakov, A. V.; Lemenovskii, D. A.; Kuzmina, L. G. *J. Organomet. Chem.* **1995**, *489*, C81–C83.
380. Ciruelos, S.; Cuenca, T.; Gómez-Sal, P.; Manzanero, A.; Royo, P. *Organometallics* **1995**, *14*, 177–185.
381. Buitrago, O.; Jiménez, G.; Cuenca, T. *J. Organomet. Chem.* **2003**, *683*, 70–76.
382. Royo, B.; Royo, P.; Cadenas, L. M. *J. Organomet. Chem.* **1998**, *551*, 293–297.
383. Vázquez, A. B.; Royo, P.; Herdtweck, E. *J. Organomet. Chem.* **2003**, *683*, 155–164.
384. Murphy, E. F.; Yu, P. H.; Dietrich, S.; Roesky, H. W.; Parisini, E.; Noltemeyer, M. *J. Chem. Soc., Dalton Trans.* **1996**, 1983–1987.
385. Gómez-García, R.; Royo, P. *J. Organomet. Chem.* **1999**, *583*, 86–93.
386. Cano, A. M.; Cano, J.; Gómez-Sal, P.; Manzanero, A.; Royo, P. *Inorg. Chim. Acta* **1998**, *280*, 1–7.
387. Mkoyan, S. G.; Aliev, Z. G.; Urazovskii, I. F.; Atovmyan, L. O.; Nifantev, I. E.; Butakov, K. A. *Russ. Chem. Bull.* **1996**, *45*, 2154–2156.
388. Jung, J.; Noh, S. K.; Lee, D. H.; Park, S. K.; Kim, H. *J. Organomet. Chem.* **2000**, *595*, 147–152.
389. Noh, S. K.; Byun, G. G.; Lee, C. S.; Lee, D.; Yoon, K. B.; Kang, K. S. *J. Organomet. Chem.* **1996**, *518*, 1–6.
390. Sudupe, M.; Cano, J.; Royo, P.; Herdtweck, E. *Eur. J. Inorg. Chem.* **2004**, 3074–3083.
391. Cano, J.; Gómez-Sal, P.; Heinz, G.; Martínez, G.; Royo, P. *Inorg. Chim. Acta* **2003**, *345*, 15–26.
392. Cermak, J.; St'astna, L.; Sykora, J.; Cisarova, I.; Kvicala, J. *Organometallics* **2004**, *23*, 2850–2854.
393. Churakov, A. V.; Kuzmina, L. G. *Acta Crystallogr., Sect. C: Cryst. Struct. Commun.* **1996**, *52*, 3037–3038.
394. Aldridge, S.; Bresner, C. *Coord. Chem. Rev.* **2003**, *244*, 71–92.
395. Duchateau, R.; Lancaster, S. J.; Thornton-Pett, M.; Bochmann, M. *Organometallics* **1997**, *16*, 4995–5005.
396. Larkin, S. A.; Golden, J. T.; Shapiro, P. J.; Yap, G. P. A.; Foo, D. M. J.; Rheingold, A. L. *Organometallics* **1996**, *15*, 2393–2398.
397. Flores, J. C.; Hernández, R.; Royo, P.; Butt, A.; Spaniol, T. P.; Okuda, J. *J. Organomet. Chem.* **2000**, *594*, 202–210.
398. Kotov, V. V.; Avtomonov, E. V.; Sundermeyer, J.; Harms, K.; Lemenovskii, D. A. *Eur. J. Inorg. Chem.* **2002**, 678–691.
399. Koch, T.; Hey-Hawkins, E.; Galan-Fereres, M.; Eisen, M. S. *Polyhedron* **2002**, *21*, 2445–2450.
400. Huang, J. L.; Wu, T. Z.; Qian, Y. L. *Chem. Commun.* **2003**, 2816–2817.
401. Ready, T. E.; Day, R. O.; Chien, J. C. W.; Rausch, M. D. *Macromolecules* **1993**, *26*, 5822–5823.
402. Shaw, S. L.; Storhoff, J. J.; Cullison, S.; Davis, C. E.; Holloway, G.; Morris, R. J.; Huffman, J. C.; Bollinger, J. C. *Inorg. Chim. Acta* **1999**, *292*, 220–224.
403. Ready, T. E.; Chien, J. C. W.; Rausch, M. D. *J. Organomet. Chem.* **1996**, *519*, 21–28.
404. Kim, Y.; Koo, B. H.; Do, Y. *J. Organomet. Chem.* **1997**, *527*, 155–161.
405. Ready, T. E.; Chien, J. C. W.; Rausch, M. D. *J. Organomet. Chem.* **1999**, *583*, 11–27.
406. Alt, H. G.; Weis, A.; Reb, A.; Ernst, R. *Inorg. Chim. Acta* **2003**, *343*, 253–274.
407. Foster, P.; Chien, J. C. W.; Rausch, M. D. *Organometallics* **1996**, *15*, 2404–2409.
408. Ohare, D.; Murphy, V.; Diamond, G. M.; Arnold, P.; Mountford, P. *Organometallics* **1994**, *13*, 4689–4694.
409. Stojkovic, O.; Kaminsky, W. *Macromol. Chem. Phys.* **2004**, *205*, 357–362.
410. Xu, G. X.; Cheng, D. L. *Macromolecules* **2000**, *33*, 2825–2831.
411. Foster, P.; Rausch, M. D.; Chien, J. C. W. *J. Organomet. Chem.* **1998**, *571*, 171–181.
412. Thomas, E. J.; Rausch, M. D.; Chien, J. C. W. *Organometallics* **2000**, *19*, 5744–5749.
413. Foster, P.; Rausch, M. D.; Chien, J. C. W. *J. Organomet. Chem.* **1997**, *527*, 71–74.
414. Tian, G. L.; Xu, S. S.; Zhang, Y. Q.; Wang, B. Q.; Zhou, X. Z. *J. Organomet. Chem.* **1998**, *558*, 231–233.
415. Knjazhanski, S. Y.; Moreno, G.; Cadenas, G.; Belsky, V. K.; Bulychev, B. M. *Tetrahedron* **1999**, *55*, 1639–1646.
416. Schneider, N.; Proscenc, M. H.; Brintzinger, H. H. *J. Organomet. Chem.* **1997**, *546*, 291–295.
417. Flores, J. C.; Ready, T. E.; Chien, J. C. W.; Rausch, M. D. *J. Organomet. Chem.* **1998**, *562*, 11–15.
418. Pevec, A. *Acta Chim. Slov.* **2003**, *50*, 199–206.
419. Erben, M.; Cisarova, I.; Vinklarek, J.; Holeccek, J. *Acta Crystallogr., Sect. E: Struct. Rep. Online* **2004**, *60*, M1120–M1121.
420. Lensink, C.; Gainsford, G. J.; Brandsma, M. *Acta Crystallogr., Sect. E: Struct. Rep. Online* **2001**, *57*, M211–M212.
421. Lensink, C.; Gainsford, G. J.; Hosie, C. F. *Acta Crystallogr., Sect. E: Struct. Rep. Online* **2001**, *57*, m293–m294.
422. Hafner, A.; Okuda, J. *Organometallics* **1993**, *12*, 949–950.

423. Fedorov, A. V.; Snively, D. L. *J. Phys. Chem. A* **1999**, *103*, 7795–7799.
424. Weiss, T.; Natarajan, K.; Lang, H.; Holze, R. *J. Electroanal. Chem.* **2002**, *533*, 127–133.
425. Kunkely, H.; Vogler, A. *J. Photochem. Photobiol. A: Chem.* **1998**, *119*, 187–190.
426. Diefenbach, A.; Bickelhaupt, F. M. *Z. Anorg. Allg. Chem.* **1999**, *625*, 892–900.
427. Pathak, A. K.; Mittal, A. K.; Shukla, P. R. *Synth. React. Inorg. Met.-Org. Chem.* **1995**, *25*, 163–181.
428. Roesky, H. W.; Leichtweis, I.; Noltemeyer, M. *Inorg. Chem.* **1993**, *32*, 5102–5104.
429. Ellis, J. E.; Frerichs, S. R.; Stein, B. K. *Organometallics* **1993**, *12*, 1048–1057.
430. Wilson, A. M.; West, F. G.; Arif, A. M.; Ernst, R. D. *J. Am. Chem. Soc.* **1995**, *117*, 8490–8491.
431. Alvanipour, A.; Atwood, J. L.; Bott, S. G.; Junk, P. C.; Kynast, U. H.; Prinz, H. *J. Chem. Soc., Dalton Trans.* **1998**, 1223–1228.
432. Seaburg, J. K.; Fischer, P. J.; Young, V. G.; Ellis, J. E. *Angew. Chem., Int. Ed.* **1998**, *37*, 155–158.
433. Liu, F. Q.; Kuhn, A.; Herbstimer, R.; Stalke, D.; Roesky, H. W. *Angew. Chem., Int. Ed. Engl.* **1994**, *33*, 555–556.
434. Pevec, A.; Demsar, A.; Gramlich, V.; Petricek, S.; Roesky, H. W. *J. Chem. Soc., Dalton Trans.* **1997**, 2215–2216.
435. Demsar, A.; Pevec, A.; Golic, L.; Petricek, S.; Petric, A.; Roesky, H. W. *Chem. Commun.* **1998**, 1029–1030.
436. Murphy, E. F.; Murugavel, R.; Roesky, H. W. *Chem. Rev.* **1997**, *97*, 3425–3468.
437. Yu, P. H.; Muller, P.; Said, M. A.; Roesky, H. W.; Uson, I.; Bai, G. C.; Noltemeyer, M. *Organometallics* **1999**, *18*, 1669–1674.
438. Yu, P. H.; Muller, P.; Roesky, H. W.; Noltemeyer, M.; Demsar, A.; Uson, I. *Angew. Chem., Int. Ed.* **1999**, *38*, 3319–3321.
439. Wessel, H.; Montero, M. L.; Rennekamp, C.; Roesky, H. W.; Yu, P. H.; Uson, I. *Angew. Chem., Int. Ed.* **1998**, *37*, 843–845.
440. Gibson, V. C.; Spitzmesser, S. K. *Chem. Rev.* **2003**, *103*, 283–315.
441. Conti, G.; Arribas, G.; Altomare, A.; Ciardelli, F. *J. Mol. Catal.* **1994**, *89*, 41–50.
442. Fukui, Y.; Murata, M. *Macromol. Chem. Phys.* **2001**, *202*, 3205–3209.
443. Tomotsu, N.; Ishihara, N.; Newman, T. H.; Malanga, M. T. *J. Mol. Catal. A: Chem.* **1998**, *128*, 167–190.
444. Kawabe, M.; Murata, M. *Macromol. Chem. Phys.* **2001**, *202*, 2440–2446.
445. Lee, D. H.; Noh, S. K.; Yoon, K. B.; Lee, E. H.; Koo, S. Y. *Polym.-Korea* **1996**, *20*, 470–475.
446. Kim, J.; Kim, K. H.; Cho, J. C.; Kwak, S.; Kim, K. U.; Jo, W. H.; Yoon, H. S.; Lim, D. S. *J. Polym. Sci. Pol. Chem.* **1998**, *36*, 1733–1741.
447. Po, R.; Cardi, N.; Abis, L. *Polymer* **1998**, *39*, 959–964.
448. Nakatani, H.; Nitta, K.; Takata, T.; Soga, K. *Polym. Bull.* **1997**, *38*, 43–48.
449. Nakatani, H.; Nitta, K.; Soga, K.; Takata, T. *Polymer* **1997**, *38*, 4751–4756.
450. Thomann, R.; Sernetz, F. G.; Heinemann, J.; Steinmann, S.; Mulhaupt, R.; Kressler, J. *Macromolecules* **1997**, *30*, 8401–8409.
451. Kaminsky, W.; Strubel, C. *Macromol. Chem. Phys.* **2000**, *201*, 2519–2531.
452. Huang, D. D.; Zhu, F. M.; Lin, S. A. *Acta Polym. Sin.* **2001**, 580–583.
453. Dias, M. L.; Bruno, M. I.; Maria, L. C. D. *Eur. Polym. J.* **1997**, *33*, 1559–1562.
454. Ricci, G.; Italia, S.; Porri, L. *Macromolecules* **1994**, *27*, 868–869.
455. Kaminsky, W. *J. Chem. Soc., Dalton Trans.* **1998**, 1413–1418.
456. Kaminsky, W.; Lenk, S.; Scholz, V.; Roesky, H. W.; Herzog, A. *Macromolecules* **1997**, *30*, 7647–7650.
457. Schellenberg, J. J. *Polym. Sci. Pol. Chem.* **2000**, *38*, 2428–2439.
458. Schellenberg, J.; Newman, T. H. *J. Polym. Sci. Pol. Chem.* **2000**, *38*, 3476–3485.
459. Schwecke, C.; Kaminsky, W. *Macromol. Rapid Commun.* **2001**, *22*, 508–512.
460. Kaminsky, W.; Hinrichs, B.; Rehder, D. *Polymer* **2002**, *43*, 7225–7229.
461. Chu, K. J.; Ha, J. W. *Mater. Lett.* **1998**, *33*, 301–304.
462. Daniello, C.; Decandia, F.; Oliva, L.; Vittoria, V. *J. Appl. Polym. Sci.* **1995**, *58*, 1701–1706.
463. Aaltonen, P.; Seppala, J. *Eur. Polym. J.* **1994**, *30*, 683–687.
464. Kim, K. H.; Jo, W. H.; Kwak, S.; Kim, K. U.; Hwang, S. S.; Kim, J. *Macromolecules* **1999**, *32*, 8703–8710.
465. Naga, N.; Imanishi, Y. *J. Polym. Sci. Pol. Chem.* **2003**, *41*, 939–946.
466. Ban, H. T.; Tsunogae, Y.; Shiono, T. *J. Polym. Sci. Pol. Chem.* **2004**, *42*, 2698–2704.
467. Endo, K.; Sendo, K. *Polym. J.* **1999**, *31*, 817–821.
468. Liu, S. S.; Huang, B. T. *Macromol. Rapid Commun.* **1999**, *20*, 484–486.
469. Oliva, H.; Leal, G.; Ismayel, A.; Arribas, G.; Bronco, S. *e-Polymers, on line computer file, Paper no. 2*, **2002**.
470. Munoz-Escalona, A.; Cruz, V.; Mena, N.; Martinez, S.; Martinez-Salazar, J. *Polymer* **2002**, *43*, 7017–7026.
471. Rabagliati, F. M.; Perez, M. A.; Cancino, R. A.; Soto, M. A.; Rodriguez, F. J.; Leon, A. G.; Ayal, H. A.; Quijada, R. *Bol. Soc. Chil. Quim.* **2000**, *45*, 219–226.
472. Rabagliati, F. M.; Cancino, R. A.; Rodriguez, F. J. *Polym. Bull.* **2001**, *46*, 427–434.
473. Rabagliati, F. M.; Perez, M. A.; Soto, M. A.; de Ilarduya, A. M.; Munoz-Guerra, S. *Eur. Polym. J.* **2001**, *37*, 1001–1006.
474. Schellenberg, J.; Newman, T. H. *Eur. Polym. J.* **2001**, *37*, 1733–1739.
475. Severn, J. R.; Chadwick, J. C. *Macromol. Chem. Phys.* **2004**, *205*, 1987–1994.
476. Fan, R.; Cao, K.; Li, B. F.; Fan, H.; Li, B. G. *Eur. Polym. J.* **2001**, *37*, 2335–2338.
477. Longo, P.; Proto, A.; Oliva, P.; Zambelli, A. *Macromolecules* **1996**, *29*, 5500–5501.
478. Kim, H. J.; Maria, L. C. D. *Eur. Polym. J.* **1994**, *30*, 1295–1299.
479. Kasi, R. M.; Coughlin, E. B. *Macromolecules* **2003**, *36*, 6300–6304.
480. Jamanek, D.; Woyda, A.; Skupinski, W. *Appl. Organomet. Chem.* **2002**, *16*, 575–579.
481. Zhu, N.; Tang, T.; Wang, L. M.; Cui, D. M.; Feng, Z. L.; Huang, B. T. *Acta Chim. Sinica.* **2001**, *59*, 426–432.
482. Cermak, J.; Kvalova, M.; Blechta, V.; Capka, M.; Bastl, Z. *J. Organomet. Chem.* **1996**, *509*, 77–84.
483. Soga, K.; Suzuki, Y.; Uozumi, T.; Kaji, E. *J. Polym. Sci., Pol. Chem.* **1997**, *35*, 291–297.
484. Forte, M. M. D.; da Cunha, F. O. V.; dos Santos, J. H. Z.; Zacca, J. J. *Polymer* **2003**, *44*, 1377–1384.
485. Miyazawa, A. *J. Chem. Res. S* **2002**, 500–502.
486. Tinkler, S.; Deeth, R. J.; Duncalf, D. J.; McCamley, A. *Chem. Commun.* **1996**, 2623–2624.
487. Duncalf, D. J.; Wade, H. J.; Waterson, C.; Derrick, P. J.; Haddleton, D. M.; McCamley, A. *Macromolecules* **1996**, *29*, 6399–6403.
488. Wu, T. Z.; Qian, Y. L.; Huang, J. L. *J. Mol. Catal. A: Chem.* **2004**, *214*, 227–229.
489. Sun, X. Q.; Xie, J.; Zhang, H.; Huang, J. L. *Eur. Polym. J.* **2004**, *40*, 1903–1908.
490. Gentil, S.; Pirio, N.; Meunier, P.; Gallou, F.; Paquette, L. A. *Eur. Polym. J.* **2004**, *40*, 2241–2246.
491. Ewart, S. W.; Sarsfield, M. J.; Jeremic, D.; Tremblay, T. L.; Williams, E. F.; Baird, M. C. *Organometallics* **1998**, *17*, 1502–1510.

492. Ready, T. E.; Gurge, R.; Chien, J. C. W.; Rausch, M. D. *Organometallics* **1998**, *17*, 5236–5239.
493. Grassi, A.; Zambelli, A.; Laschi, F. *Organometallics* **1996**, *15*, 480–482.
494. Mahanthappa, M. K.; Waymouth, R. M. *J. Am. Chem. Soc.* **2001**, *123*, 12093–12094.
495. Patten, T. E.; Novak, B. M. *J. Am. Chem. Soc.* **1996**, *118*, 1906–1916.
496. Patten, T. E.; Novak, B. M. *Macromolecules* **1993**, *26*, 436–439.
497. Goodwin, A.; Novak, B. M. *Macromolecules* **1994**, *27*, 5520–5522.
498. Willey, G. R.; Butcher, M. L.; McPartlin, M.; Scowen, I. J. *J. Chem. Soc., Dalton Trans.* **1994**, 305–309.
499. Deckers, P. J. W.; Hessen, B. *Organometallics* **2002**, *21*, 5564–5575.
500. Knjazhanski, S. Y.; Cadenas, G.; Garcia, M.; Perez, C. M.; Nifant'ev, I. E.; Kashulin, I. A.; Ivchenko, P. V.; Lyssenko, K. A. *Organometallics* **2002**, *21*, 3094–3099.
501. Skoog, S. J.; Mateo, C.; Lavoie, G. G.; Hollander, F. J.; Bergman, R. G. *Organometallics* **2000**, *19*, 1406–1421.
502. Cozzi, P. G.; Carofiglio, T.; Floriani, C.; Chiesivilla, A.; Rizzoli, C. *Organometallics* **1993**, *12*, 2845–2848.
503. Schleth, F.; Vogler, T.; Harms, K.; Studer, A. *Chem. Eur. J.* **2004**, *10*, 4171–4185.
504. Avent, A. G.; Hitchcock, P. B.; Leigh, G. J.; Togrou, M. J. *Organomet. Chem.* **2003**, *669*, 87–100.
505. Andrés, R.; Galakhov, M. V.; Martín, A.; Mena, M.; Santamaría, C. *Organometallics* **1994**, *13*, 2159–2163.
506. Andrés, R.; Gómez-Sal, P.; de Jesús, E.; Martín, A.; Mena, M.; Yélamos, C. *Angew. Chem., Int. Ed. Engl.* **1997**, *36*, 115–117.
507. Andrés, R.; Galakhov, M.; Martín, A.; Mena, M.; Santamaría, C. *J. Chem. Soc., Chem. Commun.* **1995**, 551–552.
508. Kahlert, S.; Górls, H.; Scholz, J. *Angew. Chem., Int. Ed.* **1998**, *37*, 1857–1861.
509. Buitrago, O.; de Arellano, C. R.; Jiménez, G.; Cuenca, T. *Organometallics* **2004**, *23*, 5873–5876.
510. Pellicchia, C.; Royo, P.; Cuenca, T.; Galakhov, M. *Organometallics* **2001**, *20*, 5237–5240.
511. Robertson, A. H. J.; McQuillan, G. P.; McKean, D. C. *J. Chem. Soc., Dalton Trans.* **1995**, 3941–3953.
512. Bochmann, M. In *Comprehensive Organometallic Chemistry II*; Abel, E. W., Stone, F. G. A.; Wilkinson, G., Eds.; Elsevier: Oxford, 1995; Vol. 4, p 374.
513. Andrés, R.; Galakhov, M.; Gómez-Sal, M. P.; Martín, A.; Mena, M.; Santamaría, C. *Chem. Eur. J.* **1998**, *4*, 1206–1213.
514. Tomotsu, N.; Ishihara, N. *Recent development of catalysts for syndiospecific polymerization of styrene*; Elsevier: Amsterdam, 1999; Vol. 121, pp 269–276.
515. Wang, Q. Y.; Gillis, D. J.; Quyoum, R.; Jeremic, D.; Tudoret, M. J.; Baird, M. C. *J. Organomet. Chem.* **1997**, *527*, 7–14.
516. Gillis, D. J.; Tudoret, M. J.; Baird, M. C. *J. Am. Chem. Soc.* **1993**, *115*, 2543–2545.
517. Gillis, D. J.; Quyoum, R.; Tudoret, M. J.; Wang, Q. Y.; Jeremic, D.; Roszak, A. W.; Baird, M. C. *Organometallics* **1996**, *15*, 3600–3605.
518. Ewart, S. W.; Baird, M. C. *Top. Catal.* **1999**, *7*, 1–8.
519. Wang, Q. Y.; Quyoum, R.; Gillis, D. J.; Tudoret, M. J.; Jeremic, D.; Hunter, B. K.; Baird, M. C. *Organometallics* **1996**, *15*, 693–703.
520. Pellicchia, C.; Immirzi, A.; Grassi, A.; Zambelli, A. *Organometallics* **1993**, *12*, 4473–4478.
521. Quyoum, R.; Wang, Q. Y.; Tudoret, M. J.; Baird, M. C.; Gillis, D. J. *J. Am. Chem. Soc.* **1994**, *116*, 6435–6436.
522. Murray, M. C.; Baird, M. C. *J. Polym. Sci., Pol. Chem.* **2000**, *38*, 3966–3976.
523. Sassmannshausen, J.; Bochmann, M. E.; Rosch, J.; Lilje, D. *J. Organomet. Chem.* **1997**, *548*, 23–28.
524. Pellicchia, C.; Pappalardo, D.; Oliva, L.; Zambelli, A. *J. Am. Chem. Soc.* **1995**, *117*, 6593–6594.
525. Kucht, A.; Kucht, H.; Barry, S.; Chien, J. C. W.; Rausch, M. D. *Organometallics* **1993**, *12*, 3075–3078.
526. Murray, M. C.; Baird, M. C. *J. Mol. Catal. A. Chem.* **1998**, *128*, 1–4.
527. Murray, M. C.; Baird, M. C. *Can. J. Chem., Rev. Can. Chim.* **2001**, *79*, 1012–1018.
528. Jeremic, D.; Wang, Q. Y.; Quyoum, R.; Baird, M. C. *J. Organomet. Chem.* **1995**, *497*, 143–147.
529. Liu, T. M.; Baker, W. E.; Schytt, V.; Jones, T.; Baird, M. C. *J. Appl. Polym. Sci.* **1996**, *62*, 1807–1818.
530. Kawabe, M.; Murata, M. *J. Polym. Sci., Pol. Chem.* **2001**, *39*, 3692–3706.
531. Kucht, H.; Kucht, A.; Chien, J. C. W.; Rausch, M. D. *Appl. Organomet. Chem.* **1994**, *8*, 393–396.
532. Ioku, A.; Shiono, T.; Ikeda, T. *J. Macromol. Sci., Pure Appl. Chem.* **2002**, *39*, 397–404.
533. Pellicchia, C.; Pappalardo, D.; Darco, M.; Zambelli, A. *Macromolecules* **1996**, *29*, 1158–1162.
534. Pellicchia, C.; Pappalardo, D.; Oliva, L.; Mazzeo, M.; Gruter, G. J. *Macromolecules* **2000**, *33*, 2807–2814.
535. Pellicchia, C.; Pappalardo, D.; Gruter, G. J. *Macromolecules* **1999**, *32*, 4491–4493.
536. Pellicchia, C.; Mazzeo, M.; Gruter, G. J. *Macromol. Rapid Commun.* **1999**, *20*, 337–340.
537. Song, F. Q.; Pappalardo, D.; Johnson, A. F.; Rieger, B.; Bochmann, M. *J. Polym. Sci., Pol. Chem.* **2002**, *40*, 1484–1497.
538. Bryliakov, K. P.; Semikolenova, N. V.; Zakharov, V. A.; Talsi, E. P. *J. Organomet. Chem.* **2003**, *683*, 23–28.
539. Chen, R.; Xie, M. R.; Wu, Q.; Lin, S. G. *J. Polym. Sci., Pol. Chem.* **2000**, *38*, 411–415.
540. Xu, G. X. *Macromolecules* **1998**, *31*, 586–591.
541. Jensen, T. R.; Yoon, S. C.; Dash, A. K.; Luo, L. B.; Marks, T. J. *J. Am. Chem. Soc.* **2003**, *125*, 14482–14494.
542. Barsan, F.; Karam, A. R.; Parent, M. A.; Baird, M. C. *Macromolecules* **1998**, *31*, 8439–8447.
543. Barsan, F.; Baird, M. C. *J. Chem. Soc., Chem. Commun.* **1995**, 1065–1066.
544. Wang, Q. Y.; Baird, M. C. *Macromolecules* **1995**, *28*, 8021–8027.
545. Kumar, K. R.; Hall, C.; Penciu, A.; Drewitt, M. J.; McInenly, P. J.; Baird, M. C. *J. Polym. Sci., Pol. Chem.* **2002**, *40*, 3302–3311.
546. Kumar, K. R.; Penciu, A.; Drewitt, M. J.; Baird, M. C. *J. Organomet. Chem.* **2004**, *689*, 2900–2904.
547. Pellicchia, C.; Grassi, A. *Top. Catal.* **1999**, *7*, 125–132.
548. Zambelli, A.; Pellicchia, C.; Proto, A. *Macromol. Symp.* **1995**, *89*, 373–382.
549. Zambelli, A.; Pellicchia, C.; Oliva, L.; Laschi, F. *Macromol. Chem. Phys.* **1995**, *196*, 1093.
550. Grassi, A.; Pellicchia, C.; Oliva, L.; Laschi, F. *Macromol. Chem. Phys.* **1995**, *196*, 1093–1100.
551. Grassi, A.; Lamberti, C.; Zambelli, A.; Mingozzi, I. *Macromolecules* **1997**, *30*, 1884–1889.
552. Grassi, A.; Saccheo, S.; Zambelli, A.; Laschi, F. *Macromolecules* **1998**, *31*, 5588–5591.
553. Newman, T. H.; Malanga, M. T. *J. Macromol. Sci., Pure Appl. Chem.* **1997**, *A34*, 1921–1927.
554. Campbell, R. E.; Newman, T. H.; Malanga, M. T. *Macromol. Symp.* **1995**, *97*, 151–160.
555. Williams, E. F.; Murray, M. C.; Baird, M. C. *Macromolecules* **2000**, *33*, 261–268.
556. Sarsfield, M. J.; Ewart, S. W.; Tremblay, T. L.; Roszak, A. W.; Baird, M. C. *J. Chem. Soc., Dalton Trans.* **1997**, 3097–3104.
557. Tremblay, T. L.; Ewart, S. W.; Sarsfield, M. J.; Baird, M. C. *Chem. Commun.* **1997**, 831–832.
558. Ewart, S. W.; Sarsfield, M. J.; Williams, E. F.; Baird, M. C. *J. Organomet. Chem.* **1999**, *579*, 106–113.

559. Tobisch, S.; Ziegler, T. *Organometallics* **2003**, *22*, 5392–5405.
560. Tobisch, S.; Ziegler, T. *J. Am. Chem. Soc.* **2004**, *126*, 9059–9071.
561. Blok, A. N. J.; Budzelaar, P. H. M.; Gal, A. W. *Organometallics* **2003**, *22*, 2564–2570.
562. de Bruin, T. J. M.; Magna, L.; Raybaud, P.; Toulhoat, H. *Organometallics* **2003**, *22*, 3404–3413.
563. Chen, Y. X.; Stern, C. L.; Yang, S. T.; Marks, T. J. *J. Am. Chem. Soc.* **1996**, *118*, 12451–12452.
564. Martín, A.; Mena, M.; Yélamos, C.; Serrano, R.; Raithby, P. R. *J. Organomet. Chem.* **1994**, *467*, 79–84.
565. Haaland, A.; Volden, H. V.; Ostby, K. A.; Mena, M.; Yelamos, C.; Palacios, F. J. *Mol. Struct.* **2001**, *567*, 295–301.
566. Gómez-Sal, P.; Martín, A.; Mena, M.; Yélamos, C. *J. Chem. Soc., Chem. Commun.* **1995**, 2185–2186.
567. Gómez-Sal, P.; Irigoyen, A. M.; Martín, A.; Mena, M.; Monge, M.; Yélamos, C. *J. Organomet. Chem.* **1995**, *494*, C19–C21.
568. Irigoyen, A. M.; Martín, A.; Mena, M.; Palacios, F.; Yélamos, C. *J. Organomet. Chem.* **1995**, *494*, 255–259.
569. Galakhov, M.; Martín, A.; Mena, M.; Palacios, F.; Yélamos, C.; Raithby, P. R. *Organometallics* **1995**, *14*, 131–136.
570. Galakhov, M.; Gómez-Sal, P.; Martín, A.; Mena, M.; Yélamos, C. *Eur. J. Inorg. Chem.* **1998**, 1319–1325.
571. Sinnema, P. J.; Spaniol, T. P.; Okuda, J. *J. Organomet. Chem.* **2000**, *598*, 179–181.
572. Rhodes, B.; Rausch, M. D.; Chien, J. C. W. *J. Polym. Sci., Pol. Chem.* **2001**, *39*, 313–319.
573. Laurent, F.; Legros, J. P. *Acta Crystallogr. Sect., C: Cryst. Struct. Commun.* **1993**, *49*, 540–542.
574. Pupi, R. M.; Coalter, J. N.; Petersen, J. L. *J. Organomet. Chem.* **1995**, *497*, 17–25.
575. Martins, A. M.; Ascenso, J. R.; de Azevedo, C. G.; Calhorda, M. J.; Dias, A. R.; Rodrigues, S. S.; Toupet, L.; de Leonardis, P.; Veiros, L. F. *J. Chem. Soc., Dalton Trans.* **2000**, 4332–4338.
576. Ascenso, J. R.; de Azevedo, C. G.; Correia, M. J.; Dias, A. R.; Duarte, M. T.; da Silva, J. L. F.; Gomes, P. T.; Lourenco, F.; Martins, A. M.; Rodrigues, S. S. *J. Organomet. Chem.* **2001**, *632*, 58–66.
577. Nomura, K.; Fujii, K. *Organometallics* **2002**, *21*, 3042–3049.
578. Nomura, K.; Fujii, K. *Science and Technology in Catalysis 2002*; Kodansha Ltd Eds.; Tokyo, 2003, *145*, 121–124.
579. Wraage, K.; Kunzel, A.; Noltemeyer, M.; Schmidt, H. G.; Roesky, H. W. *Angew. Chem., Int. Ed. Engl.* **1995**, *34*, 2645–2647.
580. Gómez, R.; Gómez-Sal, P.; Martín, A.; Nunez, A.; del Real, P. A.; Royo, P. *J. Organomet. Chem.* **1998**, *564*, 93–100.
581. Ciruelos, S.; Cuenca, T.; Gómez, R.; Gómez-Sal, P.; Manzanero, A.; Royo, P. *Organometallics* **1996**, *15*, 5577–5585.
582. Cano, J.; Royo, P.; Jacobsen, H.; Blaque, O.; Berke, H.; Herdtweck, E. *Eur. J. Inorg. Chem.* **2003**, 2463–2474.
583. Braunschweig, H.; Breitling, F. M.; von Koblinski, C.; White, A. J. P.; Williams, D. J. *Dalton Trans.* **2004**, 938–943.
584. Braunschweig, H.; von Koblinski, C.; Wang, R. M. *Eur. J. Inorg. Chem.* **1999**, 69–73.
585. Bochmann, M.; Bwembya, G. C.; Whilton, N.; Song, X. J.; Hursthouse, M. B.; Coles, S. J.; Karaulov, A. *J. Chem. Soc., Dalton Trans.* **1995**, 1887–1892.
586. Lee, M. H.; Hwang, J. W.; Kim, Y.; Han, Y. Y.; Do, Y. *Organometallics* **2000**, *19*, 5514–5517.
587. Wang, H. P.; Wang, Y. R.; Li, H. W.; Xie, Z. W. *Organometallics* **2001**, *20*, 5110–5118.
588. Wang, J. H.; Zheng, C.; Maguire, J. A.; Hosmane, N. S. *Organometallics* **2003**, *22*, 4839–4841.
589. Novak, B. M.; Patten, T. E.; Hoff, S. M. *J. Macromol. Sci., Pure Appl. Chem.* **1994**, *A31*, 1619–1626.
590. Maxein, G.; Mayer, S.; Zentel, R. *Macromolecules* **1999**, *32*, 5747–5754.
591. Timonen, S.; Pakkanen, T. T.; Iiskola, E. I. *J. Mol. Catal. A: Chem.* **1999**, *148*, 235–244.
592. Morillo, A.; Chirinos, J.; Rajmankina, T.; Ibarra, D.; Arevalo, J.; Parada, A. *J. Chem. Res. S* **2003**, 238–239.
593. Valade, L.; Danjoy, C.; Chansou, B.; Riviere, E.; Pellegatta, J. L.; Choukroun, R.; Cassoux, P. *Appl. Organomet. Chem.* **1998**, *12*, 173–187.
594. Scholz, J.; Kahlert, S.; Górls, H. *Organometallics* **1998**, *17*, 2876–2884.
595. Asmus, S. M. F.; Regitz, M. *Tetrahedron Lett.* **2001**, *42*, 7543–7545.
596. Scholz, J.; Hadi, G. A.; Thiele, K. H.; Górls, H.; Weimann, R.; Schumann, H.; Sieler, J. *J. Organomet. Chem.* **2001**, *626*, 243–259.
597. Amor, F.; Gómez-Sal, P.; Royo, P.; Okuda, J. *Organometallics* **2000**, *19*, 5168–5173.
598. Bottcher, P.; Wraage, K.; Roesky, H. W.; Lanfranchi, M.; Tiripicchio, A. *Chem. Ber. Recl.* **1997**, *130*, 1787–1790.
599. Tabernero, V.; Cuenca, T.; Herdtweck, E. *Eur. J. Inorg. Chem.* **2004**, 3154–3162.
600. Tabernero, V.; Cuenca, T. *Eur. J. Inorg. Chem.* **2005**, 338–346.
601. Tomaszewski, R.; Arif, A. M.; Ernst, R. D. *J. Chem. Soc., Dalton Trans.* **1999**, 1883–1890.
602. Tomaszewski, R.; Lam, K. C.; Rheingold, A. L.; Ernst, R. D. *Organometallics* **1999**, *18*, 4174–4182.
603. Mountford, P. *Chem. Commun.* **1997**, 2127–2134.
604. Dunn, S. C.; Batsanov, A. S.; Mountford, P. *J. Chem. Soc., Chem. Commun.* **1994**, 2007–2008.
605. Dunn, S. C.; Mountford, P.; Robson, D. A. *J. Chem. Soc., Dalton Trans.* **1997**, 293–304.
606. Jagirdar, B. R.; Murugavel, R.; Schmidt, H. G. *Inorg. Chim. Acta* **1999**, *292*, 105–107.
607. Grigsby, W. J.; Olmstead, M. M.; Power, P. P. *J. Organomet. Chem.* **1996**, *513*, 173–180.
608. Ascenso, J. R.; de Azevedo, C. G.; Dias, A. R.; Duarte, M. T.; Eleuterio, I.; Ferreira, M. J.; Gomes, P. T.; Martins, A. M. *J. Organomet. Chem.* **2001**, *632*, 17–26.
609. Zhang, S.; Piers, W. E.; Gao, X. L.; Parvez, M. *J. Am. Chem. Soc.* **2000**, *122*, 5499–5509.
610. Zhang, S. B.; Piers, W. E. *Organometallics* **2001**, *20*, 2088–2092.
611. Dias, A. R.; Duarte, M. T.; Fernandes, A. C.; Fernandes, S.; Marques, M. M.; Martins, A. M.; da Silva, J. F.; Rodrigues, S. S. *J. Organomet. Chem.* **2004**, *689*, 203–213.
612. Nomura, K.; Fujita, K.; Fujiki, M. *J. Mol. Catal. A: Chem.* **2004**, *220*, 133–144.
613. Nomura, K.; Fujita, K.; Fujiki, M. *Catal. Commun.* **2004**, *5*, 413–417.
614. Retboll, M.; Ishii, Y.; Hidai, M. *Organometallics* **1999**, *18*, 150–155.
615. Liu, F. Q.; Herzog, A.; Roesky, H. W.; Uson, I. *Inorg. Chem.* **1996**, *35*, 741–744.
616. Hughes, A. K.; Marsh, S. M. B.; Howard, J. A. K.; Ford, P. S. *J. Organomet. Chem.* **1997**, *528*, 195–198.
617. Lancaster, S. J.; Al-Benna, S.; Thornton-Pett, M.; Bochmann, M. *Organometallics* **2000**, *19*, 1599–1608.
618. Benito, J. M.; Arévalo, S.; de Jesús, E.; de la Mata, F. J.; Flores, J. C.; Gómez, R. *J. Organomet. Chem.* **2000**, *610*, 42–48.
619. Li, Z.; Huang, J. L.; Yao, T.; Qian, Y. L.; Leng, M. Y. *J. Organomet. Chem.* **2000**, *598*, 339–347.
620. Bai, G. C.; Roesky, H. W.; Hao, H. J.; Noltemeyer, M.; Schmidt, H. G. *Inorg. Chem.* **2001**, *40*, 2424–2426.
621. Roesky, H. W.; Bai, Y.; Noltemeyer, M. *Angew. Chem., Int. Ed. Engl.* **1989**, *28*, 754–755.
622. Abarca, A.; Gómez-Sal, P.; Martín, A.; Mena, M.; Poblet, J. M.; Yélamos, C. *Inorg. Chem.* **2000**, *39*, 642–651.
623. Martín, A.; Mena, M.; Pedrez-Redondo, A.; Yelamos, C. *Inorg. Chem.* **2004**, *43*, 2491–2498.



624. García-Castro, M.; Martín, A.; Mena, M.; Pérez-Redondo, A.; Yélamos, C. *Chem. Eur. J.* **2001**, *7*, 647–651.
625. Abarca, A.; Martín, A.; Mena, M.; Yélamos, C. *Angew. Chem., Int. Ed. Engl.* **2000**, *39*, 3460–3463.
626. Abarca, A.; Galakhov, M.; Gómez-Sal, P.; Martín, A.; Mena, M.; Poblet, J. M.; Santamaría, C.; Sarasa, J. P. *Angew. Chem., Int. Ed.* **2000**, *39*, 534–537.
627. Abarca, A.; Galakhov, M. V.; Gracia, J.; Martín, A.; Mena, M.; Poblet, J. M.; Sarasa, J. P.; Yélamos, C. *Chem. Eur. J.* **2003**, *9*, 2337–2346.
628. Freitag, K.; Gracia, J.; Martín, A.; Mena, M.; Poblet, J. M.; Sarasa, J. P.; Yélamos, C. *Chem. Eur. J.* **2001**, *7*, 3645–3651.
629. Martín, A.; Mena, M.; Pérez-Redondo, A.; Yélamos, C. *Organometallics* **2002**, *21*, 3308–3310.
630. Decker, A.; Fenske, D.; Maczek, K. *Angew. Chem., Int. Ed. Engl.* **1996**, *35*, 2863–2866.
631. Gómez-Sal, P.; Martín, A.; Mena, M.; Morales, M. D.; Santamaría, C. *Chem. Commun.* **1999**, 1839–1840.
632. Straub, B. F.; Bergman, R. G. *Angew. Chem., Int. Ed. Engl.* **2001**, *40*, 4632–4635.
633. Siebeneicher, H.; Doye, S. J. *Prakt. Chem., Chem. Ztg.* **2000**, *342*, 102–106.
634. Johnson, J. S.; Bergman, R. G. *J. Am. Chem. Soc.* **2001**, *123*, 2923–2924.
635. Stephan, D. W. *Macromol. Symp.* **2001**, *173*, 105–115.
636. Stephan, D. W. *Can. J. Chem., Rev. Can. Chim.* **2002**, *80*, 125–132.
637. Stephan, D. W. *Organometallics* **2005**, *24*, 2548–2560.
638. Beddie, C.; Hollink, E.; Wei, P. R.; Stephan, D. W. *Organometallics* **2004**, *23*, 5240–5251.
639. Stephan, D. W.; Stewart, J. C.; Guerin, F.; Spence, R.; Xu, W.; Harrison, D. G. *Organometallics* **1999**, *18*, 1116–1118.
640. Stephan, D. W.; Stewart, J. C.; Guerin, F.; Courtenay, S.; Kickham, J.; Hollink, E.; Beddie, C.; Hoskin, A.; Graham, T.; Wei, P. R., *et al.* *Organometallics* **2003**, *22*, 1937–1947.
641. Rubenstahl, T.; Weller, F.; Harms, K.; Dehnicke, K.; Fenske, D.; Baum, G. *Z. Anorg. Allg. Chem.* **1994**, *620*, 1741–1749.
642. Mikoluk, M. D.; McDonald, R.; Cavell, R. G. *Inorg. Chem.* **1999**, *38*, 2791–2801.
643. Yue, N. L. S.; Stephan, D. W. *Organometallics* **2001**, *20*, 2303–2308.
644. Hollink, E.; Wei, P. R.; Stephan, D. W. *Can. J. Chem., Rev. Can. Chim.* **2004**, *82*, 1304–1313.
645. Guerin, F.; Beddie, C. L.; Stephan, D. W.; Spence, R. E. V.; Wurz, R. *Organometallics* **2001**, *20*, 3466–3471.
646. Carraz, C. A.; Stephan, D. W. *Organometallics* **2000**, *19*, 3791–3796.
647. Babu, R. P. K.; McDonald, R.; Cavell, R. G. *J. Chem. Soc., Dalton Trans.* **2001**, 2210–2214.
648. Balakrishna, M. S.; Teipel, S.; Pinkerton, A. A.; Cavell, R. G. *Inorg. Chem.* **2001**, *40*, 1802–1808.
649. Sarsfield, M. J.; Said, M.; Thornton-Pett, M.; Gerrard, L. A.; Boehmann, M. J. *Chem. Soc., Dalton Trans.* **2001**, 822–827.
650. Brown, S. J.; Gao, X. L.; Kowalchuk, M. G.; Spence, R. E. V.; Stephan, D. W.; Swabey, J. *Can. J. Chem., Rev. Can. Chim.* **2002**, *80*, 1618–1624.
651. Guerin, F.; Stephan, D. W. *Angew. Chem., Int. Ed. Engl.* **1999**, *38*, 3698–3701.
652. Kickham, J. E.; Guerin, F.; Stewart, J. C.; Stephan, D. W. *Angew. Chem., Int. Ed.* **2000**, *39*, 3263–3266.
653. Kickham, J. E.; Guerin, F.; Stewart, J. C.; Urbanska, E.; Stephan, D. W. *Organometallics* **2001**, *20*, 1175–1182.
654. Sung, R. C. W.; Courtenay, S.; McGarvey, B. R.; Stephan, D. W. *Inorg. Chem.* **2000**, *39*, 2542–2546.
655. Graham, T. W.; Kickham, J.; Courtenay, S.; Wei, P. R.; Stephan, D. W. *Organometallics* **2004**, *23*, 3309–3318.
656. Stewart, P. J.; Blake, A. J.; Mountford, P. *J. Organomet. Chem.* **1998**, *564*, 209–214.
657. Richter, J.; Edelmann, F. T.; Noltemeyer, M.; Schmidt, H. G.; Shmulinson, M.; Eisen, M. S. *J. Mol. Catal. A: Chem.* **1998**, *130*, 149–162.
658. Gómez, R.; Duchateau, R.; Chernega, A. N.; Teuben, J. H.; Edelmann, F. T.; Green, M. L. H. *J. Organomet. Chem.* **1995**, *491*, 153–158.
659. Chernega, A. N.; Gómez, R.; Green, M. L. H. *J. Chem. Soc., Chem. Commun.* **1993**, 1415–1417.
660. Gómez, R.; Duchateau, R.; Chernega, A. N.; Meetsma, A.; Edelmann, F. T.; Teuben, J. H.; Green, M. L. H. *J. Chem. Soc., Dalton Trans.* **1995**, 217–225.
661. Guiducci, A. E.; Cowley, A. R.; Skinner, M. E. G.; Mountford, P. *J. Chem. Soc., Dalton Trans.* **2001**, 1392–1394.
662. Sita, L. R.; Babcock, J. R. *Organometallics* **1998**, *17*, 5228–5230.
663. Koterwas, L. A.; Fetting, J. C.; Sita, L. R. *Organometallics* **1999**, *18*, 4183–4190.
664. Babcock, J. R.; Incarvito, C.; Rheingold, A. L.; Fetting, J. C.; Sita, L. R. *Organometallics* **1999**, *18*, 5729–5732.
665. Hagadorn, J. R.; McNevin, M. J. *Organometallics* **2003**, *22*, 609–611.
666. Sarasa, J.; Poblet, J. M.; Benard, M. *Organometallics* **2000**, *19*, 2264–2272.
667. Ishino, H.; Takemoto, S.; Hirata, K.; Kanaizuka, Y.; Hidai, M.; Nabika, M.; Seki, Y.; Miyatake, T.; Suzuki, N. *Organometallics* **2004**, *23*, 4544–4546.
668. Mizobe, Y.; Yokobayashi, Y.; Oshita, H.; Takahashi, T.; Hidai, M. *Organometallics* **1994**, *13*, 3764–3766.
669. Ishino, H.; Nagano, T.; Kuwata, S.; Yokobayashi, Y.; Ishii, Y.; Hidai, M. *Organometallics* **2001**, *20*, 188–198.
670. Taberero, V.; Cuenca, T.; Herdtweck, E. *J. Organomet. Chem.* **2002**, *663*, 173–182.
671. Tamm, M.; Randall, S.; Bannenberg, T.; Herdtweck, E. *Chem. Commun.* **2004**, 876–877.
672. Kretschmer, W. P.; Dijkhuis, C.; Meetsma, A.; Hessen, B.; Teuben, J. H. *Chem. Commun.* **2002**, 608–609.
673. Mösch-Zanetti, N. C.; Hewitt, M.; Schneider, T. R.; Magull, J. *Eur. J. Inorg. Chem.* **2002**, 1181–1185.
674. Diamond, G. M.; Jordan, R. F.; Petersen, J. L. *Organometallics* **1996**, *15*, 4030–4037.
675. Sernetz, F. G.; Mulhaupt, R.; Waymouth, R. M. *Macromol. Chem. Phys.* **1996**, *197*, 1071–1083.
676. Okuda, J.; Eberle, T. In *Metalloenes: Synthesis, Reactivity and Applications*; Togni, A.; Halterman, R. L., Eds.; Wiley-VCH: New York, 1998; Vol. 1, pp 415–453.
677. McKnight, A. L.; Waymouth, R. M. *Chem. Rev.* **1998**, *98*, 2587–2598.
678. Braunschweig, H.; Breitling, F. M.; Gullo, E.; Kraft, M. *J. Organomet. Chem.* **2003**, *680*, 31–42.
679. Canich, J. A. M. (Exxon). U.S. Patent 5,504,169, 1996.
680. Pannell, R. B.; Canich, J. A. M.; Hlatky, G. G. (Exxon). PCT Int. Appl. WO 94/00500, 1994.
681. Turner, H. W.; Hlatky, G. G.; Canich, J. A. M. (Exxon). PCT Int. Appl. WO 93,19,103, 1993.
682. Devore, D. D.; Crawford, L. H.; Stevens, J. C.; Timmers, F. J.; Mussel, R. D.; Wilson, R. D.; Rosen, R. K. PCT Int. Appl. WO 95/00526, 1995.
683. Nickias, P. N.; McAdon, M. H.; Patton, J. T. PCT Int. Appl. WO 97/15583, 1997.
684. Rosen, R. K.; Nickias, P. N.; Devore, D. D.; Stevens, J. C.; Timmers, F. J. U.S. Patent 5374696, 1994.
685. Okuda, J.; Eberle, T.; Spaniol, T. P. *Chem. Ber. Rec.* **1997**, *130*, 209–215.
686. Amor, F.; Okuda, J. *J. Organomet. Chem.* **1996**, *520*, 245–248.
687. Resconi, L.; Camurati, I.; Grandini, C.; Rinaldi, M.; Mascellani, N.; Traverso, O. *J. Organomet. Chem.* **2002**, *664*, 5–26.

688. Xu, G. X.; Ruckenstein, E. *Macromolecules* **1998**, *31*, 4724–4729.
689. Xu, G. X.; Cheng, D. L. *Macromolecules* **2001**, *34*, 2040–2047.
690. Grandini, C.; Camurati, I.; Guidotti, S.; Mascellani, N.; Resconi, L.; Nifant'ev, I. E.; Kashulin, I. A.; Ivehenko, P. V.; Mercandelli, P.; Sironi, A. *Organometallics* **2004**, *23*, 344–360.
691. De Rosa, C.; Auriemma, F.; de Ballesteros, O. R.; Resconi, L.; Fait, A.; Ciaccia, E.; Camurati, I. *J. Am. Chem. Soc.* **2003**, *125*, 10913–10920.
692. Hagihara, H.; Shiono, T.; Ikeda, T. *Macromolecules* **1997**, *30*, 4783–4785.
693. Razavi, A.; Thewalt, U. *J. Organomet. Chem.* **2001**, *621*, 267–276.
- 693a. Busico, V.; Cipullo, R.; Cutillo, F.; Talarico, G.; Razavi, A. *Macromol. Chem. Phys.* **2003**, *204*, 1269–1274.
- 693b. Razavi, A.; Bellia, V.; De Brawer, Y.; Hortmann, K.; Peters, L.; Sirole, S.; Van Belle, S.; Thewalt, U. *Macromol. Symp.* **2004**, *213*, 157–171.
694. Dias, H. V. R.; Wang, Z. Y.; Bott, S. G. *J. Organomet. Chem.* **1996**, *508*, 91–99.
695. van Leusen, D.; Beetsma, D. J.; Hessen, B.; Teuben, J. H. *Organometallics* **2000**, *19*, 4084–4089.
696. Sinnema, P. J.; Hessen, B.; Teuben, J. H. *Macromol. Rapid Commun.* **2000**, *21*, 562–566.
697. Balboni, D.; Prini, G.; Rinaldi, M.; Resconi, L. *Polym. Prepr. (Am. Chem. Soc., Div. Polym. Chem.)* **2000**, 456–458.
698. Lavoie, A. R.; Waymouth, R. M. *Tetrahedron* **2004**, *60*, 7147–7155.
699. Hughes, A. K.; Meetsma, A.; Teuben, J. H. *Organometallics* **1993**, *12*, 1936–1945.
700. Herrmann, W. A.; Morawietz, M. J. A. *J. Organomet. Chem.* **1994**, *482*, 169–181.
701. Gauthier, W. J.; Collins, S. *Macromolecules* **1995**, *28*, 3779–3786.
702. Gauthier, W. J.; Corrigan, J. F.; Taylor, N. J.; Collins, S. *Macromolecules* **1995**, *28*, 3771–3778.
703. Diamond, G. M.; Jordan, R. F.; Petersen, J. L. *J. Am. Chem. Soc.* **1996**, *118*, 8024–8033.
704. Diamond, G. M.; Rodewald, S.; Jordan, R. F. *Organometallics* **1995**, *14*, 5–7.
705. Carpenetti, D. W.; Kloppenburg, L.; Kupec, J. T.; Petersen, J. L. *Organometallics* **1996**, *15*, 1572–1581.
706. McKnight, A. L.; Waymouth, R. M. *Macromolecules* **1999**, *32*, 2816–2825.
707. McKnight, A. L.; Masood, M. A.; Waymouth, R. M.; Straus, D. A. *Organometallics* **1997**, *16*, 2879–2885.
708. Okuda, J.; Verch, S.; Spaniol, T. P.; Sturmer, R. *Chem. Ber. Recl.* **1996**, *129*, 1429–1431.
709. Seo, W. S.; Cho, Y. J.; Yoon, S. C.; Park, J. T.; Park, Y. *J. Organomet. Chem.* **2001**, *640*, 79–84.
710. Novak, A.; Blake, A. J.; Wilson, C.; Love, J. B. *Chem. Commun.* **2002**, 2796–2797.
711. Shi, Y. H.; Hall, C.; Ciszewski, J. T.; Cao, C. S.; Odom, A. L. *Chem. Commun.* **2003**, 586–587.
712. Cao, C. S.; Li, Y. H.; Shi, Y. H.; Odom, A. L. *Chem. Commun.* **2004**, 2002–2003.
713. Lensink, C. J. *Organomet. Chem.* **1998**, *553*, 387–392.
714. Braunschweig, H.; von Koblinski, C.; Englert, U. *Chem. Commun.* **2000**, 1049–1050.
715. Chen, Y. X.; Marks, T. J. *Organometallics* **1997**, *16*, 3649–3657.
716. Cano, J.; Royo, P.; Lanfranchi, M.; Pellinghelli, M. A.; Tiripicchio, A. *Angew. Chem., Int. Ed. Engl.* **2001**, *40*, 2495–2497.
717. Sinnema, P. J.; van der Veen, L.; Spek, A. L.; Veldman, N.; Teuben, J. H. *Organometallics* **1997**, *16*, 4245–4247.
718. Gomes, P. T.; Green, M. L. H.; Martins, A. M.; Mountford, P. *J. Organomet. Chem.* **1997**, *541*, 121–125.
719. Gomes, P. T.; Green, M. L. H.; Martins, A. M. *J. Organomet. Chem.* **1998**, *551*, 133–138.
720. Alt, H. G.; Fottinger, K.; Milius, W. *J. Organomet. Chem.* **1999**, *572*, 21–30.
721. Chen, Y. X.; Stern, C. L.; Marks, T. J. *J. Am. Chem. Soc.* **1997**, *119*, 2582–2583.
722. Nomura, K.; Naga, N.; Takaoki, K. *Macromolecules* **1998**, *31*, 8009–8015.
723. Rhodes, B.; Chien, J. C. W.; Wood, J. S.; Chandrasekaran, A.; Rausch, M. D. *Appl. Organomet. Chem.* **2002**, *16*, 323–330.
724. Zemanek, J.; Stepnicka, P.; Fejfarova, K.; Gypes, R.; Cisarova, I.; Horacek, M.; Kubista, J.; Varga, V.; Mach, K. *Collect. Czech. Chem. Commun.* **2001**, *66*, 605–620.
725. Kamigaito, M.; Lal, T. K.; Waymouth, R. M. *J. Polym. Sci., Pol. Chem.* **2000**, *38*, 4649–4660.
726. Liu, T. *Pol. J. Chem.* **2001**, *75*, 1371–1375.
727. Rodriguez-Delgado, A.; Mariott, W. R.; Chen, E. Y. X. *Macromolecules* **2004**, *37*, 3092–3100.
728. Millward, D. B.; Cole, A. P.; Waymouth, R. M. *Organometallics* **2000**, *19*, 1870–1878.
729. Devore, D. D.; Timmers, F. J.; Hasha, D. L.; Rosen, R. K.; Marks, T. J.; Deck, P. A.; Stern, C. L. *Organometallics* **1995**, *14*, 3132–3134.
730. Strauch, J. W.; Petersen, J. L. *Organometallics* **2001**, *20*, 2623–2630.
731. Cowley, A. H.; Hair, G. S.; McBurnett, B. G.; Jones, R. A. *Chem. Commun.* **1999**, 437–438.
732. Dahlmann, M.; Schottek, J.; Frohlich, R.; Kunz, D.; Nissinen, M.; Erker, G.; Fink, G.; Kleinschmidt, R. *J. Chem. Soc., Dalton Trans.* **2000**, 1881–1886.
733. Spannenberg, A.; Baumann, W.; Becke, S.; Rosenthal, U. *Organometallics* **2002**, *21*, 1512–1514.
734. Okuda, J.; Musikabhumma, K.; Sinnema, P. J. *Isr. J. Chem.* **2002**, *42*, 383–392.
735. Gómez, R.; Gómez-Sal, P.; del Real, P. A.; Royo, P. *J. Organomet. Chem.* **1999**, *588*, 22–27.
736. Hair, G. S.; Jones, R. A.; Cowley, A. H.; Lynch, V. *Organometallics* **2001**, *20*, 177–181.
737. Liu, T. Q.; Guo, D. W.; Lin, Y. H.; Yang, X. Z.; Hu, Y. L. *Chin. Chem. Lett.* **2000**, *11*, 459–462.
738. Okuda, J.; Verch, S.; Sturmer, R.; Spaniol, T. P. *J. Organomet. Chem.* **2000**, *605*, 55–67.
739. Okuda, J.; Verch, S.; Sturmer, R.; Spaniol, T. P. *Chirality* **2000**, *12*, 472–475.
740. Klosin, J.; Kruper, W. J.; Nickias, P. N.; Roof, G. R.; De Waele, P.; Abboud, K. A. *Organometallics* **2001**, *20*, 2663–2665.
741. Alt, H. G.; Reb, A.; Kundu, K. *J. Organomet. Chem.* **2001**, *628*, 211–221.
742. Alt, H. G.; Reb, A.; Milius, W.; Weiss, A. *J. Organomet. Chem.* **2001**, *628*, 169–182.
743. Weiss, T.; Becke, S.; Sachse, H.; Rheinwald, G.; Lang, H. *Inorg. Chem. Commun.* **2002**, *5*, 159–162.
744. Sebastián, A.; Royo, P.; Gómez-Sal, P.; Herdtweck, E. *Inorg. Chim. Acta* **2003**, *350*, 511–519.
745. Chirinos, J.; Rajmankina, T.; Morillo, A.; Ibarra, D.; Parada, A.; Arevalo, J. *Macromol. Chem. Phys.* **2002**, *203*, 1501–1505.
746. Xu, G. X. *Macromolecules* **1998**, *31*, 2395–2402.
747. Hasan, T.; Ioku, A.; Nishii, K.; Shiono, T.; Ikeda, T. *Macromolecules* **2001**, *34*, 3142–3145.
748. Hagihara, H.; Shiono, T.; Ikeda, T. *Macromolecules* **1998**, *31*, 3184–3188.
749. Feng, S. G.; Klosin, J.; Kruper, W. J.; McAdon, M. H.; Neithamer, D. R.; Nickias, P. N.; Patton, J. T.; Wilson, D. R.; Abboud, K. A.; Stern, C. L. *Organometallics* **1999**, *18*, 1159–1167.
750. Okuda, J.; du Plooy, K. E.; Massa, W.; Kang, H. C.; Rose, U. *Chem. Ber.* **1996**, *129*, 275–277.
751. Amor, F.; Butt, A.; du Plooy, K. E.; Spaniol, T. P.; Okuda, J. *Organometallics* **1998**, *17*, 5836–5849.

752. Arndt, S.; Beckerle, K.; Hultsch, K. C.; Sinnema, P. J.; Voth, P.; Spaniol, T. P.; Okuda, J. *J. Mol. Catal. A: Chem.* **2002**, *190*, 215–223.
753. Eberle, T.; Spaniol, T. P.; Okuda, J. *Eur. J. Inorg. Chem.* **1998**, 237–244.
754. du Plooy, K. E.; Moll, U.; Wocadlo, S.; Massa, W.; Okuda, J. *Organometallics* **1995**, *14*, 3129–3131.
755. Jiménez, G.; Rodríguez, E.; Gómez-Sal, P.; Royo, P.; Cuenca, T.; Galakhov, M. *Organometallics* **2001**, *20*, 2459–2467.
756. Jiménez, G.; Royo, P.; Cuenca, T.; Herdtweck, E. *Organometallics* **2002**, *21*, 2189–2195.
757. Yoon, S. C.; Bae, B. J.; Suh, I. H.; Park, J. T. *Organometallics* **1999**, *18*, 2049–2051.
758. Park, J. T.; Yoon, S. C.; Bae, B. J.; Seo, W. S.; Suh, I. H.; Han, T. K.; Park, J. R. *Organometallics* **2000**, *19*, 1269–1276.
759. Okuda, J.; Eberle, T.; Spaniol, T. P.; Piquet-Faure, V. *J. Organomet. Chem.* **1999**, *591*, 127–137.
760. Noh, S. K.; Lee, J.; Lee, D. H. *J. Organomet. Chem.* **2003**, *667*, 53–60.
761. Lee, D. H.; Noh, S. K. *Korea Polym. J.* **2001**, *9*, 71–83.
762. Li, H. B.; Li, L. T.; Marks, T. J.; Liable-Sands, L.; Rheingold, A. L. *J. Am. Chem. Soc.* **2003**, *125*, 10788–10789.
763. Guo, N.; Li, L. T.; Marks, T. J. *J. Am. Chem. Soc.* **2004**, *126*, 6542–6543.
764. Wang, J. X.; Li, H. B.; Guo, N.; Li, L. T.; Stern, C. L.; Marks, T. J. *Organometallics* **2004**, *23*, 5112–5114.
765. Kim, T. H.; Won, Y. C.; Lee, B. Y.; Shin, D. M.; Chung, Y. K. *Eur. J. Inorg. Chem.* **2004**, 1522–1529.
766. Chirinos, J.; Rajmankina, T.; Parada, A.; Ciardelli, F. *Macromol. Chem. Phys.* **2000**, *201*, 2581–2585.
767. Kunz, K.; Erker, G.; Doring, S.; Frohlich, R.; Kehr, G. *J. Am. Chem. Soc.* **2001**, *123*, 6181–6182.
768. Kunz, K.; Erker, G.; Doring, S.; Bredeau, S.; Kehr, G.; Frohlich, R. *Organometallics* **2002**, *21*, 1031–1041.
769. Schwink, L.; Knochel, P.; Eberle, T.; Okuda, J. *Organometallics* **1998**, *17*, 7–9.
770. Bredeau, S.; Altenhoff, G.; Kunz, K.; Doring, S.; Grimme, S.; Kehr, G.; Erker, G. *Organometallics* **2004**, *23*, 1836–1844.
771. Altenhoff, G.; Bredeau, S.; Erker, G.; Kehr, G.; Kataeva, O.; Frohlich, R. *Organometallics* **2002**, *21*, 4084–4089.
772. Juvaste, H.; Pakkanen, T. T.; Iiskola, E. I. *Organometallics* **2000**, *19*, 4834–4839.
773. Galan-Fereres, M.; Koch, T.; Hey-Hawkins, E.; Eisen, M. S. *J. Organomet. Chem.* **1999**, *580*, 145–155.
774. Kasi, R. M.; Coughlin, E. B. *Organometallics* **2003**, *22*, 1534–1539.
775. Carvalho, M.; Mach, K.; Dias, A. R.; Mano, J. F.; Marques, M. M.; Soares, A. M.; Pombeiro, A. J. L. *Inorg. Chem. Commun.* **2003**, *6*, 331–334.
776. Staal, O. K. B.; Beetstra, D. J.; Jekel, A. P.; Hessen, B.; Teuben, J. H.; Stepnicka, P.; Gyepes, R.; Horacek, M.; Pinkas, J.; Mach, K. *Collect. Czech. Chem. Commun.* **2003**, *68*, 1119–1130.
777. Ioku, A.; Hasan, T.; Shiono, T.; Ikeda, T. *Macromol. Chem. Phys.* **2002**, *203*, 748–755.
778. Ewen, J. A.; Zambelli, A.; Longo, P.; Sullivan, J. M. *Macromol. Rapid Commun.* **1998**, *19*, 71–73.
779. Nomura, K.; Okumura, H.; Komatsu, T.; Naga, N.; Imanishi, Y. *J. Mol. Catal. A: Chem.* **2002**, *190*, 225–234.
780. Sernez, F. G.; Mulhaupt, R.; Amor, F.; Eberle, T.; Okuda, J. *J. Polym. Sci., Pol. Chem.* **1997**, *35*, 1571–1578.
781. Galimberti, M.; Mascellani, N.; Piemontesi, F.; Camurati, I. *Macromol. Rapid Commun.* **1999**, *20*, 214–218.
782. Naga, N.; Toyota, A. *Polymer* **2004**, *45*, 7513–7517.
783. Suhm, J.; Schneider, M. J.; Mulhaupt, R. *J. Mol. Catal. A: Chem.* **1998**, *128*, 215–227.
784. Dankova, M.; Waymouth, R. M. *Macromolecules* **2003**, *36*, 3815–3820.
785. Walter, P.; Trinkle, S.; Suhm, J.; Mader, D.; Friedrich, C.; Mulhaupt, R. *Macromol. Chem. Phys.* **2000**, *201*, 604–612.
786. Shiono, T.; Moriki, Y.; Soga, K. *Macromol. Symp.* **1995**, *97*, 161–170.
787. Schulze, U.; Fonagy, T.; Komber, H.; Pompe, G.; Pionteck, J.; Ivan, B. *Macromolecules* **2003**, *36*, 4719–4726.
788. Thorshaug, K.; Mendiachi, R.; Boggioni, L.; Tritto, I.; Trinkle, S.; Friedrich, C.; Mulhaupt, R. *Macromolecules* **2002**, *35*, 2903–2911.
789. Sukhova, T. A.; Panin, A. N.; Babkina, O. N.; Bravaya, N. M. *J. Polym. Sci., Pol. Chem.* **1999**, *37*, 1083–1093.
790. Shaffer, T. D.; Canich, J. A. M.; Squire, K. R. *Macromolecules* **1998**, *31*, 5145–5147.
791. Wakabayashi, Y.; Miyashita, A.; Nomura, K.; Nohira, H. *Kobunshi Ronbunshu* **2002**, *59*, 393–401.
792. Nishii, K.; Shiono, T.; Ikeda, T. *Kobunshi Ronbunshu* **2002**, *59*, 371–376.
793. Nishii, K.; Matsumae, T.; Dare, E. O.; Shiono, T.; Ikeda, T. *Macromol. Chem. Phys.* **2004**, *205*, 363–369.
794. Musikabhumma, K.; Spaniol, T. P.; Okuda, J. *Macromol. Chem. Phys.* **2002**, *203*, 115–121.
795. Musikabhumma, K.; Spaniol, T. P.; Okuda, J. *J. Polym. Sci., Pol. Chem.* **2003**, *41*, 528–544.
796. Musikabhumma, K.; Spaniol, T. P.; Okuda, J. *J. Mol. Catal. A: Chem.* **2004**, *208*, 73–81.
797. Markel, E. J.; Weng, W. Q.; Peacock, A. J.; Dekmezian, A. H. *Macromolecules* **2000**, *33*, 8541–8548.
798. Abramo, G. P.; Li, L. T.; Marks, T. J. *J. Am. Chem. Soc.* **2002**, *124*, 13966–13967.
799. Komon, Z. J. A.; Bazan, G. C. *Macromol. Rapid Commun.* **2001**, *22*, 467–478.
800. Chen, E. Y.-X.; Mariott, W. R. *Polym. Prepr. (Am. Chem. Soc., Div. Polym. Chem.)* **2004**, *45*, 993–994.
801. Xu, Z. T.; Vanka, K.; Ziegler, T. *Organometallics* **2004**, *23*, 104–116.
802. Xu, Z. T.; Vanka, K.; Ziegler, T. *Macromol. Symp.* **2004**, *206*, 457–469.
803. Lanza, G.; Fragala, I. L.; Marks, T. J. *J. Am. Chem. Soc.* **1998**, *120*, 8257–8258.
804. Lanza, G.; Fragala, I.; Marks, T. J. *Organometallics* **2001**, *20*, 4006–4017.
805. Lanza, G.; Fragala, I. L.; Marks, T. J. *Organometallics* **2002**, *21*, 5594–5612.
806. Woo, T. K.; Margl, P. M.; Lohrenz, J. C. W.; Blochl, P. E.; Ziegler, T. *J. Am. Chem. Soc.* **1996**, *118*, 13021–13030.
807. Woo, T. K.; Margl, P. M.; Ziegler, T.; Blochl, P. E. *Organometallics* **1997**, *16*, 3454–3468.
808. Fan, L. Y.; Harrison, D.; Woo, T. K.; Ziegler, T. *Organometallics* **1995**, *14*, 2018–2026.
809. Gilje, J. W.; Roesky, H. W. *Chem. Rev.* **1994**, *94*, 895–910.
810. Bottomley, F.; Sutin, L. *Adv. Organomet. Chem.* **1988**, *28*, 339–396.
811. Varkey, S. P.; Schormann, M.; Pape, T.; Roesky, H. W.; Noltemeyer, M.; Herbst-Irmer, R.; Schmidt, H. G. *Inorg. Chem.* **2001**, *40*, 2427–2429.
812. Gómez-Sal, P.; Martín, A.; Mena, L.; Yélamos, C. *Inorg. Chem.* **1996**, *35*, 242–243.
813. Yu, P. H.; Roesky, H. W.; Demsar, A.; Albers, T.; Schmidt, H. G.; Noltemeyer, M. *Angew. Chem., Int. Ed. Engl.* **1997**, *36*, 1766–1767.
814. Qian, Y. L.; Huang, J. L.; Yang, J. M.; Chan, A. S. C.; Chen, W. C.; Chen, X. P.; Li, G. S.; Jin, X. L.; Yang, Q. C. *J. Organomet. Chem.* **1997**, *547*, 263–279.
815. Qian, Y.; Huang, J.; Chen, X.; Li, G.; Chen, W.; Li, B.; Jin, X.; Yang, Q. *Polyhedron* **1994**, *13*, 1105–1108.
816. Andrés, R.; Galakhov, M.; Gómez-Sal, M. P.; Martín, A.; Mena, M.; Santamaría, C. *J. Organomet. Chem.* **1996**, *526*, 135–143.
817. Galakhov, M.; Mena, M.; Santamaría, C. *Chem. Commun.* **1998**, 691–692.
818. Andrés, R.; Galakhov, M. V.; Gómez-Sal, M. P.; Martín, A.; Mena, M.; Morales-Varela, M. D.; Santamaría, C. *Chem. Eur. J.* **2002**, *8*, 805–811.
819. Gracia, J.; Martín, A.; Mena, M.; Morales-Varela, M. D.; Poblet, J. M.; Santamaría, C. *Angew. Chem., Int. Ed.* **2003**, *42*, 927–930.

820. Martin, A.; Mena, M.; Morales-Varela, M. D.; Santamaria, C. *Eur. J. Inorg. Chem.* **2004**, 1914–1921.
821. Abarca, A.; Martín, A.; Mena, M.; Raithby, P. R. *Inorg. Chem.* **1995**, *34*, 5437–5440.
822. Ciruelos, S.; Cuenca, T.; Gómez, R.; Gómez-Sal, P.; Manzanero, A.; Royo, P. *Polyhedron* **1998**, *17*, 1055–1064.
823. Voigt, A.; Murugavel, R.; Montero, M. L.; Wessel, H.; Liu, F. Q.; Roesky, H. W.; Uson, I.; Albers, T.; Parisini, E. *Angew. Chem., Int. Ed. Engl.* **1997**, *36*, 1001–1003.
824. Carofiglio, T.; Floriani, C.; Roth, A.; Sgamellotti, A.; Rosi, M.; Chiesivilla, A.; Rizzoli, C. *J. Organomet. Chem.* **1995**, *488*, 141–154.
825. Heshmatpour, F.; Wocadlo, S.; Massa, W.; Dehnicke, K.; Bottomley, F.; Day, R. W. *Z. Naturforsch.(B)* **1994**, *49*, 827–830.
826. Yu, P. H.; Pape, T.; Uson, I.; Said, M. A.; Roesky, H. W.; Montero, M. L.; Schmidt, H. G.; Demsar, A. *Inorg. Chem.* **1998**, *37*, 5117–5124.
827. Kienitz, C. O.; Thone, C.; Jones, P. G. *Acta Crystallogr., Sect. C: Cryst. Struct. Commun.* **1997**, *53*, 843–845.
828. Nieuwenhuyzen, M.; Schobert, R.; Hampel, F.; Hoops, S. *Inorg. Chim. Acta* **2000**, *304*, 118–121.
829. Osella, D.; Ravera, M.; Floriani, C.; Solari, E. *J. Organomet. Chem.* **1996**, *510*, 45–50.
830. Bottomley, F. *Organometallics* **1993**, *12*, 2652–2659.
831. Fussing, I. M. M.; Pletcher, D.; Whitby, R. J. *J. Organomet. Chem.* **1994**, *470*, 109–117.
832. Sturla, S. J.; Buchwald, S. L. *J. Org. Chem.* **1999**, *64*, 5547–5550.
833. Hicks, F. A.; Kablaoui, N. M.; Buchwald, S. L. *J. Am. Chem. Soc.* **1999**, *121*, 5881–5898.
834. Hicks, F. A.; Buchwald, S. L. *J. Am. Chem. Soc.* **1999**, *121*, 7026–7033.
835. Hicks, F. A.; Buchwald, S. L. *J. Am. Chem. Soc.* **1996**, *118*, 11688–11689.
836. Sturla, S. J.; Buchwald, S. L. *Organometallics* **2002**, *21*, 739–748.
837. Nomura, K.; Komatsu, T.; Imanishi, Y. *Macromolecules* **2000**, *33*, 8122–8124.
838. Nomura, K.; Tsubota, M.; Fujiki, M. *Macromolecules* **2003**, *36*, 3797–3799.
839. Nomura, K.; Fujii, K. *Macromolecules* **2003**, *36*, 2633–2641.
840. Byun, D. J.; Fudo, A.; Tanaka, A.; Fujiki, M.; Nomura, K. *Macromolecules* **2004**, *37*, 5520–5530.
841. Nomura, K.; Oya, K.; Komatsu, T.; Imanishi, Y. *Macromolecules* **2000**, *33*, 3187–3189.
842. Nomura, K.; Naga, N.; Miki, M.; Yanagi, K. *Macromolecules* **1998**, *31*, 7588–7597.
843. Nomura, K.; Komatsu, T.; Imanishi, Y. *J. Mol. Catal. A: Chem.* **2000**, *152*, 249–252.
844. Nomura, K.; Komatsu, T.; Imanishi, Y. *J. Mol. Catal. A: Chem.* **2000**, *159*, 127–137.
845. Nomura, K.; Okumura, H.; Komatsu, T.; Naga, N. *Macromolecules* **2002**, *35*, 5388–5395.
846. Nomura, K.; Oya, K.; Imanishi, Y. *J. Mol. Catal. A: Chem.* **2001**, *174*, 127–140.
847. Nomura, K.; Naga, N.; Miki, M.; Yanagi, K.; Imai, A. *Organometallics* **1998**, *17*, 2152–2154.
848. Thorn, M. G.; Vilardo, J. S.; Lee, J.; Hanna, B.; Fanwick, P. E.; Rothwell, I. P. *Organometallics* **2000**, *19*, 5636–5642.
849. Witt, E.; Stephan, D. W. *Inorg. Chem.* **2001**, *40*, 3824–3826.
850. Thorn, M. G.; Fanwick, P. E.; Chesnut, R. W.; Rothwell, I. P. *Chem. Commun.* **1999**, 2543–2544.
851. Turner, L. E.; Thorn, M. G.; Fanwick, P. E.; Rothwell, I. P. *Chem. Commun.* **2003**, 1034–1035.
852. Turner, L. E.; Thorn, M. G.; Swartz, R. D.; Chesnut, R. W.; Fanwick, P. E.; Rothwell, I. P. *Dalton Trans.* **2003**, 4580–4589.
853. Ma, H. Y.; Zhang, Y.; Chen, B.; Huang, J. L.; Qian, Y. L. *Chem. J. Chin. Univ.* **2001**, *22*, 1259–1261.
854. Ma, H. Y.; Zhang, Y.; Chen, B.; Huang, J. L.; Qian, Y. L. *J. Polym. Sci., Pol. Chem.* **2001**, *39*, 1817–1824.
855. Mahanthappa, M. K.; Huang, K. W.; Cole, A. P.; Waymouth, R. M. *Chem. Commun.* **2002**, 502–503.
856. Huang, K. W.; Waymouth, R. M. *J. Am. Chem. Soc.* **2002**, *124*, 8200–8201.
857. Mahanthappa, M. K.; Cole, A. P.; Waymouth, R. M. *Organometallics* **2004**, *23*, 836–845.
858. Huang, K. W.; Waymouth, R. M. *Dalton Trans.* **2004**, 354–356.
859. Qian, Y. L.; Zhang, H.; Zhou, J. X.; Zhao, W.; Sun, X. Q.; Huang, J. L. *J. Mol. Catal. A: Chem.* **2004**, *208*, 45–54.
860. Lee, J.; Fanwick, P. E.; Rothwell, I. P. *Organometallics* **2003**, *22*, 1546–1549.
861. Pérez, Y.; Morante-Zarcelero, S.; del Hierro, I.; Sierra, I.; López-Solera, I.; Monari, M.; Fajardo, M.; Otero, A. *J. Organomet. Chem.* **2004**, *689*, 3492–3500.
862. Thorn, M. G.; Vilardo, J. S.; Fanwick, P. E.; Rothwell, I. P. *Chem. Commun.* **1998**, 2427–2428.
863. Vilardo, J. S.; Thorn, M. G.; Fanwick, P. E.; Rothwell, I. P. *Chem. Commun.* **1998**, 2425–2426.
864. Amor, J. I.; Burton, N. C.; Cuenca, T.; Gómez-Sal, P.; Royo, P. *J. Organomet. Chem.* **1995**, *485*, 153–160.
865. Fraenkron, M.; Tzavellas, N.; Klouras, N.; Raptopoulou, C. P. *Monatsh. Chem.* **1996**, *127*, 1137–1143.
866. Fenwick, A. E.; Phomphrai, K.; Thorn, M. G.; Vilardo, J. S.; Trefun, C. A.; Hanna, B.; Fanwick, P. E.; Rothwell, I. P. *Organometallics* **2004**, *23*, 2146–2156.
867. Nomura, K.; Fudo, A. *Inorg. Chim. Acta* **2003**, *345*, 37–43.
868. Weller, F.; Rubenstahl, T.; Dehnicke, K. *Z. Kristallogr.* **1995**, *210*, 369–370.
869. Tian, J.; Hu, N. H.; Shen, Q.; Huang, B. T. *Acta Crystallogr. Sect. C: Cryst. Struct. Commun.* **1995**, *51*, 1065–1067.
870. Firth, A. V.; Stewart, J. C.; Hoskin, A. J.; Douglas, D. W. *J. Organomet. Chem.* **1999**, *591*, 185–193.
871. Fandos, R.; Hernández, C.; Otero, A.; Rodríguez, A.; Ruiz, M. J.; Terreros, P. *Eur. J. Inorg. Chem.* **2003**, 493–498.
872. Xie, M. R.; Wu, Q.; Lin, S. G. *Macromol. Rapid Commun.* **1999**, *20*, 167–169.
873. Zhu, F. M.; Lin, S. A.; Zhou, W. L.; Tu, J. J.; Chen, D. Q. *Chem. J. Chin. Univ.* **1998**, *19*, 1844–1847.
874. Huang, Q. G.; Wu, Q.; Zhu, F. M.; Lin, S. G. *J. Polym. Sci. Pol. Chem.* **2001**, *39*, 4068–4073.
875. Wang, Z. H.; Zhang, Y. Q.; Xiao, Y. Z. *Chin. J. Org. Chem.* **1999**, *19*, 321–324.
876. Ngo, S. C.; Toscano, P. J.; Welch, J. T. *Helv. Chim. Acta* **2002**, *85*, 3366–3382.
877. Nomura, K.; Hatanaka, Y. *Inorg. Chem. Commun.* **2003**, *6*, 517–522.
878. Qian, Y. L.; Zhang, H.; Qian, X. M.; Chen, B.; Huang, J. L. *Eur. Polym. J.* **2002**, *38*, 1613–1618.
879. Okuda, J.; König, P.; Rushkin, I. L.; Kang, H. C.; Massa, W. *J. Organomet. Chem.* **1995**, *501*, 37–39.
880. Ma, H. Y.; Chen, B.; Huang, J. L.; Qian, Y. L. *J. Mol. Catal. A: Chem.* **2001**, *170*, 67–73.
881. Liu, F. Q.; Uson, I.; Roesky, H. W. *J. Chem. Soc., Dalton Trans.* **1995**, 2453–2458.
882. González-Maupocoy, M.; Cuenca, T.; Frutos, L. M.; Castaño, O.; Herdtweck, E. *Organometallics* **2003**, *22*, 2694–2704.
883. Fandos, R.; Hernández, C.; Otero, A.; Rodríguez, A.; Ruiz, M. J.; Terreros, P. *Chem. Eur. J.* **2003**, *9*, 671–677.
884. Cossy, J.; Willis, C.; Bellosta, V.; Bouzbouz, S. *Synlett* **2000**, 1461–1463.
885. Defosseux, M.; Blanchard, N.; Meyer, C.; Cossy, J. *J. Org. Chem.* **2004**, *69*, 4626–4647.
886. Bouzbouz, S.; Cossy, J. *Org. Lett.* **2001**, *3*, 3995–3998.



887. Duthaler, R. O.; Hafner, A. *Angew. Chem., Int. Ed. Engl.* **1997**, *36*, 43–45.
888. Clark, D. L.; Click, D. R.; Grumbine, S. K.; Scott, B. L.; Watkin, J. G. *Inorg. Chem.* **1998**, *37*, 6237–6243.
889. Snell, A.; Kehr, G.; Kataeva, O.; Fröhlich, R.; Erker, G. *J. Organomet. Chem.* **2003**, *687*, 171–177.
890. Lin, C. C. *Polyhedron* **1995**, *14*, 3005–3009.
891. Choquette, D. M.; Buschmann, W. E.; Graceffa, R. F.; Planalp, R. P. *Polyhedron* **1995**, *14*, 2569–2573.
892. Choquette, D. M.; Buschmann, W. E.; Olmstead, M. M.; Planalp, R. P. *Inorg. Chem.* **1993**, *32*, 1062–1063.
893. Murugavel, R.; Shete, V. S.; Baheti, K.; Davis, P. J. *J. Organomet. Chem.* **2001**, *625*, 195–199.
894. Aranson, I.; Gudnason, P. I.; Fenske, D. Z. *Anorg. Allg. Chem.* **2003**, *629*, 951–954.
895. Bott, R. K. J.; Hughes, D. L.; Schormann, M.; Bochmann, M.; Lancaster, S. J. *J. Organomet. Chem.* **2003**, *665*, 135–149.
896. Huang, J. L.; Lian, B.; Qian, Y. L.; Zhou, W. Z.; Chen, W.; Zheng, G. *Macromolecules* **2002**, *35*, 4871–4874.
897. Doherty, S.; Errington, R. J.; Jarvis, A. P.; Collins, S.; Clegg, W.; Elsegood, M. R. *J. Organometallics* **1998**, *17*, 3408–3410.
898. Fandos, R.; Hernández, C.; Otero, A.; Rodríguez, A.; Ruiz, M. J.; Terreros, P. *J. Chem. Soc., Dalton Trans.* **2000**, 2990–2995.
899. Fandos, R.; Hernández, C.; Otero, A.; Rodríguez, A.; Ruiz, M. J.; Terreros, P. *J. Chem. Soc., Dalton Trans.* **2002**, 11–13.
900. Yi, J. J.; Xu, X. X.; Jing, Z. H. *Acta Polym. Sin.* **2001**, 678–682.
901. Yi, J. J.; Yu, P.; Xu, X. X.; Zhao, W.; Jing, W. H. *Acta Polym. Sin.* **2001**, 342–346.
902. Kim, Y.; Han, Y.; Do, Y. *J. Organomet. Chem.* **2001**, *634*, 19–24.
903. Kim, Y.; Hong, E.; Lee, M. H.; Kim, J.; Han, Y.; Do, Y. *Organometallics* **1999**, *18*, 36–39.
904. Kim, Y.; Do, Y. *Macromol. Rapid Commun.* **2000**, *21*, 1148–1155.
905. Kim, Y.; Han, Y.; Lee, M. H.; Yoon, S. W.; Choi, K. H.; Song, B. G.; Do, Y. *Macromol. Rapid Commun.* **2001**, *22*, 573–578.
906. Doherty, S.; Errington, R. J.; Housley, N.; Ridland, J.; Clegg, W.; Elsegood, M. R. *J. Organometallics* **1999**, *18*, 1018–1029.
907. Kim, Y. J.; Han, Y. G.; Hwang, J. W.; Kim, M. W.; Do, Y. K. *Organometallics* **2002**, *21*, 1127–1135.
908. Kim, Y.; Do, Y. *J. Organomet. Chem.* **2002**, *655*, 186–191.
909. Michalczyk, L.; de Gala, S.; Bruno, J. W. *Organometallics* **2001**, *20*, 5547–5556.
910. Kim, Y.; Jnaneshwara, G. K.; Verkade, J. G. *Inorg. Chem.* **2003**, *42*, 1437–1447.
911. Willoughby, C. A.; Duff, R. R.; Davis, W. M.; Buchwald, S. L. *Organometallics* **1996**, *15*, 472–475.
912. Vandoorn, J. A.; Vanderheijden, H.; Orpen, A. G. *Organometallics* **1994**, *13*, 4271–4277.
913. Vandoorn, J. A.; Vanderheijden, H.; Orpen, A. G. *Organometallics* **1995**, *14*, 1278–1283.
914. Amor, F.; Fokken, S.; Kleinhenn, T.; Spaniol, T. P.; Okuda, J. *J. Organomet. Chem.* **2001**, *621*, 3–9.
915. Okuda, J.; Fokken, S.; Kang, H. C.; Massa, W. *Chem. Ber.* **1995**, *128*, 221–227.
916. Okuda, J.; Masoud, E. *Macromol. Chem. Phys.* **1998**, *199*, 543–545.
917. Nakayama, Y.; Watanabe, K.; Ueyama, N.; Nakamura, A.; Harada, A.; Okuda, J. *Organometallics* **2000**, *19*, 2498–2503.
918. Takashima, Y.; Nakayama, Y.; Watanabe, K.; Itono, T.; Ueyama, N.; Nakamura, A.; Yasuda, H.; Harada, A.; Okuda, J. *Macromolecules* **2002**, *35*, 7538–7544.
919. Friedrich, A.; Radius, U. *Eur. J. Inorg. Chem.* **2004**, 4300–4316.
920. Evans, D. R.; Huang, M. S.; Fetting, J. C.; Williams, T. L. *Inorg. Chem.* **2002**, *41*, 5986–6000.
921. Petrella, A. J.; Roberts, N. K.; Craig, D. C.; Raston, C. L.; Lamb, R. N. *Chem. Commun.* **2003**, 1014–1015.
922. Petrella, A. J.; Roberts, N. K.; Raston, C. L.; Thornton-Pett, M.; Lamb, R. N. *Chem. Commun.* **2003**, 1238–1239.
923. Kunzel, A.; Sokolow, M.; Liu, F. Q.; Roesky, H. W.; Noltemeyer, M.; Schmidt, H. G.; Uson, I. J. *J. Chem. Soc., Dalton Trans.* **1996**, 913–919.
924. Arévalo, S.; Bonillo, M. R.; de Jesús, E.; de la Mata, F. J.; Flores, J. C.; Gómez, R.; Gómez-Sal, P.; Ortega, P. *J. Organomet. Chem.* **2003**, *681*, 228–236.
925. Arévalo, S.; Benito, J. M.; de Jesús, E.; de la Mata, F. J.; Flores, J. C.; Gómez, R. *J. Organomet. Chem.* **1999**, *592*, 265–270.
926. Arévalo, S.; Benito, J. M.; de Jesús, E.; de la Mata, F. J.; Flores, J. C.; Gómez, R. *J. Organomet. Chem.* **2000**, *602*, 208–210.
927. Arévalo, S.; de Jesús, E.; de la Mata, F. J.; Flores, J. C.; Gómez, R.; Gómez-Sal, P.; Ortega, P.; Vigo, S. *Organometallics* **2003**, *22*, 5109–5113.
928. Arévalo, S.; de Jesús, E.; de la Mata, F. J.; Flores, J. C.; Gómez, R. *Organometallics* **2001**, *20*, 2583–2592.
929. Winkhofer, N.; Voigt, A.; Dorn, H.; Roesky, H. W.; Steiner, A.; Stalke, D.; Reller, A. *Angew. Chem., Int. Ed. Engl.* **1994**, *33*, 1352–1354.
930. Edelmann, F. T.; Giessmann, S.; Fischer, A. *J. Organomet. Chem.* **2001**, *620*, 80–89.
931. Edelmann, F. T.; Giessmann, S.; Fischer, A. *Chem. Commun.* **2000**, 2153–2154.
932. Duchateau, R.; Cremer, U.; Harmsen, R. J.; Mohamud, S. I.; Abbenhuis, H. C. L.; van Santen, R. A.; Meetsma, A.; Thiele, S. K. H.; van Tol, M. F. H.; Kranenburg, M. *Organometallics* **1999**, *18*, 5447–5459.
933. Buys, I. E.; Hambley, T. W.; Houlton, D. J.; Maschmeyer, T.; Masters, A. F.; Smith, A. K. *J. Mol. Catal.* **1994**, *86*, 309–318.
934. Duchateau, R.; Abbenhuis, H. C. L.; van Santen, R. A.; Thiele, S. K. H.; van Tol, M. F. H. *Organometallics* **1998**, *17*, 5222–5224.
935. Krijnen, S.; Abbenhuis, H. C. L.; Hanssen, R.; van Hooft, J. H. C.; van Santen, R. A. *Angew. Chem., Int. Ed.* **1998**, *37*, 356–358.
936. Duchateau, R.; Dijkstra, T. W.; van Santen, R. A.; Yap, G. P. A. *Chem., Eur. J.* **2004**, *10*, 3979–3990.
937. Skowronska-Ptasinska, M. D.; Vorstenbosch, M. L. W.; van Santen, R. A.; Abbenhuis, H. C. L. *Angew. Chem., Int. Ed. Engl.* **2002**, *41*, 637–639.
938. Lee, D. H.; Yoon, K. B.; Lee, E. H.; Noh, S. K.; Byun, G. G.; Lee, C. S. *Macromol. Rapid Commun.* **1995**, *16*, 265–268.
939. Severin, K.; Beck, W.; Trojandt, G.; Polborn, K.; Steglich, W. *Angew. Chem., Int. Ed. Engl.* **1995**, *34*, 1449–1451.
940. Skupinski, W.; Nicinski, K. *Polimery* **2002**, *47*, 30–33.
941. Skupinski, W.; Nicinski, K.; Maksimowski, P.; Wasek, M. *J. Mol. Catal. A: Chem.* **2002**, *178*, 73–77.
942. Wu, Q.; Ye, Z.; Gao, Q. H.; Lin, S. G. *J. Polym. Sci., Pol. Chem.* **1998**, *36*, 2051–2057.
943. Skupinski, W.; Nicinski, K. *Appl. Organomet. Chem.* **2001**, *15*, 635–638.
944. Liu, J. F.; Huang, J. L.; Qian, Y. L.; Wang, F.; Chan, A. S. C. *Polym. Bull.* **1996**, *37*, 719–721.
945. Liu, J. F.; Ma, H. Y.; Huang, J. L.; Qian, Y. L. *Eur. Polym. J.* **2000**, *36*, 2055–2058.
946. Qian, Y. L.; Zhang, H.; Qian, X. M.; Huang, J. L.; Shen, C. J. *J. Mol. Catal. A: Chem.* **2003**, *192*, 25–33.
947. Liu, J. F.; Ma, H. Y.; Huang, J. L.; Qian, Y. L.; Chan, A. S. C. *Eur. Polym. J.* **1999**, *35*, 543–545.
948. Nomura, K.; Komatsu, T.; Nakamura, M.; Imanishi, Y. *J. Mol. Catal. A: Chem.* **2000**, *164*, 131–135.
949. Nomura, K.; Fudo, A. *J. Mol. Catal. A: Chem.* **2004**, *209*, 9–17.
950. Ngo, S.; Okuda, J.; Toscano, P.; Welch, J. T. *Polym. Prepr. (Am. Chem. Soc., Div. Polym. Chem.)* **1996**, *37*, 331–333.
951. Zhu, F. M.; Lin, S. G. *Acta Polym. Sin.* **1998**, 83–89.
952. Zhu, F. M.; Lin, S. A. *Chem. J. Chin. Univ.-Chin.* **1997**, *18*, 2065–2069.

953. Quirk, R. P.; Ok, M. A. *Macromolecules* **2004**, *37*, 3976–3982.
954. Choi, K. Y.; Chung, J. S.; Woo, B. G.; Hong, M. H. *J. Appl. Polym. Sci.* **2003**, *88*, 2132–2137.
955. Ngo, S.; Okuda, J.; Toscano, P.; Welch, J. T. *Polym. Prep. (Am. Chem. Soc., Div. Polym. Chem.)* **1996**, 331–336.
956. Zhu, F. M.; Fang, Y. T.; Chen, H. B.; Lin, S. G. *Macromolecules* **2000**, *33*, 5006–5010.
957. Zhu, F. M.; Fang, Y. T.; Chen, H. B.; Lin, S. A. *Chem. J. Chin. Univ.* **2000**, *21*, 1607–1609.
958. Zhu, F. M.; Huang, Y.; Yang, Y. J.; Lin, S. G. *J. Polym. Sci., Pol. Chem.* **2000**, *38*, 4258–4263.
959. Zhu, F. M.; Wu, Q.; Fang, Y. T.; Huang, Q. F.; Lin, S. A. *Chem. Res. Chin. Univ.* **2000**, *16*, 83–89.
960. Wu, Q.; Ye, Z.; Lin, S. G. *Macromol. Chem. Phys.* **1997**, *198*, 1823–1828.
961. Huang, Q. G.; Zhu, F. M.; Wu, Q.; Lin, S. G. *Polym. Int.* **2001**, *50*, 45–48.
962. Wu, Q.; Lu, Y. Y. *J. Polym. Sci., Pol. Chem.* **2002**, *40*, 1421–1425.
963. Fang, Y. T.; Zhu, F. M.; Lin, S. G. *Acta Polym. Sin.* **2000**, 74–78.
964. Fang, Y. T.; Zhu, F. M.; Wang, Q. F.; Lin, S. G. *Acta Polym. Sin.* **2000**, 41–45.
965. Zhu, F. M.; Huang, Q. G.; Huang, D. D.; Wu, Q.; Lin, S. A. *Chem. J. Chin. Univ.* **1999**, *20*, 1156–1158.
966. Zhu, F. M.; Huang, Q. G.; Lin, S. G. *J. Polym. Sci., Pol. Chem.* **1999**, *37*, 4497–4501.
967. Fang, Y. T.; Zhu, F. M.; Lin, S. A. *Acta Polym. Sin.* **2001**, 504–508.
968. Huang, Q. G.; Lin, S. A.; Zhu, F. M.; Wu, Q. *Chem. J. Chin. Univ.* **2002**, *23*, 167–169.
969. Manders, B.; Sciandrone, L.; Hauck, G.; Kristen, M. O. *Angew. Chem., Int. Ed. Engl.* **2001**, *40*, 4006–4007.
970. Okuda, J.; Kleinhenn, T.; Konig, P.; Taden, I.; Ngo, S.; Rushkin, I. L. *Macromol. Symp.* **1995**, *95*, 195–202.
971. Okuda, J.; Rushkin, I. L. *Macromolecules* **1993**, *26*, 5530–5532.
972. Cambie, R. C.; Coddington, J. M.; Milbank, J. B. J.; Pausler, M. G.; Rustenhoven, J. J.; Rutledge, P. S.; Shaw, G. L.; Sinkovich, P. I. *Aust. J. Chem.* **1993**, *46*, 583–591.
973. Duthaler, R. O.; Hafner, A.; Alsters, P. L.; Bold, G.; Rihs, G.; Rothestreit, P.; Wyss, B. *Inorg. Chim. Acta* **1994**, *222*, 95–113.
974. Kunz, K.; Erker, G.; Kehr, G.; Fröhlich, R.; Jacobsen, H.; Berke, H.; Blacque, O. J. *Am. Chem. Soc.* **2002**, *124*, 3316–3326.
975. Trouve, G.; Laske, D. A.; Meetsma, A.; Teuben, J. H. J. *Organomet. Chem.* **1996**, *511*, 255–262.
976. Gielens, E.; Tiesnitsch, J. Y.; Hessen, B.; Teuben, J. H. *Organometallics* **1998**, *17*, 1652–1654.
977. Rau, A.; Schmitz, S.; Luft, G. *J. Organomet. Chem.* **2000**, *608*, 71–75.
978. Sumitomo, C. C. PCT Int. Appl. WO 97/03,002, 1997.
979. Zhang, Y. T.; Wang, J. H.; Mu, Y.; Shi, Z.; Lu, C. S.; Zhang, Y. R.; Qiao, L. J.; Feng, S. H. *Organometallics* **2003**, *22*, 3877–3883.
980. Zhang, Y. T.; Mu, Y.; Lu, C. S.; Li, G. H.; Xu, J. S.; Zhang, Y. R.; Zhu, D. S.; Feng, S. H. *Organometallics* **2004**, *23*, 540–546.
981. Chen, Y. X.; Fu, P. F.; Stern, C. L.; Marks, T. J. *Organometallics* **1997**, *16*, 5958–5963.
982. Bu, W. M.; Wang, J. H.; Ye, L.; Mu, Y.; Yang, G. D.; Fan, Y. G. *Acta Crystallogr., Sect. C: Cryst. Struct. Commun.* **1999**, *55*, 728–730.
983. Duda, L.; Erker, G.; Fröhlich, R.; Zippel, F. *Eur. J. Inorg. Chem.* **1998**, 1153–1162.
984. Turner, L. E.; Thorn, M. G.; Fanwick, P. E.; Rothwell, I. P. *Organometallics* **2004**, *23*, 1576–1593.
985. Wang, J.; Xu, D. M.; Liu, Z. Y.; Chen, Y. J.; Wang, D. *Chin. J. Polym. Sci.* **2002**, *20*, 213–217.
986. Sonnenberg, J. L.; Milletti, M. C. *Polyhedron* **2002**, *21*, 2699–2704.
987. Xu, X. X.; Sun, M.; Yu, P.; Jing, Z. H. *Acta Polym. Sin.* **2002**, 667–671.
988. Sun, M.; Xu, X. X.; Zhao, W.; Ji, H. B.; Jing, Z. H. *Acta Polym. Sin.* **2004**, 137–139.
989. Min, S.; Xu, X. X.; Wei, Z.; Ji, H. B.; Jing, Z. H. *Acta Polym. Sin.* **2004**, 406–409.
990. Shah, S. A. A.; Dorn, H.; Gindl, J.; Noltemeyer, M.; Schmidt, H. G.; Roesky, H. W. *J. Organomet. Chem.* **1998**, *550*, 1–6.
991. Gindl, J.; Said, M. A.; Yu, P. H.; Roesky, H. W.; Noltemeyer, M.; Schmidt, H. G. *Isr. J. Chem.* **1999**, *39*, 125–128.
992. Dorn, H.; Vejzovic, E.; Lough, A. J.; Manners, I. *Can. J. Chem., Rev. Can. Chim.* **2002**, *80*, 1650–1654.
993. Walawalkar, M. G.; Horchler, S.; Dietrich, S.; Chakraborty, D.; Roesky, H. W.; Schafer, M.; Schmidt, H. G.; Sheldrick, G. M.; Murugavel, R. *Organometallics* **1998**, *17*, 2865–2868.
994. Gianotti, E.; Oliveira, E. C.; Coluccia, S.; Pastore, H. O.; Marchese, L. *Inorg. Chim. Acta* **2003**, *349*, 259–264.
995. Wohlr, T.; Thewalt, U. J. *Organomet. Chem.* **1994**, *468*, C1–C3.
996. Agustin, D.; Rima, G.; Gornitzka, H.; Barrau, J. *Organometallics* **2000**, *19*, 4276–4282.
997. Sengupta, S. K.; Pandey, O. P.; Srivastava, A. K.; Rai, R.; Mishra, K. D. *Indian J. Chem. Sect A-Inorg. Bio-Inorg. Phys. Theor. Anal. Chem.* **1999**, *38*, 956–960.
998. Demakopoulos, I.; Klouras, N.; Raptopoulou, C. P.; Terzis, A. Z. *Anorg. Allg. Chem.* **1995**, *621*, 1761–1766.
999. Lensink, C.; Gainsford, G. J. *Acta Crystallogr., Sect. E: Struct. Rep. Online* **2002**, *58*, M296–M297.
1000. Lensink, C.; Gainsford, G. J. *Acta Crystallogr., Sect. E: Struct. Rep. Online* **2002**, *58*, M267–M268.
1001. Lensink, C.; Gainsford, G. J.; Brandsma, M. J. R. *Acta Crystallogr., Sect. E: Struct. Rep. Online* **2002**, *58*, M519–M520.
1002. Lensink, C.; Gainsford, G. J.; Brandsma, M. J. R. *Acta Crystallogr., Sect. C: Cryst. Struct. Commun.* **2002**, *58*, m529–m530.
1003. Stephan, D. W.; Nadasdi, T. T. *Coord. Chem. Rev.* **1996**, *147*, 147–208.
1004. Trnka, T. M.; Parkin, G. *Polyhedron* **1997**, *16*, 1031–1045.
1005. Firth, A. V.; Stephan, D. W. *Inorg. Chem.* **1998**, *37*, 4732–4734.
1006. Firth, A. V.; Witt, E.; Stephan, D. W. *Organometallics* **1998**, *17*, 3716–3722.
1007. Firth, A. V.; Stephan, D. W. *Inorg. Chem.* **1998**, *37*, 4726–4731.
1008. Firth, A. V.; Stephan, D. W. *Organometallics* **1997**, *16*, 2183–2188.
1009. Lundmark, P. J.; Kubas, G. J.; Scott, B. L. *Organometallics* **1996**, *15*, 3631–3633.
1010. Firth, A. V.; Stephan, D. W. *Inorg. Chem.* **1997**, *36*, 1260–1262.
1011. Fenwick, A. E.; Fanwick, P. E.; Rothwell, I. P. *Organometallics* **2003**, *22*, 535–540.
1012. Matsuzaki, K.; Kawaguchi, H.; Voth, P.; Noda, K.; Itoh, S.; Takagi, H. D.; Kashiwabara, K.; Tatsumi, K. *Inorg. Chem.* **2003**, *42*, 5320–5329.
1013. Huang, Y. J.; Stephan, D. W. *Organometallics* **1995**, *14*, 2835–2842.
1014. Nadasdi, T. T.; Huang, Y. J.; Stephan, D. W. *Inorg. Chem.* **1993**, *32*, 347–356.
1015. Huang, Y.; Drake, R. J.; Stephan, D. W. *Inorg. Chem.* **1993**, *32*, 3022–3028.
1016. Nadasdi, T. T.; Stephan, D. W. *Inorg. Chem.* **1993**, *32*, 5933–5938.
1017. Spence, M. A.; Rosair, G. M.; Lindsell, W. E. *J. Chem. Soc., Dalton Trans.* **1998**, 1581–1586.
1018. Lindsell, W. E.; Rosair, G. M.; Spence, M. A. *J. Organomet. Chem.* **1999**, *577*, 9–14.
1019. Andras, M. T.; Duraj, S. A. *Inorg. Chem.* **1993**, *32*, 2874–2880.

1020. Antiñolo, A.; Carrillo-Hermosilla, F.; Corrochano, A. E.; Fandos, R.; Fernández-Baeza, J.; Rodríguez, A. M.; Ruiz, M. J.; Otero, A. *Organometallics* **1999**, *18*, 5219–5224.
1021. Saito, K.; Nakano, M.; Tamura, H.; Matsubayashi, G. E. *Inorg. Chem.* **2000**, *39*, 4815–4820.
1022. Matsubayashi, G. E.; Nakano, M.; Saito, K.; Tamura, H. *Mol. Cryst. Liq. Cryst.* **2000**, *343*, 347–352.
1023. Huang, Y. J.; Nadasdi, T. T.; Stephan, D. W. *J. Am. Chem. Soc.* **1994**, *116*, 5483–5484.
1024. Huang, Y. J.; Etkin, N.; Heyn, R. R.; Nadasdi, T. T.; Stephan, D. W. *Organometallics* **1996**, *15*, 2320–2330.
1025. Bottomley, F.; Day, R. W. *Organometallics* **1996**, *15*, 809–813.
1026. Gindelberger, D. E. *Acta Crystallogr., Sect. C: Cryst. Struct. Commun.* **1996**, *52*, 2493–2495.
1027. Hoskin, A. J.; Stephan, D. W. *Coord. Chem. Rev.* **2002**, *233*, 107–129.
1028. Ma, K. B.; Piers, W. E.; Gao, Y.; Parvez, M. J. *Am. Chem. Soc.* **2004**, *126*, 5668–5669.
1029. Beckaus, R. In *Metalloenes: Synthesis, Reactivity and Applications*; Togni, A., Halterman, R. L., Eds.; Wiley-VCH: New York, 1998; Vol. 1, pp 153–239.
1030. Halterman, R. L. In *Metalloenes: Synthesis, Reactivity and Applications*; Togni, A., Halterman, R. L., Eds.; Wiley-VCH: New York, 1998; Vol. 1, pp 455–544.
1031. Long, N. J. *Metalloenes*; Blackwell: Malden, 1998.
1032. Leino, R.; Lehmus, P.; Lehtonen, A. *Eur. J. Inorg. Chem.* **2004**, 3201–3222.
1033. Horacek, M.; Stepnicka, P.; Gyepes, R.; Cisarova, I.; Tislerova, I.; Zemanek, J.; Kubista, J.; Mach, K. *Chem. Eur. J.* **2000**, *6*, 2397–2408.
1034. Lukesova, L.; Stepnicka, P.; Fejfarova, K.; Gyepes, R.; Cisarova, I.; Horacek, M.; Kubista, J.; Mach, K. *Organometallics* **2002**, *21*, 2639–2653.
1035. Horacek, M.; Stepnicka, P.; Kubista, J.; Cisarova, I.; Petrusova, L.; Mach, K. *J. Organomet. Chem.* **2003**, *667*, 154–166.
1036. Schmid, M. A.; Alt, H. G.; Milius, W. J. *Organomet. Chem.* **1996**, *514*, 45–49.
1037. Xu, S. S.; Yang, L.; Yuan, K.; Wang, B. Q.; Zhou, X. Z.; Li, W.; He, X. J. *Chem. J. Chin. Univ.* **2001**, *22*, 2022–2025.
1038. Bursten, B. E.; Callstrom, M. R.; Jolly, C. A.; Paquette, L. A.; Sivik, M. R.; Tucker, R. S.; Wartchow, C. A. *Organometallics* **1994**, *13*, 127–133.
1039. Horacek, M.; Polasek, M.; Kupfer, V.; Thewalt, U.; Mach, K. *Collect. Czech. Chem. Commun.* **1999**, *64*, 61–72.
1040. Cheng, Y. X.; Yu, X. Y.; Jin, G. X.; Jia, H. Q. *Acta Polym. Sin.* **2001**, 139–142.
1041. King, W. A.; Di Bella, S.; Gulino, A.; Lanza, G.; Fragala, I. L.; Stern, C. L.; Marks, T. J. *J. Am. Chem. Soc.* **1999**, *121*, 355–366.
1042. Hart, S. L.; Duncalf, D. J.; Hastings, J. J.; McCamley, A.; Taylor, P. C. *J. Chem. Soc., Dalton Trans.* **1996**, 2843–2849.
1043. Jibril, I.; Abuorabi, S. T.; Klaib, S. A.; Zsolnai, L.; Huttner, G. *J. Organomet. Chem.* **1994**, *467*, 189–194.
1044. Hughes, R. P.; Lompvey, J. R.; Rheingold, A. L.; Haggerty, B. S.; Yap, G. P. A. *J. Organomet. Chem.* **1996**, *517*, 89–99.
1045. Schmid, G.; Thewalt, U.; Polasek, M.; Mach, K.; Sedmera, P. *J. Organomet. Chem.* **1994**, *482*, 231–241.
1046. Pinkas, J.; Horacek, M.; Kubista, J.; Gyepes, R.; Cisarova, I.; Pirio, N.; Meunier, P.; Mach, K. *J. Organomet. Chem.* **2004**, *689*, 1623–1630.
1047. Qian, Y. L.; Qin, X. R.; Huang, J. L.; Chan, A. S. C.; Chen, S. S.; Wang, H. G. *Chin. J. Chem.* **2001**, *19*, 97–101.
1048. Grimmond, B. J.; Corey, J. Y.; Rath, N. P. *Organometallics* **1999**, *18*, 404–412.
1049. Licht, E. H.; Alt, H. G.; Karim, M. M. *J. Organomet. Chem.* **2000**, *599*, 275–287.
1050. Huttenloch, M. E.; Dorer, B.; Rief, U.; Prosenc, M. H.; Schmidt, K.; Brintzinger, H. H. *J. Organomet. Chem.* **1997**, *541*, 219–232.
1051. Yang, Q.; Jensen, M. D. *Synlett* **1996**, 563–565.
1052. Polo, E.; Bellabarba, R. M.; Prini, G.; Traverso, O.; Green, M. L. H. *J. Organomet. Chem.* **1999**, *577*, 211–218.
1053. Stempfle, B.; Werner, H. *Gazz. Chim. Ital.* **1995**, *125*, 287–290.
1054. Foster, P.; Chien, J. C. W.; Rausch, M. D. *Organometallics* **1996**, *15*, 4951–4953.
1055. Walawalkar, M. G.; Murugavel, R.; Roesky, H. W. *Eur. J. Solid State Inorg. Chem.* **1996**, *33*, 943–955.
1056. Brinkmann, P. H. P.; Prosenc, M. H.; Luinstra, G. A. *Organometallics* **1995**, *14*, 5481–5482.
1057. Piao, G.; Goto, H.; Akagi, K.; Shirakawa, H. *Polymer* **1998**, *39*, 3559–3564.
1058. Akagi, K.; Goto, H.; Bannai, H.; Piao, G.; Shirakawa, H. *Synth. Met.* **1997**, *86*, 1879–1880.
1059. Qian, Y. L.; Li, G. S. *Polyhedron* **1993**, *12*, 967–970.
1060. Fernandes, A. C.; Romao, C. C.; Royo, B. J. *Organomet. Chem.* **2003**, *682*, 14–19.
1061. Barrett, A. G. M.; de Miguel, Y. R. *Chem. Commun.* **1998**, 2079–2080.
1062. Horacek, M.; Gyepes, R.; Cisarova, I.; Polasek, M.; Varga, V.; Mach, K. *Collect. Czech. Chem. Commun.* **1996**, *61*, 1307–1320.
1063. Drew, M. G. B.; Delgado, E.; Hernandez, E.; Baker, P. K.; Mansilla, N. *Acta Crystallogr., Sect. C: Cryst. Struct. Commun.* **1996**, *52*, 2168–2170.
1064. Ciruelos, S.; Sebastián, A.; Cuenca, T.; Gómez-Sal, P.; Manzanero, A.; Royo, P. *J. Organomet. Chem.* **2000**, *604*, 103–115.
1065. Wolfram, R.; Ramos, C.; Royo, P.; Lanfranchi, M.; Pellingelli, M. A.; Tiripicchio, A. *Inorg. Chim. Acta* **2003**, *347*, 114–122.
1066. Deck, P. A.; Fisher, T. S.; Downey, J. S. *Organometallics* **1997**, *16*, 1193–1196.
1067. Lang, H.; Blau, S.; Muth, A.; Weiss, K.; Neugebauer, U. *J. Organomet. Chem.* **1995**, *490*, C32–C36.
1068. Corey, J. Y.; Huhmann, J. L.; Rath, N. P. *Inorg. Chem.* **1995**, *34*, 3203–3209.
1069. Weiss, K.; Wirth-Pfeifer, C.; Hofmann, M.; Botzenhardt, S.; Lang, H.; Bruning, K.; Meichel, E. *J. Mol. Catal. A: Chem.* **2002**, *182*, 143–149.
1070. Andrés, R.; de Jesús, E.; de la Mata, F. J.; Flores, J. C.; Gómez, R. *Eur. J. Inorg. Chem.* **2002**, 2281–2286.
1071. Wang, J. T.; Xu, Y. M.; Zhang, Z. D. *Heteroat. Chem.* **1995**, *6*, 601–604.
1072. Bochmann, M.; Lancaster, S. J.; Jiménez-Pindado, G.; Walker, D. A.; Al-Benna, S.; Thornton-Pett, M. In *Contemporary Boron Chemistry*; Davidson, M. G., Hughes, A. K., Marder, T. B., Wade, K., Eds.; Royal Society of Chemistry: London, 2000, p 10.
1073. Lancaster, S. J.; Mountford, A. J.; Hughes, D. L.; Schormann, M.; Bochmann, M. *J. Organomet. Chem.* **2003**, *680*, 193–205.
1074. Han, Y.; Hong, E.; Kim, Y.; Lee, M.; Kim, J.; Hwang, J. W.; Do, Y. *J. Organomet. Chem.* **2003**, *679*, 48–58.
1075. Le Gendre, P.; Maubrou, E.; Blacque, O.; Boni, G.; Moise, C. *Eur. J. Inorg. Chem.* **2001**, 1437–1440.
1076. Delgado, E.; García, M. A.; Hernández, E.; Mansilla, N.; Martínez-Cruz, L. A.; Tornero, J.; Torres, R. *J. Organomet. Chem.* **1998**, *560*, 27–33.
1077. Broussier, R.; Bourdon, C.; Blacque, O.; Vallat, A.; Kubicki, M. M.; Gautheron, B. *J. Organomet. Chem.* **1997**, *538*, 83–90.
1078. Broussier, R.; Bourdon, C.; Blacque, O.; Vallat, A.; Kubicki, M. M.; Gautheron, B. *Bull. Soc. Chim. Fr.* **1996**, *133*, 843–851.
1079. Feng, Z. F.; Xie, J.; Chen, B.; Qian, Y. L. *Chin. J. Org. Chem.* **2001**, *21*, 33–40.
1080. Cano, A.; Cuenca, T.; Rodríguez, G.; Royo, P.; Cardin, C.; Wilcock, D. J. *J. Organomet. Chem.* **1993**, *447*, 51–57.
1081. Deppner, M.; Burger, R.; Alt, H. G. *J. Organomet. Chem.* **2004**, *689*, 1194–1211.
1082. Huhmann, J. L.; Corey, J. Y.; Rath, N. P. *J. Organomet. Chem.* **1997**, *533*, 61–72.
1083. Xu, S. S.; Wu, T.; Cui, H. L.; Dai, X. L.; Wang, B. Q.; Zhou, X. Z.; Zou, F. L.; Li, Y. *Chem. J. Chin. Univ.* **2002**, *23*, 1891–1895.
1084. Thiele, K. H.; Gerstner, P.; Somoza, F. Z. *Anorg. Allg. Chem.* **2001**, *627*, 28–30.
1085. Zemanek, J.; Horacek, M.; Thewalt, U.; Stepnicka, P.; Kubista, J.; Cejka, J.; Petrusova, L.; Mach, K. *Inorg. Chem. Commun.* **2001**, *4*, 520–525.

1086. Xu, S. S.; Dai, X. L.; Wu, T.; Wang, B. Q.; Zhou, X. Z.; Weng, L. H. *J. Organomet. Chem.* **2002**, *645*, 212–217.
1087. Feng, R.; Su, L. M.; He, D. W.; Wang, B. Q.; Tian, G. L.; Xu, S. S.; Zhou, X. Z. *Acta Polym. Sin.* **1998**, 360–363.
1088. Crimmond, B. J.; Corey, J. Y.; Rath, N. P. *Acta Crystallogr., Sect. C: Cryst. Struct. Commun.* **2000**, *56*, 53–55.
1089. Kotov, V. V.; Fröhlich, R.; Kehr, G.; Erker, G. *J. Organomet. Chem.* **2003**, *676*, 1–7.
1090. Qian, Y. L.; Guo, R. W.; Huang, J. L.; Jonas, K. *Chin. Chem. Lett.* **1996**, *7*, 1139–1142.
1091. Hitchcock, P. B.; Leigh, G. J.; Togrou, M. *J. Organomet. Chem.* **2003**, *669*, 101–105.
1092. Enders, M.; Kohler, K.; Frosch, W.; Pritzkow, H.; Lang, H. *J. Organomet. Chem.* **1997**, *538*, 163–170.
1093. Beckhaus, R.; Oster, J.; Ganter, B.; Englert, U. *Organometallics* **1997**, *16*, 3902–3909.
1094. Jutzi, P.; Redeker, T.; Neumann, B.; Stämmler, H. G. *Organometallics* **1996**, *15*, 4153–4161.
1095. Jutzi, P.; Redeker, T.; Neumann, B.; Stämmler, H. G. *Chem. Ber. Rec.* **1996**, *129*, 1509–1515.
1096. McGowan, M. A. D.; McGowan, P. C. *Inorg. Chem. Commun.* **2000**, *3*, 337–340.
1097. Allen, O. R.; Croll, L.; Gott, A. L.; Knox, R. J.; McGowan, P. C. *Organometallics* **2004**, *23*, 288–292.
1098. Causey, P. W.; Baird, M. C.; Cole, S. P. C. *Organometallics* **2004**, *23*, 4486–4494.
1099. Hierländer, D.; Fröhlich, R.; Erker, G. *J. Chem. Soc., Dalton Trans.* **2002**, 1513–1520.
1100. Graham, D. W.; Llamazares, A.; McDonald, R.; Cowie, M. *Organometallics* **1999**, *18*, 3490–3501.
1101. van der Zeijden, A. A. H.; Mattheis, C. *J. Organomet. Chem.* **1998**, *555*, 5–15.
1102. Zheng, Q. H.; Liu, Y. L.; He, Z. J.; Chen, S. S. *Chem. J. Chin. Univ.* **1995**, *16*, 1706–1709.
1103. Suzuka, T.; Kawatsura, M.; Okada, A.; Hayashi, T. *Tetrahedron: Asymmetry* **2003**, *14*, 511–515.
1104. Hart, S. L.; McCamley, A.; McCormack, P. J.; Taylor, P. C. *J. Organomet. Chem.* **1998**, *553*, 507–509.
1105. Alcock, N. W.; Clase, H. J.; Duncalf, D. J.; Hart, S. L.; McCamley, A.; McCormack, P. J.; Taylor, P. C. *J. Organomet. Chem.* **2000**, *605*, 45–54.
1106. Paquette, L. A.; Sivik, M. R.; Bzowej, E. I.; Stanton, K. J. *Organometallics* **1995**, *14*, 4865–4878.
1107. Zaegel, F.; Gallucci, J. C.; Meunier, P.; Gautheron, B.; Sivik, M. R.; Paquette, L. A. *J. Am. Chem. Soc.* **1994**, *116*, 6466–6467.
1108. Zaegel, F.; Gallucci, J. C.; Meunier, P.; Gautheron, B.; Bzowej, E. I.; Paquette, L. A. *Organometallics* **1995**, *14*, 4576–4584.
1109. Fritze, C.; Knickmeier, M.; Erker, G.; Zaegel, F.; Gautheron, B.; Meunier, P.; Paquette, L. A. *Organometallics* **1995**, *14*, 5446–5449.
1110. Gobley, O.; Meunier, P.; Gautheron, B.; Gallucci, J. C.; Erker, G.; Dahlmann, M.; Schloss, J. D.; Paquette, L. A. *Organometallics* **1998**, *17*, 4897–4903.
1111. Horacek, M.; Stepnicka, P.; Gentil, S.; Fejfarova, K.; Kubista, J.; Pirio, N.; Meunier, P.; Gallou, F.; Paquette, L. A.; Mach, K. *J. Organomet. Chem.* **2002**, *656*, 81–88.
1112. Halterman, R. L.; Tretyakov, A. *Tetrahedron* **1995**, *51*, 4371–4382.
1113. Halterman, R. L.; Ramsey, T. M. *J. Organomet. Chem.* **1997**, *530*, 225–234.
1114. Gansauer, A.; Bluhm, H.; Pierobon, M.; Keller, M. *Organometallics* **2001**, *20*, 914–919.
1115. Gansauer, A.; Rinker, B.; Barchuk, A.; Nieger, M. *Organometallics* **2004**, *23*, 1168–1171.
1116. Klouras, N.; Nastopoulos, V.; Demakopoulos, I.; Leban, I. Z. *Anorg. Allg. Chem.* **1993**, *619*, 1927–1930.
1117. Jones, P. G.; Kienitz, C.; Thone, C. Z. *Kristallogr.* **1994**, *209*, 85–86.
1118. Troyanov, S. I.; Rybakov, V. B.; Thewalt, U.; Varga, V.; Mach, K. *J. Organomet. Chem.* **1993**, *447*, 221–225.
1119. Burlakov, V. V.; Dolgushin, F. M.; Yanovsky, A. I.; Struchkov, Y. T.; Shur, V. B.; Rosenthal, U.; Thewalt, U. *J. Organomet. Chem.* **1996**, *522*, 241–247.
1120. Winter, C. H.; Lewkebandara, T. S.; Shui, X. Q.; Zhou, X. X. **1993**, *23*, 685–687.
1121. Howie, R. A.; McQuillan, G. P.; Thompson, D. W. *Acta Crystallogr., Sect. E: Struct. Rep. Online* **2001**, *57*, M181–M182.
1122. Gelmini, L.; Puddephatt, R. J.; Vittal, J. J. *Acta Crystallogr., Sect. C: Cryst. Struct. Commun.* **1993**, *49*, 30–33.
1123. Yu, Y. H.; Xia, W.; Ma, H. Y.; Tao, X. C.; Huang, J. L.; Qian, Y. L. *Acta Chim. Sinica.* **2002**, *60*, 347–354.
1124. Burgess, J.; Parsons, S. A. *Appl. Organomet. Chem.* **1993**, *7*, 343–351.
1125. Johnston, R. F.; Borjas, R. E.; Furilla, J. L. *Electrochim. Acta* **1995**, *40*, 473–477.
1126. Vallat, A.; Roullier, L.; Bourdon, C. *J. Electroanal. Chem.* **2003**, *542*, 75–83.
1127. Anderson, J. E.; Sawtelle, S. M. *Inorg. Chem.* **1992**, *31*, 5345–5346.
1128. Fussing, I. M. M.; Pletcher, D.; Whitby, R. J. *J. Organomet. Chem.* **1994**, *470*, 119–125.
1129. Langmaier, J.; Samec, Z.; Varga, V.; Horacek, M.; Mach, K. *J. Organomet. Chem.* **1999**, *579*, 348–355.
1130. Zagorevskii, D. V.; Holmes, J. L. *Org. Mass Spectrom.* **1993**, *28*, 49–55.
1131. Kenney, J. W.; Boone, D. R.; Striplin, D. R.; Chen, Y. H.; Hamar, K. B. *Organometallics* **1993**, *12*, 3671–3676.
1132. Hartmann, H.; Sarkar, B.; Kaim, W.; Fiedler, J. *J. Organomet. Chem.* **2003**, *687*, 100–107.
1133. Knizhnikov, V. A.; Maier, N. A. *Usp. Khim.* **2002**, *71*, 341–362.
1134. Qian, Y. L.; Huang, J. L. *Chin. J. Chem.* **2001**, *19*, 1009–1022.
1135. Burgmayer, S. J. N. *J. Chem. Educ.* **1998**, *75*, 460–460.
1136. Yu, P. H.; Murphy, E. F.; Roesky, H. W.; Lubini, P.; Schmidt, H. G.; Noltemeyer, M. *Organometallics* **1997**, *16*, 313–316.
1137. Baum, E.; Matern, E.; Pikies, J.; Robaszkiewicz, A. Z. *Anorg. Allg. Chem.* **2004**, *630*, 1090–1095.
1138. Cano, A.; Cuenca, T.; Galakhov, M.; Rodríguez, G. M.; Royo, P.; Cardin, C. J.; Convery, M. A. *J. Organomet. Chem.* **1995**, *493*, 17–25.
1139. Cuenca, T.; Padilla, A.; Royo, P.; Parrahaque, M.; Pellinghelli, M. A.; Tiripicchio, A. *Organometallics* **1995**, *14*, 848–854.
1140. Horikawa, Y.; Nomura, T.; Watanabe, M.; Fujiwara, T.; Takeda, T. *J. Org. Chem.* **1997**, *62*, 3678–3682.
1141. Liu, F. C.; Chen, K. Y.; Chen, J. H.; Lee, G. H.; Peng, S. M. *Inorg. Chem.* **2003**, *42*, 1758–1763.
1142. Lukesova, L.; Horacek, M.; Stepnicka, P.; Gyepes, R.; Cisarova, I.; Kubista, J.; Mach, K. *J. Organomet. Chem.* **2004**, *689*, 1919–1929.
1143. Miura, K.; Funatsu, M.; Saito, H.; Ito, H.; Hosomi, A. *Tetrahedron Lett.* **1996**, *37*, 9059–9062.
1144. Troyanov, S. I.; Varga, V.; Mach, K. *Organometallics* **1993**, *12*, 2820–2824.
1145. Horacek, M.; Cisarova, I.; Cejka, J.; Karban, J.; Petrusova, L.; Mach, K. *J. Organomet. Chem.* **1999**, *577*, 103–112.
1146. Horacek, M.; Hiller, J.; Thewalt, U.; Polasek, M.; Mach, K. *Organometallics* **1997**, *16*, 4185–4191.
1147. Varga, V.; Mach, K.; Hiller, J.; Thewalt, U.; Sedmera, P.; Polasek, M. *Organometallics* **1995**, *14*, 1410–1416.
1148. Horikawa, Y.; Watanabe, M.; Fujiwara, T.; Takeda, T. *J. Am. Chem. Soc.* **1997**, *119*, 1127–1128.
1149. Yang, F. L.; Zhao, G.; Ding, Y. *Tetrahedron Lett.* **2001**, *42*, 2839–2841.
1150. Kupfer, V.; Thewalt, U.; Horacek, M.; Petrusova, L.; Mach, K. *Inorg. Chem. Commun.* **1999**, *2*, 540–544.
1151. Lukesova, L.; Horacek, M.; Stepnicka, P.; Fejfarova, K.; Gyepes, R.; Cisarova, I.; Kubista, J.; Mach, K. *J. Organomet. Chem.* **2002**, *663*, 134–144.



1152. Troyanov, S. I.; Varga, V.; Mach, K. J. *Organomet. Chem.* **1993**, *461*, 85–90.
1153. Yamamoto, Y.; Matsumi, D.; Itoh, K. *Chem. Commun.* **1998**, 875–876.
1154. Goedheijt, M. S.; Nijbacker, T.; Akkerman, O. S.; Bickelhaupt, F.; Veldman, N.; Spek, A. L. *J. Organomet. Chem.* **1997**, *527*, 1–5.
1155. Gyepes, R.; Mach, K.; Cisarova, I.; Loub, J.; Hiller, J.; Sindelar, P. *J. Organomet. Chem.* **1995**, *497*, 33–41.
1156. Troyanov, S. I.; Varga, V.; Mach, K. J. *Chem. Soc., Chem. Commun.* **1993**, 1174–1175.
1157. Varga, V.; Petrusova, L.; Cejka, J.; Mach, K. J. *Organomet. Chem.* **1997**, *532*, 251–259.
1158. Gao, Y.; Iijima, S.; Urabe, H.; Sato, F. *Inorg. Chim. Acta* **1994**, *222*, 145–153.
1159. Szymoniak, J.; Felix, D.; Moise, C. *Tetrahedron Lett.* **1994**, *35*, 8613–8616.
1160. Gansauer, A.; Lauterbach, T.; Geich-Gimbel, D. *Chem. Eur. J.* **2004**, *10*, 4983–4990.
1161. Barrero, A. F.; Rosales, A.; Cuerva, J. M.; Gansauer, A.; Oltra, J. E. *Tetrahedron Lett.* **2003**, *44*, 1079–1082.
1162. Mandal, P. K.; Maiti, G.; Roy, S. C. *J. Org. Chem.* **1998**, *63*, 2829–2834.
1163. Rajanbabu, T. V.; Nugent, W. A. *J. Am. Chem. Soc.* **1994**, *116*, 986–997.
1164. Gold, H. J. *Synlett* **1999**, 159–159.
1165. Zhou, L. H.; Hirao, T. *Tetrahedron* **2001**, *57*, 6927–6933.
1166. Yu, P. H.; Montero, M. L.; Barnes, C. E.; Roesky, H. W.; Uson, I. *Inorg. Chem.* **1998**, *37*, 2595–2597.
1167. Sizov, A. I.; Zjukova, T. M.; Bulychov, B. M.; Belsky, V. K. *J. Organomet. Chem.* **2000**, *603*, 167–173.
1168. Troyanov, S. I.; Mach, K.; Varga, V. *Organometallics* **1993**, *12*, 3387–3389.
1169. Dzhemilev, U. M.; Ibragimov, A. G.; Ramazanov, I. R.; Sultanov, R. M.; Khalilov, L. M.; Muslukhov, R. R. *Russ. Chem. Bull.* **1996**, *45*, 2610–2613.
1170. Carlin, R. T.; Fuller, J. *Inorg. Chim. Acta* **1997**, *255*, 189–192.
1171. Liu, F. C.; Plecnik, C. E.; Liu, S. M.; Liu, J. P.; Meyers, E. A.; Shore, S. G. *J. Organomet. Chem.* **2001**, *627*, 109–120.
1172. Douthwaite, R. E. *Polyhedron* **2000**, *19*, 1579–1583.
1173. Plecnik, C. E.; Liu, F. C.; Liu, S. M.; Liu, J. P.; Meyers, E. A.; Shore, S. G. *Organometallics* **2001**, *20*, 3599–3606.
1174. Ho, N. N.; Bau, R.; Plecnik, C.; Shore, S. G.; Wang, X. P.; Schultz, A. J. *J. Organomet. Chem.* **2002**, *654*, 216–220.
1175. Gansauer, A.; Bluhm, H.; Rinker, B.; Narayan, S.; Schick, M.; Lauterbach, T.; Pierobon, M. *Chem. Eur. J.* **2003**, *9*, 531–542.
1176. Rosales, A.; Oller-Lopez, J. L.; Justicia, J.; Gansauer, A.; Oltra, J. E.; Cuerva, J. M. *Chem. Commun.* **2004**, 2628–2629.
1177. Enemaerke, R. J.; Larsen, J.; Skrydstrup, T.; Daasbjerg, K. *Organometallics* **2004**, *23*, 1866–1874.
1178. Samuel, E.; Henrique, J. J. *Organomet. Chem.* **1996**, *512*, 183–187.
1179. Enemaerke, R. J.; Hjøllund, G. H.; Daasbjerg, K.; Skrydstrup, T. *C. R. Acad. Sci. Ser. II C* **2001**, *4*, 435–438.
1180. Gansauer, A.; Lauterbach, T.; Narayan, S. *Angew. Chem., Int. Ed. Engl.* **2003**, *42*, 5556–5573.
1181. Gansauer, A.; Rinker, B.; Pierobon, M.; Grimme, S.; Gerenkamp, M.; Muck-Lichtenfeld, C. *Angew. Chem., Int. Ed. Engl.* **2003**, *42*, 3687–3690.
1182. Gansauer, A.; Bluhm, H. *Chem. Commun.* **1998**, 2143–2144.
1183. Gansauer, A.; Pierobon, M.; Bluhm, H. *Angew. Chem., Int. Ed. Engl.* **1998**, *37*, 101–103.
1184. Gansauer, A.; Rinker, B. *Tetrahedron* **2002**, *58*, 7017–7026.
1185. Matkovskii, P. E.; Chernaya, L. I. *Izv. Akad. Nauk., Ser. Khim.* **1996**, *12*, 2904–2908.
1186. Hogenbirk, M.; Schat, G.; de Kanter, F. J. J.; Akkerman, O. S.; Bickelhaupt, F.; Kooijman, H.; Spek, A. L. *Eur. J. Inorg. Chem.* **2004**, 2045–2052.
1187. Vyshinskaya, L. I.; Korneva, S. P.; Kulikova, G. P. *Russ. J. Gen. Chem.* **2000**, *70*, 1281–1283.
1188. Hu, C. J.; Zhang, W. W.; Xu, Y.; Zhu, H. Z.; Ren, X. M.; Lu, C. S.; Meng, Q. J.; Wang, H. Q. *Transition Met. Chem.* **2001**, *26*, 700–703.
1189. Klouras, N.; Tzavellas, N.; Raptopoulou, C. P. *Monatsh. Chem.* **1997**, *128*, 961–967.
1190. Gao, Z. W.; Gao, L. X.; Zhang, Z. T.; Ma, B. H.; Hu, M. C.; Wang, J. Y. *Chin. J. Org. Chem.* **1999**, *19*, 309–311.
1191. Gao, Z. W.; Hu, D. D.; Gao, L. X.; Zhang, X. L.; Zhang, Z. T.; Liang, Q. Q. *J. Organomet. Chem.* **2001**, *629*, 47–53.
1192. Gao, Z. W. *Acta Chim. Sinica* **2000**, *58*, 481–485.
1193. Gao, Z. W. *Acta Chim. Sinica* **2000**, *58*, 343–346.
1194. Srivastava, A. K.; Pandey, O. P.; Sengupta, S. K. *Synth. React. Inorg. Met.-Org. Chem.* **2000**, *30*, 1405–1416.
1195. Mittal, A. K.; Shukla, A.; Shukla, P. R.; Pathak, A. K.; Ahmad, N. *Synth. React. Inorg. Met.-Org. Chem.* **1995**, *25*, 739–759.
1196. Besancon, J.; Szymoniak, J.; Moise, C.; Toupet, L.; Trimaille, B. *J. Organomet. Chem.* **1995**, *491*, 31–39.
1197. Slifirski, J.; Teyssandier, F. *Surf. Coat. Technol.* **1996**, *80*, 255–263.
1198. Weller, F.; Petz, W. Z. *Anorg. Allg. Chem.* **1994**, *620*, 343–345.
1199. Blom, R.; Follestad, A.; Rytter, E.; Tilset, M.; Ystenes, M. In *Organometallic Complexes and Olefin Polymerization*; Blom, R. F. A., Rytter, E., Tilset, M., Ystenes, M., Eds.; Springer: Berlin, 2001.
1200. Bajgur, C. S.; Sivaram, S. *Curr. Sci.* **2000**, *78*, 1325–1335.
1201. Spitz, R.; Saudemont, T. *Actual Chim.* **1996**, 5–12.
1202. Karol, F. J.; Kao, S. C. *New J. Chem.* **1994**, *18*, 97–103.
1203. Spitz, R.; Boisson, C. *Actual Chim.* **2002**, 54–58.
1204. Grimmer, N. E.; Coville, N. J. *South Afr. J. Chem.-Suid-Afr. Tydskr. Chem.* **2001**, *54*, 1–112.
1205. Fukui, Y.; Murata, M. *Macromol. Chem. Phys.* **2001**, *202*, 1473–1477.
1206. D'Agnillo, L.; Soares, J. B. P.; Penlidis, A. *Macromol. Chem. Phys.* **1998**, *199*, 955–962.
1207. D'Agnillo, L.; Soares, J. B. P.; Penlidis, A. *J. Polym. Sci. Pol. Chem.* **1998**, *36*, 831–840.
1208. Tritto, I.; Sacchi, M. C.; Li, S. X. *Macromol. Rapid Commun.* **1994**, *15*, 217–223.
1209. Tritto, I.; Sacchi, M. C.; Locatelli, P.; Li, S. X. *Macromol. Symp.* **1995**, *89*, 289–298.
1210. Tritto, I.; Li, S. X.; Boggioni, L.; Sacchi, M. C.; Locatelli, P.; Oneill, A. *Macromol. Chem. Phys.* **1997**, *198*, 1347–1361.
1211. Bryakov, K. P.; Talsi, E. P.; Bochmann, M. *Organometallics* **2004**, *23*, 149–152.
1212. Eisch, J. J.; Pombrink, S. I.; Zheng, G. X. *Makromol. Chem., Macromol. Symp.* **1993**, *66*, 109–120.
1213. Eisch, J. J.; Pombrink, S. I.; Zheng, G. X. *Organometallics* **1993**, *12*, 3856–3863.
1214. Ricci, G.; Bosio, C.; Porri, L. *Macromol. Rapid Commun.* **1996**, *17*, 781–785.
1215. Dyachkovskii, F. S. *Role of Ions in Coordination Polymerization of Olefins*; Elsevier Science: Amsterdam, **1994**; Vol. 89, pp 201–208.
1216. Tritto, I.; Locatelli, P.; Sacchi, M. C.; Li, S. X.; Zannoni, G. *Gazz. Chim. Ital.* **1996**, *126*, 383–389.
1217. Eisch, J. J.; Pombrink, S. I.; Shi, X.; Wu, S. C. *Macromol. Symp.* **1995**, *89*, 221–229.

1218. Mohring, P. C.; Vlachakis, N.; Grimmer, N. E.; Coville, N. J. *J. Organomet. Chem.* **1994**, *483*, 159–166.
1219. Qian, Y. L.; Huang, J. L.; Huang, T. S.; Chen, S. S. *Transition Met. Chem.* **1996**, *21*, 393–397.
1220. Kissin, Y. V. *Macromol. Rapid Commun.* **2004**, *25*, 1554–1557.
1221. Rabagliati, F. M.; Perez, M. A.; Quijada, R. *Polym. Bull.* **1998**, *41*, 441–446.
1222. Gupta, V. K.; Satish, S.; Bhardwaj, I. S. *J. Macromol. Sci., Pure Appl. Chem.* **1995**, *A32*, 549–558.
1223. Wang, B.; Ye, D. K.; Liu, D. Y. *Acta Polym. Sin.* **2001**, 22–26.
1224. Grishin, D. F.; Semyonycheva, L. L.; Telegina, E. V.; Smirnov, A. S.; Nevodchikov, V. I. *Russ. Chem. Bull.* **2003**, *52*, 505–507.
1225. Sato, T.; Umenoki, T.; Seno, M. *J. Appl. Polym. Sci.* **1998**, *69*, 525–531.
1226. Sato, T.; Shibata, H.; Seno, M. *J. Appl. Polym. Sci.* **2001**, *80*, 815–822.
1227. Sato, T.; Katayose, T.; Seno, M. *J. Appl. Polym. Sci.* **2001**, *79*, 166–175.
1228. Sato, T.; Umenoki, T.; Seno, M.; Tanaka, H. *J. Macromol. Sci., Pure Appl. Chem.* **1995**, *A32*, 1329–1340.
1229. Grishin, D. F.; Ignatov, S. K.; Shchepalov, A. A.; Razuvaev, A. G. *Appl. Organomet. Chem.* **2004**, *18*, 271–276.
1230. Satyanarayana, G.; Sivaram, S. *Macromolecules* **1993**, *26*, 4712–4714.
1231. Severn, J. R.; Chadwick, J. C. *Macromol. Rapid Commun.* **2004**, *25*, 1024–1028.
1232. Tao, X. C.; Qian, F.; Yong, L.; Qian, Y. L. *J. Mol. Catal. A: Chem.* **2000**, *156*, 121–126.
1233. Sensarma, S.; Sivaram, S. *Macromol. Chem. Phys.* **1997**, *198*, 495–503.
1234. Dupuy, J.; Spitz, R. *J. Appl. Polym. Sci.* **1997**, *65*, 2281–2288.
1235. Sensarma, S.; Sivaram, S. *Polym. Int.* **2002**, *51*, 417–423.
1236. Hong, S. C.; Rief, U.; Kristen, M. O. *Macromol. Rapid Commun.* **2001**, *22*, 1447–1454.
1237. Fusco, R.; Longo, L.; Masi, F.; Garbassi, F. *Macromol. Rapid Commun.* **1997**, *18*, 433–441.
1238. Estenoz, D. A.; Chiovetta, M. G. *J. Appl. Polym. Sci.* **2001**, *81*, 285–311.
1239. Qian, Y. L.; Huang, J. L. *Macromol. Symp.* **1996**, *105*, 205–210.
1240. Qian, Y. L.; Hong, K. L.; Zong, H. J.; Huang, J. L. *Polym. Adv. Technol.* **1996**, *7*, 619–624.
1241. Qian, Y. L.; Yang, J. M.; Sun, W. Q.; Ling, Y.; Huang, J. L. *Chin. Chem. Lett.* **1997**, *8*, 305–308.
1242. Qian, Y. L.; Zhang, D. F.; Huang, J. L.; Ma, H. Y.; Chan, A. S. C. *J. Mol. Catal. A: Chem.* **1998**, *133*, 135–138.
1243. Liu, J. F.; Zhang, D. F.; Huang, J. L.; Qian, Y. L.; Chan, A. S. C. *J. Mol. Catal. A: Chem.* **1999**, *142*, 301–304.
1244. Zhang, D. F.; Huang, J. L.; Qian, Y. L.; Chan, A. S. C. *J. Mol. Catal. A: Chem.* **1998**, *133*, 131–133.
1245. Hirao, T. *Synlett* **1999**, 175–181.
1246. Merlic, C. A.; Bendorf, H. D. *Organometallics* **1993**, *12*, 559–564.
1247. Nii, S.; Terao, J.; Kambe, N. *Tetrahedron Lett.* **2004**, *45*, 1699–1702.
1248. Nii, S.; Terao, J.; Kambe, N. *J. Org. Chem.* **2000**, *65*, 5291–5297.
1249. Selvakumar, K.; Harrod, J. F. *Angew. Chem., Int. Ed.* **2001**, *40*, 2129–2131.
1250. Rangareddy, K.; Selvakumar, K.; Harrod, J. F. *J. Org. Chem.* **2004**, *69*, 6843–6850.
1251. Selvakumar, K.; Rangareddy, K.; Harrod, J. F. *Can. J. Chem., Rev. Can. Chim.* **2004**, *82*, 1244–1248.
1252. Yang, W. S.; Hsieh, H. C. C.; Tsiang, R. C. C. *J. Appl. Polym. Sci.* **1999**, *72*, 1807–1815.
1253. Zhao, G.; Sun, H. G.; Qian, Z. S.; Yin, W. X. *J. Fluorine Chem.* **2001**, *111*, 217–219.
1254. Yoo, B. W.; Choi, K. H.; Ko, J. J.; Nam, G. S.; Chang, K. Y.; Choi, K. I.; Kim, J. H. *Bull. Korean Chem. Soc.* **2001**, *22*, 541–542.
1255. Gao, Y.; Sato, F. *J. Chem. Soc., Chem. Commun.* **1995**, 659–660.
1256. Hansen, T.; Daasbjerg, K.; Skrydstrup, T. *Tetrahedron Lett.* **2000**, *41*, 8645–8649.
1257. Hara, R.; Sato, K.; Sun, W. H.; Takahashi, T. *Chem. Commun.* **1999**, 845–846.
1258. Kiplinger, J. L.; Richmond, T. G. *J. Am. Chem. Soc.* **1996**, *118*, 1805–1806.
1259. Kim, B. H.; Woo, H. G.; Kim, W. G.; Yun, S. S.; Hwang, T. S. *Bull. Korean Chem. Soc.* **2000**, *21*, 211–214.
1260. Hedenstrom, E.; Andersson, F.; Hjalmarsson, M. *J. Chem. Soc., Perkin Trans. 1* **2000**, *10*, 1513–1518.
1261. Amin, S. R.; Crowe, W. E. *Tetrahedron Lett.* **1997**, *38*, 7487–7490.
1262. Verdager, X.; Lange, U. E. W.; Reding, M. T.; Buchwald, S. L. *J. Am. Chem. Soc.* **1996**, *118*, 6784–6785.
1263. Della Sala, G.; Lattanzi, A.; Severino, T.; Scettri, A. *J. Mol. Catal. A: Chem.* **2001**, *170*, 219–224.
1264. Jun, C. H.; Lee, D. Y.; Hong, J. B. *Tetrahedron Lett.* **1997**, *38*, 6673–6676.
1265. Liu, Y. M.; Schwartz, J. *Tetrahedron* **1995**, *51*, 4471–4482.
1266. Okamoto, S.; Livinghouse, T. *Organometallics* **2000**, *19*, 1449–1451.
1267. Terao, J.; Kambe, N.; Sonoda, N. *Tetrahedron Lett.* **1998**, *39*, 9697–9698.
1268. Hicks, F. A.; Berk, S. C.; Buchwald, S. L. *J. Org. Chem.* **1996**, *61*, 2713–2718.
1269. He, Z. J.; Wang, Y. M.; Chen, S. S. *Chin. Chem. Lett.* **1998**, *9*, 421–422.
1270. Negishi, E.; Kondakov, D. Y.; Vanhorn, D. E. *Organometallics* **1997**, *16*, 951–957.
1271. Yoo, B. W.; Lee, S. J.; Yoo, B. S.; Choi, K. I.; Kim, J. H. *Synth. Commun.* **2002**, *32*, 2489–2493.
1272. Yoo, B. W.; Choi, A. W.; Kim, D. Y.; Hwang, S. K.; Choi, K. I.; Kim, J. H. *Bull. Korean Chem. Soc.* **2002**, *23*, 797–798.
1273. Yoo, B. W.; Choi, K. H.; Lee, S. J.; Yoon, C. M.; Kim, S. H.; Kim, J. H. *Synth. Commun.* **2002**, *32*, 63–67.
1274. Taw, F. L.; Scott, B. L.; Kiplinger, J. L. *J. Am. Chem. Soc.* **2003**, *125*, 14712–14713.
1275. Vanderheijden, H.; Hessen, B. *J. Chem. Soc., Chem. Commun.* **1995**, 145–146.
1276. Cauzzi, D.; Graiff, C.; Marazzi, M.; Predieri, G.; Tiripicchio, A. *J. Organomet. Chem.* **2002**, *663*, 256–262.
1277. Bochmann, M.; Lancaster, S. J.; Robinson, O. B. *J. Chem. Soc., Chem. Commun.* **1995**, 2081–2082.
1278. Thewalt, U.; Wohrle, T. *Z. Naturforsch.(B)* **1993**, *48*, 603–607.
1279. Balboni, D.; Camurati, I.; Prini, G.; Resconi, L.; Galli, S.; Mercandelli, P.; Sironi, A. *Inorg. Chem.* **2001**, *40*, 6588–6597.
1280. Lang, H.; George, D. S. A.; Rheinwald, G. *Coord. Chem. Rev.* **2000**, *206*, 101–197.
1281. Rosenthal, U.; Arndt, P.; Baumann, W.; Burlakov, V. V.; Spannenberg, A. *J. Organomet. Chem.* **2003**, *670*, 84–96.
1282. Varga, V.; Hiller, J.; Polasek, M.; Thewalt, U.; Mach, K. *J. Organomet. Chem.* **1996**, *514*, 219–226.
1283. Pellny, P. M.; Kirchbauer, F. G.; Burlakov, V. V.; Baumann, W.; Spannenberg, A.; Rosenthal, U. *Chem. Eur. J.* **2000**, *6*, 81–90.
1284. Kirchbauer, F. G.; Pellny, P. M.; Sun, H. S.; Burlakov, V. V.; Arndt, P.; Baumann, W.; Spannenberg, A.; Rosenthal, U. *Organometallics* **2001**, *20*, 5289–5296.
1285. Back, S.; Gossage, R. A.; Rheinwald, G.; del Rio, I.; Lang, H.; van Koten, G. *J. Organomet. Chem.* **1999**, *582*, 126–138.
1286. Zhang, D. M.; McConville, D. B.; Hrabusa, J. M.; Tessier, C. A.; Youngs, W. J. *J. Am. Chem. Soc.* **1998**, *120*, 3506–3507.

1287. Stepnicka, P.; Gyepes, R.; Cisarova, I.; Horacek, M.; Kubista, J.; Mach, K. *Organometallics* **1999**, *18*, 4869–4880.
1288. Beckhaus, R.; Oster, J.; Loo, R. J. *Organomet. Chem.* **1995**, *501*, 321–326.
1289. Beckhaus, R.; Sang, J.; Oster, J.; Wagner, T. J. *Organomet. Chem.* **1994**, *484*, 179–190.
1290. Banger, K. K.; Brisdon, A. K. *J. Organomet. Chem.* **1999**, *582*, 301–309.
1291. Barnes, N. A.; Brisdon, A. K.; Crossley, I. R.; Pritchard, R. G.; Warren, J. E. *Organometallics* **2004**, *23*, 2680–2685.
1292. Fandos, R.; Lanfranchi, M.; Otero, A.; Pellinghelli, M. A.; Ruiz, M. J.; Teuben, J. H. *Organometallics* **1997**, *16*, 5283–5288.
1293. Luinstra, G. A.; Brinkmann, P. H. P.; Teuben, J. H. *J. Organomet. Chem.* **1997**, *532*, 125–131.
1294. Beckhaus, R.; Lutzen, A.; Haase, D.; Saak, W.; Stroot, J.; Becke, S.; Heinrichs, J. *Angew. Chem., Int. Ed.* **2001**, *40*, 2056–2058.
1295. Rottger, D.; Erker, G. *Angew. Chem., Int. Ed. Engl.* **1997**, *36*, 813–827.
1296. Binger, P.; Sandmeyer, F.; Kruger, C.; Kuhnigk, J.; Goddard, R.; Erker, G. *Angew. Chem., Int. Ed. Engl.* **1994**, *33*, 197–198.
1297. Binger, P.; Sandmeyer, F.; Kruger, C.; Erker, G. *Tetrahedron* **1995**, *51*, 4277–4290.
1298. Arndt, P.; Spannenberg, A.; Baumann, W.; Becke, S.; Rosenthal, U. *Eur. J. Inorg. Chem.* **2001**, 2885–2890.
1299. Pulst, S.; Arndt, P.; Heller, B.; Baumann, W.; Kempe, R.; Rosenthal, U. *Angew. Chem., Int. Ed. Engl.* **1996**, *35*, 1112–1115.
1300. Burlakov, V. V.; Ohff, A.; Lefebvre, C.; Tillack, A.; Baumann, W.; Kempe, R.; Rosenthal, U. *Chem. Ber.* **1995**, *128*, 967–971.
1301. Rosenthal, U.; Ohff, A.; Tillack, A.; Baumann, W.; Gols, H. J. *Organomet. Chem.* **1994**, *468*, C4–C8.
1302. Choukroun, R.; Cassoux, P. *Acc. Chem. Res.* **1999**, *32*, 494–502.
1303. Motry, D. H.; Smith, M. R. *J. Am. Chem. Soc.* **1995**, *117*, 6615–6616.
1304. Tinga, M.; Schat, G.; Akkerman, O. S.; Bickelhaupt, F.; Smeets, W. J. J.; Spek, A. L. *Chem. Ber.* **1994**, *127*, 1851–1856.
1305. Tjaden, E. B.; Casty, G. L.; Stryker, J. M. *J. Am. Chem. Soc.* **1993**, *115*, 9814–9815.
1306. Pampaloni, G.; Tripepi, G. *J. Organomet. Chem.* **2000**, *594*, 19–26.
1307. Kienitz, C. O.; Thone, C.; Jones, P. G. *Acta Crystallogr., Sect. C: Cryst. Struct. Commun.* **1996**, *52*, 2402–2404.
1308. Thewalt, U.; Wohrle, T. J. *Organomet. Chem.* **1994**, *464*, C17–C19.
1309. Zhu, Y.; Shen, X. M. *Acta Crystallogr., Sect. C: Cryst. Struct. Commun.* **1996**, *52*, 2422–2425.
1310. Baumann, W.; Pellny, P. M.; Rosenthal, U. *Magn. Reson. Chem.* **2000**, *38*, 515–519.
1311. Deck, P. A.; Beswick, C. L.; Marks, T. J. *J. Am. Chem. Soc.* **1998**, *120*, 1772–1784.
1312. Kempe, R. *Angew. Chem., Int. Ed.* **2004**, *43*, 1463–1464.
1313. Gleiter, R.; Wittwer, W. *Chem. Ber.* **1994**, *127*, 1797–1798.
1314. Xi, Z. F.; Sato, K.; Gao, Y.; Lu, J. M.; Takahashi, T. *J. Am. Chem. Soc.* **2003**, *125*, 9568–9569.
1315. Crowe, W. E.; Vu, A. T. *J. Am. Chem. Soc.* **1996**, *118*, 5508–5509.
1316. Crowe, W. E.; Vu, A. T. *J. Am. Chem. Soc.* **1996**, *118*, 1557–1558.
1317. Harrod, J. F. *Coord. Chem. Rev.* **2000**, *206*, 493–531.
1318. Harrod, J. F.; Mu, Y.; Samuel, E. *Can. J. Chem., Rev. Can. Chim.* **1992**, *70*, 2980–2984.
1319. Varga, V.; Hiller, J.; Polasek, M.; Thewalt, U.; Mach, K. J. *Organomet. Chem.* **1996**, *515*, 57–64.
1320. Varga, V.; Mach, K.; Hiller, J.; Thewalt, U. *J. Organomet. Chem.* **1996**, *506*, 109–112.
1321. Chase, P. A.; Piers, W. E.; Parvez, M. *Organometallics* **2000**, *19*, 2040–2042.
1322. Petasis, N. A.; Hu, Y. H. *J. Org. Chem.* **1997**, *62*, 782–783.
1323. Brinkmann, P. H. P.; Luinstra, G. A.; Saenz, A. J. *J. Am. Chem. Soc.* **1998**, *120*, 2854–2861.
1324. Borkowsky, S. L.; Baenziger, N. C.; Jordan, R. F. *Organometallics* **1993**, *12*, 486–495.
1325. Doxsee, K. M.; Juliette, J. J.; Mouser, J. K. M.; Zientara, K. *Organometallics* **1993**, *12*, 4682–4686.
1326. Doxsee, K. M.; Juliette, J. J.; Zientara, K.; Nieckarz, G. J. *J. Am. Chem. Soc.* **1994**, *116*, 2147–2148.
1327. Hart, S. L.; McCamley, A.; Taylor, P. C. *Synlett* **1999**, 90–92.
1328. Stroot, J.; Beckhaus, R.; Saak, W.; Haase, D.; Lutzen, A. *Eur. J. Inorg. Chem.* **2002**, 1729–1737.
1329. Stroot, J.; Saak, W.; Haase, D.; Beckhaus, R. *Z. Anorg. Allg. Chem.* **2002**, *628*, 755–761.
1330. Stroot, J.; Lutzen, A.; Friedemann, M.; Saak, W.; Beckhaus, R. *Z. Anorg. Allg. Chem.* **2002**, *628*, 797–802.
1331. Binger, P.; Sandmeyer, F.; Kruger, C. *Organometallics* **1995**, *14*, 2969–2976.
1332. Motry, D. H.; Brazil, A. G.; Smith, M. R. *J. Am. Chem. Soc.* **1997**, *119*, 2743–2744.
1333. Harmsen, D.; Erker, G.; Frohlich, R.; Kehr, G. *Eur. J. Inorg. Chem.* **2002**, 3156–3171.
1334. De Angelis, F.; Sgamellotti, A.; Re, N. *J. Chem. Soc., Dalton Trans.* **2001**, 1023–1028.
1335. Dioumaev, V. K.; Rahimian, K.; Gauvin, F.; Harrod, J. F. *Organometallics* **1999**, *18*, 2249–2255.
1336. Arndt, P.; Thomas, D.; Rosenthal, U. *Tetrahedron Lett.* **1997**, *38*, 5467–5468.
1337. Xin, S. X.; Harrod, J. F. *J. Organomet. Chem.* **1995**, *499*, 181–191.
1338. Corey, J. Y.; Rooney, S. M. *J. Organomet. Chem.* **1996**, *521*, 75–91.
1339. Tehrani, K. A.; De Kimpe, N. *Tetrahedron Lett.* **2000**, *41*, 1975–1978.
1340. Schrock, R. R. *Chem. Rev.* **2002**, *102*, 145–179.
1341. Herndon, J. W. *Coord. Chem. Rev.* **2000**, *206*, 237–262.
1342. Herndon, J. W. *Coord. Chem. Rev.* **1999**, *181*, 177–242.
1343. Herndon, J. W. *Coord. Chem. Rev.* **2000**, *209*, 387–451.
1344. Herndon, J. W. *Coord. Chem. Rev.* **2001**, *214*, 215–285.
1345. Herndon, J. W. *Coord. Chem. Rev.* **2002**, *227*, 1–58.
1346. Herndon, J. W. *Coord. Chem. Rev.* **2003**, *243*, 3–81.
1347. Herndon, J. W. *Coord. Chem. Rev.* **2004**, *248*, 3–79.
1348. Herndon, J. W. *Coord. Chem. Rev.* **2005**, *249*, 999–1084.
1349. Barluenga, J.; Fananas, F. J. *Tetrahedron* **2000**, *56*, 4597–4628.
1350. Eisch, J. J. *J. Organomet. Chem.* **2001**, *617*, 148–157.
1351. Eisch, J. J.; Gitua, J. N.; Otieno, P. O.; Shi, X. J. *Organomet. Chem.* **2001**, *624*, 229–238.
1352. Beckhaus, R.; Santamaria, C. J. *Organomet. Chem.* **2001**, *617*, 81–97.
1353. Beckhaus, R. *J. Chem. Soc., Dalton Trans.* **1997**, 1991–2001.
1354. Beckhaus, R. *Angew. Chem., Int. Ed. Engl.* **1997**, *36*, 687–713.
1355. Beckhaus, R.; Oster, J.; Sang, J.; Strauss, I.; Wagner, M. *Synlett* **1997**, 241–249.
1356. Beckhaus, R.; Strauss, I.; Wagner, T.; Kiprof, P. *Angew. Chem., Int. Ed. Engl.* **1993**, *32*, 264–266.

1357. Beckhaus, R.; Strauss, I.; Wagner, T. *Angew. Chem., Int. Ed. Engl.* **1995**, *34*, 688–690.
1358. Beckhaus, R.; Sang, J.; Wagner, T.; Ganter, B. *Organometallics* **1996**, *15*, 1176–1187.
1359. Beckhaus, R.; Sang, J.; Englert, U.; Bohme, U. *Organometallics* **1996**, *15*, 4731–4736.
1360. Beckhaus, R.; Strauss, I.; Wagner, T. *Z. Anorg. Allg. Chem.* **1997**, *623*, 654–658.
1361. Beckhaus, R.; Strauss, I.; Wagner, T. *J. Organomet. Chem.* **1994**, *464*, 155–161.
1362. Beckhaus, R.; Wagner, M.; Wang, R. *Z. Anorg. Allg. Chem.* **1998**, *624*, 277–280.
1363. Beckhaus, R.; Wagner, M.; Burlakov, V. V.; Baumann, W.; Peulecke, N.; Spannenberg, A.; Kempe, R.; Rosenthal, U. *Z. Anorg. Allg. Chem.* **1998**, *624*, 129–134.
1364. Beckhaus, R.; Wagner, M.; Wang, R. M. *Eur. J. Inorg. Chem.* **1998**, 253–256.
1365. Beckhaus, R.; Sang, J.; Wagner, T.; Bohme, U. *J. Chem. Soc., Dalton Trans.* **1997**, 2249–2255.
1366. Beckhaus, R.; Wagner, T.; Zimmermann, C.; Herdtweck, E. *J. Organomet. Chem.* **1993**, *460*, 181–189.
1367. Beckhaus, R.; Oster, J.; Wagner, T. *Chem. Ber.* **1994**, *127*, 1003–1013.
1368. Beckhaus, R.; Oster, J. *Z. Anorg. Allg. Chem.* **1995**, *621*, 359–364.
1369. Böhme, U.; Beckhaus, R. *J. Organomet. Chem.* **1999**, *585*, 179–188.
1370. Beckhaus, R.; Oster, J.; Kempe, R.; Spannenberg, A. *Angew. Chem., Int. Ed. Engl.* **1996**, *35*, 1565–1567.
1371. Beckhaus, R.; Oster, J. *J. Organomet. Chem.* **1998**, *553*, 427–432.
1372. Janssen, M. D.; Herres, M.; Zsolnai, L.; Spek, A. L.; Grove, D. M.; Lang, H.; vanKoten, G. *Inorg. Chem.* **1996**, *35*, 2476–2483.
1373. Janssen, M. D.; Kohler, K.; Herres, M.; Dedieu, A.; Smeets, W. J. J.; Spek, A. L.; Grove, D. M.; Lang, H.; vanKoten, G. *J. Am. Chem. Soc.* **1996**, *118*, 4817–4829.
1374. Beckhaus, R.; Oster, J.; Wang, R. M.; Bohme, U. *Organometallics* **1998**, *17*, 2215–2221.
1375. Takeda, T.; Watanabe, M.; Nozaki, N.; Fujiwara, T. *Chem. Lett.* **1998**, 115–116.
1376. Horikawa, Y.; Nomura, T.; Watanabe, M.; Miura, I.; Fujiwara, T.; Takeda, T. *Tetrahedron Lett.* **1995**, *36*, 8835–8838.
1377. Fujiwara, T.; Takeda, T. *Synlett* **1999**, 354–356.
1378. Rahim, M. A.; Fujiwara, T.; Takeda, T. *Synlett* **1999**, 1029–1032.
1379. Takeda, T.; Nozaki, N.; Saeki, N.; Fujiwara, T. *Tetrahedron Lett.* **1999**, *40*, 5353–5356.
1380. Takeda, T.; Fujiwara, T. *J. Synth. Org. Chem. Jpn.* **1998**, *56*, 1048–1057.
1381. Breit, B. *Angew. Chem., Int. Ed.* **1998**, *37*, 453–456.
1382. Rahim, M. A.; Fujiwara, T.; Takeda, T. *Tetrahedron* **2000**, *56*, 763–770.
1383. Fujiwara, T.; Kato, Y.; Takeda, T. *Tetrahedron* **2000**, *56*, 4859–4869.
1384. Takeda, T.; Taguchi, H.; Fujiwara, T. *Tetrahedron Lett.* **2000**, *41*, 65–68.
1385. Takeda, T.; Takagi, Y.; Saeki, N.; Fujiwara, T. *Tetrahedron Lett.* **2000**, *41*, 8377–8381.
1386. Guthrie, E. J.; Macritchie, J.; Hartley, R. C. *Tetrahedron Lett.* **2000**, *41*, 4987–4990.
1387. Rahim, A.; Taguchi, H.; Watanabe, M.; Fujiwara, T.; Takeda, T. *Tetrahedron Lett.* **1998**, *39*, 2153–2156.
1388. Takeda, T.; Watanabe, M.; Rahim, M. A.; Fujiwara, T. *Tetrahedron Lett.* **1998**, *39*, 3753–3756.
1389. Fujiwara, T.; Iwasaki, N.; Takeda, T. *Chem. Lett.* **1998**, 741–742.
1390. Takeda, T.; Shimokawa, H.; Miyachi, Y.; Fujiwara, T. *Chem. Commun.* **1997**, 1055–1056.
1391. Fujiwara, T.; Takamori, M.; Takeda, T. *Chem. Commun.* **1998**, 51–52.
1392. Tsubouchi, A.; Nishio, E.; Kato, Y.; Fujiwara, T.; Takeda, T. *Tetrahedron Lett.* **2002**, *43*, 5755–5758.
1393. Takeda, T.; Nozaki, N.; Fujiwara, T. *Tetrahedron Lett.* **1998**, *39*, 3533–3536.
1394. Fujiwara, T.; Kato, Y.; Takeda, T. *Heterocycles* **2000**, *52*, 147–150.
1395. Takeda, T.; Endo, Y.; Reddy, A. C. S.; Sasaki, R.; Fujiwara, T. *Tetrahedron* **1999**, *55*, 2475–2486.
1396. Takeda, T.; Shono, T.; Ito, K.; Sasaki, H.; Tsubouchi, A. *Tetrahedron Lett.* **2003**, *44*, 7897–7900.
1397. Takeda, T.; Saito, J.; Tsubouchi, A. *Tetrahedron Lett.* **2003**, *44*, 5571–5574.
1398. Macleod, C.; McKiernan, G. J.; Guthrie, E. J.; Farrugia, L. J.; Hamprecht, D. W.; Macritchie, J.; Hartley, R. C. *J. Org. Chem.* **2003**, *68*, 387–401.
1399. Roberts, C. F.; Hartley, R. C. *J. Org. Chem.* **2004**, *69*, 6145–6148.
1400. Macleod, C.; Hartley, R. C.; Hamprecht, D. W. *Org. Lett.* **2002**, *4*, 75–78.
1401. Hartley, R. C.; McKiernan, G. J. *J. Chem. Soc., Perkin Trans. 1* **2002**, 2763–2793.
1402. McKiernan, G. J.; Hartley, R. C. *Org. Lett.* **2003**, *5*, 4389–4392.
1403. Macleod, C.; Austin, C. A.; Hamprecht, D. W.; Hartley, R. C. *Tetrahedron Lett.* **2004**, *45*, 8879–8882.
1404. Polse, J. L.; Kaplan, A. W.; Andersen, R. A.; Bergman, R. G. *J. Am. Chem. Soc.* **1998**, *120*, 6316–6328.
1405. Kaplan, A. W.; Polse, J. L.; Ball, G. E.; Andersen, R. A.; Bergman, R. G. *J. Am. Chem. Soc.* **1998**, *120*, 11649–11662.
1406. Polse, J. L.; Andersen, R. A.; Bergman, R. G. *J. Am. Chem. Soc.* **1996**, *118*, 8737–8738.
1407. Polse, J. L.; Andersen, R. A.; Bergman, R. G. *J. Am. Chem. Soc.* **1998**, *120*, 13405–13414.
1408. Niehues, M.; Erker, G.; Kehr, G.; Schwab, P.; Fröhlich, R.; Blaque, O.; Berke, H. *Organometallics* **2002**, *21*, 2905–2911.
1409. Petasis, N. A.; Fu, D. K. *J. Am. Chem. Soc.* **1993**, *115*, 7208–7214.
1410. Petasis, N. A.; Bzowej, E. I. *Tetrahedron Lett.* **1993**, *34*, 943–946.
1411. Petasis, N. A.; Hu, Y. H.; Fu, D. K. *Tetrahedron Lett.* **1995**, *36*, 6001–6004.
1412. Petasis, N. A.; Staszewski, J. P.; Fu, D. K. *Tetrahedron Lett.* **1995**, *36*, 3619–3622.
1413. Petasis, N. A.; Lu, S. P. *Tetrahedron Lett.* **1995**, *36*, 2393–2396.
1414. Petasis, N. A.; Lu, S. P.; Bzowej, E. I.; Fu, D. K.; Staszewski, J. P.; AkritopoulouZanze, I.; Patane, M. A.; Hu, Y. H. *Pure Appl. Chem.* **1996**, *68*, 667–670.
1415. Petasis, N. A. In *Transition Metal for Organic Synthesis*; Beller, M., Bolm, C., Eds.; Wiley-VCH: Weinheim, 1998; Vol. 1, 361.
1416. Schiott, B.; Jorgensen, K. A. *J. Chem. Soc., Dalton Trans.* **1993**, 337–344.
1417. Nicolaou, K. C.; Postema, M. H. D.; Claiborne, C. F. *J. Am. Chem. Soc.* **1996**, *118*, 1565–1566.
1418. Nicolaou, K. C.; Koumbis, A. E.; Snyder, S. A.; Simonsen, K. B. *Angew. Chem., Int. Ed.* **2000**, *39*, 2529–2533.
1419. Halterman, R. L.; Ramsey, T. M. *J. Organomet. Chem.* **1997**, *547*, 41–48.
1420. Oishi, T.; Nagumo, Y.; Shoji, M.; Le Brazidec, J. Y.; Uehara, H.; Hiram, M. *Chem. Commun.* **1999**, 2035–2036.
1421. Lamberth, C. J. *Prakt. Chem., Chem. Ztg.* **1994**, *336*, 632–633.
1422. Hanzawa, Y.; Kowase, N.; Taguchi, T. *Tetrahedron Lett.* **1998**, *39*, 583–586.



1423. Hanzawa, Y.; Kowase, N.; Momose, S.; Taguchi, T. *Tetrahedron* **1998**, *54*, 11387–11398.
1424. Matsubara, S.; Ukai, K.; Mizuno, T.; Utimoto, K. *Chem. Lett.* **1999**, 825–826.
1425. Böhme, U. *J. Organomet. Chem.* **2003**, *671*, 75–90.
1426. Binger, P.; Müller, P.; Podubrin, S.; Albus, S.; Krüger, C. *J. Organomet. Chem.* **2002**, *656*, 288–298.
1427. Berk, S. C.; Grossman, R. B.; Buchwald, S. L. *J. Am. Chem. Soc.* **1993**, *115*, 4912–4913.
1428. Berk, S. C.; Grossman, R. B.; Buchwald, S. L. *J. Am. Chem. Soc.* **1994**, *116*, 8593–8601.
1429. Casty, G. L.; Stryker, J. M. *J. Am. Chem. Soc.* **1995**, *117*, 7814–7815.
1430. Ogoshi, S.; Stryker, J. M. *J. Am. Chem. Soc.* **1998**, *120*, 3514–3515.
1431. Carter, C. A. G.; McDonald, R.; Stryker, J. M. *Organometallics* **1999**, *18*, 820–822.
1432. Greidanus, G.; McDonald, R.; Stryker, J. M. *Organometallics* **2001**, *20*, 2492–2504.
1433. Maercker, A.; Groos, A. *Angew. Chem., Int. Ed. Engl.* **1996**, *35*, 210–212.
1434. Butler, I. R.; Cullen, W. R.; Einstein, F. W. B.; Jones, R. H. *J. Organomet. Chem.* **1993**, *462*, C6–C9.
1435. Erker, G.; Korek, U.; Rheingold, A. L. *J. Organomet. Chem.* **1993**, *454*, 113–116.
1436. Suzuki, N.; Watanabe, T.; Hirose, T.; Chihara, T. *Chem. Lett.* **2004**, *33*, 1488–1489.
1437. Dooze, K. M.; Juliette, J. J. *Polyhedron* **2000**, *19*, 879–890.
1438. Petasis, N. A.; Fu, D. K. *Organometallics* **1993**, *12*, 3776–3780.
1439. Dooze, K. M.; Garner, L. C.; Juliette, J. J.; Mouser, J. K. M.; Weakley, T. J. R.; Hope, H. *Tetrahedron* **1995**, *51*, 4321–4332.
1440. Carpenetti, D. W. *Inorg. Chem. Commun.* **2003**, *6*, 1287–1290.
1441. van der Heijden, H.; Hessen, B. *Inorg. Chim. Acta* **2003**, *345*, 27–36.
1442. Fox, S.; Dunne, J. P.; Tacke, M.; Gallagher, J. F. *Inorg. Chim. Acta* **2004**, *357*, 225–234.
1443. Hanna, T. E.; Keresztes, I.; Lobkovsky, E.; Bernskoetter, W. H.; Chirik, P. J. *Organometallics* **2004**, *23*, 3448–3458.
1444. Chansou, B.; Choukroun, R.; Valade, L. *Appl. Organomet. Chem.* **1997**, *11*, 195–203.
1445. Axe, F. U.; Andzelm, J. W. *J. Am. Chem. Soc.* **1999**, *121*, 5396–5402.
1446. Sato, K.; Nishihara, Y.; Huo, S. Q.; Xi, Z. F.; Takahashi, T. *J. Organomet. Chem.* **2001**, *633*, 18–26.
1447. Horacek, M.; Kupfer, V.; Thewalt, U.; Stepnicka, P.; Polasek, M.; Mach, K. *Organometallics* **1999**, *18*, 3572–3578.
1448. Rosenthal, U.; Burlakov, V. V.; Arndt, P.; Baumann, W.; Spannenberg, A. *Organometallics* **2003**, *22*, 884–900.
1449. Rosenthal, U.; Burlakov, V. V. In *Titanium and Zirconium in Organic Synthesis*; Marek, I., Ed.; Wiley-VCH: Weinheim, 2002; pp 355–389.
1450. Varga, V.; Mach, K.; Polasek, M.; Sedmera, P.; Hiller, J.; Thewalt, U.; Troyanov, S. I. *J. Organomet. Chem.* **1996**, *506*, 241–251.
1451. Lefebvre, C.; Ohff, A.; Tillack, A.; Baumann, W.; Kempe, R.; Burlakov, V. V.; Rosenthal, U.; Górls, H. *J. Organomet. Chem.* **1995**, *501*, 179–188.
1452. Burlakov, V. V.; Polyakov, A. V.; Yanovsky, A. I.; Struchkov, Y. T.; Shur, V. B.; Volpin, M. E.; Rosenthal, U.; Górls, H. *J. Organomet. Chem.* **1994**, *476*, 197–206.
1453. Peulecke, N.; Baumann, W.; Kempe, R.; Burlakov, V. V.; Rosenthal, U. *Eur. J. Inorg. Chem.* **1998**, 419–424.
1454. Burlakov, V. V.; Yanovsky, A. I.; Struchkov, Y. T.; Rosenthal, U.; Spannenberg, A.; Kempe, R.; Ellert, O. G.; Shur, V. B. *J. Organomet. Chem.* **1997**, *542*, 105–112.
1455. Thomas, D.; Peulecke, N.; Burlakov, V. V.; Baumann, W.; Spannenberg, A.; Kempe, R.; Rosenthal, U. *Eur. J. Inorg. Chem.* **1998**, 1495–1502.
1456. Pellny, P. M.; Burlakov, V. V.; Baumann, W.; Spannenberg, A.; Rosenthal, U. *Z. Anorg. Allg. Chem.* **1999**, *625*, 910–918.
1457. Rep, M.; Kaagman, J. W. F.; Elsevier, C. J.; Sedmera, P.; Hiller, J.; Thewalt, U.; Horacek, M.; Mach, K. *J. Organomet. Chem.* **2000**, *597*, 146–156.
1458. Burlakov, V. V.; Usatov, A. V.; Lyssenko, K. A.; Antipin, M. Y.; Novikov, Y. N.; Shur, V. B. *Eur. J. Inorg. Chem.* **1999**, 1855–1857.
1459. Peulecke, N.; Ohff, A.; Kosse, P.; Tillack, A.; Spannenberg, A.; Kempe, R.; Baumann, W.; Burlakov, V. V.; Rosenthal, U. *Chem. Eur. J.* **1998**, *4*, 1852–1861.
1460. Pellny, P. M.; Peulecke, N.; Burlakov, V. V.; Tillack, A.; Baumann, W.; Spannenberg, A.; Kempe, R.; Rosenthal, U. *Angew. Chem., Int. Ed. Engl.* **1997**, *36*, 2615–2617.
1461. Pulst, S.; Kirchbauer, F. G.; Heller, B.; Baumann, W.; Rosenthal, U. *Angew. Chem., Int. Ed.* **1998**, *37*, 1925–1927.
1462. Jemmis, E. D.; Giju, K. T. *J. Am. Chem. Soc.* **1998**, *120*, 6952–6964.
1463. Jemmis, E. D.; Giju, K. T. *Angew. Chem., Int. Ed. Engl.* **1997**, *36*, 606–608.
1464. Peulecke, N.; Thomas, D.; Baumann, W.; Fischer, C.; Rosenthal, U. *Tetrahedron Lett.* **1997**, *38*, 6655–6656.
1465. Ohff, A.; Kosse, P.; Baumann, W.; Tillack, A.; Kempe, R.; Górls, H.; Burlakov, V. V.; Rosenthal, U. *J. Am. Chem. Soc.* **1995**, *117*, 10399–10400.
1466. Fan, M. F.; Lin, Z. Y. *Organometallics* **1997**, *16*, 494–496.
1467. Rosenthal, U.; Lefebvre, C.; Arndt, P.; Tillack, A.; Baumann, W.; Kempe, R.; Burlakov, V. V. *J. Organomet. Chem.* **1995**, *503*, 221–223.
1468. Thomas, D.; Peulecke, N.; Burlakov, V. V.; Heller, B.; Baumann, W.; Spannenberg, A.; Kempe, R.; Rosenthal, U.; Beckhaus, R. Z. *Anorg. Allg. Chem.* **1998**, *624*, 919–924.
1469. Tillack, A.; Baumann, W.; Ohff, A.; Lefebvre, C.; Spannenberg, A.; Kempe, R.; Rosenthal, U. *J. Organomet. Chem.* **1996**, *520*, 187–193.
1470. Burlakov, V. V.; Peulecke, N.; Baumann, W.; Spannenberg, A.; Kempe, R.; Rosenthal, U. *J. Organomet. Chem.* **1997**, *536*, 293–297.
1471. Pellny, P. M.; Burlakov, V. V.; Peulecke, N.; Baumann, W.; Spannenberg, A.; Kempe, R.; Francke, V.; Rosenthal, U. *J. Organomet. Chem.* **1999**, *578*, 125–132.
1472. Ohff, A.; Pulst, S.; Lefebvre, C.; Peulecke, N.; Arndt, P.; Burlakov, V. V.; Rosenthal, U. *Synlett* **1996**, 111–118.
1473. Zippel, T.; Arndt, P.; Ohff, A.; Spannenberg, A.; Kempe, R.; Rosenthal, U. *Organometallics* **1998**, *17*, 4429–4437.
1474. Ohff, A.; Zippel, T.; Arndt, P.; Spannenberg, A.; Kempe, R.; Rosenthal, U. *Organometallics* **1998**, *17*, 1649–1651.
1475. Khedkar, V.; Tillack, A.; Michalik, M.; Beller, M. *Tetrahedron Lett.* **2004**, *45*, 3123–3126.
1476. Horacek, M.; Stepnicka, P.; Gyepes, R.; Cisarova, I.; Polasek, M.; Mach, K.; Pellny, P. M.; Burlakov, V. V.; Baumann, W.; Spannenberg, A., et al. *J. Am. Chem. Soc.* **1999**, *121*, 10638–10639.
1477. Kupfer, V.; Thewalt, U.; Tislerova, I.; Stepnicka, P.; Gyepes, R.; Kubista, J.; Horacek, M.; Mach, K. *J. Organomet. Chem.* **2001**, *620*, 39–50.
1478. Pellny, P. M.; Kirchbauer, F. G.; Burlakov, V. V.; Baumann, W.; Spannenberg, A.; Rosenthal, U. *J. Am. Chem. Soc.* **1999**, *121*, 8313–8323.
1479. Pellny, P. M.; Kirchbauer, F. G.; Burlakov, V. V.; Spannenberg, A.; Mach, K.; Rosenthal, U. *Chem. Commun.* **1999**, 2505–2506.
1480. Pellny, P. M.; Burlakov, V. V.; Baumann, W.; Spannenberg, A.; Horacek, M.; Stepnicka, P.; Mach, K.; Rosenthal, U. *Organometallics* **2000**, *19*, 2816–2819.
1481. Mach, K.; Kubista, J.; Gyepes, R.; Trojan, L.; Stepnicka, P. *Inorg. Chem. Commun.* **2003**, *6*, 352–356.
1482. Kaminsky, W.; Arndt, M. *Metallocenes for Polymer Catalysis*; Springer: Berlin, **1997**; Vol. 127, pp 143–187.

1483. Hlatky, G. G. *Coord. Chem. Rev.* **1999**, *181*, 243–296.
1484. Kaminsky, W. *Macromol. Chem. Phys.* **1996**, *197*, 3907–3945.
1485. Kaminsky, W. *Catal. Today* **2000**, *62*, 23–34.
1486. Ewen, J. A. *J. Mol. Catal. A: Chem.* **1998**, *128*, 103–109.
1487. Scheirs, J., Kaminsky, W., Eds.; *Metallocene-Based Polyolefins*; Wiley: Chichester, 2000; Vols. I and II.
1488. Gibson, V. C.; Spitzmesser, S. K. *Chem. Rev.* **2003**, *103*, 283–315.
1489. Alexiadis, A.; Andes, C.; Ferrari, D.; Korber, F.; Hauschild, K.; Bochmann, M.; Fink, G. *Macromol. Mater. Eng.* **2004**, *289*, 457–466.
1490. Song, F. Q.; Cannon, R. D.; Lancaster, S. J.; Bochmann, M. J. *Mol. Catal. A: Chem.* **2004**, *218*, 21–28.
1491. Gladysz, J. A., Ed. *Chem. Rev.* **2000**, *100*, (Thematic issue on metal-catalyzed olefin polymerization).
1492. Mohring, P. C.; Coville, N. J. *J. Organomet. Chem.* **1994**, *479*, 1–29.
1493. Bochmann, M. J. *Chem. Soc., Dalton Trans.* **1996**, 255–270.
1494. Brintzinger, H. H.; Fischer, D.; Mulhaupt, R.; Rieger, B.; Waymouth, R. M. *Angew. Chem., Int. Ed. Engl.* **1995**, *34*, 1143–1170.
1495. Britovsek, G. J. P.; Gibson, V. C.; Wass, D. F. *Angew. Chem., Int. Ed.* **1999**, *38*, 428–447.
1496. Barta, N. S.; Kirk, B. A.; Stille, J. R. *J. Am. Chem. Soc.* **1994**, *116*, 8912–8919.
1497. Li, H. Y.; Neckers, D. C. *Can. J. Chem., Rev. Can. Chim.* **2003**, *81*, 758–763.
1498. Tritto, I.; Li, S. X.; Sacchi, M. C.; Zannoni, G. *Macromolecules* **1993**, *26*, 7111–7115.
1499. Alt, H. G. *J. Chem. Soc., Dalton Trans.* **1999**, 1703–1709.
1500. Barta, N. S.; Kirk, B. A.; Stille, J. R. *J. Organomet. Chem.* **1995**, *487*, 47–53.
1501. Chan, M. S. W.; Vanka, K.; Pye, C. C.; Ziegler, T. *Organometallics* **1999**, *18*, 4624–4636.
1502. Ustynyuk, Y. A.; Ustynyuk, L. Y.; Laikov, D. N.; Lunin, V. V. *J. Organomet. Chem.* **2000**, *597*, 182–189.
1503. Fusco, R.; Longo, L.; Proto, A.; Masi, F.; Garbassi, F. *Macromol. Rapid Commun.* **1998**, *19*, 257–262.
1504. Ustynyuk, L. Y.; Ustynyuk, Y. A.; Laikov, D. N.; Lunin, V. V. *Russ. Chem. Bull.* **2001**, *50*, 376–380.
1505. Sakai, S. *THEOCHEM-J. Mol. Struct.* **2001**, *540*, 157–169.
1506. Vanka, K.; Xu, Z. T.; Ziegler, T. *Isr. J. Chem.* **2002**, *42*, 403–415.
1507. Lutz, M.; Findeis, B.; Haukka, M.; Pakkanen, T. A.; Gade, L. H. *Organometallics* **2001**, *20*, 2505–2509.
1508. Patrick, E. L.; Ray, C. J.; Meyer, G. D.; Ortiz, T. P.; Marshall, J. A.; Brozik, J. A.; Summers, M. A.; Kenney, J. W. *J. Am. Chem. Soc.* **2003**, *125*, 5461–5470.
1509. Raptopoulou, C. P.; Tzavellas, N.; Klouras, N. Z. *Anorg. Allg. Chem.* **1996**, *622*, 1387–1391.
1510. Honzicek, J.; Vinklarek, J.; Erben, M.; Cisarova, I. *Acta Crystallogr., Sect. E: Struct. Rep. Online* **2004**, *60*, M1090–M1091.
1511. Wigley, D. E. *Organonitrido Complexes of the Transition-Metals*; Wiley New York, **1994**; Vol. 42, pp 239–482.
1512. Lefebvre, C.; Arndt, P.; Tillack, A.; Baumann, W.; Kempe, R.; Burlakov, V. V.; Rosenthal, U. *Organometallics* **1995**, *14*, 3090–3093.
1513. Mountford, P. J. *Organomet. Chem.* **1997**, *528*, 15–18.
1514. Kraft, S.; Beckhaus, R.; Haase, D.; Saak, W. *Angew. Chem., Int. Ed.* **2004**, *43*, 1583–1587.
1515. Veneziani, G.; Shimada, S.; Tanaka, M. *Organometallics* **1998**, *17*, 2926–2929.
1516. Choukroun, R.; Lorber, C.; Vendier, L. *Eur. J. Inorg. Chem.* **2004**, 317–321.
1517. Chivers, T.; Hilt, R. W.; Parvez, M.; Vollmerhaus, R. *Inorg. Chem.* **1994**, *33*, 3459–3466.
1518. Ciruelos, S.; Sebastian, A.; Cuenca, T.; Gomez-Sal, P.; Manzanero, A.; Royo, P. J. *Organomet. Chem.* **2000**, *604*, 103–115.
1519. Spannenberg, A.; Zippel, T.; Rosenthal, U. *Z. Kristallogr., New Cryst. Struct.* **2000**, *215*, 365–366.
1520. Joshi, V.; Jain, S. K.; Kaushik, N. K. *Synth. React. Inorg. Met.-Org. Chem.* **1994**, *24*, 1255–1265.
1521. Joshi, V.; Jain, S. K.; Kaushik, N. K. *J. Indian Chem. Soc.* **1993**, *70*, 997–1000.
1522. Gupta, N.; Srivastava, B. K.; Rai, R.; Pandey, O. P.; Sengupta, S. K. *Synth. React. Inorg. Met.-Org. Chem.* **1995**, *25*, 1177–1189.
1523. Mishra, V.; Parmar, D. S.; Joshi, V.; Kaushik, N. K. *J. Therm. Anal.* **1995**, *45*, 1589–1596.
1524. Pathak, A. K.; Mittal, A. K.; Shukla, P. R. *J. Indian Chem. Soc.* **1996**, *73*, 227–232.
1525. Sengupta, S. K.; Pandey, O. P.; Srivastava, B. K.; Sharma, V. K. *Transition Met. Chem.* **1998**, *23*, 349–353.
1526. Srivastava, S. K.; Srivastava, B. K.; Sengupta, S. K.; Pandey, O. P. *Indian J. Chem. Sect A-Inorg. Bio-Inorg. Phys. Theor. Anal. Chem.* **1998**, *37*, 544–546.
1527. Smith, M. R.; Matsunaga, P. T.; Andersen, R. A. *J. Am. Chem. Soc.* **1993**, *115*, 7049–7050.
1528. Spannenberg, A.; Burlakov, V. V.; Rosenthal, U. *Z. Kristallogr., New Cryst. Struct.* **2001**, *216*, 616–618.
1529. Thewalt, U.; Nuding, W. *J. Organomet. Chem.* **1996**, *512*, 127–130.
1530. Klouras, N.; Nastopoulos, V.; Tzavellas, N.; Leban, I. Z. *Anorg. Allg. Chem.* **1995**, *621*, 1767–1770.
1531. Yun, S. S.; Suh, I. H.; Kim, E. H.; Choi, B. J.; Lee, S. J. *Organomet. Chem.* **2001**, *631*, 16–18.
1532. Burlakov, V. V.; Letov, A. V.; Arndt, P.; Baumann, W.; Spannenberg, A.; Fischer, C.; Strunkina, L. I.; Minacheva, M. K.; Vygodskii, Y. S.; Rosenthal, U., et al. *J. Mol. Catal. A: Chem.* **2003**, *200*, 63–67.
1533. Burlakov, V. V.; Arndt, P.; Baumann, W.; Spannenberg, A.; Rosenthal, U.; Letov, A. V.; Lyssenko, K. A.; Korlyukov, A. A.; Strunkina, L. I.; Minacheva, M. K., et al. *Organometallics* **2001**, *20*, 4072–4079.
1534. Thewalt, U.; Wohrle, T. *J. Organomet. Chem.* **1996**, *506*, 331–335.
1535. DiPasquale, A. G.; Kaminsky, W.; Mayer, J. M. *J. Am. Chem. Soc.* **2002**, *124*, 14534–14535.
1536. Gibson, D. H.; Ding, Y.; Mashuta, M. S.; Richardson, J. F. *Acta Crystallogr., Sect. C: Cryst. Struct. Commun.* **1996**, *52*, 559–560.
1537. Vongudenberg, D. W.; Kang, H. C.; Massa, W.; Dehnicke, K.; Maichle-Mossmer, C.; Strahle, J. Z. *Anorg. Allg. Chem.* **1994**, *620*, 1719–1724.
1538. Voigt, A.; Murugavel, R.; Roesky, H. W.; Schmidt, H. G. *J. Mol. Struct.* **1997**, *437*, 49–57.
1539. Hofmann, M.; Malisch, W.; Schumacher, D.; Lager, M.; Nieger, M. *Organometallics* **2002**, *21*, 3485–3488.
1540. Miquel, L.; Bassobert, M.; Choukroun, R.; Madhouni, R.; Eichhorn, B.; Sanchez, M.; Mazieres, M. R.; Jaud, J. J. *Organomet. Chem.* **1995**, *490*, 21–28.
1541. Bourg, S.; Corriu, R. J. P.; Enders, M.; Moreau, J. J. E. *Organometallics* **1995**, *14*, 564–566.
1542. Wu, S. Z.; Chen, Y.; Zhang, Y. L. *Gazz. Chim. Ital.* **1993**, *123*, 651–652.
1543. Hoffman, D.; Reinke, H.; Krempner, C. *J. Organomet. Chem.* **2002**, *662*, 1–8.
1544. Hampel, F.; Hommes, N. V.; Hoops, S.; Maeref, F.; Schobert, R. *Eur. J. Inorg. Chem.* **1998**, 1253–1262.
1545. Wada, K.; Itayama, N.; Watanabe, N.; Bundo, M.; Kondo, T.; Mitsudo, T. A. *Organometallics* **2004**, *23*, 5824–5832.
1546. Dufrenne, N. G.; Blitz, J. P.; Meverden, C. C. *Microchem. J.* **1997**, *55*, 192–199.
1547. Petrella, A. J.; Roberts, N. K.; Craig, D. C.; Raston, C. L.; Lamb, R. N. *Chem. Commun.* **2004**, 64–65.

1548. Braunstein, P.; Morise, X.; Benard, M.; Rohmer, M. M.; Welter, R. *Chem. Commun.* **2003**, 610–611.
1549. Spaether, W.; Klass, K.; Erker, G.; Zippel, F.; Fröhlich, R. *Chem. Eur. J.* **1998**, *4*, 1411–1417.
1550. Schmittl, M.; Burghart, A.; Malisch, W.; Reising, J.; Sollner, R. *J. Org. Chem.* **1998**, *63*, 396–400.
1551. Schmittl, M.; Sollner, R. *Angew. Chem., Int. Ed. Engl.* **1996**, *35*, 2107–2109.
1552. Schmittl, M.; Sollner, R. *Chem. Ber. Recl.* **1997**, *130*, 771–777.
1553. Schmittl, M.; Werner, H.; Gevert, O.; Sollner, R. *Chem. Ber. Recl.* **1997**, *130*, 195–199.
1554. Schmittl, M.; Haeuseler, A. *J. Organomet. Chem.* **2002**, *661*, 169–179.
1555. Veya, P.; Floriani, C.; Chiesivilla, A.; Rizzoli, C. *Organometallics* **1993**, *12*, 4892–4898.
1556. Adam, W.; Muller, M.; Pechtl, F. *J. Org. Chem.* **1994**, *59*, 2358–2364.
1557. Luinstra, G. A. *J. Organomet. Chem.* **1996**, *517*, 209–215.
1558. Bosnich, B. *Aldrichimica Acta* **1998**, *31*, 76–83.
1559. Ellis, W. W.; Gavrilova, A.; Liable-Sands, L.; Rheingold, A. L.; Bosnich, B. *Organometallics* **1999**, *18*, 332–338.
1560. Hollis, T. K.; Odenkirk, W.; Robinson, N. P.; Whelan, J.; Bosnich, B. *Tetrahedron* **1993**, *49*, 5415–5430.
1561. Hollis, T. K.; Robinson, N. P.; Whelan, J.; Bosnich, B. *Tetrahedron Lett.* **1993**, *34*, 4309–4312.
1562. Chang, S. J.; Liu, H. J.; Chen, C. T.; Shih, W. E.; Lin, C. C.; Gau, H. M. *J. Organomet. Chem.* **1996**, *523*, 47–52.
1563. Chen, C. T.; Gau, H. M. *J. Organomet. Chem.* **1995**, *505*, 17–21.
1564. Gau, H. M.; Chen, C. A.; Chang, S. J.; Shih, W. E.; Yang, T. K.; Jong, T. T.; Chien, M. Y. *Organometallics* **1993**, *12*, 1314–1318.
1565. Barnes, D. L.; Eilerts, N. W.; Heppert, J. A. *Polyhedron* **1994**, *13*, 743–748.
1566. Calderazzo, F.; Englert, U.; Pampaloni, G.; Passarelli, V. *J. Chem. Soc., Dalton Trans.* **2001**, 2891–2898.
1567. Qian, Y. L.; Huang, J. L.; Chen, X. P.; Li, G. S.; Chen, W. C.; Li, B. H.; Jin, X. L.; Yang, Q. C. *Polyhedron* **1994**, *13*, 1105–1108.
1568. Qian, Y. L.; Huang, J. L.; Ding, K.; Zhang, Y.; Huang, Q. L.; Chen, X. P.; Chan, A. S. C.; Wong, W. T. *J. Organomet. Chem.* **2002**, *645*, 59–64.
1569. Huang, J. L.; Huang, Q. L.; Qian, Y. L.; Chan, A. S. C.; Wong, W. T. *Polyhedron* **1998**, *17*, 2523–2527.
1570. Dang, Y. *Coord. Chem. Rev.* **1994**, *135*, 93–128.
1571. Zeng, Z. Z.; Xie, X. M. *Acta Chim. Sinica* **2000**, *58*, 862–865.
1572. Edwards, D. A.; Mahon, M. F.; Paget, T. J.; Summerhill, N. W. *Transition. Met. Chem.* **2001**, *26*, 116–119.
1573. Gao, Z. W.; Gao, L. X. *Chin. J. Org. Chem.* **1999**, *19*, 542–545.
1574. Branham, K. E.; Mays, J. W.; Gray, G. M.; Sanner, R. D.; Overturf, G. E.; Cook, R. *Appl. Organomet. Chem.* **1997**, *11*, 213–221.
1575. Gibson, D. H.; Ding, Y.; Richardson, J. F.; Mashuta, M. S. *Acta Crystallogr., Sect. C: Cryst. Struct. Commun.* **1996**, *52*, 1614–1616.
1576. Pankowski, M.; Cabestaing, C.; Jaouen, G. *J. Organomet. Chem.* **1996**, *516*, 11–16.
1577. Gupta, S. K.; Sharma, R.; Sindhu, R. S. *J. Indian Chem. Soc.* **2001**, *78*, 202–203.
1578. Sindhu, R. S.; Tikku, S.; Sharma, A. K.; Bansal, S. K. *Synth. React. Inorg. Met.-Org. Chem.* **1995**, *25*, 307–317.
1579. Bansal, S. K.; Sindhu, R. S. *J. Indian Chem. Soc.* **1994**, *71*, 39–40.
1580. Gao, L. X.; Gao, Z. W.; Wang, J. Y. *Chin. J. Org. Chem.* **1999**, *19*, 533–536.
1581. Edwards, D. A.; Mahon, M. F.; Paget, T. J. *Polyhedron* **1997**, *16*, 25–31.
1582. Spaether, W.; Rump, M.; Erker, G.; Fröhlich, R.; Hecht, J.; Kruger, C.; Kuhnigk, J. *An. Quim., Int. Ed.* **1997**, *93*, 394–403.
1583. Singh, D.; Singh, R. *Transition Met. Chem.* **1994**, *19*, 347–349.
1584. Sengupta, S. K.; Pandey, O. P.; Srivastava, A. K.; Mishra, K. D. *Indian J. Chem. Sect A-Inorg. Bio-Inorg. Phys. Theor. Anal. Chem.* **1999**, *38*, 951–955.
1585. Bina, R.; Cisarova, I.; Pavlista, M.; Pavlik, I. *Appl. Organomet. Chem.* **2004**, *18*, 262–263.
1586. Spaltenstein, E.; Palma, P.; Kreutzer, K. A.; Willoughby, C. A.; Davis, W. M.; Buchwald, S. L. *J. Am. Chem. Soc.* **1994**, *116*, 10308–10309.
1587. Shu, R. H.; Hao, L. J.; Harrod, J. F.; Woo, H. G.; Samuel, E. *J. Am. Chem. Soc.* **1998**, *120*, 12988–12989.
1588. Ignatov, S. K.; Rees, N. H.; Tyrrell, B. R.; Dubberley, S. R.; Razuvaev, A. G.; Mountford, P.; Nikonov, G. I. *Chem. Eur. J.* **2004**, *10*, 4991–4999.
1589. Diaz, A.; Radzewich, C.; Wicholas, M. *J. Chem. Educ.* **1995**, *72*, 937–938.
1590. Klouras, N.; Demakopoulos, I.; Terzis, A.; Raptopoulou, C. P. *Z. Anorg. Allg. Chem.* **1995**, *621*, 113–116.
1591. Kunkely, H.; Vogler, A. *Z. Naturforsch. (B)* **1998**, *53*, 224–226.
1592. Sweeney, Z. K.; Polse, J. L.; Andersen, R. A.; Bergman, R. G.; Kubinec, M. G. *J. Am. Chem. Soc.* **1997**, *119*, 4543–4544.
1593. Sweeney, Z. K.; Polse, J. L.; Bergman, R. G.; Andersen, R. A. *Organometallics* **1999**, *18*, 5502–5510.
1594. Sweeney, Z. K.; Polse, J. L.; Andersen, R. A.; Bergman, R. G. *J. Am. Chem. Soc.* **1998**, *120*, 7825–7834.
1595. Steudel, R.; Pridohl, M.; Buschmann, J.; Luger, P. *Chem. Ber.* **1995**, *128*, 725–728.
1596. Pridohl, M.; Steudel, R.; Baumgart, F. *Polyhedron* **1993**, *12*, 2577–2585.
1597. Steudel, R.; Bergemann, K.; Buschmann, J.; Luger, P. *Inorg. Chem.* **1996**, *35*, 2184–2188.
1598. Steudel, R. *Chem. Rev.* **2002**, *102*, 3905–3945.
1599. Kustos, M.; Pickardt, J.; Albertsen, J.; Steudel, R. *Z. Naturforsch. (B)* **1993**, *48*, 928–934.
1600. Steudel, R.; Munchow, V.; Pickardt, J. *Z. Anorg. Allg. Chem.* **1996**, *622*, 1594–1600.
1601. Steudel, R.; Kustos, M.; Prenzel, A. *Z. Naturforsch. (B)* **1997**, *52*, 79–82.
1602. Kustos, M.; Steudel, R. *J. Org. Chem.* **1995**, *60*, 8056–8061.
1603. Steudel, R.; Hassenberg, K.; Munchow, V.; Schumann, O.; Pickardt, J. *Eur. J. Inorg. Chem.* **2000**, 921–928.
1604. Pinkas, J.; Gyepes, R.; Stepnicka, P.; Kubista, J.; Horacek, M.; Mach, K. *Inorg. Chem. Commun.* **2004**, *7*, 1135–1138.
1605. Delgado, E.; Hernández, E.; Hedayat, A.; Tornero, J.; Torres, R. *J. Organomet. Chem.* **1994**, *466*, 119–123.
1606. de Lena, J. C.; Garner, C. D. *J. Braz. Chem. Soc.* **1998**, *9*, 591–597.
1607. Guyon, F.; Lenoir, C.; Fourmigue, M.; Larsen, J.; Amaudrut, J. *Bull. Soc. Chim. Fr.* **1994**, *131*, 217–226.
1608. Guyon, F.; Fourmigue, M.; Audebert, P.; Amaudrut, J. *Inorg. Chim. Acta* **1995**, *239*, 117–124.
1609. Saito, K.; Nakano, M.; Tamra, H.; Matsubayashi, G. *J. Organomet. Chem.* **2001**, *625*, 7–12.
1610. Stafford, P. R.; Rauchfuss, T. B.; Verma, A. K.; Wilson, S. R. *J. Organomet. Chem.* **1996**, *526*, 203–214.
1611. Munchow, V.; Steudel, R. *Eur. J. Inorg. Chem.* **2004**, 718–725.
1612. Bergemann, K.; Kustos, M.; Kruger, P.; Steudel, R. *Angew. Chem., Int. Ed. Engl.* **1995**, *34*, 1330–1331.
1613. Steudel, R.; Bergemann, K.; Buschmann, J.; Luger, P. *Angew. Chem., Int. Ed. Engl.* **1996**, *35*, 2537–2539.
1614. Steudel, R.; Kustos, M.; Munchow, V.; Westphal, U. *Chem. Ber.* **1997**, *130*, 757–764.
1615. Steudel, R.; Schumann, O.; Buschmann, J.; Luger, P. *Angew. Chem., Int. Ed. Engl.* **1998**, *37*, 492–494.

1616. Chaudhury, S.; Blaurock, S.; Hey-Hawkins, E. *Eur. J. Inorg. Chem.* **2001**, 2587–2596.
1617. McCullough, R. D.; Belot, J. A. *Chem. Mat.* **1994**, *6*, 1396–1403.
1618. Senocq, F.; Viguier, N.; Gleizes, A. *Eur. J. Solid State Inorg. Chem.* **1996**, *33*, 1185–1197.
1619. Fischer, J. M.; Piers, W. E.; Ziegler, T.; MacGillivray, L. R.; Zaworotko, M. J. *Chem. Eur. J.* **1996**, *2*, 1221–1229.
1620. Kisko, J. L.; Hascall, T.; Parkin, G. J. *Am. Chem. Soc.* **1997**, *119*, 7609–7610.
1621. Fischer, J. M.; Piers, W. E.; Macgillivray, L. R.; Zaworotko, M. J. *Inorg. Chem.* **1995**, *34*, 2499–2500.
1622. Fischer, J. M.; Piers, W. E.; Batchilder, S. D. P.; Zaworotko, M. J. *J. Am. Chem. Soc.* **1996**, *118*, 283–284.
1623. Christou, V.; Wuller, S. P.; Arnold, J. F. *J. Am. Chem. Soc.* **1993**, *115*, 10545–10552.
1624. Burgess, K.; Vanderdonk, W. A. *Tetrahedron Lett.* **1993**, *34*, 6817–6820.
1625. Burgess, K.; Vanderdonk, W. A. *J. Am. Chem. Soc.* **1994**, *116*, 6561–6569.
1626. He, X. M.; Hartwig, J. F. *J. Am. Chem. Soc.* **1996**, *118*, 1696–1702.
1627. Muhoro, C. N.; He, X. M.; Hartwig, J. F. *J. Am. Chem. Soc.* **1999**, *121*, 5033–5046.
1628. Muhoro, C. N.; Hartwig, J. F. *Angew. Chem., Int. Ed. Engl.* **1997**, *36*, 1510–1512.
1629. Hartwig, J. F.; Muhoro, G. N.; He, X. M.; Eisenstein, O.; Bosque, R.; Maseras, F. J. *J. Am. Chem. Soc.* **1996**, *118*, 10936–10937.
1630. Hartwig, J. F.; Muhoro, C. N. *Organometallics* **2000**, *19*, 30–38.
1631. Liu, D.; Lin, Z. Y. *Organometallics* **2002**, *21*, 4750–4755.
1632. Liu, D.; Lam, K. C.; Lin, Z. Y. *Organometallics* **2003**, *22*, 2827–2831.
1633. Bosque, R.; Maseras, F. J. *Comput. Chem.* **2000**, *21*, 562–571.
1634. Shapiro, P. J. *Coord. Chem. Rev.* **2002**, *231*, 67–81.
1635. Ringwald, M.; Sturmer, R.; Brintzinger, H. H. *J. Am. Chem. Soc.* **1999**, *121*, 1524–1527.
1636. Mikami, K.; Terada, M.; Korenaga, T.; Matsumoto, Y.; Ueki, M.; Angelaud, R. *Angew. Chem., Int. Ed.* **2000**, *39*, 3532–3556.
1637. Hoveyda, A. H.; Morken, J. P. In *Metalloenes: Synthesis, Reactivity and Applications*; Togni, A., Halterman, R. L., Eds.; Wiley-VCH: New York, 1998; Vol. 2, pp 625–683.
1638. Hoveyda, A. H.; Morken, J. P. *Angew. Chem., Int. Ed. Engl.* **1996**, *35*, 1263–1284.
1639. Luttikhedde, H. J. G.; Leino, R.; Wilen, C. E.; Laine, E.; Sillanpaa, R.; Nasman, J. H. J. *Organomet. Chem.* **1997**, *547*, 129–132.
1640. Agarkov, A. Y.; Izmer, V. V.; Riabov, A. N.; Kuz'mina, L. G.; Howard, J. A. K.; Beletskaya, I. P.; Voskoboinikov, A. Z. *J. Organomet. Chem.* **2001**, *619*, 280–286.
1641. Koch, T.; Blaurock, S.; Somoza, F. B.; Voigt, A.; Kirmse, R.; Hey-Hawkins, E. *Organometallics* **2000**, *19*, 2556–2563.
1642. Shaltout, R. M.; Corey, J. Y.; Rath, N. P. *J. Organomet. Chem.* **1995**, *503*, 205–212.
1643. Urazowski, I. F.; Atovmyan, L. O.; Mkoyan, S. G.; Broussier, R.; Perron, P.; Gautheron, B.; Robert, F. J. *Organomet. Chem.* **1997**, *536*, 531–536.
1644. Mkoyan, S. G.; Aliev, Z. G.; Atovmyan, L. O.; Ivchenko, P. V. *Russ. Chem. Bull.* **1995**, *44*, 296–299.
1645. Green, M. L. H.; Ishihara, N. J. *Chem. Soc., Dalton Trans.* **1994**, 657–665.
1646. Miyake, S.; Okumura, Y.; Inazawa, S. *Macromolecules* **1995**, *28*, 3074–3079.
1647. Fierro, R.; Rausch, M. D.; Herrman, G. S.; Alt, H. G. J. *Organomet. Chem.* **1995**, *485*, 11–17.
1648. Willoughby, C. A.; Davis, W. M.; Buchwald, S. L. J. *Organomet. Chem.* **1995**, *497*, 11–15.
1649. Erker, G.; Psiorz, C.; Frohlich, R.; Grehl, M.; Kruger, C.; Noe, R.; Nolte, M. *Tetrahedron* **1995**, *51*, 4347–4358.
1650. Atovmyan, L.; Mkoyan, S.; Urazowski, I.; Broussier, R.; Ninoreille, S.; Perron, P.; Gautheron, B. *Organometallics* **1995**, *14*, 2601–2604.
1651. Nantz, M. H.; Hitchcock, S. R.; Sutton, S. C.; Smith, M. D. *Organometallics* **1993**, *12*, 5012–5015.
1652. Sutton, S. C.; Nantz, M. H.; Parkin, S. R. *Organometallics* **1993**, *12*, 2248–2257.
1653. Kuntz, B. A.; Ramachandran, R.; Taylor, N. J.; Guan, J. Y.; Collins, S. J. *Organomet. Chem.* **1995**, *497*, 133–142.
1654. Eisch, J. J.; Shi, X.; Owuor, F. A. *Organometallics* **1998**, *17*, 5219–5221.
1655. Tacke, M.; Allen, L. T.; Cuffe, L.; Gallagher, W. M.; Ying, L.; Mendoza, O.; Muller-Bunz, H.; Rehmann, F. J. K.; Sweeney, N. J. *Organomet. Chem.* **2004**, *689*, 2242–2249.
1656. Fox, S.; Dunne, J. P.; Tacke, M.; Gallagher, J. F. *Inorg. Chim. Acta* **2004**, *357*, 225–234.
1657. Gibis, K. L.; Helmchen, G.; Huttner, G.; Zsolnai, L. J. *Organomet. Chem.* **1993**, *445*, 181–186.
1658. Xu, L.; Mikami, K. *Tetrahedron Lett.* **2004**, *45*, 9215–9217.
1659. Chin, B.; Buchwald, S. L. J. *Org. Chem.* **1996**, *61*, 5650–5651.
1660. Parkin, S.; Hitchcock, S. R.; Hope, H.; Nantz, M. H. *Acta Crystallogr., Sect. C: Cryst. Struct. Commun.* **1994**, *50*, 169–171.
1661. Xin, S. X.; Harrod, J. F. *Can. J. Chem., Rev. Can. Chim.* **1995**, *73*, 999–1002.
1662. Hansen, M. C.; Buchwald, S. L. *Tetrahedron Lett.* **1999**, *40*, 2033–2034.
1663. Hansen, M. C.; Buchwald, S. L. *Org. Lett.* **2000**, *2*, 713–715.
1664. Yanagisawa, A.; Asakawa, K.; Yamamoto, H. *Chirality* **2000**, *12*, 421–424.
1665. Jaquith, J. B.; Guan, J. Y.; Wang, S. T.; Collins, S. *Organometallics* **1995**, *14*, 1079–1081.
1666. Rahimian, K.; Harrod, J. F. *Inorg. Chim. Acta* **1998**, *270*, 330–336.
1667. Halterman, R. L.; Chen, Z. L.; Khan, M. A. *Organometallics* **1996**, *15*, 3957–3967.
1668. Halterman, R. L.; Combs, D.; Khan, M. A. *Organometallics* **1998**, *17*, 3900–3907.
1669. Kelly, P. A.; Berger, G. O.; Wyatt, J. K.; Nantz, M. H. *J. Org. Chem.* **2003**, *68*, 8447–8452.
1670. Hitchcock, S. R.; Situ, J. J.; Covell, J. A.; Olmstead, M. M.; Nantz, M. H. *Organometallics* **1995**, *14*, 3732–3740.
1671. Palandoken, H.; Wyatt, J. K.; Hitchcock, S. R.; Olmstead, M. M.; Nantz, M. H. *J. Organomet. Chem.* **1999**, *579*, 338–347.
1672. Halterman, R. L.; Tretyakov, A.; Khan, M. A. *J. Organomet. Chem.* **1998**, *568*, 41–51.
1673. Halterman, R. L.; Ramsey, T. M.; Pailles, N. A.; Khan, M. A. *J. Organomet. Chem.* **1995**, *497*, 43–53.
1674. Steinhorst, A.; Erker, G.; Grehl, M.; Fröhlich, R. J. *Organomet. Chem.* **1997**, *542*, 191–204.
1675. Dorer, B.; Prosen, M. H.; Rief, U.; Brintzinger, H. H. *Organometallics* **1994**, *13*, 3868–3872.
1676. Halterman, R. L.; Tretyakov, A.; Combs, D.; Chang, J.; Khan, M. A. *Organometallics* **1997**, *16*, 3333–3339.
1677. Grossman, R. B.; Tsai, J. C.; Davis, W. M.; Gutierrez, A.; Buchwald, S. L. *Organometallics* **1994**, *13*, 3892–3896.
1678. Halterman, R. L.; Combs, D.; Kihega, J. G.; Khan, M. A. *J. Organomet. Chem.* **1996**, *520*, 163–170.
1679. Ellis, W. W.; Hollis, T. K.; Odenkirk, W.; Whelan, J.; Ostrander, R.; Rheingold, A. L.; Bosnich, B. *Organometallics* **1993**, *12*, 4391–4401.
1680. Broene, R. D.; Buchwald, S. L. *J. Am. Chem. Soc.* **1993**, *115*, 12569–12570.
1681. Viso, A.; Lee, N. E.; Buchwald, S. L. *J. Am. Chem. Soc.* **1994**, *116*, 9373–9374.



1682. Halterman, R. L.; Zhu, C. J.; Chen, Z. L.; Dunlap, M. S.; Khan, M. A.; Nicholas, K. M. *Organometallics* **2000**, *19*, 3824–3829.
1683. Urazowski, I.; Mkoyan, S.; Atovmyan, L.; Gautheron, B.; Broussier, R.; Perron, P. *Acta Crystallogr., Sect. C: Cryst. Struct. Commun.* **1995**, *51*, 1063–1064.
1684. Alt, H. G. *Russ. Chem. Bull.* **1995**, *44*, 1–8.
1685. Male, N. A. H.; Skinner, M. E. G.; Wilson, P. J.; Mountford, P.; Schroder, M. *New J. Chem.* **2000**, *24*, 575–577.
1686. Horacek, M.; Stepnicka, P.; Fejfarova, K.; Gyepes, R.; Cisarova, I.; Kubista, J.; Mach, K. *J. Organomet. Chem.* **2002**, *642*, 148–155.
1687. Cuenca, T.; Flores, J. C.; Royo, P. *J. Organomet. Chem.* **1993**, *462*, 191–201.
1688. Cuenca, T.; Gómez, R.; Gómez-Sal, P.; Royo, P. *J. Organomet. Chem.* **1993**, *454*, 105–111.
1689. Vyshinskaya, L. I.; Korneva, S. P.; Kulikova, G. P. *Russ. J. Gen. Chem.* **2002**, *72*, 68–70.
1690. Antiñolo, A.; Fajardo, M.; Gómez-Ruiz, S.; López-Solera, I.; Otero, A.; Prashar, S.; Rodríguez, A. M. *J. Organomet. Chem.* **2003**, *683*, 11–22.
1691. Varga, V.; Hiller, J.; Gyepes, R.; Polasek, M.; Sedmera, P.; Thewalt, U.; Mach, K. *J. Organomet. Chem.* **1997**, *538*, 63–74.
1692. Lee, H.; Bonanno, J. B.; Hascall, T.; Cordaro, J.; Hahn, J. M.; Parkin, G. *J. Chem. Soc., Dalton Trans.* **1999**, 1365–1368.
1693. Tian, G. L.; Wang, B. Q.; Dai, X. L.; Xu, S. S.; Zhou, X. Z.; Sun, J. *J. Organomet. Chem.* **2001**, *634*, 145–152.
1694. Chacon, S. T.; Coughlin, E. B.; Henling, L. M.; Bercaw, J. E. *J. Organomet. Chem.* **1995**, *497*, 171–180.
1695. Douzich, B.; Choukroun, R.; Lorber, C.; Donnadieu, B. *J. Organomet. Chem.* **2002**, *649*, 15–20.
1696. Raptopoulou, C. P.; Terzis, A.; Tzavellas, N.; Klouras, N. *Z. Anorg. Allg. Chem.* **1995**, *621*, 1257–1260.
1697. Tzavellas, N.; Klouras, N.; Raptopoulou, C. P. *Z. Anorg. Allg. Chem.* **1997**, *623*, 384–388.
1698. Lang, H.; Blau, S.; Nuber, B.; Zsolnai, L. *Organometallics* **1995**, *14*, 3216–3223.
1699. Beagley, P.; Davies, P.; Adams, H.; White, C. *Can. J. Chem., Rev. Can. Chim.* **2001**, *79*, 731–741.
1700. Beagley, P.; Davies, P. J.; Blacker, A. J.; White, C. *Organometallics* **2002**, *21*, 5852–5858.
1701. Yano, A.; Yamada, S.; Akimoto, A. *Macromol. Chem. Phys.* **1999**, *200*, 1356–1362.
1702. Kim, S. J.; Lee, Y. J.; Kang, E.; Kim, S. H.; Ko, J.; Lee, B.; Cheong, M.; Suh, I. H.; Kang, S. O. *Organometallics* **2003**, *22*, 3958–3966.
1703. Jin, J. Z.; Chen, E. Y. X. *Organometallics* **2002**, *21*, 13–15.
1704. Jin, J. Z.; Chen, E. Y. X. *Macromol. Chem. Phys.* **2002**, *203*, 2329–2333.
1705. Jin, J. Z.; Mariott, W. R.; Chen, E. Y. X. *J. Polym. Sci., Pol. Chem.* **2003**, *41*, 3132–3142.
1706. Tamm, M.; Kunst, A.; Bannenberg, T.; Herdtweck, E.; Sirsch, P.; Elsevier, C. J.; Ernsting, J. M. *Angew. Chem., Int. Ed.* **2004**, *43*, 5530–5534.
1707. Antiñolo, A.; Fajardo, M.; Gómez-Ruiz, S.; López-Solera, I.; Otero, A.; Prashar, S. *Organometallics* **2004**, *23*, 4062–4069.
1708. Cano, A.; Cuenca, T.; Gómez-Sal, P.; Royo, B.; Royo, P. *Organometallics* **1994**, *13*, 1688–1694.
1709. Cuenca, T.; Galakhov, M.; Royo, E.; Royo, P. *J. Organomet. Chem.* **1996**, *515*, 33–36.
1710. Cano, A.; Cuenca, T.; Gómez-Sal, P.; Manzanero, A.; Royo, P. *J. Organomet. Chem.* **1996**, *526*, 227–235.
1711. Weiss, K.; Neugebauer, U.; Blau, S.; Lang, H. *J. Organomet. Chem.* **1996**, *520*, 171–179.
1712. Miyake, S.; Henling, L. M.; Bercaw, J. E. *Organometallics* **1998**, *17*, 5528–5533.
1713. Thiele, K. H.; Schliessburg, C.; Baumeister, K.; Hassler, K. *Z. Anorg. Allg. Chem.* **1996**, *622*, 1806–1810.
1714. Xu, S. S.; Deng, X. B.; Wang, B. Q.; Zhou, X. Z. *Acta Chim. Sinica* **1997**, *55*, 829–832.
1715. Tian, G. G.; Wang, B. Q.; Xu, S. S.; Zhang, Y. Q.; Zhou, X. Z. *J. Organomet. Chem.* **1999**, *579*, 24–29.
1716. Wang, B. Q.; Xu, S. S.; Zhou, X. Z.; Su, L. M.; Feng, R.; He, D. W. *Chem. J. Chin. Univ.* **1999**, *20*, 77–80.
1717. Sun, X. L.; Wang, B. Q.; Xu, S. S.; Zhou, X. Z.; Zhao, J.; Hu, Y. L. *Chem. J. Chin. Univ.* **2000**, *21*, 222–226.
1718. Horacek, M.; Stepnicka, P.; Kubista, J.; Gyepes, R.; Cisarova, I.; Petrusova, L.; Mach, K. *J. Organomet. Chem.* **2002**, *658*, 235–241.
1719. Song, W.; Shackett, K.; Chien, J. C. W.; Rausch, M. D. *J. Organomet. Chem.* **1995**, *501*, 375–380.
1720. Zhou, X. Z.; Wang, B. Q.; Xu, S. S. *Chem. J. Chin. Univ.* **1995**, *16*, 887–891.
1721. Alt, H. G.; Fottinger, K.; Milius, W. *J. Organomet. Chem.* **1998**, *564*, 109–114.
1722. Ciruelos, S.; Cuenca, T.; Flores, J. C.; Gómez, R.; Gómez-Sal, P.; Royo, P. *Organometallics* **1993**, *12*, 944–948.
1723. Cuenca, T.; Flores, J. C.; Gómez, R.; Gómez-Sal, P.; Parra-Hake, M.; Royo, P. *Inorg. Chem.* **1993**, *32*, 3608–3612.
1724. Ushioda, T.; Green, M. L. H.; Haggitt, J.; Yan, X. F. *J. Organomet. Chem.* **1996**, *518*, 155–166.
1725. Huang, J. L.; Feng, Z. F.; Wang, H.; Qian, Y. L.; Sun, J. Q.; Xu, Y. J.; Chen, W.; Zheng, G. J. *Mol. Catal. A: Chem.* **2002**, *189*, 187–194.
1726. Yoshida, T.; Koga, N.; Morokuma, K. *Organometallics* **1996**, *15*, 766–777.
1727. Yang, S. H.; Huh, J.; Yang, J. S.; Jo, W. H. *Macromolecules* **2004**, *37*, 5741–5751.
1728. Alonso-Moreno, C.; Antiñolo, A.; López-Solera, I.; Otero, A.; Prashar, S.; Rodríguez, A. M.; Villaseñor, E. *J. Organomet. Chem.* **2002**, *656*, 129–138.
1729. Shapiro, P. J. *Eur. J. Inorg. Chem.* **2001**, 321–326.
1730. Braunschweig, H.; von Koblinski, C.; Mamuti, M.; Englert, U.; Wang, R. M. *Eur. J. Inorg. Chem.* **1999**, 1899–1904.
1731. Zi, G. F.; Li, H. W.; Xie, Z. W. *Organometallics* **2002**, *21*, 3850–3855.
1732. Shin, J. H.; Hascall, T.; Parkin, G. *Organometallics* **1999**, *18*, 6–9.
1733. Wheatley, N.; Kalck, P. *Chem. Rev.* **1999**, *99*, 3379–3419.
1734. Gade, L. H. *Angew. Chem., Int. Ed. Engl.* **2000**, *39*, 2659–2678.
1735. Huang, J. L.; Feng, Z. F.; Wang, H.; Qian, Y. L.; Sun, J. Q.; Xu, Y. J.; Chen, W.; Zheng, G. J. *Mol. Catal. A: Chem.* **2002**, *189*, 187–194.
1736. Siddiqui, Z. A.; Khan, A. A. *Transition. Met. Chem.* **1995**, *20*, 469–471.
1737. Braunstein, P.; Cauzzi, D.; Kelly, D.; Lanfranchi, M.; Tiripicchio, A. *Inorg. Chem.* **1993**, *32*, 3373–3377.
1738. Azad, S. M.; Azam, K. A.; Das, P. C.; Kabir, S. E. *Indian J. Chem. Sect A-Inorg. Phys. Theor. Anal. Chem.* **1993**, *32*, 266–267.
1739. Bartik, T.; Windisch, H.; Sorkau, A.; Thiele, K. H.; Kriebel, C.; Herfurth, A.; Tschöerner, C. M.; Zucchi, C.; Palyi, G. *Inorg. Chim. Acta* **1994**, *227*, 201–205.
1740. Rau, M. S.; Kretz, C. M.; Geoffroy, G. L.; Rheingold, A. L.; Haggerty, B. S. *Organometallics* **1994**, *13*, 1624–1634.
1741. Calhorda, M. J. *J. Organomet. Chem.* **1994**, *475*, 149–155.
1742. Fandos, R.; Fierro, J. L. G.; Kubicki, M. M.; Otero, A.; Terreros, P.; Vivarerrato, M. A. *Organometallics* **1995**, *14*, 2162–2163.
1743. Fandos, R.; Otero, A.; Rodríguez, A.; Ruiz, M. J.; Terreros, P. *Angew. Chem., Int. Ed.* **2001**, *40*, 2884–2887.
1744. Galakhov, M.; Martín, A.; Mena, M.; Yélamos, C. *J. Organomet. Chem.* **1995**, *496*, 217–220.
1745. Matsubara, K.; Niibayashi, S.; Nagashima, H. *Organometallics* **2003**, *22*, 1376–1382.
1746. Niibayashi, S.; Mitsui, K.; Matsubara, K.; Nagashima, H. *Organometallics* **2003**, *22*, 4885–4892.
1747. Veya, P.; Cozzi, P. G.; Floriani, C.; Chiesivilla, A.; Rizzoli, C. *Organometallics* **1994**, *13*, 4939–4945.
1748. Veya, P.; Cozzi, P. G.; Floriani, C.; Rotzinger, F. P.; Chiesivilla, A.; Rizzoli, C. *Organometallics* **1995**, *14*, 4101–4108.

1749. Sabat, M.; Reynolds, K. A.; Finn, M. G. *Organometallics* **1994**, *13*, 2084–2087.
1750. Gau, H. M.; Chen, C. T.; Jong, T. T.; Chien, M. Y. *J. Organomet. Chem.* **1993**, *448*, 99–106.
1751. Huang, T. Y.; Chen, C. T.; Gau, H. M. *J. Organomet. Chem.* **1995**, *489*, 63–70.
1752. An, J.; van Niekerk, L.; Esterhuysen, C.; Raubenheimer, H. G. *J. Chem. Soc., Dalton Trans.* **2002**, 2386–2389.
1753. Berardini, M.; Emge, T. J.; Brennan, J. G. *Inorg. Chem.* **1993**, *32*, 2724–2728.
1754. Stang, P. J.; Persky, N. E. *Chem. Commun.* **1997**, 77–78.
1755. Edwards, D. A.; Mahon, M. F.; Paget, T. J. *Polyhedron* **2000**, *19*, 757–764.
1756. Shafir, A.; Power, M. P.; Whitener, G. D.; Arnold, J. *Organometallics* **2001**, *20*, 1365–1369.
1757. Shafir, A.; Arnold, J. *J. Am. Chem. Soc.* **2001**, *123*, 9212–9213.
1758. Herberhold, M. *Angew. Chem., Int. Ed.* **2002**, *41*, 956–958.
1759. Hitchcock, P. B.; Hughes, D. L.; Leigh, G. J.; Sanders, J. R.; de Souza, J. S. *Chem. Commun.* **1996**, 1985–1986.
1760. Hitchcock, P. B.; Hughes, D. L.; Leigh, G. J.; Sanders, J. R.; de Souza, J. S. *J. Chem. Soc., Dalton Trans.* **1999**, 1161–1173.
1761. Hitchcock, P. B.; Leigh, G. J.; Togrou, M. *J. Organomet. Chem.* **2003**, *667*, 73–80.
1762. Thiele, K. H.; Baumann, H. Z. *Anorg. Allg. Chem.* **1993**, *619*, 1111–1114.
1763. Mala, A.; Srivastava, A. K.; Pandey, O. P.; Sengupta, S. K. *Transition. Met. Chem.* **2000**, *25*, 613–616.
1764. Sengupta, S. K.; Pandey, O. P.; Srivastava, A. K.; Srivastava, S. K. *Indian J. Chem. Sect A-Inorg. Phys. Theor. Anal. Chem.* **1999**, *38*, 1066–1069.
1765. Srivastava, B. K.; Srivastava, S. K.; Pandey, O. P.; Sengupta, S. K. *Gazz. Chim. Ital.* **1997**, *127*, 827–830.
1766. Srivastava, S. K.; Srivastava, B. K.; Gupta, N.; Pandey, O. P.; Sengupta, S. K. *Indian J. Chem. Sect A-Inorg. Phys. Theor. Anal. Chem.* **1997**, *36*, 778–782.
1767. Srivastava, B. K.; Srivastava, S. K.; Pandey, O. P.; Sengupta, S. K. *Indian J. Chem. Sect A-Inorg. Phys. Theor. Anal. Chem.* **1996**, *35*, 57–59.
1768. Ma, C. L.; Yin, H. D.; Wang, D. Q.; Wang, S. H.; Zhang, R. F. *J. Indian Chem. Soc.* **1996**, *73*, 415–417.
1769. Ma, C. L.; Yin, H. D.; Wang, D. Q.; Zhang, R. F. *ACH-Models Chem.* **1994**, *131*, 829–834.
1770. Calvo, M.; Gómez-Sal, P.; Manzanero, A.; Royo, P. *Polyhedron* **1998**, *17*, 1081–1089.
1771. Delgado, E.; Fornies, J.; Hernández, E.; Lalinde, E.; Mansilla, N.; Moreno, M. T. *J. Organomet. Chem.* **1995**, *494*, 261–265.
1772. Delgado, E.; Hernández, E.; Mansilla, N.; Moreno, M. T.; Sabat, M. *J. Chem. Soc., Dalton Trans.* **1999**, 533–538.
1773. Graham, T. W.; Llamazares, A.; McDonald, R.; Cowie, M. *Organometallics* **1999**, *18*, 3502–3510.
1774. Le Gendre, P.; Richard, P.; Moise, C. *J. Organomet. Chem.* **2000**, *605*, 151–156.
1775. Braunstein, P.; Graiff, C.; Morise, X.; Tiripicchio, A. *J. Organomet. Chem.* **1997**, *541*, 417–422.
1776. Hidai, M.; Kuwata, S.; Mizobe, Y. *Acc. Chem. Res.* **2000**, *33*, 46–52.
1777. Kuwata, S.; Hidai, M. *Coord. Chem. Rev.* **2001**, *213*, 211–305.
1778. Oro, L. A.; Ciriano, M. A.; Pérez-Torrente, J. J.; Casado, M. A.; Hernández-Gruel, M. A. *F. C. R. Chim.* **2003**, *6*, 47–57.
1779. Nagano, T.; Kuwata, S.; Ishii, Y.; Hidai, M. *Organometallics* **2000**, *19*, 4176–4178.
1780. Kabashima, S.; Kuwata, S.; Ueno, K.; Shiro, M.; Hidai, M. *Angew. Chem., Int. Ed.* **2000**, *39*, 1128–1131.
1781. Kabashima, S.; Kuwata, S.; Hidai, M. *J. Am. Chem. Soc.* **1999**, *121*, 7837–7845.
1782. Kuwata, S.; Hidai, M. *Chem. Lett.* **1998**, 885–886.
1783. Kuwata, S.; Kabashima, S.; Sugiyama, N.; Ishii, Y.; Hidai, M. *Inorg. Chem.* **2001**, *40*, 2034–2040.
1784. Kuwata, S.; Nagano, T.; Matsubayashi, A.; Ishii, Y.; Hidai, M. *Inorg. Chem.* **2002**, *41*, 4324–4330.
1785. Amador, U.; Delgado, E.; Fornies, J.; Hernández, E.; Lalinde, E.; Moreno, M. T. *Inorg. Chem.* **1995**, *34*, 5279–5284.
1786. Khanna, A.; Khandelwal, B. L.; Gupta, S. K. *Transition. Met. Chem.* **1994**, *19*, 442–445.
1787. Fujita, K.; Ikeda, M.; Kondo, T.; Mitsudo, T. *Chem. Lett.* **1997**, 57–58.
1788. Fujita, K.; Ikeda, M.; Nakano, Y.; Kondo, T.; Mitsudo, T. *J. Chem. Soc., Dalton Trans.* **1998**, 2907–2913.
1789. Osakada, K.; Kawaguchi, Y.; Yamamoto, T. *Organometallics* **1995**, *14*, 4542–4548.
1790. Casado, M. A.; Ciriano, M. A.; Edwards, A. J.; Lahoz, F. J.; Oro, L. A.; Pérez-Torrente, J. J. *Organometallics* **1999**, *18*, 3025–3034.
1791. Casado, M. A.; Pérez-Torrente, J. J.; Ciriano, M. A.; Edwards, A. J.; Lahoz, F. J.; Oro, L. A. *Organometallics* **1999**, *18*, 5299–5310.
1792. Amemiya, T.; Kuwata, S.; Hidai, M. *Chem. Commun.* **1999**, 711–712.
1793. Casado, M. A.; Ciriano, M. A.; Edwards, A. J.; Lahoz, F. J.; Pérez-Torrente, J. J.; Oro, L. A. *Organometallics* **1998**, *17*, 3414–3416.
1794. Atencio, R.; Casado, M. A.; Ciriano, M. A.; Lahoz, F. J.; Pérez-Torrente, J. J.; Tiripicchio, A.; Oro, L. A. *J. Organomet. Chem.* **1996**, *514*, 103–110.
1795. Nadasdi, T. T.; Stephan, D. W. *Inorg. Chem.* **1994**, *33*, 1532–1538.
1796. Landman, M.; Waldbach, T.; Górls, H.; Lotz, S. *J. Organomet. Chem.* **2003**, *678*, 5–14.
1797. Komuro, T.; Matsuo, T.; Kawaguchi, H.; Tatsumi, K. *Angew. Chem., Int. Ed. Engl.* **2003**, *42*, 465–468.
1798. Casado, M. A.; Pérez-Torrente, J. J.; Ciriano, M. A.; Dobrinovitch, I. T.; Lahoz, F. J.; Oro, L. A. *Inorg. Chem.* **2003**, *42*, 3956–3964.
1799. Ara, I.; Delgado, E.; Fornies, J.; Hernández, E.; Lalinde, E.; Mansilla, N.; Moreno, M. T. *J. Chem. Soc., Dalton Trans.* **1996**, 3201–3207.
1800. Delgado, E.; Hernández, E.; Lalinde, E.; Lang, H.; Mansilla, N.; Moreno, M. T.; Rheinwald, G.; Zamora, F. *Inorg. Chim. Acta* **2001**, *315*, 1–8.
1801. Delgado, E.; García, M. A.; Gutiérrez-Puebla, E.; Hernández, E.; Mansilla, N.; Zamora, F. *Inorg. Chem.* **1998**, *37*, 6684–6689.
1802. Delgado, E.; Donnadieu, B.; Hernández, E.; Lalinde, E.; Mansilla, N.; Moreno, M. T. *J. Organomet. Chem.* **1999**, *592*, 283–289.
1803. Lang, H.; Stein, T. *J. Organomet. Chem.* **2002**, *641*, 41–52.
1804. Frosch, W.; Back, S.; Rheinwald, G.; Kohler, K.; Pritzkow, H.; Lang, H. *Organometallics* **2000**, *19*, 4016–4024.
1805. Frosch, W.; del Villar, A.; Lang, H. *J. Organomet. Chem.* **2000**, *602*, 91–96.
1806. Frosch, W.; Back, S.; Lang, H. *Organometallics* **1999**, *18*, 5725–5728.
1807. Lang, H.; Weinmann, M. *Synlett* **1996**, 1–10.
1808. Lang, H.; Kohler, K.; Rheinwald, G.; Zsolnai, L.; Buchner, M.; Driess, A.; Huttner, G.; Strahle, J. *Organometallics* **1999**, *18*, 598–605.
1809. Janssen, M. D.; Herres, M.; Zsolnai, L.; Grove, D. M.; Spek, A. L.; Lang, H.; Vankoten, G. *Organometallics* **1995**, *14*, 1098–1100.
1810. Lang, H.; Kohler, K.; Blau, S. *Coord. Chem. Rev.* **1995**, *143*, 113–168.
1811. Janssen, M. D.; Herres, M.; Spek, A. L.; Grove, D. M.; Lang, H.; Vankoten, G. *J. Chem. Soc., Chem. Commun.* **1995**, 925–926.
1812. Lang, H.; Rheinwald, G. *J. Prakt. Chem., Chem. Ztg.* **1999**, *341*, 1–19.
1813. Lang, H.; Herres, M.; Zsolnai, L. *Organometallics* **1993**, *12*, 5008–5011.
1814. Al-Anber, M.; Walfort, B.; Stein, T.; Lang, H. *Inorg. Chim. Acta* **2004**, *357*, 1675–1681.

1815. Stein, T.; Lang, H. *Chem. Commun.* **2001**, 1502–1503.
1816. Frosch, W.; Back, S.; Lang, H. *J. Organomet. Chem.* **2001**, 621, 143–152.
1817. Frosch, W.; Back, S.; Muller, H.; Kohler, K.; Driess, A.; Schiemenz, B.; Huttner, G.; Lang, H. *J. Organomet. Chem.* **2001**, 619, 99–109.
1818. Frosch, W.; Back, S.; Rheinwald, G.; Kohler, K.; Zsolnai, L.; Huttner, G.; Lang, H. *Organometallics* **2000**, 19, 5769–5779.
1819. Lang, H.; Kohler, K.; Zsolnai, L. *Chem. Ber.* **1995**, 128, 519–523.
1820. Herres, M.; Lang, H. *J. Organomet. Chem.* **1994**, 480, 235–239.
1821. Kohler, K.; Silverio, S. J.; Hyla-Kryspin, I.; Gleiter, R.; Zsolnai, L.; Driess, A.; Huttner, G.; Lang, H. *Organometallics* **1997**, 16, 4970–4979.
1822. Stein, T.; Lang, H. *J. Organomet. Chem.* **2002**, 664, 142–149.
1823. Janssen, M. D.; Smeets, W. J. J.; Spek, A. L.; Grove, D. M.; Lang, H.; vanKoten, G. *J. Organomet. Chem.* **1995**, 505, 123–126.
1824. Frosch, W.; Back, S.; Lang, H. *J. Organomet. Chem.* **2001**, 625, 140–147.
1825. Lang, H.; Herres, M.; Imhof, W. *J. Organomet. Chem.* **1994**, 465, 283–287.
1826. Lang, H.; Meichel, E.; Stein, T.; Weber, C.; Kralik, J.; Rheinwald, G.; Pritzkow, H. *J. Organomet. Chem.* **2002**, 664, 150–160.
1827. Back, S.; Stein, T.; Frosch, W.; Wu, I. Y.; Kralik, J.; Buchner, M.; Huttner, G.; Rheinwald, G.; Lang, H. *Inorg. Chim. Acta* **2001**, 325, 94–102.
1828. Back, S.; Stein, T.; Kralik, J.; Weber, C.; Rheinwald, G.; Zsolnai, L.; Huttner, G.; Lang, H. *J. Organomet. Chem.* **2002**, 664, 123–129.
1829. Berenguer, J. R.; Falvello, L. R.; Fornies, J.; Lalinde, E.; Tomás, M. *Organometallics* **1993**, 12, 6–7.
1830. Berenguer, J. R.; Fornies, J.; Lalinde, E.; Martín, A. *Angew. Chem., Int. Ed. Engl.* **1994**, 33, 2083–2085.
1831. Lang, H.; Wu, I. Y.; Weinmann, S.; Weber, C.; Nuber, B. *J. Organomet. Chem.* **1997**, 541, 157–165.
1832. Rosenthal, U.; Pulst, S.; Arndt, P.; Ohff, A.; Tillack, A.; Baumann, W.; Kempe, R.; Burlakov, V. V. *Organometallics* **1995**, 14, 2961–2968.
1833. Pulst, S.; Arndt, P.; Baumann, W.; Tillack, A.; Kempe, R.; Rosenthal, U. *J. Chem. Soc., Chem. Commun.* **1995**, 1753–1754.
1834. Zhao, J. S.; Gu, A. P.; He, S. Y.; Choukroun, R.; Valade, L.; Cassoux, P. *Acta Chim. Sinica* **2002**, 60, 687–691.
1835. Zhao, J. S.; Gu, A. P.; He, S. Y.; Choukroun, R.; Valade, L.; Cassoux, P. *Chem. J. Chin. Univ.* **2002**, 23, 1833–1836.
1836. Danjoy, C.; Zhao, J. S.; Donnadiou, B.; Legros, J. P.; Valade, L.; Choukroun, R.; Zwick, A.; Cassoux, P. *Chem., Eur. J.* **1998**, 4, 1100–1105.
1837. Köcher, S.; Lang, H. *J. Organomet. Chem.* **2002**, 641, 62–66.
1838. Back, S.; Pritzkow, H.; Lang, H. *Organometallics* **1998**, 17, 41–44.
1839. Back, S.; Rheinwald, G.; Lang, H. *Organometallics* **1999**, 18, 4119–4122.
1840. Ara, I.; Delgado, E.; Fornies, J.; Hernández, E.; Lalinde, E.; Mansilla, N.; Moreno, M. T. *J. Chem. Soc., Dalton Trans.* **1998**, 3199–3208.
1841. Zippel, T.; Arndt, P.; Ohff, A.; Spannenberg, A.; Kempe, R.; Rosenthal, U. *Organometallics* **1998**, 17, 4429–4437.
1842. Ohff, A.; Zippel, T.; Arndt, P.; Spannenberg, A.; Kempe, R.; Rosenthal, U. *Organometallics* **1998**, 17, 1649–1651.
1843. Kunkely, H.; Vogler, A. *Inorg. Chim. Acta* **1997**, 254, 195–198.
1844. Findeis, B.; Schubart, M.; Platzek, C.; Gade, L. H.; Scowen, I.; McPartlin, M. *Chem. Commun.* **1996**, 219–220.
1845. Gade, L. H.; Schubart, M.; Findeis, B.; Fabre, S.; Bezougli, I.; Lutz, M.; Scowen, I. J.; McPartlin, M. *Inorg. Chem.* **1999**, 38, 5282–5294.
1846. Friedrich, S.; Memmler, H.; Gade, L. H.; Li, W. S.; McPartlin, M. *Angew. Chem., Int. Ed. Engl.* **1994**, 33, 676–678.
1847. Selent, D.; Beckhaus, R.; Pickardt, J. *Organometallics* **1993**, 12, 2857–2860.
1848. Hollis, T. K.; Ahn, Y. J.; Tham, F. S. *Chem. Commun.* **2002**, 2996–2997.
1849. Hollis, T. K.; Ahn, Y. J.; Tham, F. S. *Organometallics* **2003**, 22, 1432–1436.
1850. Brown, S. J.; Gao, X. L.; Harrison, D. G.; Koch, L.; Spence, R. E. V.; Yap, G. P. A. *Organometallics* **1998**, 17, 5445–5447.
1851. Dodge, T.; Curtis, M. A.; Russell, J. M.; Sabat, M.; Finn, M. G.; Grimes, R. N. *J. Am. Chem. Soc.* **2000**, 122, 10573–10580.
1852. Hosmane, N. S.; Wang, Y.; Zhang, H. M.; Lu, K. J.; Maguire, J. A.; Gray, T. G.; Brooks, K. A.; Waldhor, E.; Kaim, W.; Kremer, R. K. *Organometallics* **1997**, 16, 1365–1377.
1853. Hosmane, N. S.; Wang, Y.; Zhang, H. M.; Maguire, J. A.; Waldhor, E.; Kaim, W.; Binder, H.; Kremer, R. K. *Organometallics* **1994**, 13, 4156–4158.
1854. Bowen, D. E.; Jordan, R. F.; Rogers, R. D. *Organometallics* **1995**, 14, 3630–3635.
1855. Bei, X. H.; Kreuder, C.; Swenson, D. C.; Jordan, R. F.; Young, V. G. *Organometallics* **1998**, 17, 1085–1091.
1856. Kreuder, C.; Jordan, R. F.; Zhang, H. M. *Organometallics* **1995**, 14, 2993–3001.
1857. Bei, X. H.; Young, V. G.; Jordan, R. F. *Organometallics* **2001**, 20, 355–358.
1858. Saccheo, S.; Gioia, G.; Grassi, A.; Bowen, D. E.; Jordan, R. F. *J. Mol. Catal. A: Chem.* **1998**, 128, 111–118.
1859. Kim, D. H.; Won, J. H.; Kim, S. J.; Ko, J.; Kim, S. H.; Cho, S. G. C.; Kang, S. O. *Organometallics* **2001**, 20, 4298–4300.
1860. Lee, Y. J.; Lee, J. D.; Jeong, H. J.; Son, K. C.; Ko, J. J.; Cheong, M.; Kang, S. O. *Organometallics* **2005**, 24, 3008–3019.
1861. Lee, Y. J.; Lee, J. D.; Ko, J. J.; Kim, S. H.; Kang, S. O. *Chem. Commun.* **2003**, 1364–1365.
1862. Dias, A. R.; Galvao, A. M.; Galvao, A. C.; Salema, M. S. *J. Chem. Soc., Dalton Trans.* **1997**, 1055–1061.
1863. Dias, A. R.; Galvao, A. M.; Galvao, A. C. *J. Organomet. Chem.* **2001**, 632, 157–163.
1864. Xu, X. X.; Yi, J. J.; Jing, Z. H. *Acta Polym. Sin.* **2001**, 683–686.
1865. Herberich, G. E.; Englert, U.; Schmitz, A. *Organometallics* **1997**, 16, 3751–3757.
1866. Ashe, A. J.; Fang, X. G.; Kampf, J. W. *Organometallics* **1999**, 18, 1363–1365.
1867. Troyanov, S. *J. Organomet. Chem.* **1994**, 475, 139–147.
1868. Solari, E.; Floriani, C.; Schenk, K.; Chiesivilla, A.; Rizzoli, C.; Rosi, M.; Sgamellotti, A. *Inorg. Chem.* **1994**, 33, 2018–2028.
1869. Kiprof, P.; Li, J.; Renish, C. L.; Kalombo, E. K.; Young, V. G. *J. Organomet. Chem.* **2001**, 620, 113–118.
1870. Calderazzo, F.; Ferri, I.; Pampaloni, G.; Troyanov, S. *J. Organomet. Chem.* **1996**, 518, 189–196.
1871. Calderazzo, F.; Pampaloni, G.; Vallieri, A. *Inorg. Chim. Acta* **1995**, 229, 179–186.
1872. Kiprof, P.; Steurer, B. C.; Fansler, D. D.; Erickson, M. A. *Mendeleev Commun.* **2000**, 170–170A.
1873. Fang, X. D.; Woodmansee, D.; Bu, X. H.; Bazan, G. C. *Angew. Chem., Int. Ed.* **2003**, 42, 4510–4514.
1874. King, R. B. *Appl. Organomet. Chem.* **2003**, 17, 393–397.
1875. Cloke, F. G. N.; Green, J. C.; Hitchcock, P. B.; Joseph, S. C. P.; Mountford, P.; Kaltsoyannis, N.; McCamley, A. J. *Chem. Soc., Dalton Trans.* **1994**, 2867–2874.
1876. Calderazzo, F.; Englert, U.; Pampaloni, G.; Kolle, U.; Tripepi, G. *J. Organomet. Chem.* **1997**, 543, 201–207.
1877. Jonas, K.; Korb, P.; Kollbach, G.; Gabor, B.; Mynott, R.; Angermund, K.; Heinemann, O.; Kruger, C. *Angew. Chem., Int. Ed. Engl.* **1997**, 36, 1714–1718.
1878. Gleiter, R.; Bethke, S.; Okubo, J.; Jonas, M. *Organometallics* **2001**, 20, 4274–4278.
1879. Munson, E. J.; Douskey, M. C.; De Paul, S. M.; Ziegewied, M.; Phillips, L.; Separovic, F.; Davies, M. S.; Aroney, M. J. *J. Organomet. Chem.* **1999**, 577, 19–23.

1880. Calderazzo, F.; Englert, U.; Pampaloni, G.; Tripepi, G. *J. Organomet. Chem.* **1998**, *555*, 49–56.
1881. Reetz, M. T. In *Organometallic in Synthesis*; Schlosser, M., Ed.; Wiley: Chichester, 1994.
1882. Petasis, N. A. In *Encyclopedia of Reagents for Organic Synthesis*; Paquette, L. A., Ed.; Wiley: New York, 1995; Vol. 1.
1883. Marek, I. In *Titanium and Zirconium in Organic Synthesis*; Wiley-VCH: Weinheim, 2002.
1884. Corneils, B.; Herrmann, W. A., Eds.; *Applied Homogeneous Catalysis with Organometallic Compounds*; VCH: Weinheim, 1996; Vol. I and II.
1885. Petasis, N. A.; Hu, Y. H. *Curr. Org. Chem.* **1997**, *1*, 249–286.
1886. Janiak, C. In *Metallocenes: Synthesis, Reactivity and Applications*; Togni, A.; Halterman, R. L., Eds.; Wiley-VCH: New York, 1998; Vol. 2, pp 547–624.
1887. Hoveyda, A. H.; Morken, J. P. In *Metallocenes: Synthesis, Reactivity and Applications*; Togni, A.; Halterman, R. L., Eds.; Wiley-VCH: New York, 1998; Vol. 2, pp 625–684.
1888. Negishi, E.; Kondakov, D. Y. *Chem. Soc. Rev.* **1996**, *25*, 417–426.
1889. Casey, C. P.; Strotman, N. A. *J. Am. Chem. Soc.* **2004**, *126*, 1699–1704.
1890. de Meijere, A.; Kozhushkov, S. I.; Savchenko, A. I. *J. Organomet. Chem.* **2004**, *689*, 2033–2055.
1891. Voigt, T.; Winsel, H.; de Meijere, A. *Synlett* **2002**, 1362–1364.
1892. Cozzi, P. G.; Alesi, S. *Chem. Commun.* **2004**, 2448–2449.
1893. Gensini, M.; de Meijere, A. *Chem. Eur. J.* **2004**, *10*, 785–790.
1894. Wiedemann, S.; Marek, I.; de Meijere, A. *Synlett* **2002**, 879–882.
1895. Ohff, A.; Burlakov, V. V.; Rosenthal, U. *J. Mol. Catal. A: Chem.* **1996**, *105*, 103–110.
1896. Sun, Q.; Liao, S. J.; Xu, Y.; Zhang, Y. P.; Yang, R. W.; Sun, R. A.; Chen, S. S. *Chem. J. Chin. Univ.* **1996**, *17*, 1441–1445.
1897. Della Sala, G.; Labano, S.; Lattanzi, A.; Tedesco, C.; Scettri, A. *Synthesis* **2002**, 505–510.
1898. Bijpost, E. A.; Duchateau, R.; Teuben, J. H. *J. Mol. Catal. A: Chem.* **1995**, *95*, 121–128.
1899. Wali, A.; Ganeshpure, P. A.; Pillai, S. M.; Satish, S. *Ind. Eng. Chem. Res.* **1994**, *33*, 444–447.
1900. Fairfax, D.; Stein, M.; Livinghouse, T.; Jensen, M. *Organometallics* **1997**, *16*, 1523–1525.
1901. McGrane, P. L.; Livinghouse, T. *J. Am. Chem. Soc.* **1993**, *115*, 11485–11489.
1902. Fan, Y. H.; Liao, S. J.; Xu, J.; Qian, Y. L.; Huang, J. L. *Chem. J. Chin. Univ.* **1997**, *18*, 1683–1687.
1903. Gansauer, A.; Pierobon, M. *Synlett* **2000**, 1357–1359.
1904. Raponi, E.; Pons, J. M. *Tetrahedron Lett.* **2003**, *44*, 9193–9196.
1905. Abbott, A. R.; Thompson, J.; Thompson, L. C.; Knight, K. S. *Transition. Met. Chem.* **2003**, *28*, 305–307.
1906. Millward, D. B.; Sammis, G.; Waymouth, R. M. *J. Org. Chem.* **2000**, *65*, 3902–3909.
1907. Della Sala, G.; Labano, S.; Lattanzi, A.; Scettri, A. *Tetrahedron* **2002**, *58*, 6679–6683.
1908. North, M. *Synlett* **1993**, 807–820.
1909. Lee, C. B.; Wu, Z. C.; Zhang, F.; Chappell, M. D.; Stachel, S. J.; Chou, T. C.; Guan, Y. B.; Danishefsky, S. J. *J. Am. Chem. Soc.* **2001**, *123*, 5249–5259.
1910. Verdaguer, X.; Berk, S. C.; Buchwald, S. L. *J. Am. Chem. Soc.* **1995**, *117*, 12641–12642.
1911. Hoffmann, R. W.; Polachowski, A. *Chem. Eur. J.* **1998**, *4*, 1724–1730.
1912. BouzBouz, S.; Pradaux, F.; Cossy, J.; Ferroud, C.; Falguieres, A. *Tetrahedron Lett.* **2000**, *41*, 8877–8880.
1913. Cossy, J.; BouzBouz, S.; Pradaux, F.; Willis, C.; Bellosta, V. *Synlett* **2002**, 1595–1606.
1914. Krause, N.; Laux, M.; Hoffmann-Roder, A. *Tetrahedron Lett.* **2000**, *41*, 9613–9616.
1915. Barrett, A. G. M.; Damiani, F. *J. Org. Chem.* **1999**, *64*, 1410–1411.
1916. Siebeneicher, H.; Bytschkov, I.; Doye, S. *Angew. Chem., Int. Ed. Engl.* **2003**, *42*, 3042–3044.
1917. Hoff, S. M.; Novak, B. M. *Macromolecules* **1993**, *26*, 4067–4069.
1918. Sylvestre, I.; Ollivier, J.; Salaun, J. *Tetrahedron Lett.* **2001**, *42*, 4991–4994.
1919. Racouchot, S.; Ollivier, J.; Salaun, J. *Synlett* **2000**, 1729–1732.
1920. Willoughby, C. A.; Buchwald, S. L. *J. Am. Chem. Soc.* **1994**, *116*, 11703–11714.
1921. Ibragimov, A. G.; Zagrebels'kaya, I. V.; Satenov, K. G.; Khalilov, L. M.; Dzhemilev, U. M. *Russ. Chem. Bull.* **1998**, *47*, 691–694.
1922. Gao, Y. A.; Urabe, H.; Sato, F. *J. Org. Chem.* **1994**, *59*, 5521–5523.
1923. Gao, Y.; Harada, K.; Hata, T.; Urabe, H.; Sato, F. *J. Org. Chem.* **1995**, *60*, 290–291.
1924. Larsson, M.; Galandrin, E.; Hogberg, H. E. *Tetrahedron* **2004**, *60*, 10659–10669.
1925. Verdaguer, X.; Lange, U. E. W.; Buchwald, S. L. *Angew. Chem., Int. Ed.* **1998**, *37*, 1103–1107.
1926. Yun, J.; Buchwald, S. L. *J. Am. Chem. Soc.* **1999**, *121*, 5640–5644.
1927. Carter, M. B.; Schiott, B.; Gutierrez, A.; Buchwald, S. L. *J. Am. Chem. Soc.* **1994**, *116*, 11667–11670.
1928. Imma, H.; Mori, M.; Nakai, T. *Synlett* **1996**, 1229–1233.
1929. Halterman, R. L.; Ramsey, T. M.; Chen, Z. L. *J. Org. Chem.* **1994**, *59*, 2642–2644.
1930. Colletti, S. L.; Halterman, R. L. *J. Organomet. Chem.* **1993**, *455*, 99–106.
1931. Halterman, R. L.; Ramsey, T. M. *J. Organomet. Chem.* **1994**, *465*, 175–179.
1932. Della Sala, G.; Giordano, L.; Lattanzi, A.; Proto, A.; Scettri, A. *Tetrahedron* **2000**, *56*, 3567–3573.
1933. Ghosh, P.; Kotchevar, A. T.; DuMez, D. D.; Ghosh, S.; Peiterson, J.; Uckun, F. M. *Inorg. Chem.* **1999**, *38*, 3730–3737.
1934. Klunduk, M. C.; Maschmeyer, T.; Thomas, J. M.; Johnson, B. F. G. *Chem. Eur. J.* **1999**, *5*, 1481–1485.
1935. Lattanzi, A.; Della Sala, G.; Russo, M.; Scettri, A. *Synlett* **2001**, 1479–1481.
1936. Thorimbert, S.; Klein, S.; Maier, W. F. *Tetrahedron* **1995**, *51*, 3787–3792.
1937. Yun, S. H.; Bu, J.; Rhee, H. K. *React. Kinet. Catal. Lett.* **2001**, *72*, 343–353.
1938. Guidotti, M.; Conti, L.; Fusi, A.; Ravasio, N.; Psaro, R. *J. Mol. Catal. A: Chem.* **2002**, *182*, 151–156.
1939. Sinclair, P. E.; Sankar, G.; Catlow, C. R. A.; Thomas, J. M.; Maschmeyer, T. *J. Phys. Chem. B* **1997**, *101*, 4232–4237.
1940. Ferreira, P.; Goncalves, I. S.; Kuhn, F. E.; Pillinger, M.; Rocha, J.; Santos, A. M.; Thursfield, A. *Eur. J. Inorg. Chem.* **2000**, 551–557.
1941. Corma, A.; Diaz, U.; Fornes, V.; Jorda, J. L.; Domine, M.; Rey, F. *Chem. Commun.* **1999**, 779–780.
1942. Murugavel, R.; Roesky, H. W. *Angew. Chem., Int. Ed. Engl.* **1997**, *36*, 477–479.
1943. Maschmeyer, T.; Rey, F.; Sankar, G.; Thomas, J. M. *Nature* **1995**, *378*, 159–162.
1944. Oldroyd, R. D.; Sankar, G.; Thomas, J. M.; Ozkaya, D. *J. Phys. Chem. B* **1998**, *102*, 1849–1855.
1945. Doye, S. *Synlett* **2004**, 1653–1672.
1946. Bytschkov, I.; Doye, S. *Eur. J. Org. Chem.* **2003**, 935–946.



1947. Pohlki, F.; Doye, S. *Chem. Soc. Rev.* **2003**, *32*, 104–114.
1948. Haak, E.; Bytschkov, I.; Doye, S. *Angew. Chem., Int. Ed.* **1999**, *38*, 3389–3391.
1949. Haak, E.; Siebeneicher, H.; Doye, S. *Org. Lett.* **2000**, *2*, 1935–1937.
1950. Siebeneicher, H.; Doye, S. *Eur. J. Org. Chem.* **2002**, 1213–1220.
1951. Ackermann, L.; Bergman, R. G.; Loy, R. N. *J. Am. Chem. Soc.* **2003**, *125*, 11956–11963.
1952. Pohlki, F.; Dove, S. *Angew. Chem., Int. Ed.* **2001**, *40*, 2305–2308.
1953. Pohlki, F.; Heutling, A.; Bytschkov, I.; Hotopp, T.; Doye, S. *Synlett* **2002**, 799–801.
1954. Heutling, A.; Doye, S. *J. Org. Chem.* **2002**, *67*, 1961–1964.
1955. Haak, E.; Bytschkov, I.; Doye, S. *Eur. J. Org. Chem.* **2002**, 457–463.
1956. Bytschkov, I.; Doye, S. *Eur. J. Org. Chem.* **2001**, 4411–4418.
1957. Bytschkov, T.; Doye, S. *Tetrahedron Lett.* **2002**, *43*, 3715–3718.
1958. Heutling, A.; Pohlki, F.; Doye, S. *Chem. Eur. J.* **2004**, *10*, 3059–3071.
1959. Ackermann, L.; Bergman, R. G. *Org. Lett.* **2002**, *4*, 1475–1478.
1960. Tillack, A.; Castro, I. G.; Hartung, C. G.; Beller, M. *Angew. Chem., Int. Ed. Engl.* **2002**, *41*, 2541–2543.
1961. Castro, I. G.; Tillack, A.; Hartung, C. G.; Beller, M. *Tetrahedron Lett.* **2003**, *44*, 3217–3221.
1962. Tillack, A.; Jiao, H. J.; Castro, I. G.; Hartung, C. G.; Beller, M. *Chem. Eur. J.* **2004**, *10*, 2409–2420.
1963. Gansauer, A.; Rinker, B. In *Titanium and Zirconium in Organic Synthesis*; Marek, I., Ed.; Wiley-VCH: Weinheim, 2002; pp 435–456.
1964. Gansauer, A.; Bluhm, H. *Chem. Rev.* **2000**, *100*, 2771–2788.
1965. Urabe, H.; Yoshikawa, K.; Sato, F. *Tetrahedron Lett.* **1995**, *36*, 5595–5598.
1966. Justicia, J.; Rosales, A.; Bunuel, E.; Oller-López, J. L.; Valdivia, N.; Haidour, A.; Oltra, J. E.; Barrero, A. F.; Cardenas, D. J.; Cuerva, J. M. *Chem. Eur. J.* **2004**, *10*, 1778–1788.
1967. Leca, D.; Fensterbank, L.; Lacote, E.; Malacria, M. *Angew. Chem., Int. Ed.* **2004**, *43*, 4220–4222.
1968. Zhou, L. H.; Hirao, T. *J. Org. Chem.* **2002**, *68*, 1633–1635.
1969. Gansauer, A.; Barchuk, A.; Fielenbach, D. *Synthesis* **2004**, 2567–2573.
1970. Gansauer, A.; Bluhm, H.; Pierobon, M. *J. Am. Chem. Soc.* **1998**, *120*, 12849–12859.
1971. Gansauer, A.; Lauterbach, T.; Bluhm, H.; Noltemeyer, M. *Angew. Chem., Int. Ed.* **1999**, *38*, 2909–2910.
1972. Gansauer, A.; Narayan, S. *Adv. Synth. Catal.* **2002**, *344*, 465–475.
1973. Gansauer, A.; Bluhm, H.; Lauterbach, T. *Adv. Synth. Catal.* **2001**, *343*, 785–787.
1974. Barrero, A. F.; Oltra, J. E.; Cuerva, J. M.; Rosales, A. *J. Org. Chem.* **2002**, *67*, 2566–2571.
1975. Hardouin, C.; Burgaud, L.; Valleix, A.; Doris, E. *Tetrahedron Lett.* **2003**, *44*, 435–437.
1976. Hardouin, C.; Chevallier, F.; Rousseau, B.; Doris, E. *J. Org. Chem.* **2001**, *66*, 1046–1048.
1977. Hardouin, C.; Doris, E.; Rousseau, B.; Mioskowski, C. *J. Org. Chem.* **2002**, *67*, 6571–6574.
1978. Hardouin, C.; Doris, E.; Rousseau, B.; Mioskowski, C. *Org. Lett.* **2002**, *4*, 1151–1153.
1979. Moisan, L.; Hardouin, C.; Rousseau, B.; Doris, E. *Tetrahedron Lett.* **2002**, *43*, 2013–2015.
1980. Gansauer, A.; Pierobon, M.; Bluhm, H. *Synthesis* **2001**, 2500–2520.
1981. Gansauer, A.; Bluhm, H.; Lauterbach, T. *Adv. Synth. Catal.* **2001**, 785–787.
1982. Gansauer, A.; Narayan, S. *Adv. Synth. Catal.* **2002**, 465–475.
1983. Gansauer, A.; Pierobon, M.; Bluhm, H. *Angew. Chem., Int. Ed.* **2002**, *41*, 3206–3208.
1984. Jana, S.; Guin, C.; Roy, S. C. *Tetrahedron Lett.* **2004**, *45*, 6575–6577.
1985. Roy, S. C.; Rana, K. K.; Guin, C. *J. Org. Chem.* **2002**, *67*, 3242–3248.
1986. Clive, D. L. J.; Magnuson, S. R. *Tetrahedron Lett.* **1995**, *36*, 15–18.
1987. Barrero, A. F.; Rosales, A.; Cuerva, J. M.; Oltra, J. E. *Org. Lett.* **2003**, *5*, 1935–1938.
1988. Hersant, G.; Ferjani, M. B. S.; Bennett, S. M. *Tetrahedron Lett.* **2004**, *45*, 8123–8126.
1989. Gansauer, A.; Moschioni, M.; Bauer, D. *Eur. J. Org. Chem.* **1998**, 1923–1927.
1990. Gansauer, A. *Synlett* **1997**, 363–364.
1991. Dunlap, M. S.; Nicholas, K. M. *J. Organomet. Chem.* **2001**, *630*, 125–131.
1992. Hirao, T.; Hatano, B.; Asahara, M.; Muguruma, Y.; Ogawa, A. *Tetrahedron Lett.* **1998**, *39*, 5247–5248.
1993. Dunlap, M. S.; Nicholas, K. M. *Synth. Commun.* **1999**, *29*, 1097–1106.
1994. Yamamoto, Y.; Hattori, R.; Miwa, T.; Nakagai, Y.; Kubota, T.; Yamamoto, C.; Okamoto, Y.; Itoh, K. *J. Org. Chem.* **2001**, *66*, 3865–3870.
1995. Lake, K.; Dorrell, M.; Blackman, N.; Khan, M. A.; Nicholas, K. M. *Organometallics* **2003**, *22*, 4260–4264.
1996. Gansauer, A. *Chem. Commun.* **1997**, 457–458.
1997. Gansauer, A.; Bauer, D. *Eur. J. Org. Chem.* **1998**, 2673–2676.
1998. Gansauer, A.; Bauer, D. *J. Org. Chem.* **1998**, *63*, 2070–2071.
1999. Zhang, Y. M.; Yu, Y. P.; Bao, W. L. *Synth. Commun.* **1995**, *25*, 1825–1830.
2000. Roux, P.; Pillot, J. P.; Birot, M.; Dunogues, J.; Lapouyade, P. *J. Organomet. Chem.* **1995**, *499*, 199–204.
2001. Goodson, S. H.; Novak, B. M. *Macromolecules* **2001**, *34*, 3849–3855.
2002. Myers, L. K.; Ho, D. M.; Thompson, M. E.; Langhoff, C. *Polyhedron* **1995**, *14*, 57–67.
2003. Melendez, E. *Crit. Rev. Oncol. Hemat.* **2002**, *42*, 309–315.
2004. Sun, H. Z.; Li, H. Y.; Weir, R. A.; Sadler, P. J. *Angew. Chem., Int. Ed.* **1998**, *37*, 1577–1579.
2005. Kopf-Maier, P.; Kopf, H. In *Metal Compounds in Cancer Chemotherapy*; Fricker, S. P., Ed.; Capmann and Hall: London, 1994; Vol. 1, pp 109–146.
2006. Christodoulou, C. V.; Eliopoulos, A. G.; Young, L. S.; Hodgkins, L.; Ferry, D. R.; Kerr, D. J. *Br. J. Cancer* **1998**, *77*, 2088–2097.
2007. Schwietert, C. W.; McCue, J. P. *Coord. Chem. Rev.* **1999**, *184*, 67–89.
2008. Yang, P.; Guo, M. L. *Coord. Chem. Rev.* **1999**, *186*, 189–211.
2009. Kopfmaier, P. *Eur. J. Clin. Pharmacol.* **1994**, *47*, 1–16.
2010. Ghosh, P.; D'Cruz, O. J.; Narla, R. K.; Uckun, F. M. *Clin. Cancer Res.* **2000**, *6*, 1536–1545.
2011. Mokhsi, G.; Harding, M. M. *J. Inorg. Biochem.* **2001**, *83*, 205–209.
2012. Harding, M. M.; Mokhsi, G. *Curr. Med. Chem.* **2000**, *7*, 1289–1303.
2013. Klapotke, T. M.; Kopf, H.; Tornieporthoetting, I. C.; White, P. S. *Organometallics* **1994**, *13*, 3628–3633.
2014. Klapotke, T. M.; Kopf, H.; Tornieporthoetting, I. C.; White, P. S. *Angew. Chem., Int. Ed. Engl.* **1994**, *33*, 1518–1519.

2015. Mokdsi, G.; Harding, M. M. *J. Organomet. Chem.* **1998**, *565*, 29–35.
2016. Tornieporthoetting, I. C.; White, P. S. *Organometallics* **1995**, *14*, 1632–1636.
2017. Guo, M. L.; Sadler, P. J. *J. Chem. Soc., Dalton Trans.* **2000**, 7–9.
2018. Guo, M. L.; Sun, H. Z.; Bihari, S.; Parkinson, J. A.; Gould, R. O.; Parsons, S.; Sadler, P. J. *Inorg. Chem.* **2000**, *39*, 206–215.
2019. Guo, M. L.; Sun, H. Z.; McArdle, H. J.; Gambling, L.; Sadler, P. J. *Biochemistry* **2000**, *39*, 10023–10033.
2020. Jaouen, G.; Top, S.; Vessieres, A.; Alberto, R. *J. Organomet. Chem.* **2000**, *600*, 23–36.
2021. Top, S.; Lescop, C.; Lehn, J. S.; Jaouen, G. *J. Organomet. Chem.* **2000**, *594*, 167–174.
2022. Lovejoy, D. B.; Richardson, D. R. *Expert Opin. Investig. Drugs* **2000**, *9*, 1257–1270.
2023. Shackelford, S. A.; Shellhamer, D. F.; Heasley, V. L. *Tetrahedron Lett.* **1999**, *40*, 6333–6337.
2024. Singh, Y.; Singh, M. P.; Swarup, R. *Synth. Met.* **1993**, *56*, 1878–1883.
2025. Singh, D.; Singh, R. V. *J. Inorg. Biochem.* **1993**, *50*, 227–234.
2026. Sheppeck, J. E.; Liu, W.; Chamberlin, A. R. *J. Org. Chem.* **1997**, *62*, 387–398.

## 4.06

# Complexes of Zirconium and Hafnium in Oxidation States 0 to II

---

P J Chirik, Cornell University, Ithaca, NY, USA

C A Bradley, Cornell University, Ithaca, NY, USA

© 2007 Elsevier Ltd. All rights reserved.

<b>4.06.1 Zirconium/Hafnium Complexes in Oxidation States +I and Below</b>	<b>697</b>
4.06.1.1 Bis(arene)zirconium and Hafnium Complexes	697
4.06.1.2 Subvalent Zirconium Arene, Bipyridine, and Biphosphinine Complexes	698
4.06.1.3 Zero- and Subvalent Zirconium and Hafnium Carbonyl Complexes	699
<b>4.06.2 Zirconium and Hafnium Complexes in Oxidation State +II</b>	<b>700</b>
4.06.2.1 Ligand-stabilized Zirconium/Hafnium(+II)	700
4.06.2.1.1 Dicarbonyl complexes	700
4.06.2.1.2 Phosphine complexes	702
4.06.2.1.3 Alkene complexes	704
4.06.2.1.4 Zirconacyclopentanes	714
4.06.2.1.5 Alkyne complexes	715
4.06.2.1.6 Zirconacyclopentadienes	722
4.06.2.1.7 Benzyne complexes	722
4.06.2.1.8 Zirconacyclocumulene complexes	725
4.06.2.1.9 Butadiene complexes	727
4.06.2.1.10 Bis(indenyl)zirconium sandwich complexes	728
4.06.2.2 Zirconium/Hafnium(II) Dinitrogen Complexes	730
4.06.2.2.1 Bis(cyclopentadienyl)dinitrogen complexes	730
4.06.2.2.2 Non-cyclopentadienyl dinitrogen complexes	732
4.06.2.3 Pentadienyl Complexes	734
4.06.2.4 Zirconocene-mediated C–F Activation	735
4.06.2.5 Miscellaneous Reduction Chemistry of Zirconium	735
<b>References</b>	<b>736</b>

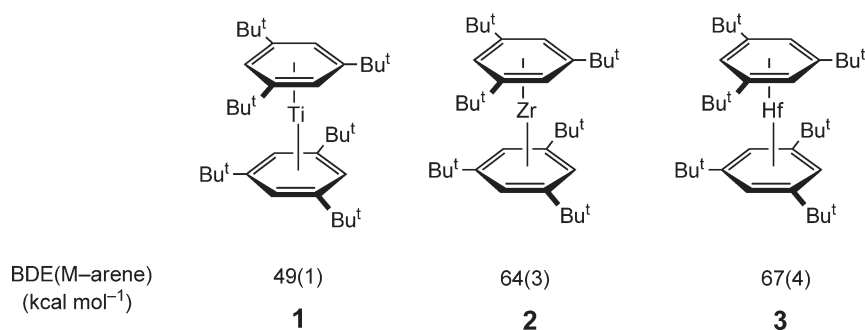
---

### 4.06.1 Zirconium/Hafnium Complexes in Oxidation States +I and Below

#### 4.06.1.1 Bis(arene)zirconium and Hafnium Complexes

Zero-valent zirconium and hafnium compounds remain relatively rare, owing to the strong thermodynamic driving force for the second and third row metals to attain a higher oxidation state. Despite this obstacle, examples of formally zero-valent compounds have been reported and characterized. The majority of these are arene complexes, whose syntheses and resulting chemistry have been reviewed.<sup>1,2</sup> In addition to arene compounds, formally zero-valent butadiene complexes have also been described and are the subject of a rather comprehensive review.<sup>3</sup> The focus of this section will be on compounds that have not been covered.

Incorporation of sterically demanding aryl substituents allows isolation of bis(arene)zirconium and hafnium complexes. The bond enthalpies of  $(\eta^6\text{-(1,3,5-}^t\text{Bu)}_3\text{C}_6\text{H}_3)_2\text{M}$  (M = Ti, **1**; Zr, **2**; Hf, **3**) have been measured by iodimetric bath calorimetry and values of 49(1), 64(3), and 67(4) kcal mol<sup>−1</sup> have been determined for the respective metal–arene bond enthalpies (Scheme 1).<sup>4</sup> Computational studies establish that the major metal–arene bonding interaction is a  $\delta$ -backbond formed from the overlap of metal  $d_{x^2-y^2}$  and  $d_{xy}$  orbitals with the appropriate linear combination of arene  $p$ -orbitals. The observed increase in metal–arene bond strength is consistent with increased backbonding down the



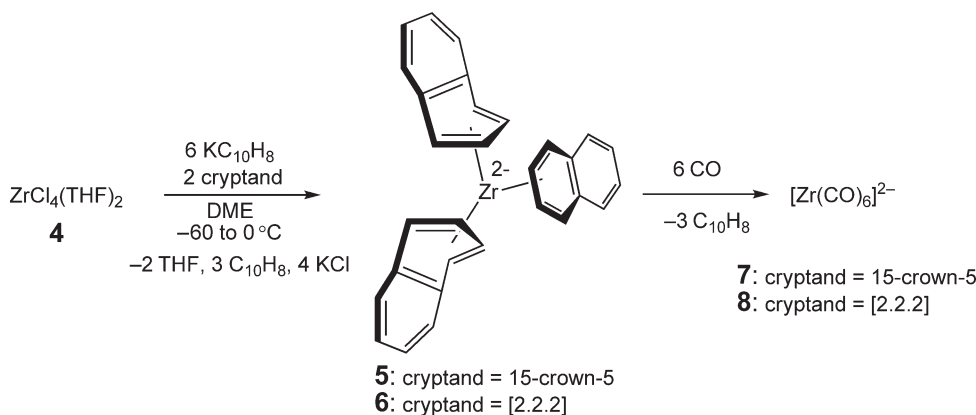
Scheme 1

triad. The values of the bond enthalpies suggest that the zirconium and hafnium complexes may serve as useful arene transfer reagents to the lanthanide metals.

#### 4.06.1.2 Subvalent Zirconium Arene, Bipyridine, and Biphosphinine Complexes

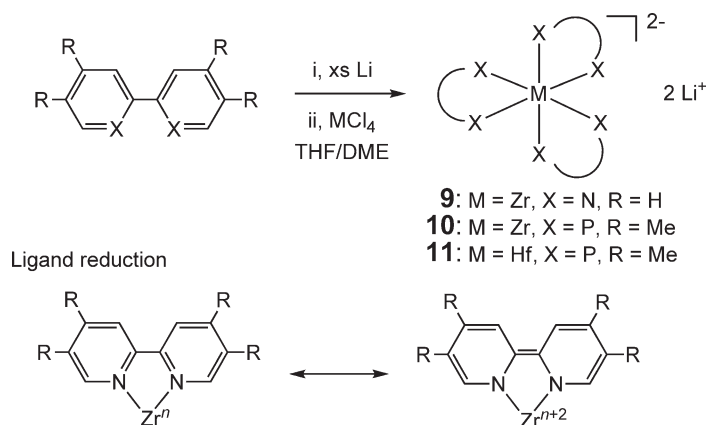
Arene ligands have also been used to stabilize zirconium complexes in oxidation states below zero. Compounds of this type have been termed “subvalent.” Treatment of a DME solution of  $\text{ZrCl}_4(\text{THF})_2$  **4** with potassium naphthalenide in the presence of a cryptand such as 15-crown-5 or [2.2.2]-cryptand at low temperature furnishes the tris( $\eta^4$ -naphthalene)zirconate( $2^-$ ) complexes (cryptand = 15-crown-5, **5**; [2.2.2]-cryptand, **6**) (Scheme 2).<sup>5</sup> The solid-state structures reveal approximate  $C_{3v}$  symmetry and are essentially isostructural with the previously characterized isoelectronic tris( $\eta^4$ -butadiene)molybdenum(0) and tris(cyclooctatetraene)niobate( $1^-$ ) derivatives. The aryl rings are significantly distorted from planarity. The carbon–carbon bond distances in the coordinated diene fragments are similar to those found in the stannyl titanate complex  $[(\eta^4\text{-naphthalene})_2\text{Ti}(\text{SnMe}_3)_2]$ . The zirconates are stable in the solid state for months if stored in an inert atmosphere. In solution, exchange with free naphthalene is not observed over a range of concentrations and temperatures, demonstrating the lack of intermolecular ring exchange. Displacement of the naphthalene ligands can be achieved upon addition of strong-field ligands such as carbon monoxide to yield the hexacarbonyl zirconate complexes  $[\text{Zr}(\text{CO})_6]^{2-}$  (cryptand = 15-crown-5, **7**; [2.2.2]-cryptand, **8**) (Scheme 2).

Addition of the dianions of 2,2'-bipyridine or 2,2'-biphosphinine to  $\text{MCl}_4$  ( $\text{M} = \text{Zr}, \text{Hf}$ ) in THF yields the hexacoordinate zirconate ( $\text{X} = \text{N}$ ,  $\text{R} = \text{H}$ , **9**;  $\text{X} = \text{P}$ ,  $\text{R} = \text{Me}$ , **10**) and hafnate ( $\text{X} = \text{P}$ ,  $\text{R} = \text{Me}$ , **11**) compounds (Scheme 3).<sup>6</sup> While electron counting and oxidation assignment schemes provide subvalent metal centers, analysis of the metrical parameters from the solid-state structures of the zirconium compounds indicates significant reduction of the aromatic rings, suggesting that assignment as  $\text{Zr}(\text{IV})$  may be more appropriate. Depending on the degree of electron transfer from the metal to the aromatic  $\pi$ -system, intermediate oxidation states are also possible. The molecular geometry about the zirconium varies from the N- to P-based ligands, where a structure intermediate



Scheme 2





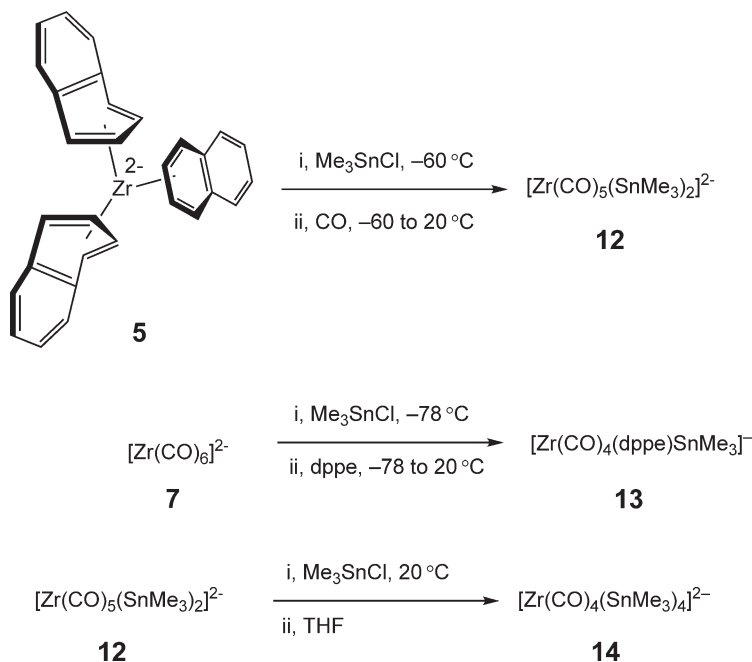
Scheme 3

between an idealized octahedron and trigonal prism is observed for **9**, while the phosphorus congener, **10**, is distinctly trigonal prismatic. Because the bite angles of the ligands in the two complexes are comparable, electronic differences have been used to account for the observed structural differences.

#### 4.06.1.3 Zero- and Subvalent Zirconium and Hafnium Carbonyl Complexes

As expected, the strong-field  $\pi$ -acidic ligand, carbon monoxide, has also been used to isolate zero-valent zirconium and hafnium complexes. This area has been a subject of relatively long-standing interest and has been reviewed.<sup>7</sup> Chemistry outside of this review will be the focus of this section.

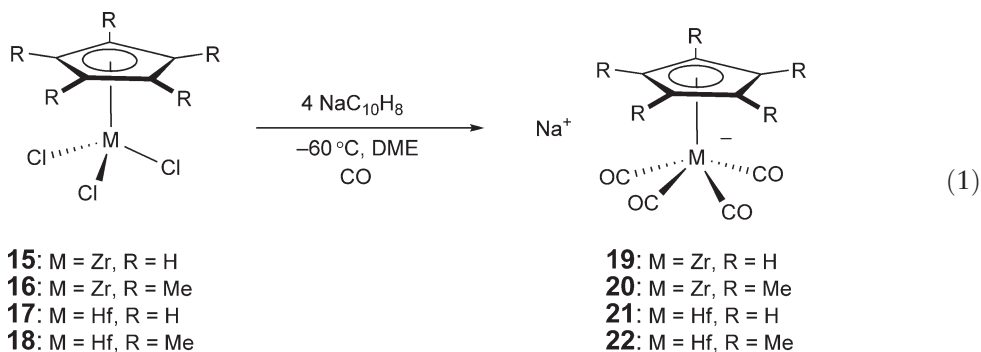
Addition of carbon monoxide to the tris( $\eta^4$ -naphthalene)zirconate(2-), **5**, in the presence of stannyl chloride affords the heptacoordinate complex  $[\text{Zr}(\text{CO})_5(\text{SnMe}_3)_2]^{2-}$  **12** (Scheme 4).<sup>8</sup> The related bis(phosphine) zirconate anion,  $[\text{Zr}(\text{CO})_4(\text{dppe})\text{SnMe}_3]^-$  **13**, has been prepared by treatment of **7** with  $\text{Me}_3\text{SnCl}$  at low temperature followed



Scheme 4

by dppe addition (Scheme 4). Carbonyl bands in the range of  $1790\text{--}1900\text{ cm}^{-1}$  are observed by infrared (IR) spectroscopy while the  $^{13}\text{C}$  NMR shifts seen above 280 ppm are typical of carbonyl complexes of this type. If the stannylation procedure is conducted at room temperature,  $[\text{K}(15\text{-crown-5})_2][\text{Zr}(\text{CO})_4(\text{SnMe}_3)_4]$  **14**, is isolated, highlighting the sensitivity of the reaction to temperature (Scheme 4).

Substituted piano stool complexes  $(\eta^5\text{-C}_5\text{R}_5)\text{MCl}_3$  ( $\text{M} = \text{Zr}$ ,  $\text{R} = \text{H}$ , **15**;  $\text{M} = \text{Zr}$ ,  $\text{R} = \text{Me}$ , **16**;  $\text{M} = \text{Hf}$ ,  $\text{R} = \text{H}$ , **17**;  $\text{M} = \text{Hf}$ ,  $\text{R} = \text{Me}$ , **18**) undergo reduction upon addition of alkali metal naphthalenides at low temperature in the presence of carbon monoxide to yield  $[(\eta^5\text{-C}_5\text{R}_5)\text{M}(\text{CO})_4]^-$  anions ( $\text{M} = \text{Zr}$ ,  $\text{R} = \text{H}$ , **19**;  $\text{M} = \text{Zr}$ ,  $\text{R} = \text{Me}$ , **20**;  $\text{M} = \text{Hf}$ ,  $\text{R} = \text{H}$ , **21**;  $\text{M} = \text{Hf}$ ,  $\text{R} = \text{Me}$ , **22**) anions (Equation (1)).<sup>9</sup> As with other low-valent carbonyl complexes, CO bands are observed between  $1770\text{--}1780$  and  $1910\text{--}1920\text{ cm}^{-1}$ , indicative of reduction of the carbonyl ligands.



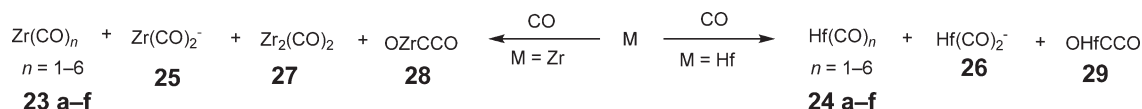
The carbonyl chemistry of atomic zirconium and hafnium has also been investigated.<sup>10</sup> Examination of laser-ablated zirconium and hafnium atoms co-condensed with 0.1% CO in neon gas by IR spectroscopy allows the identification of a series of metal carbonyl products (Scheme 5). Both  $^{13}\text{C}$  and  $^{18}\text{O}$  isotopic labeling studies, in combination with DFT calculations, have been used to assign the identity of the products as  $\text{M}(\text{CO})_n$  ( $\text{M} = \text{Zr}$ ,  $n = 1\text{--}6$ , **23 a–f**;  $\text{M} = \text{Hf}$ ,  $n = 1\text{--}6$ , **24 a–f**). In addition,  $\text{M}(\text{CO})_2^-$  ( $\text{M} = \text{Zr}$ , **25**;  $\text{M} = \text{Hf}$ , **26**) anions and the zirconium dimer,  $\text{Zr}_2(\text{CO})_2$  **27**, are also observed. Photochemical rearrangement of the  $\text{M}(\text{CO})_2$  species to OMCCO ( $\text{M} = \text{Zr}$ , **28**;  $\text{M} = \text{Hf}$ , **29**) also occurs. In general, lower carbonyl stretching frequencies are observed for the hafnium congeners, consistent with greater reduction by the third row metal center.

## 4.06.2 Zirconium and Hafnium Complexes in Oxidation State +II

### 4.06.2.1 Ligand-stabilized Zirconium/Hafnium(+II)

#### 4.06.2.1.1 Dicarbonyl complexes

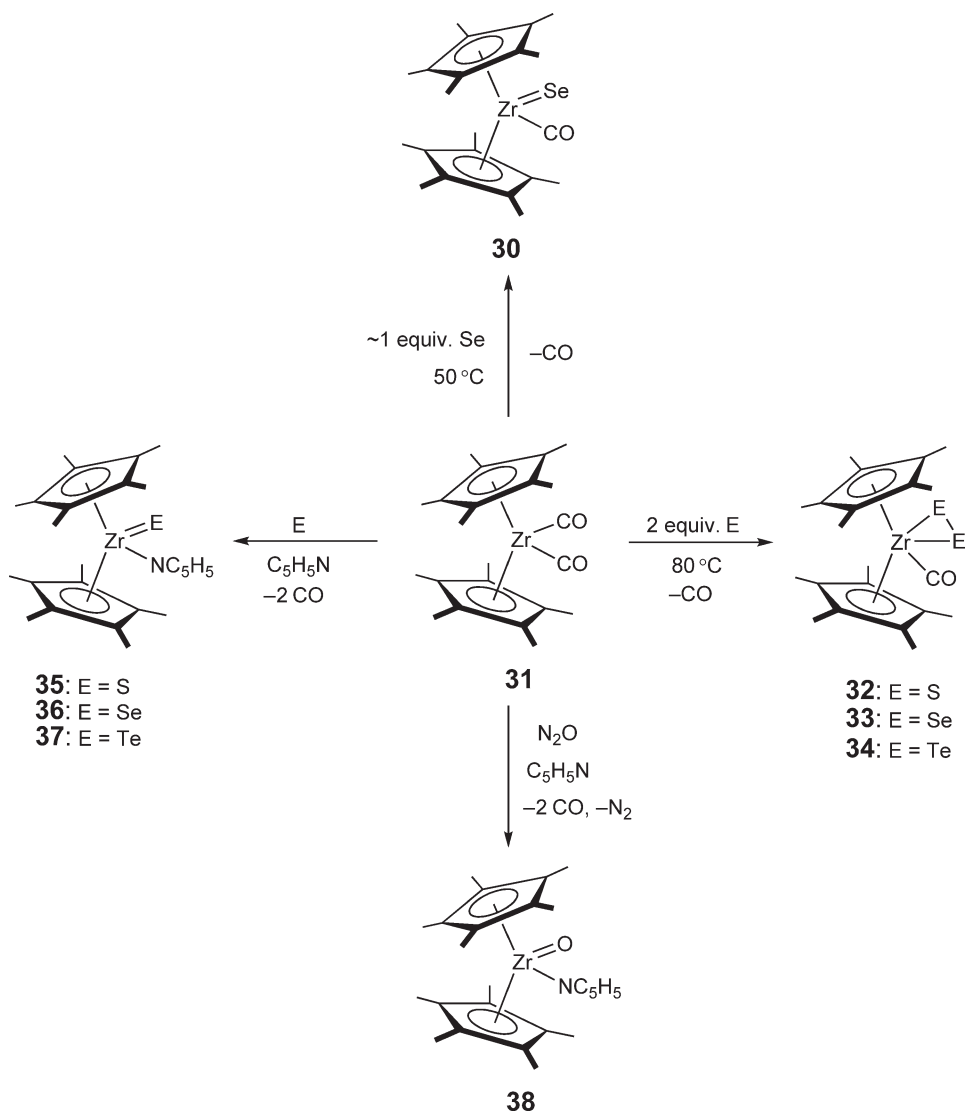
As with zero- and subvalent chemistry, stabilization of divalent zirconium and hafnium is readily achieved with strong-field,  $\pi$ -acidic ligands such as carbon monoxide. For bis(cyclopentadienyl)zirconium and hafnium compounds, dicarbonyl derivatives are typically prepared by magnesium or sodium amalgam reduction of the corresponding dichloride precursors under an atmosphere of CO. In this manner, a series of unbridged and *ansa*-zirconocene dicarbonyl complexes have been synthesized.<sup>11</sup> The CO stretching frequencies determined by pentane solution IR spectroscopy have proven to be a valuable tool in determining the electronic properties of the zirconium center. A comprehensive compilation of these values has recently appeared. For unbridged complexes, introduction of alkyl groups onto the cyclopentadienyl ligand results in relatively low carbonyl stretching frequencies, indicative of CO reduction from an electron-rich metal center. In contrast, silyl substituents are electron withdrawing, as evidenced by higher CO stretching frequencies. For *ansa*-zirconocenes, introduction of a single  $[\text{SiMe}_2]$  bridge produces a net electron-withdrawing effect whereas introduction of a second  $[\text{SiMe}_2]$  linker generates more electron-rich zirconium centers.



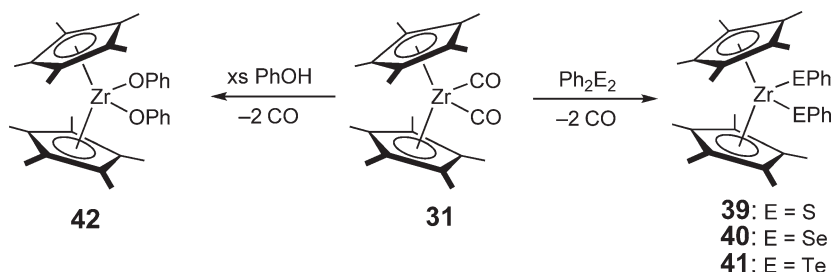
Scheme 5

Permethylzirconocene dicarbonyl complexes also serve as a source of the reactive  $[(\eta^5\text{-C}_5\text{Me}_5)_2\text{Zr}]$  fragment and can be readily oxidized with elemental chalcogens to form a family of zirconium(IV) compounds with different classes of chalcogenido ligands (Scheme 6). A non-classical zirconocene carbonyl complex,  $(\eta^5\text{-C}_5\text{Me}_5)_2\text{Zr}(\text{Se})\text{CO}$  **30**, containing a terminal selenido ligand, has been prepared by addition of approximately 1 equiv. of elemental selenium to  $(\eta^5\text{-C}_5\text{Me}_5)_2\text{Zr}(\text{CO})_2$  **31** at 50 °C. Carbonyl substitution is readily achieved by addition of pyridine.<sup>12</sup> Addition of 2 equiv. of a series of elemental chalcogens (S, Se, Te) to **31** at 80 °C also furnishes non-classical carbonyl complexes with  $\eta^2$ -dichalcogenido ligands,  $(\eta^5\text{-C}_5\text{Me}_5)_2\text{Zr}(\eta^2\text{-E}_2)(\text{CO})$  (E = S, **32**; Se, **33**; Te, **34**), demonstrating the flexibility of the zirconocene center to accommodate different modes of chalcogenido bonding.<sup>13</sup> The ditellurido derivative, **34**, has been characterized by X-ray diffraction and exists in both triclinic and tetragonal forms. The structural data reveal different Zr–CO bond lengths for the two structures while the C–O distances are similar. The origin of this difference is crystallographic disorder in the tetragonal modification, which has been successfully modeled.

Terminal chalcogenido zirconocene complexes have also been isolated as the corresponding pyridine adducts by treatment of  $(\eta^5\text{-C}_5\text{Me}_5)_2\text{Zr}(\text{CO})_2$  **31** with elemental sulfur, selenium, or tellurium in the presence of pyridine (Scheme 6).<sup>14,15</sup> The corresponding oxozirconocene pyridine compound has been prepared using  $\text{N}_2\text{O}$  as the source of the oxygen atom with the liberation of  $\text{N}_2$  upon addition to **31** (Scheme 6).<sup>16</sup> Similar synthetic routes have been



Scheme 6

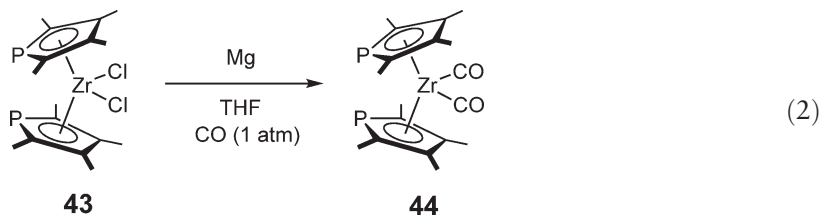


Scheme 7

used to prepare the hafnium congeners.<sup>17</sup> Significantly, the zirconocene chalcogenido complexes participate in a range of cycloaddition reactions<sup>15</sup> but this chemistry is beyond the scope of this chapter.

Formal oxidation of **31** concomitant with CO loss has been achieved by addition of a series of  $\text{Ph}_2\text{E}_2$  (E = S, Se, Te) reagents (Scheme 7).<sup>18</sup> The analogous permethylzirconocene bis(phenolate),  $(\eta^5\text{-C}_5\text{Me}_5)_2\text{Zr}(\text{OPh})_2$ , **42**, was prepared by treatment of **31** with phenol. Crystallographic characterization of **42** established a near-linear zirconium phenolate linkage with a zirconium–oxygen distance shorter than the sum of the covalent radii of the constituent atoms. The bond contraction has been attributed to steric factors rather than a bonafide  $p_\pi\text{-}d_\pi$  lone pair donation from the oxygens to the metal.

In analogy to zirconocene dicarbonyl complexes, magnesium reduction of the phosphazirconocene dichloride,  $(\eta^5\text{-C}_4\text{Me}_4\text{P})_2\text{ZrCl}_2$  **43**, in THF under an atmosphere of CO furnishes the dicarbonyl complex  $(\eta^5\text{-C}_4\text{Me}_4\text{P})_2\text{Zr}(\text{CO})_2$  **44** (Equation (2)).<sup>19</sup> Comparison of the IR stretching frequencies of the carbonyl bands of **44** to  $(\eta^5\text{-C}_5\text{H}_5)_2\text{Zr}(\text{CO})_2$  **45** and  $(\eta^5\text{-C}_9\text{H}_7)_2\text{Zr}(\text{CO})_2$  **46** suggests that the electronic properties of the phosphazirconocene are between the two species. Electrochemical reduction of the dichloride, **43**, is also in agreement with this finding.

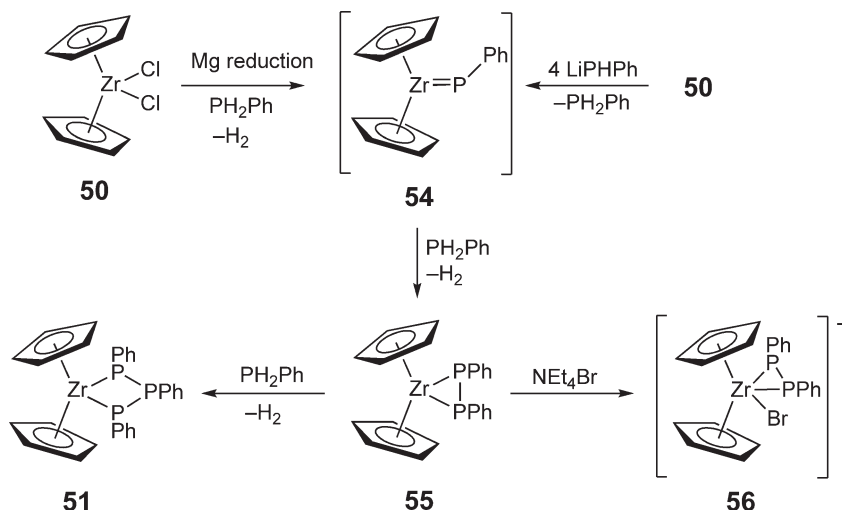


Dicarbonyl complexes of mixed cyclopentadienyl bis(phosphine)amide zirconium compounds have also been prepared by ligand-induced disproportionation of  $(\eta^5\text{-C}_5\text{H}_5)\text{ZrBH}_4[\text{N}(\text{SiMe}_2\text{CH}_2\text{PPr}^i_2)_2]$  **47**, yielding the bis(tetrahydroborate) complex  $(\eta^5\text{-C}_5\text{H}_5)\text{Zr}(\text{BH}_4)_2[\text{N}(\text{SiMe}_2\text{CH}_2\text{PPr}^i_2)_2]$  **48** and the dicarbonyl derivative  $(\eta^5\text{-C}_5\text{H}_5)\text{Zr}(\text{CO})_2[\text{N}(\text{SiMe}_2\text{CH}_2\text{PPr}^i_2)_2]$  **49**.<sup>20</sup> The toluene IR spectrum of **49** exhibits two strong CO bands at 1871 and  $1965\text{ cm}^{-1}$ . Mixed cyclopentadienyl boratabenzene zirconium dicarbonyl complexes as well as the bis(boratabenzene) derivatives have also been prepared.<sup>21</sup> These molecules are synthesized in a straightforward manner by reduction of the corresponding dichloride precursors under an atmosphere of CO. The IR stretching frequencies of the carbonyl bands have been used to assay the electronic properties of a variety of substituted boratabenzene ligands.

#### 4.06.2.1.2 Phosphine complexes

Despite being principally  $\sigma$ -donors, phosphorus-based ligands display a rich chemistry with low-valent zirconocene complexes. In some cases, phosphines are used to stabilize the low-valent metal fragment while in other instances phosphines serve as substrates for subsequent chemistry. For example, reduction of  $(\eta^5\text{-C}_5\text{H}_5)_2\text{ZrCl}_2$  **50** with magnesium metal followed by addition of the primary phosphine,  $\text{H}_2\text{PPh}$ , affords  $(\eta^5\text{-C}_5\text{H}_5)_2\text{Zr}(\text{PPh})_3$  **51** in moderate yield (Scheme 8).<sup>22</sup> The more sterically hindered zirconocene phosphide complex,  $(\eta^5\text{-C}_5\text{Me}_5)_2\text{Zr}(\text{PCy})_3$  **52**, has been prepared in a similar manner by reduction of  $(\eta^5\text{-C}_5\text{Me}_5)_2\text{ZrCl}_2$  **53**. Complications arising from incomplete reduction of the dichloride precursors by magnesium are believed to be the origin of low yields. The mechanistic pathway for product formation has been investigated by preparing potential intermediates by salt metathesis chemistry. Addition of appropriate lithium phosphide salts to the zirconocene dichlorides has implicated transient zirconium phosphinidenes such as **54** as intermediates on the reaction pathway (Scheme 8).

In contrast to primary and secondary phosphines where the P–H bond engages in chemistry with the formally divalent zirconocene, tertiary phosphines serve as stabilizing ligands allowing the isolation of  $(\eta^5\text{-C}_5\text{R}_n\text{H}_{5-n})_2\text{Zr}(\text{PR}'_3)_2$  complexes.



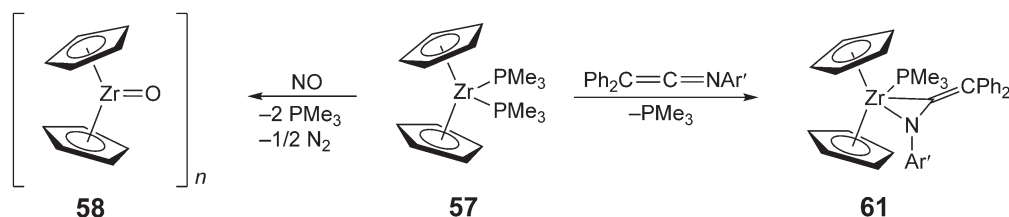
Scheme 8

Phosphine dissociation then provides access to the rich chemistry of the  $[(\eta^5\text{-C}_5\text{R}_n\text{H}_{5-n})_2\text{Zr}]$  fragment. For example, addition of NO to  $(\eta^5\text{-C}_5\text{H}_5)_2\text{Zr}(\text{PMe}_3)_2$  **57** results in reduction of the gas to  $\text{N}_2$  with the formation of an oligomeric oxozirconocene compound (**58**, Scheme 9).<sup>23</sup> A stepwise mechanism has been proposed for the reaction to account for the observed products. In the first step, 2 equiv. of nitric oxide are reduced to  $\text{N}_2\text{O}$  with the formation of the oxozirconocene compound. The intermediate nitrous oxide is then believed to undergo further reduction to  $\text{N}_2$  with the formation of another equivalent of oxozirconocene. The organometallic compound can be trapped by addition of  $\text{Me}_3\text{SiCl}$  or  $(\eta^5\text{-C}_5\text{H}_5)_2\text{ZrMe}_2$  to furnish  $(\eta^5\text{-C}_5\text{H}_5)_2\text{Zr}(\text{OSiMe}_3\text{Cl})\text{Cl}$  **59** and  $[(\eta^5\text{-C}_5\text{H}_5)_2\text{ZrMe}]_2(\mu_2\text{-O})$  **60**, respectively.

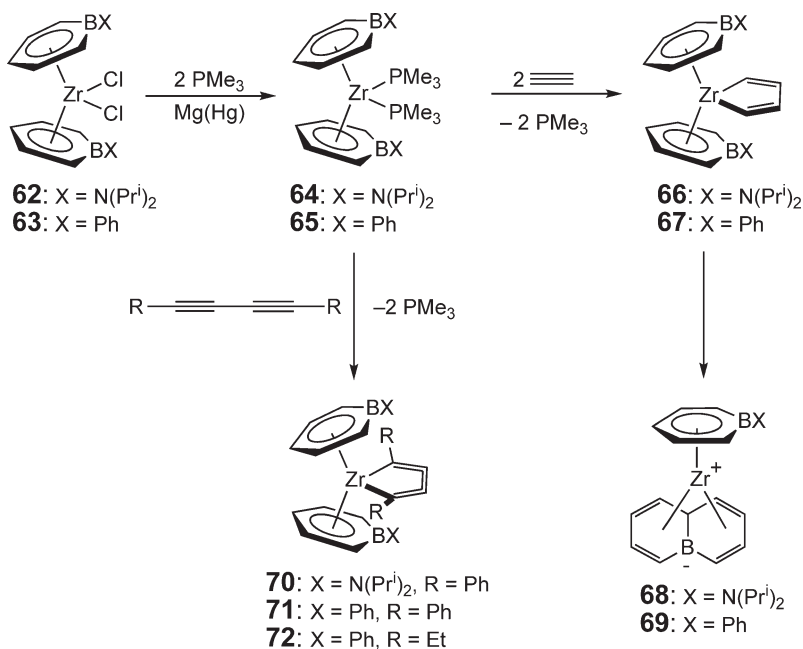
The zirconocene bis(phosphine) complex, **57**, also coordinates  $\text{Ar}'\text{N}=\text{C}=\text{CPh}_2$  ( $\text{Ar}' = p\text{-MeC}_6\text{H}_4$ ) to yield the zirconocene ketenimine derivative  $(\eta^5\text{-C}_5\text{H}_5)_2\text{Zr}(\eta^2\text{-(C, N)-Ar}'\text{N}=\text{C}=\text{CPh}_2)(\text{PMe}_3)$  **61** with loss of phosphine (Scheme 9). Similar chemistry is observed upon reduction of  $(\eta^5\text{-C}_5\text{Me}_5)_2\text{ZrCl}_2$  **53** with  $\text{LiBu}^t$  in the presence of the ketenimine.<sup>24</sup> However, in the latter example the base-free ketenimine complex is isolated.

Cyclopentadienyl ligands are not a prerequisite for phosphine-stabilized zirconium(II) complexes. Reduction of the boratabenzene zirconocene dichlorides ( $\text{X} = \text{N}(\text{Pr}^i)_2$ , **62**;  $\text{X} = \text{Ph}$ , **63**) with magnesium amalgam in the presence of  $\text{PMe}_3$  furnishes the bis(phosphine) complexes ( $\text{X} = \text{N}(\text{Pr}^i)_2$ , **64**;  $\text{X} = \text{Ph}$ , **65**). Treatment of these compounds with acetylene results in alkyne coupling followed by addition to one of the boratabenzene ligands (Scheme 10).<sup>25</sup> Similarly, 1,4-disubstituted-1,3-butadiynes also displace the phosphines to yield the zirconacyclopenta-2,3,4-triene complexes.<sup>26</sup> The lack of rearrangement in the latter case is believed to be a result of the in-plane zirconium coordination of the central double bond of the triene ligand, preventing conversion to products similar to **68** or **69**. Phosphacyclopentadienyl zirconium bis(phosphine) complexes can also be prepared using similar reduction protocols.

Hafnium tetraiodide can be reduced in benzene solvent with sodium amalgam in the presence of  $\text{PMe}_3$  to furnish the formally divalent hafnium “inverted sandwich” complex,  $(\mu_2\text{-}\eta^6, \eta^6\text{-C}_6\text{H}_6)\text{HfI}_4(\text{PMe}_3)_4 \cdot \text{C}_6\text{H}_6$  **73**, where each  $\pi$ -face of the benzene ring is complexed to a hafnium center.<sup>27</sup> The six-membered ring is significantly distorted into a twist boat conformation, arising from steric repulsion of the neighboring  $\text{PMe}_3$  ligands.



Scheme 9

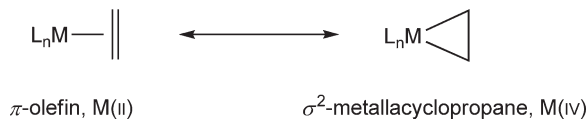


Scheme 10

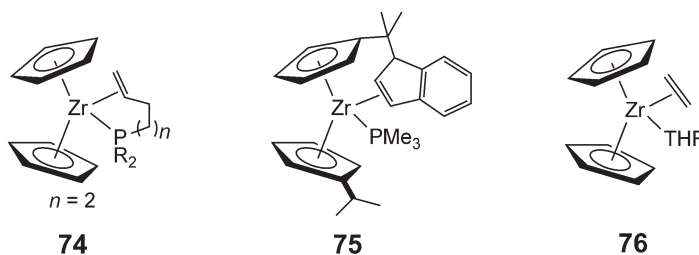
#### 4.06.2.1.3 Alkene complexes

Alkene complexes of formally low-valent zirconium and hafnium have occupied a central role in the development and utility of group IV organometallic chemistry. The stability of these species can be traced to the Dewar–Chatt–Duncanson model of olefin coordination, where the oxidation state of the metal is ambiguous, owing to a hybrid structure arising from contributions from a divalent metal–olefin complex and a tetravalent metallacyclopentane (Scheme 11). For the purpose of the present review, these compounds will be considered divalent although in most instances the metallacyclopentane canonical structure is the dominant contributor to the hybrid. Reviews focused on the general synthesis and structure of the zirconium and hafnium olefin compounds have been published<sup>28–31</sup> in addition to others devoted to synthetic applications including asymmetric transformations<sup>32</sup> and carboalumination chemistry.<sup>33,34</sup>

In general, isolable zirconium and hafnium alkene complexes are rare, as they typically undergo carbon–carbon coupling reactions with additional olefin to yield metallacyclopentanes. Addition of an exogenous donor ligand is a common strategy for stabilizing alkene complexes. Several classes of these compounds have been prepared: those with phosphalkene ligands (**74**, Scheme 12),<sup>35</sup> those with either a phosphorus donor or olefin tethered to the



Scheme 11



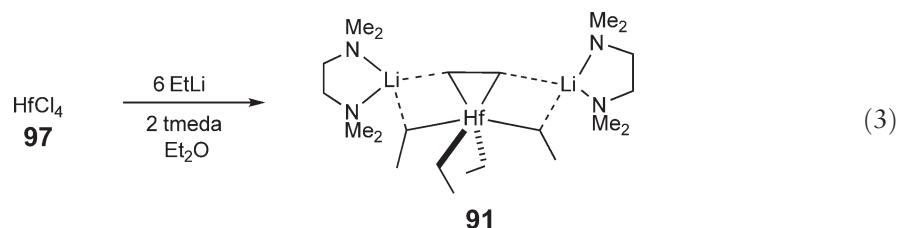
Scheme 12

ancillary ligands, typically cyclopentadienyls **75**,<sup>36</sup> or simple ligand adducts of olefin compounds **76**.<sup>37,38</sup> Examples of base-free zirconocene propene and butene compounds have been generated *in situ*, using the so-called “Negishi conditions,” and will be discussed in detail in the latter portion of this section.

Compiled in Table 1 are typical carbon–carbon bond distances and NMR shifts of the olefinic carbons in several base-stabilized olefin complexes of zirconium and hafnium. In general, the <sup>1</sup>H NMR shifts are considerably upfield of free olefin and the <sup>13</sup>C peaks are in the region typically associated with zirconium alkyls, indicative of significant zirconacyclopentane character. Consistent with this view is the elongation of the C–C bond, typically around 1.45 Å, compared to that found in free olefins. The zirconium–carbon bond distances are fairly invariant around 2.34 Å.

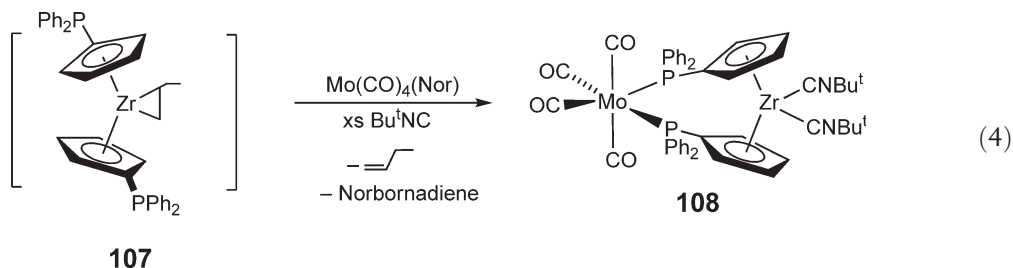
Synthesis of base-stabilized zirconocene alkene complexes is typically achieved using two common synthetic methods. In one procedure, a strong,  $\sigma$ -donating ligand such as a phosphine is added to a zirconocene dialkyl, **92**, inducing hydrogen abstraction to release alkane and produce the desired base-stabilized zirconocene olefin complex (**81**, Scheme 13).<sup>40</sup> An alternative method involves alkali metal reduction of a zirconocene dichloride precursor, **93** for example, in the presence of a donor ligand. In the case illustrated in Scheme 13, the olefin is tethered to the cyclopentadienyl ligand, facilitating coordination. Generation of transient zirconocene equivalents is also common, as in treatment of **94** with 2 equiv. of butyllithium followed by intramolecular coordination of alkene, which results in overall C–H activation to form a zirconocene phenyl alkyl complex (**96**, Scheme 13).<sup>44</sup>

Examples of “non-cyclopentadienyl” olefin compounds have also appeared. Treatment of HfCl<sub>4</sub> **97** with 6 equiv. of ethyllithium in the presence of tmeda (tmeda = N,N,N',N'-tetramethylethylenediamine) furnishes [Li(tmeda)]<sub>2</sub>[Hf( $\eta^2$ -C<sub>2</sub>H<sub>4</sub>)Et<sub>4</sub>] **91** (Equation (3)). The product is believed to arise from  $\beta$ -hydrogen elimination from an unobserved hexaethylhafnate intermediate.



Both homo- and heterobimetallic compounds have been synthesized from zirconocene olefin complexes. Homodinuclear  $\mu$ -ethylene complexes, **98** (X = Cl) and **99** (X = Br), have been prepared by ligand redistribution from mixing ( $\eta^5$ -C<sub>5</sub>H<sub>5</sub>)<sub>2</sub>Zr( $\eta^2$ -C<sub>2</sub>H<sub>4</sub>)(PR<sub>3</sub>) (PR<sub>3</sub> = PPh<sub>2</sub>Me, **78**; PR<sub>3</sub> = PBu<sup>n</sup><sub>3</sub>, **100**) with ( $\eta^5$ -C<sub>5</sub>H<sub>5</sub>)<sub>2</sub>ZrX<sub>2</sub> (X = Br, Cl) (Scheme 14).<sup>45</sup> Metathesis of the terminal halide ligands with a range of alkyllithiums affords the corresponding  $\mu$ -ethylene zirconocene alkyl compounds, **101–104**. In the case of the transient butene complex, **105**, treatment with the pentamethylcyclopentadienyl iridium imide furnishes the bridging imido species **106** arising from the loss of 1-butene.<sup>46</sup>

Heterobimetallic complexes of zirconium and molybdenum have also been prepared from zirconocene olefin complexes. Displacement of 1-butene from the phosphine-substituted zirconocene 1-butene complex, ( $\eta^5$ -C<sub>5</sub>H<sub>4</sub>PPh<sub>2</sub>)<sub>2</sub>Zr( $\eta^2$ -CH<sub>2</sub>=CHCH<sub>2</sub>CH<sub>3</sub>) **107**, by addition of *tert*-butyl isonitrile in the presence of Mo(CO)<sub>4</sub>(norbornadiene) furnishes the formal zirconium(II)–molybdenum(0) compound, **108** (Equation (4)).<sup>47</sup>



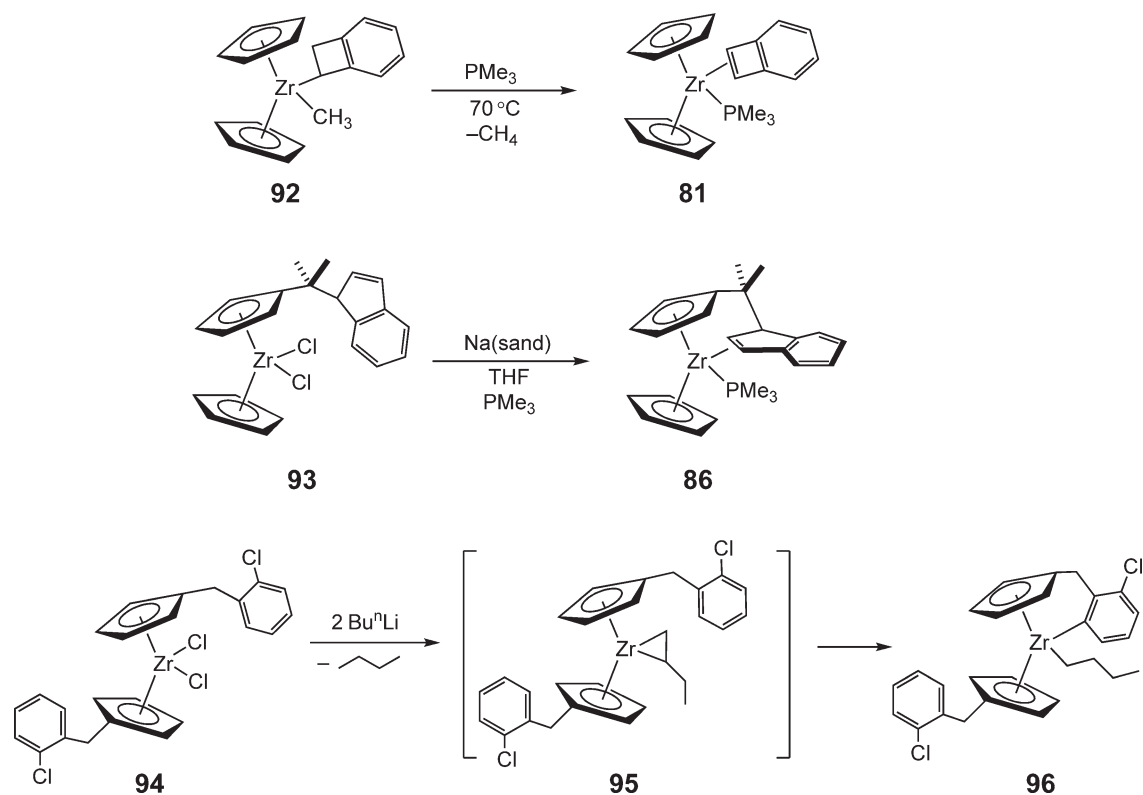
Treatment of zirconocene dichloride, **50**, with 2 equiv. of an appropriate alkyllithium or Grignard reagent generates transient zirconocene olefin complexes that upon loss of alkene provide access to “zirconocene,” **109**, and the powerful reduction chemistry of divalent zirconium.<sup>48</sup> Owing to the utility of this reagent in organic synthesis and organometallic reactions, the low-temperature alkylation of zirconocene dichloride, **50**, with Bu<sup>n</sup>Li has been

**Table 1** Selected bond distances,  $^1\text{H}$  NMR and  $^{13}\text{C}$  NMR spectroscopic data for zirconium alkene complexes

Complex	Cmpd	Zr–C distances (Å)	C–C (Å)	Zr–X (Å)	$^1\text{H}$ $\delta$ (ppm)	$^{13}\text{C}$ $\delta$ (ppm)	References
$\text{Cp}_2\text{Zr}(\eta^2\text{-CH}_2\text{=CHCH}_2\text{CH}_2\text{CH}_2\text{PPh}_2)$	<b>74</b>	2.332(3), 2.390(3)	1.435(3)	2.696(1)			35
$(\eta^5\text{-C}_5\text{H}_4\text{CMe}_2\text{H})(\eta^5\text{-}\eta^2\text{-C}_5\text{H}_4\text{CMe}_2\text{C}_9\text{H}_7)\text{Zr}(\text{PMe}_3)$	<b>75</b>	2.317(2), 2.395(2)		2.718(1)			36
$\text{Cp}_2\text{Zr}(\eta^2\text{-C}_2\text{H}_4)(\text{THF})$	<b>76</b>				0.51 <sup>a</sup>	33.5 <sup>a</sup>	38
$\text{Cp}_2\text{Zr}(\eta^2\text{-C}_2\text{H}_4)(\text{py})$	<b>77</b>	2.304(8), 2.341(6)	1.455(9)	2.487(6)	−1.43 <sup>a</sup>	49.4, 52.1 <sup>a</sup>	38
$\text{Cp}_2\text{Zr}(\eta^2\text{-C}_2\text{H}_4)(\text{PPh}_2\text{Me})$	<b>78</b>				0.36, 0.76 <sup>a</sup>		39
$\text{Cp}_2\text{Zr}(\eta^2\text{-C}_2\text{H}_3\text{Et})(\text{PPh}_2\text{Me})$	<b>79</b>				0.01, 0.69 <sup>a</sup>		39
$\text{Cp}_2\text{Zr}(\eta^2\text{-C}_2\text{H}_3\text{Ph})(\text{PPh}_2\text{Me})$	<b>80</b>				−0.19, 0.47 <sup>a</sup>		39
$\text{Cp}_2\text{Zr}(\eta^2\text{-benzocyclobutadiene})(\text{PMe}_3)$	<b>81</b>	2.339(3), 2.346(3)	1.526(4)	2.7022(9)		47.4, 47.8 <sup>b</sup>	40
$(\text{C}_5\text{H}_3\text{Me}_2)_2\text{Zr}(\eta^2\text{-CH}_2\text{=CHCH}_2\text{CH}_2\text{PPh}_2)$	<b>82</b>	2.323(5), 2.357(4)	1.432(8)	2.680(2)			35
$\text{Ind}_2\text{Zr}(\eta^2\text{-C}_2\text{H}_4)(\text{THF})$	<b>83</b>	2.292(3), 2.334(3)	1.451(5)	2.363(2)	0.69 <sup>a</sup>	27.8, 35.4 <sup>a</sup>	38
<i>Rac</i> -(EBI)Zr( $\eta^2\text{-C}_2\text{H}_4$ )(PMe <sub>3</sub> )	<b>84</b>				0.21, −2.84 <sup>b</sup>	36.7, 49.2 <sup>b</sup>	37
<i>Meso</i> -(EBI)Zr( $\eta^2\text{-C}_2\text{H}_4$ )(PMe <sub>3</sub> )	<b>85</b>	2.282(5), 2.359(6)	1.424(9)	2.667(2)	0.87, −2.79 <sup>b</sup>	31.2, 45.8 <sup>b</sup>	37
$\text{Cp}(\eta^5\text{-}\eta^2\text{-C}_5\text{H}_4\text{CMe}_2\text{C}_9\text{H}_7)\text{Zr}(\text{PMe}_3)$	<b>86</b>	2.324(6), 2.391(6)	1.49(1)	2.702(2)		51.5, 52.7 <sup>b</sup>	41
$[\eta^5\text{-C}_5\text{H}_3\text{-}(1,3\text{-}(\text{SiMe}_2\text{CH}_2\text{PPr}^i_2)_2)]\text{Zr}(\eta^2\text{-C}_2\text{H}_4)\text{Br}$	<b>87</b>				1.01 <sup>b</sup>		42
$[\eta^5\text{-C}_5\text{H}_3\text{-}(1,3\text{-}(\text{SiMe}_2\text{CH}_2\text{PMe}_2)_2)]\text{Zr}(\eta^2\text{-C}_2\text{H}_4)\text{Br}$	<b>88</b>	2.293(5), 2.312(5)	1.431(6)	2.703(1), 2.730(1)	0.88, 1.33 <sup>b</sup>		42
$[\eta^5\text{-C}_5\text{H}_3\text{-}(1,3\text{-}(\text{SiMe}_2\text{CH}_2\text{PPr}^i_2)_2)]\text{Zr}(\eta^2\text{-C}_2\text{H}_4)\text{Cp}$	<b>89</b>				0.85 <sup>b</sup>		42
$[\eta^5\text{-C}_5\text{H}_3\text{-}(1,3\text{-}(\text{SiMe}_2\text{CH}_2\text{PPr}^i_2)_2)]\text{Zr}(\eta^2\text{-C}_2\text{H}_4)\text{Me}$	<b>90</b>				1.05 <sup>b</sup>		42
$[\text{Li}(\text{tmeda})]_2[\text{Hf}(\eta^2\text{-C}_2\text{H}_4)\text{Et}_4]$	<b>91</b>	2.26(4), 2.31(4)	1.49(6)			30.5 <sup>c</sup>	43

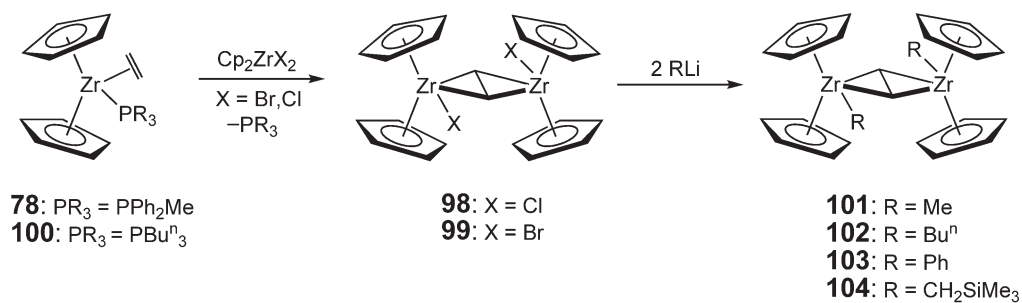
<sup>a</sup>in THF-*d*<sub>8</sub>.<sup>b</sup>in benzene-*d*<sub>6</sub>.<sup>c</sup>in toluene-*d*<sub>8</sub>.Cp =  $\eta^5\text{-C}_5\text{H}_5$ ; Ind =  $\eta^5\text{-C}_9\text{H}_7$ ; EBI = ethylenebis(indenyl).



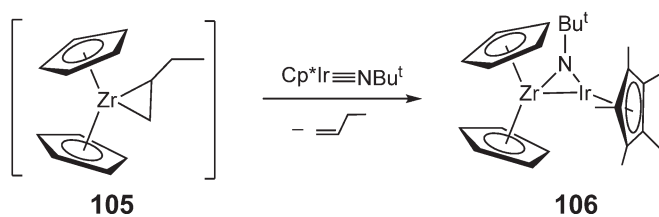


Scheme 13

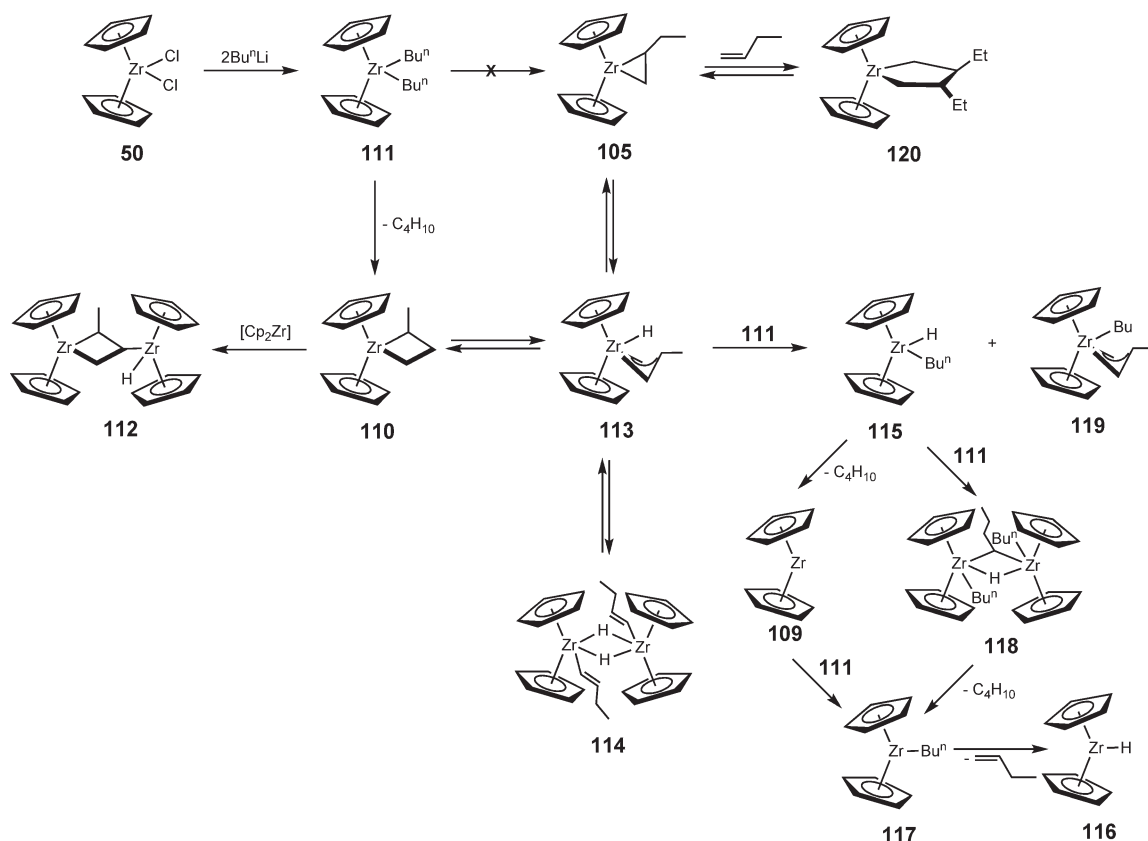
## Homobimetallic



## Heterobimetallic



Scheme 14

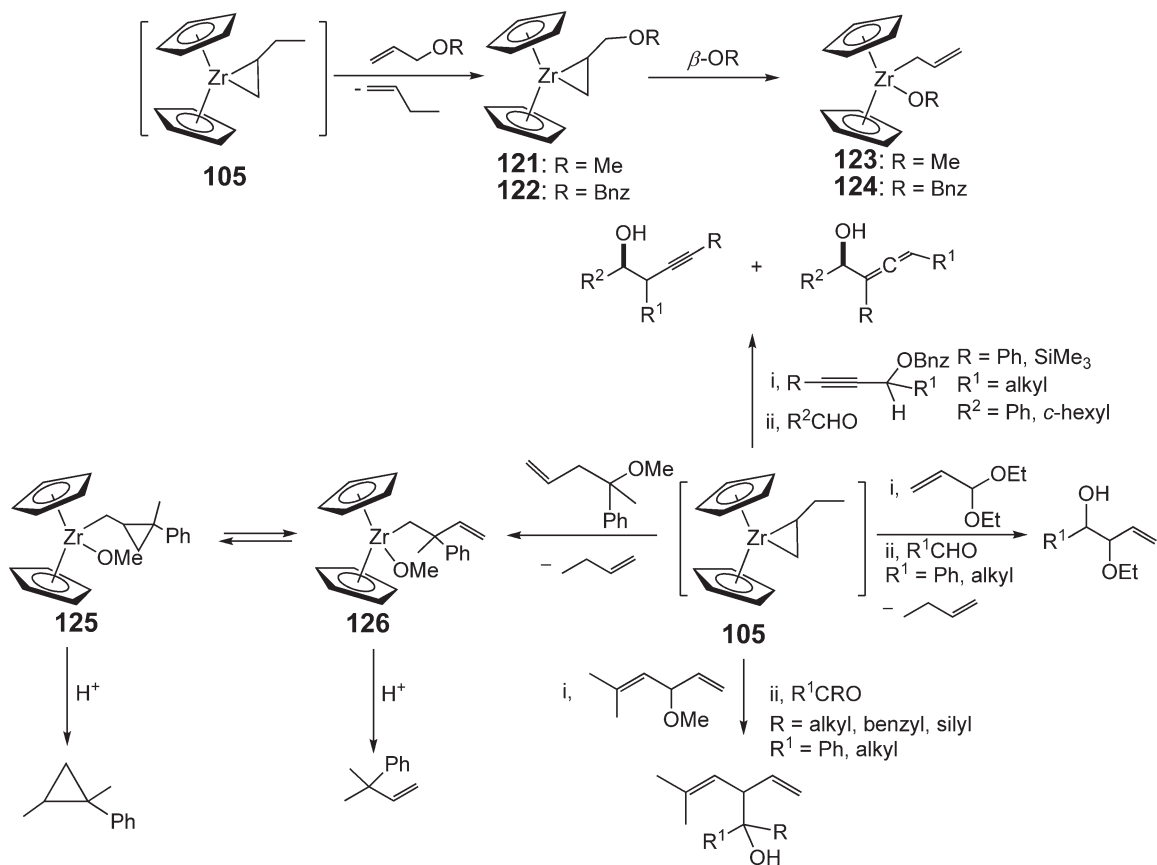


Scheme 15

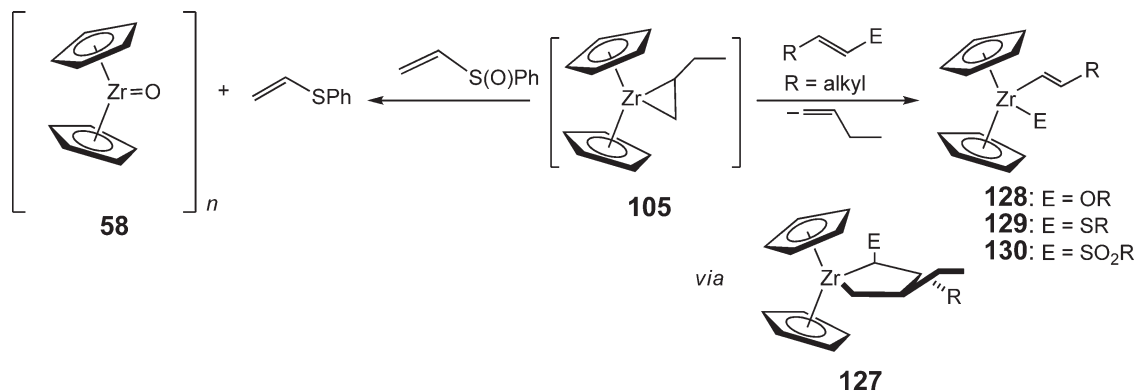
studied in detail. Initially, the dialkylation reaction was believed to generate the bis(butyl)zirconocene complex **111** that converted to the corresponding butene compound ( $(\eta^5\text{-C}_5\text{H}_5)_2\text{Zr}(\eta^2\text{-CH}_2=\text{CHCH}_2\text{CH}_3)$  **105** by  $\beta$ -hydrogen abstraction. More careful investigation of the *in situ* generated alkene complex reveals a more complicated reaction sequence (Scheme 15).<sup>49</sup> Using a combination of two-dimensional NMR experiments, it has been determined that zirconacyclobutane formation, **110**, arising from  $\gamma$ -hydrogen abstraction is favored over  $\beta$ -hydrogen abstraction. While zirconacyclopentane **110** has not been observed directly, its formation has been inferred from the products derived from its decomposition. These include the bridged zirconocene, **112**, and the crotyl hydride, **113**, which is in equilibrium with the butene complex **105**. The crotyl hydride, **113**, can undergo dimerization to form the dimeric zirconocene alkenyl hydride, **114**, or undergo transmetalation with bis(butyl)zirconocene, **111**, to form the zirconocene butyl hydride **115**. Upon extended thermolysis, zirconium(III) products are formed, including the zirconocene mono-hydride, **116**, and the monobutyl complex **117**. While this study suggests complicated chemistry upon dialkylation of zirconocene dichloride, it should be noted that these experiments were not conducted under conditions typically employed in organic transformations.

The transient zirconocene butene complex, **105**, has proved to be useful in a number of organic transformations. For example, butene substitution of zirconocene alkene complexes with alkoxy-substituted olefins results in  $\beta$ -alkoxide elimination to furnish the zirconocene alkoxy compounds ( $\text{R} = \text{Me}$ , **123**;  $\text{R} = \text{Bnz}$ , **124**) (Scheme 16).<sup>50,51</sup> Addition of propargyl alcohols to the zirconocene butene complex, **105**, affords homoallylic alcohols. These reactions are of limited utility owing to the lack of stereoselectivity or formation of multiple products. Positioning the alkoxy functional group further down the hydrocarbyl chain allows synthesis of cyclopropanes, though mixtures of the carbocycle and alkene products are obtained in some cases (Scheme 16).<sup>52</sup>

The zirconocene butene complex, **105**, also reacts with methoxy-, sulfoxy-, or sulfonyl-substituted alkenes to form a range of products (Scheme 17).<sup>53,54</sup> Vinyl sulfoxides are deoxygenated to the vinyl sulfide and the polymeric oxozirconocene compound **58**. Product labeling and selectivity studies are consistent with pathways proceeding through zirconacyclopentanes **127**. Once in hand, the allylic products are useful for preparing functionalized *trans*-alkenes as well as serving as transmetalation reagents in copper-catalyzed coupling reactions.



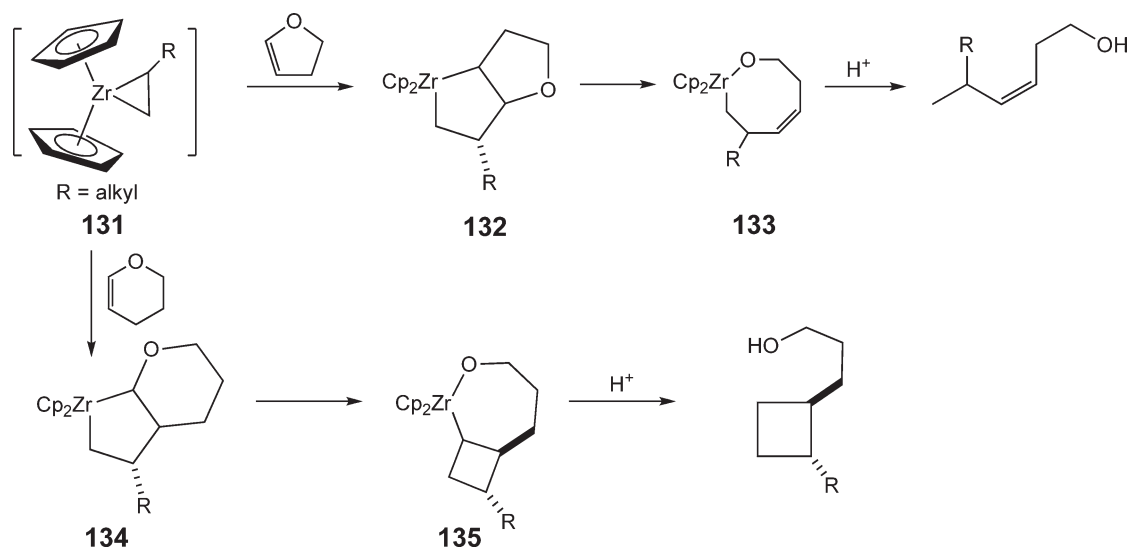
Scheme 16



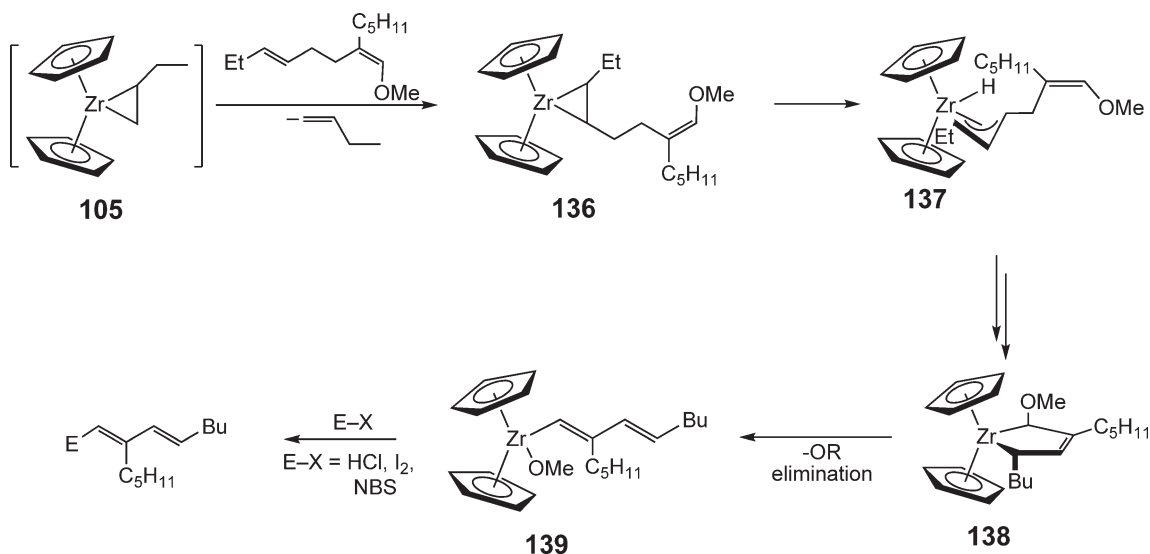
Scheme 17

Similar reactions using dihydropyrans and dihydrofurans furnish cyclobutanes or alkenol products upon hydrolysis (Scheme 18).<sup>55</sup> As with the previous applications, zirconacyclic intermediates are implicated. Differences in stereochemistry in the observed products versus the open chain vinyl substrates are thought to arise from geometric restrictions imposed by the bicyclic intermediates.

Analogous dienyl zirconium compounds can be prepared by addition of unconjugated dienes that contain enol ethers to **105** (Scheme 19).<sup>56–58</sup> These reactions are believed to proceed by initial coordination of the terminal olefin followed by isomerization via zirconocene allyl hydride intermediates to eventually yield zirconacyclopentanes that



Scheme 18



Scheme 19

can undergo irreversible alkoxide elimination. These procedures can also be used in tandem with CuCl-mediated couplings of allyl chlorides to yield stereoselective trienes.

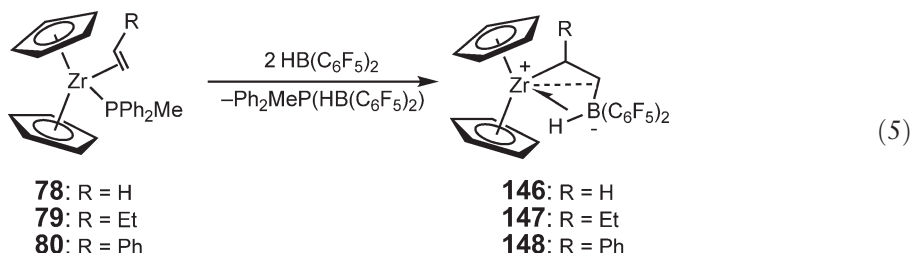
In addition, the base-free zirconocene butene intermediate, **105**, has also been used as a source of zirconocene in the preparation of 3,4-dichloro-1,2-dihydro-1,2-diphosphetes by phosphalkene coupling,<sup>59</sup> and was used in a phosphine-stabilized form **140** to prepare zirconaalkenylphosphonates by alkyne and chlorophosphate addition (Scheme 20).<sup>60</sup>

Zirconocene olefin complexes containing  $\gamma$ -hydrogens are also known to be in equilibrium with the corresponding allyl hydride compounds, making them versatile synthons for a variety of transformations.<sup>61</sup> Addition of sterically hindered carbonyls such as diisopropyl ketone to the transient zirconocene propylene complex,  $(\eta^5\text{-C}_5\text{H}_5)_2\text{Zr}(\eta^2\text{-CH}_2\text{=CHCH}_3)$  **142**, results in insertion into the zirconium hydride to reduce the carbonyl (Scheme 21). The zirconoxy allyl complex undergoes reaction with aldehydes to form allylic alcohols in good yields with reasonable *anti*-stereoselectivities.<sup>62</sup> In an analogous procedure, imine addition furnishes secondary allylamines. Reactions with  $\alpha$ -bromoketones and triethylborane afford the ketone-coupled product.<sup>63</sup> In addition to ketone reduction, **142** also reacts with aryl acid chlorides to yield allylic alcohols,<sup>64</sup> while esters form intermediate oxometallacycles which

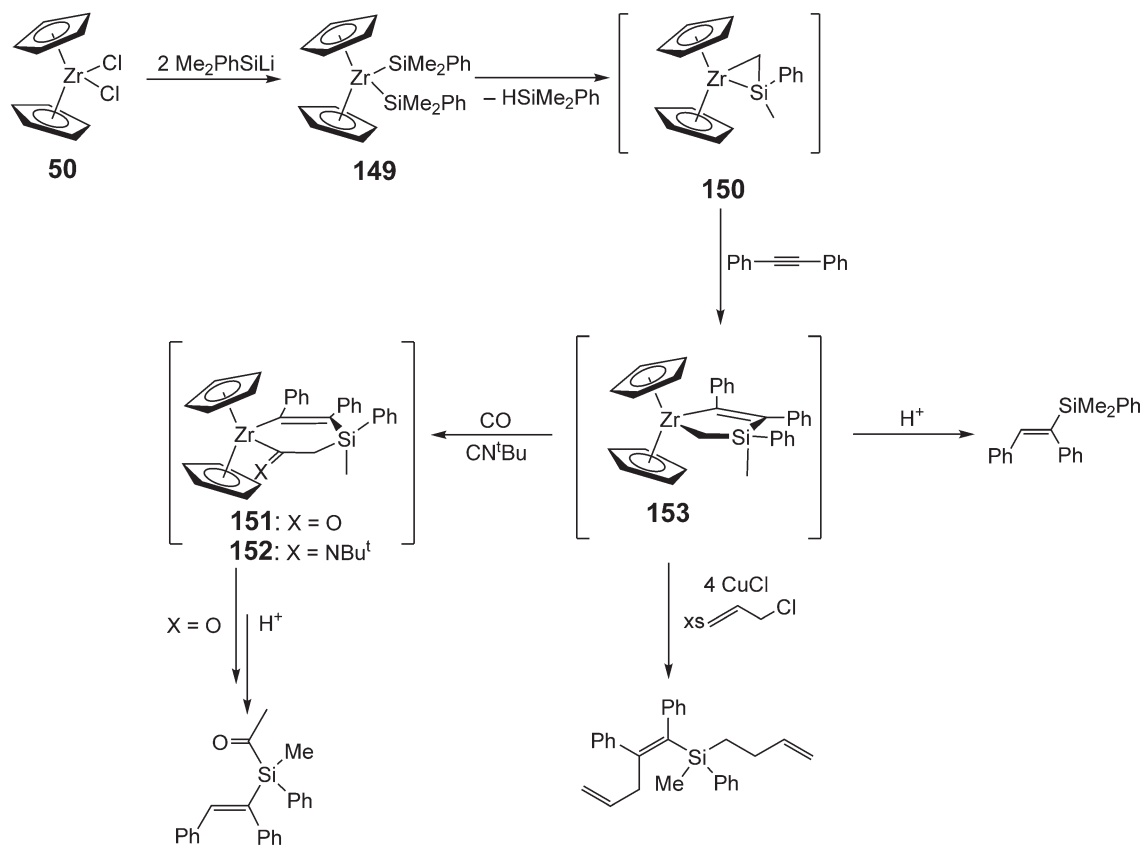


collapse to form cyclopropenes. Addition of 1,4-diketones furnishes a diol product, where the reaction is believed to proceed through a “chair-like” transition state (Scheme 21).

Hydroboration of coordinated alkenes has been achieved with the phosphine-stabilized olefin complexes,  $(\eta^5\text{-C}_5\text{H}_5)_2\text{Zr}(\eta^2\text{-CH}_2\text{=CHR})(\text{PPh}_2\text{Me})$  ( $\text{R} = \text{H}$ , **78**; Et, **79**; Ph, **80**), upon addition of the Lewis-acidic borane,  $\text{HB}(\text{C}_6\text{F}_5)_2$  (Equation (5)).<sup>37,65</sup> Solid-state characterization indicates a weak interaction between the formally positively charged zirconium center and the carbon adjacent to the borate anion. This interaction is maintained in solution, as an upfield shifted  $^{13}\text{C}$  NMR resonance is observed for this carbon, which is in agreement with previous reports of metal–carbon interactions of this type.



Divalent zirconocenes have also found application in silicon chemistry, including stabilization of silalkenes for use in coupling reactions<sup>66–68</sup> with alkynes. Treatment of zirconocene dichloride, **50**, with 2 equiv. of  $\text{LiSiPhMe}_2$  in the presence of alkyne followed by hydrolysis affords a mixture of the silyl-substituted alkene along with a diene, which arises from homocoupling of the alkyne (Scheme 22). Detection of the transient zirconocene silalkene complex, **150**, has been achieved by monitoring the alkylation reaction by NMR spectroscopy. In addition to hydrolysis, the silazirconacyclopentene, **150**, can be trapped with isocyanides or carbon monoxide forming the



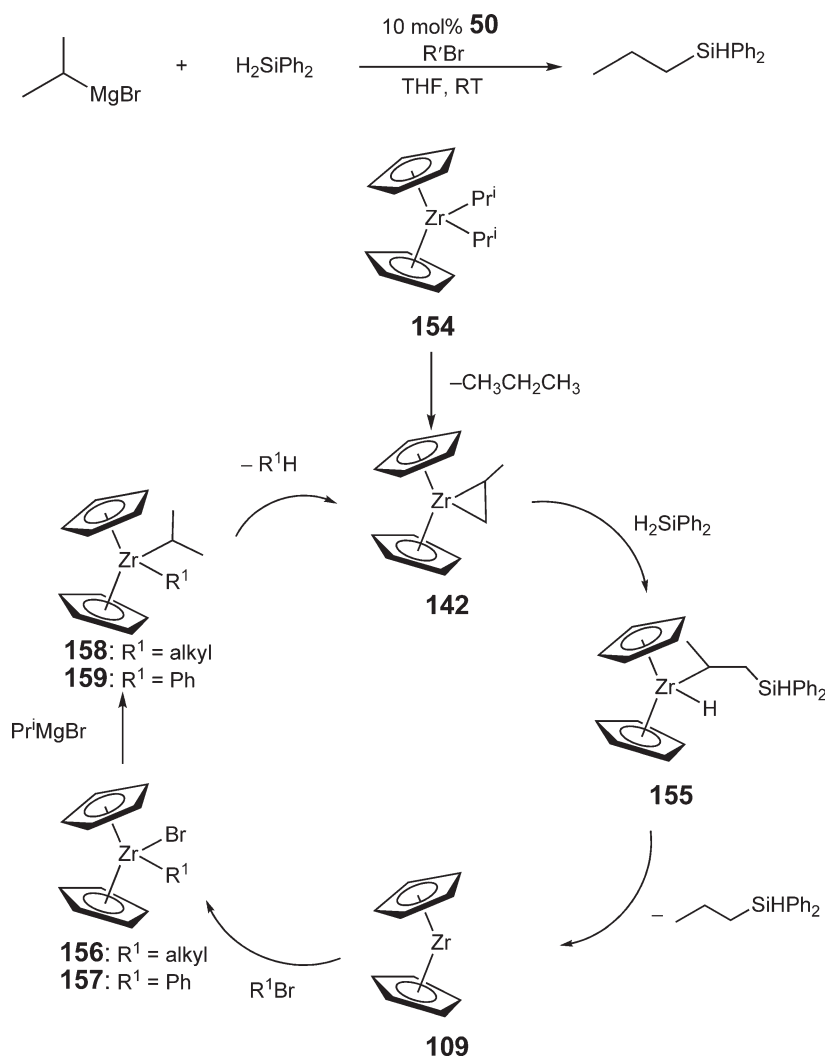
Scheme 22

silazirconacyclohexenes, **151** and **152** (Scheme 22). The silazirconacyclopentene intermediate, **153**, can also be transmetalated with copper to form other unsaturated silicon compounds.

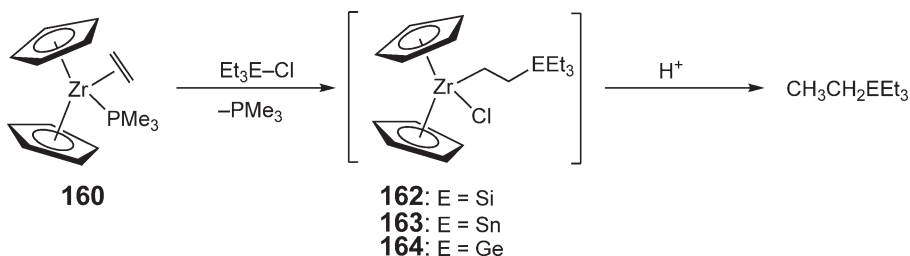
The addition of Grignard reagents to secondary silanes has been catalyzed by low-valent zirconocene compounds (Scheme 23).<sup>69</sup> Oxidative addition of an organic halide to the divalent zirconocene occurs following reductive elimination of silane. Using this procedure, silanes can be alkylated in excellent yield.

The phosphine-stabilized zirconocene ethylene complex,  $(\eta^5\text{-C}_5\text{H}_5)_2\text{Zr}(\eta^2\text{-CH}_2=\text{CH}_2)(\text{PMe}_3)$  **160**, undergoes addition of silyl, stannyl, and germyl chlorides to yield the corresponding substituted alkane upon hydrolysis (Scheme 24).<sup>70</sup> Catalytic hydrosilation with divalent zirconocene species has also been reported. In some cases, oligomerization of the silane is observed.<sup>71</sup> Significantly, the order of addition appears to influence the product distribution in catalytic hydrosilation (Scheme 25).<sup>72</sup> Both Markovnikov and anti-Markovnikov products can be accessed depending on the reaction conditions. The observed product distribution has been rationalized by the generation of a zirconate complex,  $[(\eta^5\text{-C}_5\text{H}_5)_2\text{Zr}(\text{Bu})]\text{Li}$  **161**, formed from the reaction of LiH with the zirconocene. The LiH is generated from the addition of  $\text{Bu}^n\text{Li}$  to hydrosilane. When silane is added after the alkene, the regioselectivity is reversed, most likely due to the presence of a different catalytic species.

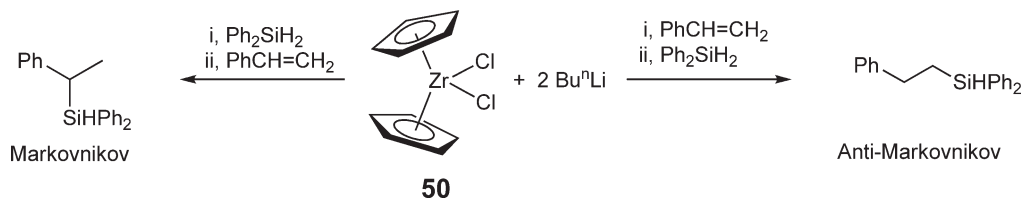
Divalent zirconocene adducts of heavy pnictogens containing double bonds have also been reported. Reduction of  $(\eta^5\text{-C}_5\text{H}_5)_2\text{ZrCl}_2$  **50** with sodium metal in the presence of 2 equiv. of  $\text{RBiCl}_2$  ( $\text{R} = \text{C}_6\text{H}_3\text{-2,6-Me}_2$ ) furnishes the adduct  $(\eta^5\text{-C}_5\text{H}_5)_2\text{Zr}(\eta^2\text{-RBiBiR})$  **165** (Equation (6)).<sup>73</sup> Although **165** may appear to resemble an alkene complex,



Scheme 23

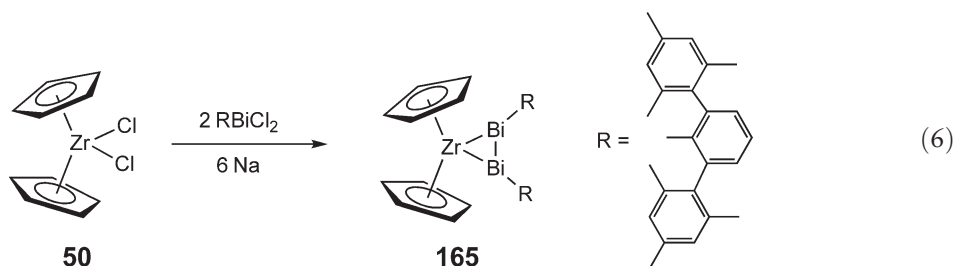


Scheme 24



Scheme 25

examination of the Zr–Bi interactions in the compound by X-ray analysis and DFT calculations indicate that the interaction is much more metallocyclopropane-like in character.

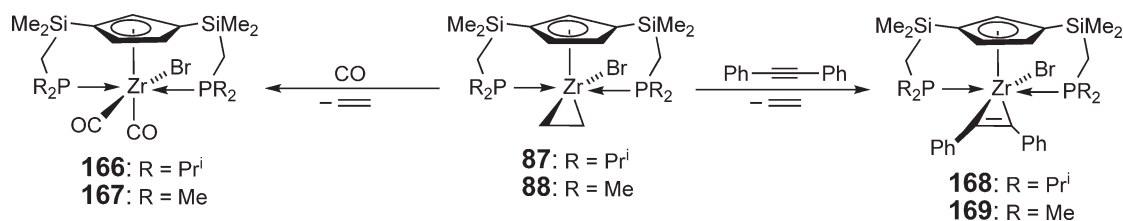


Addition of strong-field ligands such as carbon monoxide or alkynes to zirconium alkene complexes can also result in olefin displacement. Treatment of the monocyclopentadienyl complexes,  $[\eta^5\text{-C}_5\text{H}_3\text{-(1,3-(SiMe}_2\text{CH}_2\text{PR}_2)_2)]\text{Zr}(\eta^2\text{-C}_2\text{H}_4)\text{Br}$  (R = Pr<sup>i</sup>, **87**; R = Me, **88**), with CO or alkynes results in ethylene loss and the formation of the corresponding dicarbonyl (R = Pr<sup>i</sup>, **166**; R = Me, **167**) and alkyne (R = Pr<sup>i</sup>, **168**; R = Me, **169**) complexes (Scheme 26). For the alkyne addition, no metallocycle is observed, presumably due to the sterics of the ligand array.

Allenes have also been used to stabilize low-valent zirconium and hafnium compounds. This chemistry has been the subject of a recent review.<sup>74</sup>

#### 4.06.2.1.4 Zirconacyclopentanes

As was seen in the previous section, addition of excess olefin to formally divalent zirconium or hafnium alkene complexes usually induces coupling to form the corresponding metallocyclopentane. Interestingly, metallocycle



Scheme 26



formation is often reversible, suggesting that formally divalent zirconocene olefin intermediates are accessible under laboratory conditions. For example, coupling of either (*Z*)- or (*E*)- $\beta$ -methylstyrene with *in situ* generated zirconocene ultimately yields one thermodynamically favored zirconacycle over time.<sup>75</sup>

The general area of zirconacyclopentane chemistry has been reviewed.<sup>76</sup> Because these molecules are best viewed as zirconium or hafnium dialkyl complexes, and hence as tetravalent metal centers, this renders them beyond the scope of this review. It should be noted that these molecules display a rich reaction chemistry, serving as initiators for olefin polymerization,<sup>77–79</sup> reagents for organic methodology,<sup>57,80–86</sup> and key intermediates in natural product synthesis.<sup>87,88</sup>

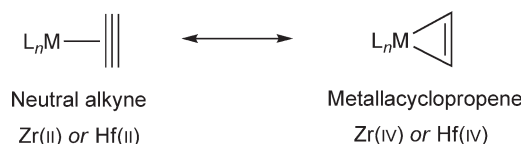
#### 4.06.2.1.5 Alkyne complexes

In analogy to carbon monoxide, the  $\pi$ -accepting ability of alkynes renders them effective ligands for stabilizing formally divalent zirconium and hafnium complexes. This chemistry is dominated by cyclopentadienyl complexes but other ligand arrays have also been employed. As with the olefin compounds, the bonding in these molecules is between a formally divalent metal center containing a neutral alkyne ligand, where the  $\pi$ -system of the alkyne is viewed as donating into an empty metal *d*-orbital, and a metallacyclopentene, where the alkyne is acting as a  $\pi$ -acceptor and the metal is in its highest oxidation state (Scheme 27).

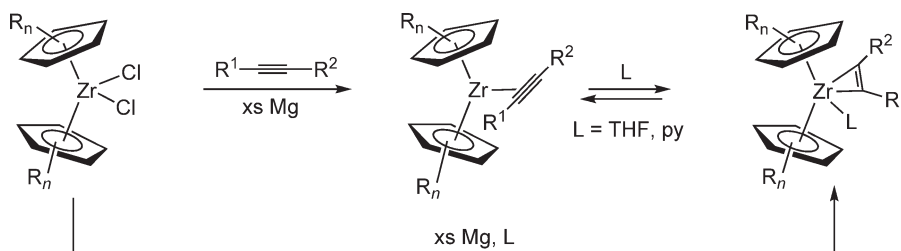
Typically, zirconocene alkyne complexes are isolated as ligand adducts,  $(CpR_n)_2Zr(\eta^2\text{-alkyne})(L)$ , prepared from reduction of the corresponding dichloride complex with magnesium in the presence of a donor solvent such as THF (Scheme 28).<sup>89,90</sup> This synthetic procedure has been extended to *ansa*-zirconocenes, unbridged tetrahydroindenyl (THI) compounds as well as non-metallocene derivatives such as  $(OEP)Zr(\eta^2\text{-PhC}\equiv\text{CPh})$  (*OEP* = octaethylporphyrinato) **170**.<sup>91–93</sup> In some instances, exchange of the THF ligand is readily achieved by addition of pyridine.<sup>94</sup>

Base-free alkyne adducts can also be synthesized, particularly when more sterically demanding ancillary ligands are employed.<sup>95</sup> Introduction of methylated cyclopentadienyl ligands has allowed a systematic study of additional ligand coordination. Reduction of the series of zirconocene dichloride compounds,  $(\eta^5\text{-C}_5\text{Me}_n\text{H}_{5-n})_2\text{ZrCl}_2$  ( $n = 2\text{--}5$ , **171**, **172**, **173**, **53**), with magnesium metal in the presence of  $\text{Me}_3\text{SiC}\equiv\text{CSiMe}_3$  with THF as the solvent allows the isolation of the corresponding base-free zirconocene alkyne adducts ( $n = 2\text{--}5$ , **174**, **175**, **176**, **177**).<sup>96</sup> When  $n = 2\text{--}4$ , color changes are observed upon cooling solutions in non-polar solvents below  $-78^\circ\text{C}$  with THF present, suggesting ligand coordination at lower temperatures. Significantly, no such color changes are observed when  $n = 5$ . Other base-free permethylzirconocene alkyne adducts,  $(\eta^5\text{-C}_5\text{Me}_5)_2\text{Zr}(\eta^2\text{-Me}_3\text{SiC}\equiv\text{CR})$  ( $R = \text{Ph}$ , **178**; *c*-C<sub>5</sub>H<sub>9</sub>, **179**; Bu<sup>t</sup>, **180**), have also been prepared by reduction of the corresponding dichloride complexes with sodium amalgam.<sup>97</sup>

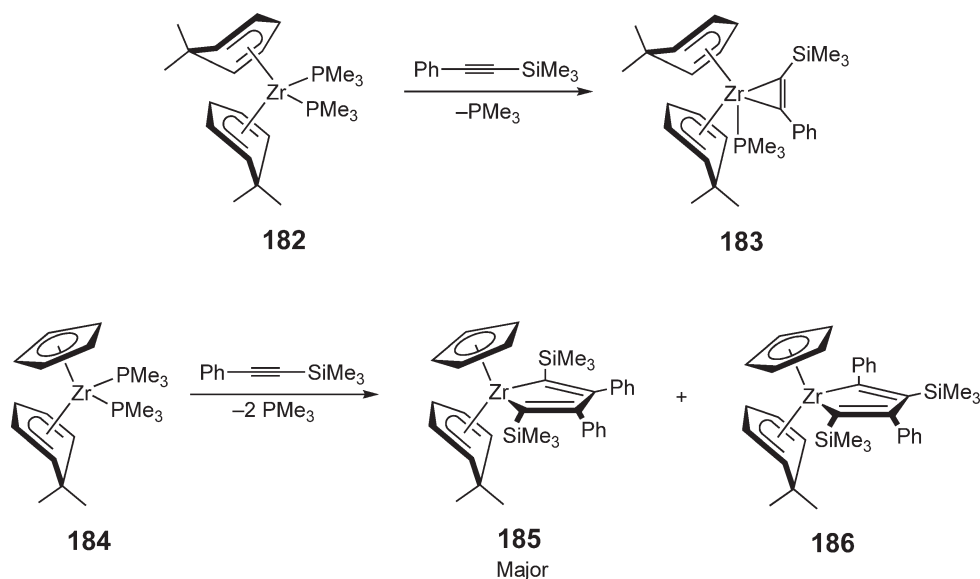
Displacement of weakly coordinating ligands is another strategy for the preparation of zirconium alkyne complexes. Addition of diphenylacetylene to the weakly activated permethylzirconocene dinitrogen complex,  $[(\eta^5\text{-C}_5\text{Me}_5)_2\text{Zr}(\eta^1\text{-N}_2)]_2(\mu_2, \eta^1, \eta^1\text{-N}_2)$  **181**, results in loss of free N<sub>2</sub> and the formation of the alkyne adduct.<sup>98</sup> Similarly, the



Scheme 27



Scheme 28



Scheme 29

bis(cyclohexadienyl)zirconium phosphine complex  $(6,6\text{-dmch})_2\text{Zr}(\text{PMe}_3)_2$  (**182**, dmch = dimethylcyclohexadienyl) undergoes displacement of one of the  $\text{PMe}_3$  ligands upon addition of  $\text{Me}_3\text{SiC}\equiv\text{CPh}$  to yield  $(6,6\text{-dmch})_2\text{Zr}(\eta^2\text{-PhC}\equiv\text{CSiMe}_3)(\text{PMe}_3)$  **183** (Scheme 29).<sup>99</sup> Replacement of a dmch ligand with a cyclopentadienyl ring results in alkyne coupling to yield the zirconacyclopentadiene upon addition of the same alkyne (Scheme 29).<sup>100</sup>

Table 2 is a compilation of pertinent  $^{13}\text{C}$  NMR chemical shifts and IR stretching frequencies of the  $\text{C}\equiv\text{C}$  fragment of zirconocene alkyne complexes. While the use of different solvents and temperatures for data collection complicates interpretation, a few trends are evident and noteworthy. In general, base-stabilized complexes display a stark downfield shift, typically greater than 10 ppm, of the alkyne carbon as compared to the base-free compounds. This chemical shift difference is reasonable, given the ability of the alkyne ligand to behave as a four-electron donor in the absence of an exogenous ligand.<sup>101</sup> In complexes where either the additional ligand or the alkyne is kept constant and the cyclopentadienyl fragment substituents are altered, the  $^{13}\text{C}$  resonance of the alkyne ligand shifts downfield as the cyclopentadienyl becomes more electron-donating. Comparing zirconocene and titanocene alkyne complexes reveals a substantial, as much as  $100\text{ cm}^{-1}$ , red shift of the  $\text{C}\equiv\text{C}$  stretching frequencies, consistent with the more reducing zirconium center. In general, base-free compounds exhibit blue-shifted acetylene IR bands, indicative of less significant reduction of the alkyne as compared to the base-stabilized compounds. A similar trend is noted in  $^{13}\text{C}$  NMR chemical shifts, as more downfield  $\text{C}\equiv\text{C}$  resonances are observed.

Also compiled in Table 2 are the metrical parameters for the crystallographically characterized alkyne adducts. Both base-free and base-stabilized compounds are included. In general, a wide array of  $\text{Zr-C}$ ,  $\text{Zr-L}$ , and  $\text{C}\equiv\text{C}$  bond distances are observed, although the carbon-carbon bond lengths typically range between 1.29 and  $1.34\text{ \AA}$ .

Zirconium and hafnium alkyne complexes display a wealth of reactivity. A comprehensive presentation of this chemistry has been the subject of several recent reviews.<sup>105–107</sup> Reactivity beyond the scope of these reviews will be the focus here.

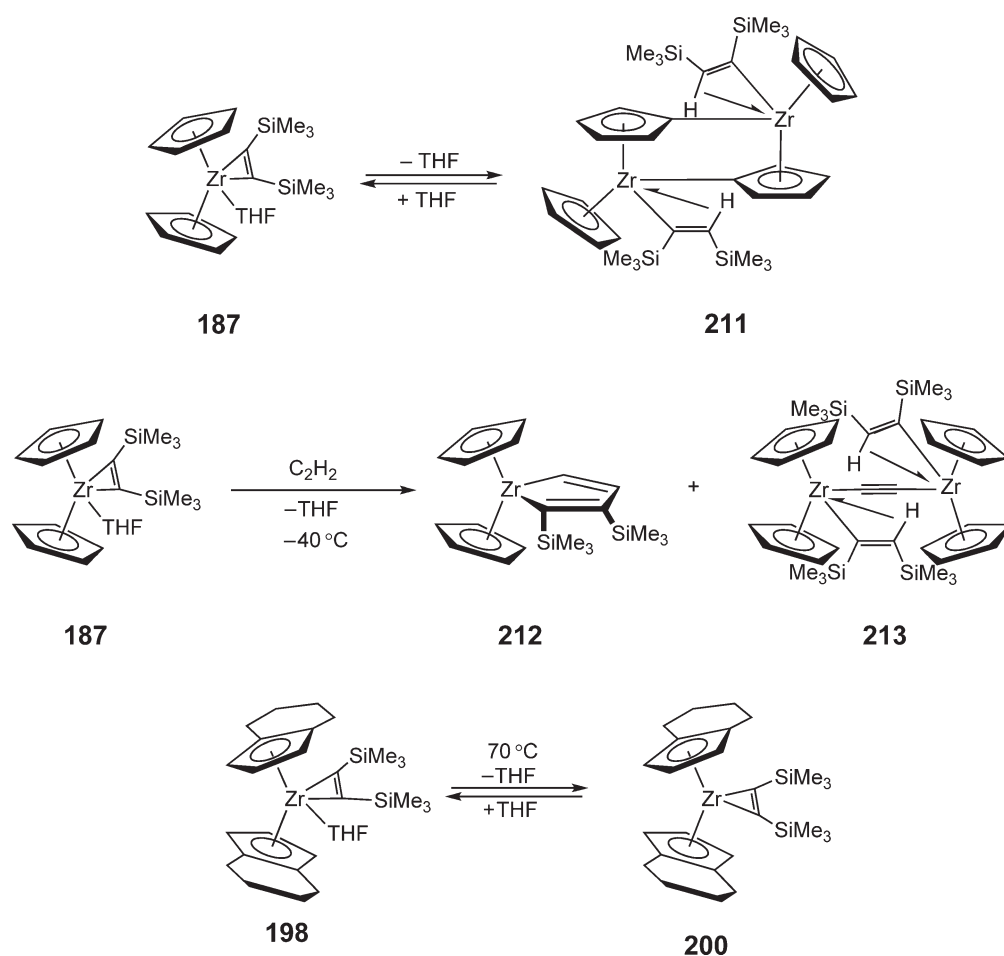
In the absence of excess donor ligand and in non-polar solvents such as benzene or pentane, the zirconocene alkyne THF complex, **187**, undergoes loss of THF and subsequent hydrogen transfer from the cyclopentadienyl ligand to the alkyne occurs, forming a bridged dinuclear complex **211** (Scheme 30). Both crystallographic and solution NMR data indicate an agostic interaction between the alkenyl ligand and the zirconium center. The reaction is reversible, as dissolving **211** in THF regenerates **187**. Addition of acetylene to **187** furnishes the product of alkyne coupling, **212**, in addition to the bridging acetylide compound **213** (Scheme 30).<sup>108</sup> As with **211**, **213** contains a  $\beta$ -agostic interaction from the alkenyl ligand. Thermolysis of the more substituted alkyne complex,  $(\text{THI})_2\text{Zr}(\eta^2\text{-Me}_3\text{SiC}\equiv\text{CSiMe}_3)(\text{THF})$  **198**, results in the dissociation of THF to form the base-free compound  $(\text{THI})_2\text{Zr}(\eta^2\text{-Me}_3\text{SiC}\equiv\text{CSiMe}_3)$  **200** (Scheme 30). **200** can be observed by  $^1\text{H}$  NMR spectroscopy and is relatively robust at elevated temperatures. In contrast, solid-state thermolysis of  $(\eta^5\text{-C}_5\text{Me}_4\text{SiMe}_3)_2\text{Zr}(\eta^2\text{-Me}_3\text{SiC}\equiv\text{CSiMe}_3)$  **214** results in intramolecular C-H activation.<sup>109</sup>

**Table 2** Selected bond distances, IR, and  $^{13}\text{C}$  NMR spectroscopic data for zirconium alkyne complexes

	<i>Cmpd</i>	<i>Zr–C distances</i> (Å)	<i>C–C</i> (Å)	<i>Zr–X</i> (Å)	$\nu_{\text{C}\equiv\text{C}}$ (cm <sup>−1</sup> )	$\delta$ (ppm)	<i>References</i>	
	[ $\eta^5\text{-C}_5\text{H}_3\text{-(1,3-(SiMe}_2\text{CH}_2\text{PPr}^i_2)_2)]\text{Zr}(\eta^2\text{-PhC}\equiv\text{CPh})\text{Br}$	<b>168</b>					42	
	(OEP)Zr( $\eta^2\text{-PhC}\equiv\text{CPh}$ )	<b>170</b>	2.160(4)	1.333(8)	1697 <sup>a</sup>	218.4 <sup>c</sup>	93	
	(C <sub>5</sub> Me <sub>2</sub> H <sub>3</sub> ) <sub>2</sub> Zr( $\eta^2\text{-Me}_3\text{SiC}\equiv\text{CSiMe}_3$ )	<b>174</b>			1535 <sup>a</sup>	260.0 <sup>c</sup>	96	
	(C <sub>5</sub> Me <sub>3</sub> H <sub>2</sub> ) <sub>2</sub> Zr( $\eta^2\text{-Me}_3\text{SiC}\equiv\text{CSiMe}_3$ )	<b>175</b>			1512, 1566 <sup>a</sup>	258.2 <sup>c</sup>	96	
	(C <sub>5</sub> Me <sub>4</sub> H) <sub>2</sub> Zr( $\eta^2\text{-Me}_3\text{SiC}\equiv\text{CSiMe}_3$ )	<b>176</b>	2.202(2)	1.316(3)	1516 <sup>a</sup>	260.2 <sup>c</sup>	96	
	Cp* <sub>2</sub> Zr( $\eta^2\text{-Me}_3\text{SiC}\equiv\text{CSiMe}_3$ )	<b>177</b>	2.216(2), 2.221(2)	1.320(3)	1516 <sup>a</sup>	260.5 <sup>c</sup>	96	
	Cp* <sub>2</sub> Zr( $\eta^2\text{-Me}_3\text{SiC}\equiv\text{CPh}$ )	<b>178</b>	2.178(6), 2.219(5)	1.340(9)	1618 <sup>a</sup>	222.5, 235.1 <sup>c</sup>	97	
	Cp* <sub>2</sub> Zr( $\eta^2\text{-Me}_3\text{SiC}\equiv\text{C-}i\text{-pentyl}$ )	<b>179</b>				220.6, 250 <sup>c</sup>	97	
	Cp* <sub>2</sub> Zr( $\eta^2\text{-Me}_3\text{SiC}\equiv\text{CCMe}_3$ )	<b>180</b>				220.8, 253.7 <sup>c</sup>	97	
	Cp <sub>2</sub> Zr( $\eta^2\text{-Me}_3\text{SiC}\equiv\text{CSiMe}_3$ )(THF)	<b>187</b>	2.204(7), 2.260(7)	1.302(9)	2.390(5)	1581 <sup>b</sup>	212.9 <sup>d</sup>	89
	Cp <sub>2</sub> Zr( $\eta^2\text{-Me}_3\text{SiC}\equiv\text{CSiMe}_3$ )(py)	<b>188</b>	2.216(2), 2.242(2)	1.312(3)	2.437(2)		208.5, 220.5 <sup>d</sup>	94
	Cp <sub>2</sub> Zr( $\eta^2\text{-Me}_3\text{CC}\equiv\text{CSiMe}_3$ )(THF)	<b>189</b>			1611 <sup>b</sup>	223.4 <sup>d</sup>	90	
	Cp <sub>2</sub> Zr( $\eta^2\text{-Me}_3\text{SiC}\equiv\text{CSiMe}_2\text{H}$ )	<b>190</b>				125.4, 194.7 <sup>c</sup>	102	
	Cp <sub>2</sub> Zr( $\eta^2\text{-Me}_3\text{CC}\equiv\text{CSiMe}_2\text{H}$ )(THF)	<b>191</b>			1688 <sup>b</sup>		102	
	Cp <sub>2</sub> Zr( $\eta^2\text{-Me}_3\text{CC}\equiv\text{CSiMe}_2\text{H}$ )	<b>192</b>			1689 <sup>b</sup>	214.7 <sup>c</sup>	102	
	Cp <sub>2</sub> Zr( $\eta^2\text{-PhC}\equiv\text{CSiMe}_2\text{H}$ )(THF)	<b>193</b>			1683 <sup>b</sup>	221.8 <sup>d</sup>	102	
	Cp <sub>2</sub> Zr( $\eta^2\text{-PhC}\equiv\text{CSiMe}_2\text{H}$ )	<b>194</b>			1686 <sup>b</sup>	201.6 <sup>c</sup>	102	
	Cp <sub>2</sub> Zr( $\eta^2\text{-HMe}_2\text{SiC}\equiv\text{CSiMe}_2\text{H}$ )(THF)	<b>195</b>				198.3, 225.7 <sup>d</sup>	102	
	Cp <sub>2</sub> Zr( $\eta^2\text{-HMe}_2\text{SiC}\equiv\text{CSiMe}_2\text{H}$ )	<b>196</b>	2.299(3), 2.407(3)	1.291(4)		127.1, 191.2 <sup>c</sup>	102	
	Cp <sub>2</sub> Zr( $\eta^2\text{-HC}\equiv\text{CBu}^u$ )(PMe <sub>3</sub> )	<b>197</b>	2.211(3), 2.244(3)	1.286(5)	2.658(1)		103	
	(THI) <sub>2</sub> Zr( $\eta^2\text{-Me}_3\text{SiC}\equiv\text{CSiMe}_3$ )(THF)	<b>198</b>	2.218(5), 2.271(5)	1.340(7)	2.404(4)	1559 <sup>b</sup>	212.9, 222 <sup>d</sup>	91
	(THI) <sub>2</sub> Zr( $\eta^2\text{-Me}_3\text{SiC}\equiv\text{CSiMe}_3$ )(py)	<b>199</b>			1548, 1595 <sup>b</sup>	207, 216.7 <sup>c</sup>	91	
	(THI) <sub>2</sub> Zr( $\eta^2\text{-Me}_3\text{SiC}\equiv\text{CSiMe}_3$ )	<b>200</b>				244 <sup>c</sup>	91	
	<i>Rac</i> -(EBTHI)Zr( $\eta^2\text{-Me}_3\text{SiC}\equiv\text{CSiMe}_3$ )(py)	<b>201</b>	2.22(1), 2.27(1)	1.34(1)	2.380(9)	1560 <sup>b</sup>	95	
	<i>Rac</i> -(EBTHI)Zr( $\eta^2\text{-Me}_3\text{SiC}\equiv\text{CSiMe}_3$ )(nic) <sup>f</sup>	<b>202</b>				1560 <sup>b</sup>	95	
	<i>Rac</i> -(EBTHI)Zr( $\eta^2\text{-Me}_3\text{SiC}\equiv\text{CSiMe}_3$ )	<b>203</b>	2.199(7), 2.211(7)	1.30(1)		1534 <sup>b</sup>	259.7 <sup>c</sup>	95
	[SiMe <sub>2</sub> ( $\eta^5\text{-C}_5\text{H}_4$ ) <sub>2</sub> ] <sub>2</sub> Zr( $\eta^2\text{-Me}_3\text{SiC}\equiv\text{CSiMe}_3$ )(py)	<b>204</b>	2.223(4), 2.258(4)	1.297(6)	2.449(3)	1579, 1597 <sup>b</sup>	193.0, 218.5 <sup>c</sup>	92
	O(SiMe <sub>2</sub> ( $\eta^5\text{-C}_5\text{H}_4$ )) <sub>2</sub> Zr( $\eta^2\text{-Me}_3\text{SiC}\equiv\text{CSiMe}_3$ )(py)	<b>205</b>				1587, 1597 <sup>b</sup>	212.5 <sup>c</sup>	92
	( $\eta^5\text{-C}_9\text{H}_5\text{-}1,3\text{-(CHMe}_2)_2$ ) <sub>2</sub> Zr( $\eta^2\text{-PhC}\equiv\text{CPh}$ )	<b>206</b>					209.38 <sup>c</sup>	104
	( $\eta^5\text{-C}_9\text{H}_5\text{-}1,3\text{-(SiMe}_2\text{Ph})_2$ ) <sub>2</sub> Zr( $\eta^2\text{-PhC}\equiv\text{CPh}$ )	<b>207</b>					217.78 <sup>c</sup>	104
	( $\eta^5\text{-C}_9\text{H}_5\text{-}1,3\text{-(SiMe}_3)_2$ ) <sub>2</sub> Zr( $\eta^2\text{-MeC}\equiv\text{CMe}$ )	<b>208</b>					227.45 <sup>c</sup>	104
	( $\eta^5\text{-C}_9\text{H}_5\text{-}1,3\text{-(SiMe}_2\text{Bu})_2$ ) <sub>2</sub> Zr( $\eta^2\text{-MeC}\equiv\text{CMe}$ )	<b>209</b>					226.03 <sup>c</sup>	104
	(C <sub>4</sub> Me <sub>4</sub> P) <sub>2</sub> Zr( $\eta^2\text{-Me}_3\text{SiC}\equiv\text{CSiMe}_3$ )	<b>210</b>					19	

<sup>a</sup>in KBr.<sup>b</sup>in Nujol.<sup>c</sup>in benzene-*d*<sub>6</sub>.<sup>d</sup>in THF-*d*<sub>8</sub>.<sup>e</sup>in toluene-*d*<sub>8</sub>.<sup>f</sup>nic = (S)-(–)-nicotine.

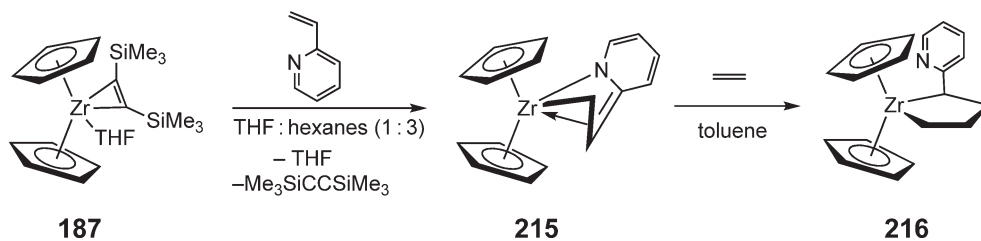
EBTHI = ethylene-bis(tetrahydroindenyl).



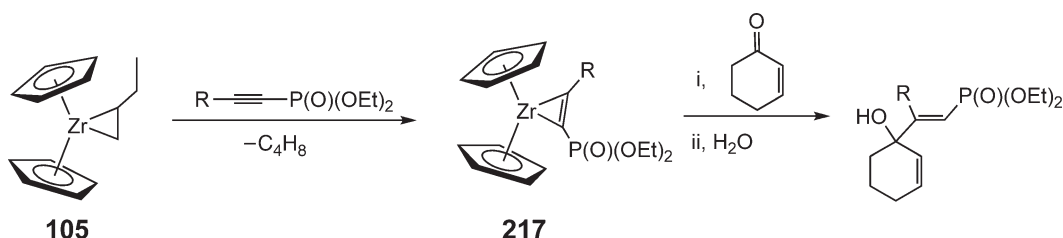
Scheme 30

The sterically demanding alkyne,  $\text{Me}_3\text{SiC}\equiv\text{CSiMe}_3$ , has been widely used to stabilize a range of zirconocene complexes while also serving as a convenient leaving group to access the rich chemistry of divalent zirconium. These results have been the subject of a comprehensive review. Representative reactivity will be presented here.

Addition of vinyl pyridine to the parent zirconocene adduct,  $(\eta^5\text{-C}_5\text{H}_5)_2\text{Zr}(\eta^2\text{-Me}_3\text{SiC}\equiv\text{CSiMe}_3)(\text{THF})$  **187**, yields an alkylamide complex, arising from reduction of the aromatic ring (**215**, Scheme 31).<sup>110</sup> Coupling of a second equivalent of vinyl pyridine is not observed and the lack of reactivity is believed to be the result of coordination of the pyridyl nitrogen. However, smaller alkenes such as ethylene are reactive, forming the corresponding zirconacycle **216**. In addition to coupling reactions, the zirconocene alkylamide compound, **215**, also displays typical reactivity of zirconocene olefin complexes, forming metallacyclic carboxylate products upon addition of carbon dioxide.



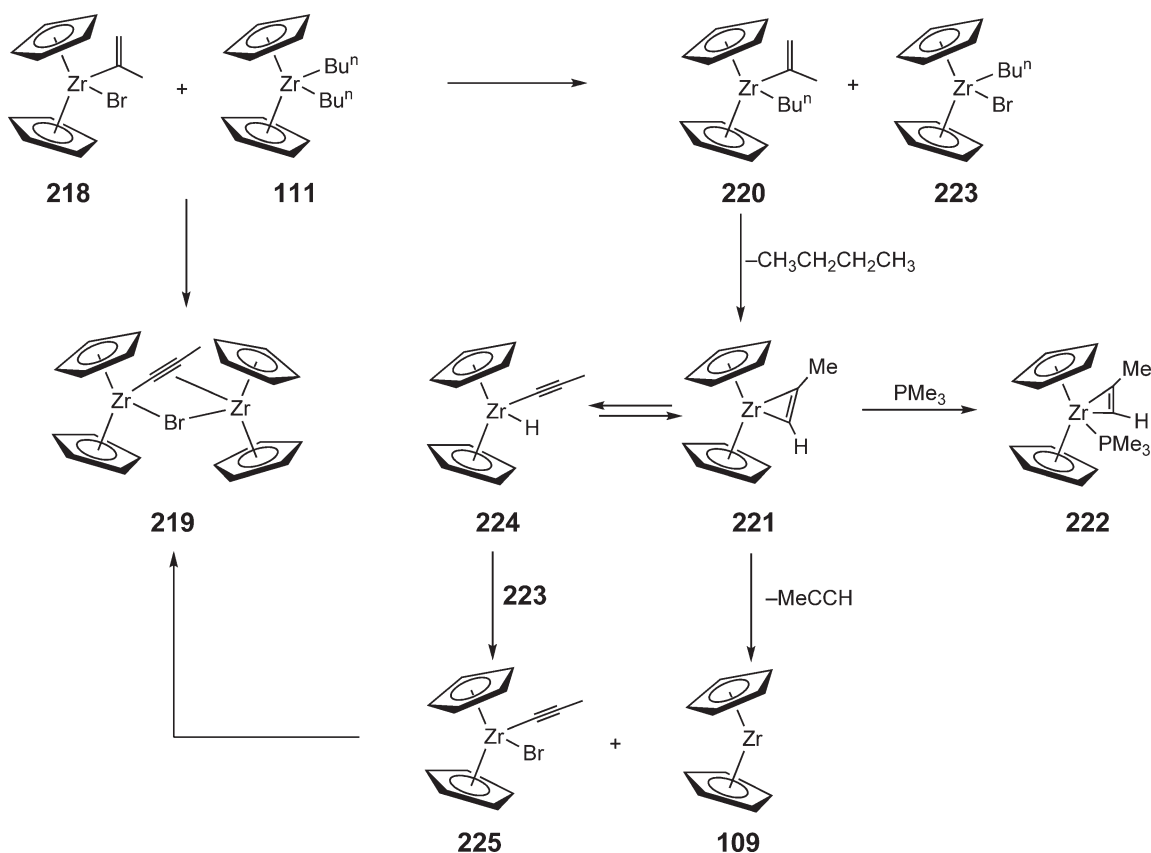
Scheme 31



Scheme 32

Another type of reactivity typical of zirconium and hafnium alkyne complexes is ring expansion to yield five-membered and larger metallacycles. A variety of unsaturated organic reagents can be added including alkenes, alkynes, and ketones. This chemistry has been reviewed in detail.<sup>105,107</sup> Heteroatom-stabilized zirconocene alkyne complexes are emerging for their potential utility in organic synthesis. For example, various 1-hexynyl-1-phosphates displace olefin from the *in situ* generated zirconocene olefin complex, **105**, to form the alkyne complex, **217** (Scheme 32).<sup>111</sup> These intermediates can be treated with 2-cyclohexen-1-one, which after hydrolysis, afford vinyl phosphates. These products are of interest due to their biological activity.

Terminal alkyne complexes of zirconium, while challenging to isolate, have been implicated in a number of organometallic transformations. Mixing an alkenyl zirconocene **218** with a transient dialkyl zirconocene **111** furnishes a  $\mu$ -acetylide complex **219** (Scheme 33).<sup>112</sup> This reaction is believed to proceed by initial transmetalation to form a zirconocene alkenyl alkyl **220**, which undergoes subsequent  $\beta$ -hydrogen abstraction to generate the terminal alkyne complex **221**. This proposed intermediate can be trapped with  $PMe_3$  **222** from the alkylation of the zirconocene alkenyl bromide with butyllithium. Comparison of the spectroscopic features of this product to the



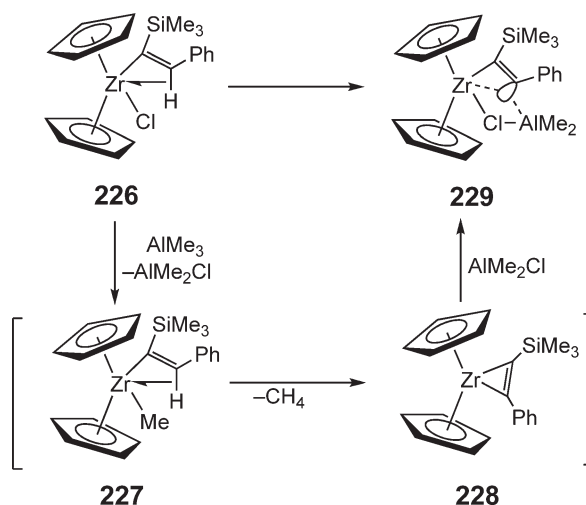
Scheme 33

previously reported  $(\eta^5\text{-C}_5\text{H}_5)_2\text{Zr}(\eta^2\text{-Bu}^t\text{C}\equiv\text{CH})(\text{PMe}_3)$  **197** indicates terminal alkyne complex formation. Transmetalation of **224** by **223** gives  $(\eta^5\text{-C}_5\text{H}_5)_2\text{Zr}(\text{C}\equiv\text{CMe})(\text{Br})$  **225**, which can be trapped by the transient “zirconocene” **109** generated from alkyne loss by **221** to afford the observed product.

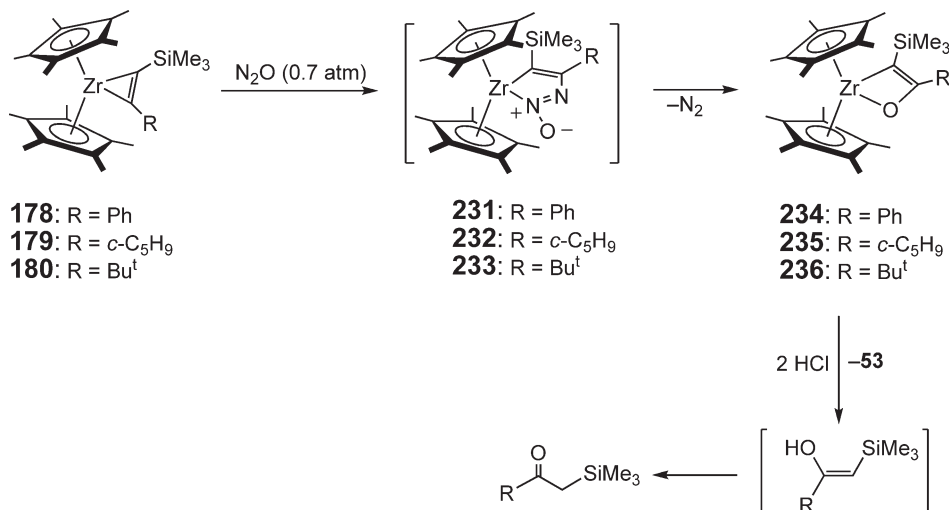
Terminal alkyne complexes have also been implicated in the generation of planar tetracoordinate carbon (**Scheme 34**). These compounds are rapidly trapped with main group organometallics, typically alkylaluminums, to afford bimetallic products.<sup>113</sup>

The coupling of vinyl bromide with *in situ* generated terminal alkyne complexes has also been accomplished by the alkylation of  $(\eta^5\text{-C}_5\text{H}_5)_2\text{Zr}(\text{Me})\text{Cl}$  **230** with terminal alkenyl lithium reagents.<sup>114</sup> The reaction products are either dienes or cyclobutenes, depending upon the substrates employed.

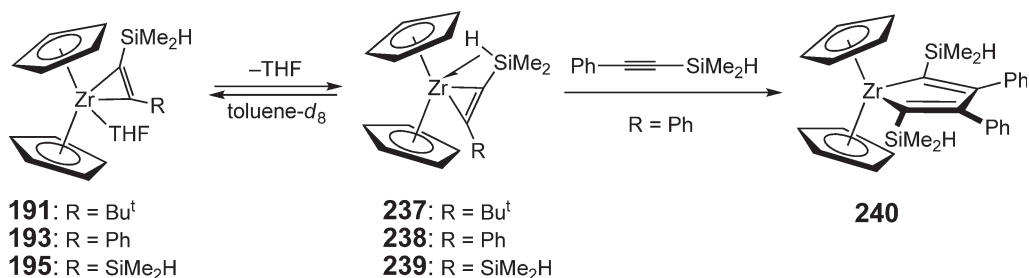
Oxidation of zirconocene alkyne complexes with  $\text{N}_2\text{O}$  has also been explored. The addition of  $\text{N}_2\text{O}$  to  $(\eta^5\text{-C}_5\text{Me}_5)_2\text{Zr}(\eta^2\text{-RC}\equiv\text{CSiMe}_3)$  ( $\text{R} = \text{Ph}$ , **178**;  $\text{c-C}_5\text{H}_9$ , **179**,  $\text{Bu}^t$ , **180**) at low temperature is believed to proceed through the azazirconacycles, ( $\text{R} = \text{Ph}$ , **231**;  $\text{c-C}_5\text{H}_9$ , **232**,  $\text{Bu}^t$ , **233**) (**Scheme 35**).<sup>97</sup> Warming the solution induces loss of dinitrogen to form the oxozirconacyclobutenes ( $\text{R} = \text{Ph}$ , **234**;  $\text{c-C}_5\text{H}_9$ , **235**,  $\text{Bu}^t$ , **236**), which have been isolated. In analogy to alkyne coupling chemistry, only one isomer of the zirconacyclobutenes is observed. These observations have been confirmed by protonolysis studies, liberating the corresponding ketone and  $(\eta^5\text{-C}_5\text{Me}_5)_2\text{ZrCl}_2$  **53**.



Scheme 34



Scheme 35

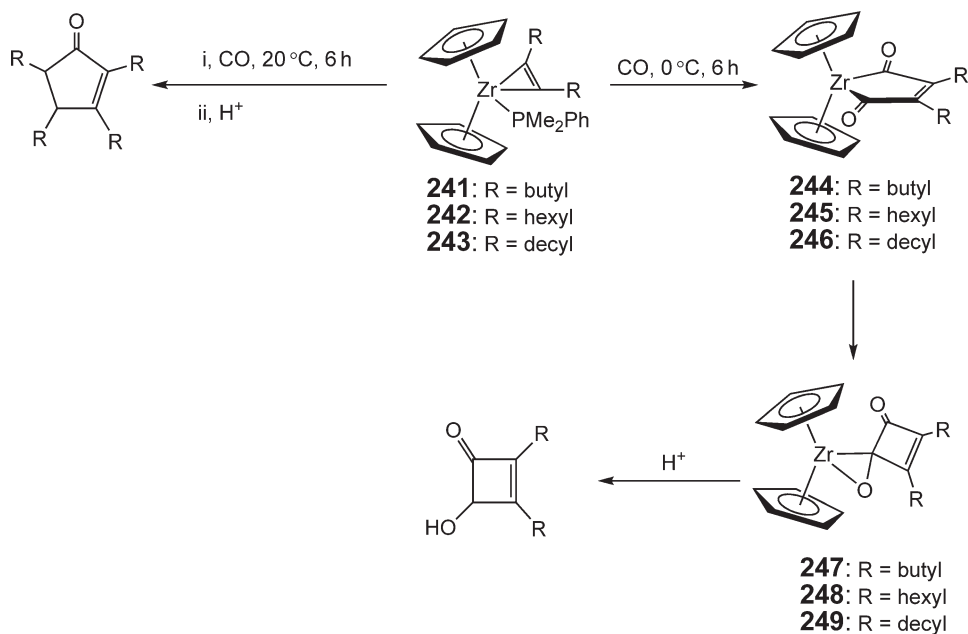


Scheme 36

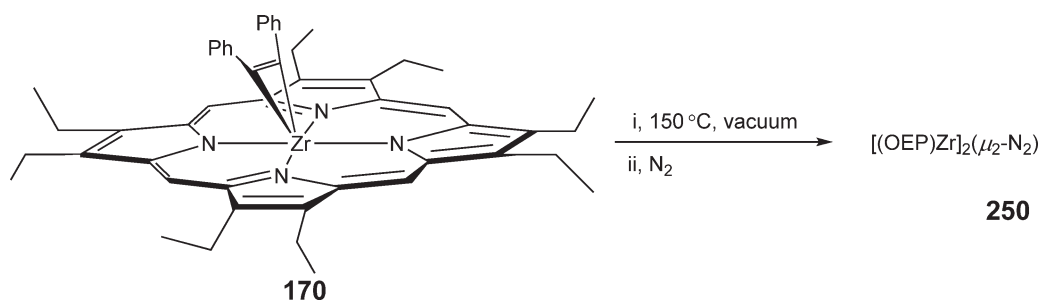
Alkyne substitution reactions have been used to prepare zirconocene complexes of alkynylsilanes (Scheme 36). In non-polar solvents, the silylalkyne compounds,  $(\eta^5\text{-C}_5\text{H}_5)_2\text{Zr}(\eta^2\text{-RC}\equiv\text{CSiMe}_2\text{H})(\text{THF})$  (R = Bu<sup>t</sup>, **191**; Ph, **193**; SiMe<sub>2</sub>H, **195**), undergo dissociation of THF to form the corresponding base-free complexes that contain Si–H agostic interactions. The agostic interactions have been observed at low temperatures and are characterized by upfield <sup>1</sup>H NMR shifts, in the range of –4 to –8 ppm, for the Si–H resonances. Displacement of the coordinated Si–H bond is readily accomplished by addition of excess alkyne, forming the corresponding zirconacyclopentadiene **240**. Initially a kinetic mixture of products is formed which converts to **240** over time.

Recently, double carbonylation of an alkyne has been accomplished using the  $(\eta^5\text{-C}_5\text{H}_5)_2\text{Zr}(\eta^2\text{-R-C}\equiv\text{C-R})$  (PMe<sub>2</sub>Ph) (R = butyl, **241**; hexyl, **242**; decyl, **243**) complexes to afford 2,3-dialkyl-4-hydroxycyclobuten-1-ones upon hydrolysis (Scheme 37).<sup>115</sup> The reaction is typically performed at 1 atm of CO at 0 °C and is temperature sensitive, as no reaction occurs below –15 °C, while at room temperature tetraalkylcyclopentenones are observed. The mechanism of carbonylation is thought to proceed through a five-membered zirconacycle that rearranges, presumably due to the oxophilicity of the zirconium, to yield the observed cyclobutene ring skeleton.

Cyclopentadienyl ligands are not a prerequisite for preparing low-valent zirconium alkyne complexes. Solid-state thermolysis of the octaethylporphyrin complex, (OEP)Zr( $\eta^2\text{-PhC}\equiv\text{CPh}$ ) **170**, results in the loss of alkyne and the formation of a paramagnetic product under vacuum (Scheme 38).<sup>116</sup> Performing a similar thermolysis procedure under an atmosphere of dinitrogen forms a diamagnetic compound, tentatively formulated as the bridging N<sub>2</sub> complex, **250**. Because both the paramagnetic product and **250** decompose rapidly in solution at room temperature,



Scheme 37



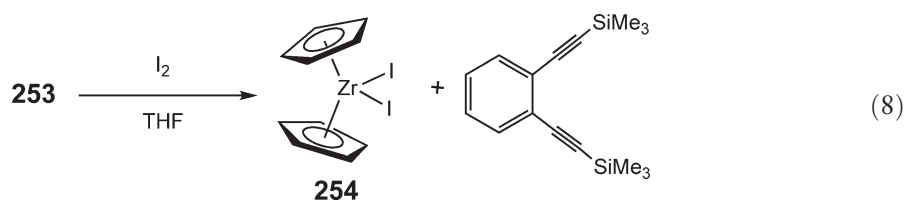
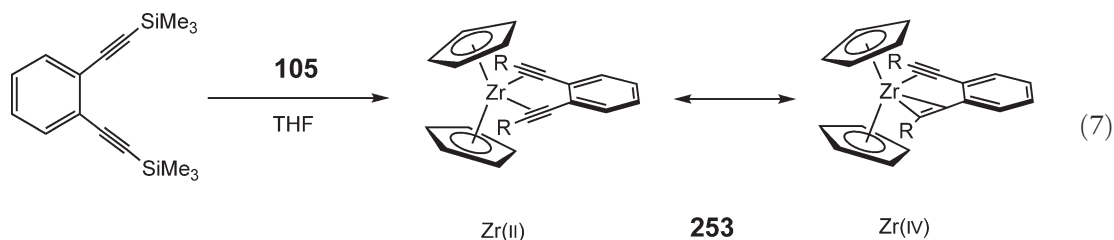
Scheme 38

few spectroscopic data are available. However, addition of dichloromethane furnishes the bridging chloride, methylene complex, **251** which yields the  $\mu$ -oxo dimer, **252**, upon hydrolysis.

#### 4.06.2.1.6 Zirconacyclopentadienes

In analogy to alkene coupling reactions, addition of excess alkyne to low-valent zirconium and hafnium complexes results in coupling of the unsaturate to form the corresponding metallacyclopentadienes.<sup>117</sup> While not formally divalent zirconium and hafnium complexes, several reactions reported with these species are worthy of comment. Zirconocene-mediated couplings have been used to prepare conjugated monomers, macrocycles, and polymers with applications to light-emitting diodes and for other non-linear optical applications.<sup>118–124</sup> Ene–yne cyclization reactions have also found use in natural product synthesis,<sup>125–127</sup> while other zirconacyclopentadiene couplings have been employed in the preparation of larger (eight- or nine-membered) bicyclic structures.<sup>128,129</sup>

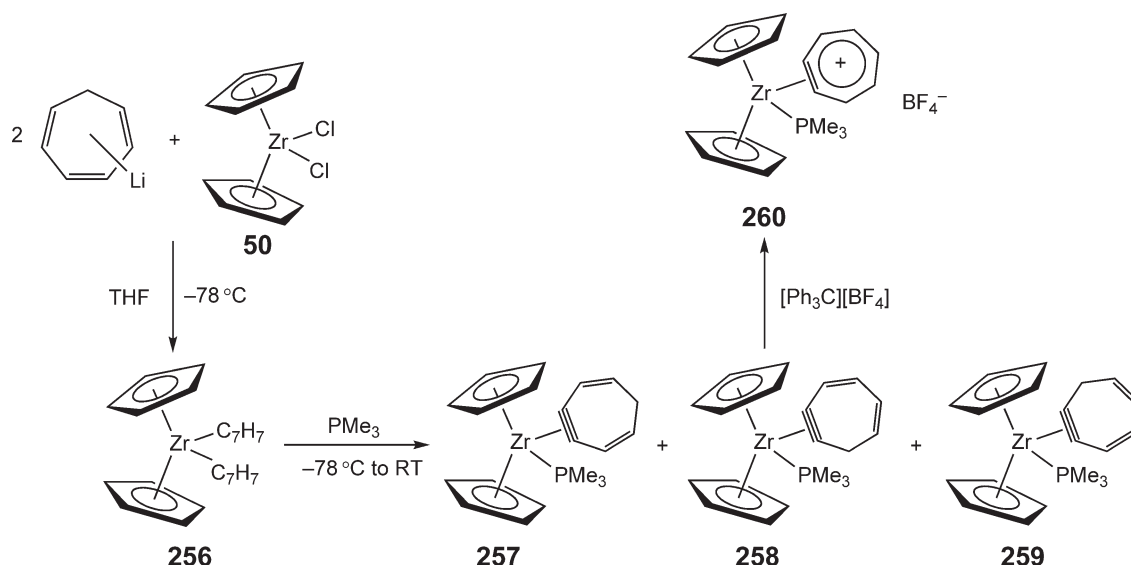
One example of a bonafide bis(alkyne) complex has recently been prepared. Reaction of the *in situ* generated olefin complex prepared by alkylation of  $(\eta^5\text{-C}_5\text{H}_5)_2\text{ZrCl}_2$  **50** with the diaryl alkyne in Equation (7) yields **253**.<sup>130</sup> In this structure, C–C coupling has not occurred, presumably a result of the steric strain associated with the zirconacyclopentadienyl fragment (Equation (7)). The solid-state structure further establishes the compound as a bis(alkyne) complex. Computational studies suggest that a Zr(IV) resonance structure is the most suitable representation of the compound. However, reaction of **253** with iodine in THF yields  $(\eta^5\text{-C}_5\text{H}_5)_2\text{ZrI}_2$  **254** and the dialkyne starting material, suggesting that the zirconium center can act as a source of Zr(II) (Equation (8)).



#### 4.06.2.1.7 Benzyne complexes

The structural characterization of  $(\eta^5\text{-C}_5\text{H}_5)_2\text{Zr}(\eta^2\text{-C}_6\text{H}_4)(\text{PMe}_3)$  **255** in 1986 established the utility of formally divalent zirconocene complexes to stabilize otherwise reactive and transient organic molecules.<sup>131</sup> The synthesis and reactivity of these species has been the subject of two recent reviews.<sup>74,132</sup> Building on these seminal discoveries, formally low-valent zirconocene fragments have been used to stabilize other aryne species. Typically, these syntheses are achieved by

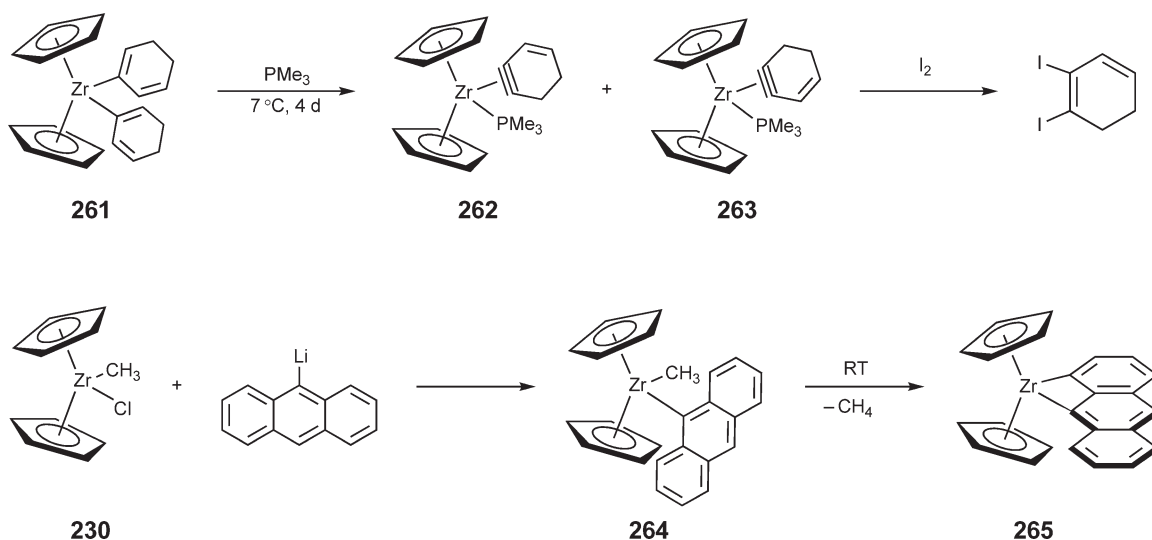




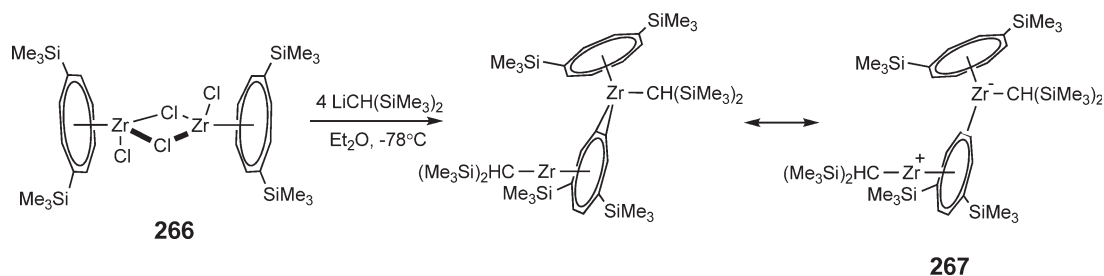
Scheme 39

ligand-induced reductive elimination from a suitable zirconocene bis(aryl) or bis(alkenyl) complex. For example, alkylation of zirconocene dichloride ( $\eta^5\text{-C}_5\text{H}_5\text{)}_2\text{ZrCl}_2$  **50** with three isomeric cycloheptatrienyllithiums furnishes the intermediate zirconocene bis(aryl) complex **256** that when warmed to room temperature in the presence of  $\text{PMe}_3$  gives an inseparable mixture of three cycloheptadienyne complexes **257–259** (Scheme 39).<sup>133</sup> Hydride abstraction with  $[\text{Ph}_3\text{C}][\text{BF}_4]$  yields the first example of a zirconocene tropyne compound **260**. This compound is thermally unstable, readily decomposing at temperatures above  $-50^\circ\text{C}$ . Replacement of the  $\text{BF}_4^-$  anion with  $\text{BPh}_4^-$  or  $\text{B}(\text{C}_6\text{F}_5)_4^-$  did not increase its stability.

Zirconocene complexes of cyclohexene-3-yne have also been prepared.<sup>134</sup> Addition of  $\text{PMe}_3$  to the zirconocene bis(alkenyl) complex, **261**, induces the elimination of 1,3-cyclohexadiene along with formation of two isomeric zirconocene cyclohexene-3-yne complexes (**262** and **263**). Iodination yields 1,2-diiodocyclohexa-1,3-diene. Treatment of the zirconocene methyl chloride complex, ( $\eta^5\text{-C}_5\text{H}_5\text{)}_2\text{Zr}(\text{Me})\text{Cl}$  **230**, with 9-lithioanthracene yields a yellow compound identified as ( $\eta^5\text{-C}_5\text{H}_5\text{)}_2\text{Zr}(\text{Me})(9\text{-anthracenyl})$  **264**.<sup>135</sup> Slow methane elimination is observed at room temperature, affording the zirconacycle, **265** (Scheme 40). This compound has been shown to participate in insertion chemistry with both alkynes and nitriles and the mechanism has been investigated with isotopic labeling studies.



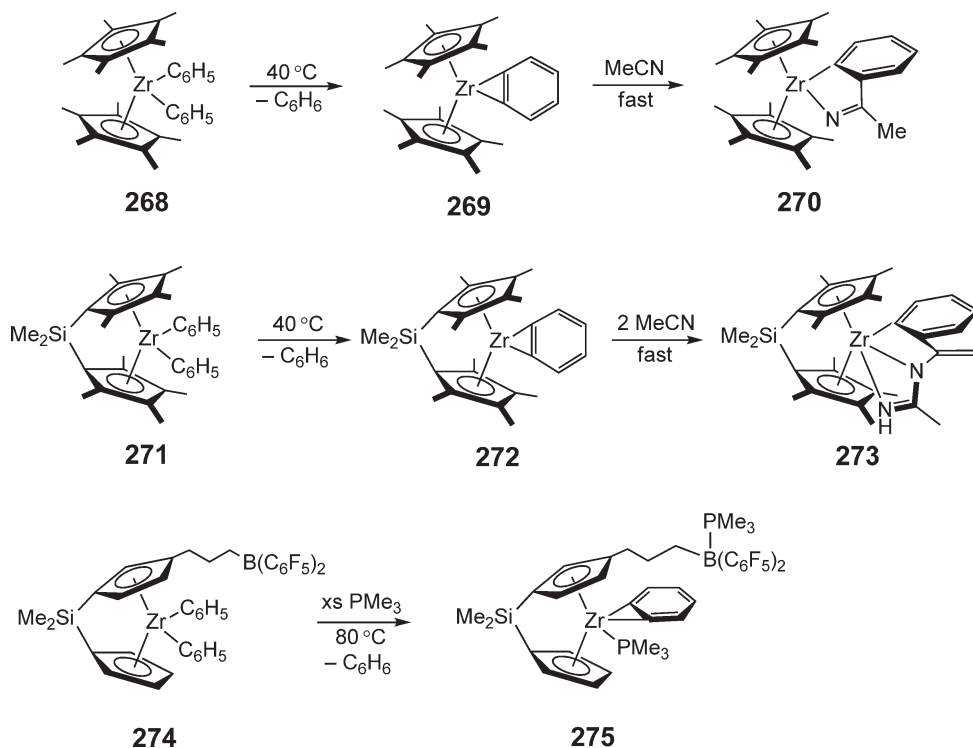
Scheme 40



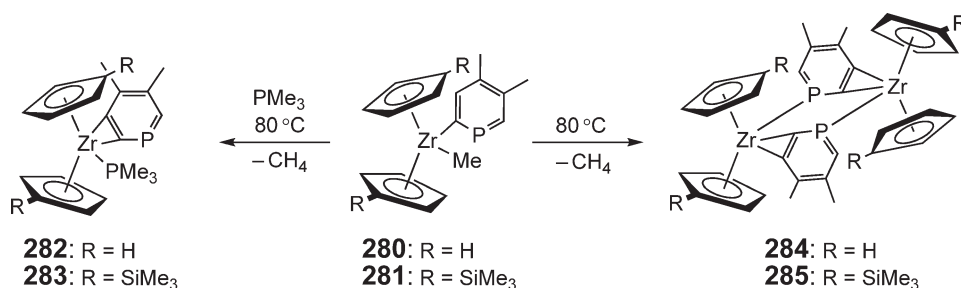
Scheme 41

A compound analogous to zirconocene benzyne complexes has been prepared with cyclooctatetraenyl ligands. Addition of 4 equiv. of the sterically demanding alkyl lithium,  $\text{LiCH}(\text{SiMe}_3)_2$ , to an ethereal solution of  $[(\text{COT}')\text{ZrCl}_2]_2$  (**266**,  $\text{COT}' = 1,4\text{-bis}(\text{trimethylsilyl})\text{cyclooctatetraenyl}$ ) furnishes a dimeric complex arising from multiple C–H activations of the COT ligand (**267**, Scheme 41).<sup>136</sup> Several resonance structures can be drawn for this complex, but based on structural data and the diamagnetism of the complex, the  $\text{Zr(II)}\text{--Zr(IV)}$  form is thought to be a dominant contributor to the overall resonance hybrid.

The influence of an  $[\text{SiMe}_2]$  *ansa*-bridge on the formation of zirconocene benzyne complexes has also been investigated. Comparing the relative rates of benzene elimination from  $(\eta^5\text{-C}_5\text{Me}_5)_2\text{Zr}(\text{C}_6\text{H}_5)_2$  **268** and  $[\text{Me}_2\text{Si}(\eta^5\text{-C}_5\text{Me}_4)_2]\text{Zr}(\text{C}_6\text{H}_5)_2$  **271** establishes more rapid product formation in the *ansa*-complex (Scheme 42).<sup>137</sup> Trapping of the intermediate permethylzirconocene benzyne complex **269** with acetonitrile affords **270**, while in the *ansa*-case 2 equiv. of MeCN trap the benzyne compound, **272**, to yield **273**. In both reactions, the rate of product formation is independent of MeCN concentration, allowing direct comparison of the rate of the elimination reactions. It is proposed that the faster reaction rate for the *ansa*-complex is a result of a lower barrier for Zr–Ph bond rotation, which allows **271** to more easily obtain the required configuration for benzene elimination. Thermal, phosphine-induced benzene elimination has also been observed from the borane-functionalized *ansa*-zirconocene,



Scheme 42



Scheme 43

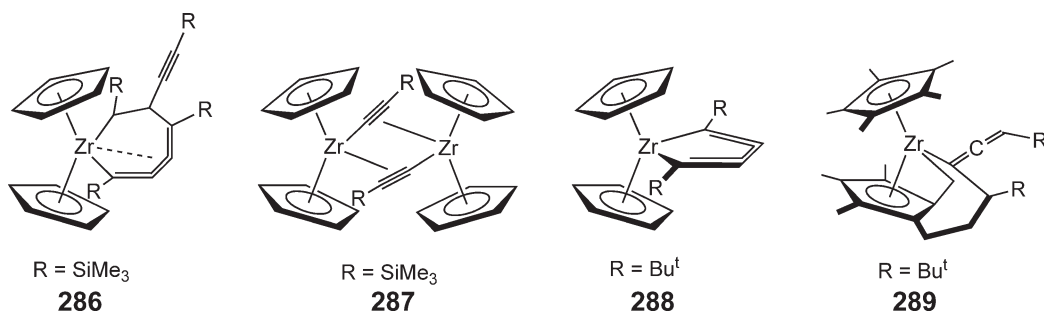
**274**, to yield the benzyne- $\text{PMe}_3$  complex, **275**, where 1 equiv. of  $\text{PMe}_3$  is coordinated to the pendant borane (Scheme 42). Synthesis of a zirconocene-1,2-dehydro-*o*-carborane complex has also been reported.<sup>138</sup>

Zirconocene-benzyne complexes have found utility in organic synthesis and this area has been recently reviewed.<sup>74,132</sup> Examples include synthesis of benzo-zirconacyclohexadiene-phospha- and silacyclobutene fused ring systems that may be used in the preparation of mono- and tricyclic heterocycles,<sup>139</sup> as well as coupling to phosphine-substituted alkynes to form zirconaindene metallacycles as a mixture of two regioisomers.<sup>140</sup> Zirconocene-benzyne compounds have also been used to prepare group 13 zirconium heterobimetallic compounds. Addition of main group (B, Al, and Ga) alkoxides to  $(\eta^5\text{-C}_5\text{H}_5)_2\text{Zr}(\text{C}_6\text{H}_5)_2$  **276** yields  $\text{R}_2\text{E}(\mu\text{-OR}')(\mu\text{-1,2-C}_6\text{H}_4)\text{Zr}(\eta^5\text{-C}_5\text{H}_5)_2$  (E = B, R = Et, R' = Me, **277**; E = B, R = Me, R' = Et, **278**; E = Al, R = Et, R' = Et, **279**) derivatives.<sup>141</sup>

Zirconocene-stabilized benzyne complexes with phosphorus-containing heterocycles have also been reported.<sup>142,143</sup> These compounds can be prepared in analogy to the parent benzyne compounds, where elimination of methane from the zirconocene aryl alkyl complex is observed upon thermolysis at 80 °C (Scheme 43). In the presence of  $\text{PMe}_3$ , monomeric complexes (R = H, **282**; R = SiMe<sub>3</sub>, **283**) are obtained whereas in the absence of a trapping ligand, dimeric compounds (R = H, **284**; R = SiMe<sub>3</sub>, **285**) result. Compounds **282–285** behave similarly to the carbon analogs, forming zirconacycles upon thermolysis in the presence of alkynes, nitriles, or aldehydes.

#### 4.06.2.1.8 Zirconacyclocumulene complexes

The interaction of tethered diynes with low-valent zirconocenes affords unique metallacyclocumulene structures. Accounts reviewing recent highlights in this area have been published.<sup>144,145</sup> Typically, substituted 1,3-butadiynes are added to a transient zirconocene,  $[(\eta^5\text{-C}_5\text{H}_5)_2\text{Zr}]$  **109**, to yield diverse products, the identity of which are dependent on reaction stoichiometry, conditions, and diyne substitution. For example, reaction of bis(trimethylsilyl)butadiyne with **105** furnishes the zirconacyclocumulene, **286**, arising from the coupling of two diyne molecules (Scheme 44). If 2 equiv. of the zirconocene are added to 1 equiv. of the diyne, carbon–carbon bond cleavage to yield the bridging acetylide complex, **287**, is observed. It is postulated that the  $[\text{SiMe}_3]$  groups activate the inner carbon–carbon bond for cleavage by inductively withdrawing electrons from the  $\beta$ -position. With 1,3-( $\text{Bu}^t$ )-butadiyne, a monomeric zirconocene complex, **288**, has been prepared (Scheme 44).



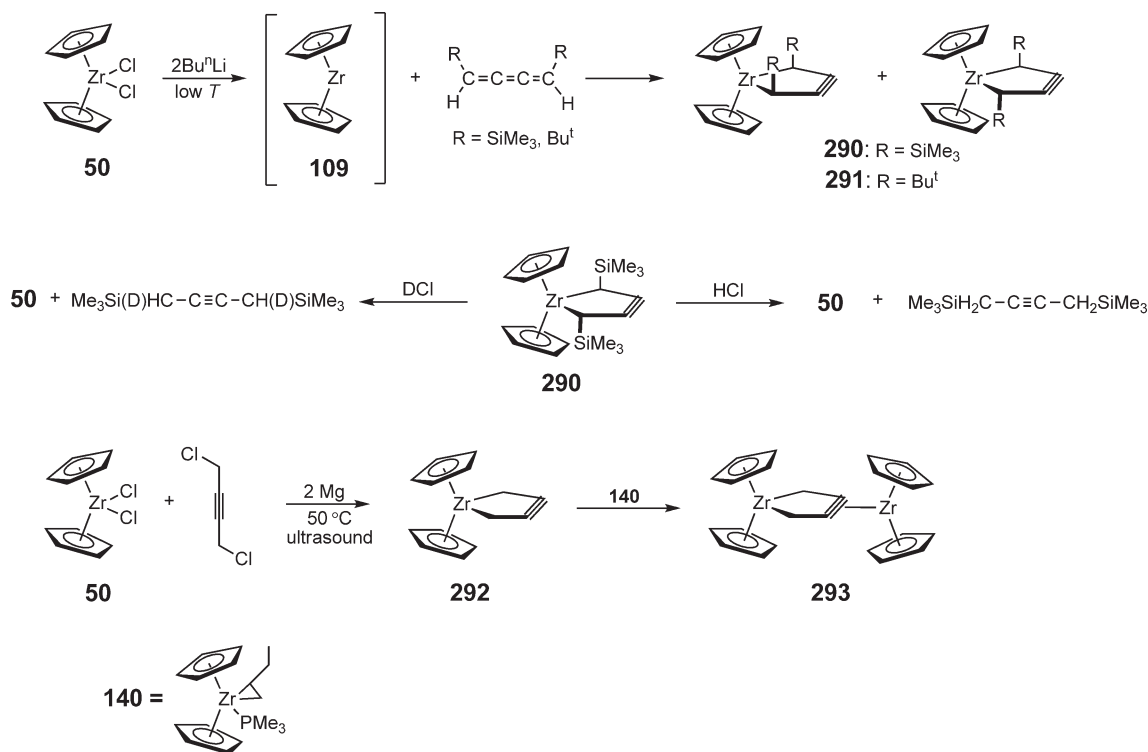
Scheme 44

The cumulene chemistry has also been extended to formally divalent permethylzirconocene complexes.<sup>146</sup> As with the parent cyclopentadienyl complexes, the fate of the reactions are sensitive to the conditions employed. In one case, unique to the permethylated complex, magnesium reduction of  $(\eta^5\text{-C}_5\text{Me}_5)_2\text{ZrCl}_2$  **53** with magnesium metal in the presence of  $\text{Bu}^t\text{C}\equiv\text{C-C}\equiv\text{CBu}^t$  results in the annulation of the pentamethylcyclopentadienyl ligand to furnish **289** (Scheme 44). Monomeric, five-membered zirconacyclocumulenes have also been prepared when the 1,3-butadiyne contains either phenyl or  $\text{SiMe}_3$  substituents.<sup>147</sup> The  $\text{SiMe}_3$  derivative reacts with 2 equiv. of carbon dioxide to yield an unusual cumulenic dicarboxylate compound. The bonding in the zirconacyclocumulenes has been studied using density functional theory (DFT) and supports highly delocalized structures. The presence of metal atoms in the five-membered ring serves to nearly eliminate strain energy.<sup>148,149</sup> Bonding in related dimeric cumulene complexes has also been examined using similar methods.<sup>149</sup>

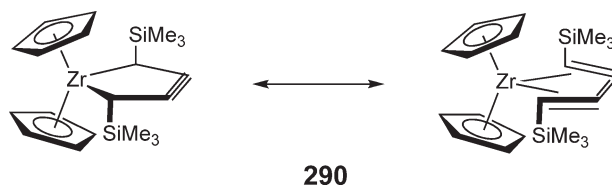
Formally divalent zirconocene fragments have also been used to stabilize purported metallacyclic alkynes, such as cyclopentyne. Treatment of the zirconocene equivalent, **109**, with a series of (*Z*)-1,4-disubstituted-1,2,3-butatrienes,  $[(Z)\text{-RCH=C=C=CHR}]$  ( $\text{R} = \text{SiMe}_3, \text{Bu}^t$ ), yields 1-zirconacyclopent-3-yne compounds as a mixture of *cis*- and *trans*-isomers (Scheme 45).<sup>150</sup> Crystallographic characterization of the *trans*-isomer of **290** ( $\text{SiMe}_3$ ) revealed a planar zirconium four-carbon core with an alkyne carbon-carbon bond distance of  $1.206(7)\text{ \AA}$ , comparable to the  $\text{C}\equiv\text{C}$  distance in cyclooctyne. Examples have also been synthesized where the bulky substituents adjacent to the carbon-carbon triple bond have been removed.<sup>151</sup> In these cases, the compounds are prepared by ultrasonic magnesium reduction of the zirconocene dichloride in the presence of 1,4-dichlorobut-2-yne (Scheme 45). These derivatives are essentially isostructural with **290**, bearing bulky  $\text{SiMe}_3$  substituents. The unsubstituted compound, **292**, reacts with  $(\eta^5\text{-C}_5\text{H}_5)_2\text{Zr}(\eta^2\text{-CH}_2=\text{CHCH}_2\text{CH}_3)(\text{PMe}_3)$  **140** to furnish the bimetallic complex **293**.

A detailed computational study of the bonding in the zirconocene cyclopentyne complex suggests that the metallacyclopentyne depiction does not adequately describe the electronic structure of the complexes.<sup>152</sup> The structure is best represented as a hybrid intermediate between the cumulene complex and the metallacyclopentyne form (Scheme 46).

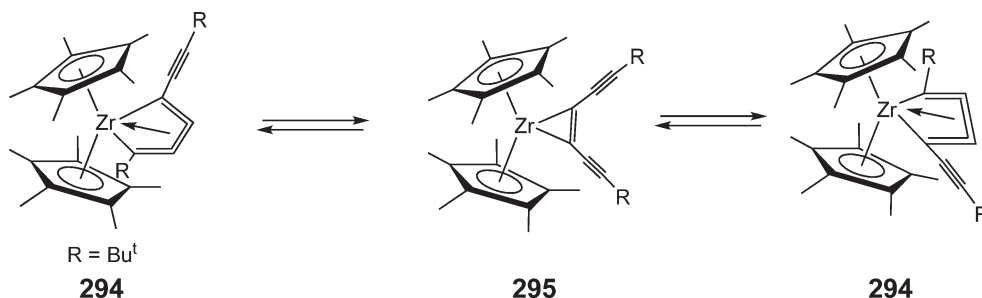
In certain cases, the  $\eta^2$ - and  $\eta^4$ -coordinated polyyne are in equilibrium.<sup>153</sup> For  $(\eta^5\text{-C}_5\text{Me}_5)_2\text{Zr}(\eta^4\text{-Bu}^t\text{C}_4\text{-C}\equiv\text{CBu}^t)$  **294**, a combination of IR and  $^{13}\text{C}$  NMR spectroscopies establish that both the free and unbound alkyne portions of the polyyne are observable. However, EXSY NMR spectra of **294** at  $30^\circ\text{C}$  reveal exchange of the free and coordinated alkyne fragments, demonstrating reversible complexation of the polyyne (Scheme 47).



Scheme 45

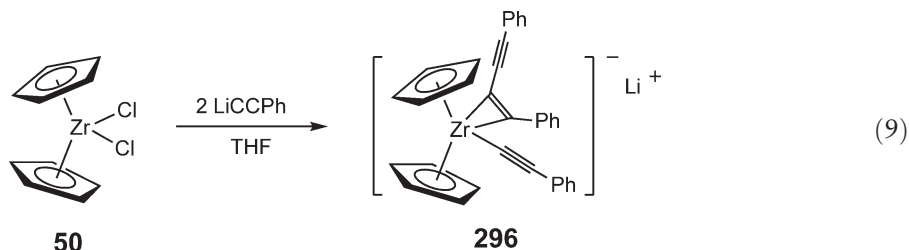


Scheme 46



Scheme 47

Reaction of  $(\eta^5\text{-C}_5\text{H}_5)_2\text{ZrCl}_2$  **50** with 2 equiv. of  $\text{LiC}\equiv\text{CPh}$  furnishes an unusual anionic  $\text{Zr(II)}$  complex,  $\text{Li}[(\eta^5\text{-C}_5\text{H}_5)_2\text{Zr}(\text{C}\equiv\text{CPh})(\eta^2\text{-1,2-PhC}_2\text{C}\equiv\text{CPh})]$  (**296**, Equation (9)), in which a C–C coupling has taken place to generate a diyne fragment. Preliminary mechanistic experiments suggest that a reaction of  $\text{LiC}\equiv\text{CPh}$  with the *in situ* generated zirconium bis(acetylide) complex triggers the C–C coupling event to give **296**.<sup>154</sup> The zirconacyclocumulene complex is not thought to be an intermediate on the pathway to **296**.



#### 4.06.2.1.9 Butadiene complexes

Zirconium and hafnium butadiene complexes have emerged as an important class of molecules, given their interesting ground-state structures and utility in both stoichiometric and catalytic bond forming reactions. In particular, the ability of these compounds to serve as precursors to olefin polymerization catalysts<sup>155–157</sup> has been a major motivation for studying butadiene compounds. This area has been the subject of recent comprehensive reviews.<sup>158,159</sup> The chemistry of zirconium and hafnium butadiene complexes is, for the most part, dominated by bis(cyclopentadienyl) compounds<sup>160,161</sup> although those with calixarene,<sup>162,163</sup> macrocyclic bis(amido)phosphines,<sup>164</sup> mixed cyclopentadienyl–amidinate<sup>165,166</sup> monocyclopentadienyl,<sup>167–171</sup> indenyl,<sup>172</sup> and *ansa*-cyclopentadienyl–amido<sup>173,174</sup> ligands have been prepared and characterized.

Using the parent zirconocene–butadiene complex as a representative example, a typical bonding situation in these types of molecules is presented in Scheme 48. For **297**, equilibration between the *s-trans* and the *s-cis* isomers occurs with a barrier of  $23\text{ kcal mol}^{-1}$  at 283 K. The  $\eta^2$ -olefin complex is believed to be a high-energy intermediate on the interconversion reaction surface. Significantly, structural data indicates that the *s-cis* complexes are best described as  $\text{Zr(IV)}$  compounds with a  $\sigma^2$ ,  $\pi$  ligand.<sup>158,175</sup> The dynamic NMR measurements have also been extended to *ansa*-zirconocene and hafnocene butadiene complexes.<sup>176</sup> Moreover, photoelectron spectroscopy has been used to determine the relative energetics of the two isomers for *ansa*-metallocenes.<sup>177</sup>

Butadiene complexes display a wealth of interesting reactivity including C–H and N–H activation,<sup>160</sup> use in the synthesis of metal-bound enamines,<sup>178</sup> oxidative addition of hypervalent organosulfur compounds to yield

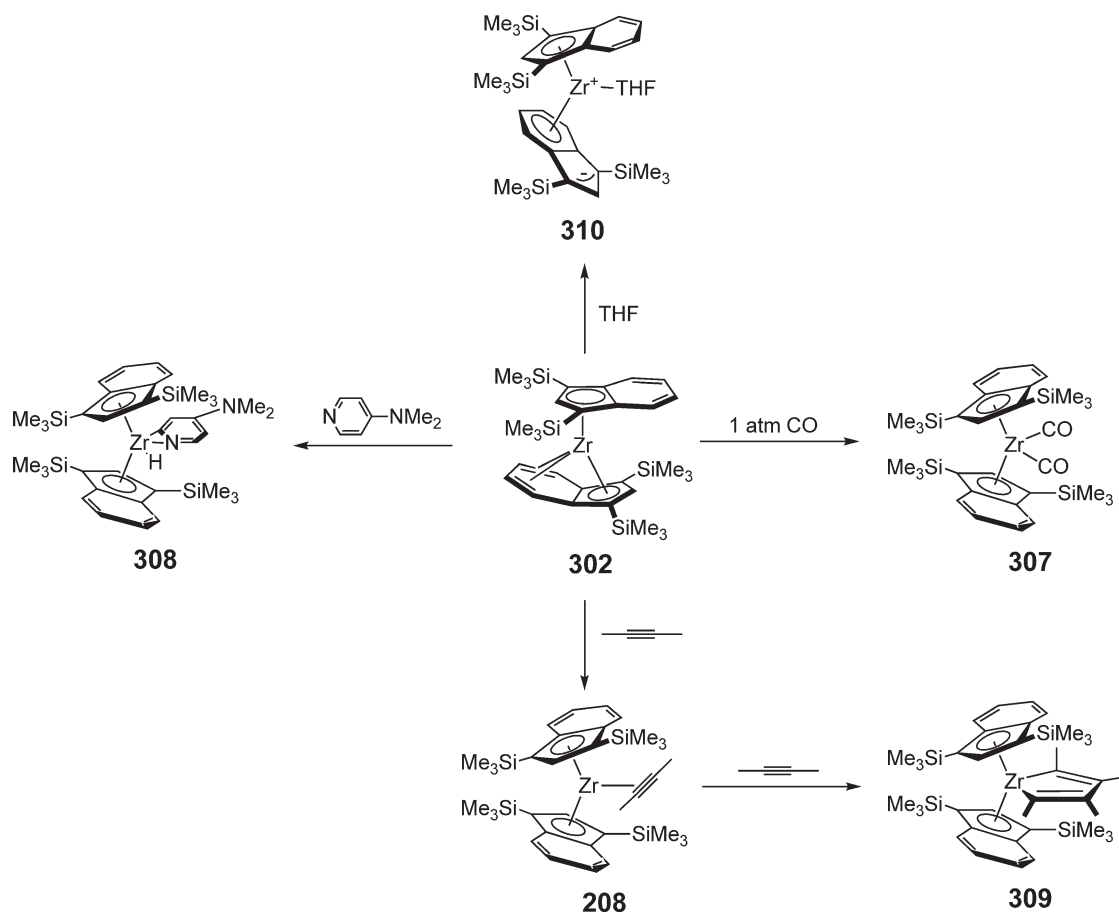


Both alkane reductive elimination and alkali metal reduction reactions have been used to prepare a family of bis(indenyl)zirconium sandwich complexes.<sup>104</sup> Crystallographic characterization of the  $\text{Pr}^{\text{I}}$  **304** and the  $\text{SiMe}_2\text{Bu}^{\text{t}}$  variants establishes an unprecedented  $\eta^9$ -hapticity of the indenyl ligand where all nine carbons of the carbocycle are engaged in bonding with the zirconium center. Interestingly, this coordination mode was computationally predicted before structural confirmation.<sup>183</sup>

Variable-temperature NMR studies establish that the  $\eta^5$ - and  $\eta^9$ -indenyl ligands interchange rapidly in solution with barriers ranging between 14 and 20  $\text{kcal mol}^{-1}$ .<sup>104</sup> Computational studies suggest that the ring exchange occurs through an  $\eta^5$ ,  $\eta^5$ -bis(indenyl)zirconium sandwich intermediate ( $\text{R} = \text{SiMe}_3$ , **305**;  $\text{R} = \text{CHMe}_2$ , **306**) with a singlet ground state (Scheme 49).<sup>183</sup> Preparation of “mixed ring” sandwiches establishes a thermodynamic preference for alkylated indenyl ligands to adopt  $\eta^9$ -coordination, although the other, minor haptomer is kinetically accessible.

Reactivity studies reveal that the bis(indenyl)zirconium sandwich complexes serve as isolable, modular precursors to the rich chemistry of divalent “zirconocene.” Addition of 1 atm of carbon monoxide generates the bis(indenyl)-zirconocene dicarbonyl complex, **307**, while treatment with *N,N*-dimethylaminopyridine results in C–H activation to form the zirconocene pyridyl hydride complex **308**. Crystallographic characterization of both complexes as well as multinuclear NMR spectroscopy establishes that the more familiar  $\eta^5$ ,  $\eta^5$  hapticity for the indenyl ligands has been restored. Alkyne coupling reactions are also observed as addition of 2-butyne to **302** allows observation of the alkyne complex, **208**, and ultimately the zirconacyclopentadiene **309** (Scheme 50).<sup>104</sup>

Addition of THF to **302** results in an unusual haptotropic rearrangement of the  $\eta^9$ -indenyl ligand to yield  $(\eta^5\text{-C}_9\text{H}_5\text{-1,3-(SiMe}_3)_2)(\eta^6\text{-C}_9\text{H}_5\text{-1,3-(SiMe}_3)_2)\text{Zr(THF)}$  **310**, where the zirconium has migrated to the benzo ring of one indenyl ligand. Crystallographic characterization of **310** reveals significant buckling of the  $\eta^6$ -indenyl ligand,



Scheme 50

suggesting an important contribution from the zirconium(IV) canonical form.<sup>182</sup> Computational studies indicate that the THF-induced haptotropic rearrangement occurs through an associative interchange-type mechanism with a low barrier, consistent with the experimental observation of facile reaction at ambient temperature.<sup>183</sup>

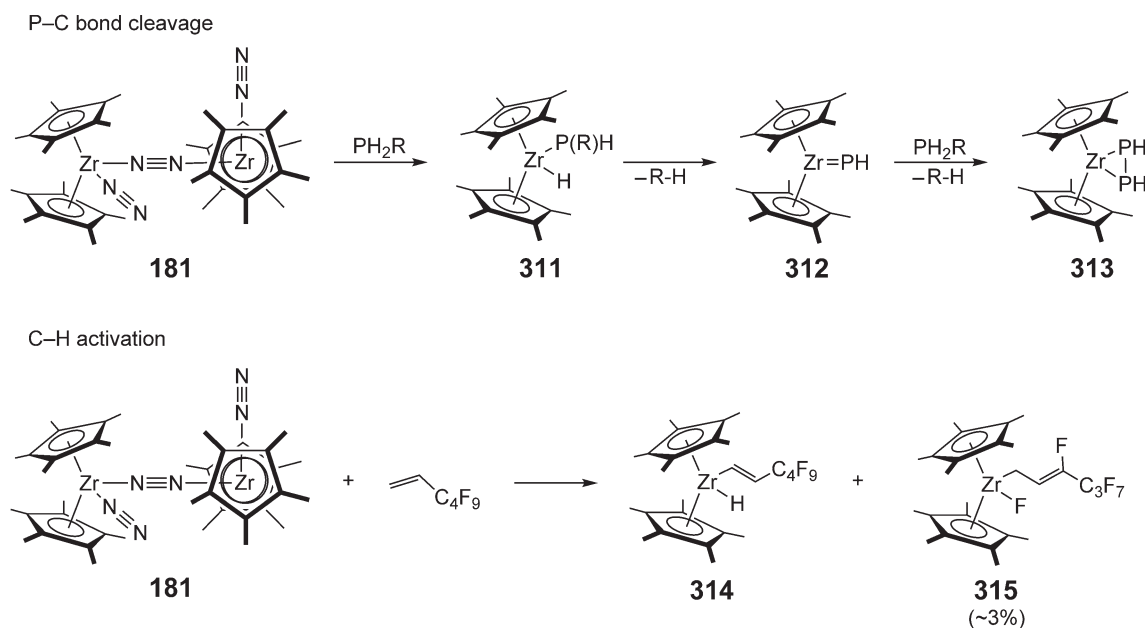
#### 4.06.2.2 Zirconium/Hafnium(II) Dinitrogen Complexes

##### 4.06.2.2.1 Bis(cyclopentadienyl)dinitrogen complexes

There has been renewed interest in zirconocene and hafnocene dinitrogen complexes for both  $N_2$  fixation and as a means for accessing the rich chemistry of the divalent metals. With respect to the latter,  $[(\eta^5\text{-C}_5\text{Me}_5)_2\text{Zr}(\eta^1\text{-N}_2)]_2$  ( $\mu_2, \eta^1, \eta^1\text{-N}_2$ ) **181** induces P–C bond cleavage upon reaction with 2 equiv. of the primary phosphine,  $\text{PH}_2(\text{C}_6\text{H}_2\text{-2,4,6-Bu}^t_3)$ , to yield  $(\eta^5\text{-C}_5\text{Me}_5)_2\text{Zr}(\text{PH})_2$  (**313**, Scheme 51).<sup>184</sup> It is proposed that the reaction proceeds via initial oxidative addition of a P–H bond followed by P–C bond cleavage and liberation of alkane, a consequence of the steric environment about the zirconium. Subsequent P–H activation and alkane liberation affords the observed product. Loss of dinitrogen and formal oxidative addition of vinylic C–H bonds has also been reported. Addition of nonafluorohexene to **181** furnishes predominantly (*E*)- $(\eta^5\text{-C}_5\text{Me}_5)_2\text{Zr}(\text{CH}=\text{CHC}_4\text{F}_9)\text{H}$  **314** along with a small amount (~3%) of (*Z*)- $(\eta^5\text{-C}_5\text{Me}_5)_2\text{Zr}(\text{CH}_2\text{CH}=\text{CFC}_3\text{F}_7)\text{F}$  **315**, arising from activation of an internal C–H bond followed by rearrangement (Scheme 51).<sup>185</sup>

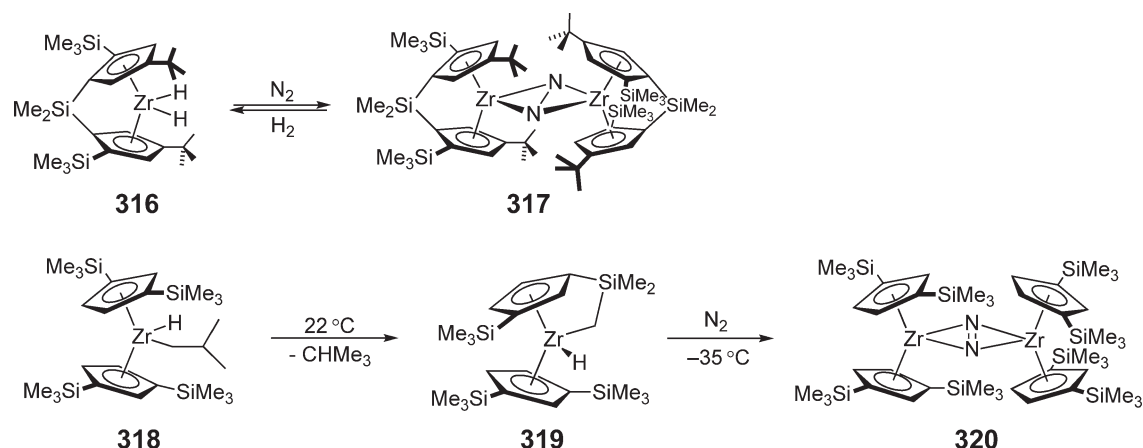
Examples of “side-on” bound zirconocene dinitrogen complexes have also been prepared. Reductive elimination of dihydrogen from the monomeric, *ansa*-zirconocene dihydride,  $\{\text{rac-Me}_2\text{Si}(\eta^5\text{-C}_5\text{H}_2\text{-2-SiMe}_3\text{-4-Bu}^t)_2\}\text{ZrH}_2$  **316**, in the presence of 1 atm of  $N_2$  furnishes  $[\{\text{rac-Me}_2\text{Si}(\eta^5\text{-C}_5\text{H}_2\text{-2-SiMe}_3\text{-4-Bu}^t)_2\}\text{Zr}]_2(\mu_2, \eta^2, \eta^2\text{-N}_2)$  (**317**, Scheme 52).<sup>186</sup> Single crystal X-ray diffraction establishes a side-on bound dinitrogen ligand with an N–N bond length of 1.241(3) Å. Similarly, alkane reductive elimination from the silylated zirconocene isobutyl hydride complex,  $(\eta^5\text{-C}_5\text{H}_3\text{-1,3-(SiMe}_3)_2\text{Zr}(\text{CH}_2\text{CHMe}_2)\text{H}$  **318**, initially yields the zirconocene cyclometalated hydride, **319**, which yields the side-on bound dinitrogen complex,  $[(\eta^5\text{-C}_5\text{H}_3\text{-1,3-(SiMe}_3)_2\text{Zr})_2(\mu_2, \eta^2, \eta^2\text{-N}_2)]$  **320**, upon exposure to  $N_2$  at  $-35^\circ\text{C}$  (Scheme 52).<sup>187</sup>

While the reduction of the “mixed ring” zirconocene dichloride,  $(\eta^5\text{-C}_5\text{Me}_5)(\eta^5\text{-C}_5\text{Me}_4\text{H})\text{ZrCl}_2$  **321**, furnishes the weakly activated “end-on” dinitrogen complex,  $[(\eta^5\text{-C}_5\text{Me}_5)(\eta^5\text{-C}_5\text{Me}_4\text{H})\text{Zr}(\eta^1\text{-N}_2)]_2(\mu_2, \eta^1, \eta^1\text{-N}_2)$  **322**,<sup>188</sup> an analogous procedure with the homoleptic zirconocene dichloride,  $(\eta^5\text{-C}_5\text{Me}_4\text{H})_2\text{ZrCl}_2$  **173**, produces the side-on dinitrogen complex  $[(\eta^5\text{-C}_5\text{Me}_4\text{H})_2\text{Zr}]_2(\mu_2, \eta^2, \eta^2\text{-N}_2)$  **323** (Scheme 53).<sup>189</sup> Significantly, the solid-state structure of **323** revealed a strongly activated  $N_2$  ligand with an elongated N–N bond length of 1.377(3) Å, consistent with an  $[\text{N}_2]^{4-}$  hydrazido-type ligand.

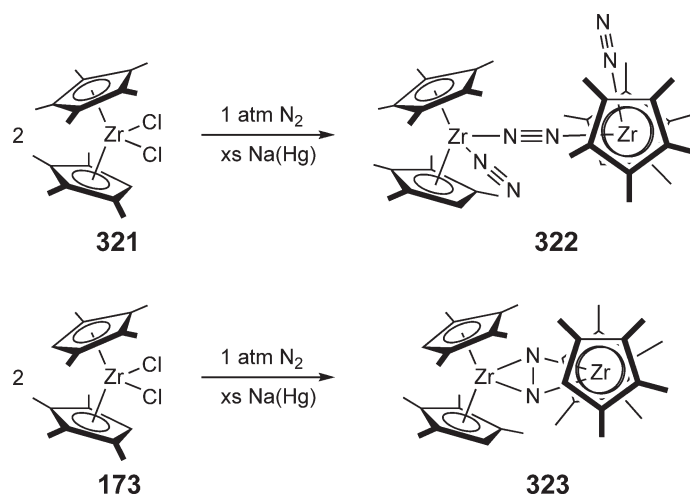


Scheme 51





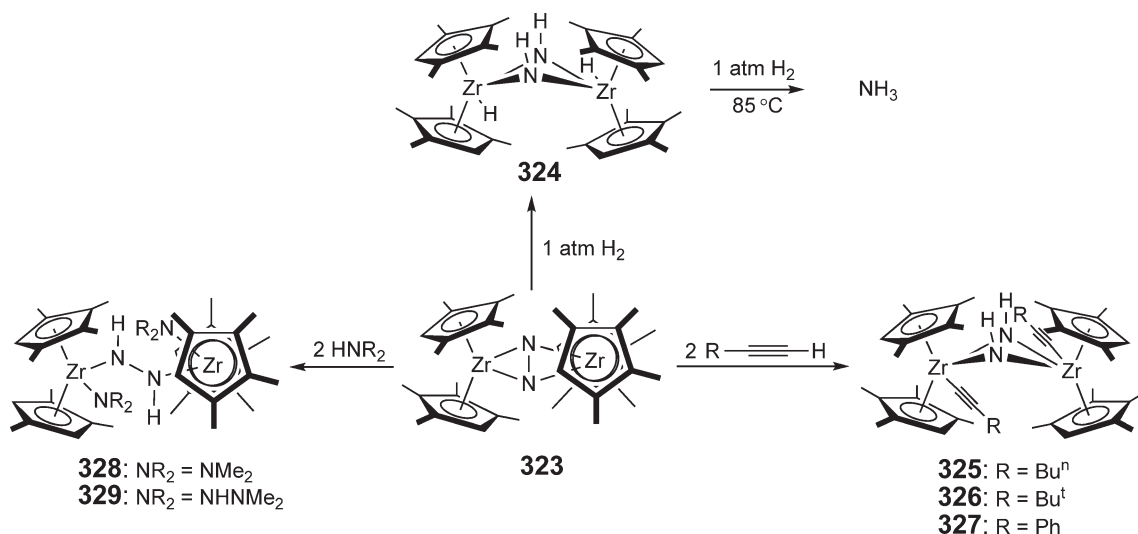
Scheme 52



Scheme 53

The side-on bound dinitrogen complex **323** serves as a platform for several nitrogen fixation reactions. Exposure of **323** to 1 atm of  $\text{H}_2$  results in rapid hydrogenation of the  $\text{N}_2$  ligand to afford the hydrido zirconocene diazenido complex,  $[(\eta^5\text{-C}_5\text{Me}_4\text{H})_2\text{ZrH}]_2(\mu_2, \eta^2, \eta^2\text{-N}_2\text{H}_2)$  **324**, providing the first example of  $\text{N}_2$  hydrogenation to coordinated hydrazine in solution (Scheme 54).<sup>189</sup> Additional hydrogenation at  $85^\circ\text{C}$  liberates small quantities of free ammonia along with a range of zirconium products derived from the reaction of  $\text{NH}_3$  with the organometallic reactants and products. The origin of this unique reactivity has been investigated through a combination of isotopic labeling experiments and DFT calculations. The results of these studies indicate that  $\text{N}_2$  hydrogenation arises from the “twisted” ground-state structure of **323** which imparts imido-like character to the zirconium–nitrogen bonds, facilitating 1,2-addition of dihydrogen.<sup>188</sup> (For references on 1,2-addition see Refs: 190, 190a, and 190b.)

The imido-like reactivity of **323** has been extended to include terminal alkynes. Addition of 2 equiv. of 1-hexyne, *tert*-butylacetylene, or phenylacetylene to **323** furnishes the acetylide zirconocene diazenido compounds,  $[(\eta^5\text{-C}_5\text{Me}_4\text{H})_2\text{Zr}(\text{C}\equiv\text{CR})]_2(\mu_2, \eta^2, \eta^2\text{-N}_2\text{H}_2)$  ( $\text{R} = \text{Bu}^n$ , **325**;  $\text{Bu}^t$ , **326**;  $\text{Ph}$ , **327**) (Scheme 54).<sup>191</sup> Variable-temperature  $^1\text{H}$  and  $^{15}\text{N}$  NMR spectroscopy reveal dynamic interconversion between the “end-on” and “side-on” diazenido compounds, where the side-on complex is favored at lower temperatures and in the solid state, while at higher temperatures significant concentrations of the end-on isomer are detected. Dinitrogen functionalization with protic sources such as amines and hydrazines has also been described, affording solely the end-on diazenido complexes  $[(\eta^5\text{-C}_5\text{Me}_4\text{H})_2\text{Zr}(\text{NR}_2)]_2(\mu_2, \eta^1, \eta^1\text{-N}_2\text{H}_2)$  ( $\text{NR}_2 = \text{NMe}_2$ , **328**;  $\text{NHNMe}_2$ , **329**). Addition of stronger acids such as ethanol, water, or  $\text{HCl}$  produces free hydrazine.



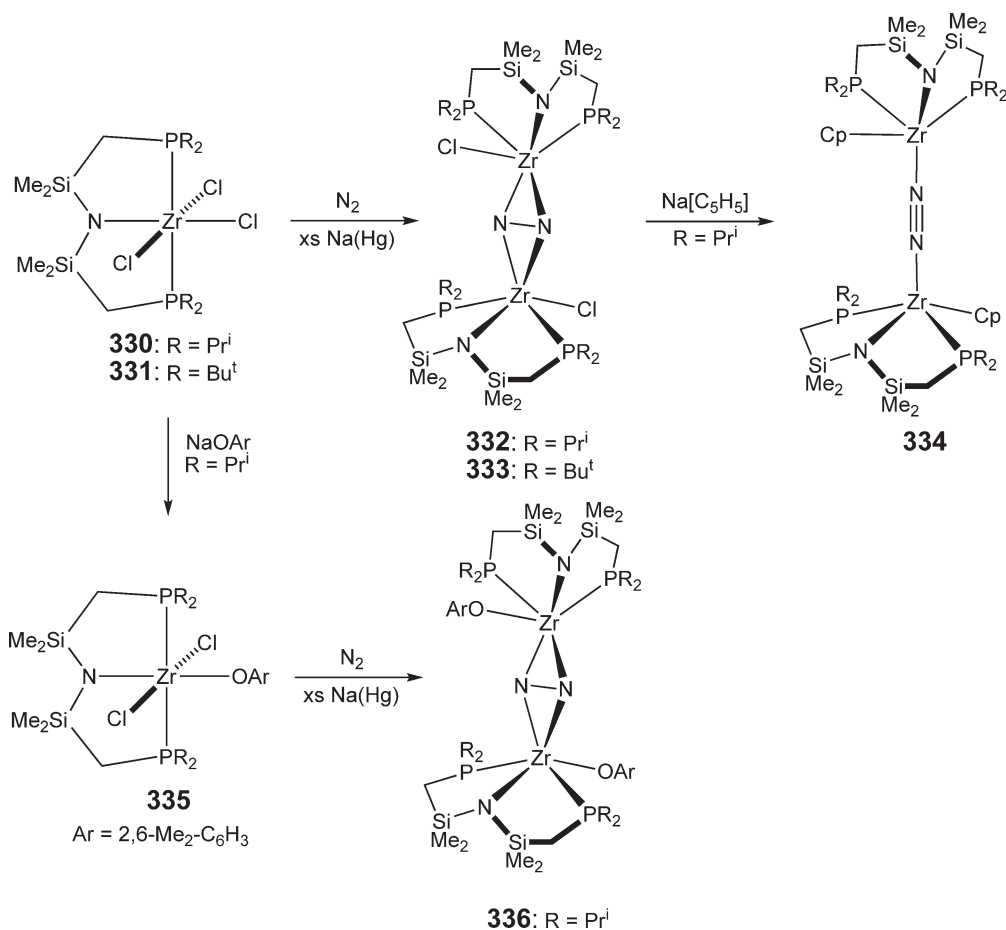
Scheme 54

#### 4.06.2.2.2 Non-cyclopentadienyl dinitrogen complexes

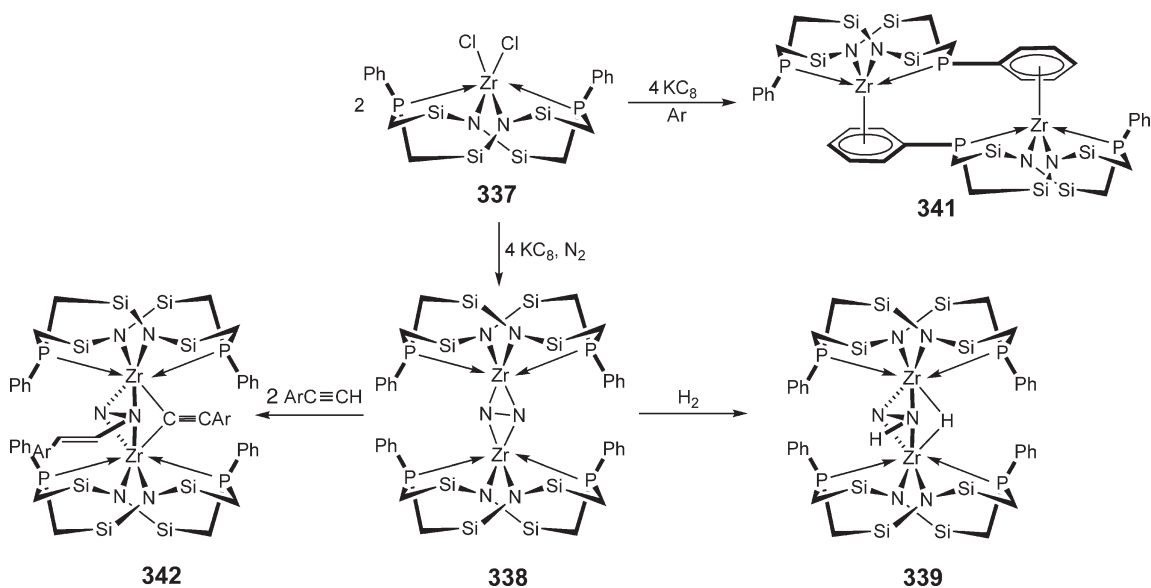
Considerable interest has been devoted to the chemistry of “non-cyclopentadienyl” zirconium dinitrogen complexes. This area has been the subject of several recent, comprehensive reviews.<sup>192–196</sup> In particular, phosphine-amido ligands have proven particularly effective for stabilizing a range of strongly activated dinitrogen compounds. For example, reduction of  $[\text{N}(\text{SiMe}_2\text{CH}_2\text{PR}_2)_2]\text{ZrCl}_3$  ( $\text{R} = \text{Pr}^i$ , **330**;  $\text{Bu}^t$ , **331**) with sodium amalgam furnishes the side-on bound dinitrogen complexes, **332** and **333**, respectively (Scheme 55).<sup>197</sup> Crystallographic characterization of the isopropyl-substituted compound established a strongly activated dinitrogen ligand with an N–N distance of 1.548(7) Å. Analysis of the molecular orbitals of the side-on compounds revealed that the amide donor on the tridentate ligand is oriented by the phosphines to form a  $\pi$ -bond to the zirconium, thereby removing one of the  $\pi$ -interactions between the zirconium and the  $\text{N}_2$  ligand which typically favors end-on coordination. Replacement of the chloride with a cyclopentadienyl ligand changes the hapticity of the  $\text{N}_2$  ligand to end-on, a result of overlap of the cyclopentadienyl molecular orbitals with a zirconium  $d$ -orbital that would otherwise form a  $\delta$ -bond with the side-on bound  $\text{N}_2$  ligand. Side-on dinitrogen coordination is also seen in the phenoxy-substituted compound  $[\text{N}(\text{SiMe}_2\text{CH}_2\text{PR}_2)_2](2,6\text{-Me}_2\text{-C}_6\text{H}_3\text{O})\text{Zr}(\mu_2, \eta^2, \eta^2\text{-N}_2)$  ( $\text{R} = \text{Pr}^i$ , **336**).<sup>198</sup> As in the chloride complex, an elongated N–N bond distance of 1.528(7) Å is observed. A detailed spectroscopic study on all three dinitrogen complexes and their vibrational spectroscopy has been reported.<sup>199</sup>

Modification of the  $\text{L}_2\text{X}$  bis(phosphine)amide ligand to an  $\text{L}_2\text{X}_2$  bis(phosphine)diamide macrocycle has produced interesting dinitrogen functionalization chemistry. Treatment of the side-on bound dinitrogen complex **338** with dihydrogen results in partial hydrogenation of the  $\text{N}_2$  ligand to form one N–H and a bridging zirconium hydride,<sup>200</sup> the structure of which has been confirmed by neutron diffraction (**339**, Scheme 56).<sup>201</sup> Dinitrogen functionalization with primary silanes has also been reported.<sup>200</sup> The vibrational and electronic structure has also been analyzed.<sup>202</sup> An N–N stretching band centered at  $775\text{ cm}^{-1}$  has been assigned on the basis of resonance Raman spectroscopy and isotopic labeling experiments. A DFT study on the ground-state structure of the compound suggests that bending of the  $\text{Zr}_2\text{N}_2$  core rotates the axial amide lone pairs by  $90^\circ$  and is approximately  $11\text{ kcal mol}^{-1}$  lower in energy than the planar core, owing to a more uniform distribution of electron density over the zirconium centers and nitrogen atoms. The mechanism of hydrogenation has been studied on the model complex,  $[(\text{p}_2\text{n}_2)\text{Zr}]_2(\mu_2, \eta^2, \eta^2\text{-N}_2)$  (**340**:  $\text{p}_2\text{n}_2 = (\text{PH}_3)_2(\text{NH}_2)_2$ ), using DFT. The calculations demonstrate that the reaction proceeds through a “metathesis-like” or cycloaddition transition state, where the Zr–H and N–H bonds are formed simultaneously. This initial product rearranges to the observed product, and the entire reaction is calculated to be exothermic by  $13\text{--}15\text{ kcal mol}^{-1}$ .<sup>203</sup> Subsequent DFT studies suggest that addition of a second equivalent of  $\text{H}_2$  is thermodynamically favored but not observed experimentally due to a high kinetic barrier.<sup>204</sup>

Performing the reduction of the dichloride under an argon rather than dinitrogen atmosphere affords a phosphorus-bridged dizirconium complex where the bridging phenyl groups are reduced to bis(allyl) anions (**341**, Scheme 56).<sup>205</sup> Addition of aryl alkynes to **338** offers another method of dinitrogen functionalization,



Scheme 55

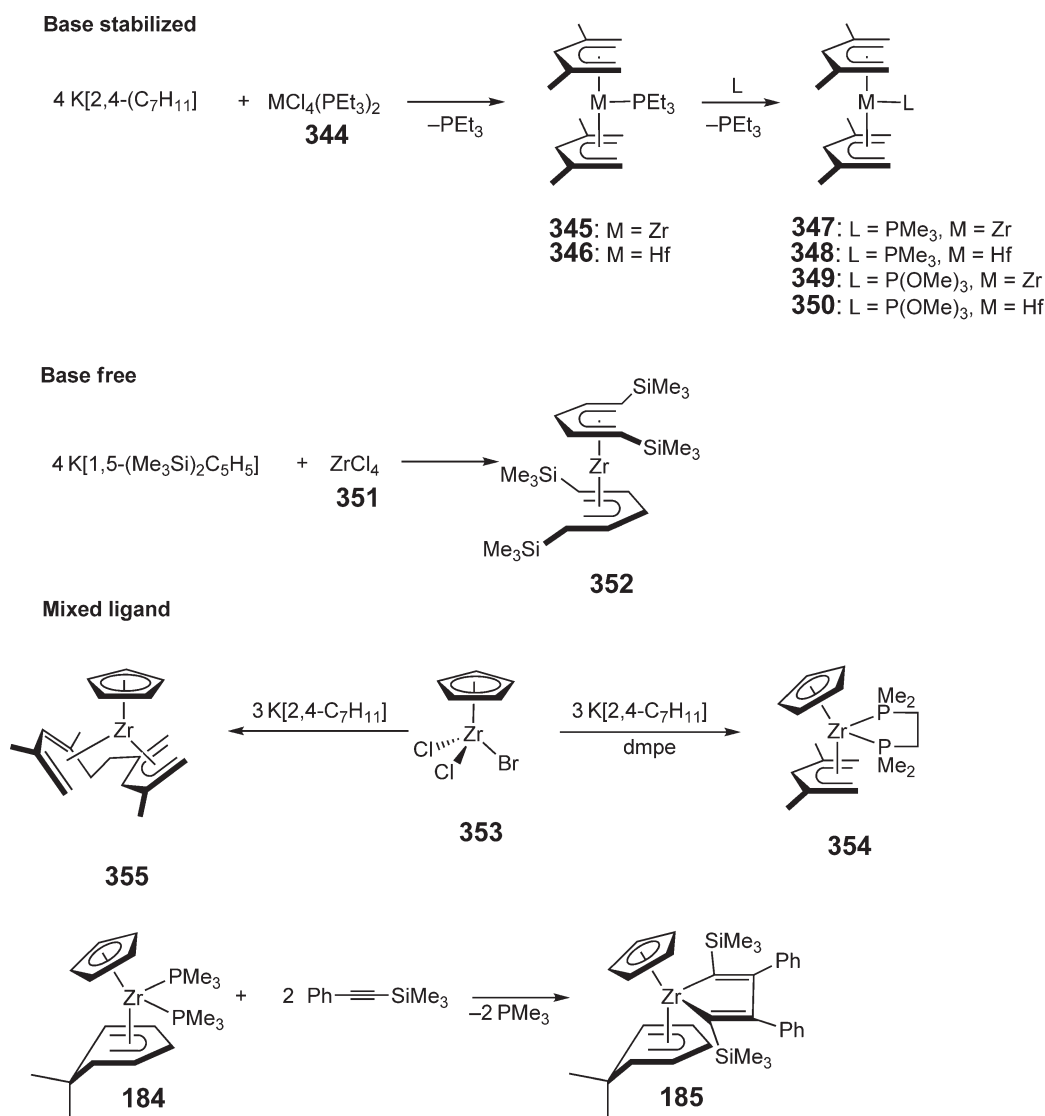


Scheme 56

where a nitrogen–carbon bond is formed to yield  $[(P_2N_2)Zr]_2(\mu, \eta^2, \eta^2-N_2CCAr)(\mu-CCAr)$  **342**.<sup>206</sup> It is proposed that dinitrogen functionalization occurs by cycloaddition of the alkyne to the side-on dinitrogen complex followed by protonation by the remaining equivalent of the terminal acetylene. The analogous hafnium dinitrogen complex,  $[(P_2N_2)Hf]_2(\mu, \eta^2, \eta^2-N_2)$  **343**, has been prepared by reduction of the corresponding diiodide compound.<sup>207</sup>

#### 4.06.2.3 Pentadienyl Complexes

The formally divalent zirconium and hafnium pentadienyl complexes,  $(2,4-C_7H_{11})_2M(PEt_3)_3$  ( $M = Zr$ , **345**;  $Hf$ , **346**), have been synthesized by reductive metallation of  $MCl_4(PEt_3)_3$  **344** with 4 equiv. of  $K(2,4-C_7H_{11})$  (Scheme 57).<sup>208,209</sup> For both metals, the compounds are diamagnetic and undergo rapid exchange with small phosphines and phosphites such as  $PMe_3$  and  $P(OMe)_3$ , respectively. This synthetic procedure has been extended to include base-free bis(pentadienyl) zirconium compounds by incorporation of sterically demanding substituents in



Scheme 57

the ancillary ligand. Addition of 4 equiv. of  $K[1,5-(\text{Me}_3\text{Si})_2\text{C}_5\text{H}_5]$  to  $\text{ZrCl}_4$  **351** furnishes the diamagnetic, formally 14-electron compound  $[1,5-(\text{Me}_3\text{Si})_2\text{C}_5\text{H}_5]_2\text{Zr}$  **352**.<sup>210</sup>

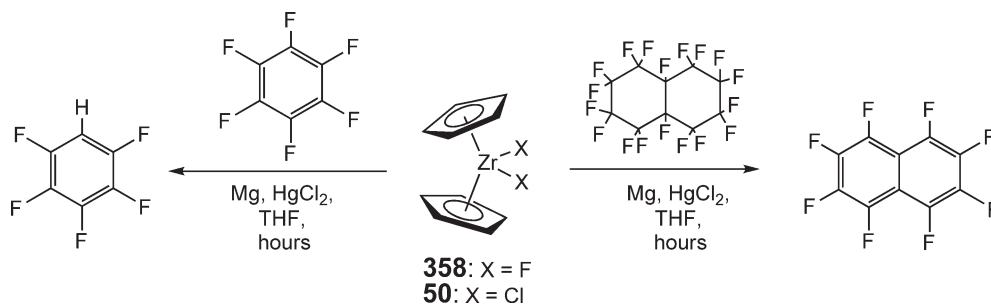
Mixed cyclopentadienyl–pentadienyl compounds have also been prepared. Addition of 3 equiv. of  $K[2,4-\text{C}_7\text{H}_{11}]$  to  $(\eta^5-\text{C}_5\text{H}_5)\text{ZrCl}_2\text{Br}$  **353** in the presence of 1,2-bis(dimethyl phosphino)ethane (dmpe) furnishes  $(\eta^5-\text{C}_5\text{H}_5)(2,4-\text{C}_7\text{H}_{11})\text{Zr}(\text{dmpe})$  **354** which has been characterized by X-ray diffraction.<sup>211</sup> Performing the same procedure without dmpe yields the unusual  $(\eta^5-\text{C}_5\text{H}_5)(\text{C}_{14}\text{H}_{21})\text{Zr}$  **355**, formed from coupling of two pentadienyl ligands followed by formal loss of one hydrogen atom in the form of free ligand. Structural data on **352** indicate that the diene coordination is more appropriately described as a  $\text{Zr}(\text{IV})$  ene–diyl complex rather than a  $\text{Zr}(\text{II})$  compound (Scheme 57). Related divalent zirconium complexes with cyclopentadienyl–dimethylcyclohexadienyl (dmch) ligands have also been prepared.<sup>100</sup> The bis(phosphine) complex  $(\eta^5-\text{C}_5\text{H}_5)(\text{dmch})\text{Zr}(\text{PMe}_3)_2$  **184** reacts readily with 2 equiv. of  $\text{PhC}\equiv\text{CSiMe}_3$  to yield the corresponding zirconacyclopentadiene complex **185** (Scheme 57).

#### 4.06.2.4 Zirconocene-mediated C–F Activation

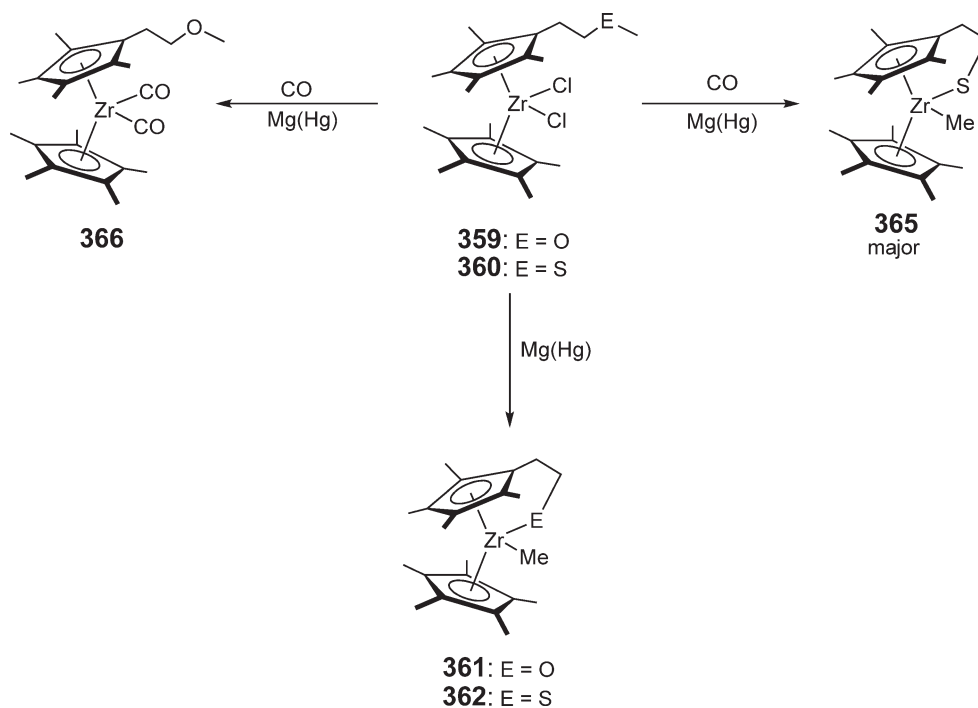
The reducing nature of formally divalent zirconocene complexes makes them attractive candidates for the activation of strong bonds by oxidative addition and other mechanistic pathways. Defluorination of both aromatic and aliphatic fluorocarbons has been accomplished by magnesium reduction of zirconocene dihalide complexes in the presence of the appropriate substrate (Scheme 58). In addition, the C–F bond activation procedure is also effective in the presence of  $\text{PMe}_3$  as well as with *in situ* generated zirconocene olefin complexes.<sup>212,213</sup> While oxidative addition reactions are likely, electron transfer pathways are also viable alternatives. C–F activation of a pentafluorophenyl ligand has also been reported and is thought to occur by oxidative addition of a  $\text{Zr}(\text{II})$  center generated by disproportionation of a  $\text{Zr}(\text{III})$  alkyl complex.<sup>214</sup> In related zirconium(IV) hydride complexes  $[(\eta^5-\text{C}_5\text{H}_5)_2\text{ZrH}_2]_n$  **356** and  $(\eta^5-\text{C}_5\text{H}_5)_3\text{ZrH}$  **357**, generation of a transient zirconium sandwich  $[(\eta^5-\text{C}_5\text{H}_5)_2\text{Zr}]$  **109** capable of C–F bond activation appears unlikely.<sup>215</sup>

#### 4.06.2.5 Miscellaneous Reduction Chemistry of Zirconium

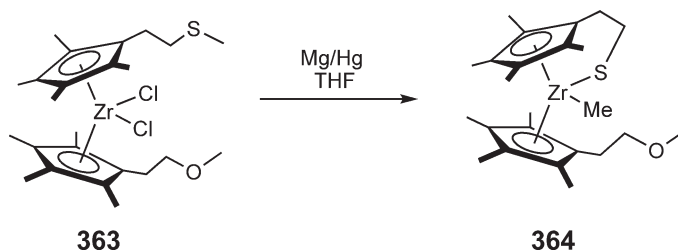
Magnesium amalgam reduction of  $(\eta^5-\text{C}_5\text{Me}_5)(\eta^5-\text{C}_5\text{Me}_4\text{CH}_2\text{CH}_2\text{OMe})\text{ZrCl}_2$  **359** and its thioether analog, **360**, results in E–R cleavage (Scheme 59).<sup>216</sup> When the mixed ether, thioether zirconocene dichloride, **363**, is reduced under similar conditions, the major product arises from cleavage of the weaker carbon–sulfur bond (Equation (10)). Interestingly, performing the reduction of the thioether substituted zirconocene **360** in the presence of CO furnishes predominantly the C–S cleavage product, with only small amounts of the corresponding zirconocene dicarbonyl being observed (Scheme 59).



Scheme 58



Scheme 59



(10)

## References

1. Troyanov, S. J. *Organomet. Chem.* **1994**, 475, 139.
2. Calderazzo, F.; Pampaloni, G. J. *Organomet. Chem.* **1995**, 500, 47.
3. Poli, R. *Chem. Rev.* **1996**, 96, 2135.
4. King, W. A.; Di Bella, S.; Lanza, G.; Khan, K.; Duncalf, D. J.; Cloke, F. G. N.; Fragala, I. L.; Marks, T. J. *J. Am. Chem. Soc.* **1996**, 118, 627.
5. Jang, M.; Ellis, J. E. *Angew. Chem., Int. Ed. Engl.* **1994**, 33, 1973.
6. Rosa, P.; Mézailles, N.; Ricard, L.; Mathey, F.; Le Floch, P. *Angew. Chem. Int. Ed.* **2000**, 39, 1823.
7. Ellis, J. E. *Organometallics* **2003**, 22, 3322.
8. Ellis, J. E.; Yuen, P.; Jang, M. J. *Organomet. Chem.* **1996**, 507, 283.
9. Ellis, J. E.; Frerichs, S. R.; Stein, B. K. *Organometallics* **1993**, 12, 1048.
10. Zhou, M.; Andrews, L. J. *Am. Chem. Soc.* **2000**, 122, 1531.
11. Zachmanoglou, C. E.; Docrat, A.; Bridgewater, B. M.; Parkin, G.; Brandow, C. G.; Bercaw, J. E.; Jardine, C. N.; Lyall, M.; Green, J. C.; Keister, J. B. *J. Am. Chem. Soc.* **2002**, 124, 9525.
12. Howard, W. A.; Trnka, T. M.; Parkin, G. *Organometallics* **1995**, 14, 4037.
13. Howard, W. A.; Parkin, G.; Rheingold, A. L. *Polyhedron* **1995**, 14, 25.
14. Howard, W. A.; Waters, M.; Parkin, G. *J. Am. Chem. Soc.* **1993**, 115, 4917.
15. Howard, W. A.; Trnka, T. M.; Waters, M.; Parkin, G. *J. Organomet. Chem.* **1997**, 528, 95.
16. Howard, W. A.; Parkin, G. *J. Am. Chem. Soc.* **1994**, 116, 606.

17. Howard, W. A.; Parkin, G. *J. Organomet. Chem.* **1994**, 472, C1.
18. Howard, W. A.; Trnka, T. M.; Parkin, G. *Inorg. Chem.* **1995**, 34, 5900.
19. Buzin, F.-X.; Nief, F.; Ricard, L.; Mathey, F. *Organometallics* **2002**, 21, 259.
20. Fryzuk, M. D.; Mylvaganam, M.; Zaworotko, M. J.; MacGillivray, L. R. *Organometallics* **1996**, 15, 1134.
21. Bazan, G. C.; Cotter, W. D.; Komon, Z. J. A.; Lee, R. A.; Lachicotte, R. J. *J. Am. Chem. Soc.* **2000**, 122, 1371.
22. Ho, J.; Breen, T. L.; Ozarowski, A.; Stephan, D. W. *Inorg. Chem.* **1994**, 33, 865.
23. McNeil, K.; Bergman, R. G. *J. Am. Chem. Soc.* **1999**, 121, 8260.
24. Fandos, R.; Lanfranchi, M.; Otero, A.; Pellinghelli, M. A.; Ruiz, M. J.; Teuben, J. H. *Organometallics* **1997**, 16, 5283.
25. Ashe, A. J.; Al-Ahmad, S.; Kampf, J. W.; Young, V. G. *Angew. Chem., Int. Ed. Engl.* **1997**, 36, 2014.
26. Ashe, A. J.; Al-Ahmad, S.; Kampf, J. W. *Organometallics* **1999**, 18, 4234.
27. Troyanov, S. I.; Meetsma, A.; Teuben, J. H. *Inorg. Chim. Acta* **1998**, 271, 180.
28. Broene, R. D.; Buchwald, S. L. *Science* **1993**, 261, 1696.
29. Negishi, E.-I.; Takahashi, T. *Acc. Chem. Res.* **1994**, 27, 124.
30. Negishi, E.-I.; Takahashi, T. *Bull. Chem. Soc. Jpn.* **1998**, 71, 755.
31. Fujita, K.; Yorimitsu, H.; Oshima, K. *Chem. Rec.* **2004**, 4, 110.
32. Hoveyda, A. H.; Morken, J. P. *Angew. Chem., Int. Ed. Engl.* **1996**, 35, 1262.
33. Marek, I. *J. Chem. Soc., Perkins Trans. 1* **1999**, 535.
34. Negishi, E.-I. *Dalton Trans.* **2005**, 827.
35. Yamazaki, A.; Nishihara, Y.; Nakajima, K.; Hara, R.; Takahashi, T. *Organometallics* **1999**, 18, 3105.
36. Licht, E. H.; Alt, H. G.; Milius, W.; Abu-Orabi, S. *J. Organomet. Chem.* **1998**, 560, 69.
37. Lee, L. W. M.; Piers, W. E.; Parvez, M.; Rettig, S. J.; Young, V. G. *Organometallics* **1999**, 18, 3904.
38. Fischer, R.; Walther, D.; Gebhardt, P.; Görls, H. *Organometallics* **2000**, 19, 2532.
39. Takahashi, T.; Murakami, M.; Kunishige, M.; Saburi, M.; Uchida, Y.; Kozawa, K.; Uchida, T. *Chem. Lett.* **1989**, 761.
40. Ramakrishna, T. V.; Lushnikova, S.; Sharp, P. R. *Organometallics* **2002**, 21, 5685.
41. Alt, H. G.; Han, J. S.; Thewalt, U. *J. Organomet. Chem.* **1993**, 456, 89.
42. Fryzuk, M. D.; Duval, P. B.; Rettig, S. J. *Can. J. Chem.* **2001**, 79, 536.
43. Spencer, M. D.; Morse, P. M.; Wilson, S. R.; Girolami, G. S. *J. Am. Chem. Soc.* **1993**, 115, 2057.
44. Licht, A. I.; Schneider, K. J.; Alt, H. G. *J. Organomet. Chem.* **2003**, 688, 254.
45. Ura, Y.; Jin, M.; Nakajima, K.; Takahashi, T. *Chem. Lett.* **2001**, 356.
46. Baranger, A. M.; Bergman, R. G. *J. Am. Chem. Soc.* **1994**, 116, 3822.
47. Schenk, W. A.; Gutmann, T. *J. Organomet. Chem.* **1998**, 552, 83.
48. Negishi, E.-I.; Montchamp, J.-L. In *The Metallocenes*; Togni, A., Haltermann, R. L., Eds.; Wiley-VCH: Weinheim, 2000; p 241.
49. Dioumaev, V. K.; Harrod, J. F. *Organometallics* **1997**, 16, 1452.
50. Ito, H.; Nakamura, T.; Taguchi, T.; Hanzawa, Y. *Tetrahedron* **1995**, 51, 4507.
51. Bertus, P.; Drouin, L.; Laroche, C.; Szymoniak, J. *Tetrahedron* **2004**, 60, 1375.
52. Gandon, V.; Laroche, C.; Szymoniak, J. *Tetrahedron Lett.* **2003**, 44, 4827.
53. Liard, A.; Marek, I. *J. Org. Chem.* **2000**, 65, 7218.
54. Farhat, S.; Zouev, I.; Marek, I. *Tetrahedron* **2004**, 60, 1329.
55. Barluenga, J.; Álvarez-Rodrigo, L.; Rodríguez, F.; Fañanás, F. J. *Angew. Chem. Int. Ed.* **2004**, 43, 3932.
56. Chinkov, N.; Majumdar, S.; Marek, I. *J. Am. Chem. Soc.* **2002**, 124, 10282.
57. Chinkov, N.; Majumdar, S.; Marek, I. *J. Am. Chem. Soc.* **2003**, 125, 13258.
58. Chinkov, N.; Majumdar, S.; Marek, I. *Synthesis* **2004**, 2411.
59. Cénac, N.; Chrostowska, A.; Sotiropoulos, J.-M.; Donnadieu, B.; Igau, A.; Pfister-Guillouzo, G.; Majoral, J.-P. *Organometallics* **1997**, 16, 4551.
60. Lai, C.; Xi, C.; Chen, C.; Ma, M.; Hong, X. *Chem. Commun.* **2003**, 2736.
61. Fujita, K.; Shinokubo, H.; Oshima, K. *Angew. Chem. Int. Ed.* **2003**, 42, 2550.
62. Fujita, K.; Yorimitsu, H.; Shinokubo, H.; Oshima, K. *J. Org. Chem.* **2004**, 69, 3302.
63. Hirano, K.; Fujita, K.; Shinokubo, H.; Oshima, K. *Org. Lett.* **2004**, 6, 593.
64. Fujita, K.; Yorimitsu, H.; Shinokubo, H.; Oshima, K. *J. Am. Chem. Soc.* **2004**, 126, 6776.
65. Sun, Y.; Piers, W. E.; Rettig, S. J. *Organometallics* **1996**, 15, 4110.
66. Mori, M.; Kuroda, S.; Dekura, F. *J. Am. Chem. Soc.* **1999**, 121, 5591.
67. Kuroda, S.; Dekura, F.; Sato, Y.; Mori, M. *J. Am. Chem. Soc.* **2001**, 123, 4139.
68. Kuroda, S.; Sato, Y.; Mori, M. *J. Organomet. Chem.* **2000**, 611, 304.
69. Ura, Y.; Hara, R.; Takahashi, T. *Chem. Commun.* **2000**, 875.
70. Ura, Y.; Hara, R.; Takahashi, T. *Chem. Lett.* **1998**, 195.
71. Corey, J. Y.; Huhmann, J. L.; Zhu, X.-H. *Organometallics* **1993**, 12, 1121.
72. Ura, Y.; Gao, G.; Bao, F.; Ogasawara, M.; Takahashi, T. *Organometallics* **2004**, 23, 4804.
73. Wang, L.; Quillan, B.; Yang, X.-J.; Wei, P.; Chen, Z.; Wannere, C. S.; Schleyer, P. R.; Robinson, G. H. *J. Am. Chem. Soc.* **2005**, 127, 7672.
74. Jones, W. M.; Klosin, J. *Adv. Organomet. Chem.* **1998**, 42, 147.
75. Negishi, E.-I.; Choueiry, D.; Nguyen, T. B.; Swanson, D. R.; Suzuki, N.; Takahashi, T. *J. Am. Chem. Soc.* **1994**, 116, 9751.
76. Negishi, E.-I.; Hou, S. In *Titanium and Zirconium in Organic Synthesis*; Marek, I., Ed.; Wiley-VCH: Weinheim, 2002; p 1.
77. Mansel, S.; Thomas, D.; Lefebvre, C.; Heller, D.; Kempe, R.; Baumann, W.; Rosenthal, U. *Organometallics* **1997**, 16, 2886.
78. Licht, A. I.; Alt, H. G. *J. Organomet. Chem.* **2002**, 648, 134.
79. Licht, A. I.; Alt, H. G. *J. Organomet. Chem.* **2003**, 684, 91.
80. Xi, Z.; Gao, G.; Kotori, M.; Takahashi, T. *J. Organomet. Chem.* **2002**, 663, 13.
81. Hanzawa, Y.; Ikeuchi, Y.; Nakamura, T.; Taguchi, T. *Tetrahedron Lett.* **1995**, 36, 6503.
82. Kasai, K.; Kotori, M.; Suzuki, N.; Takahashi, T. *J. Chem. Soc., Chem. Commun.* **1995**, 109.
83. Takahashi, T.; Kotori, M.; Xi, Z. *J. Chem. Soc., Chem. Commun.* **1995**, 1503.
84. Takahashi, T.; Xi, C.; Ura, Y.; Nakajima, K. *J. Am. Chem. Soc.* **2000**, 122, 3228.
85. Uesaka, N.; Mori, M.; Okamura, K.; Date, T. *J. Org. Chem.* **1994**, 59, 4542.
86. Zhao, C.; Lu, J.; Li, Z.; Xi, Z. *Tetrahedron* **2004**, 60, 1417.



87. Mori, M.; Saitoh, F.; Uesaka, N.; Shibasaki, M. *Chem. Lett.* **1993**, 213.
88. Mori, M.; Imai, A. E.; Uesaka, N. *Heterocycles* **1995**, *40*, 551.
89. Rosenthal, U.; Ohff, A.; Michalik, M.; Görls, H.; Burlakov, V. V.; Shur, V. B. *Angew. Chem., Int. Ed. Engl.* **1993**, *32*, 1193.
90. Lefebvre, C.; Ohff, A.; Tillack, A.; Baumann, W.; Kempe, R.; Burlakov, V. V.; Rosenthal, U. *J. Organomet. Chem.* **1995**, *501*, 189.
91. Peulecke, N.; Baumann, W.; Kempe, R.; Burlakov, V. V.; Rosenthal, U. *Eur. J. Inorg. Chem.* **1998**, 419.
92. Peulecke, N.; Lefebvre, C.; Ohff, A.; Baumann, W.; Tillack, A.; Kempe, R.; Burlakov, V. V.; Rosenthal, U. *Chem. Ber.* **1996**, *129*, 959.
93. Kim, H.-J.; Jung, S.; Jeon, Y.-M.; Whang, D.; Kim, K. *Chem. Commun.* **1997**, 2201.
94. Rosenthal, U.; Ohff, A.; Baumann, W.; Tillack, A.; Görls, H.; Burlakov, V. V.; Shur, V. B. *Z. Anorg. Allg. Chem.* **1995**, *621*, 77.
95. Lefebvre, C.; Baumann, W.; Tillack, A.; Kempe, R.; Görls, H.; Rosenthal, U. *Organometallics* **1996**, *15*, 3486.
96. Hiller, J.; Thewalt, U.; Polášek, M.; Petrusová, L.; Varga, V.; Sedmera, P.; Mach, K. *Organometallics* **1996**, *15*, 3752.
97. List, A. K.; Koo, K.; Rheingold, A. L.; Hillhouse, G. L. *Inorg. Chim. Acta* **1998**, *270*, 399.
98. Threlkel, R. S. Ph.D. Thesis, California Institute of Technology, 1980.
99. Basta, R.; Harvey, B. G.; Arif, A. M.; Ernst, R. D. *Inorg. Chim. Acta* **2004**, *357*, 3883.
100. Kulsomphob, V.; Harvey, B. G.; Arif, A. M.; Ernst, R. D. *Inorg. Chim. Acta* **2002**, *334*, 17.
101. Templeton, J. L. *Adv. Organomet. Chem.* **1989**, *29*, 1.
102. Peulecke, N.; Ohff, A.; Kosse, P.; Tillack, A.; Spannenberg, A.; Kempe, R.; Baumann, W.; Burlakov, V. V.; Rosenthal, U. *Chem. Eur. J.* **1998**, *4*, 1852.
103. Buchwald, S. L.; Watson, B. T.; Huffman, J. C. *J. Am. Chem. Soc.* **1987**, *109*, 2544.
104. Bradley, C. A.; Keresztes, I.; Lobkovsky, E.; Young, V. G.; Chirik, P. J. *J. Am. Chem. Soc.* **2004**, *126*, 16937.
105. Ohff, A.; Pulst, S.; Lefebvre, C.; Peulecke, N.; Arndt, P.; Burlakov, V. V.; Rosenthal, U. *Synlett* **1996**, 111.
106. Rosenthal, U.; Burlakov, V. V.; Arndt, P.; Baumann, W.; Spannenberg, A.; Shur, V. B. *Eur. J. Inorg. Chem.* **2004**, 4739.
107. Rosenthal, U.; Burlakov, V. V. In *Titanium and Zirconium in Organic Synthesis*; Marek, I., Ed.; Wiley-VCH: Weinheim, 2002; p 355.
108. Thomas, D.; Peulecke, N.; Burlakov, V. V.; Heller, B.; Baumann, W.; Spannenberg, A.; Kempe, R.; Rosenthal, U. *Z. Anorg. Allg. Chem.* **1998**, *624*, 919.
109. Horáček, M.; Štěpnička, P.; Kubišta, J.; Fejfarová, K.; Gyepes, R.; Mach, K. *Organometallics* **2003**, *22*, 861.
110. Thomas, D.; Baumann, W.; Spannenberg, A.; Kempe, R.; Rosenthal, U. *Organometallics* **1998**, *17*, 2096.
111. Baum, O.; Quntar, A. A.; Dembitsky, V. M.; Srebnik, M. *Tetrahedron* **2004**, *60*, 1359.
112. Takahashi, T.; Nishihara, Y.; Sun, W.-H.; Fischer, R.; Nakajima, K. *Organometallics* **1997**, *16*, 2216.
113. Röttger, D.; Erker, G. *Angew. Chem., Int. Ed. Engl.* **1997**, *36*, 812.
114. Barluenga, J.; Rodríguez, F.; Álvarez-Rodrigo, L.; Fañanás, F. J. *Chem. Eur. J.* **2004**, *10*, 101.
115. Mito, S.; Takahashi, T. *Chem. Commun.* **2005**, 2495.
116. Collman, J. P.; Boulatov, R.; Jameson, G. B.; Narang, V. *Inorg. Chem.* **2002**, *41*, 416.
117. Takahashi, T.; Li, Y. In *Titanium and Zirconium in Organic Synthesis*; Marek, I., Ed.; Wiley-VCH: Weinheim, 2002; p 50.
118. Lucht, B. L.; Mao, S. S. H.; Tilley, T. D. *J. Am. Chem. Soc.* **1998**, *120*, 4354.
119. Jiang, B.; Tilley, T. D. *J. Am. Chem. Soc.* **1999**, *121*, 9744.
120. Nitschke, J. R.; Zürcher, S.; Tilley, T. D. *J. Am. Chem. Soc.* **2000**, *122*, 10345.
121. Johnson, S. A.; Liu, F.-Q.; Suh, M. C.; Zürcher, S.; Haufe, M.; Mao, S. S. H.; Tilley, T. D. *J. Am. Chem. Soc.* **2003**, *125*, 4199.
122. Mao, S. S. H.; Liu, F.-Q.; Tilley, T. D. *J. Am. Chem. Soc.* **1998**, *120*, 1193.
123. Takahashi, T.; Tsai, F.-Y.; Li, Y. *Chem. Lett.* **1999**, 1173.
124. Lucht, B. L.; Tilley, T. D. *Chem. Commun.* **1998**, 1645.
125. Uesaka, N.; Saitoh, F.; Mori, M.; Shibasaki, M.; Okamura, K.; Date, T. *J. Org. Chem.* **1994**, *59*, 5633.
126. Mori, M.; Uesaka, N.; Saitoh, F.; Shibasaki, M. *J. Org. Chem.* **1994**, *59*, 5643.
127. Mori, M.; Kuroda, S.; Zhang, C.-S.; Sato, Y. *J. Org. Chem.* **1997**, *62*, 3263.
128. Takahashi, T.; Kitora, M.; Kasai, K.; Suzuki, N. *Organometallics* **1994**, *13*, 4183.
129. Takahashi, T.; Sun, W.-H.; Liu, Y.; Nakajima, K.; Kitora, M. *Organometallics* **1998**, *17*, 3841.
130. Warner, B. P.; Davis, W. M.; Buchwald, S. L. *J. Am. Chem. Soc.* **1994**, *116*, 5471.
131. Buchwald, S. L.; Watson, B. T.; Huffman, J. C. *J. Am. Chem. Soc.* **1986**, *108*, 7411.
132. Majoral, J.-P.; Meunier, P.; Igau, A.; Pirió, N.; Zablocka, M.; Skowronska, A.; Bredeau, S. *Coord. Chem. Rev.* **1998**, *178–180*, 145.
133. Lu, Z.; Jones, W. M. *Organometallics* **1994**, *13*, 1539.
134. Yin, J.; Abboud, K. A.; Jones, W. M. *J. Am. Chem. Soc.* **1993**, *115*, 8859.
135. Sharp, P. R. *J. Am. Chem. Soc.* **2000**, *122*, 9880.
136. Cloke, F. G. N.; Hitchcock, P. B.; Joseph, S. C. P. *Chem. Commun.* **1994**, 1207.
137. Lee, H.; Bridgewater, B. M.; Parkin, G. J. *Chem. Soc., Dalton Trans.* **2000**, 4490.
138. Wang, H.; Li, H.-W.; Huang, X.; Lin, Z.; Xie, Z. *Angew. Chem., Int. Ed.* **2003**, *42*, 4347.
139. Pirió, N.; Bredeau, S.; Dupuis, L.; Schütz, P.; Donnadieu, B.; Igau, A.; Majoral, J.-P.; Guillemin, J.-C.; Meunier, P. *Tetrahedron* **2004**, *60*, 1317.
140. Harouch, Y. E.; Cadierno, V.; Igau, A.; Donnadieu, B.; Majoral, J.-P. *J. Organomet. Chem.* **2004**, *689*, 953.
141. de Rege, F. M. G.; Davis, W. M.; Buchwald, S. L. *Organometallics* **1995**, *14*, 4799.
142. Rosa, P.; Le Floch, P.; Ricard, L.; Mathey, F. J. *J. Am. Chem. Soc.* **1997**, *119*, 9417.
143. Avarvari, N.; Rosa, P.; Mathey, F.; Le Floch, P. *J. Organomet. Chem.* **1998**, *567*, 151.
144. Rosenthal, U.; Pellny, P.-M.; Kirchbauer, F. G.; Burlakov, V. V. *Acc. Chem. Res.* **2000**, *33*, 119.
145. Rosenthal, U.; Burlakov, V. V.; Arndt, P.; Baumann, W.; Spannenberg, A. *Organometallics* **2005**, *24*, 456.
146. Pellny, P.-M.; Kirchbauer, F. G.; Burlakov, V. V.; Baumann, W.; Spannenberg, A.; Rosenthal, U. *Chem. Eur. J.* **2000**, *6*, 81.
147. Pellny, P.-M.; Kirchbauer, F. G.; Burlakov, V. V.; Baumann, W.; Spannenberg, A.; Rosenthal, U. *J. Am. Chem. Soc.* **1999**, *121*, 8313.
148. Jemmis, E. D.; Phukan, A. K.; Jiao, H.; Rosenthal, U. *Organometallics* **2003**, *22*, 4958.
149. Jemmis, E. D.; Phukan, A. K.; Rosenthal, U. *J. Organomet. Chem.* **2001**, *635*, 204.
150. Suzuki, N.; Nishiura, M.; Wakatsuki, Y. *Science* **2002**, *295*, 660.
151. Suzuki, N.; Aihara, N.; Takahara, H.; Watanabe, T.; Iwasaki, M.; Saburi, M.; Hashizume, D.; Chihara, T. *J. Am. Chem. Soc.* **2004**, *126*, 60.
152. Lam, K. C.; Lin, Z. *Organometallics* **2003**, *22*, 3466.
153. Pellny, P.-M.; Burlakov, V. V.; Arndt, P.; Baumann, W.; Spannenberg, A.; Rosenthal, U. *J. Am. Chem. Soc.* **2000**, *122*, 6317.
154. Choukroun, R.; Zhao, J.; Lorber, C.; Cassoux, P.; Donnadieu, B. *Chem. Commun.* **2000**, 1511.
155. Hessen, B.; van der Heijden, H. J. *J. Am. Chem. Soc.* **1996**, *118*, 11670.



156. Pindado, G. J.; Thornton-Pett, M.; Bouwkamp, M.; Meetsma, A.; Hessen, B.; Bochmann, M. *Angew. Chem., Int. Ed. Engl.* **1997**, *36*, 2358.
157. Karl, J.; Erker, G.; Fröhlich, R.; Zippel, F.; Bickelhaupt, F.; Goedheijt, M. S.; Akkerman, O. S.; Binger, P.; Stannek, J. *Angew. Chem., Int. Ed. Engl.* **1997**, *36*, 2771.
158. Erker, G.; Kehr, G.; Fröhlich, R. *Adv. Organomet. Chem.* **2004**, *51*, 109.
159. Erker, G.; Kehr, G.; Fröhlich, R. *J. Organomet. Chem.* **2004**, *689*, 1402.
160. Venne-Dunker, S.; Kehr, G.; Fröhlich, R.; Erker, G. *Organometallics* **2003**, *22*, 948.
161. Casty, G. L.; Lugmair, C. G.; Radu, N. S.; Tilley, T. D.; Walzer, J. F.; Zargarian, D. *Organometallics* **1997**, *16*, 8.
162. Giannini, L.; Solari, E.; Floriani, C.; Chiesi-Villa, A.; Rizzoli, C. *Angew. Chem., Int. Ed. Engl.* **1994**, *33*, 2204.
163. Giannini, L.; Solari, E.; Zanotti-Gerosa, A.; Floriani, C.; Chiesi-Villa, A.; Rizzoli, C. *Angew. Chem., Int. Ed. Engl.* **1996**, *35*, 85.
164. Fryzuk, M. D.; Love, J. B.; Rettig, S. J. *Organometallics* **1998**, *17*, 846.
165. Keaton, R. J.; Sita, L. R. *Organometallics* **2002**, *21*, 4315.
166. Keaton, R. J.; Koterwas, L. A.; Fetting, J. C.; Sita, L. R. *J. Am. Chem. Soc.* **2002**, *124*, 5932.
167. Visser, C.; van den Hende, J. R.; Meetsma, A.; Hessen, B. *Organometallics* **2003**, *22*, 615.
168. Visser, C.; Meetsma, A.; Hessen, B. *Organometallics* **2002**, *21*, 1912.
169. Pindado, G. J.; Thornton-Pett, M.; Bochmann, M. *J. Chem. Soc., Dalton Trans.* **1997**, 3115.
170. Pindado, G. J.; Thornton-Pett, M.; Bochmann, M. *J. Chem. Soc., Chem. Commun.* **1997**, 609.
171. Pindado, G. J.; Thornton-Pett, M.; Hursthouse, M. B.; Coles, S. J.; Bochmann, M. *J. Chem. Soc., Dalton Trans.* **1999**, 1663.
172. Diamond, G. M.; Green, M. L. H.; Walker, N. M.; Howard, J. A. K.; Mason, S. A. *J. Chem. Soc., Dalton Trans.* **1992**, 2641.
173. Strauch, J. W.; Petersen, J. L. *Organometallics* **2001**, *20*, 2623.
174. Dahlmann, M.; Schottek, J.; Fröhlich, R.; Kunz, D.; Nissinen, M.; Erker, G.; Fink, G.; Kleinschmidt, R. *J. Chem. Soc., Dalton Trans.* **2000**, 1881.
175. Dahlmann, M.; Erker, G.; Fröhlich, R.; Meyer, O. *Organometallics* **1999**, *18*, 4459.
176. Bürgi, T.; Berke, H.; Wingbermühle, D.; Psiorz, C.; Noe, R.; Fox, T.; Knickmeier, M.; Berlekamp, M.; Fröhlich, R.; Erker, G. *J. Organomet. Chem.* **1995**, *497*, 149.
177. Green, J. C.; Green, M. L. H.; Taylor, G. C.; Saunders, J. J. *J. Chem. Soc., Dalton Trans.* **2000**, 317.
178. Erker, G.; Pfaff, R. *Organometallics* **1993**, *12*, 1921.
179. Mashima, K.; Oshiki, T.; Matsuo, Y.; Tani, K. *Chem. Lett.* **1997**, 793.
180. Noe, R.; Wingbermühle, D.; Erker, G.; Krüger, C.; Bruckmann, J. *Organometallics* **1993**, *12*, 4993.
181. Erker, G.; Kehr, G.; Fröhlich, R. *Coord. Chem. Rev.* **2005**, *250*, 36.
182. Bradley, C. A.; Lobkovsky, E.; Chirik, P. J. *J. Am. Chem. Soc.* **2003**, *125*, 8110.
183. Veiros, L. F. *Chem. Eur. J.* **2005**, *11*, 2505.
184. Fermin, M. C.; Ho, J.; Stephan, D. W. *Organometallics* **1995**, *14*, 4247.
185. Kraft, B. M.; Jones, W. D. *J. Am. Chem. Soc.* **2002**, *124*, 8681.
186. Chirik, P. J.; Henling, L. M.; Bercaw, J. E. *Organometallics* **2001**, *20*, 534.
187. Pool, J. A.; Lobkovsky, E.; Chirik, P. J. *J. Am. Chem. Soc.* **2003**, *125*, 2241.
188. Pool, J. A.; Bernskoetter, W. H.; Chirik, P. J. *J. Am. Chem. Soc.* **2004**, *126*, 14326.
189. Pool, J. A.; Lobkovsky, E.; Chirik, P. J. *Nature* **2004**, *427*, 527.
190. Walsh, P. J.; Hollander, F. J.; Bergman, R. G. *J. Am. Chem. Soc.* **1988**, *110*, 8729.
- 190a. Cummins, C. C.; Baxter, S. M.; Wolczanski, P. T. *J. Am. Chem. Soc.* **1988**, *110*, 8731.
- 190b. Schaller, C. P.; Cummins, C. C.; Wolczanski, P. T. *J. Am. Chem. Soc.* **1996**, *118*, 591.
191. Bernskoetter, W. H.; Pool, J. A.; Lobkovsky, E.; Chirik, P. J. *J. Am. Chem. Soc.* **2005**, *127*, 7901.
192. Fryzuk, M. D. *Chem. Rev.* **2003**, *3*, 2.
193. Fryzuk, M. D.; Johnson, S. A. *Coord. Chem. Rev.* **2000**, *200*, 379.
194. Gambarotta, S.; Scott, J. *Angew. Chem. Int. Ed.* **2004**, *43*, 5298.
195. Shaver, M. P.; Fryzuk, M. D. *Adv. Synth. Catal.* **2003**, *345*, 1061.
196. MacKay, B. A.; Fryzuk, M. D. *Chem. Rev.* **2004**, *104*, 385.
197. Fryzuk, M. D.; Haddad, T. S.; Mylvaganam, M.; McConville, D. H.; Rettig, S. J. *J. Am. Chem. Soc.* **1993**, *115*, 2782.
198. Cohen, J. D.; Fryzuk, M. D.; Loehr, T. M.; Mylvaganam, M.; Rettig, S. J. *Inorg. Chem.* **1998**, *37*, 112.
199. Cohen, J. D.; Mylvaganam, M.; Fryzuk, M. D.; Loehr, T. M. *J. Am. Chem. Soc.* **1994**, *116*, 9529.
200. Fryzuk, M. D.; Love, J. B.; Rettig, S. J.; Young, V. G. *Science* **1997**, *275*, 1445.
201. Basch, H.; Musaev, D. G.; Morokuma, K.; Fryzuk, M. D.; Love, J. B.; Seidel, W. W.; Albinati, A.; Koetzle, T. F.; Klooster, W. T.; Mason, S. A.; Eckert, J. *J. Am. Chem. Soc.* **1999**, *121*, 523.
202. Studt, F.; Morello, L.; Lehnert, N.; Fryzuk, M. D.; Tuczek, F. *Chem. Eur. J.* **2003**, *9*, 520.
203. Basch, H.; Musaev, D. G.; Morokuma, K. *J. Am. Chem. Soc.* **1999**, *121*, 5754.
204. Basch, H.; Musaev, D. G.; Morokuma, K. *Organometallics* **2000**, *19*, 3393.
205. Fryzuk, M. D.; Kozaki, C. M.; Mehrkhodavandi, P.; Morello, L.; Patrick, B. O.; Rettig, S. J. *J. Am. Chem. Soc.* **2002**, *124*, 516.
206. Morello, L.; Love, J. B.; Patrick, B. O.; Fryzuk, M. D. *J. Am. Chem. Soc.* **2004**, *126*, 9480.
207. Fryzuk, M. D.; Corkin, J. R.; Patrick, B. O. *Can. J. Chem.* **2003**, *81*, 1376.
208. Waldman, T. E.; Stahl, L.; Wilson, D. R.; Arif, A. M.; Hutchinson, J. P.; Ernst, R. D. *Organometallics* **1993**, *12*, 1543.
209. Harvey, B. G.; Basta, R.; Arif, A. M.; Ernst, R. D. *Dalton Trans.* **2004**, 1221.
210. Gedridge, R. W.; Arif, A. M.; Ernst, R. D. *J. Organomet. Chem.* **1995**, *501*, 95.
211. Kulsomphob, V.; Arif, A. M.; Ernst, R. D. *Organometallics* **2002**, *21*, 3182.
212. Kiplinger, J. L.; Richmond, T. G. *J. Am. Chem. Soc.* **1996**, *118*, 1805.
213. Kiplinger, J. L.; Richmond, T. G. *Chem. Commun.* **1996**, 1115.
214. O'Connor, P. E.; Berg, D. J.; Barclay, T. *Organometallics* **2002**, *21*, 3947.
215. Edelbach, B. J.; Rahman, A. K. F.; Lachicotte, R.; Jones, W. D. *Organometallics* **1999**, *18*, 3170.
216. Krut'ko, D. P.; Borzov, M. V.; Kuz'mina, L. G.; Churakov, A. V.; Lemenovskii, D. A.; Reutov, O. A. *Inorg. Chim. Acta* **1998**, *280*, 257.

## 4.07

# Complexes of Zirconium and Hafnium in Oxidation State III

---

S J Lancaster, University of East Anglia, Norwich, UK

© 2007 Elsevier Ltd. All rights reserved.

<b>4.07.1</b>	<b>Introduction</b>	<b>741</b>
<b>4.07.2</b>	<b>Compounds with <math>\eta^1</math>-Ligands</b>	<b>742</b>
<b>4.07.3</b>	<b>Compounds with <math>\eta^3</math>-Ligands</b>	<b>742</b>
<b>4.07.4</b>	<b>Mono-cyclopentadienyl Compounds</b>	<b>743</b>
4.07.4.1	Mono-cyclopentadienyl Zirconium(III) Compounds	743
4.07.4.2	Mono-cyclopentadienyl (Pendant Phosphine) Zirconium(III) Compounds	744
4.07.4.3	Mono-cyclopentadienyl Zirconium(III) Porphyrin Complexes	745
<b>4.07.5</b>	<b>Bis-Cyclopentadienyl Compounds</b>	<b>745</b>
4.07.5.1	Electrochemical Reduction of Bis-cyclopentadienyl Zirconium(IV) to Zirconium(III)	745
4.07.5.2	Mononuclear Bis-cyclopentadienyl Zirconium(III) Compounds	746
4.07.5.3	Dinuclear Bis-cyclopentadienyl Zirconium(III) Compounds	747
4.07.5.3.1	Dinitrogen complexes	747
4.07.5.3.2	Alkynyl-bridged complexes	749
4.07.5.3.3	Phosphido-bridged complexes	750
4.07.5.4	Dinuclear Fulvalene Zirconium(III) Compounds	751
4.07.5.5	Isolated Metallate(III) Compounds	751
4.07.5.6	Heterobimetallic Bis-cyclopentadienyl Zirconium(III) Hydride Complexes	753
4.07.5.7	Bis-cyclopentadienyl Zirconium(III) Halides in Organic Synthesis	754
<b>4.07.6</b>	<b>Compounds with Metal–Metal Bonds; Mixed-Valence Compounds</b>	<b>755</b>
<b>References</b>		<b>756</b>

---

### 4.07.1 Introduction

For titanium, the lightest of the group 4 metals, there is an extensive organometallic chemistry of both oxidation states III and IV. For organotitanium(III), see Chapter 4.04 and for organotitanium(IV), see Chapter 4.05. In contrast, examples of organometallic compounds of zirconium(III) and hafnium(III) are relatively rare and oxidation state IV predominates. For organozirconium(IV), see Chapter 4.08. Prior to the publication of COMC(1982), there were only a few reports of isolated zirconium(III) compounds and much of the evidence for Zr(III) complexes resulted from ESR studies.<sup>1</sup> During the period covered by COMC(1995), there was an increased interest in organozirconium(III) chemistry, particularly dinuclear bis(cyclopentadienyl) compounds, and also mononuclear and metallate complexes.<sup>2–4</sup>

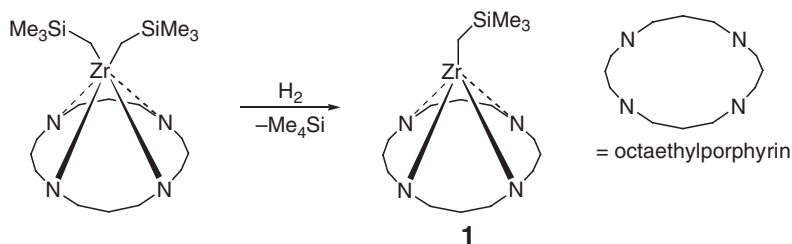
In this chapter, we present a guide to the organozirconium(III) and organohafnium(III) literature since the publication of COMC(1995) up to early 2005. During this period, the organometallic chemistry of zirconium and hafnium has continued to be dominated by oxidation state IV. However, there have been a number of reports describing the syntheses, structure, and applications of organozirconium(III) compounds, and the first isolation and structural characterization of organohafnium(III) compounds.

### 4.07.2 Compounds with $\eta^1$ -Ligands

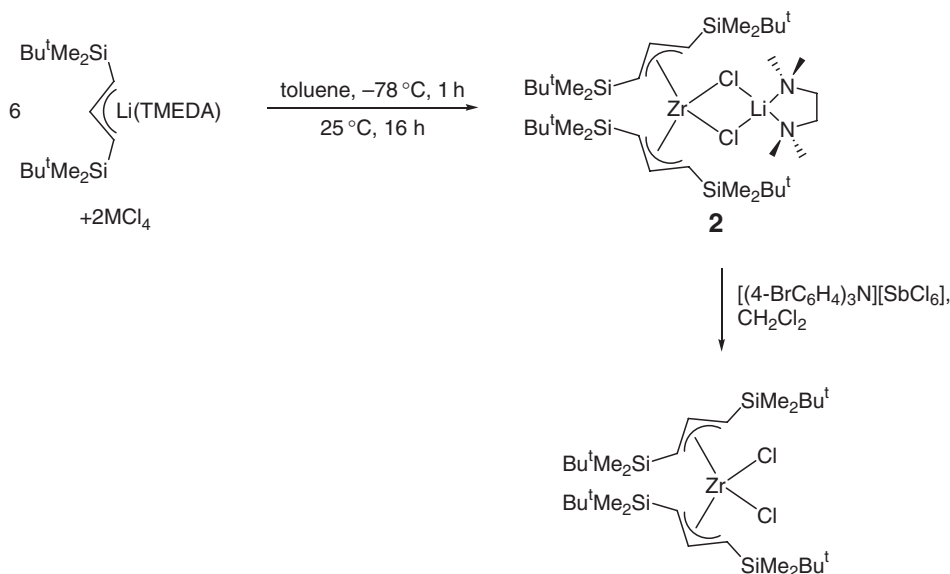
The alkylzirconium(III) octaethylporphyrin complex, (OEP)ZrCH<sub>2</sub>SiMe<sub>3</sub> **1**, was prepared from the dialkylzirconium(IV) complex by reduction with H<sub>2</sub> (1 atm) in toluene at 20 °C (Scheme 1).<sup>5</sup> This reaction therefore appears to be a rather rare example of the chemical reduction of Zr(IV) to Zr(III) by H<sub>2</sub>. The structure of **1** was elucidated by single crystal X-ray diffraction and has a Zr–C bond length of 2.216(8) Å. Although this complex formally contains zirconium in oxidation state III, careful consideration of the structural and spectroscopic data led the authors to conclude that this was an overly simplistic view. At 77 K, an EPR signal typical of a metal-centered radical was observed, while no signal was detected at 293 K. The UV/Vis spectrum of **1** contains bands typical of a porphyrin anion. The electronic structure of **1** is therefore better described as a combination of two resonance forms: a Zr(III) metal-based radical, and a zwitterionic form with a positively charged Zr(IV) center and a porphyrin radical anion.

### 4.07.3 Compounds with $\eta^3$ -Ligands

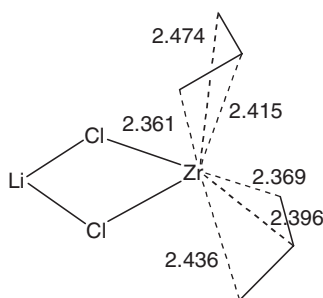
In the course of an investigation into the syntheses and polymerization activity of bis(allyl)zirconium pre-catalysts, Eisen and co-workers found that the treatment of ZrCl<sub>4</sub> with 2 equiv. of the lithium allyl, (<sup>t</sup>BuMe<sub>2</sub>SiCH<sub>2</sub>)<sub>2</sub>CHLi(TMEDA), in toluene afforded { $\eta^3$ -(<sup>t</sup>BuMe<sub>2</sub>SiCH<sub>2</sub>)<sub>2</sub>CH}<sub>2</sub>Zr( $\mu$ -Cl)<sub>2</sub>Li(TMEDA) **2** in 48% yield (Scheme 2).<sup>6</sup> The authors concluded that reduction of MCl<sub>4</sub> to MCl<sub>3</sub> with concomitant formation of the allyl dimer and LiCl occurs first, before reaction with further 2 equiv. of lithium allyl yields the bis(allyl)zirconium(III) complex **2**.



Scheme 1



Scheme 2



**Figure 1** Zr–C bond lengths (Å) for the two allyl ligands in complex **2**.

The structure of **2** was elucidated by X-ray crystallography and is the only structurally characterized example of an allyl zirconium(III) complex. The ligands are both  $\eta^3$ -allyl but they are not symmetrically bonded to the metal center, and in each case one of the terminal carbon atoms is significantly closer to the metal center (Figure 1).

Complex **2** gave an unusually strong ESR singlet ( $g_{\text{iso}} = 1.989$ ) together with an effective magnetic moment in toluene solution of  $1.5 \pm 0.8$  BM, indicating a metal-centered radical with almost no metal–metal interactions.

As is typical for organozirconium(III), **2** proved to be highly air sensitive. Exposing a brown toluene solution to dry oxygen resulted in decomposition and formation of a yellow solution. Mild chemical oxidation of **2** with [(4-BrC<sub>6</sub>H<sub>4</sub>)<sub>3</sub>N][SbCl<sub>6</sub>] in dichloromethane solution afforded a Zr(IV) complex (Scheme 2).

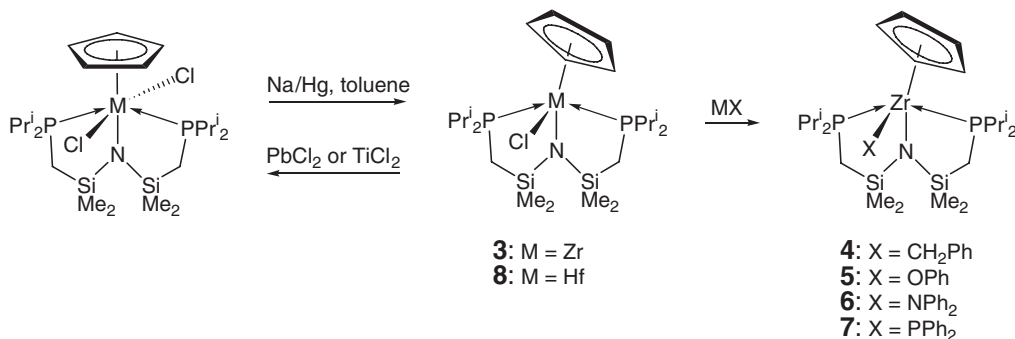
Complex **2** proved to be an effective pre-catalyst for propene polymerization, when activated with methylaluminoxane. However, very similar productivities were observed using the Zr(IV) complex as the pre-catalyst, suggesting that activation is accompanied by oxidation and that the active species contains zirconium in oxidation state IV.

#### 4.07.4 Mono-cyclopentadienyl Compounds

Despite the academic challenge presented by the scarcity of neutral mononuclear organozirconium(III) compounds, there have been a few deliberate attempts to design ligands to stabilize this oxidation state, and most Zr(III) compounds are diamagnetic and dinuclear. Fryzuk and co-workers recognized that the key to stabilizing the Zr(III) state against dimerization and disproportionation is to use sterically demanding ligands.<sup>7–9</sup> They have reported two such ligands systems: the first consists of a cyclopentadienyl ligand and a tridentate amidodiphosphine;<sup>7,8</sup> in the second, the phosphine donors are appended to the cyclopentadienyl ligand.<sup>9</sup>

##### 4.07.4.1 Mono-cyclopentadienyl Zirconium(III) Compounds

The yellow Cp{N(SiMe<sub>2</sub>CH<sub>2</sub>P<sup>*i*</sup>Pr<sub>2</sub>)<sub>2</sub>}ZrCl<sub>2</sub> was reduced with sodium amalgam to the deep green Zr(III) complex Cp{N(SiMe<sub>2</sub>CH<sub>2</sub>P<sup>*i*</sup>Pr<sub>2</sub>)<sub>2</sub>}ZrCl **3** (Scheme 3).<sup>7,8</sup> It was found that the reduction is best conducted under vacuum or an argon atmosphere, since prolonged exposure to molecular nitrogen leads to the formation of a dinitrogen complex.<sup>10</sup>



**Scheme 3**

**Table 1** Selected ESR spectral data on compounds **3–7**, **9**, and **10**

Compound	$g_{\text{iso}}$	$a(^{91}\text{Zr})$ (G)	$a(^{31}\text{P})$ (G)	$a(^{14}\text{N})$ (G)
<b>3</b>	1.955	37.2	21.1	2.9
<b>4</b>	1.956	<sup>a</sup>	18.6	3.4
<b>5</b>	1.955	<sup>a</sup>	18.7	<sup>a</sup>
<b>6</b>	1.953	<sup>a</sup>	11.2	<sup>a</sup>
<b>7</b>	1.965	<sup>a</sup>	18.6, 29.8	<sup>a</sup>
<b>9</b>	1.96	13.6	22.7	<sup>b</sup>
<b>10</b>	2.01	<sup>a</sup>	23.0	<sup>b</sup>

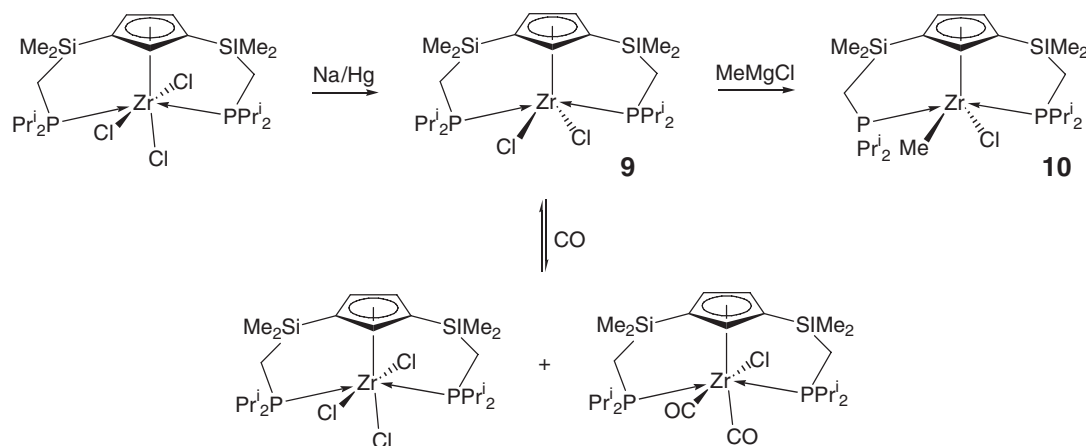
<sup>a</sup>Data not available.<sup>b</sup>Nuclei not present.

Metathesis of **3** with a variety of alkylating agents yielded a series of isolable alkyl derivatives, and the molecular structures of the trimethylsilylmethyl (and later the phenyl<sup>8</sup>) derivatives were elucidated by X-ray crystallography. This chemistry was reviewed in COMC(1995).<sup>2</sup> In 1996, the authors expanded upon their initial communication and reported the preparation of benzyl, phenoxy, amido, and phosphido derivatives **4–7** (Scheme 3).<sup>8</sup> Satisfactory elemental analyses were obtained for **4** and **5**, but the high solubility of **6** and **7** hampered purification attempts. In each case, only broad resonances were observed in the <sup>1</sup>H NMR spectra, suggesting quantitative conversion to paramagnetic products. The ESR spectra were also consistent with a paramagnetic mononuclear zirconium(III) species (Table 1).

The brown hafnium(III) analog of **3**, Cp{N(SiMe<sub>2</sub>CH<sub>2</sub>P<sup>i</sup>Pr<sub>2</sub>)<sub>2</sub>}HfCl **8**, was prepared similarly through reduction of the hafnium(IV) precursor with Na/Hg (Scheme 3). A sample pure enough to give the first satisfactory elemental analysis of an organohafnium(III) compound was separated from contamination with **3** by fractional crystallization. The EPR spectrum consisted of a broad singlet reflecting the inherently large line widths.<sup>11</sup> Both **3** and **8** are oxidized by TiCl<sub>3</sub> or PbCl<sub>2</sub> to give the corresponding M(IV) dichlorides in near quantitative yield (Scheme 3).

#### 4.07.4.2 Mono-cyclopentadienyl (Pendant Phosphine) Zirconium(III) Compounds

The doubly pendant-phosphine-substituted cyclopentadienyl ligand {η<sup>5</sup>-C<sub>5</sub>H<sub>3</sub>-1,3-(SiMe<sub>2</sub>CH<sub>2</sub>P(<sup>i</sup>Pr)<sub>2</sub>)<sub>2</sub>} has been used successfully to stabilize Zr(III).<sup>9</sup> With the exclusion of dinitrogen, {η<sup>5</sup>-C<sub>5</sub>H<sub>3</sub>-1,3-(SiMe<sub>2</sub>CH<sub>2</sub>P(<sup>i</sup>Pr)<sub>2</sub>)<sub>2</sub>}ZrCl<sub>3</sub> reacts with excess sodium amalgam to yield the dark green complex {η<sup>5</sup>-C<sub>5</sub>H<sub>3</sub>-1,3-(SiMe<sub>2</sub>CH<sub>2</sub>P(<sup>i</sup>Pr)<sub>2</sub>)<sub>2</sub>}ZrCl<sub>2</sub> **9** (Scheme 4). Compound **9** reacts with molecular nitrogen to form a dinuclear N<sub>2</sub> complex. As a consequence of its paramagnetism, **9** gives only broad <sup>1</sup>H NMR resonances and no observable signal in the <sup>31</sup>P{<sup>1</sup>H} NMR spectrum. The ESR data for **9** (Table 1), the solid-state (1.8 μ<sub>B</sub>), and solution-phase (2.0 μ<sub>eff</sub>) magnetic moments are all consistent with one

**Scheme 4**

unpaired electron, while mass spectrometry indicates that **9** is mononuclear. Compound **9** could be methylated with MeMgCl, but even the use of an excess yielded only the monomethyl derivative **10** (Scheme 4). Compound **10** was characterized by elemental analysis and ESR (Table 1). All attempts to treat complex **9** with alternative alkylating agents led only to decomposition.

Treatment of a solution of **9** with 1 atm CO at 25 °C resulted in a rapid but reversible disproportionation reaction, affording a dark brown solution containing two diamagnetic compounds: the Zr(IV) trichloride and Zr(II) dicarbonyl chloride (Scheme 4).

#### 4.07.4.3 Mono-cyclopentadienyl Zirconium(III) Porphyrin Complexes

Treatment of tetraphenylporphyrinato (tpp) zirconium dichloride with TiCp in the presence of sodium amalgam afforded (tpp)CpZr **11** (Scheme 5). The structure of **11** was elucidated by X-ray crystallography ( $\text{Zr-Cp}_{(\text{centroid})} = 2.206(6) \text{ \AA}$ ). Compound **11** was also obtained from the reaction between  $[\text{Li}(\text{THF})_4][(\text{tpp})\text{Zr}(\text{C}\equiv\text{CPh})_3]$  and  $\text{Cp}_2\text{Ti}(\text{Me}_3\text{SiC}\equiv\text{CSiMe}_3)$ . Compound **11** has a number of similarities to  $((\text{OEP})\text{ZrCH}_2\text{SiMe}_3)$  **1**; both are paramagnetic with ESR spectra consistent with metal-centered radicals at low temperature and radical anions at room temperature. As was seen for **1**, the UV/Vis spectrum of **11** also has a band (at 638 nm) characteristic of a porphyrin radical anion. So while **11** is formally an organozirconium(III) compound, it is better described as a resonance hybrid between a metal-centered radical and a zwitterion with a cationic Zr(IV) and radical porphyrin anion.

#### 4.07.5 Bis-Cyclopentadienyl Compounds

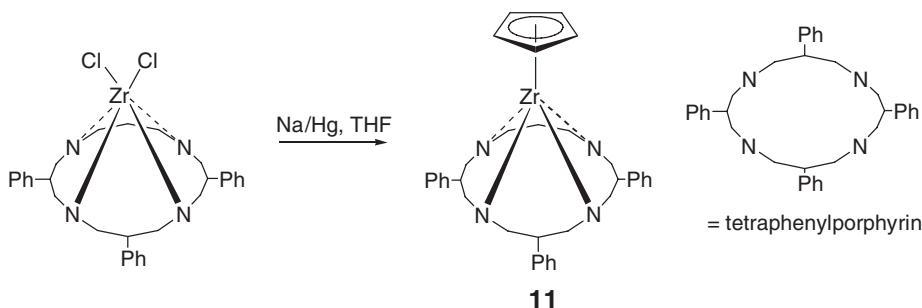
The great majority of examples of organozirconium(III) and organohafnium(III) complexes are bent metallocene derivatives. Complexes are prepared through either electrochemical or chemical reduction of M(IV) precursors, the mild oxidation of M(II) precursors, or ligand exchange at M(III) centers.

##### 4.07.5.1 Electrochemical Reduction of Bis-cyclopentadienyl Zirconium(IV) to Zirconium(III)

Lappert *et al.* first reported the one-electron electrochemical reduction of organozirconium(IV) (Equation (1)) in 1981.<sup>13</sup> The difference in reduction potential for  $\text{Cp}_2\text{ZrCl}_2$  (−1.70 V) versus  $\text{Cp}_2\text{TiCl}_2$  (−0.75 V) is striking, and explains why, for zirconium, one cannot use mild chemical reducing agents such as Zn or Al, which are effective in reducing Ti(IV) compounds. For zirconium, stronger reducing agents such as metallic Na, Li, Mg, amalgams, or naphthalene salts are generally required with the concomitant risk of further reduction and other competing side-reactions.<sup>2,3</sup> The results of a survey of reduction potentials are tabulated in COMC(1995).<sup>2</sup>



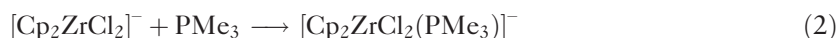
The reduction potential of a metallocene dichloride complex is one indicator of the electron density at the metal center. A systematic study of the one-electron reduction potential for the series  $(\text{C}_5\text{H}_5-n\text{Me}_n)_2\text{ZrCl}_2$  ( $n = 0-4$ ) revealed a shift to more negative potential by 0.071 V per methyl group. The deviation from this trend for  $n = 5$  was



Scheme 5

ascribed to the effect of steric hindrance on the angle between the planes of the two Cp ligands. They also reported a subtle interplay between the steric and electronic effects on the redox properties of the trimethylsilyl-substituted zirconocene dichlorides  $(C_5H_{5-n}(SiMe_3)_n)_2ZrCl_2$  ( $n=0-3$ ) and the *ansa*-analogs  $Me_2Si(C_5H_4)_2ZrCl_2$  and  $Me_2Si\{C_5H_2(SiMe_3)_2\}_2ZrCl_2$ .<sup>14</sup>

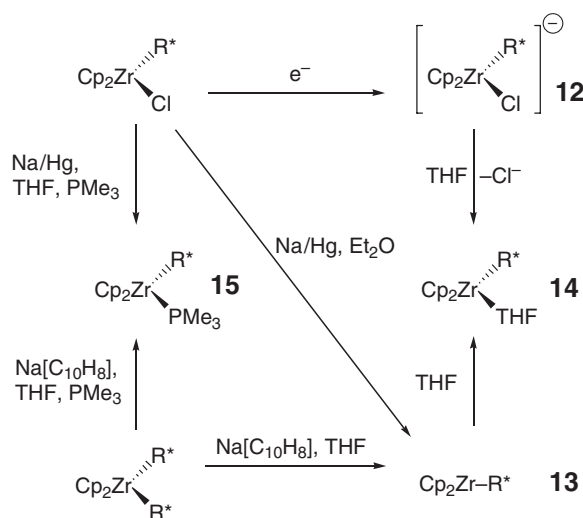
Solution-phase ESR evidence for a number of mononuclear phosphine complexes of the form  $Cp_2Zr^{III}X(PR_3)$  was summarized in COMC(1995).<sup>2</sup> In 1996, Samuel and Henique extended their own contribution to this field by reporting the ESR parameters for  $Cp_2Zr(Me)(PMe_3)$  ( $g_{iso}=1.989$ ,  $a(P)=21.1$  G), which was prepared by electrochemical reduction in the presence of  $PMe_3$ .<sup>15</sup> Since the anion radical  $[Cp_2ZrCl_2]^-$  is stable, they proposed that  $Cp_2Zr(Cl)(PMe_3)$ <sup>16</sup> was formed in a two-step process, in which the phosphine coordinates to the radical anion (Equation (2)) before cleavage of the Zr–Cl bond occurs (Equation (3)).



Lappert *et al.* reported the syntheses and the one-electron reduction chemistry of the chiral-at-carbon zirconocene complex  $Cp_2ZrR^*Cl$  (where  $R^* = CH(SiMe_3)(2-MeC_6H_4)$ ) and the related zirconocene dialkyl and hafnium monoalkyl compounds.<sup>17</sup> An electrochemical investigation revealed that the reversible one-electron reduction of  $Cp_2ZrR^*Cl$  ( $E^{red} = -1.72$  vs.  $-1.70$  V for  $Cp_2ZrCl_2$ ) initially gave the complex anion  $[Cp_2ZrR^*Cl]^-$  **12** (Scheme 6). In contrast, the hafnium analog was irreversibly reduced at  $-2.00$  V, affording an unknown product. Irreversible reduction of the diastereomers *rac*- and *meso*- $Cp_2ZrR^*_2$  ( $-2.12$  and  $-2.08$  V, respectively) leads to the identification of an intermediate,  $Cp_2ZrR^*$  **13**, which reacted with THF to give  $Cp_2ZrR^*(THF)$  **14**. The phosphine complex  $Cp_2ZrR^*(PMe_3)$  **15** could be formed through chemical reduction of  $Cp_2ZrR^*Cl$  or *rac*- and *meso*- $Cp_2ZrR^*_2$  in the presence of  $PMe_3$ . Complexes **12–15** were characterized by ESR, but attempts to isolate them were unsuccessful.

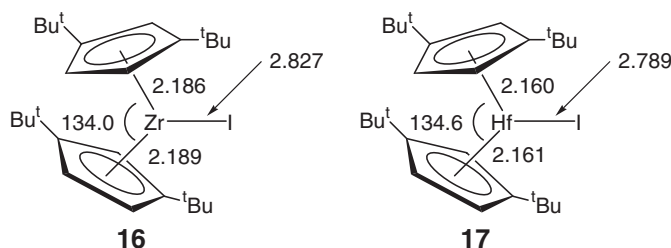
#### 4.07.5.2 Mononuclear Bis-cyclopentadienyl Zirconium(III) Compounds

The chemical reduction of zirconocene dichloride derivatives normally affords dinuclear zirconocene(III) complexes.<sup>2</sup> The bulky 1,3- $C_5H_3(^tBu)_2$  ligand is exceptional in stabilizing mononuclear metallocene(III) complexes. In 1989, the chlorides  $\{1,3-C_5H_3(^tBu)_2\}_2MCl$  ( $M = Zr, Hf$ ) were synthesized by reducing the dichlorides with potassium and the zirconium analog structurally characterized. A decade later, the iodides  $\{1,3-C_5H_3(^tBu)_2\}_2MI$  (**16**:  $M = Zr$ ; **17**:  $M = Hf$ ) were prepared through treatment of the corresponding metallocene diiodides with potassium amalgam.<sup>19</sup> Both **16** and **17** have been characterized by X-ray diffraction, and the important structural parameters are given in

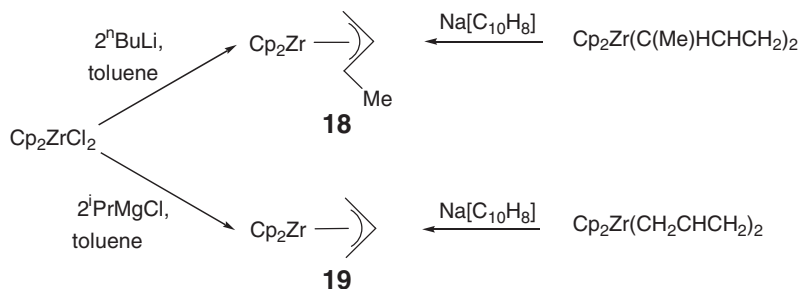


Scheme 6





**Figure 2** Selected bond lengths (Å) and angles (°) for complexes **16** and **17**.



**Scheme 7**

**Figure 2.** Compounds **16** and **17** react with  $I_2$  to regenerate the diiodide, in a process which was monitored thermochemically in order to provide a measure of the M–I bond strength.<sup>19</sup>

Thermal decomposition of the initial products from the reactions between  $Cp_2ZrCl_2$  and 2 equiv. of  $^nBuLi$  or  $^iPrMgCl$  leads to the allyl complexes  $Cp_2Zr(MeCHCHCH_2)$  **18** and  $Cp_2Zr(CH_2CHCH_2)$  **19**, respectively (Scheme 7).<sup>20</sup> The ESR spectra of solutions of **18** and **19** at room temperature and 203 K were consistent with the proposed structures (**18**:  $g = 1.994$ ,  $a(^{91}Zr) = 33.4$  G,  $a(^1H) = 0.56$  G ( $C_5H_5$ ),  $a(^1H) = 2.85$  G ( $MeCHCHCH_2$ ),  $a(^1H) = 3.705$  G ( $MeCHCHCH_2$ ); **19**:  $g = 1.994$ ,  $a(^{91}Zr) = 31.5$  G,  $a(^1H) = 0.52$  G ( $C_5H_5$ ),  $a(^1H) = 2.52$  G ( $CH_2CHCH_2$ )). Further evidence for the presence of an allyl ligand in **18** was forthcoming from the reaction with  $PhC(O)Cl$ , which yielded  $PhC(O)CH(Me)CH=CH_2$  and provided an estimate of 40–45% for the proportion of Zr(III) present. This estimate was supported through monitoring the paramagnetism by  $^1H$  NMR using the Evans method.<sup>21</sup> Complexes **18** and **19** could also be prepared through the reduction of  $Cp_2Zr(MeCHCHCH_2)_2$  and  $Cp_2Zr(CH_2CHCH_2)_2$  with sodium naphthalide (Scheme 7).

### 4.07.5.3 Dinuclear Bis-cyclopentadienyl Zirconium(III) Compounds

#### 4.07.5.3.1 Dinitrogen complexes

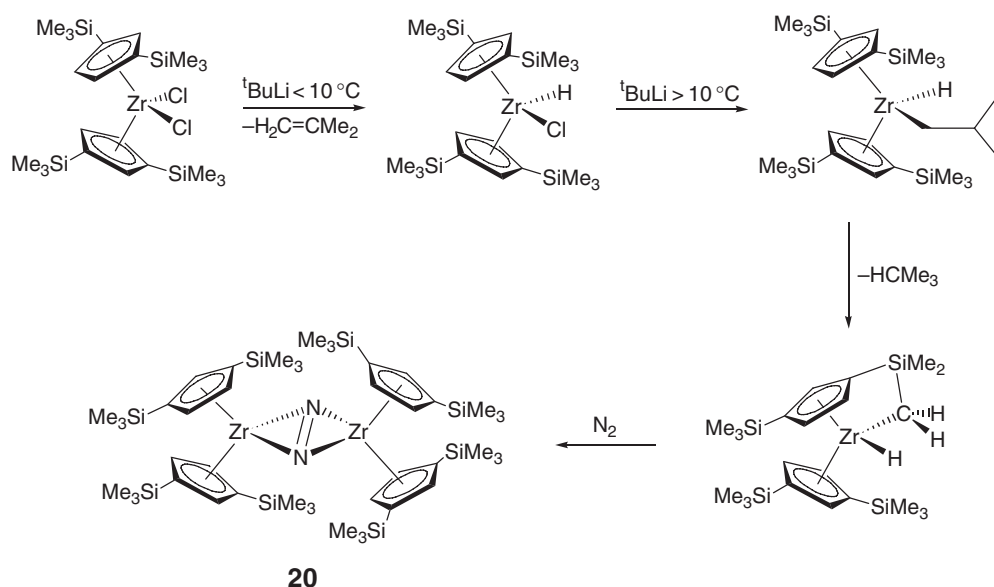
During the period documented by COMC(1995), dinuclear zirconocene(III) compounds were prepared using a variety of synthetic methods, including thermolysis of zirconocene(II) bis(phosphine) complexes and reduction of zirconocene(IV) precursors.<sup>2</sup>

In one such example, the reduction of  $\{1,3-C_5H_3(SiMe_3)_2\}_2ZrCl_2$  with sodium amalgam afforded the paramagnetic complex  $[\{1,3-C_5H_3(SiMe_3)_2\}_2Zr(\mu-Cl)]_2$ .<sup>22</sup> If, however,  $\{1,3-C_5H_3(SiMe_3)_2\}_2ZrCl_2$  is treated with 2 equiv. of  $^tBuLi$ , reduction proceeds according to Scheme 8, and dark purple  $[\{1,3-C_5H_3(SiMe_3)_2\}_2Zr]_2(\mu_2-\eta^2, \eta^2-N_2)$  **20** is formed by the reaction of dinitrogen with the cyclometallated zirconocene hydride.<sup>23</sup>

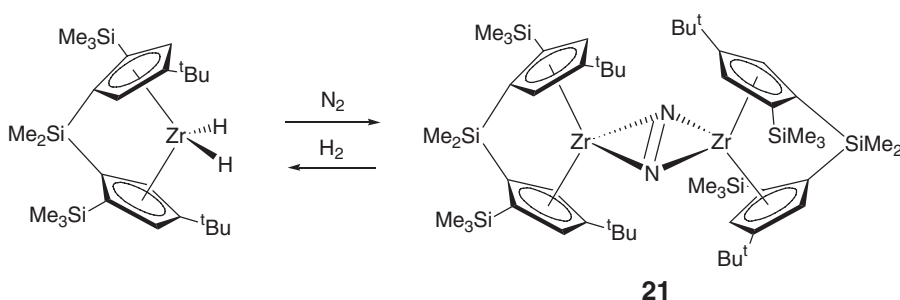
A related green *ansa*-metallocene dinitrogen complex  $[Me_2Si\{2,4-C_5H_2(SiMe_3)(^tBu)\}_2Zr]_2(\mu_2-\eta^2, \eta^2-N_2)$  **21** was (reversibly) prepared through exposure of the corresponding dihydride to an atmosphere of dinitrogen (Scheme 9).<sup>24</sup>

Confirmation of the side-on dinitrogen bonding in **20** and **21** (rather than the end-on bonding seen in the zirconocene(II) complex  $\{(C_5Me_5)_2ZrN_2\}$ )<sup>25</sup> was provided by single crystal X-ray crystallography. The bonding of the cyclopentadienyl ligands is unremarkable; therefore, only the bond lengths for the  $Zr_2N_2$  cores are represented schematically in Figure 3.

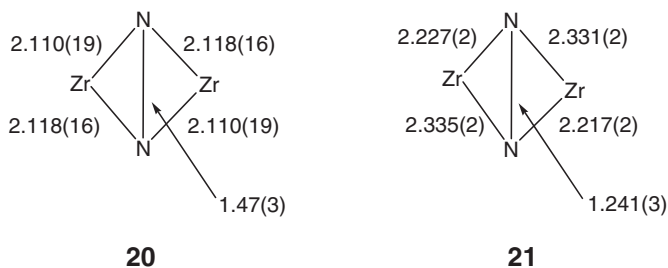




Scheme 8



Scheme 9

**Figure 3** Selected bond lengths (Å) for the  $\text{Zr}_2\text{N}_2$  cores of complexes **20** and **21**.

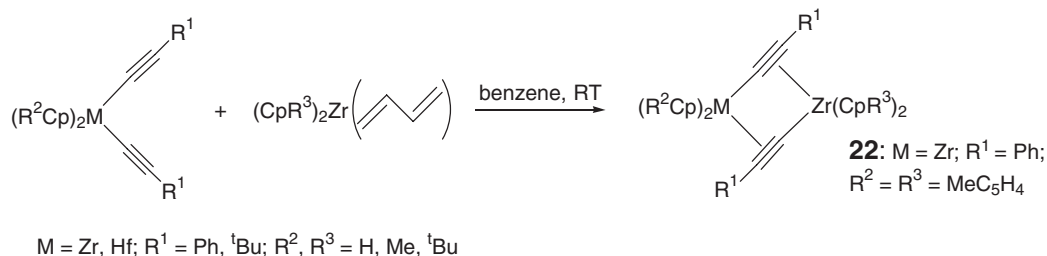
Complex **20** is paramagnetic with a magnetic moment of  $2.73 \mu_{\text{B}}$ , which is consistent with two  $d^1$ ,  $\text{Zr(III)}$  centers. Compound **21** also appears to contain two  $d^1$ ,  $\text{Zr(III)}$  centers, because although it is diamagnetic, the N–N bond length is comparable to other  $\text{N}=\text{N}$  double bonds and shorter than that for the formally dianionic  $\text{N}^{2-}=\text{N}^{2-}$  fragment in **20**. The observed diamagnetism of **21** requires antiferromagnetic coupling of the  $d^1$ ,  $\text{Zr(III)}$  centers.

#### 4.07.5.3.2 Alkynyl-bridged complexes

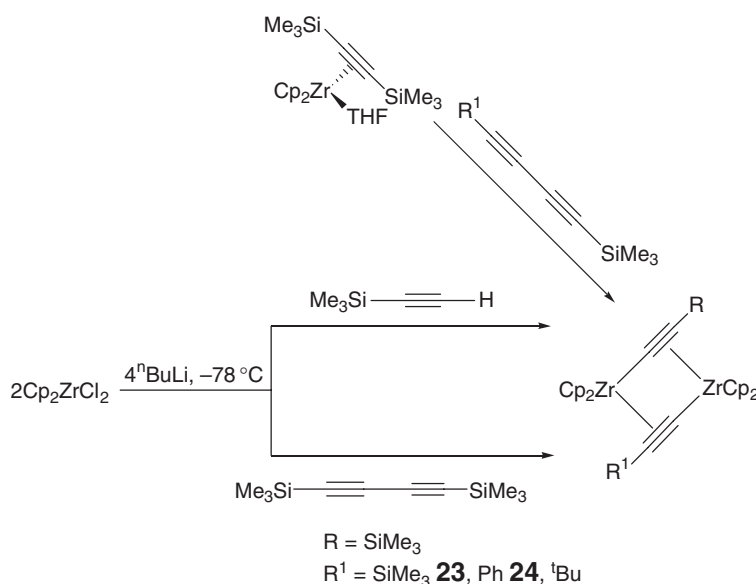
Several different methods have been described to prepare doubly alkynylide-bridged dinuclear zirconocene(III) compounds. The first approach reported was the comproportionation reaction between bis(alkynyl)metallocenes ( $M = \text{Zr, Hf}$ ) and (butadiene)zirconocene, which has been utilized to prepare the examples summarized in Scheme 10.<sup>26,27</sup> The solid-state structure of the representative example  $\{(\text{MeC}_5\text{H}_4)_2\text{Zr}(\mu\text{-C}\equiv\text{CPh})\}_2$  **22** was reported. Whereas  $\{\text{Cp}_2\text{Zr}(\mu\text{-C}\equiv\text{C-SiMe}_3)\}_2$  **23** was obtained in low yield by treating “ $\text{Cp}_2\text{Zr}$ ” with  $\text{Me}_3\text{SiC}\equiv\text{CH}$  or  $\text{Me}_3\text{SiC}\equiv\text{C-C}\equiv\text{CSiMe}_3$ , the reaction between  $\text{Cp}_2\text{Zr}(\text{THF})(\text{Me}_3\text{SiC}\equiv\text{CSiMe}_3)$  and  $\text{Me}_3\text{SiC}\equiv\text{C-C}\equiv\text{CSiMe}_3$  gave **23** in 45% yield (Scheme 11).<sup>28–30</sup> The latter method was also effective for the preparation of the mixed alkynylide complexes  $\text{Cp}_2\text{Zr}(\mu\text{-C}\equiv\text{C-SiMe}_3)(\mu\text{-C}\equiv\text{C-}^t\text{Bu})\text{ZrCp}_2$  and  $\text{Cp}_2\text{Zr}(\mu\text{-C}\equiv\text{C-SiMe}_3)(\mu\text{-C}\equiv\text{C-Ph})\text{ZrCp}_2$  **24**.

The solid-state structures of compounds **22–24** have been determined by X-ray crystallography, and the pertinent structural parameters are summarized in Table 2. In each case, zirconium is essentially symmetrically  $\pi$ -bonded to a second  $\text{Cp}_2\text{Zr-C}\equiv\text{CR}$ , forming a dimer, and the central  $\text{C}_4\text{Zr}_2$  cores are coplanar. The distance  $\text{C}_\alpha\text{-C}_{\pi\alpha}$  is too long to be regarded as a bonding interaction of the type seen in related titanium complexes (Figure 4).<sup>31</sup> Direct metal–metal interactions appear unlikely, since the Zr–Zr distances (Table 2) exceed the sum of the van der Waals radii (3.1 Å).<sup>27</sup> However, apparently there is electronic coupling via the unsaturated bridging groups, since the compounds are diamagnetic at room temperature and can be characterized by NMR spectroscopy.<sup>30</sup>

The side-on complexation mode of the metallocene to the alkyne function is easily recognized spectroscopically, since it leads to characteristic low-field shifts for the  $^{13}\text{C}$  resonances such that for complex **22**,  $\delta$  is 227.7 ( $\text{C}_\alpha$ ) and



Scheme 10

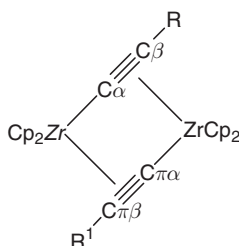


Scheme 11 Three routes to dinuclear zirconocene dialkynyl complexes.

**Table 2** Selected structural parameters for compounds **22–24** and **30**

Bond lengths (Å) and angles (°) <sup>a</sup>	<b>22</b>	<b>23</b>	<b>24</b>	<b>30</b>
Zr–Zr	3.506(1)	3.522(2)	3.528(2)	3.405(1)
Zr–C <sub>α</sub>	2.188(2)	2.191(5)	2.216(3)	2.181(9)
Zr–C <sub>πα</sub>	2.431(2)	2.420(5)	2.416(3)	2.417(8)
Zr–C <sub>πβ</sub>	2.407(2)	2.399(5)	2.354(3)	2.433(9)
Zr–C <sub>α</sub> –C <sub>β</sub>	172.3(1)	172.7(4)	173.3(3)	169.3(7)

<sup>a</sup>The atom designations are indicated schematically in Figure 4.

**Figure 4** Atom labeling system employed in Table 2: carbon atom labels are with respect to the italicized Zr atom.

155.4 (C<sub>β</sub>) ppm. This coordination mode also gives rise to prominent  $\nu(\text{C}\equiv\text{C})$  IR absorptions in the region 1875–1750 cm<sup>−1</sup>.<sup>27,30</sup>

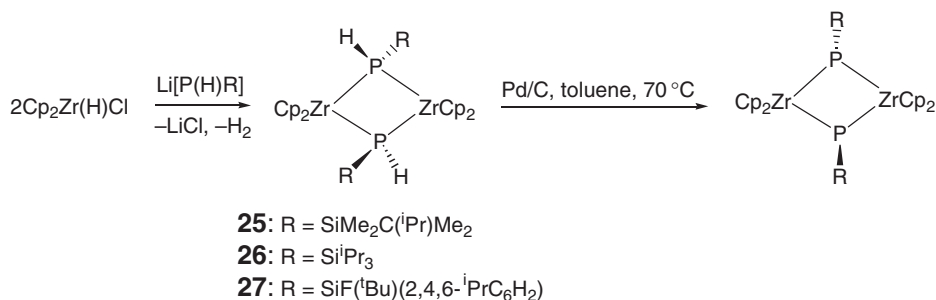
Alkynyl-bridged dinuclear zirconocene(III) compounds such as **22–24** (and **30** below) exhibit dynamic behavior and rapidly exchange alkynyl ligands between the two metal centers, in a process that can be monitored by variable-temperature NMR.<sup>27,32</sup>

#### 4.07.5.3.3 Phosphido-bridged complexes

Phosphido-bridged dinuclear zirconocene(III) complexes have been prepared through reaction of “Cp<sub>2</sub>Zr” with RPH<sub>2</sub> (R = cyclohexyl), and by treating the primary phosphine with [Cp<sub>2</sub>ZrClH]<sub>n</sub> (R = phenyl).<sup>2,33</sup> Treatment of [Cp<sub>2</sub>ZrClH]<sub>n</sub> with the lithium salts of three primary phosphines with bulky silyl substituents afforded the phosphido-bridged complexes {Cp<sub>2</sub>Zr(μ-P(H)R)}<sub>2</sub> **25–27** (Scheme 12).<sup>34</sup>

Compounds **25–27** were characterized by <sup>1</sup>H, <sup>31</sup>P NMR, and X-ray crystallography. They are diamagnetic and the large Zr–Zr separations of 3.64 Å **25**, 3.57 Å **26**, and 3.61 Å **27** indicate that there is no direct metal–metal bonding, and therefore the anti-ferromagnetic coupling must be ligand-mediated.

Heating toluene solutions of **25–27** to 70 °C in the presence of Pd/C resulted in dehydrogenation and formed neutral dinuclear phosphinidene-bridged zirconocene(IV) complexes (Scheme 12). In the case of **27**, dehydrogenation proceeded in refluxing toluene without a catalyst.

**Scheme 12**

#### 4.07.5.4 Dinuclear Fulvalene Zirconium(III) Compounds

Reduction of  $\text{Cp}_2\text{ZrCl}_2$  with 1.5 equiv. of sodium amalgam affords the fulvalene complex  $\{\text{CpZr}(\mu\text{-Cl})\}_2(\mu\text{-C}_5\text{H}_4\text{-C}_5\text{H}_4)$  **28**.<sup>35</sup> COMC(1995) summarized a number of phosphido, sulfide, imido, and alkyl complexes derived from **28**. Cuenca and co-workers have since reported further investigations into the chemistry of **28**, leading to new zirconium(IV)  $\mu$ -imido,  $\mu$ -( $\eta^2$ ,  $\eta^2$ -N,N-hydrazido), and  $\mu$ -( $\eta^1$ -C: $\eta^2$ -C,N-isocyanido) dinuclear fulvalene derivatives.<sup>36</sup>

The phosphido fulvalene zirconium(III) complex  $\{\text{CpZr}(\mu\text{-PPh}_2)\}_2(\mu\text{-C}_5\text{H}_4\text{-C}_5\text{H}_4)$  **29** was obtained by treating either **28** or the zirconium(IV) precursor  $\{\text{CpZrCl}_2\}_2(\mu\text{-C}_5\text{H}_4\text{-C}_5\text{H}_4)$  with 1 or 2 equiv. of  $\text{LiPPh}_2$  (Scheme 13).<sup>32</sup>

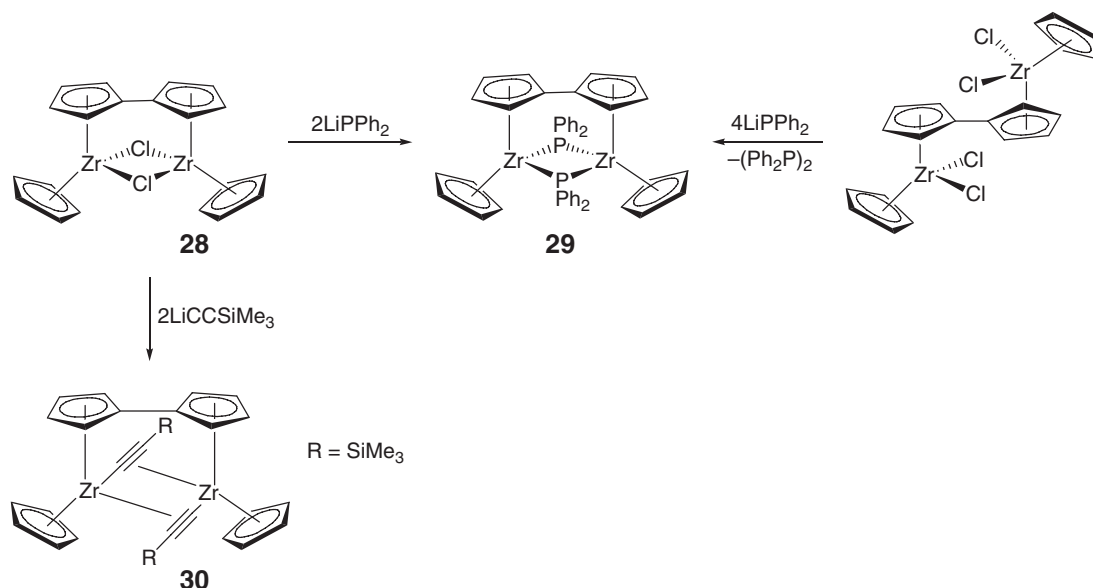
A fulvalene analog of the alkynyl-bridged complex **23**,  $\{\text{CpZr}(\mu\text{-C}\equiv\text{CSiMe}_3)\}_2(\mu\text{-C}_5\text{H}_4\text{-C}_5\text{H}_4)$  **30**, was prepared from **28** and  $\text{LiC}\equiv\text{CSiMe}_3$  (Scheme 13). Selected parameters from the structural characterization of **30** are given in Table 2. The most significant difference between the structures of **25** and **30** is the distortion from coplanar of the  $\text{Zr}_2\text{C}_4$  core, enforced by the fulvalene ligand. While the  $\text{Zr}\text{--}\text{Zr}$  distance in **30** is shorter than those found for **25**–**27**, it is still significantly longer than the sum of the van der Waals radii (3.1 Å).<sup>32</sup> Presumably, as for **25**–**27**, the diamagnetism of **30**, which was characterized by NMR spectroscopy, is the result of electronic coupling through the bridging alkynyl ligands.

The more sterically encumbered analog of **28**,  $\{[1,3\text{-C}_5\text{H}_3(\text{tBu})_2]\text{Zr}(\mu\text{-Cl})\}_2(\mu\text{-C}_5\text{H}_4\text{-C}_5\text{H}_4)$  **31**, was prepared by reduction of the mixed metallocene  $\text{Cp}\{1,3\text{-C}_5\text{H}_3(\text{tBu})_2\}\text{ZrCl}_2$  with sodium amalgam (Scheme 14).<sup>37,38</sup> Compound **31** exhibits similar reactivity to **28**, which is exemplified by oxidation with chlorine to give the zirconium(IV) dichloride, and with  $\text{CN}^t\text{Bu}$  affording the  $\mu$ -( $\eta^1$ -C: $\eta^2$ -C,N-isocyanido) complex (Scheme 14).

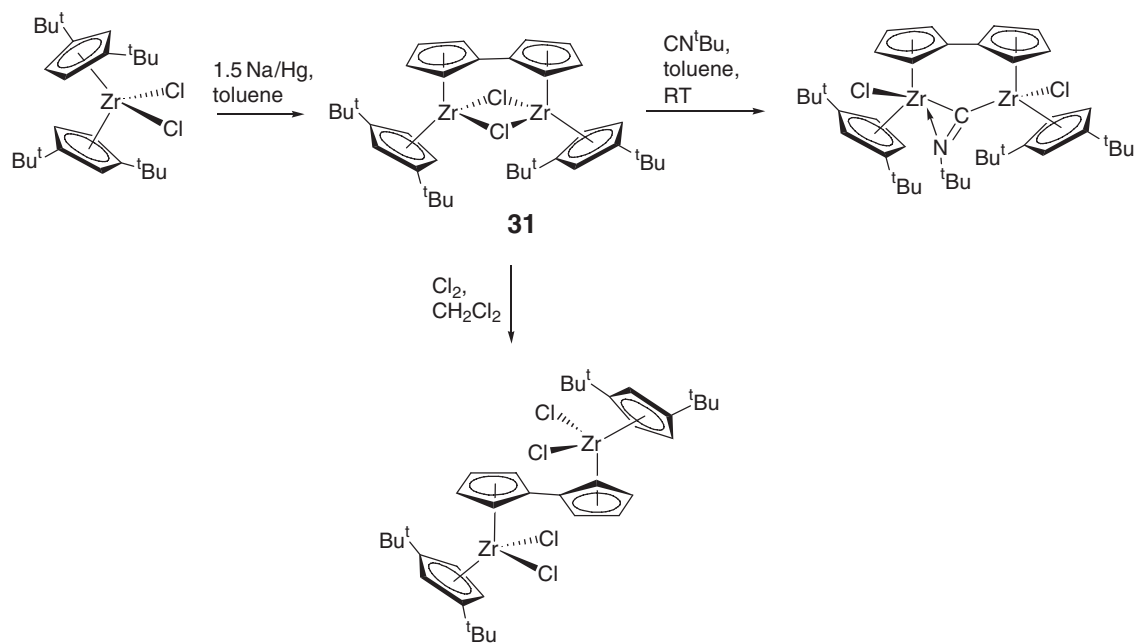
The doubly bridged zirconocene dichloride  $\{(\text{Me}_2\text{Si})_2(\text{C}_5\text{H}_3)_2\}\text{ZrCl}_2$  was reduced with 1 equiv. of sodium amalgam to give the red-brown dinuclear *ansa*-zirconocene(III)  $\{[(\text{Me}_2\text{Si})_2(\text{C}_5\text{H}_3)_2]\text{Zr}(\mu\text{-Cl})\}_2$  **32**.<sup>39</sup> The analogous compound with a single  $\text{Me}_2\text{Si}$  bridge was first reported in 1990.<sup>2,40</sup> Compound **32** is sparingly soluble in common NMR solvents and reacts immediately with halocarbons to give the  $\text{Zr(IV)}$  chloride. It is diamagnetic and has been characterized by NMR in benzene- $d_6$ .<sup>39</sup>

#### 4.07.5.5 Isolated Metallate(III) Compounds

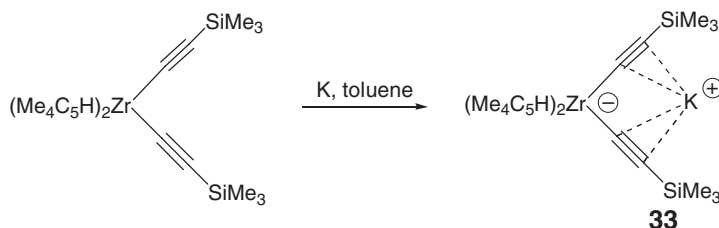
The zirconocenate(III) complex  $[\text{Bu}_4\text{N}][\{1,3\text{-C}_5\text{H}_3(\text{SiMe}_3)_2\}\text{ZrCl}_2]$  was prepared through nucleophilic attack on the dinuclear precursor  $\{[1,3\text{-C}_5\text{H}_3(\text{SiMe}_3)_2]\text{Zr}(\mu\text{-Cl})\}_2$ .<sup>22</sup> Since then, there have been only two reports of the isolation of zirconocenate(III) complexes.



Scheme 13



Scheme 14



Scheme 15

Reduction of the zirconocene(IV) dialkynyl  $(C_5HMe_4)_2Zr(C\equiv CSiMe_3)_2$  with potassium metal afforded  $K[(C_5HMe_4)_2Zr(C\equiv CSiMe_3)_2]$  **33** (Scheme 15).<sup>41</sup> Determination of the solid-state structure revealed that the potassium is intramolecularly coordinated to both alkyne functions and intermolecularly associated with the cyclopentadienyl ligand of an adjacent molecule.

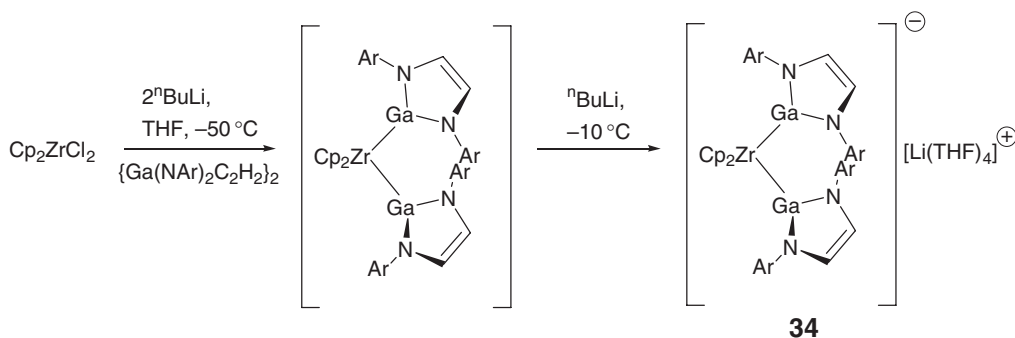
Compound **33** is paramagnetic; the ESR data are given in Table 3, and are similar to other reports of zirconocenate(III) complexes.<sup>2</sup> The UV/Vis spectrum has bands suggestive of a  $d-d$  (800–580 nm) and zirconium–alkynyl (440, 383 nm) transitions. The IR spectrum has intense  $\nu(C\equiv C)$  bands (1940 and  $1933\text{ cm}^{-1}$ ), which are shifted to low frequency relative to those in the zirconium(IV) precursor due to potassium coordination.

The di(gallyl)zirconocenate(III) complex  $[Li(THF)_4][Cp_2Zr\{Ga(NAr)_2C_2H_2\}_2]$  **34** was formed by the treatment of “ $Cp_2Zr$ ” with  $\{Ga(NAr)_2C_2H_2\}_2$  in the presence of excess  $nBuLi$  ( $Ar = 2,6\text{-}iPr_2C_6H_3$ ).<sup>42</sup> The reaction sequence is believed to proceed as depicted in Scheme 16, but attempts to isolate the Zr(IV) intermediate were not successful. It would appear that the gallyl ligands render the Zr(IV) complex more susceptible to reduction, since there is little precedent for the isolation of reduction products from the reaction of zirconocenes with alkyl lithiums.

The structure of compound **34** was elucidated by X-ray crystallography. The paramagnetism of **34** rendered NMR uninformative. Its ESR spectrum was recorded at  $25^\circ\text{C}$  and was dominated by hyperfine couplings to gallium ( $a(^{69}\text{Ga}) = 54.5\text{ G}$ ,  $a(^{71}\text{Ga}) = 70.0\text{ G}$ ), while the  $g_{iso}$  and  $a(^{91}\text{Zr})$  values are given for comparison in Table 3.<sup>42</sup>

**Table 3** Selected ESR spectral data on compounds **33** and **34**

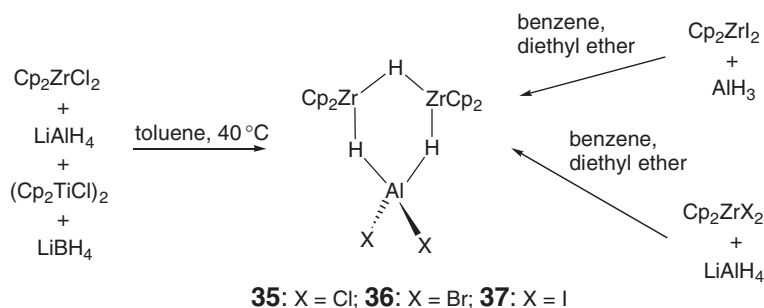
Compound	$g_{\text{iso}}$	$a(^{91}\text{Zr})$ (G)
$[\{1,3\text{-C}_5\text{H}_3(\text{SiMe}_3)_2\}_2\text{ZrCl}_2]^{-\text{a}}$	1.9856	17
<b>33</b>	1.9914	18.6
<b>34</b>	1.9735	15

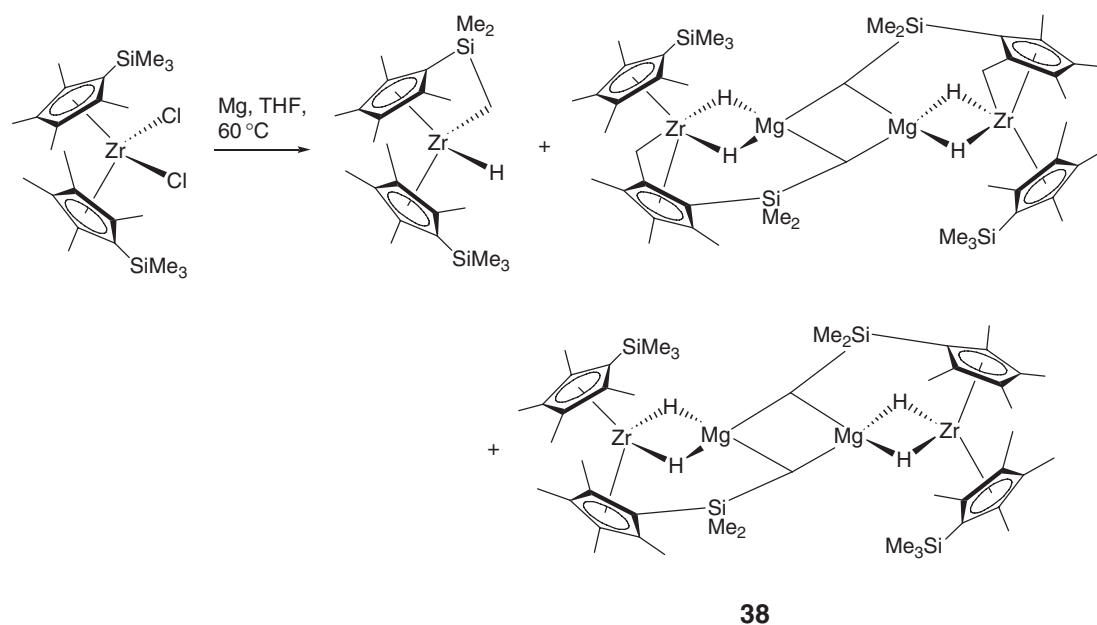
<sup>a</sup>Reference 22.**Scheme 16**

#### 4.07.5.6 Heterobimetallic Bis-cyclopentadienyl Zirconium(III) Hydride Complexes

Heterobimetallic zirconocene hydride complexes of the type  $[\text{M}][(\text{C}_5\text{H}_4\text{R})_2\text{ZrH}_2]$  were first characterized by ESR in 1991 ( $\text{M} = \text{Li}, \text{Na}, \text{K}$ ;  $\text{R} = \text{Me}, ^t\text{Bu}, \text{SiMe}_3$ ).<sup>2,43,44</sup> Aluminum–zirconium hydride complexes are involved in a number of catalytic and stoichiometric processes.<sup>4</sup> The presence of  $\text{Zr(III)}$  species in reaction mixtures has been inferred from the color<sup>45</sup> and, in the case of  $\text{Cp}_2\text{Zr}(\mu\text{-H})_2\text{Al}(\text{Me})(2,4,6\text{-}^t\text{Bu}_3\text{C}_6\text{H}_2)$ , detected by ESR.<sup>46</sup>

$\text{Cp}_2\text{ZrCl}_2$  is not reduced rapidly by  $\text{LiAlH}_4$ ; however, Bulychev and co-workers have shown that this reaction can be promoted by stoichiometric amounts of titanium compounds and catalyzed by certain other transition metal compounds.<sup>47,48</sup> For example, mixing the reagents  $\text{Cp}_2\text{ZrCl}_2$ ,  $(\text{Cp}_2\text{TiCl})_2$ ,  $\text{LiAlH}_4$ ,  $\text{LiBH}_4$  in toluene solution at  $40^\circ\text{C}$  afforded red needles of  $\{\text{Cp}_2\text{Zr}(\mu\text{-H})_2\}_2(\mu\text{-H})\text{AlCl}_2$  **35** (Scheme 17),<sup>47</sup> while treating  $\text{Cp}_2\text{ZrCl}_2$  with  $\text{LiAlH}_4$  in the presence of  $\text{CoBr}_2$  also gives compound **35**. The bromide **36** and iodide **37** analogs were also prepared using  $\text{CoBr}_2$  to catalyze reduction of the corresponding zirconocene dihalide by  $\text{AlH}_3$  or  $\text{LiAlH}_4$  (Scheme 17).

**Scheme 17**



Scheme 18

The structures of **35–37** were determined by X-ray crystallography, and all have a similar  $\text{Zr}_2\text{AlH}_3$  core, in which the Zr–Zr distances vary from 3.483 to 3.506 Å. Clearly, since the sum of the van der Waals radii is 3.1 Å, this is too long to be regarded as a Zr–Zr bond. A theoretical study of the bonding in related complexes has been reported.<sup>49,2</sup> The Zr–Al distances vary from 2.875 to 2.914 Å and are up to 0.12 Å shorter than the Zr–Al distances in comparable zirconocene(IV)–aluminum hydrides, suggesting that there may be a Zr–Al–Zr interaction. Interestingly, all three hydride bridges are retained in the presence of donor solvents such as THF and 1,4-dioxane.<sup>48</sup>

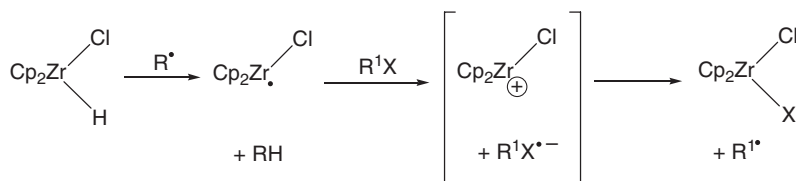
Solutions of **35** and **36** are diamagnetic and the complexes could be characterized by  $^1\text{H}$  and  $^{27}\text{Al}$  NMR.<sup>48</sup> It is not clear whether the apparent antiferromagnetic coupling of the two zirconium centers is mediated by Zr–Zr, Zr–Al–Zr interactions, or by the hydride bridges.

Mach and co-workers reported that reduction of  $(\text{C}_5\text{Me}_4(\text{SiMe}_3))_2\text{ZrCl}_2$  with excess magnesium in tetrahydrofuran afforded a mixture of products, one of which was the tetranuclear heterobimetallic organozirconium(III) complex **38** (Scheme 18).<sup>50</sup> It proved impossible to separate **38** from the doubly activated zirconium(IV) compound by fractional crystallization. Mixtures were paramagnetic, and **38** was characterized by ESR ( $g_{\text{iso}} = 1.9870$ ,  $a(^1\text{H}) = 7.1 \text{ G}$  ( $\mu\text{-H}$ )).

#### 4.07.5.7 Bis-cyclopentadienyl Zirconium(III) Halides in Organic Synthesis

$(\text{Cp}_2\text{ZrCl})_2$  was first reported by Floriani and co-workers in 1984, and can be prepared by reducing zirconocene dichloride with 1 equiv. of sodium amalgam.<sup>51,52</sup> Despite the fact that  $(\text{Cp}_2\text{ZrCl})_2$  should be a more potent reducing agent, it proved to be less reactive than  $(\text{Cp}_2\text{TiCl})_2$  in promoting certain radical reactions.<sup>53,54</sup> This was attributed to the dimer's resistance to dissociation.

Oshima and co-workers demonstrated that it is a much more effective reagent when prepared *in situ*. Alkyl radicals, generated for example by the trace oxidation of  $\text{Et}_3\text{B}$ , react with  $\text{Cp}_2\text{Zr}(\text{H})\text{Cl}$  through hydrogen abstraction to afford highly reactive  $[\text{Cp}_2\text{ZrCl}]$ .<sup>55</sup>  $[\text{Cp}_2\text{ZrCl}]$  prepared in this fashion acts as a single-electron reductant toward alkyl halides giving transient halide anions, which decompose, affording the desired alkyl radical and zirconocene(IV) dihalide (Scheme 19). Following the target radical-coupling reaction, the product radical can then react with further  $\text{Cp}_2\text{Zr}(\text{H})\text{Cl}$  forming a new Zr(III) center. This reaction sequence has been used to promote radical cyclizations and allylations.<sup>55–57</sup>

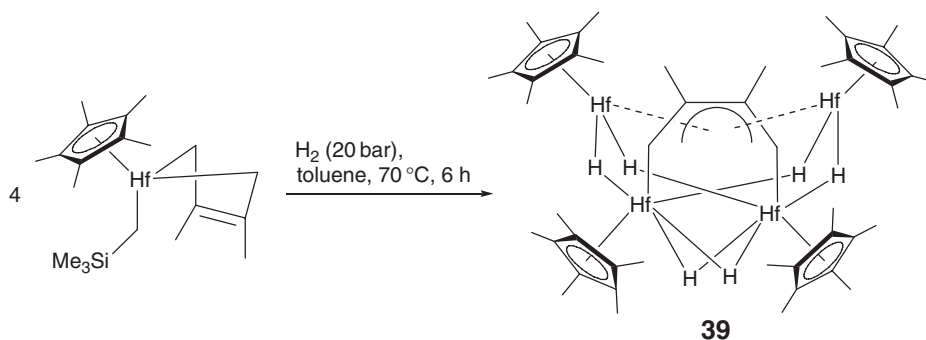


Scheme 19

#### 4.07.6 Compounds with Metal–Metal Bonds; Mixed-Valence Compounds

There have been no systematic investigations of mixed-valent polyorganometallic complexes containing zirconium or hafnium in oxidation state III. However, since 2001, one zirconium and one hafnium example have been definitively characterized by X-ray crystallography.

Treating  $(\text{C}_5\text{Me}_5)\text{Hf}(\text{2,3-dimethyl-1,3-butadiene})(\text{CH}_2\text{SiMe}_3)$  with dihydrogen at moderate temperature and pressure leads to the isolation of deep red crystals of the tetranuclear complex **39** (Scheme 20).<sup>58</sup> It is not clear how the complex is formed, but under optimized conditions the isolated yield reaches 44%. Determination of the solid-state structure revealed four hafnium atoms in a butterfly arrangement: Hf(3) and Hf(4) are  $\eta^1$ -bonded and Hf(1) and Hf(2)  $\eta^4$ -bonded to the single central 2,3-dimethyl-1,3-butadiene-1,4-diyl fragment. Selected atom–atom distances are represented schematically in Figure 5. Since the 1,4-diyl is formally a tetranionic ligand, compound **39** can be regarded as mixed-valent  $\text{Hf(III)}_2\text{Hf(IV)}_2$ . The Hf(3)–Hf(4) distance is substantially shorter than the remaining Hf–Hf distances and is the shortest reported for a molecular compound of hafnium. Compound **39** could be



Scheme 20

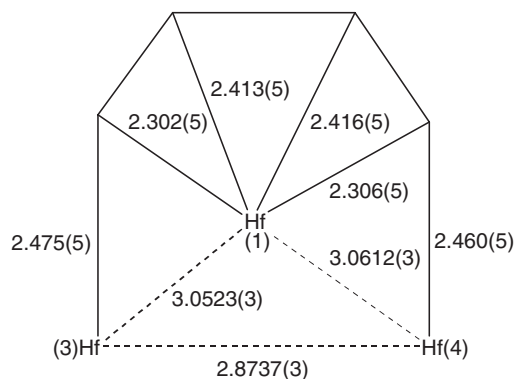
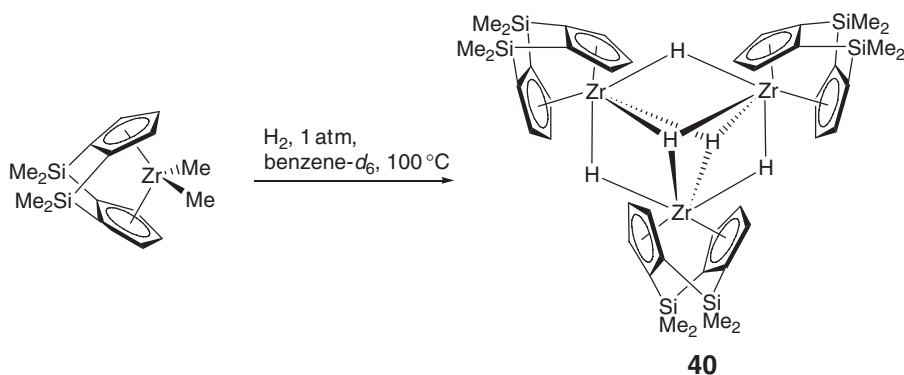
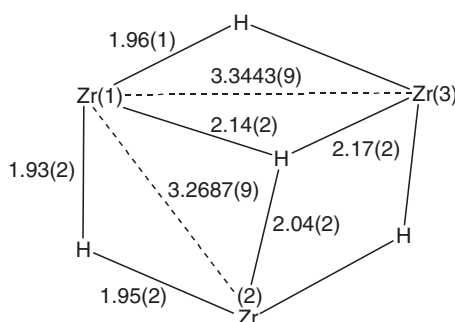


Figure 5 Selected Hf–Hf and Hf–C distances (Å) in compound **39**.





Scheme 21

Figure 6 Zr-Zr and Zr-H distances (Å) for the core of compound **40**.

characterized by NMR, indicating that it is diamagnetic as a result either of an  $\text{Hf}(3)\text{--Hf}(4)$  single bond or a ligand-mediated antiferromagnetic coupling.

The most significant feature of the reported NMR spectra was the  $^{13}\text{C}$  methyne resonance at  $\delta = 115.0$  ( $J_{\text{CH}} = 145$  Hz) ppm, which is significantly higher field than that seen in related complexes.

Heating a  $\text{benzene-}d_6$  solution of  $\{(\text{Me}_2\text{Si})_2(\text{C}_5\text{H}_3)_2\}\text{ZrMe}_2$  to  $100^\circ\text{C}$  under an atmosphere of  $\text{H}_2$  resulted in methane evolution and precipitation of crystals of **40** (Scheme 21).<sup>24</sup> Compound **40** proved to be insoluble in all common organic solvents and was therefore not characterized spectroscopically.

The trinuclear structure of **40** was elucidated by X-ray crystallography. The molecule lies on a twofold axis through  $\text{Zr}(2)$ , and the  $\text{Zr}\text{--Zr}$  and  $\text{Zr}\text{--H}$  distances are represented schematically in Figure 6. The three  $\mu^2\text{-hydride}$  ligands and three zirconium atoms are essentially coplanar, with  $\mu^3\text{-hydrides}$  above and below the plane. There are five hydrides and three zirconium atoms so compound **40** is formally mixed-valent  $\text{Zr}(\text{III})\text{Zr}(\text{IV})_2$ . The shorter  $\text{Zr}\text{--Zr}$  distances in **40** compared to those seen in  $\text{Zr}(\text{IV})$  dihydride dimers are consistent with the presence of  $\text{Zr}\text{--Zr}$  bonding.<sup>24</sup>

## References

- Cardin, D. J.; Lappert, M. F.; Raston, C. L.; Riley, P. I. In *Comprehensive Organometallic Chemistry I*; Wilkinson, G., Stone, F. G. A., Abel, E. W., Eds.; Pergamon: Oxford, 1982; Vol. 3, 549.
- Ryan, E. J. In *Comprehensive Organometallic Chemistry II*; Abel, E. W., Stone, F. G. A., Wilkinson, G., Eds.; Elsevier: Oxford, 1995; Vol. 4, Chapter 8, 465–481.
- Wielstra, Y.; Gambarotta, S.; Chiang, M. Y. *Recl. Trav. Chim. Pays-Bas* **1989**, *108*, 1–6.
- Cardin, D. J.; Lappert, M. F.; Raston, C. L. *Chemistry of Organo-Zirconium and -Hafnium Compounds*; Ellis Horwood: Chichester, 1986.
- Brand, H.; Arnold, J. *Angew. Chem., Int. Ed. Engl.* **1994**, *33*, 95–97.
- Ray, B.; Neyroud, T. G.; Kapon, M.; Eichen, Y.; Eisen, M. S. *Organometallics* **2001**, *20*, 3044–3055.
- Fryzuk, M. D.; Mylvaganam, M.; Zaworotko, M. J.; MacGillivray, L. R. *J. Am. Chem. Soc.* **1993**, *115*, 10360–10361.
- Fryzuk, M. D.; Mylvaganam, M.; Zaworotko, M. J.; MacGillivray, L. R. *Polyhedron* **1996**, *15*, 689–703.
- Fryzuk, M. D.; Jafarpour, L.; Rettig, S. J. *Organometallics* **1999**, *18*, 4050–4058.

10. Fryzuk, M. D.; Haddad, T. S.; Mylvaganam, M.; McConville, D. H.; Rettig, S. J. *J. Am. Chem. Soc.* **1993**, *115*, 2782–2792.
11. Baker, R. T.; Whitney, J. F.; Wreford, S. S. *Organometallics* **1983**, *2*, 1049–1051.
12. Kim, H.-J.; Jung, S.; Jeon, Y.-M.; Whang, D.; Kim, K. *Chem. Commun.* **1997**, 2201–2202.
13. Lappert, M. F.; Pickett, C. J.; Riley, P. I.; Yarrow, P. I. W. *J. Chem. Soc., Dalton Trans.* **1981**, 805–813.
14. Langmaier, J.; Samec, Z.; Varga, V.; Horáček, M.; Choukroun, R.; Mach, K. *J. Organomet. Chem.* **1999**, *584*, 323–328.
15. Samuel, E.; Hénique, J. *J. Organomet. Chem.* **1996**, *512*, 183–187.
16. Samuel, E.; Guery, D.; Vedel, J.; Basile, F. *Organometallics* **1985**, *4*, 1073–1077.
17. Lappert, M. F.; Raston, C. L.; Skelton, B. W.; White, A. H. *J. Chem. Soc., Dalton Trans.* **1997**, 2895–2902.
18. Urazowski, I. F.; Ponomaryev, V. I.; Nifant'ev, I. E.; Lemenovskii, D. A. *J. Organomet. Chem.* **1989**, *368*, 287–294.
19. King, W. A.; Di Bella, S.; Gulino, A.; Lanza, G.; Fragalà, I. L.; Stern, C. L.; Marks, T. J. *J. Am. Chem. Soc.* **1999**, *121*, 355–366.
20. Soleil, F.; Choukroun, R. *J. Am. Chem. Soc.* **1997**, *119*, 2938–2939.
21. Löliger, J.; Scheffold, R. *J. Chem. Edu.* **1972**, *49*, 646–647.
22. Hitchcock, P. B.; Lappert, M. F.; Lawless, G. A.; Olivier, H.; Ryan, E. J. *J. Chem. Soc., Chem. Commun.* **1992**, 474–476.
23. Pool, J. A.; Lobkovsky, E.; Chirik, P. J. *J. Am. Chem. Soc.* **2003**, *125*, 2241–2251.
24. Chirik, P. J.; Henling, L. M.; Bercaw, J. E. *Organometallics* **2001**, *20*, 534–544.
25. Sanner, R. D.; Manriquez, J. M.; Marsh, R. E.; Bercaw, J. E. *J. Am. Chem. Soc.* **1976**, *98*, 8351–8357.
26. Erker, G.; Frömberg, W.; Mynott, R.; Gabor, B.; Krüger, C. *Angew. Chem., Int. Ed. Engl.* **1986**, *25*, 463–465.
27. Erker, G.; Frömberg, W.; Benn, R.; Mynott, R.; Angermund, K.; Krüger, C. *Organometallics* **1989**, *8*, 911–920.
28. Metzler, N.; Nöth, H. *J. Organomet. Chem.* **1993**, *454*, C5–C7.
29. Hsu, D. P.; Davis, W. M.; Buchwald, S. L. *J. Am. Chem. Soc.* **1993**, *115*, 10394–10395.
30. Rosenthal, U.; Ohff, A.; Baumann, W.; Kempe, R.; Tillack, A.; Burlakov, V. V. *Organometallics* **1994**, *13*, 2903–2906.
31. Sekutowski, D. G.; Stucky, G. D. *J. Am. Chem. Soc.* **1976**, *98*, 1376–1382.
32. Cano, A.; Cuenca, T.; Galakhov, M.; Rodríguez, G. M.; Royo, P.; Cardin, C. J.; Convery, M. A. *J. Organomet. Chem.* **1995**, *493*, 17–25.
33. Ho, J.; Hou, Z.; Drake, R. J.; Stephan, D. W. *Organometallics* **1993**, *12*, 3145–3157.
34. Driess, M.; Aust, J.; Merz, K. *Eur. J. Inorg. Chem.* **2005**, 866–871.
35. Cuenca, T.; Herrmann, W. A.; Ashworth, T. V. *Organometallics* **1986**, *5*, 2514–2517.
36. González-Maupoe, M.; Rodríguez, G. M.; Cuenca, T. *Eur. J. Inorg. Chem.* **2002**, 2057–2063.
37. Royo, E.; Galakhov, M.; Royo, P.; Cuenca, T. *Organometallics* **2000**, *19*, 3347–3353.
38. González-Maupoe, M.; Rodríguez, G. M.; Cuenca, T. *J. Organomet. Chem.* **2002**, *645*, 112–117.
39. Cano, A.; Cuenca, T.; Gómez-Sal, P.; Manzanero, A.; Royo, P. *J. Organomet. Chem.* **1996**, *526*, 227–235.
40. Gomez, R.; Cuenca, T.; Royo, P.; Pellingelli, A.; Tiripicchio, A. *Organometallics* **1991**, *10*, 1505–1510.
41. Varga, V.; Hiller, J.; Thewalt, U.; Polášek, M.; Mach, K. *J. Organomet. Chem.* **1998**, *553*, 15–22.
42. Baker, R. J.; Jones, C.; Murphy, D. M. *Chem. Commun.* **2005**, 1339–1341.
43. Choukroun, R.; Dahan, F.; Larssonneur, A.; Samuel, E.; Petersen, J.; Meunier, P.; Sornay, C. *Organometallics* **1991**, *10*, 374–376.
44. Larssonneur, A.; Choukroun, R.; Jaud, J. *Organometallics* **1993**, *12*, 3216–3224.
45. Khan, K.; Raston, C. L.; McGrady, J. E.; Skelton, B. W.; White, A. H. *Organometallics* **1997**, *16*, 3252–3254.
46. Wehmschulte, R. J.; Power, P. P. *Polyhedron* **1999**, *18*, 1885–1888.
47. Sizov, A. I.; Zvukova, T. M.; Belsky, V. K.; Bulychev, B. M. *J. Organomet. Chem.* **2001**, *619*, 36–42.
48. Sizov, A. I.; Zvukova, T. M.; Khvostov, A. V.; Belsky, V. K.; Stash, A. I.; Bulychev, B. M. *J. Organomet. Chem.* **2003**, *681*, 167–173.
49. DeKock, R. L.; Peterson, M. A.; Reynolds, L. E. L.; Chen, L.-H.; Baerends, E. J.; Vernooijs, P. *Organometallics* **1993**, *12*, 2794–2805.
50. Horáček, M.; Štěpnička, P.; Kubišta, J.; Fejfarová, K.; Gyepes, R.; Mach, K. *Organometallics* **2003**, *22*, 861–869.
51. Fochi, G.; Guidi, G.; Floriani, C. *J. Chem. Soc., Dalton Trans.* **1984**, 1253–1256.
52. Cuenca, T.; Royo, P. *J. Organomet. Chem.* **1985**, *293*, 61–67.
53. Barden, M. C.; Schwartz, J. *J. Org. Chem.* **1997**, *62*, 7520–7521.
54. Spencer, R. P.; Schwartz, J. *Tetrahedron* **2000**, *56*, 2103–2112.
55. Fujita, K.; Nakamura, T.; Yorimitsu, H.; Oshima, K. *J. Am. Chem. Soc.* **2001**, *123*, 3137–3138.
56. Fujita, K.; Yorimitsu, H.; Oshima, K. *Bull. Chem. Soc. Jpn.* **2004**, *77*, 1727–1736.
57. Hirano, K.; Fujita, K.; Shinokubo, H.; Oshima, K. *Org. Lett.* **2004**, *6*, 593–595.
58. Visser, C.; van den Hende, J. R.; Meetsma, A.; Hessen, B. *Organometallics* **2003**, *22*, 615–617.

# 4.08

## Complexes of Zirconium and Hafnium in Oxidation State IV

---

E Y-X Chen and A Rodriguez-Delgado, Colorado State University, Fort Collins, CO, USA

© 2007 Elsevier Ltd. All rights reserved.

<b>4.08.1</b>	<b>Introduction</b>	<b>761</b>
<b>4.08.2</b>	<b>Complexes with <math>\eta^1</math>-Ligands</b>	<b>763</b>
4.08.2.1	Alkyl, Halide, and Amide Precursors for Complexes of Higher Ligand Hapticity	763
4.08.2.2	Alkynyl, Aryl, and Aryloxide Complexes	764
4.08.2.3	Amido Alkyls and Halides	765
4.08.2.4	Phosphinimide Complexes	767
<b>4.08.3</b>	<b>Complexes with <math>\eta^2</math>-Ligands</b>	<b>767</b>
4.08.3.1	Chelating Bis(amido) $[N^-, N^-]$ Complexes	767
4.08.3.1.1	Silylamido $[N^-, N^-]$ complexes	767
4.08.3.1.2	Arylamido $[N^-, N^-]$ complexes	771
4.08.3.1.3	Borylamido $[N^-, N^-]$ complexes	772
4.08.3.1.4	Ferrocenylamido $[N^-, N^-]$ complexes	773
4.08.3.2	Amidinate $[N_2^-]$ Complexes	774
4.08.3.3	Guanidinate $[N_2^-]$ Complexes	776
4.08.3.4	$\beta$ -diketiminato $[N_2^-]$ Complexes	779
4.08.3.5	Pyrrolide, Pyrazolato, Enamido, and Amido Nitrogen-donor $[N^-, N]$ Complexes	780
4.08.3.6	Amido Oxygen-donor $[N^-, O]$ and Amido Aryloxide $[N^-, O^-]$ Complexes	783
4.08.3.7	$\beta$ -Ketoiminato $[(N, O)^-]$ Complexes	784
4.08.3.8	Chelating Aryloxide $[O^-, O^-]$ and Thiolate $[S^-, S^-]$ Complexes	784
4.08.3.9	Aryloxide and Alkoxide Donor $[O^-, D]$ ( $D = N, O$ ) Complexes	785
4.08.3.10	Carbanion Nitrogen-donor $[C^-, N]$ and Carbanion Amido $[C^-, N^-]$ Complexes	788
4.08.3.11	Phosphinomethanide $[C^-, P]$ and $[P_2^-]$ Complexes	789
<b>4.08.4</b>	<b>Complexes with <math>\eta^3</math>-Ligands</b>	<b>789</b>
4.08.4.1	Bis(amido) Nitrogen-donor $[N^-, N, N^-]$ Complexes	790
4.08.4.1.1	Bis(amido)amine and pyridine complexes	790
4.08.4.1.2	Cyclodiphosph(III)azane-bridged bis(amido) complexes	793
4.08.4.2	Bis(amido) Oxygen-donor $[N^-, O, N^-]$ Complexes	795
4.08.4.2.1	Bis(amido)aryl ether and thioether complexes	795
4.08.4.2.2	Bis(amido)alkyl ether, thioether, and silyl ether complexes	797
4.08.4.3	Bis(amido) Carbene-donor $[N^-, C, N^-]$ and Bis(imino) Carbene $[N, C^{2-}, N]$ Complexes	798
4.08.4.4	Amido Phosphine-donor $[N^-, P, N^-]$ and $[P, N^-, P]$ Complexes	799
4.08.4.5	Tripodal Triamido $[N^-, N^-, N^-]$ Complexes	800
4.08.4.6	Tris(pyrazolyl)borate $[N_3^-]$ Complexes	803
4.08.4.7	Amido Nitrogen-donor $[N, N^-, N]$ Complexes	804
4.08.4.8	Bis(alkoxide) Nitrogen-donor $[O^-, N, O^-]$ Complexes	805
4.08.4.9	$\sigma$ -Aryl Nitrogen-donor $[C^-, N, C^-]$ and $[C^-, N, O^-]$ Complexes	806

<b>4.08.5 Complexes with <math>\eta^4</math>-Ligands</b>	<b>807</b>
4.08.5.1 Chelating $\beta$ -diketiminato [ $N_2^-$ , $N_2^-$ ] Complexes	807
4.08.5.2 Porphyrinato [ $N^-$ , $N$ , $N^-$ , $N$ ] Complexes	809
4.08.5.3 Tropocoronandato [ $N^-$ , $N$ , $N^-$ , $N$ ] Complexes	810
4.08.5.4 Triamidoamine [ $N^-$ , $N^-$ , $N$ , $N^-$ ] Complexes	811
4.08.5.5 Chelating Diamido–Diamine [ $N^-$ , $N$ , $N$ , $N^-$ ] Complexes	811
4.08.5.6 Chelating Guanidinato [ $N_2^-$ , $N_2^-$ ] Complexes	812
4.08.5.7 Chelating Bis(phenoxy) Amine-donor [ $O^-$ , $N$ , $D$ , $O^-$ ] ( $D = N, O, S$ ) Complexes	813
4.08.5.8 Chelating Bis(phenoxy) Imine-donor [ $O^-$ , $N$ , $N$ , $O^-$ ] Complexes	814
4.08.5.9 Chelating Bis(phenoxy) Sulfur-donor [ $O^-$ , $S$ , $S$ , $O^-$ ] Complexes	816
4.08.5.10 Chelating $\beta$ -Ketoiminato [ $O^-$ , $N$ , $N$ , $O^-$ ] Complexes	816
4.08.5.11 Chelating Bis(amido) Phosphine-donor [ $N^-$ , $P$ , $P$ , $N^-$ ] Complexes	816
<b>4.08.6 Complexes with Non-Cyclopentadienyl <math>\eta^5</math>-Ligands</b>	<b>817</b>
4.08.6.1 Complexes Containing Aminoquinolato [ $N$ , $N^-$ , $O$ , $N^-$ , $N$ ] Ligands	817
4.08.6.2 Complexes Containing Pyrrolyl Ligands	817
4.08.6.3 Complexes Containing Carboranyl Ligands	819
4.08.6.4 Complexes Containing Phospholyl Ligands	819
<b>4.08.7 Monocyclopentadienyl Complexes</b>	<b>820</b>
4.08.7.1 Non-functionalized Mono-Cp Complexes Containing Monodentate Ligands	820
4.08.7.1.1 Complexes containing halide, alkyl, and aryl ligands	820
4.08.7.1.2 Complexes containing nitrogen ligands	824
4.08.7.1.3 Complexes containing oxygen and sulfur ligands	827
4.08.7.2 Non-functionalized Mono-Cp Complexes Containing Multidentate Ligands	827
4.08.7.2.1 Complexes containing bidentate amidinate and guanidinate [ $N_2^-$ ] ligands	827
4.08.7.2.2 Complexes containing other bidentate ligands	831
4.08.7.2.3 Complexes containing tri-, tetra-, and pentadentate ligands	835
4.08.7.3 Silylated Mono-Cp Complexes	840
4.08.7.3.1 Bis(trimethylsilyl)cyclopentadienyl (Cp <sup>+</sup> ) complexes	840
4.08.7.3.2 Hydrido- and chlorosilyl mono-Cp complexes	843
4.08.7.4 Boryl and Borato Mono-Cp Complexes	845
4.08.7.5 Complexes of Mono-Cp Bearing Neutral Pendant Donors	846
4.08.7.5.1 Complexes with pendant <i>N</i> -donors	847
4.08.7.5.2 Complexes with pendant <i>O</i> - and <i>S</i> -donors	848
4.08.7.5.3 Complexes with pendant <i>P</i> -donors	850
<b>4.08.8 <i>ansa</i>-Monocyclopentadienyl “Constrained-Geometry” Complexes</b>	<b>851</b>
4.08.8.1 <i>ansa</i> -Cp–amido Complexes	852
4.08.8.1.1 Cp/silylamido complexes containing monodentate ligands	852
4.08.8.1.2 Cp–silylamido diene complexes	859
4.08.8.1.3 Tridentate Cp–silylamido complexes	860
4.08.8.1.4 Bimetallic <i>ansa</i> -Ind–silylamido complexes	863
4.08.8.1.5 Hydrocarbyl-bridged Cp–amido complexes	864
4.08.8.2 <i>ansa</i> -Cp–Oxo Complexes	866
4.08.8.3 <i>ansa</i> -Cp/Phosphido Complexes	869
4.08.8.4 <i>ansa</i> -Cp/Carbanionic Complexes	870
<b>4.08.9 Bis(Cyclopentadienyl) Complexes</b>	<b>870</b>
4.08.9.1 Complexes with M–X (Halide) Bonds	870

4.08.9.1.1	Non-functionalized metallocene halides	870
4.08.9.1.2	Ring-functionalized metallocene halides	874
4.08.9.2	Complexes with M–H Bonds	878
4.08.9.3	Complexes with M–C Bonds	884
4.08.9.3.1	Complexes containing M–C $sp^3$ -bonds	884
4.08.9.3.2	Complexes containing M–C $sp^2$ -bonds	887
4.08.9.3.3	Complexes containing M–C $sp$ -bonds	895
4.08.9.4	Cationic Zirconocene Complexes	896
4.08.9.5	Complexes with M–N Bonds	910
4.08.9.6	Complexes with M–O Bonds	917
4.08.9.7	Complexes with M–Si Bonds	925
4.08.9.8	Complexes with M–P Bonds	927
4.08.9.9	Complexes with M–E (S, Se, Te) Bonds	930
4.08.10	<b><i>ansa</i>-Metallocene Complexes</b>	<b>934</b>
4.08.10.1	$C_2$ -bridged Complexes	934
4.08.10.1.1	<i>ansa</i> -Cyclopentadienyl complexes	934
4.08.10.1.2	<i>ansa</i> -Bis(indenyl) complexes	935
4.08.10.1.3	<i>ansa</i> -Fluorenyl complexes	942
4.08.10.2	Si-bridged <i>ansa</i> -Zirconocene Complexes	944
4.08.10.2.1	Si-bridged cyclopentadienyl complexes	945
4.08.10.2.2	Si-bridged indenyl complexes	953
4.08.10.2.3	Si-bridged fluorenyl complexes	958
4.08.10.3	$C_1$ -bridged Complexes	960
4.08.10.3.1	$C_1$ -bridged cyclopentadienyl complexes	960
4.08.10.3.2	$C_1$ -bridged indenyl complexes	962
4.08.10.3.3	$C_1$ -bridged fluorenyl complexes	963
4.08.10.4	Other ( <i>B</i> , <i>P</i> , <i>N</i> , <i>Ge</i> , <i>Sn</i> , $C_n$ )-bridged Complexes	967
4.08.10.4.1	Cyclopentadienyl complexes with ( <i>B</i> , <i>P</i> , <i>N</i> , <i>Ge</i> , <i>Sn</i> , $C_n$ )-bridges	967
4.08.10.4.2	Indenyl complexes with ( <i>B</i> , <i>P</i> , <i>N</i> , <i>Ge</i> , <i>Sn</i> , $C_n$ )-bridges	972
4.08.10.4.3	Fluorenyl complexes with ( <i>B</i> , <i>P</i> , <i>N</i> , <i>Ge</i> , <i>Sn</i> , $C_n$ )-bridges	974
4.08.11	<b>Complexes with more than Two Cyclopentadienyl Ligands</b>	<b>975</b>
4.08.12	<b>Complexes with <math>\eta^n</math>- (<math>n \geq 6</math>) Ligands</b>	<b>978</b>
4.08.12.1	$\eta^6$ -Arene Complexes	978
4.08.12.2	Borata-benzene Complexes	978
4.08.12.3	Other Complexes with $\eta^6$ - or $\eta^7$ -Ligands	982
4.08.13	<b>Complexes with Metal–Metal Bonds</b>	<b>983</b>
4.08.13.1	M–M'-bonded Complexes	983
4.08.13.2	M–Metalloid-bonded Complexes	987
	<b>References</b>	<b>990</b>

## 4.08.1 Introduction

The organometallic chemistry of zirconium and hafnium has continued to develop rapidly since the publication of COMC (1995) in the mid-1990s. Areas of major developments and expansion during the period from the mid-1990s to the mid-2000s have been on the following four fronts: (i) synthesis and olefin polymerization catalysis of metallocenes and especially non-metallocene complexes (i.e., non-cyclopentadienyl-based, heteroatom-ligated complexes) incorporating diverse hapticities and functionalities; (ii) new synthetic methodologies for efficient and/or stereoselective

synthesis of chiral metallocene complexes; (iii) specifically designed metallocene and non-metallocene catalysts for living/controlled and/or stereospecific polymerizations of olefins and functionalized alkanes as well as applications to organic synthesis; and (iv) abstractive, oxidative, or protolytic reactions of the alkyl complexes with reagents  $\text{B}(\text{C}_6\text{F}_5)_3$ ,  $[\text{Ph}_3\text{C}][\text{B}(\text{C}_6\text{F}_5)_4]$ , and  $[\text{HNMe}_2\text{Ph}][\text{B}(\text{C}_6\text{F}_5)_4]$ , respectively, for generating the cationic complexes as mechanistic probes for a better understanding of the structure, reactivity, and deactivation of the catalytic species.

A large number of reference works and reviews have appeared since the publication of COMC (1995). The progress of the titanium, zirconium, and hafnium chemistry has been surveyed annually by Cotton,<sup>1</sup> and a book on the synthesis, reactivity, and applications of metallocenes,<sup>2</sup> and a special thematic review issue in metal-catalyzed polymerization<sup>3</sup> were published; comprehensive reviews that appeared in this special issue and are relevant to the zirconium and hafnium chemistry include effects of zirconocene and hafnocene structures on ethylene and propylene polymerization activity by Alt and Köppl,<sup>4</sup> olefin-polymerization stereochemistry using single-site metal catalysts by Coates,<sup>5</sup> applications of group 4 metallocene catalysts in propylene polymerization with an emphasis on stereo- and regioselectivity of the polymerization by Resconi *et al.*,<sup>6</sup> supported group 4 olefin polymerization catalysts by Hlatky,<sup>7</sup> co-catalytic chemistry in group 4 metal-catalyzed olefin polymerization by Chen and Marks,<sup>8</sup> and theoretic studies of group 4 metal-catalyzed olefin polymerization by Rappé *et al.*<sup>9</sup> and by Angermund *et al.*<sup>10</sup> Other reviews that appeared during the 1993–2004 time period related to the organometallic chemistry of zirconium and hafnium are listed in chronological order as follows: bis(Cp) (Cp = cyclopentadienyl) Zr(IV) and Hf(IV) compounds with Si-, Ge-, Sn-, N-, P-, As-, Sb-, O-, S-, Se-, Te-, or transition metal-centered anionic ligands by Hey-Hawkins,<sup>11</sup> influence of group 4 metallocene Cp-ring substituents on olefin polymerization activity and selectivity by Möhring and Coville,<sup>12</sup> stereospecific olefin polymerization by chiral group 4 metallocene catalysts by Brintzinger *et al.*,<sup>13</sup> recent development in the chemistry of early transition metal porphyrin compounds by Brand and Arnold,<sup>14</sup> coordination chemistry of zirconium and hafnium published during 1994 by Page and Wass,<sup>15</sup> early transition metal thiolates by Stephan and Nadasdi,<sup>16</sup> cationic group 4 metallocene complexes and their role in polymerization catalysis by Bochmann,<sup>17</sup> applications of chiral *ansa*-metallocenes in enantioselective C–C and C–H bond formation by Hoveyda and Morken,<sup>18</sup> applications of group 4 metallocene catalysts to olefin polymerization by Kaminsky and Arndt,<sup>19</sup> group 4 constrained geometry catalysts for olefin polymerization by McKnight and Waymouth,<sup>20</sup> fluorenyl complexes of zirconium and hafnium by Alt and Samuel,<sup>21</sup> zwitterionic metallocene complexes by Piers,<sup>22</sup> non-metallocene olefin polymerization catalysts (part I) by Gibson *et al.*,<sup>23</sup> early transition metal complexes incorporating polydentate amidodonor ligands by Gade,<sup>24</sup> strategies in synthesis, reactivity, catalysis, and utility of zirconium–phosphorus chemistry by Stephan,<sup>25</sup> reactivity of metallocene catalyst precursors with main group organometallic co-catalysts by Deffieux *et al.*,<sup>26</sup> single-component zirconocene– $\mu$ -butadiene–borate betaine complexes by Erker,<sup>27</sup> boron-bridged group 4 *ansa*-metallocene complexes by Shapiro,<sup>28</sup> conformationally dynamic 2-arylidene zirconocenes by Lin and Waymouth,<sup>29</sup> bis(phenoxyketimine) catalysts for olefin polymerization by Fujita *et al.*,<sup>30</sup> catalyst for the living polymerization of alkenes by Coates *et al.*,<sup>31</sup> non-metallocene olefin polymerization catalysts (part II) by Gibson and Spitzmesser,<sup>32</sup> heteroatom-substituted group 4 bis(indenyl)metallocenes by Leino *et al.*,<sup>33</sup> functionalization of group 4 bent metallocenes by Erker *et al.*,<sup>34</sup> non-Cp-type olefin polymerization catalysts by Do *et al.*,<sup>35</sup> (butadiene)-zirconocenes by Erker *et al.*,<sup>36</sup> kinetic and mechanistic studies on metallocene catalysts<sup>37</sup> and the use of spectroscopy in the study of polymerization catalysts<sup>38</sup> by Bochmann.

This chapter focuses on the synthesis, structures, and reactivity – the general thematic layout for each type of complexes – of zirconium and hafnium organometallic complexes in the oxidation state +IV (denoted as M(IV), M = Zr, Hf), and covers the literature in the peer-reviewed journals between 1993 and 2004. Works reported in patent literatures are not discussed, and the extensive use of zirconium and hafnium complexes in organic synthesis and polymerization catalysis is beyond the scope of this chapter. Applications of group IV metal complexes, including the Zr(IV) and Hf(IV) complexes reviewed in this chapter, to organic synthesis and olefin polymerization catalysis are covered in Volumes 10, 11 and Chapter 4.09, respectively. Complexes are grouped according to ligand hapticity and classified according to the ligand with the highest hapticity. To assist the reader in categorizing the metal–ligand (especially those non-Cp-based ligands) combinations, a simple ligand classification system is used for ligands of hapticity  $\geq 2$  to directly indicate the “identity, number, and formal charge” of the metal-attached ligand atoms; for example, a tridentate bis(amido) nitrogen-donor ligand, where the donor nitrogen atom is placed approximately at the central position between the two amido functionalities, is conveniently represented as  $[\text{N}^-, \text{N}, \text{N}^-]$ .

The extensive applications of the Zr(IV) and Hf(IV) complexes reviewed in this chapter in organic synthesis are included in Volume 10, while olefin polymerization catalysis beyond the scope discussed here is covered in Chapter 4.09 as well as in Chapter 11.05.



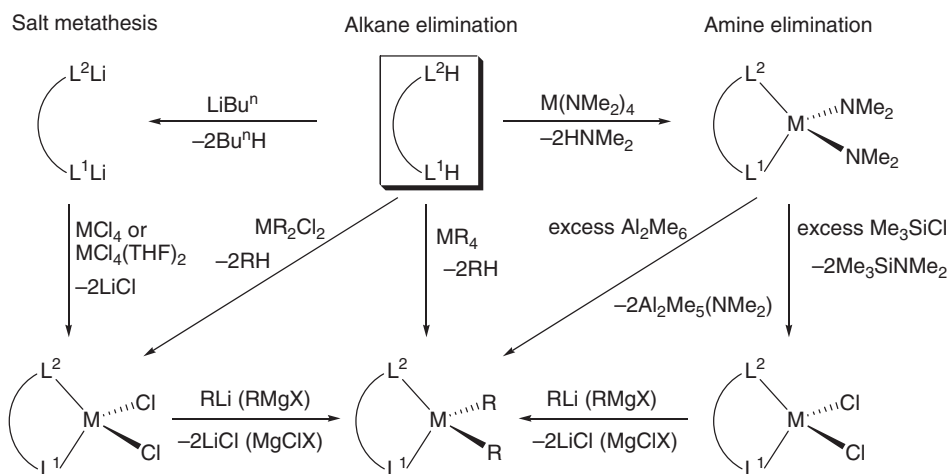
## 4.08.2 Complexes with $\eta^1$ -Ligands

### 4.08.2.1 Alkyl, Halide, and Amide Precursors for Complexes of Higher Ligand Hapticity

The organometallic chemistry of the monohapto, homoleptic Zr(IV) and Hf(IV) complexes has been dominated over the last decade by the reactivity of  $MCl_4$  ( $M = \text{Hf, Zr}$ ),  $MR_4$  ( $R = \text{CH}_2\text{Ph}$ ,  $\text{CH}_2\text{CMe}_3$ ,  $\text{CH}_2\text{SiMe}_3$ ), and  $M(\text{NR}_2)_4$  ( $R = \text{Me}$ ,  $\text{Et}$ ). These complexes and others serve as precursors for a variety of homo- and heteroleptic complexes with ligands of variable hapticity. A different  $M(\text{IV})$  precursor reagent is the *in situ*-generated “ $\text{Bu}^n_2\text{MCl}_2$ ” species at low temperatures. Zirconium and hafnium alkyl halides of the type  $\text{Bu}_2\text{MCl}_2$  ( $M = \text{Zr, Hf}$ ), generated in hydrocarbon media at  $-78^\circ\text{C}$  by treating  $MCl_4$  with 2 equiv. of  $\text{LiBu}^n$ , function as strong bases toward a variety of Brønsted acids,  $\text{EH}$ , where  $\text{E} = \text{cyclopentadienyl (Cp)}$  or substituted cyclopentadienyl, 1-alkynyl, indenyl, alkoxy, aryloxy, and disubstituted amino, to form metallocene and non-metallocene olefin polymerization pre-catalysts,  $\text{E}_2\text{MCl}_2$ , expeditiously and generally in high yield. For example,  $\text{Bu}^n_2\text{ZrCl}_2$ , formed *in situ* from  $\text{Bu}^n\text{Li}$  and  $\text{ZrCl}_4$  in hexanes or toluene at  $-78^\circ\text{C}$ , reacts with  $\text{CpH}$  to give pure  $\text{Cp}_2\text{ZrCl}_2$  in 95% yield.<sup>39</sup>

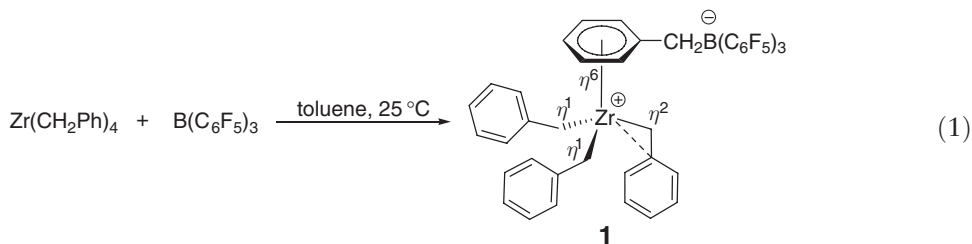
The final products produced by these monohapto reagents rarely maintain the monohapto ligand coordination. Therefore, discussions of their reactions are covered in the following sections dealing with complexes of higher hapticity. To facilitate the future discussions, Scheme 1 summarizes the commonly employed methodologies for the synthesis of zirconium and hafnium complexes using these complex precursors. The synthetic methodologies are classified into three major categories: salt metathesis, alkane elimination, and amine elimination. In a salt metathesis (elimination) approach, a neutral ligand is deprotonated by  $\text{LiBu}^n$ , followed by metallation reaction using  $\text{ZrCl}_4$  in hydrocarbons or  $\text{CH}_2\text{Cl}_2$ , or  $\text{ZrCl}_4(\text{THF})_2$  ( $\text{THF} = \text{tetrahydrofuran}$ ) in ether or related solvents. The final alkyl complex can be furnished with alkylation reaction using  $\text{RLi}$  or  $\text{RMgX}$ . Two types of alkane elimination route are possible; the first is the reaction of a neutral ligand with  $\text{MR}_4$  (typically  $R = \text{CH}_2\text{Ph}$ ,  $\text{CH}_2\text{CMe}_3$ ,  $\text{CH}_2\text{SiMe}_3$ ), leading directly to the final alkyl complex in one step. The second type involves the reaction of the neutral ligand with “ $\text{R}_2\text{MCl}_2$ ” ( $R = \text{CH}_2\text{Ph}$ ,  $\text{Bu}^n$ ,  $\text{Me}$ ), typically generated *in situ*, affording the chloride complex. The increasingly popular and highly efficient approach is the amine elimination approach. As with the alkane elimination approach, the amine elimination route uses a neutral ligand and undergoes aminolysis with  $\text{Zr}(\text{NR}_2)_4$ , yielding the amide complex. The amide complex can be readily converted to either the corresponding chloride complex upon treatment with excess of  $\text{Me}_3\text{SiCl}$  (or  $[\text{NH}_2\text{Me}_2]\text{Cl}$ ) or directly to the methyl complex when reacted with excess of  $\text{Al}_2\text{Me}_6$ . Choice of an approach that is suitable for a given metal complex synthesis depends on factors such as acidity of the ligand protons, steric bulk of the ligand, and sensitivity of functional groups present in the ligand. One or more routes work well in many syntheses, but there also exist many examples in which only one of these routes works or one approach works far better than others.

The notion of transformation to complex hapticity from a simple homoleptic tetraalkyl precursor is nicely illustrated by the reaction of  $\text{Zr}(\text{CH}_2\text{Ph})_4$  with the strongly Lewis-acidic and chemically robust activator,  $\text{B}(\text{C}_6\text{F}_5)_3$  (Equation (1)).<sup>40</sup> The mixing of these two reagents in toluene at room temperature yields, after addition of heptane, an orange-red crystalline solid, identified spectroscopically as the zwitterionic complex,



Scheme 1

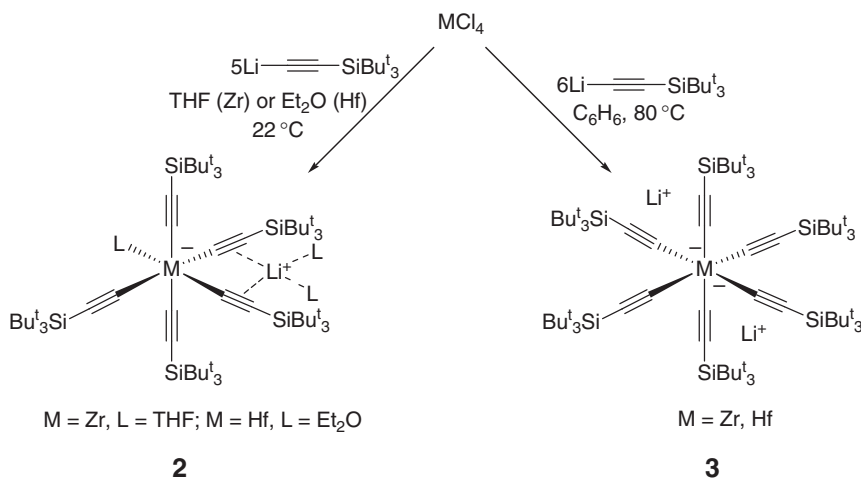
$[\text{Zr}(\text{CH}_2\text{Ph})_3][\text{PhCH}_2\text{B}(\text{C}_6\text{F}_5)_3]$  **1**. Both variable-temperature NMR studies and the solid-state structure reveal association of the cation and anion via  $\eta^6$ -coordination of the B–benzyl group; one of the benzyl groups is bound to the cationic zirconium center via  $\eta^2$ -coordination, whereas the remaining benzyl groups bind to Zr in the monohapto,  $\eta^1$ -fashion. The cationic species **1** is an active catalyst for ethylene and propylene polymerizations at 50 °C in toluene, affording polyethylene and a mixture of atactic and isotactic polypropylene, respectively. The single-propylene-insertion product can be isolated and characterized by NMR spectroscopy when the reaction of **1** with propylene is carried out at 25 °C in toluene, and the less stable single-ethylene-insertion product only detected at lower temperatures ( $< -20^\circ\text{C}$ ) by NMR.<sup>41</sup>



#### 4.08.2.2 Alkynyl, Aryl, and Aryloxide Complexes

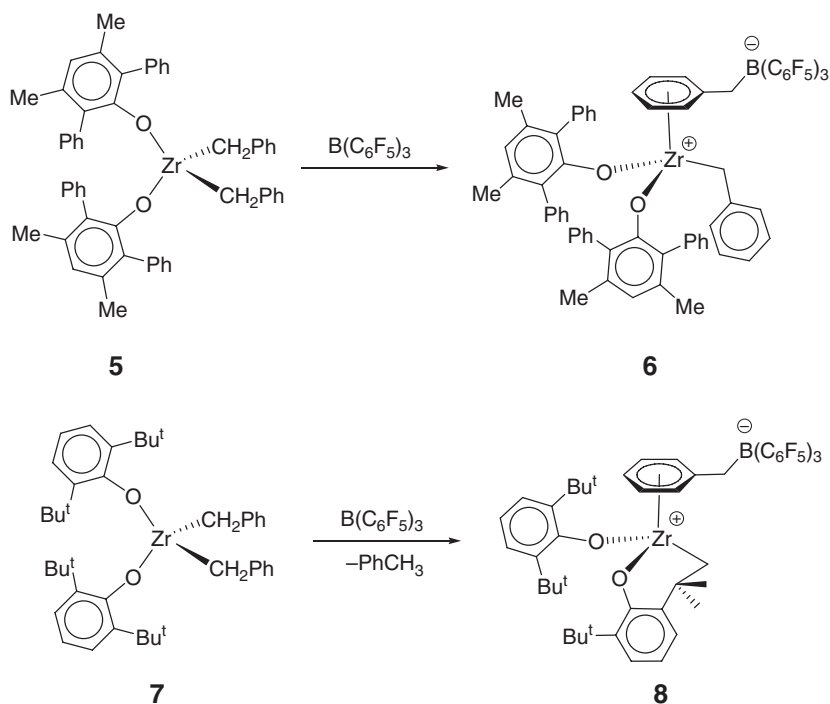
Treatment of  $\text{MCl}_4$  ( $\text{M} = \text{Zr}, \text{Hf}$ ) with 5 equiv. of  $\text{LiC}\equiv\text{CSiBu}^t_3$  in THF (Zr) or  $\text{Et}_2\text{O}$  (Hf) gives the pentaalkynyl complexes **2**<sup>42</sup> (Scheme 2). The molecular structure shows a distorted octahedral geometry about the metal which is coordinated by five alkynyls and one THF (or  $\text{Et}_2\text{O}$ ) ligands; the lithium cation resides between two of the alkynyls and is coordinated by two THF (or  $\text{Et}_2\text{O}$ ) molecules. The reaction with 6 equiv. of  $\text{LiC}\equiv\text{CSiBu}^t_3$  in benzene leads to the hexaalkynyl complexes **3**, which have near-perfect octahedral structures based on X-ray diffraction analysis. The two unusual “bare” lithium cations apparently reside in hydrophobic pockets and are surrounded by the methyl groups of the ligands whose carbons are 2.9–3.6 Å away.

The arylation of  $\text{MCl}_4$  ( $\text{M} = \text{Zr}, \text{Hf}$ ) with  $\text{LiC}_6\text{Cl}_5$  afforded lithium-containing mixtures from which no defined products can be isolated. Considering the possibility that anionic species could have been formed in this reaction,  $[\text{NBu}_4]\text{Br}$  was added after the arylation, producing heteroleptic, monohapto complexes  $[\text{NBu}_4][\text{M}(\text{C}_6\text{Cl}_5)_3\text{Cl}_2]$  (**4**;  $\text{M} = \text{Zr}, \text{Hf}$ ) in ~70% yield (Equation (2)).<sup>43</sup> Molecular structures of both complexes have been determined by



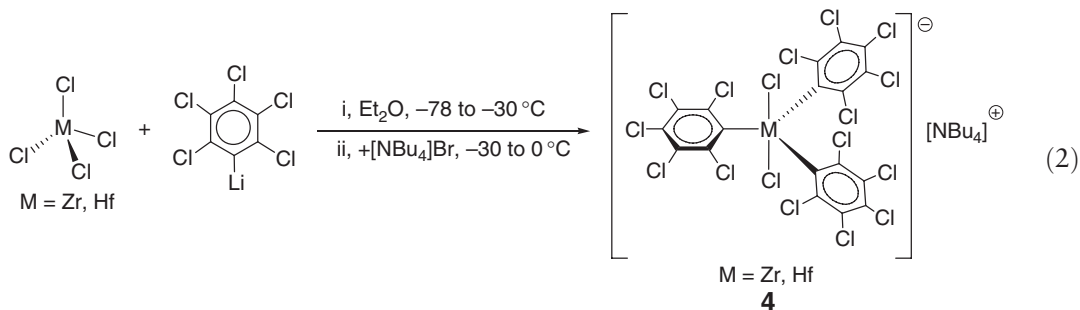
Scheme 2





Scheme 3

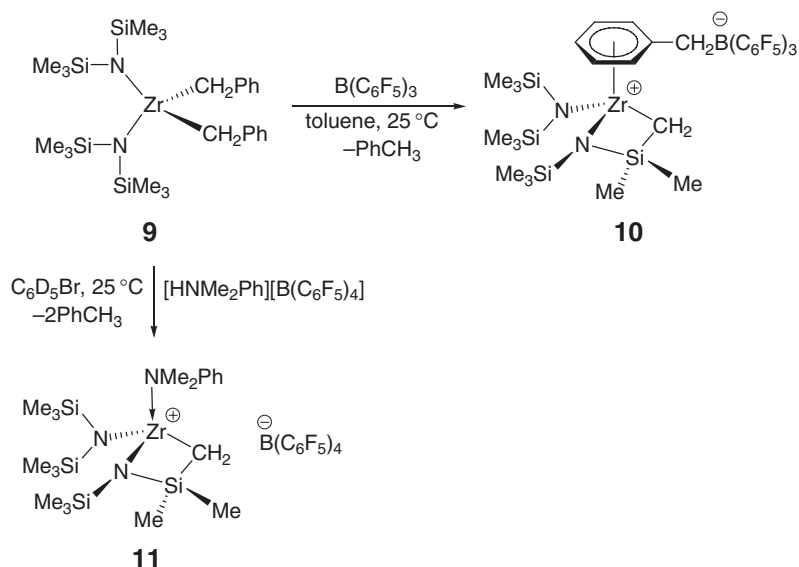
X-ray diffraction analysis, featuring anionic metal centers in trigonal-bipyramidal (tbp) geometries ( $D_{3h}$ ) defined by two axial  $\text{-Cl}$  ligands and three equatorial  $\text{-C}_6\text{Cl}_5$  groups.



Treatment of a benzene solution of the sterically crowded bis(aryloxide)zirconium dibenzyl complex **5** with  $\text{B(C}_6\text{F}_5)_3$  leads to the facile formation of the corresponding zwitterionic species **6** (Scheme 3).<sup>44</sup> The molecular structure of **6** features a three-legged piano-stool geometry about Zr with the  $\eta^1$ -bound benzyl group and the tightly associated benzyl borate anion through  $\eta^6$ -arene coordination; this complex is stable in solution in the presence of propylene and phenylpropyne. In contrast, treatment of the 2,6-di- $\text{Bu}^t$ -substituted aryloxide dibenzyl derivative **7** with  $\text{B(C}_6\text{F}_5)_3$  forms the cyclometallated compound **8** after elimination of toluene (Scheme 3);<sup>45</sup> compound **8** was structurally characterized.

#### 4.08.2.3 Amido Alkyls and Halides

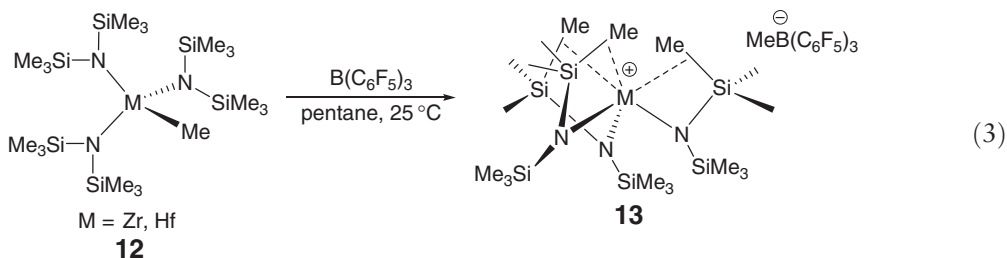
Reaction of the sterically encumbered diamido zirconium dibenzyl complex **9** with  $\text{B(C}_6\text{F}_5)_3$  in toluene at ambient temperature affords the cyclometallated product **10** after benzyl abstraction and elimination of



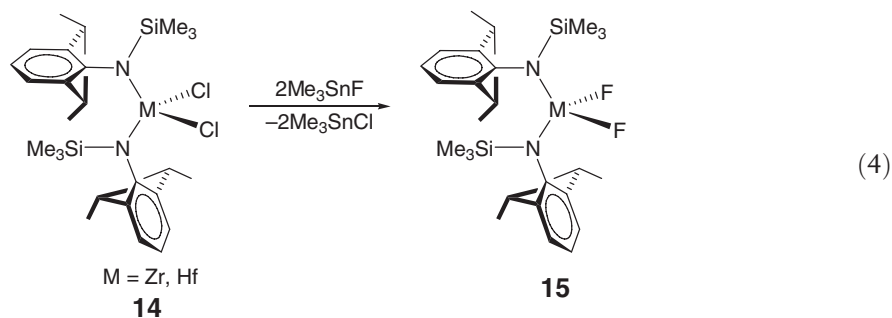
Scheme 4

toluene<sup>46</sup> (Scheme 4). This observed silyl–methyl group C–H activation in this example is a common theme for other cationic Zr(IV) and Hf(IV) complexes containing silylamido groups within the ligand framework, which leads to a ligand degradation as a catalyst decomposition pathway for such cationic complexes. Strong anion coordination to Zr in **10** suppresses alkene polymerization activity, whereas the analogous cationic amine adduct **11**, produced by protolysis of **9** with  $[\text{HNMe}_2\text{Ph}][\text{B}(\text{C}_6\text{F}_5)_4]$ , is active for both polymerizations of ethylene and propylene.

Treatment of tris(trimethylsilyl amido) methyl complexes **12** with 1 equiv. of  $\text{B}(\text{C}_6\text{F}_5)_3$  in pentane yields the corresponding ion pair **13**,  $\text{M}\{\text{N}(\text{SiMe}_3)_2\}_3^+\text{MeB}(\text{C}_6\text{F}_5)_3^-$ , as white solids that can be recrystallized from toluene.<sup>47</sup> The crystal structures reveal completely separated cations and anions, and that the cation is pyramidally coordinated by three amide ligands ( $\text{NSi}-\text{CH}_3$  moieties), in which each amide ligand has one of six  $\text{Si}-\text{CH}_3$  units located in close proximity to the metal atom (Equation (3)). These multicenter  $\text{M}-\text{Si}-\text{C}$  interactions observed in the solid-state structures may also be present in solution at low temperatures; however, the  $\text{Si}-\text{CH}_3$  groups are magnetically equivalent at room temperature.

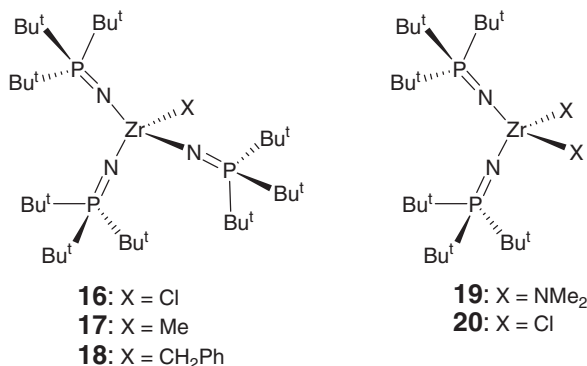


Introduction of both bulky aryl and silyl groups onto amido nitrogen results in the formation of the monodentate bis(amido)zirconium and hafnium dichlorides **14**, which are obtained by salt metathesis approach and converted to the corresponding difluoride compounds **15** using trimethyltin fluoride<sup>48</sup> (Equation (4)). The use of the  $\text{Me}_3\text{Si}$  group not only provides a sterically demanding ligand but also makes it necessary to prevent the formation of imido compounds. When activated with methylalumoxane (MAO), both the chloride and fluoride complexes exhibit moderate activity for polymerization of ethylene.



#### 4.08.2.4 Phosphinimide Complexes

Mono-anionic phosphinimide ligands can be considered as sterically equivalent to Cp, but they are monodentate and bind to a transition metal center via a linear,  $\eta^1$ -fashion, namely, conical ligands. Salt metathesis between  $\text{Bu}^t_3\text{P}=\text{NLi}$  and  $\text{ZrCl}_4$  in a 3:1 ratio affords isolable tris(phosphinimide)zirconium chloride ( $\text{Bu}^t_3\text{P}=\text{N}$ )<sub>3</sub>ZrCl **16**, which can be readily alkylated to form ( $\text{Bu}^t_3\text{P}=\text{N}$ )ZrMe **17** and ( $\text{Bu}^t_3\text{P}=\text{N}$ )ZrCH<sub>2</sub>Ph **18**.<sup>49</sup> Attempts to prepare bis(phosphinimide)zirconium dichloride using the 2:1 ratio of  $\text{Bu}^t_3\text{P}=\text{NLi}$  versus  $\text{ZrCl}_4$  in the salt metathesis reaction yielded a mixture of products; however, aminolysis of  $\text{Zr}(\text{NEt}_2)_4$  with the neutral ligand,  $\text{Bu}^t_3\text{P}=\text{NH}$ , gives bis(phosphinimide)zirconium diamide **19**, which is readily converted to the dichloride **20** upon treatment with excess of  $\text{Me}_3\text{SiCl}$ .<sup>50</sup> Attempts to alkylate the dichloride complex to give the corresponding dimethyl complex were unsuccessful, obtaining a complex mixture of unidentified compounds. This problem is reflected in the performance of the dichloride **20** as a catalyst precursor for ethylene polymerization; upon activation with methylaluminoxane (MAO), it shows only moderate activity (much lower than the titanium analog), producing polyethylene with a broad molecular weight distribution ( $\text{MWD} = \bar{M}_w/\bar{M}_n = 10.8$ ), characteristic of multi-site catalysis.

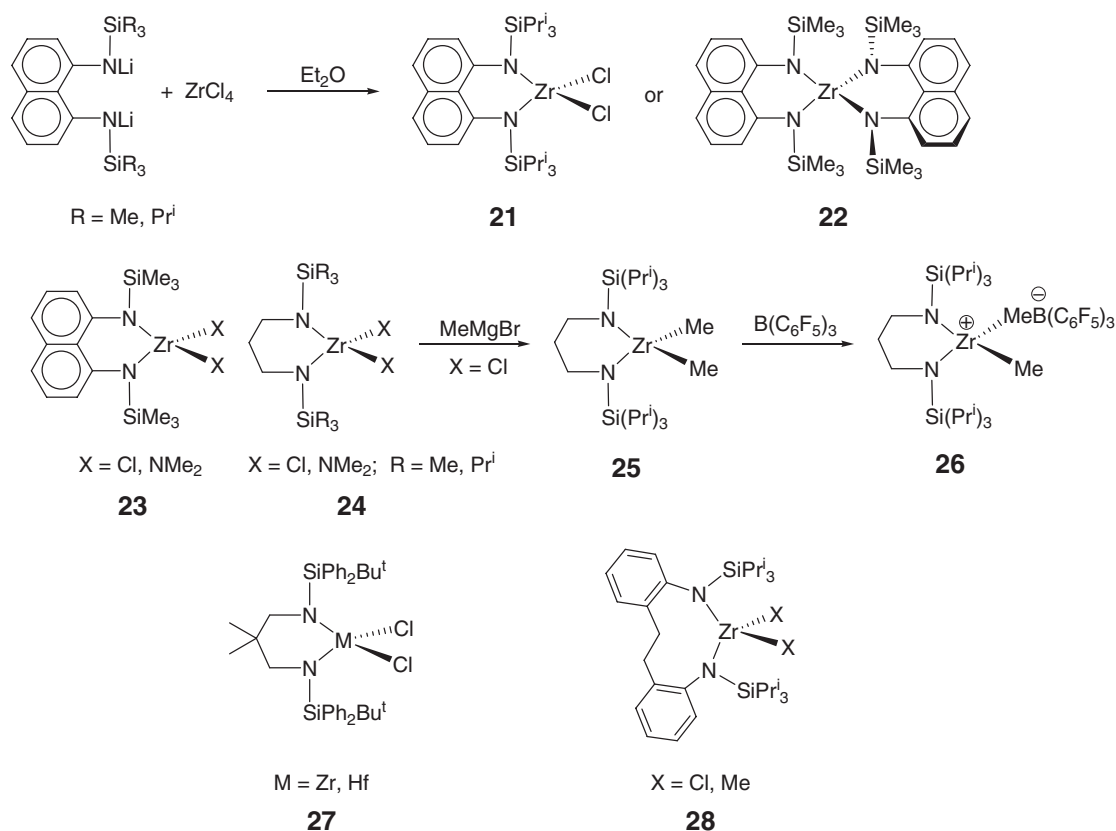


#### 4.08.3 Complexes with $\eta^2$ -Ligands

##### 4.08.3.1 Chelating Bis(amido) [ $\text{N}^-$ , $\text{N}^-$ ] Complexes

##### 4.08.3.1.1 Silylamido [ $\text{N}^-$ , $\text{N}^-$ ] complexes

Zirconium complexes **21** and **22** incorporating rigid 1,8-naphthalene-bridged bis(silylamido) ligand were synthesized by salt metathesis involving the reaction of the dilithium salt of the bis(silylamido) ligand and  $\text{ZrCl}_4$  (Scheme 5).<sup>51</sup> The structure of the salt metathesis product depends on the size of the silyl substituent. When the  $\text{Pr}^i_3\text{Si}$  group is attached to the amido N, the desired diamido dichloride complex **21** is produced; on the other hand, when the smaller  $\text{Me}_3\text{Si}$  group is attached to the amido N, the tetraamido complex **22** incorporating two bis(silylamido) ligands is obtained. Amine elimination is more selective in this example, and thus a series of chelating bis(silylamido)zirconium complexes incorporating rigid aryl **23** or flexible alkyl **24** bridging moieties was prepared by this route<sup>52</sup> (Scheme 5).

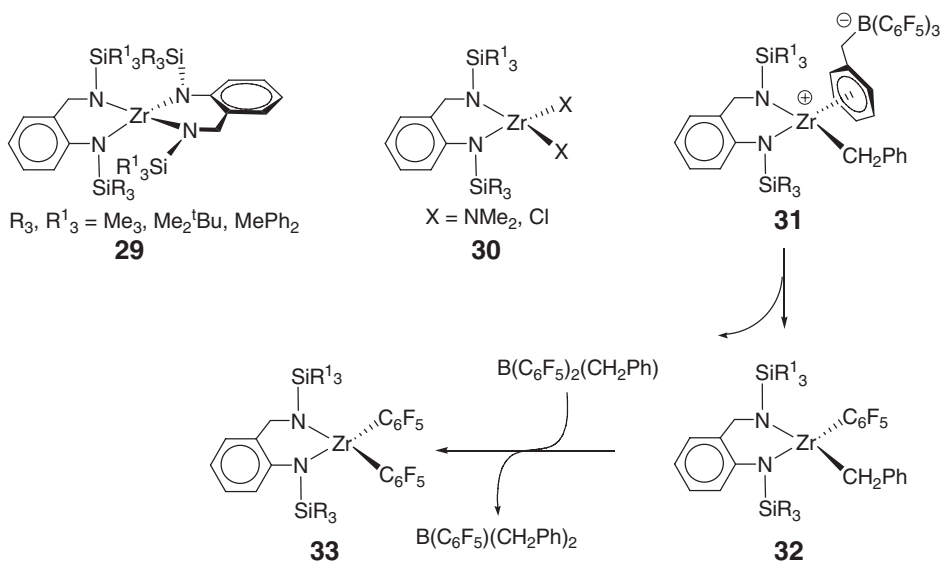


Scheme 5

The dimethyl complex **25** is isolated from the reaction of the dichloride with MeMgBr and the cationic species **26** generated *in situ* from the reaction of **25** with  $\text{B}(\text{C}_6\text{F}_5)_3$  in  $\text{CD}_2\text{Cl}_2$  at  $0^\circ\text{C}$ . The diamide and dichloride complexes, when activated with MMAO (modified MAO), exhibit moderate activity for polymerization of ethylene; the dimethyl derivative **25**, upon activation with  $[\text{Ph}_3\text{C}][\text{B}(\text{C}_6\text{F}_5)_4]$  in the presence of triisobutyl aluminum, shows substantially enhanced activity; however, the activity of this catalytic species is still considerably lower than that by the  $\text{Cp}_2\text{ZrCl}_2/\text{MMAO}$  system and inactive toward propylene and 1-hexene polymerizations. The analogous zirconium and hafnium dichlorides **27**<sup>53</sup> supported by the trimethylene-bridged bulky bis(silylamide) ligand and the related 2,2'-ethylene-bis(*ortho*-phenyl)-bridged bis(silylamido)zirconium complexes **28** are also prepared.<sup>54</sup> Complexes **28** serve as catalyst precursors for polymerizations of ethylene, propylene, and 1-hexene upon activation with a suitable activator.

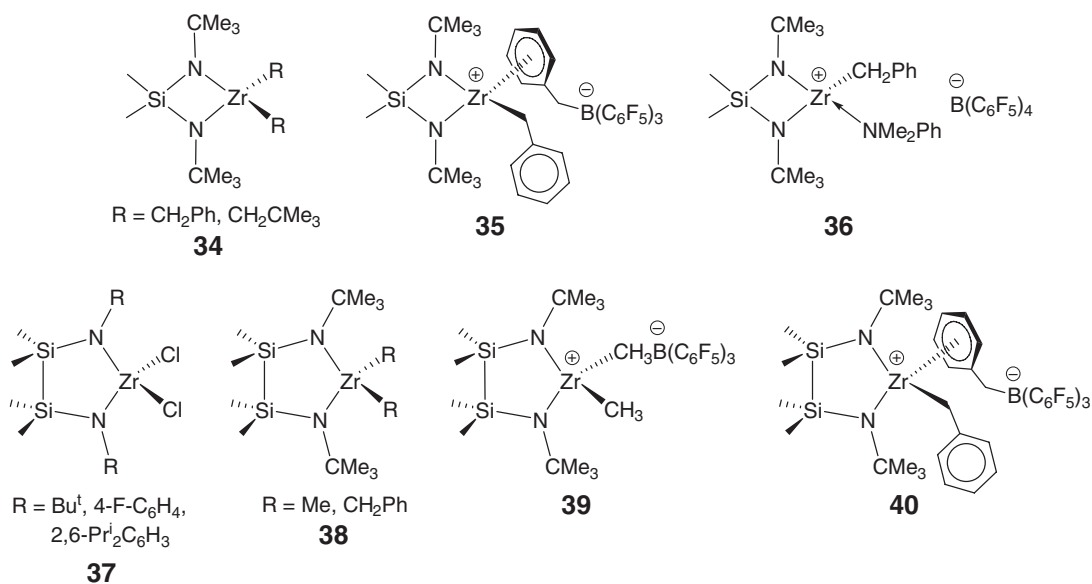
Several chelating bis(silylamido)Zr(IV) complexes **29** and **30** in which the diamide ligand is bridged by the *ortho*- $\text{C}_6\text{H}_4\text{CH}_2$  benzyl moiety were obtained by the reaction of the dilithiated amide ligand with  $\text{ZrCl}_4$ <sup>55</sup> and protolysis of  $\text{Zr}(\text{NMe}_2)_4$  with 1 equiv. of the parent diamine followed by subsequent reaction with excess  $\text{SiMe}_3\text{Cl}$ , respectively.<sup>56</sup> Upon activation with MAO, the dichloride complexes **30** polymerize ethylene to yield linear high molecular weight polyethylenes with broad molecular weight mass distributions ( $\overline{M}_w/\overline{M}_n > 27$ ) and exhibit no activity toward propylene and 1-hexene polymerizations. Reactions of the dibenzyl complexes with  $\text{B}(\text{C}_6\text{F}_5)_3$  form unstable zwitterionic adducts **31**, which decompose to the bis( $\text{C}_6\text{F}_5$ ) complexes **33**, through the mono( $\text{C}_6\text{F}_5$ ) intermediates **32** in a stepwise fashion<sup>57</sup> (Scheme 6).

Dimethylsilyl-bridged bis(amido)zirconium dialkyl complexes **34** are prepared using the standard alkylation methodology involving the reaction of the corresponding dichloride with organometallic alkyl reagents.<sup>58</sup> Alkyl abstraction of the dibenzyl species with  $\text{B}(\text{C}_6\text{F}_5)_3$  cleanly affords the cation **35** that is tightly paired with the anion via  $\eta^6$ -arene coordination. Neutral amine coordination to the cationic metal center is often observed in the activated form **36** when  $[\text{HNMe}_2\text{Ph}][\text{B}(\text{C}_6\text{F}_5)_4]$  is employed in the protonolytic activation process. The analogous disilyl-bridged bis(amido)zirconium dichlorides **37**<sup>59</sup> are also prepared from the salt metathesis approach, and the

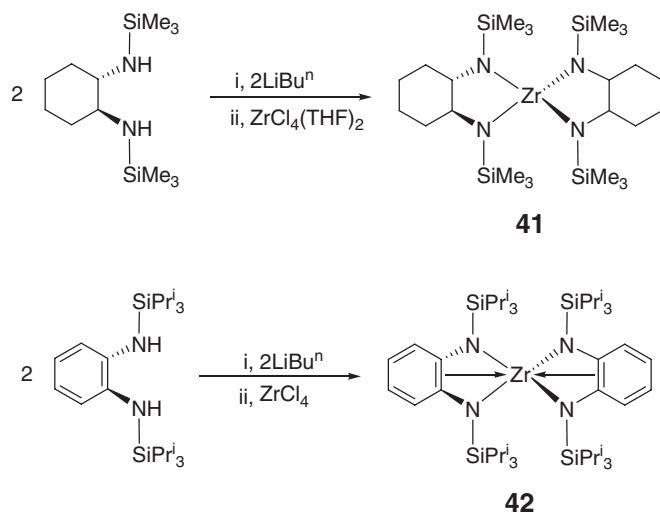


Scheme 6

corresponding dimethyl and dibenzyl complexes **38**<sup>60</sup> are obtained by standard alkylation methods. Reactions of the dimethyl and dibenzyl complexes with  $\text{B}(\text{C}_6\text{F}_5)_3$  give the zwitterions **39** and **40**, respectively, the latter of which was structurally characterized by X-ray diffraction. The dichloride **37**, when activated with MAO, is moderately active for ethylene polymerization, while **39** and **40** catalyze ethylene oligomerization affording highly linear  $\alpha$ -olefins under mild conditions ( $\text{C}_6$  fraction > 99.5% 1-hexene at 50 °C, 6 atm ethylene pressure).



The reaction of the dilithiated bisamide ligand, *trans*-1,2-( $\text{Me}_2\text{SiNLi}$ )<sub>2</sub> $\text{C}_6\text{H}_{10}$ , with  $\text{ZrCl}_4(\text{THF})_2$  in diethyl ether leads to the formation of the colorless tetraamido Zr(IV) complex **41** incorporating two bis(silylamido) ligands<sup>61</sup> (Scheme 7). Irrespective of the dilithiated ligand : Zr ratio, the desired dichloride species could not be obtained using this salt metathesis method. Nevertheless, this tetraamido complex can be activated with MAO to generate a moderately active catalyst for ethylene polymerization. A similar result is seen in the reaction of the dilithiated bis(silylamido) ligand bridged by *ortho*-phenylene with  $\text{ZrCl}_4$  in refluxing benzene, leading to the formation of the

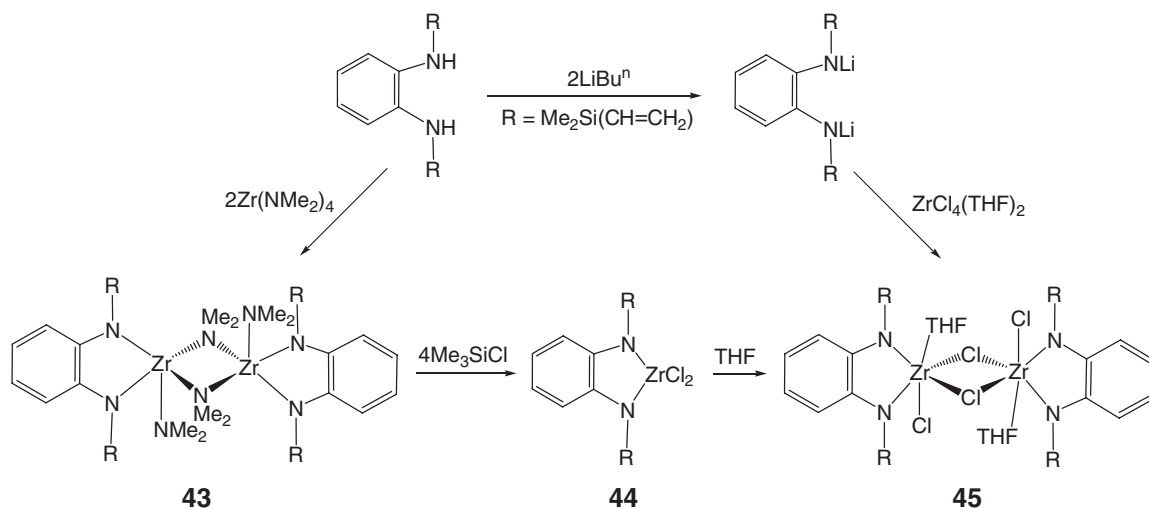


Scheme 7

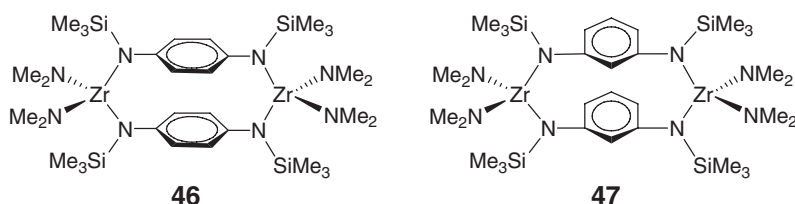
yellow crystals of the tetraamido Zr(IV) complex **42** incorporating two bis(silylamido) ligands<sup>62</sup> (Scheme 7). The X-ray crystallographic and variable-temperature NMR studies indicate this complex possesses two  $\eta^4$ -C<sub>6</sub>H<sub>4</sub>(NSiPr<sub>3</sub>)<sub>2</sub> ligands ( $\sigma^2$ ,  $\pi$ -bonds), which undergoes an  $\eta^4$ - $\eta^2$  fluxional process in solution.

Chelating diamido Zr(IV) complexes derived from *ortho*-C<sub>6</sub>H<sub>4</sub>-silyldiamines are obtained from either amine elimination starting from the neutral ligand or metallation of the dilithiated ligand.<sup>63</sup> For the former approach, the reaction of the neutral ligand with Zr(NMe<sub>2</sub>)<sub>4</sub> produces the dinuclear complex **43**, which can be converted to the mononuclear dichloride complex **44** (Scheme 8). Upon addition of THF, complex **44** is converted into the chloride-bridging dinuclear complex **45**, which is the identical product obtained directly from the metallation reaction of the dianionic ligand with ZrCl<sub>4</sub>(THF)<sub>2</sub>. These complexes, upon activation with MAO, are active for ethylene polymerization, and the resulting polymers are shown to have extremely high average molecular weights as determined by viscosity measurements.

When *para*- and *meta*-C<sub>6</sub>H<sub>4</sub>-bridged silyldiamines are used in the aminolysis reaction with Zr(NMe<sub>2</sub>)<sub>4</sub>, *para*- and *meta*-dimetallacyclophanes **46** and **47** are obtained.<sup>64</sup> Both complexes are structurally characterized by X-ray diffraction analyses and form moderately active catalysts, when treated with MAO, for polymerization ethylene.

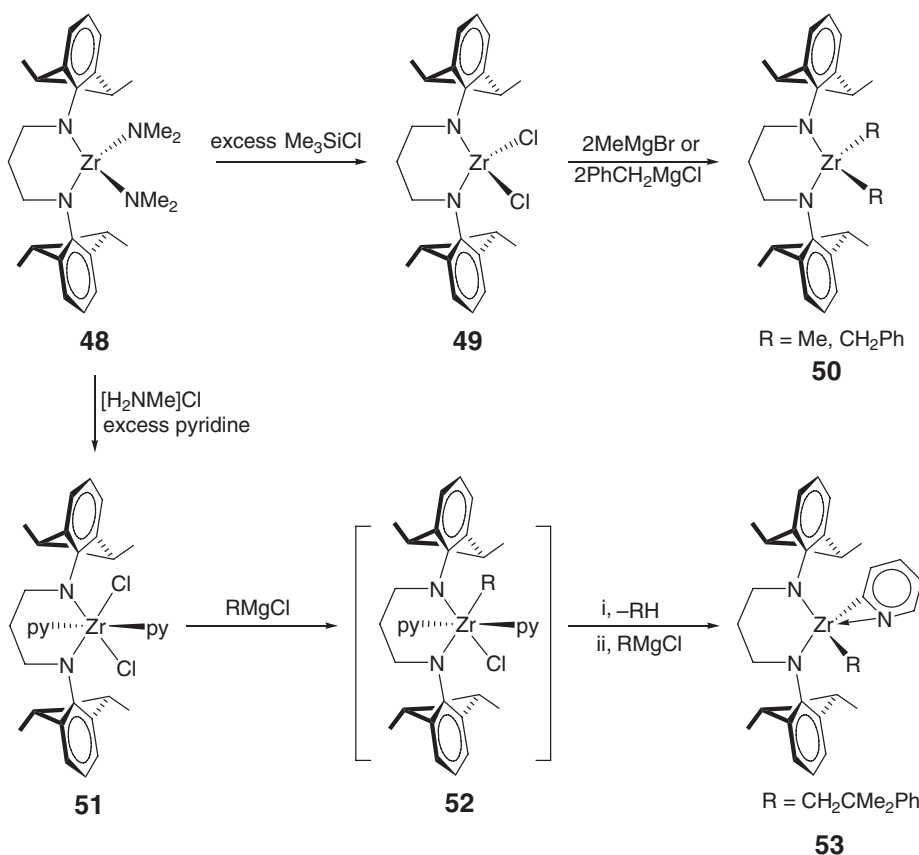


Scheme 8



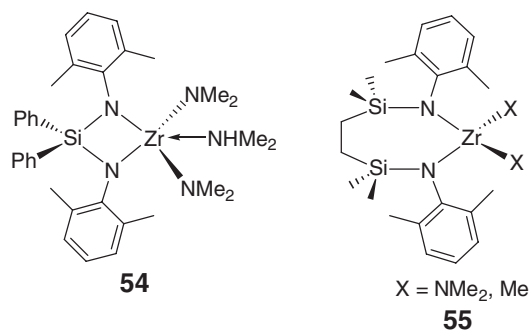
#### 4.08.3.1.2 Arylamido [ $N^-, N^-$ ] complexes

Introduction of bulky aryl groups such as 2,6- $\text{Pr}^i_2\text{C}_6\text{H}_4$  onto the heteroatom binding to the metal is a widely used strategy for providing excellent steric protection for the reactive, electrodeficient cationic metal species, and for weakening the binding of an anion to the metal center. To this end, zirconium complex diamide **48** incorporating the chelating bulky aryl diamido ligand is obtained from the aminolysis reaction between the neutral diamine ligand and  $\text{Zr}(\text{NMe}_2)_4$ <sup>65,66</sup> (Scheme 9). Treatment of diamide **48** with excess of  $\text{Me}_3\text{SiCl}$  gives the base-free dichloride **49**, which can be readily converted to the corresponding dialkyl derivatives **50**. The diamide **48** reacts with  $[\text{H}_2\text{NMe}_2]\text{Cl}$  in the presence of excess of pyridine to give the dichloride–pyridine adduct **51**, which can also be converted to the base-free dialkyl derivatives **50** as the base-free dichloride **49**. However, the reaction of **51** with 2 equiv. of  $\text{PhMe}_2\text{CCH}_2\text{MgCl}$  yields the  $\eta^2$ -pyridyl complex **53**, which was characterized by X-ray diffraction. The formation of **53** likely occurs via proton abstraction from the coordinated pyridine through the transient monoalkyl **52** (Scheme 9). The catalyst system consisting of the dimethyl complex **50** and a large excess of MAO polymerizes 1-hexene to a mixture of high polymers and oligomers. On the other hand, activation with  $[\text{Ph}_3\text{C}][\text{B}(\text{C}_6\text{F}_5)_4]$  yields only oligomers ( $n = 2\text{--}7$ ) due to rapid  $\beta$ -hydride elimination which precludes polymer formation.

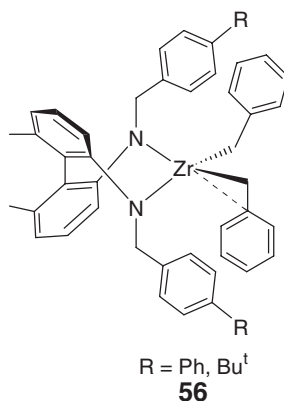


Scheme 9

Introduction of both aryl and silyl groups onto amido nitrogens results in the formation of zirconium complexes **54** and **55** bearing chelating silyl- and disilyl-bridged bis(arylamido) ligands, respectively, which are produced by the aminolysis approach in high yields.<sup>67</sup> There is a dramatic effect of chelate ring size on ethylene polymerization activity and kinetic profile. The catalytic species derived from **54** with suitable activation procedures is short-lived and moderately active. On the other hand, activation of **55** with MAO (for the diamide or dimethyl) or  $[\text{Ph}_3\text{C}][\text{B}(\text{C}_6\text{F}_5)_4]$  (for the dimethyl) gives highly active catalysts and, with MAO activation, stable kinetic profiles. The non-binding of small base molecules such as  $\text{Me}_2\text{NH}$  in the neutral complex **55** and the catalytic results indicate the improved steric protection of the zirconium center by the bulky aryl substituents of the larger-ring chelate ligand.



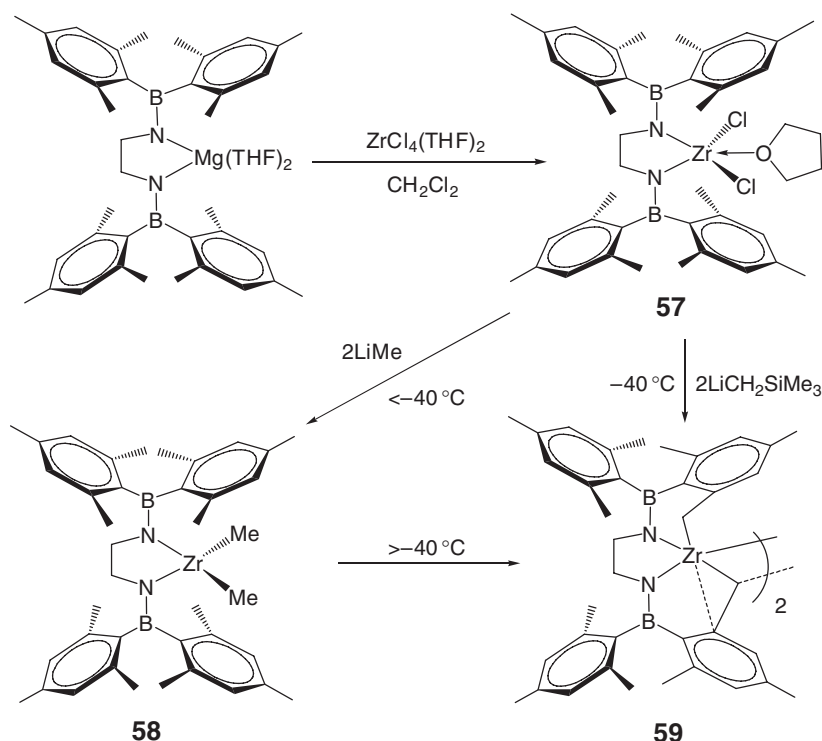
An alkane elimination approach involving the reaction between a neutral ligand and  $\text{Zr}(\text{CH}_2\text{Ph})_4$  in pentane gives chiral dibenzylzirconium complexes **56** incorporating biphenyl-bridged bis(amido) ligands.<sup>68</sup> The complex displays averaged  $C_2$ -symmetry in solution and an  $\eta^2$ -benzyl coordination mode in the solid state. When activated with MAO, this complex type shows moderate activity for the polymerization of ethylene.



#### 4.08.3.1.3 Borylamido $[\text{N}^-, \text{N}^-]$ complexes

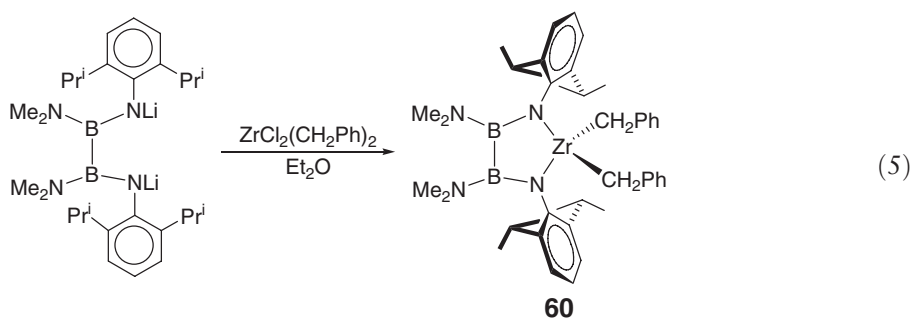
Reaction of the magnesium salt  $[\text{Mes}_2\text{BNCH}_2\text{CH}_2\text{NBMes}_2]\text{Mg}(\text{THF})_2$  with  $\text{ZrCl}_4(\text{THF})_2$  in  $\text{CH}_2\text{Cl}_2$  affords a chelating bis(borylamido)Zr(IV) complex **57**<sup>69</sup> (Scheme 10). The dimethyl derivative **58** can be obtained from the treatment of the dichloride with methyllithium at  $-40^\circ\text{C}$ , but it is thermally unstable and converts readily to, via metallation of the *ortho*-methyl groups from mesityl rings on different borons, the dicyclometallated complex **59**; this complex exists as a dimer in the solid state, with two methylene groups nearly symmetrically bridging two Zr centers. Derivatives that contain more sterically demanding alkyl derivatives are even less stable. For example, the reaction between the dichloride and 2 equiv. of  $\text{LiCH}_2\text{SiMe}_3$  yields only **59** and tetramethylsilane. Modifications of the ligand by substituting the mesityl group with 2,4,6- $\text{Pr}^i_3\text{C}_6\text{H}_2$  or cyclohexyl group yield isolable zirconium dialkyl complexes and the corresponding alkyl cations upon activation with  $\text{B}(\text{C}_6\text{F}_5)_3$  or  $[\text{Ph}_3\text{C}][\text{B}(\text{C}_6\text{F}_5)_4]$ .<sup>70</sup> The zirconium cation of the cyclohexyl derivative is active for polymerization of 1-hexene; however, the molecular weight distribution of the polymer produced is very broad.





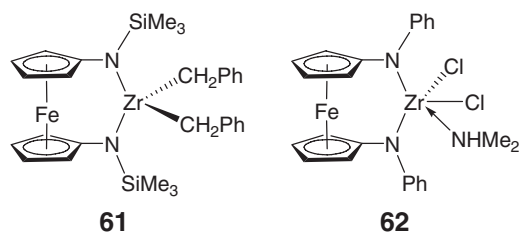
Scheme 10

Reacting the dialkyl  $\text{ZrCl}_2(\text{CH}_2\text{Ph})_2$ , the comproportionation product of  $\text{Zr}(\text{CH}_2\text{Ph})_4$  and  $\text{ZrCl}_4$ , with the dilithiated ligand, the diborane-bridged chelate bis(arylamido)Zr(IV) dibenzyl complex **60** is obtained in 20% yield<sup>71</sup> (Equation (5)). This complex, when activated with MAO, is active for the co-polymerization of ethylene and 1-octene at 70 °C, but the co-polymer produced has a broad molecular weight distribution.



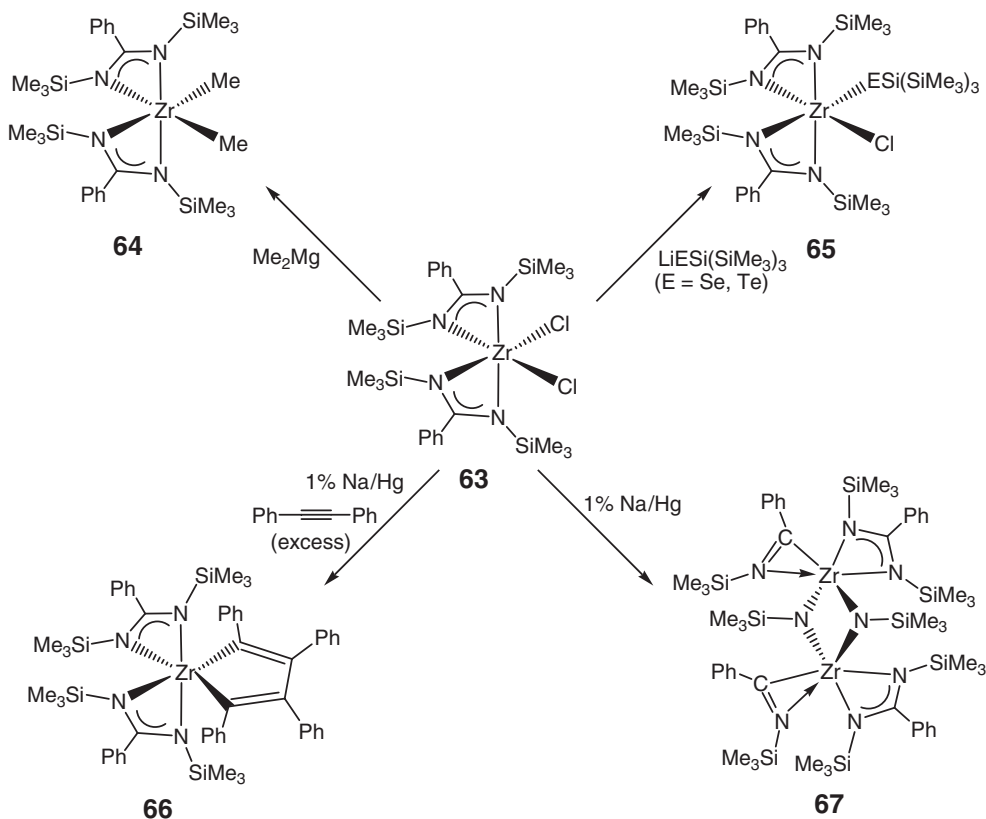
#### 4.08.3.1.4 Ferrocenylamido [ $N^-, N^-$ ] complexes

The redox-tunable ferrocenyl-bridged bis(amido)zirconium complexes **61**<sup>72</sup> and **62**<sup>73</sup> are obtained using the alkane elimination involving the reaction of the neutral silyldiamine ligand with  $\text{Zr}(\text{CH}_2\text{Ph})_4$  and the amine elimination approach involving the reaction of the neutral phenyldiamine ligand with  $\text{Zr}(\text{NMe}_2)_4$ , respectively. Although in the solid state, the average  $\text{Zr}-\text{C}-\text{C}(\text{Ph})$  angle of 98.9° in **61** is less than that expected for an  $sp^3$ -carbon, there is no evidence found spectroscopically for any  $\eta^2$ -interaction in solution. Complex **62** shows a distorted tbp geometry with the amino group and a chloride ligand occupying two axial positions.



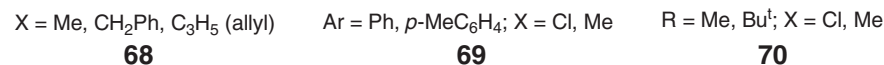
#### 4.08.3.2 Amidinate [ $N_2^-$ ] Complexes

Amidinate ligands are formally regarded as amido imine-donor ligands, thereby mono-anionic, six-electron donors. The bulky *N,N'*-bis(trimethylsilyl) benzamidinato zirconium dichloride  $[\text{PhC}(\text{NSiMe}_3)_2]_2\text{ZrCl}_2$  **63**<sup>74</sup> behaves more like  $\text{Cp}^*_2\text{ZrCl}_2$  ( $\text{Cp}^* = \eta^5\text{-Me}_5\text{C}_5$ ) than  $\text{Cp}_2\text{ZrCl}_2$ , suggesting that the  $\text{PhC}(\text{NSiMe}_3)_2$  group can also be considered as a steric equivalent of  $\text{Cp}^*$ . For example, similar to  $\text{Cp}^*_2\text{ZrCl}_2$ , the reaction of  $[\text{PhC}(\text{NSiMe}_3)_2]_2\text{ZrCl}_2$  with  $\text{Me}_2\text{Mg}$  can readily produce the corresponding dimethyl derivative **64**, whereas the reaction of the dichloride with 2 equiv. of bulky chalcogenolate reagents  $(\text{THF})_2\text{LiESi}(\text{SiMe}_3)_3$  ( $\text{E} = \text{Se}, \text{Te}$ ) affords only monosubstituted complexes **65**<sup>75</sup> (Scheme 11). The dimethyl compound reacts cleanly with  $\text{B}(\text{C}_6\text{F}_5)_3$  to form the corresponding zwitterionic complex,  $[\text{PhC}(\text{NSiMe}_3)_2]_2\text{ZrMeMeB}(\text{C}_6\text{F}_5)_3$ , which is moderately active toward ethylene polymerization.<sup>76</sup> Also similar to the metallocene dichloride, reduction of  $[\text{PhC}(\text{NSiMe}_3)_2]_2\text{ZrCl}_2$  using 1% Na/Hg in presence of excess of diphenylacetylene yields  $[\text{PhC}(\text{NSiMe}_3)_2]_2\text{Zr}(\eta^2\text{-C}_4\text{Ph}_4)$  **66**. However, in the absence of the acetylene, the reduction gives orange crystals of a dinuclear zirconium complex,  $\{[\text{PhC}(\text{NSiMe}_3)_2]_2\text{Zr}(\eta^2\text{-PhCNSiMe}_3)(\mu\text{-NSiMe}_3)\}_2$  **67**; the crystal structure shows each six-coordinate Zr being bound to two bridging imido ligands, an  $\eta^2$ -iminoacyl, and a bidentate  $[\text{PhC}(\text{NSiMe}_3)_2]_2$  ligand. Formation of the complex **67** most likely occurs via a reduced species



Scheme 11

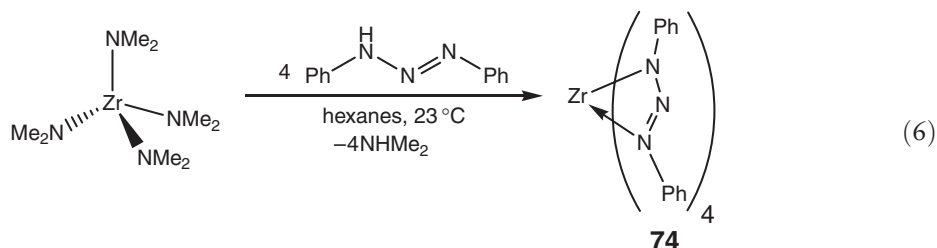
The parent benzamidinatozirconium dichloride  $[\text{PhC}(\text{NSiMe}_3)_2]_2\text{ZrCl}_2$  **63** can be further derivatized to alkyl and allyl complexes **68**,<sup>77</sup> and the phenyl group on the backbone can be substituted by the *para*-tolyl group **69**.<sup>78,79</sup> Complexes of type **69**, when activated with MAO and under high pressure conditions, effect highly isospecific propylene polymerization.<sup>79</sup> The polymerization at atmospheric pressure, however, produces atactic polymer due to faster epimerization as compared with stereospecific insertion of the monomer. There is a strong activator/anion effect on the propylene polymerization stereochemistry; unlike activation with MAO, the dimethyl compound of type **69**, when activated with  $\text{B}(\text{C}_6\text{F}_5)_3$ , produces highly isotactic polypropylene even under atmospheric pressure.<sup>80</sup> Bis(alkylamidinate)zirconium and hafnium complexes **70**, in which an alkyl group (Me or Bu<sup>t</sup>) is placed on the backbone and cyclohexyl (Cy) at nitrogen, are obtained via the salt metathesis approach.<sup>81</sup> The molecular structures of the zirconium dichloride and dimethyl complexes having the methyl substituent on the backbone confirm *cis*-arrangements of dichloride or dimethyl ligands as depicted, but the X–Zr–X angles in **70** are  $\sim 10^\circ$  smaller than those found in **63** and **64** with the *N,N'*-bis(trimethylsilyl)benzamidinate ligand. Moderate activity toward ethylene polymerization leading to polyethylene with broad molecular weight distributions by the MAO-activated species are a common feature of these bis(amidinate) complexes.



Tris(benzamidinate)zirconium chloride and methyl complexes **71** with a chiral R\* substituent at one nitrogen of the benzamidinate ligand have  $C_3$ -symmetry; when activated with MAO, the dichloride complex polymerizes propylene under pressure (>5 atm), leading to highly isotactic polypropylene via a site-controlled mechanism.<sup>82</sup> Binuclear oxalic amidinate complex **72** is obtained via the amine elimination approach; low ethylene polymerization activity is observed when activating this complex with MAO, but the activity is enhanced about 12 times after pre-alkylation treatment with AlMe<sub>3</sub> or Al(Bu<sup>i</sup>)<sub>3</sub>.<sup>83</sup> The amidinate ligand is structurally related to the iminophosphonamide ligand. Zirconium complexes **73** bearing two iminophosphonamide ligands are found to exhibit considerably higher ethylene polymerization activity upon activation with MAO than the analogous bis(amidinate) complex, and importantly, the polymers produced have narrow molecular weight distributions,<sup>84</sup> consistent with single-site polymerization catalysis.



A related zirconium complex with a  $[N_2^-]$ -type of ligation is tetrakis(1,3-diphenyltriazenido)zirconium(IV) **74**,<sup>85</sup> which is obtained from the amine elimination approach. Thus, treatment of  $Zr(NMe_2)_4$  with 4 equiv. of 1,3-diphenyltriazene in hexanes at ambient temperature affords **74** in 79% yield as a deep red crystalline solid (Equation (6)). This Zr complex is eight coordinate with four  $\eta^2$ -1,3-diphenyltriazenido ligands. Complex **74** crystallizes with a distorted dodecahedral geometry about Zr; consistent with this solid-state structure, the solution molecular weight measurements indicate a monomeric structure in benzene.



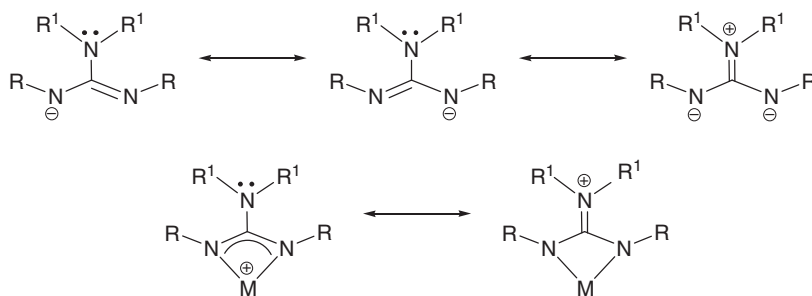
Aminooxazolines such as (*S*)-2-(3,5-dimethyl)phenylamino-4-*tert*-butyloxazoline serve as “chiral” amidinate analogs. The neutral ligands of this type have been employed to react with  $\text{ZrR}_4$  ( $\text{R} = \text{CH}_2\text{Ph}$ ,  $\text{CH}_2\text{Bu}^t$ ), affording a range of chiral zirconium *cis*-dialkyl complexes in good yields with good control over metal/ligand stoichiometry.<sup>86</sup>

#### 4.08.3.3 Guanidinate $[\text{N}_2^-]$ Complexes

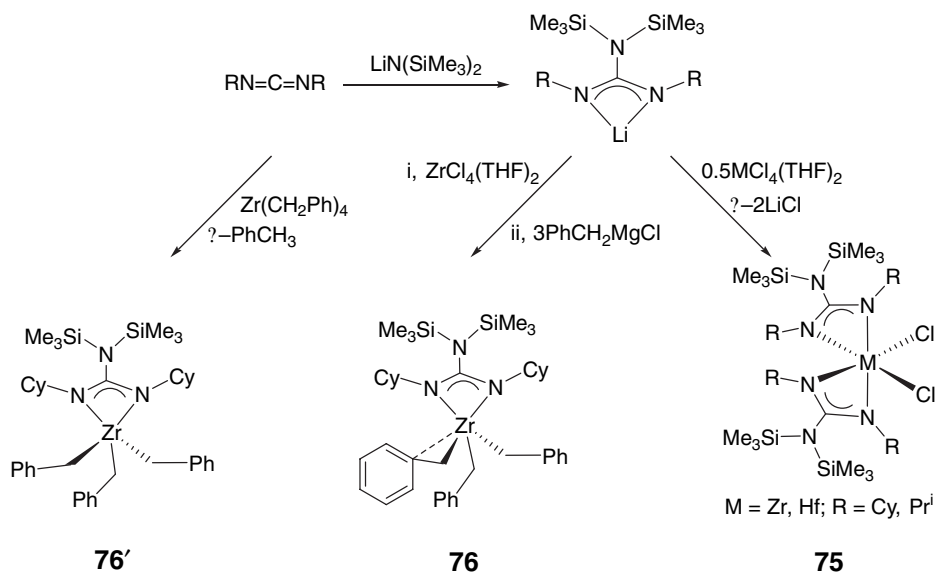
Similar to amidinate ligands, guanidines are also mono-anionic, six-electron donors; however, guanidines are zwitterionic in nature, due to the contribution from the lone pair of the  $\text{NR}'_2$  function on the backbone in the overall resonance structure. Stabilization to a cationic metal center provided by the charge delocalization to the guanidinate ligand framework can also be visualized through the participation of the  $\text{NR}'_2$  moiety (Scheme 12).

Addition of  $\text{LiN}(\text{SiMe}_3)_2$  to carbodiimides,  $\text{R}=\text{C}=\text{R}$  ( $\text{R} = \text{Cy}$ ,  $\text{Pr}^i$ ), generates tetrasubstituted guanidines which provides entry to a series of bis(guanidinate)zirconium and hafnium complexes **75** and mono(guanidinate)zirconium tribenzyl complex **76**<sup>87</sup> (Scheme 13). The molecular structures of the bis(guanidinate) complexes feature distorted pseudo-octahedral metal centers, which lie on an approximate two fold axis bisecting the  $\text{Cl-M-Cl}$  angle, with two planar bidentate guanidinate ligands and two *cis*-chloride ligands completing the coordination sphere. The mono-(guanidinate)zirconium tribenzyl complex shows that one of the benzyl groups is  $\eta^2$ -bonded to Zr in the structure determined from the single crystals from toluene, but there is no evidence for such benzyl ligation in solution. Interestingly, the same compound (denoted as **76'**), when prepared from the alkane elimination approach involving the reaction between the neutral ligand and  $\text{Zr}(\text{CH}_2\text{Ph})_4$  and recrystallized from pentane, shows no evidence for the presence of an  $\eta^2$ -benzyl coordination either in the solid state or in solution.<sup>88</sup> This variation in bonding for the same compound is attributed to crystal packing effects.

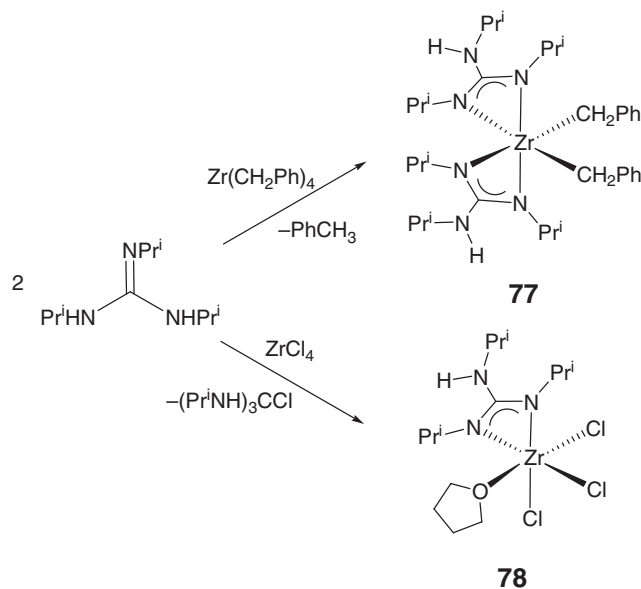
Hydrocarbyl elimination was used to synthesize bis(guanidinato)bis(benzyl)zirconium complex **77**<sup>89</sup> (Scheme 14). This complex was obtained in 88% yield from the reaction of  $\text{Zr}(\text{CH}_2\text{Ph})_4$  with 2 equiv. of *N,N',N''*-triisopropylguanidine through proton transfer and toluene elimination. The molecular structure of **77** features a distorted octahedral geometry about Zr with approximate  $C_2$ -symmetry. The two benzyl groups are bound to Zr via  $\eta^1$ -bonding, whereas the two guanidinato ligands serve as bidentate ligands via  $\pi$ -conjugated  $\text{N-C-N}$  chelates. When  $\text{ZrCl}_4$  is used, instead of  $\text{Zr}(\text{CH}_2\text{Ph})_4$ , the same reaction generates the mono(guanidinato) complex **78** and guanidinium hydrochloride, a co-product of this reaction. When crystallized from THF, complex **78** was isolated as the THF adduct (Scheme 14).



Scheme 12



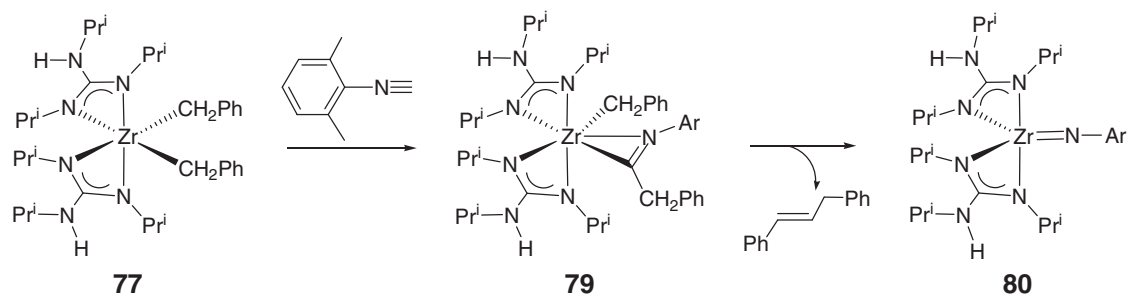
Scheme 13



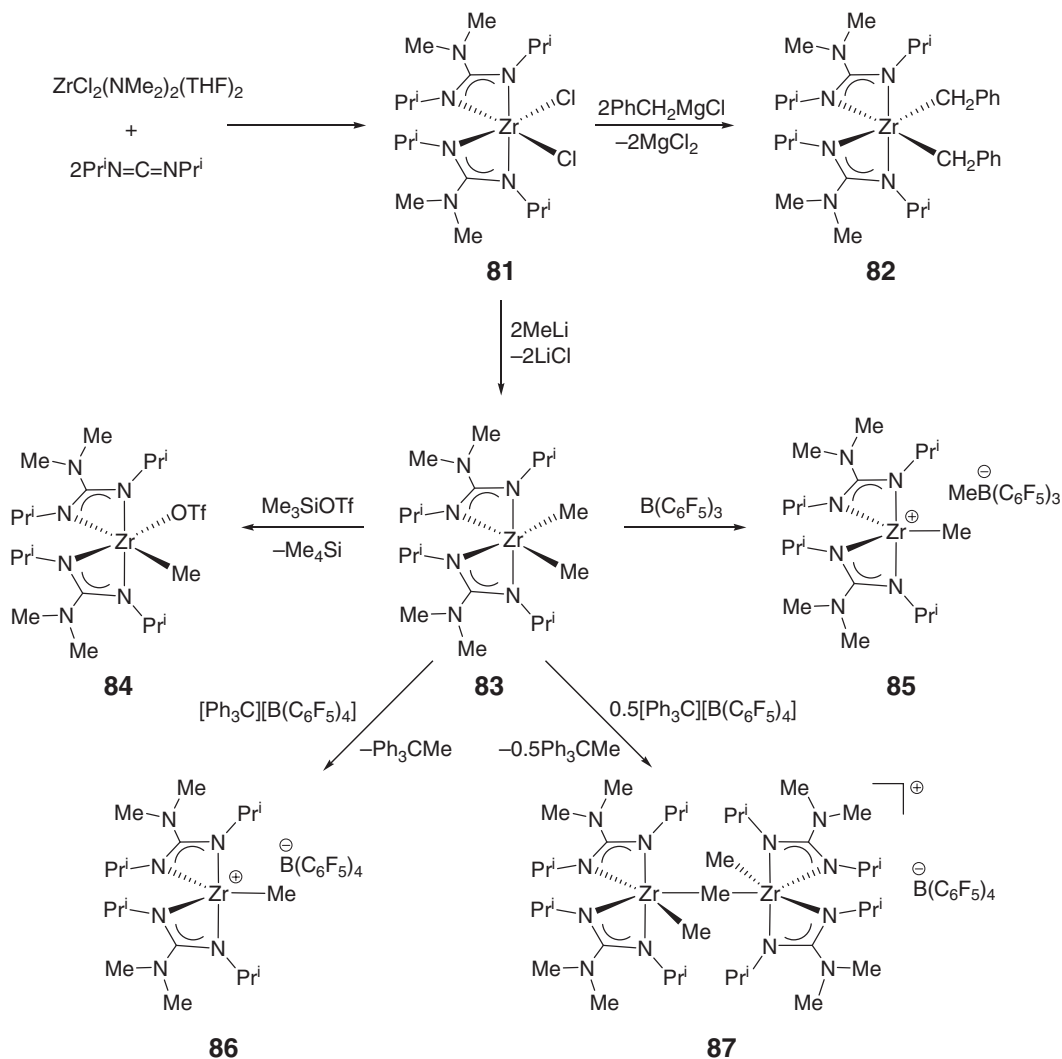
Scheme 14

Complex **77** reacts rapidly with 1 equiv. of 2,6-dimethylphenyl isocyanide to form the monoinsertion  $\eta^2$ -iminoacyl product **79**<sup>90</sup> (Scheme 15). A toluene solution of **24/79** undergoes elimination of *trans*-2-benzylstyrene at room temperature over several hours, yielding the terminal Zr imido complex **25/80**. Complex **80** adopts a *tbp* geometry, with the imido ligand occupying an equatorial site. The transformation of the  $\eta^2$ -iminoacyl **24/79** to the terminal imido **25/80** is unique, presumably occurring via a retro [2 + 2]-cycloaddition from an azametallacyclobutane intermediate.

The inert nature of guanidines as suitable spectator ligands supporting organometallic fragments is demonstrated in various types of organometallic reactions starting from the dichloride precursor **81**, which is conveniently obtained in quantitative yield from the reaction of  $ZrCl_2(NMe_2)_2(THF)_2$  with 2 equiv. of diisopropylcarbodiimide<sup>91</sup> (Scheme 16). The dichloride can be converted to the dibenzyl **82** in which both benzyl ligands adopt undistorted



Scheme 15



Scheme 16

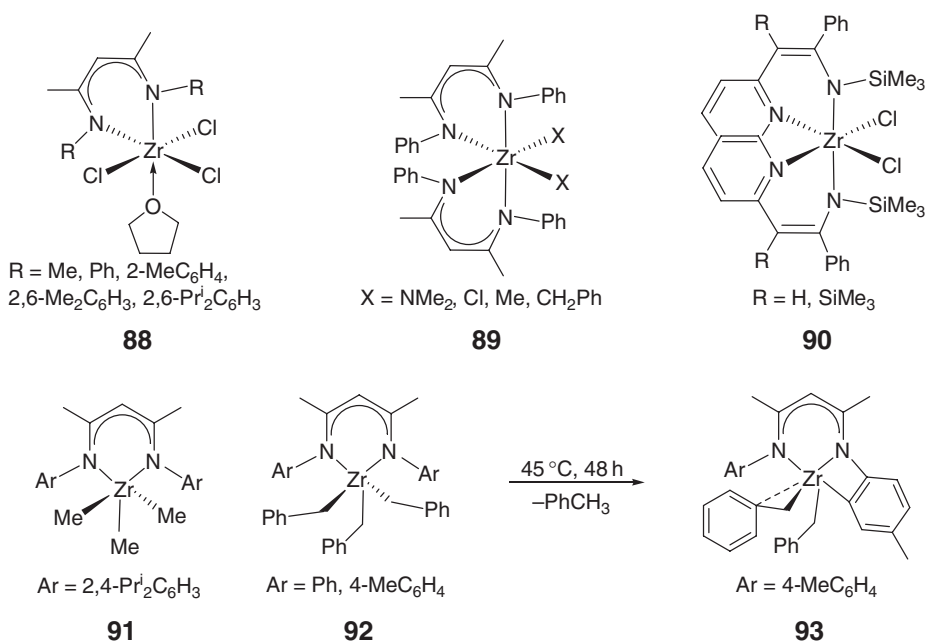
( $\eta^1$ -) coordination modes and to the dimethyl **83**. Treatment of the dimethyl **83** with 1 equiv. of  $\text{Me}_3\text{SiOTf}$  affords the lower symmetry, mono-triflate complex **84**, along with 1 equiv. of tetramethylsilane. Clean and facile methide abstraction from the dimethyl **83** is manifested by its reactions with  $\text{B}(\text{C}_6\text{F}_5)_3$  and  $[\text{Ph}_3\text{C}][\text{B}(\text{C}_6\text{F}_5)_4]$ , leading to formation of stable and isolable cationic complex **85** and **86**, respectively. The NMR data indicate the anion

$\text{MeB}(\text{C}_6\text{F}_5)_3^-$  in **85** is not strongly associated with the cationic Zr center, and remarkably, the unique donor ability of the guanidinate ligand allows for isolation and characterization of the zirconium methyl cation **86** with the extremely weakly coordinating  $[\text{B}(\text{C}_6\text{F}_5)_4]^-$  counteranion. When the dimethyl **83** reacts with 0.5 equiv. of  $[\text{Ph}_3\text{C}][\text{B}(\text{C}_6\text{F}_5)_4]$  in pentane/benzene solution, the dinuclear cation **87** is produced as a white precipitate, indicating the neutral **83** is a better ligand for the cationic zirconium center than either the weakly coordinating  $[\text{B}(\text{C}_6\text{F}_5)_4]^-$  anion or the chlorinated solvent (**87** can also be generated in chlorobenzene- $d_5$ ). The dichloride **81** and dimethyl **83**, when activated with MMAO and  $[\text{Ph}_3\text{C}][\text{B}(\text{C}_6\text{F}_5)_4]$ , respectively, as well as the preformed cation **86** showed low ethylene polymerization activity; the polymer produced exhibit broad and/or bimodal molecular weight distributions.

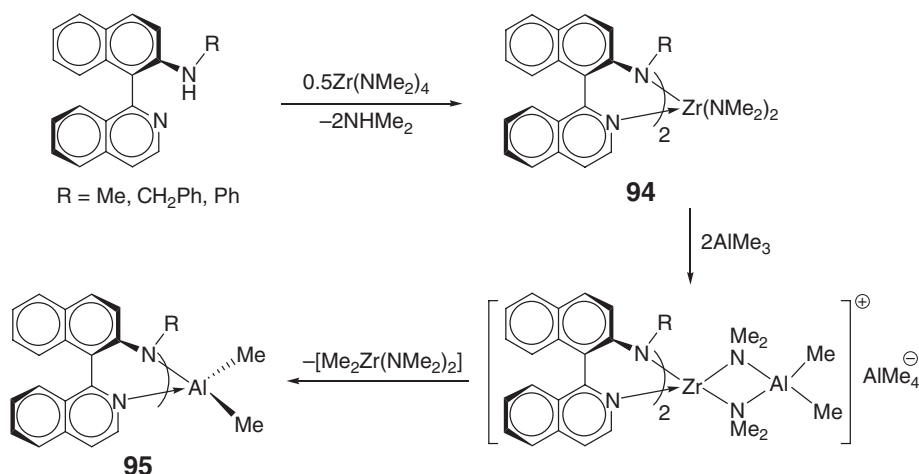
#### 4.08.3.4 $\beta$ -diketiminato $[\text{N}_2^-]$ Complexes

Scheme 17 depicts a series of zirconium complexes supported by  $\beta$ -diketiminates, formally  $\eta^2$ -,  $[\text{N}_2^-]$  ligands. Mono( $\beta$ -diketiminato) trichloride complexes **88** are prepared by the salt metathesis method;<sup>92</sup> when activated with MAO, they are active catalysts for ethylene polymerization, with the catalyst containing the *N*-methyl-substituted ligand being more active and stable than those having *N*-aryl-substituted ligands. Bis( $\beta$ -diketiminato) zirconium diamide, dichloride, and dialkyl complexes **89** are obtained by the amine elimination approach;<sup>93</sup> upon activation with MAO, these complexes exhibit considerably higher activity than the analogous mono( $\beta$ -diketiminato) complexes.<sup>94</sup> Interestingly, when one of the  $\beta$ -diketiminato ligands is replaced with a Cp or indenyl ligand, the remaining  $\beta$ -diketiminato ligand adopts an  $\eta^5$ -coordination mode in the mixed Cp and  $\beta$ -diketiminato complexes.<sup>93</sup> Dichloride complexes **90** bearing two pyridyl  $\beta$ -diketiminates are prepared using the salt metathesis method and the analogous quinolyl  $\beta$ -diketiminato complexes obtained in the same manner.<sup>95</sup> With this type of the ligand set, however these bis( $\beta$ -diketiminato) complexes exhibit marginal or no ethylene polymerization activity when activated with MAO, but the mono( $\beta$ -diketiminato)zirconium trichloride complexes have substantially higher activity.<sup>96</sup> Mono( $\beta$ -diketiminato)zirconium trimethyl complex **91**<sup>97</sup> and tribenzyl complexes **92** are also prepared.<sup>93,97</sup> The square-pyramidal tribenzyl complex **92** undergoes toluene elimination at 45 °C to give the orthometallated complex **93**.<sup>97</sup>

Racemic  $C_2$ -zirconium complexes **94** incorporating chiral  $\beta$ -diketiminato ligands are obtained by the reaction between a neutral  $\beta$ -diketimine and  $\text{Zr}(\text{NMe}_2)_4$ , via amine elimination<sup>98</sup> (Scheme 18). The solid-state structure ( $\text{R} = \text{Me}$ ) shows a *cis*-arrangement of both pyridyl and dimethylamido nitrogen atoms, which mandates a *trans*-arrangement for the anilinic nitrogen atoms. An attempt to exchange dimethylamido ligands for methyl groups



Scheme 17

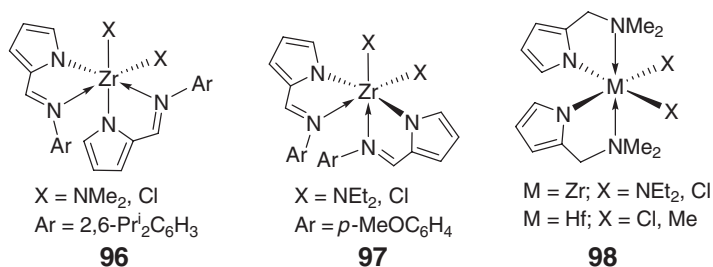


Scheme 18

using  $\text{AlMe}_3$  results in a surprisingly facile transmetalation of the bis( $\beta$ -diketiminato)Zr(IV) complex to mono-( $\beta$ -diketiminato)Al(III) dimethyl complexes **95**<sup>99</sup> (Scheme 18). These aluminum complexes, when activated with MMAO, exhibit substantial activity in the polymerization of ethylene.

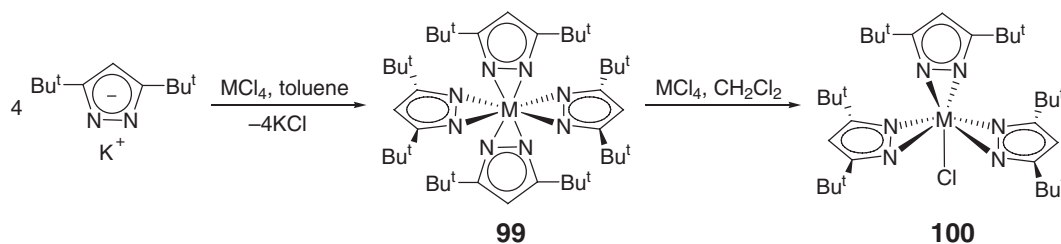
#### 4.08.3.5 Pyrrolide, Pyrazolato, Enamido, and Amido Nitrogen-donor [ $N^-,M$ ] Complexes

Zirconium complexes incorporating imino-pyrrolide ligands **96**<sup>100</sup> and **97**<sup>101</sup> and amino-pyrrolide ligands **98**<sup>102,103</sup> can be viewed as having the amido nitrogen-donor, namely, [ $N^-,M$ ], ligation. The molecular structure of the bis(dimethylamide) complex of **96** with two bulky substituents on the 2,6-positions of the aryl ring shows that all three different types of nitrogen atoms – pyrrolide, imine, and amide – are mutually *cis*. However, the pyrrolide nitrogen atoms in **97** with smaller substituents are arranged in a *trans*-configuration, reflecting the steric effect of the substituents in the aryl ring. For amino-pyrrolide complexes **98**, all structurally characterized zirconium ( $X = \text{Cl}$ ) and hafnium ( $X = \text{Cl}$  and  $\text{Me}$ ) complexes show *cis*-configurations for two  $X$  ligands and two pyrrolide nitrogens and *trans*-arrangements for two amino nitrogens. Zirconium and hafnium monochloride complexes bearing three (dimethylaminomethyl)pyrrolide ligands have also been prepared simply by adjusting the ratio of the reactants in the salt metathesis approach. The zirconium dichloride complex of types **96** and **97** catalyze the polymerization of ethylene after activation with MAO. Similarly, the zirconium complexes of type **98**, when activated with MAO, show moderate activity for ethylene polymerization; however, the polymer produced has a very broad molecular weight distribution, indicating a multi-site catalysis. The analogous hafnium complexes are also moderately active, but the property of the resulting polymer is unknown.



The salt metathesis reaction of potassium 3,5-di-*tert*-butylpyrazolate and  $\text{MCl}_4$  ( $M = \text{Zr}, \text{Hf}$ ) in toluene leads to tetrakis(3,5-di-*tert*-butylpyrazolato)zirconium and hafnium complexes **99**<sup>104</sup> (Scheme 19), in which the 3,5-di-*tert*-butylpyrazolato ligands are coordinated to  $M$  in an  $\eta^2$ -mode. Ligand redistribution between the tetrakis complexes and  $\text{MCl}_4$  in  $\text{CH}_2\text{Cl}_2$  yields the corresponding chlorotris(3,5-di-*tert*-butylpyrazolato)zirconium and hafnium complexes **100**. The molecular structure of **100** ( $M = \text{Hf}$ ) shows the pyrazolato ligands are coordinated to Hf with

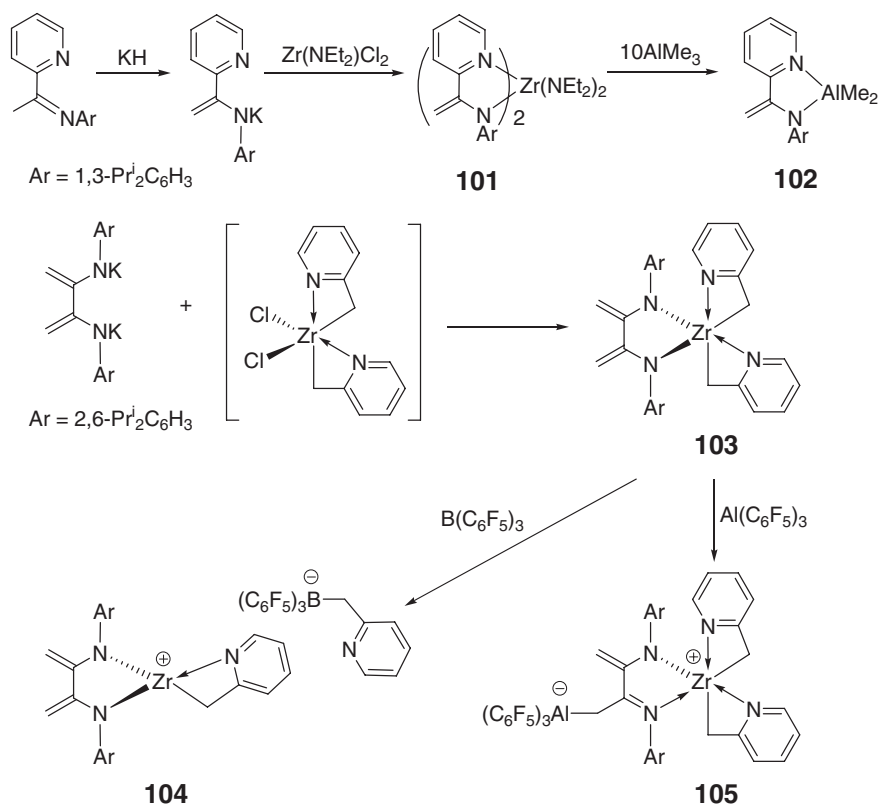




Scheme 19

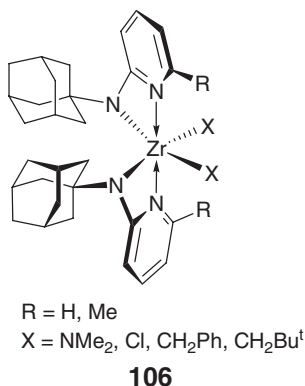
idealized  $\eta^2$ -bonding and canted with respect to each other, yielding chiral molecules; the compound crystallizes as the racemate.

The pyridine–enamido complex **101** was prepared according to Scheme 20.<sup>105</sup> In an attempt to prepare the corresponding dimethyl species, treatment of this complex with excess  $\text{AlMe}_3$  leads to transmetalation of Zr to Al, affording Al enamido complex **102**. Bis(enamido)zirconium complex **103** was synthesized by salt metathesis using the dianionic ligand and the *in situ*-generated bis(2-picoly)zirconium dichloride.<sup>106</sup> Activation of this enamido zirconium complex with Lewis acids  $\text{E}(\text{C}_6\text{F}_5)_3$  ( $\text{E} = \text{B}, \text{Al}$ ) occurs via two different pathways, dependent on E. While  $\text{B}(\text{C}_6\text{F}_5)_3$  undergoes electrophilic abstraction of the picolyl group to form ion pair **104**,  $\text{Al}(\text{C}_6\text{F}_5)_3$  undergoes electrophilic addition to the methylene carbon on the enamido ligand backbone to give zwitterionic complex **105**. The ion-paired complex **104** is sluggish for ethylene polymerization, but the zwitterionic complex **105** shows good activity. These results further highlight the importance of carrying studies of catalyst precursors with different activators, since these can change the catalyst structures and thus give different catalytic activity and chemistry.

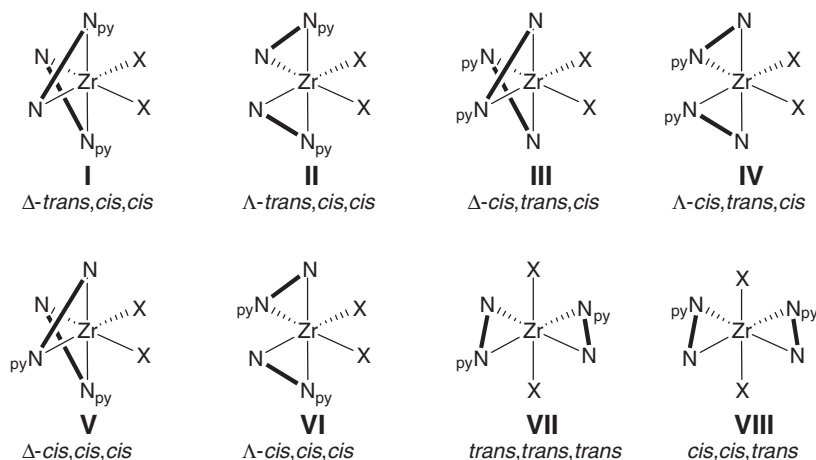


Scheme 20

A series of zirconium dichloride, diamide, and dialkyl complexes **106** supported by 1-adamantyl-2-pyridyl amido ligands was obtained using a combination of salt metathesis, amine elimination, and alkane elimination approaches.<sup>107</sup> The molecular structure of the six-coordinate bis(neopentyl) complex ( $R = H$ ,  $X = CH_2Bu^t$ ) shows mutually *cis*-arrangements for the neopentyl methylene groups and amido N atoms, whereas the two pyridine nitrogens are mutually *trans* in the axial position. The structure of the complexes in solution is similar to that observed in the solid state, as judged from NMR spectra. In all the instances, only one set of resonances for the aminopyridinato ligands is observed at accessible temperatures; thus, these complexes are stable with respect to possible ligand redistribution. The reaction of the dibenzyl complexes with  $B(C_6F_5)_3$  generates the corresponding benzyl cation; upon activation with MAO, the dichloride complex ( $R = H$ ,  $X = Cl$ ) shows similar activity toward ethylene polymerization to the related  $Zr(benzamidate)_2Cl_2$  system.

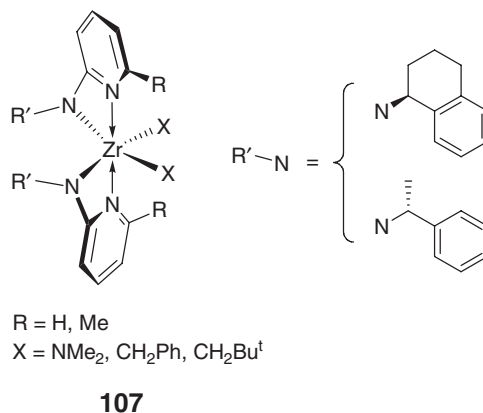


Closely related 2-pyridyl amido zirconium complexes **107** contain chiral (*S*)-1,2,3,4-tetrahydro-1-naphthyl or (*S*)- $\alpha$ -methylbenzyl substituents on the amido nitrogens.<sup>108</sup> All such complexes are in dynamic exchange between diastereomers via an *N*-dissociative mechanism – conversion from six- to five-coordinate structure followed by rapid intramolecular scrambling; surprisingly, the conformationally flexible  $\alpha$ -methylbenzyl-based pyridylamido ligands promote much better control of diastereoselectivity than do the cyclic tetrahydronaphthyl analogs in **107**. For example, although several diastereomers of the dibenzyl complex with the more rigid cyclic substituent were detected, the dibenzyl complexes with the flexible substituent exist as a ca. 9:1 mixture of two isomers ( $R = H$ ) only, or essentially complete control of stereochemistry ( $R = Me$ ) at  $-80^\circ C$  with observation of only one diastereomer out of eight possible structures – the  $\Delta$ -*cis,cis,cis*-diastereomer, structure **VI**, Scheme 21. The molecular structures determined by X-ray diffraction correspond to the  $C_2$ -symmetric  $\Lambda$ -*trans,cis,cis* diastereomer (structure **II**,



Scheme 21

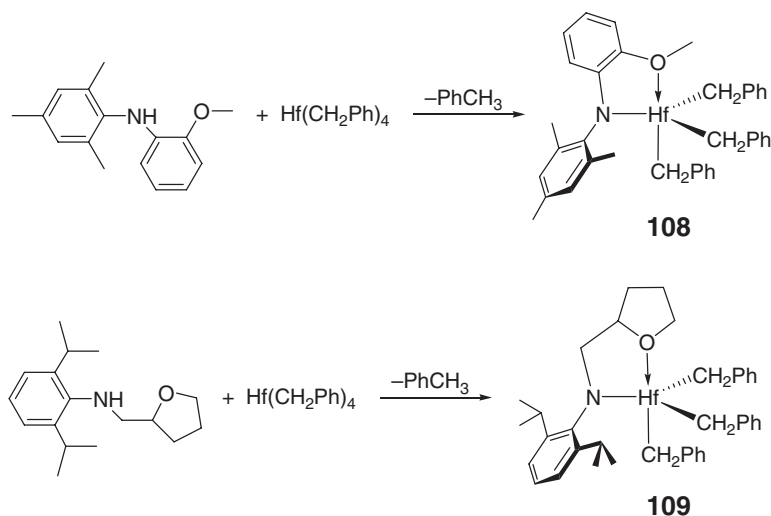
Scheme 21) for the bis(neopentyl) complex ( $R = H$ ) and the  $C_1$ -symmetric  $\Delta$ -*cis,cis,cis* diastereomer (structure VI) for the dibenzyl complex ( $R = Me$ ).



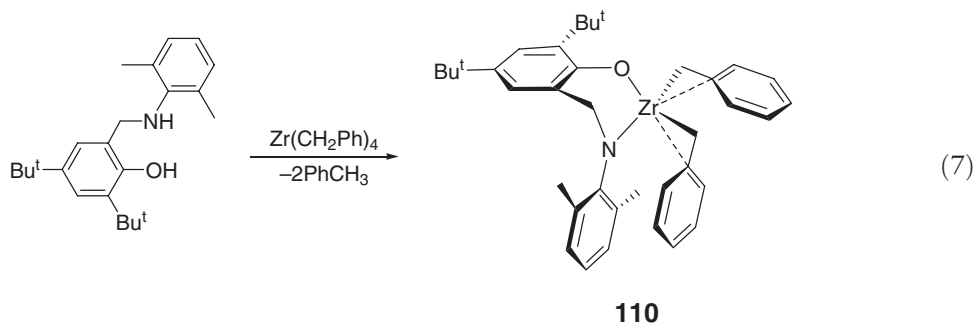
#### 4.08.3.6 Amido Oxygen-donor [ $N^-,O$ ] and Amido Aryloxide [ $N^-,O^-$ ] Complexes

Amide ether-based zirconium and hafnium complexes were discovered to be highly efficient olefin polymerization catalysts, when activated with suitable activators, through the application of fully integrated high-throughput primary and secondary screening techniques, supported by rapid polymer characterization methods. In particular, the primary screening methods rapidly identify tribenzylhafnium complex  $\{\eta^2-[N^-,O]-(2-MeO-C_6H_4)(2,4,6-Me_3C_6H_2)N\}-Hf(CH_2Ph)_3$  **108** to be capable of polymerizing 1-octene to high conversion.<sup>109</sup> This complex and its analogous complex **109** are obtained from the reaction of  $Hf(CH_2Ph)_4$  with neutral amine ligands via toluene elimination (Scheme 22).

Protolysis of  $Zr(CH_2Ph)_4$  with the 2,6-dimethylphenyl aminophenol ligand in toluene affords the mononuclear zirconium dibenzyl complex **110** bearing the chelating phenoxy amido, dianionic bidentate ligand<sup>110</sup> (Equation (7)). The molecular structure of complex **110** is that of a distorted tetrahedron, if considering the benzyl unit as monodentate. However, the angles at the two benzyl methylene carbons (that is,  $Zr-CH_2-C_{ipso}$  angles) are  $87.0(2)^\circ$  and  $91.0(2)^\circ$ , values typical of  $\eta^2$ -bonding for benzyl groups in related systems. When activated with MAO, this complex exhibits low ethylene polymerization activity.

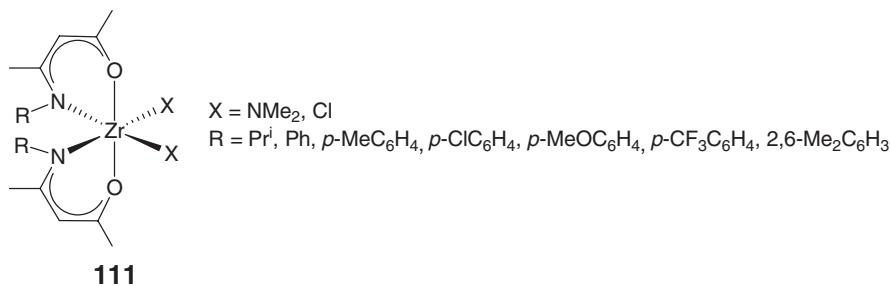


Scheme 22



#### 4.08.3.7 $\beta$ -Ketoiminate $[(N,O)^-]$ Complexes

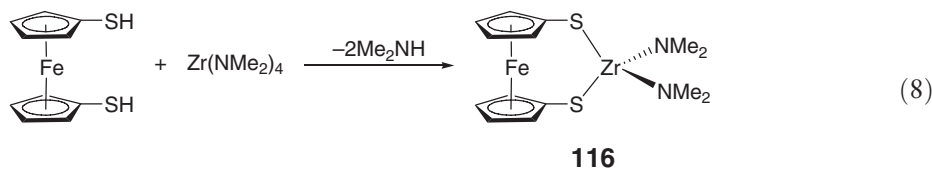
A series of bis( $\beta$ -ketoiminate)zirconium complexes with a general structure of **111** was synthesized via either salt metathesis or amine elimination.<sup>111–113</sup> The molecular structures of both dichloride complexes ( $R = \text{Ph}$ ,  $p$ -tolyl) show that the O, N, and Cl atoms are *trans*, *cis*, and *cis*, respectively. Moderate activity is observed for the complexes of this type for ethylene oligomerization when activated with an alkylaluminum chloride<sup>114</sup> and for polymerization of ethylene when activated with modified MAO.<sup>113</sup>

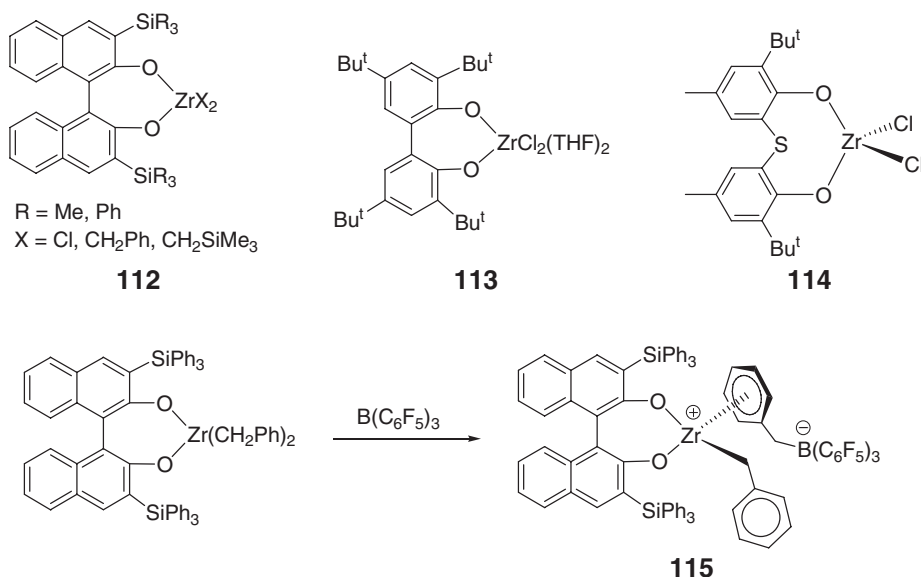


#### 4.08.3.8 Chelating Aryloxide $[\text{O}^-, \text{O}^-]$ and Thiolate $[\text{S}^-, \text{S}^-]$ Complexes

Sterically hindered, chelating phenoxide Zr(IV) complexes **112–114**<sup>115</sup> (Scheme 23), prepared by alkane elimination involving the reaction of  $\text{Zr}(\text{CH}_2\text{Ph})_4$  or  $\text{Zr}(\text{CH}_2\text{Ph})_2\text{Cl}_2(\text{OEt}_2)_2$  with the appropriate biphenol or binaphthol ligands, are active catalysts for polymerization of ethylene and oligomerization of  $\alpha$ -olefins upon activation with MAO or  $\text{B}(\text{C}_6\text{F}_5)_3$  (for benzyl precursors). Spectroscopic investigations of the reaction between the zirconium dibenzyl complex with  $\text{B}(\text{C}_6\text{F}_5)_3$  in toluene show the formation of the corresponding zwitterionic complex associated with a benzyl borate anion via  $\eta^6$ -Ph coordination (i.e., complex **115**; Scheme 23).

The ferrocenyl-bridged dithiolate zirconium diamide complex **116** is readily obtained from the reaction of the ferrocenyl dithiol ligand and  $\text{Zr}(\text{NMe}_2)_4$ <sup>116</sup> (Equation (8)). Treatment of **116** with trimethylaluminum followed by exposure to ethylene in the presence of MAO yields solid polyethylene, but the catalyst activity is low and the polymer produced has a very broad molecular weight distribution.

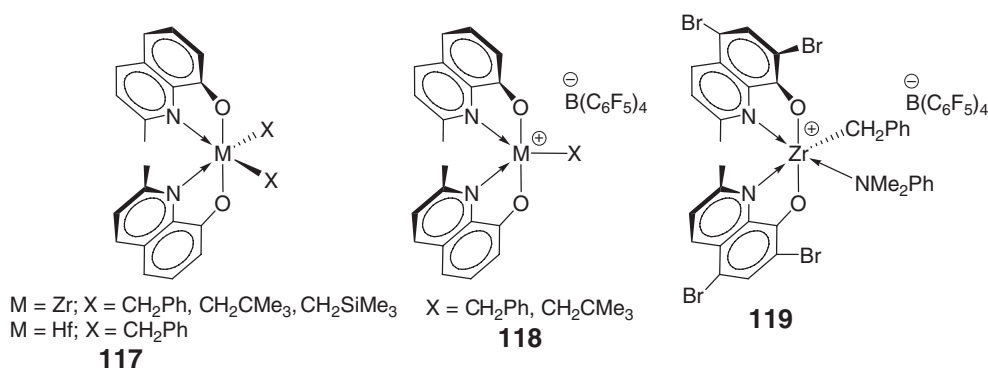




Scheme 23

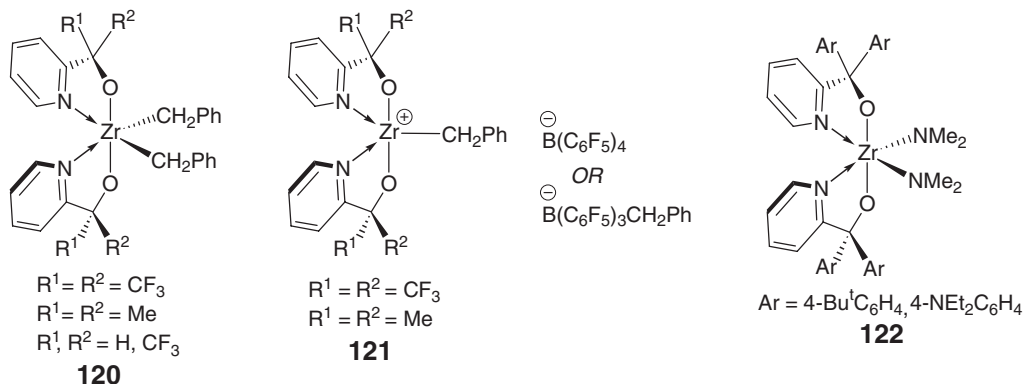
#### 4.08.3.9 Aryloxide and Alkoxide Donor $[\text{O}^-, D]$ ( $D = \text{N, O}$ ) Complexes

Zirconium and hafnium dialkyl complexes **117** incorporating 8-quinolinolato ligands are readily obtained from the alkane elimination approach involving the reaction of the neutral ligand and  $\text{ZrR}_4$  ( $R = \text{CH}_2\text{Ph, CH}_2\text{CMe}_3, \text{CH}_2\text{SiMe}_3$ ).<sup>117</sup> The solid-state structure of the Zr dibenzyl complex adopts a distorted octahedral geometry about Zr with a *trans*-O, *cis*-N, *cis*-X ligand arrangement and one of the benzyl ligands is bonded to Zr in an  $\eta^2$ -fashion. Solution NMR data are consistent with this structure, and the complexes undergo inversion of metal configuration (racemization) on the NMR timescale at elevated temperatures. Reaction of the dibenzyl and bis(neopentyl) complexes with  $[\text{HNMe}_2\text{Ph}][\text{B(C}_6\text{F}_5)_4]$  yields the base-free cationic complexes **118**, whereas the corresponding reaction of the dibromo-substituted derivative gives the labile amine adduct **119**. The base-free cationic complexes **118** are inactive in ethylene polymerizations, while the dibromo-substituted analogs exhibit moderate activity.

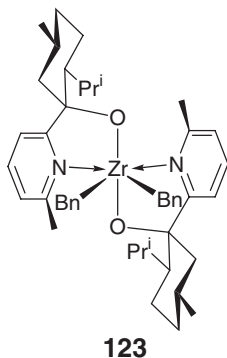


The reaction of  $\text{Zr(CH}_2\text{Ph)}_4$  with pyridine alcohols yields the zirconium dibenzyl complexes **120** incorporating bidentate pyridine-alkoxide ligands.<sup>118</sup> These complexes adopt distorted octahedral geometries about Zr with *trans*-O, *cis*-N, *cis*-C ligand arrangements but undergo rapid inversion of configurations at Zr (racemization) on the NMR timescale. Reactions with  $\text{B(C}_6\text{F}_5)_3$  and  $[\text{HNMe}_2\text{Ph}][\text{B(C}_6\text{F}_5)_4]$  yield the base-free cationic complexes **121** with loosely paired anions  $[\text{PhCH}_2\text{B(C}_6\text{F}_5)_3]^-$  and  $[\text{B(C}_6\text{F}_5)_4]^-$ . The cation with  $R^1 = R^2 = \text{CF}_3$  shows moderate activity for ethylene and 1-hexene polymerizations leading to low molecular weight polymers, whereas the cation with

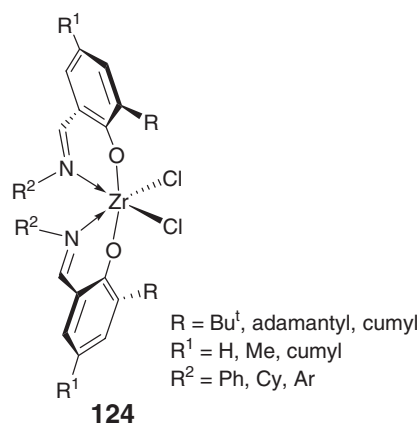
$R^1 = R^2 = \text{CH}_3$  is inactive. The closely related zirconium bis(amide) complexes **122** with aryl substitutions are conveniently obtained via amine elimination.<sup>119</sup> The *in situ* activation of these complexes with  $\text{Al}(\text{Bu}^i)_3$  and MAO yields active, multi-site ethylene polymerization catalysts.



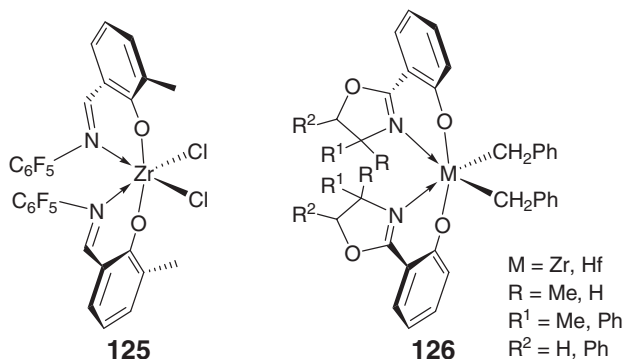
Protolysis of  $\text{Zr}(\text{CH}_2\text{Ph})_4$  using 2-( $-$ )menthyl-4-methylpyridine, an enantiomerically pure ligand, produces the chiral version of pyridine alcoholate zirconium dibenzyl complex **123** as a single product.<sup>120</sup> Only one of eight possible diastereomers is observed by NMR spectroscopy in the slow exchange regime. X-ray crystallography reveals a  $\Delta$ -*trans,cis,cis*-structure, as shown below. The geometry about Zr is strongly distorted from octahedral as a result of the ligand bite angles  $\text{N}-\text{Zr}-\text{O}$  of ca.  $70^\circ$ .



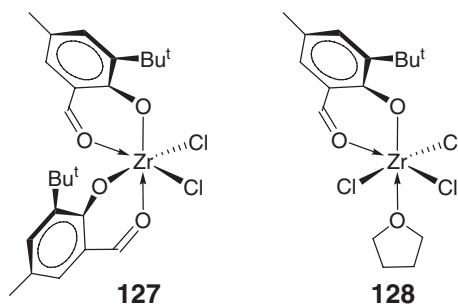
A series of zirconium complexes of the general type **124**, which incorporate two salicylaldiminato (phenoxy-imine) chelating ligands, is obtained by the salt metathesis approach.<sup>121</sup> Among five possible stereoisomers, the *trans* ( $\text{O}-\text{O}$ ), *cis* ( $\text{N}-\text{N}$ ), *cis* ( $\text{Cl}-\text{Cl}$ ), one depicted below, is the most preferred according to DFT calculations and the molecular structure of such a complex ( $\text{R} = \text{Bu}^t$ ;  $\text{R}^1 = \text{H}$ ;  $\text{R}^2 = \text{Ph}$ ). The steric bulk of the *ortho*-substituent  $\text{R}$  group and the group  $\text{R}^2$  attached to the imine nitrogen atoms substantially influence the activity of these complexes and the resulting polymer molecular weight in ethylene polymerization using MAO activator. Increasing the size of the  $\text{R}$  group leads to an increase in activity, presumably due to the enhanced steric protection of the  $\text{Zr}-\text{O}$  bond toward electrophilic attack by trimethylaluminum present in MAO and a larger degree of cation-anion separation of the active species. On the other hand, a twofold effect is expected when increasing the size of the imino substituent  $\text{R}^2$ : steric congestion in the proximity of the active site reduces both rates of polymerization and  $\beta$ -hydrogen transfer, resulting in the production of higher molecular weight polymers, but at slower rates. The catalyst that gives the highest ethylene polymerization activity with a turnover frequency of  $42\,900\text{ s}^{-1}$  is a combination of  $\text{R} = \text{cumyl}$ ,  $\text{R}^1 = \text{Me}$ ,  $\text{R}^2 = \text{cyclohexyl}$  ( $\text{Cy}$ ), whereas the catalyst with a combination of  $\text{R} = \text{Bu}^t$ ,  $\text{R}^1 = \text{H}$ ,  $\text{R}^2 = 2\text{-Bu}^t\text{C}_6\text{H}_4$  produces the polyethylene with the highest molecular weight but with a substantially reduced activity.



The pentafluorophenyl-substituted derivative **125**<sup>122</sup> was also prepared by salt metathesis and structurally characterized; it has the expected *trans* (O–O), *cis* (Cl–Cl), *cis* (N–N) ligand arrangement. Upon activation with MAO, this complex polymerizes propylene to poorly stereoregular, predominantly syndiotactic polypropylene via a chain-end control mechanism. The polymer end-group analysis indicates mainly a primary insertion mode in both initiation and propagation,<sup>122</sup> in contrast to the prevailing secondary regiochemistry established for related bis(phenoxy–imine) titanium catalysts.<sup>123</sup> Zirconium diamides and dichlorides analogous to complexes **124** but supported by bis(salicylaldiminato) ligands without substituents in the *ortho*-positions of the phenoxy rings<sup>124</sup> show only moderate activity for ethylene polymerization upon activation with MAO. An earlier version of the bis(phenoxy–imine) zirconium and hafnium dibenzyl complexes of the general type **126**, which incorporates two chiral phenoxy oxazoline ligands, is obtained via alkane elimination approach.<sup>125</sup> The *in situ*-generated benzyl cation is active for polymerization of ethylene, albeit with low activity. Six-coordinate zirconium dichloride complexes incorporating two bulky phenoxy–amine ligands, [2,4-Bu<sup>t</sup><sub>2</sub>-6-(RNCH<sub>2</sub>)C<sub>6</sub>H<sub>2</sub>O]<sub>2</sub>ZrCl<sub>2</sub> (R = C<sub>4</sub>H<sub>8</sub>, C<sub>5</sub>H<sub>10</sub>), have also been synthesized; on activation with MAO, they show negligible activity toward ethylene polymerization.<sup>126</sup>



Replacing the nitrogen donor with an oxygen donor yields bis(phenoxy–aldehyde)zirconium dichloride **127** and mono(phenoxy–aldehyde)zirconium trichloride **128**; when activated with MAO, they exhibit high catalytic activity toward polymerization of ethylene, affording high molecular weight polyethylene with a broad molecular weight distribution ( $\bar{M}_w/\bar{M}_n > 16$ ).<sup>127</sup>

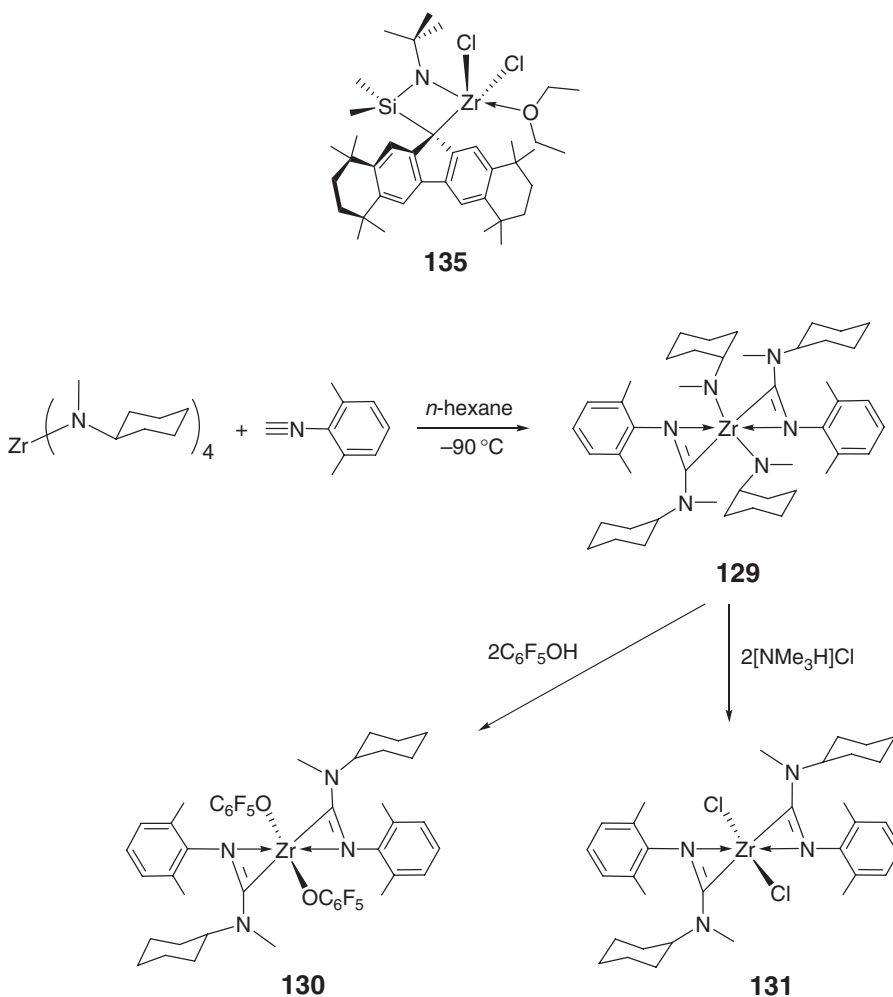


#### 4.08.3.10 Carbanion Nitrogen-donor $[C^-,M]$ and Carbanion Amido $[C^-,N^-]$ Complexes

Double insertion of 2,6-dimethyl phenyl isocyanide into the Zr–N bond in  $Zr(NMeCy)_4$  (Cy = cyclohexyl) affords  $\eta^2$ -formamidinyl Zr complex **129**<sup>128</sup> (Scheme 24); complex **129** is structurally characterized. The two anionic  $-NMeCy$  amido ligands at Zr can be readily substituted by  $-OC_6F_5$  and  $-Cl$  ligands in high-yield reactions of **129** with  $C_6F_5OH$  and  $[HNMe_3]Cl$ , producing the corresponding phenoxide and chloride derivatives of **130** and **131**, respectively. All three complexes, when treated with stoichiometric amounts of  $[HNMe_2Ph][B(C_6F_5)_4]$  as activator and with  $AlBu^i_3$  as scavenger, are active for polymerizations of 1-hexene and ethylene, although the activity is low to moderate as compared with that of  $Cp_2ZrCl_2$ .

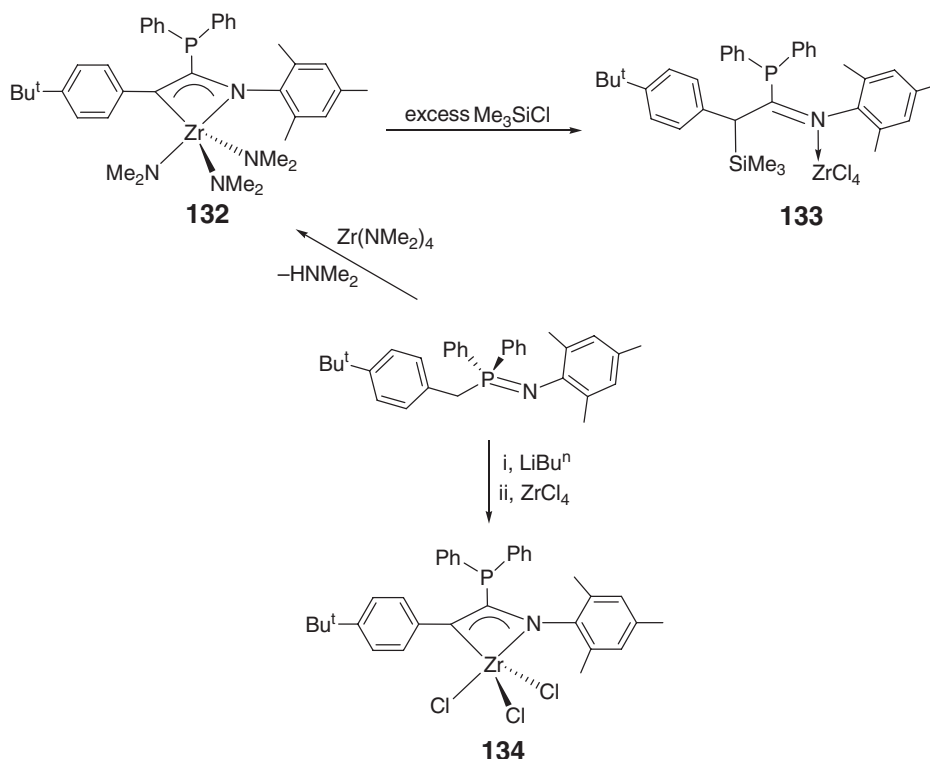
Zirconium triamide **132** bearing an iminophosphoranato ligand was obtained from the amine elimination approach<sup>129</sup> (Scheme 25). Interestingly, with this type of ligand, treatment of the triamide **132** with excess  $Me_3SiCl$  does not lead to the corresponding trichloride **134**, but a ligand silylation product **133**. Nevertheless, the trichloride can be prepared from the salt metathesis approach. These complexes upon activation with MAO are moderately active for ethylene polymerization.

The sterically expanded zirconium fluorenyl–amido complex **135** is formally a 12-electron trigonal bipyramid with the amido nitrogen and ether oxygen atoms occupying the axial positions ( $N-Zr-O = 169.9^\circ$ ).<sup>130</sup> The fluorenyl-containing  $C_{29}H_{36}$  fragment is best categorized as a simple  $\eta^1$ -C-type ligand and the whole ligand as a bidentate, dianionic  $[C^-,N^-]$  type. Upon activation with MAO, this dichloride complex is very effective in homopolymerization of  $\alpha$ -olefins and incorporates bulky  $\alpha$ -olefins at unprecedented levels; this is likely due to its spatial accessibility, rendering a sterically indiscriminate catalyst that controls selectivity by electronic considerations of  $\alpha$ -olefins.



Scheme 24





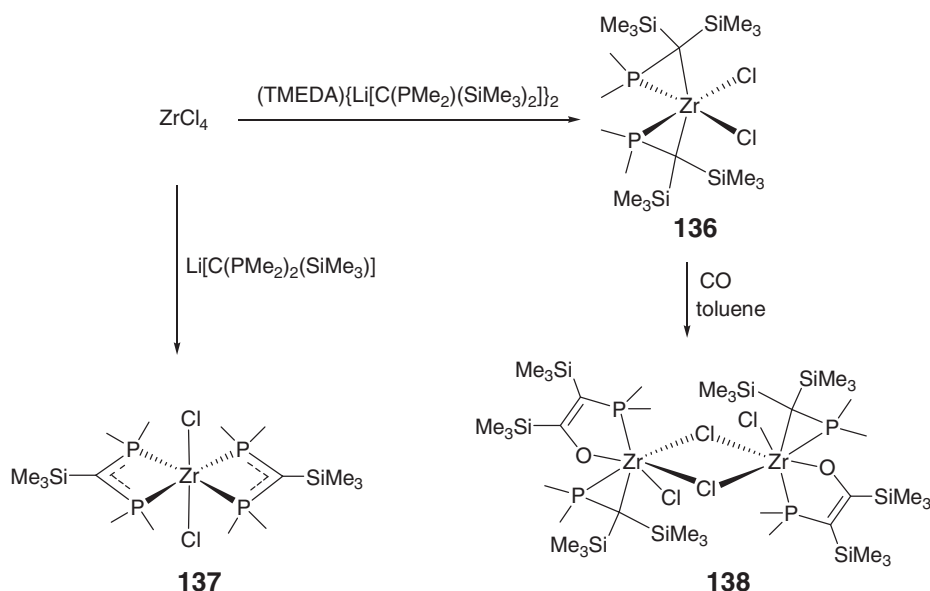
Scheme 25

#### 4.08.3.11 Phosphinomethanide $[\text{C}^-, \text{P}]$ and $[\text{P}_2^-]$ Complexes

Salt metathesis between  $\text{ZrCl}_4$  and  $(\text{TMEDA})\{\text{Li}[\text{C}(\text{PMe}_2)(\text{SiMe}_3)_2]\}_2$  (TMEDA = tetramethylethylenediamine) produces the monomeric, six-coordinate phosphinomethanide  $\text{Zr}(\text{IV})$  complex **136** in high yield as red crystals<sup>131</sup> (Scheme 26). When the fully substituted diphosphinomethanide  $\text{Li}[\text{C}(\text{PMe}_2)_2(\text{SiMe}_3)]$  is used, the reaction with  $\text{ZrCl}_4$  forms complex **137** with two diphosphinomethanide chelates. Complex **136** inserts 1 equiv. of CO in toluene into a  $\text{Zr}-\text{C}$  bond followed by a subsequent 1,2-silyl shift and dimerization, producing a phosphino enolate dinuclear complex **138**. The same insertion reaction, when carried out in THF, yields a mixture of products.

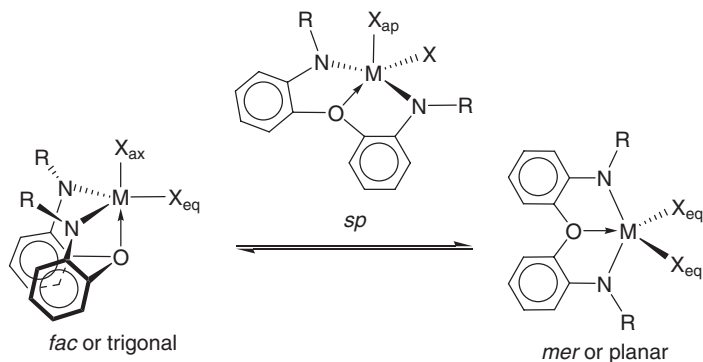
#### 4.08.4 Complexes with $\eta^3$ -Ligands

Most popular examples of the  $\text{Zr}(\text{IV})$  and  $\text{Hf}(\text{IV})$  complexes belonging to this tridentate ligand classification are a class of complexes incorporating chelating bis(amide)s bearing an additional neutral nitrogen or oxygen donor, denoted as  $[\text{N}^-, \text{N}, \text{N}^-]$  and  $[\text{N}^-, \text{O}, \text{N}^-]$ , respectively. With two additional reactive X ligands such as chlorides and alkyls bound to the neutral metal or an alkyl group and a donor ligand bound to the cationic metal center, these five-coordinate complexes typically exhibit distorted tbp geometries. By way of examining how the three heteroatoms within the supporting ligand are arranged in these trigonal bipyramids, two limiting geometries can be further described in Equation (9). When the tridentate ligand binds to the metal in a *fac*- (facial) fashion, the two nitrogen and an oxygen atoms in this example are in a trigonal arrangement with the two amido nitrogen atoms occupying approximately equatorial (eq) positions and the two X groups are non-equivalent (equatorial vs. axial). On the other hand, if the tridentate ligand binds to the metal in a *mer*- (meridional) fashion, the three heteroatoms are in a planar arrangement with the two amido nitrogen atoms occupying approximately axial (ax) positions. Intermediate geometries between these two limiting cases such as square pyramids (*sp*) in which one of



Scheme 26

the X groups is in the apical (ap) position and facile exchange between these two geometries is possible, depend on ligand features (such as rigidity) and the metal.



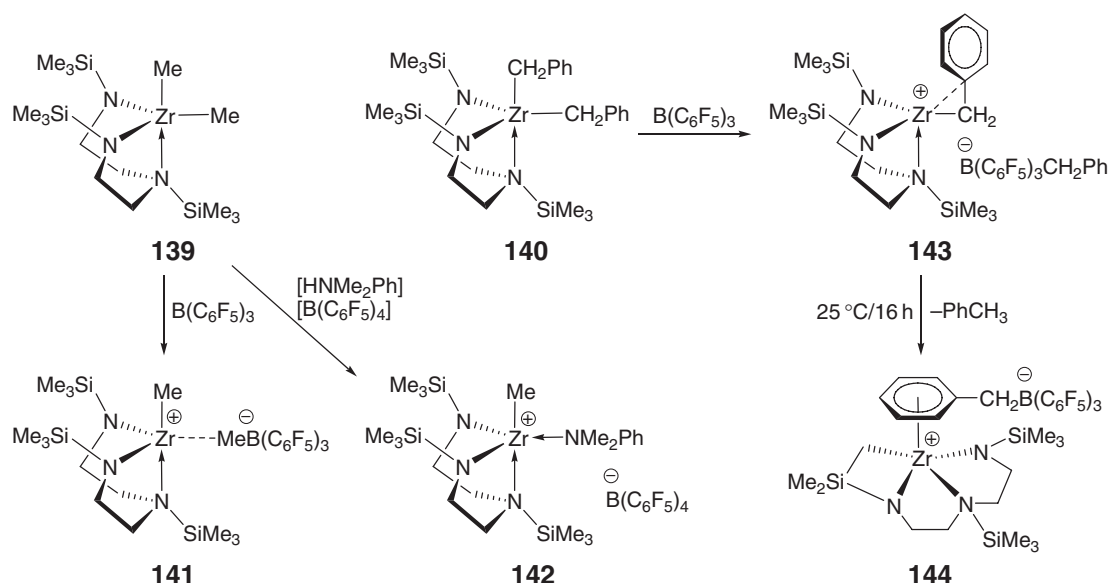
(9)

#### 4.08.4.1 Bis(amido) Nitrogen-donor [ $N^-, N, N^-$ ] Complexes

##### 4.08.4.1.1 Bis(amido)amine and pyridine complexes

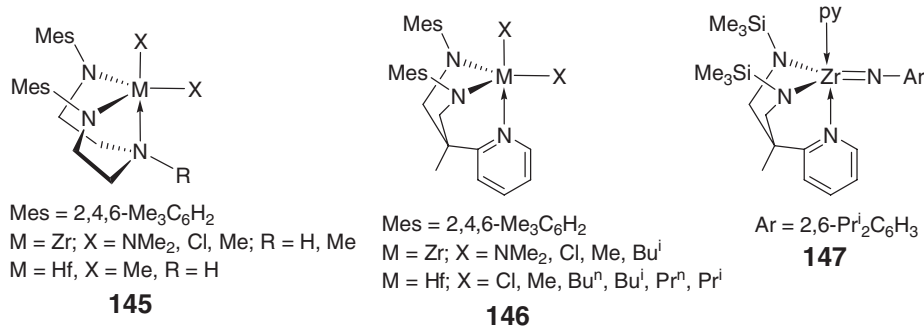
Bis(silylamido)amine zirconium dimethyl **139** and dibenzyl **140** complexes, derived from the alkylation of the dimeric dichloride precursor,<sup>132</sup> exhibit different reactivity toward alkyl abstraction. The dimethyl complex reacts with  $\text{B}(\text{C}_6\text{F}_5)_3$  to give the zwitterion **141** with coordinating methyl borate anion, whereas in the ion pair **142**, produced with  $[\text{HNMe}_2\text{Ph}][\text{B}(\text{C}_6\text{F}_5)_4]$ , the amine byproduct is coordinated to the metal center<sup>133</sup> (Scheme 27). Alkyl abstraction of the dibenzyl species with  $\text{B}(\text{C}_6\text{F}_5)_3$  affords the ion pair **143**, in which the benzyl group is bound to Zr in  $\eta^2$ -fashion; this species decomposes slowly at ambient temperature to give a zwitterionic cyclometallation product **144** with an  $\eta^6$ -arene-coordinated benzylborate anion.

To fine-tune the metal complex sterics, electronics, and geometries, as well as the stability of the resulting cationic catalysts with respect to ligand degradation due to C–H activation, a series of Zr(IV) and Hf(IV) diamide, dichloride, and dialkyl complexes incorporating tridentate bis(arylamido)amines **145**<sup>134,135</sup> and a bis(arylamido)pyridine **146**<sup>136,137</sup> has been synthesized using a combination of standard salt metathesis, amine elimination, and alkylation

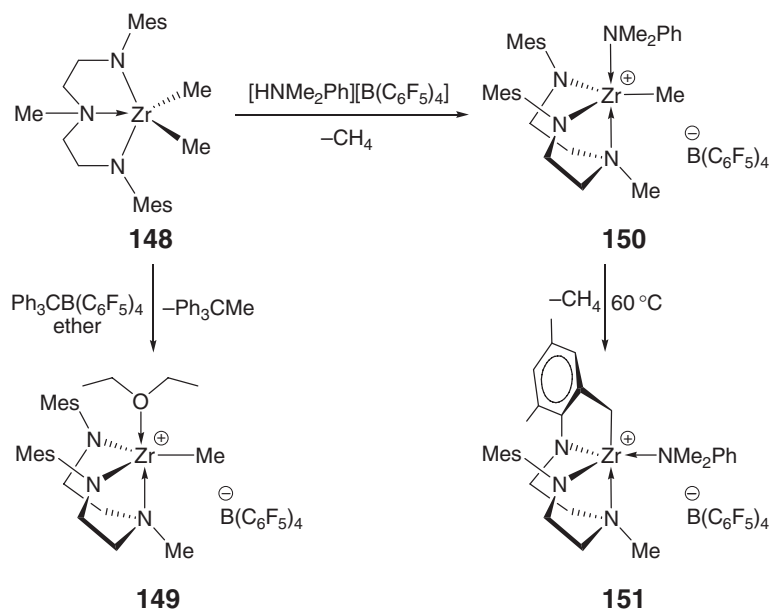


Scheme 27

methodologies. A five-coordinate imidozirconium complex **147** supported by the tridentate bis(silyl)amido)pyridine ligand was also prepared by salt metathesis.<sup>138</sup>

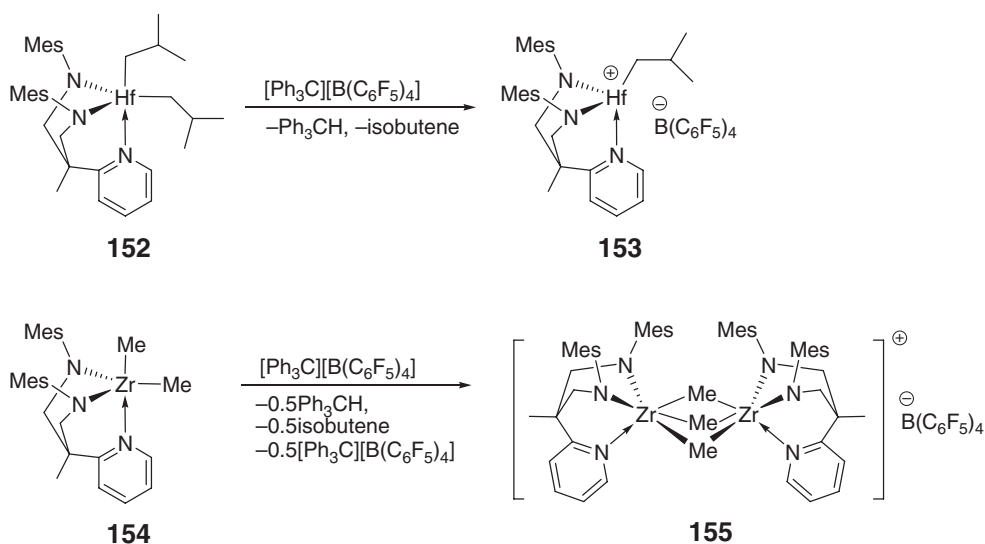


The zirconium dimethyl complex **148** adopts a *mer*-geometry in the solid state, in which the amido nitrogen atoms occupy the approximately axial positions in a trigonal bipyramid;<sup>134</sup> this contrasts with the *fac*-structures found for the analogous bis(silylamido) amine complexes  $[(\text{Me}_3\text{SiNCH}_2\text{CH}_2)_2\text{NSiMe}_3]\text{ZrX}_2$  ( $\text{X} = \text{Cl}$  or alkyl).<sup>132,133</sup> Oxidative cleavage of a Zr–Me bond in the dimethyl **148** using 1 equiv. of  $[\text{Ph}_3\text{C}][\text{B}(\text{C}_6\text{F}_5)_4]$  followed by addition of diethyl ether yields the ether adduct **149**, the structure of which is revealed to be a *fac* trigonal bipyramid in which the diethyl ether is coordinated to the Zr cation in an apical position<sup>135</sup> (Scheme 28). Using the activator  $[\text{HNMe}_2\text{Ph}][\text{B}(\text{C}_6\text{F}_5)_4]$  for generating the cationic species, the same reaction gives the corresponding adduct **150**, the solution structure of which, as illustrated by NMR studies, is consistent with that of the ether adduct **149**. Heating solutions of **150** to  $60^\circ\text{C}$  leads to C–H activation in an *ortho*-methyl group in the mesityl substituent, forming the structure **151** after release of methane (Scheme 28). The cationic species derived from the reaction of the dimethyl with 1 equiv. of  $[\text{Ph}_3\text{C}][\text{B}(\text{C}_6\text{F}_5)_4]$  in the absence of diethyl ether undergoes a similar C–H activation, catalyst decomposition reaction, accounting for its non-living behavior in the 1-hexene polymerization. This C–H activation problem is circumvented by replacing the mesityl group with a 2,6-Cl<sub>2</sub>C<sub>6</sub>H<sub>3</sub> group, which is approximately sterically equivalent; thus the cationic catalyst containing this ligand consumes 1-hexene in a strictly first-order, living manner at  $0^\circ\text{C}$  in chlorobenzene.<sup>139</sup>

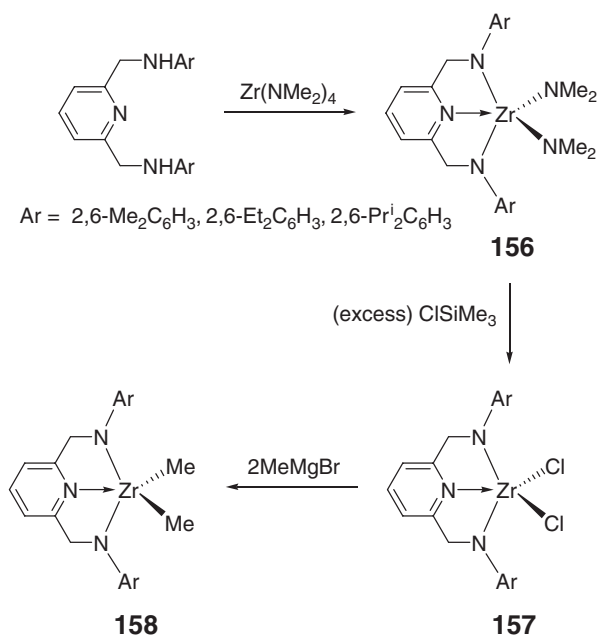


Scheme 28

The bis(arylamido)pyridine hafnium alkyl cations derived from the reaction of the dialkyl complexes of the type **146** and  $[\text{Ph}_3\text{C}][\text{B}(\text{C}_6\text{F}_5)_4]$  are readily characterizable at  $10^\circ\text{C}$  or below by NMR methods; they are active initiators for the living polymerization of 1-hexene.<sup>137</sup> Apparently, under these conditions, such cations are stable toward C–H activation involving the mesityl group and  $\beta$ -hydride elimination of the Hf–alkyl group. For example, addition of  $[\text{Ph}_3\text{C}][\text{B}(\text{C}_6\text{F}_5)_4]$  to the hafnium diisobutyl **152** yields the ion pair **153** quantitatively (Scheme 29), which decomposes in a first-order process at  $0^\circ\text{C}$  and catalyzes the well-controlled polymerization of 1-hexene at up to  $10^\circ\text{C}$ .<sup>140</sup> The hafnium diisobutyl complex **152** can also be activated with  $\text{B}(\text{C}_6\text{F}_5)_3$  to give a similar ion pair consisting of the identical cation but a different anion,  $[\text{HB}(\text{C}_6\text{F}_5)_3]^-$ . The analogous Zr dialkyls and the corresponding cations are thermally less stable and light sensitive. Significantly, reaction of the Zr (or Hf) dimethyl complex **154** with  $[\text{Ph}_3\text{C}][\text{B}(\text{C}_6\text{F}_5)_4]$  or  $\text{B}(\text{C}_6\text{F}_5)_3$  produces the catalytically inactive methyl-bridging binuclear cation **155** (Scheme 29).



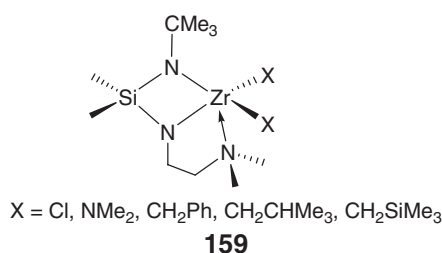
Scheme 29



Scheme 30

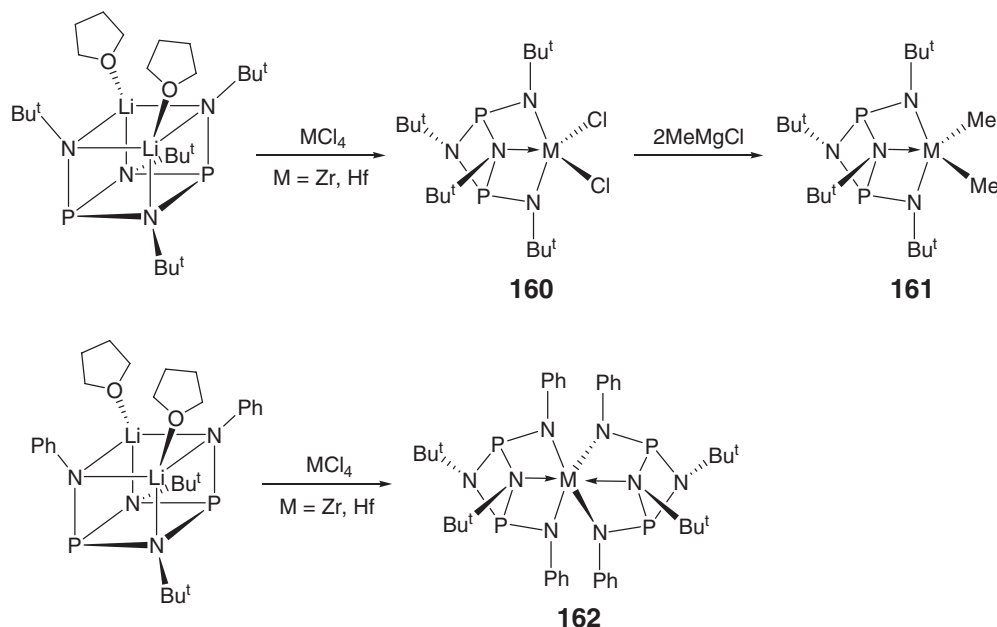
Zirconium diamide **156**, dichloride **157**, and dimethyl **158** complexes incorporating conformationally rigid pyridine–diamide ligands are synthesized in high yields according to the route depicted in Scheme 30.<sup>141</sup> The molecular structure of the dimethyl complex (Ar = 2,6-diethylphenyl) shows a distorted *tbp* structure with the amide nitrogen atoms occupying the axial positions. The pyridine–diamide ligand system exhibits coordination behavior at Zr that is very similar to the fragment [Cp<sub>2</sub>Zr].

A different type of bis(amido) amine complex is compound **159**, which bears a supporting ligand where the amine donor group is not placed in the central position between the two amido functionalities.<sup>142</sup> Importantly, this [*N*<sup>−</sup>,*N*<sup>−</sup>,*N*] nitrogen atom arrangement results in an inactive catalyst system for the polymerization of 1-hexene when the alkyl species is activated with [HNMe<sub>2</sub>Ph][B(C<sub>6</sub>F<sub>5</sub>)<sub>4</sub>] or [Ph<sub>3</sub>C][B(C<sub>6</sub>F<sub>5</sub>)<sub>4</sub>].



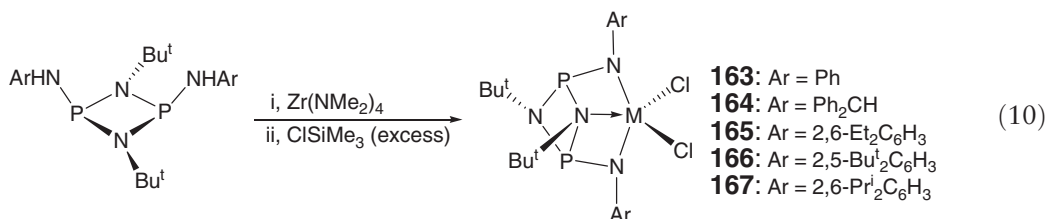
#### 4.08.4.1.2 Cyclodiphosph(III)azane-bridged bis(amido) complexes

The prolonged (24 h) reactions of the dilithium salt of bis(*tert*-butylamido)cyclodiphosph(III)azane with MCl<sub>4</sub> (M = Zr, Hf) in hot toluene at 80 °C afford thermally and chemically stable, monomeric complexes [(Bu<sup>t</sup>NP)<sub>2</sub>(Bu<sup>t</sup>N)<sub>2</sub>]MCl<sub>2</sub> **160**<sup>143</sup> (Scheme 31). Treatment of the dichloride complexes **160** with 2 equiv. of MeMgCl in ether yields the corresponding zirconium and hafnium dimethyl complexes **161**,<sup>144</sup> which are remarkably stable to atmospheric oxygen and moisture. This salt metathesis reaction is highly solvent dependent; when done in THF, the reaction leads to intractable mixtures. The reaction is also sensitive to the ligand sterics; the less bulky bis(arylamido)cyclodiphosph(III)azanes form diligand complexes **162**.<sup>145</sup>



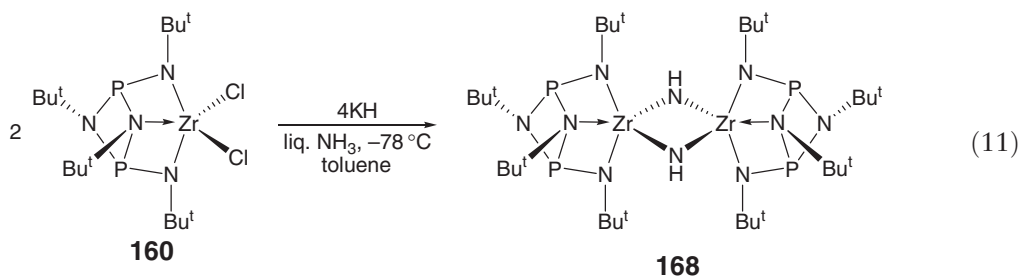
Scheme 31

Using the amine elimination approach that involves reactions of the neutral bis(arylamino)cyclodiphosph(III)azane ligands with  $\text{Zr}(\text{NMe}_2)_4$ , followed by treatment with excess of  $\text{SiMe}_3\text{Cl}$ , a series of monomeric dichloride  $\text{Zr}(\text{IV})$  complexes  $[(\text{ArN})_2(\text{Bu}^t\text{NP})_2]\text{ZrCl}_2$  [Ar = Ph **163**, diphenylmethyl **164**, 2,6-diethylphenyl **165**, 2,5-di-*tert*-butylphenyl **166**, and 2,6-diisopropylphenyl **167**] is obtained in high yields<sup>146</sup> (Equation (10)).



The molecular structures of isostructural complexes **160** feature pseudo-*ttb* geometries about the metal centers, with the  $\eta^3$ -coordinated ligand through the anionic diamido nitrogen atoms and an additional donor bond from the basal nitrogen (i.e., bis(amido)amino coordination) for a  $C_s$ -symmetric ground state, but a time-averaged  $C_{2v}$ -symmetry in solution due to the equivalence of the ring-*tert*-butyl substituents in the NMR spectra. Because of the planarity of the amido groups in **160**, it may be assumed that there is at least some  $\pi$ -bonding between ligand and metal, making these ligands possible eight-electron donors and raising the electron-count at the metal to 14 electrons. Furthermore, the steric pocket in these complexes is quite reminiscent of that in bent metallocenes and related compounds. Complexes **160**, when activated with MAO, were initially reported inactive for polymerization of ethylene at 60 °C.<sup>145</sup> However, a later and more detailed polymerization catalysis study indicates that, upon activation with MAO, complexes **163–167**, including **160**, exhibit moderate to high activities in ethylene polymerization and produce high molar mass polyethylene, with average molecular weight up to  $1100 \text{ kg mol}^{-1}$ .<sup>146</sup>

Treatment of dichloride complex **160** with 2 equiv. of KH in liquid ammonia and toluene (a two-phase reaction) at  $-78^\circ\text{C}$  yields the imido(NH)-bridged dinuclear zirconium complex **168** supported by the bis(*tert*-butylamido)cyclodiphosph(III)azane ligand<sup>147</sup> (Equation (11)). The solid state structure contains an ideally planar (centrosymmetrical) four-membered  $\text{Zr}_2(\mu\text{-N})_2$  ring, and the coordination sphere of each zirconium is completed by the  $\eta^3$ -coordinated bis(*tert*-butylamido)cyclodiphosph(III)azane ligand. The approximately triangular-planar geometry at the amido nitrogen (i.e.,  $sp^2$ -hybridized) indicates that these nitrogen atoms also donate their lone-pair electrons into the empty *d*-orbitals of zirconium.

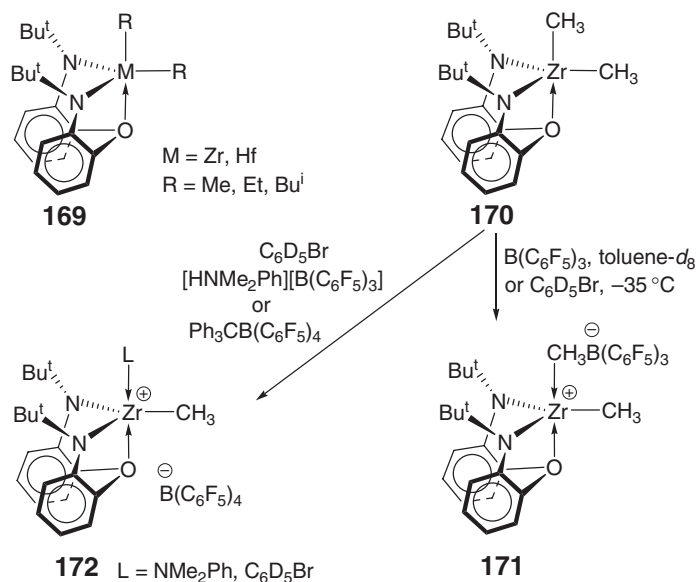


#### 4.08.4.2 Bis(amido) Oxygen-donor [ $N^-, O, N^-$ ] Complexes

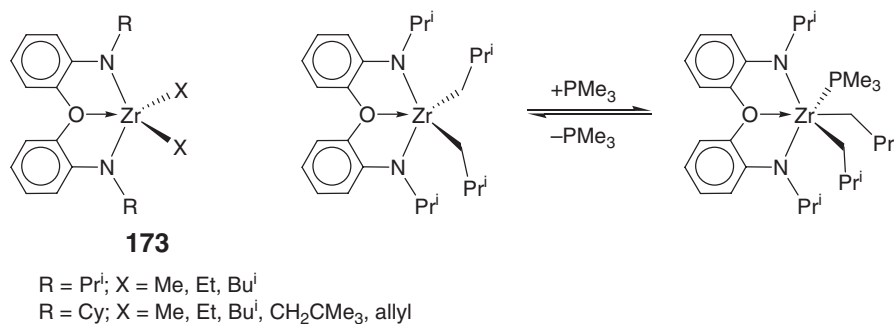
##### 4.08.4.2.1 Bis(amido)aryl ether and thioether complexes

The zirconium dialkyl complexes **169** supported by the tridentate diamido aryl ether ligand  $[(Bu^t-d_6-N-o-C_6H_4)_2O]^{2-}$  ( $[NON]^{2-}$ ) are obtained from aminolysis of  $Zr(NMe_2)_4$  by the neutral diamine ligand  $H_2[NON]$  followed by treatment of the resulting diamide  $[NON]Zr(NMe)_2$  with  $CH_3I$  or  $SiMe_3Cl$  and alkylation of the resulting  $[NON]ZrX_2$  with  $RMgX$ .<sup>148,149</sup> The dimethyl complex **170** shows a twisted *fac*-structure in the solid state in which two amido nitrogen atoms occupy equatorial positions in a distorted trigonal bipyramid. However, in solution, such species exhibit equivalent alkyl groups on the NMR timescale as a consequence of formation of an intermediate *mer*-structure that contains a planar oxygen donor. Addition of  $B(C_6F_5)_3$  to a toluene or bromobenzene solution of the dimethyl **170** results in abstraction of the “apical” methyl group of **170** to form species **171** (Scheme 32). The solid-state structure of **171** shows a *tdp* coordination geometry with elongated  $Zr-Me$  (bridge) bond of 2.487(12) Å, compared with  $Zr-Me$  (terminal) of 2.200(13) Å, as well as a single  $Zr-O$  donor bond (2.2568(8) Å). Amine- or bromobenzene-separated ion pairs **172** can be spectroscopically observed by reacting the dimethyl **170** with  $[HNMe_2Ph][B(C_6F_5)_4]$  or  $Ph_3CB(C_6F_5)_4$ , respectively.<sup>150</sup> Both **171** and **172** are active catalysts for ethylene polymerization, but **172** also catalyzes 1-hexene polymerization in a living fashion. The analogous hafnium complexes are not as well-behaved since the dimethylaniline is insufficiently labile.

Substituting the  $Bu^t$  group attached to the amido nitrogen in complexes **169** with less bulky  $Pr^i$  and cyclohexyl (Cy) alkyl groups affords the analogous zirconium dialkyl complexes **173**.<sup>151</sup> The dimethyl complex ( $R = Pr^i$ ) adopts a *mer*-configuration in the solid state as shown below. The decompositions of the dialkyl complexes ( $R = Pr^i$ ) is dramatically accelerated in the presence of  $PMe_3$ ; presumably 1 equiv. of  $PMe_3$  coordinates to give a



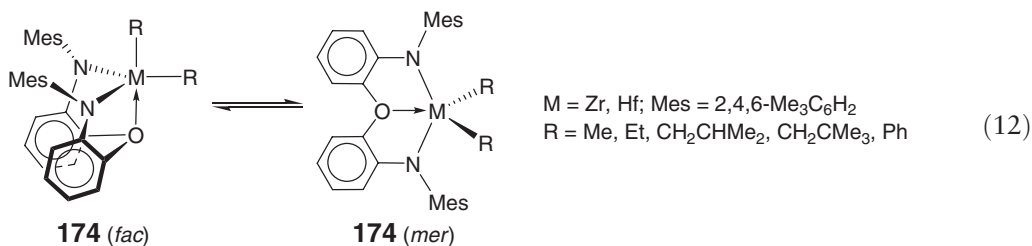
Scheme 32



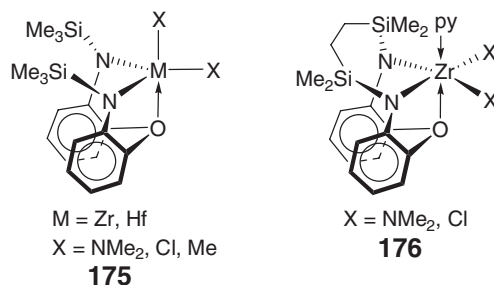
Scheme 33

pseudo-octahedral adduct, in which the two alkyl groups are pushed close to one another, and  $\beta$ -hydrogen abstraction is thereby accelerated (Scheme 33). These alkyl complexes, when activated with [HNMe<sub>2</sub>Ph][B(C<sub>6</sub>F<sub>5</sub>)<sub>4</sub>], only oligomerize 1-hexene, consistent with their relatively less crowded coordination sphere at the active center as compared with that in the Bu<sup>t</sup> amido complexes 169.

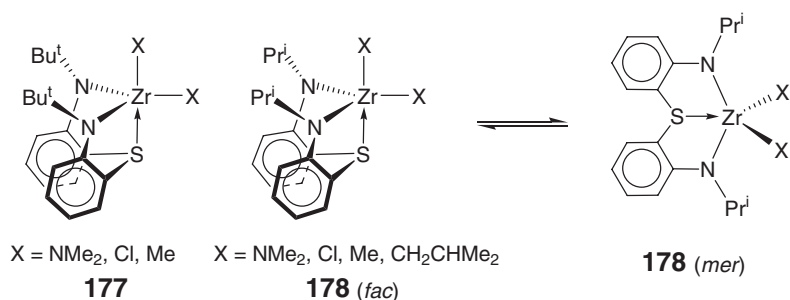
The mesityl amido complexes 174 have been also prepared.<sup>152</sup> The structure of the hafnium di(neopentyl) complex is close to a square pyramid with a neopentyl ligand in the apical position, which is approximately halfway between the two “ideal” structures for complexes of this type, the *fac*- and *mer*-geometries, as shown in Equation (12). The zirconium dialkyl complexes can be activated with either [HNMe<sub>2</sub>Ph][B(C<sub>6</sub>F<sub>5</sub>)<sub>4</sub>] or Ph<sub>3</sub>C[B(C<sub>6</sub>F<sub>5</sub>)<sub>4</sub>], but the resulting cationic species only oligomerize 1-hexene.



Substituting the amido Bu<sup>t</sup> group complexes 169 with a trimethylsilyl group generates the trimethylsilyl amido zirconium diamide, dichloride, and dimethyl complexes 175.<sup>153</sup> The cationic species derived from the activation of the dimethyl complexes with [HNMe<sub>2</sub>Ph][B(C<sub>6</sub>F<sub>5</sub>)<sub>4</sub>] or Ph<sub>3</sub>C[B(C<sub>6</sub>F<sub>5</sub>)<sub>4</sub>] cannot be observed in NMR studies; the *in situ*-generated zirconium cation exhibits no well-behaved activity for the polymerization of 1-hexene, whereas the THF adduct of the hafnium methyl cation is inactive. Bridging the two amido silyl silicon atoms with an CH<sub>2</sub>CH<sub>2</sub> linker affords zirconium complexes of the type 176. Aminolysis of the neutral diamine ligand with Zr(NMe<sub>2</sub>)<sub>4</sub> gives the six-coordinate diamide complex in which the coordinated amine can be replaced with pyridine and then converted into the pyridine-coordinated dichloride complex with excess Me<sub>3</sub>SiCl. The reaction of this dichloride with 1 or 2 equiv. of MeMgCl, PhCH<sub>2</sub>MgCl, or LiMe under a variety of conditions produces mixtures of products, none of which could be identified. However, the reaction with 2 equiv. of Me<sub>3</sub>SiCH<sub>2</sub>MgCl yields a bimetallic complex in which one of the trimethylsilyl methyl groups has been doubly C–H activated, as confirmed by its solid-state structure.





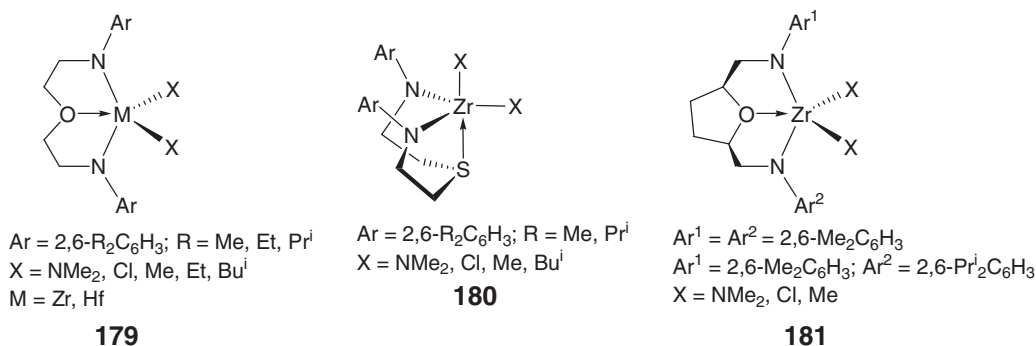


Scheme 34

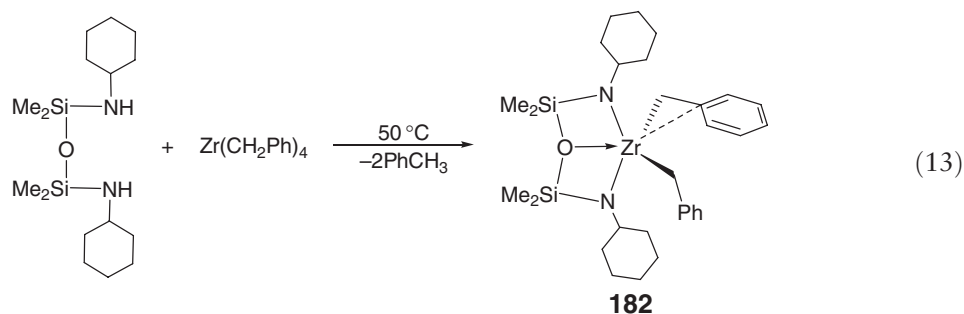
Replacing the oxygen donor with sulfur in complex **170** gives the analogous thioether complexes **177** and **178**<sup>154</sup> (Scheme 34). The dimethyl derivative of **177** is thermally unstable, but the methyl chloride complex was characterized by X-ray diffraction studies and shows an approximately *fac*-structure with the chloride and sulfur atoms occupying the axial positions. On the other hand, the dialkyl derivatives of **178** are stable, and the dimethyl complex shows a structure approximately halfway between a *fac*- and a *mer*-geometry, that is, approximately a square-pyramidal structure with a methyl group in the apical position. Cationic complexes prepared from the dimethyl derivatives of **177** and **178** are neither stable at 22 °C nor active for the polymerization of 1-hexene.

#### 4.08.4.2.2 Bis(amido)alkyl ether, thioether, and silyl ether complexes

Tridentate alkyl ether- and thioether-linked chelating bis(arylamide) ligands are also employed for the synthesis of their Zr and Hf diamide, dichloride, and dialkyl complexes. The zirconium dimethyl complex of the type **179**<sup>155,156</sup> ( $\text{Ar} = 2,6\text{-Me}_2\text{C}_6\text{H}_3$ ) exhibits a *mer*-structure in the solid state containing axial amido groups, whereas the hafnium diethyl complex ( $\text{Ar} = 2,6\text{-Pr}^i_2\text{C}_6\text{H}_3$ ) has a structure halfway between the *mer*- and *fac*-geometries, that is, a distorted square pyramid with one ethyl group in the apical position. The cationic complexes derived from the reaction of the dialkyls with  $[\text{HNMe}_2\text{Ph}][\text{B}(\text{C}_6\text{F}_5)_4]$  contain coordinated dimethylaniline, which does not exchange readily with free aniline on the NMR timescale at 60 °C. Activation of the dialkyl complexes with  $\text{Ph}_3\text{C}[\text{B}(\text{C}_6\text{F}_5)_4]$  yields efficient catalysts for the polymerization of 1-hexene. Analogous compounds **180** that contain a sulfur donor instead of oxygen were also prepared.<sup>156</sup> However, an X-ray crystallographic study reveals that the zirconium dimethyl compound of type **180** ( $\text{Ar} = 2,6\text{-Me}_2\text{C}_6\text{H}_3$ ) is closest to a *fac*-structure, as depicted. These sulfur-containing dialkyls can be activated with  $\text{Ph}_3\text{C}[\text{B}(\text{C}_6\text{F}_5)_4]$  and yield 1-hexene polymerization catalysts. Lastly, zirconium complexes **181**<sup>157</sup> incorporating chelating diamide ligands bearing a rigid oxygen donor have been prepared; the dimethyl derivative is significantly distorted toward a square pyramid with the two amido nitrogen atoms being arranged approximately *trans* to each other.



A hydrocarbyl elimination approach is used to produce the Zr(IV) dibenzyl complex incorporating a tridentate bis(amido) silylether  $[\text{N}^-, \text{O}, \text{N}^-]$  complex **182**<sup>61</sup> (Equation (13)). The molecular structure of **182** features a distorted *tbp* geometry with an approximately linear  $\text{ZrN}_2\text{O}$  unit and the two amido nitrogen atoms occupying approximately axial positions. One benzyl group is  $\eta^2$ -coordinated. When activated with MAO, complex **182** shows moderate activity for ethylene polymerization.

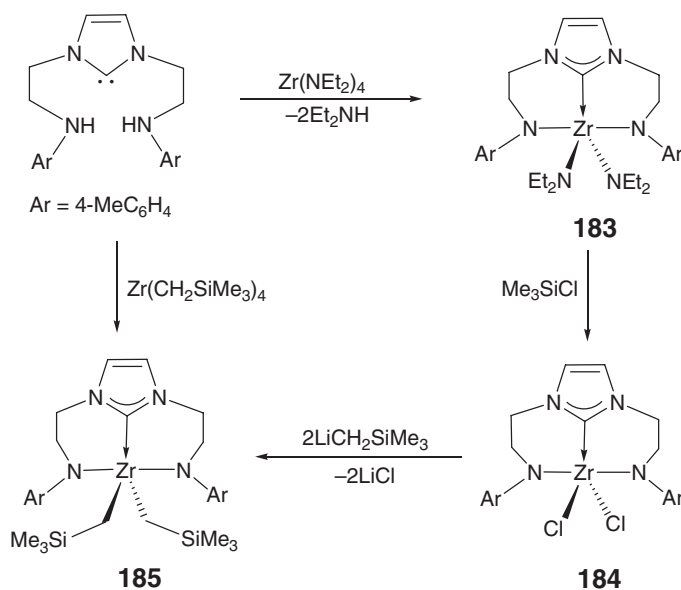


#### 4.08.4.3 Bis(amido) Carbene-donor [ $N^-, C, N^-$ ] and Bis(imino) Carbene [ $N, C^{2-}, N$ ] Complexes

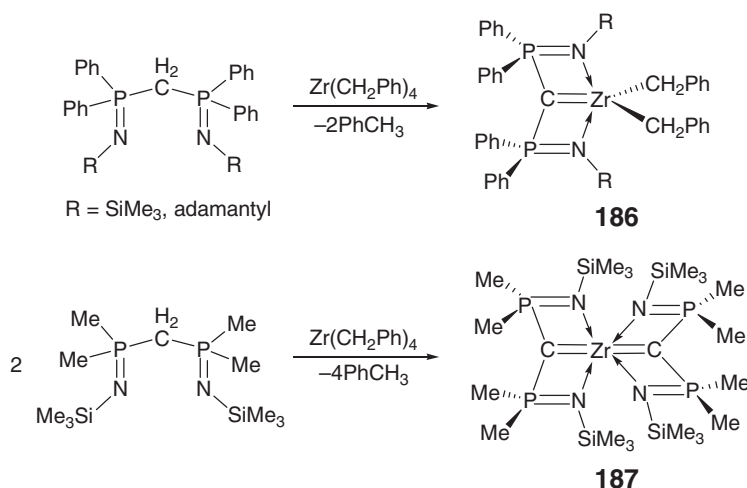
Aminolysis of  $Zr(NEt_2)_4$  with tridentate diamidocarbene imidazolydene,  $ArNHCH_2CH_2[C_3H_2N_2]CH_2CH_2NHAr$  ( $Ar = 4-MeC_6H_4$ ,  $C_3H_2N_2 =$  imidazol-1,3-diyl-2-ylidene), affords the chelating bis(amido) carbene-donor [ $N^-, C, N^-$ ] zirconium bis(amide) **183**<sup>158</sup> (Scheme 35). Chlorination of complex **183** can be achieved with  $SiMe_3Cl$ , yielding the corresponding dichloride complex **184**. Aminolysis of  $Zr(CH_2SiMe_3)_4$  with the neutral ligand gives the dialkyl derivative **185**; the same product is obtained by alkylation of **184**. The solid-state structure of **185** reveals a distorted tbp geometry about Zr. The solution NMR studies indicate that the carbene donor is rendered stable to dissociation because of its central disposition between two anionic amido units.

Protolysis of  $Zr(CH_2Ph)_4$  with bis[imino(diphenyl)phosphorano]methane  $CH_2(Ph_2P=NR)_2$  ( $R = SiMe_3$ , adamantyl) in toluene affords dibenzylzirconium phosphoranimino carbene complexes **186**<sup>159</sup> (Scheme 36). The molecular structure of the carbene complex **186** ( $R =$  adamantyl) features a distorted tbp environment about Zr that is bound to the tridentate, “pincer”-type ligand consisting of two nearly planar, fused, four-membered rings; both solution NMR data and solid state metric parameters provide strong evidence for the carbene character of the complex. This toluene elimination approach was also employed to prepare bis(phosphoranimino)carbene complex **187** by simply adjusting the ratio of two reactants.<sup>160</sup> The core structure of the highly symmetric complex **187** consists of two mutually perpendicular six-membered bicyclic planes, each containing the tridentate “pincer” methanediide ligand moiety bound to Zr in a spirocyclic fashion;  $\pi$ -electrons are indicated to delocalize within these six-membered frames.

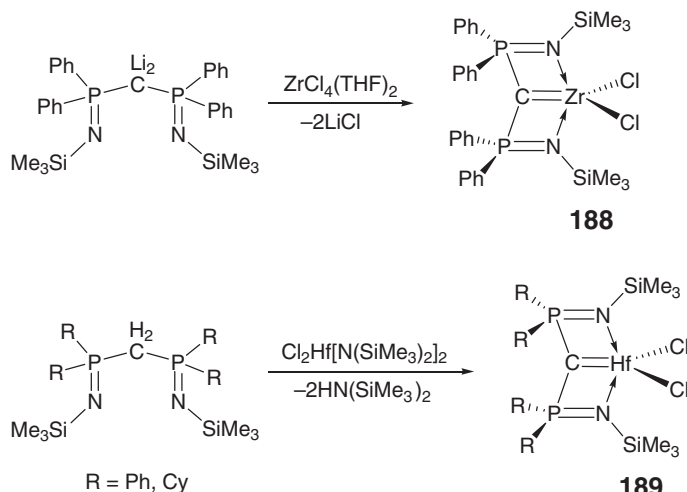
The analogous zirconium dichloride complex bearing a phosphoranimino–carbene ligand **188** was obtained from the salt metathesis reaction between the dilithiated salt of the ligand and  $ZrCl_4(THF)_2$ <sup>161</sup> (Scheme 37). The  $Zr=C$



Scheme 35



Scheme 36

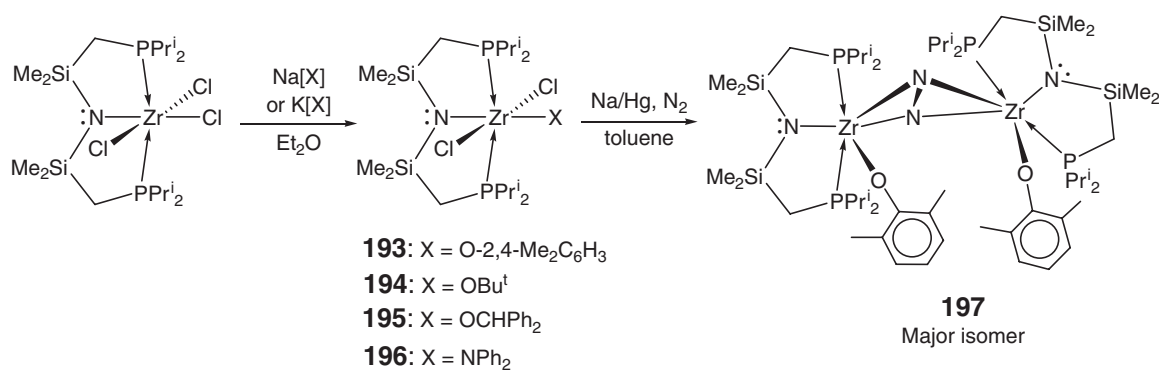


Scheme 37

bond distance (2.190(8) Å) is short compared to related alkyl complexes, which is consistent with the multiple-bond character expected for a metal carbene. To prepare the analogous hafnium complexes **189**, the amine elimination approach involving the neutral ligand and  $\text{HfCl}_2[\text{N}(\text{SiMe}_3)_2]_2$  was effective.<sup>162</sup> These zirconium and hafnium dichloride complexes incorporating the phosphoranimino–carbene ligand exhibit nucleophilic reactivity at the multiply bonded carbon center;<sup>163</sup> they form Lewis acid–base adducts with THF, nitriles, and isonitriles, and undergo 1,2-addition reactions with amines, alcohols, and alkyl iodides, and [2 + 2]-cycloaddition reactions with heteroallenes. Furthermore, the dichloride complexes can be alkylated with lithium alkyl reagents without attack at the carbene center. All these reactions are consistent with high-valent metal alkylidene character.<sup>164</sup>

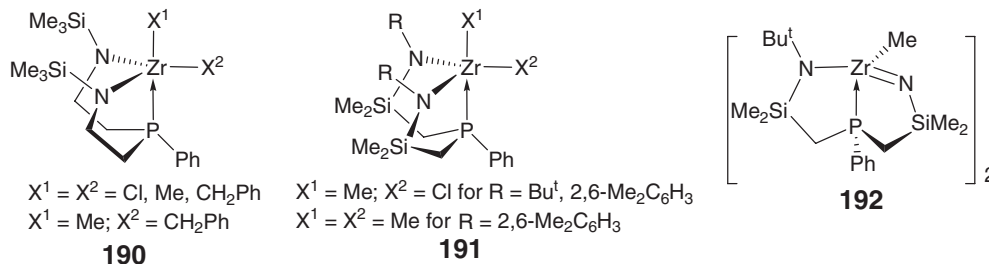
#### 4.08.4.4 Amido Phosphine-donor [ $\text{N}^-$ , $\text{P}$ , $\text{N}^-$ ] and [ $\text{P}$ , $\text{N}^-$ , $\text{P}$ ] Complexes

A tridentate bis(amido)phosphine ligand,  $(\text{Me}_3\text{SiNHCH}_2\text{CH}_2)_2\text{PPh}$ , is employed to prepare several Zr(IV) complexes including the dichloride, dialkyl, and mixed alkyl complexes **190**, via standard amine elimination and alkylation methodologies.<sup>165</sup> The mixed methyl benzyl dialkyl complex shows a distorted trigonal bipyramid in which the methyl group is in the apical position *trans* to phosphorus and the  $\eta^2$ -benzyl group is *cis* to phosphorus. Related



Scheme 38

bis(amido)phosphine ligands, (CH<sub>2</sub>SiMe<sub>2</sub>NHR)<sub>2</sub>PPh (R = Bu<sup>t</sup>, 2,6-Me<sub>2</sub>C<sub>6</sub>H<sub>3</sub>), are used to synthesize the corresponding Zr(IV) complexes **191**, including the methyl chloride and dimethyl (for R = 2,6-Me<sub>2</sub>C<sub>6</sub>H<sub>3</sub>) complexes. An attempt to prepare the dimethyl derivatives of the Bu<sup>t</sup>-substituted bis(amido) phosphine complex upon treating the dichloride compound with 2 equiv. of MeMgCl or LiMe leads to loss of a Bu<sup>t</sup> group and formation of a dimeric complex **192** containing imido-type bridging nitrogen ligands.

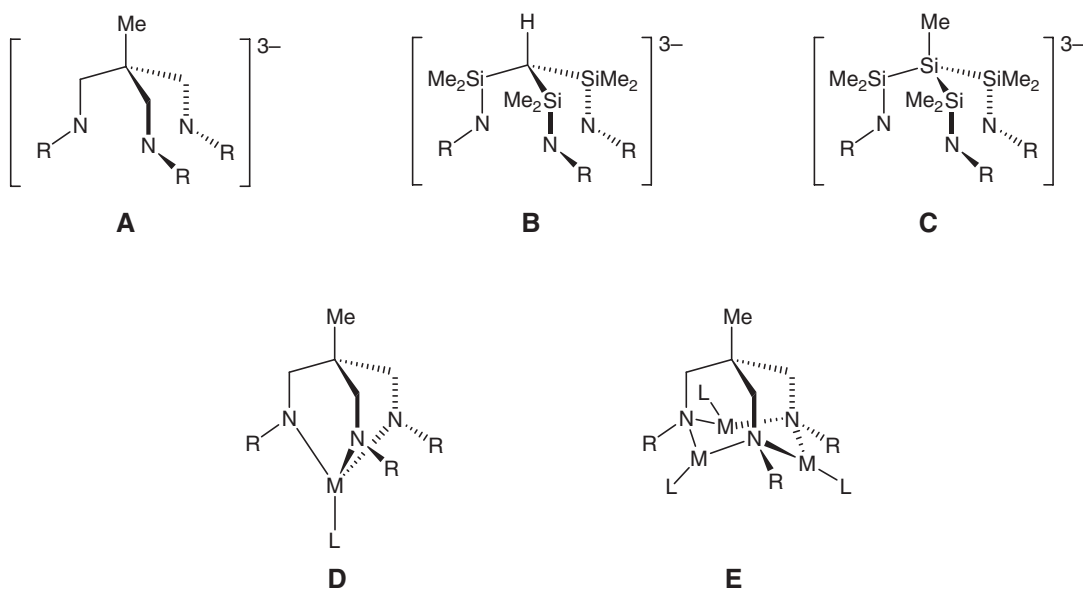


A series of six-coordinate dichlorozirconium aryloxide, alkoxide, and amide complexes **193–196** supported by the η<sup>3</sup>-N(SiMe<sub>2</sub>CH<sub>2</sub>PPr<sup>i</sup><sub>2</sub>)<sub>2</sub> amide ligand with two donor phosphine side-arms is obtained from the reaction of the trichloride precursor complex ZrCl<sub>3</sub>[N(SiMe<sub>2</sub>CH<sub>2</sub>PPr<sup>i</sup><sub>2</sub>)<sub>2</sub>] with sodium phenolate, potassium alkoxides, or sodium diphenylamide<sup>166</sup> (Scheme 38). Reduction of aryloxide **193** with > 2 equiv. of Na/Hg in toluene under 1–4 atm of N<sub>2</sub> produces the dinuclear dinitrogen complex {[(Pr<sup>i</sup><sub>2</sub>PCH<sub>2</sub>SiMe<sub>2</sub>)<sub>2</sub>N]Zr(O-2,6-Me<sub>2</sub>C<sub>6</sub>H<sub>3</sub>)<sub>2</sub>(μ-η<sup>2</sup>:η<sup>2</sup>-N<sub>2</sub>)} **197** in 40% yield. Solid state structural analysis shows that the dinitrogen unit is bound in a side-on mode, with a long N–N bond distance of 1.528(7) Å. This compares with the N–N distances of 1.0975(2) Å in N<sub>2</sub>, 1.255 Å in PhN=NPh, and 1.46 Å in H<sub>2</sub>NNH<sub>2</sub>. The resonance Raman spectrum of **197** shows a band at 751 cm<sup>–1</sup> for ν(N–N), consistent with this very long bond. Other Zr(IV) precursors ZrCl<sub>2</sub>X[N(SiMe<sub>2</sub>CH<sub>2</sub>PPr<sup>i</sup><sub>2</sub>)<sub>2</sub>] (X = OBU<sup>t</sup>, **194**; OCHPh<sub>2</sub>, **195**; NPh<sub>2</sub>, **196**) either decompose or produce a mixture of products upon reduction under N<sub>2</sub>.

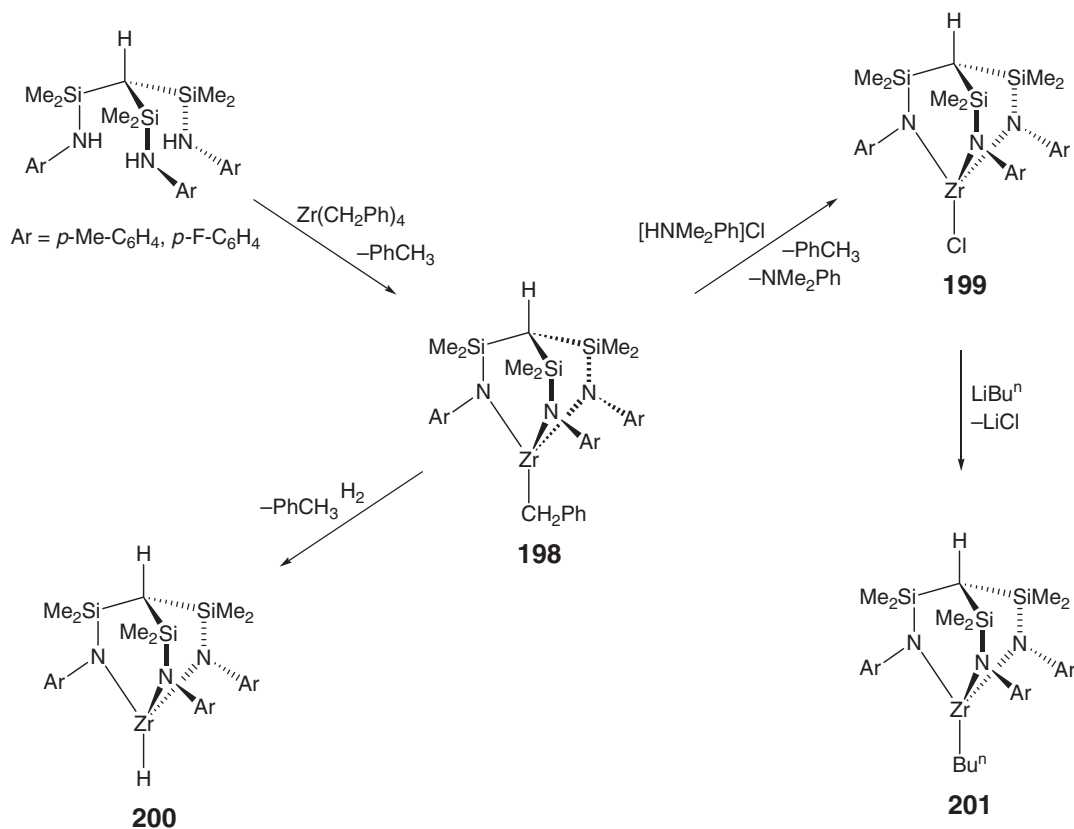
#### 4.08.4.5 Tripodal Triamido [N<sup>–</sup>,N<sup>–</sup>,N<sup>–</sup>] Complexes

There are three general types **A**, **B**, and **C** of tripodal triamido ligands available for complexes of group 4 metals (Scheme 39).<sup>167</sup> Although all three types of the ligands give essentially the same complex structures, varying the ligand from the all-carbon-based ligand backbone in **A** to the branched tetrasilane in **C** provides suitable binding pockets for different metals. The peripheral *N*-substituents add important tools for further fine-tuning sterics and electronics at the metal center. Two types of complex structures are possible, depending on the transition metal to which these ligands are coordinated: relatively rigid molecular cage of bicycle[2.2.2]-octane topology **D** and a metallaadamantane unit **E**.

Aminolysis of Zr(CH<sub>2</sub>Ph)<sub>4</sub> with the neutral tripodal amide ligand affords the benzyl complex **198** bearing the tridentate tripodal amide ligand in 90% yield<sup>168</sup> (Scheme 40). Solution and solid-state X-ray structural data indicate an η<sup>2</sup>-bonding mode for the benzyl group. Treatment of the benzyl **198** with [HNMe<sub>2</sub>Ph]Cl yields the dimeric chloride complex **199**. Hydrogenolysis of **198** gives the hydride species **200**, which also exists as a dimer bridged by two hydrides in the solid state. Metathesis of the chloride **199** with LiBu<sup>n</sup> produces the *n*-butyl complex **201**,<sup>169</sup>



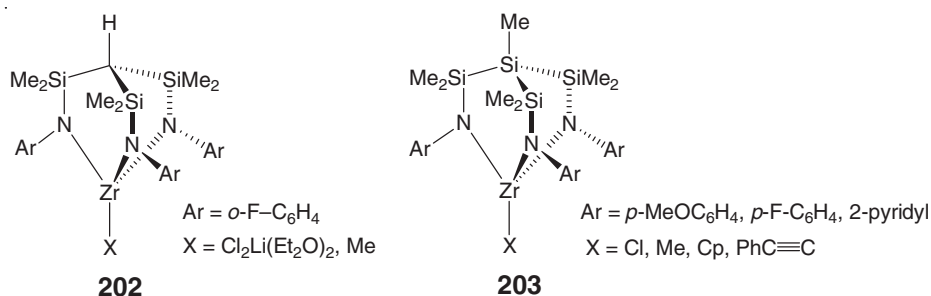
Scheme 39



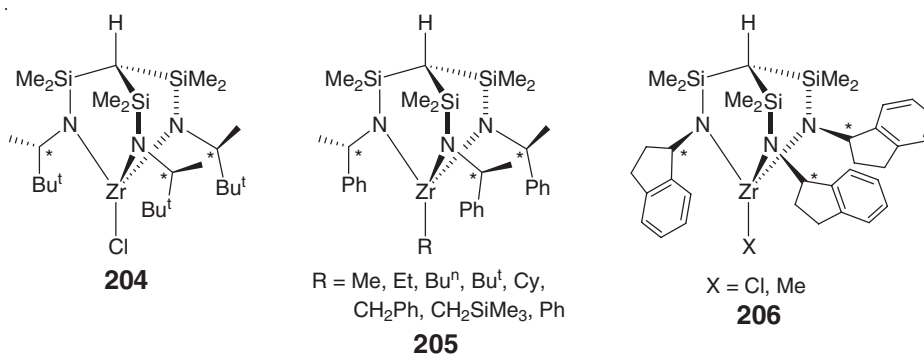
Scheme 40

which shows weak  $\beta$ -agostic interactions in the solid state; there is no evidence for such interactions in solution. The benzyl **198** and hydride **200** exhibit low activity for ethylene polymerization and diene cyclization, and the benzyl **198** and *n*-butyl **201** are active alkene hydrosilation catalysts.

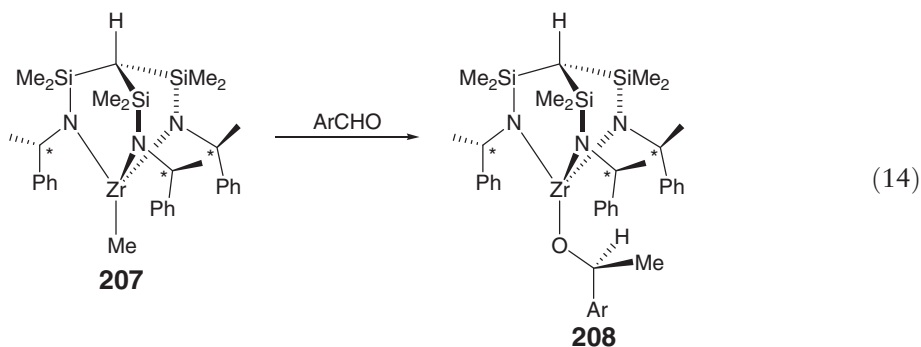
Several analogous tripodal (amido)zirconium compounds **202**<sup>170</sup> and **203**<sup>171</sup> were prepared earlier using salt metathesis. Only when X in compound **202** is small, such as Me, the spectroscopic data and structural considerations indicate all three F-donors at *ortho*-positions of the aryl rings are bonded to Zr, demonstrating the coordinative flexibility of the ancillary donor functions in the tripodal amido complexes.



Attaching peripheral chiral R\* auxiliary to the amido nitrogen creates C<sub>3</sub>-chiral tripodal amido ligands for the synthesis of chiral metal complexes. For example, the chiral zirconium chloride complex **204**, obtained from the salt metathesis approach involving the reaction of the lithium salt of the trianionic ligand with ZrCl<sub>4</sub> in toluene, contains (*S*)-3,3-dimethyl-2-butyl group as chiral R\* auxiliary.<sup>172</sup> The peripheral chiral R\* auxiliaries are (*S*)-1-phenyl ethyl and (*R*)-1-indanyl in chiral complexes **205** and **206**, respectively.<sup>173</sup>

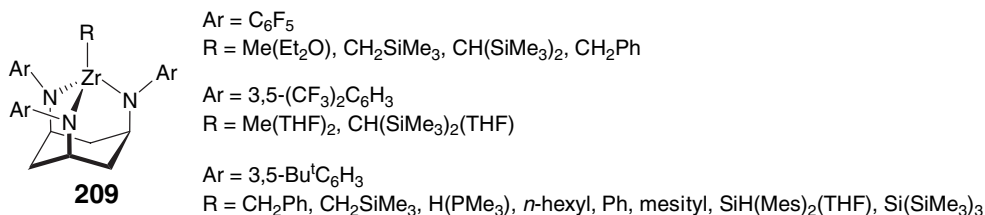


To examine the possible chiral induction effected by the C<sub>3</sub>-chiral tripodal amido ligation, the methyl complex **207** was treated with several aryl aldehydes, yielding the alkoxo complexes **208** with high stereoselectivity (Equation (14)). The chiral alcohols recovered after hydrolysis show 68–80% ee's, depending on substrate.<sup>173</sup>



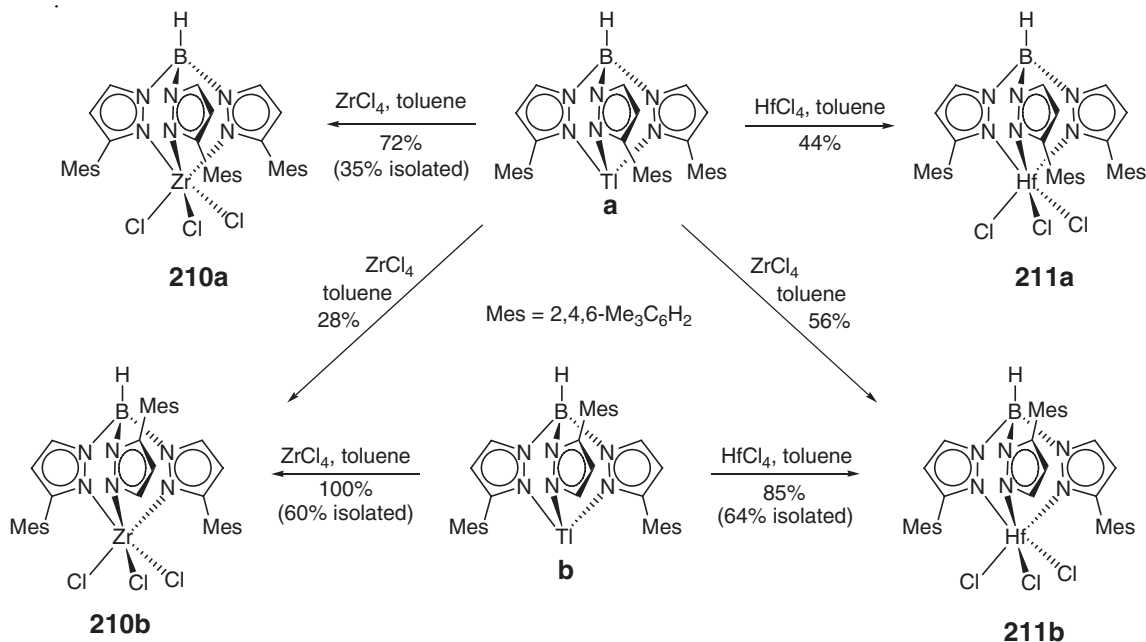
A different type of tripodal triamido ligand is based on *cis,cis*-1,3,3-triaminocyclohexane. Several ligands of this type with different peripheral *N*-substituents have been employed to synthesize a series of organometallic zirconium

complexes **209**. For fluorinated aryl substituents on the amido nitrogens, zirconium amide, halide, and alkyl complexes containing such ligands can be readily prepared.<sup>174</sup> However, attempts to produce the hydride complexes via hydrogenation of the alkyl complexes led to the isolation of Zr–F species derived from activation of the fluorinated ligand substituents, reflecting the strong fluorophilicity of these electrophilic zirconium centers. On the other hand, the zirconium complexes containing non-fluorinated aryl substituents are substantially less prone to activation, enabling the isolation of the hydride and rare examples of  $d^0$  silyl and hydrosilyl complexes featuring this non-fluorinated peripheral ligand.<sup>175</sup>



#### 4.08.4.6 Tris(pyrazolyl)borate [N<sub>3</sub><sup>−</sup>] Complexes

Zirconium **210** and hafnium **211** trichloride complexes bearing sterically crowded, tridentate mono-anionic, mesityl-substituted tris(pyrazolyl)borate ligands were synthesized by salt metathesis between MCl<sub>4</sub> and thallium salts of tris(5-mesitylpyrazolyl)borate (isomer **a**) and tris(3-mesitylpyrazolyl)borate (isomer **b**) in toluene<sup>176</sup> (Scheme 41). Using thallium salt isomer **a**, the reaction with ZrCl<sub>4</sub> yields a 72/28 mixture of **210a** and **210b**, from which **210a** was isolated by crystallization in 35% yield. The same reaction in the presence of THF (i.e., ZrCl<sub>4</sub>(THF)<sub>2</sub> in THF) gives a 35/65 mixture of **210a** and **210b**. The reaction of ZrCl<sub>4</sub> with thallium salt isomer **b** in toluene yields **210b** quantitatively, which was isolated in 60% (or 62%<sup>177</sup>) yield, whereas the same reaction in THF causes minor isomerization to **210a** (8%). Reactions of HfCl<sub>4</sub> in toluene with either thallium salt isomer **a** or isomer **b** produces **211b** as the major product (56% and 85%, respectively). Compound **211b** was isolated in 64% yield from the latter reaction.



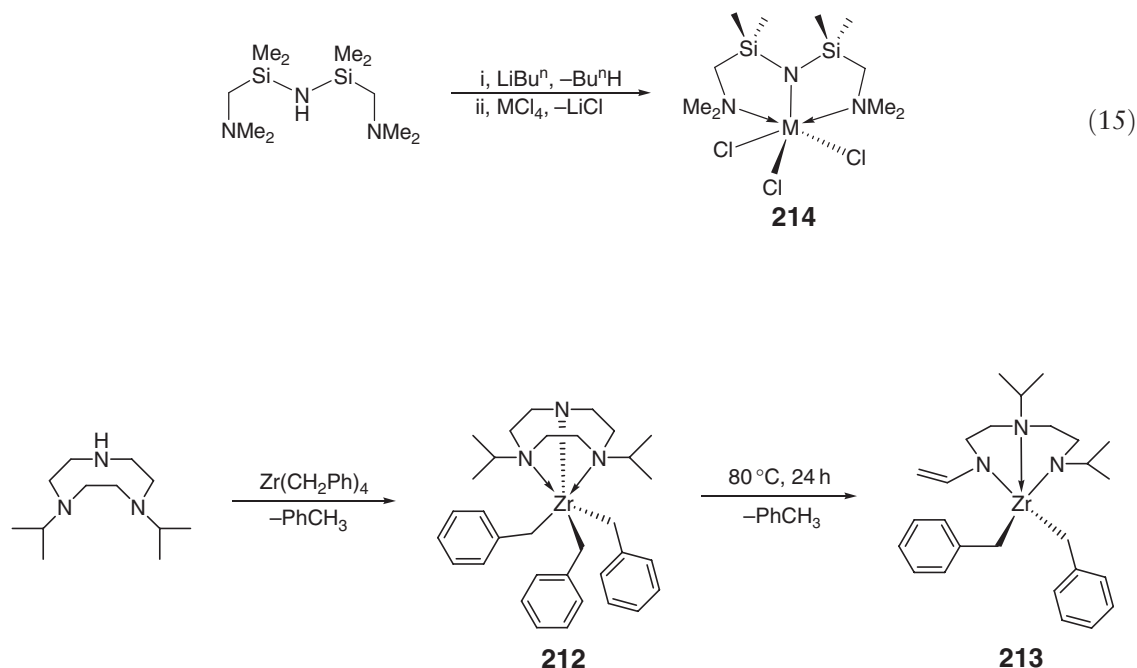
Scheme 41

The core structures of **210a**, **210b**, and **211b** are very similar, but the steric properties of these compounds differ markedly due to the different placements of the mesityl substituents on the tris(pyrazolyl)borate ligand; the three mesityl rings in **210a** form a deep pocket that shields the three chloride ligands, whereas in **210b** and **211b** the two chloride ligands that flank the 5-mesitylpyrazole ring are sterically more accessible. Upon activation with MAO at low pre-catalyst concentrations, **210a** exhibits extremely high activity for ethylene polymerization and ethylene/1-hexene co-polymerization, producing ultrahigh molecular weight polyethylene and ethylene/1-hexene co-polymers (up to 27% 1-hexene incorporation) with narrow molecular weight distributions ( $\bar{M}_w/\bar{M}_n = 1.8\text{--}2.3$ ), characteristic of single-site catalysis. Under the MAO activation conditions, **210a** is more active for ethylene polymerization than the less crowded isomer **210b**, and the hafnium complex **210b** produces polyethylene with broad molecular weight distributions.<sup>176</sup> These trends are consistent with the earlier observation that tris(3,5-dimethylpyrazolyl)borate zirconium trichloride exhibits higher olefin polymerization activity than the non-substituted tris(pyrazolyl)borate zirconium trichloride.<sup>178</sup>

#### 4.08.4.7 Amido Nitrogen-donor [ $N, N^-, N$ ] Complexes

Zirconium tribenzyl complex **212** incorporating diisopropyltriazacyclonone, a type of mono-anionic, tridentate diamino-amido [ $N, N^-, N$ ] ligand, was obtained via alkane elimination (Scheme 42); alternatively, this complex can also be prepared via either salt metathesis or amine elimination approaches.<sup>179</sup> The crystal structure of **212** reveals a monomeric form; on heating at 80 °C in benzene solution for 24 h, this complex undergoes elimination of 1 equiv. of toluene, affording complex **213** bearing a dianionic, acyclic, diamido-amino [ $N^-, N, N^-$ ] moiety.

Salt metathesis was employed to synthesize zirconium and hafnium trichloride complexes **214** incorporating a mono-anionic, tridentate diamino-amido [ $N, N^-, N$ ] ligand<sup>180</sup> (Equation (15)). In the solid state, the zirconium and hafnium complexes are isostructural. The tridentate ligand binds to the metal with *cis*-amine donors, and the overall geometry is perhaps best described as a distorted bicapped tetrahedron rather than a distorted octahedron. Diagnostic of this geometry descriptor is the observation that there is no chloride ligand *trans* to the amido nitrogen (the Cl–Hf–N(amido) angle of 143.8(1)° is much smaller than expected for a *trans*-relationship). Thus, in such a distorted bicapped tetrahedral geometry, the four formally anionic ligands, the three chlorides and the amide, generate the tetrahedral motif with the two amine donors capping two faces of the distorted tetrahedron.



Scheme 42

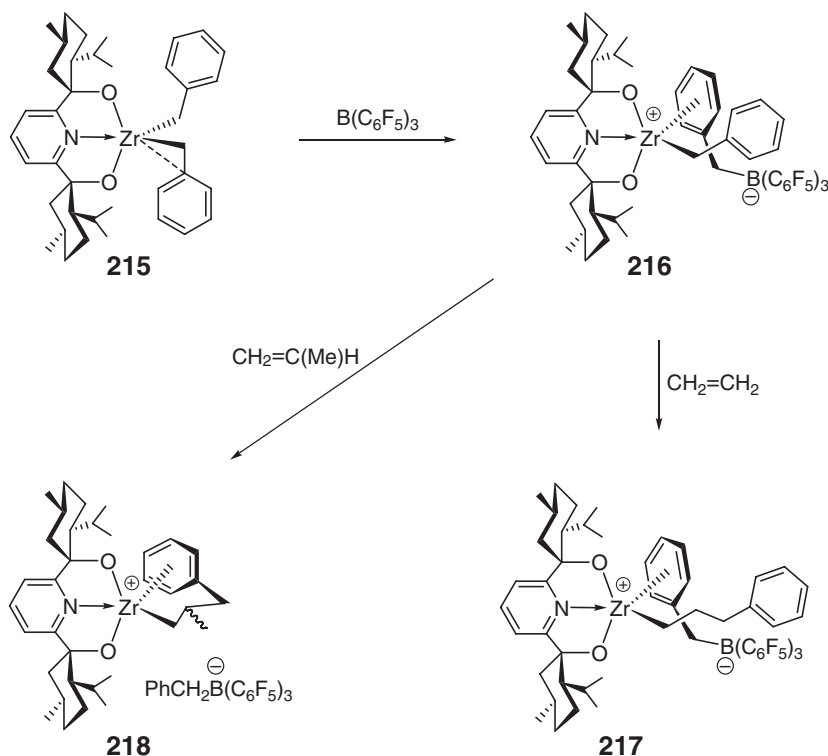


#### 4.08.4.8 Bis(alkoxide) Nitrogen-donor [O<sup>−</sup>,N,O<sup>−</sup>] Complexes

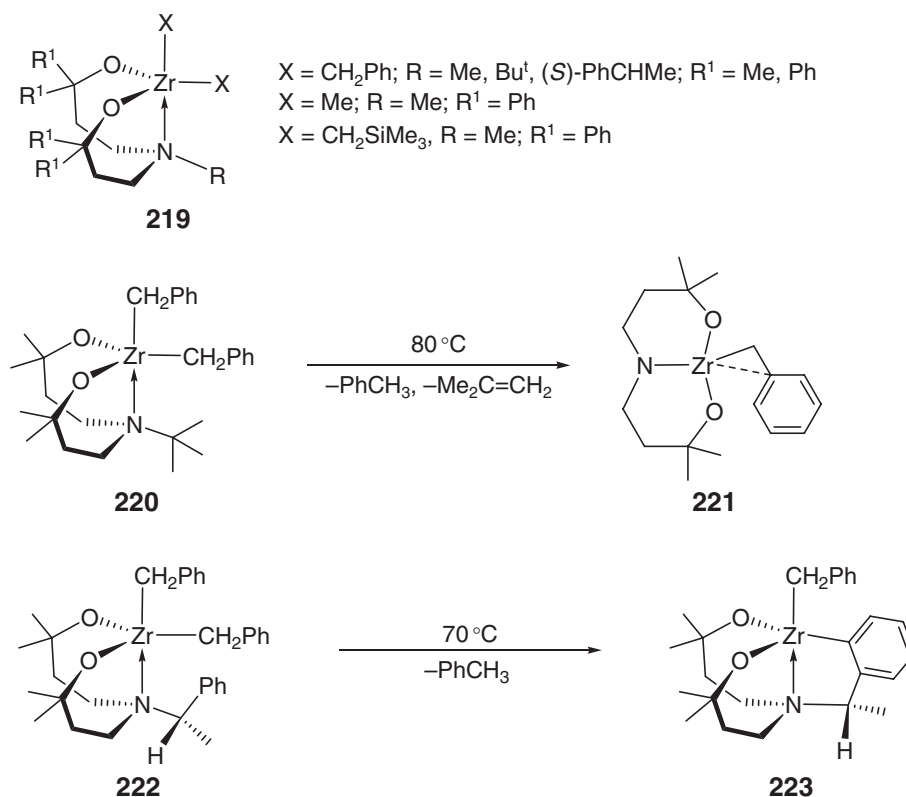
Chiral *C*<sub>2</sub>-symmetric zirconium dibenzyl complex **215** bearing the tridentate 2,6-bis[1*S*,2*S*,5*R*-(−)-menthoxy]pyridyl ligand is obtained from the protolysis of Zr(CH<sub>2</sub>Ph)<sub>4</sub> with 1 equiv. of the neutral diol ligand<sup>181</sup> (Scheme 43). The solid-state structure of this complex adopts a distorted tbp geometry with a *mer*-coordination mode of the tridentate, dianionic ligand. Addition of 1 equiv. of B(C<sub>6</sub>F<sub>5</sub>)<sub>3</sub> leads to the formation of the zwitterionic complex **216** in which the benzylborate anion is bound to the cationic Zr center through η<sup>6</sup>-arene coordination. The reaction of **216** with ethylene yields no polyethylene but the single ethylene insertion product **217**, whereas its reaction with propylene gives the regioselective, 1,2-insertion product **218** as a mixture of diastereomers. Activation of the dibenzyl complex **215** with MAO or [Ph<sub>3</sub>C][B(C<sub>6</sub>F<sub>5</sub>)<sub>4</sub>] also yields species that are inactive for ethylene polymerization.

A series of monomeric zirconium dialkyl complexes **219** incorporating aminodiolate ligands was synthesized using a combination of alkane elimination, ligand redistribution, and salt metathesis methods<sup>182</sup> (Scheme 44). The solution NMR studies of the complexes with smaller substituents at nitrogen (R = Me) are consistent with them having the pseudo-*fac*-tbp structure as shown, and stable upon heating at 100 °C for several days. In contrast, dialkyl complexes with larger substituents on nitrogen (R = Bu<sup>t</sup>, (*S*)-PhCHMe) are fluxional at room temperature and also thermally unstable at elevated temperatures. For example, complex **220** with the Bu<sup>t</sup> substituent on nitrogen decomposes at 80 °C by elimination of isobutene and toluene to form **221**, and complex **222** with the (*S*)-PhCHMe substituent at nitrogen undergoes clean *ortho*-metallation upon mild heating (70 °C, 4 h) to afford metallacycle **223** (Scheme 44).

The zirconium dichloride complex **224** incorporating a rigid tridentate pyridine-bis(phenolate) ligand was prepared by either salt metathesis involving the reaction of the dilithiated ligand with ZrCl<sub>4</sub> in toluene/THF or alkane elimination involving the reaction of the neutral ligand with Zr(CH<sub>2</sub>Ph)<sub>2</sub>Cl<sub>2</sub>(OEt<sub>2</sub>)<sub>2</sub> with the alkane elimination approach giving higher yield (>80%).<sup>183</sup> It is important to note here that in the absence of THF an intractable yellow precipitate is produced. The molecular structure of complex **224** has a pseudo-octahedral Zr center chelated by the non-planar tridentate pyridine-bis(phenolate) ligand in a *mer*-fashion, with *cis*-chloride atoms and a THF group

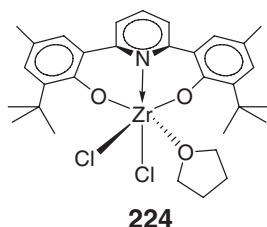


Scheme 43



Scheme 44

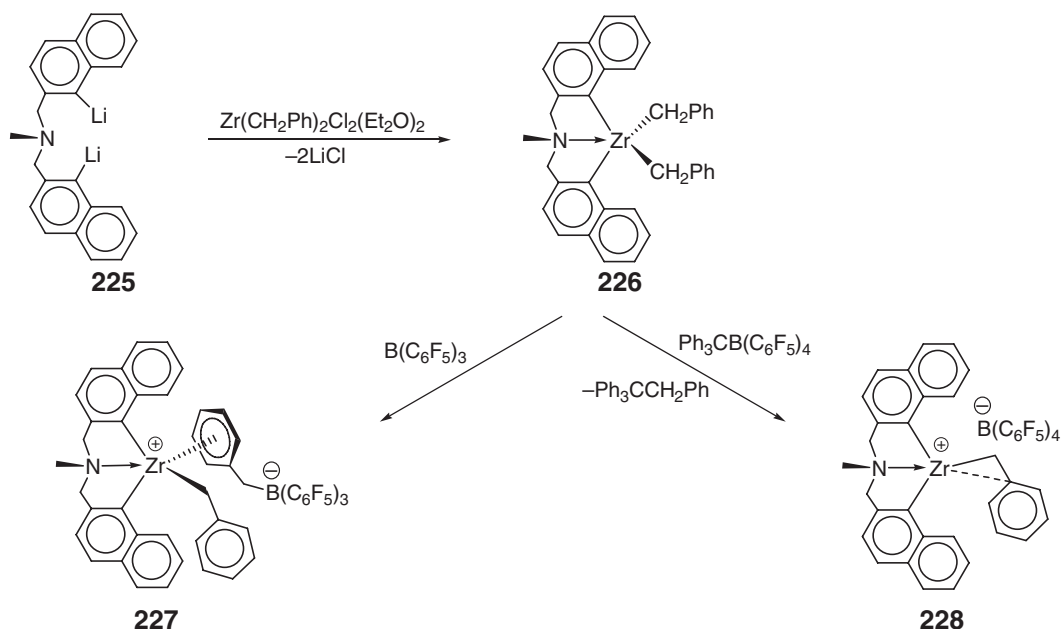
completing the coordination sphere. Upon activation with MAO, the zirconium complex **224**, despite the presence of a THF donor ligand, shows remarkably high activity for polymerization of ethylene, with exotherms of up to  $60^\circ\text{C}$  over 4–6 min.



#### 4.08.4.9 $\sigma$ -Aryl Nitrogen-donor $[\text{C}^-, \text{N}, \text{C}^-]$ and $[\text{C}^-, \text{N}, \text{O}^-]$ Complexes

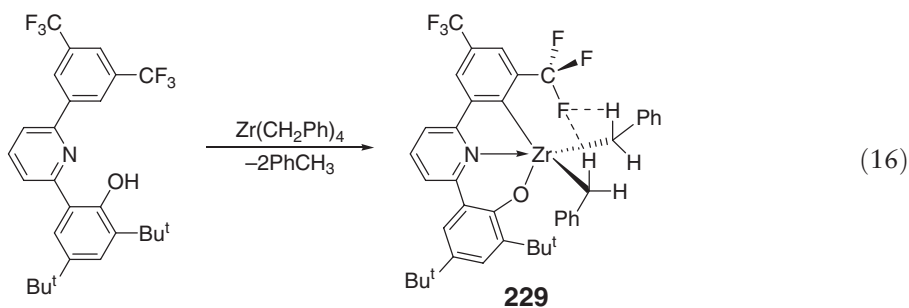
The reaction of the dilithium salt **225** with  $\text{ZrCl}_4$  yields the undesired tetraaryl complex with two dianionic ligands bound to one Zr, irrespective of the ligand-to-Zr ratio employed. However, the reaction of **225** with  $\text{Zr}(\text{CH}_2\text{Ph})_2\text{Cl}_2(\text{Et}_2\text{O})_2$  produces the desired dibenzyl complex **226** incorporating one tridentate bis( $\sigma$ -aryl)amino  $[\text{C}^-, \text{N}, \text{C}^-]$  ligand<sup>184</sup> (Scheme 45). Compound **226** possesses a strongly distorted tbp geometry with the  $\sigma$ -aryl carbons occupying the axial positions and the N and benzyl- $\text{CH}_2$  carbons in the plane. Complex **226** reacts with  $\text{B}(\text{C}_6\text{F}_5)_3$  to generate catalytically inactive **227**, with an  $\eta^6$ -bound benzylborate anion, whereas its reaction with  $[\text{Ph}_3\text{C}][\text{B}(\text{C}_6\text{F}_5)_4]$  gives the  $\eta^2$ -bound benzyl cation **228** paired with unassociated  $[\text{B}(\text{C}_6\text{F}_5)_4]^-$  anion, which polymerizes olefins with low activity.

A unique cyclometallation process was utilized to synthesize zirconium dibenzyl complex **229** involving the reaction of 2-(2'-phenol)-6-arylpyridine with  $\text{Zr}(\text{CH}_2\text{Ph})_4$ <sup>185</sup> (Equation (16)). This complex is supported by an unsymmetric tridentate, phenolate-pyridine-carbanion  $[\text{C}^-, \text{N}, \text{O}^-]$ -type ligand. Both the solution NMR data and



Scheme 45

solid-state structure metric parameters suggest weak intramolecular  $\text{C}-\text{H}\cdots\text{F}-\text{C}$  hydrogen bonding, as shown in Equation (16). This type of hydrogen bonding is thought to explain the observed fluorine substituent effect on the living  $\alpha$ -olefin polymerization behavior by related catalyst structures.

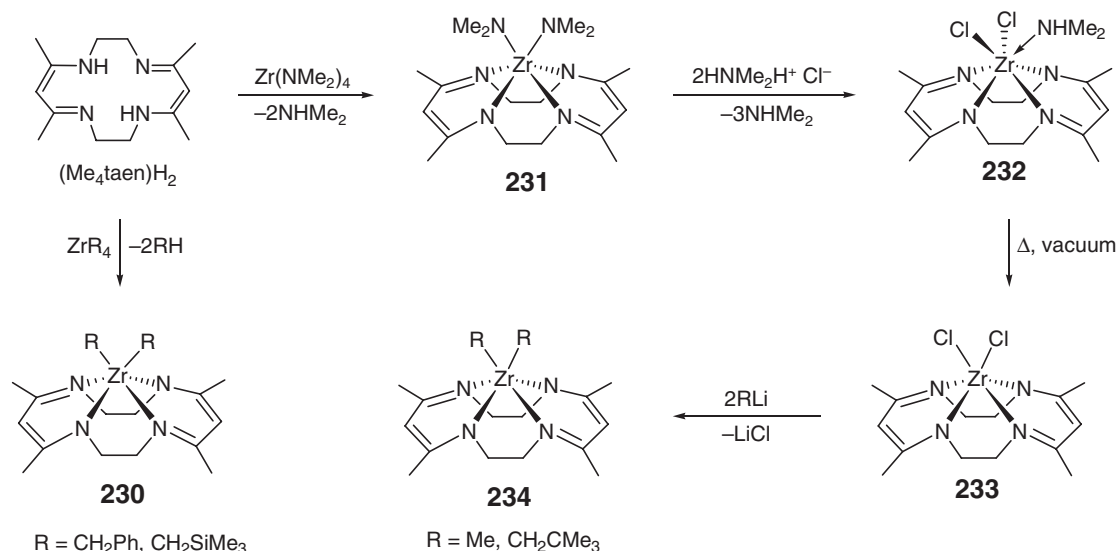


#### 4.08.5 Complexes with $\eta^4$ -Ligands

##### 4.08.5.1 Chelating $\beta$ -diketiminate $[\text{N}_2^-, \text{N}_2^-]$ Complexes

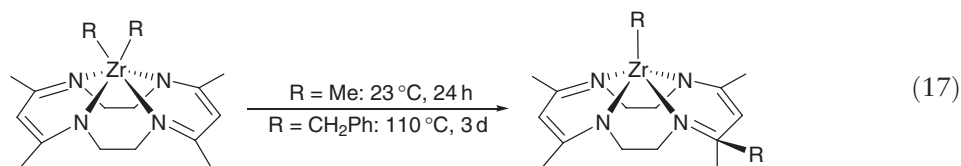
A series of out-of-plane macrocyclic complexes  $(\text{Me}_4\text{taen})\text{ZrX}_2$ , where  $\text{Me}_4\text{taen}$  = 5,7,12,14-tetramethyl-1,4,8,11-tetraazacyclotetradeca-4,6,11,13-tetraene and X is an alkyl, chloride, or amide group, were obtained via alkane or amine elimination or salt metathesis followed by alkylation reaction<sup>186,187</sup> (Scheme 46). Alkane elimination reactions of the neutral ligand  $(\text{Me}_4\text{taen})\text{H}_2$  with  $\text{ZrR}_4$  ( $\text{R} = \text{CH}_2\text{Ph}$ ,  $\text{CH}_2\text{SiMe}_3$ ) yield dialkyl complexes **230**. Aminolysis of  $\text{Zr}(\text{NMe}_2)_4$  with  $(\text{Me}_4\text{taen})\text{H}_2$  affords the bisamide complex **231**, and protolysis of **231** with  $[\text{HNHMe}_2]\text{Cl}$  yields the seven-coordinate amine adduct **232**, which loses amine under vacuum ( $120^\circ\text{C}$ , 10 h) to generate the base-free dichloride complex **233**. The reaction of **233** with  $\text{RLi}$  ( $\text{R} = \text{Me}$ ,  $\text{CH}_2\text{CMe}_3$ ) reagents in toluene produces the dialkyl complexes **234**.

Dichloride **223** adopts a trigonal prismatic structure in which the chlorides occupy adjacent edge sites, and the conformation of the  $[\text{Me}_4\text{taen}]^{2-}$  ligand is rather planar. The dibenzyl complex has a similar but more twisted trigonal prismatic structure. The bisamide **231** is a distorted octahedron in which the  $[\text{Me}_4\text{taen}]^{2-}$  ligand is significantly folded. The seven-coordinate complex **232** forms a side-capped trigonal prism with a tripodal arrangement of chloride

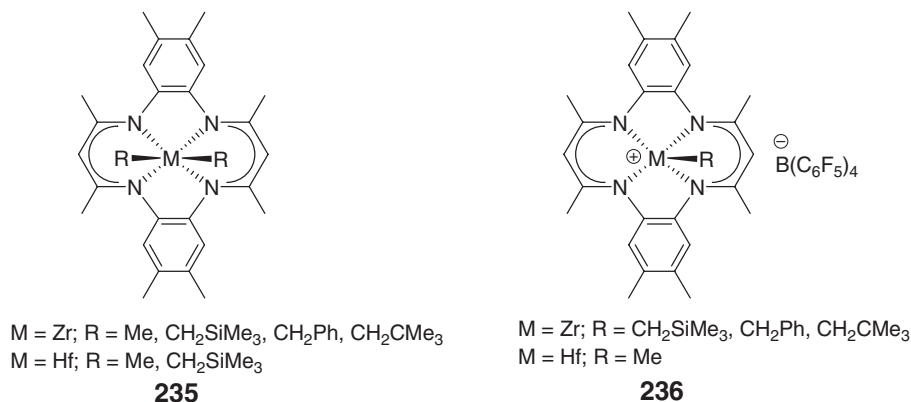


Scheme 46

and amine ligands. The properties of these tetraazamacrocyclic Zr(IV) complexes may be compared to those of  $\text{Cp}_2\text{ZrX}_2$  and other early metal analogs; however, the dimethyl and dibenzyl complexes rearrange thermally by migration of an alkyl group from Zr to a macrocycle imine carbon (Equation (17)).



The benzo derivatives **235** bearing the tetramethyldibenzo-tetramethyltetraaza[14]-annulene ( $\text{Me}_8\text{taa}$ ) ligand are also obtained from the combination of salt metathesis, alkane elimination, and amine elimination reactions.<sup>188</sup> The well-defined, square-pyramidal cationic complexes **236** are produced from the reaction of the dialkyl complex with either  $[\text{HNMe}_2\text{Ph}][\text{B}(\text{C}_6\text{F}_5)_4]$  or  $[\text{HNMePh}_2][\text{B}(\text{C}_6\text{F}_5)_4]$ . In general, these cations are significantly less reactive toward alkene and alkyne insertion than are  $\text{Cp}_2\text{MR}^+$  cations, reflecting both the lower Lewis acidity and the harder character of the metal cations **236**.



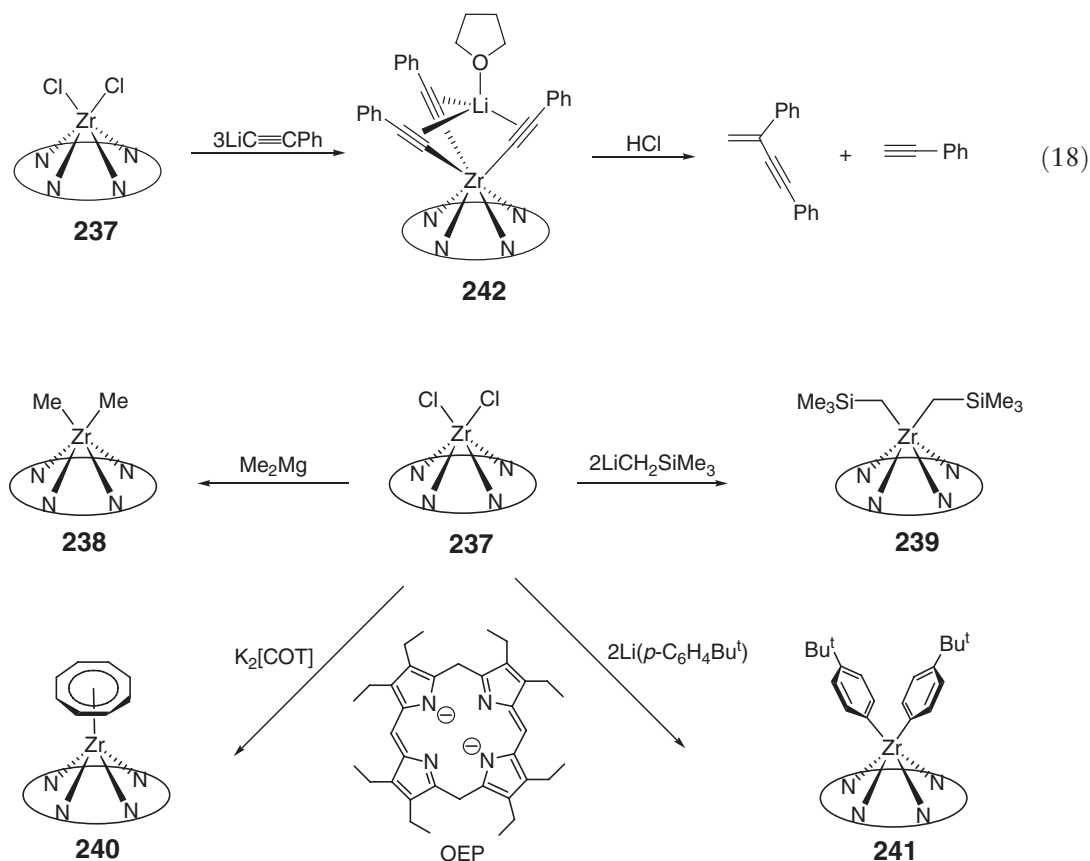
Zirconium complexes analogous to **235** but incorporating the dibenzo-tetramethyltetraaza[14]-annulene ( $\text{Me}_4\text{taa}$ ) ligand (i.e., removing the four methyl groups from the phenyl rings),  $(\text{Me}_4\text{taa})\text{ZrR}_2$ , have also been synthesized,

including complexes of  $R = \text{Me}$  or  $\text{Ph}$ ,<sup>189</sup>  $R = \text{CH}_2\text{SiMe}_3$ ,<sup>190</sup> as well as  $R_2 = \text{N-2,4-Pr}_2\text{C}_6\text{H}_3$ ,  $\text{py}$  (i.e., pyridine-stabilized Zr imido complex).<sup>191</sup> The dimethyl and dibenzyl complexes are thermally labile, and one of the alkyl groups undergoes a thermally-induced migration to one of the imino groups, leading to the complexes  $(R\text{-Me}_4\text{taa})\text{ZrR}$  bearing a trianionic ligand<sup>189</sup> (similar to Equation (17)). Nucleophiles are even more effective in inducing the alkyl migration to the ligand; in the presence of THF or pyridine, the benzyl complex  $(\text{Me}_4\text{taa})\text{Zr}(\text{CH}_2\text{Ph})_2$  is readily converted to  $[(\text{CH}_2\text{Ph})_2\text{Me}_4\text{taa}]\text{Zr}$ , in which both benzyl groups have migrated to the imino groups of the ligand.

#### 4.08.5.2 Porphyrinato $[\text{N}^-, \text{N}, \text{N}^-, \text{N}]$ Complexes

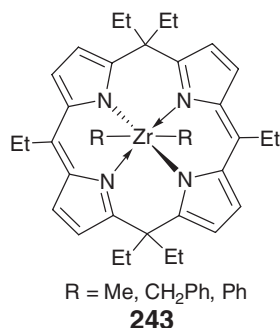
The zirconium porphyrinato dichloride  $\text{Zr}(\text{OEP})\text{Cl}_2$  (**237**, OEP = octaethylporphyrinato) serves as a versatile synthon for further functionalization. Thus, the organometallic derivatives of zirconium porphyrinates  $\text{Zr}(\text{OEP})\text{X}_2$ : dimethyl **238**, bis(trimethylsilyl)methyl **239**, cyclooctatetraenyl **240**, and aryl **241** have been synthesized<sup>192</sup> (Scheme 47). In general, the metal is displaced ca.  $0.9 \text{ \AA}$  out of the  $\text{N}_4$ -plane, and the  $\text{X-Zr-X}$  angle of the *cis*-ligated two X groups is approximately  $80^\circ$ . Alkyl derivatives of Zr and Hf porphyrinates can also be obtained directly on large scales from the dilithium porphyrinates and dialkylmetal dichlorides generated *in situ*.<sup>193</sup> The alkyl derivatives are particularly reactive toward small unsaturated molecules. The Zr(IV) dialkyls act as pre-catalysts for the hydrogenation of 1-alkenes. These studies show that the  $(\text{OEP})\text{Zr}$  fragment behaves like the well-known metallocene moiety  $\text{Cp}_2\text{Zr}$  and stabilizes a wide variety of ancillary ligands.

The reaction of  $(\text{OEP})\text{ZrCl}_2$  with 3 equiv. of  $\text{LiC}\equiv\text{CPh}$  produces the alkynyl  $(\text{OEP})\text{Zr}(\text{IV})$  porphyrin complex  $(\text{OEP})\text{Zr}(\eta^1\text{-C}\equiv\text{CPh})_3\text{Li}(\text{THF})$  **242**<sup>194</sup> (Equation (18)). The molecular structure shows that three alkynyl ligands are coordinated to the Zr center in a piano-stool fashion and that the lithium cation is bound to the pocket formed by three alkynyl ligands. Treatment of complex **242** with anhydrous  $\text{HCl}$  produces a C–C bond-coupled product  $\text{H}_2\text{C}=\text{C}(\text{Ph})\equiv\text{CPh}$  and  $\text{HC}\equiv\text{CPh}$  quantitatively. This example shows different reactivity of the zirconium porphyrin from that of analogous metallocene complexes.



Scheme 47

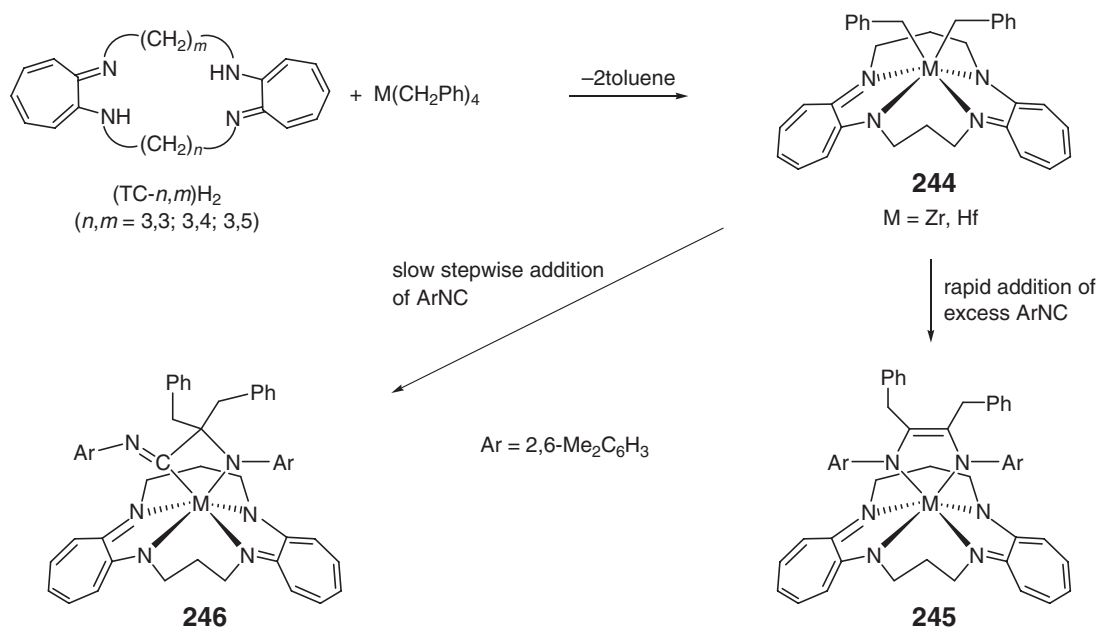
The *cis*-dichloro-*meso*-hexaethylporphodimetheneZr(IV) complex can be functionalized to the corresponding dialkyl derivatives **243**, which display a variety of migratory pathways.<sup>195</sup> In the case of benzyl complex, the spontaneous migration of the first benzyl to the ligand is followed by the second one, photochemically induced, forming a Zr-porphyrinogen complex. The methyl derivative undergoes thermally induced methane elimination with the metallation of the *meso*-ethyl chains. Migration of both methyl groups is observed in the reaction with Bu<sup>t</sup>N≡C, with the preliminary formation of  $\eta^2$ -imine, which rearranges to the corresponding enamine.



#### 4.08.5.3 Tropocoronandato [ $N^-, N, N^-, M$ ] Complexes

Zirconium(IV) and hafnium(IV) dichloride and dialkyl complexes incorporating tropocoronands, [MX<sub>2</sub>(TC-*n,m*)] (X = Cl, CH<sub>2</sub>Ph, CH<sub>2</sub>SiMe<sub>3</sub>), are synthesized and structurally characterized.<sup>196</sup> Scheme 48 depicts an example of such complexes, the dibenzyl complex **244**. These complexes exhibit variable stereochemistry, depending on the number of methylene units, *n* and *m*, in the poly(methylene) linker chains connecting the two aminotroponimate rings, although in all cases the *cis*-stereoisomer is formed. With the smallest ligand (TC-3,3), the dialkyl and dichloro complexes display slightly distorted trigonal prismatic structures; increasing the size of the macrocyclic ring substantially shifts the geometry at the metal center toward octahedral geometry.

Reactivity of the organometallic Zr(IV) and Hf(IV) tropocoronand complexes is demonstrated by their versatile isocyanide insertion reaction pathways, leading to the formation of  $\eta^2$ -iminoacyl, enediamido,  $\eta^2$ -imine, and  $\mu$ -imido



Scheme 48

products.<sup>197</sup> Alkyl isocyanides induces migration of both benzyl groups to afford the bis(iminoacyl) species. Different products are obtained with aryl isocyanides, depending on the rate of substrate addition. For example, treatment of complexes **244** with excess 2,6-dimethylphenyl isocyanide generates the enediamido compounds **245** (Scheme 48) via coupling of two bis(iminoacyl) groups. On the other hand, slow stepwise addition produces the corresponding four-membered metallacycle **246** with an iminoacyl group adopting an uncommon  $\eta^1$ -bonding mode.

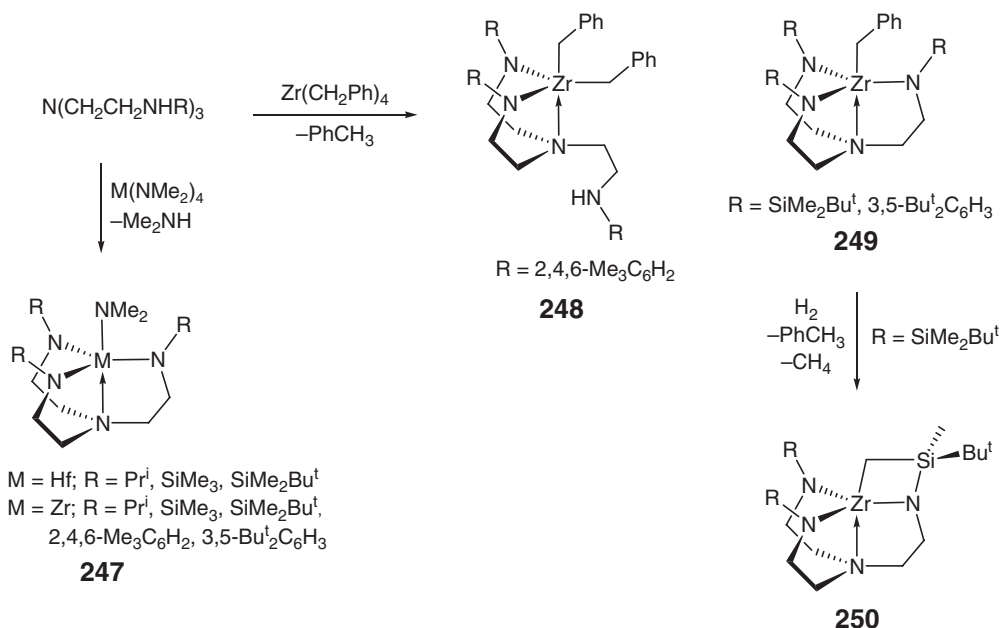
At ambient temperature and pressure, the dialkyl-ligated tropocoronand complex  $[\text{Hf}(\text{TC-3,5})(\text{CH}_2\text{Ph})_2]$  inserts CO into the metal–carbon bonds, affording the  $\eta^2$ -ketone complex  $[\text{Hf}(\text{TC-3,5})(\eta^2\text{-OC}(\text{CH}_2\text{Ph})_2)]$ .<sup>198</sup> Its crystal structure revealed a significant reduction of the bond order of the C–O moiety in the resulting metalloxirane ring of the insertion product. The dichloromethane solution of this complex reacts with 2 equiv. of cyclohexyl isocyanide, possibly via a four-membered metallacyclic ( $\eta^1$ -iminoacyl) intermediate, generating a ketenimine complex. In contrast, addition of 2 equiv. of benzyl isocyanide induces cleavage of a CN–benzyl bond, affording a rare example of group 4 complex containing a terminal cyanide ligand.

#### 4.08.5.4 Triamidoamine [ $\text{N}^-$ , $\text{N}^-$ , $\text{N}, \text{N}^-$ ] Complexes

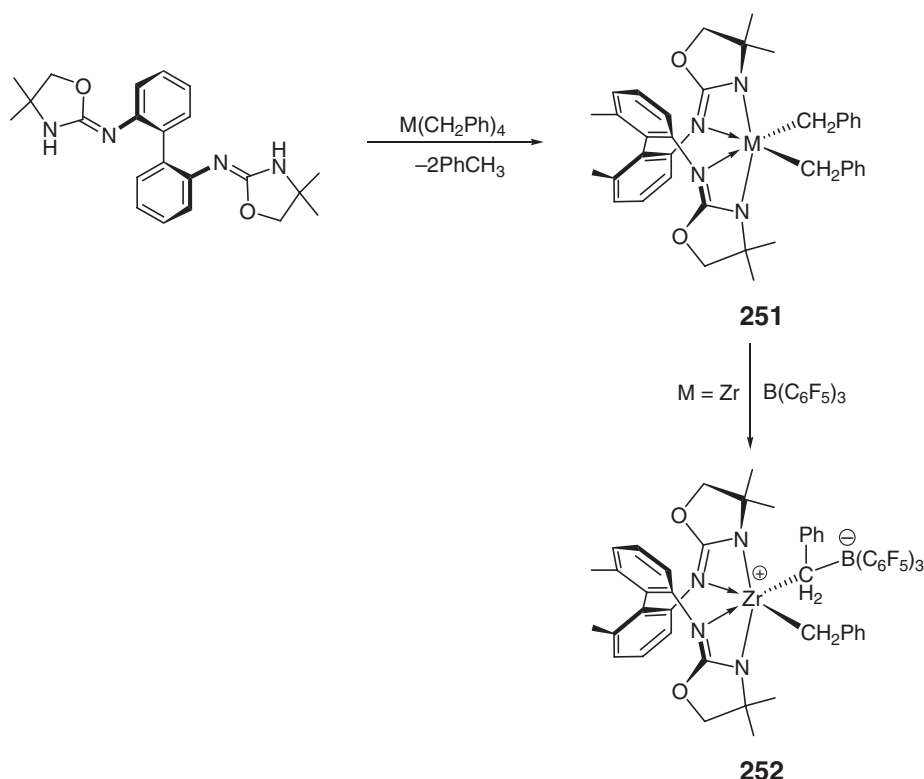
Dimethylamido zirconium and hafnium triamidoamine or azametallatrane complexes **247** are readily accessible from aminolysis of  $\text{Zr}(\text{NMe}_2)_4$  with neutral triamidoamine ligands (Scheme 49).<sup>199–201</sup> The alkane elimination approach involving reactions of  $\text{Zr}(\text{CH}_2\text{Ph})_4$  with neutral triamidoamines, however, gives either the dibenzyl product **248** with a bulky aryl substituent or the desired monobenzyl complexes **249**.<sup>200,201</sup> The molecular structures in general show the triamidoamine ligands adopt the usual threefold symmetric arrangement to give approximately *thp* geometries; for the aryl-substituted complexes, the aryl substituents form a bowl cavity with the apical ligand at the base. The monobenzyl complex with  $\text{R} = \text{SiMe}_2\text{Bu}^t$  undergoes hydrogenolysis, leading to the colorless zirconacycle **250**, with elimination of toluene and methane; sublimation of **249** also leads to pure **250**,<sup>200</sup> further highlighting the susceptibility of the silicon–methyl group subject to C–H activation.

#### 4.08.5.5 Chelating Diamido–Diamine [ $\text{N}^-$ , $\text{N}, \text{N}, \text{N}^-$ ] Complexes

Zirconium and hafnium dibenzyl complexes **251** incorporating a tetradentate, biaryl-bridged bis(iminooxazolidine) ligand were conveniently prepared using the alkane elimination approach<sup>202</sup> (Scheme 50). These six-coordinate complexes are  $C_2$ -symmetric, and the auxiliary benzyl groups occupy mutually *cis*-positions; however, upon activation



Scheme 49



Scheme 50

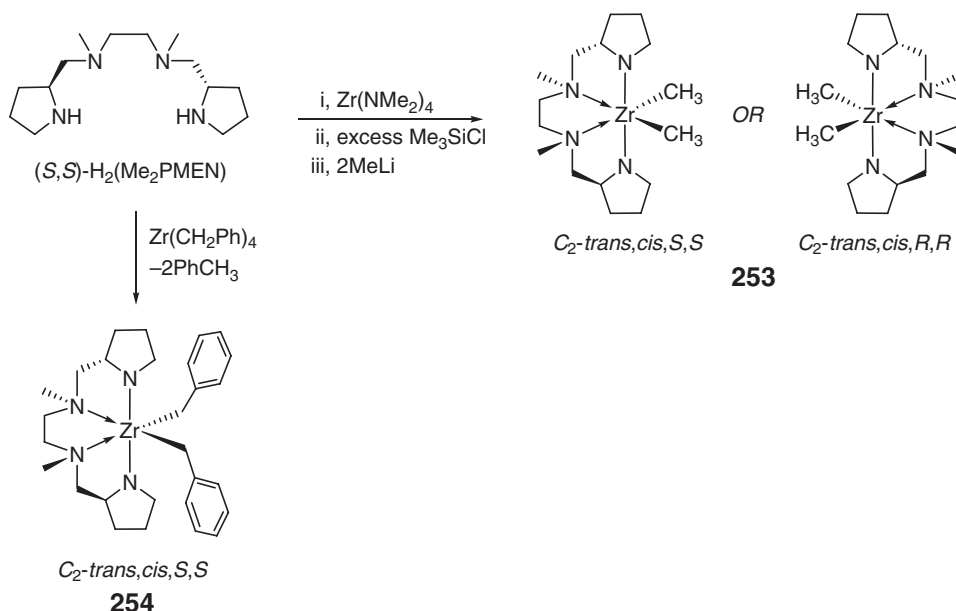
with a range of activators, they show low to no activity toward polymerizations of ethylene and 1-hexene. The reaction of the zirconium dibenzyl complex with  $\text{B}(\text{C}_6\text{F}_5)_3$  forms the tight ion pair **252**, but not the more usual zwitterion with an  $\eta^6$ -arene-coordinated anion. Related chiral bis(dimethylamido)zirconium complexes incorporating several other tetradentate biaryl-bridged bis(arylamido) ligands with addition donors (N, O) have been synthesized earlier.<sup>203</sup>

Aminolysis of  $\text{Zr}(\text{NMe}_2)_4$  with a neutral chiral tetraamine ligand,  $N,N'$ -dimethyl- $N,N'$ -bis[(*S*)-2-methylpyrrolidine]ethylenediamine [(*S,S*)- $\text{H}_2(\text{Me}_2\text{PMEN})$ ], leads to formation of  $C_2$ -symmetric  $(\text{Me}_2\text{PMEN})\text{Zr}(\text{NMe}_2)_2$ , which can be further treated with excess of  $\text{Me}_3\text{SiCl}$  followed by  $\text{MeLi}$  to afford the corresponding  $C_2$ -symmetric dimethyl complex **253**<sup>204</sup> (Scheme 51). On the basis of the solution NMR data, this complex has a structure of either *trans*-amido, *cis*-methyl, *S,S*- or *trans*-amido, *cis*-methyl, *R,R*-ligand arrangements (note that the amino nitrogens must be *cis* in these structures), whereas the transient dichloride complex is  $C_1$ -symmetric having *cis*-amido, *cis*-chloride, *S,R*-ligand arrangements in the solid state. Protolysis of  $\text{Zr}(\text{CH}_2\text{Ph})_4$  with (*S,S*)- $\text{H}_2(\text{Me}_2\text{PMEN})$  affords the desired dibenzyl complex **254**, which can be isolated as mixture of two isomers having  $C_2$ - and  $C_1$ -symmetries. Alkyl abstraction from the dimethyl **253** and the dibenzyl **254** using  $[\text{Ph}_3\text{C}][\text{B}(\text{C}_6\text{F}_5)_4]$ ,  $[\text{HNMe}_2\text{Ph}][\text{B}(\text{C}_6\text{F}_5)_4]$ , or  $\text{B}(\text{C}_6\text{F}_5)_3$  affords the corresponding cationic alkyl complexes. The *in situ*-generated methyl and benzyl cation are moderately active for ethylene polymerization.

#### 4.08.5.6 Chelating Guanidinato [ $\text{N}_2^-$ , $\text{N}_2^-$ ] Complexes

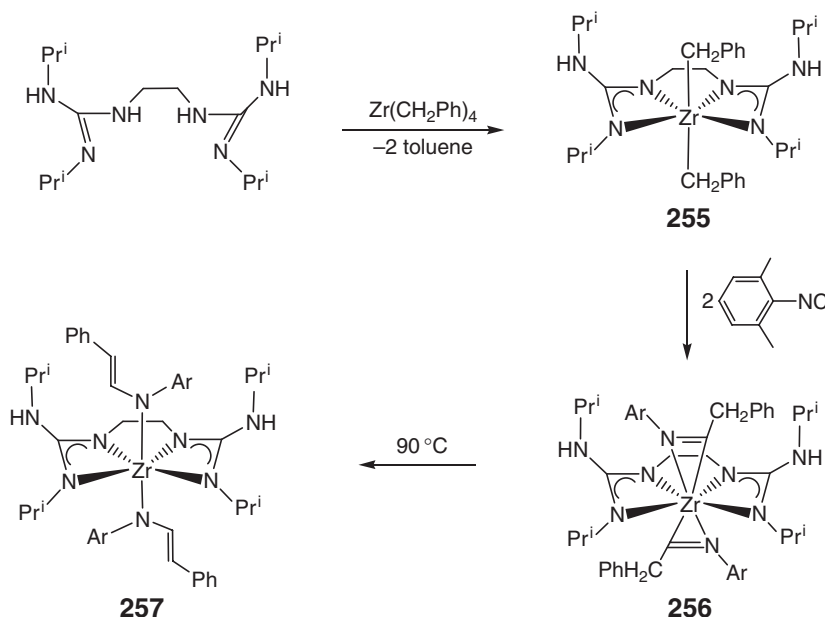
The neutral “linked” guanidinate ligand  $\text{Pr}^i\text{HN}(\text{NHPr}^i)\text{CN}(\text{CH}_2)_2\text{NC}(\text{NHPr}^i)\text{NPr}^i\text{H}$  reacts with  $\text{Zr}(\text{CH}_2\text{Ph})_4$  to give the hydrocarbyl complex **255**<sup>205</sup> (Scheme 52). The solid-state structure of this complex features a distorted octahedral geometry about Zr with the coordinated,  $\eta^4$ -linked guanidinate chelate being nearly planar. Linking the guanidinate moieties has the effect of opening up the metal coordination sphere, as indicated by an increase in the angle between the two  $\eta^1$ -bound benzyl groups, in comparison with the unlinked analogs. Treatment of this complex with 2,6-dimethylphenyl isocyanide results in aryl isocyanide insertion into  $\text{Zr}-\text{Bn}$  bonds to produce bis( $\eta^2$ -iminoacyl)Zr complex **256**,





Only one possible isomer shown

**Scheme 51**



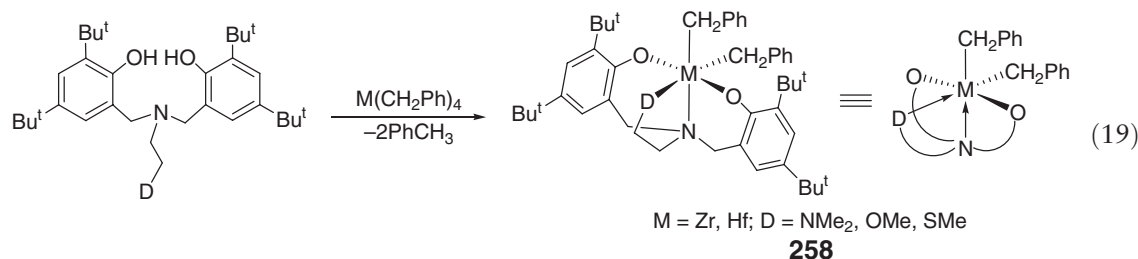
**Scheme 52**

which undergoes thermolysis at  $90^\circ\text{C}$  to form bis(ene-diamido)Zr complex **257**, involving an overall 1,2-hydrogen shift into vinylamido groups. Both complexes **256** and **257** have been characterized by X-ray diffraction analysis.

#### 4.08.5.7 Chelating Bis(phenoxy) Amine-donor $[\text{O}^-, \text{N}, \text{D}, \text{O}^-]$ ( $\text{D} = \text{N}, \text{O}, \text{S}$ ) Complexes

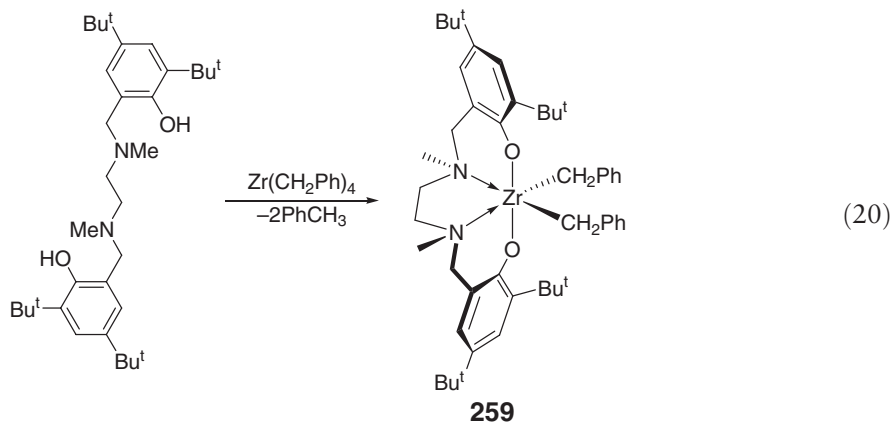
Zirconium and hafnium dibenzyl complexes **258** incorporating tetradentate bis(bulky phenoxy) amines with an additionally heteroatom ( $\text{N}$ ,  $\text{O}$ , or  $\text{S}$ )-donor containing pendant sidearm are produced from the reaction of the

corresponding neutral chelating bisphenol with  $M(\text{CH}_2\text{Ph})_4$  ( $M = \text{Zr}, \text{Hf}$ ) via elimination of toluene<sup>206,207</sup> (Equation (19)). All complexes exhibit a  $C_s$ -symmetry; two phenolate units are arranged in a *trans*-geometry, whereas the two benzyl groups are in a *cis*-configuration; this arrangement seems to be a critical requirement for olefin polymerization activity. Indeed, on treatment with  $\text{B}(\text{C}_6\text{F}_5)_3$ , all complexes are highly active for the polymerization of 1-hexene, yielding high molecular weight polymers. Interestingly, the polymerization activity order as a function of the pendant donor is different between the Zr and the Hf complexes; for the Zr series, the activity decreases in the series  $\text{OMe} > \text{NMe}_2 > \text{SMe}$ , whereas for the Hf series, the order becomes  $\text{SMe} > \text{OMe} > \text{NMe}_2$ . In the absence of this X donor on the sidearm, this type of the complexes exhibits only poor activity.<sup>208</sup>



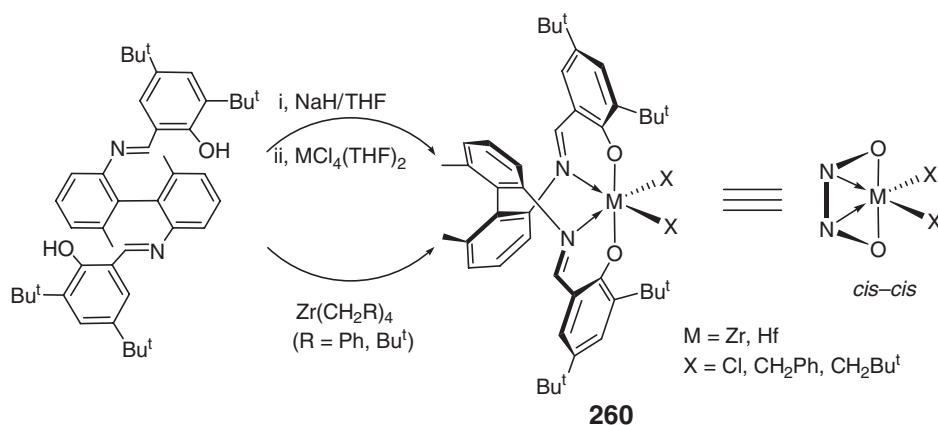
Weakening the electron-donating ability of the pendant donor sidearm of the bis(phenoxy)amine ligands affects the 1-hexene polymerization characteristics of the corresponding Zr complexes.<sup>209</sup> For example, switching from 2-tetrahydrofuranyl sidearm to the 2-furanyl sidearm (a weaker donor) does not appear to affect the polymerization activity, but it substantially reduces polymer molecular weight, reflecting enhanced chain-transfer processes with the less tightly bound sidearm donor.

A modification of the ligand by moving the donor group on the side chain to the main chain, namely bis(phenoxy)amine ligand, yields the  $C_2$ -symmetric zirconium dibenzyl complex **259** according to Equation (20).<sup>210</sup> When activated with  $\text{B}(\text{C}_6\text{F}_5)_3$ , this complex polymerizes 1-hexene in a living fashion, and the resulting polymer is >95% isotactic. This  $\text{B}(\text{C}_6\text{F}_5)_3$ -activated species is inactive toward propylene polymerization, but activation with MAO or  $[\text{HNMe}_2\text{Ph}][\text{B}(\text{C}_6\text{F}_5)_4]$  in combination with  $\text{AlBu}^t_3$  produces moderately isotactic polypropylene of low molecular weight;<sup>211</sup> the active species generated from the latter activation mode has also been used to produce polyethylene and isotactic polypropylene-block-polyethylene block co-polymers.<sup>212</sup> Fine-tuning the ligand framework by varying the substituents at the 2,4-positions on the phenoxy rings further improves the performance of catalysts of this type.<sup>213</sup>



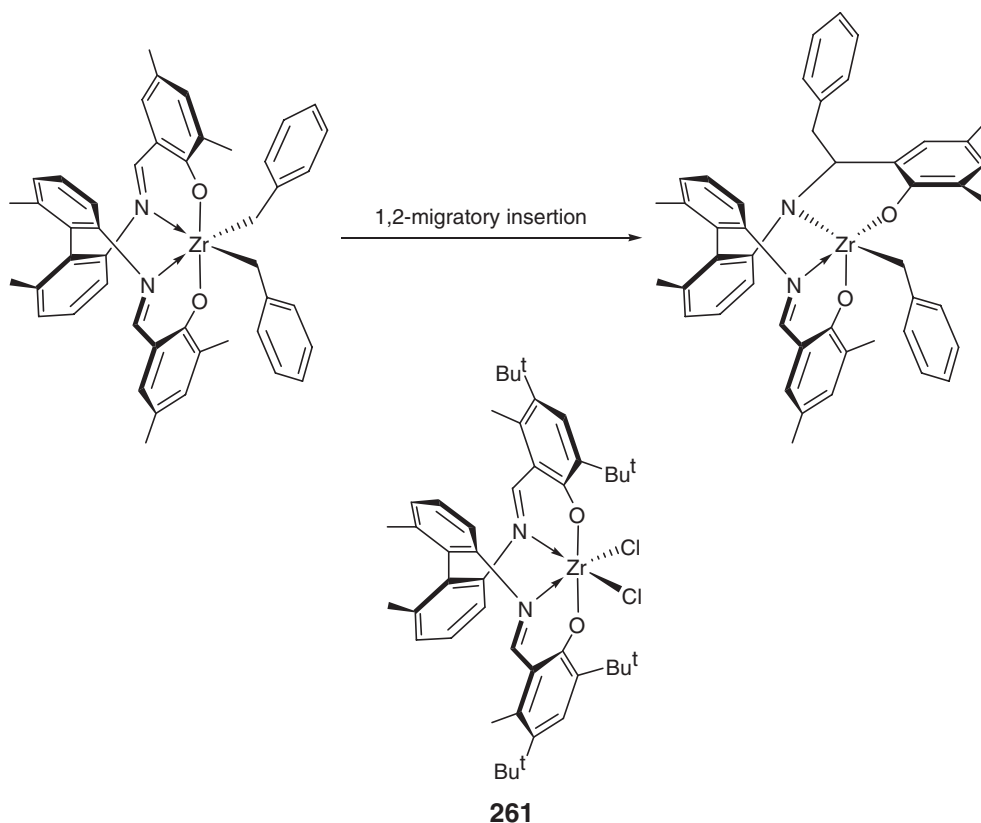
#### 4.08.5.8 Chelating Bis(phenoxy) Imine-donor $[\text{O}^-, \text{N}, \text{N}, \text{O}^-]$ Complexes

The salt metathesis of  $\text{MCl}_4(\text{THF})_2$  ( $M = \text{Zr}$  or  $\text{Hf}$ ) and the deprotonated form of the  $C_2$ -symmetric Schiff base ligand prepared by condensation of 2,2'-diamino-6,6'-dimethylbiphenyl and 3,5-di-*tert*-butylsalicylaldehyde gives the dichloride complexes **260**<sup>214,215</sup> (Scheme 53). The molecular structures of these complexes show the *cis-cis* configuration of tetradentate Schiff base complex with the two chloride ligands occupying mutually *cis*-coordination sites. The thermally unstable and light sensitive dibenzyl Zr(IV) complex can be obtained from the reaction of the



Scheme 53

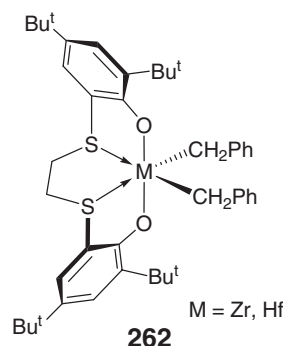
neutral ligand with Zr(CH<sub>2</sub>Ph)<sub>4</sub>; they undergo a 1,2-benzyl shift to a ligand C=N bond (Scheme 54). Alkane elimination using Zr(CH<sub>2</sub>Bu<sup>t</sup>)<sub>4</sub> gives the thermally more stable bis(neopentyl) complex, which allows isolation and crystallographic characterization of such dialkyl complexes.<sup>216</sup> Mixtures of the zirconium dichloride complex with MAO exhibit no activity for ethylene polymerization. However, introduction of a methyl group onto the phenoxy ring in order to block the intramolecular 1,2-migratory insertion of a Zr-bound benzyl group to an imine carbon leads to an active and long-lived ethylene polymerization catalyst, **261** (Scheme 54).<sup>217</sup>



Scheme 54

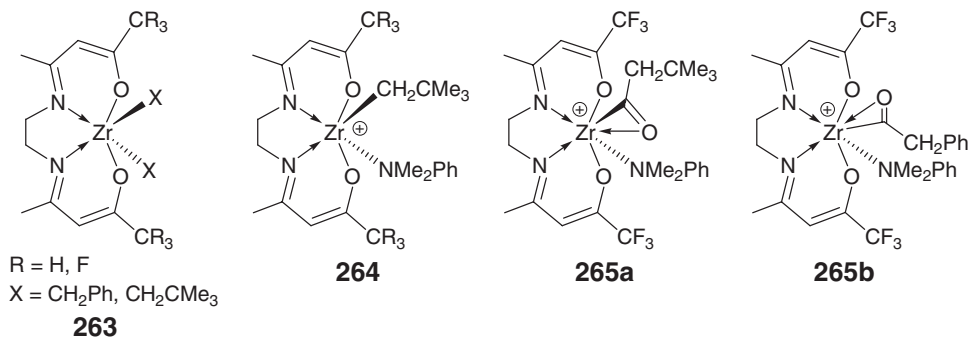
#### 4.08.5.9 Chelating Bis(phenoxy) Sulfur-donor [ $O^-$ ,S,S, $O^-$ ] Complexes

The alkane elimination was employed to synthesize the zirconium and hafnium dibenzyl complexes **262**.<sup>218</sup> The molecular structure of the hafnium complex was determined, featuring a  $C_2$ -symmetric configuration with *cis*-arranged benzyl groups and thioether donor atoms. The two bridging sulfur atoms adopt a *gauche*-conformation, evidently enforcing the *trans*-configuration of the two bulky phenoxy ligand moieties. Notably, the two benzyl groups show different coordination modes in the solid state, with one displaying an  $\eta^2$ -coordination and the other an  $\eta^1$ -coordination. Upon activation with MAO, these complexes are active for isospecific polymerization of styrene, albeit with low activity.



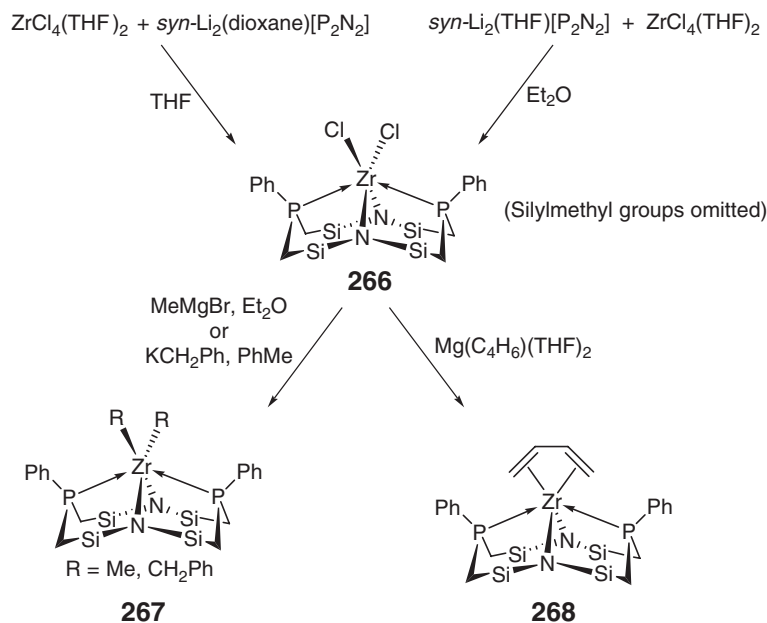
#### 4.08.5.10 Chelating $\beta$ -Ketoiminato [ $O^-$ ,N,N, $O^-$ ] Complexes

Alkane elimination reactions of the neutral acen tetradentate  $N_2O_2$  ligand and  $ZrR_4$  ( $R = CH_2Ph$ ,  $CH_2CMe_3$ ) afford the dialkylzirconium complexes **263** in high yield.<sup>219</sup> The solid state structure of the bis(neopentyl) complex shows a trigonal prismatic structure with a large angle [ $129.9(2)^\circ$ ] between the two neopentyl groups, which is substantially larger than those two alkyl angles in which the alkyl ligands are *cis*-ligated. The reaction of the bis(neopentyl) complex with  $[HNMe_2Ph][B(C_6F_5)_4]$  in  $CH_2Cl_2$  yields the cationic amine adduct **264**, whereas the same reaction in benzene gives the base-free analog which is stable in  $CH_2Cl_2$ . The amine adduct **264** inserts CO, yielding an  $\eta^2$ -acyl as two isomers **265a** and **265b**.



#### 4.08.5.11 Chelating Bis(amido) Phosphine-donor [ $N^-$ ,P,P, $N^-$ ] Complexes

Zirconium(IV) dichloride complex  $ZrCl_2[P_2N_2]$  **266** that incorporates the macrocyclic bis(amido-phosphine) ligand  $PhP(CH_2SiMe_2NSiMe_2CH_2)_2PPh$ ,  $[P_2N_2]$ , is obtained from the salt metathesis between  $ZrCl_4(THF)_2$  and *syn*- $Li_2(S)[P_2N_2]$  ( $S = \text{dioxane or THF}$ );<sup>220</sup> (Scheme 55). Subsequent alkylation of **266** with either  $MeMgBr$  or  $KCH_2Ph$  generates the corresponding dialkyl complexes  $ZrR_2[P_2N_2]$  **267**;  $R = Me$ ,  $CH_2Ph$ ). Reaction of the dichloride complex **266** with  $Mg(C_4H_6) \cdot 2THF$  gives  $\pi$ - $\eta^4$ -butadiene complex  $Zr(\eta^4-C_4H_6)[P_2N_2]$  **268**. The solid-state structures of these complexes all show that the Zr center sits above the plane defined by the donor atoms of the macrocyclic ligand, due to the fact that the Zr ion is too large to fit into the cavity of the 12-membered macrocycle. The distortions of the macrocycle observed in the solid state are not evident in solution, which suggests that these ligand backbones are rather flexible.

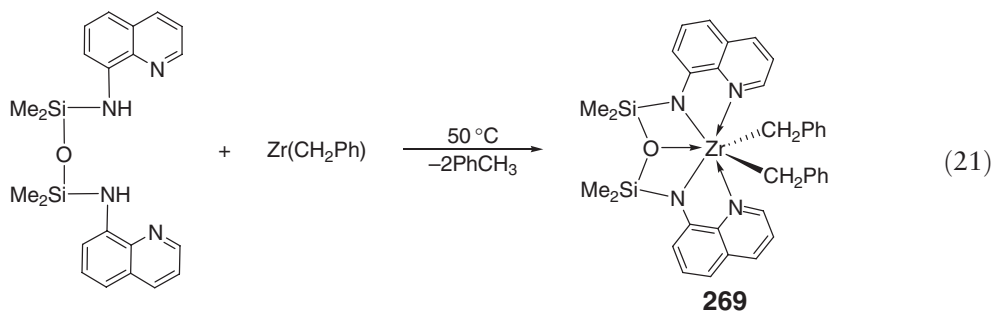


Scheme 55

#### 4.08.6 Complexes with Non-Cyclopentadienyl $\eta^5$ -Ligands

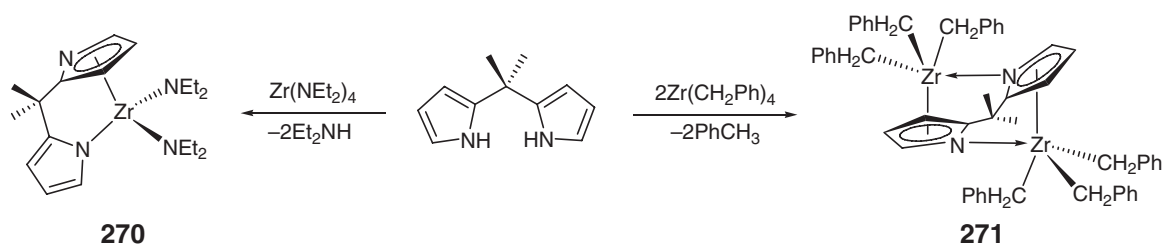
##### 4.08.6.1 Complexes Containing Aminoquinolato $[N, N^-, O, N^-, N]$ Ligands

The reaction of  $\text{Zr}(\text{CH}_2\text{Ph})_4$  with bis(aminoquinoline)  $(\text{RHNSiMe}_2)_2\text{O}$  ( $\text{R} = \text{quinolin-8-yl}$ ) leads to ruby-red Zr(IV) complex **269** via elimination of toluene<sup>61</sup> (Equation (21)). The molecular structure of **17** shows an approximately pentagonal-bipyramidal geometry with the dianionic chelating ligand bound to Zr via  $\eta^5$ -coordination  $[N, N^-, O, N^-, N]$ . Owing to the *trans*-orientation of the benzyl groups in this complex, the MAO-activated species exhibits little activity in polymerization of ethylene under either ambient or high-pressure conditions.



##### 4.08.6.2 Complexes Containing Pyrrolyl Ligands

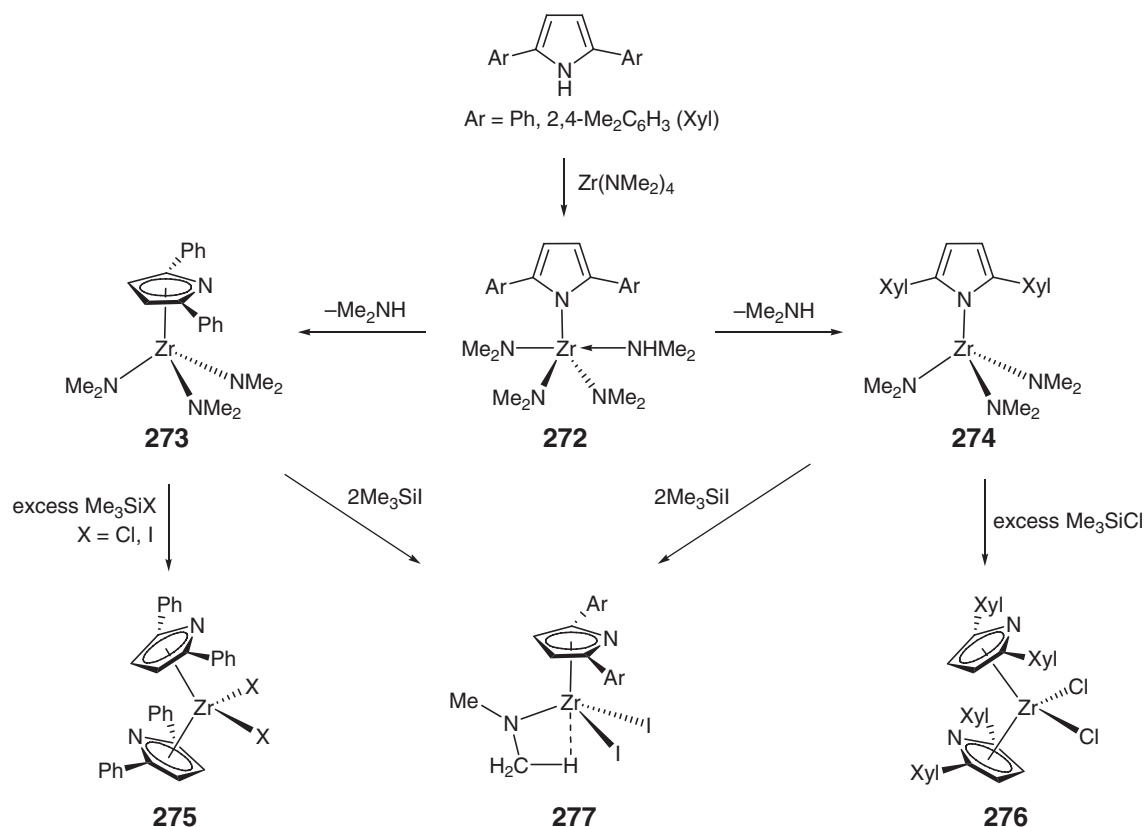
Zirconium complexes **270** and **271** supported by dipyrrolyl ligands capable of both  $\eta^1$ - and  $\eta^5$ -bonding modes were prepared from aminolysis of  $\text{Zr}(\text{NEt}_2)_4$  and protolysis of  $\text{Zr}(\text{CH}_2\text{Ph})_4$  with neutral *meso*-dimethyl dipyrromethane, respectively (Scheme 56).<sup>221</sup> Based on the structurally characterized Ti analog, the structure of **270** was first postulated to exhibit a unique  $\eta^1$ -/ $\eta^5$ -bonding mode to a single metal center; however, X-ray diffraction of **271** showed a bimetallic structure with each Zr coordinating to the dipyrrolyl ligand via a not straightforward  $\eta^1$ -/ $\eta^5$ -bonding mode because of the subtle perturbation by the benzyl ligands. Pre-treatment of **270** with  $\text{Me}_3\text{SiCl}$  followed



Scheme 56

by MAO generates a species that is moderately active for ethylene polymerization, producing polyethylene with a broad molecular weight distribution ( $\bar{M}_w/\bar{M}_n = 80$ ).

The relative stabilities of the various coordination modes involving substituted pyrrolyl ligands are influenced by both steric factors and the Lewis acidity of the metal zirconium center, such that bulky and  $\pi$ -donor ligands attached to the metal favor  $\eta^1$ -coordination; this has been demonstrated by a series of structurally characterized zirconium complexes that feature both  $\eta^1$ - and  $\eta^5$ -2,5-diaryl pyrrolyl ligands<sup>222</sup> (Scheme 57). Depending on the steric bulk of the Ar substituents, aminolysis of  $\text{Zr}(\text{NMe}_2)_4$  with the neutral 2,5-diaryl pyrrolyl ligands yields either the half-sandwich,  $\eta^5$ -pyrrolyl zirconium complex **273** (Ar = Ph) or the  $\eta^1$ -pyrrolyl zirconium complex **274** (Ar = 2,4-Me<sub>2</sub>C<sub>6</sub>H<sub>3</sub>), via the dimethylamine adducts **272**. Treatment of the triamide complexes **273** and **274** with excess of Me<sub>3</sub>SiX (X = Cl, I) produces bis( $\eta^5$ -pyrrolyl) zirconium sandwich complexes **275** and **276**. The same reaction, but with just 2 equiv. of Me<sub>3</sub>SiI, affords  $\eta^5$ -pyrrolyl half-sandwich zirconium complex **277**, which exhibits  $\beta$ -agostic interactions between the methyl group of the NMe<sub>2</sub> ligand and the zirconium center.



Scheme 57

### 4.08.6.3 Complexes Containing Carboranyl Ligands

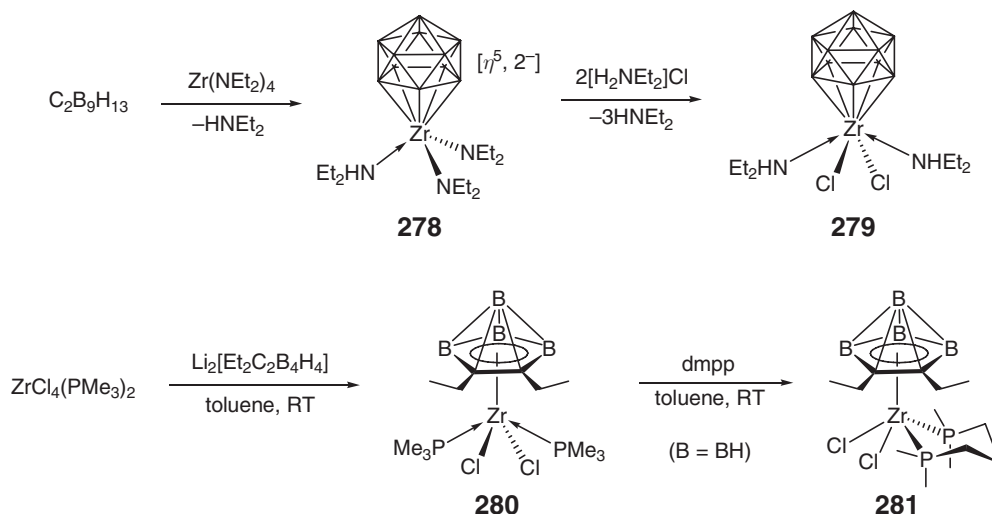
Aminolysis of  $\text{Zr}(\text{NEt}_2)_4$  with the neutral carborane  $\text{C}_2\text{B}_9\text{H}_{13}$  yields the mono-dicarbollide zirconium bis(diethyl-amido) complex **278** (Scheme 58).<sup>223</sup> The X-ray diffraction analysis of this complex reveals a three-legged piano-stool structure with the dianionic, six-electron dicarbollide ( $\text{C}_2\text{B}_9\text{H}_{11}$ ) ligand adopting an  $\eta^5$ -coordination mode. Protolysis of the amido ligands in complex **278** with 2 equiv. of  $[\text{NH}_2\text{Et}_2]\text{Cl}$  results in formation of the corresponding dichloride complex **279** as a bis(amine) adduct. When activated with either a large excess of MAO or a small amount of triisobutylaluminum, zirconium bis(diethylamido) complex **278** is active for ethylene polymerization;<sup>224</sup> however, the polymers produced have either very broad molecular weight distributions ( $\bar{M}_w/\bar{M}_n > 15$ ) (by MAO activation) or bimodal molecular weight distributions (by the triisobutylaluminum activation), indicating that at least two catalytically active species are present in this system.

Zirconium dichloride complexes **280** and **281**, prepared by the salt metathesis method (Scheme 58), incorporate a dianionic, small carborane  $\eta^5$ - $[\text{Et}_2\text{C}_2\text{B}_4\text{H}_4]^{2-}$  ligand.<sup>225</sup> Complex **280** is thermally unstable and decomposes in solution or *in vacuo* with loss of the phosphine, whereas complex **281**, obtained by immediate trapping of **280** with the chelating diphosphine dmpp, is thermally stable. When activated with MAO, complex **281** is active toward polymerization of ethylene, producing high molecular weight, linear high density polyethylene with bimodal molecular weight distribution ( $\bar{M}_w/\bar{M}_n \approx 24$ ).

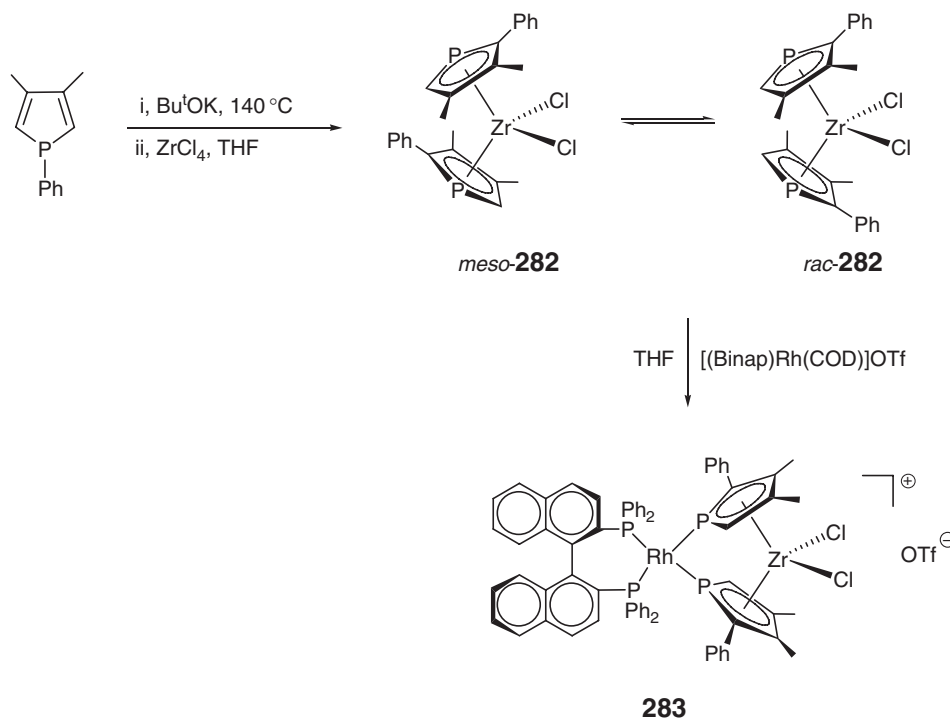
### 4.08.6.4 Complexes Containing Phospholyl Ligands

Bis(phospholyl)zirconocene **282** was obtained as a 63:37 mixture of *rac*- and *meso*-isomers in the crude product from salt metathesis of a phospholyl anion and  $\text{ZrCl}_4$  in THF (Scheme 59).<sup>226</sup> Washing the crude product with pentane enhanced the *rac*/*meso* ratio to 80:20, but a THF solution of this mixture reached back to the equilibrium ratio of 63:37 in <15 min, indicating facile isomerization processes among these diastereomers. Slow addition of a THF solution of  $[(R)\text{-Binap}]\text{Rh}(\text{COD})\text{OTf}$  to a THF solution of **282** produced a single diastereomer of the bimetallic *ansa*-phosphazirconocene **283**, which accomplishes the dynamic resolution of phosphazirconocene **282** (COD = 1,5-cyclooctadiene).

On the other hand, recrystallization of the diastereomeric product mixture of the bis(phospholyl)zirconocene afforded the pure  $C_2$ -symmetric *rac*-phosphazirconocene and phosphahafnocene **284**.<sup>227</sup> The *rac*-phosphazirconocene dichloride binds as a bidentate ligand to  $\text{Mo}(\text{CO})_4$  to give bimetallic *ansa*-phosphazirconocene **285**. Alkylation of the dichloride compounds with  $\text{MeMgBr}$  produces the dimethyl derivatives *rac*-**286** and *rac*-**287**. Upon activation with MAO, the *rac*-phosphazirconocene dichloride and dimethyl complexes exhibit high activity toward co-polymerization of ethylene and 1-hexene. Interestingly, the bimetallic *ansa*-phosphazirconocenes **285** and **287** are inactive, presumably due to decomposition of the complexes under polymerization conditions. A reactivity study and an

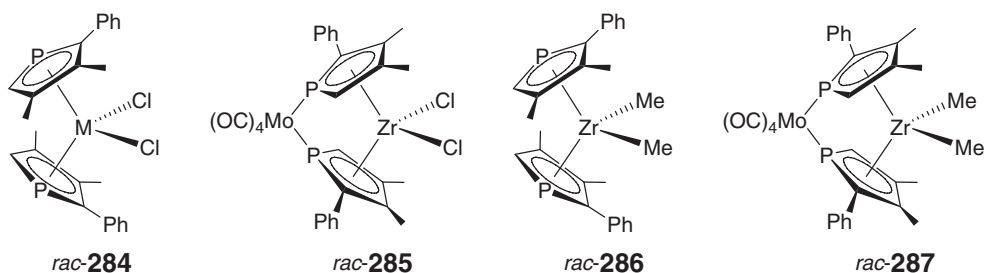


Scheme 58



Scheme 59

assessment of the  $\pi$ -basicity of the  $\eta^5$ -C<sub>4</sub>Me<sub>4</sub>P phospholyl ligand indicate that the  $\eta^5$ -C<sub>4</sub>Me<sub>4</sub>P ligand is a poorer  $\pi$ -base than the Cp ligand.<sup>228</sup>



#### 4.08.7 Monocyclopentadienyl Complexes

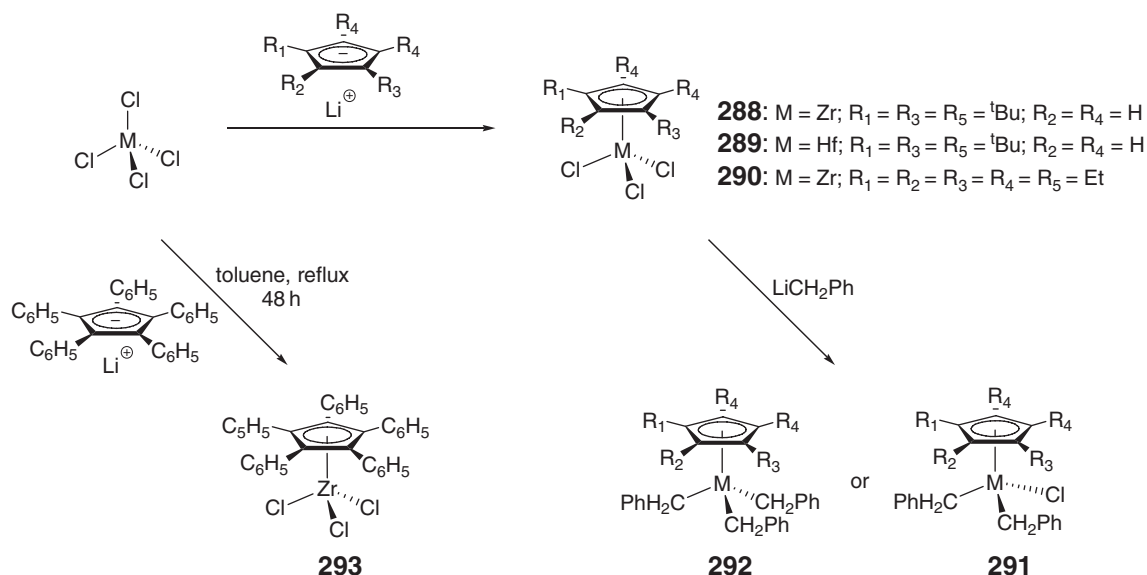
##### 4.08.7.1 Non-functionalized Mono-Cp Complexes Containing Monodentate Ligands

Complexes incorporating non-functionalized mono-Cp ligands are those complexes bearing the parent Cp, indenyl (Ind), and fluorenyl (Flu), as well as their alkylated or arylated derivatives. Complexes bearing silylated Cp ligands or other types of functionalized Cp ligands are the subject of Sections 4.08.7.3–4.08.7.5 and 4.08.8.

###### 4.08.7.1.1 Complexes containing halide, alkyl, and aryl ligands

Alkylated mono-Cp trichloride complexes Cp'MCl<sub>3</sub>, Cp' = 1,2,4-Bu<sup>t</sup><sub>3</sub>C<sub>5</sub>H<sub>2</sub>, M = Zr **288**, Hf **289**, and Cp' = Et<sub>5</sub>C<sub>5</sub>, M = Zr **290**, were synthesized by salt metathesis (Scheme 60). These compounds can be readily converted into the corresponding benzyl derivatives Cp'Zr(CH<sub>2</sub>Ph)<sub>2</sub>Cl **291** or Cp'Zr(CH<sub>2</sub>Ph)<sub>3</sub> **292**.<sup>229</sup> Refluxing a mixture of lithium



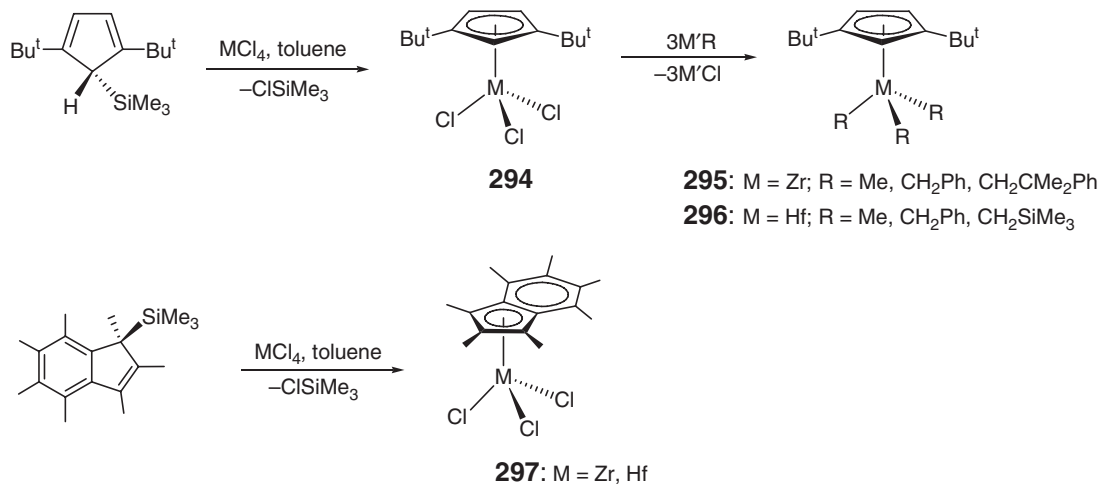


Scheme 60

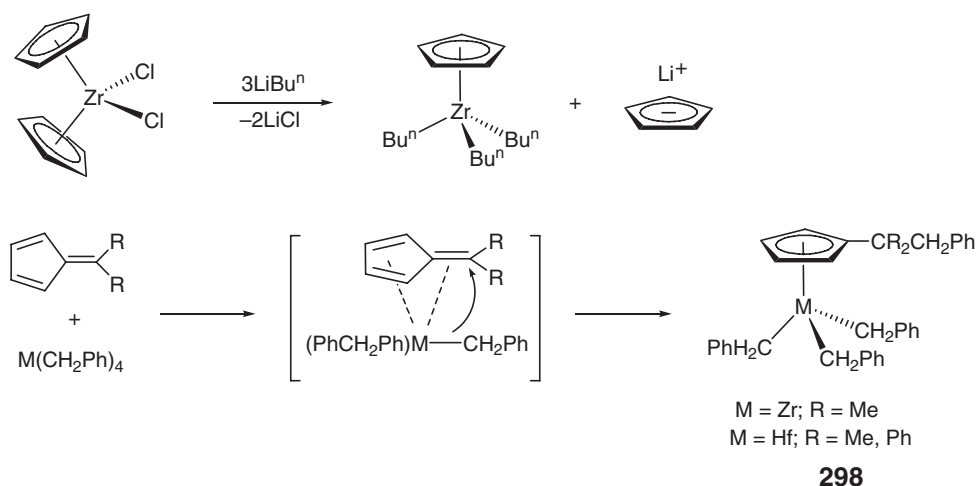
pentaphenylcyclopentadienide and ZrCl<sub>4</sub> in toluene for 48 h produces (η<sup>5</sup>-Ph<sub>5</sub>C<sub>5</sub>)ZrCl<sub>3</sub> **293**, which serves as an useful precursor for the synthesis of prochiral bis(Cp) complexes.<sup>230,231</sup>

Elimination of chlorotrimethylsilane involving the reaction of MCl<sub>4</sub> with a neutral silylated mono-Cp ligand is also an effective approach leading to substituted mono-Cp complexes or to none. For example, the reaction of (1,3-Bu<sup>t</sup><sub>2</sub>C<sub>5</sub>H<sub>3</sub>)SiMe<sub>3</sub> with MCl<sub>4</sub> (M = Zr, Hf) in toluene or hexanes at ambient temperature produces zirconium<sup>232</sup> and hafnium<sup>233</sup> trichloride complexes (1,3-Bu<sup>t</sup><sub>2</sub>C<sub>5</sub>H<sub>3</sub>)MCl<sub>3</sub> **294**, which can be readily converted using appropriate alkylating reagents to the corresponding trialkyl complexes (1,3-Bu<sup>t</sup><sub>2</sub>C<sub>5</sub>H<sub>3</sub>)MR<sub>3</sub> **295**: M = Zr, R = Me, CH<sub>2</sub>Ph, CH<sub>2</sub>CMe<sub>2</sub>Ph; **296**: M = Hf, R = Me, CH<sub>2</sub>Ph, CH<sub>2</sub>SiMe<sub>3</sub>; (Scheme 61). The presence of bulky *tert*-butyl substituents enhances the solubility of the zirconium and hafnium complexes. The permethylindenyl zirconium and hafnium trichloride complexes **297** were obtained by the same chlorotrimethylsilane elimination route.<sup>234</sup>

In addition to the two widely used synthetic routes (i.e., salt metathesis and elimination) discussed above, there are two unique approaches effectively leading to mono-Cp alkyl complexes in one step. The first utilizes a bis(Cp) complex precursor, Cp<sub>2</sub>ZrCl<sub>2</sub>, to react with 3 equiv. of LiBu<sup>n</sup>, yielding a 1:1 mixture CpZr(Bu<sup>n</sup>)<sub>3</sub> and CpLi via a facile



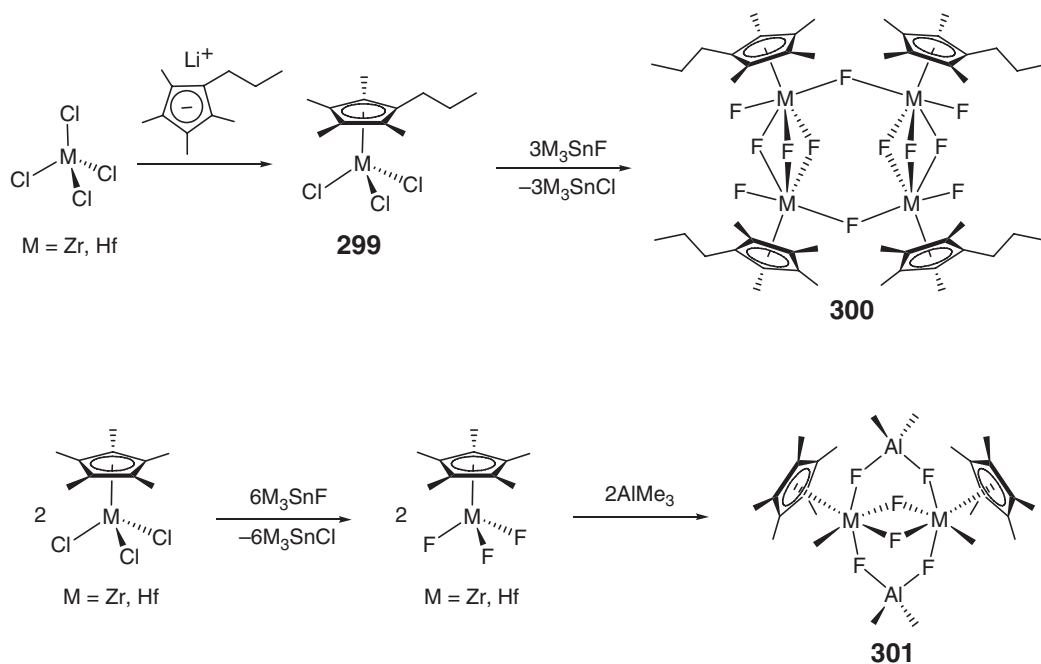
Scheme 61



Scheme 62

displacement of a Cp ring<sup>235</sup> (Scheme 62). Isolation of  $\text{CpZr}(\text{Bu}^n)_3$  from the reaction mixture is proven to be problematic; many such attempts led only to its decomposition. The second route utilizes the reaction of polar 6,6-dialkylfulvenes with  $\text{M}(\text{CH}_2\text{Ph})_4$  ( $M = \text{Zr, Hf}$ ), affording the alkylated mono-Cp tribenzyl complexes **298**, presumably via coordination of the *cis*-diene functionality in the fulvene substrate followed by migratory insertion into a metal–benzyl bond<sup>236</sup> (Scheme 62).

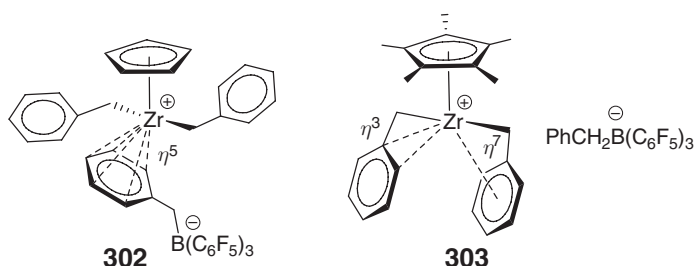
The  $\text{Me}_3\text{SnF}$  reagent is effective in the chloride-to-fluoride exchange process. For example, trifluoro zirconium and hafnium complexes **300** containing the *n*-propyltetramethyl-cyclopentadienyl ligand were synthesized by the metathesis reaction between 3 equiv. of  $\text{Me}_3\text{SnF}$  and 1 equiv. of the trichloride precursor **299**, which was prepared by salt metathesis<sup>237</sup> (Scheme 63). The tetrameric nature of these complexes was established by NMR and mass spectrometric data. This effective chloride-to-fluoride exchange process by  $\text{Me}_3\text{SnF}$  has been employed to synthesize a variety of zirconium fluoride complexes from the corresponding readily available chloride complexes, including  $\text{Cp}^*\text{MF}_3$ , which have been shown to be fluorine-bridged tetramers in the solid state.<sup>238</sup> The reaction of  $\text{Cp}^*\text{MF}_3$  with 1 equiv. of  $\text{AlMe}_3$



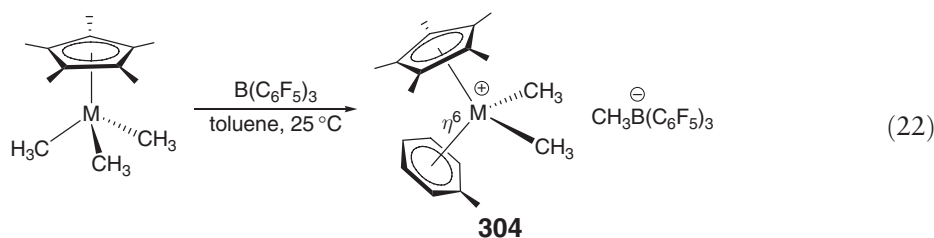
Scheme 63

in toluene or *n*-hexane leads to exchange of only one M–Me bond with an M–F bond, forming stereoselectively fluorine-bridged *cis*-dimers **301**.<sup>239</sup> On the other hand, the reaction of Cp\*ZrF<sub>3</sub> with an excess of AlMe<sub>3</sub> substitutes all the fluorines at Zr and eliminates methane; the maximum amount of methane (3.5 equiv.) can be achieved when 5 equiv. of AlMe<sub>3</sub> is reacted, producing a Zr<sub>3</sub>Al<sub>6</sub>C<sub>7</sub> cluster with a structural formula of (Cp\*Zr)<sub>3</sub>Al<sub>6</sub>Me<sub>8</sub>(CH<sub>2</sub>)<sub>7</sub>(CH)<sub>5</sub>.<sup>240</sup>

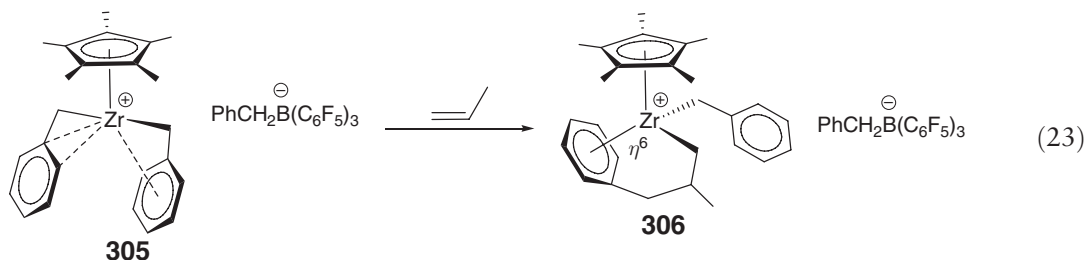
Several strategies have been employed for generating characterizable and isolable mono-Cp *d*<sup>0</sup>-metal dialkyl cationic complexes, which can serve as active, single-component catalysts for polymerizations of  $\alpha$ -olefins. The first such strategy uses a benzyl ligand to stabilize the derived cation via multi-hapto coordination. Thus, the reaction of CpZr(CH<sub>2</sub>Ph)<sub>3</sub>, the solid-state structure of which features a monomeric species with the benzyl ligands adopting  $\eta^2$ -coordination,<sup>241</sup> with 1 equiv. of B(C<sub>6</sub>F<sub>5</sub>)<sub>3</sub> in toluene at ambient temperature yields the contact ion pair CpZr(CH<sub>2</sub>Ph)<sub>2</sub><sup>(+)</sup>PhCH<sub>2</sub>B(C<sub>6</sub>F<sub>5</sub>)<sub>3</sub><sup>(-)</sup> **302** with a  $\pi$ -bonded benzylborate anion, as revealed by both solid-state structure and solution spectroscopic investigations.<sup>242</sup> In the solid state, the two benzyl groups of the cation behave as normal, undistorted  $\eta^1$ -ligands without significant Zr–C<sub>*ipso*</sub> interactions, while the phenyl ring of the anion is asymmetrically coordinated to Zr and best described as  $\eta^5$ -arene coordination (2.86(2) Å for Zr–C<sub>*ipso*</sub> and 2.68 Å (av) for the remaining Zr–C distances). In contrast, with the sterically more bulky and more electron-donating Cp\* (Cp\* = Me<sub>5</sub>C<sub>5</sub>) ligand, the crystal structure of [Cp\*Zr(CH<sub>2</sub>Ph)<sub>2</sub>][PhCH<sub>2</sub>B(C<sub>6</sub>F<sub>5</sub>)<sub>3</sub>] **303** reveals discrete ion pairs and negligible cation–anion associations.<sup>243</sup> The cation is still stabilized by a remarkable combination of  $\eta^7$ -benzyl and  $\eta^3$ -benzyl coordination modes.



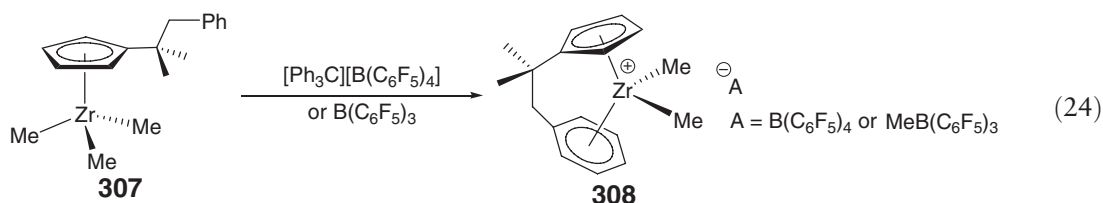
The second strategy involves stabilization of the mono-Cp *d*<sup>0</sup>-non-benzyl dialkyl metal cation with  $\pi$ -arene coordination. The arene coordination becomes the primary stabilization factor enabling the detection or isolation of the mono-Cp dimethyl cations. Thus, the reaction of Cp\*MMe<sub>2</sub> (M = Zr, Hf) with 1 equiv. of B(C<sub>6</sub>F<sub>5</sub>)<sub>3</sub> in toluene/hexanes (1 : 10) solutions at ambient temperature affords the cationic arene complexes [(Cp\*M(Me)<sub>2</sub>( $\eta^6$ -PhMe))[MeB(C<sub>6</sub>F<sub>5</sub>)<sub>3</sub>] **304** as the solvent-separated ion pairs stabilized by the coordination of the aromatic solvent (Equation (22)).<sup>244</sup> The crystal structure of the hafnium complex [(Cp\*Hf(Me)<sub>2</sub>( $\eta^6$ -PhMe))[MeB(C<sub>6</sub>F<sub>5</sub>)<sub>3</sub>] confirms the formation of the separated, discrete ion pairs in which the bent-sandwich cation is coordinated to an  $\eta^6$ -toluene ligand.<sup>245</sup>



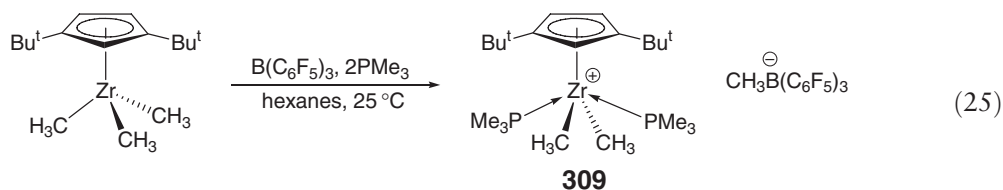
The  $\eta^6$ -arene coordination is also seen in the structurally characterized single-propylene-insertion product, [Cp\*Zr(CH<sub>2</sub>CHMeCH<sub>2</sub>Ph)(CH<sub>2</sub>Ph)][(CH<sub>2</sub>Ph)B(C<sub>6</sub>F<sub>5</sub>)<sub>3</sub>] **306**, derived from [Cp\*Zr(CH<sub>2</sub>Ph)<sub>2</sub>][PhCH<sub>2</sub>B(C<sub>6</sub>F<sub>5</sub>)<sub>3</sub>] **305** (Equation (23)). The molecular structure reveals that the unexpected stability of this first monomer insertion product is due to an unusual “back-biting”  $\eta^6$ -arene coordination from the initiating benzyl group to the *d*<sup>0</sup>-metal center.<sup>246</sup>



The  $\eta^6$ -arene stabilization strategy can be extended to intramolecular coordination of a pendant phenyl group to the cationic metal center. The reaction of a neutral Cp ligand containing a pendant phenyl substituent and a readily displaceable trimethylsilyl group,  $\text{C}_5\text{H}_4(\text{CMe}_2\text{CH}_2\text{Ph})\text{SiMe}_3$ , with  $\text{ZrCl}_4(\text{SMe}_2)_2$  affords the monomeric  $\text{C}_5\text{H}_4(\text{CMe}_2\text{CH}_2\text{Ph})\text{ZrCl}_3(\text{dme})$ , which is then converted to the corresponding trimethyl species **307** upon alkylation with MeLi.<sup>247</sup> Treatment of the trimethyl **307** with  $[\text{Ph}_3\text{C}][\text{B}(\text{C}_6\text{F}_5)_4]$  or  $\text{B}(\text{C}_6\text{F}_5)_3$  in dichloromethane at low temperatures generates the cationic complex  $[(\eta^5\text{-C}_5\text{H}_4\text{R})\text{ZrMe}_2]^+$  **308**, which is stabilized by  $\pi$ -coordination to the pendant Ph ring to give an *ansa*-Cp/arene type of complex with a two-carbon linkage (Equation (24)).



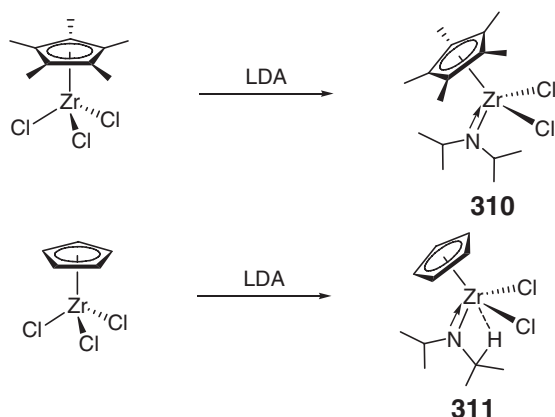
The third strategy of stabilizing the mono-Cp dialkyl metal cations is *the* addition of external donor ligands such as  $\text{PMe}_3$  and  $\text{Bu}^t\text{C}\equiv\text{N}$ . The reaction of  $(1,3\text{-Bu}^t_2\text{C}_5\text{H}_3)\text{ZrMe}_3$  with  $\text{B}(\text{C}_6\text{F}_5)_3$  in the presence of  $\text{PMe}_3$  in hexanes at ambient temperature yields the cationic dimethyl complexes  $[(1,3\text{-Bu}^t_2\text{C}_5\text{H}_3)\text{Zr}(\text{PMe}_3)_2(\text{CH}_3)_2][\text{MeB}(\text{C}_6\text{F}_5)_3]$  **309** (Equation (25)); this separated ion pair was obtained as orange-yellow solids and is stable at room temperature.<sup>248</sup>



This third strategy has been employed to synthesize the cationic dichloride, dicationic monochloride, and tricationic mono-Cp complexes. Thus, treatment of  $[\text{CpMCl}_3(\text{MeCN})_2]$  ( $\text{M} = \text{Zr}, \text{Hf}$ ) with  $\text{SbCl}_5$  in acetonitrile allows the isolation of  $[\text{CpMCl}_2(\text{MeCN})_3][\text{SbCl}_6]$ ,  $[\text{CpMCl}(\text{MeCN})_4][\text{SbCl}_6]_2$ , and  $[\text{CpM}(\text{MeCN})_6][\text{SbCl}_6]_3$ , via facile chloride abstraction.<sup>249</sup> The X-ray structure of the hafnium complex  $[\text{CpHf}(\text{MeCN})_6][\text{SbCl}_6]_3$  shows two independent seven-coordinate pentagonal-bipyramidal trications  $[\text{CpHf}(\text{MeCN})_6]^{3+}$  in which the Cp occupies an axial position, and six  $[\text{SbCl}_6]^-$  monoanions, as well as two lattice solvent ( $\text{CH}_2\text{Cl}_2$ ) molecules.

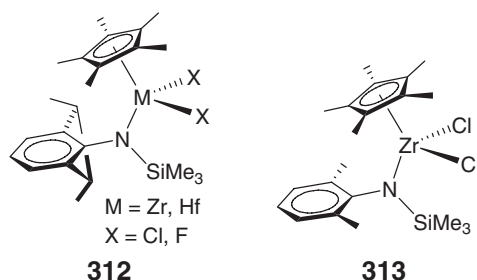
#### 4.08.7.1.2 Complexes containing nitrogen ligands

“Transamination” reaction of  $\text{CpZrCl}_3$ , a polymeric species in the solid state, or  $\text{Cp}^*\text{ZrCl}_3$ , a doubly Cl-bridged dimer in the solid state,<sup>250</sup> with lithiated nitrogen-containing nucleophiles is a most common route leading to the mono-Cp amido complexes. Thus, reactions  $\text{Cp}^*\text{ZrCl}_3$  and  $\text{CpZrCl}_3$  with 1 equiv. of  $\text{Li}[\text{N}(\text{tPr})_2]$  (LDA) generate 14-electron dichloro alkylamido complexes  $\text{Cp}^*\text{Zr}[\text{N}(\text{tPr})_2]\text{Cl}_2$  **310** and  $\text{CpZr}[\text{N}(\text{tPr})_2]\text{Cl}_2$  **311**, respectively<sup>251</sup> (Scheme 64). The Zr–N distances of 2.003(4) and 1.988(4) Å in **310** and **311**, respectively, are consistent with the presence of a Zr–N double bond. The solid-state structure of **311** is characterized by a  $\beta$ -agostic interaction involving the methine C–H bond of an isopropyl group. However, the replacement of the Cp ring in **311** by the stronger  $\pi$ -donating and bulkier  $\text{Cp}^*$  ring in **310** loses such a  $\beta$ -agostic interaction and increases the Cp(centroid)–Zr–N angle by 13.5°, reflecting a strong stereoelectronic influence of permethylated Cp ligand. A comparison of the structural parameters about the electrophilic metal centers of **310** and **311** with those of related bent metallocenes is consistent with the diisopropylamido ligand being a poorer  $\pi$ -donor than either Cp or  $\text{Cp}^*$ .



Scheme 64

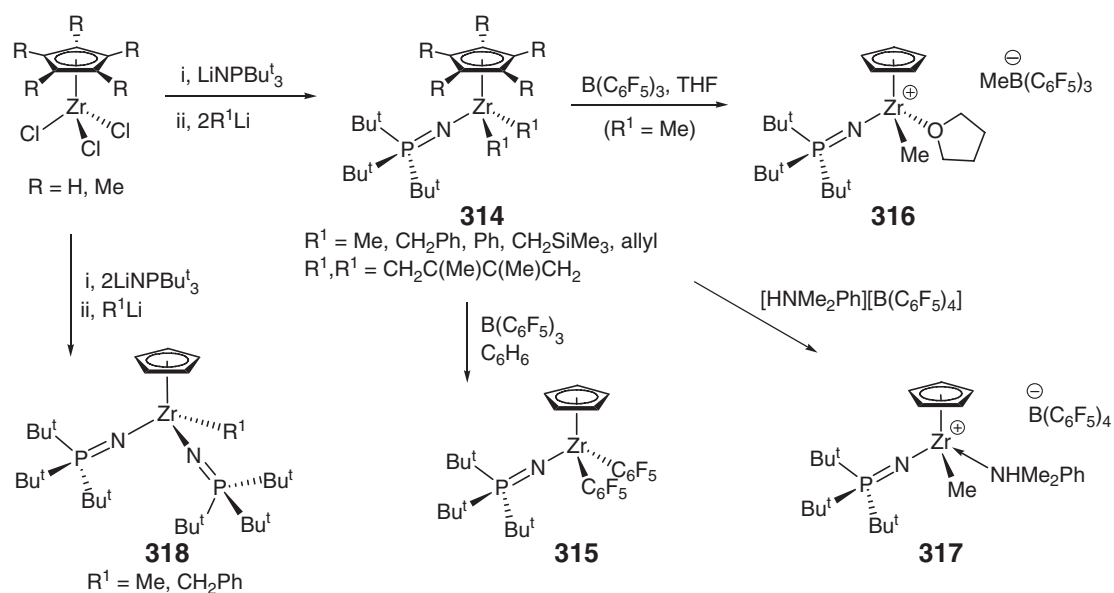
Arylamido complexes of a general formula of  $\text{Cp}^*\text{Zr}[\text{N}(\text{Ar})\text{SiMe}_3]\text{Cl}_2$  can be obtained in a similar fashion. Thus, the reaction of  $\text{Cp}^*\text{MCl}_3$  with 1 equiv. of  $\text{Li}[\text{N}(\text{Ar})\text{SiMe}_3]$  produces complexes **312**<sup>48</sup> and **313**.<sup>252</sup> The difluoride **312** was prepared by metathesis reaction of the dichloride and  $\text{Me}_3\text{SnF}$ . Upon activation with MAO, all complexes are active for polymerization of ethylene; within complexes **312**, the zirconium complexes are much more active than the analogous hafnium complexes, whereas within complexes **313**, the zirconium complex exhibits poor activity as compared with the analogous titanium complex.



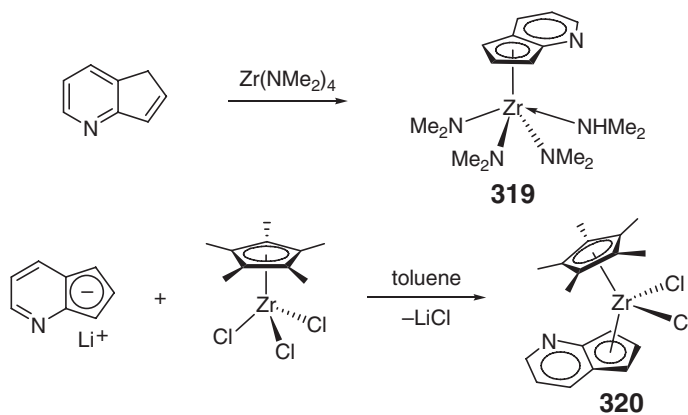
Transamination reaction of  $\text{CpZrCl}_3$  or  $\text{Cp}^*\text{ZrCl}_3$  with 1 equiv. of  $\text{LiN}=\text{P}^t\text{Bu}_3$  followed by alkylation with 2 equiv. of  $\text{R}^1\text{Li}$  reagents leads to a series of mono-Cp zirconium dialkyl phosphinimide complexes **314**<sup>253</sup> (Scheme 65). The reaction of the dimethyl complex with  $\text{B}(\text{C}_6\text{F}_5)_3$  in benzene results in aryl group transfer and formation of catalytically inactive bis(pentafluorophenyl) complex **315**. Such an aryl group transfer process can be shut down by running the same reaction in the presence of THF, thereby leading the THF-stabilized cationic complex **316**.<sup>50</sup> Activation of the dimethyl complex with  $[\text{HNMe}_2\text{Ph}][\text{B}(\text{C}_6\text{F}_5)_4]$  generates the same cation **317**, but now stabilized by the co-product amine liberated by protolysis. The bis(phosphinimide) complexes **318** were also synthesized by the same two-step process using appropriate stoichiometric ratios of the reagents.<sup>50</sup>

“Amine elimination” involving the reaction of  $\text{Zr}(\text{NR}_2)_4$  and neutral Cp-based ligands is another commonly employed approach for the synthesis of the mono-Cp amino complexes. For example, aminolysis of  $\text{Zr}(\text{NMe}_2)_4$  by cyclopenta[*b*]pyridine in toluene yields mono-Cp-based zirconium triamido complex **319** with a coordinated dimethylamine molecule<sup>254</sup> (Scheme 66). The anionic version of this ligand reacts smoothly with  $\text{Cp}^*\text{ZrCl}_3$  generating the unsymmetrical bis(Cp)-type complex **320**, in which the bifunctional ligand coordinates to Zr in an  $\eta^5$ -manner rather than via nitrogen.

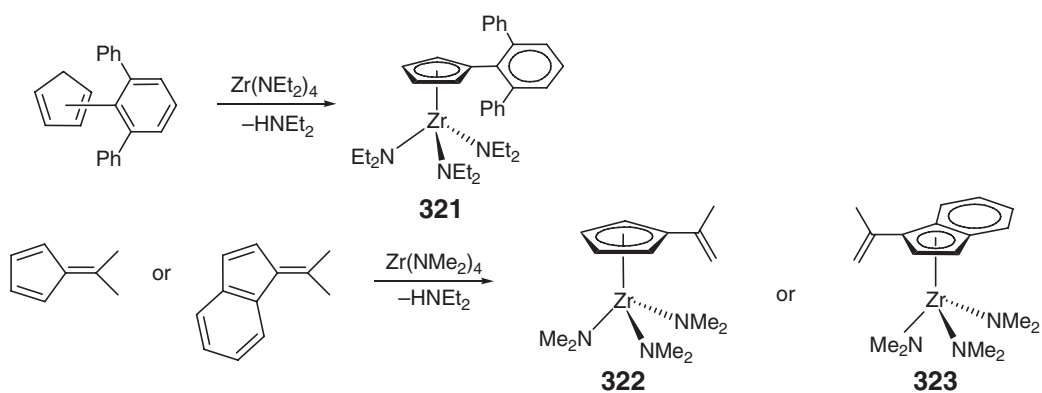
With a sterically more demanding ligand, cyclopentadienyl-2,6-diphenylbenzene, the amine elimination approach using  $\text{Zr}(\text{NEt}_2)_4$  produces the desired  $[(2,6\text{-Ph}_2\text{-C}_6\text{H}_3\text{-}\eta^5\text{-C}_5\text{H}_4)\text{Zr}(\text{NEt}_2)_3]$  **321** without an additional coordinated amine<sup>255</sup> (Scheme 67). The molecular structure of this complex features significant distortions of the three-legged piano-stool geometry as a result of steric interactions with the bulky aryl substituents. Aminolysis of  $\text{Zr}(\text{NMe}_2)_4$  with



Scheme 65



Scheme 66



Scheme 67

6,6-dimethylfulvene yields the zirconium tris(dimethylamido) complex **322** bearing a 2-propenyl-Cp ligand, presumably via deprotonation of one of the acidic 6,6-methyl protons.<sup>236</sup> The (2-propenyl)indenyl zirconium tris(dimethylamide) **323** can be obtained in the same procedure.

#### 4.08.7.1.3 Complexes containing oxygen and sulfur ligands

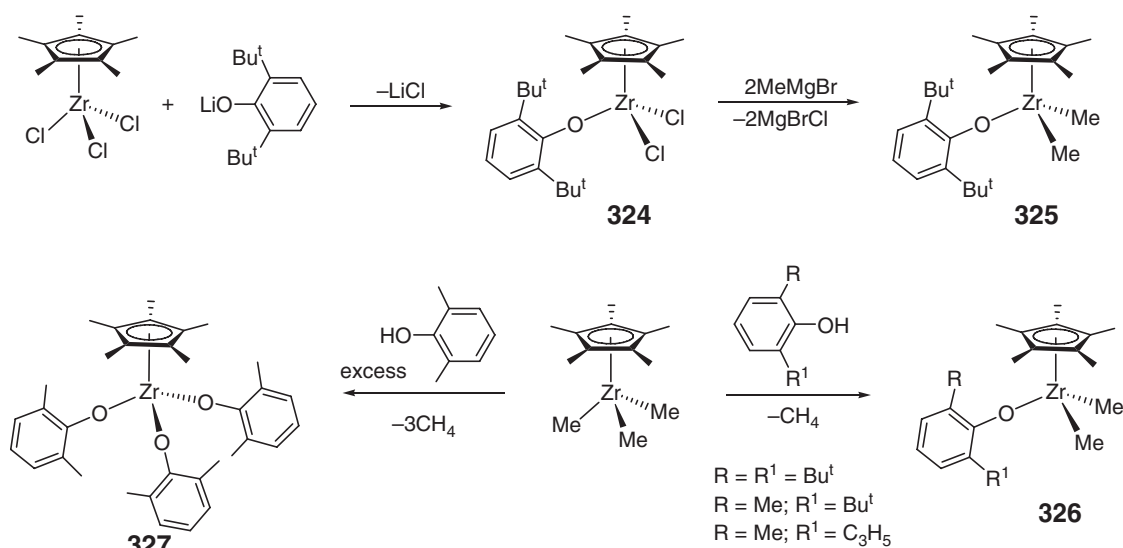
Zirconium mono-Cp\* complexes containing aryloxy ligands are readily synthesized by either salt metathesis using the Cp\*ZrCl<sub>3</sub> precursor or alkane elimination using the Cp\*ZrMe<sub>3</sub> precursor. Thus, the reaction of Cp\*ZrCl<sub>3</sub> with lithium 2,6-di-*tert*-butylphenoxide produces the dichloride complex **324** bearing one such bulky phenoxide ligand<sup>256</sup> (Scheme 68). The dichloride complex can be converted to the corresponding dimethyl complex **325**, which reacts smoothly with 1 equiv. of isocyanides to afford the Zr-C insertion products, namely, the corresponding  $\eta^2$ -iminoacyl compounds. The alkane elimination approach involves the reaction of Cp\*ZrMe<sub>3</sub> with 1 equiv. of 2,6-disubstituted phenol, affording the corresponding dimethyl complexes **326** incorporating one phenoxide ligand. When an excess of the less bulky 2,6-Me<sub>2</sub>C<sub>6</sub>H<sub>3</sub>OH phenol was used, the completely substituted complex Cp\*Zr(2,6-OC<sub>6</sub>H<sub>3</sub>Me<sub>2</sub>)<sub>3</sub> **327** was obtained (Scheme 68). The dichloride complex **324** and tris(phenoxide) complex **327** were tested for ethylene polymerization; upon activation with MAO, the former complex shows high activity similar to that found for classical metallocene catalysts, while the latter is much less active.

The reaction of Cp\*ZrCl<sub>3</sub> with a slight excess of 3 equiv. of sodium benzyl mercaptam leads to the mono-Cp zirconium benzyl thiolate compound **328**<sup>257</sup> (Scheme 69). The solution NMR data are consistent with a symmetric dimer in which two thiolate ligands bridge two Zr centers and the two Cp\* ligands adopt a *cisoid*-geometry. Treatment of **328** with PMe<sub>3</sub> results in the monomeric adduct **329**, whereas the reaction of **328** with MeOH yields the *transoid*-dimer species **330**, which was structurally characterized.

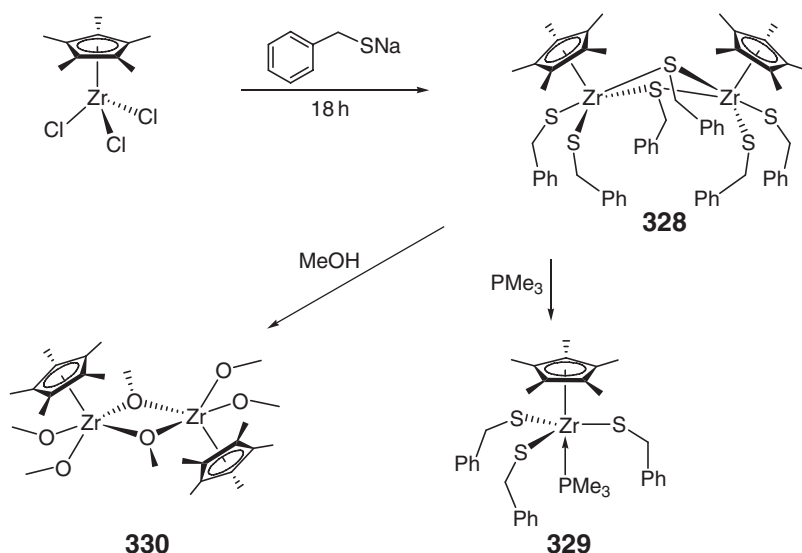
#### 4.08.7.2 Non-functionalized Mono-Cp Complexes Containing Multidentate Ligands

##### 4.08.7.2.1 Complexes containing bidentate amidinate and guanidinate [N<sub>2</sub><sup>-</sup>] ligands

Salt metathesis was employed to synthesize half-sandwich zirconium and hafnium dichloride complexes **331** incorporating the bidentate, mono-anionic benzamidinate ligand<sup>258,259</sup> (Equation (26)). The corresponding zirconium dimethyl and dibenzyl complexes have also been prepared using appropriate alkylating reagents.<sup>260</sup> The zirconium dichloride complex (R = H), upon activation with MAO, are active for both polymerizations of ethylene

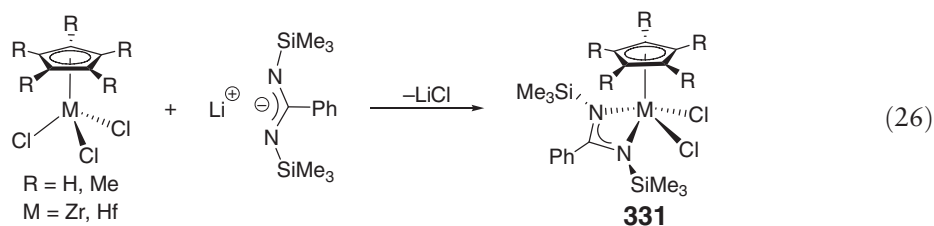


Scheme 68

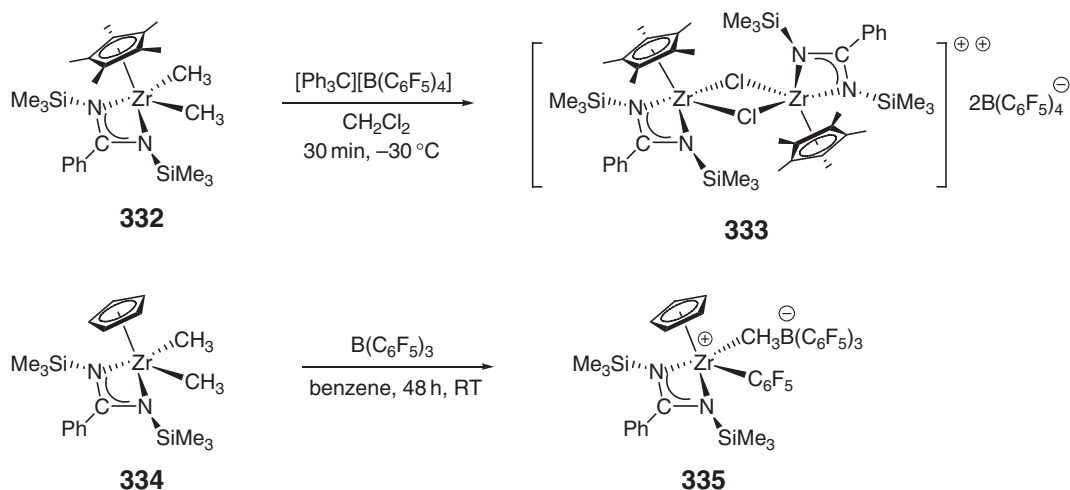


Scheme 69

and propylene; however, the activity and the molecular weight of the resulting polymer are lower than those by the systems Cp<sub>2</sub>ZrCl<sub>2</sub>/MAO or CpZrCl<sub>3</sub>/MAO.

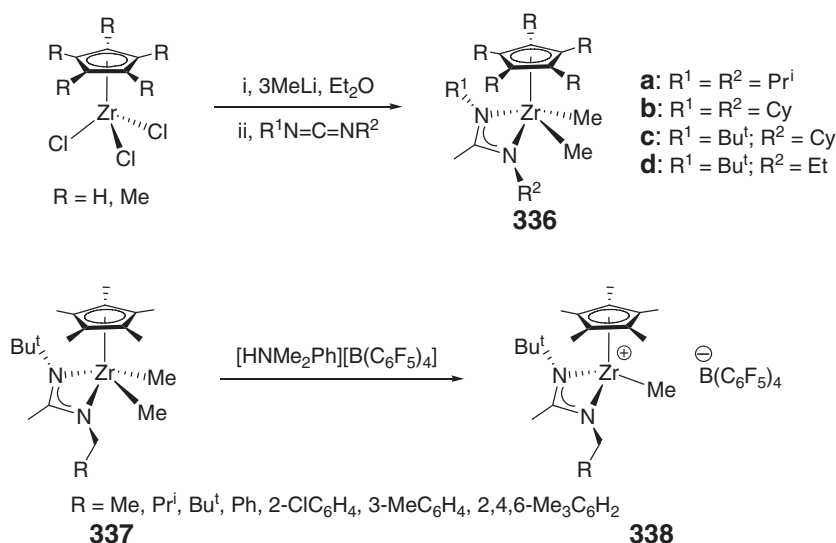


Activation of the mono-Cp\* benzamidinate zirconium dialkyls such as dimethyl **332** with [Ph<sub>3</sub>C][B(C<sub>6</sub>F<sub>5</sub>)<sub>4</sub>] halogenated solvents such as CH<sub>2</sub>Cl<sub>2</sub> results in the formation of Cl<sup>-</sup> abstraction products. In the example shown in Scheme 70, the dicationic bis(μ-Cl) product **333** has been isolated and crystallographically characterized.<sup>261</sup> The



Scheme 70





Scheme 71

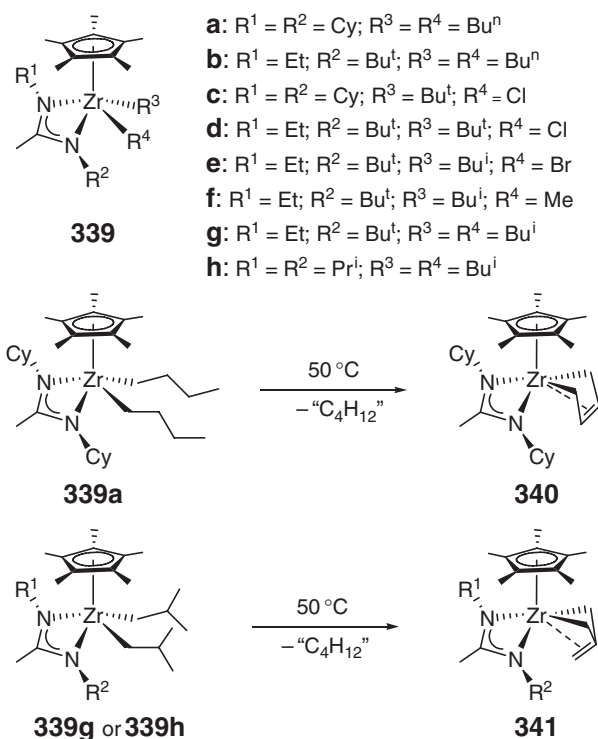
catalyst deactivation occurs also in the reaction carried out in hydrocarbon solvents. Thus, the reaction of the mono-Cp benzamidinate zirconium dimethyl complex **334** with  $\text{B}(\text{C}_6\text{F}_5)_3$  in benzene at ambient temperature results in aryl group transfer to Zr, affording the catalytically inactive perfluorophenylzirconium complex **335**.

Insertion of symmetric or unsymmetric carbodiimides into a Zr–Me bond of  $\text{Cp}^*\text{ZrMe}_3$  or  $\text{Cp}^*\text{ZrMe}_2$ , which can be generated *in situ* by the reaction of the trichloride compounds with 3 equiv. of MeLi at low temperatures, provides a facile access to a variety of half-sandwich zirconium and hafnium methyl complexes **336**<sup>262,263</sup> and **337**<sup>264</sup> incorporating diverse acetamidinate ligands (Scheme 71). The reaction of dimethyl **337** with  $[\text{HNMe}_2\text{Ph}][\text{B}(\text{C}_6\text{F}_5)_4]$  in chlorobenzene at  $-10^\circ\text{C}$  generates the corresponding cationic species **338**.<sup>264</sup> The unsymmetric acetamidinate complexes **338** ( $\text{R} = \text{Me}$  or  $\text{Ph}$ ) effect isospecific, living polymerization of 1-hexene at  $-10^\circ\text{C}$ , but the cationic complex derived from the symmetric acetamidinate complexes such as **336b** ( $\text{R} = \text{Me}$ ,  $\text{R}^1 = \text{R}^2 = \text{Cy}$ ) lacks stereocontrol of polymer microstructure.<sup>262,264</sup> The R group in complex **338** strongly affects the polymerization activity and stereospecificity; for example, when  $\text{R} = \text{Pr}^i$ , the catalyst is much less active and produces atactic polymer, whereas complexes bearing bulky R groups ( $\text{R} = \text{Bu}^t$ , mesityl) are inactive.<sup>264</sup> The Cp-based complexes **336** ( $\text{R} = \text{H}$ ), when activated with  $[\text{HNMe}_2\text{Ph}][\text{B}(\text{C}_6\text{F}_5)_4]$  at  $-10^\circ\text{C}$ , also catalyze the living polymerization of vinylcyclohexane, a sterically more encumbered monomer.<sup>263</sup>

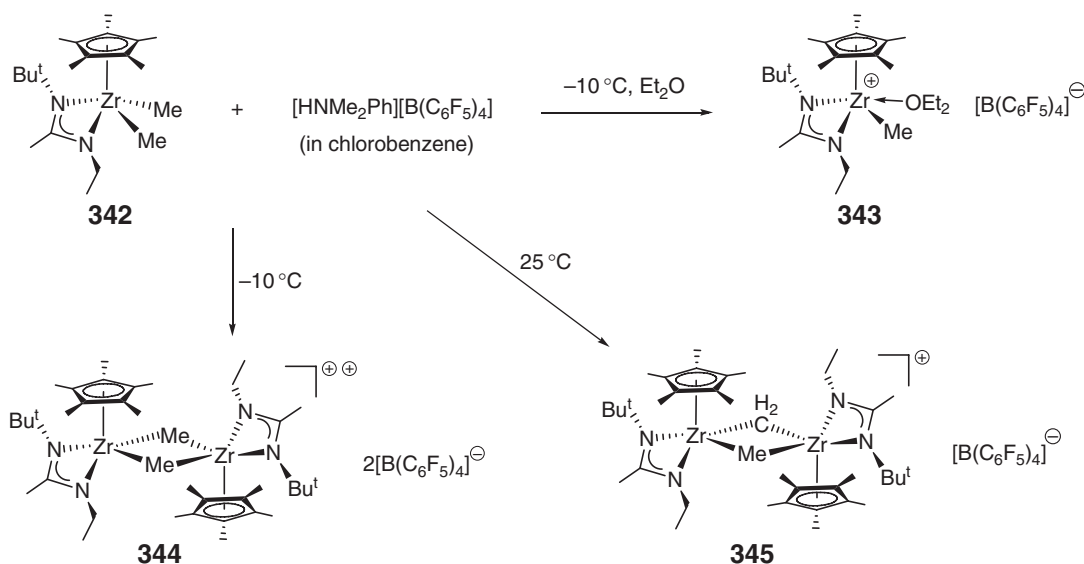
To investigate the thermal stability of mono-Cp\* zirconium acetamidinate complexes bearing alkyl substituents with  $\beta$ -hydrogen, a series of such zirconium complexes **339** has been synthesized (Scheme 72).<sup>265</sup> These complexes are found to be remarkably resistant to  $\beta$ -hydrogen eliminations/abstractions, including the *tert*-butyl derivatives **336c** and **336d**, the former of which is stable in solution to at least  $100^\circ\text{C}$ . There is an apparent preference for alternative hydrogen atom abstractions according to the alkyl substituents; complexes **339a** and **339g/h** bearing isomeric dibutyl substituents ( $\text{Bu}^n$  in **339a** vs.  $\text{Bu}^i$  in **339g/h**) are transformed at elevated temperatures to complexes **340** and **341** which contain the isomeric butadiene and trimethylenemethane  $\text{C}_4$  fragments, respectively (Scheme 72).

Three different types of the structurally characterized cationic complexes have been obtained by crystallization from the reaction of the amidinate zirconium dimethyl complex **342** with  $[\text{HNMe}_2\text{Ph}][\text{B}(\text{C}_6\text{F}_5)_4]$  in chlorobenzene, depending on the conditions<sup>266</sup> (Scheme 73). Thus, the low-temperature crystallization in the presence of a small amount of  $\text{Et}_2\text{O}$  leads to the  $\text{Et}_2\text{O}$ -separated ion pair **343**, whereas in the absence of this Lewis base, the crystallization affords the doubly methyl-bridged dinuclear dication **344** which represents the formal dimerization of the base-free version of the monocation **343** and exhibits unique intramolecular bridging  $\alpha$ -agostic interactions. The characterization of such dinuclear dications indicates the possibility of methyl group exchange within the cationic species occurring in solution and thus methyl–polymeryl transfer occurring during polymerization, providing the basis for the production of stereoblock polyolefins.<sup>267</sup> In contrast to these low-temperature crystallization results, the ambient-temperature crystallization produces the  $\mu\text{-CH}_2$ ,  $\mu\text{-CH}_3$ -bridged dinuclear monocation **345**.

Chemoselective “on-site” functionalization of half-sandwich zirconium and hafnium acetamidinates can be achieved by deprotonation of the dichloride complexes **346** using sterically encumbered bases to produce enolate

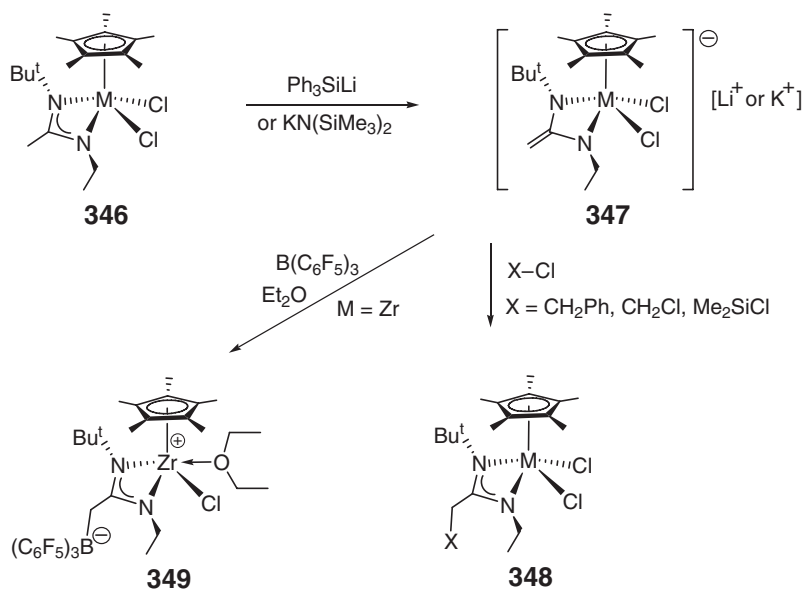


Scheme 72

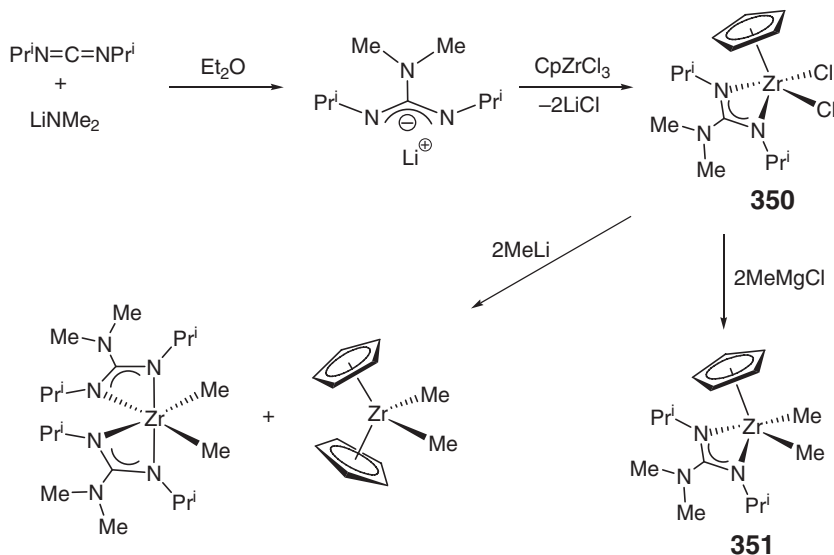


Scheme 73

complexes **347**, followed by subsequent reactions with electrophiles such as  $\text{PhCH}_2\text{Cl}$ ,  $\text{CH}_2\text{Cl}_2$ , and  $\text{Me}_2\text{SiCl}_2$  to give functionalized acetamidinate complexes **348**<sup>268</sup> (Scheme 74). These complexes are not accessible by conventional routes. The reaction of the anionic enolate intermediate **347** with  $\text{B}(\text{C}_6\text{F}_5)_3$  in  $\text{Et}_2\text{O}$  affords the “remotely activated”,  $\text{Et}_2\text{O}$ -stabilized zwitterionic complex **349**.



Scheme 74

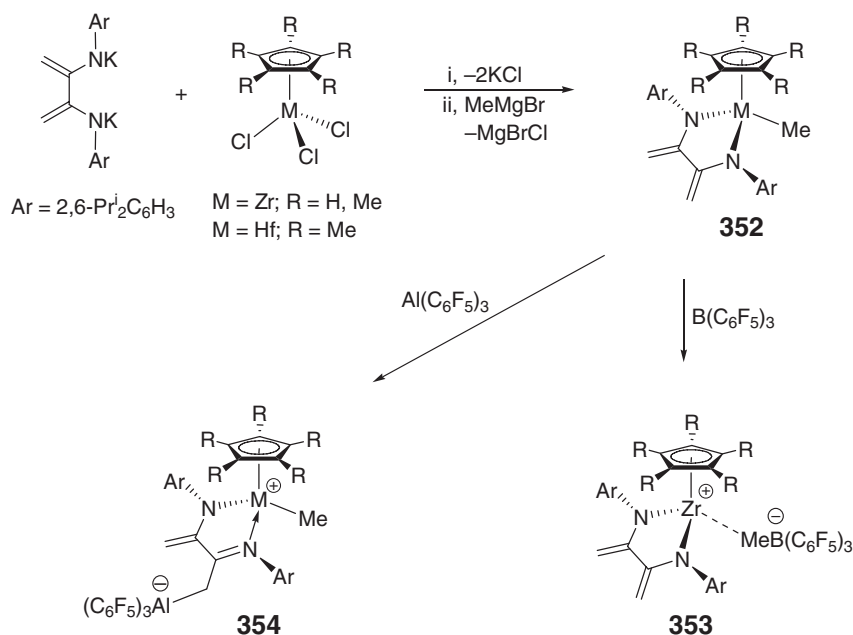


Scheme 75

Treatment of  $\text{CpZrCl}_3$  with the *in situ*-generated guanidinate lithium salt,  $\eta^2\text{-(Pr}^i\text{N)}_2\text{C(NMe}_2\text{)Li}$ , produces mono-Cp guanidinato zirconium dichloride **350** (Scheme 75). The reaction of the dichloride **350** with 2 equiv. of  $\text{MeMgCl}$  affords the corresponding dimethyl derivative **351**, but when treated with 2 equiv. of  $\text{MeLi}$ , complex **350** gives 0.5 equiv. of  $\text{Cp}_2\text{ZrMe}_2$  and 0.5 equiv. of  $[\eta^2\text{-(Pr}^i\text{N)}_2\text{C(NMe}_2\text{)}]_2\text{ZrMe}_2$ .<sup>91</sup>

#### 4.08.7.2.2 Complexes containing other bidentate ligands

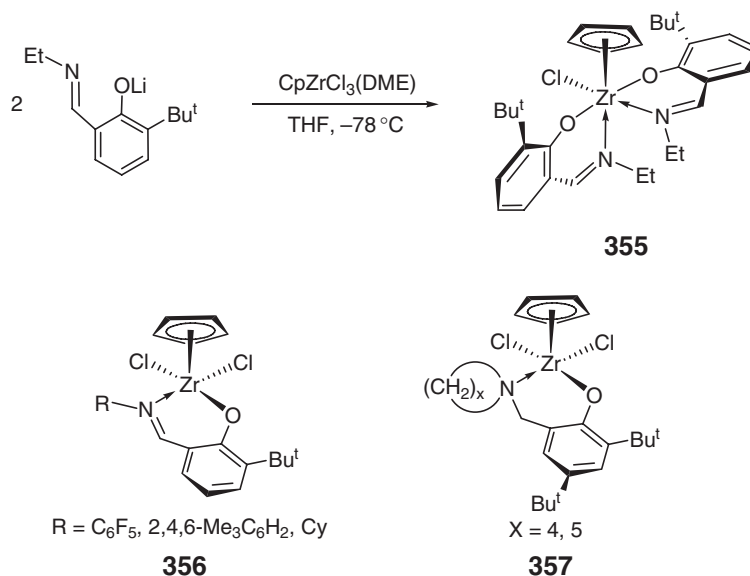
Reaction of dipotassium *N,N'*-(1,2-dimethylene-1,2-ethanediyl)bis(2,6-diisopropylanilide) with  $\text{CpZrCl}_3$  or  $\text{Cp}^*\text{MCl}_3$  (M = Zr, Hf) followed by alkylation with  $\text{MeMgBr}$  produces half-sandwich zirconium and hafnium methyl complexes **352** incorporating the bidentate, dianionic enamide  $\{[N^-, N^-]$  type} ligand<sup>106</sup> (Scheme 76). Activation of these enamido methyl complexes with Lewis acids  $\text{M}(\text{C}_6\text{F}_5)_3$  (M = B, Al) proceeds through two different pathways, dependent on the



Scheme 76

Lewis acid employed. The methyl abstraction occurs using  $\text{B}(\text{C}_6\text{F}_5)_3$  to give associated ion pair **353**, whereas the use of  $\text{Al}(\text{C}_6\text{F}_5)_3$  effects electrophilic addition to the methylene carbon on the enamide ligand backbone to give zwitterionic complex **354**. The ion-paired complexes **353** are inactive for ethylene polymerization, but the zwitterionic complex **354**, the “remotely activated” complex, rapidly consumes ethylene to form polyethylene.

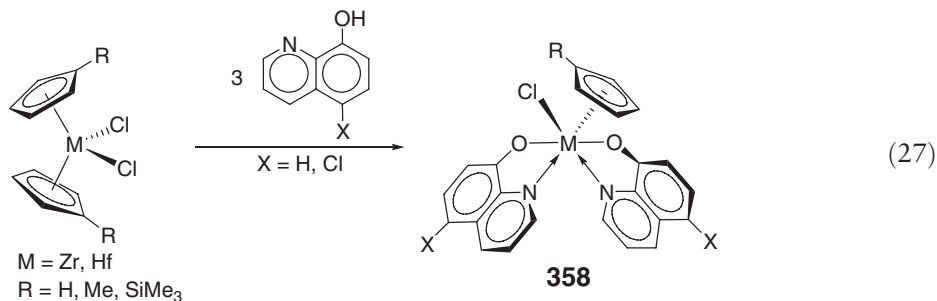
Six-coordinate mono-Cp chloride complex **355** containing two mono-anionic, *ortho*-substituted phenoxy-imine  $\{[O^-, N]\text{-type}\}$  ligands was obtained by salt metathesis involving the reaction of  $\text{CpZrCl}_3(\text{DME})$  and the lithium salt of the ligand in THF (Scheme 77).<sup>269</sup> If the centroid of the Cp ring is considered as a single coordination site, the molecular structure of this complex can be described as octahedral, with a *trans* (O–O), *cis* (N–N), and *cis* (Cl–Cp)



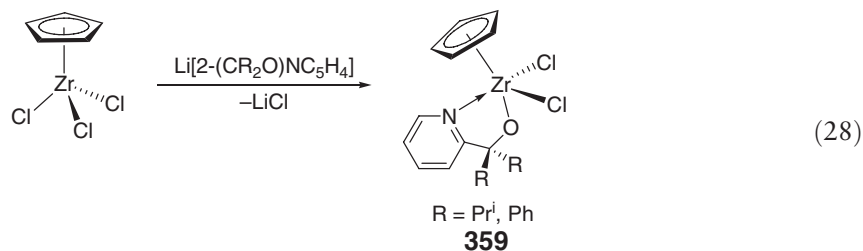
Scheme 77

ligand arrangement. Despite the presence of only one chloride ligand, this complex, when activated with MAO, exhibits high activity for polymerization of ethylene. Five-coordinate mono-Cp dichloride complexes incorporating one *ortho*-substituted phenoxy–“imine” ligand **356** or 2,4-substituted bulky phenoxy–“amine” ligand **357** were also synthesized by the salt metathesis approach.<sup>126</sup> Both types of complexes are active for polymerization of ethylene when activated with MAO.

The reaction of  $(\eta^5\text{-C}_5\text{H}_4\text{R})_2\text{MCl}_2$  ( $\text{M} = \text{Zr}, \text{Hf}$ ;  $\text{R} = \text{H}, \text{Me}, \text{SiMe}_3$ ) with 3 equiv. of 8-hydroxyquinoline (QH) or 5-chloro-8-hydroxyquinoline ( $\text{Q}^{\text{Cl}}\text{H}$ ) in polar solvents such as  $\text{CH}_2\text{Cl}_2$  produces mono-Cp bis(8-hydroxyquinolinato)-zirconium and hafnium chloride complexes  $(\eta^5\text{-C}_5\text{H}_4\text{R})\text{MCl}(\text{Q})_2$  and  $(\eta^5\text{-C}_5\text{H}_4\text{R})\text{MCl}(\text{Q}^{\text{Cl}})_2$  **358** via cleavage of an M–Cp bond<sup>270</sup> (Equation (27)). The crystal structure of the mono-Cp hafnium complex incorporating two 5-chloro-8-hydroxyquinolinato ligands shows the approximate octahedral hafnium center with a *trans* (O–O), *cis* (N–N), and *cis* (Cl–Cp) ligand arrangement. When considering that the Cp ligand occupies three coordination sites at Hf, the eight-coordinate structure is best described as approximately dodecahedral.



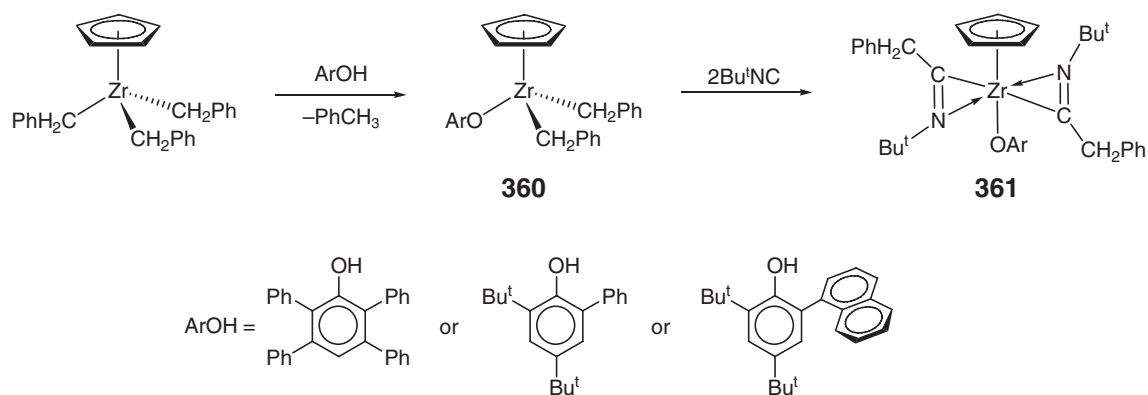
Half-sandwich zirconium complexes **359** with mixed Cp and mono-anionic bidentate alkoxy–pyridine  $\{[O^-, N]\text{-type}\}$  ligands were obtained by the straightforward salt metathesis reaction<sup>271</sup> (Equation (28)). The single crystal analysis reveals that the complex ( $\text{R} = \text{Ph}$ ) adopts a pseudo-square-pyramidal structure in which the Cp ligand is asymmetrically bonded and the pyridylalkoxide is bidentate as expected. Upon activation with MAO, these complexes catalyze ethylene polymerization to produce high molecular weight polyethylene with narrow molecular weight distributions.



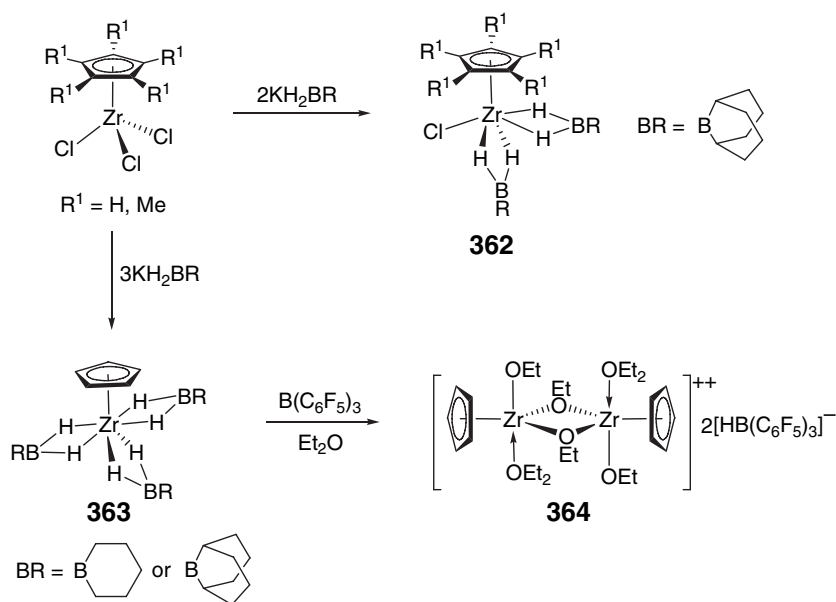
Mono-Cp zirconium dibenzyl complexes **360** bearing one bulky phenoxide ligand, which were prepared conveniently from alkane elimination involving the reaction of  $\text{CpZr}(\text{CH}_2\text{Ph})_3$  with 1 equiv. of a neutral phenol ligand (Scheme 78), react with *tert*-butylisocyanide in hydrocarbon solvents to initially produce the mono(iminoacyl) intermediate followed by the bis(iminoacyl) complexes **361**.<sup>272</sup> Solution NMR data are consistent with the  $\eta^2\text{-C}, N$ -binding for the iminoacyl ligands, which is confirmed by the solid-state structures. Rotations of the iminoacyl and aryloxy ligands in complexes **361** [except for the 2-(1-naphthyl) derivative] are facile at ambient temperature.

The reaction of  $\text{CpZrCl}_3$  or  $\text{Cp}^*\text{ZrCl}_3$  with 2 equiv. of  $\text{K}[\text{H}_2\text{BC}_8\text{H}_{14}]$  yields half-sandwich cyclic organohydroborate complexes **362** in which the  $\text{H}_2\text{BC}_8\text{H}_{14}$  moiety serves as a mono-anionic, bidentate ligand coordinated to Zr.<sup>273</sup> (Scheme 79). On the other hand, treatment of  $\text{CpZrCl}_3$  with 3 equiv. of  $\text{KH}_2\text{BR}$  ( $\text{R} = \text{C}_5\text{H}_{10}, \text{C}_8\text{H}_{14}$ ) in diethyl ether produces the tris(organohydroborate) mono-Cp complexes  $\text{CpZr}[(\mu\text{-H})_2\text{BR}]_3$  **363**. Reactions of complexes **363** with  $\text{B}(\text{C}_6\text{F}_5)_3$  in diethyl ether produce the same salt, a doubly bridged dicationic complex  $[\text{CpZr}(\text{OEt})(\text{OEt}_2)(\mu\text{-OEt})_2[\text{HB}(\text{C}_6\text{F}_5)_3]_2]$  **364**.

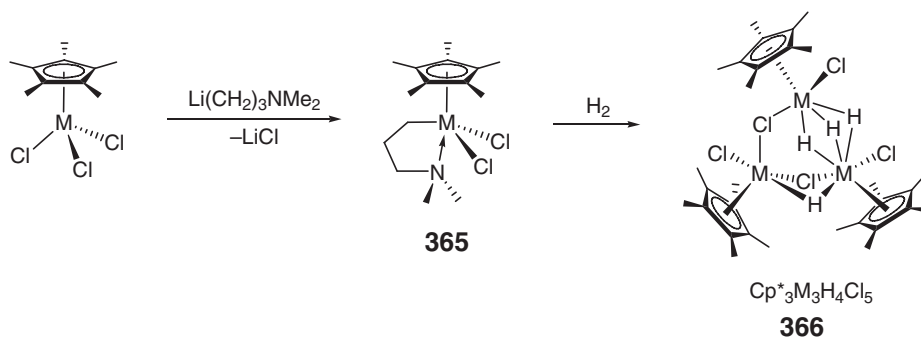
Half-sandwich zirconium and hafnium dichloride complexes **365** incorporating the bidentate *N,N*-dimethylaminopropyl ligand were obtained from alkylation reactions of  $\text{Cp}^*\text{MCl}_3$  and the lithiated ligand<sup>274</sup> (Scheme 80). Hydrogenolysis of these dichlorides results in the formation of the polyhydride complexes



Scheme 78



Scheme 79



Scheme 80

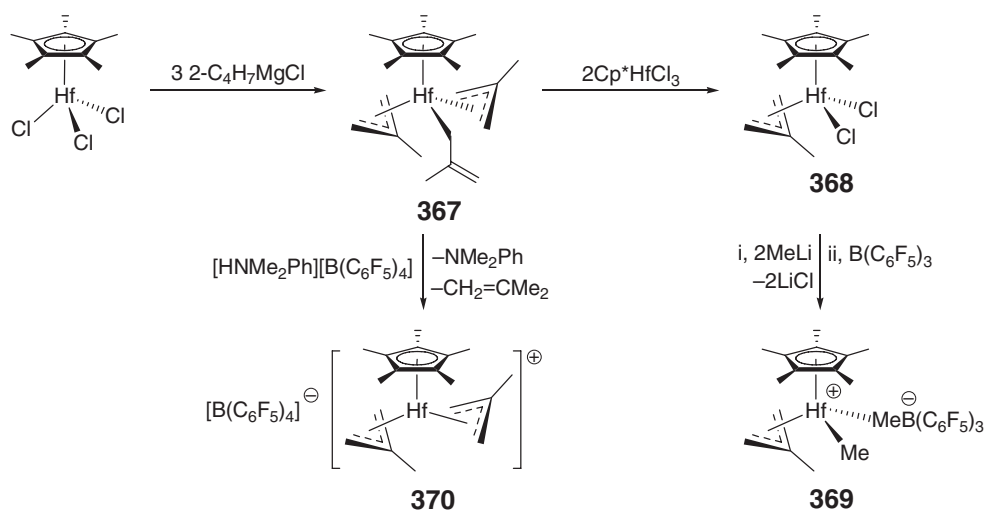
$\text{Cp}^*_3\text{M}_3(\mu\text{-H})_4(\mu\text{-Cl})_2\text{Cl}_3$  **366**. The crystal structure of the hafnium polyhydride complex reveals a fully asymmetric trinuclear structure with three widely differing Hf–Hf distances but the hydrides themselves could not be located.

Mono- $\text{Cp}^*$  zirconium complexes incorporating chelating pyrimidinethiolate, oxypyrimidine, and oxypyridine ligands have been prepared by salt metathesis involving the reaction of  $\text{Cp}^*\text{ZrCl}_3$  with lithium thiolate or alkane elimination involving the reaction of  $\text{Cp}^*\text{ZrMe}_3$  with 6-methyl-2-hydroxypyridine or 2,4-dimethyl-6-hydroxypyrimidine.<sup>275</sup> In the latter alkane elimination reactions, the methyl groups are completely replaced by the hydroxyl groups regardless of the stoichiometric ratios employed. The zirconium mono- $\text{Cp}^*$  bis(thiolate) complexes  $\text{Cp}^*\text{ZrCl}(\eta^2\text{-SR})_2$  complexes are rigid in solution at room temperature, whereas the mono- $\text{Cp}^*$  trisubstituted oxypyridine and oxypyrimidine complexes show fluxional behavior in solution. Mono- $\text{Cp}$  zirconium and hafnium complexes bearing three bidentate diethylcarbamate ligands,  $\text{CpM}(\eta^2\text{-O}_2\text{CNEt}_2)_3$  ( $\text{M} = \text{Zr}, \text{Hf}$ ), were synthesized by either the ligand-exchange reaction of 0.5 equiv. of  $\text{Cp}_2\text{Mg}$  with homoleptic zirconium or hafnium diethylcarbamates,  $\text{M}(\text{O}_2\text{CNEt}_2)_4$ , or that of  $\text{Fe}(\text{O}_2\text{CNEt}_2)_2$  with  $\text{Cp}_2\text{M}$  in the appropriate stoichiometric ratio.<sup>276</sup> The analogous mono- $\text{Cp}$  zirconium dichloride incorporating one bidentate carbamoyl ligand bound to Zr through both carbamoyl oxygens (i.e.,  $\kappa^2\text{-O}, \text{O}'$ -coordination),  $\text{CpZrCl}_2[\eta^2\text{-C}_5\text{H}_3(\text{CONH}\text{CMe}_3)_2](\text{THF})$ , was synthesized by salt metathesis.<sup>277</sup>

#### 4.08.7.2.3 Complexes containing tri-, tetra-, and pentadentate ligands

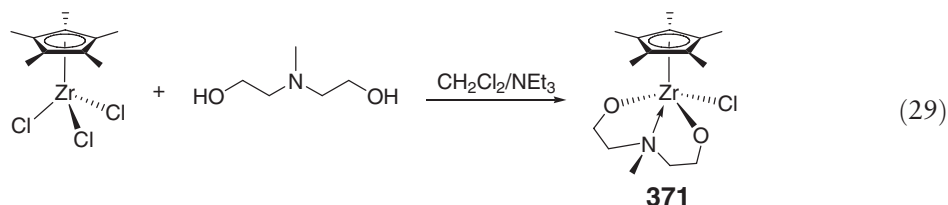
The reaction of  $\text{Cp}^*\text{HfCl}_3$  with 3 equiv. of  $(2\text{-C}_4\text{H}_7)\text{MgCl}$  yields the tris(2-methylallyl) hafnium mono- $\text{Cp}^*$  complex **367** in which two of the allyl ligands are bound to Hf in an  $\eta^3$ -fashion and the third in an  $\eta^1$ -mode (Scheme 81).<sup>278</sup> The monoallyl hafnium dichloride **368** was obtained conveniently by comproportionation of the tris(allyl) complex **367** with  $\text{Cp}^*\text{HfCl}_3$ . The dichloride **368** can be readily alkylated with 2 equiv. of  $\text{MeLi}$  to give the dimethyl derivative, which reacts with  $\text{B}(\text{C}_6\text{F}_5)_3$  to generate the corresponding zwitterionic complex **369**; this species readily polymerizes ethylene but shows no activity toward propylene. The reaction of the tris(allyl) complex **367** with  $[\text{HNMe}_2\text{Ph}][\text{B}(\text{C}_6\text{F}_5)_4]$  proceeds through attack on the nucleophilic allyl methylene group and elimination of isobutene to give bis(allyl) hafnium cation **370**, which oligomerizes propylene to atactic oligomers.

Derivatization of  $\text{Cp}^*\text{ZrCl}_3$  can be achieved in a straightforward fashion by treatment of  $\text{Cp}^*\text{ZrCl}_3$  with 1 equiv. of *N*-methyl-*N,N*-diethanolamine in the presence of triethylamine, affording the mono- $\text{Cp}^*$  zirconium chloride **371** bearing a bis(alkoxo)nitrogen-donor  $[\text{O}^-, \text{N}, \text{O}^-]$  tridentate ligand<sup>279</sup> (Equation (29)). The molecular structure of this complex with regard to whether it is a monomeric or dimeric species is currently unknown. Nevertheless, when activated with large excess of MAO, this complex is active for polymerization of ethylene, but producing polymers



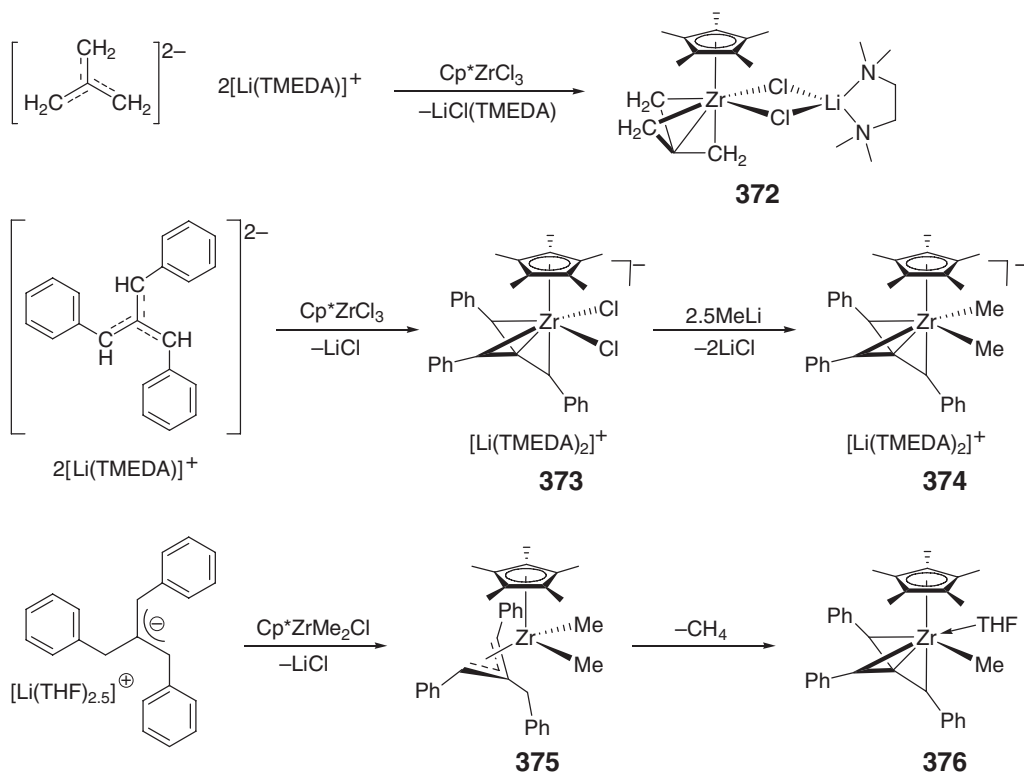
Scheme 81

with very broad molecular weight distributions ( $\overline{M}_w/\overline{M}_n = 11\text{--}38$ ) at all polymerization temperatures investigated (30–70 °C), characteristic of multi-site catalysis.



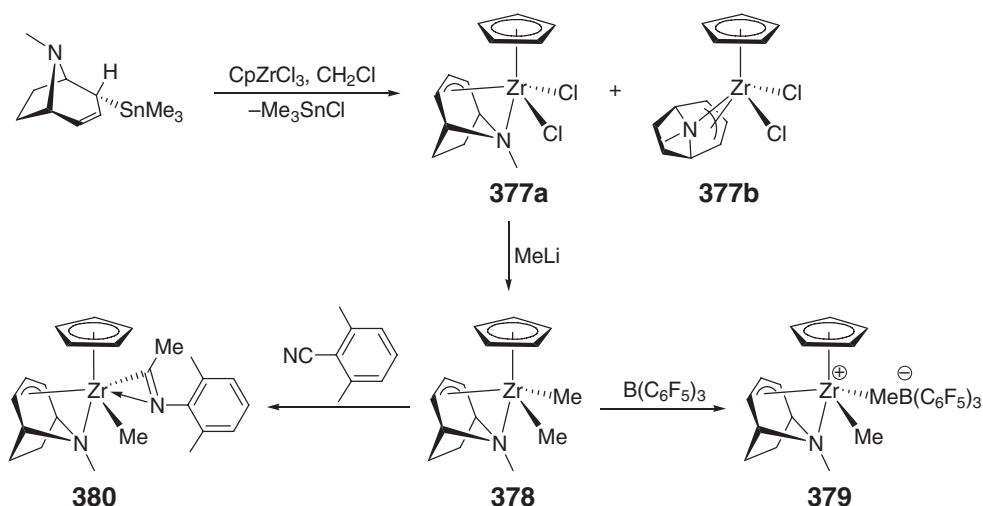
The reaction of  $\text{Cp}^*\text{ZrCl}_3$  with the dilithio salt of trimethylenemethane yields the mono- $\text{Cp}^*$  zirconium chloride **372**<sup>280</sup> as a zwitterionic adduct of  $\text{LiCl}(\text{TMEDA})$  (Scheme 82). The molecular structure shows that the dianionic trimethylenemethide ligand binds to Zr in a pyramidal  $\eta^4$ -fashion with the central carbon directed away from Zr. The analogous reaction of  $\text{Cp}^*\text{ZrCl}_3$  with the dilithio salt of tribenzylidenemethane affords, however, the mono- $\text{Cp}^*$  zirconium dichloride **373** as a discrete salt, consisting of the zirconate anion with the *syn*-coordinated dianionic tribenzylidenemethide ligand, accompanied by the tetrahedral  $[\text{Li}(\text{TMEDA})_2]$  counteranion. The Cp derivative of **373** was obtained in the same manner. Direct alkylation of these chloride complexes has proved to be difficult, and the best result was obtained when the dichlorozirconate **373** was treated with 2.5 equiv. of MeLi to give the corresponding dimethyl derivative **374** in only 10% yield.<sup>281</sup> Subsequently, a unique strategy was developed for the synthesis of the neutral alkyl complex. Thus, the reaction of  $\text{Cp}^*\text{ZrMe}_2\text{Cl}$  with *endo-endo*- $\text{Li}[\text{PhCH}_2\text{C}(\text{CHPh})_2]$  yields the corresponding dimethyl zirconium allyl species **375**, which undergoes elimination of methane via  $\sigma$ -bond metathesis to produce the desired methyl derivative **376** stabilized by coordination of THF. Upon activation with large excess of MAO, the chloride complexes **372** and **373** are active catalysts for polymerization of ethylene, co-polymerization of ethylene/1-hexene, and cyclopolymerization of 1,5-hexadiene.<sup>281</sup>

Transmetalation between  $\text{CpZrCl}_3$  and the *endo*-stannylated tropidine, with concomitant elimination of  $\text{Me}_3\text{SnCl}$ , yields mono- $\text{Cp}$  zirconium dichloride **377**<sup>282</sup> (Scheme 83), bearing the  $\eta^4$ -tropidinyl ligand which functions as a



Scheme 82

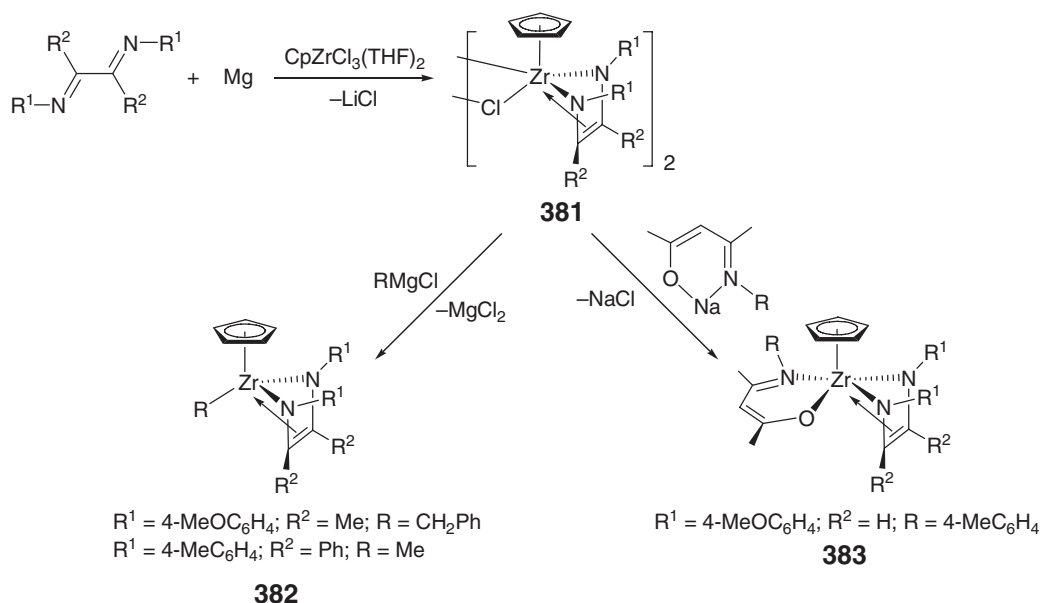




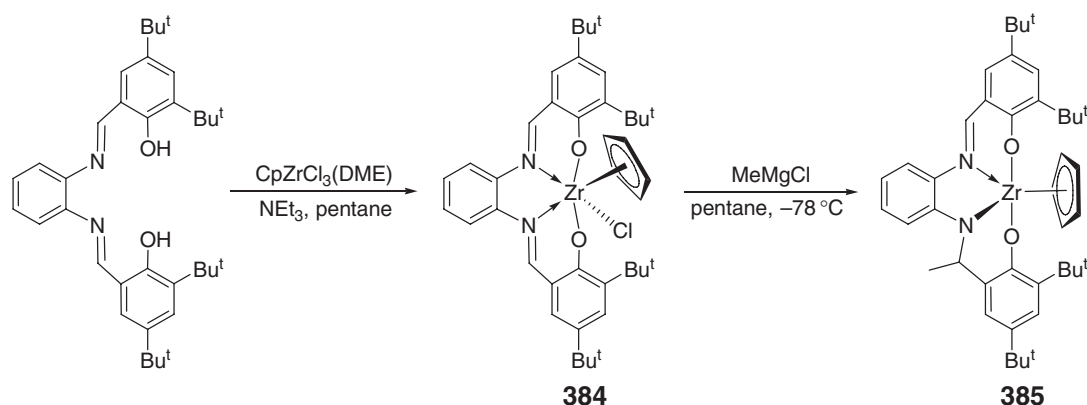
Scheme 83

$\sigma^2$ -(amine),  $\pi^4$ -(allyl) bicyclic ligand. Complex **377** was obtained as a mixture of two isomers, and the major isomer **377a** was isolated as an orange crystalline solid. Alkylation of the dichloride with MeLi affords the dimethyl derivative **378**, which reacts with  $\text{B(C}_6\text{F}_5)_3$  to generate the corresponding cationic species **379**. Reaction of dimethyl **378** with an aryl isonitrile gives the insertion product,  $\eta^2$ -iminoacyl complex **380**. The system **378**/ $\text{B(C}_6\text{F}_5)_3$  is active for ethylene polymerization, whereas the activity of the dichloride **377**/MMAO is considerably higher and similar to that observed for  $\text{Cp}_2\text{ZrCl}_2$ /MMAO. On the other hand, the activity of the analogous zirconium dichloride incorporating two such  $\eta^4$ -tropidynyl ligands, which was obtained by the reaction of  $\text{ZrCl}_4$  with 2 equiv. of the *endo*-stannylated tropidine,<sup>283</sup> is substantially lower under similar conditions.

Treatment of  $\text{CpZrCl}_3(\text{THF})_2$  with 1 equiv. of magnesium in the presence of 1,4-diaza-1,3-dienes yields the chloro-bridged dimeric half-sandwich zirconium complexes **381** bearing a heterodiene ligand that adopts a  $\sigma^2, \pi$ -coordination geometry with a *supine*-conformation (Scheme 84).<sup>284</sup> Alkylation of this dimer with Grignard reagents



Scheme 84

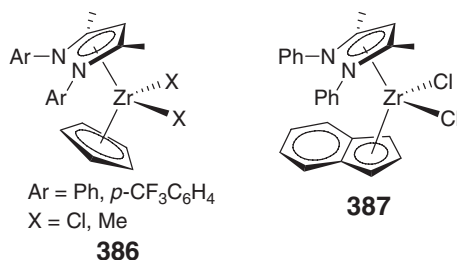


Scheme 85

affords the methyl and benzyl zirconium complexes **382**. On the other hand, treatment of the chloro-bridged dimer with chelating acetylacetonate imine sodium salts leads to the monomeric mono-Cp zirconium complex **383** incorporating two chelating ligands, one dianionic,  $\sigma^2, \pi$ -coordinated heterodiene ligand with *supine*-conformation, and the other a mono-anionic, nearly planar acetylacetonate imine ligand.

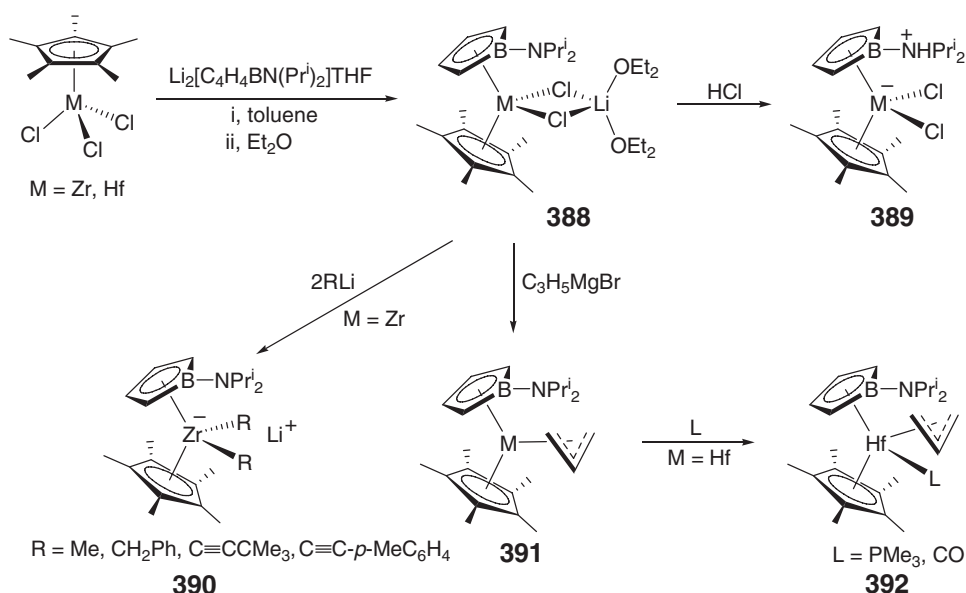
Zirconium mono-Cp chloride **384** incorporating a tetradentate, dianionic Schiff base ligand was obtained by the reaction of  $\text{CpZrCl}_3(\text{DME})$  and the neutral ligand in the presence of trimethyl amine (Scheme 85).<sup>269</sup> Attempted alkylation at metal of this chloride with  $\text{MeMgCl}$  results in alkylation of one of the  $\text{C}=\text{N}$  bonds of the Schiff base ligand, giving the bis(phenoxy)–imino–amido (i.e., a trianionic ligand) zirconium complex **385**. Both types of complexes are active for polymerization of ethylene when activated with MAO, but the activity of the amido complex **385** is roughly twice that of the imino complex **384** under comparable conditions.

Mono-Cp **386** and indenyl **387** zirconium complexes bearing a  $\beta$ -diketiminate ligand were prepared by salt metathesis.<sup>93</sup> Interestingly, the  $\beta$ -diketiminate ligand serves as a  $\pi$ -ligand, adopting a distorted,  $\eta^5$ -binding mode in these mixed Cp and  $\beta$ -diketiminate complexes, as confirmed by the solid-state structure of the indenyl derivative **387**, rather than the commonly seen  $\eta^2$ - $\sigma$ -coordination for this class of ligands.

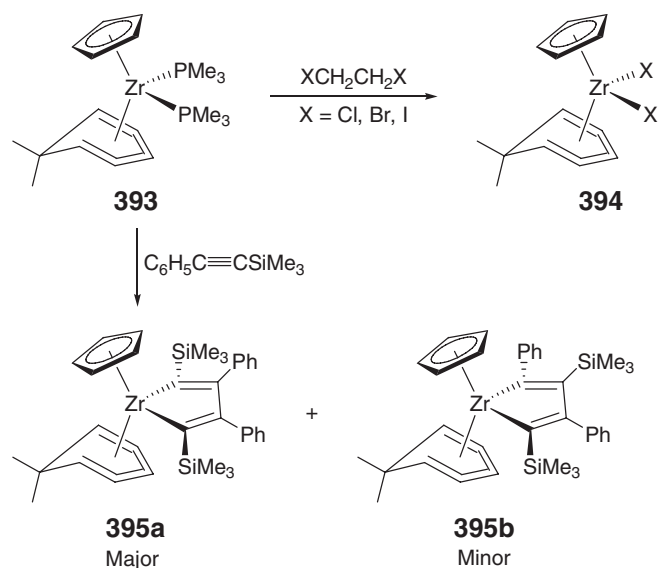


Treatment of  $\text{Cp}^*\text{MCl}_3$  ( $\text{M} = \text{Zr}, \text{Hf}$ ) with  $\text{Li}_2[\text{C}_4\text{H}_4\text{BN}(\text{Pr}^i)_2] \cdot \text{THF}$  in toluene yields the mixed  $\eta^5\text{-Cp}^*/\eta^5$ -aminoborollide mono-chloride complexes **388**, crystallographically characterized as  $\text{LiCl}(\text{Et}_2\text{O})$  adducts<sup>285</sup> (Scheme 86). The metric parameters found in the zirconium complex indicate  $p_\pi$ - $p_\pi$  interactions between the boron and nitrogen atoms so that its resonance structures can be drawn accordingly. Protonation of the borollide nitrogen with 1 equiv. of  $\text{HCl}$  affords zwitterionic dichlorides **389** with the negative charge placed on the metal center. The dialkylzirconium lithium salts **390** are obtained from the reaction of the zirconium complex **388** with 2 equiv of alkyl lithium reagents, whereas the treatment of both the zirconium and hafnium complex **388** with allylmagnesium bromide leads to the neutral allyl complexes **391**.<sup>286</sup> Addition of donor ligands, such as  $\text{PMe}_3$  and  $\text{CO}$ , to the hafnium allyl complex gives the corresponding base adducts **392**. The neutral allyl complexes **391** are active catalysts for polymerization of ethylene at room temperature.

Cyclopentadienyl–cyclohexadienyl zirconium(IV) complexes were prepared by the reaction of  $\text{Cp}(6,6\text{-dmch})\text{Zr}(\text{PMe}_3)_2$  (**393**:  $6,6\text{-dmch} = \eta^5\text{-6,6-dimethylcyclohexadienyl}$ ) with dihaloalkanes  $\text{XCH}_2\text{CH}_2\text{X}$ , yielding  $\text{Cp}(6,6\text{-dmch})\text{ZrX}_2$  (**394**:  $\text{X} = \text{Cl}, \text{Br}, \text{I}$ ; Scheme 87).<sup>287</sup> These complexes allow a comparison of the bonding and properties of  $\eta^5$ -pentadienyl and  $\eta^5$ -cyclopentadienyl ligands in the same high oxidation state metal complexes.



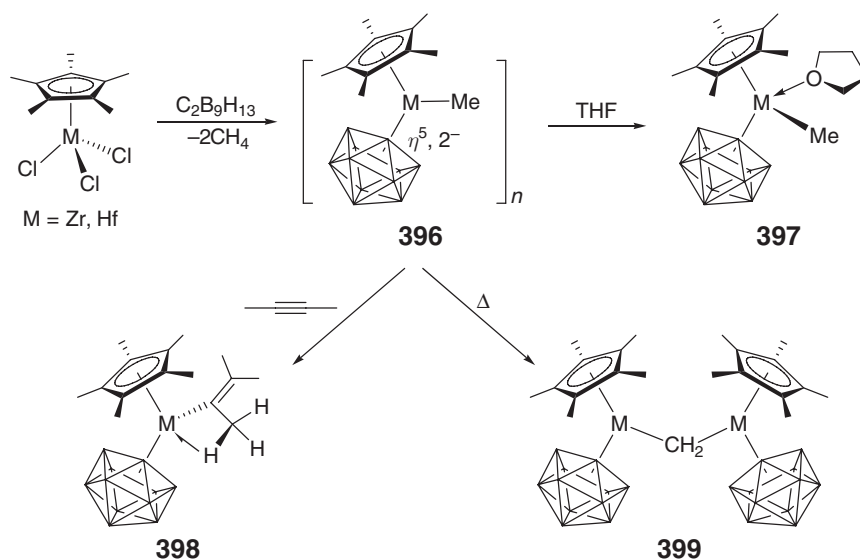
Scheme 86



Scheme 87

Unlike the Cp<sub>2</sub>ZrX<sub>2</sub> analogs, these Cp(6,6-dmch)ZrX<sub>2</sub> molecules are intensely colored, contributable to a 6,6-dmch ligand-to-metal charge-transfer band. Furthermore, the Cp(6,6-dmch)ZrX<sub>2</sub> molecules have a considerably less stable HOMO that is pentadienyl-based and an essentially unchanged metal-based LUMO, as compared with the Cp<sub>2</sub>ZrX<sub>2</sub> analogs. The Zr(II) precursor **393** can be used for the synthesis of the Zr(IV) derivatives incorporating the mixed η<sup>5</sup>-pentadienyl/η<sup>5</sup>-cyclopentadienyl ligand set. For example, complex **393** couples with 2 equiv. of the alkyne PhC≡CSiMe<sub>3</sub> to give the zirconacyclopentadiene complex **395** as a mixture of two isomers.<sup>288</sup>

Double protolysis of Cp<sup>\*</sup>MMe<sub>3</sub> (M = Zr, Hf) with the neutral carborane C<sub>2</sub>B<sub>9</sub>H<sub>13</sub> gives the mono-Cp<sup>\*</sup> zirconium and hafnium monomethyl complexes **396** of stoichiometry [Cp<sup>\*</sup>(C<sub>2</sub>B<sub>9</sub>H<sub>11</sub>)MMe]<sub>n</sub> (Scheme 88).<sup>289</sup> The C<sub>2</sub>B<sub>9</sub>H<sub>11</sub> moiety in the complex serves as a dianionic, six-electron dicarbollide ligand, the hafnium complex is crystallographically characterized to be an unsymmetric dinuclear structure with an unusual bridging dicarbollide ligand, which



Scheme 88

may be represented as the ion pair  $[\text{Cp}^*\text{HfMe}_2][\text{Cp}^*(\eta^5\text{-C}_2\text{B}_9\text{H}_{11})\text{Hf}(\eta^2\text{-C}_2\text{B}_9\text{H}_{11})]$ .<sup>290</sup> Nevertheless, complexes **396** are catalysts for polymerization of ethylene and oligomerization of propylene; they are Lewis acids and form monomeric adducts **397** with donor bases such as THF and pyridine. They also undergo rapid, single insertion of 2-butyne yielding monomeric alkenyl complexes **398**. The molecular structure of **398** ( $\text{M} = \text{Zr}$ ) reveals an  $\eta^5$ -bonded dicarbollide ligand and a normal bent-metallocene geometry at Zr with the  $\text{Cp}^*(\text{C}_2\text{B}_9\text{H}_{11})\text{Zr}$  unit being sterically similar to a  $\text{Cp}^*_2\text{Zr}$  unit; the alkenyl ligand is distorted by a  $\beta$ -agostic interaction that may inhibit further acetylene insertions. Thermolysis of complexes **396** (45 °C, 2 h for Zr; 4–75 °C, 2 d for Hf) results in methane elimination and formation of the methylene-bridged dinuclear complexes **399**.

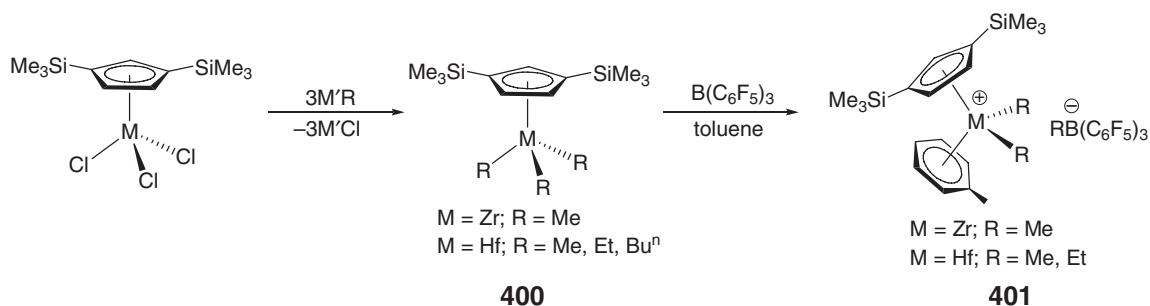
#### 4.08.7.3 Silylated Mono-Cp Complexes

Substituting one or more of the cyclopentadienyl ring hydrogen atoms or alkyl groups with heteroatoms or functional groups dramatically affects the reactivity and stability of the mono-Cp type of complexes. Owing to their significant synthetic and catalytic applications, the synthesis and development of functionalized mono-Cp group 4 complexes have represented one of the most significant advances in the early transition metal organometallic chemistry. One of the most common types of functionalization is the one that leads to silyl-functionalized mono-Cp complexes, the subject of the coverage in this section.

##### 4.08.7.3.1 Bis(trimethylsilyl)cyclopentadienyl ( $\text{Cp}^*$ ) complexes

By introducing suitable bulky, stabilizing substituents such as trimethylsilyl groups onto the spectator Cp ligand that supports the complex, alkyl complexes carrying  $\beta$ -hydrogen atoms become isolable. Thus, neutral bis(trimethylsilyl)-mono-Cp zirconium and hafnium trialkyl complexes  $\text{Cp}^*\text{MR}_3$  [**400**:  $\text{M} = \text{Zr, Hf}$ ;  $\text{Cp}^* = 1,3\text{-(SiMe}_3)_2\text{C}_5\text{H}_3$ ] are readily accessible from the reaction of the trichloride precursor  $\text{Cp}^*\text{MCl}_3$  with appropriate alkylating reagents such as RLi or EtMgBr (Scheme 89).<sup>291</sup> Treatment of the trimethyl complexes with  $\text{B}(\text{C}_6\text{F}_5)_3$  in toluene yields stable and isolable mono-Cp<sup>+</sup> dimethyl cations **401** stabilized by toluene coordination to the metal. The molecular structure of the hafnium arene complex confirms the formation of the ion pair  $[\text{Cp}^*\text{HfMe}_2(\eta^6\text{-toluene})][\text{MeB}(\text{C}_6\text{F}_5)_3]$ , which is well separated by an  $\eta^6$ -bound toluene molecule. The analogous hafnium diethyl toluene complex is thermally unstable; attempts to isolate this complex led to formation of the ethylene-bridged dication  $[\{\text{Cp}^*\text{HfEt}(\text{toluene})\}(\mu\text{-C}_2\text{H}_4)]_2^{2+}$ .

$\text{Cp}^*\text{MCl}_3$  compounds are very versatile precursors for a variety of mono-Cp<sup>+</sup> complexes with ligands of diverse hapticity. For example, mono-Cp<sup>+</sup> diene complexes  $\text{Cp}^*\text{Zr}(\eta^4\text{-butadiene})\text{Cl}$  **402** were obtained by the reaction of  $\text{Cp}^*\text{MCl}_3$  with internally substituted 1,4-butadiene in the presence of Na/Hg.<sup>292</sup> Subsequent alkylation of **402** with appropriate alkylating reagents leads to the corresponding  $\eta^3$ -allyl **403**<sup>292</sup> and  $\eta^2$ -benzyl **404** ( $\text{M} = \text{Zr}$ ) or  $\eta^1$ -benzyl

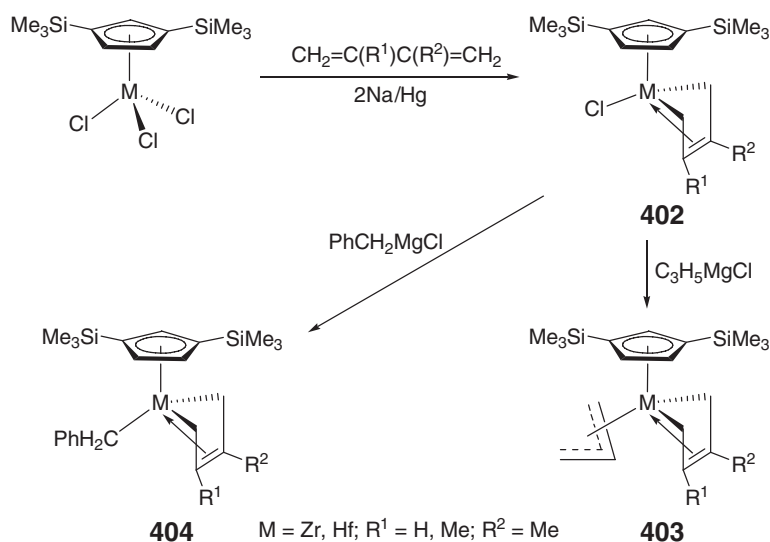


Scheme 89

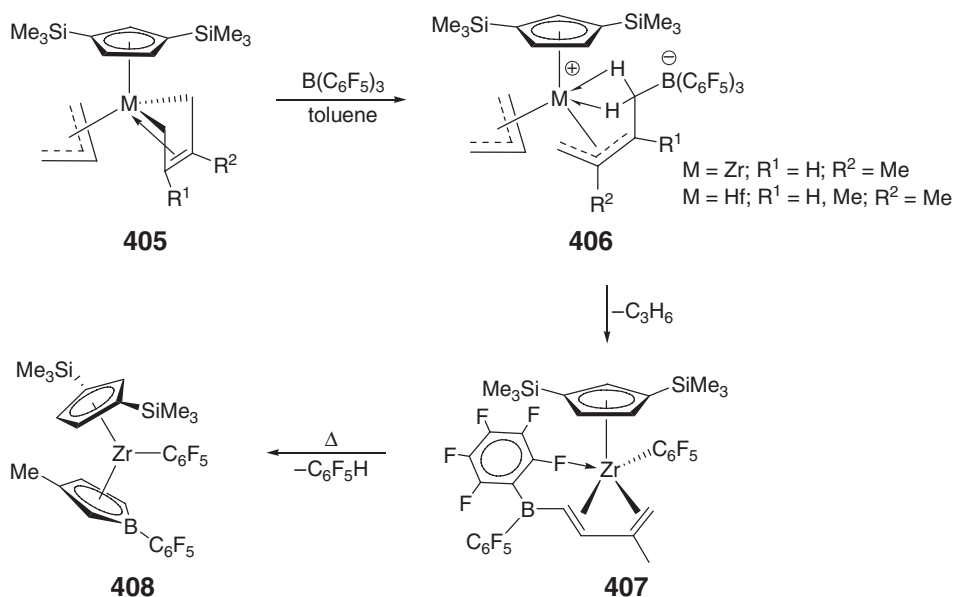
**404** ( $M = \text{Hf}$ )<sup>293</sup> complexes (Scheme 90). Analogous mono-Cp'' diazadiene (1,4-diphenyl-2,3-dimethyl-1,4-diazabuta-1,3-diene) complexes with an additional allyl, benzyl, or methyl ligand were also synthesized in a similar manner.<sup>294</sup>

The molecular structure of the zirconium allyl complex **405** ( $R^1 = R^2 = \text{Me}$ ) features essentially a square-pyramidal geometry about Zr with an apical  $\eta^5\text{-Cp''}$  and the  $\eta^3$ -allyl and  $\eta^4$ -butadiene ligands occupying the basal positions; both the allyl and butadiene ligands are oriented in the *supine*-configuration with respect to Cp''.<sup>292</sup> Allyl butadiene complexes of this type are attacked by  $\text{B}(\text{C}_6\text{F}_5)_3$  exclusively at the less-substituted terminal carbon atom of the diene ligand to give zwitterionic complexes **406** (Scheme 91), which readily polymerize ethylene to high molecular weight polymers.<sup>295</sup> The zirconium complex is thermally unstable and eliminates  $\text{C}_3\text{H}_6$  via C–H activation and concomitant migration of a  $\text{C}_6\text{F}_5$  group from boron to zirconium, yielding complex **407**; further elimination of  $\text{C}_6\text{F}_5\text{H}$  from **407** under controlled conditions affords a sandwich zirconium pentafluorophenyl complex **408** consisting of a Cp'' and a dianionic pentafluorophenyl-substituted borole ligand.<sup>296</sup> The reaction of  $\text{B}(\text{C}_6\text{F}_5)_3$  with the related benzyl complexes gives the corresponding zwitterionic complexes as a result of the benzyl abstraction, except for the isoprene Zr derivative whose reaction results in both the diene and benzyl ligand abstraction. The isoprene Zr product can undergo further elimination of toluene via C–H activation and concomitant migration of a  $\text{C}_6\text{F}_5$  group from boron to zirconium to afford the same complex **407**.<sup>293</sup>

As discussed above, the first pathway of the decomposition of the complex type **407** yields the zirconium Cp''/borole sandwich complex type **408**. When stabilized with diethyl ether, this type of mixed sandwich complexes,  $\text{Cp''Zr}(\text{C}_6\text{F}_5)(\text{OEt}_2)[\eta^5\text{-(3-RC}_4\text{H}_3\text{BC}_6\text{F}_5)]$  ( $R = \text{H, Me}$ ), react with nitriles  $\text{R}^1\text{CN}$  ( $R^1 = \text{Me, Bu}^t$ ) in aromatic solvents to produce the corresponding adducts  $\text{Cp''Zr}(\text{C}_6\text{F}_5)(\text{NCR}^1)[\eta^5\text{-(3-RC}_4\text{H}_3\text{BC}_6\text{F}_5)]$  in high yields.<sup>297</sup> Insertion of

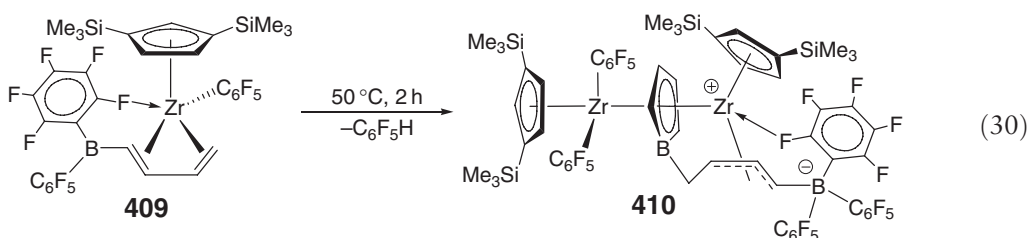


Scheme 90



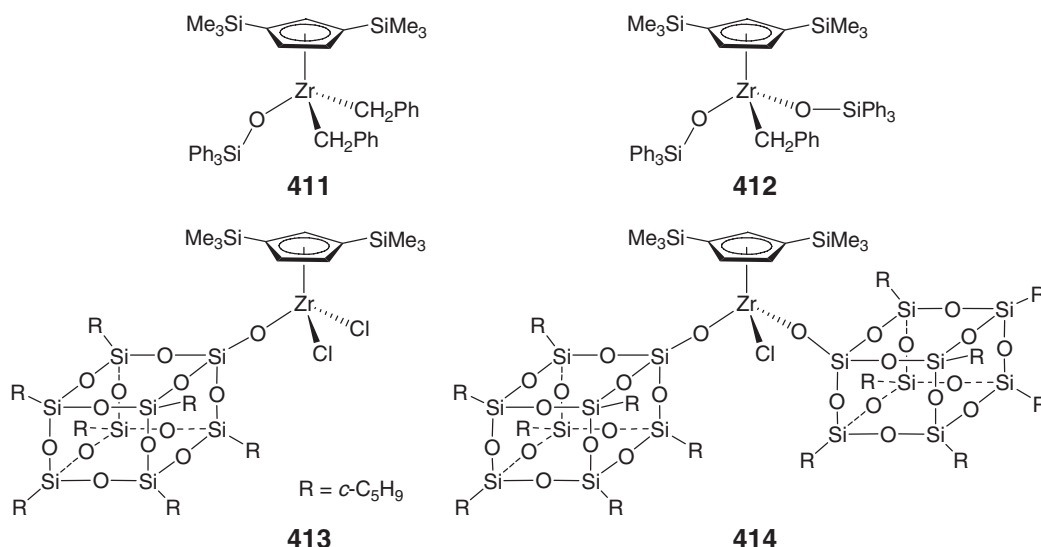
Scheme 91

isocyanides into the  $\text{Zr}-\text{C}_6\text{F}_5$  bond is also possible at ambient temperature, giving rise to the corresponding  $\eta^2$ -iminoacyl complexes. There is a second pathway associated with the decomposition of the complex **407** type, leading to a different product. Specifically, the analogous boryldiene complex  $\text{Cp}''\text{Zr}(\text{C}_6\text{F}_5)[\eta^4\text{-CH}_2\text{CHCHCHB}(\text{C}_6\text{F}_5)_2]$  **409** decomposes smoothly via elimination of  $\text{C}_6\text{F}_5\text{H}$  at  $50^\circ\text{C}$  in toluene to give the triple-decker complex  $\text{Cp}''\text{Zr}_2(\text{C}_6\text{F}_5)_2[\mu\text{-}\eta^5\text{:}\eta^5\text{-C}_4\text{H}_4\text{BCH}_2\text{-}\eta^3\text{:}\kappa F\text{-CHCHCHB}(\text{C}_6\text{F}_5)_3]$  **410** (Equation (30)), involving elimination of  $\text{C}_6\text{F}_5\text{H}$  and a complete transfer of all three  $\text{C}_6\text{F}_5$  groups of one  $\text{B}(\text{C}_6\text{F}_5)_3$  molecule.<sup>298</sup> This triple-decker complex features a  $\text{Zr}_2\text{C}_4\text{B}$  core, a zwitterionic structure, and an unusually strong  $\text{Zr}-\text{F}$  donor interaction. The first decomposition pathway, leading to **408**, seems to be specific to bulky Cp ligands such as  $\text{Cp}''$ , but the second pathway to tripledeckers can occur with Cp, methyl-Cp, and trimethylsilyl-Cp, besides  $\text{Cp}''$ .



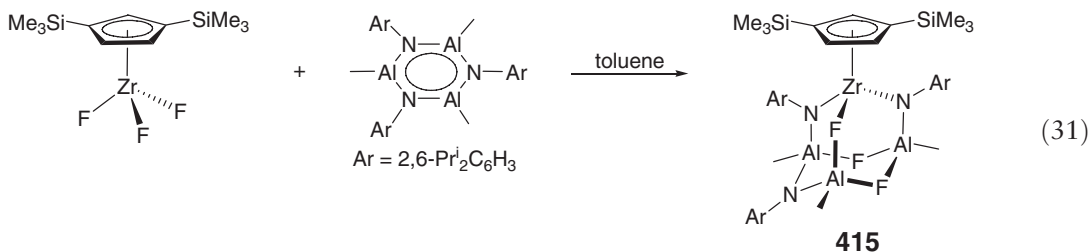
Half-sandwich  $\text{Cp}''$  zirconium siloxy and silsesquioxane complexes have been synthesized, serving as soluble model systems for silica-supported heterogeneous group 4 olefin polymerization catalysts. Thus, protolysis of  $\text{Cp}''\text{Zr}(\text{CH}_2\text{Ph})_3$  with  $\text{Ph}_3\text{SiOH}$  gives either triphenylsiloxy bis(benzyl) complex **411** or bis(triphenylsiloxy) monobenzyl complex **412**, depending on the stoichiometric ratio of the two reagents (Scheme 92).<sup>299</sup> On the other hand, salt metathesis involving the reaction of  $\text{Cp}''\text{ZrCl}_3$  with the silsesquioxane thallium salt in 1 : 1 and 1 : 2 stoichiometric ratios yields the corresponding silsesquioxane dichloride complex **413** and monochloride complex **414**, respectively. The half-sandwich  $\text{Cp}''$  zirconium complex containing a tridentate silsesquioxane ligand was also synthesized. When activated with MAO, all complexes are active for ethylene polymerization, including the complex without any alkyl or chloro ligands; this observation indicates that the silsesquioxane and siloxy ligands are easily substituted by MAO.

The reaction of  $\text{Cp}''\text{ZrF}_3$  with an alumazene,  $[\text{MeAlN}(\text{2,6-Pr}_i^2\text{C}_6\text{H}_3)]_3$ , leads to fluorine–nitrogen exchange and the formation of the bis(amido) zirconium fluoride **415**<sup>300</sup> (Equation (31)). This reaction proceeds with activation of  $\text{Zr}-\text{F}$  bonds, providing a unique route to aluminum-containing mixed zirconium amido fluorides. The molecular structure



Scheme 92

of this complex is that of isostructural adamantane-like cages; the core is built from one  $\text{Al}_3\text{F}_2\text{N}$ , one  $\text{ZrAl}_2\text{FN}_2$ , and two  $\text{ZrAl}_3\text{F}_2\text{N}$  six-membered rings in a *chair*-conformation, with bridging F and N atoms.

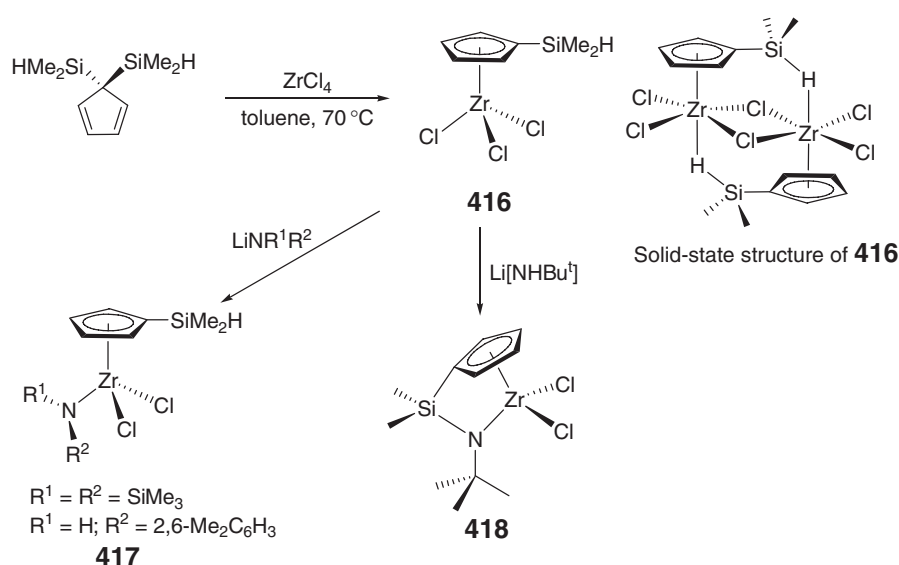


#### 4.08.7.3.2 Hydrido- and chlorosilyl mono-Cp complexes

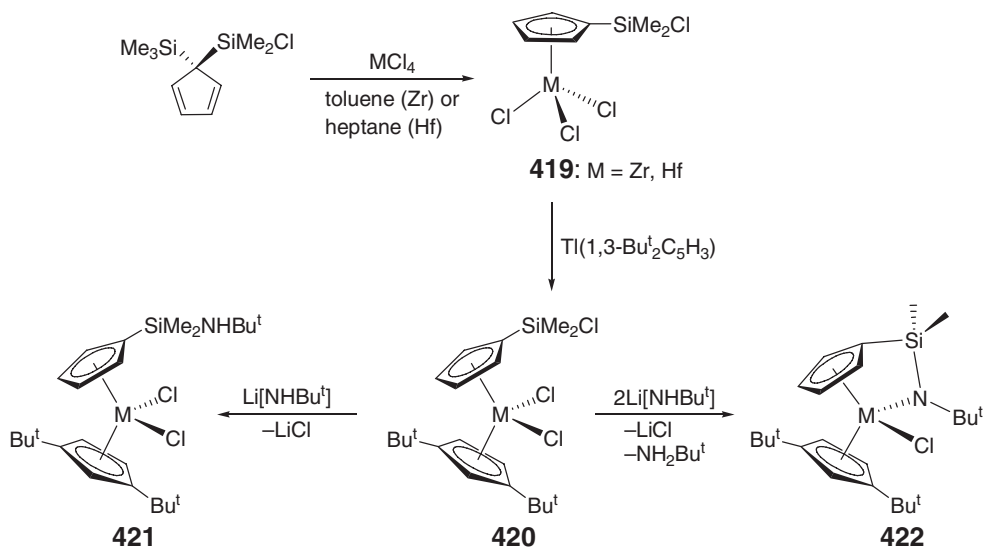
The reaction of  $\text{ZrCl}_4$  with 1 equiv. of  $\text{C}_5\text{H}_4(\text{SiMe}_2\text{H})_2$  in toluene produces an air sensitive monohydrodimethylsilyl-substituted Cp zirconium trichloride  $[\eta^5\text{-C}_5\text{H}_4(\text{SiMe}_2\text{H})]\text{ZrCl}_3$  **416**<sup>301</sup> (Scheme 93). In the solid state, complex **416** exists as a dimer through two  $\mu$ -chloro bridges and Zr–H–Si agostic interactions. Reactions of **416** with lithium amides in hexane give different products depending on the basicity of the nitrogen atom and the steric nature of the amido substituents. Thus, treatment of **416** with  $\text{LiN}(\text{SiMe}_3)_2$  or  $\text{LiNH}(2,6\text{-Me}_2\text{C}_6\text{H}_3)$  induces the normal nucleophilic ligand substitution reaction leading to the corresponding amido zirconium dichlorides **417**; however, the reaction of **416** with  $\text{LiNHBu}^t$  affords the *ansa*-Cp/silylamido zirconium dichloride **418**, presumably via a hypervalent silicon hydride intermediate.

Monochlorodimethylsilyl-substituted Cp trichlorides  $[(\eta^5\text{-C}_5\text{H}_4\text{SiMe}_2\text{Cl})\text{MCl}_3]$  (**419**:  $\text{M} = \text{Zr}$ ,<sup>302</sup>  $\text{Hf}$ <sup>303</sup>) were obtained by the reaction of  $\text{MCl}_4$  with 1 equiv. of disilylated Cp ligand  $\text{C}_5\text{H}_4(\text{SiClMe}_2(\text{SiMe}_3))$  (Scheme 94). These trichloro complexes are suitable precursors readily leading to mixed bis(Cp) metallocene derivatives. For example, the reaction of trichloro **419** with 1 equiv. of  $\text{Tl}(1,3\text{-Bu}^t_2\text{C}_5\text{H}_3)$  gives the mixed metallocene complexes **420** with one Cp bearing the chlorodimethylsilyl functionality.<sup>303</sup> The Si–Cl bond within this functionality reacts selectively with 1 equiv. of  $\text{LiNHBu}^t$  to yield the amidosilyl–Cp complexes **421**. The same reaction, but with 2 equiv. of  $\text{LiNHBu}^t$ , leads to the *ansa*-Cp/silylamido zirconium and hafnium monochloro complexes **422**; there are four non-equivalent ligands attached to the metal center in these complexes, and they can be considered as chiral-at-metal complexes.

The reactivity of the zirconium trichloride **419** bearing a chlorodimethylsilyl-substituted Cp ligand toward various nucleophilic reagents has been extensively investigated. As with **416**, the reactions of **419** with lithium amides in hexane produce diverse products. For example, its reaction with 1 equiv. of  $\text{LiN}(\text{SiMe}_3)_2$  gives the monoamido



Scheme 93

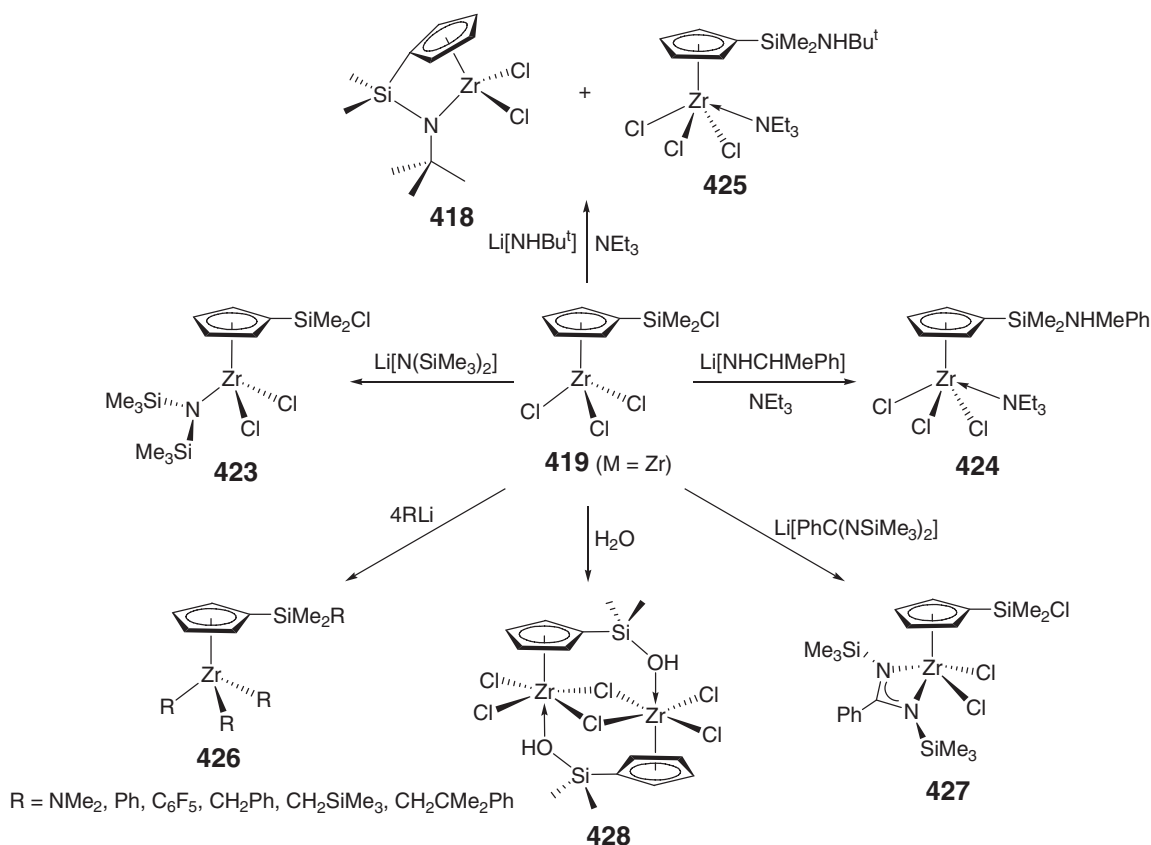


Scheme 94

zirconium dichloride **423** with the chlorosilyl functionality on the Cp ring remaining intact (Scheme 95), while the reaction with  $\text{LiNHCH}(\text{Me})\text{Ph}$  in the presence of  $\text{NEt}_3$  leads to the Cp-ring substitution product **424**.<sup>304</sup> The same reaction but with  $\text{LiNH}^t\text{Bu}$  in the presence of  $\text{NEt}_3$  is also different, affording a mixture of the *ansa*-Cp/silylamido zirconium dichloride **418** and the Cp-ring substitution product **425**.

Complete substitution of all four chloro ligands in complex **419** is readily accomplished by its reactions with 4 equiv. of appropriate nucleophilic lithium reagents (or 2 equiv. of  $\text{Mg}(\text{CH}_2\text{Ph})_2(\text{THF})_2$ ), yielding fully alkylated or amidated zirconium trialkyl or triamido complexes **426**.<sup>305</sup> (Scheme 95). The structurally characterized tribenzyl complex **426** ( $\text{R} = \text{CH}_2\text{Ph}$ ) displays three different benzyl ligands: a distorted  $\eta^2$ -benzyl group, a normal  $\eta^1$ -benzyl group, and a benzyl ligand with an intermediate coordination mode. Treatment of **419** with 1 equiv. of lithium benzamidinate affords the corresponding half-sandwich zirconium dichloride **427** with a bidentate, mono-anionic benzamidinate ligand. Lastly, the reaction of **419** with the weak nucleophile  $\text{H}_2\text{O}$  gives the dimeric silanol species **428**,<sup>306</sup> which has been crystallographically characterized and features two distorted octahedral Zr units linked by two Cl and OH bridges.

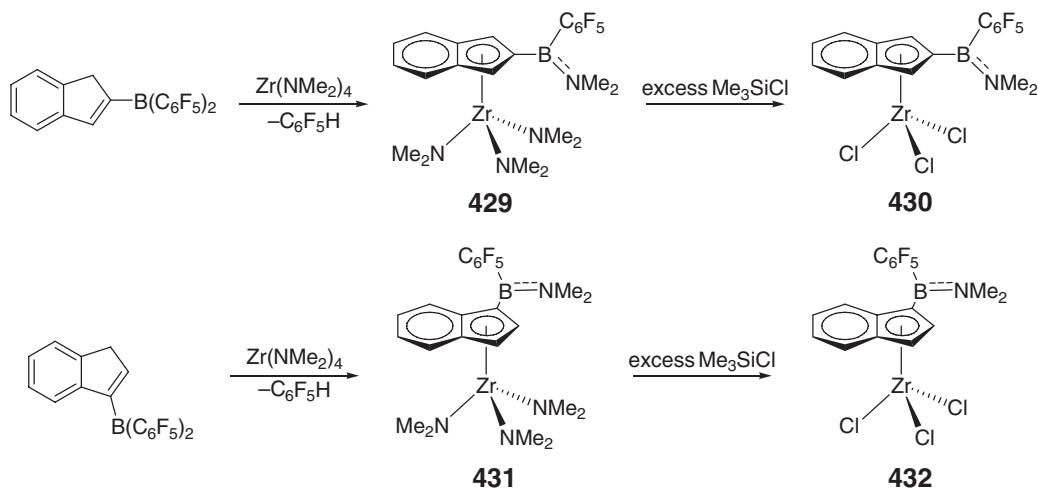




Scheme 95

#### 4.08.7.4 Boryl and Borato Mono-Cp Complexes

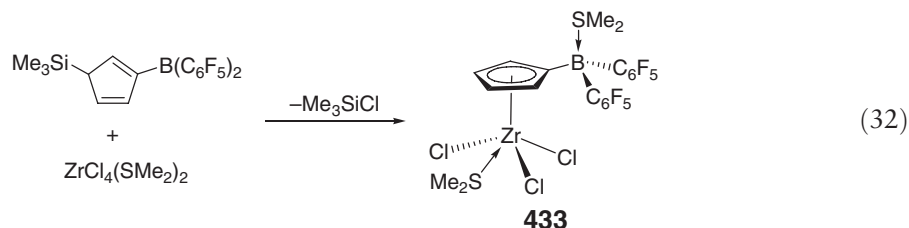
Aminolysis of  $\text{Zr}(\text{NMe}_2)_4$  with 2- $\text{B}(\text{C}_6\text{F}_5)_2$ -substituted indene at room temperature was found to be accompanied by an unexpected exchange of one  $\text{B}-\text{C}_6\text{F}_5$  substituent by  $\text{NMe}_2$ , affording the indenyl half-sandwich zirconium amido complex **429**<sup>307</sup> (Scheme 96). Treatment of the triamide **429** with excess  $\text{Me}_3\text{SiCl}$  gives the corresponding trichloride



Scheme 96

**430.** The regioisomeric 1- $\text{B}(\text{C}_6\text{F}_5)_2$ -substituted indene reacts with  $\text{Zr}(\text{NMe}_2)_4$  in an identical manner, affording **431**, and the subsequent treatment with excess  $\text{Me}_3\text{SiCl}$  yields the corresponding trichloride **432**. In the presence of low concentrations of  $\text{AlEt}_3$ , the trichloride complex **430** is active for polymerization of ethylene, whereas under comparable conditions, the mixture of  $(\text{Ind})\text{ZrCl}_3$  is inactive.

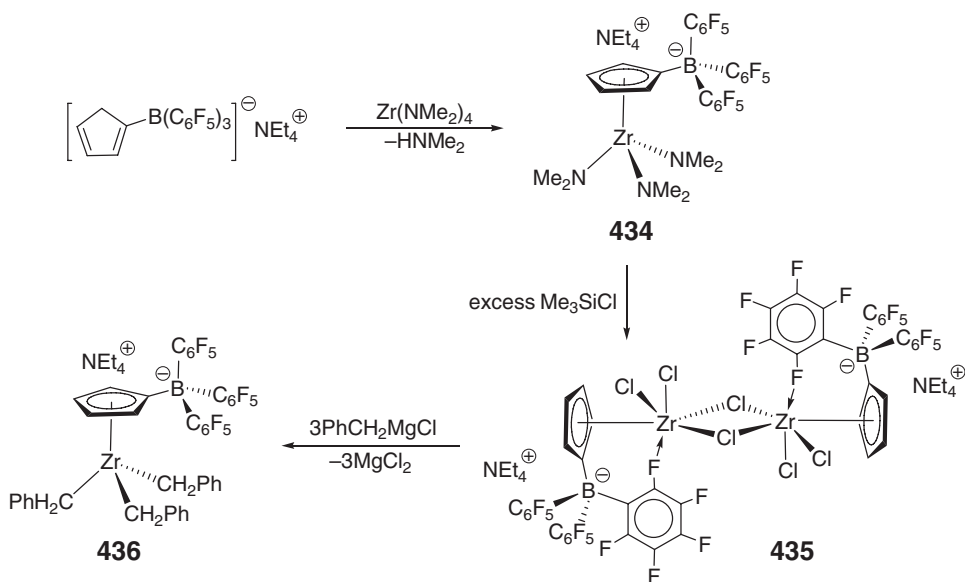
A general approach for preparation of bis(pentafluorophenyl)boryl-substituted cyclopentadienyl half-sandwich zirconium complexes is through the reaction of the trimethylsilyl derivative of the bis(pentafluorophenyl)boryl-substituted cyclopentadiene and  $\text{ZrCl}_4(\text{SMe}_2)_2$ <sup>308</sup> (Equation (32)). The trichloride product **433** from this reaction is a versatile precursor leading to many other derivatives by either replacing the coordinated  $\text{SMe}_2$  with other bases such as pyridine or substituting one of the chloride ligands with a different anionic ligand such as Cp or Ind. In the latter substitution reaction, sandwich complexes with mixed Cp-type ligands are readily obtainable.



Protonation of  $\text{Zr}(\text{NMe}_2)_4$  with the ammonium salt of the  $\text{B}(\text{C}_6\text{F}_5)_3$ -substituted cyclopentadiene,  $[\text{NEt}_4][\text{C}_5\text{H}_5\text{B}(\text{C}_6\text{F}_5)_3]$ , cleanly affords the borato-Cp half-sandwich zirconium triamido complex as an ammonium salt (**434**,<sup>309</sup> Scheme 97). Compound **434** reacts with excess  $\text{Me}_3\text{SiCl}$  to give the corresponding trichloride **435**, which exists as a doubly chloro-bridged dimer in the solid state as characterized crystallographically. The octahedral geometry is completed by a relatively strongly coordinated *o*-F atom of  $\text{C}_6\text{F}_5$ . Alkylation of the trichloride with  $\text{PhCH}_2\text{MgCl}$  produces the tribenzyl derivative **436**.

#### 4.08.7.5 Complexes of Mono-Cp Bearing Neutral Pendant Donors

Mono-Cp complexes supported by the Cp ligands bearing neutral pendant, heteroatom-containing sidearms – the  $\eta^5:\eta^1$  chelating ligand – fundamentally differ from those discussed under section 8.8, where the Cp pendant arms are anionic in nature and covalently bound to the metal center. Complexes discussed in this section belong to those with



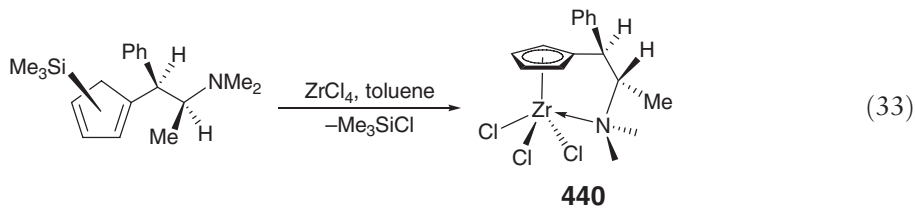
Scheme 97

neutral pendant donor groups that form dative bonds to the metal; often these bonds exhibit fluxional behavior in solution.

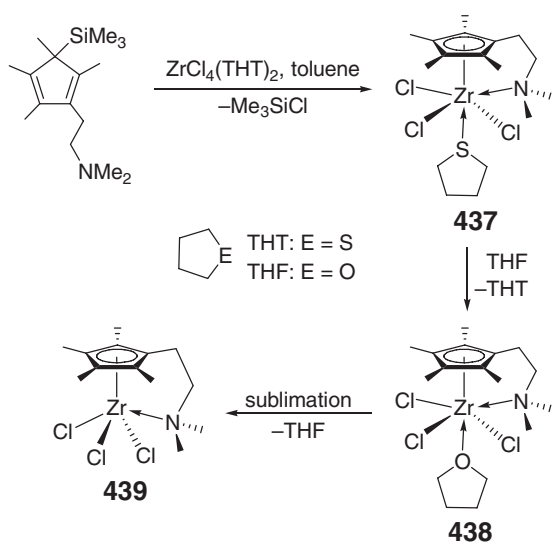
#### 4.08.7.5.1 Complexes with pendant *N*-donors

The reaction of the trimethylsilyl derivative of the substituted Cp ligand having a pendant amine sidearm with  $\text{ZrCl}_4(\text{THT})_2$  (THT = tetrahydrothiophene) produces half-sandwich zirconium trichloride complex **437** (Scheme 98).<sup>310</sup> The crystal structure of this THT adduct shows the approximate octahedral Zr center with its coordination sphere being occupied by an  $\eta^5$ -substituted Cp ligand, an  $\eta^1$ -amine donor group, three chloro ligands, and a THT molecule. The coordinated THT solvent molecule can be readily displaced by THF to give the THF adduct **438**, which can further lose the THF molecule under high-vacuum sublimation conditions to afford the base-free trichloride **439**. In the solid-state structure, the five-coordinate half-sandwich complex **439** surprisingly has a monomeric structure, not the usual chloro-bridged dimer: If one considers the substituted Cp centroid as occupying a single coordination site, its coordination polyhedron is a tetragonal pyramid.

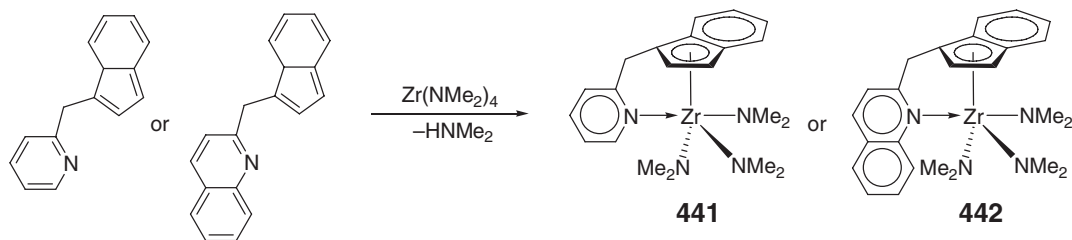
A chiral zirconium trichlorides incorporating an  $\eta^5$ -Cp: $\eta^1$ -amine chelating ligand has been synthesized. Thus, the reaction of the trimethylsilyl derivative of the *N*-functionalized Cp ligand with  $\text{ZrCl}_4$  in toluene (or dichloromethane) gives the half-sandwich zirconium trichloride complex **440** in 50% yield (Equation (33)).<sup>311</sup> The crystal structure of this complex was not obtained, but the appearance of two sharp signals for the  $\text{NMe}_2$  group in  $^1\text{H}$  and  $^{13}\text{C}$  NMR spectra suggest that the nitrogen sidearm is firmly coordinated to the metal center. However, applying this complex as a chiral Lewis acid for catalyzing the Diels–Alder reaction between methacroleine and cyclopentadiene achieved no measurable ee.



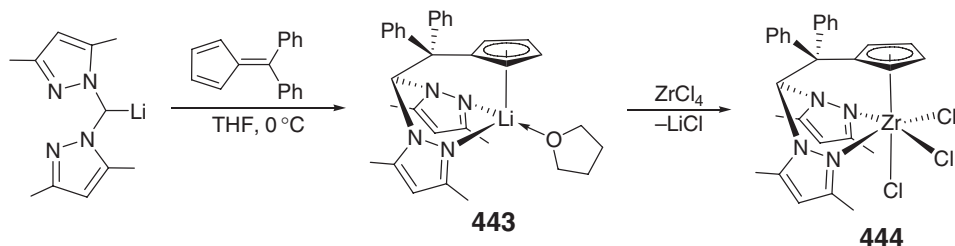
Aminolysis of  $\text{Zr}(\text{NMe}_2)_4$  with indenyl ligands having a pendant pyridylmethyl sidearm or a pendant quinolylmethyl sidearm affords indenyl half-sandwich zirconium triamido complex **441** or **442** (Scheme (99)).<sup>312</sup> The molecular structure of the complex **441** is best described as tbp with the pyridine nitrogen and one of the amido nitrogens occupying the apical positions, and the remaining nitrogens and the centroid of the five-membered ring of the  $\eta^5$ -indenyl ligand occupying the basal position.



Scheme 98



Scheme 99

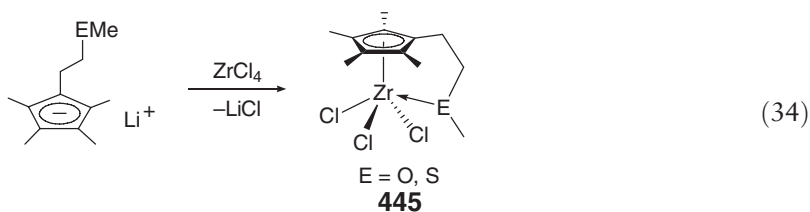


Scheme 100

The reaction of bis(3,5-dimethylpyrazol-1-yl)methyl lithium and 6,6-diphenylfulvene generates the lithium salt of a tridentate hybrid Cp/scorpionate ligand **443**, and the subsequent metathesis reaction with  $\text{ZrCl}_4$  leads to the six-coordinate zirconium trichloride **444** (Scheme 100).<sup>313</sup> Both the lithium and zirconium complexes were crystallographically characterized.

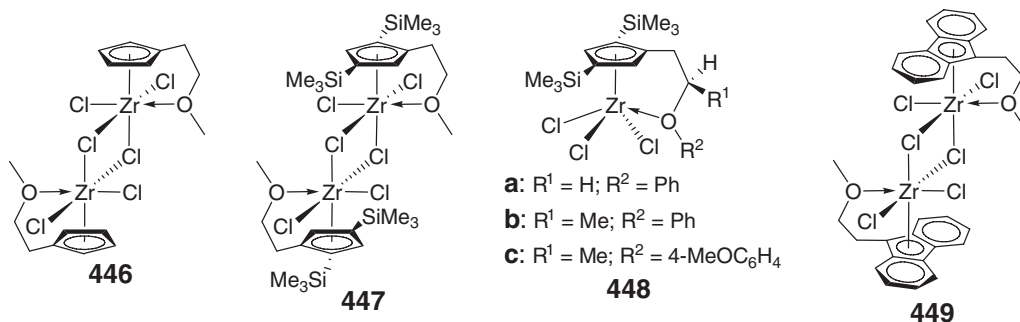
#### 4.08.7.5.2 Complexes with pendant O- and S-donors

The salt metathesis reaction of  $\text{ZrCl}_4$  and the lithium tetramethylcyclopentadienide bearing the 2-methoxyethyl or the 2-methylthioethyl donor sidearm produces half-sandwich zirconium trichloride complexes **445** (Equation (34)).<sup>314,315</sup> As expected, these complexes show monomer–dimer dynamic behavior in solution and exist as doubly chloro-bridged dimers in the solid state.



The analogous complex **446** with the parent Cp ligand was obtained by the elimination reaction involving  $\text{C}_5\text{H}_4(\text{CH}_2\text{CH}_2\text{OMe})(\text{SiMe}_3)$  and  $\text{ZrCl}_4(\text{SMe}_2)_2$ .<sup>316</sup> This complex also exists as a doubly chloro-bridged dimer (cf. the monomeric titanium analog), which is characterized by X-ray diffraction analysis as a distorted octahedron. It is monomeric in dichloromethane solution even at  $-50^\circ\text{C}$ , indicating the dimeric association is not very strong; however, the coordination of the ether moiety to Zr is very strong and is maintained in solution. Upon activation with MAO, the activity of complex **446** is several orders of magnitude lower than that of  $\text{Cp}_2\text{ZrCl}_2$ . The planar chiral bis(trimethylsilyl) derivative **447** and the aryl ether-functionalized analogs **448** were synthesized using the salt metathesis approach.<sup>317</sup> The monomeric chelate form of **447** in most organic solvents gives rise to two unequally populated conformers differing in the steric interactions between the tethering group and its neighboring trimethylsilyl groups. The aryl ether derivative **448a** behaves similarly; however, the other two of this series **448b** and **448c** contain chiral Cp ligands and were each isolated as two diastereomers in a ratio of 73:27. There is no dynamic equilibrium between the diastereomers detected in solution. In general, the pendant chelation is noticeably weaker in these aryl ether tethers as compared with the alkyl ether tether, and even weak donors such as benzaldehyde can

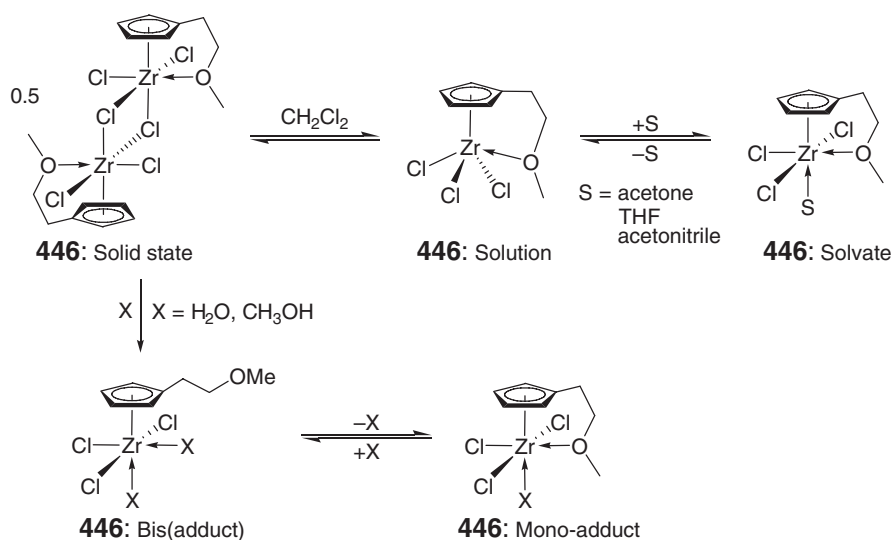
readily disrupt the chelate structure. Lastly, the fluorenyl derivative **449** was also synthesized and structurally characterized.<sup>318</sup> The fluorenyl ligand is best described as  $\eta^3$ -bound to Zr, whereas this relatively weak bond is stabilized by intramolecular coordination of the ether side chain attached to the fluorenyl backbone. Nevertheless, this bidentate ligand can easily be detached upon dissolution of this complex in THF, and a simultaneous ether cleavage leads to *spiro*-[cyclopropane-1,9'-fluorene], reflecting its high reactivity.



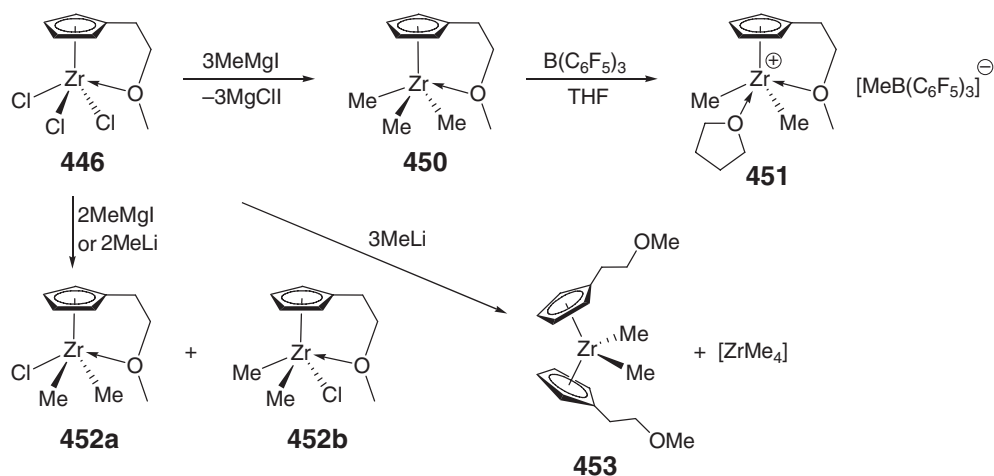
Complex **446** is a doubly chloro-bridged dimer in the solid state but is essentially monomeric in dichloromethane (or chloroform) solution (Scheme 101). Thus, coordination of an additional Lewis-basic solvent (S) molecule such as acetone, THF, and acetonitrile is feasible in a position *trans* to the Cp ligand to form a solvate, but no such stable solvates could be isolated.<sup>319</sup> Methanol or water (X) displaces the ether side chain to form the bis(solvate) adducts; however, the chelate is re-formed on removal of the solvent under vacuum to give stable methanol or water mono-adducts. The THF-solvate of the water adduct has been structurally characterized.

The methylation chemistry of **446** is interesting. Treatment of **446** with 3 equiv. of MeMgI readily affords the desired trimethyl derivative **450**, which can be converted to the methyl-abstracted cationic species **451** as a THF adduct upon addition of B(C<sub>6</sub>F<sub>5</sub>)<sub>3</sub> in THF<sup>320</sup> (Scheme 102). The methylation reaction with 2 equiv. of MeMgI or MeLi yields the corresponding dimethyl species **452** as a mixture of two rapidly exchanging isomers in solution. Surprisingly, treatment of **446** with 3 equiv. of MeLi produces bis(Cp) sandwich type complex **453** as a result of disproportionation.

This is one of the many examples where it is preferable to use Grignard reagents over alkyllithium compounds for the alkylation of the heteroatom-functionalized Cp and related halide complexes, because of the risk of possible side-reactions with lithium alkyls.



Scheme 101



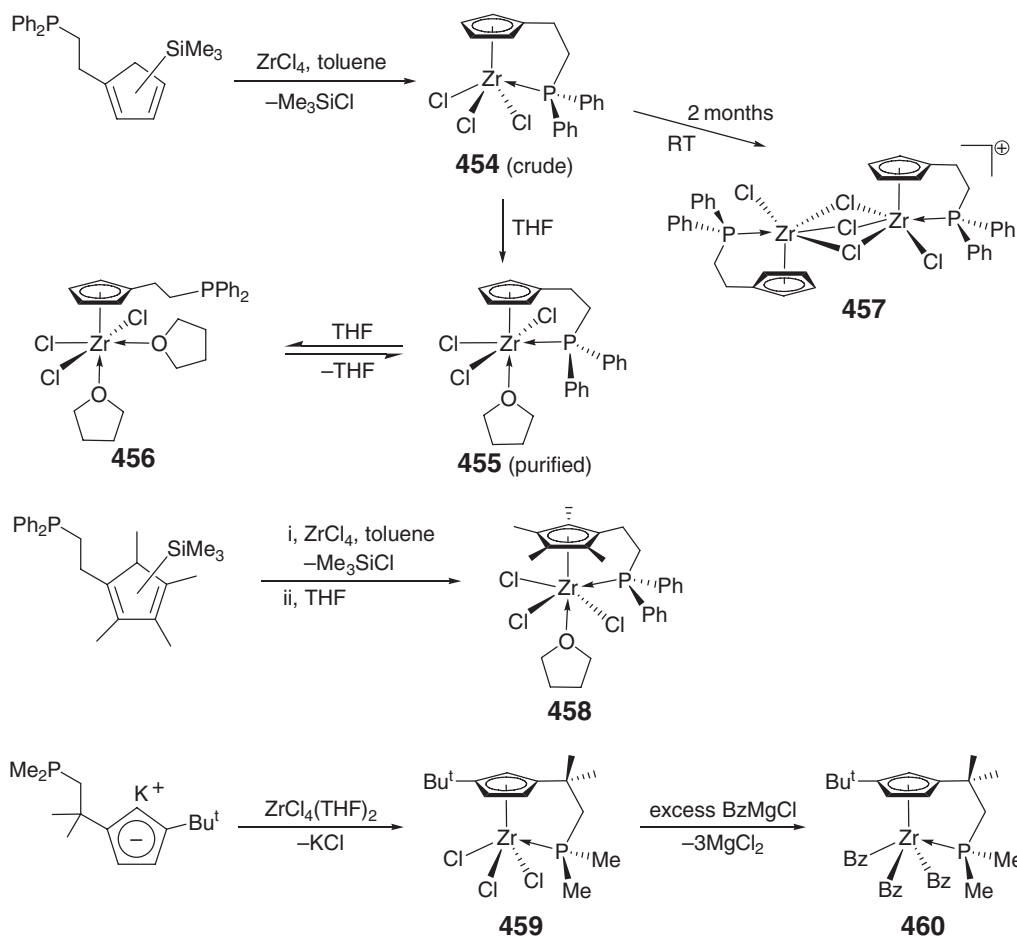
Scheme 102

#### 4.08.7.5.3 Complexes with pendant *P*-donors

Half-sandwich zirconium complexes supported by Cp ligands bearing the 2-diphenylphosphinoethyl pendant donor group were obtained by the elimination approach. Thus, the reaction of the silylated ligand with  $\text{ZrCl}_4$  in toluene yields compound **454** as a crude product; purification can be achieved by addition of THF to give the pure product **455** as a THF adduct, which was structurally characterized (Scheme 103).<sup>321</sup> As shown by variable NMR experiments, the adduct **455** displays dynamic behavior in THF solution, and further coordination of another molecule of THF by decomplexation of the phosphine sidearm to generate the bis(THF) adduct **456**. In the absence of THF, when the crude product **454** was left at room temperature for two months, a small amount of a crystalline solid was formed; its X-ray structure showed the product to be the cationic, triply  $\mu\text{-Cl}$ -bridged dimer **457** (the half of the centrosymmetric dianion  $[(\text{ZrCl}_4)_2(\mu\text{-Cl})_2]^{2-}$  is not shown). The tetramethyl-substituted Cp derivative **458** was synthesized in the same manner,<sup>322</sup> whereas the zirconium trichloride **459** supported by the *tert*-butyl-substituted Cp containing the 2-dimethylphosphino-1,1-dimethylethyl pendant donor group was prepared by the salt metathesis approach.<sup>323</sup> The corresponding tribenzyl derivative **460** was obtained by straightforward alkylation with excess (5 equiv.)  $\text{BzMgCl}$ .

Mono-bis(silyl)Cp ligands with two pendant phosphino sidearms function as tridentate mixed donor ligands. The zirconium trichloride complex bearing such a ligand,  $[\text{P}_2\text{Cp}]\text{ZrCl}_3$  **461**, was obtained by addition of  $[\text{P}_2\text{Cp}]\text{Li}$  to  $\text{ZrCl}_4(\text{THT})_2$  in toluene  $\{[\text{P}_2\text{Cp}] = [\eta^5\text{-C}_5\text{H}_3\text{-1,3-(SiMe}_2\text{CH}_2\text{PPh}_2)_2]\}$ ; THT = tetrahydrothiophene; Scheme 104).<sup>324</sup> The molecular structure of **461** is best described as a distorted, quasi-octahedron with a  $\text{P-Zr-P}$  angle of  $159.53(4)^\circ$  for approximately a *trans* (P-P) arrangement.<sup>325</sup> The solution geometry derived from NMR data is  $C_s$ -symmetric, consistent with the solid-state structure, whereas the observation that the NMR spectra are invariant with changes in temperature indicates that the phosphine arms do not undergo any detectable exchange process. The reaction of the trichloride **461** with 1 equiv. of  $\text{Mg}(\text{CH}_2\text{Ph})_2 \cdot 2\text{THF}$  leads to the formation of a 1:1 mixture of the corresponding monobenzyl and tribenzyl complexes, but not the bis(benzyl) derivative. When the mixture of the benzyl species was photolyzed or thermolyzed, the benzylidene complex  $[\text{P}_2\text{Cp}]\text{Zr}=\text{CHPh}(\text{Cl})$  **462** was obtained and isolated in 85% yield (Scheme 104).<sup>324</sup> The same reaction but with 1.5 equiv. of  $\text{Mg}(\text{CH}_2\text{Ph})_2 \cdot 2\text{THF}$  leads to a complete substitution of all three chloro ligands, yielding the four-coordinate tribenzyl complex **463** with a concomitant decomplexation of both phosphine arms.<sup>325</sup> Similarly, the reaction with 0.5 equiv. of  $\text{Mg}(\text{CH}_2\text{Ph})_2 \cdot 2\text{THF}$  affords the monobenzyl complex **464** with one phosphine arm coordinated to the metal and the other dangling. The sterically undemanding tri(methyl) derivative also exhibits a five-coordinate tdp structure in solution at low temperatures.

Mechanistic studies of the formation of the zirconium alkylidene complexes of type **462** have been carried out.<sup>326</sup> Neither the independently prepared monobenzyl complex nor the tribenzyl derivative is thermally sensitive or reacts with light as a separate species, but the equimolar mixture is thermolyzed to give the benzylidene species. The reaction of the trichloride **461** with 2 equiv. of  $\text{KCH}_2\text{Ph}$  generates an equilibrium mixture of benzyl complexes consisting of monobenzyl **464**, tribenzyl **463**, and the “bis(benzyl)” derivative. The dibenzyl complex is spectroscopically detectable, but not isolable and co-exists with the mono- and tribenzyl species; however, it is the bis(benzyl) species that is photochemically and thermally labile for a facile  $\alpha$ -hydrogen abstraction process, leading

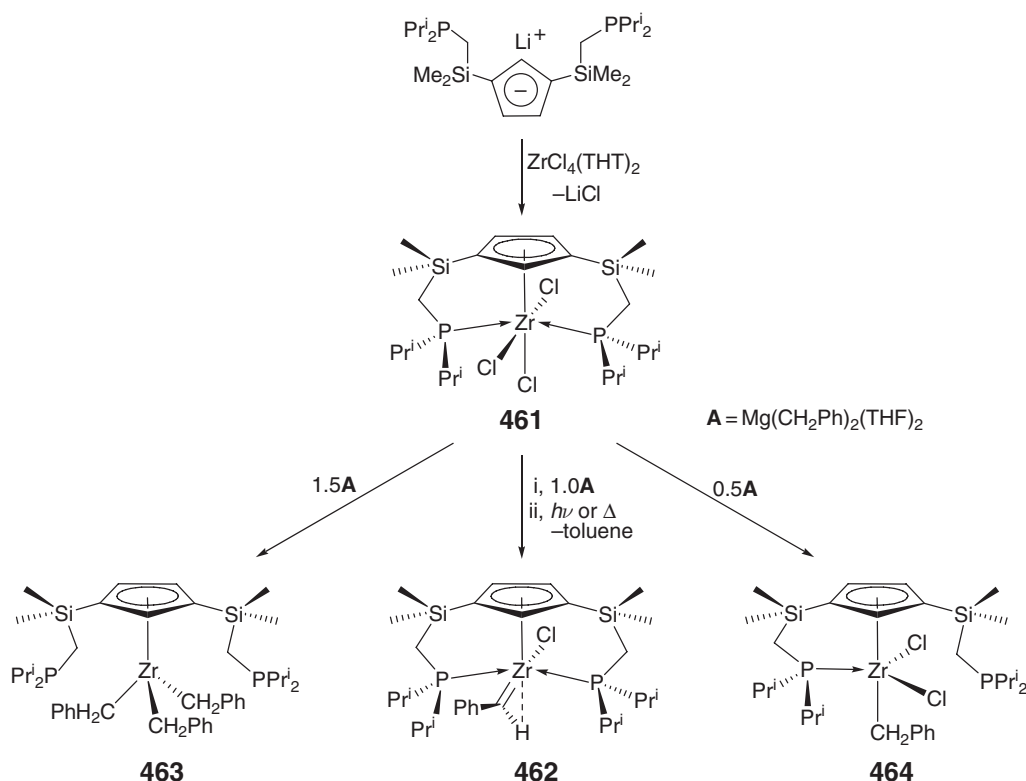


Scheme 103

to the benzyldiene species. Other alkyls such as  $\text{CH}_2\text{CMe}_3$  and  $\text{CH}_2\text{SiMe}_3$  behave similarly to  $\text{CH}_2\text{Ph}$  discussed above, leading to alkylidene derivatives  $[\text{P}_2\text{Cp}]\text{Zr}=\text{CHR}(\text{Cl})$  ( $\text{R} = \text{CMe}_3, \text{SiMe}_3$ ). The reactivity of the phenyl **462** and trimethylsilyl alkylidene complexes has been detailed.<sup>327</sup> For example, they react with ethylene and acetone to give the ethylene complex  $[\text{P}_2\text{Cp}]\text{Zr}(\eta^2\text{-C}_2\text{H}_4)\text{Cl}$  and the alkene  $\text{RCH}=\text{CMe}_2$ , respectively. An insertion of CO into the  $\text{Zr}=\text{C}$  bond yields the corresponding ketene complex  $[\text{P}_2\text{Cp}]\text{Zr}(\eta^2\text{-C}, \text{O}-\text{OC}=\text{CHR})\text{Cl}$ , while the reaction with *tert*-butyl isocyanide affords the analogous ketenimine complex  $[\text{P}_2\text{Cp}]\text{Zr}(\eta^2\text{-C}, \text{N}-\text{Bu}^t\text{NC}=\text{CHR})\text{Cl}$ .

#### 4.08.8 *ansa*-Monocyclopentadienyl “Constrained-Geometry” Complexes

A prototype constrained-geometry ligand framework is the dimethylsilylene-bridged tetramethyl-Cp/*tert*-butylamido dianion,  $[\text{Me}_2\text{Si}(\eta^5\text{-Cp})(\eta^1\text{-NBu}^t)]^{2-}$ , which serves as a bifunctional,  $\eta^5:\eta^1$ -chelating ligand when it binds to a metal.<sup>328</sup> The constrained-geometry type of group 4 complexes have a six-electron donor,  $\eta^5\text{-Cp}$  ligand and a covalently attached, sterically protected  $sp^2$ -hybridized amido *N*-donor ligand, which stabilize the electrophilic  $d^0$ -metal center electronically serving as a four-electron donor (ionic model) with an appreciable *N*  $\pi$ -donation to the metal, while the short  $\text{Me}_2\text{Si}$  bridging group considerably opens the coordination-gap aperture, compared with conventional metallocenes. The constrained geometry induced by the  $\text{Me}_2\text{Si}$  linker leads to an acute Cp(centroid)–M–N angle in group 4 metal complexes and a substantial displacement of the Si atom from the Cp ring plane; this displacement is in the range of 0.85–0.95 Å. The Cp(centroid)–M–N “bite angle” typically ranges from 100 to 110°, approximately 20–30° less than the angle in conventional bent-sandwich metallocene complexes. Consequently, typical constrained-geometry group 4 complexes exhibit remarkably open catalyst sites (surfaces), which are



Scheme 104

translated into their unique catalytic features of these complexes, one of which is the ability to incorporate high levels of even bulky  $\alpha$ -olefins in co-polymerizations with ethylene, as well as the ability to effectively polymerize such  $\alpha$ -olefins directly in homopolymerizations. Extensions to the original type of constrained-geometry complexes include indenyl and fluorenyl derivatives, as well as other types of the relatively short bridging groups and covalently bound anionic pendant chelating ligands. From a catalytic point of view, the most important constrained-geometry complexes are based on titanium, whereas zirconium derivatives tend to be rather less active.

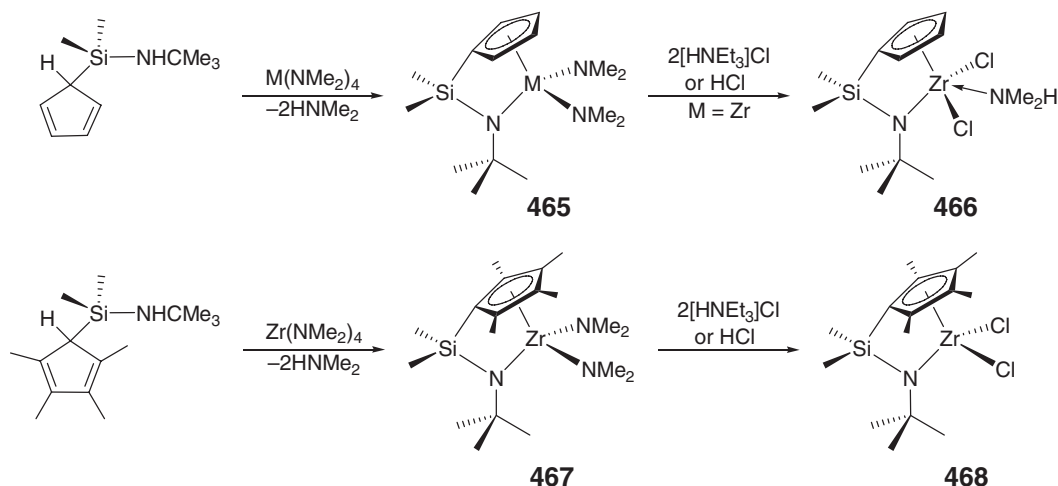
#### 4.08.8.1 *ansa*-Cp-amido Complexes

##### 4.08.8.1.1 Cp/silylamido complexes containing monodentate ligands

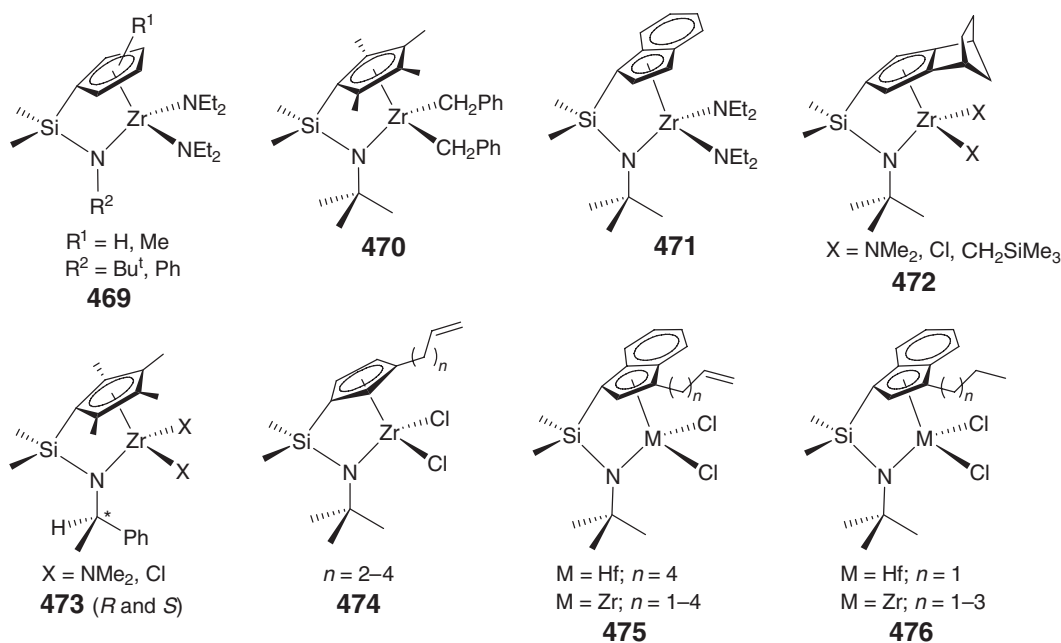
To overcome the low-yield synthesis of the *ansa*-mono-Cp-silylamido complexes (especially for the parent Cp derivative) by the salt metathesis route, the amine elimination approach was employed to produce these complexes in typically 70 to 85% yield.<sup>329</sup> Thus, heating the 1 : 1 neat reaction mixture of  $\text{Me}_2\text{Si}(\text{CpH})(\text{NHBu}^i)$  and  $\text{M}(\text{NMe}_2)_4$  ( $\text{M} = \text{Zr}, \text{Hf}$ ) at 110–120 °C affords the bis(dimethylamido) complexes **465** as a colorless waxy solid (Scheme 105). The subsequent reaction of the zirconium bis(amido) complex with 2 equiv. of  $\text{HCl}$  or  $[\text{HNEt}_3]\text{Cl}$  gives the corresponding dichloride complex **466** as the dimethylamine adduct, with the amine being placed between the two chloride ligands and lying *trans* to the appended amido group in this X-ray crystallographically characterized four-legged piano-stool type of the molecular structure. The analogous reaction using the tetramethyl-substituted Cp ligand proceeds via a similar fashion in the aminolysis step, yielding the bis(dimethylamido) analog **467**; however, the subsequent reaction with 2 equiv.  $[\text{HNEt}_3]\text{Cl}$  affords the base-free dichloride complex **468**.

Amine or hydrocarbyl elimination was also employed to prepare the following *ansa*-mono-Cp-silylamido derivatives (Scheme 106), including zirconium bis(diethylamido) complexes **469** with variations on the ring and amido substitutions,<sup>330</sup> zirconium dibenzyl complex **470**,<sup>331</sup> *ansa*-mono-Ind-silylamido zirconium complex **471**,<sup>330</sup> isodicyclopentadienyl zirconium complexes **472**,<sup>332</sup> and enantiomerically pure zirconium bis(dimethylamido) and dichloro complexes **473**<sup>333</sup> with the *R* or *S*-CH(Me)Ph group attached to the amido nitrogen; the last two complexes of this





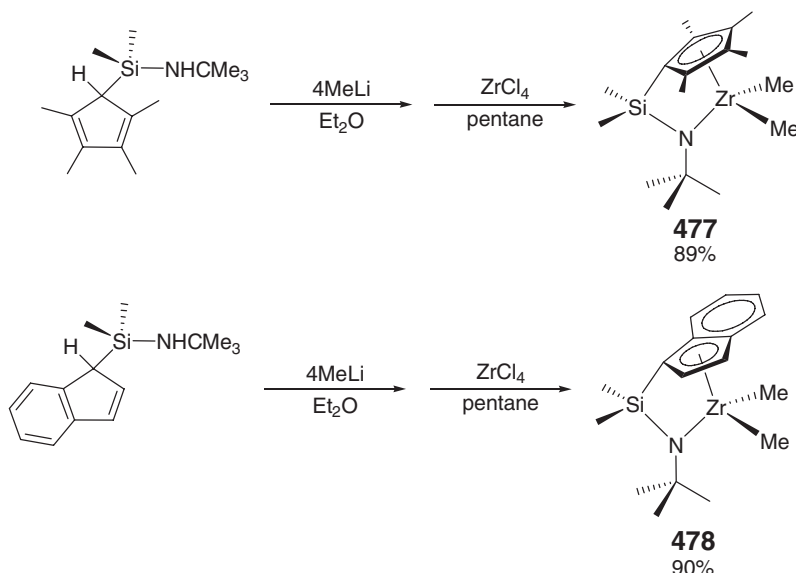
Scheme 105



Scheme 106

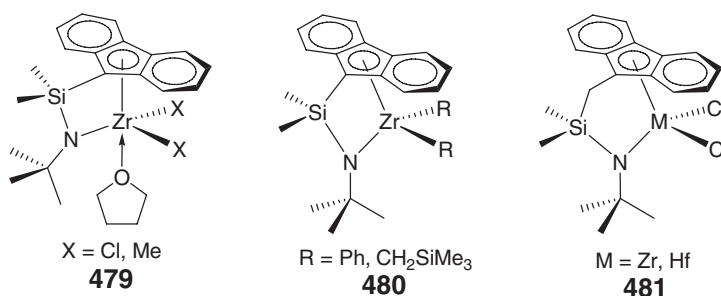
series **472**<sup>334</sup> and **473**<sup>333</sup> were also obtained by salt metathesis. A series of Cp-silylamido **474** and Ind-silylamido **475** and **476** complexes with alkyl and  $\omega$ -alkenyl substituents on the Cp and Ind rings has been prepared by the salt metathesis route.<sup>335</sup> The primary purpose of the preparation of these  $\omega$ -alkenyl-substituted complexes is to heterogenize the catalyst via self-immobilization during the course of polymerization when activated with MAO, assuming the double bond of the  $\omega$ -alkenyl substituent is co-polymerized with ethylene. Within this series, the Ind complexes exhibit much higher ethylene polymerization activity than the corresponding Cp complexes.

An improved salt metathesis route has been developed for the high-yield synthesis of *ansa*-Cp-silylamido zirconium dimethyl complexes in a one-pot fashion.<sup>336</sup> Thus, treatment of the neutral amidosilyl-functionalized tetramethyl-Cp ligand with 4 equiv. of MeLi in diethyl ether, followed by addition of ZrCl<sub>4</sub> in pentane, gives the desired zirconium dimethyl complex **477** in 89% yield (Scheme 107). The analogous reaction with the amidosilyl-functionalized Ind ligand affords the corresponding zirconium dimethyl complex **478** in 90% yield.

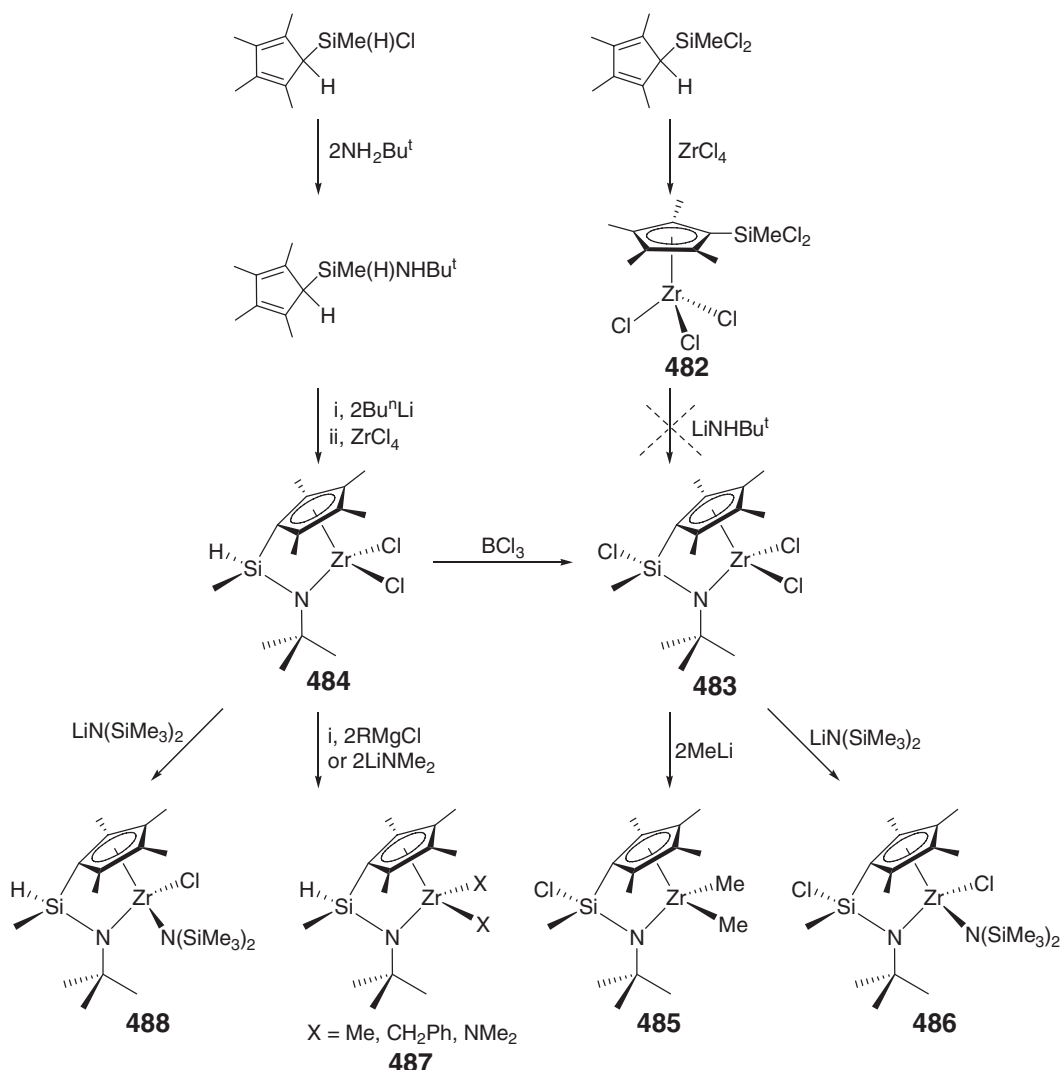


Scheme 107

Zirconium dichloride **479** containing the  $\text{Me}_2\text{Si}$ -bridged fluorenyl-amido bidentate ligand was prepared by salt metathesis and isolated as a labile solvent adduct.<sup>337</sup> The thermally sensitive dimethyl derivative was also isolated as the THF (or ether) adduct, whereas the diphenyl and bis(trimethylsilyl methyl) derivatives **480** were isolated as base-free species. The molecular structure of the trimethylsilyl methyl derivative features the rather rigid, sterically congested  $\eta^5:\eta^1$ -chelating ligand framework and shows  $\eta^5$ -to- $\eta^3$ -bonded fluorenyl ring with some variation of the Zr–ring carbon lengths. The amido nitrogen is trigonal planar as a result of significant  $\pi$ -donation to Zr, while the two trimethylsilyl methyl groups adopt a conformation in which the repulsion between the trimethylsilyl and the *tert*-butyl groups is minimized. The crystal structure of the base-free dichloride complex was determined four years later.<sup>338</sup> The analogous zirconium and hafnium complexes **481** with a  $\text{CH}_2$  extension to the silyl bridge were also synthesized by salt metathesis and structurally characterized.<sup>339</sup> The relatively longer  $-\text{CH}_2\text{SiMe}_2-$  bridge in complexes **481** releases the ring strain of the ligand backbone, but increases the effectiveness of the protection offered by the ligand to the metal ion.



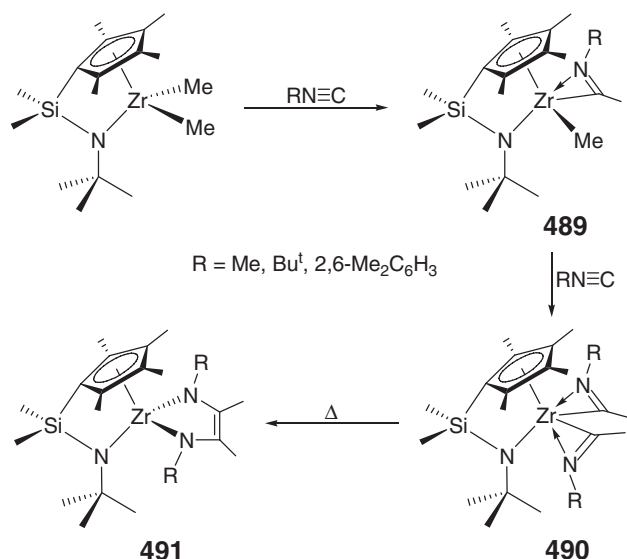
A number of *ansa*-Cp-silylamido zirconium complexes containing the hydrosilyl and chlorosilyl bridging moieties have been synthesized (Scheme 108). Thus, the reaction of  $\text{ZrCl}_4$  with 1 equiv. of the disilylated tetramethyl-Cp ligand  $\text{C}_5\text{Me}_4(\text{SiMeCl}_2)(\text{SiMe}_3)$  affords the zirconium trichloride ( $\eta^5\text{-C}_5\text{Me}_4\text{SiMeCl}_2$ ) $\text{ZrCl}_3$  **482** bearing the dichloromethylsilyl-functionalized Cp ligand.<sup>340</sup> Treatment of this trichloride with different ratios of *tert*-butylamine and its lithium salt did not produce the targeted *ansa*-tetramethyl-Cp-amido zirconium dichloride **483**, resulting in the formation of inseparable mixtures of various substituted products. However, this complex can be readily obtained by  $\text{BCl}_3$ -induced chlorination of the hydrosilyl-bridged complex **484**, which is prepared by salt metathesis using the amidohydrosilyl-functionalized tetramethyl-Cp ligand (Scheme 108). Both the hydrosilyl- and chlorosilyl-bridged



Scheme 108

*ansa*-Cp-silylamido zirconium complexes **483** and **484** can be dialkylated, mono or diamidated at Zr without affecting the functionalities on the bridge, leading to the corresponding dimethyl **485**, monoamido **486**, bis(alkyl) or bis(dimethylamido) **487**, and monoamido **488**, respectively.

Four types of reactions involving the typical *ansa*-mono-Cp-silylamido complexes are discussed here: (i) insertion into the metal-alkyl bond for the production of derivatives, (ii) hydroboration of unsaturated Cp-pendant groups for the formation of zwitterionic species, (iii) ligand substitution of the metal-chloride bond for the assembly of chiral-at-metal and ester enolate complexes, and (iv) activation of the metal alkyl complex for the generation of ion pairs. The insertion reaction involving the *ansa*-mono-Cp-silylamido dimethyl complex,  $\text{Me}_2\text{Si}(\eta^5\text{-C}_5\text{Me}_4)(\eta^1\text{-NBu}^t)\text{ZrMe}_2$ , and 2 equiv. of isocyanide RNC (R = Me, Bu<sup>t</sup>, 2,6-Me<sub>2</sub>C<sub>6</sub>H<sub>3</sub>) proceeds sequentially with isocyanide insertion into both Zr-Me bonds to afford the corresponding mono- $\eta^2$ -iminoacyl zirconium methyl complex **489** and bis( $\eta^2$ -iminoacyl) zirconium complex **490**<sup>341</sup> (Scheme 109). Subsequent thermolysis of the bis( $\eta^2$ -iminoacyl) zirconium complex **490** leads to *C,C*-coupling of the two  $\eta^2$ -iminoacyl units and proceeds exclusively with formation of the cyclic enediamidate derivative **491**. The bis( $\eta^2$ -iminoacyl) **490** (R = Bu<sup>t</sup>, 2,6-Me<sub>2</sub>C<sub>6</sub>H<sub>3</sub>) and cyclic enediamidate **491** (R = Bu<sup>t</sup>, 2,6-Me<sub>2</sub>C<sub>6</sub>H<sub>3</sub>) complexes have been structurally characterized. Interestingly, the 1,4-diaza-5-zirconacyclopentene ring conformations in structures **491** depend on the R group, adopting either a *prone*- (R = Bu<sup>t</sup>) or *supine*- (R = 2,6-Me<sub>2</sub>C<sub>6</sub>H<sub>3</sub>) conformation; this is contributable to the steric features of the substituents.

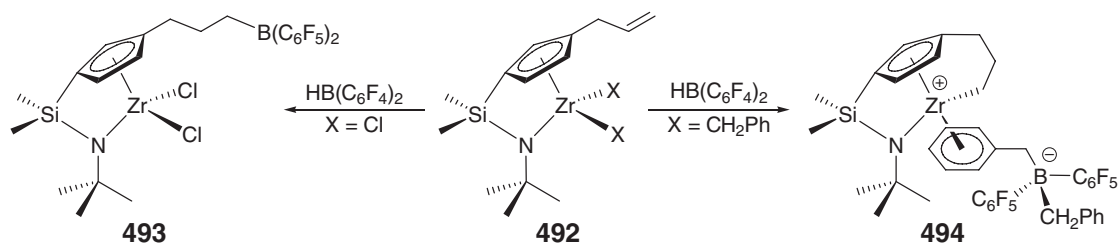


Scheme 109

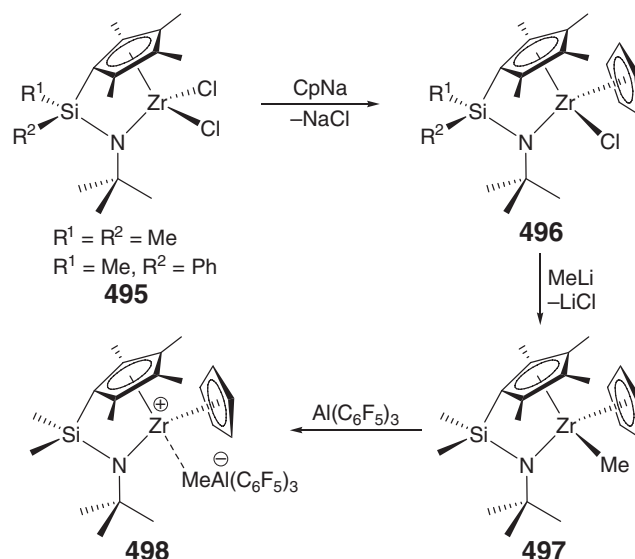
Hydroboration of the *ansa*-mono-Cp-silylamido complexes **492** containing a Cp-pendant allyl group using 1 equiv. of  $\text{HB}(\text{C}_6\text{F}_5)_2$  in hexanes proceeds rapidly to give the products dependent on the nature of the X ligand<sup>342</sup> (Scheme 110). For the dichloride precursor, the reaction yields the corresponding hydroboration product **493**, but attempts to alkylate this resulting dichloride were unsuccessful. On the other hand, the dibenzyl complex reacts with 1 equiv. of  $\text{HB}(\text{C}_6\text{F}_5)_2$  in hexanes leading to the formation of the ring-metallated, tuck-in type, tightly associated ion pair **494**. The hydroboration was assumed to occur in the initial step of the reaction, followed by double benzyl group transfer from Zr to B, giving the non-zwitterionic product in which the cation is stabilized by the typical  $\eta^6$ -coordination provided by the benzylborate anion.

Nucleophilic chloro ligand substitution of *ansa*-tetramethyl-Cp-amido zirconium dichloride complexes **495** with  $\text{CpNa}$  in THF produces the monochloro, chiral-at-metal complexes **496**, which can be methylated to the corresponding monomethyl complex **497** (Scheme 111).<sup>343</sup> Upon activation with excess of MAO, the monochloride complexes are highly active for co-polymerization of ethylene and 1-octene, despite the apparent lack of the free metal-alkyl ligand in their activated form – a requirement for a catalyst to initiate the olefin polymerization via a migratory insertion mechanism. The model activation study shows that the reaction of the monomethyl complex **497** with the strong Lewis acid  $\text{Al}(\text{C}_6\text{F}_5)_3$  cleanly generates the alkyl-free cationic species **498**. The initiation step is proposed to involve nucleophilic attack on the coordinated (thus polarized) olefin and formation of the  $\text{Zr-CH}_2(\text{R})\text{-Al}$  bimetallic intermediate.

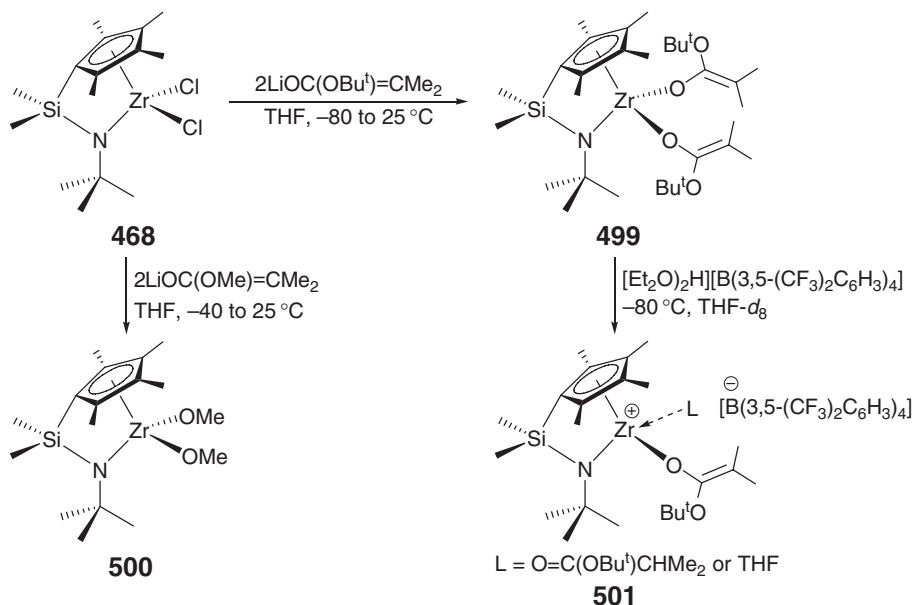
Another example of the nucleophilic chloro ligand substitution involves the reaction of the zirconium dichloride complex **468** with lithium ester enolates (Scheme 112). Its reaction with 2 equiv. of stable lithium ester enolates such as lithium *tert*-butyl isobutyrate in THF produces the bis(ester enolate) complex **499** as a crystalline solid.<sup>344</sup> The same reaction but with the unstable lithium methyl isobutyrate leads to the isolation of the decomposition product, the bis(methoxide) complex **500**, which exists as a dimer in the solid state. Treatment of the bis(ester enolate)



Scheme 110



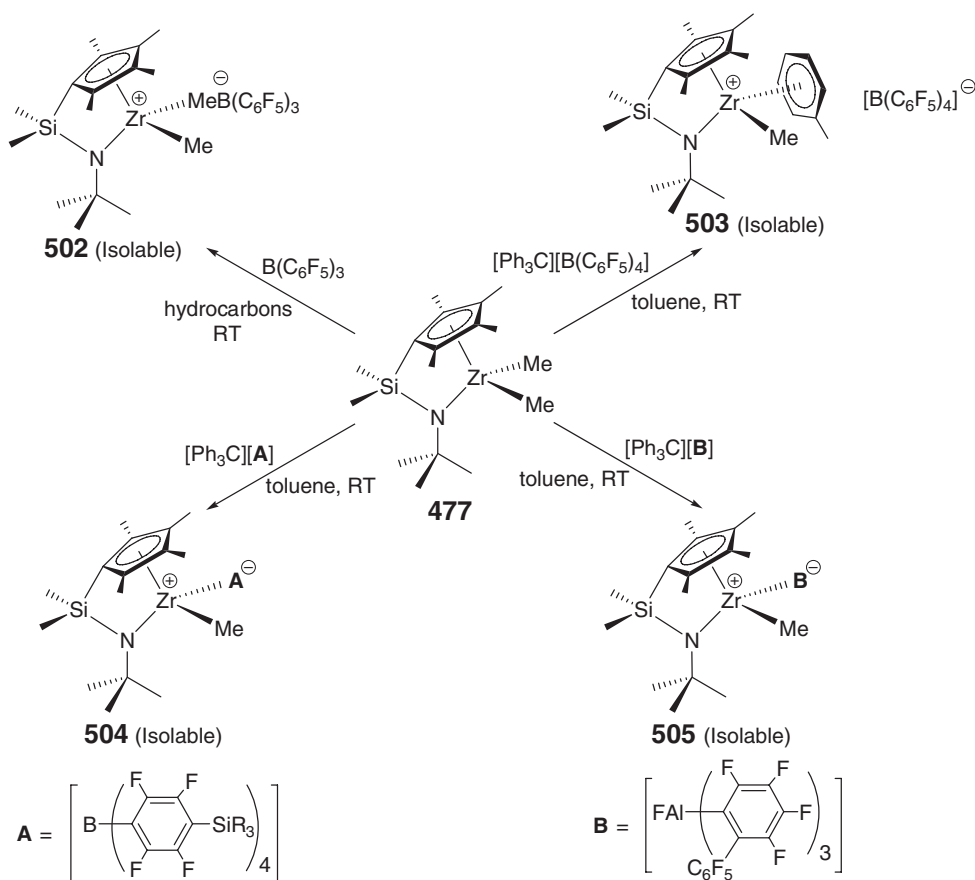
Scheme 111



Scheme 112

complex **499** with 1 equiv. of the strong oxonium acid  $[\text{H}(\text{OEt}_2)_2]^+$  in  $\text{CD}_2\text{Cl}_2$  or  $\text{THF-}d_8$  at  $-80^\circ\text{C}$  generates the corresponding cationic ester enolate complex **501**, which is stable in solution below  $-40^\circ\text{C}$ . At  $-40$  to  $-60^\circ\text{C}$ , **501** polymerizes methyl methacrylate to highly isotactic polymer.

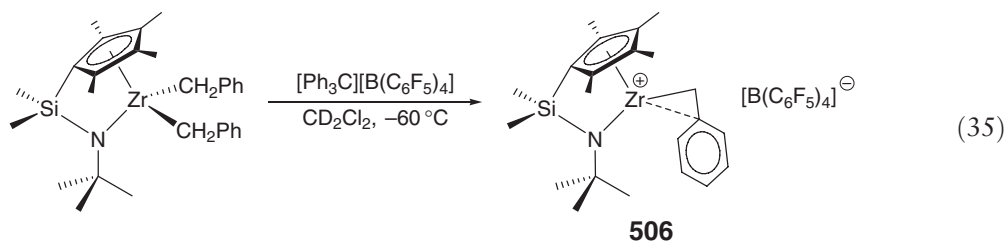
Activation of the dialkyl complexes  $\text{Me}_2\text{Si}(\eta^5\text{-C}_5\text{Me}_4)(\eta^1\text{-NBu}^t)\text{ZrR}_2$  with widely used reagents such as  $\text{B}(\text{C}_6\text{F}_5)_3$  and  $[\text{Ph}_3\text{C}][\text{B}(\text{C}_6\text{F}_5)_4]$  leads to the formation of various forms of cationic products, depending on the nature of the R group and the reagent employed. For the dimethyl complex **477**, abstractive activation with  $\text{B}(\text{C}_6\text{F}_5)_3$  in hydrocarbon solvents at ambient temperature cleanly generates the isolable cationic species **502**, but the oxidative cleavage of the Zr–Me bond with  $[\text{Ph}_3\text{C}][\text{B}(\text{C}_6\text{F}_5)_4]$  in toluene gives a cationic complex **503** stabilized by toluene instead of  $[\text{B}(\text{C}_6\text{F}_5)_4]^-$ , reflecting the extremely weak coordinating nature of this anion



Scheme 113

(Scheme 113).<sup>345</sup> The use of the trialkylsilyl-functionalized borate trityl salts  $[\text{Ph}_3\text{C}][\text{B}(\text{C}_6\text{F}_4\text{SiR}_3)_4]$ <sup>346</sup> affords the corresponding ion pair **504** stabilized by the functionalized borate anion, indicating the more coordinating nature of these trialkylsilyl-functionalized borate anions as compared with  $[\text{B}(\text{C}_6\text{F}_5)_4]$ . However, this coordination is still very weak, as evidenced by high olefin polymerization activities of their derived cationic complexes; moreover, the weak coordination extends the catalyst lifetime by preventing the cation self-destruction via various decomposition pathways, and offers the opportunity for isolation and full characterization of the cationic catalysts. In short, a balance needs to be struck in terms of anion coordination/stabilization – not too strong but not too weak. To this end, the sterically encumbered fluoroaryl aluminate-based trityl salt was introduced, and its reaction with  $\text{Me}_2\text{Si}(\eta^5\text{-C}_5\text{Me}_4)(\eta^1\text{-NBu}^t)\text{ZrMe}_2$  leads to the crystallographically characterizable tight ion pair **505** via the Zr–F–Al bridge (Scheme 113).<sup>347</sup>

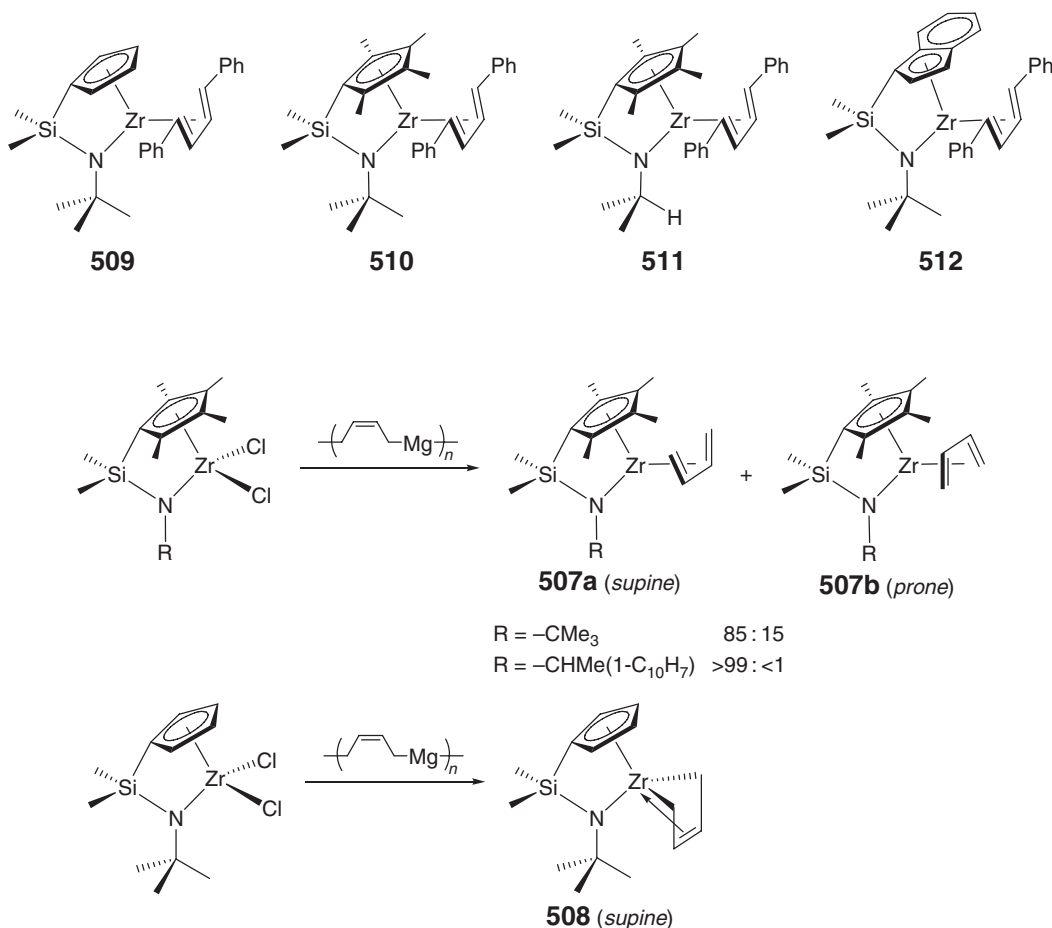
Activation of the dibenzyl complex,  $\text{Me}_2\text{Si}(\eta^5\text{-C}_5\text{Me}_4)(\eta^1\text{-NBu}^t)\text{ZrBz}_2$ , with  $[\text{Ph}_3\text{C}][\text{B}(\text{C}_6\text{F}_5)_4]$  is facile even at  $-60^\circ\text{C}$ , yielding the corresponding separated ion pair **506** in which the benzyl group in the cation is bound to Zr via an  $\eta^2$ -fashion (Equation (35)).<sup>331</sup> Attempted isolation of this complex led to the formation of the ring-metallated, tuck-in-type complex through ring-methyl C–H activation and elimination of toluene.



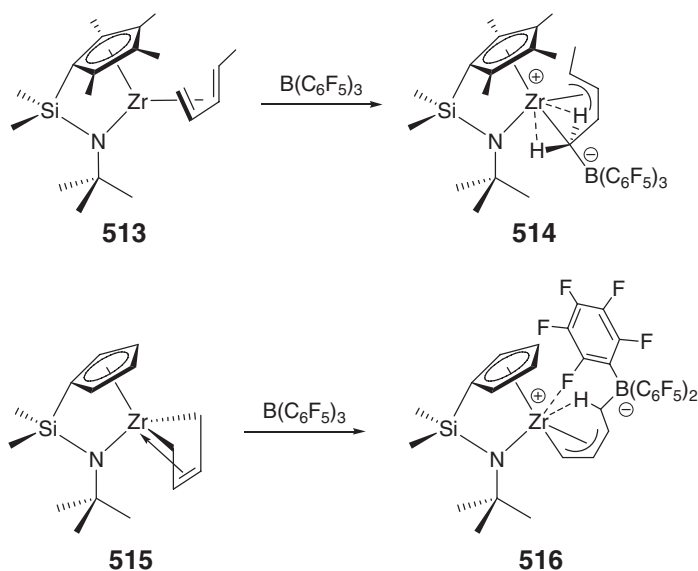
#### 4.08.8.1.2 Cp-silylamido diene complexes

Treatment of *ansa*-mono-Cp-silylamido dichlorides  $\text{Me}_2\text{Si}(\eta^5\text{-C}_5\text{Me}_4)(\eta^1\text{-NR})\text{ZrCl}_2$  ( $\text{R} = \text{Bu}^t$ ,  $\text{CHMe}(1\text{-C}_{10}\text{H}_7)$ ) with “butadienemagnesium”  $[\text{Mg}(\text{C}_4\text{H}_6)(\text{THF})_2]_n$  gives the diene complexes **507**<sup>348</sup> (Scheme 114). In solution, the ratio of *supine*- and *prone*-isomers with respect to the arrangement of the *s-cis*-coordinated  $\eta^4$ -diene moiety depends on the R group attached to the amido nitrogen; for the parent zirconium diene complex ( $\text{R} = \text{Bu}^t$ ), the equilibrium *supine*-versus *prone*-isomer ratio is 85 : 15, whereas the single *supine*-isomer is obtained when  $\text{R} = \text{CHMe}(1\text{-C}_{10}\text{H}_7)$ . In the solid state, the favored *supine*-isomers feature a central metallacyclic  $\sigma^2, \pi$ -type (*s-cis*- $\eta^4$ -diene) Zr(IV) framework; this is in sharp contrast to the titanium counterpart, which predominantly exists as a *prone*-isomer in solution and its solid-state structure is a conventional  $\pi$ -butadiene Ti(II) complex. The analogous reaction using the unmethylated Cp derivative  $\text{Me}_2\text{Si}[(\eta^5\text{-Cp})(\eta^1\text{-NBu}^t)]\text{ZrCl}_2$  also yields the *supine*-isomer **508**. This solution structure of the metallacyclic  $\sigma^2, \pi$ -type zirconacyclopentene is consistent with the X-ray crystallographic analysis, which shows actually a tetranuclear structure linked by four asymmetrically bridging butadiene groups.<sup>349</sup>

Four *ansa*-Cp-silylamido zirconium 1,4-diphenylbutadiene complexes have been synthesized by the salt metathesis route involving the reaction of the respective dichloride precursors and  $[\text{Mg}(\text{C}_4\text{H}_4\text{Ph}_2)(\text{THF})_3]_n$ .<sup>350</sup> these 1,4-diphenylbutadiene complexes include the unsubstituted Cp **509**, tetramethyl-Cp *tert*-butylamido **510**, tetramethyl-Cp isopropylamido **511**, and indenyl diene complex **512**. In solution, complex **511** exists as only the *supine*-isomer, whereas the other complexes exhibit various *supine/prone*-isomeric ratios: >20:1 for **509**, 2:1 for **510**, 6:1 for **512**. The solid-state structures of the favored *supine*-isomers show that the 1,4-diphenylbutadiene moiety is coordinated to Zr via a  $\pi$ -*cis*- $\eta^4$ -diene-type (i.e., as Zr(II)  $\eta^4$ -diene species rather than as Zr(IV) enediyl complexes) and the level of the  $\eta^4$ - $\pi$  bonding contribution is enhanced by replacement of the *tert*-butyl substituent on the amido nitrogen with the sterically less demanding isopropyl group.



Scheme 114

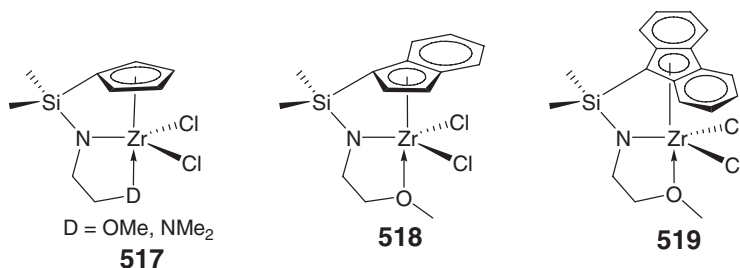


Scheme 115

Activation of the *ansa*-Cp-silylamido zirconium diene complexes with  $\text{B}(\text{C}_6\text{F}_5)_3$  can produce diverse structures. For example, the reaction of  $\text{B}(\text{C}_6\text{F}_5)_3$  and the parent tetramethyl Cp-silylamido diene complex **513**, prepared by the *in situ* reaction of  $\text{Me}_2\text{Si}(\eta^5\text{-C}_5\text{Me}_4)(\eta^1\text{-NBu}^t)\text{ZrCl}_2$  and 2 equiv. of  $\text{Bu}^n\text{Li}$  in the presence of excess of 1,3-pentadiene, generates the zirconium borate zwitterionic complex **514**<sup>351</sup> (Scheme 115). The molecular structure shows the borane is bound to the terminal methylene carbon atom of the precursory pentadiene ligand, which is now an  $\eta^3$ -allyl fragment. The hydrogen atoms on the methylene carbon have close contacts with Zr, suggesting agostic bonding. In sharp contrast, the analogous reaction with the unmethylated Cp zirconium diene complex **515** gives the zirconium borate zwitterionic complex **516** which features a dative  $\text{Zr} \leftarrow \text{F}-\text{C}(\text{ortho})$  interaction, in addition to a single  $\text{Zr}-\text{H}-\text{CH}-\text{B}(\text{C}_6\text{F}_5)_3$  agostic interaction.<sup>352</sup>

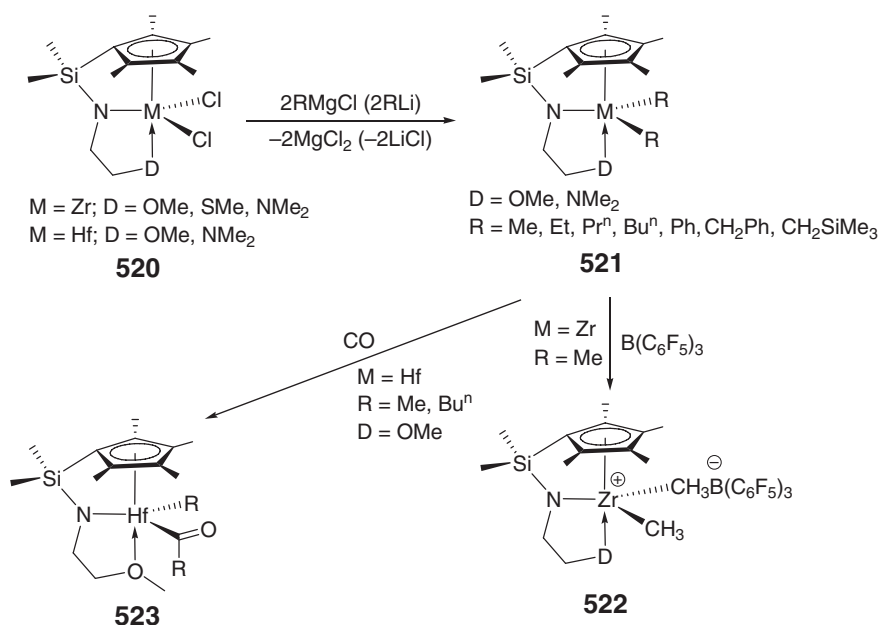
#### 4.08.8.1.3 Tridentate Cp-silylamido complexes

An extension of the bidentate,  $\text{Me}_2\text{Si}$ -bridged Cp-amido ligation is the induction of an additional tethered side chain containing donor atoms such as O and N, effectively serving as a tridentate  $\eta^5\text{-Cp}:\eta^1\text{-amido}:\eta^1\text{-N}(\text{O})$  donor chelation to support the metal center. Complexes of this class include those supported by dimethylsilyl-bridged unmethylated Cp **517**, indenyl **518**, and fluorenyl **519** amido ligands tethered with ether or amine side chain. All three complexes show a dynamic coordination behavior of the ether binding in chlorocarbon solution.<sup>353</sup>



A series of zirconium and hafnium complexes containing the tridentate tetramethyl-Cp-amido-ether, thioether or amine donor ligands has been synthesized (Scheme 116). The pseudo-tbp dichloride complexes,  $\text{Me}_2\text{Si}(\eta^5\text{-Me}_4\text{C}_5)\{\eta^2\text{-N}(\text{CH}_2)_2\text{X}\}\text{MCl}_2$  (**520**:  $\text{M} = \text{Zr}$ ,  $\text{X} = \text{OMe}$ ,  $\text{NMe}_2$ ,<sup>354</sup>  $\text{SMe}$ <sup>355</sup>;  $\text{M} = \text{Hf}$ ,  $\text{X} = \text{OMe}$ ,<sup>356</sup>  $\text{NMe}_2$ <sup>357</sup>), prepared by the salt metathesis approach involving the reactions between the lithiated ligands and  $\text{MCl}_4(\text{THF})_2$ , are versatile precursors leading to various monoalkyl<sup>356</sup> and dialkyl derivatives.<sup>357,358</sup> The dialkyl complexes **521**, including those dialkyl groups containing  $\beta$ -hydrogen atoms, can be readily obtained by straightforward alkylation, although the thermal stability of the dialkyl derivatives follows the order  $\text{Et} < \text{Pr}^n < \text{Bu}^n < \text{CH}_2\text{SiMe}_3 < \text{Me} < \text{Ph} < \text{CH}_2\text{Ph}$ , with

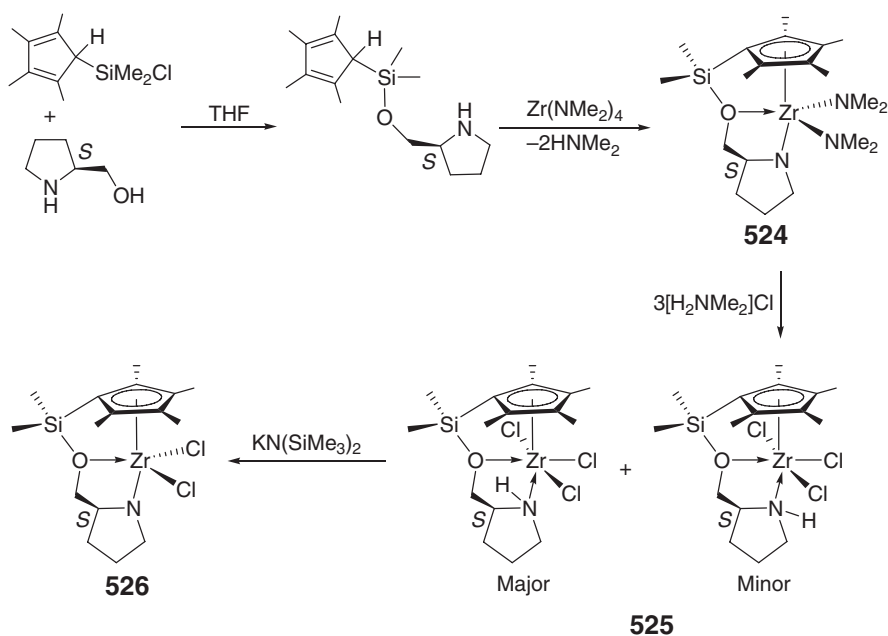




Scheme 116

the hafnium complexes being more stable than the zirconium counterparts. The reaction of the zirconium dimethyl derivative with  $\text{B}(\text{C}_6\text{F}_5)_3$  generates the contact ion pair **522**, and the insertion of CO into the Hf–R bond affords the  $\eta^1$ -monoacyl complex **523**.<sup>357</sup> Owing to the intramolecular coordination of the tethered neutral donor ligands, the MAO-activated dialkyl catalysts exhibit lower activity for ethylene polymerization than the donor-free analogs.

Aminolysis of  $\text{Zr}(\text{NMe}_2)_4$  with a chiral tridentate tetramethyl-Cp-amido-ether ligand produces the zirconium bis(amido) complex **524** in quantitative yield<sup>359</sup> (Scheme 117). Because of the ligand linkage, the amido moiety is positioned *trans* to the Cp ring, instead of the oxygen donor as in the tridentate complexes discussed above. Treatment of this bis(amido) complex with 3 equiv. of  $[\text{H}_2\text{NMe}_2]\text{Cl}$  leads to a mixture of two diastereomeric

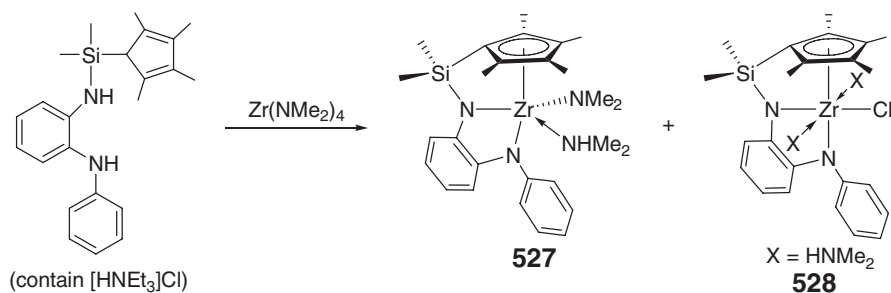


Scheme 117

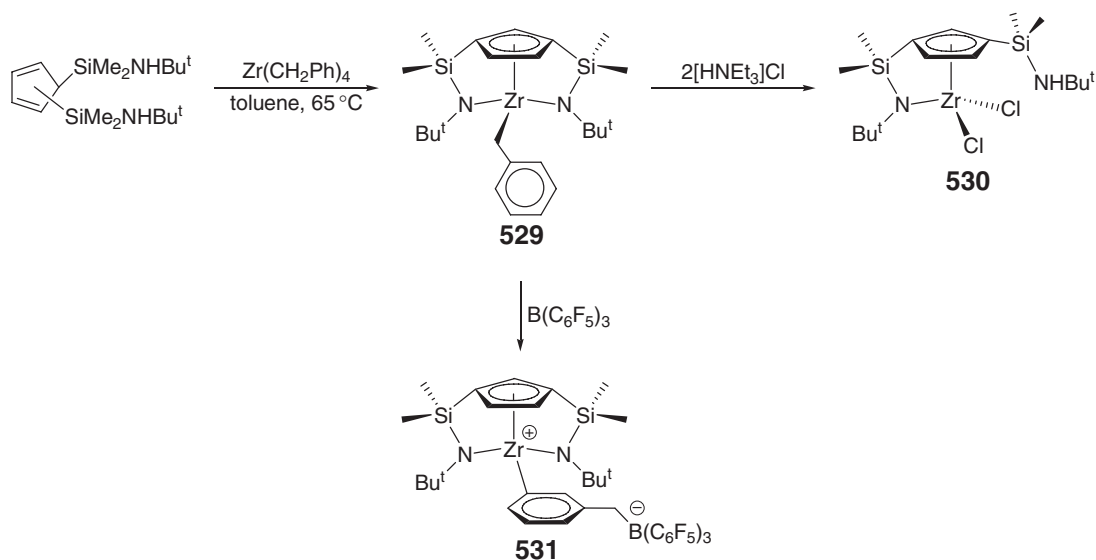
(*S,S* and *S,R*) trichloride complexes **525** in a 7:1 ratio; by limiting the amount of  $[\text{H}_2\text{NMe}_2]\text{Cl}$  employed, the concomitant protonation of the pyrrolidine amide cannot be prevented for the formation of the desired dichloride complex. However, an additional step of deprotonation of the trichloride with sterically crowded  $\text{LiN}(\text{SiMe}_3)_2$  affords the dichloride complex **526** in 80% yield. Alkylation of either the trichloride **525** or the dichloride **526** with  $\text{MeLi}$  results in Si–O bond cleavage in the chelating ligand and gives an undesired dimeric complex.

The reaction of  $\text{Zr}(\text{NMe}_2)_4$  with a tridentate tetramethyl-Cp-amido/amido-type trianionic ligand gives a mixture of two products in low yields: the zirconium dimethylamido complex **527** as a dimethylamine adduct and the zirconium chloro complex **528** as a bis(dimethylamine) adduct<sup>360</sup> (Scheme 118). The formation of the chloro complex **528** was due to the presence of the chloride impurity in the ligand, and separate isolation of this complex can be achieved by the same reaction, but with 2 equiv. of the neutral ligand. Both complexes were characterized by X-ray diffraction analysis.

A different class of the *ansa*-Cp-amido complexes is those incorporating the tridentate, trianionic Cp/bis(silylamido) ligands. The synthesis of such complexes utilizes the bis(amidosilyl)-functionalized ligand  $\text{C}_5\text{H}_4(\text{SiMe}_2\text{NHBu}^t)_2$  to protonate  $\text{Zr}(\text{CH}_2\text{Ph})_4$ , yielding the doubly silylamido-bridged Cp zirconium monobenzyl complex  $\eta^5\text{-C}_5\text{H}_3\{\text{SiMe}_2(\eta^1\text{-NBu}^t)\}_2\text{Zr}(\text{CH}_2\text{Ph})$  **529**<sup>361</sup> (Scheme 119). The reactions of the benzyl complex **529** (and its dimethylamido derivative) with  $\text{NEt}_3\cdot\text{HCl}$  yield the dichloride complex **530** containing the bidentate *ansa*-Cp-silylamido ligation, with concomitant cleavage of one of the silylamido bridges.<sup>362</sup> Treatment of the monobenzyl complex **529** with  $\text{B}(\text{C}_6\text{F}_5)_3$  generates the corresponding cationic complex **531**. The molecular structure of **531** features a pseudo-tetrahedral geometry about Zr, which is defined by the centroid of the 1,3-silylated Cp ring and the two appended silylamido sidearms, with the remaining coordination site occupied by the *meta*-C of the phenyl ring of the benzylborate anion.<sup>363</sup> Thus, the cation and anion are associated by the unusual  $\eta^1$ -coordination of the phenyl ring of the anion. Nevertheless, this cationic complex polymerizes ethylene under mild conditions (i.e., 23 °C and atmospheric pressure) despite being free of metal-alkyl



Scheme 118

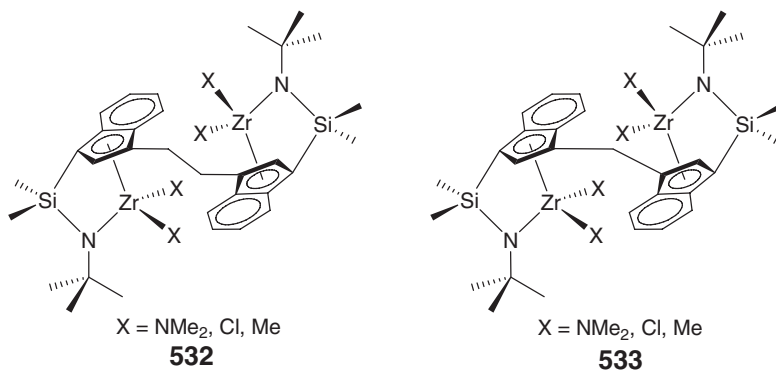


Scheme 119

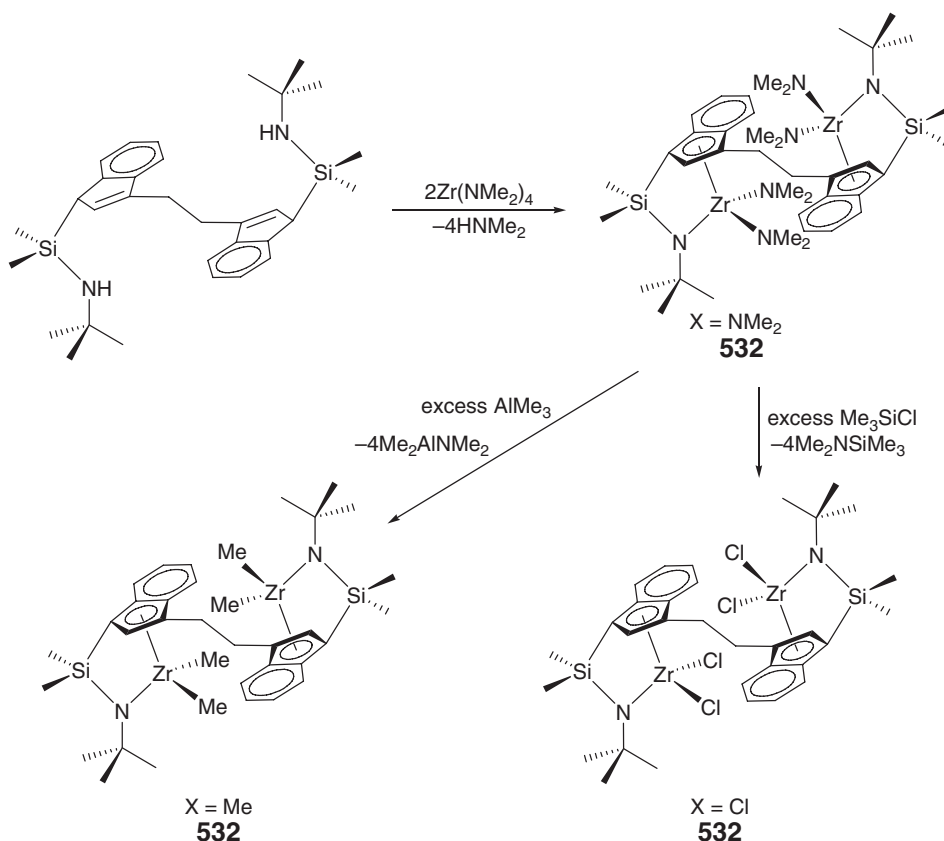
ligands in its activated, cationic form. The neutral benzyl complex **529**, when activated with MAO, is also active for polymerization of ethylene and co-polymerization of ethylene and 1-hexene.<sup>361</sup>

#### 4.08.8.1.4 Bimetallic *ansa*-Ind-silylamido complexes

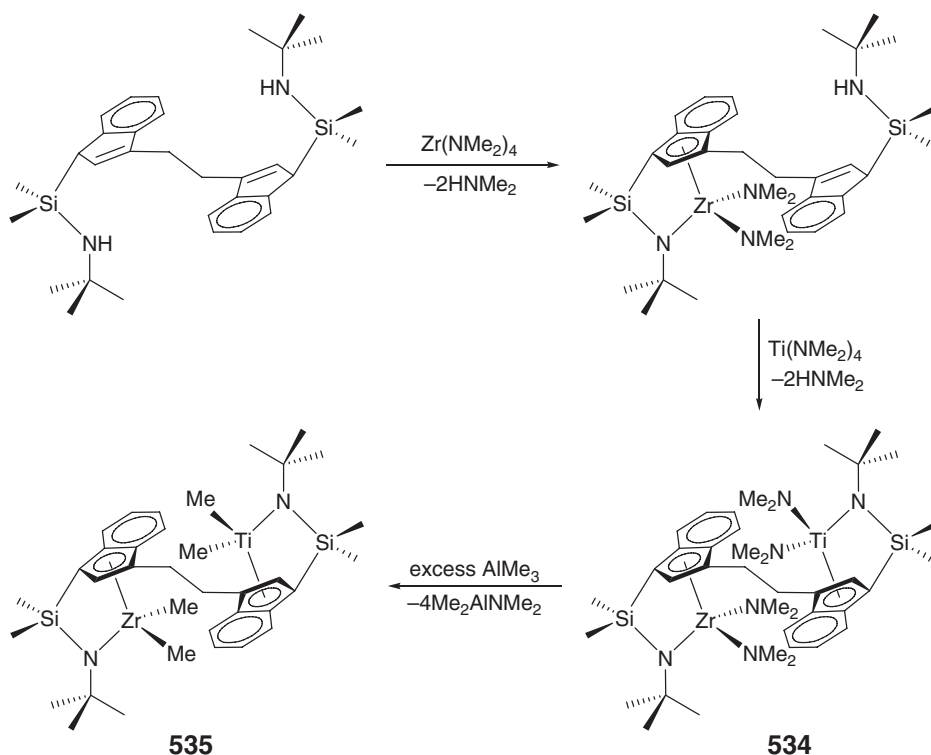
To investigate the potential cooperative effects between two proximate single-site active catalytic centers in olefin polymerization catalysis, a series of homobimetallic zirconium complexes incorporating two indenyl constrained-geometry ligand moieties linked by the ethylene bridge **532**<sup>364</sup> and the methylene bridge **533**<sup>365</sup> has been synthesized. The aim was to lock the two active centers into a spatially close proximity at all times by a covalent linker, rather than purely by electrostatic interactions, and to probe the effects of spatial proximity by changing the length of the linker.



The synthesis of the ethylene-bridged dinuclear complexes **532** employs the standard amine elimination procedures. Thus, aminolysis of Zr(NMe<sub>2</sub>)<sub>4</sub> with the neutral, C<sub>2</sub>H<sub>4</sub>-linked bis(indenyl) constrained-geometry-type ligand gives the bis(amido) bimetallic complex as a mixture of two diastereomers, in a 1 : 1.3 ratio (Scheme 120).<sup>364</sup> Treatment of this



Scheme 120



Scheme 121

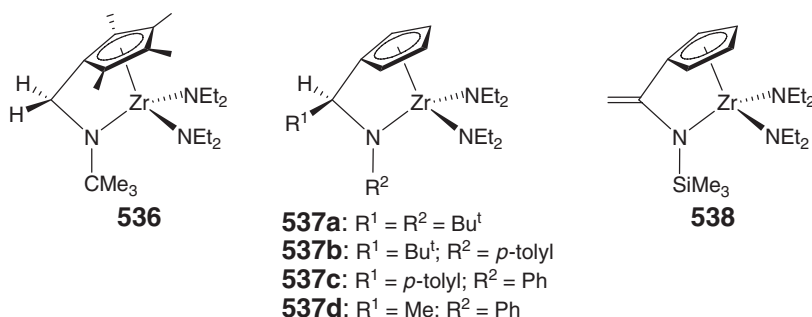
bis(amido) bimetallic complex with excess of  $\text{Me}_3\text{SiCl}$  and  $\text{AlMe}_3$  leads to the formation of the dichloride and dimethyl complex, respectively. The methylene-bridged dinuclear complexes **533** are synthesized in an analogous manner.<sup>365</sup> The active catalyst derived from the bimetallic complex **532** ( $\text{X} = \text{Me}$ ) activated with the bifunctional diborate activator,  $[\text{Ph}_3\text{C}]_2[1,4\text{-(C}_6\text{F}_5)_3\text{BC}_6\text{F}_4\text{B(C}_6\text{F}_5)_3]$ , produces  $\sim 11$  times more ethyl branches in ethylene polymerization and incorporates several times more  $\alpha$ -olefin co-monomers in ethylene co-polymerizations than the catalyst derived from the mononuclear analog combined with the monofunctional borate activator  $[\text{Ph}_3\text{C}][\text{B(C}_6\text{F}_5)_4]$ . This enhanced polyethylene branching and  $\alpha$ -olefin co-monomer enchainment are thought to occur via a process involving the second, closely held metal center. Compared with the catalyst derived from the ethylene-bridged dinuclear complex, the shorter methylene-bridged catalyst affords significantly higher molecular weight polyethylene and enhances the selectivity for  $\alpha$ -olefin co-monomer enchainment. These results support the argument that bimetallic cooperativity effects can decrease chain-transfer rates and increase selectivity for co-monomer enchainment.

In an effort to fully exploit the potential of heterodinuclear intramolecular cooperative effects in olefin polymerization catalysis, heterobimetallic zirconium and titanium complexes that contain the covalently linked Zr and Ti indenyl constrained-geometry moieties have been synthesized (Scheme 121).<sup>366</sup> The synthesis employs sequential aminolysis reactions of the neutral,  $\text{C}_2\text{H}_4$ -linked bis(indenyl) constrained-geometry-type ligand, first with  $\text{Zr(NMe}_2)_4$  and subsequently with  $\text{Ti(NMe}_2)_4$ , affording the heterobimetallic bis(amido) complex **534**. The choice of the reaction sequence employed is because the aminolysis of  $\text{Zr(NMe}_2)_4$  is faster and more selective than that of  $\text{Ti(NMe}_2)_4$ , and because a small amount of the undesired homodinuclear Zr byproduct can be readily separated by filtration. The solid-state structure of **534** reveals that the Zr and Ti are positionally disordered. The reaction of the bis(amido) complex with excess  $\text{AlMe}_3$  cleanly affords the corresponding dimethyl heterobimetallic complex **535**. Upon activation with  $[\text{Ph}_3\text{C}][\text{B(C}_6\text{F}_5)_4]$ , this dimethyl complex is active for ethylene polymerization; more significantly, it produces long-chain ( $\geq \text{C}_6$ ) branched polyethylenes, in sharp contrast to control experiments with catalyst mixtures containing mononuclear Zr and Ti analogs.

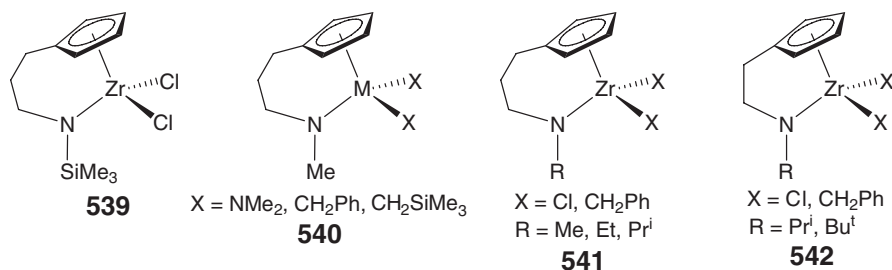
#### 4.08.8.1.5 Hydrocarbyl-bridged Cp-amido complexes

All the *ansa*-Cp-amido complexes discussed so far are based on the dimethylsilylene-bridged Cp-amido ligation. A significant extension of the constrained-geometry group 4 complexes is the development of the hydrocarbyl-bridged

Cp-amido ligation, and, subsequently, a series of complexes incorporating the bidentate *ansa*-Cp-amido ligation bridged by  $sp^3$ - and  $sp^2$ -hydrocarbyl moieties has been synthesized. Complexes with only one-carbon linker ( $C_1$ ) include the methylene-bridged complex **536**,<sup>367</sup> alkylidene-bridged complexes **537**,<sup>368</sup> with variations of the groups on the bridging carbon and the amido nitrogen, and the  $sp^2$ -carbon, 1,1-ethylene-bridged complex **538**.<sup>369</sup> These complexes were synthesized by the salt metathesis route involving the reaction of  $Cl_2Zr(NEt_2)_2(THF)_2$  with the dilithium salt of the bidentate Cp-amido ligand linked by the appropriate hydrocarbon moiety, which was prepared by addition of a lithium amide reagent to an appropriate fulvene. One of the most prominent structural features about these complexes is the observation that substituting the  $Me_2Si$  linker by the  $R(H)C$  moiety consistently results in a reduction of the Cp(centroid)–M–N angle by about  $10^\circ$ , suggesting even more constrained ligation in these  $C_1$ -bridged Cp-amido complexes and thus sterically even more open catalysts in their activated forms; this is supported by the ethylene/1-octene co-polymerization results, which show that the MAO-activated complexes generally exhibit good activity with high 1-octene incorporation.

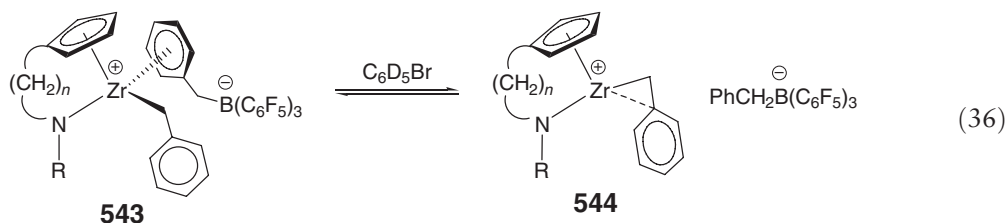


Hydrocarbyl-bridged Cp-amido complexes with ethylene ( $C_2$ ) and propylene ( $C_3$ ) linkers have also been prepared; these include the propylene-bridged zirconium dichloride **539**,<sup>370</sup> propylene-bridged Cp/methylamido zirconium and hafnium bis(dimethylamido) and dialkyl complexes **540**,<sup>371</sup> propylene-bridged Cp/methyl (ethyl, isopropyl)amido zirconium dichloride and dibenzyl complexes **541**,<sup>372</sup> and ethylene-bridged Cp/isopropyl (*tert*-butyl)amido zirconium dichloride and dibenzyl complexes **542**.<sup>372</sup> These complexes were synthesized by elimination routes involving reactions between the trimethylsilyl-substituted ligand and  $ZrCl_4$ , the neutral ligand and  $Cl_2Zr(NMe_2)_2(THF)_2$ , or the neutral ligand and  $M(NMe_2)_4$ .



Activation of the ethylene- and propylene-bridged Cp-amido zirconium dibenzyl complexes by  $B(C_6F_5)_3$  in  $C_6D_5Br$  generates the corresponding cationic benzyl complexes in which the interaction between the cationic and anionic moieties is highly dependent on the nature of the  $[Cp(CH_2)_nNR]^{2-}$  ligand.<sup>372</sup> There are two types of ion pair structures derived from *in situ* activation: contact ion pair **543** via  $\eta^6$ -arene coordination of the anion and solvent-separated ion pair **544** via  $\eta^2$ -benzyl stabilization of the cation (Equation (36)). From the low-temperature  $^{19}F$  NMR studies, it is found that for ion pairs with the  $n=2$  linker, changing the substituent  $R$  from  $^iPr$  to  $^tBu$  shifts the equilibrium from a predominantly bound to a predominantly free anion structure (i.e., to the right). There is a

comparable change induced by lengthening the bridge length from  $n = 2$  to 3 for a given R. For a comparative example, the silylene-bridged  $\text{Me}_2\text{Si}(\text{Me}_4\text{Cp})\text{Bu}^t\text{N}$  analog exists predominantly as the solvent-separated ion pair (structural type **544**). This observation further illustrates the subtle interplay of ligand steric bulk and cation–anion separation.

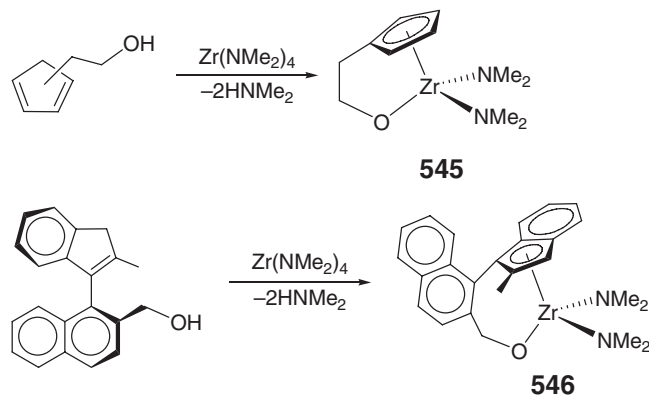


#### 4.08.8.2 *ansa*-Cp–Oxo Complexes

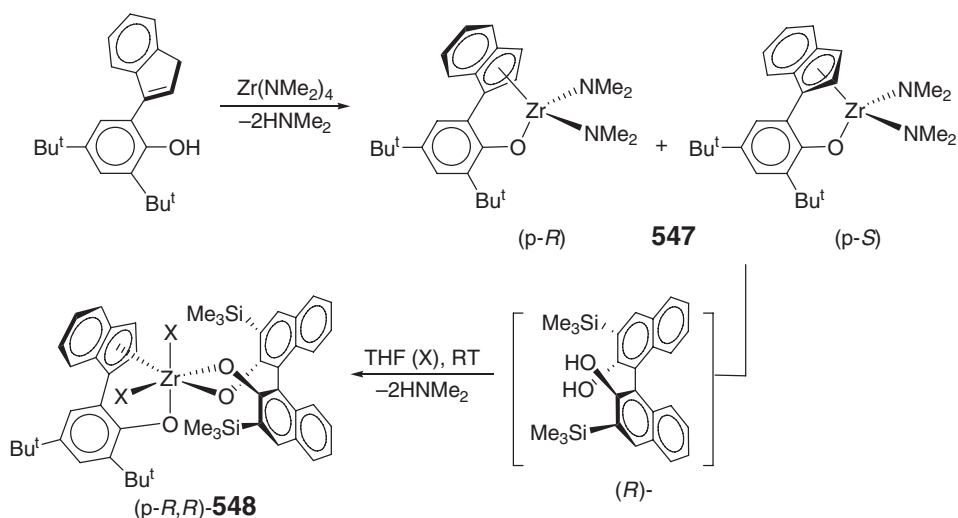
The aminolytic reaction between  $\text{Zr}(\text{NMe}_2)_4$  and the OH-functionalized Cp ligand,  $\text{C}_5\text{H}_5\text{CH}_2\text{CH}_2\text{OH}$ , which was prepared by epoxide ring opening of ethylene oxide with  $\text{CpLi}/\text{BF}_3 \cdot \text{Et}_2\text{O}$ , yields the zirconium bis(dimethylamido) complex **545** bearing the *ansa*-Cp–ethoxide chelating ligand<sup>373</sup> (Scheme 122). The structural features about this complex and its reactivity were not available. The analogous aminolytic reaction of  $\text{Zr}(\text{NMe}_2)_4$  and the enantiomerically pure, OH-functionalized indenyl ligand leads to the planar chiral *ansa*-Ind/oxido zirconium bis(amide) **546** in quantitative yield.<sup>374</sup>

Aminolysis of  $\text{Zr}(\text{NMe}_2)_4$  with 2-(indenyl)–4,6-di-*tert*-butylphenoxide ligand affords indenyl half-sandwich zirconium bis(amide) **547** (Scheme 123).<sup>375</sup> The structural studies show the presence of both the (*p*-*R*) and (*p*-*S*) enantiomers within the unit cell due to the planar chirality created by the indenyl coordination. The two remaining dimethylamido ligands can undergo protolysis reaction with (*R*)-3,3′-bis(trimethylsilyl)–1,1′-binaphthyl-2,2′-diol, forming an initial 50/50 mixture of two diastereomers. The use of THF for crystallization led to crystals of the (*p*-*R*,*R*) diastereomer **548**. The molecular structure of **548** features a pseudo-octahedral Zr center with two *cis*-coordinated THF molecules along with the (*R*)-binol ligand and the (*p*-*R*) chelated indenyl phenoxide ligand. The indenyl ring is only  $\eta^3$ -bound to Zr in the solid state of **548**. Aminolysis of  $\text{Zr}(\text{NMe}_2)_4$  with 2 equiv. of 2-(indenyl)–4,6-di-*tert*-butylphenoxide ligand yields bis(chelated indenyl–phenoxy) sandwich zirconium complexes as a mixture of two isomers.<sup>376</sup>

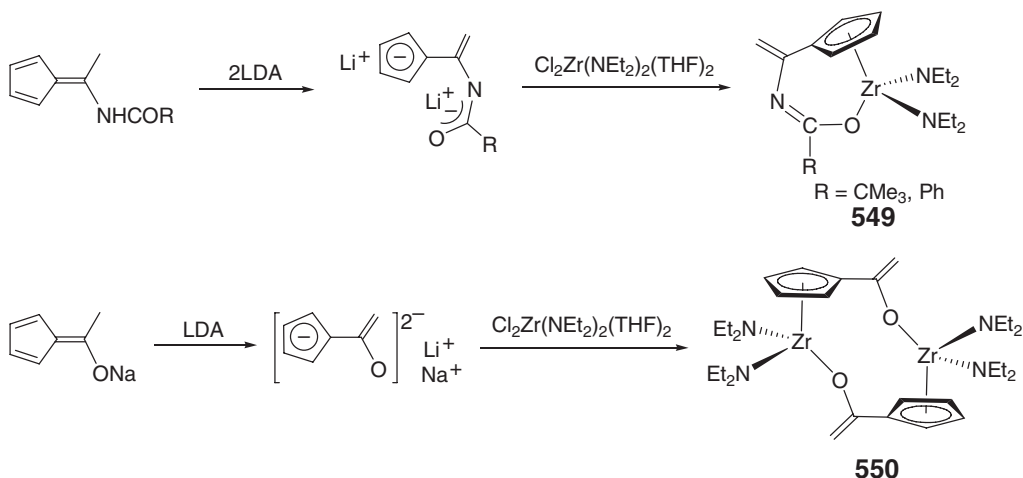
Several zirconium complexes supported by *ansa*- $\eta^5$ -Cp/ $\eta^1$ -oxo chelating ligands, including the monomeric complexes **549** ( $\text{R} = \text{Bu}^t$ ,<sup>369</sup>  $\text{Ph}$ <sup>377</sup>) and the dimeric zirconium complex **550**,<sup>378</sup> have been synthesized by the salt metathesis route involving the reaction of  $\text{Cl}_2\text{Zr}(\text{NEt}_2)_2(\text{THF})_2$  with the dilithium salt of the bidentate Cp/oxo ligand prepared from the fulvene route (Scheme 124). The crystallographically characterized dimeric structure of the



Scheme 122



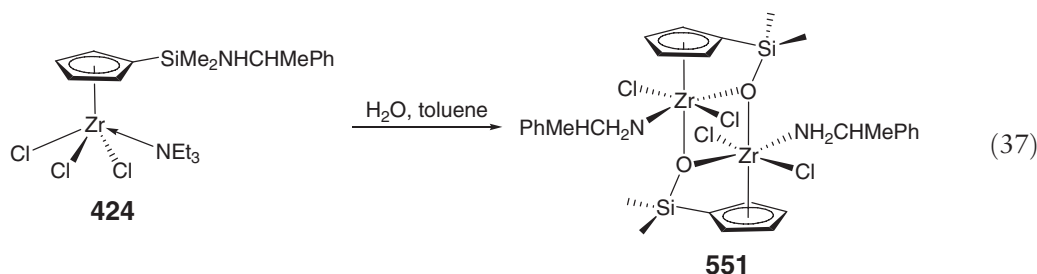
Scheme 123



Scheme 124

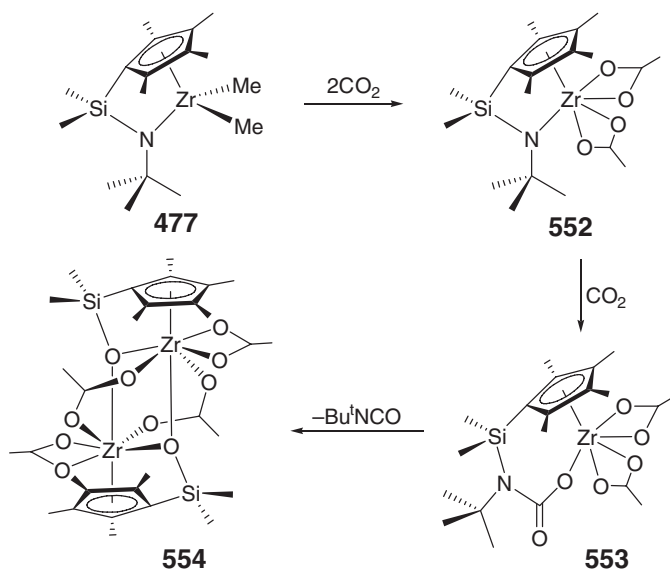
zirconium complex **550** is retained in solution as shown by cryoscopy in benzene. More significantly, the ligand backbone of this complex shows no specific steric constraints as compared with the typical constrained geometry complexes with the dimethylsilylene-bridged Cp-amido ligation. However, upon treatment with excess MAO, the unconstrained complex **550** is an active catalyst for effective ethene/1-octene co-polymerization, with up to 20% 1-octene incorporation in the resulting co-polymer at 90 °C. This complex is structurally and catalytically similar to the unbridged mono-Cp complexes which are also good catalysts for such co-polymerizations.

Hydrolysis of the amidosilyl-substituted Cp zirconium trichloride **424** in water-saturated toluene results in the slow precipitation of the oxozirconium derivative **551** as white crystals in low yield (Equation (37)).<sup>304</sup> The solid-state structure of **551** features a dimer in which the two *ansa*-Cp/oxo zirconium dichloride units are bridged by two oxygen atoms through two pseudo-octahedral zirconium centers, forming a four-membered  $\text{Zr}_2\text{O}_2$  core, instead of an eight-membered ring chelate in the case of the titanium counterpart. The formation of such a structure presumably results from the hydrolysis of the Si–N bond in the precursor trichloride **424** with the concomitant elimination of the amine  $\text{NH}_2\text{CH}(\text{Me})\text{Ph}$  which is subsequently coordinated to Zr in the product, and the simultaneous hydrolysis of one of the Zr–Cl bonds to give HCl, eliminated as the ammonium salt  $[\text{HNEt}_3]\text{Cl}$ .



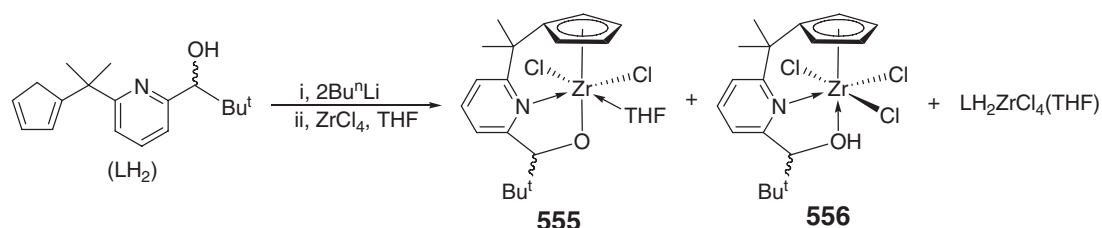
Insertion of 2 equiv. of  $\text{CO}_2$  into both the  $\text{Zr-Me}$  bonds in  $\text{Me}_2\text{Si}(\eta^5\text{-C}_5\text{Me}_4)(\eta^1\text{-NBu}^t)\text{ZrMe}_2$  **477** yields the double-insertion product **552** with a pair of chelating acetate ligands (Scheme 125).<sup>379</sup> Complex **552** exists as a dimer linked by two bridging acetate ligands in the solid state with an acute Cp(centroid)–Zr–N angle of  $99.6^\circ$ , but the IR and NMR data indicate that the monomeric structure with only chelating acetates (i.e., no bridging acetates) predominates in solution. Further reaction with  $\text{CO}_2$  affords the dimeric structure **554** with concomitant elimination of isocyanate  $\text{Bu}^t\text{NCO}$ , occurring presumably via the intermediate **553**. The molecular structure of the complex **554** shows that the two seven-coordinate Zr centers are linked by a pair of bridging acetate groups, which are positioned above and below the central  $\text{Zr}_2\text{O}_2$  unit, and by the silyloxy oxygen atoms; the coordination sphere at each Zr center is completed with a single chelated acetate ligand and the tetramethyl–Cp ring. There is a total of six Zr-bound oxygen donor atoms, five of which are located in a nearly pentagonal arrangement with the sixth one lying *trans* to the centroid of the Cp ring. The overall result of this carboxylation reaction of the *ansa*-Cp–silylamido starting structure has been converted to the *ansa*-Cp/oxo product, providing a simple route for the conversion from *N*- to *O*-functionality in these constrained-geometry type of complexes.

Double deprotonation of the bifunctional mono-CpH/alcohol racemic ligand linked by the 2,6-pyridyl unit followed by salt metathesis with  $\text{ZrCl}_4$  yielded the *ansa*-Cp/oxo zirconium dichloride complex **555**, but with the concomitant formation of the undesired complex **556** incorporating the mono-anionic form of the ligand and the simple adduct of the neutral ligand and  $\text{ZrCl}_4$ <sup>380</sup> (Scheme 126). The latter two undesired species have been structurally characterized; however, complex **555** obtained forms an insoluble oligomeric species after the loss of THF upon purification.



Scheme 125



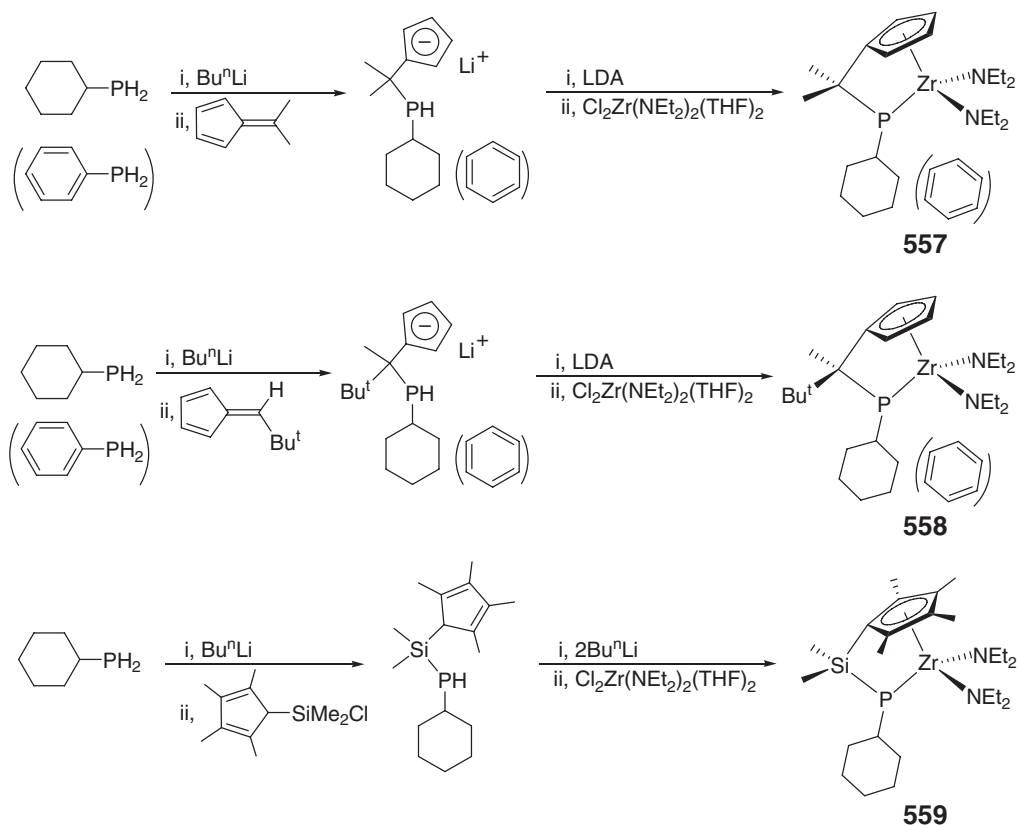


Scheme 126

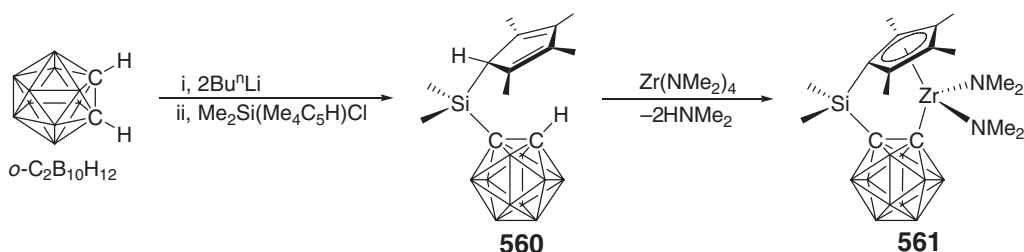
#### 4.08.8.3 *ansa*-Cp/Phosphido Complexes

Single-carbon ( $sp^3$ -C<sub>1</sub>)-bridged Cp/phosphido zirconium bis(amido) complexes **557**<sup>367</sup> were synthesized by the salt metathesis route involving the reaction of  $\text{Cl}_2\text{Zr}(\text{NEt}_2)_2(\text{THF})_2$  with the dilithium salt of bidentate Cp/phosphido ligands linked by an isopropylidene moiety. The ligands were prepared by deprotonation of cyclohexylphosphine or phenylphosphine, followed by the addition to 6,6-dimethylfulvene (Scheme 127). The same metathesis approach but with some variations in the ligand synthesis was employed to prepare its alkylidene-bridged analogs **558**<sup>381</sup> and the dimethylsilylene-bridged tetramethyl-Cp/phosphido complex **559**.<sup>382</sup>

These complexes show dynamic behavior in solution due to the stereochemical inversion at the phosphorus atom, but the barrier for such inversions is low. For example, the Gibbs activation energies for the inversion at P in **557** are  $\Delta G^\ddagger(193\text{ K}) = 8.6 \pm 0.5\text{ kcal mol}^{-1}$  (for the cyclohexyl derivative) and  $\Delta G^\ddagger(173\text{ K}) = 7.5 \pm 0.5\text{ kcal mol}^{-1}$  (for the phenyl derivative).<sup>381</sup> Upon activation with a large excess of MAO, all complexes are active for polymerization of ethylene and co-polymerization of ethylene and 1-octene. Within the alkylidene series, the isopropylidene-bridged Cp/phosphido complexes **557** exhibit high catalytic activity and are more active than the titanium counterparts,



Scheme 127



Scheme 128

which is a reversal of the trend observed typically for  $\text{Me}_2\text{Si}(\eta^5\text{-Cp})(\eta^1\text{-NBu}^t)\text{MCl}_2$  complexes. On the other hand, substituting a methyl group on the alkylidene bridging moiety by a *tert*-butyl group, which gives the closely related complexes **558**, produces substantially lower activity catalysts for these types of polymerization reactions. These results reflect the strong influence of the bridging backbone structure on the reactivity of these complexes. In the case of the  $\text{SiMe}_2$ -bridged complex **559**, the ethylene polymerization and ethylene/1-octene co-polymerization activities of the zirconium complex are comparable with its titanium counterpart.

#### 4.08.8.4 *ansa*-Cp/Carbanionic Complexes

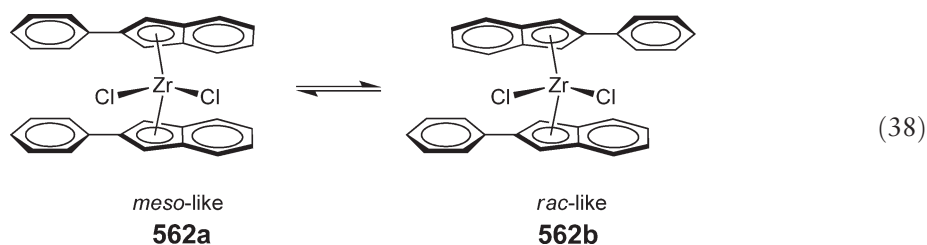
The *o*-carboranyl silyl-substituted Cp ligand (**560**, Scheme 128) was obtained by the reaction of the *in situ*-generated dilithium salt of *o*-carborane,  $\text{Li}_2\text{C}_2\text{B}_{10}\text{H}_{10}$ , and  $\text{Me}_2\text{Si}(\text{Me}_4\text{C}_5\text{H})\text{Cl}$  in refluxing benzene/diethyl ether followed by hydrolysis.<sup>383</sup> Aminolysis of  $\text{Zr}(\text{NMe}_2)_4$  with this neutral carborane-containing ligand at 70 °C in toluene produces the zirconium bis(amide) **561** incorporating a constrained-geometry-type ligand framework with a dimethylsilyl-bridged Cp/carboranyl linkage: a Cp(centroid)–Zr–C angle of 110.3°.

### 4.08.9 Bis(Cyclopentadienyl) Complexes

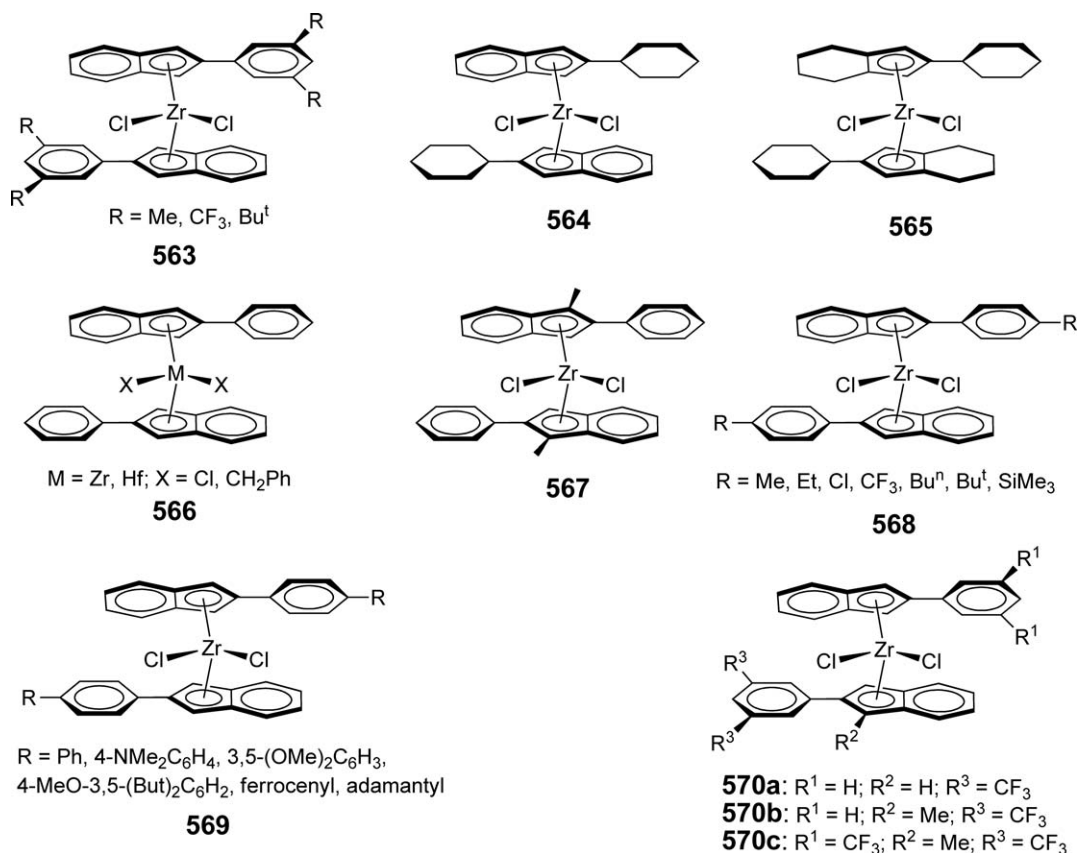
#### 4.08.9.1 Complexes with M–X (Halide) Bonds

##### 4.08.9.1.1 Non-functionalized metallocene halides

One of the major advances in the chemistry of non-bridged bis(Cp)-type metallocenes halides is the development of the so-called “oscillating” catalysts.<sup>384</sup> A prototype of such a class of complexes is bis(2-phenylindenyl)zirconium dichloride **562**, shown in Equation (38). This complex can undergo rapid isomerization between achiral, *meso*-like and chiral, *rac*-like conformational stereoisomers; upon activation with MAO, it polymerizes propylene to atactic–isotactic stereoblock poly(propylene), a thermoplastic elastomeric material. Although the formation of this polymer microstructure was originally attributed to the oscillation between aspecific (*meso*-isomer) and isospecific (*rac*-isomer) conformer geometries during the chain growth process, ligand rotation is far too fast to account for the formation of stereoblock-type polymers. Oscillation between *rac*-type conformers is more likely. The mechanism is still a subject of debate.<sup>385,386</sup> For further discussion see Chapter 4.09, section 4.09.4.2.3.



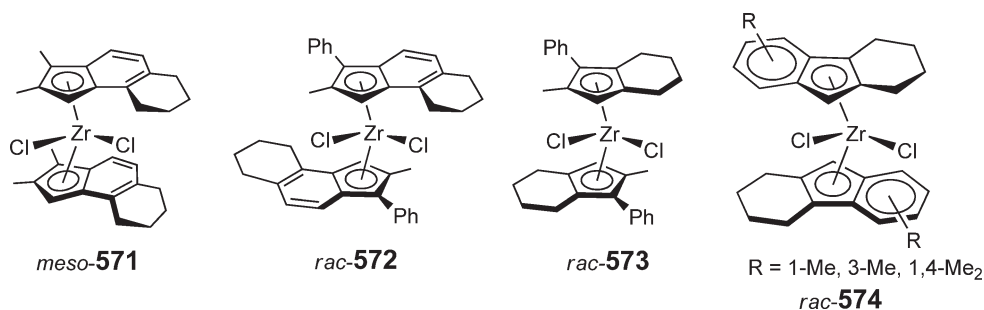
Major efforts in catalyst modification directed toward enhancement of catalyst productivity and the properties of the resulting polymer have resulted in a number of derivatives, which are summarized in Scheme 129 (only *rac*-like



Scheme 129

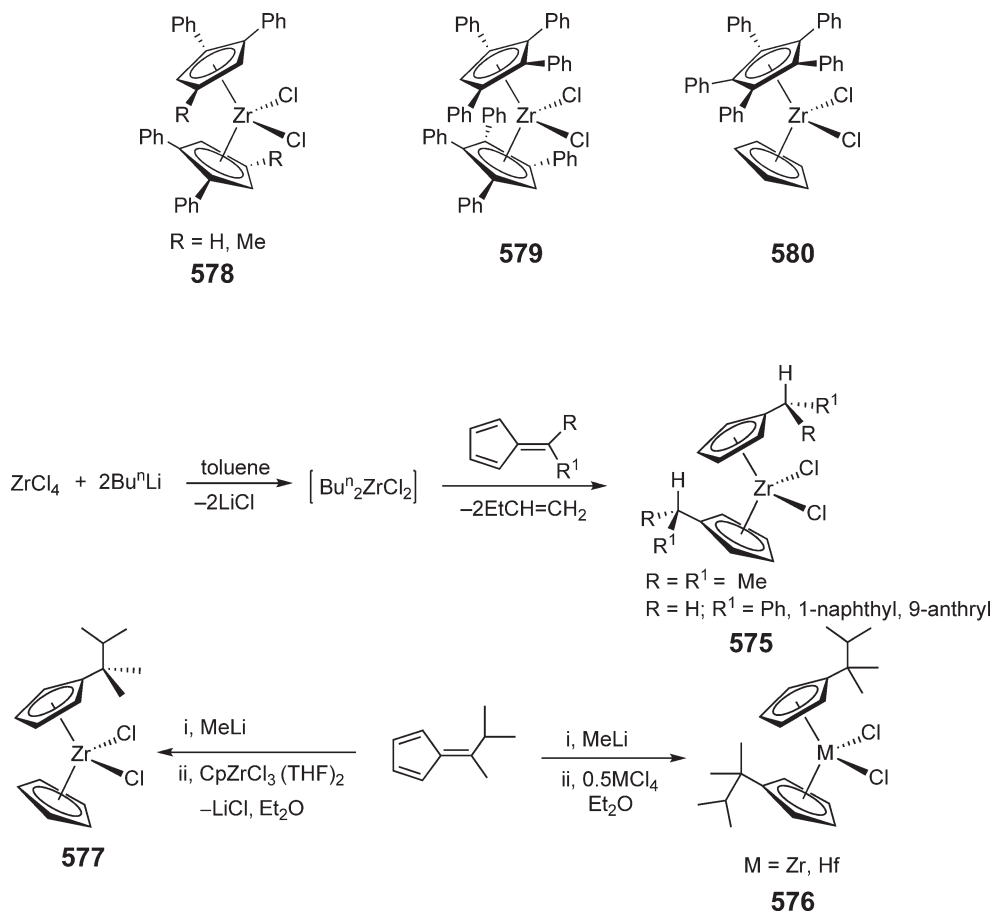
isomers shown); these include 3,5-disubstituted phenyl derivatives **563**<sup>387,388</sup> 2-cyclohexyl-substituted indenyl **564** and tetrahydroindenyl **565** derivatives,<sup>389</sup> zirconium and hafnium dichloro and dibenzyl derivatives **566**<sup>390</sup> 1-methyl-2-phenyl derivative **567**<sup>391</sup> 2-phenyl derivatives **568**<sup>392</sup> and **569**<sup>393</sup> of varying the 4-substituent on the phenyl ring, as well as complexes **570** with mixed 2-phenylindenyl ligands.<sup>394</sup>

Modification of the bis(indenyl) metallocene structure has been extended to 2-alkyl- (butyl, octyl, dodecyl) and arylalkyl- (benzyl, phenylethyl, phenylpropyl) substituted zirconocene dichlorides (2-R-Ind)<sub>2</sub>ZrCl<sub>2</sub> (R = alkyl and arylalkyl substituents)<sup>395</sup> and 1-substituted bis(indenyl) zirconocene dichlorides (1-R-Ind)<sub>2</sub>ZrCl<sub>2</sub> (R = Me, Et, Pr<sup>i</sup>, Bu<sup>t</sup>, SiMe<sub>3</sub>, Ph, CH<sub>2</sub>Ph, 1-Naph).<sup>396</sup> Bis(2-menthylindenyl)zirconocene dichloride and bis(2-menthyl-4,7-dimethylindenyl)zirconocene dichloride have also been synthesized and structurally characterized; upon activation with MAO, they are moderately active for polymerization of propylene, producing the polymer of low stereoregularity.<sup>397</sup> Aryl-substituted zirconocenes **571** containing the bis(tetrahydro-2,3-dimethylbenz[e]indenyl) and **572** containing the bis(tetrahydro-2-methyl-3-phenylbenz[e]indenyl) ligand were isolated as *meso*-like and *rac*-like isomers, respectively, by the standard salt metathesis approach.<sup>398</sup> Analogous phenyl-substituted bis(Cp) zirconocenes **573** were obtained as a *rac/meso*-isomer mixture, from which the pure *rac*-isomer was isolated by recrystallization.<sup>399</sup> Zirconocenes **574** (only racemic isomers shown) bearing the unbridged tetrahydrofluorenyl ligands were obtained as 1:1 mixtures of the *rac*- and *meso*-isomers by salt metathesis and produce mostly atactic polypropylene in polymerization of propylene when activated with suitable activators.<sup>760</sup> Interestingly, the simple unbridged bis(1-methylfluorenyl)zirconium dichloride, when activated with MAO, produces isotactic polypropylene with *[mmmm]* = 83% in the polymerization of liquid propylene at 60 °C.<sup>400</sup> On the other hand, bis((1-methyl-9-phenyl-fluorenyl)zirconium dichloride/MAO and bis((1-methyl-9-cyclohexyl-fluorenyl)zirconium dichloride/MAO were reported to exhibit no propylene polymerization activity.<sup>401</sup> Other C<sub>2</sub>-symmetric unbridged bis(fluorenyl)-zirconocene complexes such as bis(2,7-dimesitylfluorenyl)zirconium dichloride exhibit low activity in propylene polymerization, producing atactic polypropylene.<sup>402</sup>



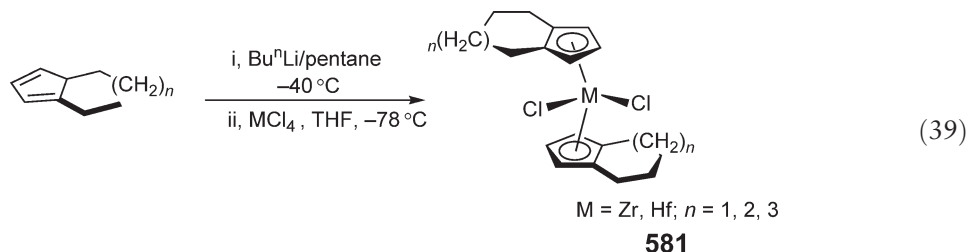
6,6-Disubstituted fulvenes are a common source for alkyl-substituted Cp ligand. The reaction of the *in-situ* generated “Bu<sup>n</sup><sub>2</sub>ZrCl<sub>2</sub>” species with 2 equiv. of substituted fulvenes in hydrocarbons produces alkyl-substituted zirconocene dichlorides **575** in high yields (Scheme 130).<sup>403</sup> 6,6-Disubstituted fulvenes were also used to synthesize sterically hindered metallocene dichlorides **576** and **577** via the salt metathesis route.<sup>404</sup>

Aryl groups such as phenyl are frequently employed to tune the sterics and electronics of the resulting zirconocene dichlorides as effective olefin polymerization pre-catalysts. For example, pseudo-*C*<sub>2</sub> *rac*-like zirconocene complexes **578** with diphenyl-substituted Cp ligands were obtained by salt metathesis; when activated with MAO, these complexes exhibit moderate activities for ethylene polymerization at relatively low Al:Zr ratios, producing high molecular weight polyethylenes with high melting transition temperatures.<sup>405</sup> Derived by the investigations of ligand effects on olefin polymerization activity of the zirconocene complexes, zirconocene dichlorides **579**<sup>406</sup> and the mixed sandwich complex **580**<sup>230</sup> with higher levels of phenyl substitution have also been prepared.



Scheme 130

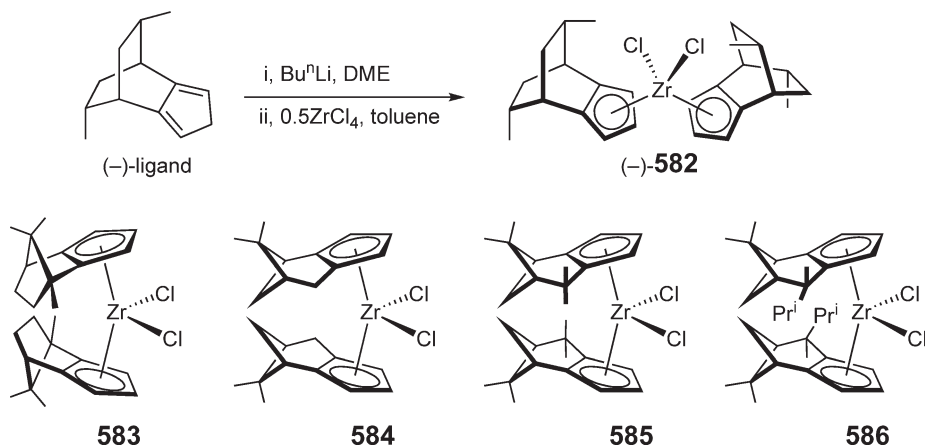
The normal route to the tetrahydroindenyl ligands is via the catalytic hydrogenation of the corresponding unsaturated  $\eta^5$ -indenyl metallocenes. A more versatile and flexible route to the tetrahydroindenyl system containing six-, seven-, and eight-membered saturated rings attached to the Cp ring has been developed.<sup>407</sup> The synthesis of fused tetrahydroindenyl-type zirconocene and hafnocene complexes **581** containing bicyclic ligands  $C_5H_3(1,2-CH_2-)_n$ , where  $n = 4, 5$ , or  $6$ , involves the standard salt metathesis approach using the tetrahydroindenyl-type ligands prepared from bicycloalkenones (Equation (39)).



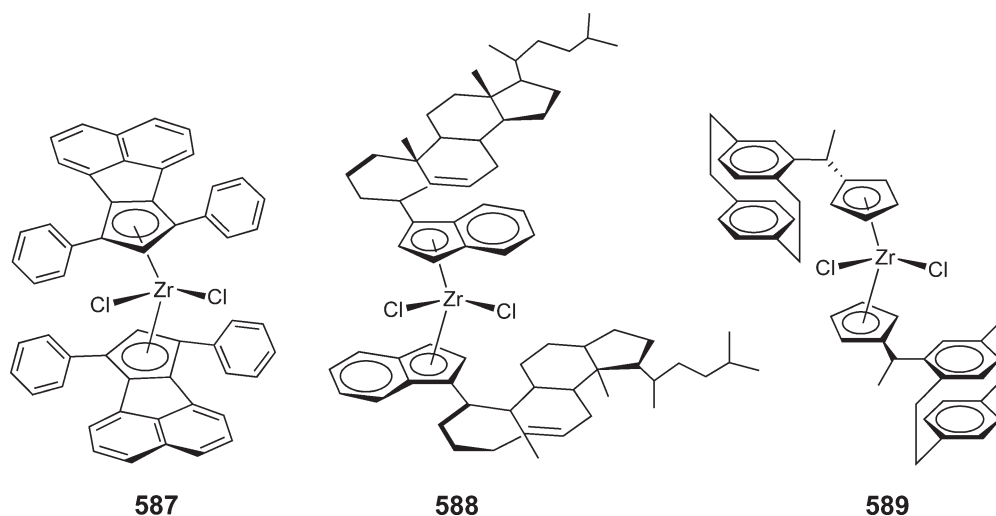
The enantiomerically pure complex **582** was obtained by salt metathesis using the enantiomerically pure lithiated ligand<sup>408</sup> (Scheme 131). The molecular structure shows that the Cp substituents are arranged in a roughly  $C_2$ -symmetric orientation and the Cp carbons are close to a synclinal orientation. Other examples of non-bridged optically active,  $C_2$ -symmetric zirconocene dichlorides containing similarly fused Cp rings include complexes **583–586**<sup>409</sup> which have been investigated as catalysts to effect the asymmetric hydrogenation of 2-phenyl-1-butene and 2-( $\alpha$ -naphthyl)-1-butene.

Zirconocenes such as complex **587** (Scheme 132) incorporating very large substituents on the Cp rings were synthesized for the purpose of examining the influence of large  $\alpha$ - and  $\beta$ -substituents on the olefin polymerization behavior.<sup>410</sup> Complexes analogous to **587** with a methyl or phenyl group substituted at the 2-cyclopenta[*l*]phenanthryl position have also been prepared; they produce polypropylene of low isotacticity in the MAO-co-catalyzed polymerization of propylene.<sup>411</sup> Non-bridged bis(indenyl)zirconocene dichlorides bearing large, optically active substituents on the indenyl rings are typically formed as a mixture of three planarly chiral diastereomers via the salt metathesis route. For example, the cholesteryl-substituted indenyllithium salt reacts with  $ZrCl_4$  to generate the bis[3-(5-cholesten-3 $\alpha$ -yl)indenyl] $ZrCl_2$  **588** as a mixture of three diastereoisomers.<sup>412</sup> Several analogous Cp complexes and Ind complexes carrying other types of optically active substituents have been reported.<sup>413–415</sup> Chiral metallocenophanes such as complex **589** were derived from [2,2]paracyclophane;<sup>416</sup> the bulky and rigid substitutions on the Cp rings are employed to reduce conformational mobility in the resulting metallocene complex, thereby presenting permanent chiral character.

Other ligand variations have resulted in a large number of metallocene dichloride complexes; these include  $\omega$ -phenylalkyl-substituted Cp zirconocenes,<sup>417</sup> mixed zirconocenes of the type (L)(Ind) $ZrCl_2$  (L =  $\omega$ -phenylalkyl-substituted Cp, 1-phenylsilyl-substituted Ind) and (L)(Flu) $ZrCl_2$  (L = 1-benzyl-substituted Ind or 2-benzyl



Scheme 131

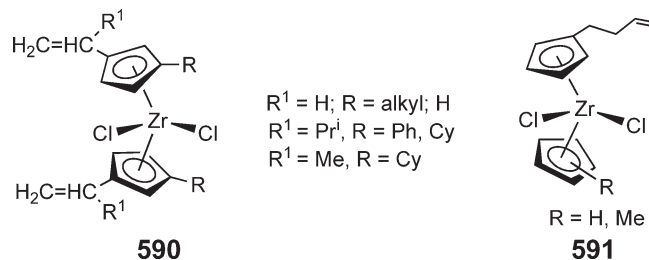


Scheme 132

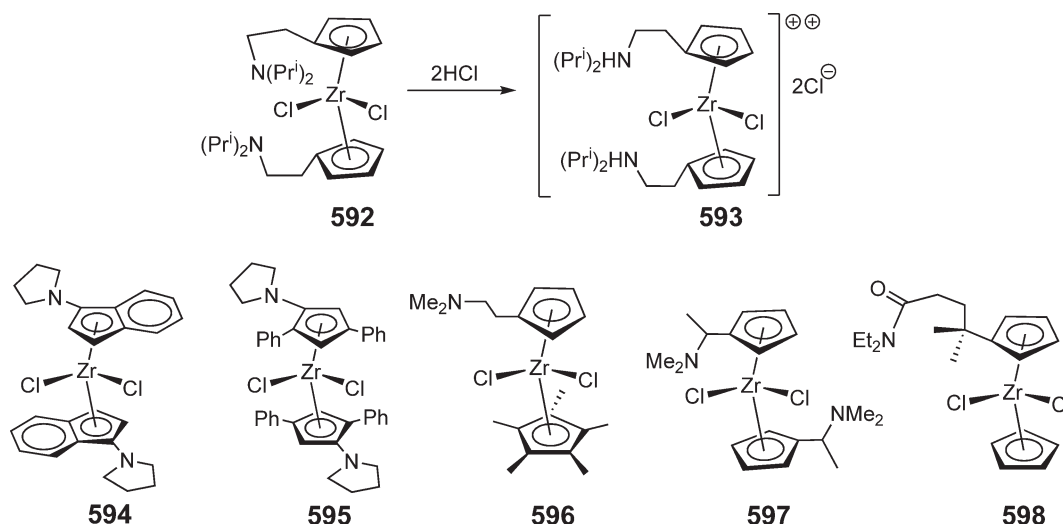
substituted Ind),<sup>418,419</sup> as well as zirconocenes carrying one or two Ph-, C<sub>6</sub>F<sub>5</sub>-, and bis- or tris(C<sub>6</sub>F<sub>5</sub>)-substituted Cp rings.<sup>420</sup> Zirconocene difluoride and alkyl monofluoride complexes can be prepared by several different approaches, depending on the precursor employed.<sup>421</sup>

#### 4.08.9.1.2 Ring-functionalized metallocene halides

Ring functionalized zirconocenes **590** contain (1-alkenyl-3-alkyl)Cp ligands, the double bonds of which, upon irradiation at 450 nm, can undergo rapid intramolecular [2 + 2]-cycloaddition to form cyclobutene-bridged *ansa*-metallocene complexes in high yield.<sup>422</sup> This photochemical coupling of readily introduced alkenyl functionalities represents a unique, alternative route leading to C<sub>2</sub>-chiral, hydrocarbyl-bridged *ansa*-zirconocenes. The functionalized Cp ligand with a longer alkenyl chain, C<sub>5</sub>Me<sub>4</sub>CH<sub>2</sub>CH<sub>2</sub>CH=CH<sub>2</sub>, was employed to prepare mixed zirconocenes **591**.<sup>423</sup>



Introduction of *N*-donor functionalities to the Cp ligands that support metallocenes is a feasible strategy to provide stabilization for the highly reactive metallocene intermediate in polymerization catalysis via reversible coordination of the *N*-donor atom to the vacant coordination site at the metal. Zirconocene dichloride **592** bearing [2-(diisopropyl-amino)ethyl]-substituted Cp ligands is one such example.<sup>424</sup> This complex is an active catalyst for ethylene polymerization, upon activation with MAO, and reacts with 2 equiv. of HCl to give the air- and moisture-stable zirconocene dichloride **593**, with protonation of the amino groups (Scheme 133). Dipyrrolidinyl-substituted indenyl zirconocene dichloride **594** crystallizes in its racemic mixture, whereas the *meso*-rotamer is not present.<sup>425</sup> The analogous dipyrrolidinyl-substituted Cp zirconocene dichloride **595** was also isolated. Nitrogen-functionalized zirconocene complexes analogous to **594**, such as bis(phenyl-3-pyrrolidinylcyclopentadienyl)zirconium dichloride and bis(2-morpholinoindenyl)zirconium dichloride, are obtained by salt metathesis. Their dynamic features with respect to conformationally rotational processes were examined by variable-temperature NMR studies.<sup>426</sup> Additionally, bis(2-furylindenyl)ZrCl<sub>2</sub>, bis[2-(5'-methyl-2'-furyl)indenyl]MCl<sub>2</sub>, and bis[2-(5'-methyl-2'-thienyl)indenyl]MCl<sub>2</sub> (M = Zr, Hf) complexes have been synthesized and used in propylene polymerizations for production of elastomeric polypropylene.<sup>427</sup> Dimethylaminoethyl-substituted Cp and Cp\* (or Ind) mixed zirconocene complexes of type **596**



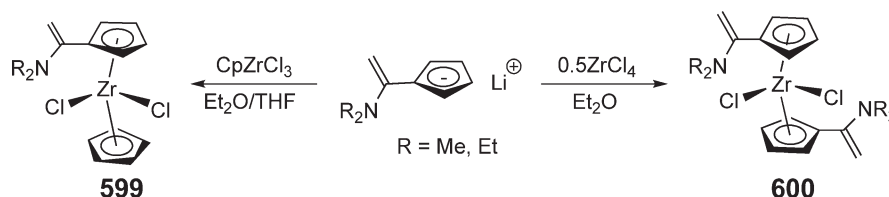
Scheme 133

catalyze, in combination with 2 equiv. of  $\text{Bu}^n\text{Li}$ , dehydrocoupling polymerization of phenylsilane to afford high molecular weight poly(phenylsilane)s.<sup>428</sup> The amino-functionalized zirconocene dichloride **597** was isolated as a mixture of *rac*- and *meso*-diastereomers.<sup>429</sup> Other substituted lithium cyclopentadienide reagents such as  $[(\text{C}_5\text{H}_4)\text{-CMe}_2\text{CH}_2\text{CH}_2\text{CONR}_2]\text{Li}$  resist intramolecular cyclization and serve as precursors of zirconocene complexes upon treatment with  $\text{CpZrCl}_3$ , leading to the formation of the mixed zirconocene **598**<sup>430</sup> (Scheme 133). The structural analysis of  $[\eta\text{-}(N,N\text{-dimethylamino})\text{fluorenyl}]_2\text{ZrCl}_2$  reveals strong Zr–N dative bonds and essentially an  $\eta^1$ -fluorenyl coordination.<sup>431</sup> The barrier to rotation around the C–N bond of  $[\eta\text{-}(N,N\text{-diisopropylamino})\text{fluorenyl}](\text{Cp}^*)\text{ZrCl}_2$  has been determined.

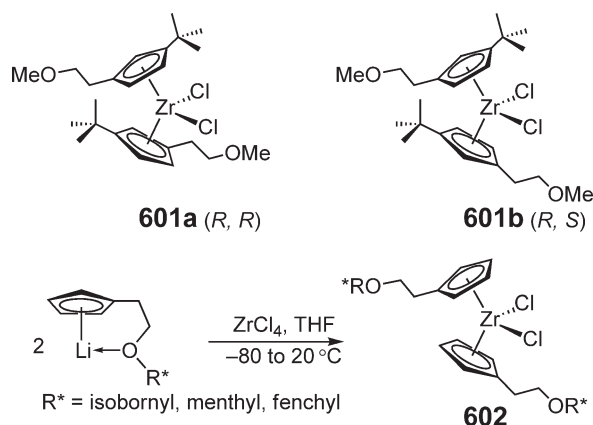
Treatment of the lithiated enamino-functionalized Cp ligand with  $\text{CpZrCl}_3$  and  $\text{ZrCl}_4$  yields the mixed zirconocene complex  $[\eta^5\text{-C}_5\text{H}_4\text{-C(=CH}_2\text{)-NR}_2]\text{CpZrCl}_2$  (**599**; R = Me, Et) and  $[\eta^5\text{-C}_5\text{H}_4\text{-C(=CH}_2\text{)-NR}_2]_2\text{ZrCl}_2$  **600**, respectively<sup>432</sup> (Scheme 134). The enamino-functionalized zirconocene **600** is rather stable at ambient conditions, but it is not completely resistant to intramolecular Mannich-type C–C coupling; thus, upon storage of this complex for 4 weeks at room temperature, ca. 50% of a sample had converted to an *ansa*-metallocene product with loss of diethylamine, presumably via a typical acid-catalyzed C–C coupling process.

Metallocenes carrying two different substituents on one or both Cp rings exhibit planar chirality. For example, two planar chiral diastereomers **601** were formed by the salt metathesis reaction between  $\text{ZrCl}_4$  and the lithiated 1-(2-methoxyethyl)-3-*tert*-butylcyclopentadiene ligand as a 3:1 mixture of **601a**:**601b**<sup>433</sup> (Scheme 135). Chiral zirconocenes **602**<sup>434</sup> contain chiral ether side arms, which can function as reversible coordinating ligand during asymmetric transformations and catalysis; however, these complexes, upon activation with MAO, exhibit no activity for olefin polymerization, presumably caused by attack of the co-catalyst MAO on the side-chains leading to immobilization of the catalyst.

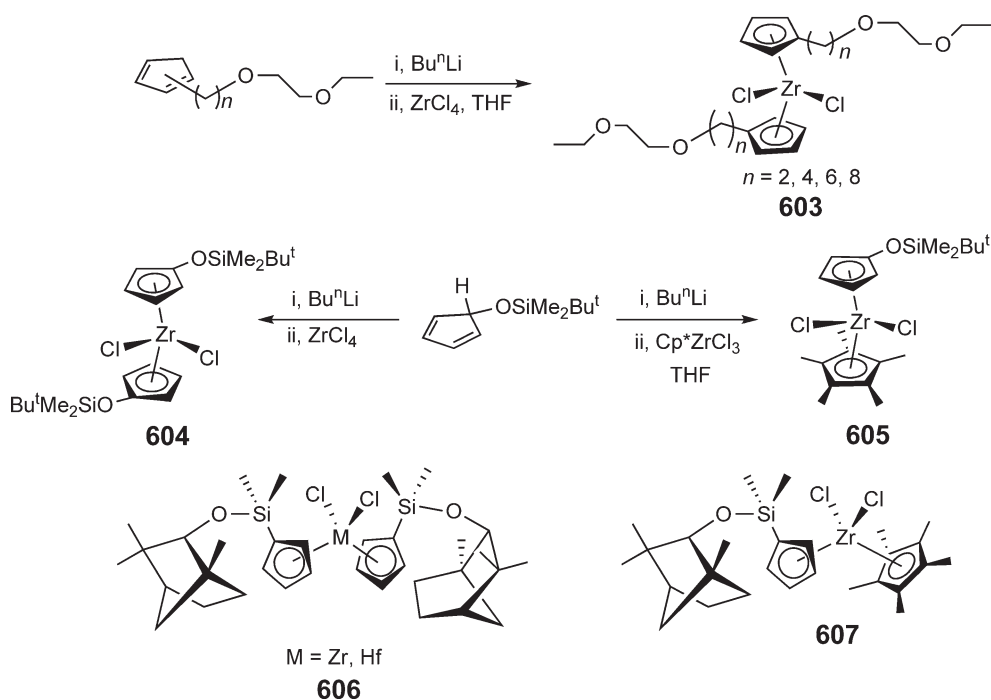
Zirconocene dichlorides having the ether functionality at the Cp substituents with variable spacing between the oxygen donor and metal center, such as complexes **603** ( $n = 2, 4, 6, 8$ ) shown in Scheme 136,<sup>435</sup> were prepared to elucidate how that spacing affects their catalytic behavior. The presence of the oxygen atom close to the metal center severely reduced the olefin polymerization activity, whereas such activity increased as the distance between



Scheme 134



Scheme 135

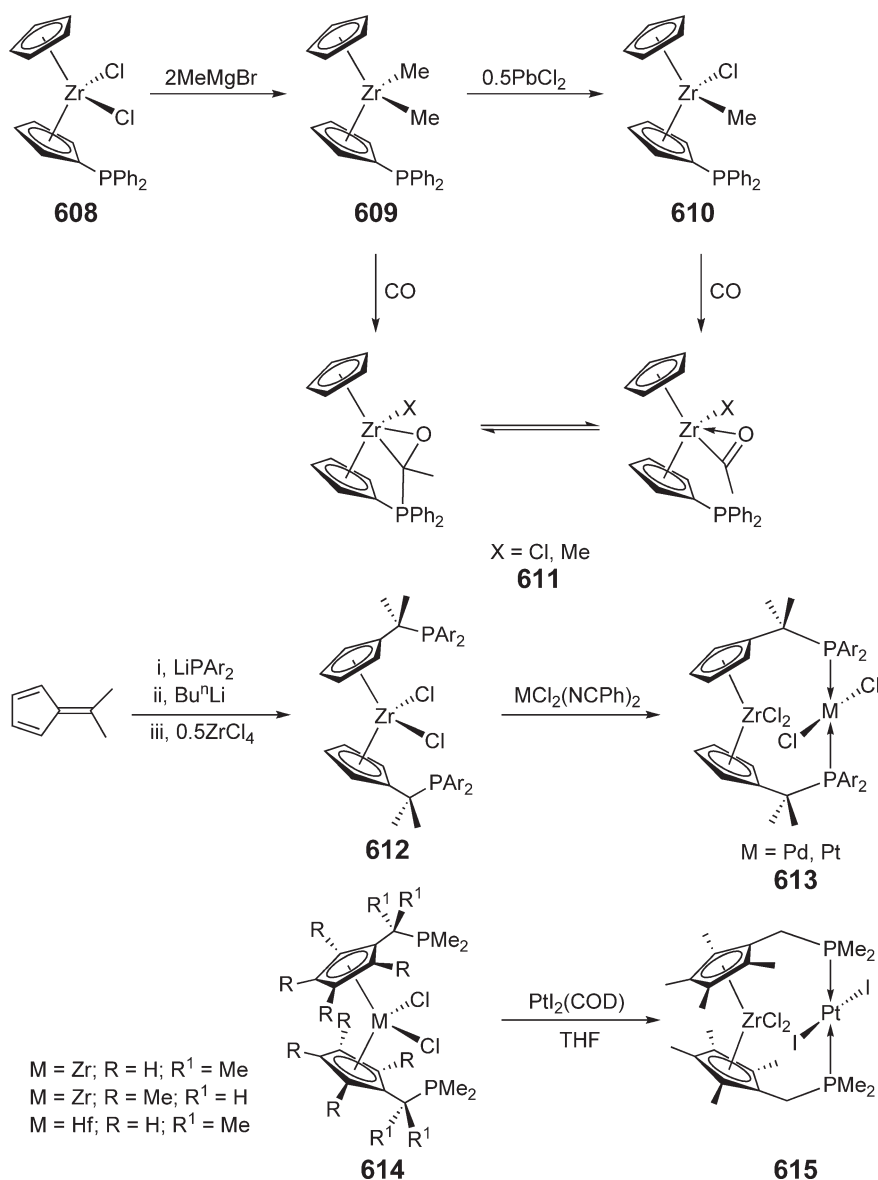


Scheme 136

zirconium and oxygen atoms increased, reaching maximum activity when  $n=6$ . Zirconocene **604** and mixed zirconocene **605** carrying the trialkylsilyl ether group on both or one of the Cp rings, respectively, have also been reported.<sup>436</sup> Replacing the *tert*-butyl group in the trialkylsilyl ether functionality contained in zirconocenes **604** and **605** with the optically active (1*R*)-*endo*-(+)-C<sub>10</sub>H<sub>17</sub> group produces chiral enantiopure *C*<sub>2</sub>-symmetric metallocene dichloride **606** and *C*<sub>1</sub>-symmetric mixed zirconocene dichloride **607**<sup>437</sup> (Scheme 136). When combined with 2 equiv. of Bu<sup>n</sup>Li, they are active catalysts for the dehydropolymerization PhSiH<sub>3</sub> leading to atactic polyphenylsilanes. A number of alkylsilyl-functionalized Cp metallocene dichlorides and mixed metallocene dichlorides have been reported; these include complexes bearing the (*p*-C<sub>6</sub>H<sub>4</sub>Br)SiMe<sub>2</sub>-Cp,<sup>438</sup> (Bu<sup>t</sup>)SiMe<sub>2</sub>-Cp,<sup>439</sup> and (CH<sub>2</sub>=CHCH<sub>2</sub>)-SiMe<sub>2</sub>Cp<sup>440</sup> ligands.

Treatment of the phosphorus-functionalized zirconocene dichloride **608** with 2 equiv. of MeMgBr affords the dimethyl complex **609**, which, on reaction with 0.5 equiv. of PbCl<sub>2</sub>, gives the monochloro methyl complex **610**<sup>441</sup> (Scheme 137). Both the dimethyl and the monochloro methyl complexes can insert one molecule of CO to afford products **611**, which interconvert between an acyl complex and a phosphonium alkoxide at ambient temperature.

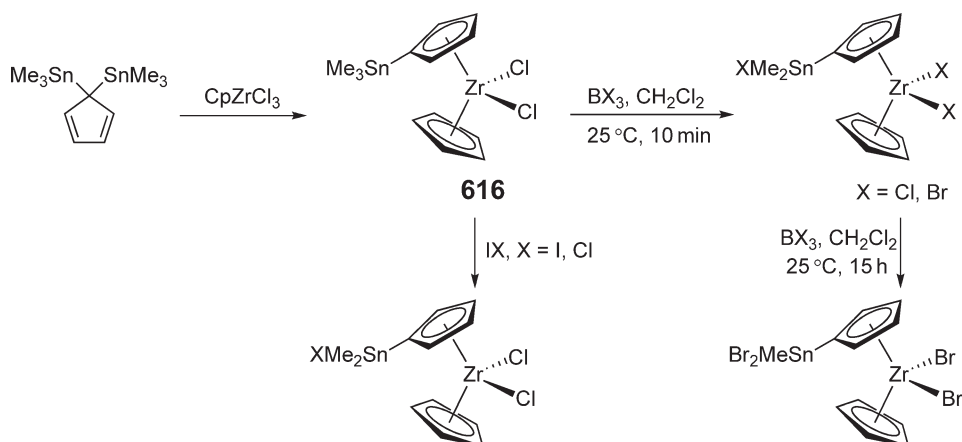




Scheme 137

Treatment of fulvenes with  $\text{LiPAR}_2$  ( $\text{Ar} = \text{Ph}$ , *p*-tolyl) yields diarylphosphinoalkyl-substituted cyclopentadienides, which undergo the metathesis reaction with  $\text{ZrCl}_4$  to give diarylphosphinoalkyl-Cp substituted zirconocene dichloride **612**.<sup>442</sup> Further reaction of this complex with  $\text{PdCl}_2(\text{NCPh})_2$  or  $\text{PtCl}_2(\text{NCPh})_2$  leads to the formation of the *trans*-(metallocene-chelate-phosphine)metal early/late transition heterobimetallic complexes **613**. In a similar fashion, the analogous early/late transition heterobimetallic complex **615** was prepared from the precursor metallocene complex carrying dimethylphosphinoalkyl-functionalized Cp ligands.<sup>443</sup> Analogous heterobimetallic complexes such as  $(\mu\text{-}\eta^5\text{-}\eta^1\text{-(C}_5\text{H}_4\text{)CH}_2\text{CH}_2\text{PPh}_2)_2\text{ZrCl}_2\text{Mo(CO)}_4$ , which link the zirconocene moiety and  $\text{Mo(CO)}_4$  fragment via the diaryl or dialkylphosphinoalkyl substituents on the Cp rings of the zirconocene, have also been synthesized.<sup>444</sup>

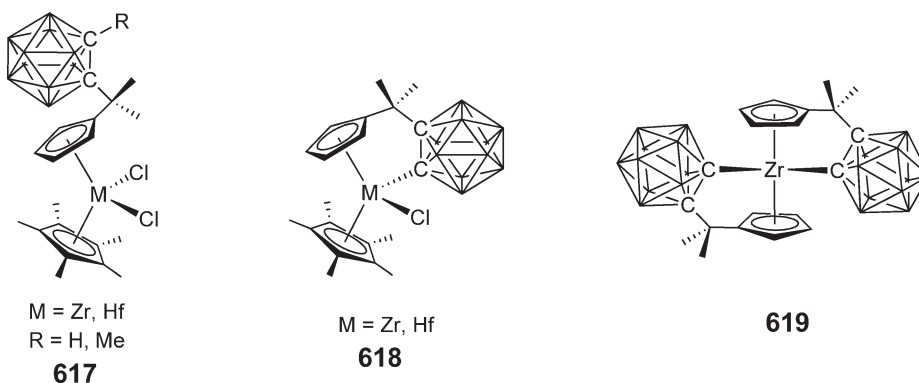
The mixed-ligand zirconocene dichloride  $(\text{Me}_3\text{SnC}_5\text{H}_4)\text{CpZrCl}_2$  **616** undergoes selective tin-carbon bond cleavage reactions with electrophiles (Scheme 138).<sup>445</sup> For example, this complex reacts with  $\text{BX}_3$  ( $\text{X} = \text{Br}$ ,  $\text{Cl}$ ) to afford the  $\text{Sn-Me}$  cleavage products  $(\text{XMe}_2\text{SnC}_5\text{H}_4)\text{CpZrX}_2$  and  $(\text{Br}_2\text{MeSnC}_5\text{H}_4)\text{CpZrBr}_2$ , depending on the reaction conditions. The analogous reaction with  $\text{IX}$  ( $\text{X} = \text{I}$ ,  $\text{Cl}$ ) gives similar products  $(\text{XMe}_2\text{SnC}_5\text{H}_4)\text{CpZrCl}_2$ . Compared with a  $\text{SiMe}_3$  substituent,<sup>446</sup> the reactivity of the  $\text{SnMe}_3$  substituent toward Lewis-acidic halodemethylation using



Scheme 138

$\text{BX}_3$  is much greater, whereas the reactivity of the halostannylated complexes toward nucleophiles such as airborne moisture is much lower. Ferrocenyldimethylsilyl ( $\text{FcSiMe}_2$ )-functionalized metallocene dichlorides, including  $(\text{FcSiMe}_2\text{C}_5\text{H}_4)\text{Cp}^*\text{ZrCl}_2$ ,  $(\text{FcSiMe}_2\text{C}_5\text{H}_4)\text{Cp}^*\text{MCl}_2$  ( $\text{M} = \text{Zr}, \text{Hf}$ ), and  $(\text{FcSiMe}_2\text{C}_5\text{H}_4)_2\text{ZrCl}_2$ , have been synthesized by salt metathesis approach and catalytic properties of their activated forms toward olefin polymerization and stereoselective cyclopolymerization of 1,5-hexadiene examined.<sup>447,448</sup>

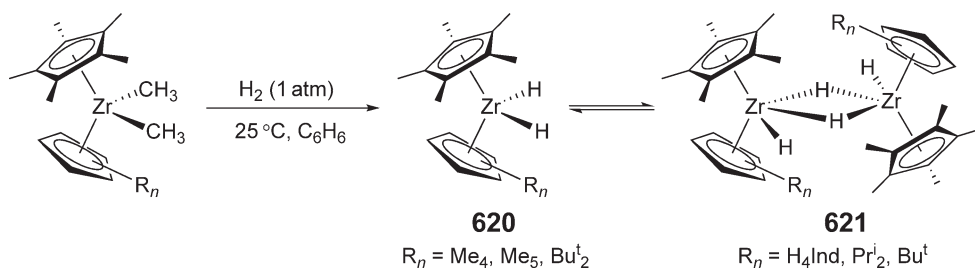
A series of metallocene complexes with *o*-carboranyl  $[\text{C}_2\text{B}_{10}\text{H}_{10}]$ -functionalized Cp ligands has been synthesized and examined as pre-catalysts for polymerization of ethylene.<sup>449</sup> These complexes include  $\text{Cp}^*[(\text{C}_5\text{H}_4)\text{CMe}_2\text{CB}_{10}\text{H}_{10}\text{CR}]\text{MCl}_2$  (**617**:  $\text{M} = \text{Zr}, \text{Hf}$ ;  $\text{R} = \text{H}, \text{Me}$ ),  $\text{Cp}^*[\eta^5\text{:}\eta^1\text{-(C}_5\text{H}_4)\text{CMe}_2\text{CB}_{10}\text{H}_{10}\text{C}]\text{MCl}$  (**618**:  $\text{M} = \text{Zr}, \text{Hf}$ ), and  $\text{C}_2$ -symmetric chelating  $[\eta^5\text{:}\eta^1\text{-(C}_5\text{H}_4)\text{CMe}_2\text{CB}_{10}\text{H}_{10}\text{C}]_2\text{Zr}$  **619**.<sup>450</sup> All complexes except the hafnium complex **617** have been structurally characterized. When activated with a large excess of MAO, the zirconium complexes are active catalysts to yield high-density polyethylene. The neutral  $\text{C}_2$ -symmetric chelate complex **619** polymerizes methylmethacrylate in THF to syndiorich polymers with low activity.



#### 4.08.9.2 Complexes with M–H Bonds

Zirconocene dihydrides **620** having substituted Cp ligands were readily prepared by hydrogenation of the corresponding dimethyl complexes<sup>451</sup> (Scheme 139). Most group 4 metallocene hydride complexes are subject to dimerization through formation of relatively robust three-center, two-electron hydride bridges. The most sterically crowded members in this  $[\text{Cp}^*(\text{Cp}^{\text{Rn}})\text{ZrH}_2]_n$  series are monomeric compounds of type **620**, including those with tetramethyl, pentamethyl, and di-*tert*-butyl substituted  $\text{Cp}^{\text{Rn}}$  rings, whereas less crowded complexes are predominantly dimeric, **621**, in benzene solution.

A convenient method for the synthesis of zirconocene hydrido chloride, isobutyl hydride, and dihydride complexes has been developed using the  $\text{Bu}^t\text{Li}$  reagent.<sup>452</sup> Thus, the reaction of  $\text{Cp}^*\text{Cp}^{\text{Rn}}\text{ZrCl}_2$  with  $\text{Bu}^t\text{Li}$  reagent gives

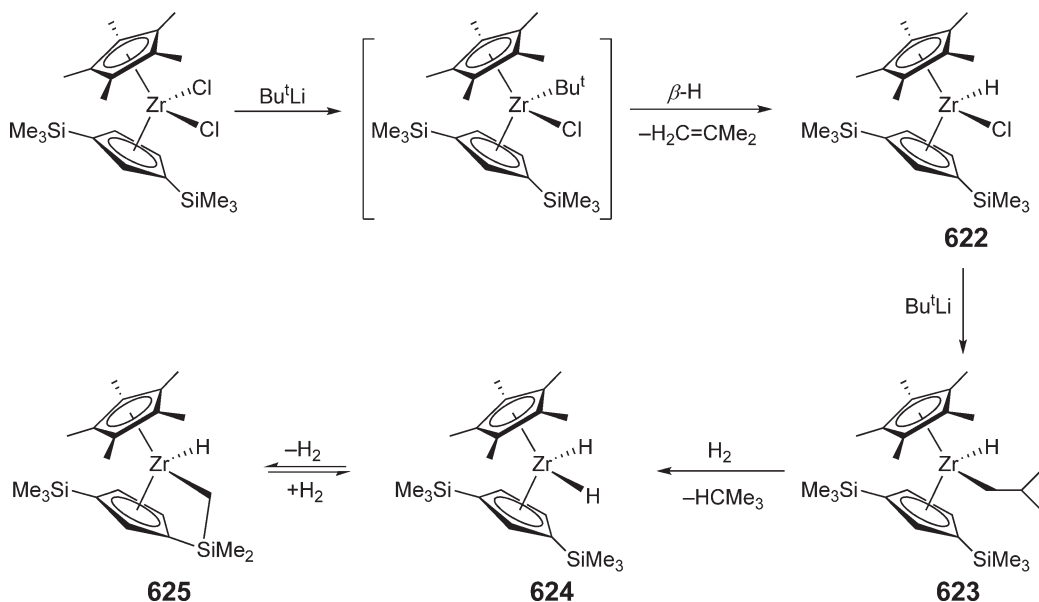


Scheme 139

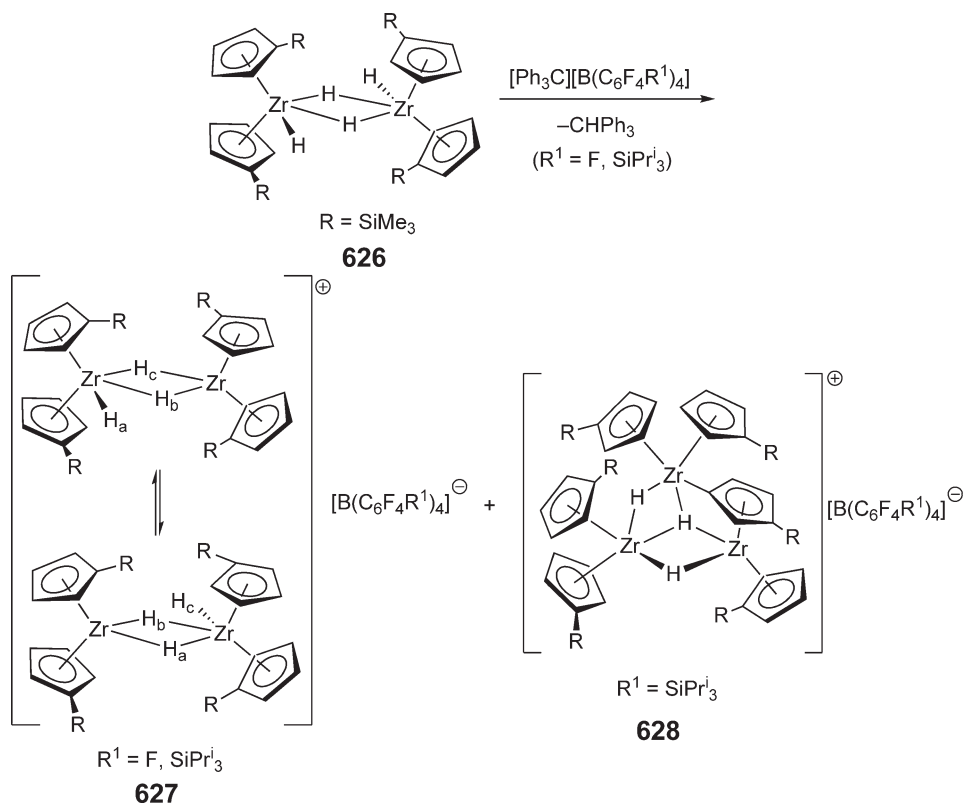
zirconocene hydrido chloride **622** in high yield (Scheme 140). Further addition of  $\text{Bu}^t\text{Li}$  to **622** affords the isobutyl hydride complex **623**, which upon addition of 1 atm of  $\text{H}_2$  undergoes rapid hydrogenolysis, yielding the monomeric dihydride **624**. In the absence of dihydrogen, the zirconocene dihydride undergoes reversible C–H activation of a Cp trimethylsilyl group, affording the tuck-in derivative **625**. The *ansa*-zirconocene  $\text{Pr}^t_2\text{Si}(\text{3-SiMe}_3\text{C}_5\text{H}_3)(\text{3,4-SiMe}_3)_2\text{C}_5\text{H}_2\text{ZrCl}_2$  and the bis(substituted)Ind zirconocene dichloride *rac*-(1- $\text{Bu}^t\text{C}_9\text{H}_6$ ) $_2\text{ZrCl}_2$  react with  $\text{Bu}^t\text{Li}$  in an analogous manner. The Cp substituent effects on reductive elimination reactions of a family of zirconocene isobutyl hydride complexes  $\text{Cp}^*(\text{Cp}R_n)\text{Zr}(\text{CH}_2\text{CHMe}_2)\text{H}$  ( $\text{Cp}R_n$  = substituted Cp) have been subsequently investigated.<sup>453</sup>

$\text{Cp}^*_2\text{ZrH}_2$  reacts with primary, secondary, and tertiary monofluorinated aliphatic hydrocarbons to give  $\text{Cp}^*_2\text{Zr}(\text{F})\text{H}$  and/or  $\text{Cp}^*_2\text{ZrF}_2$  and alkane quantitatively through a radical chain mechanism.<sup>454</sup> On the other hand, non-radical mechanisms are invoked in the aromatic C–F activation involved in the reaction of  $\text{Cp}^*_2\text{ZrH}_2$  with fluorobenzene, which gives a mixture of  $\text{Cp}^*_2\text{Zr}(\text{F})\text{H}$ , benzene, and  $\text{Cp}^*_2\text{Zr}(\text{C}_6\text{H}_5)\text{F}$ .  $\text{Cp}^*_2\text{ZrH}_2$  also reacts with excess hexafluorobenzene to produce  $\text{Cp}^*_2\text{Zr}(\text{F})\text{H}$ ,  $\text{C}_6\text{F}_5\text{H}$ , and  $\text{Cp}^*_2\text{Zr}(\text{C}_6\text{F}_5)\text{H}$  in a 2 : 1 : 1 ratio. Fluorination of  $\text{Cp}^*_2\text{Zr}(\text{C}_6\text{F}_5)\text{H}$  with HF-pyridine gives  $\text{Cp}^*_2\text{Zr}(\text{C}_6\text{F}_5)\text{F}$ , the crystal structure of which was determined.<sup>455</sup> The same starting zirconocene dihydride reacts with vinylic C–F bonds of  $\text{CF}_2=\text{CH}_2$  and 1,1-difluoromethylenecyclohexane to afford  $\text{Cp}^*_2\text{Zr}(\text{F})\text{H}$  and hydrodefluorinated products.<sup>456</sup>

Binuclear cationic zirconocene hydrides can be prepared directly from the zirconocene dihydride precursor. Thus, the reaction of the zirconocene dihydride **626** with a trityl borate salt produces the binuclear hydrido complexes **627**<sup>457</sup> (Scheme 141). The synthesis of **627** may be accompanied by the formation of cationic zirconocene hydrides of higher nuclearity. For example, cationic trinuclear hydrido complex **628** was also isolated during the recrystallization



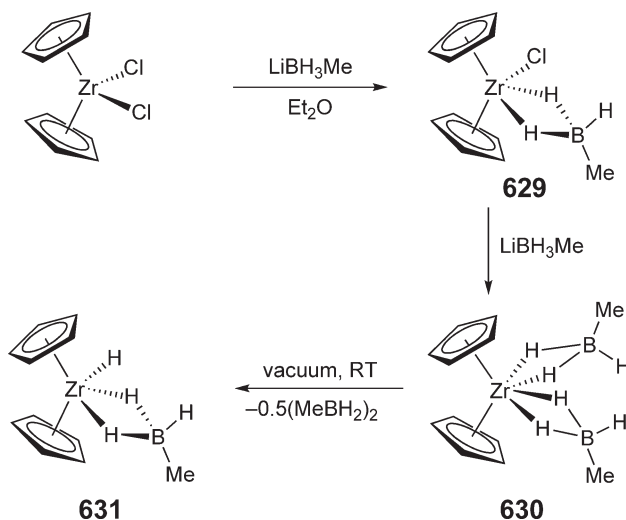
Scheme 140



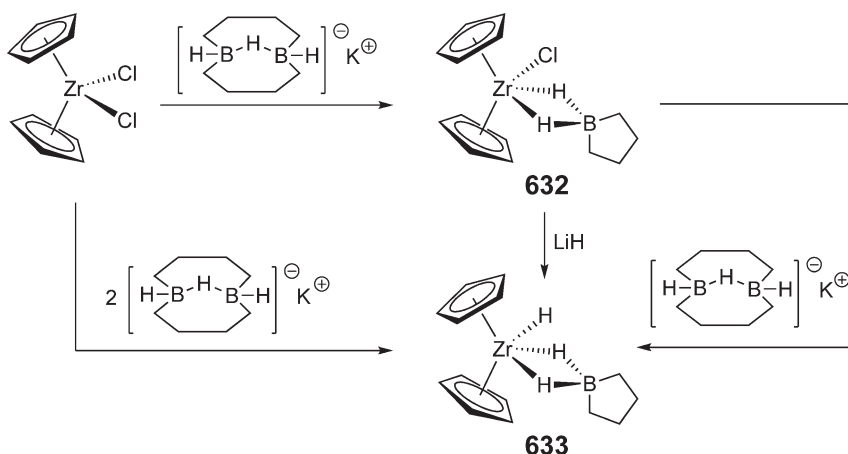
Scheme 141

of **627** ( $R^1 = \text{SiPr}^i_3$ ); complex **628** was characterized by X-ray diffraction. These binuclear cationic zirconocene hydrides are highly active initiators for the polymerization of isobutene and the co-polymerization of isobutene with isoprene.<sup>458</sup>

The zirconocene methyltrihydroborate complex **629** was obtained by the reaction of  $\text{Cp}_2\text{ZrCl}_2$  with 1 equiv. of  $\text{LiBH}_3\text{Me}$ <sup>459</sup> (Scheme 142). The same reaction with an excess amount of  $\text{LiBH}_3\text{Me}$  gives the



Scheme 142



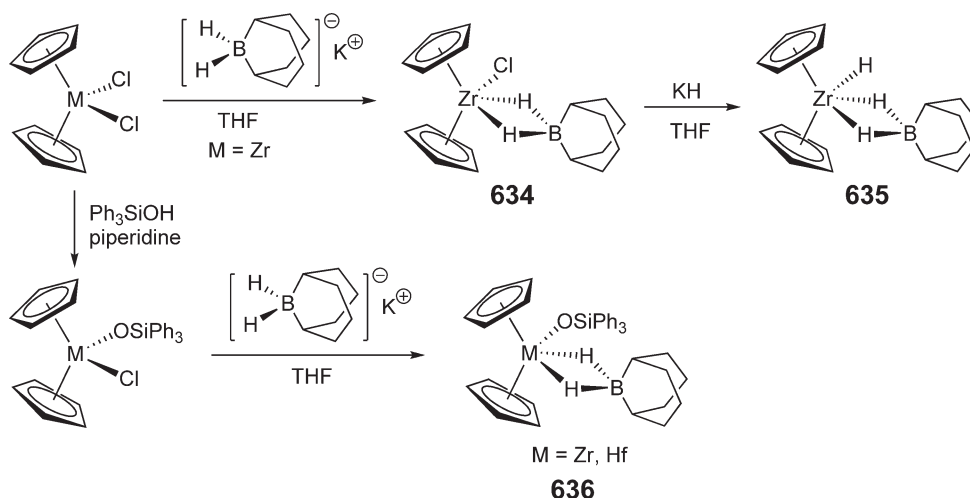
Scheme 143

bis(methyltrihydroborate) complex **630**; under a dynamic vacuum at room temperature, this complex decomposes to the zirconium hydride complex **631**.

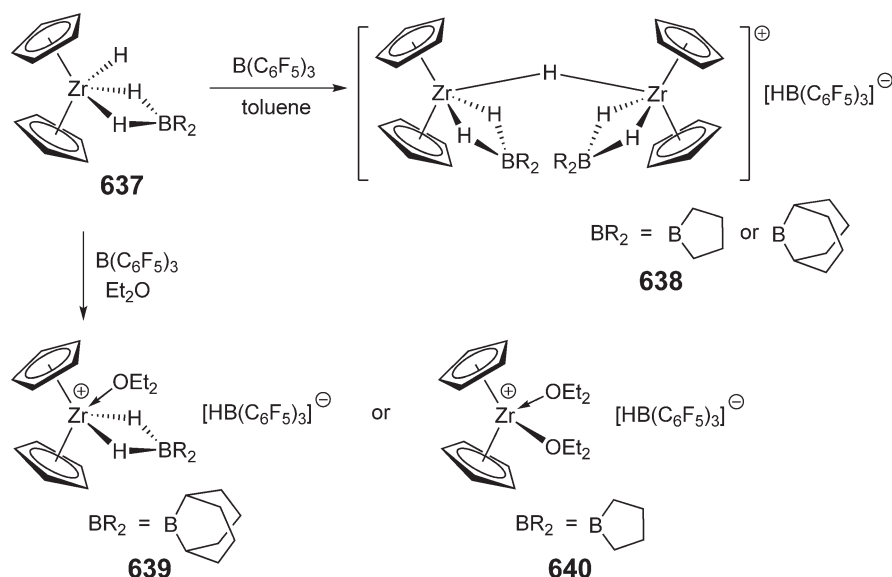
Hydrido- and bis(methyltri)hydrido-zirconocenes of cycloalkylhydridoborates such as **633** can be prepared by three routes<sup>460</sup> (Scheme 143): from the reaction of  $\text{Cp}_2\text{ZrCl}_2$  with 2 equiv. of  $\text{K}[\text{H}_2\text{B}_2(\mu\text{-H})(\mu\text{-C}_4\text{H}_8)_2]$ , the reaction of  $\text{Cp}_2\text{ZrCl}[(\mu\text{-H})_2\text{BC}_4\text{H}_8]$  **632** with 1 equiv. of  $\text{K}[\text{H}_2\text{B}_2(\mu\text{-H})(\mu\text{-C}_4\text{H}_8)_2]$ , and the reaction of **632** with 1 equiv. of  $\text{LiH}$ . The benzyl derivatives  $\text{Cp}_2\text{Zr}(\text{CH}_2\text{Ph})[(\mu\text{-H})_2\text{BC}_4\text{H}_8]$  and  $\text{Cp}_2\text{Zr}(\text{CH}_2\text{Ph})[(\mu\text{-H})_2\text{BC}_5\text{H}_{10}]$  are similarly obtained using  $\text{Cp}_2\text{ZrCl}(\text{CH}_2\text{Ph})$  instead of  $\text{Cp}_2\text{ZrCl}_2$ . Derivatives of **632**, the complexes  $\text{Cp}_2\text{MCl}[(\mu\text{-H})_2\text{BC}_5\text{H}_{10}]$  ( $\text{M} = \text{Zr}, \text{Hf}$ ), were prepared from the reaction of  $\text{Cp}_2\text{MCl}_2$  with 1 equiv. of  $\text{K}[\text{H}_2\text{BC}_5\text{H}_{10}]$ .<sup>461</sup> In general, zirconocene and hafnocene dichlorides react with potassium salts of cycloalkyldiborate anions to yield hydridoborate complexes of type **632**.<sup>462,463</sup>

Treatment of  $\text{Cp}_2\text{ZrCl}_2$  with 1 equiv. of  $\text{K}[\text{H}_2\text{BC}_8\text{H}_{14}]$  in THF yields crystalline chlorozirconocene **634**. Its subsequent reaction with  $\text{KH}$  gives the corresponding hydrido- and bis(methyltri)hydrido-zirconocene complex **635**<sup>464</sup> (Scheme 144). Complex **635** cannot be prepared directly from the 1:2 reaction of  $\text{Cp}_2\text{ZrCl}_2$  and  $\text{K}[\text{H}_2\text{BC}_8\text{H}_{14}]$ , which gives a mixture containing **634**, **635**, and an unidentified boron-containing complex. Triphenylsiloxy derivatives **636** were obtained analogously.<sup>465</sup>

Products from the hydride abstraction reactions of the zirconocene cycloalkylhydridoborate complexes **637** with  $\text{B}(\text{C}_6\text{F}_5)_3$  are a function of the solvent and the  $-\text{BR}_2$  moiety. Thus, the reaction in poorly coordinating solvents such as



Scheme 144

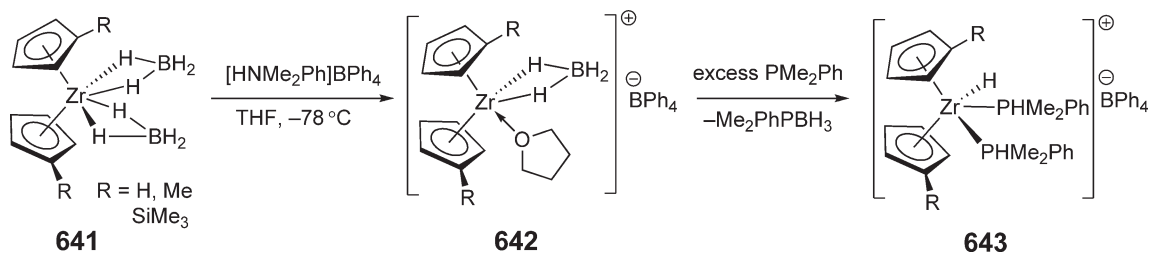


Scheme 145

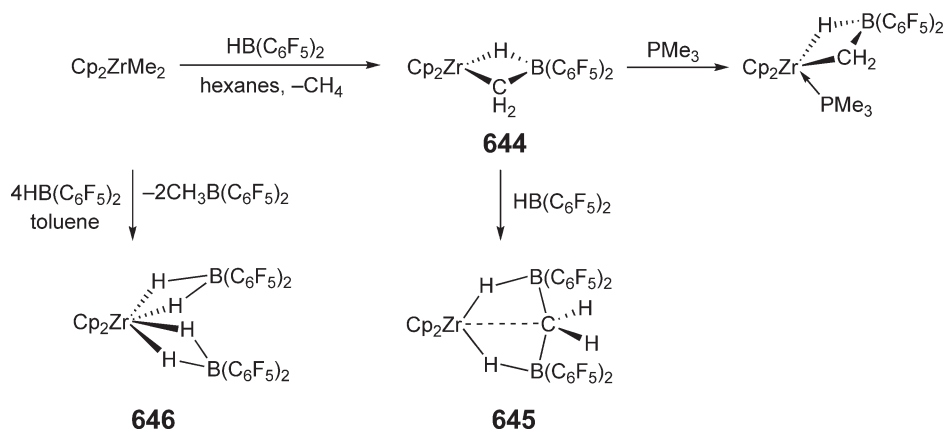
benzene and toluene forms  $\mu$ -H-bridged binuclear zirconocene borate salts **638**<sup>466,467</sup> (Scheme 145). On the other hand, the reaction in diethyl ether gives either the solvent-separated ion pair **639** ( $\text{BR}_2 = \text{BC}_8\text{H}_{14}$ ) or the cationic zirconocene ethoxide complex **640** ( $\text{BR}_2 = \text{BC}_4\text{H}_8$ ), formed presumably via hydride insertion from Zr into the carbon–oxygen bond of one of the coordinated ether molecules, resulting in the liberation of ethane and the formation of an ethoxy group covalently bound to Zr.

Protonolysis of zirconocene borohydride complexes **641** with  $[\text{HNMe}_2\text{Ph}]\text{BPh}_4$  in THF leads to the corresponding cationic zirconocenium complex **642**, the structure of which ( $\text{R} = \text{Me}$ ) has been determined by X-ray diffraction<sup>468</sup> (Scheme 146). Treatment of the cationic complex **642** with an excess of the phosphine  $\text{PMe}_2\text{Ph}$  gives the cationic hydride **643** followed by disproportionation and redox reactions, producing the neutral  $[(\text{C}_5\text{H}_4\text{R})_2\text{ZrH}(\mu\text{-H})_2]$  and the cationic Zr(III) species  $[(\text{C}_5\text{H}_4\text{R})_2\text{Zr}(\text{PMe}_2\text{Ph})_2][\text{BPh}_4]$ , implicative of a probable deactivation pathway for the cationic metallocenium hydrides.

Zirconocene hydroborate complexes can also be prepared from the reaction of zirconocene dialkyls with the electrophilic hydroborane reagent,  $\text{HB(C}_6\text{F}_5)_2$ . Thus, the stoichiometric reaction of  $\text{Cp}_2\text{ZrMe}_2$  with  $\text{HB(C}_6\text{F}_5)_2$  in hexanes gives the highly reactive borane-stabilized methyldiene complex **644**, which can be further stabilized by  $\text{PMe}_3$  to afford the isolable and X-ray crystallographically characterized complex, or reacts with another equivalent of  $\text{HB(C}_6\text{F}_5)_2$  to produce the rather unusual complex **645** containing pentacoordinate carbon<sup>469</sup> (Scheme 147). On the other hand, the reaction of  $\text{Cp}_2\text{ZrMe}_2$  with 4 equiv. of  $\text{HB(C}_6\text{F}_5)_2$  in benzene or toluene undergoes alkyl–hydride exchange, resulting in the formation of the stable zirconocene bis(dihydroborate) complex **646**. The latter pathway dominates when R is sterically bulky in the precursor  $\text{Cp}_2\text{ZrR}_2$ , and the mechanistic aspects of this reaction have been investigated.<sup>470</sup>



Scheme 146

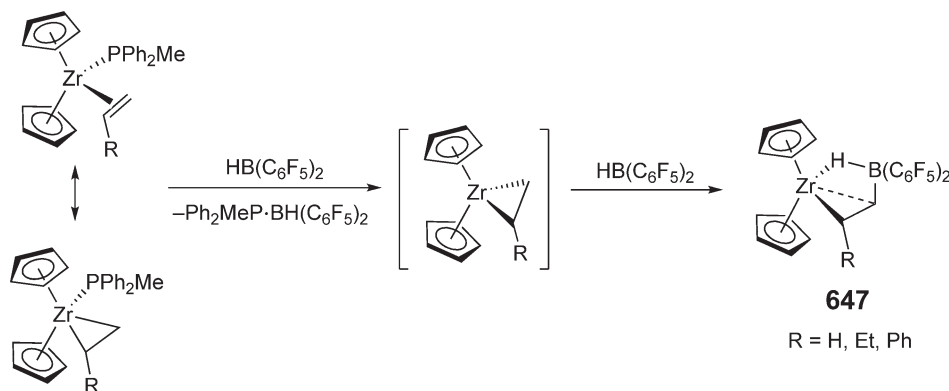


Scheme 147

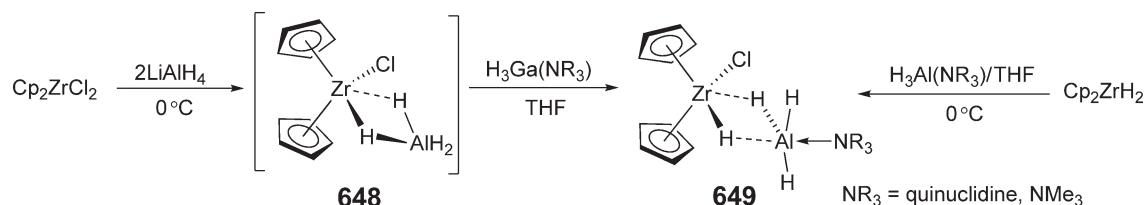
The zirconium(II) olefin complexes  $\text{Cp}_2\text{Zr}(\text{PPh}_2\text{Me})(\eta^2\text{-RCH=CH}_2)$  ( $\text{R} = \text{H, Et, Ph}$ ) react rapidly with 2 equiv. of  $\text{HB}(\text{C}_6\text{F}_5)_2$  to give the zwitterionic **647** and the borane–phosphine adduct  $\text{Ph}_2\text{MeP}\cdot\text{HB}(\text{C}_6\text{F}_5)_2$  as the byproduct<sup>471</sup> (Scheme 148). On the basis of spectroscopic and structural data, complex **647** exhibits interaction between Zr and the  $\beta$ -C attached to boron, again featuring a pentacoordinate carbon.

Although the zirconocene hydroaluminate complex **648**, generated from the reaction of  $\text{Cp}_2\text{ZrCl}_2$  with excess  $\text{LiAlH}_4$  in THF, is unstable, further treatment with  $\text{H}_3\text{Ga}(\text{NR}_3)$  produces the stable and crystallographically characterized hydride-bridged heterobimetallic zirconium–aluminum complex **649** in moderate yield (Scheme 149).<sup>472</sup> The same complex can also be obtained by the reaction of the preformed  $\text{Cp}_2\text{ZrH}_2$  with  $\text{H}_3\text{Al}(\text{NR}_3)$  in THF.

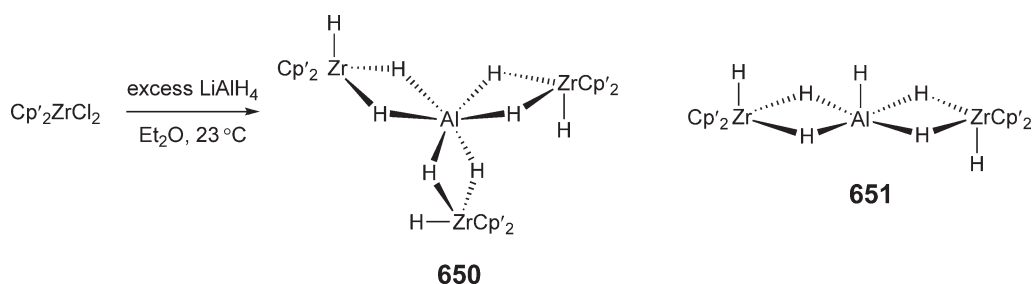
The reaction of  $\text{Cp}'_2\text{ZrCl}_2$  ( $\text{Cp}' = \text{Me}_3\text{SiC}_5\text{H}_4$ ) with excess  $\text{LiAlH}_4$  affords the dihydride–alane adduct, the structure of which reveals two types of aggregation between the  $\text{Cp}'_2\text{ZrH}_2$  and  $\text{AlH}_3$  moieties formulated as  $[\text{Cp}'_2\text{ZrH}(\mu\text{-H})_2]_3\text{Al}$  **650** and  $[\text{Cp}'_2\text{ZrH}(\mu\text{-H})_2]_2\text{AlH}$  **651**<sup>473</sup> (Scheme 150). A pseudo-octahedral environment about the Al center in the case of  $\text{Zr}_3\text{Al}$  aggregate is observed, whereas a distorted square-pyramidal geometry about Al is seen for the  $\text{Zr}_2\text{Al}$  aggregate.



Scheme 148

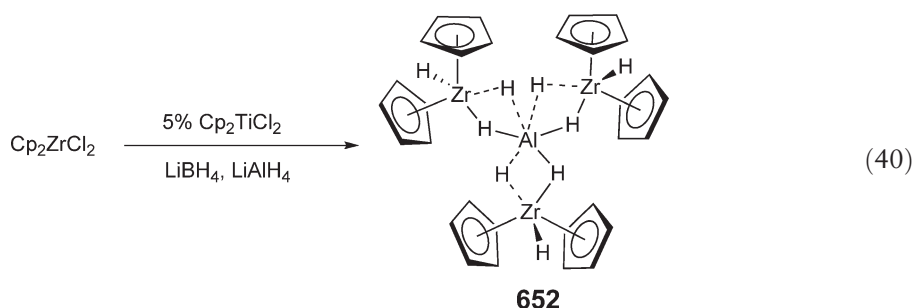


Scheme 149



Scheme 150

The trinuclear zirconocene–aluminum heterometallic hydrido complex  $[\text{Cp}_2\text{ZrH}(\mu\text{-H})_2]_3\text{Al}$  **652** was isolated in low yield from the reaction of  $\text{Cp}_2\text{ZrCl}_2$  with  $\text{LiBH}_4$ ,  $\text{LiAlH}_4$ , and a catalytic amount of  $\text{Cp}_2\text{TiCl}_2$  (Equation (40)). The molecular structure of this complex has been determined by X-ray diffraction analysis, featuring the distorted octahedral Al geometry.<sup>474</sup>



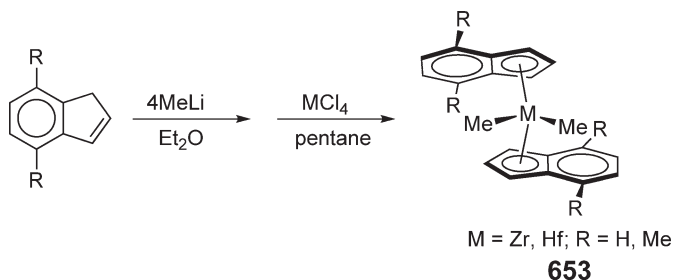
The reaction of  $\text{Cp}_2\text{ZrMe}_2$  with the sterically encumbered arylalane hydride  $(\text{MesAlH}_2)_2$  ( $\text{Mes} = 2,4,6\text{-Bu}^t_3\text{C}_6\text{H}_2$ ) affords  $\text{Cp}_2(\text{H})\text{Zr}(\mu^2\text{-H})_2\text{Al}(\text{Me})\text{Mes}$  together with  $\text{Cp}_2\text{ZrH}_2$  and  $\text{MesAlMe}_2$ , whereas the reaction of  $\text{Cp}_2\text{Zr}(\text{Cl})\text{H}$  with  $[\text{MesAlH}_3\text{Li}(\text{THF})_2]_2$  gives colorless  $\text{Cp}_2(\text{H})\text{Zr}(\mu^2\text{-H})_2\text{Al}(\text{H})\text{Mes}$  in moderate yield.<sup>475</sup>

Several Li, K, and  $\text{AlH}_2$  salts of the anion  $[\text{Cp}^*_2\text{ZrH}_3]^-$  have been prepared.<sup>476</sup> Reactions of  $\text{Cp}^*_2\text{ZrH}_2$  with  $\text{KH}$  and  $\text{LiH}$  in THF give  $[\text{Cp}^*_2\text{ZrH}_3]\text{K}$  and  $[\text{Cp}^*_2\text{ZrH}_3]\text{Li}$  in moderate yields, respectively, whereas treatment of  $\text{Cp}^*_2\text{ZrCl}_2$  with  $\text{LiAlH}_4$  affords  $\text{Cp}^*_2\text{ZrH}(\mu^2\text{-H}_2\text{AlH}_2)$  in quantitative yield. Subsequent reaction of  $\text{Cp}^*_2\text{ZrH}(\mu^2\text{-H}_2\text{AlH}_2)$  with  $\text{Bu}^n\text{Li}$  leads to  $[\text{Cp}^*_2\text{ZrH}_3]\text{Li}$ , providing a direct and high-yield conversion to the lithium salt.

#### 4.08.9.3 Complexes with M–C Bonds

##### 4.08.9.3.1 Complexes containing M–C $\text{sp}^3$ -bonds

An improved synthetic route to bis(indenyl)dimethyl metallocenes **653** involves treatment of the neutral ligand with a twofold excess of  $\text{MeLi}$  followed by the reaction of the resulting mixture with  $\text{MCl}_4$  ( $\text{M} = \text{Zr}, \text{Hf}$ ) in pentane<sup>477</sup> (Scheme 151). This simple, one-pot method produces the metallocene dimethyl complexes in high overall yields



Scheme 151

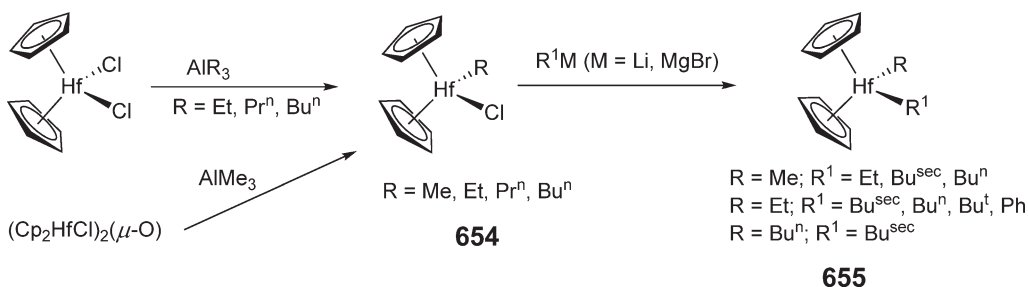


based on the neutral ligands (85% for R = H; 74% for R = Me). This synthetic methodology has also been extended to the preparation of *ansa*-metallocene dimethyl complexes.

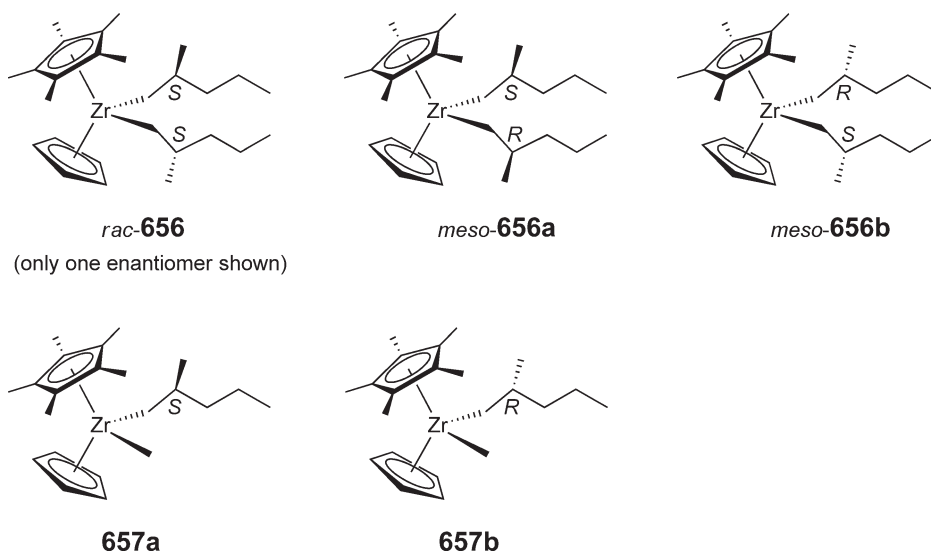
The reaction of  $\text{Cp}_2\text{HfCl}_2$  with aluminum trialkyls ( $\text{AlR}_3$ ; R = Et,  $\text{Pr}^n$ ,  $\text{Bu}^n$ ) in hexanes selectively produces monoalkyl hafnocene complexes **654** in high yields<sup>478,479</sup> (Scheme 152). Exceptionally,  $\text{Cp}_2\text{Hf}(\text{Me})\text{Cl}$  was not cleanly formed using this  $\text{AlMe}_3$ , but alternatively it can be prepared by the reaction of the hafnocene oxo-bridged chloride complex with  $\text{AlMe}_3$ . Further treatment of **654** with organolithium or Grignard alkylating reagents affords unsymmetric dialkylhafnocene complexes **655** with variable stability. Kinetic studies of the thermolysis of  $\text{Cp}_2\text{HfEtR}$  (R = Me, Et,  $\text{Bu}^n$ ,  $\text{Bu}^{\text{sec}}$ ,  $\text{Bu}^t$ , Ph) suggested that the decomposition of  $\text{Cp}_2\text{HfEt}(\text{Bu}^{\text{sec}})$  was much faster than the others;  $\text{Cp}_2\text{Hf}(\text{Bu}^{\text{sec}})_2$  can be used as a good precursor for  $\text{Cp}_2\text{Hf}(\text{II})$  species.

Alkylation of mixed-ligand zirconocene dichloride  $\text{CpCp}^*\text{ZrCl}_2$  with 1-lithio-2-methylpentane gives the corresponding dialkyl zirconocene  $\text{CpCp}^*\text{Zr}[\text{CH}_2\text{CH}(\text{CH}_3)\text{CH}_2\text{CH}_2\text{CH}_3]_2$  **656** in high yields<sup>480</sup> (Scheme 153). The mixed alkyl derivative  $\text{CpCp}^*\text{Zr}(\text{CH}_3)[\text{CH}_2\text{CH}(\text{CH}_3)\text{CH}_2\text{CH}_2\text{CH}_3]$  **657** was obtained using  $\text{CpCp}^*\text{Zr}(\text{CH}_3)\text{Cl}$ . The dialkyl complex **656** has three stereogenic centers (the metal and the two  $\beta$ -carbons) and can thus give rise to a maximum of eight different stereoisomers, whereas **657**, having two stereocenters, can give rise to four. For **656**, symmetry makes some of the eight possible stereoisomers identical, thus reducing the number of possible stereoisomers to four, as shown in Scheme 153, and they are formed in a statistical distribution. On the other hand, the diastereomers of **657** are formed in a 2:3 ratio. A most remarkable feature about these alkyl complexes is their unprecedented thermal stability despite the fact the alkyls in these complexes carry  $\beta$ -hydrogen atoms.

Chiral metallocene alkyl chlorides,  $\text{Cp}_2\text{M}(\text{Cl})\text{R}^1$  ( $\text{R}^1 = \text{CH}(\text{SiMe}_3)(o\text{-MeC}_6\text{H}_4)$ ), have been prepared by salt metathesis involving the reaction of  $\text{Cp}_2\text{MCl}_2$  with 1 equiv. of  $\text{R}^1\text{Li}(\text{TMEDA})$ .<sup>481</sup> Further alkylation occurred only for M = Zr, affording *rac*- and *meso*-dialkyl complexes  $\text{Cp}_2\text{Zr}(\text{R}^1)_2$ . In contrast, the reaction of  $\text{Cp}_2\text{ZrCl}_2$  with 2 equiv. of  $(\text{TMEDA})\text{LiCH}(\text{SiMe}_3)_2$  yielded an alkyl elimination product bearing  $(\mu\text{-}\eta^1:\eta^5\text{-C}_5\text{H}_4)^{2-}$  ligands.



Scheme 152

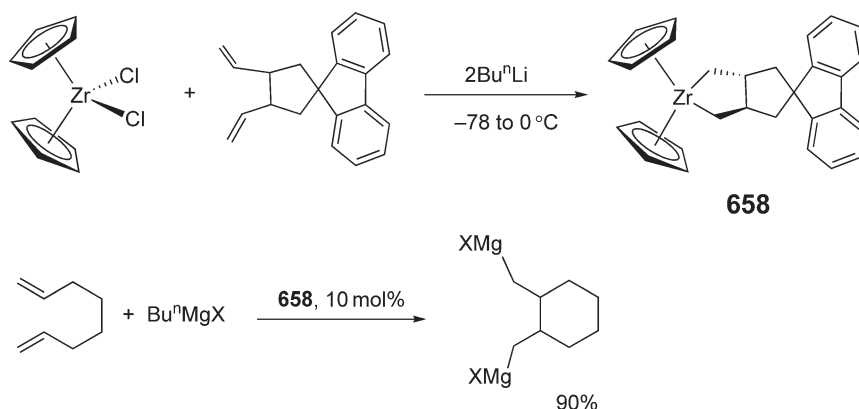


Scheme 153

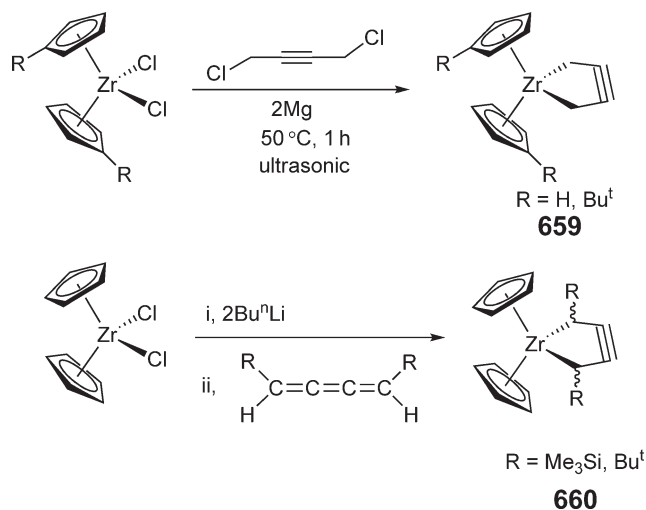
Zirconocene metallacycles are invoked as key intermediates in the catalytic cyclomagnesiation of dienes. To probe for the intermediacy of metallacycles, zirconacyclopentane derivative **658** was synthesized from the reaction of  $\text{Cp}_2\text{ZrCl}_2$  and 9,9-diallylfluorene in the presence of 2 equiv. of  $\text{Bu}^n\text{Li}$ <sup>482</sup> (Scheme 154). This structurally characterized zirconacyclopentane is a catalytically competent intermediate for the cyclization of dienes. For example, cyclomagnesiation of 1,7-octadiene occurs smoothly in the presence of 10 mol% of **658**.

Treatment of  $\text{Cp}^R_2\text{ZrCl}_2$  ( $R = \text{H}, \text{Bu}^t$ ) with 1,4-dichlorobut-2-yne in the presence of magnesium under ultrasonic conditions produces five-membered metallacyclic alkynes **659** without substituents adjacent to the triple bond<sup>483</sup> (Scheme 155). These metallacyclopentynes are stable enough to be isolated in a pure form and stored at ambient temperature under an inert atmosphere for at least a month. Further reaction of **659** with an equimolar amount of  $\text{Cp}_2\text{Zr}(\text{but-1-ene})(\text{PMe}_3)$  gives a bimetallic complex in which the zirconacyclopentyne coordinates to the other zirconocene moiety as an alkyne. The previously isolated and structurally characterized stable five-membered zirconacyclopentynes **660**, obtained from the reaction of the *in situ*-generated divalent zirconocene “ $\text{Cp}_2\text{Zr}$ ” with (*Z*)-1,4-disubstituted 1,2,3-butatrienes, contain bulky substituents adjacent to the triple bond<sup>484</sup> (Scheme 155).<sup>155</sup> Subsequent density functional theory calculations conclude, however, that the originally proposed metallacyclopentyne form cannot adequately describe the complex. Instead, a resonance hybrid between a cumulene complex form and a metallacyclopentyne Lewis structure is required to account for the structure and stability of the complex.<sup>485</sup>

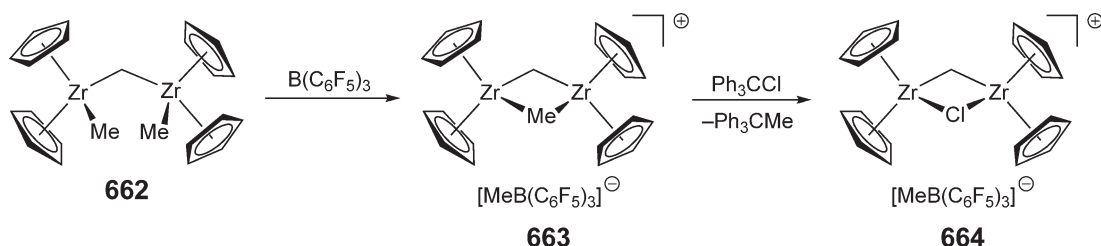
The reaction of  $\text{Cp}^R_2\text{ZrCl}_2$  ( $R = \text{H}, \text{Me}_3\text{Si}$ ) with 2 equiv. of  $\text{EtMgCl}$  in THF gives ethylene-bridged binuclear complex ( $\text{Cp}^R_2\text{ZrEt}_2$ )<sub>2</sub>( $\mu$ -ethylene) **661** in good yield<sup>486</sup> (Equation (41)). On the basis of the crystal structure, the



Scheme 154

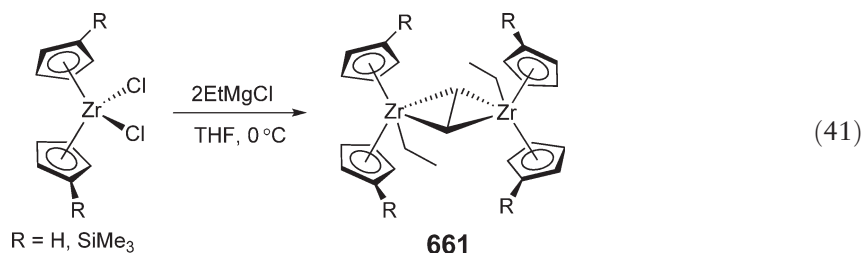


Scheme 155



Scheme 156

bridging ethylene can be considered as the dianion  $\text{C}_2\text{H}_4^{2-}$ , which is asymmetrically coordinated to the two neighboring Zr centers. The mononuclear complex  $\text{Cp}_2\text{Zr}(\text{ethylene})(\text{THF})$  was obtained by the reaction of  $\text{Cp}_2\text{ZrCl}_2$  and  $\text{Et}_2\text{Mg}(\text{dioxane})$  in THF below  $0^\circ\text{C}$ . The closely related indenyl derivative  $(\text{Ind})_2\text{Zr}(\text{ethylene})(\text{THF})$  was analogously prepared, the structure of which shows that the Zr atom, the two carbons of ethylene, and the O donor atom of THF lie in a single plane and the C–C bond of the coordinated ethylene is elongated to  $1.451(5) \text{ \AA}$ . The analogous ethylene-bridged methyl zirconium complex,  $(\text{Cp}_2\text{ZrMe})_2(\mu\text{-ethylene})$ , was prepared earlier by the reaction of  $\text{Cp}_2\text{ZrMe}_2$  with a zirconocene–ethylene complex,  $(\text{Cp}_2\text{ZrEt})(\text{CH}_2=\text{CH}_2)\text{MgBr}$ .<sup>487</sup>



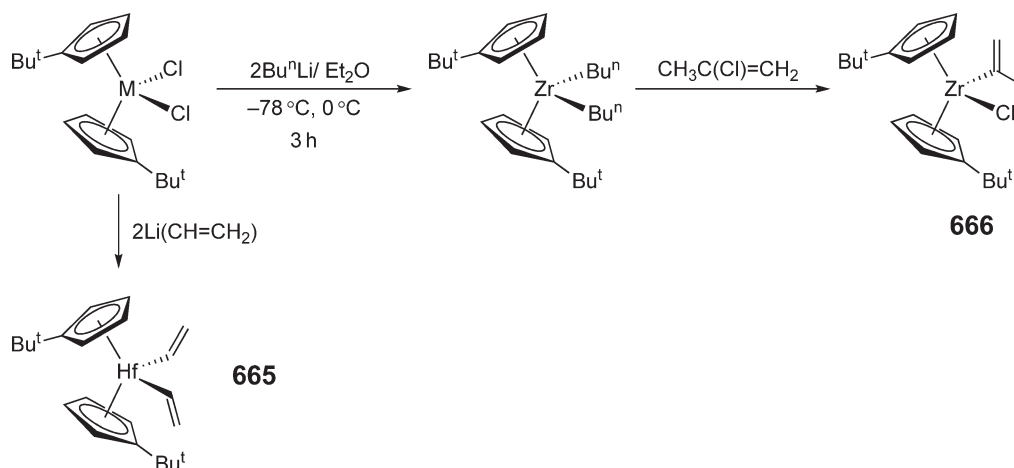
The reaction of  $\text{Cp}^{\text{P}}_2\text{ZrCl}_2$  ( $\text{Cp}^{\text{P}} = \text{C}_5\text{H}_4\text{PPh}_2$ ) with organolithium or Grignard reagents gives the corresponding dialkyl derivatives  $\text{Cp}^{\text{P}}_2\text{ZrR}_2$  ( $\text{R} = \text{Me, } p\text{-tolyl, CH}_2\text{SiMe}_3$ ), while the reaction with  $\text{AlMe}_3$  affords the monomethyl complex  $\text{Cp}^{\text{P}}_2\text{Zr}(\text{Me})\text{Cl}$  that serves as a precursor to other mixed alkyl derivatives such as  $\text{Cp}^{\text{P}}_2\text{Zr}(\text{Me})\text{Ph}$ .<sup>488</sup> Treatment of  $\text{Mo}(\text{CO})_4(\text{norbornadiene})$  with  $\text{Cp}^{\text{P}}_2\text{Zr}(\text{Me})\text{Cl}$  or  $\text{Cp}^{\text{P}}_2\text{Zr}(\text{Me})\text{Ph}$  leads to Zr–Mo binuclear tetracarbonyl complexes  $\text{Me}(\text{X})\text{ZrCp}^{\text{P}}_2\text{Mo}(\text{CO})_4$  in which the zirconocene moiety serves as a bridge through two diphenylphosphine substitutes on both Cp rings. Coupling of  $\text{Cp}_2\text{ZrEt}_2$  and  $\text{Cp}_2\text{ZrX}_2$  ( $\text{X} = \text{Cl, Br}$ ) in donor solvents gives ethylene-bridged bimetallic zirconocene halide complexes  $\text{Cp}_2\text{ZrX}(\mu\text{-C}_2\text{H}_4)\text{XZrCp}_2$ . Subsequent alkylation with  $\text{RLi}$  ( $\text{R} = \text{Me, Ph, CH}_2\text{SiMe}_3$ ) produces the corresponding ethylene-bridged bimetallic zirconocene alkyl complexes  $\text{Cp}_2\text{ZrR}(\mu\text{-C}_2\text{H}_4)\text{RZrCp}_2$ .<sup>489</sup>

$(\mu\text{-Methylene})\text{bis}(\text{methylzirconocene})$  **662** was synthesized by the reaction of  $\text{Cp}_2\text{Zr}(\text{Me})\text{Cl}$  with  $\text{CH}_2(\text{MgBr})_2$  or  $(\text{CH}_2\text{Mg})_n$ .<sup>490</sup> (Scheme 156). The X-ray structure of **662** shows that the carbon atom bridging the two zirconium atoms is not planar as might have been expected; however, the widened Zr–C–Zr angle and an asymmetric coordination of the central  $\mu\text{-CH}_2$  group indicate a tendency toward planarity. Complex **662** is relatively stable in THF solution, but disproportionates in toluene to give 1,3-dizirconacyclobutane  $(\text{Cp}_2\text{ZrCH}_2)_2$  and  $\text{Cp}_2\text{ZrMe}_2$ . Abstractive reaction with  $\text{B}(\text{C}_6\text{F}_5)_3$  yields the corresponding methylene- and methyl-bridged cationic complex **663**, which, upon treatment with trityl chloride, was transformed into the corresponding chloro-bridged complex **664**.

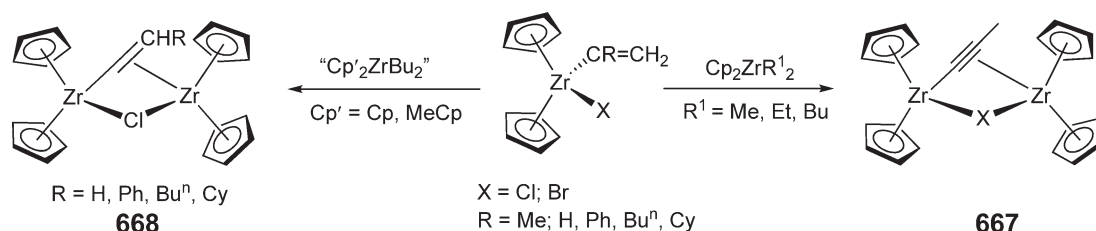
#### 4.08.9.3.2 Complexes containing M–C $sp^2$ -bonds

The reaction of  $(\text{Bu}^t\text{C}_5\text{H}_4)_2\text{HfCl}_2$  with 2 equiv. of vinyl lithium gives the divinyl complex **665**.<sup>491</sup> (Scheme 157). On the other hand, the chlorozirconocene alkenyl complex **666** was obtained by treatment of  $(\text{Bu}^t\text{C}_5\text{H}_4)_2\text{ZrCl}_2$  with 2 equiv. of  $\text{Bu}^n\text{Li}$  followed by addition of 2-chloropropene, which oxidatively adds to the dibutylzirconocene intermediate.<sup>492</sup> This oxidative addition approach to alkenyl metallocenes avoids the undesired isomerization to regioisomers usually obtained by hydrozirconation.

Alkenylzirconocenes monohalides ( $\text{X} = \text{Cl, Br}$ ) react dialkyl zirconocenes  $\text{Cp}_2\text{ZrR}_2$  ( $\text{R} = \text{Me, Et, Bu}^n$ ) to yield the bimetallic zirconocene complexes  $\text{Cp}_2\text{Zr}(\mu\text{-X})(\mu\text{-C}\equiv\text{CCH}_3)\text{ZrCp}_2$  **667**.<sup>493</sup> (Scheme 158). The first step of this reaction involves exchange of the alkyl and halide groups. Alkenylzirconocene chlorides also react with the *in situ*-generated “ $\text{Cp}'_2\text{Zr}$ ” to yield the neutral binuclear alkenyl-bridged complexes  $\text{Cp}_2\text{Zr}(\mu\text{-Cl})(\mu\text{-}\eta^1:\eta^2\text{-CH=CHR})\text{ZrCp}_2$  **668**, which



Scheme 157

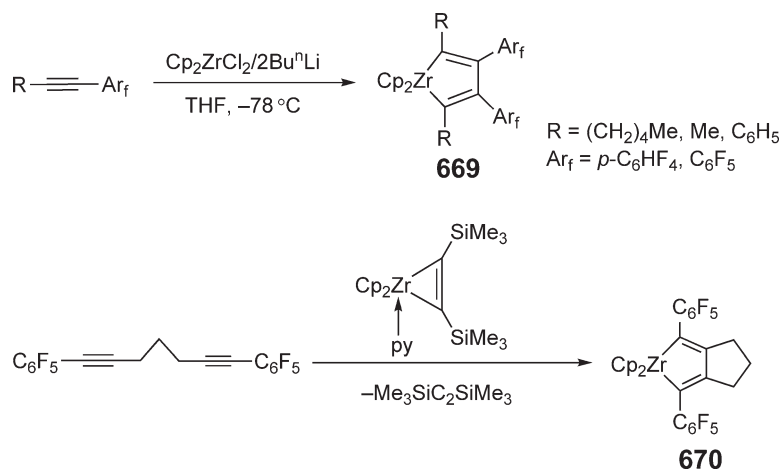


Scheme 158

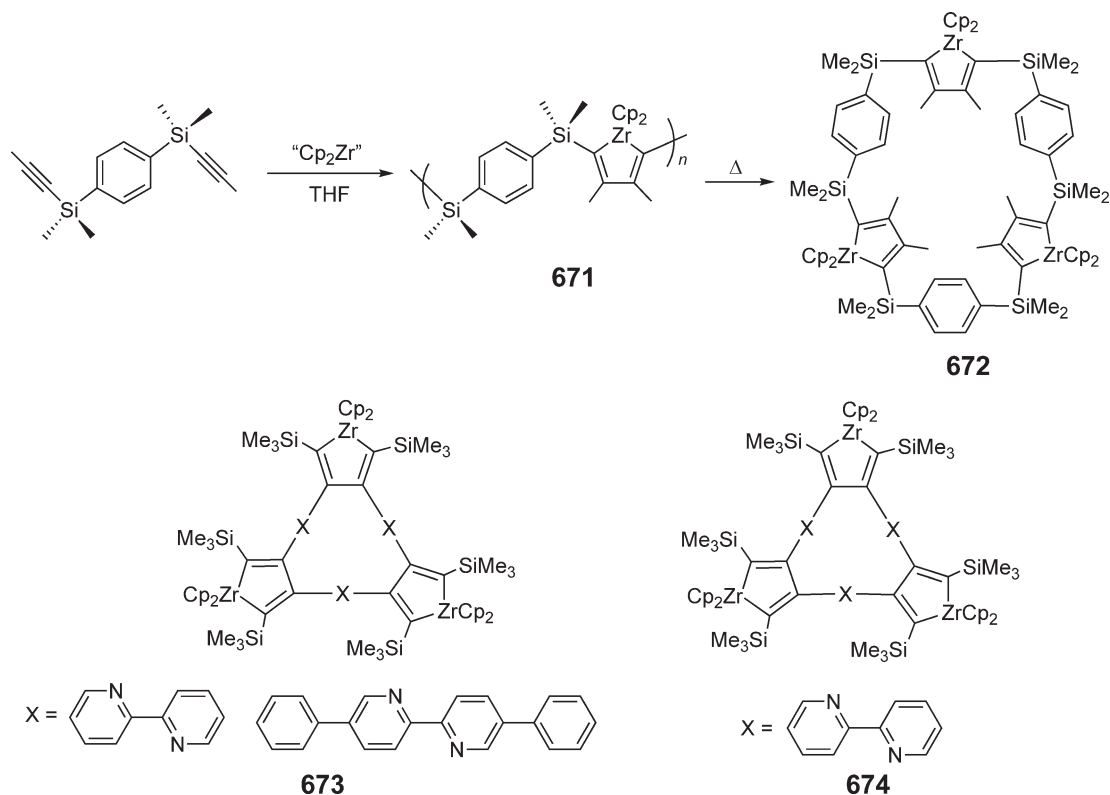
are regioselectively protonated by  $[\text{HNMe}_2\text{Ph}]\text{BPh}_4$  to yield  $[\text{Cp}_2\text{Zr}(\mu\text{-Cl})(\mu\text{-}\eta^1\text{:}\eta^2\text{-C}^1\text{H}_2\text{C}^2\text{HR})\text{ZrCp}_2]^+$ .<sup>494</sup> These unusually structured products exhibit an unsymmetric bridged hydrocarbyl ligand containing a hypercoordinated carbon center ( $\text{C}^1$ ) inside the rigid organometallic framework. In zirconocene phenylallenyl complexes such as  $\text{Cp}_2\text{ZrMe}[\eta^3\text{-C}(\text{Ph})=\text{C}=\text{CH}_2]$ , the phenylallenyl ligand is  $\eta^3$ -bound to Zr based on the X-ray crystal structure.<sup>495</sup> The related bis(allenyl) complex,  $\text{Cp}_2\text{Zr}[\text{C}(\text{Ph})=\text{C}=\text{CH}_2]_2$ , displays a dynamic solution behavior that apparently involves rapid interconversion of  $\eta^1$ - and  $\eta^3$ - $\text{C}(\text{Ph})=\text{C}=\text{CH}_2$  ligands.<sup>496</sup>

Coupling of unsymmetric tetra- or pentafluorophenyl-substituted alkynes  $\text{RC}\equiv\text{CAr}_f$  by  $\text{Cp}_2\text{ZrCl}_2/2\text{Bu}^n\text{Li}$  occurs regioselectively to give zirconacyclopentadienes **669** in which the  $\text{Ar}_f$  substituents preferentially adopt the 3,4-positions ( $\beta\beta$ ) of the zirconacyclopentadiene ring (Scheme 159).<sup>497</sup> With  $\text{Cp}_2\text{Zr}(\text{py})(\eta^2\text{-Me}_3\text{SiC}\equiv\text{CSiMe}_3)$  as the “ $\text{Cp}_2\text{Zr}$ ” reagent, the couplings can be carried out at ambient temperature; however, at higher temperatures, significant quantities of the 2,4-fluoroaryl substituted ( $\alpha\beta$ ) isomers were also formed. None of the conditions employed produced the 2,5-fluoroaryl substituted ( $\alpha\alpha$ ) isomers. However,  $\alpha\alpha$ -fluoroaryl-substituted isomers such as zirconacyclopentadiene **670** can be prepared by the reaction of  $[(\text{C}_6\text{F}_5)\text{C}\equiv\text{CCH}_2]_2\text{CH}_2$  with  $\text{Cp}_2\text{Zr}(\text{py})(\eta^2\text{-Me}_3\text{SiC}\equiv\text{CSiMe}_3)$ , forcing the  $\text{C}_6\text{F}_5$  substituents into the 2,5-positions ( $\alpha\alpha$ ).

Zirconocene-mediated polymerization and cyclotrimerization of  $1,4\text{-MeC}\equiv\text{C}(\text{Me}_2\text{Si})\text{C}_6\text{H}_4(\text{Me}_2\text{Si})\text{C}\equiv\text{CMe}$  gives high-yield polymeric zirconacyclopentadiene **671** and macrocycle **672**<sup>498</sup> respectively (Scheme 160). High-temperature conditions favor the production of the low molecular weight product **672**, identified by X-ray crystallography as a trimer, due to depolymerization of polymer **671**. Treatment of  $1,4\text{-Me}_3\text{SiC}\equiv\text{CC}_6\text{H}_4\text{C}_6\text{H}_4\text{C}\equiv\text{CSiMe}_3$  with a slight excess of “ $\text{Cp}_2\text{Zr}$ ” generated by addition of  $\text{Bu}^n\text{Li}$  to  $\text{Cp}_2\text{ZrCl}_2$ , promotes the analogous zirconocene-mediated cyclotrimerization and cyclotetramerization of  $1,4\text{-Me}_3\text{SiC}\equiv\text{CC}_6\text{H}_4\text{C}_6\text{H}_4\text{C}\equiv\text{CSiMe}_3$ , yielding trimeric and tetrameric zirconacyclopentadiene unsaturated macrocycles.<sup>499</sup> Utilizing this unique, efficient route, bicyclic cage-type macrocycles have also been prepared.<sup>500</sup> Furthermore, using a different macrocyclization reagent,  $\text{Cp}_2\text{Zr}(\text{py})(\text{Me}_3\text{SiC}\equiv\text{CSiMe}_3)$ , has allowed the preparation of two large, functionalized zirconocene macrocycles **673** and **674**<sup>501</sup> (Scheme 160).

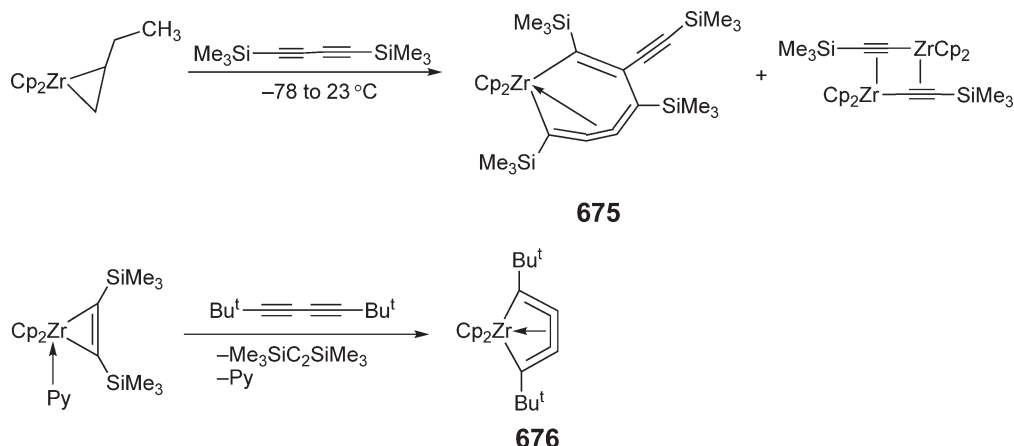


Scheme 159



Scheme 160

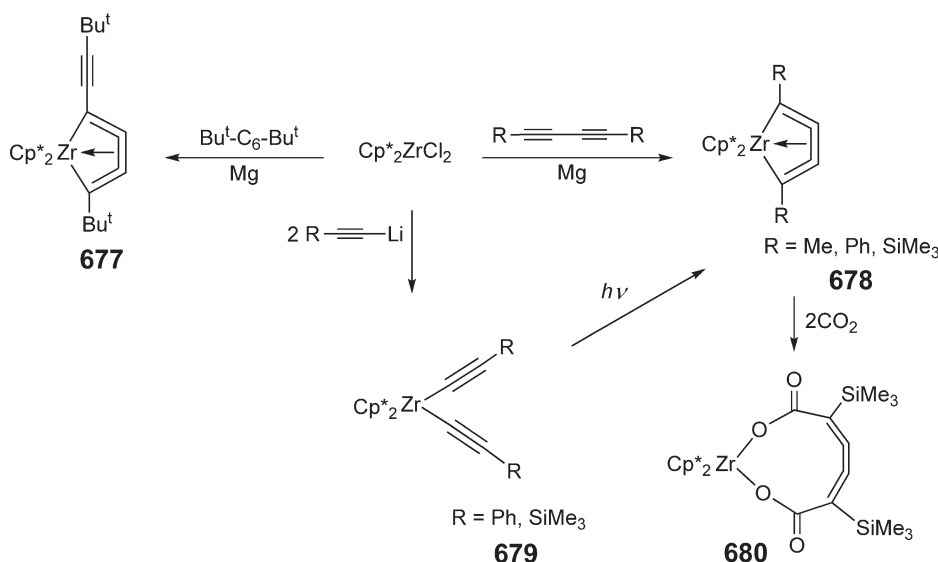
The reaction of a bis(trimethylsilyl)butadiene with the *in situ*-prepared *n*-butene zirconocene complex (as precursor to the  $\text{Cp}_2\text{Zr}$  synthon) unexpectedly yielded a distorted seven-membered cyclic cumulene **675**<sup>502</sup> (Scheme 161), together with  $[\text{Cp}_2\text{Zr}(\text{C}\equiv\text{CSiMe}_3)]_2$ , which can also be synthesized by reaction of zirconocene generated *in situ* with trimethylsilylacetylene.<sup>503</sup> Use of a different  $\text{Cp}_2\text{Zr}$  precursor, namely,  $\text{Cp}_2\text{Zr}(\text{py})(\eta^2\text{-Me}_3\text{SiC}_2\text{SiMe}_3)$  in the reaction with 1,3-butadiene  $\text{Bu}^t\text{C}\equiv\text{C}-\text{C}\equiv\text{CBu}^t$ , led to the formation of the first stable five-membered metallacyclocumulene (1-zircona- $\eta^4$ -cyclopenta-2,3,4-triene) **676**<sup>504</sup> with the concomitant elimination of pyridine and bis(trimethylsilyl)-acetylene (Scheme 161).



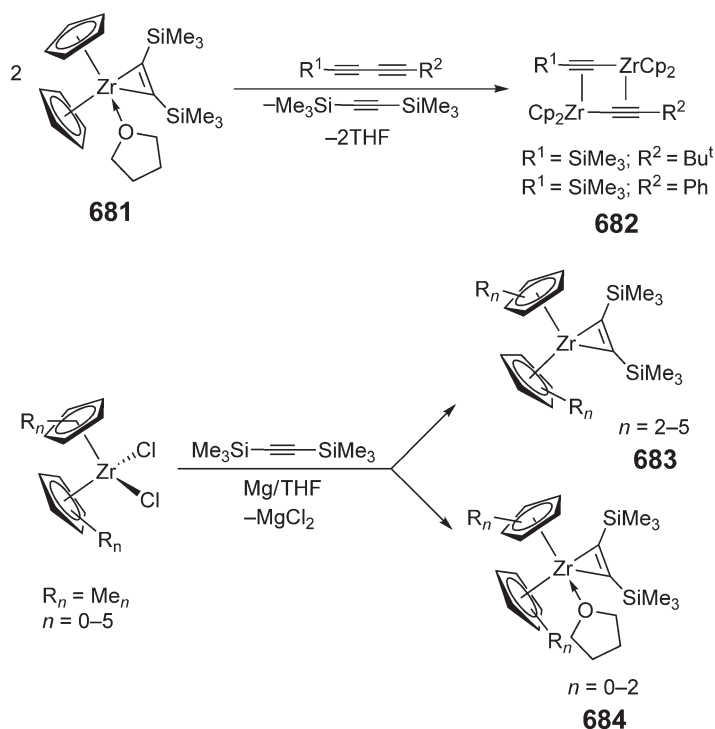
Scheme 161

Reaction of  $\text{Cp}^*_2\text{ZrCl}_2$  with magnesium in THF in the presence of hexatriynes  $\text{Bu}^t(\text{C}\equiv\text{C})_3\text{Bu}^t$  gives the  $\eta^4$ -diyne complex, zirconacyclopenta-2,3,4-triene  $\text{Cp}^*_2\text{Zr}(\eta^4\text{-Bu}^t\text{C}_4\text{-C}\equiv\text{CBu}^t)$  **677** in high yield<sup>505</sup> (Scheme 162). In general, stable, five-membered zirconacyclocumulenes of type **678** can be prepared using two effective synthetic routes.<sup>506,507</sup> The first involves reduction of  $\text{Cp}^*_2\text{ZrCl}_2$  with Mg in the presence of appropriate disubstituted butadiynes  $\text{RC}\equiv\text{C-C}\equiv\text{CR}$ , whereas the second starts with zirconocene bisacetylides  $\text{Cp}^*_2\text{Zr}(\text{C}\equiv\text{CR})_2$  (**679**;  $\text{R} = \text{Ph}, \text{SiMe}_3$ ), which rearrange in sunlight to form the stable five-membered zirconacyclocumulenes **678**. The zirconacyclocumulene ( $\text{R} = \text{SiMe}_3$ ) surprisingly inserts two molecules of  $\text{CO}_2$  to give the cumulenenic dicarboxylate **680**.

The zirconocene alkyne complex  $\text{Cp}_2\text{Zr}(\text{THF})(\eta^2\text{-Me}_3\text{SiC}_2\text{SiMe}_3)$  **681** readily reacts with disubstituted butadiynes to form the dimeric symmetric and doubly acetylide-bridged crystalline complexes **682**<sup>508</sup> (Scheme 163). Complex **681** also reacts with a nickel(0) complex of bis(trimethylsilyl)butadiyne to form the heterobimetallic, doubly acetylide-bridged complex.<sup>509</sup> The zirconocene alkyne complexes can be prepared by the reduction of the unsubstituted or methyl-substituted zirconocene dichlorides with Mg in the presence of bis(trimethylsilyl)acetylene, leading to complexes **683** with two or more methyls on the Cp rings, which are stable in the absence of THF, or complexes **684** with one or no methyl group on the Cp rings.<sup>510,511</sup> The monomethyl-substituted complex **684** was



Scheme 162



Scheme 163

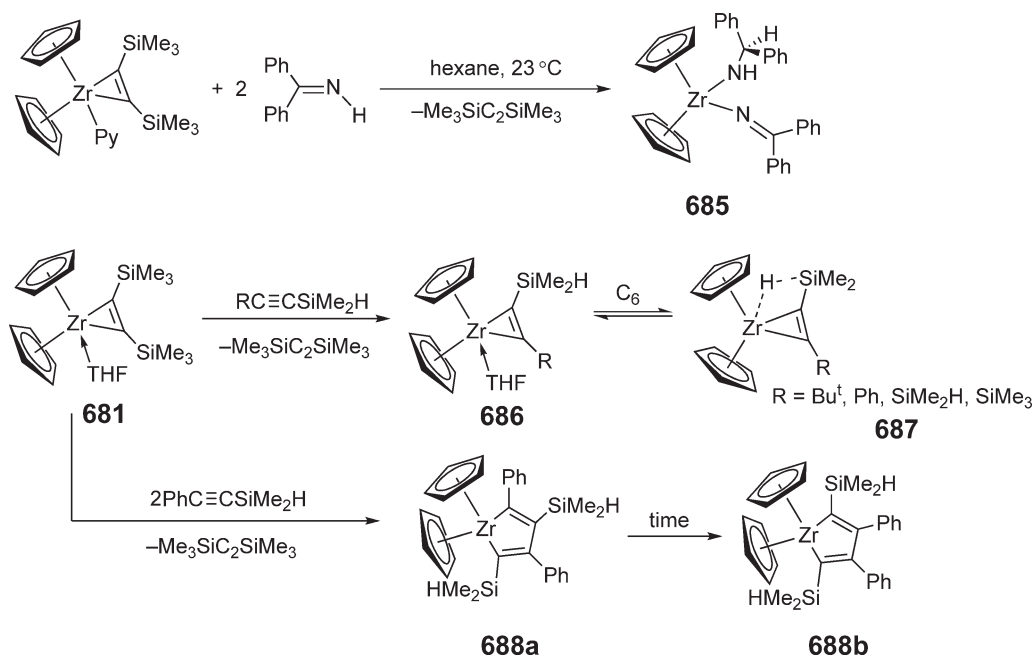
not isolated but found to rearrange after the loss of THF to give a dimeric product  $[(\eta^5\text{-C}_5\text{H}_4\text{Me})(\eta^1\text{-C}(\text{SiMe}_3)\text{CH}(\text{SiMe}_3))\text{Zr}(\mu\text{-}\eta^1\text{:}\eta^5\text{-C}_5\text{H}_3\text{Me})]_2$ .

Under mild conditions, the zirconocene alkyne complex  $\text{Cp}_2\text{Zr}(\text{py})(\eta^2\text{-Me}_3\text{SiC}\equiv\text{CSiMe}_3)$  generates the unstable zirconocene “ $\text{Cp}_2\text{Zr}$ ”, which reacts *in situ* with 2 equiv. of the ketimine  $\text{HN}=\text{CPh}_2$  to form zirconocene amido alkylideneamido complex  $\text{Cp}_2\text{Zr}(\text{NH-CHPh}_2)(\text{N}=\text{CPh}_2)$  (**685**, Scheme 164) via hydrogen transfer of the ketimine moieties.<sup>512</sup> Lactams also react with zirconocene alkyne complexes  $\text{Cp}_2\text{Zr}(\text{L})(\eta^2\text{-Me}_3\text{SiC}_2\text{SiMe}_3)$  ( $\text{L} = \text{THF}, \text{py}$ ) to yield various products.<sup>513</sup> The zirconocene alkyne complex **681** undergoes acetylene exchange reactions with 1 equiv. of alkynylsilanes  $\text{RC}\equiv\text{CSiMe}_2\text{H}$  to give the THF-stabilized alkyne complexes **686**.<sup>514</sup> Upon dissolving in *n*-hexane, complete dissociation of the THF ligand yields base-free zirconocene alkyne complexes **687**, stabilized by agostic interaction between the Si–H bonds and the metal center (Scheme 165). Coupling of 2 equiv. of  $\text{PhC}\equiv\text{CSiMe}_2\text{H}$  to alkyne complex **681** gives zirconacyclopentadiene **688**, with the unsymmetrically substituted complex **688a** being the kinetic product and the symmetrically substituted complex **688b** being the thermodynamic product.

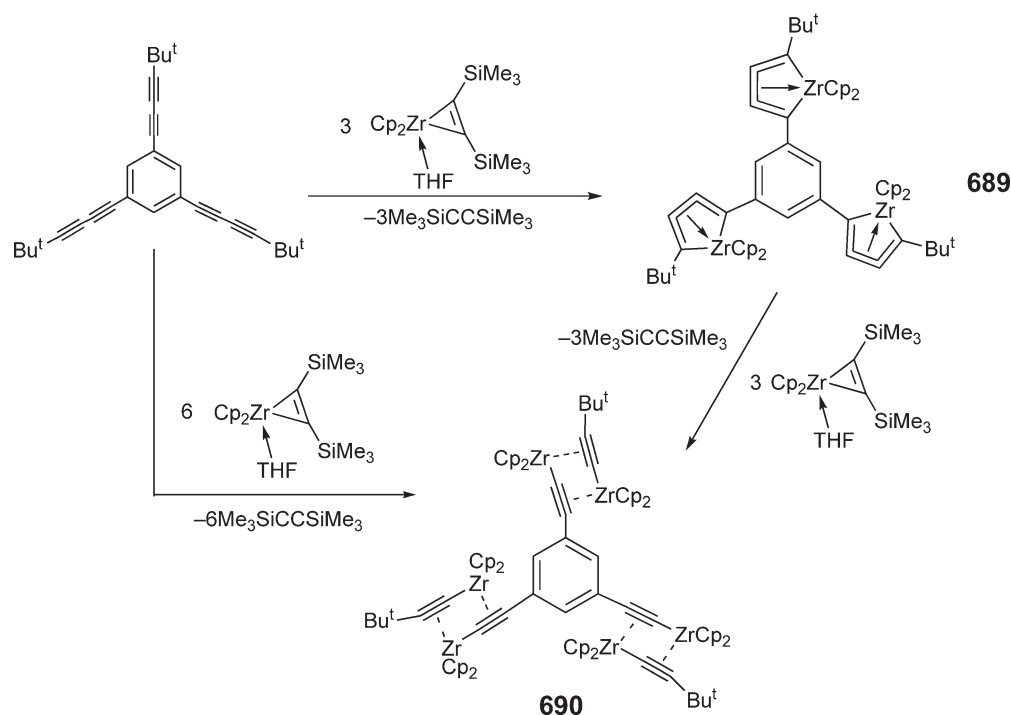
Treatment of the branched polyyne tris(*tert*-butylbutadiynyl)benzene with 3 equiv. of zirconocene alkyne complex  $\text{Cp}_2\text{Zr}(\text{THF})(\eta^2\text{-Me}_3\text{SiC}\equiv\text{CSiMe}_3)$  leads to the formation of the  $\text{Zr}_3$  complex **689**, which can be viewed as a benzene derivative substituted by three five-membered zirconacyclocumulene moieties<sup>515</sup> (Scheme 165). In contrast, the reaction with 6 equiv. of  $\text{Cp}_2\text{Zr}(\text{THF})(\eta^2\text{-Me}_3\text{SiC}\equiv\text{CSiMe}_3)$  affords the  $\text{Zr}_6$  alkyne acetylide complex **690**, which has been structurally characterized. The closely related reaction of  $\text{Cp}_2\text{Zr}(\text{THF})(\eta^2\text{-Me}_3\text{SiC}\equiv\text{CSiMe}_3)$  with branched tetraalkynylsilanes produced binuclear *spiro*-zirconocene complexes.<sup>516</sup> The reaction of  $\text{Cp}_2\text{Zr}(\text{py})(\eta^2\text{-Me}_3\text{SiC}\equiv\text{CSiMe}_3)$  with diisobutylaluminum hydride under mild conditions yields crystalline heterobimetallic  $\text{Zr}/\text{Al}$  products.<sup>517</sup>

The reactions of  $\text{Cp}_2\text{Zr}(\text{L})(\eta^2\text{-Me}_3\text{SiC}_2\text{SiMe}_3)$  with 2 equiv. or an excess of bicyclo[2.2.1]hepta-2,5-diene give five-membered,  $C_2$ -symmetric zirconacyclopentane complexes **691**<sup>518</sup> (Scheme 166). The analogous zirconacyclopentane complexes **692** are obtained from the reactions with an excess of 1,4-dihydro-1,4-methanonaphthalene. Similarly, the reactions of  $\text{Cp}_2\text{Zr}(\text{L})(\eta^2\text{-Me}_3\text{SiC}_2\text{SiMe}_3)$  with methyl vinyl ketone and 1,4-diazadienes yield 2-oxa-1-zirconacyclopent-3-ene (zirconadihydrofuran **693**)<sup>519</sup> and 1-zircona-2,5-diazacyclopent-3-ene (zirconadiazadiene **694**),<sup>520</sup> respectively.

Treatment of *o*- $\text{C}_6\text{H}_4(\text{C}\equiv\text{CSiMe}_3)_2$  with  $\text{Cp}_2\text{Zr}$  generated *in situ* from  $\text{Cp}_2\text{ZrCl}_2/2\text{Bu}^n\text{Li}$  failed to produce the anticipated zirconacyclopentene complex **695**; instead, a zirconocene dialkyne complex **696** was formed.<sup>521</sup> The



Scheme 164

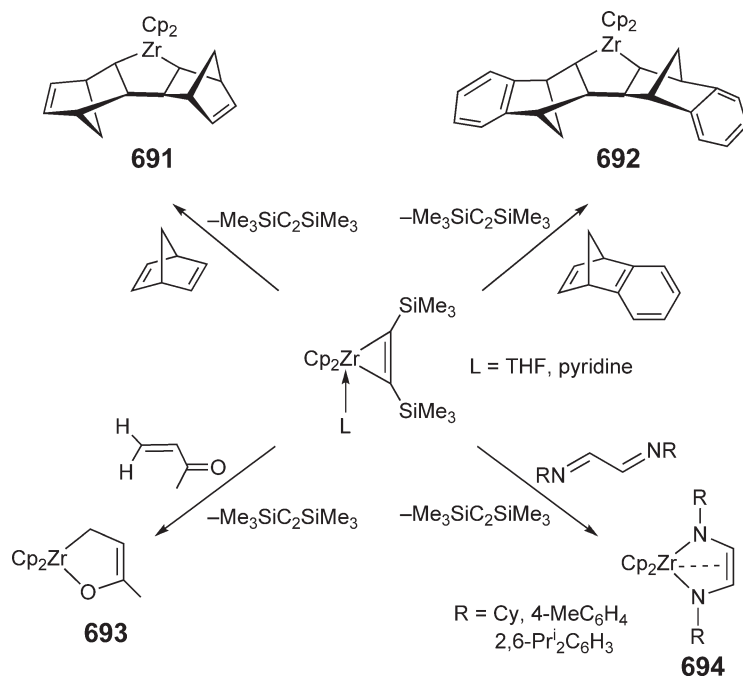


Scheme 165

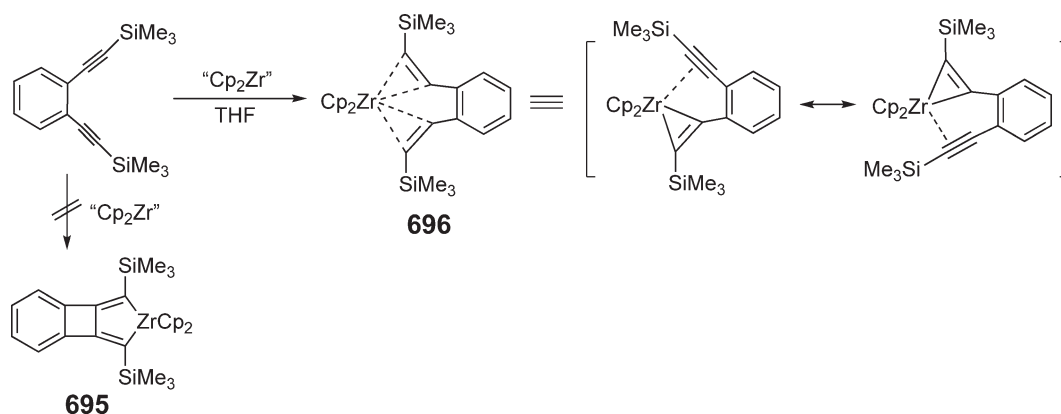
nature of **696** is best represented as the superposition of the two degenerate resonance contributors, each of which implies a  $\text{Zr}(\text{IV})$  moiety with one dative alkyne ligand and one zirconacyclopropene moiety (Scheme 167).

Treatment of bis(phenylethynyl)silanes with  $\text{Cp}_2\text{ZrEt}_2$  followed by addition of  $\text{H}_2\text{O}/\text{CuCl}$  affords (1*E*,3*E*)-1,4-diphenyl-1,3-butadienes in moderate to high yields after hydrolysis. The zirconocene complex **697** ( $\text{Bu}^t\text{C}_5\text{H}_4$ ) was



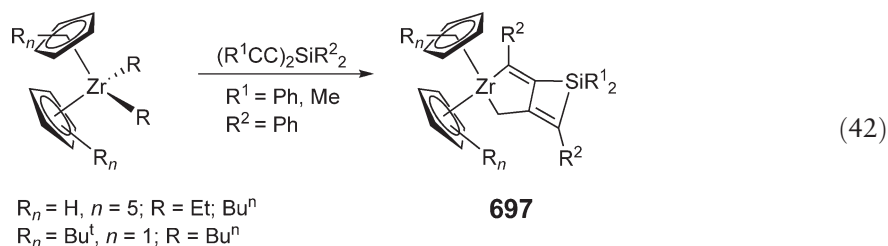


Scheme 166

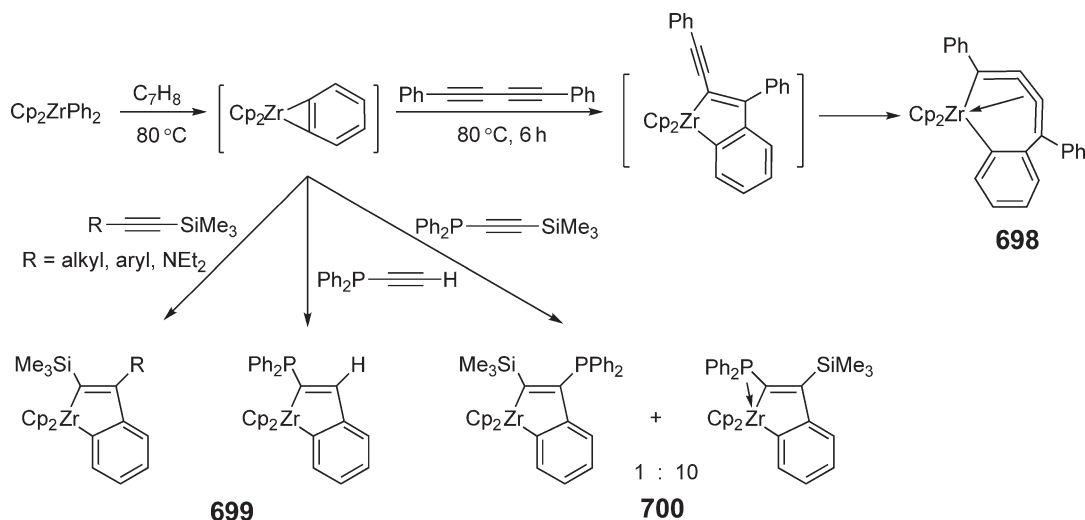


Scheme 167

obtained as orange crystals<sup>522</sup> (Equation (42)). The structure of **697** shows a zirconacyclobutene–silacyclobutene fused ring system. Accordingly, zirconacyclopentadienes with an alkynylsilyl group at the  $\alpha$ -position afforded zirconacyclohexadiene derivatives in high yields.



The thermolysis of diphenylzirconocene in the presence of 1,4-diphenyl-1,3-butadiyne gives the seven-membered zirconacyclocumulene **698** via a zirconocene benzyne intermediate, as shown in Scheme 168.<sup>523</sup> Coupling reactions



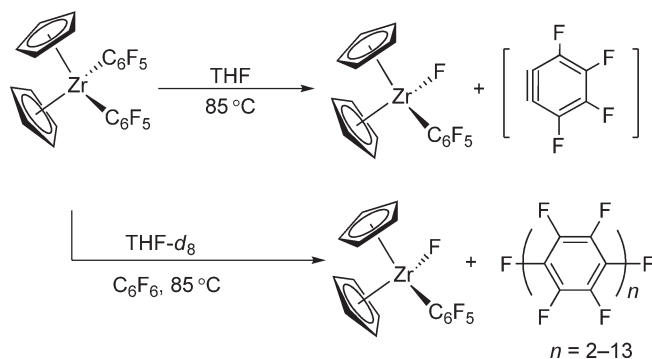
Scheme 168

of the benzyne complex  $\text{Cp}_2\text{Zr}(\eta^2\text{-C}_6\text{H}_4)$  with internal acetylenes give regioselectively the zirconaindene metallacycles **699**.<sup>524</sup> The unusual acute Zr–C–P angle and the short Zr–P distance indicate a significant Lewis-base/acid  $\sigma\text{-P-Zr}$  interaction in the  $\alpha$ -phosphino zirconaindene metallacycle **700**.

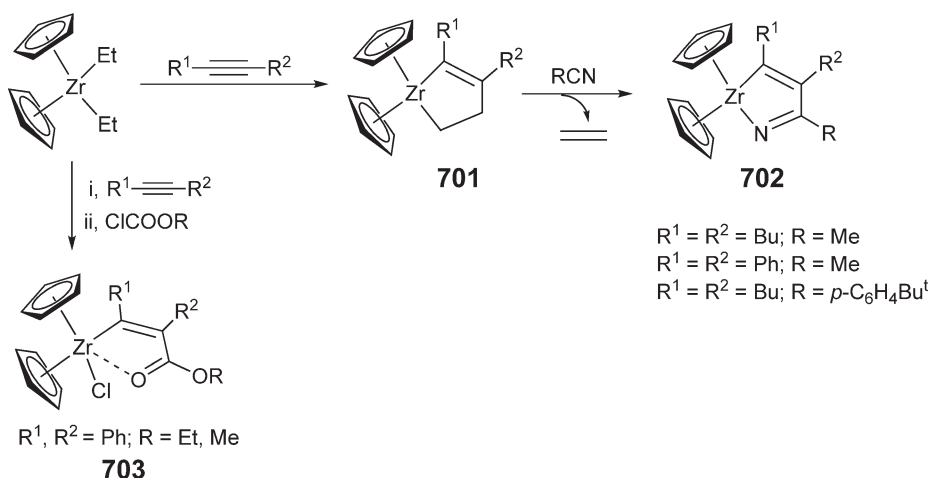
Perfluoropolyphenylene oligomers can be generated via carbon–fluorine bond activation with  $\text{Cp}_2\text{Zr}(\text{C}_6\text{F}_5)_2$ . Thermal decomposition of  $\text{Cp}_2\text{Zr}(\text{C}_6\text{F}_5)_2$  in THF results in the slow formation of  $\text{Cp}_2\text{Zr}(\text{C}_6\text{F}_5)\text{F}$  and tetrafluorobenzyne. The latter can be trapped by THF to give several products. If  $\text{Cp}_2\text{Zr}(\text{C}_6\text{F}_5)_2$  is heated in the presence of  $\text{C}_6\text{F}_6$ , perfluorophenylene linear chains are rapidly generated along with  $\text{Cp}_2\text{Zr}(\text{C}_6\text{F}_5)\text{F}$ <sup>525</sup> (Scheme 169). Dual mechanisms involving a rapid radical chain reaction and a slower tetrafluorobenzyne-producing reaction have been invoked to account for the kinetics of this reaction.

Zirconacyclopentenes **701** are obtained by the reaction of alkynes with  $\text{Cp}_2\text{ZrEt}_2$ , as shown in Scheme 170.<sup>526</sup> The X-ray structure of **701** ( $\text{R}^1 = \text{R}^2 = \text{Ph}$ ) indicates a single bond between the  $\beta$ - and  $\beta'$ -carbons of the zirconacyclopentene. The reaction of these zirconacyclopentenes with nitriles proceeds via  $\beta, \beta'$ -carbon–carbon bond cleavage of the zirconacyclopentenes to give the azazirconacyclopentadienes **702**. Alkynes also react with diethyl zirconocene and electrophiles such as  $\text{ClCO}_2\text{Et}$  to give stereodefined  $\alpha, \beta$ -unsaturated esters **703**.<sup>527</sup>

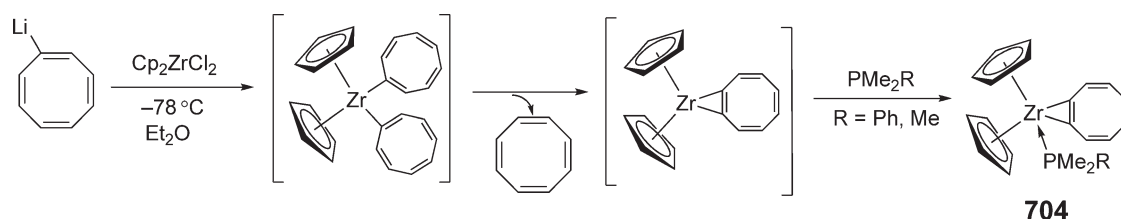
Cyclooctatrienyne zirconocene complexes of type **704** can be prepared by  $\beta$ -hydrogen elimination from zirconocene biscyclooctatetraenyl complexes (Scheme 171).<sup>528</sup> These complexes are fluxional by a ring inversion process, with activation barriers in the range typical of cyclooctatetraenes. An X-ray crystal structure ( $\text{R} = \text{Ph}$ ) reveals a boat conformation of the cyclooctatrienyne ring with no significant flattening when compared with cyclooctatetraene, thus the structure more closely resembles substituted cyclooctatetraenes than that expected of a cyclooctatrienyne.



Scheme 169



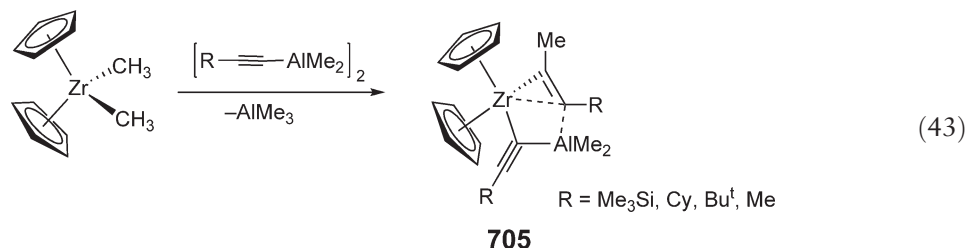
Scheme 170



Scheme 171

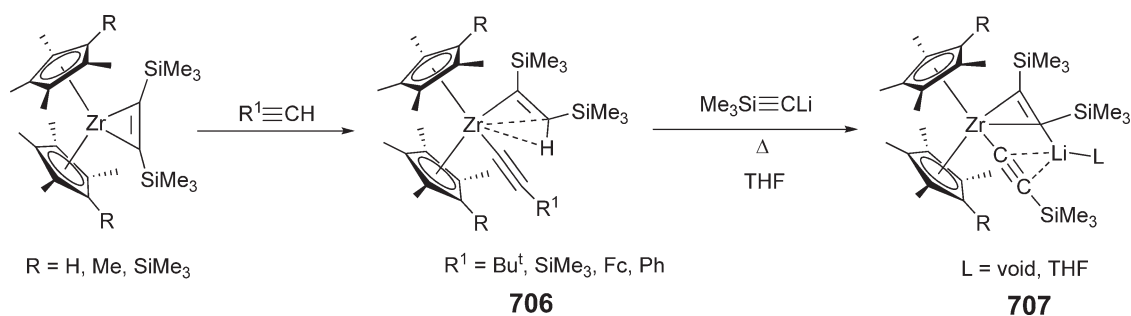
#### 4.08.9.3.3 Complexes containing M–C *sp*-bonds

Zirconocene complexes **705** that contain an acetylide ligand bridging between a main group metal (aluminum) and a transition metal (zirconium) are obtained by treatment of dimethyl zirconocene with (alkynyl)dimethylaluminum, (Equation (43)).<sup>529</sup> In this reaction, an ( $\eta^2$ -alkyne)zirconocene complex is presumably formed *in situ*, and it is then trapped by the excess (alkynyl)dimethylaluminum to yield the final product. The molecular structures of the complexes **705** ( $\text{R} = \text{SiMe}_3$ , Cy) contain a dimetallabicyclic framework, and one of the bridgehead positions is a planar tetracoordinate carbon center. In these complexes, the  $\text{C}\equiv\text{CR}$  bridge between zirconium and aluminum can be described as being mainly of  $\mu$ -( $\sigma$ -acetylide) character.



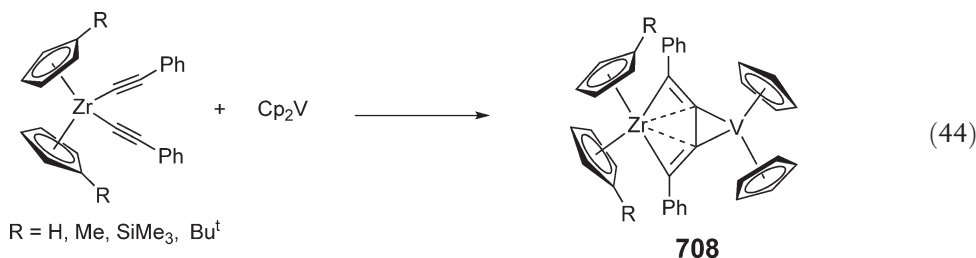
Reactions of substituted zirconocene-bis(trimethylsilyl)alkyne complexes with terminal alkynes produce the agostic-stabilized alkenyl-alkynyl complexes **706**<sup>530</sup> (Scheme 172). Heating of complexes **706** with  $\text{LiC}\equiv\text{CSiMe}_3$  in toluene or THF gives the zirconate complex **707**. On the basis of the crystal structure, the lithium cation is placed in a position at the side of the alkynyl triple bond and close to the  $\beta$ -carbon of the  $\eta^2\text{-Me}_3\text{SiC}\equiv\text{CSiMe}_3$  ligand, apparently interacting with both moieties.

The reaction of bis(phenylacetylide) zirconocenes  $(\text{C}_5\text{H}_4\text{R})_2\text{Zr}(\text{C}\equiv\text{CPh})_2$  ( $\text{R} = \text{H}, \text{Me}, \text{Bu}^t, \text{SiMe}_3$ ) with vanadocene in toluene at ambient temperature gives heterobimetallic complexes **708**<sup>531,532</sup> (Equation (44)). The molecular structures show the  $\text{Cp}_2\text{V}$  and  $\text{Cp}^R_2\text{Zr}$  metallocene moieties bonded to a butadiene framework through the two



Scheme 172

internal carbon atoms for  $\text{Cp}_2\text{V}$  and through the two internal and the two external carbon atoms for  $\text{Cp}^R_2\text{Zr}$ . The two internal carbon atoms of the butadiene skeleton are planar and tetracoordinated.



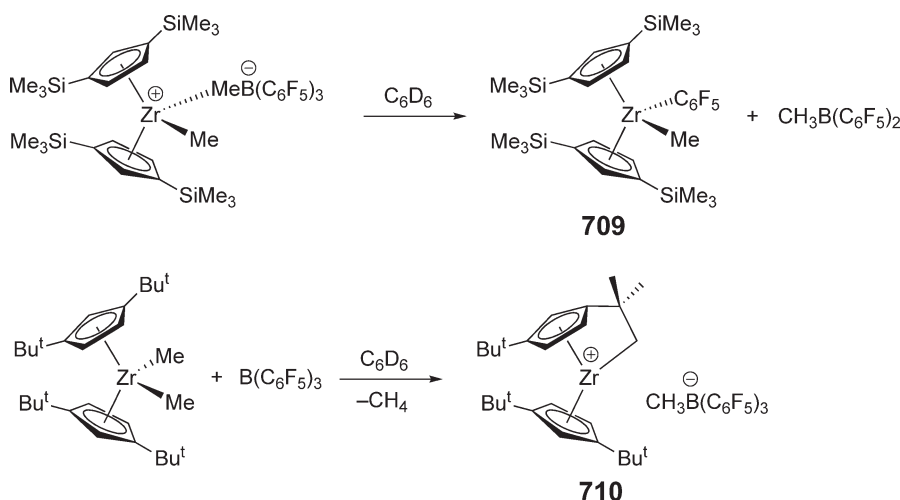
#### 4.08.9.4 Cationic Zirconocene Complexes

Alkyl or hydride abstraction of metallocene dialkyl or hydride complexes by the strongly Lewis-acidic and chemically robust borane reagent,  $\text{B}(\text{C}_6\text{F}_5)_3$ , cleanly generates the corresponding cationic metallocenium methylborate ion pairs which are typically isolable and crystallizable. Such reactions involving zirconocene dimethyl complexes and  $\text{B}(\text{C}_6\text{F}_5)_3$  in hydrocarbon solvents have been investigated in great detail.<sup>533</sup> These alkyl or hydride metallocenium methylborate complexes are highly active catalysts for olefin polymerizations as well as for hydroamination/cyclization of aminoalkenes.<sup>534</sup> As a rule, the reaction with an excess of  $\text{B}(\text{C}_6\text{F}_5)_3$  does not effect the removal of the second Zr–methyl ligand, even after extended periods of reaction. However, NMR spectroscopic evidence showed that  $\text{B}(\text{C}_6\text{F}_5)_3$  is capable of abstracting a second methide group from the benzyl-substituted zirconocenes (*p*-MeC<sub>6</sub>H<sub>4</sub>CMe<sub>2</sub>Cp)<sub>2</sub>ZrMe<sub>2</sub> at  $-60^\circ\text{C}$  in  $\text{CD}_2\text{Cl}_2$ .<sup>535</sup> Arene coordination of the Cp benzyl group to Zr is thought to stabilize the resulting dication-like structure. Above  $-40^\circ\text{C}$ , the dication-like species reverts to the normal monocationic complex and neutral  $\text{B}(\text{C}_6\text{F}_5)_3$ .

Exceptions regarding the stability of the resulting cationic zirconocenium methylborate complexes include those having bulky substituents on the Cp rings. For example, the moderately stable complex  $\text{Cp}''_2\text{ZrMe}(\mu\text{-Me})\text{B}(\text{C}_6\text{F}_5)_3$  ( $\text{Cp}'' = 1,3\text{-C}_5\text{H}_3(\text{SiMe}_3)_2$ ), which has been structurally characterized by X-ray diffraction,<sup>536</sup> slowly undergoes decomposition via  $\text{C}_6\text{F}_5$  transfer to generate the neutral zirconocene **709** and the byproduct  $\text{MeB}(\text{C}_6\text{F}_5)_2$  (Scheme 173).  $\text{Al}(\text{C}_6\text{F}_5)_3$ -derived ion pairs show much more facile  $\text{C}_6\text{F}_5$  transfer, which accounts for their poor thermal stability compared with  $\text{B}(\text{C}_6\text{F}_5)_3$ -derived analogs. For example,  $\text{Cp}_2\text{Zr}(\text{Me})(\mu\text{-Me})\text{Al}(\text{C}_6\text{F}_5)_3$  decomposes at temperatures above  $0^\circ\text{C}$  to form  $\text{Cp}_2\text{ZrMe}(\text{C}_6\text{F}_5)$ .<sup>537</sup> Decomposition products arising from fluoride abstraction to give species such as  $[(1,2\text{-Me}_2\text{Cp})_2\text{ZrMe}]_2(\mu\text{-F})^+[\text{MeB}(\text{C}_6\text{F}_5)_3]^-$  often result from prolonged standing of solutions of  $\text{L}_2\text{ZrMe}(\mu\text{-Me})\text{B}(\text{C}_6\text{F}_5)_3$  at room temperature over a period of weeks.

Another commonly observed decomposition pathway involves C–H bond activation. For example, the reaction of  $(1,3\text{-Bu}^t\text{Cp})_2\text{ZrMe}_2$  with  $\text{B}(\text{C}_6\text{F}_5)_3$  yields a C–H activated  $\eta^5, \eta^1$ -“tuck-in” cation **710** (Scheme 173), which is inert with respect to ethylene polymerization. There are also significant metal–alkyl group effects on the thermodynamic stability and stereochemical mobility of the  $\text{B}(\text{C}_6\text{F}_5)_3$ -derived Zr and Hf metallocenium ion pairs.<sup>538</sup>

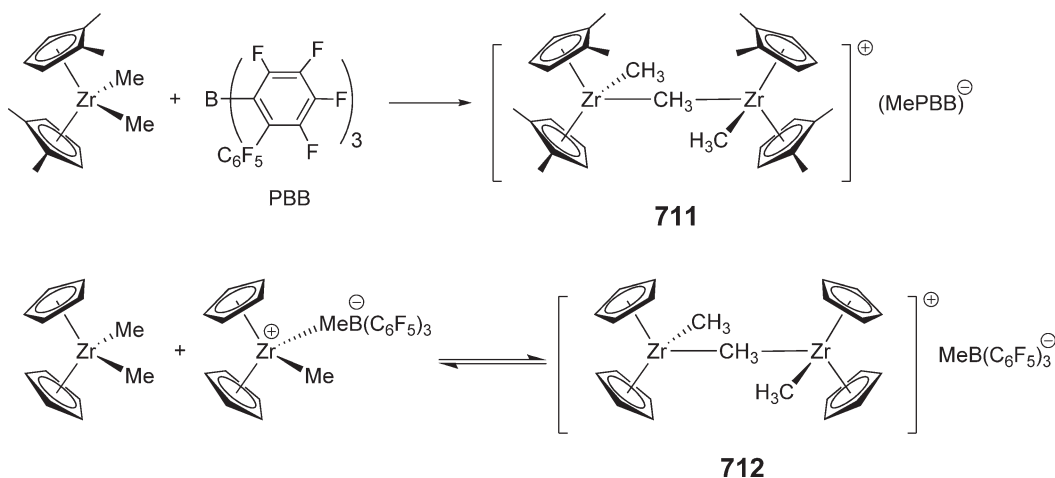
The electronic features and steric environment inherent in perfluoroaryl borane abstractors employed for alkyl abstraction reactions are key to the metallocene activation process for polymerization catalysis and the structure of the



Scheme 173

resulting products.<sup>539,540</sup> For instance, the reaction of the sterically encumbered borane tris(2,2',2''-perfluorobiphenyl)borane (PBB) with metallocene methyls affords cationic methyl-bridged binuclear complexes such as **711**<sup>541</sup> even with a stoichiometric excess of the bulky borane and extended reaction times (Scheme 174). The remarkably enhanced stability of  $\mu$ -Me bonding here likely reflects reduced coordinative tendency and greater bulk of the  $\text{CH}_3\text{PBB}^-$  anion compared to  $\text{CH}_3\text{B}(\text{C}_6\text{F}_5)_3^-$ .

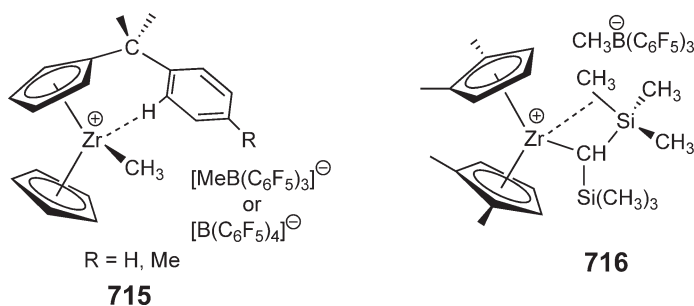
The preference of the cationic species  $[\text{Cp}_2\text{ZrMe}]^+$  to bind to  $\text{Cp}_2\text{ZrMe}_2$  as opposed to the anion, and to form  $\mu$ -Me binuclear cationic complexes, is also observed for the extremely weakly coordinating anion  $\text{B}(\text{C}_6\text{F}_5)_4^-$ . Thus, the  $\mu$ -Me binuclear complex  $[\text{Cp}_2\text{ZrMe}(\mu\text{-Me})\text{MeZrCp}_2]^+\text{B}(\text{C}_6\text{F}_5)_4^-$  is first formed in the 1:1 stoichiometric ratio reaction of  $\text{Cp}_2\text{ZrMe}_2$  with  $[\text{Ph}_3\text{C}][\text{B}(\text{C}_6\text{F}_5)_4]$ , and the quantitative formation of such binuclear species can be observed by NMR in reactions with a 2:1 ratio of  $\text{Cp}_2\text{ZrMe}_2$ : $[\text{Ph}_3\text{C}][\text{B}(\text{C}_6\text{F}_5)_4]$ .<sup>542,543</sup> For the more coordinating anion  $\text{CH}_3\text{B}(\text{C}_6\text{F}_5)_3^-$ ,  $\mu$ -Me bimetallic cationic complexes are not detected, except when an excess of neutral metallocene dimethyl is employed (Scheme 174).<sup>544</sup> This equilibrium can be utilized to stabilize the highly active form of the monomeric cations and prevent deactivation. Thus, using an excess of the neutral metallocene dimethyl versus activator often results in enhanced polymerization activity by virtue of the formation of cationic binuclear species **712**, especially for systems with  $\text{B}(\text{C}_6\text{F}_5)_4^-$ -based activators.



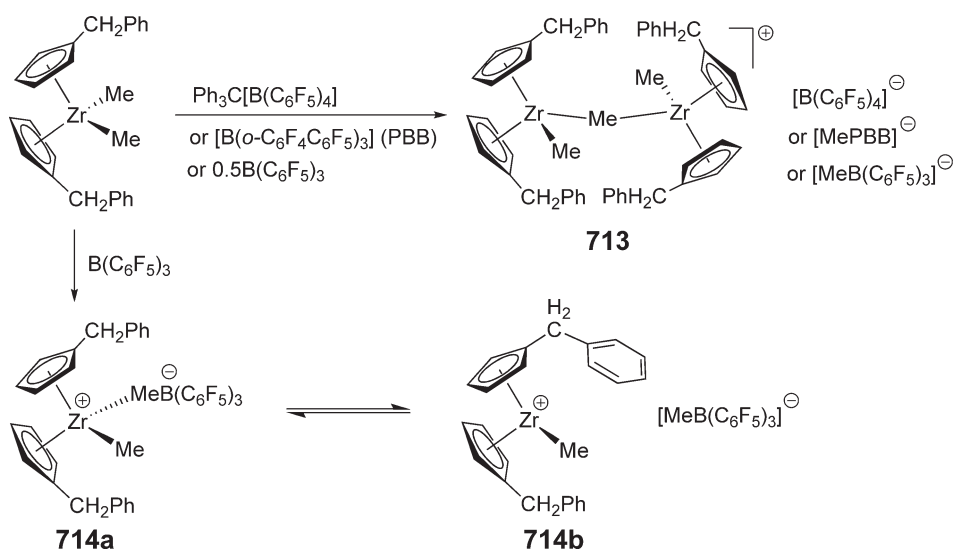
Scheme 174

The dimethyl zirconocene  $\text{Cp}^R_2\text{ZrMe}_2$  ( $R = \text{CH}_2\text{Ph}$ ) reacts with the methide abstracting agents such as  $\text{Ph}_3\text{C}[\text{B}(\text{C}_6\text{F}_5)_4]$ , PBB, or 0.5 equiv. of  $\text{B}(\text{C}_6\text{F}_5)_3$  at low temperature to form the methyl-bridged homobinuclear cations **713** paired with the respective anions (Scheme 175).<sup>545</sup> On the other hand, the reaction with 1 equiv. of  $\text{B}(\text{C}_6\text{F}_5)_3$  gives the corresponding cationic complexes which are in equilibrium between the contact ion pair **714a** and the separated (probably by intramolecular arene coordination) ion pair **714b**. Similar behavior is observed with  $\text{Cp}^{R^1}_2\text{ZrMe}_2$  ( $R^1 = \text{CHPh}_2$ ), but not with sterically more demanding ligands [ $R^1 = \text{Si}(\text{SiMe}_3)_3$ ].

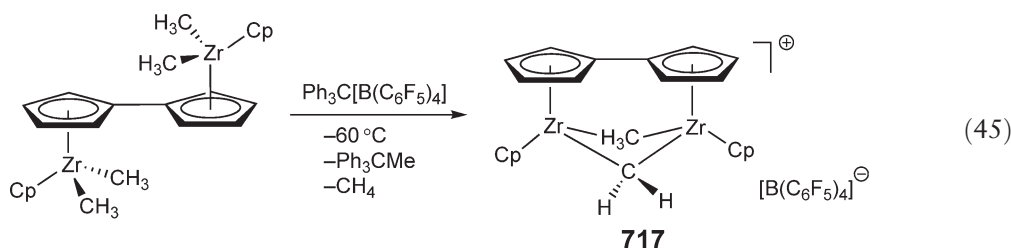
If the anion is well-separated from the cation, other types of interactions may be involved in cation stabilization. Coordination modes often observed include the solvent, a neutral metallocene alkyl, or multi-hapto benzyl interactions. Metallocene dibenzyl precursors often form more stable cationic complexes after activation, especially with activators containing weakly coordinating anions like  $\text{Ph}_3\text{C}[\text{B}(\text{C}_6\text{F}_5)_4]$ , due to  $\eta^2$ -benzyl stabilization of the cation.<sup>546</sup> Evidence for intramolecular phenyl coordination of cationic monobenzyl-substituted zirconocene complexes **715** has also been established by low-temperature NMR studies,<sup>547</sup> and the  $\beta$ -cation stabilizing effects of the silyl functionalities have been suggested in ion pair  $[(1,2\text{-Me}_2\text{Cp})_2\text{ZrCHTMS}_2]^+\text{CH}_3\text{B}(\text{C}_6\text{F}_5)_3^-$  **716** to explain the outer-sphere structure of the resulting ion pair.<sup>548</sup> Reactions of zirconocene dimethyl and dibenzyl complexes with  $[\text{Ph}_3\text{C}][\text{B}(\text{C}_6\text{F}_5)_4]$  in  $\text{C}_6\text{D}_5\text{Cl}$  afford the corresponding zirconocenium alkyl chlorobenzene complexes, in which chlorobenzene acts as an  $\eta^1$ -ligand via the chloride.<sup>549</sup> The X-ray structures, thermal and photochemical reactivity as well as hydrogenolysis and  $\beta$ -Cl elimination processes of these cationic Zr(IV) chlorobenzene complexes, have been investigated.



In the absence of donor ligands, the binuclear zirconium fulvalene complex reacts with  $\text{Ph}_3\text{C}[\text{B}(\text{C}_6\text{F}_5)_4]$  to give the relatively inert  $(\mu\text{-CH}_2)(\mu\text{-CH}_3)$  doubly-bridged binuclear cationic complex **717**<sup>550</sup> (Equation (45)). This C–H activation process via  $\alpha$ -H elimination and loss of  $\text{CH}_4$  is facile even at  $-60^\circ\text{C}$ .



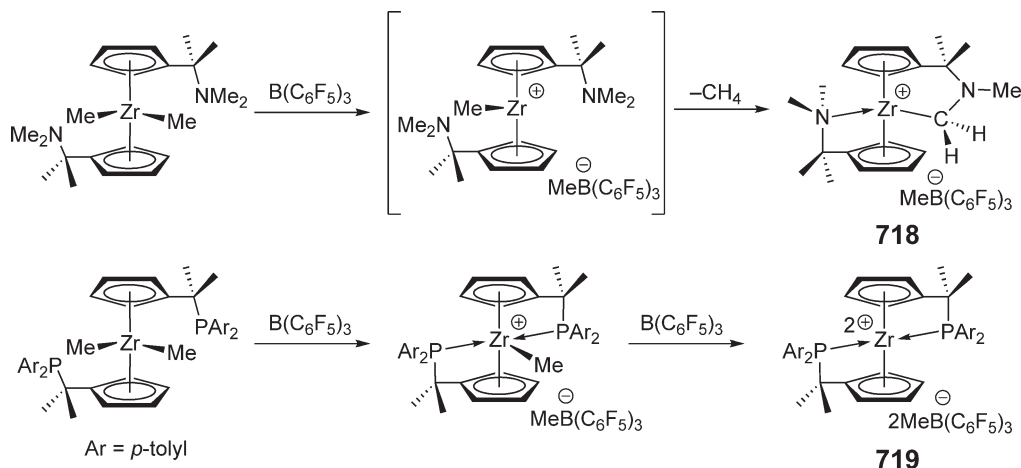
Scheme 175



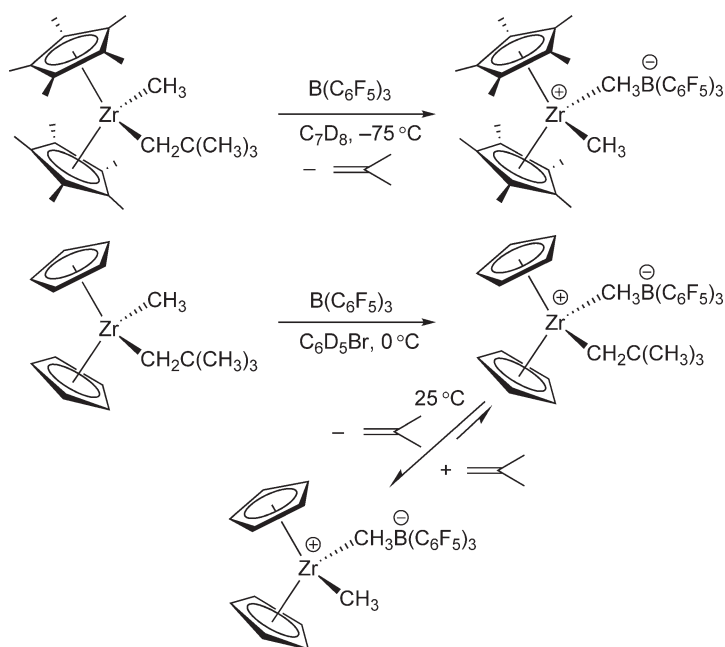
The reaction of (dimethylamino)alkyl-functionalized zirconocene dimethyl  $[\text{Me}_2\text{NC}(\text{Me})_2\text{Cp}]_2\text{ZrMe}_2$  with  $\text{B}(\text{C}_6\text{F}_5)_3$  generates the corresponding zirconocenium cation. This cationic complex is unstable at  $-20^\circ\text{C}$  and undergoes facile intramolecular C–H activation at the Cp-(dimethylamino)alkyl substituents, leading to the formation of the cyclometallated zirconocenium product **718**<sup>551</sup> (Scheme 176). The same C–H activation was also observed in the cationic species derived from the reaction of the mixed zirconocene dimethyl  $[\text{Me}_2\text{NC}(\text{Me})_2\text{Cp}]\text{CpZrMe}_2$  with  $\text{B}(\text{C}_6\text{F}_5)_3$ .<sup>552,553</sup> Treatment of (diarylphosphino)alkyl-functionalized zirconocene dimethyl  $[\text{Ar}_2\text{PC}(\text{Me})_2\text{Cp}]_2\text{ZrMe}_2$  ( $\text{Ar} = p\text{-tolyl}$ ) with 1 equiv. of  $\text{B}(\text{C}_6\text{F}_5)_3$  yields the corresponding zirconocenium cationic complex,  $[\text{Ar}_2\text{PC}(\text{Me})_2\text{Cp}]_2\text{ZrMeMeB}(\text{C}_6\text{F}_5)_3$  (Scheme 176).<sup>554</sup> The molecular structure of the cation, determined by X-ray diffraction, shows that both  $-\text{PAR}_2$  units are intramolecularly coordinated to Zr. Treatment of  $[\text{Ar}_2\text{PC}(\text{Me})_2\text{Cp}]_2\text{ZrMe}_2$  with 2 equiv. of  $\text{B}(\text{C}_6\text{F}_5)_3$  generates the highly reactive dicationic complex,  $\{\text{Ar}_2\text{PC}(\text{Me})_2\text{Cp}\}_2\text{Zr}[\text{MeB}(\text{C}_6\text{F}_5)_3]_2$  **719**, which is unstable and in  $\text{CH}_2\text{Cl}_2$  is converted to the chloride-abstraction product,  $\{\text{Ar}_2\text{PC}(\text{Me})_2\text{Cp}\}_2\text{Zr}(\text{Cl})\text{MeB}(\text{C}_6\text{F}_5)_3$ .

Direct  $\beta\text{-Me}$  elimination was observed when activating zirconocene methyl neopentyl complexes with  $\text{B}(\text{C}_6\text{F}_5)_3$ .<sup>555</sup> With sterically bulky  $\text{Cp}^*$  ligands, instantaneous isobutylene elimination is observed at  $-75^\circ\text{C}$ ; however, for the bis-(Cp) compound, the zwitterionic neopentyl complex species is stable at  $0^\circ\text{C}$  but undergoes clean and reversible  $\beta\text{-Me}$  elimination at  $25^\circ\text{C}$  (Scheme 177). This finding is consistent with  $\beta\text{-Me}$  elimination as the major chain-transfer pathway in propylene polymerizations using a sterically encumbered metallocene catalyst.

Activation of  $\eta^1, \eta^5\text{-Cp}^*$  “tuck-in” zirconocene complexes results in the formation of zwitterionic single-component olefin polymerization catalysts. Thus, the reaction of “tuck-in” zirconocene **720** with 1 equiv. of  $\text{B}(\text{C}_6\text{F}_5)_3$  in hexane initially forms a yellow kinetic product, which under mild conditions subsequently undergoes conversion to an orange thermodynamic product **721**, in which the Zr center is stabilized by interactions between the methylene carbon attached to  $\text{B}(\text{C}_6\text{F}_5)_3$  and the *ortho*-hydrogen of the phenyl group<sup>556</sup> (Scheme 178). Hydrogenolysis of **721** affords the corresponding hydride derivative, acting as an active single-component ethylene polymerization catalyst. All of these active species have been isolated and crystallographically characterized. The reaction of **720** with  $\text{B}(\text{C}_6\text{F}_5)_3$  and its ethylene polymerization activity was also examined in toluene with and without the presence of THF.<sup>557</sup> Treatment of the neopentyl “tuck-in” zirconocene **722** with 1 equiv. of  $\text{B}(\text{C}_6\text{F}_5)_3$  results in selective electrophilic attack of the borane on the methylene group of the cyclometallated ligand to give the zwitterionic zirconocene neopentyl complex **723**.<sup>558</sup> This complex is thermolabile and decomposes in bromobenzene solution at ambient temperature to give the



Scheme 176

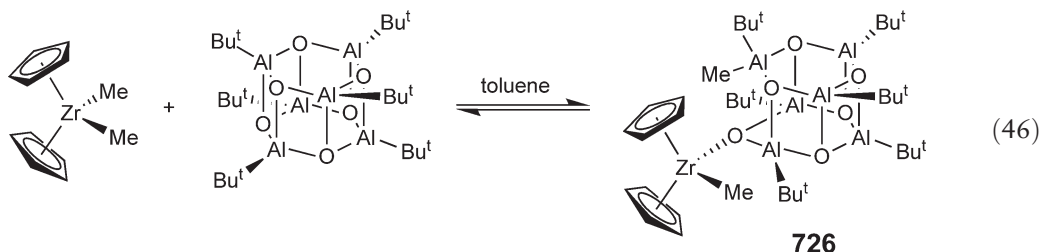


Scheme 177

unexpected  $\eta^3$ -2-methallyl complex (Scheme 178). Although no intermediates for this transformation could be detected, it presumably proceeds through initial  $\beta$ -Me elimination to give a zwitterionic methyl species and isobutene, followed by transfer of the borane to the methyl group and subsequent allylic C–H activation of the isobutene.

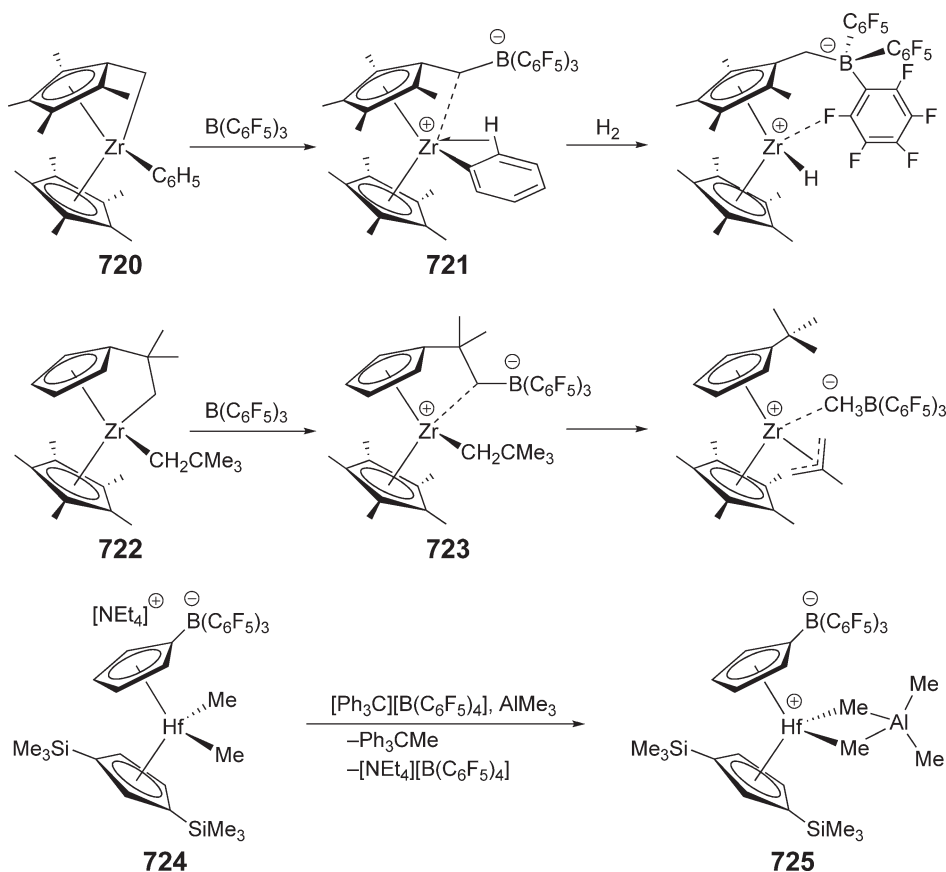
The reaction of the ammonium salt of the anionic hafnocene dimethyl complex **724**, bearing the mixed Cp'' and B(C<sub>6</sub>F<sub>5</sub>)<sub>3</sub>-substituted borato-Cp ligand, with [Ph<sub>3</sub>C][B(C<sub>6</sub>F<sub>5</sub>)<sub>4</sub>] in the presence of 1 equiv. of AlMe<sub>3</sub> produces zwitterionic metallocene complex **725** (Scheme 178).<sup>559</sup> The synthesis of anionic metallocene complexes of type **724** was accomplished by salt metathesis between [Li(THF)<sub>4</sub>][C<sub>5</sub>H<sub>4</sub>B(C<sub>6</sub>F<sub>5</sub>)<sub>3</sub>] and Cp''MCl<sub>3</sub> (M = Zr, Hf), followed by methylation with MeLi and cation exchange with [NEt<sub>4</sub>]BF<sub>4</sub>. Interestingly, the analogous reaction between base-free Li[1,3-Me<sub>3</sub>SiC<sub>5</sub>H<sub>3</sub>B(C<sub>6</sub>F<sub>5</sub>)<sub>3</sub>] and Cp\*ZrMe<sub>3</sub> leads to elimination of Li[MeB(C<sub>6</sub>F<sub>5</sub>)<sub>3</sub>] to give the neutral zirconocene dimethyl species, Cp\*(Me<sub>3</sub>SiC<sub>5</sub>H<sub>4</sub>)ZrMe<sub>2</sub>.<sup>560</sup>

Cp<sub>2</sub>ZrMe<sub>2</sub> reacts reversibly with the closed cage compound [(Bu<sup>t</sup>)Al( $\mu^3$ -O)]<sub>6</sub>, a structurally characterized model structure for MAO, to give an ion pair complex presumably having the formula [Cp<sub>2</sub>ZrMe][ (Bu<sup>t</sup>)<sub>6</sub>Al<sub>6</sub>( $\mu^3$ -O)<sub>6</sub>Me] **726**<sup>561</sup> (Equation (46)). All aluminum atoms in [(Bu<sup>t</sup>)Al( $\mu^3$ -O)]<sub>6</sub> are tetracoordinate, and thus the Lewis acidity needed for methide abstraction arises from “latent Lewis acidity” as a consequence of the ring strain present in the cluster. The resulting species **726** from this methyl transfer and cluster opening process is active for the polymerization of ethylene.



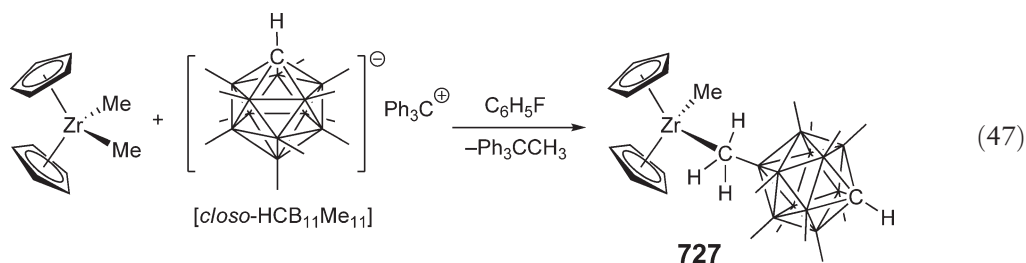
Methyl abstraction of Cp<sub>2</sub>ZrMe<sub>2</sub> with a trityl salt of a highly methylated carborane anion, [CPh<sub>3</sub>][*closo*-HCB<sub>11</sub>Me<sub>11</sub>], shown in Equation (47), leads to formation of the cationic complex **727** in which the methyl zirconocene cation is closely associated with the methylated carborane anion through the Zr( $\mu$ -CH<sub>3</sub>)B motif.<sup>562</sup> The Zr...H<sub>3</sub>C interaction is maintained in solution, as shown by a change in chemical shift for the methyl group





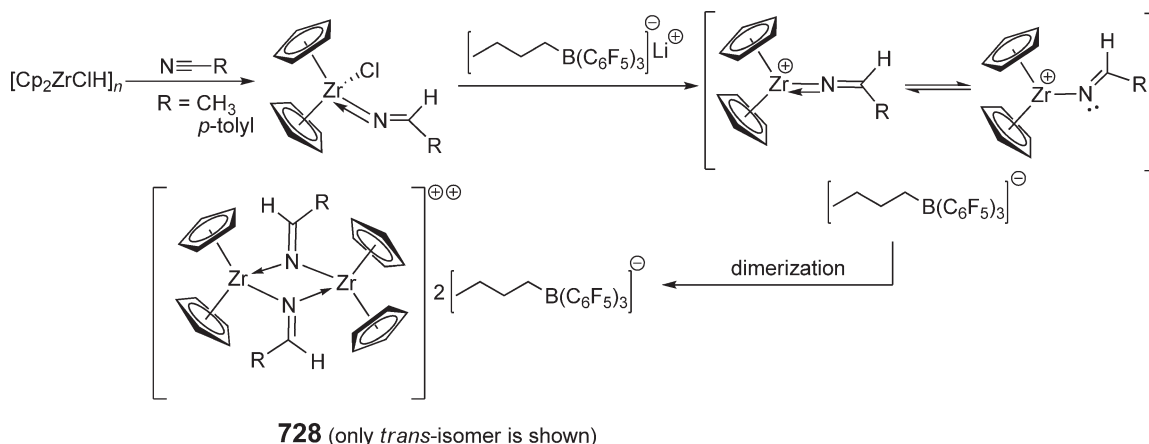
Scheme 178

which coordinates to the metal fragment relative to the [*clos*-HCB<sub>11</sub>Me<sub>11</sub>] anion when partnered with a non-coordinating cation.

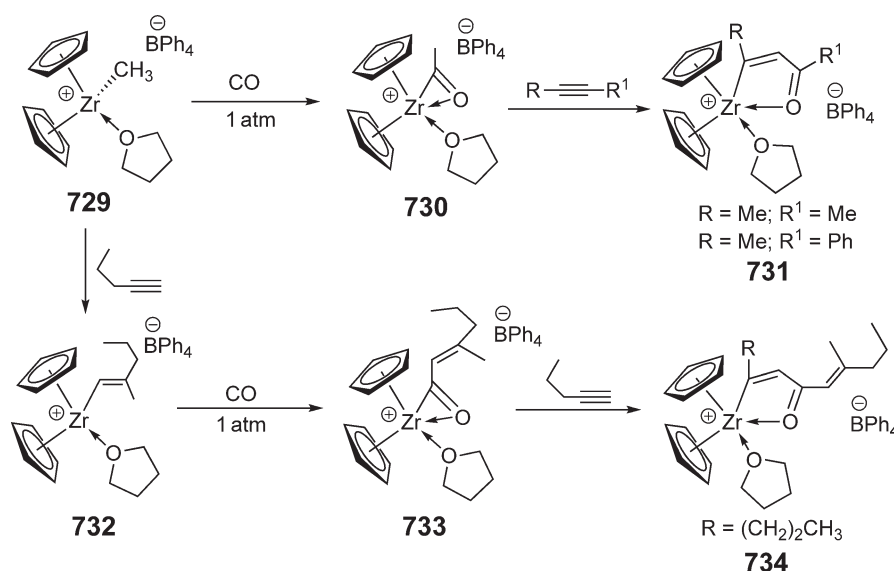


Chloride abstraction of (alkylideneamido)zirconocene chlorides  $\text{Cp}_2\text{ZrCl(N=CHR)}$  ( $\text{R} = \text{Me}, p\text{-tolyl}$ ), prepared by a hydrosilyration reaction, with lithium butylborate  $\text{Li}^+[\text{t-BuB(C}_6\text{F}_5)_3]^-$  at ambient temperature gives the transient cation  $[\text{Cp}_2\text{Zr(N=CHR)}]^+$ , which readily dimerizes under the reaction conditions to form the *cis/trans*-isomers of the dimeric  $\mu$ -alkylideneamido zirconocene dication **728**<sup>563</sup> (Scheme 179). Treatment of these dication with acetonitrile leads to the respective mononuclear monocationic adduct complexes.

The cationic complex  $[\text{Cp}_2\text{ZrMe(THF)}]^+$  **729** reacts with 1-pentyne to afford the (*E*)-alkenyl complex **732**. Complexes **729** and **732** react with carbon monoxide to afford the  $\eta^2$ -acyl complexes **730** and **733**, as summarized in Scheme 180.<sup>564</sup> Both complexes **730** and **733** are inert to carbon monoxide, but regio/stereoselectively insert terminal and internal alkynes to afford chelating  $\beta$ -ketoalkenyl complexes **731** and **734**, respectively. Hydrolysis of  $[\text{Cp}_2\text{ZrMe(THF)}]^+\text{BPh}_4^-$  **729** with excess  $\text{H}_2\text{O}$  in dichloromethane/THF at  $-78^\circ\text{C}$  yields the trinuclear metallocene oxide cationic complex  $[(\text{Cp}_2\text{Zr})_3(\mu_2\text{-OH})_3(\mu_3\text{-O})]^+\text{BPh}_4^-(\text{THF})_3$  in 72% yield.<sup>565</sup> The molecular structure of this metallocene cluster features a planar central  $\text{Zr}_3\text{O}_3$  hexagon having the  $\mu_3\text{-O}$  ligand in its center; each of the three



Scheme 179

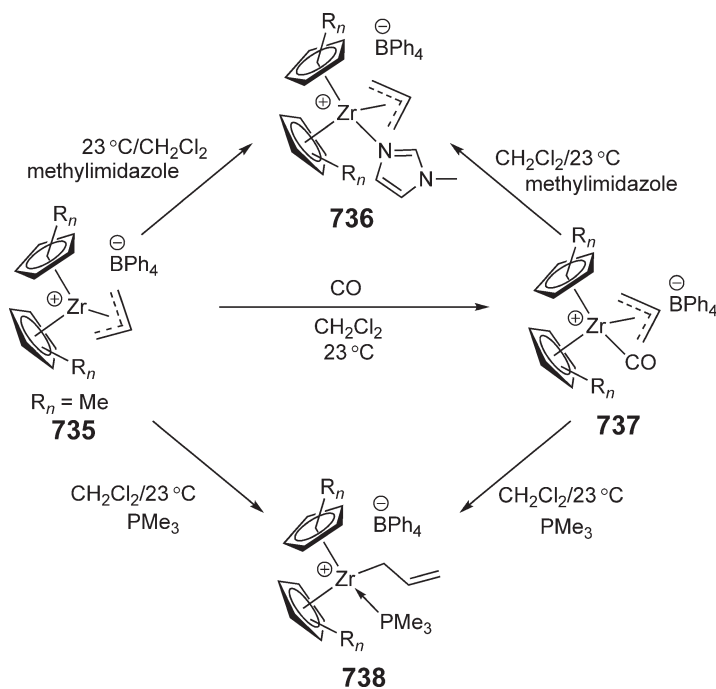


Scheme 180

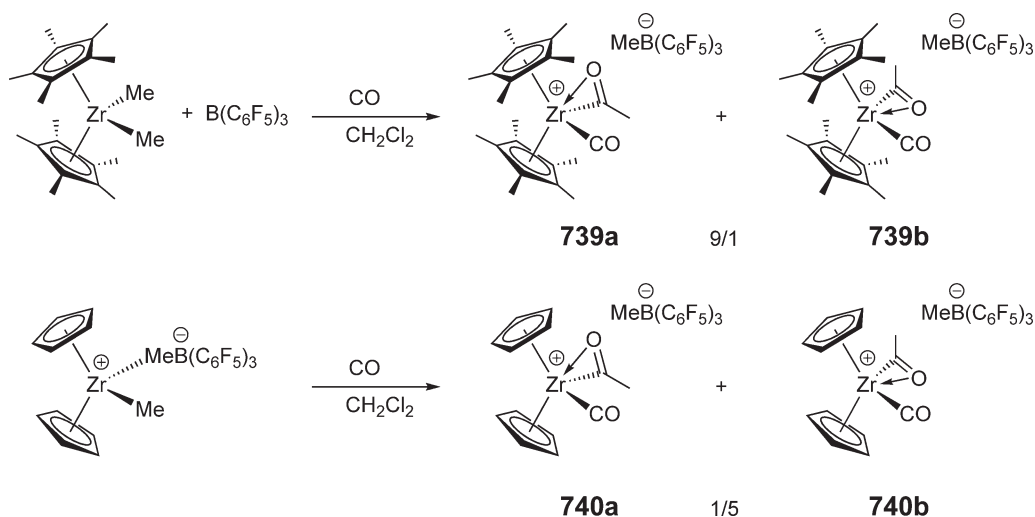
oxygen atoms at the perimeter is protonated and in the crystal connected to a THF molecule by means of a weak hydrogen bond.

Treatment of the zirconocene allyl cation **735** with CO in CH<sub>2</sub>Cl<sub>2</sub> affords the isolable *d*<sup>0</sup>-CO complex cation **737** (Scheme 181).<sup>566</sup> The remarkable stability of this complex is attributed to strong  $\sigma \rightarrow \pi^*$ -donation from the neighboring allyl ligand, which completely inhibits fluxionality in the allyl fragment. This structural feature of the allyl moiety in **737** is in sharp contrast to that in other analogs such as [Cp<sup>+</sup>Zr( $\eta^3$ -C<sub>3</sub>H<sub>5</sub>)(NC<sub>3</sub>H<sub>3</sub>NCH<sub>3</sub>)]BPh<sub>4</sub> **736**, in which the allyl ligand is fluxional and  $\eta^3$ -bound to the metal center, and [Cp<sup>+</sup><sub>2</sub>Zr( $\eta^1$ -CH<sub>2</sub>CH=CH<sub>2</sub>)(PMe<sub>3</sub>)]BPh<sub>4</sub> **738**, which has a terminally coordinated allyl ligand.

The isolation and structural characterization of a terminal carbonyl complex of Zr(IV) was achieved by the reaction of Cp<sup>+</sup><sub>2</sub>ZrMe<sub>2</sub>/B(C<sub>6</sub>F<sub>5</sub>)<sub>3</sub> with CO in CH<sub>2</sub>Cl<sub>2</sub>, which yields the  $\eta^2$ -acyl carbonyl zirconocene cations **739** as a 9:1 mixture of O-outside **739a** and O-inside **739b** isomers,<sup>567</sup> (Scheme 182). Analogous O-outside and O-inside isomers are observed for the unsubstituted zirconocene complexes **740**, prepared by the reaction of the preformed zirconocenium methylborate and CO, but the isomer preference is inverted (i.e., **740a/740b** = 1:5). The  $\nu_{\text{CO}}$  values for both O-inside isomers (**b** isomers) are higher than the free CO value, indicating that the Zr–CO bond is primarily  $\sigma$ -donor in character. On the other hand, the  $\nu_{\text{CO}}$  values for both O-outside isomers (**a** isomers) are slightly lower than the free CO value, as a result of overlap of a filled Zr–acyl bonding orbital and a CO  $\pi^*$ -orbital (i.e.,  $\sigma \rightarrow \pi^*$ -backbonding).



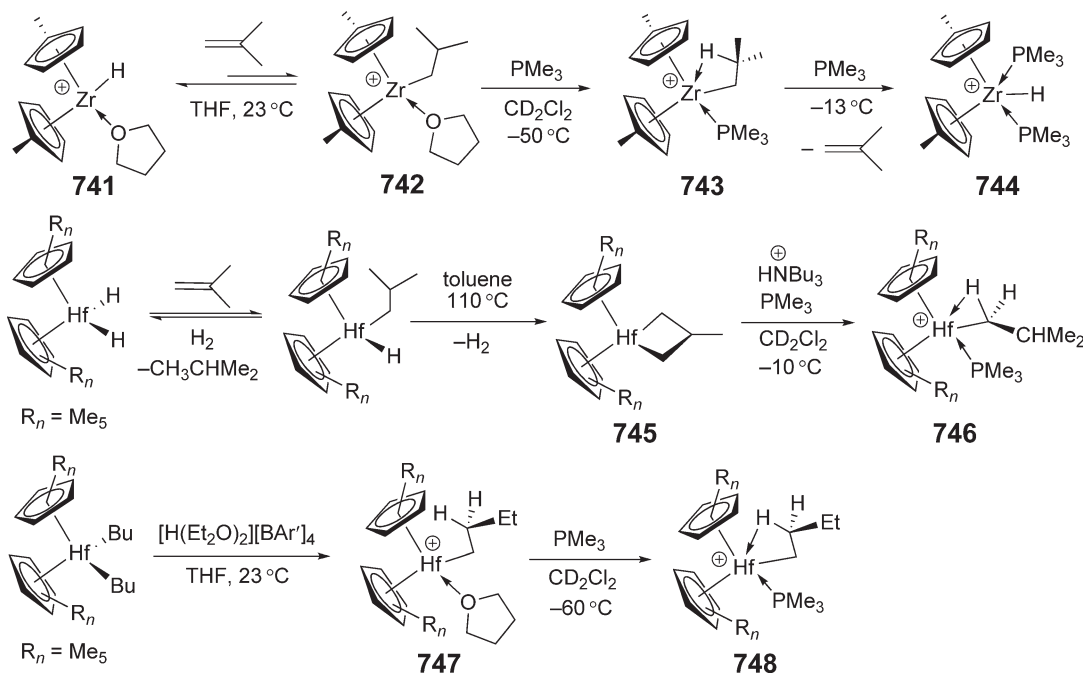
Scheme 181



Scheme 182

The reaction of the cationic Zr acyl carbonyl complex **740** with vinyl chloride yields an unusual binuclear dicationic  $\mu$ -acyl  $\mu$ -keto-alkoxide complex.<sup>568</sup>

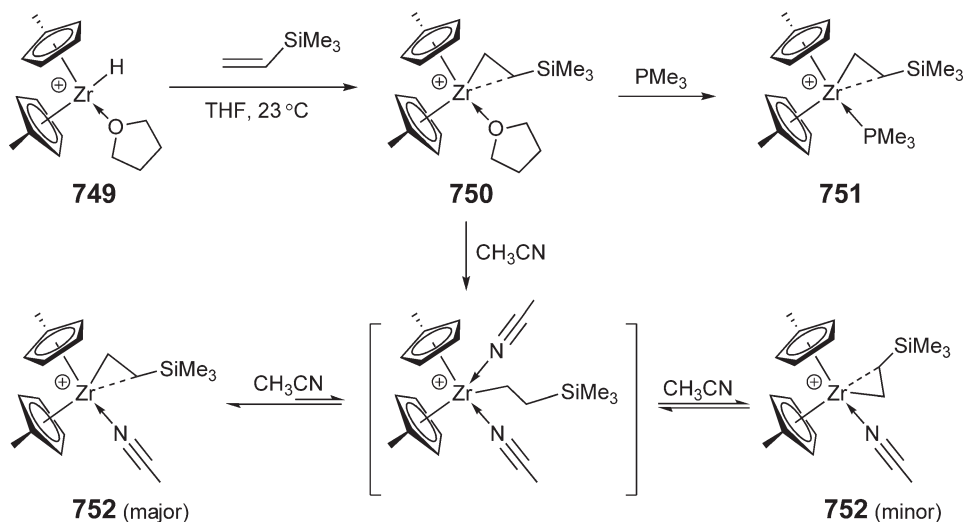
In order to model the cationic active species involved in propylene polymerizations catalyzed by cationic metallocene complexes, a series of cationic Zr and Hf isobutyl complexes have been prepared,<sup>569</sup> (Scheme 183). The cationic hydride **741**, prepared by hydrogenolysis of the corresponding methyl cation, reversibly inserts isobutylene at 23 °C to afford the THF-stabilized isobutyl complex **742**, in which the isobutyl group adopts a normal structure. Replacing the THF ligand with PMe<sub>3</sub> gives the phosphine complex **743**, in which the isobutyl moiety adopts a  $\beta$ -agostic structure. This complex undergoes  $\beta$ -H elimination above −13 °C to form the hydride complex **744** stabilized by two molecules of PMe<sub>3</sub>. The reaction of the hafnacyclobutane **745** with [HNBu<sub>3</sub>][BPh<sub>4</sub>] in the presence of PMe<sub>3</sub> yields the cationic isobutyl complex **746**, in which the isobutyl group is distorted by an  $\alpha$ -agostic interaction. The structures



Scheme 183

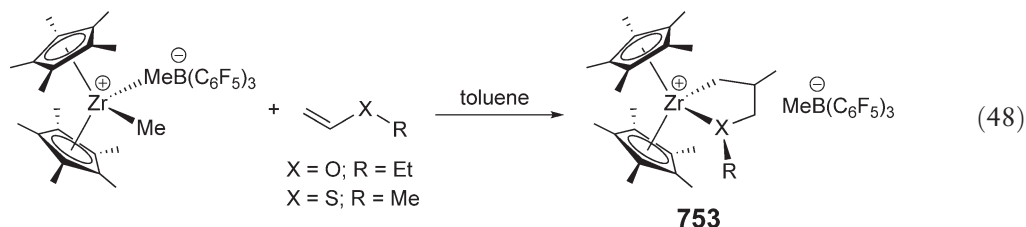
of cationic hafnocene *n*-butyl complexes are characterized as having a normal *n*-butyl ligand **747** with coordinated THF, or a  $\beta$ -agostically bonded *n*-butyl **748** with coordinated  $\text{PMe}_3$ .

The reaction of the cationic zirconocene hydrido complex **749** (the  $\text{BPh}_4$  anion is omitted) with vinyltrimethylsilane yields the corresponding cationic  $\beta$ - $\text{SiMe}_3$  alkyl complex **750**<sup>570</sup> (Scheme 184). The structural data of **750** indicate that the cationic metal center interacts primarily with the  $\beta$ -carbon rather than the  $\beta$ -hydrogen of the  $\text{CH}_2\text{CH}_2\text{SiMe}_3$  group and thus the cationic metal center is stabilized by interaction of the Zr LUMO with the backlobe of the C $\beta$ –Si bond. This direct  $\text{Zr} \cdots \text{C}\beta\text{--Si}$  interaction is analogous to the stabilization of silyl-substituted carbocations by the  $\gamma$ -silicon effect and appears to be stronger than the  $\text{Zr} \cdots \text{H}$   $\beta$ -agostic interactions observed for analogous alkyl cations. Reactions of **750** with  $\text{PMe}_3$  and  $\text{CH}_3\text{CN}$  yield complexes **751** and **752**, respectively, the latter of which exists as a mixture of two isomers shown in Scheme 184.

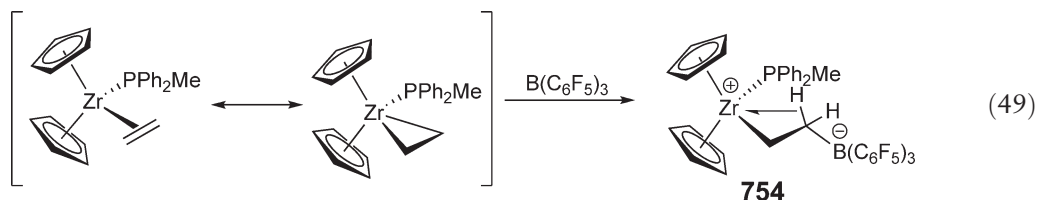


Scheme 184

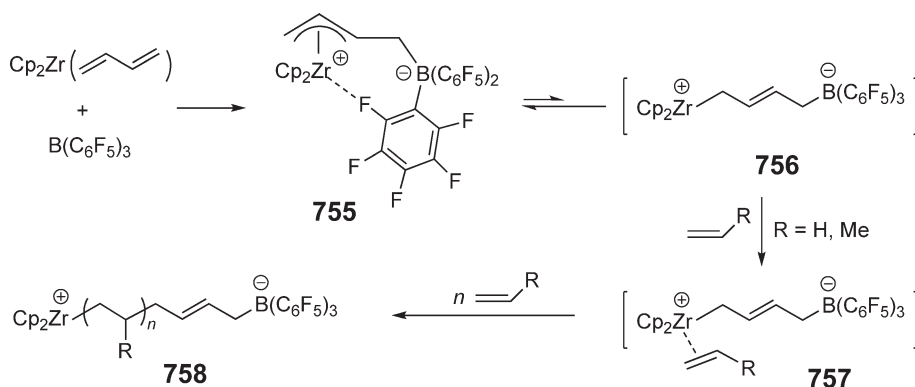
Treatment of  $\text{Cp}^*_2\text{ZrMe}(\mu\text{-Me})\text{B}(\text{C}_6\text{F}_5)_3$  with (thio)ether-functionalized alkenes gives stable insertion products **753** in which the (thio)ether function is intramolecularly coordinated to the cationic Zr center (Equation (48)).<sup>571</sup> These metallacycles are stable toward further insertion of functionalized alkenes and cannot be activated for ethene polymerization by pre-complexation of the (thio)ether function with strong Lewis acids. The cationic complex  $[\text{Cp}_2\text{Zr}(\text{OPr}^i)(\text{Pr}^i\text{OH})][\text{H}_2\text{N}\{\text{B}(\text{C}_6\text{F}_5)_3\}_2]$  was obtained from the reaction of  $\text{Cp}_2\text{Zr}(\text{OPr}^i)_2$  with  $[\text{H}(\text{OE}t_2)_2][\text{H}_2\text{N}\{\text{B}(\text{C}_6\text{F}_5)_3\}_2]$  and structurally characterized; this complex initiates the polymerization of propylene oxide, presumably via a cationic mechanism.<sup>572</sup> The reaction of  $\text{Cp}_2\text{ZrMeMeB}(\text{C}_6\text{F}_5)_3$  with an Arduengo-type carbene, 1,3-diisopropylimidazol-2-ylidene, gives the stable zirconocenium carbene methylborate complex  $[\text{Cp}_2\text{ZrMe}(\text{carbene})][\text{MeB}(\text{C}_6\text{F}_5)_3]$ .<sup>573</sup>



The phosphine-stabilized ethylene complex of zirconocene( $\eta$ ) reacts with 1 equiv. of  $\text{B}(\text{C}_6\text{F}_5)_3$  to form the girdle-type zwitterionic complex **754** (Equation (49)).<sup>574</sup> Both the solution and solid-state structures of **754** feature a strong  $\beta$ -CH agostic interaction. The zwitterion **754** is a single-component catalyst for the polymerization of ethylene under ambient conditions, although for optimal activity an additional equivalent of  $\text{B}(\text{C}_6\text{F}_5)_3$  is needed.



Activation of the zirconocene butadiene complex  $\text{Cp}_2\text{Zr}(\eta^4\text{-C}_4\text{H}_6)$  by  $\text{B}(\text{C}_6\text{F}_5)_3$  in toluene yields the zwitterionic butenylborate complex **755** (Scheme 185).<sup>575</sup> A characteristic structural feature of type **755** zirconocene and hafnocene complexes is the weak coordination of an *ortho*-fluoro substituent to the cationic metal center to give a metallacyclic structure.<sup>576</sup> This is a common structural motif in such metallocene-based zwitterions. The  $\text{Zr}\cdots\text{F}$  bond in complexes of type **755** is cleaved by THF to form 1,2- $\eta^2$ -allyl zirconocene complexes. Addition of *tert*-butylisocyanide or *tert*-butylcyanide also leads to cleavage of the  $\text{Zr}\cdots\text{F}$  linkage and formation of the corresponding adducts.<sup>577</sup> Complex **755** readily dissociates in solution, as evidenced by the dynamic behavior often observed in its  $^{19}\text{F}$  NMR spectra, with an NMR-derived  $\text{Zr}\cdots\text{F}$  bond dissociation energy of ca.  $8.5 \text{ kcal mol}^{-1}$ . This magnitude of the activation barrier for the  $\text{Zr}\cdots\text{F}$  bond dissociation makes the internal fluorocarbon coordination a very effective tool for



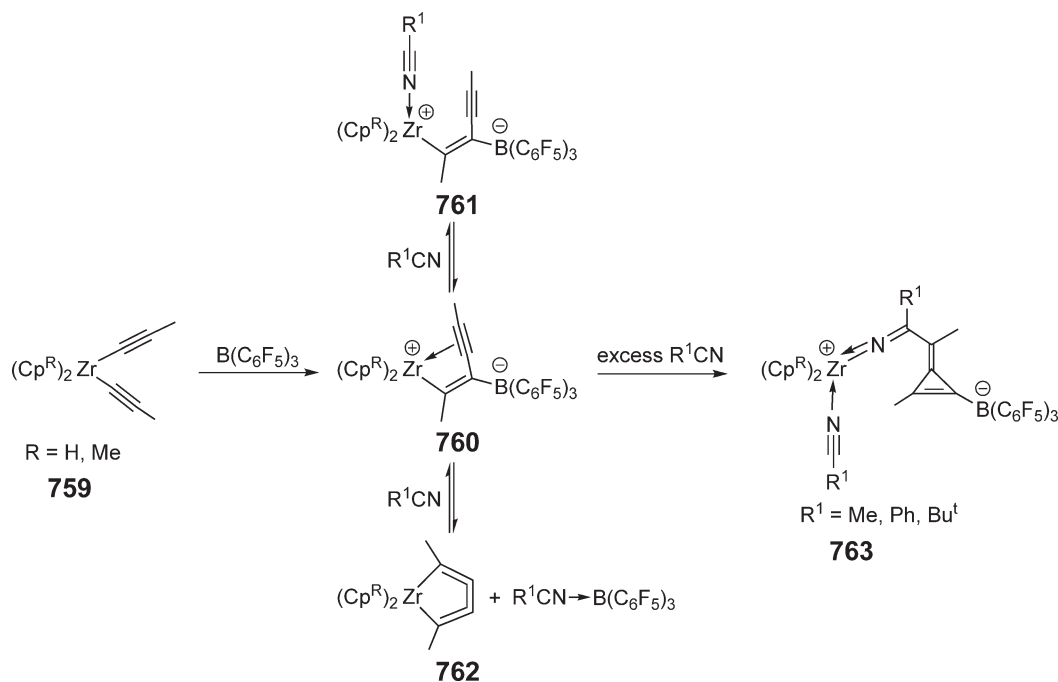
Scheme 185

protecting highly electrophilic metal catalyst centers. The dynamic process of the metallacyclic metallocene betaine in solution involves a degenerate  $\pi$  to  $\sigma$  **756** to  $\pi$ -allyl interconversion on the NMR timescale, which becomes markedly faster in the presence of added 1-alkenes. The latter observation is attributable to the increased stabilization of the  $(\sigma\text{-alkyl})(\pi\text{-alkene})\text{metallocene}$  betaine intermediate **757**.<sup>578</sup> Alkene insertion into the zirconium carbon bond of **755**, via intermediate **757**, leads to the zirconocenium cation **758**, which carries an anionic polymeryl chain during the initial phases of the catalytic process (Scheme 185). These metallocene model compounds have made possible an experimental estimate of the intrinsic activation barrier of the first olefin insertion step into the Zr–C bond of an active metallocene polymerization catalyst. Related investigations include the metallocene borate betaine derived from the reaction of zirconacyclopentadiene with  $\text{B}(\text{C}_6\text{F}_5)_3$ ,<sup>579</sup> the synthesis of metallocene borate zwitterionic in which the intramolecular metal–carbon ion pairing stabilization is controlled by the geometric features of the  $\text{CH}_2[\text{B}]$ -substituted allyl moiety,<sup>580</sup> and the isolation of a zirconocene- $(\mu\text{-hydrocarbyl})\text{borate}$  complex derived from the reaction of the zirconocene alkenyl alkynyl complex  $\text{Cp}_2\text{Zr}(\text{CH}=\text{CHMe})(\text{C}=\text{CMe})$  with  $\text{B}(\text{C}_6\text{F}_5)_3$ .<sup>581</sup>

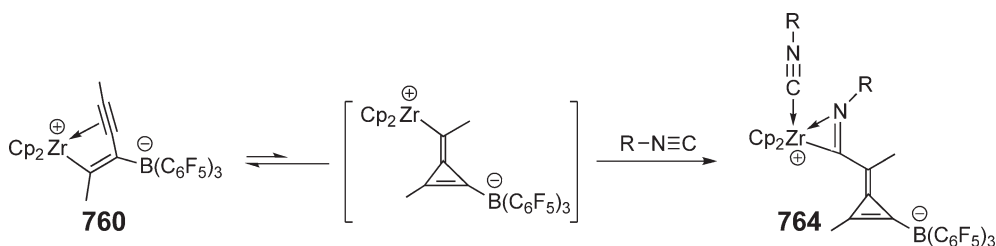
Treatment of the bis(propynyl)zirconocene **759** with  $\text{B}(\text{C}_6\text{F}_5)_3$  results in a linear C–C coupling of the alkynyl ligands to form the zwitterionic complex **760**.<sup>582,583</sup> (Scheme 186). Complex **760** reacts with nitriles  $\text{R}^1\text{CN}$  to form initially the 1:1 adduct **761** that concurrently equilibrates with **760** and the metallacyclocumulene **762** (and the nitrile–borane adduct); subsequently, irreversible reaction in the presence of excess nitrile yields the methylenecyclopropene derivative **763**.<sup>584,585</sup> Calculations have shown that the conversion **760**  $\rightarrow$  **763** is probably triggered by nitrile addition to the metal with formation of a planar-tetracoordinate carbon intermediate that features coordination of the three-membered carbocycle through one of its C–C  $\sigma$ -bonds.

The reactions of bis(alkynyl)metallocenes  $\text{Cp}_2\text{M}(\text{C}\equiv\text{CR})_2$  ( $\text{M} = \text{Zr}, \text{Hf}$ ;  $\text{R} = \text{Me}, \text{Pr}^n, \text{Bu}^n, \text{Cy}$ ) with  $\text{B}(\text{C}_6\text{F}_5)_3$  afford the corresponding metallocene borate betaines of structure type **760**.<sup>586</sup> An assumed intramolecular alkyne insertion reaction leads to their less stable methylenecyclopropene-derived isomers, which are effectively trapped by the added *tert*-butylisocyanide to yield complexes **764** which contain a methylenecyclopropene derived  $\sigma$ -ligand framework<sup>587</sup> (Scheme 187).

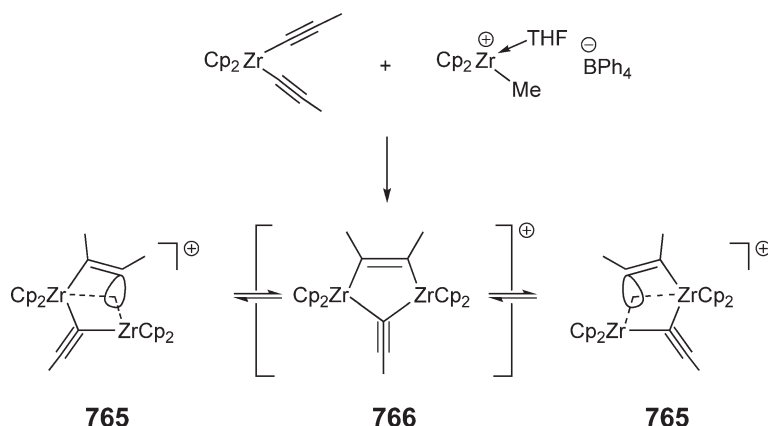
The cationic binuclear  $(\mu\text{-hydrocarbyl})\text{bis}(\text{zirconocene})$  complex **765** was obtained by the reaction of bis(propynyl)zirconocene with  $[\text{Cp}_2\text{ZrMe}(\text{THF})]\text{BPh}_4$  (Scheme 188).<sup>592</sup> The structurally characterized complex **765** contains a planar-tetracoordinate carbon atom, featuring four strong bonds to its nearest in-plane neighbors (i.e., to two carbons and two Zr centers). It is dynamic in solution; its  $C_s$ -symmetric planar-tetracoordinate carbon undergoes a thermally induced tautomerization reaction that proceeds through a  $C_{2v}$ -symmetric geometry **766** that has the characteristics of a transition state according to a theoretical analysis of this rearrangement process.



Scheme 186

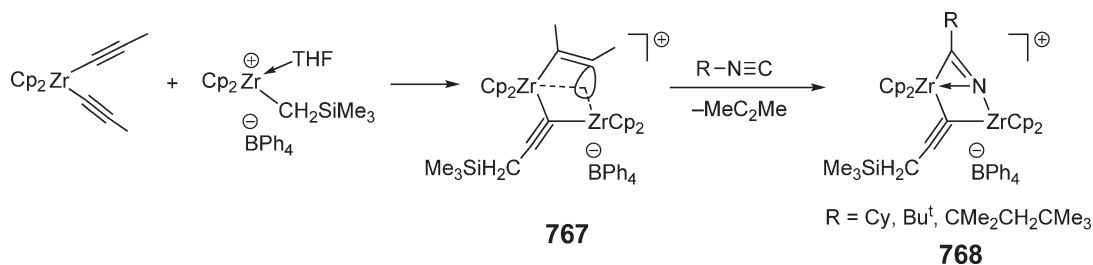


Scheme 187



Scheme 188

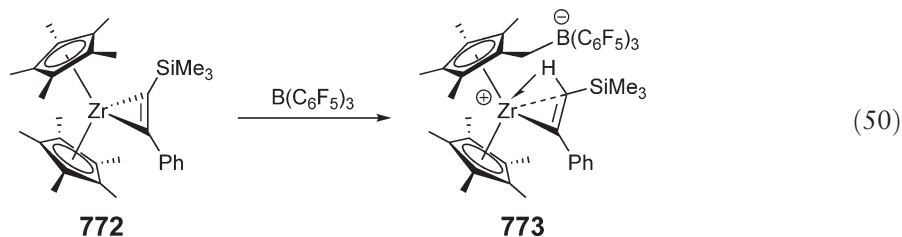
The reaction of  $\text{Cp}_2\text{Zr}(\text{Cl})(\text{C}\equiv\text{C}-\text{R})$  ( $\text{R} = \text{Me}, \text{CH}_2\text{Ph}, \text{Pr}^n$ ) with  $[\text{Cp}_2\text{ZrMe}(\text{THF})]\text{BPh}_4$  occurs analogously to yield the stable binuclear metallocene cations  $[(\text{Cp}_2\text{Zr})_2(\mu-\text{Cl})(\mu-\eta^1:\eta^2-\text{RCCCH}_3)]$  that contain planar-tetracoordinate carbon atoms.<sup>588</sup> Treatment of bis(propynyl)zirconocene with the methylhafnocene cation  $[\text{Cp}_2\text{Hf}(\text{Me})(\text{THF})]^+$  yields a heterobimetallic cation, also containing a planar-tetracoordinate carbon atom.<sup>589</sup> Similarly, bis(alkynyl) metallocene complexes,  $\text{Cp}_2\text{M}(\text{C}\equiv\text{CR})_2$  ( $\text{M} = \text{Zr}, \text{Hf}; \text{R} = \text{Me}, \text{Et}, \text{CH}_2\text{Ph}$ ), react with  $\text{Cp}_2\text{M}(\text{butadiene})$  to yield the corresponding binuclear  $\sigma,\pi$ -acetylide-bridged complexes  $[(\text{Cp}_2\text{M})_2(\mu-\text{C}\equiv\text{CR})_2]$ , which can be selectively protonated with  $[\text{PhNHMe}_2]^+\text{X}^-$  ( $\text{X} = \text{BPh}_4, \text{B}(\text{C}_6\text{F}_5)_3$ ) to yield binuclear cationic metallocene complexes with planar-tetracoordinate carbon atoms.<sup>590</sup> An unexpected alkyl-substituent exchange was observed during the formation of the planar four-coordinate carbon-containing, cationic bis(zirconocene) complex **767** using the reaction of bis(propynyl)zirconocene with  $[\text{Cp}_2\text{Zr}(\text{CH}_2\text{SiMe}_3)(\text{THF})]^+[\text{BPh}_4]^-$ <sup>591</sup> (Scheme 189). Finding the  $\text{CH}_2\text{SiMe}_3$  substituent, which originates from the alkylzirconocene reagent, attached at the  $\mu$ -acetylide ligand in the final product is unusual, but its formation can be explained by a reversible alkynyl carbometallation sequence. This complex reacts with alkyl isocyanides  $\text{RN}\equiv\text{C}$  ( $\text{R} = \text{CMe}_2\text{CH}_2\text{CMe}_3, \text{CMe}_3, \text{Cy}$ ) to form the  $\mu$ -isocyanide complexes **768**, with concomitant elimination of the  $\mu-\eta^1:\eta^2-\text{CH}_3\text{CCCH}_3$  ligand.



Scheme 189

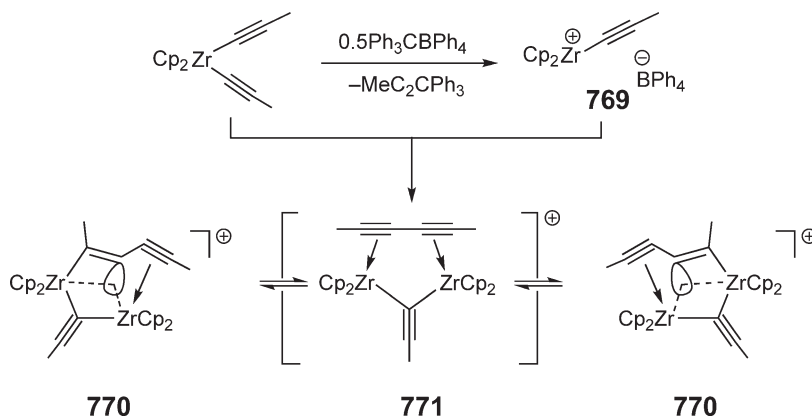
Unlike the reaction of bis(propynyl)zirconocene with  $\text{B}(\text{C}_6\text{F}_5)_3$ , where the initially formed alkynyl cation  $[\text{Cp}_2\text{ZrC}\equiv\text{CCH}_3]^+$  undergoes a rapid subsequent insertion reaction with the generated alkynyl borate anion to yield the stable betaine product **760**, the  $[\text{Cp}_2\text{ZrC}\equiv\text{CCH}_3]^+$  cation **769** generated with  $[\text{Ph}_3\text{C}]\text{BPh}_4$  is instantaneously trapped by the neutral starting reagent bis(propynyl)zirconocene to give complex **770**<sup>592</sup> (Scheme 190). The solid-state structure of **770** features an asymmetrically bridging hexadiyne ligand with a planar-tetracoordinate carbon center that is stabilized by a three-center, two-electron interaction with the two adjacent zirconocene moieties. In solution, complex **770** undergoes a tautomerization reaction, most likely via the symmetrical intermediate **771**.

Activation of the zirconocene alkyne complex  $\text{Cp}^*_2\text{Zr}(\eta^2\text{-PhC}\equiv\text{CSiMe}_3)$  **772** with  $\text{B}(\text{C}_6\text{F}_5)_3$  generates the zwitterionic complex **773** via electrophilic substitution of a hydrogen atom of a  $\text{Cp}^*$ -methyl group by  $\text{B}(\text{C}_6\text{F}_5)_3$ <sup>593</sup> (Equation (50)). This reaction is in sharp contrast to that of the titanocene analog, where dissociation of the alkyne and liberation of dihydrogen leads to a  $\text{Ti}(\text{III})$  species. The structure of **773** shows the  $\sigma$ -bonded alkenyl group with an agostic interaction to Zr.



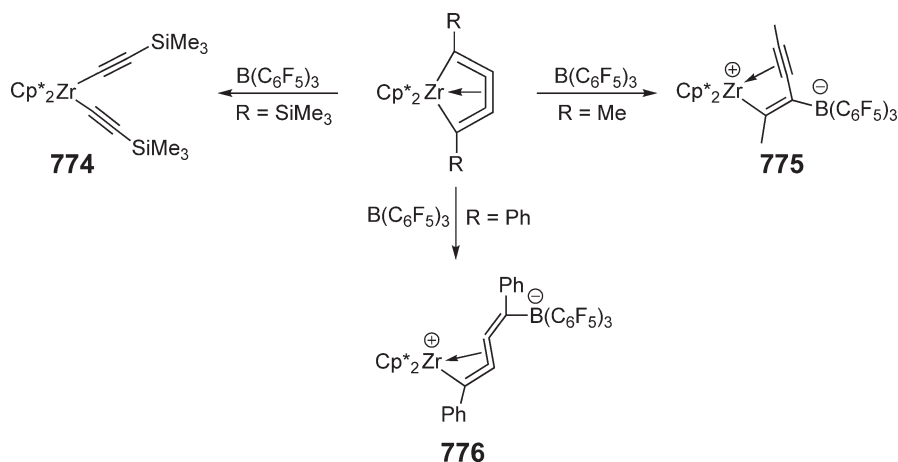
The products resulting from the activation of five-membered zirconacyclocumulenes  $\text{Cp}^*_2\text{Zr}(\eta^4\text{-1,2,3,4-RC}_4\text{R})$  with  $\text{B}(\text{C}_6\text{F}_5)_3$  depend on nature of the R group<sup>594</sup> (Scheme 191). For  $\text{R} = \text{Me}_3\text{Si}$ , bond cleavage of the central C–C double bond of the cyclocumylene occurs with 10%  $\text{B}(\text{C}_6\text{F}_5)_3$ , giving, after 6 days, a quantitative yield of the bis- $\sigma$ -alkynyl complex **774**. For  $\text{R} = \text{Me}$ , the borane attacks the  $\beta$ -C atom of the cumulene while the  $\text{C}_4$  chain remains intact, affording  $\sigma$ -alkenyl- $\pi$ -alkynyl zwitterionic complex **775**. Lastly, for  $\text{R} = \text{Ph}$ , the  $\text{C}_4$  chain also is not cleaved, but the borane attacks the  $\beta$ -C atom of the cumulene, yielding  $\sigma$ -alkenyl- $\pi$ -alkenyl zwitterionic complex **776** in which the cationic and anionic centers are bridged by the 1,4-diphenyl-1,2,3-butatrienyl ligand. Different products are also obtained from the reaction of  $\text{Cp}^*_2\text{Zr}(\eta^4\text{-1,2,3,4-RC}_4\text{R})$  with  $\text{Bu}^i_2\text{AlH}$ , again depending on the nature of the R group;<sup>595</sup> in all studied cases, the reactions occur via a *cis*-hydroalumination of the central double bond of the zirconacyclocumulenes to form zirconacyclopentadienes with the  $\text{Bu}^i_2\text{Al}$  substituent in the 3-position. These intermediates were not isolated but subsequently stabilized in a different manner, depending on the substituent R used.

There has been a growing interest in the direct observation and characterization of cationic  $d^0$ -zirconocenium alkyl or alkoxy-alkene complexes that model the unobserved cationic  $d^0$ -zirconocenium alkene complex, a proposed key intermediate in the coordination polymerization of olefins. Species like this have so far eluded direct observation because of their high reactivity and low thermodynamic stability due to the absence of  $d \rightarrow \pi^*$ -backbonding. A successful strategy for the observation and characterization of the model cationic  $d^0$ -zirconocenium-alkene complex has been the use of an olefin moiety tethered either to the alkyl (alkoxy) group at Zr or to the Cp ring



Scheme 190

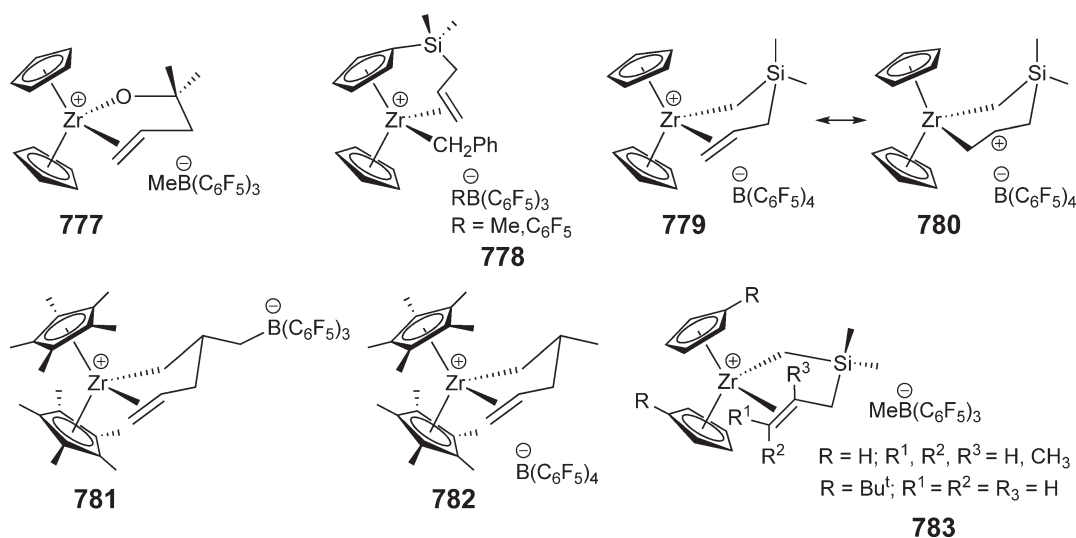




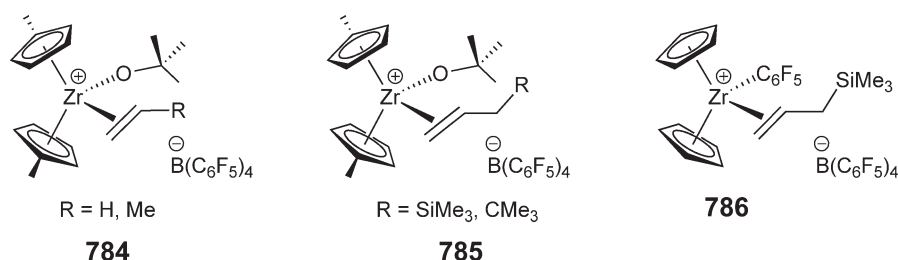
Scheme 191

(i.e., intramolecular zirconocenium–alkene complexes). A rather weak Zr–olefin bond has been identified in the crystallographically characterized alkoxy complex  $[\text{Cp}_2\text{Zr}(\text{OCMe}_2\text{CH}_2\text{CH}_2\text{CH}=\text{CH}_2)]^+\text{MeB}(\text{C}_6\text{F}_5)_3^-$  **777**<sup>596</sup> (Scheme 192). The weak interaction between the  $d^0$ -Zr(IV) cation and the double bond in the solid state is primarily through the terminal carbon atom ( $\text{Zr}-\text{C}(\text{terminal}) = 2.68(2) \text{ \AA}$  vs.  $\text{Zr}-\text{C}(\text{internal}) = 2.89(2) \text{ \AA}$ ). The presence of significant  $\text{O} \rightarrow \text{Zr}$   $\pi$ -donation in this complex may strengthen the Zr–olefin binding by increased  $d \rightarrow \pi^*$  back-bonding. The combined structural and spectroscopic data show that the Zr–olefin interaction does not significantly perturb the structure of the coordinated olefin but it does polarize the  $\text{C}=\text{C}$  double bond, such that positive charge buildup occurs at the internal carbon.<sup>597</sup> The spectroscopically characterized cationic  $d^0$ -zirconocenium–alkene complex **778** contains a coordinated Cp-tethered alkene moiety,<sup>598</sup> whereas complex **779** (resonance structure **780**) exhibits a coordinated alkene moiety which is tethered to the  $d^0$ -metal center (i.e., a cationic zirconocenium–alkyl–alkene complex).<sup>599</sup> Analogous spectroscopically characterized complexes **781** and **782** were obtained from the activation of  $\beta$ -allyl zirconacyclobutane with  $\text{B}(\text{C}_6\text{F}_5)_3$  and  $[\text{HNMePh}_2][\text{B}(\text{C}_6\text{F}_5)_4]$  in  $\text{CD}_2\text{Cl}_2$  at  $-78^\circ\text{C}$ , respectively.<sup>600</sup> Ancillary ligand and olefin substituent effects on olefin dissociation for complexes **783** bearing a coordinated pendant olefin have been examined.<sup>601</sup>

Several strategies have recently been developed for the direct observation of “non-chelated” cationic zirconocenium–alkene adducts. The first is the use of a non-inserting alkoxide ligand which lowers the metal Lewis acidity.



Scheme 192



Scheme 193

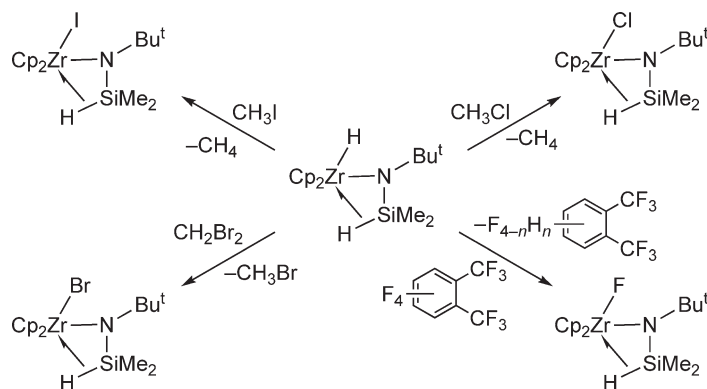
Thus, base-free zirconocene *tert*-butoxide cations as solvent adducts in  $\text{C}_6\text{D}_5\text{Cl}$  and  $\text{CD}_2\text{Cl}_2$  solutions are furnished by mixing the zirconocene dimethyl with *tert*-butyl alcohol followed by addition of  $[\text{Ph}_3\text{C}][\text{B}(\text{C}_6\text{F}_5)_4]$ .<sup>602</sup> Adding ethylene and propylene to these cations in polar solvents at  $-89^\circ\text{C}$  results in the reversible formation of the corresponding alkene adducts **784** (Scheme 193). The second strategy is the use of  $\beta$ -silicon substituents in the alkene ligand which stabilize the positive charge on the internal carbon of the double bond. For example, in structures **785**, the  $\beta$ - $\text{SiMe}_3$  substituent greatly enhances substrate binding to the cationic Zr center. The third one is the combination of  $\beta$ -silicon-substituted alkene substrate and the unreactive  $\text{C}_6\text{F}_5$  group to inhibit insertion. Utilization of both tactics enabled the direct observation of the cationic  $d^0$ -Zr-aryl-alkene complexes **786**.<sup>603</sup>

#### 4.08.9.5 Complexes with M–N Bonds

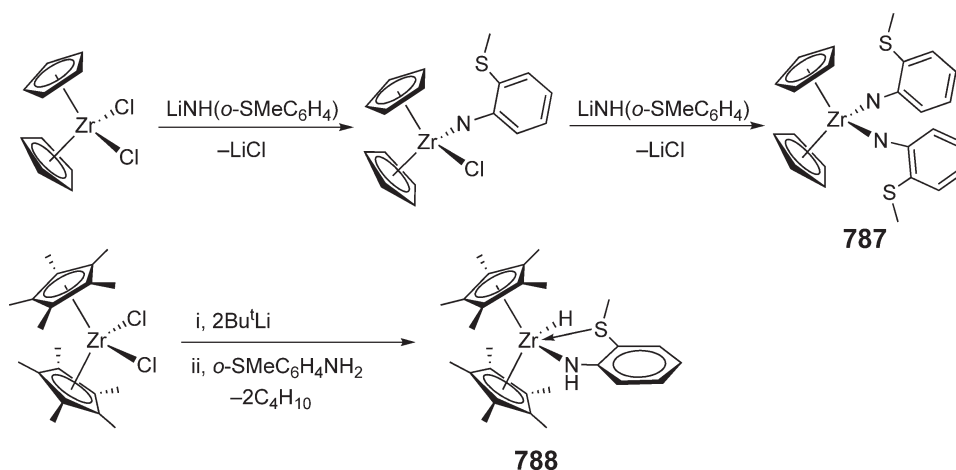
A series of silylamido complexes of zirconium,  $\text{Cp}_2\text{Zr}(\text{X})(\text{NBu}^t\text{SiMe}_2\text{H})$  ( $\text{X} = \text{H, I, Br, Cl, F}$ ), has been prepared<sup>604</sup> (Scheme 194). These complexes exhibit agostic  $\beta$ -Si–H interactions with the metal center and have been characterized by spectroscopic and structural methods. The spectroscopic data also establish a clear trend for the strength of the non-classical Zr–H–Si interaction in  $\text{Cp}_2\text{Zr}(\text{X})(\text{NBu}^t\text{SiMe}_2\text{H})$ :  $\text{X} = \text{H} > \text{I} > \text{Br} > \text{Cl} > \text{F}$ ; this ordering directly reflects the relative electrophilicity of the zirconium center. The molecular structures of the hydride and chloride derivatives as determined by X-ray diffraction are also consistent with coordination of the Si–H bond to the metal center.

The zirconocene bis(arylamido) complex **787** was obtained by the reaction of  $\text{Cp}_2\text{ZrCl}_2$  with 2 equiv. of the lithium amide<sup>605</sup> (Scheme 195). When the reaction is carried out in a 1:1 ratio, the monoamido zirconocene chloride is generated as the major product. Reaction of *in situ*-generated “ $\text{Cp}^*_2\text{Zr}$ ” with 2-(methylmercapto)aniline yields monoamido zirconocene hydride **788**, the spectroscopic data of which suggest an interaction between the S atom and the Zr center in this complex. The bis(amido) complex **787** serves as a precursor for the synthesis of amido rhodium and iridium complexes.

Zirconocene–imine complexes such as **789** insert isocyanates and cyclic carbonates and in some cases  $\text{CO}_2$ .<sup>606</sup> For example, isocyanates can insert either exclusively into the Zr–C bond, to form complexes **790** when R = bulky group such as  $\text{Bu}^t$  and  $\text{SiMe}_3$ , or preferentially into the Zr–N bond to give complexes **791** when R = Me, Et,  $\text{CH}_2\text{Ph}$ , and



Scheme 194

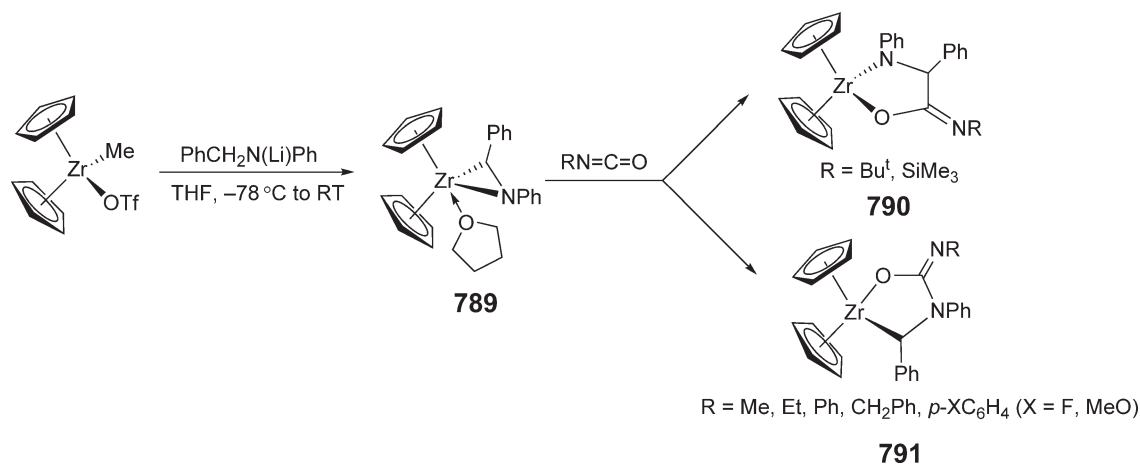


Scheme 195

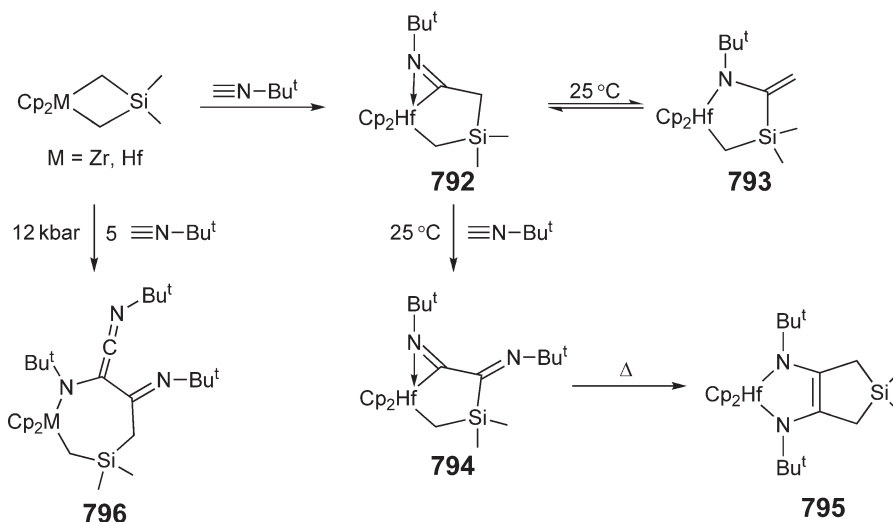
aryl groups (Scheme 196). Subsequent protonolysis of the zirconacycles **790** resulting from the Zr–C insertion gives amides, whereas protonolysis of **791** gives ureas.

Insertion of 1 equiv. of *tert*-butyl isocyanide into the metallacyclobutane  $\text{Cp}_2\text{Hf}(\text{CH}_2\text{SiMe}_2\text{CH}_2)$  affords a 1:1 equilibrium mixture of the  $\eta^2$ -iminoacyl complex **792** and the cyclic enamido complex **793**.<sup>607</sup> Subsequent addition of a second equivalent of *tert*-butyl isocyanide into this equilibrium mixture proceeds exclusively with the formation of the  $\eta^2$ -iminoacyl imine **794**, which upon heating rearranges to the bicyclic enediamido complex **795** (Scheme 197). Multiple C–C coupling of isocyanides is possible. For example, the reaction of 5 equiv. of *tert*-butyl isocyanide with metallacyclobutane  $\text{Cp}_2\text{M}(\text{CH}_2\text{SiMe}_2\text{CH}_2)$  ( $\text{M} = \text{Zr}, \text{Hf}$ ) at high-pressure conditions affords product **796** that contains three *tert*-butyl groups, two imine carbons, and a ketenimine functionality.<sup>608</sup>

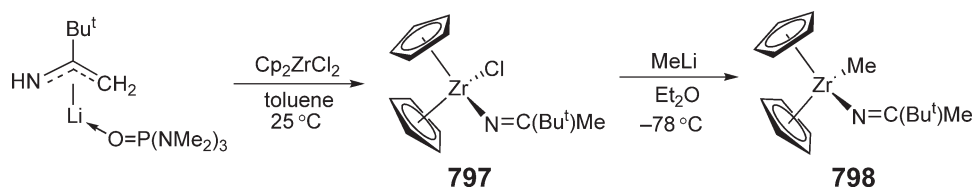
The chlorozirconocene ketimide complex **797** was prepared by the salt metathesis reaction between the lithium 1-azaallyl compound  $[(\text{HMPA})\text{LiN}(\text{H})\text{C}(\text{Bu}^t)\text{CH}_2]_2$  with zirconocene dichloride<sup>609</sup> (Scheme 198). The azaallyl ligand isomerizes to a ketimido variation when it is transferred to the transition metal due to the presence of a heteroallenic ( $\text{Zr}=\text{N}=\text{C}$ ) interaction in the ketimido isomer. Other zirconocene ketimides such as  $\text{Cp}_2\text{Zr}(\text{Cl})(\text{N}=\text{CR}^1\text{R}^2)$  ( $\text{R}^1 = \text{R}^2 = \text{CH}_2\text{Ph}$ ,  $\text{NMe}_2$ ;  $\text{R}^1 = \text{Ph}$ ,  $\text{R}^2 = \text{Bu}^t$ ) were obtained directly from the reactions between  $\text{Cp}_2\text{ZrCl}_2$  and appropriate lithiated organonitrogen compounds.<sup>610</sup> Methylation of the monochloride **797** with  $\text{MeLi}$  gives the corresponding methyl zirconocene ketimide complex **798**. NMR experiments reveal that addition of  $\text{B}(\text{C}_6\text{F}_5)_3$  to the methyl compound results in methide abstraction, with retention of the ketimide unit on the cationic zirconocene. When activated with an excess of MAO, both complexes **797** and **798** become active catalysts for the polymerization of ethylene.



Scheme 196



Scheme 197

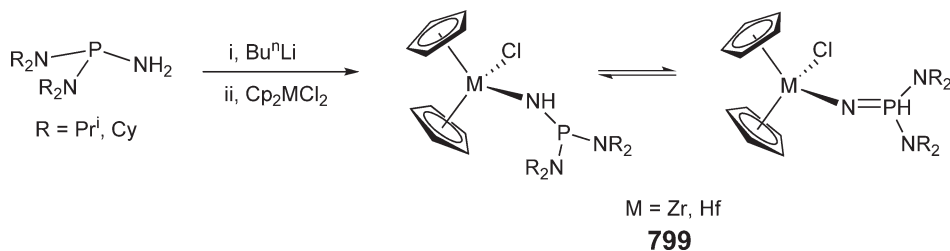


Scheme 198

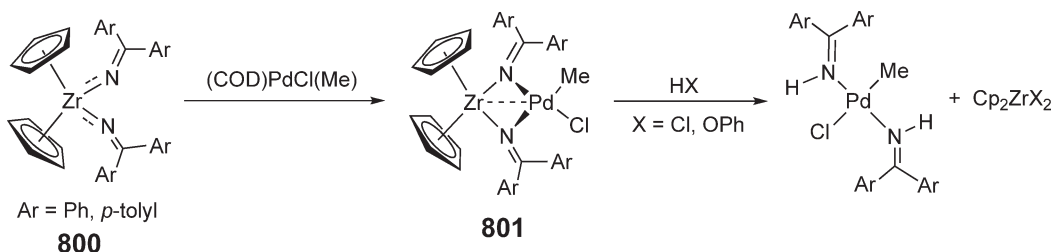
The addition of  $\text{Cp}_2\text{MCl}_2$  ( $\text{M} = \text{Zr}, \text{Hf}$ ) to a THF solution of aminobis(diorganylamino)phosphines and  $\text{Bu}^n\text{Li}$  affords metallocene (NH)-phosphanylamido and (PH)-phosphoraneiminato complexes **799**<sup>611</sup> (Scheme 199). There is a strong influence of the electronic effects of the metal fragment on the resulting equilibrium between the (NH)-phosphanylamido and the tautomeric (PH)-iminophosphorane form; a stronger acidic transition metal center stabilizes the PH form. The monoamido complex  $\text{Cp}_2\text{Zr}(\text{Cl})\text{N}(\text{PPh}_2)_2$ , in which the  $(\text{Ph}_2\text{P})_2\text{N}$  ligand is coordinated to Zr in a chelating fashion via P and N atoms, is obtained by the reaction of zirconocene dichloride with  $[\text{K}(\text{THF})_m][\text{N}(\text{PPh}_2)_2]$  ( $m = 1.25\text{--}1.5$ ).<sup>612</sup> When  $\text{K}[\text{CH}(\text{PPh}_2)_2\text{NSiMe}_3]_2$  is treated with zirconocene dichloride, the carbene-like mono-Cp complex  $\text{CpZr}(\text{Cl})\text{C}(\text{PPh}_2\text{NSiMe}_3)_2$  is formed.

The reaction of the zirconocene imido complex **800** with  $\text{PdCl}(\text{Me})(\text{COD})$  gives Zr/Pd heterobimetallic complexes **801** with bridging alkylideneamido ligands<sup>613</sup> (Scheme 200). The molecular structures of the complexes **801** have puckered  $\text{ZrN}_2\text{Pd}$  rings with Zr–Pd distances of  $2.8135(5)\text{ \AA}$  ( $\text{Ar} = \text{Ph}$ ) and  $2.8416(4)\text{ \AA}$  ( $\text{Ar} = p\text{-tolyl}$ ), respectively. Upon treatment with  $\text{HX}$  ( $\text{X} = \text{Cl}, \text{OPh}$ ), complexes **801** are converted to  $\text{Cp}_2\text{ZrX}_2$  and  $\text{trans-PdCl}(\text{Me})(\text{NH}=\text{CAr}_2)_2$ .

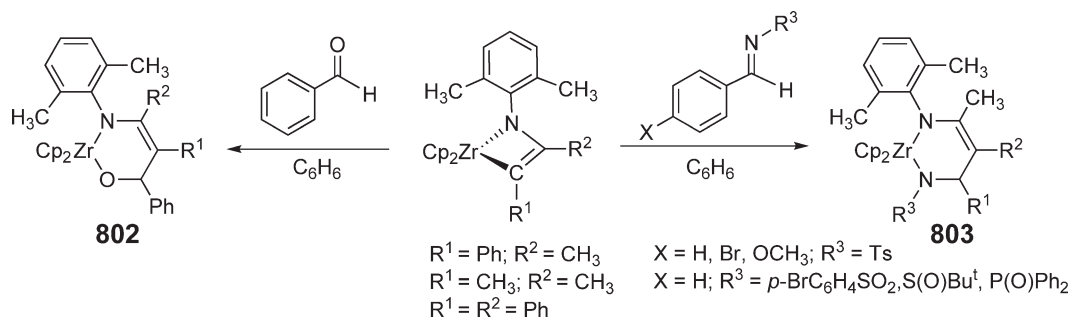
Azazirconacyclobutenes react with benzaldehyde to generate six-membered ring zirconacycle **802**<sup>614</sup> (Scheme 201). Upon heating, these metallacycles undergo a retro-[4 + 2]-cycloaddition to afford  $\alpha, \beta$ -unsaturated



Scheme 199



Scheme 200

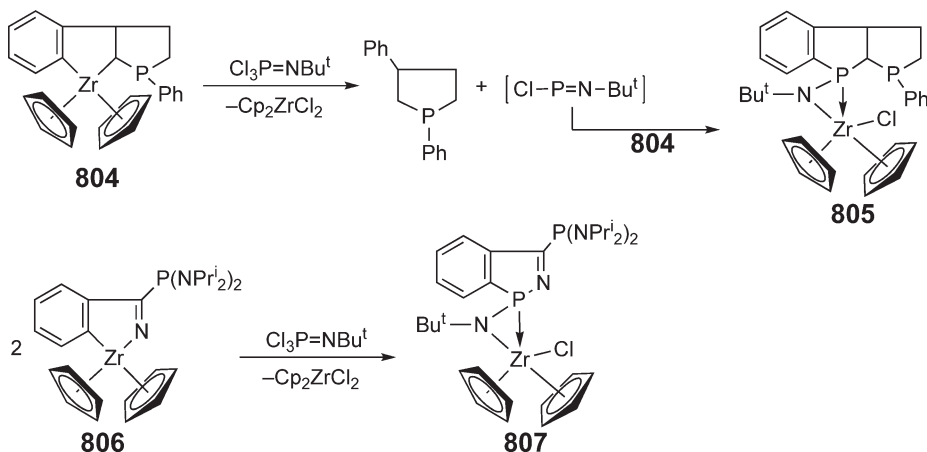


Scheme 201

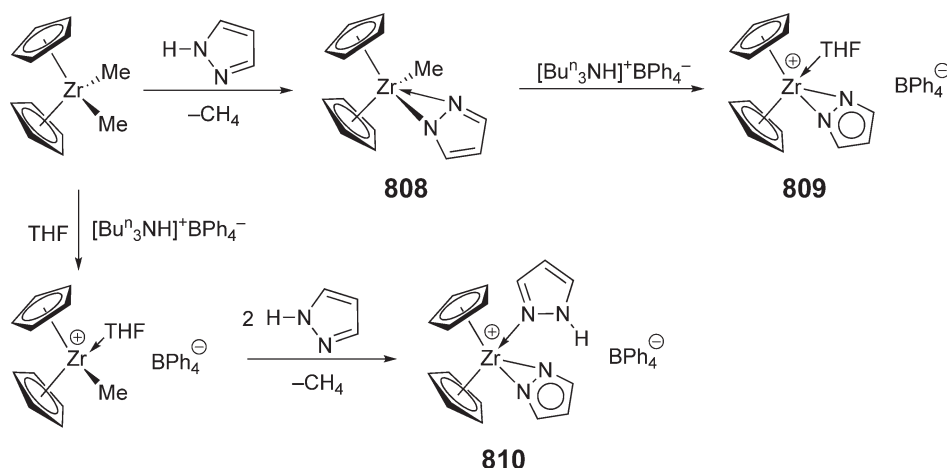
imines and (Cp<sub>2</sub>ZrO)<sub>*n*</sub>. Electron-deficient imines also insert into the zirconium–carbon bond of azazirconacyclobutenes to give six-membered ring metallacycles **803**.<sup>615</sup> On heating, these expanded zirconacycles undergo a retro-[4 + 2]-cycloaddition to generate  $\alpha,\beta$ -unsaturated imines in excellent yields and the fully characterized electron-deficient imidozirconocene complexes [Cp<sub>2</sub>Zr=N-R<sup>3</sup>].

The reaction of trichloroiminophosphorane, Bu<sup>t</sup>N=PCl<sub>3</sub>, with zirconaindane phospholane **804** leads to formation of zircona-azaspirophosphane **805**<sup>616</sup> (Scheme 202). This complex has been characterized by X-ray diffraction analysis. Other metallacyclic complexes react with Bu<sup>t</sup>N=PCl<sub>3</sub> in an analogous fashion; for example, treatment of azazirconacyclopentene **806** with Bu<sup>t</sup>N=PCl<sub>3</sub> produces metalla-azaspirophosphane **807**. The reaction of ZrCl<sub>4</sub> with 2 equiv. of the dilithium salt of the amidoboryl-indenyl ligand C<sub>9</sub>H<sub>7</sub>B(NPr<sup>i</sup>)<sub>2</sub>N(H)Ph gives the zirconocene-type complex [ $\eta^5$ : $\eta^1$ -C<sub>9</sub>H<sub>6</sub>B(NPr<sup>i</sup>)<sub>2</sub>NPh]Zr.<sup>617</sup>

The methylzirconocene pyrazolyl compound **808** was obtained by the reaction of Cp<sub>2</sub>ZrMe<sub>2</sub> with 1 equiv. of pyrazol. Subsequent treatment of **808** with tributylammonium tetraphenylborate gives the cationic



Scheme 202

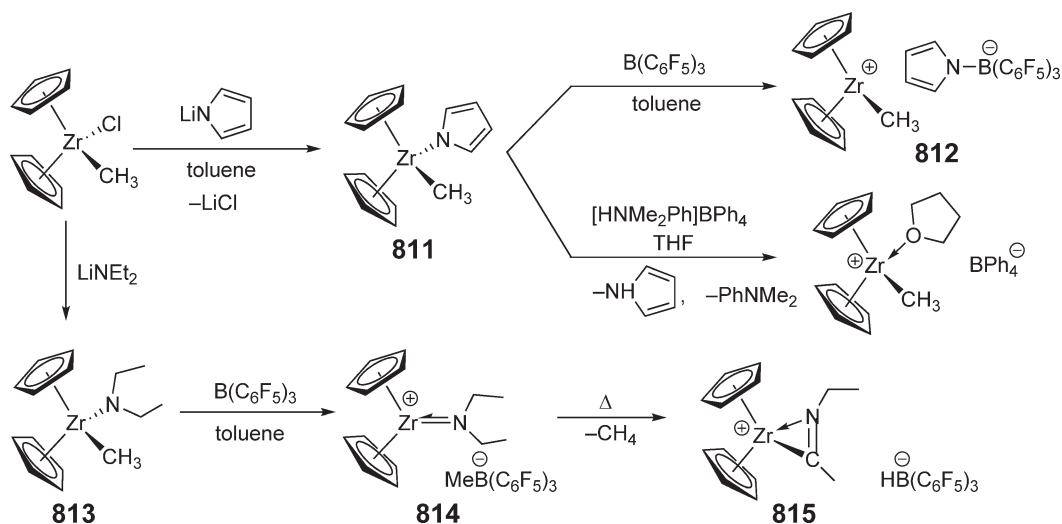


Scheme 203

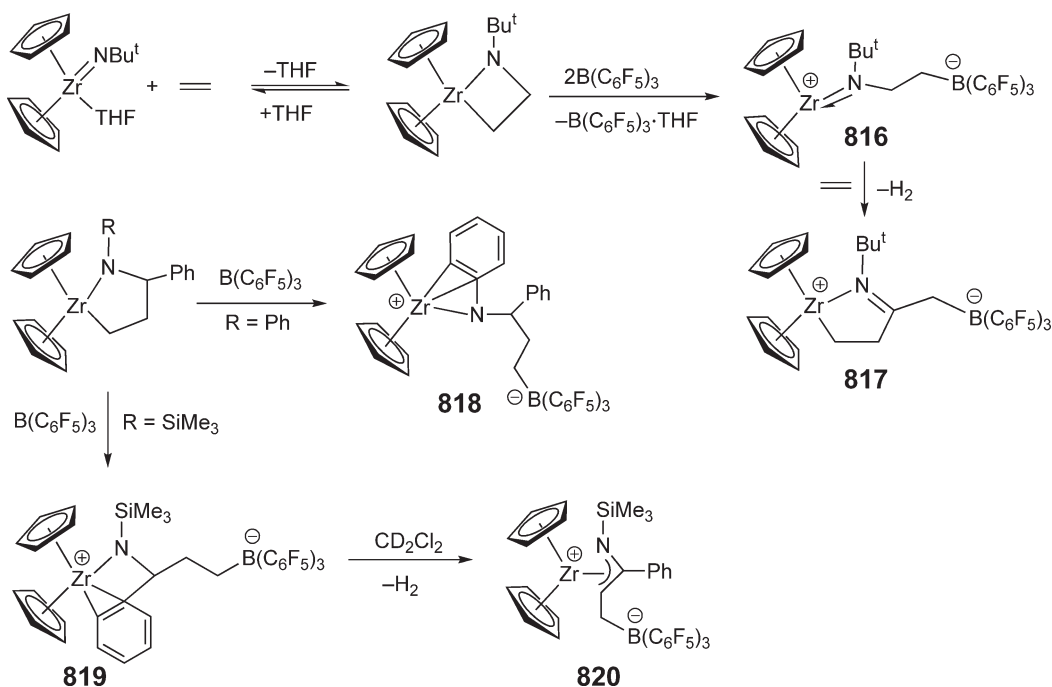
( $\eta^2$ -pyrazolyl- $N,N'$ )(THF)zirconocenium complex **809**<sup>618</sup> (Scheme 203). Treatment of the methylzirconocenium tetraphenylborate salt with 2 equiv. of pyrazol in dichloromethane gave the related ( $\eta^2$ -pyrazolyl- $N,N'$ )( $\eta^1$ -pyrazolyl- $N'$ )zirconocene tetraphenylborate salt **810**.

Activation of the ( $N$ -pyrrolyl)methylzirconocene **811** by  $\text{B}(\text{C}_6\text{F}_5)_3$  selectively transfers the heterocyclic ligand to the borane to give the salt **812**, which is an active ethylene polymerization catalyst when generated *in situ* in toluene<sup>619</sup> (Scheme 204). Protonolysis of **811** by  $[\text{HNMe}_2\text{Ph}]\text{BPh}_4$  in THF generates the same cation stabilized by THF. In contrast, activation of (diethylamido)methylzirconocene **813** by  $\text{B}(\text{C}_6\text{F}_5)_3$  selectively undergoes only transfer of the Me group to the borane, yielding the (diethylamido)zirconocene salt **814**. This is not stable and rapidly eliminates methane at ambient temperature to give the cationic ( $\eta^2$ -iminoacyl)zirconocenium hydroborate **815**. ( $N$ -piperidyl)methylzirconocene reacts similarly with  $\text{B}(\text{C}_6\text{F}_5)_3$  to give the analogous ( $\eta^2$ -iminoacyl)zirconocenium hydridoborate salt.

$\text{B}(\text{C}_6\text{F}_5)_3$ , as a strong Lewis acid, effects the ring opening of  $N\text{-Bu}^t$  azazirconacyclobutane to give the zwitterionic amido complex **816** which reacts slowly with 1 equiv. of ethylene to form a chelating  $\gamma$ -iminoalkyl zirconocene zwitterion **817**<sup>620</sup> (Scheme 205). Analogous reactions of  $\text{B}(\text{C}_6\text{F}_5)_3$  with  $N\text{-Ph}$  azazirconacyclopentane and  $N\text{-SiMe}_3$  azazirconacyclopentane in toluene proceed with removal of the carbon from the Zr centers, forming amido cations **818** and **819**, respectively, both of which are stabilized in the solid state by coordination of Ph substituents on N or C



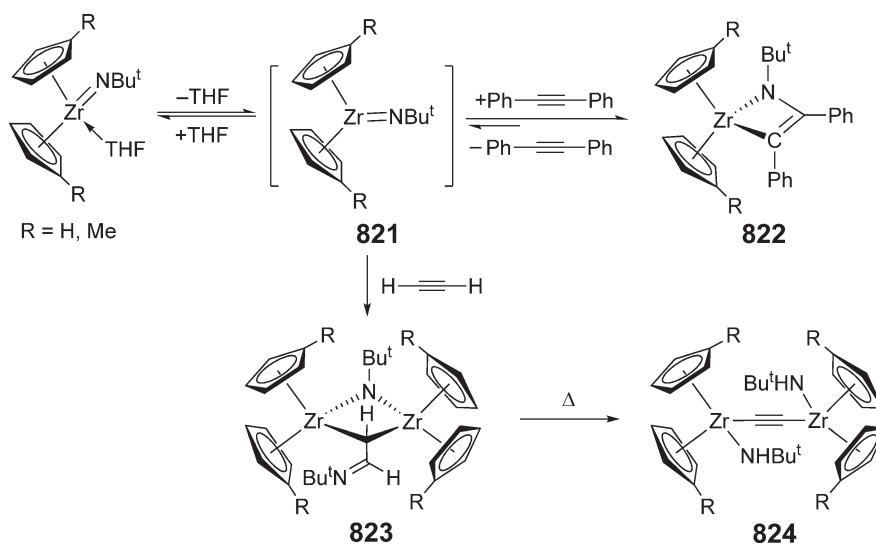
Scheme 204



Scheme 205

to the cationic Zr center. When dissolved in  $\text{CD}_2\text{Cl}_2$ , complex **819** slowly loses dihydrogen to generate an azaallyl cation **820**.

Monomeric zirconocene terminal imido complexes  $\text{Cp}_2\text{Zr}=\text{NR}(\text{THF})$  ( $\text{R} = \text{Bu}^t$ , 2,6-dimethylphenyl,  $\text{SiBu}^t\text{Me}_2$ ) are obtained by thermolysis of alkyl amides  $\text{Cp}_2\text{Zr}(\text{NHR})(\text{R}^1)$  and bis(amides)  $\text{Cp}_2\text{Zr}(\text{NHR})_2$  via  $\alpha$ -abstraction of alkane and amine, respectively.<sup>621</sup> Dissociation of THF gives the highly reactive base-free intermediate **821** which undergoes cycloaddition reactions with a variety of unsaturated organic substrates such as alkynes and certain olefins leading to azametallacyclobutenes (**822**, Scheme 206) and azametallacyclobutanes, respectively. The addition of asymmetric alkynes to  $\text{Cp}_2\text{Zr}=\text{NR}$  occurs regioselectively with the net result being an anti-Markovnikov addition to

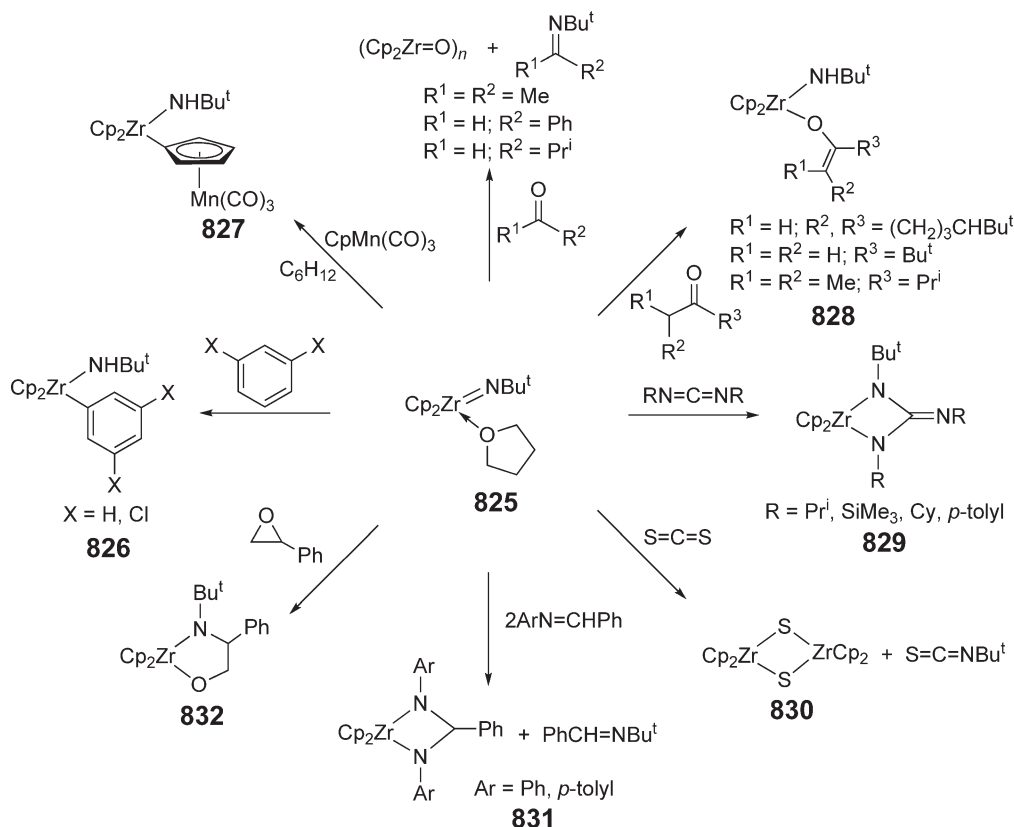


Scheme 206

the alkyne. The size of the R group on the imido ligand and the size of the alkyne are influential in determining the degree of regioselectivity.<sup>622</sup> On the other hand, treatment of the zirconocene imido complex **821** with acetylene gives a binuclear product **823**, in which the Zr centers are linked by N and C bridges<sup>623</sup> (Scheme 206). Upon heating, the binuclear complex **823** is cleaved into the azametallacyclobutene (type **822**) and the terminal imido complex **821** which can be readily trapped by Lewis bases or alkynes. Heating the binuclear complex **823** in the absence of traps cleanly produces the alkynyl-bridged dimeric species **824**.

The highly reactive, transient monomeric imidozirconocene  $[\text{Cp}_2\text{Zr}=\text{NBU}^t]$ , which is generated reversibly from isolable  $\text{Cp}_2\text{Zr}=\text{NBU}^t(\text{THF})$  **825**, reacts with a variety of unsaturated organic or organometallic substrates. The reactions are summarized in Scheme 207. Heating the imidozirconocene complex **825** in 1,3-dichlorobenzene solution at 75 °C results in selective activation of the C–H bond at the 5-position in the arene molecule to give the arylamido zirconocene complex **826**.<sup>624</sup> When **825** is heated to 75 °C in the more-hindered solvent 1,3,5-trimethylbenzene, in addition to the aryl C–H activation product  $\text{Cp}_2\text{Zr}(\text{NHBu}^t)(\text{CH}_2\text{C}_6\text{H}_3\text{Me}_2)$ , the dimeric Cp-bridged amido zirconocene complex  $[\text{CpZr}(\text{NHBu}^t)(\eta^1:\eta^5\text{-C}_5\text{H}_4)]_2$  was generated by Cp C–H activation of a second molecule of **825**. Similar intermolecular Cp C–H activation was observed in the reactions of **825** with other Cp metal complexes. For example, treatment of  $\text{CpMn}(\text{CO})_3$  in  $\text{C}_6\text{H}_{12}$  at 75 °C with the imido complex **825** resulted in metallation of the Mn–Cp ring to produce  $\text{Cp}_2\text{Zr}(\text{NHBu}^t)(\eta^1:\eta^5\text{-C}_5\text{H}_4)\text{Mn}(\text{CO})_3$  **827**.

The C=N linkage of  $\text{Cp}_2\text{Zr}=\text{NBU}^t(\text{THF})$  undergoes imido/oxo exchange reactions with the carbonyl compounds and generates several different types of oxozirconocene products.<sup>625</sup> For example, the reaction of **825** with aldehydes and simple ketones generates the corresponding imine products and oligomeric  $(\text{Cp}_2\text{Zr}=\text{O})_n$ , whereas the reaction with sterically encumbered ketones containing  $\alpha$ -protons affords zirconocene enolate complexes **828** by  $\alpha$ -hydrogen abstraction, (Scheme 207). A study has been carried out to examine the structural factors that influence the overall [2 + 2]-cycloaddition reactions between imidozirconocene complexes and heterocumulenes.<sup>626,627</sup> When  $\text{Cp}_2\text{Zr}=\text{NBU}^t(\text{THF})$  was treated with symmetric carbodiimides  $\text{RN}=\text{C}=\text{NR}$  ( $\text{R} = \text{Pr}^i$ ,  $\text{SiMe}_3$ , Cy, *p*-tolyl), the corresponding diazametallacycles **829** formed in high yields. On the other hand, the reaction with sulfur-containing heterocumulenes results in imido/sulfur exchange, leading to the immediate formation of the dimeric sulfide **830**



Scheme 207



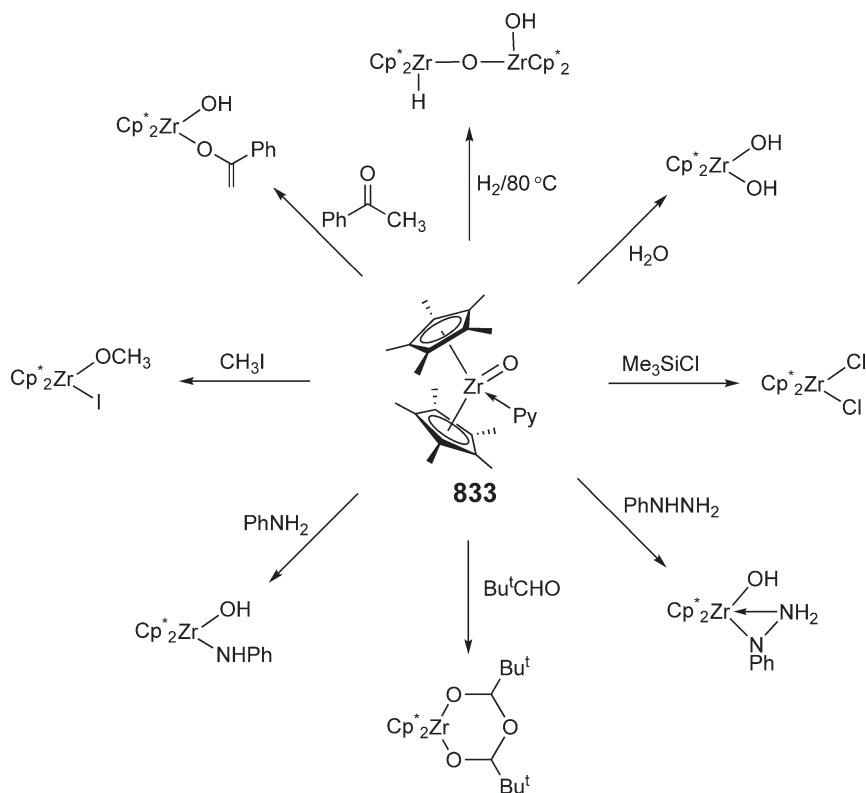
(Scheme 207). Diazametallacycles such as **831** are key intermediates involved in imine metathesis catalyzed by zirconocene imido complexes,<sup>628</sup> the authentic samples of which were synthesized independently by the reaction of **825** with 2 equiv. of the corresponding imine.<sup>629</sup> The zirconocene imido complex **825** also ring-opens epoxides such as styrene oxide regioselectively to give metallacycle **832** (Scheme 207).<sup>630</sup>

#### 4.08.9.6 Complexes with M–O Bonds

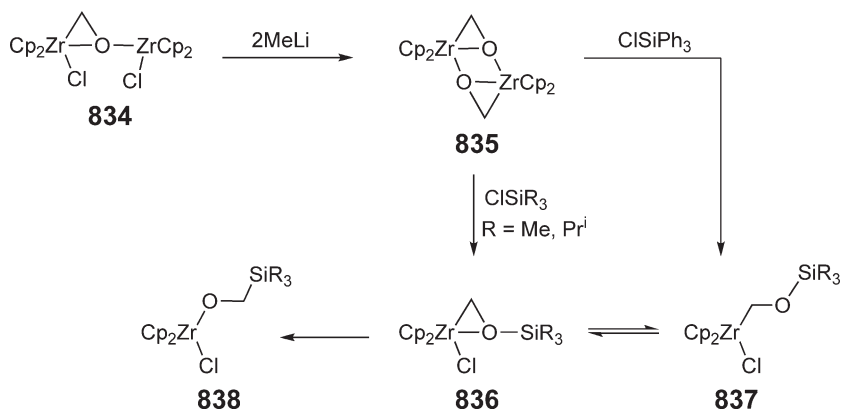
The reaction of zirconocene dicarbonyl with  $N_2O$  in the presence of pyridine yields terminal zirconium oxo complexes such as **833**. The zirconium–oxo interaction in these complexes is best represented as a  $Zr=O$  double bond, with little triple bond  $Zr\equiv O$  character. The  $[Zr=O]$  moiety in  $Cp^*_2Zr(=O)py$  reacts with a variety of both polar ( $X^{6+}-Y^{6-}$ ) and non-polar substrates to give products  $Cp^*_2Zr(OX)(Y)$  that may be considered to be derived by a formal 1,2-addition across the  $Zr=O$  double bond<sup>631</sup> (Scheme 208). The facile reaction of **833** with  $H_2$  at  $80^\circ C$  gives a  $\mu$ -O binuclear complex, whereas the reaction with  $Me_3SiCl$  results in complete abstraction of oxygen from Zr to give the zirconocene dichloride and  $(Me_3Si)_2O$ . The cycloaddition reaction with the aldehyde  $Bu^tCHO$  gives a six-membered metallacycle, but the  $Zr=O$  group deprotonates methyl ketones to afford the zirconocene enolate derivative.

The dimeric zirconocene  $\eta^2$ -formaldehyde, or metallaioxirane, complex **835**, prepared by treatment of  $(Cp_2ZrCl)_2(\mu-CH_2O)$  **834** with 2 equiv. of MeLi, reacts with trialkylsilanes  $R_3SiCl$  to give  $[\eta^2-(trialkylsiloxy)methyl]$ -zirconocene chloride complex **836**<sup>632</sup> (Scheme 209). Thermolysis of complexes **836** at  $110^\circ C$  leads to equilibration with the isomers **837** and **838**. Treatment of **835** with  $Ph_3SiCl$  results in the direct formation of the acyclic addition product  $Cp_2Zr(Cl)CH_2OSiPh_3$  **837**. Metallaioxirane-supported hydrido metallocene complexes have also been prepared by the reaction of  $(\eta^2$ -diaryl ketone)zirconocene dimers with the zirconocene and hafnocene dihydride complexes.<sup>633</sup> Treatment of these complexes with  $B(C_6F_5)_3$  results in the selective abstraction of the terminal hydride ligand to form the dimetallic cation complexes.

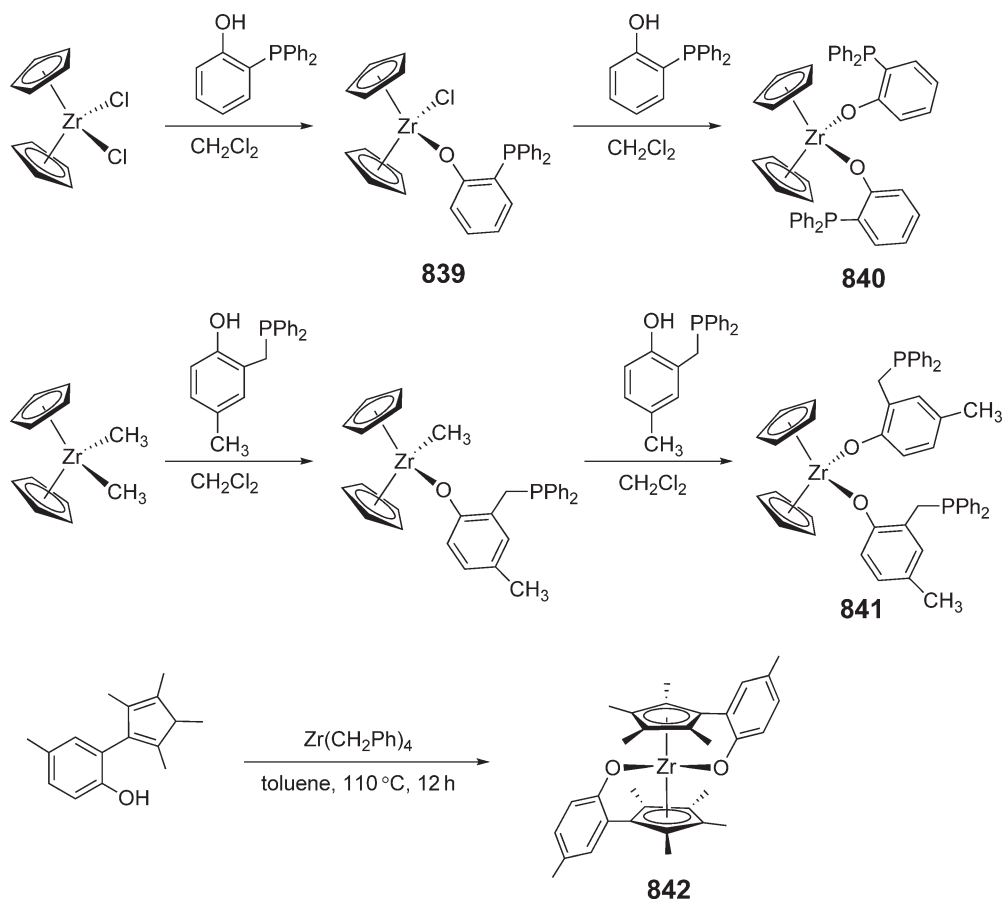
Zirconocene dichloride reacts with 1 and 2 equiv. of 2-(diphenylphosphino)phenol in the presence of imidazole to give monoaryloxy complex **839** and bis(aryloxy) complex **840**, respectively<sup>634</sup> (Scheme 210). The bulkier



Scheme 208



Scheme 209



Scheme 210

2-(diphenylphosphinomethyl)-4-methylphenol ligand failed to react with  $\text{Cp}_2\text{ZrCl}_2$ , but its reaction with  $\text{Cp}_2\text{ZrMe}_2$  yields the monoaryloxy zirconocene methyl complex and the bis(aryloxy) zirconocene methyl complex **841** according to the stoichiometric ratio of the two reagents. Modified metallocenes by incorporating aryloxy ligands showed slightly higher activity than the parent metallocene dichlorides in MAO-activated ethylene polymerization.<sup>635</sup> The reaction of zirconocene dichloride  $\text{Cp}_2\text{ZrCl}_2$  with 1 equiv. of pentafluorophenol in the presence of aniline gives a mixture of  $\text{Cp}_2\text{ZrCl}(\text{OC}_6\text{F}_5)$  and  $\text{Cp}_2\text{Zr}(\text{OC}_6\text{F}_5)_2$ , whereas the reaction with 2 equiv. of pentafluorophenol affords just

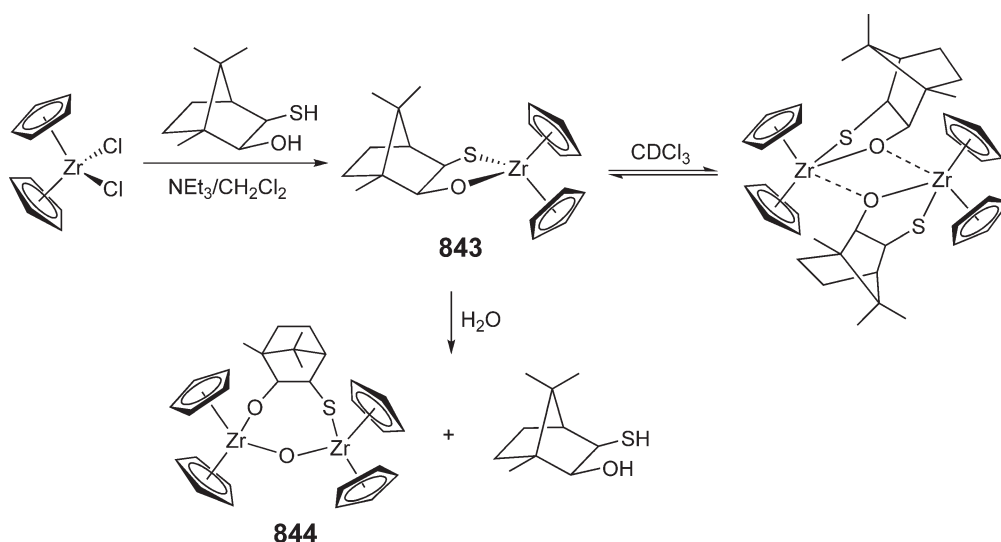
$\text{Cp}_2\text{Zr}(\text{OC}_6\text{F}_5)_2$ .<sup>636</sup> When the  $\mu$ -oxo binuclear complex  $(\text{Cp}_2\text{ZrMe})_2(\mu\text{-O})$  is treated with 2 equiv. of pentafluorophenol,  $[\text{Cp}_2\text{Zr}(\text{OC}_6\text{F}_5)]_2(\mu\text{-O})$  is formed. Zirconocene dichloride and monochloride react with benzenediols and triols, producing benzenediolate and triolate polymetallic complexes.<sup>637</sup> The alkane elimination reaction between the neutral 2-(tetramethylcyclopentadienyl)-4-methylphenol ligand with  $\text{Zr}(\text{CH}_2\text{Ph})_4$  yields chiral  $C_2$ -symmetric zirconocene complex **842** (Scheme 210) containing an *O*-donor functionalized, chelated bis(Cp) ligand.<sup>638</sup>

Zirconocene bis(triflate)  $\text{Cp}_2\text{Zr}(\text{OTf})_2$  is obtained by the reaction of  $\text{Cp}_2\text{ZrMe}_2$  with 2 equiv. of triflic acid ( $\text{HOTf}$ ), whereas zirconocene monotriflate complexes  $\text{Cp}_2\text{ZrX}(\text{OTf})$  ( $\text{X} = \text{Cl}, \text{Me}, \text{BH}_4$ ) can be conveniently prepared by comproportionation between  $\text{Cp}_2\text{Zr}(\text{OTf})_2$  and  $\text{Cp}_2\text{ZrX}_2$ .<sup>639</sup> Treatment of  $\text{Cp}_2\text{Zr}(\text{BH}_4)(\text{OTf})$  with triethylamine gives the hydrido-zirconocene monotriflate complex  $\text{Cp}_2\text{ZrH}(\text{OTf})$ .<sup>640</sup> Hexene insertion into the  $\text{Zr-H}$  bond is fast and reversible, and treatment of the hydride complex with styrene leads to a kinetically controlled mixture of  $\text{Cp}_2\text{ZrCH}_2\text{CH}_2\text{Ph}(\text{OSO}_2\text{CF}_3)$  and  $\text{Cp}_2\text{ZrCH}(\text{CH}_3)\text{Ph}(\text{OSO}_2\text{CF}_3)$  that equilibrates with a first-order rate law. The halide–triflate metathesis of zirconocene dichloride with  $\text{TeF}_5(\text{OH})$  produces  $\text{Cp}_2\text{Zr}(\text{OTeF}_5)_2$ .<sup>641</sup> Reactions of alkyl-substituted zirconocene dimethyl  $(\text{C}_5\text{EtMe}_4)_2\text{ZrMe}_2$  with thioglycolic acids result in elimination of methane and formation of the macrocyclic, dimeric zirconocene complexes which can act as metalloligands toward complex fragments of a second metal.<sup>642</sup>

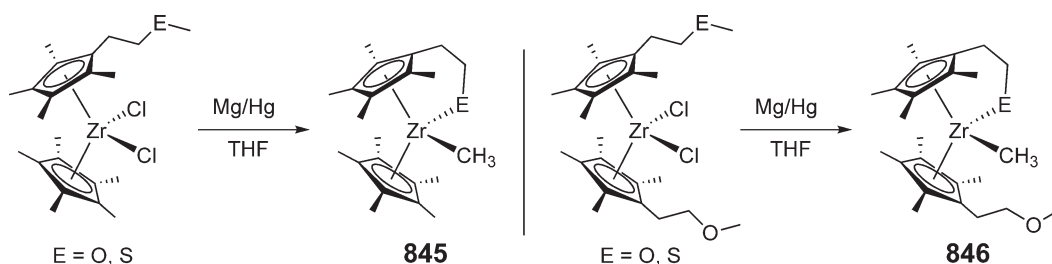
$\text{Cp}^*\text{ZrCl}_2$  reacts with hard (oxygen)–soft (sulfur) donor ligands such as 3-mercapto-1-propanol and 2-mercaptoethanol in the presence of triethylamine to form the oxygen-bonded monomeric complexes  $\text{Cp}^*\text{Zr}(\text{Cl})(\text{O}(\text{CH}_2)_n\text{SH})$  ( $n = 2, 3$ ).<sup>643</sup> The dimethyl zirconocene reacts with these donor ligands in a similar fashion to produce the oxygen-bonded monomeric zirconocene methyl complexes  $\text{Cp}^*\text{ZrMe}(\text{O}(\text{CH}_2)_n\text{SH})$  ( $n = 2, 3$ ),<sup>644</sup> which can slowly lose methane to give the monomeric chelate complexes  $\text{Cp}^*\text{Zr}(\text{O}(\text{CH}_2)_n\text{S})$ . The bis(substituted) zirconocene complex  $\text{Cp}^*\text{Zr}(\text{O}(\text{CH}_2)_n\text{SH})_2$  can also be prepared from the reaction of  $\text{Cp}^*\text{ZrMe}_2$  with 2 equiv. of the ligand. These permethylzirconocene complexes present different structural behavior, as compared with that of the parent zirconocene in which the twisted dimeric zirconocene complex  $[\text{Cp}_2\text{Zr}(\text{OCH}_2\text{CH}_2\text{S})]_2$  is isolated.<sup>646</sup> Chlorozirconocene alkoxide complexes  $\text{Cp}^R\text{ZrCl}(\text{OCH}_2\text{CH}_2\text{SPh})$  and  $\text{Cp}^R\text{ZrCl}(\text{OC}_6\text{H}_4\text{SPh})$  ( $R = \text{Me}$ ) have also been prepared by the reaction of  $\text{Cp}^R\text{ZrCl}_2$  with  $\text{HOCH}_2\text{CH}_2\text{SPh}$  or  $\text{HOC}_6\text{H}_4\text{SPh}$  in the presence of triethylamine.<sup>645</sup> Alkyl and aryl derivatives were obtained by the reaction of the corresponding dialkyl or diaryl zirconocene complexes with  $\text{HOCH}_2\text{CH}_2\text{SPh}$ , or by the reaction of  $\text{Cp}^R\text{ZrCl}(\text{OCH}_2\text{CH}_2\text{SPh})$  with  $\text{LiMe}$  or  $\text{LiPh}$ .

Treatment of  $\text{Cp}_2\text{ZrCl}_2$  with the chiral difunctional ligand (1*R*,2*S*,3*R*)-3-mercapto-1,7,7-trimethylbicyclo[2,2,1]-heptan-2-ol yields the chelate product  $\text{Cp}_2\text{Zr}(\text{OC}_{10}\text{H}_{16}\text{S})$  **843** (Scheme 211),<sup>646</sup> which exists as a mixture of monomeric and dimeric species in  $\text{CDCl}_3$  solution. This complex can be readily hydrolyzed to give the air-stable binuclear complex **844**. The related complex  $[\text{Cp}_2\text{Zr}(\mu\text{-OCH}_2\text{CH}_2\text{S})]_2$  was also prepared by the reaction of  $\text{Cp}_2\text{ZrMe}_2$  with 1 equiv. of 2-mercaptoethanol in diethyl ether; this is a zirconocene dimer bridging through the oxygen atoms.

Reduction of 2-methoxyethyl- and 2-methylthioethyl-functionalized zirconocene dichlorides with  $\text{Mg}/\text{Hg}$  in THF leads to the products of the  $\text{O-Me}$  and  $\text{S-Me}$  bond cleavage.<sup>647</sup> For example, the reduction of  $(\text{C}_5\text{Me}_4\text{CH}_2\text{CH}_2\text{EMe})(\text{C}_5\text{Me}_5)\text{ZrCl}_2$  ( $\text{E} = \text{O}, \text{S}$ ) with  $\text{Mg}/\text{Hg}$  in THF gives the chelating (ring-metallated) complex



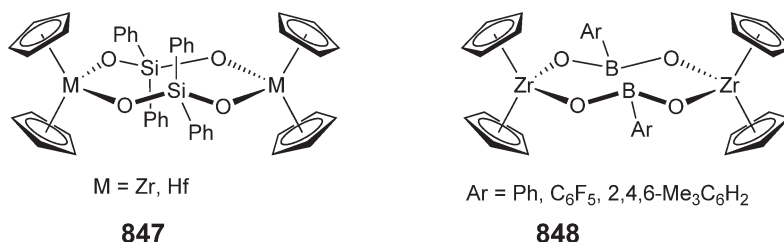
Scheme 211



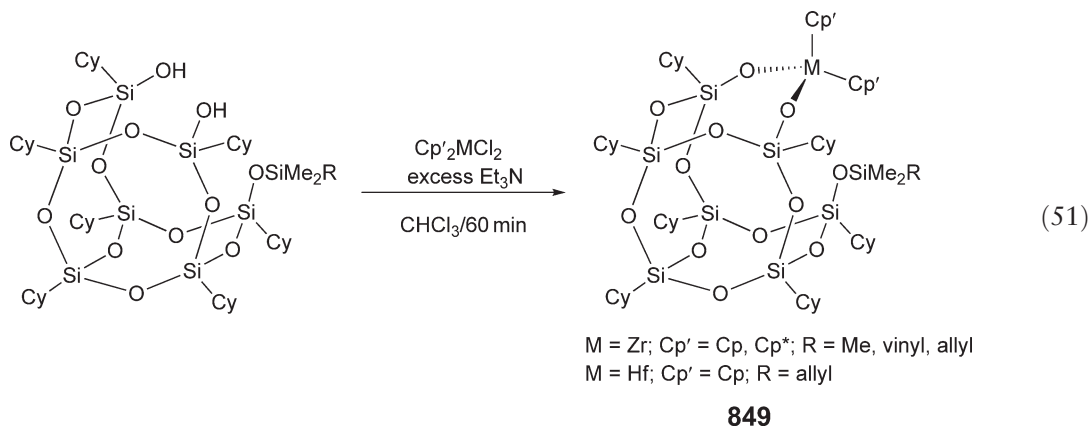
Scheme 212

**845**, and the reduction of the difunctionalized zirconocene dichloride  $(C_5Me_4CH_2CH_2EMe)(C_5Me_4CH_2CH_2OMe)ZrCl_2$  ( $E = O, S$ ) yields the analogous complex **846** (Scheme 212). On the other hand, the reduction of  $(C_5Me_4CH_2CH_2SMe)_2ZrCl_2$  results in a product where the S–Me bonds on both Cp rings have been cleaved.

The reaction of zirconocene and hafnocene dimethyl complexes with  $Ph_2Si(OH)_2$  yields the eight-membered metallacycles **847**.<sup>648</sup> The crystal structure of the zirconium derivative reveals a non-planar chelating ring; the  $Cp_2Zr$  units are bent  $20^\circ$  out of the  $Si_2O_4$  plane to give a “chaise longue” conformation. In solution, however, the molecule is fluxional on the NMR timescale. Reaction of  $Cp_2ZrMe_2$  with phenylboronic anhydride,  $(PhBO)_3$ , results in the formation of the heterocyclic dimer  $Cp_2Zr(\mu-O_2BPh)_2$  (**848**,  $Ar = Ph$ ); no reaction was observed with the mesityl derivative.<sup>649</sup> Compound **848** was also synthesized from the protonolysis reaction between  $Cp_2ZrMe_2$  and *in situ*-generated phenylboronic acid,  $PhB(OH)_2$ , the approach of which can be extended to the preparation of other aryl derivatives from the corresponding isolable arylboronic acids,  $ArB(OH)_2$ . Treatment of  $Cp_2ZrMe_2$  with P–H-functionalized phosphinoalcohol 1-PH(Ar)-2-OH-*cyclo*- $C_6H_{10}$  ( $Ar = 2,4,6-Pr^i_3C_6H_2$ ) gives exclusively the monosubstituted product  $Cp_2Zr(Me)(cyclo-1-O-2-PH(Ar)-C_6H_{10})$ , with elimination of methane.<sup>650</sup> The P(Ar)H group can serve as a ligand for the preparation of heterobimetallic complexes such as  $Cp_2Zr(Me)(cyclo-1-O-2-PH(Ar)[Mo(CO)_5]-C_6H_{10})$ .



Metallocene-containing silsesquioxanes **849** with alkenylsilyl and trimethylsilyl groups have been synthesized by the reaction of the disilanol with the corresponding metallocene dichloride in the presence of excess triethylamine (Equation (51)).<sup>651</sup> The structures of the complexes **849** ( $M = Zr, Hf$ ;  $R = CH_2CH=CH_2$ ) were established by single crystal X-ray diffraction analyses. Silylation or germylation of the zirconocene-containing silsesquioxane monosilanol  $Cp_2Zr[(\textit{c}-C_5H_9)_7Si_7O_{11}](OH)$  or its hafnocene analog yields metallocene-containing silsesquioxanes.

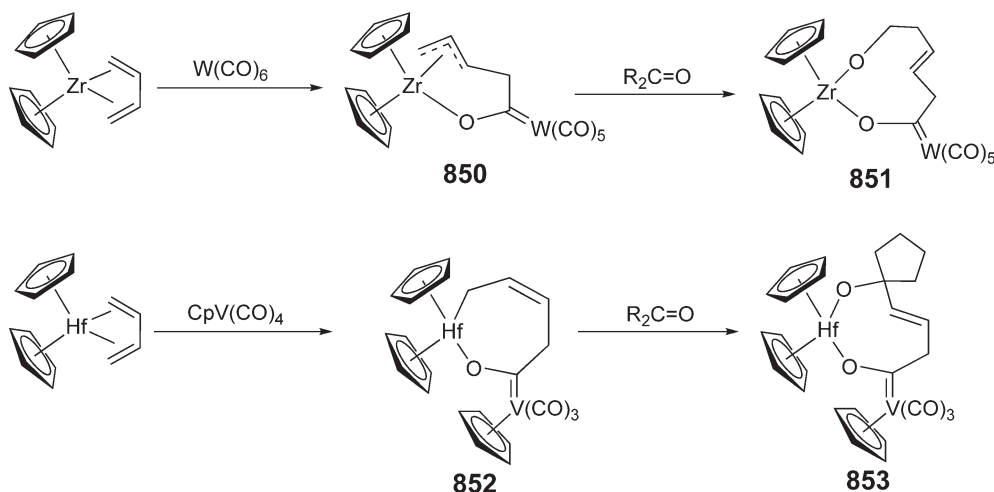


The reaction of (butadiene)zirconocene with  $\text{W}(\text{CO})_6$  gives the metallacyclic  $[(\pi\text{-allyl})\text{zirconoxyl}]$ carbene complex **850**, which couples with a variety of ketones to yield nine-membered metallacyclic ring systems **851**<sup>652</sup> (Scheme 213). The formation of these systems can be regarded as 1,4-selective coupling reactions of 1,3-butadiene with  $\text{W}(\text{CO})_6$  and an organic carbonyl compound at the zirconocene template. Treatment of (butadiene)hafnocene with  $\text{CpV}(\text{CO})_4$  formed the metaloxycarbene vanadium complex **852**, which was then trapped by coupling with cyclopentanone to give the nine-membered metallacyclic metalloxycarbene vanadium complex **853** containing a *trans*-C=C double bond in the medium-size ring system.<sup>653</sup> The formation of oxametallacycloheptene ring systems bearing the bulky 9-BBN substituent at the carbon atom adjacent to hafnium was accomplished by regioselective addition of ketones to the *s-trans* [(BBN)butadienyl]hafnocene complex generated by photolysis of the *s-cis*-isomer.<sup>654</sup>

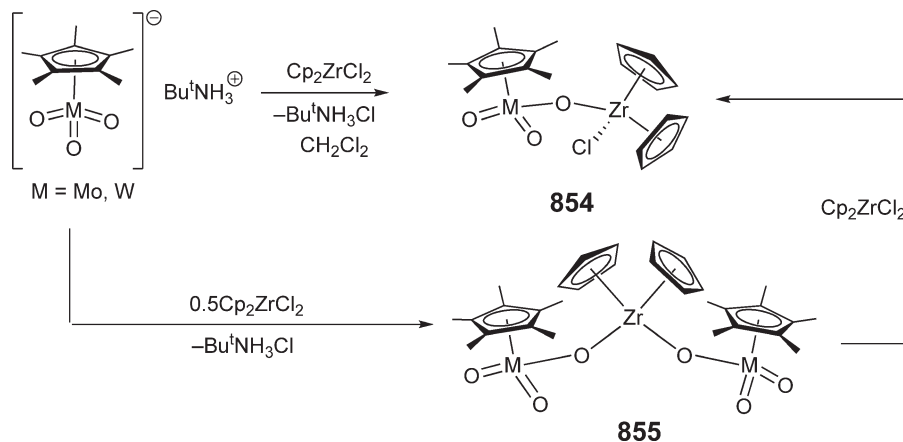
Heterobimetallic  $\mu$ -oxo complexes **854** are formed via halide displacement reactions between trioxo anions such as  $[\text{Cp}^*\text{M}(\text{O})_3]^-$  ( $\text{M} = \text{Mo}, \text{W}$ ) and  $\text{Cp}_2\text{ZrCl}_2$ <sup>655</sup> (Scheme 214). The corresponding heterotrinnuclear complexes **855** are obtained by addition of 2 equiv. of trioxoanion complexes to zirconocene dichloride. Other heterobimetallic complexes such as  $\mu^2\text{-}\eta^3\text{-CO}_2$ -bridged ruthenium–zirconium and rhenium–zirconium complexes have also been prepared.<sup>656</sup>

The salt metathesis reaction of sodium fluorenone ketyl with  $\text{Cp}^*_2\text{ZrCl}_2$  in THF produces the corresponding zirconium fluorenone ketyl complex **856**<sup>657</sup> which was structurally characterized (Scheme 215). In the case of sodium benzophenone ketyl, further reaction between the ketyl radical and a  $\text{Cp}^*$  ligand takes place to give finally the ring-metallated zirconocene bis(alkoxide) complex **857**.

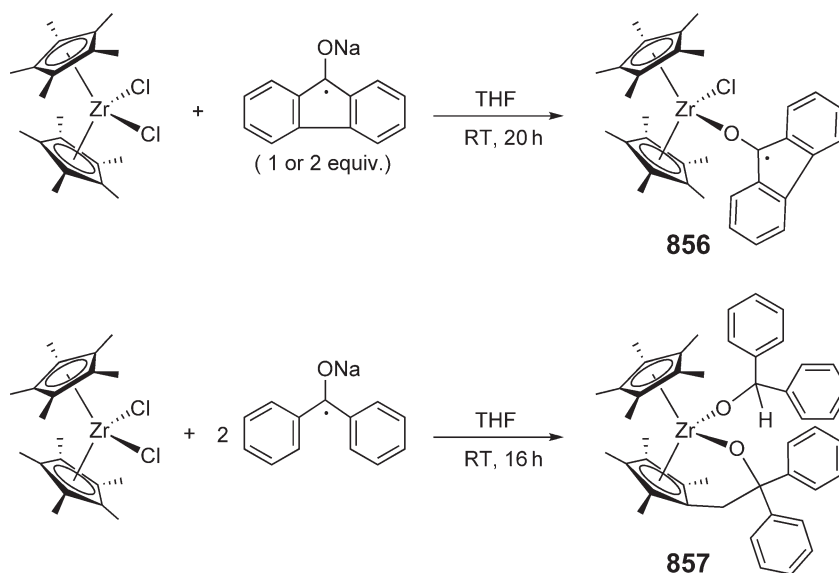
Chlorozirconocene mono(keto enolate)s can be readily obtained by the reaction of zirconocene dichloride with the *in situ*-generated or isolated lithium or potassium salt of enolates. For example, reactions of  $\text{Cp}_2\text{ZrCl}_2$  with 1 equiv. of the



Scheme 213

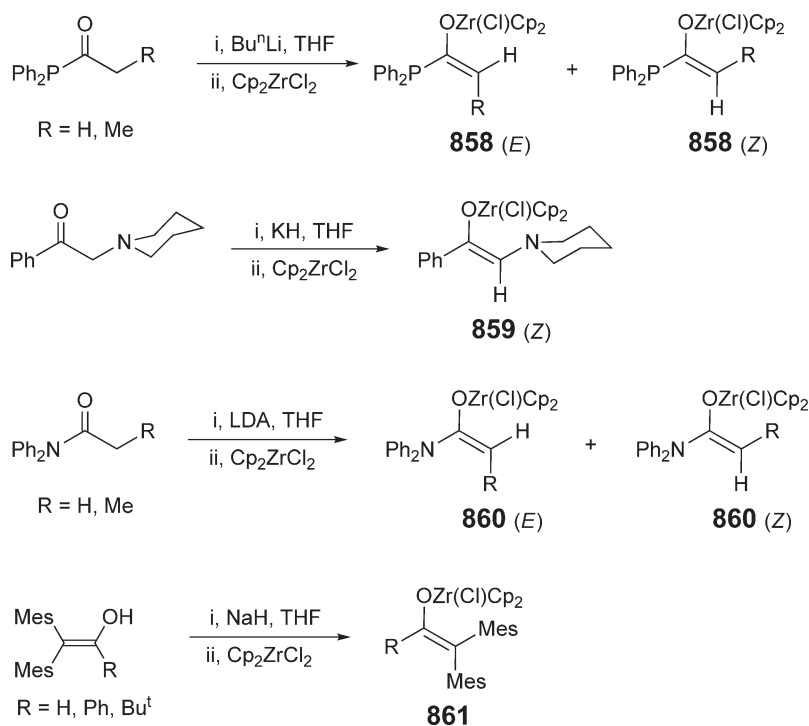


Scheme 214



Scheme 215

lithium  $\alpha$ -phosphino enolates lead to the corresponding zirconocene enolates **858** as mixtures of (*E*)- and (*Z*)-isomers<sup>658</sup> (Scheme 216). The (*E*)-isomer ( $R = \text{Me}$ ) has been structurally characterized by X-ray diffraction analysis. The reactivity of phosphino enolates **858** with benzaldehyde and acetophenone has been explored. On the other hand, the reaction of  $\text{Cp}_2\text{ZrCl}_2$  with the *in situ*-prepared potassium salt of  $\beta$ -keto amino enolate produces crystalline complex **859** as a single diastereomer (*Z*).<sup>659</sup> Chlorozirconocene amido enolates **860** as mixtures of (*E*)- and (*Z*)-isomers are obtained analogously.<sup>660</sup> With  $\beta,\beta$ -dimesitylenols, two routes can lead to the corresponding zirconocene enolates;<sup>661</sup> the first is the reaction of the  $\beta,\beta$ -dimesitylenols with  $\text{NaH}$  followed by addition of  $\text{Cp}_2\text{ZrCl}_2$ , yielding the chlorozirconocene

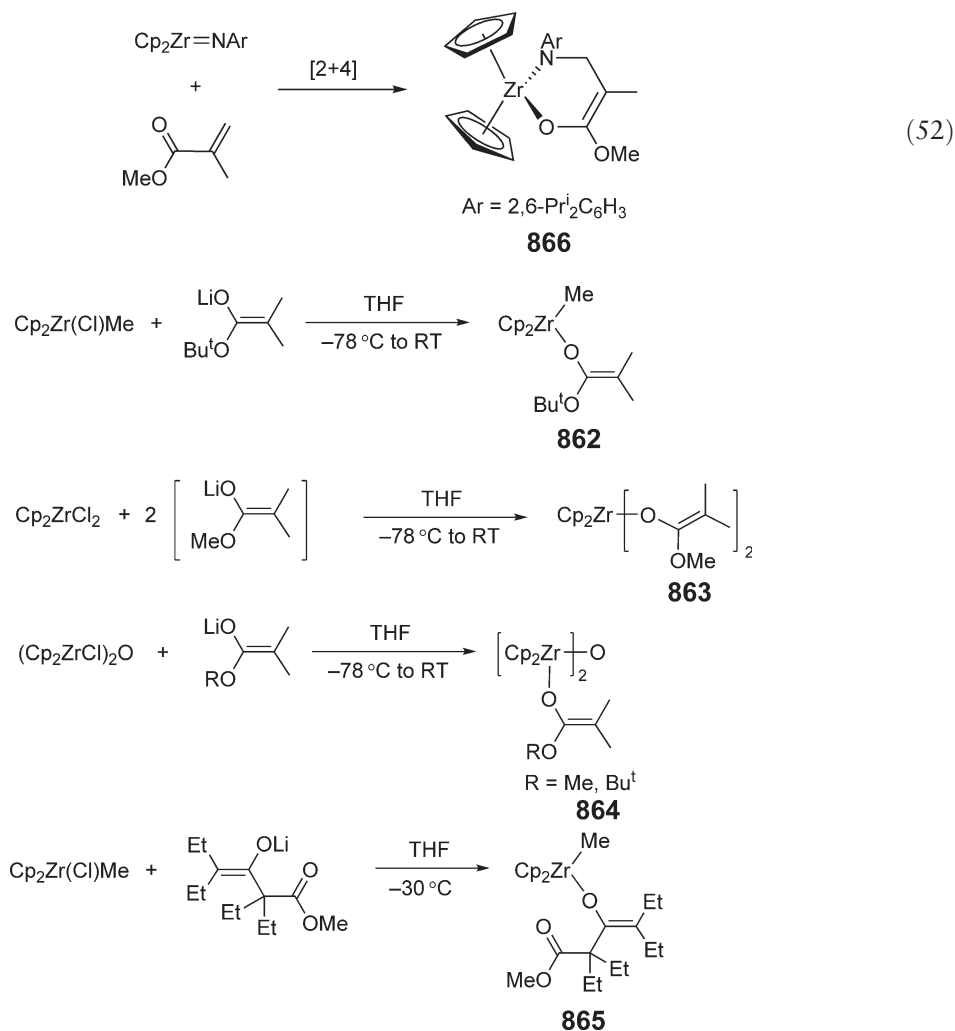


Scheme 216

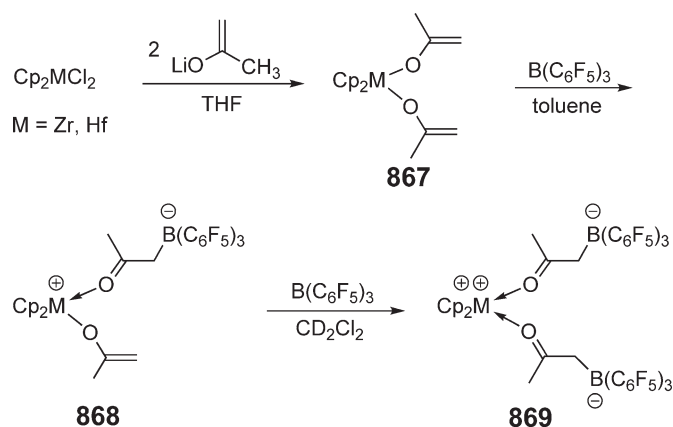
enolates **861**, (Scheme 216). The second route involves treatment of  $\beta,\beta$ -dimesitylenols directly with  $\text{Cp}_2\text{ZrMe}_2$ , affording the methyl zirconocene enolate derivative accompanied by elimination of methane.

Methyl zirconocene ester enolate  $\text{Cp}_2\text{ZrMe}[\text{OC}(\text{OBu}^t)=\text{CMe}_2]$  **862** can be readily obtained from the reaction of  $\text{Cp}_2\text{Zr}(\text{Cl})\text{Me}$  with 1 equiv. of  $\text{LiOC}(\text{OBu}^t)=\text{CMe}_2$ .<sup>662</sup> This complex exists as a viscous, yellow oil at ambient conditions; attempts to crystallize it under various conditions did not yield any success. The reaction of  $\text{Cp}_2\text{ZrCl}_2$  with 2 equiv. of  $\text{LiOC}(\text{OMe})=\text{CMe}_2$  leads to the formation of zirconocene bis(enolate) **863**, which can be converted to the corresponding cationic enolate species using  $[\text{HNEt}_3]\text{BPh}_4$  in THF at low temperatures.<sup>663</sup> Binuclear zirconocene ester enolates **864** are obtained in a similar manner using the  $\mu$ -oxo-bridged binuclear zirconocene chloride precursor<sup>664</sup> (Scheme 217). The cationic derivative of **864** ( $\text{R} = \text{Bu}^t$ ), generated by protonolysis of the bis(enolate) with  $[\text{HNMe}_2\text{Ph}][\text{B}(\text{C}_6\text{F}_5)_4]$  at low temperatures, functions as an effective initiator for the controlled polymerization of methyl methacrylate, analogous to a two-component, parent-Cp zirconocene-based initiator system. Attempts to synthesize a crystalline zirconocene ester enolate led to an unexpected result. Specifically, crystals of the zirconocene  $\beta$ -keto ester enolate **865** were obtained by using methyl 2-ethylbutyrate instead of *tert*-butylisobutyrate in the described reaction sequence for the preparation of **862**.<sup>665</sup> Treatment of methyl-2-ethylbutyrate with 1 equiv. of LDA is proposed to cause an ester condensation to form a  $\beta$ -keto ester, subsequent reaction of which with  $\text{Cp}_2\text{Zr}(\text{Cl})\text{Me}$  gives the crystalline zirconocene  $\beta$ -keto ester enolate **865**.

A convenient synthesis of zirconocene cyclic ester enolates such as complex **866** is the direct  $[2+4]$ -type cycloaddition reaction between the zirconocene imido complex and methyl methacrylate<sup>666</sup> (Equation (52)). The resulting cyclic ester enolate can be activated by the Lewis acid  $\text{Al}(\text{C}_6\text{F}_5)_3$  for efficient polymerization of methyl methacrylate.



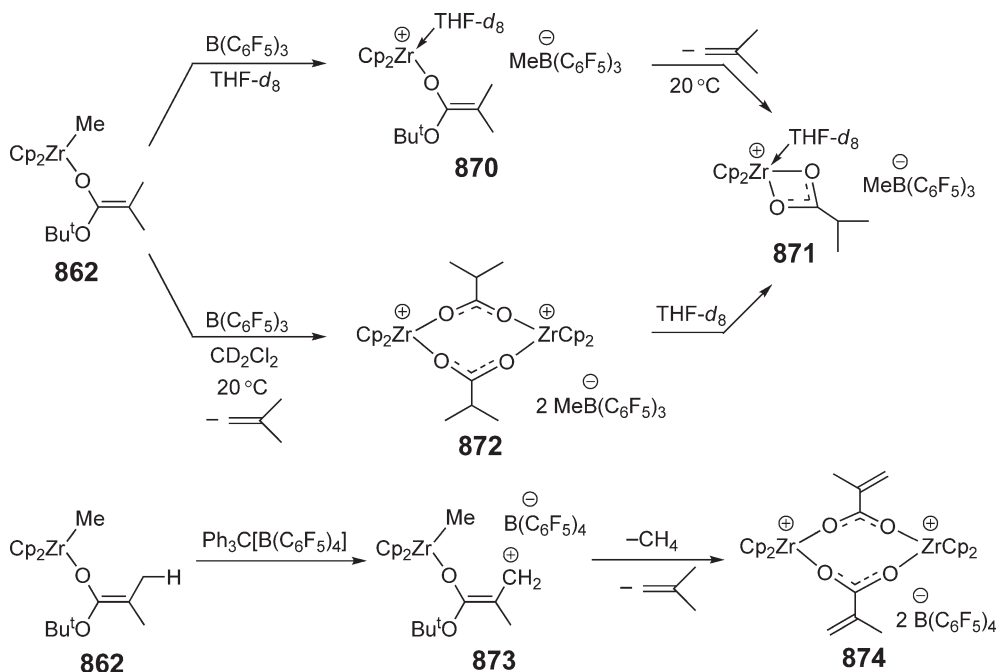
Scheme 217



Scheme 218

Electrophilic addition of 1 or 2 equiv. of  $\text{B}(\text{C}_6\text{F}_5)_3$  zirconocene and hafnocene bis(keto enolate) complexes **867** forms the corresponding addition products **868** and **869**, respectively (Scheme 218).<sup>667</sup> The molecular structure of the dication-like bis(adduct) **869** has been determined by X-ray diffraction analysis. The mono-adducts **868** undergo a thermally induced intramolecular aldol condensation. Nevertheless, mixtures of bis(enolate) **867** and  $\text{B}(\text{C}_6\text{F}_5)_3$ , in ratios ranging from 1 : 1 to 1 : 4, give increasingly active catalyst systems for the polymerization of methyl vinyl ketone which proceeds by a group-transfer mechanism.

The reaction of the methyl zirconocene ester enolate  $\text{Cp}_2\text{ZrMe}[\text{OC}(\text{O}^t\text{Bu})=\text{CMe}_2]$  **862** with 1 equiv. of  $\text{B}(\text{C}_6\text{F}_5)_3$  in THF at  $0^\circ\text{C}$  leads to the selective formation of the cationic enolate complex **870**<sup>668</sup> (Scheme 219). The cation of this ion pair decomposes rapidly at  $20^\circ\text{C}$  in THF with concomitant elimination of 1 equiv. of isobutene to form the cationic zirconocene carboxylate species **871**. The same reaction in  $\text{CD}_2\text{Cl}_2$  leads to the direct, rapid formation of the dimeric  $\mu$ -isobutyrate-zirconocene dicationic species **872**, which also gives carboxylate complex **871** upon dissolution in THF. However, when the ester enolate **862** is treated with  $[\text{Ph}_3\text{C}][\text{B}(\text{C}_6\text{F}_5)_4]$ , a 15 : 85 mixture of the dicationic



Scheme 219



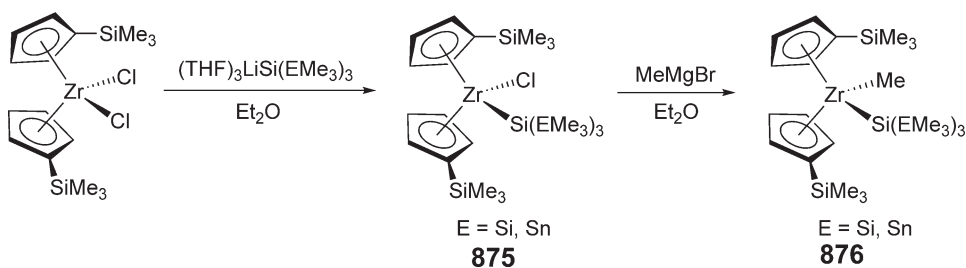
complexes **872** and **874** was obtained. The formation of **874** is proposed to arise from an initial hydride abstraction from a methyl enolate group by  $\text{Ph}_3\text{C}^+$  to give intermediate **873**, followed by subsequent elimination of methane and isobutene (Scheme 219).

#### 4.08.9.7 Complexes with M–Si Bonds

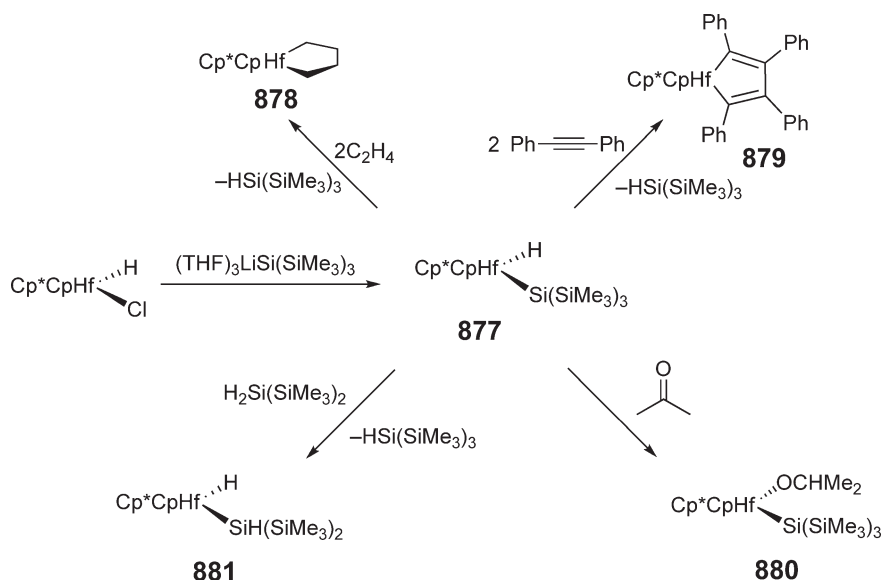
The silyl chlorozirconocene complexes **875** were obtained by the reaction of the zirconocene dichloride with a silyl Li reagent<sup>669</sup> (Scheme 220). Methylation of such complexes with  $\text{MeMgBr}$  affords silyl methylzirconocene complexes **876**. Complex **875** ( $\text{E} = \text{Si}$ ) is a catalyst for the dehydropolymerization of both  $\text{PhSiH}_3$  and  $\text{Bu}^n_2\text{SnH}_2$  to relatively low molecular weight polymers.

Mixed  $\text{Cp}^*/\text{Cp}$  hafnocene silyl hydride complex  $\text{Cp}^*\text{CpHfH}[\text{Si}(\text{SiMe}_3)_3]$  **877** was obtained by the reaction of  $\text{Cp}^*\text{CpHf}(\text{H})\text{Cl}$  with  $(\text{THF})_3\text{LiSi}(\text{SiMe}_3)_3$ <sup>670</sup> (Scheme 221). This complex reacts rapidly both ethylene and diphenylacetylene with elimination of  $\text{HSi}(\text{SiMe}_3)_3$  to afford the corresponding hafnacyclopentane **878** and tetraphenylhafnacyclopentadiene **879** complexes. The silyl hydride complex **877** also reacts with acetone to give the insertion product **880** and with the secondary silane  $\text{H}_2\text{Si}(\text{SiMe}_3)_2$  to afford the new silyl hydride complex  $\text{Cp}^*\text{CpHf}[\text{SiH}(\text{SiMe}_3)_2]\text{H}$  **881**, which was structurally characterized. The silane  $\text{H}_2\text{Si}(\text{SiMe}_3)_2$  undergoes a similar  $\sigma$ -bond metathesis reaction with  $\text{Cp}^*\text{CpHfCl}[\text{Si}(\text{SiMe}_3)_3]$  to give  $\text{Cp}^*\text{CpHfCl}[\text{SiH}(\text{SiMe}_3)_2]$ .

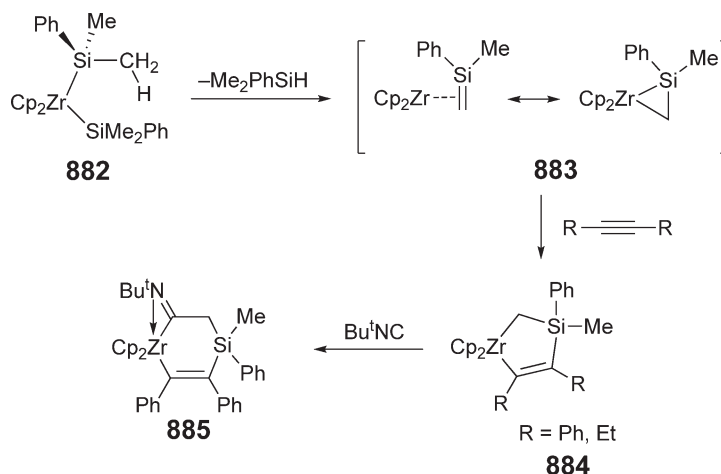
Insertion reaction of alkyne and zirconium–silene complexes **883**, which are generated from disilylzirconocenes **882** prepared from the reaction of zirconocene dichloride with 2 equiv. of  $\text{Me}_2\text{PhSiLi}$ , affords



Scheme 220



Scheme 221

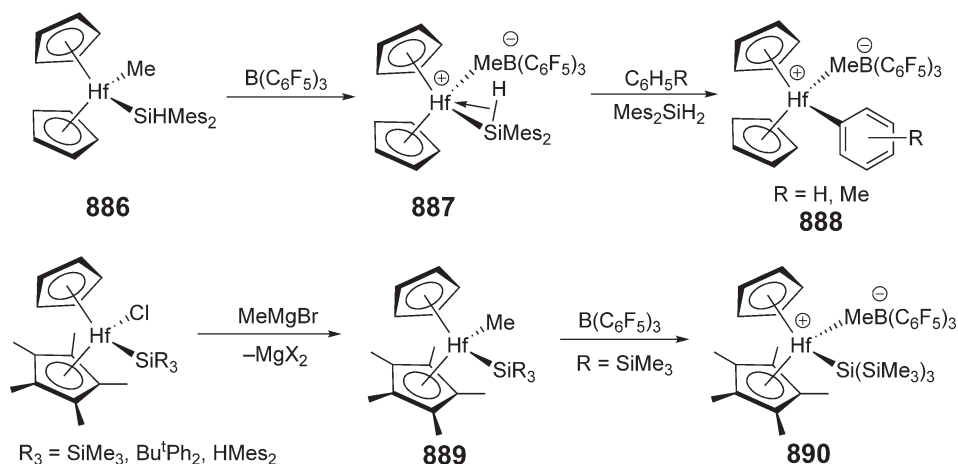


Scheme 222

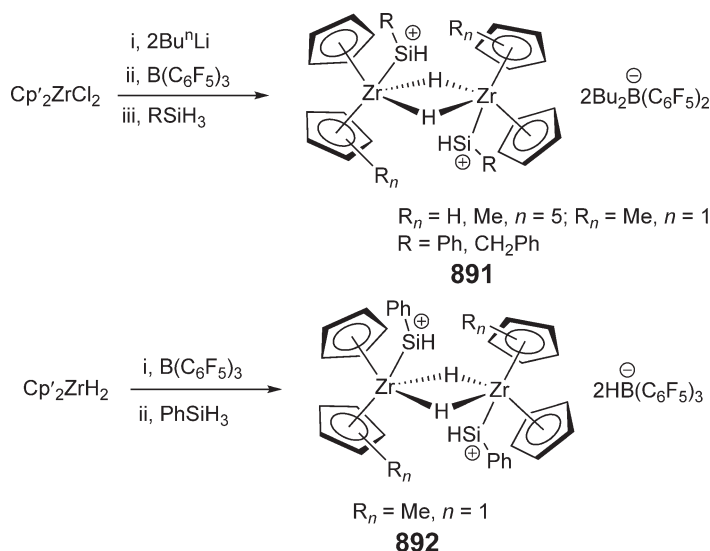
silazirconacyclopentenes **884** (Scheme 222).<sup>671</sup> The reaction of silazirconacyclopentenes **884**, with *tert*-butyl isocyanide leads to iminosilazirconacyclohexene **885**.<sup>672</sup>

The reaction of  $\text{Cp}_2\text{HfMe}(\text{SiMe}_2\text{H})$  **886** with  $\text{B}(\text{C}_6\text{F}_5)_3$  produces the corresponding zwitterionic species **887** which is stable for >8 h at  $-40^\circ\text{C}$  in toluene and possesses an  $\alpha$ -agostic Si–H interaction<sup>673</sup> (Scheme 223). At room temperature, the cationic complex **887** reacts with the C–H bonds of aromatic hydrocarbons such as benzene and toluene to produce the  $\sigma$ -bond metathesis product (**888**, all isomers with  $\text{R} = \text{Me}$ ). Activation of the mixed-ring silyl methyl complexes **889** ( $\text{R} = \text{SiMe}_3$ ) with  $\text{B}(\text{C}_6\text{F}_5)_3$  in bromobenzene-*d*<sub>5</sub> produces rapidly the corresponding zwitterionic Hf silyl complex  $[\text{CpCp}^*\text{HfSi}(\text{SiMe}_3)_3][\text{MeB}(\text{C}_6\text{F}_5)_3]$  **890**, which is stable for at least 12 h in solution.<sup>674</sup> However, reactions of the other two complexes of type **889** ( $\text{R} = \text{Bu}^t\text{Ph}_2$ ,  $\text{HMe}_2$ ) with  $\text{B}(\text{C}_6\text{F}_5)_3$  result in the formation of unidentified Hf-containing species, along with the quantitative production of  $\text{HSiR}_3$ . The same reactions with bis(Cp) hafnocene silyl methyl complexes give the corresponding cationic Hf silyl complexes. Addition of  $\text{PhSiH}_3$  to the hafnium complex **890** produces  $\text{CpCp}^*\text{HfH}(\mu\text{-H})\text{B}(\text{C}_6\text{F}_5)_3$ ,  $\text{HSi}(\text{SiMe}_3)_3$ , and oligomeric silane products.

The use of  $\text{B}(\text{C}_6\text{F}_5)_3$  as a co-catalyst in the dehydrocoupling of phenylsilane by the  $\text{Cp}'_2\text{ZrCl}_2/2\text{Bu}^n\text{Li}$  system leads to suppression of chain scission reactions and to an increase in polysilane chain length.<sup>675</sup> The formation of hydrido-bridged dimers **891**, which incorporate a cation-like silylium ligand on each zirconium, was observed spectroscopically from the reaction of dichlorozirconocenes with  $\text{Bu}^n\text{Li}$  and  $\text{B}(\text{C}_6\text{F}_5)_3$ , followed by the addition of silanes (Scheme 224). Analogous catalysts such as **892** can also be obtained by the reaction of hydridozirconocene with  $\text{B}(\text{C}_6\text{F}_5)_3$ , followed by addition of silanes.<sup>676</sup>



Scheme 223



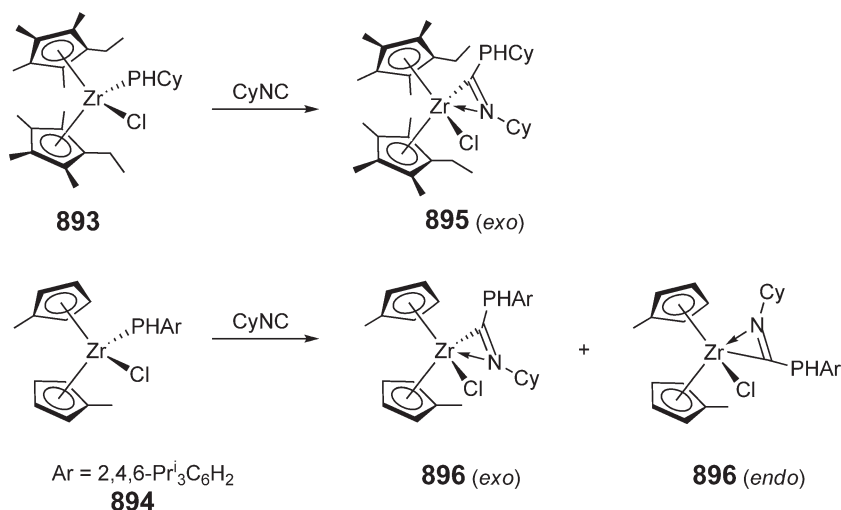
Scheme 224

#### 4.08.9.8 Complexes with M–P Bonds

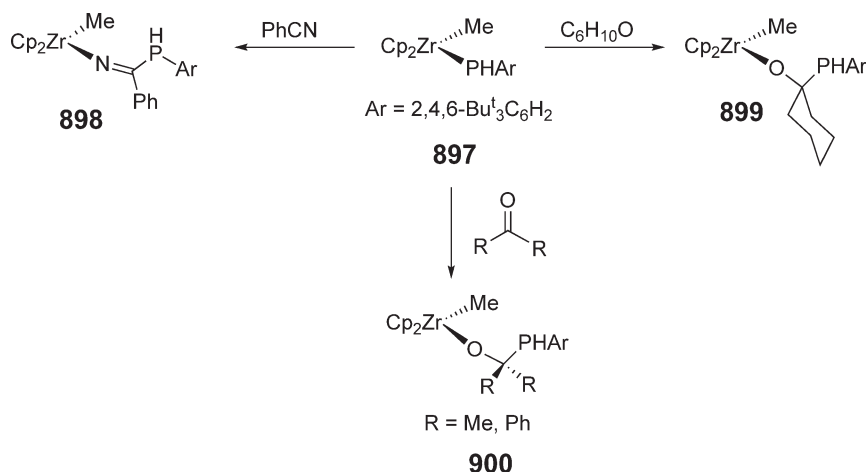
Both primary phosphido chlorozirconocene complexes **893** and **894** readily insert  $\text{CyNC}$  to give zirconocene  $\eta^2$ -iminoacyl complexes **895** and **896**<sup>677</sup> respectively (Scheme 225). Of the two possible coordination modes of the ligand, complex **895** is obtained exclusively as the *exo*-isomer, in which the  $\text{NCy}$  group is adjacent to the  $\text{Zr-Cl}$  bond, whereas for complex **896**, both isomers are formed in a ratio 1 : 1.5 whereby the *endo*-isomer is favored.

The reactivity of primary phosphido zirconocene methyl<sup>678</sup> and chloride<sup>679</sup> complexes has been investigated. For example, reactions of  $\text{Cp}_2\text{ZrMe(PHAr)}$  (**897**:  $\text{Ar} = 2,4,6\text{-Bu}_3\text{C}_6\text{H}_2$ ), prepared from the reaction of  $\text{Cp}_2\text{ZrMeCl}$  and  $\text{LiPHAr}$ , with benzonitrile, cyclohexanone, and ketones result in the insertion of these organic substrates into the  $\text{Zr-P}$  bond in **897** to form the corresponding insertion products **898**, **899**, and **900**, respectively (Scheme 226). The analogous methylzirconocene phosphide complex  $\text{Cp}_2\text{ZrMe(PHAr)}$  ( $\text{Ar} = 2,4,6\text{-Me}_3\text{C}_6\text{H}_2$ ) was also obtained reacting  $\text{Cp}_2\text{ZrMe}_2$  with  $\text{H}_2\text{PHAr}$ ; however, this complex reacts further with  $\text{Cp}_2\text{ZrMe}_2$  to generate the bimetallic species  $(\text{Cp}_2\text{ZrMe})_2(\mu\text{-PHAr})$ .

The less bulky primary phosphido methylzirconocene complex  $\text{Cp}_2\text{ZrMe(PHAr)}$  (**901**:  $\text{Ar} = 2,4,6\text{-Me}_3\text{C}_6\text{H}_2$ ) is thermally unstable with respect to methane elimination; in the presence of  $\text{PMe}_3$ , this reaction produces the terminal



Scheme 225

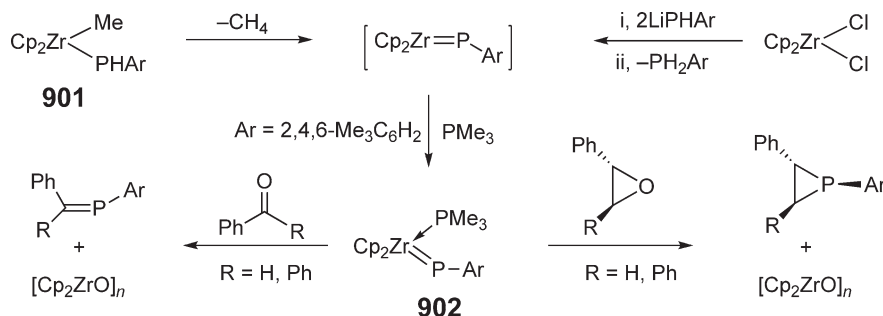


Scheme 226

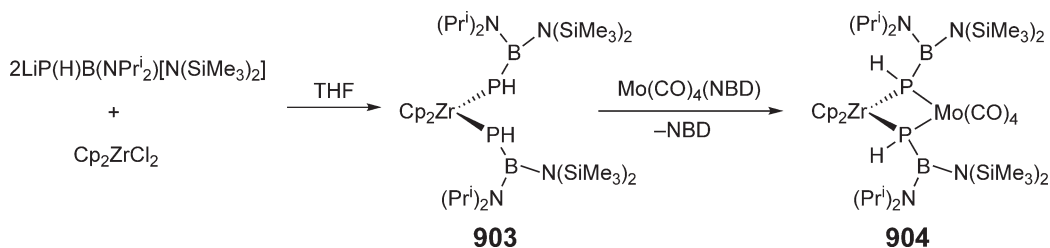
zirconocene phosphinidene complex  $\text{Cp}_2\text{Zr}=\text{PAr}(\text{PMe}_3)$  (**902**;  $\text{Ar} = 2,4,6\text{-Me}_3\text{C}_6\text{H}_2$ ).<sup>680</sup> Alternately, the phosphinidene complex **902** can also be obtained from either  $\text{Cp}_2\text{ZrCl}_2$  or  $\text{Cp}_2\text{Zr}(\text{PAr})\text{Cl}$ .<sup>681</sup> Reactions of **902** with benzophenone or benzaldehyde produce phosphalkenes and the byproduct  $[\text{Cp}_2\text{Zr}=\text{O}]_n$  (Scheme 227). Phosphinidene group transfer also takes place in the reaction of **890** with appropriate epoxides to give phosphiranes; the use of propylene oxide yields the enolate species  $\text{Cp}_2\text{Zr}(\text{PAr})(\text{OCH}_2\text{CH}=\text{CH}_2)$ . Furthermore, additions of  $\text{PhEH}$  ( $\text{E} = \text{O}, \text{S}$ ),  $\text{PhEH}_2$  ( $\text{E} = \text{N}, \text{P}$ ),  $\text{MesPH}_2$ , or  $\text{Ph}_2\text{PH}$  to  $\text{Cp}_2\text{Zr}=\text{PAr}(\text{PMe}_3)$  ( $\text{Ar} = 2,4,6\text{-Bu}_3\text{C}_6\text{H}_2$ ) provide a facile route to complexes of the form  $\text{Cp}_2\text{Zr}(\text{PAr})(\text{ER}^1\text{R}^2)$ .<sup>682</sup> These complexes show facile metal-mediated inversion at phosphorus as well as rapid rotation about the  $\text{Zr}-\text{E}$  bonds at room temperature. The terminal phosphinidene complex  $\text{Cp}_2\text{Zr}=\text{PAr}(\text{PMe}_3)$  ( $\text{Ar} = 2,6\text{-Mes}_2\text{C}_6\text{H}_3$ ) has also been prepared.<sup>683</sup>

Terminal primary arylphosphido zirconocene complexes  $\text{Cp}_2\text{ZrCl}(\text{PAr})$  ( $\text{Ar} = 2,6\text{-Mes}_2\text{C}_6\text{H}_3$ ) and  $\text{Cp}_2\text{Zr}(\text{PAr})_2$  bearing the sterically demanding  $2,6\text{-Mes}_2\text{C}_6\text{H}_3$  ligand have been synthesized and structurally characterized.<sup>684</sup> A flattened pyramidal geometry for the P atom of  $\text{Cp}_2\text{ZrCl}(\text{PAr})$  and a shortened  $\text{Zr}-\text{P}$  bond length of 2.638(1) Å provide evidence for moderate  $\text{Zr}-\text{P}$   $\pi$ -bonding. In the case of  $\text{Cp}_2\text{Zr}(\text{PAr})_2$ , both pyramidal and planar P atoms are observed. Taken together with these P geometries, the corresponding  $\text{Zr}-\text{P}$  bond lengths of 2.726(2) and 2.519(2) Å indicate that one phosphido ligand is engaged in substantial  $\pi$ -bonding to the Zr center while almost no such interactions are present for the other phosphido ligand. The solid-state structures of these two complexes are very different from the derivatives with less bulky ligands such as  $\text{Ar} = 2,4,6\text{-Bu}_3\text{C}_6\text{H}_2$ .

Zirconocene bis(phosphido) complexes  $(\text{C}_5\text{H}_4\text{SiMe}_3)_2\text{Zr}(\text{PPh}_2)_2$  and  $\text{Cp}^*\text{CpZr}(\text{PPh}_2)_2$  have been synthesized by salt metathesis.<sup>685</sup> The reaction of the structurally characterized  $(\text{C}_5\text{H}_4\text{SiMe}_3)_2\text{Zr}(\text{PPh}_2)_2$  with the rhodium complex  $\text{Rh}_2(\mu\text{-S-Bu}^t)_2(\text{CO})_4$  affords the heterometallic complex  $(\text{C}_5\text{H}_4\text{SiMe}_3)_2\text{Zr}(\mu\text{-PPh}_2)_2[\text{Rh}(\mu\text{-S-Bu}^t)_2\text{Rh}](\mu\text{-PPh}_2)_2\text{Zr}(\text{C}_5\text{H}_4\text{SiMe}_3)_2$ , which serves as catalyst for hydroformylation of 1-hexene. The reaction of  $\text{Cp}_2\text{ZrCl}_2$  with 2 equiv. of  $\text{LiP}(\text{H})\text{B}(\text{NPr}^i)_2[\text{N}(\text{SiMe}_3)_2]\text{DME}$  yields a crystalline metallobis(borylphosphane) complex **903**.<sup>686</sup>



Scheme 227

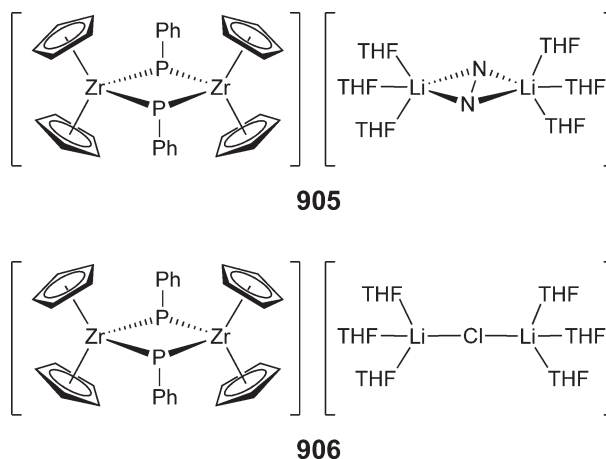


Scheme 228

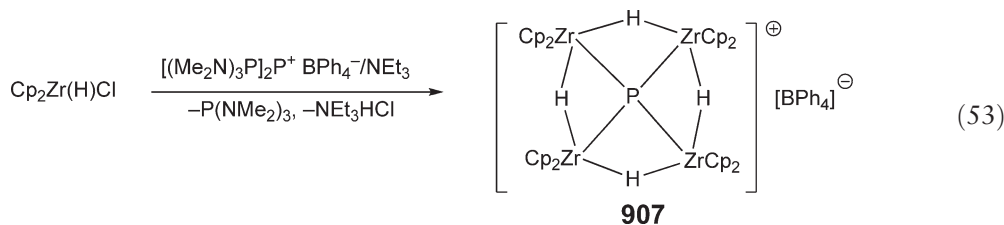
(Scheme 228). This complex acts as a chelating ligand in its reaction with  $\text{Mo(CO)}_4(\text{norbornadiene})$ , affording the heterobimetallic adduct **904**. Both complexes have been structurally characterized by X-ray diffraction analysis.

Triphosphanato zirconocene complexes  $\text{Cp}_2\text{M(P}_3\text{R}_3)$  ( $\text{M} = \text{Zr}$ ,  $\text{R} = \text{Ph}$ ;  $\text{M} = \text{Hf}$ ,  $\text{R} = \text{Cy}$ ) and  $\text{Cp}^*_2\text{Zr(P}_3\text{Cy}_3)$  have been prepared by the reaction of metallocene dihalides with appropriate primary lithium or potassium phosphides; these complexes have been structurally characterized.<sup>687</sup> These complexes are also accessible via activation of the P–H bonds of a primary phosphine by zirconocene(II). The reaction of  $\text{Cp}_2\text{ZrCl}_2$  with the phosphide  $\text{LiP(H)Ph}$  in the presence of  $\text{NEt}_4\text{Br}$  affords the species  $[\text{Cp}_2\text{ZrBr(P(H)Ph)}_2][\text{NEt}_4]$ , the results of which suggest a mechanism of formation of the  $\text{M(PR)}_3$  derivatives involving phosphinidene  $\text{M=PR}$  and  $\text{M(PR)}_2$  intermediates.

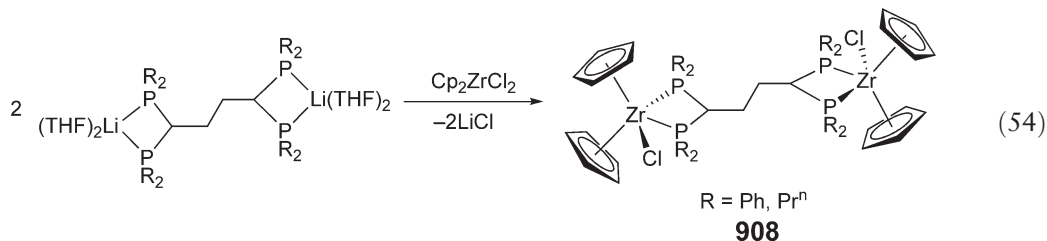
Treatment of a mixture of  $\text{PPhH}_2$  and 2 equiv. of  $\text{Bu}^n\text{Li}$  in THF with  $\text{Cp}_2\text{ZrCl}_2$  yields the dinitrogen complex  $[\text{Cp}_2\text{Zr}(\mu\text{-PPh})_2][(\text{THF})_3\text{Li}]_2(\mu\text{-N}_2)$  **905**.<sup>688</sup> This complex was initially assigned to contain a Zr(III) phosphinidene dianion,  $[\text{Cp}_2\text{Zr}(\mu\text{-PPh})_2]^{2-}$ , and the dication  $\{[(\text{THF})_3\text{Li}]_2(\mu\text{-N}_2)\}^{2+}$ ; however, a later study with  $[\text{Cp}_2\text{Zr}(\mu\text{-PPh})_2][(\text{THF})_3\text{Li}]_2(\mu\text{-Cl})$  **906**<sup>689</sup> which contains the identical anion and a similar cation, concluded that the anion part of these complexes is actually the mixed valence  $[\text{Zr(III)Zr(IV)}]$  monoanion. Therefore, the  $[(\text{THF})_3\text{Li}]_2(\mu\text{-N}_2)$  cation is also singly charged, which can be regarded as a complex of  $\text{N}_2$  with the pair  $(\text{Li} \cdots \text{Li})^+$  or that of  $\text{N}_2^-$  stabilized by two  $\text{Li}^+$  cations.



Treatment of 9 equiv. of  $[\text{Cp}_2\text{Zr(H)Cl}]$  with 1 equiv. of  $\{[(\text{Me}_2\text{N})_3\text{P}]_2\text{P}^+\}[\text{BPh}_4^-]$  in THF and the presence of  $\text{Et}_3\text{N}$  affords the cationic zirconocene phosphonium complex **907** in 11% yield<sup>690</sup> (Equation (53)). The crystal structure of this complex reveals a remarkable planar-tetracoordinate phosphorus atom in the cation, along with its isoelectronic, classical tetraphenyl borate counterion. The eight-membered  $\text{Zr}_4\text{H}_4$  cycle is almost planar and can be regarded as an “anti-crown ether” ligand for the phosphorus cation.

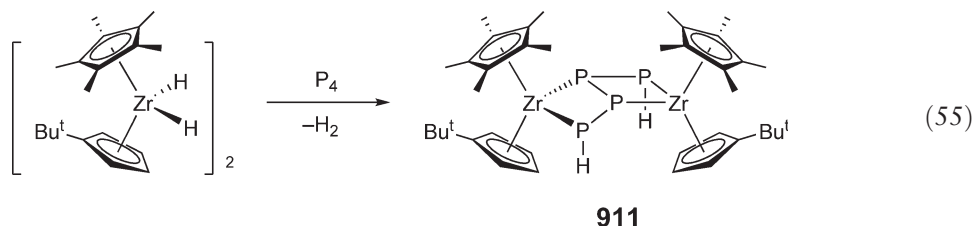


The binuclear chlorozirconocene **908** linked by the dianionic bis(diphosphinomethanide) ligand is obtained in high yield by the reaction of  $\text{Cp}_2\text{ZrCl}_2$  with the THF adduct of  $[\text{Li}\{(\text{R}_2\text{P})_2\text{CCH}_2\}]_2$  ( $\text{R} = \text{Ph}, \text{Pr}^n$ ) according to Equation (54).<sup>691</sup> The molecular structures of complexes **908** show that the zirconocenium atoms are asymmetrically bound at each end of the phosphinomethanide ligands in a *P,P*-bidentate fashion to give four-membered chelate rings.



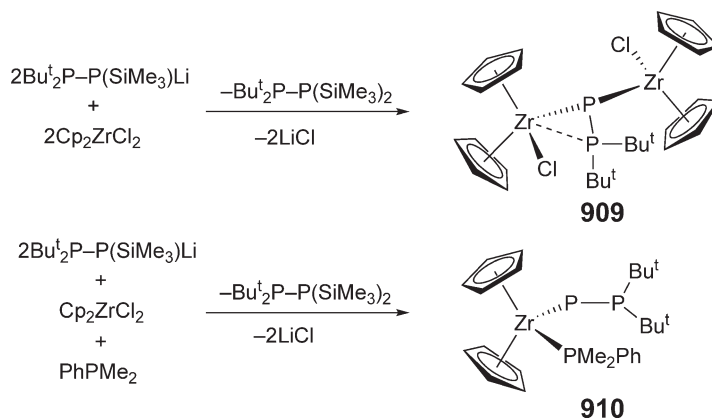
The reaction  $\text{Cp}_2\text{ZrCl}_2$  with lithiated diphosphines such as  $\text{Bu}^t_2\text{P}-\text{P}(\text{SiMe}_3)\text{Li}$  in  $\sim 1:1$  ratio produces binuclear chlorozirconocene phosphino–phosphinidene complex  $\mu-(1,2,2-\eta\text{-Bu}^t_2\text{P}=\text{P})[\text{Zr}(\text{Cl})\text{Cp}_2]_2$  **909**<sup>692</sup> (Scheme 229). The same reaction in a 1:2 molar ratio in the presence of an excess of  $\text{PPhMe}_2$  yields a terminally bonded phosphino–phosphinidene complex **910**. Both complexes have been structurally characterized.

Hydrogenation of white phosphorus ( $\text{P}_4$ ) was achieved under ambient conditions using its reaction with zirconocene dihydride complex to give the functionalized derivative **911** according to Equation (55).<sup>693</sup> The molecular structure shows a binuclear zirconium complex with a puckered, bicyclic  $\text{Zr}_2\text{P}_4$  core, having a  $[\text{P}_4\text{H}_2]^{4-}$  fragment and two formally 16-electron zirconium(IV) centers. Somewhat surprisingly, the two sterically demanding  $\text{Cp}^*$  ligands are arranged in a *cis*-like fashion, although the pyramidalization of the  $\text{P}_4\text{H}_2$  unit serves to minimize unfavorable steric interactions between the  $\text{Cp}^*$  rings.

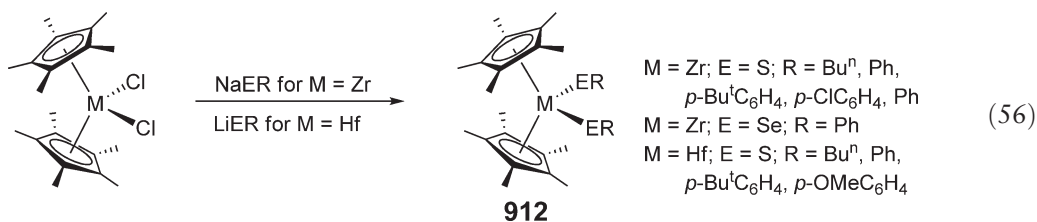


#### 4.08.9.9 Complexes with M–E (S, Se, Te) Bonds

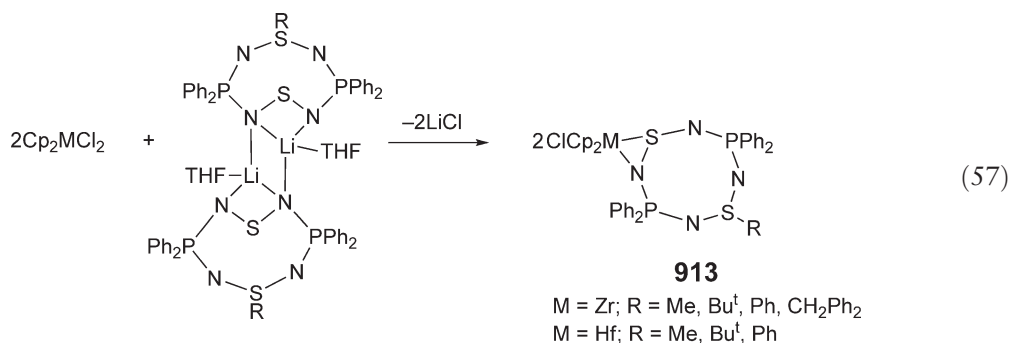
A series of zirconocene bis(thiolate) complexes (**912**, Equation (56)) has been synthesized by the reaction of  $\text{Cp}^*_2\text{ZrCl}_2$  with  $\text{NaER}$  and shown to exhibit rich luminescence behavior.<sup>694</sup> The crystal structure of  $\text{Cp}^*_2\text{Zr}(\text{SBu}^n)_2$  has been determined by X-ray diffraction. Unlike the zirconocene analogs, the reaction of  $\text{Cp}^*_2\text{HfCl}_2$  with  $\text{NaER}$  did not lead to the desired  $\text{Cp}^*_2\text{Hf}(\text{ER})_2$  complexes, but only to the monosubstituted derivatives  $\text{Cp}^*_2\text{Hf}(\text{ER})\text{Cl}$ . On the other hand, the use of  $\text{LiSR}$  in DME produces the hafnocene bis(thiolate) complexes shown in Equation (56).<sup>695</sup> The structures of these hafnocene complexes have been determined; these compounds also exhibit rich luminescence behavior.



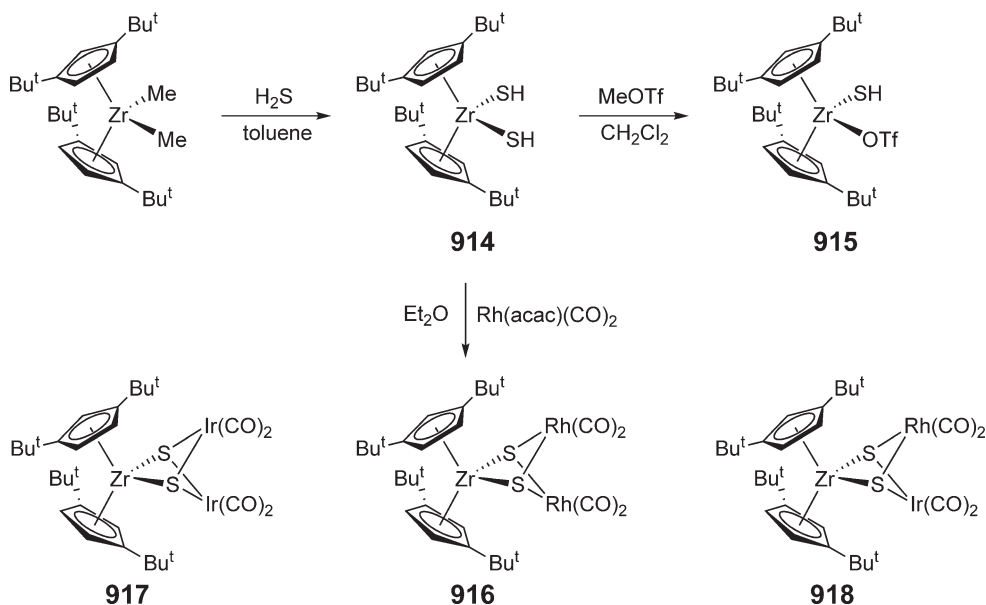
Scheme 229



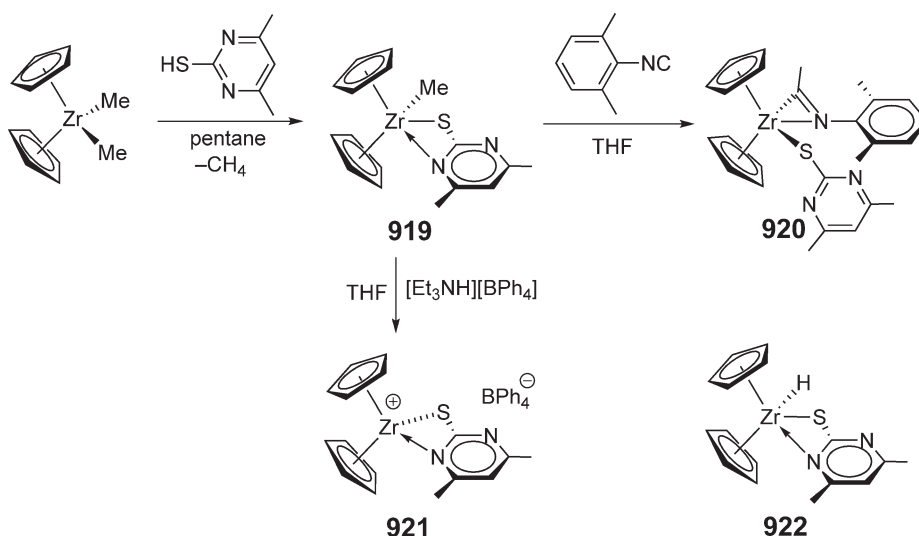
The metallocene complex **913** of the unsaturated  $\text{P}_2\text{N}_4\text{S}_2$  ring is obtained by the reaction  $\text{Cp}_2\text{ZrCl}_2$  with  $[\text{Li}(\text{Ph}_4\text{P}_2\text{N}_4\text{S}_2\text{Bu}^t)]_2$  in THF (Equation (57)).<sup>696</sup> These complexes contain a heterocyclic ring asymmetrically bonded to the metal through a bidentate- $N,S$  bonding mode. A regiospecific functionalization of the  $\text{P}_2\text{N}_4\text{S}_2$  ring is accomplished by the reaction of **913** with electrophiles such as  $\text{Br}_2$ ,  $\text{MeI}$ , and  $\text{HCl}$ . Surprisingly, zirconyl complexes of this type do not react with strong nucleophiles such as  $\text{Li}[\text{Et}_3\text{BH}]$  or  $\text{MeLi}$ .<sup>697</sup>



Zirconocene bis(hydrosulfide) complex **914** is readily accessible from treatment of the corresponding zirconocene dimethyl precursor with  $\text{H}_2\text{S}$ <sup>698</sup> (Scheme 230). The reaction of **914** with  $\text{CF}_3\text{SO}_3\text{Me}$  gives the structurally characterized monohydrosulfido complex **915**, which exists as two isomers in solution. Complex **914** serves as an effective metallaligand for the controlled synthesis of trinuclear early–late heterobimetallic complexes such as **916** with a  $\text{ZrRh}_2$  core. Analogous trinuclear early–late heterobimetallic complex **917** with a  $\text{ZrIr}_2$  core and heterotrimetallic complex **918** with a  $\text{Zr-Rh-Ir}$  core have also been synthesized.<sup>699</sup>



Scheme 230

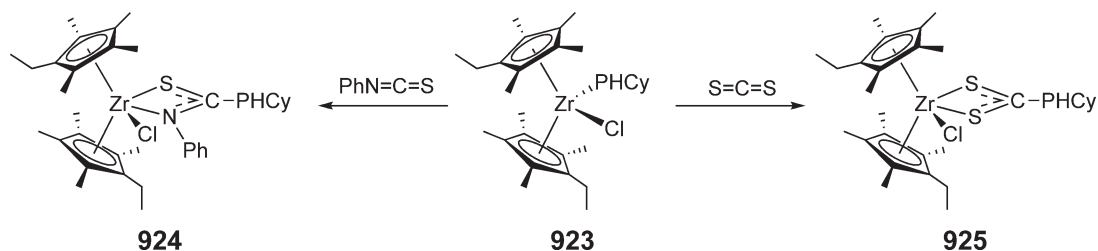


Scheme 231

The alkylzirconocene thiolate complex **919** is obtained by treatment of  $\text{Cp}_2\text{ZrMe}_2$  with 1 equiv. of 4,6-dimethyl-2-mercaptopyrimidine<sup>700</sup> (Scheme 231). The molecular structure of **919** shows that the thiolate ligand is bonded to Zr in an  $\eta^2$ -fashion through the S and one of the N atoms. Complex **919** undergoes insertion reaction with 2,6-dimethylphenyl isocyanide to yield the corresponding iminoacyl derivative **920** with the thiolate and iminoacyl ligand being  $\eta^1$ - and  $\eta^2$ -bonded, respectively. The reaction of the complex **919** with  $[\text{NHEt}_3]\text{BPh}_4$  produces the corresponding salt **921**. The hydride thiolate complex **922** is obtained by oxidative addition reaction of  $[\text{Cp}^*_2\text{Zr}]$  with 4,6-dimethyl-2-mercaptopyrimidine.

Insertion of  $\text{PhNCS}$  and  $\text{CS}_2$  into the Zr–P bond of the chlorozirconocene primary phosphido complex **923**, which is prepared by the reaction of the zirconocene dichloride with  $\text{LiPhCy}$ , yields the corresponding insertion products **924** and **925**, respectively (Scheme 232).<sup>701</sup> The molecular structure of the complex **924** confirms the  $\eta^2$ -bonding mode of the S,N-ligation.

A series of hafnium terminal chalcogenido complexes  $(\text{C}_5\text{Me}_4\text{R})_2\text{Hf}(=\text{E})(\text{NC}_5\text{H}_5)$  ( $\text{E} = \text{S}, \text{Se}, \text{Te}$ ;  $\text{R} = \text{Me}, \text{Et}$ ) was synthesized by the reactions of hafnocene dicarbonyl complexes with the chalcogens in the presence of pyridine.<sup>702</sup> The analogous zirconocene chalcogenido complexes **926** were obtained in a similar fashion (Scheme 233) and their reactivity was extensively examined, with emphasis on a variety of 1,2-addition and cycloaddition reactions to afford a diverse array of products.<sup>703</sup> The complete series of phenylchalcogenolato derivatives of permethylzirconocene  $\text{Cp}^*_2\text{Zr}(\text{EPh})_2$  (**927**:  $\text{E} = \text{O}, \text{S}, \text{Se}, \text{Te}$ ) has been prepared by the reactions of zirconocene dicarbonyl with  $\text{PhOH}$  or  $\text{Ph}_2\text{E}_2$  ( $\text{E} = \text{S}, \text{Se}, \text{Te}$ ) according to Scheme 233.<sup>704</sup> The molecular structures of all the derivatives as determined by X-ray diffraction analysis provide evidence that the nature of the bonding varies as a function of the chalcogen. Specifically, the structure of the phenoxo derivative is notably distinct from those of its heavier congeners. For example, whereas the Zr–E ( $\text{E} = \text{S}, \text{Se}, \text{Te}$ ) bond lengths are comparable to the sum of their respectively covalent radii, the Zr–O bond length is significantly shorter than the sum of the covalent radii, as would be anticipated due to an increased ionic contribution to the bonding. The Zr–O–C bond angle is effectively linear, whereas the Zr–E–C bond angles for the



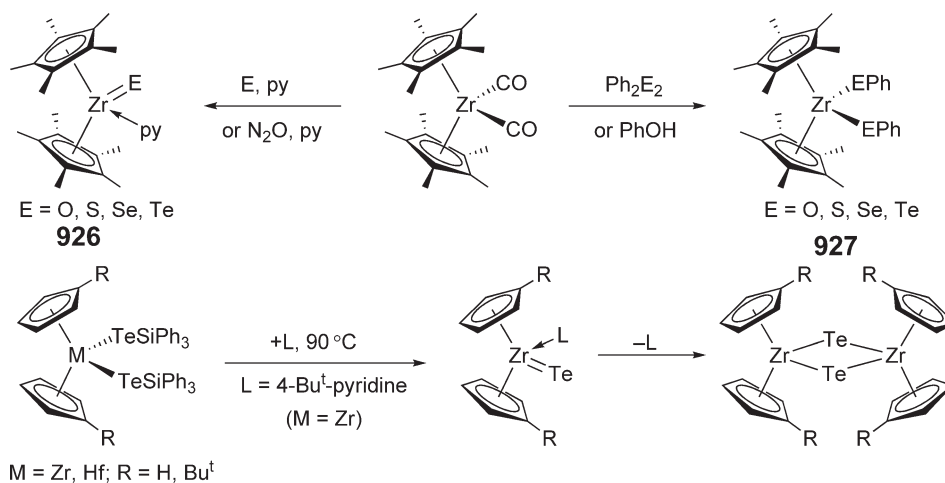
Scheme 232



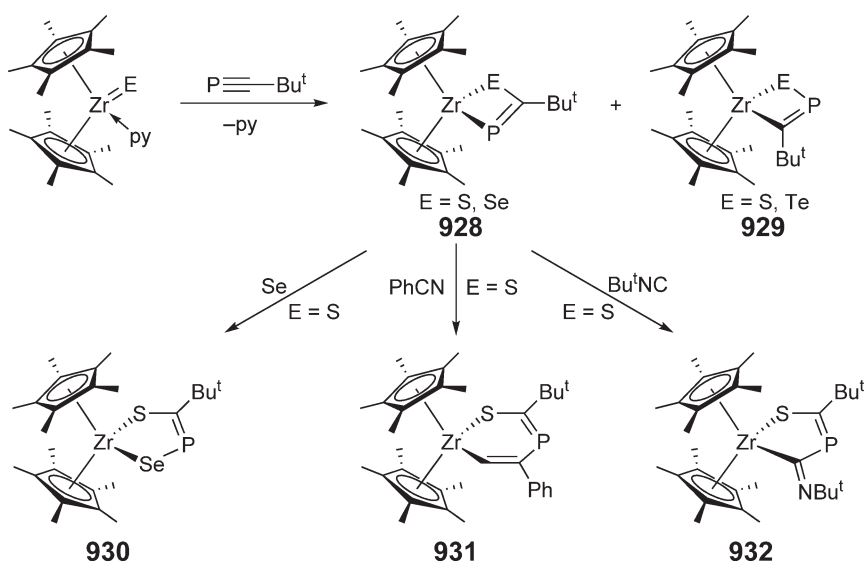
heavier congeners are significantly bent. However, comparison of the structure of  $\text{Cp}^*_2\text{Zr}(\text{OPh})_2$  with that of the less-substituted zirconocene derivative  $\text{Cp}_2\text{Zr}(\text{OPh})_2$ , which possesses a bent  $\text{Zr}-\text{O}-\text{C}$  moiety, suggests that the linearity of  $(\text{Cp}^*)_2\text{Zr}(\text{OPh})_2$  may be attributed to steric factors. Thus, short  $\text{M}-\text{OR}$  bond lengths and linear  $\text{M}-\text{O}-\text{R}$  angles are not necessarily a consequence of strong  $p\pi-d\pi$  lone pair donation from oxygen to the metal.

Treatment of  $\text{Cp}_2\text{MCl}_2$  ( $\text{M} = \text{Zr}, \text{Hf}$ ) with 2 equiv. of  $(\text{THF})_2\text{LiTeSi}(\text{SiMe}_3)_3$  produces metallocene bis(tellurolato) complexes  $\text{Cp}_2\text{M}[\text{TeSi}(\text{SiMe}_3)_3]_2$  in high yields.<sup>705</sup> The zirconium mono- and bis-tellurolates can also be obtained by tellurolysis of  $\text{Cp}_2\text{ZrMe}_2$  with 1 and 2 equiv. of  $\text{HTeSi}(\text{SiMe}_3)_3$ , respectively. Metallocene tellurolate derivatives  $\text{Cp}^R_2\text{M}(\text{TeSiPh}_3)_2$  ( $\text{M} = \text{Zr}, \text{Hf}$ ;  $\text{R} = \text{H}, \text{Bu}^t$ ) have also been prepared by treatment of the appropriate metallocene dichloride with  $(\text{THF})_3\text{LiTeSiPh}_3$ .<sup>706</sup> Addition of *tert*-butylpyridine to  $\text{Cp}^R_2\text{Zr}(\text{TeSiPh}_3)_2$  ( $\text{R} = \text{Bu}^t$ ) results in clean elimination of  $\text{Te}(\text{SiPh}_3)_2$  to form  $[\text{Cp}^R_2\text{ZrTe}]_2$  as the only metal-containing product (Scheme 233).

Zirconocene chalcogenide complexes  $\text{Cp}^*_2\text{Zr}(\text{E})(\text{py})$  ( $\text{E} = \text{S}, \text{Se}, \text{Te}$ ) undergo  $[2+2]$ -cycloaddition reactions with the phosphalkyne, liberating the pyridine and yielding four-membered zirconacyclic complexes **928** and **929**<sup>707</sup> (Scheme 234). Both isomers **928** and **929** were formed in the case of  $\text{E} = \text{S}$ , but only one of the two possible isomers is obtained when  $\text{E} = \text{Se}$  **928** and  $\text{Te}$  **929**. Complex **928** ( $\text{E} = \text{S}$ ) undergoes ring-expansion reactions with  $\text{Se}$ ,  $\text{PhCN}$ , and  $\text{Bu}^t\text{NC}$  to produce the corresponding zirconocene metallacycles **930**, **931**, and **932**, respectively.



Scheme 233



Scheme 234

## 4.08.10 *ansa*-Metallocene Complexes

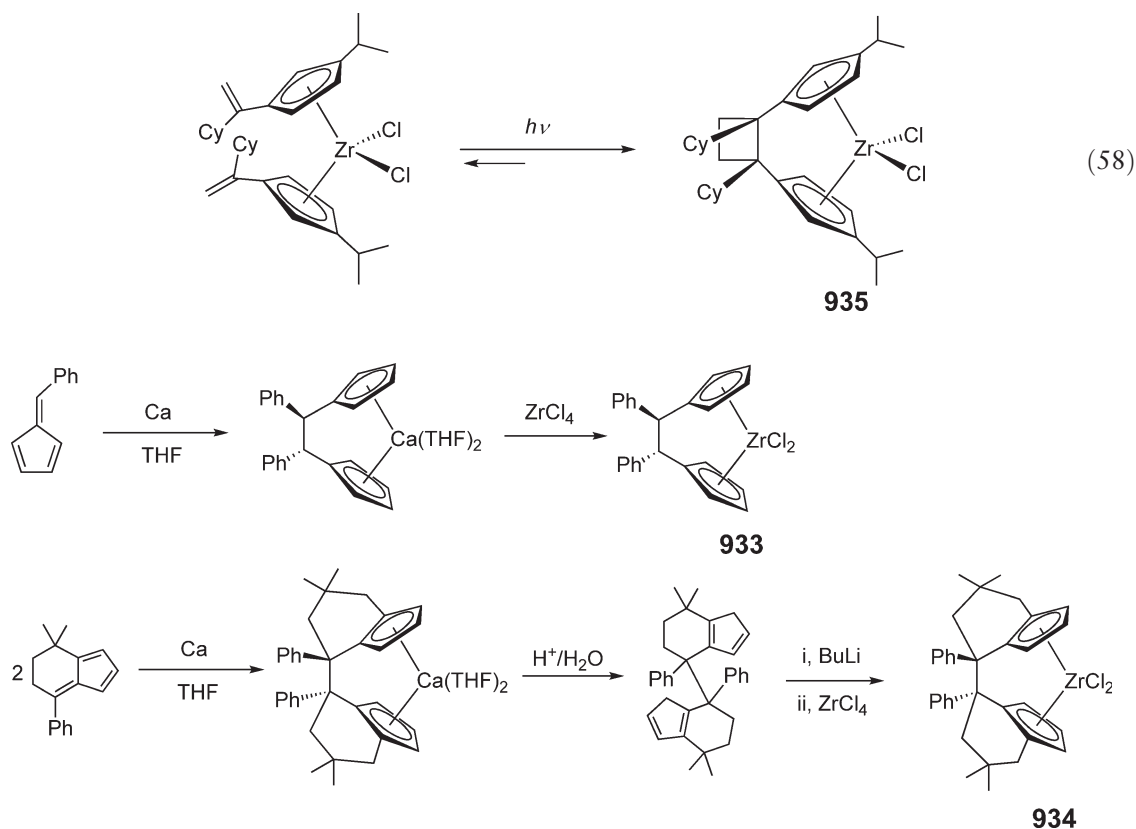
### 4.08.10.1 $C_2$ -bridged Complexes

The design of linked ligands for the synthesis of bridged *ansa*-metallocene complexes has largely been targeted at improving the catalytic characteristics of the resulting metallocene complexes, including polymerization activity, the resulting polymer molecular weight and molecular weight distribution, as well as the degree of control over the regio- and stereochemistry of the polymeric materials derived from olefins and functionalized vinyl monomers. The most studied *ansa*-metallocenes are two-carbon ( $C_2$ -) bridged bis(indenyl) zirconocenes: *rac*-(EBI)ZrX<sub>2</sub> (EBI = C<sub>2</sub>H<sub>4</sub>(1-Ind)<sub>2</sub>) and *rac*-(EBIH)ZrX<sub>2</sub> (EBIH = C<sub>2</sub>H<sub>4</sub>(1-tetrahydroindenyl)<sub>2</sub>) (X = halides, alkyls, enolates, etc.), which have been widely employed as model systems for homogenous, stereospecific polymerization of  $\alpha$ -olefins and polar vinyl monomers, as well as for asymmetric catalysis.

#### 4.08.10.1.1 *ansa*-Cyclopentadienyl complexes

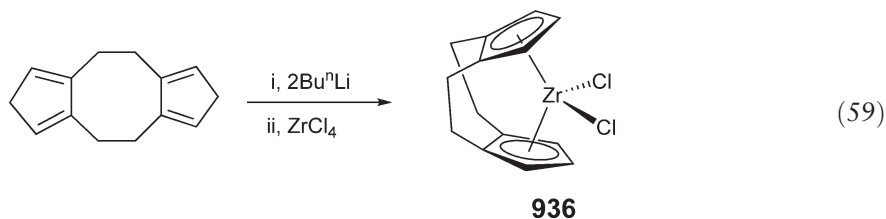
*ansa*-Calcocenes can serve as suitable precursors leading to the desired chiral *ansa*-zirconocenes. Specifically, reductive coupling of phenylfulvene with activated calcium in THF gives a mixture of *trans*- (70%) and *cis*- (30%) diphenylethanediyl-bridged *ansa*-calcocenes Ph<sub>2</sub>C<sub>2</sub>H<sub>2</sub>(Cp)<sub>2</sub>Ca(THF)<sub>2</sub>. Treatment of the isolated crystalline  $C_2$ -symmetric *trans*-isomer with ZrCl<sub>4</sub> leads to the formation of  $C_2$ -symmetric *ansa*-zirconocene **933**<sup>708</sup> (Scheme 235). In a similar fashion, racemic *ansa*-zirconocene complex **934** with a bridge as part of the fused bis(tetrahydroindenyl) ligand system is obtained via the *ansa*-calcocene intermediate.<sup>709</sup>

Photochemical [2 + 2]-cycloaddition of unbridged bis(alkenyl-Cp)zirconocene complexes provides a unique approach for the synthesis of  $C_2$ -hydrocarbyl-bridged *ansa*-zirconocenes. For example, the cyclobutene-bridged racemic *ansa*-zirconocene **935** is conveniently obtained via rapid intramolecular [2 + 2]-cycloaddition of the unbridged, racemic bis(alkenyl-substituted Cp)zirconocene precursor upon irradiation ( $\lambda = 450$  nm)<sup>710</sup> (Equation (58)). Similarly, irradiation of the *meso*-precursor leads to the corresponding *meso-ansa*-zirconocene.



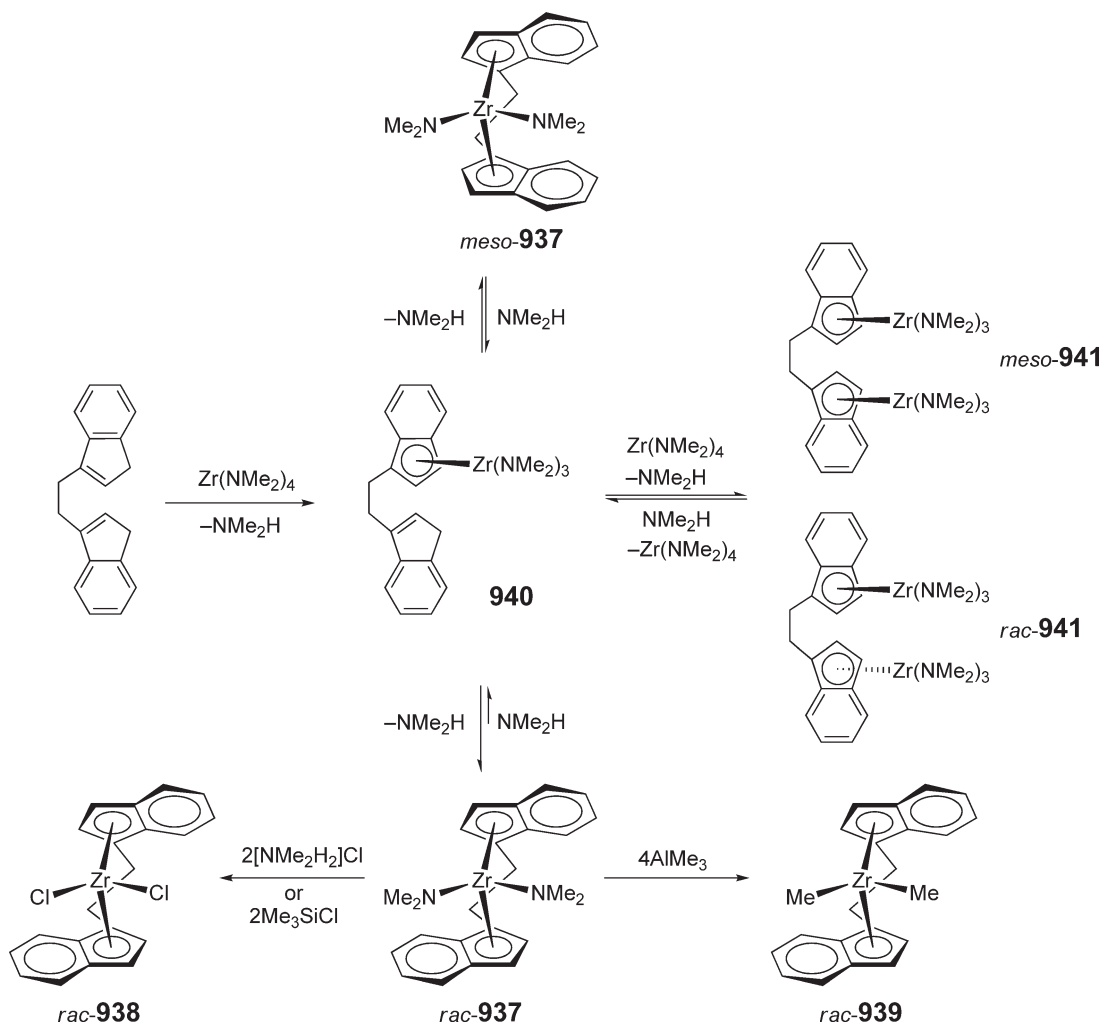
Scheme 235

A doubly  $C_2$ -bridged bis(cyclopentadienyl) ligand was obtained by Skattebøl rearrangement of the bis(dibromocarbene) adduct of 1,2,5,6-tetramethylenecyclooctane, induced by the action of MeLi. Reaction of its dilithium salt with  $ZrCl_4$  affords the corresponding zirconocene dichloride **936**<sup>711</sup> (Equation (59)); this complex has been structurally characterized. The same  $[2_2]$ zirconocenophane complex **936** has also been prepared by the reaction of the trimethylsilyl derivative of the ligand and  $ZrCl_4$  in  $CH_2Cl_2$ .<sup>712</sup>



#### 4.08.10.1.2 *ansa*-Bis(indenyl) complexes

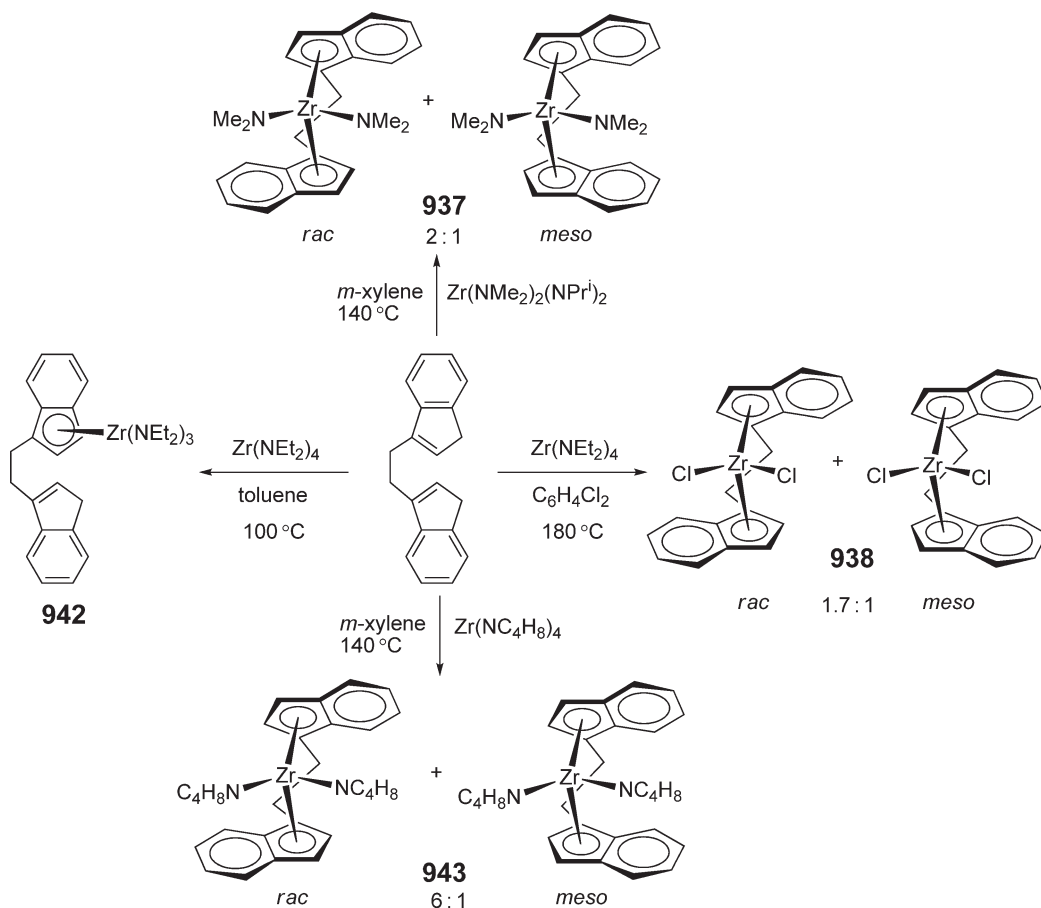
The amine elimination reactions of  $Zr(NMe_2)_4$  and the neutral (EBI) $H_2$  [1,2-bis(3-indenyl)ethane] ligand in toluene at 100 °C afford pure *rac*-(EBI) $Zr(NMe_2)_2$  **937** in 68% isolated yield.<sup>713</sup> This bis(amido) complex can be subsequently converted in high yield to the corresponding dichloride *rac*-(EBI) $ZrCl_2$  **938** and the dimethyl *rac*-(EBI) $ZrMe_2$  **939** derivatives by reactions with  $[NMe_2H_2]Cl$  or  $Me_3SiCl$  and  $AlMe_3$ , respectively (Scheme 236).



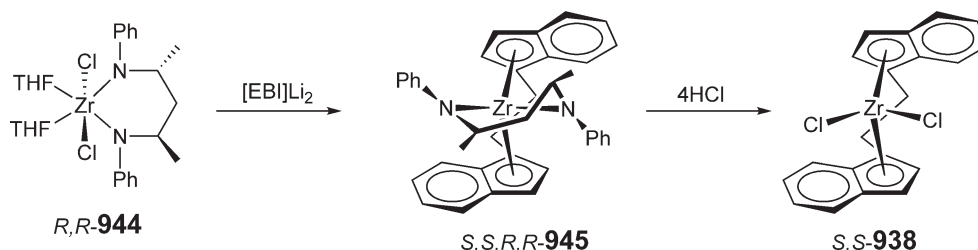
Scheme 236

This amine reaction proceeds via the rapidly formed mono-indenyl intermediate **940**, which undergoes reversible intermolecular amine elimination with a second equivalent of  $\text{Zr}(\text{NMe}_2)_4$  to give binuclear species **941** or reversible intramolecular amine elimination to give either *rac*-**937** or *meso*-**937**.<sup>714</sup> The kinetic zirconocene bis(amide) product is a 1:1 mixture of *rac*-**937** and *meso*-**937**, whereas the thermodynamic product is *rac*-**937**; the *meso*-**937** to *rac*-**937** isomerization is catalyzed by the  $\text{NMe}_2\text{H}$  byproduct. Significantly, the *rac*-**937**/*meso*-**937** product ratio can be controlled by adjusting the rate of  $\text{NMe}_2\text{H}$  removal from the reaction vessel and the steady-state concentration of amine in the reaction mixture. For example, the reaction of  $\text{Zr}(\text{NMe}_2)_4$  and  $(\text{EBI})\text{H}_2$  in toluene at  $100^\circ\text{C}$  with  $\text{N}_2$  bubbling through the reaction mixture to sweep away the volatile  $\text{NMe}_2\text{H}$  affords a 1:1 mixture of *rac*-**937** and *meso*-**937** (kinetically controlled product ratio). On the other hand, when the  $\text{N}_2$  purge is replaced with a static  $\text{N}_2$  atmosphere – the open condition that allows the evolved  $\text{NMe}_2\text{H}$  simply to escape from the reaction vessel via an oil bubbler, the stereoselectivity of this amine elimination reaction increases dramatically to a *rac*/*meso* ratio of 13/1 (thermodynamically controlled product ratio)! The amide *rac*-**937** can be used directly as a catalyst precursor for the isospecific polymerization of propylene.<sup>715</sup> The molecular structures of both *rac*-(EBI) $\text{ZrCl}_2$  and *meso*-(EBI) $\text{ZrCl}_2$  have been determined by X-ray diffraction and solution conformations investigated by NMR.<sup>716</sup>

The scope of the amine elimination reaction of the neutral  $(\text{EBI})\text{H}_2$  ligand with zirconium and hafnium amides has been investigated.<sup>718</sup> The reaction of  $(\text{EBI})\text{H}_2$  with  $\text{Zr}(\text{NEt}_2)_4$  in toluene at  $100^\circ\text{C}$  yields the mono-indenyl complex **942** via a single amine elimination (Scheme 237). At higher temperature ( $180^\circ\text{C}$ ) and using 1,2-dichlorobenzene as solvent, this reaction produces a metallocene dichloride  $(\text{EBI})\text{ZrCl}_2$  **938** *rac*/*meso* mixture in a ratio of 1.7/1. The reaction of  $(\text{EBI})\text{H}_2$  with  $\text{Zr}(\text{NMe}_2)_2(\text{NPr}^i)_2$  in *m*-xylene at  $140^\circ\text{C}$  affords the sterically least hindered *ansa*-zirconocene product,  $(\text{EBI})\text{Zr}(\text{NMe}_2)_2$  **937** (*rac*/*meso* ratio = 2/1), via  $\text{NPr}^i_2\text{H}$  elimination. Mixing  $(\text{EBI})\text{H}_2$  with the pyrrolide complex  $\text{Zr}(\text{NC}_4\text{H}_8)_4$  in *m*-xylene at  $140^\circ\text{C}$  yields  $(\text{EBI})\text{Zr}(\text{NC}_4\text{H}_8)_2$  (**943**; *rac*/*meso* ratio = 6/1), from which



Scheme 237

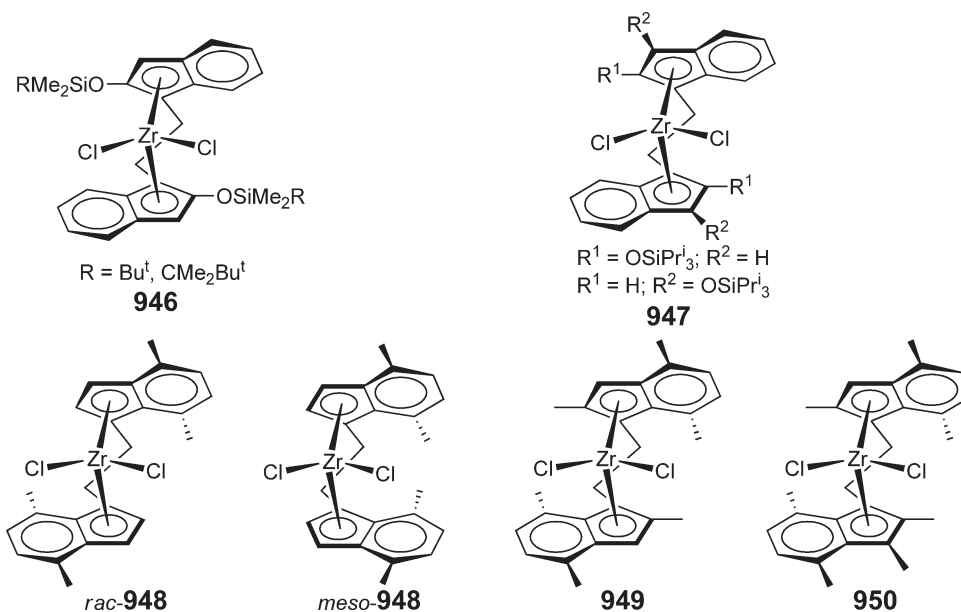


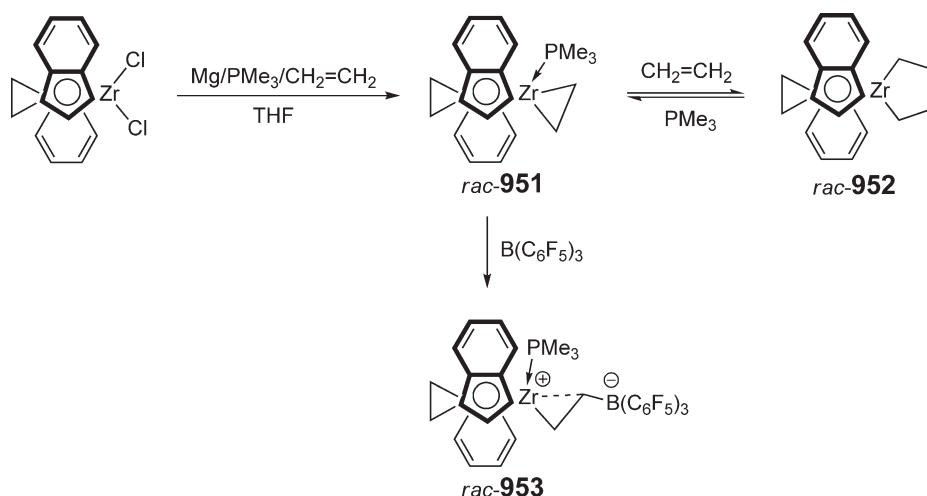
Scheme 238

the pure *rac*-**943** was isolated in 42% yield. The reaction of  $(EBI)H_2$  with  $Hf(NMe_2)_4$  in *m*-xylene at  $140^\circ C$  provides  $(EBI)Hf(NMe_2)_2$  in 85% NMR yield (*rac/meso* ratio = 6/1).

The stereospecific synthesis of enantiomerically pure *ansa*-zirconocene dichlorides has been accomplished using the enantiomerically pure chelated bis(amide)zirconium dichloride ( $R,R$ )-**944** (Scheme 238) via the “chelate-controlled” metallation process.<sup>719</sup> Thus, transmetalation of  $Li_2[EBI]$  with the optically active dichlorozirconium bis(amide) **944** affords zirconocene **945** in >95% yield and >99% ee. Bis(amide) **945** can be deaminated by treatment with  $HCl/Et_2O$  to give the corresponding enantiomerically pure dichloride ( $S,S$ )- $(EBI)ZrCl_2$  **938** in >91% isolated yield and >99% ee. The absolute configuration of ( $S,S$ )- $(EBI)ZrCl_2$  was established by X-ray crystallography.

Zirconocenes **946** supported by 2-siloxy-substituted EBI ligands have been synthesized by salt metathesis.<sup>720–722</sup> The structures of these complexes have been determined by X-ray diffraction. The propylene polymerization behavior upon activation with MAO was investigated. The analogous 1- and 2-triisopropylsiloxy-substituted bis(indenyl) zirconocenes **947** have also been synthesized.<sup>723</sup> The tetrahydro-1-indenyl derivatives are obtained by hydrogenation of **947** with  $H_2/PtO_2$ . The isolation and molecular structure determination of both *rac*-(4,7-Me<sub>2</sub>-EBI) $ZrCl_2$  and *meso*-(4,7-Me<sub>2</sub>-EBI) $ZrCl_2$  **948** have been accomplished and chain-transfer reactions in propylene polymerization with the *rac*-isomer investigated.<sup>724</sup> An additional methyl substitution at the 2-position of the Cp rings has produced highly rigid complex *rac*-(2,4,7-Me<sub>3</sub>-EBI) $ZrCl_2$  **949**; on activation with MAO for the polymerization in liquid propylene, it produces highly isotactic polypropylene with  $[mmmm] = 99\%$  and  $T_m = 163^\circ C$  at a reaction temperature of  $30^\circ C$ .<sup>725</sup> In comparison, the analogous complex **950** with an additional methyl substituent at the 3-position of the “lower” Cp ring gives isotactic polypropylene with a considerably lower isotacticity  $[mmmm] = 90\%$  and molecular weight under the same polymerization conditions; the polymerization activity is also much lower.

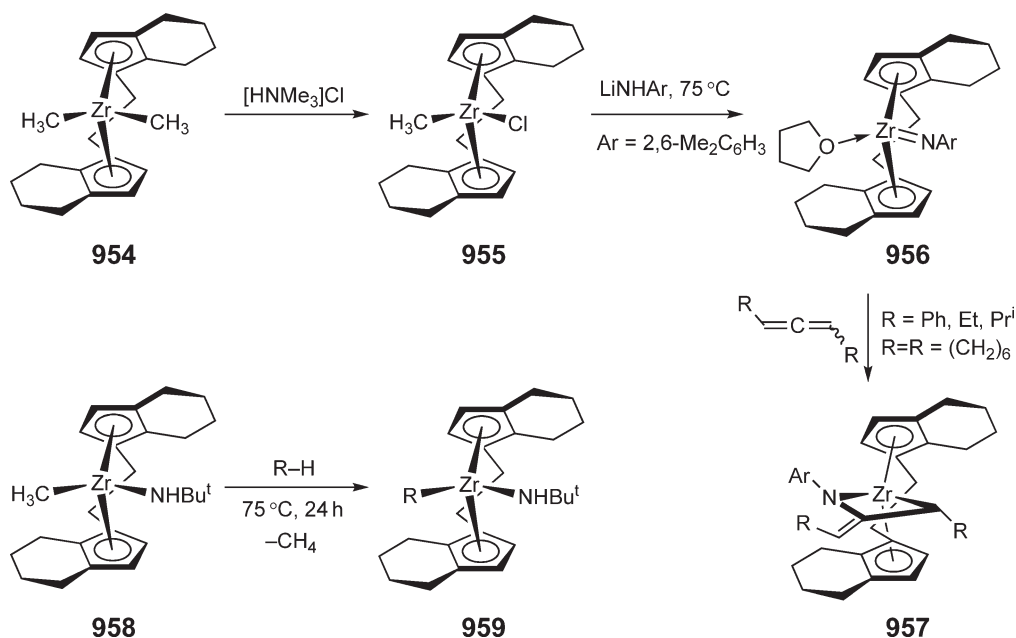




Scheme 239

The trimethylphosphine-stabilized *ansa*-zirconocene ethylene complex **951** is obtained by magnesium reduction of *rac*-(EBI)ZrCl<sub>2</sub> in the presence of ethylene and  $\text{PMe}_3$ <sup>726</sup> (Scheme 239). When the reaction is halted after 6 h, a mixture containing both **951** and the zirconacyclopentane derivative **952** is formed. This mixture can be converted to pure *rac*-**951** when treated with excess  $\text{PMe}_3$ . Upon treatment of *rac*-**951** with  $\text{B}(\text{C}_6\text{F}_5)_3$ , a charge-separated zwitterionic species *rac*-**953** is formed. This complex is stabilized by the coordinated  $\text{PMe}_3$  ligand and a strong  $\beta\text{-CH}_2$  interaction.

Treatment of *rac*-(EBIH)ZrMe<sub>2</sub> **954** with  $[\text{HNMe}_3]\text{Cl}$  yields the chlorozirconocene methyl derivative *rac*-(EBIH)Zr(Cl)Me **955**, which is subsequently treated with  $\text{LiHNAr}$  in THF to afford the *ansa*-zirconocene imido complex *rac*-(EBIH)Zr(=NAr)(THF)<sub>2</sub> **956**<sup>727</sup> (Scheme 240). This racemic imido complex undergoes highly diastereoselective cycloadditions reactions with 1 equiv. of racemic disubstituted allenes to yield single diastereomeric azametallacycle products **957**. The use of the enantiopure zirconocene imido complex

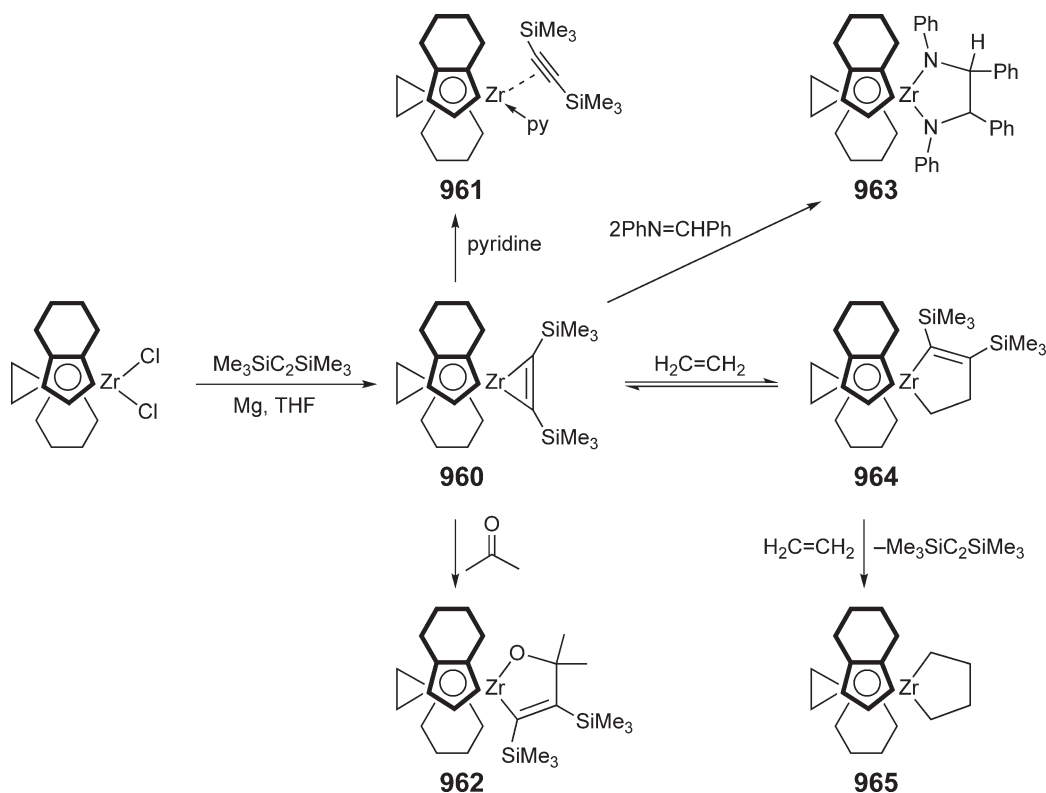


Scheme 240

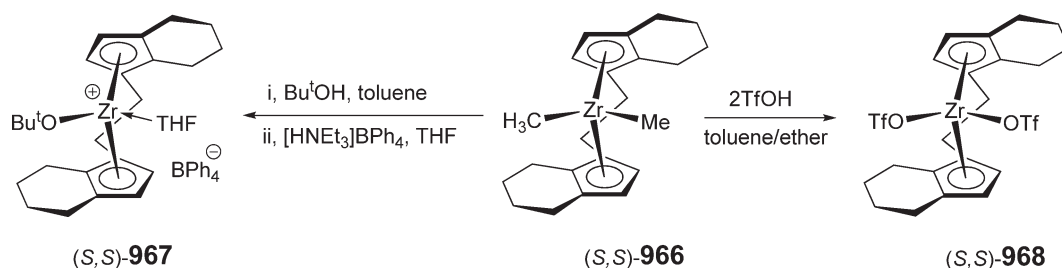
(*S,S*)-(EBIH)Zr(=NAr)(THF)<sub>2</sub> promotes highly enantioselective cycloaddition reactions with allenes and, in certain cases, this system allows conversion of an allene racemate into a mixture enriched in one enantiomer. Mechanistic studies about the enantioselective cycloaddition and stereoinversion of allenes mediated by imidozirconocenes have revealed that the initial [2 + 2]-cycloaddition to form the azazirconacyclobutane is stereospecific and is not involved in the racemization process.<sup>728</sup> The reactive zirconocene imido precursor *rac*-(EBIH)Zr(NHBu<sup>t</sup>)(Me) **958** has been shown to activate a variety of hydrocarbons R–H with primary alkyl, alkenyl, and aryl C–H bonds to form the corresponding alkyl derivative *rac*-(EBIH)Zr(NHBu<sup>t</sup>)(R) **959** with concomitant elimination of methane<sup>729</sup> (Scheme 240). Mechanistic experiments support the proposal of intramolecular elimination of methane followed by hydrocarbon C–H addition.

Reduction of *rac*-(EBIH)ZrCl<sub>2</sub> with equimolar amounts of Mg in the presence of Me<sub>3</sub>SiC≡CSiMe<sub>3</sub> in THF yields zirconocene–alkyne complex **960** without additional base ligands<sup>730</sup> (Scheme 241). Addition of pyridine forms the corresponding adduct **961**, whereas the reaction of **960** with acetone gives the insertion product **962**. Treatment of **960** with 2 equiv. of PhN=CHPh results in complete substitution of the alkyne moiety to form zirconocene diazametallacycle **963**. The reaction of the zirconocene–alkyne complex **960** with an excess of ethylene at room temperature forms the corresponding zirconacyclopentane complex **965**, which was isolated as stable yellow crystals and structurally characterized by X-ray diffraction.<sup>731</sup> The same reaction with 1 equiv. of ethylene at –70 °C gives zirconacyclopentene **964**, serving as a possible intermediate for the transformation from **960** to **965**. *In situ* activation of complex **965** with B(C<sub>6</sub>F<sub>5</sub>)<sub>3</sub> under an ethylene atmosphere generates an effective ethylene polymerization catalyst.

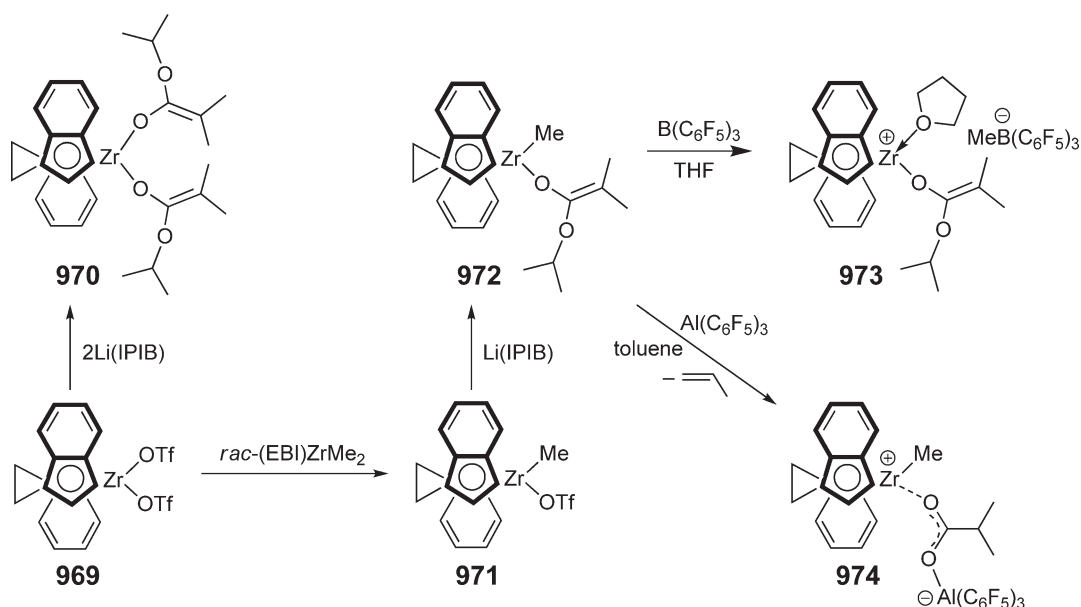
The optically pure, structurally characterized zirconocenium *tert*-butoxide complex [(*S,S*)-(EBIH)Zr(OBu<sup>t</sup>)(THF)]BPh<sub>4</sub> (**967**, Scheme 242) was prepared by treatment of the corresponding dimethyl complex (*S,S*)-(EBIH)ZrMe<sub>2</sub> **966** with *tert*-butanol in toluene followed by *in situ* protonolysis with [HNEt<sub>3</sub>]BPh<sub>4</sub> in THF. The complex catalyzes the asymmetric Diels–Alder reaction between cyclopentadiene and various dienophiles.<sup>732</sup> The enantiopure zirconocene bis(triflate) complex (*S,S*)-(EBIH)Zr(OTf)<sub>2</sub> **968** also efficiently catalyzes the asymmetric Diels–Alder reaction between cyclopentadiene and oxazolidinones.<sup>733,734</sup>



Scheme 241



Scheme 242

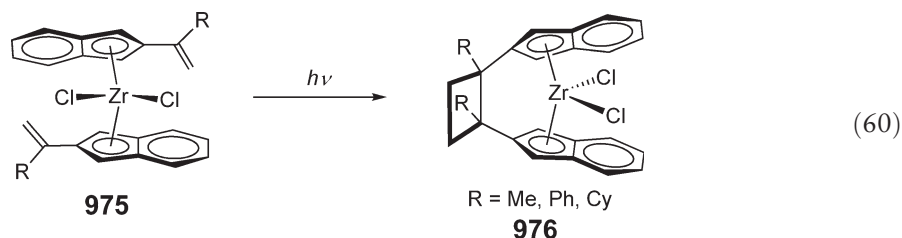


Scheme 243

Treatment of *rac*-(EBI)Zr(OTf)<sub>2</sub> **969** with 2 equiv. of lithium isopropylisobutyrate [Li(IPIB)] in toluene produces the structurally characterized *ansa*-zirconocene ester enolate complex *rac*-(EBI)Zr[OC(OP<sup>i</sup>)=CMe<sub>2</sub>]<sub>2</sub> (**970**, Scheme 243).<sup>735</sup> Comproportionation between *rac*-(EBI)Zr(OTf)<sub>2</sub> and *rac*-(EBI)ZrMe<sub>2</sub> generates *rac*-(EBI)ZrMe(OTf) **971**, which is converted to the enolate complex *rac*-(EBI)ZrMe[OC(OP<sup>i</sup>)=CMe<sub>2</sub>] **972** by treatment with 1 equiv. of Li[OC(OP<sup>i</sup>)=CMe<sub>2</sub>]. The reaction of the methylzirconocene ester enolate **972** with B(C<sub>6</sub>F<sub>5</sub>)<sub>3</sub> in THF at ambient temperature cleanly produces the corresponding isolable cationic *ansa*-zirconocene ester enolate complex **973** in quantitative yield. The analogous reaction of **972** with Al(C<sub>6</sub>F<sub>5</sub>)<sub>3</sub> in toluene, however, proceeds through a proposed intramolecular proton-transfer process in which propylene is eliminated from the isopropoxy group, subsequently producing a carboxylate-bridged tight ion pair *rac*-(EBI)Zr<sup>+</sup>(Me)OC(OP<sup>i</sup>)OAl(C<sub>6</sub>F<sub>5</sub>)<sub>3</sub><sup>-</sup> **974**. Both the isolated cationic **973** and neutral **972** compounds (the latter combined with B(C<sub>6</sub>F<sub>5</sub>)<sub>3</sub> *in situ*) are highly active and highly isospecific for polymerizations of alkyl methacrylates, via an enantiomorphic site-control mechanism in a living fashion. The aluminate complex **974**, however, produces syndiotactic polymethacrylates predominantly by chain-end control.

Photochemical [2 + 2]-cycloaddition of unbridged bis(alkenylindenyl)zirconocene complexes **975** is a unique approach leading to formation of 1,2-cyclobutylene-bridged *ansa*-bis(indenyl)zirconocenes **976** (Equation (60)).<sup>736</sup> These cycloadditions are highly efficient and complete within 2–3 h with nearly quantitative conversions. Upon activation with MAO, these *ansa*-zirconocenes are effective catalysts for ethylene/1-octene co-polymerizations at elevated temperatures.

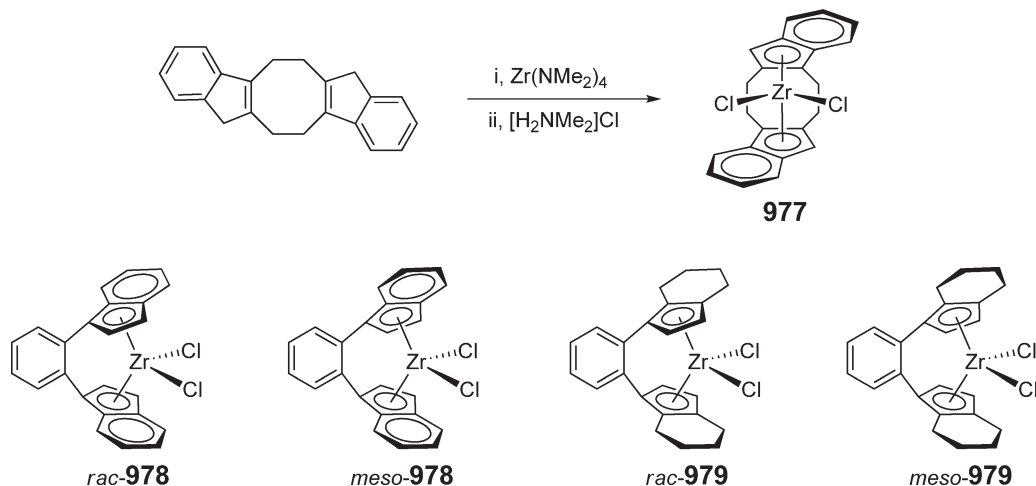




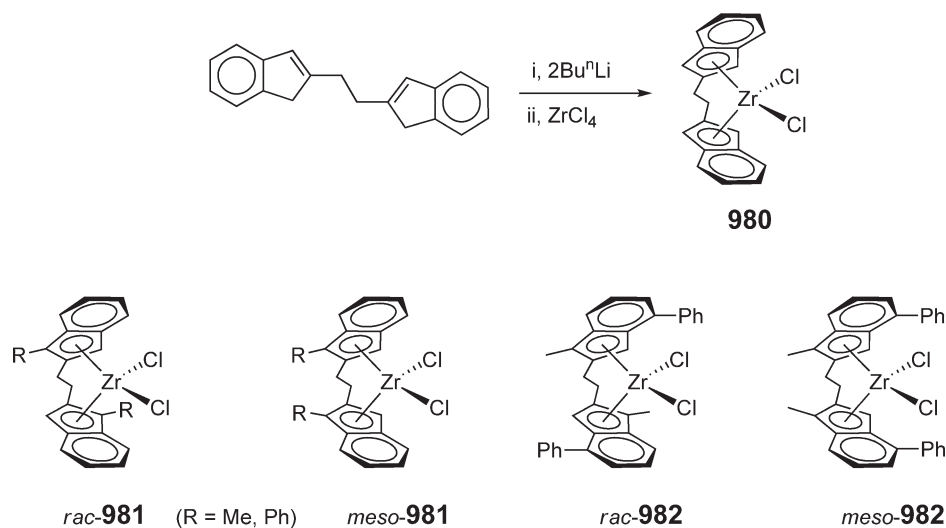
Doubly ethylene-bridged  $C_2$ -symmetric *ansa*-bis(indenyl)zirconocene dichloride **977** is obtained in 67% yield by the amine elimination approach according to Scheme 244.<sup>737</sup> This is the only bridged  $C_2$ -diastereomer formed because the geometry of the double bridge precludes formation of a *meso*-isomer, and there is no evidence of oligomeric metallocene products either. The amine elimination approach was also employed for the synthesis of the 1,2-phenylene-bridged *ansa*-bis(indenyl)zirconocenes **978** with high *rac*-selectivity, whereas the salt metathesis approach gives a 60:40 mixture of *rac*-**978** and *meso*-**978**.<sup>738</sup> The synthesis of the 1,2-phenylene-bridged *ansa*-bis(tetrahydroindenyl)zirconocene derivatives **979** salt metathesis affords a 60:40 mixture of *rac*-**979** and *meso*-**979**.<sup>739</sup> Attempts to selectively separate the *rac*- from the *meso*-isomer with hot toluene by crystallization resulted in observation of the known light-initiated isomerization of the *meso*- to the *rac*-isomer in a 93:7 ratio of *rac*-**979** to *meso*-**979**.

The achiral  $C_2$ -symmetric ethylene-bridged bis(2-indenyl)zirconocene **980** was obtained by the salt metathesis route<sup>740</sup> (Scheme 245). Incorporation of alkyl substituents such as Me and Ph at 1-position on the Cp ring affords mixtures containing *rac*- and *meso*-*ansa*-zirconocenes **981**. The disubstituted derivative **982** is also obtained as a mixture of *rac*- and *meso*-isomers. When activated with MAO, these complexes exhibit high activity for ethylene polymerization but low activity for propylene polymerization leading to low molecular weight, atactic polypropylene. The analogous titanium complexes were prepared earlier.<sup>741,742</sup>

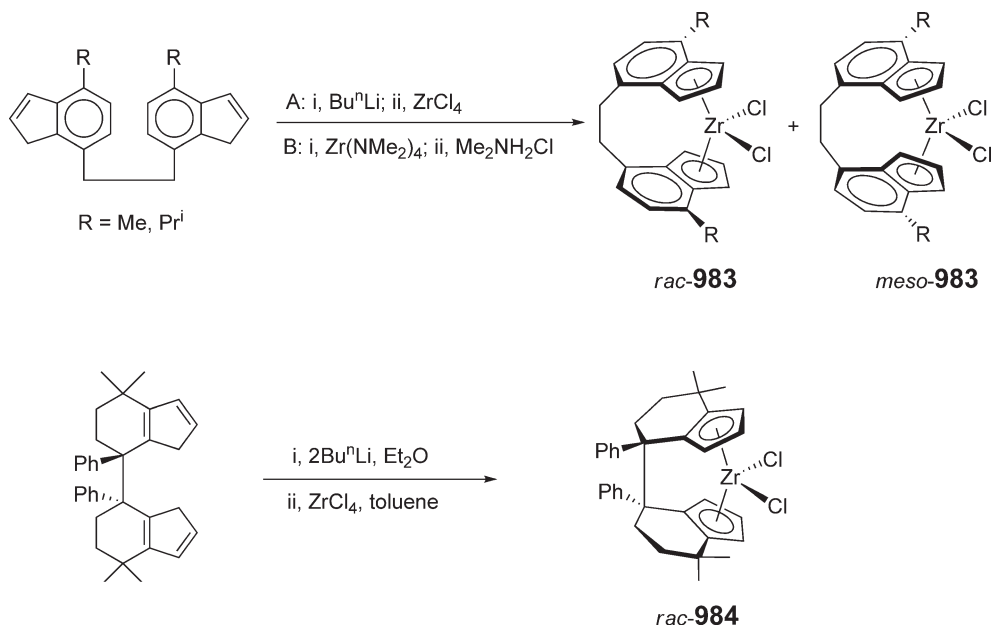
Ethylene-bridged *ansa*-bis(indenyl)zirconocenes bridged at the 7,7'-positions of  $C_6$ -ring of the indenyl moiety have been synthesized according to Scheme 246.<sup>743</sup> In the synthesis, the salt metathesis approach (route A) gives a 50:50 mixture of *rac*-**983** and *meso*-**983**, whereas the amine elimination (route B) leads to formation of only the *racemo*-isomers. In the solid state, the compounds *rac*-**983** ( $R = \text{Me}, \text{Pr}^i$ ) are found to have  $C_1$ -symmetry but in solution exhibit  $C_2$ -symmetry, as seen in the  $^1\text{H}$  NMR spectra at room temperature. Analogous methylene-bridged *ansa*-bis(indenyl)zirconocenes have also been prepared. When activated with a large excess of MAO, *rac*-**983** ( $R = \text{Me}$ ) is active for liquid propylene polymerization at  $50^\circ\text{C}$  to give a highly regioregular polymer with low isotacticity ( $[mmmm] = 65\%$ ). The compound is significantly more active for the co-polymerization of ethylene and propylene.<sup>744</sup> The closely related *ansa*-bis(tetrahydroindenyl)zirconocene *rac*-**984** with an *ansa*-fused annulated six-membered ring system has also been synthesized as a single diastereomer by the salt metathesis route according to Scheme 246.<sup>745</sup> The molecular structure of this complex has been determined by X-ray diffraction. On activation with MAO, it polymerizes propylene to moderately isotactic PP.



Scheme 244



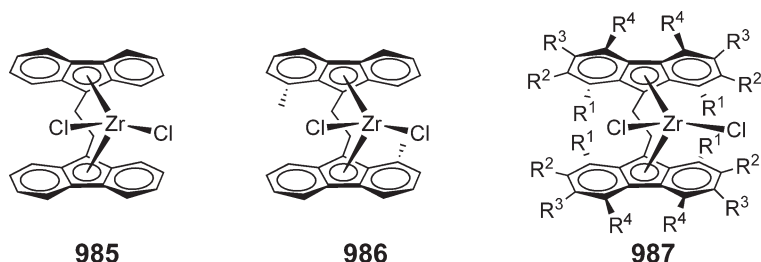
Scheme 245



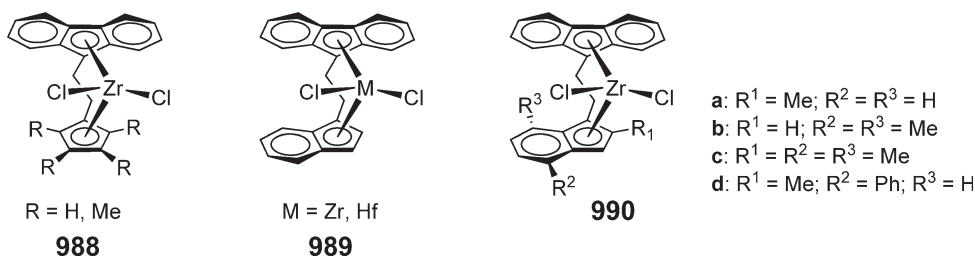
Scheme 246

#### 4.08.10.1.3 *ansa*-Fluorenyl complexes

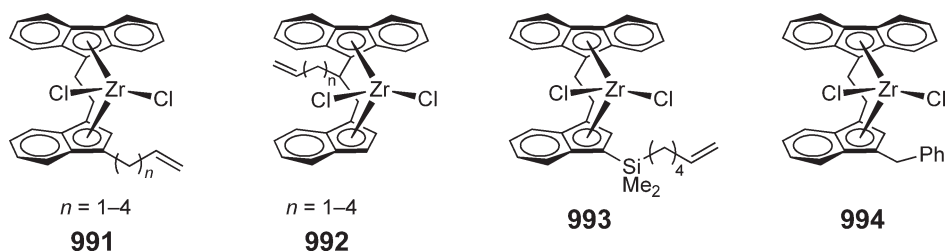
*ansa*-Bis(fluorenyl)zirconocene dichlorides **985** and **986** are obtained by the salt metathesis approach.<sup>746,747</sup> Upon activation with suitable activators, complex **985** produces high molecular weight, atactic polypropylene, whereas complex **986** employed as a *rac*- and *meso*-mixture affords anisotactic polypropylene of low stereoregularity. A large number of *ansa*-bis(fluorenyl)zirconocene dichloride derivatives, having a structure **987** by introducing various substituents at all positions of the fluorenyl rings, have been synthesized and their ethylene polymerization activities examined.<sup>748</sup>



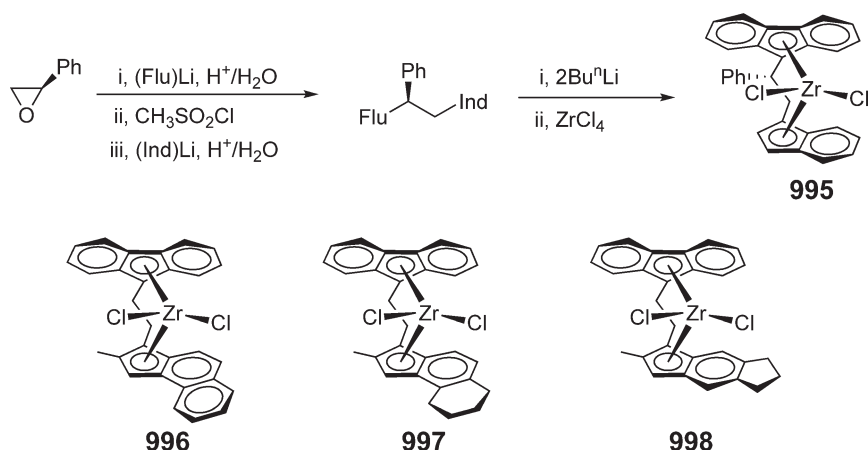
Ethylene-bridged pseudo- $C_s$ -symmetric *ansa*-(1-fluorenyl-2-cyclopentadienylethane)zirconocene dichloride complexes **988** have been synthesized and their molecular structures determined by X-ray diffraction studies.<sup>749</sup> When activated with MAO, complex **988** ( $R = H$ ) catalyzes propylene polymerization to produce syndiotactic polypropylene, whereas the  $C_5Me_4$  derivative (**988**:  $R = Me$ ) affords nearly atactic polypropylene. Ethylene-bridged,  $C_1$ -symmetric *ansa*-fluorenyl-indenyl zirconocenes **989** and **990** (which bear substituents on the indenyl moiety) have been synthesized and evaluated as ethylene and propylene polymerization catalysts.<sup>750</sup> Isotactic polypropylenes are produced by two of these complexes **990c** and **990d** when combined with excess MAO.<sup>751</sup> The hafnocene dichloride (**989**:  $M = Hf$ ) and the corresponding dimethyl derivative are also obtained, and the structure of the dimethyl complex has been determined by X-ray crystallography.<sup>752</sup>



A series of  $C_2$ -bridged fluorenyl and indenyl zirconocene and hafnocene dichloride complexes **991–994** has been synthesized.<sup>753</sup> In this study, the  $\omega$ -alkenyl substituents with various chain lengths in the  $C_2$ -bridge or in the 3-indenyl position are to effect self-immobilization during the olefin polymerization reactions by virtue of their incorporation into the backbone of a growing polymer chain, thereby providing heterogeneous catalyst systems. The impact of these substituents on the polymerization activity and the molecular weight of the produced polyethylene has also been investigated.



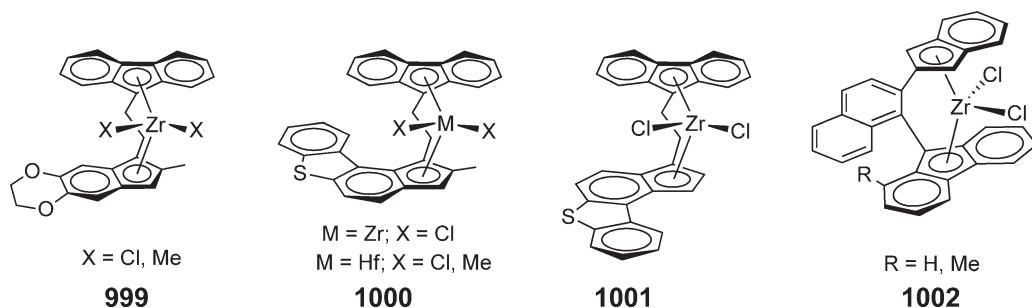
Ethylene-bridged fluorenyl-indenyl ligands are readily accessible using chiral epoxides as starting materials, from which the corresponding ethylene-bridged *ansa*-zirconocene dichlorides such as **995** are obtained<sup>754</sup> (Scheme 247). With a phenyl-substituted bridge, diastereomeric complexes are obtained which are separable by crystallization. The diastereomeric systems **995** show two different bridge conformations in the solid state (i.e.,  $\delta$ -forward and  $\lambda$ -backward) and have been employed for propylene polymerization. Under comparable conditions, they produce polypropylenes with significantly different stereoregularities. These results underscore the importance of a defined bridge conformation for the design of highly stereoselective catalysts. To this end, ethylene-bridged, the  $C_1$ -symmetric *ansa*-fluorenyl-indenyl zirconocenes **996–998** have been employed as propylene polymerization catalysts in combination with excess MAO.<sup>755</sup> The two different coordination sites of these “dual-side” catalysts lead to isotactic polypropylenes with variable amounts of stereoerrors, depending on the monomer concentration.



Scheme 247

The bulk properties of the polymer can thus be adjusted from a flexible, semicrystalline thermoplastic to an excellent thermoplastic elastomer.<sup>756</sup>

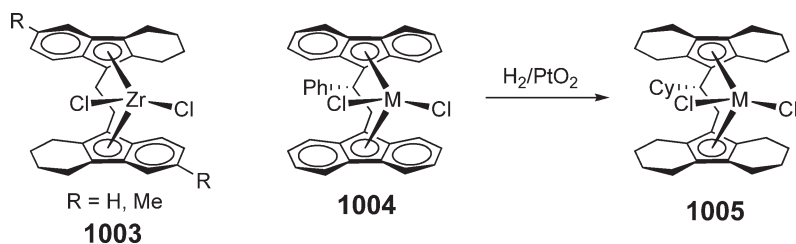
Oxygen-containing, asymmetric “dual-side” zirconocene complexes such as **999** have been prepared.<sup>757</sup> The studies show that the presence of oxygen substituents on the indenyl ring results in a strong increase of the propylene polymerization activity and also of the molecular weight of the resulting polymer with decreasing Al (MAO)/Zr ratio. Significantly higher molecular weights and activities are achieved with the dimethyl derivative which can be activated with  $\text{Ph}_3\text{C}[\text{B}(\text{C}_6\text{F}_5)_4]$  due to the absence of chain transfer to aluminum. The symmetric ethylene-bridged *ansa*-metallocenes **1000** and **1001** containing the fluorenyl and dibenzothiophene ligands have been synthesized. On MAO activation, they polymerize propylene to high molecular weight PP plastomers.<sup>758</sup> *ansa*-Fluorenyl-indenyl zirconocene dichlorides **1002** bearing the 1,2-naphthalenyl bridging moiety, including the *rac*-complex ( $\text{R} = \text{Me}$ ) and the  $C_s$ -symmetric complex ( $\text{R} = \text{H}$ ), have been synthesized and structurally characterized by X-ray diffraction.<sup>759</sup>



Ethylene-bridged *ansa*-bis(tetrahydrofluorenyl)zirconocenes **1003** have been synthesized and found to be highly stable compared to the analogous *ansa*-bis(fluorenyl)zirconocenes.<sup>760</sup> Both unsubstituted and substituted complexes are obtained as 1 : 1 mixtures of *rac*- and *meso*-isomers and produce mostly atactic polypropylene upon activation with suitable activators. The reaction of  $\text{MCl}_4$  with the dilithio salt of the optically active ligand (1*S*)-1,2-bis(9-fluorenyl)-1-phenylethane produces the enantiomerically pure *ansa*-bis(fluorenyl)metallocene dichlorides **1004**<sup>761</sup> (Scheme 248). Hydrogenation of **1004** over  $\text{PtO}_2$  gives the corresponding octahydrofluorenyl derivative **1005**, the structure of which ( $\text{M} = \text{Zr}$ ) has been determined by X-ray crystallography.<sup>762</sup>

#### 4.08.10.2 Si-bridged *ansa*-Zirconocene Complexes

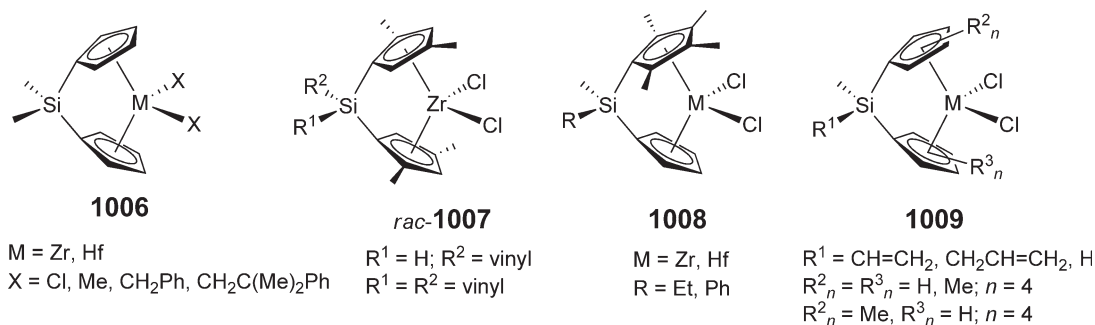
The dialkylsilylene  $[\text{R}_2\text{Si}]$  bridge imposes high rigidity and favorable electronic characteristics to *ansa*-metallocenes as suitable catalyst precursors; this bridging is often coupled with a combination of alkyl or aryl substitutions in certain positions of Cp, Ind, or Flu ligands, enabling the derived catalysts to exhibit high degrees of control over the polymerization processes, especially the stereo- and regiospecificity in propylene polymerization.



Scheme 248

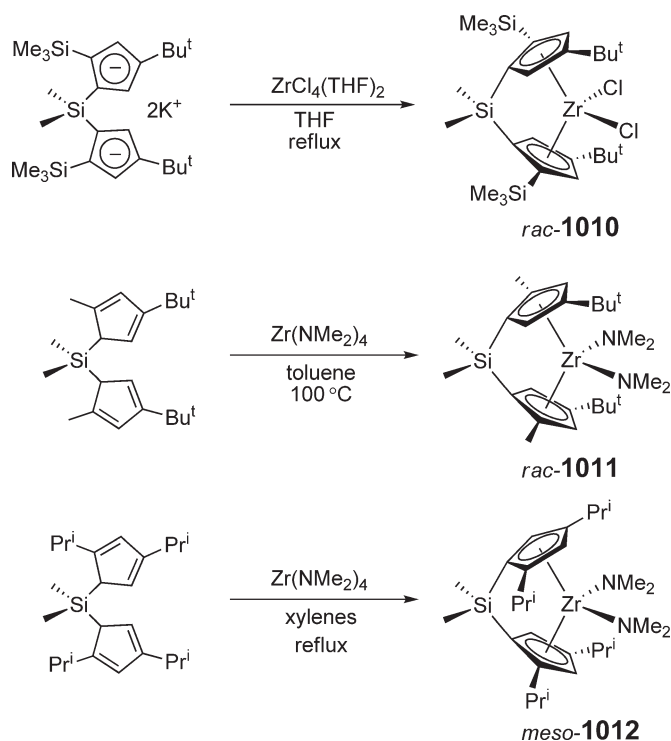
#### 4.08.10.2.1 Si-bridged cyclopentadienyl complexes

The unsubstituted  $\text{Me}_2\text{Si}$ -bridged bis(Cp) metallocene complexes,  $\text{Me}_2\text{Si}(\text{Cp})_2\text{MX}_2$  (**1006**:  $\text{M} = \text{Zr, Hf}$ ;  $\text{X} = \text{Cl, Me, CH}_2\text{Ph, CH}_2\text{C}(\text{Me})_2\text{Ph}$ ), are obtained by the conventional salt metathesis approach and standard alkylation technique.<sup>763</sup> Extension of the  $\text{R}_2\text{Si}$  bridge has produced  $[\text{Me}_2\text{SiN}(\text{R})\text{SiMe}_2]$ -bridged *ansa*-bis(Cp)metallocene complexes,  $[\text{Me}_2\text{SiN}(\text{Bu}^n)\text{SiMe}_2](\text{Cp})_2\text{MCl}_2$  ( $\text{M} = \text{Zr, Hf}$ ).<sup>764</sup> Further modifications of the silylene bridge lead to vinyl-substituted silylene-bridged *ansa*-zirconocene dichlorides **1007**.<sup>765</sup> These complexes are obtained as *rac*/*meso*-rich *rac*/*meso* mixtures; pure racemic complexes can be obtained after repeated recrystallizations. *ansa*-Zirconocene dichlorides **1008** having four different substituents at the bridge Si atom are designed to investigate the potential influence of the chirality of the bridgehead silicon on the olefin polymerization.<sup>766</sup> However, upon activation with MAO, these complexes produce atactic polypropylene, just like the unbridged or symmetrically substituted silylene-bridged zirconocene analogs. Functionalizations on the bridge Si atom by introduction of vinyl and allyl groups lead to *ansa*-zirconocene and hafnocene dichlorides **1009** which are designed for the development of supported homogeneous metallocene catalysts in a heterogeneous medium.<sup>767</sup> *ansa*-Zirconocene and hafnocene dichlorides **1009** with the  $\text{Me}(\text{H})\text{Si}$  bridge undergo hydrosilylation reactions with  $\text{Si}(\text{CH}=\text{CH}_2)_4$  and  $\text{Me}_2\text{Si}(\text{CH}=\text{CH}_2)_2$  to give the corresponding hydrosilylation products, thereby providing an alternative approach toward functionalization of *ansa*-metallocene complexes.<sup>768</sup>

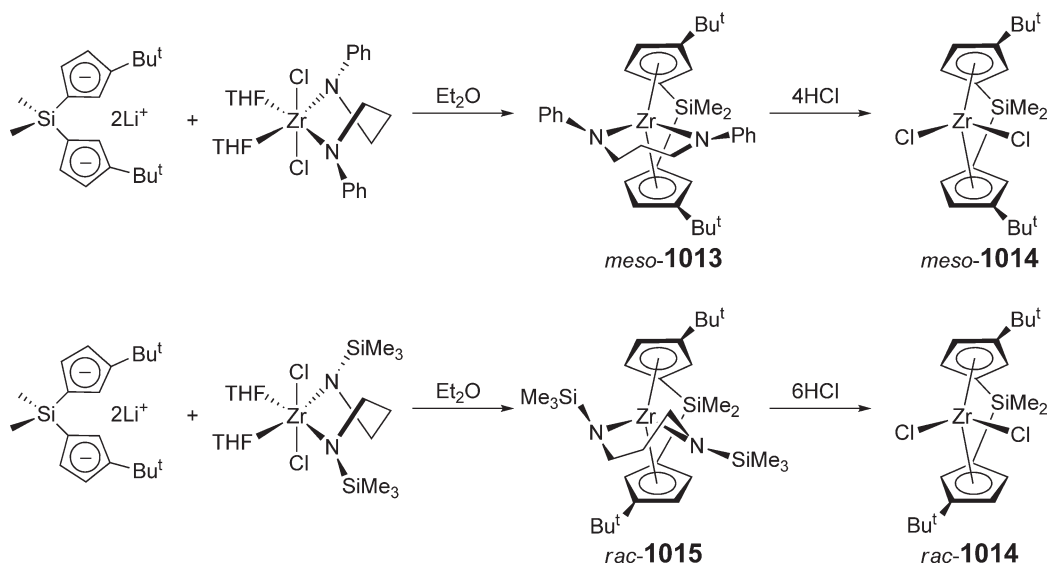


The pure racemic  $C_2$ -symmetric  $\text{Me}_2\text{Si}$ -bridged *ansa*-zirconocene dichloride **1010** is obtained by the salt metathesis approach in 15% isolated yield<sup>769</sup> (Scheme 249). Repulsions of ring substituents on opposing rings can be observed by the differing angles about the  $\alpha$ -trimethylsilyl substituents in the crystal structure. Owing to intramolecular steric repulsion, the  $[\text{ZrCl}_2]$  and  $\text{SiC}_2$  planes of the  $[\text{SiMe}_2]$  bridge are twisted by  $11^\circ$ . The amine elimination approach has been used in the reaction of the neutral ligand  $\text{Me}_2\text{Si}(1\text{-C}_5\text{H}_3\text{-2-Me-4-Bu}^t)_2$  with  $\text{Zr}(\text{NMe}_2)_4$  which gives the racemic  $\text{Me}_2\text{Si}$ -bridged *ansa*-zirconocene bis(amide) complex **1011** in 52% yield, isolated from an initially formed 2.5/1 *rac*/*meso* mixture.<sup>770</sup> Substituted silastannatetrahydro-*s*-indacene precursors, such as *meso*- $\text{Me}_2\text{Si}(\text{Bu}^t\text{C}_5\text{H}_3)_2\text{SnMe}_2$ , *meso*- $\text{Me}_2\text{Si}(\text{Me}_2\text{C}_5\text{H}_2)_2\text{SnMe}_2$ , and *meso*- $\text{Me}_2\text{Si}(\text{Me-Pr}^i\text{C}_5\text{H}_2)_2\text{SnMe}_2$ , react with  $\text{ZrCl}_4$  to give selectively the *meso*-diastereomers of the respective *ansa*-zirconocene complexes.<sup>771</sup> Also, interestingly, the amine elimination reaction of the neutral ligand  $\text{Me}_2\text{Si}(\text{C}_5\text{H}_3\text{-2,4-Pr}^i)_2$  with  $\text{Zr}(\text{NMe}_2)_4$  yields exclusively *meso*- $\text{Me}_2\text{Si}(\text{C}_5\text{H}_2\text{-2,4-Pr}^i)_2\text{Zr}(\text{NMe}_2)_2$  **1012**.<sup>772</sup>

A chelate-controlled synthesis of *rac*- and *meso*- $\text{Me}_2\text{Si}$ -bridged *ansa*-bis(Cp)zirconocenes has been developed.<sup>773</sup> Specifically, the reaction of the bis(amide) chelate complex  $\text{Zr}\{\text{PhN}(\text{CH}_2)_3\text{NPh}\}\text{Cl}_2(\text{THF})_2$  with  $\text{Li}_2[\text{Me}_2\text{Si}(3\text{-Bu}^t\text{-C}_5\text{H}_3)_2]$  yields *meso*- $\text{Me}_2\text{Si}(3\text{-Bu}^t\text{-C}_5\text{H}_3)_2\text{Zr}\{\text{PhN}(\text{CH}_2)_3\text{NPh}\}$  (*meso*-**1013**, Scheme 250) in >98% yield, which can be conveniently converted to the corresponding dichloride *meso*-**1014** upon treatment with HCl. In contrast, the reaction

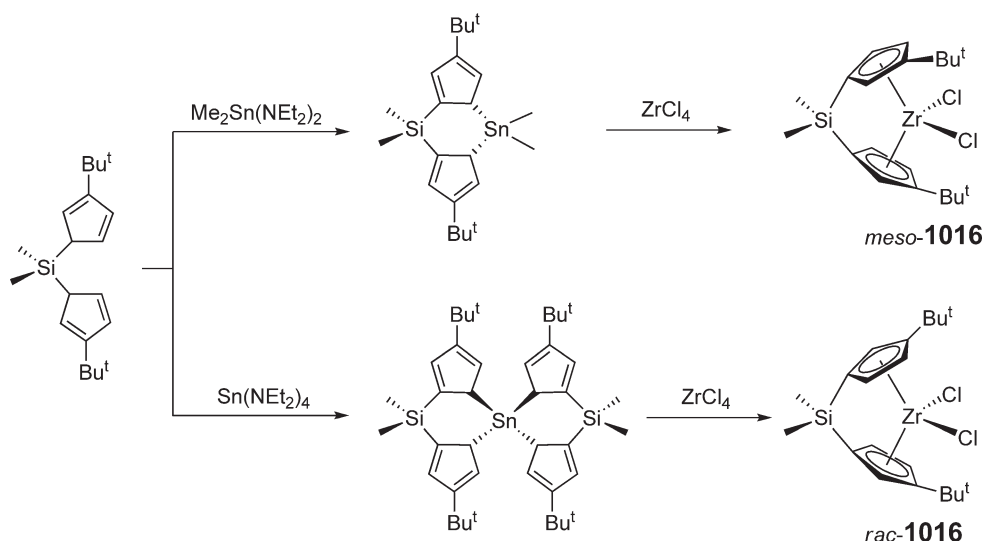


Scheme 249



Scheme 250

of Zr{Me<sub>3</sub>SiN(CH<sub>2</sub>)<sub>3</sub>NSiMe<sub>3</sub>}Cl<sub>2</sub>(THF)<sub>2</sub> or the related mono-THF adduct Zr{Me<sub>3</sub>SiN(CH<sub>2</sub>)<sub>3</sub>NSiMe<sub>3</sub>}Cl<sub>2</sub>(THF) with Li<sub>2</sub>[Me<sub>2</sub>Si(3-Bu<sup>t</sup>-C<sub>5</sub>H<sub>3</sub>)<sub>2</sub>] produces *rac*-Me<sub>2</sub>Si(3-Bu<sup>t</sup>-C<sub>5</sub>H<sub>3</sub>)<sub>2</sub>Zr{Me<sub>3</sub>SiN(CH<sub>2</sub>)<sub>3</sub>NSiMe<sub>3</sub>} *rac*-**1015**; HCl treatment generates the corresponding dichloride *rac*-**1014**. The X-ray structure shows that the chelate ring Zr{RN(CH<sub>2</sub>)<sub>3</sub>NR} in *rac*-**1015** has a pronounced twist, while that in *meso*-**1013** has a flat, envelope conformation. Thus, it is reasonable

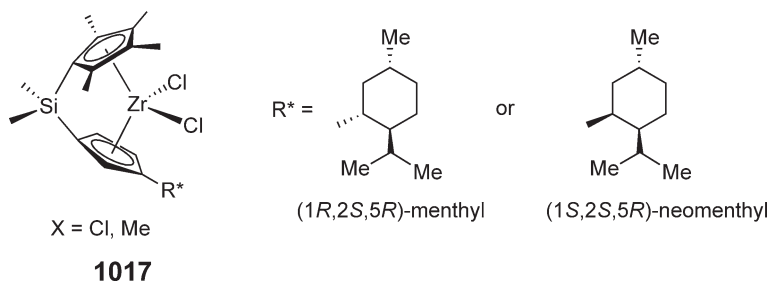


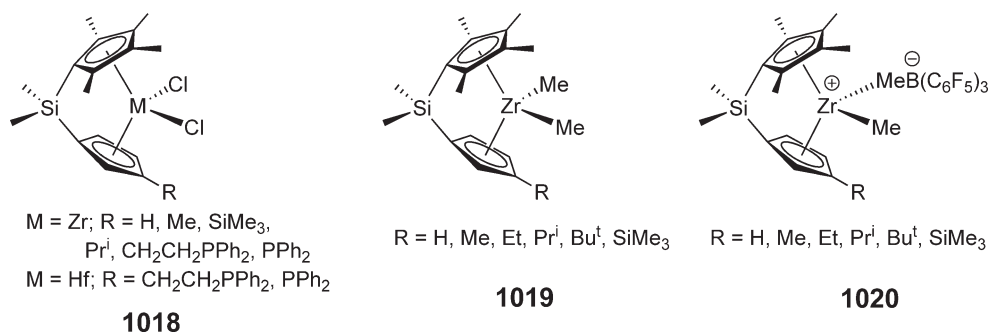
Scheme 251

to assume the conformations of the  $\text{Zr}\{\text{RN}(\text{CH}_2)_3\text{NR}\}$  chelate rings in the transition state stereochemistry for the addition of the second  $\text{Cp}^-$  ring.

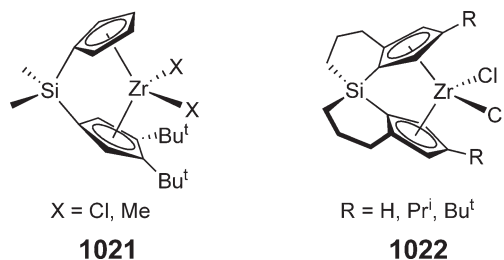
Alkyl-substituted bis(cyclopentadienyl)dimethylsilanes react with  $\text{Me}_2\text{Sn}(\text{NEt}_2)_2$  and  $(\text{Me}_2\text{N})_4\text{Sn}$  to form *meso*-configured *RS*-8-sila-4-stanna-*s*-tetrahydroindacene<sup>774</sup> and  $S_4$ -symmetric *RR,SS*-4-*spiro*-bis(8-sila-4-stanna-*s*-tetrahydroindacene)<sup>775</sup> compounds (Scheme 251), respectively; reaction with  $\text{ZrCl}_4$  converts these intermediates stereoselectively to the corresponding *meso*- and *rac*-zirconocene dichlorides  $\text{Me}_2\text{Si}(3\text{-Bu}^t\text{C}_5\text{H}_3)_2\text{ZrCl}_2$  **1016**. The stereochemistry of Sn-to-Zr transmetalation has been investigated using the reaction of *meso*-( $\text{CH}_2\text{Ph}$ ) $\text{MeSi}(3\text{-Bu}^t\text{-C}_5\text{H}_3)_2\text{SnMe}_2$  with  $\text{ZrCl}_4$ , which generates both isomers of the *C*-symmetric *ansa*-zirconocene, *meso*-( $\text{PhCH}_2$ ) $\text{MeSi}(3\text{-Bu}^t\text{-C}_5\text{H}_3)_2\text{ZrCl}_2$ , but not the  $C_1$ -symmetric, *rac*-like isomer.<sup>776</sup> The proposed mechanism envisages that the major product (70%) of the *meso*-isomers is formed under inversion at both Sn-bound carbon atoms by consecutive “back-side” attacks of  $\text{ZrCl}_4$ , while the minor product (30%) of the *meso*-isomers is formed under retention at both Sn-bound carbon atoms by a concerted “frontside” attack of  $\text{ZrCl}_4$ .

Chiral, non- $C_2$ -symmetric zirconocene dichlorides **1017** are obtained from the reaction of  $\text{ZrCl}_4$  with  $\text{Me}_2\text{Si}(\text{Me}_4\text{C}_5)(\text{C}_5\text{H}_3\text{R}^*)\text{Li}_2$ , where  $\text{R}^*$  is the chiral menthyl or neomenthyl group.<sup>777</sup> These dichlorides are converted to the corresponding dimethyl complexes by the reaction with 2 equiv. of  $\text{MeLi-LiBr}$ , from which the cationic catalysts are generated using activators such as MAO,  $\text{B}(\text{C}_6\text{F}_5)_3$ ,  $\text{Ph}_3\text{CB}(\text{C}_6\text{F}_5)_4$ , or  $[\text{HNBu}_3][\text{B}(\text{C}_6\text{F}_5)_4]$ . These chiral, non- $C_2$ -symmetric zirconocene catalysts are competent for the isospecific polymerization of propylene. The polymerization characteristics are strongly dependent on co-catalyst type and concentration, suggesting strong, structure-sensitive ion-pairing effects.<sup>778</sup> Analogous asymmetrically substituted *ansa*-zirconocene complexes  $\text{Me}_2\text{Si}(\text{Me}_4\text{C}_5)(\text{C}_5\text{H}_3\text{R})\text{ZrCl}_2$  **1018**, where R is a non-chiral substituent, have also been prepared by the salt metathesis approach.<sup>779,780</sup> Activation of a series of asymmetrically substituted *ansa*-zirconocene dimethyl complexes  $\text{Me}_2\text{Si}(\text{Me}_4\text{C}_5)(\text{C}_5\text{H}_3\text{R})\text{ZrMe}_2$  **1019** with  $\text{B}(\text{C}_6\text{F}_5)_3$  gives the corresponding zwitterionic species **1020** that are active catalysts for polymerization of ethylene.<sup>781</sup>

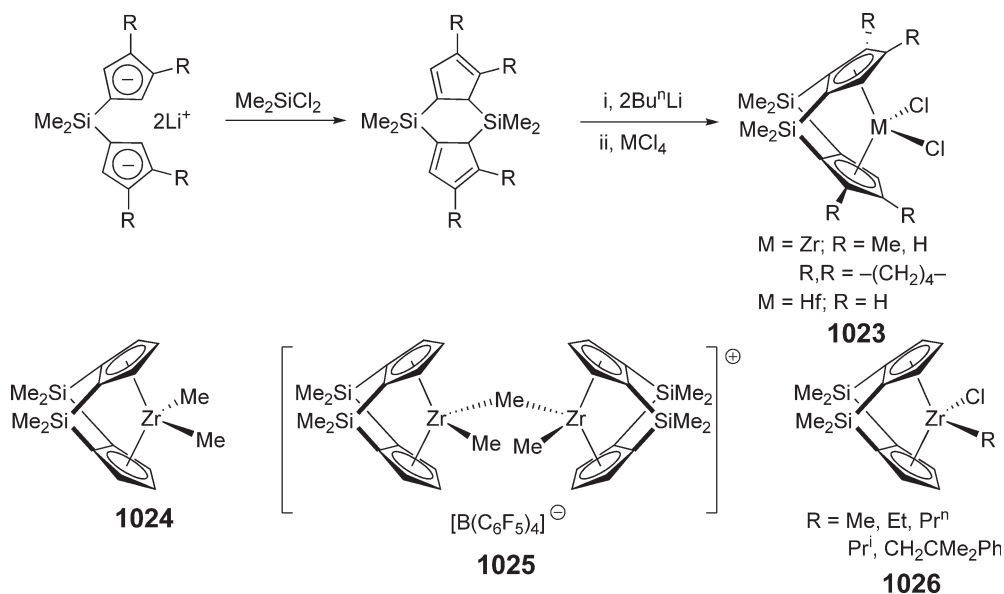




The salt metathesis route was employed to synthesize dimethylsilylene-bridged  $C_2$ -symmetric *ansa*-zirconocene dichloride  $\text{Me}_2\text{Si}(\text{Cp})(3,4\text{-Bu}^t\text{C}_5\text{H}_2)\text{ZrCl}_2$  **1021**, which was structurally characterized by X-ray diffraction.<sup>782</sup> Alkylation of the dichloride with  $\text{MeMgBr}$  gives the dimethyl derivative. The dichloride/MAO system was employed for polymerization of 1-hexene under high-pressure conditions. Compounds of type **1022** with a spiroisilane bridge have been synthesized by the salt metathesis route. The molecular structures ( $R = \text{Pr}^i, \text{Bu}^t$ ) have been determined.<sup>783</sup> When activated with MAO, the  $\text{Bu}^t$ -substituted spiroisilane complex produces polypropylenes with a relatively high content of 3,1-insertions. The increased regioirregularity was attributed to the decreased coordination gap aperture and increased lateral extension angles in the spiroisilane-bridged compounds.



The doubly  $\text{Me}_2\text{Si}$ -bridged *ansa*-metallocene **1023** ( $M = \text{Zr}; R = \text{Me}$ ) is obtained by salt metathesis as outlined in Scheme 252.<sup>784</sup> The complex incorporates  $C_2$ -symmetrically disposed methyl substituents on the Cp rings. Dithallium or dilithium salts of the bridged ligand were employed for the synthesis of unsubstituted derivatives

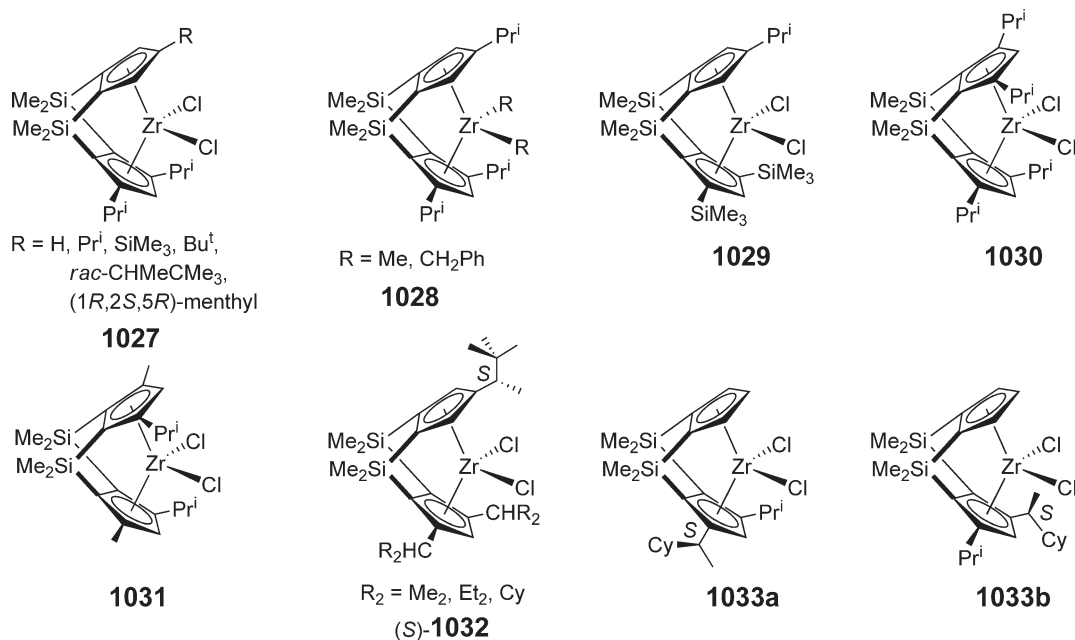


Scheme 252



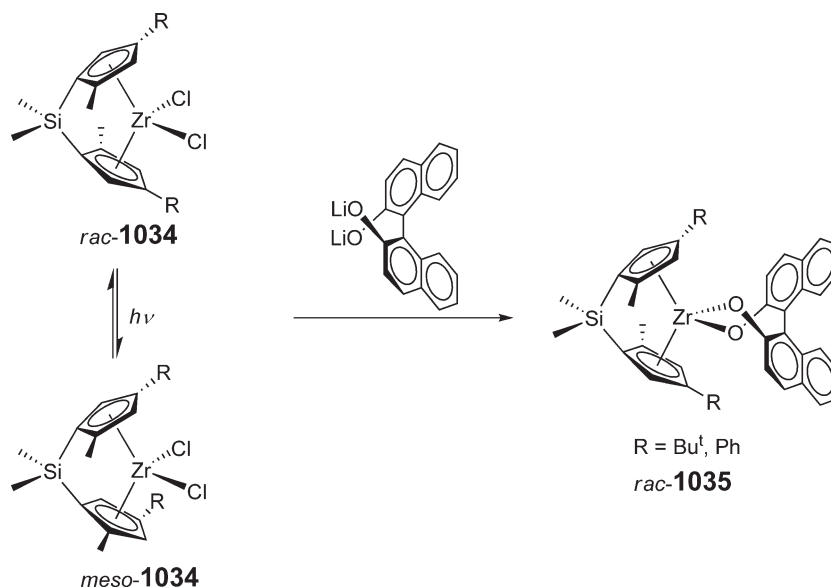
$[(\text{Me}_2\text{Si})_2(\eta^5\text{-C}_5\text{H}_3)_2]\text{MCl}_2$  (**1023**;  $\text{M} = \text{Zr}, \text{Hf}$ ;  $\text{R} = \text{H}$ ),<sup>785</sup> which can be methylated by  $\text{MeLi}$  or  $\text{MeMgCl}$  to afford the corresponding dimethyl species **1024** in moderate yield. NMR data suggest that the reaction of the dimethyl complex with  $[\text{Ph}_3\text{C}][\text{B}(\text{C}_6\text{F}_5)_4]$  in  $\text{CD}_2\text{Cl}_2$  at  $-78^\circ\text{C}$  generates the methyl-bridged binuclear cation **1025**.<sup>786</sup> Alkylation of the dichloride complex with 1 equiv. of  $\text{RMgCl}$  or  $\text{RLi}$  in THF leads to the monoalkylated complexes **1026**.<sup>787</sup> Insertion of isocyanides into the  $\text{Zr-C}$  bond of both dimethyl **1024** and monoalkyl chloride **1026** complexes yields the corresponding iminoacyl derivatives.<sup>788</sup> Zirconocene and hafnocenes complexes bearing larger, doubly disiloxanediyl  $[\text{Me}_2\text{SiOSiMe}_2]$  bridges have also been made.<sup>789</sup>

A large number of other doubly dimethylsilylene-bridged *ansa*-zirconocenes **1027–1033** with varying complex symmetry and ligand steric bulk have been synthesized. These complexes were designed specifically for systematic investigations of their activity and stereoselectivity toward  $\alpha$ -olefins. Complexes of type **1027** can be further divided into two classes:  $C_s$ -symmetric pre-catalysts ( $\text{R} = \text{H}, \text{Pr}^i, \text{SiMe}_3, \text{Bu}^t$ ) and  $C_1$ -symmetric pre-catalysts ( $\text{R} = \text{CHMeCMe}_3, (1S,2R,5R)\text{-menthyl}$ ).<sup>790,791</sup> When activated with MAO, the  $C_s$ -symmetric systems are highly regiospecific and syndiospecific in neat propylene, whereas the  $C_1$ -symmetric systems display an unusual dependence of stereospecificity on propylene concentration, switching from isospecific to syndiospecific with increasing propylene pressure, consistent with a competitive unimolecular site-epimerization process and a bimolecular chain propagation. Dialkyl complexes **1028** have been prepared and their reactivity in 1-pentene polymerization, co-catalyzed by  $[\text{Ph}_3\text{C}][\text{B}(\text{C}_6\text{F}_5)_4]$ , investigated.<sup>792</sup> Polymerizations by these two catalysts at low temperatures in liquid 1-pentene monomer produced poly(1-pentene) with syndiotactic microstructure and narrow molecular weight distribution. By contrast, in 1-pentene/toluene solutions, a broad molecular weight distribution is observed. Under all conditions examined, the **1028** ( $\text{R} = \text{Me}$ )/MAO system produced high molecular weight, highly syndiotactic poly(1-pentene) with narrow molecular weight distributions. The  $C_s$ - and  $C_{2v}$ -symmetric doubly  $\text{Me}_2\text{Si}$ -bridged zirconocenes **1029**/MAO and **1030**/MAO are active catalysts for polymerization of propylene, to produce syndiotactic and atactic polypropylenes, respectively.<sup>793</sup> The racemic  $C_2$ -zirconocene **1031** is chemically and configurationally stable in solution at room temperature for a week or to heating at  $80^\circ\text{C}$  for 24 h; in sharp contrast, the titanium complex of the same ligation undergoes facile *rac-meso*-interchange in benzene solution just above room temperature, affording an approximately 1:1 mixture of *rac*- and *meso*-isomers.<sup>794</sup> Related enantiomerically pure  $C_1$ -symmetric doubly-bridged *ansa*-zirconocenes (*S*)-**1032** that incorporate an enantiopure methylneopentyl substituent in the “upper” Cp ligand, and the diastereomerically pure *ansa*-zirconocenes (*S*)-**1033a** and (*S*)-**1033b**, which have an enantiopure, 1-cyclohexylethyl substituent on the “lower” Cp ligand, have been synthesized for use in the polymerization of chiral  $\alpha$ -olefins.<sup>795</sup> When activated with MAO, these catalysts show unprecedented activity for the polymerization of bulky racemic  $\alpha$ -olefins bearing substituents in the 3- and/or 4-positions. Owing to the optically pure nature of these single-site catalysts, they effect kinetic resolution of racemic  $\alpha$ -olefins.

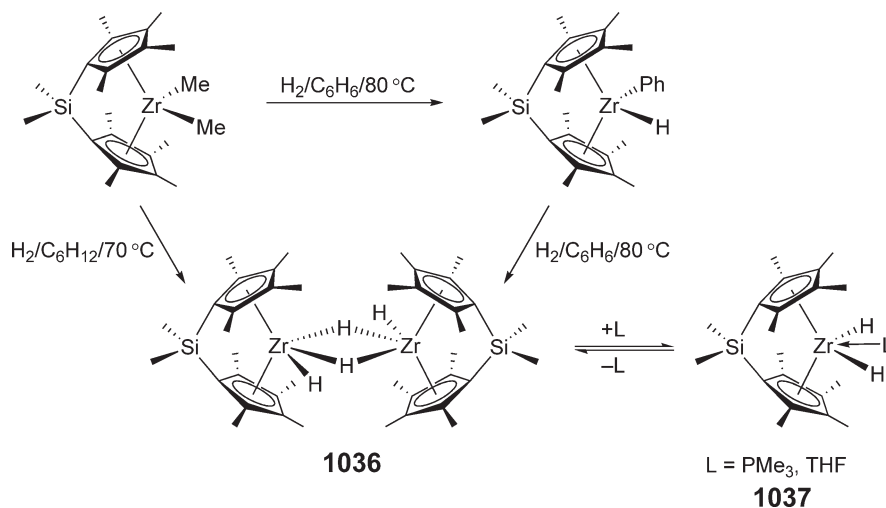


*Rac/meso*-isomers of bridged bis(indenyl) zirconium dichlorides can interconvert photochemically.<sup>796</sup> This interconversion has been utilized in the stereoselective synthesis of *ansa*-zirconocene binaphtholate stereoisomers.<sup>797</sup> Specifically, the *rac*-*meso*-mixtures **1034** induced by irradiation in toluene react with 1 equiv. of the dilithium salt of racemic binaphthol to give the racemic binaphtholate complex **1035** (Scheme 253). Analogous reactions with 1 equiv. of the *R*(+) enantiomer of dilithium binaphtholate afford the enantiomerically pure *ansa*-zirconocene binaphtholate complex. The structure of the racemic binaphtholate complex,  $\text{Me}_2\text{Si}(2\text{-Me-4-Bu}^t\text{-C}_5\text{H}_2)_2\text{Zr}(\text{binaphtholate})$ , has been crystallographically determined.

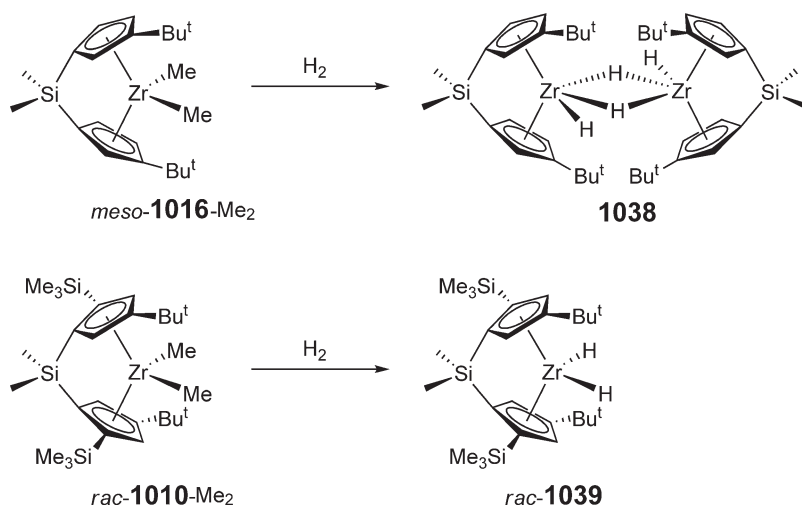
The *ansa*-effect in zirconocene chemistry has been demonstrated in the C–H activation of benzene. Specifically, the incorporation of the  $\text{Me}_2\text{Si}$  *ansa*-bridge in complexes such as  $[\text{Me}_2\text{Si}(\text{C}_5\text{Me}_4)_2]\text{ZrMe}_2$  produces a more electrophilic zirconium center and promotes C–H bond activation of  $\text{C}_6\text{H}_6$  during the hydrogenation of the dimethyl complex in benzene, yielding the corresponding phenyl hydride complex  $[\text{Me}_2\text{Si}(\text{C}_5\text{Me}_4)_2]\text{Zr}(\text{Ph})\text{H}$  (Scheme 254).<sup>798</sup> The same reaction in cyclohexane gives the dihydride complex  $[\text{Me}_2\text{Si}(\text{C}_5\text{Me}_4)_2]\text{ZrH}(\mu\text{-H})_2$  **1036**, which



Scheme 253



Scheme 254



Scheme 255

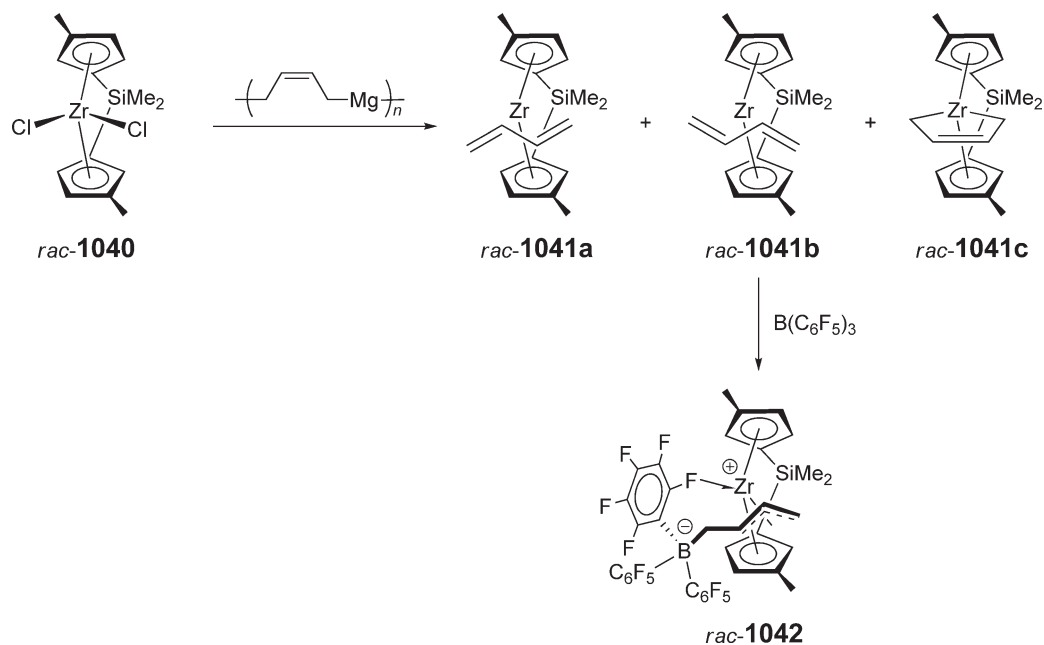
reacts readily with benzene to give  $[\text{Me}_2\text{Si}(\text{C}_5\text{Me}_4)_2]\text{Zr}(\text{Ph})\text{H}$ . Addition of Lewis bases such as  $\text{PMe}_3$  and THF traps the monomer as adducts **1037**, demonstrating the facile monomer–dimer equilibrium in the dihydride complex. The dihydride complex **1036** is an excellent precursor of the ethylene–hydride complex  $[\text{Me}_2\text{Si}(\text{C}_5\text{Me}_4)_2\text{Zr}(\eta^2\text{-C}_2\text{H}_4)\text{H}]_2\text{Mg}$  by reaction with divinylmagnesium in aromatic solvents.<sup>799</sup>

A series of singly and doubly  $\text{Me}_2\text{Si}$ -bridged *ansa*-zirconocene dihydride complexes has been synthesized via hydrogenation of the corresponding dimethyl derivatives.<sup>800</sup> The hydrogenation of the singly bridged dimethyl complexes at 25 °C is facile and affords the dihydride products, whereas for the doubly bridged analogs the reaction requires more forcing conditions and occurs over the course of days at 87 °C. Hydrogenation of *meso*- $\text{Me}_2\text{Si}(\eta^5\text{-C}_5\text{H}_3\text{-3-Bu}^t)_2\text{ZrMe}_2$  **1016-Me**<sub>2</sub> affords the isomeric dimeric dihydrides  $[\{\text{meso-Me}_2\text{Si}(\eta^5\text{-C}_5\text{H}_3\text{-3-Bu}^t)_2\text{ZrH}\}_2(\mu\text{-H})_2]$  (**1038**, Scheme 255), one of which has been characterized by X-ray diffraction. On the other hand, hydrogenation of the racemic isomer  $\text{Me}_2\text{Si}(\eta^5\text{-C}_5\text{H}_2\text{-2-SiMe}_3\text{-4-Bu}^t)_2\text{ZrMe}_2$  **1010-Me**<sub>2</sub> produces the monomeric dihydride  $\text{Me}_2\text{Si}(\eta^5\text{-C}_5\text{H}_2\text{-2-SiMe}_3\text{-4-Bu}^t)_2\text{ZrH}_2$  **1039**.

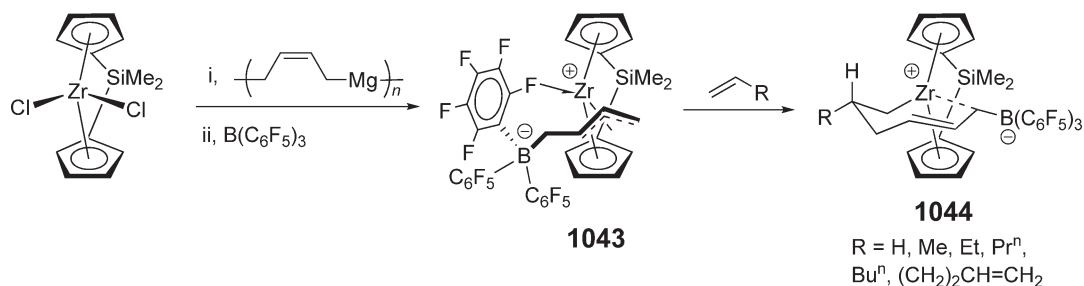
Treatment of *rac*-dimethylsilylene-bridged, methyl-substituted *ansa*-zirconocene dichloride **1040** with “butadiene–magnesium” yields a 82:8:10 mixture of (*s-trans*- $\eta^4$ -butadiene)zirconocenes **1041a** and **1041b** and (*s-cis*-butadiene)zirconocene isomer **1041c** (Scheme 256).<sup>801</sup> The structure of the *trans*-isomer **1041a** has been characterized by X-ray diffraction and features a typical *s-trans*- $\eta^4$ -butadiene moiety. Addition of  $\text{B}(\text{C}_6\text{F}_5)_3$  to the **1041** mixture gives rise to the formation of the *ansa*-zirconocene betaine system **1042**.<sup>802</sup> As the molecular structure shows, complex **1042** contains a substituted  $\eta^3$ -allyl ligand of (*E*)-configuration and a characteristic (*ortho*-aryl)  $\text{C-F} \cdots \text{Zr}$  interaction that stabilizes the electron-deficient metal center. Zwitterion **1042** and its substituted derivatives are single-component metallocene catalysts for the stereospecific polymerization of methyl methacrylate, and investigations of the alkyl substituent effect on the polymerization stereochemistry provide evidence for an anion-dependent metallocene-catalyzed polymerization process.<sup>803</sup>

The unsubstituted *ansa*-zirconocene betaine system **1043** is generated in the same fashion as *rac*-**1042** (Scheme 257). Stoichiometric insertion reactions of  $\alpha$ -olefins with **1043** at –20 °C yield the metallacyclic carbon–carbon coupling products **1044**, which feature an internal  $\text{C}=\text{C}$  alkene coordination to zirconium and an intramolecular  $\text{Zr-CH}_2\text{B}(\text{C}_6\text{F}_5)_3$  ion pair interaction.<sup>804</sup> This system made it possible to kinetically isolate a single alkene insertion step as the initiation of a chain growth sequence and to study this essential step experimentally, thereby obtaining the alkene-addition/insertion energy profile.

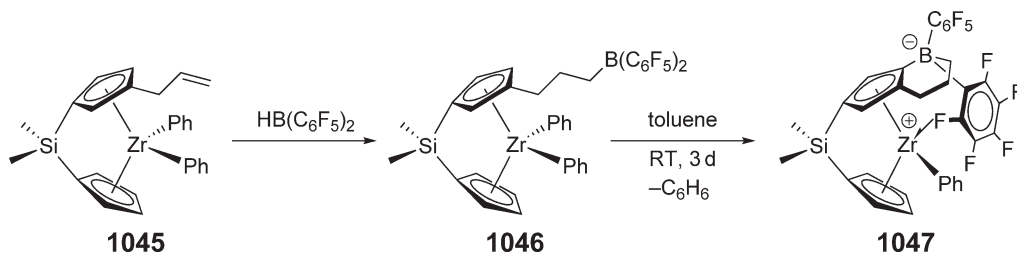
Hydroboration of the allyl-substituted  $\text{Me}_2\text{Si}$ -bridged *ansa*-zirconocene diphenyl complex **1045** with  $\text{HB}(\text{C}_6\text{F}_5)_2$  produces the [bis(pentafluorophenyl)boryl]propyl-functionalized derivative **1046**<sup>805</sup> (Scheme 258). This complex cyclizes in 3 days at room temperature, via electrophilic substitution at the Cp ring by the  $-\text{B}(\text{C}_6\text{F}_5)_2$  group and elimination of benzene, yields  $\eta^5$ -cyclopentadienoborinane zwitterionic zirconocene complex **1047** in which a pentafluorophenyl group is coordinated to zirconium as indicated by X-ray diffraction results. The  $\text{C}_6\text{F}_5 \cdots \text{Zr}$  interaction can be disrupted by addition of  $\text{PMe}_3$ , leading to the corresponding phosphine adduct.



Scheme 256

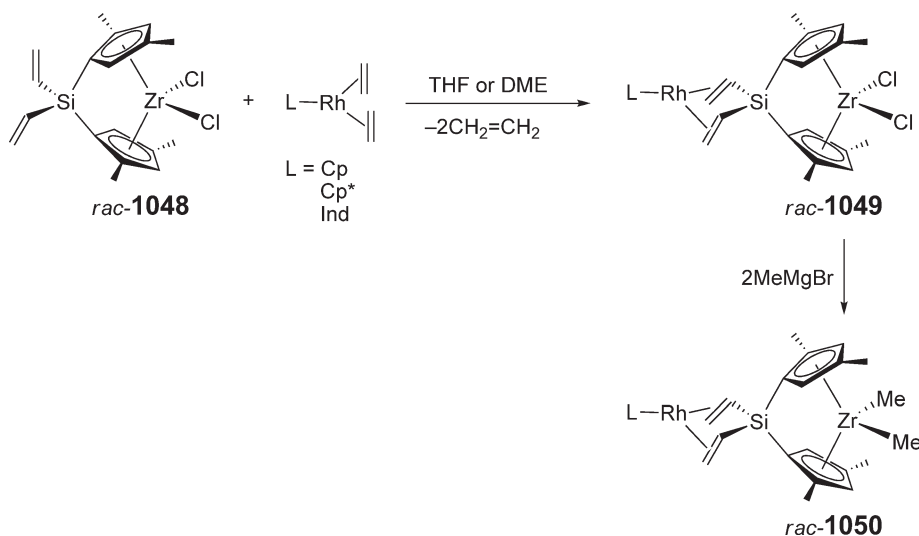


Scheme 257



Scheme 258

Heterobimetallic Zr/Rh complexes, *rac*-L Rh( $\eta^2$ -CH<sub>2</sub>=CH<sub>2</sub>) Si( $\eta^5$ -C<sub>5</sub>H<sub>2</sub>-2,4-Me<sub>2</sub>)<sub>2</sub> ZrCl<sub>2</sub> (**1049**: L = Cp, Cp<sup>\*</sup>, Ind), have been synthesized by a ligand exchange reaction between the divinylsilylene-bridged *ansa*-zirconocene dichloride complex **1048** and bis(ethylene)(L)rhodium complexes according to Scheme 259.<sup>806</sup> The molecular structures of **1049** (L = Cp) along with the dichloride precursor **1048** have been determined and the corresponding dimethyl

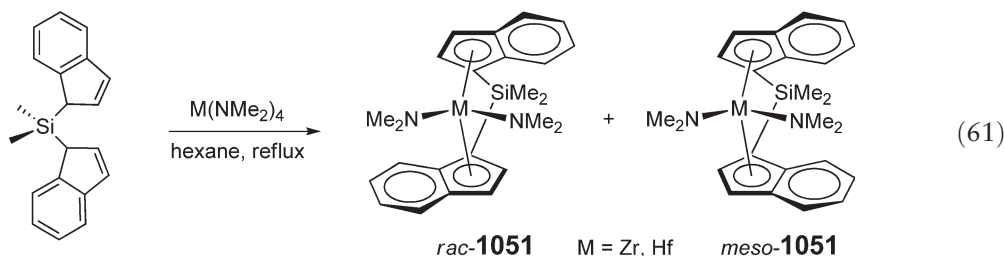


Scheme 259

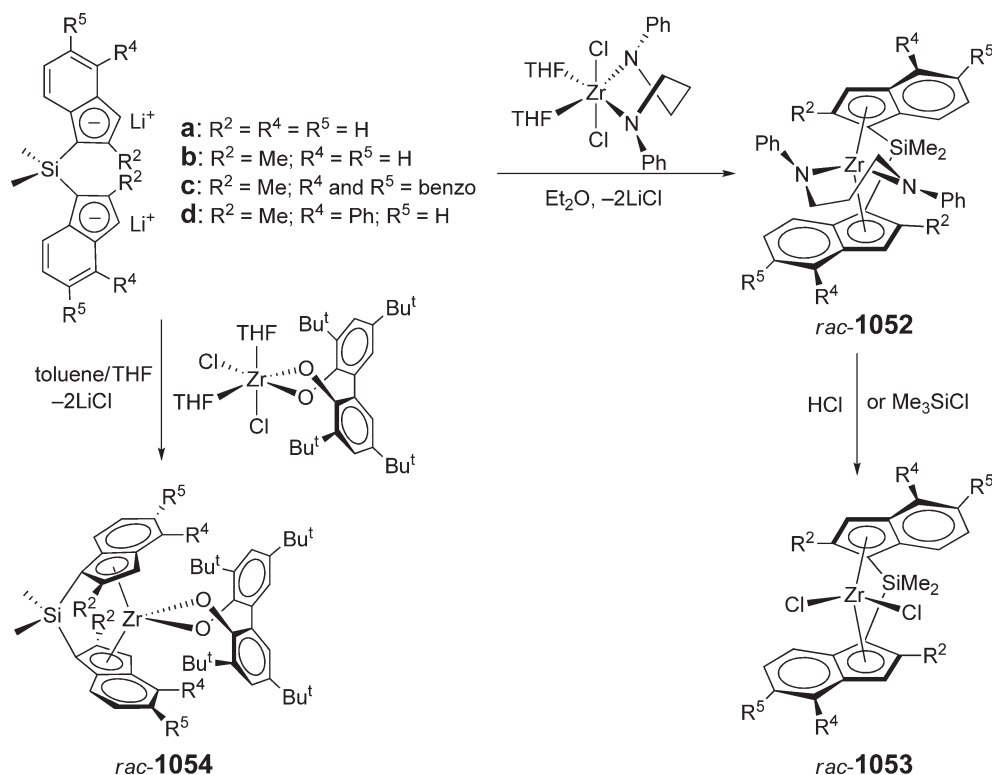
derivatives **1050** prepared. In combination with a large excess of MAO, these Zr/Rh heterobimetallic dichloride complexes **1049** catalyze the highly isospecific polymerization of propylene and 1-hexene, with their catalytic activities being higher than the parent zirconocene complex **1048**. Thus, it is interesting to see that a late transition metal fragment located far away ( $>6 \text{ \AA}$ ) from the early transition metal center can still influence the catalytic activity of the latter.

#### 4.08.10.2.2 Si-bridged indenyl complexes

Amine elimination reactions of  $(\text{SBI})\text{H}_2$  ( $\text{SBI} = \text{Me}_2\text{Si}(\text{Ind})_2$ ) and  $\text{M}(\text{NMe}_2)_4$  ( $\text{M} = \text{Zr}, \text{Hf}$ ) afford  $\text{rac}-(\text{SBI})\text{M}(\text{NMe}_2)_2$  (**1051**:  $\text{M} = \text{Zr}$ ,<sup>807</sup>  $\text{Hf}$ <sup>808</sup>) in 65% (51%)<sup>809</sup> and 20% isolated yields, respectively (Equation (61)). A general theme of these amine elimination reactions is that the reaction proceeds by initial formation of a mono(indenyl) intermediate, which reacts reversibly with a second equivalent ligand to form a binuclear complex and undergoes reversible intramolecular amine elimination to form both *rac*- and *meso*-diastereomers. With the bis[2-(*N,N*-diethyl-amino)ethyl-indenyl]dimethylsilane ligand, its amine elimination reaction with  $\text{Zr}(\text{NMe}_2)_4$  in *n*-octane under reflux conditions for 8 h results in the formation of a mixture of species, including *rac*- and *meso*-diastereomers as well as the half-sandwich complexes.<sup>810</sup>



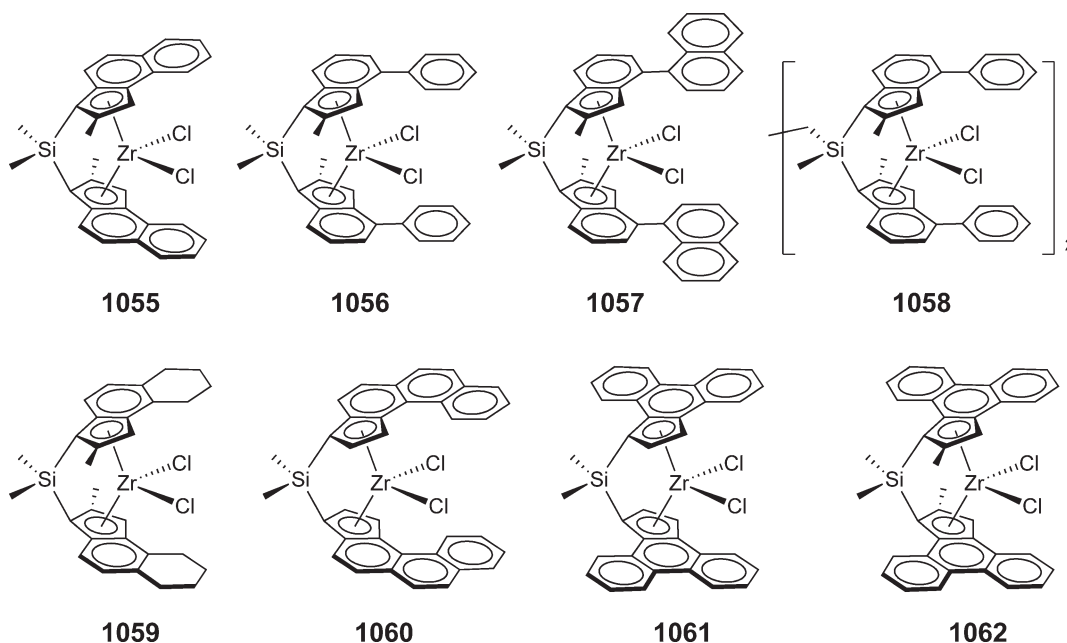
The amine elimination approach using the reagent  $\text{Zr}(\text{NR}_2)_4$  typically works well for simple *ansa*-bis(indenyl) ligands. However, this approach is not successful for sterically crowded ligands such as 2,4-substituted and related indenenes. Incorporation of such a ligand framework into a propylene polymerization catalyst structure is necessary in order to achieve high polymer isotacticity and molecular weight. To overcome this problem, a general, chelate-controlled synthesis of racemic  $\text{Me}_2\text{Si}$ -bridged *ansa*-bis(indenyl)zirconocene complexes has been developed, based on the chelate propylene-diamide zirconium dichloride precursor,  $\text{Zr}[\text{PhN}(\text{CH}_2)_3\text{NPh}]\text{Cl}_2(\text{THF})_2$ .<sup>811</sup> Thus, the reaction of  $\text{Zr}[\text{PhN}(\text{CH}_2)_3\text{NPh}]\text{Cl}_2(\text{THF})_2$  and  $\text{Li}_2[\text{SBI}](\text{Et}_2\text{O})$  in  $\text{Et}_2\text{O}$  at ambient temperature produces *rac*-**1052**, with no detectable amount of *meso*-isomer, which reacts further with  $\text{SiMe}_3\text{Cl}$  to give *rac*-( $\text{SBI}$ ) $\text{ZrCl}_2$  **1053**. This synthesis can be readily extended to other 2,4,5-substituted *ansa*-bis(indenyl) derivatives and gives high chemical



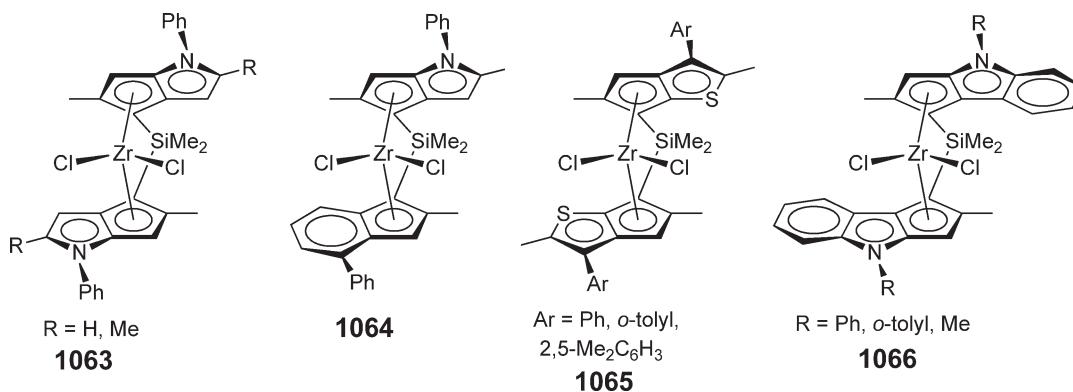
Scheme 260

yields and diastereoselectivities with no detectable amount of *meso*-isomers (Scheme 260).<sup>812</sup> The X-ray structure shows that the chelate ring  $Zr[PhN(CH_2)_3NPh]$  in racemic isomers adopts a twist conformation which complements the *rac*-orientation of the bridged bis(indenyl) ligand but destabilizes the corresponding *meso*-diastereomer. It is proposed that the  $Zr[PhN(CH_2)_3NPh]$  chelate ring adopts a similar twist conformation in the stereodetermining transition state for addition of the second indenyl ring in these reactions, to give the *rac*-product diastereoselectively. The chelating biphenolate dichlorozirconium has previously been employed to direct the *racemo*-selective synthesis of *ansa*-zirconocenes.<sup>813</sup> Using this approach, the biphenolate complexes **1054** (Scheme 260) have been isolated in yields of 60–75%.

Among many substituted silylene-bridged *ansa*-bis(indenyl)zirconocene complexes, some of the best catalysts (upon activation with suitable activators) for propylene polymerization in terms of their catalytic activity as well as the resulting polymer molecular weight and isotacticity are listed below. For example, the 2-methyl-4,5-benzo-substituted derivative **1055**, when activated with MAO, produces highly isotactic polypropylene with high molecular weight; it is proposed that the presence of the methyl group at the 2-position is responsible for the unusually high polymer molecular weight achieved as a result of a strong suppression of direct  $\beta$ -H transfer to monomer by this methyl group.<sup>814,815</sup> The 2-methyl-4-phenyl-substituted derivative **1056** and 2-methyl-4-(1-naphthyl)-substituted derivative **1057** activated with MAO are also highly effective catalysts for the polymerization of propylene in all aspects.<sup>816</sup> The binuclear derivative **1058** linked through the  $-(CH_2)_2SiMe$  bridge is a less effective catalyst than the corresponding mononuclear complex.<sup>817</sup> Further ligand modifications have produced four more derivatives **1059–1062**.<sup>818</sup> Much of the work has been devoted to the synthesis of these highly sterically demanding and annulated aromatic ligands, whereas the final metallation steps using salt metathesis are typically straightforward, giving mixtures of *rac*- and *meso*-diastereomers, from which the desirable *rac*-isomers are obtained by fractional recrystallization. On activation with MAO, these complexes are highly active for polymerization of propylene, leading to polypropylenes with high isotacticities and molecular weights. The results from co-polymerizations of ethylene with 1-octene also show that benzannulation present in these complexes substantially improves the degree and the randomness of co-monomer incorporation, whereas 2-methyl substitution promotes activity.<sup>819</sup>



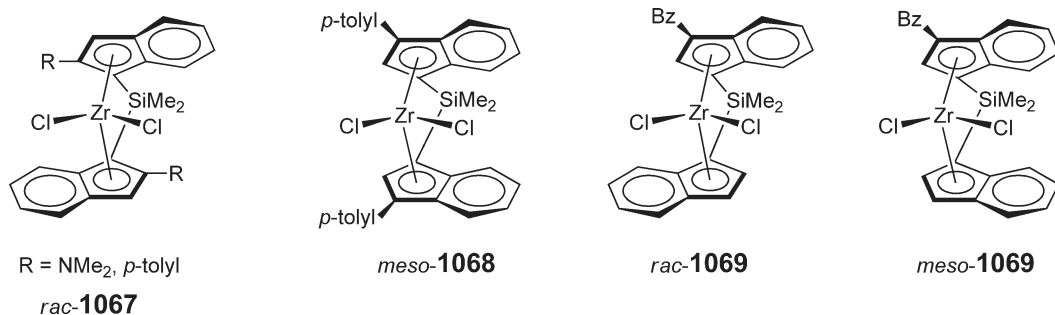
Chiral *ansa*-zirconocenes incorporating dimethylsilylene-bridged cyclopentadienyl ligands [*b*]-fused to substituted pyrrole **1063** and **1064** and thiophene **1065** heterocycles have been synthesized.<sup>820,821</sup> When activated with MAO, complex **1062** (Ar = Ph) is most reactive for polymerization of propylene, which is 3.5 times higher in activity than the benchmark catalyst  $\text{Me}_2\text{Si}(2\text{-Me-4-Ph-Ind})_2\text{ZrCl}_2$  **1056**. Though the latter is more stereospecific and less regio-specific, the sum of these two enantioface errors is the same for both catalysts.<sup>822</sup> Analogous systems **1066** incorporating *N*-substituted 2-methylcyclopenta[*b*]indolyl ligands have also been developed.<sup>823</sup> Mixtures of these complexes with MAO are also highly isospecific and regiospecific propylene polymerization catalysts, with indices comparable with those obtained by **1056**. The activity of the catalyst derived from the non-heterocene **1056** is 1–2 orders of magnitude higher than that by **1066** at high MAO/Zr ratios, but the activity is similar between these two systems at low MAO/Zr ratios.



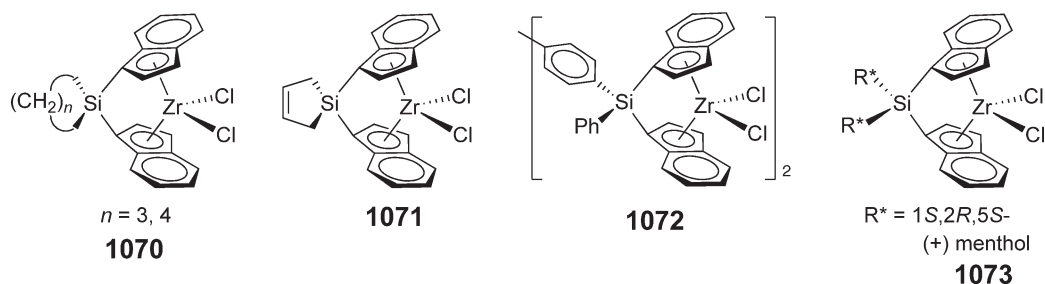
To increase electron density at the metal center, the dimethylamido group is introduced to the 2-position of the indenyl ligand, leading to the preparation of the *ansa*-(SBI)zirconocene dichloride complex **1067** (R = NMe<sub>2</sub>).<sup>824</sup> The pure *rac*-isomer was obtained in 30% yield from the initially formed diastereomeric mixture. The microstructure of the polypropylene produced by the **1067** (R = NMe<sub>2</sub>)/MAO system is comparable to that produced with unsubstituted *rac*-(SBI)ZrCl<sub>2</sub>. The salt metathesis approach was employed for the preparation of *ansa*-(SBI)zirconocene complexes with 2- and 3-*p*-tolyl substitution on the indenyl rings.<sup>825</sup> The racemic complex **1067** was isolated by fractional recrystallization from an initially formed 2:1 *rac*/*meso* mixture, whereas for the 3-aryl-substituted complex **1068** the *meso*-isomer was obtained from an initially formed 1:1 *rac*/*meso*-mixture. Dimethylsilylene-bridged *ansa*-(cyclopentadienyl-substituted-indenyl)zirconocene dichlorides,  $\text{Me}_2\text{Si}(\text{Cp})(\text{R-Ind})\text{ZrCl}_2$  (R = 2- or 3-*p*-tolyl), have



also been prepared.<sup>826</sup> The dual-site, unsymmetrically substituted *rac*- and *meso*-like  $\text{Me}_2\text{Si}(3\text{-benzylindenyl})(\text{indenyl})$  zirconocene dichloride complexes **1069** were obtained by salt metathesis and separated by fractional recrystallization.<sup>827</sup> Interestingly, these diastereomers produce isotactic polypropylenes with similar microstructures and molar masses under equivalent polymerization conditions.



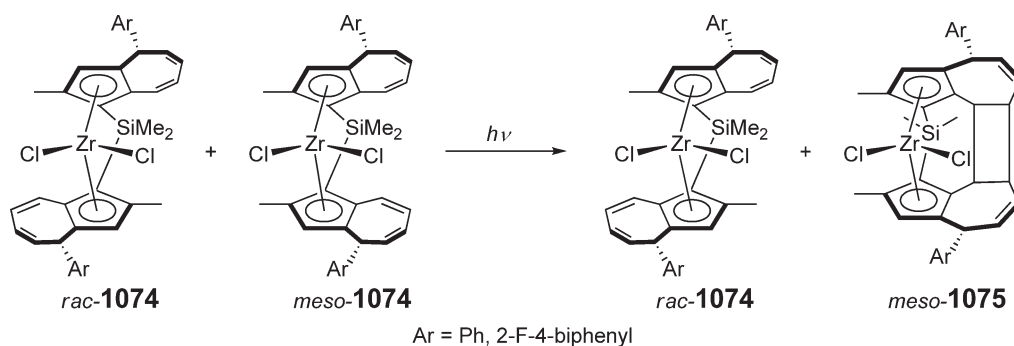
Modifications of silylene-bridging moieties have resulted in the preparation of *ansa*-bis(indenyl)zirconocenes having different silylene bridges, including (1,4-butanediyl)silylene-bis(1-indenyl)dichlorozirconium **1070** ( $n=4$ )<sup>828</sup> and its tetrahydroindenyl derivative,<sup>829</sup> (1,3-propanediyl)silylene-bis(1-indenyl)dichlorozirconium **1070** ( $n=3$ ),<sup>830</sup> 1,1'-(1-silacyclopent-3-ene-1,1-diyl)bis(indenyl)dichlorozirconium **1071**,<sup>831</sup> as well as  $\mu$ -1,4-phenylene-bridged binuclear *ansa*-bis(indenyl)zirconocenes **1072**.<sup>832</sup> These complexes were obtained mostly as mixtures of *rac*- and *meso*-diastereomers and investigated as catalysts, upon activation with suitable activators, for the polymerization of  $\alpha$ -olefins. Double deprotonation of the bis(1-indenyl)-di[(1'*S*,2'*R*,5'*S*)-menthoxy]silane ligand followed by metallation with  $\text{ZrCl}_4$  gives a mixture of two *ansa*-diastereomeric zirconocenes **1073**.<sup>833</sup> Fractional recrystallization afforded an optically active single diastereomer, which is soluble in aliphatic solvents. When activated with  $\text{Al}(\text{Bu}^i)_3$  and  $[\text{Ph}_3\text{C}][\text{B}(\text{C}_6\text{F}_5)_4]$ , this complex is a highly active homogeneous catalyst for olefin polymerization and copolymerization in both toluene and heptane solutions. Tetramethyldisilylene [ $\text{Me}_4\text{Si}_2$ ]-bridged *ansa*-bis(indenyl) and bis(Me- or  $\text{SiMe}_3$ -substituted-indenyl)zirconocenes have also been synthesized; the molecular structure of *meso*-( $\text{Me}_4\text{Si}_2$ )(3- $\text{SiMe}_3$ -Ind) $_2\text{ZrCl}_2$  was determined.<sup>834</sup>



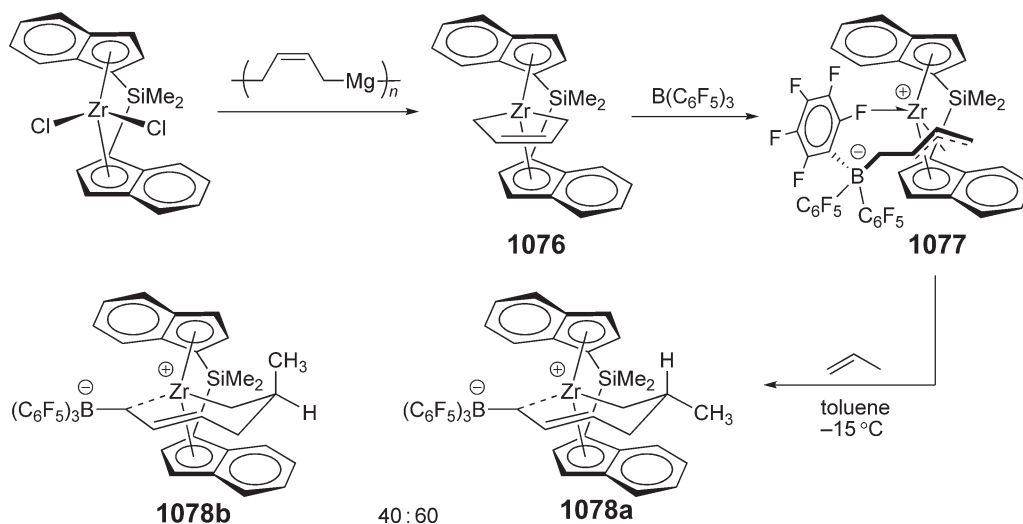
Dimethylsilylene-bridged bis(2-methyl-4-phenyl-4-*H*-azulenyl) zirconium dichlorides **1074** are obtained as a mixture of *rac*/*meso*-isomers by the salt metathesis route.<sup>835</sup> The pure *rac*-isomer has been isolated in low yield from this mixture by repeated crystallization process and also structurally characterized by X-ray diffraction. When activated with MAO, this complex showed high catalytic activity for polymerization of propylene to give isotactic polypropylene; however, both the reactivity and the polymer molecular weight by this catalyst are considerably lower than those obtained by  $\text{Me}_2\text{Si}(2\text{-Me-4-Ph-Ind})_2\text{ZrCl}_2$  **1056**. Irradiation of the *rac*/*meso*-mixture of **1074** induces a rapid conversion of only the *meso*-isomer to give *meso*-**1075** supported by the bis(azulenyl) ligand cross-linked by a cyclobutylene ring, which was produced by intramolecular [2 + 2]-cycloaddition (Scheme 261).<sup>836</sup> The *rac*-isomer, on the other hand, is stable toward photoirradiation. The molecular structure of the *meso*-**1075** (Ar = 2-F-4-biphenyl) has been determined by X-ray crystallography. Owing to the high solubility of the cyclobutylene-bridged zirconocenes, after photoirradiation of the *rac*/*meso*-mixture **1074**, the *rac*-isomers were easily isolated.

Treatment of *rac*-(SBI) $\text{ZrCl}_2$  with (butadiene)magnesium yields the corresponding *ansa*-zirconocene (*s-cis*- $\eta^4$ -butadiene) complex **1076**,<sup>837</sup> which reacts with  $\text{B}(\text{C}_6\text{F}_5)_3$  to give the *ansa*-zirconocene-( $\mu$ - $\text{C}_4\text{H}_6$ )- $\text{B}(\text{C}_6\text{F}_5)_3$  betaine **1077** (Scheme 262). This betaine complex is an active single-component catalyst and polymerizes propylene stereoselectively to isotactic polypropylene by enantiomorphic-site control. In toluene at  $-15^\circ\text{C}$ , complex **1077**





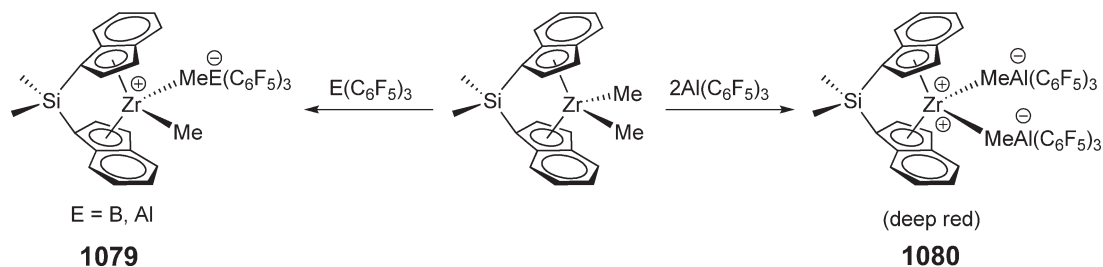
Scheme 261



Scheme 262

inserts a single propene molecule into the Zr–CH<sub>2</sub> bond; the insertion is regioselective but non-stereoselective and gives a 60:40 mixture of the metallacyclic products **1078**. Unlike the first insertion step, subsequent propylene insertions proceed with a high degree of stereoselectivity. A stereochemical “relay mechanism” is proposed to account for this behavior.

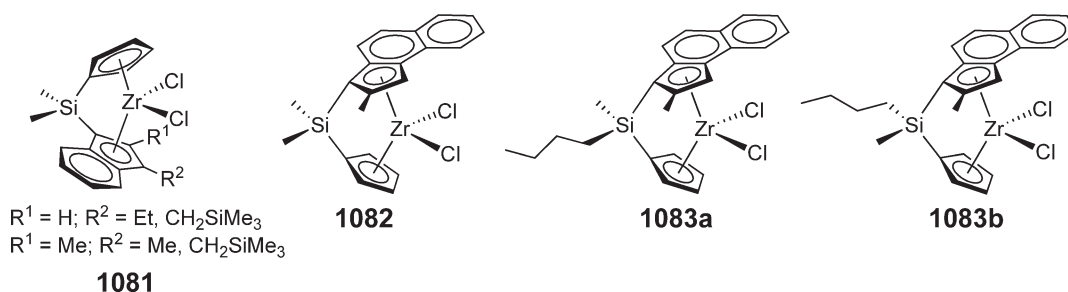
Activation of *rac*-(SBI)ZrMe<sub>2</sub> with 1 equiv. of E(C<sub>6</sub>F<sub>5</sub>)<sub>3</sub> (E = B, Al) results in the instantaneous formation of the corresponding zwitterionic species **1079** as yellow solutions in toluene<sup>838</sup> (Scheme 263). An excess of B(C<sub>6</sub>F<sub>5</sub>)<sub>3</sub> does



Scheme 263

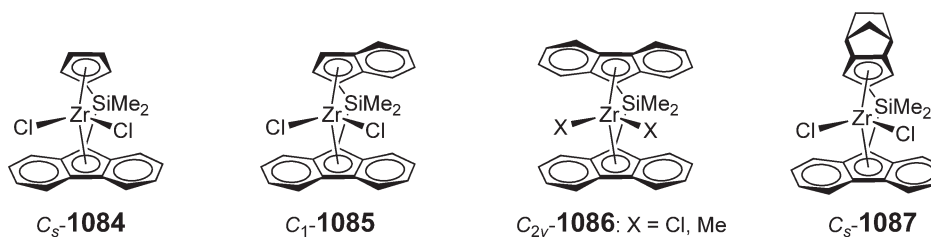
not affect the abstraction of the second methide group; however, addition of a second equiv of  $\text{Al}(\text{C}_6\text{F}_5)_3$  causes an immediate color change to deep red as a result of formation of the doubly activated dicationic species **1080**. This complex has been fully characterized, including the molecular structure by X-ray diffraction. The doubly activated complexes such as **1080** are highly active catalysts for olefin polymerizations and co-polymerizations.

A series of  $\text{Me}_2\text{Si}$ -bridged asymmetric *ansa*-(cyclopentadienyl-substituted-indenyl)zirconocene dichlorides **1081** has been prepared for the investigation of substituent effects on the syndiotactic polypropylene production using these  $C_1$ -symmetric *ansa*-zirconocene complexes in combination with MAO.<sup>839</sup> Analogous  $[\text{Me}_2\text{C}]$ -bridged zirconocenes having the same ligand framework have also been prepared for comparative studies. The polymerization results show that these systems yield polypropylenes with various degrees of syndiotacticity ( $[rrrr] = 28\text{--}66\%$ ) as a function of the substituent size, substitution pattern, and bridging moiety. The silicon-bridged systems produce polymers of higher molecular weight but lower syndiotacticity than the carbon-bridged analogs. Asymmetric *ansa*-zirconocene complexes **1082** and **1083** incorporating a dialkylsilylene-bridged methylbenz[*e*]indenyl and cyclopentadienyl ligand have been synthesized.<sup>840</sup> The preparation procedure involves the reaction of 2-methylbenz[*e*]indene with  $\text{Me}(\text{R})\text{SiCl}_2$  ( $\text{R} = \text{Me}, \text{H}$ ) and further reactions with  $\text{NaCp}$  to give the bridged ligands  $\text{MeC}_{13}\text{H}_8\text{-Si}(\text{R})\text{Me-C}_5\text{H}_5$  ( $\text{R} = \text{Me}, \text{H}$ ). Double deprotonation of the ligand  $\text{MeC}_{13}\text{H}_8\text{-SiMe}_2\text{-C}_5\text{H}_5$  with 2 equiv. of  $\text{BuLi}$  followed by the metallation step with  $\text{ZrCl}_4(\text{THF})_2$  yields complex **1082** in 23% yield. On the other hand, the same reactions using the ligand  $\text{MeC}_{13}\text{H}_8\text{-Si}(\text{H})\text{Me-C}_5\text{H}_5$  did not produce the corresponding zirconocene complex with a hydrogen atom bound to Si, but unexpectedly afforded complexes **1083** with a butyl group attached to Si, as a 1:1 mixture of two diastereomers. The molecular structures of complex **1082** and **1083a** have been determined by X-ray diffraction.

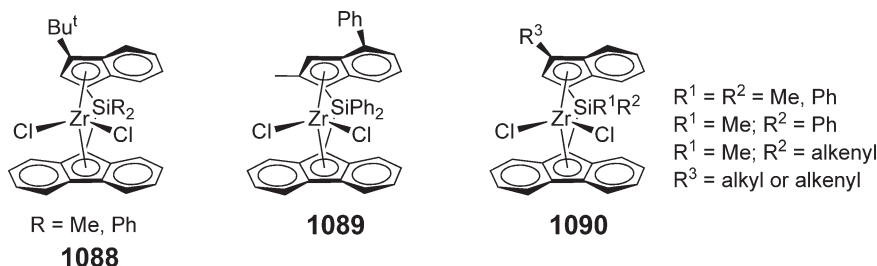


#### 4.08.10.2.3 Si-bridged fluorenyl complexes

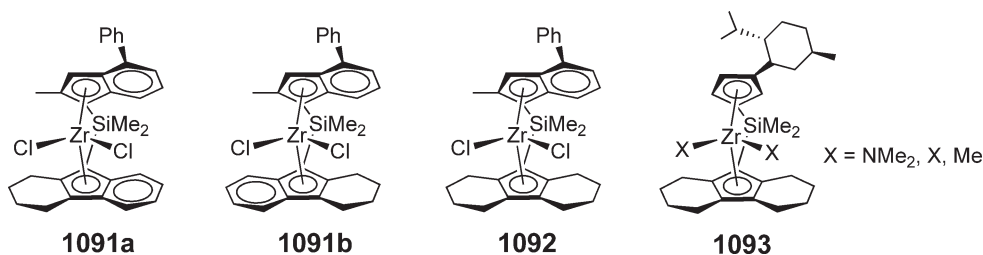
Dimethylsilylene-bridged, fluorenyl-containing *ansa*-zirconocene complexes having various symmetries have been prepared by the salt metathesis approach. Upon activation with MAO, the  $C_s$ -symmetric  $\text{Me}_2\text{Si}$ -bridged *ansa*-(Cp-Flu) zirconocene dichloride **1084** surprisingly yielded atactic polypropylene rather than syndiotactic polymer anticipated on the basis of its symmetry.<sup>841</sup> The  $C_1$ -symmetric  $\text{Me}_2\text{Si}$ -bridged *ansa*-(Ind-Flu) zirconocene dichloride **1085** produces high molecular weight, low isotactic polypropylene. On the other hand, the high molecular weight, atactic polypropylene elastomer can readily be made by the  $C_{2v}$ -symmetric  $\text{Me}_2\text{Si}$ -bridged *ansa*-bis(Flu)zirconocene dichloride **1086**.<sup>842</sup> Other silylene-bridged, fluorenyl-containing *ansa*-zirconocene derivatives include  $\text{Ph}_2\text{Si}(\text{Cp})(\text{Flu})\text{ZrCl}_2$ ,  $\text{R}_2\text{Si}(\text{Cp})(2,7\text{-Bu}^t_2\text{-Flu})\text{ZrCl}_2$  ( $\text{R} = \text{Me}, \text{Ph}$ ), and  $\text{R}_2\text{Si}(2,7\text{-Bu}^t_2\text{-Flu})_2\text{ZrCl}_2$  ( $\text{R} = \text{Me}, \text{Ph}$ );<sup>843</sup> the propylene polymerization behavior of these complexes, when activated with MAO, has been examined. Extension of the dimethylsilylene bridge has produced  $[\text{Me}_2\text{SiCH}_2]$ - and  $[\text{Me}_2\text{SiSiMe}_2]$ -bridged *ansa*-bis(Flu)zirconocene dichloride complexes<sup>844</sup> and a  $[\text{Me}_2\text{SiCH}_2]$ -bridged *ansa*-bis(octahydrofluorenyl)zirconocene dichloride.<sup>845</sup> Dimethylsilylene-bridged (isodicyclopentadienyl)-fluorenyl)zirconium dichloride **1087** was prepared via the standard salt metathesis route and structurally characterized by X-ray diffraction.<sup>846</sup> When activated with a large excess of MAO, this complex produces atactic polypropylene at  $70^\circ\text{C}$  and syndiotactic polypropylene at  $20^\circ\text{C}$ .



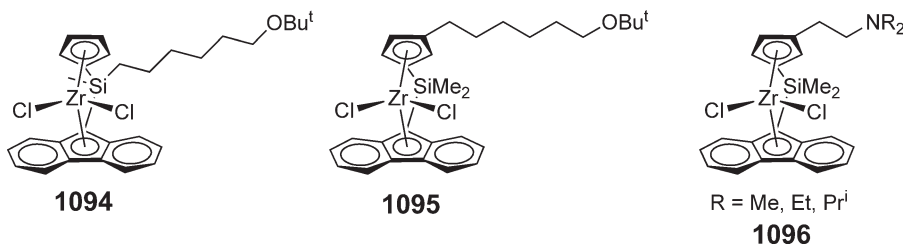
Asymmetric  $\text{Me}_2\text{Si}$ -bridged *ansa*-zirconocenes incorporating bridged fluorenyl and substituted indenyl ligands are readily accessible by the standard salt metathesis route. In complex **1088**, the *tert*-butyl group is introduced to the 3-position of the indenyl ring, whereas complex **1089** has a 2-methyl-4-phenyl substitution pattern;<sup>847</sup> when activated with MAO, **1089** produces isotactic polypropylene with  $[mmmm] = 83\%$ . A large number of other  $C_1$ -symmetric complexes of type **1090** have been prepared and their activities toward polymerization of ethylene examined.<sup>848</sup>



$\text{Me}_2\text{Si}$ -bridged *ansa*-zirconocene dichlorides **1091** incorporating the bridged 2-Me-4-Ph-substituted indenyl and tetrahydrofluorenyl ligands are obtained by salt metathesis as a mixture of two isomers;<sup>849</sup> the octahydrofluorenyl derivative **1092** is prepared in the similar fashion. Upon activation with MAO, these  $C_1$ -symmetric complexes are highly active for the polymerizations of ethylene and the isospecific polymerization of propylene. The stereo-demanding, electron-donating octahydrofluorenyl ligand has been previously employed as a supporting ligand for the synthesis of chiral  $C_1$ -symmetric zirconocenes **1093**.<sup>850</sup> The highly (*S*)-enriched ( $\geq 90\%$ ) zirconocene dichloride complex is prepared from the corresponding bis(dimethylamide) complex, obtained by the amine elimination route, with  $[\text{H}_2\text{NMe}_2]\text{Cl}$ ; subsequent alkylation of the dichloride complex proceeds with retention of configuration to yield the dimethyl complex. The cationic catalysts are generated using common activators, including MAO,  $\text{B}(\text{C}_6\text{F}_5)_3$ , and  $\text{Ph}_3\text{C}[\text{B}(\text{C}_6\text{F}_5)_4]$ , and examined for propylene polymerization. The polymerization results show that the octahydrofluorenyl catalysts exhibit activities similar to or higher than those of the  $\eta^5\text{-Me}_4\text{C}_5$  analogs. More importantly, the polypropylene produced by the former catalysts exhibit substantially higher isotacticities as well as higher molecular weights.



The alkoxy-functionalized silylene-bridged *ansa*-Cp-Flu zirconocene dichlorides bearing a 6-*tert*-butoxyhexyl pendant ligand at the bridgehead Si **1094** or the 3-position of the Cp ring **1095** have been synthesized using the standard salt metathesis techniques.<sup>851</sup> It has been shown that the ethylene polymerization activity of the catalyst derived from the MAO-activated bridge-functionalized complex **1094** is higher than the catalyst derived from the Cp-functionalized **1095**. Silylene-bridged *ansa*-Cp-Flu zirconocene complexes **1096** containing a 3-dialkyl-aminoethyl-functionalized Cp ligand have also been synthesized.<sup>852</sup> Low activities were observed for these complexes in the MAO-co-catalyzed polymerization of propylene.



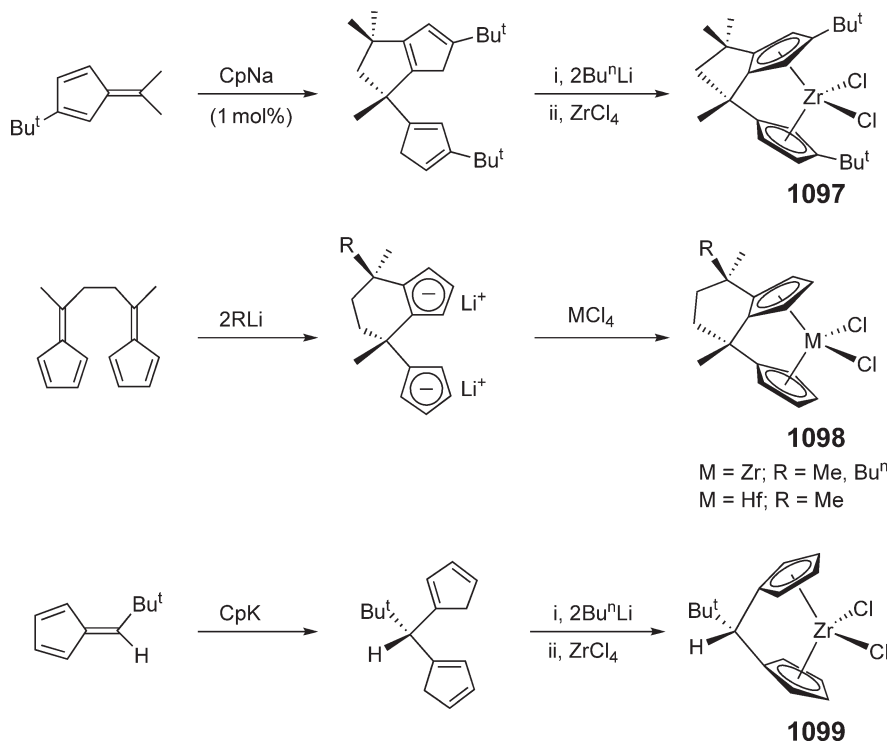
### 4.08.10.3 C<sub>1</sub>-bridged Complexes

Single carbon-atom-bridged *ansa*-metallocene systems such as methylene [R<sub>2</sub>C]-bridged complexes typically impose even higher conformational and configurational rigidity than that of the ethylene [C<sub>2</sub>]- or silylene [R<sub>2</sub>Si]-bridged congeners, which leads to different characteristics in catalytic reactions. As in the [C<sub>2</sub>]- and [R<sub>2</sub>Si]-bridging systems, designing a desired catalyst for certain applications requires the coupling of the [C<sub>1</sub>]-bridging with judicious choice of substitutions in certain positions of Cp, Ind, or Flu ligands to achieve high degrees of control over the characteristics of the employed reactions such as stereo- and regioselectivity of the reaction.

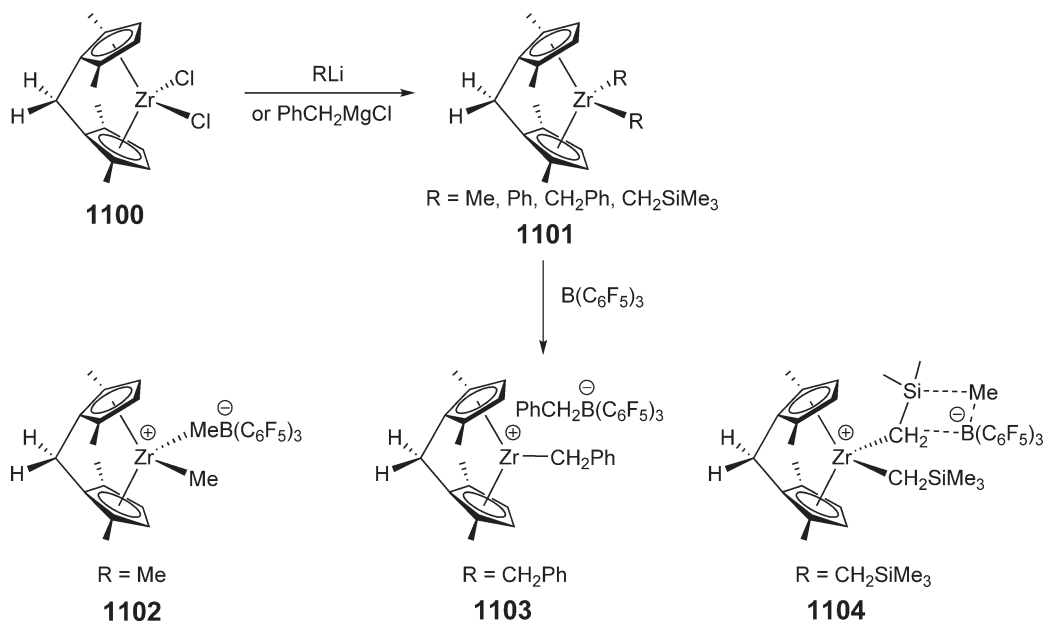
#### 4.08.10.3.1 C<sub>1</sub>-bridged cyclopentadienyl complexes

The presence of CpNa catalyzes the dimerization of 3-*tert*-butyl-6,6-dimethylfulvene to form the five-membered-ring annulated C<sub>1</sub>-bridged bis(Cp) ligand (Scheme 264); double deprotonation of this ligand by BuLi followed by metallation with ZrCl<sub>4</sub> yields the corresponding chiral *ansa*-zirconocene **1097** as a 1:2:1 mixture of two racemic pairs which can be separated by fractional recrystallization.<sup>853</sup> An *ansa*-zirconocene complex analogous to complex **1097**, with the same annulated bridging moiety but without the *tert*-butyl groups on the Cp rings, has been prepared.<sup>854</sup> Six-membered-ring annulated C<sub>1</sub>-bridged *ansa*-metallocene complexes **1098** and the corresponding butadiene complexes have also been synthesized using the substituted fulvene precursor, the reaction sequences of which are summarized in Scheme 264.<sup>855</sup> When the starting fulvene is 6-*tert*-butylfulvene, its reaction with CpK gives the 2,2-dimethylpropylidene-bridged bis(Cp) ligand, which is subsequently converted to the corresponding C<sub>1</sub>-bridged *ansa*-zirconocene dichloride **1099**.<sup>856</sup> Unsymmetric *ansa*-(Cp-Ind)- and *ansa*-(Cp-Flu)-zirconocenes with dimethylpropylidene bridges can be obtained in the similar fashion, and the corresponding dimethyl alkyl complexes can be furnished using MeLi.

The simplest bridge in *ansa*-zirconocenes is the methylene (CH<sub>2</sub>) group, and complexes with this structural motif of the type [H<sub>2</sub>C(Cp)<sub>2</sub>]ZrX<sub>2</sub> (X = Cl, I) have been recently synthesized and structurally characterized.<sup>857</sup> The C<sub>2v</sub>-symmetric methylene-bridged complex **1100** bearing 2,5-dimethyl substituents on both Cp rings (Scheme 265) has been synthesized by key steps involving catalytic Pauson–Khand and the retro-Diels–Alder reactions.<sup>858</sup> The molecular structure of **1100** shows a small Cp(centroid)–Zr–Cp(centroid) bite angle of 117.15° and a correspondingly wide open coordination gap aperture. When activated with MAO, this complex is a very effective catalyst for



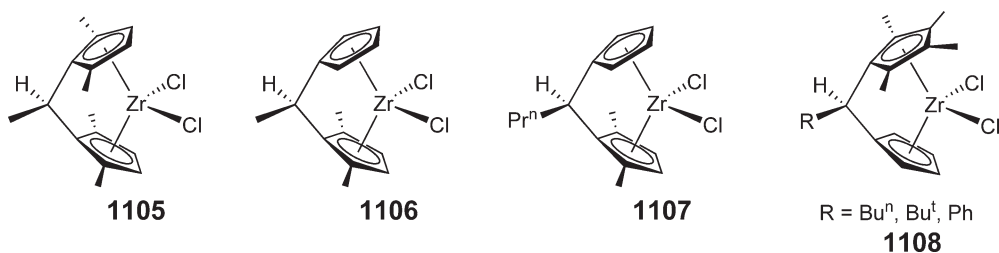
Scheme 264



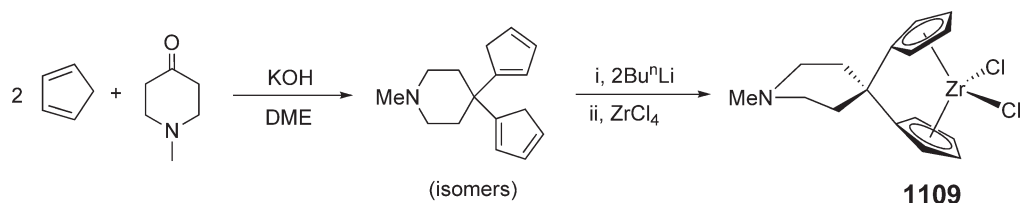
Scheme 265

co-polymerization of ethylene and norbornene, with the activity and norbornene incorporation being higher than those obtained by the benchmark catalyst  $\text{Ph}_2\text{C(Flu)(Cp)ZrCl}_2$ . Alkylation of the dichloride **1100** with suitable alkylating reagents readily affords the corresponding dialkyl complexes **1101**.<sup>859</sup> Abstractive reactions of these alkyl complexes with  $\text{B(C}_6\text{F}_5)_3$  generate different types of cationic complexes, depending on the nature of the alkyl ligand. Specifically, for  $\text{R} = \text{Me}$ , the formation of the inner-sphere (contact) ion pair **1102** is observed; for  $\text{R} = \text{CH}_2\text{Ph}$ , the outer-sphere (separated) ion pair **1103** is seen, whereas for  $\text{R} = \text{CH}_2\text{SiMe}_3$ , the zwitterionic species **1104** has been proposed, although that structure is not confirmed.

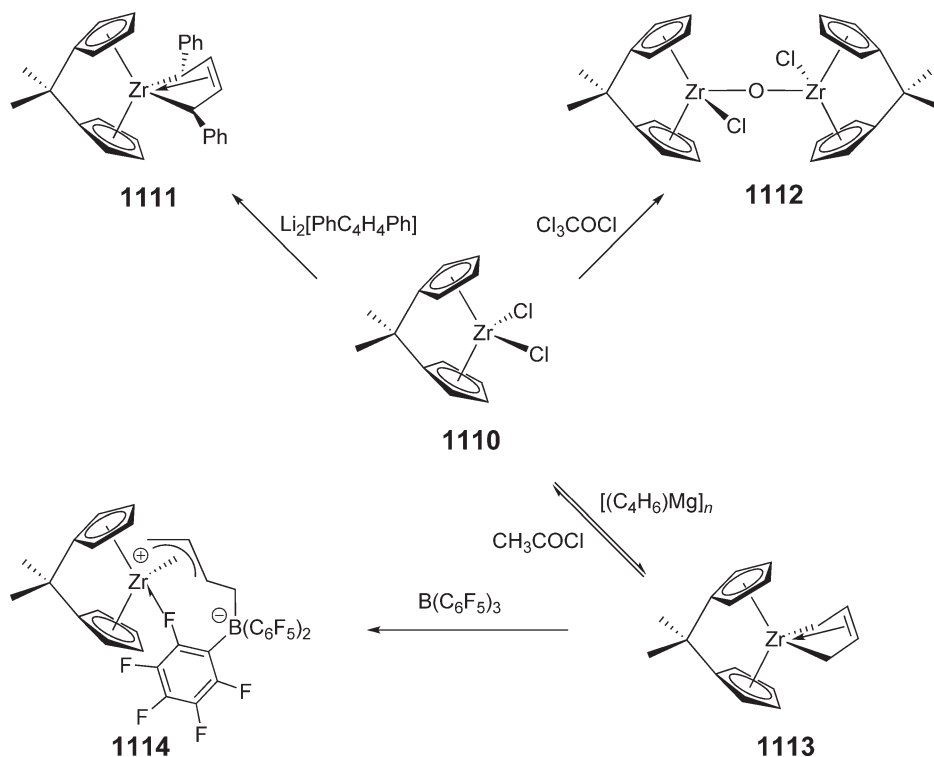
Several unsymmetric  $\text{R(H)C}$ -bridged *ansa*-zirconocene dichlorides have been synthesized. Complexes **1105–1107** contain one or two 2,5-dimethylcyclopentadienyl ligands and are obtained using 2-bromo-3-methoxy-2,5-dimethylcyclopentene as a starting material.<sup>860</sup> Upon activation with MAO, these three complexes are highly active for co-polymerization of ethylene and norbornene with large amounts (>50 mol%) of norbornene incorporation. Complexes **1108**, which combine a  $\text{C}_5\text{H}_4$  and a  $\text{C}_5\text{Me}_4$  ring, were prepared using a potassium fulvene-substituted cyclopentadienyl synthon,  $(\text{C}_5\text{Me}_4)=\text{CH}(\text{C}_5\text{H}_4)\text{K}$ , generated from the reaction of  $\text{K}[\text{C}_5\text{Me}_4\text{H}]$  and 6-(dimethylamino)fulvene in THF via  $\text{HNMe}_2$  elimination.<sup>861</sup> The reaction of the synthon  $(\text{C}_5\text{Me}_4)=\text{CH}(\text{C}_5\text{H}_4)\text{K}$  with  $\text{RLi}$  ( $\text{R} = \text{Bu}^n, \text{Bu}^t, \text{Ph}$ ) in  $\text{Et}_2\text{O}$  leads to the formation of heterobimetallic potassium lithium salts, which undergo salt metathesis reactions with  $\text{ZrCl}_4$  to give the final complexes **1108**.



Condensation of cyclopentadiene with *N*-methylpiperidone yields the bridged ligand 4,4-di(cyclopentadienyl)-*N*-methylpiperidine, which is subsequently converted to the corresponding *ansa*-zirconocene complex **1109** bearing the *N*-methylpiperidine-4-diyl bridge (Scheme 266).<sup>862</sup> No direct  $\text{Zr} \cdots \text{N}$  contact was found in the crystal structure. The analogous *ansa*-bis(indenyl)zirconocene complex carrying the *N*-methylpiperidine bridge can be obtained in a similar manner.



Scheme 266



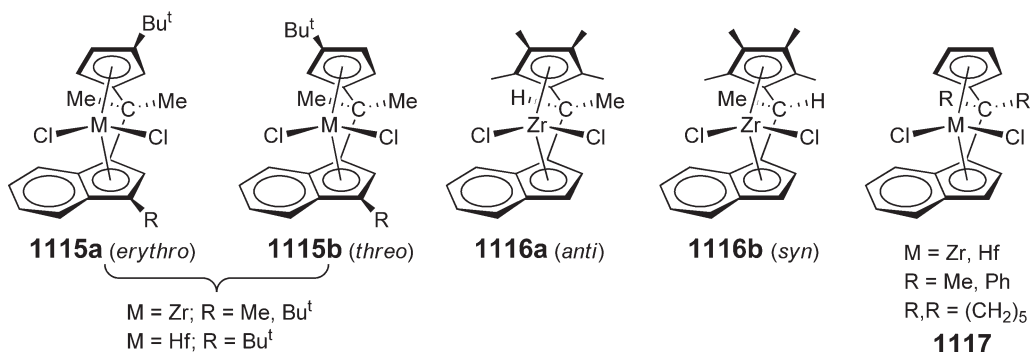
Scheme 267

The reactivity of the  $\text{Me}_2\text{C}$ -bridged *ansa*-zirconocene dichloride **1110** has been investigated with an emphasis on the formation of its diene complexes, representative results of which are summarized in Scheme 267.<sup>863</sup> Treatment of  $\text{Me}_2\text{C}(\text{Cp})_2\text{ZrCl}_2$  with 2 equiv. of  $\text{BuLi}$  at  $-78^\circ\text{C}$  followed by addition of 1,4-*trans,trans*-diphenylbutadiene gives ruby-red crystals of the 1,4-diphenylbutadiene complex **1111** in 75% yield. The reaction of a THF solution of  $\text{Me}_2\text{C}(\text{Cp})_2\text{ZrCl}_2$  with trichloroacetyl chloride  $\text{Cl}_3\text{COCl}$  affords the  $\mu$ -O-bridged binuclear chlorozirconocene complex **1112**; the oxygen is presumed to have derived from adventitious water. Treatment of  $\text{Me}_2\text{C}(\text{Cp})_2\text{ZrCl}_2$  with a suspension of butadiene magnesium in toluene at  $0^\circ\text{C}$  leads to the formation of the *cis*-butadiene complex **1113** in 90% yield. Addition of  $\text{B}(\text{C}_6\text{F}_5)_3$  to this butadiene complex results in the formation of the zwitterionic  $\eta$ -allyl species **1114**, similar to the reaction of  $\text{B}(\text{C}_6\text{F}_5)_3$  with zirconocene diene complexes.

#### 4.08.10.3.2 $\text{C}_1$ -bridged indenyl complexes

Unsymmetric,  $\text{Me}_2\text{C}$ -bridged 3-*tert*-butyl-substituted cyclopentadienyl and 3-substituted indenyl *ansa*-zirconocenes such as **1115** have been obtained using the salt metathesis route.<sup>864</sup> These complexes were isolated as a mixture of diastereomers which can be further separated into *erythro*- **1115a** and *threo*- **1115b** isomers by repeated

recrystallization. The molecular structure of the *threo*-isomer (**1115b**; M = Zr; R = Bu<sup>t</sup>) has been determined by X-ray crystallography; when activated with MAO, this complex catalyzes the polymerization of propylene, affording highly isotactic, high molecular weight polypropylene with an isotacticity [*mm*] of >99.6% and a melt transition temperature of 161 °C. In contrast, the corresponding *erythro*-isomer produces polypropylene with low molecular weight and isotacticity ([*mm*] = 51.8%). *Anti*- and *syn*-Me(H)C-bridged *ansa*-(Me<sub>4</sub>Cp-Ind) zirconocenes **1116** are obtained by salt metathesis; the *anti*-diastereomer has been structurally characterized by X-ray diffraction.<sup>865</sup> The *syn*-isomer, when activated with MAO, exhibits marginal activity, forming hemiisotactic polymer. A series of R<sub>2</sub>C-bridged unsubstituted *ansa*-(Cp-Ind) zirconocenes **1117** has also been synthesized by the standard salt metathesis route using the appropriate 6,6-substituted fulvene precursors. Their performance in MAO-co-catalyzed propylene and styrene polymerizations has been examined.<sup>866</sup> The dimethylzirconocene derivative Me<sub>2</sub>C(Cp)(Ind)ZrMe<sub>2</sub> was converted into the corresponding cationic THF-stabilized species [Me<sub>2</sub>C(Cp)(Ind)ZrMe(THF)][BPh<sub>4</sub>];<sup>867</sup> the latter was employed as catalyst for the isospecific polymerization of methyl methacrylate.<sup>868</sup> The molecular structure of the Ph<sub>2</sub>C-bridged zirconocene **1117** was determined later. The catalyst was used for co-polymerizations of ethylene and bulky cycloalkenes; large amounts of cycloalkene were incorporated to give materials with high glass transition temperatures.<sup>869</sup>

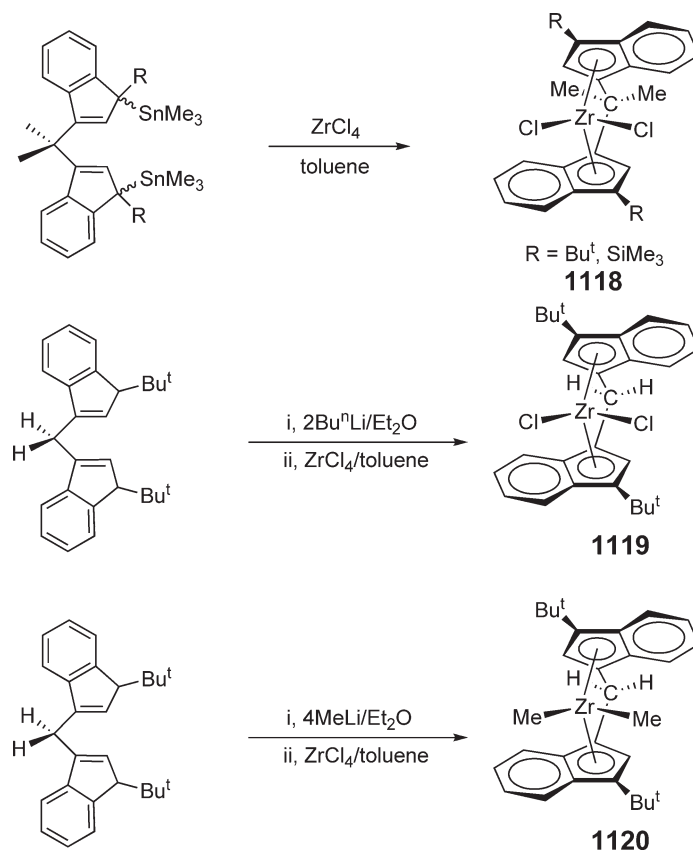


The C<sub>2</sub>-symmetric Me<sub>2</sub>C-bridged compounds **1118** with 3-substituted indenyl ligands (R = *tert*-butyl or Me<sub>3</sub>Si) have been prepared by transmetallation between the bis(trialkyltin) derivatives of the ligands and ZrCl<sub>4</sub> in non-coordinating solvents such as toluene (Scheme 268).<sup>870</sup> The molecular structures of both the *tert*-butyl and Me<sub>3</sub>Si derivatives have been determined by X-ray diffraction, revealing small Cp(centroid)–Zr–Cp(centroid) “bite” angles of 118.3° and 117.4°, respectively. Upon activation with MAO, these complexes are highly regiospecific catalysts in the isospecific polymerization of liquid propylene. For example, complex **1118** (R = *tert*-butyl) produces highly isotactic polypropylene at 50 °C with [*mmmm*] ~95% and with no detectable 2,1-regioirregular monomer units. The analogous H<sub>2</sub>C-bridged dichloride complex **1119** has also been synthesized using the standard salt metathesis approach, and the corresponding dimethyl complex **1120** was prepared by the “one-pot” metallation route.<sup>871</sup> H<sub>2</sub>C-bridged **1119** produces isotactic polypropylene with higher isotacticity ([*mmmm*] ~97%) and higher molecular weight with no regioerrors compared to the Me<sub>2</sub>C-bridged analog **1118**, although its activity in the MAO-co-catalyzed polymerization of liquid propylene is lower.

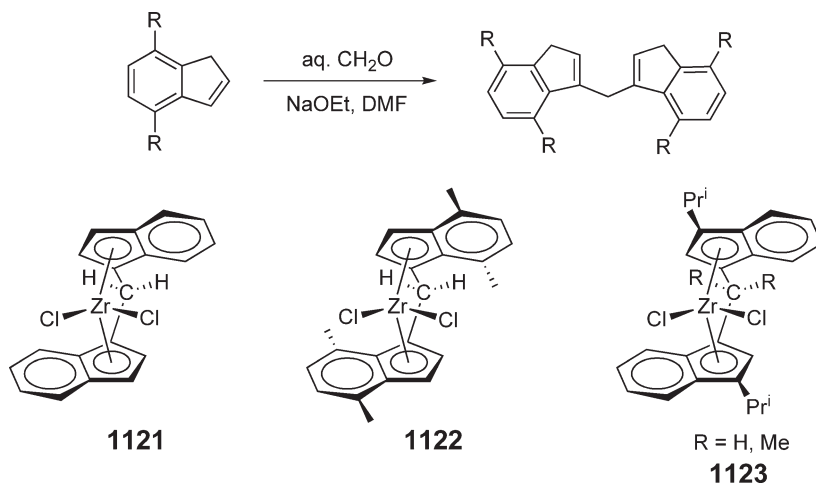
A convenient, atom-efficient route for a rapid entry into bis(3-indenyl)methanes involves the base-catalyzed condensation between formaldehyde and (substituted) indenenes (Scheme 269).<sup>872</sup> Using this route, H<sub>2</sub>C-bridged *ansa*-zirconocene complexes **1121** and **1122** have been prepared. On MAO activation, these complexes polymerize liquid propylene to low molecular weight, low isotactic polypropylene, highlighting the importance of bulky substituents at the 2-position of the Cp rings for these complexes to exhibit high stereo- and regiospecificity in propylene polymerization. To further illustrate this point, complexes **1123** with 3-isopropyl substitution on the Cp rings were made and shown to produce high molecular weight amorphous, elastic polypropylene.<sup>873</sup>

#### 4.08.10.3.3 C<sub>1</sub>-bridged fluorenyl complexes

The 6,6-substituted fulvenes are commonly employed as starting precursors for the preparation of bridged cyclopentadienyl–fluorenyl ligands, which are subsequently converted to the [C<sub>1</sub>]-bridged *ansa*-Cp-Flu metallocene complexes. Scheme 270 shows a representative example of the reaction sequence for the preparation of Ph<sub>2</sub>C-bridged *ansa*-Cp-Flu metallocene dichlorides **1124**.<sup>874</sup> When activated with MAO, the Zr complex catalyzes syndiospecific polymerization of propylene to syndiotactic polypropylene that exhibits comparable syndiotacticity with and considerably higher molecular weight than that obtained by the Me<sub>2</sub>C-bridged analog. The phosphine-stabilized



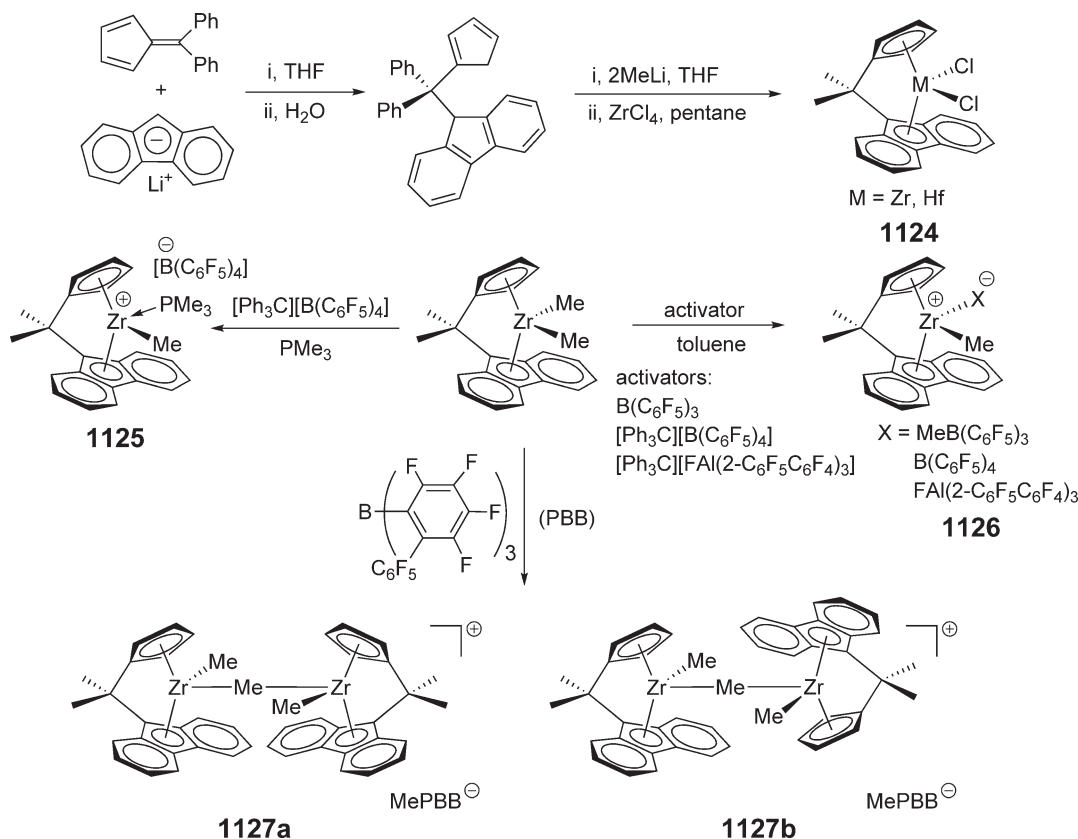
Scheme 268



Scheme 269

cationic complex **1125** can be readily generated by the reaction of the dimethyl precursor with  $\text{Ph}_3\text{C}[\text{B}(\text{C}_6\text{F}_5)_4]$ ; this stabilized cation has been isolated and structurally characterized by X-ray diffraction.<sup>875</sup> The  $^{13}\text{C}$  NMR studies show that  $\text{Me}_2\text{C}$ - and  $\text{Ph}_2\text{C}$ -bridged *ansa*-Cp-Flu zirconocene complexes exhibit fluxional hapticities in solution.<sup>876</sup> Activation of  $\text{Me}_2\text{C}(\text{Cp})(\text{Flu})\text{ZrMe}_2$  with four different co-catalysts produces ionic complexes with greatly different

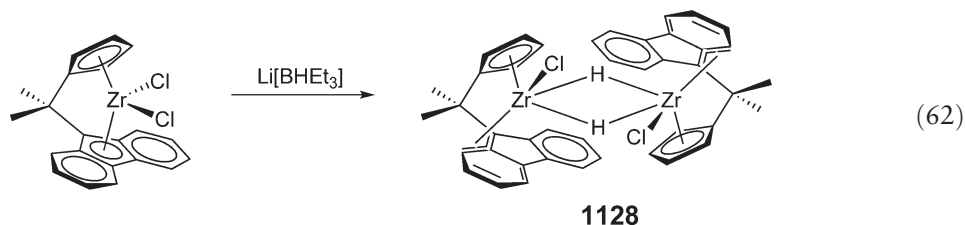




Scheme 270

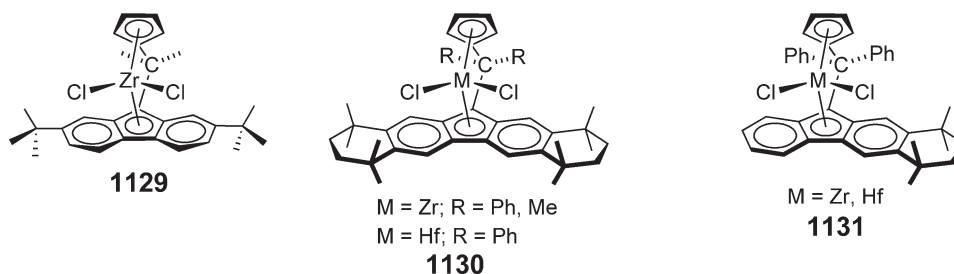
structural and ion pairing characteristics.<sup>877</sup> Thus, the reaction of Me<sub>2</sub>C(Cp)(Flu)ZrMe<sub>2</sub> with B(C<sub>6</sub>F<sub>5</sub>)<sub>3</sub>, Ph<sub>3</sub>C[B(C<sub>6</sub>F<sub>5</sub>)<sub>4</sub>], and Ph<sub>3</sub>C[FAI(2-C<sub>6</sub>F<sub>5</sub>)C<sub>6</sub>F<sub>4</sub>)<sub>3</sub>] gives the corresponding monometallic ion pairs **1126** (Scheme 270), whereas the reaction with the sterically encumbered borane PBB yields μ-methyl binuclear ion pair **1127** as a mixture of two diastereomers. The molecular structures of the two resulting ion pairs [**1126**: X = MeB(C<sub>6</sub>F<sub>5</sub>)<sub>3</sub>, FAI(2-C<sub>6</sub>F<sub>5</sub>)C<sub>6</sub>F<sub>4</sub>)<sub>3</sub>] have been determined by X-ray diffraction and correlations of ion pair structure and dynamics with propylene polymerization activity, chain transfer, and syndiospecificity carefully examined.

The dihydride complex derived from Me<sub>2</sub>C(Cp)(Flu)ZrCl<sub>2</sub> was the intended target complex by the reaction with Li[BHET<sub>3</sub>]; however, the hydrido-chloro dimeric complex **1128** was isolated as bright red crystals (Equation (62)).<sup>878</sup> The molecular structure reveals that the fluorenyl moiety adopts an unusual η<sup>3</sup>-allyl coordination mode involving both the five- and one of the six-membered rings. This structural motif is in contrast to the structures of known *ansa*-(Cp-Flu) zirconocenes, representing a unique example of the facile “ring slippage” often inferred for fluorenyl-containing complexes. The dimeric solid-state structure is maintained in solution.

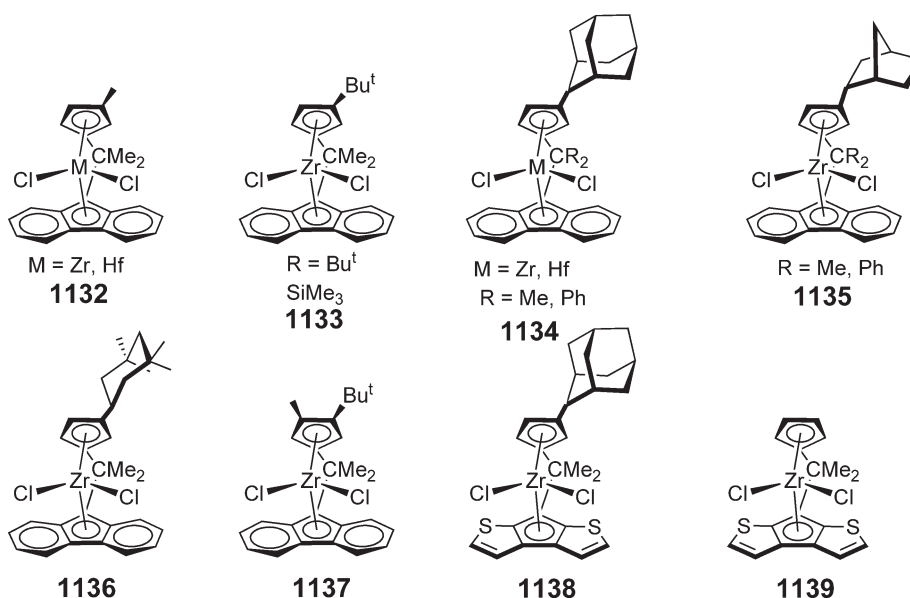


In an effort to enhance the activity and syndiospecificity of *C*<sub>s</sub>-symmetric *ansa*-Cp-Flu metallocene complexes in the MAO-co-catalyzed polymerization of propylene, a large number of fluorenyl-substituted *ansa*-Cp-Flu metallocene complexes have been prepared,<sup>879–881</sup> including the di-*tert*-butyl-substituted derivative **1129**.<sup>882</sup> The hafnocene

analogues of **1129** with  $\text{Ar}_2\text{C}$  bridges ( $\text{Ar} = 4\text{-MeC}_6\text{H}_4$ ,  $4\text{-MeOC}_6\text{H}_4$ ) have also been made and examined for MAO-co-catalyzed propylene polymerizations.<sup>883</sup> Further steric expansion of the fluorenyl ligand system has produced **1130** and **1131** which incorporate an octamethyloctahydrodibenzofluorenyl ligand and a tetramethyltetrahydrodibenzofluorenyl ligand, respectively.<sup>884</sup> The MAO-co-catalyzed propylene polymerization results reveal that the Zr complexes **1130** produce highly syndiotactic polypropylene largely devoid of stereoerrors and of significantly higher melting transition temperature as compared with *ansa*-Cp-Flu metallocene dichlorides containing other substituted fluorenyl ligands, including parent fluorenyl **1124**, tetramethyltetrahydrodibenzofluorenyl **1131**, and 2,7-di-*tert*-butylfluorenyl **1129**; these results demonstrate an influence of distal ligand substituents on polymerization characteristics.

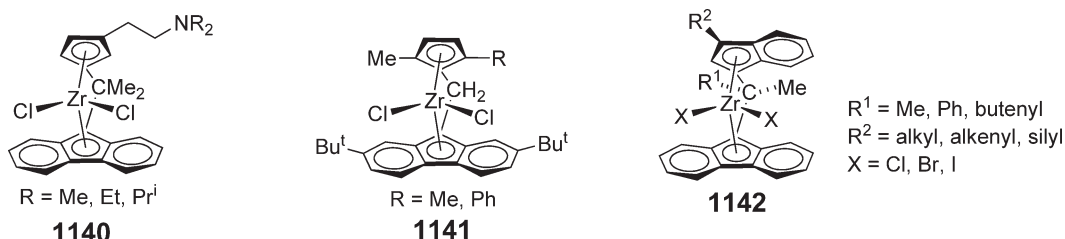


Introduction of a single alkyl substituent onto the Cp ring lowers the symmetry of the parent  $C_s$ -symmetric *ansa*-Cp-Flu complex to  $C_1$ . This change strongly affects the stereochemistry of the polymerization. Methyl and *tert*-butyl or trimethylsilyl substituents at the 3-position of the Cp ring were employed to give compounds **1132** ( $\text{R} = \text{Me}$ )<sup>885</sup> and **1133** ( $\text{R} = \text{Bu}^t$ ,<sup>886</sup>  $\text{SiMe}_3$ <sup>887</sup>), respectively. When activated with MAO, both **1132** and **1133** ( $\text{R} = \text{Bu}^t$ ) catalyze the polymerization of propylene, leading to hemiisotactic and to isotactic polypropylenes, respectively. A large number of analogous  $C_1$ -symmetric *ansa*-Cp-Flu metallocene complexes with varying steric bulk of the substituent at the 3-position of the Cp ring have been prepared, which can be used for the production of hemiisotactic, syndiotactic, isotactic, and/or stereoblock polypropylenes.<sup>888</sup> The 3-neomenthyl-substituted *ansa*-Cp-Flu zirconocene dichloride has been isolated as a 60:40 mixture of two diastereomers.<sup>889</sup> Mixed with MAO, this complex catalyzes the polymerization of propylene to isotactic-rich polymer with  $[mm]$  triad = 63%. Further fine-tuning of the R substituent on the Cp ring has produced complexes **1134–1137**.<sup>890</sup> Among these complexes, zirconium complexes **1134** with a bulky 2-adamantyl group produce isotactic-hemiisotactic stereoblock polypropylene. Such a polymer microstructure can also be produced with complex **1138** in which the fluorenyl ligand is replaced by a Cp-ring-fused dithiophene ligand.<sup>891</sup> The parent  $C_s$ -symmetric complex **1139**, when activated with MAO, catalyzes propylene-specific co-polymerization of ethylene and propylene to produce more random ethylene/propylene co-polymer than its fluorenyl analog. A series of derivatives of **1139** with alkyl or phenyl substituents on both Cp and dithiophene ligands has been synthesized and examined in propylene polymerizations.<sup>892</sup>



Aminoethyl-substituted cyclopentadienyl ligands have been employed to prepare the amino-functionalized  $\text{Me}_2\text{C}$ -bridged *ansa*-Cp-Flu zirconocene complexes such as **1140**.<sup>893</sup> These complexes have the ability to regulate the molecular weight distribution of the resulting polyethylene in the MAO-co-catalyzed ethylene polymerization.<sup>894</sup> For example, complex **1140** ( $\text{R} = \text{Me}$ ) produces polyethylene with a bimodal molecular weight distribution at 50 °C of the polymerization temperature, indicating that two different single-site catalysts are operating in the ethylene polymerization using this complex in combination with MAO.

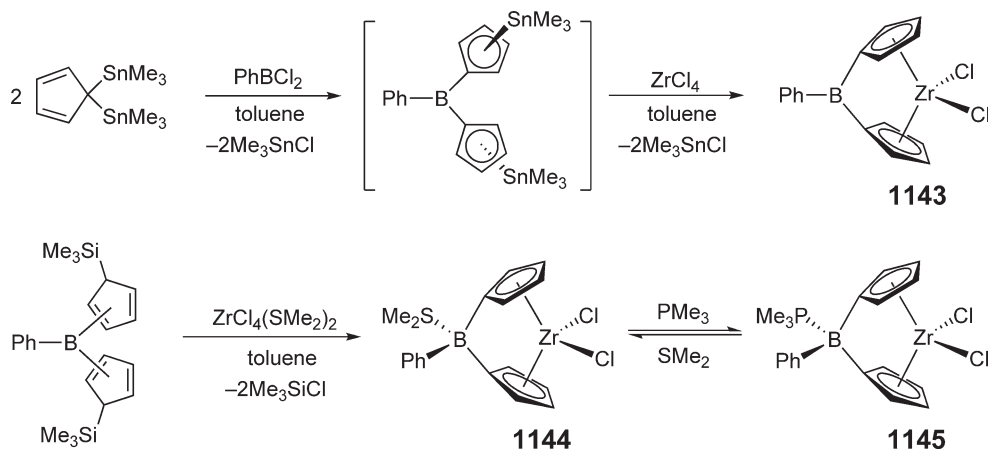
$\text{H}_2\text{C}$ -bridged *ansa*-Cp-Flu zirconocene complexes **1141** are prepared from (2,7-di-*tert*-butyl)-9-prop-2-ynyl-9H-fluorene.<sup>895</sup> The procedure of the ligand synthesis involves the use of 3-bromo-1-propyne, which affords the methylene bridging unit via an intermolecular Pauson–Khand reaction in which norbornadiene and a pendant alkyne cyclize to form a ring that later becomes a substituted cyclopentadienyl group. In the presence of a large excess of MAO as co-catalyst, these complexes catalyze the co-polymerization of ethylene and norbornene. The co-polymerization results show the effects of the R group of the Cp ring on the co-polymerization activity, with the activity of **1141** ( $\text{R} = \text{Me}$ ) being comparable to that of the benchmark catalyst  $\text{Me}_2\text{C}(\text{Cp})(\text{Flu})\text{ZrCl}_2$  but much higher than that of the phenyl-substituted **1141** ( $\text{R} = \text{Ph}$ ). Additionally, the methyl-substituted complex incorporates a larger amount of norbornene than does the phenyl-substituted derivative. A large number of asymmetric  $\text{C}_1$ -bridged *ansa*-zirconocenes of type **1142** incorporating bridged fluorenyl and substituted indenyl ligands have been prepared and their activities toward MAO-co-catalyzed polymerization of ethylene examined.<sup>896</sup>



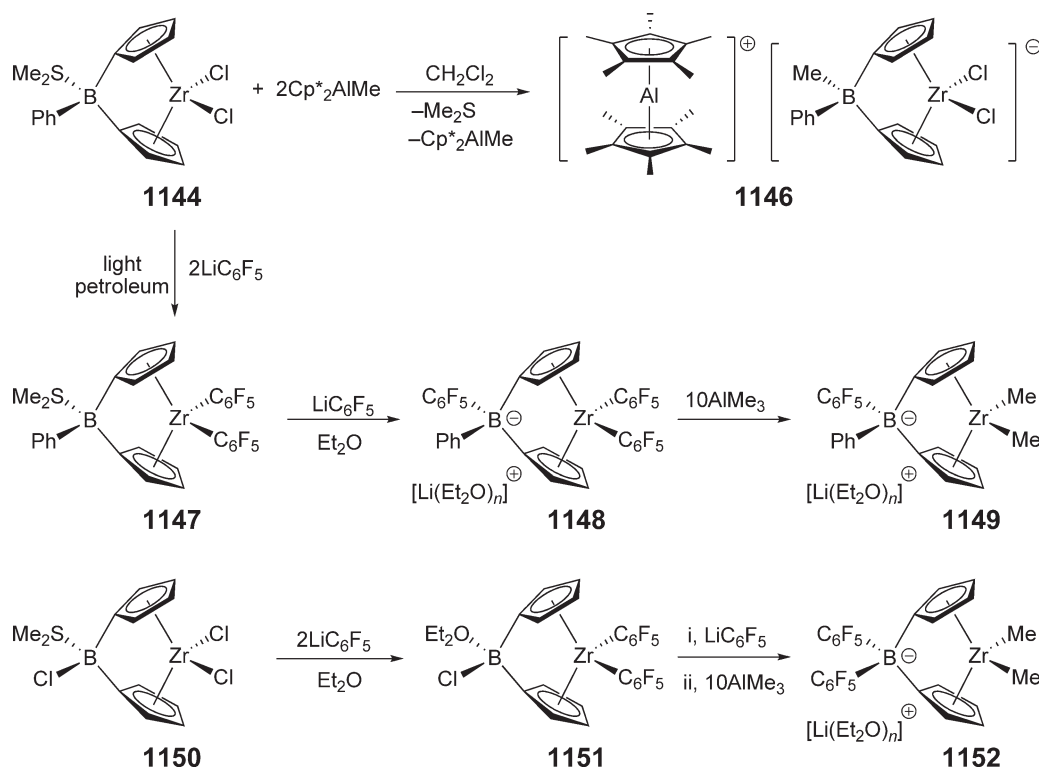
#### 4.08.10.4 Other (B, P, N, Ge, Sn, C<sub>n</sub>)-bridged Complexes

##### 4.08.10.4.1 Cyclopentadienyl complexes with (B, P, N, Ge, Sn, C<sub>n</sub>)-bridges

Successive transmetallation reactions of  $\text{C}_5\text{H}_4(\text{SnMe}_3)_2$  with  $\text{PhBCl}_2$  and  $\text{ZrCl}_4$  produce borylidene-bridged *ansa*-zirconocene dichloride **1143** (Scheme 271).<sup>897</sup> The corresponding precursor phenylbis(cyclopentadiene)borane is unstable and was isolated as a pyridine adduct. The dimethylsulfide adduct **1144** of the same complex was prepared from a double dehalodesilylation reaction between  $\text{PhB}(\text{C}_5\text{H}_4\text{SiMe}_3)_2$  and  $\text{ZrCl}_4(\text{SMe}_2)_2$ .<sup>898</sup> The dimethylsulfide in **1144** can be readily displaced by trimethylphosphine to give the corresponding  $\text{PMe}_3$  adduct **1145**; both compounds have been structurally characterized by X-ray diffraction. Whereas the alkylation of **1144** was not successful, presumably due to the lability of  $\text{Me}_2\text{S}$  that serves as the necessary protection for the boron bridge from nucleophilic



Scheme 271

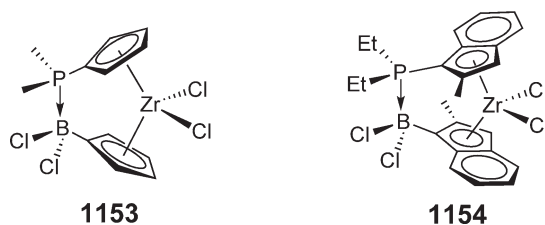


Scheme 272

attack by alkyl anions, the  $\text{PMe}_3$  derivative **1145** has been successfully alkylated by  $\text{LiR}$  ( $\text{R} = \text{Me}, \text{CH}_2\text{SiMe}_3$ ). Consistent with this finding, only the  $\text{PMe}_3$  adduct **1145** can be activated by MAO to generate an active catalyst for polymerization of ethylene.

Complex **1144** reacts with 2 equiv. of  $\text{Cp}^*\text{AlMe}$  to yield the stable borate-bridged anionic *ansa*-zirconocene complex **1146** as the  $[\text{AlCp}^*_2]^+$  salt, an example of the enhanced Lewis acidity of the boron bridge due to ring strain (Scheme 272).<sup>899</sup> The reaction of **1144** with 2 equiv. of  $\text{LiC}_6\text{F}_5$  proceeds selectively to give the pentafluorophenyl complex **1147**, while 3 equiv. of  $\text{LiC}_6\text{F}_5$  affords the borato-bridged ionic complex **1148**.<sup>900</sup> Treatment of complex **1148** with an excess of  $\text{AlMe}_3$  results in  $\text{C}_6\text{F}_5/\text{Me}$  ligand exchange to give the corresponding dimethyl complex **1149**. The chloroborane-bridged *ansa*-zirconocene derivative  $\text{Cl}(\text{Me}_2\text{S})\text{B}(\text{C}_5\text{H}_4)_2\text{ZrCl}_2$  **1150**, which was obtained by the reaction of boron trichloride with  $(\text{SiMe}_3)(\text{SnMe}_3)\text{C}_5\text{H}_4$  to generate  $\text{BCl}(\text{C}_5\text{H}_4\text{SiMe}_3)_2$  followed by dehalosilylation with  $\text{ZrCl}_4(\text{Me}_2\text{S})_2$ , undergoes successive reactions with  $\text{LiC}_6\text{F}_5$  and  $\text{AlMe}_3$  in an analogous fashion, leading to  $(\text{Et}_2\text{O})\text{ClB}(\text{C}_5\text{H}_4)_2\text{Zr}(\text{C}_6\text{F}_5)_2$  **1151** and the borato-bridged ionic dimethylzirconocene complex  $[\text{Li}(\text{Et}_2\text{O})_4][(\text{C}_6\text{F}_5)_2\text{B}(\text{C}_5\text{H}_4)_2\text{ZrMe}_2]$  (**1152**, Scheme 272).

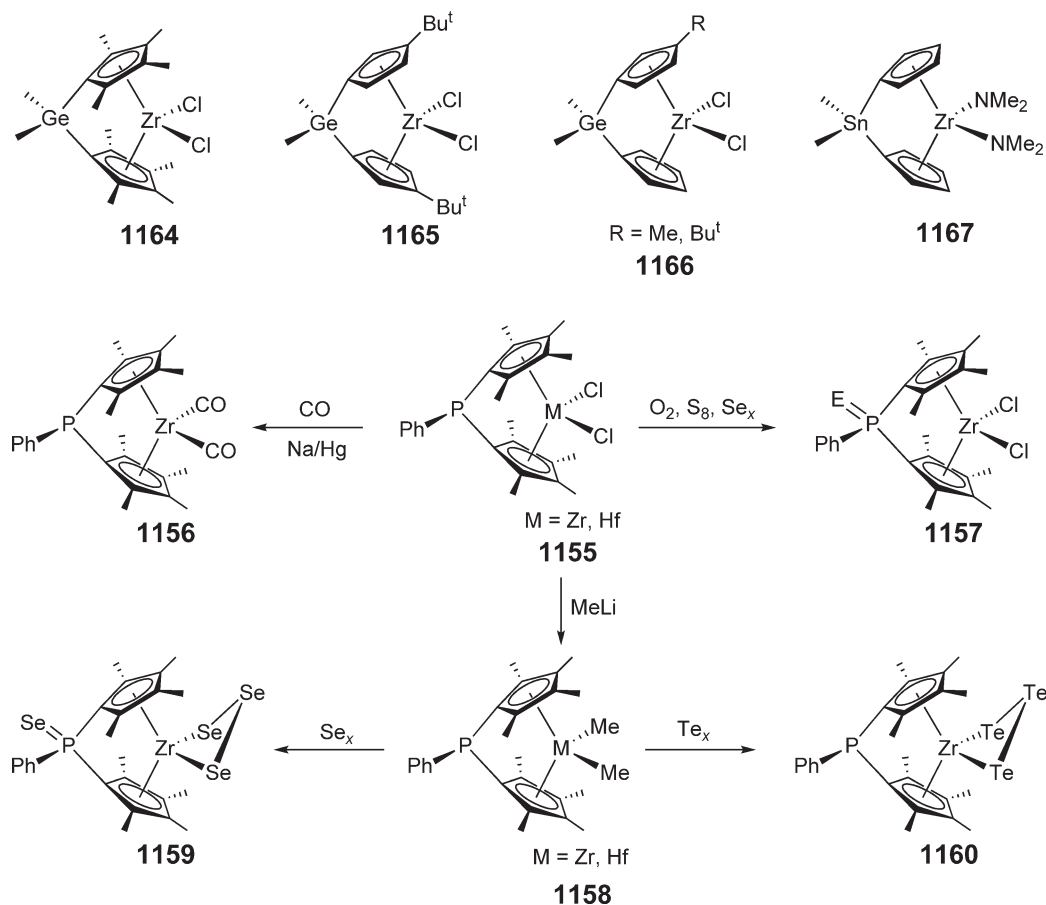
A different class of *ansa*-metallocenes of the type **1153** is based on bridge formation by a donor→acceptor dative bond between boron and a group 15 atom.<sup>901</sup> The polar  $\text{P} \rightarrow \text{B}$  bridge in **1153**, which was characterized by X-ray diffraction, is thermally very stable; thus, even at  $100^\circ\text{C}$ , the ring-bridging dative interaction still remains in solution. The chiral version of such complexes such as *rac*- $[\text{Et}_2\text{P}(2\text{-MeInd})][\text{Cl}_2\text{B}(2\text{-MeInd})]\text{ZrCl}_2$  **1154** have also been prepared. When activated with  $\text{AlBu}_3$  and  $\text{Ph}_3\text{C}[\text{B}(\text{C}_6\text{F}_5)_4]$  at room temperature under 2 atm propylene pressure, the complex produces highly isotactic polypropylene, with a relative  $[mmmm]$  pentad content of 92%.



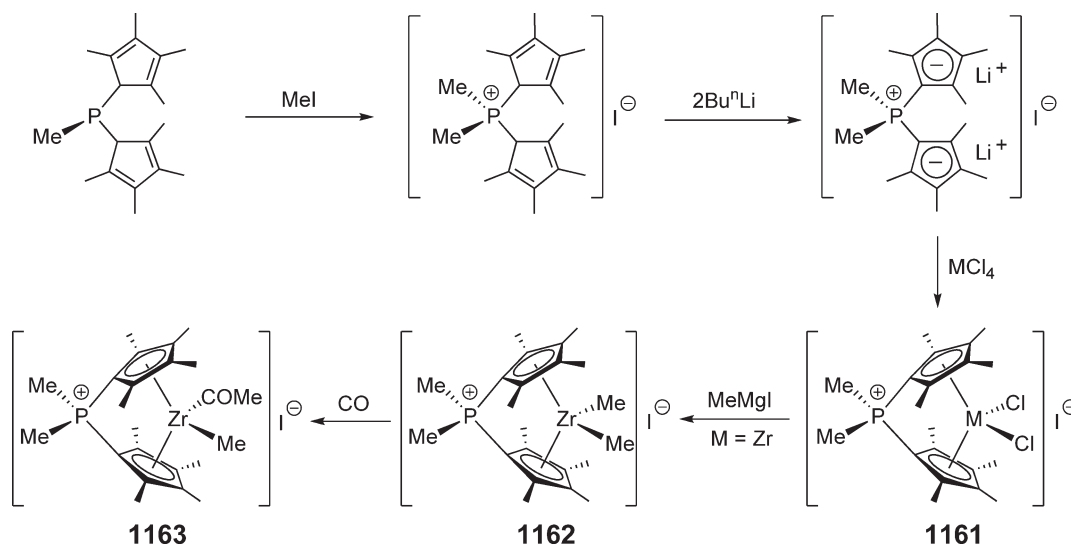
Investigations of the *ansa*-effect on the reactivity of phosphorus have yielded a series of phosphorus-bridged *ansa*-metallocenes.<sup>902</sup> The zirconocene dichloride **1155**, prepared by salt metathesis between  $[\text{PhP}(\text{C}_5\text{Me}_4)_2]\text{Li}_2$  and  $\text{ZrCl}_4$ , is a useful precursor to other zirconocene derivatives, including the dicarbonyl **1156** and the dimethyl **1158**, as illustrated in Scheme 273. The reaction of dichloride **1155** with oxygen, sulfur, and selenium readily affords four-coordinate-phosphorus  $[\text{Ph}(\text{=E})\text{P}]$ -bridged *ansa*-zirconocene dichlorides **1157**; tellurium, however, is unreactive toward this dichloride, a reflection of the lower  $\text{P}=\text{Te}$  bond energy. Furthermore, whereas elemental selenium reacts with the dimethyl **1158** to give complex **1159** with concomitant functionalization of the phosphorus bridge, the corresponding reaction with elemental tellurium does not functionalize the phosphorus atom but reacts only at the  $\text{Zr}-\text{C}$  bond to give the  $\text{Zr}$  telluride **1160**. Structural characterizations of some of these complexes by X-ray diffraction indicate that, in comparison to their non-*ansa*-counterparts  $(\text{C}_5\text{Me}_5)_2\text{ZrX}_2$ , the cyclopentadienyl ligands in the phosphorus-bridged complexes are displaced from symmetric  $\eta^5$ -coordination toward  $\eta^3$ -coordination. Such  $\eta^3, \eta^3$ -coordination creates more electrophilic metal centers.

Phosphonium-bridged cationic *ansa*-metallocenes **1161** have been synthesized by salt metathesis, as illustrated in Scheme 274.<sup>903</sup> Methylation of the zirconium complex yields the methyl derivative **1162**, which reacts rapidly with  $\text{CO}$  at room temperature to give the acyl derivative **1163**. The molecular structures of the dichloride complexes have been determined by X-ray diffraction.

Dimethylgermylene-bridged *ansa*-bis( $\text{Cp}$ )-type zirconocenes **1164–1166** with varying substituents and substitution patterns on the  $\text{Cp}$  rings have been prepared via the metathesis route from the reactions of the dilithiated ligands with  $\text{ZrCl}_4(\text{THF})_2$ .<sup>904</sup> The molecular structure of complex **1164** has been determined by X-ray diffraction. All these complexes are thermally stable and can be activated with MAO to give highly active catalysts for polymerization of ethylene at relatively high temperatures, highlighting that germylene-bridged *ansa*-zirconocene systems are thermally robust catalysts. The amine elimination reaction of  $\text{Zr}(\text{NMe}_2)_4$  with  $(\text{CH}_3)_2\text{Sn}(\text{C}_5\text{H}_5)_2$  leads to the  $\text{Sn}$ -bridged *ansa*-zirconocene **1167** in quantitative yield.<sup>905</sup> When  $\text{Sn}(\text{C}_5\text{H}_5)_4$  is employed, the reaction with  $\text{Zr}(\text{NMe}_2)_4$  gives the spirocyclic *ansa*-zirconocene complex,  $\text{Sn}[(\text{C}_5\text{H}_5)_2\text{Zr}(\text{NMe}_2)_2]_2$ .



Scheme 273

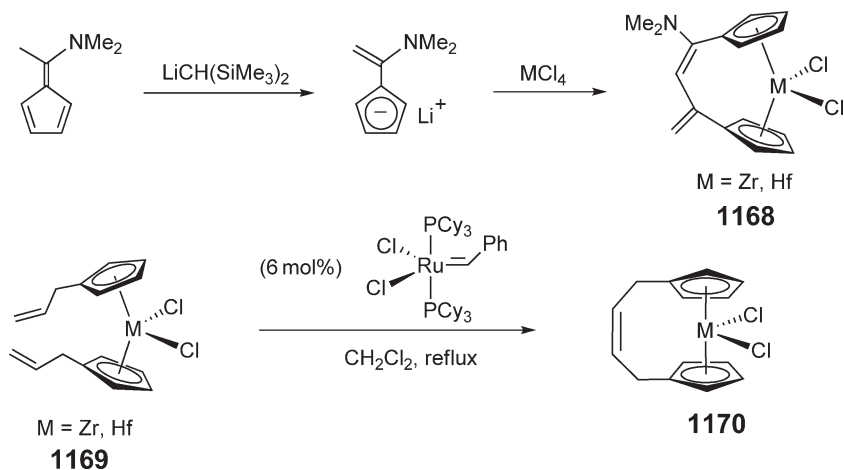


Scheme 274

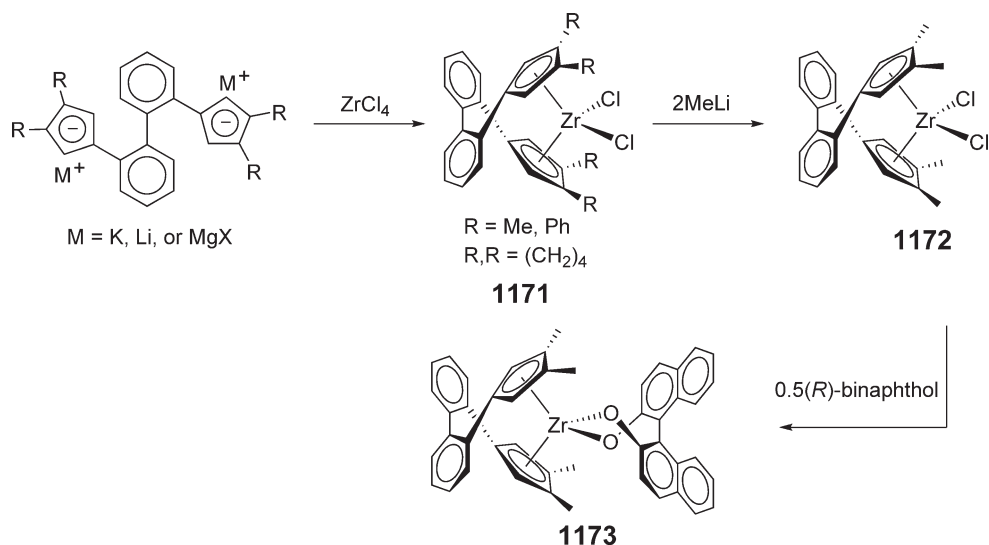
The  $C_3$ -bridged *ansa*-metalloenes **1168** were obtained unexpectedly by the transmetalation reaction between  $MCl_4$  and (1-dimethylaminoethenyl)cyclopentadienyllithium (Scheme 275).<sup>906</sup> These products are formed by a reaction sequence involving intramolecular amine elimination and fulvene coupling reactions. The olefin ring-closing metathesis reaction of bis(allyl-substituted-Cp)metalloenes **1169** catalyzed by a ruthenium carbene catalyst under high dilute conditions, has been employed to prepare the  $C_4$ -alkenyl-bridged *ansa*-metalloenes **1170**.<sup>907</sup> The use of a diastereomeric mixture of the substituted bent metalloenes shows excellent diastereoselectivity in this ring-closing metathesis route to *ansa*-metalloenes.

Chiral biphenyl-bridged *ansa*-zirconocene dichlorides **1171** and the dimethyl derivative **1172** are obtained by salt metathesis routes according to Scheme 276.<sup>908</sup> The reaction of the dimethyl complex with 0.5 equiv. of (*R*)-binaphthol gives the corresponding binaphtholate **1173**.

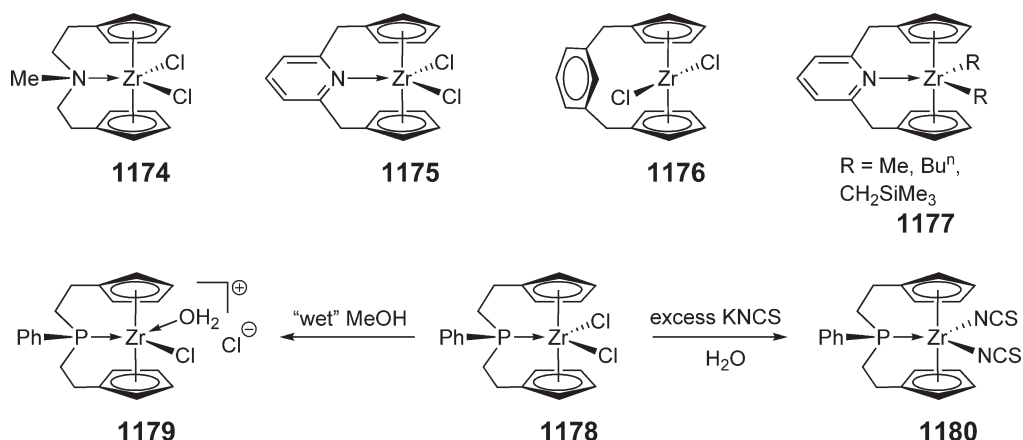
*ansa*-Zirconocene dichlorides **1174–1176** (Scheme 277) bearing interannular  $MeN(CH_2CH_2)_2$ ,  $C_5H_3N(CH_2)_2$ -2,6, and  $C_6H_4(CH_2)_2$ -1,3 bridges, respectively, were synthesized by the reaction of the corresponding disodium salts with  $ZrCl_4$ .<sup>909</sup> The crystal structure of  $[C_6H_4(CH_2C_5H_4)_2-1,3]ZrCl_2$  **1176** was determined by X-ray diffraction. Alkylation of the dichloride **1175** readily affords the corresponding trigonal-bipyramidal dialkyl complexes **1177**.<sup>910</sup> It is worth noting the isolation and structural characterization of the trigonal-bipyramidal bis(*n*-butyl) complex, since the parent complex  $Cp_2Zr(Bu)_2$  is thermally unstable and has never been isolated due to facile  $\beta$ -H elimination.



Scheme 275



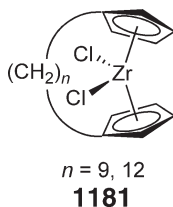
Scheme 276



Scheme 277

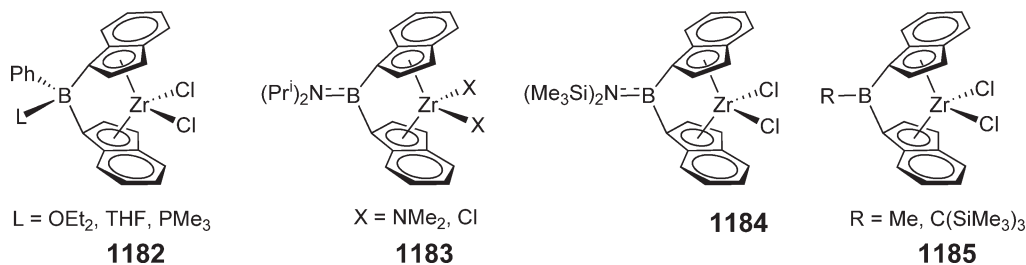
The five-coordinate zirconocene dichloride **1178** contains a tethered bis(Cp)-phosphine ligand; it was prepared by salt metathesis of  $ZrCl_4(THF)_2$  with  $Li_2[PhP(CH_2CH_2C_5H_4)_2]$ .<sup>911</sup> Coordination of the phosphorus atom to the metal center was confirmed by its X-ray structure. Dissolution of **1178** in "wet" MeOH followed by evaporation of the solvent yielded the cationic chloro-aqua complex **1179** shown in Scheme 277 as the chloride salt. Treatment of an aqueous solution of **1178** with excess potassium thiocyanate gives the bis(isothiocyanato) complex **1180**.

*ansa*-Metallocenes bearing long bridging  $-(CH_2)_n-$  chains, such as **1181**, are of interest in terms of their conformational features. Two such complexes have been synthesized by salt metathesis under dilute conditions and isolated in low yields ( $n = 9$ , 7%;  $n = 12$ , 18%).<sup>912</sup> The molecular structure of **1181** ( $n = 9$ ) reveals a metallocene conformation where the  $(CH_2)_9$ -bridge is oriented toward the lateral sector of the bent metallocene wedge. When activated with MAO, both complexes give very active catalysts for the polymerization of ethylene and the oligomerization of propylene.



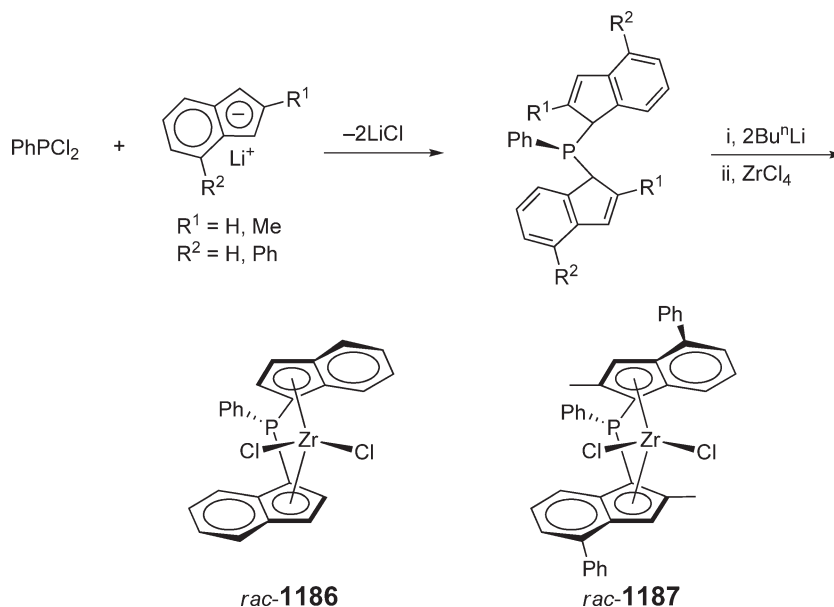
4.08.10.4.2 Indenyl complexes with (B, P, N, Ge, Sn, C<sub>n</sub>)-bridges

Boron-bridged *ansa*-bis(indenyl)zirconocenes **1182** are obtained by salt metathesis as adducts of donors such as Et<sub>2</sub>O, THF, and PMe<sub>3</sub>. The THF and PMe<sub>3</sub> adducts have been structurally characterized by X-ray diffraction.<sup>913</sup> The formation of such donor complexes constitutes chiral boron bridging and also leads to vastly different catalytic properties in the MAO-co-catalyzed polymerization of propylene, with the PMe<sub>3</sub>-containing complex being the most active and stereoselective (*[mmmm]* = 96% at 20 °C). Aminoboranediy [ (Pr<sup>i</sup>)<sub>2</sub>NB]-bridged *ansa*-bis(indenyl)zirconocenes **1183** have been prepared by the amine elimination route. The dichloride complex was characterized by X-ray crystallography;<sup>914</sup> in the MAO-co-catalyzed polymerization of propylene, it shows similar activity to the Me<sub>2</sub>Si-bridged analog. The (Me<sub>3</sub>Si)<sub>2</sub>NB-bridged *ansa*-bis(indenyl)zirconocene **1184** has been synthesized by the salt metathesis route.<sup>915</sup> The alkylboranediy [RB]-bridged *ansa*-bis(indenyl)zirconocenes **1185** have been made similarly.<sup>916</sup>



Phosphorus-bridged racemic *ansa*-bis(indenyl)zirconocenes **1186** and **1187** have been prepared by the salt metathesis route outlined in Scheme 278.<sup>917</sup> The PhP-bridge has been extended to *ansa*-bis(Flu) zirconocene dichloride and *ansa*-(Flu-Cp) zirconocene dichloride complexes. The pure *rac*-**1186** was isolated, but a 1:2 *rac*/*meso*-mixture of **1187** was obtained due to the inability to separate the two diastereomers by repeated recrystallization. Nevertheless, when activated with a large excess of MAO, the 1:2 *rac*/*meso*-mixture of the 2,4-disubstituted *ansa*-zirconocene **1187** polymerizes liquid propylene at 50 °C to highly isotactic polypropylene with *[mmmm]* > 98%.

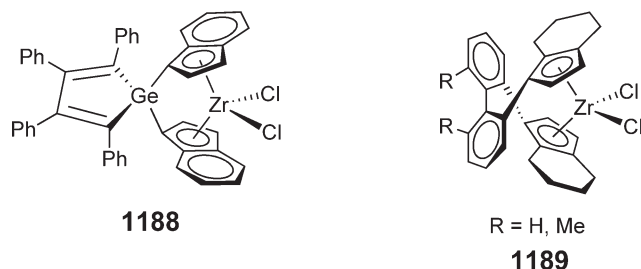
Germylene-bridged *rac*-[(1,2,3,4-tetraphenyl-1,3-butadiene-1,4-diyl)germylene-bis(indenyl)] zirconium dichloride **1188** was synthesized using the salt metathesis approach.<sup>918</sup> When combined with AlBu<sub>3</sub><sup>i</sup> and Ph<sub>3</sub>C[B(C<sub>6</sub>F<sub>5</sub>)<sub>4</sub>],



Scheme 278

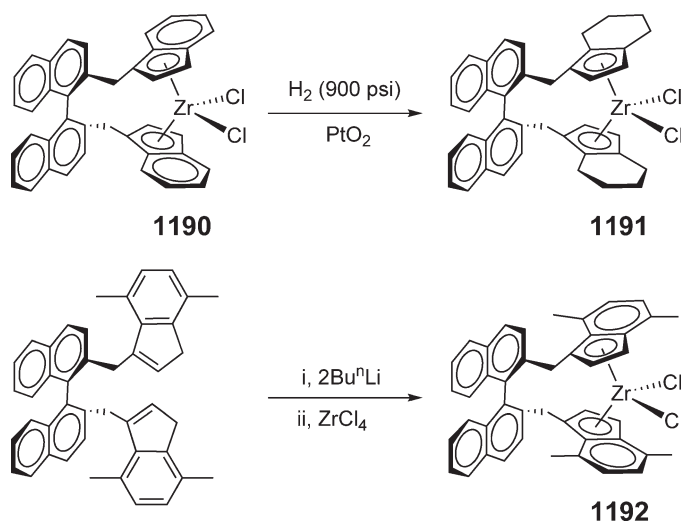


this complex polymerizes propylene with high activity and isospecificity to high molecular weight polymer. The characteristics of this polymerization catalysis by **1188** are essentially independent of polymerization temperature over a broad temperature range. *ansa*-2,2'-Bis(2-tetrahydroindenyl)biaryl zirconocene complexes **1189** which contain  $[C_4]$ -chiral biaryl bridges are obtained as single chiral diastereomers with the biaryl link determining the chirality of the complex and the tetrahydroindenyl ligands projecting the  $C_2$ -chirality directly to the site of reaction.<sup>919</sup>

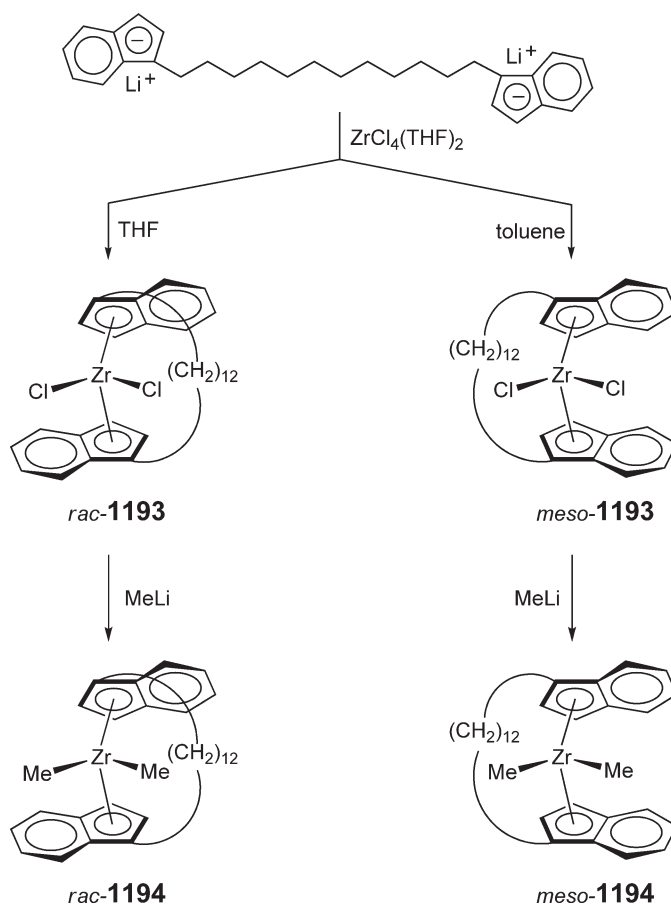


Hydrogenation of the known  $C_2$ -symmetric 2,2'-dimethyl-1,1'-binaphthyl- $[C_6]$ -bridged *ansa*-bis(1-indenyl)zirconium dichloride **1190** over  $Pt_2O$  produces the corresponding tetrahydroindenyl derivative **1191**.<sup>920</sup> Unlike the hydrogenation of the titanium analog, the hydrogenation of the zirconium is selective and does not hydrogenate the binaphthyl moiety. Salt metathesis was employed to convert the *S*-(-)-ligand to the corresponding 4,7-dimethylindenyl zirconocene complex **1192** in 21% yield (Scheme 279). As was the case for the metallation to the unsubstituted derivative **1190**, the dimethylindenyl complex **1192** was formed as conformationally mobile, diastereomerically pure,  $C_2$ -symmetric product. No evidence for the formation of the diastereomeric  $C_1$ -symmetric (*meso*-like) *ansa*-zirconocene complex was observed in the NMR spectra of the crude reaction products.

*ansa*-Bis(indenyl)metallocene systems with large bridges have been made, for example, by the reaction of dilithio salt of 1,12-bis(3-indenyl)dodecane with  $ZrCl_4(THF)_2$  in THF under high dilute conditions which gives the *rac*-dodecamethylene-bridged compound **1193** in 15% isolated yield. Alternatively, the reaction in toluene leads to the isolation of *meso*-**1193** in 11% isolated yield (Scheme 280).<sup>921</sup> Both the *rac*- and *meso*-dichloride complexes can be readily converted to the corresponding dimethyl derivatives **1194**. The molecular structure of *rac*-**1193** shows that the  $-(CH_2)_{12}$ -bridging chain is oriented in a nearly  $C_2$ -symmetric arrangement in the central position at the open "front"-side of the bent-metallocene wedge. In this orientation the mean plane of the dodecamethylene loop is arranged orthogonal to the  $ZrCl_2$   $\sigma$ -ligand plane and spatially separates the two segments in front of the bent metallocene unit.



Scheme 279

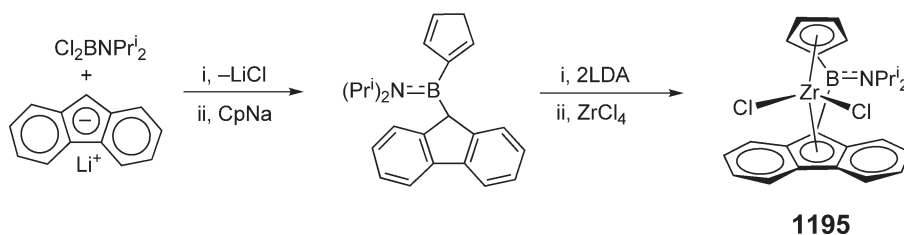


Scheme 280

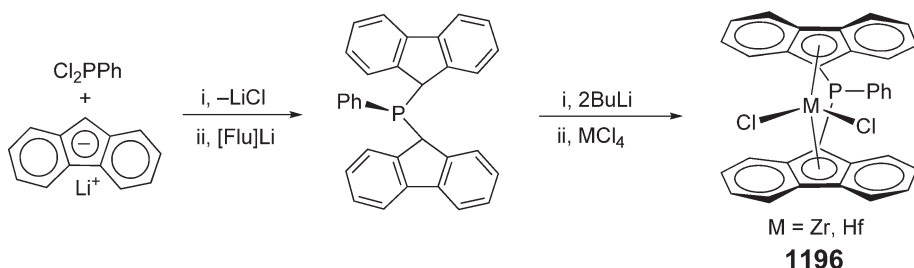
#### 4.08.10.4.3 Fluorenyl complexes with (B, P, N, Ge, Sn, C<sub>n</sub>)-bridges

Aminoboranediy-bridged *ansa*-(Cp-Flu) zirconocene dichloride **1195** has been prepared according to the salt metathesis approach shown in Scheme 281, which involves sequential reactions of 9-fluorenyllithium and CpNa with (Pr<sup>i</sup>)<sub>2</sub>NBCl<sub>2</sub>, followed by treatment with lithium diisopropylamide and ZrCl<sub>4</sub>.<sup>922</sup> The molecule has C<sub>s</sub>-symmetry; both solution spectroscopic and solid-state X-ray data reveal a partial double bond character between N and B atoms as a result of the B–N π-bonding. Upon activation with MAO, this complex polymerizes propylene to syndiotactic PP ([*rr*] = 81%).

The synthesis of the PhP-bridged bis(fluorenyl) complex **1196** is outlined in Scheme 282.<sup>923</sup> Its activity in the MAO-co-catalyzed polymerization of ethylene is substantially lower than that of the carbon- or silicon-bridged analogs; this decrease has been attributed to the increased electron density at the metal center effected by the PPh bridge.



Scheme 281

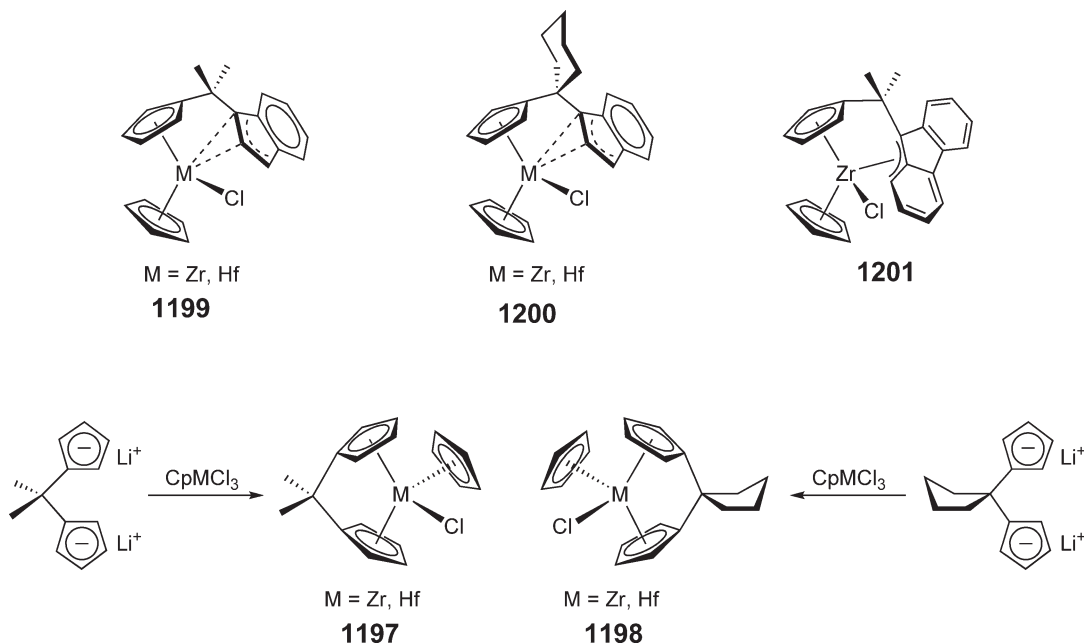


Scheme 282

#### 4.08.11 Complexes with more than Two Cyclopentadienyl Ligands

$\text{Me}_2\text{C}$ -bridged *ansa*-tris(cyclopentadienyl)metallocenes  $[\text{Me}_2\text{C}(\text{C}_5\text{H}_4)_2](\text{C}_5\text{H}_5)\text{MCl}$  **1197**: M = Zr, Hf) are obtained conveniently by the reaction of the bridged bis(Cp) dianion with  $\text{CpMCl}_3$  according to Scheme 283.<sup>924</sup> The molecular structures of both complexes have been determined by X-ray diffraction, revealing  $\eta^5$ -coordination to the metal center for all three rings; this is in sharp contrast to the unbridged Hf complex,  $[(\eta^5\text{-C}_5\text{H}_5)_2(\sigma\text{-C}_5\text{H}_5)]\text{HfCl}$ , where the third Cp adopts  $\sigma$ -bonding. Analogous  $(\text{CH}_2)_4\text{C}$ -bridged *ansa*-tris(cyclopentadienyl)metallocene chlorides **1198** and the corresponding methyl derivatives have also been synthesized.<sup>925</sup> When activated with MAO, complexes **1198** are active for polymerization of ethylene.

One-carbon-bridged *ansa*-metallocenes incorporating two cyclopentadienyl and one indenyl or fluorenyl rings have also been made by the reaction of  $\text{CpMCl}_3$  with appropriate bridged dianions.<sup>926</sup> In complex **1199** (M = Zr, Hf), the indenyl ligand is coordinated to the metal center via  $\eta^2$ -fashion, on the basis of the crystal structure of the zirconium complex; the electron donation from the  $\eta^2$ -indenyl group is intermediate between the  $\eta^1$ - ( $\sigma$ -) and  $\eta^3$ - ( $\pi$ -) coordination. The solution structure derived from the  $^1\text{H}$  NMR data is consistent with the solid-state structure. The structural features of the analogous  $(\text{CH}_2)_5\text{C}$ -bridged *ansa*-metallocenes **1200** are similar to those described for complexes **1199**. The molecular structure of the fluorenyl-containing zirconium complex **1201** shows that the fluorenyl moiety adopts an unusual  $\eta^3$ -allyl coordination mode involving both the five- and one of the six-membered rings, similar to that seen in the hydrido complex **1128**.<sup>878</sup> The spectroscopic data indicate that this structural motif is maintained in solution.



Scheme 283

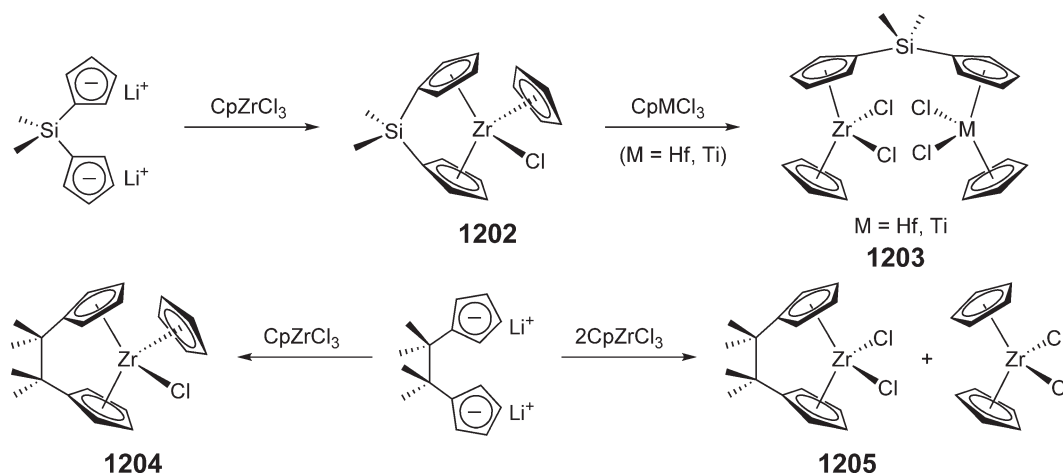
The Me<sub>2</sub>Si-bridged *ansa*-tris(cyclopentadienyl)zirconocene Me<sub>2</sub>Si(C<sub>5</sub>H<sub>4</sub>)<sub>2</sub>(C<sub>5</sub>H<sub>5</sub>)ZrCl **1202** has been prepared analogously by the reaction of the bridged bis(Cp) dianion with 1 equiv. of CpZrCl<sub>3</sub> according to Scheme 284.<sup>927</sup> The X-ray molecular structure shows that all three rings are  $\eta^5$ -coordinated to the metal center. This complex is a convenient precursor for the synthesis of Me<sub>2</sub>Si-linked heterobinuclear metallocene complexes. For example, the reaction of the *ansa*-tris(cyclopentadienyl)zirconium complex **1202** with CpMCl<sub>3</sub> (M = Hf, Ti) gives Zr/Hf and Zr/Ti heterobinuclear metallocene complexes **1203**. The reaction of the tetramethylethylene-bridged bis(Cp) dianion with 1 equiv. of CpZrCl<sub>3</sub> affords the corresponding *ansa*-tris(cyclopentadienyl)zirconocene Me<sub>4</sub>C<sub>2</sub>(C<sub>5</sub>H<sub>4</sub>)<sub>2</sub>(C<sub>5</sub>H<sub>5</sub>)ZrCl **1204**; the reaction with 2 equiv. of CpZrCl<sub>3</sub>, however, gives a mixture containing *ansa*-bis(Cp) complex **1205** and Cp<sub>2</sub>ZrCl<sub>2</sub>.

The stable tris(cyclopentadienyl)zirconium methyl complex **1206** is readily obtained by the reaction of Cp<sub>2</sub>Zr(Cl)Me with CpNa (Scheme 285).<sup>928</sup> The molecular structure of this complex shows that all three symmetry-equivalent Cp rings are  $\eta^5$ -coordinated to Zr. Abstraction of the methyl group with dimethylanilinium tetraphenylborate in THF gives the corresponding base-stabilized cationic species **1207**. The donor solvent-free cationic complex **1208** can be *in situ*-generated by the reaction with B(C<sub>6</sub>F<sub>5</sub>)<sub>3</sub> in CD<sub>2</sub>Cl<sub>2</sub> at low temperatures; it is, however, thermally unstable and cannot be isolated, though addition of nitriles to solutions of **1208** gives isolable base-stabilized cations **1209**. Other ligands such as CO and *tert*-butyl isonitrile also convert **1208** to the corresponding ligand-stabilized cationic complexes **1210**; the cationic CO and *tert*-butylisonitrile complexes were isolated and structurally characterized. Trapping **1208** with Cp<sub>2</sub>ZrCl<sub>2</sub> and Cp<sub>3</sub>ZrCl yields the chloro-bridged binuclear adducts **1211** and **1212**, respectively.<sup>929</sup> The crystal structures show a strongly bent Zr–Cl–Zr moiety in **1211** (137.15°) but a more linear arrangement in **1212** (160.88°). In **1212**, each of the two Cp<sub>3</sub>Zr units adopts an almost trigonal-pyramidal arrangement of the three  $\eta^5$ -Cp rings and the single bridging chloride around zirconium.

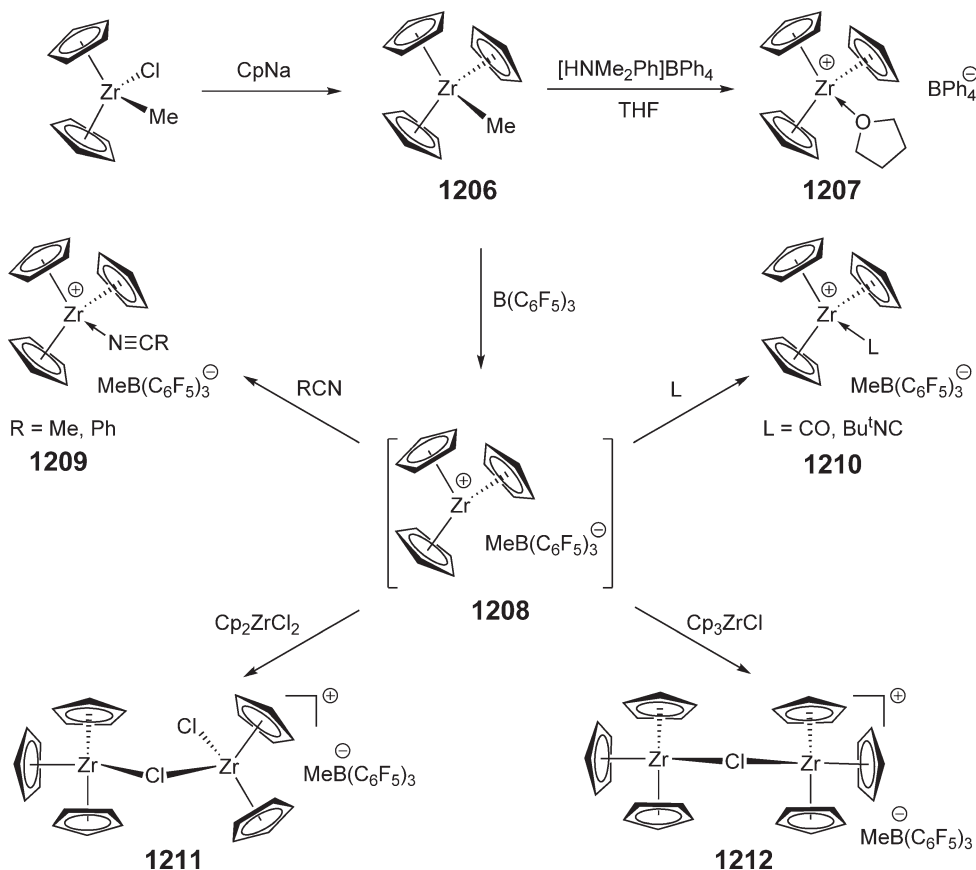
The zwitterionic tris(cyclopentadienyl)zirconocene complex **1213** is obtained by treatment of Cp<sub>2</sub>ZrCl<sub>2</sub> with the lithium, sodium salt of the B(C<sub>6</sub>F<sub>5</sub>)<sub>3</sub>-substituted borato-Cp dianion according to Scheme 286.<sup>930</sup> The X-ray crystal structure of this complex reveals that the three  $\eta^5$ -cyclopentadienyl ligands are in a nearly trigonal-planar coordination around zirconium with a pronounced Zr–F–C(aryl) coordination perpendicular to it; this Zr–F–C(aryl) coordination is persistent in solution based on solution NMR studies.

Treatment of dilithium pentalendiide with Cp<sub>2</sub>ZrCl<sub>2</sub> gives the structurally characterized, 18-electron complex **1214** bearing the bicyclic  $\eta^8$ -coordinated pentalene ligand (Scheme 287).<sup>931</sup> The reaction of Cp<sub>2</sub>MCl<sub>2</sub> (M = Zr, Hf) with 2 equiv. of dilithium pentalendiide leads to formation of homoleptic, 20-electron bis( $\eta^8$ -pentalene) zirconium and hafnium complexes **1215**. When treated with 1 equiv. of ZrCl<sub>4</sub>(THF)<sub>2</sub>, complex **1215** is converted to the monopentalene complex, ( $\eta^8$ -pentalene)ZrCl<sub>2</sub>(THF)<sub>2</sub>, with a distorted pseudo-octahedral coordination geometry around the zirconium center.

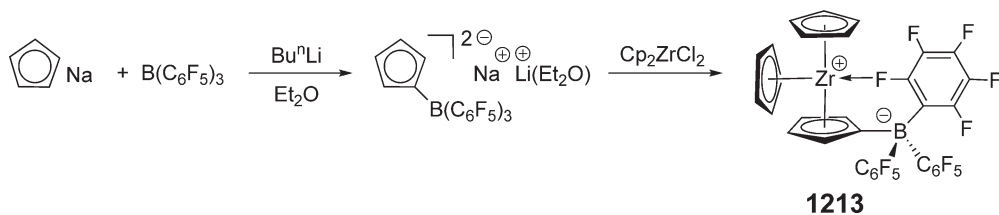
Tetrakis(cyclopentadienyl) complexes of group 4 metals, M(Cp)<sub>4</sub>, have been prepared in high yields from the reaction of Cp<sub>2</sub>MCl<sub>2</sub> and CpNa in toluene.<sup>932</sup> The reactivity of the zirconium complex **1216** with active-proton-containing species has been investigated. For example, the reaction of **1216** with 2 equiv. of Ph<sub>3</sub>SiOH forms bis(Cp) derivative **1217** according to Scheme 288. Treatment of **1216** with 2 equiv. of CF<sub>3</sub>SO<sub>3</sub>H gives the triflate derivative Cp<sub>2</sub>Zr(CF<sub>3</sub>SO<sub>3</sub>)<sub>2</sub>, but the reaction with 1 equiv. of CF<sub>3</sub>SO<sub>3</sub>H affords the tris(Cp) complex Cp<sub>3</sub>Zr(CF<sub>3</sub>SO<sub>3</sub>) **1218** as a pale yellow crystalline material, which can be hydrolyzed to give the  $\mu$ -oxo binuclear complex [Cp<sub>2</sub>Zr(CF<sub>3</sub>SO<sub>3</sub>)<sub>2</sub>]<sub>2</sub>O.



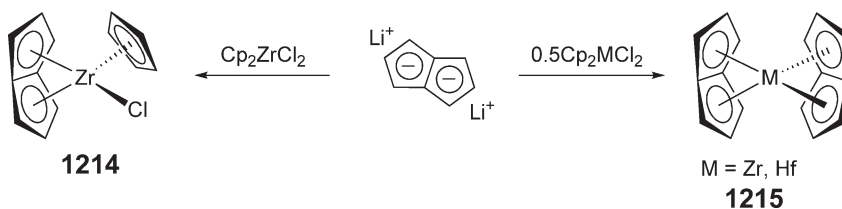
Scheme 284



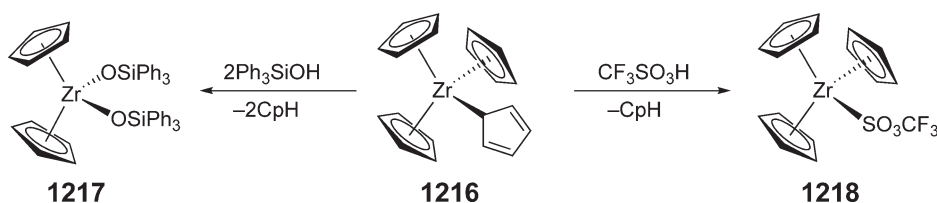
Scheme 285



Scheme 286



Scheme 287



Scheme 288

#### 4.08.12 Complexes with $\eta^n$ - ( $n \geq 6$ ) Ligands

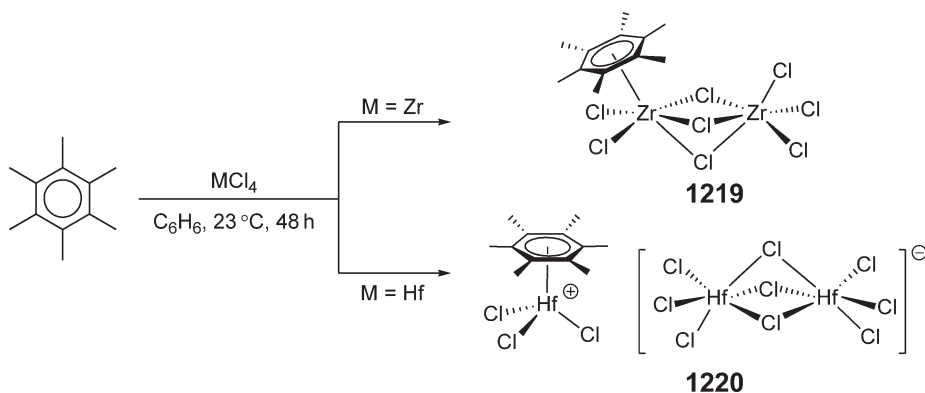
##### 4.08.12.1 $\eta^6$ -Arene Complexes

Treatment of hexamethylbenzene with  $\text{ZrCl}_4$  and  $\text{HfCl}_4$  in benzene for 48 h at room temperature gives the neutral covalent zirconium  $\eta^6$ -arene complex  $\text{Zr}(\eta^6\text{-Me}_6\text{C}_6)\text{Cl}_2(\mu\text{-Cl})_3\text{ZrCl}_3$  **1219** and the ionic hafnium complex  $[\text{Hf}(\eta^6\text{-Me}_6\text{C}_6)\text{Cl}_3][\text{Hf}_2\text{Cl}_9]$  **1220**, respectively, as illustrated in Scheme 289.<sup>933</sup> These complexes can also be obtained in the presence of aluminum trichloride that normally acts as halide abstractor for the generation of the isoelectronic titanium(IV) species. Both the zirconium and hafnium complexes have been structurally characterized. Arene complexes of titanium and zirconium reported before 1994 were surveyed in a review article.<sup>934</sup>

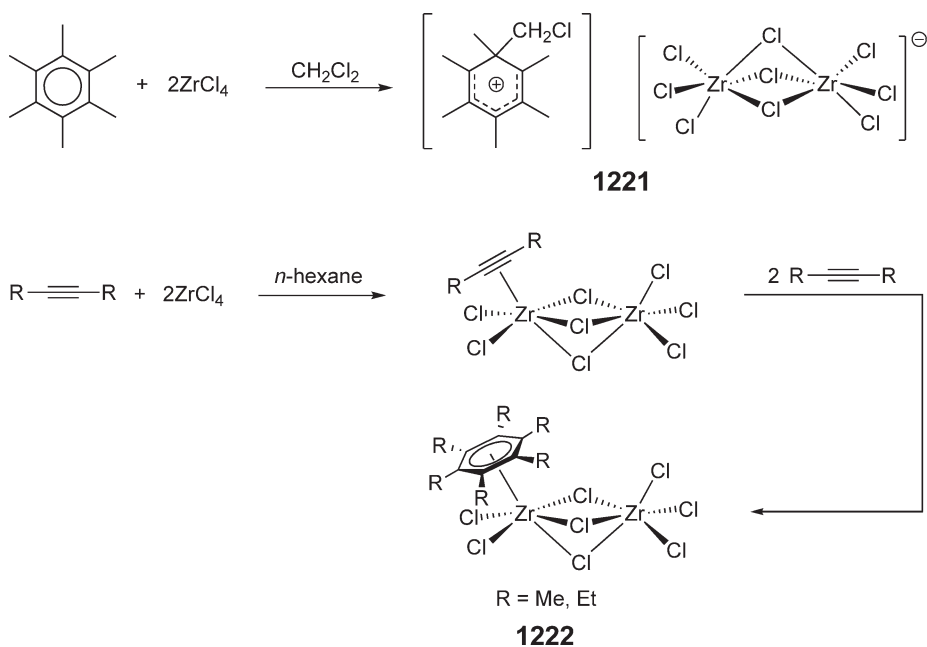
The identical zirconium  $\eta^6$ -arene complex **1219** was prepared in 90% yield and structurally characterized earlier from the reaction of hexamethylbenzene with  $\text{ZrCl}_4$  in 1,2-dichlorobenzene, along with the tetra- and pentamethylbenzene derivatives.<sup>935</sup> The initial observation of solubilization of the highly insoluble polymeric  $\text{ZrCl}_4$  using 1,2,4,5-Me<sub>4</sub>C<sub>6</sub>H<sub>2</sub> as a carrier in a halogenated solvent prompted the isolation of such zirconium  $\eta^6$ -arene complexes. As revealed by the <sup>1</sup>H NMR spectrum in CD<sub>2</sub>Cl<sub>2</sub>, complex **1219** is in equilibrium with free hexamethylbenzene and a complex of type  $(\text{C}_6\text{Me}_6)(\text{ZrCl}_4)_n$  having a higher Zr/ $\text{C}_6\text{Me}_6$  ratio.<sup>936</sup> The methyl redistribution reaction of  $\text{C}_6\text{Me}_6$  and  $\text{ZrCl}_4$  in  $\text{CH}_2\text{Cl}_2$  can result in formation of byproducts such as the structurally characterized  $[\text{C}_6\text{Me}_6\text{CHCl}_2][\text{Zr}_2\text{Cl}_9]$  (**1221**, Scheme 290), which is derived from the zirconium-assisted Friedel–Craft reaction of  $\text{CH}_2\text{Cl}_2$  on the arene. The reaction of  $\text{ZrCl}_4$  with internal alkynes such as 2-butyne and 3-hexyne in an innocent solvent (i.e., *n*-hexane) leads to the quantitative formation of the  $\text{ZrCl}_4$ -assisted trimerization products,  $\text{Zr}(\eta^6\text{-R}_6\text{C}_6)\text{Cl}_2(\mu\text{-Cl})_3\text{ZrCl}_3$  **1222**, due to the high stability of such zirconium  $\eta^6$ -arene complexes.

##### 4.08.12.2 Borata-benzene Complexes

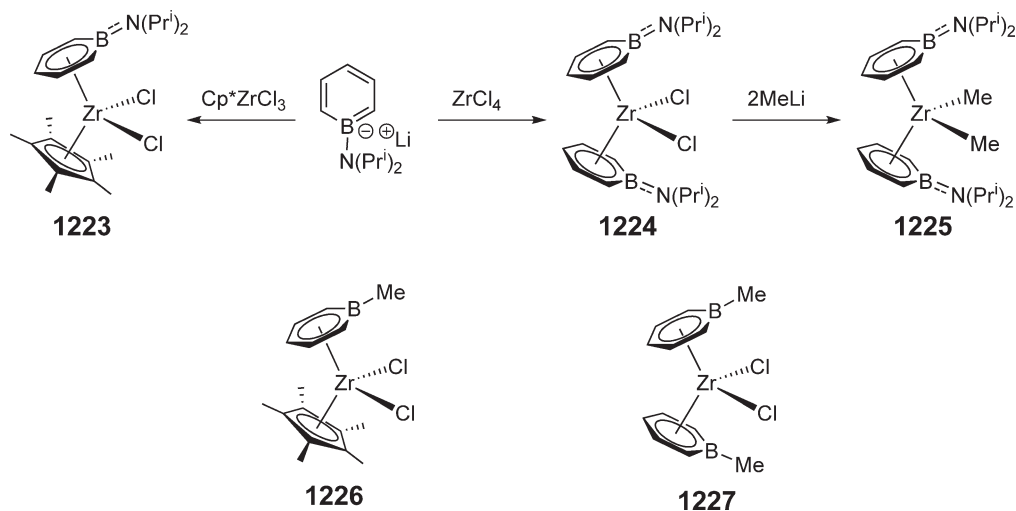
The reaction of *N,N*-diisopropylaminoboratabenzene lithium with  $\text{Cp}^*\text{ZrCl}_3$  and  $\text{ZrCl}_4$  affords aminoboratabenzene zirconium complexes **1223** and **1224** (Scheme 291), respectively.<sup>937</sup> The molecular structure of the bis(boratabenzene) complex **1224**, determined by X-ray diffraction, shows that the boratabenzene rings are  $\eta^5$ -coordinated to Zr through the five carbon atoms within the rings, in sharp contrast to the  $\eta^6$ -coordinated boratabenzene–late transition metal complexes. This distortion toward  $\eta^5$ -binding in these two zirconium complexes is presumably due to the high



Scheme 289



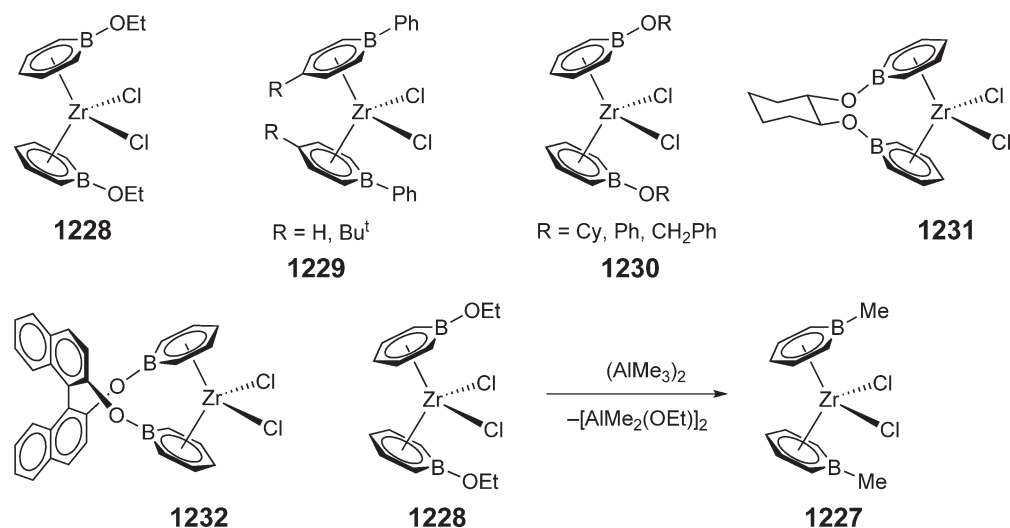
Scheme 290



Scheme 291

electron demand of Zr(IV), which prefers coordination to the more electron-rich carbons. However, the boratabenzene rings in monomethylboratabenzene and bis(methylboratabenzene) zirconium complexes **1226** and **1227** containing no stabilizing substituents at boron are characterized to have  $\eta^6$ -bonding.<sup>938</sup> There exists strong B–N  $\pi$ -bonding in complex **1224**, as evidenced by a short distance of the B–N bond of 1.396(6) Å, the  $sp^2$ -hybridized nitrogen, and the high rotational barrier about the B–N bond. Methylation of the dichloride **1224** affords the corresponding dimethyl derivative **1225** without complications. Upon activation with a large excess of MAO, both the monoboratabenzene and bis(boratabenzene) zirconium complexes polymerize ethylene with activities comparable to that of  $\text{Cp}_2\text{ZrCl}_2$ .

The sterically less demanding ethoxyboratabenzene zirconium complex **1228** (Scheme 292), when activated with MAO, produces  $\alpha$ -olefins from ethylene, as a result of the much enhanced  $\beta$ -hydrogen transfer rate as compared with the *N,N*-diisopropylaminoboratabenzene zirconium derivative.<sup>939</sup> Zirconium complexes **1229** bearing the phenylboratabenzene ligands are obtained by salt metathesis, where both boratabenzene rings in the structurally characterized **1229**

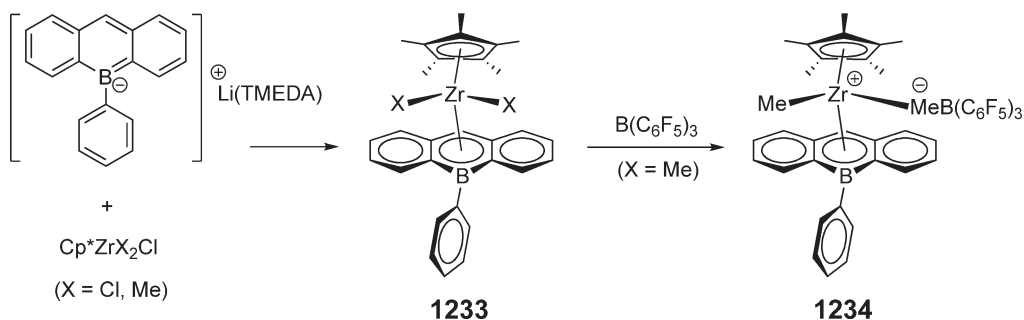


Scheme 292

( $R = Bu^t$ ) are  $\eta^6$ -coordinated to Zr.<sup>940</sup> The MAO-activated **1229** ( $R = H$ ) also affords ethylene oligomers. A tandem catalysis system has been developed by combining in one reactor two types of complexes, a constrained-geometry titanium catalyst and the ethoxyboratabenzene zirconium complex **1228**, to polymerize ethylene. This strategy utilizes the ability of complex **1228** to produce  $\alpha$ -olefins which the titanium constrained-geometry complex incorporates into the growing polymer chain, thereby leading to the formation of branched polyolefins.<sup>941</sup> Other alkoxyboratabenzene zirconium complexes have been prepared by the salt metathesis route, including cyclohexyl, phenyl, and benzyl derivatives **1230**, as well as the linked 1,2-*trans*-cyclohexanediol and binaphthol *ansa*-type complexes **1231** and **1232**.<sup>942</sup> Interestingly, treatment of the ethoxyboratabenzene complex **1228** with trimethylaluminum, which is present in large amounts in commercial MAO (up to 35 wt.%), leads preferentially to methylation at boron rather than zirconium to give the bis(methylboratabenzene) derivative **1227** (Scheme 292).

The reaction of lithium borata-anthracene with  $Cp^*ZrX_2Cl$  ( $X = Cl, Me$ ) affords 9-phenyl-9-borata-anthracene zirconium complexes **1233** (Scheme 293).<sup>943</sup> The X-ray structure of the dichloride derivative resembles a bent metallocene with a tetrahedral disposition of ligands around Zr. The borata-anthracene ligand bends significantly (approximately  $16^\circ$ ) to avoid steric contacts with the  $[Cp^*ZrCl_2]$  moiety. Treatment of the methyl derivative with  $B(C_6F_5)_3$  gives the corresponding tight ion pair **1234**. The MAO-activated dichloride derivative **1233** reacts with 1 atm of ethylene to produce a mixture of low molecular oligomers, whereas the reaction of the methylborate species **1234** with ethylene gives low molecular weight polyethylene.

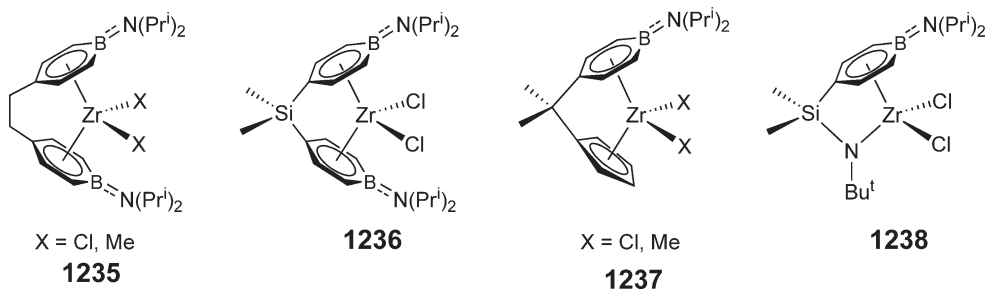
Various bridged *ansa*-boratabenzene zirconium complexes have been synthesized by salt metathesis, including ethylene-bridged bis(*N,N*-diisopropylaminoboratabenzene)zirconium complexes **1235**, dimethylsilylene-bridged bis(*N,N*-diisopropylaminoboratabenzene)zirconium dichloride **1236**, and dimethylmethylene-bridged (cyclopentadienyl)(*N,N*-diisopropylaminoboratabenzene)zirconium complexes **1237**.<sup>944</sup> As the crystal structures of the dimethyl



Scheme 293

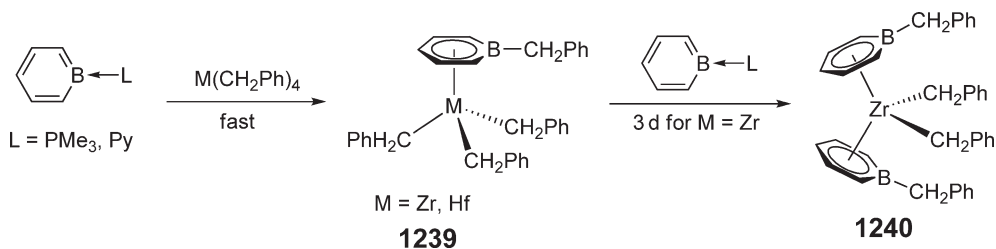


derivatives of **1235** and **1237** show, these complexes closely resemble the corresponding *ansa*-zirconocenes. The compounds are active catalysts for the MAO-co-catalyzed polymerization of olefins. The Me<sub>2</sub>Si-bridged (*tert*-butylamido)(*N,N*-diisopropyl-aminoboratabenzene) zirconium complex **1238**, a constrained-geometry-type complex, has been synthesized;<sup>945</sup> the molecular structure of this complex shows that the Zr atom is  $\eta^5$ -bound to the coplanar five ring carbon atoms, whereas the boron atom is displaced out of this plane away from Zr by 0.09 Å. On MAO activation, this complex copolymerizes ethylene with 1-octene, although with marginal activity and only 1.1 mol% of 1-octene incorporation.

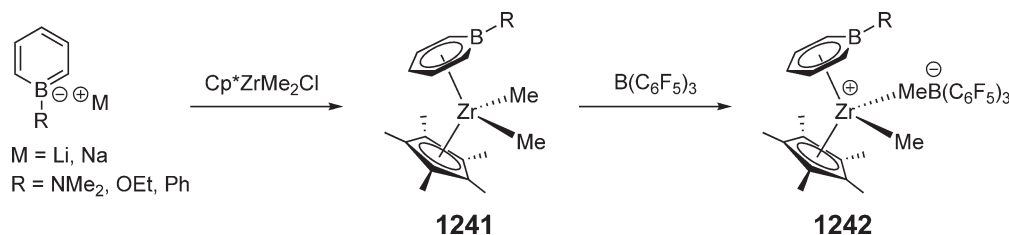


An alternative route to boratabenzene complexes involves the intramolecular nucleophilic substitution on coordinated boratabenzenes, as illustrated in Scheme 294.<sup>946</sup> Thus, the reaction of M(CH<sub>2</sub>Ph)<sub>4</sub> (M = Zr, Hf) with C<sub>5</sub>H<sub>5</sub>B ← L (L = pyridine, PMe<sub>3</sub>) in benzene quickly gives the mono(benzylboratabenzene) tribenzyl complexes **1239**, the molecular structure of which (M = Hf) has been determined by X-ray diffraction. Further reaction leading to the final bis(benzylboratabenzene)zirconium dibenzyl complex **1240** is considerably slower, requiring 3 days at room temperature, whereas there is no further reaction for mono(benzylboratabenzene) tribenzyl hafnium complex. The reaction of C<sub>5</sub>H<sub>5</sub>B ← PMe<sub>3</sub> with Zr(NMe<sub>2</sub>)<sub>4</sub> occurs analogously to form (C<sub>5</sub>H<sub>5</sub>B-NMe<sub>2</sub>)Zr(NMe<sub>2</sub>)<sub>3</sub>, but no further reaction takes place to the bis(boratabenzene) complex, even after heating to 80 °C for 48 h.

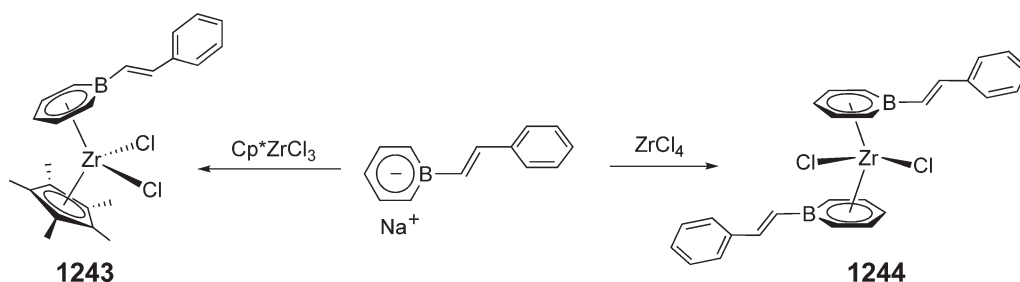
The preparation of boratabenzene-containing zirconium dimethyl complexes from their dichlorides is not straightforward because alkylation with MeMgBr or MeLi is sometimes complicated by boron's susceptibility to nucleophilic attack, which results in low yields and in the formation of side-products. The use of the Cp<sup>\*</sup>ZrMe<sub>2</sub>Cl reagent to react with an appropriate alkali boratabenzene salt gives the dimethyl complexes **1241** (Scheme 295) in modest isolated yields.<sup>947</sup> Treatment of these dimethyl complexes with B(C<sub>6</sub>F<sub>5</sub>)<sub>3</sub> rapidly and quantitatively generates the zwitterionic compounds **1242**. These are stable in toluene at room temperature for up to 1 week but decompose instantly in CH<sub>2</sub>Cl<sub>2</sub>. The molecular structure of the dimethylaminoboratabenzene complex (**1242**: R = NMe<sub>2</sub>) is similar to those observed for typical zirconocenium methylborate complexes, although the aminoboratabenzene ligand more closely



Scheme 294



Scheme 295



Scheme 296

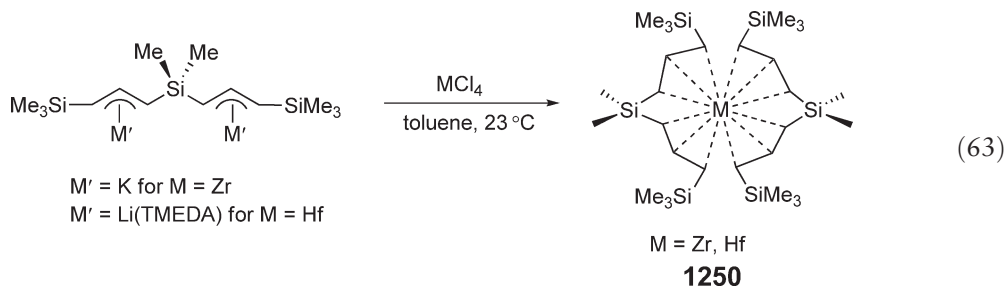
resembles an  $\eta^5$ -pentadienyl fragment than a phenylboratabenzene derivative (**1242**: R = Ph), where it is  $\eta^6$ -bound. Ion pair dissociation/recombination processes occur in solution, as evidenced by variable-temperature  $^1\text{H}$  NMR spectroscopy. On the basis of the dynamic NMR, IR, and electrochemical data, it was concluded that the donor properties in  $[\text{C}_5\text{H}_5\text{B-R}]$  ligands decrease in the order  $\text{R} = \text{NMe}_2 > \text{OEt} \sim \text{Me} > \text{Ph}$ .

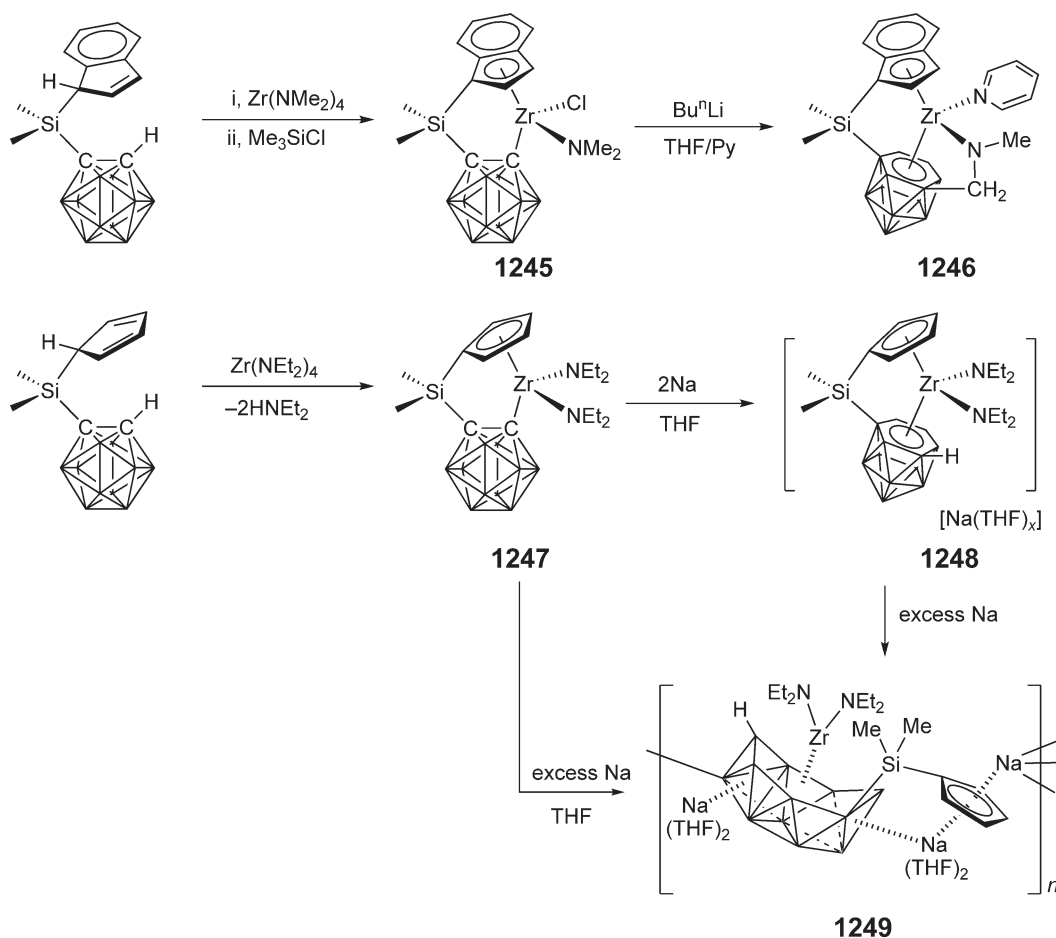
Zirconium complexes **1243** and **1244** (Scheme 296) incorporating the  $\eta^6$ -boratastilbene ligand are obtained from the reaction of the sodium salt of boratastilbene with  $\text{Cp}^*\text{ZrCl}_3$  and  $\text{ZrCl}_4$ , respectively.<sup>948</sup> Analogous zirconium complexes bearing 4-boratastyrylstilbene and 1,4-bis(boratastyryl)benzene were also synthesized. Upon activation with a large excess of MAO, the activity of the complex **1243** for polymerization of ethylene was 3 times higher than that of  $\text{Cp}_2\text{ZrCl}_2$  under similar conditions.

#### 4.08.12.3 Other Complexes with $\eta^6$ - or $\eta^7$ -Ligands

High-valent Zr(IV) metallocarboranes bearing  $[\text{C}_2\text{B}_{10}\text{H}_{10}]^{2-}$  that cannot be prepared by conventional metathesis methods have been synthesized by an unexpected oxidative-addition reaction between Zr(II) and the carborane cage as shown in Scheme 297.<sup>949</sup> Thus, treatment of the dimethylsilylene-bridged Ind/carboranyl zirconium amide complex **1245**,<sup>950</sup> prepared by aminolysis of  $\text{Zr}(\text{NMe}_2)_4$  with this neutral carborane-containing ligand followed by the reaction with an equimolar amount of  $\text{Me}_3\text{SiCl}$ , with 1 equiv. of  $\text{Bu}^n\text{Li}$  in THF/pyridine yields complex **1246** as yellow crystals in 56% yield. The molecular structure of complex **1246** reveals that the Zr atom is  $\eta^5$ -bound to the  $\text{C}_5$  ring of the indenyl moiety,  $\eta^6$ -bound to the open hexagonal  $[\text{C}_2\text{B}_4]$  bonding face of the *nido*- $[\text{C}_2\text{B}_{10}]$  moiety, and  $\sigma$ -bound to two N atoms from the appended amido group and coordinated pyridine in a distorted tetrahedral geometry. The direct reaction of the  $\text{Me}_2\text{Si}$ -bridged Cp/carboranyl zirconium amide complex **1247**, also prepared by the amine elimination route, with excess Na in THF gives the Zr(IV) metallocarborane **1249** bearing an  $\eta^7$ -carboranyl ligand in 33% isolated yield, presumably via the  $\eta^6$ -carboranyl intermediate **1248** according to Scheme 297. The molecular structure of complex **1249** shows that the Zr atom is  $\eta^7$ -bound to the open  $\text{C}_2\text{B}_5$  bonding face of the *arachno*-carboranyl tetra-anion and  $\sigma$ -bound to two N atoms of the  $\text{NEt}_2$  ligand.

The synthesis of the *ansa*-bis(allyl) zirconium and hafnium complexes **1250** has been accomplished by the reaction of the potassium or lithium salt of the  $\eta^3$ -bis(allyl) ligand linked by a  $\text{Me}_2\text{Si}$  bridge<sup>951</sup> (Equation (63)). The lithium complex  $\text{Li}(\text{TMEDA})_2\{3-(\eta^3\text{-C}_3\text{H}_3\text{SiMe}_3\text{-1})_2\text{SiMe}_2\}$  is transformed into the corresponding potassium complex  $\text{K}_2\{3-(\eta^3\text{-C}_3\text{H}_3\text{SiMe}_3\text{-1})_2\text{SiMe}_2\}$  and into the hafnium complex  $\text{Hf}\{3-(\eta^3\text{-C}_3\text{H}_3\text{SiMe}_3\text{-1})_2\text{SiMe}_2\}_2$  (**1250**: M = Hf) by reactions with  $\text{KOBu}^t$  and  $\text{HfCl}_4$ , respectively. The potassium salt serves as the precursor of the zirconium complex **1250**, which is active for ethylene polymerization upon activation with MAO.





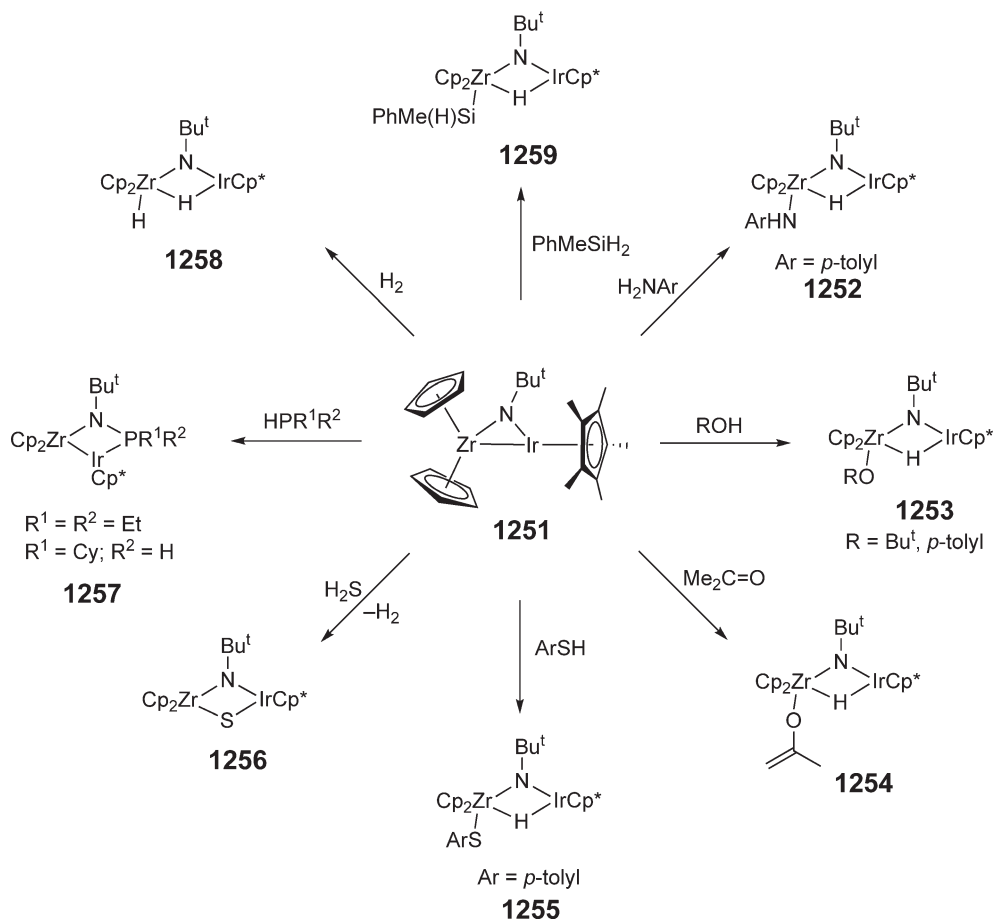
Scheme 297

### 4.08.13 Complexes with Metal–Metal Bonds

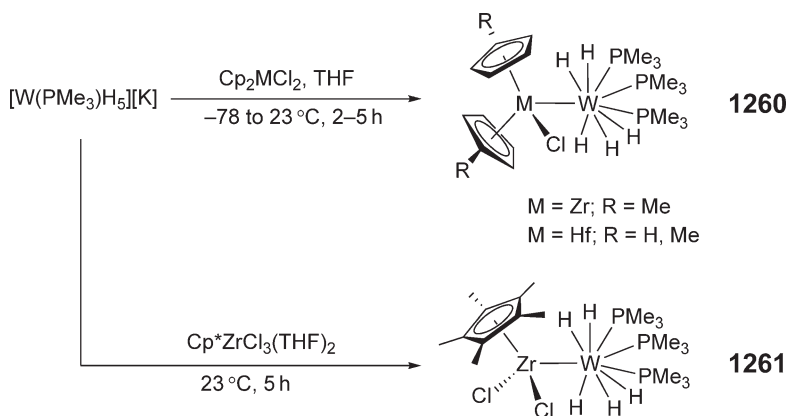
#### 4.08.13.1 M–M'-bonded Complexes

Early–late heterobimetallic bridging imido complex  $\text{Cp}_2\text{Zr}(\mu\text{-NBu}^t)\text{IrCp}^*$  **1251** was synthesized in 65% yield by the sequential addition of  $\text{Bu}^n\text{Li}$  and  $\text{Cp}^*\text{Ir}(\text{NBu}^t)$  to  $\text{Cp}_2\text{ZrCl}_2$ .<sup>952</sup> The Zr–Ir bond distance as determined by X-ray diffraction is 2.598(2) Å, and the Ir–N (1.887(13) Å) and Zr–N (2.084(13) Å) bond distances are comparable to those observed in analogous homonuclear imido dimers. This imido complex undergoes additions of both polar (N–H, O–H, S–H) and non-polar (H–H, Si–H, C–H) X–H bonds across the Zr–Ir bond, the reactions of which are summarized in Scheme 298. For example, reactions of **1251** with *p*-toluidine, *p*-cresol or *tert*-butyl alcohol, acetone, and *p*-thiocresol give the  $\mu\text{-NBu}^t\text{:}\mu\text{-H}$ -doubly bridged heterobimetallic Zr/Ir complexes **1252**, **1253**, **1254**, and **1255**, respectively. Addition of  $\text{H}_2\text{S}$  to **1251** results in formation of the bridging sulfide  $\mu\text{-NBu}^t\text{:}\mu\text{-S}$ -complex **1256**, presumably by a similar X–H addition followed by elimination of  $\text{H}_2$ . The reaction of **1251** with diethylphosphine and cyclohexylphosphine results in the unusual insertion of phosphide ( $\text{PR}_2$ ) into the Ir–N rather than the Zr–Ir bond to give complexes **1257** with the Zr–Ir bond intact. The addition of  $\text{H}_2$  to **1251** results in the reversible addition of the H–H bond across the Zr–Ir bond to form complex **1258** in which the terminal and bridging hydrides undergo exchange with each other and with excess  $\text{H}_2$ . Finally, addition of  $\text{MePhSiH}_2$  to **1251** gives complex **1259**, a product analogous to the  $\text{H}_2$  addition product.

The reaction of the potassium salt  $\text{K}[\text{W}(\text{PMe}_3)_3\text{H}_5]$  with  $\text{Cp}^R_2\text{MCl}_2$  ( $\text{M} = \text{Zr}$ ,  $\text{R} = \text{Me}$ ;  $\text{M} = \text{Hf}$ ,  $\text{R} = \text{H}$ ,  $\text{Me}$ ) gives heterobimetallic complexes  $\text{Cp}^R_2\text{M}(\text{Cl})\text{W}(\text{PMe}_3)_3\text{H}_5$  **1260** containing the M–W bond (Scheme 299).<sup>953</sup> Treatment of the same potassium salt with  $\text{Cp}^*\text{ZrCl}_3$  leads to the formation of analogous dichloride



Scheme 298



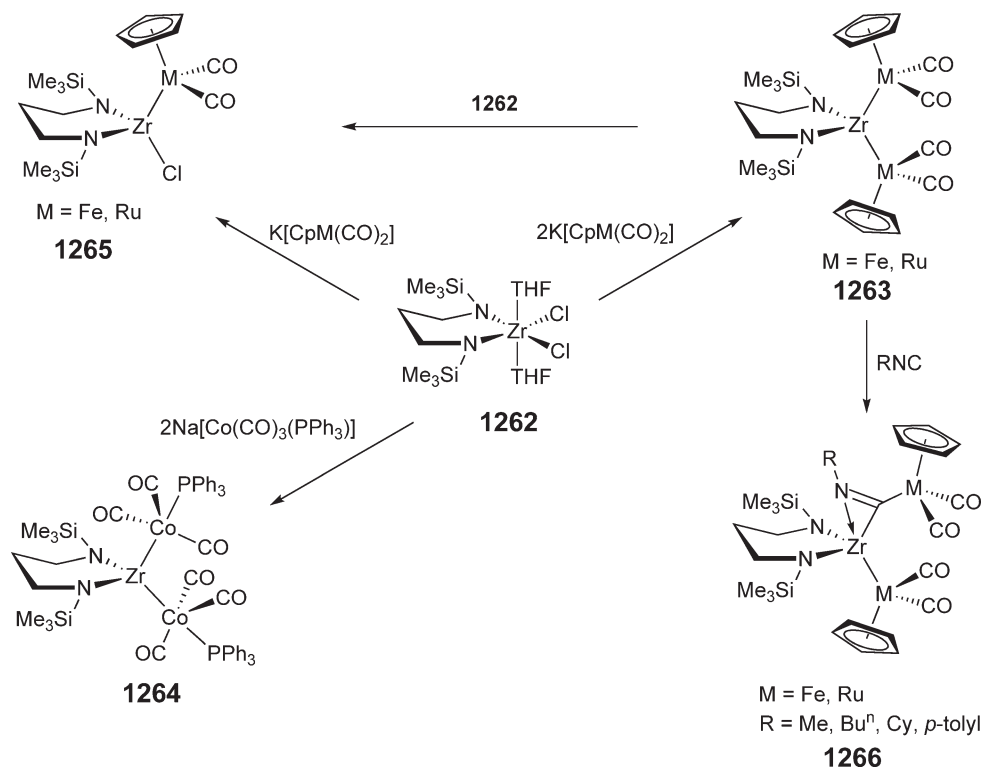
Scheme 299

heterobimetallic complex  $\text{Cp}^*\text{Zr}(\text{Cl})_2\text{W}(\text{PMe}_3)_3\text{H}_5$  **1261**, which has been structurally characterized. The Zr–W bond distance of  $2.94 \text{ \AA}$  is close to the sum of atomic radii of Zr and W ( $2.90 \text{ \AA}$ ) and less than the sum of metallic radii of  $2.99 \text{ \AA}$ . Hydrogen atoms bonded directly to the W center were not located, and thus bridging hydrogens between the two metals are possible.

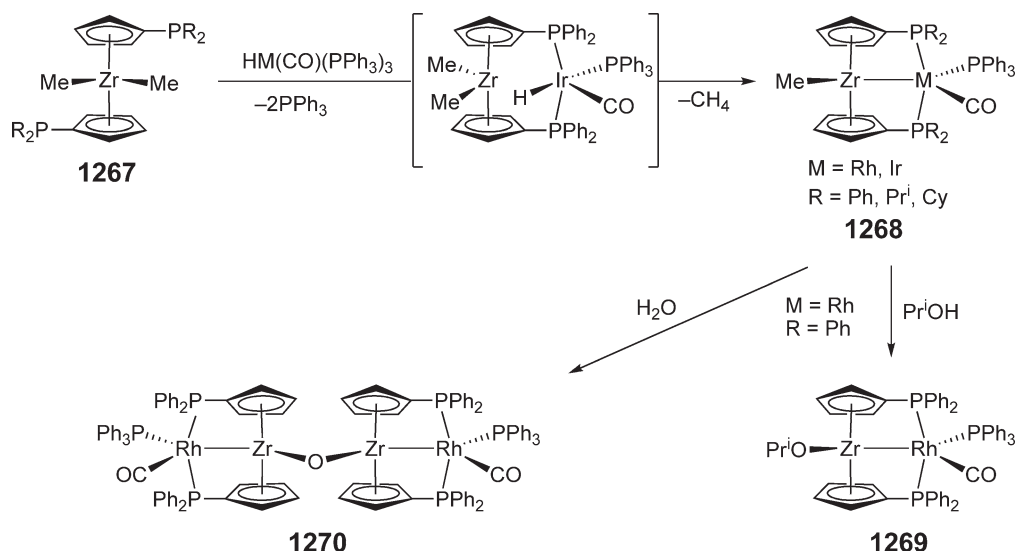
Early-late Zr-Co heterobimetallic complex  $\text{Cp}_2\text{Zr}[\text{Co}(\text{CO})_4]_2$  was prepared either by alkane elimination from the corresponding zirconocene dialkyls and  $\text{HCo}(\text{CO})_4$  or by salt elimination from zirconocene dihalide and  $\text{NaCo}(\text{CO})_4$ .<sup>954</sup> The chelate-amidozirconium dichloride derivative **1262** serves as a building block for unsupported trinuclear heterobimetallic complexes  $\text{ZrM}_2$  ( $\text{M} = \text{Fe}, \text{Ru}, \text{Co}$ ), as shown in Scheme 300.<sup>955</sup> Thus, reactions of **1262** with 2 equiv. of the carbonyl metallate derivatives  $\text{K}[\text{CpM}(\text{CO})_2]$  ( $\text{M} = \text{Fe}, \text{Ru}$ ) and  $\text{Na}[\text{Co}(\text{CO})_3(\text{PPh}_3)]$  give the heterotrinuclear complexes **1263** and **1264**, respectively. The molecular structures of the complexes **1263** determined by X-ray diffraction establish two unsupported metal-metal bonds in both the  $\text{ZrFe}_2$  [ $d(\text{Zr}-\text{Fe}) = 2.665(2), 2.664(2) \text{ \AA}$ ] and  $\text{ZrRu}_2$  [ $d(\text{Zr}-\text{Ru}) = 2.7372(7), 2.7452(7) \text{ \AA}$ ] complexes. The reaction of the trinuclear  $\text{ZrM}_2$  **1263** with the dichloride **1262** in a 1:1 molar ratio leads to a quantitative redistribution of complex fragments, yielding the binuclear complexes **1265**, which can also be obtained in moderate yield by reacting of **1262** with 1 equiv. of carbonyl metallate derivatives  $\text{K}[\text{CpM}(\text{CO})_2]$  ( $\text{M} = \text{Fe}, \text{Ru}$ ). Addition of isocyanides to the trinuclear complex **1263** results in exclusive insertion of the isocyanides into one of the metal-metal bonds, to give heterobimetallic  $\eta^2$ -metallaiminoacyl zirconium complexes **1266** (Scheme 300).<sup>956</sup>

The reaction of phosphine-substituted zirconocene dimethyl complexes **1267** with the rhodium hydride  $\text{HRh}(\text{CO})(\text{PPh}_3)_3$  proceeds with substitution of two  $\text{PPh}_3$  and instantaneous liberation of methane to give the Zr-Rh-bonded heterobimetallic complex **1268** according to Scheme 301.<sup>957</sup> The analogous reaction with the iridium hydride  $\text{HIr}(\text{CO})(\text{PPh}_3)_3$  is much slower, enabling the identification of the key reaction intermediate that still contains both methyl groups at Zr and the hydride at Ir but does not contain a metal-metal bond;<sup>958</sup> this intermediate reacts further with methane formation to eventually form the metal-metal-bonded complex type **1268**, as shown in Scheme 301. The rhodium complex **1268** ( $\text{R} = \text{Ph}$ ) reacts cleanly with isopropanol to liberate methane and yield the corresponding Rh-Zr isopropoxide complex **1269**. The tetrametallic  $\mu$ -oxo-(Zr-Rh) metallocene derivative **1270** was obtained by the reaction initiated by H-OH addition to the Zr-Rh bond followed by elimination of methane.

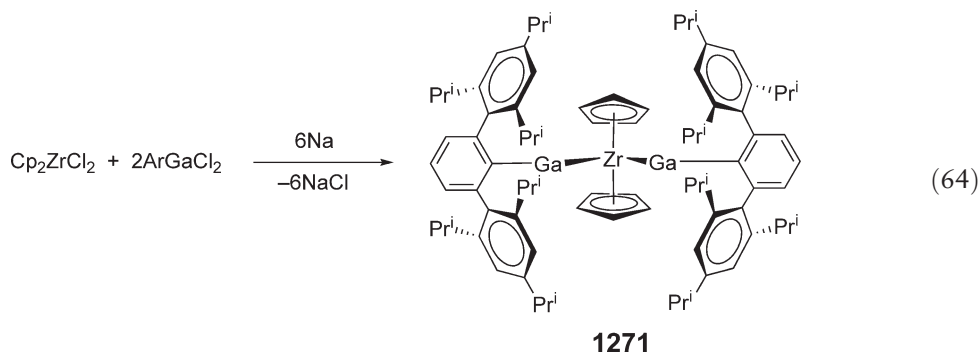
Zirconocene **1271** (Equation (64)) containing Zr-Ga bonds has been obtained by the reaction of sodium metal with  $\text{Cp}_2\text{ZrCl}_2$  and  $\text{ArGaCl}_2$  in hexane as deep green-black, air-sensitive crystals.<sup>959</sup> X-ray diffraction analysis revealed a Zr-Ga bond length of  $2.6350(8) \text{ \AA}$ ; this distance is compared with a sum of the Ga and Zr covalent radii of  $2.850 \text{ \AA}$ . Complex **1271** is isoelectronic with the well-known 18-electron zirconocene dicarbonyl complex,  $\text{Cp}_2\text{Zr}(\text{CO})_2$ , thus formally a  $\text{Zr}(\text{II})$  species.



Scheme 300

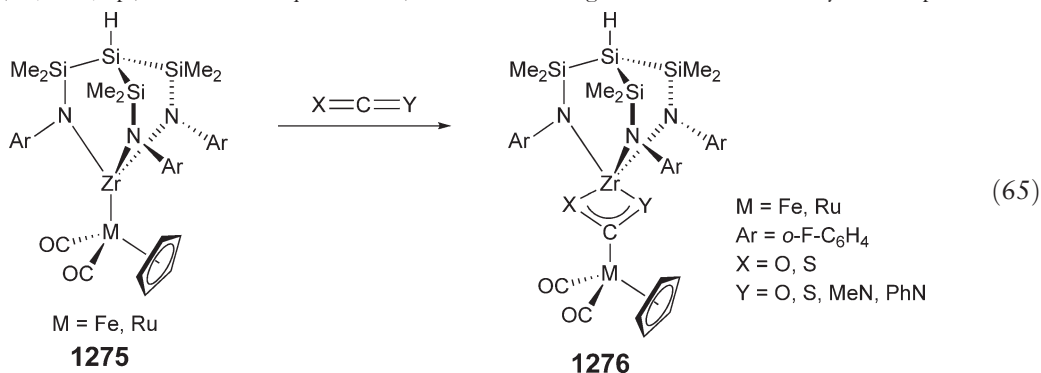


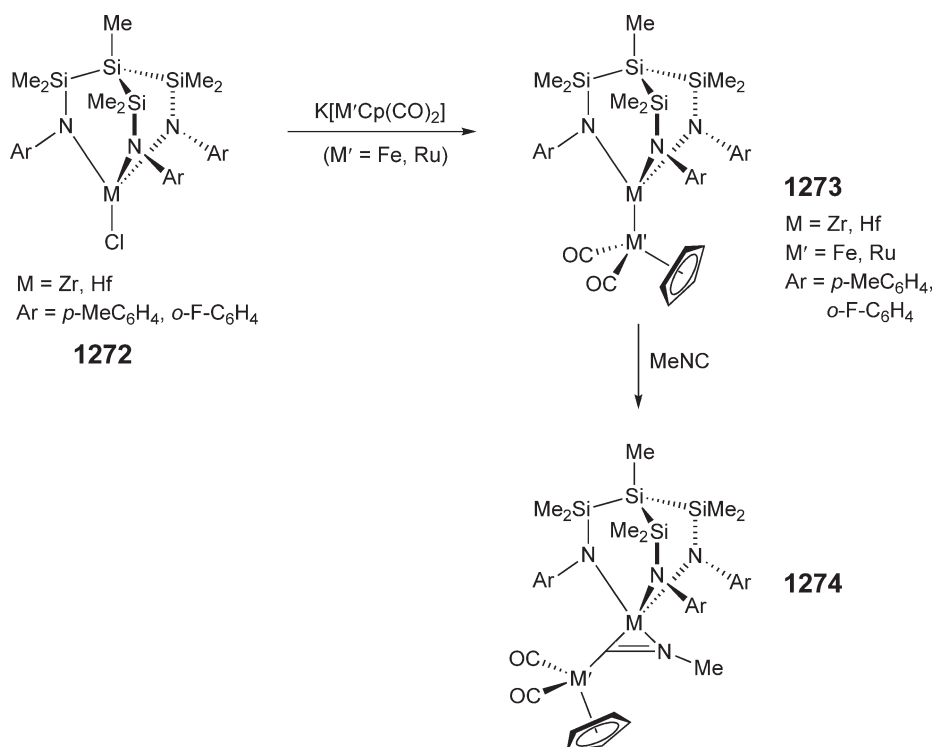
Scheme 301



Stable early-late M–M' metal-metal-bonded heterobimetallic complexes **1273** (M = Zr, Hf; M' = Fe, Ru) supported by tripodal amido ligands have been synthesized by the reaction of the zirconium and hafnium complexes MeSi(SiMe<sub>2</sub>NAr)<sub>3</sub>MCl **1272** with K[CpM'(CO)<sub>2</sub>], as shown in Scheme 302.<sup>960,961</sup> The molecular structure of the Zr–Fe complex (Ar = *p*-tolyl) determined by X-ray diffraction establishes the presence of an unsupported metal-metal bond with a Zr–Fe bond distance of 2.605(2) Å. The reaction of **1273** with isocyanides leads to insertion into the metal-metal bond and formation of metallaiminoacyl complexes **1274**.

Analogous heterobimetallic tripodal amido complexes **1275** (M = Fe, Ru) undergo highly selective reactions with heteroallenes X=C=Y (CO<sub>2</sub>, CS<sub>2</sub>, OCNPh, SCNMe, SCNPh) to yield the insertion products **1276** (Equation (65)).<sup>962</sup> Single crystal X-ray structures of the products (**1276**: M = Fe; X = Y = S; X = S, Y = NPh) established the mode of coordination of the substrates to the two metal centers as depicted in Equation (65). The Zr–Fe complex CpFe(CO)<sub>2</sub>Zr(Obu<sup>t</sup>)Cp<sub>2</sub> reacts with 1 equiv. of CS<sub>2</sub> to form the analogous stable dithiocarboxylate complex.<sup>963</sup>





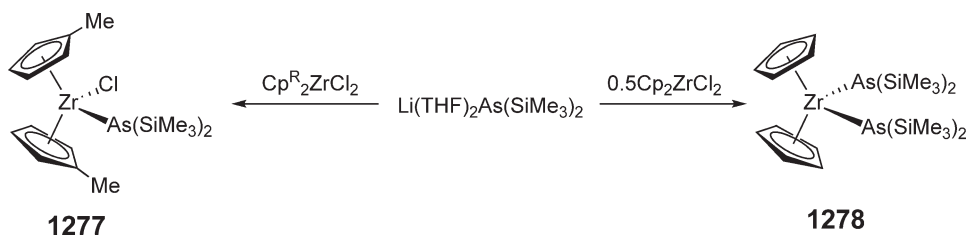
Scheme 302

#### 4.08.13.2 M–Metalloid-bonded Complexes

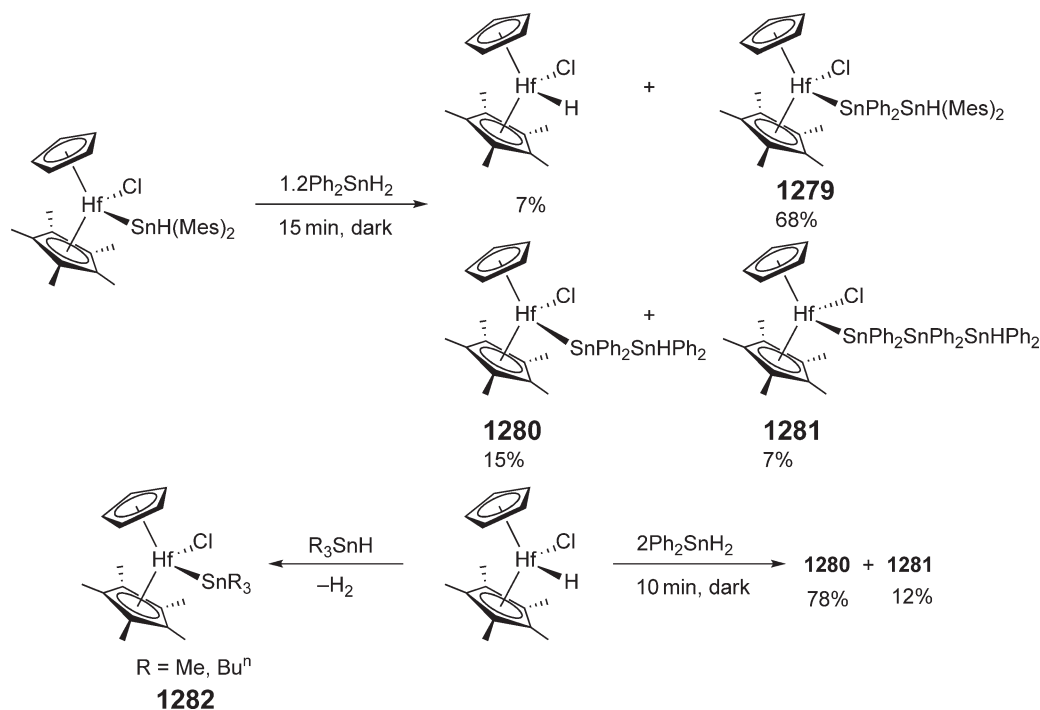
Reactions of  $\text{Li}(\text{THF})_2\text{As}(\text{SiMe}_3)_2$  with 1 equiv. of  $\text{Cp}^R_2\text{ZrCl}_2$  ( $R = \text{Me}$ ) and 0.5 equiv. of  $\text{Cp}_2\text{ZrCl}_2$  form zirconocene arsenido complexes **1277** and **1278**, respectively (Scheme 303).<sup>964</sup> Both compounds have been structurally characterized by X-ray diffraction. The bis(arsenide) complex **1278** possesses two distinctly different  $\text{As}(\text{SiMe}_3)_2$  groups and Zr–As bond lengths, Zr–As(1) = 2.799(2) and Zr–As(2) = 2.616(2) Å, indicating the presence of a Zr–As(1) single bond and a Zr–As(2) with  $\pi$ -bond character, as observed for zirconocene bis(phosphido) complexes (Section 4.08.9.8).

Treatment of the hafnocene hydrostannyl complex  $\text{CpCp}^*\text{HfCl}(\text{SnHMe}_2)$  with 1.2 equiv. of  $\text{Ph}_2\text{SnH}_2$  leads to the formation of a mixture containing  $\text{CpCp}^*\text{Hf}(\text{H})\text{Cl}$  (7%) and oligostannyl complexes  $\text{CpCp}^*\text{Hf}(\text{SnPh}_2\text{SnHMe}_2)\text{Cl}$  (**1279**, 68%),  $\text{CpCp}^*\text{Hf}(\text{SnPh}_2\text{SnHPh}_2)\text{Cl}$  (**1280**, 15%), and  $\text{CpCp}^*\text{Hf}(\text{SnPh}_2\text{SnPh}_2\text{SnHPh}_2)\text{Cl}$  (**1281**, 7%), which may be intermediates in the stannane dehydropolymerization process.<sup>965</sup> The latter two derivatives **1280** and **1281** were obtained in higher yields in the reaction of  $\text{CpCp}^*\text{Hf}(\text{H})\text{Cl}$  with 2 equiv. of  $\text{Ph}_2\text{SnH}_2$  (Scheme 304). Two trialkylstannyl complexes  $\text{CpCp}^*\text{Hf}(\text{SnR}_3)\text{Cl}$  (**1282**;  $R = \text{Me, Bu}^n$ ) were synthesized in good yields by the reaction of  $\text{CpCp}^*\text{Hf}(\text{H})\text{Cl}$  with  $\text{R}_3\text{SnH}$ .

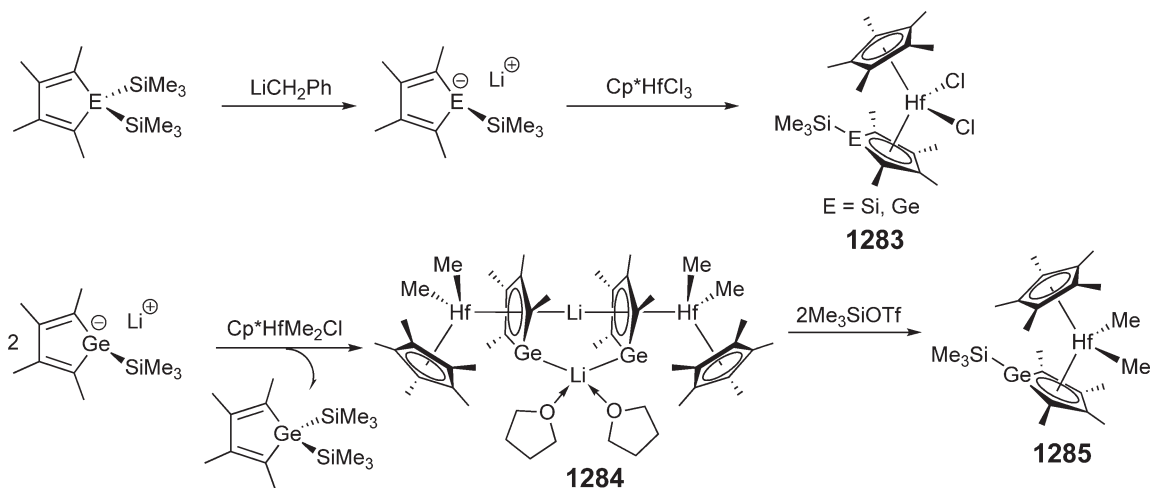
Pentahapto hafnium silolyl and germolyl complexes  $\text{Cp}^*(\eta^5\text{-C}_4\text{Me}_4\text{ESiMe}_3)\text{HfCl}_2$  (**1283**;  $E = \text{Si, Ge}$ ) are obtained in low and variable yields (5–30%) by salt metathesis according to Scheme 305.<sup>966</sup> The molecular structures of both complexes determined by X-ray diffraction show the planar silolyl and germolyl rings that are  $\eta^5$ -bound to Hf; the



Scheme 303



Scheme 304



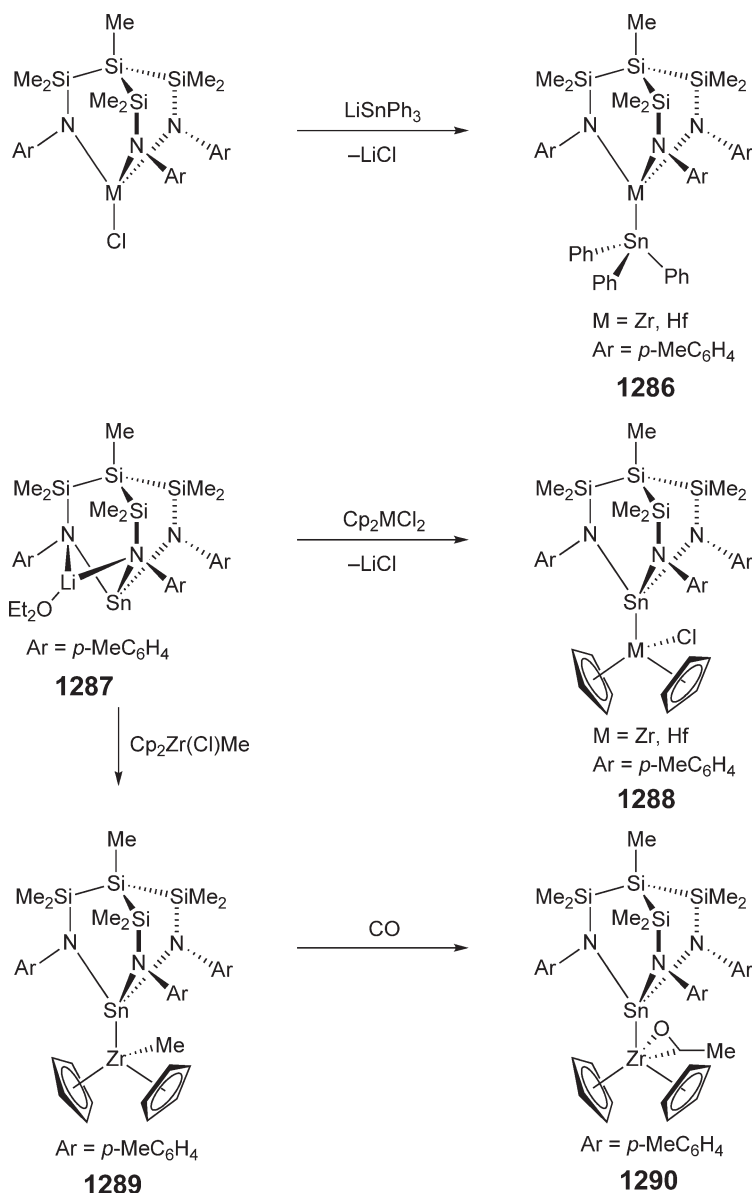
Scheme 305

Hf–Ge distance of 2.7978(7) Å is clearly bonding, given that the corresponding bond distance in  $\text{Cp}^*\text{HfCl}_2\text{Ge}(\text{SiMe}_3)_3$  is 2.740 Å. Treatment of  $\text{Cp}^*\text{HfMe}_2\text{Cl}$  with 2 equiv. of  $\text{Li}[\text{C}_4\text{Me}_4\text{Ge}(\text{SiMe}_3)_2]$  results in formation of hafnium complex of a germole dianion  $[\text{Cp}^*(\eta^5\text{-C}_4\text{Me}_4\text{Ge})\text{HfMe}_2\text{Li}(\text{THF})_2]$  **1284**, via the apparent elimination of  $\text{Me}_3\text{SiCl}$ , along with  $\text{C}_4\text{Me}_4\text{Ge}(\text{SiMe}_3)_2$  as the final  $\text{Me}_3\text{Si}$ -containing product.<sup>967</sup> The structurally characterized dimer **1284** shows that one Li atom is sandwiched in an  $\eta^5$ -fashion between two germole rings, while the other Li atom is coordinated by both germanium atoms. The reaction of **1284** with 2 equiv. of  $\text{Me}_3\text{SiOTf}$  gives the dimethylhafnium germolyl complex **1285**. Complex **1285** reacts with  $\text{H}_2$  to give  $\text{CH}_4$  and  $\text{Me}_3\text{SiH}$  as a result of



$\sigma$ -bond metathesis involving the germole-bound trimethylsilyl group and presumably an intermediate hafnium hydride species. The reaction of complex **1285** with  $\text{PhSiH}_3$  occurs analogously to form  $\text{PhMeSiH}_2$  and  $\text{Me}_3\text{SiH}$ .

Treatment of the tripodal amido zirconium and hafnium complexes  $\text{MeSi}\{\text{SiMe}_2\text{N}(4\text{-CH}_3\text{C}_6\text{H}_4)\}_3\text{MCl}$  ( $\text{M} = \text{Zr}, \text{Hf}$ ) with  $\text{LiSnPh}_3$  in toluene leads to the formation of  $\text{M-Sn}$ -bonded heterobimetallic complexes **1286** (Scheme 306).<sup>968</sup> More stable  $\text{Sn-metallocene}$ -bonded complexes  $\text{MeSi}\{\text{SiMe}_2\text{N}(4\text{-CH}_3\text{C}_6\text{H}_4)\}_3\text{SnMCp}_2(\text{Cl})$  (**1288**;  $\text{M} = \text{Zr}; \text{Hf}$ ) were obtained by the reaction of the triamido stannate complex  $\text{MeSi}\{\text{SiMe}_2\text{N}(4\text{-CH}_3\text{C}_6\text{H}_4)\}_3\text{SnLi}(\text{OEt}_2)$  **1287** with metallocene dichlorides. X-ray diffraction studies of **1288** show  $\text{Zr-Sn}$  and  $\text{Hf-Sn}$  bond lengths of 3.02313(17) and 2.9956(3) Å, respectively. The triamidostannate complex **1287** also reacts with  $\text{Cp}_2\text{ZrMeCl}$  in toluene to give the  $\text{Zr-Sn}$  complex **1289**, which possesses a  $\text{Zr-Sn}$  bond length of 3.0397(2) Å.<sup>969</sup> The CO insertion into the  $\text{Zr-Me}$  bond in **1289** results in formation of the structurally characterized acylzirconium complex **1290**, while the  $\text{Zr-Sn}$  bond remains intact.



Scheme 306

## References

1. Cotton, S. A. *Annu. Rep. Prog. Chem., Sect. A* **2005**, *101*, 139–148; **2004**, *100*, 151–161; **2003**, *99*, 139–148; **2002**, *98*, 129–137; **2001**, *97*, 133–142; **2000**, *96*, 161–173; **1999**, *95*, 105–115; **1998**, *94*, 149–160; **1997**, *93*, 143–153; **1996**, *92*, 147–156; **1995**, *91*, 153–163; **1994**, *90*, 119–130.
2. Togni, A.; Halterman, R. L., Eds. *Metallocenes: Synthesis – Reactivity – Applications*, Wiley-VCH: Weinheim, 1998.
3. Gladysz, J. A., Ed. *Frontiers in metal-catalyzed polymerization*. *Chem. Rev.* **2000**, *100*, pp 1167–1681.
4. Alt, H. G.; Köppl, A. *Chem. Rev.* **2000**, *100*, 1205–1221.
5. Coates, G. W. *Chem. Rev.* **2000**, *100*, 1223–1252.
6. Resconi, L.; Cavallo, L.; Fait, A.; Piemontesi, F. *Chem. Rev.* **2000**, *100*, 1253–1345.
7. Hlatky, G. G. *Chem. Rev.* **2000**, *100*, 1347–1376.
8. Chen, E. Y.-X.; Marks, T. J. *Chem. Rev.* **2000**, *100*, 1391–1434.
9. Rappé, A. K.; Skiff, W. M.; Casewit, C. J. *Chem. Rev.* **2000**, *100*, 1435–1456.
10. Angermund, K.; Fink, G.; Jensen, V. R.; Kleinschmidt, R. *Chem. Rev.* **2000**, *100*, 1457–1470.
11. Hey-Hawkins, E. *Chem. Rev.* **1994**, *94*, 1661–1717.
12. Möhring, P. C.; Coville, N. J. *Organomet. Chem.* **1994**, *479*, 1–29.
13. Brintzinger, H. H.; Fischer, D.; Mühlaupt, R.; Rieger, B.; Waymouth, R. M. *Angew. Chem., Int. Ed. Engl.* **1995**, *34*, 1143–1170.
14. Brand, H.; Arnold, J. *Coord. Chem. Rev.* **1995**, *140*, 137–168.
15. Page, E. M.; Wass, S. A. *Coord. Chem. Rev.* **1996**, *152*, 411–466.
16. Stephan, D. W.; Nadasdi, T. T. *Coord. Chem. Rev.* **1996**, *147*, 147–208.
17. Bochmann, M. J. *Chem. Soc., Dalton Trans.* **1996**, 255–270.
18. Hoveyda, A. H.; Morken, J. P. *Angew. Chem., Int. Ed. Engl.* **1996**, *35*, 1262–1284.
19. Kaminsky, W.; Arndt, M. *Adv. Polym. Sci.* **1997**, *127*, 143–187.
20. McKnight, A. L.; Waymouth, R. M. *Chem. Rev.* **1998**, *98*, 2587–2598.
21. Alt, H. G.; Samuel, E. *Chem. Soc. Rev.* **1998**, *27*, 323–329.
22. Piers, W. E. *Chem. Eur. J.* **1998**, *4*, 13–18.
23. Britovsek, G. J. P.; Gibson, V. C.; Wass, D. F. *Angew. Chem., Int. Ed. Engl.* **1999**, *38*, 428–447.
24. Gade, L. H. *Chem. Commun.* **2000**, 173–181.
25. Stephan, D. W. *Angew. Chem., Int. Ed. Engl.* **2000**, *39*, 314–329.
26. Pédeutour, J.-N.; Radhakrishnan, K.; Cramail, H.; Deffieux, A. *Macromol. Rapid Commun.* **2001**, *22*, 1095–1123.
27. Erker, G. *Acc. Chem. Res.* **2001**, *34*, 309–317.
28. Shapiro, P. J. *Eur. J. Inorg. Chem.* **2001**, 321–326.
29. Lin, S.; Waymouth, R. M. *Acc. Chem. Res.* **2002**, *35*, 765–773.
30. Makio, H.; Kashiwa, N.; Fujita, T. *Adv. Synth. Catal.* **2002**, *344*, 477–493.
31. Coates, G. W.; Hustad, P. D.; Reinartz, S. *Angew. Chem., Int. Ed. Engl.* **2002**, *41*, 2237–2257.
32. Gibson, V. C.; Spitzmesser, S. K. *Chem. Rev.* **2003**, *103*, 283–315.
33. Leino, R.; Lehmus, P.; Lehtonen, A. *Eur. J. Inorg. Chem.* **2004**, 3201–3222.
34. Erker, G.; Kehr, G.; Fröhlich, R. *J. Organomet. Chem.* **2004**, *689*, 1402–1412.
35. Park, S.; Han, Y.; Kim, S. K.; Lee, J.; Kim, H. K.; Do, Y. *J. Organomet. Chem.* **2004**, *689*, 4263–4276.
36. Erker, G.; Kehr, G.; Fröhlich, R. *J. Organomet. Chem.* **2004**, *689*, 4305–4418.
37. Bochmann, M. *J. Organomet. Chem.* **2004**, *689*, 3982–3998.
38. Bochmann, M. In *Catalytic Mechanisms from Spectroscopic Measurements*; Heaton, B. T., Ed.; Wiley-VCH: Weinheim, 2005; pp 311–357.
39. Eisch, J. J.; Owuor, F. A.; Otieno, P. O. *Organometallics* **2001**, *20*, 4132–4134.
40. Pellecchia, C.; Grassi, A.; Immirzi, A. *J. Am. Chem. Soc.* **1993**, *115*, 1160–1162.
41. Pellecchia, C.; Grassi, A.; Zambelli, A. *Organometallics* **1994**, *13*, 298–302.
42. Vaid, T. P.; Veige, A. S.; Lobkovsky, E. B.; Glassey, W. V.; Wolczanski, P. T.; Liable-Sands, L. M.; Rheingold, A. L.; Cundari, T. R. *J. Am. Chem. Soc.* **1998**, *120*, 10067–10079.
43. Ara, I.; Fornies, J.; Garcia-Monforte, M. A.; Martin, A.; Menjon, B. *Chem. Eur. J.* **2004**, *10*, 4186–4197.
44. Thorn, M.; Etheridge, Z. C.; Fanwick, P. E.; Rothwell, I. P. *Organometallics* **1998**, *17*, 3636–3638.
45. Thorn, M.; Etheridge, Z. C.; Fanwick, P. E.; Rothwell, I. P. *J. Organomet. Chem.* **1999**, *591*, 148–162.
46. Horton, A. D.; de With, J. *Chem. Commun.* **1996**, 1375–1376.
47. Galsworthy, J. R.; Green, M. L. H.; Maxted, N.; Muller, M. J. *Chem. Soc., Dalton Trans.* **1998**, 387–392.
48. Shah, S. A. A.; Dorn, H.; Voigt, A.; Roesky, H. W.; Parisini, E.; Schmidt, H.-G.; Noltemeyer, M. *Organometallics* **1996**, *15*, 3176–3181.
49. Guérin, F.; Stewart, J. C.; Beddie, C.; Stephan, D. W. *Organometallics* **2000**, *19*, 2994–3000.
50. Hollink, E.; Wei, P.; Stephan, D. W. *Organometallics* **2004**, *23*, 1562–1569.
51. Lee, C. H.; La, Y.-H.; Park, S. J.; Park, J. W. *Organometallics* **1998**, *17*, 3648–3655.
52. Lee, C. H.; La, Y.-H.; Park, J. W. *Organometallics* **2000**, *19*, 344–351.
53. Lorber, C.; Donnadiou, B.; Choukroun, R. *Organometallics* **2000**, *19*, 1963–1966.
54. Jeon, Y.-M.; Park, S. J.; Heo, J.; Kim, K. *Organometallics* **2000**, *17*, 3161–3163.
55. Jeon, Y.-M.; Heo, J.; Lee, W. M.; Chang, T.; Kim, K. *Organometallics* **1999**, *18*, 4107–4113.
56. Gauvin, R. M.; Lorber, C.; Choukroun, R.; Donnadiou, B.; Kress, J. *Eur. J. Inorg. Chem.* **2001**, 2337–2346.
57. Gauvin, R. M.; Mazet, C.; Kress, J. *J. Organomet. Chem.* **2002**, *658*, 1–8.
58. Horton, A. D.; de With, J. *Organometallics* **1997**, *16*, 5424–5436.
59. Jäger, F.; Roesky, H. W.; Dorn, H.; Shah, S.; Noltemeyer, M.; Schmidt, H.-G. *Chem. Ber.* **1997**, *130*, 399–403.
60. Horton, A. D.; von Hebel, K. L.; de With, J. *Macromol. Symp.* **2001**, *173*, 123–136.
61. Male, N. A. H.; Thornton-Pett, M.; Bochmann, M. J. *Chem. Soc., Dalton Trans.* **1997**, 2487–2494.
62. Aoyagi, K.; Gantzel, P. K.; Kalai, K.; Tilley, T. D. *Organometallics* **1996**, *15*, 923–927.
63. Daniele, S.; Hitchcock, P. B.; Lappert, M. F.; Merle, P. G. *J. Chem. Soc., Dalton Trans.* **2001**, 13–19.
64. Daniele, S.; Hitchcock, P. B.; Lappert, M. F. *Chem. Commun.* **1999**, 1909–1910.

65. Scollard, J. D.; McConville, D. H.; Vittal, J. J. *Organometallics* **1995**, *14*, 5478–5480.
66. Scollard, J. D.; McConville, D. H.; Vittal, J. J. *Organometallics* **1997**, *16*, 4415–4420.
67. Gibson, V. C.; Kimberley, B. S.; White, A. J. P.; Williams, D. J.; Howard, P. *Chem. Commun.* **1998**, 313–314.
68. Cloke, F. G. N.; Geldbach, T. J.; Hitchcock, P. B.; Love, J. B. *J. Organomet. Chem.* **1996**, *506*, 343–345.
69. Warren, T. H.; Schrock, R. R.; Davis, W. M. *Organometallics* **1996**, *15*, 562–569.
70. Warren, T. H.; Schrock, R. R.; Davis, W. M. *Organometallics* **1998**, *17*, 308–321.
71. Patton, J. T.; Feng, S. G.; Abboud, K. A. *Organometallics* **2001**, *20*, 3399–3405.
72. Shafrir, A.; Power, M. P.; Whitener, G. D.; Arnold, J. *Organometallics* **2001**, *20*, 1365–1369.
73. Siemeling, U.; Kuhnert, O.; Neumann, B.; Stämmler, A.; Stämmler, H.-G.; Bildstein, B.; Malaun, M.; Zanello, P. *Eur. J. Inorg. Chem.* **2001**, 913–916.
74. Roesky, H. W.; Meller, B.; Noltemeyer, M.; Schmidt, H. G.; Scholz, U.; Sheldrick, G. M. *Chem. Ber.* **1988**, *121*, 1403–1406.
75. Hagadorn, J. R.; Arnold, J. *Organometallics* **1994**, *13*, 4670–4672.
76. Hagadorn, J. R.; Arnold, J. *J. Chem. Soc., Dalton Trans.* **1997**, 3087–3096.
77. Walther, D.; Fischer, R.; Görls, H.; Koch, J.; Schweder, B. *J. Organomet. Chem.* **1996**, *508*, 13–22.
78. Herskovics-Korine, D.; Eisen, M. S. *J. Organomet. Chem.* **1995**, *503*, 307–314.
79. Volkis, V.; Shmulinson, M.; Averbuj, C.; Lisovskii, A.; Edelman, F. T.; Eisen, M. S. *Organometallics* **1998**, *17*, 3155–3157.
80. Volkis, V.; Nelkenbaum, E.; Lisovskii, A.; Hasson, G.; Semiat, R.; Kapon, M.; Botoshansky, M.; Eishen, Y.; Eisen, M. S. *J. Am. Chem. Soc.* **2003**, *125*, 2179–2194.
81. Littke, A.; Sleiman, N.; Bensimon, C.; Richeson, D.; Yap, G. P. A.; Brown, S. *Organometallics* **1998**, *17*, 446–451.
82. Averbuj, C.; Tish, E.; Eisen, M. S. *J. Am. Chem. Soc.* **1998**, *120*, 8640–8646.
83. Chen, C.-T.; Rees, L. H.; Cowley, A. R.; Green, M. L. H. *J. Chem. Soc., Dalton Trans.* **2001**, 1761–1767.
84. Vollmerhaus, R.; Shao, P.; Taylor, N. J.; Collins, S. *Organometallics* **1999**, *18*, 2731–2733.
85. Guzei, I. A.; Liable-Sands, L. M.; Rheingold, A. L.; Winter, C. H. *Polyhedron* **1997**, *16*, 4017–4022.
86. Munslow, I. J.; Wade, A. R.; Deeth, R. J.; Scott, P. *Chem. Commun.* **2004**, 2596–2597.
87. Wood, D.; Yap, G. P. A.; Richeson, D. S. *Inorg. Chem.* **1999**, *38*, 5788–5794.
88. Giesbrecht, G. R.; Whitener, G. D.; Arnold, J. *Organometallics* **2000**, *19*, 2809–2812.
89. Bazinet, P.; Wood, D.; Yap, G. P. A.; Richeson, D. S. *Inorg. Chem.* **2003**, *42*, 6225–6229.
90. Ong, T.-G.; Wood, D.; Yap, G. P. A.; Richeson, D. S. *Organometallics* **2002**, *21*, 1–3.
91. Duncan, A. P.; Mullins, S. M.; Arnold, J.; Bergman, R. G. *Organometallics* **2001**, *20*, 1808–1819.
92. Jin, X.; Novak, B. M. *Macromolecules* **2000**, *33*, 6205–6207.
93. Rahim, M.; Taylor, N. J.; Xin, S.; Collins, S. *Organometallics* **1998**, *17*, 1315–1323.
94. Vollmerhaus, R.; Rahim, M.; Tomaszewski, R.; Xin, S.; Taylor, N. J.; Collins, S. *Organometallics* **2000**, *19*, 2161–2169.
95. Deelman, B.-J.; Hitchcock, P. B.; Lappert, M. F.; Lee, H.-K.; Leung, W.-P. *J. Organomet. Chem.* **1996**, *513*, 281–285.
96. Deelman, B.-J.; Hitchcock, P. B.; Lappert, M. F.; Leung, W.-P.; Lee, H.-K.; Mak, T. C. W. *Organometallics* **1999**, *18*, 1444–1452.
97. Qian, B.; Scanlon, W. J.; Smith, M. R., III *Organometallics* **1999**, *18*, 1693–1698.
98. Cortright, S. B.; Johnston, J. N. *Angew. Chem., Int. Ed.* **2002**, *41*, 345–348.
99. Cortright, S. B.; Coalter, J. N. III; Pink, M.; Johnston, J. N. *Organometallics* **2004**, *23*, 5885–5888.
100. Dawson, D. M.; Walker, D. A.; Thornton-Pett, M.; Bochmann, M. *J. Chem. Soc., Dalton Trans.* **2000**, 459–466.
101. Matsuo, Y.; Mashima, K.; Tani, K. *Chem. Lett.* **2000**, 1114–1115.
102. Huang, J.-H.; Chi, L.-S.; Yu, R.-C.; Jiang, G. J.; Yang, W.-T.; Lee, G.-H.; Peng, S.-M. *Organometallics* **2001**, *20*, 5788–5791.
103. Hsieh, K.-C.; Chang, J.-C.; Lee, M.-T.; Hu, C.-H.; Hung, C.-H.; Lee, H. M.; Huang, J.-H.; Wang, M.-H.; Lee, T.-Y. *Inorg. Chim. Acta.* **2004**, *357*, 3517–3524.
104. Yélamos, C.; Heeg, M. J.; Winter, C. H. *Inorg. Chem.* **1999**, *38*, 1871–1878.
105. Joung, U. G.; Kim, T. H.; Joe, D. J.; Lee, B. Y.; Shin, D. M.; Chung, Y. K. *Polyhedron* **2004**, *23*, 1587–1594.
106. Kim, Y. H.; Kim, T. H.; Kim, N. Y.; Cho, E. S.; Lee, B. Y.; Shin, D. M.; Chung, Y. K. *Organometallics* **2003**, *22*, 1503–1511.
107. Morton, C.; O'Shaughnessy, P.; Scott, P. *Chem. Commun.* **2000**, 2099–2100.
108. Crust, E. J.; Clarke, A. J.; Deeth, R. J.; Morton, C.; Scott, P. *J. Chem. Soc., Dalton Trans.* **2004**, 4050–4058.
109. Boussie, T. R.; Diamond, G. M.; Goh, C.; Hall, K. A.; LaPointe, A. M.; Leclerc, M.; Lund, C.; Murphy, V.; Shoemaker, J. A. W.; Tracht, U., *et al.* *J. Am. Chem. Soc.* **2003**, *125*, 4306–4317.
110. Oakes, D. C. H.; Kimberley, B. S.; Gibson, V. C.; Jones, D. J.; White, A. J. P.; Williams, D. J. *Chem. Commun.* **2004**, 2174–2175.
111. Jones, D.; Roberts, A.; Cavell, K.; Keim, W.; Englert, U.; Skelton, B. W.; White, A. H. *J. Chem. Soc., Dalton Trans.* **1998**, 255–262.
112. Kakaliou, L.; Scanlon, W. J., IV; Qian, B.; Baek, S. W.; Smith, M. R., III; Motry, D. H. *Inorg. Chem.* **1999**, *38*, 5964–5977.
113. Kim, J.; Hwang, J.-W.; Kim, Y.; Lee, M. H.; Han, Y.; Do, Y. J. *Organomet. Chem.* **2001**, *620*, 1–7.
114. Jones, D.; Cavell, K.; Keim, W. J. *Mol. Catal.* **1999**, *138*, 37–52.
115. van der Linden, A.; Schaverien, C. J.; Meijboom, N.; Ganter, C.; Orpen, A. G. *J. Am. Chem. Soc.* **1995**, *117*, 3008–3021.
116. Gibson, V. C.; Long, N. J.; Martin, J.; Solan, G. A.; Stichbury, J. C. *J. Organomet. Chem.* **1999**, *590*, 115–117.
117. Bei, X.; Swenson, D. C.; Jordan, R. F. *Organometallics* **1997**, *16*, 3282–3302.
118. Tsukahara, T.; Swenson, D. C.; Jordan, R. F. *Organometallics* **1997**, *16*, 3303–3313.
119. Kim, I.; Nishihara, Y.; Jordan, R. J.; Rogers, R. D.; Rheingold, A. L.; Yap, G. A. *Organometallics* **1997**, *16*, 3314–3323.
120. Munslow, I. J.; Clarke, A. J.; Deeth, R. J.; Westmoreland, I.; Scott, P. *Chem. Commun.* **2002**, 1868–1869.
121. Matsui, S.; Mitani, M.; Saito, J.; Tohi, Y.; Makio, H.; Matsukawa, N.; Takagi, Y.; Tsuru, K.; Nitabar, M.; Nakano, T., *et al.* *J. Am. Chem. Soc.* **2001**, *123*, 5847–5856.
122. Lamberti, M.; Gliubizzi, R.; Mazzeo, M.; Tedesco, C.; Pellicchia, C. *Macromolecules* **2004**, *37*, 276–282.
123. Hustad, P. D.; Tian, J.; Coates, G. W. *J. Am. Chem. Soc.* **2002**, *124*, 3614–3621.
124. Strauch, J.; Warren, T. H.; Erker, G.; Fröhlich, R.; Saarenketo, P. *Inorg. Chim. Acta* **2000**, *300–302*, 810–821.
125. Cozzi, P. G.; Gallo, E.; Floriani, C.; Chiesi-Villa, A.; Rizzoli, C. *Organometallic* **1995**, *14*, 4994–4996.
126. Bott, R. K. J.; Hughes, D. L.; Schormann, M.; Bochmann, M.; Lancaster, S. J. *J. Organomet. Chem.* **2003**, *665*, 135–149.
127. Matilainen, L.; Klinga, M.; Leskelä, M. *J. Chem. Soc., Dalton Trans.* **1996**, 219–225.
128. Benetollo, F.; Carta, G.; Cavinato, G.; Crociani, L.; Paolucci, G.; Rossetto, G.; Veronese, F.; Zanello, P. *Organometallics* **2003**, *22*, 3985–3990.
129. Said, M.; Thornton-Pett, M.; Bochmann, M. *J. Chem. Soc., Dalton Trans.* **2001**, 2844–2849.

130. Irwin, L. J.; Reibenspies, J. H.; Miller, S. A. *J. Am. Chem. Soc.* **2004**, *126*, 16716–16717.
131. Karsch, H. H.; Grauvogl, G.; Kaweck, M.; Bissinger, P.; Kumberger, O.; Schier, A.; Mueller, G. *Organometallics* **1994**, *13*, 610–618.
132. Cloke, F. G. N.; Hitchcock, P. B.; Love, J. B. *J. Chem. Soc., Dalton Trans.* **1995**, 25–30.
133. Horton, A. D.; de With, J.; van der Linden, A. J.; van de Weg, H. *Organometallics* **1996**, *15*, 2672–2674.
134. Liang, L.-C.; Schrock, R. R.; Davis, W. M.; McConville, D. H. *J. Am. Chem. Soc.* **1999**, *121*, 5797–5798.
135. Schrock, R. R.; Casado, A. L.; Goodman, J. T.; Liang, L.-C.; Bonitatebus, P. J., Jr.; Davis, W. M. *Organometallics* **2000**, *19*, 5325–5341.
136. Mehrkhodavandi, P.; Bonitatebus, P. J., Jr.; Schrock, R. R. *J. Am. Chem. Soc.* **2000**, *122*, 7841–7842.
137. Mehrkhodavandi, P.; Schrock, R. R. *J. Am. Chem. Soc.* **2001**, *123*, 10746–10747.
138. Blake, A. J.; Collier, P. E.; Gade, L.; Mountford, P.; Lloyd, J.; Pugh, S. M.; Schubart, M.; Skinner, M. E. G.; Trösch, D. J. M. *Inorg. Chem.* **2001**, *40*, 870–877.
139. Schrock, R. R.; Bonitatebus, P. J., Jr.; Schrock, Y. *Organometallics* **2001**, *20*, 1056–1058.
140. Mehrkhodavandi, P.; Schrock, R. R.; Pryor, L. L. *Organometallics* **2003**, *22*, 4569–4583.
141. Guérin, F.; McConville, D. H.; Vittal, J. J. *Organometallics* **1996**, *15*, 5586–5590.
142. Schattenmann, F. J.; Schrock, R. R.; Davis, W. M. *Organometallics* **1998**, *17*, 989–992.
143. Grocholl, L.; Stahl, L.; Staples, R. J. *Chem. Commun.* **1997**, 1465–1466.
144. Grocholl, L.; Huch, V.; Stahl, L.; Staples, R. J.; Steinhart, P.; Johnson, A. *Inorg. Chem.* **1997**, *36*, 4451–4457.
145. Moser, D. F.; Grocholl, L.; Stahl, L.; Staples, R. J. *J. Chem. Soc., Dalton Trans.* **2003**, 1402–1410.
146. Axenov, K. V.; Klinga, M.; Leskelä, M.; Kotov, V.; Repo, T. *Eur. J. Inorg. Chem.* **2004**, 4702–4709.
147. Bai, G.; Roesky, H. W.; Schmidt, H.-G.; Noltemeyer, M. *Organometallics* **2001**, *20*, 2962–2965.
148. Baumann, R.; David, W. M.; Schrock, R. R. *J. Am. Chem. Soc.* **1997**, *119*, 3830–3831.
149. Schrock, R. R.; Baumann, R.; Reid, S. M.; Goodman, J. T.; Stumpf, R.; Davis, W. M. *Organometallics* **1999**, *18*, 3649–3670.
150. Baumann, R.; Schrock, R. R. *J. Organomet. Chem.* **1998**, *557*, 69–75.
151. Baumann, R.; Stumpf, R.; David, W. M.; Liang, L.-C.; Schrock, R. R. *J. Am. Chem. Soc.* **1999**, *121*, 7822–7836.
152. Liang, L.-C.; Schrock, R. R.; Davis, W. M. *Organometallics* **2000**, *19*, 2526–2531.
153. Schrock, R. R.; Liang, L.-C.; Baumann, R.; Davis, W. M. *J. Organomet. Chem.* **1999**, *591*, 163–173.
154. Graft, D. D.; Schrock, R. R.; Davis, W. M.; Stumpf, R. *Organometallics* **1999**, *18*, 843–852.
155. Schrock, R. R.; Schattenmann, F.; Aizenberg, M.; Davis, W. M. *Chem. Commun.* **1997**, 199–200.
156. Aizenberg, M.; Turculet, L.; Davis, W. M.; Schattenmann, F.; Schrock, R. R. *Organometallics* **1998**, *17*, 4795–4812.
157. Flores, M. A.; Manzoni, M. R.; Baumann, R.; Davis, W. M.; Schrock, R. R. *Organometallics* **1999**, *18*, 3220–3227.
158. Spencer, L. P.; Winston, S.; Fryzuk, M. D. *Organometallics* **2004**, *23*, 3372–3374.
159. Kamalesh Babu, R. P.; McDonald, R.; Decker, S. A.; Klobukowski, M.; Cavell, R. G. *Organometallics* **1999**, *18*, 4226–4229.
160. Aparna, K.; Kamalesh Babu, R. P.; McDonald, R.; Cavell, R. G. *Angew. Chem., Int. Ed.* **2001**, *40*, 4400–4402.
161. Cavell, R. G.; Kamalesh Babu, R. P.; Kasani, A.; McDonald, R. *J. Am. Chem. Soc.* **1999**, *121*, 5805–5806.
162. Kamalesh Babu, R. P.; McDonald, R.; Cavell, R. G. *Chem. Commun.* **2000**, 481–482.
163. Kamalesh Babu, R. P.; McDonald, R.; Cavell, R. G. *Organometallics* **2000**, *19*, 3462–3465.
164. Cavell, R. G.; Kamalesh Babu, R. P.; Kasani, A.; Aparna, K. J. *Organomet. Chem.* **2001**, *617*–618, 158–169.
165. Schrock, R. R.; Seidel, S. W.; Schrock, Y.; Davis, W. M. *Organometallics* **1999**, *18*, 428–437.
166. Cohen, J. D.; Fryzuk, M. D.; Loehr, T. M.; Mylvaganam, M.; Rettig, S. J. *Inorg. Chem.* **1998**, *37*, 112–119.
167. Gade, L. H. *Acc. Chem. Res.* **2002**, *35*, 575–582.
168. Jia, L.; Ding, E.; Rheingold, A. L.; Rhatigan, B. *Organometallics* **2000**, *19*, 963–965.
169. Jia, L.; Zhao, J.; Ding, E.; Brennessel, W. W. *J. Chem. Soc., Dalton Trans.* **2002**, 2608–2615.
170. Memmler, H.; Walsh, K.; Gade, L. H.; Lauher, J. W. *Inorg. Chem.* **1995**, *34*, 4062–4068.
171. Findeis, B.; Schubart, M.; Gade, L. H.; Möller, F.; Scowen, I.; McPartlin, M. *J. Chem. Soc., Dalton Trans.* **1996**, 125–132.
172. Renner, P.; Galka, C. H.; Gade, L. H.; Radojevic, S.; McPartlin, M. *Eur. J. Inorg. Chem.* **2001**, 1425–1430.
173. Gade, L. H.; Renner, P.; Memmler, H.; Fecher, F.; Galka, C. H.; Laubender, M.; Radojevic, S.; McPartlin, M.; Lauher, J. W. *Chem. Eur. J.* **2001**, *7*, 2563–2580.
174. Turculet, L.; Tilley, T. D. *Organometallics* **2002**, *21*, 3961–3972.
175. Turculet, L.; Tilley, T. D. *Organometallics* **2004**, *23*, 1542–1553.
176. Michiue, K.; Jordan, R. F. *Organometallics* **2004**, *23*, 460–470.
177. Furlan, L. G.; Gil, M. P.; Casagrande, O. L., Jr. *Macromol. Rapid Commun.* **2000**, *21*, 1054–1057.
178. Nakazawa, H.; Ikai, S.; Imaoka, K.; Kai, Y.; Yano, T. *J. Mol. Catal. A* **1998**, *132*, 33–41.
179. Giesbrecht, G. R.; Shafir, A.; Arnold, J. *Chem. Commun.* **2000**, 2135–2136.
180. Fryzuk, M. D.; Hoffman, V.; Kickham, J. E.; Rettig, S. J.; Gambarotta, S. *Inorg. Chem.* **1997**, *36*, 3480–3484.
181. Gauvin, R.; Osborn, J. A.; Kress, J. *Organometallics* **2000**, *19*, 2944–2946.
182. Shao, P.; Gendron, R. A. L.; Berg, D. J.; Bushnell, G. W. *Organometallics* **2000**, *19*, 509–520.
183. Chan, M. C. W.; Tam, K.-H.; Pui, Y.-L.; Zhu, N. J. *Chem. Soc., Dalton Trans.* **2002**, 3085–3087.
184. Bouwkamp, M.; van Leusen, D.; Meetsma, A.; Hessen, B. *Organometallics* **1998**, *17*, 3645–3647.
185. Kui, S. C. F.; Zhu, N.; Chan, M. C. W. *Angew. Chem., Int. Ed.* **2003**, *42*, 1628–1632.
186. Uhrhammer, R.; Black, D. G.; Gardner, T. G.; Olsen, J. D.; Jordan, R. F. *J. Am. Chem. Soc.* **1993**, *115*, 8493–8494.
187. Black, D. G.; Swenson, D. C.; Jordan, R. F. *Organometallics* **1995**, *14*, 3539–3550.
188. Martin, A.; Uhrhammer, R.; Gardner, T. G.; Jordan, R. F. *Organometallics* **1998**, *17*, 382–397.
189. Giannini, L.; Solari, E.; De Angelis, S.; Ward, T. R.; Floriani, C.; Chiesi-Villa, A.; Rizzoli, C. *J. Am. Chem. Soc.* **1995**, *117*, 5801–5811.
190. Nikonov, G. I.; Blake, A. J.; Mountford, P. *Inorg. Chem.* **1997**, *36*, 1107–1112.
191. Blake, A. J.; Mountford, P.; Nikonov, G. I.; Swallow, D. *Chem. Commun.* **1996**, 1835–1836.
192. Brand, H.; Arnold, J. *Organometallics* **1993**, *12*, 3655–3665.
193. Brand, H.; Capriotti, J. A.; Arnold, J. *Organometallics* **1994**, *13*, 4469–4473.
194. Kim, H.-J.; Jung, S.; Jeon, Y.-M.; Whang, D.; Kim, K. *Chem. Comm.* **1999**, 1033–1034.
195. Bonomo, L.; Toraman, G.; Solari, E.; Scopelliti, R.; Floriani, C. *Organometallics* **1999**, *18*, 5198–5200.
196. Scott, M. J.; Lippard, S. J. *Inorg. Chim. Acta.* **1997**, *263*, 287–299.
197. Scott, M. J.; Lippard, S. J. *Organometallics* **1997**, *16*, 5857–5868.

198. Scott, M. J.; Lippard, S. J. *J. Am. Chem. Soc.* **1997**, *119*, 3411–3412.
199. Duan, Z.; Naiini, A. A.; Lee, J.-H.; Verkade, J. G. *Inorg. Chem.* **1995**, *34*, 5477–5482.
200. Morton, C.; Munslow, I. J.; Sander, C. J.; Alcock, N. W.; Scott, P. *Organometallics* **1999**, *18*, 4608–4613.
201. Morton, C.; Gillespie, K. M.; Sanders, C. J.; Scott, P. *J. Organomet. Chem.* **2000**, *606*, 141–146.
202. Westmoreland, I.; Munslow, I. J.; Clarke, A. J.; Clarkson, G.; Scott, P. *Organometallics* **2004**, *23*, 5066–5074.
203. O'Shaughnessy, P. N.; Gillespie, K. M.; Morton, C.; Westmoreland, I.; Scott, P. *Organometallics* **2002**, *21*, 4496–4504.
204. Carpentier, J.-F.; Martin, A.; Swenson, D. C.; Jordan, R. *Organometallics* **2003**, *22*, 4999–5010.
205. Ong, T.-G.; Yap, G. P. A.; Richeson, D. S. *Organometallics* **2003**, *22*, 387–389.
206. Tshuva, E. Y.; Goldberg, I.; Kol, M.; Goldschmidt, Z. *Organometallics* **2001**, *20*, 3017–3028.
207. Tshuva, E. Y.; Groysman, S.; Goldberg, I.; Kol, M.; Goldschmidt, Z. *Organometallics* **2002**, *21*, 662–670.
208. Tshuva, E. Y.; Goldberg, I.; Kol, M.; Weitman, H.; Goldschmidt, Z. *Chem. Commun.* **2000**, 379–380.
209. Groysman, S.; Goldberg, I.; Kol, M. *Organometallics* **2003**, *22*, 3013–3015.
210. Groysman, S.; Goldberg, I.; Kol, M. *J. Am. Chem. Soc.* **2000**, *122*, 10706–10707.
211. Busico, V.; Cipullo, R.; Ronca, S.; Budzelaar, P. H. M. *Macromol. Rapid Commun.* **2001**, *22*, 1405–1410.
212. Busico, V.; Cipullo, R.; Friederichs, N.; Ronca, S.; Togrou, M. *Macromolecules* **2003**, *36*, 3806–3808.
213. Busico, V.; Cipullo, R.; Friederichs, N.; Ronca, S.; Talarico, G.; Togrou, M.; Wang, B. *Macromolecules* **2004**, *37*, 8201–8203.
214. Woodman, P. R.; Hitchcock, P. B.; Scott, P. *Chem. Commun.* **1996**, 2735–2736.
215. Woodman, P. R.; Munslow, I. J.; Hitchcock, P. B.; Scott, P. *J. Chem. Soc., Dalton Trans.* **1999**, 4069–4076.
216. Knight, P. D.; O'Shaughnessy, P. N.; Munslow, I. J.; Kimberley, B. S.; Scott, P. *J. Organomet. Chem.* **2003**, *683*, 103–113.
217. Knight, P. D.; Clarke, A. J.; Kimberley, B. S.; Jackson, R. A.; Scott, P. *Chem. Commun.* **2002**, 352–353.
218. Capacchione, C.; Proto, A.; Ebeling, H.; Mülhaupt, R.; Möller, K.; Spaniol, T. P.; Okuda, J. *J. Am. Chem. Soc.* **2003**, *125*, 4964–4965.
219. Tjaden, E. B.; Swenson, D. C.; Jordan, R. F. *Organometallics* **1995**, *14*, 371–386.
220. Fryzuk, M. D.; Love, J. B.; Rettig, S. J. *Organometallics* **1998**, *17*, 846–853.
221. Novak, A.; Blake, A. J.; Wilson, C.; Love, J. B. *Chem. Commun.* **2002**, 2796–2797.
222. Tanski, J. M.; Parkin, G. *Organometallics* **2002**, *21*, 587–589.
223. Bowen, D. E.; Jordan, R. F.; Rogers, R. *Organometallics* **1995**, *14*, 3630–3635.
224. Saccheo, S.; Gioia, G.; Grassi, A.; Bowen, D. E.; Jordan, R. F. *J. Mol. Catal.* **1998**, *128*, 111–118.
225. Dodge, T.; Curtis, M. A.; Russell, J. M.; Sabat, M.; Finn, M. G.; Grimes, R. N. *J. Am. Chem. Soc.* **2000**, *122*, 10573–10580.
226. Hollis, T. K.; Wang, L.-S.; Tham, F. J. *J. Am. Chem. Soc.* **2000**, *122*, 11737–11738.
227. Bellemine-Lapponaz, S.; Lo, M. M.-C.; Peterson, T. H.; Allen, J. M.; Fu, G. C. *Organometallics* **2001**, *20*, 3453–3458.
228. Buzin, F.-X.; Nief, F.; Ricard, L.; Mathey, F. *Organometallics* **2002**, *21*, 259–263.
229. Sitzmann, H.; Zhou, P.; Wolmershauser, G. *Chem. Ber.* **1994**, *127*, 3–9.
230. Greene, D. L.; Villalta, O. A.; Macias, D. M.; Gonzalez, A.; Tikkanen, W.; Schick, B.; Kantardjieff, K. *Inorg. Chem. Comm.* **1999**, *2*, 311–314.
231. Greene, D. L.; Chau, A.; Monreal, M.; Mendez, C.; Cruz, I.; Wenj, T.; Tikkanen, W.; Schick, B.; Kantardjieff, K. *J. Organomet. Chem.* **2003**, *682*, 8–13.
232. Amor, J. I.; Cuenca, T.; Galakhov, M.; Royo, P. *J. Organomet. Chem.* **1995**, *497*, 127–131.
233. Cuenca, T.; Montejano, C.; Royo, P. *J. Organomet. Chem.* **1996**, *514*, 93–96.
234. O'Hare, D.; Murphy, V.; Diamond, G. M.; Arnold, P.; Mountford, P. *Organometallics* **1994**, *13*, 4689–4694.
235. Kondakov, D.; Negishi, E. *Chem. Comm.* **1996**, 963–964.
236. Rogers, J. S.; Lachicotte, R. J.; Bazan, G. C. *Organometallics* **1999**, *18*, 3976–3980.
237. Kuenzel, A.; Parisini, E.; Roesky, H. W.; Sheldrick, G. M. *J. Organomet. Chem.* **1997**, *536/537*, 177–180.
238. Herzog, A.; Liu, F.-Q.; Roesky, H. W.; Demsar, A.; Keller, K.; Noltemeyer, M.; Pauer, F. *Organometallics* **1994**, *13*, 1251–1256.
239. Herzog, A.; Roesky, H. W.; Steiner, A.; Noltemeyer, M. *Organometallics* **1996**, *15*, 909–917.
240. Herzog, A.; Roesky, H. W.; Zak, Z.; Noltemeyer, M. *Angew. Chem., Int. Ed.* **1994**, *33*, 967–968.
241. Scholz, J.; Rehbaum, F.; Thiele, K.-H.; Goddard, R.; Betz, P.; Krüger, C. *J. Organomet. Chem.* **1993**, *443*, 93–99.
242. Pellicchia, C.; Immirzi, A.; Grassi, A.; Zambelli, A. *Organometallics* **1993**, *12*, 4473–4478.
243. Pellicchia, C.; Immirzi, A.; Pappalardo, D.; Peluso, A. *Organometallics* **1994**, *13*, 3773–3775.
244. Gillis, D. J.; Tudoret, M. J.; Baird, M. C. *J. Am. Chem. Soc.* **1993**, *115*, 2543.
245. Gillis, D. J.; Quyoum, R.; Tudoret, M.-J.; Wang, Q.; Jeremic, D.; Roszak, A. W.; Baird, M. C. *Organometallics* **1996**, *15*, 3600–3605.
246. Pellicchia, C.; Immirzi, A.; Zambelli, A. *J. Organomet. Chem.* **1994**, *479*, C9–C11.
247. Saßmannshausen, J.; Powell, A. K.; Anson, Ch. E.; Wocadlo, S.; Bochmann, M. *J. Organomet. Chem.* **1999**, *592*, 84–94.
248. Amor, J. I.; Cuenca, T.; Galakhov, M.; Gomez-Sal, P.; Manzanero, A.; Royo, P. *J. Organomet. Chem.* **1997**, *535*, 155–168.
249. Willey, G. R.; Butcher, M. L.; Drew, M. G. B. *J. Chem. Soc., Dalton Trans.* **1994**, 3285–3290.
250. Martin, A.; Mena, M.; Palacios, J. *J. Organomet. Chem.* **1994**, *480*, C10–C11.
251. Pupi, R. M.; Coalter, J. N.; Petersen, J. L. *J. Organomet. Chem.* **1995**, *497*, 17–25.
252. Nomura, K.; Fujii, K. *Organometallics* **2002**, *21*, 3042–3049.
253. Yue, N.; Hollink, E.; Guérin, F.; Stephan, D. W. *Organometallics* **2001**, *20*, 4424–4433.
254. Ryabov, A. N.; Izmer, V. V.; Borisenko, A. A.; Canich, J. A. M.; Kuz'mina, L. G.; Howard, J. A. K.; Voskoboinikov, A. Z. *J. Chem. Soc., Dalton Trans.* **2002**, 2995–3000.
255. Curnow, O. J.; Fern, G. M.; Woll, D. *Inorg. Chem. Comm.* **2003**, *6*, 1201–1204.
256. Antinolo, A.; Carrillo-Hermosilla, F.; Corrochano, A.; Fernandez-Baeza, J.; Lara-Sanchez, A.; Ribeiro, M. R.; Lanfranchi, M.; Otero, A.; Pellinghelli, M. A.; Portela, M. F.; Santos, J. V. *Organometallics* **2000**, *19*, 2837–2843.
257. Heyn, R. H.; Stephan, D. W. *Inorg. Chem.* **1995**, *34*, 2804.
258. Chernega, A. N.; Gómez, R.; Green, M. L. H. *Chem. Commun.* **1993**, 1415–1417.
259. Gómez, R.; Duchateau, R.; Chernega, A. N.; Teuben, J. H.; Edelmann, F. T.; Green, M. L. H. *J. Organomet. Chem.* **1995**, *491*, 153–158.
260. Gómez, R.; Duchateau, R.; Chernega, A. N.; Meetsma, A.; Edelmann, F. T.; Teuben, J. H.; Green, M. L. H. *J. Chem. Soc., Dalton Trans.* **1995**, 217–225.
261. Gómez, R.; Green, M. L. H.; Haggitt, J. L. *J. Chem. Soc., Dalton Trans.* **1996**, 939–946.
262. Jayaratne, K. C.; Sita, L. R. *J. Am. Chem. Soc.* **2000**, *122*, 958–959.
263. Keaton, R. J.; Jayaratne, K. C.; Henningsen, D. A.; Koterwas, L. A.; Sita, L. R. *J. Am. Chem. Soc.* **2001**, *123*, 6197–6198.



264. Kissounko, D. A.; Fetting, J. C.; Sita, L. R. *Inorg. Chim. Acta* **2003**, *345*, 121–129.
265. Keaton, R. J.; Koterwas, L. A.; Fetting, J. C.; Sita, L. R. *J. Am. Chem. Soc.* **2002**, *124*, 5932–5933.
266. Keaton, R. J.; Jayaratne, K. C.; Fetting, J. C.; Sita, L. R. *J. Am. Chem. Soc.* **2000**, *122*, 12909–12910.
267. Jayaratne, K. C.; Sita, L. R. *J. Am. Chem. Soc.* **2001**, *123*, 10754–10755.
268. Zhang, Y.; Kissounko, D. A.; Fetting, J. C.; Sita, L. R. *Organometallics* **2003**, *22*, 21–23.
269. Sanz, M.; Cuenca, T.; Galakhov, M.; Grassi, A.; Bott, R. K. J.; Hughes, D. L.; Lancaster, S. J.; Bochmann, M. *Organometallics* **2004**, *23*, 5324–5331.
270. Demakopoulos, I.; Klouras, N.; Raptopoulou, C. P.; Terzis, A. Z. *Anorg. Allg. Chem.* **1995**, *621*, 1761–1766.
271. Doherty, S.; Errington, R. J.; Jarvis, A. P.; Collins, S.; Clegg, W.; Elsegood, M. R. J. *Organometallics* **1998**, *17*, 3408–3410.
272. Thorn, M. G.; Lee, J.; Fanwick, P. E.; Rothwell, I. P. *J. Chem. Soc., Dalton Trans.* **2002**, 3398–3405.
273. Ding, E.; Liu, F.-C.; Liu, S.; Meyers, E. A.; Shore, S. G. *Inorg. Chem.* **2002**, *41*, 5329–5335.
274. Visser, C.; van den Hende, J. R.; Meetsma, A.; Hessen, B.; Teuben, J. H. *Organometallics* **2001**, *20*, 1620–1628.
275. Antinolo, A.; Carrillo-Hermosilla, F.; Corrochano, A. E.; Fandos, R.; Fernandez-Baeza, J.; Rodriguez, A. M.; Ruiz, M. J.; Otero, A. *Organometallics* **1999**, *18*, 5219–5224.
276. Abis, L.; Calderazzo, F.; Maichle-Mossmer, C.; Pampaloni, G.; Strahle, J.; Tripepi, G. *J. Chem. Soc., Dalton Trans.* **1998**, 841–845.
277. Klab, K.; Duda, L.; Kleigrewe, N.; Erker, G.; Fröhlich, R.; Wegelius, E. *Eur. J. Inorg. Chem.* **1999**, 11–19.
278. Hessen, B.; van der Heijden, H. J. *Organomet. Chem.* **1997**, *534*, 237–239.
279. Kim, Y.; Han, Y.; Do, Y. J. *Organomet. Chem.* **2001**, *634*, 19–24.
280. Bazan, G. C.; Rodriguez, G.; Cleary, B. P. *J. Am. Chem. Soc.* **1994**, *116*, 2177–2178.
281. Rodriguez, G.; Bazan, G. C. *J. Am. Chem. Soc.* **1997**, *119*, 343–352.
282. Skoog, S. J.; Mateo, C.; Lavoie, G. G.; Hollander, F. J.; Bergman, R. G. *Organometallics* **2000**, *19*, 1406–1421.
283. Lavoie, G. G.; Bergman, R. G. *Angew. Chem., Int. Ed.* **1997**, *36*, 2450–2452.
284. Scholz, J.; Hadi, G. A.; Thiele, K.-H.; Gols, H.; Weimann, R.; Schumann, H.; Sieler, J. J. *Organomet. Chem.* **2001**, *626*, 243–259.
285. Quan, R. W.; Bazan, G. C.; Kiely, A. F.; Schaefer, W. P.; Bercaw, J. E. *J. Am. Chem. Soc.* **1994**, *116*, 4489–4490.
286. Pastor, A.; Kiely, A. F.; Henling, L. M.; Day, M. W.; Bercaw, J. E. *J. Organomet. Chem.* **1997**, *528*, 65–75.
287. Rajapakse, A.; Gruhn, N. E.; Lichtenberger, D. L.; Basta, R.; Arif, A. M.; Ernst, R. D. *J. Am. Chem. Soc.* **2004**, *126*, 14105–14116.
288. Kulsomphob, V.; Harvey, B. G.; Arif, A. M.; Ernst, R. D. *Inorg. Chim. Acta* **2002**, *334*, 17–24.
289. Crowther, D. J.; Jordan, R. F. *Macromol. Symp.* **1993**, *66*, 121–126.
290. Crowther, D. J.; Swenson, D. C.; Jordan, R. J. *J. Am. Chem. Soc.* **1995**, *117*, 10403–10404.
291. Lancaster, S. J.; Robinson, O. B.; Bochmann, M.; Coles, S. J.; Hursthouse, M. B. *Organometallics* **1995**, *14*, 2456–2462.
292. Pindado, G. J.; Thornton-Pett, M.; Bochmann, M. *J. Chem. Soc., Dalton Trans.* **1997**, 3115–3127.
293. Pindado, G. J.; Thornton-Pett, M.; Hursthouse, M. B.; Coles, S. J.; Bochmann, M. *J. Chem. Soc., Dalton Trans.* **1999**, 1663–1668.
294. Pindado, G. J.; Thornton-Pett, M.; Bochmann, M. *J. Chem. Soc., Dalton Trans.* **1998**, 393–400.
295. Pindado, G. J.; Thornton-Pett, M.; Bouwkamp, M.; Meetsma, A.; Hessen, B.; Bochmann, M. *Angew. Chem., Int. Ed. Engl.* **1997**, *36*, 2358–2361.
296. Pindado, G. J.; Lancaster, S. J.; Thornton-Pett, M.; Bochmann, M. *J. Am. Chem. Soc.* **1998**, *120*, 6816–6817.
297. Woodman, T. J.; Thornton-Pett, M.; Hughes, D. L.; Bochmann, M. *Organometallics* **2001**, *20*, 4080–4091.
298. Woodman, T. J.; Thornton-Pett, M.; Bochmann, M. *Chem. Comm.* **2001**, 329–330.
299. Duchateau, R.; Cremer, U.; Harmsen, R. J.; Mohamud, S. I.; Abbenhuis, H. C. L.; van Santen, R. A.; Meetsma, A.; Thiele, S. K.-H.; van Tol, M. F. H.; Kranenburg, M. *Organometallics* **1999**, *18*, 5447–5459.
300. Wessel, H.; Rennekamp, C.; Roesky, H. W.; Montero, M. L.; Müller, P.; Usón, I. *Organometallics* **1998**, *17*, 1919–1921.
301. Ciruelo, G.; Cuenca, T.; Gómez, R.; Gómez-Sal, P.; Martín, A. *J. Chem. Soc., Dalton Trans.* **2001**, 1657–1663.
302. Ciruelos, S.; Cuenca, T.; Gómez-Sal, P.; Manzanero, A.; Royo, P. *Organometallics* **1995**, *14*, 177–185.
303. Ciruelo, G.; Sebastian, A.; Cuenca, T.; Gómez-Sal, P.; Manzanero, A.; Royo, P. *J. Organomet. Chem.* **2000**, *604*, 103–115.
304. Ciruelos, S.; Cuenca, T.; Gómez, R.; Gómez-Sal, P.; Manzanero, A.; Royo, P. *Organometallics* **1996**, *15*, 5577–5585.
305. Ciruelo, G.; Cuenca, T.; Gómez, R.; Gómez-Sal, P.; Martín, A.; Rodríguez, G.; Royo, P. *J. Organomet. Chem.* **1997**, *547*, 287–296.
306. Ciruelos, S.; Cuenca, T.; Gómez, R.; Gómez-Sal, P.; Manzanero, A.; Royo, P. *Polyhedron* **1998**, *17*, 1055–1064.
307. Duchateau, R.; Lancaster, S. J.; Thornton-Pett, M.; Bochmann, M. *Organometallics* **1997**, *16*, 4995–5005.
308. Lancaster, S. J.; Hughes, D. L. *J. Chem. Soc., Dalton Trans.* **2003**, 1779–1789.
309. Lancaster, S. J.; Thornton-Pett, M.; Dawson, D. M.; Bochmann, M. *Organometallics* **1998**, *17*, 3829–3831.
310. Krut'ko, D. P.; Borzov, M. V.; Kirsanov, R. S.; Antipin, M. Y.; Churakov, A. V. *J. Organomet. Chem.* **2004**, *689*, 595–604.
311. van der Zeijden, A. A. H. *J. Organomet. Chem.* **1996**, *518*, 147–153.
312. Ziniuk, Z.; Goldberg, I.; Kol, M. *J. Organomet. Chem.* **1997**, *545–546*, 441–446.
313. Otero, A.; Fernandez-Baeza, J.; Antinolo, A.; Tejada, J.; Lara-Sanchez, A.; Sanchez-Barba, L.; Rodriguez, A. M.; Maestro, M. A. *J. Am. Chem. Soc.* **2004**, *126*, 1330–1331.
314. Krut'ko, D. P.; Borzov, M. V.; Petrosyan, V. S.; Kuz'mina, L. G.; Churakov, A. V. *Russ. Chem. Bull.* **1996**, *45*, 1740–1744.
315. Krut'ko, D. P.; Borzov, M. V.; Petrosyan, V. S.; Kuz'mina, L. G.; Churakov, A. V. *Russ. Chem. Bull.* **1996**, *45*, 940–949.
316. van der Zeijden, A. A. H.; Mattheis, Ch.; Fröhlich, R. *Organometallics* **1997**, *16*, 2651–2658.
317. van der Zeijden, A. A. H.; Mattheis, C. *J. Organomet. Chem.* **1999**, *584*, 274–285.
318. van der Zeijden, A. A. H.; Mattheis, C.; Fröhlich, R. *Chem. Ber./Recueil* **1997**, *130*, 1231–1234.
319. van der Zeijden, A. A. H.; Mattheis, Ch.; Fröhlich, R.; Zippel, F. *Inorg. Chem.* **1997**, *36*, 4444–4450.
320. Mattheis, C.; van der Zeijden, A. A. H.; Fröhlich, R. *J. Organomet. Chem.* **2000**, *602*, 51–58.
321. Krut'ko, D. P.; Borzov, M. V.; Veksler, E. N.; Churakov, A. V.; Howard, J. A. K. *Polyhedron* **1998**, *17*, 3889–3901.
322. Krut'ko, D. P.; Borzov, M. V.; Veksler, E. N.; Kirsanov, R. S.; Churakov, A. V. *Eur. J. Inorg. Chem.* **1999**, 1973–1979.
323. Paisner, S. N.; Lavoie, G. G.; Bergman, R. G. *Inorg. Chim. Acta* **2002**, *334*, 253–275.
324. Fryzuk, M. D.; Mao, S. S. H.; Zaworotko, M. J.; MacGillivray, L. R. *J. Am. Chem. Soc.* **1993**, *115*, 5336–5337.
325. Fryzuk, M. D.; Mao, S. S. H.; Duval, P. B.; Retting, S. J. *Polyhedron* **1995**, *14*, 11–23.
326. Fryzuk, M. D.; Duval, P. B.; Mao, S. S. H.; Rettig, S. J.; Zaworotko, M. J.; MacGillivray, L. R. *J. Am. Chem. Soc.* **1999**, *121*, 2478–2487.
327. Fryzuk, M. D.; Duval, P. B.; Mao, S. S. H.; Rettig, S. J.; Zaworotko, M. J.; MacGillivray, L. R. *J. Am. Chem. Soc.* **1999**, *121*, 1707–1716.
328. Shapiro, P. J.; Cotter, W. D.; Schaefer, W. P.; Labinger, J. A.; Bercaw, J. E. *J. Am. Chem. Soc.* **1994**, *116*, 4623–4640.

329. Carpenetti, D. W.; Kloppenburg, L.; Kupec, J. T.; Petersen, J. L. *Organometallics* **1996**, *15*, 1572–1581.
330. Herrmann, W. A.; Morawietz, M. A. J. *Organomet. Chem.* **1994**, *482*, 169–181.
331. Chen, Y.-X.; Marks, T. J. *Organometallics* **1997**, *16*, 3649–3657.
332. Gallucci, J. C.; Gentil, S.; Prio, N.; Meunier, Ph.; Gallou, F.; Paquette, L. A. *Acta Cryst. C* **2003**, *59*, M109–M111.
333. Leung, W.-P.; Song, F.-Q.; Zhou, Z.-Y.; Xue, F.; Mak, T. C. W. *J. Organomet. Chem.* **1999**, *575*, 232–241.
334. Gentil, S.; Prio, N.; Meunier, Ph.; Gallucci, J.; Schloss, J. D.; Paquette, L. A. *Organometallics* **2000**, *19*, 4169–4172.
335. Alt, H. G.; Reb, A.; Milius, W.; Weis, A. J. *Organomet. Chem.* **2001**, *628*, 169–182.
336. Resconi, L.; Camurati, I.; Grandini, C.; Rinaldi, M.; Mascellani, N.; Traverso, O. J. *Organomet. Chem.* **2002**, *664*, 5–26.
337. Okuda, J.; Schattenmann, F. J.; Wocadlo, S.; Massa, W. *Organometallics* **1995**, *14*, 789–795.
338. Alt, H. G.; Föttinger, K.; Millius, W. J. *Organomet. Chem.* **1999**, *572*, 21–30.
339. Dias, H. V. R.; Wang, Z.; Bott, S. G. *Organometallics* **1996**, *15*, 91–99.
340. Vazquez, A. B.; Royo, P. J. *Organomet. Chem.* **2003**, *671*, 172–178.
341. Kloppenburg, L.; Petersen, J. L. *Organometallics* **1997**, *16*, 3548–3556.
342. Spence, R. E. v. H.; Piers, W. E. *Organometallics* **1995**, *14*, 4617–4624.
343. Jin, J.; Wilson, D. R.; Chen, E. Y.-X. *Chem. Commun.* **2002**, 708–709.
344. Nguyen, H.; Jarvis, A. P.; Lesley, M. J. G.; Kelly, W. M.; Reddy, S. S.; Taylor, N. J.; Collins, S. *Macromolecules* **2000**, *33*, 1508–1510.
345. Jia, L.; Yang, X.; Stern, C. L.; Marks, T. J. *Organometallics* **1997**, *16*, 842–857.
346. Jia, L.; Yang, X.; Ishihara, A.; Marks, T. J. *Organometallics* **1995**, *14*, 3135–3137.
347. Chen, Y.-X.; Metz, M. V.; Li, L.; Stern, C. L.; Marks, T. J. *J. Am. Chem. Soc.* **1998**, *120*, 6287–6305.
348. Dahlmann, M.; Schottek, J.; Fröhlich, R.; Kunz, D.; Nissinen, M.; Erker, G.; Fink, G.; Kleinschmidt, R. *J. Chem. Soc., Dalton Trans.* **2000**, 1881–1886.
349. Strauch, J. W.; Petersen, J. L. *Organometallics* **2001**, *20*, 2623–2630.
350. Braun, L. F.; Dreier, T.; Christy, M.; Petersen, J. L. *Inorg. Chem.* **2004**, *43*, 3976–3987.
351. Hair, G. S.; Jones, R. A.; Cowley, A. H.; Lynch, W. *Inorg. Chem.* **2001**, *40*, 1014–1019.
352. Hannig, F.; Fröhlich, R.; Bergander, K.; Erker, G.; Petersen, J. L. *Organometallics* **2004**, *23*, 4495–4502.
353. Alt, H. G.; Föttinger, K.; Millius, W. J. *Organomet. Chem.* **1998**, *564*, 115–123.
354. du Plooy, K. E.; Moll, U.; Wocadlo, S.; Massa, W.; Okuda, J. *Organometallics* **1995**, *14*, 3129–3131.
355. Okuda, J.; Eberle, T.; Spaniol, T. P.; Piquet-Fauré, V. J. *Organomet. Chem.* **1999**, *591*, 127–137.
356. Amor, F.; Butt, A.; du Plooy, K. E.; Spaniol, T. P.; Okuda, J. *J. Organomet. Chem.* **1998**, *558*, 139–146.
357. Amor, F.; Butt, A.; du Plooy, K. E.; Spaniol, T. P.; Okuda, J. *Organometallics* **1998**, *17*, 5836–5849.
358. Amor, F.; du Plooy, K. E.; Okuda, J. *Organometallics* **1997**, *16*, 4765–4767.
359. Mu, Y.; Piers, W. E.; MacGillivray, L. R.; Zaworotko, M. J. *Polyhedron* **1995**, *14*, 1–10.
360. Doufou, P.; Abboud, K. A.; Boncella, J. M. J. *Organomet. Chem.* **2000**, *603*, 213–219.
361. Cano, J.; Royo, P.; Lanfranchi, M.; Pellinghelli, M. A.; Tiripicchio, A. *Angew. Chem., Int. Ed.* **2001**, *40*, 2495–2497.
362. Sdupe, M.; Cano, J.; Royo, P.; Herdtweck, E. *Eur. J. Inorg. Chem.* **2004**, 3074–3083.
363. Cano, J.; Royo, P.; Jacobsen, H.; Blacque, O.; Berke, H.; Herdtweck, E. *Eur. J. Inorg. Chem.* **2003**, 2463–2474.
364. Li, L.; Metz, M. V.; Li, H.; Chen, M.-C.; Marks, T. J.; Liable-Sands, L.; Rheingold, A. L. *J. Am. Chem. Soc.* **2002**, *124*, 12725–12741.
365. Li, H.; Li, L.; Marks, T. J. *Angew. Chem. Int. Ed.* **2004**, *43*, 4937–4940.
366. Wang, J.; Li, H.; Guo, N.; Li, L.; Stern, C. L.; Marks, T. J. *Organometallics* **2004**, *23*, 5112–5114.
367. Kunz, K.; Erker, G.; Döring, S.; Fröhlich, R.; Kehr, G. *J. Am. Chem. Soc.* **2001**, *123*, 6181–6182.
368. Kunz, K.; Erker, G.; Döring, S.; Bredeau, S.; Kehr, G.; Fröhlich, R. *Organometallics* **2002**, *21*, 1031–1041.
369. Duda, L.; Erker, G.; Fröhlich, R.; Zippel, F. *Eur. J. Inorg. Chem.* **1998**, 1153–1162.
370. Gomes, P. T.; Green, M. L.; Martins, A. M. J. *Organomet. Chem.* **1998**, *551*, 133–138.
371. Hughes, A. K.; Meetsma, A.; Teuben, J. H. *Organometallics* **1993**, *12*, 1936–1945.
372. Sinnema, P.-J.; Liekelema, K.; Staal, O. K. B.; Hessen, B.; Teuben, J. H. *J. Mol. Catal.* **1998**, *128*, 143–153.
373. Herrmann, W. A.; Morawietz, M. J. A.; Priemeier, T. *Angew. Chem., Int. Ed.* **1994**, *33*, 1946–1949.
374. Baker, R. W.; Wallace, B. J. *Chem. Commun.* **1999**, 1405–1406.
375. Turner, L. E.; Thorn, M.; Fanwick, P. E.; Rothwell, I. P. *Chem. Commun.* **2003**, 1034–1035.
376. Thorn, M.; Fanwick, P. E.; Chesnut, R. W.; Rothwell, I. P. *Chem. Commun.* **1999**, 2543–2544.
377. Kunz, D.; Erker, G.; Fröhlich, R.; Kehr, G. *Eur. J. Inorg. Chem.* **2000**, 409–416.
378. Kunz, K.; Erker, G.; Kehr, G.; Fröhlich, R.; Jacobsen, H.; Berke, H.; Blacque, O. J. *Am. Chem. Soc.* **2002**, *124*, 3316–3326.
379. Kloppenburg, L.; Petersen, J. L. *Organometallics* **1996**, *15*, 7–9.
380. Paolucci, G.; Vignola, M.; Coletto, L.; Pitteri, B.; Benetollo, F. J. *Organomet. Chem.* **2003**, *687*, 161–170.
381. Bredeau, S.; Altenhoff, G.; Kunz, K.; Döring, S.; Grimme, S.; Kehr, G.; Erker, G. *Organometallics* **2004**, *23*, 1836–1844.
382. Altenhoff, G.; Bredeau, S.; Erker, G.; Kehr, G.; Kataeva, O.; Fröhlich, R. *Organometallics* **2002**, *21*, 4084–4089.
383. Lee, M. H.; Hwang, J.-W.; Kim, Y.; Han, Y.; Do, Y. *Organometallics* **2000**, *19*, 5514–5517.
384. Coates, G. W.; Waymouth, R. M. *Science* **1995**, *267*, 217–219.
385. Busico, V.; Castelli, V. V. A.; Aprea, P.; Cipullo, R.; Segre, A.; Talarico, G.; Vacatello, M. J. *Am. Chem. Soc.* **2003**, *125*, 5451–5460.
386. Busico, V.; Cipullo, R.; Kretschmer, W. P.; Talarico, G.; Vacatello, M.; Castelli, V. V. A. *Angew. Chem., Int. Ed.* **2002**, *41*, 505–508.
387. Hauptman, E.; Waymouth, R. M.; Ziller, J. W. *J. Am. Chem. Soc.* **1995**, *117*, 11586–11587.
388. Wilmes, G. M.; Lin, S.; Waymouth, R. M. *Macromolecules* **2002**, *35*, 5382–5387.
389. Maciejewski Petoff, J. L.; Bruce, M. D.; Waymouth, R. M.; Masood, A.; Lal, T. K.; Quan, R. W.; Behrend, S. J. *Organometallics* **1997**, *16*, 5909–5916.
390. Bruce, M. D.; Coates, G. W.; Hauptman, E.; Waymouth, R. M.; Ziller, J. W. *J. Am. Chem. Soc.* **1997**, *119*, 11174–11182.
391. Kravchenko, R.; Masood, A.; Waymouth, R. M. *Organometallics* **1997**, *16*, 3635–3639.
392. Lin, S.; Hauptman, E.; Lal, T. K.; Waymouth, R. M.; Quan, R. W.; Ernst, A. B. *J. Mol. Catal. A: Chem.* **1998**, *136*, 23–33.
393. Witte, P.; Lal, T. K.; Waymouth, R. M. *Organometallics* **1999**, *18*, 4147–4155.
394. Tagge, C. D.; Kravchenko, R. L.; Lal, T. K.; Waymouth, R. M. *Organometallics* **1999**, *18*, 380–388.
395. Schmidt, R.; Alt, H. G. *J. Organomet. Chem.* **2001**, *621*, 304–309.
396. Grimmer, N. E.; Coville, N. J.; de Koning, C. b.; Smith, J. M.; Cook, L. M. J. *Organomet. Chem.* **2000**, *616*, 112–127.

397. Halterman, R. L.; Fahey, D. R.; Bailly, E. F.; Dockter, D. W.; Stenzel, O.; Shipman, J. L.; Khan, M. A.; Dechert, S.; Schumann, H. *Organometallics* **2000**, *19*, 5464–5470.
398. Foster, P.; Rausch, M. D.; Chien, J. C. W. *J. Organomet. Chem.* **1998**, *571*, 171–181.
399. Batsanov, A. S.; Bridgewater, B. M.; Howard, J. A. K.; Hughes, A. K.; Wilson, C. *J. Organomet. Chem.* **1999**, *590*, 169–179.
400. Razavi, A.; Atwood, J. L. *J. Am. Chem. Soc.* **1993**, *115*, 7529–7530.
401. Patsidis, K.; Alt, H. G. *J. Organomet. Chem.* **1995**, *501*, 31–35.
402. Alt, H. G.; Zenk, R. *J. Organomet. Chem.* **1996**, *512*, 51–60.
403. Eisch, J. J.; Owuor, F. A.; Shi, X. *Organometallics* **1999**, *18*, 1583–1585.
404. Grimmond, B. J.; Corey, J. Y.; Rath, N. P. *Organometallics* **1999**, *18*, 404–412.
405. Zhang, F.; Mu, Y.; Zhao, L.; Zhang, Y.; Bu, W.; Chen, C.; Zhai, H.; Hong, H. *J. Organomet. Chem.* **2000**, *613*, 68–76.
406. Conti, G.; Arribas, G.; Altomare, A.; Mendez, B.; Ciardelli, F. Z. *Naturforsch., B: Chem. Sci.* **1995**, *50*, 411–414.
407. Polo, E.; Bellabarba, R. M.; Prini, G.; Traverso, O.; Green, M. L. H. *J. Organomet. Chem.* **1999**, *577*, 211–218.
408. Halterman, R. L.; Chen, Z. *J. Organomet. Chem.* **1995**, *503*, 53–57.
409. Paquette, L. A.; Sivik, M. R.; Bzowej, E. I.; Stanton, K. J. *Organometallics* **1995**, *14*, 4865–4878.
410. Repo, T.; Jany, G.; Hakala, K.; Klinga, M.; Polamo, M.; Leskela, M.; Rieger, B. *J. Organomet. Chem.* **1997**, *549*, 177–186.
411. Schneider, N.; Schaper, F.; Schmidt, K.; Kirsten, R.; Geyer, A.; Brintzinger, H. H. *Organometallics* **2000**, *19*, 3597–3604.
412. Erker, G.; Aulbach, M.; Wingbermuehle, D.; Krueger, C.; Werner, S. *Chem. Ber.* **1993**, *126*, 755–761.
413. Erker, G.; Mollenkopf, C. *J. Organomet. Chem.* **1994**, *483*, 173–181.
414. Erker, G.; Aulbach, M.; Knickmeier, M.; Wingbermuehle, D.; Kruger, C.; Nolte, M.; Werner, S. *J. Am. Chem. Soc.* **1993**, *115*, 4590–4601.
415. Knickmeier, M.; Erker, G.; Fox, T. *J. Am. Chem. Soc.* **1996**, *118*, 9623–9630.
416. Hopf, H.; Sankararaman, S.; Dix, I.; Jones, P. G.; Alt, H. G.; Licht, A. *Eur. J. Inorg. Chem.* **2002**, 123–131.
417. Licht, E. H.; Alt, H. G.; Karim, M. M. *J. Organomet. Chem.* **2000**, *599*, 275–287.
418. Licht, E. H.; Alt, H. G.; Karim, M. M. *J. Mol. Cat. A: Chem.* **2000**, *159*, 273–283.
419. Schmidt, R.; Deppner, M.; Alt, H. G. *J. Mol. Cat. A: Chem.* **2001**, *172*, 43–65.
420. Thornberry, M. P.; Reynolds, N. T.; Deck, P. A.; Fronczek, F. R.; Rheingold, A. L.; Liable-Sands, L. M. *Organometallics* **2004**, *23*, 1333–1339.
421. Spannenberg, A.; Arndt, P.; Baumann, W.; Burlakov, V. V.; Rosenthal, U.; Becke, S.; Weiss, T. *Organometallics* **2004**, *23*, 3819–3825.
422. Erker, G.; Wilker, S.; Krueger, C.; Nolte, M. *Organometallics* **1993**, *12*, 2140–2151.
423. Butakoff, K. A.; Lemenovskii, D. A.; Mountford, P.; Kuz'mina, L. G.; Churakov, A. V. *Polyhedron* **1996**, *15*, 489–499.
424. Jutzi, P.; Redeker, T.; Neumann, B.; Stammel, H.-G. *Organometallics* **1996**, *15*, 4153–4161.
425. Plenio, H.; Burth, D. *J. Organomet. Chem.* **1996**, *519*, 269–272.
426. Knüppel, S.; Fauré, J.-L.; Erker, G.; Kehr, G.; Nissinen, M.; Fröhlich, R. *Organometallics* **2000**, *19*, 1262–1268.
427. Dreier, T.; Erker, G.; Fröhlich, R.; Wibbeling, B. *Organometallics* **2000**, *19*, 4095–4103.
428. Choi, N.; Onozawa, S.; Sakakura, T.; Tanaka, M. *Organometallics* **1997**, *16*, 2765–2767.
429. Grimmond, B. J.; Corey, J. Y. *Inorg. Chim. Acta* **2002**, *330*, 89–94.
430. Hueerlaender, D.; Fröhlich, R.; Erker, G. *J. Chem. Soc., Dalton Trans.* **2002**, 1513–1520.
431. Miller, S. A.; Bercaw, J. E. *Organometallics* **2000**, *19*, 5608–5613.
432. Venne-Dunker, S.; Kehr, G.; Fröhlich, R.; Erker, G. *Organometallics* **2003**, *22*, 948–958.
433. Christoffers, J.; Bergman, R. G. *Angew. Chem., Int. Ed. Engl.* **1995**, *34*, 2266–2267.
434. Van der Zeijden, A. A. H.; Mattheis, C. *J. Organomet. Chem.* **1998**, *555*, 5–15.
435. Lee, B. Y.; Oh, J. S. *J. Organomet. Chem.* **1998**, *552*, 313–317.
436. Plenio, H.; Warnecke, A. *J. Organomet. Chem.* **1997**, *544*, 133–137.
437. Grimmond, B. J.; Rath, N. P.; Corey, J. Y. *Organometallics* **2000**, *19*, 2975–2984.
438. Shafiq, F. A.; Richardson, D. E.; Boncella, J. M. *J. Organomet. Chem.* **1998**, *555*, 1–4.
439. Wolgramm, R.; Ramos, C.; Royo, P.; Lanfranchi, M.; Pellinghelli, M. A.; Tiripicchio, A. *Inorg. Chim. Acta* **2003**, *347*, 114–122.
440. Cano, J.; Gomez-Sal, P.; Heinz, G.; Martinez, G.; Royo, P. *Inorg. Chim. Acta* **2003**, *345*, 5–26.
441. Tikkanen, W.; Kim, A. L.; Lam, K. B.; Ruekert, K. *Organometallics* **1995**, *14*, 1525–1528.
442. Bosch, B.; Erker, G.; Fröhlich, R. *Inorg. Chim. Acta* **1998**, *270*, 446–458.
443. Bellabarba, R. M.; Clancy, G. P.; Gomes, P. T.; Martins, A. M.; Rees, L. H.; Green, M. L. H. *J. Organomet. Chem.* **2001**, *640*, 93–112.
444. Graham, T. W.; Llamazares, A.; McDonald, R.; Cowie, M. *Organometallics* **1999**, *18*, 3490–3501.
445. Cheng, X.; Slobodnick, C.; Deck, P. A.; Billodeaux, D. R.; Fronczek, F. R. *Inorg. Chem.* **2000**, *39*, 4921–4926.
446. Deck, P. A.; Fisher, T. S.; Downey, J. S. *Organometallics* **1997**, *16*, 1193–1196.
447. Mitani, M.; Oouchi, K.; Hayakawa, M.; Yamada, T.; Mukaiyama, T. *Chem. Lett.* **1995**, 905–906.
448. Mitani, M.; Hayakawa, M.; Yamada, T.; Mukaiyama, T. *Bull. Chem. Soc. Jpn.* **1996**, *69*, 2967–2976.
449. Han, Y.; Hong, E.; Kim, Y.; Lee, M. H.; Kim, J.; Hwang, J.-W.; Do, Y. *J. Organomet. Chem.* **2003**, *679*, 48–58.
450. Hong, E.; Kim, Y.; Do, Y. *Organometallics* **1998**, *17*, 2933–2935.
451. Chirik, P. J.; Day, M. W.; Bercaw, J. E. *Organometallics* **1999**, *18*, 1873–1881.
452. Pool, J. A.; Bradley, C. A.; Chirik, P. J. *Organometallics* **2002**, *21*, 1271–1277.
453. Pool, J. A.; Lobkovsky, E.; Chirik, P. J. *J. Am. Chem. Soc.* **2003**, *125*, 2241–2251.
454. Kraft, B. M.; Lachicotte, R. J.; Jones, W. D. *J. Am. Chem. Soc.* **2001**, *123*, 10973–10979.
455. Kraft, B. M.; Jones, W. D. *J. Organomet. Chem.* **2002**, *658*, 132–140.
456. Kraft, B. M.; Jones, W. D. *J. Am. Chem. Soc.* **2002**, *124*, 8681–8689.
457. Carr, A. G.; Dawson, D. M.; Thornton-Pett, M.; Bochmann, M. *Organometallics* **1999**, *18*, 2933–2935.
458. Garratt, S.; Carr, A. G.; Langstein, G.; Bochmann, M. *Macromolecules* **2003**, *36*, 4276–4287.
459. Liu, F.-C.; Chen, K.-Y.; Chen, J.-H.; Lee, G.-H.; Peng, S.-M. *Inorg. Chem.* **2003**, *42*, 1758–1763.
460. Liu, F.-C.; Du, B.; Liu, J.; Meyers, E. A.; Shore, S. G. *Inorg. Chem.* **1999**, *38*, 3228–3234.
461. Liu, J.; Meyers, E. A.; Shore, S. G. *Inorg. Chem.* **1998**, *37*, 496–502.
462. Jordan, G. T.; Shore, S. G. *Inorg. Chem.* **1996**, *35*, 1087–1088.
463. Jordan, G. T.; Liu, F.-C.; Shore, S. G. *Inorg. Chem.* **1997**, *36*, 5597–5602.
464. Chen, X.; Liu, S.; Plecnik, C. E.; Liu, F.-C.; Fraenkel, G.; Shore, S. G. *Organometallics* **2003**, *22*, 275–283.



465. Lacroix, F.; Plecnik, C. E.; Liu, S.; Liu, F.-C.; Meyers, E. A.; Shore, S. G. *J. Organomet. Chem.* **2003**, *687*, 69–77.
466. Chen, X.; Liu, F.-C.; Plecnik, C. E.; Liu, S.; Du, B.; Meyers, E. A.; Shore, S. G. *Organometallics* **2004**, *23*, 2100–2106.
467. Liu, F.-C.; Liu, J.; Meyers, E. A.; Shore, S. G. *J. Am. Chem. Soc.* **2000**, *122*, 6106–6107.
468. Choukroun, R.; Douziech, B.; Donnadieu, B. *Organometallics* **1997**, *16*, 5517–5521.
469. Spence, R. E. H.; Parks, D. J.; Piers, W. E.; MacDonald, M.-A.; Zaworotko, M. J.; Rettig, S. J. *Angew. Chem., Int. Ed.* **1995**, *34*, 1230–1233.
470. Spence, R. E. v. H.; Piers, W. E.; Warren, E.; Sun, Y.; Parvez, M.; MacGillivray, L. R.; Zaworotko, M. J. *Organometallics* **1998**, *17*, 2459–2469.
471. Sun, Y.; Piers, W. E.; Rettig, S. J. *Organometallics* **1996**, *15*, 4110–4112.
472. Khan, K.; Raston, C. L.; McGrady, J. E.; Skelton, B. W.; White, H. A. *Organometallics* **1997**, *16*, 3252–3254.
473. Etkin, N.; Stephan, D. W. *Organometallics* **1998**, *17*, 763–765.
474. Sizov, A. I.; Zvukova, T. M.; Belsky, V. K.; Bulychev, B. M. *J. Organomet. Chem.* **2001**, *619*, 36–42.
475. Wehmschulte, R. J.; Power, P. P. *Polyhedron* **1999**, *18*, 1885–1888.
476. Etkin, N.; Hoskin, A. J.; Stephan, D. W. *J. Am. Chem. Soc.* **1997**, *119*, 11420–11424.
477. Balboni, D.; Camurati, I.; Prini, G.; Resconi, L.; Galli, S.; Mercandelli, P.; Sironi, A. *Inorg. Chem.* **2001**, *40*, 6588–6597.
478. Takahashi, T.; Nishihara, Y.; Ishida, T. *Chem. Lett.* **1995**, *2*, 159–160.
479. Nishihara, Y.; Ishida, T.; Huo, S.; Takahashi, T. *J. Organomet. Chem.* **1997**, *547*, 209–216.
480. Wendt, O. F.; Bercaw, J. E. *Organometallics* **2001**, *20*, 3891–3895.
481. Lappert, M. F.; Raston, C. L.; Skelton, B. W.; White, A. H. *J. Chem. Soc., Dalton Trans.* **1997**, 2895–2902.
482. Knight, K. S.; Wang, D.; Waymouth, R. M.; Ziller, J. *J. Am. Chem. Soc.* **1994**, *116*, 1845–1854.
483. Suzuki, N.; Aihara, N.; Takahara, H.; Watanabe, T.; Iwasaki, M.; Saburi, M.; Hashizume, D.; Chihara, T. *J. Am. Chem. Soc.* **2004**, *126*, 60–61.
484. Suzuki, N.; Nishiura, M.; Wakatsuki, Y. *Science* **2002**, *295*, 660–663.
485. Lam, K. C.; Lin, Z. *Organometallics* **2003**, *22*, 3466–3470.
486. Fischer, R.; Walther, D.; Gebhardt, P.; Goerls, H. *Organometallics* **2000**, *19*, 2532–2540.
487. Takahashi, T.; Kasai, K.; Suzuki, N. *Organometallics* **1994**, *13*, 3413–3414.
488. Schenk, W. A.; Gutmann, T. *J. Organomet. Chem.* **1997**, *544*, 69–78.
489. Ura, Y.; Jin, M.; Nakajima, K.; Takahashi, T. *Chem. Lett.* **2001**, 356–357.
490. Hogenbirk, M.; Schat, G.; Akkerman, O. S.; Bickelhaupt, F.; Schottek, J.; Albrecht, M.; Froehlich, R.; Kehr, G.; Erker, G.; Kooijman, H., *et al.* *Eur. J. Inorg. Chem.* **2004**, 1175–1182.
491. Boehme, U.; Clark, R. J. H.; Jennens, M. J. *Organomet. Chem.* **1994**, *474*, C19–C20.
492. Takahashi, T.; Kotori, M.; Fischer, R.; Nishihara, Y.; Nakajima, K. *J. Am. Chem. Soc.* **1995**, *117*, 11039–11040.
493. Takahashi, T.; Nishihara, Y.; Sun, W.-H.; Fischer, R.; Nakajima, K. *Organometallics* **1997**, *16*, 2216–2219.
494. Schottek, J.; Roettger, D.; Erker, G.; Froehlich, R. *J. Am. Chem. Soc.* **1998**, *120*, 5264–5273.
495. Blosser, P. W.; Gallucci, J. C.; Wojcicki, A. *J. Am. Chem. Soc.* **1993**, *115*, 1994–2995.
496. Blosser, P. W.; Gallucci, J. C.; Wojcicki, A. *J. Organomet. Chem.* **2000**, *597*, 125–132.
497. Johnson, S. A.; Liu, F.-Q.; Suh, M. C.; Zuercher, S.; Haufe, M. M.; Shane, S. H.; Tilley, T. D. *J. Am. Chem. Soc.* **2003**, *125*, 4199–4211.
498. Mao, S. S. H.; Tilley, T. D. *J. Am. Chem. Soc.* **1995**, *117*, 5365–5366.
499. Mao, S. S. H.; Tilley, T. D. *J. Am. Chem. Soc.* **1995**, *117*, 7031–7032.
500. Liu, F.-Q.; Harder, G.; Tilley, T. D. *J. Am. Chem. Soc.* **1998**, *120*, 3271–3272.
501. Nitschke, J. R.; Zürcher, S.; Tilley, T. D. *J. Am. Chem. Soc.* **2000**, *122*, 10345–10352.
502. Hsu, D. P.; Davis, W. M.; Buchwald, S. L. *J. Am. Chem. Soc.* **1993**, *115*, 10394–10395.
503. Metzler, N.; Noeth, H. *J. Organomet. Chem.* **1993**, *454*, C5–C7.
504. Rosenthal, U.; Ohff, A.; Baumann, W.; Kempe, R.; Tillack, A.; Burlakov, V. V. *Angew. Chem., Int. Ed.* **1994**, *33*, 1605–1607.
505. Pellny, P.-M.; Burlakov, V. V.; Arndt, P.; Baumann, W.; Spannenberg, A.; Rosenthal, U. *J. Am. Chem. Soc.* **2000**, *122*, 6317–6318.
506. Pellny, P.-M.; Kirchbauer, F. G.; Burlakov, V. V.; Baumann, W.; Spannenberg, A.; Rosenthal, U. *J. Am. Chem. Soc.* **1999**, *121*, 8313–8323.
507. Pellny, P.-M.; Kirchbauer, F. G.; Burlakov, V. V.; Baumann, W.; Spannenberg, A.; Rosenthal, U. *Chem. Eur. J.* **2000**, *6*, 81–90.
508. Rosenthal, U.; Ohff, A.; Baumann, W.; Kempe, R.; Tillack, A.; Burlakov, V. V. *Organometallics* **1994**, *13*, 2903–2906.
509. Rosenthal, U.; Pulst, S.; Arndt, P.; Ohff, A.; Tillack, A.; Baumann, W.; Kempe, R.; Burlakov, V. V. *Organometallics* **1995**, *14*, 2961–2968.
510. Rosenthal, U.; Ohff, A.; Michalik, M.; Görls, H.; Burlakov, V. V.; Shur, V. B. *Organometallics* **1993**, *12*, 5016–5019.
511. Hiller, J.; Thewalt, U.; Polasek, M.; Petrusova, L.; Varga, V.; Sedmera, P.; Mach, K. *Organometallics* **1996**, *15*, 3752–3759.
512. Lefebvre, C.; Arndt, P.; Tillack, A.; Baumann, W.; Kempe, R.; Burlakov, V. V.; Rosenthal, U. *Organometallics* **1995**, *14*, 3090–3093.
513. Arndt, P.; Lefebvre, C.; Kempe, R.; Tillack, A.; Rosenthal, U. *Chem. Ber.* **1996**, *129*, 1281–1285.
514. Peulecke, N.; Ohff, A.; Kosse, P.; Tillack, A.; Spannenberg, A.; Kempe, R.; Baumann, W.; Burlakov, V. V.; Rosenthal, U. *Chem. Eur. J.* **1998**, *4*, 1852–1861.
515. Pellny, P.-M.; Burlakov, V. V.; Baumann, W.; Spannenberg, A.; Kempe, R.; Rosenthal, U. *Organometallics* **1999**, *18*, 2906–2909.
516. Pellny, P.-M.; Peulecke, N.; Burlakov, V. V.; Baumann, W.; Spannenberg, A.; Rosenthal, U. *Organometallics* **2000**, *19*, 1198–1200.
517. Arndt, P.; Spannenberg, A.; Baumann, W.; Becke, S.; Rosenthal, U. *Eur. J. Inorg. Chem.* **2001**, 2885–2890.
518. Sun, H.; Burlakov, V. V.; Spannenberg, A.; Baumann, W.; Arndt, P.; Rosenthal, U. *Organometallics* **2001**, *20*, 5472–5477.
519. Sun, H.; Burlakov, V. V.; Spannenberg, A.; Baumann, W.; Arndt, P.; Rosenthal, U. *Organometallics* **2002**, *21*, 3360–3366.
520. Zippel, T.; Arndt, P.; Ohff, A.; Spannenberg, A.; Kempe, R.; Rosenthal, U. *Organometallics* **1998**, *17*, 4429–4437.
521. Warner, B. P.; Davis, W. M.; Buchwald, S. L. *J. Am. Chem. Soc.* **1994**, *116*, 5471–5472.
522. Xi, Z.; Fischer, R.; Hara, R.; Sun, W.-H.; Obora, Y.; Suzuki, N.; Nakajima, K.; Takahashi, T. *J. Am. Chem. Soc.* **1997**, *119*, 12842–12848.
523. Bredeau, S.; Delmas, G.; Pirio, N.; Richard, P.; Donnadieu, B.; Meunier, P. *Organometallics* **2000**, *19*, 4463–4467.
524. El Harouch, Y.; Cadierno, V.; Igau, A.; Donnadieu, B.; Majoral, J.-P. *J. Organomet. Chem.* **2004**, *689*, 953–964.
525. Edelbach, B. L.; Kraft, B. M.; Jones, W. D. *J. Am. Chem. Soc.* **1999**, *121*, 10327–10331.
526. Takahashi, T.; Xi, C.; Xi, Z.; Kageyama, M.; Fischer, R.; Nakajima, K.; Negishi, E. *J. Org. Chem.* **1998**, *63*, 6802–6806.
527. Takahashi, T.; Xi, C.; Ura, Y.; Nakajima, K. *J. Am. Chem. Soc.* **2000**, *122*, 3228–3229.
528. Yin, J.; Klosin, J.; Abboud, K. A.; Jones, W. M. *Tetrahedron Lett.* **1995**, *36*, 3107–3110.
529. Erker, G.; Albrecht, M.; Krueger, C.; Nolte, M.; Werner, S. *Organometallics* **1993**, *12*, 4979–4986.
530. Horacek, M.; Stepnicka, P.; Kubista, J.; Gyepes, R.; Mach, K. *Organometallics* **2004**, *23*, 3388–3397.
531. Danjoy, C.; Zhao, J.; Donnadieu, B.; Legros, J.-P.; Valade, L.; Choukroun, R.; Zwick, A.; Cassoux, P. *Chem. Eur. J.* **1998**, *4*, 1100–1105.
532. Choukroun, R.; Donnadieu, B.; Zhao, J.-S.; Cassoux, P.; Lepetit, C.; Silvi, B. *Organometallics* **2000**, *19*, 1901–1911.

533. Yang, X.; Stern, C. L.; Marks, T. J. *J. Am. Chem. Soc.* **1994**, *116*, 10015–10031.
534. Gribkov, D. V.; Hultsch, K. C. *Angew. Chem., Int. Ed.* **2004**, *43*, 5542–5546.
535. Green, M. L. H.; Sassmannshausen, J. *Chem. Commun.* **1999**, 115–116.
536. Bochmann, M.; Lancaster, S. J.; Hursthouse, M. B.; Malik, K. M. A. *Organometallics* **1994**, *13*, 2235–2243.
537. Bochmann, M.; Sarsfield, M. J. *Organometallics* **1998**, *17*, 5908–5912.
538. Beswick, C. L.; Marks, T. J. *J. Am. Chem. Soc.* **2000**, *122*, 10358–10370.
539. Deck, P. A.; Beswick, C. L.; Marks, T. J. *J. Am. Chem. Soc.* **1998**, *120*, 1772–1784.
540. Chen, Y.-X.; Yang, S.; Stern, C. L.; Marks, T. J. *J. Am. Chem. Soc.* **1996**, *118*, 12451–12452.
541. Chen, Y.-X.; Metz, M. V.; Li, L.; Stern, C. L.; Marks, T. J. *J. Am. Chem. Soc.* **1998**, *120*, 6287–6305.
542. Bochmann, M.; Lancaster, S. J. *Angew. Chem., Int. Ed.* **1994**, *33*, 1634–1637.
543. Lancaster, S. J.; Bochmann, M. *J. Organomet. Chem.* **2002**, *654*, 221–223.
544. Beck, S.; Prosenc, M.-H.; Brintzinger, H.-H.; Goretzki, R.; Herfert, N.; Fink, G. *J. Mol. Catal. A: Chem.* **1996**, *111*, 67–79.
545. Bochmann, M.; Green, M. L. H.; Powell, A. K.; Sassmannshausen, J.; Triller, M. U.; Wocadlo, S. *J. Chem. Soc., Dalton Trans.* **1999**, 43–49.
546. Bochmann, M.; Lancaster, S. J. *Organometallics* **1993**, *12*, 633–640.
547. Doerrer, L. H.; Green, M. L. H.; Haussinger, D.; Sassmannshausen, J. *J. Chem. Soc., Dalton Trans.* **1999**, 2111–2118.
548. Beswick, C. L.; Marks, T. J. *Organometallics* **1999**, *18*, 2410–2412.
549. Wu, F.; Dash, A. K.; Jordan, R. F. *J. Am. Chem. Soc.* **2004**, *126*, 15360–15361.
550. Bochmann, M.; Cuenca, T.; Hardy, D. T. *J. Organomet. Chem.* **1994**, *484*, C10–C12.
551. Bertuleit, A.; Fritze, C.; Erker, G.; Fröhlich, R. *Organometallics* **1997**, *16*, 2891–2899.
552. Pflug, J.; Bertuleit, A.; Kehr, G.; Fröhlich, R.; Erker, G. *Organometallics* **1999**, *18*, 3818–3826.
553. Pflug, J.; Erker, G.; Kehr, G.; Fröhlich, R. *Eur. J. Inorg. Chem.* **2000**, 1795–1801.
554. Bosch, B. E.; Erker, G.; Fröhlich, R.; Meyer, O. *Organometallics* **1997**, *16*, 5449–5456.
555. Horton, A. D. *Organometallics* **1996**, *15*, 2675–2677.
556. Sun, Y.; Spence, R. E. v. H.; Piers, W. E.; Parvez, M.; Yap, G. P. A. *J. Am. Chem. Soc.* **1997**, *119*, 5132–5143.
557. Song, X.; Bochmann, M. *J. Organomet. Chem.* **1997**, *545–546*, 597–600.
558. van der Heijden, H.; Hessen, B.; Orpen, A. G. *J. Am. Chem. Soc.* **1998**, *120*, 1112–1113.
559. Bochmann, M.; Lancaster, S. J.; Robinson, O. B. *Chem. Commun.* **1995**, 2081–2082.
560. Shafiq, F. A.; Abboud, K. A.; Richardson, D. E.; Boncella, J. M. *Organometallics* **1998**, *17*, 982–985.
561. Harlan, C. J.; Bott, S. G.; Barron, A. R. *J. Am. Chem. Soc.* **1995**, *117*, 6465–6474.
562. Ingleson, M. J.; Clarke, A.; Mahon, M. F.; Rourke, J. P.; Weller, A. S. *Chem. Commun.* **2003**, 1930–1931.
563. Doring, S.; Erker, G.; Fröhlich, R. *J. Organomet. Chem.* **2002**, *643–644*, 61–67.
564. Guram, A. S.; Guo, Z.; Jordan, R. F. *J. Am. Chem. Soc.* **1993**, *11*, 4902–4903.
565. Niehues, M.; Erker, G.; Meyer, O.; Fröhlich, R. *Organometallics* **2000**, *19*, 2813–2815.
566. Antonelli, D. M.; Tjaden, E. B.; Stryker, J. M. *Organometallics* **1994**, *13*, 763–765.
567. Guo, Z.; Swenson, D. C.; Guram, A. S.; Jordan, R. F. *Organometallics* **1994**, *13*, 766–773.
568. Shen, H.; Jordan, R. F. *Organometallics* **2003**, *22*, 2080–2086.
569. Guo, Z.; Swenson, D. C.; Jordan, R. F. *Organometallics* **1994**, *13*, 1424–1432.
570. Alelyunas, Y. W.; Baenziger, N. C.; Bradley, P. K.; Jordan, R. F. *Organometallics* **1994**, *13*, 148–156.
571. Bijpost, E. A.; Zuideveld, M. A.; Meetsma, A.; Teuben, J. H. *J. Organomet. Chem.* **1998**, *551*, 159–164.
572. Farrow, E.; Sarazin, Y.; Hughes, D. L.; Bochmann, M. *J. Organomet. Chem.* **2004**, *689*, 4624–4629.
573. Niehues, M.; Erker, G.; Kehr, G.; Schwab, P.; Fröhlich, R.; Blacque, O.; Berke, H. *Organometallics* **2002**, *21*, 2905–2911.
574. Sun, Y.; Piers, W. E.; Rettig, S. J. *Chem. Commun.* **1998**, 127–128.
575. Temme, B.; Erker, G.; Karl, J.; Luftmann, H.; Fröhlich, R.; Kotila, S. *Angew. Chem., Int.* **1995**, *34*, 1755–1757.
576. Karl, J.; Erker, G.; Fröhlich, R. *J. Am. Chem. Soc.* **1997**, *119*, 11165–11173.
577. Temme, B.; Karl, J.; Erker, G. *Chem. Eur. J.* **1996**, 919–924.
578. Karl, J.; Dahlmann, M.; Erker, G.; Bergander, K. *J. Am. Chem. Soc.* **1998**, *120*, 5643–5652.
579. Ruwwe, J.; Erker, G.; Fröhlich, R. *Angew. Chem., Int. Ed.* **1996**, *35*, 80–82.
580. Karl, J.; Erker, G.; Fröhlich, R.; Zippel, F.; Bickelhaupt, F.; Goedheijt, M. S.; Akkerman, O. S.; Binger, P.; Stannek, J. *Angew. Chem., Int. Ed.* **1997**, *36*, 2771–2774.
581. Ahlers, W.; Erker, G.; Fröhlich, R. *Eur. J. Inorg. Chem.* **1998**, 889–895.
582. Temme, B.; Erker, G.; Fröhlich, R.; Grehl, M. *Angew. Chem., Int. Ed.* **1994**, *33*, 1480–1482.
583. Ahlers, W.; Temme, B.; Erker, G.; Fröhlich, R.; Fox, T. *J. Organomet. Chem.* **1997**, *527*, 191–201.
584. Temme, B.; Erker, G.; Fröhlich, R.; Grehl, M. *J. Chem. Commun.* **1994**, *14*, 1713–1714.
585. Erker, G.; Venne-Dunker, S.; Kehr, G.; Kleigrew, N.; Fröhlich, R.; Mueck-Lichtenfeld, C.; Grimme, S. *Organometallics* **2004**, *23*, 4391–4395.
586. Ahlers, W.; Erker, G.; Fröhlich, R.; Peuchert, U. *J. Organomet. Chem.* **1999**, *578*, 115–124.
587. Erker, G.; Ahlers, W.; Fröhlich, R. *J. Am. Chem. Soc.* **1995**, *117*, 5853–5854.
588. Roettger, D.; Erker, G.; Fröhlich, R. *J. Organomet. Chem.* **1996**, *518*, 221–225.
589. Roettger, D.; Erker, G.; Fröhlich, R.; Kotila, S. *Chem. Ber.* **1996**, *129*, 1–3.
590. Schottek, J.; Erker, G.; Fröhlich, R. *Eur. J. Inorg. Chem.* **1998**, 551–558.
591. Pflug, J.; Fröhlich, R.; Erker, G. *J. Chem. Soc., Dalton Trans.* **1999**, *15*, 2551–2556.
592. Roettger, D.; Erker, G.; Fröhlich, R.; Grehl, M.; Silverio, S. J.; Gleiter, R. *J. Am. Chem. Soc.* **1995**, *117*, 10503–10512.
593. Burlakov, V. V.; Shur, V. B.; Pellny, P.-M.; Arndt, P.; Baumann, W.; Spannenberg, A.; Rosenthal, U. *Chem. Commun.* **2000**, 241–242.
594. Burlakov, V. V.; Arndt, P.; Baumann, W.; Spannenberg, A.; Rosenthal, U. *Organometallics* **2004**, *23*, 5188–5192.
595. Burlakov, V. V.; Arndt, P.; Baumann, W.; Spannenberg, A.; Rosenthal, U. *Organometallics* **2004**, *23*, 4160–4165.
596. Wu, Z.; Jordan, R. F.; Petersen, J. L. *J. Am. Chem. Soc.* **1995**, *117*, 5867–5868.
597. Carpentier, J.-F.; Wu, Z.; Lee, C. W.; Strömberg, S.; Christopher, J. N.; Jordan, R. F. *J. Am. Chem. Soc.* **2000**, *122*, 7750–7767.
598. Casey, C. P.; Carpenetti, D. W. II; Sakurai, H. *Organometallics* **2001**, *20*, 4262–4265.
599. Galakhov, M. V.; Heinz, G.; Royo, R. *Chem. Commun.* **1998**, 17–18.
600. Casey, C. P.; Carpenetti, D. W. II; *Organometallics* **2000**, *19*, 3970–3977.

601. Brandow, C. G.; Mendiratta, A.; Bercaw, J. E. *Organometallics* **2001**, *20*, 4253–4261.
602. Stoeckenau, E. J. III; Jordan, R. F. *J. Am. Chem. Soc.* **2003**, *125*, 3222–3223.
603. Stoeckenau, E. J. III; Jordan, R. F. *J. Am. Chem. Soc.* **2004**, *126*, 11170–11171.
604. Procopio, L. J.; Carroll, P. J.; Berry, D. H. *J. Am. Chem. Soc.* **1994**, *116*, 177–185.
605. Fandos, R.; Martinez-Ripoll, M.; Otero, A.; Ruiz, M. J.; Rodriguez, A.; Terreros, P. *Organometallics* **1998**, *17*, 1465–1470.
606. Gately, D. A.; Norton, J. R.; Goodson, P. A. *J. Am. Chem. Soc.* **1995**, *117*, 986–996.
607. Berg, F. J.; Petersen, J. L. *Organometallics* **1993**, *12*, 3890–3895.
608. Valero, C.; Grehl, M.; Wingermuehle, D.; Kloppenburg, L.; Carpenetti, D.; Erker, G.; Petersen, J. L. *Organometallics* **1994**, *13*, 415–417.
609. Armstrong, D. R.; Henderson, K. W.; Little, I.; Jenny, C.; Kennedy, A. R.; McKeown, A. E.; Mulvey, R. E. *Organometallics* **2000**, *19*, 4369–4375.
610. Henderson, K. W.; Hind, A.; Kennedy, A. R.; McKeown, A. E.; Mulvey, R. E. *J. Organomet. Chem.* **2002**, *656*, 63–70.
611. Raab, M.; Sundermann, A.; Schick, G.; Loew, A.; Nieger, M.; Schoeller, W. W.; Niece, E. *Organometallics* **2001**, *20*, 1770–1775.
612. Gamer, M. T.; Rastatter, M.; Roesky, P. W. *Z. Anorg. Allg. Chem.* **2002**, *628*, 2269–2272.
613. Kuwabara, J.; Takeuchi, D.; Osakada, K. *Organometallics* **2004**, *23*, 5092–5095.
614. Hanna, T. A.; Baranger, A. M.; Bergman, R. G. *J. Org. Chem.* **1996**, *61*, 4532–4541.
615. Ruck, R. T.; Bergman, R. G. *Organometallics* **2004**, *23*, 2231–2233.
616. Owsianik, K.; Zablocka, M.; Donnadiou, B.; Majoral, J.-P. *Angew. Chem., Int. Ed.* **2003**, *42*, 2176–2179.
617. Braunschweig, H.; Von Koblinski, C.; Breitling, F. M.; Radacki, K.; Hu, C.; Wesemann, L.; Marx, T.; Pantenburg, I. *Inorg. Chim. Acta* **2003**, *350*, 467–474.
618. Roettger, D.; Erker, G.; Grehl, M.; Froehlich, R. *Organometallics* **1994**, *13*, 3897–3902.
619. Temme, B.; Erker, G. *J. Organomet. Chem.* **1995**, *488*, 177–182.
620. Harlan, C. J.; Bridgewater, B. M.; Hascall, T.; Norton, J. R. *Organometallics* **1999**, *18*, 3827–3834.
621. Walsh, P. J.; Hollander, F. J.; Bergman, R. G. *Organometallics* **1993**, *12*, 3705–3723.
622. Baranger, A. M.; Walsh, P. J.; Bergman, R. G. *J. Am. Chem. Soc.* **1993**, *115*, 2753–2763.
623. Harlan, C. J.; Tunge, J. A.; Bridgewater, B. M.; Norton, J. R. *Organometallics* **2000**, *19*, 2365–2372.
624. Lee, S. Y.; Bergman, R. G. *J. Am. Chem. Soc.* **1995**, *117*, 5877–5878.
625. Lee, S. Y.; Bergman, R. G. *J. Am. Chem. Soc.* **1996**, *118*, 6396–6406.
626. Zuckerman, R. L.; Bergman, R. G. *Organometallics* **2000**, *19*, 4795–4809.
627. Zuckerman, R. L.; Bergman, R. G. *Organometallics* **2001**, *20*, 1792–1807.
628. Krska, S. W.; Zuckerman, R. L.; Bergman, R. G. *J. Am. Chem. Soc.* **1998**, *120*, 11828–11829.
629. Zuckerman, R. L.; Krska, S. W.; Bergman, R. G. *J. Am. Chem. Soc.* **2000**, *122*, 751–761.
630. Blum, S. A.; Walsh, P. J.; Bergman, R. G. *J. Am. Chem. Soc.* **2003**, *125*, 14276–14277.
631. Howard, W. A.; Waters, M.; Parkin, G. *J. Am. Chem. Soc.* **1993**, *115*, 4917–4918.
632. Erker, G.; Bendix, M.; Petrenz, R. *Organometallics* **1994**, *13*, 456–461.
633. Blaschke, U.; Erker, G.; Nissinen, M.; Wegelius, E.; Froehlich, R. *Organometallics* **1999**, *18*, 1224–1234.
634. Miquel, L.; Basso-Bert, M.; Choukroun, R.; Madhouni, R.; Eichhorn, B.; Sanchez, M.; Mazieres, M.-R.; Jaud, J. *J. Organomet. Chem.* **1995**, *490*, 21–28.
635. Firth, A. V.; Stewart, J. C.; Hoskin, A. J.; Stephan, D. W. *J. Organomet. Chem.* **1999**, *591*, 185–193.
636. Amor, J. I.; Burton, N. C.; Cuenca, T.; Gomez-Sal, P.; Royo, P. *J. Organomet. Chem.* **1995**, *485*, 153–160.
637. Arevalo, S.; Bonillo, M. R.; De Jesus, E.; De la Mata, F. J.; Flores, J. C.; Gomez, R.; Gomez-Sal, P.; Ortega, P. *J. Organomet. Chem.* **2003**, *681*, 228–236.
638. Chen, Y.-X.; Fu, P.-F.; Stern, C. L.; Marks, T. J. *Organometallics* **1997**, *16*, 5958–5963.
639. Luinstra, A. J. *Organomet. Chem.* **1996**, *517*, 209–215.
640. Huesgen, N. S.; Luinstra, G. A. *Inorg. Chim. Acta* **1997**, *259*, 185–196.
641. Crossman, M. C.; Hope, E. G.; Saunders, G. C. *J. Chem. Soc., Dalton Trans.* **1996**, 509–511.
642. Wenzel, B.; Loennecke, P.; Hey-Hawkins, E. *Organometallics* **2002**, *21*, 2070–2075.
643. Chen, C.-T.; Gau, H.-M. *J. Organomet. Chem.* **1995**, *505*, 17–21.
644. Chang, S.-J.; Liu, H.-J.; Chen, C.-T.; Shih, W.-E.; Lin, C.-C.; Gau, H.-M. *J. Organomet. Chem.* **1996**, *523*, 47–52.
645. Fandos, R.; Hernandez, C.; Otero, A.; Rodriguez, A.; Ruiz, M. J.; Terreros, P. *J. Organomet. Chem.* **2000**, *606*, 156–162.
646. Gau, H. M.; Chen, C. A.; Chang, S. J.; Shih, W. E.; Yang, T. K.; Jong, T. T.; Chien, M. Y. *Organometallics* **1993**, *12*, 1314–1318.
647. Krut'ko, D. P.; Borzov, M. V.; Kuz'mina, L. G.; Churakov, A. V.; Lemenovskii, D. A.; Reutov, O. A. *Inorg. Chim. Acta* **1998**, *280*, 257–263.
648. Samuel, E.; Harrod, J. F.; McGlinchey, M. J.; Cabestaing, C.; Robert, F. *Inorg. Chem.* **1994**, *33*, 1292–1296.
649. Balkwill, J. E.; Cole, S. C.; Coles, M. P.; Hitchcock, P. B. *Inorg. Chem.* **2002**, *41*, 3548–3552.
650. Koch, T.; Blaurock, S.; Hey-Hawkins, E.; Galan-Fereres, M.; Plat, D.; Eisen, M. S. *J. Organomet. Chem.* **2000**, *595*, 126–133.
651. Wada, K.; Itayama, N.; Watanabe, N.; Bundo, M.; Kondo, T.; Mitsudo, T. *Organometallics* **2004**, *23*, 5824–5832.
652. Berlekamp, M.; Erker, G.; Schoenecker, B.; Krieg, R.; Rheingold, A. L. *Chem. Ber.* **1993**, *126*, 2119–2126.
653. Berlekamp, M.; Erker, G.; Petersen, J. L. *J. Organomet. Chem.* **1993**, *458*, 97–103.
654. Noe, R.; Wingermuehle, D.; Erker, G.; Krueger, C.; Bruckmann, J. *Organometallics* **1993**, *12*, 4993–4999.
655. Rau, M. S.; Kretz, C. M.; Geoffroy, G. L.; Rheingold, A. L.; Haggerty, B. S. *Organometallics* **1994**, *13*, 1624–1634.
656. Gibson, D. H.; Mehta, J. M.; Sleadd, B. A.; Mashuta, M. S.; Richardson, J. F. *Organometallics* **1995**, *14*, 4886–4891.
657. Hou, Z.; Fujita, A.; Koizumi, T.; Yamazaki, H.; Wakatsuki, Y. *Organometallics* **1999**, *18*, 1979–1985.
658. Veya, P.; Floriani, C.; Chiesi-Villa, A.; Guastini, C. *Organometallics* **1994**, *13*, 208–213.
659. Cozzi, P. G.; Veya, P.; Floriani, C.; Chiesi-Villa, A.; Rizzoli, C. *Organometallics* **1994**, *13*, 1528–1532.
660. Cozzi, P. G.; Veya, P.; Floriani, C.; Rotzinger, F. P.; Chiesi-Villa, A.; Rizzoli, C. *Organometallics* **1995**, *14*, 4092–4100.
661. Schmittel, M.; Sollner, R. *Chem. Commun.* **1998**, 565–566.
662. Collins, S.; Ward, D. G.; Suddaby, K. H. *Macromolecules* **1994**, *27*, 7222–7224.
663. Li, Y.; Ward, D. G.; Reddy, S. S.; Collins, S. *Macromolecules* **1997**, *30*, 1875–1883.
664. Stojcevic, G.; Kim, H.; Taylor, N. J.; Marder, T. B.; Collins, S. *Angew. Chem., Int. Ed.* **2004**, *43*, 5523–5526.
665. Stuhldreier, T.; Keul, H.; Hoecker, H.; Englert, U. *Organometallics* **2000**, *19*, 5231–5234.
666. Jin, J.; Mariott, W. R.; Chen, E. Y.-X. *J. Polym. Sci. Part A: Polym. Chem.* **2003**, *41*, 3132–3142.

667. Spaether, W.; Klass, K.; Erker, G.; Zippel, F.; Froehlich, R. *Chem. Eur. J.* **1998**, *4*, 1411–1417.
668. Lian, B.; Toupet, L.; Carpentier, J.-F. *Chem. Eur. J.* **2004**, *10*, 4301–4307.
669. Imori, T.; Heyn, R. H.; Tilley, T. D.; Rheingold, A. L. *J. Organomet. Chem.* **1995**, *493*, 83–89.
670. Casty, G. L.; Lugmair, C. G.; Radu, N. S.; Tilley, T. D.; Walzer, J. F.; Zargarian, D. *Organometallics* **1997**, *16*, 8–12.
671. Mori, M.; Kuroda, S.; Dekura, F. *J. Am. Chem. Soc.* **1999**, *121*, 5591–5592.
672. Kuroda, S.; Sato, Y.; Mori, M. *J. Organomet. Chem.* **2000**, *611*, 304–307.
673. Sadow, A. D.; Tilley, T. D. *J. Am. Chem. Soc.* **2002**, *124*, 6814–6815.
674. Sadow, A. D.; Tilley, T. D. *J. Am. Chem. Soc.* **2003**, *125*, 9462–9475.
675. Dioumaev, V. K.; Harrod, J. F. *Organometallics* **1994**, *13*, 1548–1550.
676. Dioumaev, V. K.; Harrod, J. F. *Organometallics* **1996**, *15*, 3859–3867.
677. Segerer, U.; Blaurock, S.; Sieler, J.; Hey-Hawkins, E. *J. Organomet. Chem.* **2000**, *608*, 21–26.
678. Breen, T. L.; Stephan, D. W. *Organometallics* **1996**, *15*, 4509–4514.
679. Ho, J.; Rousseau, R.; Stephan, D. W. *Organometallics* **1994**, *13*, 1918–1926.
680. Breen, T. L.; Stephan, D. W. *J. Am. Chem. Soc.* **1995**, *117*, 11914–11921.
681. Ho, J.; Breen, T. L.; Stephan, D. W. *Organometallics* **1993**, *12*, 3158–3167.
682. Breen, T. L.; Stephan, D. W. *Organometallics* **1996**, *15*, 4223–4227.
683. Urnezis, E.; Lam, K.-C.; Rheingold, A. L.; Protasiewicz, J. D. *J. Organomet. Chem.* **2001**, *630*, 193–197.
684. Urnezis, E.; Klippenstein, S. J.; Protasiewicz, J. D. *Inorg. Chim. Acta* **2000**, *297*, 181–190.
685. Larssonneur, A.-M.; Choukroun, R.; Daran, J.-C.; Cuenca, T.; Flores, J. C.; Royo, P. J. *Organomet. Chem.* **1993**, *444*, 83–89.
686. Chen, T.; Duesler, E. N.; Noth, H.; Paine, R. T. *J. Organomet. Chem.* **2000**, *614–615*, 99–106.
687. Ho, J.; Breen, T. L.; Ozarowski, A.; Stephan, D. W. *Inorg. Chem.* **1994**, *33*, 865–870.
688. Ho, J.; Drake, R. J.; Stephan, D. W. *J. Am. Chem. Soc.* **1993**, *115*, 3792–3793.
689. Bazhenova, T. A.; Kulikov, A. V.; Shestakov, A. F.; Shilov, A. E.; Antipin, M. Yu.; Lysenko, K. A.; Struchkov, Yu. T.; Makhaev, V. D. *J. Am. Chem. Soc.* **1995**, *117*, 12176–12180.
690. Driess, M.; Aust, J.; Merz, K.; Van Wullen, C. *Angew. Chem., Int. Ed.* **1999**, *38*, 3677–3680.
691. Izod, K.; McFarlane, W.; Tyson, B. V.; Clegg, W.; Harrington, R. W. *J. Chem. Soc., Dalton Trans.* **2004**, 4074–4078.
692. Píkies, J.; Baum, E.; Matern, E.; Chojnacki, J.; Grubba, R.; Robaszkiewicz, A. *Chem. Commun.* **2004**, 2478–2479.
693. Chirik, P. J.; Pool, J. A.; Lobkovsky, E. *Angew. Chem., Int. Ed.* **2002**, *41*, 3463–3465.
694. Yam, V. W.-W.; Qi, G.-Z.; Cheung, K.-K. *J. Chem. Soc., Dalton Trans.* **1998**, 1819–1824.
695. Yam, V. W.-W.; Qi, G.-Z.; Cheung, K.-K. *Organometallics* **1998**, *17*, 5448–5453.
696. Chivers, T.; Hilt, R. W.; Parvez, M. *Inorg. Chem.* **1994**, *33*, 997–998.
697. Chivers, T.; Hilt, R. W.; Parvez, M.; Vollmerhaus, R. *Inorg. Chem.* **1994**, *33*, 3459–3466.
698. Hernandez-Gruel, M. A. F.; Perez-Torrente, J. J.; Ciriano, M. A.; Lopez, J. A.; Lahoz, F. J.; Oro, L. A. *Eur. J. Inorg. Chem.* **1999**, 2047–2050.
699. Hernandez-Gruel, M. A. F.; Perez-Torrente, J. J.; Ciriano, M. A.; Lahoz, F. J.; Oro, L. A. *Angew. Chem., Int. Ed.* **1999**, *38*, 2769–2771.
700. Fandos, R.; Lanfranchi, M.; Otero, A.; Pellinghelli, M. A.; Ruiz, M. J.; Terreros, P. *Organometallics* **1996**, *15*, 4725–4730.
701. Segerer, U.; Hey-Hawkins, E. *Polyhedron* **1997**, *16*, 2537–2545.
702. Howard, W. A.; Parkin, G. *J. Organomet. Chem.* **1994**, *472*, C1–C4.
703. Howard, W. A.; Trnka, T. M.; Waters, M.; Parkin, G. *J. Organomet. Chem.* **1997**, *528*, 95–121.
704. Howard, W. A.; Trnka, T. M.; Parkin, G. *Inorg. Chem.* **1995**, *34*, 5900–5909.
705. Christou, V.; Wuller, S. P.; Arnold, J. *J. Am. Chem. Soc.* **1993**, *115*, 10545–10552.
706. Gindlberger, D. E.; Arnold, J. *Organometallics* **1994**, *13*, 4462–4468.
707. d'Arbeloff-Wilson, S. E.; Hitchcock, P. B.; Nixon, J. F.; Kawaguchi, H.; Tatsumi, K. *J. Organomet. Chem.* **2003**, *672*, 1–10.
708. Kane, K. M.; Shapiro, P. J.; Vij, A.; Cubbon, R.; Rheingold, A. L. *Organometallics* **1997**, *16*, 4567–4571.
709. Koennemann, M.; Erker, G.; Froehlich, R.; Kotila, S. *Organometallics* **1997**, *16*, 2900–2908.
710. Erker, G.; Wilker, S.; Krueger, C.; Nolte, M. *Organometallics* **1993**, *12*, 2140–2151.
711. Dorer, B.; Prosen, M.-H.; Rief, U.; Brintzinger, H. H. *Organometallics* **1994**, *13*, 3868–3872.
712. Hafner, K.; Mink, C.; Lindner, H. J. *Angew. Chem., Int. Ed.* **1994**, *33*, 1479–1480.
713. Diamond, G. M.; Rodewald, S.; Jordan, R. F. *Organometallics* **1995**, *14*, 5–7.
714. Diamond, G. M.; Jordan, R. F.; Petersen, J. L. *J. Am. Chem. Soc.* **1996**, *118*, 8024–8033.
715. Kim, I.; Jordan, R. F. *Macromolecules* **1996**, *29*, 489–491.
716. Piemontesi, F.; Camurati, I.; Resconi, L.; Balboni, D.; Sironi, A.; Moret, M.; Ziegler, R.; Piccolrovazzi, N. *Organometallics* **1995**, *14*, 1256–1266.
717. Diamond, G. M.; Jordan, R. F.; Petersen, J. L. *Organometallics* **1996**, *15*, 4030–4037.
718. LoCoco, M. D.; Jordan, R. F. *J. Am. Chem. Soc.* **2004**, *126*, 13918–13919.
719. Leino, R.; Luttikhedde, H.; Wilen, C.-E.; Sillanpaa, R.; Nasman, J. *Organometallics* **1996**, *15*, 2450–2453.
720. Leino, R.; Luttikhedde, H. J. G.; Lehtonen, A.; Ekholm, P.; Nasman, J. H. *J. Organomet. Chem.* **1998**, *558*, 181–188.
721. Leino, R.; Luttikhedde, H. J. G.; Lehtonen, A.; Seppala, J. V.; Nasman, J. H. *J. Organomet. Chem.* **1998**, *559*, 65–72.
722. Luttikhedde, H. J. G.; Leino, R.; Lehtonen, A.; Nasman, J. H. *J. Organomet. Chem.* **1998**, *555*, 127–134.
723. Resconi, L.; Piemontesi, F.; Camurati, I.; Balboni, D.; Sironi, A.; Moret, M.; Rychlicki, H.; Ziegler, R. *Organometallics* **1996**, *15*, 5046–5059.
724. Kaminsky, W.; Rabe, O.; Schaubwienold, A.-M.; Schupfner, G. U.; Hanss, J.; Kopf, J. *J. Organomet. Chem.* **1995**, *497*, 181–193.
725. Lee, L. W. M.; Piers, W. E.; Parvez, M.; Rettig, S. J.; Young, V. G., Jr. *Organometallics* **1999**, *18*, 3904–3912.
726. Sweeney, Z. K.; Salsman, J. L.; Andersen, R. A.; Bergman, R. G. *Angew. Chem., Int. Ed.* **2000**, *39*, 2339–2343.
727. Michael, F. E.; Duncan, A. P.; Sweeney, Z. K.; Bergman, R. G. *J. Am. Chem. Soc.* **2003**, *125*, 7184–7185.
728. Hoyt, H. M.; Michael, F. E.; Bergman, R. G. *J. Am. Chem. Soc.* **2004**, *126*, 1018–1019.
729. Lefebvre, C.; Baumann, W.; Tillack, A.; Kempe, R.; Goerls, H.; Rosenthal, U. *Organometallics* **1996**, *15*, 3486–3490.
730. Mansel, S.; Thomas, D.; Lefebvre, C.; Heller, D.; Kempe, R.; Baumann, W.; Rosenthal, U. *Organometallics* **1997**, *16*, 2886–2890.
731. Hong, Y.; Kuntz, B. A.; Collins, S. *Organometallics* **1993**, *12*, 964–969.
732. Jaquith, J. B.; Guan, J.; Wang, S.; Collins, S. *Organometallics* **1995**, *14*, 1079–1081.
733. Jaquith, J. B.; Levy, C. J.; Bondar, G. V.; Wang, S.; Collins, S. *Organometallics* **1998**, *17*, 914–925.



735. Bolig, A. D.; Chen, E. Y.-X. *J. Am. Chem. Soc.* **2004**, *126*, 4897–4906.
736. Nie, W.-Li.; Erker, G.; Kehr, G.; Fröhlich, R. *Angew. Chem., Int. Ed.* **2004**, *43*, 310–313.
737. Halterman, R. L.; Tret'yakov, A.; Combs, D.; Chang, J.; Khan, M. A. *Organometallics* **1997**, *16*, 3333–3339.
738. Halterman, R. L.; Tret'yakov, A.; Khan, M. A. *J. Organomet. Chem.* **1998**, *568*, 41–51.
739. Halterman, R. L.; Ramsey, T. M.; Pailles, N. A.; Khan, M. A. *J. Organomet. Chem.* **1995**, *497*, 43–53.
740. Schaverien, C. J.; Ernst, R.; Schut, P.; Dall'Occo, T. *Organometallics* **2001**, *20*, 3436–3452.
741. Nantz, M. H.; Hitchcock, S. R.; Sutton, S. C.; Smith, M. D. *Organometallics* **1993**, *12*, 5012–5015.
742. Hitchcock, S. R.; Situ, J. J.; Covell, J. A.; Olmstead, M. M.; Nantz, M. H. *Organometallics* **1995**, *14*, 3732–3740.
743. Halterman, R. L.; Combs, D.; Khan, M. A. *Organometallics* **1998**, *17*, 3900–3907.
744. Schaverien, C. J.; Ernst, R.; Schut, P.; Skiff, W. M.; Resconi, L.; Barbassa, E.; Balboni, D.; Bubitsky, Y. A.; Orpen, A. G.; Mercandelli, P., *et al.* *J. Am. Chem. Soc.* **1998**, *120*, 9945–9946.
745. Könemann, M.; Erker, G.; Fröhlich, R.; Kotila, S. *Organometallics* **1997**, *16*, 2900–2908.
746. Chen, Y.-X.; Rausch, M. D.; Chien, J. C. W. *Macromolecules* **1995**, *28*, 5399–5404.
747. Alt, H. G.; Milius, W.; Palackal, S. J. *J. Organomet. Chem.* **1994**, *472*, 113–118.
748. Schertl, P.; Alt, H. G. *J. Organomet. Chem.* **1999**, *582*, 328–337.
749. Lee, M. H.; Park, J.-W.; Hong, C. S.; Woo, S. I.; Do, Y. J. *Organomet. Chem.* **1998**, *561*, 37–47.
750. Thomas, E. J.; Chien, J. C. W.; Rausch, M. D. *Organometallics* **1999**, *18*, 1439–1443.
751. Thomas, E. J.; Rausch, M. D.; Chien, J. C. W. *Organometallics* **2000**, *19*, 4077–4083.
752. Jany, G.; Repo, T.; Gustafsson, M.; Klinga, M.; Abu-Surrah, A. S.; Leskela, M. Z. *Anorg. Allg. Chem.* **2000**, *62*, 1897–1900.
753. Alt, H. G.; Jung, M. J. *Organomet. Chem.* **1999**, *580*, 1–16.
754. Rieger, B.; Jany, G.; Fawzi, R.; Steimann, M. *Organometallics* **1994**, *13*, 647–653.
755. Dietrich, U.; Hackmann, M.; Rieger, B.; Klinga, M.; Leskelä, M. *J. Am. Chem. Soc.* **1999**, *121*, 4348–4355.
756. Kukral, J.; Lehmus, P.; Feifel, T.; Troll, C.; Rieger, B. *Organometallics* **2000**, *19*, 3767–3775.
757. Kukral, J.; Lehmus, P.; Klinga, M.; Leskela, M.; Rieger, B. *Eur. J. Inorg. Chem.* **2002**, 1349–1356.
758. Deisenhofer, S.; Feifel, T.; Kukral, J.; Klinga, M.; Leskelä, M.; Rieger, B. *Organometallics* **2003**, *22*, 3495–3501.
759. Baker, R. W.; Foulkes, M. A.; Turner, P. *J. Chem. Soc., Dalton Trans.* **2000**, 431–433.
760. Thomas, E. J.; Rausch, M. D.; Chien, J. C. W. *Organometallics* **2000**, *19*, 5744–5748.
761. Rieger, B.; Jany, G. *Chem. Ber.* **1994**, *127*, 2417–2419.
762. Jany, G.; Fawzi, R.; Steimann, M.; Rieger, B. *Organometallics* **1997**, *16*, 544–550.
763. Cuenca, T.; Gomez-Sal, P.; Martin, C.; Royo, B.; Royo, P. *J. Organomet. Chem.* **1999**, *588*, 134–140.
764. Alt, H. G.; Föttinger, K.; Milius, W. *J. Organomet. Chem.* **1998**, *564*, 109–114.
765. Huhn, T.; Suzuki, N.; Yamaguchi, Y.; Mise, T.; Chihara, T.; Wakatsuki, Y. *Chem. Lett.* **1997**, 1201–1202.
766. Schumann, H.; Zietzke, K.; Weimann, R.; Demtschuk, J.; Kaminsky, W.; Schauwienold, A.-M. *J. Organomet. Chem.* **1999**, *574*, 228–240.
767. Antinolo, A.; Fajardo, M.; Gomez-Ruiz, S.; Lopez-Solera, I.; Otero, A.; Prashar, S.; Rodriguez, A. M. *J. Organomet. Chem.* **2003**, *683*, 11–22.
768. Antinolo, A.; Fajardo, M.; Gomez-Ruiz, S.; Lopez-Solera, I.; Otero, A.; Prashar, S. *Organometallics* **2004**, *23*, 4062–4069.
769. Chacon, S. T.; Coughlin, E. B.; Henling, L. M.; Bercaw, J. E. *J. Organomet. Chem.* **1995**, *497*, 171–180.
770. Diamond, G. M.; Jordan, R. F.; Petersen, J. L. *Organometallics* **1996**, *15*, 4045–4053.
771. Huettnerhofer, M.; Prosenc, M.-H.; Rief, U.; Schaper, F.; Brintzinger, H.-H. *Organometallics* **1996**, *15*, 4816–4822.
772. Yoder, J. C.; Day, M. W.; Bercaw, J. E. *Organometallics* **1998**, *17*, 4946–4958.
773. LoCoco, M. D.; Jordan, R. F. *Organometallics* **2003**, *22*, 5498–5503.
774. Hüttenhofer, M.; Schaper, F.; Brintzinger, H.-H. *J. Organomet. Chem.* **2002**, *660*, 85–90.
775. Hüttenhofer, M.; Schaper, F.; Brintzinger, H.-H. *Angew. Chem., Int. Ed.* **1998**, *37*, 2268–2270.
776. Hüttenhofer, M.; Weeber, A.; Brintzinger, H.-H. *J. Organomet. Chem.* **2002**, *663*, 58–62.
777. Giardello, M. A.; Eisen, M. S.; Stern, C. L.; Marks, T. J. *J. Am. Chem. Soc.* **1993**, *115*, 3326–3327.
778. Giardello, M. A.; Eisen, M. S.; Stern, C. L.; Marks, T. J. *J. Am. Chem. Soc.* **1995**, *117*, 12114–12129.
779. Antinolo, A.; Lopez-Solera, I.; Orive, I.; Otero, A.; Prashar, S.; Rodriguez, A. M.; Villasenor, E. *Organometallics* **2001**, *20*, 71–78.
780. Antinolo, A.; Fernandez-Galan, R.; Orive, I.; Otero, A.; Prashar, S. *Eur. J. Inorg. Chem.* **2002**, 2470–2476.
781. Antinolo, A.; Lopez-Solera, I.; Otero, A.; Prashar, S.; Rodriguez, A. M.; Villasenor, E. *Organometallics* **2002**, *21*, 2460–2467.
782. Suzuki, N.; Mise, T.; Yamaguchi, Y.; Chihara, T.; Ikegami, Y.; Ohmori, H.; Matsumoto, A.; Wakatsuki, Y. *J. Organomet. Chem.* **1998**, *560*, 47–54.
783. Mansel, S.; Rief, U.; Prosenc, M.-H.; Kirsten, R.; Brintzinger, H.-H. *J. Organomet. Chem.* **1996**, *512*, 225–236.
784. Mengele, W.; Diebold, J.; Troll, C.; Roell, W.; Brintzinger, H. H. *Organometallics* **1993**, *12*, 1931–1935.
785. Cano, A.; Cuenca, T.; Gomez-Sal, P.; Royo, B.; Royo, P. *Organometallics* **1994**, *13*, 1688–1694.
786. Cano, A. M.; Cuenca, T.; Gomez-Sal, P.; Manzanero, A.; Royo, P. *J. Organomet. Chem.* **1996**, *526*, 227–235.
787. Fernandez, F. J.; Gomez-Sal, P.; Manzanero, A.; Royo, P.; Jacobsen, H.; Berke, H. *Organometallics* **1997**, *16*, 1553–1561.
788. Barriola, A. M.; Cano, A. M.; Cuenca, T.; Fernandez, F. J.; Gomez-Sal, P.; Manzanero, A.; Royo, P. *J. Organomet. Chem.* **1997**, *542*, 247–253.
789. Jung, J.; Noh, S. K.; Lee, D.-H.; Park, S. K.; Kim, K. *J. Organomet. Chem.* **2000**, *595*, 147–152.
790. Herzog, T. A.; Zubris, D. L.; Bercaw, J. E. *J. Am. Chem. Soc.* **1996**, *118*, 11988–11989.
791. Veghini, D.; Henling, L. M.; Burkhardt, T. J.; Bercaw, J. E. *J. Am. Chem. Soc.* **1999**, *121*, 564–573.
792. Veghini, D.; Day, M. W.; Bercaw, J. E. *Inorg. Chim. Acta.* **1998**, *280*, 226–232.
793. Miyake, S.; Bercaw, J. E. *J. Mol. Catal. A: Chem.* **1998**, *128*, 29–39.
794. Miyake, S.; Henling, L. M.; Bercaw, J. E. *Organometallics* **1998**, *17*, 5528–5533.
795. Baar, C. R.; Levy, C. J.; Min, E. Y. J.; Henling, L. M.; Day, M. W.; Bercaw, J. E. *J. Am. Chem. Soc.* **2004**, *126*, 8216–8231.
796. Kaminsky, W.; Schauwienold, A.-M.; Freidanck, F. *J. Mol. Catal. A: Chem.* **1996**, *112*, 37–42.
797. Schmidt, K.; Reinmuth, A.; Rief, U.; Diebold, J.; Brintzinger, H. H. *Organometallics* **1997**, *16*, 1724–1728.
798. Lee, H.; Desrosiers, P. J.; Guzei, I.; Rheingold, A. L.; Parkin, G. *J. Am. Chem. Soc.* **1998**, *120*, 3255–3256.
799. Lee, H.; Hascall, T.; Desrosiers, P. J.; Parkin, G. *J. Am. Chem. Soc.* **1998**, *120*, 5830–5831.
800. Chirik, P. J.; Henling, L. M.; Bercaw, J. E. *Organometallics* **2001**, *20*, 534–544.
801. Dahlmann, M.; Erker, G.; Froehlich, R.; Meyer, O. *Organometallics* **1999**, *18*, 4459–4461.
802. Dahlmann, M.; Erker, G.; Froehlich, R.; Meyer, O. *Organometallics* **2000**, *19*, 2956–2967.

803. Strauch, J. W.; Fauré, J.-L.; Bredeau, S.; Wang, C.; Kehr, G.; Fröhlich, R.; Luftmann, H.; Erker, G. *J. Am. Chem. Soc.* **2004**, *126*, 2089–2104.
804. Dahlmann, M.; Erker, G.; Bergander, K. *J. Am. Chem. Soc.* **2000**, *122*, 7986–7998.
805. Hill, M.; Kehr, G.; Erker, G.; Kataeva, O.; Fröhlich, R. *Chem. Commun.* **2004**, 1020–1021.
806. Yamaguchi, Y.; Suzuki, N.; Mise, T.; Wakatsuki, Y. *Organometallics* **1999**, *18*, 996–1001.
807. Christopher, J. N.; Diamond, G. M.; Jordan, R. F.; Petersen, J. L. *Organometallics* **1996**, *15*, 4038–4044.
808. Christopher, J. N.; Jordan, R. F.; Petersen, J. L.; Young, V. G., Jr. *Organometallics* **1997**, *16*, 3044–3050.
809. Vogel, A.; Priemeier, T.; Herrmann, W. A. *J. Organomet. Chem.* **1997**, *527*, 297–300.
810. Hagemeister, T.; Jutzi, P.; Stämmler, A.; Stämmler, H.-G. *Can. J. Chem.* **2003**, *81*, 1255–1262.
811. Zhang, X.; Zhu, Q.; Guzei, I. A.; Jordan, R. F. *J. Am. Chem. Soc.* **2000**, *122*, 8093–8094.
812. LoCoco, M. D.; Zhang, X.; Jordan, R. F. *J. Am. Chem. Soc.* **2004**, *126*, 15231–15244.
813. Damrau, H.-R. H.; Royo, E.; Obert, S.; Schaper, F.; Weeber, A.; Brintzinger, H.-H. *Organometallics* **2001**, *20*, 5258–5265.
814. Stehling, U.; Diebold, J.; Kirsten, R.; Roll, W.; Brintzinger, H. H.; Jüngling, S.; Mülhaupt, R.; Langhauser, F. *Organometallics* **1994**, *13*, 964–970.
815. Jüngling, S.; Mülhaupt, R.; Stehling, U.; Brintzinger, H.-H.; Fischer, D.; Langhauser, F. *J. Polym. Sci. Part A: Polym. Chem.* **1995**, *33*, 1305–1317.
816. Spaleck, W.; Küber, F.; Winter, A.; Rohrmann, J.; Bachmann, B.; Antberg, M.; Dolle, V.; Paulus, E. F. *Organometallics* **1994**, *13*, 954–963.
817. Spaleck, W.; Küber, F.; Bachmann, B.; Fritze, C.; Winter, A. *J. Mol. Catal.: Chem.* **1998**, *128*, 279–287.
818. Schneider, N.; Huttenloch, M. E.; Stehling, U.; Kirsten, R.; Schaper, F.; Brintzinger, H.-H. *Organometallics* **1997**, *16*, 3413–3420.
819. Schneider, M. J.; Suhm, J.; Mülhaupt, R.; Prosenc, M.-H.; Brintzinger, H.-H. *Macromolecules* **1997**, *30*, 3164–3168.
820. Ewen, J. A.; Jones, R. L.; Elder, M. J.; Rheingold, A. L.; Liable-Sands, L. M. *J. Am. Chem. Soc.* **1998**, *120*, 10786–10787.
821. Rayabov, A. N.; Gribkov, D. V.; Izmer, V. V.; Voskoboinikov, A. A. *Organometallics* **2002**, *21*, 2842–2855.
822. Ewen, J. A.; Elder, M. J.; Jones, R. L.; Rheingold, A. L.; Liable-Sands, L. M.; Sommer, R. D. *J. Am. Chem. Soc.* **2001**, *123*, 4763–4773.
823. van Baar, J. F.; Horton, A. D.; de Kloe, K. P.; Kragt, E.; Mkooyan, S. G.; Nifant'ev, I. E.; Schut, P. A.; Taidakov, I. V. *Organometallics* **2003**, *22*, 2711–2722.
824. Barsties, E.; Schaible, S.; Prosenc, M.-H.; Rief, U.; Röhl, W.; Weyand, O.; Dorer, B.; Brintzinger, H.-H. *J. Organomet. Chem.* **1996**, *520*, 63–68.
825. Yoon, S. C.; Park, J.-W.; Jung, H. S.; Song, H.; Park, J. T.; Woo, S. I. *J. Organomet. Chem.* **1998**, *559*, 149–156.
826. Yoon, S. C.; Han, T. K.; Woo, B. W.; Song, H.; Woo, S. I.; Park, J. T. *J. Organomet. Chem.* **1997**, *534*, 81–87.
827. Puranen, A. J.; Klinga, M.; Leskelä, M.; Repo, T. *Organometallics* **2004**, *23*, 3759–3762.
828. Tsai, W. M.; Chien, J. C. W. *J. Polym. Sci., Part A: Polym. Chem.* **1994**, *32*, 149–158.
829. Luttikhedde, H. J. G.; Leino, R.; Näsman, J. H.; Ahlgrén, M.; Pakkanen, T. *J. Organomet. Chem.* **1995**, *486*, 193–198.
830. Chen, Y.-X.; Rausch, M. D.; Chien, J. C. W. *J. Organomet. Chem.* **1995**, *487*, 29–34.
831. Krut'ko, D. P.; Borzov, M. V.; Charakov, A. V.; Lemenovskii, D. A.; Reutov, A. *Russ. Chem. Bull.* **1998**, *47*, 2280–2285.
832. Soga, K.; Ban, H. T.; Uozumi, T. *J. Mol. Catal. A: Chem.* **1998**, *128*, 273–278.
833. Chen, Y.-X.; Rausch, M. D.; Chien, J. C. W. *J. Pol. Sci., Part A: Polym. Chem.* **1995**, *33*, 2093–2108.
834. Pérez-Camacho, O.; Knjazhanski, S. Y.; Cadenas, G.; Rosales-Hoz, M. J.; Leyva, M. A. *J. Organomet. Chem.* **1999**, *585*, 18–25.
835. Iwama, N.; Uchino, H.; Osano, Y. T.; Sugano, T. *Organometallics* **2004**, *23*, 3267–3269.
836. Iwama, N.; Kato, T.; Sugano, T. *Organometallics* **2004**, *23*, 5813–5817.
837. Dahlmann, M.; Erker, G.; Nissinen, M.; Fröhlich, R. *J. Am. Chem. Soc.* **1999**, *121*, 2820–2828.
838. Chen, E. Y.-X.; Kruper, W. J.; Roof, G.; Wilson, D. R. *J. Am. Chem. Soc.* **2001**, *123*, 745–746.
839. Gómez, F. J.; Waymouth, R. M. *Macromolecules* **2002**, *35*, 3358–3368.
840. Sebastian, A.; Royo, P.; Gomez-Sal, P.; Herdtweck, E. *Inorg. Chim. Acta* **2003**, *350*, 511–519.
841. Chen, Y.-X.; Rausch, M. D.; Chien, J. C. W. *J. Organomet. Chem.* **1995**, *497*, 1–9.
842. Resconi, L.; Jones, R. L.; Rheingold, A. L.; Yap, G. P. A. *Organometallics* **1996**, *15*, 998–1005.
843. Patsidis, K.; Alt, H. G.; Milius, W.; Palackal, S. J. *J. Organomet. Chem.* **1996**, *509*, 63–71.
844. Schertl, P.; Alt, H. G. *J. Organomet. Chem.* **1997**, *545–546*, 553–557.
845. Leino, R.; Luttikhedde, H. J. G.; Lehtonen, A.; Wilén, C.-E.; Näsman, J. H. *J. Organomet. Chem.* **1997**, *545–546*, 219–224.
846. Gentil, S.; Dietz, M.; Pirio, N.; Meunier, P.; Gallucci, J. C.; Gallou, F.; Paquette, L. A. *Organometallics* **2002**, *21*, 5162–5166.
847. Esteb, J. J.; Chien, J. C. W.; Rausch, M. D. *J. Organomet. Chem.* **2003**, *688*, 153–160.
848. Alt, H. G.; Jung, M. *J. Organomet. Chem.* **1998**, *562*, 229–253.
849. Thomas, E. J.; Rausch, M. D.; Chien, J. C. W. *J. Organomet. Chem.* **2001**, *631*, 29–35.
850. Obora, Y.; Stern, C. L.; Marks, T. J.; Nickias, P. N. *Organometallics* **1997**, *16*, 2503–2505.
851. Lee, H.; Lee, C. H. *J. Organomet. Chem.* **2004**, *689*, 214–223.
852. Jutzi, P.; Müller, C.; Neumann, B.; Stämmler, H.-G. *J. Organomet. Chem.* **2001**, *625*, 180–185.
853. Atovmyan, L.; Mkooyan, S.; Urazowski, I.; Broussier, R.; Ninoreille, S.; Perron, P.; Gautheron, B. *Organometallics* **1995**, *14*, 2601–2604.
854. Erker, G.; Psiorz, C.; Fröhlich, R. *Z. Naturforsch., B: Chem. Sci.* **1995**, *50*, 469–475.
855. Bürgi, T.; Berke, H.; Wingbermühle, D.; Psiorz, C.; Noe, R.; Fox, T.; Knickmeier, M.; Berlekamp, J.; Fröhlich, R.; Erker, G. *J. Organomet. Chem.* **1995**, *497*, 149–159.
856. Fierro, R.; Rausch, M. D.; Herrman, G. S.; Alt, H. G. *J. Organomet. Chem.* **1995**, *485*, 11–17.
857. Zachmanoglou, C. E.; Docrat, A.; Bridgewater, B. M.; Parkin, G.; Brandow, C. G.; Bercaw, J. E.; Jardine, C. N.; Lyall, M.; Green, J. C.; Keister, J. B. *J. Am. Chem. Soc.* **2002**, *124*, 9525–9546.
858. Lee, B. Y.; Kim, Y. H.; Won, Y. C.; Han, J. W.; Suh, W. H.; Lee, I. S.; Chung, Y. K.; Song, K. H. *Organometallics* **2002**, *21*, 1500–1503.
859. Hong, S.-D.; Park, Y.-W.; Jeon, B.-G.; Nam, D.-W.; Jung, H. Y.; Jung, M. W.; Song, K. H. *J. Organomet. Chem.* **2004**, *689*, 3402–3411.
860. Cho, E. S.; Joung, U. G.; Lee, B. Y.; Lee, H.; Park, Y.-W.; Lee, C. H.; Shin, D. M. *Organometallics* **2004**, *23*, 4693–4699.
861. Antinolo, A.; Fernandez-Galan, R.; Otero, A.; Prashar, S.; Rivilla, I.; Rodriguez, A. M.; Maestro, M. A. *Organometallics* **2004**, *23*, 5108–5111.
862. Nifant'ev, I. E.; Ivchenko, P. V.; Bagrov, V. V.; Kuz'mina, L. G. *Organometallics* **1998**, *17*, 4734–4738.
863. Green, J. C.; Green, M. L. H.; Taylor, G. C.; Saunders, J. J. *Chem. Soc., Dalton Trans.* **2000**, 317–327.
864. Miyake, S.; Okumura, Y.; Inazawa, S. *Macromolecules* **1995**, *28*, 3074–3079.
865. Llinas, G. H.; Day, R. O.; Rausch, M. D.; Chien, J. C. W. *Organometallics* **1993**, *12*, 1283–1288.
866. Green, M. L. H.; Ishihara, N. *J. Chem. Soc., Dalton Trans.* **1994**, 657–665.
867. Stuhldreier, T.; Keul, H.; Höcker, H. *Macromol. Rapid Commun.* **2000**, *21*, 1093–1098.

868. Frauenrath, H.; Keul, H.; Höcker, H. *Macromolecules* **2001**, *34*, 14–19.
869. Kaminsky, W.; Engehausen, R.; Kopf, J. *Angew. Chem., Int. Ed.* **1995**, *34*, 2273–2275.
870. Resconi, L.; Piemontesi, F.; Camurati, I.; Sudmeijer, O.; Nifant'ev, I. E.; Ivchenko, P. V.; Kuz'mina, L. G. *J. Am. Chem. Soc.* **1998**, *120*, 2308–2321.
871. Resconi, L.; Balboni, D.; Baruzzi, G.; Fiori, C.; Guidotti, S.; Mercandelli, P.; Sironi, A. *Organometallics* **2000**, *19*, 420–429.
872. Dang, V. A.; Yu, L.-C.; Balboni, D.; Dall'Occo, T.; Resconi, L.; Mercandelli, P.; Moret, M.; Sironi, A. *Organometallics* **1999**, *18*, 3781–3791.
873. Balboni, D.; Moscardi, G.; Baruzzi, G.; Braga, V.; Camurati, I.; Piemontesi, F.; Resconi, L.; Nifant'ev, I. E.; Venditto, V.; Antinucci, S. *Macromol. Chem. Phys.* **2001**, *202*, 2010–2028.
874. Razavi, A.; Atwood, J. L. *J. Organomet. Chem.* **1993**, *459*, 117–123.
875. Razavi, A.; Thewalt, J. J. *J. Organomet. Chem.* **1993**, *445*, 111–114.
876. Drago, D.; Pregosin, P. S.; Razavi, A. *Organometallics* **2000**, *19*, 1802–1805.
877. Chen, M.-C.; Roberts, J. A. S.; Marks, T. J. *J. Am. Chem. Soc.* **2004**, *126*, 4605–4625.
878. Bochmann, M.; Lancaster, S. J.; Hursthouse, M. B.; Mazid, M. *Organometallics* **1993**, *12*, 4718–4720.
879. Alt, H. G.; Zenk, R.; Milius, W. *J. Organomet. Chem.* **1996**, *514*, 257–270.
880. Alt, H. G.; Zenk, R. *J. Organomet. Chem.* **1996**, *518*, 7–15.
881. Alt, H. G.; Zenk, R. *J. Organomet. Chem.* **1996**, *526*, 295–301.
882. Ewen, J. A. *Macromol. Symp.* **1995**, *89*, 181–196.
883. Kaminsky, W.; Hopf, A.; Piel, C. *J. Organomet. Chem.* **2003**, *684*, 200–205.
884. Miller, S. A.; Bercaw, J. E. *Organometallics* **2004**, *23*, 1777–1789.
885. Razavi, A.; Atwood, J. L. *J. Organomet. Chem.* **1995**, *497*, 105–111.
886. Razavi, A.; Atwood, J. L. *J. Organomet. Chem.* **1996**, *520*, 115–120.
887. Razavi, A.; Thewalt, U. J. *J. Organomet. Chem.* **2001**, *621*, 267–276.
888. Alt, H. G.; Jung, M. J. *J. Organomet. Chem.* **1998**, *568*, 87–112.
889. Halterman, R. L.; Fahey, D. R.; Marin, V. P.; Dockter, D. W.; Khan, M. A. *J. Organomet. Chem.* **2001**, *625*, 154–159.
890. Miller, S. A.; Bercaw, J. E. *Organometallics* **2002**, *21*, 934–945.
891. Ewen, J. A.; Jones, R. L.; Elder, M. J.; Camurati, I.; Pritzkow, H. *Macromol. Chem. Phys.* **2004**, *205*, 302–307.
892. Nifant'ev, I. E.; Laishchev, I.; Ivchenko, P. V.; Kashulin, I. A.; Guidotti, S.; Piemontesi, F.; Camurati, I.; Resconi, L.; Klusener, P. A. A.; Rijsemus, J. J. H., et al. *Macromol. Chem. Phys.* **2004**, *205*, 2275–2291.
893. Jutzi, P.; Redeker, T. *Eur. J. Inorg. Chem.* **1998**, 663–674.
894. Müller, C.; Lilge, D.; Kristen, M. O.; Jutzi, P. *Angew. Chem., Int. Ed.* **2000**, *39*, 789–792.
895. Lee, S.-G.; Hong, S.-D.; Park, Y.-W.; Jeong, B.-G.; Nam, D.-W.; Jung, H. Y.; Lee, H.; Song, K. H. *J. Organomet. Chem.* **2004**, *689*, 2586–2592.
896. Alt, H. G.; Jung, M.; Kehr, G. *J. Organomet. Chem.* **1998**, *562*, 153–181.
897. Rufanov, K. A.; Kotov, V. V.; Kazennova, N. B.; Lemenovskii, D. A.; Avtomonov, E. V.; Lorberth, J. J. *J. Organomet. Chem.* **1996**, *525*, 287–289.
898. Stelck, D. S.; Shapiro, P. J.; Basicakes, N.; Rheingold, A. L. *Organometallics* **1997**, *16*, 4546–4550.
899. Burns, C. T.; Stelck, D. S.; Shapiro, P. J.; Vij, A.; Kunz, K.; Kehr, G.; Concolino, T.; Rheingold, A. L. *Organometallics* **1999**, *18*, 5432–5434.
900. Lancaster, S. J.; Bochmann, M. *Organometallics* **2001**, *20*, 2093–2101.
901. Starzewski, K. A. O.; Kelly, W. M.; Stumpf, A.; Freitag, D. *Angew. Chem., Int. Ed.* **1999**, *38*, 2439–2443.
902. Shin, J. H.; Hascall, T.; Parkin, G. *Organometallics* **1999**, *18*, 6–9.
903. Shin, J. H.; Bridgewater, B. M.; Parkin, G. *Organometallics* **2000**, *19*, 5155–5159.
904. Xu, S.; Dai, X.; Wang, B.; Zhou, X. J. *J. Organomet. Chem.* **2002**, *645*, 262–267.
905. Herrmann, W. A.; Morawietz, M. J. A.; Herrmann, H.-F.; Kueber, F. *J. Organomet. Chem.* **1996**, *509*, 115–117.
906. Bai, S.-D.; Wei, X.-H.; Guo, J.-P.; Liu, D.-S.; Zhou, Z.-Y. *Angew. Chem., Int. Ed.* **1999**, *38*, 1926–1928.
907. Ogasawara, M.; Nagano, T.; Hayashi, T. *J. Am. Chem. Soc.* **2002**, *124*, 9068–9069.
908. Huttenlocher, M. E.; Dorer, B.; Rief, U.; Prosenc, M.-H.; Schmidt, K.; Brintzinger, H.-H. *J. Organomet. Chem.* **1997**, *541*, 219–232.
909. Qian, C.; Guo, J.; Ye, C.; Sun, J.; Zheng, P. *J. Chem. Soc., Dalton Trans.* **1993**, 3441–3445.
910. Paolucci, G.; Pojana, G.; Zanon, J.; Lucchini, V.; Avtomonov, E. *Organometallics* **1997**, *16*, 5312–5320.
911. Butchard, J. R.; Cornow, O. J.; Smail, S. J. *J. Organomet. Chem.* **1997**, *541*, 407–416.
912. Jodicke, T.; Menges, F.; Kehr, G.; Erker, G.; Howeler, U.; Fröhlich, R. *Eur. J. Inorg. Chem.* **2001**, 2097–2106.
913. Reetz, M. T.; Willuhn, M.; Psiorz, C.; Goddard, R. *Chem. Commun.* **1999**, 1105–1106.
914. Ashe, A. J. III; Fang, X.; Kampf, J. W. *Organometallics* **1999**, *18*, 2288–2290.
915. Braunschweig, H.; Von Koblinski, C.; Mamuti, M.; Englert, U.; Wang, R. *Eur. J. Inorg. Chem.* **1999**, 1899–1904.
916. Rufanov, K.; Avtomonov, E.; Kazennova, N.; Kotov, V.; Khvorost, A.; Lemenovskii, D.; Lorberth, J. J. *J. Organomet. Chem.* **1997**, *536*–537, 361–373.
917. Schaverien, C. J.; Ernst, R.; Terlouw, W.; Schut, P.; Sudmeijer, O.; Budzelaar, P. H. M. *J. Mol. Catal. A: Chem.* **1998**, *128*, 245–256.
918. Chen, Y.-X.; Rausch, M. D.; Chien, J. C. W. *Organometallics* **1994**, *13*, 748–749.
919. Ellis, W. W.; Hollis, T. K.; Odenkirk, W.; Whelan, J.; Ostrander, R.; Rheingold, A. L.; Bosnich, B. *Organometallics* **1993**, *12*, 4391–4401.
920. Halterman, R. L.; Combs, D.; Kihega, J.; Khan, M. A. *J. Organomet. Chem.* **1996**, *520*, 163–170.
921. Erker, G.; Mollenkopf, C.; Grehl, M.; Fröhlich, R.; Krüger, C.; Noe, R.; Riedel, M. *Organometallics* **1994**, *13*, 1950–1955.
922. Ashe, A. J. III; Fang, X.; Hokky, A.; Kampf, J. W. *Organometallics* **2004**, *23*, 2197–2200.
923. Alt, H. G.; Jung, M. J. *J. Organomet. Chem.* **1998**, *568*, 127–131.
924. Diamond, G. M.; Green, M. L. H.; Popham, N. A.; Chernega, A. N. *J. Chem. Soc., Dalton Trans.* **1993**, 2535–2536.
925. Yan, X.; Chernega, A.; Green, M. L. H.; Sanders, J.; Souter, J.; Ushioda, T. *J. Mol. Catal. A: Chem.* **1998**, *128*, 119–141.
926. Diamond, G. M.; Chernega, A. N.; Mountford, P.; Green, M. L. H. *J. Chem. Soc., Dalton Trans.* **1996**, 921–938.
927. Ushioda, T.; Green, M. L. H.; Haggitt, J.; Yan, X. *J. Organomet. Chem.* **1996**, *518*, 155–166.
928. Brackemeyer, T.; Erker, G.; Fröhlich, R. *Organometallics* **1997**, *16*, 531–536.
929. Jacobsen, H.; Brackemeyer, T.; Berke, H.; Erker, G.; Fröhlich, R. *Eur. J. Inorg. Chem.* **2000**, 1423–1428.
930. Kleigrew, N.; Brackemeyer, T.; Kehr, G.; Fröhlich, R.; Erker, G. *Organometallics* **2001**, *20*, 1952–1955.
931. Jonas, K.; Kolb, P.; Kollbach, G.; Gabor, B.; Mynott, R.; Angermund, K.; Heinemann, O.; Kruger, C. *Angew. Chem., Int. Ed.* **1997**, *36*, 1714–1718.
932. Calderazzo, F.; Englert, U.; Pampaloni, G.; Tripepi, G. *J. Organomet. Chem.* **1998**, *555*, 49–56.

933. Calderazzo, F.; Ferri, I.; Pampaloni, G.; Troyanov, S. *J. Organomet. Chem.* **1996**, *518*, 189–196.
934. Troyanov, S. *J. Organomet. Chem.* **1994**, *475*, 139–147.
935. Solari, E.; Musso, F.; Ferguson, R.; Floriani, C.; Chiesi-Villa, A.; Rizzoli, C. *Angew. Chem., Int. Ed.* **1995**, *34*, 1510–1512.
936. Musso, F.; Solari, E.; Floriani, C.; Schenk, K. *Organometallics* **1997**, *16*, 4889–4895.
937. Bazan, G. C.; Rodriguez, G.; Ashe, A. J. III; Al-Ahmad, S.; Müller, C. *J. Am. Chem. Soc.* **1996**, *118*, 2291–2292.
938. Herberich, G. E.; Englert, U.; Schmitz, A. *Organometallics* **1997**, *16*, 3751–3757.
939. Rogers, J. S.; Bazan, G. C.; Sperry, C. K. *J. Am. Chem. Soc.* **1997**, *119*, 9305–9306.
940. Bazan, G. C.; Rodriguez, G.; Ashe, A. J. III; Al-Ahmad, S.; Kampf, J. W. *Organometallics* **1997**, *16*, 2492–2494.
941. Barnhart, R. W.; Bazan, G. C.; Mourey, T. *J. Am. Chem. Soc.* **1998**, *120*, 1082–1083.
942. Rogers, J. S.; Lachicotte, R. J.; Bazan, G. C. *J. Am. Chem. Soc.* **1999**, *121*, 1288–1298.
943. Lee, R. A.; Lachicotte, R. J.; Bazan, G. C. *J. Am. Chem. Soc.* **1998**, *120*, 6037–6046.
944. Ashe, A. J. III; Al-Ahmad, S.; Fang, X.; Kampf, J. W. *Organometallics* **1998**, *17*, 3883–3888.
945. Ashe, A. J. III; Fang, X.; Kampf, J. W. *Organometallics* **1999**, *18*, 1363–1365.
946. Putzer, M. A.; Rogers, J. S.; Bazan, G. C. *J. Am. Chem. Soc.* **1999**, *121*, 8112–8113.
947. Bazan, G. C.; Cotter, W. D.; Komon, Z. J. A.; Lee, R. A.; Lachicotte, R. J. *J. Am. Chem. Soc.* **2000**, *122*, 1371–1380.
948. Lee, B. Y.; Bazan, G. C. *J. Organomet. Chem.* **2002**, *642*, 275–279.
949. Wang, Y.; Wang, H.; Li, H.-W.; Xie, Z. *Organometallics* **2002**, *21*, 3311–3313.
950. Wang, H.; Wang, Y.; Li, H.-W.; Xie, Z. *Organometallics* **2001**, *20*, 5110–5118.
951. Fernandez-Galan, R.; Hitchcock, P. B.; Lappert, M. F.; Antinolo, A.; Rodriguez, A. M. *J. Chem. Soc., Dalton Trans.* **2000**, 1743–1749.
952. Baranger, A. M.; Bergman, R. G. *J. Am. Chem. Soc.* **1994**, *116*, 3822–3835.
953. Michaelidou, D. M.; Green, M. L. H.; Hughes, A. K.; Mountford, P.; Chernega, A. N. *Polyhedron* **1995**, *14*, 2663–2675.
954. Bartik, T.; Windisch, H.; Sorkau, A.; Thiele, K.-H.; Kriebel, C.; Herfurth, A.; Tschoerner, C. M.; Zucchi, C.; Palyi, G. *Inorg. Chim. Acta* **1994**, *227*, 201–205.
955. Friedrich, S.; Gade, L. H.; Scowen, I. J.; McPartlin, M. *Angew. Chem., Int. Ed.* **1996**, *35*, 1338–1341.
956. Gade, L. H.; Friedrich, S.; Troesch, D. J. M.; Scowen, I. J.; McPartlin, M. *Inorg. Chem.* **1999**, *38*, 5295–5307.
957. Bosch, B. E.; Brümmer, I.; Kunz, K.; Erker, G.; Kehr, G.; Fröhlich, R.; Kotila, S. *Organometallics* **2000**, *19*, 1255–1261.
958. Cornelissen, C.; Erker, G.; Kehr, G.; Fröhlich, R. *J. Chem. Soc., Dalton Trans.* **2004**, 4059–4063.
959. Yang, X.-J.; Quillian, B.; Wang, Y.; Wei, P.; Robinson, G. H. *Organometallics* **2004**, *23*, 5119–5120.
960. Findeis, B.; Schubart, M.; Platzek, C.; Gade, L. H.; Scowen, I.; McPartlin, M. *Chem. Commun.* **1996**, 219–220.
961. Gade, L. H.; Schubart, M.; Findeis, B.; Fabre, S.; Bezougli, I.; Lutz, M.; Scowen, I. J.; McPartlin, M. *Inorg. Chem.* **1999**, *38*, 5282–5294.
962. Memmler, H.; Kauper, U.; Gade, L. H.; Scowen, I. J.; McPartlin, M. *Chem. Commun.* **1996**, 1751–1752.
963. Pinkes, J. R.; Tetrick, S. M.; Landrum, B. E.; Cutler, A. R. *J. Organomet. Chem.* **1998**, *566*, 1–7.
964. Hey-Hawkins, E.; Lindenberg, F. *Organometallics* **1994**, *13*, 4643–4644.
965. Neale, N. R.; Tilley, T. D. *Tetrahedron* **2004**, *60*, 7247–7260.
966. Dysard, J. M.; Tilley, T. D. *J. Am. Chem. Soc.* **1998**, *120*, 8245–8246.
967. Dysard, J. M.; Tilley, T. D. *J. Am. Chem. Soc.* **2000**, *122*, 3097–3105.
968. Lutz, M.; Findeis, B.; Haukka, M.; Pakkanen, T. A.; Gade, L. H. *Organometallics* **2001**, *20*, 2505–2509.
969. Lutz, M.; Haukka, M.; Pakkanen, T. A.; Gade, L. H. *Organometallics* **2002**, *21*, 3477–3480.



## 4.09

# Olefin Polymerizations with Group IV Metal Catalysts

---

**L Resconi**, Basell Polyolefins, Ferrara, Italy

**J C Chadwick**, Eindhoven University of Technology, Eindhoven, The Netherlands

**L Cavallo**, University of Salerno, Salerno, Italy

© 2007 Elsevier Ltd. All rights reserved.

<b>4.09.1</b>	<b>Introduction</b>	<b>1006</b>
<b>4.09.2</b>	<b>Pre-catalysts by Chemical Type and Reaction Principles</b>	<b>1007</b>
4.09.2.1	M–C as Propagating Species/Activation	1008
4.09.2.2	Monomer Coordination and Insertion Reactions	1010
4.09.2.3	Concepts of Stereo-, Regio-, and Enantioselectivity	1015
4.09.2.3.1	Regio- and stereochemistry of monomer insertion	1015
4.09.2.3.2	Definition of stereoregular polymers	1016
4.09.2.3.3	Elements of chirality	1016
4.09.2.3.4	Mechanism of stereocontrol	1018
4.09.2.3.5	Symmetry rules for stereocontrol	1020
4.09.2.4	Mechanism of Regiocontrol and Stereochemistry of Regioirregular Insertions	1023
4.09.2.5	Chain-release and Isomerization Reactions	1023
4.09.2.6	Kinetics	1028
<b>4.09.3</b>	<b>Ziegler–Natta Polymerizations with Heterogeneous Catalysts</b>	<b>1031</b>
4.09.3.1	Catalyst Structure and Characterization	1031
4.09.3.2	Polymer Particle Growth	1033
4.09.3.3	Mechanistic Studies of Ziegler–Natta Catalysts	1034
4.09.3.3.1	Oxidation state	1034
4.09.3.3.2	Number of active centers	1035
4.09.3.3.3	Internal/external donor effects and the nature of the active species	1035
4.09.3.3.4	Effects of hydrogen	1037
4.09.3.3.5	Effects of temperature	1038
4.09.3.4	Polyolefins Accessible from Ziegler–Natta Catalysts	1038
4.09.3.5	Polymerization of Acyclic Internal Olefins	1040
4.09.3.6	Major Industrial Processes	1040
<b>4.09.4</b>	<b>Polymerizations with Metallocene Catalysts</b>	<b>1041</b>
4.09.4.1	Ethylene Polymers	1041
4.09.4.1.1	Polyethylene	1041
4.09.4.1.2	Ethylene/ $\alpha$ -olefin co-polymers	1043
4.09.4.1.3	Ethylene/propylene co-polymers and ethylene/propylene/diene terpolymers	1045
4.09.4.1.4	Ethylene co-polymerization with $\alpha,\alpha'$ -disubstituted and internal olefins	1047
4.09.4.1.5	Ethylene co-polymers with cycloolefins	1047
4.09.4.1.6	Ethylene/styrene co-polymers	1049
4.09.4.2	Propylene Polymers	1051
4.09.4.2.1	Amorphous polypropylene	1052
4.09.4.2.2	Isotactic polypropylene	1056
4.09.4.2.3	Low isotacticity: from flexible to elastomeric isotactic polypropylene	1064
4.09.4.2.4	Syndiotactic crystalline and elastomeric polypropylene	1070
4.09.4.2.5	Semicrystalline propylene/ethylene co-polymers	1073
4.09.4.2.6	Propylene/butene co-polymers	1075

4.09.4.2.7	Propylene/higher $\alpha$ -olefin co-polymers	1076
4.09.4.2.8	Propylene co-polymerization with macromonomers	1077
4.09.4.3	Polybutene	1078
4.09.4.4	Poly( $\alpha$ -olefins) from Monomers Higher than Butene	1080
4.09.4.5	Polystyrene	1081
4.09.4.6	Cyclopolymers	1084
4.09.4.7	Polymers of Cyclic Olefins	1084
4.09.4.8	Polymerization of Conjugated Dienes	1084
<b>4.09.5</b>	<b>Polymerization of Ethylene, Propylene, and Higher <math>\alpha</math>-Olefins with other Single-Center Catalysts</b>	<b>1086</b>
4.09.5.1	Complexes with Coordination Number 4	1086
4.09.5.1.1	Ligands with coordinating O–O atoms	1086
4.09.5.1.2	Ligands with coordinating N–N atoms	1087
4.09.5.1.3	Other ligands	1090
4.09.5.2	Complexes with Coordination Number 5	1091
4.09.5.2.1	Ligands with coordinating O–O atoms	1091
4.09.5.2.2	Ligands with coordinating N–O atoms	1091
4.09.5.2.3	Ligands with coordinating N–N atoms	1092
4.09.5.2.4	Other ligands	1095
4.09.5.3	Complexes with Coordination Number 6	1095
4.09.5.3.1	Ligands with coordinating O–O atoms	1095
4.09.5.3.2	Ligands with coordinating N–O atoms: phenoxy–imine-catalysts for polyethylene	1096
4.09.5.3.3	Ligands with coordinating N–O atoms: phenoxy–imine catalysts for syndiotactic polypropylene	1115
4.09.5.3.4	Ligands with coordinating N–O atoms: phenoxy–imine catalysts for isotactic polypropylene	1126
4.09.5.3.5	Other ligands with coordinating N–O atoms	1127
4.09.5.3.6	Complexes with N–N chelate ligands	1138
4.09.5.3.7	Other ligands	1142
4.09.5.3.8	Olefin co-polymerizations with post-metallocene catalysts	1143
4.09.5.3.9	Polystyrene and olefin–styrene co-polymerization with post-metallocene catalysts	1145
<b>References</b>		<b>1146</b>

## 4.09.1 Introduction

This chapter covers the polymerization of alkenes with homogeneous and heterogeneous catalysts based on group 4 metals, including the underlying reaction principles and the relationship between catalyst structure and polymer properties. Applications of related complexes in C–C bond-forming reactions in organic synthesis are covered in Chapter 00125. The use of transition metal catalysts in polymer synthesis is more widely discussed in chapter 11.06.

Catalytic olefin polymerization by means of groups 4 and 5 (Ziegler–Natta) or group 6 (Phillips) metal catalysts is one of the major chemical industries in the world. Polyethylene (PE) (both high density (HDPE) and linear low density (LLDPE) and polypropylene (PP); including propylene-rich co-polymers and heterophasic co-polymers) are the two major thermoplastic polymers, with world productions of about 40 and 36 million tons/year, respectively (2003 figures). Titanium-based, heterogeneous Ziegler–Natta catalysts dominate PP production and also play a leading role in the manufacture of HDPE and LLDPE. Chromium-based Phillips catalysts are also widely used in HDPE production, while metallocene and related “single-site” catalysts are making significant inroads in LLDPE production. The total market for industrial polyolefin catalysts is estimated to exceed 6000 tons/year.

In the last 20 years or so, thanks to the development of the metallocene and “single-site” organometallic catalysts, catalytic olefin polymerization has further evolved into one of the most actively studied branches of catalysis. (The term “single-site catalyst” is widely used; however, in order to avoid confusion with coordination sites, and to underline the chemical uniformity of the active species in metallocene catalysts, we prefer the term “single-center catalyst”.) While characterized as “mature” about 10 years ago, and despite its cyclic nature, the polyolefin business is recognized today as a healthy and growing business, thanks to continuing technology innovations, and significant

expansions in the Asian market. The huge commercial success of polyolefin materials has, in turn, fueled research activities in academia and industrial R&D institutions. In addition to the continuing expansion of established technologies, such as the Spheripol and Unipol processes, several new processes have been developed, and new plants built, in order to fulfill the ever-growing market request for new polyolefin-based materials. Most recent examples are those of Basell's new Spherizone gas-phase process for PP, Basell's new two-reactor polybutene plant, and Dow's and Exxon's solution processes for the production of propylene-based plastomers and elastomers. Without diminishing the importance of process and material design, polymer science, and obviously market economics, the success of these new technologies is to a great extent due to catalyst development.

Despite the heterogeneous and multi-component nature of the industrial  $\text{MgCl}_2$ - or silica-supported Ziegler–Natta catalysts, which hampers the understanding of the elementary steps and kinetics of monomer insertion, chain growth, and termination mechanisms, significant progress has been made, especially in the elucidation of fundamental aspects of stereoregulation and molecular mass control. New and more efficient catalyst modifiers (“donors”) that enable the tuning of chain stereoregularity, molecular mass distribution, and co-monomer incorporation in isotactic polypropylene (iPP) have been found.

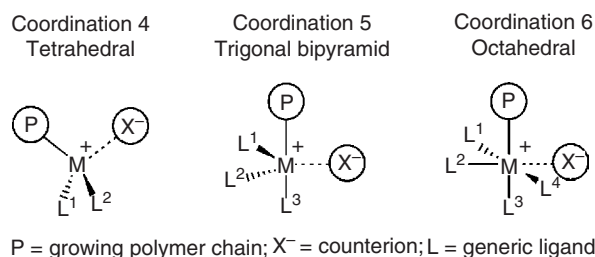
On the other hand, in order to simplify the nature of the active species and better unravel the many elementary steps simultaneously operating during catalytic polymerization, group 4 bis(cyclopentadienyl) complexes<sup>1</sup> were studied by Natta and Breslow as early as 1957 as soluble and structurally well-defined models for  $\text{TiCl}_3$ -based heterogeneous Ziegler–Natta catalysts.<sup>2,3</sup> However, for many years, these complexes remained just models due to their uncompetitively low catalytic activities. At the end of the 1970s, the pioneering work of Brintzinger on the synthesis of chiral metallocenes,<sup>4–13</sup> combined with Sinn and Kaminsky's seminal discovery of methylalumoxane (MAO) as a superior activator for metallocene catalysts,<sup>14</sup> suddenly turned zirconocenes from model catalysts into highly effective ethylene polymerization systems, endowed also with an unprecedented co-monomer incorporation ability. These discoveries, and Ewen's subsequent groundbreaking work on ligand effects in stereoselective polymerization, marked the birth of a new era in catalytic olefin polymerization: that of well-defined, purposely designed, single-center organometallic catalysts.

Organometallic chemists have played a key role in designing new ligands, organometallic complexes, and catalyst systems, understanding their activation chemistry, and determining the mechanisms of olefin interaction with transition metals and the stereochemical implications of chain growth. In addition to a much clearer understanding of the chemistry involved in polymerization catalysis, detailed mechanistic investigations have also generated a wealth of new polyolefin materials, new applications, and ultimately markets, that were inaccessible with the heterogeneous Ziegler–Natta catalysts.

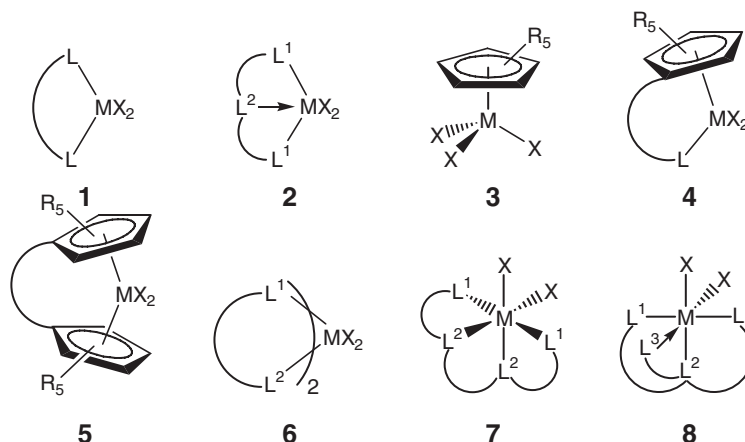
Many extensive reviews and books have been recently dedicated to the field of catalytic olefin polymerization, both for Ziegler–Natta catalysts<sup>15–17</sup> and for metallocene and other single-center catalysts.<sup>18–20</sup> Nevertheless, the pace of development is so quick that a new, comprehensive review appears timely. In the following, we describe the evolution of Ziegler–Natta catalysts, the revolution of single-center catalysts, and their application – most at laboratory level only – to the synthesis of novel or improved polyolefins in the last 10 years.

#### 4.09.2 Pre-catalysts by Chemical Type and Reaction Principles

The most common geometries adopted by group 4 catalysts are depicted in [Scheme 1](#). In all practical cases, the active center is a cationic, strongly electrophilic metal complex capable of activating the  $\text{C}=\text{C}$  double bond of the inserting monomer. This positive charge of the complex cation is counterbalanced by a weakly (or non-) coordinating



Scheme 1



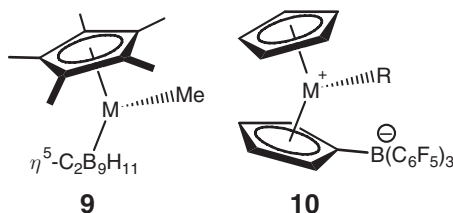
**Figure 1** Structure of the most typical pre-catalysts used in catalytic olefin polymerizations.

counteranion. The active center must have two coordination sites in mutually *cis*-positions in order to enable the transfer of the growing polymeryl chain to the coordinated monomer. In the absence of the monomer, one of these *cis*-coordination positions is usually saturated by the counterion. The ligand(s) must confer the required steric and electronic properties, which control the microstructure and the molecular mass of the produced polymers. The generic ligands L can be based on anionic aromatic groups such as the cyclopentadienyl (Cp,  $\eta^5\text{-C}_5\text{H}_5$ ) ring and its derivatives, as well as on anionic or neutral  $\sigma,\pi$ -donors usually based on heteroatoms, such as O, N, S, and P. Overall, the set of coordinating L ligands is usually dianionic. Finally, the metal atom most often is a  $d^0$ -metal in the oxidation state +IV.

A brief listing of the most typical pre-catalysts used in catalytic olefin polymerizations is represented in Figure 1. These are the systems that will be discussed in much more detail in the following sections. Examples of catalysts based on **1** are dialkoxide- and diamide-based tetrahedral systems. Introduction of an extra neutral donor ligand as in **2** results in pentacoordinate catalysts. Structures with a piano-stool geometry such as **3** are usually denominated half-sandwich complexes. Pre-catalysts such as **4** include the remarkably interesting class of *ansa*-monocyclopentadienyl amido complexes (also known as constrained-geometry catalysts or CGC), while the well-known bis-cyclopentadienyl metallocenes correspond to pre-catalysts of generic formula **5**. Systems **6–8** present an octahedral coordination geometry at the metal atom, and include systems with two unbridged chelating ligands as in **6**, and the most well-known complexes of this kind are the bis(phenoxy-imine) complexes of titanium. Pre-catalysts with tetradentate ligands as in **7** include the bridged bis(phenoxy-amine)-based catalysts, while pre-catalysts such as **8** are characterized by a tridentate ligand with an extra donor arm. Systems such as **3–5**, which contain at least one Cp ligand, are discussed in Section 4.09.4, while systems **1, 2, 6, 7, and 8**, which can be broadly defined as non-metallocene catalysts, are discussed in Section 4.09.5

#### 4.09.2.1 M–C as Propagating Species/Activation

The propagating active site in olefin polymerizations mediated by group 4 catalysts is the M–C(polymer) bond of a metal-alkyl complex.<sup>21–33</sup> Although a few neutral group 4 catalysts, such as complexes **9** ( $\text{M} = \text{Zr}, \text{Hf}^{34}$ ) and **10**,<sup>35–39</sup> have been synthesized, almost all effective group 4 complexes are inactive in polymerization if not activated by a suitable co-catalyst.



Activation and formation of the cationic species are accomplished through a suitable activating species, the co-catalyst, and thus the importance of the co-catalyst in olefin polymerizations with group 4 systems is fundamental. The activator becomes an anion after the activation process, forming a cation–anion pair, which is now accepted to be the real catalytically active polymerization species. With different activators, dramatic differences in activity are possible for a given pre-catalyst structure.<sup>40,41,86,86a</sup> Furthermore, the counteranion was demonstrated to influence the stability and activity of the catalyst, as well as the molecular masses and even stereoregularity of the polymers produced. It was the discovery of MAO by Sinn and Kaminsky<sup>14</sup> that started the metallocene revolution, although the complexity of the catalytic system did not allow conclusions about the structure of the active species. After the cationic nature of the active catalytic species was established,<sup>22–32</sup> several other activators were designed, most of them based on non-coordinating borates and aluminates. Excellent reviews on the subject have appeared.<sup>40,41</sup> Selected examples of activators are shown in Figure 2.

In order to produce an active catalyst upon reaction with the activator, the pre-catalyst has to be alkylated either during its synthesis or *in situ* by an aluminum alkyl compound. Al-alkyls and Al-alkyl chlorides are important components of heterogeneous Ziegler–Natta systems. However, their inability to efficiently activate group 4 metallocenes has for a long time limited developments in this field, until the arrival of MAO, which is now the most widely used activator. The structure of MAO is still rather undefined. In solution, MAO exists as an equilibrium of species with different aggregation numbers and structures.<sup>42–44</sup> Proposed structures include linear chains, cyclic rings, three-dimensional clusters, and cage structures.<sup>40,45–56</sup> MAO as co-catalyst has some drawbacks: low solubility in aliphatic solvents, poor long-term stability in solution, the high content of MAO residues (alumina) in the final product, and the relatively high cost, not least in view of the rather large amount needed for effective activation (the typical Al/M molar ratio needed for homogeneous systems is  $10^3$ : $1$ – $10^4$ : $1$ , although in supported systems, ratios around 100:1 are sufficient). This is especially true for systems of not very high activity.

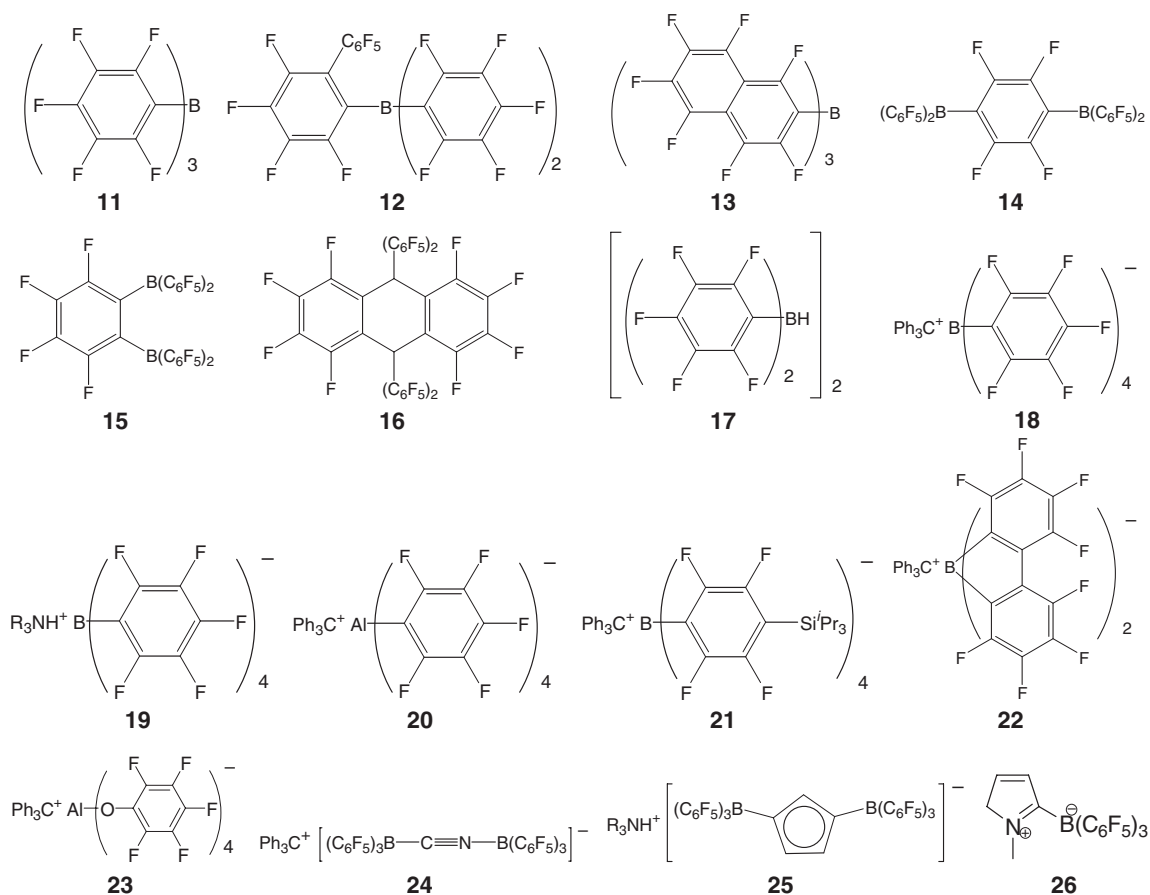


Figure 2 Selected examples of activators.

Finally, the danger inherent in the use of extremely pyrophoric  $\text{AlMe}_3$  has to be taken into account. Surrogates of MAO include ethylalumoxane and isobutylalumoxane synthesized from  $\text{AlEt}_3$  and  $\text{AlBu}^i_3$ , although they do not perform as well as MAO.<sup>57–63</sup> To solve the above problems, modified MAOs have been investigated. The patent literature reports the use of MAO/ $\text{AlBu}^i_3$  mixtures,<sup>64</sup> or the hydrolysis products of  $\text{AlBu}^i_3$  and other branched Al-alkyls.<sup>61,65,66</sup> The presence of residual  $\text{AlMe}_3$  is another problem associated with MAO. Several authors showed that increasing the  $\text{AlMe}_3/\text{MAO}$  ratio or replacing  $\text{AlMe}_3$  with  $\text{AlEt}_3$  or  $\text{AlBu}^i_3$  results in a decrease of both activity and molecular masses.<sup>44,67–72</sup> MAOs which contain much less residual  $\text{AlMe}_3$  have been developed and are claimed to exhibit better performances than conventional MAO.<sup>73,74</sup> Several other approaches have been proposed to reduce the amount of  $\text{AlMe}_3$  in MAO.<sup>75–77</sup>

A different strategy toward stoichiometric co-catalysts has been the use of perfluoroaryl boranes such as **11–15** and **17**. Ewen and Marks independently introduced the already known strongly Lewis-acidic borane  $\text{B}(\text{C}_6\text{F}_5)_3$  **11** as activator for olefin polymerizations with group 4 metallocenes.<sup>78–81</sup> Reaction of  $\text{B}(\text{C}_6\text{F}_5)_3$  with group 4 dimethyl metallocenes (Figure 3) is rapid and quantitative at room temperature in non-coordinating solvents. Crystal structures of the products show that the methyl group of the  $[\text{MeB}(\text{C}_6\text{F}_5)_3]^-$  moiety remains coordinated to the cationic metallocene.<sup>78,79</sup> Other perfluoroaryl borane activators were developed, such as the bifunctional borane  $[\text{HB}(\text{C}_6\text{F}_5)_2]_2$  **17**,<sup>82</sup> and the sterically encumbered perfluorobiphenyl and perfluoronaphthyl boranes.<sup>83–85</sup> Trityl and ammonium borates such as **18**, **19**, **21**, and **22** and aluminate salts such as **20** and **23** are other classes of widely used activators.<sup>40,83,86,86a–90</sup> Different approaches include the cyano-bridged **24**, the weakly coordinating **25**, and the pyrrole-based **26**.<sup>86,86a,91,92</sup> Although the  $[\text{B}(\text{C}_6\text{F}_5)_4]^-$ -based activators are highly effective in olefin polymerization,<sup>93–98</sup> they have some drawbacks. They are poorly soluble in many hydrocarbon solvents and can have limited thermal stability, which results in short catalytic lifetimes.<sup>89</sup> On the other hand, whereas MAO and related co-catalysts are used in large stoichiometric excess, for borane, borate, and similar co-catalysts, a 1:1 molar ratio of activator and dialkyl pre-catalyst is sufficient. In some cases,  $[\text{Ph}_3\text{C}][\text{B}(\text{C}_6\text{F}_5)_4]$  used in excess over the metallocene can significantly increase the productivity of some propylene polymerization catalysts, in particular, those with high activity systems such as “constrained-geometry” titanium complexes.<sup>99,100</sup>

Since the catalyst activator has been shown to exert a remarkable influence on the performance of olefin polymerization catalysts,<sup>41,99,101–106</sup> the search for new co-catalysts is an active field of research. This, however, is beyond the scope of this review.<sup>86,86a,107–113</sup>

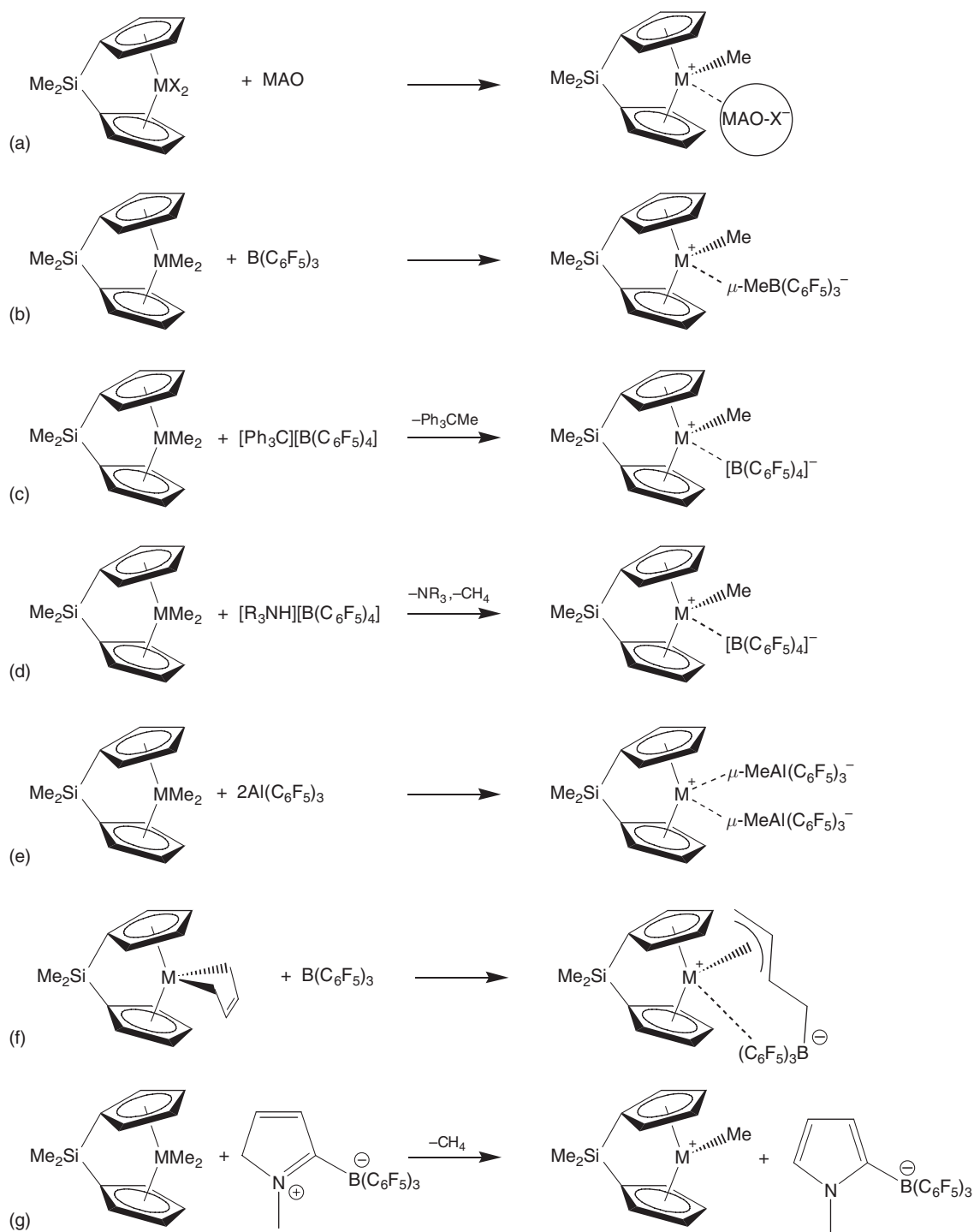
The products of activation with the three main classes of activators described above are shown in Figure 3. We only add that in order to have more reproducible results, and to reduce the amount of catalyst needed for optimum activity, adding small amounts of  $\text{AlR}_3$  (such as  $\text{AlBu}^i_3$  and  $\text{AlEt}_3$ ) to the reaction system is a common practice to scavenge impurities and, with metallocene dihalide precursors, to alkylate the metal.<sup>114,115</sup> It is worth noting that small aluminum alkyls such as  $\text{AlMe}_3$  and  $\text{AlEt}_3$  form heterobinuclear complexes with metallocene alkyl cations, of the type  $[\text{L}_2\text{M}(\mu\text{-Me})_2\text{AlMe}_2]^+$ , such that high concentrations of these aluminum alkyls reduce the catalyst activity.<sup>31,33</sup> However, there is no evidence that bulky aluminum alkyls such as  $\text{AlBu}^i_3$  form similar adducts with group 4 metallocene catalysts.

Upon activation, the metal-alkyl cation and the counteranion form an ion pair. In the low-polarity solvents used in olefin polymerizations, the interaction between the cation and the anion is rather strong. Methyl borates derived from **11** (activation reaction (b) in Figure 3) represent an example of a tight ion pair, with a bridging Me group.<sup>40,116</sup> Conversely, ion pairs with a tetrakis(perfluoroaryl) borate counterion (Figure 3, reactions (c) and (d)) represent examples of less tightly bound ion pairs and the anion in an outer-sphere position.<sup>40,101,116</sup> The exact mechanism and energetics of ion pair formation (pre-catalyst activation) have been widely investigated by several groups.<sup>40,117–120,122,126,127</sup> The structure and dynamics of ion pairs is conveniently investigated by spectroscopic NMR techniques.<sup>116</sup> Finally, the possible aggregation of ion pairs to form species such as ion quadruples, hexuples, and higher-order aggregates has also been investigated.<sup>101,105,121–125</sup> The main conclusion seems to be that, at the concentrations typically used in olefin polymerizations, catalyst ion pairs are unlikely to be present as higher aggregates.<sup>105,123,124</sup> These aspects have been summarized in pertinent reviews.<sup>41,116</sup>

#### 4.09.2.2 Monomer Coordination and Insertion Reactions

The fundamental reaction in catalytic olefin polymerizations is monomer insertion into an M–C bond, schematically described in Scheme 2. The general mechanistic features are well covered in two reviews.<sup>126,127</sup>

The mechanism generally accepted for the chain-growth reaction of Scheme 2 is reported in Figure 4. Cossee originally proposed this mechanism, now known as the Arlman–Cossee mechanism.<sup>128,129</sup> It substantially occurs in



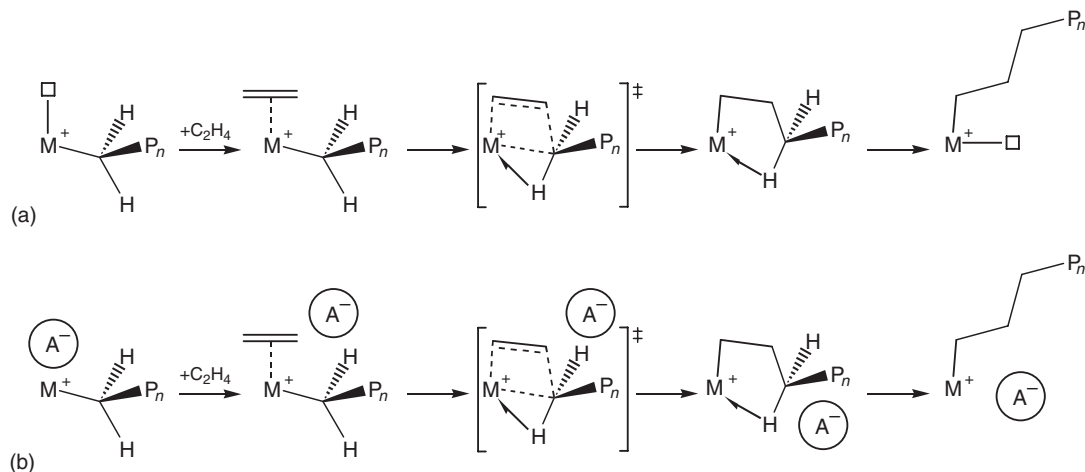
**Figure 3** Selected examples of metallocene activation processes.

two steps: (i) olefin coordination to the metal, (ii) alkyl migration of the  $\sigma$ -coordinated growing chain to the  $\pi$ -coordinated olefin. Green, Rooney, and Brookhart slightly modified this mechanism with the introduction of a stabilizing  $\alpha$ -agostic interaction,<sup>130</sup> which would facilitate the insertion reaction.<sup>131–133</sup> The role of  $\alpha$ -agostic interactions in olefin insertion has been rationalized by Grubbs and Coates.<sup>134</sup>





Scheme 2



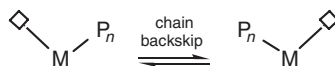
**Figure 4** (a) Modified Cossee mechanism for olefin polymerizations with group 4 transition metals; (b) modified mechanism in the presence of an anionic counterion.

The first step of the insertion reaction requires that the active metal center has an available coordination site for the incoming monomer. For many years, it was commonly accepted that olefin coordination to the cationic metal was an easy process, with a low activation energy possibly connected to the displacement of a weakly coordinated solvent molecule or of a weakly agostic interaction between the metal and a C–H bond of the growing polymer chain. In recent years, this view has changed. Certainly, with coordinating anions like  $[MeB(C_6F_5)_3]^-$ , olefin coordination requires anion displacement, and it has even been suggested that olefin coordination could represent the rate-limiting step.<sup>135,136</sup>

The second step of the chain-growth reaction, the insertion step, occurs via chain migration to the closest carbon of the olefin double bond, which undergoes *cis*-opening with formation of the new metal–carbon and carbon–carbon bonds.<sup>137</sup> Consequently, at the end of the reaction, the new M–chain  $\sigma$ -bond is on the site previously occupied by the coordinated monomer molecule (chain-migratory mechanism). At the end of the reaction, the coordination position previously occupied by the growing chain is then occupied by the counteranion. This mechanism is schematically represented in Figure 4(b). It is important to note that the inclusion of the anionic counterion does not pertain to heterogeneous Ziegler–Natta catalytic systems since no anionic co-catalysts are used in this case.

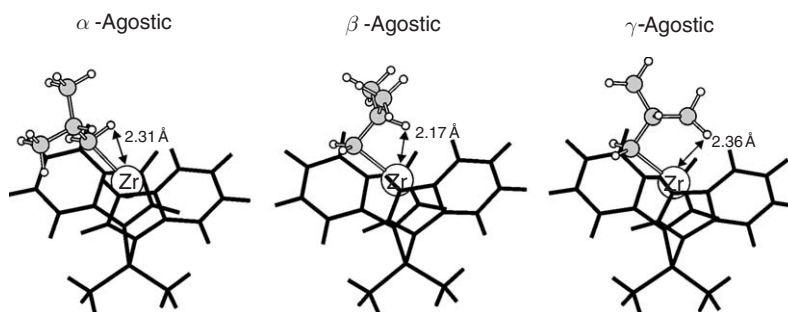
The overall activation energy of the reaction is the result of different contributions, from counterion displacement to the breaking and forming of the M–C bonds. Of course, the strength of the ion pair interaction contributes sensitively to the overall activation barrier, and it explains why catalysts with tightly bound counteranions such as  $[MeB(C_6F_5)_3]^-$  show lower activities relative to catalysts with weakly bound counteranions such as  $[B(C_6F_5)_4]^-$ . In some cases, it has been suggested that the nature of the monomer influences the position of the transition state for monomer insertion, with anion displacement being important in propene polymerization, while with 1-hexene alkyl transfer to the coordinated monomer was found to be rate determining, independent of the anion.<sup>138</sup> Further details on this topic can be found in a critical review.<sup>41</sup>

After insertion, the growing chain can swing back to the coordination position occupied before insertion. This isomerization mechanism, represented in Scheme 3, is usually referred to as “site isomerization” or “backskip of the



Scheme 3





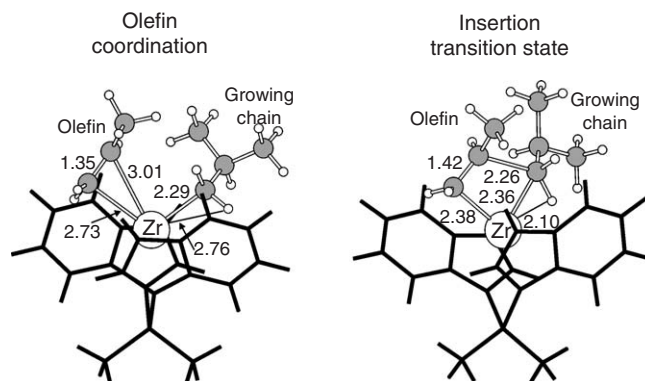
**Figure 5** Agostic interactions between an isobutyl group (simulating a growing chain) and the Zr atom in  $[\text{Me}_2\text{Si}(1\text{-Ind})_2\text{Zr-Bu}]^+$ ; distances in Å.

growing chain”.<sup>139</sup> The backskip of the growing chain can have an effect on the sequence of enantioselective steps which determine the microstructure of the resulting polymer in the case of prochiral olefins.<sup>104,139</sup> While the chain-migratory mechanism is commonly accepted, there are cases in which regular (or predominant) chain migration at each insertion step is not operative. In this case, the growing chain returns to the original coordination position at the end of each insertion reaction, and olefin coordination occurs predominantly at one coordination site. This last mechanism was shown to occur in some particular cases, and its occurrence is highly dependent on the nature of the counteranion.<sup>104</sup> We refer to it as chain-retention mechanism.

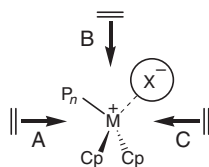
Detailed quantum mechanics calculations have indicated that agostic interactions occur between the growing chain and the metal atom. The most typical are shown in Figure 5. Calculations on gas-phase metal alkyl cations indicate that the  $\beta$ -agostic interaction is the most stable, with the  $\gamma$ -agostic interaction roughly 2–5 kcal mol<sup>−1</sup> higher in energy, and the less stable  $\alpha$ -agostic interaction about 10 kcal mol<sup>−1</sup> higher in energy.<sup>140,141</sup>

Quantum mechanics calculations indicated that olefin coordination to the naked cationic catalyst is a barrierless and exothermic process that leads to the olefin coordination intermediate of Figure 6. The coordination intermediate eventually evolves to the four-center Cossee-like transition state of Figure 6, and then collapses into the products that resemble the agostically bound alkyl species of Figure 5.<sup>140–146</sup> Interestingly, these quantum mechanics calculations confirmed that the transition state is assisted by  $\alpha$ -agostic interactions, as proposed by Green, Rooney and Brookhart.<sup>130</sup> Quite a small energy barrier (1–5 kcal mol<sup>−1</sup>) has been calculated for the insertion step in the case of the naked cationic catalyst.<sup>141,144–146</sup>

While the naked cation could be a model of a catalyst with a completely non-coordinating counteranion, the energy profile in the presence of a tightly coordinating counterion such as  $[\text{MeB}(\text{C}_6\text{F}_5)_3]^-$  is remarkably different. The first issue is how the olefin enters the metal coordination sphere. The three different olefin approaches shown in Scheme 4 have been investigated with quantum mechanics approaches.



**Figure 6** Olefin coordination intermediate and transition state for insertion of propylene into the Zr–Bu<sup>1</sup> bond of  $[\text{Me}_2\text{Si}(1\text{-Ind})_2\text{Zr-Bu}]^+$ ; the Bu<sup>1</sup> group simulates the growing chain; distances in Å.

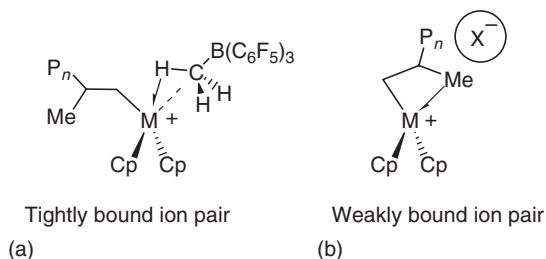


Scheme 4

For the  $[\text{H}_2\text{Si}(\text{Cp})(\text{NBu}^t)\text{TiCH}_3][\text{MeB}(\text{C}_6\text{F}_5)_3]$  system, olefin coordination/insertion along path A is slightly favored over paths B and C because it requires less cation–anion separation. In any case, olefin coordination in the presence of the counterion requires that a sizeable energy barrier must be overcome.<sup>147–149</sup> Modeling ethylene insertion on the  $[\text{Me}_2\text{Si}(\text{Cp})(\text{NBu}^t)\text{TiCH}_3][\text{MeB}(\text{C}_6\text{F}_5)_3]$  system confirmed that ethylene approach pathways A and B are of very similar energy, but they also indicated that for insertion into longer Ti–alkyl bonds, such as insertion into the Ti–Pr<sup>n</sup> bond, path B is favored.<sup>136</sup> More interestingly, they also suggested that the rate-limiting step could be olefin coordination and not olefin insertion.<sup>135,136</sup> Ethylene insertion into the  $[\text{Cp}_2\text{ZrC}_2\text{H}_5]^+$  cation with both the  $[\text{MeB}(\text{C}_6\text{F}_5)_3]^-$  and  $[\text{B}(\text{C}_6\text{F}_5)_4]^-$  counterions has been modeled; for these systems too, the approach along path B was found to be favored.<sup>117</sup>

Many experimental mechanistic studies have been devoted to clarify the role of the counterion in monomer insertion (and thus on catalyst activity).<sup>41,55,99,101–106,117,119,135,136,147,148,150–156</sup> Based on the results of studies on the competitive coordination to the metal atom of the counterion versus an added Lewis base, it has been proposed that the tight ion pair is unable to insert the monomer, and that displacement of the counterion has to occur. After dissociation, one (or possibly more) olefin molecules may insert into the M–chain bond before the counterion recoordinates to the metal, and chain growth is stopped until the counterion dissociates.<sup>157</sup> This mechanism closely resembles that proposed by Fink based on early studies on the kinetics of ethylene oligomerization, which led to a mechanistic scheme where the polymer chain-growth process could be interrupted at any stage by the reversible formation of a resting state, the so-called “intermittent” mechanism.<sup>158</sup>

On the other hand, studies on the polymerization of 1-hexene polymerization catalyzed by *rac*- $\text{C}_2\text{H}_4(\text{Ind})_2\text{ZrMe}-(\mu\text{-Me})\text{B}(\text{C}_6\text{F}_5)_3$  showed that monomer insertion, anion displacement, and anion recoordination are part of a concerted process, for which the term “continuous mechanism” was suggested.<sup>154</sup> NMR studies on metallocene ion pairs bearing a longer-chain alkyl ligand as polymeryl model,  $[\text{rac-Me}_2\text{Si}(\text{Ind})_2\text{ZrCH}_2\text{SiMe}_3^+ \cdots \text{X}^-]$ , indicated that a mechanism of the “continuous” type is operative for the tightly bound counteranion  $[\text{MeB}(\text{C}_6\text{F}_5)_3]^-$ . By contrast, if the cation is paired with the very weakly coordinating  $[\text{B}(\text{C}_6\text{F}_5)_4]^-$ , the counteranion does not enter the inner coordination sphere of the metallocenium cation, and as a result the inserting monomer does not have to compete with the counteranion for coordination to the metal. The catalysts differ therefore structurally, with  $[\text{MeB}(\text{C}_6\text{F}_5)_3]^-$  forming an inner-sphere ion pair (ISIP), while  $[\text{B}(\text{C}_6\text{F}_5)_4]^-$  gives an outer-sphere ion pair (OSIP). Nevertheless, although the degree of anion coordination and the catalyst structures are strongly anion dependent, both insertion mechanisms are similar in the sense that both involve an exchange of the alkyl ligand and anion positions after each insertion step, following the principle outlined in Figure 4(b).<sup>101</sup> This mechanistic model is in agreement with Fink’s original concept of an “intermittent” process.<sup>158</sup> On the basis of combined X-ray and NMR studies, it has been suggested that the different binding capability of the two counterions results in different resting states, involving an  $\alpha$ -agostic methyl interaction with tightly bound  $[\text{MeB}(\text{C}_6\text{F}_5)_3]^-$ , and a  $\gamma$ -agostically bonded alkyl chain in OSIPs with non-bonded counterions such as  $[\text{B}(\text{C}_6\text{F}_5)_4]^-$  (see Scheme 5).<sup>41,101</sup>



Scheme 5

### 4.09.2.3 Concepts of Stereo-, Regio-, and Enantioselectivity

While ethylene insertion can occur in a single mode, insertion of  $\alpha$ -olefins can occur in the four geometrically different modes represented in [Scheme 6](#). Thus, polymerization of prochiral monomers requires the definition of a few terms.

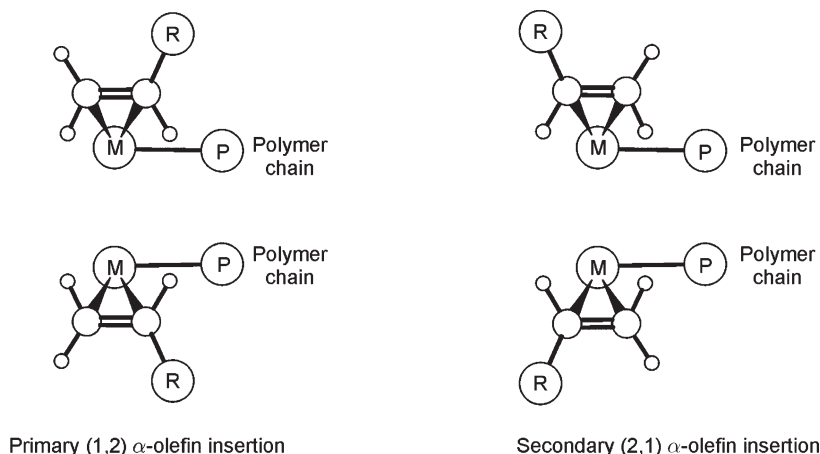
#### 4.09.2.3.1 Regio- and stereochemistry of monomer insertion

The regiochemistry of insertion (the catalyst regioselectivity) defines whether olefin insertion is primary or secondary (also called 1,2 or 2,1 insertions, respectively). Any catalyst will insert some olefin molecules with the wrong regiochemistry. Regioirregular insertions (regioerrors or regiomistakes) mean occasional secondary (primary) insertion if propagation is prevalingly primary (secondary). Monomer insertion is mostly primary for metallocene catalysts (the amount of regiomistakes being usually <1%), regioirregular for some dialkoxotitanium complexes, and mostly secondary for some non-metallocene catalysts (the amount of regiomistakes usually <1–2%).<sup>137,159–162</sup> While the preference for primary insertion in metallocenes is mainly steric in nature,<sup>163,164</sup> for most non-metallocene catalysts it is the result of a subtle interplay of steric and electronic effects.<sup>165</sup>

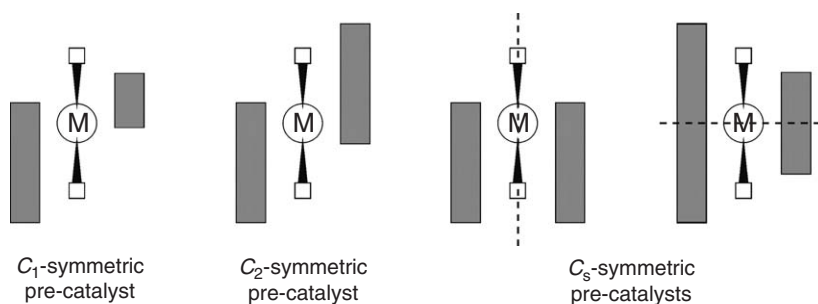
The ability to insert preferentially one and the same olefin enantioface (or enantioface selectivity) defines the stereochemistry of each insertion (the catalyst stereoselectivity). Every insertion of a monosubstituted prochiral  $\alpha$ -olefin creates a new stereogenic center, and the stereoregularity or tacticity of the polymer is determined by the stereochemical relationships between successive tertiary carbon atoms in the polymer chain. The term “stereo-specific polymerization” refers to the process leading to a tactic (stereoregular) polymer produced with a stereoselective catalyst. The terms stereoselective (or enantioselective) and regioselective are also used to refer to the single insertion event. Given their widespread use, the terms aspecific, isospecific, and syndiospecific, referring to the type of enantioselectivity of a catalyst,<sup>162</sup> are also used.

In summary, the stereoregularity or tacticity of a polymer chain is determined by the stereochemical relationship(s) between neighboring tertiary carbon atoms in the chain. The stereoselectivity of a catalyst, that is, the reactivity and selectivity of its active sites, is determined by the metal, the geometry of the ligands, and the structure of the metal-bound polymer chain end. Thus, different structures of the last inserted monomer unit, or the chirality of its stereogenic carbon (defined by the primary or secondary, left or right insertion) increase the number of active sites on a given metal center. The sites can, and often do, differ in reactivity, regioselectivity, and enantioface selectivity: as a result, the active metal center itself changes in chemical structure during a single chain growth, but statistically keeps the same overall reactivity from one polymer chain to the next. From these considerations, it appears that these catalysts are better defined as “single-center” catalysts, a term we prefer over the commonly used description as “single-site” catalysts.

In the framework of the chain-migratory mechanism, olefin insertion occurs on the two different coordination sites available. This implies that the two different geometric situations, corresponding to an exchange between the coordination positions of the growing chain and of the monomer, are related by the overall symmetry of the metal



Scheme 6



**Figure 7** Schematic representation of the most common symmetries of group 4 olefin polymerization catalysts. Gray rectangles define the space occupied by the organic ligand. Hollow squares represent the coordination positions available to the growing chain and to the monomer. Dashed lines represent the local mirror plane of the two  $C_s$ -symmetric catalysts.

$\pi$ -ligands framework. The most typical situations are shown in Figure 7. If the pre-catalyst has an overall  $C_1$ -symmetry, the two coordination positions are sterically and electronically different. The activity and catalytic properties of the two possible sites can be completely different. If the pre-catalyst has an overall  $C_2$ -symmetry, the two coordination positions are homotopic and thus the activity and catalytic properties of the two sites are identical. If the pre-catalyst has an overall  $C_s$ -symmetry, two cases are possible. If the local mirror plane contains the coordination positions available to the growing chain and the monomer, the two coordination positions are not symmetry related, and, by symmetry, they are both non enantioselective. More interesting is the case in which the local mirror plane relates the coordination positions available to the growing chain and to the monomer. In fact, in this case the two coordination positions are enantiotopic, and thus the possible asymmetric induction (in the framework of the chain-migration mechanism) is opposite at each insertion step.

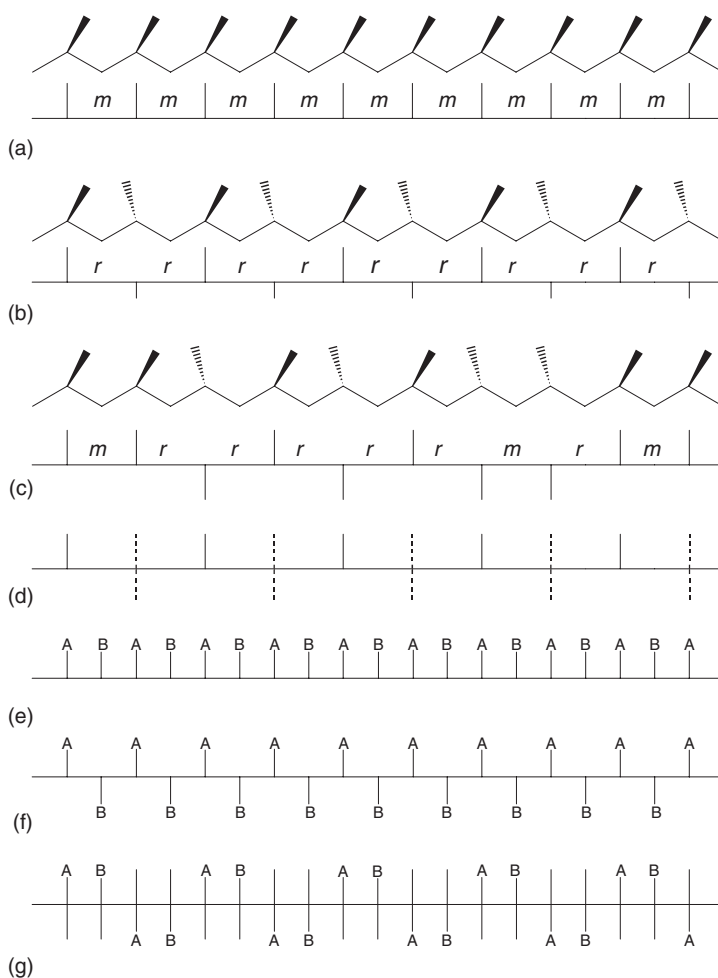
#### 4.09.2.3.2 Definition of stereoregular polymers

The structure of perfectly regular isotactic and syndiotactic PP (iPP and sPP) is shown in Figure 8. Isotactic PP is characterized by a sequence of tertiary C atoms with the same local spatial arrangement (a single configuration) in the polymer chain. Syndiotactic PP is characterized by a sequence of tertiary C atoms with alternate configuration in the polymer chain. Atactic PP (aPP) has no regularity in the sequence of the configuration of the tertiary C atoms. While the iPP is of major industrial interest, and sPP- and aPP have found some applications, hemiisotactic PP, in which one in every two tertiary C atoms is isotactic while the other is atactic, also shown in Figure 8, is an academic curiosity. If the relative configuration of two successive tertiary C atoms (a diad) is considered, an isotactic polymer can be considered as composed by a sequence of *m* (meso) diads, while a syndiotactic polymer can be considered to be composed by a sequence of *r* (racemic) diads. Finally, in the case of diolefins, stereoselective polymerization can lead to diisotactic and disyndiotactic polymers, whose structure is also reported in Figure 8.<sup>166</sup>

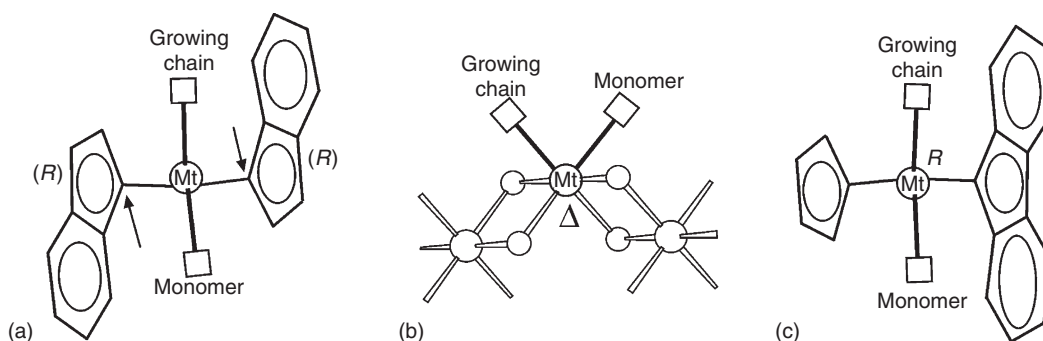
#### 4.09.2.3.3 Elements of chirality

Stereoselective  $\alpha$ -olefin polymerization is the result of a sequence of asymmetric reactions ( $\alpha$ -olefin coordination/insertion). The main elements of chirality are as follows.

- (i) Monomer coordination. Coordination of the two enantiofaces of a prochiral  $\alpha$ -olefin gives rise to chiral *si* and *re*  $\alpha$ -olefin coordinations.<sup>167</sup> Isotactic polymers are generated by multiple insertions of  $\alpha$ -olefin molecules with the same enantioface (either *re* or *si*), while syndiotactic polymers are generated by a regular alternation of insertions of *re*- and *si*-coordinated monomers.
- (ii) Chirality of the active site. Different cases are present here. (a) The chirality can arise from coordination of prochiral ligands. In this case, the notation (*R*) or (*S*), in parenthesis, according to the Cahn–Ingold–Prelog rules as extended by Schögl can be used.<sup>168,169</sup> As an example, the (*R,R*) chirality of coordination of the  $H_2C(1\text{-Ind})_2$  ligand, labeled according to the absolute configurations of the bridgehead carbon atoms marked by arrows, is shown in Figure 9(a). In the case of complexes with two bidentate ligands, the relative orientations of the two bidentate ligands can be chiral and generate chirality at the metal. This chirality can be labeled with the notation  $\Lambda$  or  $\Delta$ , defined for octahedral coordination compounds (Figure 9(b)).<sup>170</sup> (c) An intrinsic chirality at the central metal atom, which for tetrahedral or pseudo-tetrahedral situations can be labeled with the notation *R* or *S* of



**Figure 8** Segments of isotactic (a), syndiotactic (b), atactic (c), and hemiisotactic polypropylene (d) chains. Segments of erythro-diisotactic (e), threo-diisotactic (f), and disyndiotactic (g) poly-diolefin chains. The modified Fischer projection is shown. For parts, (a)–(c) a zigzag representation is also reported.



**Figure 9** Schematic representation of the chirality at the active site in the case (a) of a  $C_2$ -symmetric pseudo-tetrahedral metallocene, (b) of a  $C_2$ -symmetric octahedral model for heterogeneous catalysts, and (c) of a syndiospecific  $C_5$ -symmetric pseudo-tetrahedral metallocene.

Cahn–Ingold–Prelog rules as extended by Stanley and Baird.<sup>168,171</sup> For instance, the diastereoisomer with intrinsic *R* configuration at the central metal atom is shown in Figure 9(c), for the case of a metallocene with a  $\text{H}_2\text{C}(\text{Cp})(9\text{-Flu})$  ligand. It is important to note that chirality of type (c) requires that the two coordination positions available for the growing chain and the monomer are occupied by different ligands. This implies that compounds such as the dichloride pre-catalysts are not chiral.

One or more of these kinds of chirality of the site can be present in the active site. However, for the case of catalytic complexes in which the two ligands are tightly connected through chemical bonds and which are called hereafter as “stereorigid,” only the chirality of kind (c) can change during the polymerization reaction.

- (iii) Chirality of the growing chain. The last tertiary C atom of the growing chain is chiral, and its configuration is determined by the chirality of monomer coordination in the last insertion step. The *R/S* Cahn–Ingold–Prelog nomenclature can be used. However, it is common to label the two configurations as *si*- or *re*-ending growing chains, according to the configuration of the monomer during coordination/insertion.<sup>168,172</sup>

#### 4.09.2.3.4 Mechanism of stereocontrol

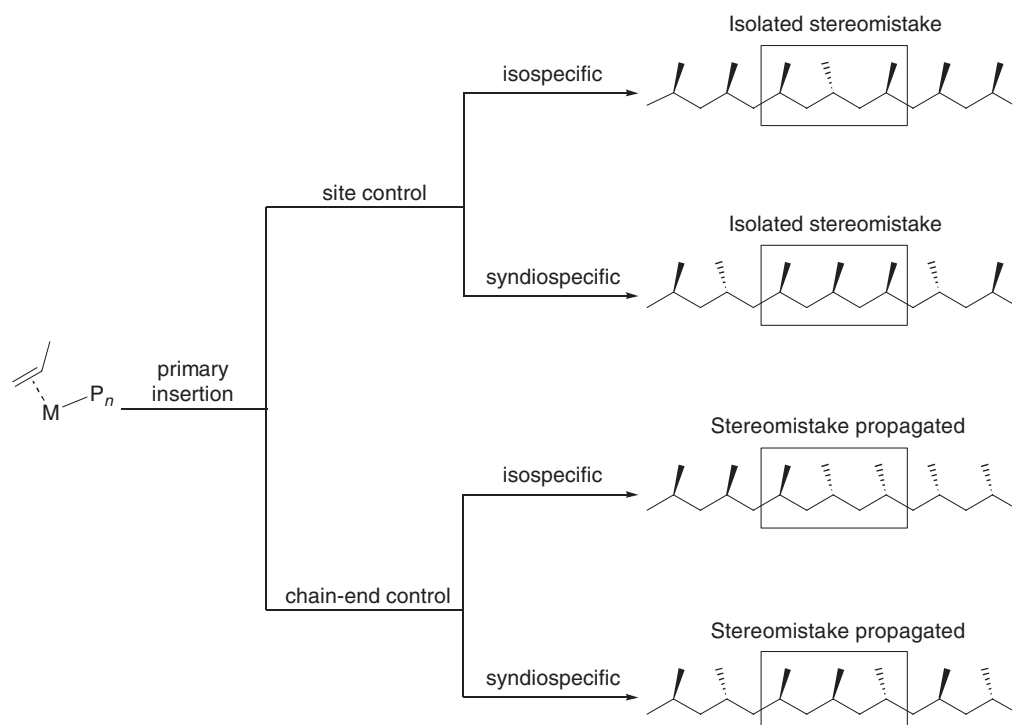
It is well accepted that two mechanisms of stereocontrol (the chiral induction responsible for selecting the monomer enantioface) are operative in stereoselective  $\alpha$ -olefin polymerizations. In the simpler cases, the discrimination between the two faces of the prochiral monomer may be dictated either by the configuration of the asymmetric tertiary C atom of the last inserted monomer unit or by the chirality of the catalytic site. These two different mechanisms of stereocontrol are named chain-end stereocontrol and enantiomorphic-site or site stereocontrol. In the case of chain-end stereocontrol, the selection between the two enantiofaces of the incoming monomer is operated by the chiral environment provided by the last inserted tertiary C atom of the growing chain, whereas in the case of site stereocontrol this selection is operated by the chirality of the catalytic site. The origin of stereocontrol in olefin polymerization has been reviewed extensively.<sup>162,172–178</sup>

The distribution of steric defects along the polymer chain may be indicative of which kind of stereocontrol is operative. The type and amount of stereomistakes (enantioface insertion errors) is measured by solution  $^{13}\text{C}$  NMR spectroscopy, a sensitive technique that is able to “see” the steric environment of a given propylene unit up to undecads (five propylene units on each side of the observed monomeric unit). Routine analysis is usually performed at the pentad level (two propylene units on each side of the observed monomeric unit).<sup>162,179</sup> The microstructures which result from stereomistakes are shown in Scheme 7.

Any catalyst will make some enantioface insertion mistakes (stereoerrors or stereomistakes). In the case of stereomistakes in propylene polymerization, the chemical shift of the methyl groups is highly sensitive to the relative stereochemistry of neighboring monomer units. The degree of tacticity can be given as the pentad, triad, or diad content (% *mmmm*, % *mm*, % *m* for isospecific polymerization, and % *rrrr*, % *rr*, % *r* for syndiospecific polymerization, respectively). In the case of low stereoregularity, the diad excess, % *m-r* (% *r-m*) better represents the degree of iso-(syndio-) tacticity.<sup>180</sup> Isolated insertion errors unambiguously identify the polymerization mechanism. Stereomistakes are easily and quantitatively detected by NMR spectroscopy, and useful relationships for the four stereospecific polymerization mechanisms discussed above are reported in Table 1. Additionally, the relationships  $2[\text{rr}]/[\text{mr}] = 1$  and  $2[\text{mm}]/[\text{mr}] = 1$  identify iso- and syndiospecific site control, respectively, whereas the relationship  $4[\text{mm}][\text{rr}]/[\text{mr}]^2 = 1$  identifies chain-end control. The average stereoregular block lengths are  $2[\text{m}]/[\text{r}] + 1$  and  $2[\text{r}]/[\text{m}] + 1$  for isotactic and syndiotactic polymers, respectively.

It is worth noting that in the case of syndiospecific propagation, the microstructure of the polymer is also affected by other secondary reactions such as the backskip of the growing chain, or backside attack of the olefin. For example, a backskip of the growing chain followed by correct enantioface selection and regular chain migration would originate a microstructure identical to that generated from a stereomistake in the case of chain-end stereocontrol.<sup>104,179,181,182</sup>

The origin of stereocontrol in  $\alpha$ -olefin polymerizations has been clarified in detail, and it was shown to be essentially driven by steric effects.<sup>172,174–176,178</sup> The commonly accepted mechanism was developed by the Corradini school, and it is called the mechanism of the “chiral orientation of the growing chain”. It was proposed at the beginning of the 1980s to explain the stereospecificity of heterogeneous catalysts.<sup>183–188</sup> In the case of primary propagation, the chiral environment provided by the chirality of the complex (in the case of site stereocontrol) or by the chirality of the tertiary C atom of the last inserted monomeric unit (in the case of chain-end stereocontrol) imposes a chiral orientation to the growing chain in order to minimize the steric interaction between the ligand skeleton and the growing chain. It is this chiral orientation of the growing chain that selects between the two enantiofaces of the incoming monomer molecule. The preferred enantioface is the one that minimizes steric



Scheme 7

**Table 1** Relationship between the microstructures which result from the stereomistakes shown in Scheme 7

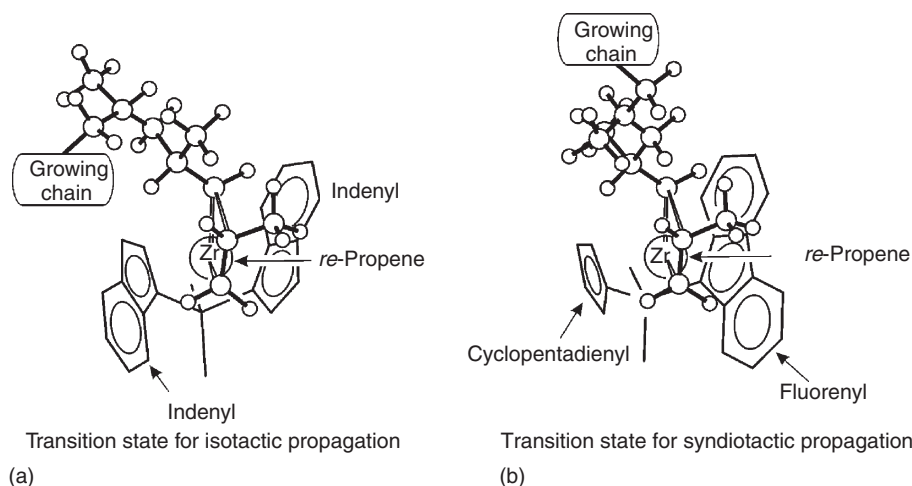
Mechanism	Misinsertions (triads)	Misinsertions (pentads)
Isospecific chiral-site control	$[mr] = 2[rr]$	$[mmmr] = [mmrr] = 2[mrrm]$
Syndiospecific chiral-site control	$[mr] = 2[mm]$	$[rrrm] = [mmrr] = 2[rmrm]$
Isospecific chain-end control	$mr$ only	$[mmmr] = [mmrm]$
Syndiospecific chain-end control	$mr$ only	$[rrrm] = [rmrm]$

interaction with the chirally oriented growing chain. Usually, this is the enantioface that places the methyl group of the propylene *trans* to (i.e., away from) the chirally oriented growing chain (Figure 10).<sup>172,174,175,183,185,187,189–192</sup>

In the case of secondary propagation, the mechanism of the chiral orientation of the growing chain is still operative for stereoflexible compounds. For example, Cavallo and Guerra suggested that for the bis(phenoxy-imine)Ti catalysts, the secondary growing chain assumes a chiral orientation in order to establish an  $\alpha$ -agostic interaction with the metal.<sup>172,193</sup> This chiral orientation imposes a configuration to the stereoflexible complex, and it is the chirality of the complex (imposed by the growing chain) that selects between the two enantiofaces of the secondary inserting propylene. This mechanism was originally proposed for the V-based systems.<sup>194</sup> Finally, in the case of secondary propagation and stereorigid complexes, stereoselectivity is simply determined by steric interactions between the ligand and the monomer molecule. The growing chain plays no role here.

The mechanism of the chiral orientation of the growing chain has strong experimental support. The  $^{13}\text{C}$  NMR analysis of the PP end groups performed by Zambelli and co-workers showed that propylene insertion is essentially non-enantioselective in the first polymerization step (when the alkyl group bonded to the metal is a methyl group), whereas it is enantioselective in successive insertion steps when an isobutyl group is bonded to the metal. This holds good for both heterogeneous<sup>195</sup> and homogeneous<sup>196</sup> Ziegler–Natta catalysts. The same mechanism predicts that *re* insertion of the monomer is favored in case of (*R,R*) chirality of coordination of the  $\text{C}_2\text{H}_4(1\text{-Ind})_2$  ligand. This is in agreement with optical activity measurements by Pino<sup>197,198</sup> on saturated propylene oligomers obtained with this





**Figure 10** Transition states for primary insertion of propylene (a) with the isospecific  $\text{Me}_2\text{Si}(\text{1-Ind})_2\text{Zr}$  system and (b) with the syndiospecific  $\text{Me}_2\text{C}(\text{Cp})(\text{9-Flu})\text{Zr}$  systems.

kind of catalyst, proving that *re* insertion of the monomer is indeed favored in case of (*R,R*) chirality of coordination of the  $\text{C}_2\text{H}_4(\text{1-Ind})_2$  ligand. Moreover, deuteration and deuterio-oligomerization studies of  $\alpha$ -olefins (propylene, 1-pentene, 4-methyl-pentene) using catalysts based on (*R,R*)  $\text{C}_2\text{H}_4(\text{H}_4\text{-1-Ind})_2$  zirconium derivatives showed that the *R* enantioface of the olefin is predominantly involved in dimerizations and oligomerizations whereas the *S* enantioface is favored in the deuterations.<sup>197</sup> These results confirm that the growing chain plays a primary role in enantioface discrimination.<sup>199</sup> Results relative to deuteration and deuterodimerization experiments on isotopically chiral 1-pentene, as well as on propylene insertion with betaine derivatives of classical metallocenes, also agree with a mechanism involving a chiral orientation of the growing chain.<sup>200,201</sup>

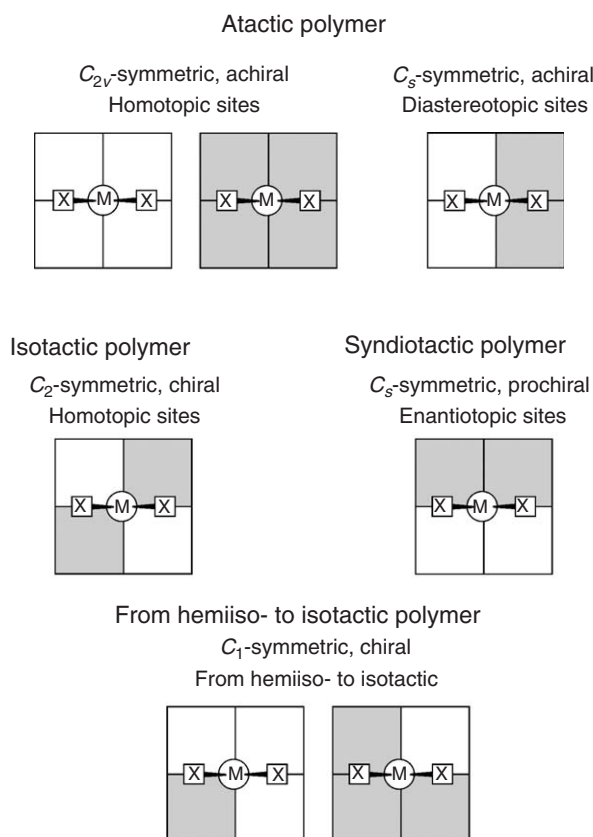
In conclusion, in site-controlled stereoselective polymerizations, it is accepted and proved that the site chirality is unable to select directly between the two enantiofaces of the inserting monomer. Instead, it is accepted and proved that the site chirality can force a chiral orientation of the growing chain, which in turn is able to select between the two enantiofaces of the inserting monomer. Thus, the growing chain acts as a messenger to transfer the chiral information from the catalytic site to the monomer.<sup>172</sup>

#### 4.09.2.3.5 Symmetry rules for stereocontrol

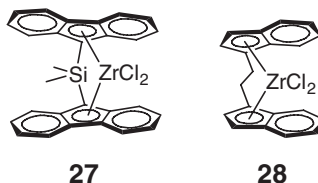
The key to understanding the variety of different tacticities obtained in  $\alpha$ -olefin polymerizations is the chain-migratory mechanism with the site-switching mechanism of Figure 4, and the fact that insertion of the olefin can actually occur on two different active sites. It is the symmetry relationship between the two situations corresponding to an exchange of the positions of the growing chain and of the monomer that determines the tacticity of the resulting poly- $\alpha$ -olefin. Considering the space around the metal center divided in four quadrants, the steric bulkiness of the ligands shapes a chiral pocket that can result in asymmetric insertion. The relationship between metallocene symmetry and polymer stereochemistry has been fully understood. In the quadrants' representation, a gray quadrant means that space in this quadrant is occupied by the ligand, and thus is scarcely accessible to either the monomer or the growing chain. In this representation, it does not matter if the geometry of coordination around the metal atom is tetrahedral or octahedral, since space occupation is relevant. The most typical symmetries and the (possibly expected) microstructures of the resulting poly- $\alpha$ -olefins are shown in Scheme 8. These rules apply to stereorigid catalysts operating under site-control mechanism, and for primary monomer insertion.

Representative examples of aspecific  $C_{2v}$ -symmetric pre-catalysts are  $\text{Me}_2\text{Si}(\text{Cp})_2\text{MCl}_2$  and  $\text{Me}_2\text{Si}(\text{9-Flu})_2\text{MCl}_2$  27. The ligands of these two catalysts have very different space occupation, and in the quadrants' representation can be considered to correspond to systems with all white quadrants or all gray quadrants, respectively. Another example of an aspecific catalyst is based on the  $C_s$ -symmetric *meso*- $\text{C}_2\text{H}_4(\text{1-Ind})_2\text{MCl}_2$  complex 28.<sup>202</sup> In the quadrant representation, this catalyst can be considered a combination of the two  $C_{2v}$ -symmetric catalysts just described, and thus it is characterized by two white quadrants on the side of the Cp rings and by two gray quadrants on the side of the six-membered rings of 28.

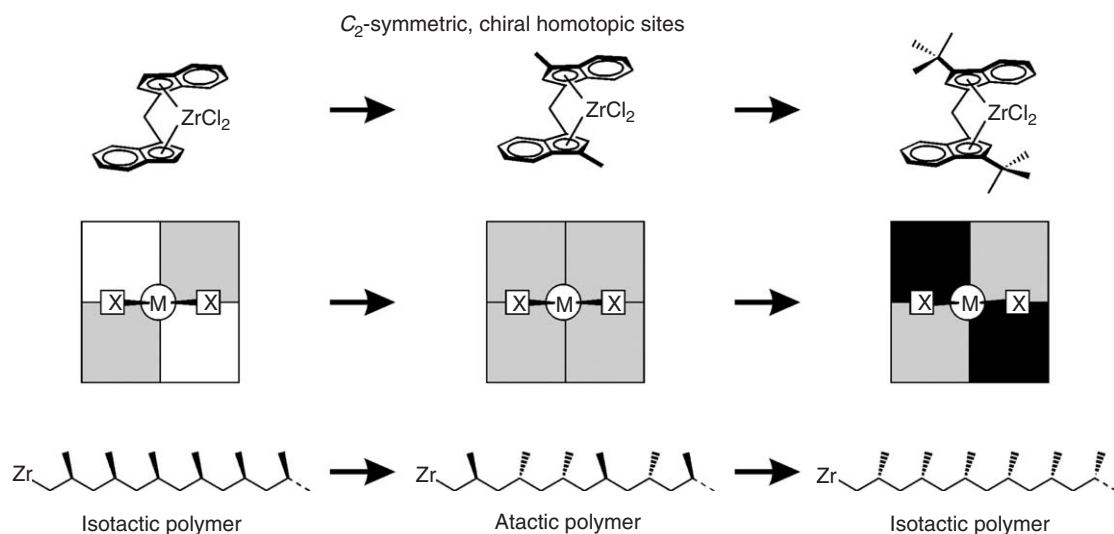




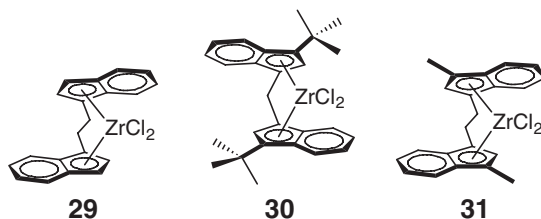
Scheme 8



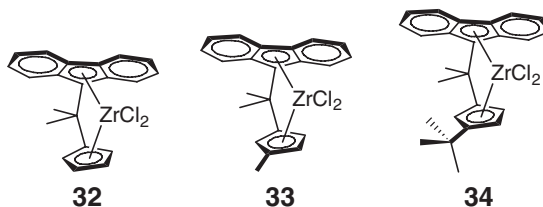
Examples of isospecific  $C_2$ -symmetric catalysts are the pseudo-tetrahedral *rac*- $C_2H_4(1\text{-Ind})_2MCl_2$  complex **29**<sup>6,202,203</sup> and the *rac*- $H_2C(3\text{-Bu}^t\text{-1-Ind})_2MCl_2$  complex **30**.<sup>204</sup> In the quadrants' representation of Scheme 8, sterically encumbered gray quadrants correspond to the six-membered rings in **29**, and to the  $Bu^t$  groups in **30**. Another relevant system is the *rac*- $C_2H_4(3\text{-Me-1-Ind})_2MCl_2$  complex **31**, which is substantially aspecific although it is  $C_2$ -symmetric.<sup>205</sup> The effect of the increase of the bulkiness in different quadrants is best understood comparing the three  $C_2$ -symmetric systems of Scheme 9. While the parent bis(indenyl)-based catalyst is isospecific, the presence of a methyl group in position 3 of the Cp ring substantially counterbalances the bulkiness of the six-membered rings. In the quadrant representation, all quadrants are gray, and the catalyst is substantially aspecific because it is unable to impose a chiral orientation on the growing chain. Further increase of the steric bulkiness by introduction of  $Bu^t$  groups in position 3 of the Cp rings again corresponds to an isospecific catalyst, but the quadrants occupied by the  $Bu^t$  groups are substantially forbidden to the growing chain (black quadrants). Theoretical calculations have in fact indicated that the  $Bu^t$  group is able to induce a stronger steric pressure on the growing chain relative to the flat indenyl group, and that for the same configuration of the complexes, catalysts based on **29** and **30** impose opposite chiral orientations to the growing chain, which results in the insertion of opposite propylene enantiofaces.<sup>206,207</sup>

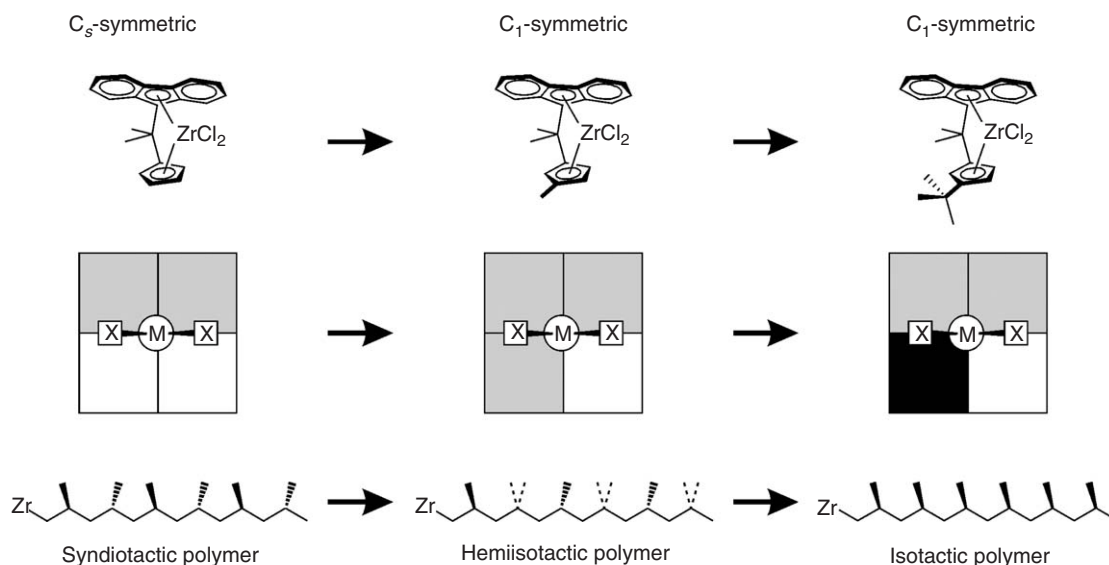


Scheme 9



Returning to Scheme 8, an example of syndiospecific  $C_s$ -symmetric catalysts is the  $\text{Me}_2\text{C}(\text{Cp})(9\text{-Flu})\text{ZrCl}_2$  system **32**,<sup>208</sup> characterized by enantiotopic coordination sites that favor opposite chiral orientations of the growing chain, which results in the insertion of opposite propylene enantiofaces. It is the (almost) regular chain migration between the two coordination sites that rationalizes the syndiospecificity of this kind of catalysts. Finally,  $C_1$ -symmetric catalysts can range from hemiispecific, as for the  $\text{Me}_2\text{C}(3\text{-MeCp})(9\text{-Flu})\text{ZrCl}_2$  system **33**,<sup>209–211</sup> to isospecific as for the  $\text{Me}_2\text{C}(3\text{-Bu}^t\text{-Cp})(9\text{-Flu})\text{ZrCl}_2$  structure, **34**.<sup>212</sup> The effect of the bulkiness of the substituents on the parent  $\text{Me}_2\text{C}(\text{Cp})(9\text{-Flu})\text{ZrCl}_2$  complex is summarized in Scheme 10. Introduction of a single methyl substituent on position 3 of the Cp ring counterbalances the steric effect of the Flu group. In the quadrants' representation, there are three gray quadrants, and when the growing chain is located in the coordination position between the Flu and the Me group, insertion is non-stereoselective because the catalyst is unable to impose a chiral orientation to the growing chain. In the framework of the chain-migratory mechanism, this  $C_1$ -symmetric catalyst is hemiispecific, because there is an (almost) regular alternance between non-selective and stereoselective propylene insertions. Instead, a single  $\text{Bu}^t$  substituent on position 3 of the Cp ring sterically dominates the Flu ligand, and the quadrant occupied by the  $\text{Bu}^t$  group is forbidden to the growing chain. Thus, at each insertion step, the catalyst imposes the same chiral orientation to the growing chain, and the same propylene enantioface is selected. This results in an isotactic polymer. Detailed theoretical calculations have rationalized these effects at molecular level.<sup>175,213,214</sup>





Scheme 10

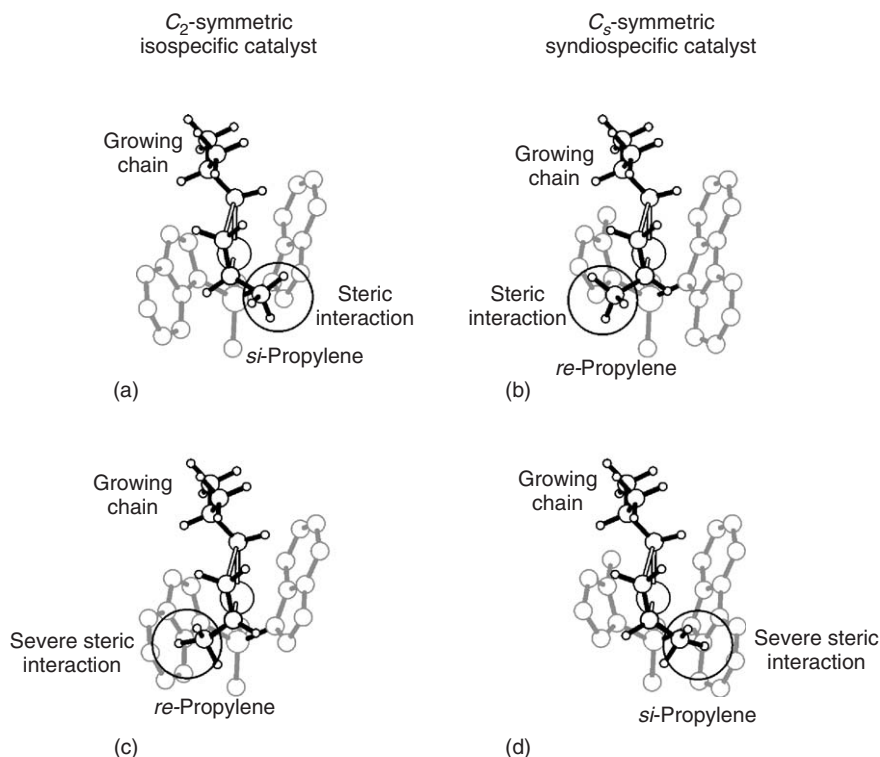
These rules, now referred to as “Ewen’s symmetry rules”, are the result of milestone papers by Brintzinger,<sup>6</sup> Ewen,<sup>181,202,205,208,215,216</sup> Kaminsky,<sup>203</sup> and co-workers. Although they have been developed for primary propylene insertion with pseudo-tetrahedral metallocenes, they can be extended to octahedral catalysts as well. On the other hand, in the case of secondary monomer insertion with unbridged octahedral systems, the tacticity of the polymer produced is the result of a delicate balance between the chiralities of the chain end and of the fluxional active species. This particular case has been discussed in a review.<sup>172</sup>

#### 4.09.2.4 Mechanism of Regiocontrol and Stereochemistry of Regioirregular Insertions

The origin of regiochemistry in propylene polymerization by group 4 catalysts has been investigated in great detail. While the preference for primary insertion in metallocenes is mainly steric in nature,<sup>163,164</sup> for most post-metallocene catalysts it is a subtle interplay of steric and electronic effects.<sup>165</sup> In the case of the prototype-based catalysts **29** and **32**, the most favored transition states leading to secondary propylene insertion are shown in Figures 11(a) and 11(b), respectively. These transition states are disfavored with respect to the corresponding transition states for primary propylene insertion due to some steric interaction between the methyl group of the inserting propylene molecule and the nearby Cp ring of the metallocene ligand. These steric interactions are at the origin of the preference for primary propagation with metallocene-based catalysts. Transition states of Figures 11(c) and 11(d) correspond to secondary insertion of the other propylene enantioface, and are much higher in energy due to strong steric interactions between the methyl group of the inserting propylene molecule and the closer and bulkier (relative to the Cp ring) six-membered ring of the metallocene ligand. This implies that insertion of the secondary propylene is enantioselective, and that for  $C_2$ -symmetric metallocenes opposite enantiofaces are favored for primary and secondary insertion (compare Figures 10(a) and 11(a)), whereas in the case of  $C_S$ -symmetric metallocenes the same propylene enantioface is favored in primary and secondary insertion (compare Figures 10(b) and 11(b)). This fact has been used to develop a kinetic model that links the regioselectivity of a given metallocene to its stereoselectivity, and that rationalizes the higher regioselectivity usually exhibited by syndiospecific  $C_S$ -symmetric metallocenes relative to  $C_2$ -symmetric metallocenes.<sup>164</sup>

#### 4.09.2.5 Chain-release and Isomerization Reactions

The average degree of polymerization  $\bar{P}_n$  of a polyolefin (its molecular mass), produced under steady-state conditions, with a non-living process, is determined by the ratio between propagation rates and chain release rates (Equation (1)).



**Figure 11** Favored transition states for the secondary insertion of propylene with (a) the isospecific  $\text{Me}_2\text{Si}(\text{1-Ind})_2\text{Zr}$  system and with (b) the syndiospecific  $\text{Me}_2\text{C}(\text{Cp})(\text{9-Flu})\text{Zr}$  system. High-energy transition states for the secondary insertion of propylene with (c) the isospecific  $\text{Me}_2\text{Si}(\text{1-Ind})_2\text{Zr}$  system and (d) the syndiospecific  $\text{Me}_2\text{C}(\text{Cp})(\text{9-Flu})\text{Zr}$  system.

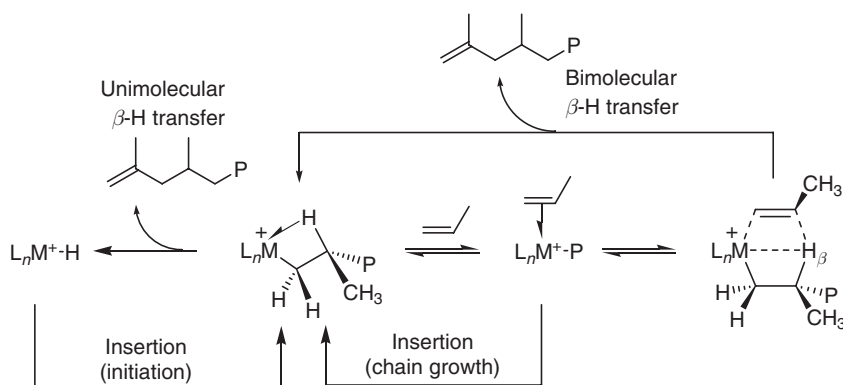
$$\bar{P}_n = \frac{\sum R_p}{\sum R_r} \quad (1)$$

The structure and the mechanisms of formation of end groups have been reviewed.<sup>217</sup> The most important chain-release reactions are  $\beta$ -H transfer after primary or secondary insertion (either to the metal or to a coordinated monomer molecule),  $\beta$ -Me transfer, and chain transfer to the aluminum co-catalyst or scavenger, when present. For a given set of polymerization conditions, the rates of these chain-release reactions are obviously inherent to the steric and electronic nature of the active species. In other words, the molecular mass, as is the case with stereoregularity, strongly depends on the structure of the catalyst. Since propagation and chain-release reaction rates often have different dependencies on temperature and monomer concentration, the molecular mass of polyolefins is also strongly affected by the polymerization conditions. This important point is further discussed in Section 4.09.4.2.2.

In cases in which the catalyst produces too high molecular mass polymers for a given process or application, molecular masses can be controlled more effectively by hydrogenolysis (chain transfer to hydrogen),<sup>218–221</sup> or, in specific cases, by chain transfer to ethylene after a primary insertion.<sup>222,223</sup> It is worth noting that the activity of most propylene polymerization catalysts is increased by both hydrogen and ethylene. Thus, designing catalysts able to produce polyolefins with much higher molecular masses than needed, then requiring hydrogen (or ethylene) for molecular mass control, provides the additional advantage of increasing the catalyst activity.<sup>224</sup>

The chain-transfer and -release reactions occurring with Ti-based heterogeneous Ziegler–Natta catalysts are discussed in Section 4.09.3. In the following, the most important chain-release reactions occurring at metallocene and other single-center group IV catalysts are summarized. Chain transfer to ethylene is also addressed in Sections 4.09.4.1 and 4.09.4.2.

For ethylene polymerization, the picture is fairly simple, including bimolecular  $\beta$ -hydride transfer to a coordinated ethylene monomer<sup>225–227</sup> and transfer to the aluminum co-catalyst.<sup>42,228</sup> Formation of internal unsaturations has been reported,<sup>227,229,230</sup> often connected to the formation of hydrogen (see below). With some catalysts, isomerization and formation of ethyl and longer branches have also been observed, as a consequence of this chain-release reaction. This aspect is described in Section 4.09.4.1.



**Scheme 11** Primary  $\beta$ -H transfer reactions.

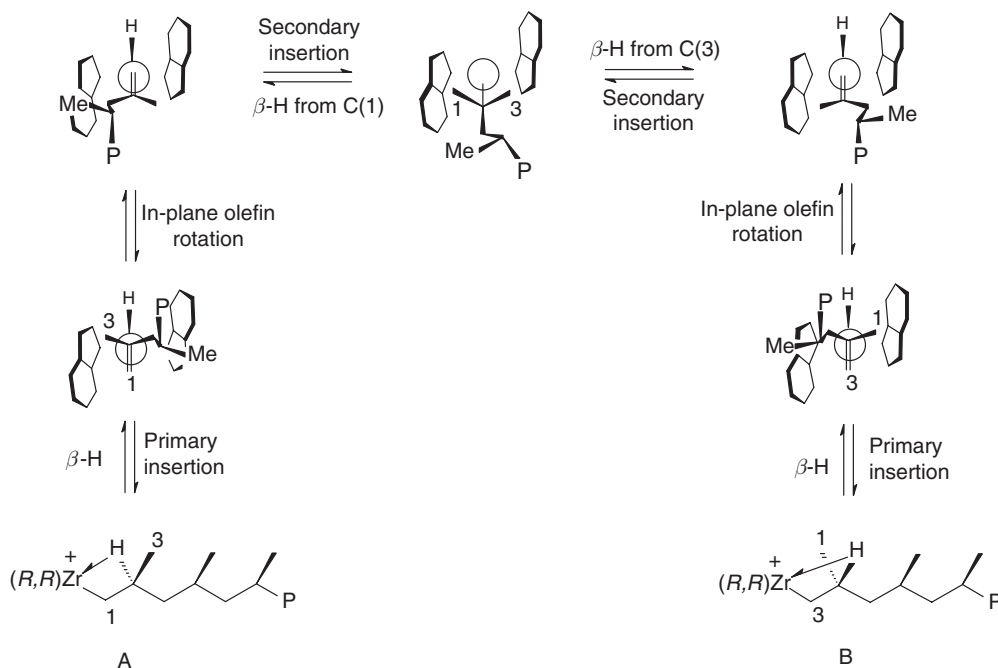
The most ubiquitous chain-release reactions occurring in  $\alpha$ -olefin polymerizations are the unimolecular and bimolecular  $\beta$ -hydride transfers after primary insertion.<sup>217,231–236</sup> These are shown in **Scheme 11**.

Unimolecular  $\beta$ -H transfer to the metal in propylene polymerization is key to understanding growing-chain-end isomerization<sup>237</sup> and formation of internal vinylidenes.<sup>217</sup>

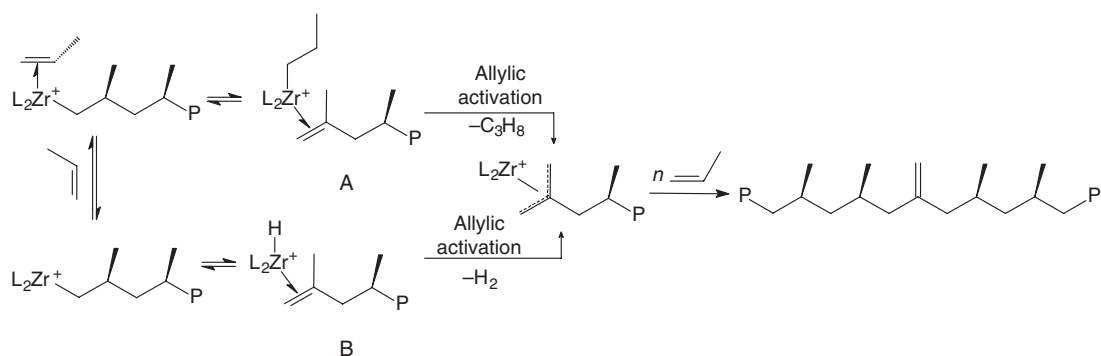
Detailed studies have unambiguously shown that in the case of zirconocenes,<sup>237–246</sup> and other single-center catalysts,<sup>247,248</sup> isotacticity decreases at lower propylene concentrations due to unimolecular primary-growing-chain-end epimerization, which scrambles the chirality of the last chirotopic methine of the growing chain.

The now-accepted mechanism of epimerization, first proposed by Busico and Cipullo,<sup>238</sup> and recently confirmed by Yoder and Bercaw by means of an elegant double-labeling study,<sup>237</sup> involves the reaction product of  $\beta$ -H transfer to the metal, a metal cation–polymeryl olefin complex, and is shown in **Scheme 12**. Allylic activation on the same metal cation–olefin complex has been proposed to generate internal double bonds in PE<sup>229</sup> and vinylidene unsaturations in PP (**Scheme 13**).<sup>249</sup>

An important phenomenon occurs in ethylene–propylene co-polymerization, especially in liquid propylene polymerization: addition of small amounts (< 30 mol%) of ethylene causes a strong decrease in PP molecular masses. This



**Scheme 12** Epimerization via unimolecular  $\beta$ -hydride transfer–double bond in-plane rotation–reinsertion.



**Scheme 13** Formation of internal vinylidene unsaturations. A: via bimolecular  $\beta$ -H transfer; B: via unimolecular  $\beta$ -H transfer.

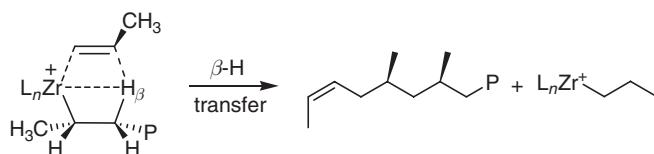
has been observed with isospecific and aspecific metallocenes,<sup>222,223,250–253</sup> and has limited the development of industrial metallocene catalysts for isotactic polypropylene (iPP).

In order to avoid this limitation, new (and more complex) bis-indenyl ligands have been developed, and are described in Section 4.09.4.2.5.

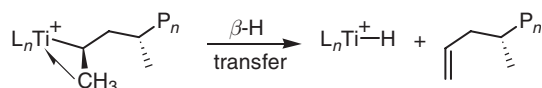
When the catalyst is not fully regioselective, chain release by a  $\beta$ -H transfer after a secondary insertion with formation of internal double bonds is often observed. This has been reported for ethylene/ $\alpha$ -olefin co-polymers,<sup>229,254</sup> PP,<sup>255</sup> and other polyolefins,<sup>232</sup> as well as for 1-hexene polymerization with dialkoxide catalysts.<sup>256</sup> The reaction is shown in Scheme 14 for the case of propylene, where kinetic studies have shown it to be a bimolecular process, following the rate law  $^sR_{\beta-H} = ^s k_{\beta-H} [^sZr][m]$ .<sup>217,257</sup> [ $^sZr$ ] refers to the concentration of active Zr centers bearing a growing chain having a secondary propylene unit linked to the metal.

Differently, in the case of secondary chain growth with bis(phenoxy-imine)titanium catalysts, Coates and co-workers reported that chain release occurs exclusively by  $\beta$ -H hydride transfer from the terminal methyl. This generates an allylic end group as shown in Scheme 15,<sup>160</sup> and it has been utilized to produce functionalized syndiotactic propylene oligomers.<sup>258</sup>

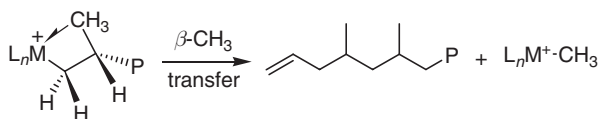
Chain release by  $\beta$ -CH<sub>3</sub> transfer to the metal is unimolecular (Scheme 16)<sup>32,207,259</sup> and obviously limited to the presence of propylene or other 2-methyl-substituted  $\alpha$ -olefins, such as isobutene,<sup>260</sup> and 2-methyl-1,5-hexadiene.<sup>261</sup> No  $\beta$ -alkyl transfer has been reported for higher alkyls, except for  $\beta$ -trimethylsilyl transfer<sup>262</sup> and cases in which a strained ring is formed.<sup>263–265</sup>  $\beta$ -Methyl transfer is an important and sometimes prevalent cause of molecular mass depression in the case of propylene polymerization with sterically hindered metallocenes<sup>262,266,267</sup> or high polymerization temperatures combined with low propylene concentrations.<sup>268</sup> Eisen reported this mechanism to be the



**Scheme 14**  $\beta$ -H transfer to a coordinated propylene monomer after a secondary propylene insertion.



**Scheme 15**  $\beta$ -H transfer to the metal from terminal methyl of a secondary chain.



**Scheme 16**

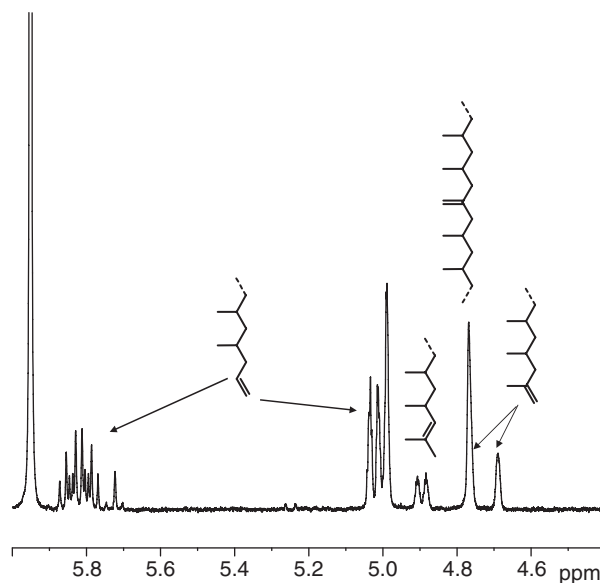
exclusive chain-release reaction with bis(benzamidinate)-based catalysts.<sup>247,248</sup>  $\beta$ -Methyl transfer has been used for the production of allyl-terminated propylene oligomers, which are themselves polymerizable monomers and have been used for the production of long-chain-branched (LCB) polyolefins.<sup>269,270</sup>

Figure 12 shows the most common terminal unsaturations of iPP, generated by chain-release reactions after primary insertion. The internal vinylidene, likely produced by allylic activation, is also shown.<sup>217,246</sup>

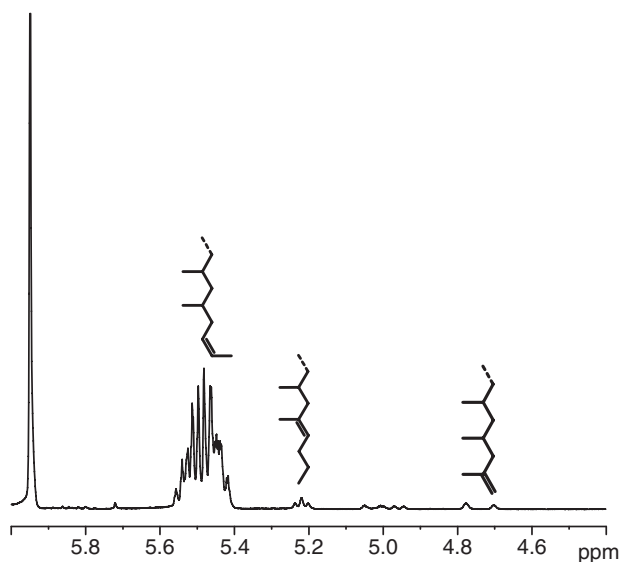
Figure 13 shows the terminal unsaturations of iPP, generated by chain-release reactions after a secondary insertion.<sup>246,257</sup>

In addition to chain transfer to the coordinated monomer, there are three other relevant chain-transfer reactions:

- (i) Chain transfer to the aluminum alkyl species (usually the co-catalyst or the  $\text{AlR}_3$  species used as scavenger of impurities) or other organometallic species, usually zinc alkyls.<sup>271,272</sup> Chain transfer to aluminum usually occurs



**Figure 12** Olefinic region of a  $^1\text{H}$  NMR spectrum ( $120^\circ\text{C}$ , solvent  $\text{C}_2\text{D}_2\text{Cl}_4$  at 5.95 ppm) showing terminal and internal unsaturations in iPP (catalyst  $\text{rac-Me}_2\text{C}(\text{3-Bu}^t\text{Ind})_2\text{ZrCl}_2/\text{MAO}$ ).



**Figure 13** Olefinic region of a  $^1\text{H}$  NMR spectrum ( $120^\circ\text{C}$ , solvent  $\text{C}_2\text{D}_2\text{Cl}_4$  at 5.95 ppm) showing terminal and internal unsaturations in iPP (catalyst  $\text{rac-C}_2\text{H}_4(4,7\text{-Me}_2\text{Ind})_2\text{ZrCl}_2/\text{MAO}$ ).

with the residual  $\text{AlMe}_3$  present in MAO, and has been used to prepare hydroxo-terminated PP.<sup>273,274</sup> Using borate activators in combination with higher Al alkyls such as  $\text{AlEt}_3$  or  $\text{AlBu}^i_3$  effectively reduces chain transfer to Al (Scheme 17).

Transfer to Al was reported to be operative with several non-metallocene catalysts. It is the only chain-release mechanism operative with the diamido complexes  $\text{MCl}_2\{\text{ArN}(\text{CH}_2)_n\text{NAr}\}$  catalysts, as well as with the mono- and tris(benzamidinate) catalysts, since no olefinic resonances were observed in the  $^1\text{H}$  or  $^{13}\text{C}$  NMR spectra of these polymers.<sup>275,276</sup> This chain-release reaction is also dominant with bis(phenoxy-imine)zirconium catalysts,<sup>277</sup> as well as with tris(pyrazolyl)borate-based catalysts.<sup>278,279</sup>

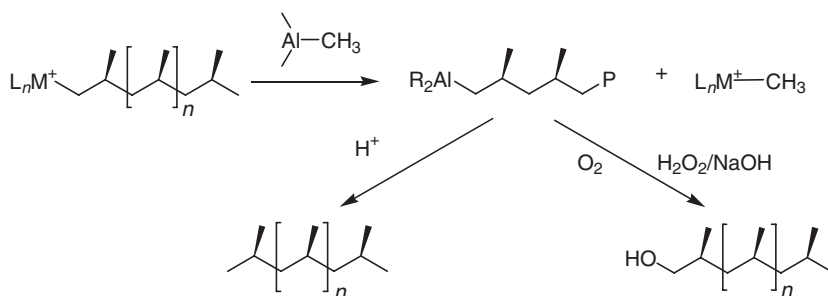
- (ii) Chain transfer to hydrogen is the most widely used means of molecular mass control, in both classic Ziegler-Natta catalysis<sup>224,280,281</sup> and metallocenes.<sup>218–221,282</sup> Although molecular masses can be reduced by either reducing monomer concentration (in propylene and higher olefin polymerizations) or increasing polymerization temperature, these two experimental parameters can be varied only within a narrow range in a given polymerization process. Hence, a good hydrogen response is a must for an industrial polymerization catalyst.
- (iii) Chain transfer to organosilanes, introduced by Marks for lanthanides, corresponds to the silanolytic M-chain reaction shown in Scheme 18. This chain-transfer process efficiently produces silyl end-capped PEs as well as ethylene/1-hexene and ethylene/styrene co-polymers.<sup>283,284</sup>

#### 4.09.2.6 Kinetics

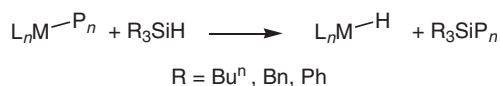
The kinetics of olefin polymerization are the subject of several studies,<sup>104,153–156,162,182,221,226,240,241,246,252,255,266,285–312</sup> and of an excellent book by Keii.<sup>17</sup> The most relevant studies will be discussed below. However, we first note that the precise description of the kinetics of catalytic olefin polymerization under industrially relevant polymerization conditions has proved to be very difficult. For a given catalytic system, one has to identify all possible insertion, chain-release, and chain-isomerization reactions, and their dependence on the polymerization parameters (most importantly, temperature and monomer concentration). Once the kinetic laws for each elementary step have been determined, they have to be combined in one model in order to be able to predict the catalyst performance. This has been attempted for both ethylene<sup>226,285</sup> and propylene polymerizations. The case of propylene polymerization with a chiral, isospecific zirconocene is shown in Figure 14.<sup>162</sup>

Both polymerization temperature and monomer concentration usually have a strong influence on catalyst activity and polyolefin molecular mass. With respect to monomer concentration, the rate of monomer insertion must obey the simple first-order law

$$R_p = k_p[\text{C}][\text{m}] \quad (2)$$

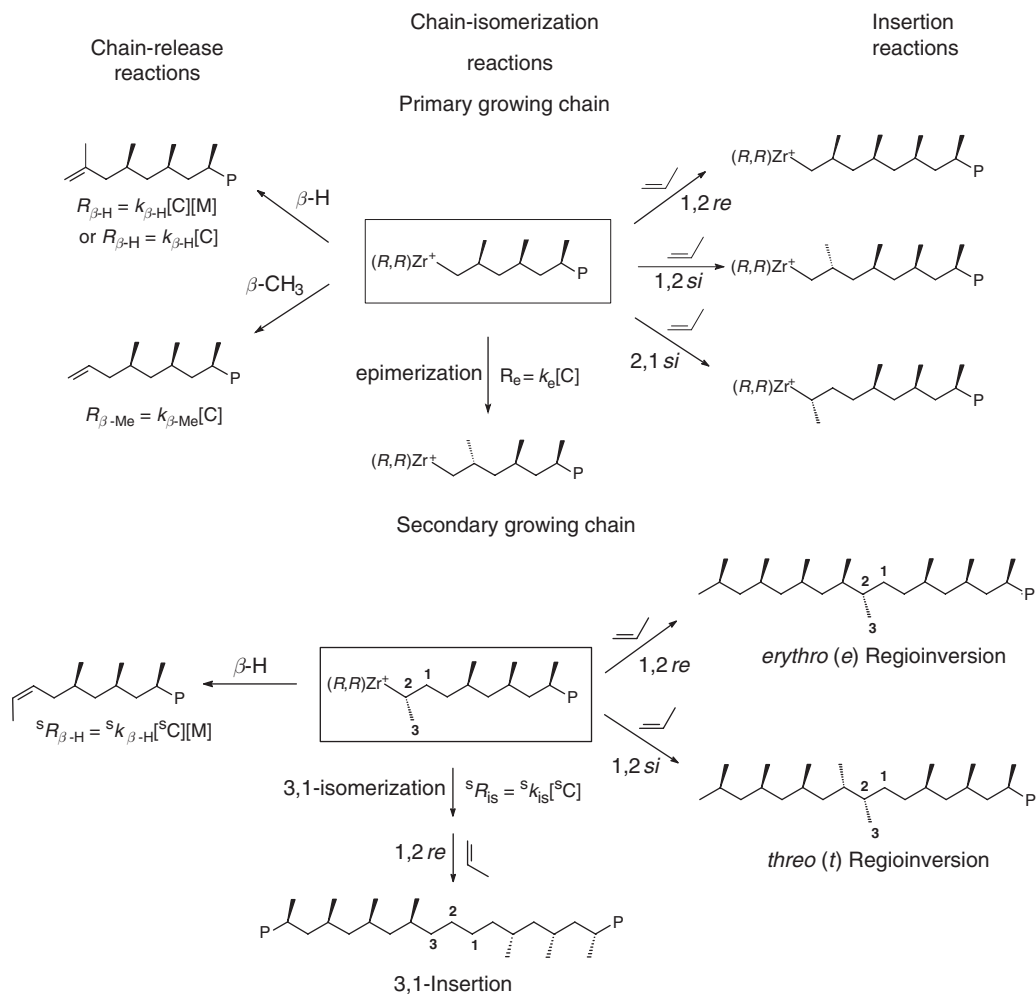


**Scheme 17** Chain transfer to aluminum (the case of methylated aluminum species, such as  $\text{Al}(\text{CH}_3)_3$ , is shown).



**Scheme 18**





**Figure 14** The most relevant elementary steps observed at the (*R,R*)-enantiomer of a chiral,  $C_2$ -symmetric, isospecific zirconium center with a primary growing chain end (top) and a secondary growing chain end (bottom). The (*S,S*)-enantiomer produces the opposite stereochemistry of each single event, but overall the same polymer chains and the same insertion mistakes. In practice, in the case of  $C_2$ -symmetric metallocenes, the racemic mixture (*R,R* + *S,S*) is always used. P = growing polypropylene chain; [C] = concentration of active primary centers; [ $^R$ C] = concentration of active secondary centers.

Here,  $[C]$  is the concentration of active catalyst and  $[m]$  is the concentration of the monomer. In practice, polymer production rates have instead been found to deviate substantially from first-order behavior, and follow the non-linear dependence on monomer concentration

$$R_p = k_p' [m]^n \quad (3)$$

for both ethylene<sup>286</sup> and propylene,<sup>241,246,255,288</sup> with  $1 < n < 2$ . This behavior has been rationalized by the coexistence of two different active species differing in monomer insertion rates.<sup>289</sup> In this model, the two species are in equilibrium with each other and the position of the equilibrium is determined by the concentration of the monomer, with each active species obeying the rate law of Equation (2). This results in the law expressed by Equation (4).

$$R_p = \frac{k_1[C][m] + k_2[C][m]^2}{k_3 + k_4[m]} \quad (4)$$

Propagation rates of first order in monomer concentration have been reported for ethylene<sup>226,287</sup> and for propylene in the case of aspecific metallocenes<sup>266</sup> as well as for propylene polymerization with isospecific metallocenes activated with MAO,  $B(C_6F_5)_3$ , and  $[Ph_3C][B(C_6F_5)_4]$ .<sup>290,297</sup> Moreover, first-order kinetics were also observed for 1-hexene polymerization with the  $[rac-C_2H_4(1-Ind)_2ZrMe][MeB(C_6F_5)_3]$ .<sup>156</sup>

Higher orders affect the laws determining the degree of polymerization as a function of propylene concentration. The dependence of molecular mass on propylene concentration is given by

$$\bar{P}_n = \frac{a[m] + b[m]^2}{c + d[m]} \quad (5)$$

If the propagation rate is first order in propylene concentration, then Equation (5) reduces to Equation (6), which can be linearized (Equation (7)).<sup>266</sup>

$$\bar{P}_n = \frac{k_p[m]}{k_{t0} + k_{t1}[m]} \quad (6)$$

$$\frac{1}{\bar{P}_n} = \frac{k_{t1}}{k_p} + \frac{k_{t0}}{k_p[m]} \quad (7)$$

Models able to rationalize and predict catalyst performances for propylene polymerization with  $C_1$ - and  $C_s$ -symmetric metallocenes such as  $Me_2C(Cp)(1-Ind)ZrMe_2$  and  $Me_2C(Cp)(9-Flu)ZrCl_2$  have been proposed.<sup>291,292</sup> A kinetic model has been proposed based on microstructural analysis, including both chain-epimerization and site-epimerization reactions in both  $C_2$ - and  $C_s$ -symmetric metallocenes, and rationalizing the observed pseudo-second-order kinetics of propylene polymerization promoted by  $C_2$ -symmetric metallocene catalysts.<sup>182,293</sup> This point has been extended to co-polymers.<sup>298</sup> A thorough study of propylene polymerization with the  $Me_2C(Cp)(9-Flu)ZrCl_2$  system in the presence of a large series of different counterions that rationalized the correlation between the nature of ion pair and the microstructure of the resulting PPs has been performed.<sup>104</sup>

As regards a comparison between initiation (i.e., insertion of the monomer into the M-CH<sub>3</sub> bond) and propagation (i.e., insertion of 1-hexene into the M-chain bond), in the case of 1-hexene polymerization with the  $[rac-C_2H_4(1-Ind)_2ZrMe][MeB(C_6F_5)_3]$  catalyst, initiation is about 70 times slower than propagation.<sup>156</sup> An even more pronounced effect was found in the polymerization of propylene with the  $rac-Me_2Si(1-Ind)_2$  zirconocene; in the presence of MAO, initiation is about 800 times slower than propagation, and this value increases to 6000 when polymerizing in the presence of the  $[B(C_6F_5)_4]^-$  counterion.<sup>290</sup>

The amount of metal centers actually active during polymerization has been investigated using quenched-flow kinetic techniques. The concentration of active sites in MAO-activated systems is significantly lower (about 10%) than the analytical concentration of the metal, and a large fraction of metal species are in a “dormant” state.<sup>290,297</sup> In the case of propylene polymerization, it was suggested that the resting state after secondary propylene insertion was a major contributor to the dormant-state concentration, since insertion of a new propylene molecule into the M-(secondary alkyl) is greatly slowed by steric effects.<sup>240,290,294,295,299–301</sup> However, any other situation that slows chain propagation may contribute to the “dormant” state. These conclusions have been extended also to  $[Ph_3C][B(C_6F_5)_4]$ -activated systems, and the higher activity exhibited by borate-activated systems relative to the MAO-activated systems has been ascribed to the weaker coordination ability of borate relative to MAO, rather than to the differences in the active site concentrations.<sup>290</sup> Finally, the mole fraction of active species is about 80% when the  $[Ph_3C][B(C_6F_5)_4]$ -activated bis(phenoxy-amine)Zr catalyst is considered.<sup>296</sup>

Using deuterium-labeling experiments, about 100% of the metal was shown to be active in 1-hexene polymerizations with the  $[rac-C_2H_4(1-Ind)_2ZrMe][MeB(C_6F_5)_3]$  catalyst,<sup>922</sup> and the reactivity of M-(secondary alkyl) bonds at  $-80^\circ C$  was comparable to that of primary alkyl metallocenes.<sup>302</sup> These relative monomer insertion rates appear strongly ligand specific. However, when these comparisons are made, it must be borne in mind that different authors use very different catalysts, as well as different definitions of the term “active center”: Landis defined the active species as the product of the first monomer insertion, whereas Bochmann<sup>290</sup> and Busico<sup>297</sup> used the term to describe the proportion of total [Zr] actively engaged in chain growth based on kinetic measurements. Similarly important is the fact that very different activities and polymerization mechanisms are operative with the weakly coordinating

MAO and  $[\text{B}(\text{C}_6\text{F}_5)_4]^-$  counterions on one hand,<sup>290,297</sup> and the tightly bound  $[\text{MeB}(\text{C}_6\text{F}_5)_3]^-$  counterion on the other.<sup>101,156,302</sup>

### 4.09.3 Ziegler–Natta Polymerizations with Heterogeneous Catalysts

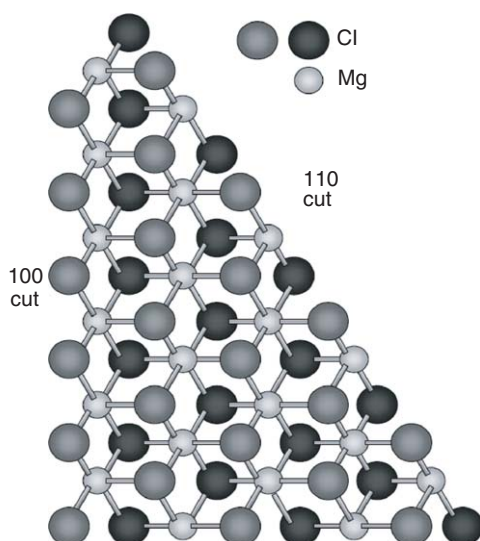
#### 4.09.3.1 Catalyst Structure and Characterization

As indicated above, Ziegler–Natta catalysts occupy a dominant position in polyolefins' manufacture, and have evolved from first- and second-generation titanium trichloride catalysts, developed up until the 1970s<sup>313–315</sup> and described in COMC (1982),<sup>316</sup> to the high-activity  $\text{MgCl}_2$ -supported catalysts used in modern industrial processes.<sup>317</sup> PP catalysts, often termed third-, fourth-, and fifth-generation, according to the catalyst performance and catalyst composition, comprise magnesium chloride as support material, a titanium component (usually  $\text{TiCl}_4$ ), and an electron donor (Lewis base). The basis for the development of the high-activity supported catalysts lay in the discovery, in the late 1960s, of “activated”  $\text{MgCl}_2$  able to support  $\text{TiCl}_4$  and give high catalyst activity, and the subsequent discovery, in the mid-1970s, of electron donors (Lewis bases) capable of increasing the stereospecificity of the catalyst so that (highly) isotactic PP could be obtained.<sup>318–321</sup> A further feature which contributed greatly to the commercial success of  $\text{MgCl}_2$ -supported catalysts was the development of spherical catalysts with controlled particle size and porosity.<sup>317</sup>

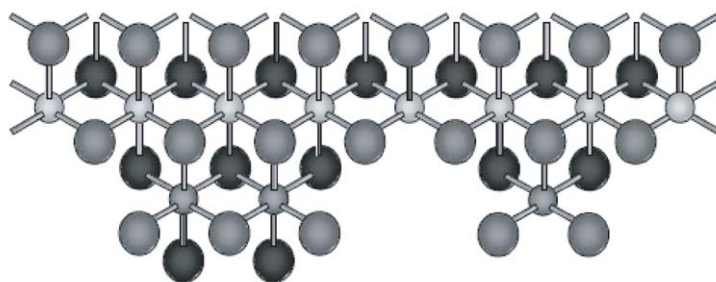
High-activity Ziegler–Natta catalysts comprising  $\text{MgCl}_2$ ,  $\text{TiCl}_4$ , and an “internal” electron donor are typically used in combination with an aluminum alkyl co-catalyst such as  $\text{AlEt}_3$  and an “external” electron donor added in polymerization. The third-generation catalyst systems contained ethyl benzoate as internal donor and a second aromatic ester as external donor, whereas the now widely used fourth-generation catalysts contain a diester (e.g., diisobutyl phthalate) as internal donor and are used in combination with an alkoxysilane external donor of type  $\text{RR}^1\text{Si}(\text{OMe})_2$  or  $\text{RSi}(\text{OMe})_3$ . The most effective alkoxysilane donors for high stereospecificity are methoxysilanes containing relatively bulky groups  $\alpha$  to the silicon atom.<sup>322–325</sup> In the early stages of  $\text{MgCl}_2$ -supported catalyst development, activated magnesium chloride was prepared by ball milling in the presence of ethyl benzoate, leading to the formation of very small ( $\leq 3$  nm thick) primary crystallites within each particle.<sup>315</sup> High resolution transmission electron microscopy has shown that the  $\text{MgCl}_2$  crystal structure is severely distorted by ball milling, changing the structure from crystalline to amorphous.<sup>326</sup> Nowadays, the activated support is prepared by chemical means, such as via complex formation of  $\text{MgCl}_2$  and an alcohol, or by reaction of a magnesium alkyl or alkoxide with a chlorinating agent or  $\text{TiCl}_4$ . A chemical rather than a physical route to catalyst preparation can also lead to a more uniform titanium distribution.<sup>327</sup> Many of these approaches are also effective for the preparation of catalysts having controlled particle size and morphology. For example, the cooling of emulsions of molten  $\text{MgCl}_2 \cdot n\text{EtOH}$  in paraffin oil gives almost perfectly spherical supports, which are then converted into the catalysts.<sup>317</sup> Characterization of a number of adducts of magnesium chloride and ethanol has been described by Bart and Roovers<sup>328</sup>, while Sozzani *et al.*<sup>329</sup> have recently reported the use of advanced solid-state NMR techniques to determine the various components present in  $\text{MgCl}_2 \cdot n\text{EtOH}$  adducts. It was found that  $n$  values of 1.5 and 2.8 represented stable and well-defined complexes.

A typical catalyst preparation involves reaction of the  $\text{MgCl}_2 \cdot n\text{EtOH}$  support with excess  $\text{TiCl}_4$  in the presence of an “internal” electron donor. Temperatures of at least  $80^\circ\text{C}$  and at least two  $\text{TiCl}_4$  treatment steps are normally used, in order to obtain high-performance catalysts in which the titanium is mainly present as  $\text{TiCl}_4$  rather than the  $\text{TiCl}_3\text{OEt}$  generated in the initial reaction with the support.

The function of the internal donor in  $\text{MgCl}_2$ -supported catalysts is twofold. One function is to stabilize small primary crystallites of magnesium chloride; the other is to control the amount and distribution of  $\text{TiCl}_4$  in the final catalyst, affecting stereoselectivity. Activated magnesium chloride has a disordered structure comprising very small lamellae. X-ray diffraction studies have revealed rotational disorder in the stacking of the  $\text{Cl-Mg-Cl}$  triple layers.<sup>330,331</sup> Small  $\text{MgCl}_2$  crystallite size and large rotational disorder appear to give high catalyst activity.<sup>332</sup> Giannini<sup>319</sup> has indicated that, on preferential lateral cleavage surfaces, the magnesium atoms are coordinated with four or five chlorine atoms, as opposed to six chlorine atoms in the bulk of the crystal. These lateral cuts correspond to the (110) and (100) faces of  $\text{MgCl}_2$ , as shown in Figure 15. It has been proposed that bridged, binuclear  $\text{Ti}_2\text{Cl}_8$  species can coordinate to the (100) face of  $\text{MgCl}_2$  and give rise to the formation of chiral, isospecific active species (Figure 16), it being pointed out that  $\text{Ti}_2\text{Cl}_6$  species formed by reduction on contact with  $\text{AlEt}_3$  would resemble analogous species in  $\text{TiCl}_3$  catalysts.<sup>333,334</sup> An extended X-ray absorption fine structure (EXAFS) investigation of a  $\text{MgCl}_2/\text{TiCl}_4$  catalyst has indicated the presence of dimeric  $\text{TiCl}_4$  complexes on the (100) face of  $\text{MgCl}_2$ .<sup>335</sup> It has been



**Figure 15** Model of a  $\text{MgCl}_2$  layer showing the (100) and (110) lateral cuts.



**Figure 16** Model showing dimeric and monomeric Ti species on a (100) lateral cut of  $\text{MgCl}_2$ .

suggested<sup>317</sup> that a possible function of the internal donor is preferential coordination on the more acidic (110) face of  $\text{MgCl}_2$ , such that this face is prevailingly occupied by donor and the (100) face is prevailingly occupied by  $\text{Ti}_2\text{Cl}_8$  dimers. However, as outlined in [Section 4.09.3.3.3](#), this is by no means the only likely mode of coordination of Ti species to the support.

Analytical studies have indicated that a monoester internal donor such as ethyl benzoate is coordinated to  $\text{MgCl}_2$  and not to  $\text{TiCl}_4$ .<sup>336</sup> In the search for donors giving catalysts with improved performance, it was considered<sup>337</sup> that bidentate donors should be able to form strong chelating complexes with tetracoordinate Mg atoms on the (110) face of  $\text{MgCl}_2$ , or binuclear complexes with two pentacoordinate Mg atoms on the (100) face. This led to the development of the  $\text{MgCl}_2/\text{TiCl}_4$ /phthalate ester catalysts, used, as indicated above, in combination with an alkoxy silane as external donor. The requirement for an external donor when using catalysts containing a benzoate or phthalate ester is due to the fact that, when the catalyst is brought into contact with the co-catalyst, a large proportion of the internal donor is lost as a result of alkylation and/or complexation reactions, which in the absence of an external donor would lead to poor stereospecificity. When the external donor is present, contact of the catalyst components leads to replacement of the internal donor by the external donor. The most active and stereospecific systems were found to be those which allowed the highest incorporation of external donor,<sup>338</sup> the effectiveness of a catalyst system depending more on the combination of donors rather than on the individual internal or external donor.

Recently, research on  $\text{MgCl}_2$ -supported catalysts has led to systems not requiring the use of an external donor. This required the identification of bidentate internal donors which not only had the right oxygen–oxygen distance for effective coordination with  $\text{MgCl}_2$  but which, unlike phthalate esters, were not removed from the support on contact with  $\text{AlEt}_3$ , and which were unreactive with  $\text{TiCl}_4$  during catalyst preparation. It was found<sup>337,339–341</sup> that certain

2,2-disubstituted-1,3-dimethoxypropanes met all these criteria. The best performance was obtained when bulky substituents in the 2-position resulted in the diether having a most probable conformation<sup>342</sup> with an oxygen–oxygen distance in the range 2.8–3.2 Å. The successive “generations” of high-activity  $\text{MgCl}_2$ -supported catalyst systems for PP are summarized below:

- (i)  $\text{MgCl}_2/\text{TiCl}_4$ /ethyl benzoate– $\text{AlR}_3$ –aromatic ester,
- (ii)  $\text{MgCl}_2/\text{TiCl}_4$ /phthalate ester– $\text{AlR}_3$ –alkoxysilane, and
- (iii)  $\text{MgCl}_2/\text{TiCl}_4$ /diether– $\text{AlR}_3$ .

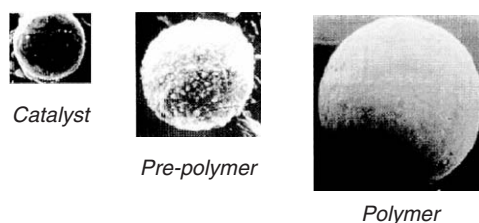
Catalyst performance has improved considerably with each generation. The PP yield obtained under typical polymerization conditions (liquid monomer, in the presence of hydrogen, 70 °C, 1–2 h) has increased from 15–30  $\text{kg g}^{-1}$  catalyst for the third-generation ethyl benzoate-containing catalysts to 30–80  $\text{kg g}^{-1}$  catalyst for the fourth-generation phthalate-based catalysts. With the recently developed fifth-generation catalysts, containing a diether as internal donor, yields of 80–160  $\text{kg g}^{-1}$  catalyst can be achieved. These different catalysts also display different kinetic profiles in propylene polymerization. The catalysts containing a diether as internal donor exhibit very stable activities during polymerization. A low rate of catalyst decay during polymerization is also obtained with the catalyst system  $\text{MgCl}_2/\text{TiCl}_4$ /phthalate ester– $\text{AlR}_3$ –alkoxysilane, whereas the system  $\text{MgCl}_2/\text{TiCl}_4$ /ethyl benzoate– $\text{AlR}_3$ –aromatic ester has a very high initial polymerization activity but also a high decay rate, limiting the final polymer yield. The rapid decay in activity can at least partially be ascribed to the use of an ester as external as well as internal donor, the ester being able to react with titanium–hydrogen bonds formed in chain transfer with hydrogen, generating Ti–O bonds inactive for chain propagation.<sup>343</sup>

Most recently, a further family of  $\text{MgCl}_2$ -supported catalysts has been developed,<sup>344,345</sup> in which the internal donor is a succinate rather than a phthalate ester. As is the case with the phthalate-based catalysts, an alkoxysilane is used as external donor. The essential difference between these catalysts is that the succinate-based systems produce PP having much broader molecular mass distribution, discussed in Section 4.09.3.4.

#### 4.09.3.2 Polymer Particle Growth

An important feature of olefin polymerization using heterogeneous catalysts concerns the characteristics of particle growth during the course of polymerization, taking into account such aspects as mass and heat transfer. Ineffective monomer mass transfer can limit the catalyst productivity, while ineffective removal of heat of polymerization from the growing particle in the early stages of polymerization can cause the formation of hot spots, which may in turn lead to catalyst decay. In the absence of pre-polymerization, exotherms of up to 20 °C have been measured for individual catalyst particles in the early stages of polymerization.<sup>346</sup>

Typically, heterogeneous Ziegler–Natta catalysts have particle sizes in the range 10–100  $\mu\text{m}$ . Each particle comprises millions of primary crystallites with sizes of up to about 15 nm. On contacting the catalyst components, at the start of polymerization, co-catalyst and monomer diffuse through the catalyst particle, and polymerization takes place on the surface of each primary crystallite within the particle. As solid, crystalline polymer is formed, the primary crystallites are pushed outward and apart as the particle grows, analogous to the expanding universe. The particle shape is retained, and this phenomenon is therefore referred to as replication (Figure 17). Ideally, the catalyst particle should have spherical morphology and controllable porosity. It is important that the mechanical strength of the catalyst is high enough to prevent disintegration, but low enough to allow progressive expansion as polymerization proceeds.<sup>347</sup>



**Figure 17** “Replication” phenomenon in polymerization.

Under appropriate polymerization conditions, polymer particles can be obtained with an internal morphology that can range from a compact to a porous structure.<sup>348</sup> In what is termed reactor granule technology, porous polymer particles can be produced which can then function as a microreactor for the polymerization of other monomers within the solid matrix. A PP skin encloses the second polymer phase, thereby preventing coalescence of particles in which the second phase is an amorphous, low-melting material. Reactor granule technology is able to provide products ranging from superstiff, high-fluidity PP homopolymers to stiff/impact or clear/impact heterophasic co-polymers and supersoft alloys, produced using the Catalloy process.<sup>345,347,348</sup> The feasibility of producing heterophasic alloys containing up to 70% of elastomeric co-polymers arises from the use of a controlled porosity catalyst and the ability to control the porosity of the growing polymer particle during the early stages of polymerization. Pre-polymerization is applied to give the particles sufficient heat capacity to withstand injection into a gas-phase polymerization step.

Various models describing particle growth during olefin polymerization have been developed and recently reviewed by McKenna and Soares.<sup>349</sup> One of the most popular models is the “multigrain model”, put forward by Ray and co-workers,<sup>350</sup> in which the monomer diffuses into the catalyst macroparticle and polymerizes on the surface of the microparticles within, causing progressive expansion of the macroparticle as polymerization proceeds. An investigation by Kakugo *et al.*<sup>351</sup> of nascent polymer morphology obtained using a  $\text{TiCl}_3$  catalyst showed that the polymer particle comprised numerous globules, each of which contained some tens of much smaller primary particles. Recently, a model for particle growth with  $\text{MgCl}_2$ -supported catalysts has been proposed by Cecchin,<sup>345,352</sup> who has also provided evidence for polymer “subglobule” formation within the growing particle. Again, these subglobules originate from clusters of primary crystallites, but the crystallites themselves are pushed to the surface of each subglobule as the polymer forms. This model explains the fact that, in the preparation of heterophasic co-polymers via propylene homopolymerization followed by ethylene–propylene co-polymerization, the rubbery E–P co-polymer is formed at the surface of the homopolymer subglobules, gradually filling up the pores within the particle. Evidence for drifting of catalyst microparticles to the surface of polymer (sub)globules has been provided by scanning electron microscopy studies of pre-polymerized catalyst particles.<sup>353</sup>

Extensive fragmentation and uniform particle growth are key features in the replication process and are dependent on a high surface area, a homogeneous distribution of catalytically active centers throughout the particle, and free access of the monomer to the innermost zones of the particle. In the case of ethylene polymerization, the latter is not always the case, and it is frequently observed that polymer growth starts at and near the particle surface, leading to the formation of a shell of PE around the catalyst particle. This imposes a diffusion limitation, preventing free access of the monomer to active sites within the particle. Polymerization then takes place layer by layer, as the monomer gradually diffuses through the outer layers to the core, resulting in an onion-type internal morphology.<sup>354</sup> This mechanism of particle growth is associated with a kinetic profile in which an initial induction period is followed by an acceleration period, after which, in the absence of chemical deactivation, a stationary rate is obtained. Each polymerizing particle can be considered as a microreactor with its own mass and heat balance.<sup>355</sup> Ethylene polymerization activity can be greatly increased by first carrying out pre-polymerization with propylene, which results in a significant lowering in the monomer diffusion barrier in the subsequent ethylene polymerization.<sup>356</sup> In a further refinement of particle growth models, effects of not only diffusion but also monomer convection have been taken into account, the convection being driven by a pressure gradient created by monomer consumption within the particle.<sup>357</sup> Serious mass-transfer limitations are less common in propylene polymerization. Studies with  $\text{MgCl}_2$ -supported Ziegler–Natta catalysts have revealed uniform polymer particle growth in the early stages of polymerization, the catalyst support undergoing even and progressive fragmentation.<sup>358</sup>

### 4.09.3.3 Mechanistic Studies of Ziegler–Natta Catalysts

#### 4.09.3.3.1 Oxidation state

It is generally accepted<sup>315</sup> that in the  $\text{TiCl}_3/\text{AlEt}_2\text{Cl}$  system, the active species are  $\text{Ti(III)}$ . In the case of  $\text{MgCl}_2$ -supported catalysts, in which the titanium is generally tetravalent prior to contact with the co-catalyst, the dominant active species in polymerization also appears to be  $\text{Ti(III)}$ , although active  $\text{Ti(IV)}$  and  $\text{Ti(II)}$  species may also be present. Most reports indicate that both  $\text{Ti(III)}$  and  $\text{Ti(II)}$  species are active for ethylene polymerization, whereas  $\text{Ti(II)}$  has little or no activity in propylene polymerization.<sup>359</sup> The immobilization of a titanium chloride on a magnesium chloride support lowers the susceptibility to (over)reduction on contact with an Al alkyl,<sup>360</sup> but Kashiwa<sup>361</sup> found that treatment of an  $\text{MgCl}_2/\text{TiCl}_4$ /ethyl benzoate catalyst with excess  $\text{AlEt}_3$  for 2 h at 60 °C resulted in reduction to 80%  $\text{Ti(II)}$  and 20%  $\text{Ti(III)}$ . The catalyst was moderately active for ethylene polymerization but not for propylene, although co-polymerization was possible. After reoxidation, the catalyst was active for



propylene polymerization and showed increased activity in ethylene polymerization. With a similar catalyst but at milder reaction conditions and in the presence of an external donor (methyl *p*-toluate), Chien<sup>362</sup> observed that 85% of the initial  $\text{Ti}^{4+}$  was reduced to  $\text{Ti}^{3+}$  and 15% to  $\text{Ti}^{2+}$ , while in subsequent studies  $\text{Ti}^{4+}$  (35%),  $\text{Ti}^{3+}$  (25%), and  $\text{Ti}^{2+}$  (40%) could be detected.<sup>363</sup> Brief (2 min) treatment of a similar catalyst with  $\text{AlBu}^i_3$ , with or without ethyl benzoate as external donor, resulted in almost exclusively  $\text{Ti}^{3+}$ , about 30% of which could be detected by ESR and the remainder only after contact with pyridine.<sup>364</sup> A combination of ESR and titration techniques was used by Chien to estimate the Ti oxidation states in a catalyst containing a phthalate as internal donor.<sup>365</sup> Contact of the catalyst with  $\text{AlEt}_3$ /phenyltriethoxysilane resulted in oxidation states  $\text{Ti}^{4+}$ :  $\text{Ti}^{3+}$ :  $\text{Ti}^{2+}$  in the proportions 28.1:38.5:33.4, whereas in the absence of phenyltriethoxysilane the proportions were 7.0:73.7:19.3.

X-ray photoelectron spectroscopy (XPS) has also been used to investigate the nature of the species formed on contacting  $\text{MgCl}_2$ -supported catalysts with Al-alkyls. Terano and co-workers<sup>366</sup> observed that the binding energy of  $\text{MgCl}_2$ -supported  $\text{TiCl}_4$  was unaffected by the presence of an internal donor, indicating no direct interaction of the donor with the titanium, but contact with  $\text{AlR}_3$  resulted in a shift to lower binding energy, indicative of reduction of  $\text{Ti}^{4+}$ .

#### 4.09.3.3.2 Number of active centers

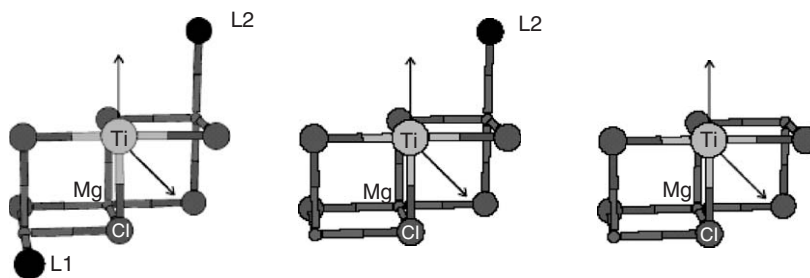
Various methods, generally based on kinetic and radiotagging methods, have been developed for the determination of the number of active centers in Ziegler–Natta catalysts.<sup>367</sup> Labeling methods determine the proportion of total metal that carries a polymeryl chain, whereas kinetic methods can be used to measure the proportion of M–polymeryl chains actively engaged in chain growth. Hence, very different values must be expected, arising from different definitions. For  $\text{MgCl}_2$ -supported catalysts, active center ( $\text{C}^*$ ) values of around 4% (of total Ti present) have been obtained from stopped-flow experiments.<sup>368</sup>  $\text{C}^*$  values obtained by other techniques, notably  $^{14}\text{CO}$  quenching of propylene polymerization, have ranged from 1% or less<sup>369</sup> to more than 20%.<sup>370</sup> Clearly, there are large differences in  $\text{C}^*$  values obtained by different groups, but it is consistently found that the major proportion of the Ti present in Ziegler–Natta catalysts is inactive. The propagation rate constant ( $k_p$ ) values for isospecific active sites are around an order of magnitude greater than those for weakly specific sites.<sup>369,370</sup> The value of  $k_p$  increases significantly in the presence of hydrogen,<sup>371</sup> in accordance with the reactivation of “dormant” (2,1-inserted) centers by chain transfer (*vide infra*).

#### 4.09.3.3.3 Internal/external donor effects and the nature of the active species

The characteristics of Ziegler–Natta catalysts for polypropylene are, to a large extent, dependent on the types of donors present, both in the solid catalyst and added as external donor in polymerization. It is well established that effective external donors not only increase the isotactic index of PP (the proportion of polymer insoluble in boiling heptane or in xylene at 25 °C), but can also increase in absolute terms the amount of isotactic polymer formed. This has been demonstrated by Kashiwa<sup>372</sup> for the catalyst system  $\text{MgCl}_2/\text{TiCl}_4\text{--AlEt}_3$ . An increase in the molecular mass and stereoregularity of the isotactic fraction was also noted. Similar trends are apparent with catalyst systems of type  $\text{MgCl}_2/\text{TiCl}_4$ /phthalate ester– $\text{AlR}_3$ –alkoxysilane.<sup>373</sup> Kakugo<sup>374</sup> has used elution fractionation to demonstrate that the external donor not only decreases “atactics” formation but also increases the degree of steric control at isospecific sites. Soga has reported that an almost aspecific  $\text{MgCl}_2/\text{TiCl}_3$  catalyst, with a very low content of (probably isolated, monomeric) Ti species, could be rendered isospecific by the addition of ethyl benzoate as external donor<sup>375</sup> or by using  $\text{Cp}_2\text{TiMe}_2$  as co-catalyst.<sup>376</sup> It was suggested<sup>377</sup> that in both cases, aspecific sites having two coordination vacancies could be converted to isospecific sites by blocking one of the two vacancies.

A powerful technique to study the effects of electron donors on site selectivity in Ziegler–Natta catalysts is the determination of the stereoregularity of the first insertion step in propylene polymerization. Sacchi *et al.*<sup>378,379</sup> have investigated the effect of Lewis bases on the first-step stereoregularity resulting from propylene insertion into a Ti–Et bond formed via chain transfer with  $^{13}\text{C}$ -enriched  $\text{AlEt}_3$ . First-step stereoregularity is particularly sensitive to the steric environment of the active center, due to the fact that the stereospecificity of the first monomer insertion is always lower than that of the following propagation steps. For example, with an  $\text{MgCl}_2/\text{TiCl}_4$ /diisobutyl phthalate catalyst, it was found<sup>379</sup> that the mole fraction of *erythro*- (isotactic) placement in the isotactic polymer fraction was 0.67 with no external donor, 0.82 with  $\text{MeSi}(\text{OEt})_3$ , and 0.92 with  $\text{PhSi}(\text{OEt})_3$ . It could be concluded that the alkoxysilane external donor was present in the environment of at least part of the isospecific centers. Subsequent studies<sup>380,381</sup> indicated that similar considerations apply to diether donors.

Recently, significant advances have been made in understanding the fundamental factors determining the performance of state-of-the-art  $\text{MgCl}_2$ -supported catalysts. Studies by Busico *et al.*<sup>382</sup> have shown that the chain irregularities in iPP prepared using heterogeneous catalysts are not randomly distributed along the chain but are



**Figure 18** Model of possible active species for highly isotactic, isotactoid, and syndiotactic propagation. Reproduced with permission from *Macromolecules* **2003**, 26, 2616–2622. © 2003, American Chemical Society.

clustered. The chain can therefore contain, in addition to highly isotactic blocks, sequences which can be attributed to weakly isotactic (isotactoid) and to syndiotactic blocks. This implies that the active site can isomerize very rapidly (during the growth time of a single polymer chain, i.e., in less than a second) between three different propagating species. The same sequences are present, but in different amounts, in both the soluble and the insoluble fractions. The polymer can therefore be considered to have a stereoblock structure in which highly isotactic sequences alternate with defective isotactic (isotactoid) and with syndiotactoid sequences. A mechanistic model has been formulated in which the relative contributions of these sequences can be related to site transformations involving the presence or absence of steric hindrance in the vicinity of the active species. The  $^{13}\text{C}$  NMR studies have indicated<sup>383</sup> the presence of  $C_1$ -symmetric active species in  $\text{MgCl}_2$ -supported catalysts, with a mechanism of isotactic propagation which is analogous to that for certain  $C_1$ -symmetric metallocenes, in the sense that propylene insertion at a highly enantioselective site tends to be followed by chain “backskip” rather than a less regio- and stereoselective insertion when the chain is in the coordination position previously occupied by the monomer. The probability of chain “backskip” will increase with decreasing monomer concentration, and it has indeed been confirmed that increased polymer isotacticity is obtained at low monomer concentration. It is proposed<sup>382</sup> that a (temporary) loss of steric hindrance from one side of an active species with local  $C_2$ -symmetry, giving a  $C_1$ -symmetric species, may result in a transition from highly isospecific to moderately isospecific propagation. Loss of steric hindrance on both sides can lead to syndiospecific propagation in which chain-end control becomes operative. The model is illustrated in Figure 18.

If it is considered that the steric hindrance in the vicinity of the active species can result from the presence of a donor molecule, and that the coordination of such a donor is reversible, the above model provides us with an explanation for the fact that strongly coordinating, stereorigid donors typically give stereoregular polymers in which the highly isotactic sequences predominate.<sup>384</sup> It has been suggested<sup>385</sup> that the high stereospecificity obtained using silanes having one or more bulky hydrocarbyl groups is due to the silane stabilizing “fluctuating” isospecific sites, the bulky hydrocarbyl groups protecting the silane from removal from the catalyst surface via complexation with aluminum alkyl.

Several types of active species in which the presence of a donor in the vicinity of the active Ti atom is necessary for high isospecificity have been proposed,<sup>386</sup> although the exact structure of the active species is still by no means resolved. In particular, it is still uncertain whether the active Ti is located on the (100) face of  $\text{MgCl}_2$ , as originally proposed,<sup>333,334</sup> or on the (110) face. There is strong evidence that the dominant coordination mode of diether donors to  $\text{MgCl}_2$  is via bidentate coordination on the (110) face.<sup>387,388</sup> It has also been shown<sup>389</sup> that the use of a diether as external donor in combination with a  $\text{MgCl}_2/\text{TiCl}_4$ /phthalate ester catalyst gives active species which are very similar to those present when the diether is used as internal donor. This could imply that the dominant coordination mode of phthalate esters is also bidentate coordination on the (110) face of  $\text{MgCl}_2$ . Bearing in mind the evidence for the presence of a donor in the environment of at least part of the isospecific active centers, it thus seems likely that active Ti is also located on the (110) face of  $\text{MgCl}_2$ , or on an edge position adjacent to the (110) face.<sup>386</sup> In contrast to the diether-based catalysts, molecular modeling studies have indicated the succinate ester complexes with both the (110) and the (100) faces of  $\text{MgCl}_2$ , via three or four different modes of interaction.<sup>390</sup> This is likely to be a contributory factor to the formation of a broad range of active species in the succinate-based system.

Isospecific active species not requiring the presence of a donor for high stereospecificity have been proposed by Boero,<sup>391</sup> while Terano<sup>392</sup> has suggested various active species in which coordination of  $\text{AlEt}_3$  or  $\text{AlEt}_2\text{Cl}$  in the vicinity of the titanium atom can lead to high stereospecificity. Pre-contact of a  $\text{MgCl}_2/\text{TiCl}_4$  catalyst with  $\text{AlEt}_3$  prior

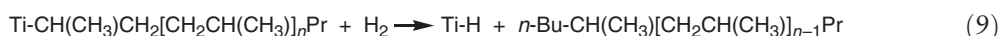
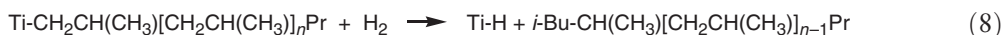


to polymerizations carried out under stopped-flow conditions led to the formation of a small proportion of highly isotactic material in the resulting polymer. Subsequent studies with a catalyst containing ethyl benzoate as internal donor showed<sup>393</sup> that the highly isotactic polymer fraction increased when the catalyst was briefly pre-contacted with  $\text{AlEt}_3$ , but extended pre-contact led to a loss of isospecificity due to extraction of the internal donor. Solid-state  $^{27}\text{Al}$  NMR spectroscopy has been used to study the surface aluminum compounds formed during the treatment of a  $\text{MgCl}_2/\text{TiCl}_4$  catalyst with aluminum alkyls; it was proposed that the proportion of Ti in active state was dependent on adsorption/desorption of Al species. Strong adsorption of  $\text{AlEt}_2\text{Cl}$ , blocking active centers, was put forward to explain the low catalytic activity obtained using  $\text{AlEt}_2\text{Cl}$  as co-catalyst.<sup>394</sup> It has also been suggested<sup>384</sup> that the catalyst system  $\text{MgCl}_2/\text{TiCl}_4$ /ethyl benzoate– $\text{AlEt}_3$ –aromatic ester contains species for which high selectivity is not dependent on the presence of an electron donor in the immediate vicinity of the active site, taking into account that it is unlikely that monoester donors can provide the stable coordination shown by highly stereoregulating diether and silane donors.

#### 4.09.3.3.4 Effects of hydrogen

In PP production, hydrogen is used as a chain-transfer agent for polymer molecular mass (melt flow rate) control. Recent work by Terano and co-workers<sup>395</sup> has shown that, under stopped-flow conditions, hydrogen is only effective as chain-transfer agent when catalyst and co-catalyst have been pre-contacted. These and subsequent<sup>396,397</sup> results indicated that effective chain transfer with hydrogen requires the presence of species able to promote the dissociation of  $\text{H}_2$  to atomic hydrogen.

The effect of hydrogen (concentration) on polymer molecular mass is dependent on the catalyst system. An advantage of catalysts containing a diether donor, in addition to very high activity, is high sensitivity to hydrogen, so that relatively little hydrogen is required for molecular mass control. This effect can be ascribed to chain transfer after the occasional secondary (2,1) rather than the usual primary (1,2) insertion, a 2,1-insertion slowing down a subsequent monomer insertion and therefore increasing the probability of chain transfer.<sup>398</sup> Reactivation of “dormant” (2,1-inserted) species via chain transfer with hydrogen also explains the frequently observed activating effect of hydrogen in propylene polymerization, giving yields which may be around 3 times those observed in the complete absence of hydrogen.<sup>399</sup> These conclusions have been based on the  $^{13}\text{C}$  NMR determination of the relative proportions of *i*-Bu- and *n*-Bu-terminated chains, resulting from chain transfer with hydrogen after primary and secondary insertion, respectively Equations (8) and (9).



The probability of the 2,1-insertion is much higher for the first insertion of propylene into a Ti–H bond. When followed by a series of 1,2-insertions, this results in the formation of a 2,3-dimethylbutyl terminal unit, as opposed to *n*-propyl when the first insertion is primary. Significant proportions of 2,3-dimethylbutyl end groups have been found in polymers prepared using both metallocene<sup>219,400</sup> and Ziegler–Natta catalysts.<sup>401</sup> The relatively low propagation rate of 2,1-inserted species also applies to the Ti-isopropyl reaction product of 2,1-insertion into Ti–H, making a further transfer reaction with hydrogen (generating propane) more probable than chain growth to form a 2,3-dimethylbutyl end group.<sup>401</sup> It has been suggested<sup>402</sup> that the hydrogen activation effect is related to the hydrogenolysis of the Ti–isopropyl unit, but this seems unlikely, as in this case hydrogen is involved in both the formation and removal of such dormant species.

The introduction of hydrogen in ethylene polymerization with a Ziegler–Natta catalyst causes a significant decrease in the polymerization rate, in contrast to what is observed in propylene polymerization. Kissin<sup>403–407</sup> has proposed that this can be explained by the formation of “dormant”  $\text{Ti-CH}_2\text{CH}_3$  species formed by insertion of ethylene into Ti–H after chain transfer with hydrogen. The low propagation activity of the Ti–Et species was ascribed to  $\beta$ -agostic stabilization. However, this proposal was not supported by Garoff,<sup>408</sup> who found that increasing the amount of hydrogen present in polymerization tended to slow down the activation of catalysts in which the titanium was present as Ti(IV).

A strong deactivating effect of hydrogen has been noted in ethylene polymerization with vanadium-based catalysts such as  $\text{MgCl}_2/\text{VCl}_4\text{-AlBu}_3$ .<sup>409</sup> This deactivation was reversible, activity being restored when hydrogen was removed. It was proposed that the deactivating effect of hydrogen arose from the reaction of V–H species with the

co-catalyst to give V–R and AlR<sub>2</sub>H, the latter component then blocking the active sites via the formation of V–H–Al bridged complexes. Hydrogen had no effect on the number of active centers but decreased the propagation rate constant, in line with the mechanism proposed.<sup>410</sup> A comparison of vanadium- and titanium-based catalysts for ethylene polymerization has shown that hydrogen is a more effective chain-transfer agent with the vanadium catalysts.<sup>411</sup> A half-order dependency of chain transfer on the hydrogen concentration was found, in line with dissociative adsorption of hydrogen.

For propylene polymerization, it has been demonstrated that the chain transfer is dependent not only on “regio”- but also on “stereo”-selectivity.<sup>412</sup> This is in keeping with the tendency that, with catalyst systems of the type MgCl<sub>2</sub>/TiCl<sub>4</sub>/phthalate ester–AlR<sub>3</sub>–alkoxysilane, the silanes which give the most stereoregular isotactic polymer also give relatively low hydrogen response.

#### 4.09.3.3.5 Effects of temperature

PP production using Ziegler–Natta catalysts is generally carried out at a polymerization temperature of around 70 °C. The effect of temperature on catalyst stereospecificity is dependent on the nature of the catalyst. With TiCl<sub>3</sub> catalysts, PP stereoregularity decreases as the polymerization temperature is increased,<sup>315</sup> but with MgCl<sub>2</sub>-supported catalysts the opposite trend has been found, an increase in polymerization temperature leading not only to higher proportions of isotactic polymer but also to increased stereoregularity of the isotactic fraction.<sup>413,414</sup> This effect was ascribed to a greater increase in productivity, with increasing temperature, for highly isospecific as opposed to weakly isospecific centers.

An increase in polymerization temperature from 70 to 100 °C has been found to lead to significant decreases in both catalyst productivity and polymer molecular mass, chain transfer to Al being particularly rapid at high temperature using AlEt<sub>3</sub> as co-catalyst in combination with a catalyst containing dioctyl phthalate as internal donor and with an alkoxysilane as external donor.<sup>415</sup> Decreased polymer melting point was also obtained, ascribed to the formation and co-polymerization of a small amount of ethylene, produced by the decomposition of AlEt<sub>3</sub>; this could be avoided by the use of AlBu<sup>i</sup><sub>3</sub> as co-catalyst.<sup>416</sup> It has recently been reported that the use of AlBu<sup>i</sup><sub>3</sub> together with a MgCl<sub>2</sub>/TiCl<sub>4</sub>/diether catalyst gives similar polymerization activities at 70 and 100 °C, whereas with AlEt<sub>3</sub> decreased activity was observed at 100 °C.<sup>417</sup>

#### 4.09.3.4 Polyolefins Accessible from Ziegler–Natta Catalysts

Ziegler–Natta catalysts are multi-site systems, which contain a range of different active centers having different relative rates of chain propagation and chain transfer. Each individual site produces a Schulz–Flory distribution with  $\bar{M}_w/\bar{M}_n = 2$  and with  $\bar{M}_z/\bar{M}_n = 1.5$ , and the overall polymer molecular mass distribution represents a combination of these individual distributions and is therefore broader than that which is produced by metallocene and related single-center catalysts. Kissin, via deconvolution of GPC traces, estimated that the overall distribution could be described by considering the presence of five different active centers.<sup>418</sup> In ethylene/1-hexene co-polymerization, the centers giving the highest molecular masses were those giving negligible hexene incorporation. That the relatively broad molecular mass distribution of Ziegler–Natta polyolefins is due to active center distribution and not to monomer diffusion or other effects has been demonstrated by the use of stopped-flow polymerization,<sup>419</sup> which showed that molecular mass distribution (MWD) was unaffected by the polymerization time.

By varying the nature of the electron donors (esters, silanes, diethers) present in Ziegler–Natta catalyst systems for PP, it is possible to control the polymer tacticity, molecular mass, and molecular mass distribution to produce a range of polymers having the processing and end-use properties required for very different applications. The donors present in the catalyst system play an active role in the formation or modification of isospecific sites, and the polymer molecular mass distribution depends on the relative contribution and hydrogen response (i.e., sensitivity to chain transfer with hydrogen) of each type of active site. The incorporation of an external donor into the catalyst system generally leads to an increase in molecular mass, the magnitude of the molecular mass (MW) increase depending on the nature of the donor. The characteristics of different catalyst systems with regard to PP molecular mass distribution are as follows.<sup>345</sup>

<i>Internal donor</i>	<i>External donor</i>	$\bar{M}_w/\bar{M}_n$
Diether		5–5.5
Phthalate	Alkoxysilane	6.5–8
Succinate	Alkoxysilane	10–15

It can be seen that the diether-based catalysts give relatively narrow molecular mass distribution. A narrow molecular mass distribution, and relatively low molecular mass, are advantageous in fiber-spinning applications. In contrast, extrusion of pipes and thick sheets requires high melt strength, and therefore relatively high molecular mass and broad molecular mass distribution. A broad molecular mass distribution, along with high isotactic stereoregularity, is also beneficial for high crystallinity and therefore high rigidity. The new succinate-based catalysts enable very broad molecular mass distribution PP homopolymers to be produced in a single reactor and are also of interest for the production of heterophasic co-polymers having an improved balance of stiffness and impact strength, taking into account that the incorporation of a rubbery (ethylene/propylene, EP) co-polymer phase into a PP homopolymer matrix increases impact strength but at the same time leads to decreased stiffness.

The relatively narrow PP molecular mass distributions obtained using diether-based catalysts can be attributed to the fact that in these systems even the most highly stereospecific active sites are not totally regiospecific. A proportion of approximately one secondary insertion for every 2000 primary insertions at highly isospecific sites has been noted for the system  $\text{MgCl}_2/\text{TiCl}_4/\text{diether-AIR}_3$ .<sup>398</sup> The probability of chain transfer with hydrogen after a secondary insertion is such that this is sufficient to prevent the formation of very high molecular mass chains, taking into account that the highest molecular mass fraction of the polymer is formed on the active species having the highest isospecificity. The broader molecular mass distributions obtained with catalysts containing ester internal donors are likely to be due to the presence of (some) isospecific active sites having very high regiospecificity and therefore lower hydrogen sensitivity.<sup>420</sup> Such results illustrate the profound effect of catalyst regio- and stereospecificity distribution on both molecular mass control and polymer molecular mass distribution and properties.

In addition to their dominant position in PP manufacture, Ziegler–Natta catalysts are widely used in the production of HDPE and LLDPE. More than half the world production of HDPE is based on Ziegler–Natta catalysts, chromium catalysts also being widely used. In LLDPE production, Ziegler–Natta catalysts account for more than 90% of the total production, although single-center catalysts are making strong inroads into this market.

In HDPE production, high-mileage Ziegler–Natta catalysts are used in the cascade process, in which polymerization reactors in series are used to give reactor blends with improved properties for film and pipe applications.<sup>421</sup> Broad molecular mass distribution can be obtained by the use of different hydrogen concentrations in each reactor. In addition, the process can be designed to give a low molecular mass homopolymer in the first reactor and a high molecular mass co-polymer in the second. The high molecular mass co-polymer chains function as tie molecules linking the crystalline, homopolymer domains, thereby leading to high stress crack resistance of the polymer. This process allows an “inverse” co-monomer distribution to be obtained, in the sense that the co-monomer is in the high molecular mass fraction, counteracting the general tendency of Ziegler–Natta catalysts to incorporate the co-monomer mainly in the low molecular mass chains. The latter feature is an important consideration in Ziegler–Natta catalyst design for LLDPE. Co-monomer incorporation is highest at the most open catalytic centers, whereas sterically hindered centers will tend to give PE chains with little or no co-monomer. The best catalysts for LLDPE are therefore those that have relatively uniform active center distribution, lacking excessively hindered or unhindered active sites.

In addition to titanium-based Ziegler–Natta catalysts, vanadium-based systems have also been developed for PE and ethylene-based co-polymers, particularly ethylene–propylene–diene rubbers (EPDM). Homogeneous (soluble) vanadium catalysts produce relatively narrow molecular mass distribution PE, whereas supported V catalysts give broad molecular mass distribution.<sup>422</sup> Polymerization activity is strongly enhanced by the use of a halogenated hydrocarbon as promoter in combination with a vanadium catalyst and aluminum alkyl co-catalyst.<sup>422,423</sup>

In addition to their widespread use in the production of PE and PP, Ziegler–Natta catalysts play an important role in the production of poly-1-butene, for which both  $\text{TiCl}_3$ -based and  $\text{MgCl}_2$ -supported catalysts have been developed.  $\text{TiCl}_3$  catalysts have been used with dialkylaluminum halide co-catalysts,  $\text{AlEt}_2\text{I}$  giving higher isotacticity than  $\text{AlEt}_2\text{Cl}$ .<sup>315</sup> Very high isotacticity has been obtained using  $\text{TiCl}_3$  in combination with  $\text{Cp}_2\text{TiMe}_2$ .<sup>424</sup> Much higher polymerization activity, as well as high isotacticity and broad molecular mass distribution, is obtained using  $\text{MgCl}_2$ -supported catalysts, for example the catalyst system  $\text{MgCl}_2/\text{TiCl}_4/\text{diisobutyl phthalate-AlEt}_3\text{-alkoxysilane}$ .<sup>425</sup>

Ziegler–Natta catalysts have also been developed for the polymerization of 4-methyl-1-pentene<sup>426</sup> and higher  $\alpha$ -olefins. Polymerization activity decreases with increasing steric bulk of the monomer. For example, with the catalyst system  $\text{MgCl}_2/\text{TiCl}_4/\text{ethyl benzoate-AlEt}_3\text{-ethyl benzoate}$ , the relative activities in propylene, 1-butene, and 4-methyl-1-pentene polymerization were 100:80:15.<sup>427</sup> For catalyst systems of type  $\text{MgCl}_2/\text{TiCl}_4/\text{phthalate ester-AIR}_3\text{-alkoxysilane}$ , the type of silane required is dependent on the steric bulk of the monomer. An active center having high stereospecificity in propylene polymerization may be too sterically hindered for effective polymerization of a bulkier monomer, propylene/1-butene co-polymerization studies having shown<sup>428</sup> that the incorporation of 1-butene into the polymer chain decreases with increasing site stereospecificity. This phenomenon is also

illustrated by the fact that non-bulky alkoxysilanes such as  $\text{Me}_3\text{SiOMe}$  are effective donors in 4-methyl-1-pentene polymerization,<sup>429</sup> whereas such donors are relatively ineffective in propylene polymerization.

#### 4.09.3.5 Polymerization of Acyclic Internal Olefins

Acyclic internal olefins such as *cis*- and *trans*-2-butene can be polymerized using Brookhart-type  $\text{Ni(II)}$  and  $\text{Pd(II)}$  complexes<sup>430</sup> but in the absence of isomerization do not homopolymerize using Ziegler–Natta catalysts, although examples of co-polymerizations of ethylene with an internal olefin are known.<sup>313</sup>

The application of Ziegler–Natta catalysts to monomer isomerization polymerization, in which an olefin such as 2-butene is first isomerized to 1-butene and then polymerized, has been described in an extensive series of papers by Endo and Otsu.<sup>431</sup> The non-participation of 2-butene in Ziegler–Natta polymerization (taking precautions to exclude the possibility of carbocationic polymerization)<sup>432</sup> also allowed the selective polymerization of 1-butene from mixtures of butene isomers.<sup>433</sup> It was proposed that isomerization and polymerization took place on  $\text{Ti(II)}$  and  $\text{Ti(III)}$  species, respectively.<sup>434</sup> The relative rates of isomerization and polymerization were dependent on the catalyst system, polymerization being more rapid with  $\text{TiCl}_3/\text{AlEt}_3$  than with  $\text{Ti(Obu)}_4/\text{AlEt}_3$ .

With the system  $\text{TiCl}_3/\text{AlEt}_3$ , the rate of isomerization of *cis*-2-butene to 1-butene can be increased by the incorporation of a late transition metal component such as  $\text{NiCl}_2$ .<sup>435</sup> Isomerization polymerization using 2-butene has also been shown to be useful for the synthesis of co-polymers of 1-butene with  $\alpha$ -carbon-branched 1-alkenes having low polymerization activity.<sup>436</sup> The difference in reactivity between the branched monomer and 1-butene is compensated for by the low concentration of 1-butene formed by isomerization from 2-butene.

#### 4.09.3.6 Major Industrial Processes

The major processes for polyolefins' production using Ziegler–Natta catalysts involve polymerization in the gas phase or in slurry, including bulk liquid monomer in the case of propylene. LLDPE is also produced via a solution process operating at temperatures in the range 130–250 °C.

Gas-phase processes operating in the range 70–115 °C and pressures of 20–30 bar are widely used for the production of LLDPE and HDPE. Fluidized bed reactors, such as those used in the Unipol process,<sup>437</sup> typically comprise a vertical cylindrical reactor containing a fluidized bed of catalyst/polymer particles above a perforated plate (gas distribution plate), the velocity of the circulating gas being sufficient to fluidize the bed but low enough to prevent particle entrainment from the reactor. Cooling is provided by the fluidizing gas stream, which is recycled to the bed by means of a compressor or blower, via one or more heat exchangers. Additional cooling can be provided by operating in the “condensed mode”, which involves the injection via the recycle stream of a condensed monomer and/or a volatile liquid such as isopentane, to give evaporative cooling.

Slurry processes in hydrocarbon diluent are used in the production of HDPE, including bimodal polymers produced in the cascade process in which different hydrogen concentrations are applied in two or more reactors in series. Liquid loop reactors are generally used with a light hydrocarbon diluent such as isobutane, whereas heavier hydrocarbon diluents are typically used in continuous stirred tank reactors.

The development of the Borstar PE process, by Borealis, is a relatively recent development in multi-reactor processes. The foundation of this process is the utilization of supercritical propane as diluent in the slurry loop reactor.<sup>438</sup> Operating the slurry loop in a supercritical condition provides several advantages over the tradition diluent (isobutane). The solubility of PE drops markedly at the supercritical point of propane, allowing the process to operate at higher temperatures and reducing the risk of reactor fouling. Supercritical process conditions have also been developed for propylene polymerization.<sup>439</sup>

In PP manufacture, modern bulk (liquid monomer) and gas-phase processes have largely replaced the earlier slurry processes in which polymerization was carried out in hydrocarbon diluent. The most widely adopted process for PP is Basell's Spheripol process.<sup>317</sup> Homopolymer production involves a pre-polymerization step at relatively low temperature, followed by polymerization in a loop reactor using liquid propylene; random co-polymers are produced by introducing small quantities of ethylene into the feed. The pre-polymerization step gives a pre-polymer particle with the capacity to withstand the reaction peak, which occurs on entering the main loop reactor. The addition of one or two gas-phase reactors for EP co-polymerization makes it possible to produce heterophasic co-polymers containing up to 40% of E/P rubber within the homopolymer matrix.

The development of the Spheripol process was based on the use of  $\text{MgCl}_2$ -supported Ziegler–Natta catalysts having spherical particle morphology. Further catalyst and process development, including the manufacture and use

of catalysts having different degrees of porosity, led to the Catalloy process. This is a highly sophisticated modular technology, based on three mutually independent gas-phase reactors in series. Random PP co-polymers containing up to 15% co-monomer can be obtained, as well as heterophasic alloys containing high proportions of multi-monomer co-polymers. The feasibility of producing reactor-grade polymer blends containing up to 65% rubber phase arises from the use of a controlled porosity catalyst and the ability to control the porosity of the growing polymer particle during the early stages of polymerization. Again, pre-polymerization is applied to give particles with sufficient heat capacity to withstand injection into a gas-phase polymerization step.

The most recent major development in polyolefin process technology has been the introduction of the Spherizone process, based on a gas-phase multi-zone circulating reactor.<sup>440</sup> In this process, the growing polymer granule is continuously circulated between two polymerization zones: upward, by fast fluidization, in the “riser” leg, and downward, by means of gravity in a packed bed, in the “downer” leg. The monomer composition and the hydrogen concentration in the two legs can be different, and the multiple short passes of the growing particle between the two zones leads to intimate and effective mixing of very different polymer compositions.

## 4.09.4 Polymerizations with Metallocene Catalysts

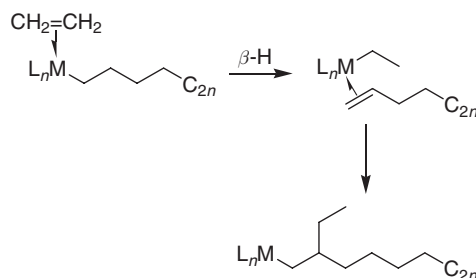
### 4.09.4.1 Ethylene Polymers

#### 4.09.4.1.1 Polyethylene

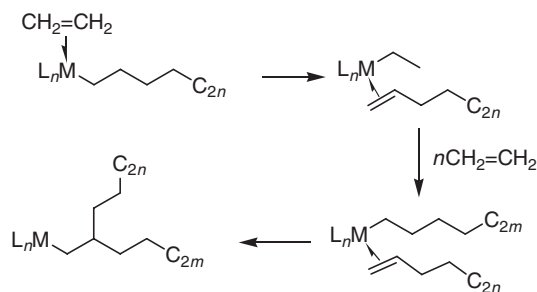
PE homopolymer (HDPE) differs from the two other major polyethylene materials, the highly branched low-density PE (LDPE, produced under supercritical conditions in high pressure reactors by means of radical initiators, and out of the scope of this review) and the LLDPE, (the family of co-polymers of ethylene with 1-butene, 1-hexene, or 1-octene, produced by both heterogeneous Ziegler–Natta and single-center catalysts, which is discussed in [Section 4.09.4.1.2](#)), by being predominantly linear. Contrary to what one might expect, however, HDPE is a rather sophisticated polymer.<sup>355</sup> Most importantly, its molecular mass distribution (width and shape of the distribution) determines the rheological behavior and mechanical properties of PE. Secondly, HDPE is seldom perfectly linear, and the number and length of the few side-branches also affect PE properties and applications. A review on metallocene-catalyzed ethylene polymerization is available.<sup>441</sup> Metallocene catalysts have been recognized early on to be capable of extremely high ethylene polymerization activities, to have excellent co-monomer incorporation ability, and to be prone to generating both long- and short-chain branches. The *ansa*-cyclopentadienyl–amido titanium complexes developed by Dow (dubbed CGCs)<sup>442,443</sup> have dominated the development of metallocene PE and are the most efficient catalysts at generating these LCBs,<sup>444–446</sup> although LCBs have been detected in HDPE from bis(cyclopentadienyl) complexes as well.<sup>446–448</sup> Methyl branches in PE made with  $\text{Me}_2\text{Si}(\text{C}_5\text{Me}_4)(\text{NBu}^t)\text{TiCl}_2$  at high temperature have also been detected.<sup>445</sup>

Formation of ethyl branches has been observed in PE from sterically encumbered complexes such as *meso*- $\text{C}_2\text{H}_4(\text{Ind})_2\text{ZrCl}_2$ ,<sup>449,450</sup> *meso*- $\text{Me}_2\text{C}(\text{Ind})_2\text{ZrCl}_2$ ,<sup>451</sup> and *rac*- $\text{CH}_2(1\text{-R-2-Ind})_2\text{ZrCl}_2$  complexes.<sup>452</sup> These branches are formed via chain transfer to ethylene followed by reinsertion of the coordinated “polymerene” chain, as shown in [Scheme 19](#).<sup>449</sup> Very likely, the bulkiness of the ligands slows release of the double-bond-terminated PE chain, increasing the chance of its reinsertion in the formed  $\text{M}-\text{C}_2\text{H}_5$  bond.

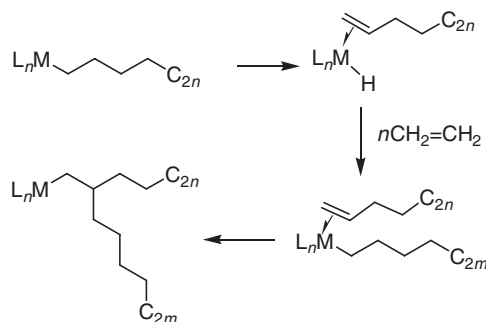
A similar mechanism can be invoked to explain formation of LCBs, as shown in [Scheme 20](#). This mechanism seems kinetically more probable than the one involving formation of a  $\text{Ti}-\text{H}$  intermediate ([Scheme 21](#)) or the  $\sigma\text{-CH}$  metathesis mechanism ([Scheme 22](#)<sup>146</sup>). In support of the mechanism of [Scheme 19](#) and [Scheme 20](#), we note that both ethyl branches



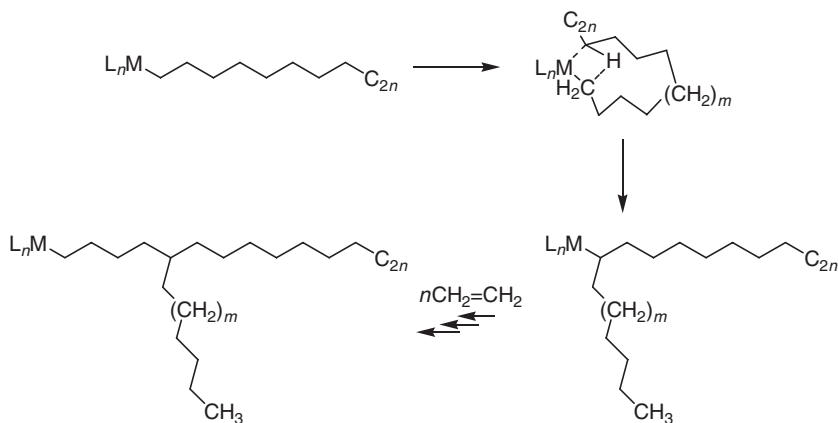
Scheme 19



**Scheme 20** LCB formation by  $\beta$ -H transfer to the ethylene monomer.



**Scheme 21** LCB formation at a site with two growing chains.



**Scheme 22** LCB formation by  $\sigma$ -bond metathesis.<sup>146</sup>

and butyl branches have been detected in PE produced with a linked homobimetallic zirconium *ansa*-Cp-amido complex,<sup>103</sup> and both ethyl branches and LCBs are formed in PE from siloxy-substituted bis(indenyl) zirconocenes.<sup>447</sup>

Concerning the performance of *ansa*-Cp-amido complexes, many papers discuss the influence of the  $\pi$ -ligand type and substitution,<sup>453–457</sup> bridge type,<sup>458–464</sup>  $\sigma$ -ligand type and substituents,<sup>463,465,466</sup> and the different metals.<sup>455</sup>

An interesting approach has been the development of linked homo- and heterobimetallic cyclopentadienyl-amido complexes, that show enhanced LCB formation<sup>467</sup> and produce higher molecular mass PE,<sup>103</sup> as well as increased co-monomer incorporation (see following section).

Several studies aimed at evaluating the influence of substituents on the cyclopentadienyl ligands,<sup>61,447,468–484</sup> of the nature of the co-catalyst,<sup>61,485</sup> and of the metal<sup>486</sup> of Cp'<sub>2</sub>MX<sub>2</sub> complexes have appeared.

Broad or bimodal molecular mass distributions have been obtained using mixtures of metallocenes,<sup>452,487–491</sup> linked homo- and heterobimetallic bis(cyclopentadienyl) complexes for broad molecular mass distribution,<sup>492</sup> or amino-functionalized bis-Cp complexes.<sup>476</sup>



In addition to *ansa*-Cp-amido and bis(cyclopentadienyl) complexes, several monocyclopentadienyl complexes have also been evaluated for ethylene polymerization.<sup>493–502</sup>

Concerning the evaluation of catalyst activity, some papers have cast a shadow on the reliability of published activity data by pointing out the dramatic influence of diffusion limitation in ethylene polymerization.<sup>86,86a,470</sup>

#### 4.09.4.1.2 Ethylene/ $\alpha$ -olefin co-polymers

Ethylene has been co-polymerized with virtually any conceivable  $\alpha$ -olefin, from propylene to vinyl-terminated PE and PP macromonomers. Ethylene/propylene (E/P) copolymerization to produce saturated rubbers and ethylene/propylene/diene (EPD) terpolymerization to produce unsaturated, vulcanizable rubbers will be discussed in Section 4.09.4.1.3. 1-Butene, 1-hexene, and 1-octene are the most commonly used co-monomers for the production of LLDPE. Ethylene/octene co-polymers, developed by Dow and marketed under the Engage tradename, have been shown to have improved thermal properties compared to ethylene/butene and ethylene/hexene co-polymers.<sup>503</sup> In ethylene/ $\alpha$ -olefin (E/O) co-polymerizations, the critical parameters are “co-monomer reactivity” and “co-monomer distribution”. The former is most conveniently described by the relative reactivity parameter,  $R$ , defined as the ratio between polymer composition and reactor medium composition.

Co-monomer distribution is defined as the product of reactivity ratios,  $r_E \times r_O$ , and describes the statistics of intramolecular co-monomer distribution in the polymer chain:

- (i) The product  $r_E \times r_O = 1$  indicates perfect randomness (Bernoullian co-monomer distribution, with diads (determined by <sup>13</sup>C NMR analysis) obeying the relationship  $4[EE][OO]/[EO]^2 = 1$ ).
- (ii) The product  $r_E \times r_O < 1$  indicates tendency to alternation (comonomer homosequences are below the Bernoullian value).
- (iii) The product  $r_E \times r_O > 1$  indicates blockiness (comonomer homosequences are above the Bernoullian value).

The product  $r_E \times r_O$  is independent of the concentration of the monomers and temperature, but the single  $r_E$  and  $r_O$  values might change with temperature.<sup>504</sup> Several  $r_E$ ,  $r_O$ , and  $r_E \times r_O$  values have been listed in the literature.<sup>229,254,505–507</sup>

There are different methods for estimating  $r_E$  and  $r_O$ . Two methods based on NMR analysis use equations based on the concentrations of diads<sup>508</sup> or triads.<sup>509,510</sup>

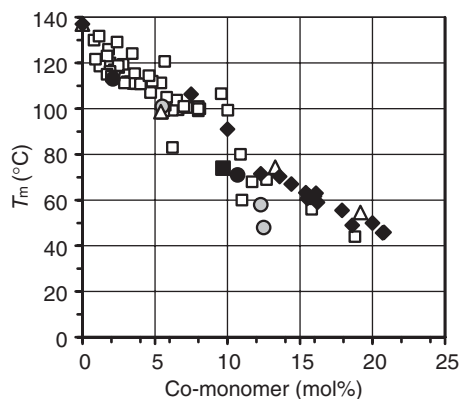
$$r_E = \frac{2[EE]}{[EO]} \times \frac{[O]}{[E]} \quad \text{and} \quad r_O = \frac{2[OO]}{[EO]} \times \frac{[E]}{O}$$

$$r_E = \frac{2[EEE] + [EEO]}{2[EOE] + [OOE]} \times \frac{\chi_O}{\chi_E} \quad \text{and} \quad r_O = \frac{2[OOO] + [OOE]}{2[EOE] + [OOE]} \times \frac{\chi_E}{\chi_O}.$$

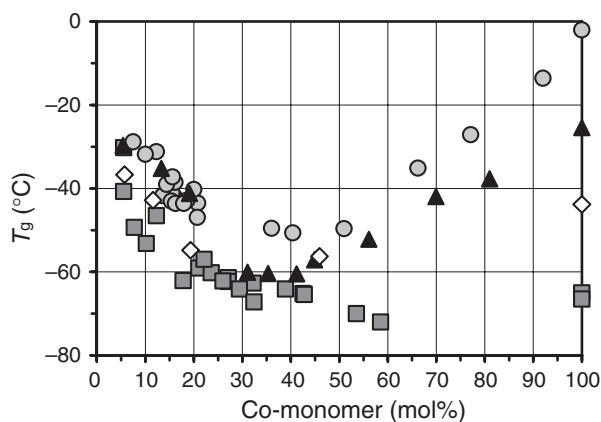
Here,  $\chi_E$  and  $\chi_O$  are the mole fractions of the two monomers in the polymerization medium.

In addition to the above, the intermolecular co-monomer distribution, that is the extent of the co-monomer's incorporation in different molecular mass fractions of the polymer, is an important aspect. When feasible, this is evaluated by fractionating the polymer and measuring the co-monomer content in each fraction, by solubility (TREF),<sup>511</sup> crystallizability (CRYSTAF),<sup>512,513</sup> or by GPC-IR.<sup>514</sup> Whereas ZN catalysts tend to produce LLDPE co-polymers of broad co-monomer distribution (with more co-monomer incorporated in the lower molecular mass fractions), single-center catalysts always have a nearly perfect intermolecular co-monomer distribution, and this aspect is taken as implicit in most co-polymerization studies with the latter systems.

Co-monomer type, amount, and distribution in turn determine the key properties of E/O co-polymers such as density, melting point ( $T_m$ ), and glass transition temperature ( $T_g$ ). A few examples of the latter two properties as a function of co-monomer type and content are shown in Figure 19 ( $T_m$ ) and Figure 20 ( $T_g$ ). It appears that differences in melting points are fairly independent of the length of the olefin, while 1-octene is superior in lowering the glass transition temperatures at low incorporation. Larger differences in  $T_g$  can be appreciated beyond 50 mol% of incorporated  $\alpha$ -olefin, where melting temperatures also become dependent on the polymer tacticity (see Section 4.09.4.2.5). The scatter of the data can be due to several factors, including different DSC instruments, scan rates, and calibrations, different co-monomer distributions produced by the different metallocene catalysts, differences between IR and NMR measurements of co-monomer contents, and last but not least, sample inhomogeneity due to possible varying monomer concentrations during the polymerization experiments.



**Figure 19** Melting point ( $T_m$ ) for ethylene/ $\alpha$ -olefin co-polymers in the range 75 mol% < ethylene < 100 mol%.<sup>254,454,484,504,507,512,515-519</sup> ◆: propylene; △: 1-butene; □: 1-hexene; ○: 1-octene; ■: 1-decene; ●: 1-dodecene.



**Figure 20** Glass transition temperature ( $T_g$ ) for ethylene/ $\alpha$ -olefin co-polymers in the range 0 mol% < ethylene < 100 mol%.<sup>454,504,507,515</sup> ○: propylene; ▲: 1-butene; ◇: 1-hexene; ■: 1-octene.

Co-monomer incorporation is highly dependent on the size of the co-monomer and the steric constraints of the active catalyst center, but also on temperature, activator, and solvent. Almost invariably, addition of  $\alpha$ -olefin co-monomers decreases molecular masses<sup>254,516</sup> and increases catalyst activity. The latter effect, for which a clear explanation is still lacking, is observed up to a given co-monomer content which depends on the type of catalyst.

E/O co-polymerization reports with bis(cyclopentadienyl) complexes include ethylene/1-butene,<sup>229,233,505,515,520,521</sup> ethylene/1-pentene,<sup>254</sup> ethylene/4-methyl-1-pentene,<sup>516,522,523</sup> ethylene/1-hexene,<sup>229,230,254,446,447,478,481,484,509,512-515,517-519,522,524-530</sup> ethylene/1-octene,<sup>254,504,505,515,522,531-535</sup> ethylene/1-decene,<sup>254,520</sup> ethylene/1-dodecene,<sup>254,536</sup> ethylene/1-tetradecene,<sup>254,532</sup> ethylene/1-hexadecene,<sup>511,512,518,525</sup> ethylene/1-octadecene.<sup>532,536</sup>

The most relevant E/O co-polymerization reports with *ansa*-Cp-amido titanium complexes include ethylene/1-butene,<sup>537,538</sup> ethylene/1-hexene,<sup>539,540</sup> and ethylene/1-octene.<sup>91,442,454,456,457,464,506,541</sup> Ethylene/4-methyl-1-pentene co-polymerizations have been reported as well.<sup>457,542</sup> The thermal and physical properties of the octene co-polymers produced with *ansa*-Cp-amido titanium complexes have been studied.<sup>543-546</sup> The importance of the activator has been pointed out in many instances.<sup>91,108</sup>

Marks has shown that linked homo- and heterobimetallic *ansa*-Cp-amido zirconium complexes produce increased co-monomer incorporation and higher molecular masses compared to their mononuclear analogs.<sup>103</sup>

The MAO-activated, unbridged  $\text{Cp}^*\text{TiCl}_2(\text{O}-2,6\text{-Pr}_2\text{C}_6\text{H}_3)$  has been reported to produce ethylene/1-butene with activities and molecular masses similar to the *ansa*-Cp-amido catalyst  $\text{Me}_2\text{Si}(\text{C}_5\text{Me}_4)(\text{NBu}^t)\text{TiCl}_2/\text{MAO}$  under similar conditions (70 °C in toluene).<sup>537</sup> A series of  $(\text{Cp}')(\text{O}-2,6\text{-Pr}_2\text{C}_6\text{H}_3)/\text{TiCl}_2$  bearing Cp with different substitution patterns have been used for the co-polymerization of ethylene with 1-hexene, 1-octene, and 1-decene.<sup>547,548</sup>



A broad range of *ansa*-(Cp')(aryloxo)TiCl<sub>2</sub> has been reported for ethylene/1-hexene co-polymerization.<sup>549</sup> Cp\*(nitroxide)TiMe<sub>2</sub> has been shown to incorporate 1-hexene efficiently, and to produce higher molecular mass co-polymer compared to Me<sub>2</sub>Si(C<sub>5</sub>Me<sub>4</sub>)(NBu<sup>t</sup>)TiMe<sub>2</sub>, although it is less active.<sup>539</sup>

More exotic co-monomers include vinylcyclohexane,<sup>550</sup> 4-vinylcyclohexene,<sup>551</sup> divinylbenzene,<sup>552</sup> *N*-(4-vinylphenyl)carbazole,<sup>553</sup> 2-vinylnaphthalene,<sup>554</sup> 5-hexen-1-ol,<sup>555</sup> 10-undecen-1-ol,<sup>556,557</sup> and dialkylaluminum-protected allyl alcohol, R<sub>2</sub>Al(OCH<sub>2</sub>CH=CH<sub>2</sub>).<sup>558</sup>

Non-conjugated dienes have also been co-polymerized with ethylene. Examples are 1,4-pentadiene,<sup>559</sup> 1,5-hexadiene,<sup>560–563</sup> 1,7-octadiene,<sup>562–564</sup> and 7-methyl-1,6-octadiene.<sup>562</sup>

In particular, ethylene co-polymerization with 1,5-hexadiene, 1,7-octadiene, and 7-methyl-1,6-octadiene using classical metallocenes such as Cp<sub>2</sub>ZrCl<sub>2</sub> and C<sub>2</sub>H<sub>4</sub>(Ind)<sub>2</sub>HfCl<sub>2</sub> has been reported.<sup>562,563,565</sup> 1,5-Hexadiene is mainly incorporated to give a cyclopentane ring, while the two octadienes are incorporated mostly as 1,2-units, thus generating branches carrying a terminal unsaturation. The vinyl-terminated branches obtained from 1,7-octadiene can cross-link different polymer chains. Similar results were obtained in the co-polymerization of ethylene with 1,4-hexadiene, that presents an internal C=C double bond. As expected, catalyst activity and co-monomer incorporation, as well as molecular masses, were low.<sup>566</sup>

Examples of terpolymerizations have also been reported: ethylene/styrene/1,5-hexadiene,<sup>561</sup> ethylene/propylene/hexene and ethylene/propylene/1-hexadecene,<sup>512</sup> ethylene/butene/1-decene,<sup>520</sup> ethylene/butene/octadecene.<sup>521</sup>

In order to introduce LCBs of different structures, vinyl-terminated olefin oligomers have been used in co-polymerization with ethylene (as well as propylene, see Section 4.09.4.2.8). Such macromonomers can be prepared by ethylene oligomerization,<sup>531,567</sup> E/P co-oligomerization,<sup>568</sup> or propylene oligomerization.<sup>569</sup> In the last case, a catalyst with a very high selectivity for  $\beta$ -Me transfer is necessary, in order to produce oligomers with the required  $\alpha$ -olefinic terminal.

Several articles deal with the so-called “tandem” co-polymerization, where two catalysts are mixed, one oligomerizing ethylene to  $\alpha$ -olefins, the second co-polymerizing these  $\alpha$ -olefins with ethylene.<sup>490,567,570–573</sup> The requirements for efficient tandem co-polymerization are quite strict: the two catalysts must have compatible activation chemistry and temperature response; the oligomerization catalyst must have a very high selectivity for  $\alpha$ -olefins to avoid formation and buildup of non-polymerizable oligomers, and no or extremely small co-polymerization capability; the polymerization catalyst on the other hand must have an extremely high capability of inserting the higher oligomers.

#### 4.09.4.1.3 Ethylene/propylene co-polymers and ethylene/propylene/diene terpolymers

Ethylene/propylene co-polymers (usually called EPRs for ethylene–propylene rubbers, or EPMS for ethylene–propylene monomers) are amorphous polyolefins when the propylene content is in the range 30–70%. Despite the typical unreactivity of saturated polyolefins, ethylene-rich EP co-polymers can be made highly elastic by radical cross-linking, but in order to make the rubber “vulcanizable”, a diene (5-ethylidene-2-norbornene, 1,4-hexadiene, or dicyclopentadiene) is added, which leaves one unreacted double bond available for subsequent cross-linking. These latter materials are called EPDMs (for ethylene–propylene–diene monomers).

Although a large share of the EP co-polymers and EPD terpolymers is still manufactured with vanadium-based catalysts at low temperature, metallocene catalysts have added a whole new dimension to EP co-polymerization, and to the range of material properties that can be achieved, as has been the case for the ethylene-based low-density co-polymers discussed in the previous section. The subject of EP co-polymerization with group 4 bis(cyclopentadienyl) complexes has been reviewed in detail up to 1998.<sup>59</sup>

The two most important properties of amorphous EP co-polymers are the molecular mass and the content of co-monomer: both strongly depend on reaction conditions (e.g., temperature and concentration of the monomers) and catalyst structure. The third parameter, that mostly depends on the catalyst structure, is the type of distribution of the co-monomers: metallocenes allow the preparation of alternating ( $r_E \times r_P < 1$ ),<sup>59,574–576</sup> random ( $r_E \times r_P \sim 1$ ),<sup>577,578</sup> and blocky ( $r_E \times r_P > 1$ )<sup>59,577,579</sup> co-polymers.

In addition to variables such as molecular mass and co-monomer distribution, metallocenes can produce EP co-polymers varying in the regiochemistry of propylene insertion<sup>578</sup> and tacticity of propylene sequences, from isotactic<sup>579</sup> to atactic.<sup>250,578,580</sup>

Alternating atactic<sup>59,574,576,581</sup> and isotactic<sup>575,576,581,582</sup> co-polymers have been produced with either *C*<sub>2v</sub>-symmetric or *C*<sub>1</sub>-symmetric *ansa*-bis(cyclopentadienyl) complexes. Quite revealing from a mechanistic standpoint is the observation that the hemiisoselective complexes Me<sub>2</sub>C(CpR)(9-Flu)ZrMe<sub>2</sub> and Me<sub>2</sub>Si(CpR)(9-Flu)ZrCl<sub>2</sub> (R = Me, Pr<sup>i</sup>) produce “isotactic” PEPEP sequences and mostly atactic EPPE sequences, and the syndiospecific metallocenes

$\text{Me}_2\text{C}(\text{Cp})(9\text{-Flu})\text{ZrMe}_2$  and  $\text{Me}_2\text{Si}(\text{Cp})(9\text{-Flu})\text{ZrCl}_2$  again produce “isotactic” PEPEP sequences (in addition to the expected syndiotactic PP and EPPE sequences).<sup>575</sup> This observation is indicative of an alternating insertion mechanism where propylene inserts only or prevailing at the most hindered stereoselective site of a  $C_1$ -symmetric metallocene, while ethylene inserts at the other. The mechanism (main reaction path only) proposed by Soga *et al.*<sup>582</sup> and Leclerc and Waymouth<sup>575,581</sup> is shown in Scheme 23. Still, the driving force for alternation, especially in the case of a  $C_s$ -symmetric ligand frame,<sup>575</sup> is not fully understood. Of more practical interest is the discovery that the *Si*-bridged complexes produce higher molecular mass co-polymers compared to their *C*-bridged analogs, although data at polymerization temperatures higher than 0 °C are not available.<sup>575</sup>

The statistics of co-polymerization are rather complicated: most of the co-polymerizations do not follow simple Bernoullian statistics, but are better described by terminal (first-order Markovian) or penultimate (second-order Markovian) statistics.<sup>59,574</sup>

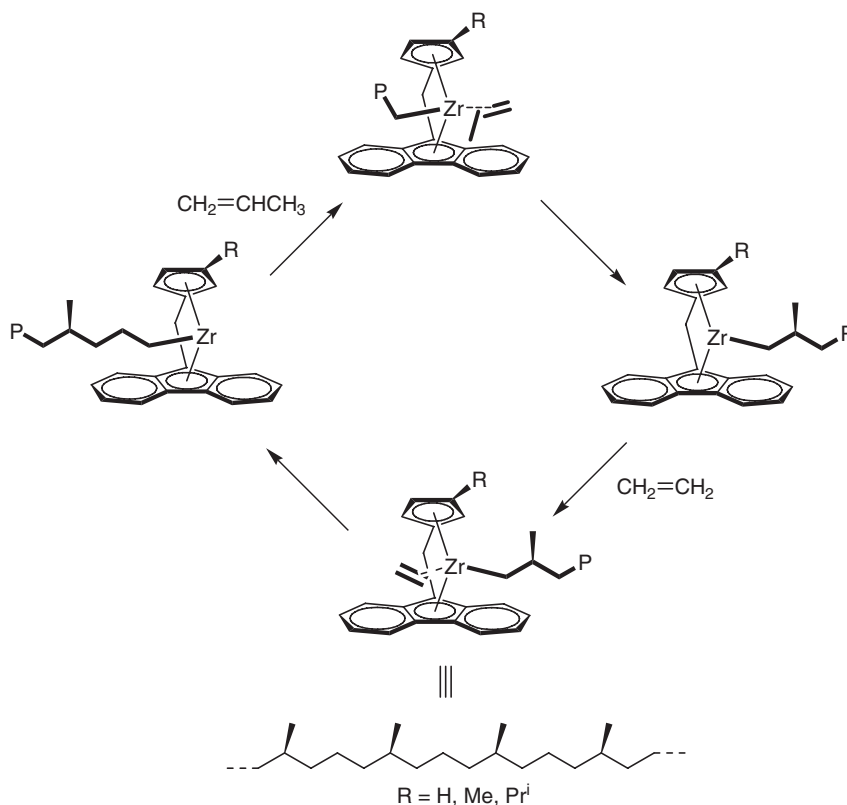
The influence of co-monomer concentration and type of solvent for the catalyst *rac*- $\text{C}_2\text{H}_4(\text{H}_4\text{Ind})_2\text{ZrCl}_2$ /tetra-*iso*octylalumoxane has been studied.<sup>583</sup>

The influence of the transition metal on a given ligand frame has been investigated for both isospecific<sup>584</sup> and syndiospecific<sup>585</sup> metallocenes, with the finding that hafnium tends to give more blocky sequences compared to zirconium, while titanium tends to be more alternating compared to zirconium in the syndiospecific systems<sup>585</sup>.

The co-polymerization with highly isoselective zirconocenes has also been studied.<sup>253</sup> Co-polymerization results with state-of-the-art highly isoselective  $C_2$ -symmetric zirconocenes providing high molecular mass co-polymers under industrially relevant conditions can be found in the patent literature.<sup>586–588</sup>

The *ansa*-Cp-amido complexes of titanium have met with the largest success in industry thanks to their high-temperature stability, which allows the use of high-temperature solution polymerization processes.<sup>442</sup> In addition to producing almost perfect random co-polymers,<sup>578</sup> they give a relatively high content of regioinverted propylene units and allow the formation of LCBs.<sup>589</sup>

Since the early report by Kaminsky and Miri on the terpolymerization of ethylene, propylene, and 5-ethylidene-2-norbornene with  $\text{Cp}_2\text{ZrMe}_2$  in 1985,<sup>590</sup> other terpolymerization studies have appeared.<sup>286</sup> Addition of a diene reduces



Scheme 23

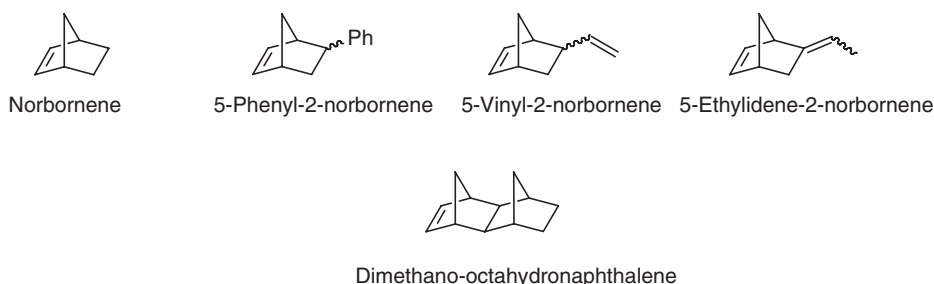
the activity of the catalyst and the molecular mass of the polymer. The best performing catalysts are again the *ansa*-Cp-amido complexes of titanium, thanks to their high diene incorporation ability.<sup>591,592</sup>

#### 4.09.4.1.4 Ethylene co-polymerization with $\alpha,\alpha'$ -disubstituted and internal olefins

Several “non-polymerizable” olefins have been successfully co-polymerized with ethylene, the most successful results being achieved with the *ansa*-Cp-amido catalysts. Relevant cases are those of isobutene,<sup>260</sup> 2-methyl-1-pentene,<sup>593</sup> and 2-butene. Typical  $C_2$ - and  $C_s$ -symmetric metallocenes like **29** and **32** have been reported to selectively co-polymerize ethylene with *cis*- and *trans*-2-butene, respectively. Working at low ethylene concentration, up to 25% and 14% mol of butene could be incorporated into the co-polymers obtained with **29** and **32**, respectively. Independent of the symmetry of the catalyst, the inserted 2-butene units undergo chain-isomerization reactions that lead to isolated methyl groups in the case of *trans*-2-butene co-polymerization, and to mainly isolated ethyl groups and a minor amount of isolated methyl groups in the case of *cis*-2-butene insertion, as shown in Scheme 24.<sup>594,595</sup>

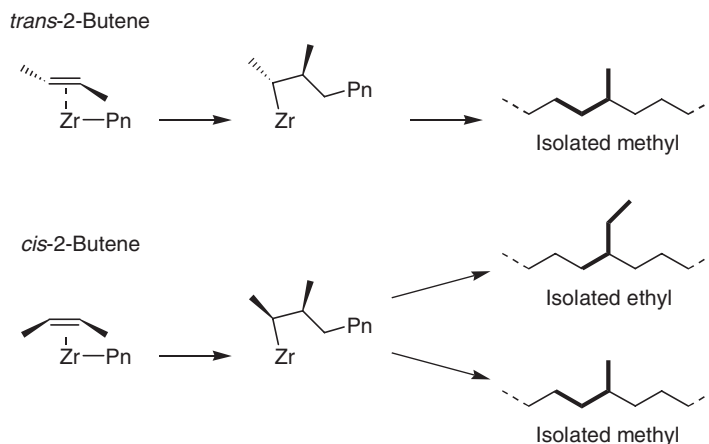
#### 4.09.4.1.5 Ethylene co-polymers with cycloolefins

Ethylene has been co-polymerized with a range of cycloolefins, including cyclobutene,<sup>596</sup> cyclopentene,<sup>596</sup> cyclohexene,<sup>597</sup> norbornene (NB),<sup>596</sup> 5-phenyl-2-norbornene,<sup>598</sup> 5-vinyl-2-norbornene,<sup>599</sup> 5-ethylidene-2-norbornene,<sup>600</sup> dimethano-octahydro-naphthalene,<sup>601</sup> phenyldimethano-octahydro-naphthalene,<sup>598</sup> and norbornadiene.<sup>602</sup> Several non-conjugated cyclo-diolefins have been co-polymerized as well.<sup>603</sup>

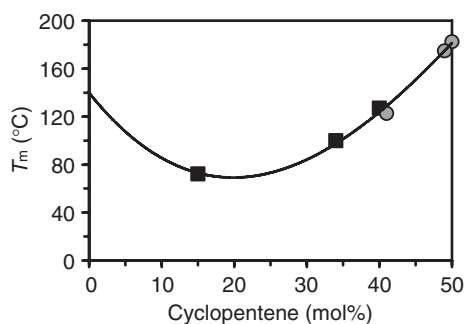


Several examples of ethylene/cyclopentene co-polymers prepared with metallocene catalysts have been reported.<sup>596,603,604</sup> As is the case of many other co-polymers, for ethylene/cyclopentene co-polymers, the glass transition temperature increases linearly with the cyclopentene content,<sup>605</sup> in the range 25–50 mol% of cyclopentane units.

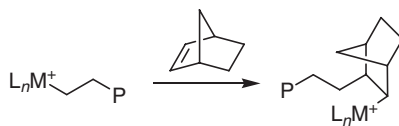
Waymouth reported the synthesis of alternating ethylene/cyclopentene co-polymers with up to 50% cyclopentane units. The achiral  $\text{Me}_2\text{Si}(\text{C}_5\text{Me}_4)(\text{NBu}^t)\text{TiCl}_2$  produces atactic poly(*cis*-1,2-cyclopentane-*alt*-ethylene) co-polymers, while the isotactic poly(*cis*-1,2-cyclopentane-*alt*-ethylene) co-polymers are obtained with the chiral  $\text{Me}_2\text{Si}(\text{Ind})(\text{NBu}^t)\text{TiCl}_2$  pre-catalyst. Remarkably, there seems to be no influence of stereoregularity on melting points (see Figure 21).<sup>606</sup>



Scheme 24



**Figure 21** Melting points of alternating ethylene/cyclopentene co-polymers, showing apparent independence of melting point from tacticity. ■: atactic poly(*cis*-cyclopentane-*alt*-ethylene) co-polymers,  $\text{Me}_2\text{Si}(\text{C}_5\text{Me}_4)(\text{NBu}^t)\text{TiCl}_2/\text{MAO}$ ; ●: isotactic poly(*cis*-cyclopentane-*alt*-ethylene) co-polymers,  $\text{Me}_2\text{Si}(\text{Ind})(\text{NBu}^t)\text{TiCl}_2/\text{MAO}$ .<sup>606</sup> The data have been fitted with a third-grade polynomial, with the only purpose of providing a guide to the eye.



**Scheme 25**

Within the family of cycloolefin co-polymers, the most important from a material properties' standpoint, are the ethylene/norbornene co-polymers. These co-polymers, dubbed “COC” for cycloolefin co-polymers, are produced by Ticona and Mitsui under the tradenames Topas® and Apel®, respectively. An overview of properties and applications (for example, blisters for pills) can be found on Ticona's Topas homepage.<sup>607</sup> Detailed ethylene/norbornene co-polymerization studies with different  $C_1$ -symmetric and *ansa*-Cp-amido catalysts, with listing of co-polymerization parameters, have been published.<sup>608–611</sup> NB is inserted exclusively in the *cis*-2,3-*exo*-mode (Scheme 25), and most of the metallocene catalysts tend to produce alternating co-polymers,<sup>609,612</sup> due to the low reactivity of the M–NB intermediate toward further NB insertion. This mode of NB insertion prevents  $\beta$ -H transfer, and thus ethylene/norbornene co-polymers have increasing molecular masses at increasing NB content.<sup>611</sup>

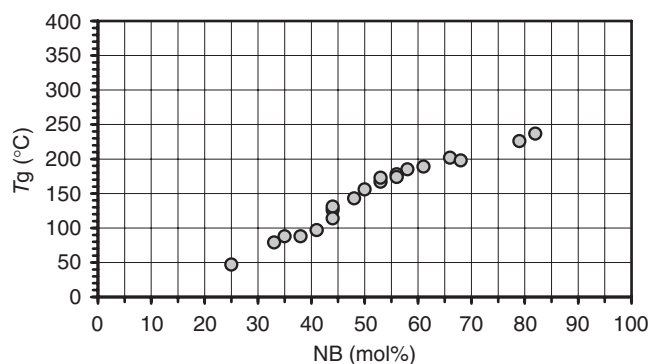
A tendency to alternation means a limitation to the amount of inserted NB co-monomer, at or slightly above 50 mol%. Some of the  $C_1$ -symmetric zirconocenes, and notably those with a higher NB homopolymerization activity, however, were found to be able to incorporate more NB (up to 70 mol% under the conditions investigated), thus leading to NB dyads and triads. The least sterically encumbered zirconocenes,  $\text{MeCH}(\text{Cp})_2\text{ZrCl}_2$ , showed the highest NB incorporation.<sup>609</sup> Analogous *ansa*-bis(cyclopentadienyl)zirconium complexes based on the 2,5-dimethylcyclopentadienyl ligand have been reported to have a good NB incorporation ability with good activities.<sup>613–616</sup>

Reviews on some catalytic aspects of ethylene/norbornene co-polymerization have appeared.<sup>596,601</sup> The influence of substituents on *ansa*-Cp-amido complexes<sup>617</sup> and the microstructure of the co-polymers,<sup>618,619</sup> have been the subject of several studies. Contrary to most *ansa*-Cp-amido complexes of titanium, which were found to produce alternating ethylene/norbornene co-polymers,<sup>609,617,620</sup> the  $\text{Me}_2\text{Si}(9\text{-Flu})(\text{NBu}^t)\text{TiMe}_2/\text{Ph}_3\text{CB}(\text{C}_6\text{F}_5)_4/\text{AlOct}_3$  catalyst has been reported to produce random ethylene/norbornene containing up to 82 mol% of NB and a correspondingly high  $T_g$  of 237 °C.<sup>621</sup>

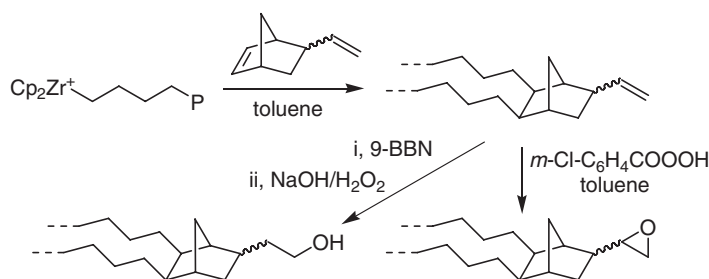
The correlation between composition and glass transition temperature in ethylene/norbornene co-polymers is shown in Figure 22.

In the ethylene/5-vinyl-2-norbornene co-polymerization, only the endocyclic double bond undergoes insertion (up to 14 mol% with the catalyst and under the conditions investigated), leaving the exocyclic vinyl bond accessible for further reactions, leading to functionalized PEs (Scheme 26).<sup>599</sup>

A similar approach uses the co-polymerization of ethylene with 5-ethylidene-2-norbornene, followed by hydroboration/oxidation of the unreacted vinyl group. The hydroxylic functions in the co-polymer are then converted into  $-\text{OAlEt}_2$  groups and used as catalysts for  $\epsilon$ -caprolactone polymerization, thus leading to poly(ethylene-*co*-ENB)-graft-polycaprolactone co-polymers.<sup>600</sup>



**Figure 22** Correlation between norbornene content and glass transition temperature in ethylene/norbornene co-polymers (○).<sup>621,622</sup>



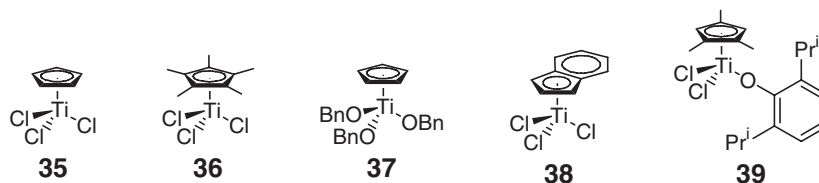
**Scheme 26**

#### 4.09.4.1.6 Ethylene/styrene co-polymers

The successful co-polymerization of ethylene with styrene is another polymeric material conquest of homogeneous catalysis. At low styrene incorporation, the co-polymer is substantially a functionalized crystalline polyethylene. Increasing the styrene content results in a decrease of crystallinity while elastomeric properties arise,<sup>623</sup> up to about 80 mol% styrene; for higher styrene contents, the co-polymer becomes a glassy amorphous material. A comprehensive review on the properties of ethylene/styrene co-polymers is available.<sup>624</sup>

The main drawback of the elastomeric co-polymers is their rather high  $T_g$ , which is always higher than LLDPE co-polymers and increases with the styrene content, reaching values above 0 °C beyond 60 wt% of styrene.<sup>624</sup> In the styrene range of 20–50 mol%, the co-polymer can be either amorphous elastomeric or crystalline. This kind of crystallinity occurs when the E–S dyad is stereoregular.<sup>625</sup> Ethylene/styrene co-polymers can act as compatibilizer for polyethylene–polystyrene blends. A review on ethylene/styrene co-polymerization has appeared.<sup>626</sup>

Even at high styrene incorporation, the co-polymers are formed by ethylene blocks and isolated styrene units.<sup>627</sup> Half-sandwich titanium complexes such as **35**–**39** have also been reported to be active in the ethylene/styrene co-polymerization. The performance of the MAO-activated complex **35** is highly dependent on the Al/Ti ratio. At a ratio of 100, a co-polymer composed of polyethylene blocks with essentially isolated styrene units could be fractionated from the homopolymers. By contrast, at Al/Ti ratios of 1000, a co-polymerization at the same feed ratio resulted in the production of only homopolymers, or co-polymers composed of long PE and sPS blocks at most.<sup>628</sup> Subsequent <sup>13</sup>C NMR analysis of the co-polymers obtained at 20 °C indicated that up to 36 mol% of styrene was incorporated.<sup>629</sup> However, under very similar conditions, only formation of the homopolymers was reported.<sup>630,631</sup> This may be reasonable since catalytic systems **35**/MAO and **36**/MAO give rise to several active species with different catalytic properties. Thus, remarkably different results can be obtained with small differences in the experimental procedure.



The  $B(C_6F_5)_3$ -activated complex **36**, which is highly active in the syndiospecific styrene polymerization, yields ethylene-styrene (E-S) copolymers at polymerization temperatures  $>25^\circ\text{C}$ . Increasing amounts of E-S units were obtained at increasing styrene concentrations in the feed. However, besides a larger amount of E-S units, the production of sPS becomes favored. Nevertheless, the THF-soluble fraction of the materials obtained comprised E-S co-polymers with a highly alternating and, interestingly, atactic microstructure.<sup>626,632</sup>

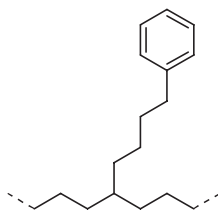
The  $B(C_6F_5)_3$ -activated complexes **35** and **36** yield PEs with 4-aryl-1-butyl branches as shown in Scheme 27. The 4-phenyl-1-butyl branches were shown to originate from the formation of ethylene/styrene co-oligomers such as 6-phenyl-1-hexene which is subsequently incorporated in the PE.<sup>633,634</sup>

Other authors have investigated titanium half-sandwich complexes by varying polymerization conditions,<sup>635,636</sup> or by varying the groups bound to the metal, or the Cp ring substitution, as in complexes, **37–39**,<sup>637–640</sup> or by using theoretical approaches.<sup>641</sup>

The above systems always yield a mixture of co-polymer and homopolymers, and the co-polymer has to be extracted with solvents such as THF or MEK. Thus, the discovery that *ansa*-Cp-amido Ti complexes are able to co-polymerize ethylene and styrene was a clear step forward. In fact, these catalysts do not homopolymerize styrene.<sup>642</sup> Structural characterization of the co-polymers obtained with the  $\text{Me}_2\text{Si}(\text{Cp})(\text{NBu}^t)\text{TiCl}_2/\text{MAO}$  catalyst showed that only 35 mol% of styrene was incorporated in the co-polymer, even at a styrene feed of 91 mol%. NMR analysis indicated the absence of S-S sequences.<sup>643</sup> A series of MAO-activated *ansa*-Cp-amido Ti complexes has been investigated, and all catalysts produced random co-polymers without any regioregular or stereoregular microstructure. The highest activity corresponds to  $\text{Me}_2\text{Si}(\text{C}_5\text{Me}_4)(\text{NBu}^t)\text{TiCl}_2$ , while the higher styrene incorporation was obtained with complexes  $\text{Me}_2\text{Si}(3\text{-Me}_3\text{Si-Indenyl})(\text{NBu}^t)\text{TiCl}_2$  and  $\text{Me}_2\text{Si}(\text{C}_5\text{Me}_4)(\text{N-Bn})\text{TiCl}_2$ .<sup>644</sup> Using a fluorenyl- and Zr-based catalyst,  $\text{Me}_2\text{Si}(\text{fluorenyl})(\text{NBu}^t)\text{ZrCl}_2/\text{MAO}$ , only 1 mol% of styrene was incorporated.<sup>644</sup> A very similar catalyst,  $\text{Me}_2\text{Si}(9\text{-Flu})(\text{NBu}^t)\text{TiMe}_2/[\text{Ph}_3\text{C}][\text{B}(\text{C}_6\text{F}_5)_4]$ , yields an almost perfectly alternating and isotactic E-S co-polymer with a  $T_m$  of  $118^\circ\text{C}$ .<sup>645</sup> Other studies on ethylene/styrene co-polymerization with *ansa*-Cp-amido complexes have been reported.<sup>646–652</sup>

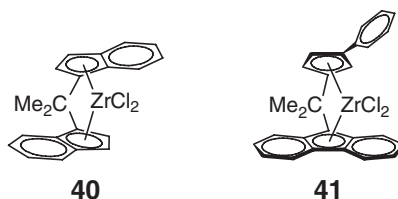
Ethylene/styrene co-polymerizations using the MAO-activated  $C_2$ -symmetric *rac*- $\text{C}_2\text{H}_4(1\text{-Ind})_2\text{ZrCl}_2$  complex **29** or the  $C_s$ -symmetric  $\text{Me}_2\text{C}(\text{Cp})(9\text{-Flu})\text{ZrCl}_2$  complex **32** lead to random co-polymers with a styrene content of up to 45 mol%.<sup>653</sup> NMR characterizations of these co-polymers indicated that insertion of styrene is not completely regioregular.<sup>654</sup> Almost perfectly stereoregular and alternating ethylene/styrene co-polymers using the same  $C_2$ - and  $C_s$ -symmetric metallocenes **29** and **32** were achieved by lowering the co-polymerization temperature to  $-25^\circ\text{C}$ . The regular microstructure allowed crystallization of the co-polymers.<sup>625</sup> Interestingly, both the co-polymers obtained with **29** and **32** resulted in an isotactic arrangement of the styrene units.<sup>655</sup> Co-polymers composed of isotactic PS and PE blocks were also synthesized utilizing the bulky  $\text{H}_2\text{C}(3\text{-Bu}^t\text{-indenyl})\text{ZrCl}_2$  complex **30**. The blocky nature of the co-polymers obtained with **30** is due to the high tendency of this complex to induce primary insertion of 1-olefins, including styrene. This is an interesting result because secondary insertion of styrene is usually favored.<sup>656</sup>

The synthesis at  $50^\circ\text{C}$  of random ethylene-styrene co-polymers using complex **40** has been reported. The resulting co-polymers showed a high content of isotactic E-S units and of occasional regioregularly arranged

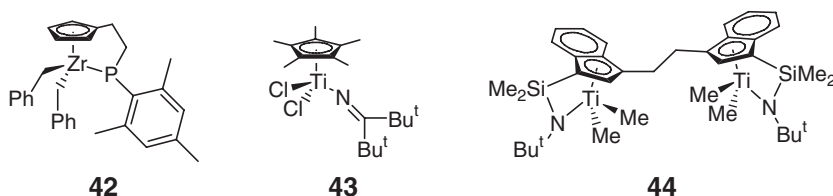


Scheme 27

head-to-tail styrene–styrene units.<sup>657</sup> The consequences of the  $C_1$ -symmetry of metallocenes such as **41** in the ethylene/styrene co-polymerization was investigated. A Ph group on the Cp ring has a beneficial effect on the activity of the catalyst, while styrene insertion is similar to that obtained with the unsubstituted analogs. Conversely, an alkyl substituent in the same position depresses styrene insertion and overall activity of the catalyst.<sup>658</sup> The mechanism of ethylene and styrene co-polymerization has also been investigated with combined experimental/theoretical approaches.<sup>648,659,660</sup> Isotactic polystyrene (iPS) polymers with ethylene units from roughly 0% to 50% can be produced using the **30**/MAO catalyst. Interestingly, at low ethylene contents, the isolated ethylene units inhibit crystallization of the iPS segments.<sup>661</sup>



Other complexes that have been used in ethylene–styrene co-polymerizations are **42**, which is inactive in styrene homopolymerization but has been claimed to produce ethylene/styrene co-polymers with styrene content in the range 35–87 mol%.<sup>662</sup> Living ethylene/styrene co-polymerization can be achieved using the MAO-activated complex **43**. Although a relatively low amount of styrene was incorporated (about 10 mol%), NMR analysis indicated that trace amounts of pseudo-random tail-to-tail S–S or S–E–S sequences were observed.<sup>663</sup> Marks and co-workers showed that bimetallic catalysts based on **44** can effectively yield ethylene/styrene co-polymers and, in contrast to the monometallic CGCs, styrene incorporation can be higher than 50%.<sup>664</sup>



Finally, it is worth noting that chloro- or methyl-substituted styrenes can be co-polymerized with ethylene using either  $\text{Me}_2\text{Si}(\text{C}_5\text{Me}_4)(\text{NBu}^t)\text{TiCl}_2$  or *rac*- $\text{C}_2\text{H}_4(1\text{-Ind})_2\text{ZrCl}_2$ . Results indicated that *p*-methyl-styrene is incorporated far more effectively than styrene.<sup>653,665,666</sup> The  $\text{Me}_2\text{Si}(\text{C}_5\text{Me}_4)(\text{NBu}^t)\text{TiCl}_2$  complex allows the terpolymerization of ethylene, propylene, and *p*-methyl-styrene as well as of ethylene 1-octene and *p*-methyl-styrene.<sup>667</sup> Besides the ethylene and styrene terpolymerization with propylene and 1-octene, the terpolymerization of ethylene and styrene with norbornene or 1,5-hexadiene has been reported.<sup>561,668</sup>

#### 4.09.4.2 Propylene Polymers

Propylene is the simplest prochiral olefin, and the different chain microstructures that can be generated by its four possible insertion modes (all made possible by single-center catalysts, albeit to largely different extents) have been described in detail in Section 4.09.2.3. Two rather different strategies can be followed in order to tailor the physical properties of PP: (i) co-polymerization with ethylene or other  $\alpha$ -olefins and (ii) varying the enantioface selectivity of the active sites of the single-center catalyst by ligand variation. The co-polymerization approach is described in Sections 4.09.4.2.5 (ethylene as co-monomer) and 4.09.4.2.6 and 4.09.4.2.7 ( $\alpha$ -olefin co-monomers). In Sections 4.09.4.2.1–4.09.4.2.4, we describe the different PP homopolymers accessible from group 4 metallocene catalysts.

The degree of PP chain stereoregularity can be modified from totally absent to almost perfect (in either direction, isotactic or syndiotactic) by altering the monomer enantioface selectivity of each active site of the catalyst: in the case of metallocenes, this means varying the substitution pattern of the two cyclopentadienyl ligands. Metallocenes are by far the most versatile systems for the production of PPs of different chain stereoregularity and molecular masses.

Controlling the type and number of monomer insertion mistakes leads to controlling the crystallinity and the melting point of PP, which, together with its molecular mass, define its physical and mechanical properties.



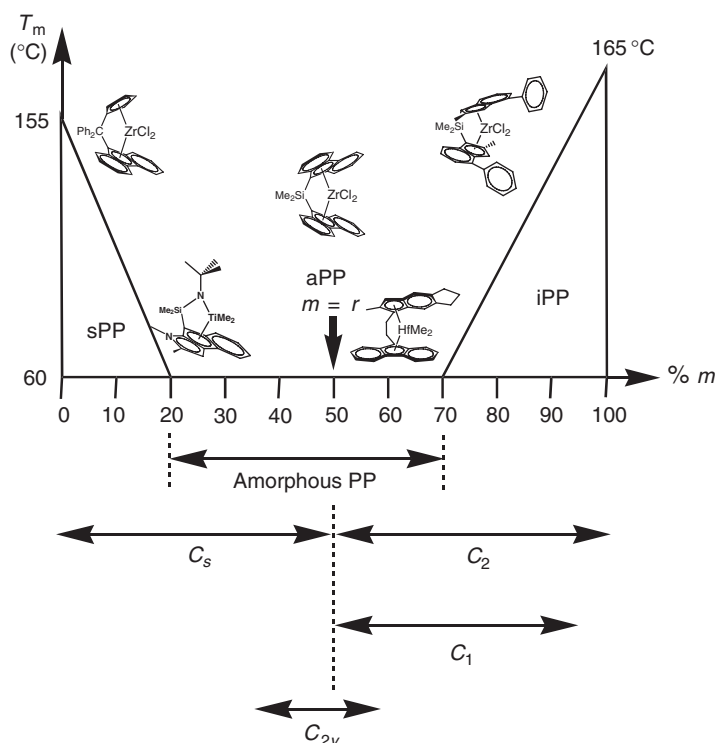
Quoting from a previous review: “in the case of highly crystalline iPP, metallocenes are unlikely to replace the newest heterogeneous Ti/MgCl<sub>2</sub> catalysts in any foreseeable future [for the production of commodity polypropylene]. So, why use metallocenes to produce polypropylene? In one sentence, because polypropylene properties can be tailored! For example, iPP can be made from fully amorphous to highly crystalline and anything in between.”<sup>162</sup> This is shown pictorially in Figure 23. In addition, the very high co-monomer incorporation ability (especially for higher  $\alpha$ -olefins) and very good inter- and intramacromolecular co-monomer distribution achievable with metallocenes represents an additional, very powerful tool for tailoring PP properties.

One additional and important requirement for a catalyst in order to make it useful in practice is its molecular mass capability, which must be as high as possible and coupled with a good hydrogen response. This simultaneous control over both the stereoselectivity and the molecular mass capability of a PP catalyst in the range of industrial polymerization temperatures, which in addition must have high activity (to give a rough indication, >100 kg PP (g metallocene)<sup>-1</sup>) and a good co-monomer incorporation ability, and last but not least, an efficient and cost-effective metallocene synthetic procedure, are the considerable challenges to be faced when developing a new catalyst.

In the following sections, we review the recent developments in metallocene catalyst structures, that made it possible to produce PPs ranging from flexible and elastomeric with varying degrees of crystallinity to highly crystalline, highly stereoregular PP on the one hand, and a very broad family of propylene-based co-polymers on the other, all these polymers having molecular masses in the range of industrial applications.

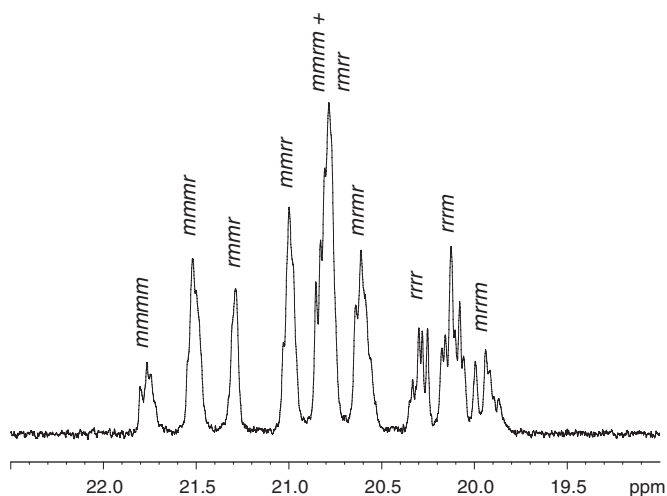
#### 4.09.4.2.1 Amorphous polypropylene

As shown in Figure 23, PP is no longer able to crystallize when the stereoregularity of the chains is reduced below a threshold value (below about 70% *m* diad, or 40% *mmmm* pentad content for iPP, or below about 60% *rrrr* pentad content for sPP), and it becomes amorphous (amPP). When statistical randomness in the sequence of chirotopic methylenes in the polymer chain is reached, the polymer is called “atactic” (aPP). In this case the pentad distribution is perfectly random Bernoullian: *mmmm* : *mmmr* : *rrrr* : *rrrm* : (*rrmr* + *rrmm*) : *rrrr* : *rrrm* : *rrmm* ~ 1 : 2 : 1 : 2 : 4 : 2 : 1 : 2 : 1.



**Figure 23** Schematic representation of melting point dependence on PP microstructure (% *m* dyads), catalyst symmetries with ranges of accessible stereoregularities, and selected examples of representative metallocene structures.





**Figure 24** Methyl pentad region of the  $^{13}\text{C}$  NMR spectrum (100 MHz, 120 °C,  $\text{C}_2\text{D}_2\text{Cl}_4$ ) of aPP with pentad assignments. Catalyst:  $\text{rac-CH}_2(1\text{-Me}_3\text{C-2-Ind})_2\text{HfMe}_2/\text{MAO}$ .<sup>669</sup>

While aPP is obviously amorphous, an aPP is not necessarily atactic. The methyl pentad region of a fully regioregular, nearly perfect aPP is shown in Figure 24 with pentad assignments.

The most important consequences of the absence of crystallinity are softness, tackiness (the property of a material to adhere to itself), a complete solubility in most low-polarity organic solvents, including ethers and aliphatic hydrocarbons, higher transparency, and lower density with respect to crystalline PP. Other physical properties depend also on the molecular mass of aPP.<sup>670</sup> Despite the insolubility of aPP in liquid propylene, its tackiness makes it impossible to produce it in bulk or gas-phase processes, with a solution process at medium temperature likely being the only viable manufacturing process.

Amorphous PP was a byproduct of iPP production in the early slurry processes, and was isolated from the aliphatic solvents in the solvent recycle section.

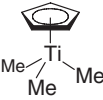
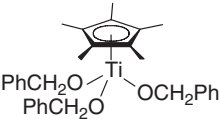
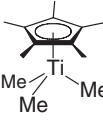
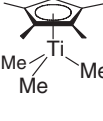
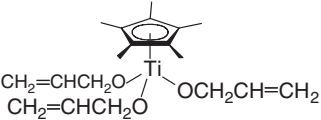
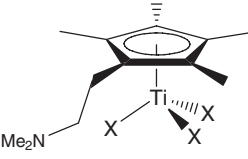
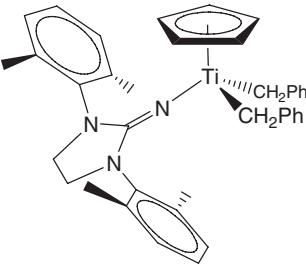
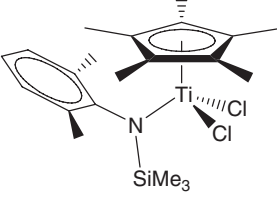
This material, often incorrectly referred to as “atactic,” is actually neither atactic nor fully amorphous, but is a mixture of chains of different stereoregularity and molecular masses, as proved by polymer fractionation.<sup>315,374,671,672</sup> The methyl pentad region of the  $^{13}\text{C}$  NMR spectrum of such a ZN PP clearly shows both isotactic and syndiotactic stereoblocks. Although the molecular masses of this material are low, amPPs have been used as bitumen additives and in hot-melt adhesives. With the improvement of the stereospecificity of the ZN catalysts for iPP, amPP was no longer available as a byproduct. Fully or largely amorphous PP from ZN has since been produced on purpose, also by adding co-monomers to further reduce crystallinity.<sup>673–680</sup>

Atactic or nearly atactic PP can be made with four types of metallocene catalysts: (i) the achiral, unbridged metallocenes lacking stereorigidity (e.g.,  $\text{Cp}_2\text{ZrCl}_2$ ,  $(\text{MeCp})_2\text{ZrCl}_2$ ,  $\text{Ind}_2\text{ZrCl}_2$ ,  $(2\text{-MeInd})_2\text{ZrCl}_2$ , and the like)<sup>180,250,681–686</sup> and the bridged, stereorigid  $C_{2v}$ -symmetric metallocenes such as  $\text{Me}_2\text{SiFlu}_2\text{ZrCl}_2$ ;<sup>250,266,687,688</sup> (ii) the *meso*-isomers of *ansa*-metallocenes (e.g., *meso*- $\text{C}_2\text{H}_4(1\text{-Ind})_2\text{ZrCl}_2$ , *meso*- $\text{C}_2\text{H}_4(\text{H}_4\text{Ind})_2\text{ZrCl}_2$ , *meso*- $\text{Me}_2\text{Si}(2\text{-Me-4-Ar-Ind})_2\text{ZrCl}_2$ );<sup>689,690</sup> (iii) the *ansa*- $C_2$ -symmetric metallocenes having the bridge between the 2,2'-position of the two indenyl moieties, such as *rac*- $\text{C}_2\text{H}_4(1\text{-R-2-indenyl})\text{MX}_2$ <sup>477</sup> and *rac*- $\text{H}_2\text{C}(1\text{-R-2-indenyl})\text{MX}_2$  ( $\text{R} = \text{Me}$ ,  $\text{CH}_2\text{Ph}$ ,  $\text{Bu}^t$ ,  $\text{Me}_3\text{Si}$ ;  $\text{M} = \text{Zr}$ ,  $\text{Hf}$ ;  $\text{X} = \text{Cl}$ ,  $\text{Me}$ )<sup>669</sup>; (iv) some monocyclopentadienyl complexes, such as  $\text{CpTiX}_3$  ( $\text{X} = \text{Me}$ ,  $\text{Cl}$ ,  $\text{OR}$ )<sup>691,692</sup> and  $\text{Cp}^*\text{TiX}_3$  ( $\text{X} = \text{Me}$ ,  $\text{Cl}$ ,  $\text{OAr}$ ,  $\text{NAr}$ ,  $\eta^2\text{-ONR}_2$ ).<sup>497,547,693–695</sup>

A selection of structures together with the most relevant polymerization results is reported in Table 2 (monocyclopentadienyl titanium complexes) and Table 3 (zirconocenes).

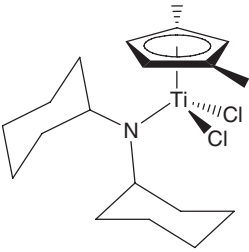
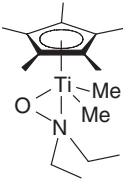
$\text{CpTiR}_3$  complexes with pendant phenyl moieties attached to the Cp show, with respect to  $\text{Cp}^*\text{TiMe}_3$ , reduced propylene polymerization activities and molecular masses upon activation with  $\text{B}(\text{C}_6\text{F}_5)_3$  in toluene at  $T_p$  –20 to 60 °C, in accordance with the formation of 16-electron resting states upon  $\eta^6$ -arene coordination.<sup>696</sup> On the other hand,  $(\text{Me}_2\text{NCH}_2\text{CH}_2\text{Cp})\text{TiCl}_3$  shows much enhanced activity with respect to the practically inactive  $\text{CpTiCl}_3/\text{MAO}$  system.<sup>286,697,698</sup> Quite interestingly, polymerization of propylene with  $(\text{Me}_2\text{NCH}_2\text{CH}_2\text{Cp})\text{TiCl}_3/\text{MAO}$  at 25 °C produces fairly high molecular mass aPP and shows a rate of polymerization with a monomer concentration dependence of 1.8, a behavior similar to that of some stereoselective *ansa*-metallocenes.<sup>289</sup>

**Table 2** Propylene polymerization with monocyclopentadienyl Ti complexes

<i>Pre-catalyst</i>	<i>Activator</i>	<i>Conditions</i>	<i>Activity</i> (kg <sub>PP</sub> mmol <sub>Ti</sub> <sup>-1</sup> h <sup>-1</sup> )	$\bar{M}_w$	<i>Tacticity</i>	<i>References</i>
	B(C <sub>6</sub> F <sub>5</sub> ) <sub>3</sub>	Toluene, propylene 1.9 mol l <sup>-1</sup> , -80 to -60 °C, 30 min	1.5	7.4 × 10 <sup>5</sup>	8.5% mm~2% 2,1	691
	MAO	Toluene, 1.30 × 10 <sup>5</sup> Pa propylene, 60 °C, 1 h	0.9	2.3 × 10 <sup>4</sup>	10% mm	692
	B(C <sub>6</sub> F <sub>5</sub> ) <sub>3</sub>	Liquid propylene, -45 °C, 240 s	5.2	4 × 10 <sup>6</sup>	amorphous	693
	B(C <sub>6</sub> F <sub>5</sub> ) <sub>3</sub>	Toluene, 1 atm propylene, 25 °C, 5 min	0.5	2.6 × 10 <sup>5</sup>	48.5% m12% 2,1	694
	Ph <sub>3</sub> C <sup>+</sup> B(C <sub>6</sub> F <sub>5</sub> ) <sub>4</sub> <sup>-</sup>	90% Propylene in toluene, 20 °C, 20 min	0.7	1.1 × 10 <sup>6</sup>	Amorphous	695
	MAO	Toluene, 1.3 atm propylene, 40 °C, 1 h	0.1	27.3 × 10 <sup>4</sup>	11% mm	702
	MAO	Toluene, 20 psi propylene, 20 °C, 30 min	1.5	4.5 × 10 <sup>5</sup>	Amorphous	698
	B(C <sub>6</sub> F <sub>5</sub> ) <sub>3</sub>	Toluene, 3 bar propylene, 50 °C, 30 min	14.4	8.1 × 10 <sup>4</sup>	23% mm	496
	MAO	Toluene, 7 atm propylene, 0 °C, 30 min	0.051	91.3 × 10 <sup>4</sup>	Atactic	497

(Continued)

Table 2 (Continued)

Pre-catalyst	Activator	Conditions	Activity (kgpp mmol <sub>Ti</sub> <sup>-1</sup> h <sup>-1</sup> )	$\bar{M}_w$	Tacticity	References
	MAO	Toluene, 7 atm propylene, 0 °C, 30 min	2.6	n.r.	Atactic	498
	Ph <sub>3</sub> C <sup>+</sup> B(C <sub>6</sub> F <sub>5</sub> ) <sub>4</sub> <sup>-</sup>	90% propylene in toluene, 20 °C, 20 min	153	2.5 × 10 <sup>6</sup>	Atactic, ~3% 2,1	695

Cp<sup>\*</sup>TiMe<sub>3</sub>/B(C<sub>6</sub>F<sub>5</sub>)<sub>3</sub> shows a quasi-living behavior at  $T_p \leq -20$  °C, producing aPP with molecular mass above 10<sup>6</sup> and very narrow molecular mass distribution.<sup>693</sup> The same system, investigated at higher temperature, was shown to produce aPP with up to 15% regioerrors;<sup>694</sup> these regioerrors do not affect the rate of further monomer insertion as evidenced by the lack of hydrogen activation, which however efficiently lowers PP molecular mass.<sup>699</sup> A similar living behavior at low temperatures has been reported for Cp′<sub>2</sub>MMe<sub>2</sub>/B(C<sub>6</sub>F<sub>5</sub>)<sub>3</sub>/AlR<sub>3</sub> (Cp′ = C<sub>5</sub>H<sub>5</sub>, C<sub>5</sub>Me<sub>5</sub>; M = Zr, Hf; R = <sup>i</sup>Bu, <sup>n</sup>Oct).<sup>700,701</sup> Interestingly, the CpTi(OR)<sub>3</sub>, CpTiX<sub>3</sub>, and Cp<sup>\*</sup>Ti(OR)<sub>3</sub> complexes produce “regio”-block aPP.<sup>692,702,703</sup>

The very high molecular mass of the aPP obtained with (2-MeInd)<sub>2</sub>ZrCl<sub>2</sub>/MAO, well above 3 × 10<sup>6</sup> at  $T_p \leq 0$  °C,<sup>250</sup> is remarkable. Amorphous PP, deviating from perfect atacticity in either direction, but still lacking any long-range stereochemical order, is obtained by several of the above four systems when different co-catalysts or low polymerization temperatures are applied,<sup>682,691,704</sup> and by three other classes of catalysts: (v) the *ansa*-Cp-amido Ti metallocenes, such as Me<sub>2</sub>Si(C<sub>5</sub>Me<sub>4</sub>)(NBu<sup>i</sup>)TiCl<sub>2</sub> and its analogs, which produce very high molecular mass amPPs with a bias toward syndiotacticity;<sup>30,705–708</sup> (vi) some C<sub>2</sub>-symmetric metallocenes, such as *rac*-Me<sub>2</sub>C(3-Pr<sup>i</sup>Ind)<sub>2</sub>ZrCl<sub>2</sub>,<sup>222,709</sup> and (vii) several C<sub>1</sub>-symmetric metallocenes.<sup>576</sup> These two latter cases will be discussed in Section 4.09.4.2.3.

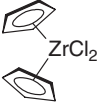
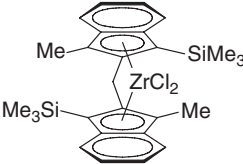
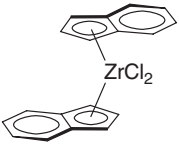



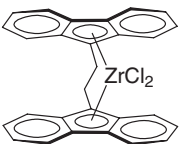
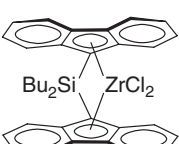
In addition to these, it is worth mentioning that also thio-bis(aryloxy)titanium compounds give aPP of high molecular masses, but with low productivities.<sup>159</sup> Regioselectivities vary widely among different catalysts, with the bis(cyclopentadienyl) complexes being the most regioselective and the thio-bis(aryloxy) compounds producing highly regioirregular aPP.

Appending asymmetric aryl groups to Cp in CpMCl<sub>3</sub> (M = Ti, Zr) has been shown to induce the formation of PP-containing aPP/iPP stereoblocks, the length of which strongly depends on the polymerization temperature.<sup>710,711</sup>

The silyl-bridged Cp-amido titanium catalysts, first developed for ethylene homo- and co-polymerization (see Section 4.09.4.1), have also been extensively studied in propylene polymerization. In general, these complexes produce remarkably high molecular mass amPP even at elevated temperatures. Microstructures are slightly biased toward either syndiotactic or isotactic, depending on the Cp substitution pattern. Significant deviations from atacticity have been reported for some complexes, and will be discussed in the next section. Variation of the substituent on the amido nitrogen also has an influence on tacticity and molecular mass.<sup>705,706,712</sup> The influence of bridge type and length has been studied by Hessen<sup>461</sup> and Marks.<sup>460</sup> Selected structures and propylene polymerization results are shown in Table 4.

The C<sub>2v</sub>-symmetric R<sub>2</sub>Si(9-Flu)<sub>2</sub>ZrCl<sub>2</sub> and the C<sub>1</sub> or C<sub>s</sub>-symmetric *ansa*-Cp-amido titanium complexes so far seem to be the most efficient catalysts for the production of high molecular mass amPP, due to their ability to maintain high activity and produce high molecular masses at relatively high polymerization temperatures ( $T_p > 50$  °C), and high molecular masses also at relatively low propylene concentration in hydrocarbon solution polymerization. The activity recently reported for Cp<sup>\*</sup>TiMe<sub>2</sub>(ONEt<sub>2</sub>)/[Ph<sub>3</sub>C][B(C<sub>6</sub>F<sub>5</sub>)<sub>4</sub>]<sup>695</sup> is clearly outstanding.

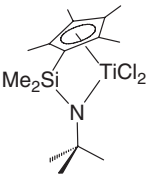
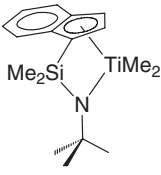
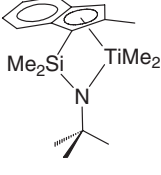
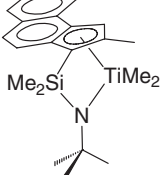
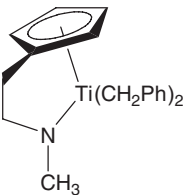
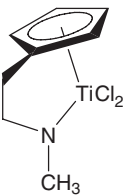
**Table 3** Propylene polymerization with bis(cyclopentadienyl) Zr complexes

<i>Pre-catalyst</i>	<i>Activator</i>	<i>Conditions</i>	<i>Activity</i> (kg <sub>PP</sub> mmol <sub>Zr</sub> <sup>-1</sup> h <sup>-1</sup> )	$\bar{M}_w$	<i>Tacticity</i>	<i>References</i>
	MAO	Liquid propylene, 50 °C, 1 h	5.7	oligomers	~25% <i>mm</i>	180
	MAO	Liquid propylene, 50 °C, 1 h	63	$3.9 \times 10^4$	17.6% <i>mm</i>	669
	MAO	Liquid propylene, 0 °C, 1 h	1.8	$2.6 \times 10^5$	56% <i>m</i>	250
	MAO	Liquid propylene, 50 °C, 1 h	18	$\sim 1 \times 10^4$	30% <i>mm</i>	180
	MAO	Liquid propylene, 0 °C, 1 h	8	$3.2 \times 10^6$	36% <i>mm</i>	250
	MAO	Liquid propylene, 50 °C, 1 h	10	$2.2 \times 10^4$	35% <i>mm</i>	250
	MAO	Liquid propylene, 50 °C, 1 h	17.7	$1.4 \times 10^5$	20% <i>mm</i>	250
	MAO	Liquid propylene, 50 °C, 1 h	32.7	$4.6 \times 10^5$	15% <i>mm</i>	250

#### 4.09.4.2.2 Isotactic polypropylene

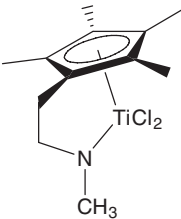
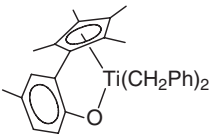
Isotactic PP is the second major thermoplastic in terms of volumes, and the vast majority of it is produced by means of heterogeneous Ti catalysts. As described in Section 4.09.3, the heterogeneous, donor-modified  $\text{MgCl}_2/\text{TiCl}_4/\text{AlR}_3$  catalysts produce very high molecular mass, highly isotactic PP with generally broad molecular mass distributions and containing small (2–10%) amounts of stereoirregular, amorphous PP, both telltales of the multi-site nature of such catalysts. Careful fractionation studies have demonstrated that, even in the more stereoregular, insoluble fraction of ZN iPP, the stereodefects are not randomly distributed in the chains but are rather cumulated in stereoblocks.<sup>713</sup> Therefore, ZN iPP has a relatively high crystallinity, a  $T_m$  of 163–167 °C, and relatively high elastic modulus (1500–2000 MPa).

**Table 4** Propylene polymerization with *ansa*-Cp-amido and related complexes

<i>Pre-catalyst</i>	<i>Activator</i>	<i>Conditions</i>	<i>Activity</i> (kg <sub>PP</sub> mmol <sub>Ti</sub> <sup>-1</sup> h <sup>-1</sup> )	$\bar{M}_w$	<i>Tacticity</i>	<i>References</i>
	MAO	Liquid propylene, 60 °C, 1 h	10.9	$650 \times 10^3$	10.5% <i>mm</i>	708
	MAO	Liquid propylene, 60 °C, 1 h	4.1	$135 \times 10^3$	24.8% <i>mm</i>	708
	MAO	Liquid propylene, 60 °C, 1 h	6.2	$550 \times 10^3$	15.6% <i>mm</i>	708
	MAO	Liquid propylene, 60 °C, 1 h	30.8	$194 \times 10^3$	13.8% <i>mm</i>	708
	B(C <sub>6</sub> F <sub>5</sub> ) <sub>3</sub>	Toluene, $4.7 \times 10^5$ Pa propylene, 30 °C, 30 min	0.72	$1,050 \times 10^3$	14% <i>mm</i>	461
	MAO	Toluene, $4.7 \times 10^5$ Pa propylene, 30 °C, 30 min	0.29	$720 \times 10^3$	17% <i>mm</i>	461

(Continued)

Table 4 (Continued)

Pre-catalyst	Activator	Conditions	Activity (kg <sub>PP</sub> mmol <sub>Ti</sub> <sup>-1</sup> h <sup>-1</sup> )	$\bar{M}_w$	Tacticity	References
	MAO	Toluene, 2 bar propylene, 50 °C, 30 min	2.4	110 × 10 <sup>3</sup>	22% mm < 0.5% 2,1	462
	Ph <sub>3</sub> C <sup>+</sup> B(C <sub>6</sub> F <sub>5</sub> ) <sub>4</sub> <sup>-</sup>	Toluene, 1 atm propylene, 25 °C, 5 min	3.8	23.6 × 10 <sup>3</sup>	22% mm	460

In the case of metallocene catalysts, due to their single-center nature, the stereochemical or regiochemical errors are randomly distributed in all PP chains. This randomness leads to PP of lower melting points ( $\leq 160^\circ\text{C}$ ) and stiffness, but at the same time better transparency, compared with ZN iPP.

The earlier, simple chiral *ansa*-bisindenyl zirconocenes and hafnocenes were found to be less stereoselective than ZN catalysts, producing PP of low melting point and very low molecular mass. The long development from the early Brintzinger and Ewen ethylene-bridged chiral *ansa*-bis(indenyl) structures<sup>202,203,714</sup> to metallocenes showing performances close to those of ZN catalysts has been described in detail up to the end of 1999.<sup>162</sup>

Since then, three major directions of industrial research have become evident: the introduction of pendant<sup>715,716</sup> or condensed heterocycles onto one or both Cp ligands,<sup>63,717–720</sup> the development of pseudo-racemic *C*<sub>1</sub>-symmetric structures aimed at removing the molecular mass drop induced by ethylene,<sup>586,721,722</sup> and the evolution of improved supportation techniques. This latter aspect has been extensively reviewed<sup>722–724</sup> and will not be further discussed here. Several new *C*<sub>2</sub>-symmetric structures have been described in recent years, mostly in the patent literature, and for the latter case polymerization results refer to the silica-supported catalysts.

A selection of these *C*<sub>2</sub>-symmetric structures, together with polymerization results, is shown in Table 5. Although structural complexity has grown considerably, no major improvement in propylene homopolymerization has been obtained so far.

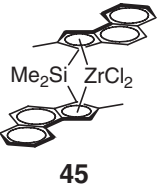
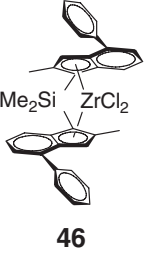


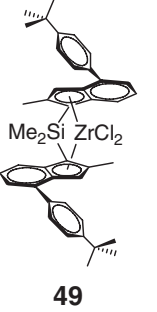
Stereoerrors in PP chains produced with catalyst systems based, for example, on Me<sub>2</sub>Si(2-Me-4-ArInd)<sub>2</sub>ZrCl<sub>2</sub> are close to the detection limit by NMR. The low melting point (*T*<sub>m</sub> 150–160 °C) of PP is due to the presence of regioirregularities (of the 2,1-*erythro*-type). Two <sup>13</sup>C NMR spectra of the methyl region of iPP having only regio-defects (2,1-*erythro*) and only stereodefects are shown in Figure 25.

It is worth noting here that in the early systems (such as *rac*-C<sub>2</sub>H<sub>4</sub>(Ind)<sub>2</sub>ZrCl<sub>2</sub>, *rac*-C<sub>2</sub>H<sub>4</sub>(H<sub>4</sub>Ind)<sub>2</sub>ZrCl<sub>2</sub>, *rac*-C<sub>2</sub>H<sub>4</sub>(4,7-Me<sub>2</sub>Ind)<sub>2</sub>ZrCl<sub>2</sub>, and their Me<sub>2</sub>Si-bridged analogs), 2,1-insertions have been indicated as the cause of lower molecular masses and activities, due to the formation of a less reactive catalyst state, and to fast β-H transfer after a 2,1-unit (see Section 4.09.2.4). On the other hand, the zirconocenes of the class Me<sub>2</sub>Si(2-Me-4-ArInd)<sub>2</sub>ZrCl<sub>2</sub>, despite an even lower regioselectivity, show the highest molecular masses and activities. In fact, the 2-Me-4-Ph substitution pattern increases stereoselectivity partially at the expense of regioselectivity,<sup>164</sup> but without increasing chain transfer rates: here, a 2,1-unit does not seem to adversely affect the rate of monomer insertion.

From the examples in Tables 5–7, it is clearly apparent that, of the different evolutionary directions of isospecific metallocene structures, the one based on the 2-methyl-4-aryl-indenyl type,<sup>734</sup> has by far been the most successful.

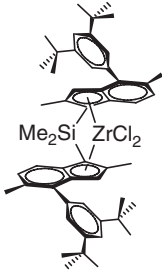
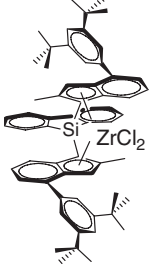
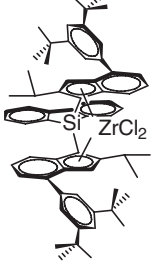
The influence of polymerization conditions on the performance of isoselective, *C*<sub>2</sub>-symmetric metallocenes has been described in detail already.<sup>162</sup> Two further studies on catalysts *rac*-Me<sub>2</sub>Si(2-Me-4-PhInd)<sub>2</sub>ZrCl<sub>2</sub> and *rac*-Me<sub>2</sub>Si(2-Me-4-NaphthInd)<sub>2</sub>ZrCl<sub>2</sub> have appeared recently.<sup>305,735</sup> Busico has investigated the kinetics of propylene polymerization with *rac*-Me<sub>2</sub>Si(2-Me-4-PhInd)<sub>2</sub>ZrCl<sub>2</sub>/MAO.<sup>297</sup>

**Table 5** Selected C<sub>2</sub>-symmetric isospecific zirconocenes with a 2-alkyl-4-aryindenyl ligand framework

Zirconocene	Activator	<i>T</i> <sub>p</sub> (°C)	<i>M</i> <sub>w</sub> (×10 <sup>-3</sup> )	<i>T</i> <sub>m</sub> (°C)	NMR <sup>a</sup>	Notes	References
 45	MAO	70	228	144	96.3% <i>mm</i> , 93.8% <i>mmmm</i> 0.4% 2,1	Unsupported, liquid propylene	725
	MAO	40	257	145.4	92.5 % <i>mmmm</i> 1% 2,1	Silica-supported, hexane, [propylene]=1.83 mol <sup>-1</sup>	726
 46	MAO	70	1,184	156	99.1% <i>mmmm</i> 0.5% 2,1	Unsupported, liquid propylene	720
	MAO	60	600	149.2		Silica-supported, liquid propylene	727
 47	MAO	50	380	156.2	98.6 % <i>mmmm</i> 0.3% 2,1	Unsupported, toluene, 1 atm propylene	728
 48	MAO	50	400	159.8	99.2% <i>mmmm</i> ca. 0.8% 2,1	Unsupported, toluene, 1 atm propylene	728
 49	MAO	70	900	151		Silica-supported, liquid propylene	729,730

(Continued)

**Table 5** (Continued)

<i>Zirconocene</i>	<i>Activator</i>	$T_p$ (°C)	$\bar{M}_w$ ( $\times 10^{-3}$ )	$T_m$ (°C)	<i>NMR</i> <sup>a</sup>	<i>Notes</i>	<i>References</i>
 <b>50</b>	MAO	70	550	152.7		Silica-supported, liquid propylene	727
 <b>51</b>	MAO	60	711	156.2		Silica-supported, liquid propylene	587
 <b>52</b>	MAO	60	381	160.8		Silica-supported, liquid propylene (low activity)	587

<sup>a</sup>When allowed by data description, %*mmmm* refers to primary insertions only.

We recall here the two major effects:

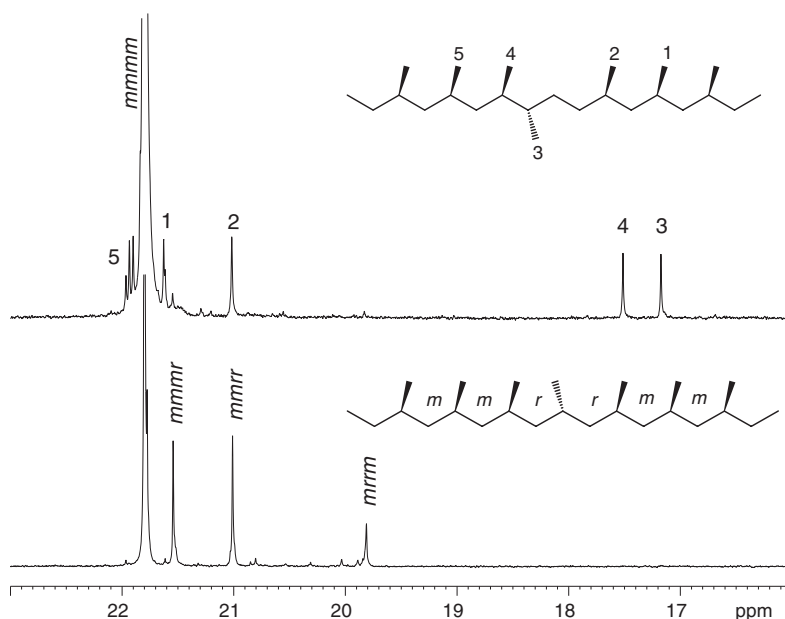
- (i) Propylene concentration has a non-linear influence on both iPP molecular mass and isotacticity. The cause of this behavior is the onset of competitive growing-chain-end epimerization. The mechanism of this reaction has been discussed in Section 4.09.2.4. Selected examples are shown in Figure 26 (isotacticity) and Figure 27 (molecular mass).

The rate of epimerization at a given monomer concentration  $[m]$  depends on the polymerization temperature and on the nature of the *ansa*- $\pi$ -ligand. The dependence of isotacticity on  $[m]$  can be described by Equation (10).<sup>162,241</sup> The equilibrium constant  $K_{eq} = [M \cdot m]/([M][m])$  is according to the model described in Ref: 162.

$$\frac{b_{obs}}{1-b_{obs}} = \frac{0.5 + bK_{eq}[m]}{0.5 + (1-b)K_{eq}[m]} \quad (10)$$

The observed (apparent) enantioselectivity parameter  $b_{obs}$  is usually lower than the true probability of a correct enantioface insertion (averaged over the two sites of the catalyst) in the absence of epimerization, defined by the





**Figure 25**  $^{13}\text{C}$  NMR spectra of the methyl region of iPP having almost only 2,1-*erythro*-regiodefects (top) and only stereodefects (bottom). The relative intensity of the *mmmr*, *mmrr*, and *mrrm* pentads is 2 : 2 : 1, the fingerprint of site-controlled isotactic chain growth.

Bernoullian probability parameter  $b$ : the value of  $b$  depends on the active site structure and  $T_p$ , but is independent of  $[\text{m}]$ . In liquid propylene, for most metallocenes  $b_{\text{obs}} \rightarrow b$ , at least at the polymerization temperature of 50 °C.

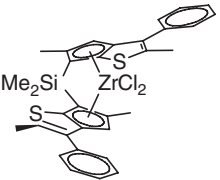
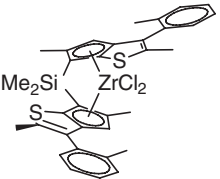
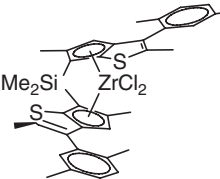
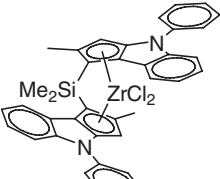
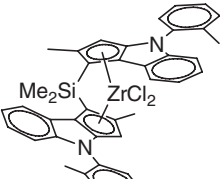
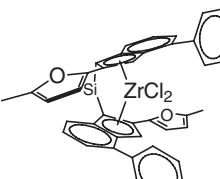
Concerning the dependence of molecular mass on monomer concentration, three examples are shown in Figure 27. In these examples, the main chain-release mechanism is different for each catalyst: Brintzinger's catalyst,  $\text{rac-C}_2\text{H}_4(\text{Ind})_2\text{ZrCl}_2/\text{MAO}$ , allows  $\beta\text{-H}$  transfer both after a 2,1-insertion; and after a 1,2-insertion; the fully regioselective catalyst,  $\text{rac-Me}_2\text{C}(\text{3-Bu}^t\text{Ind})\text{ZrCl}_2/\text{MAO}$ , shows mainly  $\beta\text{-Me}$  transfer;<sup>246</sup> while  $\text{rac-Me}_2\text{Si}(\text{2-Me-4-PhInd})\text{ZrCl}_2$ , despite being the least regioselective of the three, gives mainly  $\beta\text{-H}$  transfer after a 1,2-insertion (even in liquid monomer), with  $\beta\text{-Me}$  transfer becoming predominant at the lowest monomer concentrations.<sup>268</sup>

Two facts are worth pointing out: (a) testing metallocene catalysts under reduced pressure might lead to gross underestimation of their molecular mass capability and isoselectivity, and to missing possibly relevant differences between different catalysts; and (b) regioselectivity also affects the crystallinity of iPP.<sup>736–738</sup> For example,  $\text{rac-Me}_2\text{Si}(\text{2-Me-4-PhInd})\text{ZrCl}_2/\text{MAO}$  is more isospecific than  $\text{rac-Me}_2\text{C}(\text{3-Bu}^t\text{Ind})\text{ZrCl}_2/\text{MAO}$  at any propylene concentration, but less regioselective, the net result being that iPP from  $\text{rac-Me}_2\text{Si}(\text{2-Me-4-PhInd})\text{ZrCl}_2$  and  $\text{Me}_2\text{C}(\text{3-Bu}^t\text{Ind})\text{ZrCl}_2$  have very similar melting points.

- (ii) Increasing the polymerization temperature causes a drop, sometimes dramatic, in isoselectivity and molecular mass.<sup>267</sup> This effect has sometimes been overestimated due to concomitant decrease in monomer concentration, when the experiments were performed at constant pressure, rather than at constant monomer concentration.<sup>739</sup> Data detailing the influence of polymerization temperature for polymerizations in liquid propylene on iPP isotacticity and molecular mass are available for a few  $C_2$ -symmetric bisindenyl zirconocenes.<sup>204,267</sup>

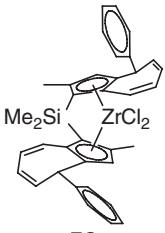
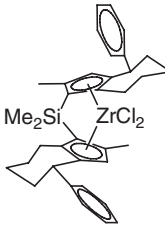
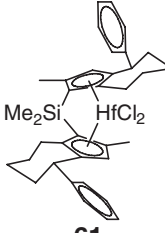
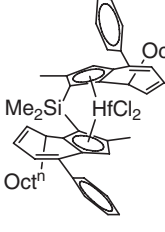
On the other hand, the above phenomena do not apply to  $C_1$ -symmetric (nor to syndiospecific  $C_s$ -symmetric) metallocenes: for these, decreasing monomer concentration either increases the isotacticity and melting point of iPP or has no relevant effect. This is due to the mechanism of site epimerization (also referred to as chain backskip, Scheme 28), in which the chain, at the lower monomer concentrations, has a higher chance to migrate to the less hindered site, which is usually also the more stereoselective. For the same reason, increasing the polymerization temperature either increases the melting point of an isotactic poly( $\alpha$ -olefin), or has no relevant effect.<sup>725</sup>

**Table 6** Selected  $C_2$ -symmetric isospecific zirconocenes containing heterocycles

<i>Zirconocene</i>	<i>Activator</i>	$T_p$ (°C)	$\bar{M}_w$ ( $\times 10^{-3}$ )	$T_m$ (°C)	<i>NMR</i> <sup>a</sup>	<i>Notes</i>	<i>References</i>
 <b>53</b>	MAO	70	445	156	0.41% <i>mrrm</i> 0.3% 2,1	Unsupported, liquid propylene	720
 <b>54</b>	MAO	70	604	160	0.35% <i>mrrm</i> 0.2% 2,1	Unsupported, liquid propylene	720
	Ph <sub>3</sub> CB(C <sub>6</sub> F <sub>5</sub> ) <sub>4</sub> /TIBA	70	1,165	162		Unsupported, liquid propylene	720
 <b>55</b>	MAO	70	795	160	0.26% <i>mrrm</i> , 0.2% 2,1	Unsupported, liquid propylene	720
 <b>56</b>	MAO	70	69.3	154.4	97% <i>mmmm</i> 0.17% 2,1	Unsupported, liquid propylene, 1% H <sub>2</sub> in gas phase	63
 <b>57</b>	MAO	70	55.5	156.3	97.7% <i>mmmm</i> 0.34% 2,1	Unsupported, liquid propylene, 1% H <sub>2</sub> in gas phase	63
 <b>58</b>	MAO	30	733, 000	159.1	97.3% <i>mmmm</i>	Toluene	716,731

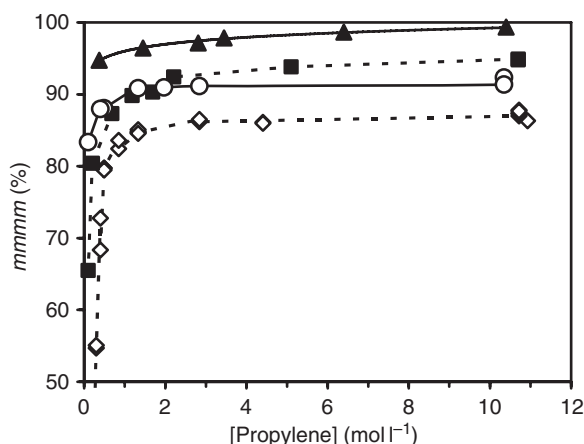
<sup>a</sup>When allowed by data description, %*mmmm* refers to primary insertions only.

**Table 7** Selected  $C_2$ -symmetric isospecific zirconocenes based on azulenyl and related rings

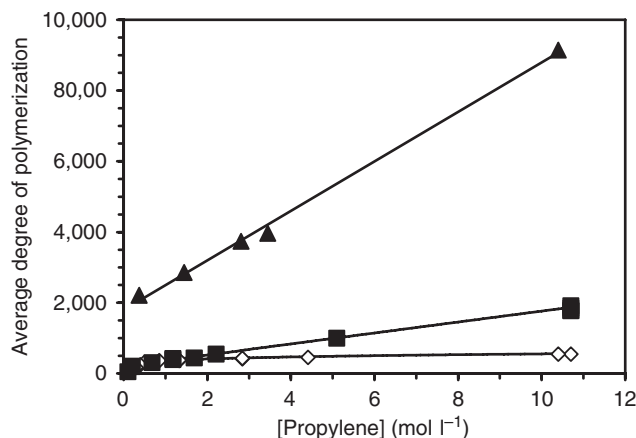
<i>Zirconocene</i>	<i>Activator</i>	$T_p$ (°C)	$(\bar{M}_w)$ ( $\times 10^{-3}$ )	$T_m$ (°C)	<i>NMR</i>	<i>Notes</i>	<i>References</i>
 <b>59</b>	MAO	70	350	151	96.8% <i>mmmm</i>	Unsupported, liquid propylene	732
 <b>60</b>	MAO	70	370	156	96.0% <i>mmmm</i>	Unsupported, liquid propylene	732
 <b>61</b>	MAO	70	2,500	160		Unsupported, liquid propylene	Iwama JOMC 2005
 <b>62</b>	MAO	70	90	Amorphous	83.5% <i>mmmm</i> 12.5% 3,1	Unsupported, liquid propylene	733

$C_1$ -symmetric structures having one of the two Cp ligands endowed with bilateral symmetry (such as fluorenyl) have several synthetic advantages, the main being the absence of a *meso*-isomer (Figure 28). We recall here that the latter is instead formed as the undesired byproduct in the synthesis of the  $C_2$ -symmetric chiral *ansa*-metallocenes.

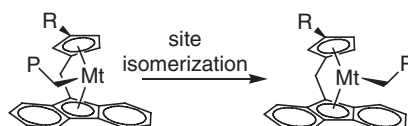
In general,  $C_1$ -symmetric structures based on fluorene give lower molecular masses than the best  $C_2$ -symmetric ones, and are also less active, with very few exceptions. Two types of  $C_1$ -symmetric structures have been developed, one based on fluorene (or related ligands with bilateral symmetry) and substituted cyclopentadienes, and the other based on the same bilaterally symmetric ligands linked to substituted indenyls. Most of the latter have been developed to generate elastomeric PPs of low isotacticity and are discussed in the next section. Zirconocene complexes containing substituted indenyls usually give higher molecular mass iPP compared to the ones having substituted cyclopentadienyls. The zirconocene complexes based on dithienocyclopentadienyl also produce higher



**Figure 26** Influence of propylene concentration on iPP isotacticity (%*mmmm*).  $\diamond$ : *rac*-C<sub>2</sub>H<sub>4</sub>(Ind)<sub>2</sub>ZrCl<sub>2</sub>/MAO at 50 °C in toluene;  $\circ$ : *rac*-C<sub>2</sub>H<sub>4</sub>(4,7-Me<sub>2</sub>Ind)<sub>2</sub>ZrCl<sub>2</sub>/MAO at 50 °C in toluene;  $\blacksquare$ : *rac*-Me<sub>2</sub>C(3-Bu<sup>1</sup>Ind)ZrCl<sub>2</sub>/MAO at 50 °C in pentane;  $\blacktriangle$ : *rac*-Me<sub>2</sub>Si(2-Me-4-PhInd)ZrCl<sub>2</sub>/MAO at 60 °C in hexane.



**Figure 27** Influence of propylene concentration on iPP molecular mass.  $\diamond$ : *rac*-C<sub>2</sub>H<sub>4</sub>(Ind)<sub>2</sub>ZrCl<sub>2</sub>/MAO at 50 °C in toluene;  $\blacksquare$ : *rac*-Me<sub>2</sub>C(3-Bu<sup>1</sup>Ind)ZrCl<sub>2</sub>/MAO at 50 °C in pentane;  $\blacktriangle$ : *rac*-Me<sub>2</sub>Si(2-Me-4-PhInd)ZrCl<sub>2</sub>/MAO at 60 °C in hexane.<sup>722</sup>

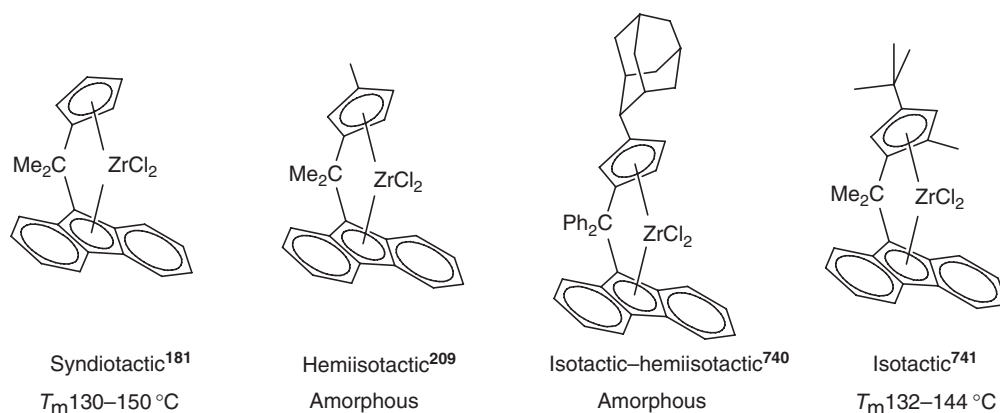


**Scheme 28**

molecular masses compared to the ones based on fluorenyl. Selected *C*<sub>1</sub>-symmetric structures and polymerization results related to the high isoselectivity structures are listed in Table 8 (cyclopentadienyls) and Table 9 (indenyls).

#### 4.09.4.2.3 Low isotacticity: from flexible to elastomeric isotactic polypropylene

Metallocenes purposely designed for the synthesis of stereodisordered, low melting, soft and highly flexible PPs have been reviewed up to the end of 1999.<sup>162</sup> In subsequent years, the line of research aimed at the preparation of low-crystallinity plastomeric or elastomeric iPP has aroused increasing interest, both from the perspective of catalyst



**Figure 28** Influence of the Cp-C(3) substituent in  $C_1$ -symmetric fluorenyl-ansa-cyclopentadienyl complexes.

design as well as from the standpoint of material properties. In addition to manufacturing difficulties of these polymers in slurry or gas-phase processes, the most important limitation to the practical use of these materials is the relatively high glass transition temperature of PP ( $T_g \sim 0^\circ\text{C}$ ), which prevents the use at sub-ambient temperatures, where PP becomes brittle. We recall that the  $T_g$  of a polyolefin, being a property of the amorphous phase, is not (or very little)<sup>222</sup> affected by tacticity.

The most successful classes of metallocene catalysts studied for low-tacticity iPP are: (i) the fluxional bis(2-aryindenyl) metallocenes first conceived and demonstrated by Waymouth and Coates<sup>748</sup> and recently reviewed;<sup>749,750</sup> (ii) a few examples of  $C_2$ -symmetric, 3-alkyl-substituted *ansa*-bis(indenyl) zirconocenes,<sup>222,709,751</sup> and (iii) several types of  $C_1$ -symmetric catalysts.

Of all the catalyst types, the sterically fluxional bis(2-aryindenyl) complexes<sup>749,752–768</sup> produce elastomeric PP with the best combination of properties, that is, relatively high melting points and very low crystallinity, due to their stereoblock nature,<sup>769–772</sup> but unfortunately their activity and molecular mass capability are too low at industrial polymerization temperatures (60–80 °C). The mechanism of stereoblock formation originally proposed by the inventors<sup>748</sup> has recently been questioned and an active role of the counterion has been proposed to better account for the heptad distribution in the  $^{13}\text{C}$  NMR spectra of the elastomeric, stereoblock PP.<sup>773,773a</sup> These polymers are PP reactor blends, since they can be fractionated with solvents into low- and high-tacticity components.<sup>162,767,769,770,774,775</sup>

The  $C_2$ -symmetric zirconocenes of type (ii) have two key structural features: a single carbon bridge, and a 3-isopropyl substituent on indene. For any alkyl substituent on C(3) of indene, all complexes are fully regioselective (through  $^{13}\text{C}$  NMR at 100 MHz), and the size of the 3-R substituent dramatically affects PP microstructure and molecular mass, as shown in Table 10.

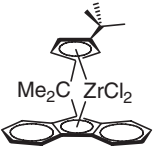
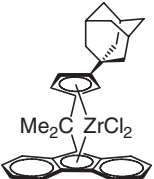
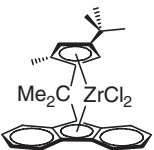
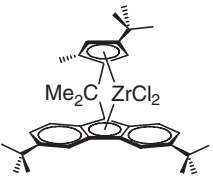
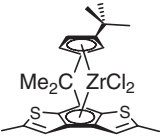
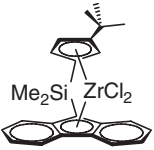
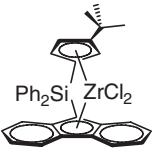
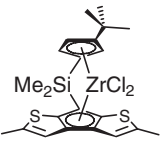

A comparison of the physical properties of these polymers with that of fully amorphous PP has been reported.<sup>722</sup>

These  $C_2$ -symmetric zirconocenes are made from relatively inexpensive ligands, but have some limitations: their synthesis produces an isomer ratio *rac*/*meso* < 1 and their catalytic activities are not very high. In addition, the elastomeric PP cannot be produced with controlled morphology in liquid propylene and, as is the case of the bis(2-aryindenyl) systems mentioned above, do not give sufficiently high molecular masses in solution at industrial polymerization temperatures.

Of the three classes designed for elastomeric or plastomeric PP, the most successful seems to be the class of  $C_1$ -symmetric structures. These are based on the bilaterally symmetric fluorenyl ligands, first developed by Ewen,<sup>209</sup> and have received a great deal of attention due mainly to three facts: (i) they are far simpler to synthesize than the chiral isospecific  $C_2$ -symmetric metallocenes; (ii) they can cover a very broad range of stereoselectivity by structural modification of one ligand only; and (iii) due to the presence of two different active sites, they offer a more potent mechanistic tool and intellectual challenge.

The propylene polymerization performances of the cyclopentadienyl-fluorenyl<sup>212,740,741,777</sup> and cyclopentadienyl-dithienocyclopentadienyl<sup>742,778,779</sup> systems have been recently reviewed.<sup>742</sup> The major drawbacks limiting the use of these catalysts are an often low activity and low molecular masses, with only a couple of exceptions. A selection of results related to the low stereoselective catalysts of this type is shown in Table 11.

**Table 8** Propylene polymerization results with MAO-activated (3-RCp) C<sub>1</sub>-symmetric structures<sup>a</sup>

Pre-catalyst	<i>T</i> <sub>p</sub> (°C)	<i>mmmm</i> (%)	<i>T</i> <sub>m</sub> (°C)	$\bar{M}_v$	References
	60	77.5	127	62,000 ( $\bar{M}_w$ )	741
	60	80.1	129	47,800	742
	60	86.3	144	402,000 ( $\bar{M}_w$ )	741
	70		154	321,000 ( $\bar{M}_w$ )	743
	60	82.9	139	50,100	742
	60		148	68,000	744
	70		144	47,000 ( $\bar{M}_w$ )	745
	60	92.1	148	11,100	742
	70	93.8	150	39,900	742

<sup>a</sup>All data from liquid propylene polymerizations.

**Table 9** Propylene polymerization results with MAO-activated indenyl C<sub>1</sub>-symmetric structures

Pre-catalyst	$T_p$ (°C)	$mm$ (%)	$T_m$ (°C)	$\bar{M}_w$	References
	70	91	151	27,000	746
	70	92	142	50,000	747
	70	93.8	148	107,400 ( $\bar{M}_v$ )	725
	70	96.2	156	139,900 ( $\bar{M}_v$ )	725

<sup>a</sup>All data from liquid propylene polymerizations.**Table 10** Influence of the bridge and indenyl C(3) substituents on PP structure. Liquid propylene polymerization results at 50 °C<sup>222,776</sup>

$mmmm$ (%)	94.8	15.6	n.a. <sup>a</sup>	80.7
$T_m$ (°C)	124.6	Amorphous	None	127
$\bar{M}_w$	111,400	164,000	~8,000	~12,000
$mmmm$ (%)	97	25.5	20.0	71.4
$T_m$ (°C)	162	Elastomeric	Amorphous	110
$\bar{M}_w$	236,800	100,600	~21,000	3,100

<sup>a</sup>n.a. = not available.

**Table 11** C<sub>1</sub>-symmetric cyclopentadienyl–fluorenyl and cyclopentadienyl–dithienocyclopentadienyl complexes

[Propylene]	2 bar	2 bar	Liquid	Liquid
T <sub>p</sub> (°C)	70	70	60	60
mm (%)	52.7	63.2	77.3	
mmmm (%)	31.4	44.0	64.4	67.0
T <sub>m</sub> (°C)				109
$\bar{M}_v$			62,000 ( $\bar{M}_w$ )	64,000 ( $\bar{M}_n$ )
References	212	212	780	781,782
[Propylene]	Liquid	1.29 mol l <sup>-1</sup>	Liquid	Liquid
T <sub>p</sub> (°C)	20	30	20	20
mm (%)	50.1	70.8	50.6	43.5
mmmm (%)	31.8	57.5	31.4	25.3
T <sub>m</sub> (°C)	149	n.r.	88	125
$\bar{M}_w$	535,000 ( $\bar{M}_w$ )	270,000 ( $\bar{M}_v$ )	81,900 ( $\bar{M}_w$ )	435,000 ( $\bar{M}_w$ )
References	740	783	740	740
[Propylene]	Liquid	Liquid	+diastereoisomer Liquid	Liquid
T <sub>p</sub> (°C)	20	40	70	20
mm (%)	45.0	44.6	60.2	38.6
mmmm (%)	24.0	23.2		18.5
T <sub>m</sub> (°C)	135			147
$\bar{M}_w$	806,000	128,000	29,000	390,000
References	740	778	784	740
[Propylene]	Liquid	Liquid	Liquid	Liquid
T <sub>p</sub> (°C)	60	60	60	60
mm (%)	58.7	84.0	73.2	66.5
mmmm (%)	42.3	73.2	59.9	49.24
$\bar{M}_n$	45,500	140,000	80,000	113,000
T <sub>m</sub> (°C)	80	123	103	80
References	742	742	742	742

Complexes based on the indenyl–fluorenyl,<sup>576,725,785,786</sup> heteroindenyl–fluorenyl,<sup>787</sup> and indenyl–dithienocyclopentadienyl systems<sup>725,738,788</sup> show improved catalytic performance, producing PPs with often higher molecular masses. Some of these catalysts have very high activities in liquid propylene. Selected structures with polymerization results are shown in Table 12.

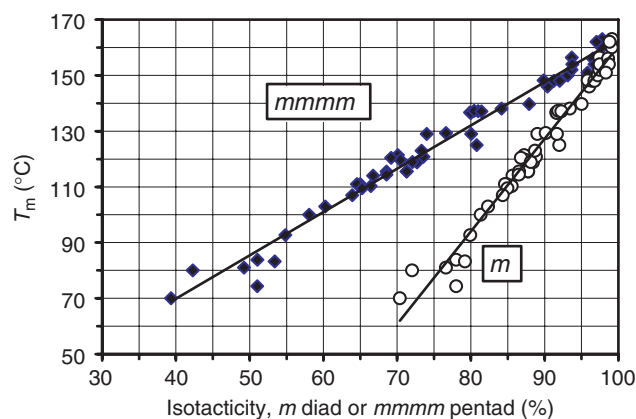


**Table 12** C<sub>1</sub>-symmetric indenyl–fluorenyl, heteroindenyl–fluorenyl, and indenyl–dithienocyclopentadienyl complexes

[Propylene]	Liquid	Liquid	Liquid <sup>a</sup>	Liquid
<i>T<sub>p</sub></i> (°C)	70	50	50	70
<i>mm</i> (%)	57			71
<i>mmmm</i> (%)		27	34	
<i>T<sub>m</sub></i> (°C)	114		117	87
<i>M<sub>w</sub></i>	40,000	200,000	700,000	50,000
References	746	789	789	747
[Propylene]	Liquid	5.1 M	5.1 M	Liquid <sup>a</sup>
<i>T<sub>p</sub></i> (°C)	70	30	30	30
<i>mm</i> (%)	77.4	62		
<i>mmmm</i> (%)	65.2	44	35.8	77.7
<i>T<sub>m</sub></i> (°C)	110			
<i>M<sub>w</sub></i>	152,000 ( <i>M<sub>v</sub></i> )	158,000	115,000	254,000
References	725	790	791	792
[Propylene]	Liquid	Liquid	Liquid	Liquid
<i>T<sub>p</sub></i> (°C)	40	40	60	70
<i>mm</i> (%)			81.7	
<i>mmmm</i> (%)	58	72	71.4	56
<i>T<sub>m</sub></i> (°C)			117	125
<i>M<sub>w</sub></i>	300,000	300,000	236,700	149,000
References	793	793	725,787	787
[Propylene]	Liquid	Liquid	Liquid	Liquid
<i>T<sub>p</sub></i> (°C)	70	70	70	70
<i>mm</i> (%)	79.8	67.0	82.2	90.2
<i>mmmm</i> (%)	68.6	51.1	72.1	84.2
<i>T<sub>m</sub></i> (°C)	116	84	119	138
<i>M<sub>v</sub></i>	231,500	123,400	209,000	169,600
References	725	725	725	725

<sup>a</sup>Activated with CPh<sub>3</sub>[B(C<sub>6</sub>F<sub>5</sub>)<sub>4</sub>].

The average isotactic sequence length determines the average crystal lamella thickness, which in turn is directly related to the heat of fusion and melting temperature of iPP. The correlation between microstructure and DSC melting point of a series of fully regioregular, as-polymerized (neither moulded nor extruded) iPP samples is shown in Figure 29. Several detailed studies on the influence of the amount and type of stereocerrors on highly defective, Bernoullian (random) PP have been reported.<sup>738,786,789,793</sup>

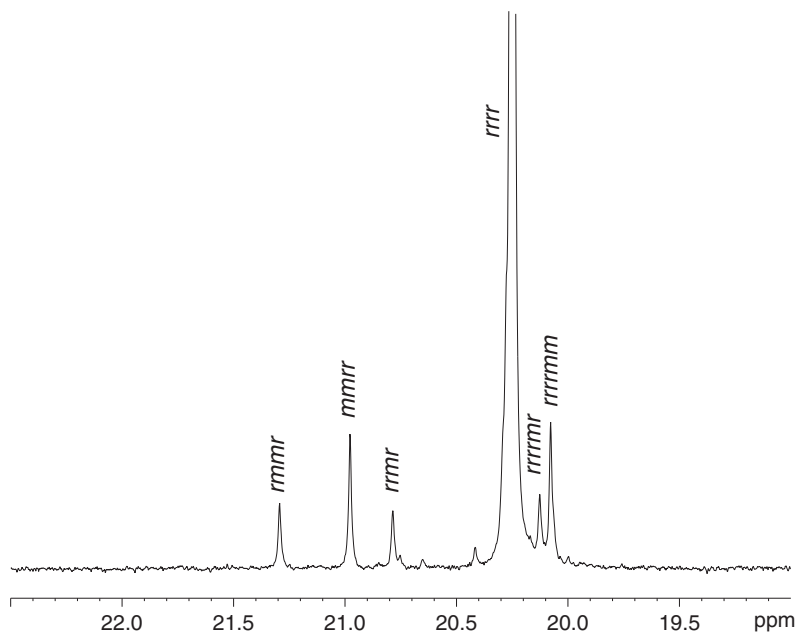


**Figure 29** Melting point,  $T_m$  (second melt, heating rate  $10^\circ \text{ min}^{-1}$ ), of regioregular iPPs made with  $C_1$ - and  $C_2$ -symmetric metallocene catalysts, as a function of isotacticity (◆:  $mmmm$  %; ○:  $m$  %).<sup>725,742</sup>

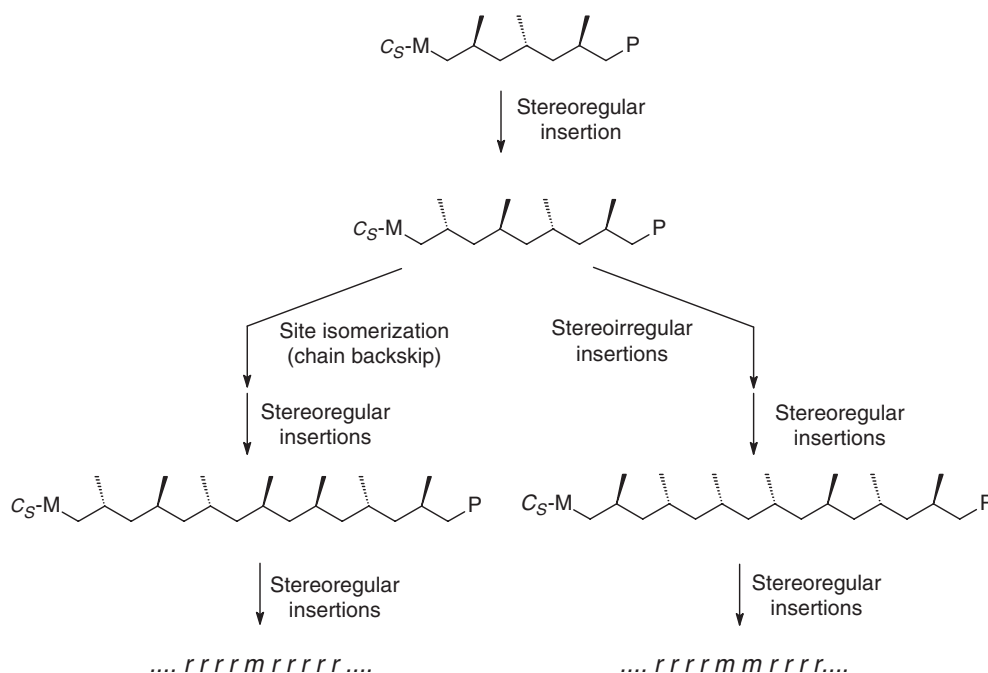
#### 4.09.4.2.4 Syndiotactic crystalline and elastomeric polypropylene

The report by Ewen and co-workers that a metallocene of  $C_s$ -symmetry was able to produce a highly syndiotactic, fully regioregular PP by site-controlled primary polyinsertion provided the first clear-cut evidence that metallocene catalysts operate by a dual-site chain-migratory mechanism.<sup>181,208</sup> Figure 30 shows the  $^{13}\text{C}$  NMR methyl region of sPP produced with **65**/MAO at  $50^\circ \text{C}$  in liquid propylene. This spectrum clearly shows the fingerprint of stereoerrors due to enantioface misinsertion ( $rrrm = rrrm = 2rrmr$ ) and of chain backskip (site isomerization) leading to the formation of an isolated  $m$  dyad ( $rrmr = rrrm$ ). Since this spectrum is at the level of heptad resolution, the  $rrrrmr$  and  $rrrrmm$  heptads are separated. The sequence of insertions leading to the different stereosequences is shown in Scheme 29. Chain-end epimerization (see Section 4.09.5.2.1) does not seem to occur with  $C_s$ -symmetric metallocenes.<sup>182,794</sup> In addition, syndiospecific catalysts are also highly regioselective.<sup>164,795</sup>

In contrast to the isospecific  $C_2$ -symmetric metallocenes, which required 20 years of structural improvement in order to achieve acceptable molecular mass capability and high isotacticity, in the case of  $C_s$ -symmetric complexes, the evolution from the original  $\text{Me}_2\text{C}(\text{Cp})(9\text{-Flu})\text{ZrCl}_2$  (**65**, Table 13) resulted very early in the complex



**Figure 30** Methyl region of  $^{13}\text{C}$  NMR spectra of sPP obtained from **65**/MAO at  $50^\circ \text{C}$  in liquid propylene (see Table 13).



**Scheme 29** Insertion sequences leading to the two major types of enchainment defects in propylene polymerization at a  $C_s$ -symmetric active center: site isomerization (left) and enantioface misinsertion (right).

$\text{Ph}_2\text{C}(\text{Cp})(9\text{-Flu})\text{ZrCl}_2$  (**66**, Table 13),<sup>745,796</sup> which on MAO activation produces sPP with very high molecular masses and requires  $\text{H}_2$  for molecular mass control. Nevertheless, the syndiospecificity of **66** not being very high, the quest for a more syndiospecific catalyst (hence producing sPP with a higher melting point and hopefully a faster sPP crystallization rate) has continued in recent years, with some improvements with respect to the parent cyclopentadienyl–fluorenyl-based structures (selected data are reported in Table 13).

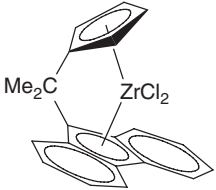
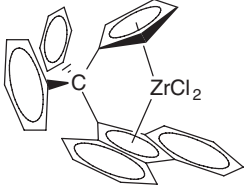
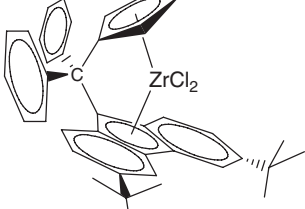
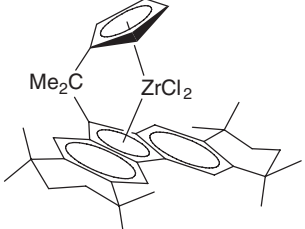
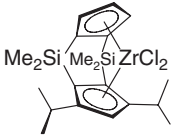
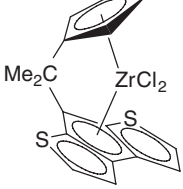
All aspects of syndiospecific propagation with  $C_s$ -symmetric catalysts, the influence of ligand,<sup>794,797–807</sup> metal,<sup>806,808,809</sup> and counteranion<sup>100,104</sup> variations, as well as the influence of the polymerization conditions,<sup>805,810</sup> have been studied in detail and reviewed.<sup>162,181,209,288,811</sup>

Syndiotactic PP is a thermoplastic with a slightly lower melting point (150–155 °C), lower crystallization rate, and higher flexibility (elastic modulus ca. 500) than iPP. It also has lower density, lower heat sealing temperature, but also better impact properties and better transparency.<sup>812,813</sup> One of the difficult aspects of sPP as a material, but a great playground for polymer chemists and physicists, is its polymorphic behavior: sPP has complex thermal properties and can crystallize in four different forms, some of which can interconvert.<sup>814–821</sup>

A different, possibly more productive, research direction has been the development of less syndiospecific catalysts, based on modifications of the silyl-bridged cyclopentadienyl–amido titanium complex.

Based on the symmetry requirements for syndiospecificity, the  $C_s$ -symmetry of most of *ansa*-Cp–amido titanium complexes should render them syndiospecific by site control. However,  $\text{Me}_2\text{Si}(\text{C}_5\text{Me}_4)(\text{NBu}^t)\text{TiCl}_2$  shows only minor syndiospecificity (about 50% *rr* triads), very likely because the bulky tetramethylcyclopentadienyl moiety cannot easily accommodate the methyl group of the coordinated propylene molecule in its syndiospecific placement (methyl opposite to the preferred conformation of the growing chain, which is away from the  $\text{C}_5\text{Me}_4$  ligand). Replacing tetramethylcyclopentadienyl by fluorenyl does increase syndiotacticity, at least for polymerizations in heptane at 0 °C.<sup>822</sup> However, several titanium complexes with more expanded Cp rings have shown improved syndiospecificity. Examples include structures with *t*-butylamide linked to 2,7-di-*tert*-butylfluorene,<sup>782</sup> 3,6-di-*tert*-butylfluorene,<sup>781,823</sup> indenoindole,<sup>824</sup> or indenopyrrole.<sup>824</sup> Syndiospecificity of these complexes never reaches that of the cyclopentadienyl–fluorenyl complexes described above, but nevertheless it is high enough to produce PP which is partially crystallizable and highly elastic due to the formation of small crystalline domains in the predominantly amorphous phase. The heterocyclic Ti complexes produce PP of very high molecular masses, even at polymerization temperatures as high as 80 °C. Syndiotactic pentad contents range from 48% to 57% *rrrr*, with very low amounts of

**Table 13** Selected results from syndiospecific bis-cyclopentadienyl complexes

<i>Pre-catalyst</i>	<i>Activator</i>	<i>Polym. conditions</i>	<i>Syndiotacticity</i>	<i>Average molecular mass</i> ( $\bar{M}_v$ or $\bar{M}_w$ )	$T_m(^{\circ}\text{C})$	<i>References</i>
 <b>65</b>	MAO	0 °C, liquid propylene	88.1 <i>rrrr</i>	140,000	145	162
		50 °C, liquid propylene	82 <i>rrrr</i>	$10^5$	137	162
 <b>66</b>	MAO	20 °C, liquid propylene	98.7 <i>rr</i>	$8.4 \times 10^5$	147	794
	MAO	40 °C, liquid propylene	92.7 <i>rr</i>	$3.8 \times 10^5$	137	794
	MAO	60 °C, liquid propylene	91.0 <i>rr</i>	$2.7 \times 10^5$	132	794
 <b>67</b>	MAO	60 °C	88.5 <i>rrrr</i>	$5.1 \times 10^5$	143	741
 <b>68</b>	MAO	0 °C, liquid propylene	95.5 <i>rr</i>	$5.3 \times 10^5$	154	806
 <b>69</b>	MAO	20 °C, liquid propylene	96.9 <i>rr</i>	$1.2 \times 10^6$	151	794
		50 °C, liquid propylene	95.5 <i>rr</i>	$3.3 \times 10^5$	140	794
		70 °C, liquid propylene	89.5 <i>rr</i>	$1.6 \times 10^5$	119	794
 <b>70</b>	MAO	50 °C, liquid propylene	84.0 <i>rr</i>	$10^5$	110	717,742

regioerrors. These PPs have been studied in detail in terms of their physical properties by De Rosa and co-workers.<sup>825–827</sup> The high molecular masses also contribute to improve elasticity. For example, catalyst **73**/MAO produces sPP with a tensile modulus < 30 MPa and elongation at break > 600%.

Some examples are shown in Table 14, together with a selection of polymerization results. It is worth noting the higher syndiospecificity of the Zr complex **74** compared to that of **73**, and the even higher syndiospecificity of the Zr complex, which bears the expanded octamethyloctahydrodibenzofluorenyl ligand (>99% *rrrr*,  $T_m = 165^\circ\text{C}$  at  $-15^\circ\text{C}$  in liquid propylene).<sup>942</sup> The very low activities and sPP molecular masses of **74**/MAO however render this complex of little interest.

Figure 31 shows the correlation between melting points and stereoregularity in the syndiotactic domain. As is the case of isoselective single-center catalysts, the degree of stereocontrol decreases by increasing the polymerization temperature for the syndiospecific ones. This behavior is shown in Figure 32.

#### 4.09.4.2.5 Semicrystalline propylene/ethylene co-polymers

On reading Section 4.09.4.2, it must have appeared evident that the very beauty of metallocene catalysts – tunability of selectivity and molecular mass by ligand design – is also their major weakness, at least from a practical (industrial) perspective. In fact, each single-center catalyst produces its own polymer, and the polymer properties can be modified only to a limited extent by varying the polymerization conditions, especially when the molecular mass of the polymer and the activity of the catalyst have to be kept within the range of practical applications. Developing a catalyst for an industrial process is a very expensive and time-consuming exercise. In addition to being highly active, toxicologically safe, inexpensive, and fit for the polymerization processes at which it is aimed, a successful catalyst must also be “versatile”. Although the dream of “one catalyst fit for all polymers and all processes” will hardly ever come true, an ideal catalyst must have high performance in both liquid and gas phase, a high molecular mass capability, a good hydrogen response, and must react efficiently with more than one monomer. In other words, it must be able to produce as many different polyolefin materials as possible.

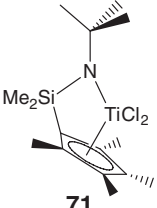
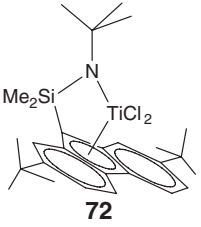
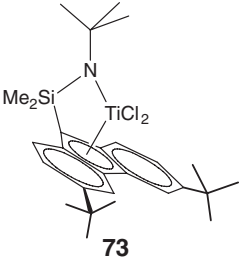
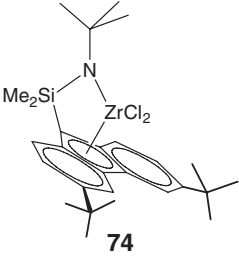
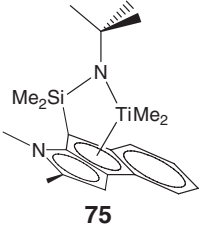
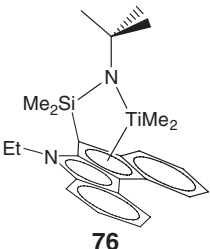
These are the main reasons that highlight the true value of single-center catalysts and metallocenes in particular, with respect to Ti-based Ziegler–Natta and Cr-based Phillips systems: a very good co-monomer distribution ability (from random to alternating), coupled with the generally much higher reactivity toward the higher and less reactive olefinic co-monomers.

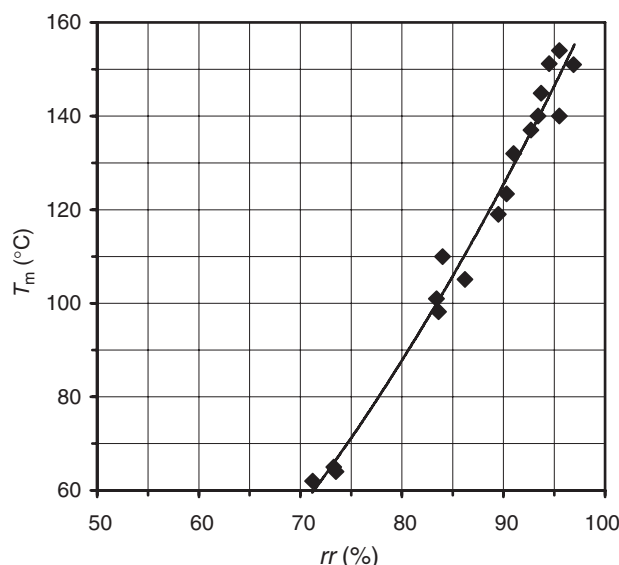
It is obviously much easier to tune polyolefin properties by adding co-monomers, rather than modifying the polymerization conditions or the catalyst itself. In addition, co-monomers enable the tuning of such properties, like the glass transition temperature, that cannot be changed by changes in tacticity, in the case of poly( $\alpha$ -olefins). This aspect has been extensively demonstrated in the case of both ethylene co-polymers (see Section 4.09.4.1) and propylene co-polymers. Below, we describe a few recent examples of the use of ethylene as co-monomer, and the following sections will cover the use of higher olefins.

Ethylene is used to modify the crystallinity of iPP: small amounts (1–10%) of ethylene reduce  $T_m$ , heat of fusion and  $T_g$  of iPP, thus increasing transparency and improving ductility, flexibility, and impact properties of iPP. This effect is stronger in metallocene-made propylene/ethylene co-polymers compared to ZN ones, due to a much better co-monomer distribution, and the absence of the highly modified, low molecular mass amorphous fraction typically formed with ZN catalysts. The co-polymer becomes soluble in hydrocarbons between 5 and 15 mol% ethylene, depending on stereoregularity, and is fully amorphous above 20 mol%. Several metallocene catalytic systems have been investigated for the production of elastomeric propylene/ethylene co-polymers, with the most relevant results being limited to the patent literature. The three key physical properties of these elastomeric co-polymers are melting point and heat of fusion (crystallinity), solubility in hydrocarbons (usually determined as the amount of co-polymer soluble in xylene at room temperature), and the glass transition temperature. The most apparent, and easier to measure, effect of ethylene on the structure of iPP is on the melting point. The decrease of melting point and heat of fusion induced by ethylene incorporation on PP from a typical highly stereoselective  $C_2$ -symmetric metallocene is shown in Figure 33.

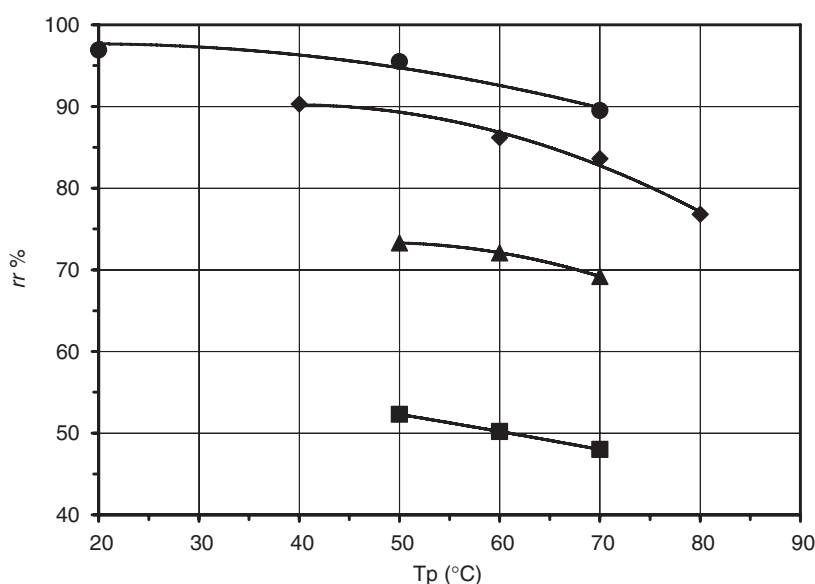
The main drawback of propylene/ethylene co-polymerization with metallocenes is the frequent strong decrease of molecular mass at increasing ethylene incorporation. The available mechanistic explanation is a fast chain transfer to ethylene after a propylene insertion (Scheme 30), and has been reported for metallocenes of different symmetries:  $C_2$ -symmetric,<sup>250</sup>  $C_2$ -symmetric,<sup>222,251–253</sup> and fluxional bis(2-aryindenyl).<sup>223</sup> This phenomenon has strongly limited the development of isoselective metallocenes for iPP until the introduction of the 2-isopropyl-indenyl ligands designed to solve the problem.<sup>586,721,722,828,829</sup> An alternative solution to low molecular masses is the use of hafnocenes, but activities are lower.<sup>584</sup>

**Table 14** Selected results from syndiospecific cyclopentadienyl amide complexes

<i>Pre-catalyst</i>	<i>Activator</i>	<i>Polym. conditions</i>	<i>Syndiotacticity</i>	<i>Average molecular mass</i> ( $\bar{M}_v$ or $\bar{M}_w$ )	$T_m(^{\circ}\text{C})$	<i>References</i>
 <b>71</b>	MAO	60 °C, liquid propylene	50.2 <i>rr</i>	$6.5 \times 10^5$	<i>Amorphous</i>	824
 <b>72</b>	MAO	60 °C, liquid propylene	63.9 <i>rrrr</i>	$5 \times 10^5$	<i>Amorphous</i>	782
 <b>73</b>	MAO	60 °C, liquid propylene	75.8 <i>rrrr</i> 86.2 <i>rr</i>	$3.5 \times 10^5$	105	781
 <b>74</b>	MAO	60 °C, liquid propylene	85.7 <i>rrrr</i> 93.7 <i>rr</i>	$6 \times 10^3$	145	781
 <b>75</b>	MAO	80 °C, liquid propylene	52 <i>rrrr</i> 71.2 <i>rr</i>	$10^6$	62	824
 <b>76</b>	MAO	70 °C, liquid propylene	54.1 <i>rrrr</i> 72.8 <i>rr</i>	$1.3 \times 10^6$		824



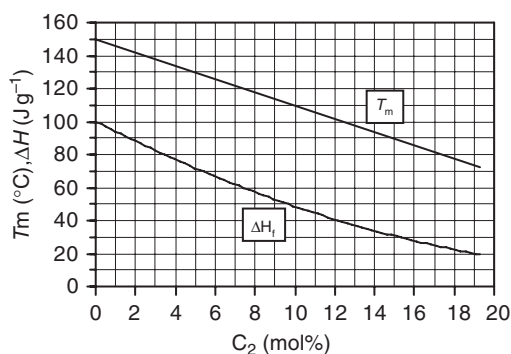
**Figure 31** Melting point of sPPs made with  $C_s$ -symmetric catalysts, versus the  $rr$  triad content. Note that samples with  $rr < 75\%$  are amorphous in the second DSC heating scan, and require several days of annealing at room temperature to develop measurable crystallinity.



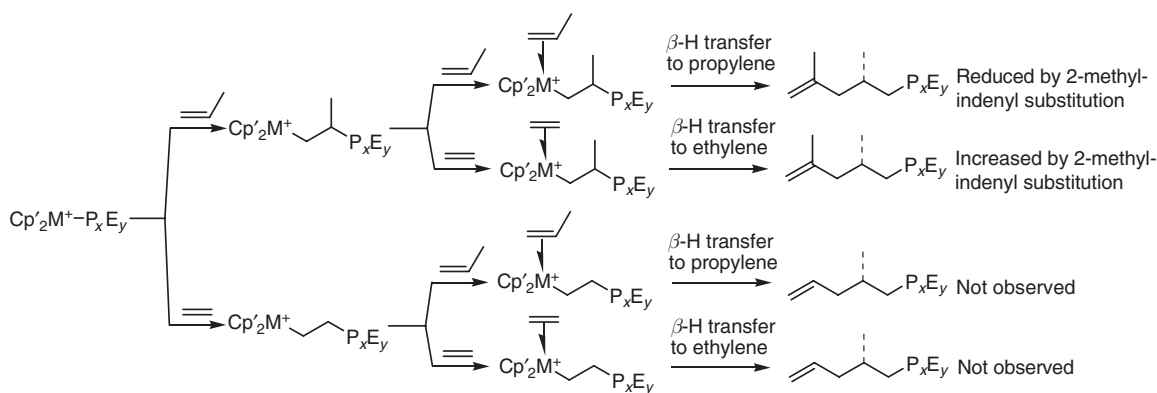
**Figure 32** Temperature dependence of the stereoselectivity of selected  $C_s$ -symmetric metallocenes. ■:  $\text{Me}_2\text{Si}(\text{C}_5\text{Me}_4)(\text{NBu}^t)\text{-TiMe}_2/\text{MAO}$ ,<sup>824</sup> ▲:  $\text{Me}_2\text{Si}(2,5\text{-dimethyl-5,6-dihydroindeno-indol-6-yl})(\text{NBu}^t)\text{-TiMe}_2/\text{MAO}$ ,<sup>824</sup> ◆:  $\text{Me}_2\text{Si}(3,6\text{-Bu}^t_2\text{Flu})(\text{NBu}^t)\text{-TiMe}_2/\text{MAO}$  63,<sup>781</sup> ●:  $(1,2\text{-SiMe}_2)_2(\text{C}_5\text{H}_2)(\text{C}_5\text{H-3,5-Pr}^i_2)\text{ZrCl}_2/\text{MAO}$  64.<sup>794</sup>

#### 4.09.4.2.6 Propylene/butene co-polymers

Isotactic  $\text{C}_3/\text{C}_4$  co-polymers with  $\text{C}_4 < 15\%$  are made with Ziegler–Natta catalysts in order to improve transparency, increase flexibility, and lower the melting point of iPP.<sup>830–832</sup>  $\text{C}_3/\text{C}_4$  co-polymers with higher content of butene are commercialized by Mitsui under the trade name TAFMER XR or XM.<sup>833</sup> According to data from the Elastomers Division of Mitsui Chemicals, such co-polymers have excellent compatibility with various polyolefins and can easily be blended with them. In general, TAFMER modifiers improve the flexibility, impact resistance, and heat sealability



**Figure 33** Isotactic propylene/ethylene co-polymers: influence of ethylene content on crystallinity (DSC data, heating rate 20 °C min<sup>-1</sup>).



**Scheme 30** Dashed bond: CH–H or CH–CH<sub>3</sub>.

of PP and PE, and are used in packaging applications such as films, extrusion laminates, and sheets. Isotactic propylene/butene co-polymers show higher melting points and higher elastic moduli at the same molar co-monomer content compared to isotactic propylene/ethylene co-polymers, allowing for higher use temperatures. On the other hand, they have higher glass transition temperatures, limiting applications at sub-ambient temperatures. Both  $T_g$  and modulus can be further lowered by addition of ethylene as termonomer.

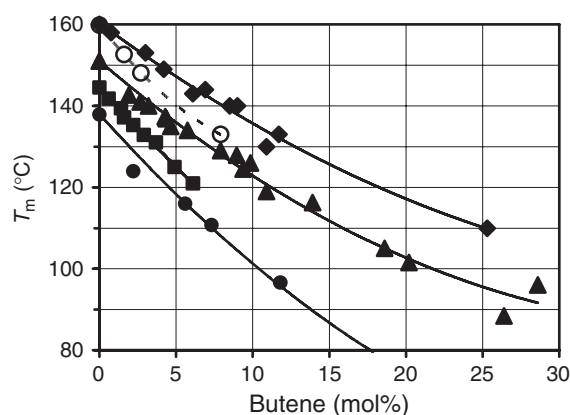
Obviously, as is the case of ethylene/propylene co-polymers, the melting point of the co-polymers is a function of both catalyst stereoselectivity and butene content. A major difference between propylene/ethylene and propylene/butene co-polymers is that while the former become amorphous at ethylene content above about 25 mol%, the latter can develop crystallinity in the whole range of composition. This is true for both the isotactic<sup>315,834</sup> and syndiotactic<sup>835,836</sup> co-polymers due to an easier inclusion of the co-monomer in the crystalline lamellae. Syndiotactic co-polymers have been prepared with both Me<sub>2</sub>C(Cp)(Flu)ZrCl<sub>2</sub> and Ph<sub>2</sub>C(Cp)(Flu)ZrCl<sub>2</sub>, and thus differ mainly by their molecular mass.

Isotactic propylene/butene co-polymers have been produced with a much broader array of metallocene catalysts, with greatly differing isotacticities and molecular masses.<sup>719,832,834,837–840</sup> The melting point/composition relationship for these isotactic co-polymers is shown in Figure 34.

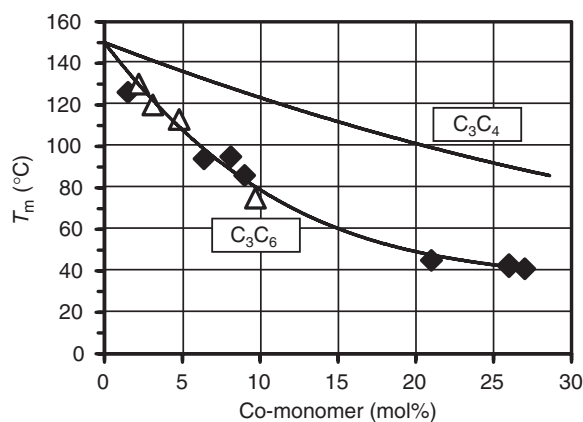
#### 4.09.4.2.7 Propylene/higher $\alpha$ -olefin co-polymers

Propylene has been co-polymerized with a broad set of higher olefins to isotactic co-polymers, including 1-pentene,<sup>842–845</sup> 4-methyl-1-pentene,<sup>842,846,847</sup> 1-hexene,<sup>834,840,842,848–852</sup> 1-heptene,<sup>842,847</sup> 1-octene,<sup>840,842,846,853–857</sup> 1-decene,<sup>856</sup> 1-tetradecene,<sup>856</sup> 1-octadecene,<sup>856,858</sup> and norbornene,<sup>859–862</sup> as well as a series of non-conjugated dienes like 1,5-hexadiene,<sup>863</sup> 7-methyl-1,6-octadiene,<sup>851,864,865</sup> 6-phenyl-1,5-hexadiene and isocitronellene,<sup>864</sup> and 1,9-decadiene.<sup>851</sup>





**Figure 34** Melting points of isotactic propylene/butene co-polymers as a function of butene molar content. ●:  $C_3/C_4$  from  $rac\text{-}C_2H_4(Ind)_2HfCl_2/MAO$ ,<sup>834,841</sup> ■:  $C_3/C_4$  from  $rac\text{-}Me_2Si(2\text{-}Me\text{-}Benz[e]ind)_2ZrCl_2$ ,<sup>837,838</sup> ▲:  $C_3/C_4$  from  $rac\text{-}Me_2Si(2\text{-}methyl\text{-}4\text{-}aryl\text{ indenyl})$  and thiopentalenyl zirconocenes,<sup>719,839,840</sup> ○:  $rac\text{-}Me_2Si(2\text{-}Me\text{-}4\text{-}NaphthInd)_2ZrCl_2/MAO$ ,<sup>832</sup> ◆:  $C_3/C_4$  from ZN catalysis.<sup>830,831,839</sup>



**Figure 35** Molecular mass depression in propylene/1-hexene copolymers compared to propylene/butene copolymers. Δ: data from Ref: 852; ◆: data from Ref: 840.

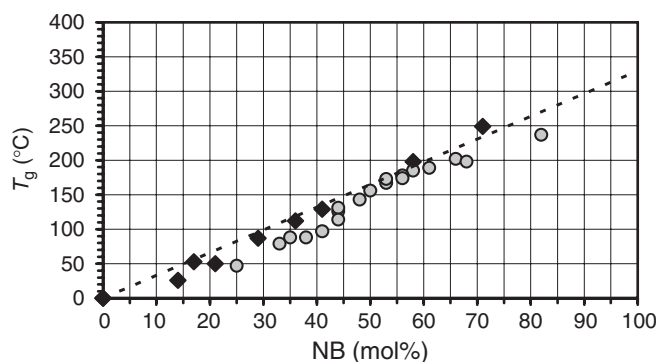
Isotactic propylene/1-hexene co-polymers have received the most attention: 1-hexene has been found to be more efficient than butene in lowering the melting point of the co-polymer<sup>840,847</sup> (see Figure 35), and their structure and physical properties have been investigated.<sup>852</sup>

Syndiotactic propylene/1-octene co-polymers have been prepared.<sup>866</sup> In propylene/norbornene co-polymerization, catalyst activity strongly decreases with the increase of norbornene in the feed. Very high  $T_g$  co-polymers have been produced at high norbornene incorporation. Surprisingly,  $T_g$  differences with the ethylene/norbornene co-polymers are small (Figure 36).

The co-polymerization between propylene and styrene is not feasible, unless minor amounts of ethylene are added to the system.<sup>867,868</sup> Several attempts at producing oxygen-functionalized polypropylenes by co-polymerization of propylene with olefinic alcohols or esters have been reported.<sup>869,870</sup>

#### 4.09.4.2.8 Propylene co-polymerization with macromonomers

LCB PP shows enhanced melt strength. Polypropylene long chain branches (PP-LCBs) are generated by electron beam irradiation of iPP in the solid state.<sup>317</sup> LCBs can also be formed by propylene co-polymerization with vinylene-terminated macromonomers, taking advantage of the high co-monomer reactivity of the *ansa*-Cp-amido Ti complexes and some chiral metallocenes. These macromonomers can be generated by different catalysts and with different monomers and microstructures. In the case of propylene, some sterically bulky metallocenes give rise to  $\beta$ -methyl elimination as the main chain-release reaction (see Section 4.09.2.4): under the proper conditions, this chain-release reaction allows the production of allyl-terminated iPP<sup>268</sup> and aPP macromonomers,<sup>871</sup> which in turn can



**Figure 36** Correlation between norbornene content and glass transition temperature in ethylene/norbornene (○)<sup>621</sup> and propylene/norbornene (◆)<sup>861,862</sup> co-polymers. The best linear fit for the propylene/norbornene data extrapolating at  $T_g = 330^\circ\text{C}$  for polynorbornene is also shown.

be used as co-monomers in propylene co-polymerization. Thus, PPs with isotactic backbone and either atactic<sup>871</sup> or isotactic PP-LCB<sup>270</sup> have been prepared, as well as PPs with atactic backbone and crystalline PP-LCB.<sup>872</sup>

Other approaches include the use of difunctional olefins such as 1,7-octadiene,<sup>873,874</sup> 1,9-decadiene,<sup>851</sup> or *para*-(3-butenyl)styrene.<sup>875</sup> While the former method also generates chain cross-linking (thus unprocessable polymer gels), the latter leads only to LCB formation through hydrogenolysis after a secondary styrene insertion. Tandem Zr/Fe catalysis has been used as well.<sup>876</sup> The preparation of iPP with PS branches has been achieved by co-polymerization of propylene with allyl-terminated PS macromonomers.<sup>877</sup>

#### 4.09.4.3 Polybutene

The major producer of isotactic poly(1-butene) (iPB) is Basell, which recently started a 45 kiloton-per-year plant in the Netherlands.<sup>878</sup> A smaller producer is Mitsui. The properties and applications of iPB, and the early process for its production have been reviewed<sup>315,879–882</sup>.

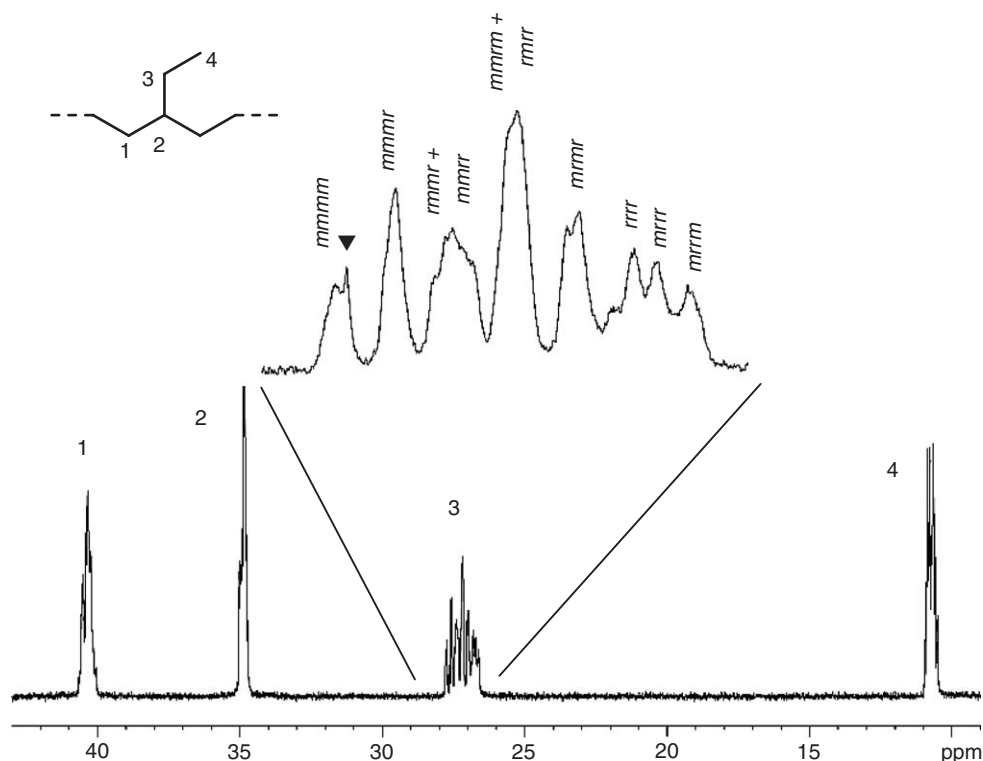
About 70% of PB production is used for the manufacturing of pipes for cold and hot water supply, and under-floor heating pipes. The remaining 30% of the production volume includes butene/ethylene random co-polymers and finds application in highly specialized and fragmented specialties markets, such as components in easy-peel films, process aids, and many others.<sup>878</sup>

$\text{TiCl}_3$  catalysts for 1-butene polymerization have relatively low activity.<sup>883</sup> The old Shell process made use of a first-generation Ziegler–Natta catalyst, and required de-ashing of the final polymer. The new Basell process makes use of a much improved high yield  $\text{MgCl}_2$ -supported Ti-based ZN catalyst and a two-reactor setup.<sup>425,884</sup> Improved distribution of co-monomer in 1-butene co-polymers with ethylene or propylene can also be achieved using such catalysts.<sup>885</sup>

Metallocenes are far more versatile in controlling polymer stereochemistry compared to Ziegler–Natta catalysts, as extensively demonstrated in the case of PP. Also in 1-butene polymerization, all kinds of chain microstructures can be obtained with different metallocenes. The  $^{13}\text{C}$  NMR pentad analysis of polybutene is somewhat less immediate than that of PP, and has been reported for both ZN<sup>886,887</sup> and metallocenes.<sup>180</sup> The  $^{13}\text{C}$  NMR spectrum of atactic polybutene, with pentad assignments of the C(3) methylene region, is shown in Figure 37.

An early report by Kaminsky and Brintzinger showed that the isospecific metallocene  $\text{rac-C}_2\text{H}_4(\text{H}_4\text{Ind})_2\text{ZrCl}_2/\text{MAO}$  catalyst is able to produce iPB.<sup>203</sup> Kaminsky also reported the influence of polymerization temperature on  $T_m$  and molecular mass, in the polymerization of 1-butene with  $\text{rac-C}_2\text{H}_4(\text{H}_4\text{Ind})_2\text{ZrCl}_2/\text{MAO}$  catalyst in the range  $-15$  to  $+60^\circ\text{C}$ . Melting points decrease with increasing  $T_p$  ( $119$ – $78^\circ\text{C}$ ), as do molecular masses ( $\bar{M}_v = 45\,000$  to  $5000$ ).<sup>888</sup> The  $\text{rac-C}_2\text{H}_4(\text{Ind})_2\text{HfCl}_2/\text{MAO}$  catalyst produces iPB of lower isotacticity ( $T_m(\text{II}) = 90^\circ\text{C}$ ), but higher molecular mass ( $\bar{M}_n = 123\,000$ ) compared to the Zr analog ( $T_m(\text{II}) = 101^\circ\text{C}$ ,  $\bar{M}_n = 12\,000$ ) at  $20^\circ\text{C}$  in 1:1 toluene:1-butene. Activities were low.<sup>889</sup>

An important observation was made by Kioka, who reported the presence of 4,1-units in iPB from  $\text{rac-C}_2\text{H}_4(\text{Ind})_2\text{ZrCl}_2/\text{MAO}$ , and a very strong hydrogen activation effect.<sup>300</sup> This fact was later confirmed by studies of



**Figure 37**  $^{13}\text{C}$  NMR spectrum (100 MHz) of atactic PB. A trace amount of iPB has been added to show the *mmmmmm* heptad, marked with ▼.

butene polymerization in the presence of hydrogen with both *rac*- $\text{C}_2\text{H}_4(\text{Ind})_2\text{ZrCl}_2/\text{MAO}$  and *rac*- $\text{Me}_2\text{Si}(\text{Ind})_2\text{ZrCl}_2/\text{MAO}$  catalysts.<sup>301,890</sup>

Low molecular mass iPB was produced with *rac*- $\text{Me}_2\text{Si}(4,5,6,7\text{-H}_4\text{Ind})\text{ZrCl}_2/\text{MAO}$  at  $100^\circ\text{C}$  in order to determine the structure of end groups and regioirregular units.<sup>232</sup> *rac*- $\text{Me}_2\text{Si}(2\text{-Me-Benz[e]ind})_2\text{ZrCl}_2/\text{MAO}$  produces iPB of low molecular mass ( $47 \times 10^3 \text{ g mol}^{-1}$ ) and melting point ( $98^\circ\text{C}$ ).<sup>515</sup> The  $C_1$ -symmetric zirconocene  $\text{Me}_2\text{C}(3\text{-MeCp})(9\text{-Flu})\text{ZrCl}_2$ , which is hemiispecific in propylene polymerization, becomes more isoselective in the case of 1-butene, producing moderately isotactic PB with 46% *mmmm*.<sup>891</sup>

Syndiotactic PB has been produced with  $\text{Me}_2\text{Si}(\text{Cp})(9\text{-Flu})\text{ZrCl}_2/\text{MAO}$  catalyst,<sup>892,893</sup> but only low molecular mass PB was obtained. sPB crystallizes very slowly and has a low melting point ( $40\text{--}50^\circ\text{C}$ ). Pure atactic, high molecular mass PB has been produced with  $\text{Me}_2\text{Si}(9\text{-Flu})_2\text{ZrCl}_2/\text{MAO}$ .<sup>894</sup>

The *rac*- and *meso*- $\text{Me}_2\text{Si}(2,3,5\text{-Me}_3\text{Cp})_2\text{ZrCl}_2$  produce isotactic/atactic PB mixtures in low yields and with rather low molecular masses.<sup>895</sup> The *meso*-isomer is less active than the racemic isomer. Interestingly,  $[\text{Ph}_3\text{C}][\text{B}(\text{C}_6\text{F}_5)_4]$  as activator coupled with TIBA as scavenger seems to produce a more active catalyst than MAO (at  $\text{Al/Zr} = 1000$ ). A similar investigation was performed by the same authors on *rac*- $\text{Me}_2\text{Si}(2\text{-MeInd})_2\text{ZrCl}_2$  (*rac*:*meso* = 17:83) at  $40^\circ\text{C}$  in toluene ( $\text{Al/Zr} = 1000$ ).<sup>896</sup> Also in this case, the *meso*-isomer was less active than the racemic isomer, the latter also producing higher molecular mass PB. The best co-catalyst, TIBA/ $[\text{Ph}_3\text{C}][\text{B}(\text{C}_6\text{F}_5)_4]$  gives iPB of  $\bar{M}_n$  250 000 and  $\bar{M}_w/\bar{M}_n = 2.9$ , with an activity of  $10 \text{ kg}_{\text{PB}} \text{ mmol}_{\text{Zr}}^{-1} \text{ h}^{-1}$  (or  $22 \text{ kg}_{\text{PB}} \text{ g}^{-1} \text{ h}^{-1}$  metallocene).

More recently, Kaminsky studied the behavior of *rac*/*meso*-mixtures of  $\text{Me}_2\text{Si}(\text{Ind})_2\text{ZrCl}_2$ ,  $\text{Me}_2\text{Si}(2\text{-Me-4,5-Benz[e]Ind})_2\text{ZrCl}_2$ , and  $\text{Me}_2\text{Si}(2\text{-Me-4-PhInd})_2\text{ZrCl}_2$  in the polymerization of 1-butene.<sup>897</sup> The most relevant observation is that, opposite to what is observed for propylene, the *meso*-isomer of the indenyl-substituted complexes are more active than the racemic ones, a fact that might be linked to the regioselectivity of the two isomers, the *meso*-isomer being likely more regioselective than the racemic one. Idemitsu Petrochemical<sup>898</sup> produced PB of low isotacticity, being low melting or amorphous, with doubly bridged metallocenes. Atactic, highly regio-irregular PB of high molecular mass has been prepared with a half-sandwich complex,  $\text{Cp}^*\text{Ti}(\text{OCH}_2\text{CH}=\text{CHPh})_3/\text{MAO}$ , at relatively low ( $0\text{--}50^\circ\text{C}$ ) polymerization temperatures.<sup>899</sup> More recently, high molecular mass, partially stereoregular

PB has been obtained with a similar catalyst system,  $\text{Cp}^*\text{Ti}(\text{OCH}_2\text{Ph})_3/\text{MAO}$ .<sup>900</sup> MAO-activated thiobis-2,2'-(4-methyl-6-*t*-butyl-phenoxy)titanium dichloride produces low molecular mass, atactic PB when the co-catalyst is MAO-modified with isobutyl groups. When MAO pretreated with water is used instead, a very high molecular weight PB is obtained, with molecular weights above 3 million at  $T_p$  of 40 °C.<sup>74</sup> In addition, this water-modified MAO endows the catalyst with a minor enantioselectivity: the polybutene produced at 25 °C has *mmmm* pentad content of 25%. A slightly higher productivity and stereoselectivity (30% *mmmm* at  $T_p$  = 40 °C) has been reported by the same authors with a MAO co-catalyst modified with water and pentafluorophenol.<sup>901</sup> The NMR data are not sufficient to determine the mechanism of enantioselectivity, and whether the microstructure is Bernoullian or stereoblock. No physical properties have been reported for these polybutenes, but given the pentad content and the molecular weight, this polymer should be amorphous with some elastomeric properties.

The above elastomeric polybutene might be similar in properties, if not in constitution, to the one produced with  $\text{Al}_2\text{O}_3$ -supported tetrabenzyl and tetraneophyl metals (Ti, Zr, Hf), which is a blend of atactic PB and isotactic-atactic stereoblock PB,<sup>902</sup> that can be fractionated by diethyl ether extraction.

A few reports have highlighted the increase in enantioface selectivity on going from propylene to 1-butene, in both chain-end-controlled<sup>180,808</sup> and site-controlled polymerizations.<sup>301,891,903</sup> Basell researchers have recently found that several  $C_2$ - and  $C_1$ -symmetric metallocenes are able to produce high molecular weight PB under industrial conditions.<sup>903–909</sup>

A few examples of 1-butene co-polymers with higher  $\alpha$ -olefins have been reported. Addition of 1-hexene stabilizes form II of polybutene and is included in the crystals.<sup>315</sup>  $C_4/C_6$  random co-polymers are soft or semirigid resins with characteristics that markedly differ from those of, for example,  $C_4/C_2$  random co-polymers.<sup>908</sup>

In general terms,  $C_4/C_6$  co-polymers have been reported to have higher crystallinity compared to  $C_4/C_2$ , that is, better thermal resistance and lower stickiness, higher flexibility and transparency, excellent workability, and good impact shock resistance. Co-polymers with 1-octene and 4-methyl-1-pentene have also been reported in the patent literature.<sup>910</sup>

#### 4.09.4.4 Poly( $\alpha$ -olefins) from Monomers Higher than Butene

As far as laboratory-scale model studies are concerned, polymers from linear  $\alpha$ -olefins higher than 1-butene combine the advantages of the liquid monomer (no high-pressure reactors needed) and polymers which are acceptably well characterizable by  $^{13}\text{C}$  NMR, having a sufficiently resolved  $\alpha$ -methylene pentad region.<sup>911</sup> In addition, 1-pentene and 1-hexene are also low boiling (easily removed after polymerization), facilitating polymer purification. However, they are amorphous and sticky, thus making their handling quite difficult and messy. Only a few 1-pentene polymerization studies have appeared,<sup>897,912–916</sup> the higher-boiling 1-hexene being largely preferred as monomer.<sup>891,913,917–919</sup>

In many instances, 1-hexene has been employed for kinetic<sup>138,154–156,920–922</sup> and activation studies,<sup>923–927</sup> and to prove the livingness of a catalyst system.<sup>700,928–931</sup> Higher  $\alpha$ -olefins like 1-octene,<sup>457,846,913–915,932</sup> 1-decene,<sup>913–915</sup> 1-tetradecene,<sup>915</sup> and 1-octadecene<sup>914,915</sup> have also been polymerized with different metallocenes. An interesting aspect of higher olefin polymerization has been the production of ultrahigh molecular weight polymers of 1-hexene and 1-octene under high pressure.<sup>933–935</sup>

Syndiotactic poly(1-pentene), poly(1-hexene), and poly(1-octene) have been described.<sup>936</sup>

Concerning the branched olefins, the most studied, and the only one with relevant industrial interest, is 4-methyl-1-pentene. Isotactic poly(4-methyl-1-pentene) has one of the highest melting points (230–240 °C) among polyolefins. Its production, properties, and uses have been reviewed.<sup>426,937</sup> As a material, such a high melting point makes it somewhat difficult to process, and hence it is produced as a co-polymer with minor amounts of higher olefins. These polymers are manufactured and commercialized by Mitsui under the tradename TPX: TPX has excellent transparency, heat resistance, and release properties, and is used in a broad range of application areas. These include industrial materials such as release film, release paper, sheath and mandrels used for the manufacture of high-pressure rubber hoses, LED molds, food-packaging materials such as heat-resistant-cooking wrap film and bags for retaining the freshness of vegetables and fruits, as well as conventional applications such as laboratory ware, medical instruments, and microwave ovenware.<sup>938</sup>

The polymerization of 4-methyl-1-pentene with metallocene catalysts has received only occasional attention.

Concerning  $^{13}\text{C}$  NMR spectroscopy, the carbon most sensitive to stereosequences seems to be the backbone methine (C2), but neither pentads nor triads have been assigned for this polymer. Also the side-group methylene (C3), which is usually the most sensitive to stereosequences in linear poly( $\alpha$ -olefins),<sup>911</sup> shows extensive overlapping

of the CH<sub>2</sub> pentad signals. Thus, stereoregularity of poly(4-methyl-1-pentene) can only be given at most at the diad level. The <sup>13</sup>C NMR spectra of the three limit structures of poly(4-methyl-1-pentene), isotactic, syndiotactic, and atactic, are shown in Figure 38. The carbons are assigned according to the literature.<sup>893,939</sup>

Isotactic poly(4-methyl-1-pentene) from C<sub>2</sub>-symmetric zirconocenes melts at lower temperature, ≤ 230 °C,<sup>846,916</sup> compared with the polymer from ZN catalysts, and has much lower molecular weights. C<sub>1</sub>-symmetric isospecific zirconocenes can produce poly(4-methyl-1-pentene) of higher isotacticity and correspondingly higher melting points, but still with low molecular weights at the higher polymerization temperatures.<sup>916</sup>

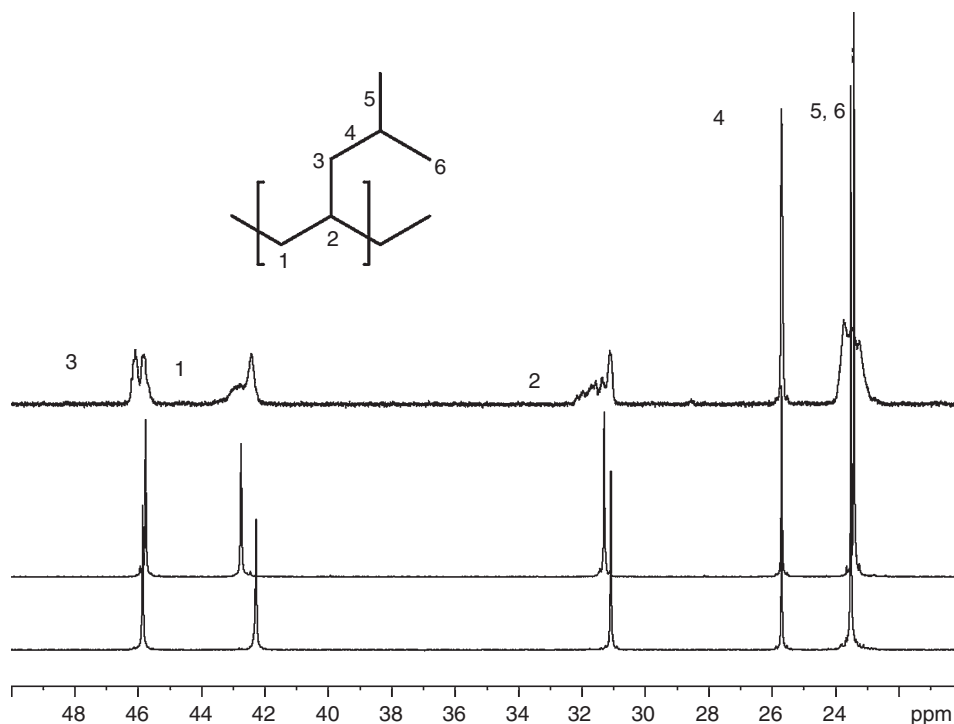
*ansa*-Indenyl-amido complexes of titanium produce poly(4-methyl-1-pentene) of low stereoregularity and molecular weights, which depend on the indenyl substitution pattern. The related fluorenyl complexes produces higher molecular weights, but with a much lower activity.<sup>542</sup>

Highly syndiotactic poly(4-methyl-1-pentene) melts at 210–215 °C and has been prepared with Ewen's catalyst Me<sub>2</sub>C(Cp)(9-Flu)ZrCl<sub>2</sub>/MAO<sup>892,893,940,941</sup> and the *ansa*-Cp-amido complex Me<sub>2</sub>Si(octamethyloctahydrodibenzofluorenyl)(NBu<sup>t</sup>)ZrCl<sub>2</sub>(OEt<sub>2</sub>).<sup>457,942</sup> Atactic poly(4-methyl-1-pentene) has been prepared with C<sub>2</sub>H<sub>4</sub>(9-Flu)<sub>2</sub>ZrCl<sub>2</sub>/MAO and is a glassy polymer with a T<sub>g</sub> of about +40 °C.

Other branched monomers that have been homopolymerized with metallocenes include 3-methyl-1-butene,<sup>943,944</sup> 3-methyl-1-pentene,<sup>943,945,946</sup> 4-methyl-1-hexene,<sup>947</sup> allylbenzene,<sup>948,949</sup> vinylcyclohexane,<sup>929</sup> and 1-vinylcyclohexene.<sup>950</sup>

#### 4.09.4.5 Polystyrene

Syndiotactic polystyrene (sPS) represents an important achievement in olefin polymerization catalysis. Syndiotactic PS is an industrially relevant thermoplastic material produced by Dow Chemical and Idemitsu Kosan Co. under the tradenames Questra™ and Xarec™, respectively. Industrial interest on sPS originates from the remarkable properties exhibited by this highly crystalline polymer. The high melting temperature, 270 °C, the relatively fast crystallization rate (at least much faster than that of iPS), the high heat resistance, the low dielectric constant, the high elastic modulus, and an excellent resistance to chemicals explain the industrial interest for this material. Syndiotactic PS was considered as an innovative new resin option for the automotive, electrical, and electronic markets, appliances such as



**Figure 38** <sup>13</sup>C NMR of poly(4-methyl-1-pentene). Isotactic, from *rac*-H<sub>2</sub>C(3-Bu<sup>t</sup>Ind)<sub>2</sub>ZrCl<sub>2</sub>/MAO (bottom); syndiotactic, from Me<sub>2</sub>C(Cp)(9-Flu)ZrCl<sub>2</sub>/MAO (middle); atactic, from C<sub>2</sub>H<sub>4</sub>(9-Flu)<sub>2</sub>ZrCl<sub>2</sub>/MAO (top).

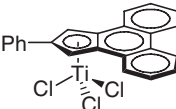
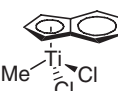
microwave oven inner parts, hot water filter and pump cases, films, fibers, packaging materials, housewares, and even medical applications. Due to low material cost and excellent properties, sPS was considered to be able to compete with most crystalline materials ranging from polybutylene terephthalate to high-temperature nylons. However, sPS did not experience the broad market penetration that was anticipated, and in December 2004 Dow Chemical announced it was going to discontinue sPS production in 2005. Conversely, Idemitsu Kosan Co. announced that it will resume a sPS plant in Japan in 2007 with a yearly production capacity of 5000 tons.

Syndiotactic PS was discovered at Idemitsu Kosan Co. in 1986.<sup>951–953</sup> The first literature report disclosed very few details about the catalyst used. Later reports indicated that MAO-activated mono-Cp Ti complexes were used. One year later, Zambelli and co-workers reported that MAO-activated  $\text{Ti}(\text{CH}_2\text{Ph})_4$  and  $\text{Zr}(\text{CH}_2\text{Ph})_4$  complexes also promote syndiospecific styrene polymerization.<sup>954,955</sup> These two groups contributed considerably to the development and mechanistic understanding of this kind of catalysis.<sup>956–964</sup> The syndiospecific polymerization of styrene has been reviewed.<sup>958,965–968</sup> Almost any Ti and many Zr compounds are able to yield sPS, although activity and syndiotacticity of the resulting polymer is dependent on the metal and on the ligands. Zr-based catalysts are usually less active and less syndiospecific than the corresponding Ti-based catalysts. Simple halide, benzyl, and alkoxides such as  $\text{TiCl}_4$ ,  $\text{TiBr}_4$ ,  $\text{Ti}(\text{OCH}_3)_4$ ,  $\text{Ti}(\text{CH}_2\text{Ph})_4$ , activated with MAO, yield sPS. Mono-Cp-based systems are however the most widely investigated systems. The performances of different half-sandwich complexes are compared in Table 15. It is clear that F atoms bound to the Ti atom in the pre-catalyst remarkably improve activity, probably a leaving group effect, although a clear rationalization has been provided yet. Permethylated Cp-based catalysts are notably less active than those with unsubstituted Cp rings. Conjugated aromatic ligands, however, improve activity and yield reasonably high molecular masses.<sup>969–971</sup> In almost all cases, rather low  $\bar{M}_w/\bar{M}_n$  values, typical of single-site catalysis, are observed.

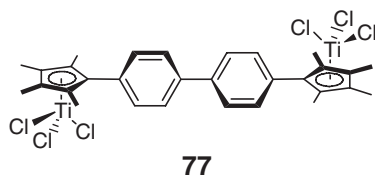
Molecular masses obtained with alkoxides such as  $\text{Ti}(\text{OBu}^n)_4$  in combination with MAO and using toluene as solvent can reach values up to  $\bar{M}_w = 600\,000$ . Considerably lower  $\bar{M}_w$  values are obtained at 87 °C, although the catalyst system still exhibits good catalytic activity.<sup>963</sup> Both MAO and fluoroborate counterions have been shown to be suitable co-catalysts for syndiotactic styrene polymerization. Activity up to  $10\text{ kg}_{\text{sPS}}\text{ mmol}^{-1}\text{ Ti}^{-1}\text{ h}^{-1}$  can be reached both with MAO and with perfluoroborate co-catalysts such as  $\text{Ph}_3\text{C}[\text{B}(\text{C}_6\text{F}_5)_4]$  or  $\text{B}(\text{C}_6\text{F}_5)_3$ . The sPS yields are substantially independent of the Al/Ti ratio, provided that ratios higher than 50:1 are used.<sup>963</sup> In all cases, the syndiotacticity of the resulting polystyrenes is remarkably high.<sup>957</sup> Styrene polymerization with bridged bis-metalloenes has also been investigated. In this case, however, very low activity was observed.<sup>956</sup>

Besides mono-Cp systems,<sup>958,959,973–989</sup> other half-sandwich complexes with different aromatic ligands were investigated.<sup>969–971,982,983,985,990–993</sup> Other studies were concerned with polymerization conditions, including catalyst heterogenization.<sup>990,994–1006</sup> Other catalysts such as mono-<sup>276</sup> and bis-benzamidinate<sup>1007</sup> complexes, bis(phenolato) Ti complexes,<sup>159,1008</sup> and salen-based Ti complexes,<sup>1009</sup> are also able to polymerize styrene to a highly syndiotactic polymer. Finally, it is noteworthy that bimetallic catalysts based on complex 44 can yield atactic

**Table 15** Polymerization of styrene in the presence of different catalytic systems in toluene

Catalyst	$T_p$ (°C)	Productivity $\text{g}_{\text{sPS}}\text{ mmol}^{-1}\text{ Ti}^{-1}\text{ h}^{-1}$	$\bar{M}_w$	$\bar{M}_w/\bar{M}_n$	$T_m$ (°C)	References
$\text{CpTiCl}_3$	50	1,100	140,000	1.9	258	972
$\text{CpTiF}_3$	50	3,000	100,000	2.0	265	972
$\text{CpTi}(\text{OBu}^n)_3$	45	1,600	40,000		258	973
$\text{Ti}(\text{OBu}^n)_4$	50		568,000	4.1		963
$(\text{C}_5\text{Me}_5)_2\text{TiCl}_2$	50	15	169,000	3.6	275	972
$(\text{C}_5\text{Me}_5)_2\text{TiF}_2$	50	690	660,000	2.0	275	972
	50	40,000	277,000		268	971
	50	38,000			270	970

polystyrene (aPS) with good activity, whereas the corresponding monometallic catalyst shows extremely low activity.<sup>664</sup> Similar results have been obtained by Do and co-workers utilizing the bimetallic complex **77**.<sup>1010</sup>



Comparison of different catalytic systems under different polymerization temperatures is reported in Table 16. It is clear that CpTiCl<sub>3</sub> is able to give quite high amounts of sPS in the polymerization temperature range from –17 to +90 °C. Remarkably, the stereoregularity and the *T<sub>m</sub>* of the sPS are quite high also at 90 °C. Although less active, the permethylated Cp\*TiCl<sub>3</sub>/MAO catalyst performs even better in terms of stereoregularity, since the resulting sPS is substantially perfectly syndiotactic whatever polymerization temperature was used. The Ti(CH<sub>2</sub>Ph)<sub>4</sub>/MAO catalyst also exhibits remarkably good performances.

Several mechanistic studies, mostly from Zambelli's school, have been devoted to understanding the syndio-specific polymerization of styrene with group-4-based catalysts.<sup>954,960,961,963,964,1011–1019</sup> Most of these mechanistic studies have been reviewed.<sup>968</sup> It has been demonstrated that the syndiospecificity is chain-end controlled, since stereomistakes occur as isolated *m* diads.<sup>954,960,1011,1012</sup> Regiochemistry of styrene propagation is secondary, and the same regiochemistry is observed in the initiation as well as in chain-end groups.<sup>960,961</sup> Solvent effects play a role in syndiospecific styrene polymerization. In the case of aromatic solvents, electron-donating groups (as in mesitylene) reduce activity, while electron-withdrawing groups (as in 1,2,4-trichlorobenzene) increase activity. Solvents of high polarity such as CH<sub>2</sub>Cl<sub>2</sub> increase activity, although they have detrimental effects on the syndiotacticity of the resulting polymers.<sup>1020</sup> As for the oxidation state of the active Ti atoms, ESR experiments, and subsequent combined ESR and NMR monitoring of the reaction with <sup>13</sup>C-enriched reactants, demonstrated that the most active Ti atoms are in the oxidation state +III.<sup>1021–1023</sup> However, this topic was rather debated in the literature.<sup>968,1017,1021,1024,1025</sup> In fact, a carbocationic mechanism was initially suggested, while subsequent investigations clearly demonstrated the occurrence of an insertion mechanism.<sup>1020,1026</sup>

Soon after syndiospecific styrene polymerization, attention was directed to the homopolymerization of substituted styrenes as well as to their co-polymerization with styrene.<sup>956,957,964,1027–1029</sup> Mono-Cp-based Ti systems are capable of homopolymerizing methyl-substituted styrenes and *p*-chlorostyrene, as well as co-polymerizing them with styrene. The general trend that emerged is that electron-withdrawing Cl substituents decrease the reactivity relative to styrene, whereas electron-releasing Me groups increase it. In both cases, syndiotactic co-polymers were obtained.

**Table 16** Polymerization of styrene in the presence of different catalytic systems in toluene (all data from Ref:1011)

Catalyst	<i>T<sub>p</sub></i> (°C)	% Atactic <sup>a</sup>	<i>P<sub>r</sub></i> <sup>b</sup>	% <i>rrr</i>	<i>T<sub>m</sub></i> (°C)
CpTiCl <sub>3</sub> /MAO	–17	Traces	1	100	257
	0	Traces	0.96	91	258
	15	14	0.96	92	255
	50	25	0.94	88	243
	70	33	0.93	81	243
	90	47	0.92	79	242
Cp*TiCl <sub>3</sub> /MAO <sup>c</sup>	50	Traces	1		265
	70	Traces	1		264
	90	Traces	1		264
Ti(CH <sub>2</sub> Ph) <sub>4</sub> /MAO	50	Traces	0.97		256
	90	10	0.98		260

<sup>a</sup>Acetone soluble fraction.

<sup>b</sup>Statistical parameter of the syndiotactic propagation.

<sup>c</sup>Cp\* = C<sub>5</sub>Me<sub>5</sub>.



#### 4.09.4.6 Cyclopolymers

The cyclopolymerization of non-conjugated terminal diolefins, such as 1,5-hexadiene, has been devised by Waymouth as an additional tool to probe the enantioselectivity of active metallocene sites, in addition to being a source of novel polyolefinic structures. The regioregular cyclopolymers have four structures of maximum order (shown in Scheme 31 for poly(methylenecyclopentane)). The *trans*-isotactic structure, having no mirror planes of symmetry, is chiral by virtue of its main-chain stereochemistry.<sup>1030</sup> Cyclopolymerization with zirconocene complexes has been reviewed.<sup>1031</sup> This reaction has also a general mechanistic importance; for example, it rules out the occurrence of two simultaneously coordinated olefins at the same site, proposed by some authors to explain higher reaction orders in monomer,<sup>313,1032</sup> since such an arrangement would lead only to *cis*-rings in the case of 1,5-hexadiene.<sup>1033</sup>

1,5-Hexadiene has also been cyclopolymerized with the CGC  $\text{Me}_2\text{Si}(\text{C}_5\text{Me}_4)(\text{NBu}^t)\text{TiCl}_2/\text{MAO}$ , with good cyclopolymerization efficiency.<sup>561</sup> A monocyclopentadienyl complex,  $\text{Cp}^*\text{TiCl}_2(\text{O}-2,6\text{-Pr}_2\text{C}_6\text{H}_3)$ , is also active in the polymerization of 1,5-hexadiene upon activation with MAO, but cyclization efficiency was rather low, producing a polymer with 25–33 mol% buten-1-yl side groups, depending on diene concentration.<sup>1034</sup> This observation contrasts an earlier report of a high cyclization efficiency shown by  $[\text{Cp}^*\text{TiMe}_2][\text{MeB}(\text{C}_6\text{F}_5)_3]$ .<sup>1035</sup>

The cyclo-co-polymerization of 1,5-hexadiene and ethylene catalyzed by  $C_1$ -symmetric *ansa*-zirconocenes gives access to alternating co-polymers,<sup>1036</sup> and lends further supporting evidence for the proposed mechanism of alternation in ethylene/propylene co-polymerization.<sup>575</sup>

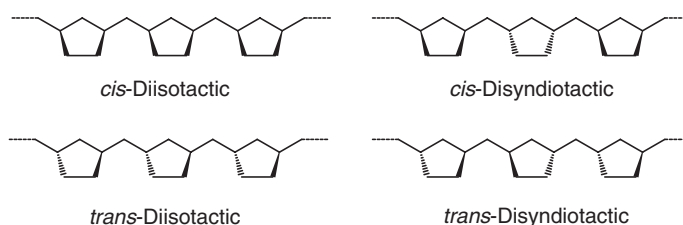
The living cyclopolymerization of 1,5-hexadiene has been achieved with monocyclopentadienyl monobenzamidinato complexes  $\text{Cp}^*\{\text{MeC}(\text{NR})_2\text{ZrMe}_2$  activated by  $[\text{PhMe}_2\text{NH}][\text{B}(\text{C}_6\text{F}_5)_4]$  at  $-10^\circ\text{C}$ .<sup>1037</sup> These catalysts also show a very high (98–100%) selectivity for cyclization. The living nature of these polymerizations allowed the preparation of iso-poly(1-hexene)/poly(methylenecyclopentane) block co-polymers. Selectivity for cyclization over insertion decreases as the monomer length increases. 1,7-Octadiene has been shown to cyclize only partially, and the selectivity is shown to be lowest for the syndiospecific zirconocene  $\text{Ph}_2\text{C}(\text{Cp})(9\text{-Flu})\text{ZrCl}_2$ .<sup>1038</sup>

#### 4.09.4.7 Polymers of Cyclic Olefins

The isomerization–polymerization of cyclopentene to poly(1,3-cyclopentane) has been reviewed.<sup>596</sup> Following the original work of Kaminsky, reviewed up to 1997,<sup>596</sup> the addition polymerization of NB has been further studied.<sup>1039–1042</sup> Polynorbornene from vinyl addition is an amorphous polymer of outstandingly high glass transition temperature, probably exceeding its decomposition temperature. For a perspective view, see Refs: 1043–1043a. Metallocene catalysts are far less active in the vinyl polymerization of NB than late transition metal catalysts.<sup>1040</sup> The co-polymerization of norbornadiene with ethylene<sup>602</sup> and 1-hexene<sup>1044</sup> has been reported.

#### 4.09.4.8 Polymerization of Conjugated Dienes

Polybutadiene rubber is a technologically important elastomer. Conjugated dienes such as butadiene and isoprene, which are typically polymerized by anionic lanthanides and late transition metal catalysts, are generally strong inhibitors for group 4 cationic metal catalysts, and even in co-polymerization with  $\alpha$ -olefins strongly depress catalyst activity. The scope of metallocene catalysts in the polymerization of butadiene, isoprene, and other conjugated dienes, and the mechanistic implications, have been reviewed in detail.<sup>1045</sup> The homopolymerization of butadiene, with a series of monocyclopentadienyl titanium trichlorides and trifluorides,<sup>1046</sup> to high molecular weight rubbers ( $\bar{M}_w < 10^6$ ), with a prevalence of 1,4-*cis*-butadiene insertion and  $T_g$  in the range  $-88$  to  $-97^\circ\text{C}$ , has been achieved.



Scheme 31



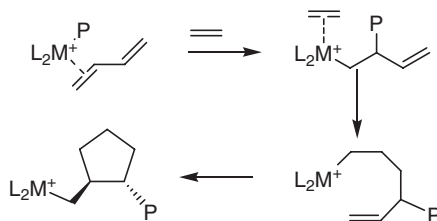
The same catalysts homopolymerize isoprene. Preparation of syndiotactic styrene/butadiene block co-polymers by means of  $\text{Cp}^*\text{TiX}_3/\text{MAO}$  catalysts ( $\text{X} = \text{Cl}, \text{F}$ ) and  $\text{Cp}^*\text{TiMe}_3/\text{MAO}$  has been reported.<sup>1047</sup>

Co-polymerization of conjugated dienes with ethylene by means of metallocene catalysts has been investigated by several authors. The co-polymerization of ethylene with 1,3-butadiene, 4-vinyl-cyclohexene, 1,4- and 1,5-hexadiene with  $\text{rac-Me}_2\text{Si}(\text{Ind})_2\text{ZrCl}_2$  has been reported.<sup>1048,1049</sup> Subsequently, a detailed  $^{13}\text{C}$  NMR analysis of ethylene/butadiene co-polymers obtained with the above-mentioned metallocenes was described, which confirmed that butadiene is incorporated in the 1,4-*trans*-configuration or is cyclopolymerized to a *trans*-1,2-methylene-cyclopentane unit, whereas 1,4-*cis*- and 1,2-units were not detected. Up to 5% mol butadiene units were incorporated.  $\text{Cp}_2\text{ZrMe}_2$  incorporated higher amounts of butadiene relative to  $\text{rac-C}_2\text{H}_4(\text{H}_4\text{Ind})_2\text{ZrCl}_2$ , but molecular masses were lower. In any case, activity was reduced.<sup>1050</sup> The cyclopentane units are formed as shown in Scheme 32.

Ethylene/butadiene co-polymers with a butadiene content up to 20% have been prepared with  $\text{Me}_2\text{Si}(\text{C}_5\text{Me}_4)(\text{NBu}^t)\text{TiCl}_2$ .<sup>1051</sup> The co-polymer with 7 mol% of butadiene has a  $T_g$  of  $-28^\circ\text{C}$ . The butadiene units are incorporated partly as 1,2-units, and mainly in the 1,4-*trans*-configuration. This was rather surprising, since the same catalyst promotes the homopolymerization of 1,3-butadiene to mainly 1,4-*cis*- and 1,2-units. The authors suggest that the relatively high amount of vinyl groups could allow vulcanization. iPP-*ran*-1,3-butadiene co-polymers have been obtained using the  $\text{rac-Me}_2\text{Si}(\text{Ind})_2\text{ZrCl}_2$  metallocene. By performing a metathesis reaction of the 1,4-butadiene units in the co-polymer with ethylene, short iPP segments with both chain ends having vinyl bonds have been obtained.<sup>1052</sup>

The synthesis of functionalized ethylene and propylene containing 1,2-methylene-cyclopropane and 1,2-methylene-cyclopentane units has been achieved, as shown in Scheme 33 for PE.<sup>1053</sup>

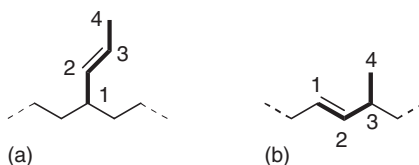
These structures were obtained from ethylene/1,3-butadiene co-polymerizations at room temperature using sterically hindered metallocenes such as  $\text{rac-H}_2\text{C}(\text{3-Bu}^t\text{-Ind})_2\text{ZrCl}_2$ . Working with ethylene and 1,3-butadiene concentrations of 0.24 and 0.62 mol  $\text{l}^{-1}$ , respectively, about 4 mol% of butadiene units are inserted in the resulting PE. About 67% of the butadiene is present as cyclopropane units, while the remaining 33% is present as cyclopentane units. In both cases, and in agreement with previous findings,<sup>590,1050</sup> a *trans*-stereochemistry of the rings, as shown in Scheme 33, was observed. By contrast, with the less hindered  $\text{H}_2\text{C}(\text{Ind})_2\text{ZrCl}_2$  metallocene, no cyclopropane units were observed in the resulting polymer. The inserted butadiene units (about 21 mol%) were present as cyclopentane (22%) and 1,4-butadiene (78%) units.<sup>1053–1055</sup> Furthermore, on increasing the polymerization temperature to  $73^\circ\text{C}$  and at low ethylene concentrations (0.05 mol  $\text{l}^{-1}$ ), the inserted butadiene units are present as 1,1- (76%) and 1,3- (24%) butadiene units, as shown in Scheme 34.<sup>1054–1056</sup>



Scheme 32



Scheme 33



Scheme 34

Co-polymerization of ethylene with different conjugated dienes, such as 1,4-pentadiene, yields methylene-1,2-cyclobutane units in the co-polymers.<sup>559</sup> In the case of propylene/1,3-butadiene co-polymerization with *rac*-H<sub>2</sub>C(3-Bu<sup>t</sup>-Ind)<sub>2</sub>ZrCl<sub>2</sub>, a low amount of butadiene units is present as cycles in the resulting co-polymer, since the butadiene inserts prevalently as an  $\alpha$ -olefin, thus resulting in 1,2-inserted butadiene units. At high butadiene concentration, sequences of *cis*-1,4-butadiene units were observed. Interestingly, the co-polymerization of butadiene forces some regioirregular secondary insertion of propylene.<sup>1057</sup>

Co-polymerization of ethylene with cyclic dienes such as 1,3-cyclopentadiene, dicyclopentadiene, and 4-vinyl-1-cyclohexene using *rac*-C<sub>2</sub>H<sub>4</sub>(Ind)<sub>2</sub>ZrCl<sub>2</sub> showed that dicyclopentadiene was the most reactive co-monomer. 1,3-Cyclopentadiene rapidly dimerizes to dicyclopentadiene, and thus ethylene/1,3-cyclopentadiene co-polymerization actually resulted in ethylene/1,3-cyclopentadiene terpolymers with dicyclopentadiene. Co-polymers with more than 9 mol% of the co-monomer did not show a melt transition.<sup>1058</sup>

Ethylene/butadiene cyclopolymerization was used to probe the dual-site nature of *C*<sub>1</sub>-symmetric *ansa*-metallocenes.<sup>1059</sup>

#### 4.09.5 Polymerization of Ethylene, Propylene, and Higher $\alpha$ -Olefins with other Single-Center Catalysts

The broadly used term “non-metallocene” (or “post-metallocene”) catalysts now comprises a large variety of different ligands and of metals with different coordination numbers. A simple classification is thus not straightforward, even if this classification is restricted to catalysts containing group 4 metals. The one we adopted here is based on the classification used by Do and co-workers in a recent review on the same topic.<sup>1060</sup> Other reviews on this subject were published a few years ago.<sup>1061,1062</sup> To keep track of the different geometrical and chemical environments in the pre-catalysts, the complexes are divided into sections according to the metal coordination number, and then into subsections according to the atoms that coordinate to the metal. However, for the sake of consistency, pre-catalysts that represent small variations from a largely explored class are discussed within the main class they were derived from, even if they should be discussed in a different section.

Before discussing catalyst activities, a caveat is in order. Experimentally determined activities strongly depend on the specific conditions (temperature, polymerization time, solvent, stirring, reactor, and even addition of the different components to the reactor) and thus a “safe” comparison of different catalysts is not easy. Following the approach used by Gibson and co-workers, we report the activities in g<sub>polymer</sub> (mmol metal)<sup>−1</sup> h<sup>−1</sup> bar<sup>−1</sup>, whenever possible, and we order the catalyst activities according to the scale reported in Table 17.<sup>1061,1062</sup> Finally, it must also be considered that under similar conditions, metallocenes can easily show activity around 10<sup>4</sup> g<sub>polymer</sub> (mmol metal)<sup>−1</sup> h<sup>−1</sup> bar<sup>−1</sup>.

##### 4.09.5.1 Complexes with Coordination Number 4

In the case of group 4 metals, coordination 4 at the metal atom corresponds to a tetrahedral or pseudo-tetrahedral geometry of coordination. This geometry is analogous to that presented by metallocenes and CGCs.

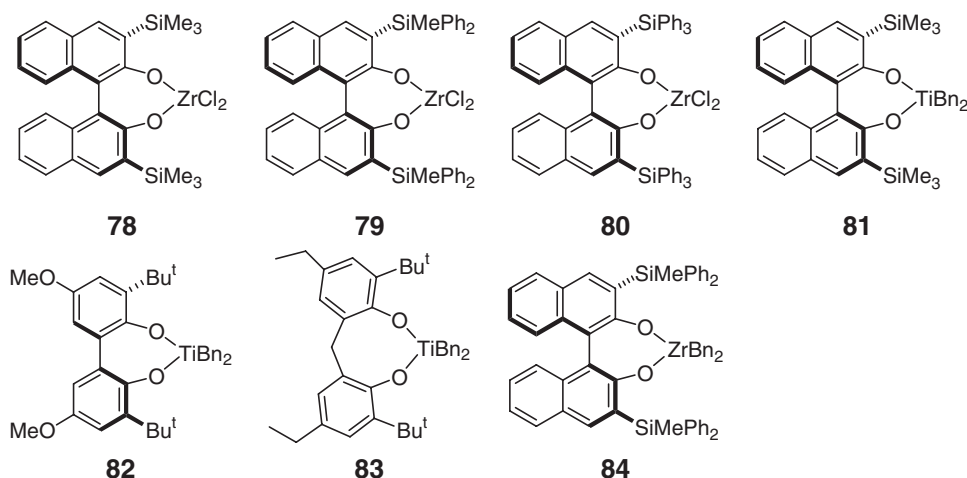
##### 4.09.5.1.1 Ligands with coordinating O–O atoms

One of the most thorough studies was performed in 1995, when the catalytic behavior of a series of MAO-activated dialkoxide complexes was tested in the polymerization of ethylene and 1-hexene.<sup>256</sup> At 20 °C, MAO-activated **78–83** and analogs exhibited the moderate average activity of about 50–90 g<sub>PE</sub> (mmol M)<sup>−1</sup> h<sup>−1</sup> bar<sup>−1</sup>. Under the same conditions, the catalyst based on **84** showed high activity, about 3 × 10<sup>2</sup> g<sub>PE</sub> (mmol M)<sup>−1</sup> h<sup>−1</sup> bar<sup>−1</sup>, whereas the catalyst based on **82** exhibited the low activity of 6 g<sub>PE</sub> (mmol M)<sup>−1</sup> h<sup>−1</sup> bar<sup>−1</sup>. Unfortunately, the few molecular

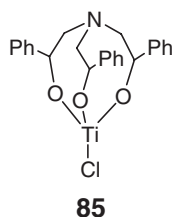
**Table 17** Qualitative performance assignment for catalyst activities

Performance	Activity (g <sub>polymer</sub> (mmol metal) <sup>−1</sup> h <sup>−1</sup> bar <sup>−1</sup> )
Very low	< 1
Low	1–10
Moderate	10–10 <sup>2</sup>
High	10 <sup>2</sup> –10 <sup>3</sup>
Very high	> 10 <sup>3</sup>

masses reported are rather low, while rather large molecular mass distributions were observed ( $\bar{M}_n < 50\,000$   $\bar{M}_w/\bar{M}_n > 7.0$ ).<sup>256</sup> Catalysts based on **78** and **79** yield highly regioregular and isotactic poly-1-hexene with rather high molecular mass and narrow molecular mass distribution ( $\bar{M}_w = 675\,000$ ,  $\bar{M}_w/\bar{M}_n = 2.2$ ). Finally, catalysts based on **82** only yield oligomers.<sup>256</sup> Theoretical DFT studies of model systems related to **82** and **83** predicted insertion barriers around 10–15 kcal mol<sup>-1</sup> for M = Ti and Zr, respectively. The presence of the CH<sub>2</sub> bridge was shown to have a minor role. Interestingly, the resting state is stabilized by a  $\gamma$ -agostic interaction between the growing chain and the metal.<sup>1063,1064</sup> This is rather different from metallocenes, where the  $\beta$ -agostic interaction is usually 4–5 kcal mol<sup>-1</sup> more stable than the  $\gamma$ -agostic interaction.<sup>141</sup>

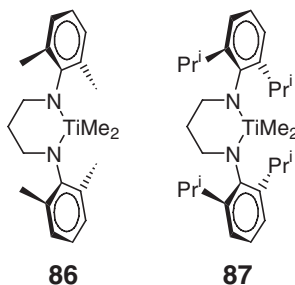


Another catalyst with coordination 4 at the metal atom and coordinating O atoms is based on complex **85**. This complex shows high activity in ethylene polymerization ( $1 \times 10^2$ – $3 \times 10^2$  g<sub>PE</sub> (mmol M)<sup>-1</sup> h<sup>-1</sup>). The tetrameric analog exhibits moderate activity.<sup>1065</sup>



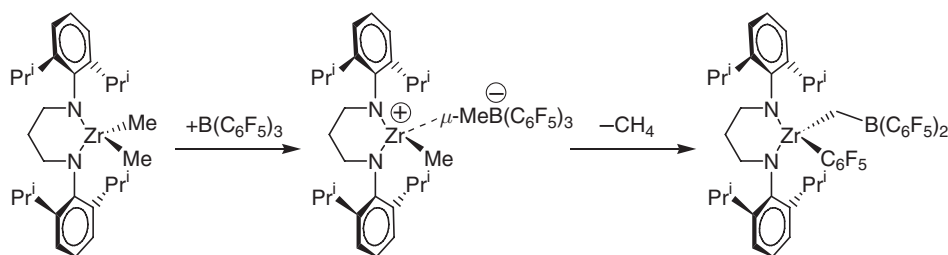
#### 4.09.5.1.2 Ligands with coordinating N–N atoms

Pre-catalysts with coordination 4 at the metal and a coordinating N–N ligand include complexes with chelating and dianionic diamide ligands. Activation of these pre-catalysts leads to a class of systems with remarkable catalytic properties and, not surprisingly, these systems have been quite deeply investigated.<sup>275,1066–1084</sup> The MAO- and B(C<sub>6</sub>F<sub>5</sub>)<sub>3</sub>-activated diamide complexes **86** and **87**, known as McConville catalysts, were introduced for 1-hexene polymerization in 1996.<sup>1066,1069</sup>

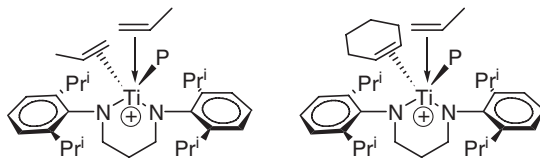


At 68 °C and with a MAO/Ti ratio of 250, these complexes yield poly-1-hexene with the remarkable activity of about  $3 \times 10^5 \text{ g}_{\text{PH}} (\text{mmol M})^{-1} \text{ h}^{-1}$ . The polymers produced had moderate molecular masses ( $\bar{M}_w = 30\,000\text{--}50\,000$ ) with  $\bar{M}_w/\bar{M}_n$  close to 2, indicative of single-site behavior.<sup>1066</sup> Activation with  $[\text{Ph}_3\text{C}][\text{B}(\text{C}_6\text{F}_5)_4]$  salts also leads to quite active catalysis (activity up to  $10^5 \text{ g}_{\text{PH}} (\text{mmol M})^{-1} \text{ h}^{-1}$ ), whereas activation with  $\text{B}(\text{C}_6\text{F}_5)_3$  is much less effective, although activity remains high ( $< 2 \times 10^3 \text{ g}_{\text{PH}} (\text{mmol M})^{-1} \text{ h}^{-1}$ ). However, it is worth noting that polymerization times were shorter than 1 min,<sup>1067</sup> and that extending the polymerization time to about 30 min resulted in only moderate activity.<sup>275</sup> Solvent effects were shown to be relevant. Activity of **87**/MAO in the presence of toluene decreases to  $8 \times 10^2 \text{ g}_{\text{PH}} (\text{mmol M})^{-1} \text{ h}^{-1}$  at 22 °C. It was hypothesized that toluene can compete with the monomer for coordination to the metal atom.<sup>1066</sup> On the other hand, small amounts of  $\text{CH}_2\text{Cl}_2$  added to the aliphatic solvent increased activity by a factor of 10. Probably, the higher polarity of the media helped to separate the borate counterion from the active species.<sup>275</sup> In the case of MAO activation,  $^1\text{H}$  and  $^{13}\text{C}$  NMR spectra of oligomers indicated that the only chain-termination mechanism is chain transfer to the Al co-catalysts, since no olefinic resonances were observed.<sup>275</sup> This could rationalize the fact that  $\text{B}(\text{C}_6\text{F}_5)_3$  and  $[\text{Ph}_3\text{C}][\text{B}(\text{C}_6\text{F}_5)_4]$  activation leads to living polymerization of  $\alpha$ -olefins such as 1-hexene, 1-octene, and 1-decene.<sup>275,1067</sup> In 10 min polymerization time, poly-1-hexene with an  $\bar{M}_n$  of 164 000 and an  $\bar{M}_w/\bar{M}_n$  ratio of 1.07 was obtained.<sup>275</sup> The  $\text{B}(\text{C}_6\text{F}_5)_3$ -activated **86** and **87** present different stabilities. While the activated **86**/ $\text{B}(\text{C}_6\text{F}_5)_3$  species is stable for days, **87**/ $\text{B}(\text{C}_6\text{F}_5)_3$  deactivates as shown in Scheme 35.<sup>1068</sup> In all cases, atactic polymers were obtained. NMR analysis of the resulting poly-1-hexenes indicated that the regiochemistry of monomer insertion into the Ti-growing-chain bond is primary.<sup>1067</sup>

McConville complexes **86** and **87** have also been used for propylene polymerization, and it has been shown that the nature of the resulting PPs is highly dependent on the polymerization conditions.<sup>1070–1072</sup> While complex **86** only yields aPP, whatever  $\text{AlR}_3$  species is used,<sup>1072</sup> catalysts based on **87**/ $\text{B}(\text{C}_6\text{F}_5)_3/\text{AlR}_3$  yield aPP only with  $\text{AlMe}_3$  and  $\text{AlEt}_3$ . Instead, with  $\text{AlBu}_3^i$  (or R bulkier than  $\text{Bu}^i$ ), the polymers produced could be fractionated into atactic and isotactic fractions.<sup>1072</sup> The weight percentage of the isotactic fraction increases with propylene concentration from roughly 0% at  $0.41 \text{ mol l}^{-1}$  up to 45% at  $2.76 \text{ mol l}^{-1}$ .<sup>1072</sup> This suggested that two propylene molecules could coordinate to the metal atom since double monomer coordination would increase steric bulkiness and could induce the stereospecific behavior.<sup>1072</sup> Further support for this hypothesis was provided by propylene polymerization in the presence of cyclohexene. NMR analysis indicated that cyclohexene was not inserted in the polymers, but even at low propylene pressure (1 atm) the iPP fraction could increase from roughly 0%, with no cyclohexene, up to 77% with a cyclohexene concentration of  $8.8 \text{ mol l}^{-1}$ . These findings added further support for the isospecific active species depicted in Scheme 36.<sup>1070</sup> To date, the origin of stereoselectivity with these catalysts is still unclear.



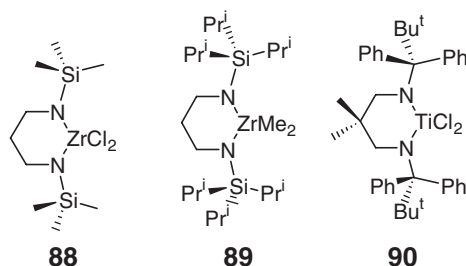
Scheme 35



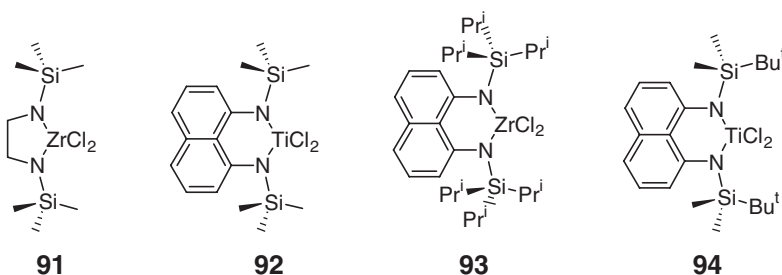
Scheme 36

NMR analysis of the iPP produced indicated that a rather good level of stereoregularity (% *mmmm* up to 80%) is reached, and that enantiomorphic site control is operative. Insertion is essentially primary and regiomistakes were not detected.<sup>1071</sup> Activity is in the range of  $4 \times 10^{-1} \times 10^3 \text{ g}_{\text{PP}} (\text{mmol M})^{-1} \text{ h}^{-1}$  when the polymerization temperature is varied between 0 and 150 °C. In the same polymerization temperature range, the  $\bar{M}_n$  of the polymers is between 194 000 and 51 000, which indicates that even at 150 °C reasonably high molecular masses are obtained. In all cases,  $\bar{M}_w/\bar{M}_n$  was slightly higher than 2. The weight percentage of the iPP fraction increases from 8% at 0 °C, reaches a maximum of 79% at 40 °C, and decreases to 36% at 150 °C.<sup>1072</sup> Since the only chain-termination mechanism operative with **86** and **87** is transfer to MAO, it was of interest to test AlMe<sub>3</sub>-free MAOs for the polymerization of propylene. Indeed, at 0 °C activation of **87** with dried MMAO leads to living propylene polymerization.<sup>1073,1074</sup>

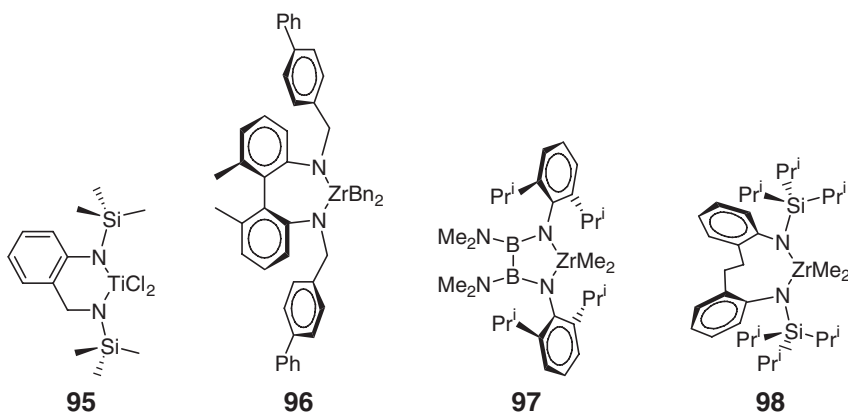
Several modifications of the aromatic rings on the N atoms as well as of the C<sub>3</sub> spacer of the classical McConville complex have been explored.<sup>1075,1076</sup> While the **89**/[Ph<sub>3</sub>C][B(C<sub>6</sub>F<sub>5</sub>)<sub>4</sub>]/AlBu<sup>i</sup><sub>3</sub> catalyst yields PE with high activity,  $3 \times 10^2 \text{ g}_{\text{PE}} (\text{mmol M})^{-1} \text{ h}^{-1} \text{ bar}^{-1}$ , the catalyst **88**/MMAO gave only moderate activity ( $15 \text{ g}_{\text{PE}} (\text{mmol M})^{-1} \text{ h}^{-1} \text{ bar}^{-1}$  at room temperature).<sup>1075</sup> Similarly, poor activity was reported for **90**/MAO, as well as for the Zr and Hf analogs.<sup>1076</sup>



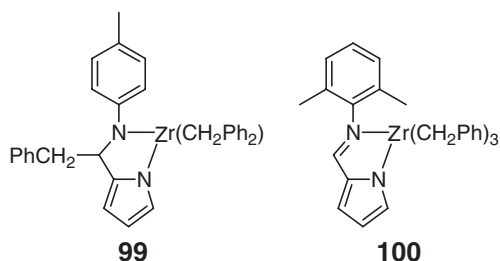
Catalysts with a rigid naphthalene bridge, such as those based on complexes **92–94**, have been also explored.<sup>1075,1077,1078</sup> MMAO-activated **92** and **93** exhibited moderate ethylene polymerization activity ( $10\text{--}40 \text{ g}_{\text{PE}} (\text{mmol M})^{-1} \text{ h}^{-1} \text{ bar}^{-1}$ ),<sup>1075,1077</sup> while **94**/MMAO in heptane showed a reasonably high activity ( $\sim 2 \times 10^2 \text{ g}_{\text{PE}} (\text{mmol M})^{-1} \text{ h}^{-1} \text{ bar}^{-1}$  at 60 °C). The PE produced had moderate molecular masses ( $\bar{M}_w = 121\,000\text{--}214\,000$ ) with rather broad and even bimodal distributions.<sup>1078</sup> Also, in this case, using toluene as solvent depresses activity, but it almost doubles the molecular masses.<sup>1078</sup>



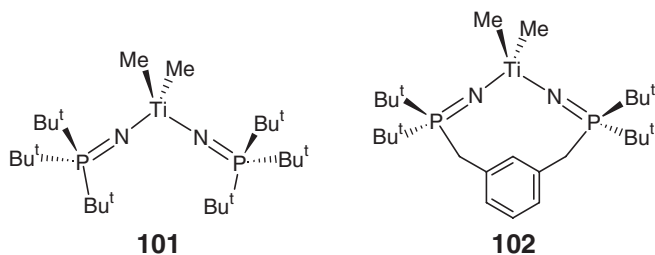
Other variations on the N–N bridge were reported.<sup>1079–1085</sup> Reducing the bridge to a C<sub>2</sub> spacer, **91**, resulted in low activity toward ethylene polymerization.<sup>1085</sup> The **95**/MMAO catalyst exhibited moderate to low activity in ethylene, propylene, and 1-hexene polymerization ( $10\text{--}30 \text{ g}_{\text{polymer}} (\text{mmol M})^{-1} \text{ h}^{-1}$ ).<sup>1079</sup> Catalysts based on **96** ( $13 \text{ g}_{\text{PE}} (\text{mmol M})^{-1} \text{ h}^{-1} \text{ bar}^{-1}$  and  $70 \text{ g}_{\text{PP}} (\text{mmol M})^{-1} \text{ h}^{-1} \text{ bar}^{-1}$ ) and **97** also exhibited moderate activity in ethylene and propylene polymerization.<sup>1080–1082</sup> Instead, the **98**/MAO catalyst exhibited high activity in ethylene, propylene, and 1-hexene polymerization ( $5 \times 10^3$ ,  $8 \times 10^2$  and  $2 \times 10^2 \text{ g}_{\text{polymer}} (\text{mmol M})^{-1} \text{ h}^{-1}$ , respectively). Unfortunately, molecular masses were rather low ( $\bar{M}_w = 161\,000$ ,  $42\,000$ , and  $26\,000$ , respectively).<sup>1083</sup> Activation of the same complexes with B(C<sub>6</sub>F<sub>5</sub>)<sub>3</sub> resulted in a remarkable decrease of activity for ethylene, while propylene and 1-hexene were polymerized with similar activity. However, molecular masses were notably higher ( $\bar{M}_w = 165\,000$ ,  $305\,000$  and  $145\,000$ , respectively).<sup>1083</sup>



The amino-pyrrolate complex **99** is another case of a complex with coordination 4 and two coordinating N atoms. In the temperature range 0–50 °C, the **99**/MAO catalyst oligomerizes ethylene ( $\bar{M}_w < 8000$ ,  $\bar{M}_w/\bar{M}_n < 2.8$ ) with high activity ( $< 8 \times 10^2 \text{ g}_{\text{PE}} (\text{mmol M})^{-1} \text{ h}^{-1} \text{ bar}^{-1}$ ), whereas the monoligated imino-pyrrolate complex **100** shows moderate polymerization activity ( $19 \text{ g}_{\text{PE}} (\text{mmol M})^{-1} \text{ h}^{-1} \text{ bar}^{-1}$ ).<sup>1086</sup>



Another class of catalysts with two coordinating N atoms is represented by the bis-phosphinimide Ti catalysts.<sup>1087–1091</sup> Complex **101** activated with either B(C<sub>6</sub>F<sub>5</sub>)<sub>3</sub> and [Ph<sub>3</sub>C][B(C<sub>6</sub>F<sub>5</sub>)<sub>4</sub>] is an highly active catalyst for ethylene polymerizations. At 25 °C and 1 bar ethylene, activity is about  $1 \times 10^3 \text{ g}_{\text{PE}} (\text{mmol M})^{-1} \text{ h}^{-1} \text{ bar}^{-1}$ . At the much more drastic conditions of about 100 bar ethylene and 160 °C, **101** still shows the interesting activity of about  $6 \times 10^2 \text{ g}_{\text{PE}} (\text{mmol M})^{-1} \text{ h}^{-1} \text{ bar}^{-1}$ . Considering the high polymerization temperature, the molecular masses obtained ( $\bar{M}_w = 80000$  and  $\bar{M}_w/\bar{M}_n = 1.9$ ) are reasonably high, while their narrow distribution indicates that single-site catalysis is achieved. Similar Zr-based catalysts showed rather lower activity.<sup>1088,1089</sup> In contrast, catalysts based on bidentate phosphinimide complexes such as **102** resulted in disappointingly lower activity.<sup>1091</sup> The reaction of **101** with AlMe<sub>3</sub> was investigated in detail, and was shown to proceed via competitive C–H activation and metathesis reactions.<sup>1090</sup>



#### 4.09.5.1.3 Other ligands

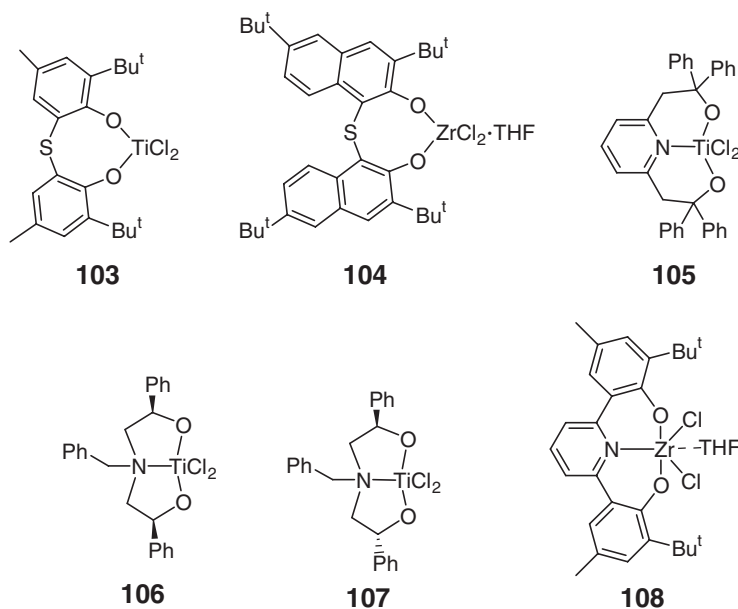
Other complexes with coordination 4 at the metal atom that have been tested in olefin polymerizations are the monodicarbollide systems of general formula  $(\eta^5\text{-C}_2\text{B}_9\text{H}_{11})(\text{C}_5\text{Me}_5)\text{M}(\text{CH}_3)$  (M = Zr, Hf) or  $(\eta^5\text{-C}_2\text{B}_9\text{H}_{11})\text{-M}(\text{NEt}_2)(\text{NHEt}_2)$ , (M = Ti, Zr). These catalyst systems were proved to be active in ethylene polymerization with a moderate activity comparable to that of CpTiCl<sub>3</sub>.<sup>34,1092</sup> Other systems investigated are ZrCl<sub>4</sub> esters or

ethers that were proved to oligomerize and polymerize ethylene and propylene,<sup>1093,1094</sup> and  $\text{TiCl}_2(2\text{-OC}_6\text{H}_4\text{OCH}_3)_2$  which was shown to polymerize propylene to an elastomeric polymer.<sup>1095</sup>

#### 4.09.5.2 Complexes with Coordination Number 5

##### 4.09.5.2.1 Ligands with coordinating O–O atoms

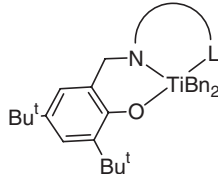

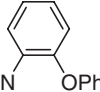
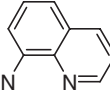
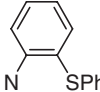
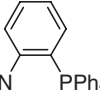
Dialkoxides with an extra donor atom have been also tested as ethylene, propylene, and 1-hexene polymerization catalysts.<sup>159,1096–1098</sup> The first reports showed that an additional sulfur donor results in quite high ethylene and propylene polymerization activity (about  $10^3 \text{ g}_{\text{PE}} (\text{mmol M})^{-1} \text{ h}^{-1} \text{ bar}^{-1}$ ), and very high molecular masses.<sup>159,1096</sup> Catalysts based on **103**, known as the Kakugo's catalysts, yield a regioregular but atactic poly-1-hexene of rather low molecular mass ( $\bar{M}_w = 10^4$ ).<sup>256</sup> Theoretical DFT studies showed that the S atom donates electron density to the metal, which reduces the activation barrier relative to the complexes with a  $\text{CH}_2$  bridge such as the simple dialkoxide **83**.<sup>1063,1064</sup> A modified version of the Kakugo catalyst, based on complex **104**, resulted in rather poor activity ( $1 \text{ g}_{\text{PE}} (\text{mmol M})^{-1} \text{ h}^{-1} \text{ bar}^{-1}$ ).<sup>1099</sup> The MAO-activated complexes **105–107** showed low activity in either ethylene or  $\alpha$ -olefin polymerization.<sup>1097,1098</sup> Nevertheless, while the *meso*-complex **106** yields atactic poly-1-hexene of low molecular mass ( $\bar{M}_n = 10^3$ ), the racemic analog **107** yields isotactic poly-1-hexene of reasonably high molecular mass ( $\bar{M}_n$  up to 300 000).<sup>1098</sup> The catalyst **108**/MAO was shown to yield polyethylene with very high activity ( $>10^3 \text{ g}_{\text{PE}} (\text{mmol M})^{-1} \text{ h}^{-1} \text{ bar}^{-1}$ ) in the polymerization temperature range 0–65 °C, whereas its Ti analog exhibited disappointingly low activity ( $4 \text{ g}_{\text{PE}} (\text{mmol M})^{-1} \text{ h}^{-1} \text{ bar}^{-1}$ ).<sup>1100</sup>



##### 4.09.5.2.2 Ligands with coordinating N–O atoms

Phenoxy–amide complexes with an extra neutral donor, such as the monometallic complexes with trichelate ligands of Figure 39, can be effective ethylene polymerization catalysts.<sup>1101</sup> The best performances were obtained with the catalyst based on the complex with a diphenylphosphine group. Besides the highest activity in the series, this complex is thermally robust and shows optimum activity at 70 °C.

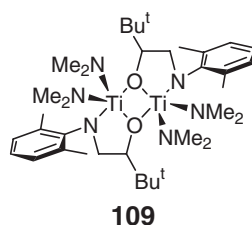
In the polymerization temperature range 25–70 °C, the catalyst based on the dimeric **109** activated with MAO exhibits moderate to high activity in ethylene polymerization (activity =  $10\text{--}10^3 \text{ g}_{\text{PE}} (\text{mmol M})^{-1} \text{ h}^{-1} \text{ bar}^{-1}$ ). The PE produced has reasonably high molecular masses ( $\bar{M}_w = 680\,000$  at 25 °C and 120 000 at 70 °C). This system was not active in propylene polymerization.<sup>1102</sup>

				
				
Activity (gPE (mmol M) <sup>-1</sup> h <sup>-1</sup> bar <sup>-1</sup> )	9 × 10	1 × 10 <sup>2</sup>	4 × 10 <sup>3</sup>	2 × 10 <sup>4</sup>
Yield (g)	0.44	0.48	3.53	1.95
$\overline{M}_w$	306,500	617,500	594,700	1,803,000
$\overline{M}_w/\overline{M}_n$	3.7	3.5	3.6	3.8

1 bar ethylene, MAO/Ti = 2,000, heptane, 25 °C, 30 min

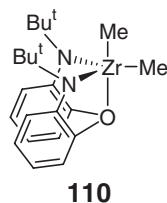
1 bar ethylene, MAO/Ti = 2,000, heptane, 25 °C, 30 min

**Figure 39** Ethylene polymerization with mono-phenoxy–amide-based catalysts.



#### 4.09.5.2.3 Ligands with coordinating N–N atoms

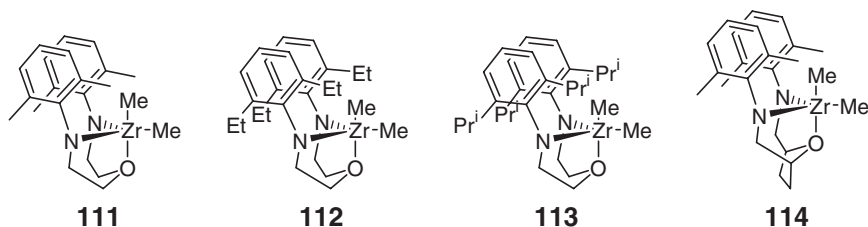
Complexes with dianionic diamide ligands show remarkable catalytic properties also in the presence of an extra neutral donor, and thus tridentate diamide systems have been extensively investigated.<sup>311,312,1103–1114</sup> The geometry of coordination at the metal atom is trigonal bipyramidal, with the two amide N atoms in the equatorial plane. Initiation consists in the reaction of a tridentate dialkyl complex with B(C<sub>6</sub>F<sub>5</sub>)<sub>3</sub> or a borate salt such as [Ph<sub>3</sub>C][B(C<sub>6</sub>F<sub>5</sub>)<sub>4</sub>] or [PhNMe<sub>2</sub>H][B(C<sub>6</sub>F<sub>5</sub>)<sub>4</sub>]. These catalysts, known as Schrock's catalysts, usually require low polymerization temperatures (around 0 °C) to avoid catalyst decomposition. Performances strongly depend on the nature of the diamide ligand, on the nature of the metal, and on the activation procedure. At 0 °C/1 h, the catalyst **110**/[PhNMe<sub>2</sub>H][B(C<sub>6</sub>F<sub>5</sub>)<sub>4</sub>] polymerizes 1-hexene in a living fashion.<sup>1112,1114</sup> The resulting poly(1-hexene)s have  $\bar{M}_n \sim 25\,000$ – $35\,000$  and  $\bar{M}_w/\bar{M}_n \sim 1.02$ – $1.05$ . Raising the polymerization temperature to 22 °C yields poly(1-hexene) with an activity of  $2 \times 10^2$  gPH (mmol M)<sup>-1</sup> h<sup>-1</sup>, and  $\bar{M}_n = 45\,000$ , but  $\bar{M}_w/\bar{M}_n$  rises to 1.2.<sup>1114</sup> The regiochemistry of 1-hexene insertion is primary.<sup>1115</sup> The Hf analog of **110** also polymerizes 1-hexene in a living fashion, while the Ti analog does not exhibit catalytic activity.<sup>1112</sup> The kinetics of these systems were investigated in detail.<sup>311</sup> At 22 °C, **110**/B(C<sub>6</sub>F<sub>5</sub>)<sub>3</sub> yields a PE with the high activity of  $1 \times 10^2$  gPE (mmol M)<sup>-1</sup> h<sup>-1</sup> bar<sup>-1</sup>, and changing the initiator to a borate salt, **110**/[PhNMe<sub>2</sub>H][B(C<sub>6</sub>F<sub>5</sub>)<sub>4</sub>], increases the activity to  $8 \times 10^2$  gPE (mmol M)<sup>-1</sup> h<sup>-1</sup> bar<sup>-1</sup>.<sup>1114</sup>



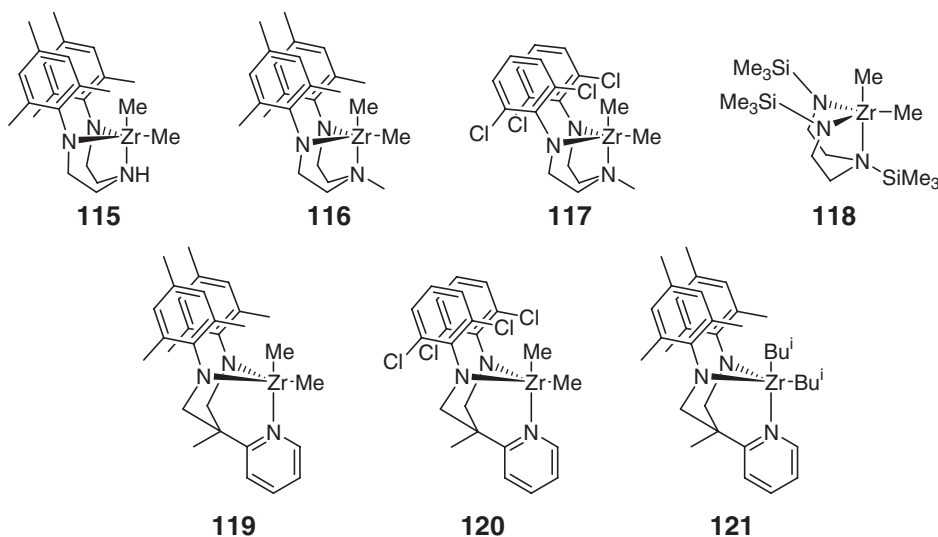
Complexes **111–114** represent other examples of Zr catalysts that contain a diamido ligand with an extra O-donor group. After activation with [Ph<sub>3</sub>C][B(C<sub>6</sub>F<sub>5</sub>)<sub>4</sub>], these systems polymerize 1-hexene at 0 °C.<sup>1111,1113</sup> Interestingly, structures **111–113** exhibit substantially similar activity, although the molecular mass decreases sensibly with the bulkiness of the substituents *ortho* to the amido N atoms **111**:  $\bar{M}_w = 18\,000$ ,  $\bar{M}_w/\bar{M}_n = 1.6$ ; **112**:  $\bar{M}_w = 11\,000$ ,



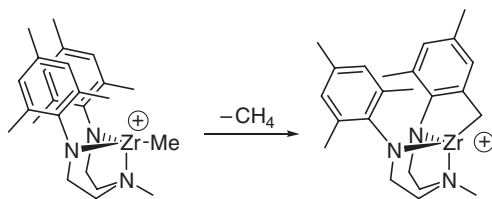
$\bar{M}_w/\bar{M}_n = 1.2$ ; **113**:  $\bar{M}_w = 400$ ,  $\bar{M}_w/\bar{M}_n = 1.7$ ). The values of  $\bar{M}_w/\bar{M}_n$  are rather narrow, but living polymerization was not reported.<sup>1113</sup> Similar behavior was observed for the Hf analogs. Introduction of the THF ring in **114** results in an increase of the molecular mass of the polymers and in narrower molecular mass distribution  $\bar{M}_n \sim 35\,000\text{--}45\,000$  and  $\bar{M}_w/\bar{M}_n \sim 1.1\text{--}1.5$ ). It was suggested that the THF ring introduces rigidity and steric hindrance, which prevents  $\beta$ -H elimination reaction.<sup>1111</sup>



Complexes **115–121** represent examples of diamido ligands with an extra *N*-donor group.<sup>1103,1105–1108,1110</sup> Both **115** and **116** exhibit reasonable activity, but molecular masses obtained with **115** ( $\bar{M}_w \sim 20\,000$ ,  $\bar{M}_w/\bar{M}_n \sim 1.3$ ) are approximately the half of those obtained with **116** ( $\bar{M}_w \sim 40\,000$ ,  $\bar{M}_w/\bar{M}_n \sim 1.4$ ). These catalysts also exhibited good stability at room temperature, while increasing the temperature to about  $65^\circ\text{C}$  resulted in rapid irreversible catalyst decomposition.<sup>1110</sup> One of the deactivation paths is a C–H activation reaction that involves an Me group of the ligand, as shown in Scheme 37.<sup>312,1107</sup> A clever and simple solution to catalyst deactivation was the synthesis of **117**, which at  $0^\circ\text{C}$  and in 1 h yields living 1-hexene polymerization ( $\bar{M}_w/\bar{M}_n \sim 1.02$ ) and  $\bar{M}_w$  up to 80 000.<sup>1103,1107</sup> The Hf analog of **117**, instead, is prone to significant  $\beta$ -H elimination which implies low molecular masses.<sup>1103</sup>

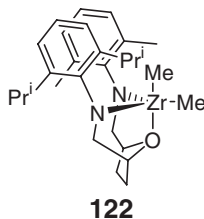


The  $\text{B}(\text{C}_6\text{F}_5)_3$ -activated complex **118** is a moderately active ethylene polymerization catalyst, although it suffers from degradation due to a C–H activation of an  $\text{SiMe}_3$  group adjacent to the metal center.<sup>1116</sup> This degradation

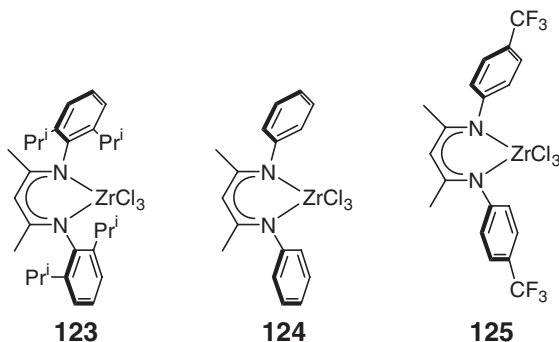


Scheme 37

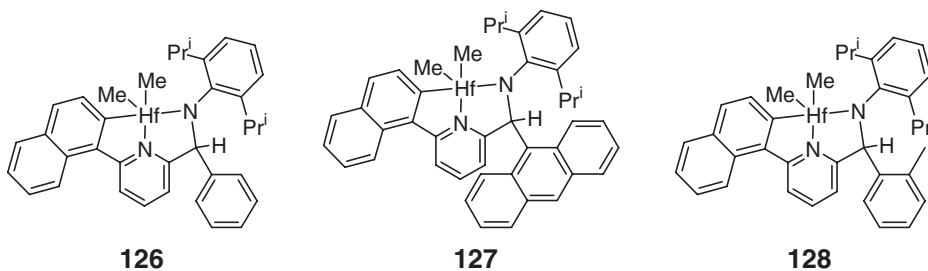
mechanism is extremely similar to that observed in related tridentate diamide complexes (see Scheme 37).<sup>1103</sup> Another variation in tridentate complexes with a diamido ligand is represented by **119** and **120**.<sup>1106,1108,1109</sup> Differently from the case of **116** and **117**, the complex **120** with halogen atoms *ortho* to the N amido atoms shows lower activity and yields polymers with lower molecular mass than the catalyst based on **119**.<sup>1106</sup> Comparison of the pyridyldiamido complex **119** with **121**, in which the two Me groups were replaced by the two *i*-Bu groups, allowed investigation of the role of the alkyl group bound to the metal. The poorer catalytic behavior of **119** was ascribed to the formation of largely inactive cationic dimeric species through Me bridges.<sup>1105,1108,1109</sup> Finally, in the attempt to achieve stereospecific polymerization, asymmetric complexes such as **122** were synthesized. Unfortunately, these complexes also only yield atactic poly(1-hexene).<sup>1104</sup>



$\beta$ -Diketiminato zirconium complexes such as **123** and **124** exhibited moderate activity in the polymerization of ethylene (about 50 gPE (mmol M)<sup>-1</sup> h<sup>-1</sup> bar<sup>-1</sup>), but molecular masses were disappointingly low ( $\bar{M}_n \sim 10\,000$ ).<sup>1117,1118</sup> Introduction of a CF<sub>3</sub> group as in **125** resulted in very high activity ( $2 \times 10^3$  gPE (mmol M)<sup>-1</sup> h<sup>-1</sup> bar<sup>-1</sup>) but still low molecular masses ( $\bar{M}_n = 80\,000$ ).<sup>1117</sup>

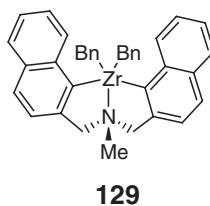


A different class of ligands with coordination 5 and two N atoms bound to the metal is represented by the Hf pyridyl amine complexes **126–128** discovered in 2003. These systems are characterized by an Hf–C  $\sigma$ -bond between the aromatic ligand and the metal. The original patent concerns the preparation of iPP co-polymers with ethylene or other unsaturated co-monomers.<sup>1119</sup> Nevertheless, a catalyst solution composed of complex **127/a** borate salt/MAO in the ratio 1 : 1 : 200 (Al) is able to homopolymerize propylene to an isotactic polymer at 110 °C for at least 10 min. The catalyst exhibited very high activity, around 5000 gPP (mmol M)<sup>-1</sup> h<sup>-1</sup> bar<sup>-1</sup>. The iPP produced had a  $T_m = 144.4^\circ\text{C}$  and high molecular mass,  $\bar{M}_w = 293\,000$ . The  $\bar{M}_w/\bar{M}_n = 2.9$  indicated that under these rather drastic conditions the catalyst shows single-site behavior. The production of a highly isotactic PP with a C<sub>1</sub>-symmetric catalyst is particularly remarkable since it is obtained at a high polymerization temperature.<sup>1119</sup>



#### 4.09.5.2.4 Other ligands

Complex **129** activated with  $[\text{Ph}_3\text{C}][\text{B}(\text{C}_6\text{F}_5)_4]$  is a catalyst for aspecific propylene polymerization. The system showed low activity ( $7 \text{ g}_{\text{PP}}(\text{mmol M})^{-1} \text{ h}^{-1} \text{ bar}^{-1}$ ) and yielded polymers of rather low molecular masses ( $\bar{M}_n = 21\,000$ ).<sup>1120</sup>



#### 4.09.5.3 Complexes with Coordination Number 6

##### 4.09.5.3.1 Ligands with coordinating O–O atoms

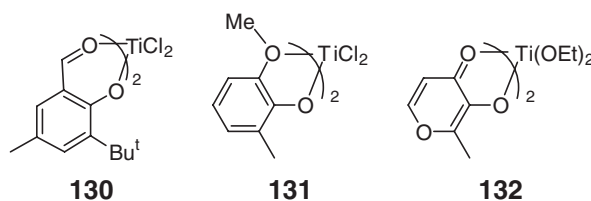
The phenoxy–ether complexes of Figure 40 are active ethylene polymerization catalysts.<sup>1121</sup> MAO- and  $[\text{Ph}_3\text{C}][\text{B}(\text{C}_6\text{F}_5)_4]/\text{Bu}^i_3\text{Al}$ -activated complexes show rather similar behavior. This is different from phenoxy–imine-based complexes, where  $\text{Bu}^i_3\text{Al}$  is accepted to react with the imine functionality. In all cases, the molecular masses of the PEs produced are very high ( $\bar{M}_v > 2 \times 10^6$ ). Activity and  $\bar{M}_v$  strongly depend on the size of the substituent R. Activity is poor with the small R = H substituent, while it is high with the bulky R = adamantyl. Bulky substituents probably prevent formation of a tightly coupled ion pair. Surprisingly, higher molecular masses are obtained with the smaller R = H substituent. This was rather unexpected, since steric congestion at the active center usually reduces chain-release reactions.

Similar complexes were investigated in less detail by other authors, although rather good performances were observed. Complex **130** is a highly active ethylene polymerization catalyst that yields very broad molecular mass distribution ( $\bar{M}_w/\bar{M}_n = 16$ ). The Zr analog of **130** behaves similarly.<sup>1122</sup> Other complexes tested in ethylene polymerization are **131** and **132**. While the  $\text{AlEt}_3/\text{AlEt}_2\text{Cl}$ -activated **131** shows high polymerization activity (about  $2 \times 10^2 \text{ g}_{\text{PE}}(\text{mmol M})^{-1} \text{ h}^{-1} \text{ bar}^{-1}$ ), the similarly activated **132** performs even better (about  $3 \times 10^3 \text{ g}_{\text{PE}}(\text{mmol M})^{-1} \text{ h}^{-1} \text{ bar}^{-1}$ ).<sup>1123</sup>

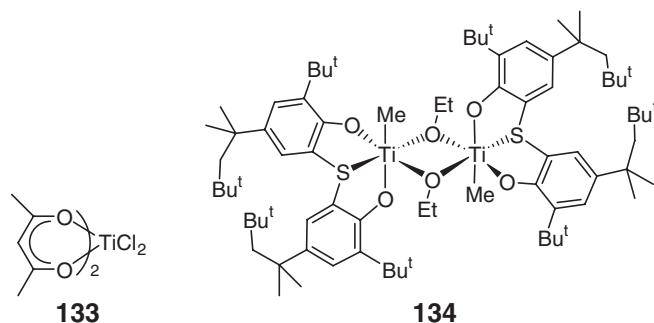
	<i>R</i>		
	H	<i>n</i> -Bu	Adamantyl
	MAO as co-catalyst		
Activity ( $\text{g}_{\text{PE}}(\text{mmol M})^{-1} \text{ h}^{-1} \text{ bar}^{-1}$ )	4.10	$3 \cdot 10^2$	$3 \cdot 10^3$
Yield (g)	0.11	0.11	1.17
$\bar{M}_v$	7,240,000	5,420,000	2,040,000
	$[\text{Ph}_3\text{C}][\text{B}(\text{C}_6\text{F}_5)_4]/\text{Bu}^i_3\text{Al}$ as co-catalyst		
Activity ( $\text{g}_{\text{PE}}(\text{mmol M})^{-1} \text{ h}^{-1} \text{ bar}^{-1}$ )	6.10	$1 \cdot 10^3$	$3 \cdot 10^3$
Yield (g)	0.14	0.61	1.45
$\bar{M}_v$	5,440,000	3,120,000	2,600,000

25 °C, 1 bar ethylene, MAO/Ti = 250,  $[\text{Ph}_3\text{C}][\text{B}(\text{C}_6\text{F}_5)_4]/\text{Ti} = 1.2$ ,  $\text{Bu}^i_3\text{Al}/\text{Ti} = 50$ , toluene, polymerization time: R = H, 30 min; R = *n*-Bu and adamantyl, 5 min

**Figure 40** Ethylene polymerization with phenoxy–ether-based catalysts.

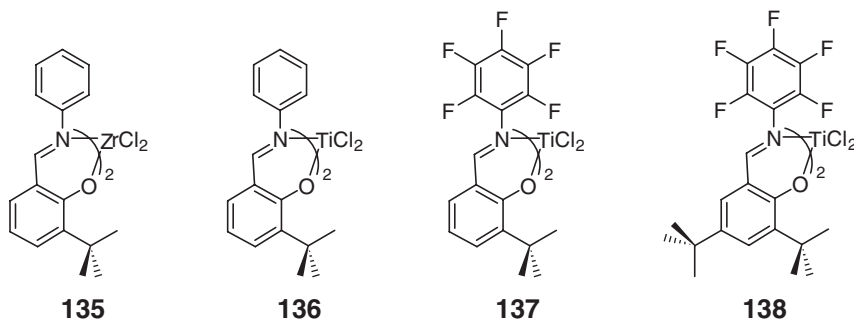


The acetylacetonate **133**/MAO catalyst, instead, yields PP with low activity ( $3\text{--}10 \text{ g}_{\text{PP}} (\text{mmol M})^{-1} \text{ h}^{-1} \text{ bar}^{-1}$ ) and moderate molecular mass ( $\bar{M}_n$  up to 125 000). The resulting PP is slightly isotactic (*mmmm* 20%) and exhibits elastomeric properties.<sup>1124</sup> Finally,  $\text{AlEt}_3/\text{AlEt}_2\text{Cl}$ -activated dimeric Ti complexes such as **134** yield PE with very high activity (about  $10^5 \text{ g}_{\text{PE}} (\text{mmol M})^{-1} \text{ h}^{-1} \text{ bar}^{-1}$ ), and with high molecular masses.<sup>1125</sup>

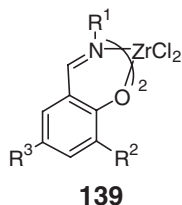


#### 4.09.5.3.2 Ligands with coordinating N–O atoms: phenoxy–imine-catalysts for polyethylene

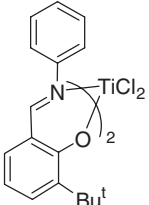
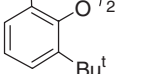
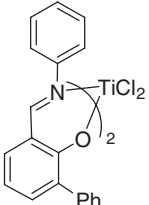
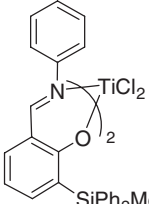
Catalysts based on salicylaldiminato ligands (commonly referred to as “phenoxy–imine” ligands) were introduced for ethylene polymerization in 1998.<sup>1126</sup> This remarkable class of highly active catalysts can lead to a unique variety of linear PEs.<sup>1121,1127–1144</sup> Several reviews have been dedicated to these systems.<sup>1140,1145–1149</sup> The performances of some of these bis(phenoxy–imine) systems are reported in Table 18. The most typical and most widely investigated systems in this class are complexes **135–138**.



The MAO-activated prototype system (**135**) exhibits an activity higher than the  $\text{Cp}_2\text{ZrCl}_2$  systems under the same conditions.<sup>1128–1130</sup> Several modifications of the basic prototype system **135** have been tested in ethylene polymerization. This class of catalysts represents by far the most widely investigated post-metallocene systems, and these modifications are centered on positions  $\text{R}^1$ ,  $\text{R}^2$ , and  $\text{R}^3$  of **139**.

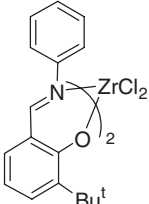
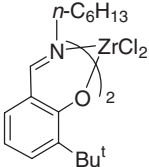
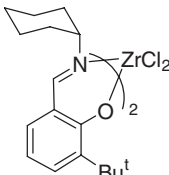
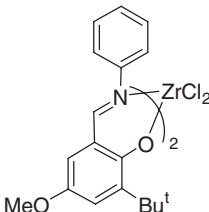


**Table 18** Ethylene polymerization with bis(phenoxy-imine)-based catalysts

Entry	Pre-catalyst	Co-catalyst	Co-catalyst M	$T_p^a$ (°C)	$P_E^b$ (bar) (Solvent)	$t_p^c$ (min)	Productivity ( $g_{PE} \text{ (mmol M)}^{-1} \text{ h}^{-1} \text{ bar}^{-1}$ )	Yield (g)	$\bar{M}_w/\bar{M}_n$	$\bar{M}_v$	References
1		MAO	250	25	1 (Tol)	10	$3 \times 10^3$	2.8		516,000	1127
2		MAO	250	50	1 (Tol)	10	$4 \times 10^3$	3.3		546,000	1127
3		MAO	250	75	1 (Tol)	10	$4 \times 10^3$	3.1		440,000	1127
4		MAO	250	25	1 (Tol)	5	$3 \times 10^3$	1.4		510,000	1127
5		MAO	6,250	25	1 (Tol)	5	$4 \times 10^3$	0.1		326,000	1133
6		MAO	1,250	75	9 ( <i>n</i> C7)	15	$5 \times 10^3$	12.0		664,000	1127
7		[Ph <sub>3</sub> C][B(C <sub>6</sub> F <sub>5</sub> ) <sub>4</sub> ]/ Bu <sub>3</sub> <sup>i</sup> Al	2/30	25	1 (Tol)	5	$2 \times 10^2$	0.1		4,810,000	1135
8		[Ph <sub>3</sub> C][B(C <sub>6</sub> F <sub>5</sub> ) <sub>4</sub> ]/ Bu <sub>3</sub> <sup>i</sup> Al	2/30	50	1 (Tol)	5	$4 \times 10^2$	0.2		5,860,000	1135
9		[Ph <sub>3</sub> C][B(C <sub>6</sub> F <sub>5</sub> ) <sub>4</sub> ]/ Bu <sub>3</sub> <sup>i</sup> Al	2/30	75	1 (Tol)	5	$7 \times 10^2$	0.3		3,920,000	1135
10		MAO	2,500	50	9 (Tol)	30	$4 \times 10^3$	11.2	2.4	464,000	1143
11		MgCl <sub>2</sub> /Bu <sub>3</sub> <sup>i</sup> Al(OR) <sub>3-<i>m</i></sub> <sup>a</sup>	800/4,800	50	9 (Tol)	30	$4 \times 10^3$	9.1	2.7	509,000	1143
12		DMAO	250	25	1 (Tol)	30	$3 \times 10^3$	8.1	2.6	$\bar{M}_w$ 1,281,000	1138
13		MAO	250	25	1 (Tol)	5	$5 \times 10^3$	1.9		604,000	1127
14		MAO	250	25	1 (Tol)	10	$3 \times 10^3$	2.1		375,000	1127

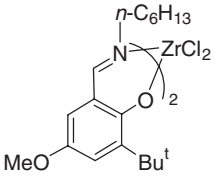
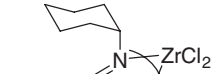
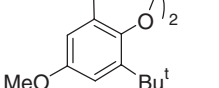
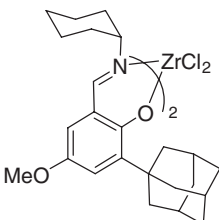
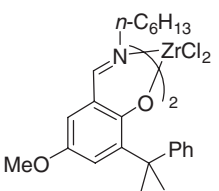
(Continued)



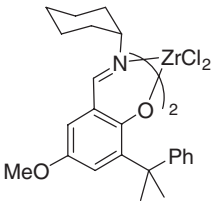
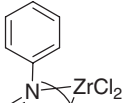
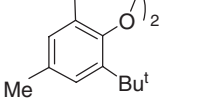
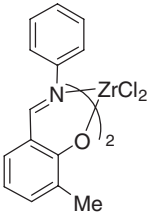
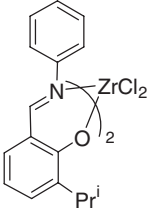
24		[Ph <sub>3</sub> C][B(C <sub>6</sub> F <sub>5</sub> ) <sub>4</sub> ]/ Bu <sup>i</sup> <sub>3</sub> Al	2/40	25	1 (Tol)	5	4 × 10 <sup>3</sup>	0.8		3,830,000	1129
25		[Ph <sub>3</sub> C][B(C <sub>6</sub> F <sub>5</sub> ) <sub>4</sub> ]/ Bu <sup>i</sup> <sub>3</sub> Al	2/40	50	1 (Tol)	5	1 × 10 <sup>4</sup>	2.3		5,050,000	1129
26		MAO	78,125	50	9 (Tol)h	30	1 × 10 <sup>5</sup>	10.3		74,000	1143
27		MgCl <sub>2</sub> / Bu <sup>i</sup> <sub>m</sub> Al(OR) <sub>3-m</sub> <sup>d</sup>	12,500/ 50,000	50	9 (Tol)h	30	2 × 10 <sup>4</sup>	2.0		91,000	1143
28		MAO	25,000	50	9 ( <i>n</i> C7)	15	1 × 10 <sup>5</sup>	14.9		47,000	1130
29		MAO	25,000	75	9 ( <i>n</i> C7)	15	2 × 10 <sup>4</sup>	2.6		100,000	1130
30		MAO	62,500	75	1 (Tol)	5	1 × 10 <sup>5</sup>		2.4	$\bar{M}_w$ 8,100	1144
31		MAO	12,500	25	1 (Tol)	5	2 × 10 <sup>5</sup>	1.9		$\bar{M}_w$ 7,300	1139
32		MAO	6,250	50	9 ( <i>n</i> C7)	15	3 × 10 <sup>4</sup>	17.3		11,000	1130
33		MAO	12,500	50	9 ( <i>n</i> C7)	15	8 × 10 <sup>4</sup>	18.8		15,000	1130
34		MAO	6,250	25	1 (Tol)	5	1 × 10 <sup>5</sup>	1.9	1.8	$\bar{M}_w$ 13,800	1152
35		MAO	12,500	50	9 ( <i>n</i> C7)	15	3 × 10 <sup>4</sup>	8.2		363,000	1130
36		MAO	62,500	75	1 (Tol)	5	8 × 10 <sup>4</sup>		11.1	$\bar{M}_w$ 28,600	1144

(Continued)

**Table 18** (Continued)

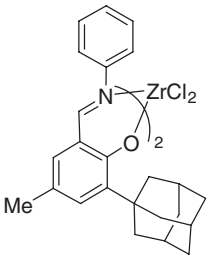
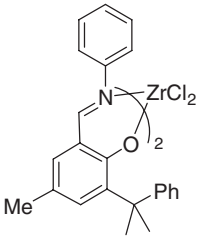
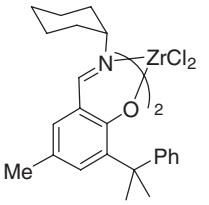
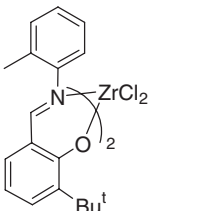
Entry	Pre-catalyst	Co-catalyst	Co-catalyst M	$T_P^a$ (°C)	$P_E^b$ (bar) (Solvent)	$t_P^c$ (min)	Productivity ( $g_{PE}$ (mmol M) $^{-1}$ h $^{-1}$ bar $^{-1}$ )	Yield (g)	$\bar{M}_w/\bar{M}_n$	$\bar{M}_v$	References
37		MAO	25,000	50	9 ( <i>n</i> C7)	15	$5 \times 10^4$	5.7		99,000	<a href="#">1130</a>
38		MAO	25,000	50	9 ( <i>n</i> C7)	15	$9 \times 10^4$	10.2		168,000	<a href="#">1130</a>
39		MAO	25,000	75	9 ( <i>n</i> C7)	15	$1 \times 10^5$	18.3		54,000	<a href="#">1130</a>
40		MAO	6,250	75	9 ( <i>n</i> C7)	15	$3 \times 10^5$	15.3		95,000	<a href="#">1130</a>
41		MAO	12,500	75	9 ( <i>n</i> C7)	15	$7 \times 10^5$	17.7		39,000	<a href="#">1130</a>

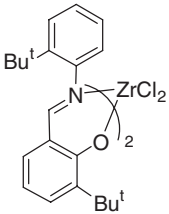
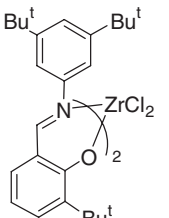
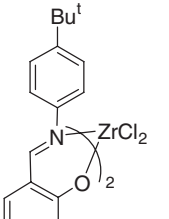
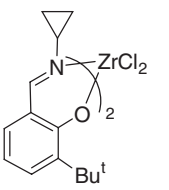


42		MAO	250,000	75	9 ( <i>n</i> C7)	15	$7 \times 10^5$	9.1		104,000	<a href="#">1130</a>
43		MAO	62,500	25	1 (Tol)	5	$3 \times 10^5$	0.5	2.0	7,000	<a href="#">1129</a>
44		MAO	62,500	75	1 (Tol)	5	$7 \times 10^4$		4.1	$\bar{M}_w$ 19,100	<a href="#">1144</a>
45		MAO	250	25	1 (Tol)	5	$4 \times 10^2$	0.2	2.3	3,000	<a href="#">1129</a>
46		MAO	250	25	1 (Tol)	5	$9 \times 10^2$	0.4	2.5	6,000	<a href="#">1129</a>

(Continued)

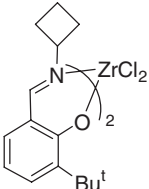
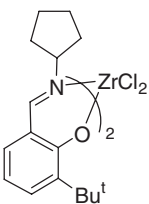
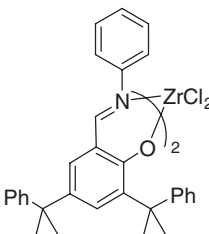
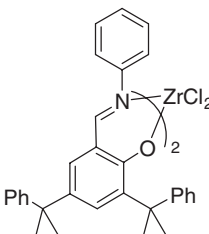
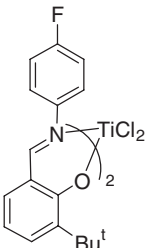
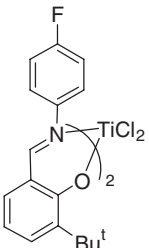
**Table 18** (Continued)

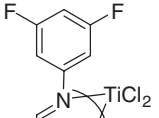
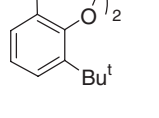
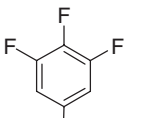
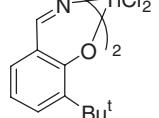
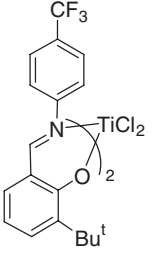
Entry	Pre-catalyst	Co-catalyst	Co-catalyst M	$T_P^a$ (°C)	$P_E^b$ (bar) (Solvent)	$t_P^c$ (min)	Productivity ( $g_{PE}$ (mmol M) <sup>-1</sup> h <sup>-1</sup> bar <sup>-1</sup> )	Yield (g)	$\bar{M}_w/\bar{M}_n$	$\bar{M}_v$	References
47		MAO	62,500	25	1 (Tol)	5	$7 \times 10^5$	1.2	2.7	12,000	<a href="#">1129</a>
48		MAO	125,000	25	1 (Tol)	5	$2 \times 10^6$	1.7	7.2	18,000	<a href="#">1129</a>
49		MAO	250,000	25	1 (Tol)	5	$4 \times 10^6$	1.8	1.9	15,000	<a href="#">1129</a>
50		MAO	2,500	25	1 (Tol)	5	$4 \times 10^4$	1.7	2.1	320,000	<a href="#">1129</a>

51		MAO	250	25	1 (Tol)	30	$1 \times 10^2$	0.2		> 2,740,000	<a href="#">1129</a>
52		MAO	12,500	25	1 (Tol)	5	$2 \times 10^5$	2.0	1.8	26,000	<a href="#">1129</a>
53		MAO	12,500	25	1 (Tol)	5	$3 \times 10^5$	2.3	2.0	7,000	<a href="#">1129</a>
54		MAO	6,250	25	1 (Tol)	5	$4 \times 10^4$	0.6	1.8	$\bar{M}_w$ 4,700	<a href="#">1152</a>

(Continued)

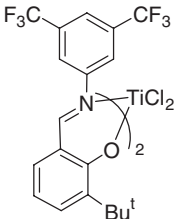
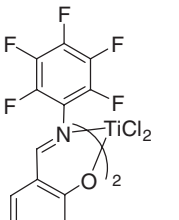
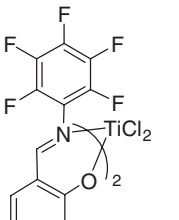
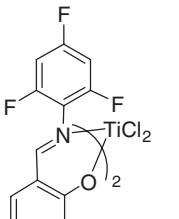
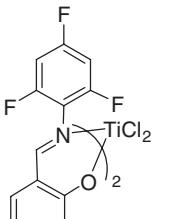
**Table 18** (Continued)

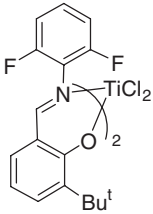
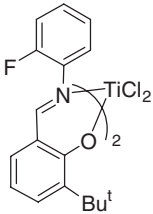
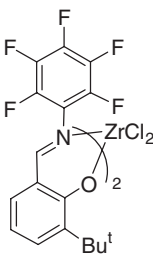
Entry	Pre-catalyst	Co-catalyst	Co-catalyst M	$T_P^a$ (°C)	$P_E^b$ (bar) (Solvent)	$t_P^c$ (min)	Productivity ( $g_{PE}$ (mmol M) $^{-1}$ h $^{-1}$ bar $^{-1}$ )	Yield (g)	$\bar{M}_w/\bar{M}_n$	$\bar{M}_v$	References
55		MAO	6,250	25	1 (Tol)	5	$3 \times 10^4$	0.5	1.5	$\bar{M}_w$ 2,100	<a href="#">1152</a>
56		MAO	6,250	25	1 (Tol)	5	$1 \times 10^5$	1.9	1.8	$\bar{M}_w$ 3,800	<a href="#">1152</a>
57		MAO	62,500	40	1 (Tol)	5	$6 \times 10^5$		24.8	133,200	<a href="#">1142</a>
58		MAO	62,500	40	1 (Tol)	8	$4 \times 10^5$		43	231,800	<a href="#">1142</a>
59		MAO	6,250	25	1 (Tol)	5	$4 \times 10^3$	0.1		419,000	<a href="#">1133</a>
60		MAO	3,125	50	1 (Tol)	5	$5 \times 10^3$	0.2	2.2	$\bar{M}_n$ 128,000	<a href="#">1134</a>

61		MAO	6,250	25	1 (Tol)	5	$3 \times 10^4$	0.6		623,000	<a href="#">1133</a>
62		MAO	2,500	50	1 (Tol)	1	$3 \times 10^4$	0.3	1.8	$\bar{M}_n$ 129,000	<a href="#">1134</a>
63		MAO	6,250	25	1 (Tol)	5	$4 \times 10^4$	0.7		378,000	<a href="#">1133</a>
64		MAO	2,500	50	1 (Tol)	1	$4 \times 10^4$	0.4	2.0	$\bar{M}_n$ 98,000	<a href="#">1134</a>
65		MAO	6,250	25	1 (Tol)	5	$3 \times 10^3$	0.1		542,000	<a href="#">1133</a>

(Continued)

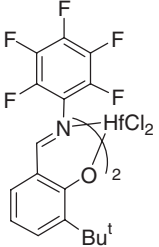
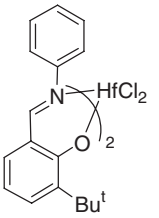
**Table 18** (Continued)

Entry	Pre-catalyst	Co-catalyst	Co-catalyst M	$T_P^a$ (°C)	$P_E^b$ (bar) (Solvent)	$t_P^c$ (min)	Productivity ( $g_{PE}$ (mmol M) $^{-1}$ h $^{-1}$ bar $^{-1}$ )	Yield (g)	$\bar{M}_w/\bar{M}_n$	$\bar{M}_v$	References
66		MAO	6,250	25	1 (Tol)	5	$4 \times 10^4$	0.7		1,365,000	<a href="#">1133</a>
67		MAO	2,500	50	1 (Tol)	1	$4 \times 10^4$	0.3	1.13	$\bar{M}_n$ 424,000	<a href="#">1134</a>
68		MAO	1,250	75	1 (Tol)	1	$3 \times 10^4$	0.5	1.15	$\bar{M}_n$ 272,000	<a href="#">1140</a>
69		MAO	625	90	1 (Tol)	1	$1 \times 10^4$	0.5	1.3	$\bar{M}_n$ 167,000	<a href="#">1140</a>
70		MAO	3,125	50	1 (Tol)	5	$2 \times 10^3$	0.1	1.3	$\bar{M}_n$ 145,000	<a href="#">1134</a>

71		MAO	1,250	50	1 (Tol)	5	$8 \times 10^2$	0.1	1.05	$\bar{M}_n$ 64,000	<a href="#">1134</a>
72		MAO	250	50	1 (Tol)	5	$1 \times 10^2$	0.1	1.06	$\bar{M}_n$ 13,000	<a href="#">1134</a>
73		MAO	12,500	25	1 (Tol)	5	$3 \times 10^5$	2.8	1.9	$\bar{M}_w$ 157,200	<a href="#">1139</a>

(Continued)

**Table 18** (Continued)

Entry	Pre-catalyst	Co-catalyst	Co-catalyst M	$T_P^a$ (°C)	$P_E^b$ (bar) (Solvent)	$t_P^c$ (min)	Productivity ( $g_{PE}$ (mmol M) $^{-1}$ h $^{-1}$ bar $^{-1}$ )	Yield (g)	$\bar{M}_w/\bar{M}_n$	$\bar{M}_v$	References
74		MAO	2,500	25	1 (Tol)	5	$3 \times 10^4$	1.2	2.7	$\bar{M}_w$ 409,600	<a href="#">1139</a>
75		MAO	2,500	25	1 (Tol)	5	$2 \times 10^4$	0.9		$\bar{M}_w$ 16,800	<a href="#">1139</a>

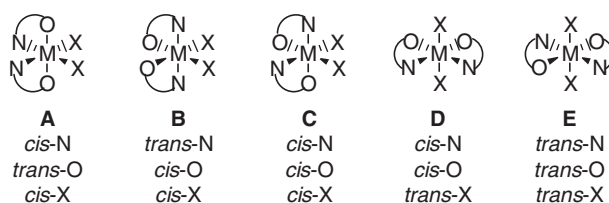
<sup>a</sup> $T_P$  = polymerization temperature.

<sup>b</sup> $P_E$  = ethylene pressure.

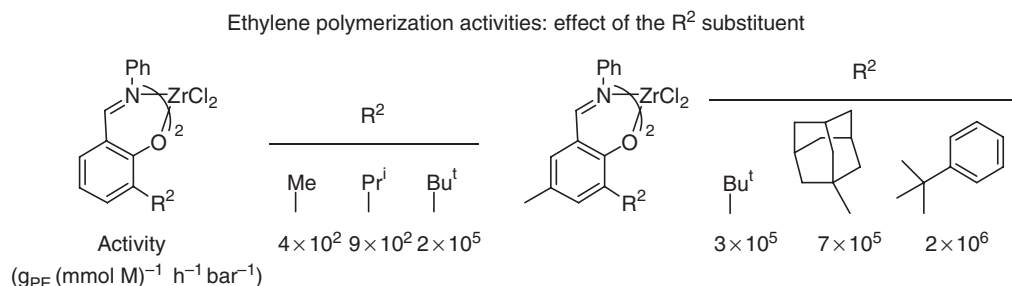
<sup>c</sup> $t_P$  = polymerization time.

<sup>d</sup>R = 2-ethyl-hexyl.





**Figure 41** Octahedral-based geometric isomers for the bis(phenoxy-imine) pre-catalysts.

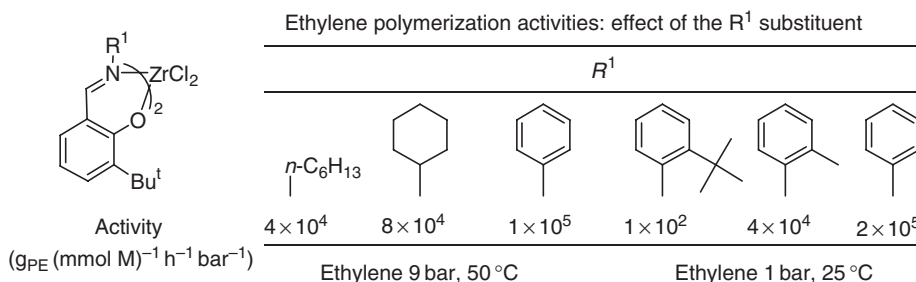


**Figure 42** Ethylene polymerization activity ( $\text{g}_{\text{PE}} (\text{mmol M})^{-1} \text{h}^{-1} \text{bar}^{-1}$ ) for a series of bis(phenoxy-imine) Zr catalysts with different  $R^2$  substituents. Left to right, the systems shown correspond to entries 45, 46, 18, 43, 47, and 48 in Table 18.

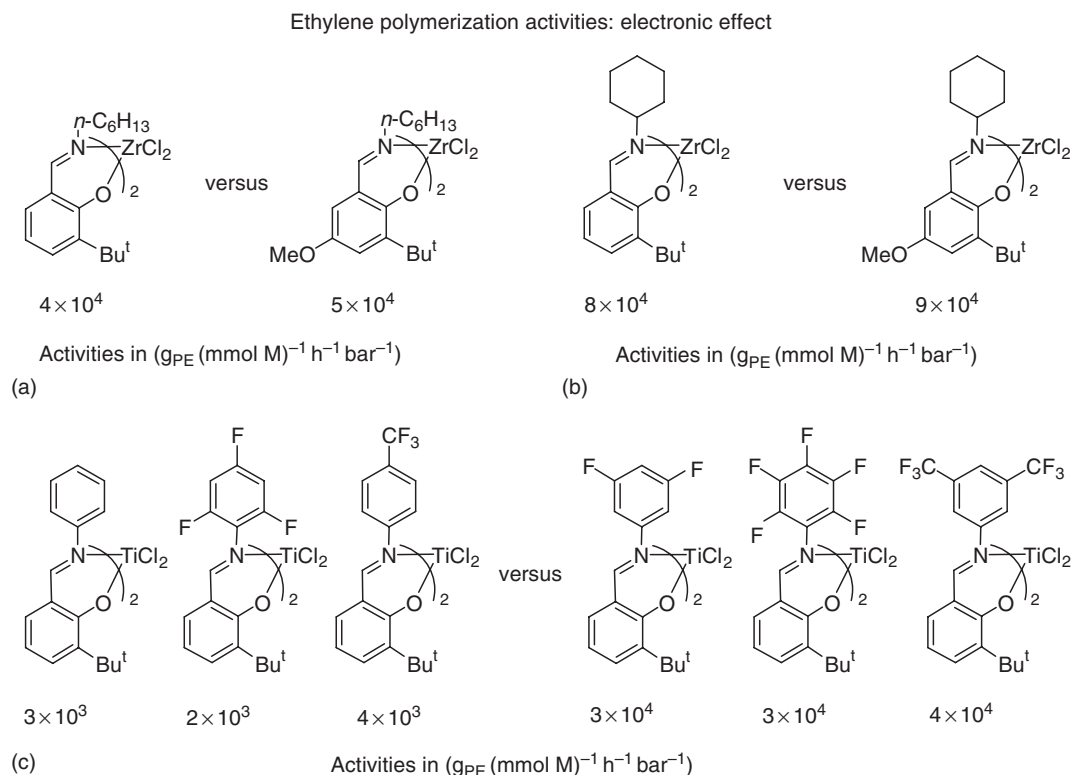
**Stereochemistry of the complex.** Bis(phenoxy-imine) and related systems are characterized by an octahedral geometry at the metal atom. The five geometrical isomers of Figure 41 are possible for octahedral complexes with two unbridged bidentate ligands. Only isomers A–C are potentially active in polymerization because they present the X groups in mutually *cis*-positions. The tendency of bis(phenoxy-imine)-based catalysts to assume a geometry with a *cis*-N, *trans*-O, and *cis*-X disposition of the coordinating atoms (isomer A in Figure 41) is proved by the X-ray structures of several pre-catalysts,<sup>1127–1129,1132,1134,1135,1145</sup> as well as by quantum mechanics calculations.<sup>1127,1129,1135,1145</sup> Nevertheless, an equilibrium between isomers A–C was invoked to explain the multimodal molecular mass distribution observed in some cases.<sup>1142,1144</sup>

**Activity: ligand-substitution effects.** Steric and electronic properties of the phenoxy-imine ligands can be tuned to regulate the catalytic behavior of the corresponding catalyst. Regarding steric effects, bulky  $R^2$  groups *ortho* to the phenoxy O atom usually enhance activity (see Figure 42).<sup>1129</sup> It was suggested that bulky  $R^2$  groups enhance catalytic activity due to a more effective separation between the cationic catalyst and the anionic counterion.<sup>1129</sup> A weakly bound ion pair results in an easier coordination of ethylene<sup>1085</sup> to a more electrophilic (and thus reactive) metal atom.<sup>1150</sup>

Conversely, the size of the  $R^1$  group has less influence on the activity of the catalyst (see Figure 43). Nevertheless, in the case of  $R^1$ =aromatic ring, bulky groups in position 2 of the phenyl ring depress activity (see Figure 43).<sup>1129,1151</sup>



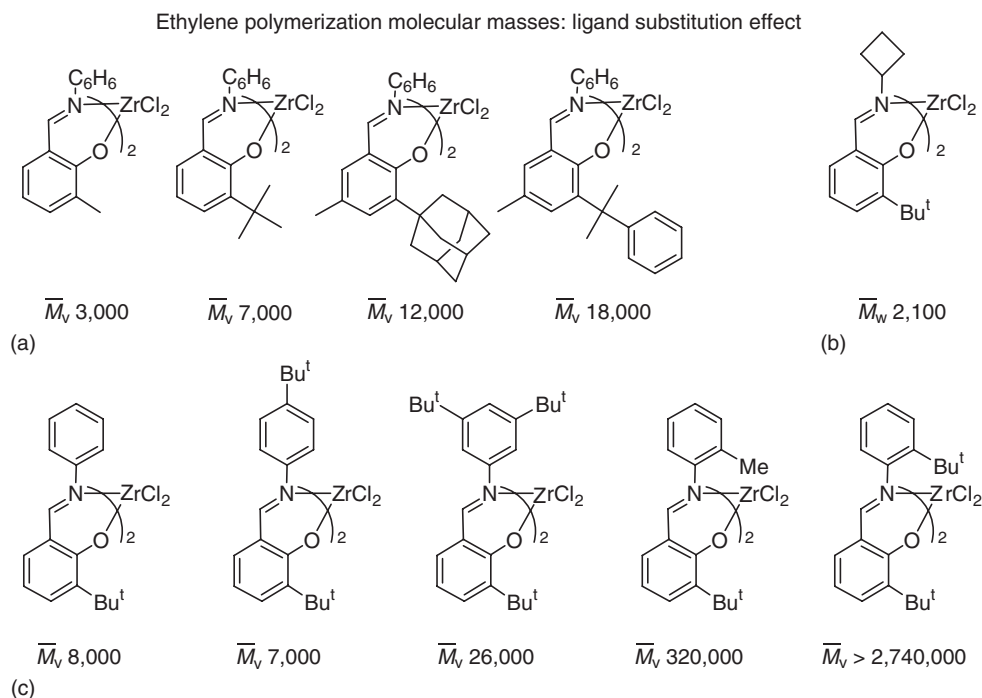
**Figure 43** Ethylene polymerization activity ( $\text{g}_{\text{PE}} (\text{mmol M})^{-1} \text{h}^{-1} \text{bar}^{-1}$ ) for a series of bis(phenoxy-imine) Zr catalysts with different  $R_1$  substituents. Left to right, the systems shown correspond to entries 32, 33, 28, 51, 50, and 18 in Table 18.



**Figure 44** Ethylene polymerization activity ( $\text{g}_{\text{PE}} (\text{mmol M})^{-1} \text{h}^{-1} \text{bar}^{-1}$ ) for a series of bis(phenoxy-imine) Zr catalysts with substituents having different electronic properties. Left to right, top to bottom, the systems shown correspond to entries 32, 37, 33, 38, 1, 70, 65, 61, 67, and 66 in Table 18.

Electronic effects have also been shown to influence catalytic properties. It has been suggested that electron-donating groups on the phenoxy-imine ligands can reduce decomposition of the active species and thus improve overall productivity. Electron-donating groups improve the stability of the active species because they can strengthen the metal-ligand bonds. This effect is particularly important at high temperature due to the low thermal stability of the active species.<sup>1130</sup> Catalysts with bis(phenoxy-imine) ligands bearing the OMe group in position  $\text{R}^3$  usually have similar activity relative to their unsubstituted analogs (see Figure 44(a) and 44(b)). Instead, electron-withdrawing groups as F or  $\text{CF}_3$  on the phenyl group in the  $\text{R}^2$  position have a profound influence on the catalyst activity.<sup>1133,1134</sup> This substitution is particularly effective when the F or  $\text{CF}_3$  groups are in the *meta*-positions (see Figure 44(c)). Moreover, it was hypothesized that electron-withdrawing groups generate a more electrophilic metal center, which results in increased reactivity.<sup>1133</sup>

**Molecular mass: ligand-substitution effects.** Steric and electronic effects can also be used to control the molecular mass of the PEs produced. Bis(phenoxy-imine)-based catalysts can yield polymers ranging from very low to extremely high molecular mass ( $\bar{M}_w < 10^4$  or  $\bar{M}_w > 10^6$ ).<sup>1152</sup> The MAO-activated prototype 135 system yields PEs with very low  $\bar{M}_v$  (about 7000–10 000; see entries 19–22 in Table 18).<sup>1128,1129</sup> As is typical for  $\alpha$ -olefin polymerizations, increasing the bulkiness around the metal atom is the key to achieving high molecular masses.<sup>1153–1155</sup> Bulkiness of the substituents *ortho* to the phenoxy O atom can be partially used to control molecular mass (see Figure 45(a)). However, the key to high molecular mass polymers is the bulkiness of the  $\text{R}^1$  group. Small  $\text{R}^1$  groups yield very low molecular mass (see Figure 45(b)). These low molecular mass ( $\bar{M}_w < 5000$ ) PEs contain a large amount of vinyl terminations (about 90% of the chain ends),<sup>1152</sup> and are potentially useful because they can be transformed by chain-end functionalization to terminally functionalized polymers.<sup>1156–1158</sup> Increasing the size of substituents on the phenyl group of the prototype 139 system yields PEs with high  $\bar{M}_v$  ( $> 200\,000$ ). Substitution on the *ortho*-position is the most effective (see Figure 45(c)). Unfortunately, as already discussed, this kind of substitution also reduces activity. It was suggested that these bulky alkyl substituents diminish chain-transfer reactions.<sup>1159</sup> This proposal is supported by theoretical calculations.<sup>1155,1159</sup> Most spectacular, however, is the effect of perfluorophenyl rings in position  $\text{R}^1$ . Molecular



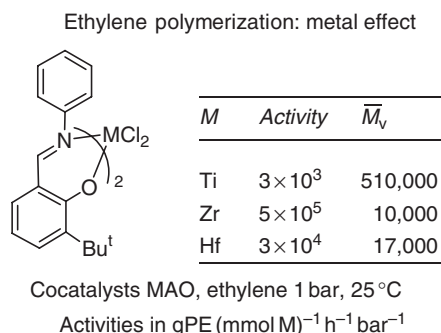
**Figure 45** PE molecular masses obtained with a series of bis(phenoxy-imine) Zr catalysts. Left to right, top to bottom, the systems shown correspond to 45, 43, 47, 48, 55, 18, 53, 52, 50, and 51 in Table 18.

masses  $>10^5$  are easily achieved with Zr- and Hf-based catalysts<sup>1139</sup> (see entries 73 and 74 in Table 18). In the case of Ti-based catalysts, chain-transfer reactions are so much depressed that living polymerization is achieved.<sup>1160</sup>

**Metal effects.** The Ti- and Hf-based catalysts are remarkably less active than the corresponding Zr-based catalysts (see Figure 46). For Ti-based catalysts, the lower activity is compensated by a remarkable increase in the molecular mass. Instead, the Hf-based catalysts yield molecular masses comparable to those obtained with the corresponding Zr-based catalyst.<sup>1149</sup>

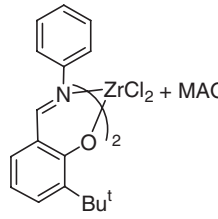
**Co-catalyst effects.** The effect of different cocatalysts on various polymerization parameters is very remarkable. The activity of MAO-activated systems shows only a small dependence on the Al/M ratio, Figure 47. Similarly, molecular mass is also substantially independent of the Al/M ratio, which suggests that transfer to MAO is not the dominant chain transfer reaction.<sup>1129</sup>

Group 4 bis(phenoxy-imine) catalysts display surprisingly different catalytic behavior when activated with  $[\text{Ph}_3\text{C}][\text{B}(\text{C}_6\text{F}_5)_4]/\text{Bu}_3\text{Al}$ .<sup>1129,1135,1161–1163</sup> While the MAO-activated prototype system 135 yields PEs with an  $\bar{M}_v$



**Figure 46** Activities ( $\text{g}_{\text{PE}} (\text{mmol M})^{-1} \text{h}^{-1} \text{bar}^{-1}$ ) and molecular masses obtained in ethylene polymerization with a series of bis(phenoxy-imine) catalysts (see Ref: 1149).

Ethylene polymerization: MAO effect



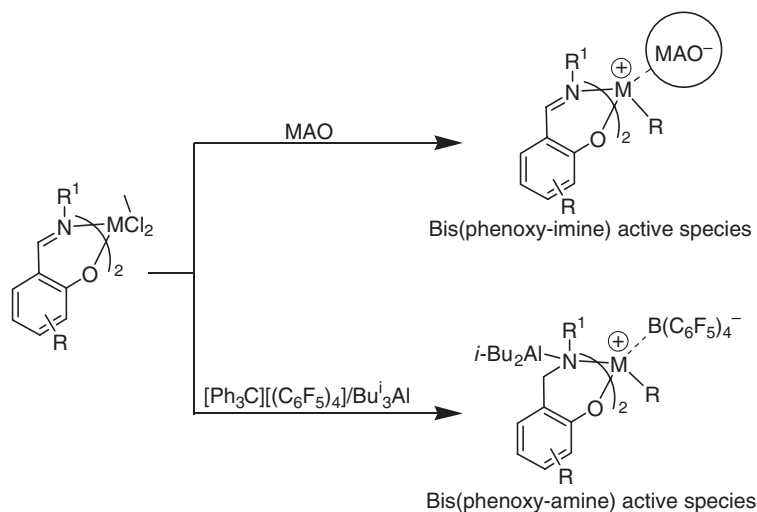
Al/Zr	Yield	Activity	$\bar{M}_v$
6,250	3.3	$2 \times 10^5$	8,000
15,625	0.9	$5 \times 10^5$	10,000
62,500	0.9	$5 \times 10^5$	9,000
125,000	0.9	$5 \times 10^5$	7,000
312,500	0.8	$5 \times 10^5$	7,000

**Figure 47** Ethylene polymerization yield (g) and activity ( $\text{g}_{\text{PE}} (\text{mmol cat})^{-1} \text{h}^{-1}$ ) and  $\bar{M}_v$  for a series of bis(phenoxy-imine) catalysts. Top to bottom, the systems shown correspond to entries 18–22 in Table 18.

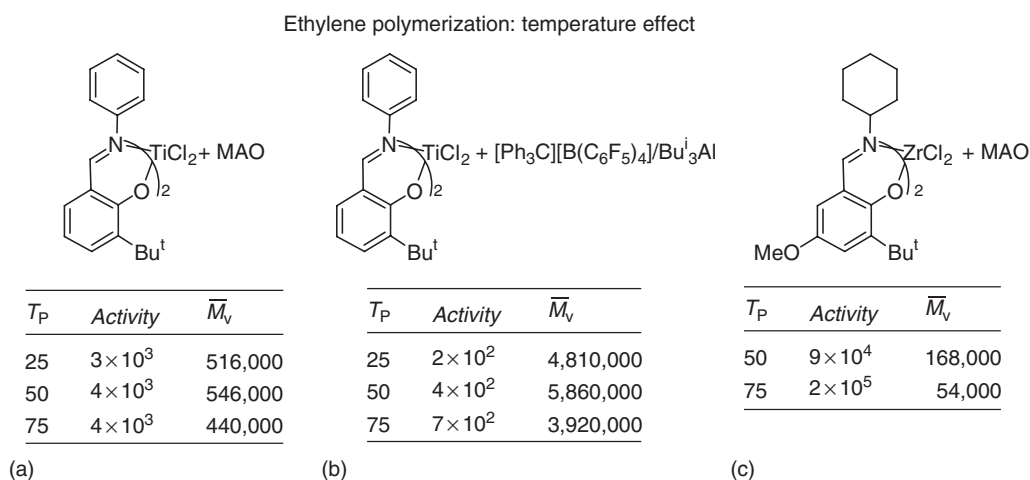
of about 7000–10 000, activation of the same system with  $[\text{Ph}_3\text{C}][\text{B}(\text{C}_6\text{F}_5)_4]/\text{Bu}^i_3\text{Al}$  yields PEs with extremely high molecular mass ( $\bar{M}_v \approx 4 \times 10^6$ – $5 \times 10^6$ ; see entries 23–25 in Table 18). The activity decreases considerably, but reasonable polymerization activity is preserved. The same behavior is observed with the corresponding Ti system **136** (entries 7–9 in Table 18).

The observed difference in the molecular masses and catalytic activity between MAO and  $[\text{Ph}_3\text{C}][\text{B}(\text{C}_6\text{F}_5)_4]/\text{Bu}^i_3\text{Al}$  co-catalysts can hardly be traced to different interaction between the cationic active species and the counterion. Consequently, it was proposed that activation with MAO and  $[\text{Ph}_3\text{C}][\text{B}(\text{C}_6\text{F}_5)_4]/\text{Bu}^i_3\text{Al}$  leads to chemically different active species.  $\text{Bu}^i_3\text{Al}$  can both alkylate and reduce the imine group. The  $^1\text{H}$  NMR experiments indicated that  $\text{Bu}^i_3\text{Al}$  reduces the phenoxy-imine ligand to a phenoxy-amine ligand, which suggests the formation of a bis(phenoxy-amine) active species. Unfortunately, the resulting phenoxy-amine complex was not isolated. Nevertheless, addition of  $[\text{Ph}_3\text{C}][\text{B}(\text{C}_6\text{F}_5)_4]$  and ethylene to the bis(phenoxy-imine) $\text{MCl}_2/\text{Bu}^i_3\text{Al}$  mixture yields PE. Following these observations, it was suggested that for bis(phenoxy-imine)-based complexes, activation with MAO and  $[\text{Ph}_3\text{C}][\text{B}(\text{C}_6\text{F}_5)_4]/\text{Bu}^i_3\text{Al}$  proceeds as shown in Scheme 38. Theoretical calculations on a model of a bis(phenoxy-amine) Zr active species suggested that the amine substituents near to the active metal atom introduce additional steric congestion that disfavors space-demanding chain-release reactions.<sup>1162</sup>

$\text{MgCl}_2/\text{R}_n\text{Al}(\text{OR}_1)_{3-n}$ -activated bis(phenoxy-imine) catalysts are highly active in ethylene polymerization (see entry 11 in Table 18). Performances of the  $\text{MgCl}_2$ -activated catalysts are rather similar to those of the corresponding MAO-activated catalysts. It was suggested that the  $\text{R}_n\text{Al}(\text{OR}_1)_{3-n}$  species act as both alkylating agents and scavengers, while  $\text{MgCl}_2$  acts as a Lewis acid to generate the cationic active species from the alkylated catalyst. Interestingly, PEs produced with the  $\text{MgCl}_2/\text{R}_n\text{Al}(\text{OR}_1)_{3-n}$ -activated bis(phenoxy-imine) Zr catalysts show morphologies with well-defined particles, whereas MAO-activated catalysts yield poorly defined morphologies. On this basis,



**Scheme 38**



**Figure 48** Ethylene polymerization activity ( $\text{g}_{\text{PE}} (\text{mmol M})^{-1} \text{h}^{-1} \text{bar}^{-1}$ ) and  $\bar{M}_v$  versus polymerization temperature,  $T_P$  ( $^{\circ}\text{C}$ ), for a series of bis(phenoxy-imine)-based catalysts. Top to bottom and left to right, the systems shown correspond to entries 1–3, 7–9, and 38 and 39 in Table 18.

it has been hypothesized that the complex exists on the surface of solid  $\text{MgCl}_2/\text{Al}$ -alkoxide crystallites.<sup>1143</sup> However, it is unclear how supportation would proceed. Finally, bis(phenoxy-imine) catalysts can be activated also by heteropoly- Mo compounds/ $\text{R}_3\text{Al}$ , and clays/ $\text{R}_3\text{Al}$ . Activating (135) with  $(\text{Ph}_3\text{C})_m\text{H}_n[\text{PMo}_{12}\text{O}_{40}]/\text{Et}_3\text{Al}$  or mica/ $\text{Et}_3\text{Al}$  results in rather active species.<sup>1137</sup>

**Temperature effects.** Bis(phenoxy-imine)-based catalysts possess considerable activity in the range 0–75  $^{\circ}\text{C}$ . The MAO-activated prototype system (135) shows a remarkable activity,  $3 \times 10^5 \text{ g}_{\text{PE}} (\text{mmol M})^{-1} \text{h}^{-1} \text{bar}^{-1}$ , already at 0  $^{\circ}\text{C}$ . The activity maximum is at ca. 40  $^{\circ}\text{C}$ ,  $\sim 6 \times 10^5 \text{ g}_{\text{PE}} (\text{mmol M})^{-1} \text{h}^{-1} \text{bar}^{-1}$ .<sup>1129</sup> Similar good activities in the range 25–75  $^{\circ}\text{C}$  are shown also by other complexes (see Figure 48), independent of the co-catalyst used. Interestingly, the low thermal stability can be alleviated by including electron-donating groups in position 4 (see Figure 48).<sup>1130</sup> Finally, although the lifetime of these catalysts tends to be limited, ethylene polymerizations over periods of 5, 15, and 30 min indicated that MAO-activated 135 has a catalytic lifetime of at least 30 min. Solvents seem to have a minor effect on the polymerization performance.

**Molecular mass distributions.** The molecular mass distributions from bis(phenoxy-imine) catalysts depend strongly on both the metal and the ligand that compose the actual catalyst. The large majority of Zr-based catalysts show  $\bar{M}_w/\bar{M}_n$  ratios around 2, typical of single-site catalysts. However, in some cases, rather large  $\bar{M}_w/\bar{M}_n$  values (from 4 to 40) have been observed (see entries 48, 57, and 58 in Table 18).<sup>1142,1144</sup> GPC curves of the PEs with high  $\bar{M}_w/\bar{M}_n$  ratios indicated multimodal (bi- and trimodal) molecular mass distribution. It was suggested that the high  $\bar{M}_w/\bar{M}_n$  values arise from an equilibrium between the three active isomers A–C that bis(phenoxy-imine) catalysts can assume (see Figure 41). The multimodality stems from the different catalytic properties of different isomers. Equilibrium between different isomers of the bis(phenoxy-imine) catalysts was confirmed by NMR experiments<sup>1142,1144</sup> and supported by DFT calculations.<sup>1144</sup> Deconvolution of the bimodal GPC peaks led to two symmetrical peaks. This indicated that the bimodal PE consists of two unimodal fractions, and both fractions are consistent with single-site polymerization behavior.<sup>1144</sup> Examination of different complexes indicated that a methyl or methoxy substituent *para* to the phenoxy-oxygen results in bimodal behavior. Cumyl substituents *ortho* and *para* to the phenoxy-oxygen result in trimodal behavior and perfluorophenyl substituents invariably lead to unimodal behavior.<sup>1142,1144</sup>

**Living polymerizations.** Of greater interest, however, is the fact that fluorophenyl-substituted bis(phenoxy-imine) Ti complexes easily show extremely narrow  $\bar{M}_w/\bar{M}_n$  ratios, around 1, indicative of living polymerization behavior.<sup>1132,1134,1140,1160</sup> At 50  $^{\circ}\text{C}$ , the perfluorophenyl-substituted complex 137 is more active than the corresponding non-fluorinated complex 136 ( $4 \times 10^4$  vs.  $3 \times 10^3 \text{ g}_{\text{PE}} (\text{mmol M})^{-1} \text{h}^{-1} \text{bar}^{-1}$ ; entries 67 and 4 in Table 18), and yields a PE with an extremely narrow molecular mass distribution ( $\bar{M}_w/\bar{M}_n$  1.13).<sup>1134</sup> Analogous perfluorophenyl Zr and Hf complexes result in  $\bar{M}_w/\bar{M}_n$  close to 2, and thus do not present living behavior (see entries 74 and 75 in Table 18). Remarkably low  $\bar{M}_w/\bar{M}_n$  values are also obtained at higher temperature ( $T_P$  75  $^{\circ}\text{C}$ ,  $\bar{M}_w/\bar{M}_n$  = 1.15;  $T_P$  90  $^{\circ}\text{C}$ ,  $\bar{M}_w/\bar{M}_n$  = 1.30). Plots of  $\bar{M}_n$  and  $\bar{M}_w/\bar{M}_n$  versus polymerization time indicate that  $\bar{M}_n$  increases linearly with time, and that  $\bar{M}_w/\bar{M}_n$  remains close to 1 for at least 15 min.<sup>1134</sup>

	$R^1$						
$\overline{M}_w/\overline{M}_n$	1.13	1.25	1.05	1.06	1.99	1.78	2.18
$\overline{M}_n$	424,000	145,000	64,000	13,000	98,000	129,000	128,000
Activity (g <sub>PE</sub> (mmol M) <sup>-1</sup> h <sup>-1</sup> bar <sup>-1</sup> )	$4 \times 10^4$	$2 \times 10^3$	$8 \times 10^2$	$1 \times 10^2$	$4 \times 10^4$	$3 \times 10^4$	$5 \times 10^3$
Polymerization time (min)	1	5	5	5	1	1	5

**Figure 49** Ethylene polymerization results with fluorinated bis(phenoxy-imine) Ti-based catalysts activated with MAO at 50 °C. Left to right, the systems shown correspond to entries 67, 70, 71, 72, 64, 62 and 60, respectively, in Table 18.

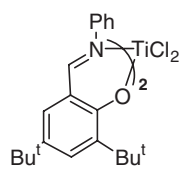
Further evidence of the living polymerization nature was obtained by the fact that the GPC peaks of the PE produced shift to higher molecular mass on increasing the polymerization time. The monomodal shape is retained, and no shoulders or low molecular mass tails are detected.<sup>1134</sup> The stability of the living polymer chain was investigated utilizing the MAO-activated complex **137** at 25 °C.<sup>1134</sup> First, the activated complex is treated with ethylene-saturated toluene for 65 min. The values of  $\overline{M}_n$  versus time clearly indicate that after 3 min all the ethylene is consumed. After 65 min under an N<sub>2</sub> atmosphere, ethylene gas was fed to the system for 2 additional min. The  $\overline{M}_w/\overline{M}_n$  value resulting after the additional 2 min ethylene feed is 1.14, which indicates that no termination reaction occurred for at least 60 min in the absence of ethylene. This remarkable result opens the route to the controlled synthesis of ethylene-based block co-polymers.

To investigate the origin of the living behavior, several differently fluoro-substituted Ti-based catalysts were synthesized.<sup>1134,1140</sup> The main results are presented in Figure 49. Most importantly, ligands without F atoms in the *ortho*-position do not exhibit living polymerization behavior (i.e.,  $\overline{M}_w/\overline{M}_n$  close to 2). By contrast, even one single F atom in an *ortho*-position confers living behavior to the corresponding catalyst, although very low activity is observed. Nevertheless, activity can easily be improved by increasing the number of F atoms on the aryl ring. The more active catalysts give marginally broader molecular mass distributions. Fujita and co-workers also remarked that a single methyl group in the *ortho*-position does not lead to living behavior, since  $\overline{M}_w/\overline{M}_n = 2.14$  after 30 min polymerization.<sup>1138</sup>

Fujita and co-workers proposed that hydrogen-bonding interactions between the *ortho*-F atoms and H atoms on the  $\beta$ -C atom of the growing chain might be responsible for the living behavior.<sup>1140</sup> This electrostatic interaction between the negatively charged F atom and the positively charged  $\beta$ -H atom of the growing chain was thought to stabilize the active species and depress the most likely  $\beta$ -H transfer termination reaction.<sup>1140</sup> The NMR and X-ray characterizations of related Zr model compounds did indeed indicate that this kind of interaction is established both in solution as well as in the solid state.<sup>1164</sup> On the other hand, based on combined quantum mechanics/molecular mechanics calculations, Talarico and co-workers suggested that the main role of the *ortho*-F substituents was to increase steric bulkiness around the metal atom, which disfavors the chain transfer to monomer, in analogy with similar calculations on metallocenes as well as on Ni-based Brookhart's type catalysts.<sup>943,1153,1154,1165</sup> Their calculations indicated the presence of an *ortho*-F... $\beta$ -H interaction in the transition state, but the strength of this interaction was estimated to be only about 1 kcal mol<sup>-1</sup>. Consistent with this, these calculations also indicated that a methyl group in the *ortho*-position should depress chain termination.<sup>1155</sup>

At the same time, Fujita and co-workers showed that a Cl atom in the *ortho*-position also yields a narrow polydispersity ( $\overline{M}_w/\overline{M}_n = 1.23$ ).<sup>1134</sup> They attributed this effect to the lone electron pairs on the Cl atom. However, it must be noted that Cl is by far less electronegative than F, and that Cl has roughly the same steric bulkiness as an Me group.

This topic has also been investigated by Coates and co-workers who reported that even the unfluorinated catalyst of Figure 50 polymerizes ethylene in a living fashion in the temperature range 0–50 °C, although the activity and the molecular masses were low compared to those obtained with the perfluorinated analog.<sup>1166</sup> These contrasting results indicate that the *ortho*-F effect cannot be considered as the only rationalization of the living behavior exhibited by bis(phenoxy-imine) Ti catalysts, and that steric effects play an important role. In conclusion, the real strength of this attractive F-interaction, as well as the real origin of the living behavior, remain an open topic.

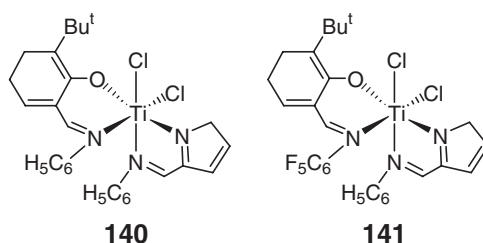


Temperature (°C)	0	20	50
Activity (g <sub>PE</sub> (mmol M) <sup>-1</sup> h <sup>-1</sup> bar <sup>-1</sup> )	2·10 <sup>3</sup>	4·10 <sup>3</sup>	3·10 <sup>3</sup>
Yield (g)	0.73	0.42	0.37
Polymerization time (min)	3	1	1
$\bar{M}_n$	78,400	48,500	44,500
$\bar{M}_w/\bar{M}_n$	1.16	1.07	1.10

MAO/Ti = 150, toluene, ethylene 0.69 bar

**Figure 50** Ethylene polymerization results with non-fluorinated bis(phenoxy-imine) Ti-based catalysts activated with MAO.

Remarkably, mixed-ligand titanium complexes with one phenoxy-imino and one imino-pyrrolato ligand, such as pre-catalysts **140** and **141**, show very high ethylene polymerization activities, about  $5 \times 10^3$  and  $9 \times 10^4$  g<sub>PE</sub> (mmol M)<sup>-1</sup> h<sup>-1</sup> bar<sup>-1</sup> (MAO, 20 °C). Thus, the heteroligated complexes, give activities substantially higher than those of the corresponding homoligated complexes, with either two phenoxy-imine or two imino-pyrrolate ligands under comparable conditions.<sup>1167</sup> A similar beneficial effect on activity, due to heteroligation, has also been reported for propylene polymerization.<sup>1168</sup>



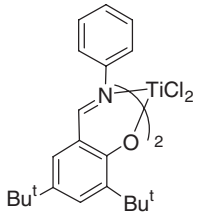
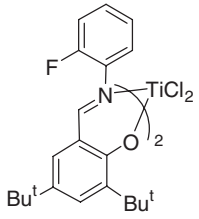
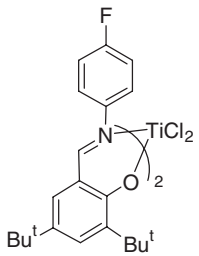
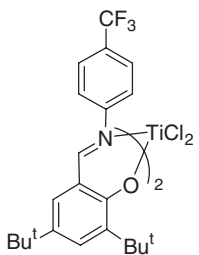
#### 4.09.5.3.3 Ligands with coordinating N–O atoms: phenoxy-imine catalysts for syndiotactic polypropylene

Bis(phenoxy-imine) catalysts have also been used extensively in the syndiotactic polymerization of propylene.<sup>160,1131,1138,1140,1147,1162,1163,1169–1177</sup> The perfluoro Ti-based complexes activated with MAO produce highly syndiotactic PP (*[r]* > 90%) in a living manner and with rather good activities (see entries 10, 11, and 17–23 in Table 19).<sup>1131,1173,1174</sup> This result was rather surprising considering that *C*<sub>2</sub>-symmetric pre-catalysts should produce iPPs. Aside from the *rrrr* pentad peak, the <sup>13</sup>C NMR analysis of the sPP revealed *rrrm* and *rmrr* peaks in a 1 : 1 ratio and no detectable *rrmmr* peak.<sup>1174</sup> The presence of isolated *m* stereomistakes indicated that these catalysts yield sPP through a chain-end stereocontrol.<sup>1173,1174</sup> Moreover, the narrow  $\bar{M}_w/\bar{M}_n$  ratio (about 1.1) indicated that living polymerization was achieved.<sup>1173</sup> Subsequent experiments indicated that the regiochemistry of chain propagation is secondary.<sup>160,161,1169,1172</sup>

**Activity and syndiospecificity: ligand effect.** The three R<sup>1</sup>, R<sup>2</sup>, and R<sup>3</sup> substituents can be used to control several properties of the PPs produced. As in the case of ethylene polymerization, the R<sup>1</sup> substituent is the key to conferring living behavior, and also has a remarkable effect on the molecular mass as well as on the stereoregularity of the PPs (see Figure 51). The perfluorophenyl-based catalyst is remarkably more syndiospecific than the non-fluorinated analog.<sup>1177</sup> The *ortho*- and *para*-F atoms seem to be important for high % *rrrr* values. This suggests that the syndiospecificity is determined by both steric and electronic effects. The presence of *ortho*-F substituents is again the key for living behavior. As for ethylene polymerization, the perfluorophenyl system is more active and yields higher  $\bar{M}_n$  than the non-fluorinated analog.<sup>1138,1172,1177</sup>

The bulkiness of the R<sup>2</sup> substituent controls several parameters of the PPs produced (see Figure 52). Generally, small R<sup>2</sup> groups result in rather active catalysts that produce low molecular mass PPs with low stereoregularity. The bulky R<sup>2</sup> substituent controls stereoregularity. In the case of the prototype **137** system, an almost linear relationship was established between the percentage of *rr* diads of the PPs and the volume occupied by the R<sup>2</sup> substituents (see Figure 52).<sup>1172</sup> The non-fluorinated analogs behave similarly (see entries 12–15 in Table 19).<sup>1138</sup> The *T*<sub>m</sub> of the resulting PPs reflects of course the high level of syndiotacticity, and the complex with R<sup>2</sup> = SiMe<sub>3</sub> at 0 °C yields an sPP with a *T*<sub>m</sub> of 156 °C (*rr* = 94%).<sup>1172</sup> Finally, the nature of the R<sup>3</sup> substituent has almost no effect on the polymerization behavior (see entries 18 and 24 in

**Table 19** Syndiospecific propylene polymerization catalyzed by bis(phenoxy-imine) catalysts

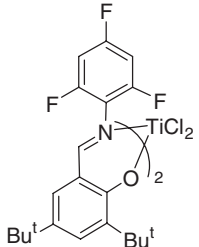
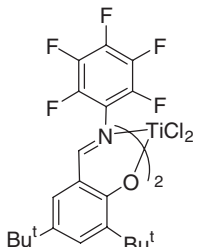
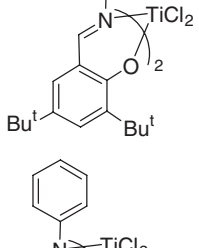
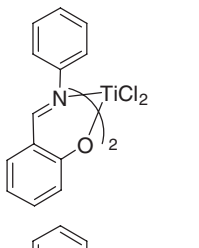
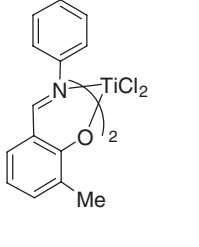
Entry	Pre-catalyst	$T_P^a$ (°C)	$P_P^b$ (bar) (Solvent)	$t_P^c$ (h)	Productivity (g <sub>PP</sub> (mol M <sup>-1</sup> ) h <sup>-1</sup> bar <sup>-1</sup> )	Yield (g)	$\bar{M}_w/\bar{M}_n$	$\bar{M}_n$	$T_m^d$ (°C)	$rr^e$ (%)	$rrrr^f$ (%)	References
1		0	2.8 (Tol)	24	600	4.20	2.14	9,910			78	1177
2		0	2.8 (Tol)	24	60	0.38	1.07	3,220			52	1177
3		0	2.8 (Tol)	24	1,100	7.20	1.75	18,600			78	1177
4		0	2.8 (Tol)	24	1,000	6.40	2.19	19,280			81	1177

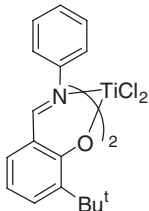
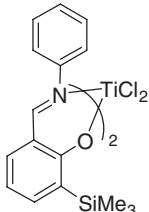
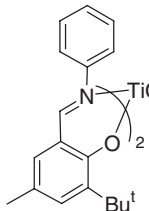
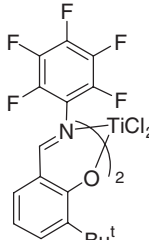


5		0	2.8 (Tol)	24	80	0.56	1.06	16,410	83	<a href="#">1177</a>
6		0	2.8 (Tol)	24	2200	14.30	2.03	9,150	83	<a href="#">1177</a>
7		0	2.8 (Tol)	24	3,600	23.40	1.91	13,580	81	<a href="#">1177</a>
8		0	2.8 (Tol)	24	1,900	12.10	2.17	14,090	51	<a href="#">1177</a>

(Continued)

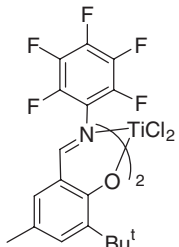
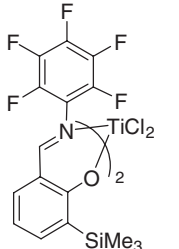
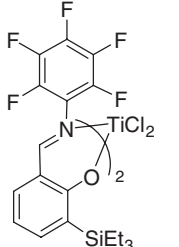
**Table 19** (Continued)

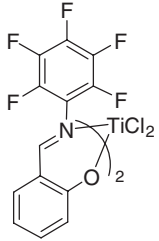
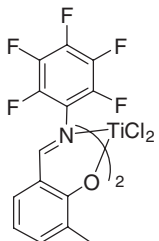
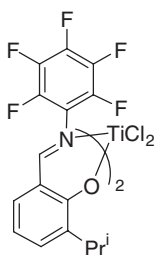
Entry	Pre-catalyst	$T_P^a$ (°C)	$P_P^b$ (bar) (Solvent)	$t_P^c$ (h)	Productivity (gPP (mol M <sup>-1</sup> ) h <sup>-1</sup> bar <sup>-1</sup> )	Yield (g)	$\bar{M}_w/\bar{M}_n$	$\bar{M}_n$	$T_m^d$ (°C)	$rr^e$ (%)	$rrrr^f$ (%)	References
9		0	2.8 (Tol)	24	400	2.48	1.08	43,420			95	<a href="#">1177</a>
10		0	2.8 (Tol)	5.2	3,800	5.34	1.11	95,900			96	<a href="#">1177</a>
11		0	2.8 (Tol)	24	2,500	16.20	1.26	216,610			96	<a href="#">1177</a>
12		1	3.7 (Tol)	6	100	0.24	2.93, 1.51	$\bar{M}_w$ 735,000 $\bar{M}_n$ 15,000	nd			<a href="#">1138</a>
13		1	3.7 (Tol)	6	1,800	4.02	1.47	$\bar{M}_w$ 101,000	nd			<a href="#">1138</a>

14		1	3.7 (Tol)	6	250	0.57	1.38	$\bar{M}_w$ 6,000	97	63	<a href="#">1138</a>
15		1	3.7 (Tol)	6	400	0.96	1.73	$\bar{M}_w$ 14,000	140	84	<a href="#">1138</a>
16		1	3.7 (Tol)	6	250	0.56	1.39	$\bar{M}_w$ 7,000	101	66	<a href="#">1138</a>
17		0	1 (Tol)	5	2,800	0.144	1.05	23,600	136		<a href="#">1172</a>
18		25	1 (Tol)	5	3,600	0.183	1.11	28,500	137	87	<a href="#">1172</a>
19		50	1 (Tol)	5	2,600	0.148	1.37	16,400	130		<a href="#">1172</a>

(Continued)

**Table 19** (Continued)

Entry	Pre-catalyst	$T_p^a$ (°C)	$P_p^b$ (bar) (Solvent)	$t_p^c$ (h)	Productivity ( $g_{PP}$ (mol $M^{-1}$ ) $h^{-1} bar^{-1}$ )	Yield (g)	$\bar{M}_w/\bar{M}_n$	$\bar{M}_n$	$T_m^d$ (°C)	$rr^e$ (%)	$rrrr^f$ (%)	References
20		25	6 (Tol)	1	2,600	0.158	1.07	30,900	135			1172
21		25	6 (Tol)	2	2,600	0.312	1.10	52,800				1172
22		25	6 (Tol)	3	2,500	0.460	1.10	73,800	135			1172
23		25	6 (Tol)	5	2,400	0.713	1.14	108,000	135			1172
24		25	1 (Tol)	5	2,300	0.115	1.11	16,500	140			1172
25		25	1 (Tol)	5	5,800	0.293	1.08	47,000	152	93		1172
26		25	1 (Tol)	5	3,500	0.174	1.16	24,400	151			1172

27		25	1 (Tol)	5	30,600	1.534	1.51	189,000	n.d.	43	<a href="#">1172</a>
28		25	1 (Tol)	5	69,000	3.440	1.22	260,000	n.d.	50	<a href="#">1172</a>
29		25	1 (Tol)	5	31,000	1.555	1.16	153,700	n.d.	75	<a href="#">1172</a>

<sup>a</sup> $T_P$  = polymerization temperature.

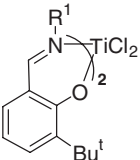
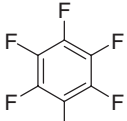
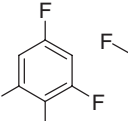
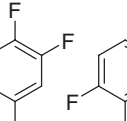
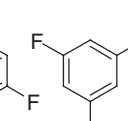
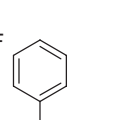

<sup>b</sup> $P_P$  = propylene pressure.

<sup>c</sup> $t_P$  = polymerization time.

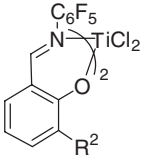
<sup>d</sup> $T_m$  = melting temperature of the PPs produced.

<sup>e</sup>%  $rr$  = amount of  $rr$  triads in the PPs produced.

<sup>f</sup>%  $rrrr$  = amount of  $rrrr$  pentads in the PPs produced.

	$R^1$					
						
% <i>rrrr</i>	96	95	83	83	81	78
$\overline{M}_w/\overline{M}_n$	1.26	1.08	2.03	1.06	1.91	2.14
$\overline{M}_n$	216,610	43,420	9,150	16,410	13,580	9,910
Activity ( $\text{g}_{\text{PP}} (\text{mmol M})^{-1} \text{h}^{-1} \text{bar}^{-1}$ )	2	$4 \times 10^{-1}$	2	$7 \times 10^{-2}$	3	$6 \times 10^{-1}$

**Figure 51** Propylene polymerization results with fluoro-substituted bis(phenoxy-imine) Ti-based catalysts activated with MAO at 0 °C. Effect of the  $R^1$  substituent.

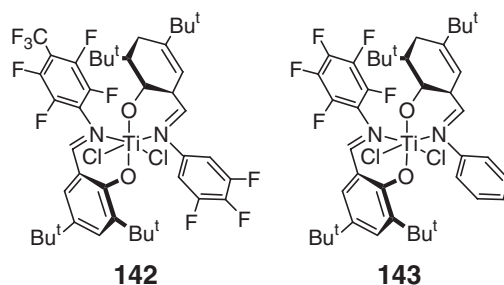
	$R^2$				
	$\text{SiMe}_3$	$\text{Bu}^t$	$\text{Pr}^i$	Me	H
$T_m$ (°C)	152	137	n.d.	n.d.	n.d.
$\overline{M}_w/\overline{M}_n$	1.08	1.11	1.16	1.22	1.51
$\overline{M}_n$	47,000	28,500	153,700	260,000	189,000
Activity $\text{g}_{\text{PP}} (\text{mmol M})^{-1} \text{h}^{-1} \text{bar}^{-1}$	6	4	$3 \times 10$	$7 \times 10$	$3 \times 10$
[ <i>rr</i> ] (%)	93	87	75	50	43
[ <i>mr</i> ] (%)	4	10	22	42	46
[ <i>mm</i> ] (%)	3	3	3	8	11
Head-to-head units (%)	3	4	8	9	10

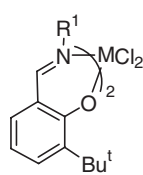
25 °C, 1 bar propylene, MAO/Ti = 250, toluene, 5 h

**Figure 52** Propylene polymerization results with fluoro-substituted bis(phenoxy-imine) Ti-based catalysts. Effect of the  $R^2$  substituent.

Table 19), probably because the  $R^3$  substituent is too distant from the metal. As in the case of ethylene, effective propylene living polymerization, or more generally low  $\overline{M}_w/\overline{M}_n$ , requires the presence of F atoms on the  $R^1$  aromatic ring (see Figure 51).<sup>1177</sup> The perfluorinated catalyst (137) exhibits living behavior for a period of at least 5 h at 25 °C.<sup>1172</sup> Moreover, longer polymerization times give higher molecular masses. Unimodal molecular mass distributions were observed in all cases.<sup>1172</sup> Bulky  $R^2$  groups also reduce the amount of regiomistakes, measured as head-to-head units.

Interestingly, heteroligated “living”/“non-living” bis(phenoxy-imine) Ti-based catalysts give higher activity and higher molecular masses relative to the symmetric and homoligated catalysts. For example, MAO-activated pre-catalysts 142 and 143 exhibit propylene polymerization activities around  $10^4 \text{ g}_{\text{PP}} (\text{mmol M})^{-1} \text{h}^{-1} \text{bar}^{-1}$ , whereas the activities of the corresponding homoligated “living” and “non-living” pre-catalysts are one order of magnitude smaller.<sup>1168</sup> Similar beneficial effect on activity, due to heteroligation, has also been reported for ethylene polymerization.<sup>1167</sup>





M	R <sup>1</sup>	Yield	Activity	$\bar{M}_n$	$\bar{M}_w/\bar{M}_n$
Ti	C <sub>6</sub> F <sub>5</sub>	0.18	4	28,500	1.11
Zr	C <sub>6</sub> H <sub>5</sub>	1.72	$7 \times 10^2$	150	1.55
Zr	C <sub>6</sub> F <sub>5</sub>	1.07	$4 \times 10^2$	1,340	2.34
Hf	C <sub>6</sub> H <sub>5</sub>	0.89	$6 \times 10$	370	1.62
Hf	C <sub>6</sub> F <sub>5</sub>	5.71	$4 \times 10^4$	9,990	2.73

Activity in  $\text{g}_{\text{PP}} (\text{mmol M})^{-1} \text{h}^{-1} \text{bar}^{-1}$ , 25 °C, 1 bar propylene,  
MAO/M = 250, toluene, Ti = 5 h, Zr = 0.5 h, Hf = 1.5 h

**Figure 53** Performance of various phenoxy-imine catalysts in propylene polymerization.

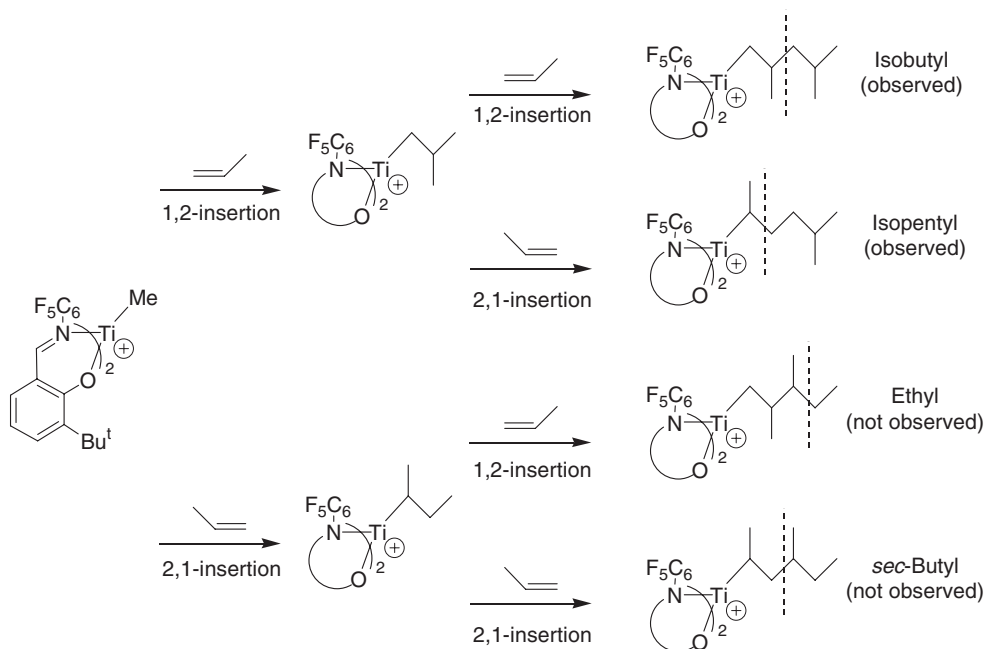
*Activity and syndiospecificity: metal effect.* Zirconium and hafnium catalysts are more active than their titanium congeners (see Figure 53).<sup>1171</sup> However, Zr and Hf only oligomerize propylene. The effect is particularly dramatic for the non-fluorinated catalysts. While consideration of tacticity in the case of the Zr/MAO systems is meaningless due to the extremely low degree of polymerization, the perfluoro Hf/MAO catalyst yields substantially atactic or slightly syndiotactic PPs (% *mm/mr*/*rr* = 9/47/44 at 25 °C and 10/48/42 at 50 °C). These data also indicate that tacticity is substantially independent of the polymerization temperature.<sup>1171</sup>

*Activity and syndiospecificity: the effect of the polymerization conditions.* The propylene pressure as well as the solvent utilized have been suggested to influence the syndiotacticity of the resulting PP.<sup>1178</sup> The *rr* of PPs produced with the MAO-activated prototype catalyst **136** decreases from 78% to 70% on increasing the propylene pressure from 2 to 6 bar. Similar behavior is shown by the fluorinated catalyst (**137**) (*rr* from 95% to 83% on increasing propylene pressure from 1 to 6 bar). Replacing the commonly used toluene with CH<sub>2</sub>Cl<sub>2</sub> results in the synthesis of substantially stereoirregular PPs (*rr* as low as 30%).<sup>1178</sup> Loss of syndiospecificity with increasing dielectric constant of the solvent was already reported for propylene polymerization with the classical Me<sub>2</sub>C(Cp)(9-Flu)ZrCl<sub>2</sub>/MAO zirconocene, and was attributed to isomerization of solvent-separated free zirconocene species via migration of the growing chain before the next insertion.<sup>1179</sup> However, it is difficult to imagine a common mechanism for these two catalysts. In fact, in the case of the bis(phenoxy-imine) systems, the regiochemistry of monomer insertion is secondary and the stereoselectivity is chain-end controlled, whereas in the case of the zirconocene the regiochemistry of monomer insertion is primary and stereoselectivity is site-controlled.

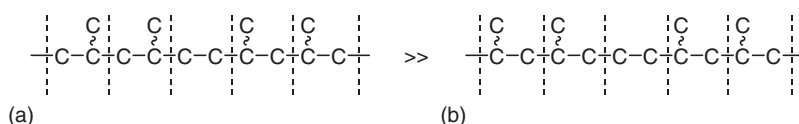
*Regiochemistry of propylene insertion.* The regiochemistry of propylene polymerization with MAO-activated bis(phenoxy-imine) Ti catalysts is prevalently secondary.<sup>160,161,1169,1172</sup> NMR analysis of chain-initiation and -termination groups indicated that the MAO-activated prototype (**137**) leads exclusively to *n*-propyl, isobutyl, and isopentyl end groups (see Scheme 39). Considering that the initiation occurs on a Ti–Me bond, it was concluded that primary propylene insertion into the Ti–Me bond is strongly favored. Moreover, the ratio of the isopentyl versus isobutyl NMR peaks also showed that the first 1,2-propylene insertion is followed by 70% of 2,1- and 30% of 1,2-propylene insertions. This indicates that propylene insertion on a Ti–primary alkyl bond is highly regioirregular. Similar analysis on the chain-end termination groups confirmed that propylene polymerization with catalysts based on (**137**) is prevalently secondary, and that the PP has a regioblock structure.<sup>1169,1172</sup>

Further NMR analysis of chain-end groups of PPs produced with similar catalysts provided additional evidence for the prevalently secondary propylene propagation with this class of catalyst. In fact, it was shown that the main chain-release reaction is  $\beta$ -H elimination, and that propylene insertion into the Ti–H bond in the initiation step is almost exclusively primary.<sup>160,161</sup> Moreover, NMR analysis of a co-polymer of propylene with a small amount (< 2 mol%) of 1-<sup>13</sup>C-ethylene, obtained with the perfluorinated catalyst (**137**), showed that the large majority of ethylene units in the co-polymer was present as two methylene units (see Scheme 40). This clearly indicated that ethylene units bridge blocks of propylene units with opposite regiochemistry, which is consistent with and further supports the whole mechanistic scenario.<sup>161</sup>

However, the regiochemistry of propylene insertion is dependent on both the metal and the bulkiness of the substituents *ortho* to the O atoms. In fact, complexes with an *ortho*-methyl group, which lead to poorly syndiotactic PPs, enchain the monomer via opposite regiochemistry<sup>277</sup> (see Figure 54). The <sup>13</sup>C NMR analysis indicated the presence of isobutyl (initiation) and *n*-propyl (termination) end groups for the Ti-based catalysts, consistent with the prevalently secondary propagation already discussed for the titanium phenoxy-imine systems, whereas the Zr analogs showed the almost exclusive presence of isobutyl end groups, indicative of primary propylene insertion in



Scheme 39



Scheme 40

	<i>M</i>	
	<i>Ti</i>	<i>Zr</i>
Yield (g)	1.40	4.95
<i>P<sub>r</sub></i>	0.71	0.67
$\bar{M}_w$	268,900	8,300
$\bar{M}_w/\bar{M}_n$	2.9	2.3
Isobutyl end groups	Yes	Yes
<i>n</i> -Propyl end groups	No	Yes

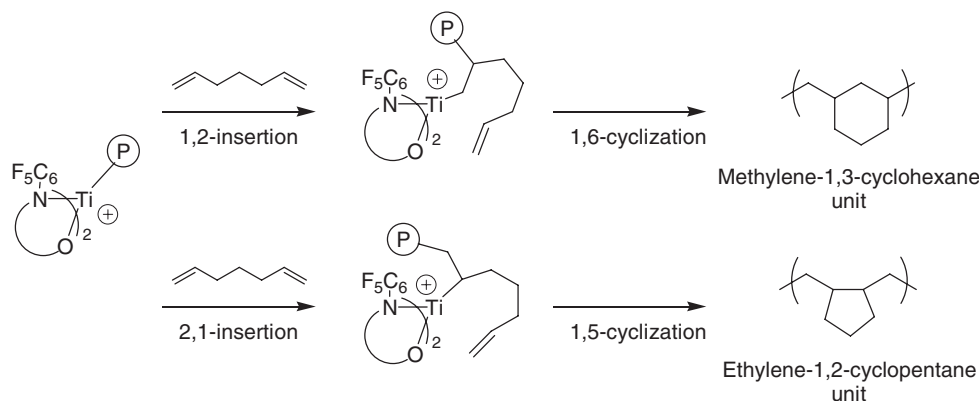
18 °C, 1 bar propylene, MAO/M = 150, toluene, 120 min

Figure 54 Propylene polymerization with methyl substituted phenoxy-imine Ti and Zr catalysts.

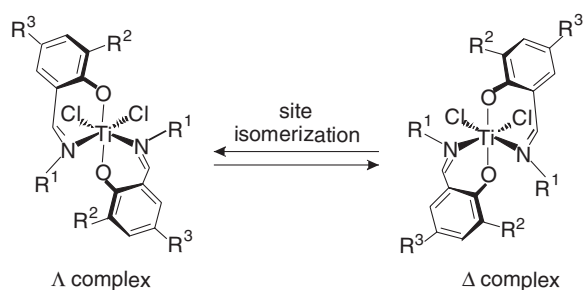
both the initiation and the termination steps. This suggested that primary insertion is also the prevailing propagation mode. Further support for this proposal was achieved by co-polymerization of propylene with small amounts ( $\approx 0.4\%$ ) of 1- $^{13}\text{C}$ -ethylene. The remarkably larger proportion of three methylene versus two methylene sequences (79% vs. 21%) was a clear indication that for the Zr-based catalysts primary propagation is favored (see Scheme 40).<sup>277</sup> The different regioselectivity exhibited by the Ti and Zr catalysts has been rationalized by DFT calculations.<sup>165</sup>

Polymerization of  $\alpha$ - $\omega$ -diolefins has also been investigated to further explore the unusual regiochemistry exhibited by bis(phenoxy-imine) Ti catalysts. Cyclopolymerization of 1,6-heptadiene (see Figure 55) produced a polymer with no observable unsaturations. This indicated quantitative cyclization of the monomer. The NMR analysis of the polymer indicated the presence of ethylene-1,2-cyclopentane units and of methylene-1,3-cyclohexane units in almost





**Figure 55** Cyclopolymerization of 1,6-heptadiene with bis(phenoxy-imine) Ti based catalysts.



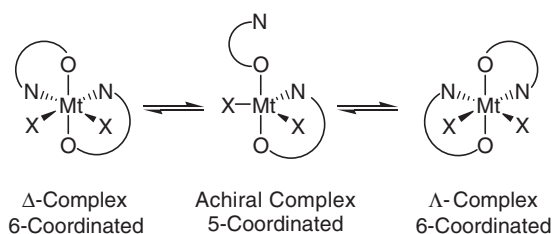
**Scheme 41**

equal amounts. The presence of both cyclopentane and cyclohexane units clearly demonstrated that secondary insertion is easy with these catalysts since cyclopentane rings can only form following a secondary insertion of the first double bond of 1,6-heptadiene.<sup>160</sup>

**Mechanism of stereocontrol.** The chain-end stereocontrol exhibited by MAO-activated bis(phenoxy-imine) Ti catalysts was rather surprising, considering the  $C_2$ -symmetry of the pre-catalyst (see Scheme 41). In fact, the PPs produced by a catalyst such as that of Scheme 41 should lead to an iPP, and stereoselectivity should be site controlled. The evidence that chain-end stereocontrol was instead operative led to the suggestion that the catalyst site could invert the configuration at each insertion step.<sup>1174</sup> This was confirmed by subsequent quantum mechanics/molecular mechanics calculations. The key of the mechanism is that the chiral chain end imposes one of the two configurations on the chiral active site. The imposed configuration of the active site in turn selects between the two enantiofaces of the incoming monomer through direct steric interaction between the  $R^1$  substituent and the methyl group of the secondary inserting propylene molecule.<sup>193</sup> Of course, this mechanism requires that site isomerization is faster than propylene insertion. A direct consequence of this mechanism is that active species that cannot isomerize rapidly should lead to isotactic polymers.<sup>193</sup>

Although for these systems inversion between the two configurations is not experimentally proved, fluxionality in solution has been reported for some Zr bis(phenoxy-imine) complexes.<sup>1142</sup> Moreover, existence of these fluxional equilibria in related neutral complexes was demonstrated by NMR experiments, which gave barriers for the interconversion close to  $15 \text{ kcal mol}^{-1}$ .<sup>1180,1181</sup> Site isomerization was proposed to occur through the dissociative mechanism of (Scheme 42). Quantum mechanics calculations have predicted a Ti–N bond-dissociation energy slightly lower than  $15 \text{ kcal mol}^{-1}$  in complexes related to those of Figure 44.<sup>172</sup>

Finally, it has been shown that some fluorinated catalysts, though not particularly effective in high molecular mass polymerization, are instead excellent catalysts for the synthesis of allyl-terminated sPP oligomers ( $\bar{M}_n \approx 3000\text{--}4000$ ). These new short sPP polymers with functionalized chain end could be used to make LCB polymers as well as other new polymeric materials with sPP segments.<sup>258</sup>



Scheme 42

#### 4.09.5.3.4 Ligands with coordinating N–O atoms: phenoxy–imine catalysts for isotactic polypropylene

While MAO activation of phenoxy–imine-based complexes results in the syndiospecific polymerization of propylene (see the previous Section), activation of the same complexes with  $[\text{Ph}_3\text{C}][\text{B}(\text{C}_6\text{F}_5)_4]/\text{Bu}^i_3\text{Al}$  shows completely different behavior.<sup>1162,1163</sup> The Ti-based catalyst leads to substantially atactic PP with extremely high molecular mass and rather broad  $\bar{M}_w/\bar{M}_n$ , while the Zr- and Hf-based analogs afford moderately isotactic PPs, with moderately high molecular masses and polydispersities typical of single-site behavior (see Figure 56).<sup>1162</sup> In agreement with this, the PP produced with the Ti-based catalyst shows no melt transition  $T_m$ , whereas PPs produced with Zr and Hf catalysts do show a  $T_m$ , indicative of stereoregular polymers. The Hf catalyst is remarkably more stereospecific than the Zr congener, although in both cases only moderately isotactic PPs are formed. The NMR analysis of the Zr- and Hf-produced PP at pentad level (Zr: *mmrr* 9.1%, *mrrm* 6.1%, *mmmr* 6.5%; Hf: *mmrr* 11.8%, *mrrm* 5.7%, *mmmr* 11.3%) revealed the presence of isolated *rr* triads, indicative of a site-controlled mechanism. Increasing propylene pressure to 4 bar resulted in a remarkable increase in molecular masses (Zr:  $\bar{M}_w = 698\,000$ ,  $\bar{M}_w/\bar{M}_n = 2.4$ ; Hf:  $\bar{M}_w = 1\,460\,000$ ,  $\bar{M}_w/\bar{M}_n = 2.3$ ).<sup>1162</sup>

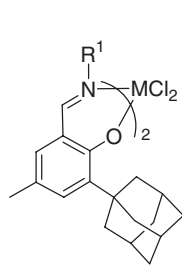
The remarkable effect of  $[\text{Ph}_3\text{C}][\text{B}(\text{C}_6\text{F}_5)_4]/\text{Bu}^i_3\text{Al}$  activation on the behavior of phenoxy–imine-based catalysts was ascribed to a reaction between  $\text{Bu}^i_3\text{Al}$  and the imino functionality of the complexes. As already discussed in Section 4.09.5.3.2, it is commonly accepted that  $\text{Bu}^i_3\text{Al}$  reduces the imino group to an amino group, thus converting a phenoxy–imine catalyst into a phenoxy–amine structure.<sup>1162</sup>

Using well-established concepts, the isotacticity of the Zr- and Hf-produced polymers was improved by increasing the bulkiness of the alkyl group *ortho* to the phenoxy O atom (see Figure 57). The resulting PPs had a multimodal MWD. Possible explanations were that the  $\text{Bu}^i_3\text{Al}$  does not completely reduce the imino functionality and/or that the active species correspond to different geometrical isomers. In all a cases, the polymers had remarkably high  $T_m$ , indicative of the high stereoregularity. The PP fraction insoluble in boiling hexane had relatively narrow  $\bar{M}_w/\bar{M}_n$  ( $< 5$ ), and NMR analysis confirmed the high isotacticity ( $R^1 = \text{Cy}$ : Zr 96.9% *mmmm*, Hf 96.8% *mmmm*). NMR analysis of the chain-end groups suggested that polymerization occurs mainly by primary monomer insertion.<sup>1163</sup>

	<i>M</i>		
	<i>Ti</i>	<i>Zr</i>	<i>Hf</i>
	$5 \times 10$	$9 \times 10$	$8 \times 10$
Activity ( $\text{g}_{\text{PP}} (\text{mmol M})^{-1} \text{h}^{-1} \text{bar}^{-1}$ )	0.08	0.16	0.13
Yield (g)	8,286,000	209,000	412,000
$\bar{M}_w$	4.15	2.42	2.15
$\bar{M}_w/\bar{M}_n$	No peak	103.5	123.8
$T_m$ (°C)	22.9	45.8	69.0
<i>mm</i> (%)	45.7	28.6	19.1
<i>mr</i> (%)	27.7	25.6	10.9
<i>rr</i> (%)			

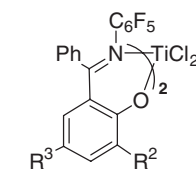
25 °C, 1 bar propylene,  $[\text{Ph}_3\text{C}][\text{B}(\text{C}_6\text{F}_5)_4]/\text{M} = 2$ ,  $\text{Bu}^i_3\text{Al}/\text{M} = 30$ , toluene, 20 min

**Figure 56** Propylene polymerization with  $[\text{Ph}_3\text{C}][\text{B}(\text{C}_6\text{F}_5)_4]/\text{Bu}^i_3\text{Al}$ -activated phenoxy–imine catalysts.

	$R^1$			
	Cy		Ph	
	Zr	Hf	Zr	Hf
Activity ( $\text{g}_{\text{PP}} (\text{mmol M})^{-1} \text{h}^{-1} \text{bar}^{-1}$ )	40	60	25	650
$\bar{M}_w$	200,000	530,000	607,000	1,453,000
$\bar{M}_w/\bar{M}_n$	4.72	14.6	18.4	2.99
$T_m$ ( $^{\circ}\text{C}$ )	163.3	164.8	154.9	160.1

25  $^{\circ}\text{C}$ , 1 bar propylene,  $[\text{Ph}_3\text{C}][\text{B}(\text{C}_6\text{F}_5)_4]/\text{M} = 2$ ,  $\text{Bu}^i_3\text{Al}/\text{M} = 30$ , toluene, 20 min

**Figure 57** PP polymerization with  $[\text{Ph}_3\text{C}][\text{B}(\text{C}_6\text{F}_5)_4]/\text{Bu}^i_3\text{Al}$ -activated phenoxy-imine catalysts. Role of the  $R^1$  substituent.

						
	$R^2 =$	$\text{Bu}^t$	$\text{Pr}^i$	Et	Me	H
	$R^3 =$	$\text{Bu}^t$	$\text{Pr}^i$	Me	Me	Me
Activity ( $\text{g}_{\text{PP}} (\text{mmol M})^{-1} \text{h}^{-1} \text{bar}^{-1}$ )		0.2	0.7	2.2	6.1	6.8
Yield (g)		0.16	0.13	0.40	1.11	1.22
$\bar{M}_n$		bimodal	2,710	7,290	27,940	35,440
$\bar{M}_w/\bar{M}_n$		broad	1.12	1.17	1.11	1.12
$T_m$ ( $^{\circ}\text{C}$ )		n.d.	n.d.	n.d.	69.5	n.d.
<i>mmmm</i> (%)		7	46	45	53	8
<i>rrrr</i> (%)		26	<1	<1	<1	13

0  $^{\circ}\text{C}$ , 2 bar propylene, toluene, MAO/Ti = 150, 3 h

**Figure 58** Propylene polymerization with MAO-activated phenoxy-ketimine catalysts. Role of the  $R^2$  substituent.

The synthesis of iPP was also achieved using the MAO-activated phenoxy-ketimine complexes of Figure 58. These complexes combine isotacticity and living behavior in propylene polymerization.<sup>1182</sup> All the catalysts except for  $R^2 = R^3 = \text{Bu}^t$  form PP with narrow molecular mass distributions indicative of living behavior ( $\bar{M}_w/\bar{M}_n < 1.17$ ). Polymerizations with  $R^2 = R^3 = \text{Me}$  at 0  $^{\circ}\text{C}$  were run for different reaction times (up to 10 h). Analysis of the resulting PPs indicated a linear relationship between  $\bar{M}_n$  and yield, which supported the living polymerization behavior. As with the aldimine catalysts, small  $R^2$  groups result in higher activity. The  $^{13}\text{C}$  NMR analysis showed the presence of stereomistakes (*mmmr*, *mmrr*, and *rrrm* pentads in a 2:2:1 ratio), consistent with an enantiomorphic site-control enchainment mechanism. Isotactic stereocontrol is only moderate, and the highest isotacticity is obtained with the relatively small  $R^2 = \text{Me}$  group. To explain the low isotacticity observed with the biggest and smallest  $R^2 = \text{Bu}^t$  and H groups, it has been suggested that the very bulky  $R^2$  groups result in unfavorable steric interaction between  $R^2$  and the incoming monomer, while  $R^2$  groups that are too small give ineffective enantioselectivity. Regioirregular insertions are not negligible (<5%). The absence of olefinic signals in the NMR spectra suggested that  $\beta$ -H and  $\beta$ -alkyl chain-release reactions do not occur. Cyclopolymerization of  $\alpha,\omega$ -dienes suggested that the regiochemistry of monomer insertion is secondary. To explain the isotacticity obtained, it has been proposed that the presence of the Ph group on the imine C atom prevents catalyst racemization.<sup>1182</sup>

#### 4.09.5.3.5 Other ligands with coordinating N–O atoms

Of course, several variations of the original bis(phenoxy-imine) ligand have been proposed. For example, the coordinating N atom can be enclosed into a pyridine ring, and it has been reported that the bis(phenoxy-pyridine) Ti complexes of Figure 59 polymerize ethylene. Although they are active catalysts, their activities are remarkably

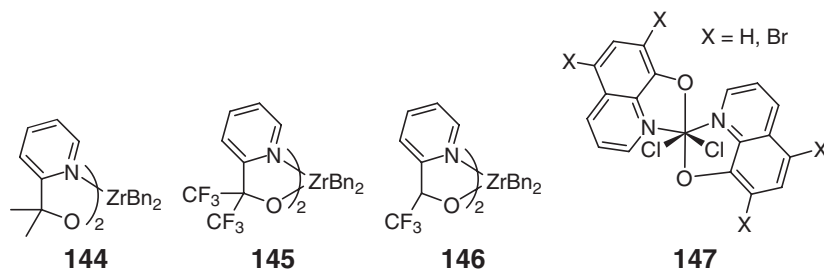
	<i>R</i>			
	<i>R</i>		<i>R</i>	
	H	Bu <sup>t</sup>	H	Bu <sup>t</sup>
	MAO as co-catalyst		[Ph <sub>3</sub> C][B(C <sub>6</sub> F <sub>5</sub> ) <sub>4</sub> ]/Bu <sup>i</sup> <sub>3</sub> Al as co-catalyst	
<i>T</i> <sub>P</sub> (°C)	25	25	25	25
Activity (g <sub>PE</sub> (mmol M) <sup>-1</sup> h <sup>-1</sup> bar <sup>-1</sup> )	4 × 10	9	2 × 10 <sup>2</sup>	6
$\overline{M}_v$	4,167,000	3,679,000	3,231,000	2,000,000
<i>T</i> <sub>P</sub> (°C)	75	75	75	75
Activity (g <sub>PE</sub> (mmol M) <sup>-1</sup> h <sup>-1</sup> bar <sup>-1</sup> )	1 × 10 <sup>2</sup>	1 × 10 <sup>2</sup>	4 × 10 <sup>2</sup>	2 × 10 <sup>2</sup>
$\overline{M}_v$	580,000	1,130,000	200,000	190,000

1 bar ethylene, MAO/Ti = 250, [Ph<sub>3</sub>C][B(C<sub>6</sub>F<sub>5</sub>)<sub>4</sub>]/Ti = 1.2, Bu<sup>i</sup><sub>3</sub>Al/Ti = 50, toluene, 30 min

**Figure 59** Ethylene polymerization with phenoxy–pyridine-based catalysts.

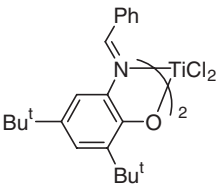
lower than those exhibited by the similarly substituted bis(phenoxy–imine)Ti catalysts. Bulky groups *ortho* to the phenoxy O atom do not improve activity. Based on the quantum mechanics calculations, it has been suggested that bis(phenoxy–pyridine) Ti-based catalysts adopt a *trans*-N, *cis*-O, *cis*-X geometry. This geometry would locate bulky groups *ortho* to the phenoxy O atoms away from the active metal center, and thus would reduce their impact on activity.<sup>1183</sup>

Poor activity is shown by other complexes with a coordinating *N*-pyridine atom. In fact, complexes **144** and **147** are not active in ethylene polymerization,<sup>1181,1184,1185</sup> whereas complexes **145** and **146** show low to moderate activity (about 10–30 g<sub>PE</sub> (mmol M)<sup>-1</sup> h<sup>-1</sup> bar<sup>-1</sup>) and yield PE with very low  $\overline{M}_n$  (<7000).<sup>1184</sup> However, these complexes also contain a more strained five-membered chelating ligand relative to the six-membered chelating ligands of bis(phenoxy–imine) catalysts.



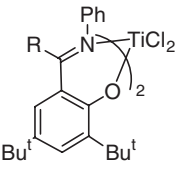
Another example of a system with a five-membered chelating ligand is the imine–phenoxy complex of Figure 60. MAO activation leads to moderately high active catalysts while the molecular masses of the PEs are very high. Activation with [Ph<sub>3</sub>C][B(C<sub>6</sub>F<sub>5</sub>)<sub>4</sub>]/Bu<sup>i</sup><sub>3</sub>Al results in slightly better activity and produces high molecular mass PEs. Thus, the polymerization behavior of the imine–phenoxy complex is totally different from that of the classical phenoxy–imine complexes, which exhibit higher activity with MAO than with [Ph<sub>3</sub>C][B(C<sub>6</sub>F<sub>5</sub>)<sub>4</sub>]/Bu<sup>i</sup><sub>3</sub>Al. In strict analogy with the phenoxy–imine complexes, NMR studies suggested that the Bu<sup>i</sup><sub>3</sub>Al reacts with the imine functionality and reduces the imine–phenoxy complex to an amine–phenoxy complex.<sup>1136</sup>

The MAO-activated phenoxy–ketimine complexes of Figure 61 are highly active ethylene polymerization catalysts, although activities are lower than those of analogous phenoxy–aldimine complexes (R = H).<sup>1166</sup> In all cases, rather low molecular masses ( $\overline{M}_n$  < 50 000) are obtained. With the exception of the complex with R = CF<sub>3</sub>, rather narrow molecular mass distributions ( $\overline{M}_w/\overline{M}_n$  < 1.1) are found, indicative of living behavior. Polymerizations with R = Ph at 0 °C were run for different reaction times. Analysis of the resulting PEs showed a linear relationship between  $\overline{M}_n$  and yield, which supported the living polymerization behavior. These experiments led to the conclusion that the presence of *ortho*-F atoms in the complex is not a mandatory requirement for living behavior.<sup>1166</sup>

	MAO as co-catalyst		[Ph <sub>3</sub> C][B(C <sub>6</sub> F <sub>5</sub> ) <sub>4</sub> ]/Bu <sup>i</sup> <sub>3</sub> Al as co-catalyst	
	50	75	50	75
	1 × 10 <sup>2</sup>	1 × 10 <sup>2</sup>	1 × 10 <sup>2</sup>	6 × 10 <sup>3</sup>
	0.25	0.27	0.58	2.41
	2,320,000	2,130,000	1,170,000	560,000

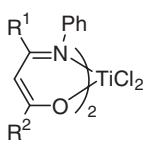
1 bar ethylene, MAO/Ti = 250, [Ph<sub>3</sub>C][B(C<sub>6</sub>F<sub>5</sub>)<sub>4</sub>]/Ti = 1.2, Bu<sup>i</sup><sub>3</sub>Al/Ti = 50, toluene

**Figure 60** Ethylene polymerization with imine-phenoxy-based catalysts.

	<i>R</i>				
	H	Me	Et	Ph	CF <sub>3</sub>
	4 · 10 <sup>3</sup>	6 · 10 <sup>2</sup>	5 · 10 <sup>2</sup>	1 · 10 <sup>3</sup>	5 · 10 <sup>2</sup>
	0.42	0.20	0.15	0.39	0.18
	48,500	24,000	21,300	44,500	28,000

0.7 bar ethylene, MAO/Ti = 150, toluene, 20 °C,  
polymerization time: R = H, 1 min; all other systems, 3 min

**Figure 61** Ethylene polymerization with phenoxy-ketimine-based catalysts.

	<i>R</i> <sup>1</sup>				
	—CF <sub>3</sub>	—CF <sub>3</sub>	—CF <sub>3</sub>	—Me	—Me
	<i>R</i> <sup>2</sup>	—Ph	—S—	—CF <sub>3</sub>	—Ph
	1 × 10 <sup>3</sup>	7 × 10 <sup>2</sup>	3 × 10 <sup>2</sup>	1 × 10 <sup>3</sup>	1 × 10 <sup>2</sup>
	0.11	0.17	0.08	0.27	0.05

25 °C, 1 bar ethylene, MAO/Ti = 2,000, toluene, 5 min

**Figure 62** Ethylene polymerization with β-enaminoketonato-based catalysts.

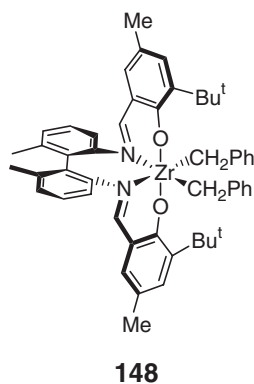
The MAO-activated β-enaminoketonato complexes of Figure 62 are moderately to highly active ethylene polymerization catalysts.<sup>1186</sup> However, molecular masses are not very high ( $\bar{M}_n < 100,000$ ). PEs produced with the first two systems, that is, R<sup>1</sup> = CF<sub>3</sub> and R<sup>2</sup> = Ph or 2-theonyl, show rather narrow molecular mass distribution ( $\bar{M}_w/\bar{M}_n < 1.35$ ), indicative of quasi-living behavior. The post-polymerization experiments indicated that the catalyst lifetime is longer than 60 min even in the absence of ethylene. On the other hand, the third system, that is, R<sup>1</sup> = CF<sub>3</sub> and R<sup>2</sup> = 2-furyl, produces PEs with rather broad polydispersities, although the only difference with the 2-theonyl-based catalyst is the replacement of an S atom with an O atom.

$T_P$ (°C)	50	50	100	50	100
Activity ( $\text{g}_{\text{PE}}$ (mmol M) $^{-1}$ h $^{-1}$ bar $^{-1}$ )		$1 \times 10^3$	$5 \times 10^2$	$4 \times 10^3$	$2 \times 10^3$
Yield (g)	Trace	1.23	0.52	0.69	0.36
$\overline{M}_w$		236,000	73,000	225,000	77,000
$\overline{M}_w/\overline{M}_n$		2.1	2.4	3.3	1.5

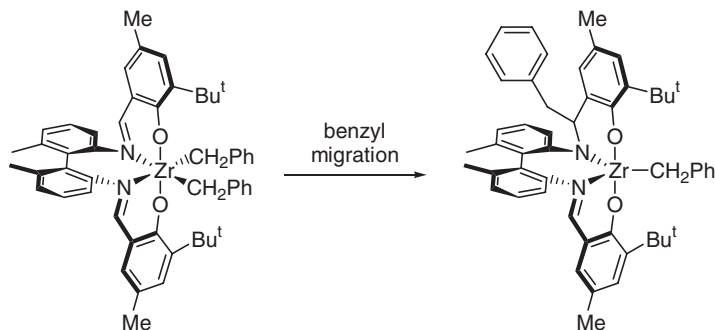
**Figure 63** Ethylene polymerization with tridentate NOP based catalysts.

The tridentate NOP complexes of [Figure 63](#) showed good performance as ethylene polymerization catalysts. Whereas the NOP complex with two chelating ligands showed no polymerization activity, the two monochelated complexes exhibited high activity even at 100 °C. Reasonably high molecular masses were obtained.<sup>1187</sup>

Some authors tried to fix the stereoflexibility of bis(phenoxy-imine) catalysts through the introduction of a bridge between the two imine N atoms. The two phenoxy-imine groups have been linked with a biaryl bridge. However, the MAO-activated [148](#) exhibited no polymerization activity.

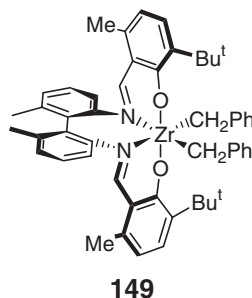


The main reason for this is that this complex decomposed through an intramolecular reduction of the imine functionality by migration of one of the benzyl groups to the C atom of the imino moiety, as shown in [Scheme 43](#).<sup>1188</sup>

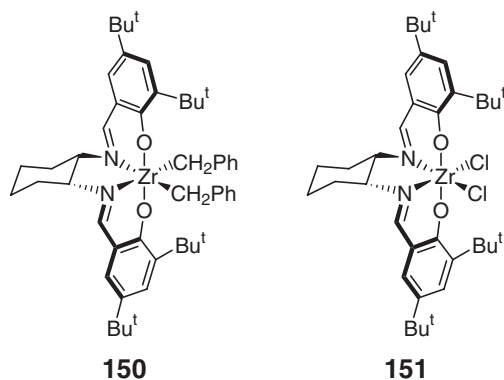


**Scheme 43**

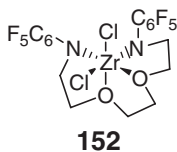
A solution to this problem was the introduction of a methyl group *ortho* to the imine group, as in complex **149**, that sterically protects the complex from benzyl migration. The MAO-activated **149** is remarkably stable, and overall activity is moderate (about  $50 \text{ g}_{\text{PE}} (\text{mmol M})^{-1} \text{ h}^{-1} \text{ bar}^{-1}$ ).<sup>1188</sup>



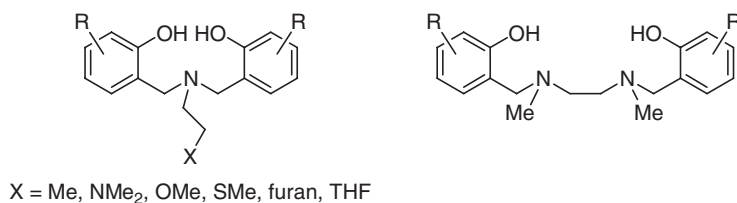
Complexes **150** and **151**, with cyclohexyl bridge between the imine groups, have also been tested. The catalyst **150**/MAO polymerized ethylene with moderate activity (up to  $30 \text{ g}_{\text{PE}} (\text{mmol M})^{-1} \text{ h}^{-1} \text{ bar}^{-1}$ ), while **151**/MAO exhibited low activity ( $10 \text{ g}_{\text{PE}} (\text{mmol M})^{-1} \text{ h}^{-1} \text{ bar}^{-1}$ ). In both cases, reasonably high molecular masses were obtained. Perfluoroborate activation was found to be quite ineffective. These catalysts were substantially inactive for propylene polymerization.<sup>1189</sup>



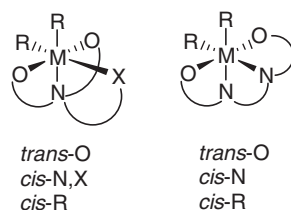
While all the 6-coordinated N–O complexes described so far have ligands with a negatively charged O and neutral N atoms, a few complexes with the N atom negatively charged and with neutral O atoms, such as **152**, have been synthesized. However, MAO activation of **152** polymerizes ethylene with rather low activity ( $3 \text{ g}_{\text{PE}} (\text{mmol M})^{-1} \text{ h}^{-1} \text{ bar}^{-1}$ ).<sup>1190</sup>



A remarkable class of catalysts with coordinating N–O atoms is that based on the ligands of Scheme 44, introduced for 1-hexene polymerization in 1999.<sup>1191–1204</sup> These catalysts differ from the bis(phenoxymethyl) catalyst and analogs



**Scheme 44**



Scheme 45

because the coordinating N atom is an amino N instead of an imino N atom. This family of catalysts can be divided into two categories depending on the topology of the ligand (see Scheme 44). In the ligands on the left, the N atom connects the two phenolate rings, and further coordination can occur through X donor atoms on the side-arm. Conversely, in the tetradentate ligand on the right, the “branched” mode of connectivity (i.e., the side-arm) is replaced with a consequential connectivity mode through the diamine bridge that connects the two phenolate rings.

In both cases, the final pre-catalysts are octahedral complexes with a *trans*-O, *cis*-N(X), *cis*-R geometry of coordination at the metal atom, as shown in Scheme 45. Of course, in the case of X = Me, the *n*-Pr side-arm is not coordinated to the metal, and the complexes present a 5-coordinated metal atom. The *cis*-disposition of the R groups is of fundamental relevance for the ability of these complexes to act as polymerization catalysts.

Activation of these complexes with equimolar amounts of B(C<sub>6</sub>F<sub>5</sub>)<sub>3</sub> at room temperature resulted in active catalysts for 1-hexene polymerization. The performance of some of the complexes with the extra side-arm is reported in Table 20. First of all, it is important to note that complexes with no donor atom in the extra side-arm give low activity, and only yield oligomers (entries 1 and 3 in Table 20).<sup>1194,1195</sup> Conversely, a donor group in the side-arm, for example, an NMe<sub>2</sub> donor group, results in catalysts that present rather different behavior. For example, the Ti complex of entry 2 in Table 20 exhibits a rather low polydispersity, indicative of quasi-living polymerization behavior,<sup>1195</sup> while the Zr complex of entry 4 is remarkably active and shows no living character.<sup>1199</sup> Comparison of the Zr and Hf series with donor groups NMe<sub>2</sub>, OMe, and SMe (Table 20; entries 4, 8, 12 for Zr, and 6, 10, 13 for Hf) revealed no clear trend in either activity or molecular mass.<sup>1199</sup> In all the cases, reasonably high molecular mass poly(1-hexene) was produced. The  $\bar{M}_w/\bar{M}_n$  values obtained were typical of single-site polymerization catalysts, and no signs of living polymerization could be observed. Diluting the monomer in heptane results in more controlled polymerization reactions, and in many instances the polymers produced exhibit remarkably high  $\bar{M}_w$ .<sup>1199</sup> Enclosing the donor O atom in a THF or furan ring has no major impact on the polymerization behavior of the Zr- and Hf-based catalysts (Table 20; entries 9, 15 for Zr, and 10, 16 for Hf). On the other hand, in the case of Ti replacement of the THF ring by furan improves the activity to about 10<sup>5</sup> g<sub>PH</sub> (mmol M)<sup>−1</sup> h<sup>−1</sup> (entries 14 and 17).

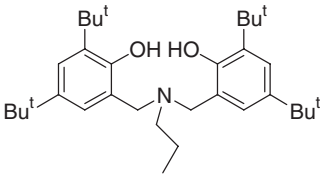
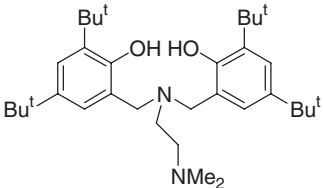
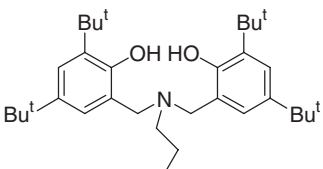
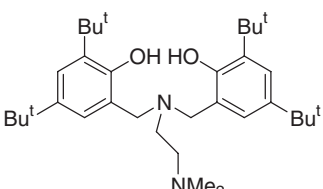
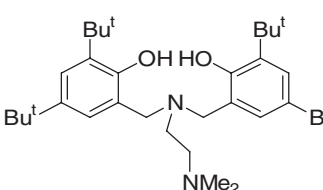
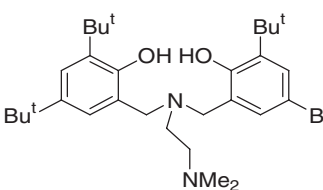
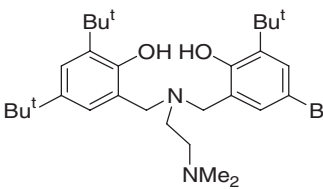
The following general conclusions emerge. Catalyst activity mostly depends on the nature of the metal atom, with the following approximate order: Zr ≥ Hf ≫ Ti. For the Zr- and Hf-based catalysts, very high activities in the range 10<sup>4</sup>–10<sup>5</sup> g<sub>PH</sub> (mmol M)<sup>−1</sup> h<sup>−1</sup> and  $\bar{M}_w$  of about 100 000 can be easily achieved. The Ti-based catalysts, on the other hand, possess moderate activity, about 10–30 g<sub>PH</sub> (mmol M)<sup>−1</sup> h<sup>−1</sup>. However, and very remarkably, while the Zr and Hf catalysts yield  $\bar{M}_w/\bar{M}_n$  values around 2, the Ti systems can exhibit living character for prolonged periods of time.

For the systems with an N-donor atom in the side-arm, the length of the side-arm or the nature of the N atom have major effects on activity.<sup>1196</sup> In comparison, steric effects of substituents *ortho* to the phenolate O atoms, although very close to the active site, have a much weaker influence. The most active catalysts contain a C<sub>2</sub> spacer between the two coordinating N atoms, which corresponds to five-membered chelate rings (compare entries 4 and 20 as well as 22 and 23 in Table 20). Changing the hybridization of the extra donor atom from *sp*<sup>3</sup> to *sp*<sup>2</sup> or reducing the size of the substituents on the aromatic rings had minor effects on reactivity (entries 4 and 22 vs. 4 and 18 in Table 20). Increasing the bulkiness of the substituents on the N-donor reduced the reactivity dramatically and led to oligomers (compare entries 4 and 21 in Table 20).

Another remarkable feature of these catalysts is their ability to promote living or quasi-living polymerization of olefins. This behavior is exhibited by almost all the B(C<sub>6</sub>F<sub>5</sub>)<sub>3</sub>-activated Ti catalysts. At room temperature, the catalyst with an NMe<sub>2</sub> group yields polymers with  $\bar{M}_w = 16\,500$  and  $\bar{M}_w/\bar{M}_n = 1.18$  after 30 min of polymerization.<sup>1195</sup> Insertion of the OMe group as donor results in much better living behavior, since the corresponding catalyst yields polymers with  $\bar{M}_w = 445\,000$  and  $\bar{M}_w/\bar{M}_n = 1.12$  after 31 h of polymerization. The effect of the polymerization temperature on the living behavior has been tested. One-hour polymerizations were carried out from room

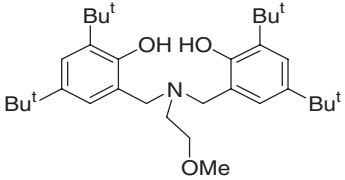
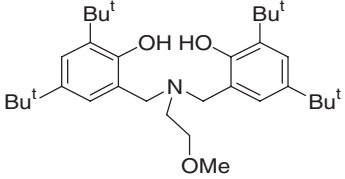
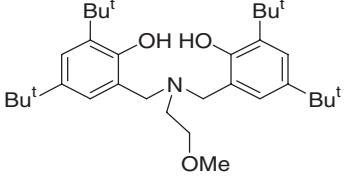
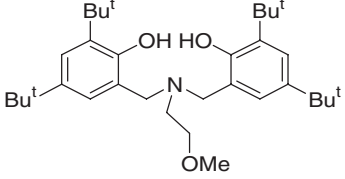
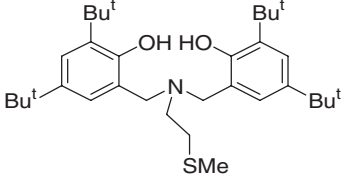
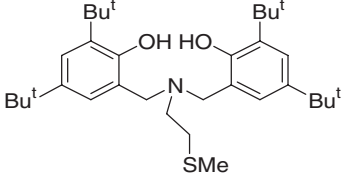
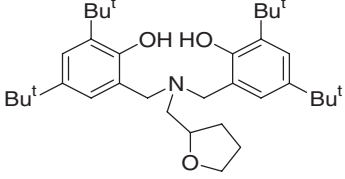


**Table 20** Selected results from bis(phenolate) complexes with an extra donor arm

Entry	Ligand	M	Solvent	Productivity (g <sub>PH</sub> (mmol M) <sup>-1</sup> h <sup>-1</sup> )	$\bar{M}_w$	$\bar{M}_w/\bar{M}_n$	References
1		Ti	1-Hexene	50	1,500	2.0	1195
2		Ti	1-Hexene	30	14,000	1.18	1195
3		Zr	1-Hexene	20	Oligomers		1194
4		Zr	1-Hexene	20,000	35,000	3.5	1199
5		Zr	n-C7	800	170,000	2.0	1199
6		Hf	1-Hexene	2,000	13,000	3.2	1199
7		Hf	n-C7	200	20,000	1.6	1199

(Continued)

Table 20 (Continued)

Entry	Ligand	M	Solvent	Productivity (g <sub>PH</sub> (mmol M) <sup>-1</sup> h <sup>-1</sup> )	$\bar{M}_w$	$\bar{M}_w/\bar{M}_n$	References
8		Zr	1-Hexene	50,000	80,000	3.0	1199
9		Zr	<i>n</i> -C7	1,000	160,000	1.4	1199
10		Hf	1-Hexene	20,000	101,000	2.2	1199
11		Hf	<i>n</i> -C7	700	140,000	1.8	1199
12		Zr	1-Hexene	9,000	195,000	2.0	1199
13		Hf	1-Hexene	30,000	66,000	2.5	1199
14		Ti	1-Hexene	10	316,000	1.05	1201

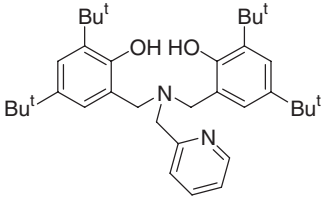
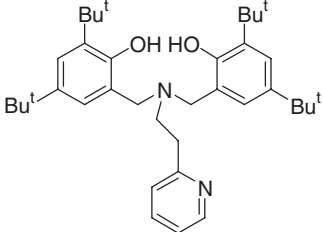
(Continued)

Table 20 (Continued)

Entry	Ligand	M	Solvent	Productivity (g <sub>PH</sub> (mmol M) <sup>-1</sup> h <sup>-1</sup> )	$\bar{M}_w$	$\bar{M}_w/\bar{M}_n$	References
15		Zr	PhCl	2,000	118,000	2.1	1201
16		Hf	PhCl	1,000	60,000	1.5	1201
17		Ti	1-Hexene	200	550,000	1.37	1205
18		Zr	1-Hexene	High	100,000	1.9	1196
19		Zr	1-Hexene	600	6,700	3.3	1196
20		Zr	1-Hexene	Negligible	Oligomers		1196
21		Zr	1-Hexene	60	1,100	1.6	1196

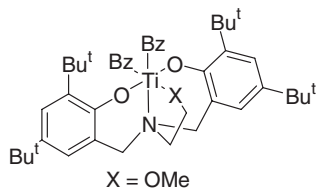
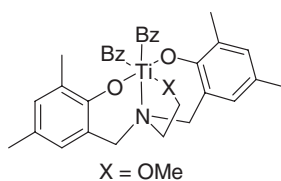
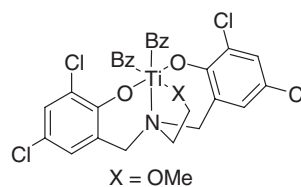
(Continued)

Table 20 (Continued)

Entry	Ligand	M	Solvent	Productivity (g <sub>PH</sub> (mmol M) <sup>-1</sup> h <sup>-1</sup> )	$\bar{M}_w$	$\bar{M}_w/\bar{M}_n$	References
22		Zr	1-Hexene	6,000	15,000	4.5	1196
23		Zr	1-Hexene	60	102,000	1.7	1196

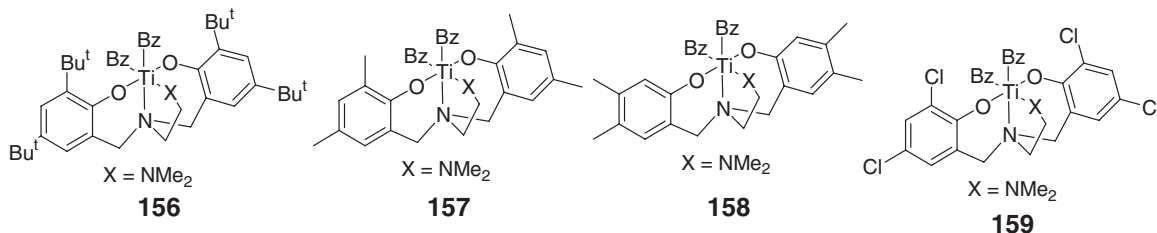
temperature up to 65 °C for the catalysts with an OMe donor group. The resulting polymers had  $\bar{M}_w$  in the range 15 000–20 000, while the  $\bar{M}_w/\bar{M}_n$  increased from 1.07 to 1.30. Thus, even at rather high polymerization temperatures, these catalysts yield narrow polydispersities.<sup>1197</sup> Exceptionally long-lived polymerization was achieved by introduction of a THF as donor group. Polymers with  $\bar{M}_w = 200\,000$  and  $\bar{M}_w/\bar{M}_n = 1.06$  were obtained after 2 days of polymerization. Extending the polymerization time to 6 days still results in extremely narrow polydispersity ( $\bar{M}_w/\bar{M}_n = 1.09$ ), with polymer growth continuing almost linearly up to  $\bar{M}_w = 816\,000$ . Considering the extremely long-living behavior of these catalysts, eventual chain-release reactions were attributed to technical sources such as water or oxygen traces.<sup>1201</sup> Even small variations in the donor group can lead to substantially different catalytic behavior. In fact, replacing the THF group with a furan group corresponds to polymers having  $\bar{M}_w > 200\,000$  after 2 h of polymerization, with very narrow molecular mass distribution  $\bar{M}_w/\bar{M}_n = 1.05$ –1.09).<sup>1200</sup>

More detailed structure/activity relationships were obtained with the pre-catalysts **153**–**155**, as well as **156**–**159**.<sup>1202</sup> In the case of X = OMe, the B(C<sub>6</sub>F<sub>5</sub>)<sub>3</sub>-activated pre-catalysts **153**–**155** exhibit rather similar activities, in the range 10–50 g<sub>PH</sub> (mmol M)<sup>-1</sup> h<sup>-1</sup>. The large *t*-Bu substituents make **153** more long-lived, with  $\bar{M}_w/\bar{M}_n = 1.12$  after more than 24 h. By contrast, complexes **154** and **155**, with smaller Me and Cl substituents, lose living character after less than 1 h. The NMR analysis of the resulting poly(1-hexene)s indicated that the polymers were substantially atactic and that a rather large fraction of regiomistakes was incorporated (4% for **153**, 16% for **154**, and 20% for **155**).

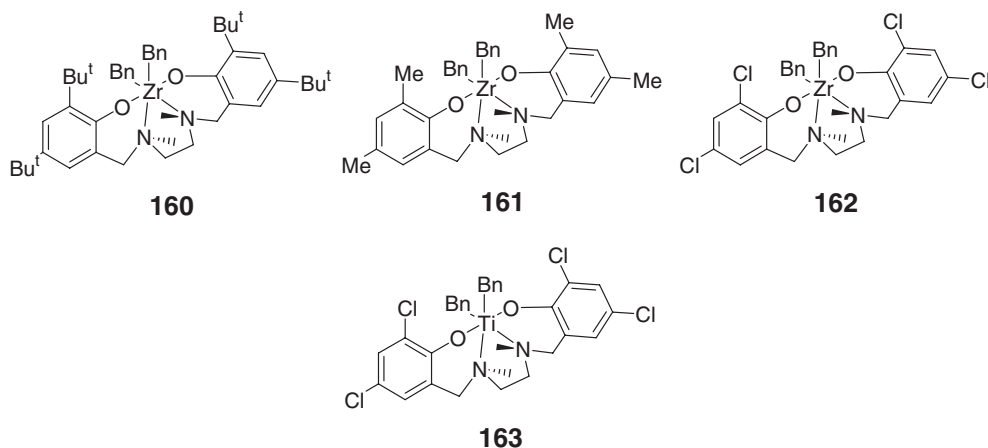
**153****154****155**

The behavior of the complexes with X = NMe<sub>2</sub> is remarkably different. First of all, complexes **157** and **158**, with relatively small substituents *ortho* to the phenolate O atom, yield very high activities (>1 kg<sub>PH</sub> (mmol M)<sup>-1</sup> h<sup>-1</sup>), noticeably higher than that of the classical complex **156** with *t*-Bu groups (about 30 g<sub>PH</sub> (mmol M)<sup>-1</sup> h<sup>-1</sup>). Even higher activity is exhibited by complex **159** (6–9 kg<sub>PH</sub> (mmol M)<sup>-1</sup> h<sup>-1</sup>), although the Cl groups are essentially similar to Me groups from a steric point of view. It has been suggested that the very high activity of **159** is due to the electron-withdrawing properties of the Cl atoms. The NMR analysis indicated that atactic polymers were also produced in these cases. On the other hand, the amount of regiomistakes is noticeably smaller relative to the related

complexes with an X=OMe group (1% for **156** and about 4–5% for **157–159**. The higher regioselectivity of the complexes with X = NMe<sub>2</sub> can be reasonably ascribed to the additional Me group on the X donor atom that increases the steric pressure on the transition state leading to a regiomistake. Interestingly, **157–159** do not show characteristics of living behavior. In fact, polymerization in chlorobenzene resulted in  $\bar{M}_w/\bar{M}_n$  in the range 1.5–2.0. However, while  $\bar{M}_w$  in the range of 25 000–50 000 was obtained with **157** and **158**, exceptionally high molecular masses ( $\bar{M}_w$  up to 4 million in 1 h) were obtained with **159**.

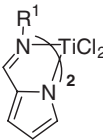
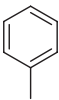
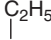
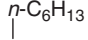
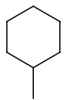


With regard to complexes with a tetradentate ligand, the *C*<sub>2</sub>-symmetric complexes **160–163** were first synthesized.<sup>1193,1204</sup> After activation with 1.1 equiv. of B(C<sub>6</sub>F<sub>5</sub>)<sub>3</sub>, **160** yields living and stereospecific 1-hexene polymerization (activity = 18 g<sub>PH</sub> (mmol M)<sup>−1</sup> h<sup>−1</sup>; reaction time = 30 min;  $\bar{M}_w$  = 12 000;  $\bar{M}_w/\bar{M}_n$  = 1.15). The NMR analysis showed that the poly-1-hexene produced was highly isotactic.<sup>1193</sup> This was a major achievement since the complexes with the extra donor on the side-arm only yield atactic polymers. Similar activation of **161** resulted in a slightly more active catalyst (activity = 35 g<sub>PH</sub> (mmol M)<sup>−1</sup> h<sup>−1</sup>) but polymerization was not living ( $\bar{M}_w$  = 23 000;  $\bar{M}_w/\bar{M}_n$  = 1.57) and the resulting polymer was atactic.<sup>1193</sup> These results clearly indicated that the living and isospecific behavior of these systems is strongly influenced by the groups *ortho* to the phenolate O atoms. As expected, further substitution of the aromatic rings with Cl atoms, as in **162** and **163**, resulted in much higher activities (5000 and 200 g<sub>PH</sub> (mmol M)<sup>−1</sup> h<sup>−1</sup>, respectively).<sup>1204</sup> However, while the Zr-based complex **162** only yields oligomers ( $\bar{M}_w$  = 9100), the Ti complex **163** yields very high molecular masses within 40 min, with some living polymerization character ( $\bar{M}_w$  > 550 000;  $\bar{M}_w/\bar{M}_n$  = 1.2). Extending the polymerization time to 19 h yielded exceedingly high molecular masses ( $\bar{M}_w$  > 1.9 million), but the living character was lost.<sup>1204</sup>



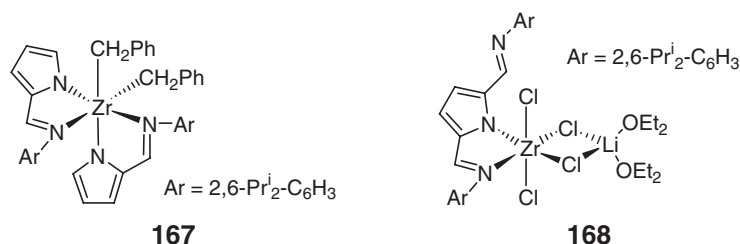
The behavior in propylene polymerization of a series of catalysts based on the bis(phenoxy–amino) skeleton has been investigated. The pre-catalyst **160**, activated with [Ph<sub>3</sub>C][B(C<sub>6</sub>F<sub>5</sub>)<sub>4</sub>] is able to polymerize propylene to an isotactic polymer with a moderate activity (about 1 g<sub>PP</sub> (mmol M)<sup>−1</sup> h<sup>−1</sup> mol(propylene)<sup>−1</sup>) in the temperature range of 0–50 °C. The <sup>13</sup>C NMR analysis showed 80% *mmmm* pentads, with randomly distributed *rr* diads, typical of site control. The *mmmr/mmrr/mrrm* pentad ratio of 2 : 2 : 1 further confirmed that the stereocontrol was determined by the catalytic site. The iPP was remarkably regioregular, and analysis of the chain-end groups indicated that propagation is primary. It has been suggested that **160** is a good model of the isotactic species active in classical Ziegler–Natta polymerization.<sup>236</sup> Once again, steric hindrance by the alkyl group *ortho* to the phenoxy O atom was found to be the key to the isotactic stereocontrol. In fact, **161**, with Me groups in place of *t*-Bu groups, yields a slightly syndiotactic



	R <sup>1</sup>			
				
	MAO as co-catalyst			
Activity (g <sub>PE</sub> (mmol M) <sup>-1</sup> h <sup>-1</sup> bar <sup>-1</sup> )	6 × 10 <sup>3</sup>	4 × 10 <sup>2</sup>	8 × 10 <sup>2</sup>	1 × 10 <sup>4</sup>
Yield (g)	0.50	0.03	0.07	1.18
M <sub>v</sub>	75,000	412,000	441,000	2,601,000
	[Ph <sub>3</sub> C][B(C <sub>6</sub> F <sub>5</sub> ) <sub>4</sub> ]/Bu <sup>i</sup> <sub>3</sub> Al as cocatalyst			
Activity (g <sub>PE</sub> (mmol M) <sup>-1</sup> h <sup>-1</sup> bar <sup>-1</sup> )	2 × 10 <sup>3</sup>	2 × 10 <sup>3</sup>	1 × 10 <sup>3</sup>	2 × 10 <sup>3</sup>
Yield (g)	0.16	0.14	0.13	0.17
M <sub>v</sub>	4,739,000	4,654,000	4,901,000	4,029,000

25 °C, 1 bar ethylene, MAO/Ti = 1,250, [Ph<sub>3</sub>C][B(C<sub>6</sub>F<sub>5</sub>)<sub>4</sub>]/Ti = 6, Bu<sup>i</sup><sub>3</sub>Al/Ti = 250, toluene, 5 min

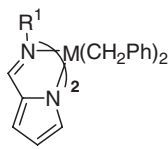
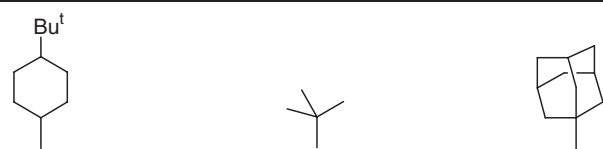
**Figure 64** Ethylene polymerization with bis(imino-pyrrolate) Ti-based catalysts.



The Zr- and Hf-based imino-pyrrolide catalysts of Figure 65 have also been investigated. While the complex with R<sup>1</sup> = 4-Bu<sup>t</sup>-C<sub>6</sub>H<sub>4</sub> is not active, the other two systems with R<sup>1</sup> = Bu<sup>t</sup> and adamantyl are active ethylene polymerization catalysts. For the Hf compounds, MAO and B(C<sub>6</sub>F<sub>5</sub>)<sub>3</sub>/Bu<sup>i</sup><sub>3</sub>Al activation results in similar activities and rather broad MWDs. In the case of the Zr catalysts, MAO activation gives slightly better activities, and the PEs had polydispersities typical of single-site catalysts. It has been suggested that the Hf catalysts produced multimodal PE by gradual generation of the active species and/or isomerization of the active species under the polymerization conditions.<sup>1212</sup> More surprisingly, in the case of M = Hf and R<sup>1</sup> = Bu<sup>t</sup> and using [Ph<sub>3</sub>C][B(C<sub>6</sub>F<sub>5</sub>)<sub>4</sub>]/Bu<sup>i</sup><sub>3</sub>Al as co-catalyst, solvent effects seem to be remarkable. Switching from toluene to *n*-heptane yields high molecular mass PE ( $\bar{M}_w = 896\,000$ ) with a very broad  $\bar{M}_w/\bar{M}_n$  of 21.<sup>1211</sup> A quantum mechanics/molecular mechanics study has indicated that in the presence of a tightly bound counterion such as [MeB(C<sub>6</sub>F<sub>5</sub>)<sub>3</sub>]<sup>−</sup>, the rate-limiting step of chain growth is probably ethylene coordination. The barrier for chain growth in the Ti-based catalysts is predicted to be around 13 kcal mol<sup>−1</sup>. A slightly lower barrier, about 9 kcal mol<sup>−1</sup>, has been predicted for the Zr analog.<sup>151</sup>

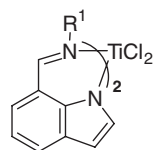
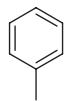
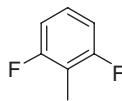
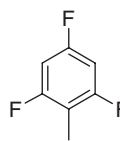
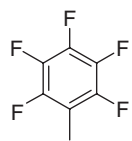
The bis(indolide-imine) Ti complexes of Figure 66 polymerize ethylene with moderate to high activities. The best performance is shown by the perfluoro-substituted complex. These complexes exhibit living polymerization behavior. Differently from bis(phenoxy-imine) Ti-based catalysts, living behavior is also shown by the system with no F atoms on the R<sup>1</sup> substituent. It was hypothesized that the bulkiness and rigidity of the indolide-imine ligand is responsible for suppressing chain-termination reactions.<sup>1160,1215</sup>

Catalysts that contain mono(benzamidinate) or bis(benzamidinate) ligands have been investigated.<sup>247,248,276,1216</sup> The bis(benzamidinate) complexes assume an octahedral geometry of coordination at the metal atom, as shown in Scheme 47. These complexes are C<sub>2</sub>-symmetric, and coordination of the benzamidinate ligands leaves two mutually *cis*-coordination positions. Thus, these complexes possess the requirements for isospecific propylene polymerization. The only drawback of these structures is the lack of stereorigidity, usually provided by a tether that bridges the two chelating ligands. In principle, there might be fast isomerization between  $\Lambda$  and  $\Delta$  configurations, as shown in

	$R^1$					
						
	M = Hf					
Co-catalyst	MAO	$B(C_6F_5)_3/Bu^i_3Al$	MAO	$B(C_6F_5)_3/Bu^i_3Al$	MAO	$B(C_6F_5)_3/Bu^i_3Al$
Activity ( $g_{PE} (mmol\ M)^{-1} h^{-1} bar^{-1}$ )			$1 \times 10^3$	$2 \times 10^3$	$6 \times 10^2$	$2 \times 10^3$
Yield (g)	Trace	Trace	0.53	0.93	0.26	0.87
$\overline{M}_w$			87,000	88,000	36,000	96,000
$\overline{M}_w/\overline{M}_n$			6.05	9.19	6.66	12.15
M = Zr						
Co-catalyst	MAO	$B(C_6F_5)_3/Bu^i_3Al$	MAO	$B(C_6F_5)_3/Bu^i_3Al$	MAO	$B(C_6F_5)_3/Bu^i_3Al$
Activity ( $g_{PE} (mmol\ M)^{-1} h^{-1} bar^{-1}$ )			$8 \times 10^3$	$7 \times 10^2$	$9 \times 10^3$	$2 \times 10^2$
Yield (g)	Trace	Trace	3.37	0.31	3.67	0.73
$\overline{M}_w$			29,000	24,000	87,000	63,000
$\overline{M}_w/\overline{M}_n$			2.25	2.25	2.08	2.05

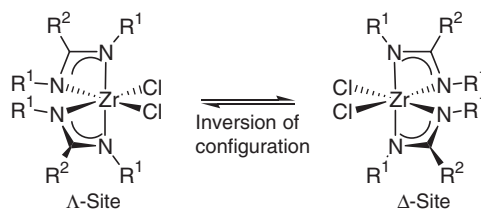
5.0  $\mu$ mol Complex, 25 °C, 1 bar ethylene, MAO/Hf = 250,  $B(C_6F_5)_3$ /Hf = 2,  $Bu^i_3Al$ /Hf = 50, toluene, 5 min

**Figure 65** Ethylene polymerization performances of Hf- and Zr-based pyrrolide-imine-based catalysts.

	$R^1$			
				
	MAO as co-catalyst			
Activity ( $g_{PE} \text{ (mmol M)}^{-1} \text{ h}^{-1} \text{ bar}^{-1}$ )	$5 \times 10$	$6 \times 10$	$3 \times 10^2$	$1 \times 10^3$
Yield (g)	0.04	0.05	0.24	0.95
$\overline{M}_w$	13,800	12,400	46,500	323,000
$\overline{M}_w/\overline{M}_n$	1.14	1.13	1.11	1.93

25 °C, 1 bar ethylene, MAO/Ti = 250, toluene, 10 min

**Figure 66** Ethylene polymerization with indolide-imine-based catalysts.

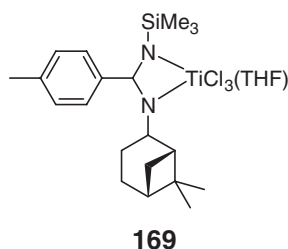


**Scheme 47**

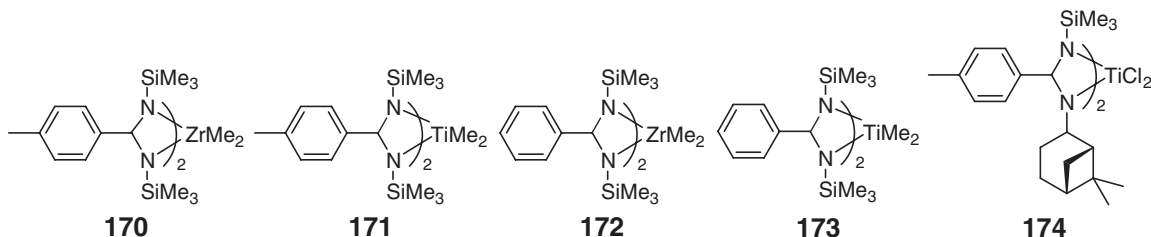


Scheme 47, which would nullify any stereinduction which might be operative at each insertion step. These systems exhibit reasonable catalytic activity only under propylene pressure ( $> 5$  bar).

At  $20^\circ\text{C}$  and at 5 bar propylene feed, the MAO-activated mono(benzamidinate) **169** yields poorly stereoregular iPP ( $mmmm \sim 25\text{--}30\%$ ) with the moderate activity of about  $20 \text{ g}_{\text{PP}} (\text{mmol M})^{-1} \text{ h}^{-1} \text{ bar}^{-1}$ , and  $\bar{M}_v = 100\,000$ . Raising the polymerization temperature to  $60^\circ\text{C}$ , and increasing the propylene pressure to 7 bar, gives very low activity ( $1 \text{ g}_{\text{PP}} (\text{mmol M})^{-1} \text{ h}^{-1} \text{ bar}^{-1}$ ) that only yields oligomers ( $\bar{M}_v = 28\,000$ ).<sup>276</sup>

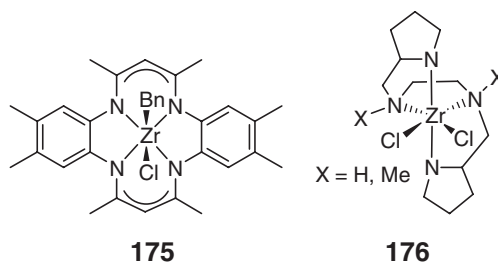


By contrast, at  $25^\circ\text{C}$  and at propylene pressures  $> 5$  bar the MAO-activated benzamidinato complex **170** in  $\text{CH}_2\text{Cl}_2$  yields substantially isotactic polymers ( $mmmm \sim 98\%$ ,  $\bar{M}_v$  in the range  $20,000\text{--}80,000$ ). Activity is moderate, about  $10\text{--}50 \text{ g}_{\text{PP}} (\text{mmol M})^{-1} \text{ h}^{-1} \text{ bar}^{-1}$ . The Ti analogue **171**, on the other hand, yields a substantially elastomeric PP ( $mmmm \sim 20\%$ ) in the same conditions.<sup>248</sup> Removing the Me substituent in the para position of the phenyl ring has beneficial effects on both activity and molecular masses (up to  $\bar{M}_w = 2$  million with **172**, and up to  $300,000$  with **173**). The resulting PP are poorly stereoregular ( $mmmm$  in the range  $10\text{--}30\%$ ), although they possess elastomeric properties. The structures of these elastomeric polymers were suggested to be consistent with longer isotactic domains disposed between domains with a large number of stereodefects.<sup>248</sup> In an attempt to explore the effects of  $C_1$ -symmetry in this class, Eisen and coworkers synthesized complex **174**. MAO activation of **174** yields highly stereoregular iPP ( $mmmm$  in the range  $93\text{--}99\%$ ) with very low activity ( $1 \text{ g}_{\text{PE}} (\text{mmol M})^{-1} \text{ h}^{-1} \text{ bar}^{-1}$ ) and  $\bar{M}_v = 10\,000\text{--}30\,000$ .<sup>276</sup>

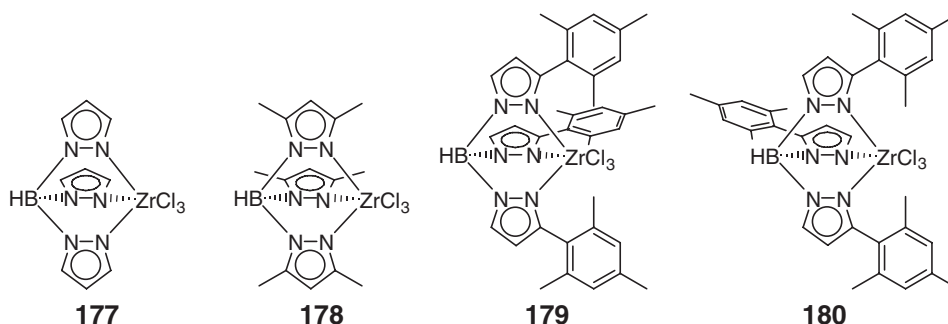


All the iPPs produced with this class of complexes had  $\bar{M}_w/\bar{M}_n$  around 2, which is consistent with the single-site behavior. The NMR analysis of the iPP revealed equal amounts of  $mmmr$  and  $mmrr$  pentads, consistent with a mechanism of enantioselectivity controlled by the site chirality.<sup>276</sup> To explain the increased isotacticity at increasing propylene pressure, it has been proposed that monomer insertion competes with chain epimerization. At increased propylene pressure, chain-epimerization reactions would be depressed by faster monomer insertion.<sup>247,248,276</sup>

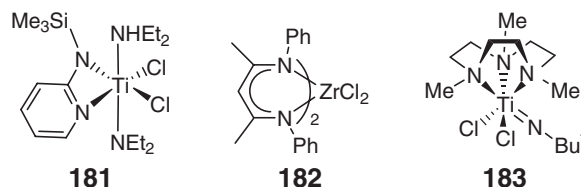
Other 6-coordinated pre-catalysts with chelating N–N atoms have been tested in olefin polymerization. However, complexes such as **175** and **176** yield PE with low to very low activity.<sup>1217,1218</sup>



Ti and Zr complexes with the tris(pyrazolyl)borate skeleton such as **177** and **178** exhibited reasonably high activity ( $< 10^3 \text{ g}_{\text{PE}} (\text{mmol M})^{-1} \text{ h}^{-1} \text{ bar}^{-1}$ ).<sup>1219</sup> Bulky mesityl groups on the tris(pyrazolyl)borate skeleton, as in the Zr complexes **179** and **180**, lead to very highly active catalysts for ethylene polymerization.<sup>278,1220</sup> The MAO-activated **179** and **180** yield PE with activity around  $10^5 \text{ g}_{\text{PE}} (\text{mmol M})^{-1} \text{ h}^{-1} \text{ bar}^{-1}$ . This activity is comparable to that of bis(phenoxy-imine)-based catalysts. Furthermore, **179** and **180** exhibit this activity at  $75^\circ\text{C}$  and for at least 20 min. The resulting PE had remarkably high molecular mass ( $\bar{M}_v$  up to  $8.5 \times 10^6$ ), while polydispersities around 2 indicated single-site behavior.<sup>278</sup> The Ti analog of **180** possesses rather low activity.<sup>279</sup> These catalysts have also been supported on silica.<sup>1221</sup>

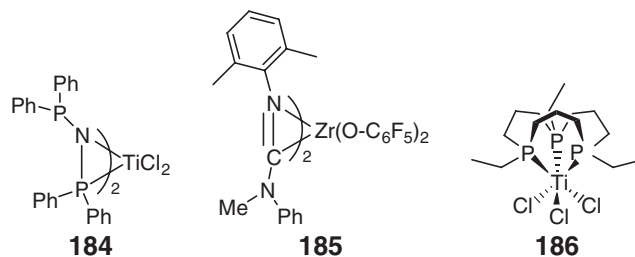


A few other complexes with N–N coordinating atoms have been tested as olefin polymerization catalysts. The aminopyridinato complex **181** is only able to oligomerize propylene and 1-butene ( $\bar{M}_n < 3500$ ) with low activity.<sup>1222</sup> The  $\beta$ -diketiminato Zr complex **182** exhibits moderate ethylene polymerization activity ( $\sim 50 \text{ g}_{\text{PE}} (\text{mmol M})^{-1} \text{ h}^{-1} \text{ bar}^{-1}$ ), but molecular masses were disappointingly low ( $\bar{M}_n$  up to 30 000).<sup>1117</sup> Finally, at  $100^\circ\text{C}$ , the MAO-activated Ti complex **183**, with a tridentate triazacyclononane ligand, yields PE with very high activity ( $10^4 \text{ g}_{\text{PE}} (\text{mmol M})^{-1} \text{ h}^{-1} \text{ bar}^{-1}$ ) but rather low molecular masses and broad polydispersity ( $\bar{M}_n = 39\,500$ ;  $\bar{M}_w/\bar{M}_n = 7.0$ ).<sup>1223</sup>



#### 4.09.5.3.7 Other ligands

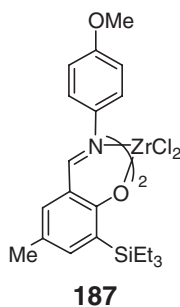
Some six-coordinate complexes have been reported that fall outside the previous sections. The catalyst **184**/MAO yields polypropylene with low activity ( $5 \text{ g}_{\text{PP}} (\text{mmol M})^{-1} \text{ h}^{-1} \text{ bar}^{-1}$ ) and moderate molecular mass ( $\bar{M}_n$  up to 105 000). The resulting PP is slightly isotactic (*mmmm* 35%) and exhibits elastomeric properties.<sup>1224</sup> The catalyst **185**/[HNMe<sub>3</sub>][B(C<sub>6</sub>F<sub>5</sub>)<sub>4</sub>]/AlBu<sub>3</sub> yields PE with very high activity ( $5 \times 10^4 \text{ g}_{\text{PE}} (\text{mmol M})^{-1} \text{ h}^{-1} \text{ bar}^{-1}$ ), rather high molecular masses ( $\bar{M}_n$  about  $10^6$ ), and low polydispersity. It also yields poly(1-hexene) with moderate activity ( $10 \text{ g}_{\text{PH}} (\text{mmol M})^{-1} \text{ h}^{-1}$ ) but with high molecular masses ( $\bar{M}_v \approx 500\,000$ ).<sup>1225</sup> The MAO-activated Ti complex **186**, with a crown-type macrocyclic phosphine ligand, yields PE with moderate activity ( $30 \text{ g}_{\text{PE}} (\text{mmol M})^{-1} \text{ h}^{-1} \text{ bar}^{-1}$ ).<sup>1226</sup>



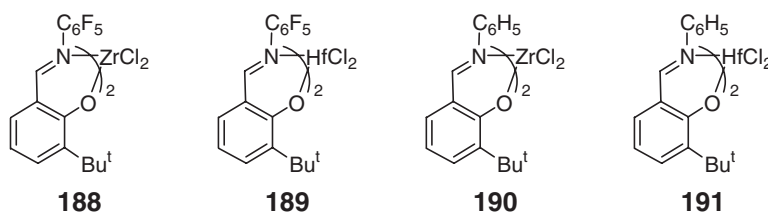
#### 4.09.5.3.8 Olefin co-polymerizations with post-metallocene catalysts

##### 4.09.5.3.8.(i) Ethylene/propylene co-polymers

Post-metallocene catalysts have been extensively used for the co-polymerization of olefins.<sup>605,1139,1175,1186,1187,1227–1231</sup> For example, the **187**/[Ph<sub>3</sub>C][B(C<sub>6</sub>F<sub>5</sub>)<sub>4</sub>]/Bu<sup>i</sup><sub>3</sub>Al catalyst is capable of co-polymerizing ethylene and propylene at 70 °C under 9 bar of total ethylene/propylene pressure with moderate activity, 70 g<sub>co-polymer</sub> (mmol M)<sup>−1</sup> h<sup>−1</sup> bar<sup>−1</sup>. The result is an amorphous ethylene/propylene co-polymer having a propylene content of 23.7 mol%. The GPC analysis indicated that the co-polymer is of extremely high molecular mass and it is produced by a single active species ( $\bar{M}_w = 10.2 \times 10^6$ ;  $\bar{M}_w/\bar{M}_n = 2.52$ ). The <sup>13</sup>C NMR spectroscopy revealed that **187** yields a substantially alternating co-polymer, indicating that the catalyst favors ethylene rather than propylene (EEE: 46.3 mol%; EEP: 28.2 mol%; PEP: 5.2 mol%; EPE: 18.5 mol%; PPE: 1.8 mol%; PPP: 0).<sup>1228</sup>



The MAO-activated complexes **188–191** have been also tested in ethylene/propylene co-polymerization.<sup>1139</sup> The perfluorinated complexes **188** and **189** resulted in somewhat higher activities and molecular masses than the corresponding non-fluorinated complexes **190** and **191** (**188**:  $\bar{M}_w = 64\,000$ ; **189**:  $\bar{M}_w = 193\,000$ ; vs. **190**:  $\bar{M}_w = 4000$ ; **191**:  $\bar{M}_w = 9000$ ). Moreover, the fluorinated complexes **188** and **189** incorporate propylene better than the non-fluorinated complexes **190** and **191** (**188**: P = 12.9 mol% **189**: P = 9.5 mol% vs. **190**: P = 6.0 mol%, **191**: P = 7.2 mol%). This finding has been correlated to the higher electrophilicity of the metal in the fluorinated complexes.<sup>1139</sup>



The MAO-activated **138** and **137**, effective in the living homopolymerization of ethylene and propylene, also promote their block co-polymerization.<sup>1175,1227</sup> This approach broadens remarkably the utility of living catalysts because it allows the preparation of block co-polymers with high glass or melting transition blocks from common commercial monomers such as ethylene and propylene. These materials could have applications as compatibilizers and elastomers.<sup>1232,1233</sup> Using complex **138**, propylene has been first homopolymerized to sPP for 2 h in toluene at 0 °C ( $\bar{M}_n = 38\,400$ ;  $\bar{M}_w/\bar{M}_n = 1.11$ ). Then, an ethylene overpressure was applied, and in 1 additional h an sPP-*block*-poly(E-*co*-P) diblock co-polymer was obtained ( $\bar{M}_n = 145\,100$ ,  $\bar{M}_w/\bar{M}_n = 1.12$ ). The microstructure of this diblock co-polymer is shown in Scheme 48. This co-polymer has a  $T_m$  of 131 °C while the ethylene–propylene block (E = 33 mol%) has a  $T_g$  of −45 °C.<sup>1175</sup> A detailed morphological and thermodynamic characterization of these co-polymers has been reported.<sup>1234</sup>

Using the MAO-activated complex **137**, an ethylene/propylene monodisperse co-polymer with a propylene content in the range 50–15 mol% has been synthesized.<sup>1227</sup> Details are shown in Figure 67.

Catalysts based on complexes **150** and **151** have also been tested for ethylene–propylene co-polymerizations but poor activity was reported. The NMR analysis of the co-polymers indicated random insertion of the monomers, with no stereoregularity in the propylene homosequences.<sup>1189</sup>

Catalysts based on the Hf pyridyl amine complexes **126–128** have been used for the preparation of ethylene/propylene co-polymers as well as of ethylene/propylene/1-octene terpolymers. These co-polymers are characterized by having at least 60 wt% propylene units,  $\bar{M}_w$  around 300 000, and  $\bar{M}_w/\bar{M}_n$  in the range 2.0–2.4. The NMR analysis of these co-polymers showed that the propylene sequences are remarkably isotactic ( $mm > 90\%$ ) and showed the presence of regioirregularly inserted propylene units ( $< 0.5\%$  mol). The most interesting property of catalysts based on **126–128** is their high thermal stability.<sup>1119</sup> Using modifications of isospecific bis(phenoxy–amine)-based catalysts, such as complex **164**, the controlled synthesis of iPP-*block*-poly(E-*co*-P) diblock co-polymers has been achieved. This is a remarkable result since iPP and PE are both polymeric materials of extreme industrial relevance.<sup>1206</sup>

#### 4.09.5.3.8.(ii) Ethylene/higher- $\alpha$ -olefin co-polymers

Using perfluorinated bis(phenoxy–imine) Ti catalysts, and techniques developed for ethylene–propylene co-polymerizations,<sup>1139,1227,1228</sup> the random and block co-polymerization of ethene with higher  $\alpha$ -olefins as 1-hexene, 1-octene, and 1-decene has been reported.<sup>1231</sup> The diamide-based catalyst **94**/MMAO was tested in ethylene–1-butene copolymerization at 70 °C. Activity and 1-butene incorporation were rather good (300–1000 g<sub>co-polymer</sub> (mmol M)<sup>−1</sup> h<sup>−1</sup> bar<sup>−1</sup>; 1-butene 12–40 mol%), but rather low molecular masses and fairly broad polydispersities were obtained ( $\bar{M}_n = 7000$ –33 000;  $\bar{M}_w/\bar{M}_n = 4.0$ –6.4). The <sup>13</sup>C NMR analysis of the random poly(ethylene-*co*-1-butene) showed regioselective insertion of 1-butene.<sup>1078</sup>

The tridentate NOP complexes of Figure 63 promote the random co-polymerization of ethylene–1-hexene with high activity. 1-Hexene incorporation was in the range 5–40 mol%.<sup>1187</sup> Catalysts based on complexes **150** and **151** have been tested for ethylene co-polymerization with 1-hexene. As for ethylene–propylene, the co-polymerization activity was poor.<sup>1189</sup> Ethylene–1-hexene co-polymers have been obtained with catalyst **179**/MAO.<sup>278</sup> This catalyst exhibits very high activity (about  $2 \times 10^5$  g<sub>co-polymer</sub> (mmol M)<sup>−1</sup> h<sup>−1</sup>) and good co-monomer incorporation (1-hexene 18–26 mol%). The resulting co-polymers have high molecular mass ( $\bar{M}_w$  up 1.5 million) with  $\bar{M}_w/\bar{M}_n = 2$ . The NMR analysis of the co-polymer indicated a tendency toward alternating ethylene and 1-hexene insertions, and no sign of head-to-head regiomistakes. The resulting co-polymers are amorphous, with  $T_g$  slightly below 0 °C.<sup>278</sup> Ethylene–1-octene co-polymers have also been prepared with bis(phosphinimide) complexes such as **101**.<sup>1089,1235</sup>



Scheme 48

E/P feed	5/95	10/90	30/70	50/50	80/20
Time (min)	20	30	10	5	5.3
Yield (g)	0.95	3.55	2.69	2.85	5.25
$\bar{M}_n$	19,600	52,300	42,500	42,700	83,600
$\bar{M}_w/\bar{M}_n$	1.07	1.11	1.08	1.08	1.13
P (mol%)	47.9	38.2	28.9	21.1	14.7

25 °C, 1 bar E/P, toluene, MAO/Ti = 100

Figure 67 Ethylene/propylene co-polymerization results using the MAO-activated complex **137**.

#### 4.09.5.3.8.(iii) Co-polymers of ethylene with internal alkenes

The co-polymerization of ethylene and 2-butene with the McConville catalyst **87** has been reported. NMR analysis of the co-polymer indicated that only the *trans*-isomer of 2-butene was incorporated.<sup>1236</sup> Ethylene and cyclopentene have been co-polymerized with the MAO-activated complex **138** working at very low ethylene pressure.<sup>605</sup> The almost regularly alternating poly(ethylene-*alt*-*cis*-1,2-cyclopentene) co-polymer exhibited a  $T_g$  of 10 °C. This co-polymer is a crystalline plastomer with high structural disorder.<sup>1237</sup> Furthermore, multi-block co-polymers were synthesized by changing the ethylene pressure during polymerization. This way, the various blocks are characterized by a different amount of cyclopentene units.<sup>605</sup>

The co-polymerization of ethylene and NB has been extensively investigated.<sup>1186,1187,1230</sup> Using the  $\beta$ -enamino-ketonato-based quasi-living catalysts of Figure 62, almost regularly alternating E/N co-polymers can be synthesized (N content in the range of 35–49%). Activities are substantially similar to those observed in the ethylene homopolymerization.<sup>1186</sup> The GPC analysis gave  $\bar{M}_n$  values in the range 150 000–570 000, while some character of quasi-living behavior was retained up to reaction times of 20 min ( $\bar{M}_w/\bar{M}_n = 1.17$ –1.35). The NMR analysis of the resulting co-polymers indicated the presence of similar amounts of iso- and syndiotactic NENEN sequences. The  $T_g$  of the co-polymers was in the range 121–135 °C. The quasi-living behavior of these catalysts was also used for the preparation of PE-*block*-poly(E-*co*-N) diblock co-polymers. After 5 min of ethylene homopolymerization, NB was added to the reaction feed for an additional 5 min. GPC profiles indicated the synthesis of a diblock co-polymer with  $\bar{M}_w/\bar{M}_n = 1.38$ . The diblock co-polymer possesses an NB content of 11 mol% and a  $T_m$  of 137 °C.<sup>1186</sup> Random ethylene/norbornene co-polymerization with the tridentate NOP-based complexes of Figure 63 gave NB incorporations in the range of 4–35 mol%.<sup>1187</sup>

The bis(pyrrolide-imine) Ti complexes of Figure 64 co-polymerize ethylene and NB with high activities.<sup>1230</sup> Changing the N/E ratio from 0.3/1 to 3/1 resulted in higher N inclusion (26 vs. 45 mol%) and lower  $\bar{M}_n$  (652 000 vs. 285 000) and  $\bar{M}_w/\bar{M}_n$  (1.28 vs. 1.11). NMR analysis revealed an almost regularly alternating structure even at 45 mol% N incorporation. Isolated N units ( $-\text{E}-\text{N}-\text{E}_{n \geq 2}-$ ) (3.7 mol%) and N–N sequences (0.9 mol%) were however detected. Almost equal amounts of alternating iso- and syndiotactic sequences were also found. NMR analysis of low molecular mass co-polymers showed the presence of  $\text{CH}_3\text{-N}$  initiation sequences, while no peaks assignable to the  $\text{CH}_3\text{-E-}$  initiation sequences were observed. Regarding the termination steps, N–E– sequences were found, while no peaks assignable to E–E– or E–N– sequences were observed. The quasi-living nature of the pyrrolide-imine catalysts was employed to synthesize PE-*block*-poly(E-*co*-N) as well as poly(E-*co*-N)<sub>1</sub>-*block*-poly(E-*co*-N)<sub>2</sub> diblock co-polymers. In the latter, each co-polymer block contains a different amount of N units. These co-polymers had  $\bar{M}_n$  in the range 424 000–783 000, with polydispersities in the range of 1.23–1.66. The resulting diblock co-polymer had two glass transitions. For example, a co-polymer with a content of N = 19 and 30 mol% in the two blocks showed a  $T_g$  of 17 °C for the first block and of 123 °C for the second block.

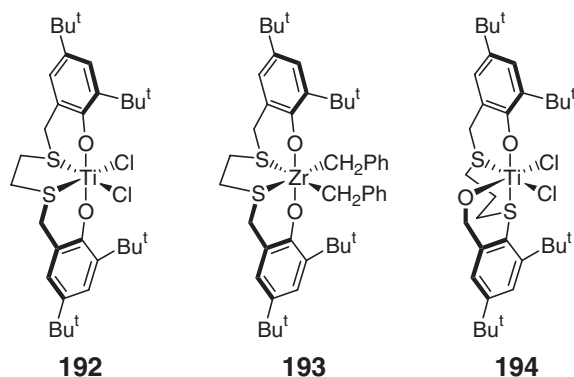
Finally, ethylene/norbornene co-polymerization with the dicarbollide Ti and Zr complexes has been also reported.<sup>1238</sup>

#### 4.09.5.3.8.(iv) Propylene/higher- $\alpha$ -olefin co-polymers

Complex **87** was used for propylene–1-hexene co-polymerization. It has been suggested that blocks of iPP and poly-1-hexene were joined to form a poly(iPP-*co*-iPH) block co-polymers.<sup>1070</sup> Propylene and 1,5-hexadiene have been co-polymerized with the **138**/MAO catalyst.<sup>1229</sup> The NMR spectroscopy indicated that the propylene homosequences are remarkably syndiotactic. As in the case of hexadiene homopolymerization with the same catalyst (see Figure 55), the hexadiene is incorporated as methylene-1,3-cyclopentane or 3-vinyl-tetramethylene units. Lower propylene concentration favored the formation of methylene-1,3-cyclopentane units, while higher propylene concentration favored 3-vinyl-tetramethylene units. Furthermore, an sPP-*block*-poly(P-*co*-HD) diblock co-polymer was synthesized by first polymerizing propylene to sPP for 2 h and then adding 1,5-hexadiene for 6 additional h.<sup>1229</sup>

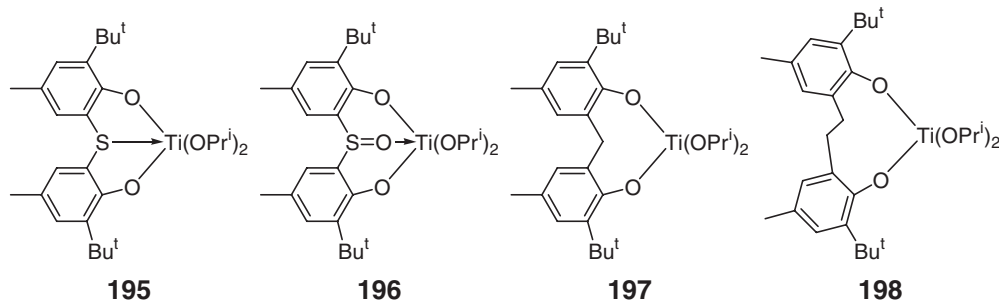
#### 4.09.5.3.9 Polystyrene and olefin–styrene co-polymerization with post-metallocene catalysts

Isotactic PS was discovered in 1955, and until a few years ago it was synthesized almost exclusively with heterogeneous Ziegler–Natta catalysts.<sup>1239</sup> Recently, it has been shown that homogeneous post-metallocene catalysts based on the MAO-activated bis(thiophenolate) complexes **192** and **193** can be used for the isospecific polymerization of styrene.<sup>1240–1243</sup> The Ti-based catalyst exhibited very high activity (more than  $1 \times 10^5 \text{ g}_{\text{PS}}(\text{mmol M})^{-1} \text{ h}^{-1}$ ) and the molecular mass of the resulting isotactic PS is remarkably high, while the molecular mass distribution indicates the single-site behavior ( $\bar{M}_n = 2\,654\,000$ ;  $\bar{M}_w/\bar{M}_n = 2.0$ ). The Zr and Hf analogs are notably less active and yield rather low molecular masses. Introduction of a longer spacer between the two S atoms such as in **194** had detrimental effects.



The catalyst system **192**/MAO has been used for the synthesis of multi-block propylene–styrene co-polymers. The resulting co-polymers have a propylene content in the range 1–33 mol%, and the molecular masses are in the range  $\bar{M}_w = 2100–60\,000$ . Lower  $\bar{M}_w$  values were observed for higher propylene content. Interestingly, NMR analysis indicated that the regiochemistry of insertion of the two monomers is opposite. In particular, the iPP blocks are formed by primary insertion of propylene, whereas the iPS blocks are formed by secondary insertion of styrene.<sup>1244</sup>

Effective ethylene–styrene co-polymerization with the post-metallocene catalysts has been achieved with the pentacoordinated complexes **195** and **196**.<sup>159,1245</sup> Pseudo-random ethylene–styrene co-polymers (i.e., co-polymers with no regioregularly arranged styrene–styrene units)<sup>642</sup> were synthesized. The synthesis of an alternating crystalline co-polymer with isotactic styrene units and a  $T_m$  of 116 °C was also claimed. In these first studies, the importance of the S atom was noted, since the CH<sub>2</sub>-bridged complex **197** showed no co-polymerization activity. However, further studies demonstrated that the S atom is not fundamental, since complex **198** also promotes ethylene–styrene co-polymerization.<sup>627,1246</sup> Moreover, it was shown that complexes **195** and **196** incorporate a rather minor amount of styrene units (about 6–10 mol%) in the co-polymer relative to complex **198** (about 35 mol%), but they are roughly 1–2 order of magnitude more active than **198**.



## References

1. Wilkinson, J.; Birmingham, J. M. *J. Am. Chem. Soc.* **1954**, *76*, 4281.
2. Natta, G.; Pino, P.; Mazzanti, G.; Giannini, U. *J. Am. Chem. Soc.* **1957**, *79*, 2975.
3. Breslow, D. S.; Newburg, N. R. *J. Am. Chem. Soc.* **1957**, *79*, 5072.
4. Schnutenhaus, H.; Brintzinger, H.-H. *Angew. Chem.* **1979**, *91*, 837.
5. Smith, J. A.; Brintzinger, H. H. *J. Organomet. Chem.* **1981**, *218*, 159.
6. Wild, F. R. W. P.; Zsolnai, L.; Huttner, G.; Brintzinger, H. H. *J. Organomet. Chem.* **1982**, *232*, 233.
7. Schwemlein, H.; Brintzinger, H. H. *J. Organomet. Chem.* **1983**, *254*, 69.
8. Schwemlein, H.; Zsolnai, L.; Huttner, G.; Brintzinger, H. H. *J. Organomet. Chem.* **1983**, *256*, 285.
9. Wild, F. R. W. P.; Wasiucionek, M.; Huttner, G.; Brintzinger, H. H. *J. Organomet. Chem.* **1985**, *288*, 63.
10. Wochner, F.; Zsolnai, L.; Huttner, G.; Brintzinger, H. H. *J. Organomet. Chem.* **1985**, *288*, 69.
11. Wochner, F.; Brintzinger, H.-H. *J. Organomet. Chem.* **1986**, *309*, 65.
12. Röhl, W.; Zsolnai, L.; Huttner, G.; Brintzinger, H.-H. *J. Organomet. Chem.* **1987**, *322*, 65.
13. Schäfer, A.; Karl, E.; Zsolnai, L.; Huttner, G.; Brintzinger, H.-H. *J. Organomet. Chem.* **1987**, *328*, 87.
14. Sinn, H. J.; Kaminsky, W. *Adv. Organomet. Chem.* **1980**, *18*, 99.
15. Cecchin, G.; Morini, G.; Piemontesi, F. Ziegler–Natta Catalysts. In *Kirk–Othmer Encyclopedia of Chemical Technology*; Wiley: New York, 2003.



16. Chadwick, J. C. Ziegler–Natta Catalysis. In *Encyclopedia of Polymer Science and Technology*; Wiley: New York, 2003.
17. Keii, T. *Heterogeneous Kinetics: Theory of Ziegler–Natta–Kaminsky Polymerization*; Springer: Berlin, 2004; Vol. 77.
18. Benedikt, G. M.; Goodall, B. L., Eds. *Metallocene-catalyzed Polymers: Materials, Properties, Processing & Markets*, Plastics Design Library: New York, 1998.
19. Scheirs, J.; Kaminsky, W., Eds. *Metallocene-based Polyolefins. Preparation: Properties and Technology*; Wiley: New York, 2000.
20. Gladysz, J. A., Ed. *Chem. Rev.* **2000**, *100*(4), **2000**.
21. Dyachkovskii, F. S.; Shilova, F. S.; Shilov, A. K. *J. Polymer Sci., Part C* **1967**, *16*, 2333.
22. Eisch, J. J.; Piotrowski, A. M.; Brownstein, S. K.; Gabe, E. J.; Lee, F. L. *J. Am. Chem. Soc.* **1985**, *107*, 7219.
23. Bochmann, M.; Wilson, L. M. *J. Chem. Soc., Chem. Commun.* **1986**, 1610.
24. Jordan, R. F.; Bajgur, C. S.; Willet, R.; Scott, B. *J. Am. Chem. Soc.* **1986**, *108*, 7410.
25. Jordan, R. F.; LaPointe, R. E.; Bajgur, C. S.; Echols, S. F.; Willett, R. *J. Am. Chem. Soc.* **1987**, *109*, 4111.
26. Jordan, R. F. *J. Chem. Ed.* **1988**, *65*, 285.
27. Bochmann, M.; Wilson, L. M.; Hursthouse, M. B.; Motevalli, M. *Organometallics* **1988**, *7*, 1148.
28. Bochmann, M.; Jaggard, A. J.; Nichols, J. C. *Angew. Chem., Int. Ed. Engl.* **1990**, *29*, 780.
29. Turner, H. W.; Hlatky, G. G.; Eckman, R. R. (Exxon Chemical). US Patent 5384299, 1993.
30. Turner, H. W.; Hlatky, G. G.; Canich, J. A. M. (Exxon Chemical). World Pat. Appl. WO 93/19103, 1993.
31. Bochmann, M.; Lancaster, S. J. *Angew. Chem., Int. Ed. Engl.* **1994**, *33*, 1634.
32. Guo, Z.; Swenson, D.; Jordan, R. F. *Organometallics* **1994**, *13*, 1424.
33. Bochmann, M.; Lancaster, S. J. *J. Organomet. Chem.* **1995**, *497*, 55.
34. Crowther, D. J.; Baenziger, N. C.; Jordan, R. F. *J. Am. Chem. Soc.* **1991**, *113*, 1455.
35. Bochmann, M.; Lancaster, S. J.; Robinson, O. B. *J. Chem. Soc., Chem. Commun.* **1995**, 2081.
36. Ruwwe, J.; Erker, G.; Fröhlich, R. *Angew. Chem., Int. Ed. Engl.* **1996**, *35*, 80.
37. Sun, Y.; Spence, R. E. v. H.; Piers, W. E.; Parvez, M.; Yap, G. P. A. *J. Am. Chem. Soc.* **1997**, *119*, 5132.
38. Song, X.; Bochmann, M. *J. Organomet. Chem.* **1997**, *545–546*, 597.
39. Lancaster, S. J.; Thornton-Pett, M.; Dawson, D. M.; Bochmann, M. *Organometallics* **1998**, *17*, 3829.
40. Chen, E. Y.-X.; Marks, T. J. *Chem. Rev.* **2000**, *100*, 1391.
41. Bochmann, M. *J. Organomet. Chem.* **2004**, *689*, 3982.
42. Resconi, L.; Bossi, S.; Abis, L. *Macromolecules* **1990**, *23*, 4489.
43. Pasynkiewicz, S. *Polyhedron* **1990**, *9*, 429.
44. Giannetti, E.; Nicoletti, G. M.; Mazzocchi, R. *J. Polym. Sci., Polym. Chem. Ed.* **1985**, *23*, 2117.
45. Sinn, H.; Kaminsky, W.; Hoker, H., Eds. *Alumoxanes*, Huthig & Wepf: Heidelberg, 1995.
46. Srinivasa Reddy, S.; Sivaram, S. *Prog. Polym. Sci.* **1995**, *20*, 309.
47. Sinn, H. *Macromol. Symp.* **1995**, *97*, 27.
48. Mason, M. R.; Smith, J. M.; Bott, S. G.; Barron, A. R. *J. Am. Chem. Soc.* **1993**, *115*, 4971.
49. Imhoff, D. W.; Simeral, L. S.; Sangokoya, S. A.; Peel, J. H. *Organometallics* **1998**, *17*, 1941.
50. Sugano, T.; Matsubara, K.; Fujita, T.; Takahashi, T. *J. Mol. Catal.* **1993**, *82*, 93.
51. Siedle, A. R.; Lamanna, W. M.; Newmark, R. A.; Stevens, J.; Richardson, D. E.; Ryan, M. F. *Makromol. Chem., Macromol. Symp.* **1993**, *66*, 215.
52. Siedle, A. R.; Newmark, R. A. *J. Organomet. Chem.* **1995**, *497*, 119.
53. Siedle, A. R.; Lamanna, W. M.; Newmark, R. A.; Schroepfer, J. N. *J. Mol. Catal. A: Chemical* **1998**, *128*, 257.
54. Zurek, E.; Woo, T. K.; Firman, T. K.; Ziegler, T. *Inorg. Chem.* **2001**, *40*, 361.
55. Zurek, E.; Ziegler, T. *Organometallics* **2002**, *21*, 83.
56. Zurek, E.; Ziegler, T. *Prog. Polym. Sci.* **2004**, *29*, 107.
57. Möhring, P. C.; Coville, N. J. *J. Organomet. Chem.* **1994**, *479*, 1.
58. Galimberti, M.; Destro, M.; Fusco, O.; Piemontesi, F.; Camurati, I. *Macromolecules* **1999**, *32*, 258.
59. Galimberti, M.; Piemontesi, F.; Fusco, O. Metallocenes as Catalysts for the Copolymerization of Ethene with Propene and Dienes. In *Metallocene-based Polyolefins: Preparation, Properties and Technology*; Scheirs, J., Kaminsky, W., Eds.; Wiley: Chichester, 2000; Vol. 1, p. 309.
60. Janiak, C.; Lange, K. C. H.; Scharmann, T. G. *Appl. Organomet. Chem.* **2000**, *14*, 316.
61. Resconi, L.; Giannini, U.; Dall’Occo, T. MAO-free Metallocene Catalysts for Ethylene (Co)Polymerization. In *Metallocene-based Polyolefins: Preparation, Properties and Technology*; Scheirs, J., Kaminsky, W., Eds.; Wiley: Chichester, 2000; Vol. 1, p. 69.
62. Kallio, K.; Kauhanen, J. Activation of Siloxy-substituted Compounds and Homopolymerization of Ethylene by Different Soluble Alumoxane Cocatalysts. In *Organometallic Catalysts and Olefin Polymerization: Catalysts for a New Millennium*; Blom, R., Follestad, A., Rytter, E., Tilsted, M., Ystenes, M., Eds.; Springer: Berlin, 2001; p 14.
63. van Baar, J. F.; Horton, A. D.; de Kloe, K. P.; Kragt, E.; Mkooyan, S. G.; Nifant’ev, I. E.; Schut, P. A.; Taidakov, I. V. *Organometallics* **2003**, *22*, 2711.
64. Tsutsui, T.; Yoshitsugu, K.; Ueda, T. (Mitsui PC). Eur. Pat. Appl. EP 452920, 1991.
65. Resconi, L.; Galimberti, M.; Piemontesi, F.; Guglielmi, F.; Albizzati, E. (Montell Technology Company). U.S. Patent 5910464, 1999.
66. Dall’Occo, T.; Galimberti, M.; Resconi, L.; Albizzati, E.; Pennini, G. (Montell Technology Company). U.S. Patent 5849653, 1998.
67. Tritto, I.; Sacchi, M. C.; Locatelli, P.; Li, S. X. *Macromol. Chem. Phys.* **1996**, *197*, 1537.
68. Tritto, I.; Mealares, C.; Sacchi, M. C.; Locatelli, P. *Macromol. Chem. Phys.* **1997**, *198*, 3963.
69. Chien, J. C. W.; Wang, B. P. *J. Polym. Sci., A: Polym. Chem.* **1988**, *26*, 3089.
70. Srinivasa Reddy, S.; Shashidhar, G.; Sivaram, S. *Macromolecules* **1993**, *26*, 1180.
71. Tritto, I.; Donetti, R.; Sacchi, M. C.; Locatelli, P.; Zannoni, G. *Macromolecules* **1997**, *30*, 1247.
72. Tomotsu, N.; Ishihara, N.; Newman, T. H.; Malanga, M. T. *J. Mol. Catal.* **1998**, *128*, 167.
73. Smith, G. M.; Palmaka, S. W.; Roger, J. S.; Malpass, D. B.; Monfiston, D. J. (Akzo-Nobel). World Pat. Appl. WO 97/23288, 1997.
74. Fujita, M.; Seki, Y.; Miyatake, T. *J. Polym. Sci. A: Polym. Chem.* **2004**, *42*, 1107.
75. Hasan, T.; Ioku, A.; Nishii, K.; Shiono, T.; Ikeda, T. *Macromolecules* **2001**, *34*, 3142.
76. Obrey, S. J.; Bott, S. J.; Barron, A. R. *Organometallics* **2001**, *20*, 5162.
77. Busico, V.; Cipullo, R.; Cutillo, F.; Friedrichs, N.; Ronca, S.; Wang, B. *J. Am. Chem. Soc.* **2003**, *125*, 12402.
78. Yang, X.; Stern, C.; Marks, T. J. *J. Am. Chem. Soc.* **1991**, *113*, 3623.

79. Yang, X.; Stern, C.; Marks, T. J. *J. Am. Chem. Soc.* **1994**, *116*, 10015.
80. Ewen, J. A.; Elder, M. J. (Fina Technology). Eur. Pat. Appl. EP 427697, 1991.
81. Ewen, J. A.; Elder, M. J. (Fina Technology). U.S. Patent US 5561092, 1996.
82. Piers, W. E.; Chivers, T. *Chem. Soc. Rev.* **1997**, *26*, 345.
83. Li, L.; Stern, C. L.; Marks, T. J. *Organometallics* **2000**, *19*, 3332.
84. Li, L.; Marks, T. J. *Organometallics* **1998**, *17*, 3996.
85. Chen, E. Y.-X.; Stern, C. L.; Yang, S.; Marks, T. J. *J. Am. Chem. Soc.* **1996**, *118*, 12451.
86. Lancaster, S. J.; Walker, D. A.; Thornton-Pett, M.; Bochmann, M. *Chem. Commun.* **1999**, 1533.
- 86a. Zhou, J.; Lancaster, S. J.; Walker, D. A.; Beck, S.; Thornton-Pett, M.; Bochmann, M. *J. Am. Chem. Soc.* **2001**, *123*, 223.
87. Metz, M. V.; Sun, Y.; Stern, C. L.; Marks, T. J. *Organometallics* **2002**, *21*, 3691.
88. Metz, M. V.; Schwartz, D. J.; Stern, C. L.; Nickias, P. N.; Marks, T. J. *Angew. Chem., Int. Ed.* **2000**, *39*, 1312.
89. Jia, L.; Yang, X.; Ishihara, A.; Marks, T. J. *Organometallics* **1995**, *14*, 3135.
90. Jia, L.; Yang, X.; Stern, C. L.; Marks, T. J. *Organometallics* **1997**, *16*, 842.
91. LaPointe, R. E.; Roof, G. R.; Abboud, K. A.; Klosin, J. J. *J. Am. Chem. Soc.* **2000**, *122*, 9560.
92. Focante, F.; Camurati, I.; Nanni, D.; Leardini, R.; Resconi, L. *Organometallics* **2004**, *23*, 5135.
93. Chien, J. C. W.; Tsai, W.-M.; Rausch, M. D. *J. Am. Chem. Soc.* **1991**, *113*, 8570.
94. Ewen, J. A.; Elder, M. J. (Fina Technology). Eur. Pat. Appl. EP 0426637, 1991.
95. Turner, H. W. (Exxon Chemical Co.). Eur. Pat. Appl. EP 0277004 A1, 1988.
96. Hlatky, G. G.; Upton, D. J.; Turner, H. W. (Exxon Chemical). World Pat. Appl. WO 91/09882, 1991.
97. Yang, X.; Stern, C. L.; Marks, T. J. *Organometallics* **1991**, *10*, 840.
98. Elder, M. J.; Ewen, J. A. (Fina Technology). Eur. Pat. Appl. EP 0573403, 1993.
99. Song, F.; Cannon, R. D.; Lancaster, S. J.; Bochmann, M. *J. Mol. Catal. A: Chem.* **2004**, *218*, 21.
100. Al-Humydi, A.; Garrison, J. C.; Youngs, W. J.; Collins, S. *Organometallics* **2005**, *24*, 193.
101. Song, F.; Lancaster, S. J.; Cannon, R. D.; Schormann, M.; Humphrey, M. B.; Zuccaccia, C.; Macchioni, A.; Bochmann, M. *Organometallics* **2005**, *24*, 1315.
102. Rodriguez-Delgado, A.; Hannant, M. D.; Lancaster, S. J.; Bochmann, M. *Macromol. Chem. Phys.* **2004**, *205*, 334.
103. Li, H.; Li, L.; Marks, T. J. *Angew. Chem., Int. Ed.* **2004**, *43*, 4937.
104. Chen, M.-C.; Roberts, J. A. S.; Marks, T. J. *J. Am. Chem. Soc.* **2004**, *126*, 4605.
105. Li, H.; Li, L.; Marks, T. J.; Liable-Sands, L. M.; Rheingold, A. L. *J. Am. Chem. Soc.* **2003**, *125*, 10788.
106. Chen, M.-C.; Marks, T. J. *J. Am. Chem. Soc.* **2001**, *123*, 11803.
107. Chakraborty, D.; Chen, E. Y.-X. *Organometallics* **2002**, *21*, 1438.
108. Chen, E. Y.-X.; Kruper, W. J.; Roof, G.; Wilson, D. R. *J. Am. Chem. Soc.* **2001**, *123*, 745.
109. Chen, E. Y.-X.; Abboud, K. A. *Organometallics* **2000**, *19*, 5541.
110. Lancaster, S. J.; Bochmann, M. *Organometallics* **2001**, *20*, 2093.
111. Dahlmann, M.; Erker, G.; Fröhlich, R.; Meyer, O. *Organometallics* **2000**, *19*, 2956.
112. Erker, G. *Acc. Chem. Res.* **2001**, *34*, 309.
113. Karl, J.; Erker, G. *J. Mol. Catal. A: Chem.* **1998**, *128*, 85.
114. Tsai, W.-M.; Rausch, M. D.; Chien, J. C. W. *Appl. Organomet. Chem.* **1993**, *7*, 71.
115. Matsumoto, J.; Okamoto, T.; Watanabe, M.; Ishihara, N. (Idemitsu Kosan Co.). Eur. Pat. Appl. EP 513380, 1992.
116. Macchioni, A. *Chem. Rev.* **2005**, *105*, 2039.
117. Nifant'ev, I. E.; Ustynyuk, L. Y.; Laikov, D. N. *Organometallics* **2001**, *20*, 5375.
118. Vanka, K.; Chan, M. S. W.; Pye, C. C.; Ziegler, T. *Organometallics* **2000**, *19*, 1841.
119. Vanka, K.; Ziegler, T. *Organometallics* **2001**, *20*, 905.
120. Xu, Z.; Vanka, K.; Firman, T.; Michalak, A.; Zurek, E.; Zhu, C.; Ziegler, T. *Organometallics* **2002**, *21*, 2444.
121. Beck, S.; Prosenc, M. H.; Brintzinger, H.-H. *J. Mol. Catal. A: Chem.* **1998**, *128*, 41.
122. Beck, S.; Lieber, S.; Schaper, F.; Geyer, A.; Brintzinger, H.-H. *J. Am. Chem. Soc.* **2001**, *123*, 1483.
123. Zuccaccia, C.; Stahl, N. G.; Macchioni, A.; Chen, M.-C.; Roberts, J. A.; Marks, T. J. *J. Am. Chem. Soc.* **2004**, *126*, 1448.
124. Stahl, N. G.; Zuccaccia, C.; Jensen, T. R.; Marks, T. J. *J. Am. Chem. Soc.* **2003**, *125*, 5256.
125. Babushkin, D. E.; Brintzinger, H.-H. *J. Am. Chem. Soc.* **2002**, *124*, 12869.
126. Brintzinger, H.-H.; Fischer, D.; Mülhaupt, R.; Rieger, B.; Waymouth, R. M. *Angew. Chem., Int. Ed.* **1995**, *34*, 1143.
127. Bochmann, M. *J. Chem. Soc., Dalton Trans.* **1996**, 255.
128. Cossee, P. *J. Catal.* **1964**, *3*, 80.
129. Cossee, P. The mechanism of Ziegler-Natta Polymerization. II. Quantum-Chemical and Crystal-Chemical aspects. In *The Stereochemistry of Macromolecules*; Ketley, A. D., Ed.; Dekker: New York, 1967; Vol. 1, pp 145–176.
130. Green, M. L. H. *Pure Appl. Chem.* **1972**, *30*, 373.
131. Dawoodi, Z.; Green, M. L. H.; Mrtwa, V. S. B.; Prout, K. J. *Chem. Soc., Chem. Commun.* **1982**, 1410.
132. Brookhart, M.; Green, M. L. H. *J. Organomet. Chem.* **1983**, *250*, 395.
133. Laverty, D. T.; Rooney, J. J. *J. Chem. Soc., Faraday Trans. 1* **1983**, *79*, 869.
134. Grubbs, R. H.; Coates, G. W. *Acc. Chem. Res.* **1996**, *29*, 85.
135. Chan, M. S. W.; Ziegler, T. *Organometallics* **2000**, *19*, 5182.
136. Xu, Z.; Vanka, K.; Ziegler, T. *Organometallics* **2004**, *23*, 104.
137. Zambelli, A.; Giongo, M. G.; Natta, G. *Makromol. Chem.* **1968**, *112*, 183.
138. Song, F.; Cannon, R. D.; Bochmann, M. *Chem. Commun.* **2004**, 542.
139. Guerra, G.; Cavallo, L.; Moscardi, G.; Vacatello, M.; Corradini, P. *Macromolecules* **1996**, *29*, 4834.
140. Yoshida, T.; Koga, N.; Morokuma, K. *Organometallics* **1995**, *14*, 746.
141. Lohrenz, J. C. W.; Woo, T. K.; Ziegler, T. *J. Am. Chem. Soc.* **1995**, *117*, 12793.
142. Kawamura-Kuribayashi, H.; Koga, N.; Morokuma, K. *J. Am. Chem. Soc.* **1992**, *114*, 8687.
143. Kawamura-Kuribayashi, H.; Koga, N.; Morokuma, K. *J. Am. Chem. Soc.* **1992**, *114*, 2359.
144. Woo, T. K.; Fan, L.; Ziegler, T. A Combined Density Functional and Molecular Mechanics Study on Olefin Polymerization by Metallocene Catalysts. In *Ziegler Catalysts*; Fink, G., Mülhaupt, R., Brintzinger, H.-H., Eds.; Springer: Berlin, 1995, p 291.



145. Woo, T. K.; Margl, P. M.; Blöchl, P. E.; Ziegler, T. *J. Am. Chem. Soc.* **1996**, *118*, 13021.
146. Woo, T. K.; Margl, P.; Ziegler, T.; Blöchl, P. E. *Organometallics* **1997**, *16*, 3454.
147. Lanza, G.; Fragalà, I. L.; Marks, T. J. *J. Am. Chem. Soc.* **1998**, *120*, 8257.
148. Lanza, G.; Fragalà, I. L.; Marks, T. J. *Organometallics* **2001**, *20*, 4006.
149. Lanza, G.; Fragalà, I. L.; Marks, T. J. *Organometallics* **2002**, *21*, 5594.
150. Lanza, G.; Fragalà, I. L.; Marks, T. J. *J. Am. Chem. Soc.* **2000**, *122*, 12764.
151. Vanka, K.; Xu, Z.; Ziegler, T. *Organometallics* **2004**, *23*, 2900.
152. Vanka, K.; Xu, Z.; Ziegler, T. *Can. J. Chem.* **2003**, *81*, 1413.
153. Sillars, D. R.; Landis, C. R. *J. Am. Chem. Soc.* **2003**, *125*, 9894.
154. Landis, C. R.; Rosaaen, K. A.; Sillars, D. R. *J. Am. Chem. Soc.* **2003**, *125*, 1710.
155. Landis, C. R.; Rosaaen, K. A.; Uddin, J. *J. Am. Chem. Soc.* **2002**, *124*, 12062.
156. Liu, Z.; Somsook, E.; White, C. B.; Rosaaen, K. A.; Landis, C. R. *J. Am. Chem. Soc.* **2001**, *123*, 11193.
157. Schaper, F.; Geyer, A.; Brintzinger, H.-H. *Organometallics* **2002**, *21*, 473.
158. Fink, G.; Fenzl, W.; Mynott, R. *Z. Naturforsch. Teil B* **1985**, *40b*, 158.
159. Miyatake, T.; Mizunuma, K.; Kakugo, M. *Makromol. Chem., Macromol. Symp.* **1993**, *66*, 203.
160. Hustad, P. D.; Tian, J.; Coates, G. W. *J. Am. Chem. Soc.* **2002**, *124*, 3614.
161. Lamberti, M.; Pappalardo, D.; Zambelli, A.; Pellicchia, C. *Macromolecules* **2002**, *35*, 658.
162. Resconi, L.; Cavallo, L.; Fait, A.; Piemontesi, F. *Chem. Rev.* **2000**, *100*, 1253.
163. Guerra, G.; Cavallo, L.; Moscardi, G.; Vacatello, M.; Corradini, P. *J. Am. Chem. Soc.* **1994**, *116*, 2988.
164. Guerra, G.; Longo, P.; Cavallo, L.; Corradini, P.; Resconi, L. *J. Am. Chem. Soc.* **1997**, *119*, 4394.
165. Talarico, G.; Busico, V.; Cavallo, L. *J. Am. Chem. Soc.* **2003**, *125*, 7172.
166. IUPAC Commission of Macromolecular Nomenclature *Pure Appl. Chem.* **1979**, *51*, 1101.
167. Corradini, P.; Paiaro, G.; Panunzi, A. *J. Polym. Sci., Polym. Symp.* **1967**, *16*, 2906.
168. Cahn, R. S.; Ingold, C.; Prelog, V. *Angew. Chem., Int. Ed. Engl.* **1966**, *5*, 385.
169. Schögl, K. *Top. Stereochem.* **1966**, *1*, 39.
170. IUPAC Nomenclature of Inorganic Chemistry *Pure Appl. Chem.* **1971**, *18*, 77.
171. Stanley, K.; Baird, M. C. *J. Am. Chem. Soc.* **1975**, *97*, 6598.
172. Corradini, P.; Guerra, G.; Cavallo, L. *Acc. Chem. Res.* **2004**, *37*, 231.
173. Farina, M. *Top. Stereochem.* **1987**, *17*, 1.
174. Corradini, P.; Guerra, G.; Cavallo, L. *Top. Stereochem.* **2003**, *24*, 1.
175. Corradini, P.; Cavallo, L.; Guerra, G. Molecular Modeling Studies on Stereospecificity and Regiospecificity of Propene Polymerization by Metallocenes. In *Metallocene-based Polyolefins: Preparation, Properties and Technology*; Scheirs, J., Kaminsky, W., Eds.; Wiley: Chichester, 2000; Vol. 2, p 3.
176. Rappé, A. K.; Skiff, W. M.; Casewit, C. J. *Chem. Rev.* **2000**, *100*, 1435.
177. Coates, G. W. *Chem. Rev.* **2000**, *100*, 1223.
178. Angermund, K.; Fink, G.; Jensen, V. R.; Kleinschmidt, R. *Chem. Rev.* **2000**, *100*, 1457.
179. Busico, V.; Cipullo, R. *Prog. Polym. Sci.* **2001**, *26*, 443.
180. Resconi, L.; Abis, L.; Francoscono, G. *Macromolecules* **1992**, *25*, 6814.
181. Ewen, J. A.; Elder, M. J.; Jones, R. L.; Curtis, S.; Cheng, H. N. Syndiospecific Propylene Polymerizations with  $\text{iPr}[\text{CpFlu}]\text{ZrCl}_2$ . In *Catalytic Olefin Polymerization, Studies in Surface Science and Catalysis*; Keii, T., Soga, K., Eds.; Elsevier: New York, 1990; p 439.
182. Busico, V.; Cipullo, R.; Cutillo, F.; Vacatello, M.; Van Axel Castelli, V. *Macromolecules* **2003**, *36*, 4258.
183. Corradini, P.; Barone, V.; Fusco, R.; Guerra, G. *Eur. Polym. J.* **1979**, *15*, 1133.
184. Corradini, P.; Guerra, G.; Fusco, R.; Barone, V. *Eur. Polym. J.* **1980**, *16*, 835.
185. Corradini, P.; Barone, V.; Fusco, R.; Guerra, G. *J. Catal.* **1982**, *77*, 32.
186. Corradini, P.; Barone, V.; Guerra, G. *Macromolecules* **1982**, *15*, 1242.
187. Corradini, P.; Barone, V.; Fusco, R.; Guerra, G. *Gazz. Chim. Ital.* **1983**, *113*, 601.
188. Corradini, P.; Guerra, G.; Barone, V. *Eur. Polym. J.* **1984**, *20*, 1177.
189. Corradini, P.; Guerra, G.; Vacatello, M.; Villani, V. *Gazz. Chim. Ital.* **1988**, *118*, 173.
190. Cavallo, L.; Corradini, P.; Guerra, G.; Vacatello, M. *Polymer* **1991**, *32*, 1329.
191. Cavallo, L.; Guerra, G.; Vacatello, M.; Corradini, P. *Macromolecules* **1991**, *24*, 1784.
192. Cavallo, L.; Guerra, G.; Corradini, P. *Gazz. Chim. Ital.* **1996**, *126*, 463.
193. Milano, G.; Cavallo, L.; Guerra, G. *J. Am. Chem. Soc.* **2002**, *124*, 13368.
194. Corradini, P.; Guerra, G.; Pucciariello, R. *Macromolecules* **1985**, *18*, 2030.
195. Zambelli, A.; Sacchi, M. C.; Locatelli, P.; Zannoni, G. *Macromolecules* **1982**, *15*, 211.
196. Longo, P.; Grassi, A.; Pellicchia, C.; Zambelli, A. *Macromolecules* **1987**, *20*, 1015.
197. Pino, P.; Galimberti, M.; Prada, P.; Consiglio, G. *Makromol. Chem.* **1990**, *191*, 1677.
198. Pino, P.; Cioni, P.; Wei, J. *J. Am. Chem. Soc.* **1987**, *109*, 6189.
199. Cavallo, L.; Guerra, G.; Corradini, P.; Vacatello, M. *Chirality* **1991**, *3*, 299.
200. Gilchrist, J. H.; Bercaw, J. E. *J. Am. Chem. Soc.* **1996**, *118*, 12021.
201. Dahlmann, M.; Erker, G.; Nissinen, M.; Fröhlich, R. *J. Am. Chem. Soc.* **1999**, *121*, 2820.
202. Ewen, J. A. *J. Am. Chem. Soc.* **1984**, *106*, 6355.
203. Kaminsky, W.; Külp, K.; Brintzinger, H. H.; Wild, F. R. W. *Angew. Chem., Int. Ed. Engl.* **1985**, *24*, 507.
204. Resconi, L.; Balboni, D.; Baruzzi, G.; Fiori, C.; Guidotti, S.; Mercandelli, P.; Sironi, A. *Organometallics* **2000**, *19*, 420.
205. Ewen, J. A.; Haspeslagh, L.; Elder, M. J.; Atwood, J. L.; Zhang, H.; Cheng, H. N. Propylene Polymerizations with Group 4 Metallocene/alumoxane Systems. In *Transition Metals and Organometallics as Catalysts for Olefin Polymerization*; Kaminsky, W., Sinn, H., Eds.; Springer: Berlin, 1988; p 281.
206. Toto, M.; Cavallo, L.; Corradini, P.; Moscardi, G.; Resconi, L.; Guerra, G. *Macromolecules* **1998**, *31*, 3431.
207. Moscardi, G.; Resconi, L.; Cavallo, L. *Organometallics* **2001**, *20*, 1918.
208. Ewen, J. A.; Jones, R. L.; Razavi, A.; Ferrara, J. D. *J. Am. Chem. Soc.* **1988**, *110*, 6255.

209. Ewen, J. A.; Elder, M. J.; Jones, R. L.; Haspeslagh, L.; Atwood, J. L.; Bott, S. G.; Robinson, K. *Makromol. Chem., Macromol. Symp.* **1991**, *48/49*, 253.
210. Antberg, M.; Dolle, V.; Klein, R.; Rohrmann, J.; Spaleck, W.; Winter, A. Propylene Polymerization by Stereorigid Metallocene Catalysts: Some New Aspects of the Metallocene Structure/polypropylene Microstructure Correlation. In *Catalytic Olefin Polymerization, Studies in Surface Science and Catalysis*; Keii, T., Soga, K., Eds.; Kodansha-Elsevier: Tokyo, 1990; p 501.
211. Dolle, V.; Rohrmann, J.; Winter, A.; Antberg, M.; Klein, R. (Hoechst). Eur. Pat. Appl. EP 399347, 1990.
212. Kleinschmidt, R.; Reffke, M.; Fink, G. *Macromol. Rapid Commun.* **1999**, *20*, 284.
213. Yoshida, T.; Koga, N.; Morokuma, K. *Organometallics* **1996**, *15*, 766.
214. van der Leek, Y.; Angermund, K.; Reffke, M.; Kleinschmidt, R.; Goretzki, R.; Fink, G. *Chem. Eur. J.* **1997**, *3*, 585.
215. Ewen, J. A.; Elder, M. J. *Makromol. Chem., Macromol. Symp.* **1993**, *66*, 179.
216. Cheng, H. N.; Ewen, J. A. *Makromol. Chem.* **1989**, *190*, 1931.
217. Resconi, L.; Camurati, I.; Sudmeijer, O. *Top. Catal.* **1999**, *7*, 145.
218. Blom, R.; Dahl, I. M. *Macromol. Chem. Phys.* **1999**, *200*, 442.
219. Moscardi, G.; Piemontesi, F.; Resconi, L. *Organometallics* **1999**, *18*, 5264.
220. Blom, R.; Dahl, I. M. *Macromol. Chem. Phys.* **2001**, *202*, 719.
221. Andersen, A.; Blom, R.; Dahl, I. M. *Macromol. Chem. Phys.* **2001**, *202*, 726.
222. Balboni, D.; Moscardi, G.; Baruzzi, G.; Braga, V.; Camurati, I.; Piemontesi, F.; Resconi, L.; Nifant'ev, I. E.; Venditto, V.; Antinucci, S. *Macromol. Chem. Phys.* **2001**, *202*, 2010.
223. Fan, W.; Waymouth, R. M. *Macromolecules* **2001**, *34*, 8619.
224. Han-Adebekun, G. C.; Hamba, M.; Ray, W. H. *J. Polym. Sci., A* **1997**, *35*, 2063.
225. Thorshaug, K.; Rytter, E.; Ystenes, M. *Macromol. Rapid Commun.* **1997**, *18*, 715.
226. Thorshaug, K.; Støvneng, J. A.; Rytter, E.; Ystenes, M. *Macromolecules* **1998**, *31*, 7149.
227. Dang, V. A.; Yu, L.-C.; Balboni, D.; Dall'Occo, T.; Resconi, L.; Mercandelli, P.; Moret, M.; Sironi, A. *Organometallics* **1999**, *18*, 3781.
228. Naga, N.; Mizunuma, K. *Polymer* **1998**, *39*, 5059.
229. Karol, F. J.; Kao, S. C.; Wasserman, E. P.; Brady, R. C. *New J. Chem.* **1997**, *21*, 797.
230. Hasegawa, S.; Sone, M.; Tanabiki, M.; Sato, M.; Yano, A. *J. Polym. Sci. A: Polym. Chem.* **2000**, *38*, 4641.
231. Janiak, C.; Lange, K. C. H.; Marquardt, P. *Macromol. Rapid Commun.* **1995**, *16*, 643.
232. Rossi, A.; Odian, G.; Zhang, J. *Macromolecules* **1995**, *28*, 1739.
233. Rossi, A.; Zhang, J.; Odian, G. *Macromolecules* **1996**, *29*, 2331.
234. Janiak, C.; Lange, K. C. H.; Marquardt, P.; Kruger, R.-P.; Hanselmann, R. *Macromol. Chem. Phys.* **2002**, *203*, 129.
235. Harney, M. B.; Keaton, R. J.; Sita, L. R. *J. Am. Chem. Soc.* **2004**, *126*, 4536.
236. Busico, V.; Cipullo, R.; Ronca, S.; Budzelaar, P. H. M. *Macromol. Rapid Commun.* **2001**, *22*, 1405.
237. Yoder, J. C.; Bercaw, J. E. *J. Am. Chem. Soc.* **2002**, *124*, 2548.
238. Busico, V.; Cipullo, R. *J. Am. Chem. Soc.* **1994**, *116*, 9329.
239. Leclerc, M. K.; Brintzinger, H.-H. *J. Am. Chem. Soc.* **1995**, *117*, 1651.
240. Busico, V.; Cipullo, R. *J. Organomet. Chem.* **1995**, *497*, 113.
241. Resconi, L.; Fait, A.; Piemontesi, F.; Colonnese, M.; Rychlicki, H.; Zeigler, R. *Macromolecules* **1995**, *28*, 6667.
242. Leclerc, M. K.; Brintzinger, H.-H. *J. Am. Chem. Soc.* **1996**, *118*, 9024.
243. Busico, V.; Caporaso, L.; Cipullo, R.; Landriani, L.; Angelini, G.; Margonelli, A.; Segre, A. L. *J. Am. Chem. Soc.* **1996**, *118*, 2105.
244. Busico, V.; Brita, D.; Caporaso, L.; Cipullo, R.; Vacatello, M. *Macromolecules* **1997**, *30*, 3971.
245. Busico, V.; Cipullo, R.; Caporaso, L.; Angelini, G.; Segre, A. L. *J. Mol. Catal. A: Chem.* **1998**, *128*, 53.
246. Camurati, I.; Fait, A.; Piemontesi, F.; Resconi, L.; Tartarini, S. Transfer and Isomerization Reactions in Propylene Polymerization with the Isospecific, Highly Regiospecific *rac*-Me<sub>2</sub>C(3-*i*-Bu-1-Ind)2ZrCl<sub>2</sub>/MAO Catalyst. In *Transition Metal Catalysis in Macromolecular Design ACS Symposium Series*; Boffa, L. S., Novak, B. M., Eds.; American Chemical Society: Washington, DC, 2000; Vol. 760, 174.
247. Volkis, V.; Shmulinson, M.; Averbuj, C.; Lisovskii, A.; Edelmann, F. T.; Eisen, M. S. *Organometallics* **1998**, *17*, 3155.
248. Volkis, V.; Nelkenbaum, E.; Lisovskii, A.; Hasson, G.; Semiat, R.; Kapon, M.; Botoshansky, M.; Eishen, Y.; Eisen, M. S. *J. Am. Chem. Soc.* **2003**, *125*, 2179.
249. Resconi, L. *J. Mol. Catal. A: Chem.* **1999**, *146*, 167.
250. Resconi, L.; Piemontesi, F.; Jones, R. L. High-molecular-weight Atactic Polypropylene from Metallocene Catalysts. Influence of Ligand Structure and Polymerization Conditions on Molecular Weight. In *Metallocene-catalyzed Polymers - Materials, Properties, Processing & Markets*; Benedikt, G. M., Goodall, B. L., Eds.; Plastics Design Library: New York, 1998.
251. Sugano, T.; Tayano, T.; Uchino, H.; Ioku, A.; Iwama, N.; Endo, J.; Osano, Y. In *Proceedings of the SPO '99*; Schotland Business Res. Ed.: Houston, 1999; p 31.
252. Voegele, J.; Troll, C.; Rieger, B. *Macromol. Chem. Phys.* **2002**, *203*, 1918.
253. Tynys, A.; Saarinen, T.; Hakala, K.; Helaja, T.; Vanne, T.; Lehmus, P.; Löfgren, B. *Macromol. Chem. Phys.* **2005**, *206*, 1043.
254. Camurati, I.; Cavicchi, B.; Dall'Occo, T.; Piemontesi, F. *Macromol. Chem. Phys.* **2001**, *202*, 701.
255. Jüngling, S.; Mülhaupt, R.; Stehling, U.; Brintzinger, H.-H.; Fischer, D.; Langhauser, F. *J. Polym. Sci. Polym. Chem.* **1995**, *33*, 1305.
256. van der Linden, A.; Schaverien, C. J.; Meijboom, N.; Ganter, C.; Guy Orpen, A. *J. Am. Chem. Soc.* **1995**, *117*, 3008.
257. Resconi, L.; Piemontesi, F.; Camurati, I.; Balboni, D.; Sironi, A.; Moret, M.; Rychlicki, H.; Zeigler, R. *Organometallics* **1996**, *15*, 5046.
258. Cherian, A. E.; Lobkovsky, E. B.; Coates, G. W. *Macromolecules* **2005**, *38*, 6259.
259. Eshuis, J. J. W.; Tan, Y. Y.; Meetsma, A.; Teuben, J. H.; Renkema, J.; Evens, G. G. *Organometallics* **1992**, *11*, 362.
260. Shaffer, T. D.; Canich, J. A. M.; Squire, K. R. *Macromolecules* **1998**, *31*, 5145.
261. Kesti, M.; Waymouth, R. M. *J. Am. Chem. Soc.* **1992**, *114*, 3565.
262. Resconi, L.; Piemontesi, F.; Franciscano, G.; Abis, L.; Fiorani, T. *J. Am. Chem. Soc.* **1992**, *114*, 1025.
263. Bunel, E.; Burger, B. J.; Bercaw, J. E. *J. Am. Chem. Soc.* **1988**, *110*, 976.
264. Yang, X.; Jia, L.; Marks, T. J. *J. Am. Chem. Soc.* **1993**, *115*, 3392.
265. Yang, X.; Seyam, A. M.; Fu, P.-F.; Marks, T. J. *Macromolecules* **1994**, *27*, 4625.
266. Resconi, L.; Jones, R. L.; Rheingold, A. L.; Yap, G. P. A. *Organometallics* **1996**, *15*, 998.
267. Resconi, L.; Piemontesi, F.; Camurati, I.; Sudmeijer, O.; Nifant'ev, I. E.; Ivchenko, P. V.; Kuz'mina, L. G. *J. Am. Chem. Soc.* **1998**, *120*, 2308.

268. Weng, W.; Markel, E. J.; Dekmezian, A. H. *Macromol. Rapid Commun.* **2000**, *21*, 103.
269. Weng, W.; Markel, E. J.; Peacock, A. J.; Dekmezian, A. H. *Macromolecules* **2000**, *33*, 8541.
270. Weng, W.; Markel, E. J.; Dekmezian, A. H. *Macromol. Rapid Commun.* **2001**, *22*, 1488.
271. Shiono, T.; Kurosawa, H.; Soga, K. *Macromolecules* **1994**, *27*, 2635.
272. Bhriain, N. N.; Brintzinger, H.-H.; Ruchatz, D.; Fink, G. *Macromolecules* **2005**, *38*, 2056.
273. Fan, G.; Dong, J.-Y. *J. Mol. Catal. A: Chem.* **2005**, *236*, 246.
274. Mogstad, A.-L.; Waymouth, R. M. *Macromolecules* **1992**, *25*, 2282.
275. Scollard, J. D.; McConville, D. H. *J. Am. Chem. Soc.* **1996**, *118*, 10008.
276. Averbuj, C.; Tish, E.; Eisen, M. S. *J. Am. Chem. Soc.* **1998**, *120*, 8640.
277. Lamberti, M.; Gliubizzi, R.; Mazzeo, M.; Tedesco, C.; Pellicchia, C. *Macromolecules* **2004**, *37*, 276.
278. Michiue, K.; Jordan, R. F. *Organometallics* **2004**, *23*, 460.
279. Michiue, K.; Jordan, R. F. *Macromolecules* **2003**, *36*, 9707.
280. Hindryckx, F.; Dubois, P.; Jerome, R.; Marti, M. G. *Polymer* **1998**, *39*, 621.
281. Kissin, Y. V.; Rishina, L. A.; Vizen, E. I. *J. Polym. Sci. A: Polym. Chem.* **2002**, *40*, 1899–1911.
282. Carvill, A.; Tritto, I.; Locatelli, P.; Sacchi, M. C. *Macromolecules* **1997**, *30*, 7056.
283. Fu, P.-F.; Marks, T. J. *J. Am. Chem. Soc.* **1995**, *117*, 10747.
284. Koo, K.; Marks, T. J. *J. Am. Chem. Soc.* **1998**, *120*, 4019.
285. Wester, T. S.; Johnsen, H.; Kittilsen, P.; Rytter, E. *Macromol. Chem. Phys.* **1998**, *199*, 1989.
286. Chien, J. C. W.; Yu, Z.; Marques, M. M.; Flores, J. C.; Rausch, M. D. *J. Polym. Sci. A: Polym. Chem.* **1998**, *36*, 319.
287. Chien, J. C. W.; Wang, B. P. *J. Polym. Sci., A: Polym. Chem.* **1990**, *28*, 15.
288. Fink, G.; Herfert, N.; Montag, P. The Relationship Between Kinetics and Mechanisms. In *Ziegler Catalysts*; Fink, G., Mülhaupt, R., Brintzinger, H.-H., Eds.; Springer: Berlin, 1995; p 159.
289. Fait, A.; Resconi, L.; Guerra, G.; Corradini, P. *Macromolecules* **1999**, *32*, 2104.
290. Song, F.; Cannon, R. D.; Bochmann, M. *J. Am. Chem. Soc.* **2003**, *125*, 7641.
291. Nele, M.; Mohammed, M.; Xin, S.; Collins, S.; Dias, M. L.; Pinto, J. C. *Macromolecules* **2001**, *34*, 3830.
292. Mohammed, M.; Nele, M.; Al-Humydi, A.; Xin, S.; Stapleton, R. A.; Collins, S. *J. Am. Chem. Soc.* **2003**, *125*, 7930.
293. Busico, V.; Cipullo, R.; Cutillo, F.; Vacatello, M. *Macromolecules* **2002**, *35*, 349.
294. Busico, V.; Cipullo, R.; Corradini, P. *Makromol. Chem., Rapid Commun.* **1993**, *14*, 97.
295. Busico, V.; Cipullo, R.; Chadwick, J. C.; Modder, J. F.; Sudmeijer, O. *Macromolecules* **1994**, *27*, 7538.
296. Busico, V.; Cipullo, R.; Romanelli, V.; Ronca, S.; Togrou, M. *J. Am. Chem. Soc.* **2005**, *127*, 1608.
297. Busico, V.; Cipullo, R.; Esposito, V. *Macromol. Rapid Commun.* **1999**, *20*, 116.
298. Monaco, G. *Macromolecules* **2001**, *34*, 4406.
299. Tsutsui, T.; Kashiwa, N.; Mizuno, A. *Makromol. Chem., Rapid Commun.* **1990**, *11*, 565.
300. Kioka, M.; Mizuno, A.; Tsutsui, T.; Kashiwa, N. 1-Butene Polymerization with Ethylenebis-(1-Indenyl)Zirconium Dichloride and Methylaluminoxane Catalyst System. In *Catalysis in Polymer Synthesis, ACS Symposium Series*; Vandenberg, E. J., Salamone, J. C., Eds.; American Chemical Society: Washington, DC, 1992; Vol. 496, p 72.
301. Borriello, A.; Busico, V.; Cipullo, R.; Fusco, O.; Chadwick, J. C. *Macromol. Chem. Phys.* **1997**, *198*, 1257.
302. Landis, C. R.; Sillars, D. R.; Batterton, J. M. *J. Am. Chem. Soc.* **2004**, *126*, 8890.
303. Mynott, R.; Fink, G.; Fenzl, W. *Angew. Makromol. Chem.* **1987**, *154*, 1.
304. Mori, H.; Terano, M. *Trends Polym. Sci.* **1997**, *5*, 314.
305. Lahelin, M.; Kokko, E.; Lehmus, P.; Pitkänen, P.; Löfgren, B.; Seppälä, J. *Macromol. Chem. Phys.* **2003**, *204*, 1323.
306. Belov, G. P.; Gyuluyan, H. R.; Khrapova, I. M.; Maryin, V. P.; Korneev, N. N. *J. Mol. Catal. A: Chem.* **1997**, *115*, 155.
307. Lin, M.; Spivak, G. J.; Baird, M. C. *Organometallics* **2002**, *21*, 2350.
308. Marques, M. M.; Costa, C.; Lemos, F.; Ribeiro, F. R.; Dias, A. R. *React. Kinet. Catal. Lett.* **1997**, *62*, 9.
309. Marques, M. M.; Tait, P. J. T.; Mejlik, J.; Dias, A. R. *J. Pol. Sci., Part A: Pol. Chem.* **1998**, *36*, 573.
310. Blom, R.; Swang, O.; Heyn, R. H. *Macromol. Chem. Phys.* **2002**, *203*, 381.
311. Goodman, J. T.; Schrock, R. R. *Organometallics* **2001**, *20*, 5205.
312. Schrodli, Y.; Schrock, R. R.; Bonitatebus, P. J., Jr. *Organometallics* **2001**, *20*, 3560.
313. Boor, J., Jr. *Ziegler-Natta Catalysts and Polymerizations*; Academic Press: New York, 1979.
314. Kissin, Y. V. *Isospecific Polymerization of Olefins*; Springer: New York, 1985.
315. van der Ven, S. *Polypropylene and other Polyolefins. Polymerization and Characterization*; Elsevier: Amsterdam, 1990.
316. Gavens, P. D.; Bottrill, M.; Kelland, J. W.; McMeeking, J. *Ziegler-Natta Catalysis*. In *Comprehensive Organometallic Chemistry I*; Wilkinson, G., Stone, F. G. A., Abel, E. W., Eds.; Pergamon: Oxford, 1982; Vol. 3, p 475.
317. Moore, E. P. Jr. *Polypropylene Handbook: Polymerization, Characterization, Properties, Applications*; Hanser: Munich, 1996.
318. Kashiwa, N. *J. Polym. Sci. A: Polym. Chem.* **2004**, *42*, 1.
319. Giannini, U. *Makromol. Chem. Suppl.* **1981**, *5*, 216.
320. Galli, P.; Luciani, L.; Cecchin, G. *Angew. Makromol. Chem.* **1981**, *94*, 63.
321. Barbè, C.; Cecchin, G.; Noristi, L. *Adv. Polym. Sci.* **1987**, *81*, 1.
322. Seppälä, J. V.; Härkönen, M.; Luciani, L. *Makromol. Chem.* **1989**, *190*, 2535.
323. Härkönen, M.; Seppälä, J. V.; Väänänen, T. In *Catalytic Olefin Polymerization*; Keii, T., Soga, K., Eds.; Elsevier: Amsterdam, 1990, p 87.
324. Proto, A.; Oliva, L.; Pellicchia, C.; Sivak, A. J.; Cullo, L. A. *Macromolecules* **1990**, *23*, 2904.
325. Okano, T.; Chida, K.; Furuhashi, H.; Nakano, A.; Ukei, S. In *Catalytic Olefin Polymerization*; Keii, T., Soga, K., Eds.; Elsevier: Amsterdam, 1990; p 177.
326. Mori, H.; Sawada, M.; Higuchi, T.; Hasebe, K.; Otsuka, N.; Terano, M. *Macromol. Rapid Commun.* **1999**, *20*, 245.
327. Mori, H.; Hasebe, K.; Terano, M. *Macromol. Chem. Phys.* **1998**, *199*, 2709.
328. Bart, J. C. J.; Roovers, W. *J. Mat. Sci.* **1995**, *30*, 2809.
329. Sozzani, P.; Bracco, S.; Comotti, A.; Simonutti, R.; Camurati, I. *J. Am. Chem. Soc.* **2003**, *125*, 12881.
330. Galli, P.; Barbè, P. C.; Guidetti, G. P.; Zannetti, R.; Martorana, A.; Marigo, A.; Bergozza, M.; Fichera, A. *Eur. Polym. J.* **1983**, *19*, 19.
331. Gerbasi, R.; Marigo, A.; Martorana, A.; Zannetti, R.; Guidetti, G. P.; Baruzzi, G. *Eur. Polym. J.* **1984**, *20*, 967.
332. Marigo, A.; Marega, C.; Zannetti, R.; Morini, G.; Ferrara, G. *Eur. Polym. J.* **2000**, *36*, 1921.

333. Corradini, P.; Busico, V.; Guerra, G. Possible Models for the Steric Control in the Heterogeneous High-yield and Homogeneous Ziegler-Natta Polymerizations of 1-Alkenes. In *Transition Metals and Organometallics as Catalysts for Olefin Polymerization*; Kaminsky, W., Sinn, H., Eds.; Springer: Berlin, 1988; p 337.
334. Busico, V.; Corradini, P.; De Martino, L.; Proto, A.; Savino, V.; Albizzati, E. *Makromol. Chem.* **1985**, *186*, 1279.
335. Potapov, A. G.; Kriventsov, V. V.; Kochubey, D. I.; Bukatov, G. D.; Zakharov, V. A. *Macromol. Chem. Phys.* **1997**, *198*, 3477.
336. Terano, M.; Kataoka, T.; Keii, T. *Makromol. Chem.* **1987**, *188*, 1477.
337. Albizzati, E.; Giannini, U.; Morini, G.; Smith, C. A.; Zeigler, R. Advances in Propylene Polymerization with  $\text{MgCl}_2$  Supported Catalysts. In *Ziegler Catalysts*; Fink, G., Mülhaupt, R., Brintzinger, H.-H., Eds.; Springer: Berlin, 1995; p 413.
338. Sacchi, M. C.; Tritto, I.; Shan, C.; Mendichi, R.; Noristi, L. *Macromolecules* **1991**, *24*, 6823.
339. Albizzati, E.; Barbé, P. C.; Noristi, L.; Scordamaglia, R.; Barino, L.; Giannini, U.; Morini, G. (Himont). Eur. Pat. Appl. EP 361494, 1989.
340. Morini, G.; Cristofori, A. (Montell). Eur. Pat. EP 361494, 1990.
341. Albizzati, E.; Giannini, U.; Morini, G.; Galimberti, M.; Barino, L.; Scordamaglia, R. *Macromol. Symp.* **1995**, *89*, 73.
342. Barino, L.; Scordamaglia, R. *Macromol. Symp.* **1995**, *89*, 101.
343. Albizzati, E.; Galimberti, M.; Giannini, U.; Morini, G. *Makromol. Chem., Macromol. Symp.* **1991**, *48/49*, 223.
344. Morini, G.; Balbontin, G.; Gulevich, Y.; Duijghuisen, H.; Kelder, R.; Klusener, P. A.; Korndorffer, F. (Basell). World Pat. Appl. WO 00/63261, 2000.
345. Cecchin, G.; Morini, G.; Pelliconi, A. *Macromol. Symp.* **2001**, *173*, 195.
346. Pater, J. T. M.; Weickert, G.; van Swaaij, W. P. M. *AIChE J.* **2003**, *49*, 450.
347. Simonazzi, T.; Giannini, U. *Gazz. Chim. Ital.* **1994**, *124*, 533.
348. Galli, P. *Prog. Polym. Sci.* **1994**, *19*, 959.
349. McKenna, T. F.; Soares, J. B. P. *Chem. Eng. Sci.* **2001**, *56*, 3931.
350. Hutchinson, R. A.; Chen, C. M.; Ray, W. H. *J. Appl. Polym. Sci.* **1992**, *44*, 1389.
351. Kakugo, M.; Sadatoshi, H.; Kojima, K.; Yokoyama, M. *Macromolecules* **1989**, *22*, 547.
352. Cecchin, G.; Marchetti, E.; Baruzzi, G. *Macromol. Chem. Phys.* **2001**, *202*, 1987.
353. Pater, J. T. M.; Weickert, G.; Loos, J.; van Swaaij, W. P. M. *Chem. Eng. Sci.* **2001**, *56*, 4107.
354. Galli, P.; Haylock, J. C. *Prog. Polym. Sci.* **1991**, *16*, 443.
355. Böhm, L. *Angew. Chem., Int. Ed.* **2003**, *42*, 5010.
356. Zakharov, V. A.; Bukatov, G. D.; Barababov, A. A. *Macromol. Symp.* **2004**, *213*, 19.
357. Parasu Veera, U.; Weickert, G.; Agarwal, U. S. *AIChE J.* **2002**, *48*, 1062.
358. Noristi, L.; Marchetti, E.; Baruzzi, G. *J. Polym. Sci. A: Polym. Chem.* **1994**, *32*, 3047.
359. Fragonese, D.; Mortara, S.; Bresadola, S. *J. Mol. Catal. A: Chem.* **2001**, *172*, 89.
360. Baulin, A. A.; Novikova, Y. I.; Mal'kova, G. Y.; Maksimov, V. L.; Vyshinskaya, L. I.; Ivanchev, S. S. *Polym. Sci. USSR* **1980**, *22*, 205.
361. Kashiwa, N.; Yoshitake, J. *Makromol. Chem.* **1984**, *185*, 1133.
362. Chien, J. C. W.; Wu, J. C. J. *Polym. Sci. A: Polym. Chem.* **1982**, *20*, 2461.
363. Weber, S.; Chien, J. C. W.; Hu, Y. J. *Polym. Sci. A: Polym. Chem.* **1989**, *27*, 1499.
364. Sergeev, S. A.; Polubayarov, V. A.; Zakharov, V. A.; Anufrienko, U. F.; Bukatov, G. D. *Makromol. Chem.* **1986**, *187*, 243.
365. Chien, J. C. W.; Hu, Y. J. *Pol. Sci., Part A: Polym. Chem.* **1989**, *27*, 897.
366. Mori, H.; Hasebe, K.; Terano, M. *J. Mol. Catal. A: Chem.* **1999**, *140*, 165.
367. Mejzlik, J.; Lesna, M.; Kratochvila, J. *Adv. Polym. Sci.* **1986**, *81*, 83.
368. Liu, B.; Matsuoka, H.; Terano, M. *Macromol. Rapid Commun.* **2001**, *22*, 1.
369. Bukatov, G. D.; Zakharov, V. A. *Macromol. Chem. Phys.* **2001**, *202*, 2003.
370. Tait, P. J. T.; Zohuri, G. H.; Kells, A. M.; McKenzie, I. D. In *Ziegler Catalysts. Recent Scientific Innovations and Technological Improvements*; Fink, G., Mülhaupt, R., Brintzinger, H. H., Eds.; Springer: Berlin, 1995; p 343.
371. Bukatov, G. D.; Goncharov, V. S.; Zakharov, V. A. *Macromol. Chem. Phys.* **1995**, *196*, 1751.
372. Kashiwa, N.; Yoshitake, J.; Toyota, A. *Polym. Bull.* **1988**, *19*, 333.
373. Chadwick, J. C. Effects of Electron Donors in Super High Activity Catalysts for Polypropylene. In *Ziegler Catalysts*; Fink, G., Mülhaupt, R., Brintzinger, H.-H., Eds.; Springer: Berlin, 1995; p 427.
374. Kakugo, M.; Miyatake, T.; Naito, Y.; Mizunuma, K. *Macromolecules* **1988**, *21*, 314.
375. Soga, K.; Park, J. R.; Shiono, T.; Kashiwa, N. *Makromol. Chem., Rapid Commun.* **1990**, *11*, 117.
376. Soga, K.; Park, J. R.; Uchino, H.; Uozumi, T.; Shiono, T. *Macromolecules* **1989**, *22*, 3824.
377. Soga, K. *Makromol. Chem., Macromol. Symp.* **1993**, *66*, 43.
378. Sacchi, M. C.; Shan, C.; Locatelli, P.; Tritto, I. *Macromolecules* **1990**, *23*, 383.
379. Sacchi, M. C.; Forlini, F.; Tritto, I.; Mendichi, R.; Zannoni, G.; Noristi, L. *Macromolecules* **1992**, *25*, 5914.
380. Sacchi, M. C.; Forlini, F.; Tritto, I.; Locatelli, P.; Morini, G.; Baruzzi, G.; Albizzati, E. *Macromol. Symp.* **1995**, *89*, 91.
381. Morini, G.; Albizzati, E.; Balbontin, G.; Mingozzi, I.; Sacchi, M. C.; Forlini, F.; Tritto, I. *Macromolecules* **1996**, *29*, 5770.
382. Busico, V.; Cipullo, R.; Monaco, G.; Talarico, G.; Vacatello, M.; Chadwick, J. C.; Segre, A. L.; Sudmeijer, O. *Macromolecules* **1999**, *32*, 4173.
383. Busico, V.; Cipullo, R.; Talarico, G.; Segre, A. L.; Chadwick, J. C. *Macromolecules* **1997**, *30*, 4786.
384. Chadwick, J. C.; Morini, G.; Balbontin, G.; Camurati, I.; Heere, J. J. R.; Mingozzi, I.; Testoni, F. *Macromol. Chem. Phys.* **2001**, *202*, 1995.
385. Härkönen, M.; Seppälä, J.; Chûjô, R.; Kogure, Y. *Polymer* **1995**, *36*, 1499.
386. Barino, L.; Scordamaglia, R. *Macromol. Theory Simul.* **1998**, *7*, 407.
387. Scordamaglia, R.; Barino, L. *Macromol. Theory Simul.* **1998**, *7*, 399.
388. Toto, M.; Morini, G.; Guerra, G.; Corradini, P.; Cavallo, L. *Macromolecules* **2000**, *33*, 1134.
389. Sacchi, M. C.; Forlini, F.; Tritto, I.; Locatelli, P.; Morini, G.; Noristi, L.; Albizzati, E. *Macromolecules* **1996**, *29*, 3341.
390. Cecchin, G.; Morini, G.; Piemontesi, F.; Ferraro, A.; News, J.; Cavallo, L. In *EUPOC 2003. European Polymer Conference on Stereospecific Polymerization and Stereoregular Polymers*; Milan, Italy, 2003.
391. Boero, M.; Parrinello, M.; Hüffer, S.; Weiss, H. J. *Am. Chem. Soc.* **2000**, *122*, 501.
392. Liu, B.; Nitta, T.; Nakatani, H.; Terano, M. *Macromol. Chem. Phys.* **2002**, *203*, 2412.
393. Liu, B.; Nitta, T.; Nakatani, H.; Terano, M. *Macromol. Chem. Phys.* **2003**, *204*, 395.
394. Potapov, A. G.; Terskikh, V. V.; Zakharov, V. A.; Bukatov, G. D. *J. Mol. Catal. A: Chem.* **1999**, *145*, 147.
395. Mori, H.; Tashino, K.; Terano, M. *Macromol. Rapid Commun.* **1995**, *16*, 651.



396. Mori, H.; Tashino, K.; Terano, M. *Macromol. Chem. Phys.* **1996**, *197*, 895.
397. Mori, H.; Iizuka, T.; Tashino, K.; Terano, M. *Macromol. Chem. Phys.* **1997**, *198*, 2499.
398. Chadwick, J. C.; Morini, G.; Albizzati, E.; Balbontin, G.; Mingozi, I.; Cristofori, A.; Sudmeijer, O.; van Kessel, G. M. M. *Macromol. Chem. Phys.* **1996**, *197*, 2501.
399. Guastalla, G.; Giannini, U. *Makromol. Chem., Rapid Commun.* **1983**, *4*, 519.
400. Randall, J. C.; Ruff, C. J.; Vizzini, J. C.; Specia, A. N.; Burkhardt, T. J. Initial Insertion in Metallocene Polymerizations of Polypropylene. In *Metalorganic Catalysts for Synthesis and Polymerisation*; Kaminsky, W., Ed. Springer: Berlin, 1999; p 601.
401. Chadwick, J. C.; Heere, J. J. R.; Sudmeijer, O. *Macromol. Chem. Phys.* **2000**, *201*, 1846.
402. Kissin, Y. V.; Rishina, L. A. *J. Polym. Sci. A: Polym. Chem.* **2002**, *40*, 1353.
403. Kissin, Y. V.; Mink, R. I.; Nowlin, T. E.; Brandolini, A. J. *Top. Catal.* **1999**, *7*, 69.
404. Kissin, Y. V.; Mink, R. I.; Nowlin, T. E. *J. Polym. Sci. A: Polym. Chem.* **1999**, *37*, 4255.
405. Kissin, Y. V.; Brandolini, A. J. *J. Polym. Sci. A: Polym. Chem.* **1999**, *37*, 4273.
406. Kissin, Y. V.; Mink, R. I.; Nowlin, T. E.; Brandolini, A. J. *J. Polym. Sci. A: Polym. Chem.* **1999**, *37*, 4281.
407. Kissin, Y. V. *Macromol. Theory Simul.* **2002**, *11*, 67.
408. Garoff, T.; Johansson, S.; Pesonen, K.; Waldvogel, P.; Lindgren, D. *Eur. Polym. J.* **2002**, *38*, 121.
409. Mikenas, T. B.; Zakharov, V. A.; Echevskaya, L. G.; Matsko, M. A. *Macromol. Chem. Phys.* **2001**, *202*, 475.
410. Matsko, M. A.; Bukatov, G. D.; Mikenas, T. B.; Zakharov, V. A. *Macromol. Chem. Phys.* **2001**, *202*, 1435.
411. Czaja, K.; Bialek, M. *J. App. Polym. Sci.* **2001**, *79*, 356.
412. Chadwick, J. C.; van Kessel, G. M. M.; Sudmeijer, O. *Macromol. Chem. Phys.* **1995**, *196*, 1431.
413. Chadwick, J. C.; Morini, G.; Balbontin, G.; Sudmeijer, O. *Macromol. Chem. Phys.* **1998**, *199*, 1873.
414. Kissin, Y. V.; Ohnishi, R.; Konakazawa, T. *Macromol. Chem. Phys.* **2004**, *205*, 284.
415. Kojoh, S.-I.; Kioka, M.; Kashiwa, N.; Itoh, M.; Mizuno, A. *Polymer* **1995**, *36*, 5015.
416. Kojoh, S.-I.; Kioka, M.; Kashiwa, N. *Eur. Polym. J.* **1999**, *35*, 751.
417. Zhong, C.; Gao, M.; Mao, B. *J. Appl. Pol. Sci.* **2003**, *90*, 3980.
418. Kissin, Y. V. *J. Polym. Sci. A: Polym. Chem.* **2003**, *41*, 1745.
419. Keii, T.; Terano, M.; Kimura, K.; Ishii, K. *Makromol. Chem., Rapid Commun.* **1987**, *8*, 583.
420. Chadwick, J. C.; van der Burgt, F. P. T. J.; Rastogi, S.; Busico, V.; Cipullo, R.; Talarico, G.; Heere, J. J. R. *Macromolecules* **2004**, *37*, 9722.
421. Böhm, L. L.; Bilda, D.; Breuers, W.; Enderle, H. F.; Lecht, R. In *Ziegler Catalysts. Recent Scientific Innovations and Technological Improvements*; Fink, G., Mühlhaupt, R., Brintzinger, H. H., Eds.; Springer: Berlin, 1995; p 387.
422. Karol, F. J.; Cann, K. J.; Wagner, B. E. In *Transition Metals and Organometallics as Catalysts for Olefin Polymerization*; Kaminsky, W., Sinn, H., Eds.; Springer: Berlin, 1988; p 149.
423. Hsieh, H. L.; McDaniel, M. P.; Martin, J. L.; Smith, P. D.; Fahey, D. R. In *Advances in Polyolefins*; Seymour, R. B., Cheng, T., Eds.; Plenum Press: New York, 1985; p 153.
424. Soga, K.; Yanagihara, H. *Makromol. Chem.* **1988**, *189*, 2839.
425. Cecchin, G.; Collina, G.; Covezzi, M. (Basell). U.S. Patent 6306996, 2001.
426. Lopez, L. C.; Wilkes, G. L.; Stricklen, P. M.; White, S. A. *J. M. S. - Rev. Macromol. Chem. Phys.* **1992**, *C32*, 301.
427. Kashiwa, N.; Yoshitake, J. *Polym. Bull.* **1984**, *11*, 485.
428. Sacchi, M. C.; Tritto, I.; Locatelli, P.; Fan, Z.-Q.; Forlini, F. *Macromol. Chem. Phys.* **1994**, *195*, 2805.
429. Kashiwa, N.; Fukui, K. (Mitsui). U.S. Patent 4659792, 1985.
430. Leatherman, M. D.; Brookhart, M. *Macromolecules* **2001**, *34*, 2748.
431. Endo, K.; Otsu, T. *J. Polym. Sci. A: Polym. Chem.* **1995**, *33*, 79.
432. Endo, K.; Otsu, T. *Makromol. Chem., Rapid Commun.* **1990**, *11*, 663.
433. Otsu, T.; Endo, K. *Makromol. Chem., Rapid Commun.* **1991**, *12*, 147.
434. Otsu, T.; Endo, K. *Makromol. Chem.* **1991**, *192*, 261.
435. Endo, K.; Ueda, R.; Otsu, T. *Makromol. Chem.* **1993**, *194*, 2623.
436. Endo, K.; Fujii, K.; Otsu, T. *Makromol. Chem., Rapid Commun.* **1991**, *12*, 409.
437. Karol, F. J. *Macromol. Symp.* **1995**, *89*, 563.
438. Ahvenainen, A.; Sarantila, K.; Andtsjo, H. (Neste Oy). World Pat. Appl. WO 92/12181, 1992.
439. Andtsjo, H.; Pentti, I.; Harlin, A. (Borealis A/S). World Pat. Appl. WO 97/13790, 1997.
440. Covezzi, M.; Mei, G. *Chem. Eng. Sci.* **2001**, *56*, 4059.
441. Hamielec, A. E.; Soares, J. B. P. *Prog. Polym. Sci.* **1996**, *21*, 651.
442. Stevens, J. C. *Stud. Surf. Sci. Catal.* **1994**, *89*, 277.
443. Stevens, J. C. *Stud. Surf. Sci. Catal.* **1996**, *101*, 11.
444. Wang, W.; Yan, D.; Charpentier, P. A.; Zhu, S.; Hamielec, A. E. *Macromol. Chem. Phys.* **1998**, *199*, 2409.
445. Wang, W.-J.; Yan, D.; Zhu, S.; Hamielec, A. E. *Macromolecules* **1998**, *31*, 8677.
446. Malmberg, A.; Liimatta, J.; Lehtinen, A.; Löfgren, B. *Macromolecules* **1999**, *32*, 6687.
447. Kokko, E.; Lehmus, P.; Leino, R.; Luttikhedde, H. J.; Ekholm, P.; Näsman, J. H.; Seppälä, J. *Macromolecules* **2000**, *33*, 9200.
448. Kokko, E.; Wang, W.-J.; Seppälä, J.; Zhu, S. *J. Polym. Sci. A: Polym. Chem.* **2002**, *40*, 3292.
449. Izzo, L.; Caporaso, L.; Senatoro, G.; Oliva, L. *Macromolecules* **1999**, *32*, 6913.
450. Melillo, G.; Izzo, L.; Zinna, M.; Tedesco, C.; Oliva, L. *Macromolecules* **2002**, *35*, 9256.
451. Izzo, L.; De Riccardis, F.; Alfano, C.; Caporaso, L.; Oliva, L. *Macromolecules* **2001**, *34*, 2.
452. Resconi, L. (Montell). World Pat. Appl. WO 00/29416, 2000.
453. Brown, S. J.; Gao, X.; Harrison, D. G.; Koch, L.; Spence, R. E. v. H.; Yap, G. P. A. *Organometallics* **1998**, *17*, 5445.
454. Xu, G.; Ruckenstein, E. *Macromolecules* **1998**, *31*, 4724.
455. Alt, H. G.; Föttinger, K.; Milius, W. *J. Organomet. Chem.* **1999**, *572*, 21.
456. Klosin, J.; Kruper, W. J., Jr.; Nickias, P. N.; Roof, G. R.; De Waele, P. *Organometallics* **2001**, *20*, 2663.
457. Irwin, L. J.; Reibenspies, J. H.; Miller, S. A. *J. Am. Chem. Soc.* **2004**, *126*, 16716.
458. Foster, P.; Chien, J. C. W.; Rausch, M. D. *J. Organomet. Chem.* **1997**, *545-546*, 35.
459. Gomes, P. T.; Green, M. L. H.; Martins, A. M.; Mountford, P. *J. Organomet. Chem.* **1997**, *541*, 121.

460. Chen, Y.-X.; Fu, P.-F.; Stern, C. L.; Marks, T. J. *Organometallics* **1997**, *16*, 5958.
461. Sinnema, P.-J.; Hessen, B.; Teuben, J. H. *Macromol. Rapid Commun.* **2000**, *21*, 562.
462. van Leusen, D.; Beetstra, D. J.; Hessen, B.; Teuben, J. H. *Organometallics* **2000**, *19*, 4084.
463. Zhang, Y.; Mu, Y.; Lu, C.; Li, G.; Xu, J.; Zhang, Y.; Zhu, D.; Feng, S. *Organometallics* **2004**, *23*, 540.
464. Ryabov, A. N.; Voskoboinikov, A. Z. *J. Organomet. Chem.* **2005**, *690*, 4213.
465. Amor, F.; Butt, A.; du Plooy, K. E.; Spaniol, T. P.; Okuda, J. *Organometallics* **1998**, *17*, 5836.
466. Okuda, J.; Eberle, T.; Spaniol, T. P.; Piquet-Fauré, V. J. *Organomet. Chem.* **1999**, *591*, 127.
467. Wang, J.; Li, H.; Guo, N.; Li, L.; Stern, C. L.; Marks, T. J. *Organometallics* **2004**, *23*, 5112.
468. Kaminsky, W.; Engehausen, R.; Zoumis, K.; Spaleck, W.; Rohrmann, J. *Makromol. Chem.* **1992**, *193*, 1643.
469. Tian, J.; Huang, B. *Macromol. Rapid Commun.* **1994**, *15*, 923.
470. Janiak, C.; Versteeg, U.; Lange, K. C. H.; Weimann, R.; Hahn, E. J. *Organomet. Chem.* **1995**, *501*, 219.
471. Reetz, M. T.; Brümmer, H.; Kessler, M.; Kuhnigk, J. *Chimia* **1995**, *49*, 501.
472. Luttikhedde, H. J. G.; Leino, R. P.; Wilén, C. E.; Näsman, J. H.; Ahlgrén, M. J.; Pakkanen, T. A. *Organometallics* **1996**, *15*, 3092.
473. Leino, R.; Luttikhedde, H.; Lehtonen, A.; Wilén, C.-E.; Näsman, J. H. *J. Organomet. Chem.* **1997**, *545–546*, 219.
474. Leino, R.; Luttikhedde, H.; Lehtonen, A.; Sillanpää, R.; Penninkangas, A.; Strandén, J.; Mattinen, J.; Näsman, J. H. *J. Organomet. Chem.* **1998**, *558*, 171.
475. Thorshaug, K.; Støvneng, J. A.; Rytter, E. *Macromolecules* **2000**, *33*, 8136.
476. Müller, C.; Lilge, D.; Kristen, M. O.; Jutzi, P. *Angew. Chem., Int. Ed.* **2000**, *39*, 789.
477. Schaverien, C. J.; Ernst, R.; Schut, P.; Dall'Occo, T. *Organometallics* **2001**, *20*, 3436.
478. Ekholm, P.; Lehmus, P.; Kokko, E.; Seppälä, J. V.; Wilén, C.-E. *J. Polym. Sci. A: Polym. Chem.* **2001**, *39*, 127.
479. Bryliakov, K. P.; Semikolenova, N. V.; Yudaev, D. V.; Zakharov, V. A.; Brintzinger, H. H.; Ystenes, M.; Rytter, E.; Talsi, E. P. *J. Organomet. Chem.* **2003**, *683*, 92.
480. Möller, A. C.; Heyn, R. H.; Blom, R.; Swang, O.; Görbitz, C. H.; Kopf, J. *J. Chem. Soc., Dalton Trans.* **2004**, 1578.
481. Thornberry, M. P.; Reynolds, N. T.; Deck, P. A.; Fronczek, F. R.; Rheingold, A. L.; Liable-Sands, L. M. *Organometallics* **2004**, *23*, 1333.
482. Aitola, E.; Surakka, M.; Repo, T.; Linnolahti, M.; Lappalainen, K.; Kervinen, K.; Klinga, M.; Pakkanen, T. A.; Leskelä, M. *J. Organomet. Chem.* **2005**, *690*, 773.
483. Wang, B.; Mu, B.; Deng, X.; Cui, H.; Xu, S.; Zhou, X.; Zou, F.; Li, Y.; Yang, L.; Li, Y., *et al.* *Chem. Eur. J.* **2005**, *11*, 669.
484. Bruaseth, I.; Bahr, M.; Gerhard, D.; Rytter, E. *J. Polym. Sci. A: Polym. Chem.* **2005**, *43*, 2584.
485. Liu, J.; Støvneng, J. A.; Rytter, E. *J. Polym. Sci. A: Polym. Chem.* **2001**, *39*, 3566.
486. Quijada, R.; Dupont, J.; Silveira, D. C.; Miranda, M. S. L.; Scipioni, R. B. *Macromol. Rapid Commun.* **1995**, *16*, 357.
487. Welch, M. B.; Palackal, S. J.; Geerts, R. L.; Pettijohn, T. M. (ConocoPhillips). Eur. Pat. Appl. EP 705851, 1996.
488. Dall'Occo, T.; Resconi, L.; Balbontin, G.; Albizzati, E. (Montell). Eur. Pat. Appl. EP 821011, 1999.
489. Lee, D. L.; Yoon, K.-B. *Macromol. Rapid Commun.* **1996**, *17*, 639.
490. Beigzadeh, D.; Soares, J. B. P.; Duever, T. A. *Macromol. Rapid Commun.* **1999**, *20*, 541.
491. Reb, A.; Alt, H. G. *J. Mol. Catal. A: Chem.* **2001**, *174*, 35.
492. Mitani, M.; Oouchi, K.; Hayakawa, M.; Yamada, T.; Mukaiyama, T. *Polym. Bull.* **1995**, *35*, 677.
493. Alt, H. G.; Föttinger, K.; Milius, W. *J. Organomet. Chem.* **1998**, *564*, 115.
494. Doherty, S.; Errington, R. J.; Jarvis, A. P.; Collins, S.; Clegg, W.; Elsegood, M. R. *J. Organometallics* **1998**, *17*, 3408.
495. Antiñolo, A.; Carrillo-Hermosilla, F.; Corrochano, A.; Fernández-Baeza, J.; Lara-Sanchez, A.; Ribeiro, M. R.; Lanfranchi, M.; Otero, A.; Pellinghelli, M. A.; Portela, M. F., *et al.* *Organometallics* **2000**, *19*, 2837.
496. Kretschmer, W. P.; Dijkhuis, C.; Meetsma, A.; Hessen, B.; Teuben, J. H. *Chem. Commun.* **2002**, 608.
497. Nomura, K.; Fujii, K. *Organometallics* **2002**, *21*, 3042.
498. Nomura, K.; Fujii, K. *Macromolecules* **2003**, *36*, 2633.
499. Hessen, B. *J. Mol. Catal. A: Chem.* **2004**, *213*, 129.
500. Sanz, M.; Cuenca, T.; Galakhov, M.; Grassi, A.; Bott, R. K. J.; Hughes, D. L.; Lancaster, S. J.; Bochmann, M. *Organometallics* **2004**, *23*, 5324.
501. Beddie, C.; Hollink, E.; Wei, P.; Gauld, J.; Stephan, D. W. *Organometallics* **2004**, *23*, 5240.
502. Martins, A. M.; Marques, M. M.; Ascenso, J. R.; Dias, A. R.; Duarte, M. T.; Fernandes, A. C.; Fernandes, S.; Ferreira, M. J.; Matos, I.; Oliveira, M. C., *et al.* *J. Organomet. Chem.* **2005**, *690*, 874.
503. Cady, L. D. *Plastics* **1987**, *25*.
504. Suhm, J.; Schneider, M. J.; Mülhaupt, R. *J. Polym. Sci. A: Polym. Chem.* **1997**, *35*, 735.
505. Suhm, J.; Schneider, M. J.; Mülhaupt, R. *J. Mol. Catal. A: Chem.* **1998**, *128*, 215.
506. Wang, W.-J.; Kolodka, E.; Zhu, S.; Hamielec, A. E. *J. Polym. Sci. A: Polym. Chem.* **1999**, *37*, 2949.
507. Bonazza, A.; Camurati, I.; Guidotti, S.; Mascellani, N.; Resconi, L. *Macromol. Chem. Phys.* **2004**, *205*, 319.
508. Uozumi, T.; Soga, K. *Makromol. Chem.* **1992**, *193*, 823.
509. Reybuck, S. E.; Meyer, A.; Waymouth, R. M. *Macromolecules* **2002**, *35*, 637.
510. Fink, G.; Richter, W. J. Copolymerization Parameters of Metallocene-catalyzed Copolymerizations. In *Polymer Handbook*; Brandrup, J., Immergut, E. H., Grulke, E. A., Eds.; Wiley: New York, 1999; Vol. 1, p 329.
511. Koivumäki, J.; Seppälä, J. V. *Polymer* **1993**, *34*, 1958.
512. Lehtinen, C.; Starck, P.; Löfgren, B. *J. Polym. Sci. A: Polym. Chem.* **1997**, *35*, 307.
513. Sarzotti, D. M.; Soares, J. B. P.; Penlidis, A. *J. Polym. Sci. B: Polym. Phys.* **2002**, *40*, 2595.
514. Miyata, H.; Yamaguchi, M.; Akashi, M. *Polymer* **2001**, *42*, 5763.
515. Mäder, D.; Heinemann, J.; Walter, P.; Mülhaupt, R. *Macromolecules* **2000**, *33*, 1254.
516. Simanke, A. G.; Galland, G. B.; Freitas, L. L.; da Jornada, J. A. H.; Quijada, R. *Macromol. Chem. Phys.* **2001**, *202*, 172.
517. Wigum, H.; Solli, K.-A.; Støvneng, J. A.; Rytter, E. *J. Polym. Sci. A: Polym. Chem.* **2003**, *41*, 1622.
518. Lehmus, P.; Härkki, O.; Leino, R.; Luttikhedde, H. J.; Näsman, J. H.; Seppälä, J. *Macromol. Chem. Phys.* **1998**, *199*, 1965.
519. Kim, I.; Kim, S. Y.; Lee, M. H.; Do, Y.; Won, M.-S. *J. Polym. Sci. A: Polym. Chem.* **1999**, *37*, 2763.
520. Seppälä, J. V.; Koivumäki, J.; Liu, X. *J. Polym. Sci. A: Polym. Chem.* **1993**, *31*, 3447.
521. Koivumäki, J.; Seppälä, J. V. *Macromolecules* **1994**, *27*, 2008.
522. Mauler, R. S.; Galland, G. B.; Scipioni, R. B.; Quijada, R. *Polym. Bull.* **1996**, *37*, 469.
523. Simanke, A. G.; Alamo, R. G.; Galland, G. B.; Mauler, R. S. *Macromolecules* **2001**, *34*, 6959.

524. Koivumäki, J.; Seppälä, J. *Macromolecules* **1993**, *26*, 5535.
525. Lehmus, P.; Kokko, E.; Härkki, O.; Leino, R.; Luttikhedde, H. J. G.; Näsman, J. H.; Seppälä, J. V. *Macromolecules* **1999**, *32*, 3547.
526. Wigum, H.; Tangen, L.; Støvneng, J. A.; Rytter, E. J. *Polym. Sci. A: Polym. Chem.* **2000**, *38*, 3161.
527. Britto, M. L.; Galland, G. B.; dos Santos, J. H. Z.; Forte, M. C. *Polymer* **2001**, 6355.
528. Dankova, M.; Waymouth, R. M. *Macromolecules* **2003**, *36*, 3815.
529. Bruaseth, I.; Rytter, E. *Macromolecules* **2003**, *36*, 3026.
530. Reybuck, S. E.; Waymouth, R. M. *Macromolecules* **2004**, *37*, 2342.
531. Soga, K.; Uozumi, T.; Nakamura, S.; Toneri, T.; Teranishi, T.; Sano, T.; Arai, T. *Macromol. Chem. Phys.* **1996**, *197*, 4237.
532. Koivumäki, J. *Polym. Bull.* **1996**, *36*, 7.
533. Schneider, M. J.; Suhm, J.; Mülhaupt, R.; Prosenc, M. H.; Brintzinger, H.-H. *Macromolecules* **1997**, *30*, 3164.
534. Kaminsky, W.; Freidanck, F. *Macromol. Symp.* **2002**, *183*, 89.
535. Kaminsky, W.; Piel, C. J. *Mol. Catal. A: Chem.* **2004**, *213*, 15.
536. Koivumäki, J.; Fink, G.; Sepp, J. *Macromolecules* **1994**, *27*, 6254.
537. Nomura, K.; Naga, N.; Miki, M.; Yanagi, K. *Macromolecules* **1998**, *31*, 7588.
538. Sahoo, S. K.; Zhang, T.; Reddy, D. V.; Rinaldi, P. L.; McIntosh, L. H.; Quirk, R. P. *Macromolecules* **2003**, *36*, 4017.
539. Mahanthappa, M. K.; Cole, A. P.; Waymouth, R. M. *Organometallics* **2004**, *23*, 836.
540. Chen, Y.-X.; Marks, T. J. *Organometallics* **1997**, *16*, 3649.
541. Ashe, A. J. III; Fang, X.; Kampf, J. W. *Organometallics* **1999**, *18*, 1363.
542. Xu, G.; Cheng, D. *Macromolecules* **2001**, *34*, 2040.
543. Sehanobish, K.; Patel, R. M.; Croft, B. A.; Chum, S.; Kao, C. I. *J. Appl. Polym. Sci.* **1994**, *51*, 887.
544. Minick, J.; Moet, A.; Hiltner, A.; Baer, E.; Chum, S. P. *J. Appl. Polym. Sci.* **1995**, *58*, 1371.
545. Bensason, S.; Minick, J.; Moet, A.; Chum, S.; Hiltner, A.; Baer, E. *J. Polym. Sci. B: Polym. Phys.* **1996**, *34*, 1301.
546. Bensason, S.; Stepanov, E. V.; Chum, S.; Hiltner, A.; Baer, E. *Macromolecules* **1997**, *30*, 2436.
547. Nomura, K.; Naga, N.; Miki, M.; Yanagi, K.; Imai, A. *Organometallics* **1998**, *17*, 2152.
548. Nomura, K.; Komatsu, T.; Imanishi, Y. *J. Mol. Catal. A: Chem.* **2000**, *159*, 127.
549. Hanaoka, H.; Senda, T.; Yoshikawa, E.; Kobayashi, S. (Sumitomo Chemical). Eur. Pat. Appl. EP 1475383, 2004.
550. Mani, R.; Burns, C. M. *Polymer* **1993**, *34*, 1941.
551. Kaminsky, W.; Arrowsmith, D.; Winkelbach, H. *Polym. Bull.* **1996**, *36*, 577.
552. Chung, T. C.; Dong, J. Y. *Macromolecules* **2002**, *35*, 2868.
553. Naga, N.; Toyota, A.; Ogino, K. *J. Polym. Sci. A: Polym. Chem.* **2005**, *43*, 911.
554. Naga, N.; Toyota, A. *Polymer* **2004**, *45*, 7513.
555. Hagihara, H.; Tsuchihara, K.; Takeuchi, K.; Murata, M. *J. Polym. Sci. A: Polym. Chem.* **2004**, *42*, 52.
556. Aaltonen, P.; Löfgren, B. *Macromolecules* **1995**, *28*, 5353.
557. Aaltonen, P.; Fink, G.; Löfgren, B.; Seppälä, J. *Macromolecules* **1996**, *29*, 5255.
558. Imuta, J.; Kashiwa, N.; Toda, Y. *J. Am. Chem. Soc.* **2002**, *124*, 1176.
559. Napoli, M.; Costabile, C.; Pragliola, S.; Longo, P. *Macromolecules* **2005**, *38*, 5493.
560. Bergemann, C.; Cropp, R.; Luft, G. *J. Mol. Catal. A: Chem.* **1997**, *116*, 317.
561. Sernetz, F. G.; Mülhaupt, R.; Waymouth, R. M. *Polym. Bull.* **1997**, *38*, 141.
562. Pietikäinen, P.; Väänänen, T.; Seppälä, J. V. *Eur. Polym. J.* **1999**, *35*, 1047.
563. Kokko, E.; Pietikäinen, P.; Koivunen, J.; Seppälä, J. *J. Polym. Sci. A: Polym. Chem.* **2001**, *39*, 3805.
564. Naga, N.; Toyota, A. *Macromol. Rapid Commun.* **2004**, *25*, 1623.
565. Pietikäinen, P.; Seppälä, J. V.; Ahjopalo, L.; Pietilä, L.-O. *Eur. Polym. J.* **2000**, *36*, 183.
566. Jin, H.-J.; Choi, C.-H.; Park, E.-S.; Lee, I.-M.; Yoon, J.-S. *J. Appl. Polym. Sci.* **2002**, *84*, 1048.
567. Barnhart, R. W.; Bazan, G. C. *J. Am. Chem. Soc.* **1998**, *120*, 1082.
568. Kolodka, E.; Wang, W.-J.; Zhu, S.; Hamielec, A. *Macromol. Rapid Commun.* **2003**, *24*, 311.
569. Shiono, T.; Moriki, Y.; Ikeda, T.; Soga, K. *Macromol. Chem. Phys.* **1997**, *198*, 3229.
570. Quijada, R.; Rojas, R.; Bazan, G.; Komon, Z. J. A.; Mauler, R. S.; Galland, G. B. *Macromolecules* **2001**, *34*, 2411.
571. Beigzadeh, D.; Soares, J. B. P.; Duever, T. A. *Macromol. Symp.* **2001**, *173*, 179.
572. de Wet-Roos, D.; Dixon, J. T. *Macromolecules* **2004**, *37*, 9314.
573. Zhang, Z.; Cui, N.; Lu, Y.; Ke, Y.; Hu, Y. *J. Polym. Sci. A: Polym. Chem.* **2005**, *43*, 984.
574. Arndt, M.; Kaminsky, W.; Schauwienold, A. M.; Weingarten, U. *Macromol. Chem. Phys.* **1998**, *199*, 1135.
575. Fan, W.; Leclerc, M. K.; Waymouth, R. M. *J. Am. Chem. Soc.* **2001**, *123*, 9555.
576. Heuer, B.; Kaminsky, W. *Macromolecules* **2005**, *38*, 3054.
577. Lehtinen, C.; Löfgren, B. *Eur. Polym. J.* **1997**, *33*, 115.
578. Galimberti, M.; Mascellani, N.; Piemontesi, F.; Camurati, I. *Macromol. Rapid Commun.* **1999**, *20*, 214.
579. Galimberti, M.; Piemontesi, F.; Mascellani, N.; Camurati, I.; Fusco, O.; Destro, M. *Macromolecules* **1999**, *32*, 7968.
580. Wang, W.-J.; Zhu, S. *Macromolecules* **2000**, *33*, 1157.
581. Leclerc, M. K.; Waymouth, R. M. *Angew. Chem., Int. Ed.* **1998**, *37*, 922.
582. Jin, J.; Uozumi, T.; Sano, T.; Teranishi, T.; Soga, K.; Shiono, T. *Macromol. Rapid Commun.* **1998**, *19*, 337.
583. Galimberti, M.; Piemontesi, F.; Baruzzi, G.; Mascellani, N.; Camurati, I.; Fusco, O. *Macromol. Chem. Phys.* **2001**, *202*, 2029.
584. Djupfors, R.; Starck, P.; Löfgren, B. *Eur. Polym. J.* **1998**, *34*, 941.
585. Longo, P.; Siani, E.; Pragliola, S.; Monaco, G. *J. Polym. Sci. A: Polym. Chem.* **2002**, *40*, 3249.
586. Schottek, J.; Oberhoff, M.; Bingel, C.; Fischer, D.; Weiss, H.; Winter, A.; Fraaije, V. (Basell). World Pat. Appl. WO 01/48034, 2001.
587. Kuchta, M. C.; Stehling, U. M.; Li, R. T.; Haygood, W. T.; Burkhardt, T. J. (Exxon-Mobil). World Pat. Appl. WO 02/02575, 2002.
588. Resconi, L.; Ferrari, P.; Cecchin, G. (Basell Polyolefins). World Pat. Appl. WO 05/023889, 2005.
589. Wang, W.-J.; Zhu, S.; Park, S.-J. *Macromolecules* **2000**, *33*, 5770.
590. Kaminsky, W.; Miri, M. *J. Polym. Sci., Part A: Polym. Chem.* **1985**, *23*, 2151.
591. Parikh, D. R.; Edmondson, M. S.; Smith, B. W.; Winter, J. M.; Castille, M. J.; Magee, J. M.; Patel, R. M.; Karajala, T. P. Structure and Properties of Single-site Constrained Geometry Ethylene-Propylene-Diene (EPDM) Elastomers. In *Metallocene-catalyzed Polymers – Materials, Properties, Processing & Markets*; Benedikt, G. M., Goodall, B. L., Eds.; Plastics Design Library: New York, 1998; p 113.

592. Ho, T.; Martin, J. M. Structure, Properties and Applications of Polyolefin Elastomers Produced by Constrained Geometry Catalysts. In *Metallocene-based Polyolefins: Preparation, Properties and Technology*; Scheirs, J., Kaminsky, W., Eds.; Wiley: Chichester, 2000; Vol. 2; 175.
593. Nomura, K.; Itagaki, K.; Fujiki, M. *Macromolecules* **2005**, *38*, 2053.
594. Guerra, G.; Longo, P.; Corradini, P.; Cavallo, L. *J. Am. Chem. Soc.* **1999**, *121*, 8651.
595. Longo, P.; Grisi, F.; Guerra, G.; Cavallo, L. *Macromolecules* **2000**, *33*, 4647.
596. Kaminsky, W.; Arndt-Rosenau, M. Homo- and Copolymerization of Cycloolefins by Metallocene Catalysts. In *Metallocene-based Polyolefins: Preparation, Properties and Technology*; Scheirs, J., Kaminsky, W., Eds.; Wiley: Chichester, 2000; Vol. 2, p 89.
597. Wang, W.; Fujiki, M.; Nomura, K. *J. Am. Chem. Soc.* **2005**, *127*, 4582.
598. Kaminsky, W.; Noll, A. Polymerization of Phenyl-substituted Cyclic Olefins with Metallocene/MAO Catalysts. In *Ziegler Catalysts*; Fink, G., Mühlaupt, R., Brintzinger, H.-H., Eds.; Springer: Berlin, 1995; p 149.
599. Marathe, S.; Sivaram, S. *Macromolecules* **1994**, *27*, 1083.
600. Wang, T.-Y.; Lin, C.-H.; Jiang, G. J. *Polym. Prepr.* **1996**, *37*, 641.
601. Kaminsky, W.; Beulich, I.; Arndt-Rosenau, M. *Macromol. Symp.* **2001**, *173*, 211.
602. Radhakrishnan, K.; Sivaram, S. *Macromol. Chem. Phys.* **1999**, *200*, 858.
603. Naga, N. *J. Polym. Sci. A: Polym. Chem.* **2005**, *43*, 1285.
604. Jerschow, A.; Ernst, E.; Wolfgang, H.; Müller, N. *Macromolecules* **1995**, *28*, 7095.
605. Fujita, M.; Coates, G. W. *Macromolecules* **2002**, *35*, 9640.
606. Lavoie, A. R.; Ho, M. H.; Waymouth, R. M. *Chem. Commun.* **2003**, 864.
607. Ticona – Engineering polymers. [www.ticona.com](http://www.ticona.com).
608. Ruchatz, D.; Fink, G. *Macromolecules* **1998**, *31*, 4669.
609. Ruchatz, D.; Fink, G. *Macromolecules* **1998**, *31*, 4674.
610. Ruchatz, D.; Fink, G. *Macromolecules* **1998**, *31*, 4681.
611. Ruchatz, D.; Fink, G. *Macromolecules* **1998**, *31*, 4684.
612. Cherdron, H.; Brekner, M.-J.; Osan, F. *Angew. Macromol. Chem.* **1994**, *223*, 121.
613. Lee, B. Y.; Kim, Y. H.; Won, Y. C.; Han, J. W.; Suh, W. H.; Lee, I. S.; Chung, Y. K.; Song, K. H. *Organometallics* **2002**, *21*, 1500.
614. Lee, H.; Hong, S.-D.; Park, Y.-W.; Jeong, B.-G.; Nam, D.-W.; Jung, Y.; Jung, M. W.; Song, K. H. *J. Organomet. Chem.* **2004**, *689*, 3402.
615. Lee, S.-G.; Hong, S.-D.; Park, Y.-W.; Jeong, B.-G.; Nam, D.-W.; Jung, H. Y.; Lee, H.; Song, K. H. *Polymer* **2004**, *45*, 2586.
616. Cho, E. S.; Jung, U. G.; Lee, B. Y.; Lee, H.; Park, Y.-W.; Lee, C. H.; Shin, D. M. *Organometallics* **2004**, *23*, 4693.
617. McKnight, A. L.; Waymouth, R. M. *Macromolecules* **1999**, *32*, 2816.
618. Arndt-Rosenau, M.; Beulich, I. *Macromolecules* **1999**, *32*, 7335.
619. Tritto, I.; Boggioni, L.; Ferro, D. R. *Macromolecules* **2004**, *37*, 9681.
620. De Rosa, C.; Buono, A.; Auriemma, F.; Grassi, A. *Macromolecules* **2004**, *37*, 9489.
621. Hasan, T.; Ikeda, T.; Shiono, T. *Macromolecules* **2004**, *37*, 8503.
622. MacKnight, W. J.; Rische, T.; Waddon, A. J.; Dickinson, L. C. *Macromolecules* **1998**, *31*, 1871.
623. D'Aniello, C.; de Candia, F.; Oliva, L.; Vittoria, V. *J. Appl. Polym. Sci.* **1995**, *58*, 1701.
624. Guest, M. J.; Cheung, Y. W.; Diehl, C. F.; Hoenig, S. M. Structure, Properties and Applications of Ethylene-Styrene Interpolymers. In *Metallocene-based Polyolefins: Preparation, Properties and Technology*; Scheirs, J., Kaminsky, W., Eds.; Wiley: Chichester, 2000; Vol. 2, p 271.
625. Venditto, V.; De Tullio, G.; Izzo, L.; Oliva, L. *Macromolecules* **1998**, *31*, 4027.
626. Pellicchia, C.; Oliva, L. *Rubber Chem. Technol.* **1999**, *72*, 553.
627. Sernetz, F. G.; Mühlaupt, R.; Fokken, S.; Okuda, J. *Macromolecules* **1997**, *30*, 1562.
628. Longo, P.; Grassi, A.; Oliva, L. *Makromol. Chem.* **1990**, *191*, 2387.
629. Oliva, L.; Mazza, S.; Longo, P. *Macromol. Chem. Phys.* **1996**, *197*, 3115.
630. Aaltonen, P.; Seppälä, J. *Eur. Polym. J.* **1994**, *30*, 683.
631. Aaltonen, P.; Seppälä, J. *Eur. Polym. J.* **1995**, *31*, 79.
632. Pellicchia, C.; Pappalardo, D.; D'Arco, M.; Zambelli, A. *Macromolecules* **1996**, *29*, 1158.
633. Pellicchia, C.; Pappalardo, D.; Oliva, L.; Mazzeo, M.; Gruter, G.-J. *Macromolecules* **2000**, *33*, 2807.
634. Pellicchia, C.; Mazzeo, M.; Gruter, G.-J. *Macromol. Rapid Commun.* **1999**, *20*, 337.
635. Xu, G.; Lin, S. *Macromolecules* **1997**, *30*, 685.
636. Chu, P. P.; Tseng, H. S.; Chen, Y. P.; Yu, D. D. *Polymer* **2000**, *41*, 8271.
637. Wu, Q.; Ye, Z.; Gao, Q. H.; Lin, S. G. *Macromol. Chem. Phys.* **1998**, *199*, 1715.
638. Lee, D.-H.; Yoon, K.-B.; Kim, H.-J.; Woo, S.-S.; Noh, S. K. *J. Appl. Polym. Sci.* **1998**, *67*, 2187.
639. Nomura, K.; Komatsu, T.; Imanishi, Y. *Macromolecules* **2000**, *33*, 8122.
640. Nomura, K.; Okumura, H.; Komatsu, T.; Naga, N. *Macromolecules* **2002**, *35*, 5388.
641. Munoz-Escalona, A.; Cruz, V.; Mena, N.; Martinez, S.; Martinez-Salazar, J. *Polymer* **2002**, *43*, 7017.
642. Stevens, J. C.; Timmers, F. J.; Wilson, D. R.; Schmidt, G. F.; Nickias, P. N.; Rosen, R. K.; Knight, G. W.; Lai, S. Y. (Dow Chemical Co.). Eur. Pat. Appl. EP 416815, 1991.
643. Sernetz, F. G.; Mühlaupt, R.; Waymouth, R. M. *Macromol. Chem. Phys.* **1996**, *197*, 1071.
644. Sernetz, F. G.; Mühlaupt, R.; Amor, F.; Eberle, T.; Okuda, J. *J. Polym. Sci. A: Polym. Chem.* **1997**, *35*, 1571.
645. Xu, G. *Macromolecules* **1998**, *31*, 2395.
646. Sukhova, T. A.; Panin, A. N.; Babkina, O. N.; Bravaya, N. M. *J. Polym. Sci. A: Polym. Chem.* **1999**, *37*, 1083.
647. Nomura, K.; Okumura, H.; Komatsu, T.; Naga, N.; Imanishi, Y. *J. Mol. Catal. A: Chem.* **2002**, *190*, 225.
648. Yang, S. H.; Jo, W. H.; Noh, S. K. *J. Chem. Phys.* **2003**, *119*, 1824.
649. Skeril, R.; Sindelar, P.; Salajka, Z.; Varga, V.; Cisarova, I.; Pinkas, J.; Horacek, M.; Mach, K. *J. Mol. Catal. A: Chem.* **2004**, *224*, 97.
650. Gentil, S.; Piriou, N.; Meunier, P.; Gallou, F.; Paquette, L. A. *Eur. Polym. J.* **2004**, *40*, 2241.
651. Martinez, S.; Exposito, M. T.; Ramos, J.; Cruz, V.; Martinez, M. C.; Lopez, M.; Munoz-Escalona, A.; Martinez-Salazar, J. *J. Polym. Sci. A: Polym. Chem.* **2005**, *43*, 711.
652. Ramos, J.; Munoz-Escalona, A.; Martinez, S.; Martinez-Salazar, J.; Cruz, V. *J. Chem. Phys.* **2005**, *122*, 074901.
653. Inoue, N.; Shiomura, T.; Kouno, M. (Mitsui Toatsu Chemicals Inc.). Eur. Pat. Appl. EP 0108824, 1993.
654. Oliva, L.; Caporaso, L.; Pellicchia, C.; Zambelli, A. *Macromolecules* **1995**, *28*, 4665.
655. Oliva, L.; Longo, P.; Izzo, L.; Di Serio, M. *Macromolecules* **1997**, *30*, 5616.



656. Caporaso, L.; Izzo, L.; Sisti, I.; Oliva, L. *Macromolecules* **2002**, *35*, 4866.
657. Arai, T.; Ohtsu, T.; Suzuki, S. *Macromol. Rapid Commun.* **1998**, *19*, 327.
658. Albers, I.; Kaminsky, W.; Weingarten, U.; Werner, R. *Catal. Commun.* **2002**, *3*, 105.
659. Martinez, S.; Cruz, V.; Munoz-Escalona, A.; Martinez-Salazar, J. *Polymer* **2002**, *43*, 295.
660. Exposito, M. T.; Martinez, S.; Ramos, J.; Cruz, V. L.; Lopez, M.; Munoz-Escalona, A.; Haider, N.; Martinez-Salazar, J. *Polymer* **2004**, *45*, 9029.
661. Capacchione, C.; D'Acunzi, M.; Motta, O.; Oliva, L.; Proto, A.; Okuda, J. *Macromol. Chem. Phys.* **2004**, *205*, 370.
662. Ishiyama, T.; Miyoshi, K.; Nakazawa, H. *J. Mol. Catal. A: Chem.* **2004**, *221*, 41.
663. Zhang, H.; Nomura, K. *J. Am. Chem. Soc.* **2005**, *127*, 9364.
664. Guo, N.; Li, L.; Marks, T. J. *J. Am. Chem. Soc.* **2004**, *126*, 6542.
665. Chung, T. C.; Lu, H. L. *J. Polym. Sci. A: Polym. Chem.* **1997**, *35*, 575.
666. Chung, T. C.; Lu, H. L. *J. Polym. Sci. A: Polym. Chem.* **1998**, *36*, 1017.
667. Lu, H. L.; Hong, S.; Chung, T. C. *Macromolecules* **1998**, *31*, 2028.
668. Sernetz, F. G.; Mülhaupt, R. *J. Polym. Sci. A: Polym. Chem.* **1997**, *35*, 2549.
669. Resconi, L. *Polym. Prepr.* **2002**, *43*, 303.
670. Resconi, L.; Silvestri, R. Polypropylene, Atactic (High Molecular Weight). In *The Polymeric Materials Encyclopedia*; Salamone, J. C., Ed. CRC Press: Boca Raton, 1996; p 6609.
671. Kawamura, H.; Hayashi, T. Y.; Inoue, Y.; Chûjô, R. *Macromolecules* **1989**, *22*, 2181.
672. Busico, V.; Corradini, P.; De Martino, L.; Graziano, F.; Iadicicco, A. *Makromol. Chem.* **1991**, *192*, 49.
673. Kakugo, M.; Miyatake, T.; Kawai, K.; Shiga, A.; Mizunuma, K. (Sumitomo Chemical). Eur. Pat. Appl. EP 241560, 1987.
674. Kakugo, M.; Miyatake, T.; Mizunuma, K.; Yagi, Y. (Sumitomo Chemical). Eur. Pat. Appl. EP 371411, 1990.
675. Smith, T.; Ames, W.; Holliday, R.; Pearson, N. (Eastman Kodak). Eur. Pat. Appl. EP 232201, 1987.
676. Smith, C. (Himont). Eur. Pat. Appl. EP 423786, 1991.
677. Pellon, B.; Allen, G. (Rexene). Eur. Pat. Appl. EP 475307, 1992.
678. Job, R. (Shell Oil). U. S. Patent 5270410, 1993.
679. Pellon, B. J. In *Proceedings of the SPO '93*; Scotland Business Res. Ed.; Skillman, 1993; p 401.
680. Robe, G. R. *Adhesive Age* **1993**, 26 February.
681. Schmidt, R.; Alt, H. G. *J. Organomet. Chem.* **2001**, *621*, 304.
682. Hagihara, H.; Shiono, T.; Ikeda, T. *Macromol. Chem. Phys.* **1998**, *199*, 2439.
683. Schmidt, R.; Deppner, M.; Alt, H. G. *J. Mol. Catal. A: Chem.* **2001**, *172*, 43.
684. Yoon, J.-S.; Kwon, O.-J.; Lee, H.-K.; Lee, I.-M.; Lee, G.-Y.; Kang, M.-S.; Xue, M. *Eur. Polym. J.* **1998**, *34*, 879.
685. Naga, N.; Mizunuma, K. *Polymer* **1998**, *39*, 2703.
686. Zhang, F.; Mu, Y.; Zhao, L.; Zhang, Y.; Bu, W.; Chen, C.; Zhai, H.; Hong, H. *J. Organomet. Chem.* **2000**, *613*, 68.
687. Chen, Y.-X.; Rausch, M. D.; Chien, J. C. W. *Macromolecules* **1995**, *28*, 5399.
688. Resconi, L. Synthesis of Atactic Polypropylene Using Metallocene Catalysts. In *Metallocene-based Polyolefins: Preparation, Properties and Technology*; Scheirs, J.; Kaminsky, W., Eds.; Wiley: Chichester, 2000; Vol. 1, p 467.
689. Collins, S.; Gauthier, W. J.; Holden, D. A.; Kuntz, B. A.; Taylor, N. J.; Ward, D. G. *Organometallics* **1991**, *10*, 2061.
690. Winter, A.; Antberg, M.; Bachmann, B.; Dolle, V.; Küber, F.; Rohrmann, J.; Spaleck, W. (Hoechst). Eur. Pat. Appl. EP 584609, 1994.
691. Csok, Z.; Liguori, D.; Sessa, I.; Zannoni, C.; Zambelli, A. *Macromol. Chem. Phys.* **2004**, *205*, 1231.
692. Wu, Q.; Ye, Z.; Gao, Q.; Lin, S. *J. Polym. Sci., A: Polym. Chem.* **1998**, *36*, 2051.
693. Sassmannshausen, J.; Bochmann, M.; Rösch, J.; Lilge, D. *J. Organomet. Chem.* **1997**, *548*, 23.
694. Ewart, S. W.; Sarsfield, M. J.; Jeremic, D.; Tremblay, T. L.; Williams, E. F.; Baird, M. C. *Organometallics* **1998**, *17*, 1502.
695. Dove, A. P.; Xie, X.; Waymouth, R. M. *Chem. Commun.* **2005**, 2152.
696. Sassmannshausen, J.; Powell, A. K.; Anson, C. E.; Wocadlo, S.; Bochmann, M. *J. Organomet. Chem.* **1999**, *592*, 84.
697. Flores, J. C.; Chien, J. C. W.; Rausch, M. D. *Organometallics* **1994**, *13*, 4140.
698. Flores, J. C.; Chien, J. C. W.; Rausch, M. D. *Macromolecules* **1996**, *29*, 8030.
699. Ewart, S. W.; Parent, M. A.; Baird, M. C. *J. Polym. Sci. A: Polym. Chem.* **1999**, *37*, 4386.
700. Fukui, Y.; Murata, M.; Soga, K. *Macromol. Rapid Commun.* **1999**, *20*, 637.
701. Fukui, Y.; Murata, M. *Appl. Catal. A: Gen.* **2002**, *237*, 1–10.
702. Xie, M.; Wu, Q.; Lin, S. *Macromol. Rapid Commun.* **1999**, *20*, 167.
703. Zambelli, A.; Csok, Z.; Sessa, I. *Macromol. Rapid Commun.* **2005**, *26*, 519.
704. Erker, G.; Fritze, C. *Angew. Chem., Int. Ed. Engl.* **1992**, *31*, 199.
705. Canich, J. A. M. (Exxon). PCT Int. Appl. WO 96/00244, 1996.
706. McKnight, A. L.; Masood, M. A.; Waymouth, R. M.; Strauss, D. A. *Organometallics* **1997**, *16*, 2879.
707. Kamigaito, M.; Lal, T. K.; Waymouth, R. M. *J. Polym. Sci. A: Polym. Chem.* **2000**, *38*, 4649–4660.
708. Resconi, L.; Camurati, I.; Grandini, C.; Rinaldi, M.; Mascellani, N.; Traverso, O. *J. Organomet. Chem.* **2002**, *664*, 5.
709. De Rosa, C.; Auriemma, F.; Perretta, C. *Macromolecules* **2004**, *37*, 6843.
710. Longo, P.; Amendola, A. G.; Fortunato, E.; Boccia, A. C.; Zambelli, A. *Macromol. Rapid Commun.* **2001**, *22*, 339.
711. De Rosa, C.; Auriemma, F.; Circelli, T.; Longo, P.; Boccia, A. C. *Macromolecules* **2003**, *36*, 3465.
712. Kleinschmidt, R.; Griebenow, Y.; Fink, G. *J. Mol. Catal. A: Chem.* **2000**, *157*, 83.
713. De Rosa, C.; Auriemma, F.; Spera, C.; Talarico, G.; Tarallo, O. *Macromolecules* **2004**, *37*, 1441.
714. Ewen, J. A.; Haspelslagh, L.; Atwood, J.; Zhang, H. *J. Am. Chem. Soc.* **1987**, *109*, 6544.
715. Ushioda, T.; Fujita, H.; Saito, J. In *Proceedings of the SPO '97*; Scotland Business Res. Ed.; Skillman, 1997, p 101.
716. Nakano, M.; Ushioda, T.; Yamazaki, H.; Uwai, T.; Kimura, M.; Ohgi, Y.; Yamamoto, K. (Chisso). German Patent DE 10125356, 2002.
717. Ewen, J. A.; Jones, R. L.; Elder, M. J.; Rheingold, A. L.; Liable-Sands, L. M. *J. Am. Chem. Soc.* **1998**, *120*, 10786.
718. Ewen, J. A.; Jones, R. L.; Elder, M. J. Expanding the Scope of Metallocene Catalysis: Beyond Indenyl and Fluorenyl Derivatives. In *Metalorganic Catalysts for Synthesis and Polymerization*; Kaminsky, W., Ed.; Springer: Berlin, 1999, p 150.
719. Ewen, J. A.; Elder, M. J.; Jones, R. L. (Basell). World Pat. Appl. WO 01/44318, 2001.
720. Ewen, J. A.; Elder, M. J.; Jones, R. L.; Rheingold, A. L.; Liable-Sands, L. M.; Sommer, R. D. *J. Am. Chem. Soc.* **2001**, *123*, 4763.
721. Elder, M. J.; Okumura, Y.; Jones, R. L.; Richter, B.; Seidel, N. *Kinet. Catal.* **2006**, *47*, 192.

722. Resconi, L.; Fritze, C. Metallocene Catalysts for Propylene Polymerization. In *Polypropylene Handbook*, 2nd ed.; Pasquini, N., Ed. Hanser: Munich, 2005, p 107.
723. Hlatky, G. G. *Chem. Rev.* **2000**, *100*, 1347.
724. Fink, G.; Steinmetz, B.; Zechlin, J.; Przybyla, C.; Tesche, B. *Chem. Rev.* **2000**, *100*, 1377.
725. Resconi, L.; Guidotti, S.; Camurati, I.; Frabetti, R.; Focante, F.; Nifant'ev, I. E.; Laishevtsev, I. P. *Macromol. Chem. Phys.* **2005**, *206*, 1405.
726. Jüngling, S.; Koltzenburg, S.; Mülhaupt, R. *J. Polym. Sci. A: Polym. Chem.* **1997**, *35*, 1.
727. Burkhardt, T. J.; Hart, J. R.; Haygood, W. T.; Li, R. T. (Exxon-Mobil). World Pat. Appl. WO 03/050131, 2003.
728. Kashiwa, N.; Kojoh, S.; Imuta, J.; Tsutsui, T. Characterization of PP Prepared with the Latest Metallocene and MgCl<sub>2</sub>-Supported TiCl<sub>4</sub> Catalyst Systems. In *Metalorganic Catalysts for Synthesis and Polymerization*; Kaminsky, W., Ed.; Springer: Berlin, 1999; p 30.
729. Bingel, C.; Goeres, M.; Fraaije, V.; Winter, A. (Targor). World Pat. Appl. WO 98/40416, 1998.
730. Resconi, L.; Ciaccia, E.; Fait, A. (Basell). World Pat. Appl. WO 04/092230, 2004.
731. Ushioda, T.; Nakano, M. In *Proceedings of the MetCon*: Houston, Texas, 2002.
732. Iwama, N.; Uchino, H.; Osano, Y. T.; Sugano, T. *Organometallics* **2004**, *23*, 3267.
733. Iwama, N.; Osano, Y. T. *Organometallics* **2005**, *24*, 132.
734. Spaleck, W.; Küber, F.; Winter, A.; Rohrmann, J.; Bachmann, B.; Antberg, M.; Dolle, V.; Paulus, E. F. *Organometallics* **1994**, *13*, 954.
735. Frediani, M.; Kaminsky, W. *Macromol. Chem. Phys.* **2003**, *204*, 1941.
736. Fischer, D.; Mülhaupt, R. *Macromol. Chem. Phys.* **1994**, *195*, 1433.
737. Thomann, R.; Wang, C.; Kressler, J.; Mülhaupt, R. *Macromolecules* **1996**, *29*, 8425.
738. De Rosa, C.; Auriemma, F.; Di Capua, A.; Resconi, L.; Guidotti, S.; Camurati, I.; Nifant'ev, I. E.; Laishevtsev, I. P. *J. Am. Chem. Soc.* **2004**, *126*, 17040.
739. Rieger, B.; Mu, X.; Mallin, D. T.; Chien, J. C. W.; Rausch, M. D. *Macromolecules* **1990**, *23*, 3559.
740. Miller, S. A.; Beraw, J. E. *Organometallics* **2002**, *21*, 934.
741. Razavi, A.; Bellia, V.; De Brauer, Y.; Hortmann, K.; Peters, L.; Sirole, S.; Van Belle, S.; Thewalt, U. *Macromol. Chem. Phys.* **2004**, *205*, 347.
742. Nifant'ev, I. E.; Laishevtsev, I.; Ivchenko, P. V.; Kashulin, I. A.; Guidotti, S.; Piemontesi, F.; Camurati, I.; Resconi, L.; Klusener, P. A. A.; Rijsemus, J. J. H., *et al.* *Macromol. Chem. Phys.* **2004**, *205*, 2275.
743. Kawai, K.; Yamashita, M.; Tohi, Y.; Kawahara, N.; Michiue, K.; Kaneyoshi, H.; Mori, R. (Mitsui Chemicals). Eur. Pat. Appl. EP 1138687, 2001.
744. Ewen, J. A.; Elder, M. J. Isospecific Pseudo-helical Zirconocenium Catalysts. In *Ziegler Catalysts*; Fink, G., Mülhaupt, R., Brintzinger, H.-H., Eds.; Springer: Berlin, 1995, p 99.
745. Spaleck, W.; Aulbach, M.; Bachmann, B.; Küber, F.; Winter, A. *Macromol. Symp.* **1995**, *89*, 237.
746. Thomas, E. J.; Chien, J. C. W.; Rausch, M. D. *Macromolecules* **2000**, *33*, 1546.
747. Thomas, E. J.; Rausch, M. D.; Chien, J. C. W. *Organometallics* **2000**, *19*, 4077.
748. Coates, G. W.; Waymouth, R. M. *Science* **1995**, *267*, 217.
749. Lin, S.; Waymouth, R. M. *Acc. Chem. Res.* **2002**, *35*, 765.
750. Bravaya, N. M.; Nedorezova, P. M.; Tsvetkova, V. I. *Russ. Chem. Rev.* **2002**, *71*, 49.
751. Auriemma, F.; De Rosa, C.; Boscato, T.; Corradini, P. *Macromolecules* **2001**, *34*, 4815.
752. Bruce, M. D.; Coates, G. W.; Hauptman, E.; Waymouth, R. M.; Ziller, J. W. *J. Am. Chem. Soc.* **1997**, *119*, 11174.
753. Kravchenko, R.; Masood, A.; Waymouth, R. M. *Organometallics* **1997**, *16*, 3635.
754. Petoff, J. L. M.; Bruce, M. D.; Waymouth, R. M.; Masood, A.; Lal, T. K.; Quan, R. W.; Behrend, S. J. *Organometallics* **1997**, *16*, 5909.
755. Kravchenko, R.; Masood, A.; Waymouth, R. M.; Myers, C. L. *J. Am. Chem. Soc.* **1998**, *120*, 2039.
756. Lin, S.; Hauptman, E.; Lal, T. K.; Waymouth, R. M.; Quan, R. W.; Ernst, A. B. *J. Mol. Catal. A: Chem.* **1998**, *136*, 23.
757. Petoff, J. L. M.; Agoston, T.; Lal, T. K.; Waymouth, R. M. *J. Am. Chem. Soc.* **1998**, *120*, 11316.
758. Lin, S.; Waymouth, R. M. *Macromolecules* **1999**, *32*, 8283.
759. Tagge, C. D.; Kravchenko, R. L.; Lal, T. K.; Waymouth, R. M. *Organometallics* **1999**, *18*, 380.
760. Witte, P.; Lal, T. K.; Waymouth, R. M. *Organometallics* **1999**, *18*, 4147.
761. Lin, S.; Kravchenko, R.; Waymouth, R. M. *J. Mol. Catal. A: Chem.* **2000**, *158*, 423.
762. Lin, S.; Tagge, C. D.; Waymouth, R. M.; Nele, M.; Collins, S.; Pinto, J. C. *J. Am. Chem. Soc.* **2000**, *122*, 11275.
763. Nele, M.; Collins, S.; Dias, M. L.; Pinto, J. C.; Lin, S.; Waymouth, R. M. *Macromolecules* **2000**, *33*, 7249.
764. Dreier, T.; Erker, G.; Fröhlich, R.; Wibbeling, B. *Organometallics* **2000**, *19*, 4095.
765. Wilmes, G. M.; Lin, S.; Waymouth, R. M. *Macromolecules* **2002**, *35*, 5382.
766. Wilmes, G. M.; Polse, J. L.; Waymouth, R. M. *Macromolecules* **2002**, *35*, 6766.
767. Wiyatno, W.; Chen, Z.-R.; Liu, Y.; Waymouth, R. M.; Krukoni, V.; Brennan, K. *Macromolecules* **2004**, *37*, 701.
768. Wilmes, G. M.; France, M. B.; Lynch, S. R.; Waymouth, R. M. *Organometallics* **2004**, *23*, 2405.
769. Carlson, E. D.; Krejchi, M. T.; Shah, C. D.; Terakawa, T.; Waymouth, R. M.; Fuller, G. G. *Macromolecules* **1998**, *31*, 5343.
770. Hu, Y.; Krejchi, M. T.; Shah, C. D.; Myers, C. L.; Segre, A. L.; Talarico, G.; Vacatello, M. *J. Am. Chem. Soc.* **1998**, *120*, 6908.
771. Schönherr, H.; Wiyatno, W.; Pople, J.; Frank, C. W.; Fuller, G. G.; Gast, A. P.; Waymouth, R. M. *Macromolecules* **2002**, *35*, 2654.
772. De Rosa, C.; Auriemma, F.; Circelli, T.; Waymouth, R. M. *Macromolecules* **2002**, *35*, 3622.
773. Busico, V.; Cipullo, R.; Kretschmer, W. P.; Talarico, G.; Vacatello, M.; Van Axel Castelli, V. *Angew. Chem., Int. Ed.* **2002**, *41*, 505.
- 773a. Busico, V.; Van Axel Castelli, V.; Aprea, P.; Cipullo, R.; Segre, A. L.; Talarico, G.; Vacatello, M. *J. Am. Chem. Soc.* **2003**, *125*, 5451.
774. Carlson, E. D.; Fuller, G. G.; Waymouth, R. M. *Macromolecules* **1999**, *32*, 8100.
775. Carlson, E. D.; Fuller, G. G.; Waymouth, R. M. *Macromolecules* **1999**, *32*, 8094.
776. Resconi, L.; Piemontesi, F.; Camurati, I.; Rychlicki, H.; Colonnese, M.; Balboni, D. *Polym. Mat. Sci. Eng.* **1995**, *73*, 516.
777. Yano, A.; Kaneko, T.; Sato, M.; Akimoto, A. *Macromol. Chem. Phys.* **1999**, *200*, 2127.
778. Ewen, J. A.; Jones, R. L.; Elder, M. J.; Camurati, I.; Pritzkow, H. *Macromol. Chem. Phys.* **2004**, *205*, 302.
779. Nifant'ev, I. E.; Guidotti, S.; Resconi, L.; Laishevtsev, I. (Montell). World Pat. Appl. WO 01/47939, 2001.
780. Spaleck, W.; Antberg, M.; Aulbach, M.; Bachmann, B.; Dolle, V.; Haftka, S.; Küber, F.; Rohrmann, J.; Winter, A. New Isotactic Polypropylenes via Metallocene Catalysts. In *Ziegler Catalysts*; Fink, G., Mülhaupt, R., Brintzinger, H.-H., Eds.; Springer: Berlin, 1995; p 83.
781. Razavi, A.; Thewalt, U. *J. Organomet. Chem.* **2001**, *621*, 267.

782. Razavi, A.; Bellia, V.; Brauwer, Y. D.; Hortmann, K.; Lambrecht, M.; Miserque, O.; Peters, L.; Belle, S. V. Syndiotactic and Isotactic Specific Metallocene Catalysts with Hapto-flexible Cyclopentadienyl-fluorenyl Ligand. In *Metalorganic Catalysts for Synthesis and Polymerization*; Kaminsky, W., Ed.; Springer: Berlin, 1999; p 236.
783. Kaminsky, W.; Werner, R. New C<sub>1</sub> Symmetric Metallocenes for the Polymerization of Olefins. In *Metalorganic Catalysts for Synthesis and Polymerization*; Kaminsky, W., Ed.; Springer: Berlin, 1999; p 170.
784. Halterman, R. L.; Fahey, D. R.; Marin, V. P.; Dockter, D. W.; Khan, M. A. *J. Organomet. Chem.* **2001**, 625, 154.
785. Voegelé, J.; Dietrich, U.; Hackmann, M.; Rieger, B. Design of Ethylene-bridged ansa-Zirconocene Dichlorides for a Controlled Propene Polymerization Reaction. In *Metallocene-based Polyolefins: Preparation, Properties and Technology*; Scheirs, J., Kaminsky, W., Eds.; Wiley: Chichester, 2000; Vol. 1, p 485.
786. Müller, G.; Rieger, B. *Prog. Polym. Sci.* **2002**, 27, 815.
787. Jones, R. L.; Elder, M. J.; Ewen, J. A. In *Ninth International Business Forum on Specialty Polyolefins*; Schotland, Ed.; Schotland: Houston, Texas, 1999; p 141.
788. Resconi, L.; Guidotti, S.; Camurati, I.; Nifant'ev, I. E.; Laishevstev, I. *Polym. Mat. Sci. Eng.* **2002**, 87, 76.
789. Rieger, B.; Troll, C.; Preuschen, J. *Macromolecules* **2002**, 35, 5742.
790. Kukral, J.; Lehmus, P.; Feifel, T.; Troll, C.; Rieger, B. *Organometallics* **2000**, 19, 3767.
791. Kukral, J.; Lehmus, P.; Klinga, M.; Leskelä, M.; Rieger, B. *Eur. J. Inorg. Chem.* **2002**, 1349.
792. Deisenhofer, S.; Feifel, T.; Kukral, J.; Klinga, M.; Leskelä, M.; Rieger, B. *Organometallics* **2003**, 22, 3495.
793. Cobzaru, C.; Deisenhofer, S.; Harley, A.; Troll, C.; Hild, S.; Rieger, B. *Macromol. Chem. Phys.* **2005**, 206, 1231.
794. Veghini, D.; Henling, L. M.; Burkhardt, T. J.; Bercaw, J. E. *J. Am. Chem. Soc.* **1999**, 121, 564.
795. Busico, V.; Cipullo, R.; Talarico, G.; Segre, A. L.; Caporaso, L. *Macromolecules* **1998**, 31, 8720.
796. Winter, A.; Rohrmann, J.; Antberg, M.; Dolle, V.; Spaleck, W. (Hoechst). Eur. Pat. Appl. EP 387690, 1990.
797. Alt, H. G.; Zenk, R. *J. Organomet. Chem.* **1996**, 522, 39.
798. Alt, H. G.; Zenk, R. *J. Organomet. Chem.* **1996**, 522, 177.
799. Alt, H. G.; Zenk, R. *J. Organomet. Chem.* **1996**, 518, 7.
800. Alt, H. G.; Zenk, R.; Milius, W. *J. Organomet. Chem.* **1996**, 514, 257.
801. Patsidis, K.; Alt, H. G.; Milius, W.; Palackal, S. *J. Organomet. Chem.* **1996**, 509, 63.
802. Miyake, S.; Bercaw, J. E. *J. Mol. Catal. A: Chem.* **1998**, 128, 29.
803. Gentil, S.; Dietz, M.; Pirio, N.; Meunier, P.; Gallucci, J. C.; Paquette, L. A. *Organometallics* **2002**, 21, 5162.
804. Razavi, A.; Bellia, V.; De Brauwer, Y.; Hortmann, K.; Peters, L.; Sirole, S.; Van Belle, S.; Marin, V.; Lopez, M. *J. Organomet. Chem.* **2003**, 684, 206.
805. Müller, F.; Hopf, A.; Kaminsky, W.; Lemstra, P. J.; Loos, J. *Polymer* **2004**, 45, 1815.
806. Miller, S. A.; Bercaw, J. E. *Organometallics* **2004**, 23, 1777.
807. Ashe, A. J. III; Fang, X.; Hokky, A.; Kampf, J. W. *Organometallics* **2004**, 23, 2197.
808. Grisi, F.; Longo, P.; Zambelli, A.; Ewen, J. A. *J. Mol. Catal. A: Chem.* **1999**, 140, 225.
809. Kaminsky, W.; Hopf, A.; Piel, C. *J. Organomet. Chem.* **2003**, 684, 200.
810. Song, W.; Rausch, M. D.; Chien, J. C. W. *J. Polym. Sci. A: Polym. Chem.* **1996**, 34, 2945.
811. Shiomura, T.; Uchikawa, N.; Asanuma, T.; Sugimoto, R.; Fujio, I.; Kimura, S.; Harima, S.; Akiyama, M.; Kohno, M.; Inoue, N. Metallocene-catalyzed Syndiotactic Polypropylene: Preparation and Properties. In *Metallocene-based Polyolefins: Preparation, Properties and Technology*; Scheirs, J., Kaminsky, W., Eds.; Wiley: Chichester, 2000; Vol. 1, p 467.
812. Shamsoum, E. S.; Sun, L.; Reddy, B. R.; Turner, D. In *Metcon 94*; Houston, TX, USA, 1994.
813. Shamsoum, E. S.; Sun, L.; Kim, S. In *Proceedings of the SPO '95*; Schotland: Houston, 1995; p 299.
814. De Rosa, C.; Corradini, P. *Macromolecules* **1993**, 26, 5711.
815. Auriemma, F.; De Rosa, C.; Corradini, P. *Macromolecules* **1993**, 26, 5719.
816. Lovinger, A. J.; Lotz, B.; Davis, D. D.; Schumacher, M. *Macromolecules* **1994**, 27, 6603.
817. Rodríguez-Arnold, J.; Bu, Z.; Cheng, S. Z. D. *J. M. S. - Rev. Macromol. Chem. Phys.* **1995**, C35, 117.
818. De Rosa, C.; Auriemma, F.; Corradini, P. *Macromolecules* **1996**, 29, 7452.
819. De Rosa, C.; Auriemma, F.; Vinti, V. *Macromolecules* **1998**, 31, 7430.
820. De Rosa, C.; Auriemma, F.; Vinti, V.; Galimberti, M. *Macromolecules* **1998**, 31, 6206.
821. Auriemma, F.; Ruiz de Ballesteros, O.; De Rosa, C. *Macromolecules* **2001**, 34, 4485.
822. Nishii, K.; Matsumae, T.; Dare, E. O.; Shiono, T.; Ikeda, T. *Macromol. Chem. Phys.* **2004**, 205, 363.
823. Busico, V.; Cipullo, R.; Cutillo, F.; Talarico, G.; Razavi, A. *Macromol. Chem. Phys.* **2003**, 204, 1269.
824. Grandini, C.; Camurati, I.; Guidotti, S.; Mascellani, N.; Resconi, L.; Nifant'ev, I. E.; Kashulin, I. A.; Ivchenko, P. V.; Mercandelli, P.; Sironi, A. *Organometallics* **2004**, 23, 344.
825. De Rosa, C.; Auriemma, F.; Ruiz de Ballesteros, O.; Resconi, L.; Fait, A.; Ciaccia, E.; Camurati, I. *J. Am. Chem. Soc.* **2003**, 125, 10913.
826. De Rosa, C.; Auriemma, F.; Ruiz de Ballesteros, O. *Macromolecules* **2003**, 36, 7607.
827. De Rosa, C.; Auriemma, F.; Ruiz de Ballesteros, O. *Macromolecules* **2004**, 37, 1422.
828. Okumura, Y.; Oberhoff, M.; Schottek, J. (Basell). World Pat. Appl. WO 03/045551, 2003.
829. Okumura, Y.; Seidel, N.; Koelling, L. (Basell). World Pat. Appl. WO 04/106351, 2004.
830. Chatterjee, A. M.; Campbell, R. N. In *52nd ANTEC*; SPE., Ed.; SPE: Houston, 1994, p 1977.
831. Chatterjee, A. M.; Campbell, R. N. *J. Plastic Film & Sheeting* **1994**, 10, p 344.
832. Hosoda, S.; Hori, H.; Yada, K.; Nakahara, S.; Tsuji, M. *Polymer* **2002**, 43, 7451.
833. Mitsui Chemicals America, INC. www.Mitsuichemicals.com.
834. Arnold, M.; Henschke, O.; Knorr, J. *Macromol. Chem. Phys.* **1996**, 197, 563.
835. De Rosa, C.; Auriemma, F.; Orlando, I.; Talarico, G.; Caporaso, L. *Macromolecules* **2001**, 34, 1663.
836. Naga, N.; Mizunuma, K.; Sadatoshi, H.; Kakugo, M. *Macromolecules* **1997**, 30, 2197.
837. Kersting, M.; Langhauser, F.; Kerth, J.; Schweier, G. (BASF). World Pat. Appl. WO 94/28039, 1994.
838. Fischer, D.; Langhauser, F.; Lilge, D.; Hingmann, R.; Schweier, G. (BASF). World Pat. Appl. WO 97/10286, 1997.
839. Ueda, T.; Mizuno, A.; Kawasaki, M.; Fukuoka, D.; Kiso, Y.; Tanizaki, T.; Hashimoto, M.; Sugi, M.; Tsutsui, T. (Mitsui Petrochemical). Eur. Pat. Appl. EP 682042, 1999.

840. Karandinos, A. G.; Lohse, D. J.; Georjon, O. J. F.; Lewtas, K.; Tancrede, J. M.; Harrington, B. A.; Nelson, K. A. (Exxon). World Pat. Appl. WO 01/46278, 2001.
841. Tsutsui, T.; Yoshitsugu, K.; Toyota, A. (Mitsui Petrochemical). Eur. Pat. Appl. EP 495 099, 1991.
842. Wahner, U. M.; Tincul, I.; Joubert, D. J.; Sadiku, E. R.; Forlini, F.; Losio, S.; Tritto, I.; Sacchi, M. C. *Macromol. Chem. Phys.* **2003**, *204*, 1738.
843. Sacchi, M. C.; Forlini, F.; Losio, S.; Tritto, I.; Wahner, U. M.; Tincul, I.; Joubert, D. J.; Sadiku, E. R. *Macromol. Chem. Phys.* **2003**, *204*, 1643.
844. Costa, G.; Stagnaro, P.; Trefiletti, V.; Sacchi, M. C.; Forlini, F.; Alfonso, G. C.; Tincul, I.; Wahner, U. M. *Macromol. Chem. Phys.* **2004**, *205*, 383.
845. Sacchi, M. C.; Forlini, F.; Tritto, I.; Stagnaro, P. *Macromol. Chem. Phys.* **2004**, *205*, 1804.
846. Arnold, M.; Bornemann, S.; Köller, F.; Menke, T. J.; Kressler, J. *Macromol. Chem. Phys.* **1998**, *199*, 2647.
847. van Reenen, A. J. *Macromol. Symp.* **2003**, *193*, 57.
848. Forlini, F.; Fan, Z. Q.; Tritto, I.; Locatelli, P.; Sacchi, M. C. *Macromol. Chem. Phys.* **1997**, *198*, 2397.
849. Forlini, F.; Tritto, I.; Locatelli, P.; Sacchi, M. C.; Piemontesi, F. *Macromol. Chem. Phys.* **2000**, *201*, 401.
850. Forlini, F.; Princi, E.; Tritto, I.; Sacchi, M. C.; Piemontesi, F. *Macromol. Chem. Phys.* **2002**, *203*, 645.
851. Song, F.; Pappalardo, D.; Johnson, A. F.; Rieger, B.; Bochmann, M. J. *Polym. Sci., Part A: Polym. Chem.* **2002**, *40*, 1484.
852. Poon, B.; Rogunova, M.; Hiltner, A.; Baer, E.; Chum, S. P.; Galeski, A.; Piorowska, E. *Macromolecules* **2005**, *38*, 1232.
853. Schneider, M. J.; Mülhaupt, R. *Macromol. Chem. Phys.* **1997**, *198*, 1121.
854. Juengling, S.; Koltzenburg, S.; Mülhaupt, R. J. *Polym. Sci. A: Polym. Chem.* **1997**, *35*, 1.
855. Fan, Z.-Q.; Yasin, T.; Feng, L.-X. *J. Polym. Sci. A: Polym. Chem.* **2000**, *38*, 4299.
856. van Reenen, A. J.; Brull, R.; Wahner, U. M.; Raubenheimer, H. G.; Sanderson, R. D.; Pasch, H. J. *Polym. Sci. A: Polym. Chem.* **2000**, *38*, 4110.
857. Poon, B.; Rogunova, M.; Chum, S. P.; Hiltner, A.; Baer, E. J. *Polym. Sci. B: Polym. Phys.* **2004**, *42*, 4357.
858. Palza, H.; Lopez-Majada, J. M.; Quijada, R.; Benavente, R.; Pérez, E.; Cerrada, M. L. *Macromol. Chem. Phys.* **2005**, *206*, 1221.
859. Henschke, O.; Koller, F.; Arnold, M. *Macromol. Rapid Commun.* **1997**, *18*, 617.
860. Naga, N.; Imanishi, Y. J. *Polym. Sci. A: Polym. Chem.* **2003**, *41*, 441.
861. Boggioni, L.; Bertini, F.; Zannoni, G.; Tritto, I.; Carbone, P.; Ragazzi, M.; Ferro, D. R. *Macromolecules* **2003**, *36*, 882.
862. Hasan, T.; Ikeda, T.; Shiono, T. *Macromolecules* **2005**, *38*, 1071.
863. Kono, H.; Ichiki, T.; Mori, H.; Nakatani, H.; Terano, M. *Polym. Int.* **2001**, *50*, 568.
864. Hackmann, M.; Repo, T.; Jany, G.; Rieger, B. *Macromol. Chem. Phys.* **1998**, *199*, 1511.
865. Hackmann, M.; Rieger, B. *Macromolecules* **2000**, *33*, 1524.
866. Jüngling, S.; Mülhaupt, R.; Fischer, D.; Langhauser, F. *Angew. Makromol. Chem.* **1995**, *229*, 93.
867. Caporaso, L.; Izzo, L.; Oliva, L. *Macromolecules* **1999**, *32*, 7329.
868. Caporaso, L.; Izzo, L.; Zappale, S.; Oliva, L. *Macromolecules* **2000**, *33*, 7275.
869. Hakala, K.; Löfgren, B.; Helaja, T. *Eur. Polym. J.* **1998**, *34*, 1093.
870. Hagihara, H.; Tsuchihara, K.; Takeuchi, K.; Murata, M.; Ozaki, H.; Shiono, T. J. *Polym. Sci. A: Polym. Chem.* **2003**, *42*, 52.
871. Shiono, T.; Azad, S. M.; Ikeda, T. *Macromolecules* **1999**, *32*, 5723.
872. Weng, W.; Dekmezian, A. H.; Markel, E. J.; Peters, D. L. (Exxon). U.S. Patent 6184327, 2001.
873. Walter, P.; Trinkle, S.; Lilge, D.; Friedrich, C.; Mülhaupt, R. *Macromol. Mater. Eng.* **2001**, *286*, 309.
874. Agarwal, P. K.; Somani, R. H.; Weng, W.; Mehta, A.; Yang, L.; Ran, S.; Liu, L.; Hsiao, B. S. *Macromolecules* **2003**, *36*, 5226.
875. Langston, J.; Dong, J. Y.; Chung, T. C. *Macromolecules* **2005**, *38*, 5849.
876. Ye, Z.; Zhu, S. J. *Polym. Sci. A: Polym. Chem.* **2003**, *41*, 1152.
877. Henschke, O.; Neubauer, A.; Arnold, M. *Macromolecules* **1997**, *30*, 8097.
878. Basell [www.basell.com](http://www.basell.com), **2004**.
879. Rubin, I. D. *Poly(1-Butene) – Its Preparation and Properties*; Gordon and Breach: New York, 1968.
880. Foglia, A. J. *Appl. Polym. Symp.* **1969**, *11*, 1.
881. Chatterjee, A. M. Butene polymers. In *Encyclopedia of Polymer Science and Engineering*; Kroschwitz, J. I., Klingsberg, A., Muldoon, J., Salvatore, A., Eds.; Wiley: New York, 1985; Vol. 2, p 590.
882. Luciani, L.; Seppälä, J.; Löfgren, B. *Prog. Polym. Sci.* **1988**, *13*, 37.
883. Abedi, S.; Sharifi-Sanjani, N. J. *Appl. Polym. Sci.* **2000**, *78*, 2533.
884. Vitale, G.; Morini, G.; Cecchin, G. (Basell). World Pat. Appl. WO 03/099883, 2003.
885. Morini, G.; Piemontesi, F.; Vitale, G.; Bigiavi, D.; Pelliconi, A.; Garagnani, E.; Baita, P. (Basell). World Pat. Appl. WO 04/048424, 2004.
886. Icenogle, R. D.; Klingensmith, G. B. *Macromolecules* **1987**, *20*, 2788.
887. Busico, V.; Corradini, P.; De Biasio, R. *Makromol. Chem.* **1992**, *193*, 897.
888. Kaminsky, W.; Niedoba, S.; Möller-Lindenhof, N.; Rabe, O. In *Catalysis in Polymer Synthesis, ACS Symposium Series*; Vandenberg, E. J., Salamone, J. C., Eds.; American Chemical Society: Washington, DC, 1992; Vol. 496, p 63.
889. Kioka, M.; Tsutsui, T.; Ueda, T.; Kashiwa, N. Stereospecific Polymerization of  $\alpha$ -Olefin with an Ethylene Bis(1-indenyl)hafnium Dichloride and Methyl-aluminoxane Catalyst System. In *Catalytic Olefin Polymerization, Studies in Surface Science and Catalysis*; Keii, T., Soga, K., Eds.; Elsevier: New York, 1990, p 483.
890. Busico, V.; Cipullo, R.; Borriello, A. *Macromol. Rapid Commun.* **1995**, *16*, 269.
891. Herfert, N.; Fink, G. *Makromol. Chem., Macromol. Symp.* **1993**, *66*, 157.
892. Albizzati, E.; Resconi, L.; Zambelli, A. (Himont). Eur. Pat. Appl. EP 387609, 1990.
893. Asanuma, T.; Nishimori, Y.; Ito, M.; Uchikawa, N.; Shiomura, T. *Polym. Bull.* **1991**, *25*, 567.
894. Resconi, L.; Jones, R. L. (Montell). Eur. Pat. Appl. EP 604908, 1994.
895. Naga, N.; Mizunuma, K. *Macromol. Rapid Commun.* **1997**, *18*, 581.
896. Naga, N.; Shiono, T.; Ikeda, T. *Macromol. Chem. Phys.* **1999**, *200*, 1587.
897. Vathauer, M.; Kaminsky, W. *Macromolecules* **2000**, *33*, 1955.
898. Minami, Y.; Kanamaru, M.; Kakigami, K.; Funabashi, H. t. (Idemitsu Petrochemical). Eur. Pat. Appl. EP 1260525, 2002.
899. Huang, Q.; Wu, Q.; Zhu, F.; Lin, S. J. *Polym. Sci. A: Polym. Chem.* **2001**, *39*, 4068.
900. Huang, Q.; Zhu, F.; Wu, Q.; Lin, S. *Polym. Int.* **2001**, *50*, 45.
901. Fujita, H.; Seki, Y.; Miyatake, T. *Macromol. Chem. Phys.* **2004**, *205*, 884.
902. Collette, J. W.; Tullock, C. W. (Du Pont). U.S. Patent 4298722, 1981.
903. Resconi, L.; Camurati, I.; Malizia, F. *Macromol. Chem. Phys.* accepted for publication.
904. Resconi, L. (Basell). *Macromol. Chem. Phys.* accepted for publication.



905. Resconi, L. (Basell). World Pat. Appl. WO 02/100909, 2002.
906. Resconi, L. (Basell). World Pat. Appl. WO 03/042258, 2003.
907. Resconi, L.; Cascio Ingurgio, A. (Basell). World Pat. Appl. WO 04/050724, 2004.
908. Resconi, L.; Pelliconi, A.; Garagnani, E. (Basell). World Pat. Appl. WO 04/050713, 2004.
909. Resconi, L. (Basell). World Pat. Appl. WO 04/099269, 2004.
910. Kohyama, M.; Muranaka, T.; Fukui, K.; Kashiwa, N. (Mitsui Petrochemical). U.S. Patent 4801672, 1989.
911. Asakura, T.; Demura, M.; Nishiyama, Y. *Macromolecules* **1991**, *24*, 2334.
912. Galimberti, M.; Balbontin, G.; Camurati, I.; Paganetto, G. *Macromol. Rapid Commun.* **1994**, *15*, 633.
913. Kim, I.; Zhou, J.-M.; Chung, H. *J. Polym. Sci. A: Polym. Chem.* **2000**, *38*, 1687.
914. Grumel, V.; Bruell, R.; Pasch, H.; Raubenheimer, H. G.; Sanderson, R.; Wahner, U. *Macromol. Mater. Eng.* **2001**, *286*, 480.
915. Bruell, R.; Kgosane, D.; Neveling, A.; Pasch, H.; Raubenheimer, H. G.; Sanderson, R.; Wahner, U. *Macromol. Symp.* **2001**, *165*, 11.
916. Mosia, M. R., Ph.D. Thesis, Eindhoven University of Technology, Eindhoven, The Netherlands, 2004.
917. Chien, J. C. W.; Gong, B. M. *J. Polym. Sci. A: Polym. Chem.* **1993**, *31*, 1747.
918. Babu, G. N.; Newmark, R. A.; Chien, J. C. W. *Macromolecules* **1994**, *27*, 3383.
919. Frauenrath, H.; Keul, H.; Höcker, H. *Macromol. Rapid Commun.* **1998**, *19*, 391.
920. Frauenrath, H.; Keul, H.; Höcker, H. *Macromol. Chem. Phys.* **2001**, *202*, 3543.
921. Frauenrath, H.; Keul, H.; Höcker, H. *Macromol. Chem. Phys.* **2001**, *202*, 3551.
922. Liu, Z.; Somsook, E.; Landis, C. R. *J. Am. Chem. Soc.* **2001**, *123*, 2915.
923. Coevoet, D.; Cramail, H.; Deffieux, A. *Macromol. Chem. Phys.* **1996**, *197*, 855.
924. Coevoet, D.; Cramail, H.; Deffieux, A. *Macromol. Chem. Phys.* **1998**, *199*, 1451.
925. Coevoet, D.; Cramail, H.; Deffieux, A. *Macromol. Chem. Phys.* **1998**, *199*, 1459.
926. Coevoet, D.; Cramail, H.; Deffieux, A. *Macromol. Chem. Phys.* **1999**, *200*, 1208.
927. Pédeutour, J.-N.; Cramail, H.; Deffieux, A. *J. Mol. Catal. A: Chem* **2001**, *176*, 87.
928. Sita, L. R.; Jayaratne, K. C. *J. Am. Chem. Soc.* **2000**, *122*, 958.
929. Keaton, R. J.; Jayaratne, K. C.; Henningsen, D. A.; Koterwas, L. A.; Sita, L. R. *J. Am. Chem. Soc.* **2001**, *123*, 6197.
930. Nomura, K.; Fudo, A. *J. Mol. Catal. A: Chem.* **2004**, *209*, 9.
931. Zhang, Y.; Sita, L. R. *J. Am. Chem. Soc.* **2004**, *126*, 7776.
932. Siedle, A. R.; Newmark, R. A.; Duerr, B. F.; Leung, P. C. *J. Mol. Catal. A: Chem.* **2004**, *214*, 187.
933. Yamaguchi, Y.; Suzuki, N.; Fries, A.; Mise, T.; Koshino, H.; Ikegami, Y.; Ohmori, H.; Matsumoto, A. *J. Polym. Sci. A: Polym. Chem.* **1999**, *37*, 283.
934. Suzuki, N.; Masubuchi, Y.; Yamaguchi, Y.; Kase, T.; Miyamoto, T. K.; Horiuchi, A.; Mise, T. *Macromolecules* **2000**, *33*, 754.
935. Suzuki, N.; Yamaguchi, Y.; Fries, A.; Mise, T. *Macromolecules* **2000**, *33*, 4602.
936. Hoff, M.; Kaminsky, W. *Macromol. Chem. Phys.* **2004**, *205*, 1167.
937. Krentsel, B. A.; Kissin, Y. V.; Kleiner, V. J.; Stotskaya, L. L. *Polymers and Copolymers of Higher  $\alpha$ -Olefins*; Hanser: Munich, 1997.
938. Mitsui Chemicals [www.mitsui-chem.co.jp](http://www.mitsui-chem.co.jp), **2005**.
939. Zambelli, A.; Ammendola, P.; Proto, A. *Macromolecules* **1989**, *22*, 2126.
940. De Rosa, C.; Venditto, V.; Guerra, G.; Corradini, P. *Macromolecules* **1992**, *25*, 6938.
941. De Rosa, C.; Grassi, A.; Capitani, D. *Macromolecules* **1998**, *31*, 3163.
942. Irwin, L. J.; Miller, S. A. *J. Am. Chem. Soc.* **2005**, *127*, 9972.
943. Stehling, U.; Diebold, J.; Kirsten, R.; Röhl, W.; Brintzinger, H.-H.; Jüngling, S.; Mülhaupt, R.; Langhauser, F. *Organometallics* **1994**, *13*, 964.
944. Borriello, A.; Busico, V.; Cipullo, R.; Chadwick, J. C.; Sudmeijer, O. *Macromol. Rapid Commun.* **1996**, *17*, 589.
945. Oliva, L.; Longo, P.; Zambelli, A. *Macromolecules* **1996**, *29*, 6383.
946. Sacchi, M. C.; Basties, E.; Tritto, I.; Locatelli, P.; Brintzinger, H.-H.; Stehling, U. *Macromolecules* **1997**, *30*, 1267.
947. Chien, J. C. W.; Vizzini, J. C.; Kaminsky, W. *Macromol. Chem. Rapid Commun.* **1992**, *13*, 479.
948. Byun, D.-J.; Shin, D.-K.; Liu, J.; Kim, S. Y. *Polym. Bull.* **1999**, *42*, 265.
949. Byun, D.-J.; Shin, D.-K.; Kim, S. Y. *Polym. Bull.* **1999**, *42*, 301.
950. Longo, P.; Grassi, A.; Grisi, F.; Milione, S. *Macromol. Rapid Commun.* **1998**, *19*, 229.
951. Ishihara, N.; Seimiya, T.; Kuramoto, M.; Uoi, U. *Macromolecules* **1986**, *19*, 2464.
952. Ishihara, N.; Kuramoto, M.; Uoi, U. Eur. Pat. EP 210615, 1987.
953. Ishihara, N.; Kuramoto, M.; Uoi, U. U.S. Patent 4680353, 1987.
954. Grassi, A.; Pellicchia, C.; Longo, P.; Zambelli, A. *Gazz. Chim. Ital.* **1987**, *117*, 249.
955. Ammendola, P.; Pellicchia, C.; Longo, P.; Zambelli, A. *Gazz. Chim. Ital.* **1987**, *117*, 65.
956. Ishihara, N.; Kuramoto, M.; Uoi, M. *Macromolecules* **1988**, *21*, 3356.
957. Ishihara, N.; Kuramoto, M. *Stud. Surf. Sci. Catal.* **1994**, *89*, 339.
958. Ishihara, N. *Macromol. Symp.* **1995**, *89*, 553.
959. Tomotsu, N.; Ishihara, N. *Stud. Surf. Sci. Catal.* **1999**, *121*, 269.
960. Pellicchia, C.; Longo, P.; Grassi, A.; Ammendola, P.; Zambelli, A. *Macromol. Chem., Rapid Commun.* **1987**, *8*, 277.
961. Zambelli, A.; Longo, P.; Pellicchia, C.; Grassi, A. *Macromolecules* **1987**, *20*, 2035.
962. Ammendola, P.; Shijing, X.; Grassi, A.; Zambelli, A. *Gazz. Chim. Ital.* **1988**, *118*, 769.
963. Oliva, L.; Pellicchia, C.; Cinquina, P.; Zambelli, A. *Macromolecules* **1989**, *22*, 1642.
964. Zambelli, A.; Pellicchia, C.; Oliva, L.; Longo, P.; Grassi, A. *Macromol. Chem.* **1991**, *192*, 223.
965. Zambelli, A.; Pellicchia, C.; Proto, A. *Macromol. Symp.* **1995**, *89*, 373.
966. Po, R.; Cardi, N. *Prog. Polym. Sci.* **1996**, *21*, 47.
967. Tomotsu, N.; Ishihara, N.; Newman, T. H.; Malanga, M. T. *J. Mol. Catal. A: Chem.* **1998**, *128*, 167.
968. Pellicchia, C.; Grassi, A. *Top. Catal.* **1999**, *7*, 125.
969. Ready, T. E.; Day, R. O.; Chien, J. C. W.; Rausch, M. D. *Macromolecules* **1993**, *26*, 5822.
970. Ready, T. E.; Chien, J. C. W.; Rausch, M. D. *J. Organomet. Chem.* **1999**, *583*, 11.
971. Schneider, N.; Proscenc, M.-H.; Brintzinger, H.-H. *J. Organomet. Chem.* **1997**, *545–546*, 291.
972. Kaminsky, W.; Lenk, S.; Scholz, V.; Roesky, H. W.; Herzog, A. *Macromolecules* **1997**, *30*, 7647.
973. Chien, J. C. W.; Salajka, Z. *J. Pol. Sci., Part A: Pol. Chem.* **1991**, *29*, 1253.

974. Sun, X.; Xie, J.; Zhang, H.; Huang, J. *Eur. Polym. J.* **2004**, *40*, 1903.
975. Schellenberg, J. *Eur. Polym. J.* **2004**, *40*, 2259.
976. Qian, Y.; Zhang, H.; Zhou, J.; Zhao, W.; Sun, X.; Huang, J. *J. Mol. Catal. A: Chem.* **2004**, *208*, 45.
977. Nomura, K.; Fujita, K.; Fujiki, M. *Catal. Commun.* **2004**, *5*, 413.
978. Qian, X.; Huang, J.; Qian, Y.; Wang, C. *Appl. Organomet. Chem.* **2003**, *17*, 277.
979. Nomura, K.; Fudo, A. *Catal. Commun.* **2003**, *4*, 269.
980. Jamanek, D.; Woyda, A.; Skupinski, W. *Appl. Organomet. Chem.* **2002**, *16*, 575.
981. Lee, B. Y.; Han, J. W.; Seo, H.; Lee, I. S.; Chung, Y. K. *J. Organomet. Chem.* **2001**, *627*, 233.
982. Soga, K.; Kawabe, M.; Murata, M.; Kase, T.; Ozaki, H.; Fukui, Y.; Hoang, T. B.; Jin, J.; Miyazawa, A.; Hagihara, H., *et al.* (Japan as Represented by Secretary of Agency of Industrial Science and Technology, Japan; Japan Chemical Innovation Institute; Soga, Hisae). World Pat. Appl. WO 0158964, 2001.
983. Xu, G.; Cheng, D. *Macromolecules* **2000**, *33*, 2825.
984. Schellenberg, J. *J. Polym. Sci. A: Polym. Chem.* **2000**, *38*, 2428.
985. Rhodes, B.; Rausch, M. D.; Chien, J. C. W. *J. Polym. Sci. A: Polym. Chem.* **2000**, *39*, 313.
986. Liu, J.; Ma, H.; Huang, J.; Qian, Y. *Eur. Polym. J.* **2000**, *36*, 2055.
987. Xu, G. *Macromolecules* **1998**, *31*, 586.
988. Liu, J.; Ma, H.; Huang, J.; Qian, Y.; Chan, A. S. C. *Eur. Polym. J.* **1998**, *35*, 543.
989. Kaminsky, W.; Lenk, S. *Macromol. Symp.* **1997**, *118*, 45.
990. Kawabe, M.; Murata, M.; Kase, T.; Ozaki, H.; Fukui, Y.; Juang, T.; Jin, J.; Miyazawa, T.; Hagiwara, H.; Tsuchihara, K., *et al.* (Agency of Industrial Sciences and Technology, Japan; Zaidan Hojin Kagaku Gijitsu Senryakusuishin Kiko). Jpn. Kokai Tokkyo Koho JP 2000319323, 2000.
991. Ready, T. E.; Chien, J. C. W.; Rausch, M. D. *J. Organomet. Chem.* **1996**, *519*, 21.
992. Tian, G.; Xu, S.; Zhang, Y.; Wang, B.; Zhou, X. *J. Organomet. Chem.* **1998**, *558*, 231.
993. Qian, Y.; Zhang, H.; Qian, X.; Chen, B.; Huang, J. *Eur. Polym. J.* **2002**, *38*, 1613.
994. Huang, B.; Cao, K.; Li, B.-G.; Zhu, S. J. *Appl. Polym. Sci.* **2004**, *94*, 1449.
995. Schellenberg, J.; Knoll, S.; Nord, G.; Leukefeld, W. *Eur. Polym. J.* **2003**, *39*, 2351.
996. Choi, K. Y.; Chung, J. S.; Woo, B. G.; Hong, M. H. *J. Appl. Polym. Sci.* **2003**, *88*, 2132.
997. Pasquet, V.; Spitz, R. *Macromol. Chem. Phys.* **2001**, *202*, 2346.
998. Kawabe, M.; Murata, M. *Macromol. Chem. Phys.* **2001**, *202*, 2440.
999. Klosin, J.; Kruper, W. J., Jr.; Nickias, P. N.; Roof, G. R.; Soto, J. (Dow Chemical). World Pat. Appl. WO 01/042315, 2001.
1000. Pasquet, V.; Spitz, R. *Macromol. Chem. Phys.* **1999**, *200*, 1453.
1001. Kaminsky, W.; Arrowsmith, D.; Strubel, C. *J. Polym. Sci. A: Polym. Chem.* **1999**, *37*, 2959.
1002. Xu, J.; Zhao, J.; Fan, Z.; Feng, L. *Eur. Polym. J.* **1998**, *35*, 127.
1003. Hu, A. T.; Lee, J. H.-J.; Chen, T.-S. *J. Appl. Polym. Sci.* **1998**, *70*, 1747.
1004. Yu, G.; Chen, H.; Zhang, X.; Jiang, Z.; Huang, B. *J. Polym. Sci. A: Polym. Chem.* **1996**, *34*, 2237.
1005. Yim, J.-H.; Chu, K.-J.; Choi, K.-W.; Ihm, S.-K. *Eur. Polym. J.* **1996**, *32*, 1381.
1006. Liu, M. T.; Baker, W. E.; Schytt, V.; Jones, T.; Baird, M. C. *J. Appl. Polym. Sci.* **1996**, *62*, 1807.
1007. Flores, J. C.; Chien, J. C. W.; Rausch, M. D. *Organometallics* **1995**, *14*, 1827.
1008. Okuda, J.; Masoud, E. *Macromol. Chem. Phys.* **1998**, *199*, 543.
1009. Kim, I.; Ha, Y. S.; Zhang, D. F.; Ha, C.-S.; Lee, U. *Macromol. Rapid Commun.* **2004**, *25*, 1319.
1010. Lee, M. H.; Kim, S. K.; Do, Y. *Organometallics* **2005**, *24*, 3618.
1011. Longo, P.; Proto, A.; Zambelli, A. *Macromol. Chem. Phys.* **1995**, *196*, 3015.
1012. Zambelli, A.; Pellicchia, C.; Oliva, L.; Han, S. *J. Polym. Sci.* **1988**, *26*, 365.
1013. Longo, P.; Grassi, A.; Proto, A.; Ammendola, P. *Macromolecules* **1988**, *21*, 24.
1014. Pellicchia, C.; Proto, A.; Zambelli, A. *Macromolecules* **1992**, *25*, 4450.
1015. Pellicchia, C.; Grassi, A.; Immirzi, A. *J. Am. Chem. Soc.* **1993**, *115*, 1160.
1016. Wang, Q.; Quyoum, R.; Gillis, D. J.; Tudoret, M.-J.; Jeremic, D.; Hunter, B. K.; Baird, M. C. *Organometallics* **1996**, *15*, 693.
1017. Williams, E. F.; Murray, M. C.; Baird, M. C. *Macromolecules* **2000**, *33*, 261.
1018. Minieri, G.; Corradini, P.; Zambelli, A.; Guerra, G.; Cavallo, L. *Macromolecules* **2001**, *34*, 2459.
1019. Minieri, G.; Corradini, P.; Guerra, G.; Zambelli, A.; Cavallo, L. *Macromolecules* **2001**, *34*, 5379.
1020. Quyoum, R.; Wang, Q.; Tudoret, M.-J.; Baird, M. C. *J. Am. Chem. Soc.* **1994**, *116*, 6435.
1021. Chien, J. C. W.; Salajka, Z.; Dong, S. *Macromolecules* **1992**, *25*, 3199.
1022. Grassi, A.; Saccheo, S.; Zambelli, A.; Laschi, F. *Macromolecules* **1998**, *31*, 5588.
1023. Grassi, A.; Zambelli, A.; Laschi, F. *Organometallics* **1996**, *15*, 480.
1024. Ready, T. E.; Gurge, R.; Chien, J. C. W.; Rausch, M. D. *Organometallics* **1998**, *17*, 5236.
1025. Mahanthappa, M. K.; Waymouth, R. M. *J. Am. Chem. Soc.* **2001**, *123*, 12093.
1026. Pellicchia, C.; Pappalardo, D.; Oliva, L.; Zambelli, A. *J. Am. Chem. Soc.* **1995**, *117*, 6593.
1027. Grassi, A.; Longo, P.; Proto, A.; Zambelli, A. *Macromolecules* **1989**, *22*, 104.
1028. Soga, K.; Nakatani, H.; Monoi, T. *Macromolecules* **1990**, *23*, 953.
1029. Zambelli, A.; Pellicchia, C. *Stud. Surf. Sci. Catal.* **1994**, *89*, 209.
1030. Coates, G. W.; Waymouth, R. M. *J. Am. Chem. Soc.* **1993**, *115*, 91.
1031. Miller, S. A.; Waymouth, R. M. Stereo- and Enantioselective Polymerization of Olefins with Homogeneous Ziegler–Natta Catalysts. In *Ziegler Catalysts*; Fink, G.; Mülhaupt, R.; Brintzinger, H.-H., Eds.; Springer: Berlin, 1995; p 441.
1032. Ystenes, M. J. *Catal.* **1991**, *129*, 383.
1033. Cheng, H. N.; Khasat, N. P. *J. Appl. Polym. Sci.* **1988**, *35*, 825.
1034. Nomura, K.; Hatanaka, Y.; Okumura, H.; Fujiki, M.; Hasegawa, K. *Macromolecules* **2004**, *37*, 1693.
1035. Jeremic, D.; Wang, Q.; Quyoum, R.; Baird, M. C. *J. Organomet. Chem.* **1995**, *497*, 143.
1036. Choo, T. N.; Waymouth, R. M. *J. Am. Chem. Soc.* **2002**, *124*, 4188.
1037. Jayaratne, K. C.; Keaton, R. J.; Henningsen, D. A.; Sita, L. R. *J. Am. Chem. Soc.* **2000**, *122*, 10490.
1038. Naga, N.; Shiono, T.; Ikeda, T. *Macromol. Chem. Phys.* **1999**, *200*, 1466.

1039. Tritto, I.; Boggioni, L.; Sacchi, M. C.; Locatelli, P. *J. Mol. Catal. A: Chem.* **1998**, *133*, 139.
1040. Arndt, M.; Gosmann, M. *Polym. Bull.* **1998**, *41*, 433.
1041. Hasan, T.; Nishii, K.; Shiono, T.; Ikeda, T. *Macromolecules* **2002**, *35*, 8933.
1042. Hasan, T.; Ikeda, T.; Shiono, T. *Macromolecules* **2004**, *37*, 7432.
1043. Mülhaupt, R. *Macromol. Chem. Phys.* **2003**, *204*, 289.
- 1043a. Janiak, C.; Lassahn, P. G. *J. Mol. Catal. A: Chem.* **2001**, *166*, 193.
1044. Yanjarappa, M. J.; Sivaram, S. *Macromol. Chem. Phys.* **2004**, *205*, 2055.
1045. Porri, L.; Giarrusso, A.; Ricci, G. Metallocene Catalysts for 1,3-Diene Polymerization. In *Metallocene-based Polyolefins: Preparation, Properties and Technology*; Scheirs, J., Kaminsky, W., Eds.; Wiley: Chichester, 2000; Vol. 2, p 115.
1046. Kaminsky, W.; Scholz, V. New Half-sandwich Titanocenes for the Polymerization of Butadiene. In *Organometallic Catalysts and Olefin Polymerization. Catalysts for a New Millennium*; Blom, R., Follestad, A., Rytter, E., Tilset, M., Ystenes, M., Eds.; Springer: Berlin, 2001; p 346.
1047. Zambelli, A.; Caprio, M.; Grassi, A.; Bowen, D. E. *Macromol. Chem. Phys.* **2000**, *201*, 393.
1048. Welborn, H. C. (Exxon). World Pat. Appl. WO 88/04672A1, 1988.
1049. Welborn, H. C.; Austin, R. G. (Exxon). World Pat. Appl. WO 8804674, 1987.
1050. Galimberti, M.; Albizzati, E.; Abis, L.; Bacchilega, G. *Makromol. Chem.* **1991**, *192*, 2591.
1051. Kaminsky, W.; Hinrichs, B. *Macromol. Symp.* **2003**, *195*, 39.
1052. Ishihara, T.; Shiono, T. *Macromolecules* **2003**, *36*, 9675.
1053. Pragliola, S.; Milano, G.; Guerra, G.; Longo, P. *J. Am. Chem. Soc.* **2002**, *124*, 3502.
1054. Pragliola, S.; Costabile, C.; Magrino, M.; Napoli, M.; Longo, P. *Macromolecules* **2004**, *37*, 238.
1055. Longo, P.; Napoli, M.; Pragliola, S.; Costabile, C.; Milano, G.; Guerra, G. *Macromolecules* **2003**, *36*, 9067.
1056. Longo, P.; Pragliola, S.; Milano, G.; Guerra, G. *J. Am. Chem. Soc.* **2003**, *125*, 4799.
1057. Pragliola, S.; Costabile, C.; Di Bartolomeo, F.; Longo, P. *Macromol. Rapid Commun.* **2004**, *25*, 995.
1058. Simanke, A. G.; Mauler, R. S.; Galland, G. B. *J. Polym. Sci. A: Polym. Chem.* **2002**, *40*, 471.
1059. Choo, T. N.; Waymouth, R. M. *J. Am. Chem. Soc.* **2003**, *125*, 8970.
1060. Park, S. J.; Han, Y.; Kim, S. K.; Lee, J. Y.; Kim, H. K.; Do, Y. *J. Organomet. Chem.* **2004**, *689*, 4263.
1061. Britovsek, G. J. P.; Gibson, V. C.; Wass, D. F. *Angew. Chem., Int. Ed.* **1999**, *38*, 428.
1062. Gibson, V. C.; Spitzmesser, S. K. *Chem. Rev.* **2003**, *103*, 283.
1063. Froese, R. D. J.; Musaev, D. G.; Matsubara, T.; Morokuma, K. *J. Am. Chem. Soc.* **1997**, *119*, 7190.
1064. Froese, R. D. J.; Musaev, D. G.; Morokuma, K. *Organometallics* **1999**, *18*, 373.
1065. Sudhakar, P.; Amburose, C. V.; Sundararajan, G.; Nethaji, M. *Organometallics* **2004**, *23*, 4462.
1066. Scollard, J. D.; McConville, D. H.; Payne, N. C.; Vittal, J. J. *Macromolecules* **1996**, *29*, 5241.
1067. Scollard, J. D.; McConville, D. H.; Vittal, J. J.; Payne, N. C. *J. Mol. Catal. A: Chem.* **1998**, *128*, 201.
1068. Scollard, J. D.; McConville, D. H.; Rettig, S. J. *Organometallics* **1997**, *16*, 1810.
1069. Scollard, J. D.; McConville, D. H.; Vittal, J. J. *Organometallics* **1997**, *16*, 4415.
1070. Uozumi, T.; Tsubaki, S.; Jin, J.; Sano, T.; Soga, K. *Macromol. Chem. Phys.* **2001**, *202*, 3279.
1071. Tsubaki, S.; Jin, J.; Ahn, C.-H.; Sano, T.; Uozumi, T.; Soga, K. *Macromol. Chem. Phys.* **2001**, *202*, 482.
1072. Jin, J.; Tsubaki, S.; Uozumi, T.; Sano, T.; Soga, K. *Macromol. Rapid Commun.* **1998**, *19*, 597.
1073. Hagimoto, H.; Shiono, T.; Ikeda, T. *Macromol. Chem. Phys.* **2004**, *205*, 19.
1074. Hagimoto, H.; Shiono, T.; Ikeda, T. *Macromol. Rapid Commun.* **2002**, *23*, 73.
1075. Lee, C. H.; La, Y.-H.; Park, J.-W. *Organometallics* **2000**, *19*, 344.
1076. Lorber, C.; Donnadiou, B.; Choukroun, R. *Organometallics* **2000**, *19*, 1963.
1077. Lee, C. H.; La, Y.-H.; Park, S. J.; Park, J. W. *Organometallics* **1998**, *17*, 3648.
1078. Nomura, K.; Naga, N.; Takaoki, K. *Macromolecules* **1998**, *31*, 8009.
1079. Jeon, Y.; Heo, J.; Lee, W.; Chang, T.; Kim, K. *Organometallics* **1999**, *18*, 4107.
1080. Cloke, F. G.; Geldbach, T. J.; Hitchcock, P. B.; Love, J. B. *J. Organomet. Chem.* **1996**, *506*, 343.
1081. Patton, J. T.; Feng, S. G.; Abboud, K. A. *Organometallics* **2001**, *20*, 3399.
1082. Patton, J. T.; Bokota, M. M.; Abboud, K. A. *Organometallics* **2002**, *21*, 2145.
1083. Jeon, Y.-M.; Park, S. J.; Heo, J.; Kim, K. *Organometallics* **1998**, *17*, 3161.
1084. Shafir, A.; Arnold, J. *Organometallics* **2003**, *22*, 567.
1085. Mack, H.; Eisen, M. S. *J. Organomet. Chem.* **1996**, *525*, 81.
1086. Tsurugi, H.; Yamagata, T.; Tani, K.; Mashima, K. *Chem. Lett.* **2003**, *32*, 756.
1087. Guérin, F.; Stewart, J. C.; Beddie, C.; Stephan, D. W. *Organometallics* **2000**, *19*, 2994.
1088. Stephan, D. W.; Guérin, F.; Spence, R. E. v. H.; Koch, L.; Gao, X.; Brown, S. J.; Swabey, J. W.; Wang, Q.; Xu, W.; Zoricak, P., *et al.* *Organometallics* **1999**, *18*, 2046.
1089. Brown, S. J.; Gao, X.; Harrison, D. G.; McKay, I.; Koch, L.; Wang, Q.; Xu, W.; Von Haken Spence, R. E.; Stephan, D. W. (Nova Chemicals Corporation). World Pat. Appl. WO 00/005238, 2000.
1090. Kickham, J. E.; Guérin, F.; Stephan, D. W. *J. Am. Chem. Soc.* **2002**, *124*, 11486.
1091. Hollink, E.; Stewart, J. C.; Wei, P.; Stephan, D. W. *J. Chem. Soc., Dalton Trans.* **2003**, 3968.
1092. Saccheo, S.; Gioia, G.; Grassi, A.; Bowen, D. E.; Jordan, R. F. *J. Mol. Catal. A: Chem.* **1998**, *128*, 111.
1093. Young, D. A. *J. Mol. Catal.* **1989**, *53*, 433.
1094. Proto, A.; Capacchione, C.; Motta, O.; De Carlo, F. *Macromolecules* **2003**, *36*, 5942.
1095. Motta, O.; Capacchione, C.; Proto, A.; Acierio, D. *Polymer* **2002**, *43*, 5847.
1096. Miyatake, T.; Mizunuma, K.; Seki, Y.; Kakugo, M. *Makromol. Chem., Rapid Commun.* **1989**, *10*, 349.
1097. Mack, H.; Eisen, M. S. *J. Chem. Soc., Dalton Trans.* **1998**.
1098. Manivannan, R.; Sundararajan, G. *Macromolecules* **2002**, *35*, 7883.
1099. Natrajan, L. S.; Wilson, C.; Okuda, J.; Arnold, P. L. *Eur. J. Inorg. Chem.* **2004**, 3724.
1100. Chan, M. C. W.; Tam, K.-H.; Pui, Y.-L.; Zhu, N. *J. Chem. Soc., Dalton Trans.* **2002**, 3085.
1101. Oakes, D. C. H.; Kimberley, B. S.; Gibson, V. C.; Jones, D. J.; White, A. J. P.; Williams, D. J. *Chem. Commun.* **2004**, 2174.
1102. Rhodes, B.; Chien, J. C. W.; Wood, J. S.; Chandrasekaran, A.; Rausch, M. D. *J. Organomet. Chem.* **2001**, *625*, 95.
1103. Schrock, R. R.; Adamchuk, J.; Ruhland, K.; Lopez, L. P. *Organometallics* **2005**, *24*, 857.

1104. Tonzetich, Z. J.; Lu, C. C.; Schrock, R. R.; Hock, A. S.; Bonitatebus, P. J., Jr. *Organometallics* **2004**, *23*, 4362.
1105. Mehrkhodavandi, P.; Schrock, R. R.; Pryor, L. L. *Organometallics* **2003**, *22*, 4569.
1106. Schrock, R. R.; Adamchuk, J.; Ruhland, K.; Lopez, L. P. H. *Organometallics* **2003**, *22*, 5079.
1107. Schrock, R. R.; Bonitatebus, P. J., Jr.; Schrodi, Y. *Organometallics* **2001**, *20*, 1056.
1108. Mehrkhodavandi, P.; Schrock, R. R. *J. Am. Chem. Soc.* **2001**, *123*, 10746.
1109. Mehrkhodavandi, P.; Bonitatebus, P. J., Jr.; Schrock, R. R. *J. Am. Chem. Soc.* **2000**, *122*, 7841.
1110. Liang, L.-C.; Schrock, R. R.; Davis, W. M.; McConville, D. H. *J. Am. Chem. Soc.* **1999**, *121*, 5797.
1111. Flores, M. A.; Manzon, M. R.; Baumann, R.; Davis, W. M.; Schrock, R. R. *Organometallics* **1999**, *18*, 3220.
1112. Schrock, R. R.; Baumann, R.; Reid, S. M.; Goodman, J. T.; Stumpf, R.; Davis, W. M. *Organometallics* **1999**, *18*, 3649.
1113. Aizenberg, M.; Turculet, L.; Davis, W. M.; Schattenmann, F.; Schrock, R. R. *Organometallics* **1998**, *17*, 4795.
1114. Baumann, R.; Davis, W. M.; Schrock, R. R. *J. Am. Chem. Soc.* **1997**, *119*, 3830.
1115. Baumann, R.; Schrock, R. R. *J. Organomet. Chem.* **1998**, *557*, 69.
1116. Horton, A. D.; de With, J.; van der Linden, A. J.; van de Weg, H. *Organometallics* **1996**, *15*, 2672.
1117. Vollmerhaus, R.; Rahim, M.; Tomaszewski, R.; Xin, S.; Taylor, N. J.; Collins, S. *Organometallics* **2000**, *19*, 2161.
1118. Jin, X.; Novak, B. M. *Macromolecules* **2000**, *33*, 6205.
1119. Stevens, J. C.; Vanderlende, D. D. (Dow Chemical). World Pat. Appl. WO 03/040201, 2003.
1120. Bouwkamp, M.; Van Leusen, D.; Meetsma, A.; Hessen, B. *Organometallics* **1998**, *17*, 3645.
1121. Suzuki, Y.; Inoue, Y.; Tanaka, H.; Fujita, T. *Macromol. Rapid Commun.* **2004**, *25*, 493.
1122. Matilainen, L.; Klinga, M.; Leskela, M. *J. Chem. Soc., Dalton Trans.* **1996**, 219.
1123. Sobota, P.; Przybylak, K.; Utko, J.; Jerzykiewicz, L. B.; Pombeiro, A. J. L.; Silva, M. F. C. G. d.; Szczegot, K. *Chem. Eur. J.* **2001**, *7*, 951.
1124. Shmulinson, M.; Galan-Fereres, M.; Lisovskii, A.; Nelkenbaum, E.; Semiat, R.; Eisen, M. S. *Organometallics* **2000**, *19*, 1208.
1125. Janas, Z.; Jerzykiewicz, L. B.; Przybylak, K.; Sobota, P.; Szczegot, K. *Eur. J. Inorg. Chem.* **2004**, 1639.
1126. Fujita, T.; Tohi, Y.; Mitani, M.; Matsui, S.; Saito, J.; Nitabaru, M.; Sugi, K.; Makio, H.; Tsutsui, T. (Mitsui Chemicals). Eur Pat. Appl. EP 874005 A1, 1998.
1127. Matsui, S.; Tohi, Y.; Mitani, M.; Saito, J.; Makio, H.; Tanaka, H.; Nitabaru, M.; Nakano, T.; Fujita, T. *Chem. Lett.* **1999**, *10*, 1065.
1128. Matsui, S.; Mitani, M.; Saito, J.; Tohi, Y.; Makio, H.; Tanaka, H.; Fujita, T. *Chem. Lett.* **1999**, *12*, 1263.
1129. Matsui, S.; Mitani, M.; Saito, J.; Tohi, Y.; Makio, H.; Matsukawa, N.; Takagi, Y.; Tsuru, K.; Nitabaru, M.; Nakano, T., *et al.* *J. Am. Chem. Soc.* **2001**, *123*, 6847.
1130. Matsukawa, N.; Matsui, S.; Mitani, M.; Saito, J.; Tsuru, K.; Kashiwa, N.; Fujita, T. *J. Mol. Catal. A: Chem.* **2001**, *169*, 99–104.
1131. Mitani, M.; Yoshida, Y.; Mohri, J.; Tsuru, K.; Ishii, S.; Kojoh, S.-I.; Matsugi, T.; Saito, J.; Matsukawa, N.; Matsui, S.; *et al.* (Mitsui Chemicals). World Pat. Appl. WO 01/55231, 2001.
1132. Saito, J.; Mitani, M.; Mohri, J.-I.; Yoshida, Y.; Matsui, S.; Ishii, S.-I.; Kojoh, S.-I.; Kashiwa, N.; Fujita, T. *Angew. Chem., Int. Ed.* **2001**, *40*, 2918.
1133. Ishii, S.-i.; Saito, J.; Mitani, M.; Mohri, J.-i.; Matsukawa, N.; Tohi, Y.; Matsui, S.; Kashiwa, N.; Fujita, T. *J. Mol. Catal. A: Chem.* **2002**, *179*, 11.
1134. Mitani, M.; Mohri, J.-I.; Yoshida, Y.; Saito, J.; Ishii, S.; Tsuru, K.; Matsui, S.; Furuyama, R.; Nakano, T.; Tanaka, H., *et al.* *J. Am. Chem. Soc.* **2002**, *124*, 3327.
1135. Saito, J.; Mitani, M.; Matsui, S.; Tohi, Y.; Makio, H.; Nakano, T.; Tanaka, H.; Kashiwa, N.; Fujita, T. *Macromol. Chem. Phys.* **2002**, *203*, 59.
1136. Suzuki, Y.; Kashiwa, N.; Fujita, T. *Chem. Lett.* **2002**, *3*, 358.
1137. Bando, H.; Nakayama, Y.; Sonobe, Y.; Fujita, T. *Macromol. Rapid Commun.* **2003**, *24*, 732.
1138. Furuyama, R.; Saito, J.; Ishii, S.-i.; Mitani, M.; Matsui, S.; Tohi, Y.; Makio, H.; Matsukawa, N.; Tanaka, H.; Fujita, T. *J. Mol. Catal. A: Chem.* **2003**, *200*, 31.
1139. Ishii, S.-i.; Furuyama, R.; Matsukawa, N.; Saito, J.; Mitani, M.; Tanaka, H.; Fujita, T. *Macromol. Rapid Commun.* **2003**, *24*, 452.
1140. Mitani, M.; Nakano, T.; Fujita, T. *Chem. Eur. J.* **2003**, *9*, 2396.
1141. Mitani, M.; Mohri, J.-i.; Furuyama, R.; Ishii, S.; Fujita, T. *Chem. Lett.* **2003**, *32*, 238.
1142. Tohi, Y.; Makio, H.; Matsui, S.; Onda, M.; Fujita, T. *Macromolecules* **2003**, *36*, 523.
1143. Nakayama, Y.; Bando, H.; Sonobe, Y.; Fujita, T. *J. Mol. Catal. A: Chem.* **2004**, *213*, 141.
1144. Tohi, Y.; Nakano, T.; Makio, H.; Matsui, S.; Fujita, T.; Yamaguchi, T. *Macromol. Chem. Phys.* **2004**, *205*, 1179.
1145. Matsui, S.; Fujita, T. *Catal. Today* **2001**, *66*, 63–73.
1146. Makio, H.; Kashiwa, N.; Fujita, T. *Adv. Synth. Catal.* **2002**, *344*, 477.
1147. Matsukawa, N.; Ishii, S.-i.; Furuyama, R.; Saito, J.; Mitani, M.; Makio, H.; Tanaka, H.; Fujita, T. *e-Polymers* **2003**, Paper No. 21.
1148. Suzuki, Y.; Terao, H.; Fujita, T. *Bull. Chem. Soc. Jpn.* **2003**, *76*, 1493.
1149. Mitani, M.; Saito, J.; Ishii, S.-I.; Nakayama, Y.; Makio, H.; Matsukawa, N.; Matsui, S.; Mohri, J.; Furuyama, R.; Terao, H., *et al.* *Chem. Rec.* **2004**, *4*, 137.
1150. Deck, P. A.; Beswick, C. L.; Marks, T. J. *J. Am. Chem. Soc.* **1998**, *120*, 1772.
1151. Strauch, J.; Warren, T. H.; Erker, G.; Fröhlich, R.; Saarenketo, P. *Inorg. Chim. Acta* **2000**, *300*, 810.
1152. Ishii, S.-I.; Mitani, M.; Saito, J.; Matsui, S.; Kojoh, S.-I.; Kashiwa, N.; Fujita, T. *Chem. Lett.* **2002**, *7*, 740.
1153. Cavallo, L.; Guerra, G. *Macromolecules* **1996**, *29*, 2729.
1154. Deng, L.; Woo, T. K.; Cavallo, L.; Margl, P. M.; Ziegler, T. *J. Am. Chem. Soc.* **1997**, *119*, 6177.
1155. Talarico, G.; Busico, V.; Cavallo, L. *Organometallics* **2004**, *23*, 5989.
1156. Mülhaupt, R.; Duschek, T.; Fischer, D.; Setz, S. *Polym. Adv. Tech.* **1993**, *4*, 439.
1157. Koo, K.; Marks, T. J. *J. Am. Chem. Soc.* **1999**, *121*, 8791.
1158. Xu, G.; Chug, T. C. *J. Am. Chem. Soc.* **1999**, *121*, 6763.
1159. Matsui, S.; Mitani, M.; Saito, J.; Matsukawa, N.; Tanaka, T.; Nakano, T.; Fujita, T. *Chem. Lett.* **2000**, *29*, 554.
1160. Matsugi, T.; Matsui, S.; Kojoh, S.-I.; Takagi, Y.; Inoue, Y.; Fujita, T.; Kashiwa, N. *Chem. Lett.* **2001**, *6*, 566.
1161. Saito, J.; Mitani, M.; Matsui, S.; Kashiwa, N.; Fujita, T. *Macromol. Rapid Commun.* **2000**, *21*, 1333.
1162. Saito, J.; Onda, M.; Matsui, S.; Mitani, M.; Furuyama, R.; Tanaka, H.; Fujita, T. *Macromol. Rapid Commun.* **2002**, *23*, 1118.
1163. Prasad, A. V.; Makio, H.; Saito, J.; Onda, M.; Fujita, T. *Chem. Lett.* **2004**, *33*, 250.
1164. Kui, S. C. F.; Zhu, N.; Chan, M. C. W. *Angew. Chem., Int. Ed.* **2003**, *42*, 1628.
1165. Ittel, S. D.; Johnson, L. K.; Brookhart, M. *Chem. Rev.* **2000**, *100*, 1169.



1166. Reinartz, S.; Mason, A. F.; Lobkovsky, E. B.; Coates, G. W. *Organometallics* **2003**, *22*, 2542.
1167. Pennington, D. A.; Coles, S. J.; Hursthouse, M. B.; Bochmann, M.; Lancaster, S. J. *Chem. Commun.* **2005**, 3150.
1168. Mason, A. F.; Coates, G. W. *J. Am. Chem. Soc.* **2004**, *126*, 10798.
1169. Saito, J.; Mitani, M.; Onda, M.; Mohri, J.-I.; Ishii, S.-I.; Yoshida, Y.; Nakano, T.; Tanaka, H.; Matsugi, T.; Kojoh, S.-I., *et al.* *Macromol. Rapid Commun.* **2001**, *22*, 1072.
1170. Mitani, M.; Furuyama, R.; Mohri, J.-I.; Saito, J.; Ishii, S.; Terao, H.; Kashiwa, N.; Fujita, T. *J. Am. Chem. Soc.* **2002**, *124*, 7888.
1171. Makio, H.; Tohi, Y.; Saito, J.; Onda, M.; Fujita, T. *Macromol. Rapid Commun.* **2003**, *24*, 894.
1172. Mitani, M.; Furuyama, R.; Mohri, J.-I.; Saito, J.; Ishii, S.; Terao, H.; Nakano, T.; Tanaka, H.; Fujita, T. *J. Am. Chem. Soc.* **2003**, *125*, 4293.
1173. Saito, J.; Mitani, M.; Mohri, J.-I.; Ishii, S.-I.; Yoshida, Y.; Matsugi, T.; Kojoh, S.-I.; Kashiwa, N.; Fujita, T. *Chem. Lett.* **2001**, *6*, 576.
1174. Coates, G. W.; Tian, J. *Angew. Chem., Int. Ed.* **2000**, *39*, 3626.
1175. Tian, J.; Hustad, P. D.; Coates, G. W. *J. Am. Chem. Soc.* **2001**, *123*, 5134.
1176. Coates, G. W.; Hustad, P. D.; Reinartz, S. *Angew. Chem., Int. Ed.* **2002**, *41*, 2236.
1177. Mason, A. F.; Tian, J.; Hustad, P. D.; Lobkovsky, E. B.; Coates, G. W. *Isr. J. Chem.* **2002**, *42*, 301.
1178. Lamberti, M.; Pappalardo, D.; Mazzeo, M.; Pellicchia, C. *Macromol. Chem. Phys.* **2004**, *205*, 486.
1179. Herfert, N.; Fink, G. *Makromol. Chem.* **1992**, *193*, 773.
1180. Harrod, J. F.; Taylor, K. J. *Chem. Soc., Chem. Commun.* **1971**, 696.
1181. Bei, X.; Swenson, D. C.; Jordan, R. F. *Organometallics* **1997**, *16*, 3282.
1182. Mason, A. F.; Coates, G. W. *J. Am. Chem. Soc.* **2004**, *126*, 16326.
1183. Inoue, Y.; Nakano, T.; Tanaka, H.; Kashiwa, N.; Fujita, T. *Chem. Lett.* **2001**, *10*, 1060.
1184. Tsukahara, T.; Swenson, D. C.; Jordan, R. F. *Organometallics* **1997**, *16*, 3303.
1185. Kim, I.; Nishihara, Y.; Jordan, R. F.; Rogers, R. D.; Rheingold, A. L.; Yap, G. P. A. *Organometallics* **1997**, *16*, 3314.
1186. Li, X.-F.; Dai, K.; Ye, W.-P.; Pan, L.; Li, Y.-S. *Organometallics* **2004**, *23*, 1223.
1187. Hu, W.-Q.; Sun, X.-L.; Wang, C.; Gao, Y.; Tang, Y.; Shi, L.-P.; Xia, W.; Sun, J.; Dai, H.-L.; Li, X.-Q., *et al.* *Organometallics* **2004**, *23*, 1684.
1188. Knight, P. D.; Clarke, A. J.; Kimberley, B. S.; Jackson, R. A.; Scott, P. *Chem. Commun.* **2002**, 352.
1189. Cuomo, C.; Strianese, M.; Cuenca, T.; Sanz, M.; Grassi, A. *Macromolecules* **2004**, *37*, 7469.
1190. O'Connor, P. E.; Morrison, D. J.; Steeves, S.; Burrage, K.; Berg, D. J. *Organometallics* **2001**, *20*, 1153.
1191. Tshuva, E. Y.; Versano, M.; Goldberg, I.; Kol, M.; Weitman, H.; Goldschmidt, Z. *Inorg. Chem. Commun.* **1999**, *2*, 371.
1192. Ziniuk, Z.; Goldberg, I.; Kol, M. *Inorg. Chem. Commun.* **1999**, *2*, 549.
1193. Tshuva, E. Y.; Goldberg, I.; Kol, M. *J. Am. Chem. Soc.* **2000**, *122*, 10706.
1194. Tshuva, E. Y.; Goldberg, I.; Kol, M.; Weitman, H.; Goldschmidt, Z. *Chem. Commun.* **2000**, 379.
1195. Tshuva, E. Y.; Goldberg, I.; Kol, M.; Goldschmidt, Z. *Inorg. Chem. Commun.* **2000**, *3*, 611.
1196. Tshuva, E. Y.; Goldberg, I.; Kol, M.; Goldschmidt, Z. *Organometallics* **2001**, *20*, 3017.
1197. Tshuva, E. Y.; Goldberg, I.; Kol, M.; Goldschmidt, Z. *Chem. Commun.* **2001**, 2120.
1198. Tshuva, E. Y.; Goldberg, I.; Kol, M.; Goldschmidt, Z. *Inorg. Chem.* **2001**, *40*, 4263.
1199. Tshuva, E. Y.; Groysman, S.; Goldberg, I.; Kol, M.; Goldschmidt, Z. *Organometallics* **2002**, *21*, 662.
1200. Groysman, S.; Goldberg, I.; Kol, M.; Genizi, E.; Goldschmidt, Z. *Organometallics* **2003**, *22*, 3013.
1201. Groysman, S.; Goldberg, I.; Kol, M.; Genizi, E.; Goldschmidt, Z. *Inorg. Chim. Acta* **2003**, *345*, 137.
1202. Groysman, S.; Tshuva, E. Y.; Goldberg, I.; Kol, M.; Goldschmidt, Z.; Shuster, M. *Organometallics* **2004**, *23*, 5291.
1203. Yeori, A.; Gendler, S.; Groysman, S.; Goldberg, I.; Kol, M. *Inorg. Chem. Commun.* **2004**, *7*, 280.
1204. Segal, S.; Goldberg, I.; Kol, M. *Organometallics* **2005**, *24*, 200.
1205. Jeske, G.; Lauke, H.; Mauermann, H.; Schumann, H.; Marks, T. J. *J. Am. Chem. Soc.* **1985**, *107*, 8111.
1206. Busico, V.; Cipullo, R.; Friederichs, N.; Ronca, S.; Talarico, G.; Togrou, M.; Wang, B. *Macromolecules* **2004**, *37*, 8201.
1207. Matsuo, Y.; Mashima, K.; Tani, K. *Chem. Lett.* **2000**, *29*, 1114.
1208. Yoshida, Y.; Matsui, S.; Takagi, Y.; Mitani, M.; Nitabaru, M.; Nakano, T.; Tanaka, H.; Fujita, T. *Chem. Lett.* **2000**, *29*, 1270.
1209. Yoshida, Y.; Saito, J.; Mitani, M.; Takagi, Y.; Matsui, S.; Ishii, S.-I.; Nakano, T.; Kashiwa, N.; Fujita, T. *Chem. Commun.* **2002**, 1298.
1210. Yoshida, Y.; Matsui, S.; Takagi, Y.; Mitani, M.; Nakano, T.; Tanaka, H.; Kashiwa, N.; Fujita, T. *Organometallics* **2001**, *20*, 4793.
1211. Matsui, S.; Spaniol, T. P.; Takagi, Y.; Yoshida, Y.; Okuda, J. *J. Chem. Soc., Dalton Trans.* **2002**, 4529.
1212. Matsui, S.; Yoshida, Y.; Takagi, Y.; Spaniol, T. P.; Okuda, J. *J. Organomet. Chem.* **2004**, *689*, 1155.
1213. Yoshida, Y.; Nakano, T.; Tanaka, H.; Fujita, T. *Isr. J. Chem.* **2002**, *42*, 353.
1214. Dawson, D. M.; Walker, D. A.; Thornton-Pett, M.; Bochmann, M. *J. Chem. Soc., Dalton Trans.* **2000**, 459.
1215. Matsugi, T.; Matsui, S.; Kojoh, S.-I.; Takagi, Y.; Inoue, Y.; Nakano, T.; Fujita, T.; Kashiwa, N. *Macromolecules* **2002**, *35*, 4880.
1216. Richter, J.; Edelmann, F. T.; Noltemeyer, M.; Schmidt, H.-G.; Shmulinson, M.; Eisen, M. S. *J. Mol. Catal. A: Chem.* **1998**, *130*, 149.
1217. Martin, A.; Uhrhammer, R.; Gardner, T. G.; Jordan, R. F.; Rogers, R. D. *Organometallics* **1998**, *17*, 382.
1218. Carpentier, J.-F.; Martin, A.; Swenson, D. C.; Jordan, R. F. *Organometallics* **2003**, *22*, 4999.
1219. Nakazawa, H.; Ikai, S.; Imaoka, K.; Kai, Y.; Yano, T. *J. Mol. Catal. A: Chem.* **1998**, *132*, 33.
1220. Murtuza, S.; Osvaldo, L.; Casagrande, J.; Jordan, R. F. *Organometallics* **2002**, *21*, 1882.
1221. Gil, M. P.; Santos, J. H. Z. d.; Osvaldo, L.; Casagrande, J. *J. Mol. Catal. A: Chem.* **2004**, *209*, 163.
1222. Fuhrmann, H.; Brenner, S.; Arndt, P.; Kempe, R. *Inorg. Chem.* **1996**, *35*, 6742.
1223. Adams, N.; Arts, H. J.; Bolton, P. D.; Cowell, D.; Dubberley, S. R.; Friederichs, N.; Grant, C. M.; Kranenburg, M.; Sealey, A. J.; Wang, B., *et al.* *Chem. Commun.* **2004**, 434.
1224. Kühl, O.; Koch, T.; Somoza, F. B., Jr.; Junk, P. C.; Hey-Hawkins, E.; Plat, D.; Eisen, M. S. *J. Organomet. Chem.* **2000**, *604*, 116.
1225. Benetollo, F.; Carta, G.; Cavinato, G.; Crociani, L.; Paolucci, G.; Rossetto, G.; Veronese, F.; Zanella, P. *Organometallics* **2003**, *22*, 3985.
1226. Baker, R. J.; Edwards, P. G. J. *J. Chem. Soc., Dalton Trans.* **2002**, 2960.
1227. Kojoh, S.-I.; Matsugi, T.; Saito, J.; Mitani, M.; Fujita, T.; Kashiwa, N. *Chem. Lett.* **2001**, *8*, 822.
1228. Ishii, S.; Saito, J.; Matsuura, S.; Suzuki, Y.; Furuyama, R.; Mitani, M.; Nakano, T.; Kashiwa, N.; Fujita, T. *Macromol. Rapid Commun.* **2002**, *23*, 693–697.
1229. Hustad, P. D.; Coates, G. W. *J. Am. Chem. Soc.* **2002**, *124*, 11578.
1230. Yoshida, Y.; Mohri, J.-I.; Ishii, S.-I.; Mitani, M.; Saito, J.; Matsui, S.; Makio, H.; Nakano, T.; Tanaka, H.; Onda, M., *et al.* *J. Am. Chem. Soc.* **2004**, *126*, 12023.
1231. Furuyama, R.; Mitani, M.; Mohri, J.; Mori, R.; Tanaka, H.; Fujita, T. *Macromolecules* **2005**, *38*, 1546.

1232. Bates, F. S. *Science* **1991**, *251*, 898.
1233. Holden, G. In *Encyclopedia of Polymer Science and Engineering*; Kroschwitz, J. I., Salvatore, A., Klingsberg, A., Muldoon, J., Eds.; Wiley: New York, 1986; Vol. 5, p 416.
1234. Ruokolainen, J.; Mezzenga, R.; Fredrickson, G. H.; Kramer, E. J.; Hustad, P. D.; Coates, G. W. *Macromolecules* **2005**, *38*, 851.
1235. Brown, S. J.; Gao, X.; Harrison, D. G.; McKay, I.; Koch, L.; Wang, Q.; Xu, W.; Von Haken Spence, R. E.; Stephan, D. W. (Nova Chemicals Corporation). U.S. Patent 2001007895, 2001.
1236. Ahn, C.-H.; Tahara, M.; Uozumi, T.; Jin, J.; Tsubaki, S.; Soga, K. *Macromol. Rapid Commun.* **2000**, *21*, 385.
1237. Auriemma, F.; Rosa, C. D.; Esposito, S.; Coates, G. W.; Fujita, M. *J. Am. Chem. Soc.* **2005**, *127*, 2850.
1238. Grassi, A.; Maffei, G.; Milione, S.; Jordan, R. F. *Macromol. Chem. Phys.* **2001**, *202*, 1239.
1239. Natta, G.; Pino, P.; Corradini, P.; Danusso, F.; Mantica, E.; Mazzanti, G.; Moraglio, G. *J. Am. Chem. Soc.* **1955**, *77*, 1708.
1240. Capacchione, C.; Proto, A.; Ebeling, H.; Mühlaupt, R.; Möller, K.; Spaniol, T. P.; Okuda, J. *J. Am. Chem. Soc.* **2003**, *125*, 4964.
1241. Beckerle, K.; Capacchione, C.; Ebeling, H.; Manivannan, R.; Mühlaupt, R.; Proto, A.; Spaniol, T. P.; Okuda, J. *J. Organomet. Chem.* **2004**, *689*, 4636.
1242. Capacchione, C.; Proto, A.; Ebeling, H.; Mühlaupt, R.; Moller, K.; Manivannan, R.; Spaniol, T. P.; Okuda, J. *J. Mol. Catal. A: Chem.* **2004**, *213*, 137.
1243. Capacchione, C.; Manivannan, R.; Barone, M.; Beckerle, K.; Centore, R.; Oliva, L.; Proto, A.; Tuzi, A.; Spaniol, T. P.; Okuda, J. *Organometallics* **2005**, *24*, 2971.
1244. Capacchione, C.; De Carlo, F.; Zannoni, C.; Okuda, J.; Proto, A. *Macromolecules* **2004**, *37*, 8918.
1245. Kakugo, M.; Miyatake, T.; Mizunuma, K. *Stud. Surf. Sci. Catal.* **1990**, *56*, 517.
1246. Fokken, S.; Spaniol, T. P.; Okuda, J.; Sernetz, F. G.; Mühlaupt, R. *Organometallics* **1997**, *16*, 4240.